Mon. May 27, 2019

[J] Oral | U (Union)：Union

9:30 AM - 10:30 AM JST | 12:30 AM - 1:30 AM UTC | 101 1F

[U-05] Large-scale Research Projects: Master Plan 2020 and its beyond

convener:Eiichi Tajika(Department of Earth and Planetary Science, Graduate School of Science, The University of Tokyo), Shigeko Haruyama(Department of Environmental Science, Graduate School of Bioresouces,Mie University), Ryoichi Fujii(Research Organization of Information and Systems), Hodaka Kawahata(Atmosphere Ocean Research Institute, the University of Tokyo), Chairperson:Eiichi Tajika, Shigeko Haruyama

9:45 AM - 10:08 AM JST | 12:45 AM - 1:08 AM UTC

[U05-01] International Astro-Bioscience Research Center

★Invited Papers

*Yukio Isozaki[1] (1.Department of Earth Science and Astronomy, Multi-disciplinary Sciences - General Systems Studies, Graduate School of Arts and Sciences, The University of Tokyo)

10:08 AM - 10:30 AM JST | 1:08 AM - 1:30 AM UTC

[U05-02] Study of coupling processes in the solar-terrestrial system

★Invited Papers

*Mamoru Yamamoto[1], Hiroyuki Hashiguchi[1], Tatsuhiro Yokoyama[1], Hiroshi Miyaoka[2], Yasunobu Ogawa[2], Kazuo Shiokawa[3], Satonori Nozawa[3], Akimasa Yoshikawa[4], Toshitaka Tsuda[5,1] (1.Research Institute for Sustainable Humanosphere, Kyoto University, 2.National Institute of Polar Research, 3.Institute for Space-Earth Environmental Laboratory, Nagoya University, 4.International Center for Space Weather Science and Education, Kyushu University, 5.Research Organization of Information and Systems)

[J] Oral | U (Union)：Union

10:45 AM - 12:15 PM JST | 1:45 AM - 3:15 AM UTC | 101 1F

[U-05] Large-scale Research Projects: Master Plan 2020 and its beyond

convener:Eiichi Tajika(Department of Earth and Planetary Science, Graduate School of Science, The University of Tokyo), Shigeko Haruyama(Department of Environmental Science, Graduate School of Bioresouces,Mie University), Ryoichi Fujii(Research Organization of Information and Systems), Hodaka Kawahata(Atmosphere Ocean Research Institute, the University of Tokyo), Chairperson:Shigeko Haruyama, Hodaka Kawahata

10:45 AM - 11:08 AM JST | 1:45 AM - 2:08 AM UTC

[U05-03] Development of the global earth observation system using satellites

★Invited Papers

*Shinichi Sobue[1], Yoshiaki HONDA[3], Shuichi Rokugawa[2], Akira Iwasaki[2], Nobuhiro Takahashi[4], Yukari Takayabu[2], Riko Oki[1], Toshiyoshi Kimura[1], Teruyuki Nakajima[1], Takeo Tadono[1], Kosuke Yamamoto[1] (1.Japan Aerospace Exploration Agency, 2.University of Tokyo, 3.Chiba University, 4.Nagoya University)

11:08 AM - 11:31 AM JST | 2:08 AM - 2:31 AM UTC

[U05-04] Promotion of Scientific Research on Climate and Earth System Sciences Using Aircrafts

★Invited Papers

*Makoto Koike[1,2] (1.Department of Earth and Planetary Science, Graduate School of Science, The University of Tokyo, 2.The Meteorological Society of Japan)

11:31 AM - 11:54 AM JST | 2:31 AM - 2:54 AM UTC

[U05-05] Global deployment of Deep Argo floats toward accurate prediction of future climate and ecosystem changes

★Invited Papers

*Toshiyuki Hibiya[1] (1. Department of Earth and Planetary Science, Graduate School of Science, The University of Tokyo)

11:54 AM - 12:15 PM JST | 2:54 AM - 3:15 AM UTC

[U05-06] A new aspect of the polar science: integrated observations of the ice sheet mass loss for better prediction of the sea level rise

★Invited Papers

*Takuji Nakamura[1], Shin Sugiyama[2], Ayako Abe-Ouchi[3], Teruo Aoki[4], Yoshifumi Nogi[1], Takeshi Tamura[1] (1.National Institute of Polar Research, 2.Institute of Low Temperature Science, Hokkaido Univ., 3.Atmosphere and Ocean Research Institute, the University of Tokyo, 4.The Graduate School of Natural Science and Technology, Okayama University)

[J] Oral | U (Union)：Union

1:45 PM - 3:15 PM JST | 4:45 AM - 6:15 AM UTC | 101 1F

[U-05] Large-scale Research Projects: Master Plan 2020 and its beyond

convener:Eiichi Tajika(Department of Earth and Planetary Science, Graduate School of Science, The University of Tokyo), Shigeko Haruyama(Department of Environmental Science, Graduate School of Bioresouces,Mie University), Ryoichi Fujii(Research Organization of Information and Systems), Hodaka Kawahata(Atmosphere Ocean Research Institute, the University of Tokyo), Chairperson:Hodaka Kawahata, Eiichi Tajika

1:45 PM - 2:08 PM JST | 4:45 AM - 5:08 AM UTC

[U05-07] New frontier of Earth, Space and Life Sciences pioneered by the innovative developments of new-generation mass spectrometry

★Invited Papers

*Kentaro Terada[1] (1.Department of Earth and Space Science, Graduate School of Science, Osaka University)

2:08 PM - 2:31 PM JST | 5:08 AM - 5:31 AM UTC

[U05-08] Building of archive and curating system for astrogeoscience materials

★Invited Papers

*Tsuyoshi Komiya[1] (1.Department of Earth Science & Astronomy Graduate School of Arts and Sciences The University of Tokyo)

2:31 PM - 2:54 PM JST | 5:31 AM - 5:54 AM UTC

[U05-09] Innovative 4D imaging of subduction-zones through real-time observatories, ultra-deep drilling and high-pressure experiments

★Invited Papers

*Masataka Kinoshita[1], Naoshi Hirata[1], Masanao Shinohara[1], Tetsuo Irifune[2], Hiroyuki Kagi[7], Teruyuki Kato[3], Shigeaki Ono[4], Katsuyoshi Michibayashi[6], Natsue Abe[4], Fumio Inagaki[4], Kentaro Omura[5], Kazushige Obara[1] (1.Earthquake Research Institute, University of Tokyo, 2.Ehime University, 3.Hot Springs Research Institute, 4.JAMSTEC, 5.NIED, 6.Nagoya Univ., 7.Geochemical Research Center, Univ. Tokyo)

2:54 PM - 3:15 PM JST | 5:54 AM - 6:15 AM UTC

[U05-10] Construction of the Cooperative Research Infrastructure for Intelligent Muography in Earth and Planetary Sciences, Other Sciences, and Society

★Invited Papers

*Hiroyuki Tanaka[1] (1.Earthquake Research Institute, the University of Tokyo)

[J] Oral | U (Union)：Union

3:30 PM - 5:00 PM JST | 6:30 AM - 8:00 AM UTC | 101 1F

[U-05] Large-scale Research Projects: Master Plan 2020 and its beyond

convener:Eiichi Tajika(Department of Earth and Planetary Science, Graduate School of Science, The University of Tokyo), Shigeko Haruyama(Department of Environmental Science, Graduate School of Bioresouces,Mie University), Ryoichi Fujii(Research Organization of Information and Systems), Hodaka Kawahata(Atmosphere Ocean Research Institute, the University of Tokyo), Chairperson:Eiichi Tajika, Shigeko Haruyama

3:30 PM - 3:53 PM JST | 6:30 AM - 6:53 AM UTC

[U05-11] Consortium for Planetary Exploration

★Invited Papers

*Yoshi-Yuki Hayashi[1], Shigeto Watanabe[2,5], Taishi Nakamoto[3,4] (1.Department of Planetology/CPS, Graduate School of Science, Kobe University, 2.SGEPSS, 3.The Japanese Society for Planetary Sciences, 4.Dept. of Earth and Planetary Sciences, Tokyo Institute of Technology, 5.Hokkaido Information University)

3:53 PM - 4:16 PM JST | 6:53 AM - 7:16 AM UTC

[U05-12] Japanese contribution to CAESAR: comet astrobiology exploration sample return

★Invited Papers

*Tomoki Nakamura[1], Kazuhiko Yamada[2], Yoshihiro Furukawa[1], Yuki Kimura[3], Aki Takigawa[4], Tomohiro Usui[2], Hitoshi Kuninaka[2], Team CAESAR SRC team (1.Tohoku University, 2.ISAS/JAXA, 3.Hokkaido University, 4.Kyoto University)

4:16 PM - 4:38 PM JST | 7:16 AM - 7:38 AM UTC

[U05-13] Strategic Mars exploration: Orbiter and EDL demonstration mission for space weather, climate, and aquatic environment

★Invited Papers

*Kanako Seki[1], Shigeto Watanabe[2], Taishi Nakamoto[3], Naoki Terada[4], Atsushi Yamazaki[5], Ayako Matsuoka[5], Tomohiro Usui[5], Yasuhito Sekine[3], Kazuhisa Fujita[5], Shoichiro Yokota[6], Satoshi Kasahara[1], Yoshifumi Saito[5], Hiromu Nakagawa[4], Atsushi Kumamoto[4], Hiroyuki Maezawa[7], Mars Orbiter and EDL Technology Demonstration Mission Planning Team (1.Graduate School of Science, University of Tokyo, 2.Department of Cosmosciences, Hokkaido University, 3.Tokyo Institute of Technology, 4.Graduate School of Science, Tohoku University, 5.ISAS, JAXA, 6.Graduate School of Science, Osaka University, 7.Department of Physical Science, Osaka Prefecture University)

[J] Poster | U (Union)：Union

5:15 PM - 6:30 PM JST | 8:15 AM - 9:30 AM UTC | Poster Hall International Exhibition Hall8, Makuhari Messe_1

[U-05] Large-scale Research Projects: Master Plan 2020 and its beyond

convener:Eiichi Tajika(Department of Earth and Planetary Science, Graduate School of Science, The University of Tokyo), Shigeko Haruyama(Department of Environmental Science, Graduate School of Bioresouces,Mie University), Ryoichi Fujii(Research Organization of Information and Systems), Hodaka Kawahata(Atmosphere Ocean Research Institute, the University of Tokyo)

[U05-P01] Planetary Exploration Roadmap from Japanese Society for Planetary Sciences

Kiyoshi Kuramoto[1], Hidenori Genda[2], *Naoki Terada[3], Hiroki Senshu[4], Taishi Nakamoto[5], Planetary Exploration Committee JSPS, Working term for revision of reply document for RFI JSPS (1.Graduate School of Sciences, Hokkaido University, 2.Earth-Life Science Institute, Tokyo Institute of Technology, 3.Graduate School of Science, Tohoku University, 4.Planetary Exploration Research Center, Chiba Institute of Technology, 5.Tokyo Institute of Technology)

[E] Oral | P (Space and Planetary Sciences)：P-PS Planetary Sciences

3:30 PM - 5:00 PM JST | 6:30 AM - 8:00 AM UTC | A03 TOKYO BAY MAKUHARI HALL

[P-PS01] Outer Solar System Exploration Today, and Tomorrow

convener:Jun Kimura(Osaka University), Yasumasa Kasaba(Planetary Plasma and Atmospheric Research Center, Tohoku University), Kunio M. Sayanagi(Hampton University), Chairperson:笠羽 康正, Kazuo Yoshioka(The University of Tokyo)

3:30 PM - 3:45 PM JST | 6:30 AM - 6:45 AM UTC

[PPS01-01] Circulation of plasma in the Jupiter's inner magnetosphere revealed from time variation in radial profile of plasma temperature and density obtained by Hisaki/EXCEED observation

*Reina Hikida[1], Kazuo Yoshioka[2], Fuminori Tsuchiya[3], Masato Kagitani[3], Go Murakami[4], Tomoki Kimura[5], Atsushi Yamazaki[4], Ichiro Yoshikawa[2] (1.Department of Earth and Planetary Science, Graduate School of Science, the University of Tokyo, 2.Department of Complexity Science and Engineering, Graduate School of Frontier Science, the University of Tokyo, 3.Planetary Plasma and Atmospheric Research Center, Graduate School of Science, Tohoku University, 4.Institute of Space and Astronautical Science (ISAS), Japan Aerospace Exploration Agency (JAXA) , 5.Frontier Research Institute for Interdisciplinary Sciences, Tohoku University)

3:45 PM - 4:00 PM JST | 6:45 AM - 7:00 AM UTC

[PPS01-02] Volcanic change of the distribution of Io’s neutral oxygen cloud observed by Hisaki

*Ryoichi Koga[1], Fuminori Tsuchiya[1], Masato Kagitani[1], Takeshi Sakanoi[1], Tomoki Kimura[1], Ichiro Yoshikawa[2], Kazuo Yoshioka[2], Go Murakami[3], Atsushi Yamazaki[3], Howard Todd Smith[4], Fran Bagenal[5] (1.Tohoku University, 2.The University of Tokyo, 3.ISAS/JAXA, 4.Johns Hopkins University, 5.University of Colorado)

4:00 PM - 4:18 PM JST | 7:00 AM - 7:18 AM UTC

[PPS01-03] New pictures of Jovian magnetosphere obtained from the Hisaki satellite observation

★Invited Papers

*Fuminori Tsuchiya[1], Kazuo Yoshioka[2], Tomoki Kimura[1], Chihiro Tao[3], Ichiro Yoshikawa[2], Go Murakami[4], Hajime Kita[4], Ryoichi Koga[1], Hikida Reina[2], Fumiharu Suzuki[2], Sooman Han[2], Masato Kagitani[1], Takeshi Sakanoi[1], Hiroaki Misawa[1], Yasumasa Kasaba[1], Atsushi Yamazaki[4] (1.Tohoku University, 2.The University of Tokyo, 3.NICT, 4.ISAS/JAXA)

4:18 PM - 4:33 PM JST | 7:18 AM - 7:33 AM UTC

[PPS01-04] Axisymmetric conductivities of Jupiter's middle- and low-latitude ionosphere

*Yuki Nakamura[1], Koichiro Terada, Chihiro Tao[2], Naoki Terada[1], Yasumasa Kasaba[3], Hajime Kita[4], Aoi Nakamizo[2], Akimasa Yoshikawa[5], Shinichi Ohtani[6], Fuminori Tsuchiya[3], Masato Kagitani[3], Takeshi Sakanoi[3], Go Murakami[4], Kazuo Yoshioka[7], Tomoki Kimura[1], Atsushi Yamazaki[4], Ichiro Yoshikawa[8] (1.Department of Geophysics, Graduate School of Science, Tohoku University, 2.National Institute of Information and Communications Technology, 3.Planetary Plasma and Atmospheric Research Center, Tohoku University, 4.Institute of Space and Astronautical Science, Japan Aerospace Exploration Agency, 5.Department of Earth and Planetary Sciences, Kyushu University, 6.The Johns Hopkins University Applied Physics Laboratory, 7.Graduate School of frontier Science, The University of Tokyo, 8.The University of Tokyo)

4:33 PM - 4:51 PM JST | 7:33 AM - 7:51 AM UTC

[PPS01-05] The magnetospheres of Saturn and Jupiter as viewed by Cassini and Juno

★Invited Papers

*G Provan[1], Stanley W. H. Cowley[1], Emma Jane Bunce[1] (1.University of Leicester)

[E] Oral | P (Space and Planetary Sciences)：P-PS Planetary Sciences

9:00 AM - 10:30 AM JST | 12:00 AM - 1:30 AM UTC | A03 TOKYO BAY MAKUHARI HALL

[P-PS05] Recent advances of Venus science

convener:Takehiko Satoh(Institute of Space and Astronautical Science, Japan Aerospace Exploration Agency), Takeshi Horinouchi(Faculty of Environmental Earth Science, Hokkaido University), Masaru Yamamoto(Research Institute for Applied Mechanics, Kyushu University), Kevin McGouldrick(University of Colorado Boulder), Chairperson:Takeshi Horinouchi

9:00 AM - 9:15 AM JST | 12:00 AM - 12:15 AM UTC

[PPS05-01] **Super-rotation of Venusian atmosphere in the equatorial region may be caused by the density driven separation**

*Adhithiyan Neduncheran[1], Ugur Guven[1,2], Ananyo Bhattacharya[3] (1.University of Petroleum and Energy Studies, India, 2.United Nations Centre for Space Science and Technology Education in Asia and the Pacific, 3.Sardar Vallabhbhai National Institute of Technology,India)

9:15 AM - 9:30 AM JST | 12:15 AM - 12:30 AM UTC

[PPS05-02] Comparison of horizontal distributions of temperature and UV absorbers at the Venus cloud-tops

*Shinichiro Kawase[1], Makoto Taguchi[1], Tetsuya Fukuhara[1], Yeon Joo Lee[2], Atsushi Yamazaki[3,4] (1.Rikkyo University, 2.Max Planck Institute for Solar System Research, 3.Institute of Space and Astronautical Science, 4.Japan Aerospace Exploration Agency)

9:30 AM - 9:45 AM JST | 12:30 AM - 12:45 AM UTC

[PPS05-03] Orographic Gravity Waves in the Venus Atmospheric

*Anna Suzuki[1], Masahiro Takagi[1], Yasumitsu Maejima[2], Hiroki Ando[1], Norihiko Sugimoto[3], Yoshihisa Matsuda[4] (1.Kyoto Sangyo University, 2.RIKEN Advanced Institute for Computational Science, 3.Keio University, 4.Tokyo Gakugei University)

9:45 AM - 10:00 AM JST | 12:45 AM - 1:00 AM UTC

[PPS05-04] Atmospheric structures simulated by T21 and T63 Venus GCMs with radiative transfer

*Masaru Yamamoto[1], Kohei Ikeda[2], Masaaki Takahashi[2] (1.Research Institute for Applied Mechanics, Kyushu University, 2.National Institute for Environmental Studies)

10:00 AM - 10:15 AM JST | 1:00 AM - 1:15 AM UTC

[PPS05-05] Thermal-tides structure at the cloud level of Venus derived from Akatsuki/LIR observations

★Invited Papers

*Toru Kouyama[1], Makoto Taguchi[2], Tetsuya Fukuhara[2], Takeshi Imamura[3], Masahiko Futaguchi[4], Takeru Yamada[2], Masahiro Akiba[2], Yeon Joo lee, Takao M. Sato[7], Shin-ya Murakami[5], George HASHIMOTO[6], Takehiko Satoh[5], Masato Nakamura[5] (1.AIST, 2.Rikkyo Univ., 3.Tokyo Univ., 4.Toho Univ., 5.JAXA, 6.Okayama Univ., 7.Hokkaido Information Univ.)

10:15 AM - 10:30 AM JST | 1:15 AM - 1:30 AM UTC

[PPS05-06] From Venus to Mars: viewpoint of comparative meteorology

★Invited Papers

*Takeshi Imamura[1], Kazunori Ogohara[2], Hiromu Nakagawa[3], Shohei Aoki[3] (1.The University of Tokyo, 2.University of Shiga Prefecture, 3.Tohoku University)

[E] Oral | P (Space and Planetary Sciences)：P-PS Planetary Sciences

10:45 AM - 12:15 PM JST | 1:45 AM - 3:15 AM UTC | A03 TOKYO BAY MAKUHARI HALL

[P-PS05] Recent advances of Venus science

convener:Takehiko Satoh(Institute of Space and Astronautical Science, Japan Aerospace Exploration Agency), Takeshi Horinouchi(Faculty of Environmental Earth Science, Hokkaido University), Masaru Yamamoto(Research Institute for Applied Mechanics, Kyushu University), Kevin McGouldrick(University of Colorado Boulder), Chairperson:Takehiko Satoh

10:45 AM - 11:05 AM JST | 1:45 AM - 2:05 AM UTC

[PPS05-07] A two-stage evolution model of Venus's mantle and its implication for the Earth

★Invited Papers

*Masaki Ogawa[1] (1.Division of General Systems Studies, Graduate School of Arts and Sciences, University of Tokyo)

11:05 AM - 11:20 AM JST | 2:05 AM - 2:20 AM UTC

[PPS05-08] Interaction between the thermosphere and the cloud-level atmosphere of Venus studied with simultaneous observations by Hisaki and Akatsuki

*Yusuke Nara[1], Takeshi Imamura[1], Ichiro Yoshikawa[1], Kazuo Yoshioka[1], Kei Masunaga[2], Atsushi Yamazaki[3], Shigeto Watanabe[4], Manabu Yamada[5], Yeon Joo Lee[1], Naoki Terada[6], Kanako Seki[1] (1.The University of Tokyo, 2.Swedish Institute of Space Physics, 3.ISAS/JAXA, 4.Hokkaido Information University, 5.Chiba Institute of Technology, 6.Tohoku University)

11:20 AM - 11:35 AM JST | 2:20 AM - 2:35 AM UTC

[PPS05-09] Mesoscale Dyanmics in the Venus Atmosphere

*Kevin McGouldrick[1], Javier Peralta[2], Takehiko Satoh[2] (1.University of Colorado Boulder, 2.Institute of Space and Astronautical Science, Japan Aerospace Exploration Agency)

11:35 AM - 11:50 AM JST | 2:35 AM - 2:50 AM UTC

[PPS05-10] Periodicity analysis of Venus' cloud-top temperature measured by Akatsuki LIR

Naoya Kajiwara[1], *Takeshi Imamura[1], Makoto Taguchi[2], Tetsuya Fukuhara[2], Toru Kouyama[3] (1.Graduate School of Frontier Sciences, The University of Tokyo, 2.College of Science, Rikkyo University, 3.National Institute of Advanced Industrial Science and Technology)

11:50 AM - 12:10 PM JST | 2:50 AM - 3:10 AM UTC

[PPS05-11] Modeling Venus-like Worlds Through Time: The habitable zone, and the evolution of Venus' atmosphere.

★Invited Papers

*Michael Way[1,2,3], Anthony Del Genio[1] (1.NASA Goddard Institute for Space Studies, 2.GSFC Sellers Exoplanet Environments Collaboration, 3.Department of Physics and Astronomy, Uppsala University, Sweden)

[E] Oral | P (Space and Planetary Sciences)：P-PS Planetary Sciences

1:45 PM - 3:15 PM JST | 4:45 AM - 6:15 AM UTC | A03 TOKYO BAY MAKUHARI HALL

[P-PS05] Recent advances of Venus science

convener:Takehiko Satoh(Institute of Space and Astronautical Science, Japan Aerospace Exploration Agency), Takeshi Horinouchi(Faculty of Environmental Earth Science, Hokkaido University), Masaru Yamamoto(Research Institute for Applied Mechanics, Kyushu University), Kevin McGouldrick(University of Colorado Boulder), Chairperson:Kevin McGouldrick

1:45 PM - 2:00 PM JST | 4:45 AM - 5:00 AM UTC

[PPS05-12] Cloud top structure of Venus retrieved from the Akatsuki IR2 dayside observations

★Invited Papers

*Takao M. Sato[1], Takehiko Satoh[2], Hideo Sagawa[3], Naohiro Manago[2], Yeon Joo Lee, Shin-ya Murakami[2], Kazunori Ogohara[4], George HASHIMOTO[5], Yasumasa Kasaba[6], Atsushi Yamazaki[2], Manabu Yamada[7], Shigeto Watanabe[1], Takeshi Imamura[8], Masato Nakamura[2] (1.Hokkaido Information University, 2.ISAS/JAXA, 3.Kyoto Sangyo University, 4.University of Shiga Prefecture, 5.Okayama University, 6.Tohoku University, 7.Chiba Institute of Technology, 8.The University of Tokyo)

2:00 PM - 2:15 PM JST | 5:00 AM - 5:15 AM UTC

[PPS05-13] Formation of superrotation studied by a TEM model

*Takeshi Horinouchi[1] (1.Faculty of Environmental Earth Science, Hokkaido University)

2:15 PM - 2:30 PM JST | 5:15 AM - 5:30 AM UTC

[PPS05-14] Morphological Feature Extraction from Venus' Cloud Images Using Principal Component Analysis

*Minori Narita[1], Takeshi Imamura[1], Yusuke Nara[1], Yeon Joo Lee, Shigeto Watanabe[2], Atsushi Yamazaki[3], Takehiko Satoh[3], Makoto Taguchi[4], Tetsuya Fukuhara[4], Manabu Yamada[5] (1.The University of Tokyo, 2.Hokkaido Information University, 3.ISAS/JAXA, 4.Rikkyo University, 5.PERC/Chiba Institute of Technology)

2:30 PM - 2:45 PM JST | 5:30 AM - 5:45 AM UTC

[PPS05-15] **Principal Components of UV Albedo Variability in Venus' Atmosphere as seen at 283 nm**

*Pushkar Kopparla[1], Yeon Joo Lee[1], Takeshi Imamura[1], Atsushi Yamazaki[2] (1.GSFS, University of Tokyo, 2.ISAS, JAXA)

2:45 PM - 3:00 PM JST | 5:45 AM - 6:00 AM UTC

[PPS05-16] Active and inactive behaviors of the planetary-scale waves on Venus cloud top

★Invited Papers

*Masataka Imai[1], Toru Kouyama[1], Yukihiro Takahashi[2], Takeshi Horinouchi[3], Takeshi Imamura[4], Atsushi Yamazaki[5], Shigeto Watanabe[6], Manabu Yamada[7], Masato Nakamura[5], Takehiko Satoh[5] (1.National Institute of Advanced Industrial Science and Technology, 2.Department of Cosmosciences, Graduate School of Science, Hokkaido University, 3.Faculty of Environmental Earth Science, Hokkaido University, 4.Graduate School of Frontier Sciences, University of Tokyo, 5.Institute of Space and Astronautical Science, Japan Aerospace Exploration Agency, 6.Space Information Center, Hokkaido Information University, 7.Planetary Exploration Research Center, Chiba Institute of Technology)

3:00 PM - 3:15 PM JST | 6:00 AM - 6:15 AM UTC

[PPS05-17] **Long-term behaviour of the morphology and dynamics of Venus's middle clouds with Akatsuki/IR1.**

★Invited Papers

*Javier Peralta[1], Naomoto Iwagami[2], Sánchez-Lavega Agustín[3], Yeon Joo Lee[4], Ricardo Hueso[3], Minori Narita[4], Takeshi Imamura[4], Phil Miles[5], Anthony Wesley[6], Emmanuel Kardasis[7], Seiko Takagi[8] (1.Institute of Space and Astronautical Science (ISAS), Japan Aerospace Exploration Agency (JAXA), Sagamihara, Japan, 2.Tokyo 156-0044, Japan, 3.Escuela de Ingeniería de Bilbao, University of the Basque Country (UPV/EHU), Bilbao, Spain, 4.Graduate School of Frontier Sciences, The University of Tokyo, Japan, 5.Rubyvale QLD, Australia, 6.Astronomical Society of Australia, Australia, 7.Hellenic Amateur Astronomy Association, Greece, 8.Research and Information Center, Tokai University, Japan)

[E] Poster | P (Space and Planetary Sciences)：P-PS Planetary Sciences

3:30 PM - 5:00 PM JST | 6:30 AM - 8:00 AM UTC | Poster Hall International Exhibition Hall8, Makuhari Messe_1

[P-PS05] Recent advances of Venus science

convener:Takehiko Satoh(Institute of Space and Astronautical Science, Japan Aerospace Exploration Agency), Takeshi Horinouchi(Faculty of Environmental Earth Science, Hokkaido University), Masaru Yamamoto(Research Institute for Applied Mechanics, Kyushu University), Kevin McGouldrick(University of Colorado Boulder)

[PPS05-P01] New thermal infrared camera for fine horizontal brightness temperature structures at the cloud-top level of Venus

*Tetsuya Fukuhara[1], Makoto Taguchi[1], Takeshi Imamura[2], Sanjay S Limaye[3] (1.Rikkyo University, 2.The University of Tokyo, 3.University of Wisconsin)

[PPS05-P02] Temperature and wind variations in Venusian mesosphere and lower thermosphere by mid-infrared heterodyne spectrometer in 2018

*Kosuke Takami[1], Hiromu Nakagawa[1], Hideo Sagawa[2], Isao Murata[1], Yasumasa Kasaba[1] (1.Graduate School of Science, Tohoku University, 2.Division of Science, Kyoto Sangyo University)

[PPS05-P03] Local time dependence of limb darkening seen in the thermal infrared Venus disk

*Masahiro Akiba[1] (1.Rikkyo University)

[PPS05-P04] Stationary wavy features and Banded structures at Venusian cloud top extracted by averaging multiple LIR images

*Kiichi Fukuya[1], Takeshi Imamura[1], Makoto Taguchi[2], Tetsuya Fukuhara[2], Toru Kouyama[3] (1.Univ. of Tokyo, 2.Rikkyo Univ., 3.AIST)

[PPS05-P05] Akatsuki's IR2 Nightside Photometry Restoration by Deconvolution

*Choon Wei Vun[1], Takehiko Satoh[2,1], Kevin McGouldrick[3], Takeshi Horinouchi[4], Takao M. Sato[5] (1.SOKENDAI, 2.ISAS/JAXA, 3.University of Colorado Boulder, 4.Hokkaido University, 5.Hokkaido Information University)

[PPS05-P06] Enormous cloud cover as seen by Akatsuki/IR2 on the night-side disk of Venus

*Takehiko Satoh[1,2], Choon Wei Vun[2], Takao M. Sato[3], Takeshi Horinouchi[4], George HASHIMOTO[5], Kevin McGouldrick[6] (1.Institute of Space and Astronautical Science, Japan Aerospace Exploration Agency, 2.Department of Space Science, SOKENDAI, 3.Department of Business and Information Systems, Hokkaido Information University, 4.Faculty of Environmental Earth Science, Hokkaido University, 5.Department of Earth Science, Okayama University, 6.LASP, University of Colorado Boulder)

[PPS05-P07] The global variation of Venus cloud obtained from IR1 camera onboard AKATSUKI

*Seiko Takagi[1], Naomoto Iwagami, Yukihiro Takahashi[1], Mitsuteru Sato[1] (1.Hokkaido University, Graduate School of Science)

[PPS05-P08] Development of a Venus' cloud formation scheme for a convection resolving model

*Ko-ichiro SUGIYAMA[1], Nozomu Fukuhara[1], Masatsugu Odaka[2], Kensuke Nakajima[3], Masaki Ishiwatari[2], Takeshi Imamura[4], Yoshi-Yuki Hayashi[5] (1.National Institute of Technology, Matsue College, 2.Department of Cosmoscience, Graduate School of Science, Hokkaido University, 3.Department of Earth and Planetary Sciences,Flculty of Sciences,Kyushu University, 4.Graduate School of Frontier Sciences, The University of Tokyo, 5.Department of Planetology, Graduate School of Science, Kobe University / Center for Planetary Science (CPS))

[PPS05-P09] Zonal mean structure of Venus atmosphere observed in a Venus general circulation model with explicit radiative transfer

★Invited Papers

*Yoshi-Yuki Hayashi[1], Chisato Shiojiri[1], Hiroki Kashimura[1], Yoshiyuki O. Takahashi[1] (1.Department of Planetology/CPS, Graduate School of Science, Kobe University)

[PPS05-P10] Gravity wave packets detected in radio occultation temperature profiles of the Venus atmosphere

*Ryota Mori[1], Takeshi Imamura[1], Javier Peralta[2] (1.The University of Tokyo, 2.Japan Aerospace Exploration Agency)

[PPS05-P11] Status of lightning hunt in Venus with Akatsuki/LAC and Pirka telescope

*Yukihiro Takahashi[1,2], Mitsuteru Sato[1,2], Masataka Imai[3], Ralph Lorenz[4], Seiko Takagi[1,2], Ono Tatsuharu[1] (1.Graduate School of Science, Hokkaido University, 2.Faculty of Science, Hokkaido University, 3.National Institute of

Advanced Industrial Science and Technology,, 4.Applied Physics Laboratory, Johns Hopkins University)

[PPS05-P12] Possibility of electric discharge in the Venusian atmosphere due to the super-rotation of clouds

*Adhithiyan Neduncheran[1], Ugur Guven[1,2], Ananyo Bhattacharya[3] (1.University of Petroleum and Energy Studies, India, 2.United Nations Centre for Space Science and Technology Education in Asia and the Pacific, 3.Sardar Vallabhbhai National Institute of Technology,India)

[E] Poster | P (Space and Planetary Sciences)：P-PS Planetary Sciences

5:15 PM - 6:30 PM JST | 8:15 AM - 9:30 AM UTC | Poster Hall International Exhibition Hall8, Makuhari Messe_2

[P-PS05] Recent advances of Venus science

convener:Takehiko Satoh(Institute of Space and Astronautical Science, Japan Aerospace Exploration Agency), Takeshi Horinouchi(Faculty of Environmental Earth Science, Hokkaido University), Masaru Yamamoto(Research Institute for Applied Mechanics, Kyushu University), Kevin McGouldrick(University of Colorado Boulder)

[PPS05-P01] New thermal infrared camera for fine horizontal brightness temperature structures at the cloud-top level of Venus

*Tetsuya Fukuhara[1], Makoto Taguchi[1], Takeshi Imamura[2], Sanjay S Limaye[3] (1.Rikkyo University, 2.The University of Tokyo, 3.University of Wisconsin)

[PPS05-P02] Temperature and wind variations in Venusian mesosphere and lower thermosphere by mid-infrared heterodyne spectrometer in 2018

*Kosuke Takami[1], Hiromu Nakagawa[1], Hideo Sagawa[2], Isao Murata[1], Yasumasa Kasaba[1] (1.Graduate School of Science, Tohoku University, 2.Division of Science, Kyoto Sangyo University)

[PPS05-P03] Local time dependence of limb darkening seen in the thermal infrared Venus disk

*Masahiro Akiba[1] (1.Rikkyo University)

[PPS05-P04] Stationary wavy features and Banded structures at Venusian cloud top extracted by averaging multiple LIR images

*Kiichi Fukuya[1], Takeshi Imamura[1], Makoto Taguchi[2], Tetsuya Fukuhara[2], Toru Kouyama[3] (1.Univ. of Tokyo, 2.Rikkyo Univ., 3.AIST)

[PPS05-P05] Akatsuki's IR2 Nightside Photometry Restoration by Deconvolution

*Choon Wei Vun[1], Takehiko Satoh[2,1], Kevin McGouldrick[3], Takeshi Horinouchi[4], Takao M. Sato[5] (1.SOKENDAI, 2.ISAS/JAXA, 3.University of Colorado Boulder, 4.Hokkaido University, 5.Hokkaido Information University)

[PPS05-P06] Enormous cloud cover as seen by Akatsuki/IR2 on the night-side disk of Venus

*Takehiko Satoh[1,2], Choon Wei Vun[2], Takao M. Sato[3], Takeshi Horinouchi[4], George HASHIMOTO[5], Kevin McGouldrick[6] (1.Institute of Space and Astronautical Science, Japan Aerospace Exploration Agency, 2.Department of Space Science, SOKENDAI, 3.Department of Business and Information Systems, Hokkaido Information University, 4.Faculty of Environmental Earth Science, Hokkaido University, 5.Department of Earth Science, Okayama University, 6.LASP, University of Colorado Boulder)

[PPS05-P07] The global variation of Venus cloud obtained from IR1 camera onboard AKATSUKI

*Seiko Takagi[1], Naomoto Iwagami, Yukihiro Takahashi[1], Mitsuteru Sato[1] (1.Hokkaido University, Graduate School of Science)

[PPS05-P08] Development of a Venus' cloud formation scheme for a convection resolving model

*Ko-ichiro SUGIYAMA[1], Nozomu Fukuhara[1], Masatsugu Odaka[2], Kensuke Nakajima[3], Masaki Ishiwatari[2], Takeshi Imamura[4], Yoshi-Yuki Hayashi[5] (1.National Institute of Technology, Matsue College, 2.Department of Cosmoscience, Graduate School of Science, Hokkaido University, 3.Department of Earth and Planetary Sciences,Flculty of Sciences,Kyushu University, 4.Graduate School of Frontier Sciences, The University of Tokyo, 5.Department of Planetology, Graduate School of Science, Kobe University / Center for Planetary Science (CPS))

[PPS05-P09] Zonal mean structure of Venus atmosphere observed in a Venus general circulation model with explicit radiative transfer

★Invited Papers

*Yoshi-Yuki Hayashi[1], Chisato Shiojiri[1], Hiroki Kashimura[1], Yoshiyuki O. Takahashi[1] (1.Department of Planetology/CPS, Graduate School of Science, Kobe University)

[PPS05-P10] Gravity wave packets detected in radio occultation temperature profiles of the Venus atmosphere

*Ryota Mori[1], Takeshi Imamura[1], Javier Peralta[2] (1.The University of Tokyo, 2.Japan Aerospace Exploration Agency)

[PPS05-P11] Status of lightning hunt in Venus with Akatsuki/LAC and Pirka telescope

*Yukihiro Takahashi[1,2], Mitsuteru Sato[1,2], Masataka Imai[3], Ralph Lorenz[4], Seiko Takagi[1,2], Ono Tatsuharu[1] (1.Graduate School of Science, Hokkaido University, 2.Faculty of Science, Hokkaido University, 3.National Institute of

Advanced Industrial Science and Technology,, 4.Applied Physics Laboratory, Johns Hopkins University)

[PPS05-P12] **Possibility of electric discharge in the Venusian atmosphere due to the super-rotation of clouds**

*Adhithiyan Neduncheran[1], Ugur Guven[1,2], Ananyo Bhattacharya[3] (1.University of Petroleum and Energy Studies, India, 2.United Nations Centre for Space Science and Technology Education in Asia and the Pacific, 3.Sardar Vallabhbhai National Institute of Technology,India)

[J] Oral | P (Space and Planetary Sciences)：P-PS Planetary Sciences

9:00 AM - 10:30 AM JST | 12:00 AM - 1:30 AM UTC | A01 TOKYO BAY MAKUHARI HALL

[P-PS06] Planetary Sciences

convener:Kenji Kurosaki(Department of Physics, Nagoya University), Yusuke Nakauchi(Japan Aerospace Exploration Agency), Chairperson:Kiyoshi Kuramoto(Hokkaido University), Takanori Sasaki(Department of Astronomy, Kyoto University)

9:00 AM - 9:15 AM JST | 12:00 AM - 12:15 AM UTC

[PPS06-01] Current status of the PLANETS telescope project for planetary and exoplanetary atmospheric monitoring

*Takeshi Sakanoi[1], Masato Kagitani[1], Yasumasa Hirahara[2], Jeffery Kuhn[3], Svetalana Berdyugina[4], Marcelo Emilio[5], Hiromu Nakagawa[6], Mikio Kurita[7], Yasumasa Kasaba[1], Takahiro Obara[1], Shoichi Okano[1] (1.Planetary Plasma and Atmospheric Research Center, Graduate School of Science, Tohoku University, 2.Graduate School of Environmental Studies, Nagoya University, 3.IfA, University of Hawaii, U.S.A., 4.KIS, Germany, 5.Universidade Estadual de Ponta Grossa, Brazil, 6.Graduate School of Science, Tohoku University, 7.Graduate School of Science, Kyoto University)

9:15 AM - 9:30 AM JST | 12:15 AM - 12:30 AM UTC

[PPS06-02] Martian Moon eXploration MMX: science objectives and their promotion

*Kiyoshi Kuramoto[1,2], Yasuhiro Kawakatsu[2], Masaki Fujimoto[2], Jean Pierre Bibring[3], David Lawrence[4], Hidenori Genda[5], Naru Hirata[6], Takeshi Imamura[7], Shingo Kameda[8], Koji Matsumoto[9], Hideaki Miyamoto[7], Tomokatsu Morota[10], Hiroshi Nagaoka[2], Hiromu Nakagawa[11], Tomoki Nakamura[11], Kazunori Ogawa[12], Hisashi Otake[2], Masanobu Ozaki[2], Sho Sasaki[13], Hiroki Senshu[14], Shogo Tachibana[7,2], Naoki Terada[11], Tomohiro Usui[2], Koji Wada[14], Sei-ichiro WATANABE[10], MMX study team (1.Hokkaido Univ., 2.JAXA, 3.IAS, 4.APL, 5.ELSI, 6.Aizu Univ., 7.Univ. of Tokyo, 8.Rikkyo Univ., 9.NAOJ, 10.Nagoya Univ., 11.Tohoku Univ., 12.Kobe Univ., 13.Osaka Univ., 14.Chiba Inst. Tech.)

9:30 AM - 9:45 AM JST | 12:30 AM - 12:45 AM UTC

[PPS06-03] **Implantation of Martian Materials in the Inner Solar System by a Mega Impact on Mars**

*Ryuki Hyodo[1], Hidenori Genda[1] (1.Tokyo Institute of Technology, Earth Life Science Institute)

9:45 AM - 10:00 AM JST | 12:45 AM - 1:00 AM UTC

[PPS06-04] Hydrodynamic escape of a reduced proto-atmosphere on early Mars

*Tatsuya Yoshida[1], Kiyoshi Kuramoto[1] (1.Hokkaido University)

10:00 AM - 10:15 AM JST | 1:00 AM - 1:15 AM UTC

[PPS06-05] Orbital evolution of Martian moons by rotating Martian proto-atmosphere with low angular momentum

*Ryo Matsuoka[1], Kiyoshi Kuramoto[1] (1.Department of Cosmosciences, Graduateschool of Science, Hokkaido University)

10:15 AM - 10:30 AM JST | 1:15 AM - 1:30 AM UTC

[PPS06-06] N-body simulations of Moon formation with cooling evolution of the protolunar disk

*Takanori Sasaki[1], Natsuki Hosono[2] (1.Department of Astronomy, Kyoto University, 2.Japan Agency for Marine-Earth Science and Technology)

[J] Oral | P (Space and Planetary Sciences)：P-PS Planetary Sciences

10:45 AM - 12:15 PM JST | 1:45 AM - 3:15 AM UTC | A01 TOKYO BAY MAKUHARI HALL

[P-PS06] Planetary Sciences

convener:Kenji Kurosaki(Department of Physics, Nagoya University), Yusuke Nakauchi(Japan Aerospace Exploration Agency), Chairperson:Hiroyuki Kurokawa(東京工業大学 地球生命研究所), Yuki Tanaka(Tokyo Institute of Technology)

10:45 AM - 11:00 AM JST | 1:45 AM - 2:00 AM UTC

[PPS06-07] Possibility of giant planet formation by pebble accretion in Class 0/I YSOs

*Yuki Tanaka[1], Yusuke Tsukamoto[2] (1.Tokyo Institute of Technology, 2.Kagoshima University)

11:00 AM - 11:15 AM JST | 2:00 AM - 2:15 AM UTC

[PPS06-08] The effect of the three-dimensional gas flow around an embedded planet on pebble accretion

*Ayumu Kuwahara[1], Hiroyuki Kurokawa[2] (1.Tokyo Institute of Technology, 2.Earth-Life Science Institute)

11:15 AM - 11:30 AM JST | 2:15 AM - 2:30 AM UTC

[PPS06-09] Icy pebble accretion onto terrestrial planets: the effect of gas flow

*Hiroyuki Kurokawa[1], Ayumu Kuwahara[2], Satoshi Okuzumi[2] (1.Earth-Life Science Institute, Tokyo Institute of Technology, 2.Tokyo Institute of Technology)

11:30 AM - 11:45 AM JST | 2:30 AM - 2:45 AM UTC

[PPS06-10] Delivery of ammonia ice to Ceres by pebble accretion

*Yuto Nara[1], Satoshi Okuzumi[1], Hiroyuki Kurokawa[2] (1.Tokyo Institute of Technology, 2.Earth-Life Science Institute, Tokyo Institute of Technology)

11:45 AM - 12:00 PM JST | 2:45 AM - 3:00 AM UTC

[PPS06-11] Volatile-driven cryovolcanic eruption on asteroid Ceres as a probe to its interior

*Koki Yumoto[1], Yuichiro Cho[1], Seiji Sugita[1] (1.Department of Earth and Planetary Science, Graduate School of Science, University of Tokyo)

12:00 PM - 12:15 PM JST | 3:00 AM - 3:15 AM UTC

[PPS06-12] Ice sheet formation on synchrnously rotating earth-like planets in M-dwarf abitable zones

Soma Arai[1], Kiyoshi Kuramoto[1], *Masaki Ishiwatari[1], Shunichi Kamata[1] (1.Department of Cosmosciences, Graduate school of Science, Hokkaido University)

[J] Oral | P (Space and Planetary Sciences)：P-PS Planetary Sciences

1:45 PM - 3:15 PM JST | 4:45 AM - 6:15 AM UTC | A01 TOKYO BAY MAKUHARI HALL

[P-PS06] Planetary Sciences

convener:Kenji Kurosaki(Department of Physics, Nagoya University), Yusuke Nakauchi(Japan Aerospace Exploration Agency), Chairperson:荻原 正博(国立天文台), Yuri Fujii(Nagoya University)

1:45 PM - 2:00 PM JST | 4:45 AM - 5:00 AM UTC

[PPS06-13] Three-dimensional linear calculation for non-isothermal type 1 planetary migration

*Kohei Okada[1], Hidekazu Tanaka[1] (1.Tohoku University)

2:00 PM - 2:15 PM JST | 5:00 AM - 5:15 AM UTC

[PPS06-14] Dependence of Central star mass on Protoplanetary disk evolution

*Ryuunosuke Nakano[1], Takeru Suzuki[1], Masahiro Ogihara[2], Eiichiro Kokubo[2] (1.University of Tokyo, 2.National Astronomical Observatory of Japan)

2:15 PM - 2:30 PM JST | 5:15 AM - 5:30 AM UTC

[PPS06-15] Radiation Hydrodynamic Simulations of the Formation of Circumplanetary Disks

*Yuri Fujii[1], Oliver Gressel[2], Kengo Tomida[3], Udo Zieglar[2] (1.Institute for Advanced Research, Nagoya University, 2.Leibniz Institute for Astrophysics Potsdam, 3.Osaka University)

2:30 PM - 2:45 PM JST | 5:30 AM - 5:45 AM UTC

[PPS06-16] Inefficient Magnetic Accretion Heating in Protoplanetary Disks: Evolution of The Snow Line

*Shoji Mori[1], Xuening Bai[2], Satoshi Okuzumi[3] (1.Department of Astronomy, The University of Tokyo, 2.Tsinghua Center for Astrophysics, Tsinghua University, 3.Department of Earth and Planetary Sciences, Tokyo Institute of Technology)

2:45 PM - 3:00 PM JST | 5:45 AM - 6:00 AM UTC

[PPS06-17] Formation of super-Earths and their atmospheres with *N*-body simulations

*Masahiro Ogihara[1], Yasunori Hori[2,1] (1.National Astronomical Observatory of Japan, 2.Astrobiology Center)

3:00 PM - 3:15 PM JST | 6:00 AM - 6:15 AM UTC

[PPS06-18] The orbital stability of planets in resonances: the evolution of mass ratio

*Yuji Matsumoto[1], Masahiro Ogihara[2] (1.Academia Sinica Institute of Astronomy and Astrophysics, 2.National Astronomical Observatory of Japan)

[J] Oral | P (Space and Planetary Sciences)：P-PS Planetary Sciences

3:30 PM - 5:00 PM JST | 6:30 AM - 8:00 AM UTC | A01 TOKYO BAY MAKUHARI HALL

[P-PS06] Planetary Sciences

convener:Kenji Kurosaki(Department of Physics, Nagoya University), Yusuke Nakauchi(Japan Aerospace Exploration Agency), Chairperson:Kenji Kurosaki(名古屋大学大学院 理学研究科), Yusuke Nakauchi(JAXA/ISAS)

3:30 PM - 3:45 PM JST | 6:30 AM - 6:45 AM UTC

[PPS06-19] Experimental study on the structure of shock remnant magnetization

*Shota Kato[1], Masahiko Sato[1], Kosuke Kurosawa[2], Masashi Ushioda[3], Sunao Hasegawa[4] (1.The University of Tokyo, 2.Planetary Exploration Research Center, Chiba Institute of Technology, 3.Geological Survey of Japan, The National Institute of Advanced Industrial Science and Technology, 4.Japan Aerospace Exploration Agency)

3:45 PM - 4:00 PM JST | 6:45 AM - 7:00 AM UTC

[PPS06-20] Low-dispersion spectra of lunar impact flashes in 2018 Geminids

*Masahisa Yanagisawa[1], Yuki Uchida[1], Seiya Kurihara[1], Shinsuke Abe[2], Ryota Fuse[2], Keisuke Onodera[3,4], Ryuhei Yamada[5] (1.The University of Electro-Communications, 2.Nihon University, 3.SOKENDAI (The Graduate University for Advanced Studies), 4.Institute of Space and Astronautical Science/Japan Aerospace Exploration Agency, 5.The University of Aizu)

4:00 PM - 4:15 PM JST | 7:00 AM - 7:15 AM UTC

[PPS06-21] High velocity cratering experiments on sand-gypsum targets simulating asteroids

*Ryo Sugimura[1], Masahiko Arakawa[1], Minami Yasui[1], Takuya Ishiguro[1] (1.Kobe University)

4:15 PM - 4:30 PM JST | 7:15 AM - 7:30 AM UTC

[PPS06-22] Experimental study on collisional processes of highly porous ice balls simulating Saturn's ring particles

*Yukari Toyoda[1], Minami Yasui[1], Masahiko Arakawa[1] (1.Graduate School of Science, Kobe University)

4:30 PM - 4:45 PM JST | 7:30 AM - 7:45 AM UTC

[PPS06-23] IN-SITU FORMATION OF THE URANIAN SATELLITES FROM WIDE DEBRIS DISK FORMED BY GIANT IMPACT

*Ishizawa Yuya[1], Takanori Sasaki[1], Natsuki Hosono[2] (1.Department of Astronomy, Kyoto University, 2.JAMSTEC)

4:45 PM - 5:00 PM JST | 7:45 AM - 8:00 AM UTC

[PPS06-24] Effect on the obliquity due to a giant impact on a rotating ice giant

*Kenji Kurosaki[1], Shu-ichiro Inutsuka[1] (1.Department of Physics, Nagoya University)

[J] Oral | P (Space and Planetary Sciences)：P-PS Planetary Sciences

9:00 AM - 10:30 AM JST | 12:00 AM - 1:30 AM UTC | A02 TOKYO BAY MAKUHARI HALL

[P-PS07] Formation and evolution of planetary materials in the Solar System

convener:Yoko Kebukawa(Faculty of Engineering, Yokohama National University), Wataru Fujiya(Ibaraki University, College of Science), Shin Ozawa(Department of Earth Science, Graduate School of Science, Tohoku University), Megumi Matsumoto(Graduate School of Science, Tohoku University), Chairperson:Wataru Fujiya, Shin Ozawa

9:00 AM - 9:15 AM JST | 12:00 AM - 12:15 AM UTC

[PPS07-07] **Evaluation of shock metamorphism of eucrites by X-ray diffraction analysis**

*Rei Kanemaru[1], Naoya Imae[2,1], Akira Yamaguchi[2,1], Hirotugu Nishido[3] (1.The Graduate University for Advanced Studyies, 2.National Institute of Polar Research, 3.Okayama University of scienece)

9:15 AM - 9:30 AM JST | 12:15 AM - 12:30 AM UTC

[PPS07-08] Hf-W dating of main-group pallasites

*Yoshitaka Homma[1], Tsuyoshi Iizuka[1], Akira Ishikawa[2] (1.Department of Earth and Planetary Science, The University of Tokyo, 2.Department of Earth and Planetary Sciences, Tokyo Institute of Technology)

9:30 AM - 9:45 AM JST | 12:30 AM - 12:45 AM UTC

[PPS07-09] Mineralogical study of TCIs in CM carbonaceous chondrites

*Akane Iemoto[1], Yusuke Seto[1], Akira Miyake[2] (1.Graduate School of Science, Kobe University, 2.Graduate School of Science, Kyoto University)

9:45 AM - 10:00 AM JST | 12:45 AM - 1:00 AM UTC

[PPS07-10] Importance of 10Be as a key indicator of (solar) cosmic ray irradiation in the early solar system

*Hajime Hiyagon[1], Yuuki Tanimura[1], Tomoya Nakamura[1], Kohei Fukuda[3], Wataru Fujiya[4], Naoji Sugiura[1], Takanori Kagoshima[2], Naoto Takahata[2], Yuji Sano[2] (1.Graduate School of Science, The University of Tokyo, 2.Atmosphere and Ocean Research Institute, the University of Tokyo, 3.Department of Geoscience, University of Wisconsin-Madison, 4.College of Science, Ibaraki University)

10:00 AM - 10:15 AM JST | 1:00 AM - 1:15 AM UTC

[PPS07-11] **3D microstructure of a cosmic symplectite in primitive carbonaceous chondrite Acfer 094**

*Megumi Matsumoto[1,2], Akira Tsuchiyama[1], Junya Matsuno[1], Aiko Nakato[1,3], Akira Miyake[1], Motoo Ito[4], Naotaka Tomioka[4], Yu Kodama[5], Kentaro Uesugi[6], Akihisa Takeuchi[6], Tsukasa Nakano[7], Epifanio Vaccaro[8] (1.Graduate School of Science, Kyoto Univ., 2.Graduate School of Science, Tohoku Univ., 3.JAXA, ISAS, 4.JAMSTEC, 5.Marine Work Japan LTD., 6.JASRI, 7.AIST, Geological Survey Japan, 8.Natural History Museum, London)

10:15 AM - 10:30 AM JST | 1:15 AM - 1:30 AM UTC

[PPS07-12] Chondrule-like objects and refractory inclusions in GEMS-bearing Antarctic micrometeorites and an interplanetary dust particle.

*Takaaki Noguchi[1], Noriaki Ohashi[2], John P. Bradley[3], Daisuke Nakashima[4], Tomoki Nakamura[4], Makoto Kimura[5], Takayuki Ushikubo[6], Noriko T. Kita[7], Naoya Imae[5] (1.Department of Arts and Science, Kyushu University, 2.NEC Networks and System Integration Co., 3.Univ. of Hawaii at Manoa, 4.Tohoku Univ., 5.National Institute of Polar Research, 6.Kochi Institute for Core Sample Research, JAMSTEC, 7.Univ. of Wisconsin-Madison)

[J] Oral | P (Space and Planetary Sciences)：P-PS Planetary Sciences

10:45 AM - 12:15 PM JST | 1:45 AM - 3:15 AM UTC | A02 TOKYO BAY MAKUHARI HALL

[P-PS07] Formation and evolution of planetary materials in the Solar System

convener:Yoko Kebukawa(Faculty of Engineering, Yokohama National University), Wataru Fujiya(Ibaraki University, College of Science), Shin Ozawa(Department of Earth Science, Graduate School of Science, Tohoku University), Megumi Matsumoto(Graduate School of Science, Tohoku University), Chairperson:Yoko Kebukawa, Shin Ozawa

10:45 AM - 11:00 AM JST | 1:45 AM - 2:00 AM UTC

[PPS07-13] Spectral and mineralogical properties of naturally-heated carbonaceous chondrites; implication to heating processes on the surface of hydrous asteroids

★Invited Papers

*Moe Matsuoka[1], Tomoki Nakamura[2], Takahiro Hiroi[3], Nobuyoshi Miyajima[4], Naoya Imae[5,6], Akira Yamaguchi[5], Hideyasu Kojima[5,6] (1.Japan Aerospace Exploration Agency(JAXA), 2.Department of Earth and Planetary Materials Sciences, Faculty of Science, Tohoku University, 3.Department of Earth, Environmental and Planetary Sciences, Brown University, 4.Bayerisches Geoinstitut, University of Bayreuth, 5.National Institute of Polar Research, 6.Department of Polar Science, School of Multidisciplinary Science, SOKENDAI)

11:00 AM - 11:15 AM JST | 2:00 AM - 2:15 AM UTC

[PPS07-14] Heterogeneity of oxygen and carbon isotopic compositions within carbonate grains in the Yamato 791198 CM chondrite and evolution of isotope ratios during aqueous alteration

*Wataru Fujiya[1], YUTO AOKI[1], Takayuki Ushikubo[2], Ko Hashizume[1] (1.Ibaraki University, College of Science, 2.Kochi Institute for Core Sample research, Japan Agency for Marine-Earth Science and Technology)

11:15 AM - 11:30 AM JST | 2:15 AM - 2:30 AM UTC

[PPS07-15] Characteristics of Oxygen isotope ratios of chondrules and isolated olivine grains from Tagish Lake C2 chondrite

*Takayuki Ushikubo[1], Makoto Kimura[2] (1.Kochi Institute for Core Sample Research, Japan Agency for Marine-Earth Science and Technology, 2.National Institute for Polar Research)

11:30 AM - 11:45 AM JST | 2:30 AM - 2:45 AM UTC

[PPS07-16] Extreme ^{16}O-rich CAIs in Isheyevo chondrite

*Naoya Sakamoto[1], Noriyuki Kawasaki[2] (1.Creative Research Institution, Hokkaido University, 2.Natural History Sciences, Hokkaido University)

11:45 AM - 12:00 PM JST | 2:45 AM - 3:00 AM UTC

[PPS07-17] Variations in initial ^{26}Al/^{27}Al ratios among fine-grained CAIs in the reduced CV chondrites

*Noriyuki Kawasaki[1], Changkun Park[2], Naoya Sakamoto[1], Hisayoshi Yurimoto[1,3] (1.Hokkaido University, 2.KOPRI, 3.ISAS/JAXA)

12:00 PM - 12:15 PM JST | 3:00 AM - 3:15 AM UTC

[PPS07-18] Petrographic study of compact type A CAIs with partial melting process

*Akimasa Suzumura[1], Yusuke Seto[2], Shoichi Itoh[1] (1.Graduate school of Science, Kyoto University, 2.Graduate school of Science, Kobe University)

[J] Poster | P (Space and Planetary Sciences)：P-PS Planetary Sciences

3:30 PM - 5:00 PM JST | 6:30 AM - 8:00 AM UTC | Poster Hall International Exhibition Hall8, Makuhari Messe_2

[P-PS07] Formation and evolution of planetary materials in the Solar System

convener:Yoko Kebukawa(Faculty of Engineering, Yokohama National University), Wataru Fujiya(Ibaraki University, College of Science), Shin Ozawa(Department of Earth Science, Graduate School of Science, Tohoku University), Megumi Matsumoto(Graduate School of Science, Tohoku University)

[PPS07-P01] Stability of Amino Acid Precursors in Simulated Extraterestrial Environments

*tomohito sato[1], Soushi Kuramoto[1], Takuya Yokoo[1], Yoshida Satoshi[2], Isao Yoda[3], Hitoshi Fukuda[3], Yoshiyuki Oguri[3], MITA Hajime[4], Kazuhiro Kanda[5], Hiromi Shibata[6], Zyunichi Takahashi[1], Yoko Kebukawa[1], Kensei Kobayashi[1] (1.yokohama national univercity, 2.QST, 3.Tokyo Institute of Technology, 4.Fukuoka Institute of Technology, 5.University of Hyogo, 6.Osaka University)

[PPS07-P02] Production of amino acids by gamma rays during aqueous alteration process in meteorite parent body

*Shinya Asano[1], Isao Yoda[2], Yasuji Muramatsu[3], Yoko Kebukawa[1], Kensei Kobayashi[1] (1.Yokohama national university, 2.Tokyo Institute of Technology, 3.University of Hyogo)

[PPS07-P03] **Kinetic approaches for the thermal history of organic matter in meteorites based on Raman spectra**

*Kento Kiryu[1], Yoko Kebukawa[1], Motoko Igisu[2], Takazo Shibuya[2], Kensei Kobayashi[1] (1.Yokohama National Univ., 2.Japan Agency for Marine-Earth Science and Technology)

[PPS07-P04] Relationship between spatial distribution of organic compounds and minerals in the Murchison meteorite

*Taiyo Sengoku[1], Minako Hashiguchi[1], Hiroshi Naraoka[1] (1.Kyushu University)

[PPS07-P05] O and Al-Mg isotope systematics of a hibonite-melilite-rich fine-grained CAI in the reduced CV chondrite NWA8613

*Sohei Wada[1], Noriyuki Kawasaki[1], Hisayoshi Yurimoto[1,2] (1.Hokkaido University, 2.ISAS/JAXA)

[PPS07-P06] Observation of Enstatite Whiskers in Fine-grained Rims in the Carbonaceous Chondrite ALH A77307

*Yasuhisa Shirota[1], Masahiro YASUTAKE[1], Satomi Enju[1], Akira Tsuchiyama[1] (1.Division of Earth and Planet, Science, Kyoto University)

[PPS07-P07] 3D observation of whisker-like material in the porous matrix of the Paris CM chondrite by SR-XCT

*Masahiro YASUTAKE[1], Epifanio Vacarro[2], Kentaro Uesugi[3], Akihisa Takeuchi[3], Tsukasa Nakano[4], Akira Tsuchiyama[1] (1.Division of Earth and Planetary Science, Graduate School of Science, Kyoto University, 2.National History Museum, London, 3.JASRI/SPring8, 4.GSJ/AIST)

[PPS07-P08] Development of cryogenic SIMS technique for isotope analysis of fluid inclusions

*Isono Yuki[1], Naoya Sakamoto[2], Hisayoshi Yurimoto[3] (1.Department of Natural History Sciences, Hokkaido University, 2.Creative Research Institusion, Hokkaido University, 3.Department of Natural History Sciences, Hokkaido University)

[PPS07-P09] X-ray diffraction study using Gandolfi attachment: Implications for small extraterrestrial materials

*Naoya Imae[1,2], Makoto Kimura[1] (1.Antarctic Meteorite Research Center, National Institute of Polar Research, 2.SOKENDAI)

[PPS07-P10] Trace elements analysis and Ar-Ar dating for microgram-scaled extraterrestrial samples

*Ryuji Okazaki[1], Sekimoto Shun[2] (1.Department of Earth and Planetary Sciences, Faculty of Science, Kyushu University, 2.Institute for Integrated Radiation and Nuclear Science, Kyoto University)

[PPS07-P11] Magnetic separation and identification of low-temperature solid particles using their translation caused by a pair of small permanent magnets

*Chiaki Uyeda[1], Wakana Yamaguchi[1], Keiji Hisayoshi[1], Kentaro Terada[1] (1.Institute of earth and Space Science Graduate School of Science Osaka University)

[PPS07-P12] The metallographic cooling rate of the Tafassasset primitive achondrite

*naoji sugiura[1], Tomoko Arai, takafumi matsui (1.Chiba Institute of Technology)

[PPS07-P13] The systematic investigations of high-pressure minerals in lunar basaltic meteorites

*Masaaki Miyahara[1], Kazunari Kozuma[1], Eiji Ohtani[2], Akira Yamaguchi[3], Takeshi Sakai[4], Hiroaki Ohfuji[4], Naotaka Tomioka[5], Yu Kodama[6] (1.Department of Earth and Planetary Systems Science, Graduate School of Science, Hiroshima University, 2.Department of Earth Sciences, Graduate School of Science, Tohoku University, 3.National Institute of Polar Research, 4.Geodynamics Research Center, Ehime University, 5.5Kochi Institute for Core Sample Research, Japan Agency for Marine-Earth Science and Technology, 6.Marine Works Japan)

[PPS07-P14] Bulk chemical analysis of iron meteorites by LA-ICP-MS

*Akira Yamaguchi[1], Naoki Shirai[2], Makiko K. Haba[3] (1.National Institute of Polar Research, 2.Tokyo Metropolitan University, 3.Tokyo Institute of Technology)

[J] Poster | P (Space and Planetary Sciences)：P-PS Planetary Sciences

5:15 PM - 6:30 PM JST | 8:15 AM - 9:30 AM UTC | Poster Hall International Exhibition Hall8, Makuhari Messe_3

[P-PS07] Formation and evolution of planetary materials in the Solar System

convener:Yoko Kebukawa(Faculty of Engineering, Yokohama National University), Wataru Fujiya(Ibaraki University, College of Science), Shin Ozawa(Department of Earth Science, Graduate School of Science, Tohoku University), Megumi Matsumoto(Graduate School of Science, Tohoku University)

[PPS07-P01] Stability of Amino Acid Precursors in Simulated Extraterestrial Environments

*tomohito sato[1], Soushi Kuramoto[1], Takuya Yokoo[1], Yoshida Satoshi[2], Isao Yoda[3], Hitoshi Fukuda[3], Yoshiyuki Oguri[3], MITA Hajime[4], Kazuhiro Kanda[5], Hiromi Shibata[6], Zyunichi Takahashi[1], Yoko Kebukawa[1], Kensei Kobayashi[1] (1.yokohama national univercity, 2.QST, 3.Tokyo Institute of Technology, 4.Fukuoka Institute of Technology, 5.University of Hyogo, 6.Osaka University)

[PPS07-P02] Production of amino acids by gamma rays during aqueous alteration process in meteorite parent body

*Shinya Asano[1], Isao Yoda[2], Yasuji Muramatsu[3], Yoko Kebukawa[1], Kensei Kobayashi[1] (1.Yokohama national university, 2.Tokyo Institute of Technology, 3.University of Hyogo)

[PPS07-P03] Kinetic approaches for the thermal history of organic matter in meteorites based on Raman spectra

*Kento Kiryu[1], Yoko Kebukawa[1], Motoko Igisu[2], Takazo Shibuya[2], Kensei Kobayashi[1] (1.Yokohama National Univ., 2.Japan Agency for Marine-Earth Science and Technology)

[PPS07-P04] Relationship between spatial distribution of organic compounds and minerals in the Murchison meteorite

*Taiyo Sengoku[1], Minako Hashiguchi[1], Hiroshi Naraoka[1] (1.Kyushu University)

[PPS07-P05] O and Al-Mg isotope systematics of a hibonite-melilite-rich fine-grained CAI in the reduced CV chondrite NWA8613

*Sohei Wada[1], Noriyuki Kawasaki[1], Hisayoshi Yurimoto[1,2] (1.Hokkaido University, 2.ISAS/JAXA)

[PPS07-P06] Observation of Enstatite Whiskers in Fine-grained Rims in the Carbonaceous Chondrite ALH A77307

*Yasuhisa Shirota[1], Masahiro YASUTAKE[1], Satomi Enju[1], Akira Tsuchiyama[1] (1.Division of Earth and Planet, Science, Kyoto University)

[PPS07-P07] 3D observation of whisker-like material in the porous matrix of the Paris CM chondrite by SR-XCT

*Masahiro YASUTAKE[1], Epifanio Vacarro[2], Kentaro Uesugi[3], Akihisa Takeuchi[3], Tsukasa Nakano[4], Akira Tsuchiyama[1] (1.Division of Earth and Planetary Science, Graduate School of Science, Kyoto University, 2.National History Museum, London, 3.JASRI/SPring8, 4.GSJ/AIST)

[PPS07-P08] Development of cryogenic SIMS technique for isotope analysis of fluid inclusions

*Isono Yuki[1], Naoya Sakamoto[2], Hisayoshi Yurimoto[3] (1.Department of Natural History Sciences, Hokkaido University, 2.Creative Research Institusion, Hokkaido University, 3.Department of Natural History Sciences, Hokkaido University)

[PPS07-P09] X-ray diffraction study using Gandolfi attachment: Implications for small extraterrestrial materials

*Naoya Imae[1,2], Makoto Kimura[1] (1.Antarctic Meteorite Research Center, National Institute of Polar Research, 2.SOKENDAI)

[PPS07-P10] Trace elements analysis and Ar-Ar dating for microgram-scaled extraterrestrial samples

*Ryuji Okazaki[1], Sekimoto Shun[2] (1.Department of Earth and Planetary Sciences, Faculty of Science, Kyushu University, 2.Institute for Integrated Radiation and Nuclear Science, Kyoto University)

[PPS07-P11] Magnetic separation and identification of low-temperature solid particles using their translation caused by a pair of small permanent magnets

*Chiaki Uyeda[1], Wakana Yamaguchi[1], Keiji Hisayoshi[1], Kentaro Terada[1] (1.Institute of earth and Space Science Graduate School of Science Osaka University)

[PPS07-P12] The metallographic cooling rate of the Tafassasset primitive achondrite

*naoji sugiura[1], Tomoko Arai, takafumi matsui (1.Chiba Institute of Technology)

[PPS07-P13] The systematic investigations of high-pressure minerals in lunar basaltic meteorites

*Masaaki Miyahara[1], Kazunari Kozuma[1], Eiji Ohtani[2], Akira Yamaguchi[3], Takeshi Sakai[4], Hiroaki Ohfuji[4], Naotaka Tomioka[5], Yu Kodama[6] (1.Department of Earth and Planetary Systems Science, Graduate School of Science, Hiroshima University, 2.Department of Earth Sciences, Graduate School of Science, Tohoku University, 3.National Institute of Polar Research, 4.Geodynamics Research Center, Ehime University, 5.5Kochi Institute for Core Sample Research, Japan Agency for Marine-Earth Science and Technology, 6.Marine Works Japan)

[PPS07-P14] Bulk chemical analysis of iron meteorites by LA-ICP-MS

*Akira Yamaguchi[1], Naoki Shirai[2], Makiko K. Haba[3] (1.National Institute of Polar Research, 2.Tokyo Metropolitan University, 3.Tokyo Institute of Technology)

[E] Poster | P (Space and Planetary Sciences)：P-EM Solar-Terrestrial Sciences, Space Electromagnetism & Space Environment

1:45 PM - 3:15 PM JST | 4:45 AM - 6:15 AM UTC | Poster Hall International Exhibition Hall8, Makuhari Messe_1

[P-EM10] Multi-scale Coupling in the Magnetosphere-Ionosphere-Thermosphere System

convener:Yue Deng(University of Texas at Arlington), Toshi Nishimura(Boston University), Huixin Liu(Earth and Planetary Science Division, Kyushu University SERC, Kyushu University), Yanshi Huang(Harbin Institute of Technology, Shenzhen)

[PEM10-P01] Atmospheric responses in both hemispheres to relativistic electron precipitation

*Yoshimasa Tanaka[1,13,14], Takanori Nishiyama[1,14], Akira Kadokura[1,13,14], Mitsunori Ozaki[2], Yoshizumi Miyoshi[3], Shin-ichiro Oyama[3,15], Ryuho Kataoka[1,14], Masaki Tsutsumi[1,14], Koji Nishimura[1,13,14], Kaoru Sato[4], Yoshiya Kasahara[2], Atsushi Kumamoto[5], Fuminori Tsuchiya[5], Mizuki Fukizawa[5], Mitsuru Hikishima[6], Shoya Matsuda[6], Ayako Matsuoka[6], Iku Shinohara[6], Masahito Nose[3], Tsutomu Nagatsuma[7], Manabu Shinohara[8], Akiko Fujimoto[9], Mariko Teramoto[3], Reiko Nomura[10], Akira Sessai Yukimatu[1,14], Keisuke Hosokawa[11], Masafumi Shoji[3], Ralph Latteck[12] (1.National Institute of Polar Research, 2.Institute of Science and Engineering, Kanazawa University, 3.Institute for Space-Earth Environmental Research, Nagoya University, 4.Graduate School of Science, The University of Tokyo, 5.Graduate School of Science, Tohoku University, 6.Japan aerospace exploration agency, Institute of space and astronautical science, 7.National Institute of Information and Communications Technology, 8.Kagoshima National College of Technology, 9.Kyushu Institute of Technology, 10.National Observatory of Japan, 11.Department of Communication Engineering and Informatics, University of Electro-Communications, 12.Leibniz-Institute of Atmospheric Physics e.V. at the University Rostock, Germany, 13.Polar Environment Data Science Center, Joint-Support Center for Data Science Research, Research Organization of Information and Systems, 14.The Graduate University for Advanced Studies (SOKENDAI), 15.University of Oulu, Finland)

[PEM10-P02] Comparison of precipitating particle energy of proton aurora at geomagnetic conjugate points

*Makoto Taguchi[1], Tatsuki Nishijima[1], Akira Kadokura[2] (1.Rikkyo University, 2.Research Organization of Information and Systems)

[PEM10-P03] A regularized deep convolutional general adversarial network (R-DCGAN) for total electron content map completion

*Mingwu Jin[1], Zhou Chen[2,3], Yue Deng[1], Yang Pan[1], Jin-Song Wang[2] (1.University of Texas at Arlington, 2.Institute of Space Science and Technology, Nanchang University, Nanchang, China, 3.Key Laboratory of Space Weather, National Center for Space Weather, China Meteorological Administration, Beijing, China)

[PEM10-P04] A long-lasting auroral bright spot around magnetic north pole: Is it the evidence of stable magnetic reconnection?

*Qing-He Zhang[1], Guo-Cheng Shen[1], Yong-Liang Zhang[2], Kjellmar Oksavik[3], Michael Lockwood[4], Zan-Yang Xing[1], Yu-Zhang Ma[1] (1.Institute of Space Sciences, Shandong University, Weihai, China, 2.The Johns Hopkins University Applied Physics Laboratory, Laurel, Maryland, USA, 3.Birkeland Centre for Space Science, University of Bergen, Bergen, Norway, 4.Department of Meteorology, University of Reading, Earley Gate, Post Office Box 243, RG6 6BB, UK.)

[PEM10-P05] Statistical study of the relationship between ion upflow and field-aligned current in the topside ionosphere for both hemispheres during disturbed and quiet times

Shan-Yu Zhou[1], *Qing-He Zhang[1], P. T. Jayachandran[2], Kjellmar Oksavik[3], Larry Lyons[4], Zan-Yang Xing[1], Yu-Zhang Ma[1], Marc Hairston[5], Yong Wang[1] (1.Institute of Space Sciences, Shandong University, Weihai, China, 2.Physics Department, University of New Brunswick, Fredericton, New Brunswick, Canada, 3.Birkeland Centre for Space Science, University of Bergen, Bergen, Norway, 4.Department of Atmospheric and Oceanic Sciences, University of California, Los Angeles, California, USA, 5.William B. Hanson Center for Space Sciences, University of Texas at Dallas, Richardson, Texas, USA)

[PEM10-P06] SAPS in the 2013 March 17 Storm Event: Initial Results from the Coupled Magnetosphere-Ionosphere-Thermosphere Model

*Dong Lin[1,2], Wenbin Wang[2], Wayne Scales[1], Kevin Pham[2], Jing Liu[2], Binzheng Zhang[2], Viacheslav Merkin[3], Xueling Shi[1] (1.Virginia Tech, 2.High Altitude Observatory, NCAR, 3.APL, John Hopkins Univ.)

[PEM10-P07] Westward turning motions of nighttime medium-scale traveling ionospheric disturbances (MSTIDs) at the equatorward side of the dusk side auroral oval associated with auroral brightening

*Sneha Yadav[1,2], Kazuo Shiokawa[1], Shin-ichiro Oyama[1,3,4], Yuichi Otsuka[1] (1.ISEE, Nagoya University, Nagoya, Japan, 2.SPL, VSSC, India, 3.Ionosphere Research Unit, University of Oulu, Oulu, Finland, 4.NIPR, Tachikawa, Japan)

[E] Poster | P (Space and Planetary Sciences)：P-EM Solar-Terrestrial Sciences, Space Electromagnetism & Space Environment

5:15 PM - 6:30 PM JST | 8:15 AM - 9:30 AM UTC | Poster Hall International Exhibition Hall8, Makuhari Messe_4

[P-EM10] Multi-scale Coupling in the Magnetosphere-Ionosphere-Thermosphere System

convener:Yue Deng(University of Texas at Arlington), Toshi Nishimura(Boston University), Huixin Liu(Earth and Planetary Science Division, Kyushu University SERC, Kyushu University), Yanshi Huang(Harbin Institute of Technology, Shenzhen)

[PEM10-P01] Atmospheric responses in both hemispheres to relativistic electron precipitation

*Yoshimasa Tanaka[1,13,14], Takanori Nishiyama[1,14], Akira Kadokura[1,13,14], Mitsunori Ozaki[2], Yoshizumi Miyoshi[3], Shin-ichiro Oyama[3,15], Ryuho Kataoka[1,14], Masaki Tsutsumi[1,14], Koji Nishimura[1,13,14], Kaoru Sato[4], Yoshiya Kasahara[2], Atsushi Kumamoto[5], Fuminori Tsuchiya[5], Mizuki Fukizawa[5], Mitsuru Hikishima[6], Shoya Matsuda[6], Ayako Matsuoka[6], Iku Shinohara[6], Masahito Nose[3], Tsutomu Nagatsuma[7], Manabu Shinohara[8], Akiko Fujimoto[9], Mariko Teramoto[3], Reiko Nomura[10], Akira Sessai Yukimatu[1,14], Keisuke Hosokawa[11], Masafumi Shoji[3], Ralph Latteck[12] (1.National Institute of Polar Research, 2.Institute of Science and Engineering, Kanazawa University, 3.Institute for Space-Earth Environmental Research, Nagoya University, 4.Graduate School of Science, The University of Tokyo, 5.Graduate School of Science, Tohoku University, 6.Japan aerospace exploration agency, Institute of space and astronautical science, 7.National Institute of Information and Communications Technology, 8.Kagoshima National College of Technology, 9.Kyushu Institute of Technology, 10.National Observatory of Japan, 11.Department of Communication Engineering and Informatics, University of Electro-Communications, 12.Leibniz-Institute of Atmospheric Physics e.V. at the University Rostock, Germany, 13.Polar Environment Data Science Center, Joint-Support Center for Data Science Research, Research Organization of Information and Systems, 14.The Graduate University for Advanced Studies (SOKENDAI), 15.University of Oulu, Finland)

[PEM10-P02] Comparison of precipitating particle energy of proton aurora at geomagnetic conjugate points

*Makoto Taguchi[1], Tatsuki Nishijima[1], Akira Kadokura[2] (1.Rikkyo University, 2.Research Organization of Information and Systems)

[PEM10-P03] A regularized deep convolutional general adversarial network (R-DCGAN) for total electron content map completion

*Mingwu Jin[1], Zhou Chen[2,3], Yue Deng[1], Yang Pan[1], Jin-Song Wang[2] (1.University of Texas at Arlington, 2.Institute of Space Science and Technology, Nanchang University, Nanchang, China, 3.Key Laboratory of Space Weather, National Center for Space Weather, China Meteorological Administration, Beijing, China)

[PEM10-P04] A long-lasting auroral bright spot around magnetic north pole: Is it the evidence of stable magnetic reconnection?

*Qing-He Zhang[1], Guo-Cheng Shen[1], Yong-Liang Zhang[2], Kjellmar Oksavik[3], Michael Lockwood[4], Zan-Yang Xing[1], Yu-Zhang Ma[1] (1.Institute of Space Sciences, Shandong University, Weihai, China, 2.The Johns Hopkins University Applied Physics Laboratory, Laurel, Maryland, USA, 3.Birkeland Centre for Space Science, University of Bergen, Bergen, Norway, 4.Department of Meteorology, University of Reading, Earley Gate, Post Office Box 243, RG6 6BB, UK.)

[PEM10-P05] Statistical study of the relationship between ion upflow and field-aligned current in the topside ionosphere for both hemispheres during disturbed and quiet times

Shan-Yu Zhou[1], *Qing-He Zhang[1], P. T. Jayachandran[2], Kjellmar Oksavik[3], Larry Lyons[4], Zan-Yang Xing[1], Yu-Zhang Ma[1], Marc Hairston[5], Yong Wang[1] (1.Institute of Space Sciences, Shandong University, Weihai, China, 2.Physics Department, University of New Brunswick, Fredericton, New Brunswick, Canada, 3.Birkeland Centre for Space Science, University of Bergen, Bergen, Norway, 4.Department of Atmospheric and Oceanic Sciences, University of California, Los Angeles, California, USA, 5.William B. Hanson Center for Space Sciences, University of Texas at Dallas, Richardson, Texas, USA)

[PEM10-P06] SAPS in the 2013 March 17 Storm Event: Initial Results from the Coupled Magnetosphere-Ionosphere-Thermosphere Model

*Dong Lin[1,2], Wenbin Wang[2], Wayne Scales[1], Kevin Pham[2], Jing Liu[2], Binzheng Zhang[2], Viacheslav Merkin[3], Xueling Shi[1] (1.Virginia Tech, 2.High Altitude Observatory, NCAR, 3.APL, John Hopkins Univ.)

[PEM10-P07] Westward turning motions of nighttime medium-scale traveling ionospheric disturbances (MSTIDs) at the equatorward side of the dusk side auroral oval associated with auroral brightening

*Sneha Yadav[1,2], Kazuo Shiokawa[1], Shin-ichiro Oyama[1,3,4], Yuichi Otsuka[1] (1.ISEE, Nagoya University, Nagoya, Japan, 2.SPL, VSSC, India, 3.Ionosphere Research Unit, University of Oulu, Oulu, Finland, 4.NIPR, Tachikawa, Japan)

[E] Oral | P (Space and Planetary Sciences)：P-EM Solar-Terrestrial Sciences, Space Electromagnetism & Space Environment

3:30 PM - 5:00 PM JST | 6:30 AM - 8:00 AM UTC | A05 TOKYO BAY MAKUHARI HALL

[P-EM10] Multi-scale Coupling in the Magnetosphere-Ionosphere-Thermosphere System

convener:Yue Deng(University of Texas at Arlington), Toshi Nishimura(Boston University), Huixin Liu(Earth and Planetary Science Division, Kyushu University SERC, Kyushu University), Yanshi Huang(Harbin Institute of Technology, Shenzhen), Chairperson:Yue Deng(University of Texas at Arlington), Huixin Liu(Kyushu University, Japan), Yanshi Huang(Harbin Institute of Technology, Shenzhen, China), Yukitoshi Nishimura(Boston University)

3:30 PM - 3:45 PM JST | 6:30 AM - 6:45 AM UTC

[PEM10-01] Auroral fragmentation into patches and pressure balance condition in the source magnetosphere

★Invited Papers

*Kazuo Shiokawa[1], Katsuki Nishi[1] (1.Institute for Space-Earth Environmental Research, Nagoya University)

3:45 PM - 4:00 PM JST | 6:45 AM - 7:00 AM UTC

[PEM10-02] Formation and Evolution of Polar Cap Ionospheric Patches and Their Associated Upflows and Scintillations: A Review

★Invited Papers

*Qing-He Zhang[1], Zan-Yang Xing[1], Yong Wang[1], Yu-Zhang Ma[1] (1.Institute of Space Sciences, Shandong University, Weihai, China)

4:00 PM - 4:15 PM JST | 7:00 AM - 7:15 AM UTC

[PEM10-03] Global ionospheric disturbances during the 6-10 September 2017 solar storms

★Invited Papers

*Shunrong Zhang[1] (1.MIT Haystack Observatory)

4:15 PM - 4:30 PM JST | 7:15 AM - 7:30 AM UTC

[PEM10-04] Multiscape Coupling of Sub-auroral Polarization Streams

*Nozomu Nishitani[1], Tomoaki Hori[1] (1.Institute for Space-Earth Environmental Research, Nagoya University)

4:30 PM - 4:45 PM JST | 7:30 AM - 7:45 AM UTC

[PEM10-05] Scale sizes of mass density enhancements inferred from accelerometer measurements

*Yanshi Huang[1], Cheryl Huang[2] (1.Harbin Institute of Technology, Shenzhen, China, 2.Space Physics Directoriate, Air Force Research Laboratory, Kirtland AFB, USA)

4:45 PM - 5:00 PM JST | 7:45 AM - 8:00 AM UTC

[PEM10-06] **Meso-scale forcing in the upper atmosphere: sources and impacts**

*Yue Deng[1], Qingyu Zhu[1], Cissi Lin[1] (1.University of Texas at Arlington)

[E] Oral | P (Space and Planetary Sciences)：P-EM Solar-Terrestrial Sciences, Space Electromagnetism & Space Environment

9:00 AM - 10:30 AM JST | 12:00 AM - 1:30 AM UTC | A04 TOKYO BAY MAKUHARI HALL

[P-EM12] Space Weather and Space Climate

convener:Ryuho Kataoka(National Institute of Polar Research), Antti A Pulkkinen(NASA Goddard Space Flight Center), Kanya Kusano(Institute for Space-Earth Environmental Research, Nagoya University), Kaori Sakaguchi(National Institute of Information and Communications Technology), Chairperson:Antti Pulkkinen(NASA/GSFC)

9:00 AM - 9:15 AM JST | 12:00 AM - 12:15 AM UTC

[PEM12-01] NASA Heliophysics Division Space Weather Update

★Invited Papers

*Nicola Justine Fox[1] (1.NASA Headquarters)

9:15 AM - 9:30 AM JST | 12:15 AM - 12:30 AM UTC

[PEM12-02] NOAA's Current and Future Space Weather Architecture

★Invited Papers

*Elsayed R Talaat[1] (1.NOAA National Environmental Satellite, Data, and Information Service)

9:30 AM - 9:45 AM JST | 12:30 AM - 12:45 AM UTC

[PEM12-03] Community Coordinating Modeling Center (CCMC): A hub for collaborative assessment and improvement of space weather capabilities.

★Invited Papers

*Maria M Kuznetsova[1], M. Leila Mays[1], Edward J Semones[2], Peter J Macneice[1], Lutz Rastaetter[1], Ja Soon Shim[1], Yihua Zheng[1], Katherine Garcia-Sage[1], Joycelyn Jones[1], Yaireshka m Collado-Vega[1], Richard E Mullinix[1], Chiu Wiegand[1] (1.NASA Goddard Space Flight Center, 2.NASA Johnson Space Center)

9:45 AM - 10:00 AM JST | 12:45 AM - 1:00 AM UTC

[PEM12-04] Different flux evolutions of relativistic electrons of the outer belt associated with high-speed coronal hole streams; Arase and Van Allen Probes observations

*Yoshizumi Miyoshi[1], Satoshi Kurita[1], Ryuho Kataoka[2], Shinji Saito[1], Vania Jordanova[3], Iku Shinohara[4], Takefumi Mitani[4], Takeshi Takashima[4], Nana Higashio[4], Satoshi Kasahara[5], Shoichiro Yokota[6], Tomoaki Hori[1], Kunihiro Keika[5], Yoshiya Kasahara[7], Shoya Matsuda[4], Atsushi Kumamoto[8], Fuminori Tsuchiya[8], Masafumi Shoji[1], Ayako Matsuoka[1], Mariko Teramoto[1], Harlan Spence[9], Geoff Reeves[3], Daniel Baker[10] (1.Institute for Space-Earth Environmental Research, Nagoya University, 2.NIPR, 3.Los Alamos National Laboratory, 4.JAXA, 5.University of Tokyo, 6.Osaka University, 7.Kanazawa University, 8.Tohoku University, 9.University of New Hampshire, 10.University of Colorado)

10:00 AM - 10:15 AM JST | 1:00 AM - 1:15 AM UTC

[PEM12-05] Study on the predictability of imminent giant solar flares based on the theory of double-arc instability

*Kanya Kusano[1], Tomoya Iju[2], Yumi Bamba[1] (1.Institute for Space-Earth Environmental Research, Nagoya University, 2.NAOJ)

10:15 AM - 10:30 AM JST | 1:15 AM - 1:30 AM UTC

[PEM12-06] Update of space weather research and operation activities in NICT

*Mamoru Ishii[1] (1.National Institute of Information and Communications Technology)

[E] Oral | P (Space and Planetary Sciences)：P-EM Solar-Terrestrial Sciences, Space Electromagnetism & Space Environment

10:45 AM - 12:15 PM JST | 1:45 AM - 3:15 AM UTC | A04 TOKYO BAY MAKUHARI HALL

[P-EM12] Space Weather and Space Climate

convener:Ryuho Kataoka(National Institute of Polar Research), Antti A Pulkkinen(NASA Goddard Space Flight Center), Kanya Kusano(Institute for Space-Earth Environmental Research, Nagoya University), Kaori Sakaguchi(National Institute of Information and Communications Technology), Chairperson:Ryuho Kataoka(National Institute of Polar Research)

10:45 AM - 11:00 AM JST | 1:45 AM - 2:00 AM UTC

[PEM12-07] Commercial Space Weather Activities From a USA small Business Perspertive

★Invited Papers

*Chigomezyo Mudala Ngwira[1], Geoff Crowley[1], Chad Fish[1] (1.Atmospheric and Space Technology Research Associates, LLC)

11:00 AM - 11:15 AM JST | 2:00 AM - 2:15 AM UTC

[PEM12-08] Development of coronal mass ejection arrival time forecasting system using interplanetary scintillation observations

★Invited Papers

*Kazumasa Iwai[1], Daikou Shiota[2], Munetoshi Tokumaru[1], Ken'ichi Fujiki[1], Mitsue Den[2], Yûki Kubo[2] (1.Institute for Space–Earth Environmental Research (ISEE), Nagoya University, 2.National Institute of Information and Communications)

11:15 AM - 11:30 AM JST | 2:15 AM - 2:30 AM UTC

[PEM12-09] Development of real-time prediction system of CME arrival and magnetic field with SUSANOO-CME MHD simulation

*Daikou Shiota[1,2], Seiji Yashiro[3], Kazumasa Iwai[2] (1.National Institute of Information and Communications Technology (NICT), 2.Institute for Space-Earth Environmental Research, Nagoya University, 3.Catholic University)

11:30 AM - 11:45 AM JST | 2:30 AM - 2:45 AM UTC

[PEM12-10] The Role of a Tiny Brightening in a Huge Geo-effective Solar Eruption Leading to the St Patrick's Day Storm

*Yumi Bamba[1,2], Satoshi Inoue[1], Keiji Hayashi[1,3,4] (1.Institute for Space-Earth Environmental Research/Nagoya University, 2.Institute if Space and Astronautical Science/Japan Aerospace Exploration Agency, 3.Key Laboratory of Solar Activity, National Astronomical Observatories, Chinese Academy of Sciences, 4.State Key Laboratory for Space Weather, National Space Science Center, Chinese Academy of Sciences)

11:45 AM - 12:00 PM JST | 2:45 AM - 3:00 AM UTC

[PEM12-11] Critical Parameters of Photospheric Magnetic Field to Produce Eruptive Solar Flares and CMEs in Active Regions

*Pei Hsuan Lin[1], Kanya Kusano[1], Daikou Shiota[2], Satoshi Inoue[1], KD Leka[1,3], Yuta Mizuno[1] (1.Institute for Space-Earth Environmental Research, Nagoya University, 2.National Institute of Information and Communications Technology, 3.NorthWest Research Associates)

12:00 PM - 12:15 PM JST | 3:00 AM - 3:15 AM UTC

[PEM12-12] Simulation study on internal velocity field variation of eruptive prominence

★Invited Papers

*Takafumi Kaneko[1], Kanya Kusano[1] (1.Institute for Space-Earth Environmental Research, Nagoya University)

[E] Oral | P (Space and Planetary Sciences)：P-EM Solar-Terrestrial Sciences, Space Electromagnetism & Space Environment

1:45 PM - 3:15 PM JST | 4:45 AM - 6:15 AM UTC | A04 TOKYO BAY MAKUHARI HALL

[P-EM12] Space Weather and Space Climate

convener:Ryuho Kataoka(National Institute of Polar Research), Antti A Pulkkinen(NASA Goddard Space Flight Center), Kanya Kusano(Institute for Space-Earth Environmental Research, Nagoya University), Kaori Sakaguchi(National Institute of Information and Communications Technology), Chairperson:Antti Pulkkinen(NASA/GSFC)

1:45 PM - 2:00 PM JST | 4:45 AM - 5:00 AM UTC

[PEM12-13] Is intensity of auroral electrojet predictable?

★Invited Papers

*Yusuke Ebihara[1], Takashi Tanaka[2], Naoki Kamiyoshikawa[3] (1.Research Institute for Sustainable Humanosphere, Kyoto University, 2.Kyushu University, 3.Mitsubishi Electric Corporation)

2:00 PM - 2:15 PM JST | 5:00 AM - 5:15 AM UTC

[PEM12-14] Geoelectromagnetics with the Geophysical Instrument Combination of Hydro-Québec, AUTUMNX, and USArray Magnetotellurics

★Invited Papers

*Martin G Connors[1], Sébastien Guillon[2], Adam Schultz[3], Naoto Imamura[3] (1.Athabasca University, 2.Hydro-Québec TransÉnergie, 3.Oregon State University)

2:15 PM - 2:30 PM JST | 5:15 AM - 5:30 AM UTC

[PEM12-15] Quantifying the Latitudinal Extent of the Aurorae During Large Geomagnetic Storms

*Sean Blake[1,2], Antti Pulkkinen[1], Pete Schuck[1] (1.NASA Goddard Space Flight Center, Space Weather Laboratory, Greenbelt, Maryland, USA, 2.Catholic University of America, Department of Physics, Washington DC, USA)

2:30 PM - 2:45 PM JST | 5:30 AM - 5:45 AM UTC

[PEM12-16] Simulation of Geomagnetically Induced Current (GIC) Flowing in 500 kV Power Grid in Japan Including a Three-Dimensional Ground Inhomogeneity

*Satoko Nakamura[1], Yusuke Ebihara[1], Shigeru Fujita[2], Tada-nori Goto[3], Shinichi Watari[4] (1.Research Institute for Sustainable Humanosphere, Kyoto University., 2.Meteorological College, Japan Meteorological Agency, 3.Graduate School of Engineering, Kyoto University, 4.National Institute of Information and Communications Technology)

2:45 PM - 3:00 PM JST | 5:45 AM - 6:00 AM UTC

[PEM12-17] Reproducibility of the geomagnetically induced currents in Hokkaido with a two-layer conductivity model

*Takashi Kikuchi[1,2], Yusuke Ebihara[2], Kumiko K. Hashimoto[3], Shinichi Watari[4] (1.Institute for Space-Earth Environmental Research, Nagoya University, 2.Institute for Sustainable Humanosphere, Kyoto University, 3.Kibi International University, 4.National Institute of Information and Communications Technology)

3:00 PM - 3:15 PM JST | 6:00 AM - 6:15 AM UTC

[PEM12-18] Fan-shaped aurora as seen from Japan during a great magnetic storm on 11 February 1958

*Ryuho Kataoka[1], Shiori Uchino[1], yasunori Fujiwara[1], Shigeru Fujita[1], Kazuaki Yamamoto[2] (1.National Institute of Polar Research, 2.National Institute of Japanese Literature)

[E] Oral | P (Space and Planetary Sciences)：P-EM Solar-Terrestrial Sciences, Space Electromagnetism & Space Environment

3:30 PM - 5:00 PM JST | 6:30 AM - 8:00 AM UTC | A04 TOKYO BAY MAKUHARI HALL

[P-EM12] Space Weather and Space Climate

convener:Ryuho Kataoka(National Institute of Polar Research), Antti A Pulkkinen(NASA Goddard Space Flight Center), Kanya Kusano(Institute for Space-Earth Environmental Research, Nagoya University), Kaori Sakaguchi(National Institute of Information and Communications Technology), Chairperson:Kanya Kusano(Nagoya University)

3:30 PM - 3:45 PM JST | 6:30 AM - 6:45 AM UTC

[PEM12-19] Application Usability Levels: Their evolution and eco-system

★Invited Papers

*Alexa Jean Halford[1], Adam Kellerman[2], Jeff Klenzing[3], Katherine Garcia-Sage[3], Brett A Carter[4], Daniel T Welling[5], Barbara Thompson[3], Antti A Pulkkinen[3] (1.The Aerospace Corporation, 2.UCLA, 3.NASA/GSFC, 4.RMIT, 5.UT Arlington)

3:45 PM - 4:00 PM JST | 6:45 AM - 7:00 AM UTC

[PEM12-20] The Operational Space Weather Forecast at NICT, Japan

★Invited Papers

*Kosuke Sakai[1], Kentaro Ukawa[1], Kentaro Kawahara[1], Mamoru Ishii[2], Yuki Kubo[2] (1.Systems Engineering Consultants Co., LTD., 2.National Institute of Information and Communications Technology)

4:00 PM - 4:15 PM JST | 7:00 AM - 7:15 AM UTC

[PEM12-21] PROGRESS: An overview of data products

*Michael A Balikhin[1], Simon N Walker[1] (1.University of Sheffield)

4:15 PM - 4:30 PM JST | 7:15 AM - 7:30 AM UTC

[PEM12-22] The Probability of Satellite Anomalies by a Disastrous Solar Flare

*Daikichi SEKI[1,2,3] (1.Graduate School of Advanced Integrated Studies in Human Survivability, Kyoto University, 2.Centre for the Study of Existential Risk, University of Cambridge, 3.Astronomical Observatory, Kyoto University)

4:30 PM - 4:45 PM JST | 7:30 AM - 7:45 AM UTC

[PEM12-23] **Operational Forecasting of Solar Flares using Deep Neural Network**

*Naoto Nishizuka[1], Yuki Kubo[1], Komei Sugiura[1], Mitsue Den[1], Mamoru Ishii[1] (1.National Institute of Information and Communications Technology)

4:45 PM - 5:00 PM JST | 7:45 AM - 8:00 AM UTC

[PEM12-24] **Spring-Autumnal asymmetry in geomagnetic activity and its origin over last 140 years**

*Hao Luo[1], Xiaoming Sha[1] (1.IGGCAS)

[E] Oral | A (Atmospheric and Hydrospheric Sciences)：A-OS Ocean Sciences & Ocean Environment

3:30 PM - 5:00 PM JST | 6:30 AM - 8:00 AM UTC | 301B 3F

[A-OS09] Ocean Mixing Processes: Impact on Biogeochemistry, Climate and Ecosystem

convener:Ichiro Yasuda(Atmosphere and Ocean Research Institute, The University of Tokyo), Toshiyuki Hibiya(Department of Earth and Planetary Science, Graduate School of Science, University of Tokyo), Jun Nishioka(Hokkaido University, Institute of low temperature sciences), Shin-ichi Ito(Atmosphere and Ocean Research Institute, The University of Tokyo), Chairperson:Toshiyuki Hibiya(Department of Earth and Planetary Science, Graduate School of Science, The University of Tokyo)

3:30 PM - 3:45 PM JST | 6:30 AM - 6:45 AM UTC

[AOS09-18] Searching 18.6 year tidal modulation impact in a global gridded ocean oxygen dataset with its improvements

*Shoshiro Minobe[1] (1.Earth and Planetary Sciences, Faculty of Science, Hokkaido University)

3:45 PM - 4:00 PM JST | 6:45 AM - 7:00 AM UTC

[AOS09-19] Contribution of tidal energy dissipation to variations of transient climate response and steric sea level rise through ocean heat uptake

*Michio Watanabe[1], Hiroaki Tatebe[1], Tatsuo Suzuki[1], Kaoru Tachiiri[1] (1.Japan Agency for Marine-Earth Science and Technology)

4:00 PM - 4:15 PM JST | 7:00 AM - 7:15 AM UTC

[AOS09-20] A Wave Resolving Simulation for Upper Ocean Turbulence Driven by Wave-Current Interaction

*Yutaka Yoshikawa[1], Yasushi Fujiwara[1], Yoshimasa Matsumura[2] (1.Graduate School of Science, Kyoto University, 2. Atmosphere and Ocean Research Institute, The University of Tokyo)

4:15 PM - 4:30 PM JST | 7:15 AM - 7:30 AM UTC

[AOS09-21] Revisiting the Characteristics of Mixing Efficiency in the Brazil Basin

*Takashi Ijichi[1], Louis St. Laurent[1], Kurt Polzin[1] (1.Woods Hole Oceanographic Institution)

4:30 PM - 4:45 PM JST | 7:30 AM - 7:45 AM UTC

[AOS09-22] Instabilities of finite-amplitude internal wave beams

*Yohei Onuki[1], Yuki Tanaka[2] (1.Research Institute for Applied Mechanics, Kyushu University, 2.Department of Earth and Planetary Science, Graduate School of Science, The University of Tokyo)

4:45 PM - 5:00 PM JST | 7:45 AM - 8:00 AM UTC

[AOS09-23] Evaluation of nutrient flux enhanced by double diffusion in the Kuroshio using glider measurements

*Keunjong Lee[1], Ryo Yamamoto[1], Ichiro Yasuda[1], Takahiro Tanaka[2] (1.Atmosphere and Ocean Research Institute, 2.Tohoku National Fisheries Research Institute, Japan Fisheries Research and Education Agency)

[E] Oral | A (Atmospheric and Hydrospheric Sciences)：A-OS Ocean Sciences & Ocean Environment

9:00 AM - 10:30 AM JST | 12:00 AM - 1:30 AM UTC | 302 3F

[A-OS12] Marine ecosystems and biogeochemical cycles: theory, observation and modeling

convener:Shin-ichi Ito(Atmosphere and Ocean Research Institute, The University of Tokyo), Takafumi Hirata(Faculty of Environmental Earth Science, Hokkaido University), Enrique N Curchitser(Rutgers University New Brunswick), Eileen E Hofmann(Old Dominion University), Chairperson:Shin-Ichi Ito(The University of Tokyo)

9:10 AM - 9:30 AM JST | 12:10 AM - 12:30 AM UTC

[AOS12-01] Projected coastal hypoxia in a coupled bio-physical model of the California Current System.

★Invited Papers

*Enrique N Curchitser[1], Raphael Dussin[1,2], Charles Stock[3], Nicoals van Oostende[4] (1.Rutgers University New Brunswick, 2.Lamont-Doherty Earth Observatory of Columbia University, 3.NOAA Geophysical Fluid Dynamics Laboratory, 4.Princeton University)

9:30 AM - 9:45 AM JST | 12:30 AM - 12:45 AM UTC

[AOS12-02] **Decadal salinity variation in the western North Pacific correlated with the strength of the Oyashio and the Kuroshio Extension**

*Hitoshi Kaneko[1], Takeshi Okunishi[2], Shinya Kouketsu[3], Sachihiko Itoh[1], Takashi Seto[4], Hiroshi Kuroda[5], Yugo Shimizu[4] (1.Atmosphere and Ocean Research Institute, The University of Tokyo, 2.Tohoku National Fisheries Research Institute, Japan Fisheries Research and Education Agency, 3.Japan Agency for Marine-Earth Science and Technology, 4.National Research Institute of Fisheries Science, Japan Fisheries Research and Education Agency, 5.Hokkaido National Fisheries Research Institute, Japan Fisheries Research and Education Agency)

9:45 AM - 10:00 AM JST | 12:45 AM - 1:00 AM UTC

[AOS12-03] **Multiscale routes to supply nutrients through the Kuroshio nutrient stream**

*Takeyoshi Nagai[1], Sophie Clayton[2], Yusuke Uchiyama[3] (1.Department of Ocean Sciences, Tokyo University of Marine Science and Technology, 2.Ocean, Earth & Atmospheric Sciences, Old Dominion University, 3.Kobe University)

10:00 AM - 10:15 AM JST | 1:00 AM - 1:15 AM UTC

[AOS12-04] **Seasonal variability of upper-ocean primary production around the Kuroshio analyzed using a ROMS-NPZD model**

*Xu Zhang[1], Yusuke Uchiyama[1,2], Yota Suzue[3], Hidekatsu Yamazaki[4] (1.Kobe University, 2.Port and Airport Research Institute, 3.Construction Technique Institute Engineering Co., Ltd., 4.Tokyo University of Marine Science and Technology)

10:15 AM - 10:30 AM JST | 1:15 AM - 1:30 AM UTC

[AOS12-05] Nutrient and light conditions at subsurface chlorophyll maximum: physical-biogeochemical observations along a mid-Pacific meridional transect

*Sachihiko Itoh[1], Hitoshi Kaneko[1], Shinya Kouketsu[2], Takeshi Okunishi[3], Hiroshi Ogawa[1], Mitsuhide Sato[4], Hiroaki Saito[1] (1.Atmosphere and Ocean Research Institute, The University of Tokyo, 2.Japan Agency for Marin-Earth Science and Technology, 3.Tohoku National Fisheries Research Institute, Fisheries Research Agency, 4.The Hong Kong University of Science and Technology)

[E] Oral | A (Atmospheric and Hydrospheric Sciences)：A-OS Ocean Sciences & Ocean Environment

10:45 AM - 12:15 PM JST | 1:45 AM - 3:15 AM UTC | 302 3F

[A-OS12] Marine ecosystems and biogeochemical cycles: theory, observation and modeling

convener:Shin-ichi Ito(Atmosphere and Ocean Research Institute, The University of Tokyo), Takafumi Hirata(Faculty of Environmental Earth Science, Hokkaido University), Enrique N Curchitser(Rutgers University New Brunswick), Eileen E Hofmann(Old Dominion University), Chairperson:Yoshimasa Matsumura(Atmosphere and Ocean Research Institute, The University of Tokyo)

10:45 AM - 11:05 AM JST | 1:45 AM - 2:05 AM UTC

[AOS12-06] A Lagrangian view of spring phytoplankton blooms

★Invited Papers

*Shinichiro Kida[1], Taka Ito[2] (1.Research Institute for Applied Mechanics, Kyushu University, 2.Georgia Institute of Technology)

11:05 AM - 11:20 AM JST | 2:05 AM - 2:20 AM UTC

[AOS12-07] Significance of acclimation process in simulating chlorophyll distribution in the Arctic Ocean

*Yoshio Masuda[1], Yasuhiro Yamanaka[1], Takafumi Hirata[1], Hideyuki Nakano[2] (1.Graduate School of Environmental Earth Science, Hokkaido University, 2.Meteorological Research Institute)

11:20 AM - 11:35 AM JST | 2:20 AM - 2:35 AM UTC

[AOS12-08] Responses of lower-trophic level ecosystem to nutrient variation in the central part of the Seto Inland Sea

*Naoki Yoshie[1], Hayato Mizuguchi[1], Xinyu Guo[1], Michio Yoneda[2], Katsuyuki Abo[2], Tomoaki Kono[2], Tatsunori Fujita[3] (1.Center for Marine Environmental Studies, Ehime University, 2.Japan Fisheries Research and Education Agency, 3.Kagawa Prefectural Fisheries Research Center)

11:35 AM - 11:50 AM JST | 2:35 AM - 2:50 AM UTC

[AOS12-09] Effects of the temperature and fish size on metabolism and swimming performance of Pacific chub mackerel *Scomber japonicus* in the Northwest Pacific

*Chenying Guo[1], Shin-ichi Ito[1], Michio Yoneda[2], Hajime Kitano[2] (1.Atmosphere and Ocean Research Institute, the University of Tokyo, 2.Fisheries Research and Education Agency Japan)

11:50 AM - 12:05 PM JST | 2:50 AM - 3:05 AM UTC

[AOS12-10] Sensitivity analyses of growth and migration of Japanese anchovy (*Engraulis japonicus*) in the East China Sea using a fish growth-migration model.

*Shin-ichi Ito[1], Takashi Setou[2], Michio Yoneda[2], Motomitsu Takahashi[2], Michiya Matsuyama[3], Chenying Guo[1], Takashi Kitagawa[1] (1.Atmosphere and Ocean Research Institute, The University of Tokyo, 2.Fisheries Research and Education Agency Japan, 3.Kyushu University)

[E] Oral | A (Atmospheric and Hydrospheric Sciences)：A-OS Ocean Sciences & Ocean Environment

1:45 PM - 3:15 PM JST | 4:45 AM - 6:15 AM UTC | 302 3F

[A-OS12] Marine ecosystems and biogeochemical cycles: theory, observation and modeling

convener:Shin-ichi Ito(Atmosphere and Ocean Research Institute, The University of Tokyo), Takafumi Hirata(Faculty of Environmental Earth Science, Hokkaido University), Enrique N Curchitser(Rutgers University New Brunswick), Eileen E Hofmann(Old Dominion University), Chairperson:Enrique Curchitser(Rutgers University)

1:45 PM - 2:05 PM JST | 4:45 AM - 5:05 AM UTC

[AOS12-11] Micro-scale patchiness enhances trophic transfer efficiency and potential plankton biodiversity

★Invited Papers

*Hidekatsu Yamazaki[1], Anupam Priyadarshi[2], Lan Smith[3], Sandip Mandal[4], Mamoru Tanaka[1] (1.Tokyo University of Marine Science and Technology, 2.Banaras Hindu University, 3.Japan Agency for Marine-Earth Science and Technology, 4.Public Health Foundation of India)

2:05 PM - 2:20 PM JST | 5:05 AM - 5:20 AM UTC

[AOS12-12] Long term observations of marine snow, using cabled observatory system

*Marika Takeuchi[1,2], Mark Doubell[3], Jim Mitchell[2], Hidekatsu Yamazaki[1] (1.Tokyo University of Marine Science and Technology, 2.Flinders University, 3.South Australia Research and Development Institute)

2:20 PM - 2:35 PM JST | 5:20 AM - 5:35 AM UTC

[AOS12-13] An insight into the area characteristic of seasonal change in nitrogen isotope ratio based on a marine nitrogen isotope model

*Chisato Yoshikawa[1], Masahito Shigemitsu[1], Akitomo Yamamoto[1], Akira Oka[2], Naohiko Ohkouchi[1] (1.JAMSTEC, 2.AORI)

2:35 PM - 2:50 PM JST | 5:35 AM - 5:50 AM UTC

[AOS12-14] Modeling variability of ^{15}N stable isotope enrichment within the planktonic food chain

*S. Lan Smith[1], Yoshikazu Sasai[1], Chisato Yoshikawa[2] (1.Marine Ecosystem Dynamics Research Group, RCGC, Japan Agency for Marine-Earth Science and Technology, Yokohama, Japan, 2.Department of Biogeochemistry, Japan Agency for Marine-Earth Science and Technology, Yokosuka, Japan)

2:50 PM - 3:05 PM JST | 5:50 AM - 6:05 AM UTC

[AOS12-15] Discussions

Shin-ichi Ito[2], *Takafumi Hirata[1] (1.Faculty of Environmental Earth Science, Hokkaido University, 2.Atmosphere and Ocean Research Institute, The University of Tokyo)

[E] Poster | A (Atmospheric and Hydrospheric Sciences)：A-OS Ocean Sciences & Ocean Environment

3:30 PM - 5:00 PM JST | 6:30 AM - 8:00 AM UTC | Poster Hall International Exhibition Hall8, Makuhari Messe_3

[A-OS12] Marine ecosystems and biogeochemical cycles: theory, observation and modeling

convener:Shin-ichi Ito(Atmosphere and Ocean Research Institute, The University of Tokyo), Takafumi Hirata(Faculty of Environmental Earth Science, Hokkaido University), Enrique N Curchitser(Rutgers University New Brunswick), Eileen E Hofmann(Old Dominion University)

[AOS12-P01] Impact of the nutrient transport through the Tsushima Strait on the ecosystem in the Japan Sea

*Ryota Shibano[1], Akihiko Morimoto[1], Katsumi Takayama[2], Tetsutaro Takikawa[3], Masashi Ito[4] (1.Center for Marine Environmental Studies, Ehime University, 2.Research Institute for Applied Mechanics, Kyushu University, 3.Graduate School of Fisheries and Environmental Sciences, Nagasaki University, 4.Fisheries Oceanography Department, Japan Sea National Fisheries Research Institute)

[AOS12-P02] Revisiting vertical variations in stoichiometry during oceanic organic matter decomposition

*Masahito Shigemitsu[1], Michio Aoyama[1], Toshimasa Doi[1], Taichi Yokokawa[1], Akihiko Murata[1] (1.Japan Agency for Marine-Earth Science and Technology)

[AOS12-P03] Reproduction of iron-rich intermediate water in the Sea of Okhotsk by high resolution biogeochemical model.

*Hatsumi Nishikawa[1], Humio Mitsudera[1], Hiroshi Yoshinari[2], Takuya Nakanowatari[3], Tomohiro Nakamura[1], Keisuke Uchimoto[4], Hiroyasu Hasumi[5] (1.Institute of Low Temperature Science, Hokkaido University, 2.National Institute for Environmental Studies, 3.Tohoku National Fisheries Research Institute, Japan Fisheries Research and Education Agency, 4.Research Institute of Innovative Technology for the Earth, 5.Atmosphere and Ocean Research Institute, University of Tokyo)

[AOS12-P04] The global oceanic iron distribution estimated by data assimilation approach

*Doi Toshimasa[1], Satoshi Osafune[1], Shuhei Masuda[1], Hajime Obata[2], Kazuhiro Misumi[3], Jun Nishioka[4] (1.Japan Agency for Marine-Earth Science and Technology, 2.The University of Tokyo, 3.Central Research Institute of Electric Power Industry, 4.Hokkaido University)

[AOS12-P05] A high-resolution multi-purpose particle tracking framework for coastal areas near Japan

*Yoshimasa Matsumura[1], Shota Katsura[1], Masao Kurogi[2], Hideyuki Nakano[3], Takateru Yamagishi[4] (1.Atmosphere and Ocean Research Institute, University of Tokyo, 2.Japan Agency for Marine-Earth Science and Technology, 3.Meteorological Research Institute, Japan Meteorological Agency , 4.Research organization for Information Science and Technology)

[AOS12-P06] Numerical study on seasonality of ocean litters collected at the Dongsha Island in the northern South China Sea

*Yi-Chia Hsin[1], Chia-Ying Ko[2], Ming-Shiou Jeng[3] (1.Research Center for Environmental Changes, Academia Sinica, 2.Institute of Fisheries Science, National Taiwan University, 3.Biodiversity Research Center, Academia Sinica)

[AOS12-P07] A key spot and timing to monitor chlorophyll-a in the Kuroshio western boundary current

*Takafumi Hirata[1] (1.Faculty of Environmental Earth Science, Hokkaido University)

[AOS12-P08] **Impacts of cyclonic eddies on phytoplankton biomass and phenology in the Kuroshio Extension region**

*Eko Siswanto[1], Yoshikazu Sasai[1] (1.Japan Agency for Marine-Earth Science and Technology)

[AOS12-P09] Diagnostic estimation and uncertainties of nutrient limitation of phytoplankton growth in Michaelis-Menten functional form

*Taketo Hashioka[1], Maki Noguchi Aita[1] (1.Japan Agency for Marine-Science and Technology)

[AOS12-P10] Modeling productivity in lower trophic levels in Otsuchi Bay, northeast of Japan, using a nested OGCM with a biogeochemical component

*Takashi T Sakamoto[1], L. Shogo Urakawa[2], Sachihiko Itoh[1], Hiroyasu Hasumi[1], Kiyoshi Tanaka[1] (1.Atmosphere and Ocean Research Institute, the University of Tokyo, 2.Meteorological Research Institute, Japan Meteorologica Agancy)

[AOS12-P11] Change in lower trophic level ecosystems to decadal scale variation of climate system in the North Pacific Ocean

*Maki Noguchi Aita[1], Kazuaki Tadokoro[2], Yoshiki Komuro[3], Taketo Hashioka[1], Naomi Harada[1] (1.Research and Development Center for Global Change, Japan Agency for Marine-Earth Science and Technology, 2.Tohoku National Fisheries Research Institute, Japan Fisheries Research and Education Agency, 3.Institute of Arctic Climate and Environment Research, Japan Agency for Marine-Earth Science and Technology)

[AOS12-P12] Estimation of experienced environment of jack mackerel in the East China Sea

*Tomihiko Higuchi[1], Motomitsu Takahashi[2], Kotaro Shirai[1], Shin-ichi Ito[1] (1.Atmosphere and Ocean Research Institute, The University of Tokyo, 2.Seikai National Fisheries Research Institute,FRA)

[E] Poster | A (Atmospheric and Hydrospheric Sciences)：A-OS Ocean Sciences & Ocean Environment

5:15 PM - 6:30 PM JST | 8:15 AM - 9:30 AM UTC | Poster Hall International Exhibition Hall8, Makuhari Messe_5

[A-OS12] Marine ecosystems and biogeochemical cycles: theory, observation and modeling

convener:Shin-ichi Ito(Atmosphere and Ocean Research Institute, The University of Tokyo), Takafumi Hirata(Faculty of Environmental Earth Science, Hokkaido University), Enrique N Curchitser(Rutgers University New Brunswick), Eileen E Hofmann(Old Dominion University)

[AOS12-P01] Impact of the nutrient transport through the Tsushima Strait on the ecosystem in the Japan Sea

*Ryota Shibano[1], Akihiko Morimoto[1], Katsumi Takayama[2], Tetsutaro Takikawa[3], Masashi Ito[4] (1.Center for Marine Environmental Studies, Ehime University, 2.Research Institute for Applied Mechanics, Kyushu University, 3.Graduate School of Fisheries and Environmental Sciences, Nagasaki University, 4.Fisheries Oceanography Department, Japan Sea National Fisheries Research Institute)

[AOS12-P02] Revisiting vertical variations in stoichiometry during oceanic organic matter decomposition

*Masahito Shigemitsu[1], Michio Aoyama[1], Toshimasa Doi[1], Taichi Yokokawa[1], Akihiko Murata[1] (1.Japan Agency for Marine-Earth Science and Technology)

[AOS12-P03] Reproduction of iron-rich intermediate water in the Sea of Okhotsk by high resolution biogeochemical model.

*Hatsumi Nishikawa[1], Humio Mitsudera[1], Hiroshi Yoshinari[2], Takuya Nakanowatari[3], Tomohiro Nakamura[1], Keisuke Uchimoto[4], Hiroyasu Hasumi[5] (1.Institute of Low Temperature Science, Hokkaido University, 2.National Institute for Environmental Studies, 3.Tohoku National Fisheries Research Institute, Japan Fisheries Research and Education Agency, 4.Research Institute of Innovative Technology for the Earth, 5.Atmosphere and Ocean Research Institute, University of Tokyo)

[AOS12-P04] The global oceanic iron distribution estimated by data assimilation approach

*Doi Toshimasa[1], Satoshi Osafune[1], Shuhei Masuda[1], Hajime Obata[2], Kazuhiro Misumi[3], Jun Nishioka[4] (1.Japan Agency for Marine-Earth Science and Technology, 2.The University of Tokyo, 3.Central Research Institute of Electric Power Industry, 4.Hokkaido University)

[AOS12-P05] A high-resolution multi-purpose particle tracking framework for coastal areas near Japan

*Yoshimasa Matsumura[1], Shota Katsura[1], Masao Kurogi[2], Hideyuki Nakano[3], Takateru Yamagishi[4] (1.Atmosphere and Ocean Research Institute, University of Tokyo, 2.Japan Agency for Marine-Earth Science and Technology, 3.Meteorological Research Institute, Japan Meteorological Agency , 4.Research organization for Information Science and Technology)

[AOS12-P06] Numerical study on seasonality of ocean litters collected at the Dongsha Island in the northern South China Sea

*Yi-Chia Hsin[1], Chia-Ying Ko[2], Ming-Shiou Jeng[3] (1.Research Center for Environmental Changes, Academia Sinica, 2.Institute of Fisheries Science, National Taiwan University, 3.Biodiversity Research Center, Academia Sinica)

[AOS12-P07] A key spot and timing to monitor chlorophyll-a in the Kuroshio western boundary current

*Takafumi Hirata[1] (1.Faculty of Environmental Earth Science, Hokkaido University)

[AOS12-P08] **Impacts of cyclonic eddies on phytoplankton biomass and phenology in the Kuroshio Extension region**

*Eko Siswanto[1], Yoshikazu Sasai[1] (1.Japan Agency for Marine-Earth Science and Technology)

[AOS12-P09] Diagnostic estimation and uncertainties of nutrient limitation of phytoplankton growth in Michaelis-Menten functional form

*Taketo Hashioka[1], Maki Noguchi Aita[1] (1.Japan Agency for Marine-Science and Technology)

[AOS12-P10] Modeling productivity in lower trophic levels in Otsuchi Bay, northeast of Japan, using a nested OGCM with a biogeochemical component

*Takashi T Sakamoto[1], L. Shogo Urakawa[2], Sachihiko Itoh[1], Hiroyasu Hasumi[1], Kiyoshi Tanaka[1] (1.Atmosphere and Ocean Research Institute, the University of Tokyo, 2.Meteorological Research Institute, Japan Meteorologica Agancy)

[AOS12-P11] Change in lower trophic level ecosystems to decadal scale variation of climate system in the North Pacific Ocean

*Maki Noguchi Aita[1], Kazuaki Tadokoro[2], Yoshiki Komuro[3], Taketo Hashioka[1], Naomi Harada[1] (1.Research and Development Center for Global Change, Japan Agency for Marine-Earth Science and Technology, 2.Tohoku National Fisheries Research Institute, Japan Fisheries Research and Education Agency, 3.Institute of Arctic Climate and Environment Research, Japan Agency for Marine-Earth Science and Technology)

[AOS12-P12] Estimation of experienced environment of jack mackerel in the East China Sea

*Tomihiko Higuchi[1], Motomitsu Takahashi[2], Kotaro Shirai[1], Shin-ichi Ito[1] (1.Atmosphere and Ocean Research Institute, The University of Tokyo, 2.Seikai National Fisheries Research Institute,FRA)

[J] Oral | A (Atmospheric and Hydrospheric Sciences)：A-OS Ocean Sciences & Ocean Environment

10:45 AM - 12:15 PM JST | 1:45 AM - 3:15 AM UTC | 102 1F

[A-OS13] Ocean circulation and material cycle in coastal seas

convener:Kiyoshi Tanaka(University of Tokyo), Akihiko Morimoto(Ehime University), Yuichi Hayami(Saga University), Kazuhiko Ichimi(Seto Inland Sea Regional Research Center, Kagawa University), Chairperson:Kiyoshi Tanaka, Akihiko Morimoto

10:45 AM - 11:00 AM JST | 1:45 AM - 2:00 AM UTC

[AOS13-01] On-demand development of bay-scale models using the Japanese Coastal Ocean Monitoring and Forecasting System

*Kei Sakamoto[1], Hideyuki Nakano[1], Shogo Urakawa[1], Takahiro Toyoda[1], Hiroyuki Tsujino[1], Goro Yamanaka[1] (1.Meteorological Research Institute)

11:00 AM - 11:15 AM JST | 2:00 AM - 2:15 AM UTC

[AOS13-02] Long term measurement of the current at the bay head in the Suruga Bay, Japan. part 2

*Takaaki Katsumata[1,4], Masato Niki[2], Akihiko Tanaka[1], Hiroyuki Tan[1,3], Kyoko Takashima[2], Takashige Sugimoto (1.Liberal Arts Education Center, Shimizu Campus, Tokai University., 2.School of Marine Science and Technology, Tokai University, 3.Japan Unmanned Vehicle exploration Agency, 4.NPO, the association for the environmental conservation of the ocean)

11:15 AM - 11:30 AM JST | 2:15 AM - 2:30 AM UTC

[AOS13-03] Bottom-water intrusion and subsequent water exchange induced by Yamase around Mutsu Bay

*Satomi Fujisaki[1], Atsuhiko Isobe[1], Izumi Ogida[2], Yuki Kosaka[2] (1.Kyushu university, 2.Aomori Prefectural Fisheries Research Institute)

11:30 AM - 11:45 AM JST | 2:30 AM - 2:45 AM UTC

[AOS13-04] The Generation Process of the Bottom Intrusion in the Bungo Channel

*Kana Maetani[1], Akihiko Morimoto[2], Xinyu Guo[2], Toru Miyama[3] (1.Graduate School of Science and Engineering, Ehime University, 2.Center for Marine Environmental Studies, Ehime University, 3.Japan Agency for Marine-Earth Science and Technology)

11:45 AM - 12:00 PM JST | 2:45 AM - 3:00 AM UTC

[AOS13-05] Characteristics of bottom intrusion in the Bungo Channel

*Akihiko Morimoto[1], Shuya Fujita[1], Hidetaka Takeoka[1], Xinyu Guo[1] (1.Ehime University)

12:00 PM - 12:15 PM JST | 3:00 AM - 3:15 AM UTC

[AOS13-06] Role of Kuroshio Current in fish resource variability off southwest Japan

*Yushi Morioka[1], Sergey Varlamov[1], Yasumasa Miyazawa[1] (1.Japan Agency for Marine-Earth Science and Technology)

[J] Oral | A (Atmospheric and Hydrospheric Sciences)：A-OS Ocean Sciences & Ocean Environment

1:45 PM - 3:15 PM JST | 4:45 AM - 6:15 AM UTC | 102 1F

[A-OS13] Ocean circulation and material cycle in coastal seas

convener:Kiyoshi Tanaka(University of Tokyo), Akihiko Morimoto(Ehime University), Yuichi Hayami(Saga University), Kazuhiko Ichimi(Seto Inland Sea Regional Research Center, Kagawa University), Chairperson:Akihiko Morimoto, Yuichi Hayami

1:45 PM - 2:00 PM JST | 4:45 AM - 5:00 AM UTC

[AOS13-07] Variation in hypoxic water mass in Ariake Sea -what consumed the dissolved oxygen?-

*Yuichi Hayami[1], Naoki Fujii[1], Hiroyuki Takasu[2], Yu Umezawa[3], Minoru Wada[2] (1.Saga University, 2.Nagasaki University, 3.Tokyo University of Agriculture and Technology)

2:00 PM - 2:15 PM JST | 5:00 AM - 5:15 AM UTC

[AOS13-08] Influence of Nori aquaculture-induced change in light environment on phytoplankton dynamics

*Naoya Minamiura[1], Soichi Yamaguchi[1] (1.Kyushu University)

2:15 PM - 2:30 PM JST | 5:15 AM - 5:30 AM UTC

[AOS13-09] **Enhanced West Philippine Sea intrusion diminishes hypoxia conditions in the Pearl River estuary**

*Hon-Kit Lui[1,2], Chen-Tung Arthur Chen[1], Wei-Ping Hou[2], Jian-Ming Liau[2] (1.Department of Oceanography, National Sun Yat-sen University, 2.Taiwan Ocean Research Institute, National Applied Research Laboratories)

2:30 PM - 2:45 PM JST | 5:30 AM - 5:45 AM UTC

[AOS13-10] North Pacific seawater radiocarbon recorded in abalone shells obtained from Otsuchi Bay, Japan

*Ota Kosuke[1], Yusuke Yokoyama[1,2], Yosuke Miyairi[2], Jun Hayakawa[2], Naomi Sato[2], Hideki Fukuda[2], Kiyoshi Tanaka[2] (1.Department of Earth and Planetary Science, Graduate School of Science, The University of Tokyo, 2.Atmosphere and Ocean Research Institute, The University of Tokyo)

2:45 PM - 3:00 PM JST | 5:45 AM - 6:00 AM UTC

[AOS13-11] Spreading of Radioactive Cesium off Joban coast through Large River Discharge

*Kiyoshi Tanaka[1], Seiya Nagao[2], Yujiro Kitade[3], Masato Niki[4], Takaaki Katsumata[4], Toru Miyama[5] (1.University of Tokyo, 2.Kanazawa University, 3.Tokyo University of Marine Science and Technology, 4.Tokai University, 5.Japan Agency for Marine-Earth Science and Technology)

3:00 PM - 3:15 PM JST | 6:00 AM - 6:15 AM UTC

[AOS13-12] Development of a river-ocean seamless model for simulating river discharges around Kyushu

*Takahiro Tsutsumi[1], Shinichiro Kida[2], Ryusuke Kuroki[3], Yosuke Alexandre Yamashiki[3] (1.Interdisciplinary Graduate School of Engineering Science, Kyushu University, 2.Research Institute for Applied Mechanics, Kyushu University, 3.Graduate School of Advanced Integrated Studies in Human Survivability, Kyoto University)

[J] Poster | A (Atmospheric and Hydrospheric Sciences)：A-OS Ocean Sciences & Ocean Environment

3:30 PM - 5:00 PM JST | 6:30 AM - 8:00 AM UTC | Poster Hall International Exhibition Hall8, Makuhari Messe_4

[A-OS13] Ocean circulation and material cycle in coastal seas

convener:Kiyoshi Tanaka(University of Tokyo), Akihiko Morimoto(Ehime University), Yuichi Hayami(Saga University), Kazuhiko Ichimi(Seto Inland Sea Regional Research Center, Kagawa University)

[AOS13-P01] An experimental study on degradation and fragmentation of marine plastic debris

*YUSEI YAMAGUCHI[1] (1.KYUSHU UNIVERSITY)

[AOS13-P02] Seafloor environment based on grain and concentrations of carbon, nitrogen and sulfur of surface sediment in Ise and Mikawa bays

*Atsuko Amano[1], Koji Seike[1] (1.National institute of Advanced Industrial Science and Technology)

[AOS13-P03] Hydrographic observations of estuarine circulation in Suruga Bay, Japan

*Kiyoshi Tanaka[1], Masato Niki[2], Kunio Kutsuwada[2], Akio Ishida[3], daisuke Takahashi[2], Takaaki Katsumata[2], Kazuyuki Uehara[2] (1.University of Tokyo, 2.Tokai University, 3.Tokoha University)

[AOS13-P04] Residence time of river water in the Jakarta Bay

*Akihiko Morimoto[1], Endro Soeyanto[2], Yuichi Hayami[3], Agus Sudaryanto[2], Suhendar Sachoemar[2] (1.Ehime University, 2.BPPT, Indonesia, 3.Saga University)

[J] Poster | A (Atmospheric and Hydrospheric Sciences)：A-OS Ocean Sciences & Ocean Environment

5:15 PM - 6:30 PM JST | 8:15 AM - 9:30 AM UTC | Poster Hall International Exhibition Hall8, Makuhari Messe_6

[A-OS13] Ocean circulation and material cycle in coastal seas

convener:Kiyoshi Tanaka(University of Tokyo), Akihiko Morimoto(Ehime University), Yuichi Hayami(Saga University), Kazuhiko Ichimi(Seto Inland Sea Regional Research Center, Kagawa University)

[AOS13-P01] An experimental study on degradation and fragmentation of marine plastic debris

*YUSEI YAMAGUCHI[1] (1.KYUSHU UNIVERSITY)

[AOS13-P02] Seafloor environment based on grain and concentrations of carbon, nitrogen and sulfur of surface sediment in Ise and Mikawa bays

*Atsuko Amano[1], Koji Seike[1] (1.National institute of Advanced Industrial Science and Technology)

[AOS13-P03] Hydrographic observations of estuarine circulation in Suruga Bay, Japan

*Kiyoshi Tanaka[1], Masato Niki[2], Kunio Kutsuwada[2], Akio Ishida[3], daisuke Takahashi[2], Takaaki Katsumata[2], Kazuyuki Uehara[2] (1.University of Tokyo, 2.Tokai University, 3.Tokoha University)

[AOS13-P04] Residence time of river water in the Jakarta Bay

*Akihiko Morimoto[1], Endro Soeyanto[2], Yuichi Hayami[3], Agus Sudaryanto[2], Suhendar Sachoemar[2] (1.Ehime University, 2.BPPT, Indonesia, 3.Saga University)

[J] Oral | A (Atmospheric and Hydrospheric Sciences)：A-OS Ocean Sciences & Ocean Environment

3:30 PM - 5:00 PM JST | 6:30 AM - 8:00 AM UTC | 102 1F

[A-OS15] Freshwater discharge through rivers and estuaries to the ocean

convener:Shinichiro Kida(Research Institute for Applied Mechanics, Kyushu University), Dai Yamazaki(Institute of Industrial Sciences, The University of Tokyo), Yosuke Alexandre Yamashiki(Earth & Planetary Water Resources Assessment Laboratory Graduate School of Advanced Integrated Studies in Human Survivability Kyoto University), Humio Mitsudera(Institute of Low Temperature Science, Hokkaido University), Chairperson:Shinichiro Kida(RIAM, Kyushu University), Humio Mitsudera(Hokkaido University, Institute of Low Temperature Science), Yosuke Yamashiki(GSAIS Kyoto University)

3:30 PM - 3:45 PM JST | 6:30 AM - 6:45 AM UTC

[AOS15-01] The forefront research for flow and water quality estimations in coastal area using geo-stationary and polar orbital satellites data

★Invited Papers

*Yuji Sakuno[1] (1.Graduate School of Engineering, Hiroshima University)

3:45 PM - 4:00 PM JST | 6:45 AM - 7:00 AM UTC

[AOS15-02] Rainfall-Runoff-Inundation Processes and Modeling in a Humid Tropical River Basin

★Invited Papers

*Takahiro Sayama[1], Kodai Yamamoto[2], Ryoko Araki[2], Apip Apip[3], Eva Mia Siska[1], Kaoru Takara[4] (1.Disaster Prevention Research Institute, Kyoto University, 2.Graduate School of Engineering, Kyoto University, 3.LIPI, Indonesia, 4.Graduate School of Advanced Integrated Studies in Human Survivability, Kyoto University)

4:00 PM - 4:15 PM JST | 7:00 AM - 7:15 AM UTC

[AOS15-03] Role of river inflows from Kamchatka Peninsula in the Okhotsk Sea

*Toru Miyama[1], Humio Mitsudera[2] (1.Application Laboratory, Japan Agency for Marine-Earth Science and Technology, , 2.Institute of Low Temperature Science, Hokkaido University)

4:15 PM - 4:30 PM JST | 7:15 AM - 7:30 AM UTC

[AOS15-04] CHLOROPHYLL ESTIMATION OF LAKE AND COASTAL WATER USING REMOTE SENSING APPROACH

*Shweta Yadav[1], Yamashiki Yosuke[1], Junichi Susaki[1], Kanako Ishikawa[2], Yoh Yamashita[1] (1.Kyoto University, 2.LBERI)

4:30 PM - 4:45 PM JST | 7:30 AM - 7:45 AM UTC

[AOS15-05] Maritime-continent coastal region as land-sea-air triple boundary layer and bio-anthroposphere

*Manabu D. Yamanaka[1] (1.Research Institute for Humanity and Nature / Professor Emeritus of Kobe University)

4:45 PM - 5:00 PM JST | 7:45 AM - 8:00 AM UTC

[AOS15-06] River-ocean interaction at the Ganges-Brahmaputra river mouth

*Shinichiro Kida[1], Dai Yamazaki[2] (1.Research Institute for Applied Mechanics, Kyushu University, 2.Institute of Industrial Sciences, The University of Tokyo)

[J] Poster | A (Atmospheric and Hydrospheric Sciences)：A-OS Ocean Sciences & Ocean Environment

5:15 PM - 6:30 PM JST | 8:15 AM - 9:30 AM UTC | Poster Hall International Exhibition Hall8, Makuhari Messe_7

[A-OS15] Freshwater discharge through rivers and estuaries to the ocean

convener:Shinichiro Kida(Research Institute for Applied Mechanics, Kyushu University), Dai Yamazaki(Institute of Industrial Sciences, The University of Tokyo), Yosuke Alexandre Yamashiki(Earth & Planetary Water Resources Assessment Laboratory Graduate School of Advanced Integrated Studies in Human Survivability Kyoto University), Humio Mitsudera(Institute of Low Temperature Science, Hokkaido University)

[AOS15-P01] MERIT Hydro: Global 90m-resolution hydrography map based on latest topography datasets.

*Dai Yamazaki[1] (1.Institute of Industrial Sciences, The University of Tokyo)

[AOS15-P02] Comparison of model performance between global- and regional-scale river models in simulating compound flooding in coastal deltas in the world's continental rivers

*Hiroaki Ikeuchi[1,2], Dai Yamazaki[2], Yukiko Hirabayashi[3] (1.Graduate School of Engineering, The University of Tokyo, 2.Institute of Industrial Science, The University of Tokyo, 3.Graduate School of Engineering and Science, Shibaura Instittute of Technology)

[AOS15-P03] Observation of a river plume by drone-mounted visible/infrared cameras

*Kenta Araki[1], Shinichiro Kida[2], Atsuhiko Isobe[2] (1.Interdisciplinary Graduate School of Engineering Sciences, Kyushu University, 2.Research Institute for Applied Mechanics, Kyushu University)

[AOS15-P04] Numerical simulation of typhoon storm surge in the LUOYUAN Bay

*Nan Yuan[1], Humio Mitsudera [1] (1.Hokkaido University, the Institute of Low Temperature Science)

[AOS15-P05] Laboratory and numerical experiments on the ballooning of river-plume bulge

*fujita yusuke[1], Atsuhiko Isobe[2] (1.interdiscipinary graduate school of engineering science, Kyushu Univercity, 2.Research Institude for Applied Mechanics Kyushu Univ)

[J] Poster | A (Atmospheric and Hydrospheric Sciences)：A-OS Ocean Sciences & Ocean Environment

1:45 PM - 3:15 PM JST | 4:45 AM - 6:15 AM UTC | Poster Hall International Exhibition Hall8, Makuhari Messe_2

[A-OS16] Chemical and Biological Oceanography

convener:Namiha Yamada(National Institute of Advanced Industrial Science and Technology), Sayaka Yasunaka(Japan Agency for Marine-Earth Science and Technology), Hiroaki Saito(Atmosphere and Ocean Research Institute, The University of Tokyo)

[AOS16-P01] **Seasonal productions of dinoflagellate cysts in relation to environmental characteristics in Jinhae-Masan Bay, Korea: One year sediment trap observation**

*Hyeon Ho Shin[1] (1.Korea Institute of Ocean Science and Technology)

[AOS16-P02] Pacific anthropogenic carbon between 1991 and 2017

*Akihiko Murata[1], Carter B.R.[2,3], Feely, R.A. Feely, R.A.[3], Wanninkhof, R. Wanninkhof, R.[3], Shinya Kouketsu[1], Sonnerup R.E.[2], Pardo P.C.[4], Sabine C.L.[5], Johnson G. C.[3], Sloyan B.M.[6], Mecking S.[2], Tilbrook B.[6], Speer K.[7], Talley L.D.[8], Millero F.J.[9], Wijffels S.E.[6,10], Macdonald A.M.[10], Gruber N.[11], Bullister J. L.[3] (1.Japan Agency for Marine-Earth Science and Technology, 2.University of Washington, 3.NOAA, 4.University of Tasmania, 5.University of Hawaii Manoa, 6.CSIRO, 7.The Florida State University, 8.University of California, 9.University of Miami, 10.Woods Hole Oceanographic Institution, 11.IBP)

[AOS16-P03] Spatio-temporal variability of surface water pCO2 and nutrients in the tropical Pacific from 1981 to 2015

*Sayaka Yasunaka[1], Shinya Kouketsu[1], P.G. Strutton[2], A.J. Sutton[3], Akihiko Murata[1], Shin-ichiro Nakaoka[4], Yukihiro Nojiri[4] (1.Japan Agency for Marine-Earth Science and Technology, 2.University of Tasmania, 3.NOAA, 4.NIES)

[J] Poster | A (Atmospheric and Hydrospheric Sciences)：A-OS Ocean Sciences & Ocean Environment

5:15 PM - 6:30 PM JST | 8:15 AM - 9:30 AM UTC | Poster Hall International Exhibition Hall8, Makuhari Messe_8

[A-OS16] Chemical and Biological Oceanography

convener:Namiha Yamada(National Institute of Advanced Industrial Science and Technology), Sayaka Yasunaka(Japan Agency for Marine-Earth Science and Technology), Hiroaki Saito(Atmosphere and Ocean Research Institute, The University of Tokyo)

[AOS16-P01] **Seasonal productions of dinoflagellate cysts in relation to environmental characteristics in Jinhae-Masan Bay, Korea: One year sediment trap observation**

*Hyeon Ho Shin[1] (1.Korea Institute of Ocean Science and Technology)

[AOS16-P02] Pacific anthropogenic carbon between 1991 and 2017

*Akihiko Murata[1], Carter B.R.[2,3], Feely, R.A. Feely, R.A.[3], Wanninkhof, R. Wanninkhof, R.[3], Shinya Kouketsu[1], Sonnerup R.E.[2], Pardo P.C.[4], Sabine C.L.[5], Johnson G. C.[3], Sloyan B.M.[6], Mecking S.[2], Tilbrook B.[6], Speer K.[7], Talley L.D.[8], Millero F.J.[9], Wijffels S.E.[6,10], Macdonald A.M.[10], Gruber N.[11], Bullister J. L.[3] (1.Japan Agency for Marine-Earth Science and Technology, 2.University of Washington, 3.NOAA, 4.University of Tasmania, 5.University of Hawaii Manoa, 6.CSIRO, 7.The Florida State University, 8.University of California, 9.University of Miami, 10.Woods Hole Oceanographic Institution, 11.IBP)

[AOS16-P03] Spatio-temporal variability of surface water pCO2 and nutrients in the tropical Pacific from 1981 to 2015

*Sayaka Yasunaka[1], Shinya Kouketsu[1], P.G. Strutton[2], A.J. Sutton[3], Akihiko Murata[1], Shin-ichiro Nakaoka[4], Yukihiro Nojiri[4] (1.Japan Agency for Marine-Earth Science and Technology, 2.University of Tasmania, 3.NOAA, 4.NIES)

[J] Oral | A (Atmospheric and Hydrospheric Sciences)：A-OS Ocean Sciences & Ocean Environment

3:30 PM - 5:00 PM JST | 6:30 AM - 8:00 AM UTC | 303 3F

[A-OS16] Chemical and Biological Oceanography

convener:Namiha Yamada(National Institute of Advanced Industrial Science and Technology), Sayaka Yasunaka(Japan Agency for Marine-Earth Science and Technology), Hiroaki Saito(Atmosphere and Ocean Research Institute, The University of Tokyo), Chairperson:Tsuneo Ono(Japan Fisheries Research and Education Agency), Naohiro Kosugi(気象研究所)

3:30 PM - 3:45 PM JST | 6:30 AM - 6:45 AM UTC

[AOS16-01] Variability of the growth rate for dissolved inorganic carbon in surface seawater along the 165°E line

*Chiho Tanizaki[1], Hisashi Ono[2], Masao Ishii[2], Atsushi Kojima[1], Shinji Masuda[1], Kazutaka Enyo[1], Daisuke Sasano[1], Toshiya NAKANO[1] (1.Japan Meteorological Agency, 2.Meteorological Research Institute, Japan Meteorological Agency)

3:45 PM - 4:00 PM JST | 6:45 AM - 7:00 AM UTC

[AOS16-02] Seasonal variations of oceanic CO_2 disequilibrium and anthropogenic CO_2 in the subarctic North Pacific

*Bofeng Li[1], Shukuta Satori[1], Kasai Hiromi[2], Hiroshi Kuroda[2], Taniuchi Yukiko[2], Daisuke Hasegawa[3], Yutaka Watanabe[1] (1.Hokkaido University, 2.Hokkaido National Fisheries Research Institute, Japan Fisheries and Education Research , 3.Tohoku National Fisheries Research Institute, Japan Fisheries and Education Research)

4:00 PM - 4:15 PM JST | 7:00 AM - 7:15 AM UTC

[AOS16-03] An evaluation of current and future ocean acidification based on pCO_2 database around Okinawa Island

*Naohiro Kosugi[1], Hiroyuki Tsujino[1], Masao Ishii[1] (1.Meteorological Research Institute)

4:15 PM - 4:30 PM JST | 7:15 AM - 7:30 AM UTC

[AOS16-04] Reconstruction of spatiotemporal change of anthropogenic fixed nitrogen in the western North Pacific

*Yutaka Watanabe[1], Kouichi Fujita[1], BOFENG LI[1] (1.Hokkaido University)

4:30 PM - 4:45 PM JST | 7:30 AM - 7:45 AM UTC

[AOS16-05] On the mechanism of significant increasing trend of silicate in intermediate layer of Oyashio region

*Tsuneo Ono[1] (1.Fisheries Research and Education Agency)

4:45 PM - 5:00 PM JST | 7:45 AM - 8:00 AM UTC

[AOS16-06] Systematics of aluminum, manganese, iron, cobalt, and lead in the North Pacific Ocean observed during ocean-section study of GEOTRACES Japan

*Yoshiki Sohrin[1], Linjie Zheng[1] (1.Institute for Chemical Research, Kyoto University)

[J] Oral | A (Atmospheric and Hydrospheric Sciences)：A-OS Ocean Sciences & Ocean Environment

9:00 AM - 10:30 AM JST | 12:00 AM - 1:30 AM UTC | 301A 3F

[A-OS19] Dynamics of oceanic and atmospheric waves, vortices, and circulations

convener:Yuki Tanaka(Graduate School of Science, The University of Tokyo), Ryo Furue(APL/JAMSTEC), Yukiharu Hisaki(University of the Ryukyus), Norihiko Sugimoto(Keio University, Department of Physics), Chairperson:Norihiko Sugimoto, Ryo Furue

9:00 AM - 9:15 AM JST | 12:00 AM - 12:15 AM UTC

[AOS19-01] Instability of Ekman pumping

★Invited Papers

*Yoshiaki Miyamoto[1], Daivd S Nolan[2], Norihiko Sugimoto[3] (1.Faculty of Environment and Information Studies, Keio University, 2.Rosenstiel School of Marine and Atmospheric Science, University of Miami, 3.Keio University, Department of Physics)

9:15 AM - 9:30 AM JST | 12:15 AM - 12:30 AM UTC

[AOS19-02] Extratropical Cyclone Structures around Japan -Comparison between Extratropical Cyclones Developing around Japan and those in Northwestern Atlantic Ocean-

*Eigo Tochimoto[1], Hiroshi Niino[1] (1.Atmosphere and Ocean Research Institute, The University of Tokyo)

9:30 AM - 9:45 AM JST | 12:30 AM - 12:45 AM UTC

[AOS19-03] Application of a new wave energy flux formulation to assessment of tropical wave propagation dynamics: Diagnostics for the tropical synoptic-scale wave disturbances in the Maritime Continent-northern Australian region

*Fukutomi Yoshiki[1], Hidenori Aiki[1] (1.Institute for Space-Earth Environmental Reasearch, Nagoya University)

9:45 AM - 10:00 AM JST | 12:45 AM - 1:00 AM UTC

[AOS19-04] Direct measurement of turbulent fluxes at sea-air interface by micrometeorological technique

★Invited Papers

*Fumiyoshi Kondo[1], Shujiro Komiya[2], Kosuke Noborio[3], Hidenori Aiki[4], Kunio Kutsuwada[5], Mitsuo Uematsu[6], Osamu Tsukamoto[7] (1.Japan Coast Guard Academy, 2.Max Planck Institute for Biogeochemistry, 3.Meiji University, 4.Nagoya University , 5.Tokai University, 6.The University of Tokyo, 7.Okayama University)

10:00 AM - 10:15 AM JST | 1:00 AM - 1:15 AM UTC

[AOS19-05] Swell-Dominant Surface Waves Inherent in the Shape of the Rias Coast facing the western North Pacific

*Kosei Komatsu[1,2], Takaki Fujii[1,2], Kiyoshi Tanaka[2] (1.Graduate School of Frontier Sciences, The University of Tokyo, 2.Atmosphere and Ocean Research Institute, The University of Tokyo)

10:15 AM - 10:30 AM JST | 1:15 AM - 1:30 AM UTC

[AOS19-06] **Variabilities of the Sea Surface Height in the Kuril Basin of the Okhotsk Sea: Coherent shelf-trapped mode and Rossby wave-like mode**

*Vigan Mensah[1], Kay I. Ohshima[1] (1.Institute of Low Temperature Science)

[J] Oral | A (Atmospheric and Hydrospheric Sciences)：A-OS Ocean Sciences & Ocean Environment

10:45 AM - 12:15 PM JST | 1:45 AM - 3:15 AM UTC | 301A 3F

[A-OS19] Dynamics of oceanic and atmospheric waves, vortices, and circulations

convener:Yuki Tanaka(Graduate School of Science, The University of Tokyo), Ryo Furue(APL/JAMSTEC), Yukiharu Hisaki(University of the Ryukyus), Norihiko Sugimoto(Keio University, Department of Physics), Chairperson:Yukiharu Hisaki(琉球大学理学部), Hidenori AIKI

10:45 AM - 11:00 AM JST | 1:45 AM - 2:00 AM UTC

[AOS19-07] Dynamics of water exchange processes at a deep submarine canyon off the western coast of the Sakhaline which causes the origin of the cold water belt along the Soya Warm Current

★Invited Papers

*Humio Mitsudera[1], Hiroyuki Iida[2] (1.Institute of Low Temperature Science, Hokkaido University, 2.Graduate School of Environmental Science)

11:00 AM - 11:15 AM JST | 2:00 AM - 2:15 AM UTC

[AOS19-08] Generation Mechanism of Tropical Instability Waves in the Equatorial Pacific Ocean

*Yuki Tanaka[1], Toshiyuki Hibiya[1] (1.Graduate School of Science, The University of Tokyo)

11:15 AM - 11:30 AM JST | 2:15 AM - 2:30 AM UTC

[AOS19-09] Annual Rossby waves below the pycnocline in the Indian Ocean

*Motoki Nagura[1] (1.Japan Agency for Marine-Earth Science and Technology)

11:30 AM - 11:45 AM JST | 2:30 AM - 2:45 AM UTC

[AOS19-10] Eddies observed by Argo floats

★Invited Papers

*Katsuro Katsumata[1] (1.JAMSTEC)

11:45 AM - 12:00 PM JST | 2:45 AM - 3:00 AM UTC

[AOS19-11] Rhythmic Phenomena in Nonlinear Systems and Oceanic General Circulation

*Shinya Shimokawa[1], Tomonori Matsuura[2] (1.National Research Institute for Earth Science and Disaster Prevention, 2.University of Toyama)

12:00 PM - 12:15 PM JST | 3:00 AM - 3:15 AM UTC

[AOS19-12] Control of the ocean circulation by bottom topography and generation of mesoscale disturbances

*Yuri Kase[1], Tomonori Matsuura[1] (1.National university corporation University of Toyama)

[J] Poster | A (Atmospheric and Hydrospheric Sciences)：A-OS Ocean Sciences & Ocean Environment

3:30 PM - 5:00 PM JST | 6:30 AM - 8:00 AM UTC | Poster Hall International Exhibition Hall8, Makuhari Messe_5

[A-OS19] Dynamics of oceanic and atmospheric waves, vortices, and circulations

convener:Yuki Tanaka(Graduate School of Science, The University of Tokyo), Ryo Furue(APL/JAMSTEC), Yukiharu Hisaki(University of the Ryukyus), Norihiko Sugimoto(Keio University, Department of Physics)

[AOS19-P01] **Atmospheric super rotation developed in a GCM (AFES-Venus)**

*Norihiko Sugimoto[1], Masahiro Takagi[2], Yoshihisa Matsuda[3] (1.Keio University, Department of Physics, 2.Kyoto Sangyo University, Department of Physics, 3.Tokyo Gakugei University, Department of Natural Sciences)

[AOS19-P02] Data assimilation of the Venus atmosphere assuming radio occultation measurement by small satellites

*Mirai Abe[1], Norihiko Sugimoto[1], Yukako Kikuchi[2], Asako Hosono[3], Hiroki Ando[4], Masahiro Takagi[4], Itziar Garate Lopez[5], Sebastien Lebonnois[6], Chi Ao[7] (1.Keio University, 2.Yokohama Futaba High School, 3.Toshimagaoka Women High School, 4.Kyoto Sangyo University, 5.Euskal Herriko Unibertsitatea, 6.Sorbonne Universite, 7.Jet Propulsion Laboratory)

[AOS19-P03] Relationship between solar wind and atmospheric circulation

*Paul Prikryl[1] (1.Physics Department University of New Brunswick and Geomagnetic Laboratory Natural Resources Canada)

[AOS19-P04] Contribution of the Atlantic storm track to the Euro-Russian blocking maintenance in summer 2010

*Akira Yamazaki[1] (1.Application Laboratory, Japan Agency for Marine-Earth Science and Technology)

[AOS19-P05] Instabilities in Ekman layer and roll structures in a tropical cyclone boundary layer

*Junshi Ito[1], Hiroshi Niino[1] (1.Atmosphere and Ocean Research Institute, The University of Tokyo)

[AOS19-P06] Mathematical description of the internal waves in a proximity of the bottom of the Ocean.

*andrei giniatoulline[1], german tobar[1] (1.Department of Mathematics, Los Andes University, Bogota, Colombia, South America)

[AOS19-P07] How deterministic are the deep zonal jets?

*Ryo Furue[1], Masami Nonaka[1], Hideharu Sasaki[1] (1.APL/JAMSTEC)

[AOS19-P08] The impact of tidal mixing on the Indonesian Throughflow

*Kohki Shiroyama[1], Shinichiro Kida[2], Hideharu Sasaki[3], Ryo Furue[3] (1.Interdisciplinary Graduate School of Engineering Sciences, Kyushu University, 2.Research Institute for Applied Mechanics Kyushu University, 3.JAMSTEC. APL)

[AOS19-P09] **Verification for subsurface oceanic structure in OFES outputs driven by different wind data sets (NCEP/NCAR and QSCAT)in the tropical Pacific Ocean**

*Hiroshige Fukunaga[1], Kunio Kutsuwada[1], Akira Kakiuchi[1], Yuma Yanagida[1], Hideharu Sasaki[2], Yoshikazu Sasai[2] (1.Tokai University, 2.JAMSTEC)

[AOS19-P10] Inter-comparison of ocean wave data from drifting buoys, moored GPS buoys and reanalysis data

*Yukiharu Hisaki[1] (1.University of the Ryukyus)

[AOS19-P11] Merge and Separation of ocean eddies around the Kuroshio Extension

*koutarou matsuhashi[1], Kazuyuki Uehara[1] (1.The Graduate School of Marine Science Technology)

[AOS19-P12] Influence of eddy-trapped water mass reaching 137E survey line using OGCM and a particle-tracking method

★Invited Papers

*Hideyuki Nakano[1], Hiroyuki Tsujino[1], Kei Sakamoto[1], Shogo Urakawa[1], Takahiro Toyoda[1], Goro Yamanaka[1], Yoshimasa Matsumura[2] (1.Meteorological Research Institute, 2.Atmosphere and ocean research Institute, the University of Tokyo)

[AOS19-P13] A study on the variability of the deep ocean circulation during glacial climate with a climate model of intermediate complexity

*Taigo Ando[1], Akira Oka[1] (1.Atmosphere and Ocean Research Institute, University of Tokyo)

[J] Poster | A (Atmospheric and Hydrospheric Sciences)：A-OS Ocean Sciences & Ocean Environment

5:15 PM - 6:30 PM JST | 8:15 AM - 9:30 AM UTC | Poster Hall International Exhibition Hall8, Makuhari Messe_9

[A-OS19] Dynamics of oceanic and atmospheric waves, vortices, and circulations

convener:Yuki Tanaka(Graduate School of Science, The University of Tokyo), Ryo Furue(APL/JAMSTEC), Yukiharu Hisaki(University of the Ryukyus), Norihiko Sugimoto(Keio University, Department of Physics)

[AOS19-P01] **Atmospheric super rotation developed in a GCM (AFES-Venus)**

*Norihiko Sugimoto[1], Masahiro Takagi[2], Yoshihisa Matsuda[3] (1.Keio University, Department of Physics, 2.Kyoto Sangyo University, Department of Physics, 3.Tokyo Gakugei University, Department of Natural Sciences)

[AOS19-P02] Data assimilation of the Venus atmosphere assuming radio occultation measurement by small satellites

*Mirai Abe[1], Norihiko Sugimoto[1], Yukako Kikuchi[2], Asako Hosono[3], Hiroki Ando[4], Masahiro Takagi[4], Itziar Garate Lopez[5], Sebastien Lebonnois[6], Chi Ao[7] (1.Keio University, 2.Yokohama Futaba High School, 3.Toshimagaoka Women High School, 4.Kyoto Sangyo University, 5.Euskal Herriko Unibertsitatea, 6.Sorbonne Universite, 7.Jet Propulsion Laboratory)

[AOS19-P03] Relationship between solar wind and atmospheric circulation

*Paul Prikryl[1] (1.Physics Department University of New Brunswick and Geomagnetic Laboratory Natural Resources Canada)

[AOS19-P04] Contribution of the Atlantic storm track to the Euro-Russian blocking maintenance in summer 2010

*Akira Yamazaki[1] (1.Application Laboratory, Japan Agency for Marine-Earth Science and Technology)

[AOS19-P05] Instabilities in Ekman layer and roll structures in a tropical cyclone boundary layer

*Junshi Ito[1], Hiroshi Niino[1] (1.Atmosphere and Ocean Research Institute, The University of Tokyo)

[AOS19-P06] Mathematical description of the internal waves in a proximity of the bottom of the Ocean.

*andrei giniatoulline[1], german tobar[1] (1.Department of Mathematics, Los Andes University, Bogota, Colombia, South America)

[AOS19-P07] How deterministic are the deep zonal jets?

*Ryo Furue[1], Masami Nonaka[1], Hideharu Sasaki[1] (1.APL/JAMSTEC)

[AOS19-P08] The impact of tidal mixing on the Indonesian Throughflow

*Kohki Shiroyama[1], Shinichiro Kida[2], Hideharu Sasaki[3], Ryo Furue[3] (1.Interdisciplinary Graduate School of Engineering Sciences, Kyushu University, 2.Research Institute for Applied Mechanics Kyushu University, 3.JAMSTEC. APL)

[AOS19-P09] **Verification for subsurface oceanic structure in OFES outputs driven by different wind data sets (NCEP/NCAR and QSCAT)in the tropical Pacific Ocean**

*Hiroshige Fukunaga[1], Kunio Kutsuwada[1], Akira Kakiuchi[1], Yuma Yanagida[1], Hideharu Sasaki[2], Yoshikazu Sasai[2] (1.Tokai University, 2.JAMSTEC)

[AOS19-P10] Inter-comparison of ocean wave data from drifting buoys, moored GPS buoys and reanalysis data

*Yukiharu Hisaki[1] (1.University of the Ryukyus)

[AOS19-P11] Merge and Separation of ocean eddies around the Kuroshio Extension

*koutarou matsuhashi[1], Kazuyuki Uehara[1] (1.The Graduate School of Marine Science Technology)

[AOS19-P12] Influence of eddy-trapped water mass reaching 137E survey line using OGCM and a particle-tracking method

★Invited Papers

*Hideyuki Nakano[1], Hiroyuki Tsujino[1], Kei Sakamoto[1], Shogo Urakawa[1], Takahiro Toyoda[1], Goro Yamanaka[1], Yoshimasa Matsumura[2] (1.Meteorological Research Institute, 2.Atmosphere and ocean research Institute, the University of Tokyo)

[AOS19-P13] A study on the variability of the deep ocean circulation during glacial climate with a climate model of intermediate complexity

*Taigo Ando[1], Akira Oka[1] (1.Atmosphere and Ocean Research Institute, University of Tokyo)

[J] Oral | A (Atmospheric and Hydrospheric Sciences)：A-HW Hydrology & Water Environment

9:00 AM - 10:30 AM JST | 12:00 AM - 1:30 AM UTC | 105 1F

[A-HW24] Isotope Hydrology 2019

convener:Masaya Yasuhara(Rissho Univ.), Kohei Kazahaya(Geological Survey of Japan, AIST), Shinji Ohsawa(Institute for Geothermal Sciences, Graduate School of Science, Kyoto University), Kazuyoshi Asai(Geo Science Laboratory), Chairperson:Masaya Yasuhara(Rissho Univ.), Noritoshi Morikawa(産業技術総合研究所活断層・火山研究部門)

9:00 AM - 9:30 AM JST | 12:00 AM - 12:30 AM UTC

[AHW24-01] The use of natural abundances of stable isotopes to elucidate the nitrogen dynamics in plant-soil systems

★Invited Papers

*Keisuke Koba[1] (1.Center for Ecological Research, Kyoto University)

9:30 AM - 9:45 AM JST | 12:30 AM - 12:45 AM UTC

[AHW24-02] Reconstruction of local temporal variation on atmospheric sulfur hexafluoride concentration in the Kyoto Basin by multiple environmental tracer and mass transport analyses

*Koki Kashiwaya[1], Taishi Hori[1], Ryuta Hazama[2], Yoichi Sakuma[3], Katsuaki Koike[1] (1.Kyoto University, 2.Osaka Sangyo University, 3.Tokyo Institute of Technology)

9:45 AM - 10:00 AM JST | 12:45 AM - 1:00 AM UTC

[AHW24-03] Quantitative reconstruction of the humidity in the moisture source region based on the ^{17}O-excess in precipitation on a subtropical island

Yuina Uechi[1], *Ryu Uemura[1] (1.University of the Ryukyus)

10:00 AM - 10:15 AM JST | 1:00 AM - 1:15 AM UTC

[AHW24-04] Identification of deep groundwater recharge system in an intermontane basin

*Takashi Nakamura[1], Kei Nishida[1], Naim Mohamad[2], Bijay Man Shakya[1], Kazuyoshi Asai[4], Sresh Das Shrestha[3] (1.ICRE, University of YAMANASHI, 2.University of Yamanashi, 3.CDG, Tribhuvan University, 4.Geo-Science Laboratory)

[J] Oral | A (Atmospheric and Hydrospheric Sciences)：A-HW Hydrology & Water Environment

10:45 AM - 12:15 PM JST | 1:45 AM - 3:15 AM UTC | 105 1F

[A-HW24] Isotope Hydrology 2019

convener:Masaya Yasuhara(Rissho Univ.), Kohei Kazahaya(Geological Survey of Japan, AIST), Shinji Ohsawa(Institute for Geothermal Sciences, Graduate School of Science, Kyoto University), Kazuyoshi Asai(Geo Science Laboratory), Chairperson:Noritoshi Morikawa(産業技術総合研究所活断層・火山研究部門), Kazuyoshi Asai(Geo-Science Laboratory), Kohei Kazahaya(Geological Survey of Japan, AIST)

10:45 AM - 11:15 AM JST | 1:45 AM - 2:15 AM UTC

[AHW24-05] The discharge rate of the Arima-type deep brine discharge in Ooshika-mura, Nagano Prefecture

★Invited Papers

*Fumitake Kusuhara[1] (1.Central Research Institute of Electric Power Industry)

11:15 AM - 11:30 AM JST | 2:15 AM - 2:30 AM UTC

[AHW24-06] Sublacustrine hydrothermal system of the active crater lake, Yudamari of Aso Volcano inferred from Mg budget of the lake

*Shinji Ohsawa[1], Takeshi Saito[2], Kazuhiro Amita[3] (1.Institute for Geothermal Sciences, Graduate School of Science, Kyoto University, 2.Academic Assembly School of Science and Technology, Shinshu University, 3.Graduate School of Engineering Science, Akita University)

11:30 AM - 11:45 AM JST | 2:30 AM - 2:45 AM UTC

[AHW24-07] Spatial distribution of chemical compositions, hydrogen and oxygen isotopic ratios of stream water of the Shimanto River area, southwestern Japan

*Masaaki Takahashi[1], Hinako Shimizu[1], Kohei Kazahaya[1], Masaya Yasuhara[2,1] (1.The National Institute of Advanced Industrial Science and Technology, 2.Rissho University)

11:45 AM - 12:00 PM JST | 2:45 AM - 3:00 AM UTC

[AHW24-08] An isotopic study on shallow groundwater origins in a densely-populated area in Shinagawa, central Tokyo, Japan

*Masaya Yasuhara[1], Akihiko Inamura[2], Takashi Nakamura[3], Kazuyoshi Asai[4] (1.Rissho Univ., 2.Geological Survey of Japan, AIST, 3.Yamanashi Univ., 4.Geo Science Laboratory)

[J] Poster | A (Atmospheric and Hydrospheric Sciences)：A-HW Hydrology & Water Environment

3:30 PM - 5:00 PM JST | 6:30 AM - 8:00 AM UTC | Poster Hall International Exhibition Hall8, Makuhari Messe_6

[A-HW24] Isotope Hydrology 2019

convener:Masaya Yasuhara(Rissho Univ.), Kohei Kazahaya(Geological Survey of Japan, AIST), Shinji Ohsawa(Institute for Geothermal Sciences, Graduate School of Science, Kyoto University), Kazuyoshi Asai(Geo Science Laboratory)

[AHW24-P01] Geochemical features for spring at Izu Peninsula

*Kazuyoshi Asai[1], Kazumi Asai[1] (1.Geo Science Laboratory)

[AHW24-P02] Acidification process of shallow groundwater in an alluvial fan in Ueda City, Nagano, Japan

Ran Takahashi[1], *Masaya Yasuhara[2], Seongwon Lee[2], Takashi Nakamura[3], Kazuyoshi Asai[4] (1.Undergraduate student, Rissho Univ., 2.Rissho Univ., 3.Yamanashi Univ., 4.Geo Science Laboratory)

[AHW24-P03] Hydroecological study on fresh water copepod in Chino-ike ('Bloody lake'), an ephemeral lake on the top of Mt. Akagi, central Japan

Hirano Yuri[1], *Masaya Yasuhara[2], Seongwon Lee[2], Yasuhiro Funyu[3], Nozomu Iwasaki[2], Natsumi Shimoda[2] (1. Undergraduate student, Rissho Univ., 2.Rissho Univ., 3.Graduate student, Rissho Univ.)

[AHW24-P04] **Cross-sectional distribution in water chemistry and oxygen and hydrogen isotopic ratios in Fuku River, Saitama, Japan**

*Manatsu Kimura[1], Yasuhara Masaya[2], Seongwon Lee[2] (1.Graduate School of Geo-Environmental Science, Rissho University, 2.Faculty of Geo-Environmental Science, Rissho University)

[AHW24-P05] On concentration and origin of chloride ion in small rivers in Jyoboji area, Fujioka, Gunma, Japan

*Taketoshi Hasegawa[1], Masaya Yasuhara[2], Seongwon Lee[2] (1.Rissho University Graduate School of Geo-environmental Science Environmental Systems Science, 2.Rissho Univ.)

[AHW24-P06] Geochemical characteristics and origin of groundwater in central to eastern Hokkaido

*Yusei Nakagaki[1] (1.Chiba University)

[AHW24-P07] Identification of hydrological characteristics on the groundwater recharge in volcanic and non-volcanic mountains

*sano anna[1], Takashi Nakamura[1], Kei Nishida[1] (1.International Research Center for River Basin Environment, University of YAMANASHI)

[AHW24-P08] Analysis of spring water formation mechanism used by ^{222}Rn concentration at Masutomi-Onsen located in Yamanashi, Japan

*Eiki Mochizuki[1], Takuya Hayakawa[1], Hiroshi Kobayashi[1] (1.Yamanashi Institute of Public Health and Environment)

[AHW24-P09] Migration Behavior of Radiocesium Derived from the Fukushima Dai-Ichi Nuclear Power Plant Accident in Natsui River and Tone River

*Deddy Irawan Permana Putra[1], Shinya Ochiai[2], Seiichi Tomihara[3], Shun Watanabe[4], Kyuma Suzuki[4], Seiya Nagao[2] (1.Kanazawa University, Graduate School of Natural Science and Technology, 2.Low Level Radioactivity Laboratory, Kanazawa University, 3.Aquamarine Fukushima, 4.Gunma Prefectural Fisheries Experiment Station)

[AHW24-P10] Estimation of excess air component in groundwater by using dissolved Argon concentration

*Kazumi Asai[1], Kazuyoshi Asai[1] (1.Chikyukagakukenkyusho inc)

[J] Poster | A (Atmospheric and Hydrospheric Sciences)：A-HW Hydrology & Water Environment

5:15 PM - 6:30 PM JST | 8:15 AM - 9:30 AM UTC | Poster Hall International Exhibition Hall8, Makuhari Messe_10

[A-HW24] Isotope Hydrology 2019

convener:Masaya Yasuhara(Rissho Univ.), Kohei Kazahaya(Geological Survey of Japan, AIST), Shinji Ohsawa(Institute for Geothermal Sciences, Graduate School of Science, Kyoto University), Kazuyoshi Asai(Geo Science Laboratory)

[AHW24-P01] Geochemical features for spring at Izu Peninsula

*Kazuyoshi Asai[1], Kazumi Asai[1] (1.Geo Science Laboratory)

[AHW24-P02] Acidification process of shallow groundwater in an alluvial fan in Ueda City, Nagano, Japan

Ran Takahashi[1], *Masaya Yasuhara[2], Seongwon Lee[2], Takashi Nakamura[3], Kazuyoshi Asai[4] (1.Undergraduate student, Rissho Univ., 2.Rissho Univ., 3.Yamanashi Univ., 4.Geo Science Laboratory)

[AHW24-P03] Hydroecological study on fresh water copepod in Chino-ike ('Bloody lake'), an ephemeral lake on the top of Mt. Akagi, central Japan

Hirano Yuri[1], *Masaya Yasuhara[2], Seongwon Lee[2], Yasuhiro Funyu[3], Nozomu Iwasaki[2], Natsumi Shimoda[2] (1. Undergraduate student, Rissho Univ., 2.Rissho Univ., 3.Graduate student, Rissho Univ.)

[AHW24-P04] **Cross-sectional distribution in water chemistry and oxygen and hydrogen isotopic ratios in Fuku River, Saitama, Japan**

*Manatsu Kimura[1], Yasuhara Masaya[2], Seongwon Lee[2] (1.Graduate School of Geo-Environmental Science, Rissho University, 2.Faculty of Geo-Environmental Science, Rissho University)

[AHW24-P05] On concentration and origin of chloride ion in small rivers in Jyoboji area, Fujioka, Gunma, Japan

*Taketoshi Hasegawa[1], Masaya Yasuhara[2], Seongwon Lee[2] (1.Rissho University Graduate School of Geo-environmental Science Environmental Systems Science, 2.Rissho Univ.)

[AHW24-P06] Geochemical characteristics and origin of groundwater in central to eastern Hokkaido

*Yusei Nakagaki[1] (1.Chiba University)

[AHW24-P07] Identification of hydrological characteristics on the groundwater recharge in volcanic and non-volcanic mountains

*sano anna[1], Takashi Nakamura[1], Kei Nishida[1] (1.International Research Center for River Basin Environment, University of YAMANASHI)

[AHW24-P08] Analysis of spring water formation mechanism used by ^{222}Rn concentration at Masutomi-Onsen located in Yamanashi, Japan

*Eiki Mochizuki[1], Takuya Hayakawa[1], Hiroshi Kobayashi[1] (1.Yamanashi Institute of Public Health and Environment)

[AHW24-P09] Migration Behavior of Radiocesium Derived from the Fukushima Dai-Ichi Nuclear Power Plant Accident in Natsui River and Tone River

*Deddy Irawan Permana Putra[1], Shinya Ochiai[2], Seiichi Tomihara[3], Shun Watanabe[4], Kyuma Suzuki[4], Seiya Nagao[2] (1.Kanazawa University, Graduate School of Natural Science and Technology, 2.Low Level Radioactivity Laboratory, Kanazawa University, 3.Aquamarine Fukushima, 4.Gunma Prefectural Fisheries Experiment Station)

[AHW24-P10] Estimation of excess air component in groundwater by using dissolved Argon concentration

*Kazumi Asai[1], Kazuyoshi Asai[1] (1.Chikyukagakukenkyusho inc)

[J] Poster | A (Atmospheric and Hydrospheric Sciences)：A-HW Hydrology & Water Environment

3:30 PM - 5:00 PM JST | 6:30 AM - 8:00 AM UTC | Poster Hall International Exhibition Hall8, Makuhari Messe_7

[A-HW25] Water Environment and Geology in Urban Areas

convener:Takeshi Hayashi(Faculty of Education and Human Studies, Akita University)

[AHW25-P01] Evaluation of regional groundwater flow system for basin water resource management

*Takeshi Hayashi[1], Akinobu Miyakoshi[2], Shoichi Hachinohe[3], Hideki Hamamoto[3] (1.Faculty of Education and Human Studies, Akita University, 2.GSJ, AIST, 3.Center for Environmental Science in Saitama)

[AHW25-P02] Integrated groundwater monitoring required for sustainable basin water resources management: Evaluation of effects of groundwater development utilized existing observation well network in the Tokyo metropolitan area

*Akinobu Miyakoshi[1], Takeshi Hayashi[2], Shoichi Hachinohe[3], Hideki Hamamoto[3] (1.Geological Survey of Japan, AIST, 2.Faculty of Education and Human Studies, Akita University, 3.Center for Environmental Science in Saitama)

[AHW25-P03] STORMWATER DRAINAGE SYSTEM OF AN INDIAN TOWN: WHETHER SUSTAINABLE?

*Rajesh Kumar Vishwakarma[1], Dr. Himanshu Joshi[1] (1.Indian Institute of Technology, Roorkee)

[AHW25-P04] Using a genetic algorithm to investigate the spatial arrangement of low impact development facilities: a case study of National Taiwan University campus.

*Chung-Yuan Liang[1], Gene Jiing-yun You[1] (1.National Taiwan University)

[J] Poster | A (Atmospheric and Hydrospheric Sciences)：A-HW Hydrology & Water Environment

5:15 PM - 6:30 PM JST | 8:15 AM - 9:30 AM UTC | Poster Hall International Exhibition Hall8, Makuhari Messe_11

[A-HW25] Water Environment and Geology in Urban Areas

convener:Takeshi Hayashi(Faculty of Education and Human Studies, Akita University)

[AHW25-P01] Evaluation of regional groundwater flow system for basin water resource management

*Takeshi Hayashi[1], Akinobu Miyakoshi[2], Shoichi Hachinohe[3], Hideki Hamamoto[3] (1.Faculty of Education and Human Studies, Akita University, 2.GSJ, AIST, 3.Center for Environmental Science in Saitama)

[AHW25-P02] Integrated groundwater monitoring required for sustainable basin water resources management: Evaluation of effects of groundwater development utilized existing observation well network in the Tokyo metropolitan area

*Akinobu Miyakoshi[1], Takeshi Hayashi[2], Shoichi Hachinohe[3], Hideki Hamamoto[3] (1.Geological Survey of Japan, AIST, 2.Faculty of Education and Human Studies, Akita University, 3.Center for Environmental Science in Saitama)

[AHW25-P03] STORMWATER DRAINAGE SYSTEM OF AN INDIAN TOWN: WHETHER SUSTAINABLE?

*Rajesh Kumar Vishwakarma[1], Dr. Himanshu Joshi[1] (1.Indian Institute of Technology, Roorkee)

[AHW25-P04] Using a genetic algorithm to investigate the spatial arrangement of low impact development facilities: a case study of National Taiwan University campus.

*Chung-Yuan Liang[1], Gene Jiing-yun You[1] (1.National Taiwan University)

[E] Oral | A (Atmospheric and Hydrospheric Sciences)：A-CG Complex & General

1:45 PM - 3:15 PM JST | 4:45 AM - 6:15 AM UTC | 104 1F

[A-CG33] Extratropical oceans and atmosphere

convener:Kazuaki Nishii(Graduate School of Bioresources, Mie University), Yoshi N Sasaki(Hokkaido University), Hatsumi Nishikawa(Institute of Low Temperature Science, Hokkaido University), Shun Ohishi(Division for Land-Ocean Ecosystem Research, Institute for Space-Earth Environmental Research, Nagoya University), Chairperson:Kazuaki Nishii(三重大学)

1:45 PM - 2:05 PM JST | 4:45 AM - 5:05 AM UTC

[ACG33-01] Gulf Stream and Kuroshio are synchronized

★Invited Papers

*Tsubasa Kohyama[1], Hiroaki Miura[1], Shoichiro Kido[1] (1.Department of Earth and Planetary Science, The University of Tokyo)

2:05 PM - 2:20 PM JST | 5:05 AM - 5:20 AM UTC

[ACG33-02] A study on mixed layer depth variability in the Kuroshio Extension region based on a frontal Ekman model

*Tomoki Tozuka[1] (1.Department of Earth and Planetary Science, Graduate School of Science, The University of Tokyo)

2:20 PM - 2:35 PM JST | 5:20 AM - 5:35 AM UTC

[ACG33-03] Mechanisms of Reemergence in the North Pacific revealed by Mixed Layer Heat Budget Analysis

*Kazumichi Murata[1], Shoichiro Kido[1], Tomoki Tozuka[1] (1.Department of Earth and Planetary Science, School of Science, The University of Tokyo)

2:35 PM - 2:50 PM JST | 5:35 AM - 5:50 AM UTC

[ACG33-04] Formation mechanism for the North Pacific Transition domain SST and SSS fronts

*Hatsumi Nishikawa[1], Humio Mitsudera[1], Takeshi Okunishi[2], Shin-ichi Ito[3], Taku Wagawa[4], Daisuke Hasegawa[2], Toru Miyama[5], Hitoshi Kaneko[2] (1.Institute of Low Temperature Science, Hokkaido University, 2.Tohoku National Fisheries Research Institute, Japan Fisheries Research and Education Agency, 3.Atmosphere and Ocean Research Institute, The University of Tokyo, 4.Japan Sea National Fisheries Research Institute, Japan Fisheries Research and Education Agency, 5.Japan Agency for Marine-Earth Science and Technology)

2:50 PM - 3:10 PM JST | 5:50 AM - 6:10 AM UTC

[ACG33-05] Impact of the Kuroshio front on frontal structure of an extratropical cyclone associated with heavy precipitation

★Invited Papers

*Hidetaka Hirata[1], Ryuichi Kawamura[2], Mayumi K Yoshioka[1], Masami Nonaka[3], Kazuhisa Tsuboki[1] (1.Institute for Space-Earth Environmental Research, Nagoya University, 2.Department of Earth and Planetary Sciences, Kyushu University, 3.Application Laboratory, Japan Agency for Marine-Earth Science and Technology)

3:10 PM - 3:15 PM JST | 6:10 AM - 6:15 AM UTC

[ACG33-06] Discussion on future studies on the role of midlatitude oceans

*Kazuaki Nishii[1] (1.Graduate School of Bioresources, Mie University)

[E] Oral | A (Atmospheric and Hydrospheric Sciences)：A-CG Complex & General

3:30 PM - 5:00 PM JST | 6:30 AM - 8:00 AM UTC | 104 1F

[A-CG33] Extratropical oceans and atmosphere

convener:Kazuaki Nishii(Graduate School of Bioresources, Mie University), Yoshi N Sasaki(Hokkaido University), Hatsumi Nishikawa(Institute of Low Temperature Science, Hokkaido University), Shun Ohishi(Division for Land-Ocean Ecosystem Research, Institute for Space-Earth Environmental Research, Nagoya University), Chairperson:Shun Ohishi

3:30 PM - 3:45 PM JST | 6:30 AM - 6:45 AM UTC

[ACG33-07] Intra-seasonal variability of oceanic low-level cloud in summertime North Pacific and its interaction with sea surface temperature

★Invited Papers

*Naoya Takahashi[1], Tadahiro Hayasaka[1] (1.Center for Atmospheric and Oceanic Studies, Graduate School of Science, Tohoku University,)

3:45 PM - 4:00 PM JST | 6:45 AM - 7:00 AM UTC

[ACG33-08] **Sea surface temperature trend in the East China Sea during the 20th century simulated by a regional ocean model**

*Yoshi N Sasaki[1], Chisato Umeda[1] (1.Hokkaido University)

4:00 PM - 4:15 PM JST | 7:00 AM - 7:15 AM UTC

[ACG33-09] Kuroshio Extension and Gulf Stream's influences on the variability of near-surface baroclinicity and the associated atmospheric fields

★Invited Papers

*Bunmei Taguchi[1], Kazuaki Nishii[2], Hisashi Nakamura[1,3] (1.Research Center for Advanced Science and Technology, The University of Tokyo, 2.Graduate School of Bioresources, Mie University, 3. Application Laboratory, Japan Agency of Marine-Earth Science and Technology)

4:15 PM - 4:30 PM JST | 7:15 AM - 7:30 AM UTC

[ACG33-10] Baroclinic Annular Mode in the Southern Hemisphere: Its Reproducibility and Sensitivity to Ocean Fronts assessed in Aqua-Planet Experiments

*Morio Nakayama[1], Masatoshi Mizukoshi[1], Hisashi Nakamura[1], Yu Kosaka[1], Bunmei Taguchi[1], Masato Mori[1], Fumiaki Ogawa[2] (1.RCAST, the University of Tokyo , 2.The University of Bergen)

4:30 PM - 4:45 PM JST | 7:30 AM - 7:45 AM UTC

[ACG33-11] **Hydro-climatic variation in northwestern China and its multi-decadal to multi-centennial teleconnection with the Pacific Ocean**

*Harry F Lee[1] (1.The Chinese University of Hong Kong)

4:45 PM - 5:00 PM JST | 7:45 AM - 8:00 AM UTC

[ACG33-12] Atmospheric zonal-mean meridional circulation and midlatitude oceanic fronts

*Kazuaki Nishii[1], Bunmei Taguchi[2], Hisashi Nakamura[2] (1.Graduate School of Bioresources, Mie University, 2.Research Center for Advanced Science and Technology, The University of Tokyo)

[E] Poster | A (Atmospheric and Hydrospheric Sciences)：A-CG Complex & General

5:15 PM - 6:30 PM JST | 8:15 AM - 9:30 AM UTC | Poster Hall International Exhibition Hall8, Makuhari Messe_12

[A-CG33] Extratropical oceans and atmosphere

convener:Kazuaki Nishii(Graduate School of Bioresources, Mie University), Yoshi N Sasaki(Hokkaido University), Hatsumi Nishikawa(Institute of Low Temperature Science, Hokkaido University), Shun Ohishi(Division for Land-Ocean Ecosystem Research, Institute for Space-Earth Environmental Research, Nagoya University)

[ACG33-P01] Analysis of water exchange processes at the Subarctic Boundary of the North Pacific using particle tracking method

*Ashida Hayato[1], Humio Mitsudera[2], Hatsumi Nishikawa[2] (1. Department of Earth and Planetary Sciences, School of Science, Hokkaido University, 2.Institute of Low Temperature Science, Hokkaido University)

[ACG33-P02] Method to evaluate the effect of obduction on properties in the ocean mixed layer

*Yoshimi Kawai[1] (1.Research and Development Center for Global Change, Japan Agency for Marine-Earth Science and Technology)

[ACG33-P03] Influence of the interannual-scale Bering Sea ice variation on cold air outbreaks

*Mizuki Iida[1], Shusaku Sugimoto[1], Toshio Suga[1] (1.Physical Oceanography Laboratory Department of Geophysics, Graduate School of Science, Tohoku University)

[E] Poster | H (Human Geosciences)：H-DS Disaster geosciences

1:45 PM - 3:15 PM JST | 4:45 AM - 6:15 AM UTC | Poster Hall International Exhibition Hall8, Makuhari Messe_3

[H-DS11] Subaqueous Landslides and Their Anthropogenic Impact for Coastal Regions

convener:Yujin Kitamura(Department of Earth and Environmental Sciences, Graduate School of Science and Engineering, Kagoshima University), Yasuhiro Yamada(Japan Agency for Marine-Earth Science and Technology (JAMSTEC), R&D Center for Ocean Drilling Science (ODS))

[HDS11-P01] Deformed sediment gravity flow deposits associated with bypassing slides:an example from the Miocene Ushikiri Formation, Southwest Japan

*Miki Kobayashi[1], Tetsuya Sakai[2] (1.Nippon Koei, 2.Shimane University)

[HDS11-P02] Submarine Landslide and Resulting Tsunami on the Continental Shelf Slope off Shikoku

*Youdai Gon[1], Toshitaka Baba[1], Tetsuo Matsuno, Mitsuru Hayashi, Hiroshi Ichihara (1.Tokushima University graduate school)

[HDS11-P03] Sedimentary environment estimated from physical properties of sediment core collected during the cruise of Hakuho-maru KH-18-3 in the South Yatsushiro sea, western Kyushu.

*Koki Hori[1], Yujin Kitamura[2], Hakuho-maru KH-18-3 Scientists (1.Department of Earth and Planetary Sciences, Graduate School of Science, Kyushu University , 2.Department of Earth and Environmental Sciences, Graduate School of Science and Engineering , Kagoshima University)

[HDS11-P04] Variation in vane shear strength and magnetic susceptibility in the cores recovered by Hakuho-maru KH-18-3 cruise in Yatsushiro sea

*Yujin Kitamura[1], Haruka Kageyama[2], Kaede Yamasaki[2], Ryoya Goto[2], Koki Hori[2], Yuta Ikebata[2], Kuniyo Kawabata[1], Daiki Oyama[2], Hakuho-maru KH-18-3 Scientists (1.Department of Earth and Environmental Sciences, Graduate School of Science and Engineering, Kagoshima University, 2.Department of Earth and Environmental Sciences, Faculty of Science, Kagoshima University)

[HDS11-P05] Identification of turbidites in the Yatsushiro Sea surface sediment core samples from non-destructive measurements: Hakuho-maru KH-18-3 Cruise, Yatsushiro Sea, Western Kyushu, Japan

*Ryoya Goto[1], Yujin Kitamura[2], Hakuho-maru KH-18-3 Cruise Scientist (1.Atmosphere and Ocean Research Institute, The University of Tokyo, 2.Department of Earth and Environmental Sciences, Graduate School of Science, Kagoshima University)

[HDS11-P06] Revised columnar section based on grain size distribution analysis of samples from Hakuho-maru KH-18-3 in Yatsushiro sea

*Yuta Ikebata[1], Yujin Kitamura[2], Hakuho-maru KH-18-3 Scientists Family (1.Kyusyu University Graduate School Of Science Earth and Planetary Science, 2.Graduate school of science, Kagoshima University)

[E] Poster | H (Human Geosciences)：H-DS Disaster geosciences

5:15 PM - 6:30 PM JST | 8:15 AM - 9:30 AM UTC | Poster Hall International Exhibition Hall8, Makuhari Messe_13

[H-DS11] Subaqueous Landslides and Their Anthropogenic Impact for Coastal Regions

convener:Yujin Kitamura(Department of Earth and Environmental Sciences, Graduate School of Science and Engineering, Kagoshima University), Yasuhiro Yamada(Japan Agency for Marine-Earth Science and Technology (JAMSTEC), R&D Center for Ocean Drilling Science (ODS))

[HDS11-P01] Deformed sediment gravity flow deposits associated with bypassing slides:an example from the Miocene Ushikiri Formation, Southwest Japan

*Miki Kobayashi[1], Tetsuya Sakai[2] (1.Nippon Koei, 2.Shimane University)

[HDS11-P02] Submarine Landslide and Resulting Tsunami on the Continental Shelf Slope off Shikoku

*Youdai Gon[1], Toshitaka Baba[1], Tetsuo Matsuno, Mitsuru Hayashi, Hiroshi Ichihara (1.Tokushima University graduate school)

[HDS11-P03] Sedimentary environment estimated from physical properties of sediment core collected during the cruise of Hakuho-maru KH-18-3 in the South Yatsushiro sea, western Kyushu.

*Koki Hori[1], Yujin Kitamura[2], Hakuho-maru KH-18-3 Scientists (1.Department of Earth and Planetary Sciences, Graduate School of Science, Kyushu University , 2.Department of Earth and Environmental Sciences, Graduate School of Science and Engineering , Kagoshima University)

[HDS11-P04] Variation in vane shear strength and magnetic susceptibility in the cores recovered by Hakuho-maru KH-18-3 cruise in Yatsushiro sea

*Yujin Kitamura[1], Haruka Kageyama[2], Kaede Yamasaki[2], Ryoya Goto[2], Koki Hori[2], Yuta Ikebata[2], Kuniyo Kawabata[1], Daiki Oyama[2], Hakuho-maru KH-18-3 Scientists (1.Department of Earth and Environmental Sciences, Graduate School of Science and Engineering, Kagoshima University, 2.Department of Earth and Environmental Sciences, Faculty of Science, Kagoshima University)

[HDS11-P05] Identification of turbidites in the Yatsushiro Sea surface sediment core samples from non-destructive measurements: Hakuho-maru KH-18-3 Cruise, Yatsushiro Sea, Western Kyushu, Japan

*Ryoya Goto[1], Yujin Kitamura[2], Hakuho-maru KH-18-3 Cruise Scientist (1.Atmosphere and Ocean Research Institute, The University of Tokyo, 2.Department of Earth and Environmental Sciences, Graduate School of Science, Kagoshima University)

[HDS11-P06] Revised columnar section based on grain size distribution analysis of samples from Hakuho-maru KH-18-3 in Yatsushiro sea

*Yuta Ikebata[1], Yujin Kitamura[2], Hakuho-maru KH-18-3 Scientists Family (1.Kyusyu University Graduate School Of Science Earth and Planetary Science, 2.Graduate school of science, Kagoshima University)

[E] Oral | H (Human Geosciences)：H-DS Disaster geosciences

3:30 PM - 5:00 PM JST | 6:30 AM - 8:00 AM UTC | 201B 2F

[H-DS11] Subaqueous Landslides and Their Anthropogenic Impact for Coastal Regions

convener:Yujin Kitamura(Department of Earth and Environmental Sciences, Graduate School of Science and Engineering, Kagoshima University), Yasuhiro Yamada(Japan Agency for Marine-Earth Science and Technology (JAMSTEC), R&D Center for Ocean Drilling Science (ODS)), Chairperson:Yujin Kitamura(Kagoshima University), Masayuki Utsunomiya(Research Institute of Geology and Geoinformation, Geological Survey of Japan, AIST), Yasuhiro Yamada(JAMSTEC)

3:30 PM - 3:45 PM JST | 6:30 AM - 6:45 AM UTC

[HDS11-01] Distribution and sedimentological characteristics of the submarine landslides filling Hidaka Trough, offshore southern Hokkaido, northern Japan with special attention to the uppermost Quaternary submarine landslide bodies

*Hiroyuki Arato[1] (1.Graduate School of International Resource Sciences, Akita University)

3:45 PM - 4:00 PM JST | 6:45 AM - 7:00 AM UTC

[HDS11-02] Origin and distribution of mass-transport deposits in the Pleistocene forearc basin, central Japan, deduced from tephro- and biostratigraphy

*Masayuki Utsunomiya[1], Yuzuru Yamamoto[2], Kiyohide Mizuno[1] (1.Geological Survey of Japan, AIST, 2.JAMSTEC)

4:00 PM - 4:15 PM JST | 7:00 AM - 7:15 AM UTC

[HDS11-03] Physico-chemical properties of sediment cores from Yatsushiro Sea, western Kyushu

*Yujin Kitamura[1], Ryoya Goto[2], Koki Hori[2], Yuta Ikebata[2], Haruka Kageyama[2], Kuniyo Kawabata[1], Daiki Oyama[1], Kaede Yamasaki[2], Hakuho-maru KH-18-3 Scientists (1.Department of Earth and Environmental Sciences, Graduate School of Science and Engineering, Kagoshima University, 2.Atmosphere and Ocean Research Institute, The University of Tokyo)

[E] Poster | H (Human Geosciences)：H-DS Disaster geosciences

1:45 PM - 3:15 PM JST | 4:45 AM - 6:15 AM UTC | Poster Hall International Exhibition Hall8, Makuhari Messe_4

[H-DS12] Advanced Remote Sensing toward Mega-Disaster Response

convener:Young-Joo Kwak(ICHARM-UNESCO: International Centre for Water Hazard And Risk Management), Wataru Takeuchi(Institute of Industrial Science, The University of Tokyo)

[HDS12-P01] Satellite-based assessment of electricity restoration efforts in Puerto Rico after Hurricane Maria

*Miguel O Roman[1], Eleanor Stokes[2,3], Zhuosen Wang[2,3], Virginia Kalb[3], Ranjay Shrestha[4,3] (1.Earth from Space Institute, Universities Space Research Association, 2.Earth System Science Interdisciplinary Center, University of Maryland, 3.NASA Goddard Space Flight Center, 4.Science Systems and Applications, Inc)

[HDS12-P02] **Flood inundation forecasting coupled with in-situ water level and satellite data**

*Young-Joo Kwak[1], Jonggeol Park[2], Wataru Takeuchi[3] (1.ICHARM-UNESCO: International Centre for Water Hazard And Risk Management, 2.Tokyo University of Information and Sciences, 3.University of Tokyo)

[HDS12-P03] Long term monitoring of flood damage in the coastal area of Bangladesh

★Invited Papers

*Park Jonggeol[1], Young-Joo Kwak[2] (1.Tokyo University of Information Sciences, 2.ICHARM-UNESCO)

[HDS12-P04] Automatic shoreline detection and coastal change detection using multiple satellite data in Bangladesh

*Young-Joo Kwak[1] (1.ICHARM-UNESCO: International Centre for Water Hazard And Risk Management)

[E] Poster | H (Human Geosciences)：H-DS Disaster geosciences

5:15 PM - 6:30 PM JST | 8:15 AM - 9:30 AM UTC | Poster Hall International Exhibition Hall8, Makuhari Messe_14

[H-DS12] Advanced Remote Sensing toward Mega-Disaster Response

convener:Young-Joo Kwak(ICHARM-UNESCO: International Centre for Water Hazard And Risk Management), Wataru Takeuchi(Institute of Industrial Science, The University of Tokyo)

[HDS12-P01] Satellite-based assessment of electricity restoration efforts in Puerto Rico after Hurricane Maria

*Miguel O Roman[1], Eleanor Stokes[2,3], Zhuosen Wang[2,3], Virginia Kalb[3], Ranjay Shrestha[4,3] (1.Earth from Space Institute, Universities Space Research Association, 2.Earth System Science Interdisciplinary Center, University of Maryland, 3.NASA Goddard Space Flight Center, 4.Science Systems and Applications, Inc)

[HDS12-P02] Flood inundation forecasting coupled with in-situ water level and satellite data

*Young-Joo Kwak[1], Jonggeol Park[2], Wataru Takeuchi[3] (1.ICHARM-UNESCO: International Centre for Water Hazard And Risk Management, 2.Tokyo University of Information and Sciences, 3.University of Tokyo)

[HDS12-P03] Long term monitoring of flood damage in the coastal area of Bangladesh

★Invited Papers

*Park Jonggeol[1], Young-Joo Kwak[2] (1.Tokyo University of Information Sciences, 2.ICHARM-UNESCO)

[HDS12-P04] Automatic shoreline detection and coastal change detection using multiple satellite data in Bangladesh

*Young-Joo Kwak[1] (1.ICHARM-UNESCO: International Centre for Water Hazard And Risk Management)

[J] Oral | H (Human Geosciences)：H-DS Disaster geosciences

10:45 AM - 12:15 PM JST | 1:45 AM - 3:15 AM UTC | 106 1F

[H-DS14] Geohazards in humid, tectonically active countries and their precursors

convener:Masahiro Chigira(Disaster Prevention Research Institute, Kyoto University), Hiroshi YAGI(Faculty of Art, Science and Education, Yamagata University), Satoru Kojima(Department of Civil Engineering, Gifu University), Taro Uchida(National Institute for Land and Infrastructure Management), Chairperson:Satoshi Ishimaru

10:45 AM - 11:00 AM JST | 1:45 AM - 2:00 AM UTC

[HDS14-01] The sources of landslides occurred by the 2018 Hokkaido Eastern Iburi Earthquake

*Satoshi Ishimaru[1], Wataru Hirose[1], Gentaro Kawakami[1], Ryo Takahashi[1], Yoshihiro Kase[1], Ken'ichi Koshimizu[1], Hiromichi Koyasu[1], Masahiro Chigira[2], Jun Tajika[3] (1.Geological Survey of Hokkaido, 2.Kyoto University, 3.Docon Co., Ltd.)

11:00 AM - 11:15 AM JST | 2:00 AM - 2:15 AM UTC

[HDS14-02] Feature of landslide of pyroclastic fall deposits induced by 2018 Hokkaido Eastern Iburi Earthquake, and its relation with damage

*Jun Tajika[1], Kazuo Amemiya[2], Masahiro Chigira[3], Satoshi Ishimaru[4], Akio Koike[1], Hidetoshi Kon[1], Kenji Kizaki[5], Nobuo Yamane[6] (1.Docon Co.,Ltd., 2.Bousai Chishitsu Kogyo Co.,Ltd., 3.Kyoto University, 4.Geological Survey of Hokkaido, HRO, 5.Kizaki PE Office, 6.Terre Research Co.)

11:15 AM - 11:30 AM JST | 2:15 AM - 2:30 AM UTC

[HDS14-03] Influence of slope cutting on failures induced by the July heavy rain, and the Iburi-tobu earthquake, 2018.

*Hidehisa Nagata[1] (1.Fu-Sui-Do Company Limited)

11:30 AM - 11:45 AM JST | 2:30 AM - 2:45 AM UTC

[HDS14-04] Slope failures occurred in the southwest part of the Izu-oshima Island in geological time, NE Japan

*Takehiko Suzuki[1], Masahiro Chigira[2] (1.Faculty of Urban Environmental Sciences, Tokyo Metropolitan University, 2.Disaster Prevention Research Institute, Kyoto University)

11:45 AM - 12:00 PM JST | 2:45 AM - 3:00 AM UTC

[HDS14-05] The strain rate observation by the borehole inclinometer on the bedrock creep slopes in Akadani-west area

*Atsuhiko Kinoshita[1,2], Yasutaka Tanaka[2], Wataru Sakurai[1], Taro Uchida[1], Koichiro Hayashi[3], Yasuuchi Kubota[3], Katsushi Kawato[4] (1.National Institute for Land and Infrastructure Management, 2.Sediment Disaster Prevention Technology Center, Kinki Developing Regional Bureau, Ministry of Land, Infrastructure, Transport and Tourism , 3.OYO Corporation, 4.NIPPON ENGINEERING CONSULTANTS CO., LTD.)

12:00 PM - 12:15 PM JST | 3:00 AM - 3:15 AM UTC

[HDS14-06] Assessing Potential Landslide Areas Due to Earthquake Using Three-Dimensional Resistivity Datasets from Across a Wide Area

*Yusuke Sakai[1], Taro Uchida[1], YASUMASA FUJIWARA[2] (1.National Institute for Land and Infrastructure Management , 2.Eight-Japan Engineering Consultants)

[J] Oral | H (Human Geosciences)：H-DS Disaster geosciences

1:45 PM - 3:15 PM JST | 4:45 AM - 6:15 AM UTC | 106 1F

[H-DS14] Geohazards in humid, tectonically active countries and their precursors

convener:Masahiro Chigira(Disaster Prevention Research Institute, Kyoto University), Hiroshi YAGI(Faculty of Art, Science and Education, Yamagata University), Satoru Kojima(Department of Civil Engineering, Gifu University), Taro Uchida(National Institute for Land and Infrastructure Management), Chairperson:Chigira Masahiro, Taro Uchida

1:45 PM - 2:00 PM JST | 4:45 AM - 5:00 AM UTC

[HDS14-07] Prediction of shallow landslides and debris flow by rainstorm: dynamic hazard mapping toward disaster mitigation

*Yuki Matsushi[1] (1.Disaster Prevention Research Institute, Kyoto University)

2:00 PM - 2:30 PM JST | 5:00 AM - 5:30 AM UTC

[HDS14-08] Land slide warning judgment mesh information of the Meteorological Agency using the Soil Water Index

★Invited Papers

*KENJI OKADA[1] (1.Japan Meteorological Agency)

2:30 PM - 3:00 PM JST | 5:30 AM - 6:00 AM UTC

[HDS14-09] A future direction of remedial measures for sediment disaster reduction from the viewpoint of enhancing a workable early warning system

★Invited Papers

*Masaru Kunitomo[1,2,3,4], Shigetaka Takiguchi[1,2,3,4], Fumiaki Akazawa[1,2,3,4], Kazuyuki Imai[1,2,3,4] (1.Ministry of Land, Infrastructure, Transport and Tourism, 2.Water and Disaster Management Bureau, 3.Sediment and Erosion Control Department, 4.Sediment and Erosion Control Planning Division)

[J] Poster | H (Human Geosciences)：H-DS Disaster geosciences

3:30 PM - 5:00 PM JST | 6:30 AM - 8:00 AM UTC | Poster Hall International Exhibition Hall8, Makuhari Messe_8

[H-DS14] Geohazards in humid, tectonically active countries and their precursors

convener:Masahiro Chigira(Disaster Prevention Research Institute, Kyoto University), Hiroshi YAGI(Faculty of Art, Science and Education, Yamagata University), Satoru Kojima(Department of Civil Engineering, Gifu University), Taro Uchida(National Institute for Land and Infrastructure Management)

[HDS14-P01] The estimation of frequency for deep-seated landslide with carbon dating in Kii mountain area

★Invited Papers

*Yasutaka Tanaka[1], Toshiaki Kotake[1], Hiroaki Sugawara[1], Atsuhiko Kinoshita[1], Yoshito Ogawauchi[2], Minami Fujiwara[2] (1.Sediment Disaster Prevention Technology Center, Kinki Regional Developing Bureau, Ministry of Land, Infrastructure, Transport and Tourism, 2.Japan Conservation Engineers & CO., LTD.)

[HDS14-P02] Tephra stratigraphy and a slope failure of about 4,000 years ago on the slope of the Late Pleistocene Janoo Volcano in the northwestern of Aso Caldera

*Yasuto Hirata[1], Keiichi Ueta[1], Riichiro Miyawaki[2], Katsutoshi Iemura[2], Toshitaka Yokoyama[2], Akiko Miyawaki[2] (1.Central Research Institute of Electric Power Industry, 2.Hanshin Consultants)

[HDS14-P03] Analysis of causal factors of landslides during 2017 northern Kyusyu torrential rainfall disaster by using decision tree

*Hiromu Daimaru[1], Wataru Murakami[1], Yuki Tsurusaki[2] (1.Forestry and Forest Products Research Institute, 2.Fukuoka Agriculture and Forestry Research Center)

[HDS14-P04] Geologic characteristics of rock mass failures caused by the heavy rain event of July 2018 in Uwajima, Ehime

*Shintaro Yamasaki[1] (1.Disaster Prevention Research Institute, Kyoto University)

[HDS14-P05] On the failure mechanism of embankments in Mabi Town during the Heavy rain of July, 2018, Japan

*Gonghui Wang[1] (1.Disaster Prevention Research Institute, Kyoto University)

[HDS14-P06] Interpretation of landslide surface deformation around the branch basins of Sun Kosi river in Nepal using InSAR images

*Otake Shunpei[1], Hiroshi, P. Sato[1] (1.College of Humanities and Sciences, Nihon University)

[HDS14-P07] The large scale landslides triggered by The 2018 Sulawesi Earthquake, Indonesia

*Masashi Omata[1], Toshiyuki Adachi[2], Takao Yamakoshi[3], Kenichi Matsui[4], Tosho Iwamatsu[1], Susumu Takagishi[1], Chiho Motojima[1], Yuu Okuizumi[1], Umito Wada[1] (1.PASCO CORPORATION, 2.LDP Upper House member, 3.SABO & LANDSLIDE TECNICAL CENTER, 4.Nobuyuki Adzchi Office)

[HDS14-P08] Relationship of the grand deformation and topography in Sapporo City at the 2018 Hokkaido Eastern Iburi Earthquake confirmed by InSAR analysis

*Akihiro Yokota[1], Tomohiro Nishimura[2], Kiyoyuki Shigeno[1], Kenichi Honda[2], Sakae Mukoyama[2] (1.Meiji Consultant Co., Ltd, 2.Kokusai Kogyo Co., Ltd)

[HDS14-P09] Estimation of co-seismic surface displacement and ground deformation associated with the 2018 Hokkaido Eastern Iburi Earthquake, based on differential InSAR and differential LiDAR DEM analysis.

*Kenichi Honda[1], Norichika Asada[1], Naruo Mushiake[1], Tomohiro Nishimura[1], Sakae Mukoyama[1] (1.Kokusai Kogyo Co.,LTD.)

[HDS14-P10] Geological features of landslides of pyroclastic fall deposits induced by the 2018 Eastern Iburi Earthquake and other previous earthquakes

*Masahiro Chigira[1], Jun Tajika[3], Satoshi Ishimaru[2], Takehiko Suzuki[4] (1.Disaster Prevention Research Institute, Kyoto University, 2.Hokkaido Geological Survey, Hokkaido Research Organization, 3.Docon Co. Ltd, 4.Tokyo Metropolitan University)

[HDS14-P11] Earthquake ground motion properties of mountainous district in Totsukawa village, Nara pref. based on the seismic observation – A fundamental study of landslides caused by earthquake –

*Tomoyuki Iida[1], Ryuji Yamada[1], Shigeki Senna[1], Hidemitsu Tokui[2], Tetsuya Onodera[2], Hiroshi Kawabe (1.National Research Institute for Earth Science and Disaster Prevention, 2.Technicallink Kabushiki kaisya)

[HDS14-P12] Study on topographic features and landslide development process in slope failure by Typhoon Talas

*Teruyuki Kikuchi[1], Teruyoshi Hatano[2], Satoshi Nishiyama[3] (1.JP-Design Co., Ltd., 2.Electric Power Development Co.,Ltd., 3.Okayama University Graduate School of Environmental and Life Science)

[HDS14-P13] Formation mechanism of bulge of slope that is sign of large-scale collapse

*tatsurou yoshimura[1] (1.Daiichi Fukken Co., Ltd.)

[HDS14-P14] Sediments accumulated in the linear depressions in the Mitsumine area, Kanto Mountains

*Masakazu Mashiko[1], Masahiro Chigira[2] (1.Graduate School of Science, kyoto University, 2.Disaster Prevention Research Institute, Kyoto University)

[J] Poster | H (Human Geosciences)：H-DS Disaster geosciences

5:15 PM - 6:30 PM JST | 8:15 AM - 9:30 AM UTC | Poster Hall International Exhibition Hall8, Makuhari Messe_15

[H-DS14] Geohazards in humid, tectonically active countries and their precursors

convener:Masahiro Chigira(Disaster Prevention Research Institute, Kyoto University), Hiroshi YAGI(Faculty of Art, Science and Education, Yamagata University), Satoru Kojima(Department of Civil Engineering, Gifu University), Taro Uchida(National Institute for Land and Infrastructure Management)

[HDS14-P01] The estimation of frequency for deep-seated landslide with carbon dating in Kii mountain area

★Invited Papers

*Yasutaka Tanaka[1], Toshiaki Kotake[1], Hiroaki Sugawara[1], Atsuhiko Kinoshita[1], Yoshito Ogawauchi[2], Minami Fujiwara[2] (1.Sediment Disaster Prevention Technology Center, Kinki Regional Developing Bureau, Ministry of Land, Infrastructure, Transport and Tourism, 2.Japan Conservation Engineers & CO., LTD.)

[HDS14-P02] Tephra stratigraphy and a slope failure of about 4,000 years ago on the slope of the Late Pleistocene Janoo Volcano in the northwestern of Aso Caldera

*Yasuto Hirata[1], Keiichi Ueta[1], Riichiro Miyawaki[2], Katsutoshi Iemura[2], Toshitaka Yokoyama[2], Akiko Miyawaki[2] (1.Central Research Institute of Electric Power Industry, 2.Hanshin Consultants)

[HDS14-P03] Analysis of causal factors of landslides during 2017 northern Kyusyu torrential rainfall disaster by using decision tree

*Hiromu Daimaru[1], Wataru Murakami[1], Yuki Tsurusaki[2] (1.Forestry and Forest Products Research Institute, 2.Fukuoka Agriculture and Forestry Research Center)

[HDS14-P04] Geologic characteristics of rock mass failures caused by the heavy rain event of July 2018 in Uwajima, Ehime

*Shintaro Yamasaki[1] (1.Disaster Prevention Research Institute, Kyoto University)

[HDS14-P05] On the failure mechanism of embankments in Mabi Town during the Heavy rain of July, 2018, Japan

*Gonghui Wang[1] (1.Disaster Prevention Research Institute, Kyoto University)

[HDS14-P06] Interpretation of landslide surface deformation around the branch basins of Sun Kosi river in Nepal using InSAR images

*Otake Shunpei[1], Hiroshi, P. Sato[1] (1.College of Humanities and Sciences, Nihon University)

[HDS14-P07] The large scale landslides triggered by The 2018 Sulawesi Earthquake, Indonesia

*Masashi Omata[1], Toshiyuki Adachi[2], Takao Yamakoshi[3], Kenichi Matsui[4], Tosho Iwamatsu[1], Susumu Takagishi[1], Chiho Motojima[1], Yuu Okuizumi[1], Umito Wada[1] (1.PASCO CORPORATION, 2.LDP Upper House member, 3.SABO & LANDSLIDE TECNICAL CENTER, 4.Nobuyuki Adzchi Office)

[HDS14-P08] Relationship of the grand deformation and topography in Sapporo City at the 2018 Hokkaido Eastern Iburi Earthquake confirmed by InSAR analysis

*Akihiro Yokota[1], Tomohiro Nishimura[2], Kiyoyuki Shigeno[1], Kenichi Honda[2], Sakae Mukoyama[2] (1.Meiji Consultant Co., Ltd, 2.Kokusai Kogyo Co., Ltd)

[HDS14-P09] Estimation of co-seismic surface displacement and ground deformation associated with the 2018 Hokkaido Eastern Iburi Earthquake, based on differential InSAR and differential LiDAR DEM analysis.

*Kenichi Honda[1], Norichika Asada[1], Naruo Mushiake[1], Tomohiro Nishimura[1], Sakae Mukoyama[1] (1.Kokusai Kogyo Co.,LTD.)

[HDS14-P10] Geological features of landslides of pyroclastic fall deposits induced by the 2018 Eastern Iburi Earthquake and other previous earthquakes

*Masahiro Chigira[1], Jun Tajika[3], Satoshi Ishimaru[2], Takehiko Suzuki[4] (1.Disaster Prevention Research Institute, Kyoto University, 2.Hokkaido Geological Survey, Hokkaido Research Organization, 3.Docon Co. Ltd, 4.Tokyo Metropolitan University)

[HDS14-P11] Earthquake ground motion properties of mountainous district in Totsukawa village, Nara pref. based on the seismic observation – A fundamental study of landslides caused by earthquake –

*Tomoyuki Iida[1], Ryuji Yamada[1], Shigeki Senna[1], Hidemitsu Tokui[2], Tetsuya Onodera[2], Hiroshi Kawabe (1.National Research Institute for Earth Science and Disaster Prevention, 2.Technicallink Kabushiki kaisya)

[HDS14-P12] Study on topographic features and landslide development process in slope failure by Typhoon Talas

*Teruyuki Kikuchi[1], Teruyoshi Hatano[2], Satoshi Nishiyama[3] (1.JP-Design Co., Ltd., 2.Electric Power Development Co.,Ltd., 3.Okayama University Graduate School of Environmental and Life Science)

[HDS14-P13] Formation mechanism of bulge of slope that is sign of large-scale collapse

*tatsurou yoshimura[1] (1.Daiichi Fukken Co., Ltd.)

[HDS14-P14] Sediments accumulated in the linear depressions in the Mitsumine area, Kanto Mountains

*Masakazu Mashiko[1], Masahiro Chigira[2] (1.Graduate School of Science, kyoto University, 2.Disaster Prevention Research Institute, Kyoto University)

[E] Oral | H (Human Geosciences)：H-CG Complex & General

1:45 PM - 3:15 PM JST | 4:45 AM - 6:15 AM UTC | 301B 3F

[H-CG26] Deltas and estuaries: multidisciplinary analyses of complex river-mouth systems

convener:Yoshiki Saito(Estuary Research Center, Shimane University), Guan-Hong Lee(Inha University), David L Dettman(University of Arizona), Kazuaki Hori(Department of Geography, Graduate School of Environmental Studies, Nagoya University), Chairperson:Yoshiki Saito(Shimane Univ/ GSJ, AIST), David Dettman(University of Arizona)

1:45 PM - 2:15 PM JST | 4:45 AM - 5:15 AM UTC

[HCG26-01] Recent Changes of the Asian Major Deltas

★Invited Papers

*Paul Liu[1] (1.North Carolina State University Raleigh)

2:15 PM - 2:30 PM JST | 5:15 AM - 5:30 AM UTC

[HCG26-02] **Matching trends in channel width, sinuosity, and depth along the fluvial to marine transition zone of tide-dominated river deltas: the need for a revision of depositional and hydraulic models**

★Invited Papers

*Marcello Gugliotta[1], Yoshiki Saito[1] (1.Shimane University)

2:30 PM - 2:45 PM JST | 5:30 AM - 5:45 AM UTC

[HCG26-03] **Effects of an Estuarine Dam on Sediment Flux Mechanisms in a Macrotidal Estuary**

Steven Miguel Figueroa[1], *Guan-Hong Lee[1] (1.Inha University)

2:45 PM - 3:00 PM JST | 5:45 AM - 6:00 AM UTC

[HCG26-04] **Late Pleistocene sedimentary evolution of the north Jiangsu coastal plain revealed by OSL dating based chronostratigraphy**

*Lei Gao[1], Hao Long[1], Ping Zhang[2], Toru Tamura[3,4], Ji Shen[1] (1.Nanjing Institute of Geography and Limnology, CAS,China, 2.Geological Survey of Jiangsu Province (GSJP), Key Lab of EFGD, Ministry of LR, China, 3.Geological Survey of Japan (GSJ), AIST, 4.Graduate School of Frontier Sciences, The University of Tokyo)

3:00 PM - 3:15 PM JST | 6:00 AM - 6:15 AM UTC

[HCG26-05] The sedimentary environments and provenance of the late Quaternary sediments, in South Yellow Sea shelf, eastern China

*Yong Yin[1] (1.School of Geography and Ocean Science, Nanjing University)

[E] Poster | H (Human Geosciences)：H-CG Complex & General

3:30 PM - 5:00 PM JST | 6:30 AM - 8:00 AM UTC | Poster Hall International Exhibition Hall8, Makuhari Messe_9

[H-CG26] Deltas and estuaries: multidisciplinary analyses of complex river-mouth systems

convener:Yoshiki Saito(Estuary Research Center, Shimane University), Guan-Hong Lee(Inha University), David L Dettman(University of Arizona), Kazuaki Hori(Department of Geography, Graduate School of Environmental Studies, Nagoya University)

[HCG26-P01] Deltafront Clinoform of Abandoned Yellow River Delta in Jiangsu Province, China

*LIANGYONG ZHOU[1] (1.Qingdao Institute of Marine Geology China Geological Survey)

[HCG26-P02] Holocene evolution and Anthropocene destruction of the Krishna delta, east coast of India: delta lobe shifts, human impact, and sea-level history

Kakani Nageswara Rao[2], *Yoshiki Saito[1], K.Ch.V. Nagakumar[4], Sumiko Kubo[3], Shilpa Pandey[5], Zhen Li[6], G. Demudu[2], A.S. Rajawat[7] (1.Estuary Research Center, Shimane University, 2.Andhra University, 3.Waseda University, 4.Centre for Water Resources and Management, 5.Birbal Sahni Institute of Palaeosciences, 6.University of Victoria, 7.Space Applications Centre)

[HCG26-P03] Offset in radiocarbon ages between marine bioclast and terrestrial plant pairs in the Holocene sediments around Japan

*Nakanishi Toshimichi[1,2], Futoshi Nanayama[3,4], Atsushi Urabe[5], Kazuaki Hori[6], Wan Hong[7] (1.Kyoto Univ., 2.JAEA, 3.AIST, 4.Kumamoto Univ., 5.Niigata Univ., 6.Nagoya Univ., 7.KIGAM)

[HCG26-P04] Assessment of MEIS for Marine Spatial Planning in the Nakdong River Estuary, Busan Metropolitan City, South Korea

*Jun-Ho Lee[1], Han Jun Woo[1], Hoi-Soo Jung[1], Chan Mi Park[1] (1.Korea Institute of Ocean Science and Technology)

[HCG26-P05] Tidal changes at Asian deltas in response to future sea-level rise

*Katsuto Uehara[1] (1.Kyushu University)

[HCG26-P06] **A governing equation of non-deltaic transgressive profile: 2D numerical simulation and flume experiments**

*Junhui Wang[1,2,3], Tetsuji Muto[3] (1.China University of Petroleum (Beijing), 2.State Key Laboratory of Petroleum Resources and Prospecting, China, 3.Nagasaki University)

[E] Poster | H (Human Geosciences)：H-CG Complex & General

5:15 PM - 6:30 PM JST | 8:15 AM - 9:30 AM UTC | Poster Hall International Exhibition Hall8, Makuhari Messe_16

[H-CG26] Deltas and estuaries: multidisciplinary analyses of complex river-mouth systems

convener:Yoshiki Saito(Estuary Research Center, Shimane University), Guan-Hong Lee(Inha University), David L Dettman(University of Arizona), Kazuaki Hori(Department of Geography, Graduate School of Environmental Studies, Nagoya University)

[HCG26-P01] Deltafront Clinoform of Abandoned Yellow River Delta in Jiangsu Province, China

*LIANGYONG ZHOU[1] (1.Qingdao Institute of Marine Geology China Geological Survey)

[HCG26-P02] Holocene evolution and Anthropocene destruction of the Krishna delta, east coast of India: delta lobe shifts, human impact, and sea-level history

Kakani Nageswara Rao[2], *Yoshiki Saito[1], K.Ch.V. Nagakumar[4], Sumiko Kubo[3], Shilpa Pandey[5], Zhen Li[6], G. Demudu[2], A.S. Rajawat[7] (1.Estuary Research Center, Shimane University, 2.Andhra University, 3.Waseda University, 4.Centre for Water Resources and Management, 5.Birbal Sahni Institute of Palaeosciences, 6.University of Victoria, 7.Space Applications Centre)

[HCG26-P03] Offset in radiocarbon ages between marine bioclast and terrestrial plant pairs in the Holocene sediments around Japan

*Nakanishi Toshimichi[1,2], Futoshi Nanayama[3,4], Atsushi Urabe[5], Kazuaki Hori[6], Wan Hong[7] (1.Kyoto Univ., 2.JAEA, 3.AIST, 4.Kumamoto Univ., 5.Niigata Univ., 6.Nagoya Univ., 7.KIGAM)

[HCG26-P04] Assessment of MEIS for Marine Spatial Planning in the Nakdong River Estuary, Busan Metropolitan City, South Korea

*Jun-Ho Lee[1], Han Jun Woo[1], Hoi-Soo Jung[1], Chan Mi Park[1] (1.Korea Institute of Ocean Science and Technology)

[HCG26-P05] Tidal changes at Asian deltas in response to future sea-level rise

*Katsuto Uehara[1] (1.Kyushu University)

[HCG26-P06] **A governing equation of non-deltaic transgressive profile: 2D numerical simulation and flume experiments**

*Junhui Wang[1,2,3], Tetsuji Muto[3] (1.China University of Petroleum (Beijing), 2.State Key Laboratory of Petroleum Resources and Prospecting, China, 3.Nagasaki University)

[E] Oral | H (Human Geosciences)：H-CG Complex & General

9:00 AM - 10:30 AM JST | 12:00 AM - 1:30 AM UTC | 301B 3F

[H-CG27] Turbidity current: from triggers for the generation to the depositional and morphologic al processes

convener:Miwa Yokokawa(Osaka Institute of Technology), Hajime Naruse(Department of Geology and Mineralogy, Graduate School of Science, Kyoto University), Norihiro Izumi(Faculty of Engineering, Hokkaido University), Ken Ikehara(Institute of Geology and Geoinformation, National Institute of Advanced Industrial Science and Technology), Chairperson:Miwa Yokokawa(Osaka Institute of Technology), Norihiro Izumi(Hokkaido University)

9:00 AM - 9:15 AM JST | 12:00 AM - 12:15 AM UTC

[HCG27-01] Inverse analysis of turbidity currents using two dimensional shallow water model

*Hajime Naruse[1] (1.Department of Geology and Mineralogy, Graduate School of Science, Kyoto University)

9:15 AM - 9:30 AM JST | 12:15 AM - 12:30 AM UTC

[HCG27-02] Inverse Analysis of Experimental Scale Turbidity Currents by Deep Learning Neural Network

*Cai Zhirong[1], Hajime Naruse[1], Qifeng Yao[1] (1.Kyoto University)

9:30 AM - 9:45 AM JST | 12:30 AM - 12:45 AM UTC

[HCG27-03] Conditions for development of depositional submarine channels: examination by flume experiments

*Justine Poppeschi[1], Kazushi Nakata[1], Hajime Naruse[1] (1.Division of Earth and Planetary Sciences, Graduate School of Science, Kyoto University)

9:45 AM - 10:00 AM JST | 12:45 AM - 1:00 AM UTC

[HCG27-04] Cyclic steps formed by long-runout turbidity currents

*Zhuyuan Wu[1], Norihiro Izumi [1] (1.Hokkaido University)

10:00 AM - 10:15 AM JST | 1:00 AM - 1:15 AM UTC

[HCG27-05] Is surface sediment remobilization more popular mechanism for generating earthquake-induced turbidity current? Evidence of radiocarbon dates from the westernmost Nankai and Japan Trench subduction zones

*Ken Ikehara[1], Toshiya Kanamatsu[3], Tobias Schwestermann[2], Arata Kioka[2], Michael Strasser[2] (1.Institute of Geology and Geoinformation, National Institute of Advanced Industrial Science and Technology, 2.Universität Innsbruck, 3.Japan Agency for Marine-Earth Science and Technology)

10:15 AM - 10:30 AM JST | 1:15 AM - 1:30 AM UTC

[HCG27-06] Shallow-subsurface event stratigraphy along the hadal trench axis of the Japan Trench

*A. Kioka[1], T. Schwestermann[1], J. Moernaut[1], K. Ikehara[2], T. Kanamatsu[3], M. Strasser[1,4] (1.Universität Innsbruck, Austria, 2.GSJ-AIST, Japan, 3.JAMSTEC, Japan, 4.MARUM-U. Bremen, Germany)

[E] Oral | H (Human Geosciences)：H-CG Complex & General

10:45 AM - 12:15 PM JST | 1:45 AM - 3:15 AM UTC | 301B 3F

[H-CG27] Turbidity current: from triggers for the generation to the depositional and morphologic al processes

convener:Miwa Yokokawa(Osaka Institute of Technology), Hajime Naruse(Department of Geology and Mineralogy, Graduate School of Science, Kyoto University), Norihiro Izumi(Faculty of Engineering, Hokkaido University), Ken Ikehara(Institute of Geology and Geoinformation, National Institute of Advanced Industrial Science and Technology), Chairperson:Hajime Naruse(Kyoto University), Ken Ikehara(AIST)

10:45 AM - 11:07 AM JST | 1:45 AM - 2:07 AM UTC

[HCG27-07] Canyon changes caused by an earthquake-triggered turbidity current in the 2016 M7.8 Kaikōura Earthquake, New Zealand

★Invited Papers

*Joshu J Mountjoy[1], Jamie D Howarth[2], Alan R Orpin[1], Philip M Barnes[1], David A Bowden[1], Ashley A Rowden[1], Alexander C. G. Schimel[1], Caroline Holden[3], Huw J Horgan[2], Scott D Nodder[1], Jayson R Patton[4], Geoffroy Lamarche[1,5], Matt Gerstenberger[3], Aaron Micallef[6], Arne Pallentin[1], Tim Kane[1] (1.NIWA, Wellington. New Zealand, 2.VUW, Wellington. New Zealand, 3.GNS Science, Lower Hutt. New Zealand, 4.HSU, Arcata CA. USA, 5.UoA, Auckland. New Zealand, 6.UoM, Msida. Malta)

11:07 AM - 11:29 AM JST | 2:07 AM - 2:29 AM UTC

[HCG27-08] Far More Prolonged Deep-sea Turbidity Currents triggered by typhoon and earthquake in the Gaoping Submarine Canyon

★Invited Papers

*Yanwei Zhang[1], Zhifei Liu[1], Yulong Zhao[1], Xiaodong Zhang[1] (1.Tongji University)

11:29 AM - 11:51 AM JST | 2:29 AM - 2:51 AM UTC

[HCG27-09] **Filling the gap between turbidity current processes and products in British Columbia fjords**

★Invited Papers

*Sophie Hage[1,2,3] (1.School of Ocean and Earth Sciences, University of Southampton, United Kingdom, 2.National Oceanography Centre Southampton, United Kingdom, 3.Department of Geography, Durham University, United Kingdom)

11:51 AM - 12:13 PM JST | 2:51 AM - 3:13 AM UTC

[HCG27-10] **Sediment transfer from shelf to abyss through giant ganyons and valleys system in deep-sea carbonate slopes (Bahamas)**

★Invited Papers

*Thierry Mulder[1], Hervé Gillet[1], Vincent Hanquiez[1], Audrey Recouvreur[1], Kelly Fauquembergue[1], Johan Le Goff[2], John J.G. Reijmer[2], Emmanuelle Ducassou[1], Margot Joumes, Thibault Cavailhes[1], Elsa Tournadour[5], Jean Borgomano[3], Emmanuelle Poli[4] (1.University of Bordeaux, UMR CNRS 5805 EPOC, Allée Geoffroy Saint Hilaire, Pessac, France, 2.King Fahd Univ. of Petroleum. and Minerals, Dhahran, Saudi Arabia., 3.Aix Marseille University, CNRS, IRD, Collège de France, CEREGE, Aix-en-Provence, France., 4.Total, CSTJF, avenue Larribau, Pau, France, 5.Ifremer, Centre de Brest, Plouzané)

[E] Poster | H (Human Geosciences)：H-CG Complex & General

5:15 PM - 6:30 PM JST | 8:15 AM - 9:30 AM UTC | Poster Hall International Exhibition Hall8, Makuhari Messe_17

[H-CG27] Turbidity current: from triggers for the generation to the depositional and morphologic al processes

convener:Miwa Yokokawa(Osaka Institute of Technology), Hajime Naruse(Department of Geology and Mineralogy, Graduate School of Science, Kyoto University), Norihiro Izumi(Faculty of Engineering, Hokkaido University), Ken Ikehara(Institute of Geology and Geoinformation, National Institute of Advanced Industrial Science and Technology)

[HCG27-P01] The Huapinghsu Canyon (SW East China Sea): morphology and sedimentary processes

*Cheng-Shing Chiang[1], Ho-Shing Yu[2] (1.National Museum of Natural Science, Taiwan, 2.Institute of Oceanography, National Taiwan University, Taipei, Taiwan)

[HCG27-P02] Towards understanding the seismic history of the Nankai Trough using fine-grained turbidites

*Natsumi Okutsu[1], Juichiro Ashi[1], Asuka Yamaguchi[1] (1.The University of Tokyo)

[HCG27-P03] Flood-induced sediment gravity-flow deposits in varved diatomites

*Hana Sasaki[1], Yoshiro Ishihara[2] (1.Graduate School of Science, Fukuoka University, 2.Department of Science, Fukuoka University)

[HCG27-P04] Features of parallel lamination in turbidite sandstones in the Upper Cretaceous Izumi Group in the southern part of the Awaji Island, southwest Japan

*Akane Okuda[1], Hajime Naruse[1] (1.Division of Earth and Planetary Sciences, Graduate school of Science, Kyoto University)

[HCG27-P05] Sediment wave formation on slope base environments: an example of the Neogene Aoshima Formation, Miyazaki Prefecture, Southwest Japan

Shiori Iwao[1], Yuri Onishi[2], *Yoshiro Ishihara[1], Miwa Yokokawa[3] (1.Department of Earth System Science Faculty of Science, Fukuoka University, 2.OYO Corporation, 3.Lab. of Geoenvironment, Osaka Institute of Technology)

[HCG27-P06] A flume experiment on sedimentary structures and grain size distribution of cyclic steps formed by surge-type turbidity currents

*Miwa Yokokawa[1], Kazunori Fujita[1], Isamu Mori[1], Robert Fernandez[2], Matt Czapiga[3], John Berrens[4], Jeffrey Kwang[4], Kensuke Naito[4], Gary Parker[4], Norihiro Izumi[5], Hajime Naruse[6] (1.Osaka Institute of Technology, 2.University of Hull, 3.Technical University of Delft, 4.University of Illinois, 5.Hokkaido University, 6.Kyoto University)

[J] Poster | S (Solid Earth Sciences)：S-GD Geodesy

10:45 AM - 12:15 PM JST | 1:45 AM - 3:15 AM UTC | Poster Hall International Exhibition Hall8, Makuhari Messe_1

[S-GD03] Geodesy General Contributions/Global Geodetic Observing System

convener:Koji Matsuo(Geospatial Information Authority of Japan), Yusuke Yokota(Institute of Industrial Science, The University of Tokyo), Takahiro Wakasugi(Geospatial Information Authority of Japan)

[SGD03-P01] The Study of Sky Condition Prediction and Combination Efficiency Estimation about Multi-GNSS

*Chieh-Ting Chou[1], Yi-Shan - Li[2], Yen-Te - Li[1], Wan-Yu - Yu[1] (1.Department of Environmental Information and Engineering, CCIT, National Defense University, Graduate Student, 2.Department of Environmental Information and Engineering, CCIT, National Defense University, Assistant Professor)

[SGD03-P02] Research on the development of rapid and accurate GNSS routine analysis system (2)

*Hiroyuki Nakagawa[1] (1.The Geospatial Information Authority of Japan)

[SGD03-P03] Characteristics of the Tenryu-Funagira laser extensometer and its detection ability of slow slips

*Akio Katsumata[1], Akiteru Takamori[2], Akito Araya[2] (1.Meteorological Research Institute, Japan Meteorological Agency, 2.Earthquake Research Institute, University of Tokyo)

[SGD03-P04] Performance evaluation of laser strainmeters

*Akiteru Takamori[1], Akito Araya[1], Akio Katsumata[2], Wataru Morii[3], Kouseki Miyo[4], Masatake Ohashi[4] (1.Earthquake Research Institute, University of Tokyo, 2.Meteorological Research Institute, 3.Disaster Prevention Research Institute, Kyoto University, 4.Institute for Cosmic Ray Research, University of Tokyo)

[SGD03-P05] Calculation Method of the Tidal Love Numbers with the Fluid Core Resonance of the Solid Earth

*Yuji Harada[1,2], Shuhei Okubo[3] (1.State Key Laboratory of Lunar and Planetary Science, Space Science Institute, Macau University of Science and Technology, 2.Ocean Hemisphere Research Center, Earthquake Research Institute, University of Tokyo, 3.Center for High Energy Geophysics Research, Earthquake Research Institute, University of Tokyo)

[SGD03-P06] Integrating PSInSAR and Hydrogeophysical Methods for the Characterization of a Earth fissure in the eastern Beijing plain

*Menglin Zhao[1], juan wang[1], wang xu[1], bing hu[1], yisheng chen[1] (1.Capitai Normal University)

[J] Poster | S (Solid Earth Sciences)：S-GD Geodesy

5:15 PM - 6:30 PM JST | 8:15 AM - 9:30 AM UTC | Poster Hall International Exhibition Hall8, Makuhari Messe_18

[S-GD03] Geodesy General Contributions/Global Geodetic Observing System

convener:Koji Matsuo(Geospatial Information Authority of Japan), Yusuke Yokota(Institute of Industrial Science, The University of Tokyo), Takahiro Wakasugi(Geospatial Information Authority of Japan)

[SGD03-P01] The Study of Sky Condition Prediction and Combination Efficiency Estimation about Multi-GNSS

*Chieh-Ting Chou[1], Yi-Shan - Li[2], Yen-Te - Li[1], Wan-Yu - Yu[1] (1.Department of Environmental Information and Engineering, CCIT, National Defense University, Graduate Student, 2.Department of Environmental Information and Engineering, CCIT, National Defense University, Assistant Professor)

[SGD03-P02] Research on the development of rapid and accurate GNSS routine analysis system (2)

*Hiroyuki Nakagawa[1] (1.The Geospatial Information Authority of Japan)

[SGD03-P03] Characteristics of the Tenryu-Funagira laser extensometer and its detection ability of slow slips

*Akio Katsumata[1], Akiteru Takamori[2], Akito Araya[2] (1.Meteorological Research Institute, Japan Meteorological Agency, 2.Earthquake Research Institute, University of Tokyo)

[SGD03-P04] Performance evaluation of laser strainmeters

*Akiteru Takamori[1], Akito Araya[1], Akio Katsumata[2], Wataru Morii[3], Kouseki Miyo[4], Masatake Ohashi[4] (1.Earthquake Research Institute, University of Tokyo, 2.Meteorological Research Institute, 3.Disaster Prevention Research Institute, Kyoto University, 4.Institute for Cosmic Ray Research, University of Tokyo)

[SGD03-P05] Calculation Method of the Tidal Love Numbers with the Fluid Core Resonance of the Solid Earth

*Yuji Harada[1,2], Shuhei Okubo[3] (1.State Key Laboratory of Lunar and Planetary Science, Space Science Institute, Macau University of Science and Technology, 2.Ocean Hemisphere Research Center, Earthquake Research Institute, University of Tokyo, 3.Center for High Energy Geophysics Research, Earthquake Research Institute, University of Tokyo)

[SGD03-P06] Integrating PSInSAR and Hydrogeophysical Methods for the Characterization of a Earth fissure in the eastern Beijing plain

*Menglin Zhao[1], juan wang[1], wang xu[1], bing hu[1], yisheng chen[1] (1.Capitai Normal University)

[J] Oral | S (Solid Earth Sciences)：S-GD Geodesy

1:45 PM - 3:15 PM JST | 4:45 AM - 6:15 AM UTC | 304 3F

[S-GD03] Geodesy General Contributions/Global Geodetic Observing System

convener:Koji Matsuo(Geospatial Information Authority of Japan), Yusuke Yokota(Institute of Industrial Science, The University of Tokyo), Takahiro Wakasugi(Geospatial Information Authority of Japan), Chairperson:Kensuke Kokado(GSI of Japan), Yusuke Yokota

1:50 PM - 2:05 PM JST | 4:50 AM - 5:05 AM UTC

[SGD03-01] Activities and future perspective of GGOS Working Group Japan

*Basara Miyahara[1] (1.GSI of Japan)

2:05 PM - 2:20 PM JST | 5:05 AM - 5:20 AM UTC

[SGD03-02] Discussion

*Koji Matsuo[1] (1.Geospatial Information Authority of Japan)

2:20 PM - 2:35 PM JST | 5:20 AM - 5:35 AM UTC

[SGD03-03] VLBI-GNSS Co-location Survey at the Ishioka Geodetic Observing Station

*Saho Matsumoto[1], Michiko Umei[1], Haruka Ueshiba[1], Shinobu Kurihara[1], Tadao Kikkawa[1], Takahiro Wakasugi[1] (1.GSI of Japan)

2:35 PM - 2:50 PM JST | 5:35 AM - 5:50 AM UTC

[SGD03-04] Research of Crustal Deformation Model for Next Version of Japanese Geodetic Datum

*Kensuke Kokado[1] (1.GSI of Japan)

2:50 PM - 3:05 PM JST | 5:50 AM - 6:05 AM UTC

[SGD03-05] Construction of a laser-strainmeter network for accurate seismic and geodetic observations

*Akito Araya[1], Akiteru Takamori[1], Wataru Morii[2], Akio Katsumata[3], Akio Kobayashi[3], Takeo Ito[4], Takashi Okuda[4], Makoto Okubo[5] (1.Earthquake Research Institute, University of Tokyo, 2.Disaster Prevention Research Institute, Kyoto University, 3.Meteorological Research Institute, Japan Meteorological Agency, 4.Graduate School of Environmental Studies, Nagoya University, 5.Natural Science Cluster, Kochi University)

[J] Oral | S (Solid Earth Sciences)：S-GD Geodesy

3:30 PM - 5:00 PM JST | 6:30 AM - 8:00 AM UTC | 304 3F

[S-GD03] Geodesy General Contributions/Global Geodetic Observing System

convener:Koji Matsuo(Geospatial Information Authority of Japan), Yusuke Yokota(Institute of Industrial Science, The University of Tokyo), Takahiro Wakasugi(Geospatial Information Authority of Japan), Chairperson:Yuji Harada(Macau University of Science and Technology), Koji Matsuo

3:35 PM - 3:50 PM JST | 6:35 AM - 6:50 AM UTC

[SGD03-06] UNAVCO GNSS Data: Real-time High-rate Streams, Geodetic Earthquake Magnitudes, Cloud Computing and Future Machine Learning Frameworks

*David A Phillips[1], Kathleen Hodgkinson[1], David Mencin[1], Charles Meertens[1], Thomas Herring[2], Walter Szeliga[3], Timothy Melbourne[3], Mark Murray[4], Glen Mattioli[1], Christine Puskas[1] (1.UNAVCO, Inc. Boulder, 2.Massachusetts Institute of Technology, 3.Central Washington University, 4.USGS)

3:50 PM - 4:05 PM JST | 6:50 AM - 7:05 AM UTC

[SGD03-07] **On application of GNSS-techniques for early tsunami warning in the Sea of Japan**

*Grigorii Viktorovich Nechaev[1,2,3], Nikolai Shestakov[2,3], Hiroaki Takahashi[1], Mako Ohzono[1] (1.Institute of Seismology and Volcanology, Graduate Schooll of Science, Hokkaido University, 2.Far Eastern Federal University, 3.Institute for Applied Mathematics FEB RAS)

4:05 PM - 4:20 PM JST | 7:05 AM - 7:20 AM UTC

[SGD03-08] Measurements of occurrence of solar conjunction with the orbits of Asian QZSS/IGSO satellites

Cancelled

*Fujinobu Takahashi[1] (1.Yokohama National University)

4:20 PM - 4:35 PM JST | 7:20 AM - 7:35 AM UTC

[SGD03-09] Sea level evaluation in northern Australian coast

*Yuta Tokui[1], Kosuke Heki[1] (1.Hokkaido University)

4:35 PM - 4:50 PM JST | 7:35 AM - 7:50 AM UTC

[SGD03-10] Implications from geomagnetic observation for the interannual fluctuations of Earth rotation

*Seiki Asari[1], Masanori Kurihara[1], Kenji Morinaga[1], Shingo Nagamachi[1] (1.Kakioka Magnetic Observatory, Japan Meteorological Agency)

[E] Poster | S (Solid Earth Sciences)：S-SS Seismology

1:45 PM - 3:15 PM JST | 4:45 AM - 6:15 AM UTC | Poster Hall International Exhibition Hall8, Makuhari Messe_5

[S-SS07] Rigorous Seismicity Modelling and Hypothesis Testing

convener:Jiancang Zhuang(Institute of Statistical Mathematics), Danijel Schorlemmer(GFZ German Research Centre for Geosciences), Matt Gerstenberger(GNS Science), Hiroshi Tsuruoka(Earthquake Research Institute, Tokyo Univ.)

[SSS07-P01] Development of Physics-based Ground Motion Simulation in A Hybrid Approach and Applications to Seismic Hazard Assessment in Taiwan

*Ming-Che Hsieh[1], Yin-Tung Yen[1], Kuo-Fong Ma[2,3] (1.Disaster Prevention Technology Research Center, Sinotech Engineering Consultants (Inc.), Taiwan, 2.Department of Earth Sciences, National Central University, Taiwan, 3.Earthquake-Disaster & Risk Evaluation and Management Center, National Central University, Taiwan)

[SSS07-P02] Increasing Earthquake Forecast Testability - CSEP Future Developments

*Danijel Schorlemmer[1], Naoshi Hirata[2], Fabrice Cotton[1], Matt Gerstenberger[3], Thomas Jordan[7], Warner Marzocchi[4], William Savran[7], Maximilian Werner[5], Stefan Wiemer[6], Thomas Beutin[1], David D Jackson[8], Philip Maechling[7], Sum Mak[1], Kazuyoshi Nanjo[9], Yosihiko Ogata[10], David Rhoades[3], Hiroshi Tsuruoka[2], Graeme Weatherill[1], Jiancang Zhuang[10] (1.GFZ German Research Centre for Geosciences, 2.Earthquake Research Institute, University of Tokyo, Japan, 3.GNS Science, Lower Hutt, New Zealand, 4.University of Naples, Naples, Italy, 5.University of Bristol, Bristol, United Kingdom, 6.ETH Zurich, Zurich, Switzerland, 7.University of Southern California, Los Angeles, USA, 8.University of California Los Angeles, Los Angeles, USA, 9.University of Shizuoka, Shizuoka, Japan, 10.Institute of Statistical Mathematics, Tachikawa, Japan)

[SSS07-P03] Precision versus uncertainty in regional seismic hazard mapping

*Matt Gerstenberger[1], Danijel Schorlemmer[2] (1.GNS Science, 2.GFZ-Potsdam)

[SSS07-P04] An extreme value analysis of seismograms designed for early forecast of aftershocks

*Kaoru Sawazaki[1] (1.National Research Institute for Earth Science and Disaster Resilience)

[SSS07-P05] Spatio-temporal clustering of successive earthquakes: data analyses of global data.

*THYSTERE MATONDO BANTIDI[1], Takeshi Nishimura[1] (1.Tohoku University)

[SSS07-P06] Kanto 3 month testing class results of CSEP Japan

*Hiroshi Tsuruoka[1], Naoshi Hirata[1] (1.Earthquake Research Institute, Tokyo Univ.)

[SSS07-P07] Long-term earthquake risk in North China estimated from a modern catalogue

Ziyao Xiong[2], *Jiancang Zhuang[1], Shiyong Zhou[2] (1.Institute of Statistical Mathematics, 2.Peking University)

[SSS07-P08] Distributions of focal mechanisms in background seismicity and earthquake clusters in Japan

*Jiancang Zhuang[1,2], Eri Maita[2] (1.Institute of Statistical Mathematics, 2.Graduate University for Advanced Studies)

[SSS07-P09] New Ground Motion Prediction Equations for Western Saudi Arabia

*Ryota Kiuchi[1,2], Walter Mooney[1], Hani Zahran[3] (1.U.S. Geological Survey, 2.Disaster Prevenetion Research Institute, Kyoto University, 3.Saudi Geological Survey)

[SSS07-P10] Study on the spatial and temporal change of velocity structure before and after 2003 Chengkung earthquake, Taiwan

*TING YA LIANG[1], Wen-Yen Chang[1,2,3], Strong Wen[4] (1.National DONG HWA University, 2.Eastern Taiwan Earthquake Research Center, 3.National Center for Research on Earthquake Engineering, 4.National Chung Cheng University)

[E] Poster | S (Solid Earth Sciences)：S-SS Seismology

5:15 PM - 6:30 PM JST | 8:15 AM - 9:30 AM UTC | Poster Hall International Exhibition Hall8, Makuhari Messe_19

[S-SS07] Rigorous Seismicity Modelling and Hypothesis Testing

convener:Jiancang Zhuang(Institute of Statistical Mathematics), Danijel Schorlemmer(GFZ German Research Centre for Geosciences), Matt Gerstenberger(GNS Science), Hiroshi Tsuruoka(Earthquake Research Institute, Tokyo Univ.)

[SSS07-P01] Development of Physics-based Ground Motion Simulation in A Hybrid Approach and Applications to Seismic Hazard Assessment in Taiwan

*Ming-Che Hsieh[1], Yin-Tung Yen[1], Kuo-Fong Ma[2,3] (1.Disaster Prevention Technology Research Center, Sinotech Engineering Consultants (Inc.), Taiwan, 2.Department of Earth Sciences, National Central University, Taiwan, 3.Earthquake-Disaster & Risk Evaluation and Management Center, National Central University, Taiwan)

[SSS07-P02] Increasing Earthquake Forecast Testability - CSEP Future Developments

*Danijel Schorlemmer[1], Naoshi Hirata[2], Fabrice Cotton[1], Matt Gerstenberger[3], Thomas Jordan[7], Warner Marzocchi[4], William Savran[7], Maximilian Werner[5], Stefan Wiemer[6], Thomas Beutin[1], David D Jackson[8], Philip Maechling[7], Sum Mak[1], Kazuyoshi Nanjo[9], Yosihiko Ogata[10], David Rhoades[3], Hiroshi Tsuruoka[2], Graeme Weatherill[1], Jiancang Zhuang[10] (1.GFZ German Research Centre for Geosciences, 2.Earthquake Research Institute, University of Tokyo, Japan, 3.GNS Science, Lower Hutt, New Zealand, 4.University of Naples, Naples, Italy, 5.University of Bristol, Bristol, United Kingdom, 6.ETH Zurich, Zurich, Switzerland, 7.University of Southern California, Los Angeles, USA, 8.University of California Los Angeles, Los Angeles, USA, 9.University of Shizuoka, Shizuoka, Japan, 10.Institute of Statistical Mathematics, Tachikawa, Japan)

[SSS07-P03] Precision versus uncertainty in regional seismic hazard mapping

*Matt Gerstenberger[1], Danijel Schorlemmer[2] (1.GNS Science, 2.GFZ-Potsdam)

[SSS07-P04] An extreme value analysis of seismograms designed for early forecast of aftershocks

*Kaoru Sawazaki[1] (1.National Research Institute for Earth Science and Disaster Resilience)

[SSS07-P05] Spatio-temporal clustering of successive earthquakes: data analyses of global data.

*THYSTERE MATONDO BANTIDI[1], Takeshi Nishimura[1] (1.Tohoku University)

[SSS07-P06] Kanto 3 month testing class results of CSEP Japan

*Hiroshi Tsuruoka[1], Naoshi Hirata[1] (1.Earthquake Research Institute, Tokyo Univ.)

[SSS07-P07] Long-term earthquake risk in North China estimated from a modern catalogue

Ziyao Xiong[2], *Jiancang Zhuang[1], Shiyong Zhou[2] (1.Institute of Statistical Mathematics, 2.Peking University)

[SSS07-P08] Distributions of focal mechanisms in background seismicity and earthquake clusters in Japan

*Jiancang Zhuang[1,2], Eri Maita[2] (1.Institute of Statistical Mathematics, 2.Graduate University for Advanced Studies)

[SSS07-P09] New Ground Motion Prediction Equations for Western Saudi Arabia

*Ryota Kiuchi[1,2], Walter Mooney[1], Hani Zahran[3] (1.U.S. Geological Survey, 2.Disaster Prevenetion Research Institute, Kyoto University, 3.Saudi Geological Survey)

[SSS07-P10] Study on the spatial and temporal change of velocity structure before and after 2003 Chengkung earthquake, Taiwan

*TING YA LIANG[1], Wen-Yen Chang[1,2,3], Strong Wen[4] (1.National DONG HWA University, 2.Eastern Taiwan Earthquake Research Center, 3.National Center for Research on Earthquake Engineering, 4.National Chung Cheng University)

[E] Oral | S (Solid Earth Sciences)：S-SS Seismology

3:30 PM - 5:00 PM JST | 6:30 AM - 8:00 AM UTC | A10 TOKYO BAY MAKUHARI HALL

[S-SS07] Rigorous Seismicity Modelling and Hypothesis Testing

convener:Jiancang Zhuang(Institute of Statistical Mathematics), Danijel Schorlemmer(GFZ German Research Centre for Geosciences), Matt Gerstenberger(GNS Science), Hiroshi Tsuruoka(Earthquake Research Institute, Tokyo Univ.), Chairperson:Matthew Gerstenberger(GNS Science, New Zealand), Danijel Schorlemmer(GFZ-Potsdam, Germany)

3:30 PM - 3:45 PM JST | 6:30 AM - 6:45 AM UTC

[SSS07-01] Improving medium-term earthquake forecasts by compensating the EEPAS model for the time-lag

★Invited Papers

David Rhoades[1], Christophersen Annemarie[1], *Matt Gerstenberger[1] (1.GNS Science)

3:45 PM - 4:00 PM JST | 6:45 AM - 7:00 AM UTC

[SSS07-02] Earthquake probability forecast incorporating non-seismic data

*Peng Han[1], Jiancang Zhuang[2], Yosihiko Ogata[2], Katsumi Hattori[3] (1.Southern University of Science and Technology, Shenzhen, China, 2.The Institute of Statistical Mathematics, Tokyo, Japan , 3.Chiba University, Chiba, Japan)

4:00 PM - 4:15 PM JST | 7:00 AM - 7:15 AM UTC

[SSS07-03] **Extended versions of the space-time ETAS model and application to the 2016 Kumamoto earthquake sequence**

★Invited Papers

*YICUN GUO[1], Jiancang Zhuang[1], Yosihiko Ogata[1] (1.The Institute of Statistical Mathematics, Tokyo, Japan)

4:15 PM - 4:30 PM JST | 7:15 AM - 7:30 AM UTC

[SSS07-04] CSEP Japan results and future developments

*Naoshi Hirata[1], Hiroshi Tsuruoka[1], Danijel Schorlemmer[3], Jiancang Zhuang[2] (1.Earthquake Research Institute, the University of Tokyo, 2.Institute of Statistical Mathematics, 3.GFZ German Research Centre for Geosciences)

4:30 PM - 4:45 PM JST | 7:30 AM - 7:45 AM UTC

[SSS07-05] From the studies of historical earthquakes to the implication of single fault to multiple fault segments ruptures in seismic hazard analysis

★Invited Papers

*Kuo-Fong Ma[1,2,3], Mingshen Yen[1], Yiwun Liao[1], Henyi Su[2] (1.Earthquake - Disaster & Risk Evaluation and Managment (E-DREaM) Center, National Central University, Taiwan, ROC, 2.Department of Earth Sciences, National Central University, Taiwan, ROC, 3.Institute of Earth Sciences, Academia Sinica, Taiwan, ROC)

4:45 PM - 5:00 PM JST | 7:45 AM - 8:00 AM UTC

[SSS07-06] **High resolution space-time models forecasting 3D seismicity beneath the Greater Tokyo Area**

★Invited Papers

*Yosihiko Ogata[1,2], Koichi Katsura, Hiroshi Tsuruoka[2], Naoshi Hirata[2] (1.Research Organization of Information and Systems, The Institute of Statistical Mathematics, 2.Earthquake Research Institute, The University of Tokyo)

[J] Oral | S (Solid Earth Sciences)：S-SS Seismology

1:45 PM - 3:15 PM JST | 4:45 AM - 6:15 AM UTC | A09 TOKYO BAY MAKUHARI HALL

[S-SS11] Seismic wave propagation: Theory and Application

convener:Kiwamu Nishida(Earthquake Research Institute, University of Tokyo), Kazuya Shiraishi(Japan Agency for Marine-Earth Science and Technology), Takao Nibe(JAPEX), Kaoru Sawazaki(National Research Institute for Earth Science and Disaster Resilience), Chairperson:Tsutomu Takahashi(JAMSTEC)

1:45 PM - 2:00 PM JST | 4:45 AM - 5:00 AM UTC

[SSS11-01] Power Spectrum of Random Heterogeneity of the Solid Earth

*Haruo Sato[1] (1.Tohoku Unvieristy)

2:00 PM - 2:15 PM JST | 5:00 AM - 5:15 AM UTC

[SSS11-02] Estimation of spatio-temporal changes of seismic scattering property associated with the 2008 Iwate-Miyagi Nairiku earthquake from sparse modeling of seismic ambient noise CCFs

*Takashi Hirose[1], Hisashi Nakahara[1], Takeshi Nishimura[1], Michel Campillo[2] (1.Graduate School of Science, Tohoku University, 2.University Grenoble Alpes, CNRS, ISTerre)

2:15 PM - 2:30 PM JST | 5:15 AM - 5:30 AM UTC

[SSS11-03] Surface roughness of the Philippine Sea plate at Nankai subduction zone

*Tsutomu Takahashi[1], Ayako Nakanishi[1], Shuichi Kodaira[1], Yoshiyuki Kaneda[2] (1.JAMSTEC, 2.Kagawa University)

2:30 PM - 2:45 PM JST | 5:30 AM - 5:45 AM UTC

[SSS11-04] Source location of volcanic earthquakes and tremors at Sakurajima volcano based on seismic correlation

*Theodorus Permana[1], Takeshi Nishimura[1], Hisashi Nakahara[1] (1.Solid Earth Physics Laboratory, Department of Geophysics, Graduate School of Science, Tohoku University)

2:45 PM - 3:00 PM JST | 5:45 AM - 6:00 AM UTC

[SSS11-05] **Crustal Structure Investigation in Northern Taiwan - Localized Wavefield Inversion of TAIGER T6 Wide Angle Refraction/Reflection Data**

*Fandy Adji Fachtony[1], How-wei Chen[1] (1.Institute of Geophysics, National Central University)

3:00 PM - 3:15 PM JST | 6:00 AM - 6:15 AM UTC

[SSS11-06] Self-organized criticality induced by randomness in block-spring models and the Gutenberg=Richter law

*Hidetsugu Sakaguchi [1] (1.Kyushi University)

[J] Oral | S (Solid Earth Sciences)：S-SS Seismology

3:30 PM - 5:00 PM JST | 6:30 AM - 8:00 AM UTC | A09 TOKYO BAY MAKUHARI HALL

[S-SS11] Seismic wave propagation: Theory and Application

convener:Kiwamu Nishida(Earthquake Research Institute, University of Tokyo), Kazuya Shiraishi(Japan Agency for Marine-Earth Science and Technology), Takao Nibe(JAPEX), Kaoru Sawazaki(National Research Institute for Earth Science and Disaster Resilience), Chairperson:Kiwamu Nishida(東京大学地震研究所)

3:30 PM - 3:45 PM JST | 6:30 AM - 6:45 AM UTC

[SSS11-07] Land-Atmosphere Interaction in the low-frequency seismic band and inversion for shallow elasticity structure

*Toshiro Tanimoto[1], Jiong Wang[1] (1.Department of Earth Science, University of California, Santa Barbara, CA93106, USA)

3:45 PM - 4:00 PM JST | 6:45 AM - 7:00 AM UTC

[SSS11-08] Noise correlation analysis of S-net records

*Ryota Takagi[1], Genti Toyokuni[1], Mare Yamamoto[1] (1.Research Center for Prediction of Earthquakes and Volcanic Eruptions, Graduate School of Science, Tohoku University)

4:00 PM - 4:15 PM JST | 7:00 AM - 7:15 AM UTC

[SSS11-09] Atmospheric waves from the gas explosion in Sapporo on December 16, 2018, recorded by seismometers

*Kazunori Yoshizawa[1] (1.Faculty of Science, Hokkaido University)

4:15 PM - 4:30 PM JST | 7:15 AM - 7:30 AM UTC

[SSS11-10] Time-lapse monitoring of seismic velocity associated with the 2011 Shinmoedake eruption using seismic interferometry

*Kiwamu Nishida[1], Yuta Mizutani[1] (1.Earthquake Research Institute, University of Tokyo)

4:30 PM - 4:45 PM JST | 7:30 AM - 7:45 AM UTC

[SSS11-11] Temporal variations of seismic velocity and azimuthal anisotropy in near-surface rock and soil at KiK-net downhole array sites

*Taka'aki Taira[1], Li-Wei Chen[1], Hiroe Miyake[2] (1.Berkeley Seismological Laboratory, University of California, Berkeley, 2.The University of Tokyo)

4:45 PM - 5:00 PM JST | 7:45 AM - 8:00 AM UTC

[SSS11-12] **Denoising Ambient Seismic Field Correlation Functions with Deep Autoencoders**

*Loic Viens[1], Chris Van Houtte[2] (1.Disaster Prevention Research Institute, Kyoto University, 2.GNS Science)

[J] Oral | S (Solid Earth Sciences)：S-SS Seismology

9:00 AM - 10:30 AM JST | 12:00 AM - 1:30 AM UTC | Convention Hall A 2F

[S-SS13] Strong Ground Motion and Earthquake Disaster

convener:Masayuki Kuriyama(Central Research Institute of Electric Power Industry), Kazuhiro Somei(Geo-Research Institute), Chairperson:Nobuyuki Morikawa(National Research Institute for Earth Science and Disaster Resilience), Ryoichi Nakamura(Earthquake Research Institute, The University of Tokyo)

9:00 AM - 9:15 AM JST | 12:00 AM - 12:15 AM UTC

[SSS13-25] **Determination of dynamic characteristics of existing buildings at various site conditions in Eskisehir, Turkey**

*Onur Kaplan[1], Seiji Tsuno[2], Hiroaki Yamanaka[3], Mehmet Safa Arslan[4], Oguz Ozel[4] (1.Eskisehir Technical University, 2.Railway Technical Research Institute , 3.Tokyo Institute of Technology , 4.Istanbul University)

9:15 AM - 9:30 AM JST | 12:15 AM - 12:30 AM UTC

[SSS13-26] **ICDP DSeis 10: Near-field Observations for the M5.5 Orkney, South Africa Earthquake**

Tatsunari Yasutomi[1], *James Mori[1], Hiroshi Ogasawara[2] (1.Earthquake Hazards Division, Disaster Prevention Research Institute, Kyoto University, 2.Ritsumeikan University)

9:30 AM - 9:45 AM JST | 12:30 AM - 12:45 AM UTC

[SSS13-27] Number of earthquakes from seismic activity model of the national seismic hazard maps for Japan

*Nobuyuki Morikawa[1], Junichi Miyakoshi[2], Hiroyuki Fujiwara[1] (1.National Research Institute for Earth Science and Disaster Resilience, 2.Ohsaki Research Institute, Inc.)

9:45 AM - 10:00 AM JST | 12:45 AM - 1:00 AM UTC

[SSS13-28] Comparative examination of the Probabilistic Seismic Hazard Maps in Japan with observed maximum seismic intensities for various periods

*Takamoto Muneta[1], Kazuki Koketsu[1] (1.Earthquake Research Institute, The University of Tokyo)

10:00 AM - 10:15 AM JST | 1:00 AM - 1:15 AM UTC

[SSS13-29] A Study on the Ground Motion Characteristics close to the Basin Edge

Ryota Hamabe[2], *Shinichi Matsushima[1], Takashi Azuma[3], Florent De Martin[4] (1.Disaster Prevention Research Institute, Kyoto University, 2.Graduate School of Engineering, Kyoto University, 3.National Institute of Advanced Industrial Science and Technology, 4.French Geological Survey)

10:15 AM - 10:30 AM JST | 1:15 AM - 1:30 AM UTC

[SSS13-30] Spectrum Characteristics of MeSO-net seismograms – Effect of Underground Installation -

*Ryoichi Nakamura[1], Hiroshi Tsuruoka[1], Aitaro Kato[1], Shin'ichi Sakai[1], Naoshi Hirata[1], Takahiro Shiina[1] (1.Earthquake Research Institute, The University of Tokyo)

[J] Oral | S (Solid Earth Sciences)：S-SS Seismology

10:45 AM - 12:15 PM JST | 1:45 AM - 3:15 AM UTC | Convention Hall A 2F

[S-SS13] Strong Ground Motion and Earthquake Disaster

convener:Masayuki Kuriyama(Central Research Institute of Electric Power Industry), Kazuhiro Somei(Geo-Research Institute), Chairperson:Yasumaro Kakehi(Department of Planetology, Graduate School of Science, Kobe University), Hisashi Nakahara(Solid Earth Physics Laboratory, Department of Geophysics, Graduate School of Science, Tohoku University)

10:45 AM - 11:00 AM JST | 1:45 AM - 2:00 AM UTC

[SSS13-31] Interpretation of attenuation of high-frequency waves from the intraslab, interplate, and outer-rise earthqukakes of Northeastern Japan

*Yasumaro Kakehi[1], Yu Ogasawara[1] (1.Graduate School of Science, Kobe University)

11:00 AM - 11:15 AM JST | 2:00 AM - 2:15 AM UTC

[SSS13-32] **Effect analysis of soil interlayer on seismic dynamic response and failure mode of metro station structure**

*Shuai Huang[1], Yuejun Lyu[1], Yanju Peng[1] (1.Institute of Crustal Dynamics,China Earthquake Administration)

11:15 AM - 11:30 AM JST | 2:15 AM - 2:30 AM UTC

[SSS13-33] **Investigation on the Applicability of V_{S30} Estimation Models for the Beijing Plain Area**

*Yi Fang, Yanju Peng, Zhijie Jiang

11:30 AM - 11:45 AM JST | 2:30 AM - 2:45 AM UTC

[SSS13-34] Early prediction of PGA and Sa using ANN

*Ting Yu Hsu[1] (1.Taiwan Tech)

11:45 AM - 12:00 PM JST | 2:45 AM - 3:00 AM UTC

[SSS13-35] Analysis of strong-motion acceleration records based on the Generalized Pareto distribution

*Hisashi Nakahara[1] (1.Solid Earth Physics Laboratory, Department of Geophysics, Graduate School of Science, Tohoku University)

[J] Poster | S (Solid Earth Sciences)：S-SS Seismology

3:30 PM - 5:00 PM JST | 6:30 AM - 8:00 AM UTC | Poster Hall International Exhibition Hall8, Makuhari Messe_10

[S-SS13] Strong Ground Motion and Earthquake Disaster

convener:Masayuki Kuriyama(Central Research Institute of Electric Power Industry), Kazuhiro Somei(Geo-Research Institute)

[SSS13-P01] Observation of Aftershock due to the 2018 Hokkaido Eastern Iburi Earthquake and Microtremor observation in the Damaged Area

*Isamu Nishimura[1], Tatsuya Noguchi[2], Yusuke Ono[2], Masanori Kohno[2], Keishin Hibi[1] (1.Graduate School of Sustainability Science,Tottori Univercity,Department of Engineering,Social Systems and Civil Engineering Program, 2.Department of Engineering Tottori Univercity)

[SSS13-P02] **Nonlinear site amplification for high intensity ground motions during the 2018 Mw 6.6 Hokkaido eastern Iburi earthquake**

*Yadab Prasad Dhakal[1], Takashi Kunugi[1], Takeshi Kimura[1], Wataru Suzuki[1], Shin Aoi[1] (1.National Research Institute for Earth Science and Disaster Resilience (NIED))

[SSS13-P03] Microtremor array measurements at strong motion recording stations, HKD127 and IBUH01, in 2018 Hokkaido Iburi earthquake.

*Takuto Kogawa[1], Koji Tokimatsu[1], Izuru Okawa[1], Hitoshi Tanaka[1], Kentaro Motoki[2] (1.TOKYO SOIL RESEARCH CO.,LTD., 2.KOBORI RESEARCH COMPLEX INC.)

[SSS13-P04] Subsurface structure model based at diffuse-field theory in Oiwake region: Simultaneous inversion analysis on adjacent two sites

*Moeko Koie[1], Kentaro Motoki[1], Kenichi Kato[1], Takuto Kogawa[2] (1.KOBORI RESEARCH COMPLEX INC., 2.TOKYO SOIL RESEARCH CO., LTD.)

[SSS13-P05] Exploration of the velocity structure model in the Mukawa town, damaged area during the 2018 Hokkaido eastern Iburi earthquake

*Michiko Shigefuji[1], Nobuo TAKAI[2], Jun Horita[3], Shingo Nomoto[3], Takahiro Maeda[4], Hiroaki Takahashi[2], Masayoshi Ichiyanagi[2], Hiroaki Yamanaka[5], Kosuke Chimoto[5], Seiji Tsuno[6], Masahiro Korenaga[6], Nobuyuki Yamada[7] (1.Kyushu University, 2.Hokkaido University, 3.Geo-Technical Research Co.,Ltd, 4.National Research Institute for Earth Science and Disaster Resilience, 5.Tokyo Institute of Technology, 6.Railway Technical Research Institute, 7.Kochi University)

[SSS13-P06] Source Process of the 2018 Hokkaido Eastern Iburi Earthquake Inferred from Strong Motion Data and Green's Functions Based on Three-Dimensional Velocity Structure Model

*Kimiyuki Asano[1], Tomotaka Iwata[1] (1.Disaster Prevention Research Institute, Kyoto University)

[SSS13-P07] Source process of the 2018 Hokkaido Eastern Iburi earthquake derived from strong motion data

*Hisahiko Kubo[1], Wataru Suzuki[1], Asako Iwaki[1], Shin Aoi[1], Haruko Sekiguchi[2] (1.National Research Institute for Earth Science and Disaster Resilience, 2.DPRI, Kyoto University)

[SSS13-P08] Broadband ground-motion simulation of the 2018 Hokkaido Eastern Iburi earthquake

*Asako Iwaki[1], Nobuyuki Morikawa[1], Takahiro Maeda[1], Hisahiko Kubo[1], Hiroyuki Fujiwara[1] (1.National Research Institute for Earth Science and Disaster Resilience)

[SSS13-P09] **Estimation of 1D S-wave velocity structures in Kumamoto plain and Mashiki town using a waveform inversion of S-wave**

*Kengo Muroi[1], Hiroaki Yamanaka[1], Kosuke Chimoto[1], Seiji Tsuno[2], Masahiro Korenaga[2], Hiroe Miyake[3], Nobuyuki Yamada[4] (1.Tokyo Institute of Technology, 2.Railway Technical Research Institute, 3.The University of Tokyo, 4.Kochi University)

[SSS13-P10] Investigation to estimate high-frequency Empirical Green’s tensor derivatives (EGTD) using aftershocks for the 2016 Kumamoto earthquake

*Sayumi Yoshida[1], Horike Masanori [1], Ken Miyakoshi[2] (1.HANSHIN CONSULTANTS Co., Ltd., 2.Geo-Research Institute)

[SSS13-P11] Estimation of Site Amplification Characteristics in Kumamoto plain by Spectral Separation Analysis Using Aftershock Records of the 2016 Kumamoto Earthquake

*Tomomi Iida[1], Hiroaki Yamanaka[1], Kosuke Chimoto[1], Daiki Shinoyama[8], Seiji Tsuno[5], Masahiro Korenaga[5], Nobuyuki Yamada[7], Hiroe Miyake[6], Tatsuo Kanno[3], Michiko Shigefuji[3], Masayuki Yoshimi[2], Shinichi Matsushima[4], Hiroshi Kawase[4], Kimiyuki Asano[4], Tomotaka Iwata[4] (1.Tokyo institute of Technology, 2.National Institute of Advanced Industrial Science and Technology, 3.Kyushu University, 4.Kyoto University, 5.Railway Technical Research Institute, 6.The University of Tokyo, 7.Kochi Unicersity, 8.Central Research Institute of Electric Power Industry)

[SSS13-P12] Kinematic and dynamic source models of the 2016 Mj6.4 Kumamoto third large earthquake

*Kunikazu Yoshida[1], Ken Miyakoshi[1] (1.Geo-Research Institute)

[SSS13-P13] Source rupture process and strong motion generation area assuming the curved fault model for the 2003 northern Miyagi prefecture earthquake

*Kazuhiro Somei[1], Ken Miyakoshi[1], Yujia Guo[1] (1.Geo-Research Institute)

[SSS13-P14] Estimation of source rupture process during the 2018 Shimane-ken seibu earthquake using strong motion data

*Susumu Kurahashi[1], Ken Miyakoshi[2] (1.Aichi Institute of Technology, 2.Geo-Research Institute)

[SSS13-P15] An estimation of SMGA of M6 class earthquakes based on strong motion records near the source regions

*Kentaro Motoki[1], Kenichi Kato[1], Tetsuo Shiota[2] (1.Kobori Research Complex, 2.Shikoku Electric Power Company)

[SSS13-P16] Difference in short-period level between the surface and buried fault rupture crustal earthquake in Japan

*Shohei Yoshida[1], Takao Kagawa[1], Tatsuya Noguchi[1] (1.Graduate School of Engineering, Tottori University)

[SSS13-P17] Probabilistic seismic hazard assessment of response spectra for whole Japan (part 1: Selection of ground motion prediction equations)

*Nobuyuki Morikawa[1], Junichi Miyakoshi[2], Hiroyuki Fujiwara[1] (1.National Research Institute for Earth Science and Disaster Resilience, 2.Ohsaki Research Institute, Inc.)

[SSS13-P18] Probabilistic seismic hazard assessment of response spectra for whole Japan (part 2: Probabilistic seismic hazard assessment)

*Junichi Miyakoshi[1], Takeshi Morii[1], Nobuyuki Morikawa[2], Hiroyuki Fujiwara[2] (1.Ohsaki Research Institute, Inc., 2.National Research Institute for Earth Science and Disaster Resilience)

[SSS13-P19] **Simulation of Long-period Ground Motion around The Fujikawa-kako Fault Zone during the 2018 Northern Osaka Earthquake**

*Seina Hashimoto[1], Hiroaki Yamanaka[1], Kosuke Chimoto[1], Masahiro Korenaga[2], Seiji Tsuno[2], Hiroe Miyake[3], Shigeki Senna[4] (1.Tokyo Institute of Technology School of Enviroment and Society, 2.Railway Technical Research Institute, 3.The University of Tokyo, 4.National Research Institute for Earth Science and Disaster Prevention)

[SSS13-P20] Site amplification factors for KiK-net stations in and around Ibaraki Prefecture estimated by the coda normalization method

*Jun Kawahara[1], Takahiro Nakamura[1], Takuji Yamada[1] (1.Graduate School of Science and Engineering, Ibaraki University)

[SSS13-P21] Estimation of earthquake ground level in Horinouchi area in the 2014 Northern Nagano earthquake

*RYOTA KAWAI[1], Hiroaki Yamanaka[1], Kosuke Chimoto[1], Seiji Tsuno[2], Masahiro Korenaga[2] (1.Interdisciplinary Graduate School of Science and Engineering,Tokyo institute of Technology, 2.Railway Technical Research Institute)

[SSS13-P22] Ground type classification for strong ground motion prediction based on characteristics of phase-velocity curves from microtremor explorations

*Atsushi Wakai[1], Shigeki Senna[1], Hisanori Matsuyama[2], Yatagai Atsushi[2], Yoshiaki Inagaki[2], Hiroyuki Fujiwara[2] (1.National Research Institute for Earth Science and Disaster Prevention, 2.OYO Corporation)

[SSS13-P23] **Establishment of the Underground Structure Model for Seismic Damage Estimation**

*Shigeki Senna[1], Atsushi Wakai[1], Hiroyuki Fujiwara[1] (1.National Research Institute for Earth Science and Disaster Resilience)

[SSS13-P24] Consideration of liquefaction damage rate based on liquefaction damage in recent years

*Shigeki Senna[1], Ozawa Kyoko[1] (1.National Research Institute for Earth Science and Disaster Resilience)

[SSS13-P25] Estimation of surface earthquake record at MeSO-NET observation points

*Shigeki Senna[1], Atsushi Wakai[1] (1.National Research Institute for Earth Science and Disaster Resilience)

[SSS13-P26] Possibility of estimating phase velocity of Love wave using Horizontal components in microtremor array surveys in the case of Nishio

*Kotoyo Tsuchida[1], Masanori Horike[1], Koji Yamada[1], Masaki Suehiro[1], Sayumi Yoshida[1] (1.HANSHIN CONSULTANTS COMPANY LIMITED)

[SSS13-P27] Enhancement of shallow velocity structure models based on array microtremor explorations for Tokai region, Central Japan

*Atsushi Wakai[1], Shigeki Senna[1], Yatagai Atsushi[2], Yoshiaki Inagaki[2], Hisanori Matsuyama[2], Hiroyuki Fujiwara[1] (1.National Research Institute for Earth Science and Disaster Prevention, 2.OYO Corporation)

[SSS13-P28] Validation of seismic bedrock structure model in the Shimousa region, Chibe prefecture, Japanusing seismic interferometry to strong motion

*Kosuke Chimoto[1], Hiroaki Yamanaka[1] (1.Tokyo Institute of Technology)

[SSS13-P29] Microtremor survey for subsurface velocity structure of Saga plain

*Masayuki Yoshimi[1], Michiko Shigefuji[2], Tadashi Maruyama[1] (1.Geological Survey of Japan, AIST, 2.Kyushu University)

[SSS13-P30] Densely microtremor observation to estimation of subsurface structure in Hane and Kute area, Ohda City, Shimane Prefecture, Japan

*Tatsuya Noguchi[1], Yoshito Yamaguchi, Yuhei Morita, Isamu Nishimura[1], Shohei Yoshida[1], Takao Kagawa[1] (1.Department of Management of Social Systems and Civil Engineering, Civil Engineering Course Graduate School of Engineering, Tottori University)

[SSS13-P31] Densely microtremor observation to estimation of subsurface structure in Nishizono and Yura area, Hokuei Town, Tottori Prefecture, Japan

*Tatsuya Noguchi[1], Katsuya Tomeoku, Isamu Nishimura[1], Shohei Yoshida[1], Takao Kagawa[1] (1.Department of Management of Social Systems and Civil Engineering, Civil Engineering Course Graduate School of Engineering, Tottori University)

[SSS13-P32] Seismic reflection survey in the Kathmandu Valley, Nepal.

*Kota Koshika[1], Yusuke Kawasaki[1], Om Pradhan[1], Masato Yamamoto[1], Dai Nobuoka[1], Yoshikazu Matsubara[1], Hisanori Matsuyama[1], Monika Jha[2], Chintan Timisina[2], Suresh Shrestha[2], Mukunda Bhattarai[2], Dinesh Nepali[2], Soma Nath Sapkota[2], Hiroe Miyake[3], Kazuki Koketsu[3] (1.OYO Corporation, 2.Department of Mines and Geology, 3.Earthquake Research Institute, University of Tokyo)

[SSS13-P33] Broadband Microtremor Array Exploration at and around Tribhuvan International Airport, Kathmandu, Nepal

*Toshiaki Yokoi[1], Takumi Hayashida[1], Mukunda Bhattarai[2], Tara Pokharel[2], Suresh Shrestha[2], Chintan Timsina[2], Sunita Bhatarrai[2], Dinesh Nepali[2] (1.International Institute of Seismology and Earthquake Engineering, Building Research Institute, Japan, 2.Department of Mines and Geology, Ministry of Industry, Commerce and Supplies, Nepal)

[SSS13-P34] Distribution of average S-wave velocities by small-scale (5 to 15 meters) microtremor arrays in and around Hue City, Thua Thien-Hue province, Vietnam

*Ikuo Cho[1], Makoto OKUBO[2] (1.National Institute of Advanced Industrial Science and Technology, 2.Kochi University)

[SSS13-P35] Microtremor Array Exploration in the Syiah Kuala University, Banda Aceh, Indonesia

*Makoto OKUBO[1] (1.Natural Science Cluster, Kochi University)

[SSS13-P36] **Turkey-Japan Joint Project on Modeling of Geological Structures for Strong Ground Motion Simulations due to Crustal Earthquakes in Eskisehir Basin, Turkey, by Using Seismic Interferometry Method**

*Mehmet Safa Arslan[1], Kosuke Chimoto[2], Asim Oguz Ozel[1], Hiroaki Yamanaka[2] (1.ISTANBUL UNIVERSITY-CERRAHPASA, 2.TOKYO INSTITUTE OF TECHNOLOGY)

[SSS13-P37] **Nonlinear Ground Motion Response During the 2016 Meinong Taiwan Earthquake**

*Kuo-Liang Wen[1], Chun-Te Chen[2] (1.National Central University, Department of Earth Sciences, 2.Academia Sinica, Institute of Earth Sciences)

[SSS13-P38] Earthquake damage of the 2017 Pohang earthquake in South Korea

*Mikyung Choi[1], Sun-Cheon Park[1], Dong-Hyo Sohn[1], Seolhan You[1], Jongsun Sun[1], Seongheum Cho[1], Duk-Kee Lee[1] (1. Korea Meteorological Administration)

[J] Poster | S (Solid Earth Sciences)：S-SS Seismology

5:15 PM - 6:30 PM JST | 8:15 AM - 9:30 AM UTC | Poster Hall International Exhibition Hall8, Makuhari Messe_20

[S-SS13] Strong Ground Motion and Earthquake Disaster

convener:Masayuki Kuriyama(Central Research Institute of Electric Power Industry), Kazuhiro Somei(Geo-Research Institute)

[SSS13-P01] Observation of Aftershock due to the 2018 Hokkaido Eastern Iburi Earthquake and Microtremor observation in the Damaged Area

*Isamu Nishimura[1], Tatsuya Noguchi[2], Yusuke Ono[2], Masanori Kohno[2], Keishin Hibi[1] (1.Graduate School of Sustainability Science,Tottori Univercity,Department of Engineering,Social Systems and Civil Engineering Program, 2.Department of Engineering Tottori Univercity)

[SSS13-P02] **Nonlinear site amplification for high intensity ground motions during the 2018 Mw 6.6 Hokkaido eastern Iburi earthquake**

*Yadab Prasad Dhakal[1], Takashi Kunugi[1], Takeshi Kimura[1], Wataru Suzuki[1], Shin Aoi[1] (1.National Research Institute for Earth Science and Disaster Resilience (NIED))

[SSS13-P03] Microtremor array measurements at strong motion recording stations, HKD127 and IBUH01, in 2018 Hokkaido Iburi earthquake.

*Takuto Kogawa[1], Koji Tokimatsu[1], Izuru Okawa[1], Hitoshi Tanaka[1], Kentaro Motoki[2] (1.TOKYO SOIL RESEARCH CO.,LTD., 2.KOBORI RESEARCH COMPLEX INC.)

[SSS13-P04] Subsurface structure model based at diffuse-field theory in Oiwake region: Simultaneous inversion analysis on adjacent two sites

*Moeko Koie[1], Kentaro Motoki[1], Kenichi Kato[1], Takuto Kogawa[2] (1.KOBORI RESEARCH COMPLEX INC., 2.TOKYO SOIL RESEARCH CO., LTD.)

[SSS13-P05] Exploration of the velocity structure model in the Mukawa town, damaged area during the 2018 Hokkaido eastern Iburi earthquake

*Michiko Shigefuji[1], Nobuo TAKAI[2], Jun Horita[3], Shingo Nomoto[3], Takahiro Maeda[4], Hiroaki Takahashi[2], Masayoshi Ichiyanagi[2], Hiroaki Yamanaka[5], Kosuke Chimoto[5], Seiji Tsuno[6], Masahiro Korenaga[6], Nobuyuki Yamada[7] (1.Kyushu University, 2.Hokkaido University, 3.Geo-Technical Research Co.,Ltd, 4.National Research Institute for Earth Science and Disaster Resilience, 5.Tokyo Institute of Technology, 6.Railway Technical Research Institute, 7.Kochi University)

[SSS13-P06] Source Process of the 2018 Hokkaido Eastern Iburi Earthquake Inferred from Strong Motion Data and Green's Functions Based on Three-Dimensional Velocity Structure Model

*Kimiyuki Asano[1], Tomotaka Iwata[1] (1.Disaster Prevention Research Institute, Kyoto University)

[SSS13-P07] Source process of the 2018 Hokkaido Eastern Iburi earthquake derived from strong motion data

*Hisahiko Kubo[1], Wataru Suzuki[1], Asako Iwaki[1], Shin Aoi[1], Haruko Sekiguchi[2] (1.National Research Institute for Earth Science and Disaster Resilience, 2.DPRI, Kyoto University)

[SSS13-P08] Broadband ground-motion simulation of the 2018 Hokkaido Eastern Iburi earthquake

*Asako Iwaki[1], Nobuyuki Morikawa[1], Takahiro Maeda[1], Hisahiko Kubo[1], Hiroyuki Fujiwara[1] (1.National Research Institute for Earth Science and Disaster Resilience)

[SSS13-P09] **Estimation of 1D S-wave velocity structures in Kumamoto plain and Mashiki town using a waveform inversion of S-wave**

*Kengo Muroi[1], Hiroaki Yamanaka[1], Kosuke Chimoto[1], Seiji Tsuno[2], Masahiro Korenaga[2], Hiroe Miyake[3], Nobuyuki Yamada[4] (1.Tokyo Institute of Technology, 2.Railway Technical Research Institute, 3.The University of Tokyo, 4.Kochi University)

[SSS13-P10] Investigation to estimate high-frequency Empirical Green’s tensor derivatives (EGTD) using aftershocks for the 2016 Kumamoto earthquake

*Sayumi Yoshida[1], Horike Masanori [1], Ken Miyakoshi[2] (1.HANSHIN CONSULTANTS Co., Ltd., 2.Geo-Research Institute)

[SSS13-P11] Estimation of Site Amplification Characteristics in Kumamoto plain by Spectral Separation Analysis Using Aftershock Records of the 2016 Kumamoto Earthquake

*Tomomi Iida[1], Hiroaki Yamanaka[1], Kosuke Chimoto[1], Daiki Shinoyama[8], Seiji Tsuno[5], Masahiro Korenaga[5], Nobuyuki Yamada[7], Hiroe Miyake[6], Tatsuo Kanno[3], Michiko Shigefuji[3], Masayuki Yoshimi[2], Shinichi Matsushima[4], Hiroshi Kawase[4], Kimiyuki Asano[4], Tomotaka Iwata[4] (1.Tokyo institute of Technology, 2.National Institute of Advanced Industrial Science and Technology, 3.Kyushu University, 4.Kyoto University, 5.Railway Technical Research Institute, 6.The University of Tokyo, 7.Kochi Unicersity, 8.Central Research Institute of Electric Power Industry)

[SSS13-P12] Kinematic and dynamic source models of the 2016 Mj6.4 Kumamoto third large earthquake

*Kunikazu Yoshida[1], Ken Miyakoshi[1] (1.Geo-Research Institute)

[SSS13-P13] Source rupture process and strong motion generation area assuming the curved fault model for the 2003 northern Miyagi prefecture earthquake

*Kazuhiro Somei[1], Ken Miyakoshi[1], Yujia Guo[1] (1.Geo-Research Institute)

[SSS13-P14] Estimation of source rupture process during the 2018 Shimane-ken seibu earthquake using strong motion data

*Susumu Kurahashi[1], Ken Miyakoshi[2] (1.Aichi Institute of Technology, 2.Geo-Research Institute)

[SSS13-P15] An estimation of SMGA of M6 class earthquakes based on strong motion records near the source regions

*Kentaro Motoki[1], Kenichi Kato[1], Tetsuo Shiota[2] (1.Kobori Research Complex, 2.Shikoku Electric Power Company)

[SSS13-P16] Difference in short-period level between the surface and buried fault rupture crustal earthquake in Japan

*Shohei Yoshida[1], Takao Kagawa[1], Tatsuya Noguchi[1] (1.Graduate School of Engineering, Tottori University)

[SSS13-P17] Probabilistic seismic hazard assessment of response spectra for whole Japan (part 1: Selection of ground motion prediction equations)

*Nobuyuki Morikawa[1], Junichi Miyakoshi[2], Hiroyuki Fujiwara[1] (1.National Research Institute for Earth Science and Disaster Resilience, 2.Ohsaki Research Institute, Inc.)

[SSS13-P18] Probabilistic seismic hazard assessment of response spectra for whole Japan (part 2: Probabilistic seismic hazard assessment)

*Junichi Miyakoshi[1], Takeshi Morii[1], Nobuyuki Morikawa[2], Hiroyuki Fujiwara[2] (1.Ohsaki Research Institute, Inc., 2.National Research Institute for Earth Science and Disaster Resilience)

[SSS13-P19] **Simulation of Long-period Ground Motion around The Fujikawa-kako Fault Zone during the 2018 Northern Osaka Earthquake**

*Seina Hashimoto[1], Hiroaki Yamanaka[1], Kosuke Chimoto[1], Masahiro Korenaga[2], Seiji Tsuno[2], Hiroe Miyake[3], Shigeki Senna[4] (1.Tokyo Institute of Technology School of Enviroment and Society, 2.Railway Technical Research Institute, 3.The University of Tokyo, 4.National Research Institute for Earth Science and Disaster Prevention)

[SSS13-P20] Site amplification factors for KiK-net stations in and around Ibaraki Prefecture estimated by the coda normalization method

*Jun Kawahara[1], Takahiro Nakamura[1], Takuji Yamada[1] (1.Graduate School of Science and Engineering, Ibaraki University)

[SSS13-P21] Estimation of earthquake ground level in Horinouchi area in the 2014 Northern Nagano earthquake

*RYOTA KAWAI[1], Hiroaki Yamanaka[1], Kosuke Chimoto[1], Seiji Tsuno[2], Masahiro Korenaga[2] (1.Interdisciplinary Graduate School of Science and Engineering,Tokyo institute of Technology, 2.Railway Technical Research Institute)

[SSS13-P22] Ground type classification for strong ground motion prediction based on characteristics of phase-velocity curves from microtremor explorations

*Atsushi Wakai[1], Shigeki Senna[1], Hisanori Matsuyama[2], Yatagai Atsushi[2], Yoshiaki Inagaki[2], Hiroyuki Fujiwara[2] (1.National Research Institute for Earth Science and Disaster Prevention, 2.OYO Corporation)

[SSS13-P23] **Establishment of the Underground Structure Model for Seismic Damage Estimation**

*Shigeki Senna[1], Atsushi Wakai[1], Hiroyuki Fujiwara[1] (1.National Research Institute for Earth Science and Disaster Resilience)

[SSS13-P24] Consideration of liquefaction damage rate based on liquefaction damage in recent years

*Shigeki Senna[1], Ozawa Kyoko[1] (1.National Research Institute for Earth Science and Disaster Resilience)

[SSS13-P25] Estimation of surface earthquake record at MeSO-NET observation points

*Shigeki Senna[1], Atsushi Wakai[1] (1.National Research Institute for Earth Science and Disaster Resilience)

[SSS13-P26] Possibility of estimating phase velocity of Love wave using Horizontal components in microtremor array surveys in the case of Nishio

*Kotoyo Tsuchida[1], Masanori Horike[1], Koji Yamada[1], Masaki Suehiro[1], Sayumi Yoshida[1] (1.HANSHIN CONSULTANTS COMPANY LIMITED)

[SSS13-P27] Enhancement of shallow velocity structure models based on array microtremor explorations for Tokai region, Central Japan

*Atsushi Wakai[1], Shigeki Senna[1], Yatagai Atsushi[2], Yoshiaki Inagaki[2], Hisanori Matsuyama[2], Hiroyuki Fujiwara[1] (1.National Research Institute for Earth Science and Disaster Prevention, 2.OYO Corporation)

[SSS13-P28] Validation of seismic bedrock structure model in the Shimousa region, Chibe prefecture, Japanusing seismic interferometry to strong motion

*Kosuke Chimoto[1], Hiroaki Yamanaka[1] (1.Tokyo Institute of Technology)

[SSS13-P29] Microtremor survey for subsurface velocity structure of Saga plain

*Masayuki Yoshimi[1], Michiko Shigefuji[2], Tadashi Maruyama[1] (1.Geological Survey of Japan, AIST, 2.Kyushu University)

[SSS13-P30] Densely microtremor observation to estimation of subsurface structure in Hane and Kute area, Ohda City, Shimane Prefecture, Japan

*Tatsuya Noguchi[1], Yoshito Yamaguchi, Yuhei Morita, Isamu Nishimura[1], Shohei Yoshida[1], Takao Kagawa[1] (1.Department of Management of Social Systems and Civil Engineering, Civil Engineering Course Graduate School of Engineering, Tottori University)

[SSS13-P31] Densely microtremor observation to estimation of subsurface structure in Nishizono and Yura area, Hokuei Town, Tottori Prefecture, Japan

*Tatsuya Noguchi[1], Katsuya Tomeoku, Isamu Nishimura[1], Shohei Yoshida[1], Takao Kagawa[1] (1.Department of Management of Social Systems and Civil Engineering, Civil Engineering Course Graduate School of Engineering, Tottori University)

[SSS13-P32] Seismic reflection survey in the Kathmandu Valley, Nepal.

*Kota Koshika[1], Yusuke Kawasaki[1], Om Pradhan[1], Masato Yamamoto[1], Dai Nobuoka[1], Yoshikazu Matsubara[1], Hisanori Matsuyama[1], Monika Jha[2], Chintan Timisina[2], Suresh Shrestha[2], Mukunda Bhattarai[2], Dinesh Nepali[2], Soma Nath Sapkota[2], Hiroe Miyake[3], Kazuki Koketsu[3] (1.OYO Corporation, 2.Department of Mines and Geology, 3.Earthquake Research Institute, University of Tokyo)

[SSS13-P33] Broadband Microtremor Array Exploration at and around Tribhuvan International Airport, Kathmandu, Nepal

*Toshiaki Yokoi[1], Takumi Hayashida[1], Mukunda Bhattarai[2], Tara Pokharel[2], Suresh Shrestha[2], Chintan Timsina[2], Sunita Bhatarrai[2], Dinesh Nepali[2] (1.International Institute of Seismology and Earthquake Engineering, Building Research Institute, Japan, 2.Department of Mines and Geology, Ministry of Industry, Commerce and Supplies, Nepal)

[SSS13-P34] Distribution of average S-wave velocities by small-scale (5 to 15 meters) microtremor arrays in and around Hue City, Thua Thien-Hue province, Vietnam

*Ikuo Cho[1], Makoto OKUBO[2] (1.National Institute of Advanced Industrial Science and Technology, 2.Kochi University)

[SSS13-P35] Microtremor Array Exploration in the Syiah Kuala University, Banda Aceh, Indonesia

*Makoto OKUBO[1] (1.Natural Science Cluster, Kochi University)

[SSS13-P36] **Turkey-Japan Joint Project on Modeling of Geological Structures for Strong Ground Motion Simulations due to Crustal Earthquakes in Eskisehir Basin, Turkey, by Using Seismic Interferometry Method**

*Mehmet Safa Arslan[1], Kosuke Chimoto[2], Asim Oguz Ozel[1], Hiroaki Yamanaka[2] (1.ISTANBUL UNIVERSITY-CERRAHPASA, 2.TOKYO INSTITUTE OF TECHNOLOGY)

[SSS13-P37] **Nonlinear Ground Motion Response During the 2016 Meinong Taiwan Earthquake**

*Kuo-Liang Wen[1], Chun-Te Chen[2] (1.National Central University, Department of Earth Sciences, 2.Academia Sinica, Institute of Earth Sciences)

[SSS13-P38] Earthquake damage of the 2017 Pohang earthquake in South Korea

*Mikyung Choi[1], Sun-Cheon Park[1], Dong-Hyo Sohn[1], Seolhan You[1], Jongsun Sun[1], Seongheum Cho[1], Duk-Kee Lee[1] (1. Korea Meteorological Administration)

[J] Oral | S (Solid Earth Sciences)：S-EM Earth's Electromagnetism

9:00 AM - 10:30 AM JST | 12:00 AM - 1:30 AM UTC | 304 3F

[S-EM19] Electromagnetic Induction in the Earth and Planetary Interiors, and Tectono-Electromagnetism

convener:Koki Aizawa(Institute of Seismology and Volcanology, Faculty of Sciences, Kyushu University), Tetsuo Matsuno(Kobe Ocean Bottom Exploration Center, Kobe University), Chairperson:Tetsuo Matsuno, Koki Aizawa

9:00 AM - 9:15 AM JST | 12:00 AM - 12:15 AM UTC

[SEM19-01] Repeated measurements of the Self-Potential at Akita-Yakeyama, Iwate and Kurikoma volcanoes

*Shin'ya Sakanaka[1], Yasiaki Sawada[3], Kenta Kato[2], Inoue Yusuke[1], Kobayashi Takuya[1], Ryuichi Takei[1], YUYA TADA[2], Muhammad Faizul Nizam Bin Zainudin[2], Tomoya Moriwaki[2] (1.Graduate school of International Resource Sciences, Akita University, 2.Faculty of International Resource Sciences, Akita University, 3.Faculty of International Resource Sciences, Akita University (gradusted in 2018))

9:15 AM - 9:30 AM JST | 12:15 AM - 12:30 AM UTC

[SEM19-02] Evaluation of surface conductivity of unsaturated Berea sandstone and porous glasses

*Ryosuke Umezawa[1], Makoto Katsura[1], Satoru Nakashima[1] (1.Department of Earth and Space Science, Graduate School of Science, Osaka University)

9:30 AM - 9:45 AM JST | 12:30 AM - 12:45 AM UTC

[SEM19-03] Observational and theoretical waveforms of electromagnetic signals generated by the motional induction effect before the arrival of seismic waves

*Ken'ichi Yamazaki[1] (1.Disaster Prevention Research Institute, Kyoto University)

9:45 AM - 10:00 AM JST | 12:45 AM - 1:00 AM UTC

[SEM19-04] Effect of reference data on geomagnetic transfer functions

*Shinya Sato[1], Tada-nori Goto[1] (1.Kyoto Univesity, Graduate School of Engineering)

10:00 AM - 10:15 AM JST | 1:00 AM - 1:15 AM UTC

[SEM19-05] Reliability estimation of magnetotelluric inversion result based on the Principle Component Analysis and Markov Chain Monte-Carlo method

Hisatoshi Koji[1], *Tada-nori Goto[1] (1.Graduate School of Engineering, Kyoto University)

10:15 AM - 10:30 AM JST | 1:15 AM - 1:30 AM UTC

[SEM19-06] Probing one-dimensional electrical anisotropy in the oceanic upper mantle from seafloor magnetotelluric array data

*Tetsuo Matsuno[1], Kiyoshi Baba[2], Hisashi Utada[2] (1.Kobe Ocean Bottom Exploration Center, Kobe University, 2.Earthquake Research Institute, The University of Tokyo)

[J] Oral | S (Solid Earth Sciences)：S-EM Earth's Electromagnetism

10:45 AM - 12:15 PM JST | 1:45 AM - 3:15 AM UTC | 304 3F

[S-EM19] Electromagnetic Induction in the Earth and Planetary Interiors, and Tectono-Electromagnetism

convener:Koki Aizawa(Institute of Seismology and Volcanology, Faculty of Sciences, Kyushu University), Tetsuo Matsuno(Kobe Ocean Bottom Exploration Center, Kobe University), Chairperson:Koki Aizawa, Tetsuo Matsuno

10:45 AM - 11:00 AM JST | 1:45 AM - 2:00 AM UTC

[SEM19-07] The Analysis of magnetotelluric sounding data on Kikai submarine caldera.

*Toki Hirose[1], Tetsuo Matsuno[2,1], Nobukazu Seama[1,2], Yuki Okizono[4], Hiroshi Ichihara[3], Hiroko Sugioka[1,2], Yoshiyuki Tatsumi[2,1] (1.Department of Planetology, Graduate School of Science, Kobe University, 2.Kobe ocean Bottom Exploration Center, Kobe University, 3.Graduate school of environmental studies, Nagoya University, 4.Department of Planetology, Faculty of Science, Kobe University)

11:00 AM - 11:15 AM JST | 2:00 AM - 2:15 AM UTC

[SEM19-08] Role of Fluids in the earthquake generation: The Nagamachi-Rifu reverse fault, NE Honshu, Japan

*Sabri Bulent Tank[1], Yasuo Ogawa[2] (1.Bogazici University, 2.Tokyo Institute of Technology)

11:15 AM - 11:30 AM JST | 2:15 AM - 2:30 AM UTC

[SEM19-09] Audio-frequency Magnetotelluric Survey of the Tsuyama-hoppou Fault, Yamasaki Fault Zone, southwest Japan.

*Satoru Yamaguchi[1], Daisuke Takakuwa[2], Akira Mimura[1], Kazuki Fkue[1], Shigehiro Katoh[3], Hideki Murakami[4], Shinichi Takakura[5] (1.Department of Geosciences, Graduate School of Science, Osaka City University, 2.Faculty of Science, Osaka City University, 3.The Museum of Nature and Human Activities, 4.Science and Technology Unit, Research and Education Faculty, Kochi University, 5.Geological Survey of Japan, Institute of Advanced Industrial Science and Technology)

11:30 AM - 11:45 AM JST | 2:30 AM - 2:45 AM UTC

[SEM19-10] Three dimensional resistivity structure around the focal region of the 2016 Kumamoto earthquakes

*Koki Aizawa[1], Hisashi Asaue[2], Katsuaki Koike[3], Shinichi Takakura[4], Toru Yoshinaga[10], Makoto Uyeshima[5], Takao Koyama[5], Ryokei Yoshimura[7], Ken'ichi Yamazaki[7], Shintaro Komatsu[7], Yusuke Yamashita[7], Hiroshi Ichihara[9], Mitsuru Utsugi[8], Kaori Tsukamoto[12], Dan Muramatsu[12], Yoshiko Teguri[1,11], Kazunari Uchida[1], Hideaki Hase[6], Azusa Shito[1], Satoshi Matsumoto[1], Takeshi Matsushima[1], Hiroshi Shimizu[1] (1.Institute of Seismology and Volcanology, Faculty of Sciences, Kyushu University, 2.Laboratory on Innovative Techniques for Infrastructures, Kyoto University, 3.Environmental Geosphere Engineering, Department of Urban Management, Graduate School of Engineering, Kyoto University, 4.Geological Survey of Japan, National Institute of Advanced Industrial Science and Technology, 5.Earthquake Research Institute, University of Tokyo, 6.GERD, 7.Disaster Prevention Research Institute, Kyoto University, 8.Aso Volcanological Laboratory, Institute for Geothermal Sciences, Graduate School of Science, Kyoto University, 9.Earthquake and Volcano Research Center, Graduate School of Environmental Studies, Nagoya University, 10.Kumamoto University, 11.Japan Meteorological Agency, 12.Department of Earth and Planetary Sciences, Graduate School of Science, Kyushu University)

11:45 AM - 12:00 PM JST | 2:45 AM - 3:00 AM UTC

[SEM19-11] **A research report on the fundamental investigations of an electrical resistivity structure beneath Chugoku and Shikoku regions, southwestern Japan(2018)**

*Ichiro Shiozaki[1], Tomofumi Uto[1], Makoto Uyeshima[2], Hiroshi Hataoka[3], Yasuo Ikezoe[3], Shinji Yamamoto[3], Tatsuya Noguchi[1], Daiki Furuichi[4], Yuki Murayama[4], Kohei Matsushita[4], Hideki Murakami[5], Naoto Oshiman[6], Yoshihisa Iio[6], Kazuya Ando[7] (1.Graduate School of Engineering, Tottori University, 2.Earthquake Research Institute, The University of Tokyo, 3.Technical Department, Tottori University, 4.Faculty of Engineering, Tottori University, 5.Research and Education Faculty , Kochi University, 6.Disaster Prevention Research Institute, Kyoto University, 7.San'in Kaigan Geopark Museum of the Earth and Sea)

12:00 PM - 12:15 PM JST | 3:00 AM - 3:15 AM UTC

[SEM19-12] Fluid distribution beneath central and southern Kyushu imaged by 3-D electrical resistivity model

*Maki Hata[1], Hiroshi Munekane[2], Hisashi Utada[1], Tsuneomi Kagiyama[3] (1.Earthquake Research Institute, the University of Tokyo , 2.Geospatial Information Aurhotiry of Japan, 3.Aso Geopark Promotion Council)

[J] Poster | S (Solid Earth Sciences)：S-EM Earth's Electromagnetism

3:30 PM - 5:00 PM JST | 6:30 AM - 8:00 AM UTC | Poster Hall International Exhibition Hall8, Makuhari Messe_11

[S-EM19] Electromagnetic Induction in the Earth and Planetary Interiors, and Tectono-Electromagnetism

convener:Koki Aizawa(Institute of Seismology and Volcanology, Faculty of Sciences, Kyushu University), Tetsuo Matsuno(Kobe Ocean Bottom Exploration Center, Kobe University)

[SEM19-P01] Effects of absolute humidity on contact resistance between dry rock sample surface and electrodes

*Takeshi Suzuki[1], Ryokei Yoshimura[2], Ken'ichi Yamazaki[2], Naoto Oshiman[2] (1.Graduate School of Science, Kyoto University, 2.Disaster Prevention Research Institute, Kyoto University)

[SEM19-P02] Japanese geomagnetic field variation model based on the IGRF (2): modeling on the oblique Mercator projection

*Tsutomu Ogawa[1] (1.Earthquake Research Institute, the University of Tokyo)

[SEM19-P03] Examination of criteria to remove the influence of the Sq-field variations from electromagnetic field spectra for a better estimation of regional electromagnetic responses

*RUIBAI LI[1], Hisayoshi Shimizu[1], Kiyoshi Baba[1], Hisashi Utada[1] (1.Earthquake Research Institute, the University of Tokyo)

[SEM19-P04] Study on long-term variation of geoelectric field observation

*Ren Ozeki[1], Ikuko Fujii[1] (1.Japan Meteorological Agency)

[SEM19-P05] Deep electrical conductivity structure of Eastern Marmara, Turkey by long period magnetotellurics

*Sabri Bulent Tank[1], Naoto Oshiman[2], Mustafa Karas[1], Ryokei Yoshimura[2], Yasuo Ogawa[3] (1.Bogazici University, 2.Kyoto University, 3.Tokyo Institute of Technology)

[SEM19-P06] Audio-frequency magnetotelluric survey on the northern edifice of the Kurikoma volcano, northeast of Japan

*Kobayashi Takuya[1], Shin'ya Sakanaka[1], Tomoki Tsutsui[1], Muhammad Faizul Nizam Bin Zinudin[1], Inoue Yusuke[1], Kenta Kato[1], Tomoya Moriwaki[1], YUYA TADA[1], Ryuichi Takei[1] (1.Akita University)

[SEM19-P07] A three-dimensional crustal electrical resistivity model beneath southern Tohoku district, NE Japan

*Aoi Motoyama[1], Yasuo Ogawa[2], Makoto Uyeshima[3], Koichi Asamori[4], Toshihiro Uchida[5], Hideaki Hase[6], Takao Koyama[3], Shin'ya Sakanaka[7], Yusuke Yamaya[5], Koki Aizawa[8], Masahiro Ichiki[1] (1.Graduate school of science, Tohoku university, 2.Volcanic Fluid Research Center, School of Science, Tokyo Institute of Technology, 3.Earthquake research institute, the university of Tokyo, 4.Japan Atomic Energy Agency, 5.National institute of advanced industrial science and technology, 6. Geothermal Energy Research & Development Co., Ltd, 7.Graduate School of International Resource Sciences Department of Earth Resource Engineering and Environmental Science, Akita University, 8.Graduate school of science, Kyusyu university)

[SEM19-P08] Magnetotelluric survey on the northern foot of Meakandake volcano

*Tomohiro Inoue[1], Takeshi Hashimoto[1] (1.Institute of Seismology and Volcanology, Faculty of Science, Hokkaido University)

[SEM19-P09] Hydrothermal system of Kuttara Volcanic Group inferred from 3D resistivity modeling (2)

*Ryo Tanaka[1], Midori Hayakawa[2], Takeshi Hashimoto[1], Wataru Kanda[3], Yuichi Morita[4], Hiroshi Aoyama[1], Makoto Uyeshima[4] (1.Institute of Seismology and Volcanology, Hokkaido University, 2.Mitsui Oil Exploration Co., Ltd. Geothermal Business Division, 3.Volcanic Fluid Research Center, School of Science, Tokyo Institute of Technology, 4.Earthquake Research Institute, The University of Tokyo)

[SEM19-P10] 3D magnetic structure of Aso volcano

*Mitsuru Utsugi[1] (1.Aso Volcanological Laboratory, Institute for Geothermal Sciences, Graduate School of Science, Kyoto University)

[SEM19-P11] The piezomagnetic field produced by an ellipsoidal pressure source: A preliminary result

*Yoichi Sasai[1] (1.Earthquake Prediction Research Center, Institute of Oceanic Research and Development, Tokai University)

[J] Poster | S (Solid Earth Sciences)：S-EM Earth's Electromagnetism

5:15 PM - 6:30 PM JST | 8:15 AM - 9:30 AM UTC | Poster Hall International Exhibition Hall8, Makuhari Messe_21

[S-EM19] Electromagnetic Induction in the Earth and Planetary Interiors, and Tectono-Electromagnetism

convener:Koki Aizawa(Institute of Seismology and Volcanology, Faculty of Sciences, Kyushu University), Tetsuo Matsuno(Kobe Ocean Bottom Exploration Center, Kobe University)

[SEM19-P01] Effects of absolute humidity on contact resistance between dry rock sample surface and electrodes

*Takeshi Suzuki[1], Ryokei Yoshimura[2], Ken'ichi Yamazaki[2], Naoto Oshiman[2] (1.Graduate School of Science, Kyoto University, 2.Disaster Prevention Research Institute, Kyoto University)

[SEM19-P02] Japanese geomagnetic field variation model based on the IGRF (2): modeling on the oblique Mercator projection

*Tsutomu Ogawa[1] (1.Earthquake Research Institute, the University of Tokyo)

[SEM19-P03] Examination of criteria to remove the influence of the Sq-field variations from electromagnetic field spectra for a better estimation of regional electromagnetic responses

*RUIBAI LI[1], Hisayoshi Shimizu[1], Kiyoshi Baba[1], Hisashi Utada[1] (1.Earthquake Research Institute, the University of Tokyo)

[SEM19-P04] Study on long-term variation of geoelectric field observation

*Ren Ozeki[1], Ikuko Fujii[1] (1.Japan Meteorological Agency)

[SEM19-P05] Deep electrical conductivity structure of Eastern Marmara, Turkey by long period magnetotellurics

*Sabri Bulent Tank[1], Naoto Oshiman[2], Mustafa Karas[1], Ryokei Yoshimura[2], Yasuo Ogawa[3] (1.Bogazici University, 2.Kyoto University, 3.Tokyo Institute of Technology)

[SEM19-P06] Audio-frequency magnetotelluric survey on the northern edifice of the Kurikoma volcano, northeast of Japan

*Kobayashi Takuya[1], Shin'ya Sakanaka[1], Tomoki Tsutsui[1], Muhammad Faizul Nizam Bin Zinudin[1], Inoue Yusuke[1], Kenta Kato[1], Tomoya Moriwaki[1], YUYA TADA[1], Ryuichi Takei[1] (1.Akita University)

[SEM19-P07] A three-dimensional crustal electrical resistivity model beneath southern Tohoku district, NE Japan

*Aoi Motoyama[1], Yasuo Ogawa[2], Makoto Uyeshima[3], Koichi Asamori[4], Toshihiro Uchida[5], Hideaki Hase[6], Takao Koyama[3], Shin'ya Sakanaka[7], Yusuke Yamaya[5], Koki Aizawa[8], Masahiro Ichiki[1] (1.Graduate school of science, Tohoku university, 2.Volcanic Fluid Research Center, School of Science, Tokyo Institute of Technology, 3.Earthquake research institute, the university of Tokyo, 4.Japan Atomic Energy Agency, 5.National institute of advanced industrial science and technology, 6. Geothermal Energy Research & Development Co., Ltd, 7.Graduate School of International Resource Sciences Department of Earth Resource Engineering and Environmental Science, Akita University, 8.Graduate school of science, Kyusyu university)

[SEM19-P08] Magnetotelluric survey on the northern foot of Meakandake volcano

*Tomohiro Inoue[1], Takeshi Hashimoto[1] (1.Institute of Seismology and Volcanology, Faculty of Science, Hokkaido University)

[SEM19-P09] Hydrothermal system of Kuttara Volcanic Group inferred from 3D resistivity modeling (2)

*Ryo Tanaka[1], Midori Hayakawa[2], Takeshi Hashimoto[1], Wataru Kanda[3], Yuichi Morita[4], Hiroshi Aoyama[1], Makoto Uyeshima[4] (1.Institute of Seismology and Volcanology, Hokkaido University, 2.Mitsui Oil Exploration Co., Ltd. Geothermal Business Division, 3.Volcanic Fluid Research Center, School of Science, Tokyo Institute of Technology, 4.Earthquake Research Institute, The University of Tokyo)

[SEM19-P10] 3D magnetic structure of Aso volcano

*Mitsuru Utsugi[1] (1.Aso Volcanological Laboratory, Institute for Geothermal Sciences, Graduate School of Science, Kyoto University)

[SEM19-P11] The piezomagnetic field produced by an ellipsoidal pressure source: A preliminary result

*Yoichi Sasai[1] (1.Earthquake Prediction Research Center, Institute of Oceanic Research and Development, Tokai University)

[E] Oral | S (Solid Earth Sciences)：S-IT Science of the Earth's Interior & Techtonophysics

9:00 AM - 10:30 AM JST | 12:00 AM - 1:30 AM UTC | A10 TOKYO BAY MAKUHARI HALL

[S-IT21] Interaction and Coevolution of the Core and Mantle in the Earth and Planets

convener:Kenji Kawai(Department of Earth and Planetary Science, School of Science, University of Tokyo), Tsuyoshi Iizuka(University of Tokyo), Kenji Ohta(Department of Earth and Planetary Sciences, Tokyo Institute of Technology), Taku Tsuchiya(Geodynamics Research Center, Ehime University), Chairperson:Anselme Borgeaud, Taku Tsuchiya

9:00 AM - 9:15 AM JST | 12:00 AM - 12:15 AM UTC

[SIT21-01] The role of stishovite as a deep nitrogen carrier indicated from high-pressure and high-temperature experiments

*Ko Fukuyama[1], Hiroyuki Kagi[1], Toru Inoue[2,3], Toru Shimei[3], Sho Kakizawa[3], Shunichi Hishita[4], Yuji Sano[5], Naoto Takahata[5] (1.Geochemical Research Center, Graduate School of Science, The University of Tokyo, 2.Department of Earth and Planetary Systems Science, Graduate School of Science, Hiroshima University, 3.Geodynamics Research Center, Ehime University, 4.National Institute for Materials Science, 5.Atmosphere and Ocean Research Institute, The University of Tokyo)

9:15 AM - 9:30 AM JST | 12:15 AM - 12:30 AM UTC

[SIT21-02] 3-D P- and S-velocity structure of the D″ layer beneath Central America and the Caribbean using waveform inversion

★Invited Papers

*Anselme F. E. Borgeaud[1,2], Kenji Kawai[1], Robert J. Geller[1] (1.Department of Earth and Planetary Science, Graduate School of Science, University of Tokyo, 2.Institute of Earth Sciences, Academia Sinica)

9:30 AM - 9:45 AM JST | 12:30 AM - 12:45 AM UTC

[SIT21-03] **Uniaxial deformation experiments of bridgmanite using D-111 type high pressure apparatus**

★Invited Papers

*Noriyoshi Tsujino[1], Daisuke Yamazaki[1], Yu Nishihara[2] (1.Institute for Planetary Materials, Okayama University, 2.Geodynamics Research Center, Ehime University)

9:45 AM - 10:00 AM JST | 12:45 AM - 1:00 AM UTC

[SIT21-04] **Waveform inversion for 3D anisotropic structure in D″ beneath the Northern Pacific: Constraints on mineralogy and flow in the lowermost mantle**

*Yuki Suzuki[1], Kenji Kawai[1], Robert J. Geller[1] (1.Department of Earth and Planetary Sciences, School of Science,The University of Tokyo)

10:00 AM - 10:15 AM JST | 1:00 AM - 1:15 AM UTC

[SIT21-05] Maximum water solubility of bridgmanite under the Earth's lower mantle conditions

*Sho Kakizawa[1], Toru Inoue[1,2,3], Ryotaro Abe[1], Minami Kuroda[4], Naoya Sakamoto[5], Hisayoshi Yurimoto[4,5,6] (1.Geodynamics Reseach Center, Ehime University, 2.Graduate School of Science, Hiroshima University, 3.Hiroshima Institute of Plate Convergence Region Research, 4.Graduate School of Science, Hokkaido University, 5.Creative Research Institution, Hokkaido University, 6.Institute of Space and Astronautical Science, Japan Aerospace Exploration Agency)

10:15 AM - 10:30 AM JST | 1:15 AM - 1:30 AM UTC

[SIT21-06] Origin and role of lost continents

*Shigenori Maruyama[1], Kenji Kawai[2], Steeve Gréaux[3], Taku Tsuchiya[3], Dapeng Zhao[4] (1.Earth-Life Science Institute, Tokyo Institute of Technology, 2.Department of Earth and Planetary Science, School of Science, University of Tokyo, 3.Ehime University, 4.Department of Geophysics, Tohoku University)

[E] Oral | S (Solid Earth Sciences)：S-IT Science of the Earth's Interior & Techtonophysics

10:45 AM - 12:15 PM JST | 1:45 AM - 3:15 AM UTC | A10 TOKYO BAY MAKUHARI HALL

[S-IT21] Interaction and Coevolution of the Core and Mantle in the Earth and Planets

convener:Kenji Kawai(Department of Earth and Planetary Science, School of Science, University of Tokyo), Tsuyoshi Iizuka(University of Tokyo), Kenji Ohta(Department of Earth and Planetary Sciences, Tokyo Institute of Technology), Taku Tsuchiya(Geodynamics Research Center, Ehime University), Chairperson:Kenji Ohta, Riko Iizuka

10:45 AM - 11:00 AM JST | 1:45 AM - 2:00 AM UTC

[SIT21-07] Thermal conductivity anomaly in spin-crossover ferropericlase under lower mantle conditions

★Invited Papers

*Zhongqing Wu[1] (1.University of Science and Technology of China)

11:00 AM - 11:15 AM JST | 2:00 AM - 2:15 AM UTC

[SIT21-08] Discussion

*Kenji Ohta[1] (1.Department of Earth and Planetary Sciences, Tokyo Institute of Technology)

11:15 AM - 11:30 AM JST | 2:15 AM - 2:30 AM UTC

[SIT21-09] ***Ab initio* anharmonic lattice dynamics for Fe-bearing lower mantle minerals**

*Haruhiko Dekura[1], Taku Tsuchiya[1] (1.Geodynamics Research Center, Ehime University)

11:30 AM - 11:45 AM JST | 2:30 AM - 2:45 AM UTC

[SIT21-10] **Measurements of high pressure-temperature thermal conductivity of the Earth's lower mantle minerals in a laser-heated diamond anvil cell**

*Kenji Ohta[1], Akira Hasegawa[1,2], Takashi Yagi[2], Yoshiyuki Okuda[1], Koutarou Onga[1], Kei Hirose[3,4], Yasuo Ohishi[5] (1.Department of Earth and Planetary Sciences, Tokyo Institute of Technology, 2.National Metrology Institute of Japan, National Institute of Advanced Industrial Science and Technology, 3.Earth-Life Science Institute, Tokyo Institute of Technology, 4.Department of Earth and Planetary Science, The University of Tokyo, 5.Japan Synchrotron Radiation Research Institute)

11:45 AM - 12:00 PM JST | 2:45 AM - 3:00 AM UTC

[SIT21-11] Is there evidence for a paleo-LLSVP beneath Eurasia?: Implications for the origin of the Siberian Traps

*Tsubasa Ue[1], Yuki Suzuki[1], Kenji Kawai[1] (1.Department of Earth and Planetary Sciences, Graduate School of Science, The University of Tokyo)

12:00 PM - 12:15 PM JST | 3:00 AM - 3:15 AM UTC

[SIT21-12] Possible compositional region of Al-bearing anhydrous bridgmanite

*Toru Inoue[1,2], Masamichi Noda[2], Sho Kakizawa[2] (1.Department of Earth and Planetary Systems Science, Graduate School of Science, Hiroshima University, 2.Geodynamics Research Center, Ehime University)

[E] Oral | S (Solid Earth Sciences)：S-IT Science of the Earth's Interior & Techtonophysics

1:45 PM - 3:15 PM JST | 4:45 AM - 6:15 AM UTC | A10 TOKYO BAY MAKUHARI HALL

[S-IT21] Interaction and Coevolution of the Core and Mantle in the Earth and Planets

convener:Kenji Kawai(Department of Earth and Planetary Science, School of Science, University of Tokyo), Tsuyoshi Iizuka(University of Tokyo), Kenji Ohta(Department of Earth and Planetary Sciences, Tokyo Institute of Technology), Taku Tsuchiya(Geodynamics Research Center, Ehime University), Chairperson:Hitoshi Gomi, Tsuyoshi Iizuka

1:45 PM - 2:00 PM JST | 4:45 AM - 5:00 AM UTC

[SIT21-13] Evolution of the Earth mantle and its possible interaction with core: view from olivine and its inclusions study

★Invited Papers

*Alexander V Sobolev[1], Valentina G. Batanova[2] (1.ISTerre Institute of Earth Sciences, 2.Vernadsky Institute of Geochemistry and Analytical Chemistry, Russian Academy of Sciences, Kosygina str. 19, Moscow 119991, Russia.)

2:00 PM - 2:15 PM JST | 5:00 AM - 5:15 AM UTC

[SIT21-14] Discussion

*Tsuyoshi Iizuka[1] (1.University of Tokyo)

2:15 PM - 2:30 PM JST | 5:15 AM - 5:30 AM UTC

[SIT21-15] Ultralow-velocity zones possibly explained by light element-enriched iron compounds

*Liang Yuan[1], Eiji Ohtani[1], Xiang Wu[2], Shengxuan Huang[3], Daijo Ikuta[1], Tatsuya Sakamaki[1], Seiji Kamada[1], Hiroshi Fukui[4,5], Satoshi Tsutsui[6], Hiroshi Uchiyama[6], Daisuke Ishikawa[5,6], Naohisa Hirao[6], Alfred Q. R. Baron[5] (1.Department of Earth and Planetary Materials Science, Graduate School of Science, Tohoku University, Sendai 980-8578, Japan, 2.State Key Laboratory of Geological Processes and Mineral Resources, China University of Geosciences, Wuhan 430074, China, 3.Key Laboratory of Orogenic Belts and Crustal Evolution, MOE, Peking University and School of Earth and Space Sciences, Peking University, Beijing 100871, China, 4.Center for Novel Material Science under Multi-Extreme Conditions, Graduate School of Material Science, University of Hyogo, Hyogo 678-1297, Japan, 5.Materials Dynamics Laboratory, RIKEN SPring-8 Center, Hyogo 679-5148, Japan, 6.Japan Synchrotron Radiation Research Institute (JASRI), SPring-8, Hyogo, 679-5198, Japan)

2:30 PM - 2:45 PM JST | 5:30 AM - 5:45 AM UTC

[SIT21-16] High-precision $^{142}W/^{144}W$ ratios of oceanic island basalts and Large Igneous Province basalts.

Asako Takamasa[1], *Katsuhiko Suzuki[1], Yusuke Fukami[2], Tsuyoshi Iizuka[3] (1.Research and Development Center for Submarine Resources, Japan Agency for Marine-Earth Science and Technology, 2.Department of Subsurface Geobiological Analysis and Research, Japan Agency for Marine-Earth Science and Technology, 3.Graduate School of Science, The University of Tokyo)

2:45 PM - 3:00 PM JST | 5:45 AM - 6:00 AM UTC

[SIT21-17] **Some technological developments in high temperature generation using KMA and precise melting/phase relations of minerals and rocks under deep mantle conditions**

*Tetsuo Irifune[1,2], Youmo Zhou[1], Takeshi Arimoto[1], Hideharu Kuwahara[1], Ryuichi Nomura[3], Masayuki Nishi[1], Momoko Yamaguchi[1], Yoshinori Tange[4], Takahiro Kuribayashi[5], Zhaodong Liu[6] (1.Geodynamics Research Center, Ehime University, 2.Eearth Life Science Institute, Tokyo Institute of Technology, 3.Hakubi Center/ Graduate School of Human and Environmental Studies, Kyoto University, 4.Research & Utilization Division, Japan Synchrotron Research Institute, 5.Graduate School of Science, Tohoku University, 6.Institute of Super Hard Materials, Jilin University)

3:00 PM - 3:15 PM JST | 6:00 AM - 6:15 AM UTC

[SIT21-18] Zr isotope constraints on early Earth differentiation

*Tsuyoshi Iizuka[1], Keita Itano[1], Shinji Yamamoto[2] (1.University of Tokyo, 2.Yokohama National University)

[E] Poster | S (Solid Earth Sciences)：S-IT Science of the Earth's Interior & Techtonophysics

3:30 PM - 5:00 PM JST | 6:30 AM - 8:00 AM UTC | Poster Hall International Exhibition Hall8, Makuhari Messe_12

[S-IT21] Interaction and Coevolution of the Core and Mantle in the Earth and Planets

convener:Kenji Kawai(Department of Earth and Planetary Science, School of Science, University of Tokyo), Tsuyoshi Iizuka(University of Tokyo), Kenji Ohta(Department of Earth and Planetary Sciences, Tokyo Institute of Technology), Taku Tsuchiya(Geodynamics Research Center, Ehime University)

[SIT21-P01] Sample-scale compositional variation of the Inada granite, Ibaraki, Japan -toward the reduction of geoneutrino flux estimation errors from the Japanese crust-

★Invited Papers

*Kenta Ueki[1], Minami Kazuki[2], Tsuyoshi Iizuka[3], Sanshiro Enomoto[4], Hiroyuki Tanaka[2] (1.Japan Agency for Marine-Earth Science and Technology, 2.Earthquake Research Institute, University of Tokyo, 3.Department of Earth and Planetary Science, University of Tokyo, 4.Center for Experimental Nuclear Physics and Astrophysics, University of Washington)

[SIT21-P02] Towards a better estimation of the temperature distribution beneath the Japanese Islands

*Akiko Tanaka[1], Makoto Yamano[2], Hideki Hamamoto[3], Shusaku Goto[4], Takumi Matsumoto[5] (1.Geological Survey of Japan, National Institute of Advanced Industrial Science and Technology, 2.Earthquake Research Institute, The University of Tokyo, 3.Center for Environmental Science in Saitama, 4.Institute for Geo-Resources and Environment National Institute of Advanced Industrial Science and Technology, 5.National Research Institute for Earth Science and Disaster Resilience)

[SIT21-P03] The estimation of the neutrino flux from the crust of the Japanese islands using the geochemical database

*Satoru Haraguchi[1], Kenta Ueki[1], Hikaru Iwamori[1,2,3] (1.Japan Agency for Marine-Earth Science and Technology, 2.Earthquake Research Institute, the University of Tokyo, 3.Tokyo Institute of Technology)

[SIT21-P04] **Viscosity of potassium titanosilicate melt at high pressure**

*Akio Suzuki[1] (1.Department of Earth Science, Graduate School of Science, Tohoku University)

[SIT21-P05] **Lattice thermal conductivity of wadsleyite and ringwoodite at the mantle transition zone pressures**

*seiji kimura[1], Kenji Ohta[6], Takaaki Kawazoe[2], Kei Hirose[3], Hiroyuki Kagi[4], Takashi Yagi[5] (1.Department of Earth and Planetary Sciences Tokyo Institute of Technology, 2.Department of Earth and Planetary Systems Science, Hiroshima University, 3.Earth-Life Science Institute, Tokyo Institute of Technology, 4.Geochemical Research Center, Graduate School of Science, University of Tokyo, 5.National Institute of Advanced Industrial Science and Technology, 6.Department of Earth and Planetary Sciences, Tokyo Institute of Technology)

[SIT21-P06] In-situ X-ray observations of the olivine-spinel transformation under shear deformation: preliminary results on the reaction-induced weakening

*Tomoaki Kubo[1], Moriyama Kazuya[1], Yuichiro Mori[1], Masahiro Imamura[1], Sanae Koizumi[2], Yu Nishihara[3], Akio Suzuki[4], Yuji Higo[5] (1.Kyushu Univ., 2.ERI, 3.GRC Ehime Univ., 4.Tohoku Univ., 5.JASRI)

[SIT21-P07] Internally resistive heated diamond anvil cell experiments with metal encapsulated minerals

*YAMAMOTO TOMONARI[1], Kenji Ohta[1], Sho Suehiro[1], Hayato Inoue[1] (1.Tokyo Institute of Technology)

[SIT21-P08] Shear deformation on post-spinel

*Daisuke Yamazaki[1], Noriyoshi Tsujino[1], Yu Nishihara[2] (1.Institute for Planetary Materials, Okayama University, 2.GRC, Ehime University)

[SIT21-P09] **Lattice thermal conductivity of $CaSiO_3$ perovskite at high pressures and high temperatures**

*Kotaro Onga[1], Kenji Ohta[1], Akira Hasegawa[1,2], Takashi Yagi[2], Kei Hirose[3,4], Yasuo Ohishi[5] (1.Department of Earth and Planetary Sciences, Tokyo Institute of Technology, 2.National Institute of Advanced Industrial Science and Technology, 3.Earth-Life Science Institute, Tokyo Institute of Technology, 4.Department of Earth and Planetary Science, The University of Tokyo, 5.Japan Synchrotron Radiation Research Institute)

[SIT21-P10] **Polycrystalline diamond sintered from ultradispersed nanodiamonds**

*Masayuki Nishi[1,2], Koichiro Yamamoto[1], Youmo Zhou[1], Tetsuo Irifune[2,1] (1.Geodynamics Research Center, Ehime University, 2.Earth-Life Science Institute, Tokyo Institute of Technology)

[SIT21-P11] Thermal conductivity measurements on iron and MgO periclase at high pressure and high temperature similar to the Earth's mid-lower mantle conditions

*Akira Hasegawa[1,2], Kenji Ohta[2], Takashi Yagi[1], Kei Hirose[3,4] (1.National Institute of Advanced Industrial Science and Technology, 2.Tokyo Institude of Technology, 3.Earth-Life Science Institute, Tokyo Institude of Technology, 4.The University of Tokyo)

[SIT21-P12] Azimuthal anisotropy in the lowermost mantle beneath Philippine from ScS-S times

*Satoru Tanaka[1] (1.Department of Deep Earth Structure and Dynamics Research Japan Agency for Marine-Earth Science and Technology)

[SIT21-P13] Detailed 3-D S-velocity structure within D" at the western Pacific LLSVP margin: smaller scale plumes and paleoslabs

*Yuki Suzuki[1], Kenji Kawai[1], Robert J. Geller[1], Satoru Tanaka[2], Weerachai Siripuvaraporn[3], Songkhun Boonchaisuku[3], Noisagool Sutthipong[3], Yasushi Ishihara[2], Taweoon Kim, Koji MIYAKAWA[4], Nozomu Takeuchi[4] (1.The University of Tokyo, 2.Japan Agency for Marine-Earth Science and Technology, 3.Mahidol University, 4.Earthquake Research Institute, The University of Tokyo)

[SIT21-P14] Possible interaction between the core and mantle inferred from a core surface flow model

*Masaki Matsushima[1] (1.Department of Earth and Planetary Sciences, School of Science, Tokyo Institute of Technology)

[SIT21-P15] Determination of the noble gas partition coefficients between metal-silicate melts under high-pressure and high-temperature conditions

*Tomotaka Tanaka[1], Hideharu Kuwahara[2], Satoshi Kishi[1], Ryuichi Nomura[3], Kenji Mibe[5], Hiroyuki Kagi[4], Shigehiko Tateno[6], Hirochika Sumino[1] (1.Department of Basic Science, Graduate School of Arts and Sciences, The University of Tokyo , 2.Geodynamics Research Center, Ehime University, 3.Kyoto University, 4.Geochemical Research Center, Graduate School of Science, University of Tokyo, 5.Earthquake Research Institute, University of Tokyo, 6.Earth-Life Science Institute, Tokyo Institute of Technology)

[SIT21-P16] **Measurement of T-dependent electrical resistivity of solid and liquid Fe and Pt at fixed P**

*Innocent Ezenwa[1], Takashi Yoshino[1] (1.Institute for Planetary Materials, Okayama University)

[SIT21-P17] Ancient, highly depleted mantle constrained by Re-Os isotope and highly-siderophile element compositions of French Polynesian xenoliths

*Norikatsu Akizawa[1], Akira Ishikawa[2], Katsuhiko Suzuki[3], Tetsu Kogiso[4] (1.Atmosphere and Ocean Research Institute, The University of Tokyo, 2.Department of Earth and Planetary Sciences, Tokyo Institute of Technology, 3.Research and Development Center for Submarine Resources, Japan Agency for Marine-Earth Science and Technology (JAMSTEC), 4.Graduate School of Human and Environmental Studies, Kyoto University)

[SIT21-P18] First-principles prediction of hydrogen partitioning between the core and mantle

*Atsuroh Ohba[1], Taku Tsuchiya[1] (1.Ehime University Geodynamics Research Center)

[SIT21-P19] Microvolume stable isotope measuremetns and its applicaiton for high-pressure high-temperature experimental run products

*Madhusoodhan Satish-Kumar[1], Shinnosuke Aoyama[1] (1.Department of Geology, Faculty of Science, Niigata University)

[SIT21-P20] Electrical resistivity of hcp Fe-Si alloys at high pressure and temperature

*Hayato Inoue[1], Sho Suehiro[1], Kenji Ohta[1], Kei Hirose[2,3], Yasuo Ohishi[4] (1.Department of Earth and Planetary Sciences, Tokyo Institute of Technology, 2.Earth-Life Science Institute, Tokyo Institute of Technology, 3.Department of Earth and Planetary Science, The University of Tokyo, 4.Japan Synchrotron Radiation Research Institute)

[SIT21-P21] Electrical resistivity and thermal conductivity of fcc Fe: Implications for the Mercury's core

★Invited Papers

*Hitoshi Gomi[1], Takashi Yoshino[1] (1.Okayama University)

[SIT21-P22] Lateral heterogeneity in the lowermost outer core (F layer) of the Earth revealed by seismic analyses

*Toshiki Ohtaki[1], Satoshi Kaneshima[2], Taku Tsuchiya[3] (1.Geological Survey of Japan, National Institute of Advanced Industrial Science and Technology (AIST), 2.Department of Earth and Planetary Sciences, Kyushu University,

3.Geodynamics Research Center, Ehime University)

[SIT21-P23] Flows and light element distribution in the outer core associated with heterogeneous growth of the inner core of the Earth

*Shin-ichi Takehiro[1], Youhei SASAKI[2] (1.Research Institute for Mathematical Sciences, Kyoto University, 2.Department of Mathematics, Kyoto University)

[SIT21-P24] Sharpness of the hemispherical boundary in the inner core beneath the northern Pacific

*Ryohei Iritani[1], Hitoshi Kawakatsu[1], Nozomu Takeuchi[1] (1.Earthquake Research Institute, Univ. of Tokyo)

[SIT21-P25] Stable carbon isotope fractionation in Fe-C system from first principles

*Haruhiko Dekura[1], Taku Tsuchiya[1] (1.Geodynamics Research Center, Ehime University)

[E] Poster | S (Solid Earth Sciences)：S-IT Science of the Earth's Interior & Techtonophysics

5:15 PM - 6:30 PM JST | 8:15 AM - 9:30 AM UTC | Poster Hall International Exhibition Hall8, Makuhari Messe_22

[S-IT21] Interaction and Coevolution of the Core and Mantle in the Earth and Planets

convener:Kenji Kawai(Department of Earth and Planetary Science, School of Science, University of Tokyo), Tsuyoshi Iizuka(University of Tokyo), Kenji Ohta(Department of Earth and Planetary Sciences, Tokyo Institute of Technology), Taku Tsuchiya(Geodynamics Research Center, Ehime University)

[SIT21-P01] Sample-scale compositional variation of the Inada granite, Ibaraki, Japan -toward the reduction of geoneutrino flux estimation errors from the Japanese crust-

★Invited Papers

*Kenta Ueki[1], Minami Kazuki[2], Tsuyoshi Iizuka[3], Sanshiro Enomoto[4], Hiroyuki Tanaka[2] (1.Japan Agency for Marine-Earth Science and Technology, 2.Earthquake Research Institute, University of Tokyo, 3.Department of Earth and Planetary Science, University of Tokyo, 4.Center for Experimental Nuclear Physics and Astrophysics, University of Washington)

[SIT21-P02] Towards a better estimation of the temperature distribution beneath the Japanese Islands

*Akiko Tanaka[1], Makoto Yamano[2], Hideki Hamamoto[3], Shusaku Goto[4], Takumi Matsumoto[5] (1.Geological Survey of Japan, National Institute of Advanced Industrial Science and Technology, 2.Earthquake Research Institute, The University of Tokyo, 3.Center for Environmental Science in Saitama, 4.Institute for Geo-Resources and Environment National Institute of Advanced Industrial Science and Technology, 5.National Research Institute for Earth Science and Disaster Resilience)

[SIT21-P03] The estimation of the neutrino flux from the crust of the Japanese islands using the geochemical database

*Satoru Haraguchi[1], Kenta Ueki[1], Hikaru Iwamori[1,2,3] (1.Japan Agency for Marine-Earth Science and Technology, 2.Earthquake Research Institute, the University of Tokyo, 3.Tokyo Institute of Technology)

[SIT21-P04] **Viscosity of potassium titanosilicate melt at high pressure**

*Akio Suzuki[1] (1.Department of Earth Science, Graduate School of Science, Tohoku University)

[SIT21-P05] **Lattice thermal conductivity of wadsleyite and ringwoodite at the mantle transition zone pressures**

*seiji kimura[1], Kenji Ohta[6], Takaaki Kawazoe[2], Kei Hirose[3], Hiroyuki Kagi[4], Takashi Yagi[5] (1.Department of Earth and Planetary Sciences Tokyo Institute of Technology, 2.Department of Earth and Planetary Systems Science, Hiroshima University, 3.Earth-Life Science Institute, Tokyo Institute of Technology, 4.Geochemical Research Center, Graduate School of Science, University of Tokyo, 5.National Institute of Advanced Industrial Science and Technology, 6.Department of Earth and Planetary Sciences, Tokyo Institute of Technology)

[SIT21-P06] In-situ X-ray observations of the olivine-spinel transformation under shear deformation: preliminary results on the reaction-induced weakening

*Tomoaki Kubo[1], Moriyama Kazuya[1], Yuichiro Mori[1], Masahiro Imamura[1], Sanae Koizumi[2], Yu Nishihara[3], Akio Suzuki[4], Yuji Higo[5] (1.Kyushu Univ., 2.ERI, 3.GRC Ehime Univ., 4.Tohoku Univ., 5.JASRI)

[SIT21-P07] Internally resistive heated diamond anvil cell experiments with metal encapsulated minerals

*YAMAMOTO TOMONARI[1], Kenji Ohta[1], Sho Suehiro[1], Hayato Inoue[1] (1.Tokyo Institute of Technology)

[SIT21-P08] Shear deformation on post-spinel

*Daisuke Yamazaki[1], Noriyoshi Tsujino[1], Yu Nishihara[2] (1.Institute for Planetary Materials, Okayama University, 2.GRC, Ehime University)

[SIT21-P09] **Lattice thermal conductivity of $CaSiO_3$ perovskite at high pressures and high temperatures**

*Kotaro Onga[1], Kenji Ohta[1], Akira Hasegawa[1,2], Takashi Yagi[2], Kei Hirose[3,4], Yasuo Ohishi[5] (1.Department of Earth and Planetary Sciences, Tokyo Institute of Technology, 2.National Institute of Advanced Industrial Science and Technology, 3.Earth-Life Science Institute, Tokyo Institute of Technology, 4.Department of Earth and Planetary Science, The University of Tokyo, 5.Japan Synchrotron Radiation Research Institute)

[SIT21-P10] **Polycrystalline diamond sintered from ultradispersed nanodiamonds**

*Masayuki Nishi[1,2], Koichiro Yamamoto[1], Youmo Zhou[1], Tetsuo Irifune[2,1] (1.Geodynamics Research Center, Ehime University, 2.Earth-Life Science Institute, Tokyo Institute of Technology)

[SIT21-P11] Thermal conductivity measurements on iron and MgO periclase at high pressure and high temperature similar to the Earth's mid-lower mantle conditions

*Akira Hasegawa[1,2], Kenji Ohta[2], Takashi Yagi[1], Kei Hirose[3,4] (1.National Institute of Advanced Industrial Science and Technology, 2.Tokyo Institude of Technology, 3.Earth-Life Science Institute, Tokyo Institude of Technology, 4.The University of Tokyo)

[SIT21-P12] Azimuthal anisotropy in the lowermost mantle beneath Philippine from ScS-S times

*Satoru Tanaka[1] (1.Department of Deep Earth Structure and Dynamics Research Japan Agency for Marine-Earth Science and Technology)

[SIT21-P13] Detailed 3-D S-velocity structure within D" at the western Pacific LLSVP margin: smaller scale plumes and paleoslabs

*Yuki Suzuki[1], Kenji Kawai[1], Robert J. Geller[1], Satoru Tanaka[2], Weerachai Siripuvaraporn[3], Songkhun Boonchaisuku[3], Noisagool Sutthipong[3], Yasushi Ishihara[2], Taweoon Kim, Koji MIYAKAWA[4], Nozomu Takeuchi[4] (1.The University of Tokyo, 2.Japan Agency for Marine-Earth Science and Technology, 3.Mahidol University, 4.Earthquake Research Institute, The University of Tokyo)

[SIT21-P14] Possible interaction between the core and mantle inferred from a core surface flow model

*Masaki Matsushima[1] (1.Department of Earth and Planetary Sciences, School of Science, Tokyo Institute of Technology)

[SIT21-P15] Determination of the noble gas partition coefficients between metal-silicate melts under high-pressure and high-temperature conditions

*Tomotaka Tanaka[1], Hideharu Kuwahara[2], Satoshi Kishi[1], Ryuichi Nomura[3], Kenji Mibe[5], Hiroyuki Kagi[4], Shigehiko Tateno[6], Hirochika Sumino[1] (1.Department of Basic Science, Graduate School of Arts and Sciences, The University of Tokyo , 2.Geodynamics Research Center, Ehime University, 3.Kyoto University, 4.Geochemical Research Center, Graduate School of Science, University of Tokyo, 5.Earthquake Research Institute, University of Tokyo, 6.Earth-Life Science Institute, Tokyo Institute of Technology)

[SIT21-P16] **Measurement of T-dependent electrical resistivity of solid and liquid Fe and Pt at fixed P**

*Innocent Ezenwa[1], Takashi Yoshino[1] (1.Institute for Planetary Materials, Okayama University)

[SIT21-P17] Ancient, highly depleted mantle constrained by Re-Os isotope and highly-siderophile element compositions of French Polynesian xenoliths

*Norikatsu Akizawa[1], Akira Ishikawa[2], Katsuhiko Suzuki[3], Tetsu Kogiso[4] (1.Atmosphere and Ocean Research Institute, The University of Tokyo, 2.Department of Earth and Planetary Sciences, Tokyo Institute of Technology, 3.Research and Development Center for Submarine Resources, Japan Agency for Marine-Earth Science and Technology (JAMSTEC), 4.Graduate School of Human and Environmental Studies, Kyoto University)

[SIT21-P18] First-principles prediction of hydrogen partitioning between the core and mantle

*Atsuroh Ohba[1], Taku Tsuchiya[1] (1.Ehime University Geodynamics Research Center)

[SIT21-P19] Microvolume stable isotope measuremetns and its applicaiton for high-pressure high-temperature experimental run products

*Madhusoodhan Satish-Kumar[1], Shinnosuke Aoyama[1] (1.Department of Geology, Faculty of Science, Niigata University)

[SIT21-P20] Electrical resistivity of hcp Fe-Si alloys at high pressure and temperature

*Hayato Inoue[1], Sho Suehiro[1], Kenji Ohta[1], Kei Hirose[2,3], Yasuo Ohishi[4] (1.Department of Earth and Planetary Sciences, Tokyo Institute of Technology, 2.Earth-Life Science Institute, Tokyo Institute of Technology, 3.Department of Earth and Planetary Science, The University of Tokyo, 4.Japan Synchrotron Radiation Research Institute)

[SIT21-P21] Electrical resistivity and thermal conductivity of fcc Fe: Implications for the Mercury's core

★Invited Papers

*Hitoshi Gomi[1], Takashi Yoshino[1] (1.Okayama University)

[SIT21-P22] Lateral heterogeneity in the lowermost outer core (F layer) of the Earth revealed by seismic analyses

*Toshiki Ohtaki[1], Satoshi Kaneshima[2], Taku Tsuchiya[3] (1.Geological Survey of Japan, National Institute of Advanced Industrial Science and Technology (AIST), 2.Department of Earth and Planetary Sciences, Kyushu University,

3.Geodynamics Research Center, Ehime University)

[SIT21-P23] Flows and light element distribution in the outer core associated with heterogeneous growth of the inner core of the Earth

*Shin-ichi Takehiro[1], Youhei SASAKI[2] (1.Research Institute for Mathematical Sciences, Kyoto University, 2.Department of Mathematics, Kyoto University)

[SIT21-P24] Sharpness of the hemispherical boundary in the inner core beneath the northern Pacific

*Ryohei Iritani[1], Hitoshi Kawakatsu[1], Nozomu Takeuchi[1] (1.Earthquake Research Institute, Univ. of Tokyo)

[SIT21-P25] Stable carbon isotope fractionation in Fe-C system from first principles

*Haruhiko Dekura[1], Taku Tsuchiya[1] (1.Geodynamics Research Center, Ehime University)

[J] Oral | S (Solid Earth Sciences)：S-GL Geology

9:00 AM - 10:30 AM JST | 12:00 AM - 1:30 AM UTC | A09 TOKYO BAY MAKUHARI HALL

[S-GL28] Regional geology and tectonics

convener:Makoto Otsubo(Geological Survey of Japan, Research Institute of Earthquake and Volcano Geology), Jun Hosoi(Geological Survey of Japan, Institute of Geology and Geoinformation, AIST), Chairperson:Makoto Otsubo(Research Institute of Earthquake and Volcano Geology, Geological Survey of Japan)

9:00 AM - 9:15 AM JST | 12:00 AM - 12:15 AM UTC

[SGL28-01] Lithology and zircon U-Pb geochronology of Paleoproterozoic and Paleozoic granitic complex in Maizuru Terrane from Tsuwano area, Shimane Prefecture, SW Japan

*Kosuke Kimura[1], Yasutaka Hayasaka[1], Tomoyuki Shibata[1], Kenta Kawaguchi[1], Hiroshi Fujiwara[1] (1.Hiroshima University)

9:15 AM - 9:30 AM JST | 12:15 AM - 12:30 AM UTC

[SGL28-02] Tectonic significance of new Zircon U-Pb ages of sedimentary complexes in the northern Hidaka Belt, central Hokkaido, northern Japan

*Futoshi Nanayama[1,5], Toru Yamasaki[1], Jun Tajika[2], Hideki Iwano[3], Tohru Danhara[3], Takafumi Hirata[4] (1.Geological Survey of Japan, AIST, 2.Docon Co. Ltd, 3.Kyoto Fission-Track Co.Ltd, 4.Tokyo Univ., 5.CWMD, Kumamoto Univ.)

9:30 AM - 9:45 AM JST | 12:30 AM - 12:45 AM UTC

[SGL28-03] New age constraints and tectonic significance of Late Oligocene marine biosiliceous deposits in the Hidaka Belt, northeastern Hokkaido, northern Japan

*Futoshi Nanayama[1,6], Hiroshi Kurita[2], Toru Yamasaki[1], Jun Tajika[3], Hideki Iwano[4], Tohru Danhara[4], Takafumi Hirata[5] (1.Geological Survey of Japan, AIST, 2.Niigata Univ., 3.Docon Co. Ltd, 4.Kyoto Fission-Track Co. Ltd, 5.Tokyo Univ., 6.CWMD, Kumamoto Univ.)

9:45 AM - 10:00 AM JST | 12:45 AM - 1:00 AM UTC

[SGL28-04] Late Cretaceous sea-level changes and tectonic history recorded in the forearc sedimentary successions of the Northeast Japan

*Jun Arimoto[1], Reishi Takashima[2], Hiroshi Nishi[2], Yuji Orihashi[3], Toshiro Yamanaka[4] (1.Department of Earth Science, Graduate School of Science, Tohoku University, 2.The Center for Academic Resources and Archives, Tohoku University, 3.Department of Earth and Environmental Sciences, Graduate School of Hirosaki University, 4.Tokyo University of Marine Science and Technology)

10:00 AM - 10:15 AM JST | 1:00 AM - 1:15 AM UTC

[SGL28-05] Paleo-stress analysis in coherent zone, an exhumed Cretacesou accretionary complex, Shimanto Belt, in Konan city and Geisei villege, Kochi prefecture, SW Japan

*Makoto Hashiguchi[1], Yoshitaka Hashimoto[1] (1.Kochi University)

10:15 AM - 10:30 AM JST | 1:15 AM - 1:30 AM UTC

[SGL28-06] Relationship between accretion of limestone blocks and subduction tectonics in Japan

*Koji Wakita[1] (1.Yamaguchi University)

[J] Oral | S (Solid Earth Sciences)：S-GL Geology

10:45 AM - 12:15 PM JST | 1:45 AM - 3:15 AM UTC | A09 TOKYO BAY MAKUHARI HALL

[S-GL28] Regional geology and tectonics

convener:Makoto Otsubo(Geological Survey of Japan, Research Institute of Earthquake and Volcano Geology), Jun Hosoi(Geological Survey of Japan, Institute of Geology and Geoinformation, AIST), Chairperson:Jun Hosoi(Geological Survey of Japan)

10:45 AM - 11:00 AM JST | 1:45 AM - 2:00 AM UTC

[SGL28-07] Discovery of faulted basin margin from the middle Miocene Tottori Grope, Tottori Prefecture, Southwest Japan and its significance

*Yuta Maruyma[1] (1.Shimane Umiversity)

11:00 AM - 11:15 AM JST | 2:00 AM - 2:15 AM UTC

[SGL28-08] Fault activity during Quaternary Period off the Shimane Peninsula based on the profiles acquired by the high-resolution seismic survey

*Masaaki Tanaka[1], Norihiro Matsuda[1], Masaru Nakamura[1], Yuichi Shimizu[1], Masanori Shimazaki[2], Kazuhito Hatakeyama[2] (1.The Chugoku Electric Power Co., Inc., 2.Sogo Geophysical Exploration Co., Ltd.)

11:15 AM - 11:30 AM JST | 2:15 AM - 2:30 AM UTC

[SGL28-09] Paleomagnetic directions of early Miocene sediments in central Japan and tectonic implications

*Hiroyuki Hoshi[1], Takuro Matsuo[2] (1.Department of Earth Sciences, Aichi University of Education, 2.Aichi Prefectural Kariya High School)

11:30 AM - 11:45 AM JST | 2:30 AM - 2:45 AM UTC

[SGL28-10] Revised Cenozoic chronostratigraphy and tectonics in the Yatsuo Area, Toyama Prefecture, central Japan

*Takeshi Nakajima[1], Hideki Iwano[2], Tohru Danhara[2], Tohru Yamashita[2], Yukio Yanagisawa[1], Yoshihiro Tanimura[3], Mahito Watanabe[1], Takayuki Sawaki[1], Satoshi Nakanishi[4], Hiroyuki Mitsuishi[4], Okiyuki Yamashina[4], Seiichi Imahori[5] (1.Geological Survey of Japan, National Institute of Advanced Industrial Science and Technology, 2.Kyoto Fission-Track Co., Ltd., 3.National Museum of Nature and Science, 4.JX Nippon Oil & Gas Exploration Corporation, 5.JX Nippon Oil & Gas Exploration Technical Services Corporation)

[J] Poster | S (Solid Earth Sciences)：S-GL Geology

3:30 PM - 5:00 PM JST | 6:30 AM - 8:00 AM UTC | Poster Hall International Exhibition Hall8, Makuhari Messe_13

[S-GL28] Regional geology and tectonics

convener:Makoto Otsubo(Geological Survey of Japan, Research Institute of Earthquake and Volcano Geology), Jun Hosoi(Geological Survey of Japan, Institute of Geology and Geoinformation, AIST)

[SGL28-P01] **Petrogenesis of Oligocene to Miocene volcanic rocks in the Tonami area, central Japan: temporal evolution of continental- to island-arc volcanism during the Japan Sea opening**

*Raiki Yamada[1], Toshiro Takahashi[2], Hayato Ueda[2] (1.Graduate school of science and technology, Niigata University, 2.Faculty of Science, Niigata University)

[SGL28-P02] Geology and post mid-Miocene tectonics of the Ogawa basin and the Atogura Nappe

*Akira Ono

[SGL28-P03] Paleostress transition estimated from small-scale deformation structures of the Sanbagawa metamorphic rocks in the Nagatoro area, Saitama Prefecture, central Japan

*Minami Nakamura[1], Aiko Takada[1,2], Hideo Takagi[1] (1.Waseda University , 2.Japan Petroleum Exploration Co., Ltd.)

[SGL28-P04] Estimation of the paleostress directions using “new dyke method” from the microcracks in the Tanzawa Tonalite

*Misaki Tomioka[1], Hideo Takagi[1] (1.Waseda University)

[SGL28-P05] Ring faults topographically discovered in the Tono-Kurihashi granitic plutonic masses by using a cnstant vertical exaggeration stereoscopic map of slope, Kitakami massif

*Nobuo Doi[1], Michio Shirasawa[2], Ryuzo Yokoyama[2] (1.Research Center for Regional Disaster Management, Iwate University, 2.Yokoyama Geo-Spatial Information Laboratory Co., Ltd.)

[SGL28-P06] **The Maizuru tectonic zone (MTZ), its formation and rearrangement as revealed by new zircon chronology data**

*Yasutaka Hayasaka[1], Kosuke Kimura[1] (1.Graduate School of Science, Hiroshima University)

[SGL28-P07] **Erosional features of Soma Slope Channel, off Miyagi, Japan**

*Jih-Hsin Chang[1], Takahiko Inoue[1], Ayanori Misawa[1], Kohsaku Arai[1] (1.Geological Survey of Japan, National Institute of Advanced Industrial and Science Technology.)

[SGL28-P08] Preliminary Analysis Result for the Integrated Lineament Map in South Korea

*Hong-Jin Lee[1], Kyoungtae Ko[2], You Hong Kihm[2] (1.Geoscience Platfrom Division, Korea Institute of Geoscience and Mineral Resources, 2.Geology Division, Korea Institute of Geoscience and Mineral Resources)

[SGL28-P09] **Seismicity along the Moradabad Basement Fault in the Central Ganga Plain: A Geological and Geophysical approach**

*ANKIT GUPTA[1], Pitambar Pati[1], Chinmay Dash[1] (1.Indian Institute of Technology Roorkee)

[SGL28-P10] Petrological and geochronological studies of the volcanic rocks in the Muslim Bagh area, Pakistan

*Masanari Arao[1,2], Takeshi Imayama[1], Koshi Yagi[3], Chiaki Ikawa[3], Yoshihiro Sawada[4], Rehanul Haq Siddiqui[5], Said Rahim Khan[5] (1.Research Institute of Natural Sciences, Okayama University of Science, 2.Faculty of Biosphere - Geosphere Science, Okayama University of Science, 3.Hiruzen Institute for Geology and Chronology, 4.Emeritus Professor of Shimane University, 5.Geoscience Laboratory, Geological Survey of Pakistan)

[J] Poster | S (Solid Earth Sciences)：S-GL Geology

5:15 PM - 6:30 PM JST | 8:15 AM - 9:30 AM UTC | Poster Hall International Exhibition Hall8, Makuhari Messe_23

[S-GL28] Regional geology and tectonics

convener:Makoto Otsubo(Geological Survey of Japan, Research Institute of Earthquake and Volcano Geology), Jun Hosoi(Geological Survey of Japan, Institute of Geology and Geoinformation, AIST)

[SGL28-P01] **Petrogenesis of Oligocene to Miocene volcanic rocks in the Tonami area, central Japan: temporal evolution of continental- to island-arc volcanism during the Japan Sea opening**

*Raiki Yamada[1], Toshiro Takahashi[2], Hayato Ueda[2] (1.Graduate school of science and technology, Niigata University, 2.Faculty of Science, Niigata University)

[SGL28-P02] Geology and post mid-Miocene tectonics of the Ogawa basin and the Atogura Nappe

*Akira Ono

[SGL28-P03] Paleostress transition estimated from small-scale deformation structures of the Sanbagawa metamorphic rocks in the Nagatoro area, Saitama Prefecture, central Japan

*Minami Nakamura[1], Aiko Takada[1,2], Hideo Takagi[1] (1.Waseda University , 2.Japan Petroleum Exploration Co., Ltd.)

[SGL28-P04] Estimation of the paleostress directions using “new dyke method” from the microcracks in the Tanzawa Tonalite

*Misaki Tomioka[1], Hideo Takagi[1] (1.Waseda University)

[SGL28-P05] Ring faults topographically discovered in the Tono-Kurihashi granitic plutonic masses by using a cnstant vertical exaggeration stereoscopic map of slope, Kitakami massif

*Nobuo Doi[1], Michio Shirasawa[2], Ryuzo Yokoyama[2] (1.Research Center for Regional Disaster Management, Iwate University, 2.Yokoyama Geo-Spatial Information Laboratory Co., Ltd.)

[SGL28-P06] **The Maizuru tectonic zone (MTZ), its formation and rearrangement as revealed by new zircon chronology data**

*Yasutaka Hayasaka[1], Kosuke Kimura[1] (1.Graduate School of Science, Hiroshima University)

[SGL28-P07] **Erosional features of Soma Slope Channel, off Miyagi, Japan**

*Jih-Hsin Chang[1], Takahiko Inoue[1], Ayanori Misawa[1], Kohsaku Arai[1] (1.Geological Survey of Japan, National Institute of Advanced Industrial and Science Technology.)

[SGL28-P08] Preliminary Analysis Result for the Integrated Lineament Map in South Korea

*Hong-Jin Lee[1], Kyoungtae Ko[2], You Hong Kihm[2] (1.Geoscience Platfrom Division, Korea Institute of Geoscience and Mineral Resources, 2.Geology Division, Korea Institute of Geoscience and Mineral Resources)

[SGL28-P09] **Seismicity along the Moradabad Basement Fault in the Central Ganga Plain: A Geological and Geophysical approach**

*ANKIT GUPTA[1], Pitambar Pati[1], Chinmay Dash[1] (1.Indian Institute of Technology Roorkee)

[SGL28-P10] Petrological and geochronological studies of the volcanic rocks in the Muslim Bagh area, Pakistan

*Masanari Arao[1,2], Takeshi Imayama[1], Koshi Yagi[3], Chiaki Ikawa[3], Yoshihiro Sawada[4], Rehanul Haq Siddiqui[5], Said Rahim Khan[5] (1.Research Institute of Natural Sciences, Okayama University of Science, 2.Faculty of Biosphere - Geosphere Science, Okayama University of Science, 3.Hiruzen Institute for Geology and Chronology, 4.Emeritus Professor of Shimane University, 5.Geoscience Laboratory, Geological Survey of Pakistan)

[J] Poster | S (Solid Earth Sciences)：S-VC Volcanology

10:45 AM - 12:15 PM JST | 1:45 AM - 3:15 AM UTC | Poster Hall International Exhibition Hall8, Makuhari Messe_2

[S-VC35] Mitigation of volcanic disasters - basic and applied researches

convener:Shinji Takarada(Geological Survey of Japan, National Institute of Advanced Industrial Science and Technology), Mitsuhiro Yoshimoto(Mount Fuji Research Institute, Yamanashi Prefectural Government), Yasuhiro Ishimine(Research and Education Center for Natural Hazards, Kagoshima University), Tomohiro Kubo(National Research Institute for Earth Science and Disaster Prevention)

[SVC35-P01] Oil paintings describing the 1914 Sakurajima eruption

*Satoko Murotani[1] (1.National Museum of Nature and Science)

[SVC35-P02] Constructing and utilizing digitized volcanic hazardmap database

*Yuhki Kohno[1], Tomohiro Kubo[1], Yosuke Miyagi[1], Toshikazu Tanada[1] (1.National Research Institute for Earth Science and Disaster Resilience)

[SVC35-P03] Pyroclastic fall simulation using Tephra2 and JRA-55

*Hisashi Sasaki[1], Shunsuke Miura[1], Shino Naruke[1] (1.Asia Air Survey Co., Ltd.)

[SVC35-P04] Research on observation method of volcanic ash-fall accumulation using spaceborne SAR

*Taku Ozawa[1], Eisuke Fujita[1] (1.National Research Institute for Earth Science and Disaster Resilience)

[SVC35-P05] Method for estimation of debris flow runout in the volcanic area

*Yusuke Yamazaki[1], Naoki Fujimura[1], Sakiko Tetsuka[1], Masaki Mizuno[1], Yasuo Ishii[1], Toshihiro Kikui[2], Shinya Yoshida[2], Yuki Igarashi[2], Takao Yamakoshi[2] (1.Public Works Research Institute, 2.STC)

[SVC35-P06] On the H_2S concentration continuous observation at Kurikoma volcano

*Hideyuki Itoh[1], Yasumichi Yamamoto[2], Kenji OOba[2], Morio Tsuji[1], Takeshi Ohba[3] (1.Faculty of policy studies, Iwate prefectural University, 2.JMS INc, 3.Tokai University)

[J] Poster | S (Solid Earth Sciences)：S-VC Volcanology

5:15 PM - 6:30 PM JST | 8:15 AM - 9:30 AM UTC | Poster Hall International Exhibition Hall8, Makuhari Messe_24

[S-VC35] Mitigation of volcanic disasters - basic and applied researches

convener:Shinji Takarada(Geological Survey of Japan, National Institute of Advanced Industrial Science and Technology), Mitsuhiro Yoshimoto(Mount Fuji Research Institute, Yamanashi Prefectural Government), Yasuhiro Ishimine(Research and Education Center for Natural Hazards, Kagoshima University), Tomohiro Kubo(National Research Institute for Earth Science and Disaster Prevention)

[SVC35-P01] Oil paintings describing the 1914 Sakurajima eruption

*Satoko Murotani[1] (1.National Museum of Nature and Science)

[SVC35-P02] Constructing and utilizing digitized volcanic hazardmap database

*Yuhki Kohno[1], Tomohiro Kubo[1], Yosuke Miyagi[1], Toshikazu Tanada[1] (1.National Research Institute for Earth Science and Disaster Resilience)

[SVC35-P03] Pyroclastic fall simulation using Tephra2 and JRA-55

*Hisashi Sasaki[1], Shunsuke Miura[1], Shino Naruke[1] (1.Asia Air Survey Co., Ltd.)

[SVC35-P04] Research on observation method of volcanic ash-fall accumulation using spaceborne SAR

*Taku Ozawa[1], Eisuke Fujita[1] (1.National Research Institute for Earth Science and Disaster Resilience)

[SVC35-P05] Method for estimation of debris flow runout in the volcanic area

*Yusuke Yamazaki[1], Naoki Fujimura[1], Sakiko Tetsuka[1], Masaki Mizuno[1], Yasuo Ishii[1], Toshihiro Kikui[2], Shinya Yoshida[2], Yuki Igarashi[2], Takao Yamakoshi[2] (1.Public Works Research Institute, 2.STC)

[SVC35-P06] On the H_2S concentration continuous observation at Kurikoma volcano

*Hideyuki Itoh[1], Yasumichi Yamamoto[2], Kenji OOba[2], Morio Tsuji[1], Takeshi Ohba[3] (1.Faculty of policy studies, Iwate prefectural University, 2.JMS INc, 3.Tokai University)

[J] Oral | S (Solid Earth Sciences)：S-VC Volcanology

1:45 PM - 3:15 PM JST | 4:45 AM - 6:15 AM UTC | 105 1F

[S-VC35] Mitigation of volcanic disasters - basic and applied researches

convener:Shinji Takarada(Geological Survey of Japan, National Institute of Advanced Industrial Science and Technology), Mitsuhiro Yoshimoto(Mount Fuji Research Institute, Yamanashi Prefectural Government), Yasuhiro Ishimine(Research and Education Center for Natural Hazards, Kagoshima University), Tomohiro Kubo(National Research Institute for Earth Science and Disaster Prevention), Chairperson:Tomohiro Kubo(防災科学技術研究所), Shinji Takarada(Geological Survey of Japan/AIST)

1:45 PM - 2:00 PM JST | 4:45 AM - 5:00 AM UTC

[SVC35-01] A working hypothesis for source craters and sequence of the 1707 Hoei eruption of Fuji Volcano, Japan

*Masato Koyama[1] (1.Shizuoka Univ.)

2:00 PM - 2:15 PM JST | 5:00 AM - 5:15 AM UTC

[SVC35-02] Consideration of the formation process of Mt.Hoei, Fuji volcano

*Akira Baba[1], Toshitsugu Fujii[1], Tatsuro Chiba[2], Mitsuhiro Yoshimoto[1], Fumikatsu NISHIZAWA[1], Hidetoshi Shibuya[3] (1.Mount Fuji Research Institute, 2.Asia Air Survey Co., Ltd., 3.Department of Earth and Environmental Sciences, Faculty of Advanced Science and Technology, Kumamoto University)

2:15 PM - 2:30 PM JST | 5:15 AM - 5:30 AM UTC

[SVC35-03] Airborne LiDAR Bathymetry reveals underwater topography of Lake Motosu - The level of water raised by lava inflow -

*Tatsuro Chiba[1], Sin-ichi kaneta[1], Makoto Ohashi[1] (1.Asia Air Survey Co., Ltd.)

2:30 PM - 2:45 PM JST | 5:30 AM - 5:45 AM UTC

[SVC35-04] Volcano monitoring using satellite thermal infrared imagery of CIRC (Compact Infrared Camera)

*Yuki Takakura[1], Koji Nakau[1], Junichiro Ishizawa[1] (1.Japan Aerospace Exploration Agency)

2:45 PM - 3:00 PM JST | 5:45 AM - 6:00 AM UTC

[SVC35-05] Impact absorption properties of wooden buildings roof subjected to ballistic block collision

*Kohei Tateyama[1], Hiroyuki Yamada[2], Mitsuhiro Yoshimoto[3], Ryo Honda[3], Toshitsugu Fujii[3] (1.Ritsumeikan University, 2.National defense academy, 3.Mount Fuji Research Institute, Yamanashi Prefectural Government)

3:00 PM - 3:15 PM JST | 6:00 AM - 6:15 AM UTC

[SVC35-06] Distribution of ballistic ejecta of the phreatic eruption at Kusatsu-Shirane volcano, on 23 Jan, 2018, part 2

*Mitsuhiro Yoshimoto[1], Ryuta FURUKAWA[2,3], Yoshihiro Ishizuka[2], Yusuke Minami[2], Masashi NAGAI[4], Shuichi Hosokawa[3], Ryo Honda[1], Taisuke Yasuda[1], Akihiko Terada[5], Tatsuji Nishizawa[5], Yasuhiro Ishimine[6], Kenichi Arai[7], Hisashi Sasaki[7], Shino Naruke[7], Yuko Sekiguchi[3], Takahiro Yanada[3], Yasuo Ishizaki[8], Nobuko Kametani[8], Fukashi Maeno[9] (1.Mount Fuji Research Institute, Yamanashi Prefectural Government, 2.Geological Survey of Japan, National Institute of Advanced Industrial Science and Technology, 3.Japan Meteorological Agency, 4.Volcano Research Department, National Research Institute for Earth Science and Disaster Resilience, 5.Volcanic Fluid Research Center, Tokyo Institute of Technology, 6.Research and Education Center for Natural Hazards, Kagoshima University, 7.Asia Air Survey Co., Ltd., 8. Graduate School of Science and Engineering, University of Toyama, 9.Earthquake Research Institute, University of Tokyo)

[J] Oral | S (Solid Earth Sciences)：S-VC Volcanology

3:30 PM - 5:00 PM JST | 6:30 AM - 8:00 AM UTC | 105 1F

[S-VC35] Mitigation of volcanic disasters - basic and applied researches

convener:Shinji Takarada(Geological Survey of Japan, National Institute of Advanced Industrial Science and Technology), Mitsuhiro Yoshimoto(Mount Fuji Research Institute, Yamanashi Prefectural Government), Yasuhiro Ishimine(Research and Education Center for Natural Hazards, Kagoshima University), Tomohiro Kubo(National Research Institute for Earth Science and Disaster Prevention), Chairperson:Mitsuhiro Yoshimoto(山梨県富士山科学研究所), Yasuhiro Ishimine(鹿児島大学地域防災教育研究センター)

3:30 PM - 3:45 PM JST | 6:30 AM - 6:45 AM UTC

[SVC35-07] Developing Ash-fall impact forecasting content.

*Tomohiro Kubo[1], Yosuke Miyagi[1], Setsuya Nakada[1], Eisuke Fujita[1], Masamitsu Miyamura[1] (1.National Research Institute for Earth Science and Disaster Prevention)

3:45 PM - 4:00 PM JST | 6:45 AM - 7:00 AM UTC

[SVC35-08] New Websites and a Pamphlet of IVHHN

*Yasuhiro Ishimine[1] (1.Research and Education Center for Natural Hazards, Kagoshima University)

4:00 PM - 4:15 PM JST | 7:00 AM - 7:15 AM UTC

[SVC35-09] State of river water pollution derived from the recent volcanic activity of Mt Iwo-Yama, Kirishima volcanoes

*Yoshikazu Kikawada[1], Haruka Yamamoto[2], Wei Deng, Megumi Fukai (1.Faculty of Science and Technology, Sophia University, 2.Graduate School of Science and Technology, Sophia University)

4:15 PM - 4:30 PM JST | 7:15 AM - 7:30 AM UTC

[SVC35-10] Development of information tools for evacuation and rescue in the event of volcanic disaster

*Yosuke Miyagi[1], Setsuya Nakada[1], Tomohiro Kubo[1], Mitsuhiro Yoshimoto[2], Ryo Honda[2] (1.National Research Institute for Earth Science and Disaster Resilience, 2.Mount Fuji Research Institute, Yamanashi Prefectural Government)

4:30 PM - 4:45 PM JST | 7:30 AM - 7:45 AM UTC

[SVC35-11] **Ignimbrite, tephra-fall, caldera and fatalities of major volcanoes in the East and Southeast Asia**

*Shinji Takarada[1], Joel Calupas Bandibas[1] (1.Geological Survey of Japan, AIST)

4:45 PM - 5:00 PM JST | 7:45 AM - 8:00 AM UTC

[SVC35-12] On the climber’s attitudes to the Volcanic mitigation for active volcanoes.

*Hideyuki Itoh[1], Chizuru Totani[2], Mizuho Arai[2] (1.Faculty of policy studies, Iwate prefectural University, 2.Asia air Survey, Co.Ltd.)

[J] Poster | S (Solid Earth Sciences)：S-VC Volcanology

10:45 AM - 12:15 PM JST | 1:45 AM - 3:15 AM UTC | Poster Hall International Exhibition Hall8, Makuhari Messe_3

[S-VC38] Active Volcanism

convener:Yuta Maeda(Nagoya University), Takahiro Miwa(National research institute for earth science and disaster prevention), Takeshi Nishimura(Department of Geophysics, Graduate School of Science, Tohoku University)

[SVC38-P01] The structure of Showa-Shinzan Yaneyama Usu by seismic reflection surveys

*Ryuichi Takei[1], Tomoki Tsutsui[1,2], Yuya Tada[2], Tomoya Moriwaki[2], Yosuke Aoki[3], Hiroshi Aoyama[4], Go Maruyama[5] (1.Graduate School of International Resource Sciences, The University of Akita, 2.Faculty of International Resource Sciences, The University of Akita, 3.Earthquake Research Institute, The University of Tokyo, 4.Graduate school of Science, The University of Hokkaido, 5.Marutec Co., Ltd.)

[SVC38-P02] Ground deformation associated with the 2014-2015 and the 2018-2019 volcanic activities at Azumayama

*Jun Okada[1], Shigeo Matsuura[2], Katsuya Ohmi[2], Takuya Yamamura[2], Yu Nihara[3], Susumu Seki[3] (1.Volcanology Research Department (Sendai Office), Meteorological Research Institute, JMA, 2.Seismology and Volcanology Division, Sendai Regional Headquarters, JMA, 3.Regional Volcanic Observation and Warning Center, Sendai Regional Headquarters, JMA)

[SVC38-P03] BP-type and BT-type volcanic earthquakes in Azumayama

*Yusuke Yoshigai[1], Yuichi Morita[2], Katsuya Ohmi[3], Yu Nihara[4], Tsukasa Kobayashi[1] (1.Volcanological Division, Japan Meteorological Agency, 2.Earthquake Research Institute, University of Tokyo, 3.Seismology and Volcanology Division, Sendai Regional Headquarters, Japan Meteorological Agency, 4.Regional Volcanic Observation and Warning Center, Sendai Regional Headquarters, Japan Meteorological Agency)

[SVC38-P04] The occurrence and petrology of the fine-grained pyroclastic materials of the Futatsudake-Shibukawa eruption in Haruna volcano.

*Teruyoshi Maruyama[1], Yuki Suzuki[2] (1.Department of Earth Sciences, School of Education , Waseda University, 2.Department of Earth Sciences, Faculty of Education and Integrated Arts of Sciences, Waseda University)

[SVC38-P05] The occurrence and petrology of the block and ash flow deposit from the Futatsudake-Shibukawa eruption, Haruna volcano

*Yuki Suzuki[1], Ryouto Fukushima[2] (1.Department of Earth Sciences, Faculty of Education and Integrated Arts of Sciences, Waseda University, 2.Department of Earth Sciences, School of Education, Waseda University)

[SVC38-P06] Report of Volcanic Activity at Kusatsu-Shiranesan in 2018

*Tsukasa Kobayashi[1], Koji Kato[1], Koichi Suemine[1], Kazuhiro Kimura[1], Yusuke Yoshigai[1], Yasuo Ogawa[2], Kenji Nogami[2], Wataru Kanda[2], Akihiko Terada[2] (1.Volcanological Division, Japan Meteorological Agency, 2.Volcanic Fluid Research Center, Tokyo Institute of Technology)

[SVC38-P07] Noble gas isotope composition of fumaroles and hydrothermal gases around Kusatsu-Shirane volcano

*Kotaro Toyama[1], Hirochika Sumino[1], Kaori Kawana[1], Yoshihide Akiyama[1], Takeshi Ohba[2], Muga Yaguchi[3], Akihiko Terada[4] (1.Department of Basic Science, Graduate School of Arts and Sciences, The University of Tokyo, 2.Department of chemistry, School of Science, Tokia University, 3.Meteorological Research Institute, 4.Volcanic Fluid Research Center, Tokyo Institute of Technology)

[SVC38-P08] Self-potential and geomagnetic total intensity observations at Motoshirane volcano after the 2018 eruption

*Akira Yamazaki[1], Hideki Iino[1], Tatsurou Tanaka[1] (1.Kakioka Magnetic Observatory)

[SVC38-P09] Eruption processes of the 3rd and 4th stage of Niigata-Yakeyama Volcano, Japan, inferred from microlite texture and chemical composition

*Takumi Yoshida[1], Takeshi Saito[1] (1.Shinshu University)

[SVC38-P10] Estimation of subsurface structure of Shinyu crater lake, Tateyama Caldera, based on the water level and seismic observation data

*Ryohei Kawaguchi[1], Naoko Saito[2], Shin'ya Onizawa[1] (1.Meteorological Research Institute, 2.Toyama local Meteorological office, Japan Meteorological Agency)

[SVC38-P11] Real time monitoring of underground temperature in Jigokudani, Midagahara volcano using LPWA devices

*Tohru Watanabe[1], Toyama branch NTT West[2] (1.Gradudate School of Science and Engineering, University of Toyama, 2.Nippon Telegraph and Telephone West Corporation)

[SVC38-P12] Varying chemical and isotopic compositions of fumarolic gases from the summit and from the 1962-63 eruptive vents at Yakedake Volcano, Japan

*Takeshi Saito[1], Shun Sawamura[2], Kazuhiro Amita[3], Taketoshi Mishima[4], Shinji Ohsawa[4] (1.Institute of Science, Academic Assembly School of Science and Technology, Shinshu University, 2.Graduate School of Science and Technology, Shinshu University, 3.Graduate School of Engineering Science, Akita University, 4.Beppu Geothermal Research Laboratory, Institute for Geothermal Sciences, Graduate School of Science, Kyoto University)

[SVC38-P13] Eruption age determination of the latest two lava flows and characteristics of volcaniclastic materials from the recent activity of Yokodake Volcano, Japan

*Hiroya Nitta[1], Takeshi Saito[1], Yorinao Shitaoka[2] (1.Shinshu University of Science and Technology, 2.Department of Environment System, Faculty of Geo-environmental Science, Rissho University)

[SVC38-P14] Estimating the date of the 2007 eruption of Mount Ontake Volcano using waveform correlation

*Shuhei Nishijima[1], Toshiko Terakawa[1], Shinichiro Horikawa[1] (1.Graduate School of Environmental Studies, Nagoya University)

[SVC38-P15] Seismic activity beneath Mt. Ontake volcano before and after the 2007 and 2014 eruptions

*Yoshiko Yamanaka[1], Shinichiro Horikawa[1], Yuta Maeda[1] (1.Graduate School of Encironmental Studies, University of NAGOYA)

[SVC38-P16] Effect of rain and snowmelt correction of tiltmeter data
- Application example for Ontakesan Volcano -

*Kazuhiro Kimura[1,5], Katsuhisa Kawashima[2], Takane Matsumoto[2], Akihiko SASAKI[4], Tsutomu Iyobe[3], Junichi Miyamura[1], Masaki Nakahashi[1] (1.Japan Meteorological Agency, 2.Research Institute for Natural Hazards and Disaster Recovery, Niigata University, 3.Faculty of Engineering, Kyoto University, 4.Department of Geography and Environmental Studies, Kokushikan University, 5.Graduate School Science and Technology, Niigata University)

[SVC38-P17] **Spatial Variation of b-value around Mt. Fuji influenced by the Eastern Shizuoka Earthquake of 15 March 2011**

*Takumi Murakoshi[1], Tomonari Miyashita[2] (1.National Defense Academy, 2.JASDF)

[SVC38-P18] Present condition of submarged volcano, Teishi Knoll, off Ito, Eastern Izu Peninsula

*Toshiro Yamanaka[1], Yoshifumi Kawada[2], Takuro Noguchi[3], Mayumi Hatta[3], Kei Okamura[3] (1.Tokyo Univ. Marine Science and Technology, 2.Tohoku University, 3.Kochi University)

[SVC38-P19] Descriptions and age of volcanic products before the caldera formation in the northern part of Izu-Oshima, off Tokyo, Pacific Ocean

*Satoshi Terayama[1], Takehiko Suzuki[1], Makoto Kobayashi[2] (1.Tokyo Metropolitan University, 2.Research Center for Volcanic Hazards and Their Mitigation, Tokyo Metropolitan University)

[SVC38-P20] Time change of p-value by Schuster method using earthquakes around Izu-Ohsima summit

*Hiroyuki Takayama[1] (1.Volcanological Division 1st labolatory, Meteorological Research Institute)

[SVC38-P21] Standard stratigraphy and characteristic properties of late Quaternary tephras on the Niijima-island: Report of geochemistry and refractive indices of volcanic glass shards, orthopyroxene, hornblende, and cummingtonite

*Kaori Aoki[1], Makoto Kobayashi[1], Fumikatsu NISHIZAWA[1,2], Masanori Murata[1], Daisuke Ishimura[1], Takehiko Suzuki[1] (1.Research Center for Volcanic Hazards and Their Mitigation, Tokyo Metropolitan University, 2.Mount Fuji Research Institute, Yamanashi Prefectural Government)

[SVC38-P22] **Tephrostratigraphy and its eruption history of the Latest Activity in the Kozushima Volcano, the Izu Islands**

*Makoto Kobayashi[1], Masanori Murata[1], Fumikatsu NISHIZAWA[2], Takehiko Suzuki[1,3] (1.Research Center for Volcanic Hazards and their mitigations, Tokyo Metropolitan Univ., 2.Fuji Research Institute, Yamanashi Prefectural

Government, 3.Department of Geography, Tokyo Metropolitan Univ.)

[SVC38-P23] Characteristics of hypocenter distribution connected with velocity structures in and around Miyakejima, Kozushima and Hachijojima volcanoes

*Hiroko Hagiwara[1], Hidefumi Watanabe[1] (1.Tokyo Metroplitan Government)

[SVC38-P24] Deformation of Miyakejima volcano measured by GNSS campaign observation (2013-2015)

*Haruna Watanabe[1], Takeshi Matsushima[2], Miyo Fukui, Atsushi Watanabe[3], Jun Oikawa[3], Takashi OKUDA[4], Taku Ozawa[5], Yosuke Miyagi[5] (1.Department of Earth and Planetary Sciences, Graduate School of Science, Kyushu University, 2.Institute of Seismology and Volcanology, Faculty of Sciences, Kyushu University, 3.Earthquake Research Institute, University of Tokyo, 4.Earthquake and Volcanology Research Center, 5.National Research Institute for Earth Science and Disaster Resilience)

[SVC38-P25] Characteristic properties of distal and proximal tephras in the Mikurajima Island, Izu Islands.

*Tomohiro Tano[1], Takehiko Suzuki[1,2], Makoto Kobayashi[2], Masanori Murata[2] (1.Faculty of Urban Environmental Sciences, Tokyo Metropolitan University, 2.Research Center for Volcanic Hazards and Their Mitigation, Tokyo Metropolitan University)

[SVC38-P26] Pseudo thermal anomalies in the shortwave infrared bands of the Himawari-8 AHI and their correction for volcano thermal observation

*Takayuki Kaneko[1], ATSUSHI YASUDA[1], Yoshizaki Yoshito[2], Takasaki Kenji[3], Yoshiaki HONDA[4] (1.Earthquake Research Institute, University of Tokyo, 2.Meteorological Satellite Center, Japan Meteorological Agency, 3.Japan Fisheries Research and Education Agency, 4.Center for Environmental Remote Sensing, Chiba University)

[SVC38-P27] Shallow earthquakes in Unzen Volcano inferred from dense seismic observation and resistivity structure

*Hashimoto Tasuku[1], Koki Aizawa[2], Takeshi Matsushima[2], Hiroshi Shimizu[2], Yuto Hayashida[1], Yuhei Yuasa[1], Kaori Tsukamoto[1], Yuto Yamamoto[3], Kanta Miyano[3], Megumi Kamizono[1], Satoshi Matsumoto[2] (1.Department of Earth and Planetary Sciences, Graduate School of Science, Kyushu University, 2.Institute of Seismology and Volcanology, Faculty of Science, Kyushu University, 3.Department of Earth and Planetary Sciences, School of Science, Kyushu University)

[SVC38-P28] Characteristics of shallow volcanic earthquakes beneath the summit of Unzen Volcano

*Kanta Miyano[1], Hiroshi Shimizu[2], Takeshi Matsushima[2], Satoshi Matsumoto[2], Koki Aizawa[2], Hashimoto Tasuku[3], Yuto Hayashida[3], Yuhei Yuasa[3] (1.Department of Earth and Planetary Sciences, School of Science, Kyushu University, 2.Institute of Seismology and Volcanology, Faculty of Science, Kyushu University, 3.Department of Earth and Planetary Sciences, Graduate School of Science, Kyushu University)

[SVC38-P29] Pyroclastic deposits and the stratigraphy on the outcrop to north east from Mt.Unzen

*Daisuke Nagai[1] (1.Mt.Unzen disaster memorial hall)

[SVC38-P30] Relative gravity changes in Aso Volcano (Kumamoto Prefecture) observed from 2015 to 2018

*Yusuke Miyauchi[1], Takahito Kazama[1], Yoichi Fukuda[1], Shin Yoshikawa[2], Takahiro Ohkura[2], Jun Nishijima[3], Yasuhiro Fujimitsu[3] (1.Graduate School of Science, Kyoto University, 2.Aso Volcanological Laboratory, Kyoto University, 3.Graduate School of Engineering, Kyushu University)

[SVC38-P31] Precise leveling survey in Aso volcano, 2018

*Takahiro Ohkura[1], Shin Yoshikawa[1], Hiroyuki Inoue[1], Akihiko Yokoo[1], Mitsuru Utsugi[1], Keigo Yamamoto[2], Kazunari Uchida[4], Yuta Maeda[5], Shinichiro Horikawa[5], Kenjiro Matsuhiro[5], Takashi OKUDA[5], Kazushi Tanoue[5], Fumiaki Kimata[7], Masayuki Murase[6], Hitoshi Mori[6], Taketoshi Mishima[3], Shintaro Komatsu[2], Masaki Takaya[3], Jun Oikawa[8], Kyoka Ishii[3], Yusuke Miyauchi[3], Ikuma Kimura[3], Masaki Uchida[3], Kazuho Nakai[3], Kosei Takishita[3], Keita Chiba[4], Hashimoto Tasuku[4], Yoshinosuke Kamiya[4], Yuto Yamamoto[4] (1.Aso Volcanological Laboratory, Institute for Geothermal Sciences, Graduate School of Science, Kyoto University, 2.DPRI, Kyoto University, 3.Graduate School of Science, Kyoto University, 4.Graduate School of Science, Kyushu University, 5.Graduate School, Nagoya University, 6.College of Human and Society, Nihon University, 7.TRIES, 8.ERI,Univ.of Tokyo)

[SVC38-P32] Magma evolution during the Aso-3 caldera-forming eruption cycle deduced from the chemistry of plagioclase phenocrysts

*yuki matsukida[1], Tsuyoshi Iizuka[1], Takayuki Ushikubo[2], Kenji Shimizu[2], Nobuo Geshi[3], Isoji MIYAGI[3], Morihisa Hamada[2] (1.the University of Tokyo, 2.Japan Agency for Marine-Earth and Science Technology, 3.The National Institute of Advanced Industrial Science and Technology)

[SVC38-P33] Relationship between duration of eruption tremor and eruption volume

*Azusa Mori[1], Hiroyuki Kumagai[1] (1.Nagoya University Environmental Studies)

[SVC38-P34] Crustal deformation accompanied with the eruption of Shinmoe-dake in early March 2018

*Tsuyoshi Watanabe[1], Takashi Yokota[1], Susumu Kurahashi[1], Kenta Enomoto[1] (1.Aichi Institute of Technology)

[SVC38-P35] Sources under Iwo-yama, Kirishima Volcanoes derived from GNSS observation and Precise leveling survey.

*Yuki Koga[1], Takeshi Matsushima[2], Kazunari Uchida[2], Dan Muramatsu[1], Yuichi Iwasa[1] (1.Department of Earth and Planetary Sciences, Graduate School of Science, Kyushu university , 2.Institute of Seismology and Volcanology, Faculty of Science, Kyushu University)

[SVC38-P36] Regional vertical deformation around Aira caldera from GNSS data

*Kazuho Nakai[1], Masato Iguchi[2], Takahiro Ohkura[3] (1.Division of Earth and Planetary Sciences, Graduate School of Science, Kyoto University, 2.Sakurajima Volcano Research Center, Disaster Prevention Research Institute, Kyoto University, 3.Aso Volcanological Laboratory, Institute for Geothermal Sciences, Graduate School of Science, Kyoto University)

[SVC38-P37] Vertical ground deformation in Sakurajima volcano measured by precise leveling survey (during Nov. 2017 - Nov. 2018)

*Keigo Yamamoto[1], Takeshi Matsushima[2], Shin Yoshikawa[3], Hiroyuki Inoue[3], Tadaomi Sonoda[1], Kosei Takishita[1], Kazuho Nakai[1], Masaki Uchida[3], Ryo Oyanagi[3], Yoshinosuke Kamiya[2], Takahiro Ohkura[3] (1.Disaster Prevention Research Institute, Kyoto University, 2.Fuculty of Sciences, Kyushu University, 3.Gruduate School of Science, Kyoto University)

[SVC38-P38] Spatiotemporal gravity variations from the 1990s in Sakurajima Volcano, revealed by repeated relative gravity measurements

*Ryo Oyanagi[1], Takahito Kazama[1], Keigo Yamamoto[2], Hiromitsu Oshima[3], Kazumi Okada[3], Tadaomi Sonoda[2], Masato Iguchi[2] (1.Graduate School of Science, Kyoto University, 2.DPRI, Kyoto University, 3.ISV, Hokkaido University)

[SVC38-P39] Investigation into the crater of Sakurajima volcano during eruption using UAV

*Shunsuke Miura[1], Takumi Mochiduki[1], Kouji Fujita[1], Toshihiro Urayama[1], Hisashi Sasaki[1], Tatsuro Chiba[1] (1.Asia Air Survey Co.,Ltd)

[SVC38-P40] **Seismic refraction and wide-angle reflection experiment in southern Kyushu, Japan: (3) the 2018 exploration report**

*Hiroki Miyamachi[1], Hiroaki Takahashi[2], Hiroshi Aoyama[2], Mako Ohzono[2], Takahiro Shiina[6], Masamitsu Takada[2], Masayoshi Ichiyanagi[2], Teruhiro Yamaguchi[2], Yuki Susukida[2], Saito Kazuma[2], Chihiro Ito[2], Yoshio Murai[2], Tatsuya Nakagaki[2], Tomoki Tsutsui[3], Ryuichi Takei[3], Yuuya Tada[3], Mare Yamamoto[4], Satoshi Hirahara[4], Takashi NAKAYAMA[4], Ryosuke Azuma[4], Syuichi Suzuki[4], Toshinori Sato[5], Eiji Kurashimo[6], Miwako Ando[6], Shinichi Tanaka[6], Satoshi Ikezawa[6], Tomoaki Yamada[6], Kazuo Nakahigashi[7], Yuta Maeda[8], Shinichiro Horikawa[8], Kenjirou Matsuhiro[8], Takashi OKUDA[8], Shuhei Tsuji[8], Naoki Sogawa[8], Hiroshi Katao[9], Takuo Shibutani[9], Tsutomu Miura[9], Nakagawa Jun[9], Itaru Yoneda[9], Takeshi Tameguri[9], Kosei Takishita[9], Kazuho Nakai[9], Yusuke Yamashita[9], Takeshi Matsushima[10], Kazunari Uchida[10], Rintaro Miyamachi[10], Hiroshi Yakiwara[1], Shuichiro Hirano[1], Takeshi Kubo[1], Kenyu Sakao[1] (1.Kagoshima University, 2.Hokkaido University, 3.Akita University, 4.Tohoku University, 5.Chiba University, 6.University of Tokyo, 7.Tokyo University of Marine Science and Technology, 8.Nagoya University, 9.Kyoto University, 10.Kyushu University)

[SVC38-P41] Flow and emplacement mechanism of Koya Ignimbrite

*Keiko Suzuki-Kamata[1], Reina NAKAOKA[1], Tomomi Yamane[2] (1.Kobe Ocean-Bottom Exploration Center , 2.Department of Planetology, Graduate School of Science, Kobe University)

[SVC38-P42] Investigating Origin of landslide-like bathymetric feature at southern Mt.Kaimon using bathymetric and multichannel seismic reflection surveys

*hiroto yamaguchi[1], Satoshi Shimizu[2], Hikaru Iwamaru[2], Mamoru Sano[2], Nobukazu Seama[3,2], Misaki Horiuchi[3], Tetsuo Matsuno[2,3], Yoshiyuki Tatsumi[2,3] (1.Department of Planetology, Faculty of Science, Kobe university, 2.Kobe ocean-bottom exploration center, 3.Department of Planetology, Graduate School of Science, Kobe university)

[SVC38-P43] Occurrence and distribution of pyroclastic fall deposits of Kuchinoerabujima volcano 2018-2019 eruption

*Masashi NAGAI[1], Shojiro Nakagawa[2], Yu Iriyama[1], Takahiro Miwa[1], Toshikazu Tanada[1], Hideki Ueda[1], Setsuya Nakada[1] (1.Volcano Research Department, National Research Institute for Earth Science and Disaster Resilience, 2.Yakushima Chigaku Club)

[SVC38-P44] Ground Deformation around Domestic Active Volcanoes detected by InSAR of ALOS-2/PALSAR-2

*Takafumi Taniguchi[1], Isao Kageyama[1], Okuyama Satoshi[2], Shinobu Ando[2] (1.Japan Meteorological Agency, 2.Meteorological Research Institute)

[SVC38-P45] **Volcano-hydrothermal inflation revealed by the spatial variation of stress field at the Tatun Volcano Group, northern Taiwan**

*Hsin-Chieh Pu[1], Cheng-Horng Lin[2,3,4,5], Ya-Ju Hsu[2], Li-Chin Chang[3] (1.Central Weather Bureau, Taiwan, ROC., 2.Institute of Earth Sciences, Academia Sinica, Taipei, Taiwan, ROC., 3.Taiwan Volcano Observatory at Tatun, Taipei, Taiwan, ROC., 4. Department of Geosciences, National Taiwan University, Taipei 10617, Taiwan, ROC., 5.National Center for Research on Earthquake Engineering, National Applied Research Laboratories, Taipei, Taiwan, ROC.)

[SVC38-P46] Topographic change and crustal deformation associated with December 2018 eruption of Krakatau volcano in Indonesia

*Hiroshi Yarai[1], Tomokazu Kobayashi[1], Shinya Yamada[1] (1.GSI of Japan)

[J] Poster | S (Solid Earth Sciences)：S-VC Volcanology

5:15 PM - 6:30 PM JST | 8:15 AM - 9:30 AM UTC | Poster Hall International Exhibition Hall8, Makuhari Messe_25

[S-VC38] Active Volcanism

convener:Yuta Maeda(Nagoya University), Takahiro Miwa(National research institute for earth science and disaster prevention), Takeshi Nishimura(Department of Geophysics, Graduate School of Science, Tohoku University)

[SVC38-P01] The structure of Showa-Shinzan Yaneyama Usu by seismic reflection surveys

*Ryuichi Takei[1], Tomoki Tsutsui[1,2], Yuya Tada[2], Tomoya Moriwaki[2], Yosuke Aoki[3], Hiroshi Aoyama[4], Go Maruyama[5] (1.Graduate School of International Resource Sciences, The University of Akita, 2.Faculty of International Resource Sciences, The University of Akita, 3.Earthquake Research Institute, The University of Tokyo, 4.Graduate school of Science, The University of Hokkaido, 5.Marutec Co., Ltd.)

[SVC38-P02] Ground deformation associated with the 2014-2015 and the 2018-2019 volcanic activities at Azumayama

*Jun Okada[1], Shigeo Matsuura[2], Katsuya Ohmi[2], Takuya Yamamura[2], Yu Nihara[3], Susumu Seki[3] (1.Volcanology Research Department (Sendai Office), Meteorological Research Institute, JMA, 2.Seismology and Volcanology Division, Sendai Regional Headquarters, JMA, 3.Regional Volcanic Observation and Warning Center, Sendai Regional Headquarters, JMA)

[SVC38-P03] BP-type and BT-type volcanic earthquakes in Azumayama

*Yusuke Yoshigai[1], Yuichi Morita[2], Katsuya Ohmi[3], Yu Nihara[4], Tsukasa Kobayashi[1] (1.Volcanological Division, Japan Meteorological Agency, 2.Earthquake Research Institute, University of Tokyo, 3.Seismology and Volcanology Division, Sendai Regional Headquarters, Japan Meteorological Agency, 4.Regional Volcanic Observation and Warning Center, Sendai Regional Headquarters, Japan Meteorological Agency)

[SVC38-P04] The occurrence and petrology of the fine-grained pyroclastic materials of the Futatsudake-Shibukawa eruption in Haruna volcano.

*Teruyoshi Maruyama[1], Yuki Suzuki[2] (1.Department of Earth Sciences, School of Education , Waseda University, 2.Department of Earth Sciences, Faculty of Education and Integrated Arts of Sciences, Waseda University)

[SVC38-P05] The occurrence and petrology of the block and ash flow deposit from the Futatsudake-Shibukawa eruption, Haruna volcano

*Yuki Suzuki[1], Ryouto Fukushima[2] (1.Department of Earth Sciences, Faculty of Education and Integrated Arts of Sciences, Waseda University, 2.Department of Earth Sciences, School of Education, Waseda University)

[SVC38-P06] Report of Volcanic Activity at Kusatsu-Shiranesan in 2018

*Tsukasa Kobayashi[1], Koji Kato[1], Koichi Suemine[1], Kazuhiro Kimura[1], Yusuke Yoshigai[1], Yasuo Ogawa[2], Kenji Nogami[2], Wataru Kanda[2], Akihiko Terada[2] (1.Volcanological Division, Japan Meteorological Agency, 2.Volcanic Fluid Research Center, Tokyo Institute of Technology)

[SVC38-P07] Noble gas isotope composition of fumaroles and hydrothermal gases around Kusatsu-Shirane volcano

*Kotaro Toyama[1], Hirochika Sumino[1], Kaori Kawana[1], Yoshihide Akiyama[1], Takeshi Ohba[2], Muga Yaguchi[3], Akihiko Terada[4] (1.Department of Basic Science, Graduate School of Arts and Sciences, The University of Tokyo, 2.Department of chemistry, School of Science, Tokia University, 3.Meteorological Research Institute, 4.Volcanic Fluid Research Center, Tokyo Institute of Technology)

[SVC38-P08] Self-potential and geomagnetic total intensity observations at Motoshirane volcano after the 2018 eruption

*Akira Yamazaki[1], Hideki Iino[1], Tatsurou Tanaka[1] (1.Kakioka Magnetic Observatory)

[SVC38-P09] Eruption processes of the 3rd and 4th stage of Niigata-Yakeyama Volcano, Japan, inferred from microlite texture and chemical composition

*Takumi Yoshida[1], Takeshi Saito[1] (1.Shinshu University)

[SVC38-P10] Estimation of subsurface structure of Shinyu crater lake, Tateyama Caldera, based on the water level and seismic observation data

*Ryohei Kawaguchi[1], Naoko Saito[2], Shin'ya Onizawa[1] (1.Meteorological Research Institute, 2.Toyama local Meteorological office, Japan Meteorological Agency)

[SVC38-P11] Real time monitoring of underground temperature in Jigokudani, Midagahara volcano using LPWA devices

*Tohru Watanabe[1], Toyama branch NTT West[2] (1.Gradudate School of Science and Engineering, University of Toyama, 2.Nippon Telegraph and Telephone West Corporation)

[SVC38-P12] Varying chemical and isotopic compositions of fumarolic gases from the summit and from the 1962-63 eruptive vents at Yakedake Volcano, Japan

*Takeshi Saito[1], Shun Sawamura[2], Kazuhiro Amita[3], Taketoshi Mishima[4], Shinji Ohsawa[4] (1.Institute of Science, Academic Assembly School of Science and Technology, Shinshu University, 2.Graduate School of Science and Technology, Shinshu University, 3.Graduate School of Engineering Science, Akita University, 4.Beppu Geothermal Research Laboratory, Institute for Geothermal Sciences, Graduate School of Science, Kyoto University)

[SVC38-P13] Eruption age determination of the latest two lava flows and characteristics of volcaniclastic materials from the recent activity of Yokodake Volcano, Japan

*Hiroya Nitta[1], Takeshi Saito[1], Yorinao Shitaoka[2] (1.Shinshu University of Science and Technology, 2.Department of Environment System, Faculty of Geo-environmental Science, Rissho University)

[SVC38-P14] Estimating the date of the 2007 eruption of Mount Ontake Volcano using waveform correlation

*Shuhei Nishijima[1], Toshiko Terakawa[1], Shinichiro Horikawa[1] (1.Graduate School of Environmental Studies, Nagoya University)

[SVC38-P15] Seismic activity beneath Mt. Ontake volcano before and after the 2007 and 2014 eruptions

*Yoshiko Yamanaka[1], Shinichiro Horikawa[1], Yuta Maeda[1] (1.Graduate School of Encironmental Studies, University of NAGOYA)

[SVC38-P16] Effect of rain and snowmelt correction of tiltmeter data
- Application example for Ontakesan Volcano -

*Kazuhiro Kimura[1,5], Katsuhisa Kawashima[2], Takane Matsumoto[2], Akihiko SASAKI[4], Tsutomu Iyobe[3], Junichi Miyamura[1], Masaki Nakahashi[1] (1.Japan Meteorological Agency, 2.Research Institute for Natural Hazards and Disaster Recovery, Niigata University, 3.Faculty of Engineering, Kyoto University, 4.Department of Geography and Environmental Studies, Kokushikan University, 5.Graduate School Science and Technology, Niigata University)

[SVC38-P17] **Spatial Variation of b-value around Mt. Fuji influenced by the Eastern Shizuoka Earthquake of 15 March 2011**

*Takumi Murakoshi[1], Tomonari Miyashita[2] (1.National Defense Academy, 2.JASDF)

[SVC38-P18] Present condition of submarged volcano, Teishi Knoll, off Ito, Eastern Izu Peninsula

*Toshiro Yamanaka[1], Yoshifumi Kawada[2], Takuro Noguchi[3], Mayumi Hatta[3], Kei Okamura[3] (1.Tokyo Univ. Marine Science and Technology, 2.Tohoku University, 3.Kochi University)

[SVC38-P19] Descriptions and age of volcanic products before the caldera formation in the northern part of Izu-Oshima, off Tokyo, Pacific Ocean

*Satoshi Terayama[1], Takehiko Suzuki[1], Makoto Kobayashi[2] (1.Tokyo Metropolitan University, 2.Research Center for Volcanic Hazards and Their Mitigation, Tokyo Metropolitan University)

[SVC38-P20] Time change of p-value by Schuster method using earthquakes around Izu-Ohsima summit

*Hiroyuki Takayama[1] (1.Volcanological Division 1st labolatory, Meteorological Research Institute)

[SVC38-P21] Standard stratigraphy and characteristic properties of late Quaternary tephras on the Niijima-island: Report of geochemistry and refractive indices of volcanic glass shards, orthopyroxene, hornblende, and cummingtonite

*Kaori Aoki[1], Makoto Kobayashi[1], Fumikatsu NISHIZAWA[1,2], Masanori Murata[1], Daisuke Ishimura[1], Takehiko Suzuki[1] (1.Research Center for Volcanic Hazards and Their Mitigation, Tokyo Metropolitan University, 2.Mount Fuji Research Institute, Yamanashi Prefectural Government)

[SVC38-P22] **Tephrostratigraphy and its eruption history of the Latest Activity in the Kozushima Volcano, the Izu Islands**

*Makoto Kobayashi[1], Masanori Murata[1], Fumikatsu NISHIZAWA[2], Takehiko Suzuki[1,3] (1.Research Center for Volcanic Hazards and their mitigations, Tokyo Metropolitan Univ., 2.Fuji Research Institute, Yamanashi Prefectural

Government, 3.Department of Geography, Tokyo Metropolitan Univ.)

[SVC38-P23] Characteristics of hypocenter distribution connected with velocity structures in and around Miyakejima, Kozushima and Hachijojima volcanoes

*Hiroko Hagiwara[1], Hidefumi Watanabe[1] (1.Tokyo Metroplitan Government)

[SVC38-P24] Deformation of Miyakejima volcano measured by GNSS campaign observation (2013-2015)

*Haruna Watanabe[1], Takeshi Matsushima[2], Miyo Fukui, Atsushi Watanabe[3], Jun Oikawa[3], Takashi OKUDA[4], Taku Ozawa[5], Yosuke Miyagi[5] (1.Department of Earth and Planetary Sciences, Graduate School of Science, Kyushu University, 2.Institute of Seismology and Volcanology, Faculty of Sciences, Kyushu University, 3.Earthquake Research Institute, University of Tokyo, 4.Earthquake and Volcanology Research Center, 5.National Research Institute for Earth Science and Disaster Resilience)

[SVC38-P25] Characteristic properties of distal and proximal tephras in the Mikurajima Island, Izu Islands.

*Tomohiro Tano[1], Takehiko Suzuki[1,2], Makoto Kobayashi[2], Masanori Murata[2] (1.Faculty of Urban Environmental Sciences, Tokyo Metropolitan University, 2.Research Center for Volcanic Hazards and Their Mitigation, Tokyo Metropolitan University)

[SVC38-P26] Pseudo thermal anomalies in the shortwave infrared bands of the Himawari-8 AHI and their correction for volcano thermal observation

*Takayuki Kaneko[1], ATSUSHI YASUDA[1], Yoshizaki Yoshito[2], Takasaki Kenji[3], Yoshiaki HONDA[4] (1.Earthquake Research Institute, University of Tokyo, 2.Meteorological Satellite Center, Japan Meteorological Agency, 3.Japan Fisheries Research and Education Agency, 4.Center for Environmental Remote Sensing, Chiba University)

[SVC38-P27] Shallow earthquakes in Unzen Volcano inferred from dense seismic observation and resistivity structure

*Hashimoto Tasuku[1], Koki Aizawa[2], Takeshi Matsushima[2], Hiroshi Shimizu[2], Yuto Hayashida[1], Yuhei Yuasa[1], Kaori Tsukamoto[1], Yuto Yamamoto[3], Kanta Miyano[3], Megumi Kamizono[1], Satoshi Matsumoto[2] (1.Department of Earth and Planetary Sciences, Graduate School of Science, Kyushu University, 2.Institute of Seismology and Volcanology, Faculty of Science, Kyushu University, 3.Department of Earth and Planetary Sciences, School of Science, Kyushu University)

[SVC38-P28] Characteristics of shallow volcanic earthquakes beneath the summit of Unzen Volcano

*Kanta Miyano[1], Hiroshi Shimizu[2], Takeshi Matsushima[2], Satoshi Matsumoto[2], Koki Aizawa[2], Hashimoto Tasuku[3], Yuto Hayashida[3], Yuhei Yuasa[3] (1.Department of Earth and Planetary Sciences, School of Science, Kyushu University, 2.Institute of Seismology and Volcanology, Faculty of Science, Kyushu University, 3.Department of Earth and Planetary Sciences, Graduate School of Science, Kyushu University)

[SVC38-P29] Pyroclastic deposits and the stratigraphy on the outcrop to north east from Mt.Unzen

*Daisuke Nagai[1] (1.Mt.Unzen disaster memorial hall)

[SVC38-P30] Relative gravity changes in Aso Volcano (Kumamoto Prefecture) observed from 2015 to 2018

*Yusuke Miyauchi[1], Takahito Kazama[1], Yoichi Fukuda[1], Shin Yoshikawa[2], Takahiro Ohkura[2], Jun Nishijima[3], Yasuhiro Fujimitsu[3] (1.Graduate School of Science, Kyoto University, 2.Aso Volcanological Laboratory, Kyoto University, 3.Graduate School of Engineering, Kyushu University)

[SVC38-P31] Precise leveling survey in Aso volcano, 2018

*Takahiro Ohkura[1], Shin Yoshikawa[1], Hiroyuki Inoue[1], Akihiko Yokoo[1], Mitsuru Utsugi[1], Keigo Yamamoto[2], Kazunari Uchida[4], Yuta Maeda[5], Shinichiro Horikawa[5], Kenjiro Matsuhiro[5], Takashi OKUDA[5], Kazushi Tanoue[5], Fumiaki Kimata[7], Masayuki Murase[6], Hitoshi Mori[6], Taketoshi Mishima[3], Shintaro Komatsu[2], Masaki Takaya[3], Jun Oikawa[8], Kyoka Ishii[3], Yusuke Miyauchi[3], Ikuma Kimura[3], Masaki Uchida[3], Kazuho Nakai[3], Kosei Takishita[3], Keita Chiba[4], Hashimoto Tasuku[4], Yoshinosuke Kamiya[4], Yuto Yamamoto[4] (1.Aso Volcanological Laboratory, Institute for Geothermal Sciences, Graduate School of Science, Kyoto University, 2.DPRI, Kyoto University, 3.Graduate School of Science, Kyoto University, 4.Graduate School of Science, Kyushu University, 5.Graduate School, Nagoya University, 6.College of Human and Society, Nihon University, 7.TRIES, 8.ERI,Univ.of Tokyo)

[SVC38-P32] Magma evolution during the Aso-3 caldera-forming eruption cycle deduced from the chemistry of plagioclase phenocrysts

*yuki matsukida[1], Tsuyoshi Iizuka[1], Takayuki Ushikubo[2], Kenji Shimizu[2], Nobuo Geshi[3], Isoji MIYAGI[3], Morihisa Hamada[2] (1.the University of Tokyo, 2.Japan Agency for Marine-Earth and Science Technology, 3.The National Institute of Advanced Industrial Science and Technology)

[SVC38-P33] Relationship between duration of eruption tremor and eruption volume

*Azusa Mori[1], Hiroyuki Kumagai[1] (1.Nagoya University Environmental Studies)

[SVC38-P34] Crustal deformation accompanied with the eruption of Shinmoe-dake in early March 2018

*Tsuyoshi Watanabe[1], Takashi Yokota[1], Susumu Kurahashi[1], Kenta Enomoto[1] (1.Aichi Institute of Technology)

[SVC38-P35] Sources under Iwo-yama, Kirishima Volcanoes derived from GNSS observation and Precise leveling survey.

*Yuki Koga[1], Takeshi Matsushima[2], Kazunari Uchida[2], Dan Muramatsu[1], Yuichi Iwasa[1] (1.Department of Earth and Planetary Sciences, Graduate School of Science, Kyushu university , 2.Institute of Seismology and Volcanology, Faculty of Science, Kyushu University)

[SVC38-P36] Regional vertical deformation around Aira caldera from GNSS data

*Kazuho Nakai[1], Masato Iguchi[2], Takahiro Ohkura[3] (1.Division of Earth and Planetary Sciences, Graduate School of Science, Kyoto University, 2.Sakurajima Volcano Research Center, Disaster Prevention Research Institute, Kyoto University, 3.Aso Volcanological Laboratory, Institute for Geothermal Sciences, Graduate School of Science, Kyoto University)

[SVC38-P37] Vertical ground deformation in Sakurajima volcano measured by precise leveling survey (during Nov. 2017 - Nov. 2018)

*Keigo Yamamoto[1], Takeshi Matsushima[2], Shin Yoshikawa[3], Hiroyuki Inoue[3], Tadaomi Sonoda[1], Kosei Takishita[1], Kazuho Nakai[1], Masaki Uchida[3], Ryo Oyanagi[3], Yoshinosuke Kamiya[2], Takahiro Ohkura[3] (1.Disaster Prevention Research Institute, Kyoto University, 2.Fuculty of Sciences, Kyushu University, 3.Gruduate School of Science, Kyoto University)

[SVC38-P38] Spatiotemporal gravity variations from the 1990s in Sakurajima Volcano, revealed by repeated relative gravity measurements

*Ryo Oyanagi[1], Takahito Kazama[1], Keigo Yamamoto[2], Hiromitsu Oshima[3], Kazumi Okada[3], Tadaomi Sonoda[2], Masato Iguchi[2] (1.Graduate School of Science, Kyoto University, 2.DPRI, Kyoto University, 3.ISV, Hokkaido University)

[SVC38-P39] Investigation into the crater of Sakurajima volcano during eruption using UAV

*Shunsuke Miura[1], Takumi Mochiduki[1], Kouji Fujita[1], Toshihiro Urayama[1], Hisashi Sasaki[1], Tatsuro Chiba[1] (1.Asia Air Survey Co.,Ltd)

[SVC38-P40] **Seismic refraction and wide-angle reflection experiment in southern Kyushu, Japan: (3) the 2018 exploration report**

*Hiroki Miyamachi[1], Hiroaki Takahashi[2], Hiroshi Aoyama[2], Mako Ohzono[2], Takahiro Shiina[6], Masamitsu Takada[2], Masayoshi Ichiyanagi[2], Teruhiro Yamaguchi[2], Yuki Susukida[2], Saito Kazuma[2], Chihiro Ito[2], Yoshio Murai[2], Tatsuya Nakagaki[2], Tomoki Tsutsui[3], Ryuichi Takei[3], Yuuya Tada[3], Mare Yamamoto[4], Satoshi Hirahara[4], Takashi NAKAYAMA[4], Ryosuke Azuma[4], Syuichi Suzuki[4], Toshinori Sato[5], Eiji Kurashimo[6], Miwako Ando[6], Shinichi Tanaka[6], Satoshi Ikezawa[6], Tomoaki Yamada[6], Kazuo Nakahigashi[7], Yuta Maeda[8], Shinichiro Horikawa[8], Kenjirou Matsuhiro[8], Takashi OKUDA[8], Shuhei Tsuji[8], Naoki Sogawa[8], Hiroshi Katao[9], Takuo Shibutani[9], Tsutomu Miura[9], Nakagawa Jun[9], Itaru Yoneda[9], Takeshi Tameguri[9], Kosei Takishita[9], Kazuho Nakai[9], Yusuke Yamashita[9], Takeshi Matsushima[10], Kazunari Uchida[10], Rintaro Miyamachi[10], Hiroshi Yakiwara[1], Shuichiro Hirano[1], Takeshi Kubo[1], Kenyu Sakao[1] (1.Kagoshima University, 2.Hokkaido University, 3.Akita University, 4.Tohoku University, 5.Chiba University, 6.University of Tokyo, 7.Tokyo University of Marine Science and Technology, 8.Nagoya University, 9.Kyoto University, 10.Kyushu University)

[SVC38-P41] Flow and emplacement mechanism of Koya Ignimbrite

*Keiko Suzuki-Kamata[1], Reina NAKAOKA[1], Tomomi Yamane[2] (1.Kobe Ocean-Bottom Exploration Center , 2.Department of Planetology, Graduate School of Science, Kobe University)

[SVC38-P42] Investigating Origin of landslide-like bathymetric feature at southern Mt.Kaimon using bathymetric and multichannel seismic reflection surveys

*hiroto yamaguchi[1], Satoshi Shimizu[2], Hikaru Iwamaru[2], Mamoru Sano[2], Nobukazu Seama[3,2], Misaki Horiuchi[3], Tetsuo Matsuno[2,3], Yoshiyuki Tatsumi[2,3] (1.Department of Planetology, Faculty of Science, Kobe university, 2.Kobe ocean-bottom exploration center, 3.Department of Planetology, Graduate School of Science, Kobe university)

[SVC38-P43] Occurrence and distribution of pyroclastic fall deposits of Kuchinoerabujima volcano 2018-2019 eruption

*Masashi NAGAI[1], Shojiro Nakagawa[2], Yu Iriyama[1], Takahiro Miwa[1], Toshikazu Tanada[1], Hideki Ueda[1], Setsuya Nakada[1] (1.Volcano Research Department, National Research Institute for Earth Science and Disaster Resilience, 2.Yakushima Chigaku Club)

[SVC38-P44] Ground Deformation around Domestic Active Volcanoes detected by InSAR of ALOS-2/PALSAR-2

*Takafumi Taniguchi[1], Isao Kageyama[1], Okuyama Satoshi[2], Shinobu Ando[2] (1.Japan Meteorological Agency, 2.Meteorological Research Institute)

[SVC38-P45] **Volcano-hydrothermal inflation revealed by the spatial variation of stress field at the Tatun Volcano Group, northern Taiwan**

*Hsin-Chieh Pu[1], Cheng-Horng Lin[2,3,4,5], Ya-Ju Hsu[2], Li-Chin Chang[3] (1.Central Weather Bureau, Taiwan, ROC., 2.Institute of Earth Sciences, Academia Sinica, Taipei, Taiwan, ROC., 3.Taiwan Volcano Observatory at Tatun, Taipei, Taiwan, ROC., 4. Department of Geosciences, National Taiwan University, Taipei 10617, Taiwan, ROC., 5.National Center for Research on Earthquake Engineering, National Applied Research Laboratories, Taipei, Taiwan, ROC.)

[SVC38-P46] Topographic change and crustal deformation associated with December 2018 eruption of Krakatau volcano in Indonesia

*Hiroshi Yarai[1], Tomokazu Kobayashi[1], Shinya Yamada[1] (1.GSI of Japan)

[J] Oral | S (Solid Earth Sciences)：S-VC Volcanology

3:30 PM - 5:00 PM JST | 6:30 AM - 8:00 AM UTC | IC 2F

[S-VC38] Active Volcanism

convener:Yuta Maeda(Nagoya University), Takahiro Miwa(National research institute for earth science and disaster prevention), Takeshi Nishimura(Department of Geophysics, Graduate School of Science, Tohoku University), Chairperson:Takehiko Suzuki, Maya Yasui

3:30 PM - 3:45 PM JST | 6:30 AM - 6:45 AM UTC

[SVC38-01] Tephrochoronology in the southwest part of basaltic Izu-oshima volcanic island during last 20,000 years, off Tokyo, Pacific Ocean

*Takehiko Suzuki[1], Satoshi Terayama[1], Jun Matsukaze[1], Yuichi Kato[1] (1.Faculty of Urban Environmental Sciences, Tokyo Metropolitan University)

3:45 PM - 4:00 PM JST | 6:45 AM - 7:00 AM UTC

[SVC38-02] **Tephrostratigraphy at Daisan-yama and Jinai-jima, and correlation with eruption deposits from Mamashitaura Volcanoes in Niijima Volcano, Izu-islands**

*Makoto Kobayashi[1], Masanori Murata[1], Kaori Aoki[1], Daisuke Ishimura[1,2], Takehiko Suzuki[1,2] (1.Research Center for Volcanic Hazards and Their Mitigations, Tokyo Metropolitan Univ., 2.Department of Geography, Tokyo Metropolitan Univ.)

4:00 PM - 4:15 PM JST | 7:00 AM - 7:15 AM UTC

[SVC38-03] Constration of pre-eruptive process using crystal clot: A case study of Unzen 1991-95 eruption

*Kurumi Iwahashi[1], ATSUSHI YASUDA[1] (1.Earthquake Research Institute,The University of Tokyo)

4:15 PM - 4:30 PM JST | 7:15 AM - 7:30 AM UTC

[SVC38-04] Petrological study of Pinatubo 1991 eruption ~ Discussions of magma plumbing model~

*Tomohisa Tamura[1,2], Mitsuhiro Nakagawa[2] (1.West Japan Engineering Consultants, Inc., 2.Earth and Planetary System Science, Hokkaido University)

4:30 PM - 4:45 PM JST | 7:30 AM - 7:45 AM UTC

[SVC38-05] Rediscovery of the Higuruma Debris Avalanche Deposit in Asama-Kurofu Volcano

*Maya Yasui[1], Masaki Takahashi[1], Tatsuo Kanamaru[1] (1.College of Humanities and Sciences, Nihon University)

[J] Oral | S (Solid Earth Sciences)：S-VC Volcanology

9:00 AM - 10:30 AM JST | 12:00 AM - 1:30 AM UTC | IC 2F

[S-VC39] Hydrothermal systems of volcanoes

convener:Yasuhiro Fujimitsu(Department of Earth Resources Engineering, Faculty of Engineering, Kyushu University), Wataru Kanda(Volcanic Fluid Research Center, School of Science, Tokyo Institute of Technology), Takeshi Ohba(Department of chemistry, School of Science, Tokia University), Chairperson:Yasuhiro Fujimitsu(Faculty of Engineering, Kyushu University), Takeshi Ohba, Wataru Kanda

9:00 AM - 9:15 AM JST | 12:00 AM - 12:15 AM UTC

[SVC39-01] Hydrothermal system of Tokachidake volcano, Japan: Examination from multi-disciplinary surveys

*Ryo Takahashi[1], Noritoshi Okazaki[1], Makoto Tamura[1] (1.Geological Survey of Hokkaido, Hokkaido Research Organization)

9:15 AM - 9:30 AM JST | 12:15 AM - 12:30 AM UTC

[SVC39-02] Fumarole and hot spring activities after the 2015 eruption of Hakone Volcano and their relationships with the seismicity and crustal deformation

*Kazutaka Mannen[1], Masatake Harada[1], Yohei Yukutake[1], George Kikugawa[1] (1.Hot Springs Research Institute of Kanagawa Prefecture)

9:30 AM - 9:45 AM JST | 12:30 AM - 12:45 AM UTC

[SVC39-03] A possible geothermal source at around 4 km depth estimated by the seismic observation in Ibusuki geothermal area

*Junzo Kasahara[1,3], Yoko Hasada[2,1], Hiroyasu Kuzume[1] (1.ENAA, 2.Daiwa Exploration and Consulting Co., 3.Shizuoka Univ.)

9:45 AM - 10:00 AM JST | 12:45 AM - 1:00 AM UTC

[SVC39-04] Time variation in the chemical and isotopic composition of fumarolic gases at Kusatsu-Shirane volcano Japan

*Takeshi Ohba[1], Muga Yaguchi[2], Nozomi Numanami[1], Kotaro Toyama[3], Hirochika Sumino[3], Urumu Tsunogai[4], Masanori Ito[4], Ryo Shingubara[4] (1.Department of chemistry, School of Science, Tokia University, 2.Meteorological Research Institute, JMA, 3.The University of Tokyo Graduate School of Arts and Sciences Department of Basic Science, 4.Nagoya University Graduate School of Environmental Studies)

10:00 AM - 10:15 AM JST | 1:00 AM - 1:15 AM UTC

[SVC39-05] Behavior of Arsenic and Mercury related to hydrothermal activities in Kirishima, Satsuma Iwojima, and Yamagawa, Kyushu Japan

*Motoya Habuchi[1], Harue Masuda[1], Tsuyoshi Shintani[1], Shuzo Furuya[1], Keigo Mori[1], Jun-ichiro Ishibashi[2], Takeshi Matsushima[2], Akinori Takeuchi[3], Syogo Oshima[4], Reo Ikawa[5] (1.Osaka City University, 2.Kyushu University, 3.National Institute for Environmental Studies, 4.West Japan Engineering Consultants, Inc., 5.National Institute of Advanced Industrial Science and Technology)

10:15 AM - 10:30 AM JST | 1:15 AM - 1:30 AM UTC

[SVC39-06] The chemical composition of thermal waters from spring and hot pool at Mt. Iwoyama of Kirishima volcano

*Muga Yaguchi[1], Takeshi Ohba[2], Kotaro Toyama[3], Fukuoka Regional Headquarters JMA[4], Kagoshima Meteorological Office JMA[4] (1.Meteorological Research Institute, 2.Tokai University, 3.Graduate School of the University of Tokyo, 4.Japan Meteorological Agency)

[J] Oral | S (Solid Earth Sciences)：S-VC Volcanology

10:45 AM - 12:15 PM JST | 1:45 AM - 3:15 AM UTC | IC 2F

[S-VC39] Hydrothermal systems of volcanoes

convener:Yasuhiro Fujimitsu(Department of Earth Resources Engineering, Faculty of Engineering, Kyushu University), Wataru Kanda(Volcanic Fluid Research Center, School of Science, Tokyo Institute of Technology), Takeshi Ohba(Department of chemistry, School of Science, Tokia University), Chairperson:Yasuhiro Fujimitsu(Faculty of Engineering, Kyushu University), Takeshi Ohba, Wataru Kanda

10:45 AM - 11:00 AM JST | 1:45 AM - 2:00 AM UTC

[SVC39-07] Re-examination of origin of the variety in magmatic-hydrothermal fluids

*Hiroshi Shinohara[1] (1.Geological Survey of Japan, AIST)

11:00 AM - 11:15 AM JST | 2:00 AM - 2:15 AM UTC

[SVC39-08] **Constraining electrical resistivity structure of volcanoes using multiphase flow modelling: an example of Miyake-jima**

*Marceau Gresse[1], Makoto Uyeshima[1], Takao Koyama[1], Maki Hata[1], Hideaki Hase[2], Koki Aizawa[3], Yusuke Yamaya[4], Yoichi Sasai[5], Jacques Zlotnicki[6], Tawat Rung-Arunwan[1], Hideki Ueda[7] (1.Earthquake Research Institute, The University of Tokyo, Tokyo, Japan, 2.Geothermal Energy Research & Development Co., Ltd., Tokyo, Japan, 3.Institute of Seismology and Volcanology, Faculty of Science, Kyushu University, Fukuoka, Japan., 4.Planning Division, National Institute of Advanced Industrial Science and Technology, Tokyo, Japan, 5.Earthquake Prediction Research Centre, Tokai University, Shizuoka, Japan, 6.CNRS, OPGC-UMR6524, Aubière, France, 7.National Research Institute for Earth Science and Disaster Resilience, Tsukuba, Japan)

11:15 AM - 11:30 AM JST | 2:15 AM - 2:30 AM UTC

[SVC39-09] MT survey and 3-D resistivity structure in the Niseko area, southwestern Hokkaido

*Makoto Tamura[1], Toru Mogi[2], Junna Kanahiro[2], Daisuke Oka[1], Junya Maruyama[1], Takahiro Suzuki[1], Noritoshi Okazaki[1] (1.Geological Survey of Hokkaido, Hokkaido Research Organization, 2.Division of Sustainable Resource Engineering, Fucluty of Engineering, Hokkaido University)

11:30 AM - 11:45 AM JST | 2:30 AM - 2:45 AM UTC

[SVC39-10] **Hydrothermal fluid activity of the Tatun Volcano Group, Taiwan, revealed by self-potentials and seismicity**

*Hong-Jia Chen[1], Zhi-Xian Yang[1], Chien-Chih Chen[1,2], Cheng-Horng Lin[3,4] (1.Department of Earth Sciences, National Central University, Taiwan., 2.Earthquake-Disaster & Risk Evaluation and Management, National Central University, Taoyuan, Taiwan., 3.Institute of Earth Sciences, Academia Sinica, Taipei, Taiwan., 4.Taiwan Volcano Observatory at Tatun, Taipei, Taiwan.)

11:45 AM - 12:00 PM JST | 2:45 AM - 3:00 AM UTC

[SVC39-11] Utilizing the electrical conductivity distribution to unravel the hydrothermal system beneath Mt.Hasan composite volcano and its vicinity, southwest Cappodocia, Turkey

*Sabri Bulent Tank[1], Mustafa Karas[1] (1.Bogazici University)

12:00 PM - 12:15 PM JST | 3:00 AM - 3:15 AM UTC

[SVC39-12] Three-dimensional Magnetotelluric Inversion to map geothermal structures in Eburru Geothermal field, Kenya.

*JUSTUS MAITHYA[1], Yasuhiro FUJIMITSU[2] (1.Graduate School of Engineering, Department of Earth Resources Engineering, Kyushu University, 2.Faculty of Engineering, Department of Earth Resources Engineering, Kyushu University)

[J] Poster | S (Solid Earth Sciences)：S-VC Volcanology

3:30 PM - 5:00 PM JST | 6:30 AM - 8:00 AM UTC | Poster Hall International Exhibition Hall8, Makuhari Messe_14

[S-VC39] Hydrothermal systems of volcanoes

convener:Yasuhiro Fujimitsu(Department of Earth Resources Engineering, Faculty of Engineering, Kyushu University), Wataru Kanda(Volcanic Fluid Research Center, School of Science, Tokyo Institute of Technology), Takeshi Ohba(Department of chemistry, School of Science, Tokia University)

[SVC39-P01] Changes in the chemistry of spring water related to the recent volcanic activity of Mt Iwo-Yama, Kirishima volcanic area

*Haruka Yamamoto[1], Yoshikazu Kikawada[2], Megumi Fukai, Wei Deng (1.Graduated school of Fuculty of Sience and Technology Sophia University, 2.Fuculty of Sience and Technology Sophia University)

[SVC39-P02] Hydrothermal circulation process related to phreatic eruption of Iwo-Yama at Kirishima volcanoes

*Keigo Mori[1], Harue Masuda[1], Tsuyoshi Shintani[1], Motoya Habuchi[1], Syuzou Furuya[1], Jun-ichiro Ishibashi[2], Takeshi Matsushima[2], Syogo Oshima[3], Reo Ikawa[4] (1.Osaka City University, 2.Kyushu University, 3.West Japan Engineering Consultants, Inc., 4.AIST)

[SVC39-P03] Determination on the stable isotopic compositions of H_2O in a volcanic plume

*Masanori Ito[1], Urumu Tsunogai[1], Koji U Takahashi[2], Fumiko Nakagawa[1] (1.Nagoya University, Graduate School of Environmental Studies, 2.Geological Survey of Japan, National Institute of Advanced Industrial Science and Technology)

[SVC39-P04] **Radon measurements at Aso volcano: an experimental automatic radon station operative within the proximal zone of Nakadake**

*Corrado CIGOLINI[1], Shin Yoshikawa[2], Tomo Shibata[3], Marco Laiolo[1], Diego Coppola[1] (1.Department of Earth Sciences, University of Torino, Italy, 2.Aso Volcanological Laboratory, Kyoto University, Japan, 3.Institute for Geothermal Sciences, Graduate school of Science, Kyoto University, Japan)

[SVC39-P05] Evolution of the hydrothermal system of Aso volcano during the 2014-2016 eruption period, as inferred by the ACTIVE observations

*Takuto Minami[1], Mitsuru Utsugi[2], Hisashi Utada[1], Tsuneomi Kagiyama[3] (1.Ocean Hemisphere Research Institute, Earthquake Research Institute,The University of Tokyo, 2.Aso Volcanological Laboratory, Institute for Geothremal Sciences, Graduate School of Science, Kyoto University, 3.Aso Geopark Promotion Council)

[SVC39-P06] 3-D Inversion of Magnetotelluric data from the Aluto-Langano Geothermal Field, Ethiopia

*Dejene Bekele[1], Yasuhiro FUJIMITSU[2] (1.Graduate School of Engineering, Department of Cooperative Resources Engineering, Kyushu University, 2.Faculty of Engineering, Department of Earth Resources Engineering, Kyushu University)

[SVC39-P07] Interpretation of Gravity Data to Delineate the Geothermal Reservoir Extent and Assess the Geothermal Resource in the Municipality of Isa, Southern Kyushu, Japan

*CARLOS OSMIN POCASANGRE[1], Yasuhiro Fujimitsu[1], Jun Nishijima[1] (1.Department of Earth Resources Engineering, Kyushu University)

[SVC39-P08] Conductive and convective heat fluxes inferred from temperature profile of a borehole in Izu-Oshima volcano

*Shin'ya Onizawa[1] (1.Volcanology Research Department, Meteorological Research Institute, JMA)

[SVC39-P09] Numerical model of the hydrothermal system at the Akakura Caldera in Kurikoma Area

*Yasuhiro Fujimitsu[1], Daichi Yoshioka[2] (1.Department of Earth Resources Engineering, Faculty of Engineering, Kyushu University, 2.Department of Earth Resources Engineering, Graduate School of Engineering, Kyushu University)

[J] Poster | S (Solid Earth Sciences)：S-VC Volcanology

5:15 PM - 6:30 PM JST | 8:15 AM - 9:30 AM UTC | Poster Hall International Exhibition Hall8, Makuhari Messe_26

[S-VC39] Hydrothermal systems of volcanoes

convener:Yasuhiro Fujimitsu(Department of Earth Resources Engineering, Faculty of Engineering, Kyushu University), Wataru Kanda(Volcanic Fluid Research Center, School of Science, Tokyo Institute of Technology), Takeshi Ohba(Department of chemistry, School of Science, Tokia University)

[SVC39-P01] Changes in the chemistry of spring water related to the recent volcanic activity of Mt Iwo-Yama, Kirishima volcanic area

*Haruka Yamamoto[1], Yoshikazu Kikawada[2], Megumi Fukai, Wei Deng (1.Graduated school of Fuculty of Sience and Technology Sophia University, 2.Fuculty of Sience and Technology Sophia University)

[SVC39-P02] Hydrothermal circulation process related to phreatic eruption of Iwo-Yama at Kirishima volcanoes

*Keigo Mori[1], Harue Masuda[1], Tsuyoshi Shintani[1], Motoya Habuchi[1], Syuzou Furuya[1], Jun-ichiro Ishibashi[2], Takeshi Matsushima[2], Syogo Oshima[3], Reo Ikawa[4] (1.Osaka City University, 2.Kyushu University, 3.West Japan Engineering Consultants, Inc., 4.AIST)

[SVC39-P03] Determination on the stable isotopic compositions of H_2O in a volcanic plume

*Masanori Ito[1], Urumu Tsunogai[1], Koji U Takahashi[2], Fumiko Nakagawa[1] (1.Nagoya University, Graduate School of Environmental Studies, 2.Geological Survey of Japan, National Institute of Advanced Industrial Science and Technology)

[SVC39-P04] **Radon measurements at Aso volcano: an experimental automatic radon station operative within the proximal zone of Nakadake**

*Corrado CIGOLINI[1], Shin Yoshikawa[2], Tomo Shibata[3], Marco Laiolo[1], Diego Coppola[1] (1.Department of Earth Sciences, University of Torino, Italy, 2.Aso Volcanological Laboratory, Kyoto University, Japan, 3.Institute for Geothermal Sciences, Graduate school of Science, Kyoto University, Japan)

[SVC39-P05] Evolution of the hydrothermal system of Aso volcano during the 2014-2016 eruption period, as inferred by the ACTIVE observations

*Takuto Minami[1], Mitsuru Utsugi[2], Hisashi Utada[1], Tsuneomi Kagiyama[3] (1.Ocean Hemisphere Research Institute, Earthquake Research Institute,The University of Tokyo, 2.Aso Volcanological Laboratory, Institute for Geothremal Sciences, Graduate School of Science, Kyoto University, 3.Aso Geopark Promotion Council)

[SVC39-P06] 3-D Inversion of Magnetotelluric data from the Aluto-Langano Geothermal Field, Ethiopia

*Dejene Bekele[1], Yasuhiro FUJIMITSU[2] (1.Graduate School of Engineering, Department of Cooperative Resources Engineering, Kyushu University, 2.Faculty of Engineering, Department of Earth Resources Engineering, Kyushu University)

[SVC39-P07] Interpretation of Gravity Data to Delineate the Geothermal Reservoir Extent and Assess the Geothermal Resource in the Municipality of Isa, Southern Kyushu, Japan

*CARLOS OSMIN POCASANGRE[1], Yasuhiro Fujimitsu[1], Jun Nishijima[1] (1.Department of Earth Resources Engineering, Kyushu University)

[SVC39-P08] Conductive and convective heat fluxes inferred from temperature profile of a borehole in Izu-Oshima volcano

*Shin'ya Onizawa[1] (1.Volcanology Research Department, Meteorological Research Institute, JMA)

[SVC39-P09] Numerical model of the hydrothermal system at the Akakura Caldera in Kurikoma Area

*Yasuhiro Fujimitsu[1], Daichi Yoshioka[2] (1.Department of Earth Resources Engineering, Faculty of Engineering, Kyushu University, 2.Department of Earth Resources Engineering, Graduate School of Engineering, Kyushu University)

[J] Oral | S (Solid Earth Sciences)：S-TT Technology & Techniques

10:45 AM - 12:15 PM JST | 1:45 AM - 3:15 AM UTC | 303 3F

[S-TT45] Synthetic Aperture Radar

convener:Youhei Kinoshita(University of Tsukuba), Yu Morishita(Geospatial Information Authority of Japan), Shoko Kobayashi(Tamagawa University), Takahiro Abe(Earth Observation Research Center, Japan Aerospace Exploration Agency), Chairperson:Shoko Kobayashi(Tamagawa University), Kazuya Ishitsuka(Kyoto University)

10:45 AM - 11:00 AM JST | 1:45 AM - 2:00 AM UTC

[STT45-01] Extraction of ground changes near the crater by the eruption of Kilauea volcano.

*Fujiyama Kaho[1], Masanobu Shimada[1], Yuki Kimoto[1], Kenta Yoshioka[1] (1.TokyoDenki University)

11:00 AM - 11:15 AM JST | 2:00 AM - 2:15 AM UTC

[STT45-02] ALOS-2 observation of the 2017 Sefidsang earthquake, northeastern Iran: a blind shallow-dipping thrust event near the Eastern Kopeh Dagh

*Nematollah Ghayournajarkar[1], Yo Fukushima[2] (1.Graduate School of Science, Tohoku University, 2.International Research Institute of Disaster Science, Tohoku University)

11:15 AM - 11:30 AM JST | 2:15 AM - 2:30 AM UTC

[STT45-03] **InSAR ground displacements and slip distribution associated with secondary fault slips of the 2016 Kumamoto earthquake**

*Yo Fukushima[1], Daisuke Ishimura[2] (1.International Research Institute of Disaster Science, Tohoku University, 2.Department of Geology, Tokyo Metropolitan University)

11:30 AM - 11:45 AM JST | 2:30 AM - 2:45 AM UTC

[STT45-04] Surface displacements at the Kumamoto plain using persistent scatterer interferometry and comparison with groundwater levels

*Kazuya Ishitsuka[1], Takeshi Tsuji[2] (1.Kyoto Univ., 2.Kyushu Univ.)

11:45 AM - 12:00 PM JST | 2:45 AM - 3:00 AM UTC

[STT45-05] Forest fire detection in the low biomass dry forest with JICA-JAXA Forest Early Warning System in the Tropics (JJ-FAST).

*Manabu Watanabe[1], Christian Naohide koyama[1], Masato Hayashi[2], Izumi Nagatani[2], Takeo Tadono[2], Masanobu Shimada[1,2] (1.School of Science and Engineering, Tokyo denki university, 2.JAXA/EORC)

12:00 PM - 12:15 PM JST | 3:00 AM - 3:15 AM UTC

[STT45-06] Nominal operation results of Japanese ALOS-2

★Invited Papers

*Shinichi Sobue[1] (1.Japan Aerospace Exploration Agency)

[J] Oral | S (Solid Earth Sciences)：S-TT Technology & Techniques

1:45 PM - 3:15 PM JST | 4:45 AM - 6:15 AM UTC | 303 3F

[S-TT45] Synthetic Aperture Radar

convener:Youhei Kinoshita(University of Tsukuba), Yu Morishita(Geospatial Information Authority of Japan), Shoko Kobayashi(Tamagawa University), Takahiro Abe(Earth Observation Research Center, Japan Aerospace Exploration Agency), Chairperson:Yohei Kinoshita(RESTEC), Takahiro Abe(JAXA)

1:45 PM - 2:00 PM JST | 4:45 AM - 5:00 AM UTC

[STT45-07] Estimation of velocity distribution of Shirase Glacier derived from SAR data obtained by ERS-1/2 tandem mission

*Koichiro Doi[1,2], Yuichi Aoyama[1,2], Kazuki Nakamura[3], Tsutomu Yamanokuchi[4], Kazuo Shibuya[1] (1.National Institute of Polar Research, 2.SOKENDAI, 3.College of Engineering, Nihon University, 4.RESTEC)

2:00 PM - 2:15 PM JST | 5:00 AM - 5:15 AM UTC

[STT45-08] Heavy rainfall-induced displacement of more than 2.5m in the Kushiro Marsh in 2016, detected by ALOS-2 SAR

*Satoshi Fujiwara[1], Yu Morishita[1], Takayuki Nakano[1], Yuji Miura[1], Yasuaki Kakiage[1], MURAMATSU Hiroki[1], Hiroshi Une[1] (1.GSI of Japan)

2:15 PM - 2:30 PM JST | 5:15 AM - 5:30 AM UTC

[STT45-09] Surface deformation of Asama Volcano, Japan, detected by time-series InSAR combining persistent and distributed scatterers, 2014-2018

*Yosuke Aoki[1], Xiaowen Wang[1] (1.Earthquake Research Institute, University of Tokyo)

2:30 PM - 2:45 PM JST | 5:30 AM - 5:45 AM UTC

[STT45-10] Improvement of Airborne L-band-SAR (Pi-SAR-L2) Coherence by Pixel by Pixel Resampling

*Makoto Murakami[1], Masato Furuya[1], Taku Ozawa[4], Youichiro Takada[1], Yosuke Aoki[3], Masanobu Shimada[2], Shohei Narita[1] (1.Hokkaido University, 2.Tokyo Denki University, School of Science and engineerring, 3.Earthquake Research Institute, The University of Tokyo, 4. National Research Institute for Earth Science and Disaster Resilience)

2:45 PM - 3:00 PM JST | 5:45 AM - 6:00 AM UTC

[STT45-11] Ionospheric delay estimation in SAR interferometry: Significance of the method using the split-spectrum double-difference interferogram

*Taku Ozawa[1] (1.National Research Institute for Earth Science and Disaster Resilience)

3:00 PM - 3:15 PM JST | 6:00 AM - 6:15 AM UTC

[STT45-12] Detecting surface displacement accosiated with the 2018 slow slip event around Boso peninsla by use of Sentinel-1 InSAR with atmospheric correction

*Youhei Kinoshita[1], Tadahiro Nimura[1], Ryoichi Furuta[1] (1.RESTEC, Remote Sensing Technology Center of Japan)

[J] Poster | S (Solid Earth Sciences)：S-TT Technology & Techniques

3:30 PM - 5:00 PM JST | 6:30 AM - 8:00 AM UTC | Poster Hall International Exhibition Hall8, Makuhari Messe_15

[S-TT45] Synthetic Aperture Radar

convener:Youhei Kinoshita(University of Tsukuba), Yu Morishita(Geospatial Information Authority of Japan), Shoko Kobayashi(Tamagawa University), Takahiro Abe(Earth Observation Research Center, Japan Aerospace Exploration Agency)

[STT45-P01] Development of InSAR tropospheric phase delay correction system at MRI (2nd report)

*Okuyama Satoshi[1], Shinobu Ando[1], Toshiki Shimbori[1] (1.Meteorological Research Institute)

[STT45-P02] Mitigation of atmospheric delay in InSAR for fair estimate of crustal deformation at Azumayama volcano

*Kana Abe[1], Yoshiko Ogawa[1], Yasuhiro Hisada[1], Hirohide Demura[1], Taku Ozawa[2], Satoshi Miura[3], Akira Kusakabe[1], Takehiro Arai[1] (1.The University of Aizu, 2.National Research Institute for Earth Science and Disaster Resilience, 3.Graduate School of Science, Tohoku University)

[STT45-P03] Unusual displacement observed in InSAR analysis results of fumarolic area of active volcanos: An example of the Kamiyu district in Hakone Volcano

*Ryosuke Doke[1], Kazuhiro Itadera[1] (1.Hot Springs Research Institute of Kanagawa Prefecture)

[STT45-P04] Detection of Deformation Signals at Mud Volcanoes in Semau Island, Indonesia

*Naufal Setiawan[1], Masato Furuya[1] (1.Hokkaido University)

[STT45-P05] Extraction of supraglacial lakes on debris-covered glacier using ALOS-2/PALSAR-2

Chikako Kinefuchi[2], *Chiyuki Narama[1], Tsutomu Yamanokuchi[3], Takeo Tadono[4] (1.Niigata University, Program of Field Research in the Environmental Sciences, 2.Graduate School of Science and Technology, Niigata University, 3.RESTEC, 4.JAXA)

[STT45-P06] **Observation of the water level fluctuation at Ozegahara by ALOS-2/PALSAR-2**

*Wataru Iwatate[1], Masanobu Shimada[1] (1.Tokyo Denki University)

[STT45-P07] The steady crustal deformation around the Omaezaki, Sionomisaki, Muroto and Ashizuri, using InSAR time-series analysis 2

*Shinobu Ando[1], Akio Kobayashi[1] (1.Seismology and Tsunami Research Department, Meteorological Research Institute)

[STT45-P08] Evaluation of InSAR analysis result using pipe strain gauge data in Otari village, Nagano prefecture, Japan

*Tomoya Kiyosawa[1], Hiroshi, P. Sato[2] (1.Department of Geography, Graduate School of Science and Technology, Nihon University , 2.College of Humanities and Science, Nihon University)

[STT45-P09] DEM creation using ALOS / PALSAR interferometric SAR and its accuracy evaluation.

*takahashi koya[1], Masanobu Shimada[1] (1.tokyo denki university)

[STT45-P10] Approach to monitoring ground deformation using InSAR time series analysis all over Japan

*Kyonosuke Hayahsi[1], Tatsuya Yamashita[1], Masaki Kuwahara[1], Masaki Honda[1], Kazuki Sakai[1], Hiroshi Munekane[1], Tomokazu Kobayashi[1] (1.GSI of Japan)

[J] Poster | S (Solid Earth Sciences)：S-TT Technology & Techniques

5:15 PM - 6:30 PM JST | 8:15 AM - 9:30 AM UTC | Poster Hall International Exhibition Hall8, Makuhari Messe_27

[S-TT45] Synthetic Aperture Radar

convener:Youhei Kinoshita(University of Tsukuba), Yu Morishita(Geospatial Information Authority of Japan), Shoko Kobayashi(Tamagawa University), Takahiro Abe(Earth Observation Research Center, Japan Aerospace Exploration Agency)

[STT45-P01] Development of InSAR tropospheric phase delay correction system at MRI (2nd report)

*Okuyama Satoshi[1], Shinobu Ando[1], Toshiki Shimbori[1] (1.Meteorological Research Institute)

[STT45-P02] Mitigation of atmospheric delay in InSAR for fair estimate of crustal deformation at Azumayama volcano

*Kana Abe[1], Yoshiko Ogawa[1], Yasuhiro Hisada[1], Hirohide Demura[1], Taku Ozawa[2], Satoshi Miura[3], Akira Kusakabe[1], Takehiro Arai[1] (1.The University of Aizu, 2.National Research Institute for Earth Science and Disaster Resilience, 3.Graduate School of Science, Tohoku University)

[STT45-P03] Unusual displacement observed in InSAR analysis results of fumarolic area of active volcanos: An example of the Kamiyu district in Hakone Volcano

*Ryosuke Doke[1], Kazuhiro Itadera[1] (1.Hot Springs Research Institute of Kanagawa Prefecture)

[STT45-P04] Detection of Deformation Signals at Mud Volcanoes in Semau Island, Indonesia

*Naufal Setiawan[1], Masato Furuya[1] (1.Hokkaido University)

[STT45-P05] Extraction of supraglacial lakes on debris-covered glacier using ALOS-2/PALSAR-2

Chikako Kinefuchi[2], *Chiyuki Narama[1], Tsutomu Yamanokuchi[3], Takeo Tadono[4] (1.Niigata University, Program of Field Research in the Environmental Sciences, 2.Graduate School of Science and Technology, Niigata University, 3.RESTEC, 4.JAXA)

[STT45-P06] **Observation of the water level fluctuation at Ozegahara by ALOS-2/PALSAR-2**

*Wataru Iwatate[1], Masanobu Shimada[1] (1.Tokyo Denki University)

[STT45-P07] The steady crustal deformation around the Omaezaki, Sionomisaki, Muroto and Ashizuri, using InSAR time-series analysis 2

*Shinobu Ando[1], Akio Kobayashi[1] (1.Seismology and Tsunami Research Department, Meteorological Research Institute)

[STT45-P08] Evaluation of InSAR analysis result using pipe strain gauge data in Otari village, Nagano prefecture, Japan

*Tomoya Kiyosawa[1], Hiroshi, P. Sato[2] (1.Department of Geography, Graduate School of Science and Technology, Nihon University , 2.College of Humanities and Science, Nihon University)

[STT45-P09] DEM creation using ALOS / PALSAR interferometric SAR and its accuracy evaluation.

*takahashi koya[1], Masanobu Shimada[1] (1.tokyo denki university)

[STT45-P10] Approach to monitoring ground deformation using InSAR time series analysis all over Japan

*Kyonosuke Hayahsi[1], Tatsuya Yamashita[1], Masaki Kuwahara[1], Masaki Honda[1], Kazuki Sakai[1], Hiroshi Munekane[1], Tomokazu Kobayashi[1] (1.GSI of Japan)

[J] Oral | S (Solid Earth Sciences)：S-TT Technology & Techniques

1:45 PM - 3:15 PM JST | 4:45 AM - 6:15 AM UTC | A08 TOKYO BAY MAKUHARI HALL

[S-TT46] Seismic Big Data Analysis Based on the State-of-the-Art of Bayesian Statistics

convener:Hiromichi Nagao(Earthquake Research Institute, The University of Tokyo), Aitaro Kato(Earthquake Research Institute, the University of Tokyo), Takuto Maeda(Graduate School of Science and Technology, Hirosaki University), Keisuke Yano(The university of Tokyo), Chairperson:Nana Yoshimitsu(Earthquake Research Institute, The University of Tokyo), Takeru Matsuda(Graduate School of Information Science and Technology, The University of Tokyo)

1:45 PM - 2:00 PM JST | 4:45 AM - 5:00 AM UTC

[STT46-01] A bad inversion result suggests bad modeling

★Invited Papers

*Yukitoshi Fukahata[1], Yuji Yagi[2] (1.Disaster Prevention Research Institute, Kyoto University, 2.Graduate School of Life and Environmental Sciences, University of Tsukuba)

2:00 PM - 2:15 PM JST | 5:00 AM - 5:15 AM UTC

[STT46-02] A seismic wavefield estimation in a dense seismograph network: An optimization for the MeSO-net

*Takahiro Shiina[1], Takuto Maeda[2], Masayuki Kano[3], Aitaro Kato[1], Naoshi Hirata[1] (1.Earthquake Research Institute, The University of Tokyo, 2.Graduate School of Science and Technology, Hirosaki University, 3.Graduate school of science, Tohoku University)

2:15 PM - 2:30 PM JST | 5:15 AM - 5:30 AM UTC

[STT46-03] Uncertainty quantification based on 4DVar data assimilation for massive simulation models

*Shin-ichi Ito[1], Masayuki Kano[2], Hiromichi Nagao[1] (1.The University of Tokyo, 2.Tohoku University)

2:30 PM - 2:45 PM JST | 5:30 AM - 5:45 AM UTC

[STT46-04] Bayesian approach for statistical modeling and forecasting of aftershock activities

★Invited Papers

*Takahiro Omi[1] (1.Institue of Industrial Science, the University of Tokyo)

2:45 PM - 3:00 PM JST | 5:45 AM - 6:00 AM UTC

[STT46-05] **Bias Correction for the Distribution of Aftershocks Within Short-Term Period Immediately After Large Main Shock**

*Kosuke Morikawa[1], Hiromichi Nagao[2], Shin-ichi Ito[2], Shin'ichi Sakai[2], Naoshi Hirata[2] (1.Osaka University, 2.Earthquake Research Institute, The University of Tokyo)

3:00 PM - 3:15 PM JST | 6:00 AM - 6:15 AM UTC

[STT46-06] Deep-learning-based Earthquake Detection for Continuous Seismic Network Records

*Keisuke Yano[1], Takahiro Shiina[2], Sumito Kurata[1], Aitaro Kato[2], Fumiyasu Komaki[1], Shin'ichi Sakai[2], Naoshi Hirata[2] (1.Graduate School of Information Science and Technology, The University of Tokyo, , 2.Earthquake Research Institute, The University of Tokyo)

[J] Poster | S (Solid Earth Sciences)：S-TT Technology & Techniques

3:30 PM - 5:00 PM JST | 6:30 AM - 8:00 AM UTC | Poster Hall International Exhibition Hall8, Makuhari Messe_16

[S-TT46] Seismic Big Data Analysis Based on the State-of-the-Art of Bayesian Statistics

convener:Hiromichi Nagao(Earthquake Research Institute, The University of Tokyo), Aitaro Kato(Earthquake Research Institute, the University of Tokyo), Takuto Maeda(Graduate School of Science and Technology, Hirosaki University), Keisuke Yano(The university of Tokyo)

[STT46-P01] P-wave Polarity Determination of Waveform Data Observed in Western Japan, Using Deep Learning

*Shota Hara[1], Yukitoshi Fukahata[2], Yoshihisa Iio[2] (1.Division of Earth and Planetary Sciences, Graduate School of Science, Kyoto University, 2.Disaster Prevention Research Institute, Kyoto University)

[STT46-P02] Trans-dimensional Bayesian inversion for a radially anisotropic S-wave velocity model in the crust and upper mantle: Application to the Australian continent

*Toru Taira[1], Kazunori Yoshizawa[2] (1.Graduate School of Science, Hokkaido University, 2.Faculty of Science, Hokkaido University)

[STT46-P03] Seismic wavefield imaging based on dense seismic networks using replica exchange Monte Carlo method

*Masayuki Kano[1], Hiromichi Nagao[2,3], Kenji Nagata[4,5], Shin-ichi Ito[2,3], Kei Hasegawa[2], Shin'ichi Sakai[2], Shigeki Nakagawa[2], Muneo Hori[2], Naoshi Hirata[2] (1.Graduate school of science, Tohoku University, 2.Earthquake Research Institute, The University of Tokyo, 3.Graduate School of Information Science and Technology, The University of Tokyo, 4.AIST, 5.Japan Science and Technology Agency)

[STT46-P04] Bayesian oscillator decomposition for seismic data

*Takeru Matsuda[1] (1.The University of Tokyo)

[STT46-P05] Uncertainty evaluation of source parameter estimates by MCMC in Oklahoma

*Nana Yoshimitsu[1], Takuto Maeda[2], William Ellsworth[3] (1.The University of Tokyo, Earthquake Research Institute, 2.Hirosaki University, 3.Stanford Univerisy)

[J] Poster | S (Solid Earth Sciences)：S-TT Technology & Techniques

5:15 PM - 6:30 PM JST | 8:15 AM - 9:30 AM UTC | Poster Hall International Exhibition Hall8, Makuhari Messe_28

[S-TT46] Seismic Big Data Analysis Based on the State-of-the-Art of Bayesian Statistics

convener:Hiromichi Nagao(Earthquake Research Institute, The University of Tokyo), Aitaro Kato(Earthquake Research Institute, the University of Tokyo), Takuto Maeda(Graduate School of Science and Technology, Hirosaki University), Keisuke Yano(The university of Tokyo)

[STT46-P01] P-wave Polarity Determination of Waveform Data Observed in Western Japan, Using Deep Learning

*Shota Hara[1], Yukitoshi Fukahata[2], Yoshihisa Iio[2] (1.Division of Earth and Planetary Sciences, Graduate School of Science, Kyoto University, 2.Disaster Prevention Research Institute, Kyoto University)

[STT46-P02] Trans-dimensional Bayesian inversion for a radially anisotropic S-wave velocity model in the crust and upper mantle: Application to the Australian continent

*Toru Taira[1], Kazunori Yoshizawa[2] (1.Graduate School of Science, Hokkaido University, 2.Faculty of Science, Hokkaido University)

[STT46-P03] Seismic wavefield imaging based on dense seismic networks using replica exchange Monte Carlo method

*Masayuki Kano[1], Hiromichi Nagao[2,3], Kenji Nagata[4,5], Shin-ichi Ito[2,3], Kei Hasegawa[2], Shin'ichi Sakai[2], Shigeki Nakagawa[2], Muneo Hori[2], Naoshi Hirata[2] (1.Graduate school of science, Tohoku University, 2.Earthquake Research Institute, The University of Tokyo, 3.Graduate School of Information Science and Technology, The University of Tokyo, 4.AIST, 5.Japan Science and Technology Agency)

[STT46-P04] Bayesian oscillator decomposition for seismic data

*Takeru Matsuda[1] (1.The University of Tokyo)

[STT46-P05] Uncertainty evaluation of source parameter estimates by MCMC in Oklahoma

*Nana Yoshimitsu[1], Takuto Maeda[2], William Ellsworth[3] (1.The University of Tokyo, Earthquake Research Institute, 2.Hirosaki University, 3.Stanford Univerisy)

[E] Oral | S (Solid Earth Sciences)：S-CG Complex & General

3:30 PM - 5:00 PM JST | 6:30 AM - 8:00 AM UTC | A07 TOKYO BAY MAKUHARI HALL

[S-CG49] Hard-Rock Drilling Science: From Continental to Deep Sea Drilling, and Oman Project

convener:Katsuyoshi Michibayashi(Department of Earth and Planetary Sciences, Nagoya University), Eiichi TAKAZAWA(Department of Geology, Faculty of Science, Niigata University), Norikatsu Akizawa(Department of Ocean Floor Geoscience, Atmosphere and Ocean Research Institute, The University of Tokyo), Chairperson:Katsuyoshi Michibayashi

3:30 PM - 3:45 PM JST | 6:30 AM - 6:45 AM UTC

[SCG49-01] **Geochemical and Geochronological Constraints on the Origin and Emplacement of the East Taiwan Ophiolite: Implication for Subduction Initiation of the South China Sea.**

*Chiou-ting Lin[1], Ron A. Harris[2], Wei-dong Sun[1], Guo-liang Zhang[1] (1.Center of Deep Sea Research, Institute of Oceanology, Chinese Academy of Sciences, 2.Department of Geology, Brigham Young University)

3:45 PM - 4:05 PM JST | 6:45 AM - 7:05 AM UTC

[SCG49-02] Towards a complete profile of hydrothermal alteration in the lower oceanic crust and uppermost mantle; Insights from the Oman Drilling Project and ChikyuOman2017 and 2018

★Invited Papers

*Damon A H Teagle[1], Michelle Harris[2], Gretchen Früh-Green[3], Eiichi TAKAZAWA[4], Katsuyoshi Michibayashi[5], Peter B Kelemen[6], Oman Drilling Project Science Team[1] (1.Ocean & Earth Science, National Oceanography Centre Southampton, University of Southampton, SO14-3ZH, Southampton, UK, 2.School of Geography, Earth and Environmental Sciences, Plymouth University, UK, 3.Earth Sciences, ETH Zürich, Switzerland, 4.Geology, Niigata University, Japan, 5.Earth and Planetary Sciences, Nagoya University, Japan, 6.LDEO, Columbia University, New York, USA)

4:05 PM - 4:25 PM JST | 7:05 AM - 7:25 AM UTC

[SCG49-03] Peridotite alteration in OmanDP cores

★Invited Papers

*Peter B Kelemen[1], Juan Carlos de Obeso[1], Craig Manning[2], Marguerite Godard[3], Wolfgang Bach[4], Merry Yue Cai[1], Saebyul Choe[5], Judith Coggon[6], Eric Ellison[7], Alireza Eslami[8], Katy Evans[9], Michelle Harris[10], Wolf-Achim Kahl[4], Jürg Matter[6], Katsu Michibayashi[11], Keichi Okazaki[12], Philippe Pézard[3], Damon A.H. Teagle[6], Alexis Templeton[7], OmanDP Oman Drilling Project Science Team (1.LDEO, 2.UCLA, 3.U. Montpellier, 4.U. Bremen, 5.AMNH, 6.U. Southampton, 7.U. Colorado, 8.U. Tehran, 9.Curtin U., 10.U. Plymouth, 11.Nagoya U., 12.JAMSTEC)

4:25 PM - 4:40 PM JST | 7:25 AM - 7:40 AM UTC

[SCG49-04] Low-salinity aqueous fluid inclusions in dolomite veins of a listvenite of Oman Drilling Project Phase 1

*Tatsuhiko Kawamoto[1], Hiroki Sato[2], Toma Takahashi[3], Juan Miguel Guotana[4], Tomoaki Morishita[4], Peter B Kelemen[5], Jude Ann Coggon[6], Michelle Harris[7], Juerg Michael Matter[6], Katsuyoshi Michibayashi[8], Eiichi TAKAZAWA[9], Damon A H Teagle[6], The Oman Drilling Project Phase 1 Science Party (1.Department of Geoscience, Faculty of Science, Shizuoka University, 2.Faculty of Science, Kyoto University, 3.Faculty of Geosciences and Civil Engineering, Kanazawa University, 4.Division of Natural Sciences, Graduate School of Natural Science and Technology, Kanazawa University, 5.Lamont-Doherty Earth Observatory, Columbia University, 6.School of Ocean and Earth Science, National Oceanography Centre Southampton, University of Southampton, 7.School of Geography, Earth and Environmental Sciences, Plymouth University, 8.Department of Earth Planetary Sciences, Graduate School of Environmental Studies, Nagoya University, 9.Institute of Science and Technology, Niigata University)

4:40 PM - 5:00 PM JST | 7:40 AM - 8:00 AM UTC

[SCG49-05] Hydration and development of fracture network within oceanic lower crust: an evidence from CM1A of Oman Drilling

★Invited Papers

*Atsushi Okamoto[1], Kazuki Yosida[1], Ryosuke Oyanagi[2], Oman Drilling Project Phase 2 Science Party[3] (1.Graduate School of Environmental Studies, 2.JAMSTEC, 3.Oman Drillng Project Phase 2 Science Party)

[J] Oral | S (Solid Earth Sciences)：S-CG Complex & General

9:00 AM - 10:30 AM JST | 12:00 AM - 1:30 AM UTC | A05 TOKYO BAY MAKUHARI HALL

[S-CG56] Ocean Floor Geosciences

convener:Kyoko Okino(Atmosphere and Ocean Research Institute, The University of Tokyo), Chairperson:Arata Kioka, Atsushi Noda

9:00 AM - 9:15 AM JST | 12:00 AM - 12:15 AM UTC

[SCG56-25] Observational plans of the South Sandwich Arc by R/V Hakuho Maru: Toward understanding formation and evolution of the world southernmost arc-trench system

*Asuka Yamaguchi[1], Kenichiro Tani[2], Minoru Ikehara[3] (1.Atomosphere and Ocean Research Institute, The University of Tokyo, 2.National Museum of Nature and Science, 3.Center for Advanced Marine Core Research, Kochi University)

9:15 AM - 9:30 AM JST | 12:15 AM - 12:30 AM UTC

[SCG56-26] Seismic imaging of the source zone of the 2011 Tohoku-oki earthquake

*Dapeng Zhao[1], Xin Liu[1] (1.Department of Geophysics, Tohoku University)

9:30 AM - 9:45 AM JST | 12:30 AM - 12:45 AM UTC

[SCG56-27] Drastic export of organic carbon to hadal trench driven by megathrust earthquake

*A. Kioka[1], T. Schwestermann[1], J. Moernaut[1], K. Ikehara[2], T. Kanamatsu[3], C. M. McHugh[4], C. dos Santos Ferreira[5], G. Wiemer[5], N. Haghipour[6], A. J. Kopf[5], T. I. Eglinton[6], M. Strasser[1,5] (1.Universität Innsbruck, Austria, 2.GSJ-AIST, Japan, 3.JAMSTEC, Japan, 4.Queens-CUNY, USA, 5.MARUM-U. Bremen, Germany, 6.ETH Zürich, Switzerland)

9:45 AM - 10:00 AM JST | 12:45 AM - 1:00 AM UTC

[SCG56-28] How do trench-fill sediments subduct under the accretionary wedge?

*Atsushi Noda[1], Hiroaki Koge[2], Yasuhiro Yamada[3], Ayumu Miyakawa[1], Juichiro Ashi[2] (1.National Institute of Advanced Industrial Science and Technology, 2.Atomosphere and Ocean Research Institute, The University of Tokyo, 3.Japan Agency for Marine-Earth Science and Technology)

10:00 AM - 10:15 AM JST | 1:00 AM - 1:15 AM UTC

[SCG56-29] Formation process of a slope basin in the Nankai Accretionary prism reconstructed from high-resolution SBP integrated with core data of ODP Site 1175 and Site 1176

*Yuichi Okuma[1], Asuka Yamaguchi[1], Hiroaki Koge[1], Rina Fukuchi[1], Juichiro Ashi[1] (1.Atmosphere and Ocean Research Institute, the University of Tokyo)

10:15 AM - 10:30 AM JST | 1:15 AM - 1:30 AM UTC

[SCG56-30] About the turbidity current considered that it occurred in the northern Suruga Bay, Central Japan by the typhoon No.24. -The traces of the accidents and the phenomenon at the sea floor detected the OBSs Array-

*Nakao Nagisa[1], Hisatoshi Baba[2], Hiroshi Sato[3], Kayoko Tsuruga[4], Izumi Sakamoto[2], Takahito Nishimiya[5], Masanao Shinohara[3], Shintaro Abe[6] (1.Tokai University, 2.Department of Marine and Earth Science, Tokai University, 3.Earthquake Research Institute, University of Tokyo, 4.Tokyo University of Marine Science and Technology, 5.Meteorological Research Institute, Japan Meteorological Agency, 6.Association for the Development of Earthquake Prediction)

[J] Poster | S (Solid Earth Sciences)：S-CG Complex & General

3:30 PM - 5:00 PM JST | 6:30 AM - 8:00 AM UTC | Poster Hall International Exhibition Hall8, Makuhari Messe_17

[S-CG56] Ocean Floor Geosciences

convener:Kyoko Okino(Atmosphere and Ocean Research Institute, The University of Tokyo)

[SCG56-P01] Signature of plume-ridge interaction on bathymetry and geochemistry along mid-ocean ridges: Insights from the Réunion Plume and Central Indian Ridge

*Clement Vincent[1], Jung-Woo Park[1], Sang-Mook Lee[1], Jonguk Kim[2], Sang-Joon Pak[2] (1.Seoul National University, 2.Korea Institute of Ocean Science and Technology)

[SCG56-P02] Spreading rate and its stability of Chile Ridge near the Chile Triple Junction

*Takanori Ishihara[1], Takeshi Matsumoto[1] (1.Ryukyu university)

[SCG56-P03] Newly Mapped Seamounts on the Antarctic Plate off Southern Chile

*Toshiya Fujiwara[1], Natsue Abe[2], Naomi Harada[3], Mirai MR16-09 Leg 2 Shipboard Science Party (1.Research and Development Center for Earthquake and Tsunami, Japan Agency for Marine-Earth Science and Technology, 2.Research and Development Center for Ocean Drilling Science, 3.Research and Development Center for Global Change)

[SCG56-P04] Surface-ship gravimetry on board MR16-09 Cruise by R/V MIRAI - Characteristrics of gravity anomaly around the Chile Triple Junction

*Takeshi Matsumoto[1], Takanori Ishihara[1] (1.Faculty of Science, University of the Ryukyus)

[SCG56-P05] Magnetic and Magnetotelluric surveys across the Afar depression, transition between continental rifting and sea-floor spreading

*Ryokei Yoshimura[1], Naoto Ishikawa[2], Tesfaye Kidane[3], Shin-ichi Kagashima[4], Nobutatsu Mochizuki[5], Ameha Atnafu Muluneh[3], Kirika Kitagawa[4], Taito Ikema[6] (1.Disaster Prevention Research Institute, Kyoto University, 2.Graduate School of Human and Environmental Studies, Kyoto University, 3.Addis Ababa University, 4.Faculty of Science, Yamagata University, 5.Priority Organization for Innovation and Excellence, Kumamoto University, 6.Faculty of Science, Kyoto University)

[SCG56-P06] **Evolution of oceanic core complexes in the Shikoku Basin: when backarc basins cease to open**

*Kyoko Okino[1], Yasuhiko Ohara[2,3], Masakazu Fujii[4], Tomoko Hanyu[1] (1.Atmosphere and Ocean Research Institute, The University of Tokyo, 2.Japan Coast Guard, 3.Japan Agency for Marine-Earth Science and Technology, 4.National Institute of Polar Research)

[SCG56-P07] Thermal evolution of the Lanzo orogenic peridotite massif in western Alps: implications on thermal structure near subcontinental lithosphere-asthenosphere boundary

*Tomo Aoki[1], Kazuhito Ozawa[1], Jean-Louis Bodinier[3], Françoise Boudier[2] (1.The University of Tokyo, 2.Montpellier 2 University, 3.Geosciences Montpellier)

[SCG56-P08] Comparison of the back-arc basins of the South and the Central Ryukyus in the northwest Pacific

*Kohsaku Arai[1], Ayanori Misawa[1], Takahiko Inoue[1] (1.Institute of Geology and Geoinformation, National Institute of Advanced Industrial and Technology)

[SCG56-P09] Geochemistry and zircon U-Pb ages of mafic rocks in the Mikabu and Sorachi-Yezo belts: Comparison with the Shatsky Rise

*Naoto Kimura[1], Yuji Ichiyama[1], Shohei Takahashi[1], Hisatoshi Ito[2], Akihiro Tamura[3], Tomoaki Morishita[3] (1.Chiba University, 2.Central Research Institute of Electric Power Industry, 3.Kanazawa University)

[SCG56-P10] Submersible magnetics reveals relationship between off-axis volcanism and hydrothermal systems of the Kairei and Yokoniwa fields at the Central Indian Ridge

*Masakazu Fujii[1], Kyoko Okino[2] (1.National Institute of Polar Research and SOKENDAI, 2.Atmosphere and Ocean Research Institute, The University of Tokyo)

[SCG56-P11] Shipboard magnetic and gravity surveys around the Iheya North Knoll and the Iheya Minor Ridge in the Mid-Okinawa Trough: Preliminary results of KR18-14 Leg1/Leg2 cruises

*Kazuya Kitada[1], Takafumi Kasaya[1], Hisanori Iwamoto[1], Yoshifumi Nogi[2] (1.Japan Agency for Marine-Earth Science and Technology, 2.National Institute of Polar Research)

[SCG56-P12] A shallow scientific drilling at Higashi Ensei Hydrothermal Field, Okinawa Trough

*Hidenori Kumagai[1], Takafumi Kasaya[1], Shuhei Totsuka[2], Shinsuke Kawagucci[1], Hideaki Machiyama[1], Koichi Iijima[1], Hirofumi Yamamoto[1], junji kaneko[1], Yusuke Ohta[3], Shohei Albert Tomita[3], Shogo Komori[4] (1.Japan Agency for Marine-Earth Science and Technology, 2.Kyushu Univ., 3.Kyoto Univ., 4.AIST)

[SCG56-P13] Mineralogical and geochemical study of sediment cores collected from the Gondou hydrothermal field in the Okinawa Trough

*Jun-ichiro Ishibashi[1,2], Shuhei Totsuka[2], Akihi Tsutsumi[2], Naru Tsukamoto[2], Yusuke Kira[2], Kazuhiko Shimada[1], Toru Yamasaki[3], Ken Ikehara[3], Toshiro Nagase[4], Yutaro Takaya[5,9], Kei Ikehata[6], Takashi Goto[7], Chitaro Gouzu[7], Ryuichi Shinjo[8], Hideaki Machiyama[9], Koichi Iijima[9], Hirofumi Yamamoto[9], Hidenori Kumagai[9] (1.Department of Earth and Planetary Sciences, Kyushu University, 2.Graduate School of Science, Kyushu University, 3.National Institute of Advanced Industrial Science and Technology, 4.Tohoku University Museum, 5.School of Creative Science and Enginerring, Waseda University, 6.Faculty of Life and Environmental Sciences, University of Tsukuba, 7.Hiruzen Institute for Geology and Chronology, 8.Faculty of Science, University of the Ryukyus, 9.Japan Agency for Marine-Earth Science and Technology)

[SCG56-P14] New type of self-potential anomaly observed near a hydrothermal site of Oomuro-dashi volcano, Izu-Ogasawara arc

*Yoshifumi Kawada[1,2], Takafumi Kasaya[2] (1.International Research Institute of Disaster Science, Tohoku University, 2.Japan Agency for Marine-Earth Science and Technology)

[SCG56-P15] Numerical simulation of submarine hydrothermal ore-deposits due to a coupled process of fluid migration and reactive geochemical transport

*Claudia Fujita[1], Hajime Yamamoto[1], Jun-ichiro Ishibashi[2], Takeshi Tsuji[3] (1.Taisei Corporation, 2. Department of Earth and Planetary Sciences, Faculty of Science, Kyushu University, 3.Department of Earth Resources Engineering, Faculty of Science, Kyushu University)

[SCG56-P16] Mineral composition and grain size distribution of REY-rich mud in the Minamitorishima EEZ: Implication for formation process of extremely REY-rich mud

*Sakai Takumi[1], Erika Tanaka[1], Kazutaka Yasukawa[1,2], Junichiro Ohta[2,1], Koichiro Fujinaga[2,1], Kentaro Nakamura[1], Yasuhiro Kato[3,1,2] (1.Department of Systems Innovation, School of Engineering, University of Tokyo, 2.Ocean Resources Research Center for Next Generation, Chiba Institute of Technology, 3.Frontier Research Center for Energy and Resources, School of Engineering, The University of Tokyo)

[SCG56-P17] **Geochemical and morphological features of manganese micronodules in REY-rich mud within the Minamitorishima EEZ, western North Pacific Ocean**

*Satoshi Kino[1], Kazutaka Yasukawa[1,2], Keishiro Azami[1], Erika Tanaka[1], Koichiro Fujinaga[2,1], Kentaro Nakamura[1], Yasuhiro Kato[1,2] (1.Department of Systems Innovation, School of Engineering, University of Tokyo, 2.Ocean Resources Research Center for Next Generation, Chiba Institute of Technology)

[SCG56-P18] Seafloor sediment thickness around the Japan and Kurile trenches obtained by traveltime analysis for PS converted wave recoded by ocean bottom seismograms

*Ryosuke Azuma[1], Genti Toyokuni[1], Ryota Takagi[1], Syuichi Suzuki[1], Makiko Sato[1], Takashi NAKAYAMA[1], Naoki Uchida[1], Ryota Hino[1] (1.Recearch Center for Prediction of Earthquake and Volcanic Eruption, Graduate School of Science, Tohoku University)

[SCG56-P19] Examination of critical taper theory based on bathymetry data in subduction zones

*Hiroaki Koge[1], Juichiro Ashi[1], Jin-Oh Park[1] (1.Atmosphere and Ocean Research Institute, The University of Tokyo)

[SCG56-P20] Active structures of the Sagami Bay Fault by high-resolution sub-bottom profiling and pin-point core sampling

*Juichiro Ashi[1], Asuka Yamaguchi[2], Natsumi Okutsu[1], Ayanori Misawa[3] (1.Graduate School of Frontier Sciences, The University of Tokyo, 2.Atmosphere and Ocean Research Institute, The University of Tokyo, 3.National Institute of Advanced Industrial Science and Technology)

[SCG56-P21] Fault Distribution and Structural Characteristic in the Nankai Trough Area, Japan

*Rei Arai[1], Narumi Takahashi[1], Minako Katsuyama[1], Shigeyoshi Tanaka[1], Hiromi Kamata[1], Tomoyuki Sato[2], Takahiko Inoue[2], Yoshiyuki Kaneda[3] (1.Japan Agency for Marine-Earth Science and Technology, 2.National Institute of Advanced Industrial Science and Technology, 3.Kagawa University)

[SCG56-P22] Seismicity in the central Ryukyu Trench by the Ocean Bottom Seismometers

*Ren Yakabu[1], Mamoru Nakamura[1], Yusuke Yamashita[2], Masanao Shinohara[3], Tomoaki Yamada[3], Hajime Shiobara[3], Kimihiro Mochizuki[3] (1.University of the Ryukyus, 2.DPRI, Kyoto University, 3.ERI, Tokyo University)

[SCG56-P23] Seismic structure of subducted Philippine Sea plate beneath Kyushu inferred from Po/So waves

*Azusa Shito[1] (1.Institute of Seismology and Volcanology, Kyushu University)

[SCG56-P24] Slope failure features and their distribution in the forearc off northwestern Sumatra

*Kenji Hirata[1], Toshiya Fujiwara[2], Ayanori Misawa[3], Kohsaku Arai[3] (1.National Research Institue for Earth Science and Diaster resilience, 2.Japan Agency for Marine-Earth Science and Technology, 3.National Institute of Advanced Industrial Science and Technology)

[SCG56-P25] Origin and migration of fluid in the Sumatra subduction input: application of a geochronological method using a long-lived radioisotope of dissolved iodine

*Satoko Owari[1], Hitoshi Tomaru[1] (1.Chiba university)

[SCG56-P26] Challenge to Future Deep-Water Mapping: Unmanned Bathymetric Survey Competition "Shell Ocean Discovery XPRIZE"

*MASANAO SUMIYOSHI[1] (1.Hydrographic and Oceanographic Department, Japan Coast Guard)

[SCG56-P27] Prototype of deep-sea ocean bottom pressure recorder with self-calibration capability using “A-0-A” approach for detection of long-term crustal deformation

*Yusaku Ohta[1], Ryota Hino[1], Syuichi Suzuki[1], Makiko Sato[1], Yui Nishimagi[1], Hiroaki Kajikawa[2], Tokihiko Kobata[2] (1.Research Center for Prediction of Earthquakes and Volcanic Eruptions, Graduate School of Science, Tohoku University, 2.National Metrology Institute of Japan, National Institute of Advanced Industrial Science and Technology)

[SCG56-P28] Noise reduction and surface wave array dispersion measurements applied to NOMan's broadband OBS data

*Yuki Kawano[1], Takehi Isse[1], Hitoshi Kawakatsu[1], Akiko Takeo[1], Hajime Shiobara[1] (1.Earthquake Research Institute, The University of Tokyo)

[SCG56-P29] High-tech dredge system for abyssal bedrock research; dredge system with acoustic real time monitoring on deep sea floor.

*Teruaki Ishii[1], Yukihiro - Kida[2], Izumi - Sakamoto[3], Shiki - - Machida[4] (1.Center for Integrated Research and Education of Natural Hazards, Sizuoka University, 2.JAMSTEC, 3.Toukai University, 4.Chiba Institute of Technology)

[SCG56-P30] Construction of Database System on Offshore Faults around Japan

*Hiromi Kamata[1], Narumi Takahashi[1,2], Shigeyoshi Tanaka[1], Rei Arai[1], Minako Katsuyama[1], Ayako Nakanishi[1], Hiroyuki Fujiwara[2], Tsuneo Ohsumi[2], Takahiko Inoue[3], Tomoyuki Sato[3], Yoshiyuki Kaneda[4] (1.Japan Agency for Marine-Earth Science and Technology, 2.National Research Institute for Earth Science and Disaster Resilience, 3.National Institute of Advanced Industrial Science and Technology, 4.Kagawa University)

[SCG56-P31] **An integration method for multiple sets of seafloor backscatter intensity data**

*Shiki Machida[1,2], Taichi Sato[3], Kazutaka Yasukawa[2] (1.Ocean Resources Research Center for Next Generation, Chiba Institute of Technology, 2.University of Tokyo, 3.AIST)

[SCG56-P32] A precise calculation of average depth for ETOPO1

*Yasushi Harada[1], Sae Horiuchi[1] (1.School of Marine Science and Technology, Tokai University)

[J] Poster | S (Solid Earth Sciences)：S-CG Complex & General

5:15 PM - 6:30 PM JST | 8:15 AM - 9:30 AM UTC | Poster Hall International Exhibition Hall8, Makuhari Messe_29

[S-CG56] Ocean Floor Geosciences

convener:Kyoko Okino(Atmosphere and Ocean Research Institute, The University of Tokyo)

[SCG56-P01] Signature of plume-ridge interaction on bathymetry and geochemistry along mid-ocean ridges: Insights from the Réunion Plume and Central Indian Ridge

*Clement Vincent[1], Jung-Woo Park[1], Sang-Mook Lee[1], Jonguk Kim[2], Sang-Joon Pak[2] (1.Seoul National University, 2.Korea Institute of Ocean Science and Technology)

[SCG56-P02] Spreading rate and its stability of Chile Ridge near the Chile Triple Junction

*Takanori Ishihara[1], Takeshi Matsumoto[1] (1.Ryukyu university)

[SCG56-P03] Newly Mapped Seamounts on the Antarctic Plate off Southern Chile

*Toshiya Fujiwara[1], Natsue Abe[2], Naomi Harada[3], Mirai MR16-09 Leg 2 Shipboard Science Party (1.Research and Development Center for Earthquake and Tsunami, Japan Agency for Marine-Earth Science and Technology, 2.Research and Development Center for Ocean Drilling Science, 3.Research and Development Center for Global Change)

[SCG56-P04] Surface-ship gravimetry on board MR16-09 Cruise by R/V MIRAI - Characteristrics of gravity anomaly around the Chile Triple Junction

*Takeshi Matsumoto[1], Takanori Ishihara[1] (1.Faculty of Science, University of the Ryukyus)

[SCG56-P05] Magnetic and Magnetotelluric surveys across the Afar depression, transition between continental rifting and sea-floor spreading

*Ryokei Yoshimura[1], Naoto Ishikawa[2], Tesfaye Kidane[3], Shin-ichi Kagashima[4], Nobutatsu Mochizuki[5], Ameha Atnafu Muluneh[3], Kirika Kitagawa[4], Taito Ikema[6] (1.Disaster Prevention Research Institute, Kyoto University, 2.Graduate School of Human and Environmental Studies, Kyoto University, 3.Addis Ababa University, 4.Faculty of Science, Yamagata University, 5.Priority Organization for Innovation and Excellence, Kumamoto University, 6.Faculty of Science, Kyoto University)

[SCG56-P06] **Evolution of oceanic core complexes in the Shikoku Basin: when backarc basins cease to open**

*Kyoko Okino[1], Yasuhiko Ohara[2,3], Masakazu Fujii[4], Tomoko Hanyu[1] (1.Atmosphere and Ocean Research Institute, The University of Tokyo, 2.Japan Coast Guard, 3.Japan Agency for Marine-Earth Science and Technology, 4.National Institute of Polar Research)

[SCG56-P07] Thermal evolution of the Lanzo orogenic peridotite massif in western Alps: implications on thermal structure near subcontinental lithosphere-asthenosphere boundary

*Tomo Aoki[1], Kazuhito Ozawa[1], Jean-Louis Bodinier[3], Françoise Boudier[2] (1.The University of Tokyo, 2.Montpellier 2 University, 3.Geosciences Montpellier)

[SCG56-P08] Comparison of the back-arc basins of the South and the Central Ryukyus in the northwest Pacific

*Kohsaku Arai[1], Ayanori Misawa[1], Takahiko Inoue[1] (1.Institute of Geology and Geoinformation, National Institute of Advanced Industrial and Technology)

[SCG56-P09] Geochemistry and zircon U-Pb ages of mafic rocks in the Mikabu and Sorachi-Yezo belts: Comparison with the Shatsky Rise

*Naoto Kimura[1], Yuji Ichiyama[1], Shohei Takahashi[1], Hisatoshi Ito[2], Akihiro Tamura[3], Tomoaki Morishita[3] (1.Chiba University, 2.Central Research Institute of Electric Power Industry, 3.Kanazawa University)

[SCG56-P10] Submersible magnetics reveals relationship between off-axis volcanism and hydrothermal systems of the Kairei and Yokoniwa fields at the Central Indian Ridge

*Masakazu Fujii[1], Kyoko Okino[2] (1.National Institute of Polar Research and SOKENDAI, 2.Atmosphere and Ocean Research Institute, The University of Tokyo)

[SCG56-P11] Shipboard magnetic and gravity surveys around the Iheya North Knoll and the Iheya Minor Ridge in the Mid-Okinawa Trough: Preliminary results of KR18-14 Leg1/Leg2 cruises

*Kazuya Kitada[1], Takafumi Kasaya[1], Hisanori Iwamoto[1], Yoshifumi Nogi[2] (1.Japan Agency for Marine-Earth Science and Technology, 2.National Institute of Polar Research)

[SCG56-P12] A shallow scientific drilling at Higashi Ensei Hydrothermal Field, Okinawa Trough

*Hidenori Kumagai[1], Takafumi Kasaya[1], Shuhei Totsuka[2], Shinsuke Kawagucci[1], Hideaki Machiyama[1], Koichi Iijima[1], Hirofumi Yamamoto[1], junji kaneko[1], Yusuke Ohta[3], Shohei Albert Tomita[3], Shogo Komori[4] (1.Japan Agency for Marine-Earth Science and Technology, 2.Kyushu Univ., 3.Kyoto Univ., 4.AIST)

[SCG56-P13] Mineralogical and geochemical study of sediment cores collected from the Gondou hydrothermal field in the Okinawa Trough

*Jun-ichiro Ishibashi[1,2], Shuhei Totsuka[2], Akihi Tsutsumi[2], Naru Tsukamoto[2], Yusuke Kira[2], Kazuhiko Shimada[1], Toru Yamasaki[3], Ken Ikehara[3], Toshiro Nagase[4], Yutaro Takaya[5,9], Kei Ikehata[6], Takashi Goto[7], Chitaro Gouzu[7], Ryuichi Shinjo[8], Hideaki Machiyama[9], Koichi Iijima[9], Hirofumi Yamamoto[9], Hidenori Kumagai[9] (1.Department of Earth and Planetary Sciences, Kyushu University, 2.Graduate School of Science, Kyushu University, 3.National Institute of Advanced Industrial Science and Technology, 4.Tohoku University Museum, 5.School of Creative Science and Enginerring, Waseda University, 6.Faculty of Life and Environmental Sciences, University of Tsukuba, 7.Hiruzen Institute for Geology and Chronology, 8.Faculty of Science, University of the Ryukyus, 9.Japan Agency for Marine-Earth Science and Technology)

[SCG56-P14] New type of self-potential anomaly observed near a hydrothermal site of Oomuro-dashi volcano, Izu-Ogasawara arc

*Yoshifumi Kawada[1,2], Takafumi Kasaya[2] (1.International Research Institute of Disaster Science, Tohoku University, 2.Japan Agency for Marine-Earth Science and Technology)

[SCG56-P15] Numerical simulation of submarine hydrothermal ore-deposits due to a coupled process of fluid migration and reactive geochemical transport

*Claudia Fujita[1], Hajime Yamamoto[1], Jun-ichiro Ishibashi[2], Takeshi Tsuji[3] (1.Taisei Corporation, 2. Department of Earth and Planetary Sciences, Faculty of Science, Kyushu University, 3.Department of Earth Resources Engineering, Faculty of Science, Kyushu University)

[SCG56-P16] Mineral composition and grain size distribution of REY-rich mud in the Minamitorishima EEZ: Implication for formation process of extremely REY-rich mud

*Sakai Takumi[1], Erika Tanaka[1], Kazutaka Yasukawa[1,2], Junichiro Ohta[2,1], Koichiro Fujinaga[2,1], Kentaro Nakamura[1], Yasuhiro Kato[3,1,2] (1.Department of Systems Innovation, School of Engineering, University of Tokyo, 2.Ocean Resources Research Center for Next Generation, Chiba Institute of Technology, 3.Frontier Research Center for Energy and Resources, School of Engineering, The University of Tokyo)

[SCG56-P17] **Geochemical and morphological features of manganese micronodules in REY-rich mud within the Minamitorishima EEZ, western North Pacific Ocean**

*Satoshi Kino[1], Kazutaka Yasukawa[1,2], Keishiro Azami[1], Erika Tanaka[1], Koichiro Fujinaga[2,1], Kentaro Nakamura[1], Yasuhiro Kato[1,2] (1.Department of Systems Innovation, School of Engineering, University of Tokyo, 2.Ocean Resources Research Center for Next Generation, Chiba Institute of Technology)

[SCG56-P18] Seafloor sediment thickness around the Japan and Kurile trenches obtained by traveltime analysis for PS converted wave recoded by ocean bottom seismograms

*Ryosuke Azuma[1], Genti Toyokuni[1], Ryota Takagi[1], Syuichi Suzuki[1], Makiko Sato[1], Takashi NAKAYAMA[1], Naoki Uchida[1], Ryota Hino[1] (1.Recearch Center for Prediction of Earthquake and Volcanic Eruption, Graduate School of Science, Tohoku University)

[SCG56-P19] Examination of critical taper theory based on bathymetry data in subduction zones

*Hiroaki Koge[1], Juichiro Ashi[1], Jin-Oh Park[1] (1.Atmosphere and Ocean Research Institute, The University of Tokyo)

[SCG56-P20] Active structures of the Sagami Bay Fault by high-resolution sub-bottom profiling and pin-point core sampling

*Juichiro Ashi[1], Asuka Yamaguchi[2], Natsumi Okutsu[1], Ayanori Misawa[3] (1.Graduate School of Frontier Sciences, The University of Tokyo, 2.Atmosphere and Ocean Research Institute, The University of Tokyo, 3.National Institute of Advanced Industrial Science and Technology)

[SCG56-P21] Fault Distribution and Structural Characteristic in the Nankai Trough Area, Japan

*Rei Arai[1], Narumi Takahashi[1], Minako Katsuyama[1], Shigeyoshi Tanaka[1], Hiromi Kamata[1], Tomoyuki Sato[2], Takahiko Inoue[2], Yoshiyuki Kaneda[3] (1.Japan Agency for Marine-Earth Science and Technology, 2.National Institute of Advanced Industrial Science and Technology, 3.Kagawa University)

[SCG56-P22] Seismicity in the central Ryukyu Trench by the Ocean Bottom Seismometers

*Ren Yakabu[1], Mamoru Nakamura[1], Yusuke Yamashita[2], Masanao Shinohara[3], Tomoaki Yamada[3], Hajime Shiobara[3], Kimihiro Mochizuki[3] (1.University of the Ryukyus, 2.DPRI, Kyoto University, 3.ERI, Tokyo University)

[SCG56-P23] Seismic structure of subducted Philippine Sea plate beneath Kyushu inferred from Po/So waves

*Azusa Shito[1] (1.Institute of Seismology and Volcanology, Kyushu University)

[SCG56-P24] Slope failure features and their distribution in the forearc off northwestern Sumatra

*Kenji Hirata[1], Toshiya Fujiwara[2], Ayanori Misawa[3], Kohsaku Arai[3] (1.National Research Institue for Earth Science and Diaster resilience, 2.Japan Agency for Marine-Earth Science and Technology, 3.National Institute of Advanced Industrial Science and Technology)

[SCG56-P25] Origin and migration of fluid in the Sumatra subduction input: application of a geochronological method using a long-lived radioisotope of dissolved iodine

*Satoko Owari[1], Hitoshi Tomaru[1] (1.Chiba university)

[SCG56-P26] Challenge to Future Deep-Water Mapping: Unmanned Bathymetric Survey Competition "Shell Ocean Discovery XPRIZE"

*MASANAO SUMIYOSHI[1] (1.Hydrographic and Oceanographic Department, Japan Coast Guard)

[SCG56-P27] Prototype of deep-sea ocean bottom pressure recorder with self-calibration capability using “A-0-A” approach for detection of long-term crustal deformation

*Yusaku Ohta[1], Ryota Hino[1], Syuichi Suzuki[1], Makiko Sato[1], Yui Nishimagi[1], Hiroaki Kajikawa[2], Tokihiko Kobata[2] (1.Research Center for Prediction of Earthquakes and Volcanic Eruptions, Graduate School of Science, Tohoku University, 2.National Metrology Institute of Japan, National Institute of Advanced Industrial Science and Technology)

[SCG56-P28] Noise reduction and surface wave array dispersion measurements applied to NOMan's broadband OBS data

*Yuki Kawano[1], Takehi Isse[1], Hitoshi Kawakatsu[1], Akiko Takeo[1], Hajime Shiobara[1] (1.Earthquake Research Institute, The University of Tokyo)

[SCG56-P29] High-tech dredge system for abyssal bedrock research; dredge system with acoustic real time monitoring on deep sea floor.

*Teruaki Ishii[1], Yukihiro - Kida[2], Izumi - Sakamoto[3], Shiki - - Machida[4] (1.Center for Integrated Research and Education of Natural Hazards, Sizuoka University, 2.JAMSTEC, 3.Toukai University, 4.Chiba Institute of Technology)

[SCG56-P30] Construction of Database System on Offshore Faults around Japan

*Hiromi Kamata[1], Narumi Takahashi[1,2], Shigeyoshi Tanaka[1], Rei Arai[1], Minako Katsuyama[1], Ayako Nakanishi[1], Hiroyuki Fujiwara[2], Tsuneo Ohsumi[2], Takahiko Inoue[3], Tomoyuki Sato[3], Yoshiyuki Kaneda[4] (1.Japan Agency for Marine-Earth Science and Technology, 2.National Research Institute for Earth Science and Disaster Resilience, 3.National Institute of Advanced Industrial Science and Technology, 4.Kagawa University)

[SCG56-P31] **An integration method for multiple sets of seafloor backscatter intensity data**

*Shiki Machida[1,2], Taichi Sato[3], Kazutaka Yasukawa[2] (1.Ocean Resources Research Center for Next Generation, Chiba Institute of Technology, 2.University of Tokyo, 3.AIST)

[SCG56-P32] A precise calculation of average depth for ETOPO1

*Yasushi Harada[1], Sae Horiuchi[1] (1.School of Marine Science and Technology, Tokai University)

[J] Oral | S (Solid Earth Sciences)：S-CG Complex & General

10:45 AM - 12:15 PM JST | 1:45 AM - 3:15 AM UTC | A05 TOKYO BAY MAKUHARI HALL

[S-CG60] Investigation of inputs to subduction zones: Influence of tectonic processes on the incoming plate

convener:Makoto Yamano(Earthquake Research Institute, the University of Tokyo), Tomoaki Morishita(School of Geoscience and Civil Engineering, College of Science and Technology, Kanazawa University), Gou Fujie(Japan Agency for Marine-Earth Science and Technology), Chairperson:Shigeaki Ono(Japan Agency for Marine-Earth Science and Technology)

10:45 AM - 11:00 AM JST | 1:45 AM - 2:00 AM UTC

[SCG60-01] Geophysical-petrological studies of the Chile triple junction and their significance: MIRAI research cruise MR-1806Leg2

*Masataka Kinoshita[1,5], Hikaru Iwamori[1,5], Tomoaki Nishikawa[2], Ryo Anma[3], Sofia Lagarrigue[4], Natsue Abe[5], Yuka Yokoyama[6], Andres Veloso Espinosa[4], Alessandra Isabella Rivero Cortes[7], Gabriela Pia Lazcano Prado[7], Ivan Andres Arriagada Bascuñan[7], Satoru Haraguchi[5], Kosuke Ota[9], Yuji Orihashi[8], Kaishi Nakao[8], Shogo Numata[8], Hajime Shiobara[1], Hiroko Sugioka[10], Aki Ito[5], Nicolás Pérez-Estay[11] (1.Earthquake Research Institute, University of Tokyo, 2.DPRI, Kyoto Univ., 3.Tokushima Univ., 4.Pontificia Universidad Catolica de Chile, 5.JAMSTEC, 6.Tokai Univ., 7.Andres Bello University, 8.Hirosaki Univ., 9.AORI, Univ. Tokyo, 10.Graduate School of Science, Kobe Univ., 11.Ministerio de relaciones exteriores, Chile)

11:00 AM - 11:15 AM JST | 2:00 AM - 2:15 AM UTC

[SCG60-02] Heat flow measurement on the seaward side of the Kuril Trench off Hokkaido

*Kouta Sasaki[1], Makoto Yamano[1], Yoshifumi Kawada[2], Masataka Kinoshita[1], Kiichiro Kawamura[3] (1.Earthquake Research Institute, the University of Tokyo, 2.International Research Institute of Disaster Science, Tohoku University, 3.Yamaguchi University)

11:15 AM - 11:30 AM JST | 2:15 AM - 2:30 AM UTC

[SCG60-03] Comparison of experimental and intermediate-depth earthquake b-value: difference in hydration degree of the oceanic mantle between Tohoku and Hokkaido

★Invited Papers

*Saeko Kita[1], Thomas P. Ferrand[2] (1.International Institute of Seismology and Earthquake Engineering, BRI, 2.ERI, University of Tokyo)

11:30 AM - 11:45 AM JST | 2:30 AM - 2:45 AM UTC

[SCG60-04] Variations in bend faulting and the nature of the incoming oceanic plate off northeast Japan arc

*Gou Fujie[1], Koichiro Obana[1], Yojiro Yamamoto[1], Tomoaki Yamada[2], Takehi Isse[2], Shuichi Kodaira[1], Seiichi Miura[1] (1.Japan Agency for Marine-Earth Science and Technology, 2.Earthquake Research Institute, Univ. of Tokyo)

11:45 AM - 12:00 PM JST | 2:45 AM - 3:00 AM UTC

[SCG60-05] Seismicity in the trench-outer rise region off Fukushima and Ibaraki, southern Japan Trench

*Koichiro Obana[1], Gou Fujie[1], Yojiro Yamamoto[1], Yuka Kaiho[1], Yasuyuki Nakamura[1], Seiichi Miura[1], Tsutomu Takahashi[1], Shuichi Kodaira[1] (1.Research and Development Center for Earthquake and Tsunami, Japan Agency for Marine-Earth Science and Technology)

12:00 PM - 12:15 PM JST | 3:00 AM - 3:15 AM UTC

[SCG60-06] Influence of water–rock interactions on the strength of outer-rise faults

★Invited Papers

*Ken-ichi Hirauchi[1] (1.Department of Geosciences, Faculty of Science, Shizuoka University)

[J] Oral | S (Solid Earth Sciences)：S-CG Complex & General

1:45 PM - 3:15 PM JST | 4:45 AM - 6:15 AM UTC | A05 TOKYO BAY MAKUHARI HALL

[S-CG60] Investigation of inputs to subduction zones: Influence of tectonic processes on the incoming plate

convener:Makoto Yamano(Earthquake Research Institute, the University of Tokyo), Tomoaki Morishita(School of Geoscience and Civil Engineering, College of Science and Technology, Kanazawa University), Gou Fujie(Japan Agency for Marine-Earth Science and Technology), Chairperson:Makoto Yamano(Earthquake Research Institute, University of Tokyo)

1:45 PM - 2:00 PM JST | 4:45 AM - 5:00 AM UTC

[SCG60-07] Seismic image of the incoming oceanic crust entering the central part of the Japan Trench: structural variation caused by petite-spot, bend fault and seamount

*Shuichi Kodaira[1,2], Akane Ohira[1,2], Gou Fujie[1], Tetsuo No[1], Yasuyuki Nakamura[1], Yuka Kaiho[1], Seiichi Miura[1] (1.R&D Center for Earthquake and Tsunami Japan Agency for Marine-Earth Science and Technology, 2.Graduate School of Environment and Information Sciences, Yokohama National University)

2:00 PM - 2:15 PM JST | 5:00 AM - 5:15 AM UTC

[SCG60-08] Dependence of calculation parameters on tsunami height from the outer-rise earthquakes

*Toshitaka Baba[1], Naotaka YAMAMOTO CHIKASADA[2], Yasuyuki Nakamura[3], Gou Fujie[3], Koichiro Obana[3], Seiichi Miura[3], Shuichi Kodaira[3] (1.Graduate School of Science and Technology, Tokushima University, 2.National Research Institute for Earth Science and Disaster Resilience, 3.Japan Agency for Marine-Earth Science and Technology)

2:15 PM - 2:30 PM JST | 5:15 AM - 5:30 AM UTC

[SCG60-09] Bathymetry data analysis and multi-channel seismic reflection survey in the 1933 Sanriku earthquake (Mw 8.4) rupture region

*Tomoko Hanyu[1], Jin-Oh Park[1], Yukari Kido[2] (1.Atmosphere and Ocean Research Institute, The University of Tokyo, 2.Japan Agency for Marine-Earth Science and Technology)

2:30 PM - 2:45 PM JST | 5:30 AM - 5:45 AM UTC

[SCG60-10] Sedimentation process and deformation process before sinking of sediment on oceanic plate: examples in northwest Pacific Ocean and Sumatra

★Invited Papers

*Kiichiro Kawamura[1] (1.Yamaguchi University)

2:45 PM - 3:00 PM JST | 5:45 AM - 6:00 AM UTC

[SCG60-11] Exploring more asthenospheric melt: the preliminary report of KS-18-9 cruise, R/V Shinseimaru

*Naoto Hirano[1], Taku Yutani[2,1], Yuki Katsuragi[1], Jeffrey Anthony Oalmann[3], Fidel Costa Rodriguez[3], KS-18-9 Onboard Scientific Party (1.Tohoku University, 2.University of Bayreuth, 3.Nanyang Technological University)

3:00 PM - 3:15 PM JST | 6:00 AM - 6:15 AM UTC

[SCG60-12] Inputs of Argon on oceanic plate at subduction zones

*Shigeaki Ono[1] (1.Japan Agency for Marine-Earth Science and Technology)

[J] Poster | S (Solid Earth Sciences)：S-CG Complex & General

3:30 PM - 5:00 PM JST | 6:30 AM - 8:00 AM UTC | Poster Hall International Exhibition Hall8, Makuhari Messe_18

[S-CG60] Investigation of inputs to subduction zones: Influence of tectonic processes on the incoming plate

convener:Makoto Yamano(Earthquake Research Institute, the University of Tokyo), Tomoaki Morishita(School of Geoscience and Civil Engineering, College of Science and Technology, Kanazawa University), Gou Fujie(Japan Agency for Marine-Earth Science and Technology)

[SCG60-P01] Tsunami Simulations of the 2006 and 2007 Kuril Earthquakes

Cancelled

*Keiji Akai[1] (1.Graduate School of Advanced Technology and Science, Tokushima University)

[SCG60-P02] The variation of seismic attributes about incoming oceanic crust in Nankai Trough using multi-channel seismic reflection data

*Mikiya Yamashita[1], Seiichi Miura[1], Ayako Nakanishi[1], Jin-Oh Park[2], Shuichi Kodaira[1] (1.Japan Agency for Marine-Earth Science and Technology, 2.Department of Ocean Floor Geoscience, Atmosphere and Ocean Research Institute, The University of Tokyo)

[SCG60-P03] Bending-Related Topographic Structures of the Subducting Plate in the Southeastern Pacific Ocean

*Reno Kotate[1], Masao Nakanishi[2] (1.Chiba University Graduate School Science and Engineering Dvision of Earth and Environmental Scienes Department of Earth Sciences, 2.Chiba University Graduate School Faculty of Science)

[SCG60-P04] **Detailed tectonic structure of the Japan Trench subduction zone off Miyagi by 2D pre-stack depth migration imaging**

*GUO CHEN[1], Jin-Oh Park[1] (1.The University of Tokyo)

[SCG60-P05] Conductive zone of incoming Pacific Plate in the outer rise region off Japan trench

*Shinya Sato[1], Tada-nori Goto[1], Takafumi Kasaya[2], Hiroshi Ichihara[3], Makoto Yamano[4] (1.Kyoto Univesity, Graduate School of Engineering, 2.Japan Agency for Marine-Earth Science and Technology, 3.Nagoya University, Graduate School of Environmental Studies, 4.University of Tokyo, Earthquake Research Institute)

[SCG60-P06] Geochemical variations of the asthenosphere inferred from the geochemistry of petit-spot lavas in the NW Pacific plate

*Yuki Katsuragi[1], Naoto Hirano[1], Kenji Shimizu[2], Fidel Costa[3], Jaffrey Oalmann[3], Taku Yutani[1] (1.Tohoku University, 2.Kochi Core Center, Kochi University / JAMSTEC, 3.Nanyang Technological University)

[J] Poster | S (Solid Earth Sciences)：S-CG Complex & General

5:15 PM - 6:30 PM JST | 8:15 AM - 9:30 AM UTC | Poster Hall International Exhibition Hall8, Makuhari Messe_30

[S-CG60] Investigation of inputs to subduction zones: Influence of tectonic processes on the incoming plate

convener:Makoto Yamano(Earthquake Research Institute, the University of Tokyo), Tomoaki Morishita(School of Geoscience and Civil Engineering, College of Science and Technology, Kanazawa University), Gou Fujie(Japan Agency for Marine-Earth Science and Technology)

[SCG60-P01] Tsunami Simulations of the 2006 and 2007 Kuril Earthquakes

*Keiji Akai[1] (1.Graduate School of Advanced Technology and Science, Tokushima University)

[SCG60-P02] The variation of seismic attributes about incoming oceanic crust in Nankai Trough using multi-channel seismic reflection data

*Mikiya Yamashita[1], Seiichi Miura[1], Ayako Nakanishi[1], Jin-Oh Park[2], Shuichi Kodaira[1] (1.Japan Agency for Marine-Earth Science and Technology, 2.Department of Ocean Floor Geoscience, Atmosphere and Ocean Research Institute, The University of Tokyo)

[SCG60-P03] Bending-Related Topographic Structures of the Subducting Plate in the Southeastern Pacific Ocean

*Reno Kotate[1], Masao Nakanishi[2] (1.Chiba University Graduate School Science and Engineering Dvision of Earth and Environmental Scienes Department of Earth Sciences, 2.Chiba University Graduate School Faculty of Science)

[SCG60-P04] **Detailed tectonic structure of the Japan Trench subduction zone off Miyagi by 2D pre-stack depth migration imaging**

*GUO CHEN[1], Jin-Oh Park[1] (1.The University of Tokyo)

[SCG60-P05] Conductive zone of incoming Pacific Plate in the outer rise region off Japan trench

*Shinya Sato[1], Tada-nori Goto[1], Takafumi Kasaya[2], Hiroshi Ichihara[3], Makoto Yamano[4] (1.Kyoto Univesity, Graduate School of Engineering, 2.Japan Agency for Marine-Earth Science and Technology, 3.Nagoya University, Graduate School of Environmental Studies, 4.University of Tokyo, Earthquake Research Institute)

[SCG60-P06] Geochemical variations of the asthenosphere inferred from the geochemistry of petit-spot lavas in the NW Pacific plate

*Yuki Katsuragi[1], Naoto Hirano[1], Kenji Shimizu[2], Fidel Costa[3], Jaffrey Oalmann[3], Taku Yutani[1] (1.Tohoku University, 2.Kochi Core Center, Kochi University / JAMSTEC, 3.Nanyang Technological University)

[J] Oral | S (Solid Earth Sciences)：S-CG Complex & General

1:45 PM - 3:15 PM JST | 4:45 AM - 6:15 AM UTC | Convention Hall A 2F

[S-CG61] Dynamics in mobile belts

convener:Yukitoshi Fukahata(Disaster Prevention Research Institute, Kyoto University), Toru Takeshita(Department of Natural History Sciences, Graduate School of Science, Hokkaido University), Hikaru Iwamori(Geochemical Evolution Research Program, Japan Agency for Marine-Earth Science and Technology), Chairperson:Toru Takeshita, Kenta Kobayashi

1:45 PM - 2:00 PM JST | 4:45 AM - 5:00 AM UTC

[SCG61-01] Fault zone development in the West Tottori area, Japan

*Kenta Kobayashi[1] (1.Department of Geology, Faculty of Science, Niigata University)

2:00 PM - 2:15 PM JST | 5:00 AM - 5:15 AM UTC

[SCG61-02] **Inerastic deformation around focal area of the 2000 Western Tottori EQ (M7.3) detected by "0.1 manten" Hyper Dense Seismic Observation (2)**

★Invited Papers

*Satoshi Matsumoto[1], Yoshihisa Iio[2], Shin'ichi Sakai[3], Aitaro Kato[3], Takuo Shibutani[2], Yuto Hayashida[4], Group for 0.1 manten Hyper dense seismic observation (1.Institute of Seismology and Volcanology, Faculty of Sciences, Kyushu University, 2.Disaster Prevention Reasearch Institute, Kyoto University, 3.Earthquake Research Institute, University of Tokyo, 4.Graduate School of Science, Kyushu University)

2:15 PM - 2:30 PM JST | 5:15 AM - 5:30 AM UTC

[SCG61-03] Non-double couple micro-earthquakes in the focal area of the 2000 Western Tottori earthquake (M7.3) by "0.1 manten" hyper dense seismic observation

*Yuto Hayashida[1], Satoshi Matsumoto[2], Yoshihisa Iio[3], Shin'ichi Sakai[4], Aitaro Kato[4], Group for "0.1 Manten" hyper dense seismic observation Group registration (1.Department of Earth and Planetary Sciences, Graduate School of Science, Kyushu University, 2.Institute of Seismology and Volcanology, Faculty of Sciences, Kyushu University, 3.Disater Prevention Research Institute, Kyoto University, 4.Earthquake Research Institute, the University of Tokyo)

2:30 PM - 2:45 PM JST | 5:30 AM - 5:45 AM UTC

[SCG61-04] Stress field in the Western Tottori and Western Shimane regions deduced by the dense seismic observations

*Yoshihisa Iio[1], Manten seicmic observation group, Manten seismic observation group in the Western Tottori region (1.Disater Prevention Research Institute, Kyoto University)

2:45 PM - 3:00 PM JST | 5:45 AM - 6:00 AM UTC

[SCG61-05] Modeling the spatiotemporal change in stress field around Hinagu fault zone through the 2016 Kumamoto earthquake sequence, in central Kyushu, Japan

*Ayaho Mitsuoka[1], Satoshi Matsumoto[2], Azusa Shito[2], Yusuke Yamashita[3], Manami Nakamoto[4], Masahiro Miyazaki[3], Shin'ichi Sakai[5], Yoshihisa Iio[3], Group for urgent joint seismic observation of the 2016 Kumamoto earthquake (1.Department of Earth and Planetary Sciences, Graduate School of Science, Kyushu University, 2.Institute of Seismology and Volcanology, Faculty of Sciences, Kyushu University, 3.Disaster Prevention Research Institute, Kyoto University, 4.Association for the Development of Earthquake Prediction, 5.Earthquake Research Institute, The University of Tokyo)

3:00 PM - 3:15 PM JST | 6:00 AM - 6:15 AM UTC

[SCG61-06] **Development of the Median Tectonic Line Fault zone in Mie Prefecture, Southwest Japan : A Possible Interpretation for Strain Localization and Softening**

*Toru Takeshita[1], Dong Van Bui[1], Thomas Anthony Czertowicz[1], Shun Arai[2], Takafumi Yamamoto[3], Jun-ichi Ando[3], Norio Shigematsu[4], Koichiro Fujimoto[5] (1.Department of Natural History Sciences, Graduate School of Science, Hokkaido University, 2.Department of Earth Science, Graduate School of Science, Tohoku University, 3.Department of Earth and Planetary Systems Science, Hiroshima University, 4.AIST, 5.Tokyo Gakugei University)

[J] Oral | S (Solid Earth Sciences)：S-CG Complex & General

3:30 PM - 5:00 PM JST | 6:30 AM - 8:00 AM UTC | Convention Hall A 2F

[S-CG61] Dynamics in mobile belts

convener:Yukitoshi Fukahata(Disaster Prevention Research Institute, Kyoto University), Toru Takeshita(Department of Natural History Sciences, Graduate School of Science, Hokkaido University), Hikaru Iwamori(Geochemical Evolution Research Program, Japan Agency for Marine-Earth Science and Technology), Chairperson:Tomomi Okada, Ryosuke Ando(Graduate School of Science, University of Tokyo)

3:30 PM - 3:45 PM JST | 6:30 AM - 6:45 AM UTC

[SCG61-07] **What caused the Main Himalayan Thrust (MHT) to ramp? Insights from analogue and numerical models**

*Subhajit Ghosh[1,2], Arijit Laik[2], Santanu Bose[2,3], Nibir Mandal[4] (1.Earthquake Research Institute, The University of Tokyo, 1-1-1 Yayoi, Bunkyo-Ku, Tokyo 113-0032, 2.Department of Geology, University of Calcutta, 35, Ballygunge Circular Road, Kolkata 700019, India, 3.Department of Geology, Presidency University, 86/1 College Street, Kolkata 700073, India, 4.Department of Geological Sciences, Jadavpur University, Kolkata 700032, India)

3:45 PM - 4:00 PM JST | 6:45 AM - 7:00 AM UTC

[SCG61-08] Control of fault weakening on the structural styles of underthrusting-dominated non-cohesive tectonic wedges

*Arthur Bauville[1], Mikito Furuichi[1] (1.Department of Mathematical Science and Advanced Techology, JAMSTEC)

4:00 PM - 4:15 PM JST | 7:00 AM - 7:15 AM UTC

[SCG61-09] **Complexity of the 2016 *M* 7.8 Kaikoura, New Zealand, earthquake from seismic observation: inferences of overpressured fluid involvement**

*Tomomi Okada[1], Satoshi Matsumoto[2], Yoshihisa Iio[3], Federica Lanza[4], Clifford H Thurber[4], Miu Matsuno[1], Yuta Kawamura[2], Tadashi Sato[1], Stephen C Bannister[5], John Ristau[5], Martha K Savage[6], John Townend[6], Jarg Petttinga[7], Francesca Ghisetti[8], Richard H Sibson[9] (1.Research Center for Prediction of Earthquakes and Volcanic Eruptions, Graduate School of Science, Tohoku University, 2. Institute of Seismology and Volcanology, Faculty of Sciences, Kyushu University, 3. Disater Prevention Research Institute, Kyoto University, 4.University of Wisconsin-Madison, U.S.A., 5.GNS Science, New Zealand, 6.Victoria University of Wellington, New Zealand, 7.University of Canterbury, New Zealand, 8.TerraGeoLogica, New Zealand, 9.University of Otago, New Zealand)

4:15 PM - 4:30 PM JST | 7:15 AM - 7:30 AM UTC

[SCG61-10] Dynamic Rupture Simulation Reproduces Spontaneous Multifault Rupture and Arrest During the 2016 Mw 7.9 Kaikoura Earthquake

*Ryosuke Ando[1], Yoshihiro Kaneko[2] (1.Graduate School of Science, University of Tokyo, 2.GNS science)

4:30 PM - 4:45 PM JST | 7:30 AM - 7:45 AM UTC

[SCG61-11] Ductile deformation explains the physics of friction and genesis of earthquakes

*James Daniel Paul Moore[1], Stefan Nielsen[2], Lars N Hansen[3] (1.Earth Observatory of Singapore, 2.University of Durham, 3.University of Oxford)

4:45 PM - 5:00 PM JST | 7:45 AM - 8:00 AM UTC

[SCG61-12] The seismic moment, stress drop, and strain energy release for the rupture of asperities

*Mitsuhiro Matsu'ura[1] (1.Institute of Statistical Mathematics)

[E] Poster | B (Biogeosciences)：B-BG Biogeosciences & Geosphere-Biosphere Interactions

1:45 PM - 3:15 PM JST | 4:45 AM - 6:15 AM UTC | Poster Hall International Exhibition Hall8, Makuhari Messe_6

[B-BG01] Elemental cycling in terrestrial and coastal ecosystems- Carbon and Nitrogen perspectives

convener:Punyasloke Bhadury(Indian Institute of Science Education and Research Kolkata)

[BBG01-P01] Forest-CEW: A Forest Ecosystems Model for Carbon-Energy-Water Processes.

*Zhenghong Tan[1] (1.Hainan University China)

[BBG01-P02] **Interdependent Dynamics of LAI-ET across Roofing Landscapes: the Mongolian and Tibetan Plateaus**

*Li Tian[1] (1.Institute of Geographic Sciences and Natural Resources Research, Chinese Academy of Sciences)

[BBG01-P03] **Particle Phase Organic compounds (PAHs and VOCs) at Two Big Cities (Dhaka and Rajshahi) in Bangladesh**

*Islam Nazrul nazrulislam6727@gmail.com[1], Tanzina Tul Karim[1], Rasheda Nahida[1], Nusrat Mousume[1], Farha Jeba[1], Abdus Salam[1] (1.Department of Chemistry, University of Dhaka, Dhaka-1000, Bangladesh)

[BBG01-P04] **Diversity and activity of diazotrophs in the coastal waters of Southeastern Arabian Sea (SEAS)**

*JABIR THAJUDEEN[1], Mohamed Hatha Abdullah (1.Cochin University of Science and Technology India)

[BBG01-P05] **Bloom of *Palmerina hardmaniana*, a marine centric planktonic diatom in a coastal mangrove ecosystem- implication for coastal carbon cycling**

*Punyasloke Bhadury[1] (1.Centre for Climate and Environmental Studies and Department of Biological Sciences, Indian Institute of Science Education and Research Kolkata)

[BBG01-P06] Dynamics of Carbon and Nitrogen influx in large river system: Isotopic study from river Ganga, India

*Anurag Kumar[1], Prasanta Sanyal[1,2], Punyasloke Bhadury[3,2] (1.Department of Earth Sciences, Indian Institute of Science Education and Research Kolkata, Mohanpur 741246, India, 2.Centre for Climate and Environmental studies, Indian Institute of Science Education and Research Kolkata, Mohanpur 741246, India, 3.Department of Biological Sciences, Indian Institute of Science Education and Research Kolkata, Mohanpur 741246, India)

[E] Poster | B (Biogeosciences)：B-BG Biogeosciences & Geosphere-Biosphere Interactions

5:15 PM - 6:30 PM JST | 8:15 AM - 9:30 AM UTC | Poster Hall International Exhibition Hall8, Makuhari Messe_31

[B-BG01] Elemental cycling in terrestrial and coastal ecosystems- Carbon and Nitrogen perspectives

convener:Punyasloke Bhadury(Indian Institute of Science Education and Research Kolkata)

[BBG01-P01] Forest-CEW: A Forest Ecosystems Model for Carbon-Energy-Water Processes.

*Zhenghong Tan[1] (1.Hainan University China)

[BBG01-P02] **Interdependent Dynamics of LAI-ET across Roofing Landscapes: the Mongolian and Tibetan Plateaus**

*Li Tian[1] (1.Institute of Geographic Sciences and Natural Resources Research, Chinese Academy of Sciences)

[BBG01-P03] **Particle Phase Organic compounds (PAHs and VOCs) at Two Big Cities (Dhaka and Rajshahi) in Bangladesh**

*Islam Nazrul nazrulislam6727@gmail.com[1], Tanzina Tul Karim[1], Rasheda Nahida[1], Nusrat Mousume[1], Farha Jeba[1], Abdus Salam[1] (1.Department of Chemistry, University of Dhaka, Dhaka-1000, Bangladesh)

[BBG01-P04] **Diversity and activity of diazotrophs in the coastal waters of Southeastern Arabian Sea (SEAS)**

*JABIR THAJUDEEN[1], Mohamed Hatha Abdullah (1.Cochin University of Science and Technology India)

[BBG01-P05] **Bloom of *Palmerina hardmaniana*, a marine centric planktonic diatom in a coastal mangrove ecosystem- implication for coastal carbon cycling**

*Punyasloke Bhadury[1] (1.Centre for Climate and Environmental Studies and Department of Biological Sciences, Indian Institute of Science Education and Research Kolkata)

[BBG01-P06] Dynamics of Carbon and Nitrogen influx in large river system: Isotopic study from river Ganga, India

*Anurag Kumar[1], Prasanta Sanyal[1,2], Punyasloke Bhadury[3,2] (1.Department of Earth Sciences, Indian Institute of Science Education and Research Kolkata, Mohanpur 741246, India, 2.Centre for Climate and Environmental studies, Indian Institute of Science Education and Research Kolkata, Mohanpur 741246, India, 3.Department of Biological Sciences, Indian Institute of Science Education and Research Kolkata, Mohanpur 741246, India)

[E] Oral | B (Biogeosciences)：B-BG Biogeosciences & Geosphere-Biosphere Interactions

3:30 PM - 5:00 PM JST | 6:30 AM - 8:00 AM UTC | 201A 2F

[B-BG01] Elemental cycling in terrestrial and coastal ecosystems- Carbon and Nitrogen perspectives

convener:Punyasloke Bhadury(Indian Institute of Science Education and Research Kolkata),
Chairperson:Punyasloke Bhadury(Indian Institute of Science Education and Research Kolkata)

3:35 PM - 4:00 PM JST | 6:35 AM - 7:00 AM UTC

[BBG01-01] **Modelling nitrogen and carbon cycles in Hooghly estuary along with adjacent mangrove ecosystem**

★Invited Papers

*Santanu Ray[1] (1.Systems ecology and ecological modelling laboratory, Dept. of Zoology, Visva-Bharati University, Santiniketan 731235, India)

4:00 PM - 4:15 PM JST | 7:00 AM - 7:15 AM UTC

[BBG01-02] ^{17}O-rich nitrate as a tracer for constraining nitrogen transformations in coastal sediments

*Chawalit Charoenpong[1,2], Scott D Wankel[2], Carolyn Buchwald[3,2], Wiebke Ziebis[4] (1.Chulalongkorn University, 2.Woods Hole Oceanographic Institution, 3.Dalhousie University, 4.University of Southern California)

4:15 PM - 4:30 PM JST | 7:15 AM - 7:30 AM UTC

[BBG01-03] **Exploring changes in bacterioplankton community structure in response to tannic acid, a major component of litterfall, in a mangrove ecosystem: a laboratory mesocosm approach**

*Anwesha Ghosh[1] (1.Integrative Tax Microb Ecol Res Group, Dept. of Biol Sci, IISERK)

4:30 PM - 4:45 PM JST | 7:30 AM - 7:45 AM UTC

[BBG01-04] **Diel variations of dissolved inorganic carbon in the Pearl River plume and the northern South China Sea shelf upwelling during summer**

*Wei-Jen Huang[1], Kai-Jung Kao[1], Yu-Shih Lin[1], James T. Liu[1], Chen-Tung Arthur Chen[1] (1.National Sun Yat-sen University)

4:45 PM - 5:00 PM JST | 7:45 AM - 8:00 AM UTC

[BBG01-05] **Spatial and vertical variations of carbon and nitrogen isotopes of larch forest and NDVI in Eastern Siberia**

*Aleksandr Nogovitcyn[1], Atsuko Sugimoto[2], Ruslan Shakhmatov[1], Tomoki Morozumi[1], Shunsuke Tei[2], Yumiko Miyamoto[2], Trofim Maximov[3,4] (1.Graduate School of Environmental Science, Hokkaido University, Sapporo, Hokkaido, Japan, 2.Arctic Research Center, Hokkaido University, Sapporo, Hokkaido, Japan, 3.Institute for Biological Problems of Cryolithozone, Siberian Blanch of Russian Academy of Sciences, Yakutsk, Yakutia, Russia, 4.International Center for Biogeoscience Educational and Scientific Trainings (BEST), North-Eastern Federal University, Yakutsk, Yakutia, Russia)

[E] Oral | M (Multidisciplinary and Interdisciplinary) : M-IS Intersection

9:00 AM - 10:30 AM JST | 12:00 AM - 1:30 AM UTC | A07 TOKYO BAY MAKUHARI HALL

[M-IS02] Drilling Earth Science

convener:Yasuhiro Yamada(Japan Agency for Marine-Earth Science and Technology (JAMSTEC), R&D Center for Ocean Drilling Science (ODS)), Yumiko Harigane(Geological Survey of Japan, National Institute of Advanced Industrial Science and Technology (AIST)), Azumi Kuroyanagi(Tohoku University Museum, The Center for Academic Resources and Archives, Tohoku University), Kosei E. Yamaguchi(Toho University and NASA Astrobiology Institute), Chairperson:Azumi Kuroyanagi(Tohoku University), Kan Hsiung(JAMSTEC)

9:00 AM - 9:15 AM JST | 12:00 AM - 12:15 AM UTC

[MIS02-01] Planktonic foraminiferal biostratigraphy in the South China Sea IODP Exp. 367 U 1499

*Akira Furusawa[1], Hiroki Hayashi[1] (1.Interdisciplinary Graduate School of Science and Engineering, Shimane University)

9:15 AM - 9:30 AM JST | 12:15 AM - 12:30 AM UTC

[MIS02-02] High heat with slow cooling of rift margin in the South China Sea, IODP Exp.368

*Arito Sakaguchi[1,2], Nobuaki Osono[1], Keita Nakano[1] (1.Yamaguchi Univ., 2.JAMSTEC)

9:30 AM - 9:45 AM JST | 12:30 AM - 12:45 AM UTC

[MIS02-03] Abundant ferromanganese microparticles in oxic pelagic sediments (IODP Exp. 329)

*Go-Ichiro Uramoto[1,2], Yuki Morono[2], Naotaka Tomioka[2], Shigeyuki Wakaki[2], Ryoichi Nakada[2], Rota Wagai[3], Kentaro Uesugi[4], Akihisa Takeuchi[4], Masato Hoshino[4], Yoshio Suzuki[4,5], Satoshi Mitsunobu[6], Fumito Shiraishi[7], Hiroki Suga[5], Yasuo Takeichi[8], Yoshio Takahashi[5], Fumio Inagaki[2] (1.Kochi University, 2.Japan Agency for Marine-Earth Science and Technology, 3.National Agriculture and Food Research Organization, 4.Japan Synchrotron Radiation Research Institute, 5.University of Tokyo, 6.Ehime University, 7.Hiroshima University, 8.High Energy Accelerator Research Organization)

9:45 AM - 10:00 AM JST | 12:45 AM - 1:00 AM UTC

[MIS02-04] **Regional stratigraphic framework, Gas Hydrate occurrence and distribution of National Gas Hydrate Program Expedition 02 (NGHP-02) Area-B, offshore eastern India**

*KanHsi Hsiung[1], Saneatsu Saito[1], Toshiya Kanamatsu[1], Yoshinori Sanada[1], Yasuhiro Yamada[1], KYAW MOE[1], Yohei Hamada[1], Yasuyuki Nakamura[1], HungYu Wu[1] (1.Japan Agency for Marine-Earth Science and Technology)

10:00 AM - 10:15 AM JST | 1:00 AM - 1:15 AM UTC

[MIS02-05] Fluid flow and diagenetic process in frontal thrust zone off Cape Muroto in the Nankai Trough

*Akira Ijiri[1], Shigeyuki Wakaki[1], Yoshiro Nishio[2], Yohei Hamada[1], Tsuyoshi Ishikawa[1], Fumio Inagaki[1] (1.Japan Agency for Marine-Earth Science and Technology, 2.Kochi University)

10:15 AM - 10:30 AM JST | 1:15 AM - 1:30 AM UTC

[MIS02-06] Recent progress and perspective on paleomagnetism by means of deep-sea drilling

*Toshitsugu Yamazaki[1], Yuhji Yamamoto[2], Toshiya Kanamatsu[3], Yuho Kumagai[4], Norihiro Nakamura[4] (1.Atmosphere and Ocean Research Institute, The University of Tokyo, 2.Center for Advanced Marine Core Research, Kochi University, 3.Japan Agency for Marine-Earth Science and Technology, 4.Tohoku University)

[E] Oral | M (Multidisciplinary and Interdisciplinary)：M-IS Intersection

10:45 AM - 12:15 PM JST | 1:45 AM - 3:15 AM UTC | A07 TOKYO BAY MAKUHARI HALL

[M-IS02] Drilling Earth Science

convener:Yasuhiro Yamada(Japan Agency for Marine-Earth Science and Technology (JAMSTEC), R&D Center for Ocean Drilling Science (ODS)), Yumiko Harigane(Geological Survey of Japan, National Institute of Advanced Industrial Science and Technology (AIST)), Azumi Kuroyanagi(Tohoku University Museum, The Center for Academic Resources and Archives, Tohoku University), Kosei E. Yamaguchi(Toho University and NASA Astrobiology Institute), Chairperson:Kosei Yamaguchi(Toho University), Yasuhiro Yamada(JAMSTEC)

10:45 AM - 11:00 AM JST | 1:45 AM - 2:00 AM UTC

[MIS02-07] Patterns in natural fractures during transitions between stress regimes

*Nikita Dubinya[1] (1.The Schmidt Institute of Physics of the Earth of the Russian Academy of Sciences)

11:00 AM - 11:15 AM JST | 2:00 AM - 2:15 AM UTC

[MIS02-08] ICDP DSeis 1: Introduction into JpGU 2019 papers on Drilling into Seismogenic zones of M2.0-5.5 earthquakes in South African gold mines

*Hiroshi Ogasawara[1], Bennie Liebenberg[2], Martin Ziegler[3], Yasuo Yabe[4], Ray Durrheim[5], Musa Manzi[5], Tullis C Onstott[6], Thomas Weirsberg[7] (1.Faculty of Science and Engineering, Ritsumeikan University, 2.Moab Khotsong mine, South Africa, 3.ETH, Zurich Dep. Earth Sciences, 4.Graduate School of Science, Tohoku Univ., 5.Univ. Witwatersrand, School of Geoscience, South Africa, 6.Princeton Univ., Dept. Geoscience, USA, 7.GFZ, Potzdam, Germany)

11:15 AM - 11:30 AM JST | 2:15 AM - 2:30 AM UTC

[MIS02-09] ICDP DSeis 2: Preliminary results of physical property measurement and XRD analysis of the M5.5 fault material recovered from DSeis Project

*Tetsuro Hirono[1], Yuki Yukoyama[1], Shunya Kaneki[2], Hiroshi Ogasawara[3], Yasuo Yabe[4], Takuya Matsuzaki[5], Yuhji Yamamoto[5], Hidekazu Tokuyama[5], Tullis C. Onstott[6], Martin Ziegler[7], Durrheim Ray[8], Esterhuizen van Heerden[9], Bennie Liebenberg[9], The ICDP DSeis team (1.Department of Earth and Space Science, Graduate School of Science, Osaka University, 2.Disaster Prevention Research Institute, Kyoto University, 3.Ritsumeikan University, 4.Tohoku University, 5.Center for Advanced Marine Core Research, Kochi University, 6.Princeton University, 7.ETH Zurich, 8.Witwatersrand University, 9.Moab Khotsong mine)

11:30 AM - 11:45 AM JST | 2:30 AM - 2:45 AM UTC

[MIS02-10] ICDP DSeis 3: Spatial variation in stress state in the source region of Orkeny earthqauke (M5.5) based on analyses of the ICDP-DSeis borehole cores

*Yasuo Yabe[1], Akimasa Ishida[2], Kosuke Sugimura[2], Kanematsu Makoto[2], Mitsuya Higashi[2], Shunsuke YOSHIDA[2], Bennie Liebenberg[7], Takatoshi Ito[3], Akio Funato[5], Bryan Watson[6], Raymond Durrheim[4], Hiroshi Ogasawara[2] (1.Research Center for Prediction of Earthquakes and Volcanic Eruptions, Graduate School of Science, Tohoku University, 2.Faculty of Science and Engeneer, Ritsumeikan University, 3.Institute of Fluid Science, Tohoku University, 4.School of Geoscience, University of the Witwatersrand, 5.Fukada Geological Institute, 6.School of Mining Engeneering, University of the Witwatersrand, 7.Moab Khotsong mine)

11:45 AM - 12:00 PM JST | 2:45 AM - 3:00 AM UTC

[MIS02-11] Applications of DCDA method for in-situ crustal stress measurement - Rock core samples from NIED seismic observation wells -

*Kentaro Omura[1], Weiren Lin[2], Takatoshi Ito[3], Akio Funato[4] (1.National Research Institute for Earth Science and Disaster Resilience, 2.Graduate School of Engineering, Kyoto University, 3.Institute of Fluid Science, Tohoku University, 4.Fukada Geological Institute)

12:00 PM - 12:15 PM JST | 3:00 AM - 3:15 AM UTC

[MIS02-12] Temperature depth profile in a 700 m deep vertical borehole in Aso volcanic zone

*Weiren Lin[1], Susumu Shibutani[1,2], Koichiro Sado[2], Nana Kamiya[1], Tatsuhiro Sugimoto[1], Terasu Sano[1], Kazuya Ishitsuka[1], Xiaoqiu Yang[4], Aiming Lin[3] (1.Graduate School of Engineering, Kyoto University, 2.Chi-ken Sogo Consultants Co., Ltd., 3.Graduate School of Science, Kyoto University, 4.South China Sea Institute of Oceanology, Chinese Academy of Sciences)

[E] Oral | M (Multidisciplinary and Interdisciplinary)：M-IS Intersection

1:45 PM - 3:15 PM JST | 4:45 AM - 6:15 AM UTC | A07 TOKYO BAY MAKUHARI HALL

[M-IS02] Drilling Earth Science

convener:Yasuhiro Yamada(Japan Agency for Marine-Earth Science and Technology (JAMSTEC), R&D Center for Ocean Drilling Science (ODS)), Yumiko Harigane(Geological Survey of Japan, National Institute of Advanced Industrial Science and Technology (AIST)), Azumi Kuroyanagi(Tohoku University Museum, The Center for Academic Resources and Archives, Tohoku University), Kosei E. Yamaguchi(Toho University and NASA Astrobiology Institute), Chairperson:Yumiko Harigane(産総研), Natsue Abe(R&D Center for Ocean Drilling Science, JAMSTEC)

1:45 PM - 2:00 PM JST | 4:45 AM - 5:00 AM UTC

[MIS02-13] Estimation of Shear Stress and Lithology Prediction Using Machine Learning and Surface Drilling Data

Tomoya Inoue[1], *Ryuta Tanaka[1], Junya Ishiwata[1] (1.Japan Agency for Marine-Earth Science and Technology)

2:00 PM - 2:15 PM JST | 5:00 AM - 5:15 AM UTC

[MIS02-14] Overview of drilling of crust-mantle boundary of Oman ophiolite: the ICDP Oman Drilling Project

*Eiichi TAKAZAWA[1,4], Damon A H Teagle[2], Katsuyoshi Michibayashi[3], Yoshihiko Tamura[4], Jude Ann Coggon[2], Juerg Matter[2], Peter B Kelemen[5], Oman Drilling Project Phase 2 Science Party (1.Department of Geology, Faculty of Science, Niigata University, 2.University of Sauthampton, 3.Nagoya University, 4.JAMSTEC, 5.Columbia University)

2:15 PM - 2:30 PM JST | 5:15 AM - 5:30 AM UTC

[MIS02-15] Geophysical Logging of Crust-Mantle boundary at Oman Ophiolite

*Yasuhiro Yamada[1], Kyaw Moe[1], Philippe Pezard[2], Juerg Matter[3], OmanDP Science Party (1.Japan Agency for Marine-Earth Science and Technology (JAMSTEC), 2.Géosciences Montpellier, Université de Montpellier, 3.Southampton University)

2:30 PM - 2:45 PM JST | 5:30 AM - 5:45 AM UTC

[MIS02-16] Overview of the physical property measurements, ChikyuOman 2017 and 2018: Crust and Mantle sections from ICDP Oman Drilling Project Phase I and II

*Natsue Abe[1], Keishi Okazaki[1,11], Ikuo Katayama[2], Kohei Hatakeyama[2], Yuya Akamatsu[2], Benoit Ildefonse[3], Ole Ivar ulven[4], Gilbert Hong[5], Wenlu Zhu[6], Benoit Cordonnier[4], Katsuyoshi Michibayashi[7], Eiichi TAKAZAWA[8], Michell Harris[12], Damon Teagle[10], Peter Kelemen[9], Marguerite Goddard[3], Jurg Matter[10], Jude Coggon[10], The Oman Drilling Project Science Party (1.Japan Agency for Marine-Earth Science and Technology, 2.Hiroshima University, 3.Universitè de Montpellier, 4.University of Oslo, 5.Seoul National University, 6.University of Maryland, 7.Nagoya University, 8.Niigata University, 9.Columbia University, 10.University of Southampton, 11.Kanazawa University, 12.Polymouth University)

2:45 PM - 3:00 PM JST | 5:45 AM - 6:00 AM UTC

[MIS02-17] Exploring the deep subseafloor biosphere and biogeochemical carbon cycling beneath the Arctic ocean

*Fumio Inagaki[1], Steffen Leth Jørgensen[2], Rolf Birger Pedersen[2] (1.Japan Agency for Marine-Earth Science and Technology (JAMSTEC), 2.Department of Earth Science, University of Bergen, Norway)

[E] Poster | M (Multidisciplinary and Interdisciplinary)：M-IS Intersection

3:30 PM - 5:00 PM JST | 6:30 AM - 8:00 AM UTC | Poster Hall International Exhibition Hall8, Makuhari Messe_19

[M-IS02] Drilling Earth Science

convener:Yasuhiro Yamada(Japan Agency for Marine-Earth Science and Technology (JAMSTEC), R&D Center for Ocean Drilling Science (ODS)), Yumiko Harigane(Geological Survey of Japan, National Institute of Advanced Industrial Science and Technology (AIST)), Azumi Kuroyanagi(Tohoku University Museum, The Center for Academic Resources and Archives, Tohoku University), Kosei E. Yamaguchi(Toho University and NASA Astrobiology Institute)

[MIS02-P01] Utilization and curation of frozen core samples in IODP and implementation of the Nagoya Protocol in ocean drilling science

*Nan XIAO[1] (1.Japan Agency for Marine Earthe Science and Technology)

[MIS02-P02] In-situ rock strength calculated from drilling parameters. Comparison of results from various sites.

*Adam Wspanialy[1], Yasuhiro Yamada[1], Saneatsu Saito[1], KYAW MOE[1] (1.Japan Agency for Marine-Earth Science and Technology)

[MIS02-P03] Interaction between submarine landslides and subseafloor sedimentary microbiome: Chikyu SCORE Expedition 910 off Cape Erimo

*Tatsuhiko Hoshino[1], Go-Ichiro Uramoto[2], Satoshi Tonai[2], Yuki Morono[1], Akira Ijiri[1], Shino Suzuki[1], Yusuke Kubo[1], Fumio Inagaki[1], Chikyu SCORE Exp. 910 Scientists . (1.Japan Agency for Marine-Earth Science and Technology, 2.Kochi University)

[MIS02-P04] High-resolution continuous records of the chemical composition of the marine sediment off Cape Erimo, Hokkaido, Japan

*Masafumi MURAYAMA[1], Shinsuke Yagyu[3], Satoshi Tonai[2], Go-Ichiro Uramoto[3], Yasuhiro Yamada[4], Fumio Inagaki[4], Yusuke Kubo[5] (1.Faculty of Agriculture and Marine Science, Kochi University, 2.Faculty of Science and Technology, Kochi University, 3.Center for Advanced Marine Core Research, Kochi University, 4.Research and Development Center for Ocean Drilling Science, JAMSTEC, 5.Center for Deep Earth Exploration, JAMSTEC)

[MIS02-P05] Thermal property measurements of core samples retrieved from Futagawa fault drilling

*Terasu Sano[1], Weiren Lin[1], Susumu Shibutani[1,2], Nana Kamiya[1], Tatsuhiro Sugimoto[1], Kazuya Ishitsuka[1], Aiming Lin[3] (1.Graduate School of Engineering, Kyoto University, 2.Chi-ken Sogo Consultants Co., Ltd.,, 3.Graduate School of Science, Kyoto University)

[MIS02-P06] Results of geotechnical tests on shallow sediment cores recovered from Lord Howe Rise, off eastern Australia: Implications for future Lord Howe Rise riser drilling

*Takamitsu Sugihara[1], Kan Aoike[1], Saneatsu Saito[2], Tatsuya Murayama[1], Kentaro Takeda[1], Takuya Onodera[3], Ayumi Sumikawa[3], Yukari Kido[1], Yoshinori Sanada[1] (1.Center for deep earth exploration, Japan Agency for Marine-Science and Technology, 2.Research and development center for ocean drilling science, Japan Agency for Marine-Science and Technology, 3.Nippon Marine Enterprises, Ltd.)

[MIS02-P07] ICDP DSeis 4: Drilling, core logging, and in-hole geophysical logging of ICDP DSeis drilling into the M5.5 aftershock zones in a South African gold mines.

*Shunsuke YOSHIDA[1], Tadokoro Ryogo[1], Kosuke Sugimura[1], Kanematsu Makoto[1], Mitsuya Higashi[1], Benni Liebenberg[2], Esterhuizen van Heerden[2], Stephen Tau[3], Siyanda Mngadi[3], Ray Durrheim[3], Martin Ziegler[4], Yusuke Mukuhira[5], Ronald Conze[6], Yasuo Yabe[7], Shunya Kaneki[8], Yuki Yokoyama[9], Nomqhele Nkosi[10], Dave Roberts[10], Sifiso Buccio[11], Hiroshi Ogasawara[1] (1.Graduate school of science and engineering, Ritsumeikan , 2.Moab Khotsong mine, Vijoenskroon, 3.Univ. Witwatersrand, School of Geoscience, 4.ETH, Zurich Dep. Earth Sciences, 5.Inst. Fluid Science, Tohoku Univ., 6.GFZ, Potzdam, 7.Graduate School of Science, Tohoku Univ., 8.Disaster Prevention Research Inst., Kyoto Univ., 9.Graduate School of Science,Osaka Univ., 10.Mandela Mining Precinct, CSIR, 11.Council for Geoscience)

[MIS02-P08] ICDP DSeis 5: Diametrical Core Deformation Analysis of the M5.5 aftershock zone core - stress concentration at reflective intrusives and transition in stress regimes.

*Kosuke Sugimura[1], Shunsuke YOSHIDA[1], Ryogo Tadokoro[1], Hiroshi Ogasawara[2], Akimasa Ishida, Yasuo Yabe[3], Takatoshi Ito[4], Akio Funato[5], Siyanda Mngadi[6], Ray Durrheim[6] (1.Graduate school of science and engineering, Ritsumeikan, 2.College of Science and Engineering, Ritsumeikan Univ., 3.Graduate School of Science, Tohoku Univ., 4.Inst. Fluid Science, Tohoku Univ., 5.Fukada Geological Institute, 6.Univ. Witwatersrand, School of Geoscience)

[MIS02-P09] ICDP DSeis 6: Deformation Rate Analysis of the M5.5 aftershock zone core - stress concentration at reflective intrusives

*Kanematsu Makoto[1], Mitsuya Higashi[1], Yasuo Yabe[2], Shuhei Abe[2], Bryan Watson[3], Ray Durrheim[3], Hiroshi Ogasawara[1] (1.Ritsumeikan Univ., 2.Tohoku Univ., 3.Univ. Witwatersrand)

[MIS02-P10] ICDP DSeis 7: compilation of stress information and comparison with calculated stresses in the M5.5 aftershock zones

*Mitsuya Higashi[1], Yasuo Yabe[2], Kosuke Sugimura[1], Akimasa Ishida, Makoto Kanematsu[1], Shunsuke YOSHIDA[1], Ryogo Tadokoro[1], Takatoshi Ito[4], Akio Funato[5], Hiroshi Ogasawara[3] (1.Graduate School of Science and Engineering, Ritsumeikan Univ., 2.Research Center for Prediction of Earthquakes and Volcanic Eruptions, Graduate School of Science, Tohoku University, 3.College of Science and Engineering, Ritsumeikan Univ., 4.Inst. Fluid Science, Tohoku Univ., 5.Fukada Geological Institute)

[MIS02-P11] ICDP DSeis 8: the M5.5 fault structure and reflective intrusives in legacy 3D seismic reflection data

*Noda Taku[1], Musa Manzi[2], Hiroyuki Ogasawara[1], Lindsay Linzer[2], Stephanie Enslin[2], Ray Durrheim[2], Hiroshi Ogasawara[1] (1.Ritsumeikan Univ., 2.Univ. Witwatersrand)

[MIS02-P12] ICDP DSeis 9: are streaks in the M5.5 aftershocks potentially located on highly stressed intrusive?

*Ryogo Tadokoro[1], Katsuya Ishibashi[2], Horiuchi Shigeki[3], Hiroshi Ogasawara[4] (1.Graduate School of Science and Engineering, Ritsumeikan Univ., 2.School of Science and Engineering, Ritsumeikan Univ., 3.Homeseismo ltd., 4.College of Science and Engineering, Ritsumeikan Univ.)

[E] Poster | M (Multidisciplinary and Interdisciplinary)：M-IS Intersection

5:15 PM - 6:30 PM JST | 8:15 AM - 9:30 AM UTC | Poster Hall International Exhibition Hall8, Makuhari Messe_32

[M-IS02] Drilling Earth Science

convener:Yasuhiro Yamada(Japan Agency for Marine-Earth Science and Technology (JAMSTEC), R&D Center for Ocean Drilling Science (ODS)), Yumiko Harigane(Geological Survey of Japan, National Institute of Advanced Industrial Science and Technology (AIST)), Azumi Kuroyanagi(Tohoku University Museum, The Center for Academic Resources and Archives, Tohoku University), Kosei E. Yamaguchi(Toho University and NASA Astrobiology Institute)

[MIS02-P01] Utilization and curation of frozen core samples in IODP and implementation of the Nagoya Protocol in ocean drilling science

*Nan XIAO[1] (1.Japan Agency for Marine Earthe Science and Technology)

[MIS02-P02] In-situ rock strength calculated from drilling parameters. Comparison of results from various sites.

*Adam Wspanialy[1], Yasuhiro Yamada[1], Saneatsu Saito[1], KYAW MOE[1] (1.Japan Agency for Marine-Earth Science and Technology)

[MIS02-P03] Interaction between submarine landslides and subseafloor sedimentary microbiome: Chikyu SCORE Expedition 910 off Cape Erimo

*Tatsuhiko Hoshino[1], Go-Ichiro Uramoto[2], Satoshi Tonai[2], Yuki Morono[1], Akira Ijiri[1], Shino Suzuki[1], Yusuke Kubo[1], Fumio Inagaki[1], Chikyu SCORE Exp. 910 Scientists . (1.Japan Agency for Marine-Earth Science and Technology, 2.Kochi University)

[MIS02-P04] High-resolution continuous records of the chemical composition of the marine sediment off Cape Erimo, Hokkaido, Japan

*Masafumi MURAYAMA[1], Shinsuke Yagyu[3], Satoshi Tonai[2], Go-Ichiro Uramoto[3], Yasuhiro Yamada[4], Fumio Inagaki[4], Yusuke Kubo[5] (1.Faculty of Agriculture and Marine Science, Kochi University, 2.Faculty of Science and Technology, Kochi University, 3.Center for Advanced Marine Core Research, Kochi University, 4.Research and Development Center for Ocean Drilling Science, JAMSTEC, 5.Center for Deep Earth Exploration, JAMSTEC)

[MIS02-P05] Thermal property measurements of core samples retrieved from Futagawa fault drilling

*Terasu Sano[1], Weiren Lin[1], Susumu Shibutani[1,2], Nana Kamiya[1], Tatsuhiro Sugimoto[1], Kazuya Ishitsuka[1], Aiming Lin[3] (1.Graduate School of Engineering, Kyoto University, 2.Chi-ken Sogo Consultants Co., Ltd.,, 3.Graduate School of Science, Kyoto University)

[MIS02-P06] Results of geotechnical tests on shallow sediment cores recovered from Lord Howe Rise, off eastern Australia: Implications for future Lord Howe Rise riser drilling

*Takamitsu Sugihara[1], Kan Aoike[1], Saneatsu Saito[2], Tatsuya Murayama[1], Kentaro Takeda[1], Takuya Onodera[3], Ayumi Sumikawa[3], Yukari Kido[1], Yoshinori Sanada[1] (1.Center for deep earth exploration, Japan Agency for Marine-Science and Technology, 2.Research and development center for ocean drilling science, Japan Agency for Marine-Science and Technology, 3.Nippon Marine Enterprises, Ltd.)

[MIS02-P07] ICDP DSeis 4: Drilling, core logging, and in-hole geophysical logging of ICDP DSeis drilling into the M5.5 aftershock zones in a South African gold mines.

*Shunsuke YOSHIDA[1], Tadokoro Ryogo[1], Kosuke Sugimura[1], Kanematsu Makoto[1], Mitsuya Higashi[1], Benni Liebenberg[2], Esterhuizen van Heerden[2], Stephen Tau[3], Siyanda Mngadi[3], Ray Durrheim[3], Martin Ziegler[4], Yusuke Mukuhira[5], Ronald Conze[6], Yasuo Yabe[7], Shunya Kaneki[8], Yuki Yokoyama[9], Nomqhele Nkosi[10], Dave Roberts[10], Sifiso Buccio[11], Hiroshi Ogasawara[1] (1.Graduate school of science and engineering, Ritsumeikan , 2.Moab Khotsong mine, Vijoenskroon, 3.Univ. Witwatersrand, School of Geoscience, 4.ETH, Zurich Dep. Earth Sciences, 5.Inst. Fluid Science, Tohoku Univ., 6.GFZ, Potzdam, 7.Graduate School of Science, Tohoku Univ., 8.Disaster Prevention Research Inst., Kyoto Univ., 9.Graduate School of Science,Osaka Univ., 10.Mandela Mining Precinct, CSIR, 11.Council for Geoscience)

[MIS02-P08] ICDP DSeis 5: Diametrical Core Deformation Analysis of the M5.5 aftershock zone core - stress concentration at reflective intrusives and transition in stress regimes.

*Kosuke Sugimura[1], Shunsuke YOSHIDA[1], Ryogo Tadokoro[1], Hiroshi Ogasawara[2], Akimasa Ishida, Yasuo Yabe[3], Takatoshi Ito[4], Akio Funato[5], Siyanda Mngadi[6], Ray Durrheim[6] (1.Graduate school of science and engineering, Ritsumeikan, 2.College of Science and Engineering, Ritsumeikan Univ., 3.Graduate School of Science, Tohoku Univ., 4.Inst. Fluid Science, Tohoku Univ., 5.Fukada Geological Institute, 6.Univ. Witwatersrand, School of Geoscience)

[MIS02-P09] ICDP DSeis 6: Deformation Rate Analysis of the M5.5 aftershock zone core - stress concentration at reflective intrusives

*Kanematsu Makoto[1], Mitsuya Higashi[1], Yasuo Yabe[2], Shuhei Abe[2], Bryan Watson[3], Ray Durrheim[3], Hiroshi Ogasawara[1] (1.Ritsumeikan Univ., 2.Tohoku Univ., 3.Univ. Witwatersrand)

[MIS02-P10] ICDP DSeis 7: compilation of stress information and comparison with calculated stresses in the M5.5 aftershock zones

*Mitsuya Higashi[1], Yasuo Yabe[2], Kosuke Sugimura[1], Akimasa Ishida, Makoto Kanematsu[1], Shunsuke YOSHIDA[1], Ryogo Tadokoro[1], Takatoshi Ito[4], Akio Funato[5], Hiroshi Ogasawara[3] (1.Graduate School of Science and Engineering, Ritsumeikan Univ., 2.Research Center for Prediction of Earthquakes and Volcanic Eruptions, Graduate School of Science, Tohoku University, 3.College of Science and Engineering, Ritsumeikan Univ., 4.Inst. Fluid Science, Tohoku Univ., 5.Fukada Geological Institute)

[MIS02-P11] ICDP DSeis 8: the M5.5 fault structure and reflective intrusives in legacy 3D seismic reflection data

*Noda Taku[1], Musa Manzi[2], Hiroyuki Ogasawara[1], Lindsay Linzer[2], Stephanie Enslin[2], Ray Durrheim[2], Hiroshi Ogasawara[1] (1.Ritsumeikan Univ., 2.Univ. Witwatersrand)

[MIS02-P12] ICDP DSeis 9: are streaks in the M5.5 aftershocks potentially located on highly stressed intrusive?

*Ryogo Tadokoro[1], Katsuya Ishibashi[2], Horiuchi Shigeki[3], Hiroshi Ogasawara[4] (1.Graduate School of Science and Engineering, Ritsumeikan Univ., 2.School of Science and Engineering, Ritsumeikan Univ., 3.Homeseismo ltd., 4.College of Science and Engineering, Ritsumeikan Univ.)

[J] Poster | M (Multidisciplinary and Interdisciplinary)：M-IS Intersection

1:45 PM - 3:15 PM JST | 4:45 AM - 6:15 AM UTC | Poster Hall International Exhibition Hall8, Makuhari Messe_7

[M-IS08] Geopark

convener:Takayuki Ogata(Disaster Prevention Research Center for Island Regions, University of the Ryukyus), Tatsuto Aoki(School of Regional Development Studies, Kanazawa University), Noritaka Matsubara(Graduate School of Regional Resource Management, University of Hyogo), Keiichi Tadokoro(Research Center for Seismology, Volcanology and Earthquake and Volcano Research Center, Nagoya University)

[MIS08-P01] The efforts of Mt.Daisetsu-Kamuymintar Geopark Project

*hideyuki kawabe[1] (1.大雪山カムイミンタラジオパーク構想推進協議会)

[MIS08-P02] Re-examination of meaning indicated by "Nigori-Sumi (Muddy and clear) Bridge"~Turbidity Characteristic of Meeting Point of the Ushikubi River and the Ozo River, in Hakusan Tedorigawa Geopark ~

*Tatsuto Aoki[1] (1.School of Regional Development Studies, Kanazawa University)

[MIS08-P03] Efforts of ‘Grant-in-aid for Science Research in San’in Kaigan UGGp’

*Suzuka Koriyama[1] (1.Sanin Kaigan Geopark Promotion Council)

[MIS08-P04] Practical applications in the Tosashimizu Geopark Plan of site monitoring by local residents: Landform change of Sakurahama Beach

*Satoru Imai[1], Hisaaki Sato[1], Yorihisa Hirano (1.Tosashimizu Geopark Promotion Council)

[MIS08-P05] Geological and geomorphological environment of the Jikumaru terraced paddy field (one of the Top 100 Terraced Paddy Fields in Japan) in the Oita Bungoono Geopark

*Toshikazu Yoshioka[1] (1.Oita Bungoono Geopark Promotion Council)

[MIS08-P06] The relationship of land utilization and vegetation at the Jikumaru terraced paddy field in the Oita Bungoono Geopark

*Miki Iwasato[1], Toshikazu Yoshioka[2] (1.Bungoono City, Trade, Industry and Tourism Division, 2.Oita Bungoono Geopark Promotion Council)

[MIS08-P07] Outreach activities of Aso UNESCO Global Geopark

*Tsuneomi Kagiyama[1], Kazunori Watanabe[1], Shinichiro Ikebe[1], Akinobu Ishimatsu[1], Katsunori Toyomura[2], Natsuko Kodama[1], Shuhei Takamori[1], Shino Miyakita[1] (1.Aso Geopark Promotion Council, 2.Aso Volcano Museum)

[MIS08-P08] Geoscientific Setting and Educational Significances of Yonaguni Island in the Ryukyu Arc, Eastern Asia

*Takayuki Ogata[1], Masakazu Nara[2], Makoto Otsubo[3], Tadahiro Shibata[4] (1.Disaster Prevention Research Center for Island Regions, University of the Ryukyus, 2.Sciences Unit, Natural Sciences Cluster, Research and Education Faculty, Kochi University, 3.Geological Survey of Japan, Research Institute of Earthquake and Volcano Geology, 4.The Unit of Natural Monuments, Monuments and Sites Division, Cultural Properties Department, Agency for Cultural Affaire)

[J] Poster | M (Multidisciplinary and Interdisciplinary)：M-IS Intersection

5:15 PM - 6:30 PM JST | 8:15 AM - 9:30 AM UTC | Poster Hall International Exhibition Hall8, Makuhari Messe_33

[M-IS08] Geopark

convener:Takayuki Ogata(Disaster Prevention Research Center for Island Regions, University of the Ryukyus), Tatsuto Aoki(School of Regional Development Studies, Kanazawa University), Noritaka Matsubara(Graduate School of Regional Resource Management, University of Hyogo), Keiichi Tadokoro(Research Center for Seismology, Volcanology and Earthquake and Volcano Research Center, Nagoya University)

[MIS08-P01] The efforts of Mt.Daisetsu-Kamuymintar Geopark Project

*hideyuki kawabe[1] (1.大雪山カムイミンタラジオパーク構想推進協議会)

[MIS08-P02] Re-examination of meaning indicated by "Nigori-Sumi (Muddy and clear) Bridge"~Turbidity Characteristic of Meeting Point of the Ushikubi River and the Ozo River, in Hakusan Tedorigawa Geopark ~

*Tatsuto Aoki[1] (1.School of Regional Development Studies, Kanazawa University)

[MIS08-P03] Efforts of ‘Grant-in-aid for Science Research in San’in Kaigan UGGp’

*Suzuka Koriyama[1] (1.Sanin Kaigan Geopark Promotion Council)

[MIS08-P04] Practical applications in the Tosashimizu Geopark Plan of site monitoring by local residents: Landform change of Sakurahama Beach

*Satoru Imai[1], Hisaaki Sato[1], Yorihisa Hirano (1.Tosashimizu Geopark Promotion Council)

[MIS08-P05] Geological and geomorphological environment of the Jikumaru terraced paddy field (one of the Top 100 Terraced Paddy Fields in Japan) in the Oita Bungoono Geopark

*Toshikazu Yoshioka[1] (1.Oita Bungoono Geopark Promotion Council)

[MIS08-P06] The relationship of land utilization and vegetation at the Jikumaru terraced paddy field in the Oita Bungoono Geopark

*Miki Iwasato[1], Toshikazu Yoshioka[2] (1.Bungoono City, Trade, Industry and Tourism Division, 2.Oita Bungoono Geopark Promotion Council)

[MIS08-P07] Outreach activities of Aso UNESCO Global Geopark

*Tsuneomi Kagiyama[1], Kazunori Watanabe[1], Shinichiro Ikebe[1], Akinobu Ishimatsu[1], Katsunori Toyomura[2], Natsuko Kodama[1], Shuhei Takamori[1], Shino Miyakita[1] (1.Aso Geopark Promotion Council, 2.Aso Volcano Museum)

[MIS08-P08] Geoscientific Setting and Educational Significances of Yonaguni Island in the Ryukyu Arc, Eastern Asia

*Takayuki Ogata[1], Masakazu Nara[2], Makoto Otsubo[3], Tadahiro Shibata[4] (1.Disaster Prevention Research Center for Island Regions, University of the Ryukyus, 2.Sciences Unit, Natural Sciences Cluster, Research and Education Faculty, Kochi University, 3.Geological Survey of Japan, Research Institute of Earthquake and Volcano Geology, 4.The Unit of Natural Monuments, Monuments and Sites Division, Cultural Properties Department, Agency for Cultural Affaire)

[J] Oral | M (Multidisciplinary and Interdisciplinary)：M-IS Intersection

3:30 PM - 5:00 PM JST | 6:30 AM - 8:00 AM UTC | 103 1F

[M-IS08] Geopark

convener:Takayuki Ogata(Disaster Prevention Research Center for Island Regions, University of the Ryukyus), Tatsuto Aoki(School of Regional Development Studies, Kanazawa University), Noritaka Matsubara(Graduate School of Regional Resource Management, University of Hyogo), Keiichi Tadokoro(Research Center for Seismology, Volcanology and Earthquake and Volcano Research Center, Nagoya University), Chairperson:Takeyuki Ueki(Faculty of Risk and Crisis Management, Chiba Institute of Science), Marekazu OHNO(Unzen Volcanic Area Geopark promotion office), Takayuki Arima(Department of Tourism Management, Faculty of Economics, Teikyo University)

3:30 PM - 3:45 PM JST | 6:30 AM - 6:45 AM UTC

[MIS08-01] Normal faults observed in the Yonaguni-jima Island, Okinawa Prefecture, southwestern Japan

*Makoto Otsubo[1], Kiyokazu Oohashi[2], Takayuki Ogata[3], Tadahiro Shibata[4] (1.Geological Survey of Japan, 2.Yamaguchi University, 3.University of the Ryukyus, 4.Agency for Cultural Affairs)

3:45 PM - 4:00 PM JST | 6:45 AM - 7:00 AM UTC

[MIS08-02] Example of Study of the Itoigawa-Shizuoka Tectonic Line using “NIED Quake map!”

*Ko Takenouchi[1], Yousuke Ibaraki[1], Takahiko Ogawara[1], Hiroshi Miyajima[1], Makoto Matsubara[2], Azusa Nishizawa[2], Shin Aoi[2], Yoshihiro Hiramatsu[3], Kazuyuki Nakagawa[4] (1.Fossa Magna Museum, 2.National Research Institute for earth Science and Disaster Resilience, 3.Kanazawa University, 4.Jiji Press)

4:00 PM - 4:15 PM JST | 7:00 AM - 7:15 AM UTC

[MIS08-03] The Opening of ‘NIED Quake map!’ and result of questionnaire survey about interest of local seismicity

*Makoto MATSUBARA[1], Azusa Nishizawa[1], Shin Aoi[1], Ko Takenouchi[2], Yoshihiro Hiramatsu[3], Kazuyuki Nakagawa[4] (1.National Research Institute for Earth Science and Disaster Resilience, 2.Fossa Magna Museum, Itoigawa City, 3.School of Geosciences and Civil Engineering, College of Science and Engineering, Kanazawa University, 4.Jiji Press)

4:15 PM - 4:30 PM JST | 7:15 AM - 7:30 AM UTC

[MIS08-04] Bandaisan Geopark's traveling exhibitions and lectures on "Debris avalanche in the world"

*Hiroshi Sato[1], Tadahide UI[2] (1.Mt.Bandai Museum, 2.CeMI)

4:30 PM - 4:45 PM JST | 7:30 AM - 7:45 AM UTC

[MIS08-05] PLANETARY SCIENCE Education in Geoparks-Science Festival for Youth Formation experiment of Izumo Plain in Shimane convention

*Kunihiro Abe[1] (1.Shimane Penunsula Shinjiko Narumi, Kuibiki Geopark Promotion Committee)

4:45 PM - 5:00 PM JST | 7:45 AM - 8:00 AM UTC

[MIS08-06] ESD in Geopark: Systems thinking and Systems competence for renovating the school curriculum of local area study.

*Ryuta YAMAMOTO[1] (1.Center for professional development of teachers Shizuoka University)

[J] Oral | M (Multidisciplinary and Interdisciplinary)：M-IS Intersection

1:45 PM - 3:15 PM JST | 4:45 AM - 6:15 AM UTC | A02 TOKYO BAY MAKUHARI HALL

[M-IS11] Aqua planetology

convener:Yasuhito Sekine(Earth-Life Science Insitute, Tokyo Institute of Technology), Tomohiro Usui(Earth-Life Science Institute, Tokyo Institute of Technology), Keisuke Fukushi(Institute of Nature & Environmental Technology, Kanazawa University), Takazo Shibuya(Japan Agency for Marine-Earth Science and Technology), Chairperson:Yasuhito Sekine(Dept. Earth & Planetary Sci., University of Tokyo), Tomohiro Usui, Takazo Shibuya(JAMSTEC)

1:45 PM - 2:00 PM JST | 4:45 AM - 5:00 AM UTC

[MIS11-01] An interior structure model of Pluto resolving its mysteries

*Shunichi Kamata[1], Francis Nimmo[2], Yasuhito Sekine[3], Kiyoshi Kuramoto[1], Naoki Noguchi[4], Jun Kimura[5], Atsushi Tani[6] (1.Hokkaido University, 2.University of California, Santa Cruz, 3.Tokyo Institute of Technology, 4.Tokushima University, 5.Osaka University, 6.Kobe University)

2:00 PM - 2:15 PM JST | 5:00 AM - 5:15 AM UTC

[MIS11-02] Isotopic measurement of gas hydrate sample simulating environment of icy satellite and icy planet: Equipment development and consideration for observation method

*Kushi Kudo[1], Atsushi Tani[1], Naohiro Yoshida[2,3] (1.Graduate School of Human Development and Environment, Kobe University, 2.Department of Chemical Science and Engineering, School of Materials and Chemical Technology, Tokyo Institute of Technology, 3.Earth–Life Science Institute)

2:15 PM - 2:30 PM JST | 5:15 AM - 5:30 AM UTC

[MIS11-03] Dynamics of icy crust of the Enceladus with tidal heating and asymmetric distribution of heat generation in the rocky core

*Kaho Harada[1,2], Takashi Nakagawa[3], Manabu Morishige[2], Shigenobu Hirose[2] (1.Keio University, 2.JAMSTEC, 3.University of Hong Kong)

2:30 PM - 2:45 PM JST | 5:30 AM - 5:45 AM UTC

[MIS11-04] Chlorine-bearing aqueous fluid at crust/mantle boundary in mid-ocean ridge hydrothermal system: a case study of crustal diopsidite from Oman ophiolite

★Invited Papers

*Norikatsu Akizawa[1], Akira Miyake[2], Akira Tsuchiyama[2] (1.Atmosphere and Ocean Research Institute, The University of Tokyo, 2.Graduate School of Science, Kyoto University)

2:45 PM - 3:00 PM JST | 5:45 AM - 6:00 AM UTC

[MIS11-05] Phase relation of the $MgSO_4$-H_2O system under high pressure

*Tadashi Kondo[1], Keita Harada[1], Miki Sirata[1], Takumi Kikegawa[2] (1.Department of Earth and Space Science, Graduate School of Science Osaka University, 2.Institute for Material Structure Science, KEK)

3:00 PM - 3:15 PM JST | 6:00 AM - 6:15 AM UTC

[MIS11-06] The Origin of Earth's Volatile Composition: Effects of Impact-induced Atmospheric Erosion and Core Formation

*Sakuraba Haruka[1], Hiroyuki Kurokawa[2], Hidenori Genda[2], Kenji Ohta[1] (1.Tokyo Institute of Technology, 2.Earth-Life Science Institute)

[J] Oral | M (Multidisciplinary and Interdisciplinary)：M-IS Intersection

3:30 PM - 5:00 PM JST | 6:30 AM - 8:00 AM UTC | A02 TOKYO BAY MAKUHARI HALL

[M-IS11] Aqua planetology

convener:Yasuhito Sekine(Earth-Life Science Insitute, Tokyo Institute of Technology), Tomohiro Usui(Earth-Life Science Institute, Tokyo Institute of Technology), Keisuke Fukushi(Institute of Nature & Environmental Technology, Kanazawa University), Takazo Shibuya(Japan Agency for Marine-Earth Science and Technology), Chairperson:Yasuhito Sekine(Dept. Earth & Planetary Sci., University of Tokyo), Keisuke Fukushi, Tomohiro Usui

3:30 PM - 3:45 PM JST | 6:30 AM - 6:45 AM UTC

[MIS11-07] Finding of oxidized sulfur species in carbonates from a Martian meteorite Allan Hills 84001 using μ-XANES

*Kajitani Iori[1], Gaku Tanabe[1], Ryoichi Nakada[2], Tomohiro Usui[3], Mizuho Koike[3], Fumihiro Matsuura[4], Tetsuya Yokoyama[1] (1.Tokyo Institute of Technology, 2.Japan Agency for Marine-Earth Science and Technology, 3.Institute of Space and Astronautical Science, 4.Earth-Life Science Institute)

3:45 PM - 4:00 PM JST | 6:45 AM - 7:00 AM UTC

[MIS11-08] A study on Martian water environment based on the μ-XRF-XANES analysis for the secondary minerals formed in a nakhlite meteorite (Y 000593) vein

*Keika Suzuki[1], Hiroki Suga[1], Akira Yamaguchi[2], Tomohiro Usui[3], Oki Sekizawa[4], Kiyofumi Nitta[4], Yoshio Takahashi[1] (1.University of Tokyo, 2.National Institute of Polar Research, 3.JAXA, ISAS, 4.JASRI/SPring-8)

4:00 PM - 4:15 PM JST | 7:00 AM - 7:15 AM UTC

[MIS11-09] Influence of water and clay minerals for slope angles on Mars

*Yuhki Matsuoka[1], Ikuo Katayama[1], Rina Noguchi[2], Tomohiro Usui[2] (1.Department of Earth and Planetary Systems Science, Hiroshima University, 2.Institute of Space and Astronautical Science, Japan Aerospace Exploration Agency)

4:15 PM - 4:30 PM JST | 7:15 AM - 7:30 AM UTC

[MIS11-10] **Dark Streak Features in Mongolia: Implications for Formation Mechanisms of Recurring Slope Lineae on Mars**

*Maya Nakamura[1,2], Yasuhito Sekine[1], Keisuke Fukushi[3], Noriko Hasebe[3], Davaadorj Davaasuren[4], Yoshio Takahashi[2], Hitoshi Hasegawa[5], Takuro Ogura[6], Koki Morida[3], Tuvshin Gerelmaa[4] (1.Earth-Life Science Institute, Tokyo Institute of Technology, 2.Department of Earth and Planetary Science, The University of Tokyo, 3.Institute of Nature & Environmental Technology, Kanazawa University, 4.Department of Geography, National University of Mongolia, 5.Department of Global Environment and Disaster Prevention, Kochi University, 6.Department of Socio-Cultural Environmental Science, The University of Tokyo)

4:30 PM - 4:45 PM JST | 7:30 AM - 7:45 AM UTC

[MIS11-11] The occurrence of perchlorate salt in and around the Taklimakan Desert, China

*Haibo Qin[1,2], Shitong Yang[1], Qing Chang[3], Chihiro Miyamoto[1], Yoshio Takahashi[1] (1.Department of Earth and Planetary Science, Graduate School of Science, 2.State Key Laboratory of Environmental Geochemistry, Institute of Geochemistry, Chinese Academy of Sciences, 3.Japan Agency for Marine-Earth Science and Technology)

4:45 PM - 5:00 PM JST | 7:45 AM - 8:00 AM UTC

[MIS11-12] Measurement technique to quantify OH radicals photochemically generated on the ice surface

*Akihiro Yabushita[1], Hiroaki Nishimoto[1], Akira Harata[1] (1.Interdisciplinary Graduate School of Engineering Sciences, Kyushu University)

[J] Oral | M (Multidisciplinary and Interdisciplinary) : M-IS Intersection

10:45 AM - 12:15 PM JST | 1:45 AM - 3:15 AM UTC | 201A 2F

[M-IS13] Biogeochemistry

convener:Keisuke Koba(Center for Ecological Research, Kyoto University), Hideaki Shibata(Field Science Center fot Northern Biosphere, Hokkaido University), Naohiko Ohkouchi(Japan Agency for Marine-Earth Science and Technology), Youhei Yamashita(Faculty of Environmental Earth Science, Hokkaido University), Chairperson:Keisuke Koba(Kyoto University), Yoshiyuki Inagaki, Kazumichi Fujii

10:45 AM - 11:00 AM JST | 1:45 AM - 2:00 AM UTC

[MIS13-01] **Root meets clays: Tree root plasticity in podzolized soil**

*Kazumichi Fujii[1], Naoki Makita[2], Martin Küttim[3], Shinya sugita[3] (1.Forestry and Forest Products Research Institute, 2.Shinshu University, 3.Tallinn University)

11:00 AM - 11:15 AM JST | 2:00 AM - 2:15 AM UTC

[MIS13-02] Nitrogen transformation process in newly created salt marsh in the aftermath of the 2011 Great East Japan Earthquake

*Keitaro Fukushima[1], Kazuma Hashimoto[2], Megumi Kuroiwa[3], Katsuhide Yokoyama[2], Yuichi Suwa[3] (1.Center for Ecological Research, Kyoto University, 2.Graduate School of Urban Environmental Sciences, Tokyo Metropolitan University, 3.Faculty of Science and Engineering, Chuo University)

11:15 AM - 11:30 AM JST | 2:15 AM - 2:30 AM UTC

[MIS13-03] Succession of soil nitrification potential at a glacier foreland in Svalbard

*Kentaro Hayashi[1], Yukiko Tanabe[2,3], Keisuke Ono[1], Maki Asano[4], Shohei Hattori[5], Masaki Uchida[2,3], Masahito Hayatsu[1] (1.Institute for Agro-Environmental Sciences, NARO, 2.National Institute of Polar Research, 3.SOKENDAI, 4.University of Tsukuba, 5.Tokyo Institute of Technology)

11:30 AM - 11:45 AM JST | 2:30 AM - 2:45 AM UTC

[MIS13-04] **Transition of soil organic carbon in a volcanic ash soil derived from Towada volcano, Japan**

*JITHYA NAWODI WIJESINGHE[1], Jun Koarashi[2], Mariko Atarashi Andoh[2], Yoko Saito Kokubu[3], Noriko Yamaguchi[4], Takashi Sase[5], Mamoru Hosono[6], Yudzuru Inoue[7], Yuki Mori[1], Syuntaro Hiradate[1] (1.Soil Science Laboratory, Faculty of Agriculture, Kyushu University, Fukuoka 819-0395, Japan, 2.Nuclear Science and Engineering Center, Japan Atomic Energy Agency, Ibaraki 319-1195, Japan, 3.Tono Geoscience Center, Japan Atomic Energy Agency,Gifu 509-5102, Japan, 4.National Agriculture and Food Research Organization, Institute for Agro-environmental Sciences, 3-1-3 Kan-nondai, Tsukuba, Ibaraki 305-8604, Japan, 5.Boreal Laboratory for Phytolith Research, Iwate 028-7302,Japan, 6.Tokyo Natural History Research Structure,Tokyo 162-0052, Japan, 7.Faculty of Applied Information Technology, Nagasaki Institute of Applied Science,Nagasaki 851-0193, Japan)

11:45 AM - 12:00 PM JST | 2:45 AM - 3:00 AM UTC

[MIS13-05] General pattern of carbon and nitrogen isotopic variation across a wide range of soils and its controlling factors

*Rota Wagai[1], Masako Kajiura[1], Yudzuru Inoue[2], Maki Asano[3], Chie Hayakawa[4] (1.NARO, Institute for Agro-Environmental Sciences, 2.Nagasaki Institute of Applied Science, 3.University of Tsukuba, 4.University of Tokyo)

12:00 PM - 12:15 PM JST | 3:00 AM - 3:15 AM UTC

[MIS13-06] Nutrient sources in some Japanese forest ecosystems: the contribution of precipitation, weathering and litter fall

*Yoshiyuki Inagaki[1], Kazumichi Fujii[1] (1.Forestry and Forest Products Research Institute)

[J] Oral | M (Multidisciplinary and Interdisciplinary)：M-IS Intersection

1:45 PM - 3:15 PM JST | 4:45 AM - 6:15 AM UTC | 201A 2F

[M-IS13] Biogeochemistry

convener:Keisuke Koba(Center for Ecological Research, Kyoto University), Hideaki Shibata(Field Science Center fot Northern Biosphere, Hokkaido University), Naohiko Ohkouchi(Japan Agency for Marine-Earth Science and Technology), Youhei Yamashita(Faculty of Environmental Earth Science, Hokkaido University), Chairperson:Keisuke Koba(Kyoto University), Yohei Yamashita, Kazuya Nishina, Kazumichi Fujii

1:45 PM - 2:00 PM JST | 4:45 AM - 5:00 AM UTC

[MIS13-07] Ultrahigh-resolution mass spectral analysis of dissolved organic matter in rainfall, throughfall and soil water in temperate forest stands, western Japan

*Junichiro Ide[1], Keitaro Yamase[2], Seonghun Jeong[3], Noki Makita[4], Hiroshi Nishimura[5], Keitaro Fukushima[6], Kyoichi Otsuki[7], Mizue Ohashi[8] (1.Institute of Decision Science for a Sustainable Society, Kyushu University, 2.Forestry and Forest Products Research Institute, Hyogo Prefectural Technology Center for Agriculture, Forestry and Fisheries, 3.Graduate School of Bioresources and Bioenvironmental Sciences, Kyushu University, 4.Faculty of Science, Shinshu University, 5.Research Institute for Sustainable Humanosphere, Kyoto University, 6.The Center for Ecological Research, Kyoto University, 7.Faculty of Agriculture, Kyushu University, 8.School of Human Science and Environment, University of Hyogo)

2:00 PM - 2:15 PM JST | 5:00 AM - 5:15 AM UTC

[MIS13-08] Basin-scale transport of allochthonous humic-like fluorescent dissolved organic matter by the North Pacific Intermediate water

*Youhei Yamashita[1], Jun Nishioka[2], Hajime Obata[3], Hiroshi Ogawa[3] (1.Faculty of Environmental and Earth Science, 2.Institute of Low Temperature Science, Hokkaido University, 3.Atmosphere and Ocean Research Institute, The University of Tokyo)

2:15 PM - 2:30 PM JST | 5:15 AM - 5:30 AM UTC

[MIS13-09] Bacterial contribution to dissolved organic matter in a large monomictic lake (Lake Biwa) indicated by amino acids enantiomers

*Yasuhiko T. Yamaguchi[1], Chikage Yoshimizu[2], Ichiro Tayasu[2], Keisuke Koba[3], Kazuhide Hayakawa[1] (1.Lake Biwa Environmental Research Institute, 2.Research Institute for Humanity and Nature, 3.Center for Ecological Research, Kyoto University)

2:30 PM - 2:45 PM JST | 5:30 AM - 5:45 AM UTC

[MIS13-10] High-sensitivity tracer assay for oxygen consumption rate in ocean and lakes using ^{17}O as a tracer

*Urumu Tsunogai[1], Shogo Kashiwagi[1], Masanori Ito[1], Fumiko Nakagawa[1], Chiho Sukigara[1] (1.Graduate School of Environmental Studies, Nagoya University)

2:45 PM - 3:00 PM JST | 5:45 AM - 6:00 AM UTC

[MIS13-11] Ecology of bacterioplankton inhabiting oxygenated hypolimnia of deep freshwater lakes

*Yusuke Okazaki[1] (1.National Institute of Advanced Industrial Science and Technology)

3:00 PM - 3:15 PM JST | 6:00 AM - 6:15 AM UTC

[MIS13-12] Nitrous oxide emission from the drainage and the production processes in oil palm plantation on peatland

*Kazuya Nishina[1], Lulie Melling[2], Ryuichi Hirata[1], Yoshiyuki Takahashi[1], Sakae Toyoda[3], Kotaro Terajima[3], Masayuki Itoh[4] (1.NIES National Institute of Environmental Studies, 2.SARAWAK Tropical Peat Research Institute, 3.Tokyo Institute of Technology, 4.University of Hyogo)

[J] Poster | M (Multidisciplinary and Interdisciplinary)：M-IS Intersection

3:30 PM - 5:00 PM JST | 6:30 AM - 8:00 AM UTC | Poster Hall International Exhibition Hall8, Makuhari Messe_20

[M-IS13] Biogeochemistry

convener:Keisuke Koba(Center for Ecological Research, Kyoto University), Hideaki Shibata(Field Science Center fot Northern Biosphere, Hokkaido University), Naohiko Ohkouchi(Japan Agency for Marine-Earth Science and Technology), Youhei Yamashita(Faculty of Environmental Earth Science, Hokkaido University)

[MIS13-P01] Biomolecular composition changes and biochemical processes associated with indicators of organic matter degradation

*Satoru Hobara[1], Hiroshi Ogawa[2] (1.Rakuno Gakuen University, 2.The University of Tokyo)

[MIS13-P02] Community and metabolic responses of marine bacteria to the dissolved organic matter derived from phytoplankton

*Yuya Tada[1], Koji Suzuki[2], Youhei Yamashita[2] (1. National Institute For Minamata Disease, 2.Hokkaido University)

[MIS13-P03] High production of benthic algae promoted by increased available phosphate in the Obitsu River tidal flat

*Yuzuki Takagai[1], Muneoki Yoh[1] (1.Tokyo University of Agriculture and Technology)

[MIS13-P04] High Concentration of Phosphate and its Mechanism in "Gomi-kui" and "Gata-do"

*KOWATA Satoshi[1], Muneoki Yoh[1] (1.Tokyo University of Agriculture and Technology)

[MIS13-P05] Estimation of the formation and reduction of organic mud in tidal river using sulfate ionic flux and principal component analysis

Hiroki Itamura[1], *Yoriko Yokoo[1] (1.Faculty of Science and Engineering, Doshisha University)

[MIS13-P06] Evaluating the relationship among energy, water and carbon in soil by using multi-layered land surface model, BEAMS

*Keisuke Komiyama[1], Takahiro Sasai[1] (1.Tohoku University Graduate School of Science)

[J] Poster | M (Multidisciplinary and Interdisciplinary)：M-IS Intersection

5:15 PM - 6:30 PM JST | 8:15 AM - 9:30 AM UTC | Poster Hall International Exhibition Hall8, Makuhari Messe_34

[M-IS13] Biogeochemistry

convener:Keisuke Koba(Center for Ecological Research, Kyoto University), Hideaki Shibata(Field Science Center fot Northern Biosphere, Hokkaido University), Naohiko Ohkouchi(Japan Agency for Marine-Earth Science and Technology), Youhei Yamashita(Faculty of Environmental Earth Science, Hokkaido University)

[MIS13-P01] Biomolecular composition changes and biochemical processes associated with indicators of organic matter degradation

*Satoru Hobara[1], Hiroshi Ogawa[2] (1.Rakuno Gakuen University, 2.The University of Tokyo)

[MIS13-P02] Community and metabolic responses of marine bacteria to the dissolved organic matter derived from phytoplankton

*Yuya Tada[1], Koji Suzuki[2], Youhei Yamashita[2] (1. National Institute For Minamata Disease, 2.Hokkaido University)

[MIS13-P03] High production of benthic algae promoted by increased available phosphate in the Obitsu River tidal flat

*Yuzuki Takagai[1], Muneoki Yoh[1] (1.Tokyo University of Agriculture and Technology)

[MIS13-P04] High Concentration of Phosphate and its Mechanism in "Gomi-kui" and "Gata-do"

*KOWATA Satoshi[1], Muneoki Yoh[1] (1.Tokyo University of Agriculture and Technology)

[MIS13-P05] Estimation of the formation and reduction of organic mud in tidal river using sulfate ionic flux and principal component analysis

Hiroki Itamura[1], *Yoriko Yokoo[1] (1.Faculty of Science and Engineering, Doshisha University)

[MIS13-P06] Evaluating the relationship among energy, water and carbon in soil by using multi-layered land surface model, BEAMS

*Keisuke Komiyama[1], Takahiro Sasai[1] (1.Tohoku University Graduate School of Science)

[J] Oral | M (Multidisciplinary and Interdisciplinary)：M-IS Intersection

9:00 AM - 10:30 AM JST | 12:00 AM - 1:30 AM UTC | Convention Hall B 2F

[M-IS14] Global climate change driven by the Southern Ocean and the Antarctic Ice Sheet

convener:Osamu Seki(Institute of Low Temperature Science, Hokkaido University), Akira Oka(Atmosphere and Ocean Research Institute, The University of Tokyo), Ryu Uemura(University of the Ryukyus), Ryosuke Makabe(National Institute of Polar Research), Chairperson:Yuji Kato(Kochi University)

9:00 AM - 9:25 AM JST | 12:00 AM - 12:25 AM UTC

[MIS14-01] Mass loss of the Antarctic ice sheet under the influence of ice-ocean interaction

★Invited Papers

*Shin Sugiyama[1] (1.Institute of Low Temperature Science, Hokkaido University)

9:25 AM - 9:40 AM JST | 12:25 AM - 12:40 AM UTC

[MIS14-02] Accurate chronology and climatic reconstruction around MIS 11 (interglacial period ~400,000 years ago) from Dome Fuji ice core, Antarctica

*Kenji Kawamura[1,2,3], Ikumi Oyabu[1], Shuji Aoki[4], Takakiyo Nakazawa[4], Ayako Abe-Ouchi[5,3], Fuyuki SAITO[3] (1.National Institute of Polar Research, Research Organization of Information and Systems, 2.SOKENDAI (The Graduate University of Advanced Studies), 3.JAMSTEC, 4.Tohoku University, 5.University of Tokyo)

9:40 AM - 9:55 AM JST | 12:40 AM - 12:55 AM UTC

[MIS14-03] Study on physics and layers of ice cores containing information of climate change over the past 720 k-years, and study on the "oldest ice"

*Shuji Fujita[1,2], Motohiro Hirabayashi[1], Iizuka Yoshinori[3], Hiroshi Ohno[4] (1.National Institute of Polar Research, Research Organization of Information and Systems(ROIS), 2.Department of Polar Science, The Graduate University for Advanced Studies (SOKENDAI), Japan, 3. Institute of Low Temperature Science, Hokkaido University, Japan, 4.Kitami Institute of Technology, Japan)

9:55 AM - 10:15 AM JST | 12:55 AM - 1:15 AM UTC

[MIS14-04] Reconstructions of the Antarctic Polar Front through the glacial/interglacials

★Invited Papers

*Hiroki Matsui[1], Yuji Kato[1,2], Itsuki Suto[3], Minoru Ikehara[1] (1.Center for Advanced Marine Core Research, Kochi University, 2.JSPS PD, 3.Graduate School of Environmental Studies, Nagoya University)

10:15 AM - 10:30 AM JST | 1:15 AM - 1:30 AM UTC

[MIS14-05] **Integrated observations for marine earth science in the Indian sector of the Southern Ocean: Preliminary results of R/V Hakuho-maru KH-19-1 cruise**

*Minoru Ikehara[1], Kay I. Ohshima[2], Takuya Itaki[3], Hiroshi Sato[4], Masakazu Fujii[5], Michiyo Yamamoto-Kawai[6], Hiroki Matsui[1], Takahito Ikenoue[7], . Scientific Party of R/V Hakuho-maru KH-19-1 cruise (1.Center for Advanced Marine Core Research, Kochi University, 2.ILTS, Hokkaido University, 3.GSJ, AIST, 4.Senshu University, 5.National Institute of Polar Research, 6.Tokyo University of Marine Science and Technology, 7.Marine Ecology Research Institute)

[J] Oral | M (Multidisciplinary and Interdisciplinary) : M-IS Intersection

10:45 AM - 12:15 PM JST | 1:45 AM - 3:15 AM UTC | Convention Hall B 2F

[M-IS14] Global climate change driven by the Southern Ocean and the Antarctic Ice Sheet

convener:Osamu Seki(Institute of Low Temperature Science, Hokkaido University), Akira Oka(Atmosphere and Ocean Research Institute, The University of Tokyo), Ryu Uemura(University of the Ryukyus), Ryosuke Makabe(National Institute of Polar Research), Chairperson:Sam Sherriff-Tadano(University of Tokyo)

10:45 AM - 11:00 AM JST | 1:45 AM - 2:00 AM UTC

[MIS14-06] **High resolution ocean temperatures reconstructions over the last glacial-interglacial in the Kerguelen region, Southern Ocean.**

*Matthieu Civel[1,2], Xavier Crosta[3], Giuseppe Cortese[4], Elisabeth Michel[5], Alain Mazaud[5], Samuel Jaccard[6], Lena Thöle[6], Minoru Ikehara[1], Takuya Itaki[2] (1.Center for Advanced Marine Core Research, Kochi University, Japan, 2.Geological Survey of Japan, AIST, Tsukuba, Japan, 3.UMR 5805 CNRS EPOC, Université de Bordeaux, France, 4.GNS Science, Lower Hutt, New Zealand, 5.LSCE-IPSL, CEA-CNRS-UVSQ, 91198 Gif-sur-Yvette, France, 6.Institute of Geological Sciences & Oeschger Centre for Climate Change Research, University of Bern, Switzerland)

11:00 AM - 11:15 AM JST | 2:00 AM - 2:15 AM UTC

[MIS14-07] Present-day crustal motion and gravity change in East Antarctica: implications for the mantle viscosity and Holocene Antarctic Ice Sheet change inferred from GIA modeling

*Jun'ichi Okuno[1,2], Koichiro Doi[1,2], Yuichi Aoyama[1,2], Takeshige Ishiwa[1], Akihisa Hattori[2], Yoichi Fukuda[3] (1.National Institute of Polar Research, 2.SOKENDAI, 3.Kyoto University)

11:15 AM - 11:30 AM JST | 2:15 AM - 2:30 AM UTC

[MIS14-08] **Reconstruction of the East Antarctic ice sheet variability during the last 3 myrs in the central & eastern Droning Maud Land, East Antarctica**

*Yusuke Suganuma[1,2], Moto Kawamata[2], Kota Katsuki[3], Tatsuo Kanamaru[4], Heitaro Kaneda[5], Takushi Koyama[6], Tanabe Yukiko[1,2], Daisuke Shibata[7], Takeshige Ishiwa[1], Takuya Itaki[8], Jun'ichi Okuno[1,2], Osamu Seki[9], Itsuki Suto[10], Masakazu Fujii[1,2], Hideki Miura[1,2] (1.National institute of Polar Research, 2.SOKENDAI, 3.Shimane University, 4.Nihon University, 5.Chiba University, 6.Oita University, 7.Tsukuba University, 8.GSJ, AIST, 9.Hokkaido University, 10.Nagoya University)

11:30 AM - 11:45 AM JST | 2:30 AM - 2:45 AM UTC

[MIS14-09] Vertical ice flow motions obtained from year-round GNSS observations on Shirase Glacier, Antarctica

*Yuichi Aoyama[1,2], Koichiro Doi[1,2], Daisuke Hirano[3], Takeshi Tamura[1,2], Shigeru Aoki[3], Kazuo Shibuya[1] (1.National Institute of Polar Research, 2.SOKENDAI, 3.Institute of Low Temperature Science, Hokkaido University)

11:45 AM - 12:00 PM JST | 2:45 AM - 3:00 AM UTC

[MIS14-10] **Operation plan and design of the Antarctic exploration AUV "MONACA"**

*Hirokazu Yamagata[1], Toshihiro Maki[1], Hiroshi Yoshida[2], Yoshifumi Nogi[3] (1.Institute of Industrial Science, The University of Tokyo, 2.Japan Marine Science and Technology Center, 3.National Institute of Polar Research)

12:00 PM - 12:15 PM JST | 3:00 AM - 3:15 AM UTC

[MIS14-11] Geophysical insights into tectonic, volcanic, sedimentation, and glacial processes in Indian and Southern Oceans: Preliminary geophysical results of R/V *Hakuho-maru* KH-19-1 cruise

*Masakazu Fujii[1], Hiroshi Sato[2], Minoru Ikehara[3], Yoshifumi Nogi[1], Taichi Sato[4], Yasuyuki Nakamura[5], Eri Helen Amsler[6], Sam Sherriff-Tadano[7] (1.National Institute of Polar Research and SOKENDAI, 2.Senshu University, 3.Kochi University, 4.AIST, 5.JAMSTEC, 6.University of Bern, 7.AORI, UTokyo)

[J] Oral | M (Multidisciplinary and Interdisciplinary)：M-IS Intersection

1:45 PM - 3:15 PM JST | 4:45 AM - 6:15 AM UTC | Convention Hall B 2F

[M-IS14] Global climate change driven by the Southern Ocean and the Antarctic Ice Sheet

convener:Osamu Seki(Institute of Low Temperature Science, Hokkaido University), Akira Oka(Atmosphere and Ocean Research Institute, The University of Tokyo), Ryu Uemura(University of the Ryukyus), Ryosuke Makabe(National Institute of Polar Research), Chairperson:Takeshige Ishiwa(National institute of Polar Research)

1:45 PM - 2:00 PM JST | 4:45 AM - 5:00 AM UTC

[MIS14-12] Simulations of glacial ocean carbon cycle with a parameterization of stratification dependence of vertical diffusivity

*Hidetaka Kobayashi[1], Akira Oka[1] (1.Atmosphere and Ocean Research Institute, The University of Tokyo)

2:00 PM - 2:15 PM JST | 5:00 AM - 5:15 AM UTC

[MIS14-13] Impacts of precession on the periodicity of climate and AMOC variabilities

*Sam Sherriff-Tadano[1] (1.Atmosphere and Ocean Research Institute, the University of Tokyo)

2:15 PM - 2:30 PM JST | 5:15 AM - 5:30 AM UTC

[MIS14-14] Warming and climate feedbacks in the southern high latitude driven by obliquity, precession-eccentricity, and atmospheric CO2

*Kanon Kino[1], Ayako Abe-Ouchi[1,2], Ryouta O'ishi[1], Fuyuki SAITO[2], Masakazu Yoshimori[1] (1.Atmosphere and Ocean Research Institute, the University of Tokyo, 2.Japan Agency for Marine-Earth Science and Technology)

2:30 PM - 2:45 PM JST | 5:30 AM - 5:45 AM UTC

[MIS14-15] Origin of Circumpolar Deep Water intruding onto the Amundsen and Bellingshausen Sea continental shelves

*Yoshihiro Nakayama[1,2], Menemenlis Dimitris[2], Hong Zhang[2], Michael Schodlok[2], Eric Rignot[2,3] (1.Institute of Low Temperature Science, Hokkaido University, 2.NASA's Jet Propulsion Laboratory, 3.Uniersity of California, Irvine)

2:45 PM - 3:00 PM JST | 5:45 AM - 6:00 AM UTC

[MIS14-16] Ocean and material circulation in the southern part of the Australian Antarctic Basin in 2018/2019 summer - preliminary results from Kaiyomaru KY18-04 cruise

*Katsuro Katsumata[1], Daisuke Hirano[2], Daiki Nomura[2], Kaihe Yamazaki[2], Yoichiro Koh[2], Masaaki Kiuchi[2], Shigeru Aoki[2], Hiroto Murase[3] (1.JAMSTEC, 2.Hokkaido Univ., 3.NRI-FSF)

3:00 PM - 3:15 PM JST | 6:00 AM - 6:15 AM UTC

[MIS14-17] Mooring observation aiming direct current measurement and quantitative evaluation of Meridional Circulation of Southern Ocean

*Kitade Yujiro[1], Kohei Mizobata[1], Kazuho Watanabe[1], Linquiao Chen[3], Gaopin Guo[3], Shigeru Aoki[2], Shyuki Ushio[4], Keishi Shimada[1], Kay I. Ohshima[2] (1.Tokyo University of Marine Science and Technology, 2.Hokkaido University, 3.Shanghi Ocean University, 4.National Institute of Polar Research)

[J] Poster | M (Multidisciplinary and Interdisciplinary) : M-IS Intersection

3:30 PM - 5:00 PM JST | 6:30 AM - 8:00 AM UTC | Poster Hall International Exhibition Hall8, Makuhari Messe_21

[M-IS14] Global climate change driven by the Southern Ocean and the Antarctic Ice Sheet

convener:Osamu Seki(Institute of Low Temperature Science, Hokkaido University), Akira Oka(Atmosphere and Ocean Research Institute, The University of Tokyo), Ryu Uemura(University of the Ryukyus), Ryosuke Makabe(National Institute of Polar Research)

[MIS14-P01] Preliminary study on the effect of low-salinity ice melting water on biomass and composition of ice algae

*Keigo Takahashi[1], Ryosuke Makabe[2,3], Shintaro Takao[2,3], Tsuneo Odate[2,3], Masato Moteki[1,2] (1.Tokyo University of Marine Science and Technology, 2.National Institute of Polar Research, 3.The Graduate University for Advanced Studies (SOKENDAI))

[MIS14-P02] Effects of lugol's fixtation on preservation of samples for carbon and nitrogen stable isotope and molecular analyses

*Masayoshi Sano[1], Ryosuke Makabe[1,2], Ayu Yamamoto[3], Norio Kurosawa[4], Masato Moteki[2,3], Tsuneo Odate[1,2] (1.National Institute of Polar Research, 2.The Graduate University for Advanced Studies, 3.Tokyo University of Marine Science and Technology, 4.Soka University)

[MIS14-P03] The application of environmental DNA for the monitoring of Antarctic marine ecosystem

*Aiko Tachibana[1], Ryosuke Makabe[2], Masato Moteki[1] (1.Tokyo University of Marine Science and Technology, 2.National Institute of Polar Research)

[MIS14-P04] Coincidental occurrence process of frazil ice and high biomass off Amery Ice Shelf

*Yoshihiko Machimura[1], Kay I. Ohshima[2], Kazuki Nakata[3], Masato Ito[2], Yasushi Fukamachi[2,4], Ryosuke Makabe[5], Shintaro Takao[5], Sohey Nihashi[6] (1.Graduate School of Environmental Sciences, Hokkaido University, 2.Institute of Low Temperature Science, Hokkaido University, 3.Remote Sensing Technology Center of Japan, 4.Arctic Research Center, Hokkaido University, 5.National Institute of Polar Research, 6.National Institute of Technology, Tomakomai College)

[MIS14-P05] Feeding habit of the Antarctic amphipod *Themisto gaudichaudii* of Vincennes Bay (East Antarctica) during austral summer

*Junji Matsushita[1], Ryosuke Makabe[2], Masato Moteki[1] (1.Tokyo University of Marine Science and Technology, 2.National Institute of Polar Research)

[MIS14-P06] Time-series observation of subsurface chlorophyll *a* maximum in the seasonal ice zone of the Southern Ocean

*Ayuko Kagesawa[1], Masayoshi Sano[2], Shintaro Takao[1,2], Ryosuke Makabe[1,2], Kohei Mizobata[3], Norio Kurosawa[4], Masato Moteki[2,3], tuneo Odate[2] (1.The Graduate University for Advanced Studies, 2.National Institute of Polar Research, 3.Tokyo University of Marine Science and Technology, 4.Soka University)

[MIS14-P07] Seasonality in sulfur isotopic compositions of atmospheric sulfate and its implications for atmospheric sulfur cycles in East Antarctica

*Sakiko Ishino[1], Shohei Hattori[1], Joel Savarino[2], Michel Legrand[2], Susanne Preunkert[2], Bruno Jourdain[2], Francis Albarede[3], Emmanuelle Albalat[3], Naohiro Yoshida[1,4] (1.Department of Chemical Science and Engineering, School of Materials and Chemical Technology, Tokyo Institute of Technology, 2.Institut des Geoscience de l'Environnement, Université Grenoble Alpes/CNRS, 3.Ecole Normale Supérieure (LGL-TPE), 4.Earth-Life Science Institute, Tokyo Institute of Technology)

[MIS14-P08] Penultimate glacial-interglacial transition viewed from the Dome Fuji ice core, Antarctica

*Ikumi Oyabu[1,2], Kenji Kawamura[1,3,4], Kyotaro Kitamura[1] (1.National Institute of Polar Research, Research Organization of Information and Systems, 2.Japan Society for the Promotion of Science, 3.SOKENDAI (The Graduate University of Advanced Studies), 4.Japan Agency for Marine Science and Technology (JAMSTEC))

[MIS14-P09] Reconstruction of Antarctic ice sheet dynamics in the Last Interglacial

*Mutsumi Iizuka[1], Osamu Seki[1], Takuya Itaki[2], Tomohisa Irino[1], Minoru Ikehara[4], Saiko Sugisaki[2], Masanobu Yamamoto[1], Keiji Horikawa[5], Yuusuke Suganuma[3] (1.Hokkaido university, 2.Geological Survey of Japan, 3.National Institute of Polar Research , 4.Center for Advanced Marine Core Research, Kochi University, 5.University of Toyama)

[MIS14-P10] Pliocene CO2 concentration estimated from Southern Ocean SST

*Osamu Seki[1], Tomohiro Shimono[2] (1.Institute of Low Temperature Science, Hokkaido University, 2.Guraduate School of Environmental Science)

[MIS14-P11] **Lithogenic fluxes across a transect in the SW Indian Ocean since the last glacial inception**

*Eri Helen Amsler[1], Walter Geibert[2], Gerhard Kuhn[2], Minoru Ikehara[3], Samuel Jaccard[1] (1.Institute of Geological Sciences and Oeschger Centre for Climate Change Research, University of Bern, Switzerland, 2.Alfred-Wegener-Institut Helmholtz-Zentrum für Polar- und Meeresforschung, Bremerhaven, Germany, 3.Center for Advanced Marine Core Research, Kochi University, Kochi, Japan)

[MIS14-P12] Changes in composition of fossil diatoms from Ross Sea under gradual warming climate from MIS M2

*Saki Ishino[1], Itsuki Suto[2], Rob M. McKay[3], Laura De Santis[4], Denise K. Kluhanek[5], Expedition 374 Scientists (1.National Institute of Advanced Industrial Science and Technology, 2.Department of Earth and Planetary Sciences Graduate School of Environmental Studies, Nagoya University, 3.Victoria University, 4.Instituto Nazionale di Oceanografia e di Geofisica Sperimentale, 5.Texas A&M University)

[MIS14-P13] Geological insights into formation of Conrad Rise, Southern Ocean: Preliminary geological results of R/V *Hakuho-maru* KH-19-1 cruise

*Hiroshi Sato[1], Masakazu Fujii[2,3], Hiroki Matsui[4], Minoru Ikehara[4] (1.School of Business Administration, Senshu University, 2.NIPR, 3.SOKENDAI, 4.Center for Advanced Marine Core Research, Kochi University)

[MIS14-P14] Fossil chrysophyte cysts as a new paleoenvironmental proxy

*Yuji Kato[1,2], Itsuki Suto[1] (1.Graduate School of Environmental Studies, Nagoya University, 2.Center for Advanced Marine Core Research, Kochi University (JSPS Research Fellowship for Young Scientists))

[MIS14-P15] Spatiotemporal variability of surface mass balance along the JARE traverse route for 1991–2019

*Shun Tsutaki[1], Hideaki Motoyama[2,3], Ayako Abe-Ouchi[1,4], Shuji Fujita[2,3], Kenji Kawamura[2,3,4] (1.The University of Tokyo, 2.National Institute of Polar Research, 3.The Graduate University for Advanced Studies, 4.Japan Agency for Marine-Earth Science and Technology)

[MIS14-P16] The weathering of granitic rocks in the Sør-Rondane Mountains, East Antarctica

*Tatsuo Kanamaru[1], Yusuke Suganuma[2], hisashi Oiwane[3], Hideki Miura[2], Makoto Miura[4], Jun'ichi Okuno[2], Hideaki Hayakawa[5] (1.Department of Earth and Environmental Sciences, College of Humanities & Sciences, Nihon University, 2.National Institute of Polar Research, 3.Musuhi LLC, 4.Department of Earth and Planetary Sciences, Kanazawa University, 5.Institute for Cosmic Ray Research, University of Tokyo)

[MIS14-P17] Summary of the 2nd Year Activities of the Project on the Interaction of the solid Earth and the
Antarctic Ice Sheet:

*Yoichi Fukuda[1], Jun Nishijima[2], Takahito Kazama[1], Kazuki Nakamura[3], Koichiro Doi[4], Yusuke Suganuma[4], Jun'ichi Okuno[4], Akito Araya[5], Heitaro Kaneda[6], Yuichi Aoyama[4], Hideki Miura[4] (1.Department of Geophysics, Graduate School of Science, Kyoto University, 2.Graduate School of Engineering, Kyushu University, 3.Faculty of Engineering, Nihon University, 4.National Institute of Polar Research, 5.ERI, University of Tokyo, 6.Graduate School of Science, Chiba University)

[MIS14-P18] Late Pleistocene to Holocene sea-level change in East Antarctica revealed by glacial isostatic adjustment modeling

*Takeshige Ishiwa[1], Jun'ichi Okuno[1,2], Yusuke Suganuma[1,2], Hideki Miura[1,2] (1.National Institute of Polar Research, 2.SOKENDAI)

[MIS14-P19] An modeling study of Antarctic ice sheet of the Last Glacial Maximum and the last deglaciation

*Takashi Obase[1], Ayako Abe-Ouchi[1,2], Ralf Greve[3], Fuyuki SAITO[2] (1.Atmosphere and Ocean Research Institute, the University of Tokyo, 2.Japan Agency for Marine-Earth Science and Technology, 3.Institute of Low Temperature Science, Hokkaido University)

[MIS14-P20] Development of a coupled ice-sheet/earth rebound model for Antarctic ice-sheet simulation

*Fuyuki SAITO[1], Ayako Abe-Ouchi[2,1], Jun'ichi Okuno[3], Takashi Obase[2] (1.Japan Agency for Marine-Earth Science and Technology, 2.Atmosphere and Ocean Research Institute, University of Tokyo, 3.National Institute of Polar Research)

[MIS14-P21] Polar amplifications in the past warm periods obtained from MIROC 4m AOGCM

*Taro Higuchi[1], Ayako Abe-Ouchi[1], Wing-Le Chan[1], Sam Sherriff-Tadano[1] (1.Atmospheric and Ocean Research Institute, the University of Tokyo)

[MIS14-P22] Using a coupled AOGCM to study the Antarctic climate of the mid-Pliocene warm period

*Wing-Le Chan[1], Ayako Abe-Ouchi[1,2] (1.Atmosphere and Ocean Research Institute, The University of Tokyo, 2.National Institute of Polar Research)

[MIS14-P23] CMIP5 model analysis of future changes in ocean net primary production by focusing on different response among the individual oceans and models

*Akira Oka[1], Yuki Nakamura[1] (1.Atmosphere and Ocean Research Institute, The University of Tokyo)

[MIS14-P24] Factor analysis of the millennial time-scale climate variability in glacial periods

*Miki Akari[1], Ayako Abe-Ouchi[2], Sam Sherriff-Tadano[2] (1.Department of Earth and Planetary Science, Graduate School of Science, The University of Tokyo, 2.Atmosphere and Ocean Research Institute, the University of Tokyo)

[MIS14-P25] First continuous profiler observation of wintertime Antarctic coastal polynya

*Shigeru Aoki[1], Kazuya Ono[1], Daisuke Hirano[1], Masato Itoh[1], Tomohide Noguchi[2], Satoshi Ozawa[2] (1.Hokkaido University, 2.Marine Works Japan)

[MIS14-P26] Surface topography survey for bared rock and accumulated snow in Antarctica by Unmanned Aero Vehicle

*Yuichi Aoyama[1,2,3], Akihisa Hattori[2,3], Hajime Oishi[3,4], Koichiro Doi[1,2,3], Yoshifumi Nogi[1,2] (1.National Institute of Polar Research, 2.SOKENDAI, 3.The 59th Japanese Antarctic Research Expedition, 4.NEC Networks & System Integration Corporation)

[MIS14-P27] The analysis of long-term Mooring observation records in the northernmost area of seasonal sea ice zone in the Southern Ocean

*Kazuho Watanabe[1], Kohei Mizobata[1], Yujiro Kitade[1] (1.Tokyo University of Marine Science and Technology)

[MIS14-P28] Preliminary observation report on chlorofluorocarbons (CFCs) and sulfur hexafluoride (SF_6) off the Cape Darnley in the summer of 2019

*Yoshihiko Ohashi[1], Michiyo Yamamoto-Kawai[1], Kenichi Sasaki[2], Sayaka Kumakawa[1], Naoyuki Tamura[1], Kay I. Ohshima[3] (1.Tokyo University of Marine Science and Technology, 2.Japan Agency for Marine-Earth Science and Technology, 3.Institute of Low Temperature Science, Hokkaido University)

[MIS14-P29] Mechanism of sea-ice production variation in Amundsen Sea Polynya

*Sohey Nihashi[1], Kouta Mine[1], Kazuki Nakata[2] (1.National Institute of Technology, Tomakomai College, 2.RESTEC)

[MIS14-P30] Estimation of thin ice thickness and discrimination of ice type from AMSR2 passive microwave data

*Kazuki Nakata[1], Tamaru Naoya[1], Sohey Nihashi[2], Kay I. Ohshima[3] (1.Remote Sensing Technology Center of Japan, 2.National Institute of Technology, Tomakomai College, 3.Institute of Low Temperature Science, Hokkaido University)

[J] Poster | M (Multidisciplinary and Interdisciplinary) : M-IS Intersection

5:15 PM - 6:30 PM JST | 8:15 AM - 9:30 AM UTC | Poster Hall International Exhibition Hall8, Makuhari Messe_35

[M-IS14] Global climate change driven by the Southern Ocean and the Antarctic Ice Sheet

convener:Osamu Seki(Institute of Low Temperature Science, Hokkaido University), Akira Oka(Atmosphere and Ocean Research Institute, The University of Tokyo), Ryu Uemura(University of the Ryukyus), Ryosuke Makabe(National Institute of Polar Research)

[MIS14-P01] Preliminary study on the effect of low-salinity ice melting water on biomass and composition of ice algae

*Keigo Takahashi[1], Ryosuke Makabe[2,3], Shintaro Takao[2,3], Tsuneo Odate[2,3], Masato Moteki[1,2] (1.Tokyo University of Marine Science and Technology, 2.National Institute of Polar Research, 3.The Graduate University for Advanced Studies (SOKENDAI))

[MIS14-P02] Effects of lugol's fixtation on preservation of samples for carbon and nitrogen stable isotope and molecular analyses

*Masayoshi Sano[1], Ryosuke Makabe[1,2], Ayu Yamamoto[3], Norio Kurosawa[4], Masato Moteki[2,3], Tsuneo Odate[1,2] (1.National Institute of Polar Research, 2.The Graduate University for Advanced Studies, 3.Tokyo University of Marine Science and Technology, 4.Soka University)

[MIS14-P03] The application of environmental DNA for the monitoring of Antarctic marine ecosystem

*Aiko Tachibana[1], Ryosuke Makabe[2], Masato Moteki[1] (1.Tokyo University of Marine Science and Technology, 2.National Institute of Polar Research)

[MIS14-P04] Coincidental occurrence process of frazil ice and high biomass off Amery Ice Shelf

*Yoshihiko Machimura[1], Kay I. Ohshima[2], Kazuki Nakata[3], Masato Ito[2], Yasushi Fukamachi[2,4], Ryosuke Makabe[5], Shintaro Takao[5], Sohey Nihashi[6] (1.Graduate School of Environmental Sciences, Hokkaido University, 2.Institute of Low Temperature Science, Hokkaido University, 3.Remote Sensing Technology Center of Japan, 4.Arctic Research Center, Hokkaido University, 5.National Institute of Polar Research, 6.National Institute of Technology, Tomakomai College)

[MIS14-P05] Feeding habit of the Antarctic amphipod *Themisto gaudichaudii* of Vincennes Bay (East Antarctica) during austral summer

*Junji Matsushita[1], Ryosuke Makabe[2], Masato Moteki[1] (1.Tokyo University of Marine Science and Technology, 2.National Institute of Polar Research)

[MIS14-P06] Time-series observation of subsurface chlorophyll *a* maximum in the seasonal ice zone of the Southern Ocean

*Ayuko Kagesawa[1], Masayoshi Sano[2], Shintaro Takao[1,2], Ryosuke Makabe[1,2], Kohei Mizobata[3], Norio Kurosawa[4], Masato Moteki[2,3], tuneo Odate[2] (1.The Graduate University for Advanced Studies, 2.National Institute of Polar Research, 3.Tokyo University of Marine Science and Technology, 4.Soka University)

[MIS14-P07] Seasonality in sulfur isotopic compositions of atmospheric sulfate and its implications for atmospheric sulfur cycles in East Antarctica

*Sakiko Ishino[1], Shohei Hattori[1], Joel Savarino[2], Michel Legrand[2], Susanne Preunkert[2], Bruno Jourdain[2], Francis Albarede[3], Emmanuelle Albalat[3], Naohiro Yoshida[1,4] (1.Department of Chemical Science and Engineering, School of Materials and Chemical Technology, Tokyo Institute of Technology, 2.Institut des Geoscience de l'Environnement, Université Grenoble Alpes/CNRS, 3.Ecole Normale Supérieure (LGL-TPE), 4.Earth-Life Science Institute, Tokyo Institute of Technology)

[MIS14-P08] Penultimate glacial-interglacial transition viewed from the Dome Fuji ice core, Antarctica

*Ikumi Oyabu[1,2], Kenji Kawamura[1,3,4], Kyotaro Kitamura[1] (1.National Institute of Polar Research, Research Organization of Information and Systems, 2.Japan Society for the Promotion of Science, 3.SOKENDAI (The Graduate University of Advanced Studies), 4.Japan Agency for Marine Science and Technology (JAMSTEC))

[MIS14-P09] Reconstruction of Antarctic ice sheet dynamics in the Last Interglacial

*Mutsumi Iizuka[1], Osamu Seki[1], Takuya Itaki[2], Tomohisa Irino[1], Minoru Ikehara[4], Saiko Sugisaki[2], Masanobu Yamamoto[1], Keiji Horikawa[5], Yuusuke Suganuma[3] (1.Hokkaido university, 2.Geological Survey of Japan, 3.National Institute of Polar Research , 4.Center for Advanced Marine Core Research, Kochi University, 5.University of Toyama)

[MIS14-P10] Pliocene CO2 concentration estimated from Southern Ocean SST

*Osamu Seki[1], Tomohiro Shimono[2] (1.Institute of Low Temperature Science, Hokkaido University, 2.Guraduate School of Environmental Science)

[MIS14-P11] **Lithogenic fluxes across a transect in the SW Indian Ocean since the last glacial inception**

*Eri Helen Amsler[1], Walter Geibert[2], Gerhard Kuhn[2], Minoru Ikehara[3], Samuel Jaccard[1] (1.Institute of Geological Sciences and Oeschger Centre for Climate Change Research, University of Bern, Switzerland, 2.Alfred-Wegener-Institut Helmholtz-Zentrum für Polar- und Meeresforschung, Bremerhaven, Germany, 3.Center for Advanced Marine Core Research, Kochi University, Kochi, Japan)

[MIS14-P12] Changes in composition of fossil diatoms from Ross Sea under gradual warming climate from MIS M2

*Saki Ishino[1], Itsuki Suto[2], Rob M. McKay[3], Laura De Santis[4], Denise K. Kluhanek[5], Expedition 374 Scientists (1.National Institute of Advanced Industrial Science and Technology, 2.Department of Earth and Planetary Sciences Graduate School of Environmental Studies, Nagoya University, 3.Victoria University, 4.Instituto Nazionale di Oceanografia e di Geofisica Sperimentale, 5.Texas A&M University)

[MIS14-P13] Geological insights into formation of Conrad Rise, Southern Ocean: Preliminary geological results of R/V *Hakuho-maru* KH-19-1 cruise

*Hiroshi Sato[1], Masakazu Fujii[2,3], Hiroki Matsui[4], Minoru Ikehara[4] (1.School of Business Administration, Senshu University, 2.NIPR, 3.SOKENDAI, 4.Center for Advanced Marine Core Research, Kochi University)

[MIS14-P14] Fossil chrysophyte cysts as a new paleoenvironmental proxy

*Yuji Kato[1,2], Itsuki Suto[1] (1.Graduate School of Environmental Studies, Nagoya University, 2.Center for Advanced Marine Core Research, Kochi University (JSPS Research Fellowship for Young Scientists))

[MIS14-P15] Spatiotemporal variability of surface mass balance along the JARE traverse route for 1991–2019

*Shun Tsutaki[1], Hideaki Motoyama[2,3], Ayako Abe-Ouchi[1,4], Shuji Fujita[2,3], Kenji Kawamura[2,3,4] (1.The University of Tokyo, 2.National Institute of Polar Research, 3.The Graduate University for Advanced Studies, 4.Japan Agency for Marine-Earth Science and Technology)

[MIS14-P16] The weathering of granitic rocks in the Sør-Rondane Mountains, East Antarctica

*Tatsuo Kanamaru[1], Yusuke Suganuma[2], hisashi Oiwane[3], Hideki Miura[2], Makoto Miura[4], Jun'ichi Okuno[2], Hideaki Hayakawa[5] (1.Department of Earth and Environmental Sciences, College of Humanities & Sciences, Nihon University, 2.National Institute of Polar Research, 3.Musuhi LLC, 4.Department of Earth and Planetary Sciences, Kanazawa University, 5.Institute for Cosmic Ray Research, University of Tokyo)

[MIS14-P17] Summary of the 2nd Year Activities of the Project on the Interaction of the solid Earth and the
Antarctic Ice Sheet:

*Yoichi Fukuda[1], Jun Nishijima[2], Takahito Kazama[1], Kazuki Nakamura[3], Koichiro Doi[4], Yusuke Suganuma[4], Jun'ichi Okuno[4], Akito Araya[5], Heitaro Kaneda[6], Yuichi Aoyama[4], Hideki Miura[4] (1.Department of Geophysics, Graduate School of Science, Kyoto University, 2.Graduate School of Engineering, Kyushu University, 3.Faculty of Engineering, Nihon University, 4.National Institute of Polar Research, 5.ERI, University of Tokyo, 6.Graduate School of Science, Chiba University)

[MIS14-P18] Late Pleistocene to Holocene sea-level change in East Antarctica revealed by glacial isostatic adjustment modeling

*Takeshige Ishiwa[1], Jun'ichi Okuno[1,2], Yusuke Suganuma[1,2], Hideki Miura[1,2] (1.National Institute of Polar Research, 2.SOKENDAI)

[MIS14-P19] An modeling study of Antarctic ice sheet of the Last Glacial Maximum and the last deglaciation

*Takashi Obase[1], Ayako Abe-Ouchi[1,2], Ralf Greve[3], Fuyuki SAITO[2] (1.Atmosphere and Ocean Research Institute, the University of Tokyo, 2.Japan Agency for Marine-Earth Science and Technology, 3.Institute of Low Temperature Science, Hokkaido University)

[MIS14-P20] Development of a coupled ice-sheet/earth rebound model for Antarctic ice-sheet simulation

*Fuyuki SAITO[1], Ayako Abe-Ouchi[2,1], Jun'ichi Okuno[3], Takashi Obase[2] (1.Japan Agency for Marine-Earth Science and Technology, 2.Atmosphere and Ocean Research Institute, University of Tokyo, 3.National Institute of Polar Research)

[MIS14-P21] Polar amplifications in the past warm periods obtained from MIROC 4m AOGCM

*Taro Higuchi[1], Ayako Abe-Ouchi[1], Wing-Le Chan[1], Sam Sherriff-Tadano[1] (1.Atmospheric and Ocean Research Institute, the University of Tokyo)

[MIS14-P22] Using a coupled AOGCM to study the Antarctic climate of the mid-Pliocene warm period

*Wing-Le Chan[1], Ayako Abe-Ouchi[1,2] (1.Atmosphere and Ocean Research Institute, The University of Tokyo, 2.National Institute of Polar Research)

[MIS14-P23] CMIP5 model analysis of future changes in ocean net primary production by focusing on different response among the individual oceans and models

*Akira Oka[1], Yuki Nakamura[1] (1.Atmosphere and Ocean Research Institute, The University of Tokyo)

[MIS14-P24] Factor analysis of the millennial time-scale climate variability in glacial periods

*Miki Akari[1], Ayako Abe-Ouchi[2], Sam Sherriff-Tadano[2] (1.Department of Earth and Planetary Science, Graduate School of Science, The University of Tokyo, 2.Atmosphere and Ocean Research Institute, the University of Tokyo)

[MIS14-P25] First continuous profiler observation of wintertime Antarctic coastal polynya

*Shigeru Aoki[1], Kazuya Ono[1], Daisuke Hirano[1], Masato Itoh[1], Tomohide Noguchi[2], Satoshi Ozawa[2] (1.Hokkaido University, 2.Marine Works Japan)

[MIS14-P26] Surface topography survey for bared rock and accumulated snow in Antarctica by Unmanned Aero Vehicle

*Yuichi Aoyama[1,2,3], Akihisa Hattori[2,3], Hajime Oishi[3,4], Koichiro Doi[1,2,3], Yoshifumi Nogi[1,2] (1.National Institute of Polar Research, 2.SOKENDAI, 3.The 59th Japanese Antarctic Research Expedition, 4.NEC Networks & System Integration Corporation)

[MIS14-P27] The analysis of long-term Mooring observation records in the northernmost area of seasonal sea ice zone in the Southern Ocean

*Kazuho Watanabe[1], Kohei Mizobata[1], Yujiro Kitade[1] (1.Tokyo University of Marine Science and Technology)

[MIS14-P28] Preliminary observation report on chlorofluorocarbons (CFCs) and sulfur hexafluoride (SF_6) off the Cape Darnley in the summer of 2019

*Yoshihiko Ohashi[1], Michiyo Yamamoto-Kawai[1], Kenichi Sasaki[2], Sayaka Kumakawa[1], Naoyuki Tamura[1], Kay I. Ohshima[3] (1.Tokyo University of Marine Science and Technology, 2.Japan Agency for Marine-Earth Science and Technology, 3.Institute of Low Temperature Science, Hokkaido University)

[MIS14-P29] Mechanism of sea-ice production variation in Amundsen Sea Polynya

*Sohey Nihashi[1], Kouta Mine[1], Kazuki Nakata[2] (1.National Institute of Technology, Tomakomai College, 2.RESTEC)

[MIS14-P30] Estimation of thin ice thickness and discrimination of ice type from AMSR2 passive microwave data

*Kazuki Nakata[1], Tamaru Naoya[1], Sohey Nihashi[2], Kay I. Ohshima[3] (1.Remote Sensing Technology Center of Japan, 2.National Institute of Technology, Tomakomai College, 3.Institute of Low Temperature Science, Hokkaido University)

[J] Poster | M (Multidisciplinary and Interdisciplinary)：M-IS Intersection

1:45 PM - 3:15 PM JST | 4:45 AM - 6:15 AM UTC | Poster Hall International Exhibition Hall8, Makuhari Messe_8

[M-IS15] Evolution of Pelagic Realm

convener:Atsushi Matsuoka(Department of Geology, Faculty of Science, Niigata University), Katsunori Kimoto(Japan Agency for Marine-Earth Science and Technology), Toshiyuki Kurihara(Graduate School of Science and Technology, Niigata University), Tetsuji Onoue(Earth and Environmental Sciences, Graduate School of Science and Technology, Kumamoto University)

[MIS15-P01] Ichthyolith stratigraphy constraints on ages and areas of REY-rich mud deposition in the South Pacific Ocean

*Shugo Minabe[1], Kazuhide Mimura[1], Kentaro Nakamura[1], Junichiro Ohta[2,1], Kazutaka Yasukawa[1,2], Koichiro Fujinaga[2,1], Shiki Machida[2], Yasuhiro Kato[3,1,2] (1.Department of Systems Innovation, School of Engineering, The University of Tokyo, 2.Ocean Resource Research Center for Next Generation, Chiba Institute of Technology, 3.Frontier Research Center for Energy and Resources, School of Engineering, The University of Tokyo)

[MIS15-P02] Radiolarian phylogeny around the Jurassic–Cretaceous boundary

*Atsushi Matsuoka[1] (1.Department of Geology, Faculty of Science, Niigata University)

[MIS15-P03] Late Silurian and Early Devonian radiolarian assemblages from the Yokokurayama and Konomori areas in the Kurosegawa belt, Southwest Japan

*Toshiyuki Kurihara[1], Kaori Tsuchiya[2] (1.Graduate School of Science and Technology, Niigata University, 2.Faculty of Science, Niigata University)

[J] Poster | M (Multidisciplinary and Interdisciplinary)：M-IS Intersection

5:15 PM - 6:30 PM JST | 8:15 AM - 9:30 AM UTC | Poster Hall International Exhibition Hall8, Makuhari Messe_36

[M-IS15] Evolution of Pelagic Realm

convener:Atsushi Matsuoka(Department of Geology, Faculty of Science, Niigata University), Katsunori Kimoto(Japan Agency for Marine-Earth Science and Technology), Toshiyuki Kurihara(Graduate School of Science and Technology, Niigata University), Tetsuji Onoue(Earth and Environmental Sciences, Graduate School of Science and Technology, Kumamoto University)

[MIS15-P01] Ichthyolith stratigraphy constraints on ages and areas of REY-rich mud deposition in the South Pacific Ocean

*Shugo Minabe[1], Kazuhide Mimura[1], Kentaro Nakamura[1], Junichiro Ohta[2,1], Kazutaka Yasukawa[1,2], Koichiro Fujinaga[2,1], Shiki Machida[2], Yasuhiro Kato[3,1,2] (1.Department of Systems Innovation, School of Engineering, The University of Tokyo, 2.Ocean Resource Research Center for Next Generation, Chiba Institute of Technology, 3.Frontier Research Center for Energy and Resources, School of Engineering, The University of Tokyo)

[MIS15-P02] Radiolarian phylogeny around the Jurassic–Cretaceous boundary

*Atsushi Matsuoka[1] (1.Department of Geology, Faculty of Science, Niigata University)

[MIS15-P03] Late Silurian and Early Devonian radiolarian assemblages from the Yokokurayama and Konomori areas in the Kurosegawa belt, Southwest Japan

*Toshiyuki Kurihara[1], Kaori Tsuchiya[2] (1.Graduate School of Science and Technology, Niigata University, 2.Faculty of Science, Niigata University)

[J] Oral | M (Multidisciplinary and Interdisciplinary)：M-IS Intersection

3:30 PM - 5:00 PM JST | 6:30 AM - 8:00 AM UTC | 302 3F

[M-IS15] Evolution of Pelagic Realm

convener:Atsushi Matsuoka(Department of Geology, Faculty of Science, Niigata University), Katsunori Kimoto(Japan Agency for Marine-Earth Science and Technology), Toshiyuki Kurihara(Graduate School of Science and Technology, Niigata University), Tetsuji Onoue(Earth and Environmental Sciences, Graduate School of Science and Technology, Kumamoto University), Chairperson:Atsushi Matsuoka, Toshiyuki Kurihara

3:30 PM - 3:45 PM JST | 6:30 AM - 6:45 AM UTC

[MIS15-01] **Environmental changes of the North Pacific Ocean through the Cenozoic era recorded in DSDP/ODP pelagic clay cores**

*Kazuhide Mimura[1], Katsushi Yamamoto[1], Kentaro Nakamura[1], Kazutaka Yasukawa[1,2], Junichiro Ohta[2], Koichiro Fujinaga[2,1], Shiki Machida[2], Yoichi Usui[3], Yasuhiro Kato[1,2] (1.Department of Systems Innovation, School of Engineering, the University of Tokyo, 2.ORCeNG, Chiba Institute of Technology, 3.JAMSTEC)

3:45 PM - 4:00 PM JST | 6:45 AM - 7:00 AM UTC

[MIS15-02] Reconstruction of oceanic redox conditions in the Lower Jurassic (Pliensbachian–Toarcian) pelagic deep-sea bedded chert sequence of the Mino Belt, central Japan

*Katsuhito Soda[1] (1.Department of Earth and Environmental Sciences, Faculty of Science, Kumamoto University)

4:00 PM - 4:15 PM JST | 7:00 AM - 7:15 AM UTC

[MIS15-03] Conodont biostratigraphy of Anisian pelagic deep-sea sedimentary rocks deposited in the pelagic Panthalassa—Integration with radiolarian biozones—

*Shun Muto[1], Satoshi Takahashi[1], Satoshi Yamakita[2], Katsuhito Soda[3], Tetsuji Onoue[3] (1.Department of Earth and Planetary Science, Graduate School of Science, University of Tokyo, 2.Faculty of Education, University of Miyazaki, 3.Faculty of Advanced Science and Technology)

4:15 PM - 4:30 PM JST | 7:15 AM - 7:30 AM UTC

[MIS15-04] Triassic marine Os isotope record reconstructed from a pelagic chert succession, Sakahogi section, Mino Belt, southwest Japan

★Invited Papers

*Tatsuo Nozaki[1,2,3,4], Takashi Nikaido[5], Tetsuji Onoue[6], Yutaro Takaya[7,1,2,4], Keiko Sato[1], Jun-Ichi Kimura[8], Qing Chang[8], Daisuke Yamashita[6], Honami Sato[4,1], Katsuhiko Suzuki[1], Yasuhiro Kato[2,4], Atsushi Matsuoka[5] (1.JAMSTEC/R&D CSR, 2.Univ. of Tokyo, 3.Kobe Univ., 4.ChibaTech, 5.Niigata Univ., 6.Kumamoto Univ., 7.Waseda Univ., 8.JAMSTEC/D-SEG)

4:30 PM - 4:45 PM JST | 7:30 AM - 7:45 AM UTC

[MIS15-05] **The preservation of radiolarians across the Jurassic-Cretaceous (J/K) boundary in the Bosso Valley section, Central Italy**

*XIN LI[1], Atsushi Matsuoka[2], Angela Bertinelli[3], Marco Chiari[4] (1.State Key Laboratory of Palaeobiology and Stratigraphy, Nanjing Institute of Geology and Palaeontology, Chinese Academy of Sciences, 2.Niigata University, 3.Università degli Studi di Perugia, 4. Istituto di Geoscienze e Georisorse)

4:45 PM - 5:00 PM JST | 7:45 AM - 8:00 AM UTC

[MIS15-06] Radiolarian faunas around the Jurassic-Cretaceous boundary in the Bosso Valley section, central Italy

*Atsushi Matsuoka[1], XIN LI[2], Marco Chiari[3], Angela Bertinelli[4] (1.Department of Geology, Faculty of Science, Niigata University, 2.Nanjing Institute of Geology and Palaeontology, Chinese Academy of Sciense, 3.C.N.R., Istituto di Geoscienze e Georisorse, sede secondaria di Firenze, 4. Dipartimento di Fisica e Geologia, Università degli Studi di Perugia)

[J] Oral | M (Multidisciplinary and Interdisciplinary)：M-IS Intersection

9:00 AM - 10:30 AM JST | 12:00 AM - 1:30 AM UTC | 201B 2F

[M-IS17] History X Earth and Planetary Science

convener:Yasuyuki Kano(Earthquake Research Institute, The University of Tokyo), Kei Yoshimura(Institute of Industrial Science, The University of Tokyo), Hiroaki Isobe(Faculty of Fine Arts, Kyoto City University of Arts), kiyomi iwahashi(National Institute of Japanese Literature), Chairperson:Yasuyuki Kano(東京大学 地震研究所), Kiyomi Iwahashi, Hiroaki Isobe, Kei Yoshimura, Harufumi Tamazawa

9:05 AM - 9:30 AM JST | 12:05 AM - 12:30 AM UTC

[MIS17-01] Document based reconstruction of environment of forests in the Edo period

★Invited Papers

*SATOSHI SHIROUZU[1] (1.Chuogakuin University)

9:30 AM - 9:45 AM JST | 12:30 AM - 12:45 AM UTC

[MIS17-02] Studies of Babylonian Astronomical Diaries: Today and the Future

*Yasuyuki Mitsuma[1] (1.The University of Tokyo)

9:45 AM - 10:00 AM JST | 12:45 AM - 1:00 AM UTC

[MIS17-03] Characteristics of the Sunspots that Produce Large Solar Flares and the Possibility to Investigate these Events Utilizing Historical Observational Records

*Shin Toriumi[1] (1.National Astronomical Observatory of Japan)

10:00 AM - 10:15 AM JST | 1:00 AM - 1:15 AM UTC

[MIS17-04] An Approach of Environmental History to the "14th Century Crisis"

*Isahaya Yoichi[1] (1.Slavic-Eurasian Research Center, Hokkaido University)

10:15 AM - 10:30 AM JST | 1:15 AM - 1:30 AM UTC

[MIS17-05] Recovery of the Asian monsoon variations since the late 19th century by the data rescue activities in ACRE-Japan

*Jun Matsumoto[1,2], Tomoshige Inoue[1], Fumiaki Fujibe[1], Jun-Ichi Hamada[1], Taiichi Hayashi[3], Toru Terao[4], Fumie Murata[5], Hisayuki Kubota[6], Ikumi Akasaka[7], Hirotaka Kamahori[8], Nobuhiko Endo[9], Haruhiko Yamamoto[10], Shigeru Kobayashi[11], Yoshitaka Muraji[12] (1.Deaprtment of Geography, Tokyo Metropolitan University, 2.Department of Coupled Ocean-Atmosphere-Land Processes Research, 3.Kyoto University, 4.Kagawa University, 5.Kochi University, 6.Hokkaido University, 7.Senshu University, 8.Meteorological Research Institute, 9.NARO/NIAES, 10.Yamaguchi University, 11.Osaka University, 12.EScoT)

[J] Oral | M (Multidisciplinary and Interdisciplinary)：M-IS Intersection

10:45 AM - 12:15 PM JST | 1:45 AM - 3:15 AM UTC | 201B 2F

[M-IS17] History X Earth and Planetary Science

convener:Yasuyuki Kano(Earthquake Research Institute, The University of Tokyo), Kei Yoshimura(Institute of Industrial Science, The University of Tokyo), Hiroaki Isobe(Faculty of Fine Arts, Kyoto City University of Arts), kiyomi iwahashi(National Institute of Japanese Literature), Chairperson:Hiroaki Isobe, Kei Yoshimura, Kiyomi Iwahashi, Yasuyuki Kano(東京大学 地震研究所), Harufumi Tamazawa

10:45 AM - 11:00 AM JST | 1:45 AM - 2:00 AM UTC

[MIS17-06] Historical big data: integrated analysis of the past world by the workflow that bridges data structuring gaps

*Asanobu Kitamoto[1,2,3], Mika Ichino[1,2] (1.National Institute of Informatics, 2.ROIS-DS Center for Open Data in the Humanities, 3.SOKENDAI)

11:00 AM - 11:15 AM JST | 2:00 AM - 2:15 AM UTC

[MIS17-07] Felt earthquakes in Tokyo (Edo) based on historical daily records and seismic intensity data

*Kenji Satake[1] (1.Earthquake Research Institute, University of Tokyo)

11:15 AM - 11:30 AM JST | 2:15 AM - 2:30 AM UTC

[MIS17-08] Climate and social changes in ancient Japan construed by use of high resolution reconstruction of the Climate in Historical Time

*Katsunori IMAZU[1], Takeshi Nakatsuka[2] (1.OKAYAMA University Graduate School of Humanities and Social Sciences, 2.Research Institute for Humanity and Nature)

11:30 AM - 11:45 AM JST | 2:30 AM - 2:45 AM UTC

[MIS17-09] Absolute ages for huge eruptions of Towada Caldera and Baitoushan volcano in the 10th century as seen from dendrochronological studies and historical documents

*Masataka Hakozaki[1], Fusa Miyake[2], Masaki Sano[3], Katsuhiko Kimura[4], Toshio Nakamura[2], Mitsuru Okuno[5], Minoru Sakamoto[1], Takeshi Nakatsuka[6,2] (1.National Museum of Japanese History, 2.Nagoya University, 3.Waseda University, 4.Fukushima University, 5.Fukuoka University, 6.Research Institute for Humanity and Nature)

11:45 AM - 12:00 PM JST | 2:45 AM - 3:00 AM UTC

[MIS17-10] How can we activate collaborations with history and archaeology? – Lesson from Historical Climate Adaptation project

★Invited Papers

*Takeshi Nakatsuka[1,2] (1.Research Institute for Humanity and Nature, 2.Graduate School of Environmental Studies, Nagoya University)

[J] Poster | M (Multidisciplinary and Interdisciplinary)：M-IS Intersection

3:30 PM - 5:00 PM JST | 6:30 AM - 8:00 AM UTC | Poster Hall International Exhibition Hall8, Makuhari Messe_22

[M-IS17] History X Earth and Planetary Science

convener:Yasuyuki Kano(Earthquake Research Institute, The University of Tokyo), Kei Yoshimura(Institute of Industrial Science, The University of Tokyo), Hiroaki Isobe(Faculty of Fine Arts, Kyoto City University of Arts), kiyomi iwahashi(National Institute of Japanese Literature)

[MIS17-P01] Perspective of 'History X Earth and Planetary Science'

*Yasuyuki Kano[1], Hiroaki Isobe[2], Kei Yoshimura[3], Kiyomi Iwahashi[4], Harufumi Tamazawa[5,2] (1.Earthquake Research Institute, The University of Tokyo, 2.Faculty of Fine Arts, Kyoto City University of Arts, 3.Institute of Industrial Science, The University of Tokyo, 4.National Institute of Japanese Literature, 5.Disaster Prevention Research Institute, Kyoto University)

[MIS17-P02] Reexamination of intensity distribution of Japanese historical earthquakes using attenuation relation

*Yasuyuki Kano[1], Junzo Ohmura[2] (1.Earthquake Research Institute, The University of Tokyo, 2.Diasaster prevention Research institute, Kyoto University)

[MIS17-P03] Rekisuke: a system for sharing bibliographic information of historical documents through Interdisciplinary collaboration

★Invited Papers

*Mika Ichino[1,2], Yukie Hashimoto, Kooiti Masuda[3], Asanobu Kitamoto[2,1], Junpei Hirano[4] (1.Center for Open Data in the Humanities, Joint Support-Center for Data Science Research, Research Organization of Information and Systems , 2.National Institute of Informatics, 3.Tokyo Metropolitan University, 4.Faculty of Liberal Arts, Teikyo University)

[MIS17-P04] Analysis of reconstruction processes after the 1707 Hoei eruption of Fuji Volcano based on old maps

*Junzo Ohmura[1] (1.Research Institute for Earthquake Prediction, Disaster Prevention Research Institute, Kyoto University)

[MIS17-P05] Workshop of Word Survey about Earth and Planetary Phenomena by Citizen

*Harufumi Tamazawa[1,2], kiyomi iwahashi[3] (1. Disaster Prevention Research Institute Kyoto University, 2.Faculty of Fine Arts, Kyoto City University of Arts, 3.National Institute of Japanese Literature)

[MIS17-P06] Observational Data in the first half of 20th century to join modern scientific Observation and historical documents: A Usage example ob Photographic Plate of Kwasan Observatory

*Harufumi Tamazawa[1], Reizaburo Kitai[4], Hiroaki Isobe[2], Satoru UeNo[3], Takahito Sakaue[3] (1. Disaster Prevention Research Institute Kyoto University, 2.Faculty of Fine Arts, Kyoto City University of Arts, 3.Astronomical Observatory, Graduate School of Science, Kyoto University, 4.Bukkyo University)

[MIS17-P07] Climate changes and lords' control in the early modern period in Japan

*Kaoru kamatani[1], Masaki Sano[2], Takeshi Nakatsuka[3] (1.Ritsumeikan University, 2.Waseda University, 3.Research Institute for Humanity and Nature)

[MIS17-P08] Intense geomagnetic storm during Maunder minimum possibly by quiescent filament eruption

*Hiroaki Isobe[1], Yusuke Ebihara[2], Harufumi Tamazawa[1], Akito Davis Kawamura[3], Hisashi Hayakawa[4] (1.Faculty of Fine Arts, Kyoto City University of Arts, 2.Research Institute for Sustainable Humanosphere, Kyoto University, 3.Graduate School of Science, Kyoto University, 4.Graduate School of Letters, Osaka University)

[MIS17-P09] Reconstructing 1931 flood in Yangtze River basin and its application to Chinese economic history

*CHANG LIU[1], Akiyuki Kawasaki[1], Tomoko Shiroyama[2] (1.Department of Civil Engineering, Graduate School of Engineering, the University of Tokyo, 2.Department of Economics, Graduate School of Economics, the University of Tokyo)

[MIS17-P10] Seismicity Analysis Using Felt Reports and Attenuation Relation of Seismic Intensity

*Takeo Ishibe[1], Koji Iwasa[1], Mitsuko Furumura[1], Ritsuko S. Matsu'ura[1] (1.Association for the Development of Earthquake Prediction)

[MIS17-P11] Radiocarbon dating of Japanese tree rings – chronological research and Japanese calibration curve

*Minoru Sakamoto[1,2], Masataka Hakozaki[1], Takumi Mitsutani[3], Takeshi Nakatsuka[4,5] (1.National Museum of Japanese History, 2.The Graduate University for Advanced Studies, 3.Nara National Research Institute for Cultural Properties, 4.Research Institute for Humanity and Nature, 5.Nagoya University)

[MIS17-P12] Usage of Historical Documents with Scientific Understandings in the field of Solar Physics

*Akito Davis Kawamura[1], Hisashi Hayakawa[2], Harufumi Tamazawa[3], Hiroaki Isobe[3], Kazunari Shibata[1] (1.Astronomical Observatory, Kyoto University, 2.Graduate School of Letters, Osaka University, 3.Faculty of Fine Arts, Kyoto City University of Arts)

[MIS17-P13] The study of the relationship between the flood of Kitakami River and sociaty in the end of Edo period

*Daisuke Sato[1], Yoshitaka Takahashi[2] (1.International Reserch Institute of Disaster Science Tohoku University , 2.Tokyo University of Agriculture and Technology)

[MIS17-P14] Reconstruction of Historical Weather with Data Assimilation Using Old Diaries

*Kei Yoshimura[1], Panduka Neluwala[2], Mika Ichino[3], Kooiti Masuda[4], Junpei Hirano[5] (1.Institute of Industrial Science, The University of Tokyo, 2.University of Peradeniya , 3.National Institute of Informatics, 4.Tokyo Metropolitan University, 5.Teikyo University)

[MIS17-P15] Examination of data range for fitting Omori-Utsu law to temporal decay of aftershocks presented in historical materials on the 1830 Kyoto earthquake: Reason for the difference of numbers of aftershocks in the same place

*Kentaro Hattori[1], Junzo Ohmura[2], Ichiro Nakanishi[1] (1.Kyoto Univ., 2.Bukkyo Univ.)

[MIS17-P16] Tsunami trace height of the AD 1854 Ansei Tokai tsunami around the lake Hamanako inferred from historical maps

*ebina yuichi[1], Kentaro Imai[2], Yoshinobu Tsuji[3], hiroyuki iwase[4] (1.International Research Institute of Disaster Science, 2.JAMSTEC, 3.Fukuda Geological Instite, 4. (C)ECOH CORPORATION)

[J] Poster | M (Multidisciplinary and Interdisciplinary)：M-IS Intersection

5:15 PM - 6:30 PM JST | 8:15 AM - 9:30 AM UTC | Poster Hall International Exhibition Hall8, Makuhari Messe_37

[M-IS17] History X Earth and Planetary Science

convener:Yasuyuki Kano(Earthquake Research Institute, The University of Tokyo), Kei Yoshimura(Institute of Industrial Science, The University of Tokyo), Hiroaki Isobe(Faculty of Fine Arts, Kyoto City University of Arts), kiyomi iwahashi(National Institute of Japanese Literature)

[MIS17-P01] Perspective of 'History X Earth and Planetary Science'

*Yasuyuki Kano[1], Hiroaki Isobe[2], Kei Yoshimura[3], Kiyomi Iwahashi[4], Harufumi Tamazawa[5,2] (1.Earthquake Research Institute, The University of Tokyo, 2.Faculty of Fine Arts, Kyoto City University of Arts, 3.Institute of Industrial Science, The University of Tokyo, 4.National Institute of Japanese Literature, 5.Disaster Prevention Research Institute, Kyoto University)

[MIS17-P02] Reexamination of intensity distribution of Japanese historical earthquakes using attenuation relation

*Yasuyuki Kano[1], Junzo Ohmura[2] (1.Earthquake Research Institute, The University of Tokyo, 2.Diasaster prevention Research institute, Kyoto University)

[MIS17-P03] Rekisuke: a system for sharing bibliographic information of historical documents through Interdisciplinary collaboration

★Invited Papers

*Mika Ichino[1,2], Yukie Hashimoto, Kooiti Masuda[3], Asanobu Kitamoto[2,1], Junpei Hirano[4] (1.Center for Open Data in the Humanities, Joint Support-Center for Data Science Research, Research Organization of Information and Systems , 2.National Institute of Informatics, 3.Tokyo Metropolitan University, 4.Faculty of Liberal Arts, Teikyo University)

[MIS17-P04] Analysis of reconstruction processes after the 1707 Hoei eruption of Fuji Volcano based on old maps

*Junzo Ohmura[1] (1.Research Institute for Earthquake Prediction, Disaster Prevention Research Institute, Kyoto University)

[MIS17-P05] Workshop of Word Survey about Earth and Planetary Phenomena by Citizen

*Harufumi Tamazawa[1,2], kiyomi iwahashi[3] (1. Disaster Prevention Research Institute Kyoto University, 2.Faculty of Fine Arts, Kyoto City University of Arts, 3.National Institute of Japanese Literature)

[MIS17-P06] Observational Data in the first half of 20th century to join modern scientific Observation and historical documents: A Usage example ob Photographic Plate of Kwasan Observatory

*Harufumi Tamazawa[1], Reizaburo Kitai[4], Hiroaki Isobe[2], Satoru UeNo[3], Takahito Sakaue[3] (1. Disaster Prevention Research Institute Kyoto University, 2.Faculty of Fine Arts, Kyoto City University of Arts, 3.Astronomical Observatory, Graduate School of Science, Kyoto University, 4.Bukkyo University)

[MIS17-P07] Climate changes and lords' control in the early modern period in Japan

*Kaoru kamatani[1], Masaki Sano[2], Takeshi Nakatsuka[3] (1.Ritsumeikan University, 2.Waseda University, 3.Research Institute for Humanity and Nature)

[MIS17-P08] Intense geomagnetic storm during Maunder minimum possibly by quiescent filament eruption

*Hiroaki Isobe[1], Yusuke Ebihara[2], Harufumi Tamazawa[1], Akito Davis Kawamura[3], Hisashi Hayakawa[4] (1.Faculty of Fine Arts, Kyoto City University of Arts, 2.Research Institute for Sustainable Humanosphere, Kyoto University, 3.Graduate School of Science, Kyoto University, 4.Graduate School of Letters, Osaka University)

[MIS17-P09] Reconstructing 1931 flood in Yangtze River basin and its application to Chinese economic history

*CHANG LIU[1], Akiyuki Kawasaki[1], Tomoko Shiroyama[2] (1.Department of Civil Engineering, Graduate School of Engineering, the University of Tokyo, 2.Department of Economics, Graduate School of Economics, the University of Tokyo)

[MIS17-P10] Seismicity Analysis Using Felt Reports and Attenuation Relation of Seismic Intensity

*Takeo Ishibe[1], Koji Iwasa[1], Mitsuko Furumura[1], Ritsuko S. Matsu'ura[1] (1.Association for the Development of Earthquake Prediction)

[MIS17-P11] Radiocarbon dating of Japanese tree rings – chronological research and Japanese calibration curve

*Minoru Sakamoto[1,2], Masataka Hakozaki[1], Takumi Mitsutani[3], Takeshi Nakatsuka[4,5] (1.National Museum of Japanese History, 2.The Graduate University for Advanced Studies, 3.Nara National Research Institute for Cultural Properties, 4.Research Institute for Humanity and Nature, 5.Nagoya University)

[MIS17-P12] Usage of Historical Documents with Scientific Understandings in the field of Solar Physics

*Akito Davis Kawamura[1], Hisashi Hayakawa[2], Harufumi Tamazawa[3], Hiroaki Isobe[3], Kazunari Shibata[1] (1.Astronomical Observatory, Kyoto University, 2.Graduate School of Letters, Osaka University, 3.Faculty of Fine Arts, Kyoto City University of Arts)

[MIS17-P13] The study of the relationship between the flood of Kitakami River and sociaty in the end of Edo period

*Daisuke Sato[1], Yoshitaka Takahashi[2] (1.International Reserch Institute of Disaster Science Tohoku University , 2.Tokyo University of Agriculture and Technology)

[MIS17-P14] Reconstruction of Historical Weather with Data Assimilation Using Old Diaries

*Kei Yoshimura[1], Panduka Neluwala[2], Mika Ichino[3], Kooiti Masuda[4], Junpei Hirano[5] (1.Institute of Industrial Science, The University of Tokyo, 2.University of Peradeniya , 3.National Institute of Informatics, 4.Tokyo Metropolitan University, 5.Teikyo University)

[MIS17-P15] Examination of data range for fitting Omori-Utsu law to temporal decay of aftershocks presented in historical materials on the 1830 Kyoto earthquake: Reason for the difference of numbers of aftershocks in the same place

*Kentaro Hattori[1], Junzo Ohmura[2], Ichiro Nakanishi[1] (1.Kyoto Univ., 2.Bukkyo Univ.)

[MIS17-P16] Tsunami trace height of the AD 1854 Ansei Tokai tsunami around the lake Hamanako inferred from historical maps

*ebina yuichi[1], Kentaro Imai[2], Yoshinobu Tsuji[3], hiroyuki iwase[4] (1.International Research Institute of Disaster Science, 2.JAMSTEC, 3.Fukuda Geological Instite, 4. (C)ECOH CORPORATION)

[J] Oral | M (Multidisciplinary and Interdisciplinary)：M-IS Intersection

1:45 PM - 3:15 PM JST | 4:45 AM - 6:15 AM UTC | 301A 3F

[M-IS18] Geophysical fluid dynamics-Transfield approach to geoscience

convener:Keita Iga(Atmosphere and Ocean Research Institute, The University of Tokyo), Shigeo Yoshida(Department of Earth and Planetary Sciences, Faculty of Sciences, Kyushu University), Takatoshi Yanagisawa(Department of Deep Earth Structure and Dynamics Research, Japan Agency for Marine-Earth Science and Technology), Hidenori AIKI(Nagoya University), Chairperson:Kensuke Nakajima

1:45 PM - 2:00 PM JST | 4:45 AM - 5:00 AM UTC

[MIS18-01] Axisymmetric disturbance on an axisymmetric shallow water vortex

*Toshihisa Itano[1] (1.National Defense Academy)

2:00 PM - 2:15 PM JST | 5:00 AM - 5:15 AM UTC

[MIS18-02] Numerical studies on the classification of flow regimes of the 3-D thermal convection of rotating fluids

*Masanori Kameyama[1,2] (1.Geodynamics Research Center, Ehime University, 2.Japan Agency for Marine-Earth Science and Technology)

2:15 PM - 2:30 PM JST | 5:15 AM - 5:30 AM UTC

[MIS18-03] Diffusive behavior of columnar vortices in rotating thermal convection

*Daisuke Noto[1], Yuji Tasaka[2], Takatoshi Yanagisawa[3], Yuichi Murai[2] (1.Graduate School of Engineering, Hokkaido University, 2.Faculty of Engineering, Hokkaido University, 3.Japan Agency for Marine-Earth Science and Technology)

2:30 PM - 2:45 PM JST | 5:30 AM - 5:45 AM UTC

[MIS18-04] Liquid metal flows driven by a rotating magnetic field

*Koki Sawada[1], Vladimir Galindo[2], Tobias Vogt[2], Sven Eckert[2], Yuji Tasaka[3], Yuichi Murai[3] (1.Graduate School of Engineering, Hokkaido University , 2.Helmholtz-Zentrum Dresden-Rossendorf, 3.Faculty of Engineering, Hokkaido University,)

2:45 PM - 3:00 PM JST | 5:45 AM - 6:00 AM UTC

[MIS18-05] A symmetry-breaking self-regulating dynamo generating Mercury’s anomalous magnetic field

*Futoshi Takahashi[1], Hisayoshi Shimizu[2], Hideo Tsunakawa[3] (1.Faculty of Sciences, Kyushu University, 2.Earthquake Research Institute, University of Tokyo , 3.Department of Earth and Planetary Sciences, School of Science, Tokyo Institute of Technology)

[J] Poster | M (Multidisciplinary and Interdisciplinary)：M-IS Intersection

3:30 PM - 5:00 PM JST | 6:30 AM - 8:00 AM UTC | Poster Hall International Exhibition Hall8, Makuhari Messe_23

[M-IS18] Geophysical fluid dynamics-Transfield approach to geoscience

convener:Keita Iga(Atmosphere and Ocean Research Institute, The University of Tokyo), Shigeo Yoshida(Department of Earth and Planetary Sciences, Faculty of Sciences, Kyushu University), Takatoshi Yanagisawa(Department of Deep Earth Structure and Dynamics Research, Japan Agency for Marine-Earth Science and Technology), Hidenori AIKI(Nagoya University)

[MIS18-P01] Numerical experiments on climate of the Earth-like extrasolar planets using one-dimensional energy balance model

*Tomohiro Oonaka[1], Toru Nozawa[2] (1.Faculty of Science, Okayama University, 2.Graduate School of Natural Science and Technology,Okayama University)

[MIS18-P02] A study on disturbances with wavenumber 2 in inner-core region of tropical cyclones.

*Yuki Kawata[1], Keita Iga[1], Sho Yokota[2], Eigo Tochimoto[1] (1.Atmosphere and Ocean Research Institute, The University of Tokyo, 2.Meteorological Reseach Institute, Japan Meteorological Agency)

[MIS18-P03] Typhoon-induced vertical mixing measured by the Kuroshio Extension Observatory buoy

*Hidenori AIKI[1], Kohei Kameyama[2] (1.Institute for Space Earth Environmental Research, Nagoya University, 2.Graduate School for Environmental Studies, Nagoya University)

[MIS18-P04] A comparison between top-down and bottom-up type convective flows in a rotating spherical shell with stress-free boundaries

*Hinami Taniguchi[1], Futoshi Takahashi[1], Shin-ichi Takehiro[2] (1.Kyushu University, 2.Kyoto University)

[MIS18-P05] Oscillation of two-dimensional roll-like convection under a strong horizontal magnetic field

*Takatoshi Yanagisawa[1], Yuji Tasaka[2], Takehiro Miyagoshi[1], Ataru Sakuraba[3] (1.Department of Deep Earth Structure and Dynamics Research, Japan Agency for Marine-Earth Science and Technology, 2.Faculty of Engineering, Hokkaido University, 3.Faculty of Science, University of Tokyo)

[MIS18-P06] Two-dimensional or shallow water MHD waves on a rotating sphere with an imposed azimuthal magnetic field

*Ryosuke Nakashima[1], Shigeo Yoshida[2] (1.Department of Earth and Planetary Sciences, Graduate School of Science, Kyushu University, 2.Department of Earth and Planetary Sciences, Faculty of Science, Kyushu University)

[J] Poster | M (Multidisciplinary and Interdisciplinary)：M-IS Intersection

5:15 PM - 6:30 PM JST | 8:15 AM - 9:30 AM UTC | Poster Hall International Exhibition Hall8, Makuhari Messe_38

[M-IS18] Geophysical fluid dynamics-Transfield approach to geoscience

convener:Keita Iga(Atmosphere and Ocean Research Institute, The University of Tokyo), Shigeo Yoshida(Department of Earth and Planetary Sciences, Faculty of Sciences, Kyushu University), Takatoshi Yanagisawa(Department of Deep Earth Structure and Dynamics Research, Japan Agency for Marine-Earth Science and Technology), Hidenori AIKI(Nagoya University)

[MIS18-P01] Numerical experiments on climate of the Earth-like extrasolar planets using one-dimensional energy balance model

*Tomohiro Oonaka[1], Toru Nozawa[2] (1.Faculty of Science, Okayama University, 2.Graduate School of Natural Science and Technology,Okayama University)

[MIS18-P02] A study on disturbances with wavenumber 2 in inner-core region of tropical cyclones.

*Yuki Kawata[1], Keita Iga[1], Sho Yokota[2], Eigo Tochimoto[1] (1.Atmosphere and Ocean Research Institute, The University of Tokyo, 2.Meteorological Reseach Institute, Japan Meteorological Agency)

[MIS18-P03] Typhoon-induced vertical mixing measured by the Kuroshio Extension Observatory buoy

*Hidenori AIKI[1], Kohei Kameyama[2] (1.Institute for Space Earth Environmental Research, Nagoya University, 2.Graduate School for Environmental Studies, Nagoya University)

[MIS18-P04] A comparison between top-down and bottom-up type convective flows in a rotating spherical shell with stress-free boundaries

*Hinami Taniguchi[1], Futoshi Takahashi[1], Shin-ichi Takehiro[2] (1.Kyushu University, 2.Kyoto University)

[MIS18-P05] Oscillation of two-dimensional roll-like convection under a strong horizontal magnetic field

*Takatoshi Yanagisawa[1], Yuji Tasaka[2], Takehiro Miyagoshi[1], Ataru Sakuraba[3] (1.Department of Deep Earth Structure and Dynamics Research, Japan Agency for Marine-Earth Science and Technology, 2.Faculty of Engineering, Hokkaido University, 3.Faculty of Science, University of Tokyo)

[MIS18-P06] Two-dimensional or shallow water MHD waves on a rotating sphere with an imposed azimuthal magnetic field

*Ryosuke Nakashima[1], Shigeo Yoshida[2] (1.Department of Earth and Planetary Sciences, Graduate School of Science, Kyushu University, 2.Department of Earth and Planetary Sciences, Faculty of Science, Kyushu University)

[J] Oral | M (Multidisciplinary and Interdisciplinary)：M-IS Intersection

9:00 AM - 10:30 AM JST | 12:00 AM - 1:30 AM UTC | 103 1F

[M-IS20] Mountain Science

convener:Keisuke Suzuki(Department of Environmental Sciences, Faculty of Science, Shinshu University), Yoshihiko Kariya(Department of Environmental Geography, Senshu University), Akihiko SASAKI(Department of Geography and Environmental Studies, Kokushikan University), Chiyuki Narama(Niigata University, Department of Science), Chairperson:Yoshihiko Kariya(専修大学)

9:00 AM - 9:15 AM JST | 12:00 AM - 12:15 AM UTC

[MIS20-01] Early Holocene landslide deposits found from Mount Honita, the upper Tama River basin, west of Tokyo

*Yoshihiko Kariya[1], Koichiro Sawabe[2] (1.Department of Environmental Geography, Senshu University, 2.Japan Conservation Engineers)

9:15 AM - 9:30 AM JST | 12:15 AM - 12:30 AM UTC

[MIS20-02] The effect of understanding of mountainous terrain using 3D maps and solid model

*Jiro Komori[1] (1.Teikyo Heisei University)

9:30 AM - 9:45 AM JST | 12:30 AM - 12:45 AM UTC

[MIS20-03] Development process of Lake Naganuma in a large-scale landslide on Hachimantai Volcano

*Natsuki Sasaki[1], Toshihiko Sugai[1] (1.Graduate School of Frontier Science, the University of Tokyo)

9:45 AM - 10:00 AM JST | 12:45 AM - 1:00 AM UTC

[MIS20-04] Air and ground temperature conditions on alpine and sub-apline zone of Norikura Volcano, Northern Japanese Alps

*Akihiko SASAKI[1], Motoshi NISHIMURA[2], Keisuke Suzuki[3] (1.Department of Geography and Environmental Studies, Kokushikan University, 2.Interdisciplinary Graduate school of Science and Technology, Shinshu University, 3.Faculty of Science, Shinshu University)

10:00 AM - 10:15 AM JST | 1:00 AM - 1:15 AM UTC

[MIS20-05] Initiation and flow characteristics of debris flows on a sediment deposition zone in a mountain area

★Invited Papers

*Fumitoshi Imaizumi[1], Yuichi S. Hayakawa[2], Haruka Tsunetaka[3], Norifumi Hotta[4] (1.Faculty of Agriculture, Shizuoka University, 2.Faculty of Environmental Earth Sciences, 3.Forestry and Forest Products Research Institute, 4.Graduate School of Agricultural and Life Sciences)

10:15 AM - 10:30 AM JST | 1:15 AM - 1:30 AM UTC

[MIS20-06] Relationships between annual landform changes of the riverbed and vegetation dynamics during recent 10 years in the upper Asusa River in Kamikochi valley in the Japan Alps

★Invited Papers

*Hiroshi Shimazu[1] (1.Department of Geography, Faculty of Geo-Environmental Science, Rissho University)

[J] Oral | M (Multidisciplinary and Interdisciplinary)：M-IS Intersection

10:45 AM - 12:15 PM JST | 1:45 AM - 3:15 AM UTC | 103 1F

[M-IS20] Mountain Science

convener:Keisuke Suzuki(Department of Environmental Sciences, Faculty of Science, Shinshu University), Yoshihiko Kariya(Department of Environmental Geography, Senshu University), Akihiko SASAKI(Department of Geography and Environmental Studies, Kokushikan University), Chiyuki Narama(Niigata University, Department of Science), Chairperson:Akihiko SASAKI

10:45 AM - 11:00 AM JST | 1:45 AM - 2:00 AM UTC

[MIS20-07] Age dating of groundwater using tritium and CFCs in headwater catchments, Fukushima after the Fukushima Dai-ichi Nuclear Power Plant accident

*Koichi Sakakibara[1], Sho Iwagami[2], Maki Tsujimura[3], Yutaka Abe[4], Manami Hada[5], Ishwar Pun[6], Yuichi Onda[3,7] (1.Faculty of Science, Shinshu University, 2.Department of Disaster Prevention, Meteorology and Hydrology, Forestry and Forest Products Research Institute, 3.Faculty of Life and Environmental Sciences, University of Tsukuba, 4.Natural Environment Conservation Center, Kanagawa, 5.Graduate School of Life and Environmental Sciences, University of Tsukuba, 6.Organization for the Strategic Coordination of Research and Intellectual Property, Meiji University, 7.Center for Research in Isotopes and Environmental Dynamics, University of Tsukuba)

11:00 AM - 11:15 AM JST | 2:00 AM - 2:15 AM UTC

[MIS20-08] Hydraulic adaptation for tree height growth in tall tree species

★Invited Papers

*Wakana Azuma[1] (1.Kyoto University)

11:15 AM - 11:30 AM JST | 2:15 AM - 2:30 AM UTC

[MIS20-09] **The molecular phylogenetic structure and biogeographic history of a alpine gravel environment specific plant *Dicentra peregrina* (Papaveraceae) in Japan**

*Takahisa Ozaki[1], Hirokazu Matsuda, Koji Tojo[2] (1.Graduate School of Science and Technology, Shinshu University, 2.Biology Department, Faculty of Science, Shinshu University)

11:30 AM - 11:45 AM JST | 2:30 AM - 2:45 AM UTC

[MIS20-10] Formation process of small stands of *Abies mariesii* forest in pseudo-alpine zone on Mt. Akita-komagatake, northern Japan

*Asaka Konno[1] (1.International Research Institute of Disaster Science, Tohoku University)

11:45 AM - 12:00 PM JST | 2:45 AM - 3:00 AM UTC

[MIS20-11] Distribution of the pinas forests including a Cryptomeria japonica and its environmental factors in Echigo mountain range.

*Masatsugu YASUDA[1] (1.Asia Air Survey Co., Ltd.)

12:00 PM - 12:15 PM JST | 3:00 AM - 3:15 AM UTC

[MIS20-12] Roles of glacier microbes in alpine ecosystems of Asian high mountains: effect of cryoconite outflow on soil development in glacier forefields

★Invited Papers

*Nozomu Takeuchi[1], Masato Shiomuki[1] (1.Chiba University)

[J] Oral | M (Multidisciplinary and Interdisciplinary)：M-IS Intersection

1:45 PM - 3:15 PM JST | 4:45 AM - 6:15 AM UTC | 103 1F

[M-IS20] Mountain Science

convener:Keisuke Suzuki(Department of Environmental Sciences, Faculty of Science, Shinshu University), Yoshihiko Kariya(Department of Environmental Geography, Senshu University), Akihiko SASAKI(Department of Geography and Environmental Studies, Kokushikan University), Chiyuki Narama(Niigata University, Department of Science), Chairperson:Chiyuki Narama(新潟大学)

1:45 PM - 2:00 PM JST | 4:45 AM - 5:00 AM UTC

[MIS20-13] Comparison of surface energy balance of seasonal snowcover for three sites in Japanese alpine region

*Motoshi NISHIMURA[1], Akihiko SASAKI[2], Keisuke Suzuki[3] (1.Interdisciplinary Graduate school of Science and Technology, Shinshu University, 2.Department of Geography and environmental Studies, Kokushikan University, 3.Faculty of Science, Shinshu University)

2:00 PM - 2:15 PM JST | 5:00 AM - 5:15 AM UTC

[MIS20-14] The influence of snow for the local wind system on the east slope of Mt.Norikura

*Genki Uehara[1], Keisuke Suzuki[2] (1.Graduate School of Science and Technology, Shinshu University, 2.Department of Environmental Science, Faculty of Science, Shinshu University)

2:15 PM - 2:30 PM JST | 5:15 AM - 5:30 AM UTC

[MIS20-15] Mass balance of "Avalanche-accumulation type"glaciers and perennial snow patches in Hida mountain range.

*Kenshiro Arie[1], Chiyuki Narama[2], Kotaro FUKUI[3], Hajime IIDA[3] (1.Graduate School of Science and Technology, Niigata University, 2.Faculty of Science, Niigata University, 3.Tateyama Caldera Sabo Museum)

2:30 PM - 2:45 PM JST | 5:30 AM - 5:45 AM UTC

[MIS20-16] Pattern of occurrence of sea of clouds and waterfall cloud near Mt.Nishihotakadake

★Invited Papers

*Toru Awazawa[1] (1.Faculty of Science, Shinshu University National University, Shinshu University Faculty of Science)

2:45 PM - 3:00 PM JST | 5:45 AM - 6:00 AM UTC

[MIS20-17] Review and prospect of strong local wind “Matsubori-kaze” blowing at the western foot of Mt. Aso.

★Invited Papers

*Hiroshi Matsuyama[1] (1.Graduate School of Urban Environmental Sciences, Tokyo Metropolitan University)

3:00 PM - 3:15 PM JST | 6:00 AM - 6:15 AM UTC

[MIS20-18] **Two decades of mountain climate monitoring and research: lessons learned and future challenges.**

*Luis Duran[1,2,3], Irene Rodríguez-Muñoz[1] (1.interMET Sistemas y Redes S.L.U. Madrid. Spain, 2.Centro de Investigación, Seguimiento y Evaluación del Parque Nacional Sierra de Guadarrama. Madrid. Spain, 3.Departamento de Física de la Tierra y Astrofísica. Facultad de Ciencias Físicas. Universidad Complutense de Madrid. Spain)

[J] Poster | M (Multidisciplinary and Interdisciplinary)：M-IS Intersection

3:30 PM - 5:00 PM JST | 6:30 AM - 8:00 AM UTC | Poster Hall International Exhibition Hall8, Makuhari Messe_24

[M-IS20] Mountain Science

convener:Keisuke Suzuki(Department of Environmental Sciences, Faculty of Science, Shinshu University), Yoshihiko Kariya(Department of Environmental Geography, Senshu University), Akihiko SASAKI(Department of Geography and Environmental Studies, Kokushikan University), Chiyuki Narama(Niigata University, Department of Science)

[MIS20-P01] Development of fluvial terraces and landslides since the late Pleistocene in the Shirata River basin, southeastern side of Amagi Volcano, Izu Peninsula, Japan

*Nao Tokumoto[1], Yoshihiko Kariya[2], Kuniyasu Mokudai[3] (1.Undegraduate, Senshu Univ., 2.Senshu Univ., 3.Japan Geoservice Inc.)

[MIS20-P02] Variation trends of air temperature and snow depth in the Japanese Alps

*Keisuke Suzuki[1], Akihiko SASAKI[2] (1.Faculty of Science, Shinshu University, 2.Faculty of Literature, Kokushikan University)

[MIS20-P03] Abundant tardigrades found in snow pack in Mt.Gassan in Yamagata Prefecture, Japan

*MASATO ONO[1] (1.Chiba University)

[MIS20-P04] Variation of stable isotope ratios of precipitation in the Japanese Alps Region

*Tsukasa Katsuragawa[1], Tsutomu Yamanaka[2], Akihiko SASAKI[3], Yuki Kurokumo[1], Motoshi NISHIMURA[1], Shimizu Hironori[1], Keisuke Suzuki[4] (1.Graduate School of Science and Technology,Shinshu University, 2.Faculty of Life and Environmental Sciences, University of Tsukuba, 3.Department of Geography and Environmental Studies, Kokushikan University, 4.Department of Environmental Sciences, Faculty of Science, Shinshu University)

[MIS20-P05] Probable glacier detritus found at downstream site of the Yokoo moraines in the northern Japanese Alps: its geological characteristics and implications

*Manami Ishibashi[1], Yoshihiko Kariya[2], Kuniyasu Mokudai[3] (1.Undergraduate Senshu Univ., 2.Senshu Univ., 3.Japan Geo serivice Inc.)

[MIS20-P06] Recent Geomorphological changes of rock slopes in Hakuba-Daisekkei

*Hirotaka Sugiyama[1], Chiyuki Narama[2], Hiroshi Inoue[3] (1.Graduate School of Science and Technology, Niigata University, 2.Faculty of Science, Niigata University, 3.National Reserch Institute for Earth Science and Disaster Resilience)

[MIS20-P07] Behavior of inorganic ions in air deposition and surface runoff water in an alpine headwater catchment of Mt. Norikura

*Hironori Shimizu[1], Akihiko Sasaki[2], Keisuke Suzuki[3] (1.Graduate School of Science and Technology, Shinshu University , 2.Department of Geography and Environmental Studies, Kokushikan University, 3.Faculty of Science, Shinshu University)

[MIS20-P08] Activity of gravity faults in the Tateyama caldera, Hida Mountains, during the past 55 years

*Kotaro FUKUI[1], Hajime IIDA[1] (1.Tateyama Caldera Sabo Museum)

[MIS20-P09] Community, population and genetic structures of benthic invertebrates in alpine and sub-alpine ponds of the Kamikochi area and the Yari-Hotaka Mountain Ranges

*Keisuke Inoue[1], Koji Tojo[1] (1.Biology Department, Faculty of Science, Shinshu University)

[MIS20-P10] Water and carbon use of fine root in four tree species at the forest limit

*Hikari Yahara[1], Wakana Azuma[2], Mai Kamakura[2], Naoki Makita[1] (1.Graduate School of Science and Technology Shinshu University, 2.Graduate School of Agriculture Kyoto University)

[MIS20-P11] Visible-near infrared spectral reflectance explains variations in fine root traits of woody species

*Natsuko Tanikawa[1], Tatsuro Nakaji[3], Miwa Kobatake[2], Naoki Makita[2] (1.Graduate School of Science and technology, Shinshu University, 2.Faculty of Science, Shinshu University, 3.Field Science Center for Northern Biosphere)

[MIS20-P12] Heat Balance Analysis of Cold Air Pool Formation in Kamikochi

*Sayuri Koyama[1], Motoshi NISHIMURA[2], Keisuke Suzuki[3] (1.Graduate school of science and technorogy, Shinshu University, 2.Interdisciplinary Graduate school of Science and Technology, Shinshu university, 3.Department of

Environmental Sciences, Faculty of Science, Shinshu University)

[MIS20-P13] A finding of fossil trees buried in dammed-lake deposits formed by the Dondokosawa rock avalanche of the late 9th century in the Akaishi Mountains, and its significance

*Takashi Kimura[1], Ryuji Yamada[1], Yoshihiko Kariya[2] (1.National Research Institute for Earth Science and Disaster Resilience, 2.Senshu University)

[MIS20-P14] What alpine plants attract visitors in the Daisetsuzan national park, northern, Japan?

*Yukihiro Amagai[1], Kota Mameno[1,2], Hiroyuki Oguma[1], Takahiro Kubo[1] (1.National Institute for Environmental Studies, 2.Hokkaido University)

[MIS20-P15] Spatio-temporal variations of algal snow in Mt. Gassan, Yamagata prefecture, Japan

*Suzuki Takumi[1], Nozomu Takeuchi[1], Tsubasa Takahashi[1] (1.Chiba University)

[MIS20-P16] Feeding of a wingless stonefly living on snow surface in Mt. Gassan, Yamagata prefecture, Japan

*Risako Yonechi[1], Nozomu Takeuchi[1] (1.Chiba University)

[MIS20-P17] Drainage from glacial lake in Achinathang village, Ladakh Range on 4 August 2017

Maho Saotome[2], *Chiyuki Narama[1], Naoki Sakurai[2] (1.Niigata University, Program of Field Research in the Environmental Sciences, 2.Graduate School of Science and Technology, Niigata University)

[MIS20-P18] Recent glacier variations at Mt. Kenya using aerial digital image

*Chiyuki Narama[1], kenshiro Arie[2], MIZUNO KAZUHARU[3] (1.Program of Field Research in the Environmental Sciences, Niigata University , 2.Graduate School of Science and Technology, Niigata University, 3.Graduate School of Letters, Kyoto University)

[J] Poster | M (Multidisciplinary and Interdisciplinary)：M-IS Intersection

5:15 PM - 6:30 PM JST | 8:15 AM - 9:30 AM UTC | Poster Hall International Exhibition Hall8, Makuhari Messe_39

[M-IS20] Mountain Science

convener:Keisuke Suzuki(Department of Environmental Sciences, Faculty of Science, Shinshu University), Yoshihiko Kariya(Department of Environmental Geography, Senshu University), Akihiko SASAKI(Department of Geography and Environmental Studies, Kokushikan University), Chiyuki Narama(Niigata University, Department of Science)

[MIS20-P01] Development of fluvial terraces and landslides since the late Pleistocene in the Shirata River basin, southeastern side of Amagi Volcano, Izu Peninsula, Japan

*Nao Tokumoto[1], Yoshihiko Kariya[2], Kuniyasu Mokudai[3] (1.Undegraduate, Senshu Univ., 2.Senshu Univ., 3.Japan Geoservice Inc.)

[MIS20-P02] Variation trends of air temperature and snow depth in the Japanese Alps

*Keisuke Suzuki[1], Akihiko SASAKI[2] (1.Faculty of Science, Shinshu University, 2.Faculty of Literature, Kokushikan University)

[MIS20-P03] Abundant tardigrades found in snow pack in Mt.Gassan in Yamagata Prefecture, Japan

*MASATO ONO[1] (1.Chiba University)

[MIS20-P04] Variation of stable isotope ratios of precipitation in the Japanese Alps Region

*Tsukasa Katsuragawa[1], Tsutomu Yamanaka[2], Akihiko SASAKI[3], Yuki Kurokumo[1], Motoshi NISHIMURA[1], Shimizu Hironori[1], Keisuke Suzuki[4] (1.Graduate School of Science and Technology,Shinshu University, 2.Faculty of Life and Environmental Sciences, University of Tsukuba, 3.Department of Geography and Environmental Studies, Kokushikan University, 4.Department of Environmental Sciences, Faculty of Science, Shinshu University)

[MIS20-P05] Probable glacier detritus found at downstream site of the Yokoo moraines in the northern Japanese Alps: its geological characteristics and implications

*Manami Ishibashi[1], Yoshihiko Kariya[2], Kuniyasu Mokudai[3] (1.Undergraduate Senshu Univ., 2.Senshu Univ., 3.Japan Geo serivice Inc.)

[MIS20-P06] Recent Geomorphological changes of rock slopes in Hakuba-Daisekkei

*Hirotaka Sugiyama[1], Chiyuki Narama[2], Hiroshi Inoue[3] (1.Graduate School of Science and Technology, Niigata University, 2.Faculty of Science, Niigata University, 3.National Reserch Institute for Earth Science and Disaster Resilience)

[MIS20-P07] Behavior of inorganic ions in air deposition and surface runoff water in an alpine headwater catchment of Mt. Norikura

*Hironori Shimizu[1], Akihiko Sasaki[2], Keisuke Suzuki[3] (1.Graduate School of Science and Technology, Shinshu University , 2.Department of Geography and Environmental Studies, Kokushikan University, 3.Faculty of Science, Shinshu University)

[MIS20-P08] Activity of gravity faults in the Tateyama caldera, Hida Mountains, during the past 55 years

*Kotaro FUKUI[1], Hajime IIDA[1] (1.Tateyama Caldera Sabo Museum)

[MIS20-P09] Community, population and genetic structures of benthic invertebrates in alpine and sub-alpine ponds of the Kamikochi area and the Yari-Hotaka Mountain Ranges

*Keisuke Inoue[1], Koji Tojo[1] (1.Biology Department, Faculty of Science, Shinshu University)

[MIS20-P10] Water and carbon use of fine root in four tree species at the forest limit

*Hikari Yahara[1], Wakana Azuma[2], Mai Kamakura[2], Naoki Makita[1] (1.Graduate School of Science and Technology Shinshu University, 2.Graduate School of Agriculture Kyoto University)

[MIS20-P11] Visible-near infrared spectral reflectance explains variations in fine root traits of woody species

*Natsuko Tanikawa[1], Tatsuro Nakaji[3], Miwa Kobatake[2], Naoki Makita[2] (1.Graduate School of Science and technology, Shinshu University, 2.Faculty of Science, Shinshu University, 3.Field Science Center for Northern Biosphere)

[MIS20-P12] Heat Balance Analysis of Cold Air Pool Formation in Kamikochi

*Sayuri Koyama[1], Motoshi NISHIMURA[2], Keisuke Suzuki[3] (1.Graduate school of science and technorogy, Shinshu University, 2.Interdisciplinary Graduate school of Science and Technology, Shinshu university, 3.Department of

Environmental Sciences, Faculty of Science, Shinshu University)

[MIS20-P13] A finding of fossil trees buried in dammed-lake deposits formed by the Dondokosawa rock avalanche of the late 9th century in the Akaishi Mountains, and its significance

*Takashi Kimura[1], Ryuji Yamada[1], Yoshihiko Kariya[2] (1.National Research Institute for Earth Science and Disaster Resilience, 2.Senshu University)

[MIS20-P14] What alpine plants attract visitors in the Daisetsuzan national park, northern, Japan?

*Yukihiro Amagai[1], Kota Mameno[1,2], Hiroyuki Oguma[1], Takahiro Kubo[1] (1.National Institute for Environmental Studies, 2.Hokkaido University)

[MIS20-P15] Spatio-temporal variations of algal snow in Mt. Gassan, Yamagata prefecture, Japan

*Suzuki Takumi[1], Nozomu Takeuchi[1], Tsubasa Takahashi[1] (1.Chiba University)

[MIS20-P16] Feeding of a wingless stonefly living on snow surface in Mt. Gassan, Yamagata prefecture, Japan

*Risako Yonechi[1], Nozomu Takeuchi[1] (1.Chiba University)

[MIS20-P17] Drainage from glacial lake in Achinathang village, Ladakh Range on 4 August 2017

Maho Saotome[2], *Chiyuki Narama[1], Naoki Sakurai[2] (1.Niigata University, Program of Field Research in the Environmental Sciences, 2.Graduate School of Science and Technology, Niigata University)

[MIS20-P18] Recent glacier variations at Mt. Kenya using aerial digital image

*Chiyuki Narama[1], kenshiro Arie[2], MIZUNO KAZUHARU[3] (1.Program of Field Research in the Environmental Sciences, Niigata University , 2.Graduate School of Science and Technology, Niigata University, 3.Graduate School of Letters, Kyoto University)

[J] Oral | M (Multidisciplinary and Interdisciplinary)：M-IS Intersection

9:00 AM - 10:30 AM JST | 12:00 AM - 1:30 AM UTC | 106 1F

[M-IS23] Planetary Volcanology

convener:Rina Noguchi(Institute of Space and Astronautical Science, Japan Aerospace Exploration Agency), Tomokatsu Morota(Graduate School of Environmental Studies, Nagoya University), Kyoko S. Kataoka(Research Institute for Natural Hazards and Disaster Recovery, Niigata University), Shizuka Otsuki(Research Institute of Earthquake and Volcano Geology, Geological Survey of Japan, Advanced Industrial Science and Technology), Chairperson:Rina Noguchi(Institute of Space and Astronautical Science, Japan Aerospace Exploration Agency), Nobuo Geshi(GSJ/AIST)

9:00 AM - 9:15 AM JST | 12:00 AM - 12:15 AM UTC

[MIS23-01] Growth and evolution of isolated volcanic island, Nishinoshima, Ogasawara

★Invited Papers

*Fukashi Maeno[1] (1.Earthquake Research Institute, University of Tokyo)

9:15 AM - 9:30 AM JST | 12:15 AM - 12:30 AM UTC

[MIS23-02] The style of magmatism on terrestrial planets of various sizes predicted from numerical models of mantle dynamics

*Masaki Ogawa[1] (1.Division of General Systems Studies, Graduate School of Arts and Sciences, University of Tokyo)

9:30 AM - 9:45 AM JST | 12:30 AM - 12:45 AM UTC

[MIS23-03] Lunar and Matian lava tubes and explorations to them through their skylight holes

*Junichi Haruyama[1], Takahiro Iwata[1], Yukio Yamamoto[1], Tetsuya Kaku[2,1], Wataru Miyake[2], Atsushi Kumamoto[3], Ken Ishiyama[1], yokota yasuhiro[4], Takumi Ono[2,1] (1.Japan Aerospace Exploration Agency, 2.Tokai University, 3.Tohoku University, 4.Kochi University)

9:45 AM - 10:00 AM JST | 12:45 AM - 1:00 AM UTC

[MIS23-04] Volcanic activity on Io, formation of the atmosphere, and escape of atmosphere to the magnetosphere

*Fuminori Tsuchiya[1], Ryoichi Koga[1], Mizuki Yoneda[2], Masato Kagitani[1], Kazuo Yoshioka[4], Reina Hikida[4], Go Murakami[3], Tomoki Kimura[1], Atsushi Yamazaki[3], Hajime Kita[3], Ichiro Yoshikawa[4] (1.Tohoku University, 2.Tadano, 3.ISAS/JAXA, 4.The University of Tokyo)

10:00 AM - 10:15 AM JST | 1:00 AM - 1:15 AM UTC

[MIS23-05] Cryovolcanism, a critical review

*Kei Kurita[1] (1.Earthquake Research Inst.,The University of Tokyo)

10:15 AM - 10:30 AM JST | 1:15 AM - 1:30 AM UTC

[MIS23-06] Cryovolcanisms on Solar System bodies: Observations, importance, and future perspectives

★Invited Papers

*Yasuhito Sekine[1] (1.Earth-Life Science Insitute, Tokyo Institute of Technology)

[J] Poster | M (Multidisciplinary and Interdisciplinary)：M-IS Intersection

3:30 PM - 5:00 PM JST | 6:30 AM - 8:00 AM UTC | Poster Hall International Exhibition Hall8, Makuhari Messe_25

[M-IS23] Planetary Volcanology

convener:Rina Noguchi(Institute of Space and Astronautical Science, Japan Aerospace Exploration Agency), Tomokatsu Morota(Graduate School of Environmental Studies, Nagoya University), Kyoko S. Kataoka(Research Institute for Natural Hazards and Disaster Recovery, Niigata University), Shizuka Otsuki(Research Institute of Earthquake and Volcano Geology, Geological Survey of Japan, Advanced Industrial Science and Technology)

[MIS23-P01] **A possible method of lava flow temperature estimation by lava tube cave of Earth,Moon and Mars**

*Tsutomu Honda[1] (1.Vulcano-speleological Society)

[MIS23-P02] Process of magma eruption on the Moon

*Tomokatsu Morota[1] (1.Graduate School of Environmental Studies, Nagoya University)

[MIS23-P03] Statistical analysis of grain morphology generated under hypervelocity impact experiment as an analog of volcanic explosion

*Rina Noguchi[1], Shizuka Otsuki[2], Ayako I Suzuki, Sunao Hasegawa[1] (1.Institute of Space and Astronautical Science, Japan Aerospace Exploration Agency, 2.Geological Survey of Japan, AIST)

[MIS23-P04] Disequilibrium precipitation of salts during rapid freezing of brine: Implications for cryovolcanisms and formation of sodium carbonate of bright spots on Ceres.

*Masahiro Yoda[1,2], Yasuhito Sekine[2], Shuya Tan[1,2] (1.Department of Earth and Planetary Science, The University of Tokyo, 2.Earth-Life Science Institute, Tokyo Institute of Technology)

[J] Poster | M (Multidisciplinary and Interdisciplinary)：M-IS Intersection

5:15 PM - 6:30 PM JST | 8:15 AM - 9:30 AM UTC | Poster Hall International Exhibition Hall8, Makuhari Messe_40

[M-IS23] Planetary Volcanology

convener:Rina Noguchi(Institute of Space and Astronautical Science, Japan Aerospace Exploration Agency), Tomokatsu Morota(Graduate School of Environmental Studies, Nagoya University), Kyoko S. Kataoka(Research Institute for Natural Hazards and Disaster Recovery, Niigata University), Shizuka Otsuki(Research Institute of Earthquake and Volcano Geology, Geological Survey of Japan, Advanced Industrial Science and Technology)

[MIS23-P01] **A possible method of lava flow temperature estimation by lava tube cave of Earth,Moon and Mars**

*Tsutomu Honda[1] (1.Vulcano-speleological Society)

[MIS23-P02] Process of magma eruption on the Moon

*Tomokatsu Morota[1] (1.Graduate School of Environmental Studies, Nagoya University)

[MIS23-P03] Statistical analysis of grain morphology generated under hypervelocity impact experiment as an analog of volcanic explosion

*Rina Noguchi[1], Shizuka Otsuki[2], Ayako I Suzuki, Sunao Hasegawa[1] (1.Institute of Space and Astronautical Science, Japan Aerospace Exploration Agency, 2.Geological Survey of Japan, AIST)

[MIS23-P04] Disequilibrium precipitation of salts during rapid freezing of brine: Implications for cryovolcanisms and formation of sodium carbonate of bright spots on Ceres.

*Masahiro Yoda[1,2], Yasuhito Sekine[2], Shuya Tan[1,2] (1.Department of Earth and Planetary Science, The University of Tokyo, 2.Earth-Life Science Institute, Tokyo Institute of Technology)

[J] Oral | M (Multidisciplinary and Interdisciplinary)：M-IS Intersection

1:45 PM - 3:15 PM JST | 4:45 AM - 6:15 AM UTC | 201B 2F

[M-IS28] Fluid-sediment migration and geo-bio interaction

convener:Robert Jenkins(School of Geosciences and Civil Engineering, College of Science and Engineering, Kanazawa University), Tomohiro Toki(Faculty of Science, University of the Ryukyus), Akira Ijiri(Japan Agency for Marine-Earth Science and Technology), Takami Nobuhara(Science Education (Geology), Faculty of Education, Shizuoka University), Hiromi Kayama WATANABE(Japan Agency for Marine-Earth Science and Technology), Miho Asada(Japan Agency for Marine-Earth Science and Technology), Chairperson:Tomohiro Toki, Robert Jenkins(Kanazawa University)

1:45 PM - 2:00 PM JST | 4:45 AM - 5:00 AM UTC

[MIS28-01] Upper Pliocene large lucinid communities with cold-seep carbonates from the Shimajiri Group in the Miyagi-jima Island off the central part of Okinawa-jima Island, Japan

*Takami Nobuhara[1], Robert Jenkins[2], Shin-ichi Nomura[3] (1.Science Education (Geology), Faculty of Education, Shizuoka University, 2.School of Natural System, College of Science and Engineering, Kanazawa University, 3.Chiba Prefectural Kisarazu High School)

2:00 PM - 2:15 PM JST | 5:00 AM - 5:15 AM UTC

[MIS28-02] Chemosynthetic fossil community in Early Cretaceous methane seep from Yubari City, Hokkaido

*Nanami Shimazu[1], Robert Jenkins[1] (1.Kanazawa University)

2:15 PM - 2:30 PM JST | 5:15 AM - 5:30 AM UTC

[MIS28-03] Marine Snow Hypothesis: What is controling faunal composition of the methane-seep since Mesozoic?

*Robert Jenkins[1] (1.School of Geosciences and Civil Engineering, College of Science and Engineering, Kanazawa University)

2:30 PM - 2:45 PM JST | 5:30 AM - 5:45 AM UTC

[MIS28-04] *In situ* Sr isotope analysis of methane-seep carbonates: insight into ancient subseafloor fluid circulation

★Invited Papers

*Yusuke Miyajima[1], Michał Jakubowicz[2,3], Takafumi Hirata[1] (1.Geochemical Research Center, Graduate School of Science, The University of Tokyo, 2.Institute of Geoecology and Geoinformation, Adam Mickiewicz University, Poland, 3.Isotope Laboratory, Adam Mickiewicz University, Poland)

2:45 PM - 3:00 PM JST | 5:45 AM - 6:00 AM UTC

[MIS28-05] Monitoring CH_4 amounts deep inside deep-water mud volcanoes

★Invited Papers

*A. Kioka[1], T. Tsuji[2], H. Otsuka[3], J. Ashi[3] (1.Universität Innsbruck, Austria, 2.Kyushu University, Japan, 3.The University of Tokyo, Japan)

3:00 PM - 3:15 PM JST | 6:00 AM - 6:15 AM UTC

[MIS28-06] Discussion

*Robert Jenkins[1] (1.School of Natural System, College of Science and Engineering, Kanazawa University)

[J] Poster | M (Multidisciplinary and Interdisciplinary)：M-IS Intersection

3:30 PM - 5:00 PM JST | 6:30 AM - 8:00 AM UTC | Poster Hall International Exhibition Hall8, Makuhari Messe_26

[M-IS28] Fluid-sediment migration and geo-bio interaction

convener:Robert Jenkins(School of Geosciences and Civil Engineering, College of Science and Engineering, Kanazawa University), Tomohiro Toki(Faculty of Science, University of the Ryukyus), Akira Ijiri(Japan Agency for Marine-Earth Science and Technology), Takami Nobuhara(Science Education (Geology), Faculty of Education, Shizuoka University), Hiromi Kayama WATANABE(Japan Agency for Marine-Earth Science and Technology), Miho Asada(Japan Agency for Marine-Earth Science and Technology)

[MIS28-P01] An offshore mud volcano that indicates a heterogeneous subseafloor geological environment: a case study along southwest Japan

*Miho Asada[1,2], Kazuya Kitada[2] (1.JSPS Research Fellow, 2.Japan Agency for Marine-Earth Science and Technology)

[MIS28-P02] **New distribution and implication of dispersal capabililty of a deep-sea chemosymbiotic squat lobster *Shinkaia crosnieri***

*Hiromi Kayama WATANABE[1], Chong Chen[1], Tin-Yam Chan[2], Chien-Hui Yang[2], Chu-Chang Wang[3], Satoshi Mitarai[4], Hiroyuki Yamamoto[1] (1.Japan Agency for Marine-Earth Science and Technology (JAMSTEC), 2.National Taiwan Ocean University, 3.Taiwan Ocean Research Institute (TORI), 4.Okinawa Institute of Science and Technology (OIST))

[MIS28-P03] Taxonomy and diet of the *Ophryotrocha* (Annelida: Dorvilleidae) from whale- falls in the Tsukumo Bay, Japan

*Midori Suzuki[1], Robert Gwyn Jenkins[1], Shouzo Ogiso[2], Nobuo Suzuki[3] (1.Division of Environmental Science and Engineering, Graduate School of Natural Science and Technology, Kanazawa University, 2.Kanazawa university, 3.Institute of Nature and Environmental Technology, Kanazawa university)

[J] Poster | M (Multidisciplinary and Interdisciplinary)：M-IS Intersection

5:15 PM - 6:30 PM JST | 8:15 AM - 9:30 AM UTC | Poster Hall International Exhibition Hall8, Makuhari Messe_41

[M-IS28] Fluid-sediment migration and geo-bio interaction

convener:Robert Jenkins(School of Geosciences and Civil Engineering, College of Science and Engineering, Kanazawa University), Tomohiro Toki(Faculty of Science, University of the Ryukyus), Akira Ijiri(Japan Agency for Marine-Earth Science and Technology), Takami Nobuhara(Science Education (Geology), Faculty of Education, Shizuoka University), Hiromi Kayama WATANABE(Japan Agency for Marine-Earth Science and Technology), Miho Asada(Japan Agency for Marine-Earth Science and Technology)

[MIS28-P01] An offshore mud volcano that indicates a heterogeneous subseafloor geological environment: a case study along southwest Japan

*Miho Asada[1,2], Kazuya Kitada[2] (1.JSPS Research Fellow, 2.Japan Agency for Marine-Earth Science and Technology)

[MIS28-P02] **New distribution and implication of dispersal capabililty of a deep-sea chemosymbiotic squat lobster *Shinkaia crosnieri***

*Hiromi Kayama WATANABE[1], Chong Chen[1], Tin-Yam Chan[2], Chien-Hui Yang[2], Chu-Chang Wang[3], Satoshi Mitarai[4], Hiroyuki Yamamoto[1] (1.Japan Agency for Marine-Earth Science and Technology (JAMSTEC), 2.National Taiwan Ocean University, 3.Taiwan Ocean Research Institute (TORI), 4.Okinawa Institute of Science and Technology (OIST))

[MIS28-P03] Taxonomy and diet of the *Ophryotrocha* (Annelida: Dorvilleidae) from whale- falls in the Tsukumo Bay, Japan

*Midori Suzuki[1], Robert Gwyn Jenkins[1], Shouzo Ogiso[2], Nobuo Suzuki[3] (1.Division of Environmental Science and Engineering, Graduate School of Natural Science and Technology, Kanazawa University, 2.Kanazawa university, 3.Institute of Nature and Environmental Technology, Kanazawa university)

[J] Oral | M (Multidisciplinary and Interdisciplinary)：M-GI General Geosciences, Information Geosciences & Simulations

10:45 AM - 12:15 PM JST | 1:45 AM - 3:15 AM UTC | A08 TOKYO BAY MAKUHARI HALL

[M-GI33] Data-driven geosciences

convener:Tatsu Kuwatani(Japan Agency for Marine-Earth Science and Technology), Hiromichi Nagao(Earthquake Research Institute, The University of Tokyo), Kenta Ueki(Japan Agency for Marine-Earth Science and Technology), Masayuki Kano(Graduate school of science, Tohoku University), Chairperson:Kenta Ueki, Masayuki Kano(東北大学大学院理学研究科 地球物理学専攻)

10:45 AM - 11:15 AM JST | 1:45 AM - 2:15 AM UTC

[MGI33-01] Forecasting volcanic eruption sequence based on field data and physical models

★Invited Papers

*Takehiro Koyaguchi[1], Kensuke Ishii[2], Kyle R. Anderson[3], Tomofumi Kozono[4] (1.Earthquake Research Institute, University of Tokyo, 2.Meteorological Research Institute, 3.US Geological Survey, 4.Graduate School of Science, Tohoku University)

11:15 AM - 11:30 AM JST | 2:15 AM - 2:30 AM UTC

[MGI33-02] Sparse modeling based feature selection of magmatic tectonic settings

*Kenta Ueki[1], Hideitsu Hino[2], Tatsu Kuwatani[1,3] (1.Japan Agency for Marine-Earth Science and Technology, 2.The Institute of Statistical Mathematics, 3.Japan Science and Technology Agency)

11:30 AM - 11:45 AM JST | 2:30 AM - 2:45 AM UTC

[MGI33-03] Automatic Detection of Stationary Gravity Waves in the Venus' Atmosphere Using Deep Generative Models

*Minori Narita[1], Daiki Kimura[2], Atsushi Yamazaki[3], Takeshi Imamura[1] (1.The University of Tokyo, 2.IBM Research AI, 3.ISAS/JAXA)

11:45 AM - 12:00 PM JST | 2:45 AM - 3:00 AM UTC

[MGI33-04] Fracture and mineral distribution analysis using hyper-resolution DEM and hyperspectral satellite imagery for detecting geothermal fluids paths

*Taiki Kubo[1], Hiroaki Gonnokami[1], Arie Naftali Hawu Hede[2], Mohamad Nur Heriawan[2], Irwan Iskandar[2], Katsuaki Koike[1], Sudarto Notosiswoyo[2] (1.Graduate School of Engineering, Kyoto University, 2.Bandung Institute of Technology)

12:00 PM - 12:15 PM JST | 3:00 AM - 3:15 AM UTC

[MGI33-05] **Geochemical characterization of deep-sea sediments in the western North Pacific Ocean by an integrated multivariate statistical technique**

*Kazutaka Yasukawa[1,2], Kentaro Nakamura[1], Koichiro Fujinaga[2,1], Hikaru Iwamori[3,4], Yasuhiro Kato[1,2] (1.School of Engineering, The University of Tokyo, 2.Ocean Resources Research Center for Next Generation, Chiba Institute of Technology, 3.Earthquake Research Institute, The University of Tokyo, 4.Department of Earth and Planetary Sciences, Tokyo Institute of Technology)

[J] Poster | M (Multidisciplinary and Interdisciplinary)：M-GI General Geosciences, Information Geosciences & Simulations

1:45 PM - 3:15 PM JST | 4:45 AM - 6:15 AM UTC | Poster Hall International Exhibition Hall8, Makuhari Messe_9

[M-GI33] Data-driven geosciences

convener:Tatsu Kuwatani(Japan Agency for Marine-Earth Science and Technology), Hiromichi Nagao(Earthquake Research Institute, The University of Tokyo), Kenta Ueki(Japan Agency for Marine-Earth Science and Technology), Masayuki Kano(Graduate school of science, Tohoku University)

[MGI33-P01] The geochemical database “DODAI” with high-precision location coordinates

*Satoru Haraguchi[1], Kenta Ueki[1], Kenta Yoshida[1], Tatsu Kuwatani[1,3], Mika Mohamed[1], Hikaru Iwamori[1,2,4] (1.Japan Agency for Marine-Earth Science and Technology, 2.Earthquake Research Insititute, the University of Tokyo, 3.PRESTO, 4.Tokyo Institute of Technology)

[MGI33-P02] Bayesian statistical evaluation method for detrital zircon geochronology

*Tan Furukawa[1], Tatsuki Tsujimori[1] (1.Tohoku University)

[MGI33-P03] Geochemical data processing using machine learning with artificial training data and proposal of environmental evaluation method considering natural background of heavy metals in river water in mining area

*Satoh Kenta[1], Kengo Sawayama[1], Noriyoshi Tsuchiya[1] (1.graduate school of environmental studies, Tohoku University)

[MGI33-P04] Quantitative Logging Unit Classification with Hidden Markov Model

*Suguru Yabe[1], Rina Fukuchi[2], Kenta Ueki[1], Yohei Hamada[1] (1.Japan Agency for Marine-Earth Science and Technology, 2.UTokyo AORI)

[MGI33-P05] Sparse Modeling of Nonlinear Dynamics in Heterogeneous Reactions

*Masaki Ito[1], Tatsu Kuwatani[2], Ryosuke Oyanagi[2], Toshiaki Omori[1] (1.Kobe University, 2.JAMSTEC)

[MGI33-P06] How to obtain a high-SNR EPMA map?: complementary roles of high-resolution imaging and subsequent binning

*Atsushi Yasumoto[1], Kenta Yoshida[2] (1.Hiruzen Institute of Geology and Chronlogy, 2.Japan Agency for Marine-earth Science and Technology)

[MGI33-P07] Data-driven estimation of material transfer from bulk compositions

*Tatsu Kuwatani[1,2], Kenta Yoshida[1], Kenta Ueki[1], Ryosuke Oyanagi[1], Masaoki Uno[3], Shotaro Akaho[4] (1.Japan Agency for Marine-Earth Science and Technology, 2.Japan Science and Technology Agency, 3.Graduate School of Environmental Studies, Tohoku University, 4.National Institute of Advanced Industrial Science and Technology)

[J] Poster | M (Multidisciplinary and Interdisciplinary)：M-GI General Geosciences, Information Geosciences & Simulations

5:15 PM - 6:30 PM JST | 8:15 AM - 9:30 AM UTC | Poster Hall International Exhibition Hall8, Makuhari Messe_42

[M-GI33] Data-driven geosciences

convener:Tatsu Kuwatani(Japan Agency for Marine-Earth Science and Technology), Hiromichi Nagao(Earthquake Research Institute, The University of Tokyo), Kenta Ueki(Japan Agency for Marine-Earth Science and Technology), Masayuki Kano(Graduate school of science, Tohoku University)

[MGI33-P01] The geochemical database “DODAI” with high-precision location coordinates

*Satoru Haraguchi[1], Kenta Ueki[1], Kenta Yoshida[1], Tatsu Kuwatani[1,3], Mika Mohamed[1], Hikaru Iwamori[1,2,4] (1.Japan Agency for Marine-Earth Science and Technology, 2.Earthquake Research Insititute, the University of Tokyo, 3.PRESTO, 4.Tokyo Institute of Technology)

[MGI33-P02] Bayesian statistical evaluation method for detrital zircon geochronology

*Tan Furukawa[1], Tatsuki Tsujimori[1] (1.Tohoku University)

[MGI33-P03] Geochemical data processing using machine learning with artificial training data and proposal of environmental evaluation method considering natural background of heavy metals in river water in mining area

*Satoh Kenta[1], Kengo Sawayama[1], Noriyoshi Tsuchiya[1] (1.graduate school of environmental studies, Tohoku University)

[MGI33-P04] Quantitative Logging Unit Classification with Hidden Markov Model

*Suguru Yabe[1], Rina Fukuchi[2], Kenta Ueki[1], Yohei Hamada[1] (1.Japan Agency for Marine-Earth Science and Technology, 2.UTokyo AORI)

[MGI33-P05] Sparse Modeling of Nonlinear Dynamics in Heterogeneous Reactions

*Masaki Ito[1], Tatsu Kuwatani[2], Ryosuke Oyanagi[2], Toshiaki Omori[1] (1.Kobe University, 2.JAMSTEC)

[MGI33-P06] How to obtain a high-SNR EPMA map?: complementary roles of high-resolution imaging and subsequent binning

*Atsushi Yasumoto[1], Kenta Yoshida[2] (1.Hiruzen Institute of Geology and Chronlogy, 2.Japan Agency for Marine-earth Science and Technology)

[MGI33-P07] Data-driven estimation of material transfer from bulk compositions

*Tatsu Kuwatani[1,2], Kenta Yoshida[1], Kenta Ueki[1], Ryosuke Oyanagi[1], Masaoki Uno[3], Shotaro Akaho[4] (1.Japan Agency for Marine-Earth Science and Technology, 2.Japan Science and Technology Agency, 3.Graduate School of Environmental Studies, Tohoku University, 4.National Institute of Advanced Industrial Science and Technology)

[J] Oral | M (Multidisciplinary and Interdisciplinary)：M-GI General Geosciences, Information Geosciences & Simulations

3:30 PM - 5:00 PM JST | 6:30 AM - 8:00 AM UTC | A08 TOKYO BAY MAKUHARI HALL

[M-GI33] Data-driven geosciences

convener:Tatsu Kuwatani(Japan Agency for Marine-Earth Science and Technology), Hiromichi Nagao(Earthquake Research Institute, The University of Tokyo), Kenta Ueki(Japan Agency for Marine-Earth Science and Technology), Masayuki Kano(Graduate school of science, Tohoku University), Chairperson:Tatsu Kuwatani(JAMSTEC), Suguru Yabe(JAMSTEC)

3:30 PM - 4:00 PM JST | 6:30 AM - 7:00 AM UTC

[MGI33-06] Markov Chain Monte Carlo: algorithms for multimodal distribution and their applications

★Invited Papers

*Yukito iba[1] (1.The Institute of Statistical Mathematics)

4:00 PM - 4:15 PM JST | 7:00 AM - 7:15 AM UTC

[MGI33-07] **Specifying rate constants and reaction path on the water-rock chemical reaction based on exchange Monte Carlo method and sparse modeling**

*Ryosuke Oyanagi[1], Tatsu Kuwatani[1], Omori Toshiaki[2] (1.Japan Agency for Marine-Earth Science and Technology, 2.Kobe University)

4:15 PM - 4:30 PM JST | 7:15 AM - 7:30 AM UTC

[MGI33-08] Superresolution of X-ray CT images of core samples for understanding the multi-scale structures of water-rock interaction

*Toshiaki Omori[1], Atsushi Okamoto[2], Katsuyoshi Michibayashi[3], Oman Drilling Project Phase 2 Science Party (1.Kobe Univ., 2.Tohoku Univ., 3.Nagoya Univ.)

4:30 PM - 4:45 PM JST | 7:30 AM - 7:45 AM UTC

[MGI33-09] 3-dimensional Fracture Network Analysis by Persistent Homology

*Miyuki Miyazawa[1], Anna Suzuki[2], Atsushi Okamoto[1], Hiroyuki Shimizu[3], Ippei Obayashi[4], Yasuaki Hiraoka[4,5], Takatoshi Ito[2] (1.Graduate School of Environmental Studies, Tohoku University, 2.Institute of Fluid Science, Tohoku University, 3.Kajima Corporation, 4.The Advanced Institute for Materials Research, Tohoku University, 5.Kyoto University)

4:45 PM - 5:00 PM JST | 7:45 AM - 8:00 AM UTC

[MGI33-10] Characteristic patterns and minimal dynamics of correlated seismicity in Japanese island region

*mitsuhiro toriumi[1] (1.Japan agency of marine science and technology)

[E] Oral | M (Multidisciplinary and Interdisciplinary) : M-TT Technology & Techniques

9:00 AM - 10:30 AM JST | 12:00 AM - 1:30 AM UTC | 104 1F

[M-TT46] New phase of GPS/GNSS application as an integrated earth observation system

convener:Yoshinori Shoji(The Second Laboratory of Meteorological Satellite and Observation System Research Department, Meteorological Research Institute), Kaoru Ichikawa(Research Institute for Applied Mechanics, Kyushu University), Yusaku Ohta(Research Center for Prediction of Earthquakes and Volcanic Eruptions, Graduate School of Science, Tohoku University), Takuya Tsugawa(National Institute of Information and Communications Technology), Chairperson:Yusaku Ohta

9:00 AM - 9:30 AM JST | 12:00 AM - 12:30 AM UTC

[MTT46-01] The latest status of Quasi-Zenith Satellite System (QZSS) and its future expansion

★Invited Papers

*Satoshi Kogure[1] (1.QZSS Straetegy Office, National Space Policy Secretariate, Cabinet Office)

9:30 AM - 9:45 AM JST | 12:30 AM - 12:45 AM UTC

[MTT46-02] Application of the GNSS-A for other academic fields and fundamental marine information network

*Yusuke Yokota[1], Tadashi Ishikawa[2], Shun-ichi Watanabe[2] (1.Institute of Industrial Science, The University of Tokyo, 2.Hydrographic and Oceanographic department, Japan Coast Guard)

9:45 AM - 10:00 AM JST | 12:45 AM - 1:00 AM UTC

[MTT46-03] Feasibility of the GNSS carrier phase to fault slip approach for the estimation of slip phenomena in subduction zone

*Yusuke Tanaka[1], Yusaku Ohta[1], SHINICHI MIYAZAKI[2] (1.Tohoku University, 2.Kyoto University)

10:00 AM - 10:15 AM JST | 1:00 AM - 1:15 AM UTC

[MTT46-04] Assimilation experiments of GNSS-derived ZTD and Sentinel-derived products into WRF to improve forecasts of severe rain events in Italy

*Eugenio Realini[1], Martina Lagasio[2], Luca Pulvirenti[2], Antonio Parodi[2], Andrea Gatti[1], Giulio Tagliaferro[1], Giovanna Venuti[3], Stefano Barindelli[3], Emanuele Passera[4], Alessio Rucci[4], Nazzareno Pierdicca[5], Bjorn Rommen[6] (1.Geomatics Research & Development srl, 2.CIMA Research Foundation, 3.Dept. of Civil and Environmental Engineering, Politecnico di Milano, 4.TRE Altamira srl, 5.Dept. of Information Engineering, Electronics and Telecommunications, Sapienza Univ. of Rome, 6.European Space Agency (ESA-ESTEC))

10:15 AM - 10:30 AM JST | 1:15 AM - 1:30 AM UTC

[MTT46-05] **An analysis of tropospheric delays using goGPS software on all GEONET stations during the passage of Typhoon Jebi in September 2018**

*Andrea Gatti[1], Eugenio Realini[1], Giulio Tagliaferro[1] (1.Geomatics Research & Development srl)

[E] Oral | M (Multidisciplinary and Interdisciplinary) : M-TT Technology & Techniques

10:45 AM - 12:15 PM JST | 1:45 AM - 3:15 AM UTC | 104 1F

[M-TT46] New phase of GPS/GNSS application as an integrated earth observation system

convener:Yoshinori Shoji(The Second Laboratory of Meteorological Satellite and Observation System Research Department, Meteorological Research Institute), Kaoru Ichikawa(Research Institute for Applied Mechanics, Kyushu University), Yusaku Ohta(Research Center for Prediction of Earthquakes and Volcanic Eruptions, Graduate School of Science, Tohoku University), Takuya Tsugawa(National Institute of Information and Communications Technology), Chairperson:Takuya Tsugawa

10:45 AM - 11:05 AM JST | 1:45 AM - 2:05 AM UTC

[MTT46-06] **A new perspective of the storm-time dynamics of the ionosphere using global GNSS-TEC observation data**

★Invited Papers

*Atsuki Shinbori[1], Yuichi Otsuka[1], Takuya Sori[1], Takuya Tsugawa[2], Michi Nishioka[2] (1.Institute for Space-Earth Environment Research (ISEE), Nagoya University, 2.National Institute of Information and Communications Technology (NICT))

11:05 AM - 11:20 AM JST | 2:05 AM - 2:20 AM UTC

[MTT46-07] Ionospheric space weather studies for GNSS users

*Takuya Tsugawa[1], Kornyanat Hozumi[1], Punyawi Jamjareegulgarn[2], Supnithi Pornchai [2], Susumu Saito[3], Yuichi Otsuka[3,4], Shinichi Hama[1], Takahiro Naoi[1], Mamoru Ishii[1] (1.NICT, 2.KMITL, 3.ENRI, 4.Nagoya Univ.)

11:20 AM - 11:35 AM JST | 2:20 AM - 2:35 AM UTC

[MTT46-08] QZSS geostationary satellite for ionospheric TEC observations

*Kosuke Heki[1] (1.Department of Earth and Planetary Sciences, Faculty of Science, Hokkaido University)

11:35 AM - 11:50 AM JST | 2:35 AM - 2:50 AM UTC

[MTT46-09] Precise estimation of total electron content by double-shell model using local receiver network

*Takashi Maruyama[1,2], Kornyanat Hozumi[1], Guanyi Ma[2], Qingtao Wan[2] (1.National Institute of Information and Communications Technology, 2.National Astronomical Observatories, Chinese Academy of Sciences)

11:50 AM - 12:05 PM JST | 2:50 AM - 3:05 AM UTC

[MTT46-10] Investigation of sea surface height detection by Global Navigation Satellite System Reflectometry (GNSS-R)

*Osamu Isoguchi[1], Kaoru Ichikawa[2], Yukihito Kitazawa[3] (1.RESTEC, 2.Kyushu Univ., 3.ISAS/JAXA)

12:05 PM - 12:15 PM JST | 3:05 AM - 3:15 AM UTC

[MTT46-11] Discussion

[E] Poster | M (Multidisciplinary and Interdisciplinary)：M-TT Technology & Techniques

1:45 PM - 3:15 PM JST | 4:45 AM - 6:15 AM UTC | Poster Hall International Exhibition Hall8, Makuhari Messe_10

[M-TT46] New phase of GPS/GNSS application as an integrated earth observation system

convener:Yoshinori Shoji(The Second Laboratory of Meteorological Satellite and Observation System Research Department, Meteorological Research Institute), Kaoru Ichikawa(Research Institute for Applied Mechanics, Kyushu University), Yusaku Ohta(Research Center for Prediction of Earthquakes and Volcanic Eruptions, Graduate School of Science, Tohoku University), Takuya Tsugawa(National Institute of Information and Communications Technology)

[MTT46-P01] Continuous acoustic ranging from a GNSS buoy for the new method of seafloor crustal deformation measurements

*Keiichi Tadokoro[1], Natsuki Kinugasa[1], Teruyuki Kato[2], Yukihiro Terada[3], Akira Futamura[4], Kenjiro Matsuhiro[1] (1.Research Center for Seismology, Volcanology and Earthquake and Volcano Research Center, Nagoya University, 2.Hot Springs Research Institute of Kanagawa Prefecture, 3.Kochi National College of Technology, 4.National Institute of Technology, Yuge College)

[MTT46-P02] Accuracy and precision assessment of the real-time kinematic GNSS time series for moored buoy using three-axis programable moving table

*Yusaku Ohta[1], Misae Imano[1], Motoyuki Kido[2] (1.Research Center for Prediction of Earthquakes and Volcanic Eruptions, Graduate School of Science, Tohoku University, 2.IRIDeS, Tohoku University)

[MTT46-P03] GNSS-R altimetry using a Geostationary Satellite

*Kaoru Ichikawa[1], Tatsuki Okumura[2], Masanori Konda[3], Yasuyuki Baba[4] (1.Res. Inst. Appl. Mech., Kyushu Univ., 2.Dept. ESST, Interdicipl. Grad. School Eng. Sc., Kyushu Univ., 3.Graduate School of Science, Kyoto Univ., 4.Disaster Prevention Res. Inst., Kyoto Univ.)

[MTT46-P04] Estimation of typhoon wind speed using CYGNSS observations: A case study of Typhoon Lan in 2017

*Kako Shinichiro[1], Hiroyuki Tomita[2], Kaoru Ichikawa[3] (1.Graduate School of Science and Engineering, Kagoshima University, 2.Institute for Space-Earth Environment, Nagoya University, 3.Research institute for Applied Mechanics, Kyushu University)

[MTT46-P05] Ionospheric and seismic effects caused by the North Korea nuclear tests realized on 2006-2017

Nataliia Perevalova[2], *Nikolai Shestakov[1], Anna Dobrynina[3,4], Dmitry Kostylev[7], Meng Guojie[5], Wei-Wei Wu[5,6] (1.Institute for Applied Mathematics FEB RAS, Vladivostok, Russia; Far Eastern Federal University, Vladivostok, Russia, 2.Institute of Solar-Terrestrial Physics SB RAS, Irkutsk, Russia, 3.Institute of the Earth's Crust SB RAS, Irkutsk, Russia , 4.Geological institute SB RAS, Ulan-Ude, Russia , 5.Institute of Earthquake Forecasting, China Earthquake Administration, Beijing, China, 6.College of Surveying and Geo-informatics, Tongji University, Shanghai, China, 7.Sakhalin Branch of Federal Research Center Geophysical Survey RAS, Yuzhno_Sakhalinsk, Russia)

[MTT46-P06] Relationships between Water Vapor Concentration Index derived from GNSS and Surface Wind Convergence during Localized Heavy Rainfall in Tokyo in Summer

*Yoshihito Seto[1], Yoshinori Shoji[2], Nobumitsu Tsunematsu[3], Hideo Takahashi[1] (1.Department of Geography, Graduate School of Urban Environmental Sciences, Tokyo Metropolitan University, 2.Meteorological Research Institute, 3.Tokyo Metropolitan Research Institute for Environmental Protection)

[MTT46-P07] Development of novel ground-based microwave radiometer for earth science -preliminary report-

*Ryuichi Ichikawa[1], Hideki Ujihara[1], Shinsuke Satoh[1], Jun Amagai[1], Yusaku Ohta[2], Basara Miyahara[3], Hiroshi Munekane[3], Taketo Nagasaki[4], Osamu Tajima[5], Kentaro Araki[6], Takuya Tajiri[6], Hiroshi Takiguchi[7], Takeshi Matsushima[8], Nobuo Matsushima[9], Tatsuya Momotani[10], Kenji Utsunomiya[10] (1.National Institute of Information and Communications Technology, 2.Tohoku University, 3.Geospatial Information Authority of Japan, 4.High Energy Accelerator Research Organization, 5.Kyoto University, 6.Meteorological Research Institute, JMA, 7.Japan Aerospace eXploration Agency, 8.Kyushu University, 9.National Institute of Advanced Industrial Science and Technology, 10.Japan Weather Association)

[MTT46-P08] Refractivity Distributions over the Kanto Plain Obtained by Dual-polarization Radar

*Hiromu Seko[1], Eiichi Sato[1], Hiroshi Yamauchi[2] (1.Meteorological Research Institute, 2.Japan Meteorological Agency)

[MTT46-P09] Spatial and temporal distribution of tropospheric water vapor observed by a Raman lidar and a GNSS receiver network over Shigaraki, Japan

*Masanori Yabuki[1], Toshitaka Tsuda[1], Yuya Kawano[2], Yusaku Tottori[2], Makoto Tsukamoto[2], Eiji Takeuchi[2] (1.Research Institute for Sustainable Humanosphere, Kyoto University, 2.EKO Instruments Co., Ltd.)

[MTT46-P10] **Study of the Mechanisms of Severe Thunderstorm in Tokyo Metropolitan Area using High Frequent Assimilation of GNSS and Other Ground-based Observations**

*Yoshinori Shoji[1], Tetsu Sakai[2], Ahoro Adachi[1], Satoru Yoshida[2], Tomohiro Nagai[2] (1.The Second Laboratory of Meteorological Satellite and Observation System Research Department, Meteorological Research Institute, 2.The Third Laboratory of Meteorological Satellite and Observation System Research Department, Meteorological Research Institute)

[E] Poster | M (Multidisciplinary and Interdisciplinary)：M-TT Technology & Techniques

5:15 PM - 6:30 PM JST | 8:15 AM - 9:30 AM UTC | Poster Hall International Exhibition Hall8, Makuhari Messe_43

[M-TT46] New phase of GPS/GNSS application as an integrated earth observation system

convener:Yoshinori Shoji(The Second Laboratory of Meteorological Satellite and Observation System Research Department, Meteorological Research Institute), Kaoru Ichikawa(Research Institute for Applied Mechanics, Kyushu University), Yusaku Ohta(Research Center for Prediction of Earthquakes and Volcanic Eruptions, Graduate School of Science, Tohoku University), Takuya Tsugawa(National Institute of Information and Communications Technology)

[MTT46-P01] Continuous acoustic ranging from a GNSS buoy for the new method of seafloor crustal deformation measurements

*Keiichi Tadokoro[1], Natsuki Kinugasa[1], Teruyuki Kato[2], Yukihiro Terada[3], Akira Futamura[4], Kenjiro Matsuhiro[1] (1.Research Center for Seismology, Volcanology and Earthquake and Volcano Research Center, Nagoya University, 2.Hot Springs Research Institute of Kanagawa Prefecture, 3.Kochi National College of Technology, 4.National Institute of Technology, Yuge College)

[MTT46-P02] Accuracy and precision assessment of the real-time kinematic GNSS time series for moored buoy using three-axis programable moving table

*Yusaku Ohta[1], Misae Imano[1], Motoyuki Kido[2] (1.Research Center for Prediction of Earthquakes and Volcanic Eruptions, Graduate School of Science, Tohoku University, 2.IRIDeS, Tohoku University)

[MTT46-P03] GNSS-R altimetry using a Geostationary Satellite

*Kaoru Ichikawa[1], Tatsuki Okumura[2], Masanori Konda[3], Yasuyuki Baba[4] (1.Res. Inst. Appl. Mech., Kyushu Univ., 2.Dept. ESST, Interdicipl. Grad. School Eng. Sc., Kyushu Univ., 3.Graduate School of Science, Kyoto Univ., 4.Disaster Prevention Res. Inst., Kyoto Univ.)

[MTT46-P04] Estimation of typhoon wind speed using CYGNSS observations: A case study of Typhoon Lan in 2017

*Kako Shinichiro[1], Hiroyuki Tomita[2], Kaoru Ichikawa[3] (1.Graduate School of Science and Engineering, Kagoshima University, 2.Institute for Space-Earth Environment, Nagoya University, 3.Research institute for Applied Mechanics, Kyushu University)

[MTT46-P05] Ionospheric and seismic effects caused by the North Korea nuclear tests realized on 2006-2017

Nataliia Perevalova[2], *Nikolai Shestakov[1], Anna Dobrynina[3,4], Dmitry Kostylev[7], Meng Guojie[5], Wei-Wei Wu[5,6] (1.Institute for Applied Mathematics FEB RAS, Vladivostok, Russia; Far Eastern Federal University, Vladivostok, Russia, 2.Institute of Solar-Terrestrial Physics SB RAS, Irkutsk, Russia, 3.Institute of the Earth's Crust SB RAS, Irkutsk, Russia , 4.Geological institute SB RAS, Ulan-Ude, Russia , 5.Institute of Earthquake Forecasting, China Earthquake Administration, Beijing, China, 6.College of Surveying and Geo-informatics, Tongji University, Shanghai, China, 7.Sakhalin Branch of Federal Research Center Geophysical Survey RAS, Yuzhno_Sakhalinsk, Russia)

[MTT46-P06] Relationships between Water Vapor Concentration Index derived from GNSS and Surface Wind Convergence during Localized Heavy Rainfall in Tokyo in Summer

*Yoshihito Seto[1], Yoshinori Shoji[2], Nobumitsu Tsunematsu[3], Hideo Takahashi[1] (1.Department of Geography, Graduate School of Urban Environmental Sciences, Tokyo Metropolitan University, 2.Meteorological Research Institute, 3.Tokyo Metropolitan Research Institute for Environmental Protection)

[MTT46-P07] Development of novel ground-based microwave radiometer for earth science -preliminary report-

*Ryuichi Ichikawa[1], Hideki Ujihara[1], Shinsuke Satoh[1], Jun Amagai[1], Yusaku Ohta[2], Basara Miyahara[3], Hiroshi Munekane[3], Taketo Nagasaki[4], Osamu Tajima[5], Kentaro Araki[6], Takuya Tajiri[6], Hiroshi Takiguchi[7], Takeshi Matsushima[8], Nobuo Matsushima[9], Tatsuya Momotani[10], Kenji Utsunomiya[10] (1.National Institute of Information and Communications Technology, 2.Tohoku University, 3.Geospatial Information Authority of Japan, 4.High Energy Accelerator Research Organization, 5.Kyoto University, 6.Meteorological Research Institute, JMA, 7.Japan Aerospace eXploration Agency, 8.Kyushu University, 9.National Institute of Advanced Industrial Science and Technology, 10.Japan Weather Association)

[MTT46-P08] Refractivity Distributions over the Kanto Plain Obtained by Dual-polarization Radar

*Hiromu Seko[1], Eiichi Sato[1], Hiroshi Yamauchi[2] (1.Meteorological Research Institute, 2.Japan Meteorological Agency)

[MTT46-P09] Spatial and temporal distribution of tropospheric water vapor observed by a Raman lidar and a GNSS receiver network over Shigaraki, Japan

*Masanori Yabuki[1], Toshitaka Tsuda[1], Yuya Kawano[2], Yusaku Tottori[2], Makoto Tsukamoto[2], Eiji Takeuchi[2] (1.Research Institute for Sustainable Humanosphere, Kyoto University, 2.EKO Instruments Co., Ltd.)

[MTT46-P10] **Study of the Mechanisms of Severe Thunderstorm in Tokyo Metropolitan Area using High Frequent Assimilation of GNSS and Other Ground-based Observations**

*Yoshinori Shoji[1], Tetsu Sakai[2], Ahoro Adachi[1], Satoru Yoshida[2], Tomohiro Nagai[2] (1.The Second Laboratory of Meteorological Satellite and Observation System Research Department, Meteorological Research Institute, 2.The Third Laboratory of Meteorological Satellite and Observation System Research Department, Meteorological Research Institute)

[E] Oral | M (Multidisciplinary and Interdisciplinary)：M-TT Technology & Techniques

3:30 PM - 5:00 PM JST | 6:30 AM - 8:00 AM UTC | 106 1F

[M-TT46] New phase of GPS/GNSS application as an integrated earth observation system

convener:Yoshinori Shoji(The Second Laboratory of Meteorological Satellite and Observation System Research Department, Meteorological Research Institute), Kaoru Ichikawa(Research Institute for Applied Mechanics, Kyushu University), Yusaku Ohta(Research Center for Prediction of Earthquakes and Volcanic Eruptions, Graduate School of Science, Tohoku University), Takuya Tsugawa(National Institute of Information and Communications Technology), Chairperson:Yoshinori Shoji(Meteorological Research Institute)

3:30 PM - 3:45 PM JST | 6:30 AM - 6:45 AM UTC

[MTT46-12] Study on tropospheric delay variations extracted from a short baseline analysis and their application to meteorological observation

*Takayuki Yoshihara[1], Susumu Saito[1], Atsushi Kezuka[1], Shinji Saitoh[1] (1.Electronic Navigation Research Institute, National Institute of Maritime, Port and Aviation Technology)

3:45 PM - 4:00 PM JST | 6:45 AM - 7:00 AM UTC

[MTT46-13] Water vapor estimation using digital terrestrial broadcasting waves
- Field test in Tokyo metropolitan area and trial production of small devices -

*Seiji Kawamura[1], Hiroshi HANADO[1], Hiroki Ohta[1], Yoshinobu Matsumura[2], Ryosuke Mori[2], Kazuyoshi Noda[2], Teruaki Hasegawa[2] (1.National Institute of Information and Communications Technology, 2.Socionext Inc.)

4:00 PM - 4:15 PM JST | 7:00 AM - 7:15 AM UTC

[MTT46-14] Water vapor estimation via propagation delay of 920MHz wireless communication signal

*Nobuyasu Shiga[1], Satoshi Yasuda[1], Seiji Kawamura[1], Hiroshi HANADO[1], Ryuichi Ichikawa[1], Hironori Iwai[1], Shinsuke Satoh[1] (1.National Institute of Information and communications technology)

4:15 PM - 4:30 PM JST | 7:15 AM - 7:30 AM UTC

[MTT46-15] Comparison of a water vapor observation with GPS and high sensitivity microwave radiometer, KUMODeS

*Taketo Nagasaki[1], Osamu Tajima[2], Ryuichi Ichikawa[3], Hiroshi Takiguchi[4], Kentaro Araki[5], Hiroshi Ishimoto[5] (1.High Energy Accelerator Research Organization, IPNS, 2.Kyoto University, 3.National Institute of Information and Communications Technology, 4.Japan Aerospace Exploration Agency, 5.Meteorological Research Institute)

4:30 PM - 4:45 PM JST | 7:30 AM - 7:45 AM UTC

[MTT46-16] Development and Observation of Water Vapor Raman Lidars for Localized Torrential Rainfall Prediction

*Tomohiro Nagai[1], Tetsu Sakai[1], Satoru Yoshida[1], Toshiharu Izumi[2], Sho Yokota[1], Hiromu Seko[1], Yoshinori Shoji[1], Koichi Shiraishi[3] (1.Meteorological Research Institute, Japan Meteorological Agency, 2.Japan Meteorological Agency, 3.Fukuoka University)

4:45 PM - 5:00 PM JST | 7:45 AM - 8:00 AM UTC

[MTT46-17] Study of Water Vapor Monitoring in the Open Ocean using Kinematic Precise Point Positioning

*Yoshinori Shoji[1], Teruyuki Kato[2], Yukihiro Terada[3], Toshitaka Tsuda[4], Masanori Yabuki[4] (1.The Second Laboratory of Meteorological Satellite and Observation System Research Department, Meteorological Research Institute, 2.Hot Springs Research Institute/Kanagawa Prefectural Government, 3.Natinal Institute of Technology, Kochi College, 4.Research Institute for Sustainable Humanosphere/Kyoto Unversity)

[E] Poster | M (Multidisciplinary and Interdisciplinary)：M-TT Technology & Techniques

1:45 PM - 3:15 PM JST | 4:45 AM - 6:15 AM UTC | Poster Hall International Exhibition Hall8, Makuhari Messe_11

[M-TT47] GEOSCIENTIFIC APPLICATIONS OF HIGH-DEFINITION TOPOGRAPHY AND GEOPHYSICAL DATA IN THE ANTHROPOCENE

convener:Yuichi S. Hayakawa(Faculty of Environmental Earth Science, Hokkaido University), Shigekazu Kusumoto(Graduate School of Science and Engineering for Research, University of Toyama), Christopher A Gomez(Kobe University Faculty of Maritime Sciences Volcanic Risk at Sea Research Group)

[MTT47-P01] High-definition topography monitoring after riverbed cultivation in the Echi River, central Japan

*Takuro Ogura[1,2], Satoshi Asano[3], Toshiaki Mizuno[3], Yoshihiro Azuma[3], Takeshi Kitai[4], Yuichi S Hayakawa[5,6], Kotaro Iizuka[6] (1.Graduate School of Frontier Sciences, The University of Tokyo, 2.Graduate School of Environmental Science, Hokkaido University, 3.Lake Biwa Environmental Research Institute , 4.Lake Biwa Museum, 5.Faculty of Environmental Earth Science, Hokkaido University, 6.Center for Spatial information Science, The University of Tokyo)

[MTT47-P02] **Spatial distribution of land surface displacements in the crater of Tateyama Midagahara Volcano using high-definition topographic data**

*Yuichi S. Hayakawa[1], Shigekazu Kusumoto[2], Takuro Ogura[3,4] (1.Faculty of Environmental Earth Science, Hokkaido University, 2.Graduate School of Science and Engineering for Research, University of Toyama, 3.Graduate School of Frontier Science, The University of Tokyo, 4.Graduate School of Environmental Science, Hokkaido University)

[MTT47-P03] Study on a simplified measurement of water depth and reconstruction of the riverbed form by using SfM and MVS.

*OSAWA KOTA[1], Tadafumi Niizato [2], Katsuaki Mitachi[3], Makoto Kawamura[1], Masahiro Ohkawa[1] (1.Mitsubishi Materials Techno corporation , 2.Japan Atomic Energy Agency, 3.ATOM TRANSPORT SERVICE CO., LTD)

[MTT47-P04] Ground Penetrating Radar Imaging of Moisture and Water movement in volcanic soil

*Christopher A Gomez[1] (1.Kobe University Faculty of Maritime Sciences Volcanic Risk at Sea Research Group)

[MTT47-P05] **Estimating Eruptive Volumes of Mud Volcano Southwestern Taiwan by Using UAV and SfM-MVS Photogrammetry**

*CHIA-YING LIU[1], Ray Y Chuang[1], Horng-Yue Chen[2] (1.Department of Geography, National Taiwan University, 2.Academia Sinica, Institute of Earth Sciences)

[MTT47-P06] Increasing temporal depth of urban Land-Use Regression Models by wind-data driven dynamic buffer generation

*Tilman Leo Hohenberger[1], King Wai Leung[1] (1.Division of Environment and Sustainability, Hong Kong University of Science and Technology)

[E] Poster | M (Multidisciplinary and Interdisciplinary)：M-TT Technology & Techniques

5:15 PM - 6:30 PM JST | 8:15 AM - 9:30 AM UTC | Poster Hall International Exhibition Hall8, Makuhari Messe_44

[M-TT47] GEOSCIENTIFIC APPLICATIONS OF HIGH-DEFINITION TOPOGRAPHY AND GEOPHYSICAL DATA IN THE ANTHROPOCENE

convener:Yuichi S. Hayakawa(Faculty of Environmental Earth Science, Hokkaido University), Shigekazu Kusumoto(Graduate School of Science and Engineering for Research, University of Toyama), Christopher A Gomez(Kobe University Faculty of Maritime Sciences Volcanic Risk at Sea Research Group)

[MTT47-P01] High-definition topography monitoring after riverbed cultivation in the Echi River, central Japan

*Takuro Ogura[1,2], Satoshi Asano[3], Toshiaki Mizuno[3], Yoshihiro Azuma[3], Takeshi Kitai[4], Yuichi S Hayakawa[5,6], Kotaro Iizuka[6] (1.Graduate School of Frontier Sciences, The University of Tokyo, 2.Graduate School of Environmental Science, Hokkaido University, 3.Lake Biwa Environmental Research Institute , 4.Lake Biwa Museum, 5.Faculty of Environmental Earth Science, Hokkaido University, 6.Center for Spatial information Science, The University of Tokyo)

[MTT47-P02] **Spatial distribution of land surface displacements in the crater of Tateyama Midagahara Volcano using high-definition topographic data**

*Yuichi S. Hayakawa[1], Shigekazu Kusumoto[2], Takuro Ogura[3,4] (1.Faculty of Environmental Earth Science, Hokkaido University, 2.Graduate School of Science and Engineering for Research, University of Toyama, 3.Graduate School of Frontier Science, The University of Tokyo, 4.Graduate School of Environmental Science, Hokkaido University)

[MTT47-P03] Study on a simplified measurement of water depth and reconstruction of the riverbed form by using SfM and MVS.

*OSAWA KOTA[1], Tadafumi Niizato [2], Katsuaki Mitachi[3], Makoto Kawamura[1], Masahiro Ohkawa[1] (1.Mitsubishi Materials Techno corporation , 2.Japan Atomic Energy Agency, 3.ATOM TRANSPORT SERVICE CO., LTD)

[MTT47-P04] Ground Penetrating Radar Imaging of Moisture and Water movement in volcanic soil

*Christopher A Gomez[1] (1.Kobe University Faculty of Maritime Sciences Volcanic Risk at Sea Research Group)

[MTT47-P05] **Estimating Eruptive Volumes of Mud Volcano Southwestern Taiwan by Using UAV and SfM-MVS Photogrammetry**

*CHIA-YING LIU[1], Ray Y Chuang[1], Horng-Yue Chen[2] (1.Department of Geography, National Taiwan University, 2.Academia Sinica, Institute of Earth Sciences)

[MTT47-P06] Increasing temporal depth of urban Land-Use Regression Models by wind-data driven dynamic buffer generation

*Tilman Leo Hohenberger[1], King Wai Leung[1] (1.Division of Environment and Sustainability, Hong Kong University of Science and Technology)

[J] Poster | M (Multidisciplinary and Interdisciplinary)：M-ZZ Others

3:30 PM - 5:00 PM JST | 6:30 AM - 8:00 AM UTC | Poster Hall International Exhibition Hall8, Makuhari Messe_27

[M-ZZ51] Geoscience Studies: historical, philosophical and STS studies

convener:Michiko Yajima(College of Humanity and Science, Nihon University), Shigeyuki Aoki(Faculty of Letters, Chuo University), Toshihiro Yamada(Research Fellow, Graduate School of Education, University of Tokyo), Shigeo Yoshida(Department of Earth and Planetary Sciences, Faculty of Sciences, Kyushu University)

[MZZ51-P01] Cosmic skepticism on meaning of life

*Shigeyuki Aoki[1] (1.School of Computer Science and Engineering, University of Aizu)

[MZZ51-P02] Rethinking 'Stenonian Revolution' in stratigraphy: From *Prodromus* (1669) to 'Anthropocene'

*Toshihiro Yamada[1] (1.Research Fellow, Graduate School of Education, University of Tokyo)

[MZZ51-P03] How Edmund Naumann made the Geologic Map of Japan in 1885?

*Michiko Yajima[1] (1.College of Humanity and Science, Nihon University)

[MZZ51-P04] The role of the private sector in the formation of the meteorological observation network of Japan in the nineteenth century

*Akira Yamamoto[1] (1.Meteorological Research Institute)

[MZZ51-P05] "Thyco Brahe" in the Geology; The Compromise Models on the Plate Tectonics Revolution.

*Jun'ichi Chiba[1] (1.O-hara Business College)

[MZZ51-P06] Contributions of Tatsuro Matsumoto (1913-2009) to plate tectonics, a signifcant paradigm shift in earth sicence

*Hidehisa Mashima[1] (1.Center for Obsidian and Lithic Studies, Meiji University)

[MZZ51-P07] Online Community Responses to Volcanic Disaster: A Study of Yahoo! News Comments on the 2018 Mt. Kusatsu-Shirane eruption

*Kou Yamada[1] (1.Waseda University)

[J] Poster | M (Multidisciplinary and Interdisciplinary)：M-ZZ Others

5:15 PM - 6:30 PM JST | 8:15 AM - 9:30 AM UTC | Poster Hall International Exhibition Hall8, Makuhari Messe_45

[M-ZZ51] Geoscience Studies: historical, philosophical and STS studies

convener:Michiko Yajima(College of Humanity and Science, Nihon University), Shigeyuki Aoki(Faculty of Letters, Chuo University), Toshihiro Yamada(Research Fellow, Graduate School of Education, University of Tokyo), Shigeo Yoshida(Department of Earth and Planetary Sciences, Faculty of Sciences, Kyushu University)

[MZZ51-P01] Cosmic skepticism on meaning of life

*Shigeyuki Aoki[1] (1.School of Computer Science and Engineering, University of Aizu)

[MZZ51-P02] Rethinking 'Stenonian Revolution' in stratigraphy: From *Prodromus* (1669) to 'Anthropocene'

*Toshihiro Yamada[1] (1.Research Fellow, Graduate School of Education, University of Tokyo)

[MZZ51-P03] How Edmund Naumann made the Geologic Map of Japan in 1885?

*Michiko Yajima[1] (1.College of Humanity and Science, Nihon University)

[MZZ51-P04] The role of the private sector in the formation of the meteorological observation network of Japan in the nineteenth century

*Akira Yamamoto[1] (1.Meteorological Research Institute)

[MZZ51-P05] "Thyco Brahe" in the Geology; The Compromise Models on the Plate Tectonics Revolution.

*Jun'ichi Chiba[1] (1.O-hara Business College)

[MZZ51-P06] Contributions of Tatsuro Matsumoto (1913-2009) to plate tectonics, a signifcant paradigm shift in earth sicence

*Hidehisa Mashima[1] (1.Center for Obsidian and Lithic Studies, Meiji University)

[MZZ51-P07] Online Community Responses to Volcanic Disaster: A Study of Yahoo! News Comments on the 2018 Mt. Kusatsu-Shirane eruption

*Kou Yamada[1] (1.Waseda University)

[J] Oral | U (Union)：Union

Mon. May 27, 2019 9:30 AM - 10:30 AM JST | Mon. May 27, 2019 12:30 AM - 1:30 AM UTC | 101 1F

[U-05] Large-scale Research Projects: Master Plan 2020 and its beyond

convener:Eiichi Tajika(Department of Earth and Planetary Science, Graduate School of Science, The University of Tokyo), Shigeko Haruyama(Department of Environmental Science, Graduate School of Bioresouces,Mie University), Ryoichi Fujii(Research Organization of Information and Systems), Hodaka Kawahata(Atmosphere Ocean Research Institute, the University of Tokyo), Chairperson:Eiichi Tajika, Shigeko Haruyama

Many of top sciences in Earth and Planetary Science (EPS) are progressed by big projects that require 10 billion JPY or more in 10 years or so. In order to realize such projects, we need an arena where they are brushed up through critical reviews among various fields in EPS. Deeper mutual understandings through serious discussions there will enable us to reach a final consensus on the priorities of the projects. The Master Plan (MP) of Large-scale Research issued by the Science Council of Japan strongly motivates us to follow the process described above. Indeed some of the selected projects have been funded by the Ministry of Education, Culture, Sports, Science & Technology since 2010.
Since the current Master Plan 2017 is going to be thoroughly revised in 2020, we propose to hold a session in which large-scale research projects are concisely introduced and critically reviewed. This session is to be convened by JpGU and EPS Committee of Science Council of Japan.

9:30 AM - 9:45 AM JST | 12:30 AM - 12:45 AM UTC

Introduction

9:45 AM - 10:08 AM JST | 12:45 AM - 1:08 AM UTC

[U05-01] International Astro-Bioscience Research Center

★Invited Papers

*Yukio Isozaki[1] (1.Department of Earth Science and Astronomy, Multi-disciplinary Sciences - General Systems Studies, Graduate School of Arts and Sciences, The University of Tokyo)

10:08 AM - 10:30 AM JST | 1:08 AM - 1:30 AM UTC

[U05-02] Study of coupling processes in the solar-terrestrial system

★Invited Papers

*Mamoru Yamamoto[1], Hiroyuki Hashiguchi[1], Tatsuhiro Yokoyama[1], Hiroshi Miyaoka[2], Yasunobu Ogawa[2], Kazuo Shiokawa[3], Satonori Nozawa[3], Akimasa Yoshikawa[4], Toshitaka Tsuda[5,1] (1.Research Institute for Sustainable Humanosphere, Kyoto University, 2.National Institute of Polar Research, 3.Institute for Space-Earth Environmental Laboratory, Nagoya University, 4.International Center for Space Weather Science and Education, Kyushu University, 5.Research Organization of Information and Systems)

International Astro-Bioscience Research Center

*Yukio Isozaki[1]

1. Department of Earth Science and Astronomy, Multi-disciplinary Sciences - General Systems Studies, Graduate School of Arts and Sciences, The University of Tokyo

“Large Scientific Research Projects” under national strategic perspectives naturally comprise multidisciplinary efforts of Japanese scientists, by aggregating cutting-edge technology and knowledge to tackle research issues that had yet to be explored by anyone and bringing about dramatic development of those fields. Such projects will continue to necessiate strategic, systematic promotion through a long-term outlook, while garnering the support and understanding of the general public and society overall. As to the earth and planetary sciences in Japan during the late 20th and early 21st centuries, most researches focused on individual fields, such as studies on atmosphere, ocean, surface environment, solid earth (plate, plume, geomagnetism etc.). Nonetheless, in the views from abroad, most of efforts appear to have been concentrated in transplanting ideas and technology from western communities without nurturing domestic original ones. Under the limited financial budget of Japan, there is one hopeful possibility in earth science, which enables multispheric system studies involving core, mantle, surface crust, biosphere, and outer space. The most advantageous estate in Japan is the “earth history samples” collected from various countries during the last 30 years bu Japanese earth scientists. As there is non-such analogue in the rest of the world, we should build a new project centered by a research center “Astro-Bioscience”, which promote intimate network with many countries centered in Japan in order to reveal the entire history of the Earth and life. This project is directly linked to the sustainability of our planet, to which all humans on the Earth are facing today.

Keywords: Astro-Bioscience, Earth history

©2019. Japan Geoscience Union. All Right Reserved.

Study of coupling processes in the solar-terrestrial system

*Mamoru Yamamoto[1], Hiroyuki Hashiguchi[1], Tatsuhiro Yokoyama[1], Hiroshi Miyaoka[2], Yasunobu Ogawa[2], Kazuo Shiokawa[3], Satonori Nozawa[3], Akimasa Yoshikawa[4], Toshitaka Tsuda[5,1]

1. Research Institute for Sustainable Humanosphere, Kyoto University, 2. National Institute of Polar Research, 3. Institute for Space-Earth Environmental Laboratory, Nagoya University, 4. International Center for Space Weather Science and Education, Kyushu University, 5. Research Organization of Information and Systems

Energy from the sun is divided into radiation and solar wind (high-speed particles), which are maximum at the equatorial and polar regions, respectively. We study the flow of the energy and materials in the whole atmosphere by establishing following two large atmospheric radars at these singular points, and global observation network.
(1) Equatorial fountain
The energy and material flows that occur in all height regions of the equatorial atmosphere are named as "Equatorial Fountain." These processes from the bottom also cause various effects in the upper atmosphere. We establish Equatorial MU Rdar (EMU radar) in Indonesia as main instrument for the studies.
(2) Energy inputs into polar upper atmosphere and its response
The energy/particle inflow results in auroral Joule heating and ion drag of the atmosphere. The ion outflow from the polar ionosphere controls ambient plasma constituents in the magnetosphere. We will contribute the international EISCAT_3D radar project that has started in northern Scandinavia since 2017.
(3) Global network of observation and data
We develop a global observation network of compact radio and optical remote sensing equipment from the equator to polar region. Data from the observations will be archived and utilized by the data exchange framework of IUGONET.

This project was selected as one of important projects in both Masterplan 2014 and 2017. It was also selected as a new project in the roadmap 2014 by the Japanese Ministry of Education, Culture, Sports, Science and Technology. We continue proposing the project to Masterplan 2020.

Keywords: Equatorial MU Radar, EISCAT_3D Radar, International Observation Network, IUGONET

©2019. Japan Geoscience Union. All Right Reserved.

[J] Oral | U (Union)：Union

Mon. May 27, 2019 10:45 AM - 12:15 PM JST | Mon. May 27, 2019 1:45 AM - 3:15 AM UTC | 101 1F

[U-05] Large-scale Research Projects: Master Plan 2020 and its beyond

convener:Eiichi Tajika(Department of Earth and Planetary Science, Graduate School of Science, The University of Tokyo), Shigeko Haruyama(Department of Environmental Science, Graduate School of Bioresouces,Mie University), Ryoichi Fujii(Research Organization of Information and Systems), Hodaka Kawahata(Atmosphere Ocean Research Institute, the University of Tokyo), Chairperson:Shigeko Haruyama, Hodaka Kawahata

Many of top sciences in Earth and Planetary Science (EPS) are progressed by big projects that require 10 billion JPY or more in 10 years or so. In order to realize such projects, we need an arena where they are brushed up through critical reviews among various fields in EPS. Deeper mutual understandings through serious discussions there will enable us to reach a final consensus on the priorities of the projects. The Master Plan (MP) of Large-scale Research issued by the Science Council of Japan strongly motivates us to follow the process described above. Indeed some of the selected projects have been funded by the Ministry of Education, Culture, Sports, Science & Technology since 2010.
Since the current Master Plan 2017 is going to be thoroughly revised in 2020, we propose to hold a session in which large-scale research projects are concisely introduced and critically reviewed. This session is to be convened by JpGU and EPS Committee of Science Council of Japan.

10:45 AM - 11:08 AM JST | 1:45 AM - 2:08 AM UTC

[U05-03] Development of the global earth observation system using satellites

★Invited Papers

*Shinichi Sobue[1], Yoshiaki HONDA[3], Shuichi Rokugawa[2], Akira Iwasaki[2], Nobuhiro Takahashi[4], Yukari Takayabu[2], Riko Oki[1], Toshiyoshi Kimura[1], Teruyuki Nakajima[1], Takeo Tadono[1], Kosuke Yamamoto[1] (1.Japan Aerospace Exploration Agency, 2.University of Tokyo, 3.Chiba University, 4.Nagoya University)

11:08 AM - 11:31 AM JST | 2:08 AM - 2:31 AM UTC

[U05-04] Promotion of Scientific Research on Climate and Earth System Sciences Using Aircrafts

★Invited Papers

*Makoto Koike[1,2] (1.Department of Earth and Planetary Science, Graduate School of Science, The University of Tokyo, 2.The Meteorological Society of Japan)

11:31 AM - 11:54 AM JST | 2:31 AM - 2:54 AM UTC

[U05-05] Global deployment of Deep Argo floats toward accurate prediction of future climate and ecosystem changes

★Invited Papers

*Toshiyuki Hibiya[1] (1. Department of Earth and Planetary Science, Graduate School of Science, The University of Tokyo)

11:54 AM - 12:15 PM JST | 2:54 AM - 3:15 AM UTC

[U05-06] A new aspect of the polar science: integrated observations of the ice sheet mass loss for better prediction of the sea level rise

★Invited Papers

*Takuji Nakamura[1], Shin Sugiyama[2], Ayako Abe-Ouchi[3], Teruo Aoki[4], Yoshifumi Nogi[1], Takeshi Tamura[1] (1.National Institute of Polar Research, 2.Institute of Low Temperature Science, Hokkaido Univ., 3.Atmosphere and Ocean Research Institute, the University of Tokyo, 4.The Graduate School of Natural Science and Technology, Okayama University)

Development of the global earth observation system using satellites

*Shinichi Sobue[1], Yoshiaki HONDA[3], Shuichi Rokugawa[2], Akira Iwasaki[2], Nobuhiro Takahashi[4], Yukari Takayabu[2], Riko Oki[1], Toshiyoshi Kimura[1], Teruyuki Nakajima[1], Takeo Tadono[1], Kosuke Yamamoto[1]

1. Japan Aerospace Exploration Agency, 2. University of Tokyo, 3. Chiba University, 4. Nagoya University

Global efforts to solve social and scientific issues related to the earth environment are ongoing globally and it is critical to develop and operate a global earth observation system. Especially, as also shown in “Yume road map”, the satellite-based observation system is indispensable tool from present to future. However, the Earth Observation Satellite, which simultaneously realizes the two functions of both scientific and practical observation, such as the GCOM series and the TRMM / GPM series, is marked as the "advancement of other remote sensing and sensor technologies" and there is no long-term plan beyond 2020 in the chart of the space basic program.

"Advanced Earth Science Research Working Group (WG)", one of the working groups of Task Force Remote Sensing Subcommittee (TF; 23 academic societies + 2 organizations), we created the "Earth Observation Grand Design" which shows the strategies for realizing the proposals of the Science Council of the scientific community and various institutions concerning Earth Observation after the successful endorsement at the TF general assembly. The purpose of this “Earth Observation Grand Design” is aimed at proposing Earth observation mission towards the space related ministries and agencies’ with brining consensus of new earth observation satellites missions from the academic societies and organizations in TF.

In the Earth Observation Grand Design published in 2018, the following five missions are proposing through a simple selection / review process as a mission to be realized in the short term, in addition to the mission described in the chart of space basic plan.

A) Mission on elucidating global climate change / water circulation mechanism

B) Mission for forest biomass estimation

C) Mission to reduce short life air pollution

D) Mission concerning elucidation of cloud and rainfall process

E) Mission concerning monitoring and elucidation of global environmental change (global radiation enforcement force and ecosystem change affecting global warming)

Based on the consent of the TF Executive Committee in late 2018, as a first step to evolve the above selection process with revision of Earth Observation Grand Design, we called for new satellite earth observation missions from a wider field and selected those missions, including ongoing satellites series missions such as high resolution optical and SAR mission, GHGs missions and geostationary observation missions, while ensuring fairness and transparency. We will make a primary selection of the proposal and

©2019. Japan Geoscience Union. All Right Reserved.

will discuss further by JpGU 's special session coming. As a result, we will select additional missions as well as deepen consideration of promising proposals and establish a feedback process from experts toward realizing the mission.

By using those proposed missions, global climate change and water circulation mechanism will be studied to solve various social problems such as improvement of accuracy of global warming prediction, high accuracy of weather forecast, disaster, etc. These missions will also be expected to contribute to the achievement of Society 5.0 and UN / SDGs that compatibility of social tasks.

Keywords: Earth observation, Space basic plan, climate change

©2019. Japan Geoscience Union. All Right Reserved.

Promotion of Scientific Research on Climate and Earth System Sciences Using Aircrafts

*Makoto Koike[1,2]

1. Department of Earth and Planetary Science, Graduate School of Science, The University of Tokyo, 2. The Meteorological Society of Japan

The aim of this proposal is to promote climate and earth system research in the area of atmospheric science, oceanography, glaciology, volcanology, and ecology by introducing a dedicated aircraft for Earth observations.

The Earth’s environment has been changing rapidly, particularly as manifested by global warming, and the changes are imposing large impacts on the fundamental structures of our lives, including socio-economic activities and supplies of water and food. It is critically important to fully understand the current status of the changes and to investigate the controlling processes, in order to predict future changes and protect human society and ecosystems from serious damage. At present, direct atmospheric observations by aircraft are lacking in important geographical regions; they are needed for understanding greenhouse gases, aerosol-cloud interactions, and the hydrologic cycle, including predictions of typhoons and torrential downpours. Japan lacks an aircraft dedicated to scientific measurements, so Japanese scientists have been obliged to charter commercial aircraft for their experiments. Therefore it has been difficult to plan and conduct systematic aircraft experiments, which are indispensable for studies of climate and Earth system science.

In this study, we plan to acquire a dedicated aircraft and outfit it with an observation system that will be designed and utilized by scientists from a variety of fields and institutions on a long-term basis. Our aim is to enable the systematic planning of next-generation Earth observations and research activities by operating instrumented aircraft platforms on a long-term basis and attaining the highest levels of scientific outcome and impacts. We plan to provide today’s scientists and the next generation of scientists with exciting opportunities to use aircraft platforms to pursue new scientific ideas and to develop and use new technologies and methodologies. It is also planned to extend these new research opportunities to foreign scientists so that this Japanese system serves as a center of research and promotes Earth observations throughout Asia. The basic scientific knowledge obtained by this program will be made public in order to contribute to the welfare of world societies. All the processes involved in this research plan, including organizing scientists and activities, selection and scheduling of instruments, soliciting proposals, making field measurements, data archiving, and using the data, will be transparent to all scientific communities.

We plan to use the Gulfstream IV type aircraft as rental from a private company such as Diamond Air Service. The total cost is 15.5 billion Japanese yen for ten year project. The Institute for Space-Earth Environmental Research of Nagoya University has established the “Center for Orbital and Suborbital Observations” in order to play a central role in aircraft observations. This center will organize and manage activities related to aircraft observations in close cooperation with scientists from several institutions in Japan, such as the University of Tokyo, Chiba University, the Meteorological Research Institute, the National Institute for Environmental Studies, the National Institute of Polar Research, and the National Institute of Information and Communications Technology. We can receive advice and support aeronautical section of JAXA on determination of test plan and flight conditions in the flight test to realize more efficient and safety flight experiment. Through this study, we will contribute to SDSs and Future

©2019. Japan Geoscience Union. All Right Reserved.

Earth project.

Keywords: climate, Earth system, aircraft observations, atmosphere, ocean, ecosystem

©2019. Japan Geoscience Union. All Right Reserved.

Global deployment of Deep Argo floats toward accurate prediction of future climate and ecosystem changes

*Toshiyuki Hibiya[1]

1. Department of Earth and Planetary Science, Graduate School of Science, The University of Tokyo

Long-term assessment and conservation of marine bio-resources are crucial in securing the global food supply. Given the very rapid warming of global climate at present, however, marine environmental changes could be a very serious threat to human beings. Actually, acidification of surface seawater and decrease of dissolved oxygen in subsurface layers have been detected recently; if these trends are significant, an irreversible global/oceanic change in a longer time scale would be realistic. The deep oceanic circulation plays a key role in the marine environmental change. A recent numerical model suggests a global temperature change of more than 4°C and a decrease of marine biological production by 20% under a condition of weakened deep oceanic circulation. The actual feature and mechanism of the deep oceanic circulation are still largely unknown, and the comprehensive observation of deep sea would be also important in the assessment of oceanic ecosystem.

The Oceanographic Society of Japan submitted a research proposal in association with the 16 academic societies in theFisheries/Oceanography Research Liaison Counciland the Paleontological Society of Japan.The proposal aims to unveil the deep oceanic circulation, which is currently acting as the bottleneck in reproducingpast and future climate variability and global environmental changes in numerical models.More specifically, the proposal focuses on observation of turbulence in the deep sea with a turbulence sensor attached to the deep-sea Argo float (target depth more than 4000 meters) or "Deep NINJA". More than 10 floats of this type with conventional temperature and salinity sensors are in actual operation in the Southern Ocean. By deploying approximately 1000 floats, observation of temperature, salinity and turbulence will be conducted globally from the ocean surface to seafloor. The obtained data will be incorporated into a coupled atmosphere-ocean global climate model, and the simulation conducted using the leading Japanese supercomputer facility would yield an accurate reproduction and prediction of the past and future climate. Responses of biological community to the reproduced paleo-environmental changes can be validated by paleontological data such as microfossil record in sediment core, and the validation further refine the model prediction. A far more accurate prediction of future climate, marine biological production and marine bio-resources will be achieved through the proposed research project.

Keywords: Deep Argo floats, Turbulence in the deep ocean, Deep ocean circulation, Prediction of future climate changes, Prediction of future ecosystem changes

©2019. Japan Geoscience Union. All Right Reserved.

A new aspect of the polar science: integrated observations of the ice sheet mass loss for better prediction of the sea level rise

*Takuji Nakamura[1], Shin Sugiyama[2], Ayako Abe-Ouchi[3], Teruo Aoki[4], Yoshifumi Nogi[1], Takeshi Tamura[1]

1. National Institute of Polar Research, 2. Institute of Low Temperature Science, Hokkaido Univ., 3. Atmosphere and Ocean Research Institute, the University of Tokyo, 4. The Graduate School of Natural Science and Technology, Okayama University

Recently the global environmental change is of great interest for the governments and general public, as well as scientists on the earth and planets. The Arctic and the Antarctic regions significantly affect global environment and also provide invaluable information on its variation. In the Arctic region, for example, temperature increase due to the global warming is the largest on the globe. The climate change is most significantly emerging which causes change of ecology, human economic activity and life. On the other hand, very little is known on the response of the huge Antarctic ice sheet to the global warming, and hence a possible change in Antarctic region on a global scale and its prediction are of greatest interest. Variations in both polar regions are not independent but connected through the ocean and atmosphere circulations, and therefore it is necessary to consider them to be one unified system. Moreover, the Arctic and Antarctic regions are the best observation and/or investigation field for space/planetary sciences, atmospheric/hydrospheric sciences, and solid earth sciences, indicating that the polar regions are important windows for earth and planetary sciences.

Greenland Ice Sheet amounts about 9 % of total ice mass on the glove, and its mass loss is becoming faster due to the rapid warming in the Arctic region. This causes acceleration of the global sea level rise. On the other hand, the Antarctic Ice Sheet, which as about an order larger mass, also indicating a significant mass loss in the western part. Once the East Antarctic Ice Sheet also started to melt quickly, which has much larger mass than the West Antarctic Ice Sheet, the sea level rise would become fatal. Thus, it is very important to understand the current variation of the ice sheets, which could cause more than 60 m of sea level rise as a total amount, and monitor its trend.

This proposal focuses on the sea level rise due to the ice sheet mass loss. We propose to carry out integrated observations at remote sites in the Antarctica and Greenland, by deploying new technical challenge with un-manned and remote controlled system. Then, by unifying in-situ observations, detailed analyses, satellite observations and numerical modelings, we plan to clarity variations of the ice sheet and ocean in the past and at present, then improve the forecast of future sea level rise, which might rapidly proceed even within this century.

Keywords: Polar Science, Arctic, Antarctic, Sea level rise, Ice sheet

©2019. Japan Geoscience Union. All Right Reserved.

[J] Oral | U (Union)：Union

Mon. May 27, 2019 1:45 PM - 3:15 PM JST | Mon. May 27, 2019 4:45 AM - 6:15 AM UTC | 101 1F

[U-05] Large-scale Research Projects: Master Plan 2020 and its beyond

convener:Eiichi Tajika(Department of Earth and Planetary Science, Graduate School of Science, The University of Tokyo), Shigeko Haruyama(Department of Environmental Science, Graduate School of Bioresouces,Mie University), Ryoichi Fujii(Research Organization of Information and Systems), Hodaka Kawahata(Atmosphere Ocean Research Institute, the University of Tokyo), Chairperson:Hodaka Kawahata, Eiichi Tajika

Many of top sciences in Earth and Planetary Science (EPS) are progressed by big projects that require 10 billion JPY or more in 10 years or so. In order to realize such projects, we need an arena where they are brushed up through critical reviews among various fields in EPS. Deeper mutual understandings through serious discussions there will enable us to reach a final consensus on the priorities of the projects. The Master Plan (MP) of Large-scale Research issued by the Science Council of Japan strongly motivates us to follow the process described above. Indeed some of the selected projects have been funded by the Ministry of Education, Culture, Sports, Science & Technology since 2010.
Since the current Master Plan 2017 is going to be thoroughly revised in 2020, we propose to hold a session in which large-scale research projects are concisely introduced and critically reviewed. This session is to be convened by JpGU and EPS Committee of Science Council of Japan.

1:45 PM - 2:08 PM JST | 4:45 AM - 5:08 AM UTC

[U05-07] New frontier of Earth, Space and Life Sciences pioneered by the innovative developments of new-generation mass spectrometry

★Invited Papers

*Kentaro Terada[1] (1.Department of Earth and Space Science, Graduate School of Science, Osaka University)

2:08 PM - 2:31 PM JST | 5:08 AM - 5:31 AM UTC

[U05-08] Building of archive and curating system for astrogeoscience materials

★Invited Papers

*Tsuyoshi Komiya[1] (1.Department of Earth Science & Astronomy Graduate School of Arts and Sciences The University of Tokyo)

2:31 PM - 2:54 PM JST | 5:31 AM - 5:54 AM UTC

[U05-09] Innovative 4D imaging of subduction-zones through real-time observatories, ultra-deep drilling and high-pressure experiments

★Invited Papers

*Masataka Kinoshita[1], Naoshi Hirata[1], Masanao Shinohara[1], Tetsuo Irifune[2], Hiroyuki Kagi[7], Teruyuki Kato[3], Shigeaki Ono[4], Katsuyoshi Michibayashi[6], Natsue Abe[4], Fumio Inagaki[4], Kentaro Omura[5], Kazushige Obara[1] (1.Earthquake Research Institute, University of Tokyo, 2.Ehime University, 3.Hot Springs Research Institute, 4.JAMSTEC, 5.NIED, 6.Nagoya Univ., 7.Geochemical Research Center, Univ. Tokyo)

2:54 PM - 3:15 PM JST | 5:54 AM - 6:15 AM UTC

[U05-10] Construction of the Cooperative Research Infrastructure for Intelligent Muography in Earth and Planetary Sciences, Other Sciences, and Society

★Invited Papers

*Hiroyuki Tanaka[1] (1.Earthquake Research Institute, the University of Tokyo)

New frontier of Earth, Space and Life Sciences pioneered by the innovative developments of new-generation mass spectrometry

*Kentaro Terada[1]

1. Department of Earth and Space Science, Graduate School of Science, Osaka University

So far, various mass spectrometers, which can determine elemental abundance, isotopic composition and molecular weight of macromolecule have greatly contributed to understanding of the Earth, Space and Life sciences. Above all, high-precision isotopic measurements of natural samples using sensitive mass spectrometers provide us an important clue to decipher the origin and evolution of the Earth and/or Solar system. Whereas, it is also known that many unresolved scientific issues are still remained because of technical restrains of “general-purpose” commercially-available mass spectrometers. Therefore, the “science-oriented” development of mass spectrometer has been highly desired.

Here, Osaka University, Geochemical Society Japan, and Mass Spectrometry Society of Japan collectively propose the ideas of an innovative development of mass spectrometers that are specialized for the “Scientific issues”, which consists of two directions; (1) high-sensitive and high-spacial resolution and/or (2) reduction in size and weight with high-mass resolution. These innovative development conducted by Osaka University would pioneer a new horizon of the Earth and Planetary Science such a decipher of the pre-solar history, on-site real–time geo-cosmo-chemistry so on. These technical innovation of mass spectrometers designed for the cruel Earth and space Science would also promote the other science such as agriculture, material science and life science, so on.

Keywords: Mass spectrometer, Isotope measurement, innovative development

©2019. Japan Geoscience Union. All Right Reserved.

新しいサイエンスへの挑戦。他分野への波及効果

前太陽系史を含む、太陽系史の高精度解読
(高空間分解能、高感度磁場型CQHによる)

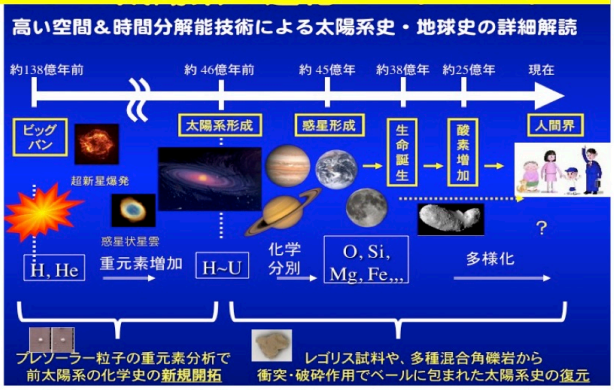

オンサイト・リアルタイム同位体分析
(小型飛行時間型MULTUMによる)

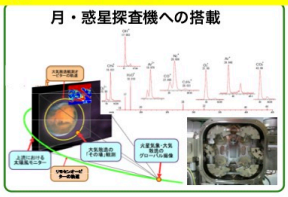

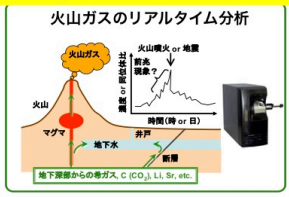

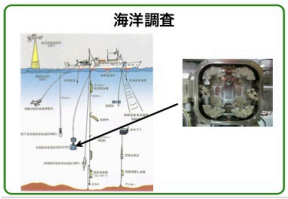

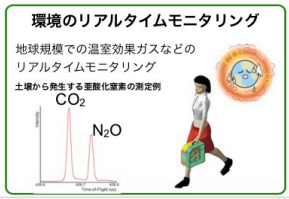

異分野への応用

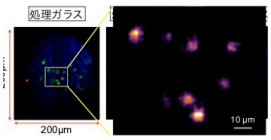

有機材料などの高品質データ評価
（工学、材料科学への応用）

呼気、唾液、歯肉溝滲出液
などオンサイト診断
（医学、歯学への応用）

土壌のリアルタイムモニター
(農学への応用)

©2019. Japan Geoscience Union. All Right Reserved.

Building of archive and curating system for astrogeoscience materials

*Tsuyoshi Komiya[1]

1. Department of Earth Science & Astronomy Graduate School of Arts and Sciences The University of Tokyo

We, Geological Society of Japan, propose “Building of archive and curating system for astrogeoscience materials” for Master Plan 2020.

Approximately 150 years passed after foundation of modern science in Japan. The Japanese researchers collected great amounts of terrestrial samples and meteorites, from over the world as well as Japan, using national and private funds during this period. Natural history is traditionally regarded as important in European countries and USA, but it is neglected more or less in Japan. As a result, Japan is far behind the European countries and USA as regards the preservation of the samples for future work, and curating system of the samples.

However, many paradigms were born from the well-organized sample archive such as Burgess Shale collection for the Cambrian Explosion and recent discovery of deep-sea economic deposit, and so on.

In addition, social responsibility of science is often emphasized in many European courtiers and USA: Open access of scientific journals, data and original samples, and guarantee of reliability of original data. However, Japan is also far behind other countries including China regards the open access.

We would like to propose building of archive and curating system for astrogeoscience materials for the future works and social responsibility.

This program is proposed by Geological society of Japan, and supported by AIST (Geological survey of Japan), National Institute of Polar Research, National Museum of Nature and Science, JAMSTEC, Kanagawa Prefectural museum of Natural History, and departments of Earth and Planetary sciences of 28 universities.

Keywords: Astrogeoscience materials, Archive and curating system

©2019. Japan Geoscience Union. All Right Reserved.

Innovative 4D imaging of subduction-zones through real-time observatories, ultra-deep drilling and high-pressure experiments

*Masataka Kinoshita[1], Naoshi Hirata[1], Masanao Shinohara[1], Tetsuo Irifune[2], Hiroyuki Kagi[7], Teruyuki Kato[3], Shigeaki Ono[4], Katsuyoshi Michibayashi[6], Natsue Abe[4], Fumio Inagaki[4], Kentaro Omura[5], Kazushige Obara[1]

1. Earthquake Research Institute, University of Tokyo, 2. Ehime University, 3. Hot Springs Research Institute, 4. JAMSTEC, 5. NIED, 6. Nagoya Univ., 7. Geochemical Research Center, Univ. Tokyo

In 2017, we submitted a proposal for the Masterplan for Advancing Major Academic Research, entitled “Earthquake and volcanic eruption prediction science through integrated onland, seafloor and ocean drilling observations -Challenge of the spatio-temporal informatics in subduction zones- “, to the Science Council of Japan. Here, we integrate this plan with the ocean-buoy GNSS observatory project and high-pressure (down to the mantle) experiments project to create a high-precision, time-lapse imaging around the subduction zones, in order to delineate the earthquake and volcanic eruption scenarios and eventually to predict the far fate of the Earth and ocean. For this purpose, we propose to construct a real-time observatory network for earthquake and crustal deformation monitoring through seafloor cables and GNSS buoys. We also propose to obtain (and try to reproduce) the state and property around the subduction zones and in the mantle, by means of ultra-deep drilling and ultra-high pressure experiments. We are extremely interested in the mantle rheology, which is primarily controlled by the thermal structure and the abundance in volatiles (e.g. water), which we believe is only possible by integration of geophysical observation and by ground-truthing, insitu experiments.

Keywords: Seafloor cable network, Ultra-deep drilling, High pressure experiments, GNSS buoy, Subduction zone, Mantle rheology

©2019. Japan Geoscience Union. All Right Reserved.

Construction of the Cooperative Research Infrastructure for Intelligent Muography in Earth and Planetary Sciences, Other Sciences, and Society

*Hiroyuki Tanaka[1]

1. Earthquake Research Institute, the University of Tokyo

Since 10 years ago when Japan first used muography to visualise the internal structure of volcanoes for the first time (with elementary particle originated in the universe), this technique has been evolving. In 2019, at least 7 ventures were generated in Canada, Finland, France, Israel, Spain, UK, and USA. Japan still holds the technological initiative in this field, and based on this advantageous position, we will construct the cooperative research infrastructure for intelligent muography in earth and planetary sciences, other sciences, and society by adding the artificial intelligent function.

Keywords: muography

©2019. Japan Geoscience Union. All Right Reserved.

[J] Oral | U (Union)：Union

Mon. May 27, 2019 3:30 PM - 5:00 PM JST | Mon. May 27, 2019 6:30 AM - 8:00 AM UTC | 101 1F

[U-05] Large-scale Research Projects: Master Plan 2020 and its beyond

convener:Eiichi Tajika(Department of Earth and Planetary Science, Graduate School of Science, The University of Tokyo), Shigeko Haruyama(Department of Environmental Science, Graduate School of Bioresouces,Mie University), Ryoichi Fujii(Research Organization of Information and Systems), Hodaka Kawahata(Atmosphere Ocean Research Institute, the University of Tokyo), Chairperson:Eiichi Tajika, Shigeko Haruyama

Many of top sciences in Earth and Planetary Science (EPS) are progressed by big projects that require 10 billion JPY or more in 10 years or so. In order to realize such projects, we need an arena where they are brushed up through critical reviews among various fields in EPS. Deeper mutual understandings through serious discussions there will enable us to reach a final consensus on the priorities of the projects. The Master Plan (MP) of Large-scale Research issued by the Science Council of Japan strongly motivates us to follow the process described above. Indeed some of the selected projects have been funded by the Ministry of Education, Culture, Sports, Science & Technology since 2010.
Since the current Master Plan 2017 is going to be thoroughly revised in 2020, we propose to hold a session in which large-scale research projects are concisely introduced and critically reviewed. This session is to be convened by JpGU and EPS Committee of Science Council of Japan.

3:30 PM - 3:53 PM JST | 6:30 AM - 6:53 AM UTC

[U05-11] Consortium for Planetary Exploration

★Invited Papers

*Yoshi-Yuki Hayashi[1], Shigeto Watanabe[2,5], Taishi Nakamoto[3,4] (1.Department of Planetology/CPS, Graduate School of Science, Kobe University, 2.SGEPSS, 3.The Japanese Society for Planetary Sciences, 4.Dept. of Earth and Planetary Sciences, Tokyo Institute of Technology, 5.Hokkaido Information University)

3:53 PM - 4:16 PM JST | 6:53 AM - 7:16 AM UTC

[U05-12] Japanese contribution to CAESAR: comet astrobiology exploration sample return

★Invited Papers

*Tomoki Nakamura[1], Kazuhiko Yamada[2], Yoshihiro Furukawa[1], Yuki Kimura[3], Aki Takigawa[4], Tomohiro Usui[2], Hitoshi Kuninaka[2], Team CAESAR SRC team (1.Tohoku University, 2.ISAS/JAXA, 3.Hokkaido University, 4.Kyoto University)

4:16 PM - 4:38 PM JST | 7:16 AM - 7:38 AM UTC

[U05-13] Strategic Mars exploration: Orbiter and EDL demonstration mission for space weather, climate, and aquatic environment

★Invited Papers

*Kanako Seki[1], Shigeto Watanabe[2], Taishi Nakamoto[3], Naoki Terada[4], Atsushi Yamazaki[5], Ayako Matsuoka[5], Tomohiro Usui[5], Yasuhito Sekine[3], Kazuhisa Fujita[5], Shoichiro Yokota[6], Satoshi Kasahara[1], Yoshifumi Saito[5], Hiromu Nakagawa[4], Atsushi Kumamoto[4], Hiroyuki Maezawa[7], Mars Orbiter and EDL Technology Demonstration Mission Planning Team (1.Graduate School of Science, University of Tokyo, 2.Department of Cosmosciences, Hokkaido University, 3.Tokyo Institute of Technology, 4.Graduate School of Science, Tohoku University, 5.ISAS, JAXA, 6.Graduate School of Science, Osaka University, 7.Department of Physical Science, Osaka Prefecture University)

4:38 PM - 4:53 PM JST | 7:38 AM - 7:53 AM UTC

Discussion

Consortium for Planetary Exploration

*Yoshi-Yuki Hayashi[1], Shigeto Watanabe[2,5], Taishi Nakamoto[3,4]

1. Department of Planetology/CPS, Graduate School of Science, Kobe University, 2. SGEPSS, 3. The Japanese Society for Planetary Sciences, 4. Dept. of Earth and Planetary Sciences, Tokyo Institute of Technology, 5. Hokkaido Information University

Consortium for Planetary Exploration is planed to establish a set of distributed infrastructures in the fields of solar system sciences in Japan to plan, promote, and realize Japanese solar system exploration missions by supporting, cooperating and/or leading the mission implementing agency, JAXA, from the viewpoint of sciences, and also promoting international corporations among other organizations in the world, and help the science community maximize scientific outcomes from those missions. The consortium is to fulfill the lack of scientific leaders of such fields as data reduction, simulation modeling, instrument development, material analyses who have good experience and expertise both of the solar system sciences and the mission planning and driving, and also fundamental environments for research and development. More importantly, the focus of the consortium plan is not only to improve the number of researchers and the fundamental environments, but to cultivate graduate students and young scientist to be working on those places. The requirement for the consortium will be briefly summarized in the presentation.

Keywords: planetary exploration, infrastructure for research and dvelopment , cultivating human resources

©2019. Japan Geoscience Union. All Right Reserved.

Japanese contribution to CAESAR: comet astrobiology exploration sample return

*Tomoki Nakamura[1], Kazuhiko Yamada[2], Yoshihiro Furukawa[1], Yuki Kimura[3], Aki Takigawa[4], Tomohiro Usui[2], Hitoshi Kuninaka[2], Team CAESAR SRC team

1. Tohoku University, 2. ISAS/JAXA, 3. Hokkaido University, 4. Kyoto University

Comet is the most ideal target for Japanese planetary scientists who investigate the origin of the solar systems, particularly the origin of habitable planets. However, the mission scale of the comet sample return exceeds the Japanese space mission capability. Thus, the involvements to an international mission is more realistic strategy to share the science values of cometary sample return. A NASA NEW Frontier 4 cometary sample return proposal team requested JAXA to participate in the proposal, providing key devices and knowledge which have acquired in previous successful missions. This Master Plan proposal explains the science and engineering contributions to the NEW Frontier 4 proposal from Japan so far and in the future and how this mission provides valuable opportunities to the Japanese planetary science community.

Comets contain minerals, volatiles, and organic compounds that formed before the formation of the solar system. Thus, the cometary sample is a key material to access the origin of our solar system and the origin of life’s building blocks in space. Comet astrobiology exploration sample return (CAESAR) is the first mission to bring the macro cometary materials to the Earth without significant alteration. Japanese planetary science community have a strategy to promote the missions which investigate the formation of habitable planetary environments and its continuation. The target of CAESAR fits the strategy and particularly, investigates the materials which formed our planetary system and the origin of prebiotic organic compounds. This mission is one of the two finalist of NASA New Frontier 4 mission that has been selected from 12 proposals. JAXA is a major partner in the CAESAR mission, developing a sample return capsule based on the heritage of Hayabusa mission. Japanese sciences have also involved in the proposal planning and will be responsible for several sample analysis. The sample return of CAESAR is the most challenging among of the history of human’s sample return mission, trying to get the most abundant sample form the most far objects with the lowest temperature. This provides significant science values and also provides significant engineering heritage for Japanese communities

The early evolution of solar system stars from the conversion of interplanetary dusts into planetary materials. Hayabusa and Hayabusa 2 have strategy to investigate materials formed in the inner region of the solar system. CAESAR have complementary strategy to investigate the samples form outer region of the solar system in which material before the formation of the solar system present abundantly than inner solar system. In the astrobiological motivation, CAESAR has complementary strategy to Hayabusa 2 mission. CAESAR investigates cometary organics which have been provided mostly with micrometeorites to the Earth whereas Hayabusa 2 investigates organic compounds which have been provided mostly with meteorites. These achievements will contribute significantly to understand the origin of solar system and the origin of prebiotic organic compounds on the Earth.

CAESAR-JAPAN is working as a preproject (Phase A), developing components of sample return capsule and revising the proposal. The final selection for NASA New Frontier 4 will be open this summer. After the first step analysis, the CAESAR sample will be distributed to international science community including Japan. This will contribute significantly in planetary science, astrobiology, astronomy, and related

©2019. Japan Geoscience Union. All Right Reserved.

disciples.

Keywords: Comet sample return

©2019. Japan Geoscience Union. All Right Reserved.

Strategic Mars exploration: Orbiter and EDL demonstration mission for space weather, climate, and aquatic environment

*Kanako Seki[1], Shigeto Watanabe[2], Taishi Nakamoto[3], Naoki Terada[4], Atsushi Yamazaki[5], Ayako Matsuoka[5], Tomohiro Usui[5], Yasuhito Sekine[3], Kazuhisa Fujita[5], Shoichiro Yokota[6], Satoshi Kasahara[1], Yoshifumi Saito[5], Hiromu Nakagawa[4], Atsushi Kumamoto[4], Hiroyuki Maezawa[7], Mars Orbiter and EDL Technology Demonstration Mission Planning Team

1. Graduate School of Science, University of Tokyo, 2. Department of Cosmosciences, Hokkaido University, 3. Tokyo Institute of Technology, 4. Graduate School of Science, Tohoku University, 5. ISAS, JAXA, 6. Graduate School of Science, Osaka University, 7. Department of Physical Science, Osaka Prefecture University

This presentation will report on outline of the strategic Mars exploration with an orbiter and EDL technology demonstration to investigate the space weather, climate, and aqua-environment at Mars, which is to be submitted to the Master Plan 2020 of the Science Council of Japan. The research project was previously proposed from Society of Geomagnetism and Earth, Planetary and Space Sciences (SGEPSS) as “Exploration of the space weather and climate at Mars,” which is listed in the Master Plan 2017 of the Science Council of Japan as the large scientific research project number 79, category number 24-2. The project has been developed since then through discussions over larger related academic communities including the planetary science. Here we propose the renewed project as a joint proposal between SGEPSS and the Japanese Society for Planetary Sciences.
In the roadmap of the solar system exploration in coming 20 years, understanding of the formation and evolution of the habitable environment is regarded as an essential goal of the planetary science. Among various targets, Mars is an idealtarget for comparative planetology and astrobiological researches, since it once had a habitable environment with an abundant water on its surface. Mars sample return mission with international collaborations is under planning for the 2030’s. In order for Japan to play a leading role there,implementation of our original strategic Mars exploration missions in 2020’s is under vital demands from both the scientific and technological points of view.
As an important step in the Japanese strategic Mars exploration to strengthen our ability to contribute the future Martian exploration scenario by ISECG (international space exploration coordination group), this project combines the orbiter and EDL (entry, descending, and landing) technology demonstration, focusing on the responses of Martian environment to extreme solar variations and its co-evolution with subsurface aquatic environment.The mission will elucidate influence of the active sun on the habitable environment and provide the basis for our future landing exploration in 2030’s. In particular, by investigating the instantaneous response to extreme solar variations, which can be usual conditions in ancient sun, we will obtain the key knowledge to understand how atmospheric escape to space contributes to the loss of habitable environment from ancient Mars. The project will also provide knowledge about Martian radiation environment and will achieve demonstration of key technologies for the future landing exploration as well as important information of possible landing sites.In order to achieve the goal, we identified three observational requirements and 11 model payloads for the mission. In the presentation, details of these items will be also introduced.

Keywords: Mars, Exploration, Master Plan, space weather, space climate, Water

©2019. Japan Geoscience Union. All Right Reserved.

[J] Poster | U (Union) : Union

Mon. May 27, 2019 5:15 PM - 6:30 PM JST | Mon. May 27, 2019 8:15 AM - 9:30 AM UTC | Poster Hall International Exhibition Hall8, Makuhari Messe_1

[U-05] Large-scale Research Projects: Master Plan 2020 and its beyond

convener:Eiichi Tajika(Department of Earth and Planetary Science, Graduate School of Science, The University of Tokyo), Shigeko Haruyama(Department of Environmental Science, Graduate School of Bioresouces,Mie University), Ryoichi Fujii(Research Organization of Information and Systems), Hodaka Kawahata(Atmosphere Ocean Research Institute, the University of Tokyo)

Many of top sciences in Earth and Planetary Science (EPS) are progressed by big projects that require 10 billion JPY or more in 10 years or so. In order to realize such projects, we need an arena where they are brushed up through critical reviews among various fields in EPS. Deeper mutual understandings through serious discussions there will enable us to reach a final consensus on the priorities of the projects. The Master Plan (MP) of Large-scale Research issued by the Science Council of Japan strongly motivates us to follow the process described above. Indeed some of the selected projects have been funded by the Ministry of Education, Culture, Sports, Science & Technology since 2010. Since the current Master Plan 2017 is going to be thoroughly revised in 2020, we propose to hold a session in which large-scale research projects are concisely introduced and critically reviewed. This session is to be convened by JpGU and EPS Committee of Science Council of Japan.

[U05-P01] Planetary Exploration Roadmap from Japanese Society for Planetary Sciences

Kiyoshi Kuramoto[1], Hidenori Genda[2], *Naoki Terada[3], Hiroki Senshu[4], Taishi Nakamoto[5], Planetary Exploration Committee JSPS, Working term for revision of reply document for RFI JSPS (1.Graduate School of Sciences, Hokkaido University, 2.Earth-Life Science Institute, Tokyo Institute of Technology, 3.Graduate School of Science, Tohoku University, 4.Planetary Exploration Research Center, Chiba Institute of Technology, 5.Tokyo Institute of Technology)

Planetary Exploration Roadmap from Japanese Society for Planetary Sciences

Kiyoshi Kuramoto[1], Hidenori Genda[2], *Naoki Terada[3], Hiroki Senshu[4], Taishi Nakamoto[5], Planetary Exploration Committee JSPS, Working term for revision of reply document for RFI JSPS

1. Graduate School of Sciences, Hokkaido University, 2. Earth-Life Science Institute, Tokyo Institute of Technology, 3. Graduate School of Science, Tohoku University, 4. Planetary Exploration Research Center, Chiba Institute of Technology, 5. Tokyo Institute of Technology

The previous version of reply document for the Request For Information (RFI) on "the purpose, strategy, and roadmap of each committee" released by ISAS was submitted on Feb. 2015, and then revised on Jan. 2018. The document has been revised again following the change in circumstances surrounding our community regarding solar and extra-solar system exploration. The revision has been conducted by recommended or self appointed members of the Japanese Society for Planetary Sciences. The new version of the reply document of the RFI will be published on the web site of the Japanese Society for Planetary Sciences after the request for public comments from the members of Japanese Society for Planetary Sciences.
The reply document contains the status of domestic and international planetary exploration programs, brief explanation on on-going and near-future missions, a list of instruments under development in Japan, and the roadmap of planetary explorations proposed by the Japanese Society for Planetary Sciences.
In this presentation we will present our roadmap of planetary explorations in coming 20 years.

Keywords: Planetary Exploration, Roadmap, Japanese Society for Planetary Sciences

©2019. Japan Geoscience Union. All Right Reserved.

[E] Oral | P (Space and Planetary Sciences)：P-PS Planetary Sciences

Mon. May 27, 2019 3:30 PM - 5:00 PM JST | Mon. May 27, 2019 6:30 AM - 8:00 AM UTC | A03 TOKYO BAY MAKUHARI HALL

[P-PS01] Outer Solar System Exploration Today, and Tomorrow

convener:Jun Kimura(Osaka University), Yasumasa Kasaba(Planetary Plasma and Atmospheric Research Center, Tohoku University), Kunio M. Sayanagi(Hampton University), Chairperson:笠羽 康正, Kazuo Yoshioka(The University of Tokyo)

The giant planets provide many keys to understanding planetary processes. They play an important role in shaping our solar system, and the physical and chemical processes they harbor also provide a unique opportunity to study the phenomena relevant for studying Earth and other planets, including exoplanetary systems. In this session, we discuss a wide range of topics encompassing the giant planets and their moons, including their origins, interiors, atmospheres, compositions, surface features, and electromagnetic fields. To advocate for current and future outer planets exploration (Cassini, Juno, New Horizons, JUICE, and beyond), we also call for discussions on future missions to explore giant planet systems, including how to develop better international cooperation. Discussion in this latter category will include progress in developing a solar sail mission concept for observing the Jupiter system and its trojan asteroids.

3:30 PM - 3:45 PM JST | 6:30 AM - 6:45 AM UTC

[PPS01-01] Circulation of plasma in the Jupiter's inner magnetosphere revealed from time variation in radial profile of plasma temperature and density obtained by Hisaki/EXCEED observation

*Reina Hikida[1], Kazuo Yoshioka[2], Fuminori Tsuchiya[3], Masato Kagitani[3], Go Murakami[4], Tomoki Kimura[5], Atsushi Yamazaki[4], Ichiro Yoshikawa[2] (1.Department of Earth and Planetary Science, Graduate School of Science, the University of Tokyo, 2.Department of Complexity Science and Engineering, Graduate School of Frontier Science, the University of Tokyo, 3.Planetary Plasma and Atmospheric Research Center, Graduate School of Science, Tohoku University, 4.Institute of Space and Astronautical Science (ISAS), Japan Aerospace Exploration Agency (JAXA) , 5.Frontier Research Institute for Interdisciplinary Sciences, Tohoku University)

3:45 PM - 4:00 PM JST | 6:45 AM - 7:00 AM UTC

[PPS01-02] Volcanic change of the distribution of Io’s neutral oxygen cloud observed by Hisaki

*Ryoichi Koga[1], Fuminori Tsuchiya[1], Masato Kagitani[1], Takeshi Sakanoi[1], Tomoki Kimura[1], Ichiro Yoshikawa[2], Kazuo Yoshioka[2], Go Murakami[3], Atsushi Yamazaki[3], Howard Todd Smith[4], Fran Bagenal[5] (1.Tohoku University, 2.The University of Tokyo, 3.ISAS/JAXA, 4.Johns Hopkins University, 5.University of Colorado)

4:00 PM - 4:18 PM JST | 7:00 AM - 7:18 AM UTC

[PPS01-03] New pictures of Jovian magnetosphere obtained from the Hisaki satellite observation

★Invited Papers

*Fuminori Tsuchiya[1], Kazuo Yoshioka[2], Tomoki Kimura[1], Chihiro Tao[3], Ichiro Yoshikawa[2], Go Murakami[4], Hajime Kita[4], Ryoichi Koga[1], Hikida Reina[2], Fumiharu Suzuki[2], Sooman Han[2], Masato Kagitani[1], Takeshi Sakanoi[1], Hiroaki Misawa[1], Yasumasa Kasaba[1], Atsushi Yamazaki[4] (1.Tohoku University, 2.The University of Tokyo, 3.NICT, 4.ISAS/JAXA)

4:18 PM - 4:33 PM JST | 7:18 AM - 7:33 AM UTC

[PPS01-04] Axisymmetric conductivities of Jupiter's middle- and low-latitude ionosphere

*Yuki Nakamura[1], Koichiro Terada, Chihiro Tao[2], Naoki Terada[1], Yasumasa Kasaba[3], Hajime Kita[4], Aoi Nakamizo[2], Akimasa Yoshikawa[5], Shinichi Ohtani[6], Fuminori Tsuchiya[3], Masato Kagitani[3], Takeshi Sakanoi[3], Go Murakami[4], Kazuo Yoshioka[7], Tomoki Kimura[1], Atsushi Yamazaki[4], Ichiro Yoshikawa[8] (1.Department of Geophysics, Graduate School of Science, Tohoku University, 2.National Institute of Information and Communications Technology, 3.Planetary Plasma and Atmospheric Research Center,

Tohoku University, 4.Institute of Space and Astronautical Science, Japan Aerospace Exploration Agency, 5.Department of Earth and Planetary Sciences, Kyushu University, 6.The Johns Hopkins University Applied Physics Laboratory, 7.Graduate School of frontier Science, The University of Tokyo, 8.The University of Tokyo)

4:33 PM - 4:51 PM JST | 7:33 AM - 7:51 AM UTC

[PPS01-05] The magnetospheres of Saturn and Jupiter as viewed by Cassini and Juno

★Invited Papers

*G Provan[1], Stanley W. H. Cowley[1], Emma Jane Bunce[1] (1.University of Leicester)

4:51 PM - 5:00 PM JST | 7:51 AM - 8:00 AM UTC

Discussion

Circulation of plasma in the Jupiter's inner magnetosphere revealed from time variation in radial profile of plasma temperature and density obtained by Hisaki/EXCEED observation

*Reina Hikida[1], Kazuo Yoshioka[2], Fuminori Tsuchiya[3], Masato Kagitani[3], Go Murakami[4], Tomoki Kimura[5], Atsushi Yamazaki[4], Ichiro Yoshikawa[2]

1. Department of Earth and Planetary Science, Graduate School of Science, the University of Tokyo, 2. Department of Complexity Science and Engineering, Graduate School of Frontier Science, the University of Tokyo, 3. Planetary Plasma and Atmospheric Research Center, Graduate School of Science, Tohoku University, 4. Institute of Space and Astronautical Science (ISAS), Japan Aerospace Exploration Agency (JAXA) , 5. Frontier Research Institute for Interdisciplinary Sciences, Tohoku University

The satellite Io, which has many volcanoes and is located at 5.9 R_J from the center of Jupiter, is a powerful plasma source in the magnetosphere. The resulting specificity of the Jupiter's magnetosphere is the magnitude of energy that circulates internally. Previous researches, using data obtained by Voyager and Cassini spacecraft and chemical models complementarily, showed that the pickup energy of heavy ions originating from volcanoes on Io and the energy of hot electrons are converted into radiation reaching ~3 TW. However, the origins of hot electrons, that is, heating and/or transport mechanisms are still unrevealed. Therefore, in this research, we focus on the response to the change in the amount of plasma supplied to the magnetosphere and explore the above problem. In this study, the radial distributions of plasma density and temperature were derived from the intensities of emission lines in the extreme ultraviolet range obtained by Hisaki satellite. In this presentation, we will show the results using data obtained from December 2014 to May 2015. The activation of volcanoes on Io in early January 2015 was confirmed by ground-based infrared observations.

©2019. Japan Geoscience Union. All Right Reserved.

Volcanic change of the distribution of Io's neutral oxygen cloud observed by Hisaki

*Ryoichi Koga[1], Fuminori Tsuchiya[1], Masato Kagitani[1], Takeshi Sakanoi[1], Tomoki Kimura[1], Ichiro Yoshikawa[2], Kazuo Yoshioka[2], Go Murakami[3], Atsushi Yamazaki[3], Howard Todd Smith[4], Fran Bagenal[5]

1. Tohoku University, 2. The University of Tokyo, 3. ISAS/JAXA, 4. Johns Hopkins University, 5. University of Colorado

Io has a thin atmosphere created by volcanism and sublimation from the surface frost. Io's atmospheric oxygen atoms are heated by atmospheric sputtering, and escape from Io's gravity, forming a neutral oxygen cloud around Io's orbit. The neutral cloud is important as a source of the Io plasma torus. Previous studies derived the distribution and density of the equilibrium neutral oxygen cloud, and showed changes in Io's volcanism can lead to increase densities of both neutral clouds and Io plasma torus. Koga et al (2018) showed the distribution of Io's neutral oxygen cloud from Hisaki observation data during a volcanically quiet period (November and December in 2014). The equilibrium neutral oxygen cloud consists of a dense region distributed around Io (the "banana cloud") and a longitudinally uniform, diffuse region distributed along Io's orbit. However, the evolution of the distribution of neutral clouds was not understood. In this study, we analyzed the Hisaki satellite observations of the spatial distribution of OI 130.4 nm emissions around Io's orbit during a volcanic event in 2015.
The radial distribution shows the oxygen cloud spread outward during the volcanically active period. The outer edge of the OI emission was 7 R_J (Jupiter radii) before the volcanic activity, but it spread to around 8-8.6 R_J during the volcanically active period. We also estimated the oxygen number density outward Io's orbit represented as $n(r)=n_0(r/r_0)^{\gamma}$, where r is radial distnace from Jupiter, r_0 is 5.9 R_J (orbit of Io), n_0 is a number density at 5.9 R_J, γ is a power law slope of the profile. The number density at Io's orbit (where north-south thickness is 1.2 R_J) increased to 88±9 cm^{-3} during the active period that is more than twice as large as the number density during the quiet period (40 cm^{-3}). The power law slope outward Io's orbit during the active period (γ=-5.5±1.3) is similar to that during the quiet period (γ=-5.3). The azimuthal distribution shows the neutral oxygen cloud during the active period also consists of the banana cloud and diffuse region distributed along Io's orbit, but both of the regions enlarge. The observation results show the main escape process of neutrals from Io's graivity remains atmospheric sputtering, but the escape rate of them significantly increased during a volcanically active period. One of the possible mechanisms to increase the escape rate is that the sublimation frost area increases and the density of sublimation driven atmosphere also increases. Another mechanism is that plumes increase the height of the exobase, and the area of atmospheric sputtering increases.

Keywords: Jupiter moon Io, Neutral oxygen, Ultraviolet observation

©2019. Japan Geoscience Union. All Right Reserved.

New pictures of Jovian magnetosphere obtained from the Hisaki satellite observation

*Fuminori Tsuchiya[1], Kazuo Yoshioka[2], Tomoki Kimura[1], Chihiro Tao[3], Ichiro Yoshikawa[2], Go Murakami[4], Hajime Kita[4], Ryoichi Koga[1], Hikida Reina[2], Fumiharu Suzuki[2], Sooman Han[2], Masato Kagitani[1], Takeshi Sakanoi[1], Hiroaki Misawa[1], Yasumasa Kasaba[1], Atsushi Yamazaki[4]

1. Tohoku University, 2. The University of Tokyo, 3. NICT, 4. ISAS/JAXA

In 2013, we got an opportunity to have an extreme ultra-violet (EUV) space telescope orbiting around the Earth, the Hisaki satellite. The strong EUV emissions come from both magnetospheric plasma and aurora through electron impact excitation of ions and molecular hydrogen, respectively. From the spectral observation, we can obtain not only total amount of energy deposited in each region but characteristic energy of electrons. Hisaki is dedicated for observing solar system planets. The monitoring capability of HISAKI provided us discoveries of dynamical behavior of the giant magnetosphere. Here, we show new pictures of Jovian magnetosphere obtained from the Hisaki satellite observation. This paper includes following topics: (1) Origin of hot electron in the inner magnetosphere, (2) Transient brightening of Jovian aurora and subsequent global expansion of the disturbance in the whole magnetosphere, (3) Global response of the magnetosphere to volcanic activity of the satellite Io, (4) Solar wind effects on the inner and middle magnetospheres, (5) Driver of radial diffusion in the Jovian radiation belt, (6) Electromagnetic magnetosphere-satellite interaction, and (7) Identification of new emission lines and new energy states of ion.

©2019. Japan Geoscience Union. All Right Reserved.

Axisymmetric conductivities of Jupiter's middle- and low-latitude ionosphere

*Yuki Nakamura[1], Koichiro Terada, Chihiro Tao[2], Naoki Terada[1], Yasumasa Kasaba[3], Hajime Kita[4], Aoi Nakamizo[2], Akimasa Yoshikawa[5], Shinichi Ohtani[6], Fuminori Tsuchiya[3], Masato Kagitani[3], Takeshi Sakanoi[3], Go Murakami[4], Kazuo Yoshioka[7], Tomoki Kimura[1], Atsushi Yamazaki[4], Ichiro Yoshikawa[8]

1. Department of Geophysics, Graduate School of Science, Tohoku University, 2. National Institute of Information and Communications Technology, 3. Planetary Plasma and Atmospheric Research Center, Tohoku University, 4. Institute of Space and Astronautical Science, Japan Aerospace Exploration Agency, 5. Department of Earth and Planetary Sciences, Kyushu University, 6. The Johns Hopkins University Applied Physics Laboratory, 7. Graduate School of frontier Science, The University of Tokyo, 8. The University of Tokyo

Ionospheric Hall and Pedersen conductivities are important parameters in determining the electric potential distribution and plasma convection in a magnetosphere-ionosphere system. At Jupiter, meteoric ions deposited by meteoroid ablation are expected to play a major role in the ionospheric conductivities [e.g., Cloutier et al., 1978]. Hall and Pedersen conductivities are expected to be axisymmetric at Jupiter due to the long lifetime of meteoric ions. This study evaluates the modification of the potential distribution and plasma convection in the inner magnetosphere caused by the axisymmetric ionospheric conductivities at Jupiter.

We have developed a photochemical model and an ionospheric potential solver to evaluate the contributions of meteoric ions to the Jovian ionospheric conductivities and dawn-to-dusk electric field in the inner magnetosphere. Our photochemical model includes chemical reactions taken from Kim et al. [1994, 2001], mass deposition of meteoric atoms and ions by meteoroid ablation, ionizations by precipitating electrons, and ambipolar diffusion of ions. The input parameters of field-aligned currents are taken from the Region 2-like current in Khurana [2001] and axisymmetric Hill current. Our ionospheric potential solver has been developed using the methods in Nakamizo et al. [2012]. We calculate the global distribution of ionospheric conductivities using ion and electron density profiles acquired from the photochemical model. The ionospheric potential distribution and the resulting dawn-to-dusk electric field in the inner magnetosphere are obtained by the ionospheric potential solver.

Our simulation results reveal that the largest contributions to the Hall and Pedersen conductivities occur in the meteoric ion layer, and the resulting height-integrated conductivities are axisymmetric in the middle- and low- latitudes. Meteoric ions dominate the ion densities in the altitude region of 350 - 450 km with a peak electron number density of ~10^{11} [m^{-3}]. The obtained electron density profile is almost constant at any local time in the middle- and low-latitudes because the lifetimes of H^+ in the high altitude and meteoric ions in the lower altitude ionosphere are sufficiently longer than the half Jovian day (~ 5h). The ionospheric conductivities reach their maxima at the meteoric ion layer, and the height-integrated Hall and Pedersen conductivities become axisymmetric in the middle- and low- latitudes. At high latitudes, the conductance are enhanced at dawn side associated with the Region 2-like upward field-aligned current. The dawn-to-dusk electric field generated in the inner magnetosphere is 4 - 27 [mV/m] around Io’ s orbit. For comparison, we model another case of ionosphere without H^+ and meteoric ions. In this case, the ionospheric conductance are entirely smaller than the former case, and diminished at night side. The resulting dawn-to-dusk electric field is 45 - 270 [mV/m] around Io’ s orbit in this case.

©2019. Japan Geoscience Union. All Right Reserved.

In order to evaluate the validity of our results, we compare our results to observations. Observations by the Hisaki satellite revealed that the variation of dawn-to-dusk brightness intensity ratio of Io plasma torus coincided with a rapid increase in the solar wind dynamic pressure. The correlation between them can be explained by the existence of a dawn-to-dusk electric field of ~4 - 9 [mV/m] around Io's orbit [Murakami et al., 2016]. Our model results are almost consistent with the Hisaki observations in the case of the existence of meteoric ions in the lower ionosphere. It is concluded that the existence of meteoric ions in the lower ionosphere causes the axisymmetric enhanced ionospheric conductance at Jupiter. The large axisymmetric conductance results in the small dawn-to-dusk electric field in the inner magnetosphere, and our model results can be supported by the Hisaki observations.

Keywords: Jupiter, Meteoric ion, M-I coupling

©2019. Japan Geoscience Union. All Right Reserved.

The magnetospheres of Saturn and Jupiter as viewed by Cassini and Juno

*G Provan[1], Stanley W. H. Cowley[1], Emma Jane Bunce[1]

1. University of Leicester

The magnetospheres of the gas giants Saturn and Jupiter are believed to be driven to varying degrees by external drivers, planetary rotation and internal plasma sources. Both planets are rapid rotators with active volcanic moons and complicated ring systems. Their auroras are key indicators to the magnetosphere-ionosphere coupling at the giant planets. At Saturn Planetary Period Oscillations (PPOs) are observed throughout the magnetosphere, including during Cassini’ s Grand Finale on field lines mapping to Saturn’ s rings. In this paper we will report on the latest results from the Cassini and Juno missions, including both the latest observations and theoretical modelling. We will elucidate on a series of studies determining properties of Saturn’ s PPOs throughout the Cassini mission, and compare our results with those derived from analysis of Saturn kilometric radiation emissions from the Voyager, Ulysses, and Cassini mission. We will further model the magnetosphere-ionosphere coupling current at Jupiter and compare these results with observations from the Juno spacecraft and HST observations. We will finish by detailing some of the outstanding questions in the field.

Keywords: Saturn, Jupiter, Juno

©2019. Japan Geoscience Union. All Right Reserved.

[E] Oral | P (Space and Planetary Sciences)：P-PS Planetary Sciences

Mon. May 27, 2019 9:00 AM - 10:30 AM JST | Mon. May 27, 2019 12:00 AM - 1:30 AM UTC | A03 TOKYO BAY MAKUHARI HALL

[P-PS05] Recent advances of Venus science

convener:Takehiko Satoh(Institute of Space and Astronautical Science, Japan Aerospace Exploration Agency), Takeshi Horinouchi(Faculty of Environmental Earth Science, Hokkaido University), Masaru Yamamoto(Research Institute for Applied Mechanics, Kyushu University), Kevin McGouldrick(University of Colorado Boulder), Chairperson:Takeshi Horinouchi

Akatsuki, being in Venus orbit since December 2015, has acquired a volume of high-quality data, unveiled many new phenomena and is allowing researchers to investigate the underlying mechanisms. As the data accumulate, numerical models and theories are being advanced as well. We are no doubt living in the new golden era of Venus studies. This session invites papers of the new scientific results with Akatsuki data and the latest results of theoretical and numerical works. We expect participants of this session share the latest research results through presentations and discussion.

9:00 AM - 9:15 AM JST | 12:00 AM - 12:15 AM UTC

[PPS05-01] Super-rotation of Venusian atmosphere in the equatorial region may be caused by the density driven separation

*Adhithiyan Neduncheran[1], Ugur Guven[1,2], Ananyo Bhattacharya[3] (1.University of Petroleum and Energy Studies, India, 2.United Nations Centre for Space Science and Technology Education in Asia and the Pacific, 3.Sardar Vallabhbhai National Institute of Technology,India)

9:15 AM - 9:30 AM JST | 12:15 AM - 12:30 AM UTC

[PPS05-02] Comparison of horizontal distributions of temperature and UV absorbers at the Venus cloud-tops

*Shinichiro Kawase[1], Makoto Taguchi[1], Tetsuya Fukuhara[1], Yeon Joo Lee[2], Atsushi Yamazaki[3,4] (1.Rikkyo University, 2.Max Planck Institute for Solar System Research, 3.Institute of Space and Astronautical Science, 4.Japan Aerospace Exploration Agency)

9:30 AM - 9:45 AM JST | 12:30 AM - 12:45 AM UTC

[PPS05-03] Orographic Gravity Waves in the Venus Atmospheric

*Anna Suzuki[1], Masahiro Takagi[1], Yasumitsu Maejima[2], Hiroki Ando[1], Norihiko Sugimoto[3], Yoshihisa Matsuda[4] (1.Kyoto Sangyo University, 2.RIKEN Advanced Institute for Computational Science, 3.Keio University, 4.Tokyo Gakugei University)

9:45 AM - 10:00 AM JST | 12:45 AM - 1:00 AM UTC

[PPS05-04] Atmospheric structures simulated by T21 and T63 Venus GCMs with radiative transfer

*Masaru Yamamoto[1], Kohei Ikeda[2], Masaaki Takahashi[2] (1.Research Institute for Applied Mechanics, Kyushu University, 2.National Institute for Environmental Studies)

10:00 AM - 10:15 AM JST | 1:00 AM - 1:15 AM UTC

[PPS05-05] Thermal-tides structure at the cloud level of Venus derived from Akatsuki/LIR observations

★Invited Papers

*Toru Kouyama[1], Makoto Taguchi[2], Tetsuya Fukuhara[2], Takeshi Imamura[3], Masahiko Futaguchi[4], Takeru Yamada[2], Masahiro Akiba[2], Yeon Joo lee, Takao M. Sato[7], Shin-ya Murakami[5], George HASHIMOTO[6], Takehiko Satoh[5], Masato Nakamura[5] (1.AIST, 2.Rikkyo Univ., 3.Tokyo Univ., 4.Toho Univ., 5.JAXA, 6.Okayama Univ., 7.Hokkaido Information Univ.)

10:15 AM - 10:30 AM JST | 1:15 AM - 1:30 AM UTC

[PPS05-06] From Venus to Mars: viewpoint of comparative meteorology

★Invited Papers

*Takeshi Imamura[1], Kazunori Ogohara[2], Hiromu Nakagawa[3], Shohei Aoki[3] (1.The University of Tokyo, 2.University of Shiga Prefecture, 3.Tohoku University)

Super-rotation of Venusian atmosphere in the equatorial region may be caused by the density driven separation

*Adhithiyan Neduncheran[1], Ugur Guven[1,2], Ananyo Bhattacharya[3]

1. University of Petroleum and Energy Studies, India, 2. United Nations Centre for Space Science and Technology Education in Asia and the Pacific, 3. Sardar Vallabhbhai National Institute of Technology,India

On Venus, the clouds move nearly 60 times faster than the rotation of the planet. Super-rotation of the Venusian atmosphere is an intriguing phenomena and the reasons are still unclear. The super-rotation is possibly due to Venus being tidally locked to Sun as a consequence of which the planet experiences maximum heating in the equatorial zones causing meridional flows in the lower latitudes. The latent heat trapped by the Carbon dioxide gradually rises above due to its increased kinetic energy, which increases the motion of the cloud layers over time. Previous works done shows that the clouds are highly unstable in the altitude ranging from 49-55Km and below 30Km as per *Zasova et al* 2006 (doi:10.1016/j.pss.2007.01.011). This work shall put forth a possibility of density driven separation of cloud layers and its viscosity which helps in the super-rotation of the clouds. Similar hypothesis were presented by *Lebonnois et al* 2017 (DOI: 10.1038/NGEO2971). Using the known densities of atmospheric constituents, and applying the principles of viscosity and fluid dynamics, a simulation in COMSOL Multiphysics is done and analyzed for the flow behavior in the atmospheric layers ranging between 20Km and 80Km with respect to it’ s horizontal distance. The possible reasons regarding the flow will be discussed considering the solar convection in the equatorial region.

Keywords: Venus, atmosphere, super-rotation, clouds, flow simulation

©2019. Japan Geoscience Union. All Right Reserved.

Comparison of horizontal distributions of temperature and UV absorbers at the Venus cloud-tops

*Shinichiro Kawase[1], Makoto Taguchi[1], Tetsuya Fukuhara[1], Yeon Joo Lee[2], Atsushi Yamazaki[3,4]

1. Rikkyo University, 2. Max Planck Institute for Solar System Research, 3. Institute of Space and Astronautical Science, 4. Japan Aerospace Exploration Agency

Venus is the nearest neighbor planet, which has a size similar to that of the earth. However, unlike the earth, Venus is covered with thick - clouds floating at 45-70 km altitudes (Nakamura et al. 2011). It is considered that the clouds are photochemically generated by oxidation of and . In the visible region, light reflected by the clouds are poorly absorbed and few structures are noticeable. On the other hand, in the ultraviolet (UV) region, inhomogeneity of albedo has been identified to be inhomogeneous distribution of UV absorbers above the layer of UV scattering. It has been identified that in the Venusian atmosphere absorbs light in the wavelength region between 200 nm and 320 nm, but chemical species responsible for the absorption in the wavelength region longer than 320 nm is still unidentified. and are candidates (Perez et al. 2018). The UV absorbers play an important role in the atmospheric dynamics, controlling vertical thermal stability by heating at the top of convection layer. The dynamics may feedback the distribution of the UV absorbers by transport of them from the lower atmosphere. Details of the chemical and dynamical coupling are still unknown.

We analyzed images obtained by the Longwave Infrared Camera (LIR) and Ultraviolet Imager (UVI) onboard the Venus orbiter Akatsuki. LIR takes images of thermal radiation in the wavelength range of 8-12 μm emitted from the cloud-tops (Fukuhara et al., 2011). Temperature distributions are derived from the images. Disturbances seen in the temperature distributions are thought to be caused by atmospheric waves and tides, changes in the cloud-top altitude and adiabatic heating and cooling due to convection, direct heating by the UV absorbers, and so on. UVI takes images of the solar radiation reflected by the clouds with narrow bandpass filters centered at the 283 and 365 nm wavelengths, which correspond to the absorption bands of and unknown absorbers (Yamazaki et al., 2018).

Observations at 365 nm often find clouds with a little radiation in the middle latitudes. Such clouds with low radiation (bright) are covering on the clouds with high radiation (dark). The bright clouds are hard to receive the supply of UV absorbers from the lower layer (Titov et al., 2008). We found such bright distributions in the middle latitudes of images taken by LIR and UVI. Examples (on January 26, 2017) are shown in figures. The fact that we can see the similar distributions at different wavelengths means that two cameras observe clouds almost the same altitude. Therefore, we are studying of the dynamics of cloud top distributions at middle latitudes to use data taken by LIR and UVI.

We converted the UV radiation obtained into the absorption rate. Furthermore, we compared by combining the absorption rate and the temperature. The combined image is displayed more reddish when the temperature is higher and it is displayed more blueish when UV absorption rate is higher. Example are shown in figures. The figure is displayed blackish in the equatorial region and whitish in the polar region. In the middle latitudes where we pay attention, the temperature is high and the amount of absorption is small, so it is displayed reddish. In this presentation, we will introduce some examples like this, and will present relationships between temperature and , temperature and unknown absorbers.

As a next step, we will further study the relationship between temperature and UV absorbers for each

©2019. Japan Geoscience Union. All Right Reserved.

latitude and local time, and will clarify what atmospheric dynamics is occurring at the cloud top.

Keywords: Venus, Akatsuki, unknown UV absorber

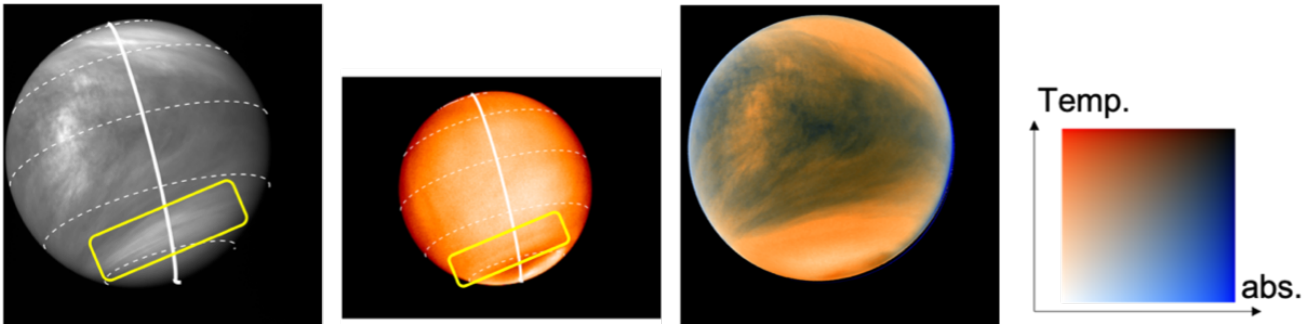

©2019. Japan Geoscience Union. All Right Reserved.

Orographic Gravity Waves in the Venus Atmospheric

*Anna Suzuki[1], Masahiro Takagi[1], Yasumitsu Maejima[2], Hiroki Ando[1], Norihiko Sugimoto[3], Yoshihisa Matsuda[4]

1. Kyoto Sangyo University, 2. RIKEN Advanced Institute for Computational Science, 3. Keio University, 4. Tokyo Gakugei University

Fast zonal winds called “super-rotation” are predominant globally in the Venus atmosphere, whose wind speed reaches ~100 m/s at ~70 km level (Schubert et al., 1980). Based on the zonal winds inferred from UV cloud images taken by the Venus Monitoring Camera onboard the Venus Express orbiter, Bertaux et al. (2016) pointed out that the zonal wind at ~70 km might be decreased by about 20 m/s over the Aphrodite terra, and suggested that the gravity waves generated by the Venus topography propagate upward, breaking at the cloud levels, giving their momentum to the atmosphere and decreasing of zonal wind. Young et al. (1987, 1994) numerically investigated the excitation and propagation processes of the gravity waves. Their results show that the gravity waves with horizontal wavelengths of 50 –800 km can propagate to the cloud levels if the zonal wind near the surface is of 2.2–3.0 m/s. However, the momentum transfer by the gravity waves is not examined. In the present study, we investigate the gravity waves in the Venus atmosphere with a focus on their momentum transfer using a cloud resolving numerical model named Cloud Resolving Storm Simulator (CReSS). Our preliminary results suggest that the orographic gravity waves can propagate upward and reach the cloud levels, as shown by Young et al. (1987, 1994). We will examine the momentum transfer by the gravity waves and discuss its effect on the super-rotation.

Keywords: Venus atmosphere, orographic gravity wave

©2019. Japan Geoscience Union. All Right Reserved.

Atmospheric structures simulated by T21 and T63 Venus GCMs with radiative transfer

*Masaru Yamamoto[1], Kohei Ikeda[2], Masaaki Takahashi[2]

1. Research Institute for Applied Mechanics, Kyushu University, 2. National Institute for Environmental Studies

Radiative forcing and topography are important in the formations of the thermal and wind structures on Venus. The surface topography forces stationary waves, which induce large-scale stationary bow-shaped wave pattern (Fukuhara et al. 2017) and conspicuous variation of cloud-top zonal flow (Bertaux et al. 2016) over the Aphrodite Terra. The topographical and radiative effects on Venus' atmosphere general circulation have been investigated using a T21L52 Venus AGCM at Atmosphere and Ocean Research Institute, Univ. Tokyo (Ikeda 2011). Our Venus GCM with the topographical data and radiative code simulated solar-locked and geographical atmospheric structures on Venus (Yamamoto et al. 2019). The model reproduced the wind structure near the subsolar point and the slowness of zonal wind over the Aphrodite Terra. Furthermore it showed that (1) the sub-rotation is formed near the surface in and around high land and mountains, (2) weakly stable layer is formed at 10-20 km at low latitudes, and (3) the zonal wind is weakened at the cloud top over the Aphrodite Terra. The third result implies that the negative wind deviation of the topographically forced stationary wave produces the slowness of the cloud-top zonal wind around the Aphrodite Terra. The GCM with the radiative code estimated the heat budget in the lower and middle atmospheres and reproduced the static stability similar to the observation. For the simulated zonal-mean structure, an equatorial fast flow of ~90 m/s and mid-latitude jets of ~120 m/s are formed around the cloud top. A poleward flow of >8 m/s is formed above the cloud layer, where the imbalance between solar and infrared radiative heating is large. Around the cloud top where the solar radiative heating balances the infrared one, a poleward flow is small (~1 m/s) and confined within the equatorward flank of the jet core. In and around the jet core, indirect circulations are formed by the eddy heat fluxes owing to the thermal tide and baroclinic waves. In solar-fixed coordinates, differences are significant between the zonal and dayside averages of the meridional wind and its related fluxes within the cloud layer. This suggests that we must carefully estimate the zonal-mean Hadley circulation, eddy momentum flux, and eddy heat flux from the one-side hemisphere. Most of the abovementioned features obtained from the T21 GCM are also seen in the T63 GCM. In this presentation, under the realistic thermal and topographical condition, the effects of the high resolution are also discussed. If we have room or time in this presentation, we briefly show the momentum budget, together with the heat budget shown in Yamamoto et al. (2019).

©2019. Japan Geoscience Union. All Right Reserved.

Thermal-tides structure at the cloud level of Venus derived from Akatsuki/LIR observations

*Toru Kouyama[1], Makoto Taguchi[2], Tetsuya Fukuhara[2], Takeshi Imamura[3], Masahiko Futaguchi[4], Takeru Yamada[2], Masahiro Akiba[2], Yeon Joo lee, Takao M. Sato[7], Shin-ya Murakami[5], George HASHIMOTO[6], Takehiko Satoh[5], Masato Nakamura[5]

1. AIST, 2. Rikkyo Univ., 3. Tokyo Univ., 4. Toho Univ., 5. JAXA, 6. Okayama Univ., 7. Hokkaido Information Univ.

Atmospheric acceleration due to thermal-tides excited in the cloud layer has been considered as one of main contributors for maintaining the atmospheric super-rotation in Venus, where zonal wind speed of the atmosphere at the cloud top (~70 km) rotates more than 60 times faster than the rotation speed of the solid body of Venus. The structures of the thermal-tides have been confirmed firstly in a temperature field and in zonal and meridional wind fields at the cloud top level by tracking cloud motions in several Venus exploration missions. In numerical studies, it has been confirmed that the thermal-tides structure is composed of diurnal, semi-diurnal, and higher frequent components which enhance at different altitudes and latitudes. Since they may contribute atmospheric acceleration according to their enhancement, observational monitoring should be important to understand what components of thermal-tides are dominant in different latitudes. On the other hand, there have been less observational studies about the latitudinal structures of thermal-tides in temperature fields due to time limitation for ground-based observations and limitation of spatial coverage for previous satellite observations.

In this study, we investigated latitudinal profiles of diurnal, semi-diurnal, and higher frequent components of thermal-tides in the temperature field obtained from long-term observation data by Longwave Infrared Camera (LIR) onboard Akatsuki that catches thermal emission from Venusian cloud layer (60-70km). We used the LIR data from October 2016 to December 2018 in which LIR had been remained to be turned on to prevent unexpected temperature increasing in LIR images, and we selected a specified emission angle (60˚) in the analysis to minimize emission angle dependence of a limb darkening effect.

Thanks to the global coverage of LIR observation in both dayside and night side, a global thermal-tides structure (local time-latitude coordinate) was firstly obtained by averaging the long-term LIR observation. By applying Fourier analysis to the thermal-tides structure, we found that the semi-diurnal component was clearly dominant in lower latitudes (< 30˚) whereas the diurnal component became significant in higher latitudes (> 45˚), and both diurnal and semi-diurnal tides showed almost equatorial symmetric profiles. These characteristics were consistent with a numerical expectation in a global circulation model by Takagi et al. (2018). In addition, the diurnal component showed clear phase tilting in mid-latitudes, which may indicate latitudinal energy transportation due to the diurnal component, while the semi-diurnal and other components with higher wavenumbers did not show such clear phase tilting in low-mid latitudes.

In this presentation, we will provide the structures of each thermal tide components, and latitudinal profiles of their amplitudes and phases, and we will also discuss thermal-tides structures at different

©2019. Japan Geoscience Union. All Right Reserved.

periods for more detail discussion about variability of the tides.

Keywords: Venus, Thermal tides, LIR

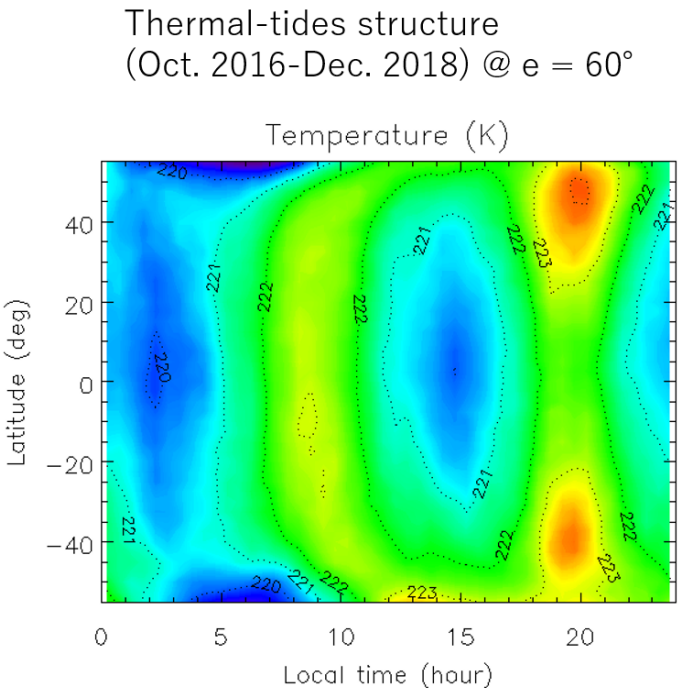

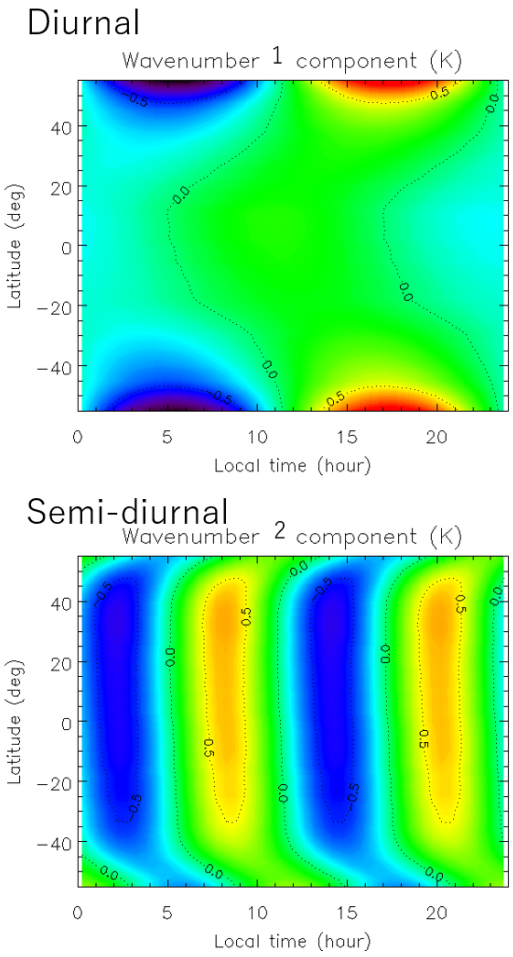

©2019. Japan Geoscience Union. All Right Reserved.

From Venus to Mars: viewpoint of comparative meteorology

*Takeshi Imamura[1], Kazunori Ogohara[2], Hiromu Nakagawa[3], Shohei Aoki[3]

1. The University of Tokyo, 2. University of Shiga Prefecture, 3. Tohoku University

The next Japanese planetary mission focusing on atmospheric science will be the Mars observation in the MMX (Martian Moons eXploration) mission. The spacecraft will enter a near-equatorial, high-altitude, circular orbit around Mars in 2025 and stay in orbit for 3 years. During this Mars-orbiting phase, the spacecraft will collect samples from Phobos and remotely observe Phobos, Deimos and Mars. Continuous, high-resolution, multi-wavelength, global observations of the Mars atmosphere enable monitoring of meteorological processes driving dust/water cycle in the atmosphere-surface system. The instruments used will be a near-infrared imaging spectrometer and multi-band cameras.

The Mars observation in MMX is considered a natural extension of the Venus orbiter Akatsuki. The observation sequence of MMX is similar to that of Akatsuki in that global images are acquired at short time intervals from an equatorial orbit similarly to Earth's meteorological satellites. From the viewpoint of comparative meteorology, Martian meteorology is contrasted with Venusian meteorology in many aspects. Examples include: superrotation on Venus vs. strong high-latitude jets on Mars; weak thermal forcing on Venus vs. strong thermal forcing on Mars; internal oscillation on Venus vs. seasonal cycle on Mars; wave-driven circulation on Venus vs. heat-driven circulation on Mars; slow convection on Venus vs. fast convection on Mars; uniform aerosols on Venus vs. variable aerosols on Mars; weak vertical coupling on Venus vs. strong vertical coupling on Mars. In order to maximize scientific achievements, feedbacks from Akatsuki to MMX are required.

Keywords: Venus, Mars, meteorology

©2019. Japan Geoscience Union. All Right Reserved.

[E] Oral | P (Space and Planetary Sciences)：P-PS Planetary Sciences

Mon. May 27, 2019 10:45 AM - 12:15 PM JST | Mon. May 27, 2019 1:45 AM - 3:15 AM UTC | A03 TOKYO BAY MAKUHARI HALL

[P-PS05] Recent advances of Venus science

convener:Takehiko Satoh(Institute of Space and Astronautical Science, Japan Aerospace Exploration Agency), Takeshi Horinouchi(Faculty of Environmental Earth Science, Hokkaido University), Masaru Yamamoto(Research Institute for Applied Mechanics, Kyushu University), Kevin McGouldrick(University of Colorado Boulder), Chairperson:Takehiko Satoh

Akatsuki, being in Venus orbit since December 2015, has acquired a volume of high-quality data, unveiled many new phenomena and is allowing researchers to investigate the underlying mechanisms. As the data accumulate, numerical models and theories are being advanced as well. We are no doubt living in the new golden era of Venus studies. This session invites papers of the new scientific results with Akatsuki data and the latest results of theoretical and numerical works. We expect participants of this session share the latest research results through presentations and discussion.

10:45 AM - 11:05 AM JST | 1:45 AM - 2:05 AM UTC

[PPS05-07] A two-stage evolution model of Venus's mantle and its implication for the Earth

★Invited Papers

*Masaki Ogawa[1] (1.Division of General Systems Studies, Graduate School of Arts and Sciences, University of Tokyo)

11:05 AM - 11:20 AM JST | 2:05 AM - 2:20 AM UTC

[PPS05-08] Interaction between the thermosphere and the cloud-level atmosphere of Venus studied with simultaneous observations by Hisaki and Akatsuki

*Yusuke Nara[1], Takeshi Imamura[1], Ichiro Yoshikawa[1], Kazuo Yoshioka[1], Kei Masunaga[2], Atsushi Yamazaki[3], Shigeto Watanabe[4], Manabu Yamada[5], Yeon Joo Lee[1], Naoki Terada[6], Kanako Seki[1] (1.The University of Tokyo, 2.Swedish Institute of Space Physics, 3.ISAS/JAXA, 4.Hokkaido Information University, 5.Chiba Institute of Technology, 6.Tohoku University)

11:20 AM - 11:35 AM JST | 2:20 AM - 2:35 AM UTC

[PPS05-09] Mesoscale Dyanmics in the Venus Atmosphere

*Kevin McGouldrick[1], Javier Peralta[2], Takehiko Satoh[2] (1.University of Colorado Boulder, 2.Institute of Space and Astronautical Science, Japan Aerospace Exploration Agency)

11:35 AM - 11:50 AM JST | 2:35 AM - 2:50 AM UTC

[PPS05-10] Periodicity analysis of Venus' cloud-top temperature measured by Akatsuki LIR

Naoya Kajiwara[1], *Takeshi Imamura[1], Makoto Taguchi[2], Tetsuya Fukuhara[2], Toru Kouyama[3] (1.Graduate School of Frontier Sciences, The University of Tokyo, 2.College of Science, Rikkyo University, 3.National Institute of Advanced Industrial Science and Technology)

11:50 AM - 12:10 PM JST | 2:50 AM - 3:10 AM UTC

[PPS05-11] Modeling Venus-like Worlds Through Time: The habitable zone, and the evolution of Venus' atmosphere.

★Invited Papers

*Michael Way[1,2,3], Anthony Del Genio[1] (1.NASA Goddard Institute for Space Studies, 2.GSFC Sellers Exoplanet Environments Collaboration, 3.Department of Physics and Astronomy, Uppsala University, Sweden)

12:10 PM - 12:15 PM JST | 3:10 AM - 3:15 AM UTC

Discussion

A two-stage evolution model of Venus’ s mantle and its implication for the Earth

*Masaki Ogawa[1]

1. Division of General Systems Studies, Graduate School of Arts and Sciences, University of Tokyo

There are two elementary processes that exert control over the evolution of the mantle in Venus and the Earth. The first is the magmatism-mantle upwelling (MMU) feedback: Suppose an upwelling flow in the solid mantle generates magma by decompression melting. The buoyancy of the magma boosts the upwelling flow itself. This positive feedback makes the magmatism and the upwelling flow vigorous. The second is mantle burst. The solid-solid phase transitions at the top of the lower mantle makes the convective flow across the phase boundaries pulsating, provided that the mantle is hot enough to cause an active magmatism. When coupled with the MMU feedback, this pulse of mantle upwelling flow causes an extensive magmatism in the upper mantle. Because of these two elementary processes, the mantle of Venus evolves in two stages. On the earlier stage when the mantle is strongly heated by radioactive elements, mantle bursts repeatedly occurs to episodically resurface Venus. As the radioactive elements decay, however, the mantle evolves into the later stage. Mantle bursts subside, and only a mild magmatism occurs at the top of the mantle to continuously resurface the planet. When a model of tectonic plates is added to this model of Venus, I obtained a two-stage evolution model of the Earth. On the earlier stage, mantle bursts repeatedly occur to make plate motion chaotic and the mantle compositionally rather homogeneous. On the later stage, in contrast, mantle bursts subside, and plate motion becomes more steady; ridge magmatism differentiates the mantle, and basaltic materials accumulate on the core-mantle boundary to form thermo-chemical piles similar to the Large Low Shear wave Velocity Provinces.

Keywords: Venus, Evolution of the interior, numerical simulation

©2019. Japan Geoscience Union. All Right Reserved.

Interaction between the thermosphere and the cloud-level atmosphere of Venus studied with simultaneous observations by Hisaki and Akatsuki

*Yusuke Nara[1], Takeshi Imamura[1], Ichiro Yoshikawa[1], Kazuo Yoshioka[1], Kei Masunaga[2], Atsushi Yamazaki[3], Shigeto Watanabe[4], Manabu Yamada[5], Yeon Joo Lee[1], Naoki Terada[6], Kanako Seki[1]

1. The University of Tokyo, 2. Swedish Institute of Space Physics, 3. ISAS/JAXA, 4. Hokkaido Information University, 5. Chiba Institute of Technology, 6. Tohoku University

In the thermosphere of Venus, the flow directing from sub-solar to anti-solar (SS-AS) is dominant driven by large temperature gradient associated with a long Venusian solar day which is ~117 Earth days. According to a numerical study by Mayr et al. (1985), the SS-AS flow without drag would exceed 300 m s^{-1} at the maximum.
It is believed that the drag force generated by gravity waves breaking effectively decelerates the thermospheric wind speed. Zalcucha et al. (2013) developed a Venus Thermosphere General Circulation Model in the presence of the gravity wave-drag, which accelerates the atmosphere when the gravity waves are broken. The model showed the SS-AS flow speed of 100-200 m s^{-1}.
The periodical variation that indicates the atmospheric waves in the thermosphere was observed by Masunaga et al. (2017). They analyzed OI dayglow variation using data obtained by the Extreme Ultraviolet Spectroscope for Exospheric Dynamics (EXCEED) on-board the Hisaki spacecraft and detected the periodicity of ~4 days only on the dawn side. They pointed out planetary-scale waves in the middle atmosphere which are expected to be exist in Venus might responsible for the variations in the thermosphere, while the existence of the planetary-scale waves at that time was not confirmed.
In this study, we investigated the vertical coupling between cloud-level atmosphere and the thermosphere of Venus, focusing on the role of atmospheric waves. To find the evidence for the wave propagation, we used data that are obtained simultaneously by Hisaki and Akatsuki spacecraft on the dawn side of Venus in June 2017.
Analyzing the time series of the atomic O dayglow emissions measured by the EXCEED and the UV images which reflect the spatial distribution of unidentified absorbers at the cloud top (~70 km) obtained by the Ultraviolet Imager (UVI), we identified characteristic periodicities of 3.5 days in both data. The wind velocity deduced with cloud tracking from UV images suggests that the 3.5-day periodicity can be associated with Kelvin waves at the cloud top; however, Kelvin waves should decay with height through radiative damping and will not reach the thermosphere. We propose an indirect process in which the Kelvin waves change the wind field periodically and examine how the vertically propagating small-scale gravity waves influence the thermospheric dayglow with a simplified numerical model.

Keywords: Venus, Thermosphere, Cloud level, Vertical coupling, Gravity waves

©2019. Japan Geoscience Union. All Right Reserved.

Mesoscale Dyanmics in the Venus Atmosphere

*Kevin McGouldrick[1], Javier Peralta[2], Takehiko Satoh[2]

1. University of Colorado Boulder, 2. Institute of Space and Astronautical Science, Japan Aerospace Exploration Agency

The Akatsuki Spacecraft is capable of observing the full disk of Venus at a number of filter-specified wavelengths, with time cadence on the order of an hour, and for up to nine days at a time (until the orbit brings the spacecraft so close that Venus exceeds the instrumental fields of view). Because of this, it is capable of supporting the elucidiation of both global atmospheric dynamics (i.e., the super-rotation) and mesoscale atmospheric dynamics. Here, we describe the analysis of the driving dynamics associated with mesoscale features observed in the Akatsuki IR2 camera data. This work focuses on just a single orbit of Akatsuki, but the features and behaviors we describe appear to be common in the Venus atmosphere. We make comparisons with similar terrestrial phenomena; and assess the implications for energy and momentum transport that may affect the overall global atmospheric dynamics. Three of the four filters in Akatsuki's IR2 camera image the night side of the planet in emitted radiation. These filters have central wavelegnths of 1.74 micron, 2.26 micron, and 2.32 micron, which are most sensitive to the conditions between about 50 km and 60 km altitude, in the midst of the lower and middle, condensational, cloud deck of Venus.

Keywords: Venus, Akatsuki, Meteorology, Clouds, Atmospheric Dynamics, Infrared Observations

©2019. Japan Geoscience Union. All Right Reserved.

Periodicity analysis of Venus' cloud-top temperature measured by Akatsuki LIR

Naoya Kajiwara[1], *Takeshi Imamura[1], Makoto Taguchi[2], Tetsuya Fukuhara[2], Toru Kouyama[3]

1. Graduate School of Frontier Sciences, The University of Tokyo, 2. College of Science, Rikkyo University, 3. National Institute of Advanced Industrial Science and Technology

Planetary-scale waves are thought to play crucial roles in the maintenance of the general circulation of the Venusian atmosphere. However, observational clues are limited, and the nature of such waves is poorly constrained. Here we analyze for the first time the cloud-top temperature field to deduce the periods (frequency) and the spatial structures of planetary-scale waves using LIR image data acquired continuously. Since the systematic (absolute) error in LIR data of around 3 K is larger than the expected amplitudes of the temperature oscillations of around 1 K, the waves are hard to detect by deducing temperature variations with time. In this study, we analyze oscillations of the zonal gradient of the temperature in each image associated with planetary-scale waves. The small random (relative) error in LIR data of 0.3 K enables detection of such small-amplitude waves with this method. Through spectral analyses of the time series of the temperature gradient spanning 142 Earth days from 18 May 2017, distinct oscillations with periods of 3.5 days, 4.9 days and 5.2 days were discovered. All of these modes show almost constant phases along the latitude, indicating that they are planetary-scale waves. Based on the wave period and the latitude dependence of the amplitude, the 3.5-day wave is identified as a Kelvin wave and the 4.9-day and 5.2-day waves seem to be hemispherically-symmetric Rossby waves. The amplitudes of these waves changed with time during the observation period.

Keywords: Venus, Akatsuki, atmosphere

©2019. Japan Geoscience Union. All Right Reserved.

Modeling Venus-like Worlds Through Time: The habitable zone, and the evolution of Venus' atmosphere.

*Michael Way[1,2,3], Anthony Del Genio[1]

1. NASA Goddard Institute for Space Studies, 2. GSFC Sellers Exoplanet Environments Collaboration, 3. Department of Physics and Astronomy, Uppsala University, Sweden

Using a modern three-dimensional general circulation coupled atmosphere/ocean model [1] we recently demonstrated [2] that climatic conditions may have permitted liquid water on Venus' surface for ~2 billion years in its early history. Similar such conditions on Earth are believed amenable to the rise of life. Several assumptions were made based on what little data we have for early Venus such as; the type of solar spectrum extant at that time, orbital parameters, estimates of a shallow ocean from Pioneer Venus D/H ratios, and topography from the Magellan Mission. We also assumed that it would have had an atmosphere similar to modern day Earth: 1 bar N2, 400ppmv CO2, 1ppmv CH4. I will discuss the motivations behind these assumptions and additional parameter space studies with direct relevance to hypothetical exoplanetary Venus-like worlds found at the inner edge of the liquid water habitable zone. Finally, I will show how our studies demonstrate that the reason for Venus' present climatic state is unlikely to be related to the gradual warming of our sun over the past 4Gyr as is commonly believed

[1] Way, M.J. et al. (2017) Astroph Journ Suppl, 231, 1
[2] Way, M. J., et al. (2016) Geophy Res Lett, 43, 8376-838

Keywords: Venus, Habitabilty, Exoplanets

©2019. Japan Geoscience Union. All Right Reserved.

[E] Oral | P (Space and Planetary Sciences)：P-PS Planetary Sciences

Mon. May 27, 2019 1:45 PM - 3:15 PM JST | Mon. May 27, 2019 4:45 AM - 6:15 AM UTC | A03 TOKYO BAY MAKUHARI HALL

[P-PS05] Recent advances of Venus science

convener:Takehiko Satoh(Institute of Space and Astronautical Science, Japan Aerospace Exploration Agency), Takeshi Horinouchi(Faculty of Environmental Earth Science, Hokkaido University), Masaru Yamamoto(Research Institute for Applied Mechanics, Kyushu University), Kevin McGouldrick(University of Colorado Boulder), Chairperson:Kevin McGouldrick

Akatsuki, being in Venus orbit since December 2015, has acquired a volume of high-quality data, unveiled many new phenomena and is allowing researchers to investigate the underlying mechanisms. As the data accumulate, numerical models and theories are being advanced as well. We are no doubt living in the new golden era of Venus studies. This session invites papers of the new scientific results with Akatsuki data and the latest results of theoretical and numerical works. We expect participants of this session share the latest research results through presentations and discussion.

1:45 PM - 2:00 PM JST | 4:45 AM - 5:00 AM UTC

[PPS05-12] Cloud top structure of Venus retrieved from the Akatsuki IR2 dayside observations

★Invited Papers

*Takao M. Sato[1], Takehiko Satoh[2], Hideo Sagawa[3], Naohiro Manago[2], Yeon Joo Lee, Shin-ya Murakami[2], Kazunori Ogohara[4], George HASHIMOTO[5], Yasumasa Kasaba[6], Atsushi Yamazaki[2], Manabu Yamada[7], Shigeto Watanabe[1], Takeshi Imamura[8], Masato Nakamura[2] (1.Hokkaido Information University, 2.ISAS/JAXA, 3.Kyoto Sangyo University, 4.University of Shiga Prefecture, 5.Okayama University, 6.Tohoku University, 7.Chiba Institute of Technology, 8.The University of Tokyo)

2:00 PM - 2:15 PM JST | 5:00 AM - 5:15 AM UTC

[PPS05-13] Formation of superrotation studied by a TEM model

*Takeshi Horinouchi[1] (1.Faculty of Environmental Earth Science, Hokkaido University)

2:15 PM - 2:30 PM JST | 5:15 AM - 5:30 AM UTC

[PPS05-14] Morphological Feature Extraction from Venus' Cloud Images Using Principal Component Analysis

*Minori Narita[1], Takeshi Imamura[1], Yusuke Nara[1], Yeon Joo Lee, Shigeto Watanabe[2], Atsushi Yamazaki[3], Takehiko Satoh[3], Makoto Taguchi[4], Tetsuya Fukuhara[4], Manabu Yamada[5] (1.The University of Tokyo, 2.Hokkaido Information University, 3.ISAS/JAXA, 4.Rikkyo University, 5.PERC/Chiba Institute of Technology)

2:30 PM - 2:45 PM JST | 5:30 AM - 5:45 AM UTC

[PPS05-15] **Principal Components of UV Albedo Variability in Venus' Atmosphere as seen at 283 nm**

*Pushkar Kopparla[1], Yeon Joo Lee[1], Takeshi Imamura[1], Atsushi Yamazaki[2] (1.GSFS, University of Tokyo, 2.ISAS, JAXA)

2:45 PM - 3:00 PM JST | 5:45 AM - 6:00 AM UTC

[PPS05-16] Active and inactive behaviors of the planetary-scale waves on Venus cloud top

★Invited Papers

*Masataka Imai[1], Toru Kouyama[1], Yukihiro Takahashi[2], Takeshi Horinouchi[3], Takeshi Imamura[4], Atsushi Yamazaki[5], Shigeto Watanabe[6], Manabu Yamada[7], Masato Nakamura[5], Takehiko Satoh[5] (1.National Institute of Advanced Industrial Science and Technology, 2.Department of Cosmosciences, Graduate School of Science, Hokkaido University, 3.Faculty of Environmental Earth Science, Hokkaido University, 4.Graduate School of Frontier Sciences, University of Tokyo, 5.Institute of Space and Astronautical Science, Japan Aerospace Exploration Agency, 6.Space Information Center, Hokkaido Information University, 7.Planetary Exploration Research Center, Chiba Institute of Technology)

3:00 PM - 3:15 PM JST | 6:00 AM - 6:15 AM UTC

[PPS05-17] **Long-term behaviour of the morphology and dynamics of Venus's middle clouds with Akatsuki/IR1.**

★Invited Papers

*Javier Peralta[1], Naomoto Iwagami[2], Sánchez-Lavega Agustín[3], Yeon Joo Lee[4], Ricardo Hueso[3], Minori Narita[4], Takeshi Imamura[4], Phil Miles[5], Anthony Wesley[6], Emmanuel Kardasis[7], Seiko Takagi[8] (1.Institute of Space and Astronautical Science (ISAS), Japan Aerospace Exploration Agency (JAXA), Sagamihara, Japan, 2.Tokyo 156-0044, Japan, 3.Escuela de Ingeniería de Bilbao, University of the Basque Country (UPV/EHU), Bilbao, Spain, 4.Graduate School of Frontier Sciences, The University of Tokyo, Japan, 5.Rubyvale QLD, Australia, 6.Astronomical Society of Australia, Australia, 7.Hellenic Amateur Astronomy Association, Greece, 8.Research and Information Center, Tokai University, Japan)

Cloud top structure of Venus retrieved from the Akatsuki IR2 dayside observations

*Takao M. Sato[1], Takehiko Satoh[2], Hideo Sagawa[3], Naohiro Manago[2], Yeon Joo Lee, Shin-ya Murakami[2], Kazunori Ogohara[4], George HASHIMOTO[5], Yasumasa Kasaba[6], Atsushi Yamazaki[2], Manabu Yamada[7], Shigeto Watanabe[1], Takeshi Imamura[8], Masato Nakamura[2]

1. Hokkaido Information University, 2. ISAS/JAXA, 3. Kyoto Sangyo University, 4. University of Shiga Prefecture, 5. Okayama University, 6. Tohoku University, 7. Chiba Institute of Technology, 8. The University of Tokyo

We present the cloud top structure of Venus retrieved from a total of 93 dayside images acquired at a wide variety of solar phase angles (0-120 deg) by the 2.02-μm channel of the 2-μm Camera (IR2) onboard Japanese Venus orbiter, Akatsuki, during the period from April 4 to May 25, 2016. Since the 2.02-μm channel locates in a CO_2 absorption band, the sunlight reflected from Venus allows us to determine the cloud top altitude corresponding to unit aerosol optical depth at 2.02 μm with radiative transfer calculation. Firstly, the observed solar phase angle dependence and zonal variation of the reflected sunlight in the equatorial region were used to construct a baseline model characterized by cloud top altitude , Mode 2 radius , and cloud scale height which are 70.287 km, 1.26 μm and 5.1 km, respectively. Secondly, individual cloud top altitudes were retrieved with the assumption that the last two values are valid for the entire planet. The latitudinal structure of cloud top altitude is symmetrical with respect to the equator: the averaged cloud top locates at a constant altitude of 68-70 km equatorward of ±45 deg but rapidly drops in latitudes of 50-60 deg and reaches 61 km poleward of ±70 deg. The averaged cloud top in the equatorial region indicates the tendency to increase from early morning (~7 h) and reach a maximum near early afternoon (~14 h) and decrease toward late afternoon (~17 h). The magnitude of the change is in the order of 1 km. After high-pass filtering of the cloud top altitude maps, small-amplitude features including stationary structures occur within several hundred meters and typically show less contrast than those at two channels (283 and 365 nm) of the Ultraviolet Imager (UVI). Although the long, zonal or tilted streaky features poleward of ~45 deg are clearly identifiable, the features in low and middle latitudes are usually faint and do not necessarily appear as the local variation in cloud top altitude where mottled and patchy patterns are seen in the UV channels, suggesting the existence of convection and turbulence at the cloud top level.

Keywords: Venus, atmosphere, clouds, Akatsuki, near-infrared, radiative transfer

©2019. Japan Geoscience Union. All Right Reserved.

Formation of superrotation studied by a TEM model

*Takeshi Horinouchi[1]

1. Faculty of Environmental Earth Science, Hokkaido University

Recently, a number of studies have reported the formation of atmospheric superrotation in three-dimensional Venus GCMs. However, its mechanism has not been fully understood, which is partly due to the difficulty of model data analysis and possible numerical problems (Lebonnois et al 2012). Earlier studies with two-dimensional models by Matsuda (1980, 1982) and Yamamoto and Yoden (2013) provided useful insights, but to assess their applicability is not straightforward, since these studies are based on the Boussinesq approximation and use fixed uniform eddy diffusivity and Newtonian cooling rate. Here, I present the results of numerical simulations with a two-dimensional axi-symmetric model to overcome these difficulties. The model is based on the transformed Eulerian mean (TEM) equations supporting deep atmosphere over multiple scale heights, and it conserves total zonal angular momentum very well when surface friction is tuned off. The model does not use prescribed eddy diffusivity. Instead, effects of dynamical instabilities (convective, symmetric, barotropic-baroclinic instabilities) are parameterized. The model was initialized with the uniform solid-body rotation at the rate of the planetary rotation and run under radiative forcing similar to that in the recent Venus AFES simulations. A realistic superrotation emerged, and it reached a statistical steady state. It is revealed that the dynamical disturbances associated with dynamical instabilities can work like eddy diffusivity in the Gierasch mechanism to create a local maximum of the angular momentum within the atmosphere. The steady-state meridional circulation is multi-layered. The surface friction works to keep the angular momentum at low levels. Effects of thermal tides will be investigated elsewhere.

Keywords: Venus, superrotation

©2019. Japan Geoscience Union. All Right Reserved.

Morphological Feature Extraction from Venus' Cloud Images Using Principal Component Analysis

*Minori Narita[1], Takeshi Imamura[1], Yusuke Nara[1], Yeon Joo Lee, Shigeto Watanabe[2], Atsushi Yamazaki[3], Takehiko Satoh[3], Makoto Taguchi[4], Tetsuya Fukuhara[4], Manabu Yamada[5]

1. The University of Tokyo, 2. Hokkaido Information University, 3. ISAS/JAXA, 4. Rikkyo University, 5. PERC/Chiba Institute of Technology

We applied principal component analysis (PCA) to Venus' multi-wavelength image data obtained by Venus orbiter Akatsuki, to extract latent morphological patterns for each wavelength and compare them to reveal similarities and dissimilarities between the wavelengths. Statistical approaches that extract latent features using massive amounts of data have hardly been done in Venus researches. The new analysis showed that tilted streaky features are dominant at all wavelengths, especially in mid-latitudes; this feature can be explained by the combination of the latitudinal gradient of the mean zonal velocity and the meridional circulation. Moreover, the result shows a strong morphological similarity between cloud height and ultraviolet absorbers.

We preprocessed images as follows. We used data in which images have been projected onto the latitude-longitude coordinate (Level-3 data). We used the following four wavelengths; near-infrared 2.02 μm (cloud height), thermal infrared 10 μm (cloud top temperature), ultraviolet 283 nm (SO_2 distribution at the cloud top), and ultraviolet 365 nm (an unknown UV absorber). First, we performed photometric correction using Minnaert Law (except for 10 μm images). Then these images are high-pass filtered by subtracting a Gaussian-smoothed image from each original image to extract scales smaller than 6 degrees both in latitude and longitude. Lastly, we extracted image patches from these images to increase the number of samples and extract specific spatial scale. The size of the image patches is 12 degrees in latitude/longitude. The total number of image patches is around 60,000 for each wavelength. Also, we analyzed images in low-latitudes and mid-latitudes separately.

We performed PCA for the image patches. PCA converts a set of observational data into a set of linearly uncorrelated variables called principal components and enables to extract spatial features that appear in data frequently. We focus on 20 most major principal components for each wavelength, and we also calculated the contribution ratios. As a result, it turned out that tilted streaky features are dominant both in low and middle latitudes. Considering that zonal winds have a latitudinal gradient and that a slow, poleward meridional circulation exists, cloud parcels are stretched obliquely while drifting from low latitudes to middle latitudes. Moreover, we found that SO_2 (283 nm) and the unknown UV absorber (365 nm) have spatial patterns similar to that of the cloud height (2.02 μm). It indicates that mechanisms that make the distribution of clouds and these chemical compounds in low latitudes are common. As unique patterns for a specific wavelength, it is worth noting that streaks in the north-south direction prevail in patterns of the cloud top temperature (10 μm). Considering that meridional bow-shaped structures are observed at this wavelength, it seems that these structures are appearing as the main principal component. Besides, the statistical approach could successfully extract streaky features from 10 μm as well, while we cannot recognize such features at this wavelength by our eyes because of apparent dominance of random, patchy features. In conclusion, we successfully extracted statistical spatial patterns in Venus' clouds and enabled further discussions about physical properties corresponding to each wavelength more in detail.

©2019. Japan Geoscience Union. All Right Reserved.

Keywords: Venus, Principal Component Analysis, Image

©2019. Japan Geoscience Union. All Right Reserved.

Principal Components of UV Albedo Variability in Venus' Atmosphere as seen at 283 nm

*Pushkar Kopparla[1], Yeon Joo Lee[1], Takeshi Imamura[1], Atsushi Yamazaki[2]

1. GSFS, University of Tokyo, 2. ISAS, JAXA

We explore the dominant modes of variability in the observed albedo at the cloud tops of Venus using the Akatsuki UVI 283 nm observations over the period Dec 2016 to May 2018. The observations consist of images of the dayside of Venus, most often observed at intervals of 2 hours, but interspersed with longer gaps. The orbit of the spacecraft does not allow for continuous observation of the full dayside, and the unobserved regions cause significant gaps in the dataset. The missing data are interpolated and the dataset is then subjected to a principal component analysis (PCA) to find six oscillating patterns in the albedo. Some of the spatial patterns and the time scales of these modes correspond to well known physical processes in the atmosphere of Venus such as short period atmospheric waves and the overturning circulation, while others defy a simple explanation. We also a find a hemispheric mode that has not been identified before and discuss its implications.

Keywords: Venus atmosphere, Clouds, UV Observations

©2019. Japan Geoscience Union. All Right Reserved.

Active and inactive behaviors of the planetary-scale waves on Venus cloud top

*Masataka Imai[1], Toru Kouyama[1], Yukihiro Takahashi[2], Takeshi Horinouchi[3], Takeshi Imamura[4], Atsushi Yamazaki[5], Shigeto Watanabe[6], Manabu Yamada[7], Masato Nakamura[5], Takehiko Satoh[5]

1. National Institute of Advanced Industrial Science and Technology, 2. Department of Cosmosciences, Graduate School of Science, Hokkaido University, 3. Faculty of Environmental Earth Science, Hokkaido University, 4. Graduate School of Frontier Sciences, University of Tokyo, 5. Institute of Space and Astronautical Science, Japan Aerospace Exploration Agency, 6. Space Information Center, Hokkaido Information University, 7. Planetary Exploration Research Center, Chiba Institute of Technology

Planetary-scale waves on Venus cloud top cause periodical fluctuations in winds and also UV brightness. The candidates of these waves are 4-day Kelvin wave and 5-day Rossby wave of zonal wavenumber 1, however, their temporal evolutions are poorly understood. In this work, we conducted time-resolved periodical analysis in 365 nm brightness and cloud tracking wind fluctuations obtained by UVI onboard AKATUSKI Japanese Venus Climate Orbiter from January to September 2017, and we have revealed the dramatical evolution of planetary-scale waves and the dynamical connection between wave and planetary-scale UV features.

During the observation season, we could find prominent ~5-day periodicity in both wind and brightness fluctuations, whose phase velocity was slower than dayside mean zonal winds (or the super-rotation) by > 35 ms^{-1}. We succeeded to reconstruct the horizontal wind field related to the observed 5-day mode, and since planetary-scale vortices, whose the center existed ~35° latitudes, having large equatorial symmetric structures in the latitudinal direction were found, it can be a strong manifestation of the retrograde propagating Rossby wave. The observed Rossby wave subjected to temporal changes of enhancing and attenuating in the amplitude of wind fluctuations with ~100-day time scale. According to the temporal evolution of the Rossby wave, white cloud belts in 45° --60° latitudinal regions began rippling synchronously in both hemispheres. Moreover, the Rossby wave deformed the planetary-scale dark UV feature in the equatorial region, and that should be the reason for significant 5.1-day periodicity in brightness variation. Before the Rossby wave enhancement, weak 3.8-day periodical signals can be observed in zonal wind and brightness variations in the equatorial region. This is a suggestive prograde propagating Kelvin wave, and this might be the reason for the origin of dark clusters in the equatorial region.

While wave activities during the observation season from January to September 2017 were clear, significant periodical wind or brightness fluctuations were not always confirmed in the other observation seasons. In orther to investigate the reason for active and inactive behaviors in planetary-scale waves, we will compare seasons when significant planetary-scale waves were observed and they were not focusing on the connection with mean zonal wind speed, global UV albedo, and cloud top temperature.

Keywords: Venus, AKATSUKI, Rossby wave, Kelvin wave

©2019. Japan Geoscience Union. All Right Reserved.

Long-term behaviour of the morphology and dynamics of Venus's middle clouds with Akatsuki/IR1.

*Javier Peralta[1], Naomoto Iwagami[2], Sánchez-Lavega Agustín[3], Yeon Joo Lee[4], Ricardo Hueso[3], Minori Narita[4], Takeshi Imamura[4], Phil Miles[5], Anthony Wesley[6], Emmanuel Kardasis[7], Seiko Takagi[8]

1. Institute of Space and Astronautical Science (ISAS), Japan Aerospace Exploration Agency (JAXA), Sagamihara, Japan, 2. Tokyo 156-0044, Japan, 3. Escuela de Ingeniería de Bilbao, University of the Basque Country (UPV/EHU), Bilbao, Spain, 4. Graduate School of Frontier Sciences, The University of Tokyo, Japan, 5. Rubyvale QLD, Australia, 6. Astronomical Society of Australia, Australia, 7. Hellenic Amateur Astronomy Association, Greece, 8. Research and Information Center, Tokai University, Japan

The Venusian atmosphere is covered by clouds with super-rotating winds whose accelerating mechanism is still not well understood. Fastest wind speeds occur at the top of the clouds (about 70 km height), and they have been studied for decades thanks to their visual contrast in dayside ultraviolet images caused by the presence of a yet unknown absorber. The middle clouds (at about 50-55 km) can be observed using near-infrared wavelengths (800-950 nm) and they exhibit much weaker contrasts. Here we present the first long-term study of the dayside middle clouds of Venus at middle to low latitudes thanks to the combination of the full dataset of Akatsuki/IR1 images acquired at 900 nm during the year 2016 (A-I), complemented with observations of Venus with small telescopes and band-pass filters 1.0-1.1 μm and 884-900 nm (J-L). Thanks to the analysis of more than 1,000 images, we report the discovery of new cloud morphologies, like fast sharp discontinuities (C), elongated "hook-like" stripes (B,J) and a single case of mesoscale wave packet (I). Surprisingly, the albedo of Venus at 900 nm exhibit periodical hemispherical asymmetry (E-F), and clouds' contrasts varying from 3% to 21%. These contrasts are larger than reported in previous missions, and they are suggestive of important changes in the optical thickness of the clouds or they might imply the presence of a new atmospheric absorber at near-infrared wavelengths. Finally, we also present more than 500 wind measurements from IR1 images and —for the first time— with ground-based observations. The mean zonal winds are observed to peak at the equator, while the combination with data from Venus Express reveals long-term variations in the zonal winds of ˜20 m/s along 10 years.

Keywords: Venus, Atmosphere, Clouds, Atmospheric dynamics, Remote sensing

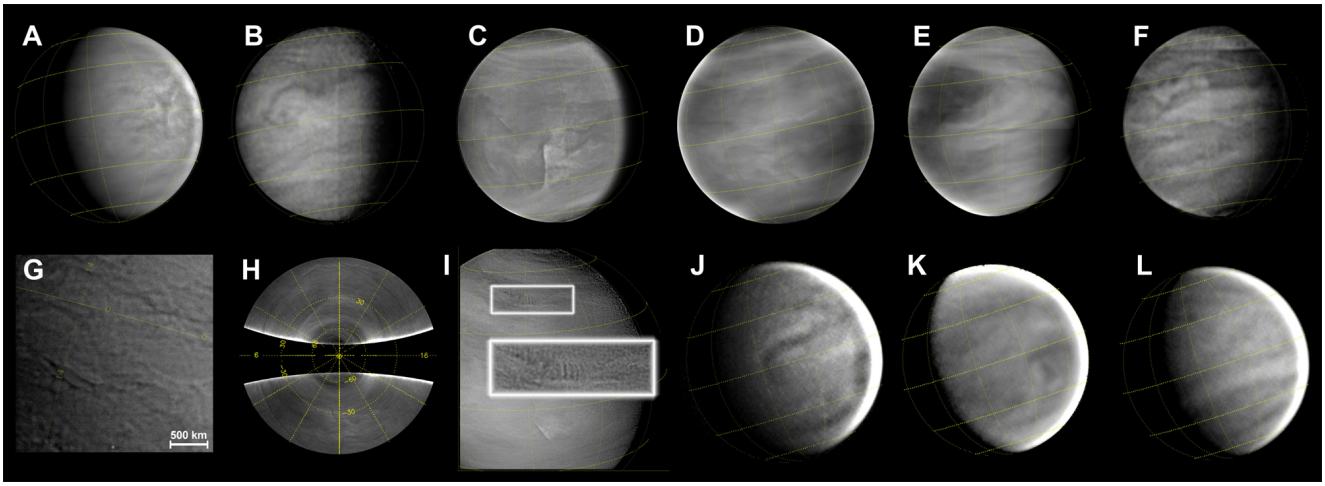

©2019. Japan Geoscience Union. All Right Reserved.

[E] Poster | P (Space and Planetary Sciences)：P-PS Planetary Sciences

Mon. May 27, 2019 3:30 PM - 5:00 PM JST | Mon. May 27, 2019 6:30 AM - 8:00 AM UTC | Poster Hall International Exhibition Hall8, Makuhari Messe_1

[P-PS05] Recent advances of Venus science

convener:Takehiko Satoh(Institute of Space and Astronautical Science, Japan Aerospace Exploration Agency), Takeshi Horinouchi(Faculty of Environmental Earth Science, Hokkaido University), Masaru Yamamoto(Research Institute for Applied Mechanics, Kyushu University), Kevin McGouldrick(University of Colorado Boulder)

Akatsuki, being in Venus orbit since December 2015, has acquired a volume of high-quality data, unveiled many new phenomena and is allowing researchers to investigate the underlying mechanisms. As the data accumulate, numerical models and theories are being advanced as well. We are no doubt living in the new golden era of Venus studies. This session invites papers of the new scientific results with Akatsuki data and the latest results of theoretical and numerical works. We expect participants of this session share the latest research results through presentations and discussion.

[PPS05-P01] New thermal infrared camera for fine horizontal brightness temperature structures at the cloud-top level of Venus

*Tetsuya Fukuhara[1], Makoto Taguchi[1], Takeshi Imamura[2], Sanjay S Limaye[3] (1.Rikkyo University, 2.The University of Tokyo, 3.University of Wisconsin)

[PPS05-P02] Temperature and wind variations in Venusian mesosphere and lower thermosphere by mid-infrared heterodyne spectrometer in 2018

*Kosuke Takami[1], Hiromu Nakagawa[1], Hideo Sagawa[2], Isao Murata[1], Yasumasa Kasaba[1] (1.Graduate School of Science, Tohoku University, 2.Division of Science, Kyoto Sangyo University)

[PPS05-P03] Local time dependence of limb darkening seen in the thermal infrared Venus disk

*Masahiro Akiba[1] (1.Rikkyo University)

[PPS05-P04] Stationary wavy features and Banded structures at Venusian cloud top extracted by averaging multiple LIR images

*Kiichi Fukuya[1], Takeshi Imamura[1], Makoto Taguchi[2], Tetsuya Fukuhara[2], Toru Kouyama[3] (1.Univ. of Tokyo, 2.Rikkyo Univ., 3.AIST)

[PPS05-P05] Akatsuki's IR2 Nightside Photometry Restoration by Deconvolution

*Choon Wei Vun[1], Takehiko Satoh[2,1], Kevin McGouldrick[3], Takeshi Horinouchi[4], Takao M. Sato[5] (1.SOKENDAI, 2.ISAS/JAXA, 3.University of Colorado Boulder, 4.Hokkaido University, 5.Hokkaido Information University)

[PPS05-P06] Enormous cloud cover as seen by Akatsuki/IR2 on the night-side disk of Venus

*Takehiko Satoh[1,2], Choon Wei Vun[2], Takao M. Sato[3], Takeshi Horinouchi[4], George HASHIMOTO[5], Kevin McGouldrick[6] (1.Institute of Space and Astronautical Science, Japan Aerospace Exploration Agency, 2.Department of Space Science, SOKENDAI, 3.Department of Business and Information Systems, Hokkaido Information University, 4.Faculty of Environmental Earth Science, Hokkaido University, 5.Department of Earth Science, Okayama University, 6.LASP, University of Colorado Boulder)

[PPS05-P07] The global variation of Venus cloud obtained from IR1 camera onboard AKATSUKI

*Seiko Takagi[1], Naomoto Iwagami, Yukihiro Takahashi[1], Mitsuteru Sato[1] (1.Hokkaido University, Graduate School of Science)

[PPS05-P08] Development of a Venus' cloud formation scheme for a convection resolving model

*Ko-ichiro SUGIYAMA[1], Nozomu Fukuhara[1], Masatsugu Odaka[2], Kensuke Nakajima[3], Masaki Ishiwatari[2], Takeshi Imamura[4], Yoshi-Yuki Hayashi[5] (1.National Institute of Technology, Matsue College, 2.Department of Cosmoscience, Graduate School of Science, Hokkaido University, 3.Department of Earth and Planetary Sciences,Flculty of Sciences,Kyushu University, 4.Graduate School of Frontier Sciences, The University of Tokyo, 5.Department of Planetology, Graduate School of Science, Kobe University / Center for Planetary Science (CPS))

[PPS05-P09] Zonal mean structure of Venus atmosphere observed in a Venus general circulation model with explicit radiative transfer

★Invited Papers

*Yoshi-Yuki Hayashi[1], Chisato Shiojiri[1], Hiroki Kashimura[1], Yoshiyuki O. Takahashi[1] (1.Department of Planetology/CPS, Graduate School of Science, Kobe University)

[PPS05-P10] Gravity wave packets detected in radio occultation temperature profiles of the Venus atmosphere

*Ryota Mori[1], Takeshi Imamura[1], Javier Peralta[2] (1.The University of Tokyo, 2.Japan Aerospace Exploration Agency)

[PPS05-P11] **Status of lightning hunt in Venus with Akatsuki/LAC and Pirka telescope**

*Yukihiro Takahashi[1,2], Mitsuteru Sato[1,2], Masataka Imai[3], Ralph Lorenz[4], Seiko Takagi[1,2], Ono Tatsuharu[1] (1.Graduate School of Science, Hokkaido University, 2.Faculty of Science, Hokkaido University, 3.National Institute of Advanced Industrial Science and Technology,, 4.Applied Physics Laboratory, Johns Hopkins University)

[PPS05-P12] **Possibility of electric discharge in the Venusian atmosphere due to the super-rotation of clouds**

*Adhithiyan Neduncheran[1], Ugur Guven[1,2], Ananyo Bhattacharya[3] (1.University of Petroleum and Energy Studies, India, 2.United Nations Centre for Space Science and Technology Education in Asia and the Pacific, 3.Sardar Vallabhbhai National Institute of Technology,India)

New thermal infrared camera for fine horizontal brightness temperature structures at the cloud-top level of Venus

*Tetsuya Fukuhara[1], Makoto Taguchi[1], Takeshi Imamura[2], Sanjay S Limaye[3]

1. Rikkyo University, 2. The University of Tokyo, 3. University of Wisconsin

The Longwave Infrared Camera (LIR), which is an uncooled microbolometer camera, is currently acquiring thermal infrared images (8-12 μm) of Venus and depicting the cloud-top brightness temperatures from Akatsuki orbiter around Venus since December 2015. The outstanding result of LIR has been the discovery of an interhemispheric bow-shaped structure meridionally stretching 10,000 km across the equator at the Venus cloud-top. Over several days of observations, the bow-shaped structure remains relatively fixed in position above the highland on the slowly rotating surface, despite the background atmospheric super rotation at ~100 m/s. We infer that the bow-shaped structure is the result of an atmospheric gravity wave generated in the lower atmosphere by mountain topography that then propagated upwards [1]. This indicates that the horizontal temperature distribution seen at the cloud-top level represents not only direct physical property at the cloud-top but also influence of dynamics in the lower atmosphere. In fact, preliminary observation of LIR has detected fine structure (~100 km) in temperature distribution from close-up observations near the periapsis. We suggest that this may be caused by the upward propagation of a gravity wave, which is generated by the convection layer at ~40 km altitude. However, the spatial resolution of LIR seems insufficient to understand the origins of such a fine structure. We need better observations at higher spatial resolution than possible from LIR in Akatsuki's orbit.

We propose that a future Venus orbiter carries an updated version of the uncooled microbolometer camera (BOL) with 1024x768 pixels and angular resolution of ~0.01 deg/pixel to detect fine temperature structure on the cloud-tops. When the orbiter is typically injected to a high-inclined elliptical orbit with altitude of 500-50,000 km, BOL provides a spatial resolution of 8.5 km at apoapsis and 0.08 km at periapsis, respectively. It will be enough to observe the fine temperature structure at the cloud-top. Further, BOL will capture the fine temperature structure at polar region near the "eye" of the hemispheric vortex situated over the poles, where the horizontal temperature varies drastically near the Venus cloud-tops. VIRTIS instrument on Venus Express orbiter showed complex structures at near infrared wavelengths [2]. Akatsuki from its near equatorial elliptical orbit cannot observe the fine structure in polar regions.

During 2012-2014, we developed an uncooled micro-bolometer array (UMBA) camera for the 50 kg class Earth observing satellite based on the experience of LIR development [3]. The camera with the pixel size of 640 ×480 was launched in 2014 and successfully detect a small wildfire which was main observation target for the mission. The results showed that its performance was better than expected. Furthermore, the newest UMBA camera with the pixel size increased to 1024 ×768 has been developed for the next wildfire mission to take finer spatial resolution image with ~0.01 deg/pixel. Unfortunately, this camera has lost the launch opportunity. However, the flight-model has been assembled and has passed function tests. Since BOL does not need heavy cryogenic systems, its mass and size are less than ~1 kg and 100 mm x 100 mm x 120 mm, respectively; it would be a relatively small mass increment for the future Venus mission.

References

[1] Fukuhara, T., et al., 2017, Large stationary gravity wave in the atmosphere of Venus, Nature Geoscience, Vol. 10, 85–88.

©2019. Japan Geoscience Union. All Right Reserved.

[2] Garate-Lopez, I., et al., 2015, Atmospheric dynamics at the southern pole of Venus: Three-dimensional winds, temperature and vorticity, AGU Fall Meeting Abstracts, 23.
[3] Fukuhara, T., et al., 2017, Detection of small wildfire by thermal infrared camera with the uncooled microbolometer array for 50 kg class satellite, IEEE Transactions on Geoscience and Remote Sensing, 2017, Vol. 55, No. 8, 4314-4324

Keywords: Venus, atmosphere, Akatsuki

©2019. Japan Geoscience Union. All Right Reserved.

Temperature and wind variations in Venusian mesosphere and lower thermosphere by mid-infrared heterodyne spectrometer in 2018

*Kosuke Takami[1], Hiromu Nakagawa[1], Hideo Sagawa[2], Isao Murata[1], Yasumasa Kasaba[1]

1. Graduate School of Science, Tohoku University, 2. Division of Science, Kyoto Sangyo University

The most extensive observations of Venusian mesosphere have been performed by Venus Express (VEX) up to 2014 (e.g., Patzold et al., 2007; Mahieux et al., 2015). These observations have found the highly spatial and temporal variations in the thermal structure. The temperature discrepancies between observations by VEX/SOIR and general circulation models in the altitude of 80 - 100 km have not been properly interpreted (Bougher et al., 2015; Gilli et al., 2017). In addition, the mesospheric dynamics located between retrograde superrotational zonal wind (cloud deck) and subsolar-to-antisolar flow (above 120 km altitude) have not been well understood due to lack of observations. On the other hand, the lower thermosphere has been observed by mid-infrared heterodyne spectrometer (MIR-HS). Temperature in this region varied extensively between 140 K and 240 K, and wind velocity changed intensely from 130 m/s to 190 m/s for a terrestrial day (Sornig et al., 2013; Krause et al., 2018). Temperature and wind variations such as periodicity and locality in Venusian mesosphere and lower thermosphere have not been comprehended. The purpose of our observations is to solve it with continuous observations by MIR-HS.
Our Mid-Infrared Laser Heterodyne Instrument (MILAHI) have been inserted to Tohoku 60 cm telescope located the summit of Mt. Haleakala in Maui, Hawaii (Nakagawa et al., 2016). MILAHI has 10 um CO_2 laser as local oscillator. The field of view is 4 arcsec with 60 cm telescope and in the wavelength of 10 um. MIR-HS can retrieve temperature and wind in different altitude between dayside observations and nightside observations. CO_2 emerge non-local thermodynamic equilibrium emission from 100 –120 km altitude in dayside (Lopez-Valverde et al., 2011). Temperature and wind are derived from Doppler width and Doppler shift of the emission spectra, respectively. In nightside, CO_2 in the mesosphere absorbs background radiation from the cloud deck. Temperature profile and wind are retrieved from this absorption spectra with radiative transfer equation and inverse method of AMATERASU developed in National Institute of Information and Communications Technology.
Dayside observations were conducted between 24th and 27th in June, 2018. Apparent diameter was 15 arcsec and apparent dayside was half of the disk in this term. Observed points were North, South, disk center, and equator with integration times of 30 - 55 minutes. Each observed point gave different temperature variation feature. Temperature variation range was 170 - 220 K in agreement with Sonnabend et al. (2010). Temperature distribution showed both latitudinal dependence in 25th and convergence at 200 K in 26th.
Nightside observations were conducted from 11th to 13th, 19th, and 20th in November, 2018. Apparent diameter of Venus changed between 55.4 and 49.4 arcsec after inferior conjunction. We observed equator with three days, north 33 degree and south 33 degree for diurnal and latitudinal variations with integration times of 80 - 130 minutes. The observed spectra in the unit of relative intensity are under conversion because the retrieval with AMATERASU is necessary to use absolute radiation. We will show retrieved temperature profile and wind velocity at this presentation.

Keywords: Venus, Mesosphere, mid-infrared spectroscopy

©2019. Japan Geoscience Union. All Right Reserved.

Local time dependence of limb darkening seen in the thermal infrared Venus disk

*Masahiro Akiba[1]

1. Rikkyo University

Brightness temperature of the Venus disk obtained by Longwave Infrared Camera (LIR) onboard Akatuski shows clear limb darkening in the low and middle latitudes. Limb darkening is an apparent temperature decrease from the center to the limb of the Venus disk. It is caused by thermal and radiative characteristics that the sensing altitude of LIR increases as an emission angle, which is a zenith angle of direction of emission from the Venus atmosphere to the sensor, increases and that the atmospheric temperature monotonically decreases with altitude. In higher latitudes limb brightening is observed, because an inversion layer exists at the cloud-top altitudes in higher latitudes. In other word a profile of the limb darkening reflects vertical distributions of atmospheric temperature and optical thickness of cloud particles. Taylor et al. [1980] presented local time dependence of limb darkening using brightness temperature data obtained by the Pioneer Venus orbiter, but did not mention its physical mechanism. In this study brightness temperature distributions obtained by LIR when Akatsuki was in the altitude range from 60,000 to 100,000 km during the period from October 19, 2016 to July 17, 2018 were analyzed to investigate temperature and cloud particle property at the cloud-tops. Each brightness temperature image with 328 x 248 pixels was divided into 3280 x 2480 sub-pixels, and 32 successive images were accumulated after precise adjustment of the Venus disk position to improve S/N. Brightness temperature profiles as a function of the emission angle were derived for 24 local time zones and 9 zonal belts with a latitudinal width of 10˚ within ±45˚. A degree of limb darkening and a brightness temperature at the disk center were determined by least-square function fitting. As a result, the degree of limb darkening shows a clear semi-diurnal variation, and is the strongest at 11h and 22h and the weakest at 7h and 18h in local time. The amplitude of semi-diurnal variation peaks at the equator, whereas its phase seems constant in all latitudes. The temperature at the disk center also shows a semi-diurnal variation with a phase shift of approximately two hours earlier than the phase of the degree of limb darkening and a slight diurnal variation in higher latitudes. These semi-diurnal and diurnal components observed by LIR are consistent with the past observation of thermal tides in the Venus atmosphere by VENERA 15 [Zasova et al., 2007]. The physical mechanism of the semi-diurnal and diurnal thermal tide components seen in the degree of limb darkening and cloud-top temperature will be discussed.

©2019. Japan Geoscience Union. All Right Reserved.

Local time dependence of limb darkening seen in the thermal infrared Venus disk

Masahiro Akiba, Tetsuya Fukuhara, and Makoto Taguchi
Rikkyo University

Brightness temperature of the Venus disk obtained by Longwave Infrared Camera (LIR) onboard Akatuski shows clear limb darkening in the low and middle latitudes. Limb darkening is an apparent temperature decrease from the center to the limb of the Venus disk. It is caused by thermal and radiative characteristics that the sensing altitude of LIR increases as an emission angle, which is a zenith angle of direction of emission from the Venus atmosphere to the sensor, increases and that the atmospheric temperature monotonically decreases with altitude. In higher latitudes limb brightening is observed, because an inversion layer exists at the cloud-top altitudes in higher latitudes. In other word a profile of the limb darkening reflects vertical distributions of atmospheric temperature and optical thickness of cloud particles. Taylor et al. [1980] presented local time dependence of limb darkening using brightness temperature data obtained by the Pioneer Venus orbiter, but did not mention its physical mechanism. In this study brightness temperature distributions obtained by LIR when Akatsuki was in the altitude range from 60,000 to 100,000 km during the period from October 19, 2016 to July 17, 2018 were analyzed to investigate temperature and cloud particle property at the cloud-tops. Each brightness temperature image with 328 x 248 pixels was divided into 3280 x 2480 sub-pixels, and 32 successive images were accumulated after precise adjustment of the Venus disk position to improve S/N. Brightness temperature profiles as a function of the emission angle were derived for 24 local time zones and 9 zonal belts with a latitudinal width of 10° within ±45°. A degree of limb darkening and a brightness temperature at the disk center were determined by least-square function fitting. As a result, the degree of limb darkening shows a clear semi-diurnal variation, and is the strongest at 11h and 22h and the weakest at 7h and 18h in local time. The amplitude of semi-diurnal variation peaks at the equator, whereas its phase seems constant in all latitudes. The temperature at the disk center also shows a semi-diurnal variation with a phase shift of approximately two hours earlier than the phase of the degree of limb darkening and a slight diurnal variation in higher latitudes. These semi-diurnal and diurnal components observed by LIR are consistent with the past observation of thermal tides in the Venus atmosphere by VENERA 15 [Zasova et al., 2007]. The physical mechanism of the semi-diurnal and diurnal thermal tide components seen in the degree of limb darkening and cloud-top temperature will be discussed.

©2019. Japan Geoscience Union. All Right Reserved.

Stationary wavy features and Banded structures at Venusian cloud top extracted by averaging multiple LIR images

*Kiichi Fukuya[1], Takeshi Imamura[1], Makoto Taguchi[2], Tetsuya Fukuhara[2], Toru Kouyama[3]

1. Univ. of Tokyo, 2. Rikkyo Univ., 3. AIST

Venus' cloud-top temperature distribution is now continuously mapped by LIR (Long-wave Infrared camera) mounted on the Venus orbiter Akatsuki. Fukuhara et al. (2017) analyzed LIR data and reported the existence of bow-shaped structures extending over 10,000 km in the north-south direction. The features are fixed in position without flowing with the super-rotation and appear above highlands with altitudes higher than 3 km. It was suggested based on a comparison with numerical simulations that the features are gravity waves generated by near-surface flows impinging on mountains. Kouyama et al. (2017) observed stationary features over 4 Venus days and revealed that the features tend to occur in the local afternoon. Gravity waves, whose restoring force is buoyancy, transport horizontal momentum in the vertical direction and accelerate or decelerate the background wind when they dissipate. Therefore, stationary gravity waves influence the general circulation of the atmosphere. In order to estimate the influence, it is essential to reveal the spatial and temporal distributions of gravity waves.
In the previous studies using LIR data, only planetary-scale stationary features have been investigated. On the other hand, Peralta et al. (2017) analyzed the data taken by VIRTIS onboard Venus Express, and reported the existence of many small-scale stationary features; however, VIRTIS can observe the night side only, and the observations were confined to the high latitude of the southern hemisphere because of the geometry of the orbit. Therefore, we intend to investigate with a new analysis method the topographical and local time dependency of small-scale, weak stationary features by using LIR data, which can observe all latitude regions at any local time. Though the S/N ratio of LIR is lower than VIRTIS, averaging of multiple images can suppress noises and at the same time emphasize stationary patterns. By using this method, small-scale, stationary wave trains were newly found above relatively-low topographic rises with altitudes of 1-3 km. In addition to stationary features, zonally-elongated banded structures were also found in averaged LIR images. Such structures have once been detected in LIR images taken during Akatsuki's Venus flyby in 2010 (Taguchi et al., 2012); the new analysis confirmed that banded structures are ubiquitous at the cloud top. The orientations of the banded structures are different from those of dark streaks found in ultraviolet images.

Keywords: Stationary gravity waves, Venus, Akatsuki

©2019. Japan Geoscience Union. All Right Reserved.

Akatsuki's IR2 Nightside Photometry Restoration by Deconvolution

*Choon Wei Vun[1], Takehiko Satoh[2,1], Kevin McGouldrick[3], Takeshi Horinouchi[4], Takao M. Sato[5]

1. SOKENDAI, 2. ISAS/JAXA, 3. University of Colorado Boulder, 4. Hokkaido University, 5. Hokkaido Information University

Akatsuki’ s IR2 camera captures images of Venus at different filters: 1.735um, 2.26um, and 2.32um. At near-dawn/dusk views (phase angles ~90 to 115 degree) of these images, the nightside photometry is contaminated by the intense dayside reflectance. As the potential well of a pixel is overfilled with incoming generated photoelectrons, the pixel is saturated and hence no longer contain information. This saturation can occur in the dayside and nightside near the terminator.
Owing to the saturation problem, main task of the restoration process is thus to simulate both day and night sides to replace the information loss in saturation. Point spread function (PSF) of the IR2 camera was modeled using Moffat function with observation of experimental image taken of point source street light before launch. Then, deconvolution by model-PSF can restore the nightside photometry of unsaturated pixels. Dayside reflectance was modeled with Lambert’ s law, where its distribution is multiplied by an F factor (W m^{-2} sr^{-1} um^{-1}). Methods of finding the F factor will be shown.
We present our Restoration by Deconvolution (RD) results of the selected dates. The restored images were limb darkening corrected. Efficiency of RD can be restored to ~0.005 sigma in standard deviation accuracy when performed on synthetic image with known answer image.
Correlation plot of unsaturated nightside radiances between two filters (2.26mm and 1.735mm) were produced to extract possible ‘branch’ phenomena. The branching in the correlation plot indicates the differences in optical depths of different particle size modes [1].
Restoration of nightside pixels also opens up the opportunity to study the cloud dynamics transiting from the dayside into the nightside. Moreover, interesting cloud features such as vortices, instabilities, and streaks are more distinct in recovered images. This in overall opens up new window to understanding the evolution of cloud motion in the middle layer.
References: [1] Carlson R.W. et al. (1993) *Planet. Space Sci., 41,* No. 7, 477-485. [2] Grinspoon D.H. et al. (1993) *Planet. Spce Sci, 41,* No. 7, 515-542. [3] Nakamura M. et al. (2011)*Earth, Planets and Space, 63,* 443-457. [4] Satoh T. et al. (2016) *Earth, Planets and Space 68:74*. [5] Satoh T. et al. (2017) *Earth, Planets and Space 69:154.* [6] Wilson C.F. et al. (2008) *JGR, 113,* E00B13

Keywords: Venus, atmosphere, image restoration, infrared

©2019. Japan Geoscience Union. All Right Reserved.

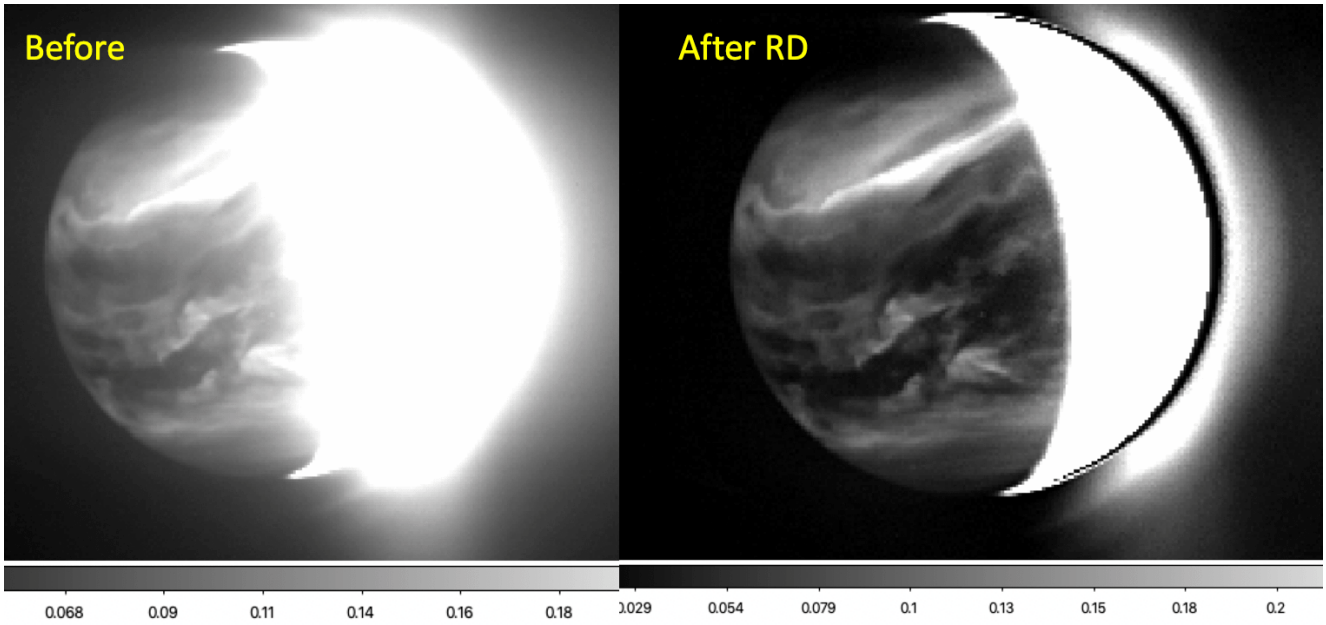

©2019. Japan Geoscience Union. All Right Reserved.

Enormous cloud cover as seen by Akatsuki/IR2 on the night-side disk of Venus

*Takehiko Satoh[1,2], Choon Wei Vun[2], Takao M. Sato[3], Takeshi Horinouchi[4], George HASHIMOTO[5], Kevin McGouldrick[6]

1. Institute of Space and Astronautical Science, Japan Aerospace Exploration Agency, 2. Department of Space Science, SOKENDAI, 3. Department of Business and Information Systems, Hokkaido Information University, 4. Faculty of Environmental Earth Science, Hokkaido University, 5. Department of Earth Science, Okayama University, 6. LASP, University of Colorado Boulder

Night-side observations in transparency windows of CO_2 atmosphere of Venus allow visualizing inhomogeneous clouds in ~50 to ~60 km altitudes. The IR2 camera on board Akatsuki captured such images at 1.735, 2.26, and 2.32 um wavelengths. In the IR2 night-side data, an enormous cloud of greater opacity and very sharp edge in the front (western end) is seen repeatedly. This feature seems to encircle the planet with a period of ~4.5 days (Peralta).
Although interesting, property of particles in this feature was not studied before due to difficulty of photometric measurements in IR2 night-side data. This difficulty comes from a combination of the intense day crescent and extended tail of IR2 point-spread function (multiple reflection in the detector is the cause). We have developed a technique to restore the contrast of the night-side data by deconvolution so that the photometric studies can be done with IR2 night-side data.
The data acquired on 18th and 27th August 2016 are analyzed. We have performed a series of radiative transfer computations to reproduce both 1.735- and 2.26-um opacities in this enormous cloud. Properties of the cloud partices will be presented and possible mechanism of this remarkable phenomenon will be discussed.

Keywords: Akatsuki IR2, Venus night-side, Cloud opacity

©2019. Japan Geoscience Union. All Right Reserved.

The global variation of Venus cloud obtained from IR1 camera onboard AKATSUKI

*Seiko Takagi[1], Naomoto Iwagami, Yukihiro Takahashi[1], Mitsuteru Sato[1]

1. Hokkaido University, Graduate School of Science

Venus is our nearest neighbor, and has a size very similar to the Earth's. However, previous observations discovered an extremely dense (92 bar at the surface) and CO_2-rich atmosphere, with H_2SO_4 thick clouds. The Venus cloud consists of H_2SO_4 main cloud deck at 47 −70 km, with thinner hazes above and below. The upper haze on Venus lies above the main cloud surrounding the planet, ranging from the top of the cloud (70 km) up to as high as 90 km. Near infrared (0.986 um) dayside image of Venus has taken by solid state imaging (SSI) of the Galileo spacecraft (NASA). It appears almost flat, there are some small scale features with a contrast of 3 %[Belton et al., 1991]. In Takagi and Iwagami. (2011), it may be calculated that the source of the contrast of the order of 3 % in near infrared Venus dayside image is due to variation in the cloud optical thickness. On December 7, 2015, AKATSUKI (JAXA) approached Venus and the Venus orbit insertion was successful. After the Venus orbit insertion, many 0.90 um Venus dayside images were taken by the 1 um near infrared camera (IR1) onboard AKATSUKI. In this study, Venus cloud variations are investigated from 0.90 um Venus dayside images taken by IR1 camera globally. Further, meteorological some changes that contribute to cloud variation are examined in using radiative transfer calculation with high altitude cloud model obtained from Venus Express/SOIR observation. Furthermore, I will introduce observation plan with PIRKA telescope of Hokkaido University.

Keywords: Venus, cloud, near infrared

©2019. Japan Geoscience Union. All Right Reserved.

Development of a Venus' cloud formation scheme for a convection resolving model

*Ko-ichiro SUGIYAMA[1], Nozomu Fukuhara[1], Masatsugu Odaka[2], Kensuke Nakajima[3], Masaki Ishiwatari[2], Takeshi Imamura[4], Yoshi-Yuki Hayashi[5]

1. National Institute of Technology, Matsue College, 2. Department of Cosmoscience, Graduate School of Science, Hokkaido University, 3. Department of Earth and Planetary Sciences,Flculty of Sciences,Kyushu University, 4. Graduate School of Frontier Sciences, The University of Tokyo, 5. Department of Planetology, Graduate School of Science, Kobe University / Center for Planetary Science (CPS)

Although convection has been suggested to occur in the lower part of Venus' cloud layer by some observational evidences, its structure remains to be clarified. In the previous studies, Baker et al. (1998, 2000), Imamura et al. (2014), and Lefevre et al. (2017) try to simulate Venus' cloud-level convection, but their models they utilized do not consider cloud formation process. Our purpose is to develop new cloud formation scheme and to perform numerical simulation using the scheme in order to investigate a possible structure of Venus' cloud-level convection and clouds distribution.

Our cloud formation scheme is based on Imamura and Hashimoto (1998). The number densities of sulfuric acid (H2SO4) and water (H2O) in the gas and liquid phases are calculated. Sedimentation of H2SO4-H2O solution droplets and chemical reactions of sulfuric acid are also considered. The scheme is implemented into our convection resolving model developed by Sugiyama et al. (2009). The model is based on the quasi-compressible system (Klemp and Wilhelmson, 1978), and is used in the simulations of the atmospheric convections of Jupiter (Sugiyama et al., 2011, 2014) and Mars (Yamashita et al. 2017).

In our poster, we will show the details of our cloud formation scheme and demonstrate some results of our calculation using similar settings of Imamura et al. (2014).

Keywords: Venus atmosphere, convection, cloud formation, numerical modeling

©2019. Japan Geoscience Union. All Right Reserved.

Zonal mean structure of Venus atmosphere observed in a Venus general circulation model with explicit radiative transfer

*Yoshi-Yuki Hayashi[1], Chisato Shiojiri[1], Hiroki Kashimura[1], Yoshiyuki O. Takahashi[1]

1. Department of Planetology/CPS, Graduate School of Science, Kobe University

Zonal mean zonal wind in Venus atmosphere is different from those in other planetary atmospheres. It is a strong prograde wind in all latitudinal ranges and is referred to as super-rotation. This unique zonal wind has been investigated by a lot of previous researchers with numerical simulations as well as ground-based and spacecraft observations. Among the studies with numerical simulations, in 2010s, Lebonnois et al. (2010) and Ikeda (2010) performed general circulation model simulations with an explicit radiative transfer model and successfully represented strong prograde zonal wind. These studies overcome a shortcoming of previous studies, in which models use Newtonian cooling as a radiative forcing.

In our group, we have been developing a general circulation model for planetary atmospheres. In addition, we have just developed a Venus radiation model, which can be used in a general circulation model. In this study, by implementing the radiation model into our general circulation model, we try to perform general circulation model simulations of Venus atmosphere and investigate the zonal mean structure of Venus atmosphere and evaluate differences between previous studies.

The general circulation model used in this study is DCPAM (http://www.gfd-dennou.org/library/dcpam/). The model is based on primitive equation system and the equation system is solved by a spectral transform method. The DCPAM includes physical processes of radiation and turbulent mixing processes. In addition, heat diffusion in soil is considered to evaluate surface temperature. The radiation model implemented into the DCPAM has also been developed in our group, and is based on a correlated k-distribution method. Radiative fluxes calculated by this radiation model are compared well with observed ones. By the use of the model, we performed two experiments with and without surface orographic variation. Resolution of experiments is T15L52, in which the model has 48 (longitude) times 24 (latitude) grids in horizontal direction and 52 layers in vertical direction. Initial conditions for those experiments are the same, and are
motionless atmospheres with horizontally uniform temperature distribution based on VIRA. With this initial condition, the model is integrated for 150000 Earth days with diurnal variation and with no seasonal variation, i.e. zero
obliquity.

Statistically steady states are achieved after about 100000 Earth days from the start of integrations. In steady state, prograde zonal winds with velocity of about 50 m/s in low and middle latitude are maintained at cloud layer in both experiments with and without orographic variation, although the velocity is about a half of that observed in Venus
atmosphere.

Meridional circulation observed in the model has large direct cells in both hemispheres. The direct cells in the experiment without surface orography have vertical extent from the ground up to top of the model, except for low latitude region just above the ground where indirect cells form. However, in the experiment with surface orography, the cells are split in the vertical direction at bottom of cloud layer. In addition to direct cells, several indirect cells are also observed in the experiments. One of those is indirect cell at

©2019. Japan Geoscience Union. All Right Reserved.

cloud layer in high latitude. Other ones are several indirect cells which extends from the ground up to bottom of cloud layer in the experiment with surface orography. These indicate that the effects of surface orography can be observed below the cloud layer, clearly.

In the presentation, results of analysis on zonal mean structure observed in the model, such as angular momentum, will also be presented.

Keywords: Venus, planetary atmosphere, general circulation model, explicit calculation of radiative transfer

©2019. Japan Geoscience Union. All Right Reserved.

Gravity wave packets detected in radio occultation temperature profiles of the Venus atmosphere

*Ryota Mori[1], Takeshi Imamura[1], Javier Peralta[2]

1. The University of Tokyo, 2. Japan Aerospace Exploration Agency

Temperature profiles has been obtained from 2016 by the radio occultation experiment in the Venus orbiter mission Akatsuki. The radio occultation experiment is a method that measures the change of the atmospheric refractive index as a change of the frequency of the signal received on the ground. At the opportunity when the radio wave transmitted from Akatsuki toward the Earth pass through the planetary atmosphere, the wave is refracted and then reaches the receiving station. We can retrieve the vertical profiles of the pressure and the temperature from each refractive index profiles. In the temperature profile obtained in this way, variations due to various atmospheric disturbances are observed. We focus on gravity waves which are thought to play an import role in driving the general atmosphere circulation.

Gravity waves are small-scale waves with the restoring force being the buoyancy in the atmosphere. Gravity waves play a role in carrying the momentum in the vertical direction. So, it results in acceleration or deceleration of the mean wind by passing momentum on the background atmosphere while dissipating. This process should affect the global structure of the high-speed zonal wind. However, since gravity waves have properties that the spatial scale is small and the wave period is relatively short, it is difficult to capture the spatial structure by observation. The latitudinal profile of the amplitude of short vertical-scale temperature disturbances, which are thought to be associated with gravity waves, has been investigated; however, the dominant wavelength and the typical vertical extent have not been studied.

In this study, we applied wavelet analysis to the temperature profiles and extracted spatially localized temperature disturbances. Though there have been studies that apply Fourier transform to the temperature data, Fourier transform assumes infinitely lasting waves and it is not suitable for extracting spatially localized wave packets. Wavelet analysis is an effective way of obtaining the periods and the amplitudes of waves in such finite intervals. In this presentation, we report the result of wavelet analysis applied to the temperature data obtained with high vertical resolution by radio holographic method. From the obtained results, we also report the relationship between the length and the packet length of gravity wave in the atmosphere.

Keywords: Akatsuki, Gravity wave in the atmosphere, The radio occultation experiment

©2019. Japan Geoscience Union. All Right Reserved.

Status of lightning hunt in Venus with Akatsuki/LAC and Pirka telescope

*Yukihiro Takahashi[1,2], Mitsuteru Sato[1,2], Masataka Imai[3], Ralph Lorenz[4], Seiko Takagi[1,2], Ono Tatsuharu[1]

1. Graduate School of Science, Hokkaido University, 2. Faculty of Science, Hokkaido University, 3. National Institute of Advanced Industrial Science and Technology,, 4. Applied Physics Laboratory, Johns Hopkins University

The existence of lightning discharge in Venus has been controversial for three decades, which might be attributed to the luck of conclusive observational evidence. There had been no satellite payload intentionally designed for the detection of lightning phenomena using radio wave or optical sensor. LAC, lightning and airglow camera, on board Akatsuki spacecraft, is the first sensor optimized for the lightning optical flash measurement in planets other than the Earth. It is expected that LAC could conclude this 30-year discussion on the existence of lightning in Venus. Unique performance of LAC compared to other equipment used in the previous exploration of Venus is the high-speed sampling rate at 20 kHz with 32 pixels of Avalanche Photo Diode (APD) matrix, enabling us to distinguish the natural optical lightning flash from other pulsing noises, including artificial electrical noise and cosmic rays. We selected OI 777 nm line for lightning detection, which is expected to be the most prominent emission in CO2-dominant atmosphere based on the laboratory experiments.

The triggering parameter was set so as to optimize for the light curve similar to the normal lightning in the Earth and data obtained totally for about 4 hours were examined. However, we couldn’ t find any lightning signals. Adding to this triggering parameter set, we added one more parameter set, optimized for sprite type emission with duration of up to 10s of ms. Furthermore, in order to investigate fainter emissions, we are now conducting successive force triggering recordings without any threshold, achieving 5 times better sensitivity than the intensity of 1 digital unit at best.

The total coverage of the LAC lightning hunt became 81.6 [million km2-hr], meaning 81 percent detectability of previous results with ground-based telescope by Hansell et al. (1995). Here we report the detailed strategy and the latest status of the LAC observation in 2018, and discuss the future observation plan.

Also we will make ground observation with a high-speed photometer installed at Pirka telescope, a 1.6-m reflector deployed by Hokkaido University. Here we report the initial results of lightning flash observation with it.

Keywords: lightning, Venus, Akatsuki, Pirka telescope

©2019. Japan Geoscience Union. All Right Reserved.

Possibility of electric discharge in the Venusian atmosphere due to the super-rotation of clouds

*Adhithiyan Neduncheran[1], Ugur Guven[1,2], Ananyo Bhattacharya[3]

1. University of Petroleum and Energy Studies, India, 2. United Nations Centre for Space Science and Technology Education in Asia and the Pacific, 3. Sardar Vallabhbhai National Institute of Technology,India

Several evidences of electromagnetic bursts were measured by various landers and orbiters studying Venus atmosphere (Venera landers, Venus Express and the Pioneer Venus Orbiter). The electromagnetic bursts that are taking place in the cloud region in the form of lightning or fluorescence might be a result of momentum transfer, solar convection and charge dispersion in the clouds of Venus. While the lightning in Earth takes place mostly in the equatorial region, in case of Venus it is possible for lightning to occur in the polar regions, considering the kinetic energy transfer and the formation of dipoles in both hemispheres of Venus. The meridional and zonal flows can interact and cause the charge separation which possibly lead to electromagnetic bursts in different spectrum and in different regions in Venus. In labs, it is observed that SO2 emissions in UV region cause fluorescence which is one of the major phenomena taking place in the cloud tops. Based on the photochemical model published by *Krasnopolsky 2011(*doi:10.1016/j.icarus.2011.11.012) and the principle of refraction, we present the possibility of lightning/fluorescence phenomena being caused by the super-rotation of the clouds in the Venusian atmosphere.

Keywords: Venus , Super-rotation, lightning, electric discharge, atmosphere

©2019. Japan Geoscience Union. All Right Reserved.

[E] Poster | P (Space and Planetary Sciences)：P-PS Planetary Sciences

Mon. May 27, 2019 5:15 PM - 6:30 PM JST | Mon. May 27, 2019 8:15 AM - 9:30 AM UTC | Poster Hall International Exhibition Hall8, Makuhari Messe_2

[P-PS05] Recent advances of Venus science

convener:Takehiko Satoh(Institute of Space and Astronautical Science, Japan Aerospace Exploration Agency), Takeshi Horinouchi(Faculty of Environmental Earth Science, Hokkaido University), Masaru Yamamoto(Research Institute for Applied Mechanics, Kyushu University), Kevin McGouldrick(University of Colorado Boulder)

Akatsuki, being in Venus orbit since December 2015, has acquired a volume of high-quality data, unveiled many new phenomena and is allowing researchers to investigate the underlying mechanisms. As the data accumulate, numerical models and theories are being advanced as well. We are no doubt living in the new golden era of Venus studies. This session invites papers of the new scientific results with Akatsuki data and the latest results of theoretical and numerical works. We expect participants of this session share the latest research results through presentations and discussion.

[PPS05-P01] New thermal infrared camera for fine horizontal brightness temperature structures at the cloud-top level of Venus

*Tetsuya Fukuhara[1], Makoto Taguchi[1], Takeshi Imamura[2], Sanjay S Limaye[3] (1.Rikkyo University, 2.The University of Tokyo, 3.University of Wisconsin)

[PPS05-P02] Temperature and wind variations in Venusian mesosphere and lower thermosphere by mid-infrared heterodyne spectrometer in 2018

*Kosuke Takami[1], Hiromu Nakagawa[1], Hideo Sagawa[2], Isao Murata[1], Yasumasa Kasaba[1] (1.Graduate School of Science, Tohoku University, 2.Division of Science, Kyoto Sangyo University)

[PPS05-P03] Local time dependence of limb darkening seen in the thermal infrared Venus disk

*Masahiro Akiba[1] (1.Rikkyo University)

[PPS05-P04] Stationary wavy features and Banded structures at Venusian cloud top extracted by averaging multiple LIR images

*Kiichi Fukuya[1], Takeshi Imamura[1], Makoto Taguchi[2], Tetsuya Fukuhara[2], Toru Kouyama[3] (1.Univ. of Tokyo, 2.Rikkyo Univ., 3.AIST)

[PPS05-P05] Akatsuki's IR2 Nightside Photometry Restoration by Deconvolution

*Choon Wei Vun[1], Takehiko Satoh[2,1], Kevin McGouldrick[3], Takeshi Horinouchi[4], Takao M. Sato[5] (1.SOKENDAI, 2.ISAS/JAXA, 3.University of Colorado Boulder, 4.Hokkaido University, 5.Hokkaido Information University)

[PPS05-P06] Enormous cloud cover as seen by Akatsuki/IR2 on the night-side disk of Venus

*Takehiko Satoh[1,2], Choon Wei Vun[2], Takao M. Sato[3], Takeshi Horinouchi[4], George HASHIMOTO[5], Kevin McGouldrick[6] (1.Institute of Space and Astronautical Science, Japan Aerospace Exploration Agency, 2.Department of Space Science, SOKENDAI, 3.Department of Business and Information Systems, Hokkaido Information University, 4.Faculty of Environmental Earth Science, Hokkaido University, 5.Department of Earth Science, Okayama University, 6.LASP, University of Colorado Boulder)

[PPS05-P07] The global variation of Venus cloud obtained from IR1 camera onboard AKATSUKI

*Seiko Takagi[1], Naomoto Iwagami, Yukihiro Takahashi[1], Mitsuteru Sato[1] (1.Hokkaido University, Graduate School of Science)

[PPS05-P08] Development of a Venus' cloud formation scheme for a convection resolving model

*Ko-ichiro SUGIYAMA[1], Nozomu Fukuhara[1], Masatsugu Odaka[2], Kensuke Nakajima[3], Masaki Ishiwatari[2], Takeshi Imamura[4], Yoshi-Yuki Hayashi[5] (1.National Institute of Technology, Matsue College, 2.Department of Cosmoscience, Graduate School of Science, Hokkaido University, 3.Department of Earth and Planetary Sciences,Flculty of Sciences,Kyushu University, 4.Graduate School of Frontier Sciences, The University of Tokyo, 5.Department of Planetology, Graduate School of Science, Kobe University / Center for Planetary Science (CPS))

[PPS05-P09] Zonal mean structure of Venus atmosphere observed in a Venus general circulation model with explicit radiative transfer

★Invited Papers

*Yoshi-Yuki Hayashi[1], Chisato Shiojiri[1], Hiroki Kashimura[1], Yoshiyuki O. Takahashi[1] (1.Department of Planetology/CPS, Graduate School of Science, Kobe University)

[PPS05-P10] Gravity wave packets detected in radio occultation temperature profiles of the Venus atmosphere

*Ryota Mori[1], Takeshi Imamura[1], Javier Peralta[2] (1.The University of Tokyo, 2.Japan Aerospace Exploration Agency)

[PPS05-P11] **Status of lightning hunt in Venus with Akatsuki/LAC and Pirka telescope**

*Yukihiro Takahashi[1,2], Mitsuteru Sato[1,2], Masataka Imai[3], Ralph Lorenz[4], Seiko Takagi[1,2], Ono Tatsuharu[1] (1.Graduate School of Science, Hokkaido University, 2.Faculty of Science, Hokkaido University, 3.National Institute of Advanced Industrial Science and Technology,, 4.Applied Physics Laboratory, Johns Hopkins University)

[PPS05-P12] **Possibility of electric discharge in the Venusian atmosphere due to the super-rotation of clouds**

*Adhithiyan Neduncheran[1], Ugur Guven[1,2], Ananyo Bhattacharya[3] (1.University of Petroleum and Energy Studies, India, 2.United Nations Centre for Space Science and Technology Education in Asia and the Pacific, 3.Sardar Vallabhbhai National Institute of Technology,India)

New thermal infrared camera for fine horizontal brightness temperature structures at the cloud-top level of Venus

*Tetsuya Fukuhara[1], Makoto Taguchi[1], Takeshi Imamura[2], Sanjay S Limaye[3]

1. Rikkyo University, 2. The University of Tokyo, 3. University of Wisconsin

The Longwave Infrared Camera (LIR), which is an uncooled microbolometer camera, is currently acquiring thermal infrared images (8-12 μm) of Venus and depicting the cloud-top brightness temperatures from Akatsuki orbiter around Venus since December 2015. The outstanding result of LIR has been the discovery of an interhemispheric bow-shaped structure meridionally stretching 10,000 km across the equator at the Venus cloud-top. Over several days of observations, the bow-shaped structure remains relatively fixed in position above the highland on the slowly rotating surface, despite the background atmospheric super rotation at ~100 m/s. We infer that the bow-shaped structure is the result of an atmospheric gravity wave generated in the lower atmosphere by mountain topography that then propagated upwards [1]. This indicates that the horizontal temperature distribution seen at the cloud-top level represents not only direct physical property at the cloud-top but also influence of dynamics in the lower atmosphere. In fact, preliminary observation of LIR has detected fine structure (~100 km) in temperature distribution from close-up observations near the periapsis. We suggest that this may be caused by the upward propagation of a gravity wave, which is generated by the convection layer at ~40 km altitude. However, the spatial resolution of LIR seems insufficient to understand the origins of such a fine structure. We need better observations at higher spatial resolution than possible from LIR in Akatsuki's orbit.

We propose that a future Venus orbiter carries an updated version of the uncooled microbolometer camera (BOL) with 1024x768 pixels and angular resolution of ~0.01 deg/pixel to detect fine temperature structure on the cloud-tops. When the orbiter is typically injected to a high-inclined elliptical orbit with altitude of 500-50,000 km, BOL provides a spatial resolution of 8.5 km at apoapsis and 0.08 km at periapsis, respectively. It will be enough to observe the fine temperature structure at the cloud-top. Further, BOL will capture the fine temperature structure at polar region near the "eye" of the hemispheric vortex situated over the poles, where the horizontal temperature varies drastically near the Venus cloud-tops. VIRTIS instrument on Venus Express orbiter showed complex structures at near infrared wavelengths [2]. Akatsuki from its near equatorial elliptical orbit cannot observe the fine structure in polar regions.

During 2012-2014, we developed an uncooled micro-bolometer array (UMBA) camera for the 50 kg class Earth observing satellite based on the experience of LIR development [3]. The camera with the pixel size of 640 ×480 was launched in 2014 and successfully detect a small wildfire which was main observation target for the mission. The results showed that its performance was better than expected. Furthermore, the newest UMBA camera with the pixel size increased to 1024 ×768 has been developed for the next wildfire mission to take finer spatial resolution image with ~0.01 deg/pixel. Unfortunately, this camera has lost the launch opportunity. However, the flight-model has been assembled and has passed function tests. Since BOL does not need heavy cryogenic systems, its mass and size are less than ~1 kg and 100 mm x 100 mm x 120 mm, respectively; it would be a relatively small mass increment for the future Venus mission.

References

[1] Fukuhara, T., et al., 2017, Large stationary gravity wave in the atmosphere of Venus, Nature Geoscience, Vol. 10, 85–88.

©2019. Japan Geoscience Union. All Right Reserved.

[2] Garate-Lopez, I., et al., 2015, Atmospheric dynamics at the southern pole of Venus: Three-dimensional winds, temperature and vorticity, AGU Fall Meeting Abstracts, 23.
[3] Fukuhara, T., et al., 2017, Detection of small wildfire by thermal infrared camera with the uncooled microbolometer array for 50 kg class satellite, IEEE Transactions on Geoscience and Remote Sensing, 2017, Vol. 55, No. 8, 4314-4324

Keywords: Venus, atmosphere, Akatsuki

©2019. Japan Geoscience Union. All Right Reserved.

Temperature and wind variations in Venusian mesosphere and lower thermosphere by mid-infrared heterodyne spectrometer in 2018

*Kosuke Takami[1], Hiromu Nakagawa[1], Hideo Sagawa[2], Isao Murata[1], Yasumasa Kasaba[1]

1. Graduate School of Science, Tohoku University, 2. Division of Science, Kyoto Sangyo University

The most extensive observations of Venusian mesosphere have been performed by Venus Express (VEX) up to 2014 (e.g., Patzold et al., 2007; Mahieux et al., 2015). These observations have found the highly spatial and temporal variations in the thermal structure. The temperature discrepancies between observations by VEX/SOIR and general circulation models in the altitude of 80 - 100 km have not been properly interpreted (Bougher et al., 2015; Gilli et al., 2017). In addition, the mesospheric dynamics located between retrograde superrotational zonal wind (cloud deck) and subsolar-to-antisolar flow (above 120 km altitude) have not been well understood due to lack of observations. On the other hand, the lower thermosphere has been observed by mid-infrared heterodyne spectrometer (MIR-HS). Temperature in this region varied extensively between 140 K and 240 K, and wind velocity changed intensely from 130 m/s to 190 m/s for a terrestrial day (Sornig et al., 2013; Krause et al., 2018). Temperature and wind variations such as periodicity and locality in Venusian mesosphere and lower thermosphere have not been comprehended. The purpose of our observations is to solve it with continuous observations by MIR-HS.
Our Mid-Infrared Laser Heterodyne Instrument (MILAHI) have been inserted to Tohoku 60 cm telescope located the summit of Mt. Haleakala in Maui, Hawaii (Nakagawa et al., 2016). MILAHI has 10 um CO_2 laser as local oscillator. The field of view is 4 arcsec with 60 cm telescope and in the wavelength of 10 um. MIR-HS can retrieve temperature and wind in different altitude between dayside observations and nightside observations. CO_2 emerge non-local thermodynamic equilibrium emission from 100 –120 km altitude in dayside (Lopez-Valverde et al., 2011). Temperature and wind are derived from Doppler width and Doppler shift of the emission spectra, respectively. In nightside, CO_2 in the mesosphere absorbs background radiation from the cloud deck. Temperature profile and wind are retrieved from this absorption spectra with radiative transfer equation and inverse method of AMATERASU developed in National Institute of Information and Communications Technology.
Dayside observations were conducted between 24th and 27th in June, 2018. Apparent diameter was 15 arcsec and apparent dayside was half of the disk in this term. Observed points were North, South, disk center, and equator with integration times of 30 - 55 minutes. Each observed point gave different temperature variation feature. Temperature variation range was 170 - 220 K in agreement with Sonnabend et al. (2010). Temperature distribution showed both latitudinal dependence in 25th and convergence at 200 K in 26th.
Nightside observations were conducted from 11th to 13th, 19th, and 20th in November, 2018. Apparent diameter of Venus changed between 55.4 and 49.4 arcsec after inferior conjunction. We observed equator with three days, north 33 degree and south 33 degree for diurnal and latitudinal variations with integration times of 80 - 130 minutes. The observed spectra in the unit of relative intensity are under conversion because the retrieval with AMATERASU is necessary to use absolute radiation. We will show retrieved temperature profile and wind velocity at this presentation.

Keywords: Venus, Mesosphere, mid-infrared spectroscopy

©2019. Japan Geoscience Union. All Right Reserved.

Local time dependence of limb darkening seen in the thermal infrared Venus disk

*Masahiro Akiba[1]

1. Rikkyo University

Brightness temperature of the Venus disk obtained by Longwave Infrared Camera (LIR) onboard Akatuski shows clear limb darkening in the low and middle latitudes. Limb darkening is an apparent temperature decrease from the center to the limb of the Venus disk. It is caused by thermal and radiative characteristics that the sensing altitude of LIR increases as an emission angle, which is a zenith angle of direction of emission from the Venus atmosphere to the sensor, increases and that the atmospheric temperature monotonically decreases with altitude. In higher latitudes limb brightening is observed, because an inversion layer exists at the cloud-top altitudes in higher latitudes. In other word a profile of the limb darkening reflects vertical distributions of atmospheric temperature and optical thickness of cloud particles. Taylor et al. [1980] presented local time dependence of limb darkening using brightness temperature data obtained by the Pioneer Venus orbiter, but did not mention its physical mechanism. In this study brightness temperature distributions obtained by LIR when Akatsuki was in the altitude range from 60,000 to 100,000 km during the period from October 19, 2016 to July 17, 2018 were analyzed to investigate temperature and cloud particle property at the cloud-tops. Each brightness temperature image with 328 x 248 pixels was divided into 3280 x 2480 sub-pixels, and 32 successive images were accumulated after precise adjustment of the Venus disk position to improve S/N. Brightness temperature profiles as a function of the emission angle were derived for 24 local time zones and 9 zonal belts with a latitudinal width of 10˚ within ±45˚. A degree of limb darkening and a brightness temperature at the disk center were determined by least-square function fitting. As a result, the degree of limb darkening shows a clear semi-diurnal variation, and is the strongest at 11h and 22h and the weakest at 7h and 18h in local time. The amplitude of semi-diurnal variation peaks at the equator, whereas its phase seems constant in all latitudes. The temperature at the disk center also shows a semi-diurnal variation with a phase shift of approximately two hours earlier than the phase of the degree of limb darkening and a slight diurnal variation in higher latitudes. These semi-diurnal and diurnal components observed by LIR are consistent with the past observation of thermal tides in the Venus atmosphere by VENERA 15 [Zasova et al., 2007]. The physical mechanism of the semi-diurnal and diurnal thermal tide components seen in the degree of limb darkening and cloud-top temperature will be discussed.

©2019. Japan Geoscience Union. All Right Reserved.

Local time dependence of limb darkening seen in the thermal infrared Venus disk

Masahiro Akiba, Tetsuya Fukuhara, and Makoto Taguchi
Rikkyo University

Brightness temperature of the Venus disk obtained by Longwave Infrared Camera (LIR) onboard Akatuski shows clear limb darkening in the low and middle latitudes. Limb darkening is an apparent temperature decrease from the center to the limb of the Venus disk. It is caused by thermal and radiative characteristics that the sensing altitude of LIR increases as an emission angle, which is a zenith angle of direction of emission from the Venus atmosphere to the sensor, increases and that the atmospheric temperature monotonically decreases with altitude. In higher latitudes limb brightening is observed, because an inversion layer exists at the cloud-top altitudes in higher latitudes. In other word a profile of the limb darkening reflects vertical distributions of atmospheric temperature and optical thickness of cloud particles. Taylor et al. [1980] presented local time dependence of limb darkening using brightness temperature data obtained by the Pioneer Venus orbiter, but did not mention its physical mechanism. In this study brightness temperature distributions obtained by LIR when Akatsuki was in the altitude range from 60,000 to 100,000 km during the period from October 19, 2016 to July 17, 2018 were analyzed to investigate temperature and cloud particle property at the cloud-tops. Each brightness temperature image with 328 x 248 pixels was divided into 3280 x 2480 sub-pixels, and 32 successive images were accumulated after precise adjustment of the Venus disk position to improve S/N. Brightness temperature profiles as a function of the emission angle were derived for 24 local time zones and 9 zonal belts with a latitudinal width of 10° within ±45°. A degree of limb darkening and a brightness temperature at the disk center were determined by least-square function fitting. As a result, the degree of limb darkening shows a clear semi-diurnal variation, and is the strongest at 11h and 22h and the weakest at 7h and 18h in local time. The amplitude of semi-diurnal variation peaks at the equator, whereas its phase seems constant in all latitudes. The temperature at the disk center also shows a semi-diurnal variation with a phase shift of approximately two hours earlier than the phase of the degree of limb darkening and a slight diurnal variation in higher latitudes. These semi-diurnal and diurnal components observed by LIR are consistent with the past observation of thermal tides in the Venus atmosphere by VENERA 15 [Zasova et al., 2007]. The physical mechanism of the semi-diurnal and diurnal thermal tide components seen in the degree of limb darkening and cloud-top temperature will be discussed.

©2019. Japan Geoscience Union. All Right Reserved.

Stationary wavy features and Banded structures at Venusian cloud top extracted by averaging multiple LIR images

*Kiichi Fukuya[1], Takeshi Imamura[1], Makoto Taguchi[2], Tetsuya Fukuhara[2], Toru Kouyama[3]

1. Univ. of Tokyo, 2. Rikkyo Univ., 3. AIST

Venus' cloud-top temperature distribution is now continuously mapped by LIR (Long-wave Infrared camera) mounted on the Venus orbiter Akatsuki. Fukuhara et al. (2017) analyzed LIR data and reported the existence of bow-shaped structures extending over 10,000 km in the north-south direction. The features are fixed in position without flowing with the super-rotation and appear above highlands with altitudes higher than 3 km. It was suggested based on a comparison with numerical simulations that the features are gravity waves generated by near-surface flows impinging on mountains. Kouyama et al. (2017) observed stationary features over 4 Venus days and revealed that the features tend to occur in the local afternoon. Gravity waves, whose restoring force is buoyancy, transport horizontal momentum in the vertical direction and accelerate or decelerate the background wind when they dissipate. Therefore, stationary gravity waves influence the general circulation of the atmosphere. In order to estimate the influence, it is essential to reveal the spatial and temporal distributions of gravity waves.
In the previous studies using LIR data, only planetary-scale stationary features have been investigated. On the other hand, Peralta et al. (2017) analyzed the data taken by VIRTIS onboard Venus Express, and reported the existence of many small-scale stationary features; however, VIRTIS can observe the night side only, and the observations were confined to the high latitude of the southern hemisphere because of the geometry of the orbit. Therefore, we intend to investigate with a new analysis method the topographical and local time dependency of small-scale, weak stationary features by using LIR data, which can observe all latitude regions at any local time. Though the S/N ratio of LIR is lower than VIRTIS, averaging of multiple images can suppress noises and at the same time emphasize stationary patterns. By using this method, small-scale, stationary wave trains were newly found above relatively-low topographic rises with altitudes of 1-3 km. In addition to stationary features, zonally-elongated banded structures were also found in averaged LIR images. Such structures have once been detected in LIR images taken during Akatsuki's Venus flyby in 2010 (Taguchi et al., 2012); the new analysis confirmed that banded structures are ubiquitous at the cloud top. The orientations of the banded structures are different from those of dark streaks found in ultraviolet images.

Keywords: Stationary gravity waves, Venus, Akatsuki

©2019. Japan Geoscience Union. All Right Reserved.

Akatsuki's IR2 Nightside Photometry Restoration by Deconvolution

*Choon Wei Vun[1], Takehiko Satoh[2,1], Kevin McGouldrick[3], Takeshi Horinouchi[4], Takao M. Sato[5]

1. SOKENDAI, 2. ISAS/JAXA, 3. University of Colorado Boulder, 4. Hokkaido University, 5. Hokkaido Information University

Akatsuki’ s IR2 camera captures images of Venus at different filters: 1.735um, 2.26um, and 2.32um. At near-dawn/dusk views (phase angles ~90 to 115 degree) of these images, the nightside photometry is contaminated by the intense dayside reflectance. As the potential well of a pixel is overfilled with incoming generated photoelectrons, the pixel is saturated and hence no longer contain information. This saturation can occur in the dayside and nightside near the terminator.
Owing to the saturation problem, main task of the restoration process is thus to simulate both day and night sides to replace the information loss in saturation. Point spread function (PSF) of the IR2 camera was modeled using Moffat function with observation of experimental image taken of point source street light before launch. Then, deconvolution by model-PSF can restore the nightside photometry of unsaturated pixels. Dayside reflectance was modeled with Lambert’ s law, where its distribution is multiplied by an F factor (W m^{-2} sr^{-1} um^{-1}). Methods of finding the F factor will be shown.
We present our Restoration by Deconvolution (RD) results of the selected dates. The restored images were limb darkening corrected. Efficiency of RD can be restored to ~0.005 sigma in standard deviation accuracy when performed on synthetic image with known answer image.
Correlation plot of unsaturated nightside radiances between two filters (2.26mm and 1.735mm) were produced to extract possible ‘branch’ phenomena. The branching in the correlation plot indicates the differences in optical depths of different particle size modes [1].
Restoration of nightside pixels also opens up the opportunity to study the cloud dynamics transiting from the dayside into the nightside. Moreover, interesting cloud features such as vortices, instabilities, and streaks are more distinct in recovered images. This in overall opens up new window to understanding the evolution of cloud motion in the middle layer.
References: [1] Carlson R.W. et al. (1993) *Planet. Space Sci., 41,* No. 7, 477-485. [2] Grinspoon D.H. et al. (1993) *Planet. Spce Sci, 41,* No. 7, 515-542. [3] Nakamura M. et al. (2011)*Earth, Planets and Space, 63,* 443-457. [4] Satoh T. et al. (2016) *Earth, Planets and Space 68:74*. [5] Satoh T. et al. (2017) *Earth, Planets and Space 69:154.* [6] Wilson C.F. et al. (2008) *JGR, 113,* E00B13

Keywords: Venus, atmosphere, image restoration, infrared

©2019. Japan Geoscience Union. All Right Reserved.

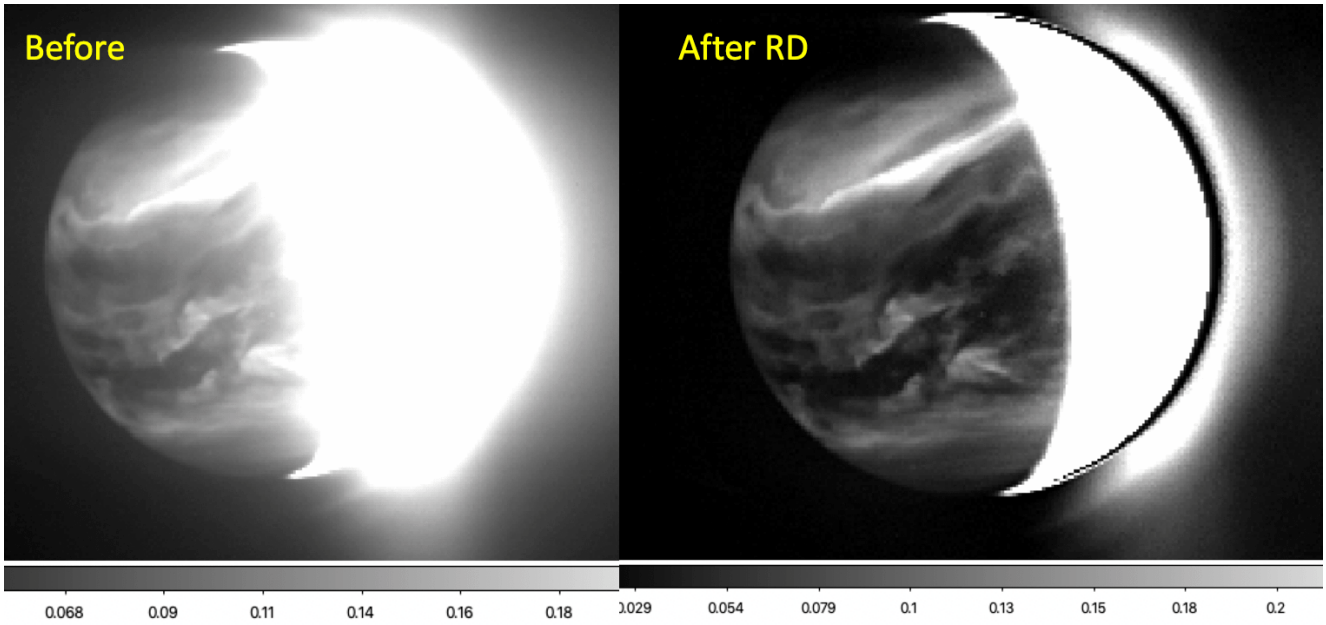

©2019. Japan Geoscience Union. All Right Reserved.

Enormous cloud cover as seen by Akatsuki/IR2 on the night-side disk of Venus

*Takehiko Satoh[1,2], Choon Wei Vun[2], Takao M. Sato[3], Takeshi Horinouchi[4], George HASHIMOTO[5], Kevin McGouldrick[6]

1. Institute of Space and Astronautical Science, Japan Aerospace Exploration Agency, 2. Department of Space Science, SOKENDAI, 3. Department of Business and Information Systems, Hokkaido Information University, 4. Faculty of Environmental Earth Science, Hokkaido University, 5. Department of Earth Science, Okayama University, 6. LASP, University of Colorado Boulder

Night-side observations in transparency windows of CO_2 atmosphere of Venus allow visualizing inhomogeneous clouds in ~50 to ~60 km altitudes. The IR2 camera on board Akatsuki captured such images at 1.735, 2.26, and 2.32 um wavelengths. In the IR2 night-side data, an enormous cloud of greater opacity and very sharp edge in the front (western end) is seen repeatedly. This feature seems to encircle the planet with a period of ~4.5 days (Peralta).
Although interesting, property of particles in this feature was not studied before due to difficulty of photometric measurements in IR2 night-side data. This difficulty comes from a combination of the intense day crescent and extended tail of IR2 point-spread function (multiple reflection in the detector is the cause). We have developed a technique to restore the contrast of the night-side data by deconvolution so that the photometric studies can be done with IR2 night-side data.
The data acquired on 18th and 27th August 2016 are analyzed. We have performed a series of radiative transfer computations to reproduce both 1.735- and 2.26-um opacities in this enormous cloud. Properties of the cloud partices will be presented and possible mechanism of this remarkable phenomenon will be discussed.

Keywords: Akatsuki IR2, Venus night-side, Cloud opacity

©2019. Japan Geoscience Union. All Right Reserved.

The global variation of Venus cloud obtained from IR1 camera onboard AKATSUKI

*Seiko Takagi[1], Naomoto Iwagami, Yukihiro Takahashi[1], Mitsuteru Sato[1]

1. Hokkaido University, Graduate School of Science

Venus is our nearest neighbor, and has a size very similar to the Earth's. However, previous observations discovered an extremely dense (92 bar at the surface) and CO_2-rich atmosphere, with H_2SO_4 thick clouds. The Venus cloud consists of H_2SO_4 main cloud deck at 47 −70 km, with thinner hazes above and below. The upper haze on Venus lies above the main cloud surrounding the planet, ranging from the top of the cloud (70 km) up to as high as 90 km. Near infrared (0.986 um) dayside image of Venus has taken by solid state imaging (SSI) of the Galileo spacecraft (NASA). It appears almost flat, there are some small scale features with a contrast of 3 %[Belton et al., 1991]. In Takagi and Iwagami. (2011), it may be calculated that the source of the contrast of the order of 3 % in near infrared Venus dayside image is due to variation in the cloud optical thickness. On December 7, 2015, AKATSUKI (JAXA) approached Venus and the Venus orbit insertion was successful. After the Venus orbit insertion, many 0.90 um Venus dayside images were taken by the 1 um near infrared camera (IR1) onboard AKATSUKI. In this study, Venus cloud variations are investigated from 0.90 um Venus dayside images taken by IR1 camera globally. Further, meteorological some changes that contribute to cloud variation are examined in using radiative transfer calculation with high altitude cloud model obtained from Venus Express/SOIR observation. Furthermore, I will introduce observation plan with PIRKA telescope of Hokkaido University.

Keywords: Venus, cloud, near infrared

©2019. Japan Geoscience Union. All Right Reserved.

Development of a Venus' cloud formation scheme for a convection resolving model

*Ko-ichiro SUGIYAMA[1], Nozomu Fukuhara[1], Masatsugu Odaka[2], Kensuke Nakajima[3], Masaki Ishiwatari[2], Takeshi Imamura[4], Yoshi-Yuki Hayashi[5]

1. National Institute of Technology, Matsue College, 2. Department of Cosmoscience, Graduate School of Science, Hokkaido University, 3. Department of Earth and Planetary Sciences,Flculty of Sciences,Kyushu University, 4. Graduate School of Frontier Sciences, The University of Tokyo, 5. Department of Planetology, Graduate School of Science, Kobe University / Center for Planetary Science (CPS)

Although convection has been suggested to occur in the lower part of Venus' cloud layer by some observational evidences, its structure remains to be clarified. In the previous studies, Baker et al. (1998, 2000), Imamura et al. (2014), and Lefevre et al. (2017) try to simulate Venus' cloud-level convection, but their models they utilized do not consider cloud formation process. Our purpose is to develop new cloud formation scheme and to perform numerical simulation using the scheme in order to investigate a possible structure of Venus' cloud-level convection and clouds distribution.

Our cloud formation scheme is based on Imamura and Hashimoto (1998). The number densities of sulfuric acid (H2SO4) and water (H2O) in the gas and liquid phases are calculated. Sedimentation of H2SO4-H2O solution droplets and chemical reactions of sulfuric acid are also considered. The scheme is implemented into our convection resolving model developed by Sugiyama et al. (2009). The model is based on the quasi-compressible system (Klemp and Wilhelmson, 1978), and is used in the simulations of the atmospheric convections of Jupiter (Sugiyama et al., 2011, 2014) and Mars (Yamashita et al. 2017).

In our poster, we will show the details of our cloud formation scheme and demonstrate some results of our calculation using similar settings of Imamura et al. (2014).

Keywords: Venus atmosphere, convection, cloud formation, numerical modeling

©2019. Japan Geoscience Union. All Right Reserved.

Zonal mean structure of Venus atmosphere observed in a Venus general circulation model with explicit radiative transfer

*Yoshi-Yuki Hayashi[1], Chisato Shiojiri[1], Hiroki Kashimura[1], Yoshiyuki O. Takahashi[1]

1. Department of Planetology/CPS, Graduate School of Science, Kobe University

Zonal mean zonal wind in Venus atmosphere is different from those in other planetary atmospheres. It is a strong prograde wind in all latitudinal ranges and is referred to as super-rotation. This unique zonal wind has been investigated by a lot of previous researchers with numerical simulations as well as ground-based and spacecraft observations. Among the studies with numerical simulations, in 2010s, Lebonnois et al. (2010) and Ikeda (2010) performed general circulation model simulations with an explicit radiative transfer model and successfully represented strong prograde zonal wind. These studies overcome a shortcoming of previous studies, in which models use Newtonian cooling as a radiative forcing.

In our group, we have been developing a general circulation model for planetary atmospheres. In addition, we have just developed a Venus radiation model, which can be used in a general circulation model. In this study, by implementing the radiation model into our general circulation model, we try to perform general circulation model simulations of Venus atmosphere and investigate the zonal mean structure of Venus atmosphere and evaluate differences between previous studies.

The general circulation model used in this study is DCPAM (http://www.gfd-dennou.org/library/dcpam/). The model is based on primitive equation system and the equation system is solved by a spectral transform method. The DCPAM includes physical processes of radiation and turbulent mixing processes. In addition, heat diffusion in soil is considered to evaluate surface temperature. The radiation model implemented into the DCPAM has also been developed in our group, and is based on a correlated k-distribution method. Radiative fluxes calculated by this radiation model are compared well with observed ones. By the use of the model, we performed two experiments with and without surface orographic variation. Resolution of experiments is T15L52, in which the model has 48 (longitude) times 24 (latitude) grids in horizontal direction and 52 layers in vertical direction. Initial conditions for those experiments are the same, and are
motionless atmospheres with horizontally uniform temperature distribution based on VIRA. With this initial condition, the model is integrated for 150000 Earth days with diurnal variation and with no seasonal variation, i.e. zero
obliquity.

Statistically steady states are achieved after about 100000 Earth days from the start of integrations. In steady state, prograde zonal winds with velocity of about 50 m/s in low and middle latitude are maintained at cloud layer in both experiments with and without orographic variation, although the velocity is about a half of that observed in Venus
atmosphere.

Meridional circulation observed in the model has large direct cells in both hemispheres. The direct cells in the experiment without surface orography have vertical extent from the ground up to top of the model, except for low latitude region just above the ground where indirect cells form. However, in the experiment with surface orography, the cells are split in the vertical direction at bottom of cloud layer. In addition to direct cells, several indirect cells are also observed in the experiments. One of those is indirect cell at

©2019. Japan Geoscience Union. All Right Reserved.

cloud layer in high latitude. Other ones are several indirect cells which extends from the ground up to bottom of cloud layer in the experiment with surface orography. These indicate that the effects of surface orography can be observed below the cloud layer, clearly.

In the presentation, results of analysis on zonal mean structure observed in the model, such as angular momentum, will also be presented.

Keywords: Venus, planetary atmosphere, general circulation model, explicit calculation of radiative transfer

©2019. Japan Geoscience Union. All Right Reserved.

Gravity wave packets detected in radio occultation temperature profiles of the Venus atmosphere

*Ryota Mori[1], Takeshi Imamura[1], Javier Peralta[2]

1. The University of Tokyo, 2. Japan Aerospace Exploration Agency

Temperature profiles has been obtained from 2016 by the radio occultation experiment in the Venus orbiter mission Akatsuki. The radio occultation experiment is a method that measures the change of the atmospheric refractive index as a change of the frequency of the signal received on the ground. At the opportunity when the radio wave transmitted from Akatsuki toward the Earth pass through the planetary atmosphere, the wave is refracted and then reaches the receiving station. We can retrieve the vertical profiles of the pressure and the temperature from each refractive index profiles. In the temperature profile obtained in this way, variations due to various atmospheric disturbances are observed. We focus on gravity waves which are thought to play an import role in driving the general atmosphere circulation.

Gravity waves are small-scale waves with the restoring force being the buoyancy in the atmosphere. Gravity waves play a role in carrying the momentum in the vertical direction. So, it results in acceleration or deceleration of the mean wind by passing momentum on the background atmosphere while dissipating. This process should affect the global structure of the high-speed zonal wind. However, since gravity waves have properties that the spatial scale is small and the wave period is relatively short, it is difficult to capture the spatial structure by observation. The latitudinal profile of the amplitude of short vertical-scale temperature disturbances, which are thought to be associated with gravity waves, has been investigated; however, the dominant wavelength and the typical vertical extent have not been studied.

In this study, we applied wavelet analysis to the temperature profiles and extracted spatially localized temperature disturbances. Though there have been studies that apply Fourier transform to the temperature data, Fourier transform assumes infinitely lasting waves and it is not suitable for extracting spatially localized wave packets. Wavelet analysis is an effective way of obtaining the periods and the amplitudes of waves in such finite intervals. In this presentation, we report the result of wavelet analysis applied to the temperature data obtained with high vertical resolution by radio holographic method. From the obtained results, we also report the relationship between the length and the packet length of gravity wave in the atmosphere.

Keywords: Akatsuki, Gravity wave in the atmosphere, The radio occultation experiment

©2019. Japan Geoscience Union. All Right Reserved.

Status of lightning hunt in Venus with Akatsuki/LAC and Pirka telescope

*Yukihiro Takahashi[1,2], Mitsuteru Sato[1,2], Masataka Imai[3], Ralph Lorenz[4], Seiko Takagi[1,2], Ono Tatsuharu[1]

1. Graduate School of Science, Hokkaido University, 2. Faculty of Science, Hokkaido University, 3. National Institute of Advanced Industrial Science and Technology,, 4. Applied Physics Laboratory, Johns Hopkins University

The existence of lightning discharge in Venus has been controversial for three decades, which might be attributed to the luck of conclusive observational evidence. There had been no satellite payload intentionally designed for the detection of lightning phenomena using radio wave or optical sensor. LAC, lightning and airglow camera, on board Akatsuki spacecraft, is the first sensor optimized for the lightning optical flash measurement in planets other than the Earth. It is expected that LAC could conclude this 30-year discussion on the existence of lightning in Venus. Unique performance of LAC compared to other equipment used in the previous exploration of Venus is the high-speed sampling rate at 20 kHz with 32 pixels of Avalanche Photo Diode (APD) matrix, enabling us to distinguish the natural optical lightning flash from other pulsing noises, including artificial electrical noise and cosmic rays. We selected OI 777 nm line for lightning detection, which is expected to be the most prominent emission in CO2-dominant atmosphere based on the laboratory experiments.

The triggering parameter was set so as to optimize for the light curve similar to the normal lightning in the Earth and data obtained totally for about 4 hours were examined. However, we couldn’ t find any lightning signals. Adding to this triggering parameter set, we added one more parameter set, optimized for sprite type emission with duration of up to 10s of ms. Furthermore, in order to investigate fainter emissions, we are now conducting successive force triggering recordings without any threshold, achieving 5 times better sensitivity than the intensity of 1 digital unit at best.

The total coverage of the LAC lightning hunt became 81.6 [million km2-hr], meaning 81 percent detectability of previous results with ground-based telescope by Hansell et al. (1995). Here we report the detailed strategy and the latest status of the LAC observation in 2018, and discuss the future observation plan.

Also we will make ground observation with a high-speed photometer installed at Pirka telescope, a 1.6-m reflector deployed by Hokkaido University. Here we report the initial results of lightning flash observation with it.

Keywords: lightning, Venus, Akatsuki, Pirka telescope

©2019. Japan Geoscience Union. All Right Reserved.

Possibility of electric discharge in the Venusian atmosphere due to the super-rotation of clouds

*Adhithiyan Neduncheran[1], Ugur Guven[1,2], Ananyo Bhattacharya[3]

1. University of Petroleum and Energy Studies, India, 2. United Nations Centre for Space Science and Technology Education in Asia and the Pacific, 3. Sardar Vallabhbhai National Institute of Technology,India

Several evidences of electromagnetic bursts were measured by various landers and orbiters studying Venus atmosphere (Venera landers, Venus Express and the Pioneer Venus Orbiter). The electromagnetic bursts that are taking place in the cloud region in the form of lightning or fluorescence might be a result of momentum transfer, solar convection and charge dispersion in the clouds of Venus. While the lightning in Earth takes place mostly in the equatorial region, in case of Venus it is possible for lightning to occur in the polar regions, considering the kinetic energy transfer and the formation of dipoles in both hemispheres of Venus. The meridional and zonal flows can interact and cause the charge separation which possibly lead to electromagnetic bursts in different spectrum and in different regions in Venus. In labs, it is observed that SO2 emissions in UV region cause fluorescence which is one of the major phenomena taking place in the cloud tops. Based on the photochemical model published by *Krasnopolsky 2011(*doi:10.1016/j.icarus.2011.11.012) and the principle of refraction, we present the possibility of lightning/fluorescence phenomena being caused by the super-rotation of the clouds in the Venusian atmosphere.

Keywords: Venus , Super-rotation, lightning, electric discharge, atmosphere

©2019. Japan Geoscience Union. All Right Reserved.

[J] Oral | P (Space and Planetary Sciences)：P-PS Planetary Sciences

Mon. May 27, 2019 9:00 AM - 10:30 AM JST | Mon. May 27, 2019 12:00 AM - 1:30 AM UTC | A01 TOKYO BAY MAKUHARI HALL

[P-PS06] Planetary Sciences

convener:Kenji Kurosaki(Department of Physics, Nagoya University), Yusuke Nakauchi(Japan Aerospace Exploration Agency), Chairperson:Kiyoshi Kuramoto(Hokkaido University), Takanori Sasaki(Department of Astronomy, Kyoto University)

We call for general interest papers for Planetary Scienses. Planetary Sciences consist of a variety of studies on the past, present, and future of our solar system and exoplanetary systems, Discussions based on various backgrounds are encouraged.

9:00 AM - 9:15 AM JST | 12:00 AM - 12:15 AM UTC

[PPS06-01] Current status of the PLANETS telescope project for planetary and exoplanetary atmospheric monitoring

*Takeshi Sakanoi[1], Masato Kagitani[1], Yasumasa Hirahara[2], Jeffery Kuhn[3], Svetalana Berdyugina[4], Marcelo Emilio[5], Hiromu Nakagawa[6], Mikio Kurita[7], Yasumasa Kasaba[1], Takahiro Obara[1], Shoichi Okano[1] (1.Planetary Plasma and Atmospheric Research Center, Graduate School of Science, Tohoku University, 2.Graduate School of Environmental Studies, Nagoya University, 3.IfA, University of Hawaii, U.S.A., 4.KIS, Germany, 5.Universidade Estadual de Ponta Grossa, Brazil, 6.Graduate School of Science, Tohoku University, 7.Graduate School of Science, Kyoto University)

9:15 AM - 9:30 AM JST | 12:15 AM - 12:30 AM UTC

[PPS06-02] Martian Moon eXploration MMX: science objectives and their promotion

*Kiyoshi Kuramoto[1,2], Yasuhiro Kawakatsu[2], Masaki Fujimoto[2], Jean Pierre Bibring[3], David Lawrence[4], Hidenori Genda[5], Naru Hirata[6], Takeshi Imamura[7], Shingo Kameda[8], Koji Matsumoto[9], Hideaki Miyamoto[7], Tomokatsu Morota[10], Hiroshi Nagaoka[2], Hiromu Nakagawa[11], Tomoki Nakamura[11], Kazunori Ogawa[12], Hisashi Otake[2], Masanobu Ozaki[2], Sho Sasaki[13], Hiroki Senshu[14], Shogo Tachibana[7,2], Naoki Terada[11], Tomohiro Usui[2], Koji Wada[14], Sei-ichiro WATANABE[10], MMX study team (1.Hokkaido Univ., 2.JAXA, 3.IAS, 4.APL, 5.ELSI, 6.Aizu Univ., 7.Univ. of Tokyo, 8.Rikkyo Univ., 9.NAOJ, 10.Nagoya Univ., 11.Tohoku Univ., 12.Kobe Univ., 13.Osaka Univ., 14.Chiba Inst. Tech.)

9:30 AM - 9:45 AM JST | 12:30 AM - 12:45 AM UTC

[PPS06-03] Implantation of Martian Materials in the Inner Solar System by a Mega Impact on Mars

*Ryuki Hyodo[1], Hidenori Genda[1] (1.Tokyo Institute of Technology, Earth Life Science Institute)

9:45 AM - 10:00 AM JST | 12:45 AM - 1:00 AM UTC

[PPS06-04] Hydrodynamic escape of a reduced proto-atmosphere on early Mars

*Tatsuya Yoshida[1], Kiyoshi Kuramoto[1] (1.Hokkaido University)

10:00 AM - 10:15 AM JST | 1:00 AM - 1:15 AM UTC

[PPS06-05] Orbital evolution of Martian moons by rotating Martian proto-atmosphere with low angular momentum

*Ryo Matsuoka[1], Kiyoshi Kuramoto[1] (1.Department of Cosmosciences, Graduateschool of Science, Hokkaido University)

10:15 AM - 10:30 AM JST | 1:15 AM - 1:30 AM UTC

[PPS06-06] N-body simulations of Moon formation with cooling evolution of the protolunar disk

*Takanori Sasaki[1], Natsuki Hosono[2] (1.Department of Astronomy, Kyoto University, 2.Japan Agency for Marine-Earth Science and Technology)

Current status of the PLANETS telescope project for planetary and exoplanetary atmospheric monitoring

*Takeshi Sakanoi[1], Masato Kagitani[1], Yasumasa Hirahara[2], Jeffery Kuhn[3], Svetalana Berdyugina[4], Marcelo Emilio[5], Hiromu Nakagawa[6], Mikio Kurita[7], Yasumasa Kasaba[1], Takahiro Obara[1], Shoichi Okano[1]

1. Planetary Plasma and Atmospheric Research Center, Graduate School of Science, Tohoku University, 2. Graduate School of Environmental Studies, Nagoya University, 3. IfA, University of Hawaii, U.S.A., 4. KIS, Germany, 5. Universidade Estadual de Ponta Grossa, Brazil, 6. Graduate School of Science, Tohoku University, 7. Graduate School of Science, Kyoto University

We are conducting a 1.8-m aperture off-axis telescope project PLANETS under international collaborations. In this presentation, we report the current status of PLANETS project and our scientific targets, and also promote use cases in other research fields in astronomy and planetary/exoplanetary sciences. PLANETS is characterized by low-scattering and high-contrast capability thanks to off-axis mirror system, and also by monitoring observation. We mainly concern variations in planetary atmospheres, faint gases produced from satellites, exoplanetary atmosphere, and also welcome other targets that match to the advantages of PLANETS. Continuous monitoring is essential to understanding the planetary atmospheric phenomena, and therefore, own facilities with even small- and medium sized telescopes and instruments are important. We have demonstrated that continuous monitoring is effective for understanding planetary and satellite phenomena using small telescopes at the summit of Mt. Haleakala, Hawaii (3050 m altitudes). We are now operating 40 cm (T40) and 60 cm (T60) telescopes at Haleakala combined with high-resolution spectrometers in visible and infrared ranges to observe faint atmospheric emissions/absorptions, such as plasma and neutral torus produced by Jupiter’s satellite Io, neutral torus produced by Saturn’s satellite Enceladus, gases in Venus and Mars, sodium gasses of Mercury, and so on. The polarization imager DIPOL-2 is also installed to measure the weak polarization of exoplanetary light. Our and guest investigators’ observations are also linked to Mercury, Venus (Akatsuki), Mars (Mars Express, MAVEN) and Jupiter (Juno) missions.
To achieve precise spectroscopy and polarimetry for faint emissions/absorption in planetary/exoplanetary atmospheres and satellites, PLANET’s a 1.8-m aperture with low-scattered light optics is necessary. PLANETS project is managed by the PLANETS Foundation (www.planets.life), which is an internationally organized entity whose board members are from several institutes in Japan, USA, Germany, Brazil, and France. This off-axis optical system brings us unrivaled high-dynamic range scientific capabilities on coronagraphy and polarimetry. It will have a Gregoian focus with a FOV of 6' (Fno=13) and a Coude focus with a FOV of 20" (Fno=49). The main mirror is Clearceram Z-HS with a diameter of 1850 mm, which is now on the final polishing process. We are designing mechanical structure of telescope for both cases of equatorial mount and azimuthal-elevation mount. We are also designing a mirror support structure in two ways, active support and passive support. We are aiming to get first light with PLANETS telescope within next several years.

Keywords: PLANETS, planet, exoplanet

©2019. Japan Geoscience Union. All Right Reserved.

Martian Moon eXploration MMX: science objectives and their promotion

*Kiyoshi Kuramoto[1,2], Yasuhiro Kawakatsu[2], Masaki Fujimoto[2], Jean Pierre Bibring[3], David Lawrence[4], Hidenori Genda[5], Naru Hirata[6], Takeshi Imamura[7], Shingo Kameda[8], Koji Matsumoto[9], Hideaki Miyamoto[7], Tomokatsu Morota[10], Hiroshi Nagaoka[2], Hiromu Nakagawa[11], Tomoki Nakamura[11], Kazunori Ogawa[12], Hisashi Otake[2], Masanobu Ozaki[2], Sho Sasaki[13], Hiroki Senshu[14], Shogo Tachibana[7,2], Naoki Terada[11], Tomohiro Usui[2], Koji Wada[14], Sei-ichiro WATANABE[10], MMX study team

1. Hokkaido Univ., 2. JAXA, 3. IAS, 4. APL, 5. ELSI, 6. Aizu Univ., 7. Univ. of Tokyo, 8. Rikkyo Univ., 9. NAOJ, 10. Nagoya Univ., 11. Tohoku Univ., 12. Kobe Univ., 13. Osaka Univ., 14. Chiba Inst. Tech.

Martian Moons eXploration, the next Japanese sample return mission following Hayabusa 2, is under extensive study for the upshift to phase B with a schedule to be launched in 2024 and return to Earth in 2029. MMX will make close-up observations of Phobos and Deimos over ~3 years and sample return from a moon, from which the origin of the Martian moons will be conclusively revealed. Simultaneously, the formation and evolution of a habitable planet having liquid water and atmosphere will be elucidated from the deep search for both moons and parallel Mars atmosphere observations, by making the best use of the inherent nature of the moons that have long history since the formation stage of Mars and orbits near the parent planet. Particularly, MMX will shed light on the formation and early evolution of Mars and the volatile transport from the outer planet region to inner one in early solar system, which are hardly assessed from the survey of Martian surface geology alone. Mission instruments to be on board are telescope camera (TENGOO), multiband visible camera (OROCHI), infrared spectroscopic imager (MacrOmega), gamma-ray and neutron spectrometer (MEGANE), light detection and ranging (LIDAR), dust monitor (CMDM), ion mass spectrum analyzer (MSA) and sampler. A rover is also under study as an additional science instrument to probe the moon’s surface microscopic structure and composition. To achieve the mission science objectives, it is essentially important to conduct close interplay among analyses of data from multi-instruments, sample analyses, and theoretical studies. To traverse the instrument development teams and data analysis, sample analysis and theoretical scientists, the MMX science board is going to be organized the sub-science teams, which will produce the best initial scientific results fully answering the mission objectives and conduct preparations for observations, data analyses, sample analyses in parallel with theoretical studies.

Keywords: MMX, sample return, Phobos, Deimos, Mars, Early solar system

©2019. Japan Geoscience Union. All Right Reserved.

Implantation of Martian Materials in the Inner Solar System by a Mega Impact on Mars

*Ryuki Hyodo[1], Hidenori Genda[1]

1. Tokyo Institute of Technology, Earth Life Science Institute

The rare asteroids, called A-type asteroids, orbit within the Hungarian region and within the main asteroid belt region. They have olivine-rich spectral features [DeMeo&Carry 2013]. Their origin is still under debate even though some could be mantle materials fragmented and ejected by a catastrophic impact of differentiated primordial asteroid [Sanchez et al. 2014]. On the other hand, olivine is a major mineral of the Martian upper mantle with ~60 wt% [e.g. Bertka&Fei 1997, Zuber 2001]. Also, at the surface of Martian grabens, such as Nili Fossae, an olivine-rich signature is detected [Hoefen et al. 2003, Mustard et al. 2009].

Recent studies showed that a giant impact may occur on Mars and it produced Mars-orbiting debris from which Martian moons, Phobos and Deimos, acreete [Rosenblatt et al. 2016, Hesselbrock&Minton 2017, Hyodo et al. 2017, Canup&Salmon 2018]. Recently, Polishook et al. (2017) suggested that such Martian-moon forming impact may also produce debris that escapes from Mars' gravitational field, and some of them may have delivered to the asteroid region. However, quantitative arguments such as mass, composition and orbits of the impact ejecta have been not studied yet.

In this talk, we will present our recent work [Hyodo&Genda 2018, ApJL] that investigated the compositional and thermodynamic properties of the impact ejecta produced by a giant impact that forms Martian moons [Hyodo et al. 2017]. We also present their mass and heliocentric orbits and discuss the possibility of forming rare A-type asteroids.

We perform high-resolution SPH simulations of Mars' giant impact (impactor mass of ~0.03 mass of Mars, impact velocity of ~6 km/s and impact angle of 45 degrees without pre-impact Martian spin). We found that the giant impact produced the following escaping debris [Hyodo&Genda 2018, ApJL]:

1. Mass of ~$10^{-2}M_{Mars}$
2. ~20wt% originates from Mars and the rest originates from the impactor
3. ~50% of the Martian material originates from Martian mantle (between 50 and 200 km in depth)
4. Temperature ranges between 1000 and 4000K with a peak around 2000 K

Assuming the Mg# (=Mg/(Mg+Fe) in mol) of bulk silicate Mars of ~75% [Elkins-Tanton et al. 2003] and thus ($Mg_{0.75}$, $Fe_{0.25}$) SiO_4olivine solid solution as a major mineral of the Martian upper mantle, solidus and liquidus temperatures are about 1850 K and 2000 K [Bowen&Schairer 1935]. Then, using our SPH simulations, we found that ~10% of escaping Martian mantle debris does not melt but ~70% of the debris completely melts. In the case of partial melting (2000 K), ~20% of the Martian mantle debris avoids melting and thus they would preserve their primitive minerarogy. Hence, the unmelted Martian mantle material (olivine-rich material) is estimated to be about ~2% of the total ejected mass (~1.7×10^{20}kg). This mass is much larger than those of current A-type asteroids found in the Hungarian region (~2.8×10^{15}kg) and the current main asteroid belt (~8.9×10^{18}kg).

The orbits of the ejected particles are distributed between ~0.5-3.0 AU with eccentricity upto ~0.6 and

©2019. Japan Geoscience Union. All Right Reserved.

inclination up to ~0.3 radian. Detailed stidues on the long-term evolution of the debris is required but the initial orbits of the debris shows that they can easily reach the asteroid belt region and thus unmelted Martian mantle material (a maximum of ~2% of the total debris mass) is potentially expected to settle into stable orbits as rare A-type asteroids found in the Hungarian and main asteroid belt regions.

We also expect that the debris hit the pre-existing asteroids with impact velocity larger than 5 km/s. The nominal collision velocity between existing asteroid is ~5km/s [Bottke et al. 1994]. Such high-velocity collision between the debris and pre-existing asteroid may record a reset of ^{40}Ar–^{39}Ar age and/or impact melts [Kurosawa&Genda 2018] and thus the timing of the giant impact on Mars may be recorded in some chondrite.

Keywords: Mars, A-type asteroids, Asteroids

©2019. Japan Geoscience Union. All Right Reserved.

Hydrodynamic escape of a reduced proto-atmosphere on early Mars

*Tatsuya Yoshida[1], Kiyoshi Kuramoto[1]

1. Hokkaido University

The short growth time of proto-Mars inferred from analyses of Martian meteorites implies that the proto-Mars likely gravitationally maintained both the solar nebula component and the impact degassed component as a proto-atmosphere. Planetary building blocks containing metallic iron should induce production of reduced volatiles such as H_2, CH_4 and CO because metallic iron acts as a reductant for the degassed component (Kuramoto and Matsui, 1996). Atmospheres with reduced compositions are promising sites for photochemical production of organic matters precursory for life (Schlesinger and Miller, 1983). If a reduced proto-atmosphere was formed and maintained on early Mars, it may be important as a field for synthesis of organic matters linked to the emergence of life organisms.

However, the reduced proto-atmosphere once possibly formed on a rocky planet has been considered to be rapidly lost by hydrodynamic escape. Hydrodynamic escape occurs when radiative heating of an atmosphere accelerates a radial outflow of an atmosphere against the planetary gravity and it is possibly induced by the extreme ultraviolet (EUV) flux of the young Sun. Previous numerical studies (Lammer et al., 2013; Erkaev et al., 2014) estimate the atmospheric escape rate of an oxidized Martian proto-atmosphere, suggesting that the proto-atmosphere with the amount equivalent to ~100 bar could have been lost per 10 Myr under the EUV flux 100 times the present. But their result likely depends on the assumption that molecules are fully dissociated into atoms. Since the gravity on Mars is small, it is likely that a considerable fraction of molecules stays undissociated in the escape outflow. If infrared active molecules are included in the atmosphere, they may reduce the atmospheric escape rate by radiative cooling. If the atmospheric escape rate decreases, the reduced environment that is suitable for producing organic matters likely continues for a long time. So far, the effect of radiative cooling on hydrodynamic escape remains poorly understood. Here, we develop a one-dimensional hydrodynamic escape model which include radiative cooling processes and photochemical processes for a multi-component atmosphere. We calculate the escape rate of a reduced Martian proto-atmosphere and estimate the duration of the reduced environment on early Mars.

We solved the fluid equations for a multi-component gas assuming spherical symmetry considering radiative processes and photochemical processes. These equations are solved by numerical integration about time until the physical quantities settle into steady profiles. We use the UV spectrum 100 Myr after the birth of the Sun estimated by the observations of solar-type G stars. We consider CO and CH_4 as radiative coolant, and consider their energy transitions with high emissivity. We calculate the radiative cooling rate by using the photon escape probability. In this modeling, a hybrid-type atmosphere in which the degassed component and solar nebula component are mixed is supposed with 18 chemical components including photolysis products.

The mass escape rate decreases more than one order as the mixing fraction of CO and CH_4 increases > 10% because of the energy loss by radiative cooling of CO and CH_4. Concurrently, the mass fractionation between H_2 and other heavier species occurs more remarkably. Time scale for H_2 loss may be longer than 100 Myr when the the degassed component is larger than ~1.0×10^{21} kg equivalent to ~100 bar atmosphere. In many simulation cases, CO and CH_4 are left behind implying that the reduced environment further continues until these reduced species are oxidized by photolysis. Our result suggests

©2019. Japan Geoscience Union. All Right Reserved.

a reduced environment on early Mars may have continued more than 100 Myr and played an important role producing organic matters.

Keywords: hydrodynamic escape, early Mars, reduced atmosphere

©2019. Japan Geoscience Union. All Right Reserved.

Orbital evolution of Martian moons by rotating Martian proto-atmosphere with low angular momentum

*Ryo Matsuoka[1], Kiyoshi Kuramoto[1]

1. Department of Cosmosciences, Graduateschool of Science, Hokkaido University

Martian moons, Phobos and Deimos has radii about several km to 10 km, and irregular shapes. Their low albedos and reflectance spectra are similar to those of primitive carbonaceous asteroid which supports “capture scenario” for their origin.

In previous studies considering the capture due to energy dissipation by gas drag from the Martian proto-atmosphere caused by the gravitational bound of the nebula gas, it is possible to circularize the moons’ orbit (Hunten 1979, Sasaki 1990). While this spherically symmetric atmospheric structure can make moon’s orbit circular, it is impossible to attenuate the orbital inclination of the moon. Also, the satellite constantly receives atmospheric drag and cause moons to fall into Mars eventually. Although the giant impact theory (e.g. Rosenblatt+ 2016) explains such moons’ orbital feature, it is difficult to form moons with carbonaceous composition because of high temperature environment during moon formation. On the other hand, in context of capture scenario, Matsuoka & Kuramoto (2018, JpGU) considered the atmospheric rotation and showed that the attenuation of inclination occurred and the orbital shrinking was inhibited. However, since this atmosphere has extremely large angular momentum (1.3 times the Martian spin anugular momentum) due to Keplerian rotation beyond the co-rotational radii, thus it seems difficult to realize to form. Also, there is a problem that moons are formed and stay beyond Deimos’ orbit. In this study, we construct models of rotating atmosphere with much small anugular momentm and show that it is more advantageous in explaining the orbital features of the current Martian moons.

This study assumed that atmospheric rotation is limited within the Bondi radii and the velocity field is modeled as follows so that the rotational velocity becomes continuous by changes with distance. (1) Mars surface to co-rotational radii R_C: co-rotational atmosphere with Mars’ spin. (2) co-rotational radii to Bondi radii R_B: attenuated atmospheric rotation with distance given by $v(r)=((R_B-r)/(R_B-R_C))^{\Gamma} v_K(r)$ (v_K is a Keplerian velocity, Γ is a constant which we set unity in this study). (3) Bondi radii to Hill radii: stationary atmosphere connecting nebula at Hill radii. Such atmosphere can be regarded as a case that has not enough angular momentum to make Keplerian rotation outside the co-rotational radii. The density field of the atmosphere was determined by the balance of centrifugal force by this velocity field, Mars gravity and pressure gradient, and the drag force by these velocity field and density field were given to the equation of motion of moons. This atmosphere has low angular momentum of only 0.14 % of the Martian spin angular momentum.

In numerical experiments, moons have the inward radial velocity component in all regions, but the orbital shrinkage is suppressed near the co-rotational radii due to small speed difference between moons and atmosphere. The typical timescale of attenuation of semi-major axes of Phobos size moons is the order of 10^4 yr or more. This timescale sharply increased as approaching the co-rotational radii, indicating that the moons stay well in this region. This result naturally explains the initial position near the co-rotational radii of moons before tidal orbital evolution. Since there is a speed difference between moons and the atmosphere even if the inclination takes small value, the attenuation of inclination occurs efficiently. In contrast to timescale of inclination decay derived in our previous study that is rapidly increasing with the

©2019. Japan Geoscience Union. All Right Reserved.

decay of inclination, timescale derived in this study has an upper limit of several thousand years for a Phobos size moon. This result explains small orbital inclination of the current Martian moons. Such tendencies are recognized in the same way when Γ has different positive values, and in the cases of the Deimos size moons, such orbital evolution occur more rapidly than those of Phobos size moons.

Keywords: Martian moons, Satellite formation

©2019. Japan Geoscience Union. All Right Reserved.

N-body simulations of Moon formation with cooling evolution of the protolunar disk

*Takanori Sasaki[1], Natsuki Hosono[2]

1. Department of Astronomy, Kyoto University, 2. Japan Agency for Marine-Earth Science and Technology

The previous studies about Moon formation focused on the first and last stages: the giant impact process (~1 day) has been investigated by SPH simulations, and the lunar accretion process (~1 month) from the circumterrestrial particulate disk has been investigated by N-body simulations. Although the Moon formation process should proceed on the cooling timescale of the protolunar disk (~100 years), there has been no study to simulate the long-term evolution of the disk. In this study, we developed an N-body code to simulate the cooling evolution of a protolunar disk in vapor/melt equilibrium, and executed long-term N-body simulations for the disk evolution and lunar accretion processes simultaneously with PEZY-SC processors. Our result showed that "mini-Moons" system would form instead of forming a single Moon.

Keywords: Moon, formation, N-body simulation, protolunar disk, PEZY-SC

©2019. Japan Geoscience Union. All Right Reserved.

[J] Oral | P (Space and Planetary Sciences)：P-PS Planetary Sciences

Mon. May 27, 2019 10:45 AM - 12:15 PM JST | Mon. May 27, 2019 1:45 AM - 3:15 AM UTC | A01 TOKYO BAY MAKUHARI HALL

[P-PS06] Planetary Sciences

convener:Kenji Kurosaki(Department of Physics, Nagoya University), Yusuke Nakauchi(Japan Aerospace Exploration Agency), Chairperson:Hiroyuki Kurokawa(東京工業大学 地球生命研究所), Yuki Tanaka(Tokyo Institute of Technology)

We call for general interest papers for Planetary Scienses. Planetary Sciences consist of a variety of studies on the past, present, and future of our solar system and exoplanetary systems, Discussions based on various backgrounds are encouraged.

10:45 AM - 11:00 AM JST | 1:45 AM - 2:00 AM UTC

[PPS06-07] Possibility of giant planet formation by pebble accretion in Class 0/I YSOs

*Yuki Tanaka[1], Yusuke Tsukamoto[2] (1.Tokyo Institute of Technology, 2.Kagoshima University)

11:00 AM - 11:15 AM JST | 2:00 AM - 2:15 AM UTC

[PPS06-08] The effect of the three-dimensional gas flow around an embedded planet on pebble accretion

*Ayumu Kuwahara[1], Hiroyuki Kurokawa[2] (1.Tokyo Institute of Technology, 2.Earth-Life Science Institute)

11:15 AM - 11:30 AM JST | 2:15 AM - 2:30 AM UTC

[PPS06-09] Icy pebble accretion onto terrestrial planets: the effect of gas flow

*Hiroyuki Kurokawa[1], Ayumu Kuwahara[2], Satoshi Okuzumi[2] (1.Earth-Life Science Institute, Tokyo Institute of Technology, 2.Tokyo Institute of Technology)

11:30 AM - 11:45 AM JST | 2:30 AM - 2:45 AM UTC

[PPS06-10] Delivery of ammonia ice to Ceres by pebble accretion

*Yuto Nara[1], Satoshi Okuzumi[1], Hiroyuki Kurokawa[2] (1.Tokyo Institute of Technology, 2.Earth-Life Science Institute, Tokyo Institute of Technology)

11:45 AM - 12:00 PM JST | 2:45 AM - 3:00 AM UTC

[PPS06-11] Volatile-driven cryovolcanic eruption on asteroid Ceres as a probe to its interior

*Koki Yumoto[1], Yuichiro Cho[1], Seiji Sugita[1] (1.Department of Earth and Planetary Science, Graduate School of Science, University of Tokyo)

12:00 PM - 12:15 PM JST | 3:00 AM - 3:15 AM UTC

[PPS06-12] Ice sheet formation on synchrnously rotating earth-like planets in M-dwarf abitable zones

Soma Arai[1], Kiyoshi Kuramoto[1], *Masaki Ishiwatari[1], Shunichi Kamata[1] (1.Department of Cosmosciences, Graduate school of Science, Hokkaido University)

Possibility of giant planet formation by pebble accretion in Class 0/I YSOs

*Yuki Tanaka[1], Yusuke Tsukamoto[2]

1. Tokyo Institute of Technology, 2. Kagoshima University

Recently, pebble accretion in protoplanetary disks attracts attention in theoretical works of planet formation. In this process, it is thought that cm-sized particles, so-called pebbles, drift inward in the disk, and growth of planets will be accelerated due to accretion of pebbles onto proto-planets. Various theoretical works which assume pebble accretion, such as giant planet formation and formation of super-Earths systems, have been done so far.

Meanwhile, recent radio observations by ALMA have revealed that existence of clear gaps and rings in many very young protoplanetary disks. Mechanisms to generate these structures of gaps and rings are yet to be investigated, and many theoretical models have been proposed. One of these hypotheses is that gas giants in the disks carve gaps in the dust disks and create such structures. Numerical simulations which assumed the existence of the planet have been shown that gaps and rings similar to the observations can be represented. However, a time-scale for planet formation will be long because the observed radii of gaps and rings are relatively large, so it is unclear whether the planet with enough mass to create a gap can form in very young disks.

Here we focus on planet formation in much earlier stages, Class 0/I phases. Combining an analytical model of a gravitationally unstable disk around Class 0/I YSOs with a model of pebble accretion, we investigate possibility of giant planet formation in the early stages of disk evolution. We find that in many cases a time-scale of pebble accretion in the condition of Class 0/I YSOs is much shorter compared to that in a typical protoplanetary disk, because of larger mass accretion rates. We also find, however, the accretion time-scale is not always a decreasing function of the gas accretion rate, and the time-scale can be longer as the increase of the gas accretion rate depending on parameters. Using derived time-scales, we investigate growth of proto-planets with different parameters such as the gas accretion rate and dust-to-gas mass ratio. Based on our results, we discuss a required initial mass of the proto-planets to form cores of the giant planets within Class 0/I phases.

Keywords: Planet formation, Protoplanetary disk, Pebble accreton, Class 0/I YSOs

©2019. Japan Geoscience Union. All Right Reserved.

The effect of the three-dimensional gas flow around an embedded planet on pebble accretion

*Ayumu Kuwahara[1], Hiroyuki Kurokawa[2]

1. Tokyo Institute of Technology, 2. Earth-Life Science Institute

Pebble accretion is a new model of planet formation, which may overcome several problems remaining in conventional planetesimal accretion theory. Accreting mm—cm-sized particles, called pebbles, onto the proto-cores can form the massive cores faster than accreting the planetesimals. In addition to the formation of the Jovian cores in a realistic timescale, pebble accretion scenario can explain the formation of various types of planets—for instance, close-in super Earths, water-rich planets, and the size distribution of terrestrial planets in the solar system. The key point of this scenario is that the pebbles experience not only the gravitational interaction with the proto-cores but also gas drag. The hydrodynamic effect is important when we consider the planet formation via pebble accretion.

Previous works have found the three-dimensional flow field around an embedded planet. Gas from the protoplanetary disk enters the Bondi or Hill sphere of the planet at high latitude and exits through the mid-plane region in the isothermal condition (Kuwahara et al. 2019). This recycling mechanism may have both positive and negative effect on the accretion of solid materials. When the particles are moving in the region at high latitude of the planet, the accretion may be promoted by the inflow of gas. On the other hand, if the particles are in the mid-plane region, the accretion of the particles can be suppressed by the outflow barrier. Though some studies considered the accretion of dust particles in the realistic flow field (Ormel 2013; Popovas et al. 2018ab), the effect on the accretion efficiency is not fully understood. This study aims to understand the hydrodynamic effect and to obtain the accretion efficiency of particles for the range of planetary masses and particle sizes.

In this study, using the numerical data obtained from three-dimensional hydrodynamical simulations, we numerically integrated the equation of motion of pebbles including the gravitational interactions and gas drag under the influence of the flow field in three dimensions. We also performed the similar calculations on the Keplerian shear flow field without the effect of planet gravity on the flow, then investigated how the description of the pebble accretion changed on the flow pattern, pebble size, and dimensionless planetary mass, $m=R_{\mathrm{Bondi}}/H$, where R_{Bondi} and H are the Bondi radius of the planet and disk scale height, respectively.

In the flow field, we found that the description of pebble accretion differs from that of in the Keplerian shear flow. Pebbles at high altitude tend to descend toward the planet because of the downward stream of gas. The accretion rate of pebbles became smaller than in the Keplerian shear flow. In spite of the pebbles descend toward the planet, the accretion of pebbles can be suppressed because of the effect of the flow field. Since the gas flows rapidly in the vicinity of the planet, the gas flow field deflects the trajectories of the pebble in the vicinity of the planet and reduces its accretion rate. The flow field has the stronger effect on the smaller pebbles. Based on these results, we will discuss the implications for planet formation via pebble accretion.

References:
Kuwahara, A., Kurokawa, H., & Ida, S. 2019, accepted for publication in A&A
Ormel, C. W. 2013, MNRAS, 428, 3526

©2019. Japan Geoscience Union. All Right Reserved.

Popovas, A., Nordlund, Å., Ramsey, J. P., & Ormel, C. W. 2018, MNRAS, 479, 5136
Popovas, A., Nordlund, Å., & Ramsey, J. P. 2018, MNRAS: Letters, 482, L107

Keywords: hydrodynamics, protoplanetary disk, planet formation

©2019. Japan Geoscience Union. All Right Reserved.

Icy pebble accretion onto terrestrial planets: the effect of gas flow

*Hiroyuki Kurokawa[1], Ayumu Kuwahara[2], Satoshi Okuzumi[2]

1. Earth-Life Science Institute, Tokyo Institute of Technology, 2. Tokyo Institute of Technology

Earth, the only life-hosting planet we know, is characterized by the small water fraction in the bulk composition: the ocean mass being 0.023% of the Earth mass. Because the abundance of water control the physical and chemical evolution of planets by atmosphere-hydrosphere-lithosphere interactions and by changing the mantle properties, unveiling how water-depleted planets form is crucial for understanding the emergence of habitability on them. Pevious studies have pointed out that icy pebble accretion following the snow line migration in protoplanetary disks typically deliver an excess amount of water to terrestrial planets unless the initial size of the disk is small (30--50 au) or a giant planet in the outer orbit (e.g., Jupiter in our solar system) formed early (Morbidelli et al. 2016; Sato et all. 2016; Ida et al. 2019). In contrast to the previous studies where the accretion rate derived for pebbles moving in (sub-) Keplerian flow, we used the accretion rate derived for pebbles moving in the gas flow perturbed by the gravity of the planet (Kuwahara et al. 2019; Kuwahara et al. in prep.). The presence of horseshoe region and outflow shuts off the accretion of small pebbles. We show that, because migrating icy pebbles at ~1 au are small, the gas flow significantly suppress the accretion onto Earth-sized planets, whereas Mars-sized planets accretes a significant amount of icy pebbles. Our results suggest that Earth-like, water-depleted rocky planets may form in a disk-size range wider than previously considered and in the systems where no giant planet exists.

Keywords: Planet formation, Origin of water, Pebble accretion

©2019. Japan Geoscience Union. All Right Reserved.

Delivery of ammonia ice to Ceres by pebble accretion

*Yuto Nara[1], Satoshi Okuzumi[1], Hiroyuki Kurokawa[2]

1. Tokyo Institute of Technology, 2. Earth-Life Science Institute, Tokyo Institute of Technology

Recent studies with the spectrometer onboard the Dawn spacecraft detected the presence of ammoniated phyllosilicates on the surface of Ceres. It is presumed that ammonia may have reacted with the phyllosilicates on Ceres during differentiation. Ammonia can not exist alone as a solid in the current temperature at the location of Ceres. It has yet to be shown how ammonia is delivered to Ceres.

In this study, by adopting a theory "Ceres formed a protoplanetary core around the current main asteroid belt and accreted ammonia-bearing ice pebbles there", we aim to give constraints on the free parameters of the protosolar nebula. We numerically calculate the growth and radial inward drift of icy dust particles, and the evolution of the surface density of the gas flow and the disk temperature in a viscous disk. We employ a formula of pebble accretion presented by a previous study to quantify the amount of ammonia-bearing ice pebbles delivered to asteroids at 2.8 au.

We find that when the free parameters of the protosolar nebula satisfy certain conditions, Ceres accretes ammonia-bearing ice pebbles with ~ 10 –100 km thickness on its surface by pebble accretion. This result can explain the observations that there is ~ 15km of relief with craters on the surface of Ceres, and the ammoniated phyllosilicates on its surface were formed globally. In our result, we support the disk model with strong turbulence. Moreover, we suggest if ammoniated phyllosilicates come from pebble accretion, the amount of ammoniated phyllosilicates on planets' surface strongly depends on accreting planet masses.

Keywords: pebble accretion, asteroid, protosolar nebula

©2019. Japan Geoscience Union. All Right Reserved.

Volatile-driven cryovolcanic eruption on asteroid Ceres as a probe to its interior

*Koki Yumoto[1], Yuichiro Cho[1], Seiji Sugita[1]

1. Department of Earth and Planetary Science, Graduate School of Science, University of Tokyo

Introduction: Imageries from NASA's DAWN mission revealed the presence of localized bright spots (or faculae) exhibiting brighter materials with likely composition of anhydrous sodium carbonate (De Sanctis et al., 2016) within the dark Ceres surface. These materials are assumed to be remnants of cryovolcanic ejecta which ascended from brine reservoirs thorough impact induced fractures. Quick et al., (2018) showed that excess pressure caused by the gradual freezing chamber could be a driving source for its ascent. However, DAWN image revealed the presence of both explosive (e.g. Vinalia faculae) and effusive (i.e. Cerealia facula and Ahuna Mons) eruptions, implying the possibility that fragmentations of cryomagma are induced by exsolved volatiles and this could be a primal driving source.
Objectives: Volatile exsolution are known to play an important role in ascent dynamics of silicate volcanism, and it enables ascent of relatively high density cryomagmas, but their contributions to cryovolcanism are not well understood. This study attempts to obtain new constraints on the properties of a subsurface brine reservoir and conduit geometry based on phase equilibria and model calculations.
Model: The equilibrium composition of CO_2-H_2O-NaCl system by Akinfiev & Diamond (2010) was used as the cryomagma composition. The cryomagma is assumed to have a viscosity of 10^5-10^8 Pa s (Quick et al., 2018), and this slurry-like rheology constrains the temperature within the solidus and liquidus curves along decompression. If we assume ascents to be isothermal at velocity $>10^{-3}$ m/s (Quick et al., 2018) and salinity lower than the stability region of hydrohalites, then the temperature of cryomagma should be within ~260 - 270 K, consistent with impact simulation (Bowling et al., 2018), and salinity <~20 wt%. One-dimensional 2-phase (i.e. cryomagma and exsolved gaseous volatile) steady flow in a cryovolcanic conduit was modelled with the theory developed by Kozono & Koyaguchi (2009) for terrestrial volcanoes. Major modifications in our model were, adjustment of the henry's law, application of choking condition at the surface, and the liquid stability of CO_2. The depth, volatile content, viscosity of brine reservoir, and conduit radius were constrained from the estimated explosive eruption velocity of Vinalia faculae 26 - 54 m/s (Quick et al., 2018) derived from its emplaced radius.
Result and Discussion: Calculation results indicated that for a given viscosity (e.g, 10^5 Pa s), a series of combinations of conduit radius and volatile content, ranging from 10 m and 4 - 7 wt% to 50 m and 0.8 - 3 wt%, 200 m and 0.7 - 3 wt%, can achieve the above eruption velocity. Note that plausible conduit radii should lie within 1 - 100 m (Fagents 2003) and robust upper limit is given by observed radii of vent-like feature ~200 m. We found that reservoir depths have little influence on eruption velocities. For a given viscosity (10^6 Pa s), similar combinations of conduit radius and volatile content ranging from 50 m and 2 - 3 wt% to 200 m and 0.7 - 3 wt% can achieve the eruption velocity. Although higher viscosity $>10^7$ Pa s can achieve similar eruption velocity when a larger conduit radius >100 m is assumed, such large conduits are not consistent with estimations (Quick & Marsh, 2016). Results for explosive eruptions experienced fragmentation at >100 m depth and showed that volatiles could drive the ascent and cause fragmentation of cryomagmas. If effusive eruptions occurred from the same reservoir, conduit radii should be <1 m. However, the probable abundance of such conduits is inconsistent with the lack of effusive eruptions on Ceres and thus could have formed differently, such as diapiric ascents (Buczkowski et al., 2018). Our model calculations showed that cryomagmas could be volatile-driven and may cause fragmentations to erupt explosively. Also, constraints from our calculation showed that Ceres subsurface could be volatile-rich than previously assumed.

©2019. Japan Geoscience Union. All Right Reserved.

Keywords: Ceres, cryovolcano, DAWN, facula, eruption

©2019. Japan Geoscience Union. All Right Reserved.

Ice sheet formation on synchrnously rotating earth-like planets in M-dwarf abitable zones

Soma Arai[1], Kiyoshi Kuramoto[1], *Masaki Ishiwatari[1], Shunichi Kamata[1]

1. Department of Cosmosciences, Graduate school of Science, Hokkaido University

It is considered that terrestrial planets near M-dwarf are synchronously rotating (Von Bloh et al, 2007). Some of such planets exist in the habitable zone defined by vertical one-dimensional atmospheric models and are expected to have liquid water on their surface. However, in synchronously rotating planets, there is a possibility that all of liquid water are lost since water vapor transported form warm day-side to cold night-side is condensed on night-side surface as ice. In order to examine this problem, Menou (2013) conducted atmospheric general circulation model (AGCM) experiments using a synchronously rotating planet configuration with surface water of 50m depth. He estimated ice sheet thickness formed on the planet surface based on the calculated amounts of precipitation and surface evaporation. The result is that the amount of ice sheet on night-side can reach the all amount of surface water given to the planet. In his estimation, GCM results obtained without topography were utilized. Since surface height will change according to the growth of ice sheet, atmospheric circulation are influenced by topography of ice sheet and distributions of precipitation and surface evaporation are also changed. Therefore, the ice sheet thickness can be different from the values estimated by Menou (2013). In this study, in order to consider the effect of the topography produced by ice sheet formation in the night-side, we perform GCM experiment with changing surface height distribution.

The model utilized is DCPAM5(https://www.gfd-dennou.org/library/dcpam/). Atmospheric constituents and parameters such as planet radius are same as those of Earth. We perform two kinds of experiments: one is aqua-planet experiment in which all surface are covered with water or ice, the another is land-planet experiment in which initial water of 20cm depth is given to day-side surface and water transport on the surface is neglected. In land-planet experiment, surface liquid water distribution is determined by atmospheric transport. The value of surface albedo is fixed to 0.15. First, integration for 1500 days with no topography is performed, then thickness of ice sheet is prognosed with considering melting of ice at the bottom of ice sheet and condensation of ice on the surface calculated from distributions of precipitation and surface evaporation. Then, using the horizontal distribution of surface height estimated by the above method, integration for 1500 days is performed and ice sheet height is prognosed again. With repeating these procedures, we search for equilibrium states in which ice sheet thickness becomes constant in time. The results of land planet experiment show that an equilibrium state with ice sheet over 4000m height can be obtained. Contrary to this, in aqua-planet experiment, equilibrium state are not been obtained in our experiment. Ice sheets with height over 10000m are formed in the night-side, although the value of ice sheet height is transient. The result of the experiment with topography determined by the above estimated ice sheet height show that day-side surface temperature become lower than 273K, and therefore, globally ice-covered state can emerge. As for the reason, we consider that day-side surface is cooled by cold air blowing from night-side with high elevation to day-side with low elevation. Since albedo change due to the ice sheet formation is neglected in our experiments, our result suggests that the atmospheric circulation influenced by ice sheet topography can produce globally ice-covered state.

Keywords: synchronously rotating planets, atmospheric general circulation model, ice sheet, globally ice-covered state, existence of liquid water

©2019. Japan Geoscience Union. All Right Reserved.

©2019. Japan Geoscience Union. All Right Reserved.

[J] Oral | P (Space and Planetary Sciences)：P-PS Planetary Sciences

Mon. May 27, 2019 1:45 PM - 3:15 PM JST | Mon. May 27, 2019 4:45 AM - 6:15 AM UTC | A01 TOKYO BAY MAKUHARI HALL

[P-PS06] Planetary Sciences

convener:Kenji Kurosaki(Department of Physics, Nagoya University), Yusuke Nakauchi(Japan Aerospace Exploration Agency), Chairperson:荻原 正博(国立天文台), Yuri Fujii(Nagoya University)

We call for general interest papers for Planetary Scienses. Planetary Sciences consist of a variety of studies on the past, present, and future of our solar system and exoplanetary systems, Discussions based on various backgrounds are encouraged.

1:45 PM - 2:00 PM JST | 4:45 AM - 5:00 AM UTC

[PPS06-13] Three-dimensional linear calculation for non-isothermal type 1 planetary migration

*Kohei Okada[1], Hidekazu Tanaka[1] (1.Tohoku University)

2:00 PM - 2:15 PM JST | 5:00 AM - 5:15 AM UTC

[PPS06-14] Dependence of Central star mass on Protoplanetary disk evolution

*Ryuunosuke Nakano[1], Takeru Suzuki[1], Masahiro Ogihara[2], Eiichiro Kokubo[2] (1.University of Tokyo, 2.National Astronomical Observatory of Japan)

2:15 PM - 2:30 PM JST | 5:15 AM - 5:30 AM UTC

[PPS06-15] Radiation Hydrodynamic Simulations of the Formation of Circumplanetary Disks

*Yuri Fujii[1], Oliver Gressel[2], Kengo Tomida[3], Udo Zieglar[2] (1.Institute for Advanced Research, Nagoya University, 2.Leibniz Institute for Astrophysics Potsdam, 3.Osaka University)

2:30 PM - 2:45 PM JST | 5:30 AM - 5:45 AM UTC

[PPS06-16] Inefficient Magnetic Accretion Heating in Protoplanetary Disks: Evolution of The Snow Line

*Shoji Mori[1], Xuening Bai[2], Satoshi Okuzumi[3] (1.Department of Astronomy, The University of Tokyo, 2.Tsinghua Center for Astrophysics, Tsinghua University, 3.Department of Earth and Planetary Sciences, Tokyo Institute of Technology)

2:45 PM - 3:00 PM JST | 5:45 AM - 6:00 AM UTC

[PPS06-17] Formation of super-Earths and their atmospheres with *N*-body simulations

*Masahiro Ogihara[1], Yasunori Hori[2,1] (1.National Astronomical Observatory of Japan, 2.Astrobiology Center)

3:00 PM - 3:15 PM JST | 6:00 AM - 6:15 AM UTC

[PPS06-18] The orbital stability of planets in resonances: the evolution of mass ratio

*Yuji Matsumoto[1], Masahiro Ogihara[2] (1.Academia Sinica Institute of Astronomy and Astrophysics, 2.National Astronomical Observatory of Japan)

Three-dimensional linear calculation for non-isothermal type 1 planetary migration

*Kohei Okada[1], Hidekazu Tanaka[1]

1. Tohoku University

Planet migration is one of the serious problems in the standard theory of planet formation. A planet excites density waves, that causes a rapid inward migration in a protoplanetary disk. In this study, we formulate the linear wave excitation by a planet in three-dimensional non-isothermal gaseous disks and calculate the torque on the planet more correctly than previous studies.
The torque on a planet has been studied by linear and non-linear calculations. In previous three-dimensional linear calculations the torque was calculated only for isothermal disks. This is because the three-dimensional linear equation has the term that is strongly divergent at corotation in non-isothermal disks. This problem has not been resolved yet and we cannot test non-linear three-dimensional calculations with linear calculations.
In linear studies of gravitational interaction between a planet and a three-dimensional gaseous disk, there are two-dimensional waves that do not have the z-component of velocity and three-dimensional waves that have non-zero v_z. Only three-dimensional waves have a divergent term but it is known that the absolute values of the torque in three-dimensional waves are much small than those of two-dimensional waves in the isothermal disk. In this study, therefore, we ignored three-dimensional waves and examined the torque on a planet in three-dimensional non-isothermal disk approximately. Actually since there is no sign of divergent in previous non-linear hydro-dynamical simulations, this approximation seems good.
With this approximation, we carry out the three-dimensional non-isothermal linear calculation. The obtained torque coincides with non-linear three-dimensional hydro-dynamical simulations. Because of this, we confirmed that our three-dimensional linear calculation is accurate.

Keywords: Protoplanetary disks, Planetary migration, Linear theory

©2019. Japan Geoscience Union. All Right Reserved.

Dependence of Central star mass on Protoplanetary disk evolution

*Ryuunosuke Nakano[1], Takeru Suzuki[1], Masahiro Ogihara[2], Eiichiro Kokubo[2]

1. University of Tokyo, 2. National Astronomical Observatory of Japan

More than 4000 outer planets have been discovered in recent years. The discovery of rocky planets such as the Earth is increasing with this. On the other hand, how such a planetary system was born and evolved has a big uncertainty factor. Understanding the evolution of protoplanetary disks are fundamentally important in considering the formation and evolution of planets. The disk is made of dust and gas and plays a central role in the formation and evolution of rocks and planets, but in order to clarify the dynamics and growth of dust, it is necessary to understand the physical state of the background gas component. It is still unknown how the dissipation of the disk is done by photoevaporation from the central star and by the wind of the magnetically driven disk wind but how they contribute over time and also depend on the difference in mass of the central star.

In this study, a one-dimensional radial simulation of gas components of protoplanetary disks was done in consideration of photoevaporation by X-ray (Owen et al. 2010) and magnetically driven disk wind (Suzuki & Inutsuka et al., 2009). We investigated how the evolution of the disk changes by the difference of the central star mass.

We performed the evolution of protoplanetary disks with different masses of the central stars. If we define the evaporation time at 1au as the time when the surface density there falls below the observable level, it is shorter for a more massive central star, because the photoevaporation is more efficient.

In contrast, the evaporation time at the snowline shows the opposite trend; the evaporation is more rapid for disks with less massive central stars. This is because the location of the snowline has a very sensitive dependence on the mass of a central star.

Keywords: Protoplanetary disk, Low mass stars

©2019. Japan Geoscience Union. All Right Reserved.

Radiation Hydrodynamic Simulations of the Formation of Circumplanetary Disks

*Yuri Fujii[1], Oliver Gressel[2], Kengo Tomida[3], Udo Zieglar[2]

1. Institute for Advanced Research, Nagoya University, 2. Leibniz Institute for Astrophysics Potsdam, 3. Osaka University

Formation of regular moons and/or planetary atmospheres are governed by the gas flow into the vicinity of forming giant planets. Gas around a sufficiently massive planet is thought to form a circumplanetary disk instead of falling directly onto the planet. Recent studies, however, have shown that the circumplanetary gas forms an expanded envelope rather than a thin, rotationally supported Keplerian disk in cases where the gas temperature is very high. Thus, calculating the temperature of the accretion flow properly is important to determine the disk structure. We performed three-dimensional radiation hydrodynamic simulations of the formation of circumplanetary disks with an equation of states that considers effects such as hydrogen dissociation and helium and hydrogen ionization. The region within the deep potential of the planet reached very high temperature regime, however, we observe a disk to form in our simulations.

Keywords: circumplanetary disks, radiation hydrodynamic simulations, satellite formation

©2019. Japan Geoscience Union. All Right Reserved.

Inefficient Magnetic Accretion Heating in Protoplanetary Disks: Evolution of The Snow Line

*Shoji Mori[1], Xuening Bai[2], Satoshi Okuzumi[3]

1. Department of Astronomy, The University of Tokyo, 2. Tsinghua Center for Astrophysics, Tsinghua University, 3. Department of Earth and Planetary Sciences, Tokyo Institute of Technology

The structures of the inner region of protoplanetary disks are essential for understanding the formation process of terrestrial planets. The gas temperature in the region is thought to be determined by accretion heating, which is conventionally attributed to turbulent dissipation. Because the turbulent dissipation occurs in the disk, the released heat accumulates in the disk and thereby effectively increases the disk temperature. However, recent studies have suggested that the inner disk (a few AU) is largely laminar, with accretion primarily driven by magnetized disk winds, as a result of nonideal magnetohydrodynamic (MHD) effects from weakly ionized gas, suggesting an alternative heating mechanism by Joule dissipation.

Purpose of this study is to investigate the accretion heating with the nonideal MHD effects and to understand thermal structure in the inner disk region. We perform local stratified MHD simulations including nonideal MHD effects and investigate the role of Joule heating and the resulting disk vertical temperature profiles. We find that Joule heating occurs at several scale heights above the midplane, making the midplane temperature much lower than that with the conventional viscous heating model. Also, 80 % of the accretion energy is flown out by the disk wind. Our results further suggest that the midplane temperature in the inner region is almost entirely determined by irradiation heating. We also discuss the evolution of the water snow line based on our results and the formation process of the earth.

Keywords: Protoplanetary disks, Magnetohydrodynamic simulation, Snow line

©2019. Japan Geoscience Union. All Right Reserved.

Formation of super-Earths and their atmospheres with *N*-body simulations

*Masahiro Ogihara[1], Yasunori Hori[2,1]

1. National Astronomical Observatory of Japan, 2. Astrobiology Center

A large number of super-Earths have been discovered by various exoplanet search programs that include the Kepler mission, which provide the perfect opportunity for a development of planet formation theory. In fact, recent *N*-body simulations have made major progress in understanding the origin of close-in super-Earths (e.g., Izidoro et al. 2017; Ogihara et al. 2018). In these previous studies, they focus on orbital properties (e.g., period-ratio distribution) and aim to reproduce them.

In this study, we also pay attention to the amount of atmospheres and make further progress in formation models of super-Earths. According to the mass-radius relation of transiting super-Earths, it is unlikely that they generally possess massive atmospheres. This is consistent with the fact that the occurrence rate of hot Jupiters is considerably smaller than that of close-in super-Earths. The amount of atmospheres would provide useful constraints on the development of formation models of super-Earths. The gas accretion onto super-Earth cores depends on several factors (e.g., formation history, disk evolution); therefore it is crucial to follow the planetary growth, the orbital evolution, and the atmospheric accretion self-consistently.

We perform *N*-body simulations of super-Earth formation in an evolving disk considering the accretion of atmospheres. In our simulations, we also consider the pebble accretion, which is a physical process in which protoplanets grow rapidly through accumulation of small particles under gas drag. The pebble accretion would help to accelerate the core formation of gas giants in the outer region. Moreover, the pebble accretion may play an important role in the accretion of close-in super-Earths.

In this presentation, we are going to discuss several important questions about the origin of super-Earths. For example, we aim to reveal realistic formation processes by results of *N*-body simulations that include the atmospheric accretion, the pebble accretion, and the disk evolution. Then we discuss properties of formed super-Earths and compare with observed super-Earth systems. We also determine whether the pebble accretion can prevent the accumulation of massive atmospheres.

Keywords: Super-Earths, N-body simulation, Planet formation, Pebble accretion

©2019. Japan Geoscience Union. All Right Reserved.

The orbital stability of planets in resonances: the evolution of mass ratio

*Yuji Matsumoto[1], Masahiro Ogihara[2]

1. Academia Sinica Institute of Astronomy and Astrophysics, 2. National Astronomical Observatory of Japan

Many systems composed of Earth or super-Earth sized planets are observed to date (e.g., Gillon et al., 2017). In some systems, three or four adjacent planets are in a series of mean motion resonances, called resonant chains (Mills et al., 2016; Luger et al., 2017). The resonant chain can be reproduced when the planets migrate inward (e.g., Ogihara & Ida 2009; Izidoro et al., 2017; Bitsch et al., 2019). After gas depletion, planets in resonant chain become orbitally unstable when their number exceeds the critical number that the planets are stable in resonance (Matsumoto et al., 2012). Izidoro et al. (2017) showed over half systems hold more than five planets in their simulations that planets are stable in resonant chain after gas depletion. The disagreement of the number of planets in resonant chain between observations and simulations can be explained by some mechanism reduces the orbital stability of planets in resonances.

The mass ratios between planets in close-in orbits and their central stars would not keep the same value after their formation. There are some mechanisms that super-Earths lose their envelopes, e.g., energy limited escape (Owen 2018). Also, young stars lose their mass by the stellar wind and coronal mass ejection (Cranmer 2017).

We perform simulations that the planets trapped in the first order resonant chain considering their mass ratio change. At first, planets migrate in the disk gas and are trapped in the resonant chain composed of the same resonant commensurability. Then, the disk gas is removed and the mass ratio between planets and the central star is changed, exponentially. When the number of planets in resonant chain exceeds the critical number corresponding resonant chain, their crossing time increases as the mass ratio decreases since the separation normalized by Hill radii becomes larger. In the cases that the resonant systems hold less planets than the critical number, planets sometimes cause orbital instability when their mass ratios change. In some conditions, the orbits of planets in resonant chain become unstable, when their mass ratios decrease only a few percent. Such instabilities tend to occur in systems that hold more planets.

Keywords: orbital stability, mean motion resonance

©2019. Japan Geoscience Union. All Right Reserved.

[J] Oral | P (Space and Planetary Sciences)：P-PS Planetary Sciences

Mon. May 27, 2019 3:30 PM - 5:00 PM JST | Mon. May 27, 2019 6:30 AM - 8:00 AM UTC | A01 TOKYO BAY MAKUHARI HALL

[P-PS06] Planetary Sciences

convener:Kenji Kurosaki(Department of Physics, Nagoya University), Yusuke Nakauchi(Japan Aerospace Exploration Agency), Chairperson:Kenji Kurosaki(名古屋大学大学院 理学研究科), Yusuke Nakauchi(JAXA/ISAS)

We call for general interest papers for Planetary Scienses. Planetary Sciences consist of a variety of studies on the past, present, and future of our solar system and exoplanetary systems, Discussions based on various backgrounds are encouraged.

3:30 PM - 3:45 PM JST | 6:30 AM - 6:45 AM UTC

[PPS06-19] Experimental study on the structure of shock remnant magnetization

*Shota Kato[1], Masahiko Sato[1], Kosuke Kurosawa[2], Masashi Ushioda[3], Sunao Hasegawa[4] (1.The University of Tokyo, 2.Planetary Exploration Research Center, Chiba Institute of Technology, 3.Geological Survey of Japan, The National Institute of Advanced Industrial Science and Technology, 4.Japan Aerospace Exploration Agency)

3:45 PM - 4:00 PM JST | 6:45 AM - 7:00 AM UTC

[PPS06-20] Low-dispersion spectra of lunar impact flashes in 2018 Geminids

*Masahisa Yanagisawa[1], Yuki Uchida[1], Seiya Kurihara[1], Shinsuke Abe[2], Ryota Fuse[2], Keisuke Onodera[3,4], Ryuhei Yamada[5] (1.The University of Electro-Communications, 2.Nihon University, 3.SOKENDAI (The Graduate University for Advanced Studies), 4.Institute of Space and Astronautical Science/Japan Aerospace Exploration Agency, 5.The University of Aizu)

4:00 PM - 4:15 PM JST | 7:00 AM - 7:15 AM UTC

[PPS06-21] High velocity cratering experiments on sand-gypsum targets simulating asteroids

*Ryo Sugimura[1], Masahiko Arakawa[1], Minami Yasui[1], Takuya Ishiguro[1] (1.Kobe University)

4:15 PM - 4:30 PM JST | 7:15 AM - 7:30 AM UTC

[PPS06-22] Experimental study on collisional processes of highly porous ice balls simulating Saturn's ring particles

*Yukari Toyoda[1], Minami Yasui[1], Masahiko Arakawa[1] (1.Graduate School of Science, Kobe University)

4:30 PM - 4:45 PM JST | 7:30 AM - 7:45 AM UTC

[PPS06-23] IN-SITU FORMATION OF THE URANIAN SATELLITES FROM WIDE DEBRIS DISK FORMED BY GIANT IMPACT

*Ishizawa Yuya[1], Takanori Sasaki[1], Natsuki Hosono[2] (1.Department of Astronomy, Kyoto University, 2.JAMSTEC)

4:45 PM - 5:00 PM JST | 7:45 AM - 8:00 AM UTC

[PPS06-24] Effect on the obliquity due to a giant impact on a rotating ice giant

*Kenji Kurosaki[1], Shu-ichiro Inutsuka[1] (1.Department of Physics, Nagoya University)

Experimental study on the structure of shock remnant magnetization

*Shota Kato[1], Masahiko Sato[1], Kosuke Kurosawa[2], Masashi Ushioda[3], Sunao Hasegawa[4]

1. The University of Tokyo, 2. Planetary Exploration Research Center, Chiba Institute of Technology, 3. Geological Survey of Japan, The National Institute of Advanced Industrial Science and Technology, 4. Japan Aerospace Exploration Agency

The history of planetary magnetism is a key to understanding the evolution of planets. We focus on shock remnant magnetization (SRM) as a record of the magnetic field of planets: the magnetic anomaly field from SRM of a planetary crust can be measured by spacecraft magnetometers. It is essential to understand the structure of SRM for estimating planetary paleofield from magnetic field data because the observed magnetic anomaly field above craters is determined by the sum of the contribution of the materials beneath the crater with the SRM. In this study, the structure of SRM is experimentally investigated by using a two-stage light gas gun placed at the Institute of Space and Astronautical Science(ISAS) of Japan Aerospace and Exploration Agency(JAXA). We measured the SRM of 3 mm cube samples cut from basalt cylinders shocked in the weak magnetic field. The characteristic features of SRM structure are as follows: (1) The intensity of SRM tends to increase with increasing the distance in less than ~10 mm from the collision point. (2) The intensity of SRM tends to decrease with increasing the distance in more than ~10 mm from the collision point. Then the intensity of SRM of blocks are compared with the pressure and temperature from iSALE (Impact-SALE) calculation. In this talk, we will discuss the structure of SRM and the relationship between the SRM structure and the calculated change in pressure and temperature.

Acknowledgement: We appreciate the developers of iSALE, including G. Collins, K. Wünnemann, B. Ivanov, J. Melosh, and D. Elbeshausen.

Keywords: shock remnant magnetization, planetary paleofield, magnetic anomaly

©2019. Japan Geoscience Union. All Right Reserved.

Low-dispersion spectra of lunar impact flashes in 2018 Geminids

*Masahisa Yanagisawa[1], Yuki Uchida[1], Seiya Kurihara[1], Shinsuke Abe[2], Ryota Fuse[2], Keisuke Onodera[3,4], Ryuhei Yamada[5]

1. The University of Electro-Communications, 2. Nihon University, 3. SOKENDAI (The Graduate University for Advanced Studies), 4. Institute of Space and Astronautical Science/Japan Aerospace Exploration Agency, 5. The University of Aizu

In the collisions in the solar system, there are many cases where the collisions occur at speeds exceeding 10 km/s, which are difficult to reproduce in laboratory experiments. In such a collision, melting, evaporation, and ionization of silicate, iron, etc. which do not occur at a speed lower than this occur. Understanding of high-speed collisions accompanying such processes is an important issue for planetary sciences. However, it is not clear yet what kind of phenomenon actually occurs. We can approach this problem from the observation of lunar impact flashes.

Several research results have been reported on the occurrence frequency and brightness of lunar impact flashes and their time variations. However, there are few reports on their spectra. As part of the SAKURA Japan-France joint observation project, that is, the joint observation of meteoroids' impacts as lunar seismic sources, we observed the flashes due to the collisions of December Geminids' meteoroids by simple spectral cameras for visible wavelength (Fig. 1) [1]. At the University of Electro-Communications (Chofu-shi, Tokyo), observations were made with two spectral cameras attached to a Newtonian telescope with an aperture of 450 mm and a focal length of 2015 mm and a Schmidt–Cassegrain telescope with an aperture of 280 mm and an effective focal length of 920 mm. At Nihon University (Funabashi-shi, Chiba Prefecture), observations were carried out mainly with an ordinary movie camera attached to a telescope with a 400 mm aperture.

Thirteen flashes were detected by the observations at the University of Electro-Communications on 15th December, 2018 (JST) and nine of them were detected simultaneously at Nihon University. For those that were not detected at the same time, it is conceivable that there are differences in the sensitivity of the observation devices and temporary interruptions of observation, but the examination in detail is a future task. We named these 13 events from A to M. Their locations on the lunar surface are shown in Fig. 2 [2]. Their spectra were obtained by comparing their spectral images with those of comparison stars which were observed every 30 minutes [2, 3]. An example is shown in Fig. 3. Most of the flash spectra can be approximated well by the blackbody radiation spectrum of about 3000 K, but some are not. For the former, they would be due to the blackbody radiations from micro-droplets of melted rocks generated at the impacts. On the other hand, there is a possibility that the latter may be reflection of sunlight by space debris.

References (in Japanese): [1] Kakinuma, F., A spectral camera for observing lunar impact flashes, Master thesis, the University of Electro-Communications, 2016, http://id.nii.ac.jp/1438/00008427/. [2] Uchida, Y., Low-dispersion spectra of lunar impact flashes I, Master thesis, the University of Electro-Communications, 2018. [3] Kurihara, S., Low-dispersion spectra of lunar impact flashes II, Master thesis, the University of Electro-Communications, 2018.

©2019. Japan Geoscience Union. All Right Reserved.

Keywords: lunar impact flash, spectrum, impact

©2019. Japan Geoscience Union. All Right Reserved.

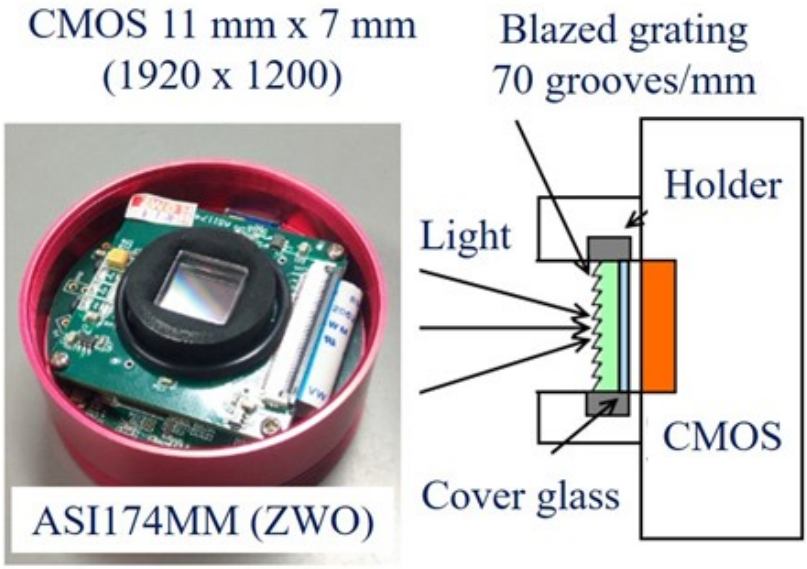

Figure 1. A simple spectral camera [1]. A grating is glued on the cover glass of a CMOS image sensor.

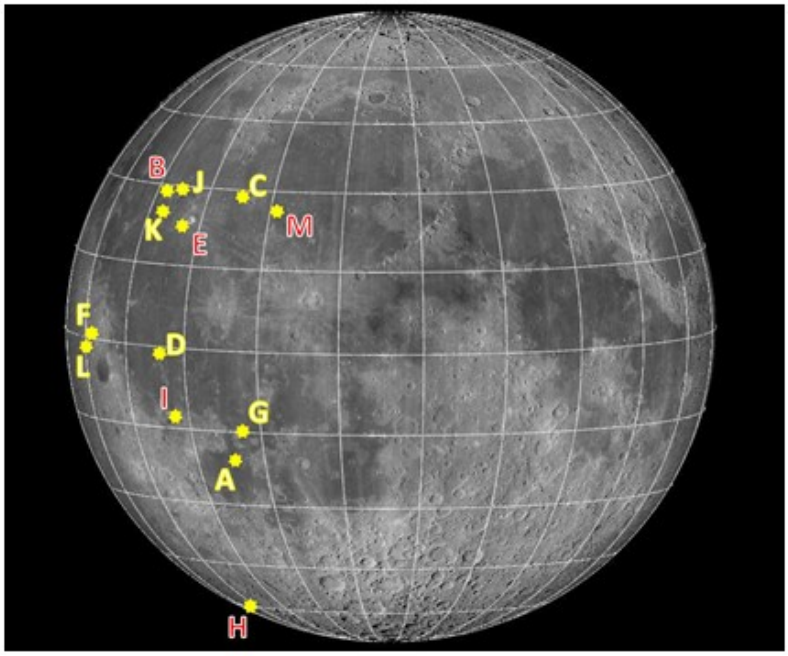

Figure 2. Locations of impact flashes (A-M) observed on December 15, 2018 [2].

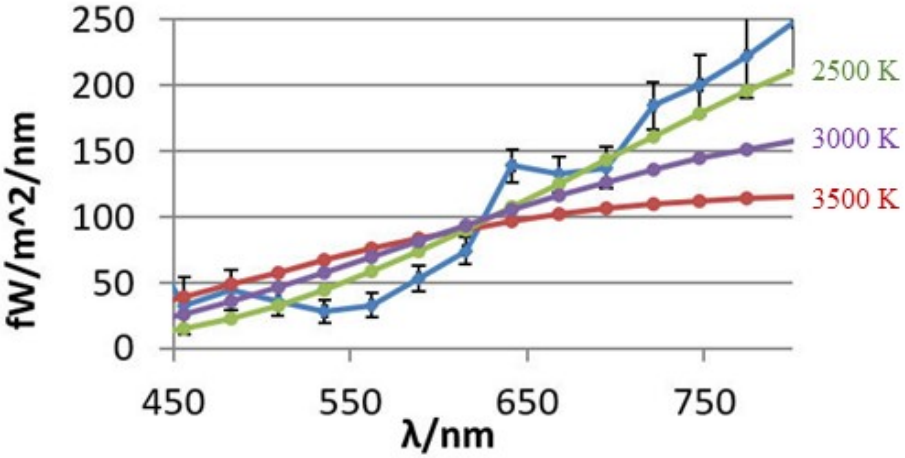

Figure 3. The spectrum of H impact flash. Black body spectra are shown with smooth lines [2].

©2019. Japan Geoscience Union. All Right Reserved.

High velocity cratering experiments on sand-gypsum targets simulating asteroids

*Ryo Sugimura[1], Masahiko Arakawa[1], Minami Yasui[1], Takuya Ishiguro[1]

1. Kobe University

A lot of impact craters are found on asteroids. To clarify the impact cratering processes on asteroids, many researchers conducted impact cratering experiments using various materials such as sand, ice, and basalt. Housen and Holsapple (2011) proposed crater scaling laws and it enable us to extrapolate experimental results to asteroid impact results on the surface. They referred rocky materials having the compressive strength larger than several MPa to constructed the crater scaling laws, but it is unclear whether these scaling laws can be applied to porous materials having low strength or not. Therefore, we conducted impact cratering experiments in order to study the cratering processes on porous rocky asteroids with low strength and the effects of the strength on the crater size and the ejecta velocity. Then, we propose the crater scaling laws applicable to low strength porous materials.

A low strength target was made by mixing quart sands with the diameter of 100 μm with porous gypsum. The mixing ratio of sand to gypsum was changed from 2:1 to 30:1 in the wt.%, and the measured tensile strength was found to change with this mixing ratio. Impact experiments were conducted by using a two-stage light gas gun, and an Al spherical projectile with the size of 2mm was launched at the velocity of 2, 4 and 6km/s. The impact-cratering process was observed by using a high-speed video camera at the framing speed of 10^5fps. Furthermore, we set a 1cm-slit on the target surface to observe 2-dimensional ejecta flow: the slit can exclude most of the ejecta covering through the line of sight of the high-speed camera. This 2-dimensional ejecta observation gave us an accurate relationship between the initial position and the velocity of ejecta fragments.

The tensile strength of the porous mixed sample was measured by a Brazilian test and we found that the tensile strength was changed in the three orders of magnitude from 1MPa to 1kPa with the increase of the sand volume content from 30 to 50%.

The morphology of the recovered crater was characterized by two regions: they are a spall region and a pit region. The spall region looks rough circle but actually it has a polygonal shape with a shallow depth, and it is formed by tensile wave reflected from the surface. The pit region exists at the center of the crater and it has a semi-spherical shape with the diameter rather smaller than the spall region. This spherical region could be formed by the compressive wave and the shear failure was expected in this region. The spall diameter was found to increase with the decrease of the target tensile strength, however the crater depth, which is defined as the depth from the initial surface to the pit floor, showed constant, irrespective of the tensile strength. Moreover, it is very difficult to recognize features characterizing a pit and a spall region in the crater interior for the low strength target as low as 1kPa.

We constructed a crater size scaling law on the strength regime by using our results and compared it to the previous studies obtained for a high strength material. Then, the obtained scaling law for a weak target was written by , where $\pi_R$is the scaled crater radius and $\pi_Y$is the scaled strength in the conventional scaling laws. We found that our $\pi_R$was smaller than the $\pi_R$of frozen sand but larger than the $\pi_R$of porous gypsum. We also constructed the crater scaling law for the crater depth, and it was written by , where π_d is the scaled crater depth, and then it is obvious that $\pi_d$was almost constant, irrespective of

©2019. Japan Geoscience Union. All Right Reserved.

the tensile strength. The reason why our π_R is smaller than the result of frozen sand is considered to be due to the impact energy being consumed by collapsing tiny porous in the gypsum in the target.

Keywords: cratering experiment, strength, porosity, crater scaling law, ejecta velocity

©2019. Japan Geoscience Union. All Right Reserved.

Experimental study on collisional processes of highly porous ice balls simulating Saturn's ring particles

*Yukari Toyoda[1], Minami Yasui[1], Masahiko Arakawa[1]

1. Graduate School of Science, Kobe University

Introduction: Saturn's rings consist of mm- to meter-sized particles of water ice, and they collide with each other at the relative speed slower than a few cm/s. After the collisions, the ring particles coagulate or rebound or fracture, and it could affect the evolution and the structure of Saturn's rings. Saturn's rings were a very thin disk (the thickness thinner than 100-200 m) and this is because the particles collide with each other inelastically so the kinetic energy might dissipate effectively. Therefore, in order to clarify the formation processes and the evolution of Saturn's rings, it is necessary to investigate the collisional properties of the ring particles. In particular, it is very important to examine the effects of material properties of the ring particles and the impact velocity on the coefficient of restitution (*e*).

It is estimated from ground observations and planetary explorations that the ring particles are speculated to be a non-porous ice, porous ice (snow), non-porous ice covered with frost etc. Previous studies have investigated the e of non-porous ice and that covered by the frost, but the e of porous ice (snow) has not been investigated yet in detail. In this study, we focused on the porosity of Saturn's ring particles and examined the dependence of the porosity on the relationship between the *e* and the impact velocity.

Experimental methods: We used ice balls with a smooth surface and snowballs with the porosity of 45, 50, 60% having the diameter of 3 cm to simulate the Saturn's ring particles. We conducted free fall experiments of the balls on an ice plate with a smooth surface and a granite plate. The impact velocity changed from 0.8 to 280 cm/s. We measured the e by two methods. One is an acoustic emission (AE) method. The AE sensor was attached on the plate and it could detect the elastic wave by each collision of the ball. So the impact and the rebound velocities of the ball could be calculated by measuring the time interval between the collisions. Another is a laser displacement meter method. A laser displacement meter was used to measure the position of the free falling ball with time. The e was calculated from the time interval between the collisions of the ball, as same as AE method.

Experimental Results: In the case of ice ball- ice plate collision, the e was almost constant (~0.9) at low impact velocity (quasi-elastic region), while as the impact velocity exceeded a critical velocity, the e decreased drastically (inelastic region). This critical velocity, v_c, was obtained to be 24.5 cm/s. In the inelastic region, the relationship between the e and the impact velocity could be fitted by using the empirical equation, $e=e_{qe}(v_i/v_c)^{-\log(v_i/v_c)}$, where v_i is the impact velocity and e_{qe} is the average value of the e in the quasi-elastic region. In the case of ice ball-granite plate collision, the relationship between the e and the impact velocity was similar to that of ice ball-ice plate collision, but the v_c was obtained to be 11.2 cm/s, which is almost a half of the ice ball-ice plate collision result.

The e of the snowball continued to decrease as the impact velocity increased and the critical velocity, v_c, could not be appeared for both collisions on the granite plate and the ice plate. Furthermore, the e of the

©2019. Japan Geoscience Union. All Right Reserved.

snowball decreased as the porosity increased monotonically, but they merged with each other at the impact velocity lower than 10 cm/s. This is because the kinetic energy of the snowball was consumed by crushing the pores near the impact point on the snowball surface at higher impact velocities. We found that the relationship between the impact velocity and the e could be shown by $e=a\cdot v_i^{-b}$ where a and b are constant. The a was obtained as 0.9 - 0.97, irrespective of the porosity, while the b increased with the increase of the porosity.

©2019. Japan Geoscience Union. All Right Reserved.

IN-SITU FORMATION OF THE URANIAN SATELLITES FROM WIDE DEBRIS DISK FORMED BY GIANT IMPACT

*Ishizawa Yuya[1], Takanori Sasaki[1], Natsuki Hosono[2]

1. Department of Astronomy, Kyoto University, 2. JAMSTEC

We adopted the so-called giant impact scenario to explain both the large axial tilt of Uranus and the formation of the Uranian regular satellites simultaneously. Hydrodynamic simulations for a giant impact onto proto-Uranus have been carried out, which showed that the giant impact can explain the large axial tilt of Uranus and also suggested that ejected materials produced by the giant impact could be distributed throughout the current orbits of the Uranian regular satellites.
In this study, we modeled wide debris disks of solids with several conditions, and performed N-body simulations to investigate the in-situ satellite formation from the wide debris disks to constrain the parameters of debris disks for the in-situ satellite formation. We found that the five major satellites formed around the current orbits from wide debris disks with several times the total satellite mass. Although one or two large satellites usually form inside the current orbits of the major satellites, such satellites would migrate inward due to the tidal torque from the planet and finally be disrupted by the planetary tides or fall onto the planet over several hundred million years. We also propose that the Uranian rings could form from the disrupted satellites and the inner regular satellites could form by use of the ring materials.

Keywords: Satellite formation, Uranus, Giant impact

©2019. Japan Geoscience Union. All Right Reserved.

Effect on the obliquity due to a giant impact on a rotating ice giant

*Kenji Kurosaki[1], Shu-ichiro Inutsuka[1]

1. Department of Physics, Nagoya University

Solar system planets have intrinsic rotation period and obliquity. Especially, Uranus's obliquity is 98 degrees, which is larger than Jupiter, Saturn, and Neptune. Obliquity of Uranus is to the giant impact event. However, previous studies ignored the pre-impact rotation of Uranus. To understand the tilted rotation axis via a giant impact, we calculate the giant impact on a rotating target. We use Godunov Smoothed Particle Hydrodynamics simulation. We include that a giant impact can reproduce the present obliquity of Uranus if the impactor collides on anti-rotating direction.

Keywords: Ice giant, Giant impact, Uranus

©2019. Japan Geoscience Union. All Right Reserved.

[J] Oral | P (Space and Planetary Sciences)：P-PS Planetary Sciences

Mon. May 27, 2019 9:00 AM - 10:30 AM JST | Mon. May 27, 2019 12:00 AM - 1:30 AM UTC | A02 TOKYO BAY MAKUHARI HALL

[P-PS07] Formation and evolution of planetary materials in the Solar System

convener:Yoko Kebukawa(Faculty of Engineering, Yokohama National University), Wataru Fujiya(Ibaraki University, College of Science), Shin Ozawa(Department of Earth Science, Graduate School of Science, Tohoku University), Megumi Matsumoto(Graduate School of Science, Tohoku University), Chairperson:Wataru Fujiya, Shin Ozawa

This session will focus on the evolution in the Solar System with interaction and co-evolution in minerals, water, organic matter, and noble gas in meteorites and interplanetary dust particles. New innovative analytical and theoretical techniques in various fields will be discussed. The developing methods are welcome to submit for the future mainstream of meteorite study. In order to explore the planetary materials and their evolution, both meteorite studies and experimental approaches are necessary. In this session, we will discuss these topics from extraterrestrial sample analyses and experimental works. Research works on undifferentiated and differentiated meteorites and parent body processes such as aqueous alteration, thermal metamorphism, shock metamorphism, volcanic activity, and core-mantle-crust differentiation are especially included in this session.

9:00 AM - 9:15 AM JST | 12:00 AM - 12:15 AM UTC

[PPS07-07] **Evaluation of shock metamorphism of eucrites by X-ray diffraction analysis**

*Rei Kanemaru[1], Naoya Imae[2,1], Akira Yamaguchi[2,1], Hirotugu Nishido[3] (1.The Graduate University for Advanced Studyies, 2.National Institute of Polar Research, 3.Okayama University of scienece)

9:15 AM - 9:30 AM JST | 12:15 AM - 12:30 AM UTC

[PPS07-08] Hf-W dating of main-group pallasites

*Yoshitaka Homma[1], Tsuyoshi Iizuka[1], Akira Ishikawa[2] (1.Department of Earth and Planetary Science, The University of Tokyo, 2.Department of Earth and Planetary Sciences, Tokyo Institute of Technology)

9:30 AM - 9:45 AM JST | 12:30 AM - 12:45 AM UTC

[PPS07-09] Mineralogical study of TCIs in CM carbonaceous chondrites

*Akane Iemoto[1], Yusuke Seto[1], Akira Miyake[2] (1.Graduate School of Science, Kobe University, 2.Graduate School of Science, Kyoto University)

9:45 AM - 10:00 AM JST | 12:45 AM - 1:00 AM UTC

[PPS07-10] Importance of 10Be as a key indicator of (solar) cosmic ray irradiation in the early solar system

*Hajime Hiyagon[1], Yuuki Tanimura[1], Tomoya Nakamura[1], Kohei Fukuda[3], Wataru Fujiya[4], Naoji Sugiura[1], Takanori Kagoshima[2], Naoto Takahata[2], Yuji Sano[2] (1.Graduate School of Science, The University of Tokyo, 2.Atmosphere and Ocean Research Institute, the University of Tokyo, 3.Department of Geoscience, University of Wisconsin-Madison, 4.College of Science, Ibaraki University)

10:00 AM - 10:15 AM JST | 1:00 AM - 1:15 AM UTC

[PPS07-11] **3D microstructure of a cosmic symplectite in primitive carbonaceous chondrite Acfer 094**

*Megumi Matsumoto[1,2], Akira Tsuchiyama[1], Junya Matsuno[1], Aiko Nakato[1,3], Akira Miyake[1], Motoo Ito[4], Naotaka Tomioka[4], Yu Kodama[5], Kentaro Uesugi[6], Akihisa Takeuchi[6], Tsukasa Nakano[7], Epifanio Vaccaro[8] (1.Graduate School of Science, Kyoto Univ., 2.Graduate School of Science, Tohoku Univ., 3.JAXA, ISAS, 4.JAMSTEC, 5.Marine Work Japan LTD., 6.JASRI, 7.AIST, Geological Survey Japan, 8.Natural History Museum, London)

10:15 AM - 10:30 AM JST | 1:15 AM - 1:30 AM UTC

[PPS07-12] Chondrule-like objects and refractory inclusions in GEMS-bearing Antarctic micrometeorites and an interplanetary dust particle.

*Takaaki Noguchi[1], Noriaki Ohashi[2], John P. Bradley[3], Daisuke Nakashima[4], Tomoki Nakamura[4], Makoto Kimura[5], Takayuki Ushikubo[6], Noriko T. Kita[7], Naoya Imae[5] (1.Department of Arts and Science, Kyushu University, 2.NEC Networks and System Integration Co., 3.Univ. of Hawaii at Manoa, 4.Tohoku Univ., 5.National Institute of Polar Research, 6.Kochi Institute for Core Sample Research, JAMSTEC, 7.Univ. of Wisconsin-Madison)

Evaluation of shock metamorphism of eucrites by X-ray diffraction analysis

*Rei Kanemaru[1], Naoya Imae[2,1], Akira Yamaguchi[2,1], Hirotugu Nishido[3]

1. The Graduate University for Advanced Studyies, 2. National Institute of Polar Research, 3. Okayama University of scienece

Introduction

Eucrites have been considered to come from the surface crust of asteroid 4 Vesta. Eucrites experienced varying degrees of shock and thermal metamorphism. The scaling of the degree of shock metamorphism necessary for the understanding of the formation history of Vesta. However, the degree of shock metamorphism has not been established. Recent studies of X-ray diffraction (XRD) analyses using the in-plane rotation of polished thin sections (PTSs) for ordinary chondrites [2] showed that the XRD technique has a potential for the classification and identification of shock and metamorphic stages. In this study, we applied this technique for the thin or thick sections of 13 basaltic and 3 cumulate eucrites. We show that the bulk XRD data may be a useful indicator for characterizing the shock degree for eucrites.

Measurement and analytical methods

We performed X-ray measurement by SmartLab (RIGAKU) at National Institute of Polar Research, Tokyo, on the condition of Cu Kα with 40 kV and 40 mA through the slit of 10 x 5 mm in size.

We defined the shock degrees of studied eucrites from A to D by the petrographic and mineralogical features of thin and thick sections: shock degree A (unshocked) = sharp optical extinction of plagioclase and pyroxenes, shock degree B (low) = weak undulatory extinction or mosaicism of plagioclase and pyroxene, shock degree C (moderate) = the presence of maskelynite, and shock degree D (high) = most (>70-80 vol%) of the plagioclase converted to maskelynite. The degrees of A, B, and C, D for eucrites roughly correspond to 0, 1 and 2 of shock stage for basaltic meteorites defined by Bischoff and Stöffler. (1992) [3], and S1, S2-4, and S5 for enstatite chondrites by defined Rubin et al. (1997) [4], respectively.

Results

We obtained the XRD patterns of 12 eucrites exhibiting the high degree of randomness (e.g., Agoult), whereas four eucrites show the feature of the crystal orientation (e.g., Moama). We identified the peaks of plagioclase, pigeonite, and augite from the XRD patterns of eucrites. The bulk XRD data of each eucrite shows the positive correlation between the full width at half maximum (FWHM) values (for both mean and total) and the shock degree estimated from the textures. On the other hand, the number of the peak in the XRD pattern shows a negative correlation for the increasing of shock degree.

The specific peaks of plagioclase (especially -202) show the decreasing peak intensity and the increasing FWHM values for the increasing shock degree. The peak of pyroxene (pigeonite 310 and augite -311) (2theta = ~30.7º) also shows the increasing FWHM value of pyroxenes for the increasing shock degree.

Discussion

The increase of the averaged FWHM values for each eucrite are related to the shock metamorphism of pyroxene and plagioclase. The negative correlation between the peak intensities of plagioclase and shock degree implies the maskelynitization of plagioclase by shock metamorphism. In particular, most of the plagioclase peaks in A-87272, the strongest shocked sample (D) studied here, have disappeared. The pyroxene peaks show a positive correlation between the FWHM value and shock degree, whereas there is no correlation between the peak intensity and shock degree. This indicates that the shock metamorphism produces the strain in pyroxenes.

In-plane rotation of PTSs method of XRD analysis for eucrites is affected by the crystal orientation in the meteorites, especially coarse-grained unbrecciated rocks and crystalline portions in brecciated rocks.

©2019. Japan Geoscience Union. All Right Reserved.

Nevertheless, we suggest that the FWHM is a useful indicator for measurements of the shock degree of eucrites, since this factor is not affected by the randomness of the crystal orientation of the meteorites.

References

[1] Imae N. et al. (2019) Meteoritics & Planetary Science (in press).
[2] Bischoff A. and Stöffler D. (1992) European Journal of Mineralogy, 4, 707-755.
[3] Rubin A. et al. (1997) Geochimica et Cosmochimica Acta, 61, 847-858.

Keywords: Eucrites, Shock degree, XRD analysis

©2019. Japan Geoscience Union. All Right Reserved.

Hf-W dating of main-group pallasites

*Yoshitaka Homma[1], Tsuyoshi Iizuka[1], Akira Ishikawa[2]

1. Department of Earth and Planetary Science, The University of Tokyo, 2. Department of Earth and Planetary Sciences, Tokyo Institute of Technology

Pallasites are stony-iron meteorites consisting mainly of olivine and FeNi metal, providing us a unique opportunity to study an interior of their parent body. Classically, pallasites have been thought to represent the core-mantle boundary of their parent body, since there are some links with IIIAB irons, which are the representative of the core (e.g. Clayton & Mayeda, 1996). Yet, some recent studies suggest pallasite formed at a shallower region than the core-mantle boundary likely by impact mixing (e.g. Yang et al., 2010; Tarduno et al., 2012). Chronological investigations of pallasites are important since they enable to determine the ages and the timescales of crystallization of pallasite minerals. Although the Al-Mg dating of pallasite olivine yielded a model age of 1.27 Myrs after the CAI formation (Baker et al., 2012), other chronological constraints are still required for resolving the two contrasting models of pallasite formation. Here we apply the Hf-W chronology to four pallasites to constrain when the metal segregated on their parent body. Previously reported W isotopic data of pallasites show a large variation in $\varepsilon^{182/184}$W (Quitté et al., 2005), some of which correspond to the model ages older than CAIs. These isotopic data may reflect multiple causes and effects, such as a nucleosynthetic anomaly, radiogenic and neutron capture effects. We combined the W and the Pt isotopic measurements to evaluate the neutron capture effect which may lead to misinterpretation in age. Also, we measured unradiogenic W isotopes to estimate if the nucleosynthetic anomaly existed in the pallasite parent body. The obtained $\varepsilon^{182/184}$W values corrected for the neutron capture effect by using Pt isotope data range from -3.53 ±0.14 to -3.45 ±0.18, which correspond to the model Hf-W ages of -0.30 ±1.43 to 0.31 ±1.74 Myrs after the CAI formation. Moreover, the $\varepsilon^{183/184}$W values are indistinguishable from the terrestrial value, suggesting that the pallasite parent body accreted in the inner solar system. The model Hf-W ages obtained in this study are coincident with the model Hf-W ages of magmatic irons (Kruijer et al., 2013) and the model Al-Mg age of pallasite olivine, suggesting its magmatic origin rather than impact origin. The implication is that the pallasite metal was originated from the planetary core and was segregated within first 2 Myrs of the solar system evolution.

Keywords: Pallasite, Hf-W chronology, Neutron capture effect, Nucleosynthesis, Core-mantle boundary

©2019. Japan Geoscience Union. All Right Reserved.

Mineralogical study of TCIs in CM carbonaceous chondrites

*Akane Iemoto[1], Yusuke Seto[1], Akira Miyake[2]

1. Graduate School of Science, Kobe University, 2. Graduate School of Science, Kyoto University

Introduction

TCIs, intergrowths of tochilinite ($6(Fe_{0.9}S)\cdot 5[(Mg,Fe)(OH)_2]$) and cronstedtite (Fe-bearing serpentine) occur in most of CM chondrites, which are considered to be aqueous alteration products on the chondrite parent bodies. Based on the textures and chemistries, they can be divided into two types. Type I appears as massive and are generally found in chondrules, while type II exhibits fibrous textures and are generally found within the matrix. Many researchers support that kamacite in chondrules had been altered into type-I TCIs. However, precursors or alteration processes of type-II TCIs are still remains unknown. TCIs potentially provide important information regarding aqueous environments on chondrite parent bodies. Here, we report microtextures of type-II TCIs in 4 CM chondrites and review the formation process.

Materials and methods

We observed the following CM chondrites; QUE97990 (2.6), Murchison (2.5), Nogoya (2.2), Cold Bokkeveld (2.2). The number in parenthesis are the alteration index for CM chondrites proposed by Rubin et al. (2007), in which they defined the index ranging from 2.6 (moderately altered) to 2.0 (highly altered). Textural observation and chemical analyses were performed using an SEM-EDS (JEOL, JSM6480LAII), and nanometer-scale observations using an STEM-EDS (JEOL, JEM2100F) after processing into thin films using an FIB (FEI, Quanta 3Di).

Results and discussion

In QUE97990 and Murchison, less altered meteorites in this study, the type-II TCIs are distributed in the matrices. They are aggregates of a few μm-sized tochilinite and cronstedtite, where thin tochilinite veins occurred inside cronstedtite, suggesting that tochilinite had formed after the formation of cronstedtite. This gives us a constraint on the aqueous condition of CM chondrites. In Nogoya, the TCIs texture showed that very fine serpentine-rich region is located at core, and toward rim, gradually changed to fibrous cronstedtite and mixed-layer phase (alternate layer phase of tochilinite and cronstedtite structure in nanometer scale). The TCIs of Cold Bokkeveld also showed the core-rim structure, where core is often rich in mixed layer phase, and rim is consists of relatively coarse-grained tochilinite and cronstedtite. In the latter two highly altered CM chondrites, the both core showed very fine, fibrous, and fluffy texture, and no evidence of precursor material, suggesting that type-II TCIs were directly formed from water solution.

Keywords: CM carbonaceous chondrites, aqueous alteration, TCIs, STEM

©2019. Japan Geoscience Union. All Right Reserved.

Importance of 10Be as a key indicator of (solar) cosmic ray irradiation in the early solar system

*Hajime Hiyagon[1], Yuuki Tanimura[1], Tomoya Nakamura[1], Kohei Fukuda[3], Wataru Fujiya[4], Naoji Sugiura[1], Takanori Kagoshima[2], Naoto Takahata[2], Yuji Sano[2]

1. Graduate School of Science, The University of Tokyo, 2. Atmosphere and Ocean Research Institute, the University of Tokyo, 3. Department of Geoscience, University of Wisconsin-Madison, 4. College of Science, Ibaraki University

Beryllium-10, which decays to ^{10}B with a half-life of 1.4 Myr, is produced mainly by spallation reactions of solar system materials induced by solar or galactic cosmic rays, but not by thermonuclear reactions in stars. Possible existence of ^{10}Be in the early solar system materials, therefore, has significant importance in considering irradiation processes near the early Sun or in the molecular cloud [1].

Excesses in ^{10}B correlated with Be/B ratios in a number of CAIs from CV chondrites [2-9] suggest the presence of live ^{10}Be at the time of CAI formation. The inferred initial ^{10}Be/^{9}Be ratios are mostly within the range of (0.5-1) x 10^{-3}, though the data are restricted to coarse-grained CAIs from CV chondrites. Recent studies including small CAIs from CH/CB chondrites [10-12] show that the initial ^{10}Be/^{9}Be ratios may be much higher and more variable (from ~10^{-4} to ~10^{-2}), suggesting that the origin of ^{10}Be in CAIs is spallation reactions induced by solar cosmic rays.

Data for chondrules are scarce. Sugiura (2001) [13] analyzed anorthite in chondrules from the Y82094 (ungrouped C3.2) chondrite and found a possible correlation between ^{10}B excesses and Be/B ratios, but the results are not conclusive due to relatively large errors. We further conducted Be-B isotope analyses for chondrules in Y82094 chondrite using NanoSIMS at the Atmosphere and Ocean Research Institute, The University of Tokyo [14]. Resolvable excesses in ^{10}B are found in some of the Y82094 chondrules, but ^{10}Be was probably not alive at the time of the chondrule formation. Some carriers of excess ^{10}B are required in the precursor materials of these chondrules.

Here we review recent progress in Be-B isotopic studies and discuss their importance in understanding the irradiation processes in the early solar system. We will also show our some new results on Be-B systematics for chondrules from Y82094 (C 3.2) and NWA7936 (LL 3.15) chondrite.

References

[1] Chaussidon M. and Gounelle M. (2006) in *Meteorites and the Early Solar System II*, pp. 323-339. [2] McKeegan K. D. et al. (2000) *Science*, 289, 1334-1337. [3] Sugiura N. et al. (2001) *Meteoritics & Planet. Sci.*, 36, 1397-1408. [4] MacPherson G. J. et al. (2002) *Geochim. Cosmochim. Acta*, 67, 3165-3179. [5] Chaussidon M. et al. (2006) *Geochim. Cosmochim. Acta*, 70, 224-245. [6] Wielandt D. et al. (2012) *Astrophys. J. Lett.* 748, L25-L29. [7] Srinivasan G. and Chaussidon M. (2013) *Earth Planet. Sci. Lett.,* 374, 11-23. [8] Liu M. C. et al. (2009) *Geochim. Cosmochim. Acta*, 73, 5051-5079. [9] Liu M. C. et al. (2010) *Astrophys. J. Lett.*, 719, L99-L103. [10] Gounelle M. et al (2013) *Astrophys. J. Lett.*, 763, L33-L37. [11] Fukuda et al. (2017) *80th Ann. Meeting of the Meteoritical Society* (Abstract) #6210. [12] Fukuda et al. (2019) *Astrophys. J.* (submitted). [13] Sugiura N. et al. *Lunar and Planetary Science* XXXII, Abstract #1277, 2001. [14] Hiyagon et al. (2018) *NIPR Symposium on Antarctic Meteorites* (Abstract).

©2019. Japan Geoscience Union. All Right Reserved.

Keywords: Beryllium-10, early solar system, cosmic ray, irradiation, CAIs, chondrules

©2019. Japan Geoscience Union. All Right Reserved.

3D microstructure of a cosmic symplectite in primitive carbonaceous chondrite Acfer 094

*Megumi Matsumoto[1,2], Akira Tsuchiyama[1], Junya Matsuno[1], Aiko Nakato[1,3], Akira Miyake[1], Motoo Ito[4], Naotaka Tomioka[4], Yu Kodama[5], Kentaro Uesugi[6], Akihisa Takeuchi[6], Tsukasa Nakano[7], Epifanio Vaccaro[8]

1. Graduate School of Science, Kyoto Univ., 2. Graduate School of Science, Tohoku Univ., 3. JAXA, ISAS, 4. JAMSTEC, 5. Marine Work Japan LTD., 6. JASRI, 7. AIST, Geological Survey Japan, 8. Natural History Museum, London

Introduction

Oxygen isotopic compositions can be used to identify the origins of planetary materials. Components of carbonaceous chondrites show wide range of oxygen isotopic compositions ($\delta^{17,18}$O: ~-50–0 ‰) that keep nearly constant δ^{17}O/ δ^{18}O ratio of ~1 [e.g.,[1]]. The isotopic variation is thought to be resulted from both mass-dependent isotope fractionation and mixing of two distinct reservoirs of ^{16}O-rich and ^{17,18}O-rich in the solar nebula. The composition of the ^{16}O-rich reservoir has been estimated from the isotopic compositions of CAIs and AOAs which were originated from the reservoir [e.g.,[2]]. Recently, Fe-rich material originated from the ^{17,18}O-rich reservoir, called cosmic symplectite (COS), has been reported from the primitive carbonaceous chondrite Acfer 094 [3]. COS have the heaviest oxygen isotopic composition ($\delta^{17,18}$O: ~180 ‰) among solar materials and consist of nanometer-scaled symplectitically intergrowth of magnetite and Fe-Ni sulfides [3,4]. They are thought to have formed by oxidation of Fe-Ni metal and sulfides by ^{17,18}O-rich water or water vapor in the early Solar System. However, petrological and mineralogical information of COS still remain limited. In this study, we performed synchrotron radiation-based X-ray computed tomography (SR-XCT) and NanoSIMS analysis to investigate the origin of COS.

Results and discussion

First, we observed a polished Acfer 094 section (~2.2 mm^2) by FE-SEM and found five COS grains. The COS grains (~10 μm) show rope-like structure like as COS reported by Abe et al. (2017) [5]. One of the five COS grains was extracted as a block (~25×25×30 μm) using FIB and analyzed by high spatial resolution (~100 nm) SR-XCT at SPring-8 BL47XU. The 3D image shows that the COS grain has irregular shape with many topographic depressions on the surface and contains small (<1 μm) inclusions. The inclusions are not connected to the outside of the COS by clack, ensuring that they were trapped when the host COS formed. We made a cross section surface of the inclusions using FIB and analyzed it by FE-SEM. The inclusions have Na, S, O rich compositions, and such material was not observed in the surrounding matrix. We confirmed that the COS, host of the inclusions, consist of symplectitically intergrowth of magnetite and Fe-Ni sulfides.

We obtained oxygen isotopic composition of the COS gain using NanoSIMS. The COS grain has ^{17,18}O-rich composition (δ^{17}O = 159.06 ±5.79 (1 σ) ‰, δ^{18}O = 166.31 ±3.18 (1 σ) ‰) which is similar to the COS grains reported by previous study [3]. We could not check the difference in oxygen isotopic compositions between the inclusions and the host COS because the inclusions were too small to obtain their compositions.

The inclusions found in this study have not been reported from other COS grains. It is possible that

©2019. Japan Geoscience Union. All Right Reserved.

previous studies could not find the inclusions because most of the inclusions were plucked from the host COS during sample polishing. In fact, many COS grains reported in previous studies contain abundant pores which probably formed by plucking of inclusions. If inclusion is common in COS, it is important to constrain the origin of COS. We will present the results of further TEM analysis of the COS and their inclusions, and discuss the origin of them.

References: [1] Clayton (1993), *Annu. Rev. Earth Planet. Sci.*, **21**, 115–149. [2] Krot et al. (2002), *Science*, **295**, 1051–1054. [3] Sakamoto et al. (2007), *Science*, **317**, 231–233. [4] Seto et al. (2008), *GCA*, **72**, 2723–2734. [5] Abe et al. (2017), *Geochem. J.*, **51**, 3–15.

Keywords: Acfer 094, Cosmic symplectite, SR-XCT, NanoSIMS

©2019. Japan Geoscience Union. All Right Reserved.

Chondrule-like objects and refractory inclusions in GEMS-bearing Antarctic micrometeorites and an interplanetary dust particle.

*Takaaki Noguchi[1], Noriaki Ohashi[2], John P. Bradley[3], Daisuke Nakashima[4], Tomoki Nakamura[4], Makoto Kimura[5], Takayuki Ushikubo[6], Noriko T. Kita[7], Naoya Imae[5]

1. Department of Arts and Science, Kyushu University, 2. NEC Networks and System Integration Co., 3. Univ. of Hawaii at Manoa, 4. Tohoku Univ., 5. National Institute of Polar Research, 6. Kochi Institute for Core Sample Research, JAMSTEC, 7. Univ. of Wisconsin-Madison

Glass with embedded metal and sulfide (GEMS) is regarded as a characteristic component of cometary dust. GEMS-bearing Antarctic micrometeorites (AMMs) and interplanetary dust particles (IDPs) containing chondrules and refractory inclusions are important to understand comets as well as P- and D-type asteroids.

We found three chondrules and a refractory inclusion (RI) in GEMS-bearing AMMs and IDP. We investigated them by TEM, FE-SEM, FE-EPMA, and SIMS. All the chondrules belong to type II (Mg# <90). An AMM contains a spinel-hibonite-perovskite (sp-hb-pv) inclusion, in which spinel contains tiny (<100 nm) Ti-bearing Zr oxides and Mo- and Ru-bearing Ir-Os alloy and that perovskite contains Y and Zr, suggestive of ultra-refractory nature. All the fine-grained matrices are highly porous and contain GEMS, olivine, low-Ca pyroxene including enstatite whisker, high-Ca pyroxene, pyrrhotite. In addition, the matrix and the embedded RI contains minor phyllosilicate. Oxygen isotopic ratios of olivine and pyroxene in two chondrules are plotted 0.7‰ below and 2.7‰ above the terrestrial fractionation line on the three-oxygen isotope diagram, respectively. Oxygen isotope ratios of spinel in the RI are $\delta^{18}O$ of -43.8‰ to -45.1‰ and $\delta^{17}O$ of -44.8‰ to -46.8‰, respectively. Resolvable ^{26}Mg excesses ($\delta^{26}Mg^*$ ~ 13±2‰ and 14±3‰) are observed in hibonite with $^{27}Al/^{24}Mg$ ratios of 35-43, while spinel show marginal excess (~1‰).

The olivine/(olivine + low-Ca pyroxene) ratios were deduced from the mid-infrared spectra of asteroids and comets; those of B-, G-, and C-type asteroids, P- and D-type asteroids, and comets are <12%, 36-52%, and >50%, respectively. The ratios of the matrices in the samples range from 0.4 to 0.61, which are well above the values of B-, G-, and C-type asteroids and comparable with those of P- and D-type asteroids and comets. Therefore, P- and D-type asteroids and comets seem to be more plausible as parent bodies of these AMMs and an IDP than B-, G-, and C-type asteroids. If that is the case, P- and D-type asteroids and comets contain abundant GEMS. Ferromagnesian silicates with Mg#<90 in the chondrules distribute around $\Delta^{17}O$ ~0‰ in the Mg# vs $\Delta^{17}O$ diagram like those in the Stardust samples. This seems to be consistent with the hypothesis that P- and D-type asteroids were migrated from the Kuiper belt. The chondrules were formed in more oxidizing conditions than chondrules in CR chondrites because type II chondrules in them occupy only ~1%.

Keywords: chondrule, refractory inclusion, GEMS

©2019. Japan Geoscience Union. All Right Reserved.

[J] Oral | P (Space and Planetary Sciences)：P-PS Planetary Sciences

Mon. May 27, 2019 10:45 AM - 12:15 PM JST | Mon. May 27, 2019 1:45 AM - 3:15 AM UTC | A02 TOKYO BAY MAKUHARI HALL

[P-PS07] Formation and evolution of planetary materials in the Solar System

convener:Yoko Kebukawa(Faculty of Engineering, Yokohama National University), Wataru Fujiya(Ibaraki University, College of Science), Shin Ozawa(Department of Earth Science, Graduate School of Science, Tohoku University), Megumi Matsumoto(Graduate School of Science, Tohoku University), Chairperson:Yoko Kebukawa, Shin Ozawa

This session will focus on the evolution in the Solar System with interaction and co-evolution in minerals, water, organic matter, and noble gas in meteorites and interplanetary dust particles. New innovative analytical and theoretical techniques in various fields will be discussed. The developing methods are welcome to submit for the future mainstream of meteorite study. In order to explore the planetary materials and their evolution, both meteorite studies and experimental approaches are necessary. In this session, we will discuss these topics from extraterrestrial sample analyses and experimental works. Research works on undifferentiated and differentiated meteorites and parent body processes such as aqueous alteration, thermal metamorphism, shock metamorphism, volcanic activity, and core-mantle-crust differentiation are especially included in this session.

10:45 AM - 11:00 AM JST | 1:45 AM - 2:00 AM UTC

[PPS07-13] Spectral and mineralogical properties of naturally-heated carbonaceous chondrites; implication to heating processes on the surface of hydrous asteroids

★Invited Papers

*Moe Matsuoka[1], Tomoki Nakamura[2], Takahiro Hiroi[3], Nobuyoshi Miyajima[4], Naoya Imae[5,6], Akira Yamaguchi[5], Hideyasu Kojima[5,6] (1.Japan Aerospace Exploration Agency(JAXA), 2.Department of Earth and Planetary Materials Sciences, Faculty of Science, Tohoku University, 3.Department of Earth, Environmental and Planetary Sciences, Brown University, 4.Bayerisches Geoinstitut, University of Bayreuth, 5.National Institute of Polar Research, 6.Department of Polar Science, School of Multidisciplinary Science, SOKENDAI)

11:00 AM - 11:15 AM JST | 2:00 AM - 2:15 AM UTC

[PPS07-14] Heterogeneity of oxygen and carbon isotopic compositions within carbonate grains in the Yamato 791198 CM chondrite and evolution of isotope ratios during aqueous alteration

*Wataru Fujiya[1], YUTO AOKI[1], Takayuki Ushikubo[2], Ko Hashizume[1] (1.Ibaraki University, College of Science, 2.Kochi Institute for Core Sample research, Japan Agency for Marine-Earth Science and Technology)

11:15 AM - 11:30 AM JST | 2:15 AM - 2:30 AM UTC

[PPS07-15] Characteristics of Oxygen isotope ratios of chondrules and isolated olivine grains from Tagish Lake C2 chondrite

*Takayuki Ushikubo[1], Makoto Kimura[2] (1.Kochi Institute for Core Sample Research, Japan Agency for Marine-Earth Science and Technology, 2.National Institute for Polar Research)

11:30 AM - 11:45 AM JST | 2:30 AM - 2:45 AM UTC

[PPS07-16] Extreme ^{16}O-rich CAIs in Isheyevo chondrite

*Naoya Sakamoto[1], Noriyuki Kawasaki[2] (1.Creative Research Institution, Hokkaido University, 2.Natural History Sciences, Hokkaido University)

11:45 AM - 12:00 PM JST | 2:45 AM - 3:00 AM UTC

[PPS07-17] Variations in initial ^{26}Al/^{27}Al ratios among fine-grained CAIs in the reduced CV chondrites

*Noriyuki Kawasaki[1], Changkun Park[2], Naoya Sakamoto[1], Hisayoshi Yurimoto[1,3] (1.Hokkaido University, 2.KOPRI, 3.ISAS/JAXA)

12:00 PM - 12:15 PM JST | 3:00 AM - 3:15 AM UTC

[PPS07-18] Petrographic study of compact type A CAIs with partial melting process

*Akimasa Suzumura[1], Yusuke Seto[2], Shoichi Itoh[1] (1.Graduate school of Science, Kyoto University, 2.Graduate school of Science, Kobe University)

Spectral and mineralogical properties of naturally-heated carbonaceous chondrites; implication to heating processes on the surface of hydrous asteroids

*Moe Matsuoka[1], Tomoki Nakamura[2], Takahiro Hiroi[3], Nobuyoshi Miyajima[4], Naoya Imae[5,6], Akira Yamaguchi[5], Hideyasu Kojima[5,6]

1. Japan Aerospace Exploration Agency(JAXA), 2. Department of Earth and Planetary Materials Sciences, Faculty of Science, Tohoku University, 3. Department of Earth, Environmental and Planetary Sciences, Brown University, 4. Bayerisches Geoinstitut, University of Bayreuth, 5. National Institute of Polar Research, 6. Department of Polar Science, School of Multidisciplinary Science, SOKENDAI

The parent bodies of carbonaceous chondrites are thought to be C-type asteroids based on the similarity of visible (Vis) -infrared (IR) spectra between carbonaceous chondrites and C-type asteroids [e.g., 1-5]. Several C-type asteroids are thought to have been heated and dehydrated judging from their spectra which are similar to the spectra of experimentally-heated chondrites [1,6]. The Hayabusa2 spacecraft of the Japan Aerospace Exploration Agency (JAXA) was arrived at the target C-type asteroid 162173 Ryugu in June 2018. Ryugu spectra exhibit a weak 2.72-μm OH absorption band that is present across the surface of the asteroid, and nearly always darker than values typical for carbonaceous chondrites [7,8]. The meteorites whose spectral features are most similar to Ryugu are shocked or moderately-heated carbonaceous chondrites. In this study, we performed spectral analysis in Vis-NIR range and mineralogical analysis in micro scale using carbonaceous chondrites that heated dehydrated on their parent bodies.

Spectral and mineralogical analyses were performed using nine naturally-heated and dehydrated carbonaceous chondrite samples (seven CM, one CI, and one CV chondrites), which classified into heating stages (HS) from I to IV based on X-ray diffraction results [9]. In-situ heating of samples at 120–400 ˚C was performed during spectral measurements and successfully removed absorption water and part of rehydrated water from chondrite samples. Lewis Cliff (LEW) 87022 (unheated CM), Jbilet Winselwan, and Dhofar 735 (heated at 600–900 ˚C [10]) were used for transmission electron microscope (TEM) analysis.

Reflectance spectra of HS-I samples show the positive slope in Vis- IR range and the significant 0.7- and 3-μm absorption bands. The 0.7-μm band appears in only HS-I sample spectra. With increasing heating degree, (1) Vis-IR slope decreases, (2) the 0.7- and 3-μm bands decrease, and (3) Mid-IR spectral feature (i.e. Christiansen feature (CF) and Reststrahlen bands (RB)) shifts toward longer wavelength. TEM/EDX analyses showed that the matrix of severely-heated chondrites consists of tiny olivine, low-Ca pyroxene, and fine Fe- and Ni-rich metal grains (<1 μm). It is indicated that in proportion to the heating degree, amorphization and dehydration of serpentine and tochilinite from HS-I to HS-II might cause the 0.7- and 3-μm band weakening, and spectral slope and albedo decreasing of spectra. Then, formation of secondary olivine and pyroxene, and FeNi-rich metal grains at HS-IV would be responsible for the 3-μm band depth decreasing, spectral slope and albedo increasing, CF peak shift, and RB changes of chondrite spectra.

We plan to compare other IR reflectance spectra of asteroids, such as those acquired by AKARI [11], to better interpret remotely sensed data of Bennu (NASA’s OSIRIS-REx mission target) and Ryugu. Future NIRS3 observations before/after the Small Carry-on Impactor (SCI) crater experiment and lab analyses of returned samples will reveal additional compositional properties of Ryugu.

©2019. Japan Geoscience Union. All Right Reserved.

References: [1] Hiroi T. et al. (1996) LPSC XXVII, Abstract #551. [2] Yamashita S. et al. (2015) 78th Met. Soc., Abstract #5154. [3] Mogi K. et al. (2017) 80th Met. Soc., Abstract #6225. [4] McBride K. et al. (2003) Antarct. Meteorite Newsl. 26 (1). [5] Cloutis E.A. et al. (2011) Icarus, 216, 309-346. [6] Hiroi, T. et al. (1993) Science, 261, 1016-1018. [7] Sugita et al. (2019) Science, under review. [8] Kitazato et al. (2019) Science, under review. [9] Nakamura, T. (2005) J. Miner. Petrol. Sci., 100, 260-272. [10] Nakato A. et al. (2009) 72nd Met. Soc., Abstract #5336. [11] Usui F. et al. (2018) arXiv:1810.03828.

Acknowledgements: We appreciate support from the National Institute of Polar Research for providing carbonaceous chondrites, the JSPS Japanese-German Graduate Externship for Research on Deep Earth Volatile Cycle, and the JSPS Core-to-Core Program "International Network of Planetary Sciences”.

Keywords: carbonaceous chondrite, C-type asteroid, reflectance spectra, TEM analysis, Hayabusa2

©2019. Japan Geoscience Union. All Right Reserved.

Heterogeneity of oxygen and carbon isotopic compositions within carbonate grains in the Yamato 791198 CM chondrite and evolution of isotope ratios during aqueous alteration

*Wataru Fujiya[1], YUTO AOKI[1], Takayuki Ushikubo[2], Ko Hashizume[1]

1. Ibaraki University, College of Science, 2. Kochi Institute for Core Sample research, Japan Agency for Marine-Earth Science and Technology

Carbonate minerals are ubiquitous in CM chondrites and formed by aqueous alteration in their parent body [1]. Previous studies have revealed a large variation in C isotope ratios of CM carbonates with $\delta^{13}C$ values ranging from ~20 to ~90 ‰[e.g., 2,3]. However, the reason for this variability has remained poorly understood. Here, we conducted in-situ C- and O-isotope measurements by SIMS along crystal growth within single carbonate grains in Yamato 791198 (CM 2.4) to trace the change in $\delta^{13}C$ values during aqueous alteration.

First, we obtained color CL images of seven calcite ($CaCO_3$) grains with an FE-EPMA. Then, we measured O and C isotope ratios of the calcite grains with the CAMECA ims-1280HR. Typically, the isotope measurements were carried out on three different points for each calcite grain. Finally, we obtained quantitative chemical compositions and elemental maps of Mg, Si, Ca, Mn, and Fe of the calcite grains using the same FE-EPMA as that for the CL images.

All grain analysed exhibit a clear zoning of Mn, Mg, and Fe. The zoning is well correlated with CL images. The heterogeneous distribution of minor elements and CL intensity likely reflects the crystal growth of these grains.

The O isotope ratios of the calcite grains significantly vary with the $\delta^{18}O$ values ranging from ~22 to ~38 ‰. The O isotope ratios plot on a single trend line in an O three-isotope plot with a slope of ~0.61, slightly steeper than the terrestrial fractionation line, reflecting a progressive O-isotope exchange between initially ^{16}O-poor water and ^{16}O-rich rock [4,5]. The $\delta^{18}O$ values also vary within single calcite grains, demonstrating crystal growth from a relatively dark CL core to a red CL periphery.

The $\delta^{13}C$ values of the calcite grains range from 17 to 32 ‰. This range is much smaller than that observed for different carbonate grains or bulk meteorite samples by previous studies. Especially, the $\delta^{13}C$ variations within individual grains are only 4 ‰at most except for one grain. Previous studies have suggested that the observed $\delta^{13}C$ variation was produced by the Rayleigh-type isotopic fractionation by the escape of ^{13}C-poor methane [2], or equilibrium isotopic fractionation reflecting variable formation temperatures of carbonates [3]. However, the small intra-grain $\delta^{13}C$ variations associated with the large $\delta^{18}O$ change observed in this study cannot be explained by such processes. Instead, here we propose that the $\delta^{13}C$ values of dissolved carbon species in aqueous solutions were locally heterogeneous, and did not significantly change during carbonate formation.

References: [1] Brearley A. J. (2006) in Meteorites and the Early Solar System II, 587-624. [2] Guo W. and Eiler J. M. (2007) GCA, 71, 5565-5575. [3] Alexander C. M. O' D. et al. (2015) Meteoritics & Planet. Sci.,

©2019. Japan Geoscience Union. All Right Reserved.

50, 810-833. [4] Clayton R. N. and Mayeda T. K. (1984) EPSL, 67, 151-161. [5] Fujiya W. (2018) EPSL, 481, 264-272.

Keywords: Carbonate mineral, Carbonaceous chondrite, Oxygen isotope, Carbon isotope

©2019. Japan Geoscience Union. All Right Reserved.

Characteristics of Oxygen isotope ratios of chondrules and isolated olivine grains from Tagish Lake C2 chondrite

*Takayuki Ushikubo[1], Makoto Kimura[2]

1. Kochi Institute for Core Sample Research, Japan Agency for Marine-Earth Science and Technology, 2. National Institute for Polar Research

Recent studies on oxygen isotope systematics of chondrules show that chondrules in individual chondrite groups have characteristic distributions in their oxygen isotope ratios and Mg# (molar % of MgO/(MgO+FeO)) [1, 2]. The correlations between Mg# and $D^{17}O$ values (= $d^{17}O_{VSMOW}$ - 0.52 ×$d^{18}O_{VSMOW}$) of chondrules can be explained by mixing of ^{16}O-rich anhydrous dusts and an ^{16}O-poor oxidizing agent (most likely H_2O ice) in chondrule forming regions [3]. Based on similar Mg# - $D^{17}O$ correlations between CR chondrite chondrules and cometary silicate particles from comet Wild 2, it has been proposed that many of cometary silicate particles formed in the outer regions of the asteroid belt [e.g. 4, 5]. The Tagish Lake meteorite (ungrouped C2) is an appropriate sample to investigate the Mg# - $D^{17}O$ systematics of silicate particles formed in the outer regions of the asteroid belt because the Tagish Lake meteorite probably derived from a D-type asteroid [6]. Previous oxygen isotope studies on olivine grains from Tagish Lake and Tagish Lake-like meteorites [e.g. 7] show that their Mg# - $D^{17}O$ systematics are similar to that of CR chondrite chondrules. Here, we report new oxygen isotope data of olivine grains from the Tagish Lake meteorite for better understandings of the Mg# - $D^{17}O$ systematics of silicate particles in the outer regions of the asteroid belt.

Two polished epoxy mounts of the Tagish Lake meteorite, TL-KC-1 (8mm ×5mm) and TL-KC-2 (4mm × 3mm), were prepared for this study. Due to extensive aqueous alteration in the Tagish Lake parent body, phyllosilicates and other secondary phases such as magnetite and carbonates replace primary anhydrous phases. However, remaining olivine grains in chondrules and matrix tend to have sharp grain boundaries and no apparent evidence for the Mg-Fe exchange between olivine grains and matrix was observed. No alteration features were observed in these grains. Forty chondrules and isolated olivine grains (hereafter “ferromagnesian inclusions”) were selected for oxygen isotope measurements (34 type I [Mg#>= 90] and 6 type II [Mg#<90]). Oxygen isotope ratios of olivine grains were measured with an ion microprobe, CAMECA IMS 1280-HR at Kochi Institute. A 20 kV accelerated Cs^+ primary beam (~30 pA, ~3 um in diameter) was used. The analytical conditions were similar to those in [1].

Oxygen three-isotope ratios of ferromagnesian inclusions from Tagish Lake are distributed along the PCM (primitive chondrule minerals) line [1]. Most type I ferromagnesian inclusions are relatively ^{16}O-rich ($D^{17}O$ = -7.4 to -3.9‰) and type II ferromagnesian inclusions are relatively ^{16}O-poor ($D^{17}O$ >= -3‰). Of six type II ferromagnesian inclusions, two inclusions have $D^{17}O$ ~ 0‰, which are recognized in in Tagish Lake-like meteorites, CR chondrites, and cometary silicate particles, but are almost absent in other carbonaceous chondrites [e.g., 2-5, 7]. The present results are further evidence for the link between ferromagnesian inclusions accumulated into asteroids in the outer regions of the asteroid belt (possibly D-type asteroids) and silicate particles accumulated into cometary nuclei in the Kuiper belt. As discussed in [4, 5, 8], type II silicates are common in cometary silicate particles, which is distinct from ferromagnesian inclusions in Tagish Lake(-like) meteorites and CR chondrites. Most cometary silicate particles formed in H_2O ice enriched oxidizing regions. Such regions were probably farther than where typical ^{16}O-rich type I chondrules of carbonaceous chondrites formed.

References:

[1] Ushikubo T. et al. (2012) GCA, 90, 242-240

©2019. Japan Geoscience Union. All Right Reserved.

[2] Tenner T. J. et al. (2018) Chapter 8 in Chondrules (Cambridge Univ. press)
[3] Tenner T. J. et al. (2015) GCA, 148, 228-250
[4] Nakashima D. et al. (2012) EPSL, 357-358, 355-365
[5] Defouilloy C. et al. (2017) EPSL, 465, 145-154
[6] Hiroi T. (2001) Science, 293, 2234-2236
[7] Yamanobe M. et al. (2018) Polar Sci., 15, 29-38
[8] Frank D. R. et al. (2014) GCA, 142, 240-259

Keywords: Tagish Lake meteorite, Chondrule, Oxygen isotope, SIMS

©2019. Japan Geoscience Union. All Right Reserved.

Extreme ^{16}O-rich CAIs in Isheyevo chondrite

*Naoya Sakamoto[1], Noriyuki Kawasaki[2]

1. Creative Research Institution, Hokkaido University, 2. Natural History Sciences, Hokkaido University

Oxygen in the solar system is believed to be formed by mixing of ^{16}O-rich and ^{16}O-poor reservoirs [e.g. 1 and references therein]. The ^{16}O-poor end member ($\Delta^{17}O$ = +85‰) was found from magnetite in cosmic symplectite and infers that the ^{16}O-poor reservor is H_2O [2]. Nevertheless candidates of ^{16}O-rich end member were reported from one chondrule named a006 ($\Delta^{17}O$ = -37‰) [3], 4 Ca-Al-rich inclusions (CAIs) ($\Delta^{17}O$ = -37 to -32‰) [4,5] and the Sun ($\Delta^{17}O$ = -28‰) [6] relative to other CAIs ($\Delta^{17}O$ = -23‰) [e.g. 7], characteristics of the reservoir are unclear because of the diversity of few samples. In this study, we surveyed extreme ^{16}O-rich CAIs in Isheyevo chondrites to investigate the ^{16}O-rich end menber.

Thirteenthick sections of Isheyevo chondrite were newly prepared. X-ray elemental maps were obtaind for whole sections by FE-SEM-EDS. Al-rich inclusions on the sections were picked up as many as possible for isotope analysis in order to prevent biased sample selection. Oxygen isotope analysis for the inclusions were performed by SIMS.

Oxygen isotopic compositions of 263 CAIs were measured and 4 extreme ^{16}O-rich CAIs were found. Two CAIs are composed of grossite core rimmed by spinel, melilite and Ti-rich diopside layer and others lack diopside and/or melilite. While the heterogeneous composition of grossite ($\Delta^{17}O$ = -36 to -32‰) would be affected by altered feature of grossite, the spinel grains have uniform ^{16}O-rich compsition ($\Delta^{17}O$ = -37‰). If we draw a line in 3 oxygen isotope diagram with the extreme ^{16}O-rich spinel and spinel in chondules near the CAI, the slope is in good agreement with a slope of olivine in a006 chondrule and porphiritic olivine chondrule infer that the oxygen isotopic composition of the spinel grains maintain the signature of an^{16}O-rich end member of the Solar System.

References:[1] Yurimoto *et al.* (2008)*Reviews in Mineralogy and Geochemistry* 68, 141–186. [2] Sakamoto *et al.* (2007) *Science*317, 231-233. [3] Kobayashi *et al.* (2003) *Geochemical J.* 37, 663–669. [4] Gounell *et al.* (2009) *ApJ*698, L18-L22.[5] Krot *et al.* (2017) *GCA* 201, 185-223. [6] McKeegan *et al.* (2011) *Science*332, 1528-1532. [7] Kawasaki *et al.* (2018) *GCA* 221, 318-341.

Keywords: Oxygen isotope, Isheyevo chondrite, CAI, SIMS

©2019. Japan Geoscience Union. All Right Reserved.

Variations in initial $^{26}Al/^{27}Al$ ratios among fine-grained CAIs in the reduced CV chondrites

*Noriyuki Kawasaki[1], Changkun Park[2], Naoya Sakamoto[1], Hisayoshi Yurimoto[1,3]

1. Hokkaido University, 2. KOPRI, 3. ISAS/JAXA

Ca-Al-rich inclusions (CAIs) are oldest solids formed in the Solar System [1] and composed of high-temperature condensates from a solar-composition gas [2]. Most of CAIs are thought to have contained detectable amounts of live ^{26}Al, a short-lived radionuclide with a half-life of ~0.7 Myr, at their formation [3]. Recent high-precision $^{26}Al–^{26}Mg$ mineral isochron studies using secondary ion mass spectrometry (SIMS) revealed detailed distributions of initial $^{26}Al/^{27}Al$ values, $(^{26}Al/^{27}Al)_0$, for individual CAIs in the reduced CV chondrites [e.g., 4–9]; coarse-grained, igneous CAIs and fluffy Type A CAIs show similar variations in $(^{26}Al/^{27}Al)_0$ respectively, which range from ~5.2 to ~4.2 $\times10^{-5}$. In this study, we obtained new $^{26}Al–^{26}Mg$ mineral isochrons of five fine-grained, spinel-rich CAIs (FGIs) from the reduced CV chondrites Efremovka, Vigarano and TIL 07007 by *in situ* measurements using a SIMS instrument (CAMECA ims-1280HR installed at Hokkaido University). Since FGIs are likely to be condensates from a solar nebular gas, $^{26}Al–^{26}Mg$ mineral isochrons of them enable a more systematic comparison of $(^{26}Al/^{27}Al)_0$ between CAIs formed by condensation and by melt crystallization than has previously been achieved. The obtained $^{26}Al–^{26}Mg$ mineral isochrons for five FGIs give $(^{26}Al/^{27}Al)_0$ of (5.19 ±0.17) $\times10^{-5}$, (5.00 ± 0.17) $\times10^{-5}$, (4.53 ±0.18) $\times10^{-5}$, (4.43 ±0.31) $\times10^{-5}$, and (3.35 ±0.21) $\times10^{-5}$. The $(^{26}Al/^{27}Al)_0$ for two FGIs are essentially identical to the whole-rock CAI value of $(^{26}Al/^{27}Al)_0$ ~ 5.2 $\times10^{-5}$ [10, 11], while those for other three FGIs are clearly lower than the whole-rock CAI value. The range of $(^{26}Al/^{27}Al)_0$ values for the FGIs, from (5.19 ±0.17) to (3.35 ±0.21) $\times10^{-5}$, corresponds to a formation age spread of 0.44 ±0.07 Myr. These variations are slightly larger than those for igneous CAIs ranging from ~5.2 to ~4.2 $\times10^{-5}$ [5, 6]. Our data imply that CAI condensation events continued for, at least, ~0.4 Myr at the very beginning of our Solar System, if ^{26}Al was distributed homogeneously in the forming region. Alternatively, the observed variations would also raise a possibility of heterogeneous distributions of ^{26}Al in the forming region, corresponding to a range over, at least, $3.4 \times10^{-5} < (^{26}Al/^{27}Al)_0 < 5.2 \times10^{-5}$.

[1] Connelly et al. (2012) *Science* 338, 651–655. [2] Grossman (1972) *GCA* 86, 597–619. [3] MacPherson et al. (1995) *Meteoritics* 30, 365–386. [4] MacPherson et al. (2010) *ApJL* 711, L117–L121. [5] MacPherson et al. (2012) *EPSL* 331–332, 43–54. [6] MacPherson et al. (2017) *GCA* 201, 65–82. [7] Kawasaki et al. (2017) *GCA* 201, 83–102. [8] Kawasaki et al. (2018) *GCA* 221, 318–341. [9] Kawasaki et al. (2019) *EPSL* 511, 25–35. [10] Jacobsen et al. (2008) *EPSL* 272, 353–364. [11] Larsen et al. (2011) *ApJL* 735, L37–L43.

©2019. Japan Geoscience Union. All Right Reserved.

Petrographic study of compact type A CAIs with partial melting process

*Akimasa Suzumura[1], Yusuke Seto[2], Shoichi Itoh[1]

1. Graduate school of Science, Kyoto University, 2. Graduate school of Science, Kobe University

Refractory inclusions (Ca-Al-rich inclusions (CAIs)) in chondritic meteorites are the oldest substances formed in the Solar System (Connelly et al., 2012). Coarse-grained CAIs are classified into three subtypes, type A, B and C, according to their petrologic features (e.g., Grossman 1975). Compact type A CAIs (CTAs) are expected to be formed in the earliest stage of solar nebula and experienced a partial melting at least once (e.g., Simon et al., 1999). Yurimoto et al. (1998) have explained the heterogeneous oxygen isotope distributions among constituent minerals in Compact Type A CAIs have formed by the partial melting model. The indicator of partial melting is necessary to discuss the formation of the entire CAIs. However, there are only a few studies that referring to the formation processes of CTAs from the perspective of crystal growth in partial melting states (Ito et al., 2004, Park et al., 2012, Kawasaki et al., 2017). Generally, spinel in CTAs are poikilitically enclosed by melilite or fassaite, and estimated to be first crystallized mineral from CAI melt (Stolper, 1982). Namely, spinel in CTAs is expected to preserve valuable information of the thermal histories such as partial melting processes. Therefore, we focus on the petrological and mineralogical feature of spinel grains in CTAs. The studied CTA (KU-N) is included in a polished thin section of North West Africa 7865 reduced CV3 carbonaceous chondrite. Yoneyama et al. (2016) had studied the same CTA, and concluded that they experienced multiple partial melting. We have undertaken petrographic and mineralogical investigations of the CTA (KU-N-02) focusing on micro-textures resulting from partial melting (local compositional zoning, grain morphology and relationships of crystallographic orientation), using a polarizing microscope, scanning electron microscope (SEM) and electron back scatter diffraction (EBSD).

In the KU-N-02 CTA, spinel crystals are enclosed by melilite or fassaite. The former (up to 50 μm in size) is substantially euhedral but the edges are rounded, while the latter (about 10 - 100 μm in size) are almost euhedral with sharp edges. On the surfaces of both type of spinel grains, small perovskite particles with sizes of several μm are ubiquitously present.

In interior KU-N-02 CAI, single crystal melilite with spinel inclusions showed a remarkable compositional zoning Single crystal melilite show core-to-rim normal zoning, with decreasing Al and increasing Mg from core to rim. In the melilite single crystal, the area of about 10 μm wide around the spinel surfaces has Åk-rich compositions in comparison. By EBSD analyses, Åk-rich melilite crystal orientation and Åk-poor melilite crystal orientation is same. Therefore, Åk-rich melilite part (~10μm) surrounding spinel are crystallized after Åk-poor melilite. Because of these results, it is difficult to explain how Åk-rich part surrounding spinel in a melilite crystal crystallized by a single stage cooling. This texture indicates that the boundary area between spinel and melilite had eutectically melted at high temperature by some heating process, and then Mg/Al contents had been redistributed to melilite and spinel during rapid cooling. Accordingly, this partial melting probably resulted in the unique morphology and the crystallographic orientation relationship of the spinel enclosed by melilite and Local composition zoning of the melilite.

Keywords: Compact Type A CAIs, partial melting, petrographic study

©2019. Japan Geoscience Union. All Right Reserved.

[J] Poster | P (Space and Planetary Sciences)：P-PS Planetary Sciences

Mon. May 27, 2019 3:30 PM - 5:00 PM JST | Mon. May 27, 2019 6:30 AM - 8:00 AM UTC | Poster Hall International Exhibition Hall8, Makuhari Messe_2

[P-PS07] Formation and evolution of planetary materials in the Solar System

convener:Yoko Kebukawa(Faculty of Engineering, Yokohama National University), Wataru Fujiya(Ibaraki University, College of Science), Shin Ozawa(Department of Earth Science, Graduate School of Science, Tohoku University), Megumi Matsumoto(Graduate School of Science, Tohoku University)

This session will focus on the evolution in the Solar System with interaction and co-evolution in minerals, water, organic matter, and noble gas in meteorites and interplanetary dust particles. New innovative analytical and theoretical techniques in various fields will be discussed. The developing methods are welcome to submit for the future mainstream of meteorite study. In order to explore the planetary materials and their evolution, both meteorite studies and experimental approaches are necessary. In this session, we will discuss these topics from extraterrestrial sample analyses and experimental works. Research works on undifferentiated and differentiated meteorites and parent body processes such as aqueous alteration, thermal metamorphism, shock metamorphism, volcanic activity, and core-mantle-crust differentiation are especially included in this session.

[PPS07-P01] Stability of Amino Acid Precursors in Simulated Extraterestrial Environments

*tomohito sato[1], Soushi Kuramoto[1], Takuya Yokoo[1], Yoshida Satoshi[2], Isao Yoda[3], Hitoshi Fukuda[3], Yoshiyuki Oguri[3], MITA Hajime[4], Kazuhiro Kanda[5], Hiromi Shibata[6], Zyunichi Takahashi[1], Yoko Kebukawa[1], Kensei Kobayashi[1] (1.yokohama national univercity, 2.QST, 3.Tokyo Institute of Technology, 4.Fukuoka Institute of Technology, 5.University of Hyogo, 6.Osaka University)

[PPS07-P02] Production of amino acids by gamma rays during aqueous alteration process in meteorite parent body

*Shinya Asano[1], Isao Yoda[2], Yasuji Muramatsu[3], Yoko Kebukawa[1], Kensei Kobayashi[1] (1.Yokohama national university, 2.Tokyo Institute of Technology, 3.University of Hyogo)

[PPS07-P03] Kinetic approaches for the thermal history of organic matter in meteorites based on Raman spectra

*Kento Kiryu[1], Yoko Kebukawa[1], Motoko Igisu[2], Takazo Shibuya[2], Kensei Kobayashi[1] (1.Yokohama National Univ., 2.Japan Agency for Marine-Earth Science and Technology)

[PPS07-P04] Relationship between spatial distribution of organic compounds and minerals in the Murchison meteorite

*Taiyo Sengoku[1], Minako Hashiguchi[1], Hiroshi Naraoka[1] (1.Kyushu University)

[PPS07-P05] O and Al-Mg isotope systematics of a hibonite-melilite-rich fine-grained CAI in the reduced CV chondrite NWA8613

*Sohei Wada[1], Noriyuki Kawasaki[1], Hisayoshi Yurimoto[1,2] (1.Hokkaido University, 2.ISAS/JAXA)

[PPS07-P06] Observation of Enstatite Whiskers in Fine-grained Rims in the Carbonaceous Chondrite ALH A77307

*Yasuhisa Shirota[1], Masahiro YASUTAKE[1], Satomi Enju[1], Akira Tsuchiyama[1] (1.Division of Earth and Planet, Science, Kyoto University)

[PPS07-P07] 3D observation of whisker-like material in the porous matrix of the Paris CM chondrite by SR-XCT

*Masahiro YASUTAKE[1], Epifanio Vacarro[2], Kentaro Uesugi[3], Akihisa Takeuchi[3], Tsukasa Nakano[4], Akira Tsuchiyama[1] (1.Division of Earth and Planetary Science, Graduate School of Science, Kyoto University, 2.National History Museum, London, 3.JASRI/SPring8, 4.GSJ/AIST)

[PPS07-P08] Development of cryogenic SIMS technique for isotope analysis of fluid inclusions

*Isono Yuki[1], Naoya Sakamoto[2], Hisayoshi Yurimoto[3] (1.Department of Natural History Sciences, Hokkaido University, 2.Creative Research Institusion, Hokkaido University, 3.Department of Natural History Sciences, Hokkaido University)

[PPS07-P09] X-ray diffraction study using Gandolfi attachment: Implications for small extraterrestrial materials

*Naoya Imae[1,2], Makoto Kimura[1] (1.Antarctic Meteorite Research Center, National Institute of Polar Research, 2.SOKENDAI)

[PPS07-P10] Trace elements analysis and Ar-Ar dating for microgram-scaled extraterrestrial samples

*Ryuji Okazaki[1], Sekimoto Shun[2] (1.Department of Earth and Planetary Sciences, Faculty of Science, Kyushu University, 2.Institute for Integrated Radiation and Nuclear Science, Kyoto University)

[PPS07-P11] Magnetic separation and identification of low-temperature solid particles using their translation caused by a pair of small permanent magnets

*Chiaki Uyeda[1], Wakana Yamaguchi[1], Keiji Hisayoshi[1], Kentaro Terada[1] (1.Institute of earth and Space Science Graduate School of Science Osaka University)

[PPS07-P12] The metallographic cooling rate of the Tafassasset primitive achondrite

*naoji sugiura[1], Tomoko Arai, takafumi matsui (1.Chiba Institute of Technology)

[PPS07-P13] The systematic investigations of high-pressure minerals in lunar basaltic meteorites

*Masaaki Miyahara[1], Kazunari Kozuma[1], Eiji Ohtani[2], Akira Yamaguchi[3], Takeshi Sakai[4], Hiroaki Ohfuji[4], Naotaka Tomioka[5], Yu Kodama[6] (1.Department of Earth and Planetary Systems Science, Graduate School of Science, Hiroshima University, 2.Department of Earth Sciences, Graduate School of Science, Tohoku University, 3.National Institute of Polar Research, 4.Geodynamics Research Center, Ehime University, 5.5Kochi Institute for Core Sample Research, Japan Agency for Marine-Earth Science and Technology, 6.Marine Works Japan)

[PPS07-P14] Bulk chemical analysis of iron meteorites by LA-ICP-MS

*Akira Yamaguchi[1], Naoki Shirai[2], Makiko K. Haba[3] (1.National Institute of Polar Research, 2.Tokyo Metropolitan University, 3.Tokyo Institute of Technology)

Stability of Amino Acid Precursors in Simulated Extraterestrial Environments

*tomohito sato[1], Soushi Kuramoto[1], Takuya Yokoo[1], Yoshida Satoshi[2], Isao Yoda[3], Hitoshi Fukuda[3], Yoshiyuki Oguri[3], MITA Hajime[4], Kazuhiro Kanda[5], Hiromi Shibata[6], Zyunichi Takahashi[1], Yoko Kebukawa[1], Kensei Kobayashi[1]

1. yokohama national univercity, 2. QST, 3. Tokyo Institute of Technology, 4. Fukuoka Institute of Technology, 5. University of Hyogo, 6. Osaka University

Since a wide variety of organic compounds have been detected in extraterrestrial bodies like carbonaceous chondrites [1] and comets [2], extraterrestrial organics could be essential sources for the first life on the Earth. Amino acids in carbonaceous chondrites increased after acid-hydrolysis, which suggested that not only free amino acids but also amino acid precursors were present in them. Laboratory experiments simulating extraterrestrial environments showed that not free amino acids but amino acid precursors were mainly formed [3, 4]. Though amino acid precursors in meteorites and products of laboratory simulations have not been well identified, aminonitriles and hydantoins could be candidates. On the other hands, proton irradiation of a mixture of CO, NH_3 and H_2O, which simulated possible reactions among interstellar media, gave complex amino acid precursors with large molecular weights [5]. Such amino acids and amino acid precursors that were formed abiotically in space environments would be exposed to various energy sources in prior to delivery to the primitive Earth. For example, organics in molecular clouds were exposed to galactic cosmic rays (protons and heavy ions). Interstellar organic compounds were irradiated with strong VUV/X-rays from the young Sun. Organic compounds in small bodies were irradiated with gamma rays from such nuclides as ^{26}Al in the earlier stage of the solar system. Organic compounds in interplanetary dust particles were exposed to solar UV/VUV before delivery to Earth atmosphere. Thus it is important to examine stability of amino acids and their precursors against energetic particles and photons. We experimentally investigated the stability of amino acids and their precursors against heavy ions, gamma-rays, UV and soft X-rays.

Target molecules used in the present study were (i) glycine (Gly), (ii) hydantoin (Hyd; a precursor of Gly), and (iii) aminoacetonitrile (AAN; the Strecker-type precursor of Gly). They are used as 5 mM solutions in ammonia water (pH 9). In addition to them, we chose (iv) organic material synthesized from a mixture of CO, NH_3 and H_2O by 2.5 MeV protons from a Tandem accelerator (Tokyo Tech). We will call them CAW. CAW contained complex amino acid precursors with large molecular weights [3].

Experimental: *Heavy ions irradiation*: Aqueous solution of each target molecule was frozen in liquid nitrogen, and was irradiated with 290 MeV/u carbon ions from HIMAC (NIRS, Japan) at 7.5-15 kGy. *Gamma-rays irradiation*: Aqueous solution of each target molecule was irradiated with gamma rays (5-10 kGy) from a ^{60}Co source (Tokyo Tech, Japan). *UV irradiation*: Each target molecule was irradiated with UV from a xenon lamp after dried in pits of an aluminum plate. *Soft X-rays irradiation*: Each target molecule was irradiated with soft X-rays from a synchrotron (NewSUBARU BL-6) for 10 min after dried on aluminum plates. Amino acid analysis: all the target materials were recovered as aqueous solutions, were acid-hydrolyzed (6 M HCl, 110℃, 24 h), and amino acids in them were determined by reversed-phase HPLC after pre-column derivatization with *o*-phthalaldehyde and mercaptoethanol.

Results and Discussion: Since glycine was always major amino acids after acid hydrolysis of all the target materials after irradiation yielded glycine, we will discuss stability of target molecules by using the glycine

©2019. Japan Geoscience Union. All Right Reserved.

yields.

Heavy ions irradiation: Recoveries at 15 kGy were as follows. CAW (95.1%), Hyd (93.6%), Gly (91.8%) and AAN (77.5%). AAN was least stable among all. *Gamma-rays irradiation*: Decomposition of AAN, CAW and Hyd at 10 kGy was not detected, while recovery of Gly was 79.5%. *Soft X-rays irradiation*: recovery ratios were less than 10 % in the case of Gly, Hyd and AAN, while that of CAW was 51.1%. UV-irradiated samples were now under analysis.

Free amino acid (glycine) was generally less stable than amino acid precursors (CAW and Hyd), and CAW was most stable among 4 compounds tested against all the energies. Thus it was suggested that complex amino acid precursors were robust molecules in space, while free amino acids were easy to decompose even if they were formed from their precursors in space.

References

[1] K. Kvenvolden *et al.*, *Nature*, **228**, 923-926 (1970).

[2] J. Kissel and F. R. Krueger, *Nature*, **326**, 755-760 (1987).

[3] Y. Takano *et al.*, *Appl. Phys. Lett.*, **84**, 1410-1412 (2004).

[4] Y. Kebukawa et al., *Sci. Adv.*, **3**, e1602093 (2017).

[5] S. Kuramoto *et al.*, *2019 JpGU Meeting*, Chiba (2019).

[6] S. Iglesias-Groth et al., *Mon. Not. R. Astron. Soc.,* **410**, 1447-1453 (2011).

Keywords: Amino Acid Precursors, Radiation, Stability

©2019. Japan Geoscience Union. All Right Reserved.

Production of amino acids by gamma rays during aqueous alteration process in meteorite parent body

*Shinya Asano[1], Isao Yoda[2], Yasuji Muramatsu[3], Yoko Kebukawa[1], Kensei Kobayashi[1]

1. Yokohama national university, 2. Tokyo Institute of Technology, 3. University of Hyogo

[Introduction]Organic compounds such as amino acids are necessary for the birth of life on the earth. Extraterrestrial materials such as meteorites are considered as one of the sources of these amino acids. Since most of these meteorites originated from asteroids, we need to consider the origins of organic matter in asteroids. In the early stage of solar system formation, asteroids beyond the snow line contained ice and low molecular weight organic matter derived from dust. The ice melted due to the heat generated by the radioactive decay of ^{26}Al and aqueous alteration occurred. It is pointed out the complex macromolecular organic materials (insoluble organic matter, IOM) in meteorites may have formed during aqueous alteration (approximately 0 to 150 ˚C.) [1]. Based on this hypothesis, experiments simulating aqueous alteration on asteroids showed that amino acids and high molecular weight organic compounds similar to IOM in meteorites was formed after heating of formaldehyde, ammonia, water [2]. In this study, we aimed to investigate effect of gamma rays generated by radioactive decay of ^{26}Al during aqueous alteration for organic synthesis.
[Experimental]^{60}Co gamma ray source (Tokyo Institute of Technology) was irradiated to glass tubes containing 200 μl of water: formaldehyde: ammonia = 100: 5: 5 (molar ratio). Six different irradiation conditions were applied: 3 kGy/h ×2.5 h, 3 kGy/h ×4 h, 3 kGy/h ×5 h, 1.5 kGy/h ×5 h, 1.5 kGy/h ×8 h, and 1.5 kGy/h ×10 h. For comparison, the same solutions were heated in an oven at 150 ˚C for 24 h. The samples after irradiation were placed on CaF_2 plate and dried, then analyzed by FT-IR. The samples after irradiation were placed on gold plate and dried, then analyzed by X-ray absorption edge near structure analysis (XANES) of Hyogo prefectural university. Also, the samples were subjected to acid hydrolysis (6 M hydrochloric acid, 24 h, 110℃) and analyzed amino acid concentrations by cation exchange HPLC.
[Results and Discussion]<Cation exchange HPLC>Various amino acids such as glycine, alanine, β-alanine were detected from the gamma-ray irradiated samples after acid hydrolysis. Relatively large amount of alanine was produced from the irradiated samples compared to the heated samples. It suggests that the formation path ways of amino acids differ between the irradiated samples and the heated samples.
[Future plan]We are planning to extrapolate the gamma-ray induced amino acid yields to the meteorite parent body environments by extending the irradiation conditions (total dose and irradiation rate) using the calculated value of total dose of gamma ray from ^{26}Al during aqueous alteration. In addition, macromolecular organic compounds will be analyzed using LC-MS.
[Reference]
[1] G.D.Cody et al.,*PNAS*,108,19171-19176 (2011)
[2] Y.Kebukawa et al.,*Astrophysical J.*, 771, 19 (2013)

©2019. Japan Geoscience Union. All Right Reserved.

Kinetic approaches for the thermal history of organic matter in meteorites based on Raman spectra

*Kento Kiryu[1], Yoko Kebukawa[1], Motoko Igisu[2], Takazo Shibuya[2], Kensei Kobayashi[1]

1. Yokohama National Univ., 2. Japan Agency for Marine-Earth Science and Technology

CI, CM, and CR chondrites experienced aqueous alteration in their parent bodies, and contain organic carbon up to a few wt%. More than 70 wt% of it exists in the form of insoluble organic matter (IOM) (e.g., Pizzarello et al., 2006). Organic matter (OM) is susceptible to heating, and changes their structures, reflecting aqueous alteration and/or thermal metamorphisms. Thus, it attracts attention as the index of the parent body processes.

Kebukawa et al. (2010) estimated kinetic parameters for thermal degradation of aliphatic C-H through in-situ heating experiments of IOM and bulk of the Murchison meteorite (CM2) using the Fourier transform infrared micro-spectroscopy (microFTIR) combined with heating stage. They revealed that the peak intensity of aliphatic C-H is a good index of low-temperature and/or short-duration heating in the parent bodies. However, microFTIR is not enough for estimating thermal process of OM under high-temperature and long-duration heating which IR signals of aliphatic C-H are unlikely to be detected. Raman spectroscopy is a complementary tool to IR spectroscopy, since their spectral features of OM in the chondrites reflect thermal changes in aromatic structure in the complex OM (Quirico et al. 2003; Bonal et al., 2006, 2007; Busemann et al., 2007). When chondritic OM is heated, its aromatic structure will be more ordered to graphitic structure. This process is an irreversible, and results in changes of disordered (D_1-: ~1350 cm^{-1}) and graphite bands (G: ~1590 cm^{-1}) in Ramn spectra. Therefore, D_1- and G-bands were often used as indicators of degree of thermal metamorphism, but understanding of kinetic behaviors of the Raman spectral parameters is still limited. Thus, in order to evaluate thermal history of OM in chondrites under high-temperature and/or long-duration heating, we performed a series of heating experiments of the Murchison meteorite powders and kinetic analyses of their Raman spectral parameters.

The Murchison meteorite powders were heated under low oxygen condition in a vacuum furnace for 3-48 h at 600-900˚C. The low-oxygen condition was maintained by a gas mixture of N_2 and H_2 (99:1, v/v). The samples after heating were analyzed using Raman spectrometer with a 532 nm laser (RAMANtouch; Nanophoton). The Raman spectra of all the samples show D_1- and G-bands. We determined 5 Raman spectral parameters: the full width at half maximum (FWHM) and the peak positions of D_1- and G-bands, and the ratio of the peak intensity of D_1- to G-band. The changes in these Raman parameters with time at each temperature will be fitted with algebraic kinetic equations deduced by possible physical mechanisms, and estimate reaction rate constant. Then the apparent activation energies and frequency factors will be calculated by the reaction rates using the Arrhenius equation. Finally, we will establish the Raman parameters as functions of heating temperature and time. Combining previously reported kinetics of aliphatic C-H (Kebukawa et al. 2010), it may allow us to calculate precise time and temperature of thermal processes for chondrites.

Keywords: Organic matter in meteorites, Thermal history, Kinetics, Raman spectroscopy

©2019. Japan Geoscience Union. All Right Reserved.

Relationship between spatial distribution of organic compounds and minerals in the Murchison meteorite

*Taiyo Sengoku[1], Minako Hashiguchi[1], Hiroshi Naraoka[1]

1. Kyushu University

[Introduction]

Primitive meteorites contain a wide variety of organic compounds. More than 600 species of CHN compounds were identified in the methanol extract of the Murchison meteorite (CM2), in which saturated- and unsaturated-alkylated pyridines ($C_nH_{2n-4}N^+$ and $C_nH_{2n-6}N^+$) as well as alkylimidazoles ($C_nH_{2n-1}N_2^+$) are predominant (Naraoka et al., 2017). Interaction between organic matter and minerals during aqueous alteration is very important in the chemical evolution (e.g. Kebukawa et al., 2010), therefore, it is necessary to investigate the spatial distribution of the organic matter and minerals in the meteorites. In the previous studies, chemical imaging of soluble organic matter (SOM) was performed on the Murray and Murchison meteorites (CM2) by desorption electrospray ionization/high-resolution mass spectrometry (DESI/HRMS), and the different spatial distribution was observed among the different CHN species and/or their alkylated homologues (Naraoka & Hashiguchi, 2018, Hashiguchi & Naraoka, 2018). However, the relationship between the organic compounds and minerals is still unresolved. In this study, the DESI-HRMS imaging and detailed mineralogical observation were performed on fragments of the Murchison meteorite.

[Sample & Method]

Two fragments designated as “np15" (2x3 mm^2) and “np16” (2x2 mm^2) were obtained by chipping from different large fragments of the Murchison meteorite. These fragments were embedded in indium or metal with low-melting point for DESI-HRMS imaging. The DESI-HRMS imaging was performed on each sample for three times. Methanol was used as a spray solvent with the flow rate of 2 μL/min. The electrospray voltage was set to 3 kV. The nebulizer N_2 gas pressure was ~100 psi. The positive ions were collected in a full scan mode (m/z 50-500) with mass resolution of about 140,000 ($m/\Delta m$ at m/z 200) on the sample surface of np15 (4x4 mm^2) and np16 (3.8x3.8 mm^2). For the fragment np16, dry polishing was performed on the sample to remove ~250 μm from the surface and the imaging was performed again, because no signals of CHN compounds were obtained by the 1st set of DESI-HRMS imaging. After the DESI-HRMS imaging, the same sample surface was used to obtain backscattered electron images (BSE) and X-ray elemental maps using SEM/EDS.

[Results & Discussion]

Some alkylated homologues of CHN compounds were detected from np15 by DESI-HRMS imaging. Their exact masses correspond to alkylimidazole ($C_nH_{2n-1}N_2^+$) and saturated- or unsaturated-alkylated pyridine ($C_nH_{2n-4}N^+$ or $C_nH_{2n-6}N^+$) within 3 ppm of mass precision. The spatial distribution was different between $C_nH_{2n-1}N_2^+$ and $C_nH_{2n-4}N^+$, which is consistent with the previous study (Naraoka & Hashiguchi, 2018). On the other hand, no CHN compounds were detected from np16. After removing ~250 μm of the surface of np16 by polishing, some CHN compounds corresponding to $C_nH_{2n-1}N_2^+$ and $C_nH_{2n-6}N^+$ were detected in 3rd DESI-HRMS imaging finally, however, these compounds were not detected by 1st and 2nd analyses. These results indicated that the CHN compounds might have been volatilized from the sample surface

©2019. Japan Geoscience Union. All Right Reserved.

during its storage, and that repeated DESI-HRMS imaging is important to obtain clear signals of SOM from inside of meteorite. The detected CHN compounds showed heterogeneous spatial distribution in the sample surface, which indicate that dry polishing does not affect the spatial distribution of SOM significantly.

In both np15 and polished np16 samples, the CHN compounds distribute mainly in the matrix region (~ few hundreds of square meters) of the meteorite. Although the X-ray elemental mapping showed that CHN compounds-rich region seemed to contain abundant Ca-containing minerals in both fragments, no clear relationship was observed between the averaged chemical compositions of matrix region and the spatial distribution of the CHN compounds. Further detailed analysis will be performed on tiny minerals in the matrix.

Keywords: carbonaceous chondrite, chemical imaging , soluble organic compounds

©2019. Japan Geoscience Union. All Right Reserved.

O and Al-Mg isotope systematics of a hibonite-melilite-rich fine-grained CAI in the reduced CV chondrite NWA8613

*Sohei Wada[1], Noriyuki Kawasaki[1], Hisayoshi Yurimoto[1,2]

1. Hokkaido University, 2. ISAS/JAXA

Ca–Al-rich inclusions (CAIs) in meteorites are composed of high-temperature condensate minerals from the solar nebular gas [1]. CAIs in CV chondrites are petrographically divided into the coarse-grained CAIs and fine-grained CAIs (FG-CAIs). Complex layer structures of constituent minerals and REE patterns of FG-CAIs suggest they are condensates from the nebular gas [2, 3]. Igneous CAIs that experienced melting and crystallization, such as coarse-grained Type B CAIs, have been extensively studied their formation processes, O-isotope compositions of minerals, and formation ages [4, 5]. On the other hand, such systematic investigations for the formation of FG-CAIs have been poorly conducted. Here, we investigated O- and Al–Mg isotope systematics of a hibonite-melilite-rich FG-CAI from the reduced CV chondrite NWA8613 as well as detailed petrographic observations. The O- and Al–Mg isotope measurements were conducted using SIMS instruments of Hokkaido University (Cameca ims-1270 and ims-1280HR).

The FG-CAI has an irregular shape with a size of approximately 10 ×12 mm and composed mainly of melilite, hibonite, and spinel. O-isotope compositions of the constituent minerals plot along the CCAM line, ranging between $\Delta^{17}O \sim -23‰$ and 0‰. The FG-CAI is petrographically divided into hibonite-rich core, spinel-rich core, melilite-rich inner-mantle, and hibonite-spinel-rich outer mantle. The CAI is rimmed by thin spinel and diopside layers. Melilite crystals are contained in core and mantle. Melilite crystals in the core exhibit normal chemical zoning and O-isotope compositions from $\Delta^{17}O \sim -23‰$ to −10‰ with increasing Åk composition. The melilite crystals in the inner-mantle show chemically complex, oscillatory zoning patterns, but are uniformly ^{16}O-poor ($\Delta^{17}O \sim 0‰$) despite their chemical variations (Åk2–14). Melilite crystals in the outer-mantle exhibit normal chemical zoning and variable O-isotope compositions from $\Delta^{17}O \sim -17‰$ to 0‰ with increasing Åk composition. The spinel and hibonite grains in the FG-CAI are uniformly ^{16}O-rich ($\Delta^{17}O = -23‰$). Al–Mg isotopic compositions of hibonite in the outer-mantle and in the core and melilite in the inner-mantle plot on a single straight line within error; an Al–Mg mineral isochron can be defined to give an initial $^{26}Al/^{27}Al$ value of $(4.50 \pm 0.09) \times 10^{-5}$. Given that the constituent minerals formed by condensation and were accumulated to form the FG-CAI, the nebular gas, from which they condensed, had variable O-isotope compositions between $\Delta^{17}O \sim -23‰$ and 0‰. The Al–Mg systematics of the FG-CAI indicate that these formation events occurred at 0.16 ±0.02 Myr after the formation of canonical CAIs [7], if ^{26}Al was homogeneously distributed. Our data support the presence of the nebular gas with variable O-isotope compositions during the first ~0.2 Myr of the Solar System formation [8].

References: [1] Grossman (1972) *GCA* 36, 597–619. [2] Boynton (1975) *GCA* 39, 569–584. [3] Krot et al. (2010) *MaPS* 39, 1517–1553. [4] Kawasaki et al. (2018) *GCA* 221, 318–341. [5] Yurimoto et al. (1998) *Science* 282, 1874–1877. [6] Beckett and Stolper (1994) *MaPS* 29, 41–65. [7] Larsen et al. (2011) *ApJL* 735 L37–L43. [8] Kawasaki et al. (2017) *GCA* 201, 83–102.

©2019. Japan Geoscience Union. All Right Reserved.

Observation of Enstatite Whiskers in Fine-grained Rims in the Carbonaceous Chondrite ALH A77307

*Yasuhisa Shirota[1], Masahiro YASUTAKE[1], Satomi Enju[1], Akira Tsuchiyama[1]

1. Division of Earth and Planet, Science, Kyoto University

Introduction Chondritic porous -interplanetary dust particles (CP-IDPs) are material that are suggested to be originated from comets and to be one of the most primitive materials in the solar system (Bradley et al., 1983). CP-IDPs include enstatite ($MgSiO_3$) whiskers. They are thought to be formed by condensation in the solar nebula (Bradley et al., 1983).

Primitive carbonaceous chondrites are affected by little aqueous alteration. Recent studies have discovered enstatite whiskers in matrices in primitive carbonaceous chondrites (Vaccaro et al., 2017; Matsumoto et al., 2018). If such crystals have similar formation processes to those of enstatite whiskers in CP-IDPs, it will constrain the formation processes of not only asteroids but also CP-IDPs. However, only a few enstatite whiskers are observed in carbonaceous chondrites. Therefore, it is not certain whether or not enstatite whiskers are common in carbonaceous chondrites and have same formation processes in CP-IDP.

We conducted a detail petrological observation of matrix in ALH A77307 (CO3.0) to understand distribution of whisker-like enstatite crystals using a scanning electron microscopy (SEM) and to constrain the formation process using a transmission electron microscopy (TEM).

Sample and Methods We observed one of the most primitive CO chondrites ALH A77307. Vaccaro et al. (2017) reported whisker-like enstatite crystals in ALH A77307. SEM/EDS analysis was carried out with an FE-SEM (JEOL JSM-7001F, Kyoto University, Hitachi HT SU6600, ISAS, JAXA) operating at 100 pA probe current and 8 kV accelerating voltage. A TEM thin section including one whisker was extracted using focus ion beam (FIB) (FEI, Helios NanoLab 3G, Kyoto University). TEM analysis was carried out with a (S)TEM/EDS (JEOL JEM-2100T, Kyoto University) operating at 200 kV accelerating voltage.

Result and Discussion We observed fine-grained rims around three chondrules. These rims consist mainly of amorphous silicate, olivine, pyroxene, and Fe,Ni metal, and similar to primitive matrix. The whisker-like enstatite crystals occur in all regions observed and the total number of whiskers found are 12. The maximum size of the whisker is 11.91 μm in length and 0.27 μm in width. We classified whiskers based on criterion the aspect ratio, p, by Bradley et al. (1983). The whiskers are classified as 4 Rods (p>20) and 8 Ribbons (p<20). The abundance of whiskers is >40 mm^{-2}, suggesting that whisker-like enstatite is common in chondrule rims in primitive carbonaceous chondrites although the abundance in CP-IDPs is higher. The aspect ratios are similar to those of enstatite whisker in CP-IDPs. In contrast to enstatite whiskers in CP-IDPs, some whiskers are curved and/or broken. It may be the result of deformation during accumulation on the parent body.

We have observed one ribbon crystal (length 1.21 μm, width 0.16 μm) using TEM. The ribbon crystal was orthoenstatite elongated along [001] axis based on electron diffraction patterns. Three dimensionally, this crystal is thought to be a columnar crystal elongated along [001] or a plate crystal with flattened (010) plane. From this results, this crystal is thought to be a platelet crystal formed by condensation in the solar nebula like enstatite whiskers in CP-IDPs (Bradley et al., 1983) or crystal formed by annealing of

©2019. Japan Geoscience Union. All Right Reserved.

amorphous silicate (Brearley, 1993). To constrain more detail formation process of the whisker-like material in carbonaceous chondrites, mineralogical investigation of whisker-like material, especially rod crystals is needed.

[1] Vaccaro E. (2017) PhD thesis. The Open University. [2] Bradley J. P. et al. (1983) Nature. 301, 473-477. [3] Matsumoto M. et al. (2018) 81st Annual Meeting of the Meteoritical Society [4] Brearley. (1993) Geochim. Cosmochim. Acta 57, 1521-1550

Keywords: Enstatite whisker, Primitive Carbonaceous Chondrite

©2019. Japan Geoscience Union. All Right Reserved.

3D observation of whisker-like material in the porous matrix of the Paris CM chondrite by SR-XCT

*Masahiro YASUTAKE[1], Epifanio Vacarro[2], Kentaro Uesugi[3], Akihisa Takeuchi[3], Tsukasa Nakano[4], Akira Tsuchiyama[1]

1. Division of Earth and Planetary Science, Graduate School of Science, Kyoto University, 2. National History Museum, London, 3. JASRI/SPring8, 4. GSJ/AIST

Introduction The chondritic-porous interplanetary dust particles (CP-IDPs) are well-known material, that preserves primitive and pristine features of the early solar system. Enstatite whisker is one of the materials that characterizes CP-IDPs. It is thought that enstatite whiskers are condensates formed in the inner solar system and transferred to the outer regions, where comets formed [e.g. 1, 2]. Recently, whisker-like enstatite crystals were found in the primitive carbonaceous chondrites [3, 4]. However, the whisker-like materials they found could be a cut-plane of thin enstatite plate. By the 2D observation, it is hard to solve this matter. 3D observation based on synchrotron radiation X-ray nano-CT is a strong tool to understand the crystal shape, mineral phase, and rough composition. We conducted a 3D observation to better understand the characteristics of whisker-like materials in primitive carbonaceous chondrites.

Methods We investigated the Paris primitive CM chondrite. Paris was reported to have a very primitive matrix that includes GEMS-like materials [5]. A section of this meteorite was observed and elemental maps of the primitive matrix were obtained by FE-SEM/EDS. A house-shaped CT sample (~25 x 25 x 30 μm) was extracted from the primitive matrix by using a FIB-SEM. CT data of the micro-samples were conducted at beamline BL47XU, SPring-8. CT images were acquired at energies of 7 keV and 7.35 keV with voxel sizes of ~32.2 nm and ~ 33.9 nm, respectively. Mineral phases were estimated using dual-energy tomography (DET) method using the X-ray linear attenuation coefficient (LAC) [6].

Result and Discussion The observed matrix is a part of the fine-grained rim of Type I porphyritic olivine pyroxene chondrule. The matrix is porous and consists mainly of amorphous silicates that include sub-micron sized Fe-rich phases. Whisker-shaped materials are abundant in the CT sample observed. However, fibrous alteration materials were also reported in the matrix of Paris [5]. The whisker-like materials observed might include such products in addition to enstatite. The size of the largest whisker is ~6 μm x ~700 nm x ~350 nm (Fig. 1) and similar to ribbon-type enstatite whisker in the CP-IDPs [1]. This whisker has a curved shape unlike those in CP-IDPs. Probably it reflects deformation during accretion to the parent body and/or planetary processes such as planetary collision.

The LAC values of most whisker materials are hard to obtain quantitatively because refraction of X-ray at the edges of the narrow whiskers enhanced their LAC values. The LAC values of the largest whisker are less affected by refraction and have the range of ~170-180 cm^{-1} and ~250-270 cm^{-1} at 7.00 and 7.35 keV, respectively. These values are consistent with those of pyroxene ($En_{80}Fs_{20}$) and clearly distinguishable from the values of fibrous alteration products (cronstedtite, tochilinite, and ferrihydrite) [5]. The above results suggest that this whisker material is an enstatite whisker. The possibility of olivine whisker (~Fo_{85}) cannot be excluded but forsterite whiskers have not been reported so far. Thus, it is reasonable to consider that the enstatite whiskers accreted to the carbonaceous chondrite parent body.

Crystallographic features such as defects and direction of elongation are still not examined. Investigation of crystallography is required to constrain the formation processes of whiskers, and it will enable us to

©2019. Japan Geoscience Union. All Right Reserved.

compare the enstatite whiskers in carbonaceous chondrites with those in CP-IDPs.

Reference [1] Bradley (1983) *Nature*, 301, 473-477. [2] Bradley, J. P. (2003) *Treatise on geochemistry*, 1, 711. [3] Vaccaro (2017) PhD thesis, The Open University. [4] Matsumoto et al. (2017) abstract JAMS annual meeting. [5] Leroux et al. (2015) *GCA*, 170, 247-265. [6] Tsuchiyama et al, (2013) *GCA*, 116, 5-16.

Keywords: CM chondrite, Paris meteortite, Primitive matrix, Enstatite whisker, SR-XCT

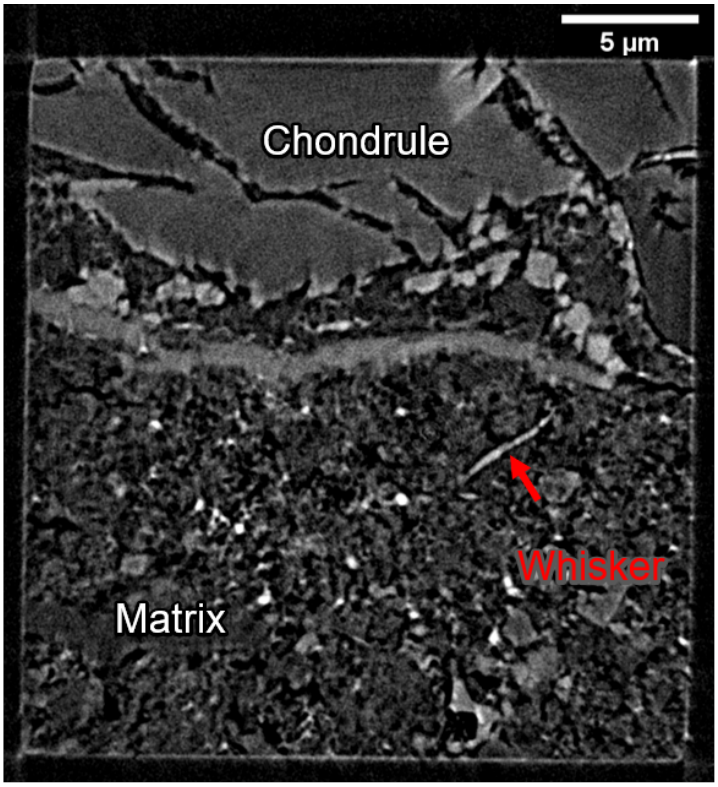

Fig. 1. CT image of porous matrix in Paris acquired at 7 keV. Silicates are shown in light grey. Amorphous silicates are shown in dark grey. Metal and sulfide are shown in white. The enstatite whisker is shown by red arrow.

©2019. Japan Geoscience Union. All Right Reserved.

Development of cryogenic SIMS technique for isotope analysis of fluid inclusions

*Isono Yuki[1], Naoya Sakamoto[2], Hisayoshi Yurimoto[3]

1. Department of Natural History Sciences, Hokkaido University, 2. Creative Research Institusion, Hokkaido University, 3. Department of Natural History Sciences, Hokkaido University

Introduction: Fluid inclusions in halite crystals from meteorites provide direct information of extraterrestrial liquid water [1]. In-situ isotope analysis of the fluid inclusions was realized by SIMS equipped with a cold-stage [2]. However, the analytical precision is limited to ±14 ‰(1 σ) for $\delta^{18}O$ due to deep sputter crater to excavate fluid inclusions. One of the methods to improve the analytical precision would be expose fluid inclusions on the sample surface. We froze the fluid inclusions and polish under cryogenic condition in nitrogen atmosphere [3, 4]. In order to measure frozen polished fluid inclusions by SIMS, the surface should be coated by conductive thin layer such as Au. However, the Au thin layer was not enough conducted because condensation of frost particles occurred before introduce the polished sample into Au coater. The sample temperature was −100 ˚C while the dew point in the glove box (−60˚C) was higher than the sample temperature [4]. Therefore we changed the sample temperature.

Changes of sample preparation procedures: The sample preparation system for cryogenic SIMS is composed of a cryo-polisher and Au ion-coater in a glove box [3]. The temperature of polishing set to −35 ˚C. Thus frost condensation on the polished surface was prevented. After polishing, the sample was settled on the bottom of deep well of new designed cryo-coating stage. The cryo-coating stage was precooled to −196 ˚C by liquid nitrogen and the deep well was filled with cool nitrogen gas evaporated from liquid nitrogen in order to prevent frost formation on sample surface. This cooling process is necessary because sublimation temperature of ice is −50 ˚C during Au coating. The sample temperature was estimated to −196 ˚C before taking into the Au coater and warmed up −130 ˚C at taking from the Au coater after Au coating for 4 minutes.
The polished ice embedded in an epoxy disk was set to the cryo-holder and transferred to cryo-stage (−190 ˚C) of Cameca ims-1270 instrument using cryo-transfer system [3]. The liquid nitrogen was supplied by a roots pump to reduce the sample stage vibration. The measurement methods for oxygen isotopes were similar to those of [2].
We obtained mass spectra of oxygen isotopes from H_2O-ice. Intensity of ^{16}O peak was about 2.8 $\times 10^5$ cps and a tale was observed symmetrically at both side of the peak below 3 cps. The interference of tail from $^{16}OH^-$ to $^{17}O^-$ was estimated to be about 10 ‰because the intensity of $^{16}OH^-$ is comparable to ^{16}O peak. Oxygen isotope analysis using $^{16}OH^-$ and $^{17,18}OH^-$ signal would be effective for further high precision oxygen isotope analysis for H_2O ice as well as the tail correction method used in [2].
References: [1] Zolensky M. et al. (1999) Science, 285, 1377-1379. [2] Yurimoto H. et al. (2014) Geochem. J, 48, 549-56. [3] A. Ishibashi (2014) Master thesis [4] J. Song (2017) Master thesis.

Keywords: Fluid inclusion, Cryogenic SIMS, Oxygen isotope

©2019. Japan Geoscience Union. All Right Reserved.

X-ray diffraction study using Gandolfi attachment: Implications for small extraterrestrial materials

*Naoya Imae[1,2], Makoto Kimura[1]

1. Antarctic Meteorite Research Center, National Institute of Polar Research, 2. SOKENDAI

Introduction

Recent studies have established the bulk features of various chondrite species based on the X-ray diffraction patterns (Howard et al. 2009; Imae and Nakamuta 2018; Imae et al. 2019). In the present study, X-ray diffraction experiments were carried out using Gandolfi attachment in order to apply for small extraterrestrial materials of various kinds of stony meteorites. The present technique is convenient in the laboratory and also useful for rapidly identifying the mineral species without any significant sample loss.

Experiments

We used the X-ray diffractometer in air with the goniometer radius of 30 cm (RIGAKU, SmartLab) at NIPR on the following conditions: (1) CuKa1 with 40 kV, and 30 mA for glass X-ray tube and 40 mA for ceramic X-ray tube, (2) the X-ray beam of 0.4 mm in diameter obtained from the polycapillary focusing optics (CBO-f unit), (3) the strip detector (D/teX Ultra 250) for counting diffracted X-rays, (4) the revolution rate of the goniometer head on the Gandolfi attachment at 30 rpm, and (5) the scan speed of normally 0.2 º/min or 0.5 º/min with the step of 0.01º and the average of the repeated analyses.

Glass fiber (13 μm in diameter) attached with glass rod (1 mm in diameter) was mainly used for holding samples. Both powder and grain samples with the diameter of ~0.2-0.8 mm were used for the measurements.

Powders and single grains for San Carlos olivine and NWA 4719 L6 chondrite were used for the calibration focused on olivine 130 index. So far, 36 stony meteorites have been measured and they are 27 ordinary chondrites (mostly Antarctic meteorites), 5 carbonaceous chondrites, an E chondrite (NWA 7401), a eucrite (Cachari), a diogenite (Bilanga), and an aubrite (Pena Blanca Spring).

Results and discussion

Calibration: The two-theta position of the olivine 130 peak for the powder samples of San Carlos olivine shows nearly consistent value by Yoder and Sahama (1957), on the contrary, the intensity of the San Carlos olivine grains is lower than that of powder on the similar measurement condition, and in addition the position of the two-theta is slightly higher than that of powder. In case of chondrite (NWA 4719 L6), the intensity is significantly lower than San Carlos olivine. Although the two-theta values for powder samples and grain samples are within the mean Fa# range of L group, the intensity of grain is significantly lower than that of powder.

©2019. Japan Geoscience Union. All Right Reserved.

Samples: The systematic differences of olivine 130 two-theta values were observed among ordinary chondrites: 32.18º-32.29º for H, 32.15º-32.21º for L, and 32.13º-32.16º for LL. These ranges include that the two-theta values are obviously higher than the ranges expected from the mean Fa# for three chemical groups (32.18º-32.21º for H, 32.12º-32.16º for L, and 32.08-32.12 for LL, Yoder and Sahama 1957). The existence of orthoenstatite 511 peak is an indicator for equilibrated ordinary chondrites but not definite, since the peak intensity is normally low. More ferroan olivine peak than ordinary chondrites appears from carbonaceous chondrites. EL6 consists of orthoenstatite. Diffraction patterns of achondrites are different from those of chondrites: pigeonite and anorthite peaks for eucrite and dominant orthopyroxene for diogenite, and dominant clinoenstatite for an aubrite. Fine-grained powder samples may represent the bulk chondrite compositions, but not for grains. This may lead to the different diffraction pattern.

Summary

The present technique is useful conveniently for examining limited or small extraterrestrial materials, when we take into consideration the variations for chondrite species depending on the different sample conditions of powder or grain and the relative modal abundance of olivines and pyroxenes for grains with the limited range of variation of the chemical groups.

Acknowledgements

NI is grateful to Dr. Yoshihiro Nakamuta for discussions, and the study is partly supported by NIPR and KAKENHI (17K05721).

References

Howard K. T., Benedix G. K., Bland P. A., and Cressey G. 2009. Geochimica et Cosmochimica Acta 73: 4576-4589.

Imae N. and Nakamuta Y. 2018. Meteoritics & Planetary Science 53: 232-248.

Imae N., Kimura M., Yamaguchi A., and Kojima H. 2019. Meteoritics & Planetary Science (In press).

Yoder Jr. H. S. and Sahama T. G. 1957. American Mineralogist 42: 475-491.

Keywords: X-ray diffraction study, Gandolfi attachment, small extraterrestrial materials, meteorites

©2019. Japan Geoscience Union. All Right Reserved.

Trace elements analysis and Ar-Ar dating for microgram-scaled extraterrestrial samples

*Ryuji Okazaki[1], Sekimoto Shun[2]

1. Department of Earth and Planetary Sciences, Faculty of Science, Kyushu University, 2. Institute for Integrated Radiation and Nuclear Science, Kyoto University

In order to elucidate the origin and evolution of planetary materials, it is important to determine the chemical composition and timing of geological events for specific minerals and microscopic portions, such as impact melt pockets, CAIs (Ca- and Al-rich Inclusion), and chondrules. Combination of EMPA, INAA, and noble gas analysis are one of the best way to determine chemical and isotopic compositions of extraterrestrial dust particles (micrometeorites) and spacecraft-returned samples.
As a first step, we have analyzed rock fragments (<several hundreds of micrometer in diameter) recovered from Holbrook L6 chondrite. Neutron irradiation and NAA experiments were conducted at Institute of Integrated Radiation and Nuclear Science, Kyoto Univ. Allende CV3 and Madagascar feldspar were used for standardization of INAA and Ar-Ar analyses, respectively. Each of the sample particles was individually placed in a conical dimple (ϕ1, depth ~ 0.5 mm) of a sapphire disk (ϕ5.5, 1.5 mm thick), and covered with a sapphire disk (ϕ5.5, 0.3 mm thick). Each of the sapphire container was wrapped with pure aluminum foil. These Al-wrapped containers were stacked and sealed in aluminum capsules to perform neutron irradiation at the hydro-irradiation port. After irradiation, the samples were recovered from irradiated glass containers, and moved to non-irradiated containers in order to reduce the radioactivity from the sapphire containers and Al foil. Gamma-ray measurements for short half-life nuclides were performed promptly after collection of the samples. Several months after the irradiation, some of the Holbrook samples were transported to Kyushu Univ. to measure noble gas isotopes.
Concentrations of Co and Ni in two Holbrook samples were determined to be 57 and 157, and 1260 and 13400 ppm, respectively. The Ni/Co ratios of the Holbrook samples are 22 and 85, which are similar to those observed in iron meteorites and chondrites (e.g., Ebihara et al., 2011). The result guarantees our NAA measurement.
Noble gas isotopes (^{36}Ar, ^{38}Ar, ^{39}Ar, and ^{40}Ar) were determined for different two Holbrook samples using stepwise heating method. The bulk ^{39}Ar concentration in the irradiated standard feldspar (K: 12.6 wt%) is 7E-6 cm^{3}STP/g, and the bulk ^{39}Ar/^{40}Ar ratio is 0.026. The result indicates that the neutron flux of KURRI is enough to determine ^{39}Ar for microgram samples with K>0.1 wt%. Using the neutron flux determined by the standard feldspar, with 450 Ma of K-Ar age (ranging 435-461 Ma; Flude et al, 2014), we calculated the Ar-Ar ages for two Holbrook samples (9.4 and 16.8 μg) to be 3795±368Ma (based on 3 plateau ages of 4 stepwise extractions) and 3714±128Ma (based on 4 plateau ages of 7 stepwise extractions). Noble gases extracted at the lowest and highest temperature steps are influenced by atmospheric Ar, resulting unreasonable old Ar-Ar age. Based on these results, we found appropriate extraction temperature for plagioclase-rich microgram samples to be 600, 800, 900, 1000, 1100, 1200, 1400, and 1600 ˚C.
Through this study we have established an analytical method that consists of a combination of EPMA, INAA, and noble gas analyses. The new method will be applied for Antarctic micrometeorites and the Hayabusa2 samples.

Keywords: Ar-Ar age, meteorite, micrometeorite, INAA, Hayabusa2

©2019. Japan Geoscience Union. All Right Reserved.

Magnetic separation and identification of low-temperature solid particles using their translation caused by a pair of small permanent magnets

*Chiaki Uyeda[1], Wakana Yamaguchi[1], Keiji Hisayoshi[1], Kentaro Terada[1]

1. Institute of earth and Space Science Graduate School of Science Osaka University

Most solid particles in nature are categorized as diamagnetic or weak paramagnetic materials; they are commonly believed to be magnetically inert, and cannot attain strong magnetization to cause specific magnetic motions at practical field intensity. Indeed, strong magnetic field above the level of 10 T were applied in previous studies to induce magnetic levitations. A method to separate solid particles by a field gradient produced by small NdFeB magnets was recently proposed and experimentally approved using a setup operated in microgravity condition [1]. By improving this system, magnetic separation was realized on volatile solid particles, namely H2O and CO2, for the first time [2]. In addition, it was possible to estimate the material of the particle in a non-destructing manner by comparing the experimental value of magnetic susceptibility with a list of published values [1][2]: here the susceptibility was obtained from the velocity of the translating particle without the knowledge of particle mass.

In the present experimental present setup, a pair of small NdFeB plates was attached in a double glass container. A microgravity condition is produced inside the box by free fall from a height of 180 cm. An ensemble of heterogeneous particles translates and separates by magnetic field gradient in free fall. The Hi-vision camera observed the translation and susceptibility is calculated by obtained terminal velocity [1]. The obtained susceptibility of the particle is compared with literature data and materials of particles are estimated.

The field-induced translational motions realized in μg condition can be utilized in various space missions in future; this is because the small but rigid apparatus can separate and identify the heterogeneous particles that is expected to be collected in an on-site mission. One of the major purposes to perform space explorations to the outer solar system was to identify the solid materials that are observed on satellite surfaces or ring. It is concluded by recent observation that the solid particles were mainly composed of ice (Ih) with high purity; previously it was considered that the icy particles of the rings contain significant amount of rock-forming silicates. Hence, for a future task, quantitative information of the minor silicate composition included in the icy particle is required in studying the origin of the Saturn rings.

An efficient method that can non-destructively identify the components of a heterogeneous aggregate sample is desired in various research fields of material science. Using an infrared optical analysis, for example, the material composition of the particle interior is difficult to determine when the sample is larger than 100 μm in diameter. In the case of a conventional mass spectrometer, it is difficult to identify the composition of solid particles without destructing the sample. Although various microprobe devices are effective in performing refined survey on aggregate samples, it is difficult to conclude by these methods whether small particles included in the aggregate are completely discovered and identified without omission. In such cases, the particles should be definitely separated into groups of different materials before performing refined analysis [1-3]. Note that the present proposal of magnetic separation can overcome the abovementioned limitations of the conventional methods, and in future, it may serve as

©2019. Japan Geoscience Union. All Right Reserved.

a standard pretreatment tool of material analysis.

[1] Hisayoshi, Uyeda & Terada (2016) Sci., Reps., 6, 38431.

[2] Yamaguchi, Hisayoshi, Uyeda & Terada (2017) J. Phys., Conf. Ser.903, 012026.

[3] Hitomi, Yamaguchi, Hisayoshi, Uyeda (2018) Planet Space Sci., available online.

Keywords: magnetic separation, diamagnetic material, low temperature solid

©2019. Japan Geoscience Union. All Right Reserved.

The metallographic cooling rate of the Tafassasset primitive achondrite

*naoji sugiura[1], Tomoko Arai, takafumi matsui

1. Chiba Institute of Technology

Tafassasset (Tafa) is a primitive achondrite with carbonaceous chondrite-like (CC) isotopic (Cr etc.) signatures. Cooling rates and chronological information give valuable insight on the evolution of achondrite parent bodies. Brent et al. [1] constructed an evolutionary model (the parent body with a radius ~17 km, accreted at ~1 Ma after CAI; Tafa is located in the middle of the mantle). It is mainly based on the chronology, but is considered to be supported by the metallographic cooling rate (100~200 C/Ma). But it is said to require refinement. Here we report observations of the metal texture and compositions, based on which a cooling history is derived.

Observation

Fe-Ni grains (average composition ~10 mol.% Ni) in Tafa show various textures. Many grains show kamacite that nucleated on the metal-silicate boundary and expanded inward during cooling. The central part is zoneless plessite which must be martensite at higher temperatures but now is made of kamacite and taenite. An interesting feature is that the boundary of kamacite and interior plessite is made of thin (~a few mm wide) taenite wall, suggesting rapid coolig. The compositions range from 17 to 31 % Ni and the average is ~26% Ni. Considering the difficulties in measuring compositions of thin taenite rim, the real value could be ~31% Ni. The zoneless plessite interior (average composition ~10 mol% Ni) is made of taenite islands in kamacite matrix. The taenite island sizes are usually only a few mm or less and the compositions range, if measurable, from 28 to 39% Ni, and the average is ~34% Ni. Again, the real value is considered to be close to ~39% Ni. A typical distance between taenite islands is ~10 mm. There are isolated zoned taenite grains, the central compositions of which are correlated with the size. There are zoned taenite grains which are surrounded by kamacite. Their compositions at the center mostly do not depend on the size, and is ~10 mol.% Ni. We note that cloudy taenite is not observed in any taenite grains. It is also to be noted that the phosphorous content in metal is nearly zero because phosphide is not observed.

Cooling rates

Estimates of the cooling rates can be made based on the above observations. Plotting on Fig.1 of [2], the isolated taenite data suggest a cooling rate slightly faster than 10^4 C/Ma. The data from zoned taenite surrounded by kamacite, when plotted on the same diagram, suggests a much faster cooling rate, but this may be artifact due to late nucleation of kamacite. Using the concept of closure, the thin taenite wall with ~31% Ni suggests a cooling rate ~10^4 C/Ma. Similarly, taenite islands with ~39% Ni in zoneless plessite suggest a cooling rate ~10^3 C/Ma. Distance between taenite islands could also be used for the cooling rate estimate. Assuming that diffusion in kamacite controls the island separation, a cooling rate of ~10^4 C/Ma is obtained. Absence of cloudy taenite is also consistent with rapid cooling.

Discussion

Although there are variations in the cooling rates depending on the features used for the calculation, it is

©2019. Japan Geoscience Union. All Right Reserved.

clear that the cooling rate of Tafa (~10^4 C/Ma) is much faster than previously considered [2]. In order to cool at this rate, Tafa has to be located at a shallow depth (~1km from the surface). Because of this, the parent body size cannot be constrained well, except that it is much larger than 10 km in order to be kept warm at ~3.5 Ma (Mn-Cr age [3]). The rapid cooling is consistent with the chronological data. All (Hf-W, Pb-Pb, Mn-Cr and Al-Mg) ages may be identical. Or, the Hf-W age may be older than the rest because of the higher closure temperature.

[1] Brent et al., 2015, EPSL, 45, 193.

[2] Taylor et al., 1987, Icarus, 69, 1.

[3] Gopel et al., 2015, GCA,156,1.

Keywords: primitive achondrite, metallographic cooling rate, parent body

©2019. Japan Geoscience Union. All Right Reserved.

The systematic investigations of high-pressure minerals in lunar basaltic meteorites

*Masaaki Miyahara[1], Kazunari Kozuma[1], Eiji Ohtani[2], Akira Yamaguchi[3], Takeshi Sakai[4], Hiroaki Ohfuji[4], Naotaka Tomioka[5], Yu Kodama[6]

1. Department of Earth and Planetary Systems Science, Graduate School of Science, Hiroshima University, 2. Department of Earth Sciences, Graduate School of Science, Tohoku University, 3. National Institute of Polar Research, 4. Geodynamics Research Center, Ehime University, 5. 5Kochi Institute for Core Sample Research, Japan Agency for Marine-Earth Science and Technology, 6. Marine Works Japan

The Moon has recorded the impact history for ca. 4.5 Ga, which is closely related with the orbit evolution of asteroids and planets in the solar system. The impact events occurred on the moon can be clarified using lunar meteorites. The lunar meteorites have several kinds of evidence for the impact events: e.g., brecciation, shock-induced melting, and high-pressure polymorphs. The high-pressure polymorph is one of the important clues for clarifying the impact events because we can constrain several physical parameters (e.g., shock pressure) for the impact events. However, only a few lunar meteorites were investigated about the high-pressure polymorphs. Several radio-isotope ages in the lunar meteorites were measured to deduce when the impact events occurred. However, the relevance between the radio-isotope ages and the shock features has not been clear. Accordingly, we initiated to investigate the shock features, especially the shock-induced melting and high-pressure polymorphs in the lunar mare basalt, NWA 032, NWA 479, NWA 2727, NWA 2977, and NWA 4898 using FE-SEM, Raman, EMPA, and FIB-TEM techniques to obtain the clues for clarifying the impact events occurred on the moon.

NWA 032 consisted of a basaltic portion and a small amount of breccia. Olivine, Ca-pyroxene, and low-Ca pyroxene occurred as phenocrysts in the basaltic portion. The matrix was filled with spherulitic textures consisting of plagioclase and Ca-pyroxene. Several shock-melt veins and melt-pockets occurred in the basaltic portion. Several olivine grains next to the shock-met veins have transformed into ringwoodite. The estimated shock pressure is ~13 GPa at least. The petrological and mineralogical features of NWA 479 were similar to those of NWA 032. Olivine grains entrained in the shock-melt veins dissociated into bridgmanite + (Mg, Fe)O. The estimated shock pressure is ~23 GPa at least. NWA 4898 showed the basaltic texture. Olivine occurred as phenocrysts. The matrix portion consisted mainly of Ca-pyroxene and plagioclase. A trace amount of silica minerals was entrained in the shock-melt veins. Some silica minerals in the shock-melt veins were stishovite. Ca-pyroxene next to the shock-melt veins dissociated into ahrensite, pyroxene-glass, and (probably) silicate titanite. The estimated shock pressure is ~9 GPa at least. NWA 2977 showed a gabbroitic texture and consisted mainly of olivine, low-Ca pyroxene, Ca-pyroxene, and plagioclase. Olivine grains next to or entrained in the shock-melt veins have transformed into ringwoodite. The estimated shock pressure is ~16 GPa at least. Two third of NWA 2727 was breccia and the other was gabbroitic. The gabbroitic portion consisted of olivine, low-Ca pyroxene, Ca-pyroxene, and plagioclase. The breccia portion included silica besides the fragments of the gabbroitic portions. Silica minerals entrained in the shock-melt veins or melt-pockets have transformed into coesite. The estimated shock pressure is ~3 GPa at least.

The shock-induced melting textures were observed in all investigated lunar mare basalt samples. Although the high-pressure polymorphs of olivine, Ca-pyroxene, and silica minerals were identified, the high-pressure polymorphs of plagioclase, which are abundant in other shocked meteorites, were not identified. In addition to previous studies [1–3], the present study reveals that many kinds of

©2019. Japan Geoscience Union. All Right Reserved.

high-pressure polymorphs occur in the lunar mare basalt, implying that most lunar mare basalts have experienced the heavy impact events.

References

[1] Ohtani E. et al. *PNAS* 108, 463–46, 2011.

[2] Miyahara M. et al. *NatureGeosci* 4:1737, 2013.

[3] Kayama M. et al. Sci.Adv. 4: eaar4378, 2018.

Keywords: Moon, Lunar mare basalt, High-pressure minerals

©2019. Japan Geoscience Union. All Right Reserved.

Bulk chemical analysis of iron meteorites by LA-ICP-MS

*Akira Yamaguchi[1], Naoki Shirai[2], Makiko K. Haba[3]

1. National Institute of Polar Research, 2. Tokyo Metropolitan University, 3. Tokyo Institute of Technology

Iron meteorites are Fe-Ni alloys with minor elements such as Co, P, S, and C. They are classified on the basis of textures (e.g., Widmanstatten pattern) and bulk chemical compositions (e.g., Ni, Ge, Ir). We performed bulk chemical analysis of iron meteorites by using an LA-ICP-MS and compared with the data obtained by INAA.

We measured five iron meteorites, Canyon Diablo (IAB, coarse octahedrite), Toluca (IAB, coarse octahedrite), Cape York (IIIAB, medium octahedrite), Muonionalusta (IV, fine octahedrite) and Dronino (ungrouped, ataxite) by using an LA-ICP-MS and INAA. Polished thick sections are prepared for LA-ICP-MS analysis. Polished thick sections of the meteorites were examined using an optical microscope, a scanning electron microscope, and an electron microprobe analyzer to observe the textures. A Thermo Element XR ICP-MS coupled to a CETAC LSX-213 laser was operated in low resolution mode (R = 300). The peaks monitored are ^{31}P, ^{34}S, ^{57}Fe, ^{59}Co, ^{60}Ni, ^{65}Cu, ^{69}Ga, ^{74}Ge, ^{95}Mo, ^{99}Ru, ^{103}Rh, ^{105}Pd, ^{182}W, ^{185}Re, ^{189}Os, ^{193}Ir, ^{194}Pt and ^{197}Au. Analyses in line and/or scanning modes were performed on a representative area of polished sections, using a 100 μm beam spot at 20 μm/sec., 20 Hz repetition rate. Typical analytical time was several minutes. Elemental abundances were obtained using Hoba (IVB, ataxite) and North Chile (IIAB, hexahedrite) iron meteorites as standard reference samples.

In INAA, samples weighing about 150 mg were firstly irradiated for 10 sec. at a neutron flux of 4.6 x 1012 $cm^{-2}s^{-1}$ at Institute for Integrated Radiation and Nuclear Science, Kyoto University for the determination of Co, Ni, Cu, Ge, and Rh. The same samples were reirradiated for 4 hrs at a neutron flux of 5.6 x 1012 $cm^{-2}s^{-1}$ at Institute for Integrated Radiation and Nuclear Science, Kyoto University for the determination of Cr, Fe, Co, Ni, Ga, As, Mo, Ru, Sb, W, Re, Os, Ir, Pt and Au.

We determined twenty elements (P, S, Fe, Co, Ni, Cu, Ga, Ge, As, Mo, Ru, Rh, Pd, Sb, W, Re, Os, Ir, Pt, and Au) for the five iron meteorites. Our results obtained by using two analytical methods were generally consistent with each other. However, our data of Muonionalusta are slightly different from literature values due to the large-scale heterogeneity of the meteorite (e.g., due to magmatic process). The abundance of some elements (e.g., Ru, Rh, Re, Ir) obtained from LA-ICP-MS data are higher than those from INAA due to the sample heterogeneity. It is possible to avoid this problem by choosing representative areas of the surface. Our study demonstrates that LA-ICP-MS has the potential to analyze a large number of iron meteorites.

Keywords: Iron meteorites, Bulk chemical analysis

©2019. Japan Geoscience Union. All Right Reserved.

[J] Poster | P (Space and Planetary Sciences)：P-PS Planetary Sciences

Mon. May 27, 2019 5:15 PM - 6:30 PM JST | Mon. May 27, 2019 8:15 AM - 9:30 AM UTC | Poster Hall International Exhibition Hall8, Makuhari Messe_3

[P-PS07] Formation and evolution of planetary materials in the Solar System

convener:Yoko Kebukawa(Faculty of Engineering, Yokohama National University), Wataru Fujiya(Ibaraki University, College of Science), Shin Ozawa(Department of Earth Science, Graduate School of Science, Tohoku University), Megumi Matsumoto(Graduate School of Science, Tohoku University)

This session will focus on the evolution in the Solar System with interaction and co-evolution in minerals, water, organic matter, and noble gas in meteorites and interplanetary dust particles. New innovative analytical and theoretical techniques in various fields will be discussed. The developing methods are welcome to submit for the future mainstream of meteorite study. In order to explore the planetary materials and their evolution, both meteorite studies and experimental approaches are necessary. In this session, we will discuss these topics from extraterrestrial sample analyses and experimental works. Research works on undifferentiated and differentiated meteorites and parent body processes such as aqueous alteration, thermal metamorphism, shock metamorphism, volcanic activity, and core-mantle-crust differentiation are especially included in this session.

[PPS07-P01] Stability of Amino Acid Precursors in Simulated Extraterestrial Environments

*tomohito sato[1], Soushi Kuramoto[1], Takuya Yokoo[1], Yoshida Satoshi[2], Isao Yoda[3], Hitoshi Fukuda[3], Yoshiyuki Oguri[3], MITA Hajime[4], Kazuhiro Kanda[5], Hiromi Shibata[6], Zyunichi Takahashi[1], Yoko Kebukawa[1], Kensei Kobayashi[1] (1.yokohama national univercity, 2.QST, 3.Tokyo Institute of Technology, 4.Fukuoka Institute of Technology, 5.University of Hyogo, 6.Osaka University)

[PPS07-P02] Production of amino acids by gamma rays during aqueous alteration process in meteorite parent body

*Shinya Asano[1], Isao Yoda[2], Yasuji Muramatsu[3], Yoko Kebukawa[1], Kensei Kobayashi[1] (1.Yokohama national university, 2.Tokyo Institute of Technology, 3.University of Hyogo)

[PPS07-P03] Kinetic approaches for the thermal history of organic matter in meteorites based on Raman spectra

*Kento Kiryu[1], Yoko Kebukawa[1], Motoko Igisu[2], Takazo Shibuya[2], Kensei Kobayashi[1] (1.Yokohama National Univ., 2.Japan Agency for Marine-Earth Science and Technology)

[PPS07-P04] Relationship between spatial distribution of organic compounds and minerals in the Murchison meteorite

*Taiyo Sengoku[1], Minako Hashiguchi[1], Hiroshi Naraoka[1] (1.Kyushu University)

[PPS07-P05] O and Al-Mg isotope systematics of a hibonite-melilite-rich fine-grained CAI in the reduced CV chondrite NWA8613

*Sohei Wada[1], Noriyuki Kawasaki[1], Hisayoshi Yurimoto[1,2] (1.Hokkaido University, 2.ISAS/JAXA)

[PPS07-P06] Observation of Enstatite Whiskers in Fine-grained Rims in the Carbonaceous Chondrite ALH A77307

*Yasuhisa Shirota[1], Masahiro YASUTAKE[1], Satomi Enju[1], Akira Tsuchiyama[1] (1.Division of Earth and Planet, Science, Kyoto University)

[PPS07-P07] 3D observation of whisker-like material in the porous matrix of the Paris CM chondrite by SR-XCT

*Masahiro YASUTAKE[1], Epifanio Vacarro[2], Kentaro Uesugi[3], Akihisa Takeuchi[3], Tsukasa Nakano[4], Akira Tsuchiyama[1] (1.Division of Earth and Planetary Science, Graduate School of Science, Kyoto University, 2.National History Museum, London, 3.JASRI/SPring8, 4.GSJ/AIST)

[PPS07-P08] Development of cryogenic SIMS technique for isotope analysis of fluid inclusions

*Isono Yuki[1], Naoya Sakamoto[2], Hisayoshi Yurimoto[3] (1.Department of Natural History Sciences, Hokkaido University, 2.Creative Research Institusion, Hokkaido University, 3.Department of Natural History Sciences, Hokkaido University)

[PPS07-P09] X-ray diffraction study using Gandolfi attachment: Implications for small extraterrestrial materials

*Naoya Imae[1,2], Makoto Kimura[1] (1.Antarctic Meteorite Research Center, National Institute of Polar Research, 2.SOKENDAI)

[PPS07-P10] Trace elements analysis and Ar-Ar dating for microgram-scaled extraterrestrial samples

*Ryuji Okazaki[1], Sekimoto Shun[2] (1.Department of Earth and Planetary Sciences, Faculty of Science, Kyushu University, 2.Institute for Integrated Radiation and Nuclear Science, Kyoto University)

[PPS07-P11] Magnetic separation and identification of low-temperature solid particles using their translation caused by a pair of small permanent magnets

*Chiaki Uyeda[1], Wakana Yamaguchi[1], Keiji Hisayoshi[1], Kentaro Terada[1] (1.Institute of earth and Space Science Graduate School of Science Osaka University)

[PPS07-P12] The metallographic cooling rate of the Tafassasset primitive achondrite

*naoji sugiura[1], Tomoko Arai, takafumi matsui (1.Chiba Institute of Technology)

[PPS07-P13] The systematic investigations of high-pressure minerals in lunar basaltic meteorites

*Masaaki Miyahara[1], Kazunari Kozuma[1], Eiji Ohtani[2], Akira Yamaguchi[3], Takeshi Sakai[4], Hiroaki Ohfuji[4], Naotaka Tomioka[5], Yu Kodama[6] (1.Department of Earth and Planetary Systems Science, Graduate School of Science, Hiroshima University, 2.Department of Earth Sciences, Graduate School of Science, Tohoku University, 3.National Institute of Polar Research, 4.Geodynamics Research Center, Ehime University, 5.5Kochi Institute for Core Sample Research, Japan Agency for Marine-Earth Science and Technology, 6.Marine Works Japan)

[PPS07-P14] Bulk chemical analysis of iron meteorites by LA-ICP-MS

*Akira Yamaguchi[1], Naoki Shirai[2], Makiko K. Haba[3] (1.National Institute of Polar Research, 2.Tokyo Metropolitan University, 3.Tokyo Institute of Technology)

Stability of Amino Acid Precursors in Simulated Extraterestrial Environments

*tomohito sato[1], Soushi Kuramoto[1], Takuya Yokoo[1], Yoshida Satoshi[2], Isao Yoda[3], Hitoshi Fukuda[3], Yoshiyuki Oguri[3], MITA Hajime[4], Kazuhiro Kanda[5], Hiromi Shibata[6], Zyunichi Takahashi[1], Yoko Kebukawa[1], Kensei Kobayashi[1]

1. yokohama national univercity, 2. QST, 3. Tokyo Institute of Technology, 4. Fukuoka Institute of Technology, 5. University of Hyogo, 6. Osaka University

Since a wide variety of organic compounds have been detected in extraterrestrial bodies like carbonaceous chondrites [1] and comets [2], extraterrestrial organics could be essential sources for the first life on the Earth. Amino acids in carbonaceous chondrites increased after acid-hydrolysis, which suggested that not only free amino acids but also amino acid precursors were present in them. Laboratory experiments simulating extraterrestrial environments showed that not free amino acids but amino acid precursors were mainly formed [3, 4]. Though amino acid precursors in meteorites and products of laboratory simulations have not been well identified, aminonitriles and hydantoins could be candidates. On the other hands, proton irradiation of a mixture of CO, NH_3 and H_2O, which simulated possible reactions among interstellar media, gave complex amino acid precursors with large molecular weights [5]. Such amino acids and amino acid precursors that were formed abiotically in space environments would be exposed to various energy sources in prior to delivery to the primitive Earth. For example, organics in molecular clouds were exposed to galactic cosmic rays (protons and heavy ions). Interstellar organic compounds were irradiated with strong VUV/X-rays from the young Sun. Organic compounds in small bodies were irradiated with gamma rays from such nuclides as ^{26}Al in the earlier stage of the solar system. Organic compounds in interplanetary dust particles were exposed to solar UV/VUV before delivery to Earth atmosphere. Thus it is important to examine stability of amino acids and their precursors against energetic particles and photons. We experimentally investigated the stability of amino acids and their precursors against heavy ions, gamma-rays, UV and soft X-rays.

Target molecules used in the present study were (i) glycine (Gly), (ii) hydantoin (Hyd; a precursor of Gly), and (iii) aminoacetonitrile (AAN; the Strecker-type precursor of Gly). They are used as 5 mM solutions in ammonia water (pH 9). In addition to them, we chose (iv) organic material synthesized from a mixture of CO, NH_3 and H_2O by 2.5 MeV protons from a Tandem accelerator (Tokyo Tech). We will call them CAW. CAW contained complex amino acid precursors with large molecular weights [3].

Experimental: *Heavy ions irradiation*: Aqueous solution of each target molecule was frozen in liquid nitrogen, and was irradiated with 290 MeV/u carbon ions from HIMAC (NIRS, Japan) at 7.5-15 kGy. *Gamma-rays irradiation*: Aqueous solution of each target molecule was irradiated with gamma rays (5-10 kGy) from a ^{60}Co source (Tokyo Tech, Japan). *UV irradiation*: Each target molecule was irradiated with UV from a xenon lamp after dried in pits of an aluminum plate. *Soft X-rays irradiation*: Each target molecule was irradiated with soft X-rays from a synchrotron (NewSUBARU BL-6) for 10 min after dried on aluminum plates. Amino acid analysis: all the target materials were recovered as aqueous solutions, were acid-hydrolyzed (6 M HCl, 110℃, 24 h), and amino acids in them were determined by reversed-phase HPLC after pre-column derivatization with *o*-phthalaldehyde and mercaptoethanol.

Results and Discussion: Since glycine was always major amino acids after acid hydrolysis of all the target materials after irradiation yielded glycine, we will discuss stability of target molecules by using the glycine

©2019. Japan Geoscience Union. All Right Reserved.

yields.

Heavy ions irradiation: Recoveries at 15 kGy were as follows. CAW (95.1%), Hyd (93.6%), Gly (91.8%) and AAN (77.5%). AAN was least stable among all. *Gamma-rays irradiation*: Decomposition of AAN, CAW and Hyd at 10 kGy was not detected, while recovery of Gly was 79.5%. *Soft X-rays irradiation*: recovery ratios were less than 10 % in the case of Gly, Hyd and AAN, while that of CAW was 51.1%. UV-irradiated samples were now under analysis.

Free amino acid (glycine) was generally less stable than amino acid precursors (CAW and Hyd), and CAW was most stable among 4 compounds tested against all the energies. Thus it was suggested that complex amino acid precursors were robust molecules in space, while free amino acids were easy to decompose even if they were formed from their precursors in space.

References

[1] K. Kvenvolden *et al.*, *Nature*, **228**, 923-926 (1970).

[2] J. Kissel and F. R. Krueger, *Nature*, **326**, 755-760 (1987).

[3] Y. Takano *et al.*, *Appl. Phys. Lett.*, **84**, 1410-1412 (2004).

[4] Y. Kebukawa et al., *Sci. Adv.*, **3**, e1602093 (2017).

[5] S. Kuramoto *et al.*, *2019 JpGU Meeting*, Chiba (2019).

[6] S. Iglesias-Groth et al., *Mon. Not. R. Astron. Soc.,* **410**, 1447-1453 (2011).

Keywords: Amino Acid Precursors, Radiation, Stability

©2019. Japan Geoscience Union. All Right Reserved.

Production of amino acids by gamma rays during aqueous alteration process in meteorite parent body

*Shinya Asano[1], Isao Yoda[2], Yasuji Muramatsu[3], Yoko Kebukawa[1], Kensei Kobayashi[1]

1. Yokohama national university, 2. Tokyo Institute of Technology, 3. University of Hyogo

[Introduction]Organic compounds such as amino acids are necessary for the birth of life on the earth. Extraterrestrial materials such as meteorites are considered as one of the sources of these amino acids. Since most of these meteorites originated from asteroids, we need to consider the origins of organic matter in asteroids. In the early stage of solar system formation, asteroids beyond the snow line contained ice and low molecular weight organic matter derived from dust. The ice melted due to the heat generated by the radioactive decay of ^{26}Al and aqueous alteration occurred. It is pointed out the complex macromolecular organic materials (insoluble organic matter, IOM) in meteorites may have formed during aqueous alteration (approximately 0 to 150 ˚C.) [1]. Based on this hypothesis, experiments simulating aqueous alteration on asteroids showed that amino acids and high molecular weight organic compounds similar to IOM in meteorites was formed after heating of formaldehyde, ammonia, water [2]. In this study, we aimed to investigate effect of gamma rays generated by radioactive decay of ^{26}Al during aqueous alteration for organic synthesis.
[Experimental]^{60}Co gamma ray source (Tokyo Institute of Technology) was irradiated to glass tubes containing 200 μl of water: formaldehyde: ammonia = 100: 5: 5 (molar ratio). Six different irradiation conditions were applied: 3 kGy/h ×2.5 h, 3 kGy/h ×4 h, 3 kGy/h ×5 h, 1.5 kGy/h ×5 h, 1.5 kGy/h ×8 h, and 1.5 kGy/h ×10 h. For comparison, the same solutions were heated in an oven at 150 ˚C for 24 h. The samples after irradiation were placed on CaF_2 plate and dried, then analyzed by FT-IR. The samples after irradiation were placed on gold plate and dried, then analyzed by X-ray absorption edge near structure analysis (XANES) of Hyogo prefectural university. Also, the samples were subjected to acid hydrolysis (6 M hydrochloric acid, 24 h, 110℃) and analyzed amino acid concentrations by cation exchange HPLC.
[Results and Discussion]<Cation exchange HPLC>Various amino acids such as glycine, alanine, β-alanine were detected from the gamma-ray irradiated samples after acid hydrolysis. Relatively large amount of alanine was produced from the irradiated samples compared to the heated samples. It suggests that the formation path ways of amino acids differ between the irradiated samples and the heated samples.
[Future plan]We are planning to extrapolate the gamma-ray induced amino acid yields to the meteorite parent body environments by extending the irradiation conditions (total dose and irradiation rate) using the calculated value of total dose of gamma ray from ^{26}Al during aqueous alteration. In addition, macromolecular organic compounds will be analyzed using LC-MS.
[Reference]
[1] G.D.Cody et al.,*PNAS*,108,19171-19176 (2011)
[2] Y.Kebukawa et al.,*Astrophysical J.*, 771, 19 (2013)

©2019. Japan Geoscience Union. All Right Reserved.

Kinetic approaches for the thermal history of organic matter in meteorites based on Raman spectra

*Kento Kiryu[1], Yoko Kebukawa[1], Motoko Igisu[2], Takazo Shibuya[2], Kensei Kobayashi[1]

1. Yokohama National Univ., 2. Japan Agency for Marine-Earth Science and Technology

CI, CM, and CR chondrites experienced aqueous alteration in their parent bodies, and contain organic carbon up to a few wt%. More than 70 wt% of it exists in the form of insoluble organic matter (IOM) (e.g., Pizzarello et al., 2006). Organic matter (OM) is susceptible to heating, and changes their structures, reflecting aqueous alteration and/or thermal metamorphisms. Thus, it attracts attention as the index of the parent body processes.

Kebukawa et al. (2010) estimated kinetic parameters for thermal degradation of aliphatic C-H through in-situ heating experiments of IOM and bulk of the Murchison meteorite (CM2) using the Fourier transform infrared micro-spectroscopy (microFTIR) combined with heating stage. They revealed that the peak intensity of aliphatic C-H is a good index of low-temperature and/or short-duration heating in the parent bodies. However, microFTIR is not enough for estimating thermal process of OM under high-temperature and long-duration heating which IR signals of aliphatic C-H are unlikely to be detected. Raman spectroscopy is a complementary tool to IR spectroscopy, since their spectral features of OM in the chondrites reflect thermal changes in aromatic structure in the complex OM (Quirico et al. 2003; Bonal et al., 2006, 2007; Busemann et al., 2007). When chondritic OM is heated, its aromatic structure will be more ordered to graphitic structure. This process is an irreversible, and results in changes of disordered (D_1-: ~1350 cm^{-1}) and graphite bands (G: ~1590 cm^{-1}) in Ramn spectra. Therefore, D_1- and G-bands were often used as indicators of degree of thermal metamorphism, but understanding of kinetic behaviors of the Raman spectral parameters is still limited. Thus, in order to evaluate thermal history of OM in chondrites under high-temperature and/or long-duration heating, we performed a series of heating experiments of the Murchison meteorite powders and kinetic analyses of their Raman spectral parameters.

The Murchison meteorite powders were heated under low oxygen condition in a vacuum furnace for 3-48 h at 600-900˚C. The low-oxygen condition was maintained by a gas mixture of N_2 and H_2 (99:1, v/v). The samples after heating were analyzed using Raman spectrometer with a 532 nm laser (RAMANtouch; Nanophoton). The Raman spectra of all the samples show D_1- and G-bands. We determined 5 Raman spectral parameters: the full width at half maximum (FWHM) and the peak positions of D_1- and G-bands, and the ratio of the peak intensity of D_1- to G-band. The changes in these Raman parameters with time at each temperature will be fitted with algebraic kinetic equations deduced by possible physical mechanisms, and estimate reaction rate constant. Then the apparent activation energies and frequency factors will be calculated by the reaction rates using the Arrhenius equation. Finally, we will establish the Raman parameters as functions of heating temperature and time. Combining previously reported kinetics of aliphatic C-H (Kebukawa et al. 2010), it may allow us to calculate precise time and temperature of thermal processes for chondrites.

Keywords: Organic matter in meteorites, Thermal history, Kinetics, Raman spectroscopy

©2019. Japan Geoscience Union. All Right Reserved.

Relationship between spatial distribution of organic compounds and minerals in the Murchison meteorite

*Taiyo Sengoku[1], Minako Hashiguchi[1], Hiroshi Naraoka[1]

1. Kyushu University

[Introduction]

Primitive meteorites contain a wide variety of organic compounds. More than 600 species of CHN compounds were identified in the methanol extract of the Murchison meteorite (CM2), in which saturated- and unsaturated-alkylated pyridines ($C_nH_{2n-4}N^+$ and $C_nH_{2n-6}N^+$) as well as alkylimidazoles ($C_nH_{2n-1}N_2^+$) are predominant (Naraoka et al., 2017). Interaction between organic matter and minerals during aqueous alteration is very important in the chemical evolution (e.g. Kebukawa et al., 2010), therefore, it is necessary to investigate the spatial distribution of the organic matter and minerals in the meteorites. In the previous studies, chemical imaging of soluble organic matter (SOM) was performed on the Murray and Murchison meteorites (CM2) by desorption electrospray ionization/high-resolution mass spectrometry (DESI/HRMS), and the different spatial distribution was observed among the different CHN species and/or their alkylated homologues (Naraoka & Hashiguchi, 2018, Hashiguchi & Naraoka, 2018). However, the relationship between the organic compounds and minerals is still unresolved. In this study, the DESI-HRMS imaging and detailed mineralogical observation were performed on fragments of the Murchison meteorite.

[Sample & Method]

Two fragments designated as “np15" (2x3 mm^2) and “np16” (2x2 mm^2) were obtained by chipping from different large fragments of the Murchison meteorite. These fragments were embedded in indium or metal with low-melting point for DESI-HRMS imaging. The DESI-HRMS imaging was performed on each sample for three times. Methanol was used as a spray solvent with the flow rate of 2 μL/min. The electrospray voltage was set to 3 kV. The nebulizer N_2 gas pressure was ~100 psi. The positive ions were collected in a full scan mode (m/z 50-500) with mass resolution of about 140,000 ($m/\Delta m$ at m/z 200) on the sample surface of np15 (4x4 mm^2) and np16 (3.8x3.8 mm^2). For the fragment np16, dry polishing was performed on the sample to remove ~250 μm from the surface and the imaging was performed again, because no signals of CHN compounds were obtained by the 1st set of DESI-HRMS imaging. After the DESI-HRMS imaging, the same sample surface was used to obtain backscattered electron images (BSE) and X-ray elemental maps using SEM/EDS.

[Results & Discussion]

Some alkylated homologues of CHN compounds were detected from np15 by DESI-HRMS imaging. Their exact masses correspond to alkylimidazole ($C_nH_{2n-1}N_2^+$) and saturated- or unsaturated-alkylated pyridine ($C_nH_{2n-4}N^+$ or $C_nH_{2n-6}N^+$) within 3 ppm of mass precision. The spatial distribution was different between $C_nH_{2n-1}N_2^+$ and $C_nH_{2n-4}N^+$, which is consistent with the previous study (Naraoka & Hashiguchi, 2018). On the other hand, no CHN compounds were detected from np16. After removing ~250 μm of the surface of np16 by polishing, some CHN compounds corresponding to $C_nH_{2n-1}N_2^+$ and $C_nH_{2n-6}N^+$ were detected in 3rd DESI-HRMS imaging finally, however, these compounds were not detected by 1st and 2nd analyses. These results indicated that the CHN compounds might have been volatilized from the sample surface

©2019. Japan Geoscience Union. All Right Reserved.

during its storage, and that repeated DESI-HRMS imaging is important to obtain clear signals of SOM from inside of meteorite. The detected CHN compounds showed heterogeneous spatial distribution in the sample surface, which indicate that dry polishing does not affect the spatial distribution of SOM significantly.

In both np15 and polished np16 samples, the CHN compounds distribute mainly in the matrix region (~ few hundreds of square meters) of the meteorite. Although the X-ray elemental mapping showed that CHN compounds-rich region seemed to contain abundant Ca-containing minerals in both fragments, no clear relationship was observed between the averaged chemical compositions of matrix region and the spatial distribution of the CHN compounds. Further detailed analysis will be performed on tiny minerals in the matrix.

Keywords: carbonaceous chondrite, chemical imaging , soluble organic compounds

©2019. Japan Geoscience Union. All Right Reserved.

O and Al-Mg isotope systematics of a hibonite-melilite-rich fine-grained CAI in the reduced CV chondrite NWA8613

*Sohei Wada[1], Noriyuki Kawasaki[1], Hisayoshi Yurimoto[1,2]

1. Hokkaido University, 2. ISAS/JAXA

Ca–Al-rich inclusions (CAIs) in meteorites are composed of high-temperature condensate minerals from the solar nebular gas [1]. CAIs in CV chondrites are petrographically divided into the coarse-grained CAIs and fine-grained CAIs (FG-CAIs). Complex layer structures of constituent minerals and REE patterns of FG-CAIs suggest they are condensates from the nebular gas [2, 3]. Igneous CAIs that experienced melting and crystallization, such as coarse-grained Type B CAIs, have been extensively studied their formation processes, O-isotope compositions of minerals, and formation ages [4, 5]. On the other hand, such systematic investigations for the formation of FG-CAIs have been poorly conducted. Here, we investigated O- and Al–Mg isotope systematics of a hibonite-melilite-rich FG-CAI from the reduced CV chondrite NWA8613 as well as detailed petrographic observations. The O- and Al–Mg isotope measurements were conducted using SIMS instruments of Hokkaido University (Cameca ims-1270 and ims-1280HR).

The FG-CAI has an irregular shape with a size of approximately 10 ×12 mm and composed mainly of melilite, hibonite, and spinel. O-isotope compositions of the constituent minerals plot along the CCAM line, ranging between $\Delta^{17}O \sim -23‰$ and 0‰. The FG-CAI is petrographically divided into hibonite-rich core, spinel-rich core, melilite-rich inner-mantle, and hibonite-spinel-rich outer mantle. The CAI is rimmed by thin spinel and diopside layers. Melilite crystals are contained in core and mantle. Melilite crystals in the core exhibit normal chemical zoning and O-isotope compositions from $\Delta^{17}O \sim -23‰$ to −10‰ with increasing Åk composition. The melilite crystals in the inner-mantle show chemically complex, oscillatory zoning patterns, but are uniformly ^{16}O-poor ($\Delta^{17}O \sim 0‰$) despite their chemical variations (Åk2–14). Melilite crystals in the outer-mantle exhibit normal chemical zoning and variable O-isotope compositions from $\Delta^{17}O \sim -17‰$ to 0‰ with increasing Åk composition. The spinel and hibonite grains in the FG-CAI are uniformly ^{16}O-rich ($\Delta^{17}O = -23‰$). Al–Mg isotopic compositions of hibonite in the outer-mantle and in the core and melilite in the inner-mantle plot on a single straight line within error; an Al–Mg mineral isochron can be defined to give an initial $^{26}Al/^{27}Al$ value of $(4.50 \pm 0.09) \times 10^{-5}$. Given that the constituent minerals formed by condensation and were accumulated to form the FG-CAI, the nebular gas, from which they condensed, had variable O-isotope compositions between $\Delta^{17}O \sim -23‰$ and 0‰. The Al–Mg systematics of the FG-CAI indicate that these formation events occurred at 0.16 ±0.02 Myr after the formation of canonical CAIs [7], if ^{26}Al was homogeneously distributed. Our data support the presence of the nebular gas with variable O-isotope compositions during the first ~0.2 Myr of the Solar System formation [8].

References: [1] Grossman (1972) *GCA* 36, 597–619. [2] Boynton (1975) *GCA* 39, 569–584. [3] Krot et al. (2010) *MaPS* 39, 1517–1553. [4] Kawasaki et al. (2018) *GCA* 221, 318–341. [5] Yurimoto et al. (1998) *Science* 282, 1874–1877. [6] Beckett and Stolper (1994) *MaPS* 29, 41–65. [7] Larsen et al. (2011) *ApJL* 735 L37–L43. [8] Kawasaki et al. (2017) *GCA* 201, 83–102.

©2019. Japan Geoscience Union. All Right Reserved.

Observation of Enstatite Whiskers in Fine-grained Rims in the Carbonaceous Chondrite ALH A77307

*Yasuhisa Shirota[1], Masahiro YASUTAKE[1], Satomi Enju[1], Akira Tsuchiyama[1]

1. Division of Earth and Planet, Science, Kyoto University

Introduction Chondritic porous -interplanetary dust particles (CP-IDPs) are material that are suggested to be originated from comets and to be one of the most primitive materials in the solar system (Bradley et al., 1983). CP-IDPs include enstatite ($MgSiO_3$) whiskers. They are thought to be formed by condensation in the solar nebula (Bradley et al., 1983).

Primitive carbonaceous chondrites are affected by little aqueous alteration. Recent studies have discovered enstatite whiskers in matrices in primitive carbonaceous chondrites (Vaccaro et al., 2017; Matsumoto et al., 2018). If such crystals have similar formation processes to those of enstatite whiskers in CP-IDPs, it will constrain the formation processes of not only asteroids but also CP-IDPs. However, only a few enstatite whiskers are observed in carbonaceous chondrites. Therefore, it is not certain whether or not enstatite whiskers are common in carbonaceous chondrites and have same formation processes in CP-IDP.

We conducted a detail petrological observation of matrix in ALH A77307 (CO3.0) to understand distribution of whisker-like enstatite crystals using a scanning electron microscopy (SEM) and to constrain the formation process using a transmission electron microscopy (TEM).

Sample and Methods We observed one of the most primitive CO chondrites ALH A77307. Vaccaro et al. (2017) reported whisker-like enstatite crystals in ALH A77307. SEM/EDS analysis was carried out with an FE-SEM (JEOL JSM-7001F, Kyoto University, Hitachi HT SU6600, ISAS, JAXA) operating at 100 pA probe current and 8 kV accelerating voltage. A TEM thin section including one whisker was extracted using focus ion beam (FIB) (FEI, Helios NanoLab 3G, Kyoto University). TEM analysis was carried out with a (S)TEM/EDS (JEOL JEM-2100T, Kyoto University) operating at 200 kV accelerating voltage.

Result and Discussion We observed fine-grained rims around three chondrules. These rims consist mainly of amorphous silicate, olivine, pyroxene, and Fe,Ni metal, and similar to primitive matrix. The whisker-like enstatite crystals occur in all regions observed and the total number of whiskers found are 12. The maximum size of the whisker is 11.91 μm in length and 0.27 μm in width. We classified whiskers based on criterion the aspect ratio, p, by Bradley et al. (1983). The whiskers are classified as 4 Rods (p>20) and 8 Ribbons (p<20). The abundance of whiskers is >40 mm^{-2}, suggesting that whisker-like enstatite is common in chondrule rims in primitive carbonaceous chondrites although the abundance in CP-IDPs is higher. The aspect ratios are similar to those of enstatite whisker in CP-IDPs. In contrast to enstatite whiskers in CP-IDPs, some whiskers are curved and/or broken. It may be the result of deformation during accumulation on the parent body.

We have observed one ribbon crystal (length 1.21 μm, width 0.16 μm) using TEM. The ribbon crystal was orthoenstatite elongated along [001] axis based on electron diffraction patterns. Three dimensionally, this crystal is thought to be a columnar crystal elongated along [001] or a plate crystal with flattened (010) plane. From this results, this crystal is thought to be a platelet crystal formed by condensation in the solar nebula like enstatite whiskers in CP-IDPs (Bradley et al., 1983) or crystal formed by annealing of

©2019. Japan Geoscience Union. All Right Reserved.

amorphous silicate (Brearley, 1993). To constrain more detail formation process of the whisker-like material in carbonaceous chondrites, mineralogical investigation of whisker-like material, especially rod crystals is needed.

[1] Vaccaro E. (2017) PhD thesis. The Open University. [2] Bradley J. P. et al. (1983) Nature. 301, 473-477. [3] Matsumoto M. et al. (2018) 81st Annual Meeting of the Meteoritical Society [4] Brearley. (1993) Geochim. Cosmochim. Acta 57, 1521-1550

Keywords: Enstatite whisker, Primitive Carbonaceous Chondrite

©2019. Japan Geoscience Union. All Right Reserved.

3D observation of whisker-like material in the porous matrix of the Paris CM chondrite by SR-XCT

*Masahiro YASUTAKE[1], Epifanio Vacarro[2], Kentaro Uesugi[3], Akihisa Takeuchi[3], Tsukasa Nakano[4], Akira Tsuchiyama[1]

1. Division of Earth and Planetary Science, Graduate School of Science, Kyoto University, 2. National History Museum, London, 3. JASRI/SPring8, 4. GSJ/AIST

Introduction The chondritic-porous interplanetary dust particles (CP-IDPs) are well-known material, that preserves primitive and pristine features of the early solar system. Enstatite whisker is one of the materials that characterizes CP-IDPs. It is thought that enstatite whiskers are condensates formed in the inner solar system and transferred to the outer regions, where comets formed [e.g. 1, 2]. Recently, whisker-like enstatite crystals were found in the primitive carbonaceous chondrites [3, 4]. However, the whisker-like materials they found could be a cut-plane of thin enstatite plate. By the 2D observation, it is hard to solve this matter. 3D observation based on synchrotron radiation X-ray nano-CT is a strong tool to understand the crystal shape, mineral phase, and rough composition. We conducted a 3D observation to better understand the characteristics of whisker-like materials in primitive carbonaceous chondrites.

Methods We investigated the Paris primitive CM chondrite. Paris was reported to have a very primitive matrix that includes GEMS-like materials [5]. A section of this meteorite was observed and elemental maps of the primitive matrix were obtained by FE-SEM/EDS. A house-shaped CT sample (~25 x 25 x 30 μm) was extracted from the primitive matrix by using a FIB-SEM. CT data of the micro-samples were conducted at beamline BL47XU, SPring-8. CT images were acquired at energies of 7 keV and 7.35 keV with voxel sizes of ~32.2 nm and ~ 33.9 nm, respectively. Mineral phases were estimated using dual-energy tomography (DET) method using the X-ray linear attenuation coefficient (LAC) [6].

Result and Discussion The observed matrix is a part of the fine-grained rim of Type I porphyritic olivine pyroxene chondrule. The matrix is porous and consists mainly of amorphous silicates that include sub-micron sized Fe-rich phases. Whisker-shaped materials are abundant in the CT sample observed. However, fibrous alteration materials were also reported in the matrix of Paris [5]. The whisker-like materials observed might include such products in addition to enstatite. The size of the largest whisker is ~6 μm x ~700 nm x ~350 nm (Fig. 1) and similar to ribbon-type enstatite whisker in the CP-IDPs [1]. This whisker has a curved shape unlike those in CP-IDPs. Probably it reflects deformation during accretion to the parent body and/or planetary processes such as planetary collision.

The LAC values of most whisker materials are hard to obtain quantitatively because refraction of X-ray at the edges of the narrow whiskers enhanced their LAC values. The LAC values of the largest whisker are less affected by refraction and have the range of ~170-180 cm^{-1} and ~250-270 cm^{-1} at 7.00 and 7.35 keV, respectively. These values are consistent with those of pyroxene ($En_{80}Fs_{20}$) and clearly distinguishable from the values of fibrous alteration products (cronstedtite, tochilinite, and ferrihydrite) [5]. The above results suggest that this whisker material is an enstatite whisker. The possibility of olivine whisker (~Fo_{85}) cannot be excluded but forsterite whiskers have not been reported so far. Thus, it is reasonable to consider that the enstatite whiskers accreted to the carbonaceous chondrite parent body.

Crystallographic features such as defects and direction of elongation are still not examined. Investigation of crystallography is required to constrain the formation processes of whiskers, and it will enable us to

©2019. Japan Geoscience Union. All Right Reserved.

compare the enstatite whiskers in carbonaceous chondrites with those in CP-IDPs.

Reference [1] Bradley (1983) *Nature*, 301, 473-477. [2] Bradley, J. P. (2003) *Treatise on geochemistry*, 1, 711. [3] Vaccaro (2017) PhD thesis, The Open University. [4] Matsumoto et al. (2017) abstract JAMS annual meeting. [5] Leroux et al. (2015) *GCA*, 170, 247-265. [6] Tsuchiyama et al, (2013) *GCA*, 116, 5-16.

Keywords: CM chondrite, Paris meteortite, Primitive matrix, Enstatite whisker, SR-XCT

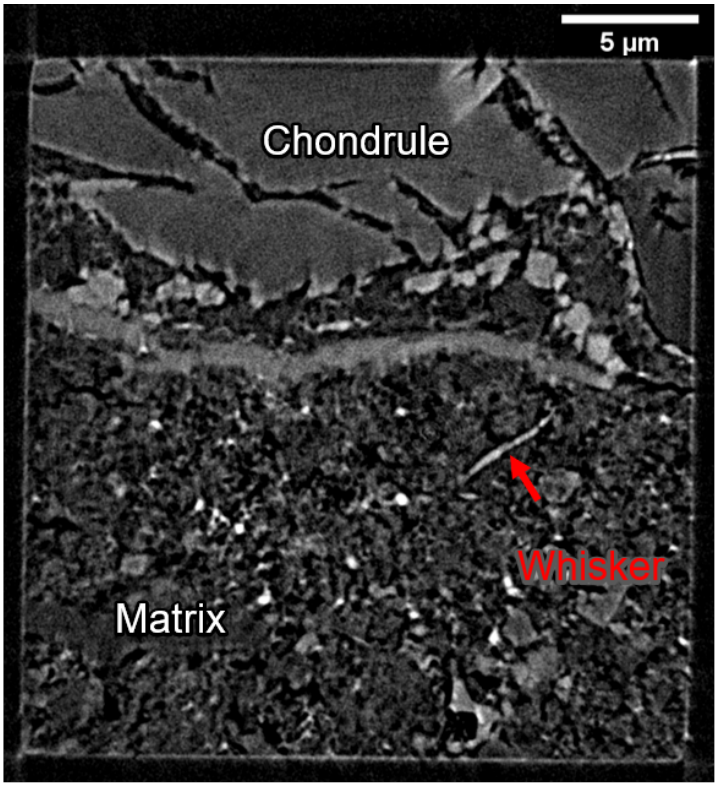

Fig. 1. CT image of porous matrix in Paris acquired at 7 keV. Silicates are shown in light grey. Amorphous silicates are shown in dark grey. Metal and sulfide are shown in white. The enstatite whisker is shown by red arrow.

©2019. Japan Geoscience Union. All Right Reserved.

Development of cryogenic SIMS technique for isotope analysis of fluid inclusions

*Isono Yuki[1], Naoya Sakamoto[2], Hisayoshi Yurimoto[3]

1. Department of Natural History Sciences, Hokkaido University, 2. Creative Research Institusion, Hokkaido University, 3. Department of Natural History Sciences, Hokkaido University

Introduction: Fluid inclusions in halite crystals from meteorites provide direct information of extraterrestrial liquid water [1]. In-situ isotope analysis of the fluid inclusions was realized by SIMS equipped with a cold-stage [2]. However, the analytical precision is limited to ±14 ‰(1 σ) for $\delta^{18}O$ due to deep sputter crater to excavate fluid inclusions. One of the methods to improve the analytical precision would be expose fluid inclusions on the sample surface. We froze the fluid inclusions and polish under cryogenic condition in nitrogen atmosphere [3, 4]. In order to measure frozen polished fluid inclusions by SIMS, the surface should be coated by conductive thin layer such as Au. However, the Au thin layer was not enough conducted because condensation of frost particles occurred before introduce the polished sample into Au coater. The sample temperature was −100 ˚C while the dew point in the glove box (−60˚C) was higher than the sample temperature [4]. Therefore we changed the sample temperature.

Changes of sample preparation procedures: The sample preparation system for cryogenic SIMS is composed of a cryo-polisher and Au ion-coater in a glove box [3]. The temperature of polishing set to −35 ˚C. Thus frost condensation on the polished surface was prevented. After polishing, the sample was settled on the bottom of deep well of new designed cryo-coating stage. The cryo-coating stage was precooled to −196 ˚C by liquid nitrogen and the deep well was filled with cool nitrogen gas evaporated from liquid nitrogen in order to prevent frost formation on sample surface. This cooling process is necessary because sublimation temperature of ice is −50 ˚C during Au coating. The sample temperature was estimated to −196 ˚C before taking into the Au coater and warmed up −130 ˚C at taking from the Au coater after Au coating for 4 minutes.
The polished ice embedded in an epoxy disk was set to the cryo-holder and transferred to cryo-stage (−190 ˚C) of Cameca ims-1270 instrument using cryo-transfer system [3]. The liquid nitrogen was supplied by a roots pump to reduce the sample stage vibration. The measurement methods for oxygen isotopes were similar to those of [2].
We obtained mass spectra of oxygen isotopes from H_2O-ice. Intensity of ^{16}O peak was about 2.8 $\times 10^5$ cps and a tale was observed symmetrically at both side of the peak below 3 cps. The interference of tail from $^{16}OH^-$ to $^{17}O^-$ was estimated to be about 10 ‰because the intensity of $^{16}OH^-$ is comparable to ^{16}O peak. Oxygen isotope analysis using $^{16}OH^-$ and $^{17,18}OH^-$ signal would be effective for further high precision oxygen isotope analysis for H_2O ice as well as the tail correction method used in [2].
References: [1] Zolensky M. et al. (1999) Science, 285, 1377-1379. [2] Yurimoto H. et al. (2014) Geochem. J, 48, 549-56. [3] A. Ishibashi (2014) Master thesis [4] J. Song (2017) Master thesis.

Keywords: Fluid inclusion, Cryogenic SIMS, Oxygen isotope

©2019. Japan Geoscience Union. All Right Reserved.

X-ray diffraction study using Gandolfi attachment: Implications for small extraterrestrial materials

*Naoya Imae[1,2], Makoto Kimura[1]

1. Antarctic Meteorite Research Center, National Institute of Polar Research, 2. SOKENDAI

Introduction

Recent studies have established the bulk features of various chondrite species based on the X-ray diffraction patterns (Howard et al. 2009; Imae and Nakamuta 2018; Imae et al. 2019). In the present study, X-ray diffraction experiments were carried out using Gandolfi attachment in order to apply for small extraterrestrial materials of various kinds of stony meteorites. The present technique is convenient in the laboratory and also useful for rapidly identifying the mineral species without any significant sample loss.

Experiments

We used the X-ray diffractometer in air with the goniometer radius of 30 cm (RIGAKU, SmartLab) at NIPR on the following conditions: (1) CuKa1 with 40 kV, and 30 mA for glass X-ray tube and 40 mA for ceramic X-ray tube, (2) the X-ray beam of 0.4 mm in diameter obtained from the polycapillary focusing optics (CBO-f unit), (3) the strip detector (D/teX Ultra 250) for counting diffracted X-rays, (4) the revolution rate of the goniometer head on the Gandolfi attachment at 30 rpm, and (5) the scan speed of normally 0.2 º/min or 0.5 º/min with the step of 0.01º and the average of the repeated analyses.

Glass fiber (13 μm in diameter) attached with glass rod (1 mm in diameter) was mainly used for holding samples. Both powder and grain samples with the diameter of ~0.2-0.8 mm were used for the measurements.

Powders and single grains for San Carlos olivine and NWA 4719 L6 chondrite were used for the calibration focused on olivine 130 index. So far, 36 stony meteorites have been measured and they are 27 ordinary chondrites (mostly Antarctic meteorites), 5 carbonaceous chondrites, an E chondrite (NWA 7401), a eucrite (Cachari), a diogenite (Bilanga), and an aubrite (Pena Blanca Spring).

Results and discussion

Calibration: The two-theta position of the olivine 130 peak for the powder samples of San Carlos olivine shows nearly consistent value by Yoder and Sahama (1957), on the contrary, the intensity of the San Carlos olivine grains is lower than that of powder on the similar measurement condition, and in addition the position of the two-theta is slightly higher than that of powder. In case of chondrite (NWA 4719 L6), the intensity is significantly lower than San Carlos olivine. Although the two-theta values for powder samples and grain samples are within the mean Fa# range of L group, the intensity of grain is significantly lower than that of powder.

©2019. Japan Geoscience Union. All Right Reserved.

Samples: The systematic differences of olivine 130 two-theta values were observed among ordinary chondrites: 32.18º-32.29º for H, 32.15º-32.21º for L, and 32.13º-32.16º for LL. These ranges include that the two-theta values are obviously higher than the ranges expected from the mean Fa# for three chemical groups (32.18º-32.21º for H, 32.12º-32.16º for L, and 32.08-32.12 for LL, Yoder and Sahama 1957). The existence of orthoenstatite 511 peak is an indicator for equilibrated ordinary chondrites but not definite, since the peak intensity is normally low. More ferroan olivine peak than ordinary chondrites appears from carbonaceous chondrites. EL6 consists of orthoenstatite. Diffraction patterns of achondrites are different from those of chondrites: pigeonite and anorthite peaks for eucrite and dominant orthopyroxene for diogenite, and dominant clinoenstatite for an aubrite. Fine-grained powder samples may represent the bulk chondrite compositions, but not for grains. This may lead to the different diffraction pattern.

Summary

The present technique is useful conveniently for examining limited or small extraterrestrial materials, when we take into consideration the variations for chondrite species depending on the different sample conditions of powder or grain and the relative modal abundance of olivines and pyroxenes for grains with the limited range of variation of the chemical groups.

Acknowledgements

NI is grateful to Dr. Yoshihiro Nakamuta for discussions, and the study is partly supported by NIPR and KAKENHI (17K05721).

References

Howard K. T., Benedix G. K., Bland P. A., and Cressey G. 2009. Geochimica et Cosmochimica Acta 73: 4576-4589.

Imae N. and Nakamuta Y. 2018. Meteoritics & Planetary Science 53: 232-248.

Imae N., Kimura M., Yamaguchi A., and Kojima H. 2019. Meteoritics & Planetary Science (In press).

Yoder Jr. H. S. and Sahama T. G. 1957. American Mineralogist 42: 475-491.

Keywords: X-ray diffraction study, Gandolfi attachment, small extraterrestrial materials, meteorites

©2019. Japan Geoscience Union. All Right Reserved.

Trace elements analysis and Ar-Ar dating for microgram-scaled extraterrestrial samples

*Ryuji Okazaki[1], Sekimoto Shun[2]

1. Department of Earth and Planetary Sciences, Faculty of Science, Kyushu University, 2. Institute for Integrated Radiation and Nuclear Science, Kyoto University

In order to elucidate the origin and evolution of planetary materials, it is important to determine the chemical composition and timing of geological events for specific minerals and microscopic portions, such as impact melt pockets, CAIs (Ca- and Al-rich Inclusion), and chondrules. Combination of EMPA, INAA, and noble gas analysis are one of the best way to determine chemical and isotopic compositions of extraterrestrial dust particles (micrometeorites) and spacecraft-returned samples.
As a first step, we have analyzed rock fragments (<several hundreds of micrometer in diameter) recovered from Holbrook L6 chondrite. Neutron irradiation and NAA experiments were conducted at Institute of Integrated Radiation and Nuclear Science, Kyoto Univ. Allende CV3 and Madagascar feldspar were used for standardization of INAA and Ar-Ar analyses, respectively. Each of the sample particles was individually placed in a conical dimple (ϕ1, depth ~ 0.5 mm) of a sapphire disk (ϕ5.5, 1.5 mm thick), and covered with a sapphire disk (ϕ5.5, 0.3 mm thick). Each of the sapphire container was wrapped with pure aluminum foil. These Al-wrapped containers were stacked and sealed in aluminum capsules to perform neutron irradiation at the hydro-irradiation port. After irradiation, the samples were recovered from irradiated glass containers, and moved to non-irradiated containers in order to reduce the radioactivity from the sapphire containers and Al foil. Gamma-ray measurements for short half-life nuclides were performed promptly after collection of the samples. Several months after the irradiation, some of the Holbrook samples were transported to Kyushu Univ. to measure noble gas isotopes.
Concentrations of Co and Ni in two Holbrook samples were determined to be 57 and 157, and 1260 and 13400 ppm, respectively. The Ni/Co ratios of the Holbrook samples are 22 and 85, which are similar to those observed in iron meteorites and chondrites (e.g., Ebihara et al., 2011). The result guarantees our NAA measurement.
Noble gas isotopes (^{36}Ar, ^{38}Ar, ^{39}Ar, and ^{40}Ar) were determined for different two Holbrook samples using stepwise heating method. The bulk ^{39}Ar concentration in the irradiated standard feldspar (K: 12.6 wt%) is 7E-6 cm^{3}STP/g, and the bulk ^{39}Ar/^{40}Ar ratio is 0.026. The result indicates that the neutron flux of KURRI is enough to determine ^{39}Ar for microgram samples with K>0.1 wt%. Using the neutron flux determined by the standard feldspar, with 450 Ma of K-Ar age (ranging 435-461 Ma; Flude et al, 2014), we calculated the Ar-Ar ages for two Holbrook samples (9.4 and 16.8 μg) to be 3795±368Ma (based on 3 plateau ages of 4 stepwise extractions) and 3714±128Ma (based on 4 plateau ages of 7 stepwise extractions). Noble gases extracted at the lowest and highest temperature steps are influenced by atmospheric Ar, resulting unreasonable old Ar-Ar age. Based on these results, we found appropriate extraction temperature for plagioclase-rich microgram samples to be 600, 800, 900, 1000, 1100, 1200, 1400, and 1600 ˚C.
Through this study we have established an analytical method that consists of a combination of EPMA, INAA, and noble gas analyses. The new method will be applied for Antarctic micrometeorites and the Hayabusa2 samples.

Keywords: Ar-Ar age, meteorite, micrometeorite, INAA, Hayabusa2

©2019. Japan Geoscience Union. All Right Reserved.

Magnetic separation and identification of low-temperature solid particles using their translation caused by a pair of small permanent magnets

*Chiaki Uyeda[1], Wakana Yamaguchi[1], Keiji Hisayoshi[1], Kentaro Terada[1]

1. Institute of earth and Space Science Graduate School of Science Osaka University

Most solid particles in nature are categorized as diamagnetic or weak paramagnetic materials; they are commonly believed to be magnetically inert, and cannot attain strong magnetization to cause specific magnetic motions at practical field intensity. Indeed, strong magnetic field above the level of 10 T were applied in previous studies to induce magnetic levitations. A method to separate solid particles by a field gradient produced by small NdFeB magnets was recently proposed and experimentally approved using a setup operated in microgravity condition [1]. By improving this system, magnetic separation was realized on volatile solid particles, namely H2O and CO2, for the first time [2]. In addition, it was possible to estimate the material of the particle in a non-destructing manner by comparing the experimental value of magnetic susceptibility with a list of published values [1][2]: here the susceptibility was obtained from the velocity of the translating particle without the knowledge of particle mass.

In the present experimental present setup, a pair of small NdFeB plates was attached in a double glass container. A microgravity condition is produced inside the box by free fall from a height of 180 cm. An ensemble of heterogeneous particles translates and separates by magnetic field gradient in free fall. The Hi-vision camera observed the translation and susceptibility is calculated by obtained terminal velocity [1]. The obtained susceptibility of the particle is compared with literature data and materials of particles are estimated.

The field-induced translational motions realized in μg condition can be utilized in various space missions in future; this is because the small but rigid apparatus can separate and identify the heterogeneous particles that is expected to be collected in an on-site mission. One of the major purposes to perform space explorations to the outer solar system was to identify the solid materials that are observed on satellite surfaces or ring. It is concluded by recent observation that the solid particles were mainly composed of ice (Ih) with high purity; previously it was considered that the icy particles of the rings contain significant amount of rock-forming silicates. Hence, for a future task, quantitative information of the minor silicate composition included in the icy particle is required in studying the origin of the Saturn rings.

An efficient method that can non-destructively identify the components of a heterogeneous aggregate sample is desired in various research fields of material science. Using an infrared optical analysis, for example, the material composition of the particle interior is difficult to determine when the sample is larger than 100 μm in diameter. In the case of a conventional mass spectrometer, it is difficult to identify the composition of solid particles without destructing the sample. Although various microprobe devices are effective in performing refined survey on aggregate samples, it is difficult to conclude by these methods whether small particles included in the aggregate are completely discovered and identified without omission. In such cases, the particles should be definitely separated into groups of different materials before performing refined analysis [1-3]. Note that the present proposal of magnetic separation can overcome the abovementioned limitations of the conventional methods, and in future, it may serve as

©2019. Japan Geoscience Union. All Right Reserved.

a standard pretreatment tool of material analysis.

[1] Hisayoshi, Uyeda & Terada (2016) Sci., Reps., 6, 38431.

[2] Yamaguchi, Hisayoshi, Uyeda & Terada (2017) J. Phys., Conf. Ser.903, 012026.

[3] Hitomi, Yamaguchi, Hisayoshi, Uyeda (2018) Planet Space Sci., available online.

Keywords: magnetic separation, diamagnetic material, low temperature solid

©2019. Japan Geoscience Union. All Right Reserved.

The metallographic cooling rate of the Tafassasset primitive achondrite

*naoji sugiura[1], Tomoko Arai, takafumi matsui

1. Chiba Institute of Technology

Tafassasset (Tafa) is a primitive achondrite with carbonaceous chondrite-like (CC) isotopic (Cr etc.) signatures. Cooling rates and chronological information give valuable insight on the evolution of achondrite parent bodies. Brent et al. [1] constructed an evolutionary model (the parent body with a radius ~17 km, accreted at ~1 Ma after CAI; Tafa is located in the middle of the mantle). It is mainly based on the chronology, but is considered to be supported by the metallographic cooling rate (100~200 C/Ma). But it is said to require refinement. Here we report observations of the metal texture and compositions, based on which a cooling history is derived.

Observation

Fe-Ni grains (average composition ~10 mol.% Ni) in Tafa show various textures. Many grains show kamacite that nucleated on the metal-silicate boundary and expanded inward during cooling. The central part is zoneless plessite which must be martensite at higher temperatures but now is made of kamacite and taenite. An interesting feature is that the boundary of kamacite and interior plessite is made of thin (~a few mm wide) taenite wall, suggesting rapid coolig. The compositions range from 17 to 31 % Ni and the average is ~26% Ni. Considering the difficulties in measuring compositions of thin taenite rim, the real value could be ~31% Ni. The zoneless plessite interior (average composition ~10 mol% Ni) is made of taenite islands in kamacite matrix. The taenite island sizes are usually only a few mm or less and the compositions range, if measurable, from 28 to 39% Ni, and the average is ~34% Ni. Again, the real value is considered to be close to ~39% Ni. A typical distance between taenite islands is ~10 mm. There are isolated zoned taenite grains, the central compositions of which are correlated with the size. There are zoned taenite grains which are surrounded by kamacite. Their compositions at the center mostly do not depend on the size, and is ~10 mol.% Ni. We note that cloudy taenite is not observed in any taenite grains. It is also to be noted that the phosphorous content in metal is nearly zero because phosphide is not observed.

Cooling rates

Estimates of the cooling rates can be made based on the above observations. Plotting on Fig.1 of [2], the isolated taenite data suggest a cooling rate slightly faster than 10^4 C/Ma. The data from zoned taenite surrounded by kamacite, when plotted on the same diagram, suggests a much faster cooling rate, but this may be artifact due to late nucleation of kamacite. Using the concept of closure, the thin taenite wall with ~31% Ni suggests a cooling rate ~10^4 C/Ma. Similarly, taenite islands with ~39% Ni in zoneless plessite suggest a cooling rate ~10^3 C/Ma. Distance between taenite islands could also be used for the cooling rate estimate. Assuming that diffusion in kamacite controls the island separation, a cooling rate of ~10^4 C/Ma is obtained. Absence of cloudy taenite is also consistent with rapid cooling.

Discussion

Although there are variations in the cooling rates depending on the features used for the calculation, it is

©2019. Japan Geoscience Union. All Right Reserved.

clear that the cooling rate of Tafa (~10^4 C/Ma) is much faster than previously considered [2]. In order to cool at this rate, Tafa has to be located at a shallow depth (~1km from the surface). Because of this, the parent body size cannot be constrained well, except that it is much larger than 10 km in order to be kept warm at ~3.5 Ma (Mn-Cr age [3]). The rapid cooling is consistent with the chronological data. All (Hf-W, Pb-Pb, Mn-Cr and Al-Mg) ages may be identical. Or, the Hf-W age may be older than the rest because of the higher closure temperature.

[1] Brent et al., 2015, EPSL, 45, 193.

[2] Taylor et al., 1987, Icarus, 69, 1.

[3] Gopel et al., 2015, GCA,156,1.

Keywords: primitive achondrite, metallographic cooling rate, parent body

©2019. Japan Geoscience Union. All Right Reserved.

The systematic investigations of high-pressure minerals in lunar basaltic meteorites

*Masaaki Miyahara[1], Kazunari Kozuma[1], Eiji Ohtani[2], Akira Yamaguchi[3], Takeshi Sakai[4], Hiroaki Ohfuji[4], Naotaka Tomioka[5], Yu Kodama[6]

1. Department of Earth and Planetary Systems Science, Graduate School of Science, Hiroshima University, 2. Department of Earth Sciences, Graduate School of Science, Tohoku University, 3. National Institute of Polar Research, 4. Geodynamics Research Center, Ehime University, 5. 5Kochi Institute for Core Sample Research, Japan Agency for Marine-Earth Science and Technology, 6. Marine Works Japan

The Moon has recorded the impact history for ca. 4.5 Ga, which is closely related with the orbit evolution of asteroids and planets in the solar system. The impact events occurred on the moon can be clarified using lunar meteorites. The lunar meteorites have several kinds of evidence for the impact events: e.g., brecciation, shock-induced melting, and high-pressure polymorphs. The high-pressure polymorph is one of the important clues for clarifying the impact events because we can constrain several physical parameters (e.g., shock pressure) for the impact events. However, only a few lunar meteorites were investigated about the high-pressure polymorphs. Several radio-isotope ages in the lunar meteorites were measured to deduce when the impact events occurred. However, the relevance between the radio-isotope ages and the shock features has not been clear. Accordingly, we initiated to investigate the shock features, especially the shock-induced melting and high-pressure polymorphs in the lunar mare basalt, NWA 032, NWA 479, NWA 2727, NWA 2977, and NWA 4898 using FE-SEM, Raman, EMPA, and FIB-TEM techniques to obtain the clues for clarifying the impact events occurred on the moon.

NWA 032 consisted of a basaltic portion and a small amount of breccia. Olivine, Ca-pyroxene, and low-Ca pyroxene occurred as phenocrysts in the basaltic portion. The matrix was filled with spherulitic textures consisting of plagioclase and Ca-pyroxene. Several shock-melt veins and melt-pockets occurred in the basaltic portion. Several olivine grains next to the shock-met veins have transformed into ringwoodite. The estimated shock pressure is ~13 GPa at least. The petrological and mineralogical features of NWA 479 were similar to those of NWA 032. Olivine grains entrained in the shock-melt veins dissociated into bridgmanite + (Mg, Fe)O. The estimated shock pressure is ~23 GPa at least. NWA 4898 showed the basaltic texture. Olivine occurred as phenocrysts. The matrix portion consisted mainly of Ca-pyroxene and plagioclase. A trace amount of silica minerals was entrained in the shock-melt veins. Some silica minerals in the shock-melt veins were stishovite. Ca-pyroxene next to the shock-melt veins dissociated into ahrensite, pyroxene-glass, and (probably) silicate titanite. The estimated shock pressure is ~9 GPa at least. NWA 2977 showed a gabbroitic texture and consisted mainly of olivine, low-Ca pyroxene, Ca-pyroxene, and plagioclase. Olivine grains next to or entrained in the shock-melt veins have transformed into ringwoodite. The estimated shock pressure is ~16 GPa at least. Two third of NWA 2727 was breccia and the other was gabbroitic. The gabbroitic portion consisted of olivine, low-Ca pyroxene, Ca-pyroxene, and plagioclase. The breccia portion included silica besides the fragments of the gabbroitic portions. Silica minerals entrained in the shock-melt veins or melt-pockets have transformed into coesite. The estimated shock pressure is ~3 GPa at least.

The shock-induced melting textures were observed in all investigated lunar mare basalt samples. Although the high-pressure polymorphs of olivine, Ca-pyroxene, and silica minerals were identified, the high-pressure polymorphs of plagioclase, which are abundant in other shocked meteorites, were not identified. In addition to previous studies [1–3], the present study reveals that many kinds of

©2019. Japan Geoscience Union. All Right Reserved.

high-pressure polymorphs occur in the lunar mare basalt, implying that most lunar mare basalts have experienced the heavy impact events.

References

[1] Ohtani E. et al. *PNAS* 108, 463–46, 2011.

[2] Miyahara M. et al. *NatureGeosci* 4:1737, 2013.

[3] Kayama M. et al. Sci.Adv. 4: eaar4378, 2018.

Keywords: Moon, Lunar mare basalt, High-pressure minerals

©2019. Japan Geoscience Union. All Right Reserved.

Bulk chemical analysis of iron meteorites by LA-ICP-MS

*Akira Yamaguchi[1], Naoki Shirai[2], Makiko K. Haba[3]

1. National Institute of Polar Research, 2. Tokyo Metropolitan University, 3. Tokyo Institute of Technology

Iron meteorites are Fe-Ni alloys with minor elements such as Co, P, S, and C. They are classified on the basis of textures (e.g., Widmanstatten pattern) and bulk chemical compositions (e.g., Ni, Ge, Ir). We performed bulk chemical analysis of iron meteorites by using an LA-ICP-MS and compared with the data obtained by INAA.

We measured five iron meteorites, Canyon Diablo (IAB, coarse octahedrite), Toluca (IAB, coarse octahedrite), Cape York (IIIAB, medium octahedrite), Muonionalusta (IV, fine octahedrite) and Dronino (ungrouped, ataxite) by using an LA-ICP-MS and INAA. Polished thick sections are prepared for LA-ICP-MS analysis. Polished thick sections of the meteorites were examined using an optical microscope, a scanning electron microscope, and an electron microprobe analyzer to observe the textures. A Thermo Element XR ICP-MS coupled to a CETAC LSX-213 laser was operated in low resolution mode (R = 300). The peaks monitored are ^{31}P, ^{34}S, ^{57}Fe, ^{59}Co, ^{60}Ni, ^{65}Cu, ^{69}Ga, ^{74}Ge, ^{95}Mo, ^{99}Ru, ^{103}Rh, ^{105}Pd, ^{182}W, ^{185}Re, ^{189}Os, ^{193}Ir, ^{194}Pt and ^{197}Au. Analyses in line and/or scanning modes were performed on a representative area of polished sections, using a 100 μm beam spot at 20 μm/sec., 20 Hz repetition rate. Typical analytical time was several minutes. Elemental abundances were obtained using Hoba (IVB, ataxite) and North Chile (IIAB, hexahedrite) iron meteorites as standard reference samples.

In INAA, samples weighing about 150 mg were firstly irradiated for 10 sec. at a neutron flux of 4.6 x 1012 $cm^{-2}s^{-1}$ at Institute for Integrated Radiation and Nuclear Science, Kyoto University for the determination of Co, Ni, Cu, Ge, and Rh. The same samples were reirradiated for 4 hrs at a neutron flux of 5.6 x 1012 $cm^{-2}s^{-1}$ at Institute for Integrated Radiation and Nuclear Science, Kyoto University for the determination of Cr, Fe, Co, Ni, Ga, As, Mo, Ru, Sb, W, Re, Os, Ir, Pt and Au.

We determined twenty elements (P, S, Fe, Co, Ni, Cu, Ga, Ge, As, Mo, Ru, Rh, Pd, Sb, W, Re, Os, Ir, Pt, and Au) for the five iron meteorites. Our results obtained by using two analytical methods were generally consistent with each other. However, our data of Muonionalusta are slightly different from literature values due to the large-scale heterogeneity of the meteorite (e.g., due to magmatic process). The abundance of some elements (e.g., Ru, Rh, Re, Ir) obtained from LA-ICP-MS data are higher than those from INAA due to the sample heterogeneity. It is possible to avoid this problem by choosing representative areas of the surface. Our study demonstrates that LA-ICP-MS has the potential to analyze a large number of iron meteorites.

Keywords: Iron meteorites, Bulk chemical analysis

©2019. Japan Geoscience Union. All Right Reserved.

[E] Poster | P (Space and Planetary Sciences)：P-EM Solar-Terrestrial Sciences, Space Electromagnetism & Space Environment

Mon. May 27, 2019 1:45 PM - 3:15 PM JST | Mon. May 27, 2019 4:45 AM - 6:15 AM UTC | Poster Hall International Exhibition Hall8, Makuhari Messe_1

[P-EM10] Multi-scale Coupling in the Magnetosphere-Ionosphere-Thermosphere System

convener:Yue Deng(University of Texas at Arlington), Toshi Nishimura(Boston University), Huixin Liu(Earth and Planetary Science Division, Kyushu University SERC, Kyushu University), Yanshi Huang(Harbin Institute of Technology, Shenzhen)

Determining the effects of energy deposition and transport, and momentum exchange across different spatial and temporal scales is an important objective in the M-I-T system, due to the clear evidence of multi-scale forcing. Coupling over multiple scales is also a critical challenge since observational and modeling methodologies for bridging different scales do not presently exist. This session solicits presentations on a wide range of coupling processes in the high-latitude M-I-T system from global to small-scale processes and related solar wind forcing. Relevant topics include (but are not limited to) (1) density structures and temperature gradients (polar cap, cusp, plume, trough, irregularities); (2) convection (flow channels, SAPS) and FAC; (3) energy transfer and deposition by precipitation and ULF waves, conductivity, aurora, and heating; and (4) coupling and feedback into the magnetosphere. Discussions of relevant multi-scale observations by means of multiple instruments, including space and ground-based, modeling and data science are encouraged.

[PEM10-P01] Atmospheric responses in both hemispheres to relativistic electron precipitation

*Yoshimasa Tanaka[1,13,14], Takanori Nishiyama[1,14], Akira Kadokura[1,13,14], Mitsunori Ozaki[2], Yoshizumi Miyoshi[3], Shin-ichiro Oyama[3,15], Ryuho Kataoka[1,14], Masaki Tsutsumi[1,14], Koji Nishimura[1,13,14], Kaoru Sato[4], Yoshiya Kasahara[2], Atsushi Kumamoto[5], Fuminori Tsuchiya[5], Mizuki Fukizawa[5], Mitsuru Hikishima[6], Shoya Matsuda[6], Ayako Matsuoka[6], Iku Shinohara[6], Masahito Nose[3], Tsutomu Nagatsuma[7], Manabu Shinohara[8], Akiko Fujimoto[9], Mariko Teramoto[3], Reiko Nomura[10], Akira Sessai Yukimatu[1,14], Keisuke Hosokawa[11], Masafumi Shoji[3], Ralph Latteck[12] (1.National Institute of Polar Research, 2.Institute of Science and Engineering, Kanazawa University, 3.Institute for Space-Earth Environmental Research, Nagoya University, 4.Graduate School of Science, The University of Tokyo, 5.Graduate School of Science, Tohoku University, 6.Japan aerospace exploration agency, Institute of space and astronautical science, 7.National Institute of Information and Communications Technology, 8.Kagoshima National College of Technology, 9.Kyushu Institute of Technology, 10.National Observatory of Japan, 11.Department of Communication Engineering and Informatics, University of Electro-Communications, 12.Leibniz-Institute of Atmospheric Physics e.V. at the University Rostock, Germany, 13.Polar Environment Data Science Center, Joint-Support Center for Data Science Research, Research Organization of Information and Systems, 14.The Graduate University for Advanced Studies (SOKENDAI), 15.University of Oulu, Finland)

[PEM10-P02] Comparison of precipitating particle energy of proton aurora at geomagnetic conjugate points

*Makoto Taguchi[1], Tatsuki Nishijima[1], Akira Kadokura[2] (1.Rikkyo University, 2.Research Organization of Information and Systems)

[PEM10-P03] A regularized deep convolutional general adversarial network (R-DCGAN) for total electron content map completion

*Mingwu Jin[1], Zhou Chen[2,3], Yue Deng[1], Yang Pan[1], Jin-Song Wang[2] (1.University of Texas at Arlington, 2.Institute of Space Science and Technology, Nanchang University, Nanchang, China, 3.Key Laboratory of Space Weather, National Center for Space Weather, China Meteorological Administration, Beijing, China)

[PEM10-P04] A long-lasting auroral bright spot around magnetic north pole: Is it the evidence of stable magnetic reconnection?

*Qing-He Zhang[1], Guo-Cheng Shen[1], Yong-Liang Zhang[2], Kjellmar Oksavik[3], Michael Lockwood[4], Zan-Yang Xing[1], Yu-Zhang Ma[1] (1.Institute of Space Sciences, Shandong University, Weihai, China, 2.The Johns Hopkins University Applied Physics Laboratory, Laurel, Maryland, USA, 3.Birkeland Centre for Space

Science, University of Bergen, Bergen, Norway, 4.Department of Meteorology, University of Reading, Earley Gate, Post Office Box 243, RG6 6BB, UK.)

[PEM10-P05] Statistical study of the relationship between ion upflow and field-aligned current in the topside ionosphere for both hemispheres during disturbed and quiet times

Shan-Yu Zhou[1], *Qing-He Zhang[1], P. T. Jayachandran[2], Kjellmar Oksavik[3], Larry Lyons[4], Zan-Yang Xing[1], Yu-Zhang Ma[1], Marc Hairston[5], Yong Wang[1] (1.Institute of Space Sciences, Shandong University, Weihai, China, 2.Physics Department, University of New Brunswick, Fredericton, New Brunswick, Canada, 3.Birkeland Centre for Space Science, University of Bergen, Bergen, Norway, 4.Department of Atmospheric and Oceanic Sciences, University of California, Los Angeles, California, USA, 5.William B. Hanson Center for Space Sciences, University of Texas at Dallas, Richardson, Texas, USA)

[PEM10-P06] SAPS in the 2013 March 17 Storm Event: Initial Results from the Coupled Magnetosphere-Ionosphere-Thermosphere Model

*Dong Lin[1,2], Wenbin Wang[2], Wayne Scales[1], Kevin Pham[2], Jing Liu[2], Binzheng Zhang[2], Viacheslav Merkin[3], Xueling Shi[1] (1.Virginia Tech, 2.High Altitude Observatory, NCAR, 3.APL, John Hopkins Univ.)

[PEM10-P07] **Westward turning motions of nighttime medium-scale traveling ionospheric disturbances (MSTIDs) at the equatorward side of the dusk side auroral oval associated with auroral brightening**

*Sneha Yadav[1,2], Kazuo Shiokawa[1], Shin-ichiro Oyama[1,3,4], Yuichi Otsuka[1] (1.ISEE, Nagoya University, Nagoya, Japan, 2.SPL, VSSC, India, 3.Ionosphere Research Unit, University of Oulu, Oulu, Finland, 4.NIPR, Tachikawa, Japan)

Atmospheric responses in both hemispheres to relativistic electron precipitation

*Yoshimasa Tanaka[1,13,14], Takanori Nishiyama[1,14], Akira Kadokura[1,13,14], Mitsunori Ozaki[2], Yoshizumi Miyoshi[3], Shin-ichiro Oyama[3,15], Ryuho Kataoka[1,14], Masaki Tsutsumi[1,14], Koji Nishimura[1,13,14], Kaoru Sato[4], Yoshiya Kasahara[2], Atsushi Kumamoto[5], Fuminori Tsuchiya[5], Mizuki Fukizawa[5], Mitsuru Hikishima[6], Shoya Matsuda[6], Ayako Matsuoka[6], Iku Shinohara[6], Masahito Nose[3], Tsutomu Nagatsuma[7], Manabu Shinohara[8], Akiko Fujimoto[9], Mariko Teramoto[3], Reiko Nomura[10], Akira Sessai Yukimatu[1,14], Keisuke Hosokawa[11], Masafumi Shoji[3], Ralph Latteck[12]

1. National Institute of Polar Research, 2. Institute of Science and Engineering, Kanazawa University, 3. Institute for Space-Earth Environmental Research, Nagoya University, 4. Graduate School of Science, The University of Tokyo, 5. Graduate School of Science, Tohoku University, 6. Japan aerospace exploration agency, Institute of space and astronautical science, 7. National Institute of Information and Communications Technology, 8. Kagoshima National College of Technology, 9. Kyushu Institute of Technology, 10. National Observatory of Japan, 11. Department of Communication Engineering and Informatics, University of Electro-Communications, 12. Leibniz-Institute of Atmospheric Physics e.V. at the University Rostock, Germany, 13. Polar Environment Data Science Center, Joint-Support Center for Data Science Research, Research Organization of Information and Systems, 14. The Graduate University for Advanced Studies (SOKENDAI), 15. University of Oulu, Finland

Relativistic electron precipitation (REP) in the polar atmosphere has been paid attention to because it changes atmospheric composition, causing ozone depletion after migrating to the lower altitude during polar winter. A plausible mechanism for REP is the interaction with magnetospheric plasma waves, such as electromagnetic ion cyclotron (EMIC) waves and whistler-mode chorus waves. Previous studies have already shown that EMIC waves can effectively drive REP, however, observational evidence that chorus waves can drive REP was lacking. In this study we present direct comparison between magnetospheric plasma waves and polar mesosphere winter echoes (PMWE) simultaneously observed with the Arase satellite and high-power Mesosphere, Stratosphere and Troposphere (MST) radars in both hemispheres, PANSY and MAARSY. PMWE can be related to the ionization in the mesosphere due to REP. The PMWE were observed at 03-07 UT on March 21, 2017 during the passage of corotating interaction region (CIR), during which the Arase footprints were close to Syowa Station (SYO; −69.00S, 39.58E), Antarctica, and Husafell (HUS; 65.67N, −21.03E), Iceland.
The observational results are summarized as follows. (1) EMIC waves and whistler-mode chorus waves were observed by Arase near the equatorial magnetosphere during 02:30-04:45 UT and 04:45-07:00 UT, respectively. (2) PMWE were detected with both the MAARSY radar at Andøya (AND; 69.30N, 16.04E), Norway, and the PANSY radar at SYO, Antarctica, during 04:45-07:00 UT, which was the recovery phase of an isolated substorm. We believe this is the first time PMWE have been observed in both hemispheres at exactly the same time. (3) During 04:45-07:00 UT, the temporal variation of the chorus wave power was similar to those of the PMWE power in the both hemispheres. (4) The PMWE observed at SYO during 03:00-04:00 UT before the substorm onset was consistent with the occurrence of the EMIC waves. The item (2) shows direct evidence that chorus waves during the substorm recovery phase cause REP. We estimated the resonance energy of electrons interacting with the observed LBC waves, however, the estimated energy was too low to cause PMWE at an altitude lower than 70 km. However, we found that the resonance energy becomes greater than 1 MeV, if LBC waves propagate to the magnetic latitude greater than 30 degrees and resonate with energetic electrons there. As for item (4), the PMWE observed at SYO during 03:00-04:00 can be related to wave-particle interaction with EMIC waves, which may be generated inside the plasmapause by ring-current hot ions with temperature anisotropy. This anisotropy

©2019. Japan Geoscience Union. All Right Reserved.

was caused by magnetospheric compression due to increasing solar wind dynamic pressure during 01:00–06:00 UT just after the arrival of the CIR. Since CIRs are main sources of geomagnetic disturbances during the declining phase of the solar cycle and solar minimum, this event is not rare but rather a common atmospheric response caused by interaction between recurrent large-scale solar wind structures and geospace.

Keywords: Polar Mesosphere Winter Echoes, Arase satellite, PANSY radar, MAARSY radar, relativistic electron precipitation, magnetospheric plasma waves

©2019. Japan Geoscience Union. All Right Reserved.

Comparison of precipitating particle energy of proton aurora at geomagnetic conjugate points

*Makoto Taguchi[1], Tatsuki Nishijima[1], Akira Kadokura[2]

1. Rikkyo University, 2. Research Organization of Information and Systems

It is expected that mirror images of aurora are observed at geomagnetic conjugate points in the northern and southern auroral zones connected by a geomagnetic field line. However, geomagnetic conjugate auroras often show non-conjugacy, which reflects north-south asymmetry of the solar wind, the magnetosphere and the ionospheres. In other words acceleration mechanism of auroral particles may be studied by comparing aurora simultaneously occurring at geomagnetic conjugate points. A hydrogen Balmer beta emission at the wavelength of 486.1 nm which is the brightest among the proton auroral lines was observed at a pair of geomagnetic conjugate points to compare precipitating particle energy. Two identical Proton Auroral Specrographs (PASs) which obtain auroral spectra along a geomagnetic meridian at a rate of 1 image/min were installed at Tjornes in Iceland and Syowa Station in Antarctica. Data obtained during a period from September 4, 2018 to October 9, 2018 were analyzed to derive an average kinetic energy of precipitating protons along a local geomagnetic field line from a Doppler shift of the H beta line. As a result we are succeeded in simultaneous observations of proton auroras at both conjugate points in 5 nights on September 4, 5, 6, 7 , and 10. The average energies of precipitating protons range from 0 keV to 7 keV, and sometimes show a periodical variation with a period of 4 - 5 min. Conjugacy of precipitating particle energy will be discussed in the presentation.

©2019. Japan Geoscience Union. All Right Reserved.

A regularized deep convolutional general adversarial network (R-DCGAN) for total electron content map completion

*Mingwu Jin[1], Zhou Chen[2,3], Yue Deng[1], Yang Pan[1], Jin-Song Wang[2]

1. University of Texas at Arlington, 2. Institute of Space Science and Technology, Nanchang University, Nanchang, China, 3. Key Laboratory of Space Weather, National Center for Space Weather, China Meteorological Administration, Beijing, China

Observations with a complete global coverage are important for space physics research and applications. However, due to the technical limitations and costs, such a complete global coverage is often unavailable. Thus, data filling algorithms are often pursued to fill missing data gaps to create a global map from the incomplete data. In this work, a novel deep learning algorithm, regularized deep convolutional generative adversarial network (R-DCGAN), is developed by adding an extra discriminator to the conventional DCGAN to fill the missing data of total electron content (TEC) map images. R-DCGAN incorporates the knowledge from reference TEC maps of the International Global Navigation Satellite Systems Service Ionosphere Working Group to achieve much better TEC map completion performance than the conventional DCGAN as demonstrated by both synthetic and real data. The R-DCGAN framework can be extended to other fields of space sciences to address the missing observation data issues.

Keywords: Deep learning method, TEC , map completion

©2019. Japan Geoscience Union. All Right Reserved.

A long-lasting auroral bright spot around magnetic north pole: Is it the evidence of stable magnetic reconnection?

*Qing-He Zhang[1], Guo-Cheng Shen[1], Yong-Liang Zhang[2], Kjellmar Oksavik[3], Michael Lockwood[4], Zan-Yang Xing[1], Yu-Zhang Ma[1]

1. Institute of Space Sciences, Shandong University, Weihai, China, 2. The Johns Hopkins University Applied Physics Laboratory, Laurel, Maryland, USA, 3. Birkeland Centre for Space Science, University of Bergen, Bergen, Norway, 4. Department of Meteorology, University of Reading, Earley Gate, Post Office Box 243, RG6 6BB, UK.

An intense and large auroral bright spot appears around the magnetic north pole observed by the Special Sensor Ultraviolet Spectrographic Imager (SSUSI) on board four different Defense Meteorological Satellite Program (DMSP) satellites during long time northward IMF conditions. The bright spot is even brighter than aurora in the auroral oval which is about 5-10˚ magnetic latitude equatorward of the bright spot. The bright spot is lasting about 8 hours, and sometimes appears as a cyclone-shape with a clockwise rotation. The DMSP in situ plasma observations suggest that the bright spot is clear associated with electron invert-V acceleration with 10s keV energy electron precipitations around the center regions and 1s keV energy electron precipitations around the egde regions. There are also strong flow shears between the two sides of the bright spot: strong sunward flows on the duskside and antisunward flows on the dawnside. These types of plasma should come from the high-latitude lobe region of the magnetotail due to the high-latitude lobe magnetic reconnections. Is it the evidence of stable lobe reconnection during long time northward IMF conditions? The detail and further analysis should be pursued in the following studies.

Keywords: Auroral bright spot, Magnetosphere-ionosphere coupling, High-latitude lobe magnetic reconnection, Stable reconnection

©2019. Japan Geoscience Union. All Right Reserved.

Statistical study of the relationship between ion upflow and field-aligned current in the topside ionosphere for both hemispheres during disturbed and quiet times

Shan-Yu Zhou[1], *Qing-He Zhang[1], P. T. Jayachandran[2], Kjellmar Oksavik[3], Larry Lyons[4], Zan-Yang Xing[1], Yu-Zhang Ma[1], Marc Hairston[5], Yong Wang[1]

1. Institute of Space Sciences, Shandong University, Weihai, China, 2. Physics Department, University of New Brunswick, Fredericton, New Brunswick, Canada, 3. Birkeland Centre for Space Science, University of Bergen, Bergen, Norway, 4. Department of Atmospheric and Oceanic Sciences, University of California, Los Angeles, California, USA, 5. William B. Hanson Center for Space Sciences, University of Texas at Dallas, Richardson, Texas, USA

A statistical study of ion upflow and field-aligned currents (FACs) has been performed in the topside ionosphere of both hemispheres for magnetic quiet and disturbed times by using DMSP satellite observations from 2010-2013. Distributions in MLT/MLAT reveal that ion upflow shows a dawn-dusk asymmetry distribution that corresponds well with the region 1 field-aligned currents. In addition, there are highest occurrence regions near noon and within the near midnight auroral disturbance area. These correspond to cusp and nightside dynamical processes, respectively. Both the ion upflow occurrence and FAC regions expand equatorward to a wider area during disturbed times.

Keywords: Ion upflows, Field-aligned current, Magnetosphere-ionosphere coupling

©2019. Japan Geoscience Union. All Right Reserved.

SAPS in the 2013 March 17 Storm Event: Initial Results from the Coupled Magnetosphere-Ionosphere-Thermosphere Model

*Dong Lin[1,2], Wenbin Wang[2], Wayne Scales[1], Kevin Pham[2], Jing Liu[2], Binzheng Zhang[2], Viacheslav Merkin[3], Xueling Shi[1]

1. Virginia Tech, 2. High Altitude Observatory, NCAR, 3. APL, John Hopkins Univ.

Subauroral polarization stream (SAPS) are latitudinally narrow flow channels of large westward plasma drifts in the subauroral ionosphere. In this study, the global structure and dynamic evolution of SAPS are investigated by using the National Center for Atmospheric Research (NCAR) Coupled Magnetosphere-Ionosphere-Thermosphere (CMIT) model with Ring Current extension, namely the LFM-TIEGCM-RCM (LTR) model, to simulate the 2013 St. Patrick's Day storm event. This is the first time that the global distribution and temporal evolution of SAPS are investigated using first-principle models. The model shows a strong westward ion drift channel formed equatorward of the auroral electron precipitation boundary on the duskside, which is identified as the SAPS structure. The simulated ion drift velocity and auroral electron precipitation sampled along the trajectory of the DMSP F18 satellite are in good agreement with the satellite measurements. SAPS initiate in the pre-dusk sector when the interplanetary magnetic field (IMF) turns southward. SAPS latitude generally decreases with magnetic local time (MLT) from dusk to midnight. The SAPS channel shows wedge, inverse wedge, and crescent morphologies during the storm, and becomes discontinuous when the IMF is weakly southward. The SAPS mean latitude has a correlation coefficient of 0.77 with the Dst index. The mean latitude moves equatorward and the flow channel broadens in the storm main phase. The simulation results are consistent with observational studies. They also illustrate the global distributions and highly dynamic behaviors of SAPS that are not readily apparent from observation data.

Keywords: SAPS, Magnetosphere-Ionosphere-Thermosphere coupling, LFM-TIEGCM-RCM

©2019. Japan Geoscience Union. All Right Reserved.

Westward turning motions of nighttime medium-scale traveling ionospheric disturbances (MSTIDs) at the equatorward side of the dusk side auroral oval associated with auroral brightening

*Sneha Yadav[1,2], Kazuo Shiokawa[1], Shin-ichiro Oyama[1,3,4], Yuichi Otsuka[1]

1. ISEE, Nagoya University, Nagoya, Japan, 2. SPL, VSSC, India, 3. Ionosphere Research Unit, University of Oulu, Oulu, Finland, 4. NIPR, Tachikawa, Japan

The characteristics of high-latitude nighttime medium-scale traveling ionospheric disturbances (MSTIDs) have not been well investigated using all-sky imagers because of the hindrance caused by the bright aurora. The limited results on the propagation characteristics of MSTIDs over high-latitudes hindered the progress in our understanding on these dynamical structure. In a case study carried out by Shiokawa et al. (JGR, 2012), an event of oscillating MSTIDs was reported over Tromsø (69.6˚N, 19.2˚E; corrected geomagnetic latitude: 66.6˚N), which was observed to be associated with auroral brightening. However, after this case study, which comprised of only one event, no observations showing oscillating motion of MSTIDs have been reported till date. In this study, for the first time, the comprehensive investigation on the westward turning of the MSTIDs in the equatorward side of the dusk side auroral oval has been performed. The all-sky imaging data of 630.0 nm airglow emissions during 2010-2018 are used to study the motions of MSTIDs over Tromsø. The results indicate that the nighttime MSTIDs primarily exhibit eastward motion under quiet magnetic conditions but turned in the westward direction during the active geomagnetic conditions. The turning of MSTIDs in the westward direction were invariably associated with the auroral brightening observed at the poleward edge of the all-sky image and localized magnetic field perturbations observed by ground-based magnetometers at Tromsø. The interesting aspect of the observations is the fact that these westward moving MSTIDs again turned in the eastward direction when the geomagnetic disturbance ceases. The SuperDARN (Super Dual Auroral Radar Network) convection maps revealed that the location of Tromsø was inside/outside the convection cell region during the time of appearance of westward/eastward moving MSTIDs. The Doppler shift measurement of the 630-nm airglow by a Fabry-Perot interferometer at Tromsø showed that northeastward winds were predominant during the appearance of eastward moving MSTIDs. The cause of the observed MSTIDs remains in question as they might either be triggered by atmospheric gravity waves or by Perkins instability. These experimental evidences suggest that the MSTIDs tend to move eastward in accordance with the background F-region dynamo electric field, but show westward motion under the influence of electric field associated with auroral activities in the dusk side of two-cell convection pattern.

Keywords: MSTIDs, Auroral oval, Airglow

©2019. Japan Geoscience Union. All Right Reserved.

[E] Poster | P (Space and Planetary Sciences)：P-EM Solar-Terrestrial Sciences, Space Electromagnetism & Space Environment

Mon. May 27, 2019 5:15 PM - 6:30 PM JST | Mon. May 27, 2019 8:15 AM - 9:30 AM UTC | Poster Hall International Exhibition Hall8, Makuhari Messe_4

[P-EM10] Multi-scale Coupling in the Magnetosphere-Ionosphere-Thermosphere System

convener:Yue Deng(University of Texas at Arlington), Toshi Nishimura(Boston University), Huixin Liu(Earth and Planetary Science Division, Kyushu University SERC, Kyushu University), Yanshi Huang(Harbin Institute of Technology, Shenzhen)

Determining the effects of energy deposition and transport, and momentum exchange across different spatial and temporal scales is an important objective in the M-I-T system, due to the clear evidence of multi-scale forcing. Coupling over multiple scales is also a critical challenge since observational and modeling methodologies for bridging different scales do not presently exist. This session solicits presentations on a wide range of coupling processes in the high-latitude M-I-T system from global to small-scale processes and related solar wind forcing. Relevant topics include (but are not limited to) (1) density structures and temperature gradients (polar cap, cusp, plume, trough, irregularities); (2) convection (flow channels, SAPS) and FAC; (3) energy transfer and deposition by precipitation and ULF waves, conductivity, aurora, and heating; and (4) coupling and feedback into the magnetosphere. Discussions of relevant multi-scale observations by means of multiple instruments, including space and ground-based, modeling and data science are encouraged.

[PEM10-P01] Atmospheric responses in both hemispheres to relativistic electron precipitation

*Yoshimasa Tanaka[1,13,14], Takanori Nishiyama[1,14], Akira Kadokura[1,13,14], Mitsunori Ozaki[2], Yoshizumi Miyoshi[3], Shin-ichiro Oyama[3,15], Ryuho Kataoka[1,14], Masaki Tsutsumi[1,14], Koji Nishimura[1,13,14], Kaoru Sato[4], Yoshiya Kasahara[2], Atsushi Kumamoto[5], Fuminori Tsuchiya[5], Mizuki Fukizawa[5], Mitsuru Hikishima[6], Shoya Matsuda[6], Ayako Matsuoka[6], Iku Shinohara[6], Masahito Nose[3], Tsutomu Nagatsuma[7], Manabu Shinohara[8], Akiko Fujimoto[9], Mariko Teramoto[3], Reiko Nomura[10], Akira Sessai Yukimatu[1,14], Keisuke Hosokawa[11], Masafumi Shoji[3], Ralph Latteck[12] (1.National Institute of Polar Research, 2.Institute of Science and Engineering, Kanazawa University, 3.Institute for Space-Earth Environmental Research, Nagoya University, 4.Graduate School of Science, The University of Tokyo, 5.Graduate School of Science, Tohoku University, 6.Japan aerospace exploration agency, Institute of space and astronautical science, 7.National Institute of Information and Communications Technology, 8.Kagoshima National College of Technology, 9.Kyushu Institute of Technology, 10.National Observatory of Japan, 11.Department of Communication Engineering and Informatics, University of Electro-Communications, 12.Leibniz-Institute of Atmospheric Physics e.V. at the University Rostock, Germany, 13.Polar Environment Data Science Center, Joint-Support Center for Data Science Research, Research Organization of Information and Systems, 14.The Graduate University for Advanced Studies (SOKENDAI), 15.University of Oulu, Finland)

[PEM10-P02] Comparison of precipitating particle energy of proton aurora at geomagnetic conjugate points

*Makoto Taguchi[1], Tatsuki Nishijima[1], Akira Kadokura[2] (1.Rikkyo University, 2.Research Organization of Information and Systems)

[PEM10-P03] A regularized deep convolutional general adversarial network (R-DCGAN) for total electron content map completion

*Mingwu Jin[1], Zhou Chen[2,3], Yue Deng[1], Yang Pan[1], Jin-Song Wang[2] (1.University of Texas at Arlington, 2.Institute of Space Science and Technology, Nanchang University, Nanchang, China, 3.Key Laboratory of Space Weather, National Center for Space Weather, China Meteorological Administration, Beijing, China)

[PEM10-P04] A long-lasting auroral bright spot around magnetic north pole: Is it the evidence of stable magnetic reconnection?

*Qing-He Zhang[1], Guo-Cheng Shen[1], Yong-Liang Zhang[2], Kjellmar Oksavik[3], Michael Lockwood[4], Zan-Yang Xing[1], Yu-Zhang Ma[1] (1.Institute of Space Sciences, Shandong University, Weihai, China, 2.The Johns Hopkins University Applied Physics Laboratory, Laurel, Maryland, USA, 3.Birkeland Centre for Space

Science, University of Bergen, Bergen, Norway, 4.Department of Meteorology, University of Reading, Earley Gate, Post Office Box 243, RG6 6BB, UK.)

[PEM10-P05] Statistical study of the relationship between ion upflow and field-aligned current in the topside ionosphere for both hemispheres during disturbed and quiet times

Shan-Yu Zhou[1], *Qing-He Zhang[1], P. T. Jayachandran[2], Kjellmar Oksavik[3], Larry Lyons[4], Zan-Yang Xing[1], Yu-Zhang Ma[1], Marc Hairston[5], Yong Wang[1] (1.Institute of Space Sciences, Shandong University, Weihai, China, 2.Physics Department, University of New Brunswick, Fredericton, New Brunswick, Canada, 3.Birkeland Centre for Space Science, University of Bergen, Bergen, Norway, 4.Department of Atmospheric and Oceanic Sciences, University of California, Los Angeles, California, USA, 5.William B. Hanson Center for Space Sciences, University of Texas at Dallas, Richardson, Texas, USA)

[PEM10-P06] SAPS in the 2013 March 17 Storm Event: Initial Results from the Coupled Magnetosphere-Ionosphere-Thermosphere Model

*Dong Lin[1,2], Wenbin Wang[2], Wayne Scales[1], Kevin Pham[2], Jing Liu[2], Binzheng Zhang[2], Viacheslav Merkin[3], Xueling Shi[1] (1.Virginia Tech, 2.High Altitude Observatory, NCAR, 3.APL, John Hopkins Univ.)

[PEM10-P07] **Westward turning motions of nighttime medium-scale traveling ionospheric disturbances (MSTIDs) at the equatorward side of the dusk side auroral oval associated with auroral brightening**

*Sneha Yadav[1,2], Kazuo Shiokawa[1], Shin-ichiro Oyama[1,3,4], Yuichi Otsuka[1] (1.ISEE, Nagoya University, Nagoya, Japan, 2.SPL, VSSC, India, 3.Ionosphere Research Unit, University of Oulu, Oulu, Finland, 4.NIPR, Tachikawa, Japan)

Atmospheric responses in both hemispheres to relativistic electron precipitation

*Yoshimasa Tanaka[1,13,14], Takanori Nishiyama[1,14], Akira Kadokura[1,13,14], Mitsunori Ozaki[2], Yoshizumi Miyoshi[3], Shin-ichiro Oyama[3,15], Ryuho Kataoka[1,14], Masaki Tsutsumi[1,14], Koji Nishimura[1,13,14], Kaoru Sato[4], Yoshiya Kasahara[2], Atsushi Kumamoto[5], Fuminori Tsuchiya[5], Mizuki Fukizawa[5], Mitsuru Hikishima[6], Shoya Matsuda[6], Ayako Matsuoka[6], Iku Shinohara[6], Masahito Nose[3], Tsutomu Nagatsuma[7], Manabu Shinohara[8], Akiko Fujimoto[9], Mariko Teramoto[3], Reiko Nomura[10], Akira Sessai Yukimatu[1,14], Keisuke Hosokawa[11], Masafumi Shoji[3], Ralph Latteck[12]

1. National Institute of Polar Research, 2. Institute of Science and Engineering, Kanazawa University, 3. Institute for Space-Earth Environmental Research, Nagoya University, 4. Graduate School of Science, The University of Tokyo, 5. Graduate School of Science, Tohoku University, 6. Japan aerospace exploration agency, Institute of space and astronautical science, 7. National Institute of Information and Communications Technology, 8. Kagoshima National College of Technology, 9. Kyushu Institute of Technology, 10. National Observatory of Japan, 11. Department of Communication Engineering and Informatics, University of Electro-Communications, 12. Leibniz-Institute of Atmospheric Physics e.V. at the University Rostock, Germany, 13. Polar Environment Data Science Center, Joint-Support Center for Data Science Research, Research Organization of Information and Systems, 14. The Graduate University for Advanced Studies (SOKENDAI), 15. University of Oulu, Finland

Relativistic electron precipitation (REP) in the polar atmosphere has been paid attention to because it changes atmospheric composition, causing ozone depletion after migrating to the lower altitude during polar winter. A plausible mechanism for REP is the interaction with magnetospheric plasma waves, such as electromagnetic ion cyclotron (EMIC) waves and whistler-mode chorus waves. Previous studies have already shown that EMIC waves can effectively drive REP, however, observational evidence that chorus waves can drive REP was lacking. In this study we present direct comparison between magnetospheric plasma waves and polar mesosphere winter echoes (PMWE) simultaneously observed with the Arase satellite and high-power Mesosphere, Stratosphere and Troposphere (MST) radars in both hemispheres, PANSY and MAARSY. PMWE can be related to the ionization in the mesosphere due to REP. The PMWE were observed at 03-07 UT on March 21, 2017 during the passage of corotating interaction region (CIR), during which the Arase footprints were close to Syowa Station (SYO; −69.00S, 39.58E), Antarctica, and Husafell (HUS; 65.67N, −21.03E), Iceland.
The observational results are summarized as follows. (1) EMIC waves and whistler-mode chorus waves were observed by Arase near the equatorial magnetosphere during 02:30-04:45 UT and 04:45-07:00 UT, respectively. (2) PMWE were detected with both the MAARSY radar at Andøya (AND; 69.30N, 16.04E), Norway, and the PANSY radar at SYO, Antarctica, during 04:45-07:00 UT, which was the recovery phase of an isolated substorm. We believe this is the first time PMWE have been observed in both hemispheres at exactly the same time. (3) During 04:45-07:00 UT, the temporal variation of the chorus wave power was similar to those of the PMWE power in the both hemispheres. (4) The PMWE observed at SYO during 03:00-04:00 UT before the substorm onset was consistent with the occurrence of the EMIC waves. The item (2) shows direct evidence that chorus waves during the substorm recovery phase cause REP. We estimated the resonance energy of electrons interacting with the observed LBC waves, however, the estimated energy was too low to cause PMWE at an altitude lower than 70 km. However, we found that the resonance energy becomes greater than 1 MeV, if LBC waves propagate to the magnetic latitude greater than 30 degrees and resonate with energetic electrons there. As for item (4), the PMWE observed at SYO during 03:00-04:00 can be related to wave-particle interaction with EMIC waves, which may be generated inside the plasmapause by ring-current hot ions with temperature anisotropy. This anisotropy

©2019. Japan Geoscience Union. All Right Reserved.

was caused by magnetospheric compression due to increasing solar wind dynamic pressure during 01:00–06:00 UT just after the arrival of the CIR. Since CIRs are main sources of geomagnetic disturbances during the declining phase of the solar cycle and solar minimum, this event is not rare but rather a common atmospheric response caused by interaction between recurrent large-scale solar wind structures and geospace.

Keywords: Polar Mesosphere Winter Echoes, Arase satellite, PANSY radar, MAARSY radar, relativistic electron precipitation, magnetospheric plasma waves

©2019. Japan Geoscience Union. All Right Reserved.

Comparison of precipitating particle energy of proton aurora at geomagnetic conjugate points

*Makoto Taguchi[1], Tatsuki Nishijima[1], Akira Kadokura[2]

1. Rikkyo University, 2. Research Organization of Information and Systems

It is expected that mirror images of aurora are observed at geomagnetic conjugate points in the northern and southern auroral zones connected by a geomagnetic field line. However, geomagnetic conjugate auroras often show non-conjugacy, which reflects north-south asymmetry of the solar wind, the magnetosphere and the ionospheres. In other words acceleration mechanism of auroral particles may be studied by comparing aurora simultaneously occurring at geomagnetic conjugate points. A hydrogen Balmer beta emission at the wavelength of 486.1 nm which is the brightest among the proton auroral lines was observed at a pair of geomagnetic conjugate points to compare precipitating particle energy. Two identical Proton Auroral Specrographs (PASs) which obtain auroral spectra along a geomagnetic meridian at a rate of 1 image/min were installed at Tjornes in Iceland and Syowa Station in Antarctica. Data obtained during a period from September 4, 2018 to October 9, 2018 were analyzed to derive an average kinetic energy of precipitating protons along a local geomagnetic field line from a Doppler shift of the H beta line. As a result we are succeeded in simultaneous observations of proton auroras at both conjugate points in 5 nights on September 4, 5, 6, 7 , and 10. The average energies of precipitating protons range from 0 keV to 7 keV, and sometimes show a periodical variation with a period of 4 - 5 min. Conjugacy of precipitating particle energy will be discussed in the presentation.

©2019. Japan Geoscience Union. All Right Reserved.

A regularized deep convolutional general adversarial network (R-DCGAN) for total electron content map completion

*Mingwu Jin[1], Zhou Chen[2,3], Yue Deng[1], Yang Pan[1], Jin-Song Wang[2]

1. University of Texas at Arlington, 2. Institute of Space Science and Technology, Nanchang University, Nanchang, China, 3. Key Laboratory of Space Weather, National Center for Space Weather, China Meteorological Administration, Beijing, China

Observations with a complete global coverage are important for space physics research and applications. However, due to the technical limitations and costs, such a complete global coverage is often unavailable. Thus, data filling algorithms are often pursued to fill missing data gaps to create a global map from the incomplete data. In this work, a novel deep learning algorithm, regularized deep convolutional generative adversarial network (R-DCGAN), is developed by adding an extra discriminator to the conventional DCGAN to fill the missing data of total electron content (TEC) map images. R-DCGAN incorporates the knowledge from reference TEC maps of the International Global Navigation Satellite Systems Service Ionosphere Working Group to achieve much better TEC map completion performance than the conventional DCGAN as demonstrated by both synthetic and real data. The R-DCGAN framework can be extended to other fields of space sciences to address the missing observation data issues.

Keywords: Deep learning method, TEC , map completion

©2019. Japan Geoscience Union. All Right Reserved.

A long-lasting auroral bright spot around magnetic north pole: Is it the evidence of stable magnetic reconnection?

*Qing-He Zhang[1], Guo-Cheng Shen[1], Yong-Liang Zhang[2], Kjellmar Oksavik[3], Michael Lockwood[4], Zan-Yang Xing[1], Yu-Zhang Ma[1]

1. Institute of Space Sciences, Shandong University, Weihai, China, 2. The Johns Hopkins University Applied Physics Laboratory, Laurel, Maryland, USA, 3. Birkeland Centre for Space Science, University of Bergen, Bergen, Norway, 4. Department of Meteorology, University of Reading, Earley Gate, Post Office Box 243, RG6 6BB, UK.

An intense and large auroral bright spot appears around the magnetic north pole observed by the Special Sensor Ultraviolet Spectrographic Imager (SSUSI) on board four different Defense Meteorological Satellite Program (DMSP) satellites during long time northward IMF conditions. The bright spot is even brighter than aurora in the auroral oval which is about 5-10˚ magnetic latitude equatorward of the bright spot. The bright spot is lasting about 8 hours, and sometimes appears as a cyclone-shape with a clockwise rotation. The DMSP in situ plasma observations suggest that the bright spot is clear associated with electron invert-V acceleration with 10s keV energy electron precipitations around the center regions and 1s keV energy electron precipitations around the egde regions. There are also strong flow shears between the two sides of the bright spot: strong sunward flows on the duskside and antisunward flows on the dawnside. These types of plasma should come from the high-latitude lobe region of the magnetotail due to the high-latitude lobe magnetic reconnections. Is it the evidence of stable lobe reconnection during long time northward IMF conditions? The detail and further analysis should be pursued in the following studies.

Keywords: Auroral bright spot, Magnetosphere-ionosphere coupling, High-latitude lobe magnetic reconnection, Stable reconnection

©2019. Japan Geoscience Union. All Right Reserved.

Statistical study of the relationship between ion upflow and field-aligned current in the topside ionosphere for both hemispheres during disturbed and quiet times

Shan-Yu Zhou[1], *Qing-He Zhang[1], P. T. Jayachandran[2], Kjellmar Oksavik[3], Larry Lyons[4], Zan-Yang Xing[1], Yu-Zhang Ma[1], Marc Hairston[5], Yong Wang[1]

1. Institute of Space Sciences, Shandong University, Weihai, China, 2. Physics Department, University of New Brunswick, Fredericton, New Brunswick, Canada, 3. Birkeland Centre for Space Science, University of Bergen, Bergen, Norway, 4. Department of Atmospheric and Oceanic Sciences, University of California, Los Angeles, California, USA, 5. William B. Hanson Center for Space Sciences, University of Texas at Dallas, Richardson, Texas, USA

A statistical study of ion upflow and field-aligned currents (FACs) has been performed in the topside ionosphere of both hemispheres for magnetic quiet and disturbed times by using DMSP satellite observations from 2010-2013. Distributions in MLT/MLAT reveal that ion upflow shows a dawn-dusk asymmetry distribution that corresponds well with the region 1 field-aligned currents. In addition, there are highest occurrence regions near noon and within the near midnight auroral disturbance area. These correspond to cusp and nightside dynamical processes, respectively. Both the ion upflow occurrence and FAC regions expand equatorward to a wider area during disturbed times.

Keywords: Ion upflows, Field-aligned current, Magnetosphere-ionosphere coupling

©2019. Japan Geoscience Union. All Right Reserved.

SAPS in the 2013 March 17 Storm Event: Initial Results from the Coupled Magnetosphere-Ionosphere-Thermosphere Model

*Dong Lin[1,2], Wenbin Wang[2], Wayne Scales[1], Kevin Pham[2], Jing Liu[2], Binzheng Zhang[2], Viacheslav Merkin[3], Xueling Shi[1]

1. Virginia Tech, 2. High Altitude Observatory, NCAR, 3. APL, John Hopkins Univ.

Subauroral polarization stream (SAPS) are latitudinally narrow flow channels of large westward plasma drifts in the subauroral ionosphere. In this study, the global structure and dynamic evolution of SAPS are investigated by using the National Center for Atmospheric Research (NCAR) Coupled Magnetosphere-Ionosphere-Thermosphere (CMIT) model with Ring Current extension, namely the LFM-TIEGCM-RCM (LTR) model, to simulate the 2013 St. Patrick's Day storm event. This is the first time that the global distribution and temporal evolution of SAPS are investigated using first-principle models. The model shows a strong westward ion drift channel formed equatorward of the auroral electron precipitation boundary on the duskside, which is identified as the SAPS structure. The simulated ion drift velocity and auroral electron precipitation sampled along the trajectory of the DMSP F18 satellite are in good agreement with the satellite measurements. SAPS initiate in the pre-dusk sector when the interplanetary magnetic field (IMF) turns southward. SAPS latitude generally decreases with magnetic local time (MLT) from dusk to midnight. The SAPS channel shows wedge, inverse wedge, and crescent morphologies during the storm, and becomes discontinuous when the IMF is weakly southward. The SAPS mean latitude has a correlation coefficient of 0.77 with the Dst index. The mean latitude moves equatorward and the flow channel broadens in the storm main phase. The simulation results are consistent with observational studies. They also illustrate the global distributions and highly dynamic behaviors of SAPS that are not readily apparent from observation data.

Keywords: SAPS, Magnetosphere-Ionosphere-Thermosphere coupling, LFM-TIEGCM-RCM

©2019. Japan Geoscience Union. All Right Reserved.

Westward turning motions of nighttime medium-scale traveling ionospheric disturbances (MSTIDs) at the equatorward side of the dusk side auroral oval associated with auroral brightening

*Sneha Yadav[1,2], Kazuo Shiokawa[1], Shin-ichiro Oyama[1,3,4], Yuichi Otsuka[1]

1. ISEE, Nagoya University, Nagoya, Japan, 2. SPL, VSSC, India, 3. Ionosphere Research Unit, University of Oulu, Oulu, Finland, 4. NIPR, Tachikawa, Japan

The characteristics of high-latitude nighttime medium-scale traveling ionospheric disturbances (MSTIDs) have not been well investigated using all-sky imagers because of the hindrance caused by the bright aurora. The limited results on the propagation characteristics of MSTIDs over high-latitudes hindered the progress in our understanding on these dynamical structure. In a case study carried out by Shiokawa et al. (JGR, 2012), an event of oscillating MSTIDs was reported over Tromsø (69.6˚N, 19.2˚E; corrected geomagnetic latitude: 66.6˚N), which was observed to be associated with auroral brightening. However, after this case study, which comprised of only one event, no observations showing oscillating motion of MSTIDs have been reported till date. In this study, for the first time, the comprehensive investigation on the westward turning of the MSTIDs in the equatorward side of the dusk side auroral oval has been performed. The all-sky imaging data of 630.0 nm airglow emissions during 2010-2018 are used to study the motions of MSTIDs over Tromsø. The results indicate that the nighttime MSTIDs primarily exhibit eastward motion under quiet magnetic conditions but turned in the westward direction during the active geomagnetic conditions. The turning of MSTIDs in the westward direction were invariably associated with the auroral brightening observed at the poleward edge of the all-sky image and localized magnetic field perturbations observed by ground-based magnetometers at Tromsø. The interesting aspect of the observations is the fact that these westward moving MSTIDs again turned in the eastward direction when the geomagnetic disturbance ceases. The SuperDARN (Super Dual Auroral Radar Network) convection maps revealed that the location of Tromsø was inside/outside the convection cell region during the time of appearance of westward/eastward moving MSTIDs. The Doppler shift measurement of the 630-nm airglow by a Fabry-Perot interferometer at Tromsø showed that northeastward winds were predominant during the appearance of eastward moving MSTIDs. The cause of the observed MSTIDs remains in question as they might either be triggered by atmospheric gravity waves or by Perkins instability. These experimental evidences suggest that the MSTIDs tend to move eastward in accordance with the background F-region dynamo electric field, but show westward motion under the influence of electric field associated with auroral activities in the dusk side of two-cell convection pattern.

Keywords: MSTIDs, Auroral oval, Airglow

©2019. Japan Geoscience Union. All Right Reserved.

[E] Oral | P (Space and Planetary Sciences)：P-EM Solar-Terrestrial Sciences, Space Electromagnetism & Space Environment

Mon. May 27, 2019 3:30 PM - 5:00 PM JST | Mon. May 27, 2019 6:30 AM - 8:00 AM UTC | A05 TOKYO BAY MAKUHARI HALL

[P-EM10] Multi-scale Coupling in the Magnetosphere-Ionosphere-Thermosphere System

convener:Yue Deng(University of Texas at Arlington), Toshi Nishimura(Boston University), Huixin Liu(Earth and Planetary Science Division, Kyushu University SERC, Kyushu University), Yanshi Huang(Harbin Institute of Technology, Shenzhen), Chairperson:Yue Deng(University of Texas at Arlington), Huixin Liu(Kyushu University, Japan), Yanshi Huang(Harbin Institute of Technology, Shenzhen, China), Yukitoshi Nishimura(Boston University)

Determining the effects of energy deposition and transport, and momentum exchange across different spatial and temporal scales is an important objective in the M-I-T system, due to the clear evidence of multi-scale forcing. Coupling over multiple scales is also a critical challenge since observational and modeling methodologies for bridging different scales do not presently exist. This session solicits presentations on a wide range of coupling processes in the high-latitude M-I-T system from global to small-scale processes and related solar wind forcing. Relevant topics include (but are not limited to) (1) density structures and temperature gradients (polar cap, cusp, plume, trough, irregularities); (2) convection (flow channels, SAPS) and FAC; (3) energy transfer and deposition by precipitation and ULF waves, conductivity, aurora, and heating; and (4) coupling and feedback into the magnetosphere. Discussions of relevant multi-scale observations by means of multiple instruments, including space and ground-based, modeling and data science are encouraged.

3:30 PM - 3:45 PM JST | 6:30 AM - 6:45 AM UTC

[PEM10-01] Auroral fragmentation into patches and pressure balance condition in the source magnetosphere

★Invited Papers

*Kazuo Shiokawa[1], Katsuki Nishi[1] (1.Institute for Space-Earth Environmental Research, Nagoya University)

3:45 PM - 4:00 PM JST | 6:45 AM - 7:00 AM UTC

[PEM10-02] Formation and Evolution of Polar Cap Ionospheric Patches and Their Associated Upflows and Scintillations: A Review

★Invited Papers

*Qing-He Zhang[1], Zan-Yang Xing[1], Yong Wang[1], Yu-Zhang Ma[1] (1.Institute of Space Sciences, Shandong University, Weihai, China)

4:00 PM - 4:15 PM JST | 7:00 AM - 7:15 AM UTC

[PEM10-03] Global ionospheric disturbances during the 6-10 September 2017 solar storms

★Invited Papers

*Shunrong Zhang[1] (1.MIT Haystack Observatory)

4:15 PM - 4:30 PM JST | 7:15 AM - 7:30 AM UTC

[PEM10-04] Multiscape Coupling of Sub-auroral Polarization Streams

*Nozomu Nishitani[1], Tomoaki Hori[1] (1.Institute for Space-Earth Environmental Research, Nagoya University)

4:30 PM - 4:45 PM JST | 7:30 AM - 7:45 AM UTC

[PEM10-05] Scale sizes of mass density enhancements inferred from accelerometer measurements

*Yanshi Huang[1], Cheryl Huang[2] (1.Harbin Institute of Technology, Shenzhen, China, 2.Space Physics Directoriate, Air Force Research Laboratory, Kirtland AFB, USA)

4:45 PM - 5:00 PM JST | 7:45 AM - 8:00 AM UTC

[PEM10-06] **Meso-scale forcing in the upper atmosphere: sources and impacts**

*Yue Deng[1], Qingyu Zhu[1], Cissi Lin[1] (1.University of Texas at Arlington)

Auroral fragmentation into patches and pressure balance condition in the source magnetosphere

*Kazuo Shiokawa[1], Katsuki Nishi[1]

1. Institute for Space-Earth Environmental Research, Nagoya University

The auroral fragmentation into patches has been reported by Shiokawa et al. (JGR, 2010; 2014) as finger-like structures developed in the diffuse aurora with horizontal scale sizes of 5-25 km (small scale) and 40-100 km (large scale). The development of these finger-like structures divides the diffuse aurora into patches. Thus we call it as the auroral fragmentation which is a cause of the patchy auroral structures in the diffuse aurora. Hashimoto et al. (JGR, 2015) made a statistical analysis of these auroral finger-like structures and found their occurrence rates of 13% and 4 % for large- and small-scale events, respectively. They also indicated that the finger-like structures tend to occur at the beginning of the substorm recovery phase in the post-midnight and dawn sectors. The auroral finger-like structure suggests the development of pressure-driven instability in the magnetosphere. Recently Nishi et al. (JGR, 2017) made the first conjugate measurement of the auroral finger-like structures with the THEMIS-E satellite at ~8 Re in the magnetosphere. They found clear anti-phase oscillations between the magnetic and plasma pressures in the post-midnight plasma sheet. This anti-phase variation is consistent with the idea of the pressure-driven instability. On the other hand, Nishi et al. (JGR, 2018a) reported that a conjugate event with the RBSP-A satellite at ~5.5 Re does not show systematic phase relationship between the magnetic and plasma pressures. Then Nishi et al. (JGR, 2018b) investigate statistical features of the phase relationship between magnetic and plasma pressures using two-year THEMIS-E observations in the nightside plasma sheet and obtained a high occurrence of the anti-phase oscillations between the magnetic and plasma pressures. In the presentation, we will review these recent results on the auroral fragmentation and pressure balance condition in the source magnetosphere, and discuss possible physical mechanism that contributes these phenomena.

References:
1. Shiokawa, K., A. Nakajima, A. Ieda, K. Sakaguchi, R. Nomura, T. Aslaksen, M. Greffen, and E. Donovan (2010), Rayleigh-Taylor type instability in auroral patches, J. Geophys. Res., 115, A02211, doi:10.1029/2009JA014273.
2. Shiokawa, K., et al. (2014), Auroral fragmentation into patches, J. Geophys. Res. Space Physics, 119, doi:10.1002/2014JA020050.
3. Hashimoto, A., K. Shiokawa, Y. Otsuka, S.-i. Oyama, S. Nozawa, T. Hori, M. Lester, and M. G. Johnsen (2015), Statistical study of auroral fragmentation into patches, J. Geophys. Res. Space Physics, 120, 6207-6217, doi:10.1002/2015JA021000.
4. Nishi, K., K. Shiokawa, and D. Fruehauff (2017), Conjugate observation of auroral finger-like structures by ground-based all-sky cameras and THEMIS satellites, J. Geophys. Res. Space Physics, 122, doi:10.1002/2016JA023774.
5. Nishi, K., K. Shiokawa, and H. Spence (2018a), Magnetospheric source region of auroral finger-like structures observed by the RBSP-A satellite, J. Geophys. Res., 123, doi: 10.0002/2018JA025480.
6. Nishi, K., K. Shiokawa, K.-H. Glassmeier, and J. Z. D. Mieth (2018b), Statistical study of phase relationship between magnetic and plasma pressures in the near-earth nightside magnetosphere using the THEMIS-E satellite, J. Geophys. Res., 123, doi: 10.0002/2018JA025846.

©2019. Japan Geoscience Union. All Right Reserved.

Keywords: auroral fragmentation into patches, pressure balance in the magnetosphere, diffuse aurora

©2019. Japan Geoscience Union. All Right Reserved.

Formation and Evolution of Polar Cap Ionospheric Patches and Their Associated Upflows and Scintillations: A Review

*Qing-He Zhang[1], Zan-Yang Xing[1], Yong Wang[1], Yu-Zhang Ma[1]

1. Institute of Space Sciences, Shandong University, Weihai, China

Polar cap patches are common phenomena, especially during southward interplanetary magnetic field (IMF) conditions, in the polar ionosphere. We summarized the recent new progress about the formation and evolution of patches as well as their impact on the magnetosphere-ionosphere-thermosphere (M-I-T) coupling processes and space weather. The dayside reconnection and bursty sunward return flows produced by the modulation of nightside reconnection, are confirmed as the dominated mechanisms to separate the entering ionization into islands (patches). The patches evolve along streamlines of the Dungey convection cycle from the dayside to the nightside and exit the polar cap modulated by pulsed nightside reconnection. However, they slowly move and rapidly fade away behind a lobe “reverse” convection cell when the IMF suddenly changed to northward. Rapidly moving patches are associated with clear ion upflows due to frictional heating and offer more upwelling ion fluxes. Patches often produce significant scintillations due to strong density gradients at their edges, especially during their merging into the auroral oval, which will result in variable disturbances to High Frequency (HF) radio communications, over-the-horizon radar location errors, disruption and errors to satellite navigation and communication.

Keywords: Polar cap patches, Magnetosphere-ionosphere coupling, Ion upflows, Ionospheric scintillations

©2019. Japan Geoscience Union. All Right Reserved.

Global ionospheric disturbances during the 6-10 September 2017 solar storms

*Shunrong Zhang[1]

1. MIT Haystack Observatory

Solar activity during the period of 6-10 September 2017 is characterized with a series of very strong flares and powerful coronal mass ejections (CMEs). Observations indicate more than two dozens of M-class and 4 X-class flares being emmitted from the solar Active Region 12673. In particular, one of these flares led to a halo-type CME which traveled earth-bound at ~1570 km/s apparent speed. With the arrival of this CME, IMF Bz turned to southward and reached a minimum of -30 nT at 23:25 UT on 7 September, triggering a Kp 8 geomagnetic storm with a sudden commencerment at ~2300 UT and a minimum Dst ~ -150 nT near 0100 UT on 8 September. These conditions caused very significant geospace disturbances, in particular, ionospheric disturbances with various spatial and temporal scales. In this presentation, we report flare induced ionospheric perturbations and post-flare traveling ionospheric disturbances (TIDs), storm-enhanced density (SED) plumes at subauroral and high latitudes of the dayside ionosphere, subauroral polarization streams (SAPs), and large scale TIDs over the globe. Our discussion will focus on some unique post-flare ionospheric oscillation and TID features, TIDs at high latitudes, and gigantic cross-hemispheric ionospheric electron density depletion channels. This study is based primarily on ground-based GNSS and Millstone Hill incoherent scatter radar observations.

Keywords: geospace storm, solar flare, traveling ionospheric disturbance

©2019. Japan Geoscience Union. All Right Reserved.

Multiscape Coupling of Sub-auroral Polarization Streams

*Nozomu Nishitani[1], Tomoaki Hori[1]

1. Institute for Space-Earth Environmental Research, Nagoya University

Sub-Auroral Polarization Streams (SAPS) are fast westward flows slightly equatorward of the auroral precipitation boundary, and manifestations of magnetosphere-coupling processes. Recenty it was shown that SAPS sometimes contain perturbation in westward speed, typically with temporal scale of a few minutes (e.g., Hori et al., GRL, 2018). However, it has not yet been clear how small the temporal scales of these perturbations can be and how perturbations with different temporal scales are related to each other. In this paper, multiscape coupling of the sub-auroral polarization streams will be studied, using multiple events observed mainly by the SuperDARN Hokkaido East / West radars.

Keywords: multiscale coupling, SuperDARN Hokkaido East / West radars, sub-auroral polarization stream (SAPS)

©2019. Japan Geoscience Union. All Right Reserved.

Scale sizes of mass density enhancements inferred from accelerometer measurements

*Yanshi Huang[1], Cheryl Huang[2]

1. Harbin Institute of Technology, Shenzhen, China, 2. Space Physics Directoriate, Air Force Research Laboratory, Kirtland AFB, USA

The spatial scale sizes of neutral mass density enhancements inferred from the accelerometer measurements on CHAMP and GRACE satellites are analyzed. Density enhancements are found as the peaks with more than 30% above the average density baseline fitted over a 90 degree magnetic latitude window. The widths of mass density peaks are defined in two different methods, one using the maximum above the average density baseline, the other method using the two minima surrounding each one density peak above a threshold value. We study various cases including one-peak and multi-peak cases using high-resolution density data from year 2002 to 2010. The results give a statistical understanding of the scale sizes of the density enhancements observed at high and polar latitudes. The scale sizes using the baseline are rather independent of solar activity, and the average is over 2500 km, whereas the scale sizes using adjacent density minima vary with solar activity, and the mean value is more than 1000 km. No significant different results are found between northern and southern hemisphere. We also investigate the impact of these mass density peaks on the orbit-averaged densities.

Keywords: neutral mass density , accelerometer measurements , CHAMP and GRACE satellites , spatial scale sizes

©2019. Japan Geoscience Union. All Right Reserved.

Meso-scale forcing in the upper atmosphere: sources and impacts

*Yue Deng[1], Qingyu Zhu[1], Cissi Lin[1]

1. University of Texas at Arlington

We present a systematical study crossing both data analysis and model simulation to improve the specification of the energy and momentum inputs into the ionosphere-thermosphere (IT) system, especially at the meso-scale, and the system response. Our results are organized in two parts. First, two-years of Swarm satellite field-aligned current (FAC) data have been analyzed in order to study the distributions of mean pattern and variability of FACs on different scales (small scale: <150 km; mesoscale: 100~500 km; large scale: >500 km). The FAC distributions are then implemented in the Global Ionosphere-Thermosphere Model (GITM) to assess relative contributions of FACs at different scales to Joule heating. To enhance our capability to directly simulate the meso- and small-scale structures, GITM has been improved with a local patch grid refinement capability. Utilizing GITM with the new grid structure, the meso- and small-scale gravity wave perturbations have been included at the lower boundary of GITM to simulate the influence of meso- and small-scale gravity waves on the upper atmosphere.

Keywords: Meso-scale forcing , upper atmosphere, Joule heating, Gravity waves

©2019. Japan Geoscience Union. All Right Reserved.

[E] Oral | P (Space and Planetary Sciences)：P-EM Solar-Terrestrial Sciences, Space Electromagnetism & Space Environment

Mon. May 27, 2019 9:00 AM - 10:30 AM JST | Mon. May 27, 2019 12:00 AM - 1:30 AM UTC | A04 TOKYO BAY MAKUHARI HALL

[P-EM12] Space Weather and Space Climate

convener:Ryuho Kataoka(National Institute of Polar Research), Antti A Pulkkinen(NASA Goddard Space Flight Center), Kanya Kusano(Institute for Space-Earth Environmental Research, Nagoya University), Kaori Sakaguchi(National Institute of Information and Communications Technology), Chairperson:Antti Pulkkinen(NASA/GSFC)

We share the latest scientific papers to understand how the solar-terrestrial environment changes in various time scales, and to discuss how we will react via international and interdisciplinary collaborations. More specifically, welcomed papers include space climate studies to reconstruct long-term variations from radio isotopes; cutting-edge observational and modeling studies of the ionosphere, geospace, heliosphere and the sun; simulation and statistical studies to predict the future space weather and space climate; applied science such as operational space weather forecast and mitigation of the social impact due to extreme space hazards.

9:00 AM - 9:15 AM JST | 12:00 AM - 12:15 AM UTC

[PEM12-01] NASA Heliophysics Division Space Weather Update

★Invited Papers

*Nicola Justine Fox[1] (1.NASA Headquarters)

9:15 AM - 9:30 AM JST | 12:15 AM - 12:30 AM UTC

[PEM12-02] NOAA's Current and Future Space Weather Architecture

★Invited Papers

*Elsayed R Talaat[1] (1.NOAA National Environmental Satellite, Data, and Information Service)

9:30 AM - 9:45 AM JST | 12:30 AM - 12:45 AM UTC

[PEM12-03] Community Coordinating Modeling Center (CCMC): A hub for collaborative assessment and improvement of space weather capabilities.

★Invited Papers

*Maria M Kuznetsova[1], M. Leila Mays[1], Edward J Semones[2], Peter J Macneice[1], Lutz Rastaetter[1], Ja Soon Shim[1], Yihua Zheng[1], Katherine Garcia-Sage[1], Joycelyn Jones[1], Yaireshka m Collado-Vega[1], Richard E Mullinix[1], Chiu Wiegand[1] (1.NASA Goddard Space Flight Center, 2.NASA Johnson Space Center)

9:45 AM - 10:00 AM JST | 12:45 AM - 1:00 AM UTC

[PEM12-04] Different flux evolutions of relativistic electrons of the outer belt associated with high-speed coronal hole streams; Arase and Van Allen Probes observations

*Yoshizumi Miyoshi[1], Satoshi Kurita[1], Ryuho Kataoka[2], Shinji Saito[1], Vania Jordanova[3], Iku Shinohara[4], Takefumi Mitani[4], Takeshi Takashima[4], Nana Higashio[4], Satoshi Kasahara[5], Shoichiro Yokota[6], Tomoaki Hori[1], Kunihiro Keika[5], Yoshiya Kasahara[7], Shoya Matsuda[4], Atsushi Kumamoto[8], Fuminori Tsuchiya[8], Masafumi Shoji[1], Ayako Matsuoka[1], Mariko Teramoto[1], Harlan Spence[9], Geoff Reeves[3], Daniel Baker[10] (1.Institute for Space-Earth Environmental Research, Nagoya University, 2.NIPR, 3.Los Alamos National Laboratory, 4.JAXA, 5.University of Tokyo, 6.Osaka University, 7.Kanazawa University, 8.Tohoku University, 9.University of New Hampshire, 10.University of Colorado)

10:00 AM - 10:15 AM JST | 1:00 AM - 1:15 AM UTC

[PEM12-05] Study on the predictability of imminent giant solar flares based on the theory of double-arc instability

*Kanya Kusano[1], Tomoya Iju[2], Yumi Bamba[1] (1.Institute for Space-Earth Environmental Research, Nagoya University, 2.NAOJ)

10:15 AM - 10:30 AM JST | 1:15 AM - 1:30 AM UTC

[PEM12-06] Update of space weather research and operation activities in NICT

*Mamoru Ishii[1] (1.National Institute of Information and Communications Technology)

NASA Heliophysics Division Space Weather Update

*Nicola Justine Fox[1]

1. NASA Headquarters

NASA is a mission driven agency whose science mission is focused on discovering the secrets of the universe, looking for life elsewhere, and safeguarding and improving life on Earth. Heliophysics plays a key role in every aspect of the NASA science mission, including understanding the drivers of and enabling the prediction of space weather. Heliophysics has an established research program that motivates and funds solar and space physics, which is the essence and foundation of space weather research. Recently, the Heliophysics Division established a Space Weather Science Applications Program, SnAP. The objective of this competed program is to enable the transition of the knowledge and understanding of space weather to operation environments, by partnering with sister agencies, the commercial sector, and academia. SnAP leverages relevant NASA capabilities to reach this objective. This talk provides an overview of space weather research and SnAP in the NASA Heliophysics Division

Keywords: Heliophysics, Space Weather, Sun Earth Connections, Sun, Solar Wind, Magnetosphere

©2019. Japan Geoscience Union. All Right Reserved.

NOAA's Current and Future Space Weather Architecture

*Elsayed R Talaat[1]

1. NOAA National Environmental Satellite, Data, and Information Service

NOAA observational responsibilities in support of space weather forecasting are in the context of significant, numerous, complementary international and domestic efforts. Each measurement plays a unique role at different phases of the forecasting or event characterization process. This paper overviews the current suite of observation that NOAA maintains and utilizes on various platforms, NOAA's forecasting capability, contributions to research efforts, and the status of the NOAA/NESDIS plan forward efforts for the Space Weather Follow-On (SWFO) program to provide needed continuity. This paper will also brief the NOAA space weather goals within the NOAA Satellite Observing System Architecture.

Keywords: space weather, coronagraph, energetic particles

©2019. Japan Geoscience Union. All Right Reserved.

Community Coordinating Modeling Center (CCMC): A hub for collaborative assessment and improvement of space weather capabilities.

*Maria M Kuznetsova[1], M. Leila Mays[1], Edward J Semones[2], Peter J Macneice[1], Lutz Rastaetter[1], Ja Soon Shim[1], Yihua Zheng[1], Katherine Garcia-Sage[1], Joycelyn Jones[1], Yaireshka m Collado-Vega[1], Richard E Mullinix[1], Chiu Wiegand[1]

1. NASA Goddard Space Flight Center, 2. NASA Johnson Space Center

The Community Coordinated Modeling Center (CCMC, http://ccmc.gsfc.nasa.gov) was established at the end of past millennium as a multi-agency strategic investment in the US space weather program. The CCMC has two main goals: 1) to support space weather research and model development aiming to advance understanding of space weather phenomena and to improve forecasting; 2) to facilitate development of space weather applications and deployment of operational capabilities. The CCMC hosts a rapidly growing collection of space weather models and applications, provides simulations services to the international research community through a one-of-a-kind runs-on-request system, and maintains real-time simulations and perpetual archives of space weather information streams. In support of NASA missions, the CCMC provides support for mission planning, develops applications for space weather monitoring and forecasting, and provides space environment analysis services. In partnership with NASA Space Radiation Analysis Group (SRAG) and international modeling community the CCMC is building a flexible system for Solar Proton Event (SPE) risk assessment and forecasting in support of human exploration. Unbiased testing, evaluating and prototyping of new models and forecasting techniques for potential transition to operational organizations (R2O) is one of the primary CCMC functions. To establish internationally recognized metrics and benchmarks the CCMC initiated an international community-wide Forum for Space Weather Capabilities Assessment. Guided by the unfolding activities of Forum working teams as well as by the needs of operational agencies and end users to quantify and track improvements over time, the CCMC has begun to develop an extensive information technology infrastructure to support validation activities through a centralized database and an interactive web-based framework. The presentation will highlight the recent progress and discuss opportunities for international research initiatives aiming to improve space weather forecasting capabilities.

Keywords: space weather, models, assessment, Solar Proton Event

©2019. Japan Geoscience Union. All Right Reserved.

Different flux evolutions of relativistic electrons of the outer belt associated with high-speed coronal hole streams; Arase and Van Allen Probes observations

*Yoshizumi Miyoshi[1], Satoshi Kurita[1], Ryuho Kataoka[2], Shinji Saito[1], Vania Jordanova[3], Iku Shinohara[4], Takefumi Mitani[4], Takeshi Takashima[4], Nana Higashio[4], Satoshi Kasahara[5], Shoichiro Yokota[6], Tomoaki Hori[1], Kunihiro Keika[5], Yoshiya Kasahara[7], Shoya Matsuda[4], Atsushi Kumamoto[8], Fuminori Tsuchiya[8], Masafumi Shoji[1], Ayako Matsuoka[1], Mariko Teramoto[1], Harlan Spence[9], Geoff Reeves[3], Daniel Baker[10]

1. Institute for Space-Earth Environmental Research, Nagoya University, 2. NIPR, 3. Los Alamos National Laboratory, 4. JAXA, 5. University of Tokyo, 6. Osaka University, 7. Kanazawa University, 8. Tohoku University, 9. University of New Hampshire, 10. University of Colorado

Relativistic and ultra-relativistic electrons increase largely during the high-speed coronal hole streams, and the enhanced flux levels are controlled by the solar wind speed and the prolonged southward IMF. Such flux enhancements associated with high-speed streams have been observed by Arase/HEP and XEP instruments as well as Van Allen Probes/MagEIS and REPT. Some coronal hole streams produce large flux enhancement of both relativistic and ultra-relativistic electrons, while other coronal holes produce large flux enhancement of relativistic electrons (~2 MeV) but do not produce enhancement of ultra-relativistic electrons. In this presentation, we will show evolutions of the energy spectrum of relativistic electrons during the coronal hole streams and discuss how evolutions of the energy spectrum are related to chorus wave activities that are derived from Arase/PWE measurements and the proxy data from the low-altitude satellite data.

Keywords: radiation belts, Arase, Sun-Earth Connection

©2019. Japan Geoscience Union. All Right Reserved.

Study on the predictability of imminent giant solar flares based on the theory of double-arc instability

*Kanya Kusano[1], Tomoya Iju[2], Yumi Bamba[1]

1. Institute for Space-Earth Environmental Research, Nagoya University, 2. NAOJ

Solar flares are catastrophic explosions in the solar corona and sometimes may cause a severe space weather disaster in geo-space and the infrastructure. Although many efforts have been taken for understanding and predicting the onset of solar flares, it is still difficult to accurately predict when, where and how large giant solar flares will occur. Here, we propose a new type of solar flare prediction scheme called the κ-scheme. The κ-scheme is the totally physics-based prediction, and it is capable of providing the information of the location as well as the energy of imminent giant solar flares. The prediction is performed by evaluating how small reconnection can trigger the onset of the double-arc instability, which was recently proposed as the initial driver of solar flares by Ishiguro and Kusano (2017), using the nonlinear force-free field extrapolation. We carried out the analysis of more than 200 active regions in the solar cycle 24 by applying the κ-scheme to the SDO/HMI data. The result shows that most of the imminent giant solar flares larger than the GOES X2 class are predictable with the κ-scheme.

Keywords: solar flares, prediction, space weather

©2019. Japan Geoscience Union. All Right Reserved.

Update of space weather research and operation activities in NICT

*Mamoru Ishii[1]

1. National Institute of Information and Communications Technology

Since September 6 2017, when X9.3 solar flare occured most of Japanese people were scared of it, the situation of Japanese spacw weather operation has been changed so much. The ionosphere observing network has been set more robustly with dual systems. A back up center of space weather information service has been installed at NICT Kobe branch. In addition, we will begin 24/7 operation of space weather forecast services in FY2019.We have been collaborating with academic researchers under the framework of PSTEP which will finish the end of FY2019. Through the activities, we have provided some applications for better service than before. A radio propagatoin simulator, HF-START, and the estimation system of human radiation on flight, WASAVIES will be up on our web soon. In addition, we continue to discuss hazardous map against severe space weather disasters, which will be published within a year.I would like to share our information and have close cooperation with Asia Oceania space weather researchers and operators.

Keywords: Space Weather forecast, AOSWA, social impact

©2019. Japan Geoscience Union. All Right Reserved.

[E] Oral | P (Space and Planetary Sciences)：P-EM Solar-Terrestrial Sciences, Space Electromagnetism & Space Environment

Mon. May 27, 2019 10:45 AM - 12:15 PM JST | Mon. May 27, 2019 1:45 AM - 3:15 AM UTC | A04 TOKYO BAY MAKUHARI HALL

[P-EM12] Space Weather and Space Climate

convener:Ryuho Kataoka(National Institute of Polar Research), Antti A Pulkkinen(NASA Goddard Space Flight Center), Kanya Kusano(Institute for Space-Earth Environmental Research, Nagoya University), Kaori Sakaguchi(National Institute of Information and Communications Technology), Chairperson:Ryuho Kataoka(National Institute of Polar Research)

We share the latest scientific papers to understand how the solar-terrestrial environment changes in various time scales, and to discuss how we will react via international and interdisciplinary collaborations. More specifically, welcomed papers include space climate studies to reconstruct long-term variations from radio isotopes; cutting-edge observational and modeling studies of the ionosphere, geospace, heliosphere and the sun; simulation and statistical studies to predict the future space weather and space climate; applied science such as operational space weather forecast and mitigation of the social impact due to extreme space hazards.

10:45 AM - 11:00 AM JST | 1:45 AM - 2:00 AM UTC

[PEM12-07] Commercial Space Weather Activities From a USA small Business Perspertive

★Invited Papers

*Chigomezyo Mudala Ngwira[1], Geoff Crowley[1], Chad Fish[1] (1.Atmospheric and Space Technology Research Associates, LLC)

11:00 AM - 11:15 AM JST | 2:00 AM - 2:15 AM UTC

[PEM12-08] Development of coronal mass ejection arrival time forecasting system using interplanetary scintillation observations

★Invited Papers

*Kazumasa Iwai[1], Daikou Shiota[2], Munetoshi Tokumaru[1], Ken'ichi Fujiki[1], Mitsue Den[2], Yûki Kubo[2] (1.Institute for Space–Earth Environmental Research (ISEE), Nagoya University, 2.National Institute of Information and Communications)

11:15 AM - 11:30 AM JST | 2:15 AM - 2:30 AM UTC

[PEM12-09] Development of real-time prediction system of CME arrival and magnetic field with SUSANOO-CME MHD simulation

*Daikou Shiota[1,2], Seiji Yashiro[3], Kazumasa Iwai[2] (1.National Institute of Information and Communications Technology (NICT), 2.Institute for Space-Earth Environmental Research, Nagoya University, 3.Catholic University)

11:30 AM - 11:45 AM JST | 2:30 AM - 2:45 AM UTC

[PEM12-10] The Role of a Tiny Brightening in a Huge Geo-effective Solar Eruption Leading to the St Patrick's Day Storm

*Yumi Bamba[1,2], Satoshi Inoue[1], Keiji Hayashi[1,3,4] (1.Institute for Space-Earth Environmental Research/Nagoya University, 2.Institute if Space and Astronautical Science/Japan Aerospace Exploration Agency, 3.Key Laboratory of Solar Activity, National Astronomical Observatories, Chinese Academy of Sciences, 4.State Key Laboratory for Space Weather, National Space Science Center, Chinese Academy of Sciences)

11:45 AM - 12:00 PM JST | 2:45 AM - 3:00 AM UTC

[PEM12-11] Critical Parameters of Photospheric Magnetic Field to Produce Eruptive Solar Flares and CMEs in Active Regions

*Pei Hsuan Lin[1], Kanya Kusano[1], Daikou Shiota[2], Satoshi Inoue[1], KD Leka[1,3], Yuta Mizuno[1] (1.Institute for Space-Earth Environmental Research, Nagoya University, 2.National Institute of Information and Communications Technology, 3.NorthWest Research Associates)

12:00 PM - 12:15 PM JST | 3:00 AM - 3:15 AM UTC

[PEM12-12] Simulation study on internal velocity field variation of eruptive prominence

★Invited Papers

*Takafumi Kaneko[1], Kanya Kusano[1] (1.Institute for Space-Earth Environmental Research, Nagoya University)

Commercial Space Weather Activities From a USA small Business Perspertive

*Chigomezyo Mudala Ngwira[1], Geoff Crowley[1], Chad Fish[1]

1. Atmospheric and Space Technology Research Associates, LLC

This talk offers a brief overview of ASTRA (Atmospheric and Space Technology Research Associates), a small business company based in Louisville, Colorado USA. ASTRA was born out of the vision for applying fundamental space physics knowledge to real-world problems. Its motto is Science + Technology + Applications –Bringing it all together. Founded in 2005, ASTRA has become a system design and technology development company. ASTRA is a leader in the “New Space” small satellite revolution specializing in miniaturized sensors, and data modeling and analytics for the government and commercial customers. ASTRA leverages its scientific and engineering expertise to develop unique solutions in HF radar and radio, GPS systems, satellite remote sensing, CubeSats/Smallsats, and LiDAR. ASTRA's technical background spans fundamental space physics disciplines of the upper atmosphere, data analysis and modeling of the complex coupling of the meso-iono- thermosphere, as well as LEO constellation design, spacecraft design, instrument sensor design and manufacture, and space to earth communications.

Keywords: Space Weather, Commercial activities

©2019. Japan Geoscience Union. All Right Reserved.

Development of coronal mass ejection arrival time forecasting system using interplanetary scintillation observations

*Kazumasa Iwai[1], Daikou Shiota[2], Munetoshi Tokumaru[1], Ken'ichi Fujiki[1], Mitsue Den[2], Yûki Kubo[2]

1. Institute for Space–Earth Environmental Research (ISEE), Nagoya University, 2. National Institute of Information and Communications

Coronal mass ejections (CMEs) sometimes cause disturbances in the environment of the Earth. However, prediction of the arrival of CMEs still remains a challenge. We have developed a data assimilation forecasting system of the CME arrival time by combining radio interplanetary scintillation (IPS) observations and a global magnetohydrodynamic (MHD) simulation of the inner heliosphere. In this system, the initial speed of a CME is roughly derived from the white light coronagraph observations. Then, the propagation of the CME is calculated by global MHD simulation (Shiota et al. submitted in this session). The IPS is estimated by the three-dimensional density distribution of the inner heliosphere derived from the MHD simulation. The estimated IPS is compared with the actual IPS observation made by the Institute for Space-Earth Environmental Research, Nagoya University. The estimated IPS shows good agreement with the observed IPS. We demonstrated the working of the simulation system using a typical halo CME event generated by a X9.3 flare observed on September 5, 2017. We found that the CME simulation that estimates IPS most similar to the observation can most accurately predict the time of arrival of the CME to the Earth. These results suggest that the accuracy of the CME arrival time will be improved if the current MHD simulations include IPS data.

Keywords: coronal mass ejection (CME), space weather forecasting, interplanetary scintillation (IPS), data assimilation

©2019. Japan Geoscience Union. All Right Reserved.

Development of real-time prediction system of CME arrival and magnetic field with SUSANOO-CME MHD simulation

*Daikou Shiota[1,2], Seiji Yashiro[3], Kazumasa Iwai[2]

1. National Institute of Information and Communications Technology (NICT), 2. Institute for Space-Earth Environmental Research, Nagoya University, 3. Catholic University

The predictions of CME arrival to the Earth and the southward magnetic field brought by the CMEs are one of crucial tasks for space weather forecast.
We have developed an MHD simulation capable of reproducing the interplanetary propagation of multiple CMEs with internal magnetic flux rope (Shiota & Kataoka 2016) called as SUSANOO-CME. The simulation solves propagation of solar wind and CMEs in the inner heliosphere from 25 solar radii where all the balk flow exceeds fast mode speed. The information of solar wind and CME is specified at the inner boundary with empirical and analytical models using real-time observations of the Sun and the corona.
Recently, we have been constructing a new prediction system of CME impacts (CME arrival and magnetic field) utilizing SUSANOO-CME with the real-time solar observations for the purpose of use in space weather forecast in NICT. The system is capable of preforming ensemble simulation with different sets of multiple CME input parameters, which is controlled from web-browser based interfaces. The results of ensemble simulation can be evaluated with real-time IPS observation in Nagoya University (the detail is reported by Iwai et al. submitted in this session). We will report the current status of the development and discuss the future directions.

Keywords: Space weather forecast, CME, solar wind

©2019. Japan Geoscience Union. All Right Reserved.

The Role of a Tiny Brightening in a Huge Geo-effective Solar Eruption Leading to the St Patrick's Day Storm

*Yumi Bamba[1,2], Satoshi Inoue[1], Keiji Hayashi[1,3,4]

1. Institute for Space-Earth Environmental Research/Nagoya University, 2. Institute if Space and Astronautical Science/Japan Aerospace Exploration Agency, 3. Key Laboratory of Solar Activity, National Astronomical Observatories, Chinese Academy of Sciences, 4. State Key Laboratory for Space Weather, National Space Science Center, Chinese Academy of Sciences

The largest magnetic storm in solar cycle 24 was caused by a fast coronal mass ejection (CME) that was related to a small C9.1 flare that occurred on 15 March 2015 in solar active region (AR) NOAA 12297. The purpose of this study is to understand the onset mechanism of the geo-effective huge solar eruption. We focused on the C2.4 flare that occurred prior to the C9.1 flare of the filament eruption. The magnetic field structure in the AR was complicated: there were several filaments including the one that erupted and caused the CME. We hence carefully investigated the photospheric magnetic field, brightenings observed in the solar atmosphere, and the three-dimensional coronal magnetic field extrapolated from nonlinear force-free field modeling, using data from *Hinode* and *Solar Dynamics Observatory*. We found three intriguing points : (1) There was a compact but noticeably highly twisted magnetic field structure that is represented by a small filament in the C2.4 flaring region, where a tiny precursor brightening was observed before the C2.4 flare. (2) The C2.4 flaring region is located in the vicinity of a foot point of the closed field that prohibits the filament from erupting. (3) The filament shows a sudden eruption after the C2.4 flare and accompanying small filament eruption. From our analysis, we suggest that a small magnetic disturbance that was represented by the tiny precursor brightening at the time of the C2.4 flare is related to the trigger of the huge filament eruption.

Keywords: St Patrick's Day Storm, Solar Flares, Filament Eruption, Hinode, Solar Dynamics Observatory

©2019. Japan Geoscience Union. All Right Reserved.

Critical Parameters of Photospheric Magnetic Field to Produce Eruptive Solar Flares and CMEs in Active Regions

*Pei Hsuan Lin[1], Kanya Kusano[1], Daikou Shiota[2], Satoshi Inoue[1], KD Leka[1,3], Yuta Mizuno[1]

1. Institute for Space-Earth Environmental Research, Nagoya University, 2. National Institute of Information and Communications Technology, 3. NorthWest Research Associates

Solar flares and coronal mass ejections (CMEs) are eruptive phenomena caused by magnetic field in the solar corona. In particular, large eruptive events originate in active regions (AR) on the solar surface. However, it is still unclear what determines the capability of an AR to produce eruptive flares and CMEs, and it hinders our ability to predict CMEs. In this study, we propose a new parameter r_m to measure the possibility that a flare on an AR can be eruptive and produce a CME. The parameter r_m is defined by the ratio of the magnetic flux of twist higher than a threshold T_c to the overlying magnetic flux. The value of rm for each AR can be estimated using the nonlinear force-free field (NLFFF) extrapolation. Based on the data obtained by the Solar Dynamics Observatory (SDO)/Helioseismic and Magnetic Imager (HMI), we calculated the values of r_m for 29 ARs at 51 times before to flares larger than M5.0 class. We find that the foot-point of field lines with twist larger than 0.2 can well represent the flare ribbons, and we thus evaluated r_m for T_c=0.2 as a critical parameter for producing eruptive flares and CMEs using discriminant analysis. The result shows that r_m is moderately able to discriminate ARs which have capability to produce CME-accompanied flares.

Keywords: solar physics, coronal magnetic field, coronal mass ejection, solar flare

©2019. Japan Geoscience Union. All Right Reserved.

Simulation study on internal velocity field variation of eruptive prominence

*Takafumi Kaneko[1], Kanya Kusano[1]

1. Institute for Space-Earth Environmental Research, Nagoya University

Solar prominences, cool dense plasma clouds in the hot tenuous corona, sometimes erupt and evolve into coronal mass ejections. Prominence eruptions have attracted interest in the researches of space weather as well as solar physics. It is known that the interior of prominences is turbulent. Recent observational statistical studies reported that standard deviation of the Doppler velocity in the eruptive prominences started to increase several hours before eruptions even when the mean velocity was nearly zero. This finding is useful to predict prominence eruptions; however, the physical relationship between the magnetically-driven eruptive mechanisms (i.e., magnetohydrodynamic instabilities) and the internal velocity field variation of prominence has not been revealed.
In this study, we performed three-dimensional magnetohydrodynamic simulation including gravity, radiative cooling, and thermal conduction to reproduce eruption of turbulent prominence. In our simulation, a bipolar magnetic field is randomly introduced along the polarity inversion line of the sheared coronal arcade field. A magnetic flux rope is created by reconnection between the bipole and the coronal arcade field. Cool dense prominence is formed in the flux rope by radiative condensation. The prominence erupts after the flux rope exceeds the critical height of torus instability. Before the eruption, the height of flux rope axis monotonically increases; however, the velocity field inside the prominence has complicated distribution containing both upflows and downflows. We confirmed that the increase in standard deviation of the vertical velocity is quantitatively consistent with the observational results. To investigate the relationship with the magnetic field, we compared the histogram of the velocity components perpendicular and parallel to the magnetic field. As a result, we found that the upflows and downflows stem from perpendicular and parallel velocity, respectively. This result indicates that upflows and downflows are driven by Lorentz force and gravity along magnetic field, respectively. We also found that the increase in standard deviation of perpendicular velocity is larger than that of parallel velocity, suggesting that the increase in standard deviation of vertical velocity is caused mainly by increase in Lorentz force.

Keywords: solar prominences, filaments, prominence eruption

©2019. Japan Geoscience Union. All Right Reserved.

[E] Oral | P (Space and Planetary Sciences)：P-EM Solar-Terrestrial Sciences, Space Electromagnetism & Space Environment

Mon. May 27, 2019 1:45 PM - 3:15 PM JST | Mon. May 27, 2019 4:45 AM - 6:15 AM UTC | A04 TOKYO BAY MAKUHARI HALL

[P-EM12] Space Weather and Space Climate

convener:Ryuho Kataoka(National Institute of Polar Research), Antti A Pulkkinen(NASA Goddard Space Flight Center), Kanya Kusano(Institute for Space-Earth Environmental Research, Nagoya University), Kaori Sakaguchi(National Institute of Information and Communications Technology), Chairperson:Antti Pulkkinen(NASA/GSFC)

We share the latest scientific papers to understand how the solar-terrestrial environment changes in various time scales, and to discuss how we will react via international and interdisciplinary collaborations. More specifically, welcomed papers include space climate studies to reconstruct long-term variations from radio isotopes; cutting-edge observational and modeling studies of the ionosphere, geospace, heliosphere and the sun; simulation and statistical studies to predict the future space weather and space climate; applied science such as operational space weather forecast and mitigation of the social impact due to extreme space hazards.

1:45 PM - 2:00 PM JST | 4:45 AM - 5:00 AM UTC

[PEM12-13] Is intensity of auroral electrojet predictable?

★Invited Papers

*Yusuke Ebihara[1], Takashi Tanaka[2], Naoki Kamiyoshikawa[3] (1.Research Institute for Sustainable Humanosphere, Kyoto University, 2.Kyushu University, 3.Mitsubishi Electric Corporation)

2:00 PM - 2:15 PM JST | 5:00 AM - 5:15 AM UTC

[PEM12-14] Geoelectromagnetics with the Geophysical Instrument Combination of Hydro-Québec, AUTUMNX, and USArray Magnetotellurics

★Invited Papers

*Martin G Connors[1], Sébastien Guillon[2], Adam Schultz[3], Naoto Imamura[3] (1.Athabasca University, 2.Hydro-Québec TransÉnergie, 3.Oregon State University)

2:15 PM - 2:30 PM JST | 5:15 AM - 5:30 AM UTC

[PEM12-15] Quantifying the Latitudinal Extent of the Aurorae During Large Geomagnetic Storms

*Sean Blake[1,2], Antti Pulkkinen[1], Pete Schuck[1] (1.NASA Goddard Space Flight Center, Space Weather Laboratory, Greenbelt, Maryland, USA, 2.Catholic University of America, Department of Physics, Washington DC, USA)

2:30 PM - 2:45 PM JST | 5:30 AM - 5:45 AM UTC

[PEM12-16] Simulation of Geomagnetically Induced Current (GIC) Flowing in 500 kV Power Grid in Japan Including a Three-Dimensional Ground Inhomogeneity

*Satoko Nakamura[1], Yusuke Ebihara[1], Shigeru Fujita[2], Tada-nori Goto[3], Shinichi Watari[4] (1.Research Institute for Sustainable Humanosphere, Kyoto University., 2.Meteorological College, Japan Meteorological Agency, 3.Graduate School of Engineering, Kyoto University, 4.National Institute of Information and Communications Technology)

2:45 PM - 3:00 PM JST | 5:45 AM - 6:00 AM UTC

[PEM12-17] Reproducibility of the geomagnetically induced currents in Hokkaido with a two-layer conductivity model

*Takashi Kikuchi[1,2], Yusuke Ebihara[2], Kumiko K. Hashimoto[3], Shinichi Watari[4] (1.Institute for Space-Earth Environmental Research, Nagoya University, 2.Institute for Sustainable Humanosphere, Kyoto University, 3.Kibi International University, 4.National Institute of Information and Communications Technology)

3:00 PM - 3:15 PM JST | 6:00 AM - 6:15 AM UTC

[PEM12-18] Fan-shaped aurora as seen from Japan during a great magnetic storm on 11 February 1958

*Ryuho Kataoka[1], Shiori Uchino[1], yasunori Fujiwara[1], Shigeru Fujita[1], Kazuaki Yamamoto[2] (1.National Institute of Polar Research, 2.National Institute of Japanese Literature)

Is intensity of auroral electrojet predictable?

*Yusuke Ebihara[1], Takashi Tanaka[2], Naoki Kamiyoshikawa[3]

1. Research Institute for Sustainable Humanosphere, Kyoto University, 2. Kyushu University, 3. Mitsubishi Electric Corporation

A large amount of energy (of the order of 10^{11} W) is consumed in the auroral ionosphere as Joule dissipation during the substorm expansion phase. The origin of the energy consumed in the auroral ionosphere is in the solar wind, but the energy flow and conversion in between are problematic. Previously, the energy consumed in the ionosphere is thought to consist of the directly driven (DD) component and the loading and unloading (UL) component. The DD component is thought to respond to the magnetic energy entering the magnetosphere, and hence, the DD component is probably predictable. The UL component, on the other hand, is thought to be unpredictable because it might depend on the amount of released energy in the lobe. On the basis of the global magnetohydrodynamics (MHD) simulation, we show that the maximum intensity of the auroral electrojet (and the Joule dissipation rate) during the substorm expansion is well correlated with the magnetic energy entering the magnetosphere. The correlation coefficient between them is 0.90 (and 0.97). There are a few key reasons. First, the amount of the released energy from the lobe increases with the southward component of interplanetary magnetic field (SBZ) and the solar wind velocity, meaning that the amount of the released energy is regulated by the solar wind parameters. Secondly, the magnetic energy released from the lobe goes into the near-Earth reconnection region, and seems not to contribute significantly to the generation of the field-aligned current associated with the substorm expansion. Thirdly, the release of the energy lasts for ~10 minutes, whereas the auroral electrojet keeps developing for 15 minutes and more. Fourthly, 40-90% of the magnetic energy entering the magnetosphere comes from the solar wind kinetic energy for the southward IMF. About 2% of the entering energy goes into the ionosphere during the expansion phase. The ratio is almost independent of the solar wind condition. These simulation results may suggest that the maximum intensity of the auroral electrojet (and the Joule dissipation rate) is predictable when the magnetic energy entering the magnetosphere is adequately predicted.

Keywords: Substorm, Auroral electrojet, MHD simulation

©2019. Japan Geoscience Union. All Right Reserved.

Geoelectromagnetics with the Geophysical Instrument Combination of Hydro-Québec, AUTUMNX, and USArray Magnetotellurics

*Martin G Connors[1], Sébastien Guillon[2], Adam Schultz[3], Naoto Imamura[3]

1. Athabasca University, 2. Hydro-Québec TransÉnergie, 3. Oregon State University

Geoelectromagnetics is a term used by Bolduc et al. (2000) regarding a pioneering study in which electric fields near a part of the Hydro-Québec transmission network were measured during an intense auroral event. To fully characterize space weather effects on an electric power transmission network, we must proceed from the source currents and their variations, through the changing magnetic fields near Earth's surface, to the electric fields induced in the Earth and to some extent in the conducting structures directly, to electric currents flowing in the grid, and finally to the effects of such currents, ranging from voltage distortion to possible equipment damage. The more data can be measured at each link in this complex chain, the better will be our ability to monitor current events in a precautionary manner and assess the robustness of the grid to varying levels of stress.

The Hydro-Québec network has had enhanced monitoring capabilities (as well as improved ability to deal with geomagnetic stresses) since 1989 (Guillon et al., 2016). The last link of the chain, effects, is able to be well quantified, especially through measures of voltage distortion. Direct measurements of transformer grounding currents, essentially the geomagnetically induced currents (GIC) themselves, are available at a few points. The AUTUMNX magnetic network (Connors et al., 2015) complemented grid instrumentation in Québec starting in 2014, and has produced a new view of the association of magnetic variations with signals in the grid. Magnetotellurics (MT) tends to operate in campaign mode, but also measures the electric field, including at relevant low frequencies, giving a more complete indication of the geoelectromagnetic environment while also providing measurements of the frequency dependent electromagnetic impedance of the ground, which can be used to reconstruct the electrical conductivity structure of the Earth's crust and mantle.

We illustrate these comprehensive geoelectromagnetic measurements with the case of the magnetic storm of September 7-9 2017, during which the NSF EarthScope MT array installed by Oregon State University was operating in the northeastern US, near the Hydro-Québec grid, at a time when the electrojet had expanded southward. We find a close correlation of times of large magnetic field variation, measured electric fields, and harmonic distortion in the grid.

While we note the complications stressed by Love et al. (2018), we feel that the enhanced MT monitoring advocated by Love et al. (2016), would give more knowledge of geological structure and geoelectric response in northeastern North America. In this way, our understanding of GIC would be greatly improved, in the areas of understanding basic processes and hazard assessment.

Bolduc et al., A Study of Geoelectromagnetic Disturbances in Québec, 2. Detailed Analysis of a Large Event, IEEE Trans. Power Delivery, 15, 272-278 (2000)
Connors et al., The AUTUMNX Magnetometer Meridian Chain in Québec, Canada, Earth, Planets and Space, 68:2(21pp.) , doi:10.1186/s40623-015-0354-4 (2015)
Guillon et al., A Colorful Blackout: The Havoc Caused by Auroral Electrojet Generated Magnetic Field Variations in 1989, IEEE Power and Energy, doi: 10.1109/MPE.2016.2591760 (2016)
Love et al. Geoelectric hazard maps for the continental United States, Geophys. Res. Lett., 43, 9415–9424

©2019. Japan Geoscience Union. All Right Reserved.

(2016)
Love et al. Geoelectric hazard maps for the Pacific Northwest. Sp. Weather, 16, 1114–1127 (2018)

Keywords: space weather, geomagnetically induced currents, magnetometry, magnetotellurics, geomagnetic storms, instrument networks

©2019. Japan Geoscience Union. All Right Reserved.

Quantifying the Latitudinal Extent of the Aurorae During Large Geomagnetic Storms

*Sean Blake[1,2], Antti Pulkkinen[1], Pete Schuck[1]

1. NASA Goddard Space Flight Center, Space Weather Laboratory, Greenbelt, Maryland, USA, 2. Catholic University of America, Department of Physics, Washington DC, USA

As geomagnetic storms grow larger, the extent of the auroral ovals can be seen to travel further towards the equator. During the famous Carrington event for example, the aurora was reportedly seen as far South as Cuba. Accompanying the auroras are large electric currents in the ionosphere. The magnetic signature of these ionospheric currents can be detected on the ground in magnetic observatories around the world in the form of increased magnetic variations. These variations can lead to large local geoelectric fields, posing a risk to the operation of power networks around the world.

It is therefore necessary to estimate the extent of the aurora and accompanying geoelectric fields during infrequent and large-scale (1-in-100 year) events. Using three decades of historical geomagnetic data from around the world, we have developed a method to detect and quantify the extent of the auroral oval (or latitude threshold) using ground-based data. We use this to statistically estimate the southernmost extent for storms with Dst values < -600 nT, as well as the geoelectric field strengths at these latitude thresholds.

In addition, building on the work by Ngwira et al. (2014) by using magnetospheric and ionospheric magnetohydrodynamic simulations, we simulate 'worst-case' scenario superstorms of different magnitudes. Applying our threshold detecion to the magnetic field outputs of these simulations enable us to estimate the latitude thresholds for storms of magnitudes not seen in the modern era.

Keywords: Aurora, Geomagnetism, Geostorms

©2019. Japan Geoscience Union. All Right Reserved.

Simulation of Geomagnetically Induced Current (GIC) Flowing in 500 kV Power Grid in Japan Including a Three-Dimensional Ground Inhomogeneity

*Satoko Nakamura[1], Yusuke Ebihara[1], Shigeru Fujita[2], Tada-nori Goto[3], Shinichi Watari[4]

1. Research Institute for Sustainable Humanosphere, Kyoto University., 2. Meteorological College, Japan Meteorological Agency, 3. Graduate School of Engineering, Kyoto University, 4. National Institute of Information and Communications Technology

We evaluate geomagnetically induced currents (GICs) flowing in the Japanese power grid during severe space weather by using several methods. First, the three-dimensional distribution of the geomagnetically induced electric field (GIE) was calculated by using the 3D finite-difference time-domain (FDTD) method with a three-dimensional electrical conductivity model constructed from a global relief model and a global map of sediment thickness. To simulate a time evolution of magnetic storms, the sheet current with its intensity inferred from the ground magnetic disturbance for famous magnetic storms is imposed. We compared the calculated GICs with the observed ones at substations around Tokyo, and found a certain agreement when the uneven distribution of GIE is incorporated with the simulation. The simulation result shows that GIE exhibits localized, uneven distribution that can be attributed to charge accumulation due to the inhomogeneous conductivity below the Earth's surface. The charge accumulation becomes large when the conductivity gradient vector is parallel, or anti-parallel to the incident electric field. For given GIE, we calculated the GICs flowing in a simplified 500 kV power grid network in Japan. The influence of the inhomogeneous ground conductivity on GIC appears to depend on a combination of the location of substations and the direction of the source current. Second, we assume conductivity anomaly simulating a plate boundary to test the effect of large-scale underground structure on GICs. We find that these structures may strongly enhance GIC just above them. Finally, we derive transfer functions between the GIC observation at 4 substations in Japan and geomagnetic field recorded at the Kakioka station. The transfer functions are not always applicable for Japanese GIC. We will discuss the validity of the assumption of uniform ground and influence of the time variation of earthing resistance of substations.

©2019. Japan Geoscience Union. All Right Reserved.

Reproducibility of the geomagnetically induced currents in Hokkaido with a two-layer conductivity model

*Takashi Kikuchi[1,2], Yusuke Ebihara[2], Kumiko K. Hashimoto[3], Shinichi Watari[4]

1. Institute for Space-Earth Environmental Research, Nagoya University, 2. Institute for Sustainable Humanosphere, Kyoto University, 3. Kibi International University, 4. National Institute of Information and Communications Technology

Watari et al. [SW 2009], based on the GIC measurements in Hokkaido, Japan (35.7 GM Lat), found that the GIC is well correlated with the y-component magnetic field (By) (correlation coefficients > 0.8) and poor correlations with Bx,z and dBx,y,z/dt. The good correlation between the GIC and By would help predict the GIC if we have capabilities of reproducing the magnetosphere-ionosphere currents responsible for ground magnetic disturbances. To use the GIC- By relationship for the GIC prediction, we need to clarify if the good correlation is valid for any period/time scale (T) of disturbances. To address this issue, we made correlation analyses for the geomagnetic sudden commencements and pulsations (T=1-10m), substorm positive bays (30m), quasi-periodic DP2 fluctuations (20-60m), and geomagnetic storms (1-20h) as well as quiet-time diurnal variations (3-12h). We found that the correlation is good for short period (cc > 0.8 for T < 1 h), but poor for long periods (cc < 0.3 for T > 6 hours). Using the conventional induction theory based on the Faraday’s, Ampere’s and Ohm’s laws, we calculated the electric field (GIE) induced by By as a convolution of dBy/dt and step response of a uniform conductor. The GIE is found to be better correlated with the GIC for the long-period disturbances (cc > 0.9), whereas the correlation with By remains better for short period disturbances. This result requires us to use two models depending on the period of disturbances. To obtain a model applicable to any period, we made constructed a two-layer model with higher conductivity on the top. We show that the two-layer model is capable of reproducing the GIC with high correlations (cc > 0.9) for any period of disturbances ranging from 1 min to 10 hours. It should be noted; however, the capability of the model may depend on the direction of the power transmission line relative to the coast line and also depend on the structure of the Earth’s conductivity.

Keywords: geomagnetically induced current, Hokkaido, two-layer conductivity model

©2019. Japan Geoscience Union. All Right Reserved.

Fan-shaped aurora as seen from Japan during a great magnetic storm on 11 February 1958

*Ryuho Kataoka[1], Shiori Uchino[1], yasunori Fujiwara[1], Shigeru Fujita[1], Kazuaki Yamamoto[2]

1. National Institute of Polar Research, 2. National Institute of Japanese Literature

A fan-shaped aurora was photographed at Memambetsu, Hokkaido Japan during a great magnetic storm on Feb 11, 1958. This is the first and oldest photograph record of auroras as observed in Japan, and many hand-written drawings were also recorded at the same time during the February 1958 event, giving a rare opportunity of the coexistence of photograph images and hand-written drawings. In fact, the combination of photographs and drawings of the 1958 event reminds us of the great red aurora with fan-shaped white pillars as illustrated during other great magnetic storms in 1872 and in 1770. From the analysis of newly digitized microfilm data, it is also found that the fan-shaped aurora appeared during the peak activity of magnetic storm, and moved westward at 0.4 km/s at 400 km altitude at 38-40 deg magnetic latitudes, which is consistent with the enhanced convection pattern in middle latitude during storm time. Such a fan-shaped aurora can be a fundamental characteristic of middle-latitude evening-to-midnight auroras during great magnetic storms, which show the most destabilized transient appearance of the inner magnetosphere.

Keywords: aurora, magnetic storm, historical records

©2019. Japan Geoscience Union. All Right Reserved.

[E] Oral | P (Space and Planetary Sciences)：P-EM Solar-Terrestrial Sciences, Space Electromagnetism & Space Environment

Mon. May 27, 2019 3:30 PM - 5:00 PM JST | Mon. May 27, 2019 6:30 AM - 8:00 AM UTC | A04 TOKYO BAY MAKUHARI HALL

[P-EM12] Space Weather and Space Climate

convener:Ryuho Kataoka(National Institute of Polar Research), Antti A Pulkkinen(NASA Goddard Space Flight Center), Kanya Kusano(Institute for Space-Earth Environmental Research, Nagoya University), Kaori Sakaguchi(National Institute of Information and Communications Technology), Chairperson:Kanya Kusano(Nagoya University)

We share the latest scientific papers to understand how the solar-terrestrial environment changes in various time scales, and to discuss how we will react via international and interdisciplinary collaborations. More specifically, welcomed papers include space climate studies to reconstruct long-term variations from radio isotopes; cutting-edge observational and modeling studies of the ionosphere, geospace, heliosphere and the sun; simulation and statistical studies to predict the future space weather and space climate; applied science such as operational space weather forecast and mitigation of the social impact due to extreme space hazards.

3:30 PM - 3:45 PM JST | 6:30 AM - 6:45 AM UTC

[PEM12-19] Application Usability Levels: Their evolution and eco-system

★Invited Papers

*Alexa Jean Halford[1], Adam Kellerman[2], Jeff Klenzing[3], Katherine Garcia-Sage[3], Brett A Carter[4], Daniel T Welling[5], Barbara Thompson[3], Antti A Pulkkinen[3] (1.The Aerospace Corporation, 2.UCLA, 3.NASA/GSFC, 4.RMIT, 5.UT Arlington)

3:45 PM - 4:00 PM JST | 6:45 AM - 7:00 AM UTC

[PEM12-20] The Operational Space Weather Forecast at NICT, Japan

★Invited Papers

*Kosuke Sakai[1], Kentaro Ukawa[1], Kentaro Kawahara[1], Mamoru Ishii[2], Yuki Kubo[2] (1.Systems Engineering Consultants Co., LTD., 2.National Institute of Information and Communications Technology)

4:00 PM - 4:15 PM JST | 7:00 AM - 7:15 AM UTC

[PEM12-21] PROGRESS: An overview of data products

*Michael A Balikhin[1], Simon N Walker[1] (1.University of Sheffield)

4:15 PM - 4:30 PM JST | 7:15 AM - 7:30 AM UTC

[PEM12-22] The Probability of Satellite Anomalies by a Disastrous Solar Flare

*Daikichi SEKI[1,2,3] (1.Graduate School of Advanced Integrated Studies in Human Survivability, Kyoto University, 2.Centre for the Study of Existential Risk, University of Cambridge, 3.Astronomical Observatory, Kyoto University)

4:30 PM - 4:45 PM JST | 7:30 AM - 7:45 AM UTC

[PEM12-23] **Operational Forecasting of Solar Flares using Deep Neural Network**

*Naoto Nishizuka[1], Yuki Kubo[1], Komei Sugiura[1], Mitsue Den[1], Mamoru Ishii[1] (1.National Institute of Information and Communications Technology)

4:45 PM - 5:00 PM JST | 7:45 AM - 8:00 AM UTC

[PEM12-24] **Spring-Autumnal asymmetry in geomagnetic activity and its origin over last 140 years**

*Hao Luo[1], Xiaoming Sha[1] (1.IGGCAS)

Application Usability Levels: Their evolution and eco-system

*Alexa Jean Halford[1], Adam Kellerman[2], Jeff Klenzing[3], Katherine Garcia-Sage[3], Brett A Carter[4], Daniel T Welling[5], Barbara Thompson[3], Antti A Pulkkinen[3]

1. The Aerospace Corporation, 2. UCLA, 3. NASA/GSFC, 4. RMIT, 5. UT Arlington

As space physics becomes both more interdisciplinary and more intertwined with commercial and government operations, there is a need for a framework to easily identify what projects can be used for specific applications and how close each project is to routine autonomous or on-demand implementation and operation. We have developed the Application Usability Level (AUL) framework and encourage publication of instrument-like papers for delivering and publicizing AULs to help the community quantify the progress of successful applications, metrics, and validation efforts.

In a given project within the AUL framework, there is typically a diverse eco-system of individuals necessary to ultimately produce a useful space weather product or productive research collaboration. For example, in the case of non-academic fields, users and researchers alike may benefit from a translator, i.e. a *broker*, who may help with the effective transition from research to operations. *Independent validators* are another essential player for validation efforts and comparing like products for a specified application. In many cases, the different players throughout the process will act in multiple roles as well as act in different roles for different projects and AUL pathways.

This paper we discuss the collaborative roles that lead from basic research to successful application within or outside the scientific community and provide examples of how this collaborative application ecosystem is maintained. We will also provide examples of space weather projects using the AUL framework, and show how it can contribute to the project's success. As always, a healthy eco-system can result in benefits for the end user and new exciting research opportunities.

This work has been completed as part of the activities of the Assessment of Understanding and Quantifying Progress working group which is part of the International Forum for Space Weather Capabilities Assessment.

Keywords: Tracking progress, Research to operations, Space Weather

©2019. Japan Geoscience Union. All Right Reserved.

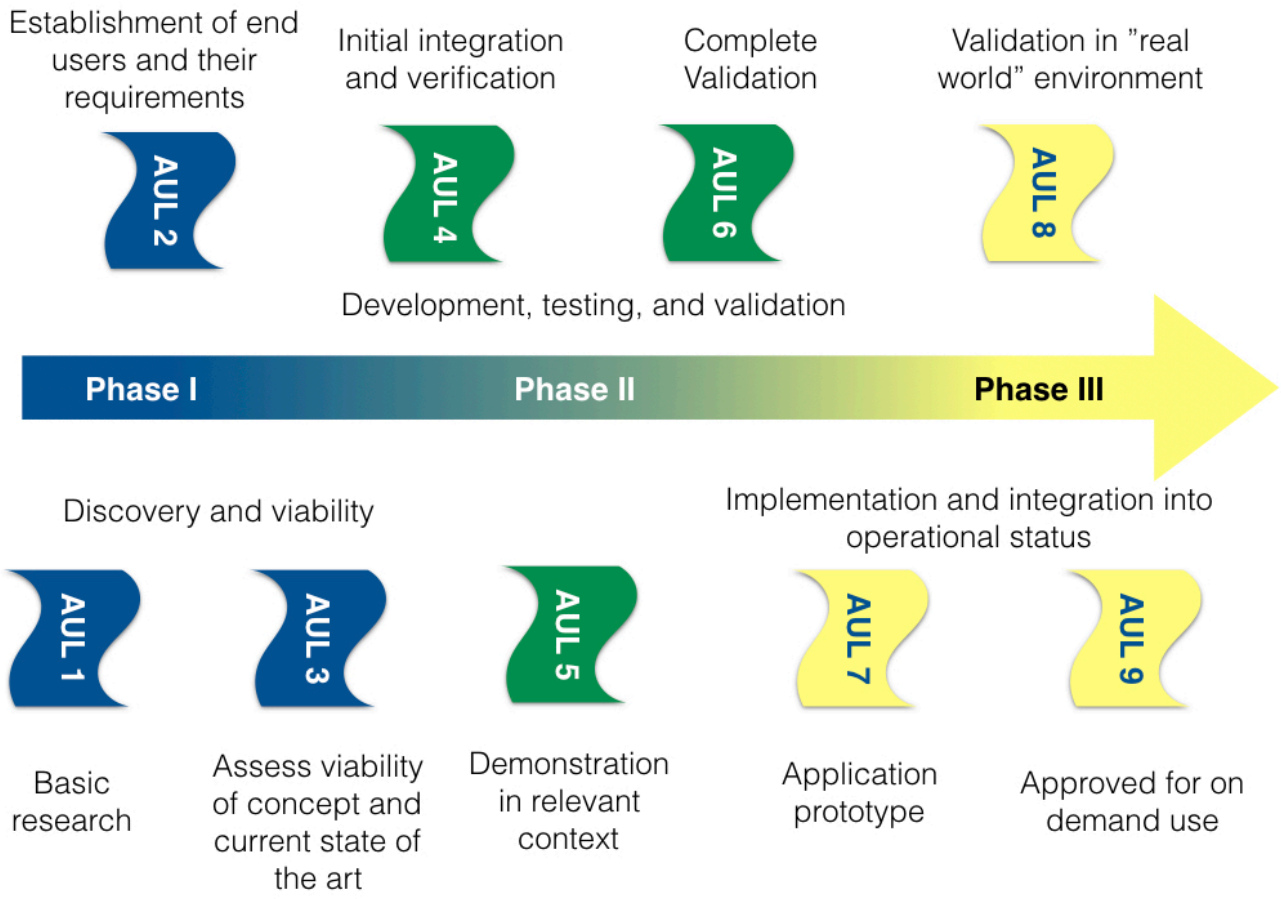

©2019. Japan Geoscience Union. All Right Reserved.

The Operational Space Weather Forecast at NICT, Japan

*Kosuke Sakai[1], Kentaro Ukawa[1], Kentaro Kawahara[1], Mamoru Ishii[2], Yuki Kubo[2]

1. Systems Engineering Consultants Co., LTD., 2. National Institute of Information and Communications Technology

At the Space Weather Forecast Center of the National Institute of Information and Communications Technology, the latest 24-hour outlines and forecasts of space weather are provided to space weather users every day.
Delivers of space weather information have been continuously performed for over 50 years as ISES Regional Warning Center, Japan, and operators in the space weather forecast center are in charge of this task.
The operational work is conducted 7 days a week. Operators collect and analyze various observation data and simulation results provided from domestic and overseas collaborators, and summarize current space weather conditions before daily briefing at 14:30 JST.
In order to determine the next 24-hour forecast, operators organize a discussion meeting with specialists, and deliver forecasts before the due at 16 JST.
In addition, operators hold regular monthly meetings, consider the results of the forecasts, and feed back to improve next forecast accuracy.
When a remarkable space weather phenomenon occurs, operators has a responsibility to deliver alerts information immediately.
In this presentation, we introduce the daily work content of the space weather forecaster and the procedure up to deciding the content of the forecast with actual case examples.
In addition, we will also introduce contrivances and other measures to operate 365 days a year without breaks.

Keywords: Space Weather

©2019. Japan Geoscience Union. All Right Reserved.

PROGRESS: An overview of data products

*Michael A Balikhin[1], Simon N Walker[1]

1. University of Sheffield

PROGRESS, an EC Horizon 2020 funded project, used state of the art modelling techiniques inorder to derive forecasts for the evolution of geomagnetoc indices, and the fluxes of electrons at geostationary orbit and within the inner magnetosphere. This presentation provides a review of the aims of PROGRESS and an overview of the tools developed to meet these aims.

Keywords: radiation belt forecasts, geomagnetic index forecasts

©2019. Japan Geoscience Union. All Right Reserved.

The Probability of Satellite Anomalies by a Disastrous Solar Flare

*Daikichi SEKI[1,2,3]

1. Graduate School of Advanced Integrated Studies in Human Survivability, Kyoto University, 2. Centre for the Study of Existential Risk, University of Cambridge, 3. Astronomical Observatory, Kyoto University

The Sun has a potential risk of various socioeconomic impacts on our human society. It often produces various eruptive phenomena such as a solar flare and a coronal mass ejection, which sometimes bring adverse effect to us like satellite anomalies, radiation exposure, and huge blackouts. Recently, it was revealed that a “super-flare”, a flare whose energy is 100 times larger than X10-class flare, can occur once in 1000 years from statistical and theoretical points of view [Maehara et al. 2012, Shibayama et al. 2013, Shibata et al. 2013].

However, though there are many assessment studies of “moderate” solar eruptive phenomena, the assessment of “disastrous” solar eruptive phenomena like a super-flare has been little conducted. For this reason, this research aims to evaluate the frequency (or probability) and the possible socioeconomic damage of a super-flare, especially focusing on satellite anomalies.

Using various data sets about satellites, their anomalies, flares, and plasma environment around the Earth*, 154 X-class flare events with 9 relating parameters (peak flux of X-ray (0.1–0.8 nm), integral fluxes of electron (> 2 MeV) and of proton (> 1, 5, 10, 30, 50, 60, 100 MeV)) were selected. To avoid multi-collinearity, Ridge regression model was used to compute the regression to the satellite anomaly rate (1/satellite/event). Also 10-fold cross validation was performed. After obtaining the model, the possible plasma parameters in case of X1000-class flare assumed by Takahashi et al. 2016 were input into the model.

As a result, we obtained the model with its coefficient of determination of 0.607 and its Pearson correlation coefficients of 0.691 ±0.212 (for 100 times randomly chosen dataset). Assuming that electron and proton with any energy follow the same scaling law, with applying scaling law by Takahashi et al. 2016, 0.573 satellite anomaly rate (57.3% per satellite per event) was obtained. It should be noted that the scaling law provided by Takahashi et al. 2016 is upper limit, so in the actual case, rate should be lower. The validity of assumption, the comparison between this research and others (Pilipenko et al. 2006; Iucci et al. 2005; Odenwald et al, 2006, 2007), and the possible socioeconomic loss will be also discussed.

* NOAA NGDC Spacecraft Anomaly Data, Satellite Catalogue (https://www.celestrak.com/satcat/search.php), NOAA GOES flare report (https://www.ngdc.noaa.gov/stp/space-weather/solar-data/solar-features/solar-flares/x-rays/goes/xrs/) , and OMNI 2 database

Keywords: space weather, satellite anomaly, super-flare

©2019. Japan Geoscience Union. All Right Reserved.

Operational Forecasting of Solar Flares using Deep Neural Network

*Naoto Nishizuka[1], Yuki Kubo[1], Komei Sugiura[1], Mitsue Den[1], Mamoru Ishii[1]

1. National Institute of Information and Communications Technology

Solar flares are the largest explosive phenomena in the Heliosphere. They affect the earth by X-ray and UV emissions, high energy particles, and magnetic storms, causing troubles of satellites and blackout in a large area. To reduce the risk of social impact caused by solar flares and space weather, it is very important to predict solar flares with high accuracy. In our institute NICT, we have predicted solar flares in the daily forecasting meeting by an empirical method. However, the amount of solar observation data is so huge that we cannot deal with all the data by hands.

Here we developed an operational system of solar flare prediction using a deep neural network (DNN), named Deep Flare Net (DeFN; Nishizuka et al. 2018 ApJ), and we started to run it in the operation. The model can predict probabilities of the maximum class of flares occurring in the following 24 hr. The training dataset is maded by 3x10^5 images during 2010-2015 taken by SDO, from which we detected active regions and calculated 79 features for each region attached with the flare occurrence labels (X, M, C). We used features in our previous work (Nishizuka et al. 2017) and added novel features for operational prediction: coronal hot brightening at 131 A (T=10^7 K) and the histories of X-ray and 131 A emissions 1 and 2 hr before an image. The prediction data in the near real-time is downloaded from JSOC server operated by Stanford University and NASA, and all the active regions and features are automatically detected and calculated. The prediction results will be shown in the web site of NICT. In this talk, we will introduce our DeFN model and operational forecasting system and would like to discuss how it works in the daily operations.

Keywords: Solar Flare , Space Weather, Machine Learning, prediction, Operation

©2019. Japan Geoscience Union. All Right Reserved.

Spring-Autumnal asymmetry in geomagnetic activity and its origin over last 140 years

*Hao Luo[1], Xiaoming Sha[1]

1. IGGCAS

Spring-Autumnal asymmetry (SA asymmetry) from years 1873-2010 in the geomagnetic activity is investigated based on the geomagnetic indices (aa, Ap and Kp). Results have shown that in general the SA asymmetry of the geomagnetic activity appears to be alternation, except for the interval during which the change of dominant solar dipole magnetic field polarity occurs. Our study implies that both the polarity of the main solar dipole field and the north-south asymmetry of the sunspot area in the two solar hemispheres control the strength of the south component (*Bs*) of the interplanetary magnetic field (IMF) near the Earth and the resulting SA asymmetry of the geomagnetic activity in the corresponding seasons. A simple sector structure model is devised to establish the relationship between the polarity of solar main dipole magnetic field, the IMF *Bs* component and the corresponding SA asymmetry in the geomagnetic activity. This is confirmed by examining the solar wind parameters from the spacecraft observations during the recent decades.

Keywords: Spring-Autumnal asymmetry, Solar magnetic polarity

©2019. Japan Geoscience Union. All Right Reserved.

[E] Oral | A (Atmospheric and Hydrospheric Sciences)：A-OS Ocean Sciences & Ocean Environment

Mon. May 27, 2019 3:30 PM - 5:00 PM JST | Mon. May 27, 2019 6:30 AM - 8:00 AM UTC | 301B 3F

[A-OS09] Ocean Mixing Processes: Impact on Biogeochemistry, Climate and Ecosystem

convener:Ichiro Yasuda(Atmosphere and Ocean Research Institute, The University of Tokyo), Toshiyuki Hibiya(Department of Earth and Planetary Science, Graduate School of Science, University of Tokyo), Jun Nishioka(Hokkaido University, Institute of low temperature sciences), Shin-ichi Ito(Atmosphere and Ocean Research Institute, The University of Tokyo), Chairperson:Toshiyuki Hibiya(Department of Earth and Planetary Science, Graduate School of Science, The University of Tokyo)

The interdisciplinary study on ocean diapycnal mixing and its impacts (Ocean Mixing Processes: Impact on Biogeochemistry, Climate and Ecosystem (OMIX) 2015-2020) is opening the integrated sciences from physical, chemical, biological oceanography to climate and fisheries sciences. In this section, results during the four years of OMIX projects and other related presentations are all welcome to be summarized and to facilitate plans of next projects.

3:30 PM - 3:45 PM JST | 6:30 AM - 6:45 AM UTC

[AOS09-18] Searching 18.6 year tidal modulation impact in a global gridded ocean oxygen dataset with its improvements

*Shoshiro Minobe[1] (1.Earth and Planetary Sciences, Faculty of Science, Hokkaido University)

3:45 PM - 4:00 PM JST | 6:45 AM - 7:00 AM UTC

[AOS09-19] Contribution of tidal energy dissipation to variations of transient climate response and steric sea level rise through ocean heat uptake

*Michio Watanabe[1], Hiroaki Tatebe[1], Tatsuo Suzuki[1], Kaoru Tachiiri[1] (1.Japan Agency for Marine-Earth Science and Technology)

4:00 PM - 4:15 PM JST | 7:00 AM - 7:15 AM UTC

[AOS09-20] A Wave Resolving Simulation for Upper Ocean Turbulence Driven by Wave-Current Interaction

*Yutaka Yoshikawa[1], Yasushi Fujiwara[1], Yoshimasa Matsumura[2] (1.Graduate School of Science, Kyoto University, 2. Atmosphere and Ocean Research Institute, The University of Tokyo)

4:15 PM - 4:30 PM JST | 7:15 AM - 7:30 AM UTC

[AOS09-21] **Revisiting the Characteristics of Mixing Efficiency in the Brazil Basin**

*Takashi Ijichi[1], Louis St. Laurent[1], Kurt Polzin[1] (1.Woods Hole Oceanographic Institution)

4:30 PM - 4:45 PM JST | 7:30 AM - 7:45 AM UTC

[AOS09-22] Instabilities of finite-amplitude internal wave beams

*Yohei Onuki[1], Yuki Tanaka[2] (1.Research Institute for Applied Mechanics, Kyushu University, 2.Department of Earth and Planetary Science, Graduate School of Science, The University of Tokyo)

4:45 PM - 5:00 PM JST | 7:45 AM - 8:00 AM UTC

[AOS09-23] Evaluation of nutrient flux enhanced by double diffusion in the Kuroshio using glider measurements

*Keunjong Lee[1], Ryo Yamamoto[1], Ichiro Yasuda[1], Takahiro Tanaka[2] (1.Atmosphere and Ocean Research Institute, 2.Tohoku National Fisheries Research Institute, Japan Fisheries Research and Education Agency)

Searching 18.6 year tidal modulation impact in a global gridded ocean oxygen dataset with its improvements

*Shoshiro Minobe[1]

1. Earth and Planetary Sciences, Faculty of Science, Hokkaido University

The 18.6 year modulation of tidal mixing plays important roles in the ocean as reported by regional analyses by Osafune and Yasuda (2006, 2010) and others. In those studies, they found that ocean water properties including dissolved oxygen concentration vary at the 18.6 year period in a manner consistent with the vertical mixing changes due to the tidal mixing modulation. Dissolved oxygen concentration is interesting not only as a tracer but also because it is important in marine ecosystems. In particular, superposition of 18.6 year variability in addition to the oxygen decline trend known as the ocean deoxygenation due to the global warming can cause more serious damages for marine animals in the specific phase of tidal modulation.

The present study aims to understand the impacts of 18.6 year tidal mixing modulation in the ocean oxygen field more systematically than the previous studies did by analyzing a global gridded dataset of dissolved oxygen concentration. A preliminary analysis using the dataset used by Ito et al. (2017 GRL) for upper 1,000 m indicates that the 18.6 year variation of oxygen concentration also occurs in regions where previous studies did not reported tidal modulation influence, including a region near the Izu-Ogasawa Ridge. In order to obtain the better spatial and temporal coverage, the dataset is and will be improved with two steps. One is to expand its vertical coverage to the top 1,000 m to 6,000 m, and the other is to use the latest version of the World Ocean Database released in September 2018. The first step has been completed, and the second step is planned to be completed in this summer. At the presentation, the analysis results based on the latest gridded dataset will be shown.

Keywords: decadal variability, biogeochemistry, climate variability and change

©2019. Japan Geoscience Union. All Right Reserved.

Contribution of tidal energy dissipation to variations of transient climate response and steric sea level rise through ocean heat uptake

*Michio Watanabe[1], Hiroaki Tatebe[1], Tatsuo Suzuki[1], Kaoru Tachiiri[1]

1. Japan Agency for Marine-Earth Science and Technology

Micro-scale turbulent mixing due to tide-induced internal wave breaking is a key process to determine the strength and pattern of the global ocean overturning circulation, that redistributes the heat all over the world ocean. Heat redistribution in the ocean have a strong impact on ocean heat uptake (OHU), thus transient climate response (TCR) and steric sea level rise (SLR) under the global warming. To study the impact of the vertical diffusivity distribution on the TCR and steric SLR, we ran a climate model of which value of CO_2 concentration is increased by 1% yr^{-1} for 150 years, employing each of two vertical diffusivity distributions in the ocean, an empirical one-dimensional one (CTRL) and a three-dimensional one considering tidal energy dissipation (TED). In TED under the pre-industrial forcing, the larger sea ice in the Southern Ocean prevents the air-sea heat flux, leading to weaker bottom water formation and lower air temperature than in CTRL. The less effective heat transport to the deep layers in TED causes less OHU and larger TCR than in CTRL by about 0.16˚C. In addition, smaller ocean heat content change in TED than in CTRL leads to significant future sea-level depression of ~0.4 m in the Southern Ocean. Since OHU under the global warming is controlled by the distribution of vertical diffusivity, it is necessary to clarify its global distribution in the real ocean for reliable TCR estimation and future SLR projection.

Keywords: diapycnal diffusivity, transient climate response, sea level rise, global warming, climate model, ocean heat uptake

©2019. Japan Geoscience Union. All Right Reserved.

A Wave Resolving Simulation for Upper Ocean Turbulence Driven by Wave-Current Interaction

*Yutaka Yoshikawa[1], Yasushi Fujiwara[1], Yoshimasa Matsumura[2]

1. Graduate School of Science, Kyoto University, 2. Atmosphere and Ocean Research Institute, The University of Tokyo

Turbulence in the upper ocean sets bulk properties of the upper ocean. For example, turbulence deepens the surface mixed layer (ML) and entrains low-temperature water below the layer to determine the ML depth and sea surface temperature (SST), which are key parameters for large-scale ocean and climate processes. Quantitative evaluation and parameterization of the upper ocean turbulence thus have crucial importance on the large-scale studies.

Recent studies revealed that turbulence induced by the surface wave has larger impact on the ML deepening than ever considered. Good example is drastic deepening of the ML and significant decrease in SST simulated in the summer Southern Ocean if parameterized wave-induced mixing is included in the simulation (e.g., Li et al. 2016). Among three types of wave-induced turbulence, surface wave breaking, Langmuir turbulence (LT) and nonbreaking-wave induced turbulence (NBWT), the latter two are considered to have significant impacts on the ML deepening. LT is associated with Langmuir circulations (LCs), the secondary circulations driven by the surface waves interacted with the wind-driven currents (e.g., Leibovich 1980). Previous theoretical studies (Craik and Leibovich 1976) showed that the interaction can be represented solely by the vortex force, vortex tilting by the Stokes drift (the Lagrangian velocity due to the surface wave) in the wave-filtered momentum equation. Many simulations with this vortex force representation have been performed so far (e.g., Skyllingstad and Denbo 1995). However, this theoretically-derived representation has not been validated by field or numerical experiments. As a consequence, there are controversial discussions about the validity of the representation and hence the simulation results with the representaion (e.g., Mellor 2016 and Ardhuin et al. 2017). NBWT on the other hand is suggested to be caused without winds (e.g., Qiao et al. 2004; Babanin 2006), but no detailed mechanism was proposed for the turbulence generation. As a result, some people consider that NBWT is the same as LT, even though LT is dependent on winds while NBWT is not. Thus, mechanism of the wave-induced turbulence is not clearly understood.

The present study is intended to clarify dynamics involved in the wave-induced turbulence. To this aim, we developed a new numerical model in which surface waves are explicity and accurately simulated. This wave-resolving simulation provides an unique opportunity to investigate how the surface waves drive / induce turbulence. We used this model to simulate LC at first (Fujiwara et al. 2018). A wave-tank simulation was performed in which a monochromatic surface wave propagated in the surface wind direction. We found that LCs were successfully reproduced through the wave-current interaction (see attached figure). Vorticity analysis showed that the interaction is well represented by the vortex force. We also performed the simulation without the surface wind, and found that NBWT was certainly generated. The virtual wave stress was found to be a key for NBWT generation in our simulation, which induced velocity shear near the surface that interacted with the surface wave as was found in the LC simulation. The wave-resolving simulation also provided an alternative Eulerian view of the vortex force that was originally viewed from the Lagrangian frame (Stokes drift), that is, rectified vortex tilting/shrinking/streatching by orbital motions of the surface waves.

©2019. Japan Geoscience Union. All Right Reserved.

Keywords: Upper Ocean Turbulence, Surface Wave - Current Interaction, Langmuir Circulation, Non-Breaking Wave Turbulence

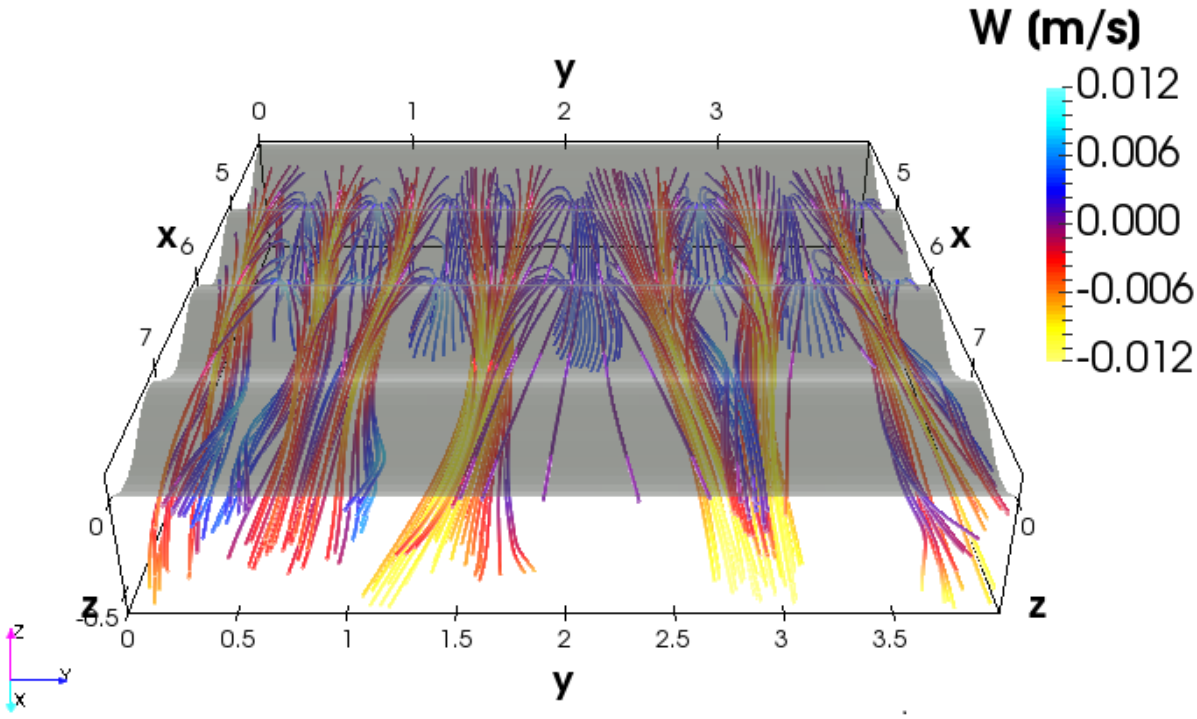

©2019. Japan Geoscience Union. All Right Reserved.

Revisiting the Characteristics of Mixing Efficiency in the Brazil Basin

*Takashi Ijichi[1], Louis St. Laurent[1], Kurt Polzin[1]

1. Woods Hole Oceanographic Institution

It is still controversial whether or not the dissipation flux coefficient Γ, often referred to as the “mixing efficiency”, is a global constant of 0.2. A primary justification for continuing to use this conventional value comes from a number of dedicated tracer-release/microstructure surveys done over the past three decades. Most notably, studies in the Brazil Basin have been the basis for examining the characteristics of mixing in the abyssal interior of the global ocean. Here, using recent microstructure data also collected in the Brazil Basin, we revisit the characteristics of Γ in the abyssal interior. It is shown that Γ, estimated from averaged profiles of the TKE dissipation rate and the thermal variance dissipation rate, actually lies around 0.2 in the pycnocline, but on the other hand, it tends to increase up to 0.4-0.8 toward the bottom. Such near-bottom high efficiency appears to be associated with weak stratification in the bottom water. Furthermore, one microstructure profile appears to reach down to within the thin bottom boundary layer: Γ abruptly decreases to $O(10^{-2})$ within 50 m above the bottom, which is reasonable given the no buoyancy flux condition at the bottom. We will also examine these results using the earlier generation microstructure datasets collected in the Brazil Basin.

©2019. Japan Geoscience Union. All Right Reserved.

Instabilities of finite-amplitude internal wave beams

*Yohei Onuki[1], Yuki Tanaka[2]

1. Research Institute for Applied Mechanics, Kyushu University, 2. Department of Earth and Planetary Science, Graduate School of Science, The University of Tokyo

Previous studies have shown that instability of small-amplitude internal wave beams, generated by a surface tide flowing over topography, is most significant at a particular latitude where parametric subharmonic instability (PSI) excites inertial oscillations. Here we extend the discussion to the case of finite-amplitude beams using a new kind of Floquet approach. The disturbance growth rate obtained is quantified in terms of two non-dimensional parameters A and F: velocity shear divided by the buoyancy frequency and the Coriolis parameter divided by the beam frequency. If A is small, PSI is indeed the principle mode under the condition $F < 0.5$ with the maximum growth rate achieved when the equality holds. As A is increased, however, instability comes to occur even for $F > 0.5$ but the location of the maximum instability shifts towards lower F, thus totally changing its latitudinal dependence. The resulting energy spectrum is significantly Doppler shifted, and therefore distinguished from that made by PSI. These findings are useful to quantify the energy loss of internal wave beams that causes water mixing prevailing in the major generation sites of internal tides.

Keywords: internal wave, instability, ocean mixing

©2019. Japan Geoscience Union. All Right Reserved.

Evaluation of nutrient flux enhanced by double diffusion in the Kuroshio using glider measurements

*Keunjong Lee[1], Ryo Yamamoto[1], Ichiro Yasuda[1], Takahiro Tanaka[2]

1. Atmosphere and Ocean Research Institute, 2. Tohoku National Fisheries Research Institute, Japan Fisheries Research and Education Agency

Kuroshio is a very strong current, western boundary current of North Pacific subtropical current system. Strong vertical mixing intensifies through various physical processes were reported in the vicinity of the Kuroshio system. Consequently, this enhanced mixing is considered to supply the nutrients from the lower layer to the euphotic layer and improve the biological productivity.

Extensive measurements were carried out to investigate the detailed structures of turbulence, hydrography, chlorophyll-a using a glider, SeaExplorer manufactured by Alseamar whose 1st science mission, equipped with two shear probes, fast response thermistor, CTD, dissolved oxygen sensor, fluorometer. The fine measurement of 66 casts lasted for 7 days during 20-27, June 2017. Although only 30 % of data acquired by shear probe were survived under the criterion following Peterson et al., (2014), a newly developed method estimating turbulent intensity using a FP07 sensor was introduced.

While, calculated vertical nutrient flux is not quite high supporting biological productivity as we expected. Contribution of double diffusion which intensify the vertical diffusivity could be considered as development of chlorophyll-a patch at subsurface. Previous research already introduced the possibility of enhanced mixing from double diffusion (Nagai et al., 2015, Inoue et al., 2007) and Hamilton et al., (1989) showed underestimation of vertical nutrient flux without using vertical eddy diffusivity for salt in case of salt finger. Interacted with low salinity water which was occurred during our mission show another evidence for supporting this hypothesis.

Following the parameterization of McDougall and Ruddick (1992), mixing efficiency for salt finger and enhancement of salt(nutrient) flux were estimated to be somewhat effective. Parameterized nutrient flux in salt finger favorable layer is 37% larger than the turbulent nutrient flux accepting mixing efficiency 0.2 proposed by Osborn et al., (1980). This value needs to be examined through statistical approach or more careful insight and will be discussed later.
The full path of glider shows Kuroshio interact with various waters with different salinity and temperature. For example, low salinity and low temperature water intruded at subsurface during 23-24, June. Around 600 m during 26-27, June we also found salinity minimum which was assumed with North Pacific Intermediate Water. This feature reminds us considerable nutrient flux with vertical mixing by double diffusive processes in addition to mechanical turbulence. Double diffusive process might be attributed to the intrusion, development, modification of relatively low salinity waters. We found double diffusive regime occurs especially at upper boundary of relatively low salinity layer.

Keywords: Vertical mixing, Double diffusion, nutrient flux, Kuroshio

©2019. Japan Geoscience Union. All Right Reserved.

[E] Oral | A (Atmospheric and Hydrospheric Sciences)：A-OS Ocean Sciences & Ocean Environment

Mon. May 27, 2019 9:00 AM - 10:30 AM JST | Mon. May 27, 2019 12:00 AM - 1:30 AM UTC | 302 3F

[A-OS12] Marine ecosystems and biogeochemical cycles: theory, observation and modeling

convener:Shin-ichi Ito(Atmosphere and Ocean Research Institute, The University of Tokyo), Takafumi Hirata(Faculty of Environmental Earth Science, Hokkaido University), Enrique N Curchitser(Rutgers University New Brunswick), Eileen E Hofmann(Old Dominion University), Chairperson:Shin-Ichi Ito(The University of Tokyo)

The ocean accounts for about 50% of global net primary production. This production is significant for carbon cycling and ecosystem functioning, and is related directly or indirectly to a variety of climatic and ecological phenomena. The responses to natural and anthropogenic environmental stressors that influence marine production and diversity can cause perturbations to marine ecosystems that alter trophic dependencies and interactions among organisms at a range of space and time scales. Quantification of the principal mechanisms driving spatio-temporal variability of marine ecosystem remains to be done, especially in terms of evaluation of uncertainty in responses. As a result, evaluating vulnerability of marine ecosystems to environmental change requires systematic and holistic approaches that integrate physics to ecology and are based in observations and modelling. In addition, expectations to deliver these science to public society is raising. This session aims to provide a venue for not only discussing recent advances in understanding marine biogeochemical cycles, ecosystems and their interactions, but also networking with a variety of people to seed new ideas in marine ecological research. Observational, modeling and conceptual studies, including technological development and operational applications, that consider linkages among biogeochemical and ecosystem processes, biodiversity, and the effects of multiple stressors from molecular to planetary scales are encouraged.

9:00 AM - 9:10 AM JST | 12:00 AM - 12:10 AM UTC

Introduction

9:10 AM - 9:30 AM JST | 12:10 AM - 12:30 AM UTC

[AOS12-01] Projected coastal hypoxia in a coupled bio-physical model of the California Current System.

★Invited Papers

*Enrique N Curchitser[1], Raphael Dussin[1,2], Charles Stock[3], Nicoals van Oostende[4] (1.Rutgers University New Brunswick, 2.Lamont-Doherty Earth Observatory of Columbia University, 3.NOAA Geophysical Fluid Dynamics Laboratory, 4.Princeton University)

9:30 AM - 9:45 AM JST | 12:30 AM - 12:45 AM UTC

[AOS12-02] **Decadal salinity variation in the western North Pacific correlated with the strength of the Oyashio and the Kuroshio Extension**

*Hitoshi Kaneko[1], Takeshi Okunishi[2], Shinya Kouketsu[3], Sachihiko Itoh[1], Takashi Seto[4], Hiroshi Kuroda[5], Yugo Shimizu[4] (1.Atmosphere and Ocean Research Institute, The University of Tokyo, 2.Tohoku National Fisheries Research Institute, Japan Fisheries Research and Education Agency, 3.Japan Agency for Marine-Earth Science and Technology, 4.National Research Institute of Fisheries Science, Japan Fisheries Research and Education Agency, 5.Hokkaido National Fisheries Research Institute, Japan Fisheries Research and Education Agency)

9:45 AM - 10:00 AM JST | 12:45 AM - 1:00 AM UTC

[AOS12-03] **Multiscale routes to supply nutrients through the Kuroshio nutrient stream**

*Takeyoshi Nagai[1], Sophie Clayton[2], Yusuke Uchiyama[3] (1.Department of Ocean Sciences, Tokyo University of Marine Science and Technology, 2.Ocean, Earth & Atmospheric Sciences, Old Dominion University, 3.Kobe University)

10:00 AM - 10:15 AM JST | 1:00 AM - 1:15 AM UTC

[AOS12-04] **Seasonal variability of upper-ocean primary production around the Kuroshio analyzed using a ROMS-NPZD model**

*Xu Zhang[1], Yusuke Uchiyama[1,2], Yota Suzue[3], Hidekatsu Yamazaki[4] (1.Kobe University, 2.Port and Airport Research Institute, 3.Construction Technique Institute Engineering Co., Ltd., 4.Tokyo University of Marine Science and Technology)

10:15 AM - 10:30 AM JST | 1:15 AM - 1:30 AM UTC

[AOS12-05] Nutrient and light conditions at subsurface chlorophyll maximum: physical-biogeochemical observations along a mid-Pacific meridional transect

*Sachihiko Itoh[1], Hitoshi Kaneko[1], Shinya Kouketsu[2], Takeshi Okunishi[3], Hiroshi Ogawa[1], Mitsuhide Sato[4], Hiroaki Saito[1] (1.Atmosphere and Ocean Research Institute, The University of Tokyo, 2.Japan Agency for Marin-Earth Science and Technology, 3.Tohoku National Fisheries Research Institute, Fisheries Research Agency, 4.The Hong Kong University of Science and Technology)

Projected coastal hypoxia in a coupled bio-physical model of the California Current System.

*Enrique N Curchitser[1], Raphael Dussin[1,2], Charles Stock[3], Nicoals van Oostende[4]

1. Rutgers University New Brunswick, 2. Lamont-Doherty Earth Observatory of Columbia University, 3. NOAA Geophysical Fluid Dynamics Laboratory, 4. Princeton University

Recent observations have shown an increase of the hypoxic area on the shelf in the California upwelling system. Climate projections suggest this increase would continue over the 21st century. However, the low-resolution ocean component of today’ s climate models in this region are hampered by the flawed representation of upwelling and coastal processes.To achieve a more realistic solution, we ported the NOAA-GFDL biogeochemical model COBALT into the regional ocean model ROMS permitting a seamless representation of the biogeochemistry across scales. With the 7km California Current implementation, we carry out sensitivity experiments for the projected changes in biogeochemical and physical drivers of coastal hypoxia : oxygen and nutrients in source waters, solubility and upwelling-favorable wind. We describe here the results obtained and assess the relative impact of drivers of coastal hypoxia in this system.

©2019. Japan Geoscience Union. All Right Reserved.

Decadal salinity variation in the western North Pacific correlated with the strength of the Oyashio and the Kuroshio Extension

*Hitoshi Kaneko[1], Takeshi Okunishi[2], Shinya Kouketsu[3], Sachihiko Itoh[1], Takashi Seto[4], Hiroshi Kuroda[5], Yugo Shimizu[4]

1. Atmosphere and Ocean Research Institute, The University of Tokyo, 2. Tohoku National Fisheries Research Institute, Japan Fisheries Research and Education Agency, 3. Japan Agency for Marine-Earth Science and Technology, 4. National Research Institute of Fisheries Science, Japan Fisheries Research and Education Agency, 5. Hokkaido National Fisheries Research Institute, Japan Fisheries Research and Education Agency

Decadal changes in salinity around the density (~1026.8 kg m^{-3}) of North Pacific Intermediate Water (NPIW) were investigated in the regions from the Oyashio to the Kuroshio Extension (KE), called as the Mixed Water Region (MWR), based on the long-term-data-sets provided from numerical reanalysis. Based on the reanalysis data provided by an ocean forecast system of the Japan Fisheries Research and Education Agency (FRA-ROMS; 1992–2012, horizontal resolutions of 0.1˚), we found that during increase of the Oyashio velocity in the upstream region, negative salinity anomaly accompanied with the southward velocity at the density was enhanced between 144–145˚E just south of 40˚N. In addition, to examine influences from the downstream region of the Oyashio, we made a lag-correlation analysis focusing on the decadal variation of KE stability calculated from the zonal average (142–165˚E) of the meridional gradient of the sea surface height (34.5–37.0˚E) as the KE strength (KES). The result showed that signals of significant negative correlation appeared around the density from Hokkaido to the north region of KE. Through the composite analysis based on the KE stability, we found that the stable KE could also lead similar anomaly distribution around the north region of KE. We examined relationships between decadal tendency and each component of salinity fluxes at the density along the north-south boundary of the region of 38–40˚N, and 142–145˚E. Concerning estimation of the salinity fluxes, we employed time-mean components (S, V) and eddy components (s', v'), and then, we calculated products of them (Sv', $s'V$, $s'v'$). Decadal tendency of salinity (ds'/dt) was negatively correlated with the meridional difference of Sv' ($-0.5 < r < -0.47$, 95% confidence interval). Whereas Sv' at northern boundary was also negatively correlated with ds'/dt ($-0.45 < r < -0.42$), the correlation between ds'/dt and Sv' at southern boundary was small ($0.03 < r < 0.07$). The result suggested that the southward Oyashio would play an important role for decadal salinity variation in the MWR.

Keywords: North Pacific Intermediate Water , Decadal variation, Oyashio, Kuroshio Extension

©2019. Japan Geoscience Union. All Right Reserved.

Multiscale routes to supply nutrients through the Kuroshio nutrient stream

*Takeyoshi Nagai[1], Sophie Clayton[2], Yusuke Uchiyama[3]

1. Department of Ocean Sciences, Tokyo University of Marine Science and Technology, 2. Ocean, Earth & Atmospheric Sciences, Old Dominion University, 3. Kobe University

In this study, the role of the Kuroshio as a nutrient conduit is discussed using results from eddy-resolving, and nested high-resolution numerical simulations using Regional Oceanic Modeling System (ROMS) coupled with a N^2PZD^2 ecosystem model, and results from recent in-situ observations. The eddy-resolving simulation can reproduce the elevated nutrient concentrations along the Kuroshio compared to those in ambient waters of the same density, similar to the Gulf Stream. The nested simulations show that nutrients in the upstream Kuroshio can be supplied to euphotic zone by strong diapycnal mixing associated with the Kuroshio over topography. This large nutrient input is consistent with the very strong turbulent mixing observed directory in the upstream Kuroshio regions, where the Kuroshio flows over the seamounts and on the continental slope. The autonomous microstructure float observations also suggest that the large turbulent nitrate diffusive flux occurs in the Izu Ridge, along the Kuroshio. These diapycnal processes may explain why the basin scale nutrient elevation on the density surface along the Kuroshio path is maintained. During winter-spring, in the model downstream Kuroshio Extension, a large nitrate induction of O(10 mmol N m^2day^{-1}), comparable to or greater than wintertime diffusive nitrate flux, occurs through the inclined mixed layer base, which is strongly influenced by the mesoscale structures.

Keywords: Kuroshio, Nutrient stream, Nutrient flux

©2019. Japan Geoscience Union. All Right Reserved.

Seasonal variability of upper-ocean primary production around the Kuroshio analyzed using a ROMS-NPZD model

*Xu Zhang[1], Yusuke Uchiyama[1,2], Yota Suzue[3], Hidekatsu Yamazaki[4]

1. Kobe University, 2. Port and Airport Research Institute, 3. Construction Technique Institute Engineering Co., Ltd., 4. Tokyo University of Marine Science and Technology

Biological processes have significant influences on the global carbon cycle on all time scales. In the coastal regions, nutrient supply to the surface by river discharge and coastal upwelling leads to active primary production. The Kuroshio, one of the strongest western boundary currents, flows off the Japan, accompanied by intense eddy activities influencing on biogeochemical processes around its path. In general, localized upwelling due to mesoscale cyclonic eddies brings nutrient-rich subsurface water to the nutrient-depleted upper ocean to enhance near-surface primary productivity. In the present study, a climatological ocean modeling is developed for the marginal seas along the Kuroshio off Japan based on ROMS (Shchepetkin and McWilliams, 2005; 2008) coupled with an NPZD biogeochemical model (Fasham *et al.*, 1990; Gruber *et al.*, 2006). The model domain encompasses both the Kuroshio and its Extension regions in a submesoscale eddy-permitting configuration with a horizontal grid spacing of 3 km. The simulation is conducted for 10 years and the results for the 10th year are used for our analysis. A nitrogen budget analysis indicates that nitrogen exists mostly in the phyto- and zooplankton compartments in both the Kuroshio and Kuroshio Extension regions during the spring bloom. The increased zooplankton further enriches detritus that settles down by about 100 m, leading to an increase of ammonium below the mixed layer. In winter, eddy-induced nitrate transport is enhanced in the region about 1˚ away from the Kuroshio axis. The baroclinic instability due to the surface cooling in winter generates meso- and submesoscale eddies and substantially promotes eddy-induced vertical nitrate transport.

Keywords: Kuroshio, eddy-induced nitrate flux, submesoscale eddies, baroclinic instability

©2019. Japan Geoscience Union. All Right Reserved.

Nutrient and light conditions at subsurface chlorophyll maximum: physical-biogeochemical observations along a mid-Pacific meridional transect

*Sachihiko Itoh[1], Hitoshi Kaneko[1], Shinya Kouketsu[2], Takeshi Okunishi[3], Hiroshi Ogawa[1], Mitsuhide Sato[4], Hiroaki Saito[1]

1. Atmosphere and Ocean Research Institute, The University of Tokyo, 2. Japan Agency for Marin-Earth Science and Technology, 3. Tohoku National Fisheries Research Institute, Fisheries Research Agency, 4. The Hong Kong University of Science and Technology

Subsurface chlorophyll maximum (SCM) occurs in a stratified water column that nutrient is depleted in the surface layer. When fully developed, such as those in calm subtropical regions, SCMs were often observed at depth where both nutrient and light availabilities are at a marginal level. Following resource competition theory, the low resource condition is likely generated by a group of phytoplankton with a low resource requirement, which expels other groups through decreasing nutrients and/or deepening the nutricline. Numerical models formulating the phytoplankton dependency on nutrients and light can reproduce some of characteristics of SCM including seasonal and geographical variability. However, comprehensive observations of the SCM and environmental conditions are still limited especially in the open ocean. In the present study, shipboard physical and biogeochemical observations were conducted along 170˚W from the South Pacific Subtropical Front up to Bering Sea during Boreal and Austral summers.

Characteristics of SCMs were estimated from multiple vertical profiles of chlorophyll fluorescence attached to a Conductivity Temperature Depth profiler (CTD), and nutrient concentrations were determined from water samples. Depths of profiles by sensors and water sample data were determined through projections onto potential density coordinate to eliminate effects of internal wave heaving, which are critical in analyzing processes around SCMs. To evaluate diffusive nutrient flux, vertical diffusivity was calculated using a microstructure profiler and multiplied by vertical gradient of nutrient concentrations. Vertical profiles of photosynthetically available radiation (PAR) were estimated using surface PAR from Moderate Resolution Imaging Spectroradiometer (MODIS), averaged over two weeks until shipboard observation, and diffuse attenuation coefficients of downwelling irradiance calculated from *in situ* PAR measurements.

In subtropical regions from 40˚S to 30˚N, except for that at the equator, SCMs were found in 80–150 m, around or slightly deeper than 1% light level relative to the surface. Depth of SCM was deepest in the middle of subtropical gyres, no shallower than 100 m in 15–25˚. Although considerably shallower than subtropical regions, SCMs were also observed at the equator and temperate and subpolar regions in the range of 15–40 m. There are significant positive correlations between the depths of SCM and 1% light level, where SCM depth was generally deeper than the 1% light level in the subtropical regions. However, PAR at SCMs was not uniform but ranged from 0.1–0.7 mol photon m^{-2} day^{-1} within the subtropical regions, and shows a negative correlation with the SCM depth. The SCM depth also shows a strong positive correlation with the depth of maximum subsurface nitrate flux. Considering effects of pure external factors that are not affected by phytoplankton to the SCM depth, we found a positive relationship with absolute dynamic topography indicating the depth of pycnocline.

©2019. Japan Geoscience Union. All Right Reserved.

Although 1% light levels can indicate the SCM depth through the linear correlation for the wide geographical range in the mid-Pacific, it is not concluded that SCM was formed under the limitation of light alone. This is followed by a fact that PAR at the 1% levels is not uniform but depends on the surface PAR, by which the relationship between PAR values at SCMs and depths of SCMs become insignificant. As deep penetration of light is caused by the low productivity in the surface water, we cannot simply consider cause and effect for the above relationship. On the other hand, as the dynamic topography is not affected by phytoplankton, its relationship between the SCM depth suggests that the large-scale hydrographic structure has some influences on the formation of SCMs. In the presentation, we will further discuss the details of the physical processes and their possible impacts on subsurface phytoplankton production.

Keywords: Subsurface chlorophyll maximum, Diffusive nutrient flux, colimitation

©2019. Japan Geoscience Union. All Right Reserved.

[E] Oral | A (Atmospheric and Hydrospheric Sciences)：A-OS Ocean Sciences & Ocean Environment

Mon. May 27, 2019 10:45 AM - 12:15 PM JST | Mon. May 27, 2019 1:45 AM - 3:15 AM UTC | 302 3F

[A-OS12] Marine ecosystems and biogeochemical cycles: theory, observation and modeling

convener:Shin-ichi Ito(Atmosphere and Ocean Research Institute, The University of Tokyo), Takafumi Hirata(Faculty of Environmental Earth Science, Hokkaido University), Enrique N Curchitser(Rutgers University New Brunswick), Eileen E Hofmann(Old Dominion University), Chairperson:Yoshimasa Matsumura(Atmosphere and Ocean Research Institute, The University of Tokyo)

The ocean accounts for about 50% of global net primary production. This production is significant for carbon cycling and ecosystem functioning, and is related directly or indirectly to a variety of climatic and ecological phenomena. The responses to natural and anthropogenic environmental stressors that influence marine production and diversity can cause perturbations to marine ecosystems that alter trophic dependencies and interactions among organisms at a range of space and time scales. Quantification of the principal mechanisms driving spatio-temporal variability of marine ecosystem remains to be done, especially in terms of evaluation of uncertainty in responses. As a result, evaluating vulnerability of marine ecosystems to environmental change requires systematic and holistic approaches that integrate physics to ecology and are based in observations and modelling. In addition, expectations to deliver these science to public society is raising. This session aims to provide a venue for not only discussing recent advances in understanding marine biogeochemical cycles, ecosystems and their interactions, but also networking with a variety of people to seed new ideas in marine ecological research. Observational, modeling and conceptual studies, including technological development and operational applications, that consider linkages among biogeochemical and ecosystem processes, biodiversity, and the effects of multiple stressors from molecular to planetary scales are encouraged.

10:45 AM - 11:05 AM JST | 1:45 AM - 2:05 AM UTC

[AOS12-06] A Lagrangian view of spring phytoplankton blooms

★Invited Papers

*Shinichiro Kida[1], Taka Ito[2] (1.Research Institute for Applied Mechanics, Kyushu University, 2.Georgia Institute of Technology)

11:05 AM - 11:20 AM JST | 2:05 AM - 2:20 AM UTC

[AOS12-07] Significance of acclimation process in simulating chlorophyll distribution in the Arctic Ocean

*Yoshio Masuda[1], Yasuhiro Yamanaka[1], Takafumi Hirata[1], Hideyuki Nakano[2] (1.Graduate School of Environmental Earth Science, Hokkaido University, 2.Meteorological Research Institute)

11:20 AM - 11:35 AM JST | 2:20 AM - 2:35 AM UTC

[AOS12-08] Responses of lower-trophic level ecosystem to nutrient variation in the central part of the Seto Inland Sea

*Naoki Yoshie[1], Hayato Mizuguchi[1], Xinyu Guo[1], Michio Yoneda[2], Katsuyuki Abo[2], Tomoaki Kono[2], Tatsunori Fujita[3] (1.Center for Marine Environmental Studies, Ehime University, 2.Japan Fisheries Research and Education Agency, 3.Kagawa Prefectural Fisheries Research Center)

11:35 AM - 11:50 AM JST | 2:35 AM - 2:50 AM UTC

[AOS12-09] Effects of the temperature and fish size on metabolism and swimming performance of Pacific chub mackerel *Scomber japonicus* in the Northwest Pacific

*Chenying Guo[1], Shin-ichi Ito[1], Michio Yoneda[2], Hajime Kitano[2] (1.Atmosphere and Ocean Research Institute, the University of Tokyo, 2.Fisheries Research and Education Agency Japan)

11:50 AM - 12:05 PM JST | 2:50 AM - 3:05 AM UTC

[AOS12-10] Sensitivity analyses of growth and migration of Japanese anchovy (*Engraulis japonicus*) in the East China Sea using a fish growth-migration model.

*Shin-ichi Ito[1], Takashi Setou[2], Michio Yoneda[2], Motomitsu Takahashi[2], Michiya Matsuyama[3], Chenying Guo[1], Takashi Kitagawa[1] (1.Atmosphere and Ocean Research Institute, The University of Tokyo, 2.Fisheries Research and Education Agency Japan, 3.Kyushu University)

12:05 PM - 12:15 PM JST | 3:05 AM - 3:15 AM UTC

Discussion

A Lagrangian view of spring phytoplankton blooms

*Shinichiro Kida[1], Taka Ito[2]

1. Research Institute for Applied Mechanics, Kyushu University, 2. Georgia Institute of Technology

The basic mechanism behind spring phytoplankton blooms is investigated using a 1-dimensional Lagrangian NPZD model, where the movement and transfers of nutrient parcels are solved by tracking a nitrogen parcel. The Lagrangian framework is useful for understanding how the nitrogen cycle works in the ocean since it naturally follows the movement of materials through the turbulent ocean environment. The model reveals that the onset of spring blooms depends on the cumulative euphotic age, which is the total time that inorganic nutrient is exposed to light before the photosynthetic conversion to phytoplankton biomass. This is regardless of the underlying mechanism, such as critical depth hypothesis or critical turbulence hypothesis. The difference between the two modes lies in how cumulative euphotic age is accumulated and this can be distinguished by examining the cumulative euphotic age spectrum. We further examined the impact of mortality by comparing the model experiments with and without mortality. The cumulative euphotic age necessary for a spring bloom is found to increase, as expected, but the spectral shapes remained similar.

Keywords: Spring Bloom, Lagrangian model

©2019. Japan Geoscience Union. All Right Reserved.

Significance of acclimation process in simulating chlorophyll distribution in the Arctic Ocean

*Yoshio Masuda[1], Yasuhiro Yamanaka[1], Takafumi Hirata[1], Hideyuki Nakano[2]

1. Graduate School of Environmental Earth Science, Hokkaido University, 2. Meteorological Research Institute

Recently, our team has developed a new oceanic ecosystem model (FlexPFT-3D) based on a novel theory for phytoplankton physiology (Smith et al. 2015). Different from our previous models (NEMURO, MEM), the model represents phytoplankton acclimation processes in which phytoplankton change their stoichiometry (nitrogen:carbon:chlorophyll:iron) according to the change of a surrounding environment. A clear improvement was found in chlorophyll distributions in oceanic interior and the Arctic Ocean. Arctic chlorophyll concentration in the new model is comparable to the observation, while it is underestimated in the previous models. In the Arctic Ocean, significant seasonal environmental change exists especially in a light condition. The new model can represent increase in the rate of chlorophyll to carbon biomass in the summer and resulting increase in the phytoplankton specific growth rate; those contribute to the improvement in simulating Arctic chlorophyll concentration.

Keywords: Phytoplankton, Ecosystem model, FlexPFT

©2019. Japan Geoscience Union. All Right Reserved.

Responses of lower-trophic level ecosystem to nutrient variation in the central part of the Seto Inland Sea

*Naoki Yoshie[1], Hayato Mizuguchi[1], Xinyu Guo[1], Michio Yoneda[2], Katsuyuki Abo[2], Tomoaki Kono[2], Tatsunori Fujita[3]

1. Center for Marine Environmental Studies, Ehime University, 2. Japan Fisheries Research and Education Agency, 3. Kagawa Prefectural Fisheries Research Center

The Seto Inland Sea is a representative coastal sea in Japan, and various environmental problems such as harmful algae bloom and hypoxia associated with the eutrophication have occurred during 50 years. The nutrient supplies from the terrestrial region related to the human activity have been reduced through the efforts for environmental cleanup over the last several decades. As a result of such excessive environmental cleanup, oligotrophic condition frequently occurred in this region in recent years. The relationships among oligotrophication, primary productivity, and fishery resources such as anchovy in this region are not clear. In this study, we investigated the responses of the lower-trophic level ecosystem in the central Seto Inland Sea to the nutrient variations using a plankton functional types model eNEMURO (4N-4P-4Z-3D). We used two different nutrient conditions for the model based on the time series observations, one was in 2005 with the good catch of anchovy larvae, and another was in 2011 with the poor catch of them. The model results showed that the spring diatom bloom in 2011 was much lower than those in 2005 due to the low nutrient concentrations in the spring of 2011. The meso-zooplankton biomass in the spring of 2011 was also lower than those in 2005 associated with the reduced spring diatom bloom in 2011. We summarized that the interannual variation of nutrient concentrations in the spring may control the interannual variation of anchovy stocks by regulating the scale of the spring diatom bloom in this region.

Keywords: ecosystem model, nutrient, diatom, meso-zooplankton, anchovy

©2019. Japan Geoscience Union. All Right Reserved.

Effects of the temperature and fish size on metabolism and swimming performance of Pacific chub mackerel *Scomber japonicus* in the Northwest Pacific

*Chenying Guo[1], Shin-ichi Ito[1], Michio Yoneda[2], Hajime Kitano[2]

1. Atmosphere and Ocean Research Institute, the University of Tokyo, 2. Fisheries Research and Education Agency Japan

Pacific chub mackerel (*Scomber japonicus*) is a small pelagic and important commercial fish species widely distributed throughout the coastal areas of the Northwestern, Northeastern, and Southeastern Pacific. Swimming energetic and metabolic data of Northwestern stock at two growth stage (young juvenile of 6.1±0.3 cm and immature of 16.5±1.4 cm fork length) were measured under various temperature (18˚C and 24˚C for young juvenile, 14˚C and 18˚C for immature) using a variable-speed swim-tunnel respirometer, and the new data were compared with the previous data from Northeastern Pacific stocks. For young juveniles, the maximum sustainable swimming speeds (U_{max}) was 50.0±6.5 cm s^{-1} at 24˚C, significantly higher than at 18˚C of 30.7±2.5 cm s^{-1}. For the immature individuals, U_{max} showed no significant increase while temperature changed from 14 to 18˚C, and did not vary significantly from Northeastern Pacific individuals within the same size range. At a given temperature of 18˚C, U_{max} of immatures was significantly higher than those of young juveniles. For all individuals, the mass-specific oxygen consumption rate (V_{O2}) increased exponentially with swimming speed (U, in cm s^{-1}). At a given speed, V_{O2} increased with temperature; at a given temperature of 18˚C, V_{O2} of immature individuals were lower than those of young juveniles. These effects of the temperature and fish size on V_{O2} were consistent with previous studies of chub mackerel of Northeastern stocks, however, compared with Northeastern stocks within the same size range, V_{O2} of Northwestern individuals acclimated to 14˚C did not vary at a given speed, while those acclimated to 18˚C showed higher V_{O2} , indicating the Northwestern stock was more sensitive for temperature on metabolism.

Keywords: Pacific chub mackerel, Scomber japonicus, swimming speed, metabolism, respirometer

©2019. Japan Geoscience Union. All Right Reserved.

Sensitivity analyses of growth and migration of Japanese anchovy (*Engraulis japonicus*) in the East China Sea using a fish growth-migration model.

*Shin-ichi Ito[1], Takashi Setou[2], Michio Yoneda[2], Motomitsu Takahashi[2], Michiya Matsuyama[3], Chenying Guo[1], Takashi Kitagawa[1]

1. Atmosphere and Ocean Research Institute, The University of Tokyo, 2. Fisheries Research and Education Agency Japan, 3. Kyushu University

Japanese anchovy (Engraulis japonicus) is an important species not only as an exploited species but also as prey for variety of predators including marine mammals, tunas, mackerels, flounders, etc. However, the biomass of Japanese anchovy have shown large fluctuation and is one of the main actors of the fish species alternation responding to basin scale climate variabilities. From the stock management views, three sub-populations are defined in Japan: Pacific stock, Tsushima stock (also called the East China Sea stock), and Seto-inland Sea stock. There is evidence (different weights-at-age and longevity) of three sub-populations of anchovy within the Japan system. While he three sub-populations of anchovy share their spawning grounds, the migration route and nursery grounds are divided. In addition, while Seto-inland Sea sub-populations do not show a large migration, Pacific and Tsushima sub-populations make long distance ontogenetic migrations, On the contrary, there is no evidence of a similar migration of juvenile anchovies in the California Current system. Therefore, we are focusing on the movement (advection and migration) routes of eggs, larvae, and juveniles from the spawning grounds to the adult grounds. We developed a fish-migration and growth model using environmental conditions derived from simulations of a coupled ocean circulation and ecosystem model. For the ocean circulation model, a high resolution (1/10 deg.) FRA-ROMS (Fisheries Research Agency - Regional Ocean Modeling System) was used. For the marine ecosystem model, eNEMURO, an extended version of NEMURO (North Pacific Ecosystem Model for Understanding Regional Oceanography) was used. The larvae transported to southern part of Kyushu Island in Japan (current main fisheries ground for anchovy larvae) were reasonably reproduced in the model. The sensitivity analyses of swimming efficiency will be conducted respect to the migration route of anchovy.

Keywords: marine ecosystem model, fish growth-migration model, Japanese anchovy

©2019. Japan Geoscience Union. All Right Reserved.

[E] Oral | A (Atmospheric and Hydrospheric Sciences)：A-OS Ocean Sciences & Ocean Environment

Mon. May 27, 2019 1:45 PM - 3:15 PM JST | Mon. May 27, 2019 4:45 AM - 6:15 AM UTC | 302 3F

[A-OS12] Marine ecosystems and biogeochemical cycles: theory, observation and modeling

convener:Shin-ichi Ito(Atmosphere and Ocean Research Institute, The University of Tokyo), Takafumi Hirata(Faculty of Environmental Earth Science, Hokkaido University), Enrique N Curchitser(Rutgers University New Brunswick), Eileen E Hofmann(Old Dominion University), Chairperson:Enrique Curchitser(Rutgers University)

The ocean accounts for about 50% of global net primary production. This production is significant for carbon cycling and ecosystem functioning, and is related directly or indirectly to a variety of climatic and ecological phenomena. The responses to natural and anthropogenic environmental stressors that influence marine production and diversity can cause perturbations to marine ecosystems that alter trophic dependencies and interactions among organisms at a range of space and time scales. Quantification of the principal mechanisms driving spatio-temporal variability of marine ecosystem remains to be done, especially in terms of evaluation of uncertainty in responses. As a result, evaluating vulnerability of marine ecosystems to environmental change requires systematic and holistic approaches that integrate physics to ecology and are based in observations and modelling. In addition, expectations to deliver these science to public society is raising. This session aims to provide a venue for not only discussing recent advances in understanding marine biogeochemical cycles, ecosystems and their interactions, but also networking with a variety of people to seed new ideas in marine ecological research. Observational, modeling and conceptual studies, including technological development and operational applications, that consider linkages among biogeochemical and ecosystem processes, biodiversity, and the effects of multiple stressors from molecular to planetary scales are encouraged.

1:45 PM - 2:05 PM JST | 4:45 AM - 5:05 AM UTC

[AOS12-11] Micro-scale patchiness enhances trophic transfer efficiency and potential plankton biodiversity

★Invited Papers

*Hidekatsu Yamazaki[1], Anupam Priyadarshi[2], Lan Smith[3], Sandip Mandal[4], Mamoru Tanaka[1] (1.Tokyo University of Marine Science and Technology, 2.Banaras Hindu University, 3.Japan Agency for Marine-Earth Science and Technology, 4.Public Health Foundation of India)

2:05 PM - 2:20 PM JST | 5:05 AM - 5:20 AM UTC

[AOS12-12] Long term observations of marine snow, using cabled observatory system

*Marika Takeuchi[1,2], Mark Doubell[3], Jim Mitchell[2], Hidekatsu Yamazaki[1] (1.Tokyo University of Marine Science and Technology, 2.Flinders University, 3.South Australia Research and Development Institute)

2:20 PM - 2:35 PM JST | 5:20 AM - 5:35 AM UTC

[AOS12-13] An insight into the area characteristic of seasonal change in nitrogen isotope ratio based on a marine nitrogen isotope model

*Chisato Yoshikawa[1], Masahito Shigemitsu[1], Akitomo Yamamoto[1], Akira Oka[2], Naohiko Ohkouchi[1] (1.JAMSTEC, 2.AORI)

2:35 PM - 2:50 PM JST | 5:35 AM - 5:50 AM UTC

[AOS12-14] Modeling variability of ^{15}N stable isotope enrichment within the planktonic food chain

*S. Lan Smith[1], Yoshikazu Sasai[1], Chisato Yoshikawa[2] (1.Marine Ecosystem Dynamics Research Group, RCGC, Japan Agency for Marine-Earth Science and Technology, Yokohama, Japan, 2.Department of Biogeochemistry, Japan Agency for Marine-Earth Science and Technology, Yokosuka, Japan)

2:50 PM - 3:05 PM JST | 5:50 AM - 6:05 AM UTC

[AOS12-15] Discussions

Shin-ichi Ito[2], *Takafumi Hirata[1] (1.Faculty of Environmental Earth Science, Hokkaido University, 2.Atmosphere and Ocean Research Institute, The University of Tokyo)

3:05 PM - 3:15 PM JST | 6:05 AM - 6:15 AM UTC

Discussion

Micro-scale patchiness enhances trophic transfer efficiency and potential plankton biodiversity

*Hidekatsu Yamazaki[1], Anupam Priyadarshi[2], Lan Smith[3], Sandip Mandal[4], Mamoru Tanaka[1]

1. Tokyo University of Marine Science and Technology, 2. Banaras Hindu University, 3. Japan Agency for Marine-Earth Science and Technology, 4. Public Health Foundation of India

Recent observations have revealed ubiquitous intermittency in phytoplankton distributions at the micro (mm) scale, and a few recent modelling studies have suggested that this micro-scale variability impacts plankton ecosystem dynamics and biodiversity. Modelling is an essential tool for studying complex food webs, by linking the observed ecological patterns with experimental findings to understand mechanisms and make future predictions. However, so far almost all ecosystem models have been developed based on the mean-field approach, i.e. assuming well mixed environmental conditions within each discretely resolved grid cell. Although this is reasonable for examining patterns at the meso- (km) to global scales, it is not realistic for plankton, which experience micro-scale variability in aquatic environments where predator-prey overlap can substantially enhance trophic transfer. Similar to a recent study that addressed variability at the scale of ocean fronts, we have recently used Reynolds decomposition and truncated Taylor series to develop ‘moment closure’ models accounting for micro-scale variability in the distributions of Nutrients and Phytoplankton (NP closure model), and also Zooplankton (NPZ closure model). Compared to conventional ecosystem models based on the mean-field approach, these closure models yield qualitatively different dynamics.

Using a generalized plankton ecosystem modelling framework, including models of differing trophic complexity and with different grazing functional responses, we investigate how micro-scale variability affects plankton biodiversity and ecosystem function. Specifically, we apply the closure modelling approach to test the functional forms often assumed in ecosystem models against observed micro-scale intermittency as quantified by the coefficient of variation (CV) (ratio of standard deviation to mean) of micro-scale fluorescence field, which is a proxy for phytoplankton biomass. With both saturating and non-saturating grazing functions and in all model configurations considered, we find that micro-scale variability consistently supports the highest trophic level present, i.e. enhances Tansfer Efficiency, and expands the model stability domain, potentially sustaining biodiversity by allowing species with a wider range of trait values to coexist. Based on our observations and model results we hypothesise a novel answer to the “paradox of the plankton” (Hutchinson, 1961) for such calm, low-nutrient oceanic environments: Heretofore under-appreciated high levels of micro-scale variability may explain the great diversity of plankton present in these vast low-nutrient regions of the ocean.

Keywords: plankton, turbulence, microstructures, ecosystem models

©2019. Japan Geoscience Union. All Right Reserved.

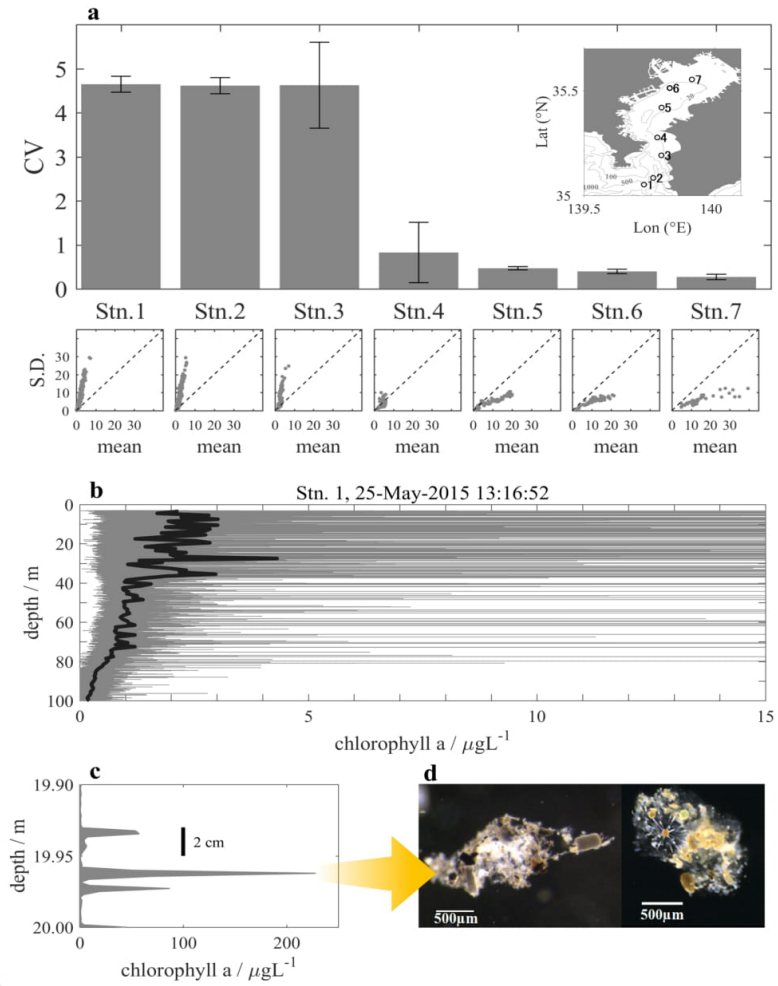

Figure: (a) Observation stations (open, numbered circles) in Tokyo bay, *CV* estimates (bar heights, with error bars indicating 99% confidence intervals) and corresponding scatter plots of observed standard deviation vs. mean of fluorescence data from each station (dotted lines showing one-to-one relationships). (b) Raw data (thin grey lines) and 1 m average values (thick black lines) from a vertical fluorescence profile acquired at stn. 1 by the laser sensor, which was calibrated with *in situ* water samples to obtain values in g chl L^{-1}. (c) A subset of peaks from the same profile around 20 m depth. Vertical thick black bar indicates a scale bar of 2 cm height. (d) Images of typical aggregates.

©2019. Japan Geoscience Union. All Right Reserved.

Long term observations of marine snow, using cabled observatory system

*Marika Takeuchi[1,2], Mark Doubell[3], Jim Mitchell[2], Hidekatsu Yamazaki[1]

1. Tokyo University of Marine Science and Technology, 2. Flinders University, 3. South Australia Research and Development Institute

Marine aggregates are formed through coagulation of small biogenic and non-biogenic components. Visible ones, known as marine snow, are typically larger than 0.5mm. Aggregates are well recognised as hotspots of microbial and planktonic activities. Aggregates formation is an important pathway for transferring organic matter from surface to deep ocean, hence the impatcs of aggregates in carbon flux is significant. However, field observations of aggregates have been challenging and not many long-term observational results have been reported.
In this study, we analysed in-situ observations of aggregates using a high-resolution plankton camera mounted on cabled observatory OCEANS. OCEANS has been continuously collecting hydrographic data and images of aggregates simultaneously since 2014. Here we will present a few months of in-situ observations results to show aggregates size and population change over time. Turbulence and other plankton distributions are compared to aggregates.

Keywords: Marine snow, Turbulence, Size distribution

©2019. Japan Geoscience Union. All Right Reserved.

An insight into the area characteristic of seasonal change in nitrogen isotope ratio based on a marine nitrogen isotope model

*Chisato Yoshikawa[1], Masahito Shigemitsu[1], Akitomo Yamamoto[1], Akira Oka[2], Naohiko Ohkouchi[1]

1. JAMSTEC, 2. AORI

The condition of nitrogenous nutrient in the surface water is an important factor that determines the primary production and the carbon cycle in the ocean. Nitrogen isotope ratios ($\delta^{15}N$) of nitrate, sinking particles, sediments have been widely used as a proxy for the condition of nitrogenous nutrient in the surface water. However, the interpretation of $\delta^{15}N$ values are not simple. The $\delta^{15}N$ value of surface primary producer records $\delta^{15}N$ value of nitrate supplied to the euphotic layer, nitrate utilization efficiency and rate of N_2 fixation. As there are multiple possibilities for the interpretation, $\delta^{15}N$ values should be interpreted with ample consideration of the characteristics of surface nitrogen cycle by region. In this study we show the area characteristic of seasonal change in $\delta^{15}N$ value by using a global ocean nitrogen isotope model in order to improve the interpretation of observed $\delta^{15}N$ values. We installed a marine nitrogen isotope model (Yoshikawa et al., 2005) with denitrification (Shigemitsu et al., 2016) and N_2 fixation (Coles et al., 2007) schemes into an off-line biogeochemical model that is driven by climatological monthly mean physical fields obtained from the outputs of a preindustrial control simulation performed with MIROC 3.2 (K-1 Model Developers, 2004). The simulated $\delta^{15}N$ of sinking particles had a global distribution similar to the observed $\delta^{15}N$ of surface sediments (Tesdal et al., 2013). The simulated sinking particles were enriched in ^{15}N in the eastern and western tropical North Pacific and the Indian Ocean where water column denitrification occurs and were depleted in ^{15}N in the Sargasso Sea, the Kuroshio extension region, and the Indian Ocean where N_2 fixation occurs. The seasonal variations in $\delta^{15}N$ of sinking particles vary considerably from one region to another. In this talk, we will report the seasonal $\delta^{15}N$ patterns categorized by region and the factors in the determination of those seasonal patterns.

Keywords: Marine nitrogen cycle, Nitrogen isotope ratio, Marine ecosystem model

©2019. Japan Geoscience Union. All Right Reserved.

Modeling variability of ^{15}N stable isotope enrichment within the planktonic food chain

*S. Lan Smith[1], Yoshikazu Sasai[1], Chisato Yoshikawa[2]

1. Marine Ecosystem Dynamics Research Group, RCGC, Japan Agency for Marine-Earth Science and Technology, Yokohama, Japan, 2. Department of Biogeochemistry, Japan Agency for Marine-Earth Science and Technology, Yokosuka, Japan

The stable isotope ^{15}N is widely used an indicator of trophic level, and has been incorporated into ecosystem models in order to understand nitrogen cycling and trophic transfer. However, such studies typically consider only the average enrichment per trophic level. We present a recently developed model of the dynamic fractionation of the stable isotope ^{15}N in lower-trophic ecosystems of the North Pacific. The model accounts for the dynamics of trophic transfer from nutrients (nitrate and ammonium) to phytoplankton, and to two idealized zooplankton compartments representing herbivores and carnivores, respectively. The $d^{15}N$ signal of herbivores tracks that of phytoplankton, with a nearly constant offset, i.e., enrichment by a nearly constant factor. However, the modeled $d^{15}N$ difference between carnivores and herbivores varies seasonally, and depends on the mortality rate (turnover time or effective lifespan) of the carnivores. Seasonal variations of modeled $d^{15}N$ signals differ with trophic level because carnivores integrate the signal from their ^{15}N uptake over longer timescales compared to herbivores. Thus, the model reproduces the lower observed variability of $d^{15}N$ for carnivorous zooplankton (chaetognaths) and the more variable $d^{15}N$ for largely herbivorous zooplankton (copepods). Our results imply that for interpreting observed $d^{15}N$ values, it is important to consider not only the average enrichment per trophic level, but also the dynamics of ^{15}N fractionation and the timing of observations, e.g. to avoid unrealistic estimates of trophic linkages based on seasonally biased observations.

Keywords: nutrients, predation, zooplankton, production, transfer efficiency

©2019. Japan Geoscience Union. All Right Reserved.

Discussions

Shin-ichi Ito[2], *Takafumi Hirata[1]

1. Faculty of Environmental Earth Science, Hokkaido University, 2. Atmosphere and Ocean Research Institute, The University of Tokyo

Discussions

Keywords: Marine Ecosystems, Biogeochemistry

©2019. Japan Geoscience Union. All Right Reserved.

[E] Poster | A (Atmospheric and Hydrospheric Sciences)：A-OS Ocean Sciences & Ocean Environment

Mon. May 27, 2019 3:30 PM - 5:00 PM JST | Mon. May 27, 2019 6:30 AM - 8:00 AM UTC | Poster Hall International Exhibition Hall8, Makuhari Messe_3

[A-OS12] Marine ecosystems and biogeochemical cycles: theory, observation and modeling

convener:Shin-ichi Ito(Atmosphere and Ocean Research Institute, The University of Tokyo), Takafumi Hirata(Faculty of Environmental Earth Science, Hokkaido University), Enrique N Curchitser(Rutgers University New Brunswick), Eileen E Hofmann(Old Dominion University)

The ocean accounts for about 50% of global net primary production. This production is significant for carbon cycling and ecosystem functioning, and is related directly or indirectly to a variety of climatic and ecological phenomena. The responses to natural and anthropogenic environmental stressors that influence marine production and diversity can cause perturbations to marine ecosystems that alter trophic dependencies and interactions among organisms at a range of space and time scales. Quantification of the principal mechanisms driving spatio-temporal variability of marine ecosystem remains to be done, especially in terms of evaluation of uncertainty in responses. As a result, evaluating vulnerability of marine ecosystems to environmental change requires systematic and holistic approaches that integrate physics to ecology and are based in observations and modelling. In addition, expectations to deliver these science to public society is raising. This session aims to provide a venue for not only discussing recent advances in understanding marine biogeochemical cycles, ecosystems and their interactions, but also networking with a variety of people to seed new ideas in marine ecological research. Observational, modeling and conceptual studies, including technological development and operational applications, that consider linkages among biogeochemical and ecosystem processes, biodiversity, and the effects of multiple stressors from molecular to planetary scales are encouraged.

[AOS12-P01] Impact of the nutrient transport through the Tsushima Strait on the ecosystem in the Japan Sea

*Ryota Shibano[1], Akihiko Morimoto[1], Katsumi Takayama[2], Tetsutaro Takikawa[3], Masashi Ito[4] (1.Center for Marine Environmental Studies, Ehime University, 2.Research Institute for Applied Mechanics, Kyushu University, 3.Graduate School of Fisheries and Environmental Sciences, Nagasaki University, 4.Fisheries Oceanography Department, Japan Sea National Fisheries Research Institute)

[AOS12-P02] Revisiting vertical variations in stoichiometry during oceanic organic matter decomposition

*Masahito Shigemitsu[1], Michio Aoyama[1], Toshimasa Doi[1], Taichi Yokokawa[1], Akihiko Murata[1] (1.Japan Agency for Marine-Earth Science and Technology)

[AOS12-P03] Reproduction of iron-rich intermediate water in the Sea of Okhotsk by high resolution biogeochemical model.

*Hatsumi Nishikawa[1], Humio Mitsudera[1], Hiroshi Yoshinari[2], Takuya Nakanowatari[3], Tomohiro Nakamura[1], Keisuke Uchimoto[4], Hiroyasu Hasumi[5] (1.Institute of Low Temperature Science, Hokkaido University, 2.National Institute for Environmental Studies, 3.Tohoku National Fisheries Research Institute, Japan Fisheries Research and Education Agency, 4.Research Institute of Innovative Technology for the Earth, 5.Atmosphere and Ocean Research Institute, University of Tokyo)

[AOS12-P04] The global oceanic iron distribution estimated by data assimilation approach

*Doi Toshimasa[1], Satoshi Osafune[1], Shuhei Masuda[1], Hajime Obata[2], Kazuhiro Misumi[3], Jun Nishioka[4] (1.Japan Agency for Marine-Earth Science and Technology, 2.The University of Tokyo, 3.Central Research Institute of Electric Power Industry, 4.Hokkaido University)

[AOS12-P05] A high-resolution multi-purpose particle tracking framework for coastal areas near Japan

*Yoshimasa Matsumura[1], Shota Katsura[1], Masao Kurogi[2], Hideyuki Nakano[3], Takateru Yamagishi[4] (1.Atmosphere and Ocean Research Institute, University of Tokyo, 2.Japan Agency for Marine-Earth Science and Technology, 3.Meteorological Research Institute, Japan Meteorological Agency , 4.Research organization for Information Science and Technology)

[AOS12-P06] Numerical study on seasonality of ocean litters collected at the Dongsha Island in the northern South China Sea

*Yi-Chia Hsin[1], Chia-Ying Ko[2], Ming-Shiou Jeng[3] (1.Research Center for Environmental Changes, Academia Sinica, 2.Institute of Fisheries Science, National Taiwan University, 3.Biodiversity Research Center, Academia Sinica)

[AOS12-P07] A key spot and timing to monitor chlorophyll-a in the Kuroshio western boundary current

*Takafumi Hirata[1] (1.Faculty of Environmental Earth Science, Hokkaido University)

[AOS12-P08] **Impacts of cyclonic eddies on phytoplankton biomass and phenology in the Kuroshio Extension region**

*Eko Siswanto[1], Yoshikazu Sasai[1] (1.Japan Agency for Marine-Earth Science and Technology)

[AOS12-P09] Diagnostic estimation and uncertainties of nutrient limitation of phytoplankton growth in Michaelis-Menten functional form

*Taketo Hashioka[1], Maki Noguchi Aita[1] (1.Japan Agency for Marine-Science and Technology)

[AOS12-P10] Modeling productivity in lower trophic levels in Otsuchi Bay, northeast of Japan, using a nested OGCM with a biogeochemical component

*Takashi T Sakamoto[1], L. Shogo Urakawa[2], Sachihiko Itoh[1], Hiroyasu Hasumi[1], Kiyoshi Tanaka[1] (1.Atmosphere and Ocean Research Institute, the University of Tokyo, 2.Meteorological Research Institute, Japan Meteorologica Agancy)

[AOS12-P11] Change in lower trophic level ecosystems to decadal scale variation of climate system in the North Pacific Ocean

*Maki Noguchi Aita[1], Kazuaki Tadokoro[2], Yoshiki Komuro[3], Taketo Hashioka[1], Naomi Harada[1] (1.Research and Development Center for Global Change, Japan Agency for Marine-Earth Science and Technology, 2.Tohoku National Fisheries Research Institute, Japan Fisheries Research and Education Agency, 3.Institute of Arctic Climate and Environment Research, Japan Agency for Marine-Earth Science and Technology)

[AOS12-P12] Estimation of experienced environment of jack mackerel in the East China Sea

*Tomihiko Higuchi[1], Motomitsu Takahashi[2], Kotaro Shirai[1], Shin-ichi Ito[1] (1.Atmosphere and Ocean Research Institute, The University of Tokyo, 2.Seikai National Fisheries Research Institute,FRA)

Impact of the nutrient transport through the Tsushima Strait on the ecosystem in the Japan Sea

*Ryota Shibano[1], Akihiko Morimoto[1], Katsumi Takayama[2], Tetsutaro Takikawa[3], Masashi Ito[4]

1. Center for Marine Environmental Studies, Ehime University, 2. Research Institute for Applied Mechanics, Kyushu University, 3. Graduate School of Fisheries and Environmental Sciences, Nagasaki University, 4. Fisheries Oceanography Department, Japan Sea National Fisheries Research Institute

The Japan Sea is a semi-closed sea with narrow and shallow straits such as the Tsushima/Korea Strait. The nutrient transports through the Tsushima Strait have an impact the ecosystem around the coast of Japan. The nutrient transports are originated in the sources from the sea, Kuroshio (Pacific), Taiwan Strait, and Yellow Sea, and the sources from the land, Changjiang river, Yellow river, and dusts. We investigated the ship cruise data in the strait from 2005 to 2017 to reveal the interannual variations in the volume transport, nutrient concentration, and nutrient transport. The nutrient transport in the strait has large interannual variations of ±50% compared to the average transport.

The recently studies indicated the contribution ratio in the nutrient transports on the sources from the Kuroshio and the rivers also change, when the yearly nutrient transport changes (e.g. Morimoto et al., 2012).

We developed a coupled ocean circulation and ecosystem model, in which the lateral boundary condition is applied based on observation data, and investigated the biogeochemical responses in the Japan Sea and the East China Sea to the interannual variations in the nutrient flux through the Tsushima Strait. We discussed about the contribution ratio in the nutrient flux on the 6 sources from Kuroshio, Taiwan Strait, Changjiang river, Yellow river, the dust, and the bottom (Yellow Sea).

Keywords: Tsushima Warm Current, nutrient transport, the Sea of Japan

©2019. Japan Geoscience Union. All Right Reserved.

Revisiting vertical variations in stoichiometry during oceanic organic matter decomposition

*Masahito Shigemitsu[1], Michio Aoyama[1], Toshimasa Doi[1], Taichi Yokokawa[1], Akihiko Murata[1]

1. Japan Agency for Marine-Earth Science and Technology

Using the new global nutrient data set, we re-evaluate basin-wide stoichiometric ratios of remineralization estimated by Anderson and Sarmiento (1994) (hereinafter, AS94). For the same latitudinal ranges of the Atlantic, Indian and Pacific Oceans as in AS94, we construct one or two end-member mixing models on 14 neutral surfaces and estimate the stoichiometric ratios with a probabilistic approach. Unlike the results of AS94, significant vertical variations in the stoichiometry are found in the Atlantic and Pacific, while relatively constant stoichiometry with depth is found in the Indian Ocean, similar to AS94. The decreases in the C/P and $-O_2$/P ratios with depth in the Atlantic could be caused via dark DIC fixation by chemoautotrophs in the deep waters. In the Pacific, changes in organic matter composition with depth would be the most important factor in the increases in stoichiometry with depth. In all the basins, the N/P ratios are probably affected by benthic denitrification, as in AS94. The P/C/-O_2ratios (mean and $5^{th}$to 95^{th} percentile) are estimated to be 1/111(97 to 129)/155(149 to 163) in the depths below 2000 m of the Indian and Pacific Oceans, where DIC fixation and vertical change in organic matter composition have little influence on the stoichiometry estimates. We suggest that chemoautotrophic DIC fixation and the effect of change in organic matter composition with depth on the stoichiometry in waters above 2000 m should be considered for large-scale biogeochemical modeling and estimation of oceanic uptake of anthropogenic carbon from observational data.

Keywords: nutrients, stoichiometric ratios, remineralization of organic matter

©2019. Japan Geoscience Union. All Right Reserved.

Reproduction of iron-rich intermediate water in the Sea of Okhotsk by high resolution biogeochemical model.

*Hatsumi Nishikawa[1], Humio Mitsudera[1], Hiroshi Yoshinari[2], Takuya Nakanowatari[3], Tomohiro Nakamura[1], Keisuke Uchimoto[4], Hiroyasu Hasumi[5]

1. Institute of Low Temperature Science, Hokkaido University, 2. National Institute for Environmental Studies, 3. Tohoku National Fisheries Research Institute, Japan Fisheries Research and Education Agency, 4. Research Institute of Innovative Technology for the Earth, 5. Atmosphere and Ocean Research Institute, University of Tokyo

Recent observation studies suggest that iron supply from sediment on the northwest continental shelf the Okhotsk Sea plays an important role for the subarctic primary production (e.g. Nishioka et al., 2013). Dense shelf water (DSW) takes up iron from sediment, thereby transporting iron into the Okhotsk Sea intermediate water. However, observational data is still limited.

To clarify detailed structure of iron circulation in the North Pacific, we develop the high-resolution biogeochemical model. However, our model did not reproduce high iron concentration in the intermediate water the Sea of Okhotsk. We use biogeochemical model developed by Parekh et al. (2005). They set the value of total ligand concentration to constant value in all place. Recent observations, however, suggest that ligand concentration varies with sea area and depth. Then, we conducted a new experiment with the ligand concentration changed in the vertical direction. The iron concentration intermediate water of the new experiment becaame higher than before.

Keywords: High-resolution modeling, Iron-rich intermediate water, Ligand concentration

©2019. Japan Geoscience Union. All Right Reserved.

The global oceanic iron distribution estimated by data assimilation approach

*Doi Toshimasa[1], Satoshi Osafune[1], Shuhei Masuda[1], Hajime Obata[2], Kazuhiro Misumi[3], Jun Nishioka[4]

1. Japan Agency for Marine-Earth Science and Technology, 2. The University of Tokyo, 3. Central Research Institute of Electric Power Industry, 4. Hokkaido University

Since distribution of oceanic iron is considered as one of the restriction factors of phytoplankton activity, it is necessary for a pelagic lower trophic level ecosystem model to take into account the effect of iron. In this study, we constructed a three dimensional gridded data of oceanic iron concentration by using both available in situ observation and simple iron cycle model. For the physical process of iron transport, the advection/diffusion model was used along with the flow field of ESTOC (Estimated State of Global Ocean for Climate Research). The falling atmospheric dust in the sea-surface and flux from the sediment at sea floor of the coast were set as the input of the iron. The scavenging or desorption by particulate matter in the water column were employed as the control variables and we constructed the simple iron cycle model. The optimized set of control parameters was obtained based on a Green's function approach by using available in situ iron concentration observations. The results showed that the iron concentration in the southern hemisphere is lower than northern hemisphere, and the low iron regions were well reproduced around the regions of high nutrient / low chlorophyll. Moreover, it is suggested that the Atlantic Ocean is more affected by the atmospheric dust compared with the Pacific Ocean.

Keywords: oceanic iron, data assimilation

©2019. Japan Geoscience Union. All Right Reserved.

A high-resolution multi-purpose particle tracking framework for coastal areas near Japan

*Yoshimasa Matsumura[1], Shota Katsura[1], Masao Kurogi[2], Hideyuki Nakano[3], Takateru Yamagishi[4]

1. Atmosphere and Ocean Research Institute, University of Tokyo, 2. Japan Agency for Marine-Earth Science and Technology, 3. Meteorological Research Institute, Japan Meteorological Agency , 4. Research organization for Information Science and Technology

A comprehensive and multi-purpose particle tracking framework using latest high resolution velocity field in the coastal regions near Japan is developed.
The particle tracking system uses accurate fourth order Runge-Kutta method and implements random-walk based diffusivity, and is built-in the recent versions of MRI.com (an OGCM developed in Meteorological Research Institute, Japan Meteorological Agency) and kinaco (a non-hydrostatic ocean model developed in Atmosphere and Ocean Research Institute, University of Tokyo) for *on-line* use. Each particle is able to store up to seven arbitrary properties (such as size, age, exposed temperature, orientation, mass and buoyancy, etc.) and record the history of them.

The code is effectively parallelized (using MPI and OpenMP hybrid technique) and allows ~O(10^{10}) particles on modern massive-parallel supercomputers, and is also ported to GPU architecture using CUDA language.

This particle tracking framework has no particular target in a priori, and can be applied to various purposes for both physical oceanography (from large scale tracking of water masses to small scale modeling of suspended sediment matter or frazil ice crystals) and ocean biogeochemistry (tracking of trace elements, Laglangian modeling of plankton and detritus, individual based modeling of fishes and marine resources), only by defining appropriate properties and inserting a few lines of code that manipulats them corresponding to the particular target use.

In the presentation, we will introduce an application of this framework to the tracking of passive particles scattered in the coastal areas near Japan using velocity field provided by the latest very high resolution ocean modeling (~300 m mesh). Each model particle records its trajectory and the history of exposed environment, and can be interpreted as eggs or larvae (before acquiring swimming ability) of species of corresponding spawning areas and seasons as well as the tracers for small scale water mass exchanges.

Keywords: Particle tracking system

©2019. Japan Geoscience Union. All Right Reserved.

Numerical study on seasonality of ocean litters collected at the Dongsha Island in the northern South China Sea

*Yi-Chia Hsin[1], Chia-Ying Ko[2], Ming-Shiou Jeng[3]

1. Research Center for Environmental Changes, Academia Sinica, 2. Institute of Fisheries Science, National Taiwan University, 3. Biodiversity Research Center, Academia Sinica

Distribution of ocean litters collected at the Dongsha Island, an isolated island in the northern South China Sea, shows a significant seasonal change. More litters were accumulated in the northern (southern) part of the island in winter (summer). By means of backward-tracking simulation by considering the effect of both ocean currents and winds (i.e., windage), a series of numerical experiments are carried out to clarify the possible source and mechanisms for the observational seasonal change of litters. Results exhibit that, in winter, low-windage litters are mainly from the western Philippine Sea via the Luzon Strait while the high-windage ones are contributed from the Taiwan Strait. In summer, litters from the southwestern South China Sea, i.e. east of Vietnam, could be a major origin.

Keywords: ocean litters, numercial study, South China Sea

©2019. Japan Geoscience Union. All Right Reserved.

A key spot and timing to monitor chlorophyll-a in the Kuroshio western boundary current

*Takafumi Hirata[1]

1. Faculty of Environmental Earth Science, Hokkaido University

The Kuroshio western boundary current originates from the subtropics in the Western Pacific and carries a thermal energy and oceanic water mass towards the north, including the south coasts and offshore islands of Japan. In spite of the oligotrophy of the origin water that the Kuroshio carries, the Kuroshio water is known for spawning and feeding grounds of commercial/non-commercial fish larvae, explaining a higher fisheries production in the region. Thus, it puzzles an oceanographic and ecological relationships among nutrient fields, standing stock and productivity of organisms. In order to understand the complex Kuroshio ecosystems, phytoplankton dynamics is investigated using remote sensing data, namely phytoplankton pigment or chlorophyll-a observed by Advanced Himawari Imager (AHI) onboard Himawari-8. The area-integrated, and the area average of, Kuroshio chlorophyll-a was found predictable from a chlorophyll-a measurement in the 134-136 ˚E, where the Kuroshio current direction is most stable between 130-150 ˚E . An analysis of short term variability (< 1 year) of the Kuroshio chlorophyll-a concentration revealed that a cumulative, and monthly average of, chlorophyll-a over a month in the Kuroshio surface water could be estimated from a chlorophyll-a measurement at a single day in the month. These results suggest that there is a key spot and timing to monitor the phytoplankton activities in the Kuroshio current.

Keywords: Kuroshio, Chlorophyll, Remote Sensing

©2019. Japan Geoscience Union. All Right Reserved.

Impacts of cyclonic eddies on phytoplankton biomass and phenology in the Kuroshio Extension region

*Eko Siswanto[1], Yoshikazu Sasai[1]

1. Japan Agency for Marine-Earth Science and Technology

Two-decade ocean color chlorophyll-a concentration (CHL, a metric of phytoplankton biomass) data from 1997 to 2017 were used to comprehend the impact of cyclonic eddies on phytoplankton biomass and phenology in the Kuroshio Extension region (KE) of the western North Pacific Ocean. The CHL data have 4-km and 8-day spatiotemporal resolution and were acquired from the ESA Ocean Colour-Climate Change Initiative (http://www.esa-oceancolour-cci.org/). Prior to defining spring bloom onset, spatiotemporal gaps in CHL data were filled by applying empirical orthogonal function-based interpolation. The analysis was mainly focused on the winter season (January-March) as oceanographic conditions during the winter largely control phytoplankton spring bloom in terms of both magnitude and onset. Based on winter sea surface height anomaly (SSHa), cyclonic eddies (negative SSHa) were dominant mainly within the periods from 1998 to 2001 and from 2005 to 2009, whereas anti-cyclonic eddies (positive SSHa) were dominant mainly within the periods from 2002 to 2004 and from 2011 to 2015. Based on datasets from all seasons, the concurrences of negative SSHa and positive phytoplankton chlorophyll anomaly (CHLa) were observed, albeit not always. This indicates an eddy-induced upwelling supplies nutrients to the near-surface layer. Upwelled nutrients eventually promote phytoplankton growth. Such a concurrence of low SSHa and high CHLa was less obvious during the winter indicating that another factor (such as intense winter vertical mixing) also non-trivially controlled nutrient input to the surface layer, and hence CHLa variability. Overall temporal mean indeed showed that the active cyclonic eddy area (approximately south of the Kuroshio Current main axis) was characterized by high CHLa, low SSHa, and shoaled mixed layer. In this study, a Cumulative Sum method was applied to find phytoplankton spring bloom onset. Correlation between SSHa and spring bloom onset time was investigated, and it was found that approximately over the active cyclonic eddy area, positive correlation between winter/late winter SSHa and time of spring bloom onset was observed. Such a positive correlation indicates that cyclonic eddies during the winter likely tended to advance phytoplankton spring bloom onset.

Keywords: Ocean color, Phytoplankton, Bloom onset, Upwelling

©2019. Japan Geoscience Union. All Right Reserved.

Diagnostic estimation and uncertainties of nutrient limitation of phytoplankton growth in Michaelis-Menten functional form

*Taketo Hashioka[1], Maki Noguchi Aita[1]

1. Japan Agency for Marine-Science and Technology

Michaelis-Menten functional form (MM) is most widely used relationship of nutrient limitation of phytoplankton growth in large-scale ecosystem models. In MM functional form, the choice of parameter value of a half-saturation constant is a key point for controlling the strength of nutrient limitation. In general, the half-saturation constant increase with the size of the phytoplankton cell depending on the surface-to-volume ratio by diffusive hypothesis, and wide ranges of values are reported from observational studies. On the other hand, the most of Plankton Functional Types (PFT) models represent a phytoplankton type as one representative PFT with one global parameter. The parameter value is chosen in the observed range as a most reasonable value that could reproduce observed chl-a or nutrient concentration in each model. As a result, there are uncertainties of the global pattern of nutrient limitation among models. In this study, we diagnostically estimated the nutrient limitation using various parameter set of different global PFT models form CMIP5 together with the observation based nutrient concentrations (World Ocean Atlas for macro nutrient and multi-model median for dissolved iron and ammonium concentration). Then we show uncertainties and robustness of estimation of nutrient limitation in the current PFT models with MM functional form.

Keywords: Plankton Functional Types model, Michaelis-Menten functional form

©2019. Japan Geoscience Union. All Right Reserved.

Modeling productivity in lower trophic levels in Otsuchi Bay, northeast of Japan, using a nested OGCM with a biogeochemical component

*Takashi T Sakamoto[1], L. Shogo Urakawa[2], Sachihiko Itoh[1], Hiroyasu Hasumi[1], Kiyoshi Tanaka[1]

1. Atmosphere and Ocean Research Institute, the University of Tokyo, 2. Meteorological Research Institute, Japan Meteorologica Agancy

Otsuchi Bay is located on the northeast coast of Honshu Island, Japan, where was extensively damaged by the huge tsunamis caused by the 2011 off the Pacific coast of Tohoku Earthquake. Motivated by how the biogeochemical circumstance and fishery resource recover, some observations have been conducted in the bay, but those have not been enough because of several restrictions and human resources. Aimed at filling the observational shortage and the acquirement of some information about physical and low trophic fields, a modeling approach has been discussed. Using a triply-nested OGCM and a downscaling method, the authors succeeded to reproduce seasonal variability of the circulation in the bay, and also showed a seasonality of the water exchange mechanism between the bay and the open ocean (Sakamoto et al. 2017). In order to know the low trophic processes in the bay, a numerical simulation using a nested OGCM with a NPZD model is conducted. The OGCM is an improved version of Sakamoto et al’ s (2017) model, and the NPZD one is based on Nagata and Hasumi (2014). In this poster, our modeling strategy and some results will be presented. The final goal of this study is to perform hindcasting simulations of the bay with realistic boundary conditions, that are the river runoff, the atmospheric forcings, and the open ocean states.

Keywords: downscaling, nest-modeling, NPZD model

©2019. Japan Geoscience Union. All Right Reserved.

Change in lower trophic level ecosystems to decadal scale variation of climate system in the North Pacific Ocean

*Maki Noguchi Aita[1], Kazuaki Tadokoro[2], Yoshiki Komuro[3], Taketo Hashioka[1], Naomi Harada[1]

1. Research and Development Center for Global Change, Japan Agency for Marine-Earth Science and Technology, 2. Tohoku National Fisheries Research Institute, Japan Fisheries Research and Education Agency, 3. Institute of Arctic Climate and Environment Research, Japan Agency for Marine-Earth Science and Technology

The changes related to interdecadal climate variations, such as the Pacific Decadal Oscillation and the 18.6-y tidal cycle, have been discussed in many marine ecosystem studies. By analyzing data from observation of nutrient concentrations, decreasing and increasing trends of nutrients in the surface and subsurface layers, have been reported in many studies. Changes have also been observed in the biomass of phytoplankton and zooplankton. To clarify variability of lower trophic level productivity and its controlling factor, we simulated changes in the marine ecosystem caused by interdecadal climate variability, using the JRA55-do (Japanese 55-year atmospheric reanalysis) dataset from 1958 to 2017 to drive an ecosystem model, NEMURO, embedded in a global three-dimensional physical-biological coupled model, ‘COCO-NEMURO’. We compared and verified ecosystem model results with observations of phytoplankton and zooplankton species composition data collected by the Tohoku National Fisheries Research Institute, Japan Fisheries Research and Education Agency (FRA). Our model results showed that changes in biomass and nutrient concentration greatly differ depending on the region. According to our model results, sea surface temperature (SST) was very low during mid 1960s to mid 1970s, then SST increased after the mid 1970s to the end of 1990s in the western subarctic North Pacific. Changes in phytoplankton biomass was follow to this. However, the change in SST and phytoplankton and zooplankton biomass were contrary to this in the western subtropical North Pacific. We also checked decadal time series of annual mean sea ice concentration, SST, and phytoplankton biomass in the eastern Bering Sea and the western Arctic. The simulated sea ice concentration in the eastern Bering Sea decreased from the late 1970s to the early 1980s, while it was higher in the early 1990s and the late 2000s. The SST had its peaks in the late 1970s and the early 2000s. The phytoplankton biomass was inversely correlated with the sea ice concentration. In the western Arctic, the simulated sea ice concentration (SST) showed negative (positive) trends on the decadal timescale. The phytoplankton biomass has also been increasing, but its trend was not so simple. To elucidate the mechanism that sustains marine ecosystems, we will also analyze focusing on primary producers and zooplankton to key link to higher trophic levels.

Keywords: Climate change, decadal change, lower trophic marine ecosystem, marine ecosystem model 'NEMURO'

©2019. Japan Geoscience Union. All Right Reserved.

Estimation of experienced environment of jack mackerel in the East China Sea

*Tomihiko Higuchi[1], Motomitsu Takahashi[2], Kotaro Shirai[1], Shin-ichi Ito[1]

1. Atmosphere and Ocean Research Institute, The University of Tokyo, 2. Seikai National Fisheries Research Institute,FRA

Jack mackerel *Trachurus japonicus* is distributed on the continental shelf waters along the subtropical Kuroshio Current and the Tsushima Warm Current in the western North Pacific. The East China Sea (ECS) is one of major region for jack mackerel and understanding the recruitment processes of jack mackerel into the fishing grounds in the ECS is important. However, marine environment such as water temperature that jack mackerel actually experiences is not directly observed yet. In this study, oxygen ($\delta^{18}O$) and carbon ($\delta^{13}C$) stable isotope of jack mackerel otolith were analyzed and the experienced environment was estimated. When we compared $\delta^{18}O$ of otolith caught in between three different station with different temperature, average of $\delta^{18}O$ varied and was negatively correlated with water temperature of sampling station. Most of individual indicated that $\delta^{13}C$ relatively increased from core part to edge in otolith. Thus, these results suggest that otolith of jack mackerel recorded experienced environment. However, because jack mackerel migrate vertically, it needs to consider vertical profile of seawater temperature and other parameters such as salinity and prey availability. A combination with fish distribution information and ecological modeling may help the improvement of estimation for detail experienced environment.

Keywords: fish otolith, isotope analysis, experienced environment, fish migration

©2019. Japan Geoscience Union. All Right Reserved.

[E] Poster | A (Atmospheric and Hydrospheric Sciences)：A-OS Ocean Sciences & Ocean Environment

Mon. May 27, 2019 5:15 PM - 6:30 PM JST | Mon. May 27, 2019 8:15 AM - 9:30 AM UTC | Poster Hall International Exhibition Hall8, Makuhari Messe_5

[A-OS12] Marine ecosystems and biogeochemical cycles: theory, observation and modeling

convener:Shin-ichi Ito(Atmosphere and Ocean Research Institute, The University of Tokyo), Takafumi Hirata(Faculty of Environmental Earth Science, Hokkaido University), Enrique N Curchitser(Rutgers University New Brunswick), Eileen E Hofmann(Old Dominion University)

The ocean accounts for about 50% of global net primary production. This production is significant for carbon cycling and ecosystem functioning, and is related directly or indirectly to a variety of climatic and ecological phenomena. The responses to natural and anthropogenic environmental stressors that influence marine production and diversity can cause perturbations to marine ecosystems that alter trophic dependencies and interactions among organisms at a range of space and time scales. Quantification of the principal mechanisms driving spatio-temporal variability of marine ecosystem remains to be done, especially in terms of evaluation of uncertainty in responses. As a result, evaluating vulnerability of marine ecosystems to environmental change requires systematic and holistic approaches that integrate physics to ecology and are based in observations and modelling. In addition, expectations to deliver these science to public society is raising. This session aims to provide a venue for not only discussing recent advances in understanding marine biogeochemical cycles, ecosystems and their interactions, but also networking with a variety of people to seed new ideas in marine ecological research. Observational, modeling and conceptual studies, including technological development and operational applications, that consider linkages among biogeochemical and ecosystem processes, biodiversity, and the effects of multiple stressors from molecular to planetary scales are encouraged.

[AOS12-P01] Impact of the nutrient transport through the Tsushima Strait on the ecosystem in the Japan Sea

*Ryota Shibano[1], Akihiko Morimoto[1], Katsumi Takayama[2], Tetsutaro Takikawa[3], Masashi Ito[4] (1.Center for Marine Environmental Studies, Ehime University, 2.Research Institute for Applied Mechanics, Kyushu University, 3.Graduate School of Fisheries and Environmental Sciences, Nagasaki University, 4.Fisheries Oceanography Department, Japan Sea National Fisheries Research Institute)

[AOS12-P02] Revisiting vertical variations in stoichiometry during oceanic organic matter decomposition

*Masahito Shigemitsu[1], Michio Aoyama[1], Toshimasa Doi[1], Taichi Yokokawa[1], Akihiko Murata[1] (1.Japan Agency for Marine-Earth Science and Technology)

[AOS12-P03] Reproduction of iron-rich intermediate water in the Sea of Okhotsk by high resolution biogeochemical model.

*Hatsumi Nishikawa[1], Humio Mitsudera[1], Hiroshi Yoshinari[2], Takuya Nakanowatari[3], Tomohiro Nakamura[1], Keisuke Uchimoto[4], Hiroyasu Hasumi[5] (1.Institute of Low Temperature Science, Hokkaido University, 2.National Institute for Environmental Studies, 3.Tohoku National Fisheries Research Institute, Japan Fisheries Research and Education Agency, 4.Research Institute of Innovative Technology for the Earth, 5.Atmosphere and Ocean Research Institute, University of Tokyo)

[AOS12-P04] The global oceanic iron distribution estimated by data assimilation approach

*Doi Toshimasa[1], Satoshi Osafune[1], Shuhei Masuda[1], Hajime Obata[2], Kazuhiro Misumi[3], Jun Nishioka[4] (1.Japan Agency for Marine-Earth Science and Technology, 2.The University of Tokyo, 3.Central Research Institute of Electric Power Industry, 4.Hokkaido University)

[AOS12-P05] A high-resolution multi-purpose particle tracking framework for coastal areas near Japan

*Yoshimasa Matsumura[1], Shota Katsura[1], Masao Kurogi[2], Hideyuki Nakano[3], Takateru Yamagishi[4] (1.Atmosphere and Ocean Research Institute, University of Tokyo, 2.Japan Agency for Marine-Earth Science and Technology, 3.Meteorological Research Institute, Japan Meteorological Agency , 4.Research organization for Information Science and Technology)

[AOS12-P06] Numerical study on seasonality of ocean litters collected at the Dongsha Island in the northern South China Sea

*Yi-Chia Hsin[1], Chia-Ying Ko[2], Ming-Shiou Jeng[3] (1.Research Center for Environmental Changes, Academia Sinica, 2.Institute of Fisheries Science, National Taiwan University, 3.Biodiversity Research Center, Academia Sinica)

[AOS12-P07] A key spot and timing to monitor chlorophyll-a in the Kuroshio western boundary current

*Takafumi Hirata[1] (1.Faculty of Environmental Earth Science, Hokkaido University)

[AOS12-P08] **Impacts of cyclonic eddies on phytoplankton biomass and phenology in the Kuroshio Extension region**

*Eko Siswanto[1], Yoshikazu Sasai[1] (1.Japan Agency for Marine-Earth Science and Technology)

[AOS12-P09] Diagnostic estimation and uncertainties of nutrient limitation of phytoplankton growth in Michaelis-Menten functional form

*Taketo Hashioka[1], Maki Noguchi Aita[1] (1.Japan Agency for Marine-Science and Technology)

[AOS12-P10] Modeling productivity in lower trophic levels in Otsuchi Bay, northeast of Japan, using a nested OGCM with a biogeochemical component

*Takashi T Sakamoto[1], L. Shogo Urakawa[2], Sachihiko Itoh[1], Hiroyasu Hasumi[1], Kiyoshi Tanaka[1] (1.Atmosphere and Ocean Research Institute, the University of Tokyo, 2.Meteorological Research Institute, Japan Meteorologica Agancy)

[AOS12-P11] Change in lower trophic level ecosystems to decadal scale variation of climate system in the North Pacific Ocean

*Maki Noguchi Aita[1], Kazuaki Tadokoro[2], Yoshiki Komuro[3], Taketo Hashioka[1], Naomi Harada[1] (1.Research and Development Center for Global Change, Japan Agency for Marine-Earth Science and Technology, 2.Tohoku National Fisheries Research Institute, Japan Fisheries Research and Education Agency, 3.Institute of Arctic Climate and Environment Research, Japan Agency for Marine-Earth Science and Technology)

[AOS12-P12] Estimation of experienced environment of jack mackerel in the East China Sea

*Tomihiko Higuchi[1], Motomitsu Takahashi[2], Kotaro Shirai[1], Shin-ichi Ito[1] (1.Atmosphere and Ocean Research Institute, The University of Tokyo, 2.Seikai National Fisheries Research Institute,FRA)

Impact of the nutrient transport through the Tsushima Strait on the ecosystem in the Japan Sea

*Ryota Shibano[1], Akihiko Morimoto[1], Katsumi Takayama[2], Tetsutaro Takikawa[3], Masashi Ito[4]

1. Center for Marine Environmental Studies, Ehime University, 2. Research Institute for Applied Mechanics, Kyushu University, 3. Graduate School of Fisheries and Environmental Sciences, Nagasaki University, 4. Fisheries Oceanography Department, Japan Sea National Fisheries Research Institute

The Japan Sea is a semi-closed sea with narrow and shallow straits such as the Tsushima/Korea Strait. The nutrient transports through the Tsushima Strait have an impact the ecosystem around the coast of Japan. The nutrient transports are originated in the sources from the sea, Kuroshio (Pacific), Taiwan Strait, and Yellow Sea, and the sources from the land, Changjiang river, Yellow river, and dusts. We investigated the ship cruise data in the strait from 2005 to 2017 to reveal the interannual variations in the volume transport, nutrient concentration, and nutrient transport. The nutrient transport in the strait has large interannual variations of ±50% compared to the average transport.

The recently studies indicated the contribution ratio in the nutrient transports on the sources from the Kuroshio and the rivers also change, when the yearly nutrient transport changes (e.g. Morimoto et al., 2012).

We developed a coupled ocean circulation and ecosystem model, in which the lateral boundary condition is applied based on observation data, and investigated the biogeochemical responses in the Japan Sea and the East China Sea to the interannual variations in the nutrient flux through the Tsushima Strait. We discussed about the contribution ratio in the nutrient flux on the 6 sources from Kuroshio, Taiwan Strait, Changjiang river, Yellow river, the dust, and the bottom (Yellow Sea).

Keywords: Tsushima Warm Current, nutrient transport, the Sea of Japan

©2019. Japan Geoscience Union. All Right Reserved.

Revisiting vertical variations in stoichiometry during oceanic organic matter decomposition

*Masahito Shigemitsu[1], Michio Aoyama[1], Toshimasa Doi[1], Taichi Yokokawa[1], Akihiko Murata[1]

1. Japan Agency for Marine-Earth Science and Technology

Using the new global nutrient data set, we re-evaluate basin-wide stoichiometric ratios of remineralization estimated by Anderson and Sarmiento (1994) (hereinafter, AS94). For the same latitudinal ranges of the Atlantic, Indian and Pacific Oceans as in AS94, we construct one or two end-member mixing models on 14 neutral surfaces and estimate the stoichiometric ratios with a probabilistic approach. Unlike the results of AS94, significant vertical variations in the stoichiometry are found in the Atlantic and Pacific, while relatively constant stoichiometry with depth is found in the Indian Ocean, similar to AS94. The decreases in the C/P and $-O_2$/P ratios with depth in the Atlantic could be caused via dark DIC fixation by chemoautotrophs in the deep waters. In the Pacific, changes in organic matter composition with depth would be the most important factor in the increases in stoichiometry with depth. In all the basins, the N/P ratios are probably affected by benthic denitrification, as in AS94. The P/C/-O_2ratios (mean and $5^{th}$to 95^{th} percentile) are estimated to be 1/111(97 to 129)/155(149 to 163) in the depths below 2000 m of the Indian and Pacific Oceans, where DIC fixation and vertical change in organic matter composition have little influence on the stoichiometry estimates. We suggest that chemoautotrophic DIC fixation and the effect of change in organic matter composition with depth on the stoichiometry in waters above 2000 m should be considered for large-scale biogeochemical modeling and estimation of oceanic uptake of anthropogenic carbon from observational data.

Keywords: nutrients, stoichiometric ratios, remineralization of organic matter

©2019. Japan Geoscience Union. All Right Reserved.

Reproduction of iron-rich intermediate water in the Sea of Okhotsk by high resolution biogeochemical model.

*Hatsumi Nishikawa[1], Humio Mitsudera[1], Hiroshi Yoshinari[2], Takuya Nakanowatari[3], Tomohiro Nakamura[1], Keisuke Uchimoto[4], Hiroyasu Hasumi[5]

1. Institute of Low Temperature Science, Hokkaido University, 2. National Institute for Environmental Studies, 3. Tohoku National Fisheries Research Institute, Japan Fisheries Research and Education Agency, 4. Research Institute of Innovative Technology for the Earth, 5. Atmosphere and Ocean Research Institute, University of Tokyo

Recent observation studies suggest that iron supply from sediment on the northwest continental shelf the Okhotsk Sea plays an important role for the subarctic primary production (e.g. Nishioka et al., 2013). Dense shelf water (DSW) takes up iron from sediment, thereby transporting iron into the Okhotsk Sea intermediate water. However, observational data is still limited.

To clarify detailed structure of iron circulation in the North Pacific, we develop the high-resolution biogeochemical model. However, our model did not reproduce high iron concentration in the intermediate water the Sea of Okhotsk. We use biogeochemical model developed by Parekh et al. (2005). They set the value of total ligand concentration to constant value in all place. Recent observations, however, suggest that ligand concentration varies with sea area and depth. Then, we conducted a new experiment with the ligand concentration changed in the vertical direction. The iron concentration intermediate water of the new experiment becaame higher than before.

Keywords: High-resolution modeling, Iron-rich intermediate water, Ligand concentration

©2019. Japan Geoscience Union. All Right Reserved.

The global oceanic iron distribution estimated by data assimilation approach

*Doi Toshimasa[1], Satoshi Osafune[1], Shuhei Masuda[1], Hajime Obata[2], Kazuhiro Misumi[3], Jun Nishioka[4]

1. Japan Agency for Marine-Earth Science and Technology, 2. The University of Tokyo, 3. Central Research Institute of Electric Power Industry, 4. Hokkaido University

Since distribution of oceanic iron is considered as one of the restriction factors of phytoplankton activity, it is necessary for a pelagic lower trophic level ecosystem model to take into account the effect of iron. In this study, we constructed a three dimensional gridded data of oceanic iron concentration by using both available in situ observation and simple iron cycle model. For the physical process of iron transport, the advection/diffusion model was used along with the flow field of ESTOC (Estimated State of Global Ocean for Climate Research). The falling atmospheric dust in the sea-surface and flux from the sediment at sea floor of the coast were set as the input of the iron. The scavenging or desorption by particulate matter in the water column were employed as the control variables and we constructed the simple iron cycle model. The optimized set of control parameters was obtained based on a Green's function approach by using available in situ iron concentration observations. The results showed that the iron concentration in the southern hemisphere is lower than northern hemisphere, and the low iron regions were well reproduced around the regions of high nutrient / low chlorophyll. Moreover, it is suggested that the Atlantic Ocean is more affected by the atmospheric dust compared with the Pacific Ocean.

Keywords: oceanic iron, data assimilation

©2019. Japan Geoscience Union. All Right Reserved.

A high-resolution multi-purpose particle tracking framework for coastal areas near Japan

*Yoshimasa Matsumura[1], Shota Katsura[1], Masao Kurogi[2], Hideyuki Nakano[3], Takateru Yamagishi[4]

1. Atmosphere and Ocean Research Institute, University of Tokyo, 2. Japan Agency for Marine-Earth Science and Technology, 3. Meteorological Research Institute, Japan Meteorological Agency , 4. Research organization for Information Science and Technology

A comprehensive and multi-purpose particle tracking framework using latest high resolution velocity field in the coastal regions near Japan is developed.
The particle tracking system uses accurate fourth order Runge-Kutta method and implements random-walk based diffusivity, and is built-in the recent versions of MRI.com (an OGCM developed in Meteorological Research Institute, Japan Meteorological Agency) and kinaco (a non-hydrostatic ocean model developed in Atmosphere and Ocean Research Institute, University of Tokyo) for *on-line* use. Each particle is able to store up to seven arbitrary properties (such as size, age, exposed temperature, orientation, mass and buoyancy, etc.) and record the history of them.

The code is effectively parallelized (using MPI and OpenMP hybrid technique) and allows ~O(10^{10}) particles on modern massive-parallel supercomputers, and is also ported to GPU architecture using CUDA language.

This particle tracking framework has no particular target in a priori, and can be applied to various purposes for both physical oceanography (from large scale tracking of water masses to small scale modeling of suspended sediment matter or frazil ice crystals) and ocean biogeochemistry (tracking of trace elements, Laglangian modeling of plankton and detritus, individual based modeling of fishes and marine resources), only by defining appropriate properties and inserting a few lines of code that manipulats them corresponding to the particular target use.

In the presentation, we will introduce an application of this framework to the tracking of passive particles scattered in the coastal areas near Japan using velocity field provided by the latest very high resolution ocean modeling (~300 m mesh). Each model particle records its trajectory and the history of exposed environment, and can be interpreted as eggs or larvae (before acquiring swimming ability) of species of corresponding spawning areas and seasons as well as the tracers for small scale water mass exchanges.

Keywords: Particle tracking system

©2019. Japan Geoscience Union. All Right Reserved.

Numerical study on seasonality of ocean litters collected at the Dongsha Island in the northern South China Sea

*Yi-Chia Hsin[1], Chia-Ying Ko[2], Ming-Shiou Jeng[3]

1. Research Center for Environmental Changes, Academia Sinica, 2. Institute of Fisheries Science, National Taiwan University, 3. Biodiversity Research Center, Academia Sinica

Distribution of ocean litters collected at the Dongsha Island, an isolated island in the northern South China Sea, shows a significant seasonal change. More litters were accumulated in the northern (southern) part of the island in winter (summer). By means of backward-tracking simulation by considering the effect of both ocean currents and winds (i.e., windage), a series of numerical experiments are carried out to clarify the possible source and mechanisms for the observational seasonal change of litters. Results exhibit that, in winter, low-windage litters are mainly from the western Philippine Sea via the Luzon Strait while the high-windage ones are contributed from the Taiwan Strait. In summer, litters from the southwestern South China Sea, i.e. east of Vietnam, could be a major origin.

Keywords: ocean litters, numercial study, South China Sea

©2019. Japan Geoscience Union. All Right Reserved.

A key spot and timing to monitor chlorophyll-a in the Kuroshio western boundary current

*Takafumi Hirata[1]

1. Faculty of Environmental Earth Science, Hokkaido University

The Kuroshio western boundary current originates from the subtropics in the Western Pacific and carries a thermal energy and oceanic water mass towards the north, including the south coasts and offshore islands of Japan. In spite of the oligotrophy of the origin water that the Kuroshio carries, the Kuroshio water is known for spawning and feeding grounds of commercial/non-commercial fish larvae, explaining a higher fisheries production in the region. Thus, it puzzles an oceanographic and ecological relationships among nutrient fields, standing stock and productivity of organisms. In order to understand the complex Kuroshio ecosystems, phytoplankton dynamics is investigated using remote sensing data, namely phytoplankton pigment or chlorophyll-a observed by Advanced Himawari Imager (AHI) onboard Himawari-8. The area-integrated, and the area average of, Kuroshio chlorophyll-a was found predictable from a chlorophyll-a measurement in the 134-136 ˚E, where the Kuroshio current direction is most stable between 130-150 ˚E . An analysis of short term variability (< 1 year) of the Kuroshio chlorophyll-a concentration revealed that a cumulative, and monthly average of, chlorophyll-a over a month in the Kuroshio surface water could be estimated from a chlorophyll-a measurement at a single day in the month. These results suggest that there is a key spot and timing to monitor the phytoplankton activities in the Kuroshio current.

Keywords: Kuroshio, Chlorophyll, Remote Sensing

©2019. Japan Geoscience Union. All Right Reserved.

Impacts of cyclonic eddies on phytoplankton biomass and phenology in the Kuroshio Extension region

*Eko Siswanto[1], Yoshikazu Sasai[1]

1. Japan Agency for Marine-Earth Science and Technology

Two-decade ocean color chlorophyll-a concentration (CHL, a metric of phytoplankton biomass) data from 1997 to 2017 were used to comprehend the impact of cyclonic eddies on phytoplankton biomass and phenology in the Kuroshio Extension region (KE) of the western North Pacific Ocean. The CHL data have 4-km and 8-day spatiotemporal resolution and were acquired from the ESA Ocean Colour-Climate Change Initiative (http://www.esa-oceancolour-cci.org/). Prior to defining spring bloom onset, spatiotemporal gaps in CHL data were filled by applying empirical orthogonal function-based interpolation. The analysis was mainly focused on the winter season (January-March) as oceanographic conditions during the winter largely control phytoplankton spring bloom in terms of both magnitude and onset. Based on winter sea surface height anomaly (SSHa), cyclonic eddies (negative SSHa) were dominant mainly within the periods from 1998 to 2001 and from 2005 to 2009, whereas anti-cyclonic eddies (positive SSHa) were dominant mainly within the periods from 2002 to 2004 and from 2011 to 2015. Based on datasets from all seasons, the concurrences of negative SSHa and positive phytoplankton chlorophyll anomaly (CHLa) were observed, albeit not always. This indicates an eddy-induced upwelling supplies nutrients to the near-surface layer. Upwelled nutrients eventually promote phytoplankton growth. Such a concurrence of low SSHa and high CHLa was less obvious during the winter indicating that another factor (such as intense winter vertical mixing) also non-trivially controlled nutrient input to the surface layer, and hence CHLa variability. Overall temporal mean indeed showed that the active cyclonic eddy area (approximately south of the Kuroshio Current main axis) was characterized by high CHLa, low SSHa, and shoaled mixed layer. In this study, a Cumulative Sum method was applied to find phytoplankton spring bloom onset. Correlation between SSHa and spring bloom onset time was investigated, and it was found that approximately over the active cyclonic eddy area, positive correlation between winter/late winter SSHa and time of spring bloom onset was observed. Such a positive correlation indicates that cyclonic eddies during the winter likely tended to advance phytoplankton spring bloom onset.

Keywords: Ocean color, Phytoplankton, Bloom onset, Upwelling

©2019. Japan Geoscience Union. All Right Reserved.

Diagnostic estimation and uncertainties of nutrient limitation of phytoplankton growth in Michaelis-Menten functional form

*Taketo Hashioka[1], Maki Noguchi Aita[1]

1. Japan Agency for Marine-Science and Technology

Michaelis-Menten functional form (MM) is most widely used relationship of nutrient limitation of phytoplankton growth in large-scale ecosystem models. In MM functional form, the choice of parameter value of a half-saturation constant is a key point for controlling the strength of nutrient limitation. In general, the half-saturation constant increase with the size of the phytoplankton cell depending on the surface-to-volume ratio by diffusive hypothesis, and wide ranges of values are reported from observational studies. On the other hand, the most of Plankton Functional Types (PFT) models represent a phytoplankton type as one representative PFT with one global parameter. The parameter value is chosen in the observed range as a most reasonable value that could reproduce observed chl-a or nutrient concentration in each model. As a result, there are uncertainties of the global pattern of nutrient limitation among models. In this study, we diagnostically estimated the nutrient limitation using various parameter set of different global PFT models form CMIP5 together with the observation based nutrient concentrations (World Ocean Atlas for macro nutrient and multi-model median for dissolved iron and ammonium concentration). Then we show uncertainties and robustness of estimation of nutrient limitation in the current PFT models with MM functional form.

Keywords: Plankton Functional Types model, Michaelis-Menten functional form

©2019. Japan Geoscience Union. All Right Reserved.

Modeling productivity in lower trophic levels in Otsuchi Bay, northeast of Japan, using a nested OGCM with a biogeochemical component

*Takashi T Sakamoto[1], L. Shogo Urakawa[2], Sachihiko Itoh[1], Hiroyasu Hasumi[1], Kiyoshi Tanaka[1]

1. Atmosphere and Ocean Research Institute, the University of Tokyo, 2. Meteorological Research Institute, Japan Meteorologica Agancy

Otsuchi Bay is located on the northeast coast of Honshu Island, Japan, where was extensively damaged by the huge tsunamis caused by the 2011 off the Pacific coast of Tohoku Earthquake. Motivated by how the biogeochemical circumstance and fishery resource recover, some observations have been conducted in the bay, but those have not been enough because of several restrictions and human resources. Aimed at filling the observational shortage and the acquirement of some information about physical and low trophic fields, a modeling approach has been discussed. Using a triply-nested OGCM and a downscaling method, the authors succeeded to reproduce seasonal variability of the circulation in the bay, and also showed a seasonality of the water exchange mechanism between the bay and the open ocean (Sakamoto et al. 2017). In order to know the low trophic processes in the bay, a numerical simulation using a nested OGCM with a NPZD model is conducted. The OGCM is an improved version of Sakamoto et al’ s (2017) model, and the NPZD one is based on Nagata and Hasumi (2014). In this poster, our modeling strategy and some results will be presented. The final goal of this study is to perform hindcasting simulations of the bay with realistic boundary conditions, that are the river runoff, the atmospheric forcings, and the open ocean states.

Keywords: downscaling, nest-modeling, NPZD model

©2019. Japan Geoscience Union. All Right Reserved.

Change in lower trophic level ecosystems to decadal scale variation of climate system in the North Pacific Ocean

*Maki Noguchi Aita[1], Kazuaki Tadokoro[2], Yoshiki Komuro[3], Taketo Hashioka[1], Naomi Harada[1]

1. Research and Development Center for Global Change, Japan Agency for Marine-Earth Science and Technology, 2. Tohoku National Fisheries Research Institute, Japan Fisheries Research and Education Agency, 3. Institute of Arctic Climate and Environment Research, Japan Agency for Marine-Earth Science and Technology

The changes related to interdecadal climate variations, such as the Pacific Decadal Oscillation and the 18.6-y tidal cycle, have been discussed in many marine ecosystem studies. By analyzing data from observation of nutrient concentrations, decreasing and increasing trends of nutrients in the surface and subsurface layers, have been reported in many studies. Changes have also been observed in the biomass of phytoplankton and zooplankton. To clarify variability of lower trophic level productivity and its controlling factor, we simulated changes in the marine ecosystem caused by interdecadal climate variability, using the JRA55-do (Japanese 55-year atmospheric reanalysis) dataset from 1958 to 2017 to drive an ecosystem model, NEMURO, embedded in a global three-dimensional physical-biological coupled model, ‘COCO-NEMURO’. We compared and verified ecosystem model results with observations of phytoplankton and zooplankton species composition data collected by the Tohoku National Fisheries Research Institute, Japan Fisheries Research and Education Agency (FRA). Our model results showed that changes in biomass and nutrient concentration greatly differ depending on the region. According to our model results, sea surface temperature (SST) was very low during mid 1960s to mid 1970s, then SST increased after the mid 1970s to the end of 1990s in the western subarctic North Pacific. Changes in phytoplankton biomass was follow to this. However, the change in SST and phytoplankton and zooplankton biomass were contrary to this in the western subtropical North Pacific. We also checked decadal time series of annual mean sea ice concentration, SST, and phytoplankton biomass in the eastern Bering Sea and the western Arctic. The simulated sea ice concentration in the eastern Bering Sea decreased from the late 1970s to the early 1980s, while it was higher in the early 1990s and the late 2000s. The SST had its peaks in the late 1970s and the early 2000s. The phytoplankton biomass was inversely correlated with the sea ice concentration. In the western Arctic, the simulated sea ice concentration (SST) showed negative (positive) trends on the decadal timescale. The phytoplankton biomass has also been increasing, but its trend was not so simple. To elucidate the mechanism that sustains marine ecosystems, we will also analyze focusing on primary producers and zooplankton to key link to higher trophic levels.

Keywords: Climate change, decadal change, lower trophic marine ecosystem, marine ecosystem model 'NEMURO'

©2019. Japan Geoscience Union. All Right Reserved.

Estimation of experienced environment of jack mackerel in the East China Sea

*Tomihiko Higuchi[1], Motomitsu Takahashi[2], Kotaro Shirai[1], Shin-ichi Ito[1]

1. Atmosphere and Ocean Research Institute, The University of Tokyo, 2. Seikai National Fisheries Research Institute,FRA

Jack mackerel *Trachurus japonicus* is distributed on the continental shelf waters along the subtropical Kuroshio Current and the Tsushima Warm Current in the western North Pacific. The East China Sea (ECS) is one of major region for jack mackerel and understanding the recruitment processes of jack mackerel into the fishing grounds in the ECS is important. However, marine environment such as water temperature that jack mackerel actually experiences is not directly observed yet. In this study, oxygen ($\delta^{18}O$) and carbon ($\delta^{13}C$) stable isotope of jack mackerel otolith were analyzed and the experienced environment was estimated. When we compared $\delta^{18}O$ of otolith caught in between three different station with different temperature, average of $\delta^{18}O$ varied and was negatively correlated with water temperature of sampling station. Most of individual indicated that $\delta^{13}C$ relatively increased from core part to edge in otolith. Thus, these results suggest that otolith of jack mackerel recorded experienced environment. However, because jack mackerel migrate vertically, it needs to consider vertical profile of seawater temperature and other parameters such as salinity and prey availability. A combination with fish distribution information and ecological modeling may help the improvement of estimation for detail experienced environment.

Keywords: fish otolith, isotope analysis, experienced environment, fish migration

©2019. Japan Geoscience Union. All Right Reserved.

[J] Oral | A (Atmospheric and Hydrospheric Sciences)：A-OS Ocean Sciences & Ocean Environment

Mon. May 27, 2019 10:45 AM - 12:15 PM JST | Mon. May 27, 2019 1:45 AM - 3:15 AM UTC | 102 1F

[A-OS13] Ocean circulation and material cycle in coastal seas

convener:Kiyoshi Tanaka(University of Tokyo), Akihiko Morimoto(Ehime University), Yuichi Hayami(Saga University), Kazuhiko Ichimi(Seto Inland Sea Regional Research Center, Kagawa University), Chairperson:Kiyoshi Tanaka, Akihiko Morimoto

Coastal seas have high biodiversity and high productivity, while various environmental problems such as eutrophication, red tide, and hypoxia are caused by human activity. In order to understand material cycle and various phenomena and to maintain sustainable environment in coastal seas, interdisciplinary research is needed. In the present session, we invite researchers who are interested in physical phenomena, material cycle, biological responsive dynamics, and their interactions in coastal seas. Neither study area nor study method is confined. We welcome presentations of wide-range topics to communize our knowledge in coastal seas.

10:45 AM - 11:00 AM JST | 1:45 AM - 2:00 AM UTC

[AOS13-01] On-demand development of bay-scale models using the Japanese Coastal Ocean Monitoring and Forecasting System

*Kei Sakamoto[1], Hideyuki Nakano[1], Shogo Urakawa[1], Takahiro Toyoda[1], Hiroyuki Tsujino[1], Goro Yamanaka[1] (1.Meteorological Research Institute)

11:00 AM - 11:15 AM JST | 2:00 AM - 2:15 AM UTC

[AOS13-02] Long term measurement of the current at the bay head in the Suruga Bay, Japan. part 2

*Takaaki Katsumata[1,4], Masato Niki[2], Akihiko Tanaka[1], Hiroyuki Tan[1,3], Kyoko Takashima[2], Takashige Sugimoto (1.Liberal Arts Education Center, Shimizu Campus, Tokai University., 2.School of Marine Science and Technology, Tokai University, 3.Japan Unmanned Vehicle exploration Agency, 4.NPO, the association for the environmental conservation of the ocean)

11:15 AM - 11:30 AM JST | 2:15 AM - 2:30 AM UTC

[AOS13-03] Bottom-water intrusion and subsequent water exchange induced by Yamase around Mutsu Bay

*Satomi Fujisaki[1], Atsuhiko Isobe[1], Izumi Ogida[2], Yuki Kosaka[2] (1.Kyushu university, 2.Aomori Prefectural Fisheries Research Institute)

11:30 AM - 11:45 AM JST | 2:30 AM - 2:45 AM UTC

[AOS13-04] The Generation Process of the Bottom Intrusion in the Bungo Channel

*Kana Maetani[1], Akihiko Morimoto[2], Xinyu Guo[2], Toru Miyama[3] (1.Graduate School of Science and Engineering, Ehime University, 2.Center for Marine Environmental Studies, Ehime University, 3.Japan Agency for Marine-Earth Science and Technology)

11:45 AM - 12:00 PM JST | 2:45 AM - 3:00 AM UTC

[AOS13-05] Characteristics of bottom intrusion in the Bungo Channel

*Akihiko Morimoto[1], Shuya Fujita[1], Hidetaka Takeoka[1], Xinyu Guo[1] (1.Ehime University)

12:00 PM - 12:15 PM JST | 3:00 AM - 3:15 AM UTC

[AOS13-06] Role of Kuroshio Current in fish resource variability off southwest Japan

*Yushi Morioka[1], Sergey Varlamov[1], Yasumasa Miyazawa[1] (1.Japan Agency for Marine-Earth Science and Technology)

On-demand development of bay-scale models using the Japanese Coastal Ocean Monitoring and Forecasting System

*Kei Sakamoto[1], Hideyuki Nakano[1], Shogo Urakawa[1], Takahiro Toyoda[1], Hiroyuki Tsujino[1], Goro Yamanaka[1]

1. Meteorological Research Institute

We have developed the "Japanese Coastal Ocean Monitoring and Forecasting System" (MOVE/MRI.COM-JPN) to reproduce oceanic conditions across the coastal seas around Japan, based on an ocean model with horizontal resolution of approximately 2 km and a 4-dimensional variational data assimilation system. The Japan Meteorological Agency plans to use this system as a platform for various coastal marine operations, and details of the system are explained in Sakamoto et al. (2019) and Hirose et al. (2019) (submitted to Ocean Dynamics). However, the model resolution of 2 km is a minimum necessary requirement for continental shelf regions in contact with open oceans and relatively large inland seas such as the Seto Inland Sea, and it is a future task to provide information targeting bay-scale regions which are more closely related to society, including small bays, inland seas and straits. As a solution, a model covering the entire coastal seas around Japan with a resolution of several hundred meters is planned, but a current ordinary computer cannot perform its enormous calculations. In this respect, it seems feasible to deploy an array of bay-scale models of high resolution and small domain, which are nested from MOVE/MRI.COM-JPN, but management costs of a lot of models are concerned in that case. Therefore, we are considering an approach to develop bay-scale models on demand for a future expansion of MOVE/MRI.COM-JPN. As a first step towards this, we began developing a package that can quickly build a bay-scale model. Currently, the package consists mainly of three elements. The first is our numerical model MRI.COM. In addition to an offline-nesting function, it is possible to introduce dynamics important in coastal seas of Japan, such as river runoff, sea ice, tides and the inverse barometer effect. The second is a package of pre-processing and analysis tools named "MRI.COM eXperimental Environment". This helps a model developer to easily create model configurations such as topography data. The third is analysis data of the coastal seas around Japan produced by MOVE/MRI.COM-JPN. By using this data for the initial value and lateral boundary condition of a bay model, we can start a model experiment anytime after 2008. Using this package, we have created a Nagasaki Bay model with resolution of 100 m and an Osaka Bay model with resolution of 200 m. We reproduced seiches called "Abiki" by the Nagasaki Bay model, and the storm surge caused by Typhoon Jebi in September 2018 by the Osaka Bay model. The poster presentation will also show these results.

Keywords: coastal model, operational model, Japanese coastal seas, nesting, model development

©2019. Japan Geoscience Union. All Right Reserved.

Long term measurement of the current at the bay head in the Suruga Bay, Japan. part 2

*Takaaki Katsumata[1,4], Masato Niki[2], Akihiko Tanaka[1], Hiroyuki Tan[1,3], Kyoko Takashima[2], Takashige Sugimoto

1. Liberal Arts Education Center, Shimizu Campus, Tokai University., 2. School of Marine Science and Technology, Tokai University, 3. Japan Unmanned Vehicle exploration Agency, 4. NPO, the association for the environmental conservation of the ocean

The Suruga Bay is located on a southern coast in the main island of Japan, and the bay facing to the Kuroshio front. Fishery in the bay are strongly influenced by a variables of rivers inflows and intruding of Kuroshio water (Sugimoto et al., 2009; Tanaka et al.,2009; Katsumata, 2016). But we have a little knowledge for these variations. Therefore, we measured the profile of the current by ferry mounted ADCP, at the line of the “Suruga Bay Ferry” cruise cross the bay head from a western coast to eastern coast, i.e., Shimizu Port to Toi Port, since 2008. We currently continuing measuring the current in the bay about near 10 years. The anticlockwise circulation at the bay head of the Suruga Bay has at least 100 m thick from surface layer. The circulation in bay head has clearly seasonal variation, it is relate difference of stratified period and non-stratified one. This current data include the period of typical large meander of Kuroshio.

Keywords: Ferry mount ADCP, Suruga Bay, typical large meander path of Kuroshio

©2019. Japan Geoscience Union. All Right Reserved.

Bottom-water intrusion and subsequent water exchange induced by Yamase around Mutsu Bay

*Satomi Fujisaki[1], Atsuhiko Isobe[1], Izumi Ogida[2], Yuki Kosaka[2]

1. Kyushu university, 2. Aomori Prefectural Fisheries Research Institute

Bottom-water intrusion in the Bungo channel, which is the cold-water intrusion onto the continental shelf from the Kuroshio intermediate layer, was studied by Takeoka et al. (2000). The bottom-water intrusion in the Bungo channel occurs when the Kuroshio Current passes along the Kyushu of the Bungo channel (Kaneda et al., 2002). In the case of Mutsu Bay, bottom-water temperature fluctuated by more than 3 degree Celsius during summer (June –September). However, Tsugaru Warm Current is not so strong compared with Kuroshio and, thus, we had to find other mechanisms for the bottom-water intrusion to occur. We here focused on Yamase which is a cold, moist and westward wind blowing from the Okhotsk Sea during summer and analyzed water temperature, current velocity and wind velocity.

Ocean buoy automatic monitoring system (hereinafter, buoy system) at three points of Mutsu Bay (Tairadate, Aomori, Higashiwan) have observed water temperature, current velocity, salinity, and so forth at a depth of 1m, 15m, 30m every single hour. An observation ship “Natsudomari” records water temperature, salinity, and so forth at eleven points of Mutsu Bay once a month. Water temperature and current velocity from 2008 to 2017 (buoy system), water temperature from 1981 to 2016 (Natsudomari), water temperature from 1981 to 2010 (Japan Oceanographic Data Center (J-DOSS)) and water temperature deviation in August from 2008 to 2017 in Tsugaru Strait (Hokkaido Research Organization) were obtained. Wind data at Oma observatory free of terrain-derived disturbances was obtained from the Japan Meteorological Agency.
A correlation analysis of time series between water temperature (5 –15 days) at Tairadate, Aomori, Higashiwan and zonal wind at Oma was performed. The days when daily average easterly (westerly) wind velocity was greater than 2 m/s was referred to as “eastern (western) wind day”. Composite maps of cross sections of water temperature in Tsugaru Strait and Mutsu Bay was created on the eastern and western wind day, respectively. The relationship between annually average bottom-water temperature at Aomori and Higashiwan and eastern winds at Oma was investigated during summer (June –September) from 2008 to 2017. Water temperature in 2011 was excluded because water temperature in Tsugaru Strait was extraordinarily low.

Long-period bottom-water temperature (about 10 days) at Tairadate and Aomori, both of which are located in western Mutsu Bay, remarkably fluctuated, that is, bottom-water intrusion occurred in the western part of Mutsu Bay. The correlation coefficients between the bottom temperature and Oma winds were 0.68 at Tairadate (a significance level of 0.05) and 0.75 at Aomori (a significance level of 0.05). Consequently, it was suggested that zonal wind induced bottom-water intrusion in western Mutsu Bay. Moreover, the composite maps stated that cold-water < 10 degree Celsius intruded onto the bottom of Mutsu Bay from Tsugaru Strait during eastern wind days. These findings suggest that westward Yamase triggers bottom-water intrusion in Mutsu Bay. However, as bottom-water temperature become lower, bottom-water intrusion was prevented even when Yamase blows continuously.

Keywords: Bottom-water intrusion, Mutsu Bay, Yamase

©2019. Japan Geoscience Union. All Right Reserved.

The Generation Process of the Bottom Intrusion in the Bungo Channel

*Kana Maetani[1], Akihiko Morimoto[2], Xinyu Guo[2], Toru Miyama[3]

1. Graduate School of Science and Engineering, Ehime University, 2. Center for Marine Environmental Studies, Ehime University, 3. Japan Agency for Marine-Earth Science and Technology

Introduction

The Bungo Channel is one of the two channels that connect to the Pacific Ocean and the Seto Inland Sea, and located between Kyushu and Shikoku Islands. Marine environment in the Bungo Channel is strongly influenced by the disturbances from open ocean. It is known that a cold-water intrusion from open sea, called a “Bottom Intrusion”, occurs in the lower layer from summer to autumn (Kaneda *et al.,* 2002). Since the Bottom Intrusion is difficult to observe because of its occurrence position, generation mechanism and intrusion process of the Bottom Intrusion have not been revealed yet. However, recently the Bottom Intrusion has been reproduced in numerical models with high resolution and high accuracy. Therefore, there is a possibility that we can figure out its three-dimensional structure and generation processes by analyzing model outputs. However, there is a possibility that the Bottom Intrusion and the intrusion of the cold-water in the numerical model do not have the same mechanism in real ocean. At first, we compare model output and observed data that derived from a mooring system at the central part of the Bungo Channel. After conforming reproduction of the model in terms of the Bottom Intrusion, we analyze the model output to understand the intrusion process of cold-water into the Bungo Channel.

Data

The observation data used in this study were measured by ADCP (Acoustic Doppler Current Profiler), thermometer and salinometer that were moored at the central part of the Bungo Channel, from 6 July to 17 October, 2016. We also used a model output of JCOPE-T-NEDO that is developed by JAMSTEC.

Results and Discussion

We analyzed two cases of the Bottom Intrusion that occurred 14 August and 10 September in 2016 because variations in current velocity and water temperature in the model consist well with those in observation. In these two cases, the cold-water mass was supplied to the shelf slope nearby N32.72˚, E132.45˚, and was crossed the 200m isobath by the anticlockwise flow in the shelf slope. As a result, a density gradient between the cold-water mass and relatively light water in the Bungo Channel was generated. The density gradient makes a northeastward density driven current in the lower layer in the Bungo Channel, and the current advects the cold-water mass into the Bungo Channel.

Furthermore, it is found from observation data that there is a case that northward flow became stronger in not lower layer but middle layer. When the northward flows became stronger in middle layer, a northeast flow also developed in northwestern part of the Bungo Channel. When strong northward flow occurred in the middle layer, water temperature in the central part of the Bungo Channel was not always dropped. This might be because the water mass transported by the strong northward flow in the middle layer came from shallower depth in the shelf edge compared with the case of Bottom Intrusion. However, the reason why velocity increased at middle layer is not clear at the moment, so that proceeding analysis is needed in addition to the Bottom Intrusion.

Keywords: Bottom Intrusion, Bungo Channel, continental shelf

©2019. Japan Geoscience Union. All Right Reserved.

Characteristics of bottom intrusion in the Bungo Channel

*Akihiko Morimoto[1], Shuya Fujita[1], Hidetaka Takeoka[1], Xinyu Guo[1]

1. Ehime University

Bungo Channel is located between Kyushu and Shikoku and faces to the Pacific Ocean. A cold water mass with high nutrients intermittently intrudes into the Bungo Channel from summer to autumn. The phenomenon is called “Bottom Intrusion (BI)”. According to Kaneda et al., (2002), the BI occurs in neap tide of summer with the current of 15 cm/s. However, when we analyzed moored current and water temperature data at the central part of the Bungo Channel, we could not see the relation between the BI and moon age. There is a possibility that the discrepancy between our analysis and Kaneda et al. (2002) is caused by the different year data. In the present study, we reexamine the characteristics of the BI, especially relationship between the BI and moon age, using long-term water temperature data.

At the Uchiumi in the central part of the Bungo Channel, multilayer water temperature has observed since 1995. At other five stations (Hoketsu, Yusu, Shitaba, Fukuura, Okinoshima), Ehime University has also observed multilayer water temperature since 2008. In the present study, we analyze the deepest data at each station to understand the characteristics of the BI. We defined the BI as follows. Water temperature continually drops for 30 hours and its drop range is more than 0.5 ℃. At first, we analyzed water temperature data at 60 m depth in Uchiumi from 1997 to 2011. The BI occurred evenly in every moon age, we could not recognize the relation between BI and neap tide as Kaneda et al, (2002) pointed out. In addition, such kind of relation was not seen in other stations except in Yusu. Water temperature drops in Uchiumi were from 0.5 –7.0 ℃. We thought range of water temperature drop might affect to the relation. Therefore, we divided two cases, drop range is more or less than 2 ℃. We could not see the relation of neap tide in both cases. Furthermore, we investigated the relation between the BI and neap tide in each year, but we could not recognize the relation.

From the above analysis, it was found that the BI occurs without relation of moon age. However there is the relation only in Yusu. A vertical mixing area is located west of Yusu. Therefore, the BI might be blocked by the strong mixing associated with spring tide. This is why the BI occurs in neap tide in Yusu. Kaneda et al., (2002) clearly showed the relation between BI and moon age. The relation at Uchiumi was for only two years of 17 years. We will discuss why there was the relation in 1995-1996.

Keywords: Bottom Intrusion, Bungo Channel

©2019. Japan Geoscience Union. All Right Reserved.

Role of Kuroshio Current in fish resource variability off southwest Japan

*Yushi Morioka[1], Sergey Varlamov[1], Yasumasa Miyazawa[1]

1. Japan Agency for Marine-Earth Science and Technology

Western boundary currents in the subtropics play a pivotal role in transporting warm water from the tropics that contribute to development of highly diverse marine ecosystem in the coastal regions. As one of the western boundary currents in the North Pacific, the Kuroshio Current (hereafter the Kuroshio) exerts great influences on biological resource variability off southwest Japan, but few studies have examined physical processes that attribute the coastal fish resource variability to the basin-scale Kuroshio variability. Using the high-quality fish catch data and high-resolution ocean reanalysis results, this study identifies statistical links of interannual fish resource variability off Sukumo Bay, Shikoku island of Japan, to subsurface ocean temperature variability in the Kuroshio. The subsurface ocean temperature variability off the south of Sukumo Bay exhibits vertically coherent structure with sea-surface height variability, which originates from the westward-propagating oceanic Rossby waves generated through surface wind anomalies in the Northwest Pacific. Although potential sources of the atmospheric variability remain unclarified, the remotely-induced oceanic Rossby waves contribute to fish resource variability off Sukumo Bay. These findings have potential applications to other coastal regions along the western boundary currents in the subtropics where the westward-propagating oceanic Rossby waves contribute to the coastal ocean temperature variability.

Keywords: Kuroshio, Fish catch variability, Sukumo Bay

©2019. Japan Geoscience Union. All Right Reserved.

[J] Oral | A (Atmospheric and Hydrospheric Sciences)：A-OS Ocean Sciences & Ocean Environment

Mon. May 27, 2019 1:45 PM - 3:15 PM JST | Mon. May 27, 2019 4:45 AM - 6:15 AM UTC | 102 1F

[A-OS13] Ocean circulation and material cycle in coastal seas

convener:Kiyoshi Tanaka(University of Tokyo), Akihiko Morimoto(Ehime University), Yuichi Hayami(Saga University), Kazuhiko Ichimi(Seto Inland Sea Regional Research Center, Kagawa University), Chairperson:Akihiko Morimoto, Yuichi Hayami

Coastal seas have high biodiversity and high productivity, while various environmental problems such as eutrophication, red tide, and hypoxia are caused by human activity. In order to understand material cycle and various phenomena and to maintain sustainable environment in coastal seas, interdisciplinary research is needed. In the present session, we invite researchers who are interested in physical phenomena, material cycle, biological responsive dynamics, and their interactions in coastal seas. Neither study area nor study method is confined. We welcome presentations of wide-range topics to communize our knowledge in coastal seas.

1:45 PM - 2:00 PM JST | 4:45 AM - 5:00 AM UTC

[AOS13-07] Variation in hypoxic water mass in Ariake Sea -what consumed the dissolved oxygen?-

*Yuichi Hayami[1], Naoki Fujii[1], Hiroyuki Takasu[2], Yu Umezawa[3], Minoru Wada[2] (1.Saga University, 2.Nagasaki University, 3.Tokyo University of Agriculture and Technology)

2:00 PM - 2:15 PM JST | 5:00 AM - 5:15 AM UTC

[AOS13-08] Influence of Nori aquaculture-induced change in light environment on phytoplankton dynamics

*Naoya Minamiura[1], Soichi Yamaguchi[1] (1.Kyushu University)

2:15 PM - 2:30 PM JST | 5:15 AM - 5:30 AM UTC

[AOS13-09] **Enhanced West Philippine Sea intrusion diminishes hypoxia conditions in the Pearl River estuary**

*Hon-Kit Lui[1,2], Chen-Tung Arthur Chen[1], Wei-Ping Hou[2], Jian-Ming Liau[2] (1.Department of Oceanography, National Sun Yat-sen University, 2.Taiwan Ocean Research Institute, National Applied Research Laboratories)

2:30 PM - 2:45 PM JST | 5:30 AM - 5:45 AM UTC

[AOS13-10] North Pacific seawater radiocarbon recorded in abalone shells obtained from Otsuchi Bay, Japan

*Ota Kosuke[1], Yusuke Yokoyama[1,2], Yosuke Miyairi[2], Jun Hayakawa[2], Naomi Sato[2], Hideki Fukuda[2], Kiyoshi Tanaka[2] (1.Department of Earth and Planetary Science, Graduate School of Science, The University of Tokyo, 2.Atmosphere and Ocean Research Institute, The University of Tokyo)

2:45 PM - 3:00 PM JST | 5:45 AM - 6:00 AM UTC

[AOS13-11] Spreading of Radioactive Cesium off Joban coast through Large River Discharge

*Kiyoshi Tanaka[1], Seiya Nagao[2], Yujiro Kitade[3], Masato Niki[4], Takaaki Katsumata[4], Toru Miyama[5] (1.University of Tokyo, 2.Kanazawa University, 3.Tokyo University of Marine Science and Technology, 4.Tokai University, 5.Japan Agency for Marine-Earth Science and Technology)

3:00 PM - 3:15 PM JST | 6:00 AM - 6:15 AM UTC

[AOS13-12] Development of a river-ocean seamless model for simulating river discharges around Kyushu

*Takahiro Tsutsumi[1], Shinichiro Kida[2], Ryusuke Kuroki[3], Yosuke Alexandre Yamashiki[3] (1.Interdisciplinary Graduate School of Engineering Science, Kyushu University, 2.Research Institute for Applied Mechanics, Kyushu University, 3.Graduate School of Advanced Integrated Studies in Human Survivability, Kyoto University)

Variation in hypoxic water mass in Ariake Sea -what consumed the dissolved oxygen?-

*Yuichi Hayami[1], Naoki Fujii[1], Hiroyuki Takasu[2], Yu Umezawa[3], Minoru Wada[2]

1. Saga University, 2. Nagasaki University, 3. Tokyo University of Agriculture and Technology

In the inner most area of Ariake Sea, the estuarine circulation is dominated in summer. Therefore, the suspended material is transported toward offshore in the surface layer and toward inward and accumulated in the bottom layer. Simultaneously, there is a conspicuous spring-neap variation where stratification is enhanced and bottom water hypoxia develops in neap tide and stratification is reduced and hypoxia is moderated in spring tide. However, it was not clarified that such variation in hypoxia was driven only by the physical process or affected by some biological process such as biological oxygen demand. In order to clarify the variation in mass transport and ecosystem, we made surveys in the inner most area of Ariake Sea in the summer of 2018. We made 6 transect surveys with a boat during a spring-neap cycle during continuous measurements of temperature, salinity, currents, DO and turbidity with moorings.

During the mooring observation period, as a typhoon attacked Ariake Sea on 27 July, most of the mooring instruments were once recovered. The surface mooring instruments was set again on 30 July, and other ones were set again on 1 August. Another typhoon attacked on 14 August but the mooring observation was continued. Between these 2 typhoons, transect surveys were conducted on 1, 5, 8 and 12 August during low tide. It was in neap tide on 5 August and in spring tide on 12 August. The water column was well mixed in the morning of 1 August at the mooring station (Stn. 3) due to strong tidal mixing in spring tide and wind induced mixing by the typhoon. The temperature decreased and salinity increased in the bottom layer toward neap tide. Stratification was strongest on 8 August. Then the stratification became weaker and the water column was entirely mixed again on 11 August. The bottom water DO decreased from 1 August and became lower than 3 mg/L on 4 August. The bottom DO was kept lower than 3 mg/L until 10 August. In the surface layer, the bloom of *Chattonella* sp. occurred from late July. It continued at least until 13 August. The results of the transect survey indicated that the cold and saline water intruded from offshore to enhance the stratification and formed hypoxic water mass. On 12 August, stratification weakened and the hypoxic water mass was disappeared in the coastal area. But, in the offshore area, weak hypoxic water mass was formed. High turbidity layer was formed over the bottom in the coastal area on 1 August. But the turbidity decreased on 5 and 8 August. The turbidity increased again and became highest on 12 August. The experiment to estimate the oxygen demand of the bottom water was conducted on the each survey day. The oxygen demand decreased from 1 to 5 August then increased and became maximum on 12 August. In order to estimate the contribution of bacterial respiration and chemical oxygen consumption to the total oxygen demand in water, we made incubation experiment with Chloramphenicol and formalin. Chloramphenicol was added to stop the bacterial respiration. Formalin was added to measure the chemical oxygen consumption. The bacterial respiration occupied about 80 % of the total oxygen demand on 6 August. However, almost all the oxygen demand was occupied by the respiration except for the bacterial respiration on 13 August. There was almost no chemical oxygen demand on each date. There was a high correlation between chlorophyll a concentration and oxygen demand (R=0.90). There was a correlation between turbidity and oxygen demand. But it was weaker than chlorophyll a (R=0.61).

The hypoxic water mass was generated by the cold and saline water intrusion occurred between spring

©2019. Japan Geoscience Union. All Right Reserved.

tide and neap tide. However, the oxygen demand in the bottom water decreased in this period. It indicated that the formation of hypoxia was generated by the physical process and the change in oxygen demand did not affected. The oxygen demand in spring tide was larger than in neap tide. It would be due to the active resuspension of organic matter by the strong tidal mixing. There was a high correlation between chlorophyll a and oxygen demand of water. But most of the oxygen demand when the hypoxic water mass was formed was bacterial respiration. The contribution of the phytoplankton respiration was small. They suggested the oxygen demand was mainly generated by the decomposition of organic matter derived from phytoplankton by bacteria. The red tide of *Chattonella* sp occurred continuously during the observation period. The maximum chlorophyll a concentration reached 72.3 ug/L. The organic matter supply from the red tide would fuel the oxygen consumption in the bottom layer.

Keywords: Ariake Sea, hypoxia, spring-neap variation, water oxygen demand, Chattonella red-tide

©2019. Japan Geoscience Union. All Right Reserved.

Influence of Nori aquaculture-induced change in light environment on phytoplankton dynamics

*Naoya Minamiura[1], Soichi Yamaguchi[1]

1. Kyushu University

In the Ariake Sea in winter, Nori aquaculture is conducted actively, and its production is the largest in Japan. On the other hand, color bleaching of Nori due to red tide occurrence has become a big problem. From previous research, it is known that the red tide occurrence involves the improvement of the light environment. At the time of Nori aquaculture season, Nori aquaculture net is set densely in the coastal area, and leaf blade is attached to the net and it grows. It can be easily imagined that such net and leaf blade have great influence on the light environment in water, but there are no examples studied so far. In this study, by continuous on-site observation of the photon quantum amount in the Nori aquaculture area and the non-Nori aquaculture area, the influence of Nori aquaculture on the light environment is evaluated, and the influence is evaluated by dynamic growth of leaf blade as a function. We investigated how phytoplankton dynamics by incorporating these results into numerical simulation changes.
We installed a photon meter (DEFI2-L by JFE Advantech Co., Ltd.) and pressure gauge (DEFI2-D10 by JFE Advantech Co., Ltd.) respectively in the sea area just under the Nori aquaculture and in the non-Nori aquaculture area possessed by the Saga Prefecture Fisheries Experiment from January 15 to 25 in 2019. This continuous observation was carried out at 5 second intervals. As a result of the observation, it was revealed that the photon quantum amount decreased by about 75% on average just under Nori aquaculture area. The reduction of this photon (light shielding factor y) was expressed as a function of the leaf length (x unit: cm), and the following equation was obtained.

$y=0.86e^{-0.1\times x}$

Next, we developed a numerical ecosystem model that takes this light shielding factor into consideration and examined how it affects phytoplankton dynamics. Calculation was carried out separately into two patterns with and without light shielding factor in Nori aquaculture area. In consideration of the light shielding factor, the phytoplankton biomass was reduced in the vicinity of the Nori aquaculture area in the inner part of Ariake sea, compared to the case without consideration. This indicates that Nori aquaculture suppresses the growth of phytoplankton by deteriorating the light environment in water.

Keywords: Aquaculture, Ariake Sea, Light environment

©2019. Japan Geoscience Union. All Right Reserved.

Enhanced West Philippine Sea intrusion diminishes hypoxia conditions in the Pearl River estuary

*Hon-Kit Lui[1,2], Chen-Tung Arthur Chen[1], Wei-Ping Hou[2], Jian-Ming Liau[2]

1. Department of Oceanography, National Sun Yat-sen University, 2. Taiwan Ocean Research Institute, National Applied Research Laboratories

The hypoxia condition (dissolved oxygen <2 mg/L) in the Pearl River estuary is worsening in the past decade, partly due to the rising anthropogenic activities. For instance, excess nutrients cause enhanced biological productivity in the surface ocean. Yet, dead phytoplankton sink to the bottom of the coastal zone, where they decompose and consume oxygen. If the oxygen consumption rate exceeds the supply rate, then hypoxia or even anoxia may develop, leading to so-called dead zones. Here we show that a strong invasion of high dissolved oxygen but low nutrients West Philippine Sea seawater into the South China Sea in the form of Kuroshio occurred around 2003-2004. Apparently due to the oxygen supply carried by the remnants of the intruded Kuroshio, little hypoxia developed off the Pearl River estuary, where the anoxic condition develops in some years with weak Kuroshio intrusion.

Keywords: hypoxia, Kuroshio, Pearl River estuary, West Philippine Sea, intrusion, South China Sea

©2019. Japan Geoscience Union. All Right Reserved.

North Pacific seawater radiocarbon recorded in abalone shells obtained from Otsuchi Bay, Japan

*Ota Kosuke[1], Yusuke Yokoyama[1,2], Yosuke Miyairi[2], Jun Hayakawa[2], Naomi Sato[2], Hideki Fukuda[2], Kiyoshi Tanaka[2]

1. Department of Earth and Planetary Science, Graduate School of Science, The University of Tokyo, 2. Atmosphere and Ocean Research Institute, The University of Tokyo

Reconstructing past ocean currents in the coastal regions is needed to better understand the relationship between oceanographic changes and coastal ecosystems. Seawater radiocarbon is a unique proxy to understand the properties of water masses. However, the knowledge of the water mass distribution is limited to the low latitude regions as the only well-established proxy for it is reef-building corals. Alternative archives are required for high latitude regions. Here we measured $\Delta^{14}C$ values of three abalone shells using accelerator mass spectrometry (AMS) and counted the shell growth checks which were made in the winter season. Abalone shells were obtained from Otsuchi Bay, where the cold Oyashio Current and the warm Kuroshio Current converge. The Oyashio Current has more depleted radiocarbon than the Kuroshio Current. We compared $\Delta^{14}C$ values of abalone shells with the sea surface temperature anomaly in Sanriku region. $\Delta^{14}C$ values of abalone shells range from 5.4 ‰to 31‰ and indicated seasonal variations. $\Delta^{14}C$ values decreased by about 5 ‰in shell growth checks that indicates winter season.We found this decrease of $\Delta^{14}C$ values of abalone shells are consistent with the significantly mixing of water brought by the Oyashio Current. $\Delta^{14}C$ value of abalone shells clearly shows the Oyashio Current inflow in 2013, 2015 and 2017 and it can be used to reconstruct fluctuations between past water masses. In addition, the $\Delta^{14}C$ values of abalone shells are possibly affected by their habitat. Abalone at 2 m to 6 m depth exhibited higher $\Delta^{14}C$ values than those in abalone at 6 m to 10 m depth. This trend resulted from cold water from the Oyashio Current having a greater influence on deeper water. These radiocarbon records indicate past seawater conditions in northern Japan, where the Oyashio and Kuroshio currents converge, can be reconstructed using abalone shells.

Keywords: Radiocarbon, AMS, Abalone, Otsuchi Bay, Oyashio Current, Ocean circulation

©2019. Japan Geoscience Union. All Right Reserved.

Spreading of Radioactive Cesium off Joban coast through Large River Discharge

*Kiyoshi Tanaka[1], Seiya Nagao[2], Yujiro Kitade[3], Masato Niki[4], Takaaki Katsumata[4], Toru Miyama[5]

1. University of Tokyo, 2. Kanazawa University, 3. Tokyo University of Marine Science and Technology, 4. Tokai University, 5. Japan Agency for Marine-Earth Science and Technology

A hydrographic observation was conducted off the Joban coast during September 7 to 12, 2011 (six months after the 2011 Great East Japan Earthquake), using a CTD profiler and a ship-mounted ADCP (R/V Tansei-Maru cruise KT-11-22). At the same time, water-samplings for radioactive cesium measurements were conducted at a depth of 10 m. The radioactivity of cesium (134Cs and 137Cs) was measured for the AMP/Cs compound using gamma-ray spectrometry at the Low Level Radioactivity Laboratory of Kanazawa University. There was a negative correlation between the radioactive cesium and salinity in the sea surface (at the depth of 10 m), indicating more radioactive cesium was included in less saline water. Abundant freshwater is discharged from three large rivers (Tone, Naka, and Kuji Rivers) into the observational area. What is important is that several days before the observation, there was extremely heavy rainfall in the upper reaches of the rivers, which resulted in that discharge of the Tone River exceeded 2000 m^3/s on September 4. Therefore, it was suggested that the highly concentrated radioactive cesium in the sea surface originated from the land through the rivers. Moreover, it was shown that spreading of the river water and radioactive cesium is strongly influenced by the Kuroshio Current.

Keywords: radioactive cesium, river discharge, 2011 Great East Japan Earthquake, off the Joban coast

©2019. Japan Geoscience Union. All Right Reserved.

Development of a river-ocean seamless model for simulating river discharges around Kyushu

*Takahiro Tsutsumi[1], Shinichiro Kida[2], Ryusuke Kuroki[3], Yosuke Alexandre Yamashiki[3]

1. Interdisciplinary Graduate School of Engineering Science, Kyushu University, 2. Research Institute for Applied Mechanics, Kyushu University, 3. Graduate School of Advanced Integrated Studies in Human Survivability, Kyoto University

Regional-scale torrential rainfalls cause river discharges that are capable of abruptly changing the oceanic condition over a wide area. It is necessary to simultaneously solve multiple rivers for capturing such events that are also often associated with flooding over land. Many coastal areas are also affected by multiple rivers but many of the conventional river-models to simulate the influence of rivers on a regional scale. The object of this research is to develop a river-ocean seamless model for simulating river discharges around Kyushu during and after weather events. By using an Isopycnal-Layered model following Kida and Yamashiki (2015), we developed a model that focuses on the island of Kyushu and the heavy rain event in September 2015. The model reproduces the increase in river flow due to the heavy rain and when compared to observations, we found some rivers to show slow water propagation speed from upstream to downstream, while some rivers reproduce the actual observation well. We plan to conduct a sensitively experiment to verify the cause behind this difference in the reproducibility of the model.

©2019. Japan Geoscience Union. All Right Reserved.

[J] Poster | A (Atmospheric and Hydrospheric Sciences)：A-OS Ocean Sciences & Ocean Environment

Mon. May 27, 2019 3:30 PM - 5:00 PM JST | Mon. May 27, 2019 6:30 AM - 8:00 AM UTC | Poster Hall International Exhibition Hall8, Makuhari Messe_4

[A-OS13] Ocean circulation and material cycle in coastal seas

convener:Kiyoshi Tanaka(University of Tokyo), Akihiko Morimoto(Ehime University), Yuichi Hayami(Saga University), Kazuhiko Ichimi(Seto Inland Sea Regional Research Center, Kagawa University)

Coastal seas have high biodiversity and high productivity, while various environmental problems such as eutrophication, red tide, and hypoxia are caused by human activity. In order to understand material cycle and various phenomena and to maintain sustainable environment in coastal seas, interdisciplinary research is needed. In the present session, we invite researchers who are interested in physical phenomena, material cycle, biological responsive dynamics, and their interactions in coastal seas. Neither study area nor study method is confined. We welcome presentations of wide-range topics to communize our knowledge in coastal seas.

[AOS13-P01] An experimental study on degradation and fragmentation of marine plastic debris

*YUSEI YAMAGUCHI[1] (1.KYUSHU UNIVERSITY)

[AOS13-P02] Seafloor environment based on grain and concentrations of carbon, nitrogen and sulfur of surface sediment in Ise and Mikawa bays

*Atsuko Amano[1], Koji Seike[1] (1.National institute of Advanced Industrial Science and Technology)

[AOS13-P03] Hydrographic observations of estuarine circulation in Suruga Bay, Japan

*Kiyoshi Tanaka[1], Masato Niki[2], Kunio Kutsuwada[2], Akio Ishida[3], daisuke Takahashi[2], Takaaki Katsumata[2], Kazuyuki Uehara[2] (1.University of Tokyo, 2.Tokai University, 3.Tokoha University)

[AOS13-P04] Residence time of river water in the Jakarta Bay

*Akihiko Morimoto[1], Endro Soeyanto[2], Yuichi Hayami[3], Agus Sudaryanto[2], Suhendar Sachoemar[2] (1.Ehime University, 2.BPPT, Indonesia, 3.Saga University)

An experimental study on degradation and fragmentation of marine plastic debris

*YUSEI YAMAGUCHI[1]

1. KYUSHU UNIVERSITY

Marine contamination due to plastic debris,especially microplastics, is attracting worldwide attention at the present time. It has already been reported that microplastics are present over the world's ocean, but the process of their formation has not been clarified in detail.In this study, we aim to elucidate the process in which plastics drifting on the surface of the sea are degraded by ultraviolet rays and fragmentized by physical processes such as waves. We attempt to reproduce the regradation and fragmentationan processes in a laboratory experiment. First, an ultraviolet irradiation experiment was conducted. The ratio of the ultraviolet intensity between a high-pressure UV lamp irradiated and sunlight was measured under the sunny, cloudy, and rainy conditions.Thereafter, plastic (polyethylene without additives) pieces of the same size were irradiated with ultraviolet rays under a high-pressure UV lamp. The degraded plastic pieces were entered into a plastic tube wite seawater and sand, which was rotated to represented motion by waves in shorelines to fragmentize. The change of fragmentation rate of the plastic pieces will be examined by varying the irradiation time and the rotating times, respectively.

Keywords: microplastics, rubbish, ultraviolet ray

©2019. Japan Geoscience Union. All Right Reserved.

Seafloor environment based on grain and concentrations of carbon, nitrogen and sulfur of surface sediment in Ise and Mikawa bays

*Atsuko Amano[1], Koji Seike[1]

1. National institute of Advanced Industrial Science and Technology

This study reconstructed seafloor environment based on the spatial distribution of grain size and concentrations of total organic carbon (TOC), total nitrogen (TN) and total sulfur (TS) in the surface sediments collected at 44 sites of Ise and Mikawa bays. Silt sediments with 6-8ϕ deposit in the interior and central parts of these bays and values of grain size decrease to sand sediment with 1-4ϕi toward the bay mouth from the central part. Concentrations of TOC, TN and TS show relatively higher values at the interior and central parts and decrease at the bay mouth. Ratios of TOC and TN (C/N) are 8-9 at the most parts of the bays and increase to over 10 in the offshore part of Kiso river mouth at Ise Bay. The distribution pattern of grain size indicates that tidal current velocity decrease from the bay mouth to the central part of the bay and hydrodynamic condition is a stagnant in the interior and central parts. The patterns of TOC, TN and TS concentrations means that organic matter likely deposit and become a reductive condition in the interior and central part of the bays. Values of C/N indicate organic matter originated from marine plankton mainly deposit, however the amount of terrestrial organic matter in sediments increases the offshore of Kiso river mouth.

Keywords: grain size, CNS elements, surface sediment of seafloor

©2019. Japan Geoscience Union. All Right Reserved.

Hydrographic observations of estuarine circulation in Suruga Bay, Japan

*Kiyoshi Tanaka[1], Masato Niki[2], Kunio Kutsuwada[2], Akio Ishida[3], daisuke Takahashi[2], Takaaki Katsumata[2], Kazuyuki Uehara[2]

1. University of Tokyo, 2. Tokai University, 3. Tokoha University

Sergestid shrimp (‘Sakura-ebi’ in Japanese), *Sergia lucens*, is an important marine product in Suruga Bay, south coast of Japan. Large-scale commercial catch of *Sergia lucens* is conducted only in Suruga Bay and around Taiwan. Although the reason abundant catch of *Sergia lucens* is limited to these areas has not yet been clarified thoroughly, two factors likely play important roles: One is a steep continental slope adjacent to a deep basin, and the other is large volume of river discharge. Therefore, we made a high-resolution hydrographic observation (shipboard ADCP and CTD) in the innermost region of Suruga Bay, where the mouth of the Fuji River is connected directly to the steep continental slope and an anticyclonic (clockwise) eddy tends to form. The observation suggested that an estuarine baroclinic circulation formed there. It is likely that a counter flow of subsurface water located around a depth of 20 m is entrained into the surface river plume at the river mouth.

Keywords: Suruga Bay, Sergia lucens, estuarine circulation, hydrographic observation

©2019. Japan Geoscience Union. All Right Reserved.

Residence time of river water in the Jakarta Bay

*Akihiko Morimoto[1], Endro Soeyanto[2], Yuichi Hayami[3], Agus Sudaryanto[2], Suhendar Sachoemar[2]

1. Ehime University, 2. BPPT, Indonesia, 3. Saga University

Jakarta bay faces to capital city of Indonesia, and its width and length are about 30km and 10km, respectively. The Jakarta Bay is shallow with maximum depth of 20m and opens to Java Sea. Massive materials supply through rivers into the bay. Since maintenance rate of sewage system is a few percentages, enormous nutrients, organic matters, and garbage. It is expected that marine environment in the Jakarta Bay has become worse. However, we do not know the environment at the moment because of lack of observed data. We have conducted hydrographic survey since December 2015 to capture current status of marine environment in the Jakarta Bay. It was found from our observation that hypoxia occurred throughout the year. Magnitude of hypoxia was small in rainy season but large in dry and transition seasons. Since tropical region like Jakarta Bay is heated at the sea surface during all seasons, water temperature becomes homogenous in vertical. Therefore, density stratification is controlled by fresh water supply from rivers. Considering this fact, it is expected that stratification develops in rainy season, and hypoxia occurs due to decreasing of vertical flux of oxygen. However, our observation did not show the situation.

In the present study, we develop a three dimensional model to understand seasonal variation in density stratification in the Jakarta Bay and to know residence time of river water in the bay. We developed a model based on POM. The model is driven by tidal forcing, surface wind, and river discharge from 10 rivers, and we reproduced physical field in 2016. Calculated sea surface salinity distributions coincided well with observations except in dry season. Sea surface current shows eastward or northeastward currents in February and May, and westward and northwestward in September and December. From the sea surface current pattern, it is implied that fresh water supplied from Citarum river might flow out to Java Sea immediately. In order to know residence time of river waters, we calculated age of river water using CART theory (Deleersnijder et al., 2001). Age of river water in May was about 15 days and that in September was about 50 days. This result suggests that density stratification in the Jakarta Bay might be controlled by not only total river discharge but also residence time of river water. At the presentation, we will introduce a result of contribution ratio of each river to salinity in the Jakarta Bay

Keywords: Residence time of river water, Jakarta Bay

©2019. Japan Geoscience Union. All Right Reserved.

[J] Poster | A (Atmospheric and Hydrospheric Sciences)：A-OS Ocean Sciences & Ocean Environment

Mon. May 27, 2019 5:15 PM - 6:30 PM JST | Mon. May 27, 2019 8:15 AM - 9:30 AM UTC | Poster Hall International Exhibition Hall8, Makuhari Messe_6

[A-OS13] Ocean circulation and material cycle in coastal seas

convener:Kiyoshi Tanaka(University of Tokyo), Akihiko Morimoto(Ehime University), Yuichi Hayami(Saga University), Kazuhiko Ichimi(Seto Inland Sea Regional Research Center, Kagawa University)

Coastal seas have high biodiversity and high productivity, while various environmental problems such as eutrophication, red tide, and hypoxia are caused by human activity. In order to understand material cycle and various phenomena and to maintain sustainable environment in coastal seas, interdisciplinary research is needed. In the present session, we invite researchers who are interested in physical phenomena, material cycle, biological responsive dynamics, and their interactions in coastal seas. Neither study area nor study method is confined. We welcome presentations of wide-range topics to communize our knowledge in coastal seas.

[AOS13-P01] An experimental study on degradation and fragmentation of marine plastic debris

*YUSEI YAMAGUCHI[1] (1.KYUSHU UNIVERSITY)

[AOS13-P02] Seafloor environment based on grain and concentrations of carbon, nitrogen and sulfur of surface sediment in Ise and Mikawa bays

*Atsuko Amano[1], Koji Seike[1] (1.National institute of Advanced Industrial Science and Technology)

[AOS13-P03] Hydrographic observations of estuarine circulation in Suruga Bay, Japan

*Kiyoshi Tanaka[1], Masato Niki[2], Kunio Kutsuwada[2], Akio Ishida[3], daisuke Takahashi[2], Takaaki Katsumata[2], Kazuyuki Uehara[2] (1.University of Tokyo, 2.Tokai University, 3.Tokoha University)

[AOS13-P04] Residence time of river water in the Jakarta Bay

*Akihiko Morimoto[1], Endro Soeyanto[2], Yuichi Hayami[3], Agus Sudaryanto[2], Suhendar Sachoemar[2] (1.Ehime University, 2.BPPT, Indonesia, 3.Saga University)

An experimental study on degradation and fragmentation of marine plastic debris

*YUSEI YAMAGUCHI[1]

1. KYUSHU UNIVERSITY

Marine contamination due to plastic debris,especially microplastics, is attracting worldwide attention at the present time. It has already been reported that microplastics are present over the world's ocean, but the process of their formation has not been clarified in detail.In this study, we aim to elucidate the process in which plastics drifting on the surface of the sea are degraded by ultraviolet rays and fragmentized by physical processes such as waves. We attempt to reproduce the regradation and fragmentationan processes in a laboratory experiment. First, an ultraviolet irradiation experiment was conducted. The ratio of the ultraviolet intensity between a high-pressure UV lamp irradiated and sunlight was measured under the sunny, cloudy, and rainy conditions.Thereafter, plastic (polyethylene without additives) pieces of the same size were irradiated with ultraviolet rays under a high-pressure UV lamp. The degraded plastic pieces were entered into a plastic tube wite seawater and sand, which was rotated to represented motion by waves in shorelines to fragmentize. The change of fragmentation rate of the plastic pieces will be examined by varying the irradiation time and the rotating times, respectively.

Keywords: microplastics, rubbish, ultraviolet ray

©2019. Japan Geoscience Union. All Right Reserved.

Seafloor environment based on grain and concentrations of carbon, nitrogen and sulfur of surface sediment in Ise and Mikawa bays

*Atsuko Amano[1], Koji Seike[1]

1. National institute of Advanced Industrial Science and Technology

This study reconstructed seafloor environment based on the spatial distribution of grain size and concentrations of total organic carbon (TOC), total nitrogen (TN) and total sulfur (TS) in the surface sediments collected at 44 sites of Ise and Mikawa bays. Silt sediments with 6-8ϕ deposit in the interior and central parts of these bays and values of grain size decrease to sand sediment with 1-4ϕi toward the bay mouth from the central part. Concentrations of TOC, TN and TS show relatively higher values at the interior and central parts and decrease at the bay mouth. Ratios of TOC and TN (C/N) are 8-9 at the most parts of the bays and increase to over 10 in the offshore part of Kiso river mouth at Ise Bay. The distribution pattern of grain size indicates that tidal current velocity decrease from the bay mouth to the central part of the bay and hydrodynamic condition is a stagnant in the interior and central parts. The patterns of TOC, TN and TS concentrations means that organic matter likely deposit and become a reductive condition in the interior and central part of the bays. Values of C/N indicate organic matter originated from marine plankton mainly deposit, however the amount of terrestrial organic matter in sediments increases the offshore of Kiso river mouth.

Keywords: grain size, CNS elements, surface sediment of seafloor

©2019. Japan Geoscience Union. All Right Reserved.

Hydrographic observations of estuarine circulation in Suruga Bay, Japan

*Kiyoshi Tanaka[1], Masato Niki[2], Kunio Kutsuwada[2], Akio Ishida[3], daisuke Takahashi[2], Takaaki Katsumata[2], Kazuyuki Uehara[2]

1. University of Tokyo, 2. Tokai University, 3. Tokoha University

Sergestid shrimp (‘Sakura-ebi’ in Japanese), *Sergia lucens*, is an important marine product in Suruga Bay, south coast of Japan. Large-scale commercial catch of *Sergia lucens* is conducted only in Suruga Bay and around Taiwan. Although the reason abundant catch of *Sergia lucens* is limited to these areas has not yet been clarified thoroughly, two factors likely play important roles: One is a steep continental slope adjacent to a deep basin, and the other is large volume of river discharge. Therefore, we made a high-resolution hydrographic observation (shipboard ADCP and CTD) in the innermost region of Suruga Bay, where the mouth of the Fuji River is connected directly to the steep continental slope and an anticyclonic (clockwise) eddy tends to form. The observation suggested that an estuarine baroclinic circulation formed there. It is likely that a counter flow of subsurface water located around a depth of 20 m is entrained into the surface river plume at the river mouth.

Keywords: Suruga Bay, Sergia lucens, estuarine circulation, hydrographic observation

©2019. Japan Geoscience Union. All Right Reserved.

Residence time of river water in the Jakarta Bay

*Akihiko Morimoto[1], Endro Soeyanto[2], Yuichi Hayami[3], Agus Sudaryanto[2], Suhendar Sachoemar[2]

1. Ehime University, 2. BPPT, Indonesia, 3. Saga University

Jakarta bay faces to capital city of Indonesia, and its width and length are about 30km and 10km, respectively. The Jakarta Bay is shallow with maximum depth of 20m and opens to Java Sea. Massive materials supply through rivers into the bay. Since maintenance rate of sewage system is a few percentages, enormous nutrients, organic matters, and garbage. It is expected that marine environment in the Jakarta Bay has become worse. However, we do not know the environment at the moment because of lack of observed data. We have conducted hydrographic survey since December 2015 to capture current status of marine environment in the Jakarta Bay. It was found from our observation that hypoxia occurred throughout the year. Magnitude of hypoxia was small in rainy season but large in dry and transition seasons. Since tropical region like Jakarta Bay is heated at the sea surface during all seasons, water temperature becomes homogenous in vertical. Therefore, density stratification is controlled by fresh water supply from rivers. Considering this fact, it is expected that stratification develops in rainy season, and hypoxia occurs due to decreasing of vertical flux of oxygen. However, our observation did not show the situation.

In the present study, we develop a three dimensional model to understand seasonal variation in density stratification in the Jakarta Bay and to know residence time of river water in the bay. We developed a model based on POM. The model is driven by tidal forcing, surface wind, and river discharge from 10 rivers, and we reproduced physical field in 2016. Calculated sea surface salinity distributions coincided well with observations except in dry season. Sea surface current shows eastward or northeastward currents in February and May, and westward and northwestward in September and December. From the sea surface current pattern, it is implied that fresh water supplied from Citarum river might flow out to Java Sea immediately. In order to know residence time of river waters, we calculated age of river water using CART theory (Deleersnijder et al., 2001). Age of river water in May was about 15 days and that in September was about 50 days. This result suggests that density stratification in the Jakarta Bay might be controlled by not only total river discharge but also residence time of river water. At the presentation, we will introduce a result of contribution ratio of each river to salinity in the Jakarta Bay

Keywords: Residence time of river water, Jakarta Bay

©2019. Japan Geoscience Union. All Right Reserved.

[J] Oral | A (Atmospheric and Hydrospheric Sciences)：A-OS Ocean Sciences & Ocean Environment

Mon. May 27, 2019 3:30 PM - 5:00 PM JST | Mon. May 27, 2019 6:30 AM - 8:00 AM UTC | 102 1F

[A-OS15] Freshwater discharge through rivers and estuaries to the ocean

convener:Shinichiro Kida(Research Institute for Applied Mechanics, Kyushu University), Dai Yamazaki(Institute of Industrial Sciences, The University of Tokyo), Yosuke Alexandre Yamashiki(Earth & Planetary Water Resources Assessment Laboratory Graduate School of Advanced Integrated Studies in Human Survivability Kyoto University), Humio Mitsudera(Institute of Low Temperature Science, Hokkaido University), Chairperson:Shinichiro Kida(RIAM, Kyushu University), Humio Mitsudera(Hokkaido University, Institute of Low Temperature Science), Yosuke Yamashiki(GSAIS Kyoto University)

The water cycle from land to the ocean involves complex dynamics of rivers and buoyancy driven flows in estuaries and the ocean. Recent progress in satellite observations and numerical models are beginning to illuminate how this water cycle occurs on various time scales globally and regionally. This session welcomes various process studies that investigate the dynamics and material circulation related to the freshwater cycle from land to the ocean such as surface runoff, river transport, estuarine circulation, and coastal river plumes based on numerical, observational, or theoretical studies.

3:30 PM - 3:45 PM JST | 6:30 AM - 6:45 AM UTC

[AOS15-01] The forefront research for flow and water quality estimations in coastal area using geo-stationary and polar orbital satellites data

★Invited Papers

*Yuji Sakuno[1] (1.Graduate School of Engineering, Hiroshima University)

3:45 PM - 4:00 PM JST | 6:45 AM - 7:00 AM UTC

[AOS15-02] Rainfall-Runoff-Inundation Processes and Modeling in a Humid Tropical River Basin

★Invited Papers

*Takahiro Sayama[1], Kodai Yamamoto[2], Ryoko Araki[2], Apip Apip[3], Eva Mia Siska[1], Kaoru Takara[4] (1.Disaster Prevention Research Institute, Kyoto University, 2.Graduate School of Engineering, Kyoto University, 3.LIPI, Indonesia, 4.Graduate School of Advanced Integrated Studies in Human Survivability, Kyoto University)

4:00 PM - 4:15 PM JST | 7:00 AM - 7:15 AM UTC

[AOS15-03] Role of river inflows from Kamchatka Peninsula in the Okhotsk Sea

*Toru Miyama[1], Humio Mitsudera[2] (1.Application Laboratory, Japan Agency for Marine-Earth Science and Technology, , 2.Institute of Low Temperature Science, Hokkaido University)

4:15 PM - 4:30 PM JST | 7:15 AM - 7:30 AM UTC

[AOS15-04] CHLOROPHYLL ESTIMATION OF LAKE AND COASTAL WATER USING REMOTE SENSING APPROACH

*Shweta Yadav[1], Yamashiki Yosuke[1], Junichi Susaki[1], Kanako Ishikawa[2], Yoh Yamashita[1] (1.Kyoto University, 2.LBERI)

4:30 PM - 4:45 PM JST | 7:30 AM - 7:45 AM UTC

[AOS15-05] Maritime-continent coastal region as land-sea-air triple boundary layer and bio-anthroposphere

*Manabu D. Yamanaka[1] (1.Research Institute for Humanity and Nature / Professor Emeritus of Kobe University)

4:45 PM - 5:00 PM JST | 7:45 AM - 8:00 AM UTC

[AOS15-06] River-ocean interaction at the Ganges-Brahmaputra river mouth

*Shinichiro Kida[1], Dai Yamazaki[2] (1.Research Institute for Applied Mechanics, Kyushu University, 2.Institute of Industrial Sciences, The University of Tokyo)

The forefront research for flow and water quality estimations in coastal area using geo-stationary and polar orbital satellites data

*Yuji Sakuno[1]

1. Graduate School of Engineering, Hiroshima University

Continuous estimation of the flow velocity and water quality distribution in a wide area at high resolution is extremely important in order to understand the natural phenomena occurring at the interface between the river and the ocean. In recent years,satellite remote sensing is expected as a powerful tool to grasp such phenomena. In this presentation, a case study of flow velocity estimation using the stationary meteorological satellite "Himawari-8" data, which observes sea surface temperature (SST) at 10 minute intervals at first. A strong flow velocity distribution of about 0.5 m/s was detected by applying the image correlation method to continuous SST images in the southern part of the Lombok Straits of Indonesia in the study area. Such a method can measure the flow velocity distribution of wide channel at low cost, so it is particularly effective in waters where there is a remarkable water temperature difference. Meanwhile, the heavy rain in western Japan occurred in July 2018, and a large amount of sediment from the land flowed out to the Seto Inland Sea. As a result, oyster beds for aquaculture were broken or red tide damage caused by a large amount of nutrient salt was occurred. The state of such huge flood were monitored by the polar orbital earth observation satellite such as Landsat-8, Sentinel-2 (10 m to 30 m spatial resolution) and GCOM-C (250 m spatial resolution). The polar orbital satellite has lower observation frequency than geostationary satellite, but there is an advantage that detailed distribution of sediment discharge from river and red tide distribution can be visualized. Combining such stationary / polar orbital satellite data, measured data, numerical model and other technologies will make it possible to monitor coastal environments connecting the open ocean and rivers more quickly and in detail in the future.

Keywords: satellite, flow, water quality

©2019. Japan Geoscience Union. All Right Reserved.

Rainfall-Runoff-Inundation Processes and Modeling in a Humid Tropical River Basin

*Takahiro Sayama[1], Kodai Yamamoto[2], Ryoko Araki[2], Apip Apip[3], Eva Mia Siska[1], Kaoru Takara[4]

1. Disaster Prevention Research Institute, Kyoto University, 2. Graduate School of Engineering, Kyoto University, 3. LIPI, Indonesia, 4. Graduate School of Advanced Integrated Studies in Human Survivability, Kyoto University

Large-scale plantations of palm and acacia trees have caused 50 % reduction of natural forests in the 25 years between 1985 to 2009 in Sumatra, Indonesia. Deforestation of natural forest might have changed water cycle in the area including runoff and evapotranspiration, which may lead to possible changes in flood and drought conditions. Downstream parts of river basins in Sumatra spreads wetlands with rich ecosystems, though such environment have degraded due to land cover changes over the last few decades to agricultural areas. Drying the wetlands by drainage for rice cropping and other agricultures caused various issues including peatland fire and haze in surrounding regions. In addition to the land cover change, climate change may give significant impact on the hydrologic cycle in this region. Climate change in humid tropical region in South East Asia has been difficult to be predicted due to local atmospheric cycle. Furthermore, hydrologic process understandings and their representations by simulation models are the important scientific step toward adequate assessment of land cover and climate changes. Among various hydrologic processes, rainfall-runoff processes in tropical climate conditions characterized also by deep weathered soil layers have been poorly understood. Our study is conducted based on field investigation with respect to rainfall-runoff processes in the mountainous hillslope in Sumatra to understand the fundamental characteristics of rainfall-runoff in this region, and to represent the feature particularly with a thick soil layer, in our distributed hydrologic model. After the calibration and validation of the model at the river basin scale in the Batanghari River basin, we assess the impact of the climate change by inputting the rainfall.

Some findings from the field monitoring are summarized below. According to a simple cone penetration experiment, the soil depths in the hillslope were estimated to be about 1.5 ~ 4.5 meters. Furthermore, the soil sample experiment at surface, 30 cm and 60 cm depths showed that saturated hydraulic conductivities were as high as 7,200 mm/h while the volumetric water content maintain also high (0.45~0.50) with negative suction between 1~10 m. Such characteristics should be explained due to the aggregated soil in humid tropics. In our site, the foot of the slope (SK1) has thicker soil layer (4.5 m), while it is reduced to 1.5 m about 20 m upstream along the hillslope (SK3). Groundwater table exists at the depths of about 3 ~ 4 m depth consistently at SK1 (bottom) and SK2 (middle) and the groundwater table responses rapidly to rainfall. With the high saturated hydraulic conductivity and high infiltration rate, especially in the natural forest area, we conceptualize the rainfall-runoff in this region is dominated by fairly quick vertical infiltration into the thick soil layer and the recharge to the groundwater table. Based on the above process understandings, we represent the process in the Rainfall-Runoff-Inundation (RRI) model to the entire Batanghari River basin to simulate streamflow at the river basin scale.

Keywords: Tropical Forest, Rainfall-Runoff, RRI Model, Landuse Change, Climate Change, Sumatra Island

©2019. Japan Geoscience Union. All Right Reserved.

Role of river inflows from Kamchatka Peninsula in the Okhotsk Sea

*Toru Miyama[1], Humio Mitsudera[2]

1. Application Laboratory, Japan Agency for Marine-Earth Science and Technology, , 2. Institute of Low Temperature Science, Hokkaido University

The Okhotsk Sea is a unique ocean in that sea ice forms at the lowest latitude in the world. The sea ice formation plays important roles in water mass formations not only in the Okhotsk Sea but also in the North Pacific Ocean. The river inflows from the surrounding coasts affect the sea ice formation by changing stratification. Especially, the contribution from the river inflow from the Amur River on the western side of the Okhotsk Sea has been widely discussed. The roles of the Amur River in chemical and biological cycles have been also investigated. On the hand, the role of the river inflows from the Kamchatka Peninsula on the eastern side of the Okhotsk Sea is not well known.
In this study, we simulated the northern part of the Okhotsk Sea to investigate the roles of river inflows from the Kamchatka Peninsula. FVCOM (Finite-Volume, Primitive equation Community Ocean Model; Chen et al. 2003) was used. JRA55-do (Tsujino et al., 2018) was used for the atmospheric forcing. The river inflow dataset also came from JRA55-do based on Suzuki et al. (2017). The unstructured horizontal grid spacing was decreased from about 9.0 km at the southern boundary to about 1.4 km along the northern boundary.
The model runs with and without the river inflows from the Kamchatka Peninsula were compared. The salinity significantly increased without the river inflow along the coast of Kamchatka (by more than 1 unit at maximum). The salinity increase also spread toward the western Okhotsk Sea. With these changes in salinity, ice formation in the Okhotsk Sea was also affected.

Keywords: Okhotsk Sea, sea ice, river inflow

©2019. Japan Geoscience Union. All Right Reserved.

CHLOROPHYLL ESTIMATION OF LAKE AND COASTAL WATER USING REMOTE SENSING APPROACH

*Shweta Yadav[1], Yamashiki Yosuke[1], Junichi Susaki[1], Kanako Ishikawa[2], Yoh Yamashita[1]

1. Kyoto University, 2. LBERI

Chlorophyll-a is an optically active compound (OAC) commonly used as a proxy for phytoplankton biomass in an aquatic environment. Retrieving the concentration of chlorophyll-a remains a challenge due to the presence of several OAC particularly in water bodies which are in proximity to the land-based activities. In this study, an effort has been made to estimate the chlorophyll-a concentration of both the freshwater Lake Biwa and the coastal water of Wakasa Bay in Japan. A spectral decomposition algorithm was used to determine the chlorophyll-a using the satellite images. The algorithm was applied to the satellite images from two different sensors namely Landsat-8 /OLI and Sentinel-2A/MSI. The satellite-derived chlorophyll-a concentration for the lake and coastal water from two different sensors were compared to assess the performance of both the sensors. The accuracy of the chlorophyll-a results derived from the images was evaluated with the in-situ measurement data of the chlorophyll-a for the Lake Biwa and the coastal water of Wakasa Bay. Both satellite sensors appear to give the best results for the coastal water ($R^2 > 0.80$) with an RMSE < 0.3 μg/L. However, slight underestimation of chlorophyll-a noted for the Landsat-8 image with an increase in chlorophyll-a concentration. For the lake water, Sentinel-2A results were relatively better ($R^2 > 0.70$) than Landsat-8, with an RMSE of < 1.0 μg/L. The obtained results will be useful to evaluate the primary productivity of both freshwater and coastal water body.

Keywords: Chlorophyll-a, Lake and Coastal Water, Satellite-Remote Sensing

©2019. Japan Geoscience Union. All Right Reserved.

Maritime-continent coastal region as land-sea-air triple boundary layer and bio-anthroposphere

*Manabu D. Yamanaka[1]

1. Research Institute for Humanity and Nature / Professor Emeritus of Kobe University

Imbalance of radiative processes determining climate is compensated by atmospheric-oceanic circulations and latent heating. The latent heat generated mainly by equatorial cumulonimbus clouds concerns both overheating and circulation pumping. Since the equatorial atmosphere is almost free from Coriolis force making cyclones, the diurnal-cycle sea-land heat contrast is the most principal mechanism to generate cumulonimbus and thus rainfall. The earth’ s longest coastline of Indonesian maritime continent (IMC) generates the largest regional rainfall and latent heat controlling the global climate (Yamanaka et al., 2018, *Prog. Earth Planet. Sci.*, **5**(21), 1-28). Massive fresh water sustains the biosphere with biodiversity over the peatland of major islands of the IMC, which also concern the carbon cycle through making peats and coals as geologically long-term reservoirs. We homo sapiens originated from the tropical Africa and evacuated to the temperate zone, where coexistence with other species was easier and thus proliferation and civilization were achieved with making the tropics a field for grabbing both alive and fossilized bio-resources. On one hand, the human population is governed by the rain water for survival, agricultural and industrial use. On the other hand, the human activity after the industrial revolution has been consuming the fossil fuels, and has been modifying the peatland for plantations, which release massive greenhouse gases. Such interactions are being studied mainly in the eastern coast of Sumatera and the southern coast of Kalimantan, under an interdisciplinary project (RIHN Tropical Peatland Society Project, 2017-21). Based on rainfall variabilities of mesoscale (with radars, and as functions of coastal distance), intraseasonal to interannual scales (based on operational data) and interdecadal to centennial scales (by historical data rescue), we may discuss a “saturation” of anthroposphere in the tropical coastal region such as the IMC peatland.

Keywords: cosatal region, sea-land breeze and monsoon circulations , hydrologic cycle, bio-anthroposphere, maritime-continent peatland

©2019. Japan Geoscience Union. All Right Reserved.

River-ocean interaction at the Ganges-Brahmaputra river mouth

*Shinichiro Kida[1], Dai Yamazaki[2]

1. Research Institute for Applied Mechanics, Kyushu University, 2. Institute of Industrial Sciences, The University of Tokyo

The Ganges-Brahmaputra river is a major source of freshwater for the Bay of Bengal. River discharge occurs through the Ganges-Brahmaputra Delta, which consists of multiple river mouths. The seasonal cycle of this river discharge is observed with a minimum from late winter to early spring and a maximum from late summer to early fall. The seasonal cycle of the sea surface height for the Bay of Bengal, on the other hand, shows the presence of the Kelvin waves propagating from the equatorial Indian Ocean. We investigated how these two processes may interact at the river mouths based on a high-resolution numerical model that resolves the various channels of the Ganges-Brahmaputra Delta. The model simulates the basic seasonal cycle of the river discharge that is comparable to observations, with a river plume forming from the major river mouth and along the coast. Preliminary results suggest significant river-ocean interaction in narrow channels and, at times, reverse the direction of the river flow.

Keywords: River discharge, water cycle, Bay of Bengal

©2019. Japan Geoscience Union. All Right Reserved.

[J] Poster | A (Atmospheric and Hydrospheric Sciences)：A-OS Ocean Sciences & Ocean Environment

Mon. May 27, 2019 5:15 PM - 6:30 PM JST | Mon. May 27, 2019 8:15 AM - 9:30 AM UTC | Poster Hall International Exhibition Hall8, Makuhari Messe_7

[A-OS15] Freshwater discharge through rivers and estuaries to the ocean

convener:Shinichiro Kida(Research Institute for Applied Mechanics, Kyushu University), Dai Yamazaki(Institute of Industrial Sciences, The University of Tokyo), Yosuke Alexandre Yamashiki(Earth & Planetary Water Resources Assessment Laboratory Graduate School of Advanced Integrated Studies in Human Survivability Kyoto University), Humio Mitsudera(Institute of Low Temperature Science, Hokkaido University)

The water cycle from land to the ocean involves complex dynamics of rivers and buoyancy driven flows in estuaries and the ocean. Recent progress in satellite observations and numerical models are beginning to illuminate how this water cycle occurs on various time scales globally and regionally. This session welcomes various process studies that investigate the dynamics and material circulation related to the freshwater cycle from land to the ocean such as surface runoff, river transport, estuarine circulation, and coastal river plumes based on numerical, observational, or theoretical studies.

[AOS15-P01] MERIT Hydro: Global 90m-resolution hydrography map based on latest topography datasets.

*Dai Yamazaki[1] (1.Institute of Industrial Sciences, The University of Tokyo)

[AOS15-P02] Comparison of model performance between global- and regional-scale river models in simulating compound flooding in coastal deltas in the world’s continental rivers

*Hiroaki Ikeuchi[1,2], Dai Yamazaki[2], Yukiko Hirabayashi[3] (1.Graduate School of Engineering, The University of Tokyo, 2.Institute of Industrial Science, The University of Tokyo, 3.Graduate School of Engineering and Science, Shibaura Instittute of Technology)

[AOS15-P03] Observation of a river plume by drone-mounted visible/infrared cameras

*Kenta Araki[1], Shinichiro Kida[2], Atsuhiko Isobe[2] (1.Interdisciplinary Graduate School of Engineering Sciences, Kyushu University, 2.Research Institute for Applied Mechanics, Kyushu University)

[AOS15-P04] Numerical simulation of typhoon storm surge in the LUOYUAN Bay

*Nan Yuan[1], Humio Mitsudera [1] (1.Hokkaido University, the Institute of Low Temperature Science)

[AOS15-P05] Laboratory and numerical experiments on the ballooning of river-plume bulge

*fujita yusuke[1], Atsuhiko Isobe[2] (1.interdiscipinary graduate school of engineering science, Kyushu Univercity, 2.Research Institude for Applied Mechanics Kyushu Univ)

MERIT Hydro: Global 90m-resolution hydrography map based on latest topography datasets.

*Dai Yamazaki[1]

1. Institute of Industrial Sciences, The University of Tokyo

High-resolution raster hydrography maps are a fundamental data source for many geoscience applications. Here we introduce MERIT Hydro, a new global flow direction map at 3 arc-second resolution (~90 m at the equator) derived from the latest elevation data (MERIT DEM) and water body datasets (G1WBM, GSWO, and OpenStreetMap). We developed a new algorithm to extract river networks near-automatically by separating actual inland basins from dummy depressions caused by the errors in input elevation data. After a minimum amount of hand-editing, the constructed hydrography map shows good agreement with existing quality-controlled river network datasets in terms of flow accumulation area and inland basin distribution. The location of river streamlines was realistically aligned with existing satellite-based global river channel data. Comparison to GRDC gauges confirmed the accuracy of drainage basin delineation for global river networks in most cases. Discrepancies in flow accumulation area were found mostly in arid river basins containing depressions that are occasionally connected at high water levels and thus resulting in uncertain watershed boundaries. MERIT Hydro improves on existing global hydrography datasets in terms of spatial coverage (between N90 and S60) and representation of small streams, mainly due to increased availability of high-quality baseline geospatial datasets. The new flow direction and flow accumulation maps, along with accompanying supplementary layers on hydrologically adjusted elevation and channel width, will advance geoscience studies related to river hydrology at both global and local scales.

Keywords: Global Hydrology, River dataset

©2019. Japan Geoscience Union. All Right Reserved.

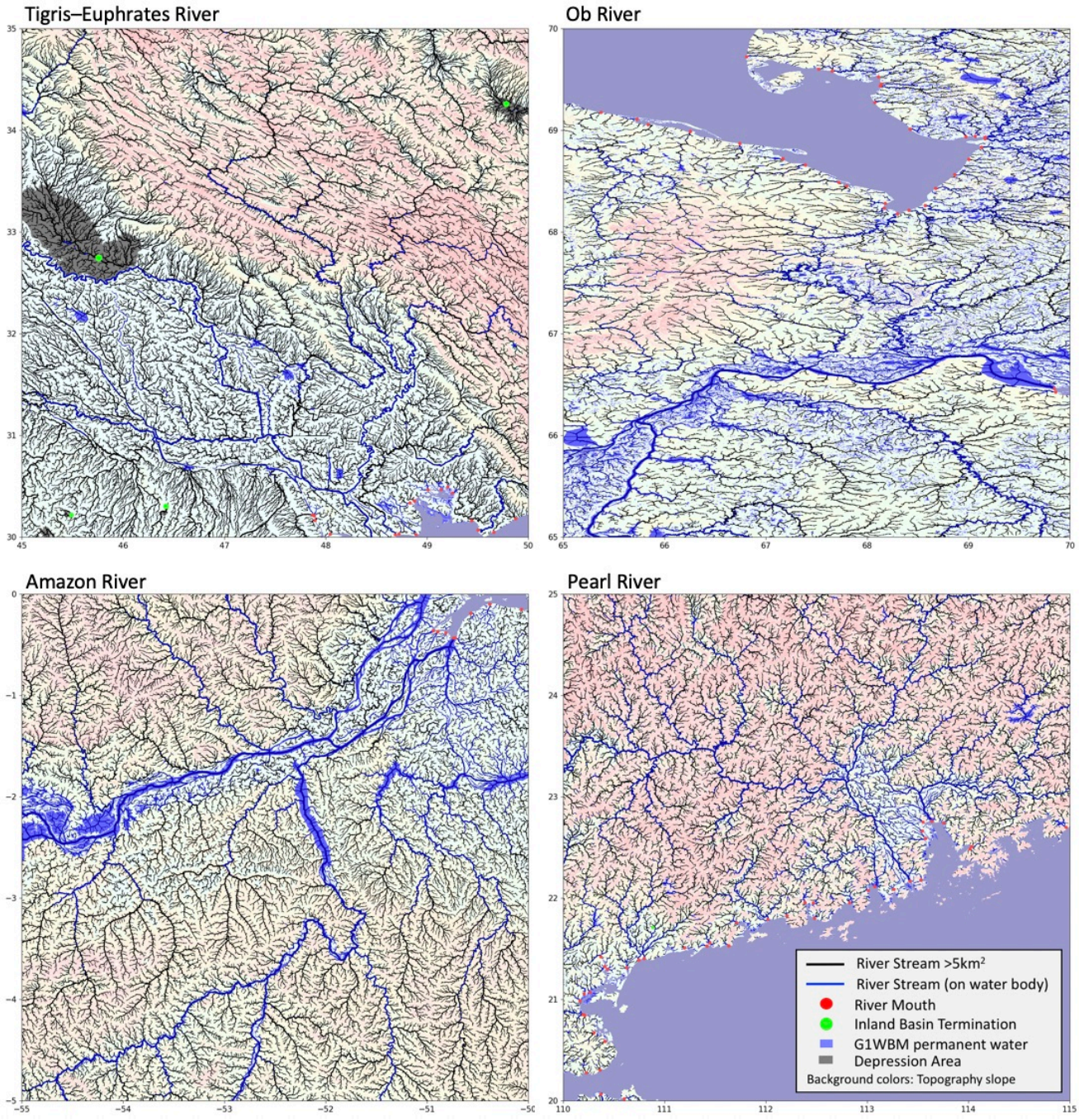

©2019. Japan Geoscience Union. All Right Reserved.

Comparison of model performance between global- and regional-scale river models in simulating compound flooding in coastal deltas in the world’s continental rivers

*Hiroaki Ikeuchi[1,2], Dai Yamazaki[2], Yukiko Hirabayashi[3]

1. Graduate School of Engineering, The University of Tokyo, 2. Institute of Industrial Science, The University of Tokyo, 3. Graduate School of Engineering and Science, Shibaura Instittute of Technology

Compound flooding, the co-occurrence of river and coastal flooding, is a major threat for delta regions and is rapidly gaining both social and academic attention. Global river models are widely used these days for various purposes such as flood forecast, flood risk assessment, and earth system sciences, and they can be used for flood risk assessment in delta regions as well. CaMa-Flood is a state-of-the-art global hydrodynamic model replicating river routing and floodplain inundation dynamics, and recently it has been applied to conduct compound flooding simulation by coupling a global tide and surge reanalysis data for the first time. However, because the model solves 1 dimensional momentum equations, complex water flow processes in river-coast interface may not be fully expressed.

The objective of this study is to enhance our understanding on issues in modelling compound flooding in the framework of global river models. To achieve this, we compare the difference in model performance between a global- and a regional-scale river model for the simulation of flood inundation in delta regions. We selected CaMa-Flood as a global model and LISFLOOD-FP as a regional model respectively. The reason for the choice of these models is that both the momentum equation and the sub-grid approximation of floodplain inundation dynamics are the same in the models, which enables us to compare the model performance in terms of dimensions, i.e., 1 dimensional flow equation for CaMa-Flood, and 2 dimension for LISFLOOD-FP. We proposed a method to construct LISFLOOD-FP model based on the topography and river channel bathymetry taken in CaMa-Flood to make the input topographical data as similar as possible. Simulation results suggest that while the overall flood extent was similar for both models, the spatial pattern of floodplain inundation depth differed because of the unit-catchment shape, i.e., the spatial unit of calculation taken in the CaMa-Flood model.

Keywords: compound flooding, global models, coastal deltas

©2019. Japan Geoscience Union. All Right Reserved.

Observation of a river plume by drone-mounted visible/infrared cameras

*Kenta Araki[1], Shinichiro Kida[2], Atsuhiko Isobe[2]

1. Interdisciplinary Graduate School of Engineering Sciences, Kyushu University, 2. Research Institute for Applied Mechanics, Kyushu University

Introduction

Thermal infrared observations of the sea surface temperature (SST) from satellites are important for understanding the ocean. However, the use of satellites is still difficult for observing coastal oceanic process with small spatio-temporal scales. The purpose of this study is to use drones and observe ocean color and SST distributions of the coastal area with a spatial resolution of about a few centimeters. Drones can be used for remote sensing of the sea surface from an altitude less than 150m.

Observation

On September 11, 2018, we conducted observations of the coastal ocean at the Iyonada of the western Seto inland sea and the Hiji river using the Ehime University research ship “Isana”. We used drone-mounted visible and infrared cameras and took images of the sea surface from 100m above the sea level. A total of 18 images were acquired over the observation time of about 7 minutes. The area covered by each image of the visible image and the infrared image are 100 m ×70 m and 80 m ×60 m, respectively. We also pursued CTD observations at the same time to examine the oceanic structure across the front.

Result and Discussion

In the observed infrared image, we found vignetting, which is a difference in brightness from the center to the periphery of the image. Therefore, we will need to remove this impact of vignetting to understand the actual SST distribution. Observed visible image showed the river plume clearly so we are currently working to detect the location of the front that matches with the infrared image. We plan to present the microstructure of the front found in the visible and infrared images. We also plan to compare the vertical cross section of the front obtained from CTD data with the sea surface temperature observed in the infrared image.

Keywords: drone, sea surface temperature, river plume

©2019. Japan Geoscience Union. All Right Reserved.

Numerical simulation of typhoon storm surge in the LUOYUAN Bay

*Nan Yuan[1], Humio Mitsudera [1]

1. Hokkaido University, the Institute of Low Temperature Science

According to the statistics of China Marine Disaster Bulletin published in May 2018, from 2008 to 2017, around 100 billion financial loss happened in each year due to marine disasters. Over 80% loss was caused by storm surges. Further, unfortunately, the FUJIAN Province is a place they prefer to visit. The research area, the LUOYUAN bay, is located on the northeastern area of the FUJIAN Province, which was so inconspicuous that not so many researchers concerned the storm surges happened there. However, it brings demands of study with the increase of financial developments and people’s settling down in this area. Therefore, this research started.

For studying the response of the sea level in this area to a storm, a high-resolution model with the ADvanced CIRCulation model (ADCIRC) was established first. It used unstructured fine grids, and the topography from electronical chart partially and coastline data with resolution 1:10000. By comparing the simulated water level with the observation, we can see that both match with each other quite well. Furthermore, via harmonic analysis and contrasting with previous studies, the accuracy of this model was verified.

Based on the model, some experiments were conducted to assess the response inside of the bay to different kinds of typhoon, primarily with different intensities on the north-south (N-S) moving path, and the northwest-southeast (NW-SE) moving path. Results are as follows. On the one hand, there are common features we can understand easily: the surge increases gradually with the strength of typhoons, and the peak-value surge can reach approximately 3 meters if a typhoon landed as a SUPER TYPHOON; the low pressure of a typhoon and strong wind will lead to a surge, and this surge would be more obvious when the typhoon passes near coastal areas; because of the cyclonic structure of a typhoon, it is easier for a typhoon that moves on an offshore path to induce the rising of water level on the southern part of bay than the northern part. On the other hand, there are also other findings that might be difficult to understand just by imagination: for the N-S path, there is a steep reduction of the sea level inside of the bay after the peak-value time. Such a rapid reduction of sea levels does not happen for the NW-SE path but for those in the southern area along the FUJIAN Province. By analyzing the data, we consider that wind direction and the shape of the bay would be the main reasons causing this phenomenon. Further, there is an oscillation in the sea level after peak-value time for the typhoon on the N-S path, and a larger reduction exists inside of the bay than the outside. Resonance between the different frequency of sea level changes, caused by various moving speeds of typhoons, and the local natural frequency of the bay might have some effects. We attempt to investigate resonance for the future study. The experiments with various parallel paths to the N-S path, as well as those parallel to the NW-SE path, also give similar results.

Keywords: Luoyuan Bay, typhoon, storm surge, marine disaster prevention and mitigation

©2019. Japan Geoscience Union. All Right Reserved.

Laboratory and numerical experiments on the ballooning of river-plume bulge

*fujita yusuke[1], Atsuhiko Isobe[2]

1. interdiscipinary graduate school of engineering science, Kyushu Univercity, 2. Research Institude for Applied Mechanics Kyushu Univ

Ballooning (infinitely growing) of river-plume bulges are observed only in laboratory and numerical experiments, but in the actual ocean we have no infinitely growing bulges. Thus, the mechanism of river-plume bulges remains obscure in detail. In this study, we focus on the dependence of growing rate of a bulge on the curvature of the line connecting estuary axis and coastline (i.e., the curvature of river-plume release) to elucidate the mechanism to cause the ballooning. First, we conducted a rotating water tank experiments under an extreme condition. Namely, we adopted two curvature: The one is that a coastline lies in parallel with the estuary axis (infinite curvature radius), and the other is that the coastline takes a right angle to the estuarine axis (null curvature radius). In the experiment with the right angle, the ballooning of river-plume bulge was observed as observed in conventional experiments. Meanwhile, when the angle between the coastline and estuarine axis was parallel, the bulge formation was not observed. We next conducted experiments using a numerical model that we could control the parameters governing fluid motion to clarify the mechanism of the ballooning. We adopted unstructured Finite Volume Coastal Ocean Model in which we can freely change the curvature using triangle cell grids.

©2019. Japan Geoscience Union. All Right Reserved.

[J] Poster | A (Atmospheric and Hydrospheric Sciences)：A-OS Ocean Sciences & Ocean Environment

Mon. May 27, 2019 1:45 PM - 3:15 PM JST | Mon. May 27, 2019 4:45 AM - 6:15 AM UTC | Poster Hall International Exhibition Hall8, Makuhari Messe_2

[A-OS16] Chemical and Biological Oceanography

convener:Namiha Yamada(National Institute of Advanced Industrial Science and Technology), Sayaka Yasunaka(Japan Agency for Marine-Earth Science and Technology), Hiroaki Saito(Atmosphere and Ocean Research Institute, The University of Tokyo)

This session invites presentations on a wide variety of topics related to chemical and biological oceanography.

[AOS16-P01] Seasonal productions of dinoflagellate cysts in relation to environmental characteristics in Jinhae-Masan Bay, Korea: One year sediment trap observation

*Hyeon Ho Shin[1] (1.Korea Institute of Ocean Science and Technology)

[AOS16-P02] Pacific anthropogenic carbon between 1991 and 2017

*Akihiko Murata[1], Carter B.R.[2,3], Feely, R.A. Feely, R.A.[3], Wanninkhof, R. Wanninkhof, R.[3], Shinya Kouketsu[1], Sonnerup R.E.[2], Pardo P.C.[4], Sabine C.L.[5], Johnson G. C.[3], Sloyan B.M.[6], Mecking S.[2], Tilbrook B.[6], Speer K.[7], Talley L.D.[8], Millero F.J.[9], Wijffels S.E.[6,10], Macdonald A.M.[10], Gruber N.[11], Bullister J. L.[3] (1.Japan Agency for Marine-Earth Science and Technology, 2.University of Washington, 3.NOAA, 4.University of Tasmania, 5.University of Hawaii Manoa, 6.CSIRO, 7.The Florida State University, 8.University of California, 9.University of Miami, 10.Woods Hole Oceanographic Institution, 11.IBP)

[AOS16-P03] Spatio-temporal variability of surface water pCO2 and nutrients in the tropical Pacific from 1981 to 2015

*Sayaka Yasunaka[1], Shinya Kouketsu[1], P.G. Strutton[2], A.J. Sutton[3], Akihiko Murata[1], Shin-ichiro Nakaoka[4], Yukihiro Nojiri[4] (1.Japan Agency for Marine-Earth Science and Technology, 2.University of Tasmania, 3.NOAA, 4.NIES)

Seasonal productions of dinoflagellate cysts in relation to environmental characteristics in Jinhae-Masan Bay, Korea: One year sediment trap observation

*Hyeon Ho Shin[1]

1. Korea Institute of Ocean Science and Technology

To investigate dinoflagellate cyst production and seasonality in relation to major environmental factors, such as water temperature, salinity, chlorophyll-*a* (chl-*a*) and dissolved nutrients, and to propose dinoflagellate cysts as possible biological indicators for the reconstruction of past environmental conditions, a sediment trap study was conducted for one year, from March 2011 to February 2012, in Jinhae-Masan Bay, Korea. Marked increases in dinoflagellate cyst production were documented in Jinhae-Masna Bay during two distinct seasons (summer and late autumn) characterized by different environmental conditions. Summer (July and August) was characterized by relatively high water temperature, dissolved inorganic nitrogen (DIN), and chl-*a* concentrations and low salinity, whereas late autumn (November and December) exhibited high dissolved inorganic phosphorus, low water temperature and high salinity, compared to those of the summer. Fourteen dinoflagellate cyst taxa were identified. These assemblages were dominated by *Brigantedinium* species (round brown cyst), cysts of *Scrippsiella* species, *Spiniferites* species and cysts of *Alexandrium* species (ellipsoidal cyst). The total flux of dinoflagellate cysts ranged from 781 cysts m^{-2} day^{-1} to 5,602 cysts m^{-2} day^{-1}, and the production of autotrophic dinoflagellate cysts was mainly restricted to the warmest months (July-September) and autumn. Multivariable analysis revealed that the production of major dinoflagellate cysts, excluding those of *Brigantedinium* species, can be enhanced by environmental conditions during summer in Jinhae-Masan Bay. In particular, the increased production of cysts of *Scrippsiella* species was related to increased water temperature, and the increased production production of *Spiniferites* species was associated with lower salinity. Two peaks in cyst production of *Alexandrium* species in August and November corresponded with significant increases in DIN and DIP; however, no significant relationship was found between the production of *Brigantedinium* species and environmental factors in Jinhae-Masan Bay. These results suggest that the cysts of *Scrippsiella* species, *Spiniferites* species and cysts of *Alexandrium* species present in sediment samples from Jinhae-Masan Bay can be used as biological indicators to reconstruct past environmental conditions involving relatively high water temperature, low salinity and enhanced nutrient level.

Keywords: Scrippsiella, Spiniferites, Alexandrium, phytoplankton, summer, Late autumn

©2019. Japan Geoscience Union. All Right Reserved.

Pacific anthropogenic carbon between 1991 and 2017

*Akihiko Murata[1], Carter B.R.[2,3], Feely, R.A. Feely, R.A.[3], Wanninkhof, R. Wanninkhof, R.[3], Shinya Kouketsu[1], Sonnerup R.E.[2], Pardo P.C.[4], Sabine C.L.[5], Johnson G. C.[3], Sloyan B.M.[6], Mecking S.[2], Tilbrook B.[6], Speer K.[7], Talley L.D.[8], Millero F.J.[9], Wijffels S.E.[6,10], Macdonald A.M.[10], Gruber N.[11], Bullister J. L.[3]

1. Japan Agency for Marine-Earth Science and Technology, 2. University of Washington, 3. NOAA, 4. University of Tasmania, 5. University of Hawaii Manoa, 6. CSIRO, 7. The Florida State University, 8. University of California, 9. University of Miami, 10. Woods Hole Oceanographic Institution, 11. IBP

The ocean is storing between a fourth and a third of anthropogenic CO_2 (C_{anth}) emissions. Monitoring the oceanic CO_2 sink is critical to assessing the global carbon budget. We estimate total C_{anth} storage and accumulation rates from 14 Pacific hydrographic sections that have been occupied two to four times over the past decades, with most sections having been recently measured as part of the Global Ocean Hydrographic Investigations Program (GO-SHIP). The C_{anth} sink over the top 1500 m of the Pacific increased from 8.6 (±1.1, 1 σ) Pg of carbon decade^{-1} from 1995 to 2005 to 10.8 (±1.1) PgC decade^{-1} from 2005 to 2015. We estimate 1.2 of this observed 2.2 PgC decade^{-1} increase in the rate of accumulation between decades is attributable to atmospheric anthropogenic CO_2 increases alone, while the remaining increase is consistent with recent literature suggesting there was an increase in the ocean carbon sink during the mid-2000s. Methods that allow for analysis of multiple occupations of sections and comparisons between different sections spaced irregularly in time are introduced. The accuracy of the resulting C_{anth} accumulation reconstructions is limited by the accuracy of the data, suggesting that a continuation of repeat hydrographic surveys with a high emphasis on obtaining multiple independent realizations of the most accurate possible measurements is a critical piece of future carbon cycle monitoring.

©2019. Japan Geoscience Union. All Right Reserved.

Spatio-temporal variability of surface water pCO2 and nutrients in the tropical Pacific from 1981 to 2015

*Sayaka Yasunaka[1], Shinya Kouketsu[1], P.G. Strutton[2], A.J. Sutton[3], Akihiko Murata[1], Shin-ichiro Nakaoka[4], Yukihiro Nojiri[4]

1. Japan Agency for Marine-Earth Science and Technology, 2. University of Tasmania, 3. NOAA, 4. NIES

We present a synthesis of surface water partial pressure of CO_2 (pCO_2) and nutrient observations in the tropical Pacific from 1981 to 2015. The e-folding scale for interannual variability of pCO_2 is estimated to be 6˚ in latitude, 13˚ in longitude, and 2 months with a signal-to-noise ratio of 4. When El Niño occurs, pCO_2 along the equator is reduced due to weakening of the easterly wind and reduced upwelling of CO_2 rich subsurface water. The surface seawater pCO_2 trend is positive in all regions with an area average of 1.8 ±0.1 μatm/yr. However, along the equator the trend is > 2 μatm/yr linked to the Pacific Decadal Oscillation forcing. Surface nutrient concentrations in the central to eastern tropics along the equator decreased during El Niño periods, but there are not enough data to characterize the trends of nutrients in the tropical Pacific.

©2019. Japan Geoscience Union. All Right Reserved.

[J] Poster | A (Atmospheric and Hydrospheric Sciences)：A-OS Ocean Sciences & Ocean Environment

Mon. May 27, 2019 5:15 PM - 6:30 PM JST | Mon. May 27, 2019 8:15 AM - 9:30 AM UTC | Poster Hall International Exhibition Hall8, Makuhari Messe_8

[A-OS16] Chemical and Biological Oceanography

convener:Namiha Yamada(National Institute of Advanced Industrial Science and Technology), Sayaka Yasunaka(Japan Agency for Marine-Earth Science and Technology), Hiroaki Saito(Atmosphere and Ocean Research Institute, The University of Tokyo)

This session invites presentations on a wide variety of topics related to chemical and biological oceanography.

[AOS16-P01] Seasonal productions of dinoflagellate cysts in relation to environmental characteristics in Jinhae-Masan Bay, Korea: One year sediment trap observation

*Hyeon Ho Shin[1] (1.Korea Institute of Ocean Science and Technology)

[AOS16-P02] Pacific anthropogenic carbon between 1991 and 2017

*Akihiko Murata[1], Carter B.R.[2,3], Feely, R.A. Feely, R.A.[3], Wanninkhof, R. Wanninkhof, R.[3], Shinya Kouketsu[1], Sonnerup R.E.[2], Pardo P.C.[4], Sabine C.L.[5], Johnson G. C.[3], Sloyan B.M.[6], Mecking S.[2], Tilbrook B.[6], Speer K.[7], Talley L.D.[8], Millero F.J.[9], Wijffels S.E.[6,10], Macdonald A.M.[10], Gruber N.[11], Bullister J. L.[3] (1.Japan Agency for Marine-Earth Science and Technology, 2.University of Washington, 3.NOAA, 4.University of Tasmania, 5.University of Hawaii Manoa, 6.CSIRO, 7.The Florida State University, 8.University of California, 9.University of Miami, 10.Woods Hole Oceanographic Institution, 11.IBP)

[AOS16-P03] Spatio-temporal variability of surface water pCO2 and nutrients in the tropical Pacific from 1981 to 2015

*Sayaka Yasunaka[1], Shinya Kouketsu[1], P.G. Strutton[2], A.J. Sutton[3], Akihiko Murata[1], Shin-ichiro Nakaoka[4], Yukihiro Nojiri[4] (1.Japan Agency for Marine-Earth Science and Technology, 2.University of Tasmania, 3.NOAA, 4.NIES)

Seasonal productions of dinoflagellate cysts in relation to environmental characteristics in Jinhae-Masan Bay, Korea: One year sediment trap observation

*Hyeon Ho Shin[1]

1. Korea Institute of Ocean Science and Technology

To investigate dinoflagellate cyst production and seasonality in relation to major environmental factors, such as water temperature, salinity, chlorophyll-*a* (chl-*a*) and dissolved nutrients, and to propose dinoflagellate cysts as possible biological indicators for the reconstruction of past environmental conditions, a sediment trap study was conducted for one year, from March 2011 to February 2012, in Jinhae-Masan Bay, Korea. Marked increases in dinoflagellate cyst production were documented in Jinhae-Masna Bay during two distinct seasons (summer and late autumn) characterized by different environmental conditions. Summer (July and August) was characterized by relatively high water temperature, dissolved inorganic nitrogen (DIN), and chl-*a* concentrations and low salinity, whereas late autumn (November and December) exhibited high dissolved inorganic phosphorus, low water temperature and high salinity, compared to those of the summer. Fourteen dinoflagellate cyst taxa were identified. These assemblages were dominated by *Brigantedinium* species (round brown cyst), cysts of *Scrippsiella* species, *Spiniferites* species and cysts of *Alexandrium* species (ellipsoidal cyst). The total flux of dinoflagellate cysts ranged from 781 cysts m^{-2} day^{-1} to 5,602 cysts m^{-2} day^{-1}, and the production of autotrophic dinoflagellate cysts was mainly restricted to the warmest months (July-September) and autumn. Multivariable analysis revealed that the production of major dinoflagellate cysts, excluding those of *Brigantedinium* species, can be enhanced by environmental conditions during summer in Jinhae-Masan Bay. In particular, the increased production of cysts of *Scrippsiella* species was related to increased water temperature, and the increased production production of *Spiniferites* species was associated with lower salinity. Two peaks in cyst production of *Alexandrium* species in August and November corresponded with significant increases in DIN and DIP; however, no significant relationship was found between the production of *Brigantedinium* species and environmental factors in Jinhae-Masan Bay. These results suggest that the cysts of *Scrippsiella* species, *Spiniferites* species and cysts of *Alexandrium* species present in sediment samples from Jinhae-Masan Bay can be used as biological indicators to reconstruct past environmental conditions involving relatively high water temperature, low salinity and enhanced nutrient level.

Keywords: Scrippsiella, Spiniferites, Alexandrium, phytoplankton, summer, Late autumn

©2019. Japan Geoscience Union. All Right Reserved.

Pacific anthropogenic carbon between 1991 and 2017

*Akihiko Murata[1], Carter B.R.[2,3], Feely, R.A. Feely, R.A.[3], Wanninkhof, R. Wanninkhof, R.[3], Shinya Kouketsu[1], Sonnerup R.E.[2], Pardo P.C.[4], Sabine C.L.[5], Johnson G. C.[3], Sloyan B.M.[6], Mecking S.[2], Tilbrook B.[6], Speer K.[7], Talley L.D.[8], Millero F.J.[9], Wijffels S.E.[6,10], Macdonald A.M.[10], Gruber N.[11], Bullister J. L.[3]

1. Japan Agency for Marine-Earth Science and Technology, 2. University of Washington, 3. NOAA, 4. University of Tasmania, 5. University of Hawaii Manoa, 6. CSIRO, 7. The Florida State University, 8. University of California, 9. University of Miami, 10. Woods Hole Oceanographic Institution, 11. IBP

The ocean is storing between a fourth and a third of anthropogenic CO_2 (C_{anth}) emissions. Monitoring the oceanic CO_2 sink is critical to assessing the global carbon budget. We estimate total C_{anth} storage and accumulation rates from 14 Pacific hydrographic sections that have been occupied two to four times over the past decades, with most sections having been recently measured as part of the Global Ocean Hydrographic Investigations Program (GO-SHIP). The C_{anth} sink over the top 1500 m of the Pacific increased from 8.6 (±1.1, 1 σ) Pg of carbon decade^{-1} from 1995 to 2005 to 10.8 (±1.1) PgC decade^{-1} from 2005 to 2015. We estimate 1.2 of this observed 2.2 PgC decade^{-1} increase in the rate of accumulation between decades is attributable to atmospheric anthropogenic CO_2 increases alone, while the remaining increase is consistent with recent literature suggesting there was an increase in the ocean carbon sink during the mid-2000s. Methods that allow for analysis of multiple occupations of sections and comparisons between different sections spaced irregularly in time are introduced. The accuracy of the resulting C_{anth} accumulation reconstructions is limited by the accuracy of the data, suggesting that a continuation of repeat hydrographic surveys with a high emphasis on obtaining multiple independent realizations of the most accurate possible measurements is a critical piece of future carbon cycle monitoring.

©2019. Japan Geoscience Union. All Right Reserved.

Spatio-temporal variability of surface water pCO2 and nutrients in the tropical Pacific from 1981 to 2015

*Sayaka Yasunaka[1], Shinya Kouketsu[1], P.G. Strutton[2], A.J. Sutton[3], Akihiko Murata[1], Shin-ichiro Nakaoka[4], Yukihiro Nojiri[4]

1. Japan Agency for Marine-Earth Science and Technology, 2. University of Tasmania, 3. NOAA, 4. NIES

We present a synthesis of surface water partial pressure of CO_2 (pCO_2) and nutrient observations in the tropical Pacific from 1981 to 2015. The e-folding scale for interannual variability of pCO_2 is estimated to be 6˚ in latitude, 13˚ in longitude, and 2 months with a signal-to-noise ratio of 4. When El Niño occurs, pCO_2 along the equator is reduced due to weakening of the easterly wind and reduced upwelling of CO_2 rich subsurface water. The surface seawater pCO_2 trend is positive in all regions with an area average of 1.8 ±0.1 μatm/yr. However, along the equator the trend is > 2 μatm/yr linked to the Pacific Decadal Oscillation forcing. Surface nutrient concentrations in the central to eastern tropics along the equator decreased during El Niño periods, but there are not enough data to characterize the trends of nutrients in the tropical Pacific.

©2019. Japan Geoscience Union. All Right Reserved.

[J] Oral | A (Atmospheric and Hydrospheric Sciences)：A-OS Ocean Sciences & Ocean Environment

Mon. May 27, 2019 3:30 PM - 5:00 PM JST | Mon. May 27, 2019 6:30 AM - 8:00 AM UTC | 303 3F

[A-OS16] Chemical and Biological Oceanography

convener:Namiha Yamada(National Institute of Advanced Industrial Science and Technology), Sayaka Yasunaka(Japan Agency for Marine-Earth Science and Technology), Hiroaki Saito(Atmosphere and Ocean Research Institute, The University of Tokyo), Chairperson:Tsuneo Ono(Japan Fisheries Research and Education Agency), Naohiro Kosugi(気象研究所)

This session invites presentations on a wide variety of topics related to chemical and biological oceanography.

3:30 PM - 3:45 PM JST | 6:30 AM - 6:45 AM UTC

[AOS16-01] Variability of the growth rate for dissolved inorganic carbon in surface seawater along the 165°E line

*Chiho Tanizaki[1], Hisashi Ono[2], Masao Ishii[2], Atsushi Kojima[1], Shinji Masuda[1], Kazutaka Enyo[1], Daisuke Sasano[1], Toshiya NAKANO[1] (1.Japan Meteorological Agency, 2.Meteorological Research Institute, Japan Meteorological Agency)

3:45 PM - 4:00 PM JST | 6:45 AM - 7:00 AM UTC

[AOS16-02] Seasonal variations of oceanic CO_2 disequilibrium and anthropogenic CO_2 in the subarctic North Pacific

*Bofeng Li[1], Shukuta Satori[1], Kasai Hiromi[2], Hiroshi Kuroda[2], Taniuchi Yukiko[2], Daisuke Hasegawa[3], Yutaka Watanabe[1] (1.Hokkaido University, 2.Hokkaido National Fisheries Research Institute, Japan Fisheries and Education Research , 3.Tohoku National Fisheries Research Institute, Japan Fisheries and Education Research)

4:00 PM - 4:15 PM JST | 7:00 AM - 7:15 AM UTC

[AOS16-03] An evaluation of current and future ocean acidification based on pCO_2 database around Okinawa Island

*Naohiro Kosugi[1], Hiroyuki Tsujino[1], Masao Ishii[1] (1.Meteorological Research Institute)

4:15 PM - 4:30 PM JST | 7:15 AM - 7:30 AM UTC

[AOS16-04] Reconstruction of spatiotemporal change of anthropogenic fixed nitrogen in the western North Pacific

*Yutaka Watanabe[1], Kouichi Fujita[1], BOFENG LI[1] (1.Hokkaido University)

4:30 PM - 4:45 PM JST | 7:30 AM - 7:45 AM UTC

[AOS16-05] On the mechanism of significant increasing trend of silicate in intermediate layer of Oyashio region

*Tsuneo Ono[1] (1.Fisheries Research and Education Agency)

4:45 PM - 5:00 PM JST | 7:45 AM - 8:00 AM UTC

[AOS16-06] Systematics of aluminum, manganese, iron, cobalt, and lead in the North Pacific Ocean observed during ocean-section study of GEOTRACES Japan

*Yoshiki Sohrin[1], Linjie Zheng[1] (1.Institute for Chemical Research, Kyoto University)

Variability of the growth rate for dissolved inorganic carbon in surface seawater along the 165˚E line

*Chiho Tanizaki[1], Hisashi Ono[2], Masao Ishii[2], Atsushi Kojima[1], Shinji Masuda[1], Kazutaka Enyo[1], Daisuke Sasano[1], Toshiya NAKANO[1]

1. Japan Meteorological Agency, 2. Meteorological Research Institute, Japan Meteorological Agency

The atmospheric concentration of carbon dioxide (CO_2) has reached 146% of the pre-industrial level resulting from the increase of CO_2 emissions by human activities. On the other hand, the ocean has absorbed about 30% of the anthropogenic CO_2, which leads to the regulation of the atmospheric CO_2 increase (IPCC, 2013). Midorikawa et al. (2012) found that the increase of the partial pressure of oceanic CO_2 (pCO_2^{sea}) along 137˚E recently decelerates though that of atmospheric CO_2 accelerates. The variability of pCO_2^{sea} is affected by the changes in sea surface temperature and salinity, dissolved inorganic carbon (DIC), and total alkalinity, and the investigation of the DIC changes in the surface seawater helps us to understand the oceanic absorption of atmospheric CO_2. In this study, the variability of DIC in surface seawater is examined from subarctic to equatorial region along 165˚E, one of the repeat hydrographic sections of Japan Meteorological Agency (JMA).

Using the observation data collected by JMA’ s Research Vessels in the 165˚E section and surface ocean CO_2 atlas (SOCAT) version 6, we calculated the mean trend of DIC in surface seawater during the period of 1996-2017. We found that DIC increases slower around 10˚N, and faster around 30˚N than atmospheric CO_2. Also, DIC growth rate is similar to the rate of atmospheric CO_2 increase in the equatorial region.

The variability of the DIC trend averaged for 10 years indicates that the DIC growth rate has increased in the equatorial region and decreased around 30˚N.

Keywords: 165˚E section, Dissolved Inorganic Carbon, growth rate

©2019. Japan Geoscience Union. All Right Reserved.

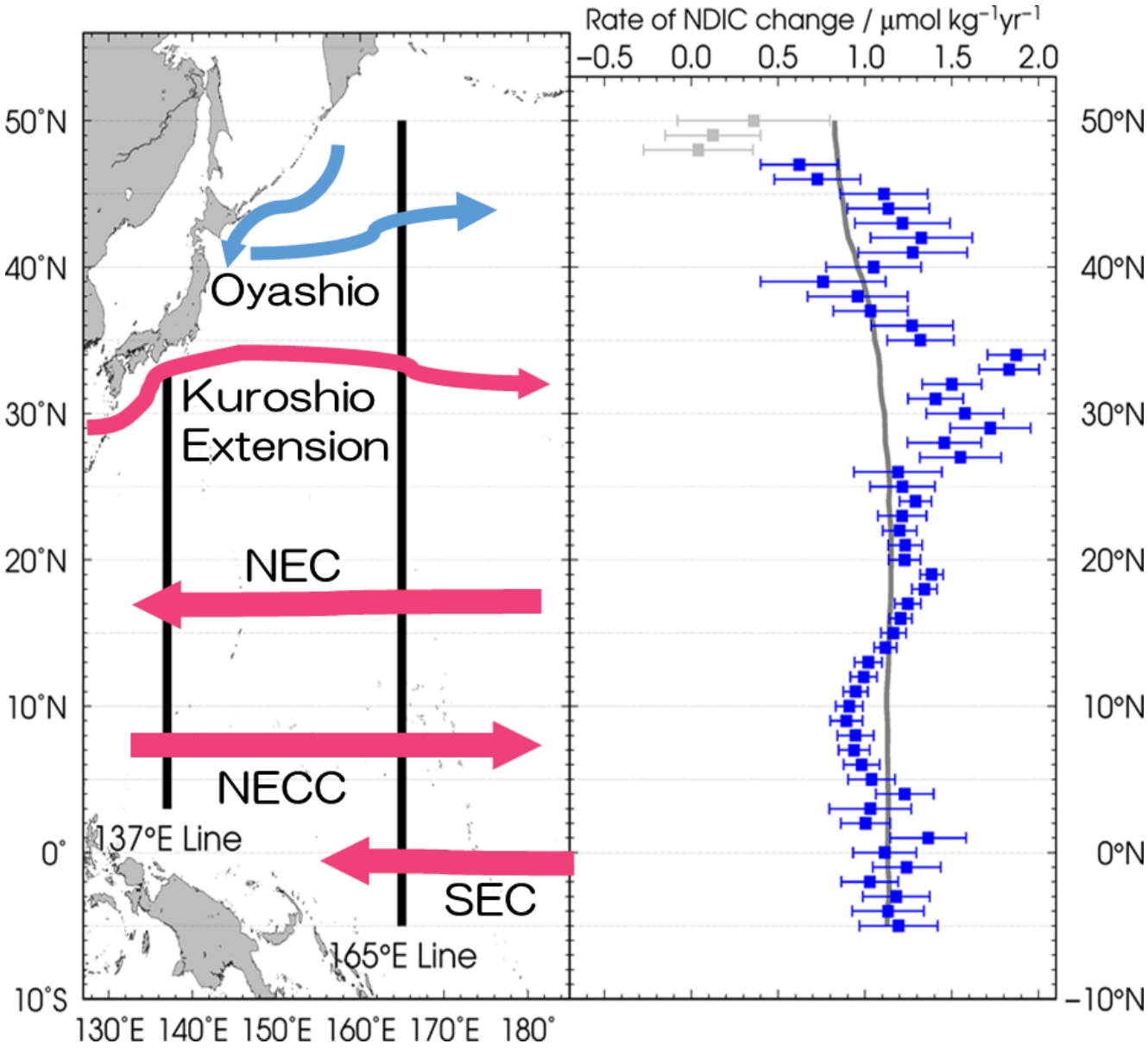

©2019. Japan Geoscience Union. All Right Reserved.

Seasonal variations of oceanic CO_2 disequilibrium and anthropogenic CO_2 in the subarctic North Pacific

*Bofeng Li[1], Shukuta Satori[1], Kasai Hiromi[2], Hiroshi Kuroda[2], Taniuchi Yukiko[2], Daisuke Hasegawa[3], Yutaka Watanabe[1]

1. Hokkaido University, 2. Hokkaido National Fisheries Research Institute, Japan Fisheries and Education Research , 3. Tohoku National Fisheries Research Institute, Japan Fisheries and Education Research

Assuming that the CO_2 above the surface mixed layer depth (MLD) mixes very well with air, we used a simple and new method to estimate air-sea CO_2 disequilibrium value at the MLD (C_{diseq}) as follow [*Li et al.*, 2019];

$$C_{diseq} = C_{MLD} - C_{sat,\,MLD} - C_{soft,\,MLD} - C_{carb,\,MLD}$$

where C_{MLD} is the observed dissolved inorganic carbon (DIC); $C_{sat,\,MLD}$ is saturated DIC; $C_{soft,\,MLD}$ is derived from the remineralization of organic matter; $C_{carb,\,MLD}$ is derived from the dissolution of $CaCO_3$ in the MLD. We collected the DIC and total alkalinity (TA) samples in the subarctic North Pacific in four seasons, and measured all the DIC and TA by using semi-closed cell simultaneous method [*Li et al.*, 2016].

C_{diseq} in this region changed from −38.29 to −56.93 μmol kg^{-1} in wintertime and from −9.65 to 1.02 μmol kg^{-1} summertime, indicating a strong seasonal change in C_{diseq}. Appling these values of C_{diseq} to the approach for estimating C_{ant} in this region, we also found a strong seasonal variation in C_{ant}.

Keywords: Air-sea CO2 disequilibrium, Anthropogenic CO2, Subarctic North Pacific

©2019. Japan Geoscience Union. All Right Reserved.

An evaluation of current and future ocean acidification based on pCO_2 database around Okinawa Island

*Naohiro Kosugi[1], Hiroyuki Tsujino[1], Masao Ishii[1]

1. Meteorological Research Institute

1. Introduction

Ocean acidification is caused by the dissolution of anthropogenic CO_2 into seawater. When CO_2 is dissolved in seawater, pH and the carbonate ion concentration decrease. A variety of marine organisms may be adversely affected since they use calcium carbonate as the main component of hard tissues such as shells and skeletons.

Coral reefs in the tropical zone are thought to be vulnerable to ocean acidification as they have a skeleton of aragonite which is a form of calcium carbonate. Ocean acidification will have adverse impacts on not only coral reefs but also whole tropical ecosystem since coral reefs are important for spawning, hatching, and habitat for many organisms.

Many coral reefs exist around Okinawa and bring a lot of benefits there by fishery and tourism. Geographically, coral reefs around Okinawa are located at the higher latitudinal area where the water temperature drops largely in winter.

In this study, we use the Surface Ocean CO_2 Atlas (SOCAT) database to evaluate the progress of ocean acidification around Okinawa from the 1980s to the present. Based on the results, we project the progress of acidification under future CO_2 concentration scenarios. This projection will reproduce seasonal variation in pCO_2 and aragonite saturation (Ω_A) there more realistically than existing predictions on a global scale.

2. Methods

The data of surface water temperature (SST), salinity (SSS) and pCO_2 around Okinawa (24-30˚N, 123-130˚E) were extracted from SOCAT database. We used the results of hydrographic observations conducted by the Japan Meteorological Agency in the same area between 2010 and 2017 in order to derive an empirical equation between salinity and total alkalinity (TA). Ω_A were calculated from pCO_2 and estimated TA using the CO2SYS program.

3. Results

In 1982-2016, pCO_2 showed a long-term trend of increase (Fig. a). At the same time, pCO_2 was high in summer and low in winter. Long-term and seasonal variation in pCO_2 was separated by using the method by Ishii et al., [2011]. As a result, the component of the long-term trend was +1.49±0.26 μatm/year (95% CI). This was as high as the rate of increase in atmospheric pCO_2 at Mauna Loa in Hawaii in the same period (+1.73±0.04 μatm/year).

TA was basically proportional to salinity (TA = 2297.1 / SSS * 35). In some areas near the shelf in the East China Sea, however, there was a positive anomaly from this relation. This may be due to the influence of river water originated from the Changjiang River. Another equation was applied (TA = 1347 + 897.6 / 34.2 * SSS) to the data to the north of 26˚N with SSS < 34.2 from July to September.

As for Ω_A, a long-term trend -0.0102±0.0018/year was calculated in the same manner as pCO_2. Previous studies showed that the coral reef habitat coincided with the area where Ω_A does not fall seasonally below 3.0 [Kleypas et al., 1999]. In the present situation, Ω_A around Okinawa island (SST > 21˚C in winter) was kept at 3.0 or more throughout the year.

©2019. Japan Geoscience Union. All Right Reserved.

4. Future projections
We can project the fluctuation in the ocean pCO_2 and Ω_A under future CO_2 concentration scenarios assuming that the current difference between in pCO_2 in the atmosphere and the ocean (ΔpCO_2) will not change in the future. Monthly ΔpCO_2 was averaged from the SOCAT database. CO_2 concentrations for the Representative Concentration Pathways (RCPs) were used to calculate atmospheric pCO_2 up to 2100 [Meinshausen et al., 2011]. Climatology of SST and SSS from 1982 to 2014 was calculated from Northwest Pacific Ocean Long-term Reanalysis Data Set (FORA-WNP30) and applied to the prediction. In the RCP 2.6 scenario, Ω_A will be at 3.0 or larger during this century. However, in the RCP 8.5 scenario, Ω_A will drop seasonally below 3.0 in the north of Okinawa island around 2030. In that scenario, Ω_A will be lower than 3.0 throughout the year in the 2060s (Fig. C). If the current increase in atmospheric CO_2 continues, coral reefs around Okinawa will be seriously affected by ocean acidification in the near future. On the other hand, there is a possibility that a suitable environment for coral reefs around Okinawa can be maintained under a strict emission reduction.

5. Figure captions
(a) pCO_2 around Okinawa during 1982-2016 from SOCAT database. SST is shown in color. Black line indicates the deseasonalized trend of pCO_2.
(b) Ω_A around Okinawa during 1982-2016 calculated from pCO_2 and estimated TA. SST is shown in color. Black line indicates the deseasonalized trend of Ω_A.
(c) Projected Ω_A in the coast of northern Okinawa Island (26.8˚N, 128.1˚E) during 2015-2100.

Keywords: ocean acidification, coral reef, SOCAT database, Future prediction

©2019. Japan Geoscience Union. All Right Reserved.

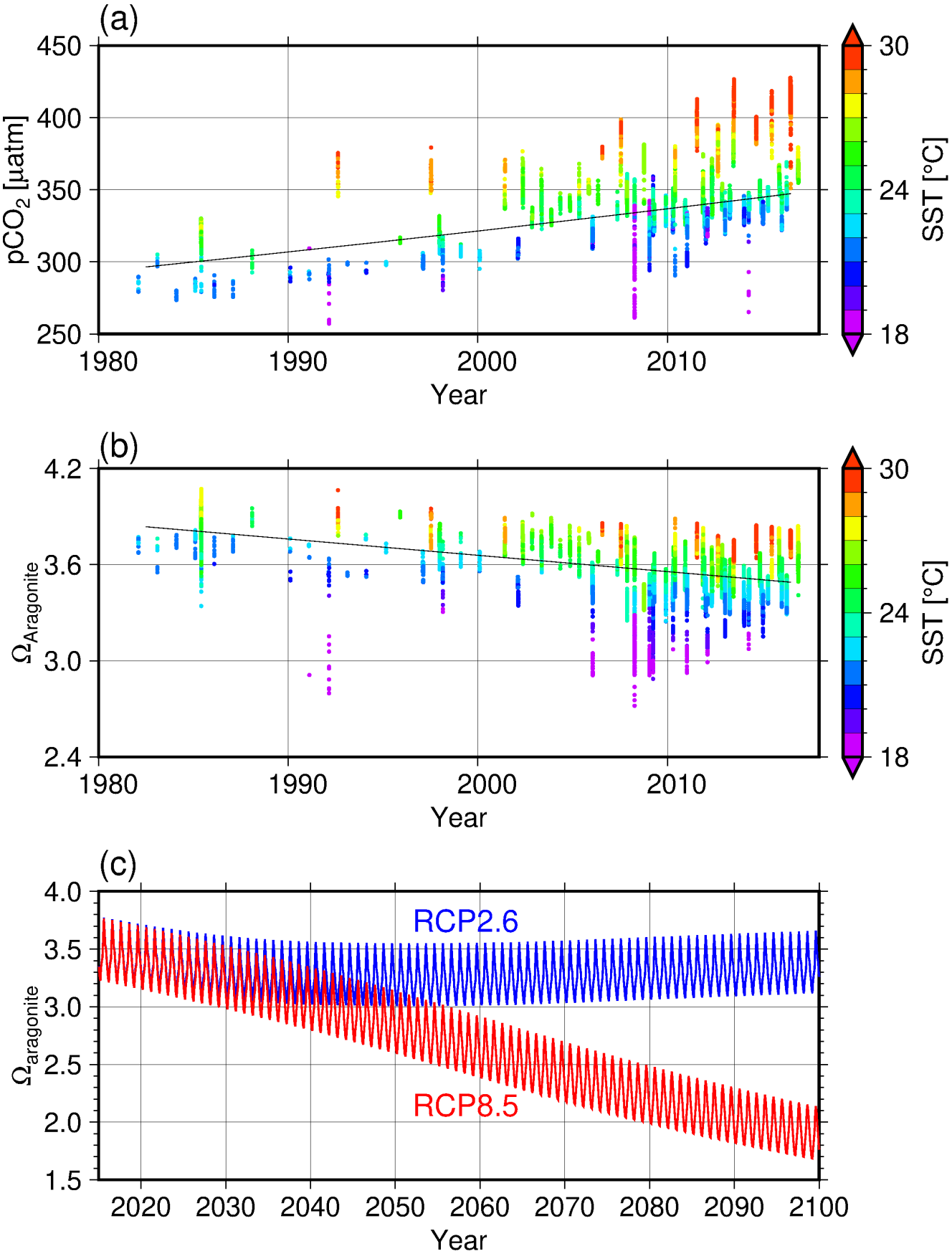

©2019. Japan Geoscience Union. All Right Reserved.

Reconstruction of spatiotemporal change of anthropogenic fixed nitrogen in the western North Pacific

*Yutaka Watanabe[1], Kouichi Fujita[1], BOFENG LI[1]

1. Hokkaido University

We constructed parameterizations for the estimation of ocean fixed nitrogen (N) in the western North Pacific. Parameterizations (N_p), determined as a function of temperature (T), potential density (sigma-theta) and dissolved oxygen (DO), provided strong correlations with direct measurements for ocean nitrogen (N_p = −2.24T −4.70sigma-theta −0.0970DO + 182.2; the coefficient of determination (r^2) = 0.988; the root mean square error (RMSE) = 1.25 umol kg^{-1}). Predicted N values were consistent with previous independent hydrographic observations, generally within the above error. By applying T, sigma-theta and DO time-series data from ship observations to our parameterization, large seasonal variations in N were demonstrated in detail. Using the parameterization technique along with the time series of observed N (N_{obs}) found the significant increasing rate of oceanic anthropogenic fixed nitrogen (N_{anth}) in the past four decades in the western North Pacific subtropical region.

Keywords: anthropogenic fixed nitrogen, western North Pacific, parameterization

©2019. Japan Geoscience Union. All Right Reserved.

On the mechanism of significant increasing trend of silicate in intermediate layer of Oyashio region

*Tsuneo Ono[1]

1. Fisheries Research and Education Agency

A large multi-decadal increasing trend of Silicate was found in the intermediate later of Oyashio region [Whitney et al., 2013]. The rate of silicate increase was significantly rather than those observed in other nutrients under the asamption of normal Redfield ratio, but mechanism of such large Si increase has long remaind unknown.
Here, I demonstrate that the observed silicate increase can be exprained by the facts that 1)Rapid warming of intermediate waters of Okhotsk Sea had deepen isopycnal surfaces and 2)this causes steep increase of silicate concentration in the water that mixes with Oyashio waters on a same density surface.

Keywords: long-term trend, silicate, Oyashio, Okhotsk Sea

©2019. Japan Geoscience Union. All Right Reserved.

Systematics of aluminum, manganese, iron, cobalt, and lead in the North Pacific Ocean observed during ocean-section study of GEOTRACES Japan

*Yoshiki Sohrin[1], Linjie Zheng[1]

1. Institute for Chemical Research, Kyoto University

Trace metals in seawater are critical parameters in oceanography as trace nutrients for organisms, tracers in the modern ocean, and proxies in paleoceanography [1]. The international study programme GEOTRACES based on intercalibrated methods is revealing global distributions and temporal variations of trace metals in the ocean (http://www.geotraces.org). We have developed a method for multielemental determination of Al, Mn, Fe, Co, Ni, Cu, Zn, Cd, and Pb in seawater using NOBIS Chelate-PA1 resin [2, 3], and revealed basin-scale and full-depth sectional distributions of the trace metals in the North Pacific during three GEOTRACES Japan cruises of R/V Hakuho Maru: a 160°W section during KH-05-2, a 165°E section (GP18) during KH-11-7, and a 47°N section (GP02) during KH-12-4. The elements showed different speciations and distributions. The fraction of labile particulate (lp) species was calculated as the difference between the total dissolvable (td) species and dissolved (d) species. The lpM/tdM ratio, where M refers to an element, is highest for Al, at 0.66 ±0.31 (average ±sd, *n*= 489), and lowest for Pb, at 0.02 ± 0.08 (*n*= 575). The distribution of each element is uniquely related to ocean circulation. We propose that the enrichment factor of dM, defined as *EF*(dM) = $(dM/dAl)_{seawater}/(M/Al)_{upper\ crust}$, where $(M/Al)_{upper\ crust}$ is the molar ratio in upper crustal abundance, can be a good parameter for the sources. As an example, the *EF*(dPb) found in this study is on the same order of magnitude as the *EF* values for aerosols found in the literature, suggesting that the deposition of aerosols is a major source for dPb. The lpFe dominates tdFe and is strongly correlated with lpAl: lpFe = 0.543 lpAl −0.12, r^2= 0.968, *n*= 510. The results also indicate that the dFe concentration corrected for lithogenic contribution improves the linear relationship with phosphate. Thus, we suggest that the mechanism controlling a scavenged element of Al significantly affects the biogeochemistry of Fe. Based on the concurrent observation of these metals, we confirm that the width of the boundary scavenging zone is approximately 500 km off the Aleutian shelf. We estimate an inventory of tdFe in the North Pacific as 1.1 ×10^{12}mol, and this is approximately four times that of dFe. The results emphasise the potential importance of lpFe in the ocean iron cycle.

1. Y. Sohrin and K. W. Bruland, Trends Anal. Chem., 2011, 30, 1291-1307.
2. Y. Sohrin, S. Urushihara, S. Nakatsuka, T. Kono, E. Higo, T. Minami, K. Norisuye and S. Umetani, Anal. Chem., 2008, 80, 6267-6273.
3. T. Minami, W. Konagaya, L. Zheng, S. Takano, M. Sasaki, R. Murata, Y. Nakaguchi and Y. Sohrin, Anal. Chim. Acta, 2015, 854, 183-190.

Keywords: trace metals, seawater, multielemental determination, GEOTRACES, North Pacific Ocean

©2019. Japan Geoscience Union. All Right Reserved.

[J] Oral | A (Atmospheric and Hydrospheric Sciences)：A-OS Ocean Sciences & Ocean Environment

Mon. May 27, 2019 9:00 AM - 10:30 AM JST | Mon. May 27, 2019 12:00 AM - 1:30 AM UTC | 301A 3F

[A-OS19] Dynamics of oceanic and atmospheric waves, vortices, and circulations

convener:Yuki Tanaka(Graduate School of Science, The University of Tokyo), Ryo Furue(APL/JAMSTEC), Yukiharu Hisaki(University of the Ryukyus), Norihiko Sugimoto(Keio University, Department of Physics), Chairperson:Norihiko Sugimoto, Ryo Furue

Oceanic and atmospheric dynamics aims at abstracting general principles from observed phenomena and constructing a system of mathematical models, thereby leading to the understanding, prediction, and parameterization of those phenomena. It provides perspectives for the advancement of sciences in various areas such as wind waves, swells, internal waves, Rossby waves, equatorial waves, tides, eddies, meandering of jets and fronts, general circulation, boundary layers, and ocean-atmosphere coupled modes. It has also been and will continue to be benefited by new uses of ideas and methods from such theories as resonance, nonlinear interaction, spectral analysis, probability, statistics, and dynamical systems. In this session, we solicit presentations on observational, experimental, numerical, and theoretical studies of oceanic and atmospheric dynamics and on exploratory use of new ideas and methods. We also welcome presentations on interdisciplinary studies in fields such as ecosystems, climate, and environment.

9:00 AM - 9:15 AM JST | 12:00 AM - 12:15 AM UTC

[AOS19-01] Instability of Ekman pumping

★Invited Papers

*Yoshiaki Miyamoto[1], Daivd S Nolan[2], Norihiko Sugimoto[3] (1.Faculty of Environment and Information Studies, Keio University, 2.Rosenstiel School of Marine and Atmospheric Science, University of Miami, 3.Keio University, Department of Physics)

9:15 AM - 9:30 AM JST | 12:15 AM - 12:30 AM UTC

[AOS19-02] Extratropical Cyclone Structures around Japan -Comparison between Extratropical Cyclones Developing around Japan and those in Northwestern Atlantic Ocean-

*Eigo Tochimoto[1], Hiroshi Niino[1] (1.Atmosphere and Ocean Research Institute, The University of Tokyo)

9:30 AM - 9:45 AM JST | 12:30 AM - 12:45 AM UTC

[AOS19-03] Application of a new wave energy flux formulation to assessment of tropical wave propagation dynamics: Diagnostics for the tropical synoptic-scale wave disturbances in the Maritime Continent-northern Australian region

*Fukutomi Yoshiki[1], Hidenori Aiki[1] (1.Institute for Space-Earth Environmental Reasearch, Nagoya University)

9:45 AM - 10:00 AM JST | 12:45 AM - 1:00 AM UTC

[AOS19-04] Direct measurement of turbulent fluxes at sea-air interface by micrometeorological technique

★Invited Papers

*Fumiyoshi Kondo[1], Shujiro Komiya[2], Kosuke Noborio[3], Hidenori Aiki[4], Kunio Kutsuwada[5], Mitsuo Uematsu[6], Osamu Tsukamoto[7] (1.Japan Coast Guard Academy, 2.Max Planck Institute for Biogeochemistry, 3.Meiji University, 4.Nagoya University , 5.Tokai University, 6.The University of Tokyo, 7.Okayama University)

10:00 AM - 10:15 AM JST | 1:00 AM - 1:15 AM UTC

[AOS19-05] Swell-Dominant Surface Waves Inherent in the Shape of the Rias Coast facing the western North Pacific

*Kosei Komatsu[1,2], Takaki Fujii[1,2], Kiyoshi Tanaka[2] (1.Graduate School of Frontier Sciences, The University of Tokyo, 2.Atmosphere and Ocean Research Institute, The University of Tokyo)

10:15 AM - 10:30 AM JST | 1:15 AM - 1:30 AM UTC

[AOS19-06] **Variabilities of the Sea Surface Height in the Kuril Basin of the Okhotsk Sea: Coherent shelf-trapped mode and Rossby wave-like mode**

*Vigan Mensah[1], Kay I. Ohshima[1] (1.Institute of Low Temperature Science)

Instability of Ekman pumping

*Yoshiaki Miyamoto[1], Daivd S Nolan[2], Norihiko Sugimoto[3]

1. Faculty of Environment and Information Studies, Keio University, 2. Rosenstiel School of Marine and Atmospheric Science, University of Miami, 3. Keio University, Department of Physics

This study derived Ekman pumping velocity without assuming that the velocity in the free atmosphere is not slow to be neglected and not homogeneous. Unlike the classic solution that is widely recognized, the solution can be unstable when the flow in the free atmosphere satisfies some conditions. The solution shows that the flow is more likely unstable when the velocity is fast and spatial variation of relative vorticity is large. One example that would be applied to Earth’ s atmosphere is secondary eyewall formation in tropical cyclone, which has been one of the hottest topics in typhoon research field in the last decades. The authors successfully showed the secondary eyewall formation in simulated cyclones is attributed to the Ekman pumping instability.

Keywords: Ekman pumping

©2019. Japan Geoscience Union. All Right Reserved.

Extratropical Cyclone Structures around Japan -Comparison between Extratropical Cyclones Developing around Japan and those in Northwestern Atlantic Ocean-

*Eigo Tochimoto[1], Hiroshi Niino[1]

1. Atmosphere and Ocean Research Institute, The University of Tokyo

Extratropical cyclones (ECs), which have horizontal scale of several thousands and time scale of a week, develop mainly in mid-latitude. They affect daily weather and sometimes cause extreme rainfall and severe winds, which result in meteorological disasters. ECs also affect climate variability: They interact with low-frequency variability such as North Atlantic oscillation. It is also pointed out that diabatic effects associated with ECs contribute to the initiation of atmospheric blocking.

Generally, there are two major conceptual model of ECs. The first model is Norwegian model, which was proposed in the beginning of 20 century. In this model, cold fronts catch up with warm fronts, and then occluded fronts form in the mature stage of ECs. The second model is Shapiro-Keyser model, which was proposed in 1990’s. In this model, an occluded front does not form, and bentback fronts extending rearward from the EC center develop. These two conceptual models are proposed mainly with the results of studies in the Northwestern Atlantic Ocean and Europe. Although the Northwestern Pacific is one of the major storm tracks, difference in EC structures between Northwestern Atlantic and Northwestern Pacific Oceans have not been well understood. In addition, a considerable number of ECs also passes over the Sea of Japan and Okhotsk Sea. Thus, the objective of our study is to clarify the differences in structures between ECs that develop around Japan and those develop in Atlantic Ocean

Firstly, ECs are automatically detected with the tracking method developed by Hodges (1994, 1995, 1999). Secondly, ECs that develop in Okhotsk Sea or the Sea of Japan (OJC), Northwestern Pacific (POC) and Northwestern Atlantic (AOC) were selected based on the locations where the ECs underwent the maximum deepening rate (in Bergeron; Sanders and Gyakum 1980). In the present study, only ECs with Bergeron larger than 0.5 are used to examine the structures of fully-developing ECs. In the composite analysis, physical variables are superposed with respect to the cyclone center. Furthermore, to examine differences in frontal characteristics between POCs and AOCs, atmospheric fronts are objectively detected with a method using thermal front parameter (e.g., Schemm et al. 2015).

The composite analysis shows clear differences in structures between OJCs, POCs and AOCs: OJCs have relatively strong cold fronts compared to warm fronts at KT, especially in Spring. On the other hand, both warm and cold fronts develop well for POCs and AOCs. Differences in frontal characteristics between POCs and AOCs are most notable in warm fronts. Warm fronts for AOCs tend to extend eastward or east-northeastward from the EC center, while those for POCs southeastward. It is also noted that bentback fronts for AOCs are stronger than those for POCs.

An analysis using a frontogenesis function shows that this difference in warm front is mainly due to the effect of shear deformation: the shear deformation in the southeast quadrant of POCs is larger than that of AOCs, resulting in development of the warm fronts in the southeast quadrant of the EC center for POCs, which are most notable in warm fronts.

©2019. Japan Geoscience Union. All Right Reserved.

Keywords: Extratropical cyclones, Front, Jetstream

©2019. Japan Geoscience Union. All Right Reserved.

Application of a new wave energy flux formulation to assessment of tropical wave propagation dynamics: Diagnostics for the tropical synoptic-scale wave disturbances in the Maritime Continent-northern Australian region

*Fukutomi Yoshiki[1], Hidenori Aiki[1]

1. Institute for Space-Earth Environmental Reasearch, Nagoya University

A two-dimensional (horizontal) wave energy flux (WEF) formulation derived by Aiki et al. (2017, PEPS) is used to diagnose the dynamics of the tropical synoptic-scale waves (TSWs) propagating across the Maritime Continent and northern Australian (MCNA) region. The new WEF vectors are considered to be useful to assess energy dispersion characteristics of various types of waves in both the tropics and extratropics. The WEF is defined by adding a rotational flux term that includes Ertel potential vorticity (EPV)-based flow to the eddy geopotential flux. We computed eddy components of EPV-based stream function and corresponding wind fields from the atmospheric reanalysis (JRA-55) data using a numerical inversion technique to estimate the additional rotational flux term. The TSWs analyzed in this study have periods of about 2-8 days and zonal wavelengths of about 3000-4000 km (Fukutomi 2018, submitted to JGR). These waves propagate westward at approximately 8 m/s along the mean monsoon westerly flow extending from the Indian Ocean to the western Pacific. Wave troughs and ridges form a well-organized wave train in the MCNA region. Eastward amplification of wave troughs and ridges due to group propagation occurs along the monsoon westerly flow. WEF diagnostics confirm that wave energy propagation facilitates the downstream development of the synoptic-scale wave train and the mean monsoon westerly flow acts as a tropical waveguide. Distribution and behavior of the WEF vectors are compared with those of traditional wave activity and energy flux vectors. Applicability of this new tool to other types of the tropical waves and extratropical waves is also discussed.

Keywords: Tropical wave disturbances, Wave energy flux, Wave enegy dispersion

©2019. Japan Geoscience Union. All Right Reserved.

Direct measurement of turbulent fluxes at sea-air interface by micrometeorological technique

*Fumiyoshi Kondo[1], Shujiro Komiya[2], Kosuke Noborio[3], Hidenori Aiki[4], Kunio Kutsuwada[5], Mitsuo Uematsu[6], Osamu Tsukamoto[7]

1. Japan Coast Guard Academy, 2. Max Planck Institute for Biogeochemistry, 3. Meiji University, 4. Nagoya University , 5. Tokai University, 6. The University of Tokyo, 7. Okayama University

Accurate parameterizations of sea–air momentum, sensible and latent heats, trace gases (e.g. greenhouse gases including CO_2 and CH_4), and aerosol fluxes are important in sea–air interaction. Coupled ocean–atmosphere global climate models require high accuracy of the net surface heat flux for the prediction of climate change, and process–based understanding of particle formation from bubble bursting to realistically predict the climate effect of marine aerosols. Precise measurements of the CO_2 gas transfer across the air–sea interface provide a better understanding of the global carbon cycle. The eddy covariance technique is the definitive method to directly determine these sea–air fluxes, but it requires measurements of the vertical and downwind components of air velocity, air temperature, humidity, trace gases, and aerosol over a sufficiently long averaging period (> 30 min) and with sufficient frequency response (< 10 Hz). One of the greatest difficulties in measuring sea–air flux by the eddy covariance technique over the open ocean is the apparent wind velocity caused by the wave–induced platform motion. As a result, the uncorrected eddy covariance results are all strongly biased, and especially represent unrealistic momentum fluxes. Improved ship motion correction scheme with Kalman filter results in a significant reduction in both the bias and the scatter of momentum fluxes. Previous studies over the oceans have shown that the eddy covariance CO_2 flux was larger than the bulk CO_2 flux estimated by the mass balance technique. Our results suggest that the density correction due to the air pressure fluctuation, which is assumed to be negligible in the WPL correction, is required to evaluate the accurate eddy covariance CO_2 flux over the ocean.

Keywords: air-sea flux, air-sea interaction, eddy covariance technique

©2019. Japan Geoscience Union. All Right Reserved.

Swell-Dominant Surface Waves Inherent in the Shape of the Rias Coast facing the western North Pacific

*Kosei Komatsu[1,2], Takaki Fujii[1,2], Kiyoshi Tanaka[2]

1. Graduate School of Frontier Sciences, The University of Tokyo, 2. Atmosphere and Ocean Research Institute, The University of Tokyo

Real-time monitoring of wind and surface waves in Otsuchi Bay, a ria located in the northeastern portion of Japan, had been continued over four years since October 2012, using a mooring buoy with an ultrasonic anemometer and a single-mode GPS wave sensor. The monitoring revealed that waves in the bay were dominated by swells propagated from the northeastern offshore region in all seasons. Time-lag correlation coefficient between the significant wave height in the bay and the offshore wind velocity component blowing in the direction to the bay was maximized in the region approximately 300 km northeast of the bay, from which waves developed by the local wind are accessible within the corresponding time-lag to the bay at a speed of the group velocity of the swell observed in the bay. As an interesting feature common to swell-dominant waves observed in the rias bays adjacent to Otsuchi Bay, the region of the significant correlation between the wave height and the offshore wind velocity extends to the direction that faces the bay mouth. It implies that the source region of the swell depends heavily on the coastal shape of the bay. Consequently, the relation between the offshore wind field and the decay-rate of the swells propagating to Otsuchi Bay indicates that the source region of the swell influential in the bay is located in the offshore region several hundreds of kilometers northeast of the bay, which is on the typical migration route of high and low pressures in the Northern temperate zone.

Keywords: swell, surface wave, rias coast, offshore surface wind, coastal shape

©2019. Japan Geoscience Union. All Right Reserved.

Variabilities of the Sea Surface Height in the Kuril Basin of the Okhotsk Sea: Coherent shelf-trapped mode and Rossby wave-like mode

*Vigan Mensah[1], Kay I. Ohshima[1]

1. Institute of Low Temperature Science

Time series analysis of Sea Surface Height anomaly (SSHa) is conducted in the Kuril Basin of the Sea of Okhotsk. The mapping methodology of the satellite-derived SSHa data is optimized to mitigate the effects of sea ice on the SSHa field during winter and the early spring. In particular, we found that conducting an objective mapping of along-track SSHa data with correlation length and time scales adapted to the Kuril Basin considerably reduces the number of missing data days in this region. A Complex Empirical Orthogonal Functions (CEOF) is then used to analyze the SSHa field, and the first 3 modes, representing 54 % of the total variability are delineated here. The focus is brought on the first and third modes. The first mode mainly represents the coherent variability trapped over the shelves all along the coast and Kuril Islands. Both seasonal (high over the shelves in winter) and interannual variations are strongly correlated with the alongshore wind stress. These variations can be well explained by the arrested topographic waves. The third mode is a propagating mode, with trains of southwestward propagating anomalies. Their characteristics are consistent with those of westward propagating Rossby waves, whose energy propagates from the Kuril Straits towards the Kuril Basin.

Keywords: Okhotsk Sea, SSHa, Circulation, Interannual variability, Dynamics, Rossby Waves

©2019. Japan Geoscience Union. All Right Reserved.

[J] Oral | A (Atmospheric and Hydrospheric Sciences)：A-OS Ocean Sciences & Ocean Environment

Mon. May 27, 2019 10:45 AM - 12:15 PM JST | Mon. May 27, 2019 1:45 AM - 3:15 AM UTC | 301A 3F

[A-OS19] Dynamics of oceanic and atmospheric waves, vortices, and circulations

convener:Yuki Tanaka(Graduate School of Science, The University of Tokyo), Ryo Furue(APL/JAMSTEC), Yukiharu Hisaki(University of the Ryukyus), Norihiko Sugimoto(Keio University, Department of Physics), Chairperson:Yukiharu Hisaki(琉球大学理学部), Hidenori AIKI

Oceanic and atmospheric dynamics aims at abstracting general principles from observed phenomena and constructing a system of mathematical models, thereby leading to the understanding, prediction, and parameterization of those phenomena. It provides perspectives for the advancement of sciences in various areas such as wind waves, swells, internal waves, Rossby waves, equatorial waves, tides, eddies, meandering of jets and fronts, general circulation, boundary layers, and ocean-atmosphere coupled modes. It has also been and will continue to be benefited by new uses of ideas and methods from such theories as resonance, nonlinear interaction, spectral analysis, probability, statistics, and dynamical systems. In this session, we solicit presentations on observational, experimental, numerical, and theoretical studies of oceanic and atmospheric dynamics and on exploratory use of new ideas and methods. We also welcome presentations on interdisciplinary studies in fields such as ecosystems, climate, and environment.

10:45 AM - 11:00 AM JST | 1:45 AM - 2:00 AM UTC

[AOS19-07] Dynamics of water exchange processes at a deep submarine canyon off the western coast of the Sakhaline which causes the origin of the cold water belt along the Soya Warm Current

★Invited Papers

*Humio Mitsudera[1], Hiroyuki Iida[2] (1.Institute of Low Temperature Science, Hokkaido University, 2.Graduate School of Environmental Science)

11:00 AM - 11:15 AM JST | 2:00 AM - 2:15 AM UTC

[AOS19-08] Generation Mechanism of Tropical Instability Waves in the Equatorial Pacific Ocean

*Yuki Tanaka[1], Toshiyuki Hibiya[1] (1.Graduate School of Science, The University of Tokyo)

11:15 AM - 11:30 AM JST | 2:15 AM - 2:30 AM UTC

[AOS19-09] Annual Rossby waves below the pycnocline in the Indian Ocean

*Motoki Nagura[1] (1.Japan Agency for Marine-Earth Science and Technology)

11:30 AM - 11:45 AM JST | 2:30 AM - 2:45 AM UTC

[AOS19-10] Eddies observed by Argo floats

★Invited Papers

*Katsuro Katsumata[1] (1.JAMSTEC)

11:45 AM - 12:00 PM JST | 2:45 AM - 3:00 AM UTC

[AOS19-11] Rhythmic Phenomena in Nonlinear Systems and Oceanic General Circulation

*Shinya Shimokawa[1], Tomonori Matsuura[2] (1.National Research Institute for Earth Science and Disaster Prevention, 2.University of Toyama)

12:00 PM - 12:15 PM JST | 3:00 AM - 3:15 AM UTC

[AOS19-12] Control of the ocean circulation by bottom topography and generation of mesoscale disturbances

*Yuri Kase[1], Tomonori Matsuura[1] (1.National university corporation University of Toyama)

Dynamics of water exchange processes at a deep submarine canyon off the western coast of the Sakhaline which causes the origin of the cold water belt along the Soya Warm Current

*Humio Mitsudera[1], Hiroyuki Iida[2]

1. Institute of Low Temperature Science, Hokkaido University, 2. Graduate School of Environmental Science

A cold water belt (CWB) is observed off the Soya Warm Current, the former of which appears from the west coast of the Sakhaline Island. Observations of the CWB (Kuma et al., 2016; Iida et al., 2018) indicates that the CWB, characterized by a cold and saline water (temperature 7℃, and salinity 34.0), is derived from the lower part of the thermocline in the Japan Sea basin. This implies that the cold and saline water in the Japan Sea basin should overcome the shelf break, which is not easy in general, and be transported to the vicinity of the coast of Sakhaline. The aim of this study is to elucidate mechanisms of water exchange between the Japan Sea basin (continental slope) and the continental shelf.

We first analyzed the output of a general circulation model OFES with the 1/30° resolution. It was found that the water over the continental slope enters the continental slope at a deep submarine canyon off the Kholmsk city on the west coast of the Sakhaline. Further, a barotropic model using Princeton Ocean Model (POM) with a realistic topography shows the exchange at the canyon in a similar manner to OFES, even though water exchange would not readily occur at the shelf break because of a potential vorticity (PV) barrier. We thus conducted numerical experiments using idealized topographic features mimicing the canyon off the Kholmsk in order to understand the barotropic exchange processes. The throughflow across the Soya Strait occurs owing to the adjustment of sea level difference between the Japan Sea and the Sea of Okhotsk by long shelf waves. It was found that the shelf waves are scattered into the second and third mode waves at the canyon, which have large transport over the continental slope; the scattered flow over the continental slope directed southward, and enters the continental shelf at the canyon. Further, nonlinearity is important in the vicinity of the canyon during the scattering process. Specifically: 1) nonlinearity produces a wave guide across the shelf break overcoming the PV barrier, by bringing low PV water from the continental slope to the continental shelf; 2) High-order mode waves (higher than 4^{th} mode) are retarded from propagation because of the background flow caused by 1^{st} -3^{rd} modes, making the flow over the continental slope steady. The nonlinear steady flow over the slope upwells at the canyon and connects to the flow over the shelf, and consequently flows through the strait.

Finally. hydrographic data during 1960-1985, archived at the Japan Hydrographic Data Center, was analyzed. Potential temperature and salinity from July to October was used. It was confirmed that the upwelling occurs at the canyon off the Kholmsk.

Keywords: water exchange across the shelf break, continental shelf wave, submarine canyon, cold water belt along the Soya Warm Current

©2019. Japan Geoscience Union. All Right Reserved.

Generation Mechanism of Tropical Instability Waves in the Equatorial Pacific Ocean

*Yuki Tanaka[1], Toshiyuki Hibiya[1]

1. Graduate School of Science, The University of Tokyo

Tropical instability waves (TIWs) are prominent features observed in the eastern to central equatorial Pacific, which typically have a wavelength of ~1000 km and a period of ~25 days, propagating westward at a speed of ~0.5 m/s. Although TIWs are thought to be generated by meridional shear between the westward-flowing South Equatorial Current (SEC) and the eastward-flowing North Equatorial Countercurrent (NECC), the decisive parameter responsible for the occurrence of the instability has not yet been fully understood. Because the meridional and vertical momentum and heat transfer by TIWs are essential to drive the equatorial ocean circulation and affect the air-sea interactions related to the global climate, a better understanding of the generation mechanism of the TIWs is prerequisite for improving models' capability to predict climate variations.

In this study, we show that a linear stability analysis using a 1.5-layer shallow water model with a zonal mean flow on the equatorial beta plane can successfully predict an unstable mode whose phase speed and meridional structure are both very similar to those of the TIWs simulated in an eddy-resolving ocean general circulation model (OGCM), although the wavelength and the growth rate are somewhat larger and smaller, respectively. This unstable mode can be interpreted as resulting from a coupling between a Rossby wave propagating eastward in the negative potential vorticity (PV) gradient just north of the equator (~1°–3.5°N) while advected westward by the SEC, and a Rossby wave propagating westward in the positive PV gradient further north (~3.5°–8°N) while weakly advected eastward by the NECC. The unstable mode tends to have smaller growth rate as the negative PV gradient becomes weaker, and even disappears when it is completely absent.

The negative PV gradient just north of the equator thus plays an essential role in forming the unstable mode. Actually, the seasonal and interannual variability of the TIWs simulated in the OGCM is shown to be significantly controlled by the strength of the negative PV gradient, suggesting the possibility that it can serve as a key parameter for a dynamically based parameterization of the heat and momentum transfer associated with TIWs in coarse-resolution OGCMs.

Keywords: Tropical Instability Wave, Equatorial Pacific Ocean, Potential Vorticity Gradient, Rossby Wave, 1.5-Layer Shallow Water Model, Linear Stability Analysis

©2019. Japan Geoscience Union. All Right Reserved.

Annual Rossby waves below the pycnocline in the Indian Ocean

*Motoki Nagura[1]

1. Japan Agency for Marine-Earth Science and Technology

In-situ observations in the Indian Ocean had long been limited to sporadic ship observations, which hampered the progress of observational research of basin-wide circulation and variability. The implementation of Argo profiling float program since 2004 dramatically improved this situation, and now abundant in-situ observations obtained from Argo floats are available. This study uses the resulting temperature and salinity observations between the sea surface and 2000 m depth and float trajectories at 1000 m depth to examine annual variability in pressure and horizontal velocity. Annual variability below the pycnocline is large in amplitude in the Arabian Sea and between 10˚S and 20˚S in the South Indian Ocean. Wavenumbers were estimated by fitting a straight line to annual harmonic phase. Results showed that vertical wavenumber tends to decrease poleward in both hemispheres, and vertical wavelength is more than tripled from about 5,000 m at 5˚N/S to 16,000 m at 20˚N/S. The inverse radius of deformation squared (defined as f^2m^2/N^2) does not show clear dependence on latitude, because poleward increase in the magnitude of the Coriolis parameter (f) compensates for poleward decrease in vertical wavenumber (m), and Brunt-Väisälä frequency (N) varies little meridionally in the analysis domain. According to the dispersion relation of linear, quasi-geostrophic Rossby waves at a rest state, these meridional structures in m and deformation radius result in steeper angle of ray trajectory at a higher latitude in the longitude-depth plane. Energy estimated from in situ observations shows a consistent pattern with this expectation. The line of constant phase of annual pressure harmonic is steeper in angle at higher latitudes, which is also expected from the uniform deformation radius and constant N. This result indicates that energy penetrates deeper at higher latitudes.

Keywords: Indian Ocean, mid-depth, Linear, quasi-geostrophic Rossby waves

©2019. Japan Geoscience Union. All Right Reserved.

Eddies observed by Argo floats

*Katsuro Katsumata[1]

1. JAMSTEC

Eddies play an important role in the oceanic general circulation theory, specifically its meridional overturning component. Due to the limited spatial extent, however, synoptic observation of the eddy field has been difficult and its quantitative arguments have depended mostly on numerical simulation outputs. Argo floats, which revolutionalised phycical oceanographic observations, demonstrate their capability in the eddy observation (albeit at limited depths).
Under the Temporal Residual Mean framework, the most natural coordinate system for ocean circulation theories, we estimated the eddy transport above the mean 1000 dbar surface by using the hydrographic and drift velocity data from Argo floats. Eddy transport is strong in the western boundaries and in the Southern Ocean. In the midlatitude oceans, it is weaker and equatorwords. In the southern part of the Antarctic Circumpolar Current (ACC), it is larger than 10 Sv poleward.
In the Southern Ocean, we can discuss the vertical transport of zonal momentum input by the westerly wind and responses of the ACC to variable wind localised to topographic features.

Keywords: Eddy, Southern Ocean

©2019. Japan Geoscience Union. All Right Reserved.

Rhythmic Phenomena in Nonlinear Systems and Oceanic General Circulation

*Shinya Shimokawa[1], Tomonori Matsuura[2]

1. National Research Institute for Earth Science and Disaster Prevention, 2. University of Toyama

Various oscillation phenomena such as transition between meander and non- meander paths of western boundary current such as the Kuroshio exist in the oceanic general circulation. These phenomena can be related to nonlinear rhythmic phenomena such as synchronization, stochastic resonance and stochastic synchronization. Synchronization 1) is a phenomenon for an adjustment of rhythms of two or more self-sustained oscillating systems, which have different periods. Stochastic resonance 2) is a phenomenon in which a kind of noise amplifies and elicits weak signals under detection thresholds. Both phenomena are observed in various nonlinear systems such as climate system, living system, and electric circuits. Also, the coupling of both phenomena was found and is called stochastic synchronization 3).

Thus, we investigate the responses of oceanic double-gyre to external wind forcing with and without noise using a 1.5 layer quasi-geostrophic model, and considered the possible role of nonlinear rhythmic phenomena in oceanic general circulation 4)-7). The variable parameter is the amplitude of external seasonal forcing, α, the amplitude of red noise, ε, and the Reynolds number, Re.

Synchronization at two times the period of the forcing occurs at a parameter range of α and Re without noise (ε =0). For cases with adequate (not too weak and not too strong) noise, potential signals in the system appear at the front as actual signals (i.e., stochastic resonance) such as intermittent large variations in energy. Also, by adding red noise to external forcing, synchronization (i.e., stochastic synchronization) occurs when the amplitude of external forcing is smaller than that in the case without noise. These results suggest that potential signals in the system are amplified and appear as stochastic resonance or synchronization in relation to the added noise.

References:

1) Kuramoto, Y., “Chemical Oscillations, Waves, and Turbulence”, (Springer, 1984), p.156.

2) Benzi, R., A. Sutera and A. Vulpiani, “The Mechanism of Stochastic Resonance”, J. Phys., Vol.14A (1981), pp.L453-L457.

3) Fukuda, H., H. Nagano, and S. Kai, “Stochastic Synchronization in Two-Dimensional Coupled Lattice Oscillators in the Belousov–Zhabotinsky Reaction”, J. Phys. Soc. Jpn., Vol.72 (2003), pp.487-490.

4) Shimokawa, S. and T. Matsuura, “Chaotic Behaviors in the Response of Q-G Oceanic Double-Gyre to Seasonal External Forcing”, J. Phys. Oceanogr., Vol.40 (2010), pp.1458-1472.

5) Shimokawa, S., K. Shiratori, and T. Matsuura, “Responses of Oceanic Double-Gyre to External Wind Forcing with Noise”, Theor. Appl. Mech. Jpn., Vol.62 (2014), pp.49-57.

©2019. Japan Geoscience Union. All Right Reserved.

6) Shimokawa, S. and T. Matsuura, “Stochastic Synchronization in an Oceanic Double Gyre”, Theor. Appl. Mech. Jpn., Vol.63 (2015), pp.99-107.

7) Shimokawa, S and T. Matsuura, “Chaos excitation and stochastic synchronization in an oceanic double gyre”, Theor. Appl. Mech. Jpn., Vol. 64 (2018), pp. 15-22.

Keywords: Oceanic general circulation, Nonlinear systems, Synchronization, Stochastic resonance, Stochastic synchronization

©2019. Japan Geoscience Union. All Right Reserved.

Control of the ocean circulation by bottom topography and generation of mesoscale disturbances

*Yuri Kase[1], Tomonori Matsuura[1]

1. National university corporation University of Toyama

One of the representative ocean current in the North Pacific is the Kuroshio. The Kuroshio which is the western boundary current of the North Pacific subtropical gyre leaves off the coast of Choshi, Chiba Prefecture, and it will be the eastward Kuroshio extension. At about 160° E, the Kuroshio-extension current encounters the Shatsky rise extending north and south, and fluctuation of flow path and generation of mesoscale disturbances due to flow-topography interaction is seen around this topography. We study the mechanism of phenomena as geophysical fluid dynamics in the North Pacific, mainly generation of mesoscale disturbances due to flow-topography interaction in rotating stratified fluid, by modeling which is target of the North Pacific.

We simulated four cases with different ocean bottom topography using the eddy resolving 3-layer QG model (Hogg et al., 2010) based on the quasi-geostrophic vorticity equation for the generation of the mesoscale disturbances accompanied the main flow path variation.

In Figure 1, the strong flow in each case is seen near the west-coast and mid-latitudes, and in case 1 where no topography is given, the most noticeable double gyre and the zonal strong flow as the gyre's front are seen. It can be inferred that this double gyre corresponds to the North Pacific subtropical gyre / subpolar gyre, and the flow on the front corresponds to the Kuroshio extension because we give the wind stress corresponding to the North Pacific about this time. On the other hand, in case 2, 3, and 4, which topography is given in each case, the strong flow near the mid-latitude is obstructed or meandered depending on the topography, and there is the long-lived eddy as an anticyclonic eddy over the topography. Especially, paying attention to the meandering flow behind the topography, and comparing case 3 and case 4, we can see that the addition of "corn" to "kamaboko" strengthens the flow of two wavelengths behind "kamaboko" (in case 4 of Figure 1).

Figure 2 shows the spatial patterns of the 10 years mean values of the squared disturbances of the potential vorticity in layer 1. The higher value area has the stronger and finer mesoscale disturbances. The development of the mesoscale disturbances in each case is seen at the west-coast, the mid-latitude area and the area surrounding the topography, corresponding to the strong flow as seen in Figure 1. In addition, when comparing case 3 and case 4, the addition of "corn" to "kamaboko" strengthens the meandering flow which has two wavelengths behind "kamaboko" (in case 4 of Figure 1), and the mesoscale disturbances are developed along the flow (in case 4 of Figure 2). From these results, it is suggested that the baroclinic instability is strengthened around the topography. We think the mechanism as described later; flow is disturbed by the influence of the topography, and the interface (of two layers) height anomaly increases, so the potential energy becomes large (strengthened baroclinic instability), and then the enlarged potential energy is released as kinetic energy (resolution of the baroclinic instability), and the mesoscale disturbances develop. It was suggested that how to change the flow and the degree of strengthened its baroclinic instability depend on the shape, arrangement and combination of the topography. And it was found that the bottom topography plays an important role in the generation of mesoscale disturbances.

©2019. Japan Geoscience Union. All Right Reserved.

Hereafter, by modeling which is given “kamaboko”, “corn” as a bottom topography imitating the Izu Ridge and the Shatsky rise (Tam massif) in the North Pacific, respectively, and simulating in some cases which have defferent positions (latitude / longitude) and heights of the topography, we presume that it is possible to realize the application of the mechanism of phenomena from the simulation results to the real phenomena.

Keywords: mesoscale disturbance, bottom topography, western boundary current, Kuroshio, Kuroshio extension

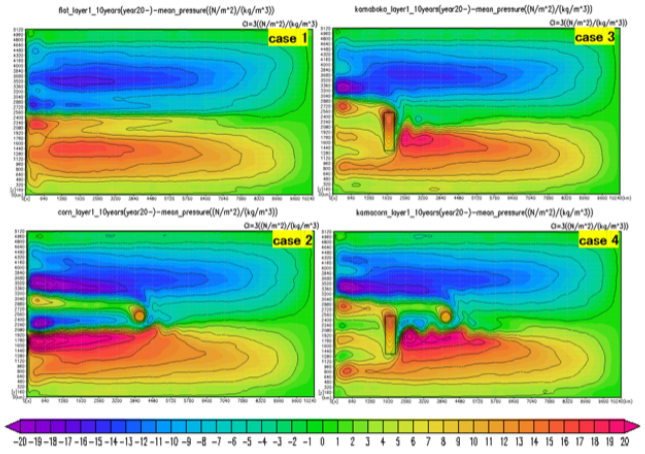

Figure 1: the four cases' spatial patterns of the 10 years mean values of the pressure in layer 1 ($\overline{p_1}(10)$) (superimposed the horizontal section of the bottom topography in each case)

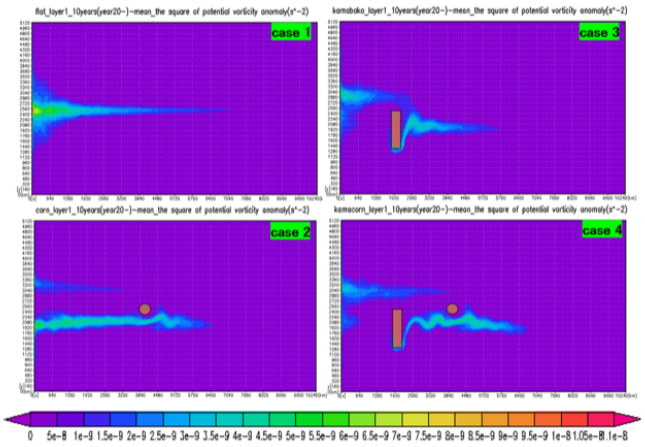

Figure 2: the four cases' spatial patterns of the 10 years mean values of the squared disturbances of the potential vorticity in layer 1 ($\overline{(q_1')^2}(10)$) (superimposed the horizontal section of the bottom topography in each case)

©2019. Japan Geoscience Union. All Right Reserved.

[J] Poster | A (Atmospheric and Hydrospheric Sciences)：A-OS Ocean Sciences & Ocean Environment

Mon. May 27, 2019 3:30 PM - 5:00 PM JST | Mon. May 27, 2019 6:30 AM - 8:00 AM UTC | Poster Hall International Exhibition Hall8, Makuhari Messe_5

[A-OS19] Dynamics of oceanic and atmospheric waves, vortices, and circulations

convener:Yuki Tanaka(Graduate School of Science, The University of Tokyo), Ryo Furue(APL/JAMSTEC), Yukiharu Hisaki(University of the Ryukyus), Norihiko Sugimoto(Keio University, Department of Physics)

Oceanic and atmospheric dynamics aims at abstracting general principles from observed phenomena and constructing a system of mathematical models, thereby leading to the understanding, prediction, and parameterization of those phenomena. It provides perspectives for the advancement of sciences in various areas such as wind waves, swells, internal waves, Rossby waves, equatorial waves, tides, eddies, meandering of jets and fronts, general circulation, boundary layers, and ocean-atmosphere coupled modes. It has also been and will continue to be benefited by new uses of ideas and methods from such theories as resonance, nonlinear interaction, spectral analysis, probability, statistics, and dynamical systems. In this session, we solicit presentations on observational, experimental, numerical, and theoretical studies of oceanic and atmospheric dynamics and on exploratory use of new ideas and methods. We also welcome presentations on interdisciplinary studies in fields such as ecosystems, climate, and environment.

[AOS19-P01] Atmospheric super rotation developed in a GCM (AFES-Venus)

*Norihiko Sugimoto[1], Masahiro Takagi[2], Yoshihisa Matsuda[3] (1.Keio University, Department of Physics, 2.Kyoto Sangyo University, Department of Physics, 3.Tokyo Gakugei University, Department of Natural Sciences)

[AOS19-P02] Data assimilation of the Venus atmosphere assuming radio occultation measurement by small satellites

*Mirai Abe[1], Norihiko Sugimoto[1], Yukako Kikuchi[2], Asako Hosono[3], Hiroki Ando[4], Masahiro Takagi[4], Itziar Garate Lopez[5], Sebastien Lebonnois[6], Chi Ao[7] (1.Keio University, 2.Yokohama Futaba High School, 3.Toshimagaoka Women High School, 4.Kyoto Sangyo University, 5.Euskal Herriko Unibertsitatea, 6.Sorbonne Universite, 7.Jet Propulsion Laboratory)

[AOS19-P03] Relationship between solar wind and atmospheric circulation

*Paul Prikryl[1] (1.Physics Department University of New Brunswick and Geomagnetic Laboratory Natural Resources Canada)

[AOS19-P04] Contribution of the Atlantic storm track to the Euro-Russian blocking maintenance in summer 2010

*Akira Yamazaki[1] (1.Application Laboratory, Japan Agency for Marine-Earth Science and Technology)

[AOS19-P05] Instabilities in Ekman layer and roll structures in a tropical cyclone boundary layer

*Junshi Ito[1], Hiroshi Niino[1] (1.Atmosphere and Ocean Research Institute, The University of Tokyo)

[AOS19-P06] Mathematical description of the internal waves in a proximity of the bottom of the Ocean.

*andrei giniatoulline[1], german tobar[1] (1.Department of Mathematics, Los Andes University, Bogota, Colombia, South America)

[AOS19-P07] How deterministic are the deep zonal jets?

*Ryo Furue[1], Masami Nonaka[1], Hideharu Sasaki[1] (1.APL/JAMSTEC)

[AOS19-P08] The impact of tidal mixing on the Indonesian Throughflow

*Kohki Shiroyama[1], Shinichiro Kida[2], Hideharu Sasaki[3], Ryo Furue[3] (1.Interdisciplinary Graduate School of Engineering Sciences, Kyushu University, 2.Research Institute for Applied Mechanics Kyushu University, 3.JAMSTEC. APL)

[AOS19-P09] **Verification for subsurface oceanic structure in OFES outputs driven by different wind data sets (NCEP/NCAR and QSCAT)in the tropical Pacific Ocean**

*Hiroshige Fukunaga[1], Kunio Kutsuwada[1], Akira Kakiuchi[1], Yuma Yanagida[1], Hideharu Sasaki[2], Yoshikazu Sasai[2] (1.Tokai University, 2.JAMSTEC)

[AOS19-P10] Inter-comparison of ocean wave data from drifting buoys, moored GPS buoys and reanalysis data

*Yukiharu Hisaki[1] (1.University of the Ryukyus)

[AOS19-P11] Merge and Separation of ocean eddies around the Kuroshio Extension

*koutarou matsuhashi[1], Kazuyuki Uehara[1] (1.The Graduate School of Marine Science Technology)

[AOS19-P12] Influence of eddy-trapped water mass reaching 137E survey line using OGCM and a particle-tracking method

★Invited Papers

*Hideyuki Nakano[1], Hiroyuki Tsujino[1], Kei Sakamoto[1], Shogo Urakawa[1], Takahiro Toyoda[1], Goro Yamanaka[1], Yoshimasa Matsumura[2] (1.Meteorological Research Institute, 2.Atmosphere and ocean research Institute, the University of Tokyo)

[AOS19-P13] A study on the variability of the deep ocean circulation during glacial climate with a climate model of intermediate complexity

*Taigo Ando[1], Akira Oka[1] (1.Atmosphere and Ocean Research Institute, University of Tokyo)

Atmospheric super rotation developed in a GCM (AFES-Venus)

*Norihiko Sugimoto[1], Masahiro Takagi[2], Yoshihisa Matsuda[3]

1. Keio University, Department of Physics, 2. Kyoto Sangyo University, Department of Physics, 3. Tokyo Gakugei University, Department of Natural Sciences

The generation mechanism of the atmospheric super rotation on Venus is one of the most important topics in the Earth and planetary sciences. Here we reproduced the fully developed super-rotation for the first time in a Venus general circulation model (GCM) driven by a zonally-averaged component of the *realistic* solar heating only. Our GCM enables us to perform long term simulations with medium resolution higher than those used in previous studies. It is newly found that mean meridional circulation driven by the *realistic* solar heating can generate the fully developed super-rotation of ~100 m s^{-1} with the vertical eddy viscosity smaller than 0.02 m^2 s^{-1} (see below Figure). Existence of the range of the vertical eddy viscosity in which the fast super-rotation can be generated by the reasonable solar heating has broad implications for the atmospheric sciences in light of optimal parameters for the GCMs.

Fully developed super-rotation driven by the mean meridional circulation in a Venus GCM, Norihiko Sugimoto, Masahiro Takagi, and Yoshihisa Matsuda, *Geophysical Research Letters*, (2019), doi.org/10.1029/2018GL080917.

Keywords: General circulation, Super rotation, Venus

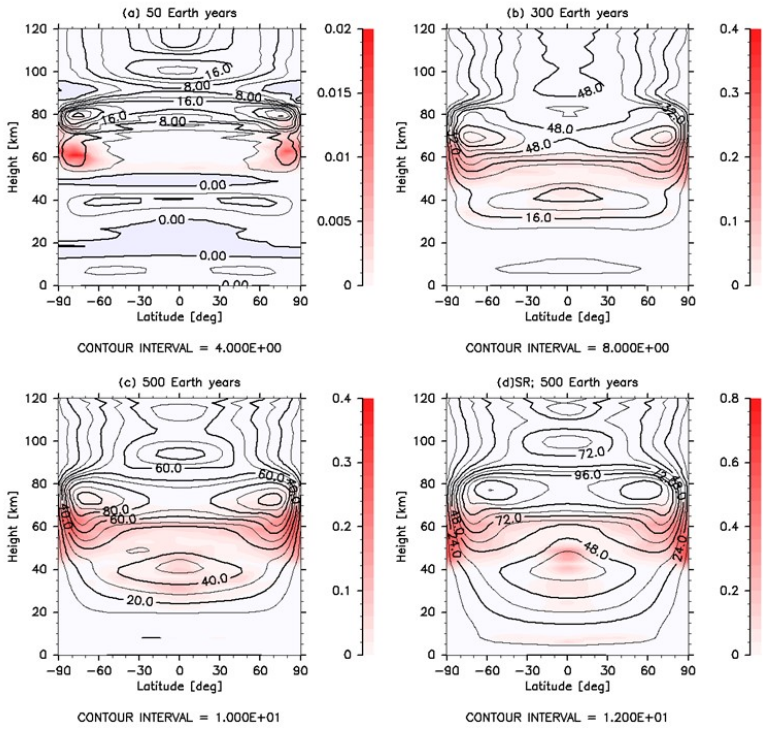

©2019. Japan Geoscience Union. All Right Reserved.

Data assimilation of the Venus atmosphere assuming radio occultation measurement by small satellites

*Mirai Abe[1], Norihiko Sugimoto[1], Yukako Kikuchi[2], Asako Hosono[3], Hiroki Ando[4], Masahiro Takagi[4], Itziar Garate Lopez[5], Sebastien Lebonnois[6], Chi Ao[7]

1. Keio University, 2. Yokohama Futaba High School, 3. Toshimagaoka Women High School, 4. Kyoto Sangyo University, 5. Euskal Herriko Unibertsitatea, 6. Sorbonne Universite, 7. Jet Propulsion Laboratory

At the altitude of approximately 60-70 km in the Venus atmosphere, there is an interesting phenomenon called “cold collar” where the temperature of the polar region is higher than that of the surroundings (latitude of about 60-80 degrees). The Japanese Venus Atmospheric GCM For the Earth Simulator (AFES-Venus) succeeded for the first time in the reproduction of cold collar[1]. However, the temperature difference between the pole and the surroundings is small compared with that observed. Recently, using the Local Ensemble Transform Kalman Filter (LETKF), we have succeeded in developing the Venus AFES LETKF Data Assimilation System (VALEDAS)[2]. In this study, we investigated the reproducibility of cold collar by the data assimilation of French Venus Atmospheric GCM(LMD/VGCM) in which cold collar is realistically reproduced[3]. We prepared idealized observation data assuming radio occultation measurement by small satellites. We will report the reproducibility of cold collar by changing the conditions such as observation point, observation number, and time interval. Figure shows three vertical profiles of temperature observations at 85 degrees North every Earth hour (obtained by temperature field from 30-90 degrees North at the altitude of about 66 km). Therefore, such kind of future mission would be promising.

[1] The puzzling Venusian polar atmospheric structure reproduced by a general circulation model,
Hiroki Ando, Norihiko Sugimoto, Masahiro Takagi, Hiroki Kashimura, Takeshi Imamura, and Yoshihisa Matsuda, *Nature Communications*, Vol. 7, (2016), 10398, 8pp.
[2] Development of an ensemble Kalman filter data assimilation system for the Venusian atmosphere,
Norihiko Sugimoto, Akira Yamazaki, Toru Kouyama, Hiroki Kashimura, Takeshi Enomoto, and Masahiro Takagi, *Scientific Reports*, Vol. 7, (2017), 9321, 9pp
[3] Latitudinal variation of clouds’ structure responsible for Venus’ cold collar,
Itziar Garate-Lopez, Sébastien Lebonnois, *Icarus*, Vol. 314, (2018), p1-11.

Keywords: Data assimilation, Venus, Radio occultation

©2019. Japan Geoscience Union. All Right Reserved.

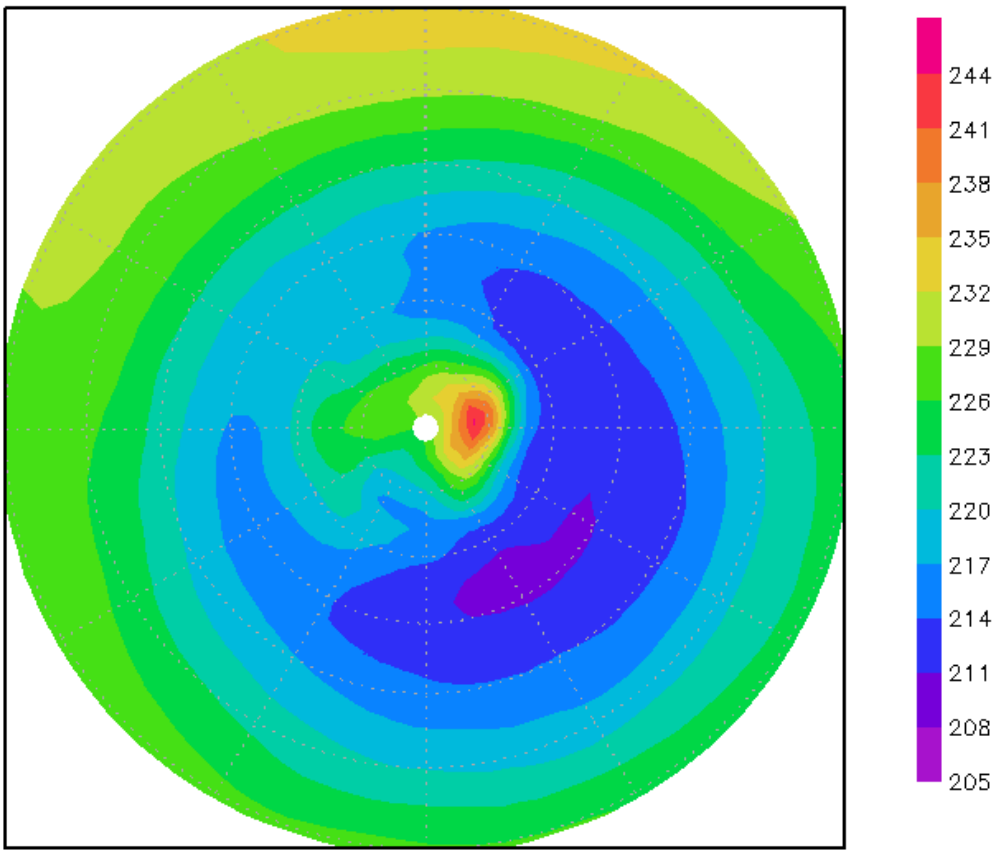

©2019. Japan Geoscience Union. All Right Reserved.

Relationship between solar wind and atmospheric circulation

*Paul Prikryl[1]

1. Physics Department University of New Brunswick and Geomagnetic Laboratory Natural Resources Canada

More than four decades have passed since the discovery of a relationship between solar wind magnetic sector boundary structure and the winter mid-latitude upper-tropospheric vorticity/circulation [1,2]. These results have been later confirmed and various physical mechanisms proposed [3,4]. Solar wind to magnetosphere - ionosphere - atmosphere (MIA) coupling process generates internal atmospheric gravity waves propagating upward and downward from the lower thermosphere sources at high latitudes [5]. If ducted over long distances in the lower atmosphere they can reach troposphere [6,7]. Despite significantly reduced wave amplitude, but subject to amplification upon over-reflection in the upper troposphere, the gravity waves can trigger moist instabilities to initiate convective bursts [4]. The latent heat release is the source of energy leading to intensification of extratropical storms and convective bursts have been linked to rapid intensification of tropical cyclones. Recent studies [8,9,10] showed that explosive extratropical cyclones and rapid intensification of tropical cyclones tend to follow arrivals of solar wind high-speed streams and interplanetary coronal mass ejections. The solar wind MIA coupling is most intense during the arrivals of co-rotating interaction regions and interplanetary shocks at the leading edge of high-speed solar wind when the amplitudes of aurorally-generated gravity waves are largest. If these gravity waves trigger moist instabilities in extratropical and tropical cyclones to initiate convective bursts the intensification of cyclones leads to enhanced atmospheric circulation.

[1] Wilcox J. M., et al., Science, 180, 185-186, 1973.
[2] Wilcox J. M., et al., J. Atmos. Sci. 31, 581–588, 1974.
[3] Prikryl P., et al., Ann. Geophys. 27, 1–30, 2009. https://doi.org/10.5194/angeo-27-1-2009
[4] Prikryl P., et al., Ann. Geophys. 27, 31–57, 2009. https://doi.org/10.5194/angeo-27-31-2009.
[5] Hines, C.O., Can. J. Phys. 38, 1441–1481, 1960.
[6] Mayr H.G., et al., J. Geophys. Res., 89, 10929–10959, 1984.
[7] Prikryl P., et al., Ann. Geophys., 23, 401-417, 2005. doi:10.5194/angeo-23-401-2005
[8] Prikryl P., et al., J. Atmos. Sol.-Terr. Phys., 149, 219–231, 2016.
[9] Prikryl P., et al., J. Atmos. Sol.-Terr. Phys., 171, 94–110, 2018.
[10] Prikryl P., et al., J. Atmos. Sol.-Terr. Phys., 183, 36-60, 2019.
https://doi.org/10.1016/j.jastp.2018.12.009.

Keywords: Solar wind-magnetosphere-ionosphere-atmosphere coupling, High-speed solar wind, Internal gravity waves, Atmospheric circulation, Extratropical and tropical cyclones

©2019. Japan Geoscience Union. All Right Reserved.

Contribution of the Atlantic storm track to the Euro-Russian blocking maintenance in summer 2010

*Akira Yamazaki[1]

1. Application Laboratory, Japan Agency for Marine-Earth Science and Technology

A long-lived blocking anticyclone occurred over western Russia during summer of 2010. This blocking persisted especially during the whole July over the western Russia and caused various weather extremes in the Eurasian continent. In this study, we investigate the mechanism and predictability of Euro-Russian blocking in terms of the interaction between blocking and synoptic eddies or storm tracks, that is, the eddy feedback mechanism. The author adopts the selective absorption mechanism (SAM, Yamazaki and Itoh 2013) to explain the maintenance mechanism and predictability of Euro-Russian blocking during July. Using an ensemble data assimilation system and an AGCM with the same forecast model, we conducted ensemble medium-range (7 days) forecast experiments. Isentropic trajectory analyses suggested that the SAM can work even in the summertime blocking event and the mechanism is more effective for forecast members in which the blocking is successfully forecast. We also conducted a sensitivity experiments in which the Atlantic storm track was suppressed by a piecewise potential vorticity inversion method to evaluate the impact of the storm track on the maintenance of the blocking. The result indicates that the blocking can be substantially maintained by the feedback from the storm track. The results suggested that the Atlantic storm track can substantially contribute to the maintenance of Euro-Russian blocking and its predictability.

Keywords: atmospheric blocking, storm tracks, ensemble forecasting

©2019. Japan Geoscience Union. All Right Reserved.

Instabilities in Ekman layer and roll structures in a tropical cyclone boundary layer

*Junshi Ito[1], Hiroshi Niino[1]

1. Atmosphere and Ocean Research Institute, The University of Tokyo

Taking advantage of the huge computational power of a massive parallel supercomputer (K-supercomputer), a large eddy simulation of entire tropical cyclones by use of a numerical weather prediction model was conducted. In the numerical results, three kinds of roll structures are found in the boundary layer (See figure; Ito et al., 2017). An analysis of linear instabilities in Ekman layer suggests that the mechanisms to form the rolls are associated with two kinds of growth modes (inflection point and parallel instabilities) of the Ekman layer.

Keywords: Tropical cyclone boundary layer, Roll structure, Linear Instability, Ekman Layer

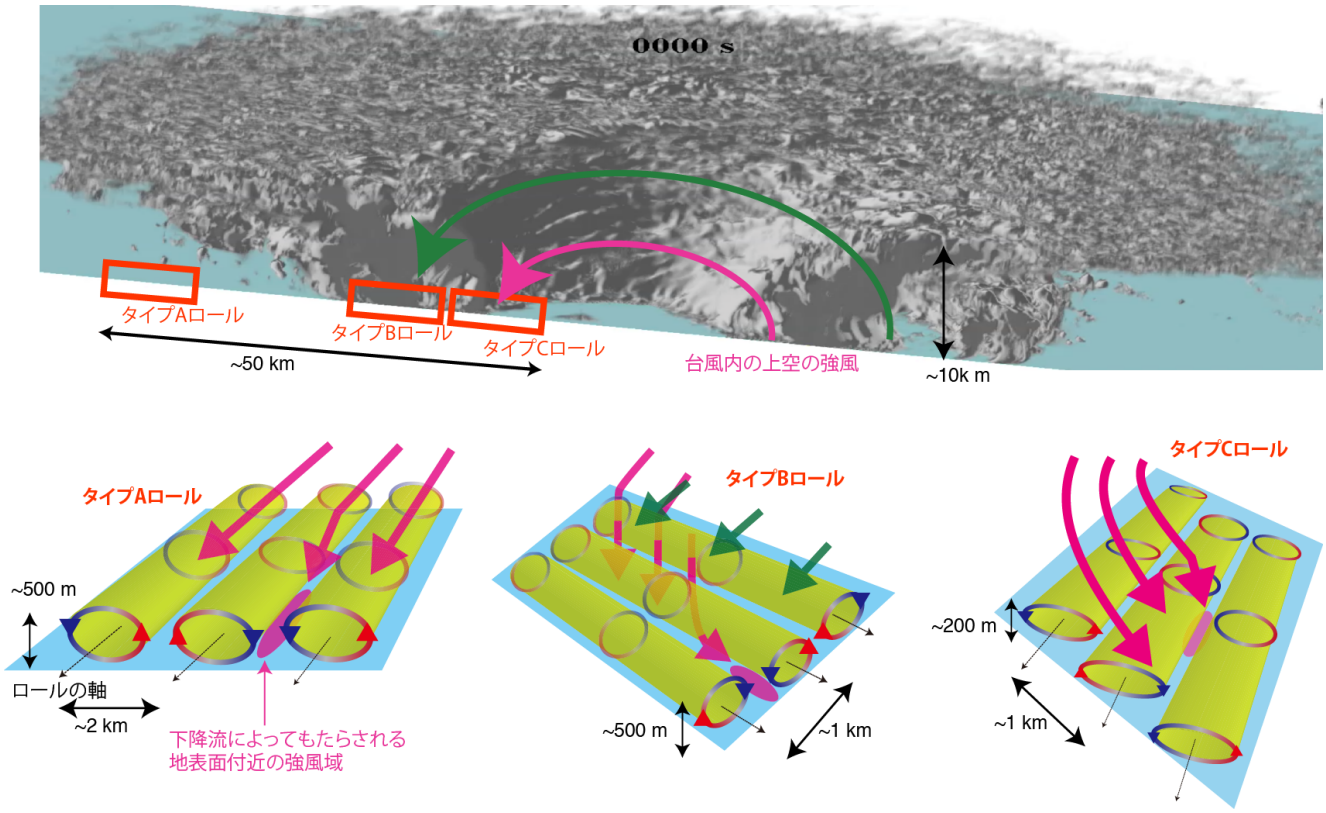

©2019. Japan Geoscience Union. All Right Reserved.

Mathematical description of the internal waves in a proximity of the bottom of the Ocean.

*andrei giniatoulline[1], german tobar[1]

1. Department of Mathematics, Los Andes University, Bogota, Colombia, South America

We construct an explicit solution for a boundary value problem in a layer at the bottom of the Ocean for a system of partial differential equations which describes the motion of a viscous rotating stratified fluid. As an effect of Coriolis and gravitational forces, there arise internal waves in the fluid. We prove the existence and uniqueness of the solution.
For a model in the half-space, for the constructed solutions we find the asymptotical behavior for large values of t. We prove the existence of the following boundary layer phenomena: the asymptotical decay of the solution is slower as we approach the boundary plane of the bottom.
The obtained results can be used not only for modeling the flows at the bottom of the Ocean, but also for the flows in the lower Atmosphere.

Keywords: Internal waves, Stratified fluid, Rotating fluid, Boundary layer

©2019. Japan Geoscience Union. All Right Reserved.

How deterministic are the deep zonal jets?

*Ryo Furue[1], Masami Nonaka[1], Hideharu Sasaki[1]

1. APL/JAMSTEC

Eddy-resolving oceanic general circulation models (OGCMs) often show eastward and westward alternating flows below the main thermocline in the velocity field averaged over one year or longer. They are commonly termed the “deep jets”. They are fairly coherent zonally, extending tens of degrees, and vertically, extending down to 1000–2000 m. Their meridional wavelength (distance between eastward flows) is typically 3º–5º. Although they tend to be masked by the general circulation near the surface, their pressure anomalies exist there and has been detected in satellite-observed sea-surface height fields. Recently, a compilation of high-resolution ADCP sections and an analysis on geostrophic velocity based on Argo showed the horizontal and vertical structure of the jets (Cravatte et al. 2017).

In an analysis of OFES , an eddy resolving model, deep jets tend to systematically migrate toward the equator between 20º–30ºN and S (Richards et al. 2006) with a period of approximately 4 years. On the other hand, Qiu et al. (2013) proposed a mechanism that generates a series of stationary deep jets at fixed distances from the equator.

A number of mechanisms have been proposed to explain the existence and the properties of these deep jets, some of them suggesting that the positions and strengths of the jets are determined by external forcing (“deterministic”) and others, that they are (or should be) only statistically determined (“stochastic”).

To determine how deterministic the deep jets are, we use a 10-member ensemble of runs of OFES 2, an OGCM for the Earth Simulator version 2, which is a semi-global model with a 0.1º horizontal resolution. Its surface forcing is based on JRA55-do, a timeseries of atmospheric conditions derived from a reanalysis product. The ensemble runs are started from the beginning of 1965 and extended to the end of 2016; their difference comes solely from slight differences in their initial conditions.

As the left panel of the figure below shows, equatorward phase propagation of deep jets is clear between 20º–30ºN, whereas poleward propagation is discernible between 5º–15ºN. Along 33º and 40ºN are rather persistent eastward jets flanked by westward jets on their equatorward sides. North of 40ºN, the jets tend to be somewhat stronger and less stable and to have shorter meridional wavelengths.

The variance among the ensemble members initially grows rapidly but stabilizes in 5–10 years (not shown). The right panel of the figure below indicates how well the positions of eastward jets agree among the ensemble members. Except for the equatorial currents (like the primary and secondary Tsuchiya Jets) and those stable jets near 33º and 40ºN, the axes of the jets more or less vary among ensemble members. Nevertheless, some coherence is also evident; in particular, the poleward-propagating jets in the 5º–15ºN band tend to agree among themselves. In the equatorward-propagating regime 20º–30ºN, coherent propagation sometimes emerges. If the tropical (equatorward of 15ºN) jets are deterministic, their migration may be due to some slow change in external forcing.

Keywords: deep jets, chaos, eddy-resolving OGCM

©2019. Japan Geoscience Union. All Right Reserved.

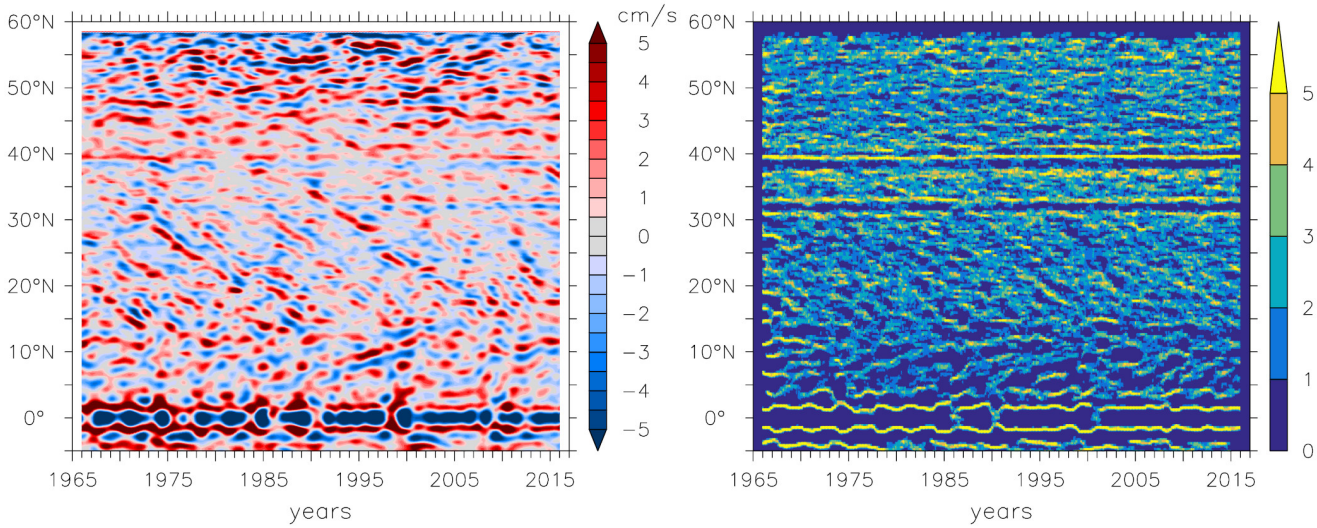

©2019. Japan Geoscience Union. All Right Reserved.

The impact of tidal mixing on the Indonesian Throughflow

*Kohki Shiroyama[1], Shinichiro Kida[2], Hideharu Sasaki[3], Ryo Furue[3]

1. Interdisciplinary Graduate School of Engineering Sciences, Kyushu University, 2. Research Institute for Applied Mechanics Kyushu University, 3. JAMSTEC. APL

The Indonesian Seas are where the Indonesian Throughflow (ITF) flows from the Pacific to the Indian Ocean. The sea surface temperature of the ITF plays an important role in the development of the atmospheric deep convection above these seas. In the Indonesian Seas, the bottom topography is rough and likely induces strong tidal mixing. To examine the impact of tidal mixing on the water mass properties of the ITF, we examined the temperature, salinity, and velocity of the ITF by using OFES2, a quasi-global ocean circulation model that includes global tidal mixing parameterization. We find the impact of tidal mixing to change the water mass properties of the ITF and its flow structure, especially above seamounts and at the straits. The vertical distribution of water mass properties at these location shows more uniform profile. This is considered that tidal mixing has a strong effect on the ITF at narrow location like Straits. We plan to analysis more to investigate the cause of these changes.

Keywords: tidal mixing, Indonesian Throughflow

©2019. Japan Geoscience Union. All Right Reserved.

Verification for subsurface oceanic structure in OFES outputs driven by different wind data sets (NCEP/NCAR and QSCAT)in the tropical Pacific Ocean

*Hiroshige Fukunaga[1], Kunio Kutsuwada[1], Akira Kakiuchi[1], Yuma Yanagida[1], Hideharu Sasaki[2], Yoshikazu Sasai[2]

1. Tokai University, 2. JAMSTEC

1 Introduction
OFES is a numerical model that reproduces oceanic circulation and structure with high resolution by inputting sea surface flux (momentum heat and freshwater). Intercomparison between two types of OFESruns (NCEPrun and QSCATrun) driven by different wind datasets with no different surface heat flux revealed that the thermocline depth near 10˚N is about 50m shallower in the NCEPrun than that in the QSCATrun. The integrated meridional geostrophic transports from the east boundary in the NCEPrun are about 10Sv larger than in the QSCATrun (Kutsuwada et al 2018).
In this study we examine oceanic structures and zonally-integrated meridional geostrophic transports in the southern hemisphere by making intercomparison between the two OFES runs together with comparison with the MOAA-GPV data set constructed by Argo float observations.
2 Data
OFES is high resolution semi-global ocean circulation model developed by JAMSTEC based on Modular Ocean Model ver.3 developed by NOAA. It can reproduce ocean circulation and structure with high resolution. As the external force driving the model we use two different types of wind data sets by numerical re-analysis (NCEP NCAR) and satellite measurement (QuikSCAT).
We averaged spatially for horizontal resolution from 0.1˚x0.1˚to 1˚x1˚. In the vertical direction we converted all simulated data such as temperature salinity and current with depth interval of 10m using Akima-method from sea surface(2.5m) to 6065m.
3 Method
Using dynamic height anomaly we calculate geostrophic current that is integrated vertically from sea surface to depth h (m). We use the depth of no motion of 2000m.The meridional Sverdrup transport corresponds vertically integrated flow from sea surface to depth of no motion (the maximum depth of wind driven circulation) and is given by the sum of the Ekman transport (calculated from Coriolis parameter and zonal wind-stress) and geostrophic transport.
In this study we verify the correspondence between geostrophic transports which are obtained from oceanic data and wind-driven transports calculated from sea surface wind data.
4 Result
The thermocline depth near 10S in the NCEPrun is about 50m shallower than that in the QSCATrun. The zonally-integrated meridional geostrophic transports from the east boundary in the NCEPrun is 10 Sv smaller than in the QSCATrun. Comparison of the two runs with the MOAA-GPV showed that the temperatures in the NCEPrun are lower than those in the MOAA-GPV at 50-400m depth while the QSCATruns is almost similar to the MOAA-GPV above 200m. In comparison for the integrated meridional geostrophic transports the values in the QSCATrun are smaller than those in the NCEPrun and similar to those in the MOAA-GPV. These results mean that in the southern hemisphere the QSCATrun reproduces real oceanic structures with higher reliability than the NCEPs one the same as that in the northern hemisphere.
Comparison in the meridional profile of zonally-averaged wind stress curl (WSC) showed that the NCEPs

©2019. Japan Geoscience Union. All Right Reserved.

WSC has larger values in a zone of 10˚S corresponding to negative maximum than the QSCAT and also the same differences as that in a zone of 10˚N corresponding to positive maximum. The geostrophic transports from the QSCATrun correspond the wind-driven flow calculated from QSCATs wind data closely at low latitude which suggests that the Sverdrup balance holds in these regions.

©2019. Japan Geoscience Union. All Right Reserved.

Inter-comparison of ocean wave data from drifting buoys, moored GPS buoys
and reanalysis data

*Yukiharu Hisaki[1]

1. University of the Ryukyus

Observation of surface wave data such as wave height and period are important for practical and scientific purposes. However, wave observations by moored buoys around Japan are only by GPS buoys, which are located about 10 km from the coast. The observations of wave heights and periods by Japan Meteorological Agency (JMA) drifting buoys were conducted from 2000. Wave data from drifting buoys are inter-compared with GPS buoys and ERA-Interim reanalysis data. The GPS wave data are compared with those from drifting buoys and ERA-Interim data, when a drifting buoy is close to a GPS buoy position, and the number of comparison is limited. The data period of wave data of drifting buoys and ERA-Interim data is from 2000 to 2018. The agreement of wave heights between from GPS and drifting buoys is better than that between from GPS and ERA-Interim data. The agreement of wave periods between from GPS and drifting buoys is not much better than that between from GPS and ERA-Interim data. There are cases that wave periods by drifting buoys are much longer than those from GPS buoys. The dependency of wave parameter differences between from drifting buoys and ERA-Interim data on drifting buoy speeds is investigated.
The drifting current components to the mean wave directions are evaluated from the drifting currents estimated from the drifting buoy positions and the ERA interim mean wave directions.
The differences of wave heights between from drifting buoys and ERA-Interim data are larger as faster current speeds.
The ERA-Interim wave heights are underestimated when current directions are opposite to mean wave directions. The ERA-Interim wave heights are overestimated current directions are following to wave directions. The ratio as drifting wave period/ERA-Interim wave period is smaller as increasing opposing current component, which is consistent with the Doppler shift.

Keywords: wave height, wave period, drifting buoy

©2019. Japan Geoscience Union. All Right Reserved.

Merge and Separation of ocean eddies around the Kuroshio Extension

*koutarou matsuhashi[1], Kazuyuki Uehara[1]

1. The Graduate School of Marine Science Technology

Oceanic mesoscale eddies make ow complicate and produce non-steady states in the ocean general circulation. These eddies are in addition considered to play a important role of heat and material transports. Therefore understanding of dynamics of mesoscale eddies and its roles are one of main tasks in Physical Oceanography. In particular the area around the Kuroshio Extension has very high activity of mesoscale eddies due to the Kuroshio Extension meanderings. Therefore, phenonmena of merging and seperating eddies frequently are observed in this area. Matsuoka et al.(2016) classified events of eddy merges and separations using a high resolution ocean general circulation model. In this study, at first we define mesoscale eddies using the second invariant of the velocity gradient tensor(this is equivalent with the Okubo-Weiss parameter) computed from sea surface height anomalies (AVISO), secondly we track the eddies, and finally, we discuss changes in physical parameters on events of eddy merging and seperating.

Keywords: messoscale eddy

©2019. Japan Geoscience Union. All Right Reserved.

Influence of eddy-trapped water mass reaching 137E survey line using OGCM and a particle-tracking method

*Hideyuki Nakano[1], Hiroyuki Tsujino[1], Kei Sakamoto[1], Shogo Urakawa[1], Takahiro Toyoda[1], Goro Yamanaka[1], Yoshimasa Matsumura[2]

1. Meteorological Research Institute, 2. Atmosphere and ocean research Institute, the University of Tokyo

Mesoscale eddies are known to play a major role in water mass formation and transport. In recent years, several studies have estimated eddy-trapped transport (e.g., Zhang et al 2014), arguing that this can be comparable to the mean-flow transport. However, these estimates are based on satellite observation and ideal vortex vertical structure of eddies, not based on direct ones. In this study, we directly diagnose the eddy-trapped transport by using eddy-resolving Ocean General Circulation Model (OGCM) and off-line particle tracking method. We focus on the eddy-trapped watermass reaching the 137E survey line, which is maintained for more than 50 years by the Japan Meteorological Agency and the importance of eddy activity is pointed out. Along 137E meridional section, a total of about 1 million particles are released every August during 1993 to 2017. Using daily output and offline-particle tracking method, reverse tracking is performed until each particle reaches the mixed-layer, where each particle is ventilated and its properties significantly change due to air-sea interaction. Each particle is divided into typical water mass categories, judging from its temperature, salinity, potential vorticity and location during the ventilation. Whether or not each particle is trapped in the mesoscale eddies is judged by Okubo-Weiss parameter. Distribution of ventilated areas of typical water masses such as Tropical Water (TW), Subtropical Mode Water (STMW), Eastern Subtropical Mode Water (ESTMW), Lighter variety of Central Mode Water (L-CMW) is realistically reproduced. About 20% of TW are present in mesoscale eddies during ventilation, and 60% of the them are present in anticyclonic ones. About half of them (~10% of the total TW) reach137E in a state trapped in the eddies. Their trajectories are almost westward, whereas the trajectories not trapped in eddies are the west-southwest direction reflecting the subtropical circulation. Arrival times from the ventilated area nearly the same for the both, except for the subtropical countercurrent where the average flow is eastward and the arrival time is shorter for those trapped in the eddies. About 30% of STMW are present in eddies during ventilation, and about 80% of them are present in anticyclonic ones. About 1/3 of them (~10% of total STMW) reach 137E in a state trapped in eddies. For the STMW, the arrival time is longer for those trapped in the eddies, and their trajectories are not simple westward. Less than 20% of ESTMW and L-CMW are present in eddies during ventilation, and the ratio between the anticyclonic and cyclonic eddies is almost the same. Only 1/4 of them (5% of the total water masses) reach 137E in a state trapped in eddies. Even though the trajectory of the water mass trapped in the eddies show a clear east-west direction like TW, the arrival time is longer for the water mass trapped in the eddies. This estimate that 5-10% of these water masses reaching 137E trapped in a state eddies may be smaller than the recent estimate in past studies. These differences are also discussed.

Keywords: mesoscale eddy, watermass, particle tracking

©2019. Japan Geoscience Union. All Right Reserved.

A study on the variability of the deep ocean circulation during glacial climate with a climate model of intermediate complexity

*Taigo Ando[1], Akira Oka[1]

1. Atmosphere and Ocean Research Institute, University of Tokyo

Ice core reconstructions show that there were abrupt climate changes termed Dansgaard-Oscillation (D-O) oscillations during glacial period, which are most characterized by about 10 ℃ of temperature changes in Greenland within a few decades. Many studies have pointed out the connection between D-O oscillations and changes in the Atlantic Meridional Overturning Circulation (AMOC), while details of its variability is still missing. Previous modeling studies have suggested that the variability of the AMOC including D-O oscillations are invoked by freshwater input from melted ice-sheets into the deep-water formation region in the North Atlantic (e.g. Rahmstrf, 2002). However, some recent model simulations exhibit abrupt and spontaneous oscillations without freshwater forcing in glacial climate (Peltier and Vettoretti, 2014; Brown and Galbraith, 2016), and more researchers are considering that the mechanism of D-O oscillations is involved within the ocean dynamics and its interactions with the atmosphere and sea ice. Since global coupled models usually used in previous simulations contain many processes of the atmosphere and the ocean, they require high computational costs and it is difficult to identify the processes contributing to D-O oscillations from the model simulations. On the other hand, earth system models of intermediate complexity with lighter computational costs have difficulties in reproducing climate features.
In this study, we modified the model in which the atmosphere component is simplified to the energy-balanced model (MIROC-lite, Oka et al., 2011, 2017) by using results of a full-coupled model (MIROC, Hasumi and Emori, 2001) as parameters so as to have equivalent performance to the full-coupled model, then conducted simulations of glacial climate with the model. This model is expected to be effective for investigating the cause of the spontaneous oscillations of full-coupled models since it can better represent thermal feedback between the atmosphere and the ocean by predicting atmosphere temperature from energy balance compared to ocean-only models. In our presentation, we discuss the performance of the model and its implications for the mechanism of D-O oscillations.

Keywords: glacial climate, deep ocean circulation, climate model

©2019. Japan Geoscience Union. All Right Reserved.

[J] Poster | A (Atmospheric and Hydrospheric Sciences)：A-OS Ocean Sciences & Ocean Environment

Mon. May 27, 2019 5:15 PM - 6:30 PM JST | Mon. May 27, 2019 8:15 AM - 9:30 AM UTC | Poster Hall International Exhibition Hall8, Makuhari Messe_9

[A-OS19] Dynamics of oceanic and atmospheric waves, vortices, and circulations

convener:Yuki Tanaka(Graduate School of Science, The University of Tokyo), Ryo Furue(APL/JAMSTEC), Yukiharu Hisaki(University of the Ryukyus), Norihiko Sugimoto(Keio University, Department of Physics)

Oceanic and atmospheric dynamics aims at abstracting general principles from observed phenomena and constructing a system of mathematical models, thereby leading to the understanding, prediction, and parameterization of those phenomena. It provides perspectives for the advancement of sciences in various areas such as wind waves, swells, internal waves, Rossby waves, equatorial waves, tides, eddies, meandering of jets and fronts, general circulation, boundary layers, and ocean-atmosphere coupled modes. It has also been and will continue to be benefited by new uses of ideas and methods from such theories as resonance, nonlinear interaction, spectral analysis, probability, statistics, and dynamical systems. In this session, we solicit presentations on observational, experimental, numerical, and theoretical studies of oceanic and atmospheric dynamics and on exploratory use of new ideas and methods. We also welcome presentations on interdisciplinary studies in fields such as ecosystems, climate, and environment.

[AOS19-P01] Atmospheric super rotation developed in a GCM (AFES-Venus)

*Norihiko Sugimoto[1], Masahiro Takagi[2], Yoshihisa Matsuda[3] (1.Keio University, Department of Physics, 2.Kyoto Sangyo University, Department of Physics, 3.Tokyo Gakugei University, Department of Natural Sciences)

[AOS19-P02] Data assimilation of the Venus atmosphere assuming radio occultation measurement by small satellites

*Mirai Abe[1], Norihiko Sugimoto[1], Yukako Kikuchi[2], Asako Hosono[3], Hiroki Ando[4], Masahiro Takagi[4], Itziar Garate Lopez[5], Sebastien Lebonnois[6], Chi Ao[7] (1.Keio University, 2.Yokohama Futaba High School, 3.Toshimagaoka Women High School, 4.Kyoto Sangyo University, 5.Euskal Herriko Unibertsitatea, 6.Sorbonne Universite, 7.Jet Propulsion Laboratory)

[AOS19-P03] Relationship between solar wind and atmospheric circulation

*Paul Prikryl[1] (1.Physics Department University of New Brunswick and Geomagnetic Laboratory Natural Resources Canada)

[AOS19-P04] Contribution of the Atlantic storm track to the Euro-Russian blocking maintenance in summer 2010

*Akira Yamazaki[1] (1.Application Laboratory, Japan Agency for Marine-Earth Science and Technology)

[AOS19-P05] Instabilities in Ekman layer and roll structures in a tropical cyclone boundary layer

*Junshi Ito[1], Hiroshi Niino[1] (1.Atmosphere and Ocean Research Institute, The University of Tokyo)

[AOS19-P06] Mathematical description of the internal waves in a proximity of the bottom of the Ocean.

*andrei giniatoulline[1], german tobar[1] (1.Department of Mathematics, Los Andes University, Bogota, Colombia, South America)

[AOS19-P07] How deterministic are the deep zonal jets?

*Ryo Furue[1], Masami Nonaka[1], Hideharu Sasaki[1] (1.APL/JAMSTEC)

[AOS19-P08] The impact of tidal mixing on the Indonesian Throughflow

*Kohki Shiroyama[1], Shinichiro Kida[2], Hideharu Sasaki[3], Ryo Furue[3] (1.Interdisciplinary Graduate School of Engineering Sciences, Kyushu University, 2.Research Institute for Applied Mechanics Kyushu University, 3.JAMSTEC. APL)

[AOS19-P09] **Verification for subsurface oceanic structure in OFES outputs driven by different wind data sets (NCEP/NCAR and QSCAT)in the tropical Pacific Ocean**

*Hiroshige Fukunaga[1], Kunio Kutsuwada[1], Akira Kakiuchi[1], Yuma Yanagida[1], Hideharu Sasaki[2], Yoshikazu Sasai[2] (1.Tokai University, 2.JAMSTEC)

[AOS19-P10] Inter-comparison of ocean wave data from drifting buoys, moored GPS buoys and reanalysis data

*Yukiharu Hisaki[1] (1.University of the Ryukyus)

[AOS19-P11] Merge and Separation of ocean eddies around the Kuroshio Extension

*koutarou matsuhashi[1], Kazuyuki Uehara[1] (1.The Graduate School of Marine Science Technology)

[AOS19-P12] Influence of eddy-trapped water mass reaching 137E survey line using OGCM and a particle-tracking method

★Invited Papers

*Hideyuki Nakano[1], Hiroyuki Tsujino[1], Kei Sakamoto[1], Shogo Urakawa[1], Takahiro Toyoda[1], Goro Yamanaka[1], Yoshimasa Matsumura[2] (1.Meteorological Research Institute, 2.Atmosphere and ocean research Institute, the University of Tokyo)

[AOS19-P13] A study on the variability of the deep ocean circulation during glacial climate with a climate model of intermediate complexity

*Taigo Ando[1], Akira Oka[1] (1.Atmosphere and Ocean Research Institute, University of Tokyo)

Atmospheric super rotation developed in a GCM (AFES-Venus)

*Norihiko Sugimoto[1], Masahiro Takagi[2], Yoshihisa Matsuda[3]

1. Keio University, Department of Physics, 2. Kyoto Sangyo University, Department of Physics, 3. Tokyo Gakugei University, Department of Natural Sciences

The generation mechanism of the atmospheric super rotation on Venus is one of the most important topics in the Earth and planetary sciences. Here we reproduced the fully developed super-rotation for the first time in a Venus general circulation model (GCM) driven by a zonally-averaged component of the *realistic* solar heating only. Our GCM enables us to perform long term simulations with medium resolution higher than those used in previous studies. It is newly found that mean meridional circulation driven by the *realistic* solar heating can generate the fully developed super-rotation of ~100 m s^{-1} with the vertical eddy viscosity smaller than 0.02 m^2 s^{-1} (see below Figure). Existence of the range of the vertical eddy viscosity in which the fast super-rotation can be generated by the reasonable solar heating has broad implications for the atmospheric sciences in light of optimal parameters for the GCMs.

Fully developed super-rotation driven by the mean meridional circulation in a Venus GCM, Norihiko Sugimoto, Masahiro Takagi, and Yoshihisa Matsuda, *Geophysical Research Letters*, (2019), doi.org/10.1029/2018GL080917.

Keywords: General circulation, Super rotation, Venus

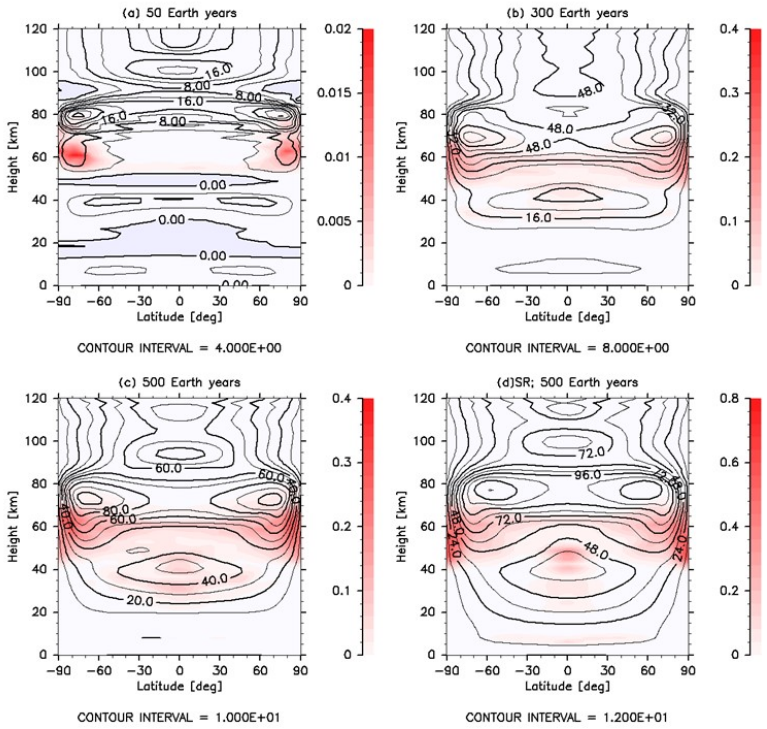

©2019. Japan Geoscience Union. All Right Reserved.

Data assimilation of the Venus atmosphere assuming radio occultation measurement by small satellites

*Mirai Abe[1], Norihiko Sugimoto[1], Yukako Kikuchi[2], Asako Hosono[3], Hiroki Ando[4], Masahiro Takagi[4], Itziar Garate Lopez[5], Sebastien Lebonnois[6], Chi Ao[7]

1. Keio University, 2. Yokohama Futaba High School, 3. Toshimagaoka Women High School, 4. Kyoto Sangyo University, 5. Euskal Herriko Unibertsitatea, 6. Sorbonne Universite, 7. Jet Propulsion Laboratory

At the altitude of approximately 60-70 km in the Venus atmosphere, there is an interesting phenomenon called “cold collar” where the temperature of the polar region is higher than that of the surroundings (latitude of about 60-80 degrees). The Japanese Venus Atmospheric GCM For the Earth Simulator (AFES-Venus) succeeded for the first time in the reproduction of cold collar[1]. However, the temperature difference between the pole and the surroundings is small compared with that observed. Recently, using the Local Ensemble Transform Kalman Filter (LETKF), we have succeeded in developing the Venus AFES LETKF Data Assimilation System (VALEDAS)[2]. In this study, we investigated the reproducibility of cold collar by the data assimilation of French Venus Atmospheric GCM(LMD/VGCM) in which cold collar is realistically reproduced[3]. We prepared idealized observation data assuming radio occultation measurement by small satellites. We will report the reproducibility of cold collar by changing the conditions such as observation point, observation number, and time interval. Figure shows three vertical profiles of temperature observations at 85 degrees North every Earth hour (obtained by temperature field from 30-90 degrees North at the altitude of about 66 km). Therefore, such kind of future mission would be promising.

[1] The puzzling Venusian polar atmospheric structure reproduced by a general circulation model,
Hiroki Ando, Norihiko Sugimoto, Masahiro Takagi, Hiroki Kashimura, Takeshi Imamura, and Yoshihisa Matsuda, *Nature Communications*, Vol. 7, (2016), 10398, 8pp.
[2] Development of an ensemble Kalman filter data assimilation system for the Venusian atmosphere,
Norihiko Sugimoto, Akira Yamazaki, Toru Kouyama, Hiroki Kashimura, Takeshi Enomoto, and Masahiro Takagi, *Scientific Reports*, Vol. 7, (2017), 9321, 9pp
[3] Latitudinal variation of clouds’ structure responsible for Venus’ cold collar,
Itziar Garate-Lopez, Sébastien Lebonnois, *Icarus*, Vol. 314, (2018), p1-11.

Keywords: Data assimilation, Venus, Radio occultation

©2019. Japan Geoscience Union. All Right Reserved.

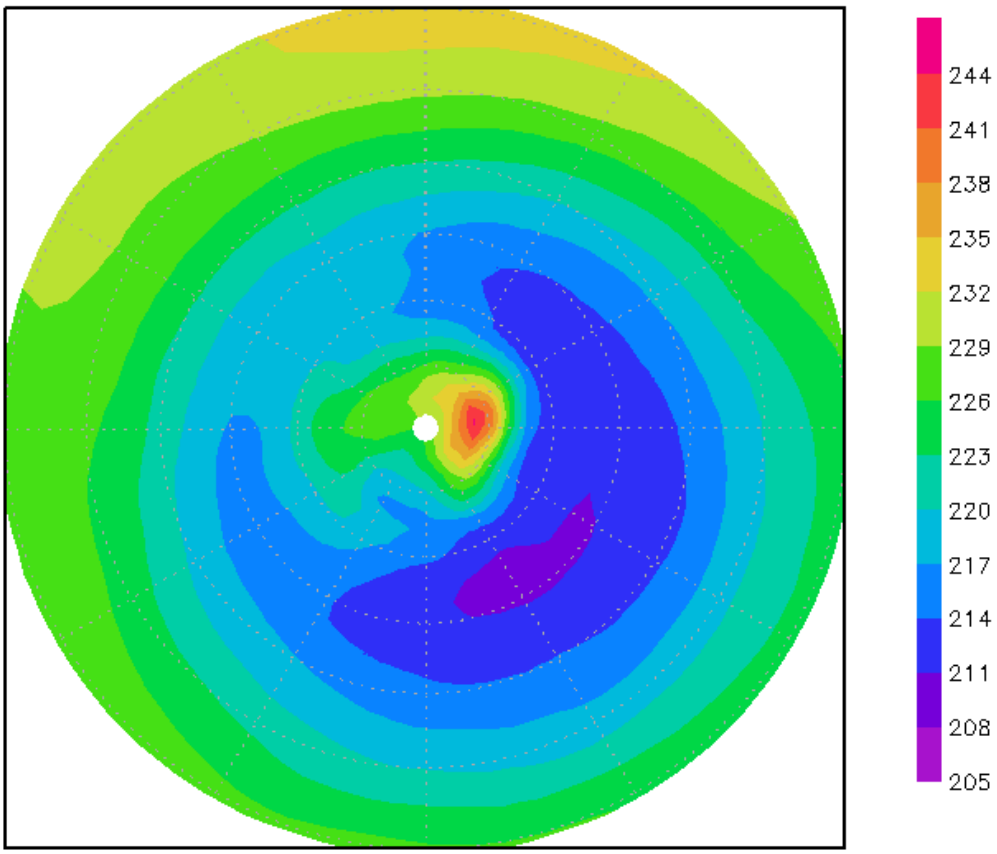

©2019. Japan Geoscience Union. All Right Reserved.

Relationship between solar wind and atmospheric circulation

*Paul Prikryl[1]

1. Physics Department University of New Brunswick and Geomagnetic Laboratory Natural Resources Canada

More than four decades have passed since the discovery of a relationship between solar wind magnetic sector boundary structure and the winter mid-latitude upper-tropospheric vorticity/circulation [1,2]. These results have been later confirmed and various physical mechanisms proposed [3,4]. Solar wind to magnetosphere - ionosphere - atmosphere (MIA) coupling process generates internal atmospheric gravity waves propagating upward and downward from the lower thermosphere sources at high latitudes [5]. If ducted over long distances in the lower atmosphere they can reach troposphere [6,7]. Despite significantly reduced wave amplitude, but subject to amplification upon over-reflection in the upper troposphere, the gravity waves can trigger moist instabilities to initiate convective bursts [4]. The latent heat release is the source of energy leading to intensification of extratropical storms and convective bursts have been linked to rapid intensification of tropical cyclones. Recent studies [8,9,10] showed that explosive extratropical cyclones and rapid intensification of tropical cyclones tend to follow arrivals of solar wind high-speed streams and interplanetary coronal mass ejections. The solar wind MIA coupling is most intense during the arrivals of co-rotating interaction regions and interplanetary shocks at the leading edge of high-speed solar wind when the amplitudes of aurorally-generated gravity waves are largest. If these gravity waves trigger moist instabilities in extratropical and tropical cyclones to initiate convective bursts the intensification of cyclones leads to enhanced atmospheric circulation.

[1] Wilcox J. M., et al., Science, 180, 185-186, 1973.
[2] Wilcox J. M., et al., J. Atmos. Sci. 31, 581–588, 1974.
[3] Prikryl P., et al., Ann. Geophys. 27, 1–30, 2009. https://doi.org/10.5194/angeo-27-1-2009
[4] Prikryl P., et al., Ann. Geophys. 27, 31–57, 2009. https://doi.org/10.5194/angeo-27-31-2009.
[5] Hines, C.O., Can. J. Phys. 38, 1441–1481, 1960.
[6] Mayr H.G., et al., J. Geophys. Res., 89, 10929–10959, 1984.
[7] Prikryl P., et al., Ann. Geophys., 23, 401-417, 2005. doi:10.5194/angeo-23-401-2005
[8] Prikryl P., et al., J. Atmos. Sol.-Terr. Phys., 149, 219–231, 2016.
[9] Prikryl P., et al., J. Atmos. Sol.-Terr. Phys., 171, 94–110, 2018.
[10] Prikryl P., et al., J. Atmos. Sol.-Terr. Phys., 183, 36-60, 2019.
https://doi.org/10.1016/j.jastp.2018.12.009.

Keywords: Solar wind-magnetosphere-ionosphere-atmosphere coupling, High-speed solar wind, Internal gravity waves, Atmospheric circulation, Extratropical and tropical cyclones

©2019. Japan Geoscience Union. All Right Reserved.

Contribution of the Atlantic storm track to the Euro-Russian blocking maintenance in summer 2010

*Akira Yamazaki[1]

1. Application Laboratory, Japan Agency for Marine-Earth Science and Technology

A long-lived blocking anticyclone occurred over western Russia during summer of 2010. This blocking persisted especially during the whole July over the western Russia and caused various weather extremes in the Eurasian continent. In this study, we investigate the mechanism and predictability of Euro-Russian blocking in terms of the interaction between blocking and synoptic eddies or storm tracks, that is, the eddy feedback mechanism. The author adopts the selective absorption mechanism (SAM, Yamazaki and Itoh 2013) to explain the maintenance mechanism and predictability of Euro-Russian blocking during July. Using an ensemble data assimilation system and an AGCM with the same forecast model, we conducted ensemble medium-range (7 days) forecast experiments. Isentropic trajectory analyses suggested that the SAM can work even in the summertime blocking event and the mechanism is more effective for forecast members in which the blocking is successfully forecast. We also conducted a sensitivity experiments in which the Atlantic storm track was suppressed by a piecewise potential vorticity inversion method to evaluate the impact of the storm track on the maintenance of the blocking. The result indicates that the blocking can be substantially maintained by the feedback from the storm track. The results suggested that the Atlantic storm track can substantially contribute to the maintenance of Euro-Russian blocking and its predictability.

Keywords: atmospheric blocking, storm tracks, ensemble forecasting

©2019. Japan Geoscience Union. All Right Reserved.

Instabilities in Ekman layer and roll structures in a tropical cyclone boundary layer

*Junshi Ito[1], Hiroshi Niino[1]

1. Atmosphere and Ocean Research Institute, The University of Tokyo

Taking advantage of the huge computational power of a massive parallel supercomputer (K-supercomputer), a large eddy simulation of entire tropical cyclones by use of a numerical weather prediction model was conducted. In the numerical results, three kinds of roll structures are found in the boundary layer (See figure; Ito et al., 2017). An analysis of linear instabilities in Ekman layer suggests that the mechanisms to form the rolls are associated with two kinds of growth modes (inflection point and parallel instabilities) of the Ekman layer.

Keywords: Tropical cyclone boundary layer, Roll structure, Linear Instability, Ekman Layer

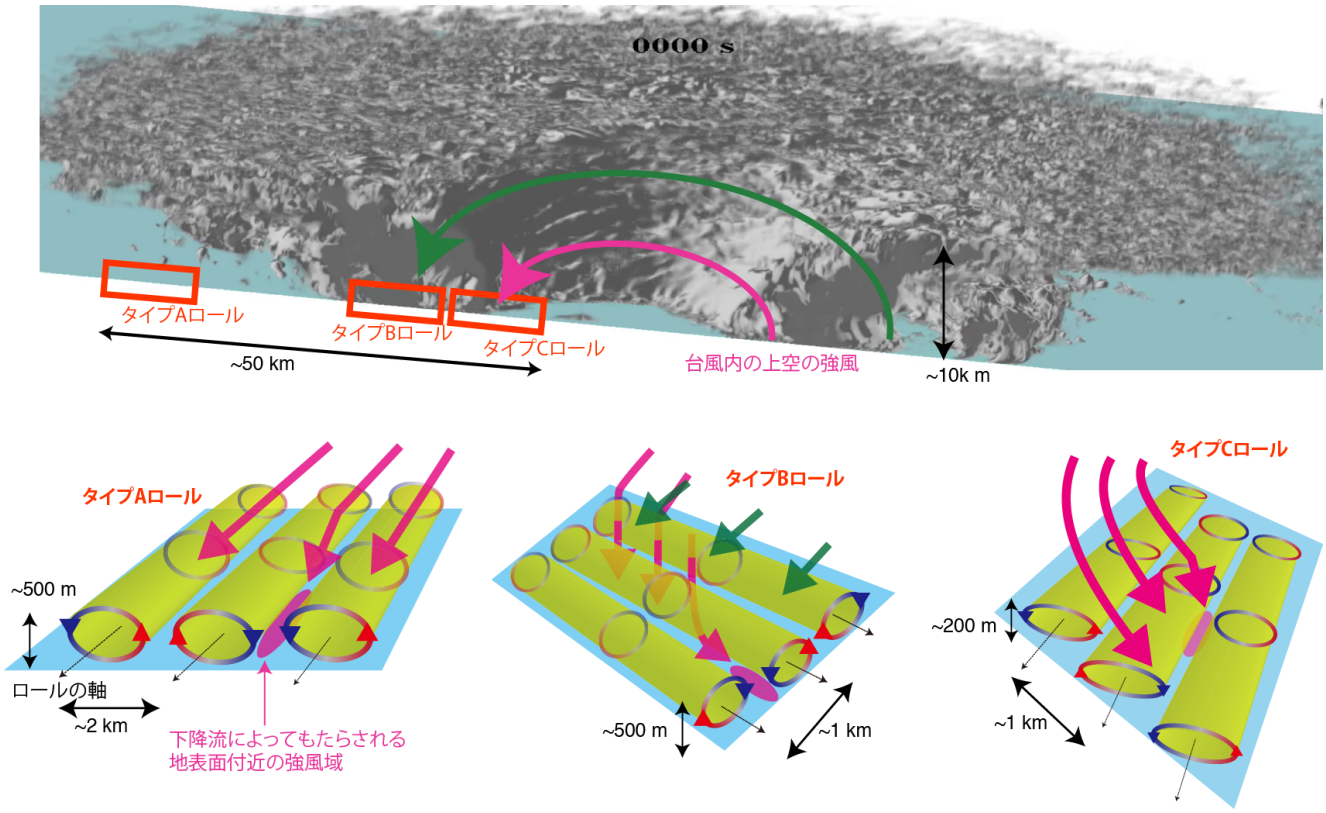

©2019. Japan Geoscience Union. All Right Reserved.

Mathematical description of the internal waves in a proximity of the bottom of the Ocean.

*andrei giniatoulline[1], german tobar[1]

1. Department of Mathematics, Los Andes University, Bogota, Colombia, South America

We construct an explicit solution for a boundary value problem in a layer at the bottom of the Ocean for a system of partial differential equations which describes the motion of a viscous rotating stratified fluid. As an effect of Coriolis and gravitational forces, there arise internal waves in the fluid. We prove the existence and uniqueness of the solution.
For a model in the half-space, for the constructed solutions we find the asymptotical behavior for large values of t. We prove the existence of the following boundary layer phenomena: the asymptotical decay of the solution is slower as we approach the boundary plane of the bottom.
The obtained results can be used not only for modeling the flows at the bottom of the Ocean, but also for the flows in the lower Atmosphere.

Keywords: Internal waves, Stratified fluid, Rotating fluid, Boundary layer

©2019. Japan Geoscience Union. All Right Reserved.

How deterministic are the deep zonal jets?

*Ryo Furue[1], Masami Nonaka[1], Hideharu Sasaki[1]

1. APL/JAMSTEC

Eddy-resolving oceanic general circulation models (OGCMs) often show eastward and westward alternating flows below the main thermocline in the velocity field averaged over one year or longer. They are commonly termed the “deep jets”. They are fairly coherent zonally, extending tens of degrees, and vertically, extending down to 1000–2000 m. Their meridional wavelength (distance between eastward flows) is typically 3º–5º. Although they tend to be masked by the general circulation near the surface, their pressure anomalies exist there and has been detected in satellite-observed sea-surface height fields. Recently, a compilation of high-resolution ADCP sections and an analysis on geostrophic velocity based on Argo showed the horizontal and vertical structure of the jets (Cravatte et al. 2017).

In an analysis of OFES , an eddy resolving model, deep jets tend to systematically migrate toward the equator between 20º–30ºN and S (Richards et al. 2006) with a period of approximately 4 years. On the other hand, Qiu et al. (2013) proposed a mechanism that generates a series of stationary deep jets at fixed distances from the equator.

A number of mechanisms have been proposed to explain the existence and the properties of these deep jets, some of them suggesting that the positions and strengths of the jets are determined by external forcing (“deterministic”) and others, that they are (or should be) only statistically determined (“stochastic”).

To determine how deterministic the deep jets are, we use a 10-member ensemble of runs of OFES 2, an OGCM for the Earth Simulator version 2, which is a semi-global model with a 0.1º horizontal resolution. Its surface forcing is based on JRA55-do, a timeseries of atmospheric conditions derived from a reanalysis product. The ensemble runs are started from the beginning of 1965 and extended to the end of 2016; their difference comes solely from slight differences in their initial conditions.

As the left panel of the figure below shows, equatorward phase propagation of deep jets is clear between 20º–30ºN, whereas poleward propagation is discernible between 5º–15ºN. Along 33º and 40ºN are rather persistent eastward jets flanked by westward jets on their equatorward sides. North of 40ºN, the jets tend to be somewhat stronger and less stable and to have shorter meridional wavelengths.

The variance among the ensemble members initially grows rapidly but stabilizes in 5–10 years (not shown). The right panel of the figure below indicates how well the positions of eastward jets agree among the ensemble members. Except for the equatorial currents (like the primary and secondary Tsuchiya Jets) and those stable jets near 33º and 40ºN, the axes of the jets more or less vary among ensemble members. Nevertheless, some coherence is also evident; in particular, the poleward-propagating jets in the 5º–15ºN band tend to agree among themselves. In the equatorward-propagating regime 20º–30ºN, coherent propagation sometimes emerges. If the tropical (equatorward of 15ºN) jets are deterministic, their migration may be due to some slow change in external forcing.

Keywords: deep jets, chaos, eddy-resolving OGCM

©2019. Japan Geoscience Union. All Right Reserved.

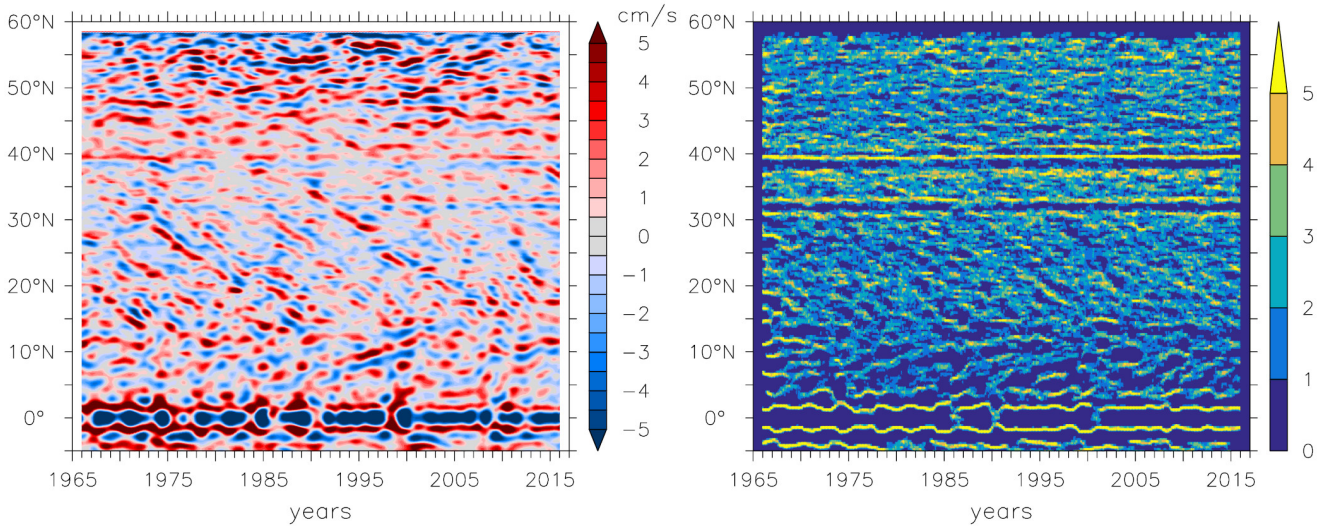

©2019. Japan Geoscience Union. All Right Reserved.

The impact of tidal mixing on the Indonesian Throughflow

*Kohki Shiroyama[1], Shinichiro Kida[2], Hideharu Sasaki[3], Ryo Furue[3]

1. Interdisciplinary Graduate School of Engineering Sciences, Kyushu University, 2. Research Institute for Applied Mechanics Kyushu University, 3. JAMSTEC. APL

The Indonesian Seas are where the Indonesian Throughflow (ITF) flows from the Pacific to the Indian Ocean. The sea surface temperature of the ITF plays an important role in the development of the atmospheric deep convection above these seas. In the Indonesian Seas, the bottom topography is rough and likely induces strong tidal mixing. To examine the impact of tidal mixing on the water mass properties of the ITF, we examined the temperature, salinity, and velocity of the ITF by using OFES2, a quasi-global ocean circulation model that includes global tidal mixing parameterization. We find the impact of tidal mixing to change the water mass properties of the ITF and its flow structure, especially above seamounts and at the straits. The vertical distribution of water mass properties at these location shows more uniform profile. This is considered that tidal mixing has a strong effect on the ITF at narrow location like Straits. We plan to analysis more to investigate the cause of these changes.

Keywords: tidal mixing, Indonesian Throughflow

©2019. Japan Geoscience Union. All Right Reserved.

Verification for subsurface oceanic structure in OFES outputs driven by different wind data sets (NCEP/NCAR and QSCAT)in the tropical Pacific Ocean

*Hiroshige Fukunaga[1], Kunio Kutsuwada[1], Akira Kakiuchi[1], Yuma Yanagida[1], Hideharu Sasaki[2], Yoshikazu Sasai[2]

1. Tokai University, 2. JAMSTEC

1 Introduction
OFES is a numerical model that reproduces oceanic circulation and structure with high resolution by inputting sea surface flux (momentum heat and freshwater). Intercomparison between two types of OFESruns (NCEPrun and QSCATrun) driven by different wind datasets with no different surface heat flux revealed that the thermocline depth near 10˚N is about 50m shallower in the NCEPrun than that in the QSCATrun. The integrated meridional geostrophic transports from the east boundary in the NCEPrun are about 10Sv larger than in the QSCATrun (Kutsuwada et al 2018).
In this study we examine oceanic structures and zonally-integrated meridional geostrophic transports in the southern hemisphere by making intercomparison between the two OFES runs together with comparison with the MOAA-GPV data set constructed by Argo float observations.
2 Data
OFES is high resolution semi-global ocean circulation model developed by JAMSTEC based on Modular Ocean Model ver.3 developed by NOAA. It can reproduce ocean circulation and structure with high resolution. As the external force driving the model we use two different types of wind data sets by numerical re-analysis (NCEP NCAR) and satellite measurement (QuikSCAT).
We averaged spatially for horizontal resolution from 0.1˚x0.1˚to 1˚x1˚. In the vertical direction we converted all simulated data such as temperature salinity and current with depth interval of 10m using Akima-method from sea surface(2.5m) to 6065m.
3 Method
Using dynamic height anomaly we calculate geostrophic current that is integrated vertically from sea surface to depth h (m). We use the depth of no motion of 2000m.The meridional Sverdrup transport corresponds vertically integrated flow from sea surface to depth of no motion (the maximum depth of wind driven circulation) and is given by the sum of the Ekman transport (calculated from Coriolis parameter and zonal wind-stress) and geostrophic transport.
In this study we verify the correspondence between geostrophic transports which are obtained from oceanic data and wind-driven transports calculated from sea surface wind data.
4 Result
The thermocline depth near 10S in the NCEPrun is about 50m shallower than that in the QSCATrun. The zonally-integrated meridional geostrophic transports from the east boundary in the NCEPrun is 10 Sv smaller than in the QSCATrun. Comparison of the two runs with the MOAA-GPV showed that the temperatures in the NCEPrun are lower than those in the MOAA-GPV at 50-400m depth while the QSCATruns is almost similar to the MOAA-GPV above 200m. In comparison for the integrated meridional geostrophic transports the values in the QSCATrun are smaller than those in the NCEPrun and similar to those in the MOAA-GPV. These results mean that in the southern hemisphere the QSCATrun reproduces real oceanic structures with higher reliability than the NCEPs one the same as that in the northern hemisphere.
Comparison in the meridional profile of zonally-averaged wind stress curl (WSC) showed that the NCEPs

©2019. Japan Geoscience Union. All Right Reserved.

WSC has larger values in a zone of 10˚S corresponding to negative maximum than the QSCAT and also the same differences as that in a zone of 10˚N corresponding to positive maximum. The geostrophic transports from the QSCATrun correspond the wind-driven flow calculated from QSCATs wind data closely at low latitude which suggests that the Sverdrup balance holds in these regions.

©2019. Japan Geoscience Union. All Right Reserved.

Inter-comparison of ocean wave data from drifting buoys, moored GPS buoys
and reanalysis data

*Yukiharu Hisaki[1]

1. University of the Ryukyus

Observation of surface wave data such as wave height and period are important for practical and scientific purposes. However, wave observations by moored buoys around Japan are only by GPS buoys, which are located about 10 km from the coast. The observations of wave heights and periods by Japan Meteorological Agency (JMA) drifting buoys were conducted from 2000. Wave data from drifting buoys are inter-compared with GPS buoys and ERA-Interim reanalysis data. The GPS wave data are compared with those from drifting buoys and ERA-Interim data, when a drifting buoy is close to a GPS buoy position, and the number of comparison is limited. The data period of wave data of drifting buoys and ERA-Interim data is from 2000 to 2018. The agreement of wave heights between from GPS and drifting buoys is better than that between from GPS and ERA-Interim data. The agreement of wave periods between from GPS and drifting buoys is not much better than that between from GPS and ERA-Interim data. There are cases that wave periods by drifting buoys are much longer than those from GPS buoys. The dependency of wave parameter differences between from drifting buoys and ERA-Interim data on drifting buoy speeds is investigated.
The drifting current components to the mean wave directions are evaluated from the drifting currents estimated from the drifting buoy positions and the ERA interim mean wave directions.
The differences of wave heights between from drifting buoys and ERA-Interim data are larger as faster current speeds.
The ERA-Interim wave heights are underestimated when current directions are opposite to mean wave directions. The ERA-Interim wave heights are overestimated current directions are following to wave directions. The ratio as drifting wave period/ERA-Interim wave period is smaller as increasing opposing current component, which is consistent with the Doppler shift.

Keywords: wave height, wave period, drifting buoy

©2019. Japan Geoscience Union. All Right Reserved.

Merge and Separation of ocean eddies around the Kuroshio Extension

*koutarou matsuhashi[1], Kazuyuki Uehara[1]

1. The Graduate School of Marine Science Technology

Oceanic mesoscale eddies make ow complicate and produce non-steady states in the ocean general circulation. These eddies are in addition considered to play a important role of heat and material transports. Therefore understanding of dynamics of mesoscale eddies and its roles are one of main tasks in Physical Oceanography. In particular the area around the Kuroshio Extension has very high activity of mesoscale eddies due to the Kuroshio Extension meanderings. Therefore, phenonmena of merging and seperating eddies frequently are observed in this area. Matsuoka et al.(2016) classified events of eddy merges and separations using a high resolution ocean general circulation model. In this study, at first we define mesoscale eddies using the second invariant of the velocity gradient tensor(this is equivalent with the Okubo-Weiss parameter) computed from sea surface height anomalies (AVISO), secondly we track the eddies, and finally, we discuss changes in physical parameters on events of eddy merging and seperating.

Keywords: messoscale eddy

©2019. Japan Geoscience Union. All Right Reserved.

Influence of eddy-trapped water mass reaching 137E survey line using OGCM and a particle-tracking method

*Hideyuki Nakano[1], Hiroyuki Tsujino[1], Kei Sakamoto[1], Shogo Urakawa[1], Takahiro Toyoda[1], Goro Yamanaka[1], Yoshimasa Matsumura[2]

1. Meteorological Research Institute, 2. Atmosphere and ocean research Institute, the University of Tokyo

Mesoscale eddies are known to play a major role in water mass formation and transport. In recent years, several studies have estimated eddy-trapped transport (e.g., Zhang et al 2014), arguing that this can be comparable to the mean-flow transport. However, these estimates are based on satellite observation and ideal vortex vertical structure of eddies, not based on direct ones. In this study, we directly diagnose the eddy-trapped transport by using eddy-resolving Ocean General Circulation Model (OGCM) and off-line particle tracking method. We focus on the eddy-trapped watermass reaching the 137E survey line, which is maintained for more than 50 years by the Japan Meteorological Agency and the importance of eddy activity is pointed out. Along 137E meridional section, a total of about 1 million particles are released every August during 1993 to 2017. Using daily output and offline-particle tracking method, reverse tracking is performed until each particle reaches the mixed-layer, where each particle is ventilated and its properties significantly change due to air-sea interaction. Each particle is divided into typical water mass categories, judging from its temperature, salinity, potential vorticity and location during the ventilation. Whether or not each particle is trapped in the mesoscale eddies is judged by Okubo-Weiss parameter. Distribution of ventilated areas of typical water masses such as Tropical Water (TW), Subtropical Mode Water (STMW), Eastern Subtropical Mode Water (ESTMW), Lighter variety of Central Mode Water (L-CMW) is realistically reproduced. About 20% of TW are present in mesoscale eddies during ventilation, and 60% of the them are present in anticyclonic ones. About half of them (~10% of the total TW) reach137E in a state trapped in the eddies. Their trajectories are almost westward, whereas the trajectories not trapped in eddies are the west-southwest direction reflecting the subtropical circulation. Arrival times from the ventilated area nearly the same for the both, except for the subtropical countercurrent where the average flow is eastward and the arrival time is shorter for those trapped in the eddies. About 30% of STMW are present in eddies during ventilation, and about 80% of them are present in anticyclonic ones. About 1/3 of them (~10% of total STMW) reach 137E in a state trapped in eddies. For the STMW, the arrival time is longer for those trapped in the eddies, and their trajectories are not simple westward. Less than 20% of ESTMW and L-CMW are present in eddies during ventilation, and the ratio between the anticyclonic and cyclonic eddies is almost the same. Only 1/4 of them (5% of the total water masses) reach 137E in a state trapped in eddies. Even though the trajectory of the water mass trapped in the eddies show a clear east-west direction like TW, the arrival time is longer for the water mass trapped in the eddies. This estimate that 5-10% of these water masses reaching 137E trapped in a state eddies may be smaller than the recent estimate in past studies. These differences are also discussed.

Keywords: mesoscale eddy, watermass, particle tracking

©2019. Japan Geoscience Union. All Right Reserved.

A study on the variability of the deep ocean circulation during glacial climate with a climate model of intermediate complexity

*Taigo Ando[1], Akira Oka[1]

1. Atmosphere and Ocean Research Institute, University of Tokyo

Ice core reconstructions show that there were abrupt climate changes termed Dansgaard-Oscillation (D-O) oscillations during glacial period, which are most characterized by about 10 ℃ of temperature changes in Greenland within a few decades. Many studies have pointed out the connection between D-O oscillations and changes in the Atlantic Meridional Overturning Circulation (AMOC), while details of its variability is still missing. Previous modeling studies have suggested that the variability of the AMOC including D-O oscillations are invoked by freshwater input from melted ice-sheets into the deep-water formation region in the North Atlantic (e.g. Rahmstrf, 2002). However, some recent model simulations exhibit abrupt and spontaneous oscillations without freshwater forcing in glacial climate (Peltier and Vettoretti, 2014; Brown and Galbraith, 2016), and more researchers are considering that the mechanism of D-O oscillations is involved within the ocean dynamics and its interactions with the atmosphere and sea ice. Since global coupled models usually used in previous simulations contain many processes of the atmosphere and the ocean, they require high computational costs and it is difficult to identify the processes contributing to D-O oscillations from the model simulations. On the other hand, earth system models of intermediate complexity with lighter computational costs have difficulties in reproducing climate features.
In this study, we modified the model in which the atmosphere component is simplified to the energy-balanced model (MIROC-lite, Oka et al., 2011, 2017) by using results of a full-coupled model (MIROC, Hasumi and Emori, 2001) as parameters so as to have equivalent performance to the full-coupled model, then conducted simulations of glacial climate with the model. This model is expected to be effective for investigating the cause of the spontaneous oscillations of full-coupled models since it can better represent thermal feedback between the atmosphere and the ocean by predicting atmosphere temperature from energy balance compared to ocean-only models. In our presentation, we discuss the performance of the model and its implications for the mechanism of D-O oscillations.

Keywords: glacial climate, deep ocean circulation, climate model

©2019. Japan Geoscience Union. All Right Reserved.

[J] Oral | A (Atmospheric and Hydrospheric Sciences)：A-HW Hydrology & Water Environment

Mon. May 27, 2019 9:00 AM - 10:30 AM JST | Mon. May 27, 2019 12:00 AM - 1:30 AM UTC | 105 1F

[A-HW24] Isotope Hydrology 2019

convener:Masaya Yasuhara(Rissho Univ.), Kohei Kazahaya(Geological Survey of Japan, AIST), Shinji Ohsawa(Institute for Geothermal Sciences, Graduate School of Science, Kyoto University), Kazuyoshi Asai(Geo Science Laboratory), Chairperson:Masaya Yasuhara(Rissho Univ.), Noritoshi Morikawa(産業技術総合研究所活断層・火山研究部門)

The purpose of the session is to review the present state of knowledge of isotope hydrology,
by bringing together hydrologists, geologists, volcanologists, geochemists, agronomists, ecologists, engineers and so on.

9:00 AM - 9:30 AM JST | 12:00 AM - 12:30 AM UTC

[AHW24-01] The use of natural abundances of stable isotopes to elucidate the nitrogen dynamics in plant-soil systems

★Invited Papers

*Keisuke Koba[1] (1.Center for Ecological Research, Kyoto University)

9:30 AM - 9:45 AM JST | 12:30 AM - 12:45 AM UTC

[AHW24-02] Reconstruction of local temporal variation on atmospheric sulfur hexafluoride concentration in the Kyoto Basin by multiple environmental tracer and mass transport analyses

*Koki Kashiwaya[1], Taishi Hori[1], Ryuta Hazama[2], Yoichi Sakuma[3], Katsuaki Koike[1] (1.Kyoto University, 2.Osaka Sangyo University, 3.Tokyo Institute of Technology)

9:45 AM - 10:00 AM JST | 12:45 AM - 1:00 AM UTC

[AHW24-03] Quantitative reconstruction of the humidity in the moisture source region based on the ^{17}O-excess in precipitation on a subtropical island

Yuina Uechi[1], *Ryu Uemura[1] (1.University of the Ryukyus)

10:00 AM - 10:15 AM JST | 1:00 AM - 1:15 AM UTC

[AHW24-04] Identification of deep groundwater recharge system in an intermontane basin

*Takashi Nakamura[1], Kei Nishida[1], Naim Mohamad[2], Bijay Man Shakya[1], Kazuyoshi Asai[4], Sresh Das Shrestha[3] (1.ICRE, University of YAMANASHI, 2.University of Yamanashi, 3.CDG, Tribhuvan University, 4.Geo-Science Laboratory)

10:15 AM - 10:30 AM JST | 1:15 AM - 1:30 AM UTC

Discussion

The use of natural abundances of stable isotopes to elucidate the nitrogen dynamics in plant-soil systems

*Keisuke Koba[1]

1. Center for Ecological Research, Kyoto University

Nitrogen (N) dynamics in terrestrial ecosystems are quite complex because of its high turnover due to the high biological N demand by plants and microbes. The uses of the natural abundance of stable N and oxygen (O) isotopes have been carried out in many ways to elucidate the N dynamics in intact terrestrial ecosystems. The methodological progress ("denitrifier method") can allow us to measure not only N but also O isotope ratios with samples with low N amounts. We applied this analytical method to elucidate the fate of nitrate. Among many fates of nitrate in terrestrial ecosystems, plant nitrate uptake is quite difficult to evaluate. In this talk, I will introduce our results on the uptake of the soil nitrate by tundra plants where soil net nitrification rates are quite low.

Keywords: stable isotopes, soil nitrate

©2019. Japan Geoscience Union. All Right Reserved.

Reconstruction of local temporal variation on atmospheric sulfur hexafluoride concentration in the Kyoto Basin by multiple environmental tracer and mass transport analyses

*Koki Kashiwaya[1], Taishi Hori[1], Ryuta Hazama[2], Yoichi Sakuma[3], Katsuaki Koike[1]

1. Kyoto University, 2. Osaka Sangyo University, 3. Tokyo Institute of Technology

Groundwater is a valuable water resource and understanding groundwater flow regime is indispensable to maintain its quantity and quality at favorable conditions and to achieve its sustainable use. Residence time is an indicator reflecting flow regime of groundwater and various environmental tracers can be used to estimate residence time. Sulfur hexafluoride (SF_6) is one of such dating tracer and is frequently used to estimate residence time of relatively young groundwater. SF_6 residence time is estimated by comparing temporal variation curve of atmospheric SF_6 concentration with concentration obtained from measurement of groundwater sample. Groundwater dating with SF_6 is sometimes difficult in urban areas because of locally elevated atmospheric SF_6 concentration and/or contamination. If local temporal change of atmospheric SF_6 concentration can be reconstructed, and if contaminated samples can be detected, they help to increase accuracy of groundwater dating with SF_6. Therefore, we tried to estimate local temporal change of atmospheric SF_6 concentration in the Kyoto Basin. Groundwater samples were collected from 47 wells in the basin and concentrations of tritium and SF_6 were determined. Air samples were also collected at three points to reconstruct the variation curve. Additionally, groundwater flow and mass transport analyses were conducted using MODFLOW and MT3DMS. The groundwater flow and mass transport models were calibrated by comparisons with actually measured water levels and tritium concentrations. Several temporal variation curves of local temporal variation on atmospheric SF_6 concentration were considered, and using these curves, mass transport analysis of SF_6 was conducted. Finally, the calculated and actually measured SF_6 concentrations in groundwater were compared and the temporal variation curve with which error between the calculated and measured values was minimum was selected. In the presentation, residence time of groundwater in the Kyoto Basin is presented and plausibility of the selected temporal curve is discussed.

Keywords: Groundwater, Residence time, Sulfur hexafluoride, Tritium, Mass transport analysis

©2019. Japan Geoscience Union. All Right Reserved.

Quantitative reconstruction of the humidity in the moisture source region based on the ^{17}O-excess in precipitation on a subtropical island

Yuina Uechi[1], *Ryu Uemura[1]

1. University of the Ryukyus

A high-precision analysis of the triple oxygen isotope composition of water provides a new tracer denoted as ^{17}O-excess. In theory, the ^{17}O-excess can be interpreted as variations in the relative humidity in moisture source regions for precipitation. However, recent studies on ^{17}O-excess in the precipitation in polar and dry regions suggest the importance of snow formation and raindrop re-evaporation processes. To date, whether humidity in the moisture source region can be quantified based on observations of ^{17}O-excess in precipitation has not been proven. Here, we show a 2 year record of the ^{17}O-excess in precipitation on a maritime island in the East Asian monsoon region, Okinawa, Japan. We demonstrate that the reconstructed relative humidity is quantitatively consistent with observations in the oceanic moisture source region. This result suggests that the ^{17}O-excess in precipitation on the subtropical island is determined largely by diffusional fractionation during evaporation in the ocean. These results suggest that the ^{17}O-excess in precipitation in tropical and subtropical regions is a unique quantitative tracer for the relative humidity in oceanic moisture source regions and thus will be a useful tracer and proxy for hydrological and paleoclimate studies.

Reference:
Uechi, Y. and R. Uemura, Dominant influence of the humidity in the moisture source region on the ^{17}O-excess in precipitation on a subtropical island, Earth and Planetary Science Letters, in press.

Keywords: 17O, stable isotope, monsoon, precipitation

©2019. Japan Geoscience Union. All Right Reserved.

Identification of deep groundwater recharge system in an intermontane basin

*Takashi Nakamura[1], Kei Nishida[1], Naim Mohamad[2], Bijay Man Shakya[1], Kazuyoshi Asai[4], Sresh Das Shrestha[3]

1. ICRE, University of YAMANASHI, 2. University of Yamanashi, 3. CDG, Tribhuvan University, 4. Geo-Science Laboratory

This study focuses on identifying the deep groundwater recharge system in Kathmandu Valley, Nepal using various environmental tracers. The Kathmandu Valley is one of the largest intermontane basin that covers an area of 625 km^2. The average altitude of the valley floor is 1350 m above sea level and is surrounded by the hills rising more than 2800 m. Rainfall in the basin is mostly seasonal with roughly 80% of the 1755 mm average annual total arriving between June and September during monsoon season. Groundwater samples were collected from 10 deep tube wells covering almost all parts of the valley and 2 shallow dug wells located at the central part of the valley. All the collected samples were then subjected to the analysis of major dissolved ions, hydrogen and oxygen stable isotopes and radiocarbon.

Groundwater ion composition using Hexa-diagram showed that the deep groundwater of the Kathmandu Valley tends to be relatively young in the outer peripheral area. Meanwhile for the groundwater located in the central area tends to be older. However, for the shallow wells located at the central area, the higher values of ion composition were derived from the effect of human activities. Relatively high pMC values obtained from radiocarbon were detected from the shallow groundwater at central part of the valley and from the deep groundwater samples those were collected from the peripheral area. On the other hand, the deep groundwater at the central part of valley was observed with low pMC values.

Relatively heavier stable isotopes of hydrogen were observed from both the deep groundwater and the shallow groundwater in the central part of the valley. Along with the pMC values, these results also suggests the possibility of vertical groundwater recharge from the shallow groundwater to the deep groundwater in central part of the valley. However, isotopically depleted groundwater recorded from the peripheral areas also concludes the recharge in this basin occurs from the mountain areas.

AKNOWLEDGMENTS: This study was supported by the JSPS KAKENHI Grant Number is 18K11617. It was also partly supported by the Science and Technology Research Partnership for Sustainable Development Program (SATREPS, Project Manager: Professor Narendra Man Shakya and Professor Futaba Kazama) of the Japan International Cooperation Agency (JICA)/Japan Science and Technology Agency (JST).

Keywords: Groundwater recharge, water quality, Hydrogen and oxygen stable isotope, Radiocarbon, Kathmandu Valley, Nepal

©2019. Japan Geoscience Union. All Right Reserved.

[J] Oral | A (Atmospheric and Hydrospheric Sciences)：A-HW Hydrology & Water Environment

Mon. May 27, 2019 10:45 AM - 12:15 PM JST | Mon. May 27, 2019 1:45 AM - 3:15 AM UTC | 105 1F

[A-HW24] Isotope Hydrology 2019

convener:Masaya Yasuhara(Rissho Univ.), Kohei Kazahaya(Geological Survey of Japan, AIST), Shinji Ohsawa(Institute for Geothermal Sciences, Graduate School of Science, Kyoto University), Kazuyoshi Asai(Geo Science Laboratory), Chairperson:Noritoshi Morikawa(産業技術総合研究所活断層・火山研究部門), Kazuyoshi Asai(Geo-Science Laboratory), Kohei Kazahaya(Geological Survey of Japan, AIST)

The purpose of the session is to review the present state of knowledge of isotope hydrology,
by bringing together hydrologists, geologists, volcanologists, geochemists, agronomists, ecologists, engineers and so on.

10:45 AM - 11:15 AM JST | 1:45 AM - 2:15 AM UTC

[AHW24-05] The discharge rate of the Arima-type deep brine discharge in Ooshika-mura, Nagano Prefecture

★Invited Papers

*Fumitake Kusuhara[1] (1.Central Research Institute of Electric Power Industry)

11:15 AM - 11:30 AM JST | 2:15 AM - 2:30 AM UTC

[AHW24-06] Sublacustrine hydrothermal system of the active crater lake, Yudamari of Aso Volcano inferred from Mg budget of the lake

*Shinji Ohsawa[1], Takeshi Saito[2], Kazuhiro Amita[3] (1.Institute for Geothermal Sciences, Graduate School of Science, Kyoto University, 2.Academic Assembly School of Science and Technology, Shinshu University, 3.Graduate School of Engineering Science, Akita University)

11:30 AM - 11:45 AM JST | 2:30 AM - 2:45 AM UTC

[AHW24-07] Spatial distribution of chemical compositions, hydrogen and oxygen isotopic ratios of stream water of the Shimanto River area, southwestern Japan

*Masaaki Takahashi[1], Hinako Shimizu[1], Kohei Kazahaya[1], Masaya Yasuhara[2,1] (1.The National Institute of Advanced Industrial Science and Technology, 2.Rissho University)

11:45 AM - 12:00 PM JST | 2:45 AM - 3:00 AM UTC

[AHW24-08] An isotopic study on shallow groundwater origins in a densely-populated area in Shinagawa, central Tokyo, Japan

*Masaya Yasuhara[1], Akihiko Inamura[2], Takashi Nakamura[3], Kazuyoshi Asai[4] (1.Rissho Univ., 2.Geological Survey of Japan, AIST, 3.Yamanashi Univ., 4.Geo Science Laboratory)

12:00 PM - 12:15 PM JST | 3:00 AM - 3:15 AM UTC

Discussion

The discharge rate of the Arima-type deep brine discharge in Ooshika-mura, Nagano Prefecture

*Fumitake Kusuhara[1]

1. Central Research Institute of Electric Power Industry

Arima-type hot spring water is thought to originate from the dehydration from the hydrous minerals in a subducting slab. In the present research, this dehydrated saline water is called “ADB (Arima-type Deep Brine)”. It is important to estimate the amount of the discharge of ADB in order to understand the water circulation in subduction zones. Few studies, however, have been conducted on such estimation because the chemical and isotopic compositions of the ADB is unknown.Ooshika-Mura is located at the southern part of Nagano prefecture, central Japan. It is thought that the ADB is diluted by local meteoric water, gushes out at several points (e.g. the Kashio hot spring, famous as the Arima-type hot spring), and flows into the 4 rivers in the region. In the present research, the flow rate and Cl- concentration of river water is measured at several points along each river. The flow rate of the ADB is estimated at each observation point, based on the results of above measurements and the previous study on the chemical and isotopic composition of the ADB in the researched region. These estimated flow rate values are regarded as the discharge rate of the ADB discharge inside the upstream watershed areas. The ADB discharge rate over the whole area of Ooshika-Mura is estimated approximately 0.8 L/s, by summing up each flow rate at the most downstream point of each river. The estimation is consistent with previous calculation of the dehydration rate from subducting slabs. More than 50% of the discharged ADB in the whole area concentrates within a few kilometers of the confluence of Kashio River and Shiokawa River. The fault plane of the MTL intersects with the Shiokawa River at the area, which is consistent with the ADB discharging model in Kii peninsula, shown by the previous study.

Keywords: slab-derived fluid, discharge rate, Median Tectonic Line, geologic structure, Kashio

©2019. Japan Geoscience Union. All Right Reserved.

Sublacustrine hydrothermal system of the active crater lake, Yudamari of Aso Volcano inferred from Mg budget of the lake

*Shinji Ohsawa[1], Takeshi Saito[2], Kazuhiro Amita[3]

1. Institute for Geothermal Sciences, Graduate School of Science, Kyoto University, 2. Academic Assembly School of Science and Technology, Shinshu University, 3. Graduate School of Engineering Science, Akita University

The crater lake, Yudamari, formed in the first crater of Mt. Nakadake, Aso Volcano, contains a large amount of dissolved components such as chloride ion (Cl) and magnesium ion (Mg), without the surface outflow of the lake. This kind of water quality is formed under the influence of subaqueous volcanic gas flowing into the lake. From analysis of the isotope composition of the Yudamari water samples (δ D and δ^{18}O), it was found that a large change occurred in the water isotope composition when the lake which became extremely acidic caused the dissolution of chemical components from rocks (oral presentation in the same session last year). In the period when the lake became extremely acidic, the volume of the lake and the water budget were demanded in detail (Saito et al., 2008). We calculated the Mg balance of the lake including the hydrological parameters reported there, and found that a large amount of Mg from 5 to 10 tons per day was eluted from the rock to the lake. Assuming chemical composition and density of the original rock subjected to the acid leaching and converting the Mg leaching amount to the volume of the rock, it is 50 to 200 cubic meters. This is an amazing phenomenon in which a cubic rock from 3 to 6 m is completely altered in one day. The elution of such a large amount of rock components is not caught up in the dissolution reaction only on the bottom surface of the lake. It strongly supports the existence of the subaqueous hydrothermal system that the lake water circulates continuously and reacts with the rock, for example, it is often assumed under the lake of a high temperature and strongly acidic crater lake called active crater lake similar to Yudamari.

Keywords: Aso volcano, active crater lake, magnesium budget, acid leaching, sublacustrine hydrothermal system

©2019. Japan Geoscience Union. All Right Reserved.

Spatial distribution of chemical compositions, hydrogen and oxygen isotopic ratios of stream water of the Shimanto River area, southwestern Japan

*Masaaki Takahashi[1], Hinako Shimizu[1], Kohei Kazahaya[1], Masaya Yasuhara[2,1]

1. The National Institute of Advanced Industrial Science and Technology, 2. Rissho University

109 river water samples were collected from 101 locations in the Shimanto River system and adjacent streams in the western part of Kochi Prefecture and southern part of Ehime Prefecture in December 2007, November 2008, and December 2009, for the purpose of understanding how the distribution of δD and δ^{18}O can be explained by geographical parameters (latitude (LAT), altitude (ELV) and inland degree (Distance from the nearest seashore; DS)) and meteorological parameters (mean annual temperature (MAT) and mean annual precipitation (MAP)), and what is the difference in those explanatory variables of the distribution of δD and δ^{18}O compared to the national level. As a result, it was found that the spatial distribution of δD, δ18O of stream water in the Shimanto area can be shown in detail by using ELV and DS as geographical parameters and MAP as meteorological parameters as explanatory variables.

Keywords: stream water of the Shimanto River, hydrogen and oxygen isotopic ratio, altitude effect, amount effect, inland effect

©2019. Japan Geoscience Union. All Right Reserved.

An isotopic study on shallow groundwater origins in a densely-populated area in Shinagawa, central Tokyo, Japan

*Masaya Yasuhara[1], Akihiko Inamura[2], Takashi Nakamura[3], Kazuyoshi Asai[4]

1. Rissho Univ., 2. Geological Survey of Japan, AIST, 3. Yamanashi Univ., 4. Geo Science Laboratory

Stable isotopes (δ D and δ^{18}O) and hydrochemical tracers (electric conductivity, NH_4^+, NO_3^-, Cl^-) of water were applied to quantify 1) rainfall infiltration (natural recharge), 2) water supply leakage, and 3) sewage leakage in a shallow aquifer in a densely-populated area in Shinagawa, central Tokyo, Japan. Despite of a quite small area about 0.5 km (E-W) by 1 km (N-S), shallow groundwater took on a wide range of values: 28 ~70 mS/m electric conductivity, 0.0 ~9.1 mg/L NH_4^+, 0.1 ~ 36.2 mg/L NO_3^-, 4.8 ~46.6 mg/L Cl^-, and -8.7 ~-7.4‰ δ^{18}O. A ternary mixing model was used based on the Cl^-concentration and d^{18}O of three plausible origins of groundwater to estimate fractions of each component in shallow groundwater in the study area. As a result, a fraction of sewage leakage in groundwater proved large for one well as much as 70%, while for some wells rainfall infiltration contributed more than 80% of water to the formation of groundwater. These remarkable differences in contribution of urban leakage to the shallow aquifer may result from the different state of the water infrastructure in the vicinity of the respective wells.

Keywords: Tokyo, shallow groundwater, origins of groundwater, water leakage, sewage leakage, isotope

©2019. Japan Geoscience Union. All Right Reserved.

[J] Poster | A (Atmospheric and Hydrospheric Sciences)：A-HW Hydrology & Water Environment

Mon. May 27, 2019 3:30 PM - 5:00 PM JST | Mon. May 27, 2019 6:30 AM - 8:00 AM UTC | Poster Hall International Exhibition Hall8, Makuhari Messe_6

[A-HW24] Isotope Hydrology 2019

convener:Masaya Yasuhara(Rissho Univ.), Kohei Kazahaya(Geological Survey of Japan, AIST), Shinji Ohsawa(Institute for Geothermal Sciences, Graduate School of Science, Kyoto University), Kazuyoshi Asai(Geo Science Laboratory)

The purpose of the session is to review the present state of knowledge of isotope hydrology,
by bringing together hydrologists, geologists, volcanologists, geochemists, agronomists, ecologists, engineers and so on.

[AHW24-P01] Geochemical features for spring at Izu Peninsula

*Kazuyoshi Asai[1], Kazumi Asai[1] (1.Geo Science Laboratory)

[AHW24-P02] Acidification process of shallow groundwater in an alluvial fan in Ueda City, Nagano, Japan

Ran Takahashi[1], *Masaya Yasuhara[2], Seongwon Lee[2], Takashi Nakamura[3], Kazuyoshi Asai[4] (1.Undergraduate student, Rissho Univ., 2.Rissho Univ., 3.Yamanashi Univ., 4.Geo Science Laboratory)

[AHW24-P03] Hydroecological study on fresh water copepod in Chino-ike ('Bloody lake'), an ephemeral lake on the top of Mt. Akagi, central Japan

Hirano Yuri[1], *Masaya Yasuhara[2], Seongwon Lee[2], Yasuhiro Funyu[3], Nozomu Iwasaki[2], Natsumi Shimoda[2] (1. Undergraduate student, Rissho Univ., 2.Rissho Univ., 3.Graduate student, Rissho Univ.)

[AHW24-P04] Cross-sectional distribution in water chemistry and oxygen and hydrogen isotopic ratios in Fuku River, Saitama, Japan

*Manatsu Kimura[1], Yasuhara Masaya[2], Seongwon Lee[2] (1.Graduate School of Geo-Environmental Science, Rissho University, 2.Faculty of Geo-Environmental Science, Rissho University)

[AHW24-P05] On concentration and origin of chloride ion in small rivers in Jyoboji area, Fujioka, Gunma, Japan

*Taketoshi Hasegawa[1], Masaya Yasuhara[2], Seongwon Lee[2] (1.Rissho University Graduate School of Geo-environmental Science Environmental Systems Science, 2.Rissho Univ.)

[AHW24-P06] Geochemical characteristics and origin of groundwater in central to eastern Hokkaido

*Yusei Nakagaki[1] (1.Chiba University)

[AHW24-P07] Identification of hydrological characteristics on the groundwater recharge in volcanic and non-volcanic mountains

*sano anna[1], Takashi Nakamura[1], Kei Nishida[1] (1.International Research Center for River Basin Environment, University of YAMANASHI)

[AHW24-P08] Analysis of spring water formation mechanism used by ^{222}Rn concentration at Masutomi-Onsen located in Yamanashi, Japan

*Eiki Mochizuki[1], Takuya Hayakawa[1], Hiroshi Kobayashi[1] (1.Yamanashi Institute of Public Health and Environment)

[AHW24-P09] Migration Behavior of Radiocesium Derived from the Fukushima Dai-Ichi Nuclear Power Plant Accident in Natsui River and Tone River

*Deddy Irawan Permana Putra[1], Shinya Ochiai[2], Seiichi Tomihara[3], Shun Watanabe[4], Kyuma Suzuki[4], Seiya Nagao[2] (1.Kanazawa University, Graduate School of Natural Science and Technology, 2.Low Level Radioactivity Laboratory, Kanazawa University, 3.Aquamarine Fukushima, 4.Gunma Prefectural Fisheries Experiment Station)

[AHW24-P10] Estimation of excess air component in groundwater by using dissolved Argon concentration

*Kazumi Asai[1], Kazuyoshi Asai[1] (1.Chikyukagakukenkyusho inc)

Geochemical features for spring at Izu Peninsula

*Kazuyoshi Asai[1], Kazumi Asai[1]

1. Geo Science Laboratory

IZU Peninsula is mainly composed of volcanic rocks and hot springs are located all over the area. This study focused on shallow groundwater with high circulation rate. Spring water was collected from 18 site and its dissolved ion, stable isotopes, CFCs and SF6 were determined. Based on the analysis results, we discuss charactaristics of water chemistry, origin and residence time.

Keywords: IZU Peninsula , spring, water chemistry, origin, residence time

©2019. Japan Geoscience Union. All Right Reserved.

Acidification process of shallow groundwater in an alluvial fan in Ueda City, Nagano, Japan

Ran Takahashi[1], *Masaya Yasuhara[2], Seongwon Lee[2], Takashi Nakamura[3], Kazuyoshi Asai[4]

1. Undergraduate student, Rissho Univ., 2. Rissho Univ., 3. Yamanashi Univ., 4. Geo Science Laboratory

The Koganezawa River water in Ueda City, Nagano Prefecture, has strong acidic nature under the influence of pyrite ore deposits once mined in its upstream reach. Sulfate-rich acidified shallow groundwater with pH range of 5 to 6 in the Koganezawagawa River alluvial fan has long been attributed to the infiltration of river water into shallow aquifers beneath the fan (Akutsu, 1958). This study, with the help of a multi-tracer method, aims to improve the information on the present hydrological environment of the Koganezawa River alluvial fan and to clarify its groundwater quality formation process with emphasis on the acidification process of shallow groundwater.
Survey on the Koganezawa River water and shallow groundwater (well water and spring water) of the alluvial fan was conducted from August to November 2018. As a result, 1) groundwater acidity is associated with nitrate and sulfate ions for the left and right banks of the river, respectively, 2) groundwater in the right bank shows lower pH than that in the left bank, and 3) oxygen ($\delta^{18}O$) and hydrogen (δD) isotopic ratios are low for the groundwater in the right bank, compared with that in the left bank. These results strongly suggest the sulfate-rich acidified and isotopically depleted river water infiltrates mainly into the right bank, affecting its shallow groundwater quality. The two end-member mixing analysis, based on the concentration of sulfate (SO_4^{2-}) and nitrate (NO_3^-) ions, indicates a contribution of the infiltrated river water to the formation of the groundwater in the right bank is in the range 8 to 31 %. Furthermore, from the nitrogen ($\delta^{15}N$) and sulfur ($\delta^{34}S$) stable isotopic ratios, it is estimated that nitrogen and sulfur in groundwater in the left bank is likely to be of manure origin. It can be concluded that acidification of shallow groundwater in the Koganezawa River alluvial fan is due to river water infiltration for the right bank, while manuring for the left bank.

Keywords: acidified river water, alluvial fan, river water infiltration, shallow groundwater, groundwater acidification, multi-tracer method

©2019. Japan Geoscience Union. All Right Reserved.

Hydroecological study on fresh water copepod in Chino-ike ('Bloody lake'), an ephemeral lake on the top of Mt. Akagi, central Japan

Hirano Yuri[1], *Masaya Yasuhara[2], Seongwon Lee[2], Yasuhiro Funyu[3], Nozomu Iwasaki[2], Natsumi Shimoda[2]

1. Undergraduate student, Rissho Univ., 2. Rissho Univ., 3. Graduate student, Rissho Univ.

Chino-ike, located on the top of Mt. Akagi at an elevation of ca. 1400 m, is known as an ephemeral lake in which water only appears from early summer to late autumn. Because of being an ephemeral lake, no fish exists there and its ecosystem is mainly composed of plankton. The representative species of plankton in Chino-ike is Acanthodiaptomus pacificus (A. pacificus). Chino-ike is also called “Blood lake” because its water surface used to turn red due to an outbreak of A. pacificus in autumn. This study aims to clarify the ecosystem in Chino-ike with special emphasis on the life cycle of A. pacificus.
The survey was conducted in June, October and December of 2018. In 2018, lake water appeared at 0:00 on October 1 and lasted until 10:00 on October 19. The maximum water depth of 98 cm was recorded at 5:00 on October 3 (Y. Funyu, unpublished data). At the time of the survey on October 16, the maximum water depth was 37 cm, when plankton samples was collected at 17 points of 13 locations including those from different depths at specific locations. The number of plankton in a given volume of lake water was counted on the samples in the laboratory. For the surveys in June and December when the lake dried up, surface soil samples were collected at the same locations for counting the number of dormant eggs and individuals of plankton.
On October 16, most of the collected A. pacificus was copepodite larva. Higher population density was foundat deeper water depths with a maximum density of 477 individuals per litre at 32 cm depth in the center of the lake. From Kadota (1971), it takes at least four months for A. pacificus to develop from an egg to a copepodite larva. But the growth of A. pacificus in Chino-ike was found to be much faster. Because of short-term persistence of water in 2018, it is estimated that A. pacificus in Chino-ike shortened its life cycle and is likely to spend a dry winter in the form of a diapausing larva. From now on, we are elucidating to clarify food habits of A. pacificus on the basis of carbon and nitrogen isotopes as well as to find dormant eggs and individuals in the Chino-ike surface soils .

Keywords: Mt. Akagi, ephemeral lake, Acanthodiaptomus pacificus, aquatic ecology, diapause, carbon and nitrogen isotopes

©2019. Japan Geoscience Union. All Right Reserved.

Cross-sectional distribution in water chemistry and oxygen and hydrogen isotopic ratios in Fuku River, Saitama, Japan

*Manatsu Kimura[1], Yasuhara Masaya[2], Seongwon Lee[2]

1. Graduate School of Geo-Environmental Science, Rissho University, 2. Faculty of Geo-Environmental Science, Rissho University

When discussing water environment of a river, it is essential to know not only the concentration of substances contained in river water but also the dissolved load which is a product of concentration of a given substance and river flow rate. It is therefore important to measure river flow rate and concentration of a given substance with accuracy. In the case of estimating the dissolved load, however, concentration of the substance is often represented by that at a single point in a river cross section, generally by the surface water sample at the center of flow, and less attention has not been paid to its representativeness in a river cross section. It also has been the case with hydrogen and oxygen isotopes, which are often used as tracers in the study on water environment of a river.
In this context, we carried out a field survey in December 2018 to elucidate a detailed concentration distribution of water chemistry (dissolved major ions and heavy metals) and isotopes (dD and $d^{18}O$) for the river cross section 7.7 m wide and ca. 0.5 m deep in Fuku River, Saitama, Japan. As a result, the difference in concentration over the whole cross section of the river was found to be 7.2 % or less for each of the dissolved major ions, whereas as much as 95 % for the dissolved heavy metals. For dD and $d^{18}O$ isotopes, there were differences in those ratios of some ‰and ca. 0.3‰, respectively. It should therefore be noted that considerable over- or underestimation in the dissolved load of substances is likely to happen when estimation is made by a conventional way in which the concentration of substances over the whole cross section is represented by a single surface water sample at the center of flow. This is particularly pronounced for the dissolved heavy metals. When evaluating the dissolved loads in rivers, it is therefore necessary to pay much more attention on where to sample water in a river cross section as well as how to measure the river flow rate accurately.

Keywords: River water, River cross section, Water chemistry, Oxygen and hydrogen isotope, Cross-sectional distribution, Dissolved load

©2019. Japan Geoscience Union. All Right Reserved.

On concentration and origin of chloride ion in small rivers in Jyoboji area, Fujioka, Gunma, Japan

*Taketoshi Hasegawa[1], Masaya Yasuhara[2], Seongwon Lee[2]

1. Rissho University Graduate School of Geo-environmental Science Environmental Systems Science, 2. Rissho Univ.

Ten short streams including Minamizawa-gawa, each of them is about 1 km long, in Joboji area on the left bank of Kanna River, Fujioka City, were investigated in July and December 2018 for the chloride ion concentration, load of chloride ion, and origin of chloride ion in stream waters. Saline low-temperature small springs (“Yashio mineral springs”) are seeping naturally on some spots in the area.

The concentration of chloride ion of Yashio mineral springs were between 4,798 mg/L and 11,892 mg/L in August, and between 5,162 mg/L and 11,032 mg/L in December. The concentration of chloride ion was very high in the streams; for example, in Minamizawa-gawa, the maximum concentration of chloride ion ranged up to 632.5 mg/L in July, while up to 213.7 mg/L in December. The load of chloride ion in Minamizawa-gawa was calculated to be as much as 45 kg/day in December, accounting for 90 % of the total load of chloride ion transported by these ten streams. In spite of being a short stream 1 km long, the hydrogen (δ D) and oxygen (δ 18O) isotopic ratios of Minamizawa-gawa in December showed a sharp increase from -54.5 ‰and -8.0 ‰in headwaters to -46.7 ‰and -7.3 ‰at a downstream end portion, respectively. In addition, the Li/Cl ratio of Minamisawa-gawa was found to be more than 0.001 for most of its watercourse with a maximum ratio of 0.0018 at a downstream end portion. These characteristics of the chloride ion, δ D and δ 18O isotopes, and Li/Cl ratio are attributed to the deep-seated fluid which flows upward through the Sambagawa crystalline schists and mixes with shallow water bodies.

Keywords: stream water, chloride ion, dissolved load, stable isotopes of water, Yasio mineral springs, deep-seated fluid

©2019. Japan Geoscience Union. All Right Reserved.

Geochemical characteristics and origin of groundwater in central to eastern Hokkaido

*Yusei Nakagaki[1]

1. Chiba University

Japanese island arc is located in the subduction system where the groundwater migration/circulation is significant. Groundwater has chemical history of dissolved components that come from deep part. There are many reports about chemical composition of groundwater in Hokkaido. However, there is little geochemical research about chemical constituents derived from deep in the groundwater in Hokkaido. The relationship between geological features and chemical characteristics of groundwater remains unknown. This study focused on the geochemistry of deep fluid collected from hot springs in central to eastern Hokkaido area to understand the origin and underground geochemical processes by analyzing main and trace elements, hydrocarbon gas, and oxygen-hydrogen isotopes.

The concentrations of dissolved major elements such as Cl, suggested that groundwater in Hokkaido is mainly of seawater origin. The δ18O and δD values, however, indicate that the fluid also contains meteoric water. The redox condition of deep environment had changed the concentrations of Mn and SO4, and the weathering of sedimentary rocks had increased the amount of Si, respectively. Iodine was significantly enriched compared to seawater, resulting from the deposition of I-rich marine algae in the internal shallow water zone. Concentrations of trace elements such as Pb, Zn, and Li vary among sampling locations, which indicates elution of Pb and Zn by the weathering of minerals, and release of Li from clay minerals in high temperature environment.

©2019. Japan Geoscience Union. All Right Reserved.

Identification of hydrological characteristics on the groundwater recharge in volcanic and non-volcanic mountains

*sano anna[1], Takashi Nakamura[1], Kei Nishida[1]

1. International Research Center for River Basin Environment, University of YAMANASHI

Kofu basin is located at the central part of Japan, Yamanashi and lies 300 km away from Japan Sea. 80% of this basin area is covered by the mountains that are originated from the volcanism and diastrophism with various geological settings. This study focuses on identifying the groundwater recharge processes in Kai city derived from volcanic mountain and Minami Alps city formed from the fault block mountains, located at the western Kofu basin of Yamanashi prefecture. Water samples were collected from major river, deep tube wells and mountain springs at 2011 to 2013 and 2018.
Spring water collected from the mountains and river water were observed with almost similar depleted value ranges. However, in both cities, the high d-excess values are detected. Higher d-excess value in the mountain might occur from the higher rainfall and snow during winter season, whereas the low d-excess values detected on the alluvial fan might be due to the less winter rainfall and snow in comparison with mountain area. The spatial distributions of the d-excess values and the Cl^- concentrations suggested the Minami Alps city is recharged from the water infiltrated at the mountain to the alluvial fan. Meanwhile, water originated from mountain is recharged to the hill, but it is not recharged to the alluvial fan in Kai city. Thus, the combination of d-excess value and Cl- tracer is useful in identifying the groundwater recharge process of areas with different geological origin.

Keywords: stable isotope of water, Water quality, Groundwater recharge, Mountain block recharge

©2019. Japan Geoscience Union. All Right Reserved.

Analysis of spring water formation mechanism used by ^{222}Rn concentration at Masutomi-Onsen located in Yamanashi, Japan

*Eiki Mochizuki[1], Takuya Hayakawa[1], Hiroshi Kobayashi[1]

1. Yamanashi Institute of Public Health and Environment

The ^{222}Rn content of Masutomi-Onsen in the northern part of Yamanashi Prefecture is one of the best in the country and many users are visiting as spa resort areas. In order to use this hot spring for a long term, planned use, it is important to clarify the current formation mechanism of spring water.
In Masutomi-Onsen, it is reported that the sedimentary rock near the surface of the earth is a source of ^{222}Rn. Therefore, the behaviors of the ^{222}Rn concentration and other component concentrations except ^{222}Rn are considered to be different. Therefore, we attempted to estimate the formation mechanism of spring water based on ^{222}Rn concentration and other component concentration.
In this study, we regularly monitored Nyuzawa spring in the Masutomi-Onsen area for 2 years from April, 2016 to March, 2018, about discharge amount , ^{222}Rn concentration , other component concentrations, and water temperature.
As a result, periodic fluctuations were observed in ^{222}Rn concentration range from 3,700 to 7,800 Bq / kg. However, except for Unusual decrease in concentration at October 2017 and March 2018, other component concentrations, discharge amount, and water temperature were constant.
In October 2017 and March 2018 in which Unusual decrease in other component concentration was observed, both were consistent with the time when the periodic fluctuation of ^{222}Rn concentration showed minimum. lot of rain was observed immediately before monitoring, and it seemed that this was related to ^{222}Rn and other component concentration reduction. From this, we analyzed the variation of ^{222}Rn concentration , Unusual decrease of other component concentrations and the relevance of precipitation.
When water was supplied to the surface by rainfall, ^{222}Rn concentration decreased, and Then it took 4 months to recover. other component concentrations were constant regardless of the amount of precipitation except Unusual decrease.
I set the following hypothesis to explain this. ^{222}Rn arising from sedimentary rocks becomes ^{222}Rn gas in the soil, and this ^{222}Rn gas is one of ^{222}Rn sources in spring water. Normally, shallow groundwater does not intersect with spring water, but shallow groundwater deprives ^{222}Rn gas according to its amount, so ^{222}Rn concentration in spring water fluctuates.
In order to verify this hypothesis, we confirmed the relationship between shallow groundwater level estimated from precipitation and ^{222}Rn concentration, and as a result, a significant negative correlation was observed, and a result supporting the hypothesis was obtained.
From these facts, it was possible to explain formation mechanism of spring water based on ^{222}Rn concentration, other component concentrations and precipitation in Nyuzawa spring.

Keywords: hot spring, Masutomi-Onsen, Yamanashi prefecture, Radon-222, formation mechanism

©2019. Japan Geoscience Union. All Right Reserved.

Migration Behavior of Radiocesium Derived from the Fukushima Dai-Ichi Nuclear Power Plant Accident in Natsui River and Tone River

*Deddy Irawan Permana Putra[1], Shinya Ochiai[2], Seiichi Tomihara[3], Shun Watanabe[4], Kyuma Suzuki[4], Seiya Nagao[2]

1. Kanazawa University, Graduate School of Natural Science and Technology, 2. Low Level Radioactivity Laboratory, Kanazawa University, 3. Aquamarine Fukushima, 4. Gunma Prefectural Fisheries Experiment Station

The accident of Fukushima Dai-ichi Nuclear Power Plant due to the Tohoku earthquake, which occurred on 11 March 2011, has released a large amount of radioactive materials to the atmosphere. This accident resulted contamination of radioactive cesium (^{134}Cs and ^{137}Cs) on land, rivers and sea around Fukushima Prefecture. Radioactive cesium widely deposited on land and transported from watershed through river system to the ocean. In this study concentration of ^{134}Cs and ^{137}Cs in river water has been investigated for dissolved and particulate phase. River water sample was collected at a fixed station from the Tone River and the Natsui River at normal and high flow condition during 2018-2019. Suspended solids were separated using continuous flow centrifugation and dissolved cesium were co-precipitated using ammonium molybdophosphate (AMP) method.
The AMP precipitated and suspended solids were dried to determined radioactive cesium concentration using HPGe gamma spectrometry. Investigations of cesium concentration in the rivers have been performed to understand factors controlling transport of radiocesium during different condition. The maximum concentration of ^{134}Cs and ^{137}Cs at normal condition was 0.7 mBq $L^{-1}$and 7.9 mBq L^{-1}in the Tone River, and 1.1 mBq $L^{-1}$and 11 mBq L^{-1}in the Natsui River, respectively. After the rainy events and typhoon, the concentration of ^{134}Cs and ^{137}Cs in river water was increased. Total concentration of ^{134}Cs after the rainy events in the Tone River and the Natsui River was 18 –37 mBq $L^{-1}$and 40 mBq L^{-1} respectively, and concentration for ^{137}Cs was 211 –411 mBq $L^{-1}$and 447 mBq L^{-1}respectively. During the study period, 97-100 % of ^{134}Cs and ^{137}Cs was distributed by suspended solid in the Tone River and 95-100 % of ^{134}Cs and ^{137}Cs in the Natsui River after the rainy events. These results indicate that behavior of suspended solids is a main factor controlling variation of concentration of ^{134}Cs and ^{137}Cs in both rivers.

Keywords: Radioactive Cesium, River water, Suspended solids, Fukushima Dai-ichi Nuclear Power Plant

©2019. Japan Geoscience Union. All Right Reserved.

Estimation of excess air component in groundwater by using dissolved Argon concentration

*Kazumi Asai[1], Kazuyoshi Asai[1]

1. Chikyukagakukenkyusho inc

Estimation of excess air component in groudwater sample is vital for precise groundwater dating using SF_6. In this study, dissolved argon concentration was used for the estimation. We will report distriution of the excess air content in groudwater samples in central Japan, and discuss the impact for the SF6 dating.

Keywords: excess air, dissolved argon, groundwater, SF6 dating, Central Japan

©2019. Japan Geoscience Union. All Right Reserved.

[J] Poster | A (Atmospheric and Hydrospheric Sciences)：A-HW Hydrology & Water Environment

Mon. May 27, 2019 5:15 PM - 6:30 PM JST | Mon. May 27, 2019 8:15 AM - 9:30 AM UTC | Poster Hall International Exhibition Hall8, Makuhari Messe_10

[A-HW24] Isotope Hydrology 2019

convener:Masaya Yasuhara(Rissho Univ.), Kohei Kazahaya(Geological Survey of Japan, AIST), Shinji Ohsawa(Institute for Geothermal Sciences, Graduate School of Science, Kyoto University), Kazuyoshi Asai(Geo Science Laboratory)

The purpose of the session is to review the present state of knowledge of isotope hydrology,
by bringing together hydrologists, geologists, volcanologists, geochemists, agronomists, ecologists, engineers and so on.

[AHW24-P01] Geochemical features for spring at Izu Peninsula

*Kazuyoshi Asai[1], Kazumi Asai[1] (1.Geo Science Laboratory)

[AHW24-P02] Acidification process of shallow groundwater in an alluvial fan in Ueda City, Nagano, Japan

Ran Takahashi[1], *Masaya Yasuhara[2], Seongwon Lee[2], Takashi Nakamura[3], Kazuyoshi Asai[4] (1.Undergraduate student, Rissho Univ., 2.Rissho Univ., 3.Yamanashi Univ., 4.Geo Science Laboratory)

[AHW24-P03] Hydroecological study on fresh water copepod in Chino-ike ('Bloody lake'), an ephemeral lake on the top of Mt. Akagi, central Japan

Hirano Yuri[1], *Masaya Yasuhara[2], Seongwon Lee[2], Yasuhiro Funyu[3], Nozomu Iwasaki[2], Natsumi Shimoda[2] (1. Undergraduate student, Rissho Univ., 2.Rissho Univ., 3.Graduate student, Rissho Univ.)

[AHW24-P04] Cross-sectional distribution in water chemistry and oxygen and hydrogen isotopic ratios in Fuku River, Saitama, Japan

*Manatsu Kimura[1], Yasuhara Masaya[2], Seongwon Lee[2] (1.Graduate School of Geo-Environmental Science, Rissho University, 2.Faculty of Geo-Environmental Science, Rissho University)

[AHW24-P05] On concentration and origin of chloride ion in small rivers in Jyoboji area, Fujioka, Gunma, Japan

*Taketoshi Hasegawa[1], Masaya Yasuhara[2], Seongwon Lee[2] (1.Rissho University Graduate School of Geo-environmental Science Environmental Systems Science, 2.Rissho Univ.)

[AHW24-P06] Geochemical characteristics and origin of groundwater in central to eastern Hokkaido

*Yusei Nakagaki[1] (1.Chiba University)

[AHW24-P07] Identification of hydrological characteristics on the groundwater recharge in volcanic and non-volcanic mountains

*sano anna[1], Takashi Nakamura[1], Kei Nishida[1] (1.International Research Center for River Basin Environment, University of YAMANASHI)

[AHW24-P08] Analysis of spring water formation mechanism used by ^{222}Rn concentration at Masutomi-Onsen located in Yamanashi, Japan

*Eiki Mochizuki[1], Takuya Hayakawa[1], Hiroshi Kobayashi[1] (1.Yamanashi Institute of Public Health and Environment)

[AHW24-P09] Migration Behavior of Radiocesium Derived from the Fukushima Dai-Ichi Nuclear Power Plant Accident in Natsui River and Tone River

*Deddy Irawan Permana Putra[1], Shinya Ochiai[2], Seiichi Tomihara[3], Shun Watanabe[4], Kyuma Suzuki[4], Seiya Nagao[2] (1.Kanazawa University, Graduate School of Natural Science and Technology, 2.Low Level Radioactivity Laboratory, Kanazawa University, 3.Aquamarine Fukushima, 4.Gunma Prefectural Fisheries Experiment Station)

[AHW24-P10] Estimation of excess air component in groundwater by using dissolved Argon concentration

*Kazumi Asai[1], Kazuyoshi Asai[1] (1.Chikyukagakukenkyusho inc)

Geochemical features for spring at Izu Peninsula

*Kazuyoshi Asai[1], Kazumi Asai[1]

1. Geo Science Laboratory

IZU Peninsula is mainly composed of volcanic rocks and hot springs are located all over the area. This study focused on shallow groundwater with high circulation rate. Spring water was collected from 18 site and its dissolved ion, stable isotopes, CFCs and SF6 were determined. Based on the analysis results, we discuss charactaristics of water chemistry, origin and residence time.

Keywords: IZU Peninsula , spring, water chemistry, origin, residence time

©2019. Japan Geoscience Union. All Right Reserved.

Acidification process of shallow groundwater in an alluvial fan in Ueda City, Nagano, Japan

Ran Takahashi[1], *Masaya Yasuhara[2], Seongwon Lee[2], Takashi Nakamura[3], Kazuyoshi Asai[4]

1. Undergraduate student, Rissho Univ., 2. Rissho Univ., 3. Yamanashi Univ., 4. Geo Science Laboratory

The Koganezawa River water in Ueda City, Nagano Prefecture, has strong acidic nature under the influence of pyrite ore deposits once mined in its upstream reach. Sulfate-rich acidified shallow groundwater with pH range of 5 to 6 in the Koganezawagawa River alluvial fan has long been attributed to the infiltration of river water into shallow aquifers beneath the fan (Akutsu, 1958). This study, with the help of a multi-tracer method, aims to improve the information on the present hydrological environment of the Koganezawa River alluvial fan and to clarify its groundwater quality formation process with emphasis on the acidification process of shallow groundwater.
Survey on the Koganezawa River water and shallow groundwater (well water and spring water) of the alluvial fan was conducted from August to November 2018. As a result, 1) groundwater acidity is associated with nitrate and sulfate ions for the left and right banks of the river, respectively, 2) groundwater in the right bank shows lower pH than that in the left bank, and 3) oxygen ($\delta^{18}O$) and hydrogen (δD) isotopic ratios are low for the groundwater in the right bank, compared with that in the left bank. These results strongly suggest the sulfate-rich acidified and isotopically depleted river water infiltrates mainly into the right bank, affecting its shallow groundwater quality. The two end-member mixing analysis, based on the concentration of sulfate (SO_4^{2-}) and nitrate (NO_3^-) ions, indicates a contribution of the infiltrated river water to the formation of the groundwater in the right bank is in the range 8 to 31 %. Furthermore, from the nitrogen ($\delta^{15}N$) and sulfur ($\delta^{34}S$) stable isotopic ratios, it is estimated that nitrogen and sulfur in groundwater in the left bank is likely to be of manure origin. It can be concluded that acidification of shallow groundwater in the Koganezawa River alluvial fan is due to river water infiltration for the right bank, while manuring for the left bank.

Keywords: acidified river water, alluvial fan, river water infiltration, shallow groundwater, groundwater acidification, multi-tracer method

©2019. Japan Geoscience Union. All Right Reserved.

Hydroecological study on fresh water copepod in Chino-ike ('Bloody lake'), an ephemeral lake on the top of Mt. Akagi, central Japan

Hirano Yuri[1], *Masaya Yasuhara[2], Seongwon Lee[2], Yasuhiro Funyu[3], Nozomu Iwasaki[2], Natsumi Shimoda[2]

1. Undergraduate student, Rissho Univ., 2. Rissho Univ., 3. Graduate student, Rissho Univ.

Chino-ike, located on the top of Mt. Akagi at an elevation of ca. 1400 m, is known as an ephemeral lake in which water only appears from early summer to late autumn. Because of being an ephemeral lake, no fish exists there and its ecosystem is mainly composed of plankton. The representative species of plankton in Chino-ike is Acanthodiaptomus pacificus (A. pacificus). Chino-ike is also called “Blood lake” because its water surface used to turn red due to an outbreak of A. pacificus in autumn. This study aims to clarify the ecosystem in Chino-ike with special emphasis on the life cycle of A. pacificus.
The survey was conducted in June, October and December of 2018. In 2018, lake water appeared at 0:00 on October 1 and lasted until 10:00 on October 19. The maximum water depth of 98 cm was recorded at 5:00 on October 3 (Y. Funyu, unpublished data). At the time of the survey on October 16, the maximum water depth was 37 cm, when plankton samples was collected at 17 points of 13 locations including those from different depths at specific locations. The number of plankton in a given volume of lake water was counted on the samples in the laboratory. For the surveys in June and December when the lake dried up, surface soil samples were collected at the same locations for counting the number of dormant eggs and individuals of plankton.
On October 16, most of the collected A. pacificus was copepodite larva. Higher population density was foundat deeper water depths with a maximum density of 477 individuals per litre at 32 cm depth in the center of the lake. From Kadota (1971), it takes at least four months for A. pacificus to develop from an egg to a copepodite larva. But the growth of A. pacificus in Chino-ike was found to be much faster. Because of short-term persistence of water in 2018, it is estimated that A. pacificus in Chino-ike shortened its life cycle and is likely to spend a dry winter in the form of a diapausing larva. From now on, we are elucidating to clarify food habits of A. pacificus on the basis of carbon and nitrogen isotopes as well as to find dormant eggs and individuals in the Chino-ike surface soils .

Keywords: Mt. Akagi, ephemeral lake, Acanthodiaptomus pacificus, aquatic ecology, diapause, carbon and nitrogen isotopes

©2019. Japan Geoscience Union. All Right Reserved.

Cross-sectional distribution in water chemistry and oxygen and hydrogen isotopic ratios in Fuku River, Saitama, Japan

*Manatsu Kimura[1], Yasuhara Masaya[2], Seongwon Lee[2]

1. Graduate School of Geo-Environmental Science, Rissho University, 2. Faculty of Geo-Environmental Science, Rissho University

When discussing water environment of a river, it is essential to know not only the concentration of substances contained in river water but also the dissolved load which is a product of concentration of a given substance and river flow rate. It is therefore important to measure river flow rate and concentration of a given substance with accuracy. In the case of estimating the dissolved load, however, concentration of the substance is often represented by that at a single point in a river cross section, generally by the surface water sample at the center of flow, and less attention has not been paid to its representativeness in a river cross section. It also has been the case with hydrogen and oxygen isotopes, which are often used as tracers in the study on water environment of a river.
In this context, we carried out a field survey in December 2018 to elucidate a detailed concentration distribution of water chemistry (dissolved major ions and heavy metals) and isotopes (dD and $d^{18}O$) for the river cross section 7.7 m wide and ca. 0.5 m deep in Fuku River, Saitama, Japan. As a result, the difference in concentration over the whole cross section of the river was found to be 7.2 % or less for each of the dissolved major ions, whereas as much as 95 % for the dissolved heavy metals. For dD and $d^{18}O$ isotopes, there were differences in those ratios of some ‰and ca. 0.3‰, respectively. It should therefore be noted that considerable over- or underestimation in the dissolved load of substances is likely to happen when estimation is made by a conventional way in which the concentration of substances over the whole cross section is represented by a single surface water sample at the center of flow. This is particularly pronounced for the dissolved heavy metals. When evaluating the dissolved loads in rivers, it is therefore necessary to pay much more attention on where to sample water in a river cross section as well as how to measure the river flow rate accurately.

Keywords: River water, River cross section, Water chemistry, Oxygen and hydrogen isotope, Cross-sectional distribution, Dissolved load

©2019. Japan Geoscience Union. All Right Reserved.

On concentration and origin of chloride ion in small rivers in Jyoboji area, Fujioka, Gunma, Japan

*Taketoshi Hasegawa[1], Masaya Yasuhara[2], Seongwon Lee[2]

1. Rissho University Graduate School of Geo-environmental Science Environmental Systems Science, 2. Rissho Univ.

Ten short streams including Minamizawa-gawa, each of them is about 1 km long, in Joboji area on the left bank of Kanna River, Fujioka City, were investigated in July and December 2018 for the chloride ion concentration, load of chloride ion, and origin of chloride ion in stream waters. Saline low-temperature small springs (“Yashio mineral springs”) are seeping naturally on some spots in the area.

The concentration of chloride ion of Yashio mineral springs were between 4,798 mg/L and 11,892 mg/L in August, and between 5,162 mg/L and 11,032 mg/L in December. The concentration of chloride ion was very high in the streams; for example, in Minamizawa-gawa, the maximum concentration of chloride ion ranged up to 632.5 mg/L in July, while up to 213.7 mg/L in December. The load of chloride ion in Minamizawa-gawa was calculated to be as much as 45 kg/day in December, accounting for 90 % of the total load of chloride ion transported by these ten streams. In spite of being a short stream 1 km long, the hydrogen (δ D) and oxygen (δ 18O) isotopic ratios of Minamizawa-gawa in December showed a sharp increase from -54.5 ‰and -8.0 ‰in headwaters to -46.7 ‰and -7.3 ‰at a downstream end portion, respectively. In addition, the Li/Cl ratio of Minamisawa-gawa was found to be more than 0.001 for most of its watercourse with a maximum ratio of 0.0018 at a downstream end portion. These characteristics of the chloride ion, δ D and δ 18O isotopes, and Li/Cl ratio are attributed to the deep-seated fluid which flows upward through the Sambagawa crystalline schists and mixes with shallow water bodies.

Keywords: stream water, chloride ion, dissolved load, stable isotopes of water, Yasio mineral springs, deep-seated fluid

©2019. Japan Geoscience Union. All Right Reserved.

Geochemical characteristics and origin of groundwater in central to eastern Hokkaido

*Yusei Nakagaki[1]

1. Chiba University

Japanese island arc is located in the subduction system where the groundwater migration/circulation is significant. Groundwater has chemical history of dissolved components that come from deep part. There are many reports about chemical composition of groundwater in Hokkaido. However, there is little geochemical research about chemical constituents derived from deep in the groundwater in Hokkaido. The relationship between geological features and chemical characteristics of groundwater remains unknown. This study focused on the geochemistry of deep fluid collected from hot springs in central to eastern Hokkaido area to understand the origin and underground geochemical processes by analyzing main and trace elements, hydrocarbon gas, and oxygen-hydrogen isotopes.

The concentrations of dissolved major elements such as Cl, suggested that groundwater in Hokkaido is mainly of seawater origin. The δ18O and δD values, however, indicate that the fluid also contains meteoric water. The redox condition of deep environment had changed the concentrations of Mn and SO4, and the weathering of sedimentary rocks had increased the amount of Si, respectively. Iodine was significantly enriched compared to seawater, resulting from the deposition of I-rich marine algae in the internal shallow water zone. Concentrations of trace elements such as Pb, Zn, and Li vary among sampling locations, which indicates elution of Pb and Zn by the weathering of minerals, and release of Li from clay minerals in high temperature environment.

©2019. Japan Geoscience Union. All Right Reserved.

Identification of hydrological characteristics on the groundwater recharge in volcanic and non-volcanic mountains

*sano anna[1], Takashi Nakamura[1], Kei Nishida[1]

1. International Research Center for River Basin Environment, University of YAMANASHI

Kofu basin is located at the central part of Japan, Yamanashi and lies 300 km away from Japan Sea. 80% of this basin area is covered by the mountains that are originated from the volcanism and diastrophism with various geological settings. This study focuses on identifying the groundwater recharge processes in Kai city derived from volcanic mountain and Minami Alps city formed from the fault block mountains, located at the western Kofu basin of Yamanashi prefecture. Water samples were collected from major river, deep tube wells and mountain springs at 2011 to 2013 and 2018.
Spring water collected from the mountains and river water were observed with almost similar depleted value ranges. However, in both cities, the high d-excess values are detected. Higher d-excess value in the mountain might occur from the higher rainfall and snow during winter season, whereas the low d-excess values detected on the alluvial fan might be due to the less winter rainfall and snow in comparison with mountain area. The spatial distributions of the d-excess values and the Cl^- concentrations suggested the Minami Alps city is recharged from the water infiltrated at the mountain to the alluvial fan. Meanwhile, water originated from mountain is recharged to the hill, but it is not recharged to the alluvial fan in Kai city. Thus, the combination of d-excess value and Cl- tracer is useful in identifying the groundwater recharge process of areas with different geological origin.

Keywords: stable isotope of water, Water quality, Groundwater recharge, Mountain block recharge

©2019. Japan Geoscience Union. All Right Reserved.

Analysis of spring water formation mechanism used by ^{222}Rn concentration at Masutomi-Onsen located in Yamanashi, Japan

*Eiki Mochizuki[1], Takuya Hayakawa[1], Hiroshi Kobayashi[1]

1. Yamanashi Institute of Public Health and Environment

The ^{222}Rn content of Masutomi-Onsen in the northern part of Yamanashi Prefecture is one of the best in the country and many users are visiting as spa resort areas. In order to use this hot spring for a long term, planned use, it is important to clarify the current formation mechanism of spring water.
In Masutomi-Onsen, it is reported that the sedimentary rock near the surface of the earth is a source of ^{222}Rn. Therefore, the behaviors of the ^{222}Rn concentration and other component concentrations except ^{222}Rn are considered to be different. Therefore, we attempted to estimate the formation mechanism of spring water based on ^{222}Rn concentration and other component concentration.
In this study, we regularly monitored Nyuzawa spring in the Masutomi-Onsen area for 2 years from April, 2016 to March, 2018, about discharge amount , ^{222}Rn concentration , other component concentrations, and water temperature.
As a result, periodic fluctuations were observed in ^{222}Rn concentration range from 3,700 to 7,800 Bq / kg. However, except for Unusual decrease in concentration at October 2017 and March 2018, other component concentrations, discharge amount, and water temperature were constant.
In October 2017 and March 2018 in which Unusual decrease in other component concentration was observed, both were consistent with the time when the periodic fluctuation of ^{222}Rn concentration showed minimum. lot of rain was observed immediately before monitoring, and it seemed that this was related to ^{222}Rn and other component concentration reduction. From this, we analyzed the variation of ^{222}Rn concentration , Unusual decrease of other component concentrations and the relevance of precipitation.
When water was supplied to the surface by rainfall, ^{222}Rn concentration decreased, and Then it took 4 months to recover. other component concentrations were constant regardless of the amount of precipitation except Unusual decrease.
I set the following hypothesis to explain this. ^{222}Rn arising from sedimentary rocks becomes ^{222}Rn gas in the soil, and this ^{222}Rn gas is one of ^{222}Rn sources in spring water. Normally, shallow groundwater does not intersect with spring water, but shallow groundwater deprives ^{222}Rn gas according to its amount, so ^{222}Rn concentration in spring water fluctuates.
In order to verify this hypothesis, we confirmed the relationship between shallow groundwater level estimated from precipitation and ^{222}Rn concentration, and as a result, a significant negative correlation was observed, and a result supporting the hypothesis was obtained.
From these facts, it was possible to explain formation mechanism of spring water based on ^{222}Rn concentration, other component concentrations and precipitation in Nyuzawa spring.

Keywords: hot spring, Masutomi-Onsen, Yamanashi prefecture, Radon-222, formation mechanism

©2019. Japan Geoscience Union. All Right Reserved.

Migration Behavior of Radiocesium Derived from the Fukushima Dai-Ichi Nuclear Power Plant Accident in Natsui River and Tone River

*Deddy Irawan Permana Putra[1], Shinya Ochiai[2], Seiichi Tomihara[3], Shun Watanabe[4], Kyuma Suzuki[4], Seiya Nagao[2]

1. Kanazawa University, Graduate School of Natural Science and Technology, 2. Low Level Radioactivity Laboratory, Kanazawa University, 3. Aquamarine Fukushima, 4. Gunma Prefectural Fisheries Experiment Station

The accident of Fukushima Dai-ichi Nuclear Power Plant due to the Tohoku earthquake, which occurred on 11 March 2011, has released a large amount of radioactive materials to the atmosphere. This accident resulted contamination of radioactive cesium (^{134}Cs and ^{137}Cs) on land, rivers and sea around Fukushima Prefecture. Radioactive cesium widely deposited on land and transported from watershed through river system to the ocean. In this study concentration of ^{134}Cs and ^{137}Cs in river water has been investigated for dissolved and particulate phase. River water sample was collected at a fixed station from the Tone River and the Natsui River at normal and high flow condition during 2018-2019. Suspended solids were separated using continuous flow centrifugation and dissolved cesium were co-precipitated using ammonium molybdophosphate (AMP) method.
The AMP precipitated and suspended solids were dried to determined radioactive cesium concentration using HPGe gamma spectrometry. Investigations of cesium concentration in the rivers have been performed to understand factors controlling transport of radiocesium during different condition. The maximum concentration of ^{134}Cs and ^{137}Cs at normal condition was 0.7 mBq $L^{-1}$and 7.9 mBq L^{-1}in the Tone River, and 1.1 mBq $L^{-1}$and 11 mBq L^{-1}in the Natsui River, respectively. After the rainy events and typhoon, the concentration of ^{134}Cs and ^{137}Cs in river water was increased. Total concentration of ^{134}Cs after the rainy events in the Tone River and the Natsui River was 18 –37 mBq $L^{-1}$and 40 mBq L^{-1} respectively, and concentration for ^{137}Cs was 211 –411 mBq $L^{-1}$and 447 mBq L^{-1}respectively. During the study period, 97-100 % of ^{134}Cs and ^{137}Cs was distributed by suspended solid in the Tone River and 95-100 % of ^{134}Cs and ^{137}Cs in the Natsui River after the rainy events. These results indicate that behavior of suspended solids is a main factor controlling variation of concentration of ^{134}Cs and ^{137}Cs in both rivers.

Keywords: Radioactive Cesium, River water, Suspended solids, Fukushima Dai-ichi Nuclear Power Plant

©2019. Japan Geoscience Union. All Right Reserved.

Estimation of excess air component in groundwater by using dissolved Argon concentration

*Kazumi Asai[1], Kazuyoshi Asai[1]

1. Chikyukagakukenkyusho inc

Estimation of excess air component in groudwater sample is vital for precise groundwater dating using SF_6. In this study, dissolved argon concentration was used for the estimation. We will report distriution of the excess air content in groudwater samples in central Japan, and discuss the impact for the SF6 dating.

Keywords: excess air, dissolved argon, groundwater, SF6 dating, Central Japan

©2019. Japan Geoscience Union. All Right Reserved.

[J] Poster | A (Atmospheric and Hydrospheric Sciences)：A-HW Hydrology & Water Environment

Mon. May 27, 2019 3:30 PM - 5:00 PM JST | Mon. May 27, 2019 6:30 AM - 8:00 AM UTC | Poster Hall International Exhibition Hall8, Makuhari Messe_7

[A-HW25] Water Environment and Geology in Urban Areas

convener:Takeshi Hayashi(Faculty of Education and Human Studies, Akita University)

The scope of this session is to create an interdisciplinary forum on the most recent advances in water environment and environmental geology research in urban areas. Various kinds of studies concerning environmental issues on water and geology in urban areas (e.g. water balance, water cycle, water resource development and management, inundations, hydrogeology, pollution and remediation, geohazard, basic law on the water cycle) are welcome from academia, industry, and government as well as wider geographic diversity.

[AHW25-P01] Evaluation of regional groundwater flow system for basin water resource management

*Takeshi Hayashi[1], Akinobu Miyakoshi[2], Shoichi Hachinohe[3], Hideki Hamamoto[3] (1.Faculty of Education and Human Studies, Akita University, 2.GSJ, AIST, 3.Center for Environmental Science in Saitama)

[AHW25-P02] Integrated groundwater monitoring required for sustainable basin water resources management: Evaluation of effects of groundwater development utilized existing observation well network in the Tokyo metropolitan area

*Akinobu Miyakoshi[1], Takeshi Hayashi[2], Shoichi Hachinohe[3], Hideki Hamamoto[3] (1.Geological Survey of Japan, AIST, 2.Faculty of Education and Human Studies, Akita University, 3.Center for Environmental Science in Saitama)

[AHW25-P03] STORMWATER DRAINAGE SYSTEM OF AN INDIAN TOWN: WHETHER SUSTAINABLE?

*Rajesh Kumar Vishwakarma[1], Dr. Himanshu Joshi[1] (1.Indian Institute of Technology, Roorkee)

[AHW25-P04] Using a genetic algorithm to investigate the spatial arrangement of low impact development facilities: a case study of National Taiwan University campus.

*Chung-Yuan Liang[1], Gene Jiing-yun You[1] (1.National Taiwan University)

Evaluation of regional groundwater flow system for basin water resource management

*Takeshi Hayashi[1], Akinobu Miyakoshi[2], Shoichi Hachinohe[3], Hideki Hamamoto[3]

1. Faculty of Education and Human Studies, Akita University, 2. GSJ, AIST, 3. Center for Environmental Science in Saitama

In the Kanto plain, which has the Tokyo metropolitan area, one of the world's largest urban areas, groundwater has been developed extensively in various places as an important water resource. While groundwater development has supported the development and expansion of urban areas, it has led to decreases in groundwater resource and land subsidence. As the measures, the national government and municipalities have regulated groundwater pumping by laws and ordinances. However, in recent years, groundwater demands have been increasing again as private water sources at facilities such as hospitals, as responding to the increase in the burden of maintenance cost of water supply and sewage infrastructure due to the declining population, and as water resource against for emergent water source for natural disasters. Responding to these groundwater demands, basin-scale water resources management is required in order to properly use of groundwater without reoccurring land subsidence. In addition, in order to properly manage water resources, it is essential to grasp the influence of the use of groundwater in each region and to grasp changes in regional groundwater flow.

The authors have carried out the studies on groundwater flow system in the plain part of Saitama prefecture, located in the central Kanto plain, to clarify the process and the mechanism of the transition of groundwater flow accompanying groundwater development. Groundwater flow in this area has been changing due to the groundwater development and the pumping restrictions. In order to respond to the future groundwater demand, that is, to predict how the groundwater flow will change with future groundwater re-development in various places, it is necessary not only to grasp the current state of groundwater flow but also to understand the mechanism of the historical change of groundwater flow due to groundwater development. In addition, in this area, the groundwater flow has been also affected by the groundwater use in the surrounding prefectures. Thus, it is also required to grasp the regional groundwater flow in regional scale.

In this area, hydraulic heads in the developed aquifers have recovered due to groundwater pumping regulation. In this process, although the overall hydraulic head distribution of the area has not changed, the difference of water heads in the area has decreased. These results show that although the mechanism of groundwater flow has not changed significantly, the groundwater flux may have decreased. However, the current hydraulic head distribution and the groundwater flow mechanism are quite different from the original ones (state before large-scale development). This suggests that groundwater flow in the area is just a state in which land subsidence is kept and it is becoming a new steady state. In this presentation, based on the results of our studies, we will discuss the groundwater flow in the current condition and in the historical changes with human activities in the area, and issues to grasp regional groundwater flow appropriately.

Keywords: basin water resource management, sustainable groundwater development, regional groundwater flow system, Tokyo metropolitan area

©2019. Japan Geoscience Union. All Right Reserved.

Integrated groundwater monitoring required for sustainable basin water resources management: Evaluation of effects of groundwater development utilized existing observation well network in the Tokyo metropolitan area

*Akinobu Miyakoshi[1], Takeshi Hayashi[2], Shoichi Hachinohe[3], Hideki Hamamoto[3]

1. Geological Survey of Japan, AIST, 2. Faculty of Education and Human Studies, Akita University, 3. Center for Environmental Science in Saitama

Three-dimensional subsurface temperature distribution and its long-term change were examined by repeated observations of temperature-depth profiles at monitoring wells since 2000 in order to evaluate effects of regional-local groundwater flow change due to groundwater development and pumping regulation, urbanization and climate change on groundwater and subsurface thermal environment in the Tokyo metropolitan area, Japan. Results of these studies have suggested that groundwater and subsurface thermal environment shows complex changes over a long term, wide area and deep part in the metropolis. Miyakoshi et al. (2017) have reported the subsurface warming at the shallow part in the southern part of the Kanto Plain from the comparison of temperature-depth profiles measured at the land subsidence and groundwater level observation well distributed in Tokyo and Saitama prefecture in the past 10 years. It was considered that effect of the subsurface warming reaches deeper at the upland corresponding to groundwater recharge area in comparison with the lowland. Miyakoshi et al. (2016) have reported the temperature changes was found at 100 to 300m deep in the southern part of Gunma and Tochigi prefecture by the comparison between present data and past data measured in 1960s and 1970s in the northern part of the plain. This temperature change at the deep part was induced by the effects of groundwater flow changes due to groundwater development and pumping regulation in this area. These results show that the changes in groundwater flow is detected as an anomaly of subsurface temperature distribution and its change.

These previous studies are based on the intermittent repeated measurement in several years. On the other hand, groundwater development shows changes according to social groundwater demand by different periods, and recent demand shows increasing tendency. Groundwater monitoring which respond quickly to its environmental change is required at the regional scale in addition to water resource management at the basin scale, in order to sustainable management of groundwater resource. The groundwater environmental change includes subsurface thermal environmental changes caused by waste heat from surface/underground buildings and climate change. Subsurface temperature monitoring has been conducted since 2012 at 6 wells in Tokyo (Miyakoshi et al., 2017) and since 2007 at 4 wells in Saitama prefecture. These monitoring results showed the continues warming tendency at the shallow part, however differences in the rates of warming and seasonal fluctuation trend were found and it was shown the effects of reginal groundwater flow changes due to artificial effects.

Additionally, it is assumed that not only pumping volume and time but also depth of groundwater development will change with diversified groundwater demand. In order to accord such diversification of groundwater development, it is required to integrate usage of current observation wells and to accumulate efficiently groundwater data. Monitoring of temperature-depth profile by using distributed temperature sensing technology (Yamano and Goto, 2001; Bense et al., 2016) is cited as an example of integrated subsurface temperature observation at the observation wells in addition to temperature monitoring at the several depths by using temperature data loggers, and these monitoring results are expected to detect changes of groundwater flux at the several aquifers. It is possible to detect and

©2019. Japan Geoscience Union. All Right Reserved.

evaluate quickly to respond effects of groundwater development and urbanization by analyzing the observed temperature fluctuation in comparison with hydrogeological information and local groundwater flow changes. Establishment of groundwater monitoring system respond quickly to groundwater development is considered to required for the basin water resource management and sustainable groundwater usage. This study was conducted as a part of Saitama Pref. –Akita Univ.– AIST Joint Research.

Keywords: Basin water resources management, Sustainable groundwater development, Groundwater and subsurface temperature monitoring, Land subsidence and groundwater level observation well network, , Tokyo metropolitan area

©2019. Japan Geoscience Union. All Right Reserved.

STORMWATER DRAINAGE SYSTEM OF AN INDIAN TOWN: WHETHER SUSTAINABLE?

*Rajesh Kumar Vishwakarma[1], Dr. Himanshu Joshi[1]

1. Indian Institute of Technology, Roorkee

In the last few decades, the world has witnessed rapid urbanization. One of the many complex problems which have come up with increased urbanization is that of rapid drainage of storm water from the inhabited areas. This paper presents sustainability evaluation of storm water drainage system of an Indian urban town and interpretation of the findings in order to explore solution. To determine and monitor the implementation of sustainable storm water paradigm, the sub-committee for development of “National (Indian) sustainable habitat parameters on urban storm water management” has developed the key parameters and indicators which are: Natural drainage system index, Drainage coverage (constructed) index, Permeability index, Water bodies rejuvenation index, water body vulnerability index, Water logging index, Area vulnerability index, Storm water discharge quality index and Rainfall intensity index etc. The sustainability indices for the storm water have been computed within the limit on 0 to 1 scale. Interpretation of the computed indices has thrown light on the current status of the system and the desired developments.

Keywords: Storm water, Drainage system, SuDS, Indicators

©2019. Japan Geoscience Union. All Right Reserved.

Using a genetic algorithm to investigate the spatial arrangement of low impact development facilities: a case study of National Taiwan University campus.

*Chung-Yuan Liang[1], Gene Jiing-yun You[1]

1. National Taiwan University

With urban development, surface runoff and peak flow in cites continuously increase and the insufficient capacity of the sewer system induces more and more urban flooding problems. Low Impact Development (LID), one of the source control strategies, uses functionally equivalent hydrologic landscape to improve the ability of infiltration and retention so that the hydrologic condition of the urban surface can be more returned to the pre-development state. Although LID is a kind of the source control strategies, previous studies seldom focus on the spatial arrangement of LID in an urban watershed but only focus on the mechanism units of LID facilities or simple case studies of its implications. This study took the main campus of National Taiwan University (NTU) as a case study. We combined SWMM and a genetic algorithm (GA) to simulate under 36 different rainfall scenarios. The program optimizes installed area size of LID in each sewershed with two different budgetary constraints. By this way, we can know what kind of watershed allocation of LID is more effective for reducing peak flow. In addition, statistical and hydrologic methods are used to analyze the results of optimization. Through analyzing the mechanism of a single unit of LID and optimizing the installed area size of LID in each subcatchment, we can find out how LID reduce peak flow from the microscale and the macroscale. This mechanism of LID also corresponds to the analysis results from optimization, which elaborated that the first priority of setting LID is located at the midstream of the main line where the peak flow concentrates on the peak outflow of the basin rather than before it or after it. In the end, we suggest a LID spatial arrangement strategy for the reference to further city planning.

Keywords: Low Impact Development (LID), Optimization, Genetic Algorithm (GA), SWMM, Urban Hydrology, Urban Drainage

©2019. Japan Geoscience Union. All Right Reserved.

[J] Poster | A (Atmospheric and Hydrospheric Sciences)：A-HW Hydrology & Water Environment

Mon. May 27, 2019 5:15 PM - 6:30 PM JST | Mon. May 27, 2019 8:15 AM - 9:30 AM UTC | Poster Hall International Exhibition Hall8, Makuhari Messe_11

[A-HW25] Water Environment and Geology in Urban Areas

convener:Takeshi Hayashi(Faculty of Education and Human Studies, Akita University)

The scope of this session is to create an interdisciplinary forum on the most recent advances in water environment and environmental geology research in urban areas. Various kinds of studies concerning environmental issues on water and geology in urban areas (e.g. water balance, water cycle, water resource development and management, inundations, hydrogeology, pollution and remediation, geohazard, basic law on the water cycle) are welcome from academia, industry, and government as well as wider geographic diversity.

[AHW25-P01] Evaluation of regional groundwater flow system for basin water resource management

*Takeshi Hayashi[1], Akinobu Miyakoshi[2], Shoichi Hachinohe[3], Hideki Hamamoto[3] (1.Faculty of Education and Human Studies, Akita University, 2.GSJ, AIST, 3.Center for Environmental Science in Saitama)

[AHW25-P02] Integrated groundwater monitoring required for sustainable basin water resources management: Evaluation of effects of groundwater development utilized existing observation well network in the Tokyo metropolitan area

*Akinobu Miyakoshi[1], Takeshi Hayashi[2], Shoichi Hachinohe[3], Hideki Hamamoto[3] (1.Geological Survey of Japan, AIST, 2.Faculty of Education and Human Studies, Akita University, 3.Center for Environmental Science in Saitama)

[AHW25-P03] STORMWATER DRAINAGE SYSTEM OF AN INDIAN TOWN: WHETHER SUSTAINABLE?

*Rajesh Kumar Vishwakarma[1], Dr. Himanshu Joshi[1] (1.Indian Institute of Technology, Roorkee)

[AHW25-P04] Using a genetic algorithm to investigate the spatial arrangement of low impact development facilities: a case study of National Taiwan University campus.

*Chung-Yuan Liang[1], Gene Jiing-yun You[1] (1.National Taiwan University)

Evaluation of regional groundwater flow system for basin water resource management

*Takeshi Hayashi[1], Akinobu Miyakoshi[2], Shoichi Hachinohe[3], Hideki Hamamoto[3]

1. Faculty of Education and Human Studies, Akita University, 2. GSJ, AIST, 3. Center for Environmental Science in Saitama

In the Kanto plain, which has the Tokyo metropolitan area, one of the world's largest urban areas, groundwater has been developed extensively in various places as an important water resource. While groundwater development has supported the development and expansion of urban areas, it has led to decreases in groundwater resource and land subsidence. As the measures, the national government and municipalities have regulated groundwater pumping by laws and ordinances. However, in recent years, groundwater demands have been increasing again as private water sources at facilities such as hospitals, as responding to the increase in the burden of maintenance cost of water supply and sewage infrastructure due to the declining population, and as water resource against for emergent water source for natural disasters. Responding to these groundwater demands, basin-scale water resources management is required in order to properly use of groundwater without reoccurring land subsidence. In addition, in order to properly manage water resources, it is essential to grasp the influence of the use of groundwater in each region and to grasp changes in regional groundwater flow.

The authors have carried out the studies on groundwater flow system in the plain part of Saitama prefecture, located in the central Kanto plain, to clarify the process and the mechanism of the transition of groundwater flow accompanying groundwater development. Groundwater flow in this area has been changing due to the groundwater development and the pumping restrictions. In order to respond to the future groundwater demand, that is, to predict how the groundwater flow will change with future groundwater re-development in various places, it is necessary not only to grasp the current state of groundwater flow but also to understand the mechanism of the historical change of groundwater flow due to groundwater development. In addition, in this area, the groundwater flow has been also affected by the groundwater use in the surrounding prefectures. Thus, it is also required to grasp the regional groundwater flow in regional scale.

In this area, hydraulic heads in the developed aquifers have recovered due to groundwater pumping regulation. In this process, although the overall hydraulic head distribution of the area has not changed, the difference of water heads in the area has decreased. These results show that although the mechanism of groundwater flow has not changed significantly, the groundwater flux may have decreased. However, the current hydraulic head distribution and the groundwater flow mechanism are quite different from the original ones (state before large-scale development). This suggests that groundwater flow in the area is just a state in which land subsidence is kept and it is becoming a new steady state. In this presentation, based on the results of our studies, we will discuss the groundwater flow in the current condition and in the historical changes with human activities in the area, and issues to grasp regional groundwater flow appropriately.

Keywords: basin water resource management, sustainable groundwater development, regional groundwater flow system, Tokyo metropolitan area

©2019. Japan Geoscience Union. All Right Reserved.

Integrated groundwater monitoring required for sustainable basin water resources management: Evaluation of effects of groundwater development utilized existing observation well network in the Tokyo metropolitan area

*Akinobu Miyakoshi[1], Takeshi Hayashi[2], Shoichi Hachinohe[3], Hideki Hamamoto[3]

1. Geological Survey of Japan, AIST, 2. Faculty of Education and Human Studies, Akita University, 3. Center for Environmental Science in Saitama

Three-dimensional subsurface temperature distribution and its long-term change were examined by repeated observations of temperature-depth profiles at monitoring wells since 2000 in order to evaluate effects of regional-local groundwater flow change due to groundwater development and pumping regulation, urbanization and climate change on groundwater and subsurface thermal environment in the Tokyo metropolitan area, Japan. Results of these studies have suggested that groundwater and subsurface thermal environment shows complex changes over a long term, wide area and deep part in the metropolis. Miyakoshi et al. (2017) have reported the subsurface warming at the shallow part in the southern part of the Kanto Plain from the comparison of temperature-depth profiles measured at the land subsidence and groundwater level observation well distributed in Tokyo and Saitama prefecture in the past 10 years. It was considered that effect of the subsurface warming reaches deeper at the upland corresponding to groundwater recharge area in comparison with the lowland. Miyakoshi et al. (2016) have reported the temperature changes was found at 100 to 300m deep in the southern part of Gunma and Tochigi prefecture by the comparison between present data and past data measured in 1960s and 1970s in the northern part of the plain. This temperature change at the deep part was induced by the effects of groundwater flow changes due to groundwater development and pumping regulation in this area. These results show that the changes in groundwater flow is detected as an anomaly of subsurface temperature distribution and its change.

These previous studies are based on the intermittent repeated measurement in several years. On the other hand, groundwater development shows changes according to social groundwater demand by different periods, and recent demand shows increasing tendency. Groundwater monitoring which respond quickly to its environmental change is required at the regional scale in addition to water resource management at the basin scale, in order to sustainable management of groundwater resource. The groundwater environmental change includes subsurface thermal environmental changes caused by waste heat from surface/underground buildings and climate change. Subsurface temperature monitoring has been conducted since 2012 at 6 wells in Tokyo (Miyakoshi et al., 2017) and since 2007 at 4 wells in Saitama prefecture. These monitoring results showed the continues warming tendency at the shallow part, however differences in the rates of warming and seasonal fluctuation trend were found and it was shown the effects of reginal groundwater flow changes due to artificial effects.

Additionally, it is assumed that not only pumping volume and time but also depth of groundwater development will change with diversified groundwater demand. In order to accord such diversification of groundwater development, it is required to integrate usage of current observation wells and to accumulate efficiently groundwater data. Monitoring of temperature-depth profile by using distributed temperature sensing technology (Yamano and Goto, 2001; Bense et al., 2016) is cited as an example of integrated subsurface temperature observation at the observation wells in addition to temperature monitoring at the several depths by using temperature data loggers, and these monitoring results are expected to detect changes of groundwater flux at the several aquifers. It is possible to detect and

©2019. Japan Geoscience Union. All Right Reserved.

evaluate quickly to respond effects of groundwater development and urbanization by analyzing the observed temperature fluctuation in comparison with hydrogeological information and local groundwater flow changes. Establishment of groundwater monitoring system respond quickly to groundwater development is considered to required for the basin water resource management and sustainable groundwater usage. This study was conducted as a part of Saitama Pref. –Akita Univ.– AIST Joint Research.

Keywords: Basin water resources management, Sustainable groundwater development, Groundwater and subsurface temperature monitoring, Land subsidence and groundwater level observation well network, , Tokyo metropolitan area

©2019. Japan Geoscience Union. All Right Reserved.

STORMWATER DRAINAGE SYSTEM OF AN INDIAN TOWN: WHETHER SUSTAINABLE?

*Rajesh Kumar Vishwakarma[1], Dr. Himanshu Joshi[1]

1. Indian Institute of Technology, Roorkee

In the last few decades, the world has witnessed rapid urbanization. One of the many complex problems which have come up with increased urbanization is that of rapid drainage of storm water from the inhabited areas. This paper presents sustainability evaluation of storm water drainage system of an Indian urban town and interpretation of the findings in order to explore solution. To determine and monitor the implementation of sustainable storm water paradigm, the sub-committee for development of “National (Indian) sustainable habitat parameters on urban storm water management” has developed the key parameters and indicators which are: Natural drainage system index, Drainage coverage (constructed) index, Permeability index, Water bodies rejuvenation index, water body vulnerability index, Water logging index, Area vulnerability index, Storm water discharge quality index and Rainfall intensity index etc. The sustainability indices for the storm water have been computed within the limit on 0 to 1 scale. Interpretation of the computed indices has thrown light on the current status of the system and the desired developments.

Keywords: Storm water, Drainage system, SuDS, Indicators

©2019. Japan Geoscience Union. All Right Reserved.

Using a genetic algorithm to investigate the spatial arrangement of low impact development facilities: a case study of National Taiwan University campus.

*Chung-Yuan Liang[1], Gene Jiing-yun You[1]

1. National Taiwan University

With urban development, surface runoff and peak flow in cites continuously increase and the insufficient capacity of the sewer system induces more and more urban flooding problems. Low Impact Development (LID), one of the source control strategies, uses functionally equivalent hydrologic landscape to improve the ability of infiltration and retention so that the hydrologic condition of the urban surface can be more returned to the pre-development state. Although LID is a kind of the source control strategies, previous studies seldom focus on the spatial arrangement of LID in an urban watershed but only focus on the mechanism units of LID facilities or simple case studies of its implications. This study took the main campus of National Taiwan University (NTU) as a case study. We combined SWMM and a genetic algorithm (GA) to simulate under 36 different rainfall scenarios. The program optimizes installed area size of LID in each sewershed with two different budgetary constraints. By this way, we can know what kind of watershed allocation of LID is more effective for reducing peak flow. In addition, statistical and hydrologic methods are used to analyze the results of optimization. Through analyzing the mechanism of a single unit of LID and optimizing the installed area size of LID in each subcatchment, we can find out how LID reduce peak flow from the microscale and the macroscale. This mechanism of LID also corresponds to the analysis results from optimization, which elaborated that the first priority of setting LID is located at the midstream of the main line where the peak flow concentrates on the peak outflow of the basin rather than before it or after it. In the end, we suggest a LID spatial arrangement strategy for the reference to further city planning.

Keywords: Low Impact Development (LID), Optimization, Genetic Algorithm (GA), SWMM, Urban Hydrology, Urban Drainage

©2019. Japan Geoscience Union. All Right Reserved.

[E] Oral | A (Atmospheric and Hydrospheric Sciences)：A-CG Complex & General

Mon. May 27, 2019 1:45 PM - 3:15 PM JST | Mon. May 27, 2019 4:45 AM - 6:15 AM UTC | 104 1F

[A-CG33] Extratropical oceans and atmosphere

convener:Kazuaki Nishii(Graduate School of Bioresources, Mie University), Yoshi N Sasaki(Hokkaido University), Hatsumi Nishikawa(Institute of Low Temperature Science, Hokkaido University), Shun Ohishi(Division for Land-Ocean Ecosystem Research, Institute for Space-Earth Environmental Research, Nagoya University), Chairperson:Kazuaki Nishii(三重大学)

The extratopical ocean had been considered passive to atmospheric variability. Recent studies, however, revealed some active role of the extratopical ocean in modulating the atmosphere. The goal of this session is to deepen our understanding of the air-sea interaction in the extratropics. A wide variety of researches whose topics range from mesoscale to basin-scale, and from daily to global warming are welcomed. Researches on cloud, aerosol, and ecosystem related to the extratopical air-sea interaction are also welcomed.

1:45 PM - 2:05 PM JST | 4:45 AM - 5:05 AM UTC

[ACG33-01] Gulf Stream and Kuroshio are synchronized

★Invited Papers

*Tsubasa Kohyama[1], Hiroaki Miura[1], Shoichiro Kido[1] (1.Department of Earth and Planetary Science, The University of Tokyo)

2:05 PM - 2:20 PM JST | 5:05 AM - 5:20 AM UTC

[ACG33-02] A study on mixed layer depth variability in the Kuroshio Extension region based on a frontal Ekman model

*Tomoki Tozuka[1] (1.Department of Earth and Planetary Science, Graduate School of Science, The University of Tokyo)

2:20 PM - 2:35 PM JST | 5:20 AM - 5:35 AM UTC

[ACG33-03] Mechanisms of Reemergence in the North Pacific revealed by Mixed Layer Heat Budget Analysis

*Kazumichi Murata[1], Shoichiro Kido[1], Tomoki Tozuka[1] (1.Department of Earth and Planetary Science, School of Science, The University of Tokyo)

2:35 PM - 2:50 PM JST | 5:35 AM - 5:50 AM UTC

[ACG33-04] Formation mechanism for the North Pacific Transition domain SST and SSS fronts

*Hatsumi Nishikawa[1], Humio Mitsudera[1], Takeshi Okunishi[2], Shin-ichi Ito[3], Taku Wagawa[4], Daisuke Hasegawa[2], Toru Miyama[5], Hitoshi Kaneko[2] (1.Institute of Low Temperature Science, Hokkaido University, 2.Tohoku National Fisheries Research Institute, Japan Fisheries Research and Education Agency, 3.Atmosphere and Ocean Research Institute, The University of Tokyo, 4.Japan Sea National Fisheries Research Institute, Japan Fisheries Research and Education Agency, 5.Japan Agency for Marine-Earth Science and Technology)

2:50 PM - 3:10 PM JST | 5:50 AM - 6:10 AM UTC

[ACG33-05] Impact of the Kuroshio front on frontal structure of an extratropical cyclone associated with heavy precipitation

★Invited Papers

*Hidetaka Hirata[1], Ryuichi Kawamura[2], Mayumi K Yoshioka[1], Masami Nonaka[3], Kazuhisa Tsuboki[1] (1.Institute for Space-Earth Environmental Research, Nagoya University, 2.Department of Earth and Planetary Sciences, Kyushu University, 3.Application Laboratory, Japan Agency for Marine-Earth Science and Technology)

3:10 PM - 3:15 PM JST | 6:10 AM - 6:15 AM UTC

[ACG33-06] Discussion on future studies on the role of midlatitude oceans

*Kazuaki Nishii[1] (1.Graduate School of Bioresources, Mie University)

Gulf Stream and Kuroshio are synchronized

*Tsubasa Kohyama[1], Hiroaki Miura[1], Shoichiro Kido[1]

1. Department of Earth and Planetary Science, The University of Tokyo

The Gulf Stream and the Kuroshio transport heat from the tropics to the extratropics, and their temperature variations affect densely-populated areas in the northern hemisphere through extreme weather and fisheries production. The two warm ocean currents are separated by the North American continent, and thus, they cannot exchange heat by the oceanic circulation within a few years.

In this presentation, however, we show that sea surface temperatures (SST) of the two warm currents are synchronized for interannual to decadal time scales. This synchronization, which we refer to as the Boundary Current Synchronization (BCS), is associated with the meridional migrations of the atmospheric jet stream. The singular value decomposition (SVD) analysis between SST and zonal wind shows that, from the conventional viewpoint, BCS is explained as the covariability shared by the Pacific Decadal Oscillation and the Northern Annular Mode. Nevertheless, the SVD time series exhibit high correlations with the zonal-mean meridional SST difference between subtropics and midlatitudes, which supports the notion that BCS may be understood better as the annular mode of the upper ocean.

We also discuss some implications for extreme weather and climate change. The regression map of 2-meter temperature on the BCS index exhibits a similar pattern to the temperature pattern in July 2018, which implies an essential relationship between BCS and the abnormally hot summer. BCS also connects two apparently unrelated global warming responses: the western boundary currents warm faster than the global mean, and that the atmospheric jet stream shifts poleward.

Keywords: Atmosphere-Ocean interactions, Kuroshio, Gulf Stream, Atmospheric jet stream

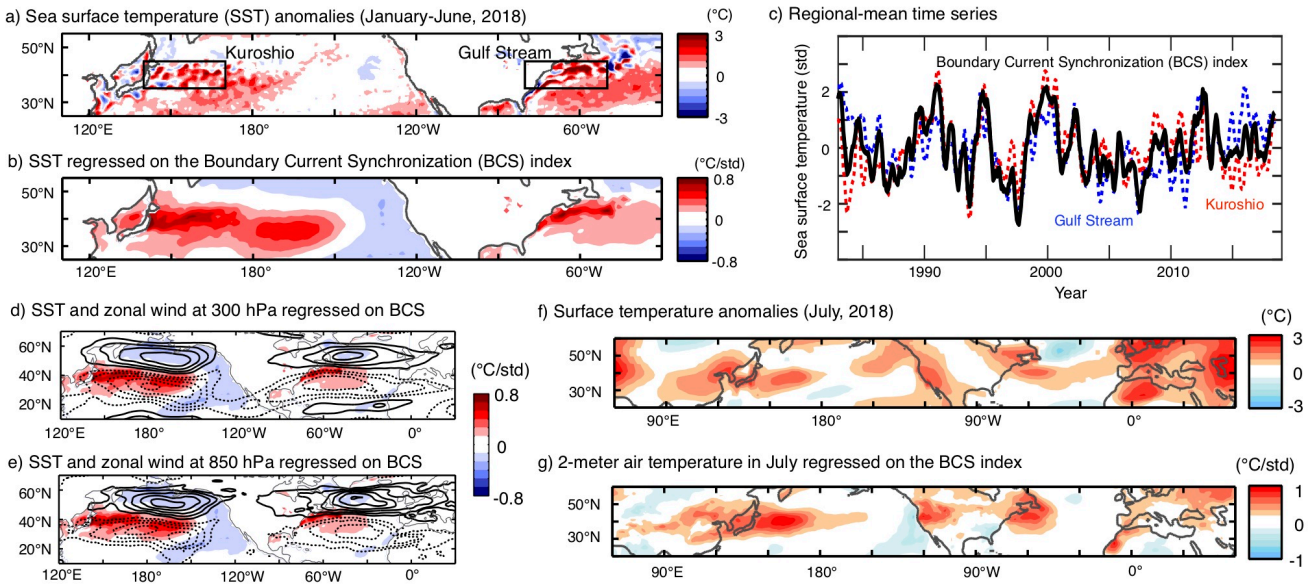

©2019. Japan Geoscience Union. All Right Reserved.

A study on mixed layer depth variability in the Kuroshio Extension region based on a frontal Ekman model

*Tomoki Tozuka[1]

1. Department of Earth and Planetary Science, Graduate School of Science, The University of Tokyo

In oceanic frontal regions, surface geostrophic currents have a vertical shear aligned with the density front that can balance a portion of the surface wind stress, and only the portion of the wind stress that is not in balance with the surface geostrophic shear (i.e. "effective wind stress") forces an ageostrophic Ekman spiral. Thus, if the front were uniform with depth, it is expected that the vertical velocity at tthe mixed layer base is better represented by the curl of the effective wind stress, rather than the full wind stress. In this study, we have examined the above in the Kuroshio Extension region, where a prominent sea surface temperature front exists, and some preliminary results based on an analysis of a high-resolution ocean assimilation product are presented.

Keywords: Mixed layer depth, Frontal Ekman model, Ekman pumping, Kuroshio Extension

©2019. Japan Geoscience Union. All Right Reserved.

Mechanisms of Reemergence in the North Pacific revealed by Mixed Layer Heat Budget Analysis

*Kazumichi Murata[1], Shoichiro Kido[1], Tomoki Tozuka[1]

1. Department of Earth and Planetary Science, School of Science, The University of Tokyo

Wintertime sea surface temperature (SST) anomalies that disappear in summer and recur in the following winter is called “reemergence”. Previous studies suggested that temperature anomalies that subduct into the subsurface during the shoaling phase of the mixed layer are preserved under the mixed layer due to isolation from atmospheric forcing and reentrained into the surface mixed layer. Since reemergence is considered to play an important role in the Pacific Decadal Oscillation, it is important to understand its mechanisms, but past studies are mostly based on statistical analyses. Therefore, in this thesis, the mechanisms of reemergence in the North Pacific is clarified quantitatively by an online mixed layer heat budget analysis with an ocean model simulation.

Following a method proposed by a previous study, areas with reemergence are detected and the focus of this study is the Reemergence Area (RA, 35˚-40˚N, 155˚-145˚W) in the central North Pacific. In the RA, the Reemergence Years (RYs) are determined and the mixed layer heat budget analysis is conducted with the integration of the Regional Ocean Model System (ROMS) covering the RA. In contrast to past studies that suggested importance of anomalous entrainment term, it is shown that several mechanisms are operating in reemergence. In particular, the anomalous Ekman meridional advection of the mean meridional temperature gradient induced by zonal wind stress anomalies plays an important role in many RYs. Also, coincidence in the sign of SST anomalies in winter and surface heat flux anomalies in the following autumn leads to recurrence of SST anomalies in some RYs. On the other hand, the conventional

©2019. Japan Geoscience Union. All Right Reserved.

mechanism related to the mean entrainment of anomalous temperature contributes to reemergence in two RYs.

Keywords: Reemergence, North Pacific, mixed layer heat budget analysis

©2019. Japan Geoscience Union. All Right Reserved.

Formation mechanism for the North Pacific Transition domain SST and SSS fronts

*Hatsumi Nishikawa[1], Humio Mitsudera[1], Takeshi Okunishi[2], Shin-ichi Ito[3], Taku Wagawa[4], Daisuke Hasegawa[2], Toru Miyama[5], Hitoshi Kaneko[2]

1. Institute of Low Temperature Science, Hokkaido University, 2. Tohoku National Fisheries Research Institute, Japan Fisheries Research and Education Agency, 3. Atmosphere and Ocean Research Institute, The University of Tokyo, 4. Japan Sea National Fisheries Research Institute, Japan Fisheries Research and Education Agency, 5. Japan Agency for Marine-Earth Science and Technology

The North Pacific Transition Domain is the area where water exchange between subtropical and subarctic is carried out and there are SST and SSS fronts. The Transition domain is very important area for air-sea interaction, ocean mixed layer formation, biological production, and so on. In this study, to clarify SST and SSS fronts structure and its formation mechanism in the transition domain, we analyzed the data of drifting buoys observation in 2015 and 2017 and modelled particles trajectory.

The buoy trajectories and the modelled trajectories captured the flow structure (i.e. front structure) in detail. They suggest that the flow structure in the transition domain is dominated by low rise bottom topography. We also showed mixing ratio of the subarctic and the subtropical seawater in the Transition domain using the particle tracking. In addition, it was also found that the place where the sea water tends to stagnate well corresponds to the place where the SST deviation appears due to the variation of the Isojet jet J1 indicated by Mitsudera et al. (2018).

Keywords: bottom topography, SST front, SSS front , Subtropical-Subarctic Seawater exchange

©2019. Japan Geoscience Union. All Right Reserved.

Impact of the Kuroshio front on frontal structure of an extratropical cyclone associated with heavy precipitation

*Hidetaka Hirata[1], Ryuichi Kawamura[2], Mayumi K Yoshioka[1], Masami Nonaka[3], Kazuhisa Tsuboki[1]

1. Institute for Space-Earth Environmental Research, Nagoya University, 2. Department of Earth and Planetary Sciences, Kyushu University, 3. Application Laboratory, Japan Agency for Marine-Earth Science and Technology

It is well known that sea surface temperature (SST) fronts associated with warm ocean currents create horizontal thermal gradients in the near-surface atmosphere in the mid-latitudes. These thermal gradients may affect frontal structure of extratropical cyclones passing near warm currents. Moreover, fronts influenced by the mid-latitude ocean may be related to the occurrence of heavy precipitation. To answer these questions, we examined the impact of the SST front along the Kuroshio Current (Kuroshio front) on the frontal structure of an extratropical cyclone associated with heavy precipitation by utilizing observational data, objective analysis data, and regional cloud-resolving numerical experiments. This study paid special attention to an extratropical cyclone and related heavy precipitation on Miyake Island in early January 2017. When the cyclone intensified around the Kuroshio front, two surface fronts developed around the cyclone center. One was a warm front. The other was a non-classic front, which was called the outer front in this study, forming on the northern side of the warm front. A line-shaped precipitation band and a comma head-shaped precipitation band appeared along the outer front and along the bent-back warm front, respectively. During the passage of these bands, heavy precipitation was observed on Miyake Island. Looking at the evolution of the outer front, we found that it was located just along the Kuroshio front in its early life. During the formation stage of the incipient outer front, sensible heat supply was evident from the Kuroshio Current, whereas it was small on the northern side of the oceanic front. This meridional difference in sensible heating caused frontogenesis along the Kuroshio front, which led to the initial formation of the front. Thus, the Kuroshio front played an important role in the formation of the incipient outer front, contributing to the occurrence of the heavy precipitation.

Keywords: extratropical cyclone, Kuroshio, heavy precipitation

©2019. Japan Geoscience Union. All Right Reserved.

Discussion on future studies on the role of midlatitude oceans

*Kazuaki Nishii[1]

1. Graduate School of Bioresources, Mie University

Here, we will discuss future plans of studies on the role of midlatitude oceans in driving the atmospheric variability, and its feedback onto the midlatitude oceans.

©2019. Japan Geoscience Union. All Right Reserved.

[E] Oral | A (Atmospheric and Hydrospheric Sciences)：A-CG Complex & General

Mon. May 27, 2019 3:30 PM - 5:00 PM JST | Mon. May 27, 2019 6:30 AM - 8:00 AM UTC | 104 1F

[A-CG33] Extratropical oceans and atmosphere

convener:Kazuaki Nishii(Graduate School of Bioresources, Mie University), Yoshi N Sasaki(Hokkaido University), Hatsumi Nishikawa(Institute of Low Temperature Science, Hokkaido University), Shun Ohishi(Division for Land-Ocean Ecosystem Research, Institute for Space-Earth Environmental Research, Nagoya University), Chairperson:Shun Ohishi

The extratopical ocean had been considered passive to atmospheric variability. Recent studies, however, revealed some active role of the extratopical ocean in modulating the atmosphere. The goal of this session is to deepen our understanding of the air-sea interaction in the extratropics. A wide variety of researches whose topics range from mesoscale to basin-scale, and from daily to global warming are welcomed. Researches on cloud, aerosol, and ecosystem related to the extratopical air-sea interaction are also welcomed.

3:30 PM - 3:45 PM JST | 6:30 AM - 6:45 AM UTC

[ACG33-07] Intra-seasonal variability of oceanic low-level cloud in summertime North Pacific and its interaction with sea surface temperature

★Invited Papers

*Naoya Takahashi[1], Tadahiro Hayasaka[1] (1.Center for Atmospheric and Oceanic Studies, Graduate School of Science, Tohoku University,)

3:45 PM - 4:00 PM JST | 6:45 AM - 7:00 AM UTC

[ACG33-08] **Sea surface temperature trend in the East China Sea during the 20th century simulated by a regional ocean model**

*Yoshi N Sasaki[1], Chisato Umeda[1] (1.Hokkaido University)

4:00 PM - 4:15 PM JST | 7:00 AM - 7:15 AM UTC

[ACG33-09] Kuroshio Extension and Gulf Stream's influences on the variability of near-surface baroclinicity and the associated atmospheric fields

★Invited Papers

*Bunmei Taguchi[1], Kazuaki Nishii[2], Hisashi Nakamura[1,3] (1.Research Center for Advanced Science and Technology, The University of Tokyo, 2.Graduate School of Bioresources, Mie University, 3. Application Laboratory, Japan Agency of Marine-Earth Science and Technology)

4:15 PM - 4:30 PM JST | 7:15 AM - 7:30 AM UTC

[ACG33-10] Baroclinic Annular Mode in the Southern Hemisphere: Its Reproducibility and Sensitivity to Ocean Fronts assessed in Aqua-Planet Experiments

*Morio Nakayama[1], Masatoshi Mizukoshi[1], Hisashi Nakamura[1], Yu Kosaka[1], Bunmei Taguchi[1], Masato Mori[1], Fumiaki Ogawa[2] (1.RCAST, the University of Tokyo , 2.The University of Bergen)

4:30 PM - 4:45 PM JST | 7:30 AM - 7:45 AM UTC

[ACG33-11] **Hydro-climatic variation in northwestern China and its multi-decadal to multi-centennial teleconnection with the Pacific Ocean**

*Harry F Lee[1] (1.The Chinese University of Hong Kong)

4:45 PM - 5:00 PM JST | 7:45 AM - 8:00 AM UTC

[ACG33-12] Atmospheric zonal-mean meridional circulation and midlatitude oceanic fronts

*Kazuaki Nishii[1], Bunmei Taguchi[2], Hisashi Nakamura[2] (1.Graduate School of Bioresources, Mie University, 2.Research Center for Advanced Science and Technology, The University of Tokyo)

Intra-seasonal variability of oceanic low-level cloud in summertime North Pacific and its interaction with sea surface temperature

*Naoya Takahashi[1], Tadahiro Hayasaka[1]

1. Center for Atmospheric and Oceanic Studies, Graduate School of Science, Tohoku University,

Oceanic low-level cloud (i.e. fog, stratus, and stratocumulus) properties are important to determine radiative cooling at the sea surface via reflecting incident solar radiation, and they strongly interact with sea surface temperature (SST) with positive feedback process (Norris et al. 1998). Despite the importance of the role of low-level cloud in climate change or air-sea interaction, the mechanism of cloud evolution on short time-scale is not well investigated. Thus, the objective of this study is to reveal the evolution of low-level cloud cover (LCC) associated with cloud controlling parameters (e.g. SST, horizontal temperature advection, relative humidity in atmospheric boundary layer, and so on) on short time scale which cannot be revealed by monthly-mean dataset.

For cloud data, we used the level-3 daily gridded data product from MODIS imager (MYD08_D3) with 1 degree of horizontal resolution. OISST and ERA-Interim are used for SST and meteorological parameters, respectively. Spatial and temporal resolutions of these dataset are interpolated into that of MODIS. Target region is western North Pacific (150E-180E, 30N-40N) where standard deviation of LCC in summertime (JJASO) is large. Target period is each summertime from 2003 to 2016. To extract the shorter time-scale variability, we applied Lanczos band-pass filter for each variable. The extracted time scale by the band-pass filter is discussed in the next paragraph.

To investigate dominant time scales of LCC and SST, Fast Fourie Transform (FFT) analysis is applied. The results of FFT analysis for each variable show that 3-7-day and 20-100-day are dominant time-scale for LCC. The dominant time scale of temperature advection (Tadv) is similar to shorter one of LCC, which implies that Tadv is a key factor to control LCC on synoptic time scale rather than SST. On the other hand, for more longer time scale (20-100-day; intra-seasonal time scale), the correlation between SST and LCC is consistent with the previous studies (Norris 2000). To investigate the evolution process of LCC and SST on both time-scale, we applied the band-pass filter to them with two time-scale; (1) 3-7 day and (2) 20-100 day.

We further conducted phase composite analysis for each time scale. The result shows that (1) variation of SST (Tadv) lags (leads) to that of LCC on both time scales but (2) propagating direction of LCC anomaly and associated specific and relative humidity is eastward (westward) on synoptic (intra-seasonal) time scale. The difference in amplitude and propagation direction of LCC on each time-scale depend on different atmospheric dynamics and variation of associated moisture field. The above results also suggest that anomalous dry-cold Tadv is a trigger to increasing in LCC and SST decreasing is followed by them. This lead-lag relationship among each variable is clear on the intra-seasonal time scale. Temperature budget analysis for ocean mixed-layer shows that the SST decreasing is caused by shortwave cooling due to low-level cloud radiative effect and enhanced latent heat release. It emphasizes an importance of anomalous Tadv for the intra-seasonal variations of not only LCC but also SST.

Keywords: Summertime North Pacific, Oceanic low-level cloud, Synoptic and intra-seasonal variabilities, Air-sea interaction, Satellite observations

©2019. Japan Geoscience Union. All Right Reserved.

©2019. Japan Geoscience Union. All Right Reserved.

Sea surface temperature trend in the East China Sea during the 20th century simulated by a regional ocean model

*Yoshi N Sasaki[1], Chisato Umeda[1]

1. Hokkaido University

It has been reported that the East China Sea is one of the region where the sea surface temperature (SST) trend during the 20th century is a couple of times larger than the global mean SST trend. However, the detailed spatial structure of the SST trend in the East China Sea, especially in the early 20th century, and its quantitative mechanism have not been understood. The present study examines the SST trend in the East China Sea from 1901 to 2010 by using a regional ocean modeling system (ROMS) with an eddy-resolving horizontal resolution (0.1˚) from 1871 to 2010. The spatial pattern of our simulation resembles that of the observations. That is, our simulation can reproduce the SST rise along the Kuroshio axis and over the continental shelf along the coast of China. The amplitude of the SST trend in the simulation is within the range between the two observations. The heat budget analysis revealed that the oceanic advection induced the SST rise in both regions. More specifically, the acceleration of the ocean currents plays an important role in the warming of the SST in both regions. In contrast, surface net heat flux acted as the damping of the SST rise.

Keywords: Kuroshio, global warming, ocean model

©2019. Japan Geoscience Union. All Right Reserved.

Kuroshio Extension and Gulf Stream's influences on the variability of near-surface baroclinicity and the associated atmospheric fields

*Bunmei Taguchi[1], Kazuaki Nishii[2], Hisashi Nakamura[1,3]

1. Research Center for Advanced Science and Technology, The University of Tokyo, 2. Graduate School of Bioresources, Mie University, 3. Application Laboratory, Japan Agency of Marine-Earth Science and Technology

Evidence is mounting that mid-latitude western boundary currents (WBCs) can influence large-scale atmospheric circulation variability on interannual-to-decadal time scales. It is, however, still unclear how significantly such extra-tropical oceanic influences stand out of the intense variability intrinsic to the mid-latitude atmosphere. Here we examine the influences of extra-tropical oceanic frontal zone and its variability in the Gulf Stream (GS) and Kuroshio Extension (KE) regions on winter-season atmospheric variability in 20-member ensemble historical AGCM simulations with a horizontal resolution about 100km prescribed with satellite-observed, high-resolution sea surface temperature (SST) and sea-ice variability for the period 1982-2013. We focus on the near-surface baroclinicity $\boldsymbol{B}$ at 925 hPa as the quantity that is crucial for baroclinic eddy growth in the troposphere and is likely to be highly constrained by underlying oceanic frontal zones via air-sea heat exchange. We characterize the $\boldsymbol{B}$ variability separately in the GS and KE regions by applying EOF analysis to DJF-mean $\boldsymbol{B}$ across all the ensemble members and to that based on JRA55 reanalysis and then examine atmospheric and sea surface fields associated with their leading modes.

The simulations capture well the spatial structure of the observed $\boldsymbol{B}$ variability in both the WBC regions. Their leading modes (EOF1), explaining 42% (35%) of the total variance, represents intensifications of $\boldsymbol{B}$ over the GS (KE). While the EOF1 in the GS region is associated with enhanced storm track activity and westerly jet aloft, and geopotential height anomalies that resemble the negative phase of North Atlantic Oscillation (NAO), the EOF1 in the KE region is associated with a meridional dipole in height anomalies that resembles Western Pacific pattern. Further analysis of surface heat flux and SST anomalies contrasts the role of the two WBCs in the variability of $\boldsymbol{B}$ and the associated atmospheric features. Specifically, the enhanced $\boldsymbol{B}$ in the GS region is associated with enhanced heat release from the ocean, but with no SST anomalies, when cold air outbreaks spread across the sharp SST front over the GS. Over the KE, on the other hand, ocean-induced warm SST anomalies enhance heat release from the ocean, strengthening the overlying $\boldsymbol{B}$. Consistently, the evolution of observed PC1 time series is captured by the ensemble mean of the simulated PC1 in the KE region (r=0.46) but not in GS region (r=0.05). The former indicates the KE-induced SST anomalies adds a predictable component to $\boldsymbol{B}$ and the associated atmospheric variability in the North Pacific, while the latter reflects the variability mainly initiated by intrinsic NAO.

Keywords: Atmospheric storm track , Western boundary currents , interannual-to-decadal variability, westerly jet

©2019. Japan Geoscience Union. All Right Reserved.

Baroclinic Annular Mode in the Southern Hemisphere: Its Reproducibility and Sensitivity to Ocean Fronts assessed in Aqua-Planet Experiments

*Morio Nakayama[1], Masatoshi Mizukoshi[1], Hisashi Nakamura[1], Yu Kosaka[1], Bunmei Taguchi[1], Masato Mori[1], Fumiaki Ogawa[2]

1. RCAST, the University of Tokyo , 2. The University of Bergen

Large-scale tropospheric variability in the extratropical Southern Hemisphere is characterized by two major and independent modes. One is the barotropic annular mode or the Southern Annular Mode (SAM), which represents meridional shifts of the eddy-driven polar front jet (PFJ; Thompson and Wallace, 2000). The other is the Baroclinic Annular Mode (BAM), which represents pulsing of stormtrack activity (Thompson and Woodworth, 2014).

In this study, the sensitivity of BAM to the midlatitude oceanic frontal zone is assessed through aqua-planet experiments in which, after the removal of landmasses, zonally symmetric distributions of sea-surface temperature (SST) are prescribed as the lower boundary condition of an atmospheric general circulation model AFES. In our control experiment, climatological SST profiles observed over the South Indian Ocean in austral summer and winter are prescribed in the model northern and southern hemispheres, respectively. The profiles are characterized by frontal SST gradient at 45˚ latitude. In our NF experiment, the frontal SST gradients are removed by raising SST artificially poleward of the front. The two experiments are both conducted over 3600 days under a perpetual condition with insolation fixed to the boreal summer solstice.
As in the observations, BAM signatures in the control experiment represent pulsing of the climatological stormtrack anchored in the vicinity of the oceanic front. By contrast, in the NF experiment without the oceanic frontal zone, BAM cannot be reproduced: BAM-associated anomalies of eddy kinetic energy and poleward eddy heat flux are reduced by ~30% and ~50%, respectively, and their peaks are displaced equatorward by ~5˚ from the oceanic frontal zone. Our experiments therefore suggest that the oceanic frontal zone enhances and anchors the BAM variability by strengthening stormtrack activity through maintaining near-surface baroclinicity. Specifically, anomalous sensible heat flux from the ocean acts to restore the meridional gradients in surface air temperature modified by anomalous meridional eddy heat flux associated with BAM, and this effect is greatly enhanced under the frontal SST gradient.

Keywords: Annular mode, Oceanic frontal zone, Aqua-planet experiment

©2019. Japan Geoscience Union. All Right Reserved.

Hydro-climatic variation in northwestern China and its multi-decadal to multi-centennial teleconnection with the Pacific Ocean

*Harry F Lee[1]

1. The Chinese University of Hong Kong

Northwestern (NW) China region locates in the boundary region between the Westerlies and the Asian Monsoon. Due to its unique geographical setting, scientific studies that examine the long-term dynamics of the hydro-climate there have received particular attention in recent years. However, these studies are often constrained by the availability of instrumental precipitation records. The present study seeks to address this issue. I based on historical drought/flood records to trace the geographic extent of drought anomalies as well as the intra-regional precipitation variability in NW China in AD580–2008, covering the periods with and without instrumental precipitation records. Moving correlation and wavelet analyses were applied to find their significant determinants. Results show that El Niño Southern Oscillation (Indo-Pacific warm pool sea surface temperature) is the major multi-decadal to centennial (centennial to multi-centennial) determinant of the hydro-climatic variability in NW China. The associated mechanism is anchored with the change of Asian Summer Monsoonal precipitation, while it is driven by different factors at different time-scales. The above findings may help predict the occurrence of drought in the boundary region between the Westerlies and the Asian Monsoon in the extratropics.

Keywords: Hydro-climate, northwestern China, Pacific Ocean

©2019. Japan Geoscience Union. All Right Reserved.

Atmospheric zonal-mean meridional circulation and midlatitude oceanic fronts

*Kazuaki Nishii[1], Bunmei Taguchi[2], Hisashi Nakamura[2]

1. Graduate School of Bioresources, Mie University, 2. Research Center for Advanced Science and Technology, The University of Tokyo

It is known that, in the zonal-mean tropospheric circulation, diabatic heating drives a thermally direct meridional overturning circulation (MOC) called the Hadley cell. While in the midlatitudes, zonal-mean vertical motion is driven mainly by atmospheric eddies, forming a thermally indirect MOC called the Ferrel cell where warmer (cooler) air apparently sinks (rises) in lower (higher) latitudes. Here we found a thermally-direct, shallow MOC embedded in the downward branch of the zonal mean Ferrel cell in the wintertime northern hemisphere in most of the latest generation reanalysis datasets. AGCM simulations reveal that this local MOC, made of upward (downward) motion around latitudes to the equatorward (poleward) side of midlatitude oceanic fronts, is driven by differential diabatic heating across the ocean fronts due to surface turbulent heat flux from the ocean and precipitation brought by synoptic-scale eddies. The compensating meridional flow in the lowermost atmosphere is northerlies, which decelerates surface westerlies just over the oceanic fronts through the Coriolis force. The decelerated surface westerlies by oceanic fronts in turn exert wind-stress curl forcing that tends to weaken oceanic subpolar and subtropical gyres, indicative of an air-sea coupled feedback that would destruct, rather than maintain, the oceanic fronts.

Keywords: Midlatitude oceanic front, vertical motion, baroclinicity

©2019. Japan Geoscience Union. All Right Reserved.

[E] Poster | A (Atmospheric and Hydrospheric Sciences)：A-CG Complex & General

Mon. May 27, 2019 5:15 PM - 6:30 PM JST | Mon. May 27, 2019 8:15 AM - 9:30 AM UTC | Poster Hall International Exhibition Hall8, Makuhari Messe_12

[A-CG33] Extratropical oceans and atmosphere

convener:Kazuaki Nishii(Graduate School of Bioresources, Mie University), Yoshi N Sasaki(Hokkaido University), Hatsumi Nishikawa(Institute of Low Temperature Science, Hokkaido University), Shun Ohishi(Division for Land-Ocean Ecosystem Research, Institute for Space-Earth Environmental Research, Nagoya University)

The extratopical ocean had been considered passive to atmospheric variability. Recent studies, however, revealed some active role of the extratopical ocean in modulating the atmosphere. The goal of this session is to deepen our understanding of the air-sea interaction in the extratropics. A wide variety of researches whose topics range from mesoscale to basin-scale, and from daily to global warming are welcomed. Researches on cloud, aerosol, and ecosystem related to the extratopical air-sea interaction are also welcomed.

[ACG33-P01] Analysis of water exchange processes at the Subarctic Boundary of the North Pacific using particle tracking method

*Ashida Hayato[1], Humio Mitsudera[2], Hatsumi Nishikawa[2] (1. Department of Earth and Planetary Sciences, School of Science, Hokkaido University, 2.Institute of Low Temperature Science, Hokkaido University)

[ACG33-P02] Method to evaluate the effect of obduction on properties in the ocean mixed layer

*Yoshimi Kawai[1] (1.Research and Development Center for Global Change, Japan Agency for Marine-Earth Science and Technology)

[ACG33-P03] Influence of the interannual-scale Bering Sea ice variation on cold air outbreaks

*Mizuki Iida[1], Shusaku Sugimoto[1], Toshio Suga[1] (1.Physical Oceanography Laboratory Department of Geophysics, Graduate School of Science, Tohoku University)

Analysis of water exchange processes at the Subarctic Boundary of the North Pacific using particle tracking method

*Ashida Hayato[1], Humio Mitsudera[2], Hatsumi Nishikawa[2]

1. Department of Earth and Planetary Sciences, School of Science, Hokkaido University, 2. Institute of Low Temperature Science, Hokkaido University

The Mixed Waters Region (MWR) of the North Pacific are thought to be an important region for climate change and ecological fluctuations. In the MWR, two quasi stationary jets are formed away from the Western Boundary [Isoguchi et al., 2006]. Mitsudera et al. [2018] showed the relationship between the jets and the topography of only 500 m near the jets.

Contours of the average sea surface height indicates bifurcation between the subarctic and the subtropical circulation on the west coast of the North American continent. The boundary passes through J2 that is the eastern quasi stationary jet [Isoguchi et al., 2006] and coincide with the latitude line of 40˚N near 160˚E which is known as the Subarctic Boundary. Focusing on the area of 38 - 42˚N, 155 - 165˚E (referred to as Box), we set particles in Box and tracked them.

J2 is a noticeable flow in the vicinity of the Box, which is formed due to the presence of a low topography at 43˚N 167˚E north east of Box. Particle pathways are greatly affected by J2. Nevertheless, a majority of the water that passes south of 40˚N in the Box goes to the subtropical region and is not affected by J2.

The water of Kuroshio origin (Kuro) is accounted for the majority of the water entering the Box, and the water of Oyashio origin (Oya) is a little. Kuro that enters the Box exceeds 60% in south of 40˚N in the Box. Most of Kuro flowed out from the southern side of the Box goes to the subtropical circulation, but Kuro flowed out from north of 40˚N in the Box enters the subarctic circulation. Since particles emanated from the northern side of the Box is thought to be susceptible to J2, J2 would play a great role in transporting Kuro to the subarctic region. The proportion of Oya coming into the Box is about 10% to the south of 40˚N, while 30 to 40% to the north of 40˚N. Therefore, Oya also changes its proportion at 40˚N as a boundary. Oya is likely to return to the subarctic circulation, but Oya entering subtropical circulation is also seen.
J2 therefore plays a role of carrying water out from the Box, which has high temperature and high salinity derived from subtropical circulation, to the subarctic circulation where temperature and salinity is low. It is thought that the topography of only 500m in the North Pacific, where the depth is about 6000m, affects the ocean circulation.

©2019. Japan Geoscience Union. All Right Reserved.

Method to evaluate the effect of obduction on properties in the ocean mixed layer

*Yoshimi Kawai[1]

1. Research and Development Center for Global Change, Japan Agency for Marine-Earth Science and Technology

Repeat hydrographic surveys revealed that the warming already extended to the global abyssal waters. The circulation of heat, freshwater and materials absorbed into the ocean, however, has not been investigated enough. The ocean mixed layer in the extratropics usually becomes deepest in winter or early spring due to strong surface cooling and wind stress. In the following warm season, the seasonal pycnocline is formed in the upper layer, and the remnant of the winter mixed layer below the seasonal pycnocline is isolated from the atmosphere. While some part of the isolated layer is entrained into the mixed layer again in the following winter, the other part is transported along an isopycnal surface into the permanent pycnocline irreversibly. The latter process is referred to as “subduction”, and one of the major processes by which properties of the upper layer facing the atmosphere are transferred into the ocean interior. The opposite process of subduction is “obduction”: water of the permanent pycnocline is entrained into the mixed layer when it deepens in autumn and winter. This process is also expected to be important for the atmosphere, especially its long-term variations, since it brings anomalies of temperature, carbon dioxide, and other properties in the ocean interior to the surface layer. Subduction and obduction rates are great in regions where the winter mixed layer becomes deeper.
The budget of the ocean mixed layer consists of five components: surface forcing, Ekman advection, geostrophic advection, entrainment, and residual. The sum of these five terms is equal to the temporal change rate of a quantity such as temperature and salinity. The entrainment in mixed-layer deepening is further separated into two components: the erosion of the permanent pycnocline, and the erosion of water mass that was within the mixed layer in the previous winter. The former is just obduction, and the latter means that the water mass that was in contact with the atmosphere in the previous winter is again entrained into the mixed layer within one year, which is referred to as “re-entrainment” in this paper expediently. The contribution of the obduction on the ocean mixed layer budget has not been examined. The authors proposes a method to evaluate it, and examines the budget by using the Argo MOAA GPV dataset. The effect of the obduction on temperature and salinity in the ocean mixed layer is notably large in the Bering Sea and around 40ºN west of the Date Line.

Keywords: Obduction, Ocean mixed layer, Entrainment

©2019. Japan Geoscience Union. All Right Reserved.

Influence of the interannual-scale Bering Sea ice variation on cold air outbreaks

*Mizuki Iida[1], Shusaku Sugimoto[1], Toshio Suga[1]

1. Physical Oceanography Laboratory Department of Geophysics, Graduate School of Science, Tohoku University

In the Northern Hemisphere winter, cold air outbreaks occur over East Asia and the eastern North America. Quantitative estimation of a cold air mass was developed recently and this allowed us to detect two climatological cold air streams (Iwasaki et al., 2014): the East Asian stream and the North American stream. Cold air incursions are strongly affected by the terrain and land–sea distributions, and the cold air mass is lost due to diabatic heating over the northwestern parts of the North Pacific and the North Atlantic, which are downstream regions of the two streams (Kanno et al., 2015). The East Asian stream passes over the Bering Sea covered by ice. It is expected that the Bering Sea ice would affect the path and formation/loss of cold air mass. However, the influence of sea ice, including the Bering Sea, on the cold air mass has been unclear. We investigate a temporal relationship between the Bering Sea ice and the cold air mass and discuss its cause from the view point of large-scale atmosphere patterns, by applying statistical methods. In addition, we try to describe an influence of cold air mass on ocean mixed layer temperature and depth. Following a pioneering work by Iwasaki et al. (2014), we calculate negative heat content (NHC), which is regarded as a cold air mass amount below potential temperature of 280K, by using ERA-Interim data. We use the Bering Sea ice concentration from NOAA OISST v2 dataset. Analysis period is 37 years of 1982-2018, and we focus on February because the Bering Sea ice concentration has the largest value and the largest variance. In order to extract the NHC and atmosphere patterns related to the Bering Sea ice variation, we perform a composite analysis. Here, we define two categories (high and low ice concentration years) based on the regional time series of Bering Sea ice concentration (160˚ E-150˚W, 55˚N-65˚N); high (low) ice concentration years are defined as years in which sea ice concentration is above (below) plus (minus) one standard deviation from the long-term mean. In high ice concentration years, NHC is found in the Bering Sea and the Bering Strait, showing southward NHC flux. NHC loss is dominated over a region south of the Bering Sea. Composite maps of sea level pressure and geopotential height show remarkably large amplitude in the central North Pacific, indicating a change of the Aleutian Low intensity. We checked a relationship between the Bering Sea ice concentration and large-scale atmospheric patterns such as Pacific/North Atlantic pattern, West Pacific pattern, and El Nino. Interestingly, the Bering Sea ice concentration is not significantly correlated with climate indices representing the atmosphere patterns mentioned above. Our result implies that the Bering Sea ice concentration has a potential to affect the cold air mass outbreak and the NHC. In the presentation, we introduce an impact of the NHC loss on the underlying ocean.

Keywords: Cold air outbreaks, Air-sea interaction, Air-sea heat exchange, Sea ice concentration

©2019. Japan Geoscience Union. All Right Reserved.

[E] Poster | H (Human Geosciences)：H-DS Disaster geosciences

Mon. May 27, 2019 1:45 PM - 3:15 PM JST | Mon. May 27, 2019 4:45 AM - 6:15 AM UTC | Poster Hall International Exhibition Hall8, Makuhari Messe_3

[H-DS11] Subaqueous Landslides and Their Anthropogenic Impact for Coastal Regions

convener:Yujin Kitamura(Department of Earth and Environmental Sciences, Graduate School of Science and Engineering, Kagoshima University), Yasuhiro Yamada(Japan Agency for Marine-Earth Science and Technology (JAMSTEC), R&D Center for Ocean Drilling Science (ODS))

A large number of people inhabit coastal areas around the world that are susceptible to natural catastrophes and subaqueous landslides are one of such hazards as demostrated recently. The risk associated with the occurrence of subaqueous landslides is not only constrained to passive margins or subduction zones but any of water areas is also susceptible to their occurrence since subaqueous failures can be triggered at very low slope angles. This realization poses a significant challenge that requires the collection of vast amounts of information and data to unravel the true nature of these events and their potential risk to coastal communities. Despite these challenges, recent technical and engineering advances in the acquisition and processing of sea floor and shallow subsurface data are encouraging. There has also been a concerted effort by scientists from different earth-science disciplines to increase interdisciplinary cooperation at an international level to advance our collective understanding of subaqueous landslides and their consequences.
This session calls for technical contributions covering all aspects of subaqueous landslide research including but not limited to: physical properties of deformed sediments (pre- and post- deformation), role of interstitial fluids in subaqueous landslide development, slope stability and risk assessments, geomorphological and sedimentological/stratigraphic descriptions, tsunamigenic risk and modeling, description of ancient subaqueous landslides, sand-box models and numerical simulations of subaqueous landslides. Case studies from lacustrine landslides and subaerial coastal landslides transitioning into the marine realm are also welcome. Case studies associated with the broader topic of subaqueous gravity-driven flows (e.g.: turbidites and transitional flows) and their relationship with seafloor faulting are also of interest to this session. Participants of IUGS project S4SLIDE IGCP-640 sponsor this session.

[HDS11-P01] Deformed sediment gravity flow deposits associated with bypassing slides:an example from the Miocene Ushikiri Formation, Southwest Japan

*Miki Kobayashi[1], Tetsuya Sakai[2] (1.Nippon Koei, 2.Shimane University)

[HDS11-P02] Submarine Landslide and Resulting Tsunami on the Continental Shelf Slope off Shikoku

*Youdai Gon[1], Toshitaka Baba[1], Tetsuo Matsuno, Mitsuru Hayashi, Hiroshi Ichihara (1.Tokushima University graduate school)

[HDS11-P03] Sedimentary environment estimated from physical properties of sediment core collected during the cruise of Hakuho-maru KH-18-3 in the South Yatsushiro sea, western Kyushu.

*Koki Hori[1], Yujin Kitamura[2], Hakuho-maru KH-18-3 Scientists (1.Department of Earth and Planetary Sciences, Graduate School of Science, Kyushu University , 2.Department of Earth and Environmental Sciences, Graduate School of Science and Engineering , Kagoshima University)

[HDS11-P04] Variation in vane shear strength and magnetic susceptibility in the cores recovered by Hakuho-maru KH-18-3 cruise in Yatsushiro sea

*Yujin Kitamura[1], Haruka Kageyama[2], Kaede Yamasaki[2], Ryoya Goto[2], Koki Hori[2], Yuta Ikebata[2], Kuniyo Kawabata[1], Daiki Oyama[2], Hakuho-maru KH-18-3 Scientists (1.Department of Earth and Environmental Sciences, Graduate School of Science and Engineering, Kagoshima University, 2.Department of Earth and Environmental Sciences, Faculty of Science, Kagoshima University)

[HDS11-P05] Identification of turbidites in the Yatsushiro Sea surface sediment core samples from non-destructive measurements: Hakuho-maru KH-18-3 Cruise, Yatsushiro Sea, Western

Kyushu, Japan

*Ryoya Goto[1], Yujin Kitamura[2], Hakuho-maru KH-18-3 Cruise Scientist (1.Atmosphere and Ocean Research Institute, The University of Tokyo, 2.Department of Earth and Environmental Sciences, Graduate School of Science, Kagoshima University)

[HDS11-P06] Revised columnar section based on grain size distribution analysis of samples from Hakuho-maru KH-18-3 in Yatsushiro sea

*Yuta Ikebata[1], Yujin Kitamura[2], Hakuho-maru KH-18-3 Scientists Family (1.Kyusyu University Graduate School Of Science Earth and Planetary Science, 2.Graduate school of science, Kagoshima University)

Deformed sediment gravity flow deposits associated with bypassing slides: an example from the Miocene Ushikiri Formation, Southwest Japan

*Miki Kobayashi[1], Tetsuya Sakai[2]

1. Nippon Koei, 2. Shimane University

The Middle Miocene Ushikiri Formation in Shimane Peninsula, southwest Japan, is interpreted to have been deposited on the shelf margin to the middle continental shelf, and is known to contain unique sediment gravity flow deposits, similar to hybrid sediment gravity flow deposits (turbidite + debrite). Intensely deformed mud clasts have been described from this formation. However, their formation has not been focused on previous studies. The present study aims to characterize the deformation of sandstone beds and mud clasts contained within the sediment gravity flow deposits and to discuss of the deformation process of the sediments.

Many of the sandstone beds in the upper Ushikiri Formation (averaging 0.6 m thick) are bipartite, with lower parts showing characteristics similar to Ta or Ta-b turbidites with rich mud clasts. The upper parts of the sandstone beds are represented by poorly-sorted muddy sand with scattered mud clasts having debrite-like features. The small mud clasts in the lower part show features different from those in ordinary turbidites: some are subject to injection of surrounding sand and some scattered in sands show jigsaw-puzzle patterns, suggesting in situ mud clast fragmentation. Some mud clasts are intensely stretched. The beds also host large mud clasts (maximum length: ca 3 m), in which deformation structures, such as slump folds, are well developed. Mud clast shapes are not consistent with internal deformation structures and the most of them have sharp margins. The sand around some large mud clasts shows local liquefaction. Local grading is also found above the large mud clasts and does not continue beyond the edge of the mud clasts.

The injection of sand into mud clasts and their in situ fragmentation into jigsaw-puzzle patterns can be explained by liquefaction of beds with overburden pressure. A possible pressure source is slides that passed over a freshly deposited turbidite bed. When a slide bypassed the sand bed, the bed once deposited as turbidite easily liquefied under the moving slide mass, having led overburden pressure in the bed that caused injection and in situ fragmentation. On the contrary, the large mud clasts may have been fragments ripped from a major sliding body that bypassed the studied locality. Local liquefaction around large mud clasts indicates they sank or were forced into the bed from above. The presence of local grading above the mud clasts can be explained by local resuspension of sand around the mud clasts when they sank into the sand. The above mentioned sediment deformation process is supported by beds with a slide deposit above a sandy part having similar mud clast deformation.
The bypassing of the slide may have been due to hydroplaning of the slide mass. The slide deposits are represented by up to 2 m thick of large mud block rich sediments with variety of deformation structures, which grades from an underlying debrite-like bed that consists of poorly-sorted muddy sand with rich mud clasts with injection of surrounding muddy sand. Some mud clasts in the muddy sandstone beds are intensely stretched, implying that shear stress exerted within the beds. The poorly-sorted muddy sand is thus interpreted as a fluid layer, which has been existed below the moving landslide mass, having triggered the hydroplaning.

©2019. Japan Geoscience Union. All Right Reserved.

Keywords: submarine landslide deposit, bypassing of landslide mass, Shamane

©2019. Japan Geoscience Union. All Right Reserved.

Submarine Landslide and Resulting Tsunami on the Continental Shelf Slope off Shikoku

*Youdai Gon[1], Toshitaka Baba[1], Tetsuo Matsuno, Mitsuru Hayashi, Hiroshi Ichihara

1. Tokushima University graduate school

Submarine landslide occurs mainly due to earthquake shaking damaging marine infrastructure such as submarine communication and causing tsunami. The bathymetry in the Nankai Trough has traces of numerous submarine landslides. One of them is located on the continental shelf 24 km off the Shikoku coast. The submarine landslide off Shikoku would have a potential causing tsunami. Therefore, in this study, with the purpose revealing the topographical features of the submarine landslide off Shikoku in detail, multi-narrow beam surveys were conducted. We also discuss the tsunami potential of the submarine landslide from numerical simulations.

The multi-narrow beam surveys were conducted once in 2017 and twice in 2018 covering an area 30 km x 20 km by a training ship, Kobe University Graduate School of Maritime Sciences Attachment Practice Ship Fukae Maru. The acquired bathymetric map indicated four head scarps neighboring to each other (hereafter scarp A, B, C, D from the west). Sediment deposition was confirmed below scarp A. The scarp A seems to be younger than the other scarps. The slopes collapsed multiple times implying occurrence of a new collapse in the future.

Tsunami calculations were carried out for slump A, B and C. But, from the topographic features, slump B and C were assumed to be a simultaneous collapse. We also assumed new two submarine landslides (slump E and F) to the east of slump D with the same size of sump A. In the calculation results, the tsunamis arrive at about 15 min. after the initiation of slump A and the simultaneous slump B and C. For slump E and F, tsunami arrives at about 20 min. The maximum tsunami heights were estimated to be about 2 m, 2 m, 4.5 m and 5 m for slump A, B-C, E and F, respectively. We are going to conduct more simulations to evaluate risk of tsunami caused by the submarine landslide tsunamis in the study area.

Keywords: The submarine landslide off Shikoku, Tsunami simulation

©2019. Japan Geoscience Union. All Right Reserved.

Sedimentary environment estimated from physical properties of sediment core collected during the cruise of Hakuho-maru KH-18-3 in the South Yatsushiro sea, western Kyushu.

*Koki Hori[1], Yujin Kitamura[2], Hakuho-maru KH-18-3 Scientists

1. Department of Earth and Planetary Sciences, Graduate School of Science, Kyushu University , 2. Department of Earth and Environmental Sciences, Graduate School of Science and Engineering , Kagoshima University

The research cruise KH-18-3 was carried out in the South Yatsushiro sea from 27th to 30th July 2018. The purpose of this cruise is to clarify the occurrence history of the submarine landslides in the Yatsushiro sea. In this survey, bottom surface sediment samples were collected by using Piston corer which is 6 meters long.
The study on physical properties of event sediment using core samples are conducted in ocean areas around the world. For example, Prior et al. (1984) reported that Mass transport deposits (MTD) commonly have a higher density than surrounding, sediments that are not submarine landslide origin. Therefore, in this study, the physical properties that serve as the basic information of the core samples were measured. In addition, we estimated the sedimentary environment in the survey area by applying tidal current, sedimentation rate, and bottom surface muddy rate in the south Yatsushiro sea (Rifardi et al.,1998) and conventional radiocarbon ages of piston core samples recovered in the same area reported by Inoue et al. (2011).

Core samples were collected from 11 sites (core name:PC01 to PC11) in the south Yatsushiro sea where the Taura-Tsunagi Oki fault group and Minamata Oki fault group are distributed.
All analyses other than the grain size distribution analysis were conducted at the Center for Advanced Marine Core Research, Kochi University. Initially, GRA density, Magnetic susceptibility and fractional porosity were measured using Whole round multi sensor core logger (MSCL-W). After the analysis, core samples were divided vertically and visual observation and color measurement of them were performed. Subsequently, a vane shear test and sub-samples which were used for MAD measurements and grain size distribution analysis collecting were performed at approximately 50 cm intervals, respectively, and the test and two sampling location were the same points.

Area 1 is under condition of rather stagnant water masses or rather weak tidal current system and is characterized fine-grained sediments. We estimated age of core samples by comparing physical properties reported by Inoue et al. (2011) because sampling point in this area matched with piston coring points of Inoue et al. (2011) and the behaviors of both physical properties were similar. As a result, a gap of more than 7000 years of sediment age is estimated at depth of 2 to 3 meters in area 1a (PC01 to PC03) and it is presumed that sediments indicating the age of about 10,000 years BP exist at depth of several tens of centimeters from the seabed surface in area 1b (PC06, PC07). In addition, K-Ah volcanic ash layer (7.3ka) could not be confirmed from sediments in both sea areas. From this, it is assumed that there was an event such as a submarine landslide or erosion with the lower part of the tephra as a sliding or eroding surface.
Since we could not obtain an index to estimate the age of the PC 08 to PC 11, we estimated the sedimentary environment using only the physical properties of sediments. PC08 and PC10 (Area 2) is located near the strait of Goshoura-jima and sisi-jima island, under influence of strong tidal and bottom currents, and is characterized by coarse sediments. Especially, upward grain refinement was observed and

©2019. Japan Geoscience Union. All Right Reserved.

the tendency that the porosity decreases within each monolayer is repeated in PC10. From this, it is assumed that the upper sediment functions as an impermeable layer against the lower sediment, and the drainage is difficult to proceed. PC 09 and PC 11 (Area 3) are relatively close to supply sources such as Minamata River and Komenotsu River, and are characterized as relatively coarse sediments. From the depth of 60 cm of PC09, and from the outermost surface layer in PC 11, the porosity does not decrease almost from around 60%. From this, it is estimated that the new sediment has been recently cleared recently.

Keywords: Piston coring, Yatsushiro sea

©2019. Japan Geoscience Union. All Right Reserved.

Variation in vane shear strength and magnetic susceptibility in the cores recovered by Hakuho-maru KH-18-3 cruise in Yatsushiro sea

*Yujin Kitamura[1], Haruka Kageyama[2], Kaede Yamasaki[2], Ryoya Goto[2], Koki Hori[2], Yuta Ikebata[2], Kuniyo Kawabata[1], Daiki Oyama[2], Hakuho-maru KH-18-3 Scientists

1. Department of Earth and Environmental Sciences, Graduate School of Science and Engineering, Kagoshima University, 2. Department of Earth and Environmental Sciences, Faculty of Science, Kagoshima University

Introduction

The 2016 Kumamoto Earthquake was sourced from a part of active faults of the Futagawa-Hinagu fault zones. The southwestern part of Hinagu fault zone forms the Yatsushiro section as a group of submarine active faults. Earthquake shaking occasionally triggers submarine landslide, however, any record of submarine landslide in this area has not been reported. We therefore conducted research cruise with R/V Hakuho-maru and recovered sediment cores in Yatsushiro sea. As it is known that the shear strength decreases at the bottom of mass transport deposits, we conducted vane shear test with the cores. We also referred the variation of magnetic susceptibility to establish core correlation with previous works.

Method

Here we conducted four-days research cruise with R/V Hakuho-maru (KH-18-3) in July, 2018 to reveal submarine landslide records and benthic environment in Yatsushiro sea. We used six-meters-long piston corers and cored at 11 sites and recovered cores were cut into 6 sections onboard. Cores were analyzed at Kochi Kore Center using X-ray CT scanner, multi-sensor core logger (gamma ray density: GRD; and magnetic susceptibility: MS), core imaging apparatus, visual core description, color spectroscope, X-ray fluorescence core scanner (Itrax). Vane shear apparatus is used with split core section and tested every about 50 cm.

Results and Discussion

Sediments are dominated by matrices of olive gray to black sand or mud. CT value, MS and GRD generally increase with depth. As MS shows cyclic fluctuation, we classified into several MS units by defining units with each broad peak. Our MS units was correlated with previous studies of high resolution seismic profile by Yagi et al. (2016) and piston cores by Inoue et al. (2011). MS units was in good agreement with Yagi's seismic profile. It is inferred that our samples include the sediments during Late Glacial Maximum to Jomon Transgression below hiatus. MS data by Inoue et al. (2011) and this study are in accordance with each other. The event layers Inoue suggested are discriminable in our cores which are characterized as local maximum of MS. Iron shows high concentration around the event layers so that the iron is a candidate for indicator for searching the events. We assume that this iron anomaly is caused by the rapid deposition during eventic turbidites.

The results of vane shear test showed that the strength increases with depth with a change in its rate at assumed hiatus. This shows that the sediments below hiatus was further deeply buried and compacted. At sites PC04 to PC06, the strength is low at their surface, indicating that the hiatus at these sites are very shallow and thus the recent surface erosion is assumed.

©2019. Japan Geoscience Union. All Right Reserved.

Keywords: turbidites, shallow marine deposits, 2016 Kumamoto earthquake

©2019. Japan Geoscience Union. All Right Reserved.

Identification of turbidites in the Yatsushiro Sea surface sediment core samples from non-destructive measurements: Hakuho-maru KH-18-3 Cruise, Yatsushiro Sea, Western Kyushu, Japan

*Ryoya Goto[1], Yujin Kitamura[2], Hakuho-maru KH-18-3 Cruise Scientist

1. Atmosphere and Ocean Research Institute, The University of Tokyo, 2. Department of Earth and Environmental Sciences, Graduate School of Science, Kagoshima University

Submarine active faults in Yatsusiro Sea, western Kyushu, Japan, constitute the Yatsushiro section of Hinagu fault zone in its southwest end (AIST et al., 2011). The 2016 Kumamoto Earthquake was sourced from a part of active faults of the Futagawa-Hinagu fault zones (JMA, 2018), and survey has hardly conducted in the sea area after the earthquake occurrence. Earthquake shaking occasionally triggers turbidity currents by submarine landslides and resuspension of unconsolidated sediments on the seafloor (Ikehara et al., 2018). In recent years, the study of earthquake occurrence history using earthquake turbidites formed by turbidity currents is being conducted throughout the world. As earthquake-origin turbidity currents can take place in very gentle slope (e.g. the Mississippi-Delta 0.01°: D. B. Prior et al., 1978), its occurrence is sufficiently thought even in Yatsushiro Sea. However, any record of earthquake turbidites in this area has not been reported. In this study, identification of turbidites in the Yatsushiro Sea surface sediment core samples from non-destructive measurements.

Here we conducted four-days research cruise Hakuho-maru KH-18-3 in July, 2018. We conducted sub-bottom profiling on eight lines, piston coring at 11 sites in Yatsushiro Sea, western Kyushu, Japan. Recovered cores are analyzed by X-ray CT scanner, multi-sensor core logger, core imaging apparatus, visual core description, color spectroscope and X-ray fluorescence core scanner (Itrax) in the Center for Advanced Marine Core Research, Kochi University. With reference to the previous studies (Iwai et al., 2014, JGS abstract; Isabel Rodríguez-Germade et al, 2015; Okutsu et al., 2017, JGS abstract), the behavior of Ca/Ti and Fe/Ti where the peak was observed at the base of turbidites, and the behavior of Fe/Ti and Zr/Ti where the peak was observed at the base of volcaniclastics turbidites.

Our results revealed turbidites and volcaniclastics turbidites in six piston coring sites (PC01 to PC06). As all of sites are located in the Taura-Tsunagioki fault group or Minamataoki fault group, turbidites were considered to be present in all of sites. However, turbidites were identified from PC01 to PC06, but not identified from PC07 to PC11. According to Rifardi et al. (1998), PC01 to PC06 are located in the sea area where the deposition rate is high, and PC07 to PC11 are located in the sea area where the deposition rate is slow.

As turbidite is formed by various factors besides earthquakes, it is necessary to consider whether the turbidites identified in this study are earthquake turbidites. In addition, to investigate the history of earthquakes, it is also a future task to conduct individual sample measurements (such as grain size distribution analysis) and dating.

Hakuho-maru KH-18-3 Cruise Scientists: Takashi Tomiyasu, Hitoshi Kodamatani, Kuniyo Kawabata, Daiki Oyama, Haruka Kageyama, Kaede Yamasaki (Kagoshima Univ.), Yuta Ikebata, Koki Hori (Kyushu Univ.), Asuka Yamaguchi, Fumiaki Tsunomori, Kameo Katsura, Tsubasa Miki, Natsumi Okutsu, Hiroaki Koge,

©2019. Japan Geoscience Union. All Right Reserved.

Kotaro Fujita, Ayaka Nakazawa, Yuichi Okuma, Genki Kobayashi, Rina Fukuchi (Tokyo Univ.), Jun Kameda, Tomonori Morisaki (Hokkaido Univ.)

Keywords: submarine landslides, turbidites, shallow sea deposits, Yatsushiro Sea, 2016 Kumamoto Earthquake

©2019. Japan Geoscience Union. All Right Reserved.

Revised columnar section based on grain size distribution analysis of samples from Hakuho-maru KH-18-3 in Yatsushiro sea

*Yuta Ikebata[1], Yujin Kitamura[2], Hakuho-maru KH-18-3 Scientists Family

1. Kyusyu University Graduate School Of Science Earth and Planetary Science, 2. Graduate school of science, Kagoshima University

Hakuho-maru KH-18-3 was held in the Yatsushiro Sea from 27th to 30th July 2018 for clarifying history of occurrence of submarine landslides. Earthquake is a one of big trigger of submarine landslides, and submarine landslides occurs in an very easy slope. Kumamoto earthquake occurred at April, 2016 and a lot of surveys in the land area were conducted but survey in the sea area weren't conducted much. In the Yatsushiro sea, the occurrence of submarine landslides caused by earthquake of the Futagawa-Hinagu fault zones can be considered sufficiently. Therefore, in this study, the creation of the columnar section which is the basic information of the submarine landslide accreditation was made based on the grain size distribution analysis.

In the Expedition, eleven piston cores(6m) from PC01 to PC11 were collected in the southern part of Yatsushiro sea, and the obtained core was subjected to non-destructive measurement and individual sample measurement at the Kochi Core Center. For non-destructive measurement, CT images and core continuous images were taken, and for individual sample measurement, Density, Magnetic susceptibility, porosity, vane shear strength, color, concentration change of major elements were examined. Grain size distribution analysis was conducted at Kagoshima University. Samples used for grain size distribution analysis were collected every 50 cm and analyzed with a laser diffraction type grain size distribution analyzer. Since it is difficult to judge the stratum boundary only with the result of grain size distribution measurement at intervals of 50 cm, it was judged by using γ ray density, magnetic susceptibility and color measurement result which are continuous data.

Grain size distribution analysis revealed PC01 to PC07 are muddy cores and PC08 to PC11 contains much sand. Grain size of PC01, PC04, PC06, PC07, PC09, PC11 are very different in Grain size distribution analysis and visual core description. Based on the results of the grain size distribution analysis, the stratum boundary was determined from the change commonly seen in the γ ray density, magnetic susceptibility and color, and a columnar section was prepared. In Rifardi et al.(1998), the distribution of mud content in the Yatsushiro Sea has been surveyed. As a result of comparing the columnar map of this study with its distribution for each sampling point, cores excluding PC08 corresponded well. It is thought that it is influenced by the supply of sediment by river and stagnant water mass, tide current as in previous research. Also, in Inoue et al.(2011), which was a reference for determining the core harvest point, dating is done in the same area. At Hori(2019MS), we compare the data with Inoue et al.(2011) and estimate the core age of this research. We also compare the columnar section made in this study with the columnar section of Inoue et al.(2011), using the comparative categories determined at the time of estimating the age. As a result, PC01 and PC02 were in good agreement, PC06 and PC07 had different stratum in the surface layer. This is probably because the sampling site of PC06 is actually about 150 m far from Inoue et al.(2011) and the sampling site of PC07 is actually about 111 m far from Inoue et al.(2011), and the sedimentary environment is slightly different. Also, in the grain size distribution analysis of this study, there is a possibility that coarse grains may be selectively left out when putting the sample into the machine, and it may be doubtful in accuracy.

©2019. Japan Geoscience Union. All Right Reserved.

Keywords: Submarine landslide

©2019. Japan Geoscience Union. All Right Reserved.

[E] Poster | H (Human Geosciences)：H-DS Disaster geosciences

Mon. May 27, 2019 5:15 PM - 6:30 PM JST | Mon. May 27, 2019 8:15 AM - 9:30 AM UTC | Poster Hall International Exhibition Hall8, Makuhari Messe_13

[H-DS11] Subaqueous Landslides and Their Anthropogenic Impact for Coastal Regions

convener:Yujin Kitamura(Department of Earth and Environmental Sciences, Graduate School of Science and Engineering, Kagoshima University), Yasuhiro Yamada(Japan Agency for Marine-Earth Science and Technology (JAMSTEC), R&D Center for Ocean Drilling Science (ODS))

A large number of people inhabit coastal areas around the world that are susceptible to natural catastrophes and subaqueous landslides are one of such hazards as demostrated recently. The risk associated with the occurrence of subaqueous landslides is not only constrained to passive margins or subduction zones but any of water areas is also susceptible to their occurrence since subaqueous failures can be triggered at very low slope angles. This realization poses a significant challenge that requires the collection of vast amounts of information and data to unravel the true nature of these events and their potential risk to coastal communities. Despite these challenges, recent technical and engineering advances in the acquisition and processing of sea floor and shallow subsurface data are encouraging. There has also been a concerted effort by scientists from different earth-science disciplines to increase interdisciplinary cooperation at an international level to advance our collective understanding of subaqueous landslides and their consequences.
This session calls for technical contributions covering all aspects of subaqueous landslide research including but not limited to: physical properties of deformed sediments (pre- and post- deformation), role of interstitial fluids in subaqueous landslide development, slope stability and risk assessments, geomorphological and sedimentological/stratigraphic descriptions, tsunamigenic risk and modeling, description of ancient subaqueous landslides, sand-box models and numerical simulations of subaqueous landslides. Case studies from lacustrine landslides and subaerial coastal landslides transitioning into the marine realm are also welcome. Case studies associated with the broader topic of subaqueous gravity-driven flows (e.g.: turbidites and transitional flows) and their relationship with seafloor faulting are also of interest to this session. Participants of IUGS project S4SLIDE IGCP-640 sponsor this session.

[HDS11-P01] Deformed sediment gravity flow deposits associated with bypassing slides:an example from the Miocene Ushikiri Formation, Southwest Japan

*Miki Kobayashi[1], Tetsuya Sakai[2] (1.Nippon Koei, 2.Shimane University)

[HDS11-P02] Submarine Landslide and Resulting Tsunami on the Continental Shelf Slope off Shikoku

*Youdai Gon[1], Toshitaka Baba[1], Tetsuo Matsuno, Mitsuru Hayashi, Hiroshi Ichihara (1.Tokushima University graduate school)

[HDS11-P03] Sedimentary environment estimated from physical properties of sediment core collected during the cruise of Hakuho-maru KH-18-3 in the South Yatsushiro sea, western Kyushu.

*Koki Hori[1], Yujin Kitamura[2], Hakuho-maru KH-18-3 Scientists (1.Department of Earth and Planetary Sciences, Graduate School of Science, Kyushu University , 2.Department of Earth and Environmental Sciences, Graduate School of Science and Engineering , Kagoshima University)

[HDS11-P04] Variation in vane shear strength and magnetic susceptibility in the cores recovered by Hakuho-maru KH-18-3 cruise in Yatsushiro sea

*Yujin Kitamura[1], Haruka Kageyama[2], Kaede Yamasaki[2], Ryoya Goto[2], Koki Hori[2], Yuta Ikebata[2], Kuniyo Kawabata[1], Daiki Oyama[2], Hakuho-maru KH-18-3 Scientists (1.Department of Earth and Environmental Sciences, Graduate School of Science and Engineering, Kagoshima University, 2.Department of Earth and Environmental Sciences, Faculty of Science, Kagoshima University)

[HDS11-P05] Identification of turbidites in the Yatsushiro Sea surface sediment core samples from non-destructive measurements: Hakuho-maru KH-18-3 Cruise, Yatsushiro Sea, Western

Kyushu, Japan

*Ryoya Goto[1], Yujin Kitamura[2], Hakuho-maru KH-18-3 Cruise Scientist (1.Atmosphere and Ocean Research Institute, The University of Tokyo, 2.Department of Earth and Environmental Sciences, Graduate School of Science, Kagoshima University)

[HDS11-P06] Revised columnar section based on grain size distribution analysis of samples from Hakuho-maru KH-18-3 in Yatsushiro sea

*Yuta Ikebata[1], Yujin Kitamura[2], Hakuho-maru KH-18-3 Scientists Family (1.Kyusyu University Graduate School Of Science Earth and Planetary Science, 2.Graduate school of science, Kagoshima University)

Deformed sediment gravity flow deposits associated with bypassing slides: an example from the Miocene Ushikiri Formation, Southwest Japan

*Miki Kobayashi[1], Tetsuya Sakai[2]

1. Nippon Koei, 2. Shimane University

The Middle Miocene Ushikiri Formation in Shimane Peninsula, southwest Japan, is interpreted to have been deposited on the shelf margin to the middle continental shelf, and is known to contain unique sediment gravity flow deposits, similar to hybrid sediment gravity flow deposits (turbidite + debrite). Intensely deformed mud clasts have been described from this formation. However, their formation has not been focused on previous studies. The present study aims to characterize the deformation of sandstone beds and mud clasts contained within the sediment gravity flow deposits and to discuss of the deformation process of the sediments.

Many of the sandstone beds in the upper Ushikiri Formation (averaging 0.6 m thick) are bipartite, with lower parts showing characteristics similar to Ta or Ta-b turbidites with rich mud clasts. The upper parts of the sandstone beds are represented by poorly-sorted muddy sand with scattered mud clasts having debrite-like features. The small mud clasts in the lower part show features different from those in ordinary turbidites: some are subject to injection of surrounding sand and some scattered in sands show jigsaw-puzzle patterns, suggesting in situ mud clast fragmentation. Some mud clasts are intensely stretched. The beds also host large mud clasts (maximum length: ca 3 m), in which deformation structures, such as slump folds, are well developed. Mud clast shapes are not consistent with internal deformation structures and the most of them have sharp margins. The sand around some large mud clasts shows local liquefaction. Local grading is also found above the large mud clasts and does not continue beyond the edge of the mud clasts.

The injection of sand into mud clasts and their in situ fragmentation into jigsaw-puzzle patterns can be explained by liquefaction of beds with overburden pressure. A possible pressure source is slides that passed over a freshly deposited turbidite bed. When a slide bypassed the sand bed, the bed once deposited as turbidite easily liquefied under the moving slide mass, having led overburden pressure in the bed that caused injection and in situ fragmentation. On the contrary, the large mud clasts may have been fragments ripped from a major sliding body that bypassed the studied locality. Local liquefaction around large mud clasts indicates they sank or were forced into the bed from above. The presence of local grading above the mud clasts can be explained by local resuspension of sand around the mud clasts when they sank into the sand. The above mentioned sediment deformation process is supported by beds with a slide deposit above a sandy part having similar mud clast deformation.
The bypassing of the slide may have been due to hydroplaning of the slide mass. The slide deposits are represented by up to 2 m thick of large mud block rich sediments with variety of deformation structures, which grades from an underlying debrite-like bed that consists of poorly-sorted muddy sand with rich mud clasts with injection of surrounding muddy sand. Some mud clasts in the muddy sandstone beds are intensely stretched, implying that shear stress exerted within the beds. The poorly-sorted muddy sand is thus interpreted as a fluid layer, which has been existed below the moving landslide mass, having triggered the hydroplaning.

©2019. Japan Geoscience Union. All Right Reserved.

Keywords: submarine landslide deposit, bypassing of landslide mass, Shamane

©2019. Japan Geoscience Union. All Right Reserved.

Submarine Landslide and Resulting Tsunami on the Continental Shelf Slope off Shikoku

*Youdai Gon[1], Toshitaka Baba[1], Tetsuo Matsuno, Mitsuru Hayashi, Hiroshi Ichihara

1. Tokushima University graduate school

Submarine landslide occurs mainly due to earthquake shaking damaging marine infrastructure such as submarine communication and causing tsunami. The bathymetry in the Nankai Trough has traces of numerous submarine landslides. One of them is located on the continental shelf 24 km off the Shikoku coast. The submarine landslide off Shikoku would have a potential causing tsunami. Therefore, in this study, with the purpose revealing the topographical features of the submarine landslide off Shikoku in detail, multi-narrow beam surveys were conducted. We also discuss the tsunami potential of the submarine landslide from numerical simulations.

The multi-narrow beam surveys were conducted once in 2017 and twice in 2018 covering an area 30 km x 20 km by a training ship, Kobe University Graduate School of Maritime Sciences Attachment Practice Ship Fukae Maru. The acquired bathymetric map indicated four head scarps neighboring to each other (hereafter scarp A, B, C, D from the west). Sediment deposition was confirmed below scarp A. The scarp A seems to be younger than the other scarps. The slopes collapsed multiple times implying occurrence of a new collapse in the future.

Tsunami calculations were carried out for slump A, B and C. But, from the topographic features, slump B and C were assumed to be a simultaneous collapse. We also assumed new two submarine landslides (slump E and F) to the east of slump D with the same size of sump A. In the calculation results, the tsunamis arrive at about 15 min. after the initiation of slump A and the simultaneous slump B and C. For slump E and F, tsunami arrives at about 20 min. The maximum tsunami heights were estimated to be about 2 m, 2 m, 4.5 m and 5 m for slump A, B-C, E and F, respectively. We are going to conduct more simulations to evaluate risk of tsunami caused by the submarine landslide tsunamis in the study area.

Keywords: The submarine landslide off Shikoku, Tsunami simulation

©2019. Japan Geoscience Union. All Right Reserved.

Sedimentary environment estimated from physical properties of sediment core collected during the cruise of Hakuho-maru KH-18-3 in the South Yatsushiro sea, western Kyushu.

*Koki Hori[1], Yujin Kitamura[2], Hakuho-maru KH-18-3 Scientists

1. Department of Earth and Planetary Sciences, Graduate School of Science, Kyushu University , 2. Department of Earth and Environmental Sciences, Graduate School of Science and Engineering , Kagoshima University

The research cruise KH-18-3 was carried out in the South Yatsushiro sea from 27th to 30th July 2018. The purpose of this cruise is to clarify the occurrence history of the submarine landslides in the Yatsushiro sea. In this survey, bottom surface sediment samples were collected by using Piston corer which is 6 meters long.
The study on physical properties of event sediment using core samples are conducted in ocean areas around the world. For example, Prior et al. (1984) reported that Mass transport deposits (MTD) commonly have a higher density than surrounding, sediments that are not submarine landslide origin. Therefore, in this study, the physical properties that serve as the basic information of the core samples were measured. In addition, we estimated the sedimentary environment in the survey area by applying tidal current, sedimentation rate, and bottom surface muddy rate in the south Yatsushiro sea (Rifardi et al.,1998) and conventional radiocarbon ages of piston core samples recovered in the same area reported by Inoue et al. (2011).

Core samples were collected from 11 sites (core name:PC01 to PC11) in the south Yatsushiro sea where the Taura-Tsunagi Oki fault group and Minamata Oki fault group are distributed.
All analyses other than the grain size distribution analysis were conducted at the Center for Advanced Marine Core Research, Kochi University. Initially, GRA density, Magnetic susceptibility and fractional porosity were measured using Whole round multi sensor core logger (MSCL-W). After the analysis, core samples were divided vertically and visual observation and color measurement of them were performed. Subsequently, a vane shear test and sub-samples which were used for MAD measurements and grain size distribution analysis collecting were performed at approximately 50 cm intervals, respectively, and the test and two sampling location were the same points.

Area 1 is under condition of rather stagnant water masses or rather weak tidal current system and is characterized fine-grained sediments. We estimated age of core samples by comparing physical properties reported by Inoue et al. (2011) because sampling point in this area matched with piston coring points of Inoue et al. (2011) and the behaviors of both physical properties were similar. As a result, a gap of more than 7000 years of sediment age is estimated at depth of 2 to 3 meters in area 1a (PC01 to PC03) and it is presumed that sediments indicating the age of about 10,000 years BP exist at depth of several tens of centimeters from the seabed surface in area 1b (PC06, PC07). In addition, K-Ah volcanic ash layer (7.3ka) could not be confirmed from sediments in both sea areas. From this, it is assumed that there was an event such as a submarine landslide or erosion with the lower part of the tephra as a sliding or eroding surface.
Since we could not obtain an index to estimate the age of the PC 08 to PC 11, we estimated the sedimentary environment using only the physical properties of sediments. PC08 and PC10 (Area 2) is located near the strait of Goshoura-jima and sisi-jima island, under influence of strong tidal and bottom currents, and is characterized by coarse sediments. Especially, upward grain refinement was observed and

©2019. Japan Geoscience Union. All Right Reserved.

the tendency that the porosity decreases within each monolayer is repeated in PC10. From this, it is assumed that the upper sediment functions as an impermeable layer against the lower sediment, and the drainage is difficult to proceed. PC 09 and PC 11 (Area 3) are relatively close to supply sources such as Minamata River and Komenotsu River, and are characterized as relatively coarse sediments. From the depth of 60 cm of PC09, and from the outermost surface layer in PC 11, the porosity does not decrease almost from around 60%. From this, it is estimated that the new sediment has been recently cleared recently.

Keywords: Piston coring, Yatsushiro sea

©2019. Japan Geoscience Union. All Right Reserved.

Variation in vane shear strength and magnetic susceptibility in the cores recovered by Hakuho-maru KH-18-3 cruise in Yatsushiro sea

*Yujin Kitamura[1], Haruka Kageyama[2], Kaede Yamasaki[2], Ryoya Goto[2], Koki Hori[2], Yuta Ikebata[2], Kuniyo Kawabata[1], Daiki Oyama[2], Hakuho-maru KH-18-3 Scientists

1. Department of Earth and Environmental Sciences, Graduate School of Science and Engineering, Kagoshima University, 2. Department of Earth and Environmental Sciences, Faculty of Science, Kagoshima University

Introduction

The 2016 Kumamoto Earthquake was sourced from a part of active faults of the Futagawa-Hinagu fault zones. The southwestern part of Hinagu fault zone forms the Yatsushiro section as a group of submarine active faults. Earthquake shaking occasionally triggers submarine landslide, however, any record of submarine landslide in this area has not been reported. We therefore conducted research cruise with R/V Hakuho-maru and recovered sediment cores in Yatsushiro sea. As it is known that the shear strength decreases at the bottom of mass transport deposits, we conducted vane shear test with the cores. We also referred the variation of magnetic susceptibility to establish core correlation with previous works.

Method

Here we conducted four-days research cruise with R/V Hakuho-maru (KH-18-3) in July, 2018 to reveal submarine landslide records and benthic environment in Yatsushiro sea. We used six-meters-long piston corers and cored at 11 sites and recovered cores were cut into 6 sections onboard. Cores were analyzed at Kochi Kore Center using X-ray CT scanner, multi-sensor core logger (gamma ray density: GRD; and magnetic susceptibility: MS), core imaging apparatus, visual core description, color spectroscope, X-ray fluorescence core scanner (Itrax). Vane shear apparatus is used with split core section and tested every about 50 cm.

Results and Discussion

Sediments are dominated by matrices of olive gray to black sand or mud. CT value, MS and GRD generally increase with depth. As MS shows cyclic fluctuation, we classified into several MS units by defining units with each broad peak. Our MS units was correlated with previous studies of high resolution seismic profile by Yagi et al. (2016) and piston cores by Inoue et al. (2011). MS units was in good agreement with Yagi's seismic profile. It is inferred that our samples include the sediments during Late Glacial Maximum to Jomon Transgression below hiatus. MS data by Inoue et al. (2011) and this study are in accordance with each other. The event layers Inoue suggested are discriminable in our cores which are characterized as local maximum of MS. Iron shows high concentration around the event layers so that the iron is a candidate for indicator for searching the events. We assume that this iron anomaly is caused by the rapid deposition during eventic turbidites.

The results of vane shear test showed that the strength increases with depth with a change in its rate at assumed hiatus. This shows that the sediments below hiatus was further deeply buried and compacted. At sites PC04 to PC06, the strength is low at their surface, indicating that the hiatus at these sites are very shallow and thus the recent surface erosion is assumed.

©2019. Japan Geoscience Union. All Right Reserved.

Keywords: turbidites, shallow marine deposits, 2016 Kumamoto earthquake

©2019. Japan Geoscience Union. All Right Reserved.

Identification of turbidites in the Yatsushiro Sea surface sediment core samples from non-destructive measurements: Hakuho-maru KH-18-3 Cruise, Yatsushiro Sea, Western Kyushu, Japan

*Ryoya Goto[1], Yujin Kitamura[2], Hakuho-maru KH-18-3 Cruise Scientist

1. Atmosphere and Ocean Research Institute, The University of Tokyo, 2. Department of Earth and Environmental Sciences, Graduate School of Science, Kagoshima University

Submarine active faults in Yatsusiro Sea, western Kyushu, Japan, constitute the Yatsushiro section of Hinagu fault zone in its southwest end (AIST et al., 2011). The 2016 Kumamoto Earthquake was sourced from a part of active faults of the Futagawa-Hinagu fault zones (JMA, 2018), and survey has hardly conducted in the sea area after the earthquake occurrence. Earthquake shaking occasionally triggers turbidity currents by submarine landslides and resuspension of unconsolidated sediments on the seafloor (Ikehara et al., 2018). In recent years, the study of earthquake occurrence history using earthquake turbidites formed by turbidity currents is being conducted throughout the world. As earthquake-origin turbidity currents can take place in very gentle slope (e.g. the Mississippi-Delta 0.01°: D. B. Prior et al., 1978), its occurrence is sufficiently thought even in Yatsushiro Sea. However, any record of earthquake turbidites in this area has not been reported. In this study, identification of turbidites in the Yatsushiro Sea surface sediment core samples from non-destructive measurements.

Here we conducted four-days research cruise Hakuho-maru KH-18-3 in July, 2018. We conducted sub-bottom profiling on eight lines, piston coring at 11 sites in Yatsushiro Sea, western Kyushu, Japan. Recovered cores are analyzed by X-ray CT scanner, multi-sensor core logger, core imaging apparatus, visual core description, color spectroscope and X-ray fluorescence core scanner (Itrax) in the Center for Advanced Marine Core Research, Kochi University. With reference to the previous studies (Iwai et al., 2014, JGS abstract; Isabel Rodríguez-Germade et al, 2015; Okutsu et al., 2017, JGS abstract), the behavior of Ca/Ti and Fe/Ti where the peak was observed at the base of turbidites, and the behavior of Fe/Ti and Zr/Ti where the peak was observed at the base of volcaniclastics turbidites.

Our results revealed turbidites and volcaniclastics turbidites in six piston coring sites (PC01 to PC06). As all of sites are located in the Taura-Tsunagioki fault group or Minamataoki fault group, turbidites were considered to be present in all of sites. However, turbidites were identified from PC01 to PC06, but not identified from PC07 to PC11. According to Rifardi et al. (1998), PC01 to PC06 are located in the sea area where the deposition rate is high, and PC07 to PC11 are located in the sea area where the deposition rate is slow.

As turbidite is formed by various factors besides earthquakes, it is necessary to consider whether the turbidites identified in this study are earthquake turbidites. In addition, to investigate the history of earthquakes, it is also a future task to conduct individual sample measurements (such as grain size distribution analysis) and dating.

Hakuho-maru KH-18-3 Cruise Scientists: Takashi Tomiyasu, Hitoshi Kodamatani, Kuniyo Kawabata, Daiki Oyama, Haruka Kageyama, Kaede Yamasaki (Kagoshima Univ.), Yuta Ikebata, Koki Hori (Kyushu Univ.), Asuka Yamaguchi, Fumiaki Tsunomori, Kameo Katsura, Tsubasa Miki, Natsumi Okutsu, Hiroaki Koge,

©2019. Japan Geoscience Union. All Right Reserved.

Kotaro Fujita, Ayaka Nakazawa, Yuichi Okuma, Genki Kobayashi, Rina Fukuchi (Tokyo Univ.), Jun Kameda, Tomonori Morisaki (Hokkaido Univ.)

Keywords: submarine landslides, turbidites, shallow sea deposits, Yatsushiro Sea, 2016 Kumamoto Earthquake

©2019. Japan Geoscience Union. All Right Reserved.

Revised columnar section based on grain size distribution analysis of samples from Hakuho-maru KH-18-3 in Yatsushiro sea

*Yuta Ikebata[1], Yujin Kitamura[2], Hakuho-maru KH-18-3 Scientists Family

1. Kyusyu University Graduate School Of Science Earth and Planetary Science, 2. Graduate school of science, Kagoshima University

Hakuho-maru KH-18-3 was held in the Yatsushiro Sea from 27th to 30th July 2018 for clarifying history of occurrence of submarine landslides. Earthquake is a one of big trigger of submarine landslides, and submarine landslides occurs in an very easy slope. Kumamoto earthquake occurred at April, 2016 and a lot of surveys in the land area were conducted but survey in the sea area weren't conducted much. In the Yatsushiro sea, the occurrence of submarine landslides caused by earthquake of the Futagawa-Hinagu fault zones can be considered sufficiently. Therefore, in this study, the creation of the columnar section which is the basic information of the submarine landslide accreditation was made based on the grain size distribution analysis.

In the Expedition, eleven piston cores(6m) from PC01 to PC11 were collected in the southern part of Yatsushiro sea, and the obtained core was subjected to non-destructive measurement and individual sample measurement at the Kochi Core Center. For non-destructive measurement, CT images and core continuous images were taken, and for individual sample measurement, Density, Magnetic susceptibility, porosity, vane shear strength, color, concentration change of major elements were examined. Grain size distribution analysis was conducted at Kagoshima University. Samples used for grain size distribution analysis were collected every 50 cm and analyzed with a laser diffraction type grain size distribution analyzer. Since it is difficult to judge the stratum boundary only with the result of grain size distribution measurement at intervals of 50 cm, it was judged by using γ ray density, magnetic susceptibility and color measurement result which are continuous data.

Grain size distribution analysis revealed PC01 to PC07 are muddy cores and PC08 to PC11 contains much sand. Grain size of PC01, PC04, PC06, PC07, PC09, PC11 are very different in Grain size distribution analysis and visual core description. Based on the results of the grain size distribution analysis, the stratum boundary was determined from the change commonly seen in the γ ray density, magnetic susceptibility and color, and a columnar section was prepared. In Rifardi et al.(1998), the distribution of mud content in the Yatsushiro Sea has been surveyed. As a result of comparing the columnar map of this study with its distribution for each sampling point, cores excluding PC08 corresponded well. It is thought that it is influenced by the supply of sediment by river and stagnant water mass, tide current as in previous research. Also, in Inoue et al.(2011), which was a reference for determining the core harvest point, dating is done in the same area. At Hori(2019MS), we compare the data with Inoue et al.(2011) and estimate the core age of this research. We also compare the columnar section made in this study with the columnar section of Inoue et al.(2011), using the comparative categories determined at the time of estimating the age. As a result, PC01 and PC02 were in good agreement, PC06 and PC07 had different stratum in the surface layer. This is probably because the sampling site of PC06 is actually about 150 m far from Inoue et al.(2011) and the sampling site of PC07 is actually about 111 m far from Inoue et al.(2011), and the sedimentary environment is slightly different. Also, in the grain size distribution analysis of this study, there is a possibility that coarse grains may be selectively left out when putting the sample into the machine, and it may be doubtful in accuracy.

©2019. Japan Geoscience Union. All Right Reserved.

Keywords: Submarine landslide

©2019. Japan Geoscience Union. All Right Reserved.

[E] Oral | H (Human Geosciences)：H-DS Disaster geosciences

Mon. May 27, 2019 3:30 PM - 5:00 PM JST | Mon. May 27, 2019 6:30 AM - 8:00 AM UTC | 201B 2F

[H-DS11] Subaqueous Landslides and Their Anthropogenic Impact for Coastal Regions

convener:Yujin Kitamura(Department of Earth and Environmental Sciences, Graduate School of Science and Engineering, Kagoshima University), Yasuhiro Yamada(Japan Agency for Marine-Earth Science and Technology (JAMSTEC), R&D Center for Ocean Drilling Science (ODS)), Chairperson:Yujin Kitamura(Kagoshima University), Masayuki Utsunomiya(Research Institute of Geology and Geoinformation, Geological Survey of Japan, AIST), Yasuhiro Yamada(JAMSTEC)

A large number of people inhabit coastal areas around the world that are susceptible to natural catastrophes and subaqueous landslides are one of such hazards as demostrated recently. The risk associated with the occurrence of subaqueous landslides is not only constrained to passive margins or subduction zones but any of water areas is also susceptible to their occurrence since subaqueous failures can be triggered at very low slope angles. This realization poses a significant challenge that requires the collection of vast amounts of information and data to unravel the true nature of these events and their potential risk to coastal communities. Despite these challenges, recent technical and engineering advances in the acquisition and processing of sea floor and shallow subsurface data are encouraging. There has also been a concerted effort by scientists from different earth-science disciplines to increase interdisciplinary cooperation at an international level to advance our collective understanding of subaqueous landslides and their consequences.
This session calls for technical contributions covering all aspects of subaqueous landslide research including but not limited to: physical properties of deformed sediments (pre- and post- deformation), role of interstitial fluids in subaqueous landslide development, slope stability and risk assessments, geomorphological and sedimentological/stratigraphic descriptions, tsunamigenic risk and modeling, description of ancient subaqueous landslides, sand-box models and numerical simulations of subaqueous landslides. Case studies from lacustrine landslides and subaerial coastal landslides transitioning into the marine realm are also welcome. Case studies associated with the broader topic of subaqueous gravity-driven flows (e.g.: turbidites and transitional flows) and their relationship with seafloor faulting are also of interest to this session. Participants of IUGS project S4SLIDE IGCP-640 sponsor this session.

3:30 PM - 3:45 PM JST | 6:30 AM - 6:45 AM UTC

[HDS11-01] Distribution and sedimentological characteristics of the submarine landslides filling Hidaka Trough, offshore southern Hokkaido, northern Japan with special attention to the uppermost Quaternary submarine landslide bodies

*Hiroyuki Arato[1] (1.Graduate School of International Resource Sciences, Akita University)

3:45 PM - 4:00 PM JST | 6:45 AM - 7:00 AM UTC

[HDS11-02] Origin and distribution of mass-transport deposits in the Pleistocene forearc basin, central Japan, deduced from tephro- and biostratigraphy

*Masayuki Utsunomiya[1], Yuzuru Yamamoto[2], Kiyohide Mizuno[1] (1.Geological Survey of Japan, AIST, 2.JAMSTEC)

4:00 PM - 4:15 PM JST | 7:00 AM - 7:15 AM UTC

[HDS11-03] Physico-chemical properties of sediment cores from Yatsushiro Sea, western Kyushu

*Yujin Kitamura[1], Ryoya Goto[2], Koki Hori[2], Yuta Ikebata[2], Haruka Kageyama[2], Kuniyo Kawabata[1], Daiki Oyama[1], Kaede Yamasaki[2], Hakuho-maru KH-18-3 Scientists (1.Department of Earth and Environmental Sciences, Graduate School of Science and Engineering, Kagoshima University, 2.Atmosphere and Ocean Research Institute, The University of Tokyo)

4:15 PM - 5:00 PM JST | 7:15 AM - 8:00 AM UTC

Discussion

Distribution and sedimentological characteristics of the submarine landslides filling Hidaka Trough, offshore southern Hokkaido, northern Japan with special attention to the uppermost Quaternary submarine landslide bodies

*Hiroyuki Arato[1]

1. Graduate School of International Resource Sciences, Akita University

In the last few years, many examples of submarine landslides have been reported worldwide, and their systematic and genetic researches have been initiated. The studies in distribution, sedimentary pattern and mechanism of submarine landslides are remarkably important mainly from the following two reasons: (1) Submarine landslides affect significantly the state of surrounding water mass due to long distance migration of huge volume sediment mass within relatively short time period. One of the critical phenomena is megatsunami induced by submarine landslides, (2) Secondly nature of submarine landslides is deeply related to transportation mechanisms of siliciclastic sediments into tectonically formed sedimentary basins and their burial processes. In this study, two dataset of 3D seismic survey are utilized to describe some submarine landslide examples, under the owner’ s permission. They are Geophysical Survey and Basin Evaluation Projects “2013FY Hidaka Shujo Kaibon 3D”(hereinafter, called HSK-3D) and “2014FY Hidaka Shujo Kaibon Seibu 3D” (HSKW-3D), acquired at the offshore southern Hokkaido by Ministry of Economy, Trade and Industry (METI).
The surveys cover the northeastern marginal slope and a part of central basin floor of Hidaka Trough elongated NW-SE direction. Water depth of covering area ranges from 577 to 1,156 mBMSL. The seismic reflector indicating seabed have been traced by using “seeded autotracking” function of PETREL, then a time structural contour map for the surface, which is equivalent to bathymetric map, have been drawn. Based on the topographic features, the survey area can be subdivided broadly into two types; one is characterized generally by smooth sea bottom surface, and another by irregular or rough surface in seismic scale. The area of smooth sea bottom cover approximately southwestern two thirds portion of HSKW-3D and a part of the western HSK-3D areas. On the other hand, northeastern one thirds of HSKW-3D, northwestern corner of HSK-3D, and northeastern portion and some extending areas are characterized by irregularly swollen, or roughly heaped unsmooth sea bottom surface. Such irregular topographic features of the seabed can be interpreted formed by Holocene or the youngest Quaternary submarine landslides from the point of view of their distribution within the basin. Within cross sectional views of the seismic data, those landslide bodies are observed as externally discontinuous and internally chaotic layers within orderly stacking parallel layered succession in seismic facies. These youngest submarine landslides seen in recent topography can largely be classified into 4 groups; called i) Shizunai, ii) Urakawa, iii) Samani and iv) Erimo Submarine Landslide, and they are laterally arrayed from northwest to southeast and running down generally from northeast to southwest on the continental slope of Hidaka Trough (Figure).
In addition, many buried submarine landslide bodies in the sediments filling the Hidaka Trough (e.g., Monbetsu SLS) can be recognized by seismic facies interpretation in the cross sections and time slice images. In the Hidaka Trough, Cretaceous to Quaternary sediments ranging up to 10km in thickness are present. Four horizons, A, B, C and D had been selected and traced within the sedimentary succession in this study. On the basis of chronostratigraphic correlation to the preceding studies, B, C, and D are correlative to intra-middle Pleistocene equivalent to the base of NPD12, base of middle Pleistocene Calabrian, and base of Pliocene, respectively. Horizon A is inferred as a horizon in the upper Pleistocene

©2019. Japan Geoscience Union. All Right Reserved.

or Holocene. At least more than 3 landslide events can be detected in the stratigraphic unit between seabed and horizon A. In the unit between horizons A and B, 3 to 5 events are recognized, and there are equivalent numbers of landslide events in the unit between horizons B and C. Almost sediments are interpreted as chaotic seismic facies below horizon D.

Keywords: submarine landslide, Hidaka Trough, submarine landslide-induced tsunami, 3D seismic survey

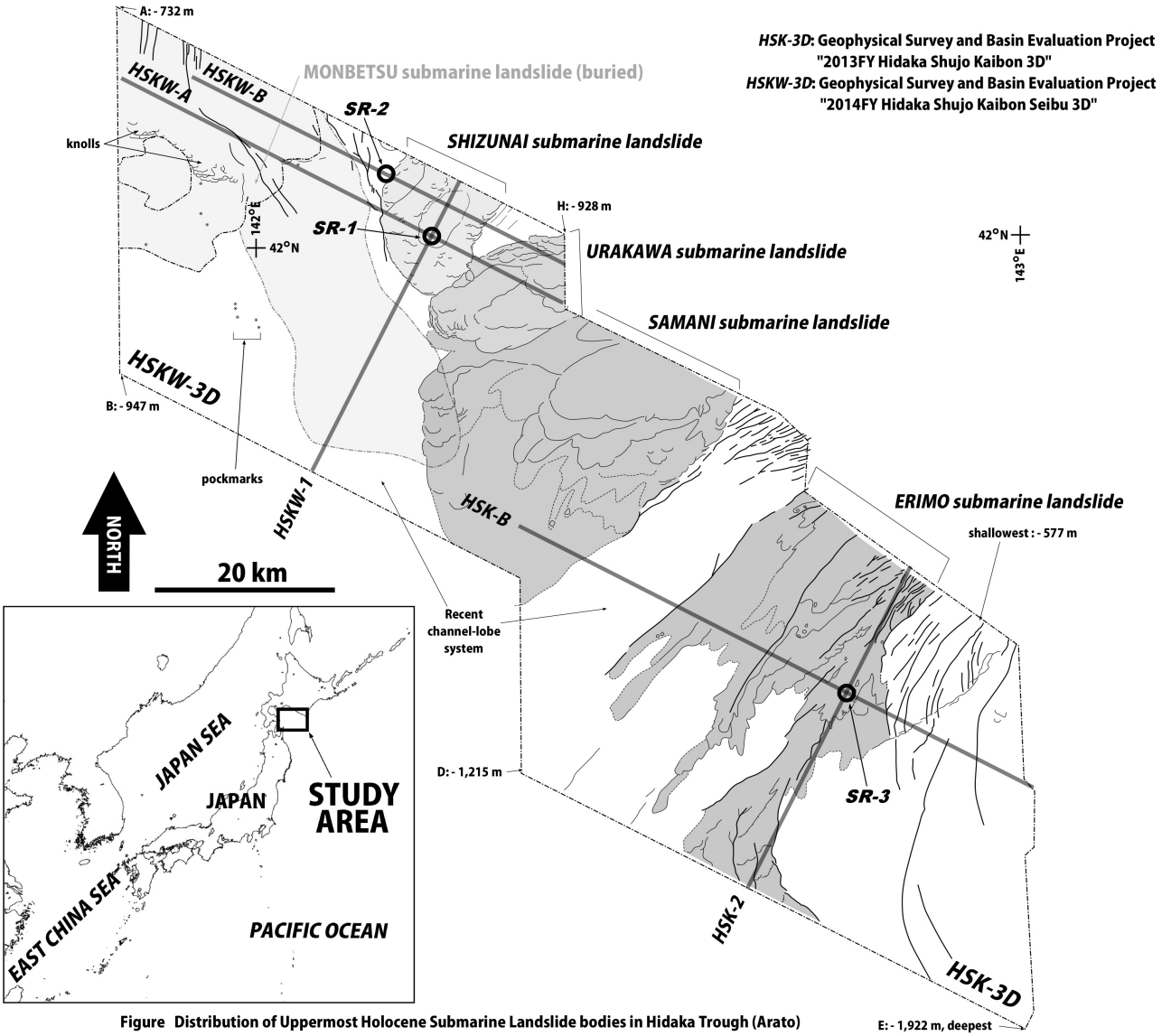

Figure Distribution of Uppermost Holocene Submarine Landslide bodies in Hidaka Trough (Arato)

©2019. Japan Geoscience Union. All Right Reserved.

Origin and distribution of mass-transport deposits in the Pleistocene forearc basin, central Japan, deduced from tephro- and biostratigraphy

*Masayuki Utsunomiya[1], Yuzuru Yamamoto[2], Kiyohide Mizuno[1]

1. Geological Survey of Japan, AIST, 2. JAMSTEC

We introduce a field-based study on the basin-wide mass-transport deposits (MTDs) by means of biostratigraphy and the marker tephra beds. The Kazusa Group, the Pleistocene forearc-basin fill exposed in central Japan, is characterized by high sedimentation rate and its stratigraphy is well-established. We focused on three MTDs referred to as MTDs-8–10. They consist of folded blocks that range from tens of centimeters to more than tens of meters in width and thickness, in a sandy mud matrix commonly containing volcaniclastics (e.g., pumice grains and euhedral crystals). The overall thickness of these MTDs ranges from ~20 to 100 m. Based on the lateral correlation of the tephra marker beds, these MTDs can be traced laterally for more than several tens of kilometers. MTD-8 (1.3 Ma) and MTD-9 (1.2 Ma) contain blocks characterized by folding, internal minor faulting, different attitude of bedding planes from the general trend, and occasionally overturned. The blocks in MTD-8 contain tephra beds and calcareous nannofossils that are typically found in the older strata down to 250 m below it, which suggest that the blocks are considered to have originated from the upstream excavated area and spread out laterally to cover the open seabed. On the other hand, MTD-10 (1.2 Ma) is characterized by a laterally-stacking pattern showing lamp-flat geometry, and the original stratigraphic positions of the blocks are consistent with the host strata, indicative of translational movement. The sedimentary dykes were observed in the basal slide plane, suggesting excess pore pressure within the slip zone. The different modes of occurrence are likely to be a result of local variation in slope gradient and distance of downslope migration. That is, initial phase of mass transportation on low-gradient slope represented a slide (MTD-10), whereas moving over a sufficiency long distance exhibited more mixtured and deformed slump (MTDs-8 and 9). Combination of studies on MTD textures, tephro- and biostratigraphy has great advantage to know their spatial distribution, original stratigraphic position where the MTDs were initiated, and mechanism to generate variable occurrence of MTDs.

Keywords: submarine landslide, mass-transport deposit, Kazusa Group, calcareous nannofossils, tephra

©2019. Japan Geoscience Union. All Right Reserved.

Physico-chemical properties of sediment cores from Yatsushiro Sea, western Kyushu

*Yujin Kitamura[1], Ryoya Goto[2], Koki Hori[2], Yuta Ikebata[2], Haruka Kageyama[2], Kuniyo Kawabata[1], Daiki Oyama[1], Kaede Yamasaki[2], Hakuho-maru KH-18-3 Scientists

1. Department of Earth and Environmental Sciences, Graduate School of Science and Engineering, Kagoshima University, 2. Atmosphere and Ocean Research Institute, The University of Tokyo

Submarine active faults in Yatsushiro sea, western Kyushu, constitute the Yatsushiro section of Hinagu fault zone in its southwest end. The 2016 Kumamoto Earthquake was sourced from a part of active faults of the Futagawa-Hinagu fault zones. Earthquake shaking occasionally triggers submarine landslide. As submarine landslide can take place in very gentle slope (< 1˚), Yatsushiro sea is yet to be a scene for it although the area is a shallow and relatively small sedimentary basin. However, any record of submarine landslide in this area has not been reported.

Minamata bay, southern Yatsushiro sea, is known to be mercury pollution from a chemical plant drainage. A complex space-time distribution of mercury content in the sediments has been revealed (Tomuyasu et al., 2014). As the transportation of the mercury-containing clastics depends on sedimentation rate and/or water current, submarine landslide is a candidate for the factor of drastic change in benthic environment.

Here we conducted four-days research cruise Hakuho-maru KH-18-3 in July, 2018 to reveal submarine landslide records and benthic environment in Yatsushiro sea. We conducted subbottom profiling, piston coring at 11 sites, and multiple coring at 13 sites). Recovered cores are analyzed by X-ray CT scanner, multi-sensor core logger, core imaging apparatus, visual core description, color spectroscope, X-ray fluorescence core scanner (Itrax), and so do discrete samples by vane shear tester, picnometer with sediments and by Radon monitor with sea water and pore water.

Our results revealed clear difference in the lower part of each core compared to the upper part. By referring piston cores and their age data by Inoue et al. (2011), these distinctive units is caused by hiatus between about 3 to 8 ka. The lower sediments below the hiatus are characterized by rather high vane shear strength, low porosity and abundant terrigenous sediments. The depth of hiatus varies in site by site, which suggests difference in local depositional environment. Sedimentation rate of recent 50 years which Rifardi et al. (1998) inferred from superficial sediments cannot be applied for whole core, but the rate in longer time scale must be further smaller.

Keywords: turbidites, shallow marine deposit, 2016 Kumamoto earthquake, mercury, Yatsushiro sea, Minamata bay

©2019. Japan Geoscience Union. All Right Reserved.

[E] Poster | H (Human Geosciences)：H-DS Disaster geosciences

Mon. May 27, 2019 1:45 PM - 3:15 PM JST | Mon. May 27, 2019 4:45 AM - 6:15 AM UTC | Poster Hall International Exhibition Hall8, Makuhari Messe_4

[H-DS12] Advanced Remote Sensing toward Mega-Disaster Response

convener:Young-Joo Kwak(ICHARM-UNESCO: International Centre for Water Hazard And Risk Management), Wataru Takeuchi(Institute of Industrial Science, The University of Tokyo)

Natural disaster under climate change is a serious threat to sustainable development, and in recent years natural disasters, i.e., hydro-geo-meteorological hazards and risks, have been frequently experienced in many countries by both developing and developed countries.
To achieve Sustainable Development Goals (SDGs), this session introduces papers focused on both principles and applications of remote sensing to promote investment in disaster risk reduction using integrated GIS and space infra data. Advanced remote sensing with Earth observation (EO) data appears to be the way forward in reducing damages and the death toll or affected people at local, national, regional and global levels.
We encourage the presentation of new research findings and novel approaches on land surface dynamics due to mega disasters between near-real time observation and long-term trends with water/hydrological cycle, such as floods, tropical cyclones (typhoons), storm surges, earthquakes, tsunamis, landslides, and wildfires.

[HDS12-P01] Satellite-based assessment of electricity restoration efforts in Puerto Rico after Hurricane Maria

*Miguel O Roman[1], Eleanor Stokes[2,3], Zhuosen Wang[2,3], Virginia Kalb[3], Ranjay Shrestha[4,3] (1.Earth from Space Institute, Universities Space Research Association, 2.Earth System Science Interdisciplinary Center, University of Maryland, 3.NASA Goddard Space Flight Center, 4.Science Systems and Applications, Inc)

[HDS12-P02] **Flood inundation forecasting coupled with in-situ water level and satellite data**

*Young-Joo Kwak[1], Jonggeol Park[2], Wataru Takeuchi[3] (1.ICHARM-UNESCO: International Centre for Water Hazard And Risk Management, 2.Tokyo University of Information and Sciences, 3.University of Tokyo)

[HDS12-P03] Long term monitoring of flood damage in the coastal area of Bangladesh

★Invited Papers

*Park Jonggeol[1], Young-Joo Kwak[2] (1.Tokyo University of Information Sciences, 2.ICHARM-UNESCO)

[HDS12-P04] Automatic shoreline detection and coastal change detection using multiple satellite data in Bangladesh

*Young-Joo Kwak[1] (1.ICHARM-UNESCO: International Centre for Water Hazard And Risk Management)

Satellite-based assessment of electricity restoration efforts in Puerto Rico after Hurricane Maria

*Miguel O Roman[1], Eleanor Stokes[2,3], Zhuosen Wang[2,3], Virginia Kalb[3], Ranjay Shrestha[4,3]

1. Earth from Space Institute, Universities Space Research Association, 2. Earth System Science Interdisciplinary Center, University of Maryland, 3. NASA Goddard Space Flight Center, 4. Science Systems and Applications, Inc

Understanding the distribution and duration of power outages after a disaster is a precursor to minimizing their harmful consequences, especially to vulnerable communities. Here, we use satellite-derived daily estimates of lights to monitor electricity restoration efforts in Puerto Rico following Hurricane Maria, which caused the longest blackout in US history. Within all settlements, we track how long it took to restore electricity, and assess the characteristics of communities that shouldered the most extended outages. Our results show an 80% decrease in lights, in total, immediately after Hurricane Maria. During the recovery, a disproportionate share of long-duration power failures (> 120 days) occurred in rural municipalities (41% of rural municipalities vs. 29% of urban municipalities), and in the northern and eastern districts. Unexpectedly, we also identify significant disparities in electricity recovery within municipalities. Land use, proximity to highways, and the structure and density of the built environment were all factors that influenced restoration times. For many urban municipalities, poor residents lived in less dense, detached housing—where power restoration lagged. The results demonstrate the capability of nighttime satellite imagery to monitor power availability at a high spatial resolution, linking monitoring efforts to neighborhood-scale demographic data. They also identify the unintended consequences of current density-based power restoration protocols. Through the integration of in-situ, satellite, and socioeconomic data products, disaster responses to long-term events can become more strategic to minimize harm, incorporating adaptive community capacity as an additional variable to determine where power should be restored.

Keywords: VIIRS DNB, Black Marble, nighttime lights, power outage detection, energy access, disaster risk reduction

©2019. Japan Geoscience Union. All Right Reserved.

Flood inundation forecasting coupled with in-situ water level and satellite data

*Young-Joo Kwak[1], Jonggeol Park[2], Wataru Takeuchi[3]

1. ICHARM-UNESCO: International Centre for Water Hazard And Risk Management, 2. Tokyo University of Information and Sciences, 3. University of Tokyo

With extreme weather events, catastrophic floods occur as one of the major disasters in the world. With the development of spaceborne optical and SAR (synthetic aperture radar) sensors, flood detection algorithms should be progressively developed to produce more accurate flood maps

Despite very limited satellite-based data, this study introduces good examples of snapshot flood detection and flood inundation forecasting focusing on short-term flood extent change using a new index-based flood algorithm with a synchronized floodwater index ($SfWI^2$). MODIS (MODerate resolution Imaging Spectroradiometer, NASA-USGS) time series data were mainly employed to detect the annual and potential flood extent of 2017. The pilot study was selected in the mega deltas over vast low-lying areas of Bangladesh and India (i.e., the 2017 flood in the basins of the Ganges, Brahmaputra and Magna rivers) As preliminary results, the resultant maps represented the dynamics of flood extent and flood propagation process. This approach shows a methodological possibility for instant and comprehensive flood mapping at the international river-basin level. For application to a global flood mapping, reliable satellite-derived flood maps will contribute flood risk management. In order to improve the accuracy of rapid flood mapping, we should solve many ambiguities in particular, surface complexity, i.e., urbanized mega-delta floodplains.

Keywords: Flood detection, Inundation forecasting, MODIS

©2019. Japan Geoscience Union. All Right Reserved.

Long term monitoring of flood damage in the coastal area of Bangladesh

*Park Jonggeol[1], Young-Joo Kwak[2]

1. Tokyo University of Information Sciences, 2. ICHARM-UNESCO

The major natural hazards which Bangladesh has to confront regularly include floods, cyclones and accompanying storm surge. Flooding from river waters overflowing the banks, particularly during monsoon, is an annual phenomenon. On average, one-third of the country goes under water every year. In this study, we investigated the flooding area of Bangladesh using time series MOD13A2 data of 15 years. Discriminant analysis using both NDVI and MDWI is more effective than extracting water bodies using existing NDWI only. The flash flood was from the Indian plateau bordering the northern part of Bangladesh to flow from April to May and a wide wetland was formed and the longest flooding period in Bangladesh was revealed as it is as it is the rainy season.

Keywords: Flood, MODIS, NDWI

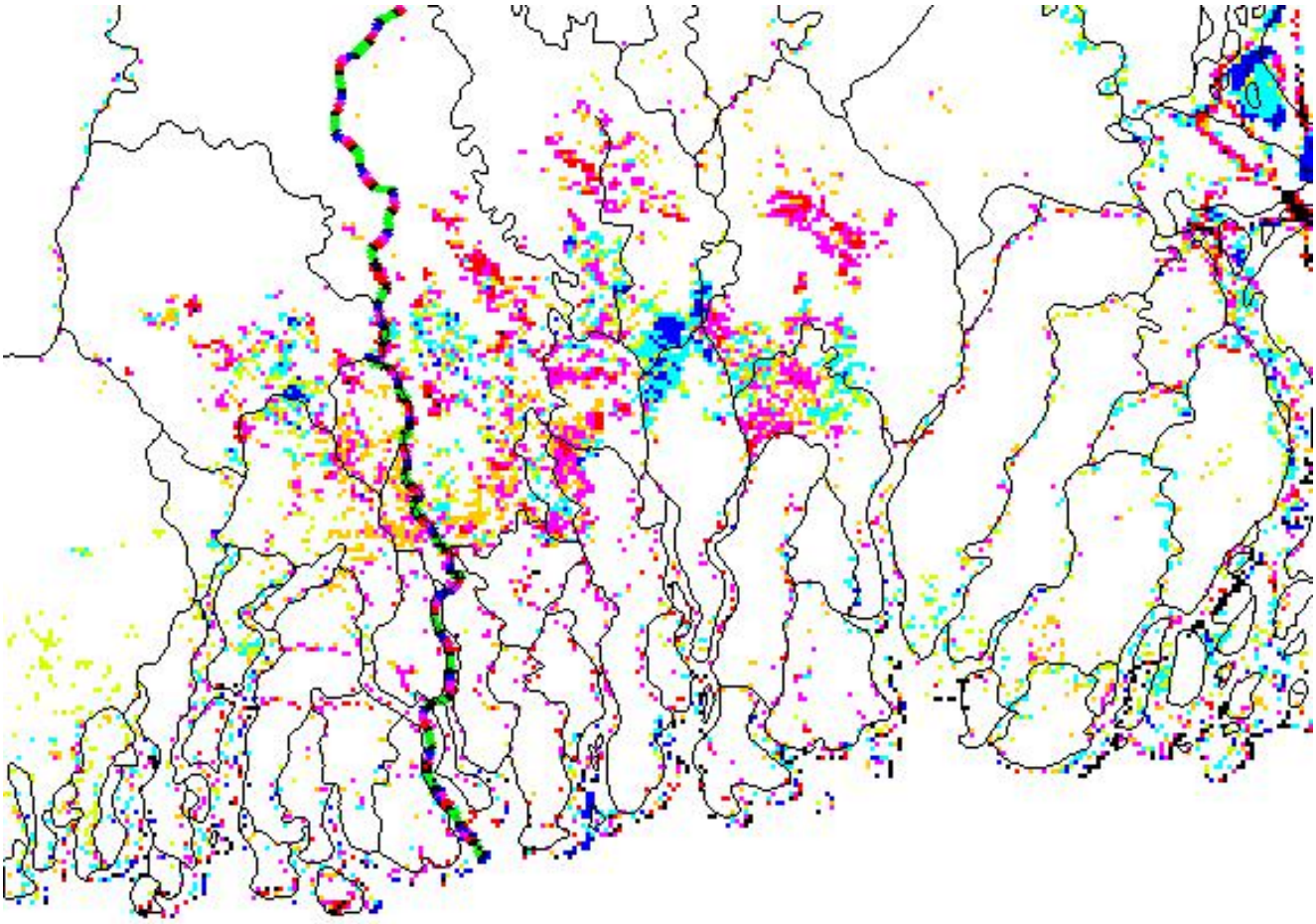

©2019. Japan Geoscience Union. All Right Reserved.

Automatic shoreline detection and coastal change detection using multiple satellite data in Bangladesh

*Young-Joo Kwak[1]

1. ICHARM-UNESCO: International Centre for Water Hazard And Risk Management

The Bangladesh government has been faced with the risk of coastal erosion as one of the urgent issues in land use planning and coastal management. As a preliminary investigation, an automated algorithm was proposed focusing on shoreline detection using multiple satellite data. The selected study site is located in the estuary of the Meghna River around the Gulf of Bengal in Bangladesh.

We employed Landsat-7, -8 data (90m and 30m spatial resolution, respectively) and ALOS, ALOS-2 (12.5m and 25m spatial resolution, respectively) to detect accurate coastal lines during the similar snapshot period.

As a result of automatic shoreline detection and coastal change detection by the interpretation and classification, the average rate of coastal line change was 0.5km (eroded) per year for the period between 2010 and 2019 in case of Meghna River along Noahkali (Noler Char). In addition, the resultant coastal change line was also verified by ground truth and field survey data using a small unmanned aerial vehicle (sUAV: Quadcopter with a flight control system, ©DJI Technology Co. Ltd., China) for comprehensive validation.

This feasibility study will continually investigate the characteristics of short-term and long-term changes with the relationship between hydrological parameters such as precipitation, river discharge, wave, and tidal effect.

Keywords: Shoreline detection, Coastal change

©2019. Japan Geoscience Union. All Right Reserved.

[E] Poster | H (Human Geosciences)：H-DS Disaster geosciences

Mon. May 27, 2019 5:15 PM - 6:30 PM JST | Mon. May 27, 2019 8:15 AM - 9:30 AM UTC | Poster Hall International Exhibition Hall8, Makuhari Messe_14

[H-DS12] Advanced Remote Sensing toward Mega-Disaster Response

convener:Young-Joo Kwak(ICHARM-UNESCO: International Centre for Water Hazard And Risk Management), Wataru Takeuchi(Institute of Industrial Science, The University of Tokyo)

Natural disaster under climate change is a serious threat to sustainable development, and in recent years natural disasters, i.e., hydro-geo-meteorological hazards and risks, have been frequently experienced in many countries by both developing and developed countries.
To achieve Sustainable Development Goals (SDGs), this session introduces papers focused on both principles and applications of remote sensing to promote investment in disaster risk reduction using integrated GIS and space infra data. Advanced remote sensing with Earth observation (EO) data appears to be the way forward in reducing damages and the death toll or affected people at local, national, regional and global levels.
We encourage the presentation of new research findings and novel approaches on land surface dynamics due to mega disasters between near-real time observation and long-term trends with water/hydrological cycle, such as floods, tropical cyclones (typhoons), storm surges, earthquakes, tsunamis, landslides, and wildfires.

[HDS12-P01] Satellite-based assessment of electricity restoration efforts in Puerto Rico after Hurricane Maria

*Miguel O Roman[1], Eleanor Stokes[2,3], Zhuosen Wang[2,3], Virginia Kalb[3], Ranjay Shrestha[4,3] (1.Earth from Space Institute, Universities Space Research Association, 2.Earth System Science Interdisciplinary Center, University of Maryland, 3.NASA Goddard Space Flight Center, 4.Science Systems and Applications, Inc)

[HDS12-P02] **Flood inundation forecasting coupled with in-situ water level and satellite data**

*Young-Joo Kwak[1], Jonggeol Park[2], Wataru Takeuchi[3] (1.ICHARM-UNESCO: International Centre for Water Hazard And Risk Management, 2.Tokyo University of Information and Sciences, 3.University of Tokyo)

[HDS12-P03] Long term monitoring of flood damage in the coastal area of Bangladesh

★Invited Papers

*Park Jonggeol[1], Young-Joo Kwak[2] (1.Tokyo University of Information Sciences, 2.ICHARM-UNESCO)

[HDS12-P04] Automatic shoreline detection and coastal change detection using multiple satellite data in Bangladesh

*Young-Joo Kwak[1] (1.ICHARM-UNESCO: International Centre for Water Hazard And Risk Management)

Satellite-based assessment of electricity restoration efforts in Puerto Rico after Hurricane Maria

*Miguel O Roman[1], Eleanor Stokes[2,3], Zhuosen Wang[2,3], Virginia Kalb[3], Ranjay Shrestha[4,3]

1. Earth from Space Institute, Universities Space Research Association, 2. Earth System Science Interdisciplinary Center, University of Maryland, 3. NASA Goddard Space Flight Center, 4. Science Systems and Applications, Inc

Understanding the distribution and duration of power outages after a disaster is a precursor to minimizing their harmful consequences, especially to vulnerable communities. Here, we use satellite-derived daily estimates of lights to monitor electricity restoration efforts in Puerto Rico following Hurricane Maria, which caused the longest blackout in US history. Within all settlements, we track how long it took to restore electricity, and assess the characteristics of communities that shouldered the most extended outages. Our results show an 80% decrease in lights, in total, immediately after Hurricane Maria. During the recovery, a disproportionate share of long-duration power failures (> 120 days) occurred in rural municipalities (41% of rural municipalities vs. 29% of urban municipalities), and in the northern and eastern districts. Unexpectedly, we also identify significant disparities in electricity recovery within municipalities. Land use, proximity to highways, and the structure and density of the built environment were all factors that influenced restoration times. For many urban municipalities, poor residents lived in less dense, detached housing—where power restoration lagged. The results demonstrate the capability of nighttime satellite imagery to monitor power availability at a high spatial resolution, linking monitoring efforts to neighborhood-scale demographic data. They also identify the unintended consequences of current density-based power restoration protocols. Through the integration of in-situ, satellite, and socioeconomic data products, disaster responses to long-term events can become more strategic to minimize harm, incorporating adaptive community capacity as an additional variable to determine where power should be restored.

Keywords: VIIRS DNB, Black Marble, nighttime lights, power outage detection, energy access, disaster risk reduction

©2019. Japan Geoscience Union. All Right Reserved.

Flood inundation forecasting coupled with in-situ water level and satellite data

*Young-Joo Kwak[1], Jonggeol Park[2], Wataru Takeuchi[3]

1. ICHARM-UNESCO: International Centre for Water Hazard And Risk Management, 2. Tokyo University of Information and Sciences, 3. University of Tokyo

With extreme weather events, catastrophic floods occur as one of the major disasters in the world. With the development of spaceborne optical and SAR (synthetic aperture radar) sensors, flood detection algorithms should be progressively developed to produce more accurate flood maps

Despite very limited satellite-based data, this study introduces good examples of snapshot flood detection and flood inundation forecasting focusing on short-term flood extent change using a new index-based flood algorithm with a synchronized floodwater index ($SfWI^2$). MODIS (MODerate resolution Imaging Spectroradiometer, NASA-USGS) time series data were mainly employed to detect the annual and potential flood extent of 2017. The pilot study was selected in the mega deltas over vast low-lying areas of Bangladesh and India (i.e., the 2017 flood in the basins of the Ganges, Brahmaputra and Magna rivers) As preliminary results, the resultant maps represented the dynamics of flood extent and flood propagation process. This approach shows a methodological possibility for instant and comprehensive flood mapping at the international river-basin level. For application to a global flood mapping, reliable satellite-derived flood maps will contribute flood risk management. In order to improve the accuracy of rapid flood mapping, we should solve many ambiguities in particular, surface complexity, i.e., urbanized mega-delta floodplains.

Keywords: Flood detection, Inundation forecasting, MODIS

©2019. Japan Geoscience Union. All Right Reserved.

Long term monitoring of flood damage in the coastal area of Bangladesh

*Park Jonggeol[1], Young-Joo Kwak[2]

1. Tokyo University of Information Sciences, 2. ICHARM-UNESCO

The major natural hazards which Bangladesh has to confront regularly include floods, cyclones and accompanying storm surge. Flooding from river waters overflowing the banks, particularly during monsoon, is an annual phenomenon. On average, one-third of the country goes under water every year. In this study, we investigated the flooding area of Bangladesh using time series MOD13A2 data of 15 years. Discriminant analysis using both NDVI and MDWI is more effective than extracting water bodies using existing NDWI only. The flash flood was from the Indian plateau bordering the northern part of Bangladesh to flow from April to May and a wide wetland was formed and the longest flooding period in Bangladesh was revealed as it is as it is the rainy season.

Keywords: Flood, MODIS, NDWI

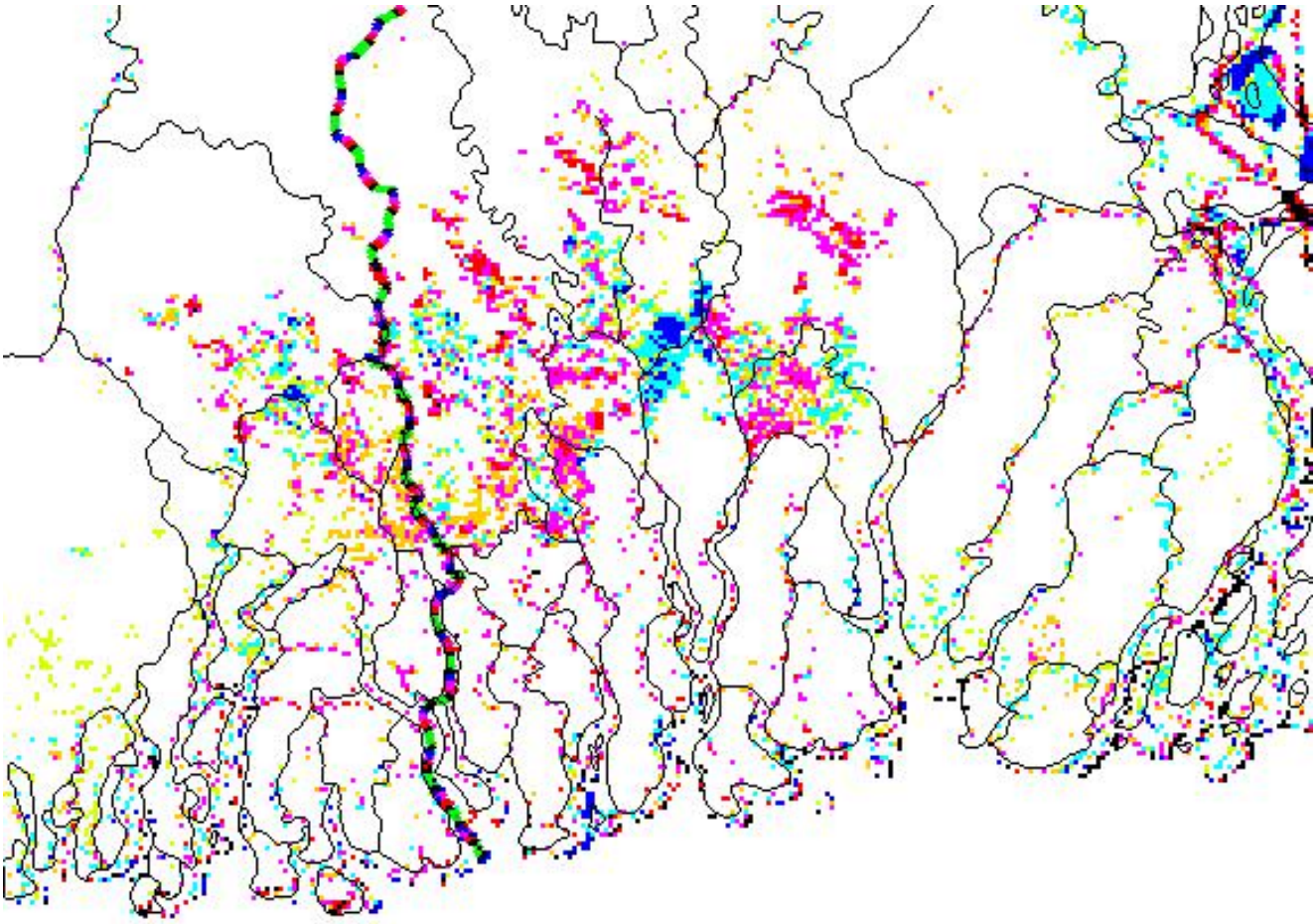

©2019. Japan Geoscience Union. All Right Reserved.

Automatic shoreline detection and coastal change detection using multiple satellite data in Bangladesh

*Young-Joo Kwak[1]

1. ICHARM-UNESCO: International Centre for Water Hazard And Risk Management

The Bangladesh government has been faced with the risk of coastal erosion as one of the urgent issues in land use planning and coastal management. As a preliminary investigation, an automated algorithm was proposed focusing on shoreline detection using multiple satellite data. The selected study site is located in the estuary of the Meghna River around the Gulf of Bengal in Bangladesh.

We employed Landsat-7, -8 data (90m and 30m spatial resolution, respectively) and ALOS, ALOS-2 (12.5m and 25m spatial resolution, respectively) to detect accurate coastal lines during the similar snapshot period.

As a result of automatic shoreline detection and coastal change detection by the interpretation and classification, the average rate of coastal line change was 0.5km (eroded) per year for the period between 2010 and 2019 in case of Meghna River along Noahkali (Noler Char). In addition, the resultant coastal change line was also verified by ground truth and field survey data using a small unmanned aerial vehicle (sUAV: Quadcopter with a flight control system, ©DJI Technology Co. Ltd., China) for comprehensive validation.

This feasibility study will continually investigate the characteristics of short-term and long-term changes with the relationship between hydrological parameters such as precipitation, river discharge, wave, and tidal effect.

Keywords: Shoreline detection, Coastal change

©2019. Japan Geoscience Union. All Right Reserved.

[J] Oral | H (Human Geosciences)：H-DS Disaster geosciences

Mon. May 27, 2019 10:45 AM - 12:15 PM JST | Mon. May 27, 2019 1:45 AM - 3:15 AM UTC | 106 1F

[H-DS14] Geohazards in humid, tectonically active countries and their precursors

convener:Masahiro Chigira(Disaster Prevention Research Institute, Kyoto University), Hiroshi YAGI(Faculty of Art, Science and Education, Yamagata University), Satoru Kojima(Department of Civil Engineering, Gifu University), Taro Uchida(National Institute for Land and Infrastructure Management), Chairperson:Satoshi Ishimaru

This session covers mass movements of landslide, slope failure, debris flow, and gravitational slope deformation in tectonically active, humid countries, and aims to discuss on their mechanisms, characteristics of occurrence sites, the significance in geological time scale, and the methodology to mitigate their affects by researchers with various related research fields. In particular, papers about 2017 northern Kyushu rainstorm, 2018 Osaka earthquake, 2018 Western Japan rainstorm, and 2018 Hokkaido earthquake are welcome

10:45 AM - 11:00 AM JST | 1:45 AM - 2:00 AM UTC

[HDS14-01] The sources of landslides occurred by the 2018 Hokkaido Eastern Iburi Earthquake

*Satoshi Ishimaru[1], Wataru Hirose[1], Gentaro Kawakami[1], Ryo Takahashi[1], Yoshihiro Kase[1], Ken'ichi Koshimizu[1], Hiromichi Koyasu[1], Masahiro Chigira[2], Jun Tajika[3] (1.Geological Survey of Hokkaido, 2.Kyoto University, 3.Docon Co., Ltd.)

11:00 AM - 11:15 AM JST | 2:00 AM - 2:15 AM UTC

[HDS14-02] Feature of landslide of pyroclastic fall deposits induced by 2018 Hokkaido Eastern Iburi Earthquake, and its relation with damage

*Jun Tajika[1], Kazuo Amemiya[2], Masahiro Chigira[3], Satoshi Ishimaru[4], Akio Koike[1], Hidetoshi Kon[1], Kenji Kizaki[5], Nobuo Yamane[6] (1.Docon Co.,Ltd., 2.Bousai Chishitsu Kogyo Co.,Ltd., 3.Kyoto University, 4.Geological Survey of Hokkaido, HRO, 5.Kizaki PE Office, 6.Terre Research Co.)

11:15 AM - 11:30 AM JST | 2:15 AM - 2:30 AM UTC

[HDS14-03] Influence of slope cutting on failures induced by the July heavy rain, and the Iburi-tobu earthquake, 2018.

*Hidehisa Nagata[1] (1.Fu-Sui-Do Company Limited)

11:30 AM - 11:45 AM JST | 2:30 AM - 2:45 AM UTC

[HDS14-04] Slope failures occurred in the southwest part of the Izu-oshima Island in geological time, NE Japan

*Takehiko Suzuki[1], Masahiro Chigira[2] (1.Faculty of Urban Environmental Sciences, Tokyo Metropolitan University, 2.Disaster Prevention Research Institute, Kyoto University)

11:45 AM - 12:00 PM JST | 2:45 AM - 3:00 AM UTC

[HDS14-05] The strain rate observation by the borehole inclinometer on the bedrock creep slopes in Akadani-west area

*Atsuhiko Kinoshita[1,2], Yasutaka Tanaka[2], Wataru Sakurai[1], Taro Uchida[1], Koichiro Hayashi[3], Yasuuchi Kubota[3], Katsushi Kawato[4] (1.National Institute for Land and Infrastructure Management, 2.Sediment Disaster Prevention Technology Center, Kinki Developing Regional Bureau, Ministry of Land, Infrastructure, Transport and Tourism , 3.OYO Corporation, 4.NIPPON ENGINEERING CONSULTANTS CO., LTD.)

12:00 PM - 12:15 PM JST | 3:00 AM - 3:15 AM UTC

[HDS14-06] Assessing Potential Landslide Areas Due to Earthquake Using Three-Dimensional Resistivity Datasets from Across a Wide Area

*Yusuke Sakai[1], Taro Uchida[1], YASUMASA FUJIWARA[2] (1.National Institute for Land and Infrastructure Management , 2.Eight-Japan Engineering Consultants)

The sources of landslides occurred by the 2018 Hokkaido Eastern Iburi Earthquake

*Satoshi Ishimaru[1], Wataru Hirose[1], Gentaro Kawakami[1], Ryo Takahashi[1], Yoshihiro Kase[1], Ken'ichi Koshimizu[1], Hiromichi Koyasu[1], Masahiro Chigira[2], Jun Tajika[3]

1. Geological Survey of Hokkaido, 2. Kyoto University, 3. Docon Co., Ltd.

An earthquake of M6.7 was occurred at 37km depth in East Iburi, Hokkaido, on September 6, 2018. This earthquake caused numerous landslides in Azuma town with seismic intensities of 7 or 6+. The number of landslides reached 8000 in area of 20km by 20km. The type of these landslides is almost debris slide on the base of tephra layers, excluding rock slide and rock fall near the epicenter.

1 Distribution of tephra layers

Thick tephra layers interleaved with kuroboku, cover on hill slopes in the area of numerous landslides. The tephras derived from Shikotsu caldera and surrounding volcanoes, about 50 km west of Atsuma town. Main tephra layers in the hillslope are Spfa1 pumice of 48ka from Shikotsu caldera, En-a pumice of 20ka from Eniwa volcano, and Ta-d pumice of 9ka, Ta-c pumice of 3ka, Ta-b pumice of AD1667, and Ta-a pumice of 1739 from Tarumai volcano. En-a layer is thick, 1m more, in the northern area with numerous landslides, and Ta-d layer is thick, 1m more, in the southern area. These tephra layers are the main parts of landslides by this earthquake.

2 Tephras on hillslope with geomorphological evolution

Slope surficial deposit moved active affected by solifluction due to freeze-thaw cycles in the last glacial period, more than 10ka. For the reason, Spfa1 and En-a could not remain on hillslopes, except for valley head slopes and the foot of the slope accumulated surficial deposits, or crest slopes. On the other hand, the lower part of slopes was eroded by increased fluvial activity related to warmer and wetter during the late glacial period. Therefore, Spfa1 and En-a from the last glacial period do not cover on the lower valley-side slopes, but Ta-d covers on slope deposits on weathered rock there.

En-a covering the slope, for example valley head slope, is underlain by the reworked Spfa1. The volcanic soil with Spfa1 contains easily water and has slippery. On the other hand, Ta-d often is underlain by reworked En-a on the lower valley-side slope. These reworked tephras and the unit of the base of Ta-d layer with high absorbability, described below, would be slide layers in this earthquake.

3 Cases of landslides

Cases of landslides of thick Ta-d in the southern area of the disaster area and of thick En-a in the northern area are shown below.

3.1 The southern part covered thick Ta-d

A landslide at Asahi, located at the west side of Yoshino at the most severe disaster, was occurred on a flat slope at the lower valley-side slope. The collapse was occurred from the lower convex break of slope. It is 35m high, 35m wide, and 90m long. The vertical surface of the 3m thick soil layers with tephras, is exposed at the both sides of the landslide. Pale yellowish water-rich volcanic ash with striations adhere to the slip surface on thin slope deposit on weathered rock. The sliding surface was in a fine-pumice layer containing much moisture at the lowest part of Ta-d layer, according to outcrop observation of both sides of this failure. The upper part of Ta-d layer of 130cm thick, is redish brown pumice with weathered clay, and the lower part of it is dull gray coarse pumice with high permeability. The moving body slid and deposited as almost kept stratigraphic structure.

3.2 The northern area covered thick En-a

A landslide at the right bank of the upper Abira river is at 80m high, 45m wide, and 230m long. The collapsed debris buried the Abira river. The landform of the slope was divided into upper and lower parts

©2019. Japan Geoscience Union. All Right Reserved.

by a break line of inclination. The source of collapse was mainly the upper, a valley head slope, shaped shallow flat slope which is covered by En-a. The lower part was a V-shaped valley before the earthquake. The moving body run on the upper of V-shaped slope along the valley and deposited over the Abira river. Acording to observation of the exposed outcrops by the failure, thin Ta-d and the above layers cover on En-a of 130cm thick. En-a is pumice of 1-2mm diameter with rich-pyroxene. The sliding surface was on the lower volcanic ash, mixed glassy Spfa1, beneath En-a.

4 Shapes of slope failures in each southern and northern area of the disaster area

In the southern part of the disaster area, almost slopes except of steep are covered thick Ta-d. The main source of collapses is thick Ta-d by the earthquake. Therefore, the collapses were occurred numerous on the slope covered by thick Ta-d, especially the lower valley-side slope, which is steep. On the other hand, in the northern area of disaster area, because Ta-d layer is thin, even though it is on the lower valley-side slope, the collapse of Ta-d is rare. The collapses of thick En-a on the valley head slopes are unevenly distributed. Because each geomorphological unit at the source of collapses in the northern and the southern is different, their shapes are different in each region.

Keywords: the 2018 Hokkaido Eastern Iburi Earthquake, tephra layer, valley head slope, lower valley-side slope

©2019. Japan Geoscience Union. All Right Reserved.

Feature of landslide of pyroclastic fall deposits induced by 2018 Hokkaido Eastern Iburi Earthquake, and its relation with damage

*Jun Tajika[1], Kazuo Amemiya[2], Masahiro Chigira[3], Satoshi Ishimaru[4], Akio Koike[1], Hidetoshi Kon[1], Kenji Kizaki[5], Nobuo Yamane[6]

1. Docon Co.,Ltd., 2. Bousai Chishitsu Kogyo Co.,Ltd., 3. Kyoto University, 4. Geological Survey of Hokkaido, HRO, 5. Kizaki PE Office, 6. Terre Research Co.

Many landslides occurred by the 2018 Hokkaido Eastern Iburi Earthquake around Atsuma-cho . Rapid landslide consisting of Holocene pyroclastic fall deposit (Debris slide by the classification of Varnes, 1978) gave the human damage of 36 above all. We show the topographical and geological cause and morphological characteristic of the landslides and discuss about relations with the human damage.

Tephra mainly derived from Shikotsu, Eniwa and Tarumai volcanos cover on sedimentary rocks for Neogene of the base in Atsuma area. Among these tephra, the Tarumai d pyroclastic fall deposit (Ta-d: 9ka) thickly distributes in this area as a central axis of distribution. Ta-d (thickness 1-2m), the tephra (Ta-c,-b,-a) and black soil (total thickness approximately 1.5-3m) which did mantle bedding was translationally sliding as landslide body. The sliding layer was formed in several centimeters above from the base of the Ta-d pumice at the slope where Ta-d directly covered the mudstone and mudstone rubble. The thickness of the layer was 1-3cm and is made of creamy clay including the halloysite. In addition, the sliding layer was formed in the weathered volcanic soil including pumice derived from Eniwa a and Shikotsu 1 Tephra in the area where the Ta-d covers up the volcanic soil.

The landslides in Atsuma area into following 7 types based from form and another feature of the slide, i.e. 1) Type Gv: Extremely gentle, shallow valley from, 2) Type Sv: Gently shallow valley form. 3) Type Dv: Deep valley form with alluvial cone or landslip lobe 4) Type Hv: Hanging valley form, 5) Type Ps: Planer slope, 6) Type Cf: Complex of Some valley form collapses along the small stream, and 7) type Ol: Gently landslide caused by overlapping of other slides.

Although there is difference in some clarity, the cutting of the layered bedding of Ta-d is often seen at the slope end in these slopes. The valley wall slope that Ta-d covers is eroded by small stream in the Type Cf. Because the thinning and omission of Ta-d occur at an exit of the hanging valley in the Type Hv , it is in a near condition for "lower part cutting". In addition, the convex break of slope angle and a man-made small cut is often observed in the foot of the collapse scarp with the Types Sv, Dv and Ps.

The landslide body of each type was moved with mostly maintaining of bedding form from the source area to the depositional area. The terminal form of slides has many variations, i.e. from stacking of plural sliding bodies which make thrust on the front, to separating and crushed into many blocks. Fluidized slide material such as the Type Cf made depositional lobes like a debris-avalanche or a debris-flow deposit in the terminal area. The distance from the base of slope to the tip of the sliding body of Types Cf, Hv and Dv were generally longer than the type Ps. The thickness of landslide body was about 1.5-3m which was reflected from the total thickness of stratified Ta-d and other tephra and black soil, and reaches 3-5m in the part which some bodies stacked at the terminal. The damaged buildings were located at the mouth of small stream and were located in the accumulation area of the landslides. Height of the first floor of the house is almost about 3m.

©2019. Japan Geoscience Union. All Right Reserved.

The geological cause of landslide is that The Ta-d tephra distributes widely with the mantle bedding. The pumice of Ta-d is weathered and halloysite formed in it. Furthermore, the tephra was cutting in the foot of slope in many places by natural and artificial process. On the other hand, the Eastern Eburi Earthquake showed that a landslide will occur by all means in the sloping ground including extremely gentle area that pyroclastic fall deposit cover with mantle bedding when the large-scale inland earthquake occurs. Because it is impossible to predict earthquake, inhabitants of the slope area cannot evacuate beforehand. The preventive measures construction is not necessarily realistic. It is necessary to avoid building house at the mouth of small valley and to make a bedroom in the places more than second floor for reducing human damage.

Keywords: landslide induced by earthquake, tephra, landslide body, Lower cutting, weathering

©2019. Japan Geoscience Union. All Right Reserved.

Influence of slope cutting on failures induced by the July heavy rain, and the Iburi-tobu earthquake, 2018.

*Hidehisa Nagata[1]

1. Fu-Sui-Do Company Limited

Many cases of failure induced by slope cutting have been also reported in the past. Some examples are added here by the July heavy rain from June 28 to July 8 and the Hokkaido Iburi-tobu earthquake on September 6, 2018. In the July heavy rain, many slope failures occurred widely main in western part of Japan including Hiroshima, Ehime and Gifu Prefectures. The Iburi-tobu earthquake caused collapses in high density in the hilly area around at Atsuma Town, Hokkaido.

Case A (Hokkaido): a failure that 20 m in width and 50 m in length caused by the Iburi-tobu earthquake. It is smaller scale one in the many failures by the earthquake. Similar to many other cases, sliding surface is the base of Tarumai-d tephra (9ka) lying under 2.5 m from the earth surface. The slope toe has been cut about 3 m in height for a hut. As a result, inclined weak layer became to daylight in the cutting slope.

Case B (Ehime Prefecture): a 30 m wide failure occurred on an orange grove slope by the July heavy rain. It is initially surface failure 0.5 m in depth, although the secondary 2 m deep failure continued on the left side. A trail for working passes at the top of the failure, and a pipe for sprinkling was buried along the trail. Leaked water from the pipe might cause the initial failure, so many small gullies run from the top. Otherwise, groove into strongly weathered Cretaceous sandstone is possible factor of the failure.

Case C (Gifu Prefecture): a forest road shoulder composed of highly weathered Jurassic Hida Granite was collapsed 25 m in width. The failure occurred on a shallow valley slope and the road passes through the upper part of the slope in up-hill grade. Although this valley has only small catchment area originally, rain water was drained from upper neighboring valley through the road and flowed out to the road shoulder along small undulations on the road. This large quantity of water caused the failure. Involving catchment area was enlarged at least 8.5 times than before the road opened.
There are many sites needed slope cutting for architecture and civil structure and dense network of forest road is required for proper management of forestry and agriculture. However, any slope cutting causes hydrological and geomorphological changes despite of its scale. When large impacts like heavy rain or earthquake occur, modified landforms can be a factor of landslide. Slope failures are induced by daylighting of weak layer in the case A, and by flowing water in the upper part of slope in the cases B and C. Moreover, construction of the forest road made drainage area increase by capture of the upper neighboring valley in the case C. On the planning of slope cutting, appropriate design, construction and maintenance should be taken considering microlandforms, subsurface geological properties and structures.

Keywords: 2018 July heavy rain, 2018 Iburi-tobu earthquake, slope failure, cutting

©2019. Japan Geoscience Union. All Right Reserved.

Slope failures occurred in the southwest part of the Izu-oshima Island in geological time, NE Japan

*Takehiko Suzuki[1], Masahiro Chigira[2]

1. Faculty of Urban Environmental Sciences, Tokyo Metropolitan University, 2. Disaster Prevention Research Institute, Kyoto University

So-called “loam” composed of primary fall-out tephras and tephric soil deposits (tephric loess) is one of the factors cause earthquake-induced landslide. To evaluate potential of slope failure by this combination in the Japanese Island, earthquake-induced landslides potential assessment should be examined in relevant areas, considering frequency of landslides in geological time. To estimate this, we examined unconformities within “loam” on the Izu-oshima Island, Tokyo, where thick loam has been formed during last 19 ka. We identified at a maximum six unconformities suggesting possibility of occurrences of landslides during the period between 19-1.8 ka.

Keywords: Slope failure, Tephric soil deposits, Izu-oshima Island

©2019. Japan Geoscience Union. All Right Reserved.

The strain rate observation by the borehole inclinometer on the bedrock creep slopes in Akadani-west area

*Atsuhiko Kinoshita[1,2], Yasutaka Tanaka[2], Wataru Sakurai[1], Taro Uchida[1], Koichiro Hayashi[3], Yasuuchi Kubota[3], Katsushi Kawato[4]

1. National Institute for Land and Infrastructure Management, 2. Sediment Disaster Prevention Technology Center, Kinki Developing Regional Bureau, Ministry of Land, Infrastructure, Transport and Tourism , 3. OYO Corporation, 4. NIPPON ENGINEERING CONSULTANTS CO., LTD.

In the disaster around Kii Peninsula in 2011, many deep-seated landslides were occurred. In order to reduce the damage, it is necessary to establish the method of the extracting dangerous slopes and to consider the countermeasures in advance. So far, the method of reading the micro topography from the topographic map such as the laser profiler, the method of judging the degree of danger from geological / topographical overview have been proposed. On the other hand, there are few cases where the strain rate was observed at the landslide dangerous slope such as the bedrock creep slope. For this reason, the validity of the past method has not been fully verified. In this study, we conducted the boring survey and observed the strain rate by borehole inclinometer on two slopes of Akadani-west area. Also, based on this observation value, the validity of the risk method by the past study was examined.

First, we calculated the strain rate (the value obtained by dividing the length of the landslide scarp by the slope length) from the topographical data obtained by the laser profiler at the two slopes in Akadani-west area. We also evaluated the risk of the two slopes using the method to evaluate the risk from geology and topography by Chigira et al. In addition, we conducted the airborne electromagnetic survey, and the degree of strain was also investigated from the resistivity distribution of the ground. By these methods, after evaluating the degree of risk, two boring investigations were conducted on each of the two slopes. At the borehole location, the strain rate was observed by the borehole inclinometer. Through these, the consistency of the observed data and the risk assessment results was verified.

The strain rate of Akadani-west I district was 4.1%, and the risk by the method by geology / topography was IV. The strain rate of Akadani-west II district was 2.7%, and the risk by the method by geology / topography was II. From this, we have found that the degree of the risk in the Akadani-west I district is higher than that of II by the risk assessment by the past research. In addition, the strain rate by the borehole inclinometer was 0.6mm/year, 1.0mm/year in Akadani I and II districts, respectively. For this reason, we have found that the danger level in the Akadani-west II district is higher by the observed data. On the other hand, in the resistivity distribution by the airborne electromagnetic survey, a large change in resistivity was seen in Akadani-west II area, and it was found that the consistency with the actual observed data was obtained. From this, we have found that there is a possibility that the degree of the risk can be accurately evaluated by combining the plural methods.

Keywords: Bedrock creep, Borehole inclinometer, Strain rate

©2019. Japan Geoscience Union. All Right Reserved.

Assessing Potential Landslide Areas Due to Earthquake Using Three-Dimensional Resistivity Datasets from Across a Wide Area

*Yusuke Sakai[1], Taro Uchida[1], YASUMASA FUJIWARA[2]

1. National Institute for Land and Infrastructure Management , 2. Eight-Japan Engineering Consultants

In recent years, sediment disasters due to earthquake have often occurred, including in the 2011 Great East Japan Earthquake, the 2016 Kumamoto Earthquake, the 2018 Hokkaido Eastern Iburi Earthquake. Measures for preventing and reducing the damage of sediment disaster due to earthquake are an urgent issue, because Nankai Trough Earthquakes are expected in the future. A variety of methods for assessing seismic landslide susceptibility have been proposed and their accuracy verified. In those methods, topographic parameters such as inclination of slope, curvature of slope, and relief are commonly used as controlling factors.

It has also been reported that underground structure has a large impact on seismic landslide occurrence, as in the case of the landslide that occurred around the Aso Volcanological Laboratory of Kyoto University in the 2016 Kumamoto Earthquake. Therefore, underground structure can be considered critical information for improving the predictability of potential landslide areas. However, geological maps only plot spatial patterns of the underground condition, and boring is required to obtain point information of underground structure in the depth direction. This lack of three-dimensional information of underground structures is one of key obstacles to evaluating potential landslide areas due to earthquake across a wide area.

Therefore, we used resistivity spatial patterns measured by airborne electromagnetic survey (AES). Airborne electromagnetic survey Based on electromagnetic induction, AES is an exploration technique for obtaining three-dimensional resistivity across a wide area by measuring the response to an induced electromagnetic field with an electromagnetic sensor from a helicopter.

The purpose of this study was to test the applicability of three-dimensional resistivity data to assessing seismic landslide susceptibility. We used three-dimensional resistivity data from the central cone of Aso Volcano measured before the 2016 Kumamoto Earthquake and landslide distribution maps made from airborne laser scanner datasets and orthoimages from before and after the earthquake. We identified the three-dimensional resistivity patterns in seismic landslide areas before landslide occurrence. Based on our findings, we argue the applicability of three-dimensional data for assessing seismic landslide susceptibility.

Keywords: resistivity, airborne electromagnetic survey, landslide, earthguake

©2019. Japan Geoscience Union. All Right Reserved.

[J] Oral | H (Human Geosciences)：H-DS Disaster geosciences

Mon. May 27, 2019 1:45 PM - 3:15 PM JST | Mon. May 27, 2019 4:45 AM - 6:15 AM UTC | 106 1F

[H-DS14] Geohazards in humid, tectonically active countries and their precursors

convener:Masahiro Chigira(Disaster Prevention Research Institute, Kyoto University), Hiroshi YAGI(Faculty of Art, Science and Education, Yamagata University), Satoru Kojima(Department of Civil Engineering, Gifu University), Taro Uchida(National Institute for Land and Infrastructure Management), Chairperson:Chigira Masahiro, Taro Uchida

This session covers mass movements of landslide, slope failure, debris flow, and gravitational slope deformation in tectonically active, humid countries, and aims to discuss on their mechanisms, characteristics of occurrence sites, the significance in geological time scale, and the methodology to mitigate their affects by researchers with various related research fields. In particular, papers about 2017 northern Kyushu rainstorm, 2018 Osaka earthquake, 2018 Western Japan rainstorm, and 2018 Hokkaido earthquake are welcome

1:45 PM - 2:00 PM JST | 4:45 AM - 5:00 AM UTC

[HDS14-07] Prediction of shallow landslides and debris flow by rainstorm: dynamic hazard mapping toward disaster mitigation

*Yuki Matsushi[1] (1.Disaster Prevention Research Institute, Kyoto University)

2:00 PM - 2:30 PM JST | 5:00 AM - 5:30 AM UTC

[HDS14-08] Land slide warning judgment mesh information of the Meteorological Agency using the Soil Water Index

★Invited Papers

*KENJI OKADA[1] (1.Japan Meteorological Agency)

2:30 PM - 3:00 PM JST | 5:30 AM - 6:00 AM UTC

[HDS14-09] A future direction of remedial measures for sediment disaster reduction from the viewpoint of enhancing a workable early warning system

★Invited Papers

*Masaru Kunitomo[1,2,3,4], Shigetaka Takiguchi[1,2,3,4], Fumiaki Akazawa[1,2,3,4], Kazuyuki Imai[1,2,3,4] (1.Ministry of Land, Infrastructure, Transport and Tourism, 2.Water and Disaster Management Bureau, 3.Sediment and Erosion Control Department, 4.Sediment and Erosion Control Planning Division)

3:00 PM - 3:15 PM JST | 6:00 AM - 6:15 AM UTC

Discussion

Prediction of shallow landslides and debris flow by rainstorm: dynamic hazard mapping toward disaster mitigation

*Yuki Matsushi[1]

1. Disaster Prevention Research Institute, Kyoto University

This study demonstrates a strategy for predicting location, timing, and magnitude of rainfall-induced shallow landslides and areas affected by subsequent debris flows. Spatial distribution of soil layers was modeled for evaluating thickness of sliding material on hillslopes, which provides a basis for predicting source area and volume of shallow landslides and simulating subsurface hydrological processes. Soil accumulation in hollows was calculated on a geographic information system using a 1 m-meshed digital terrain model with soil production by bedrock weathering and transport by soil creep. The output was validated by a ground-based survey in the actual terrain in a selected watershed. The shear strength of the bulk soil was evaluated by direct shear tests using undisturbed specimens, and quantification of soil reinforcement by tree roots through an in-situ survey at soil pits. Hydrological monitoring was carried out at representative hillslopes for modeling fluctuation in subsurface pore-water pressure by rainwater infiltration. By coupling all of those data and modeling, we analyzed the hillslope instability, and then compared the output with a landslide inventory map to confirm the accuracy and precision of the prediction. Time-series change in areas of debris flow runout was estimated based on assumed equivalent coefficient of friction as a function of hillslope wetness in the watershed. Such dynamic mapping of geohazard fills a demand in disaster mitigation in local communities for increasing events of heavy rainfall.

Keywords: Soil thickness, Tree roots, Pore-water pressure, Slope stability, Equivalent coefficient of friction

©2019. Japan Geoscience Union. All Right Reserved.

Land slide warning judgment mesh information of the Meteorological Agency using the Soil Water Index

*KENJI OKADA[1]

1. Japan Meteorological Agency

Soil Water Index shows the risk of land slide disasters caused by rain in real time and the land slide warning judgment mesh information released by the Japan Meteorological Agency using it.
Most of the dead due to land slide disasters in the last two decades occurred with the Soil Water Index value updating the maximum value in the last 10 years.

Keywords: land slide, Soil Water Index, Land slide warning judgment mesh information

©2019. Japan Geoscience Union. All Right Reserved.

A future direction of remedial measures for sediment disaster reduction from the viewpoint of enhancing a workable early warning system

*Masaru Kunitomo[1,2,3,4], Shigetaka Takiguchi[1,2,3,4], Fumiaki Akazawa[1,2,3,4], Kazuyuki Imai[1,2,3,4]

1. Ministry of Land, Infrastructure, Transport and Tourism, 2. Water and Disaster Management Bureau, 3. Sediment and Erosion Control Department, 4. Sediment and Erosion Control Planning Division

Due to “Heavy rain of July 2018”, more than 2500 sediment disasters occurred mainly in the western part of Japan. The number is equivalent to approximately 2.3 times of the annual average. Why were such a lot of people killed in this disaster, despite various measures for precaution?

The Ministry of Land, Infrastructure, Transport and Tourism (MLIT) established a committee in order to take remedial measures for sediment disaster reduction from the view point of enhancing a workable early warning system, after not only revealing the facts on cause of the disaster but reviewing our measure have been taken.

With understanding that the lack of residents’ awareness of sediment disaster risk may be a major cause of this disaster, on the other hand, mutual assistance plan among local community may work well for evacuation at the sites with no victim, the committee proposed the MLIT to;
Build the early warning system nationwide based on a community mutual assistance plan for evacuation, Get residents to aware of their risk on sediment disasters, Enhance the national and prefectural support system to build the capacity of municipalities and residents, Improve the accuracy of sediment disaster alert to encourage residents at risk to evacuate precautionary, Build disaster-prevention facilities such as debris basins to reduce evacuation risk and to prevent crucial infrastructures from debris flows as well as sediment-rich flood, with the object of climate change adaptation. As a remedial measures for sediment disaster reduction from the viewpoint of enhancing a workable early warning system.

Keywords: Sediment Disasters, Early Warning

©2019. Japan Geoscience Union. All Right Reserved.

[J] Poster | H (Human Geosciences)：H-DS Disaster geosciences

Mon. May 27, 2019 3:30 PM - 5:00 PM JST | Mon. May 27, 2019 6:30 AM - 8:00 AM UTC | Poster Hall International Exhibition Hall8, Makuhari Messe_8

[H-DS14] Geohazards in humid, tectonically active countries and their precursors

convener:Masahiro Chigira(Disaster Prevention Research Institute, Kyoto University), Hiroshi YAGI(Faculty of Art, Science and Education, Yamagata University), Satoru Kojima(Department of Civil Engineering, Gifu University), Taro Uchida(National Institute for Land and Infrastructure Management)

This session covers mass movements of landslide, slope failure, debris flow, and gravitational slope deformation in tectonically active, humid countries, and aims to discuss on their mechanisms, characteristics of occurrence sites, the significance in geological time scale, and the methodology to mitigate their affects by researchers with various related research fields. In particular, papers about 2017 northern Kyushu rainstorm, 2018 Osaka earthquake, 2018 Western Japan rainstorm, and 2018 Hokkaido earthquake are welcome

[HDS14-P01] The estimation of frequency for deep-seated landslide with carbon dating in Kii mountain area

★Invited Papers

*Yasutaka Tanaka[1], Toshiaki Kotake[1], Hiroaki Sugawara[1], Atsuhiko Kinoshita[1], Yoshito Ogawauchi[2], Minami Fujiwara[2] (1.Sediment Disaster Prevention Technology Center, Kinki Regional Developing Bureau, Ministry of Land, Infrastructure, Transport and Tourism, 2.Japan Conservation Engineers & CO., LTD.)

[HDS14-P02] Tephra stratigraphy and a slope failure of about 4,000 years ago on the slope of the Late Pleistocene Janoo Volcano in the northwestern of Aso Caldera

*Yasuto Hirata[1], Keiichi Ueta[1], Riichiro Miyawaki[2], Katsutoshi Iemura[2], Toshitaka Yokoyama[2], Akiko Miyawaki[2] (1.Central Research Institute of Electric Power Industry, 2.Hanshin Consultants)

[HDS14-P03] Analysis of causal factors of landslides during 2017 northern Kyusyu torrential rainfall disaster by using decision tree

*Hiromu Daimaru[1], Wataru Murakami[1], Yuki Tsurusaki[2] (1.Forestry and Forest Products Research Institute, 2.Fukuoka Agriculture and Forestry Research Center)

[HDS14-P04] Geologic characteristics of rock mass failures caused by the heavy rain event of July 2018 in Uwajima, Ehime

*Shintaro Yamasaki[1] (1.Disaster Prevention Research Institute, Kyoto University)

[HDS14-P05] On the failure mechanism of embankments in Mabi Town during the Heavy rain of July, 2018, Japan

*Gonghui Wang[1] (1.Disaster Prevention Research Institute, Kyoto University)

[HDS14-P06] Interpretation of landslide surface deformation around the branch basins of Sun Kosi river in Nepal using InSAR images

*Otake Shunpei[1], Hiroshi, P. Sato[1] (1.College of Humanities and Sciences, Nihon University)

[HDS14-P07] The large scale landslides triggered by The 2018 Sulawesi Earthquake, Indonesia

*Masashi Omata[1], Toshiyuki Adachi[2], Takao Yamakoshi[3], Kenichi Matsui[4], Tosho Iwamatsu[1], Susumu Takagishi[1], Chiho Motojima[1], Yuu Okuizumi[1], Umito Wada[1] (1.PASCO CORPORATION, 2.LDP Upper House member, 3.SABO & LANDSLIDE TECNICAL CENTER, 4.Nobuyuki Adzchi Office)

[HDS14-P08] Relationship of the grand deformation and topography in Sapporo City at the 2018 Hokkaido Eastern Iburi Earthquake confirmed by InSAR analysis

*Akihiro Yokota[1], Tomohiro Nishimura[2], Kiyoyuki Shigeno[1], Kenichi Honda[2], Sakae Mukoyama[2] (1.Meiji Consultant Co., Ltd, 2.Kokusai Kogyo Co., Ltd)

[HDS14-P09] Estimation of co-seismic surface displacement and ground deformation associated with the 2018 Hokkaido Eastern Iburi Earthquake, based on differential InSAR and differential LiDAR DEM analysis.

*Kenichi Honda[1], Norichika Asada[1], Naruo Mushiake[1], Tomohiro Nishimura[1], Sakae Mukoyama[1] (1.Kokusai Kogyo Co.,LTD.)

[HDS14-P10] Geological features of landslides of pyroclastic fall deposits induced by the 2018 Eastern Iburi Earthquake and other previous earthquakes

*Masahiro Chigira[1], Jun Tajika[3], Satoshi Ishimaru[2], Takehiko Suzuki[4] (1.Disaster Prevention Research Institute, Kyoto University, 2.Hokkaido Geological Survey, Hokkaido Research Organization, 3.Docon Co. Ltd, 4.Tokyo Metropolitan University)

[HDS14-P11] Earthquake ground motion properties of mountainous district in Totsukawa village, Nara pref. based on the seismic observation – A fundamental study of landslides caused by earthquake –

*Tomoyuki Iida[1], Ryuji Yamada[1], Shigeki Senna[1], Hidemitsu Tokui[2], Tetsuya Onodera[2], Hiroshi Kawabe (1.National Research Institute for Earth Science and Disaster Prevention, 2.Technicallink Kabushiki kaisya)

[HDS14-P12] Study on topographic features and landslide development process in slope failure by Typhoon Talas

*Teruyuki Kikuchi[1], Teruyoshi Hatano[2], Satoshi Nishiyama[3] (1.JP-Design Co., Ltd., 2.Electric Power Development Co.,Ltd., 3.Okayama University Graduate School of Environmental and Life Science)

[HDS14-P13] Formation mechanism of bulge of slope that is sign of large-scale collapse

*tatsurou yoshimura[1] (1.Daiichi Fukken Co., Ltd.)

[HDS14-P14] Sediments accumulated in the linear depressions in the Mitsumine area, Kanto Mountains

*Masakazu Mashiko[1], Masahiro Chigira[2] (1.Graduate School of Science, kyoto University, 2.Disaster Prevention Research Institute, Kyoto University)

The estimation of frequency for deep-seated landslide with carbon dating in Kii mountain area

*Yasutaka Tanaka[1], Toshiaki Kotake[1], Hiroaki Sugawara[1], Atsuhiko Kinoshita[1], Yoshito Ogawauchi[2], Minami Fujiwara[2]

1. Sediment Disaster Prevention Technology Center, Kinki Regional Developing Bureau, Ministry of Land, Infrastructure, Transport and Tourism, 2. Japan Conservation Engineers & CO., LTD.

Typhoon 12 in 2011 induced deep-seated landslides in Kii mountain area. In Kii mountain area, heavy rainfall also induced great damage by large scale landslide in 1889. From above we need the frequency of deep-seated landslide to construct countermeasure for sediment disaster in Kii mountain area.

Although previous report shows the method to use tephra for estimation of frequency of deep-seated landslide, in Kii mountain area we can find few point of tephra sedimentation. In recent years some study shows the methods to estimate frequency of sediment disaster with chips of wood and carbides. In this study we applied the method with chips of wood and carbides to estimation of frequency of deep-seated landslide in Kii mountain area.

In this study we proposed the research flow to pick sample shown as below;

a) Extracting landslide deposit by LiDAR

b) Preliminary research in field

c) Main research in field and picking sample up

d) Analysis sample with carbon dating

In a) we extracted the site where landslide dams may have been as landslide deposit to observe along river side closely with topographic map by LiDAR. In b) we investigate access route to the research site and whether chip of wood and carbide are or are not roughly. In c) we investigated closely and picked sample up with special sampler we developed for this research. This sampler can collect sample including soil. In d) we analyzed samples and organized carbon dating data.
We collected 28 samples in 11 landslide deposits. Especially it was easier to collect samples in upper and bottom of landslide deposits and underwater deposits than other sites. The research flow and special sampler we developed can help to collect sample effectively. In addition we found deep-seated landslide occurred once in 100 ~ 150 years in Kii mountain area from analysis of carbon date. This result isn't inconsistent with the past disaster reports. However, carbon dating has some error. To estimate accurately we need more investigation.

Keywords: deep-seated landslide, carbon dating, Kii mountain area

©2019. Japan Geoscience Union. All Right Reserved.

Tephra stratigraphy and a slope failure of about 4,000 years ago on the slope of the Late Pleistocene Janoo Volcano in the northwestern of Aso Caldera

*Yasuto Hirata[1], Keiichi Ueta[1], Riichiro Miyawaki[2], Katsutoshi Iemura[2], Toshitaka Yokoyama[2], Akiko Miyawaki[2]

1. Central Research Institute of Electric Power Industry, 2. Hanshin Consultants

In the west part of Aso Caldera, the 2016 Kumamoto Earthquake caused surface earthquake faults along the Futagawa and Hinagu fault zone, triggering numerous landslides and some lateral spreads on tephra. Janoo Volcano is located on the line that extrapolates from the end of the earthquake fault zone to the northeast in the disaster area. We carried out an excavation and boring exploration at the south slope of Janoo Volcano and measured chemical compositions of lava and radiocarbon ages of volcanic soil. The results elucidated the succession of volcanic products after the formation of Janoo Scoria Cone and showed a slope failure about 4,000 years ago. The eruption ages of key beds were estimated with calibrated method as follows: Janoo Scoria (>15.5 ka), ACP1: Aso Central Pumice 1 (~4.0 ka), Kishimadake Lava and Kishimadake Scoria (~3.7 ka), Ojodake Scoria (3.5±0.1 ka), and Kometsuka Lava (3.0±0.1 ka). Fine sandy ashes deeper than 8 m and the surface part of Janoo Scoria weathered to become yellowish and included small dislocations that are the normal sense and parallel to the surface of Janoo Scoria. The volcanic soil layer on the sandy ash was separated as 1-meter-tall blocks, and they were arranged into an imbricated form of overturned strata. This deposit was covered with a 2 m thick of soft volcanic soil moved from the upper slope. All the above tephra layers were consistently covered with ACP1. Consequently, these deformation and sedimentary structures suggest that the tephra on Janoo Scoria sild down successively from the slope toe toward the top just before the eruption of ACP1. This ancient slope failure seems to be triggered by earthquake because its depth and material are similar to those of landslides by the 2016 Kumamoto Earthquake.

Keywords: Aso Caldera, eruptive history, landslide, non-tectonic faulting, trench survey

©2019. Japan Geoscience Union. All Right Reserved.

Analysis of causal factors of landslides during 2017 northern Kyusyu torrential rainfall disaster by using decision tree

*Hiromu Daimaru[1], Wataru Murakami[1], Yuki Tsurusaki[2]

1. Forestry and Forest Products Research Institute, 2. Fukuoka Agriculture and Forestry Research Center

Causal factors of landslides induced by torrential rainfall in July 2017 in Kyushu Island were analyzed by decision tree. The landslides were mapped from orthophotos produced by GSI and overlay analysis with radar-AMeDAS rainfall data, slope, geology tree age and vegetation were conducted by using the decision tree classifier of the Scikit-learn Python module. Landslide map was defined by existence or non-existence of landslide in each 200m size grid and overlain by geological map by AIST, slope map from 10m DEM by GSI and digital forest map by Fukuoka Prefecture. The distribution of landslides was principally controlled by rainfall distribution. Slope was the secondary factor on landslide susceptibility and threshold slope decreased with rainfall intensity. Geology was the third factor. granite area was rather vulnerable comparing with metamorphic rocks and Tertiary volcanic rocks. Effect of tree age was evident in where 12hr rainfall was less than 500mm. On the other hand, effect of tree species seemed to be minor factor comparing with other factors.

Keywords: 2017 northern Kyusyu torrential rainfall disaster, landslide, decision tree

©2019. Japan Geoscience Union. All Right Reserved.

Geologic characteristics of rock mass failures caused by the heavy rain event of July 2018 in Uwajima, Ehime

*Shintaro Yamasaki[1]

1. Disaster Prevention Research Institute, Kyoto University

The heavy rain event of July 2018 caused many rock mass failures around Hokezu bay area in Uwajima city and Seiyo city, Ehime. This paper reports geologic characteristics of those failures. The rock mass failures are relatively small, because they occur on relatively low relief topography. The scarps of failures are weathered, and have dense cracks and separating planes cutting slope or mountain flanks. Webby weak mineral veins and fault fractures are found at some failure sites. These characteristics have lowered strength of the rock mass microscopically and macroscopically in the area. Because of the low strength, gravitational deformation probably proceeds in small slope, and it forms flow path to penetrate with abundant rain water in the slope before collapse. The Hokezu bay area is a characteristic low relief area in Shimanto belt in Sikoku. Similar low relief topographic areas are distributed along Butsuzo tectonic line traversing Shikoku island.

Keywords: heavy rain event, landslide, deep-seated landslide, rock control, Shimanto belt

©2019. Japan Geoscience Union. All Right Reserved.

On the failure mechanism of embankments in Mabi Town during the Heavy rain of July, 2018, Japan

*Gonghui Wang[1]

1. Disaster Prevention Research Institute, Kyoto University

From late June to mid-July, 2018, successive heavy rainfall hit a wide area of southwestern Japan, resulting in widespread sediment-related disasters and devastating floods. Among these disasters, the flooding resulting from the failures of embankments along Oda River and some other tributary rivers in Mabi Town, Okayama Prefecture, was the deadliest. To understand the possible failure mechanisms of these embankment, field geotechnical investigation and geophysical surveys were conducted. Centrifuge tests were also performed to examine the instability processes of embankment with increase of water level on the river. The results indicate that the leakage in the embankments along the tributary rivers may have resulted in retrogressive failures on the embankments, while overtopping may have played a key role in the final rapid breaching of the embankment.

Keywords: failure of embankment, failure mechanism, Internal structure of embankement, foundation of embankment, Centrifuge test

©2019. Japan Geoscience Union. All Right Reserved.

Interpretation of landslide surface deformation around the branch basins of Sun Kosi river in Nepal using InSAR images

*Otake Shunpei[1], Hiroshi, P. Sato[1]

1. College of Humanities and Sciences, Nihon University

On 25 Apr 2015, Gorkha earthquake (Mw 7.8) occurred at 80 km NW from Kathmandu, Nepal. After that, the largest aftershock (Mw 7.3) occurred on 12 May 2015 at 75 km ENE from Kathmandu. These earthquakes caused landslide disasters and big damages. Nepal has wide mountain area, and landslides disasters tend to be induced by both conditions as follows. On the one hand many earthquakes occur in Nepal, where is on the collision and subduction area related Indo-Australian and Eurasian plate. On the other hand they have much rain in monsoon season there. Therefore, landslide caused by these earthquakes may be reactivated. It is important to monitor landslide surface deformation because it contributes to prevent landslide disasters after these earthquakes. In this study we focused on the area where the largest aftershock occurred, and tried to detect landslide surface deformations after the largest aftershock.

Recently InSAR (Synthetic Aperture Rader interferometry) has been used to detect landslide surface deformation. Then, we used and adopt it for the study area, where is the watershed of Sun Koshi river branches which includes epicenter of the largest aftershock. In this study two InSAR images were produced, which was taken on 12 Sep 2016/30 Jan 2017 and on 30 Jan 2017 /11 Sep 2017. Then, landslide surface deformations were interpreted on the two InSAR images, and the interpreted areas were delineated and the center of the area were mapped. And location of such the detected sites were analyzed related with distance from the epicenter, elevation, slope aspect, deformation amount along LoS (line of sight) known from InSAR image, interpreted deformation area, lithological units of geology, and the watersheds of the branches.

As a result of the interpretation, 29 and 25 deformation sites were detected on InSAR image taken on 12 Sep 2016/30 Jan 2017 and on 30 Jan 2017 /11 Sep 2017, respectively. As a result of the analysis, it was found that ca. 70 % of the detected sites locate in the elevation of 1,500-2,999 m, and that the averaged area of deformation per one site was larger on 30 Jan 2017 /11 Sep 2017 image than on 12 Sep 2016/30 Jan 2017 image. For the former result, it is thought that low Himalayan meta-sedimentary rocks gave more detected sites than other lithological units and the rocks tend to be widely distributed in this elevation belt. For the latter result, it is thought that effect of precipitation in rainy season are related more closely with landslide surface deformation interpreted on 30 Jan 2017 /11 Sep 2017 image than on 12 Sep 2016/30 Jan 2017 image.

Keywords: Landslide, SAR, Earthquake, Nepal

©2019. Japan Geoscience Union. All Right Reserved.

The large scale landslides triggered by The 2018 Sulawesi Earthquake, Indonesia

*Masashi Omata[1], Toshiyuki Adachi[2], Takao Yamakoshi[3], Kenichi Matsui[4], Tosho Iwamatsu[1], Susumu Takagishi[1], Chiho Motojima[1], Yuu Okuizumi[1], Umito Wada[1]

1. PASCO CORPORATION, 2. LDP Upper House member, 3. SABO & LANDSLIDE TECNICAL CENTER, 4. Nobuyuki Adzchi Office

On 28 September 2018, a large earthquake occurred near Palu City, Sulawesi, Indonesia. The magnitude of the earthquake was 7.5. According to the information broadcast after the earthquake, the nearly flat terrain greatly moved laterally. The authors carried out a satellite imagery interpretation survey with using the post-earthquake imageries of Pleiades and SPOT-7. The survey revealed that there are at least three areas which seem to have moved laterally with long distance. It seems to be lateral spread in view of situations reported in the press information. Two large lateral spreads stand in the eastern side of the city and one in the western side. The two lateral spreads in the east side are 1.5 km wide and 2.5 km long and 1 km wide and 3.5 km long, respectively while the one in the western side is 0.4 km wide and 1 km long. In the upper part of the spreads, there is area of brown bare soil while there seems ropy in the lower part of the spreads. One of them seemed to be greatly fluidized and reached further in the down streams. These spreads seem to initiate from the knick point near lower edge of fluvial fans where a lot of subsurface flow is likely to return onto ground surface. A press says that local people call these phenomena as "nalodo", which means "get absorbed into mud". This implies that similar disasters repeated in the past.

Keywords: lateral spread, satellite imagery, earthquake, SPOT-7, Pleiades, Indonesia

©2019. Japan Geoscience Union. All Right Reserved.

Relationship of the grand deformation and topography in Sapporo City at the 2018 Hokkaido Eastern Iburi Earthquake confirmed by InSAR analysis

*Akihiro Yokota[1], Tomohiro Nishimura[2], Kiyoyuki Shigeno[1], Kenichi Honda[2], Sakae Mukoyama[2]

1. Meiji Consultant Co., Ltd, 2. Kokusai Kogyo Co., Ltd

In the 2018 Hokkaido Eastern Iburi Earthquake, ground displacement and building damage occurred extensively. It is thought that it is important to promptly grasp the damage caused by a natural disaster in order to advance disaster reduction. In this study, the results of SAR analysis using Sentinel - 1 satellite were investigated for validity and cause using interpretation of aerial photograph and field survey.

As a result of SAR analysis, displacement was observed in Satozuka・Utsukushigaoka・Kiyota, Kiyota Ward, Hiragishi, Toyohira Ward, and Fushiko・Naebo, Higashi Ward in Sapporo City. For these districts, I performed an investigation by the local survey and aerial photo reading.

As a result of investigation, the spot that ground movement produced confirmed that I agreed with the spot where big displacement was estimated on InSAR analysis. The correlation with the old topography and the Embankment place is high in the ground change confirmed this time

It was revealed that I could grasp the damage situation of the wide area in a short time by using the inSAR data with the, Sentinel-1 satellite about the ground damage after the 2018 Hokkaido Eastern Iburi Earthquake.

Keywords: Interferometric SAR, Ground displacement, 2018 Hokkaido Eastern Iburi Earthquake

©2019. Japan Geoscience Union. All Right Reserved.

Estimation of co-seismic surface displacement and ground deformation associated with the 2018 Hokkaido Eastern Iburi Earthquake, based on differential InSAR and differential LiDAR DEM analysis.

*Kenichi Honda[1], Norichika Asada[1], Naruo Mushiake[1], Tomohiro Nishimura[1], Sakae Mukoyama[1]

1. Kokusai Kogyo Co.,LTD.

It is important to detect the damage situation of the building quickly when an earthquake occurs for the initial response. Satellite remote sensing can measure a wide area, and is expected to obtain the damage at the time of a disaster. However, the observation frequency of the satellite, the analysis processing time, selection of information required at the beginning are suggested as problems for practical use.
This paper introduces information which can be provided by Coherence Change Detection and differential LiDAR DEM analysis when an earthquake occurs. Especially, it will introduce the earthquakes which occurred in 2018, the 2018 Hokkaido Eastern Iburi Earthquake.
On 6 September 2018, an earthquake of magnitude 6.7 hit southern Hokkaido, which is the largest and northernmost prefecture of Japan. Interferometric analysis was carried out using images of Sentinel-1 before (August 25) and after (September 6) the earthquake to estimate the damage of the building due to the ground deformation and the deterioration of the coherence. In addition, the same analysis was carried out using the image of ALOS-2.
Figure shows an example of Kiyota Ward in Sapporo City where liquefaction occurred. In the interferometry image using Sentinel-1, deviation was discontinuous or shown as noise, so extraction of the deviation was difficult. However, the area which buildings were damaged could be extracted from the coherence change detection.
On the other hand, the degradation of coherence when using ALOS-2 is Low, so the damage area can be extracted from the deviation of the interferometry image as a ground deformation. This difference is thought to be due to the difference in the sensitivity of the observation wavelength band.
For comparison, the particle image velocimetry method was applied to calculate 3-D vectors of co-seismic deformation. The result shows deformation of the housing area, which was developed over the valley that was filled up with soil, agrees with SAR analysis result.
In this case, since Sentinel-1 observed the disaster area about 3 hours after the earthquake, the image was analyzed on the day and the results were provided to local staff. Field confirmation was carried out the day after the earthquake, and the results were provided to the affected local governments. Except for the day of the earthquake, the weather was bad for the disaster area for several days, so it was not possible to take aerial photos using the aircraft. 2018 Hokkaido Eastern Iburi Earthquake is a case where utilization of the satellite SAR, which can quickly extracts damaged area, became advantageous.
Obtaining disaster damage by satellite remote sensing is effective. However, field survey and aircraft surveillance are carried out as soon as the disaster occurred in Japan, and satellite remote sensing has not be practically used in many situations. However, similar to the 2018 Hokkaido Eastern Iburi Earthquake, if acquiring the satellite data and providing analysis results could be carried out quickly, satellite remote sensing can be an option for understanding the damage at early disaster response stage. Furthermore, estimation the light damaged area is difficult by aerial photographs, therefore estimation by SAR coherence change detection are considered importance.
Finally, I wish to express my deepest condolences to those who lost loved ones in these disasters, and also to express my sympathy to all who were affected.

©2019. Japan Geoscience Union. All Right Reserved.

Keywords: Earthquake, SAR, LiDAR

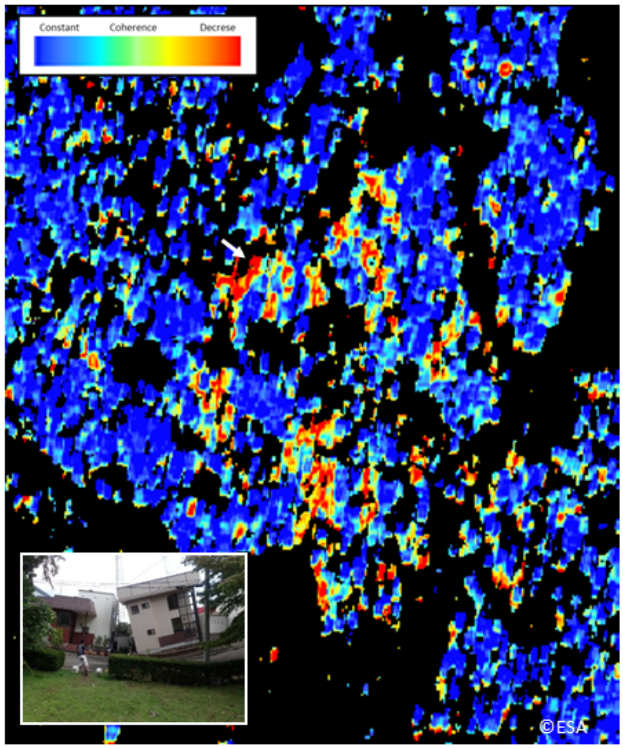

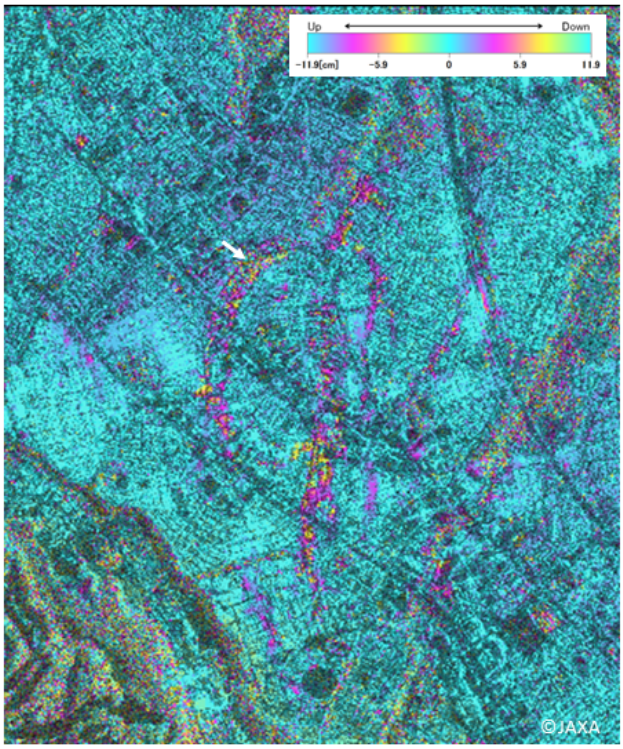

©2019. Japan Geoscience Union. All Right Reserved.

Geological features of landslides of pyroclastic fall deposits induced by the 2018 Eastern Iburi Earthquake and other previous earthquakes

*Masahiro Chigira[1], Jun Tajika[3], Satoshi Ishimaru[2], Takehiko Suzuki[4]

1. Disaster Prevention Research Institute, Kyoto University, 2. Hokkaido Geological Survey, Hokkaido Research Organization, 3. Docon Co. Ltd, 4. Tokyo Metropolitan University

2018 Eastern Iburi Earthquake induced numerous numbers of landslides in Atsuma town and its neighborhood with the seismic intensities of 7 and 6+. This was one of the most devastating earthquake-induced landslide hazards in Japan. Geographical Information Authority of Japan published a map showing the distribution of landslides, which counted 8000 in an area of 400 km^2. Most of the landslides were of pyroclastic fall deposits and highly mobile. Those deposits were of Ta-d pumice of 9 ka and En-a pumice of 20 ka, and their sliding surfaces were made within specific beds, which were the bottom of Ta-d, reworked Ta-d in its base or reworked En-a beneath Ta-d, or volcanic soil with pumice grains beneath the Ta-d or volcanic soil beneath En-a. The materials that accommodated the sliding surfaces were heavily weathered to be rich in halloysite, which mineral has been found from the sliding surface materials of previous earthquake-induced landslides of pyroclastic fall deposits and is supposed to be very weak to earthquake shaking. The depths of the landslides varied from 2 to 3 m. Most of the beds that slid were undercut at the lower portion of the slopes, because of man-made cutting or convex slope breaks of which origin is in dispute.

Landslides similar to the landslides stated above have previously occurred in Japan, Indonesia, and El Salvador. They were 1923 Kanto, 1949 Imaichi, 1968 Tokachi-Oki, 1978 Izu-Oshima-Kinkai, 1984 Naganoken-Seibu, and 2011 Tohoku earthquakes in Japan, 2001 El Salvador earthquake, and 2009 Padang earthquake in Indonesia (Chigira and Suzuki 2016). The oldest beds that accommodated a sliding surface and was dated was 330 ka and the youngest was 9 ka of Ta-d. The beds of the sliding surfaces were rich in halloysite and most of the landslides were undercut like those by Eastern Iburi earthquake.

Chigira, M. & Suzuki, T. 2016. Prediction of earthquake-induced landslides of pyroclastic fall deposits. In: Aversa, S., Cascini, L., Picarelli, L. & Scavia, C. (eds.) Landslides and Engineered Slopes. Experience, Theory and Practice. Associone Geotecnica Italiana, Rome, 93-100

Keywords: Earthquake, Landslide, Pyroclastic fall deposits

©2019. Japan Geoscience Union. All Right Reserved.

Earthquake ground motion properties of mountainous district in Totsukawa village, Nara pref. based on the seismic observation –A fundamental study of landslides caused by earthquake –

*Tomoyuki Iida[1], Ryuji Yamada[1], Shigeki Senna[1], Hidemitsu Tokui[2], Tetsuya Onodera[2], Hiroshi Kawabe

1. National Research Institute for Earth Science and Disaster Prevention, 2. Technicallink Kabushiki kaisya

The quantity of seismic information has been accumulated enormously in Japan since seismometer networks, such as K-NET or KiK-net, were completed nationwide. However, most of seismometers are installed in the plain area or hill area, and there are extremely few seismometers installed in the mountainous area where landslides may occur. Therefore, the information about earthquake ground motion properties in the mountainous area, such as the amplification characteristic which may greatly influence landslides, is not enough. It is expected that factors such as the relative position of topography will affect earthquake ground motion properties in the mountainous area together with the ground structure such as AVS30 (the average shear-wave velocity in the upper 30 m). Therefore, we pay particular attention to the influence of topography on earthquake ground motion properties and continuously observe earthquake ground motions at the ridge.

NARH01, one of the KiK-net observation spots, is situated on the ridge which extends to the east and west direction. Two seismometers are installed on NARH01, one is on the surface and another one is underground of approximately 100-m depth. The geology of this area is accretionary wedge called the Shimanto layer. We installed accelerometers (Hakusan industry JU210) in four places of around NARH01 and started the earthquake observation continuously from November, 2017, in order to supplement the observation data of NARH01 and grasp earthquake ground motion properties at each part of the slope. Setting points of the accelerometers are located at the direct perigee of the NARH01 (823 m above sea level), the east-west point on the eastern ridge along the extension of the ridge line (733 m), the north-south point on the northern slope perpendicular to the ridge line (670 m), and the valley bottom (565 m).

During the observation period over one year, we could observe four small earthquakes that were also observed by NARH01 (one of them is the North Osaka earthquake on June 18th, 2018). The result of Fourier spectrum analysis shows that amplification properties of the earthquake ground motion will be affected by the topography, ground structure, and relative position of epicenter.

Keywords: earthquake ground motion, landslide, seismic observation, amplification property, Totsukawa-village, Nara pref.

©2019. Japan Geoscience Union. All Right Reserved.

Study on topographic features and landslide development process in slope failure by Typhoon Talas

*Teruyuki Kikuchi[1], Teruyoshi Hatano[2], Satoshi Nishiyama[3]

1. JP-Design Co., Ltd., 2. Electric Power Development Co.,Ltd., 3. Okayama University Graduate School of Environmental and Life Science

1. Introduction

We have not established a prediction of landslide. The cause of this landslide is complicatedly related to the predisposition.In order to clarify the process leading to the slope failure, accumulation and analysis of cases and long-term observation and evaluation are necessary.The microtopography before disaster occurrence can clarify the process of collapse occurrence.Therefore, we tried to examine the topographic features and the landslide development process of the place where the collapse occurred, by micro-topography interpretation on the location of the slope failure occurrence site.

2. Location

Typhoon Talus crossing western Japan from 2 September to 5 September 2011 brought rain close to 2000 mm to the Kii mountain range, causing more than 50 deep-seated landslides. The scope covered by this research is the upper Totsu-gawa. In this basin, the LiDAR-data before and after the disaster is being carried out by the Kinki Regional Development Bureau, Ministry of Land, Infrastructure and Transport. Particularly in areas where many collapses occurred, the accumulated rainfall exceeded 600 mm. In addition, it corresponds to the distribution area of the Shimanto belt in the upper reaches of the Totsu-gawa, and the north to northwest slope is the dip slope.

3. Method

The verification, 38 places with a collapse area of 1,000 m^2 or more that collapsed due to the Talus. We tried micro topography interpretation of the aerial laser topographic map before the collapse. The authors chose main scarp, flank, and knickpoint, which are topographies showing the gravitational deformation of the mountain body as the topography of micro topography interpretation. In addition, as the characteristic topography recognized in the deep layer collapse in the Kii mountain range, the terminal cliff and the gravitationaldeformation appeared surface in which the back slope and the moving rock body are not completely separated are targeted. In addition, the gully was the topography showing the influence of surface water and groundwater. These micro topographies were classified into three types of "nothing", "unclear" and "clear". Next, as an index showing the developmental state of the collapsed terrain, we consider it in relation with the landslide topography development process.

4. Result

As a result of micro-topography interpretation in Table 1, seven places with the topographical features total as 1 to 3 were observed as the first group. For these, the clear of main scarp, flank is not recognized, and the gravitationaldeformation at the top of the slope is the subject. Comparing the collapsed range, the moving body is unclear. This can be classified as the earliest gravity deformation in the landslide topography development process shown in Table 2, which is very close to the initial stage. I concluded

©2019. Japan Geoscience Union. All Right Reserved.

that this is also the stage of the earlier stage in the transitional stage. The topographical features of the second group are total number 3 to 7, including main scarp,flank or include clear topographical features. Since the gravitationaldeformation, knickpoint,terminal cliff is remarkable, it can be considered that gravity deformation is being clarified. The whole contour is partially clear. Although they are transitional stage, they are thought to be close to the main moving stage. It was separated from the late stage of the transitional stage. The third group has a total number of topographical features of 4 to 12, and it is a group including main scarp. Terminal cliff and accompanying knickpoint are also often clear. Gravitationaldeformation and knickpoint are clear in the slope. This is thought to be due to weight deformation progressing, juvenile landslide sliding surface connected and "main moving stage" equivalent.

5. Discussion

According to this study, the appearance of main scarp, gully, flank is uncertain though topographic features in the early and late stages of the transitional stage, but the appearance of gravitationaldeformation and terminal cliff was high probability. In addition, if it is a landslide slide in a narrow sense, it is thought that it undergoes a stepwise development process from the early stage to the late stage of the transitional stage, but in Talus in 2011 it has collapsed even at the earlier stage. The gravitational deformation which is frequently observed at this stage is thought to have appeared on the surface because it corresponds to gravitational rock creep and the structure of the basement rock is sound. Focusing on such gravitationaldeformation, we think that there is a possibility of predicting collapse by understanding the features.

Keywords: slope failure, development of landslide process, microtopography

©2019. Japan Geoscience Union. All Right Reserved.

表-1 崩壊地の解析結果
Table-2 Data used for microtopographic features analysis

No.	面積 (m2)	比高 (m)	最大傾斜方向	崩壊範囲内の平均傾斜 (°)	地形的特徴 [0 無 ,1 有(不明瞭), 2 有(明瞭)] 滑落崖	側方崖	小崖	末端崩壊	ガリー	不規則凹凸	合計	地質 (*1)	地すべり地形発達過程
1	7,500	112	NNE	36.5	0	0	0	0	0	1	1	Ob	漸移期[前期]
2	5,100	96	E	37.7	0	0	0	0	0	1	1	My3	〃
3	48,000	56	N	38.3	0	0	0	1	0	1	2	My2	〃
4	28,700	176	WSW	35.3	0	0	0	1	0	1	2	My3	〃
5	26,400	124	SSE	32.8	0	0	0	1	0	1	2	H4	〃
6	6,600	108	NE	37.3	0	0	0	1	0	1	2	My2	〃
7	35,900	176	SW	31.1	0	0	1	0	1	1	3	Yk2	〃
8	29,900	254	NE	38.4	0	0	0	2	0	1	3	My3	漸移期[後期]
9	9,200	128	E	37.3	0	1	1	0	0	1	3	My1	〃
10	9,400	92	SW	38.8	0	1	0	1	0	1	3	My1	〃
11	14,000	114	NW	34.6	1	0	0	1	0	1	3	My3	〃
12	4,500	94	NNE	33.7	1	0	1	1	0	1	4	My4	〃
13	20,600	154	N	35.3	1	0	0	2	0	1	4	My3	〃
14	8,500	165	NW	39.8	0	1	0	1	1	1	4	Ry	〃
15	42,100	174	N	32.6	0	0	1	1	1	1	4	H4	〃
16	48,100	308	NW	38.5	0	0	0	2	1	1	4	My2	〃
17	5,044	103	W	39.8	0	0	0	1	2	1	4	Yk3	〃
18	14,300	154	NNW	38.2	1	0	1	1	1	1	5	My4	〃
19	34,100	234	NE	38.3	1	1	0	1	1	1	5	Ry	〃
20	13,500	136	ENE	39.6	1	1	1	0	1	1	5	Yk2	〃
21	7,400	64	W	41.8	1	1	0	2	1	1	6	My3	〃
22	14,700	126	NNW	37.8	0	2	1	2	2	0	7	My3	〃
23	42,300	218	WSW	38.8	1	1	1	2	1	1	7	My3	〃
24	5,100	158	NW	40.9	0	1	2	2	1	1	7	My3	〃
25	48,000	226	WSW	30.0	0	1	0	2	2	2	7	My2	〃
26	18,200	134	NNW	38.1	2	1	0	1	0	1	5	gc	滑動期
27	1,400	32	NE	39.9	0	2	0	2	1	0	5	My2	〃
28	51,700	227	NNW	32.2	1	0	1	2	0	2	6	Ry	〃
29	22,500	92	NNW	36.8	0	1	1	2	0	2	6	Ry	〃
30	77,200	124	ESE	29.6	0	0	2	2	1	1	6	H4	〃
31	38,600	120	NNW	35.1	2	0	1	1	1	1	6	H4	〃
32	59,000	254	ENE	37.3	1	1	1	1	1	1	6	My1	〃
33	86,300	396	NNE	42.1	1	1	0	2	2	1	7	My4	〃
34	10,300	144	SW	41.3	0	2	0	2	2	1	7	My2	〃
35	254,900	592	NW	38.3	2	1	1	1	1	2	8	My2	〃
36	19,200	120	NNE	34.2	0	2	0	2	2	2	8	My3	〃
37	182,700	400	NW	39.0	2	1	1	2	1	2	9	My2	〃
38	195,100	446	NNW	36.2	2	1	2	2	2	2	11	My2	〃

*1) 地質
Ry: 竜神層, H1～4: 花園層(ユニット1～4), gc 花園層緑色岩チャート, My1～4: 美山層(ユニット1～4)

表-2 崩壊事例の地すべり地形発達過程における検討結果
Conceptual map of Landslide developing history of slopes at micro-topography interpretation

先行研究		本研究							
大八木[4]		新区分	地形的特徴の傾向	合計点数と箇所数	上段:具体的な事例(それぞれ5箇所) ／下段:通しNo.と地形的特徴合計点 [先滑動期と後滑動期には崩壊事例がない]				
先滑動期	対象斜面に地すべりによる変形や運動が全体のみならず部分にも発生していない期間。地質時代に形成された地質構造が地表環境下の諸営力によって変化する。特定の構造や地層が地すべり構造の基本的な要素に移化する。	先滑動期	本研究では事例はないが、重力変形が生じる前段階の組織地形から生じる小崖地形が断続的に分布する これ以外の地形変状は認められない.	地形的特徴は認められない	–	–	–	–	–
漸移期	対象斜面の一部に小さい変形が生じているが、変動部分全体がまだ基岩から分離していない。全体の輪郭となる構造がまだ形成されていない	漸移期[前期]	初期的な重力変形によって生じる不規則凹凸、末端崩壊が主体. 滑落崖・側方崖が認められない. また明瞭な地形的特徴が認められない 特定の外的要因によって急激に不安定化する全体の輪郭は不明瞭	合計数:1～3 箇所数:7	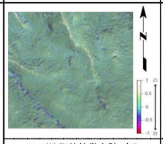 No.2(地形的特徴合計1点)	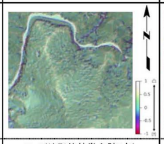 No.3(地形的特徴合計2点)	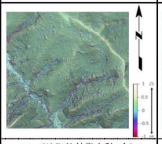 No.4(地形的特徴合計2点)	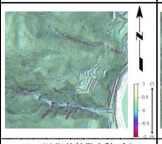 No.5(地形的特徴合計2点)	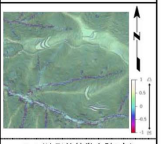 No.7(地形的特徴合計3点)
		漸移期[後期]	重力変形が明瞭化. 不規則凹凸・小崖地形・末端崩壊が顕著. 滑落崖・側方崖を含むか、明瞭な地形的特徴を含む. 全体の輪郭は部分的に明瞭	合計数:3～7 箇所数:17	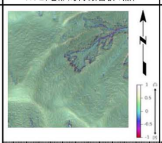 No.8(地形的特徴合計3点)	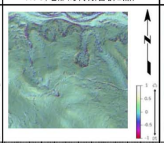 No.13(地形的特徴合計4点)	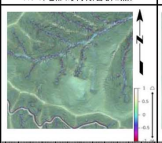 No.15(地形的特徴合計4点)	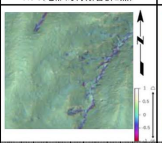 No.20(地形的特徴合計5点)	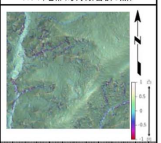 No.23(地形的特徴合計7点)
滑動期	対象斜面の変動域構成体とその下位の非変動域構成体とを限る輪郭構造が形成されて変動域構成体は非変動域から独立して運動しているか、運動できる状態になっている。活層、休止、再活動、移行拡大に細分も可能	滑動期	滑落崖、側方崖は明瞭. 移動体の輪郭は明瞭. 移動体内のガリー地形の進行が顕著 末端崩壊やこれに伴う小崖地形も明瞭なことが多い. 斜面内に不規則凹凸や小崖が明瞭となる	合計数:4～12 箇所数:13	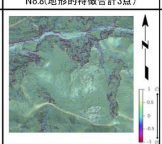 No.26(地形的特徴合計6点)	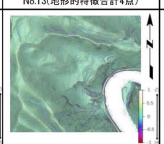 No.30(地形的特徴合計6点)	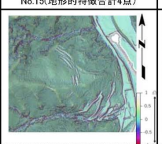 No.32(地形的特徴合計6点)	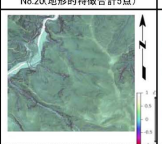 No.35(地形的特徴合計8点)	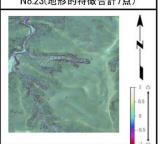 No.37(地形的特徴合計9点)
後滑動期	対象斜面における地すべり移動体が運動を完全に停止し、移動体の移動・活動中に形成された構造が運動を停止(休積)下状態において削剥される状態	後滑動期	滑落崖を含むが、一部消失している場合もある. エッジが消失することがある. 移動体の輪郭は明瞭. 移動体内のガリー地形の進行が顕著 移動体内の不規則凹凸やは拡大しないため不明瞭化する. 削剥が進行するため、末端崩壊は明瞭なことがある.	–	–	–	–	–	–

©2019. Japan Geoscience Union. All Right Reserved.

Formation mechanism of bulge of slope that is sign of large-scale collapse

*tatsurou yoshimura[1]

1. Daiichi Fukken Co., Ltd.

The fracture is distributed around main scarp and side cliff in slope failure. The formation of landslide mass results from dividing into parts by fracture. "Landslide mass formation model by dividing into fracture" was verified in large-scale landslide. The thick debris is distributed in the center part of the landslide mass. Bulge of slope is admitted before collapses. Bulge of slope is caused by seismic motion and the thick debris.

Keywords: large-scale collapse, bulge of slope, seismic motion, relief inversion, gamma-ray survey

©2019. Japan Geoscience Union. All Right Reserved.

Sediments accumulated in the linear depressions in the Mitsumine area, Kanto Mountains

*Masakazu Mashiko[1], Masahiro Chigira[2]

1. Graduate School of Science, kyoto University, 2. Disaster Prevention Research Institute, Kyoto University

Many problems about the mechanisms of an occurrence or a development of deep-seated gravitational slope deformations (DGSDs) are left behind. We are now researching in the Mitsumine area, Kanto Mountains, where is occupied by the Shimanto accretionary complex, in other to resolve the problems about the mechanisms of DGSDs. As a part of the research, simplified boring are executed in linear depressions near a ridge and boring cores composed by accumulated sediments are acquired.

Boring are operated in two different linear depressions and cores have reached the bedrock at the depth of 6.75 m to 6.95 m. Both cores have almost same characteristics; from the surface to the depth of 1.0 m, these are blackish brown humified soil or clay, and other parts deeper than 1.0 m are occupied by brown clay.
The date when the linear depressions or DGSDs on the hillslope emergenced will be estimated by specifying the tephras included in the boring cores. We have observed the ratio of volcanic glasses in the cores every 20 cm and have recognized three peaks; the depth of 2.20 m in P1 (upstream side), 2.40 m in P2 (downstream side), and 6.00 m in P2. Other researches performed in the Mitsumine area have revealed that the depositions include several tephras, such as Aira-Tn (AT) tephra (26~29 ka), Ontake-Pumice 1 (On-Pm1) (100 ka), and Yatsugatake-Kawakami (Yt-Kw) tephra (170 ka). It is likely that each volcanic glasses in the boring cores originated in one of these tephras. We are now trying to observate the refractive index of volcanic glasses to identify the tephras in the core completely.

For the explication of the mechanism of DGSDs in this area, it is indispensable to reveal the geomophological and geological characteristics in the area. We carry on not only analysis of the sediments accumulated in the linear depositions but also geological site investigations.

Keywords: Deep-seated gravitational slope deformations, Linear depressions, Sediments, Boring core, Tephra

©2019. Japan Geoscience Union. All Right Reserved.

[J] Poster | H (Human Geosciences)：H-DS Disaster geosciences

Mon. May 27, 2019 5:15 PM - 6:30 PM JST | Mon. May 27, 2019 8:15 AM - 9:30 AM UTC | Poster Hall International Exhibition Hall8, Makuhari Messe_15

[H-DS14] Geohazards in humid, tectonically active countries and their precursors

convener:Masahiro Chigira(Disaster Prevention Research Institute, Kyoto University), Hiroshi YAGI(Faculty of Art, Science and Education, Yamagata University), Satoru Kojima(Department of Civil Engineering, Gifu University), Taro Uchida(National Institute for Land and Infrastructure Management)

This session covers mass movements of landslide, slope failure, debris flow, and gravitational slope deformation in tectonically active, humid countries, and aims to discuss on their mechanisms, characteristics of occurrence sites, the significance in geological time scale, and the methodology to mitigate their affects by researchers with various related research fields. In particular, papers about 2017 northern Kyushu rainstorm, 2018 Osaka earthquake, 2018 Western Japan rainstorm, and 2018 Hokkaido earthquake are welcome

[HDS14-P01] The estimation of frequency for deep-seated landslide with carbon dating in Kii mountain area

★Invited Papers

*Yasutaka Tanaka[1], Toshiaki Kotake[1], Hiroaki Sugawara[1], Atsuhiko Kinoshita[1], Yoshito Ogawauchi[2], Minami Fujiwara[2] (1.Sediment Disaster Prevention Technology Center, Kinki Regional Developing Bureau, Ministry of Land, Infrastructure, Transport and Tourism, 2.Japan Conservation Engineers & CO., LTD.)

[HDS14-P02] Tephra stratigraphy and a slope failure of about 4,000 years ago on the slope of the Late Pleistocene Janoo Volcano in the northwestern of Aso Caldera

*Yasuto Hirata[1], Keiichi Ueta[1], Riichiro Miyawaki[2], Katsutoshi Iemura[2], Toshitaka Yokoyama[2], Akiko Miyawaki[2] (1.Central Research Institute of Electric Power Industry, 2.Hanshin Consultants)

[HDS14-P03] Analysis of causal factors of landslides during 2017 northern Kyusyu torrential rainfall disaster by using decision tree

*Hiromu Daimaru[1], Wataru Murakami[1], Yuki Tsurusaki[2] (1.Forestry and Forest Products Research Institute, 2.Fukuoka Agriculture and Forestry Research Center)

[HDS14-P04] Geologic characteristics of rock mass failures caused by the heavy rain event of July 2018 in Uwajima, Ehime

*Shintaro Yamasaki[1] (1.Disaster Prevention Research Institute, Kyoto University)

[HDS14-P05] On the failure mechanism of embankments in Mabi Town during the Heavy rain of July, 2018, Japan

*Gonghui Wang[1] (1.Disaster Prevention Research Institute, Kyoto University)

[HDS14-P06] Interpretation of landslide surface deformation around the branch basins of Sun Kosi river in Nepal using InSAR images

*Otake Shunpei[1], Hiroshi, P. Sato[1] (1.College of Humanities and Sciences, Nihon University)

[HDS14-P07] The large scale landslides triggered by The 2018 Sulawesi Earthquake, Indonesia

*Masashi Omata[1], Toshiyuki Adachi[2], Takao Yamakoshi[3], Kenichi Matsui[4], Tosho Iwamatsu[1], Susumu Takagishi[1], Chiho Motojima[1], Yuu Okuizumi[1], Umito Wada[1] (1.PASCO CORPORATION, 2.LDP Upper House member, 3.SABO & LANDSLIDE TECNICAL CENTER, 4.Nobuyuki Adzchi Office)

[HDS14-P08] Relationship of the grand deformation and topography in Sapporo City at the 2018 Hokkaido Eastern Iburi Earthquake confirmed by InSAR analysis

*Akihiro Yokota[1], Tomohiro Nishimura[2], Kiyoyuki Shigeno[1], Kenichi Honda[2], Sakae Mukoyama[2] (1.Meiji Consultant Co., Ltd, 2.Kokusai Kogyo Co., Ltd)

[HDS14-P09] Estimation of co-seismic surface displacement and ground deformation associated with the 2018 Hokkaido Eastern Iburi Earthquake, based on differential InSAR and differential LiDAR DEM analysis.

*Kenichi Honda[1], Norichika Asada[1], Naruo Mushiake[1], Tomohiro Nishimura[1], Sakae Mukoyama[1] (1.Kokusai Kogyo Co.,LTD.)

[HDS14-P10] Geological features of landslides of pyroclastic fall deposits induced by the 2018 Eastern Iburi Earthquake and other previous earthquakes

*Masahiro Chigira[1], Jun Tajika[3], Satoshi Ishimaru[2], Takehiko Suzuki[4] (1.Disaster Prevention Research Institute, Kyoto University, 2.Hokkaido Geological Survey, Hokkaido Research Organization, 3.Docon Co. Ltd, 4.Tokyo Metropolitan University)

[HDS14-P11] Earthquake ground motion properties of mountainous district in Totsukawa village, Nara pref. based on the seismic observation – A fundamental study of landslides caused by earthquake –

*Tomoyuki Iida[1], Ryuji Yamada[1], Shigeki Senna[1], Hidemitsu Tokui[2], Tetsuya Onodera[2], Hiroshi Kawabe (1.National Research Institute for Earth Science and Disaster Prevention, 2.Technicallink Kabushiki kaisya)

[HDS14-P12] Study on topographic features and landslide development process in slope failure by Typhoon Talas

*Teruyuki Kikuchi[1], Teruyoshi Hatano[2], Satoshi Nishiyama[3] (1.JP-Design Co., Ltd., 2.Electric Power Development Co.,Ltd., 3.Okayama University Graduate School of Environmental and Life Science)

[HDS14-P13] Formation mechanism of bulge of slope that is sign of large-scale collapse

*tatsurou yoshimura[1] (1.Daiichi Fukken Co., Ltd.)

[HDS14-P14] Sediments accumulated in the linear depressions in the Mitsumine area, Kanto Mountains

*Masakazu Mashiko[1], Masahiro Chigira[2] (1.Graduate School of Science, kyoto University, 2.Disaster Prevention Research Institute, Kyoto University)

The estimation of frequency for deep-seated landslide with carbon dating in Kii mountain area

*Yasutaka Tanaka[1], Toshiaki Kotake[1], Hiroaki Sugawara[1], Atsuhiko Kinoshita[1], Yoshito Ogawauchi[2], Minami Fujiwara[2]

1. Sediment Disaster Prevention Technology Center, Kinki Regional Developing Bureau, Ministry of Land, Infrastructure, Transport and Tourism, 2. Japan Conservation Engineers & CO., LTD.

Typhoon 12 in 2011 induced deep-seated landslides in Kii mountain area. In Kii mountain area, heavy rainfall also induced great damage by large scale landslide in 1889. From above we need the frequency of deep-seated landslide to construct countermeasure for sediment disaster in Kii mountain area.

Although previous report shows the method to use tephra for estimation of frequency of deep-seated landslide, in Kii mountain area we can find few point of tephra sedimentation. In recent years some study shows the methods to estimate frequency of sediment disaster with chips of wood and carbides. In this study we applied the method with chips of wood and carbides to estimation of frequency of deep-seated landslide in Kii mountain area.

In this study we proposed the research flow to pick sample shown as below;

a) Extracting landslide deposit by LiDAR

b) Preliminary research in field

c) Main research in field and picking sample up

d) Analysis sample with carbon dating

In a) we extracted the site where landslide dams may have been as landslide deposit to observe along river side closely with topographic map by LiDAR. In b) we investigate access route to the research site and whether chip of wood and carbide are or are not roughly. In c) we investigated closely and picked sample up with special sampler we developed for this research. This sampler can collect sample including soil. In d) we analyzed samples and organized carbon dating data.
We collected 28 samples in 11 landslide deposits. Especially it was easier to collect samples in upper and bottom of landslide deposits and underwater deposits than other sites. The research flow and special sampler we developed can help to collect sample effectively. In addition we found deep-seated landslide occurred once in 100 ~ 150 years in Kii mountain area from analysis of carbon date. This result isn't inconsistent with the past disaster reports. However, carbon dating has some error. To estimate accurately we need more investigation.

Keywords: deep-seated landslide, carbon dating, Kii mountain area

©2019. Japan Geoscience Union. All Right Reserved.

Tephra stratigraphy and a slope failure of about 4,000 years ago on the slope of the Late Pleistocene Janoo Volcano in the northwestern of Aso Caldera

*Yasuto Hirata[1], Keiichi Ueta[1], Riichiro Miyawaki[2], Katsutoshi Iemura[2], Toshitaka Yokoyama[2], Akiko Miyawaki[2]

1. Central Research Institute of Electric Power Industry, 2. Hanshin Consultants

In the west part of Aso Caldera, the 2016 Kumamoto Earthquake caused surface earthquake faults along the Futagawa and Hinagu fault zone, triggering numerous landslides and some lateral spreads on tephra. Janoo Volcano is located on the line that extrapolates from the end of the earthquake fault zone to the northeast in the disaster area. We carried out an excavation and boring exploration at the south slope of Janoo Volcano and measured chemical compositions of lava and radiocarbon ages of volcanic soil. The results elucidated the succession of volcanic products after the formation of Janoo Scoria Cone and showed a slope failure about 4,000 years ago. The eruption ages of key beds were estimated with calibrated method as follows: Janoo Scoria (>15.5 ka), ACP1: Aso Central Pumice 1 (~4.0 ka), Kishimadake Lava and Kishimadake Scoria (~3.7 ka), Ojodake Scoria (3.5±0.1 ka), and Kometsuka Lava (3.0±0.1 ka). Fine sandy ashes deeper than 8 m and the surface part of Janoo Scoria weathered to become yellowish and included small dislocations that are the normal sense and parallel to the surface of Janoo Scoria. The volcanic soil layer on the sandy ash was separated as 1-meter-tall blocks, and they were arranged into an imbricated form of overturned strata. This deposit was covered with a 2 m thick of soft volcanic soil moved from the upper slope. All the above tephra layers were consistently covered with ACP1. Consequently, these deformation and sedimentary structures suggest that the tephra on Janoo Scoria sild down successively from the slope toe toward the top just before the eruption of ACP1. This ancient slope failure seems to be triggered by earthquake because its depth and material are similar to those of landslides by the 2016 Kumamoto Earthquake.

Keywords: Aso Caldera, eruptive history, landslide, non-tectonic faulting, trench survey

©2019. Japan Geoscience Union. All Right Reserved.

Analysis of causal factors of landslides during 2017 northern Kyusyu torrential rainfall disaster by using decision tree

*Hiromu Daimaru[1], Wataru Murakami[1], Yuki Tsurusaki[2]

1. Forestry and Forest Products Research Institute, 2. Fukuoka Agriculture and Forestry Research Center

Causal factors of landslides induced by torrential rainfall in July 2017 in Kyushu Island were analyzed by decision tree. The landslides were mapped from orthophotos produced by GSI and overlay analysis with radar-AMeDAS rainfall data, slope, geology tree age and vegetation were conducted by using the decision tree classifier of the Scikit-learn Python module. Landslide map was defined by existence or non-existence of landslide in each 200m size grid and overlain by geological map by AIST, slope map from 10m DEM by GSI and digital forest map by Fukuoka Prefecture. The distribution of landslides was principally controlled by rainfall distribution. Slope was the secondary factor on landslide susceptibility and threshold slope decreased with rainfall intensity. Geology was the third factor. granite area was rather vulnerable comparing with metamorphic rocks and Tertiary volcanic rocks. Effect of tree age was evident in where 12hr rainfall was less than 500mm. On the other hand, effect of tree species seemed to be minor factor comparing with other factors.

Keywords: 2017 northern Kyusyu torrential rainfall disaster, landslide, decision tree

©2019. Japan Geoscience Union. All Right Reserved.

Geologic characteristics of rock mass failures caused by the heavy rain event of July 2018 in Uwajima, Ehime

*Shintaro Yamasaki[1]

1. Disaster Prevention Research Institute, Kyoto University

The heavy rain event of July 2018 caused many rock mass failures around Hokezu bay area in Uwajima city and Seiyo city, Ehime. This paper reports geologic characteristics of those failures. The rock mass failures are relatively small, because they occur on relatively low relief topography. The scarps of failures are weathered, and have dense cracks and separating planes cutting slope or mountain flanks. Webby weak mineral veins and fault fractures are found at some failure sites. These characteristics have lowered strength of the rock mass microscopically and macroscopically in the area. Because of the low strength, gravitational deformation probably proceeds in small slope, and it forms flow path to penetrate with abundant rain water in the slope before collapse. The Hokezu bay area is a characteristic low relief area in Shimanto belt in Sikoku. Similar low relief topographic areas are distributed along Butsuzo tectonic line traversing Shikoku island.

Keywords: heavy rain event, landslide, deep-seated landslide, rock control, Shimanto belt

©2019. Japan Geoscience Union. All Right Reserved.

On the failure mechanism of embankments in Mabi Town during the Heavy rain of July, 2018, Japan

*Gonghui Wang[1]

1. Disaster Prevention Research Institute, Kyoto University

From late June to mid-July, 2018, successive heavy rainfall hit a wide area of southwestern Japan, resulting in widespread sediment-related disasters and devastating floods. Among these disasters, the flooding resulting from the failures of embankments along Oda River and some other tributary rivers in Mabi Town, Okayama Prefecture, was the deadliest. To understand the possible failure mechanisms of these embankment, field geotechnical investigation and geophysical surveys were conducted. Centrifuge tests were also performed to examine the instability processes of embankment with increase of water level on the river. The results indicate that the leakage in the embankments along the tributary rivers may have resulted in retrogressive failures on the embankments, while overtopping may have played a key role in the final rapid breaching of the embankment.

Keywords: failure of embankment, failure mechanism, Internal structure of embankement, foundation of embankment, Centrifuge test

©2019. Japan Geoscience Union. All Right Reserved.

Interpretation of landslide surface deformation around the branch basins of Sun Kosi river in Nepal using InSAR images

*Otake Shunpei[1], Hiroshi, P. Sato[1]

1. College of Humanities and Sciences, Nihon University

On 25 Apr 2015, Gorkha earthquake (Mw 7.8) occurred at 80 km NW from Kathmandu, Nepal. After that, the largest aftershock (Mw 7.3) occurred on 12 May 2015 at 75 km ENE from Kathmandu. These earthquakes caused landslide disasters and big damages. Nepal has wide mountain area, and landslides disasters tend to be induced by both conditions as follows. On the one hand many earthquakes occur in Nepal, where is on the collision and subduction area related Indo-Australian and Eurasian plate. On the other hand they have much rain in monsoon season there. Therefore, landslide caused by these earthquakes may be reactivated. It is important to monitor landslide surface deformation because it contributes to prevent landslide disasters after these earthquakes. In this study we focused on the area where the largest aftershock occurred, and tried to detect landslide surface deformations after the largest aftershock.

Recently InSAR (Synthetic Aperture Rader interferometry) has been used to detect landslide surface deformation. Then, we used and adopt it for the study area, where is the watershed of Sun Koshi river branches which includes epicenter of the largest aftershock. In this study two InSAR images were produced, which was taken on 12 Sep 2016/30 Jan 2017 and on 30 Jan 2017 /11 Sep 2017. Then, landslide surface deformations were interpreted on the two InSAR images, and the interpreted areas were delineated and the center of the area were mapped. And location of such the detected sites were analyzed related with distance from the epicenter, elevation, slope aspect, deformation amount along LoS (line of sight) known from InSAR image, interpreted deformation area, lithological units of geology, and the watersheds of the branches.

As a result of the interpretation, 29 and 25 deformation sites were detected on InSAR image taken on 12 Sep 2016/30 Jan 2017 and on 30 Jan 2017 /11 Sep 2017, respectively. As a result of the analysis, it was found that ca. 70 % of the detected sites locate in the elevation of 1,500-2,999 m, and that the averaged area of deformation per one site was larger on 30 Jan 2017 /11 Sep 2017 image than on 12 Sep 2016/30 Jan 2017 image. For the former result, it is thought that low Himalayan meta-sedimentary rocks gave more detected sites than other lithological units and the rocks tend to be widely distributed in this elevation belt. For the latter result, it is thought that effect of precipitation in rainy season are related more closely with landslide surface deformation interpreted on 30 Jan 2017 /11 Sep 2017 image than on 12 Sep 2016/30 Jan 2017 image.

Keywords: Landslide, SAR, Earthquake, Nepal

©2019. Japan Geoscience Union. All Right Reserved.

The large scale landslides triggered by The 2018 Sulawesi Earthquake, Indonesia

*Masashi Omata[1], Toshiyuki Adachi[2], Takao Yamakoshi[3], Kenichi Matsui[4], Tosho Iwamatsu[1], Susumu Takagishi[1], Chiho Motojima[1], Yuu Okuizumi[1], Umito Wada[1]

1. PASCO CORPORATION, 2. LDP Upper House member, 3. SABO & LANDSLIDE TECNICAL CENTER, 4. Nobuyuki Adzchi Office

On 28 September 2018, a large earthquake occurred near Palu City, Sulawesi, Indonesia. The magnitude of the earthquake was 7.5. According to the information broadcast after the earthquake, the nearly flat terrain greatly moved laterally. The authors carried out a satellite imagery interpretation survey with using the post-earthquake imageries of Pleiades and SPOT-7. The survey revealed that there are at least three areas which seem to have moved laterally with long distance. It seems to be lateral spread in view of situations reported in the press information. Two large lateral spreads stand in the eastern side of the city and one in the western side. The two lateral spreads in the east side are 1.5 km wide and 2.5 km long and 1 km wide and 3.5 km long, respectively while the one in the western side is 0.4 km wide and 1 km long. In the upper part of the spreads, there is area of brown bare soil while there seems ropy in the lower part of the spreads. One of them seemed to be greatly fluidized and reached further in the down streams. These spreads seem to initiate from the knick point near lower edge of fluvial fans where a lot of subsurface flow is likely to return onto ground surface. A press says that local people call these phenomena as "nalodo", which means "get absorbed into mud". This implies that similar disasters repeated in the past.

Keywords: lateral spread, satellite imagery, earthquake, SPOT-7, Pleiades, Indonesia

©2019. Japan Geoscience Union. All Right Reserved.

Relationship of the grand deformation and topography in Sapporo City at the 2018 Hokkaido Eastern Iburi Earthquake confirmed by InSAR analysis

*Akihiro Yokota[1], Tomohiro Nishimura[2], Kiyoyuki Shigeno[1], Kenichi Honda[2], Sakae Mukoyama[2]

1. Meiji Consultant Co., Ltd, 2. Kokusai Kogyo Co., Ltd

In the 2018 Hokkaido Eastern Iburi Earthquake, ground displacement and building damage occurred extensively. It is thought that it is important to promptly grasp the damage caused by a natural disaster in order to advance disaster reduction. In this study, the results of SAR analysis using Sentinel - 1 satellite were investigated for validity and cause using interpretation of aerial photograph and field survey.

As a result of SAR analysis, displacement was observed in Satozuka・Utsukushigaoka・Kiyota, Kiyota Ward, Hiragishi, Toyohira Ward, and Fushiko・Naebo, Higashi Ward in Sapporo City. For these districts, I performed an investigation by the local survey and aerial photo reading.

As a result of investigation, the spot that ground movement produced confirmed that I agreed with the spot where big displacement was estimated on InSAR analysis. The correlation with the old topography and the Embankment place is high in the ground change confirmed this time

It was revealed that I could grasp the damage situation of the wide area in a short time by using the inSAR data with the, Sentinel-1 satellite about the ground damage after the 2018 Hokkaido Eastern Iburi Earthquake.

Keywords: Interferometric SAR, Ground displacement, 2018 Hokkaido Eastern Iburi Earthquake

©2019. Japan Geoscience Union. All Right Reserved.

Estimation of co-seismic surface displacement and ground deformation associated with the 2018 Hokkaido Eastern Iburi Earthquake, based on differential InSAR and differential LiDAR DEM analysis.

*Kenichi Honda[1], Norichika Asada[1], Naruo Mushiake[1], Tomohiro Nishimura[1], Sakae Mukoyama[1]

1. Kokusai Kogyo Co.,LTD.

It is important to detect the damage situation of the building quickly when an earthquake occurs for the initial response. Satellite remote sensing can measure a wide area, and is expected to obtain the damage at the time of a disaster. However, the observation frequency of the satellite, the analysis processing time, selection of information required at the beginning are suggested as problems for practical use.
This paper introduces information which can be provided by Coherence Change Detection and differential LiDAR DEM analysis when an earthquake occurs. Especially, it will introduce the earthquakes which occurred in 2018, the 2018 Hokkaido Eastern Iburi Earthquake.
On 6 September 2018, an earthquake of magnitude 6.7 hit southern Hokkaido, which is the largest and northernmost prefecture of Japan. Interferometric analysis was carried out using images of Sentinel-1 before (August 25) and after (September 6) the earthquake to estimate the damage of the building due to the ground deformation and the deterioration of the coherence. In addition, the same analysis was carried out using the image of ALOS-2.
Figure shows an example of Kiyota Ward in Sapporo City where liquefaction occurred. In the interferometry image using Sentinel-1, deviation was discontinuous or shown as noise, so extraction of the deviation was difficult. However, the area which buildings were damaged could be extracted from the coherence change detection.
On the other hand, the degradation of coherence when using ALOS-2 is Low, so the damage area can be extracted from the deviation of the interferometry image as a ground deformation. This difference is thought to be due to the difference in the sensitivity of the observation wavelength band.
For comparison, the particle image velocimetry method was applied to calculate 3-D vectors of co-seismic deformation. The result shows deformation of the housing area, which was developed over the valley that was filled up with soil, agrees with SAR analysis result.
In this case, since Sentinel-1 observed the disaster area about 3 hours after the earthquake, the image was analyzed on the day and the results were provided to local staff. Field confirmation was carried out the day after the earthquake, and the results were provided to the affected local governments. Except for the day of the earthquake, the weather was bad for the disaster area for several days, so it was not possible to take aerial photos using the aircraft. 2018 Hokkaido Eastern Iburi Earthquake is a case where utilization of the satellite SAR, which can quickly extracts damaged area, became advantageous.
Obtaining disaster damage by satellite remote sensing is effective. However, field survey and aircraft surveillance are carried out as soon as the disaster occurred in Japan, and satellite remote sensing has not be practically used in many situations. However, similar to the 2018 Hokkaido Eastern Iburi Earthquake, if acquiring the satellite data and providing analysis results could be carried out quickly, satellite remote sensing can be an option for understanding the damage at early disaster response stage. Furthermore, estimation the light damaged area is difficult by aerial photographs, therefore estimation by SAR coherence change detection are considered importance.
Finally, I wish to express my deepest condolences to those who lost loved ones in these disasters, and also to express my sympathy to all who were affected.

©2019. Japan Geoscience Union. All Right Reserved.

Keywords: Earthquake, SAR, LiDAR

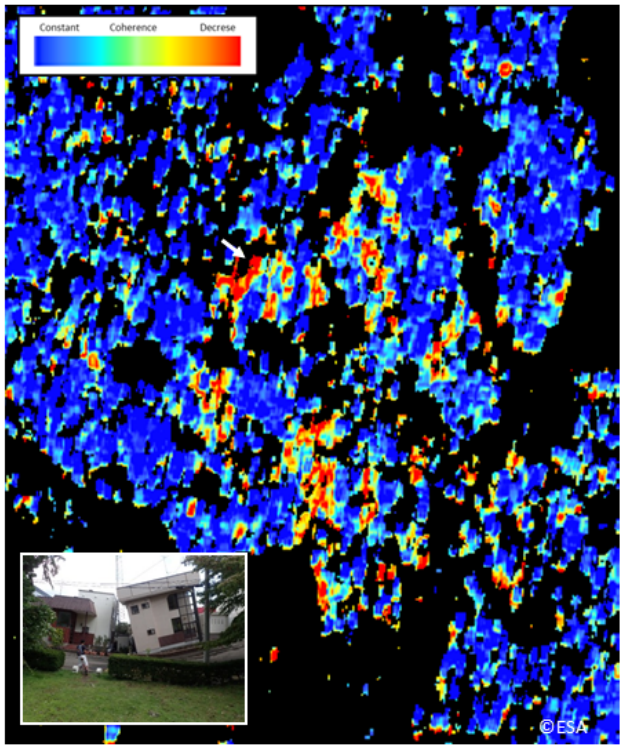

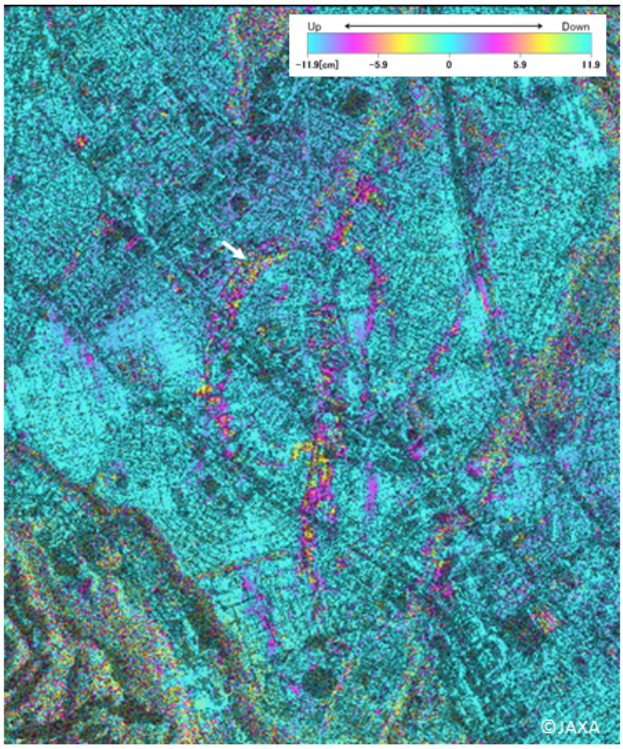

©2019. Japan Geoscience Union. All Right Reserved.

Geological features of landslides of pyroclastic fall deposits induced by the 2018 Eastern Iburi Earthquake and other previous earthquakes

*Masahiro Chigira[1], Jun Tajika[3], Satoshi Ishimaru[2], Takehiko Suzuki[4]

1. Disaster Prevention Research Institute, Kyoto University, 2. Hokkaido Geological Survey, Hokkaido Research Organization, 3. Docon Co. Ltd, 4. Tokyo Metropolitan University

2018 Eastern Iburi Earthquake induced numerous numbers of landslides in Atsuma town and its neighborhood with the seismic intensities of 7 and 6+. This was one of the most devastating earthquake-induced landslide hazards in Japan. Geographical Information Authority of Japan published a map showing the distribution of landslides, which counted 8000 in an area of 400 km^2. Most of the landslides were of pyroclastic fall deposits and highly mobile. Those deposits were of Ta-d pumice of 9 ka and En-a pumice of 20 ka, and their sliding surfaces were made within specific beds, which were the bottom of Ta-d, reworked Ta-d in its base or reworked En-a beneath Ta-d, or volcanic soil with pumice grains beneath the Ta-d or volcanic soil beneath En-a. The materials that accommodated the sliding surfaces were heavily weathered to be rich in halloysite, which mineral has been found from the sliding surface materials of previous earthquake-induced landslides of pyroclastic fall deposits and is supposed to be very weak to earthquake shaking. The depths of the landslides varied from 2 to 3 m. Most of the beds that slid were undercut at the lower portion of the slopes, because of man-made cutting or convex slope breaks of which origin is in dispute.

Landslides similar to the landslides stated above have previously occurred in Japan, Indonesia, and El Salvador. They were 1923 Kanto, 1949 Imaichi, 1968 Tokachi-Oki, 1978 Izu-Oshima-Kinkai, 1984 Naganoken-Seibu, and 2011 Tohoku earthquakes in Japan, 2001 El Salvador earthquake, and 2009 Padang earthquake in Indonesia (Chigira and Suzuki 2016). The oldest beds that accommodated a sliding surface and was dated was 330 ka and the youngest was 9 ka of Ta-d. The beds of the sliding surfaces were rich in halloysite and most of the landslides were undercut like those by Eastern Iburi earthquake.

Chigira, M. & Suzuki, T. 2016. Prediction of earthquake-induced landslides of pyroclastic fall deposits. In: Aversa, S., Cascini, L., Picarelli, L. & Scavia, C. (eds.) Landslides and Engineered Slopes. Experience, Theory and Practice. Associone Geotecnica Italiana, Rome, 93-100

Keywords: Earthquake, Landslide, Pyroclastic fall deposits

©2019. Japan Geoscience Union. All Right Reserved.

Earthquake ground motion properties of mountainous district in Totsukawa village, Nara pref. based on the seismic observation –A fundamental study of landslides caused by earthquake –

*Tomoyuki Iida[1], Ryuji Yamada[1], Shigeki Senna[1], Hidemitsu Tokui[2], Tetsuya Onodera[2], Hiroshi Kawabe

1. National Research Institute for Earth Science and Disaster Prevention, 2. Technicallink Kabushiki kaisya

The quantity of seismic information has been accumulated enormously in Japan since seismometer networks, such as K-NET or KiK-net, were completed nationwide. However, most of seismometers are installed in the plain area or hill area, and there are extremely few seismometers installed in the mountainous area where landslides may occur. Therefore, the information about earthquake ground motion properties in the mountainous area, such as the amplification characteristic which may greatly influence landslides, is not enough. It is expected that factors such as the relative position of topography will affect earthquake ground motion properties in the mountainous area together with the ground structure such as AVS30 (the average shear-wave velocity in the upper 30 m). Therefore, we pay particular attention to the influence of topography on earthquake ground motion properties and continuously observe earthquake ground motions at the ridge.

NARH01, one of the KiK-net observation spots, is situated on the ridge which extends to the east and west direction. Two seismometers are installed on NARH01, one is on the surface and another one is underground of approximately 100-m depth. The geology of this area is accretionary wedge called the Shimanto layer. We installed accelerometers (Hakusan industry JU210) in four places of around NARH01 and started the earthquake observation continuously from November, 2017, in order to supplement the observation data of NARH01 and grasp earthquake ground motion properties at each part of the slope. Setting points of the accelerometers are located at the direct perigee of the NARH01 (823 m above sea level), the east-west point on the eastern ridge along the extension of the ridge line (733 m), the north-south point on the northern slope perpendicular to the ridge line (670 m), and the valley bottom (565 m).

During the observation period over one year, we could observe four small earthquakes that were also observed by NARH01 (one of them is the North Osaka earthquake on June 18th, 2018). The result of Fourier spectrum analysis shows that amplification properties of the earthquake ground motion will be affected by the topography, ground structure, and relative position of epicenter.

Keywords: earthquake ground motion, landslide, seismic observation, amplification property, Totsukawa-village, Nara pref.

©2019. Japan Geoscience Union. All Right Reserved.

Study on topographic features and landslide development process in slope failure by Typhoon Talas

*Teruyuki Kikuchi[1], Teruyoshi Hatano[2], Satoshi Nishiyama[3]

1. JP-Design Co., Ltd., 2. Electric Power Development Co.,Ltd., 3. Okayama University Graduate School of Environmental and Life Science

1. Introduction

We have not established a prediction of landslide. The cause of this landslide is complicatedly related to the predisposition.In order to clarify the process leading to the slope failure, accumulation and analysis of cases and long-term observation and evaluation are necessary.The microtopography before disaster occurrence can clarify the process of collapse occurrence.Therefore, we tried to examine the topographic features and the landslide development process of the place where the collapse occurred, by micro-topography interpretation on the location of the slope failure occurrence site.

2. Location

Typhoon Talus crossing western Japan from 2 September to 5 September 2011 brought rain close to 2000 mm to the Kii mountain range, causing more than 50 deep-seated landslides. The scope covered by this research is the upper Totsu-gawa. In this basin, the LiDAR-data before and after the disaster is being carried out by the Kinki Regional Development Bureau, Ministry of Land, Infrastructure and Transport. Particularly in areas where many collapses occurred, the accumulated rainfall exceeded 600 mm. In addition, it corresponds to the distribution area of the Shimanto belt in the upper reaches of the Totsu-gawa, and the north to northwest slope is the dip slope.

3. Method

The verification, 38 places with a collapse area of 1,000 m^2 or more that collapsed due to the Talus. We tried micro topography interpretation of the aerial laser topographic map before the collapse. The authors chose main scarp, flank, and knickpoint, which are topographies showing the gravitational deformation of the mountain body as the topography of micro topography interpretation. In addition, as the characteristic topography recognized in the deep layer collapse in the Kii mountain range, the terminal cliff and the gravitationaldeformation appeared surface in which the back slope and the moving rock body are not completely separated are targeted. In addition, the gully was the topography showing the influence of surface water and groundwater. These micro topographies were classified into three types of "nothing", "unclear" and "clear". Next, as an index showing the developmental state of the collapsed terrain, we consider it in relation with the landslide topography development process.

4. Result

As a result of micro-topography interpretation in Table 1, seven places with the topographical features total as 1 to 3 were observed as the first group. For these, the clear of main scarp, flank is not recognized, and the gravitationaldeformation at the top of the slope is the subject. Comparing the collapsed range, the moving body is unclear. This can be classified as the earliest gravity deformation in the landslide topography development process shown in Table 2, which is very close to the initial stage. I concluded

©2019. Japan Geoscience Union. All Right Reserved.

that this is also the stage of the earlier stage in the transitional stage. The topographical features of the second group are total number 3 to 7, including main scarp,flank or include clear topographical features. Since the gravitationaldeformation, knickpoint,terminal cliff is remarkable, it can be considered that gravity deformation is being clarified. The whole contour is partially clear. Although they are transitional stage, they are thought to be close to the main moving stage. It was separated from the late stage of the transitional stage. The third group has a total number of topographical features of 4 to 12, and it is a group including main scarp. Terminal cliff and accompanying knickpoint are also often clear. Gravitationaldeformation and knickpoint are clear in the slope. This is thought to be due to weight deformation progressing, juvenile landslide sliding surface connected and "main moving stage" equivalent.

5. Discussion

According to this study, the appearance of main scarp, gully, flank is uncertain though topographic features in the early and late stages of the transitional stage, but the appearance of gravitationaldeformation and terminal cliff was high probability. In addition, if it is a landslide slide in a narrow sense, it is thought that it undergoes a stepwise development process from the early stage to the late stage of the transitional stage, but in Talus in 2011 it has collapsed even at the earlier stage. The gravitational deformation which is frequently observed at this stage is thought to have appeared on the surface because it corresponds to gravitational rock creep and the structure of the basement rock is sound. Focusing on such gravitationaldeformation, we think that there is a possibility of predicting collapse by understanding the features.

Keywords: slope failure, development of landslide process, microtopography

©2019. Japan Geoscience Union. All Right Reserved.

表-1 崩壊地の解析結果
Table-2 Data used for microtopographic features analysis

No.	面積 (m2)	比高 (m)	最大傾斜方向	崩壊範囲内の平均傾斜 (°)	地形的特徴 [0 無 ,1 有(不明瞭), 2 有(明瞭)] 滑落崖	側方崖	小崖	末端崩壊	ガリー	不規則凹凸	合計	地質 (*1)	地すべり地形発達過程
1	7,500	112	NNE	36.5	0	0	0	0	0	1	1	Ob	漸移期[前期]
2	5,100	96	E	37.7	0	0	0	0	0	1	1	My3	〃
3	48,000	56	N	38.3	0	0	0	1	0	1	2	My2	〃
4	28,700	176	WSW	35.3	0	0	0	1	0	1	2	My3	〃
5	26,400	124	SSE	32.8	0	0	0	1	0	1	2	H4	〃
6	6,600	108	NE	37.3	0	0	0	1	0	1	2	My2	〃
7	35,900	176	SW	31.1	0	0	1	0	1	1	3	Yk2	〃
8	29,900	254	NE	38.4	0	0	0	2	0	1	3	My3	漸移期[後期]
9	9,200	128	E	37.3	0	1	1	0	0	1	3	My1	〃
10	9,400	92	SW	38.8	0	1	0	1	0	1	3	My1	〃
11	14,000	114	NW	34.6	1	0	0	1	0	1	3	My3	〃
12	4,500	94	NNE	33.7	1	0	1	1	0	1	4	My4	〃
13	20,600	154	N	35.3	1	0	0	2	0	1	4	My3	〃
14	8,500	165	NW	39.8	0	1	0	1	1	1	4	Ry	〃
15	42,100	174	N	32.6	0	0	1	1	1	1	4	H4	〃
16	48,100	308	NW	38.5	0	0	0	2	1	1	4	My2	〃
17	5,044	103	W	39.8	0	0	0	1	2	1	4	Yk3	〃
18	14,300	154	NNW	38.2	1	0	1	1	1	1	5	My4	〃
19	34,100	234	NE	38.3	1	1	0	1	1	1	5	Ry	〃
20	13,500	136	ENE	39.6	1	1	1	0	1	1	5	Yk2	〃
21	7,400	64	W	41.8	1	1	0	2	1	1	6	My3	〃
22	14,700	126	NNW	37.8	0	2	1	2	2	0	7	My3	〃
23	42,300	218	WSW	38.8	1	1	1	2	1	1	7	My3	〃
24	5,100	158	NW	40.9	0	1	2	2	1	1	7	My3	〃
25	48,000	226	WSW	30.0	0	1	0	2	2	2	7	My2	〃
26	18,200	134	NNW	38.1	2	1	0	1	0	1	5	gc	滑動期
27	1,400	32	NE	39.9	0	2	0	2	1	0	5	My2	〃
28	51,700	227	NNW	32.2	1	0	1	2	0	2	6	Ry	〃
29	22,500	92	NNW	36.8	0	1	1	2	0	2	6	Ry	〃
30	77,200	124	ESE	29.6	0	0	2	2	1	1	6	H4	〃
31	38,600	120	NNW	35.1	2	0	1	1	1	1	6	H4	〃
32	59,000	254	ENE	37.3	1	1	1	1	1	1	6	My1	〃
33	86,300	396	NNE	42.1	1	1	0	2	2	1	7	My4	〃
34	10,300	144	SW	41.3	0	2	0	2	2	1	7	My2	〃
35	254,900	592	NW	38.3	2	1	1	1	1	2	8	My2	〃
36	19,200	120	NNE	34.2	0	2	0	2	2	2	8	My3	〃
37	182,700	400	NW	39.0	2	1	1	2	1	2	9	My2	〃
38	195,100	446	NNW	36.2	2	1	2	2	2	2	11	My2	〃

*1) 地質
Ry: 竜神層, H1～4: 花園層(ユニット1～4), gc 花園層緑色岩チャート, My1～4: 美山層(ユニット1～4)

表-2 崩壊事例の地すべり地形発達過程における検討結果
Conceptual map of Landslide developing history of slopes at micro-topography interpretation

先行研究		本研究							
大八木[4]		新区分	地形的特徴の傾向	合計点数と箇所数	上段:具体的な事例(それぞれ5箇所) ／下段:通しNo.と地形的特徴合計点 [先滑動期と後滑動期には崩壊事例がない]				
先滑動期	対象斜面に地すべりによる変形や運動が全体のみならず部分にも発生していない期間。地質時代に形成された地質構造が地表環境下の諸営力によって変化する。特定の構造や地層が地すべり構造の基本的な要素に移化する。	先滑動期	本研究では事例はないが、重力変形が生じる前段階の組織地形から生じる小崖地形が断続的に分布する これ以外の地形変状は認められない.	地形的特徴は認められない	–	–	–	–	–
漸移期	対象斜面の一部に小さい変形が生じているが、変動部分全体がまだ基岩から分離していない。全体の輪郭となる構造がまだ形成されていない	漸移期[前期]	初期的な重力変形によって生じる不規則凹凸、末端崩壊が主体. 滑落崖・側方崖が認められない. また明瞭な地形的特徴が認められない 特定の外的要因によって急激に不安定化する全体の輪郭は不明瞭	合計数:1～3 箇所数:7	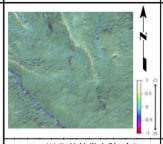 No.2(地形的特徴合計1点)	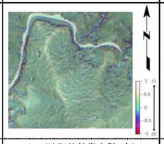 No.3(地形的特徴合計2点)	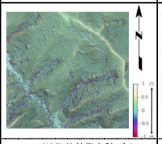 No.4(地形的特徴合計2点)	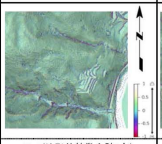 No.5(地形的特徴合計2点)	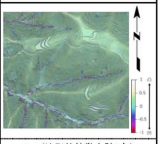 No.7(地形的特徴合計3点)
		漸移期[後期]	重力変形が明瞭化. 不規則凹凸・小崖地形・末端崩壊が顕著. 滑落崖・側方崖を含むか、明瞭な地形的特徴を含む. 全体の輪郭は部分的に明瞭	合計数:3～7 箇所数:17	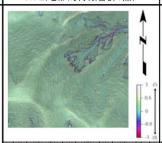 No.8(地形的特徴合計3点)	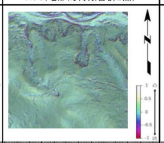 No.13(地形的特徴合計4点)	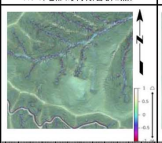 No.15(地形的特徴合計4点)	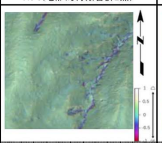 No.20(地形的特徴合計5点)	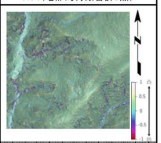 No.23(地形的特徴合計7点)
滑動期	対象斜面の変動域構成体とその下位の非変動域構成体とを限る輪郭構造が形成されて変動域構成体は非変動域から独立して運動しているか、運動できる状態になっている。活層、休止、再活動、移行拡大に細分も可能	滑動期	滑落崖、側方崖は明瞭. 移動体の輪郭は明瞭. 移動体内のガリー地形の進行が顕著 末端崩壊やこれに伴う小崖地形も明瞭なことが多い. 斜面内に不規則凹凸や小崖が明瞭となる	合計数:4～12 箇所数:13	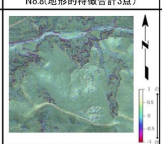 No.26(地形的特徴合計6点)	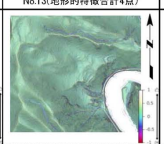 No.30(地形的特徴合計6点)	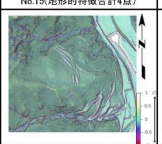 No.32(地形的特徴合計6点)	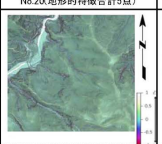 No.35(地形的特徴合計8点)	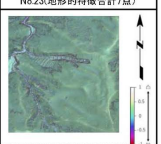 No.37(地形的特徴合計9点)
後滑動期	対象斜面における地すべり移動体が運動を完全に停止し、移動体の移動・活動中に形成された構造が運動を停止(休積)下状態において削剥される状態	後滑動期	滑落崖を含むが、一部消失している場合もある. エッジが消失することがある. 移動体の輪郭は明瞭. 移動体内のガリー地形の進行が顕著 移動体内の不規則凹凸やは拡大しないため不明瞭化する. 削剥が進行するため、末端崩壊は明瞭なことがある.	–	–	–	–	–	–

©2019. Japan Geoscience Union. All Right Reserved.

Formation mechanism of bulge of slope that is sign of large-scale collapse

*tatsurou yoshimura[1]

1. Daiichi Fukken Co., Ltd.

The fracture is distributed around main scarp and side cliff in slope failure. The formation of landslide mass results from dividing into parts by fracture. "Landslide mass formation model by dividing into fracture" was verified in large-scale landslide. The thick debris is distributed in the center part of the landslide mass. Bulge of slope is admitted before collapses. Bulge of slope is caused by seismic motion and the thick debris.

Keywords: large-scale collapse, bulge of slope, seismic motion, relief inversion, gamma-ray survey

©2019. Japan Geoscience Union. All Right Reserved.

Sediments accumulated in the linear depressions in the Mitsumine area, Kanto Mountains

*Masakazu Mashiko[1], Masahiro Chigira[2]

1. Graduate School of Science, kyoto University, 2. Disaster Prevention Research Institute, Kyoto University

Many problems about the mechanisms of an occurrence or a development of deep-seated gravitational slope deformations (DGSDs) are left behind. We are now researching in the Mitsumine area, Kanto Mountains, where is occupied by the Shimanto accretionary complex, in other to resolve the problems about the mechanisms of DGSDs. As a part of the research, simplified boring are executed in linear depressions near a ridge and boring cores composed by accumulated sediments are acquired.

Boring are operated in two different linear depressions and cores have reached the bedrock at the depth of 6.75 m to 6.95 m. Both cores have almost same characteristics; from the surface to the depth of 1.0 m, these are blackish brown humified soil or clay, and other parts deeper than 1.0 m are occupied by brown clay.
The date when the linear depressions or DGSDs on the hillslope emergenced will be estimated by specifying the tephras included in the boring cores. We have observed the ratio of volcanic glasses in the cores every 20 cm and have recognized three peaks; the depth of 2.20 m in P1 (upstream side), 2.40 m in P2 (downstream side), and 6.00 m in P2. Other researches performed in the Mitsumine area have revealed that the depositions include several tephras, such as Aira-Tn (AT) tephra (26~29 ka), Ontake-Pumice 1 (On-Pm1) (100 ka), and Yatsugatake-Kawakami (Yt-Kw) tephra (170 ka). It is likely that each volcanic glasses in the boring cores originated in one of these tephras. We are now trying to observate the refractive index of volcanic glasses to identify the tephras in the core completely.

For the explication of the mechanism of DGSDs in this area, it is indispensable to reveal the geomophological and geological characteristics in the area. We carry on not only analysis of the sediments accumulated in the linear depositions but also geological site investigations.

Keywords: Deep-seated gravitational slope deformations, Linear depressions, Sediments, Boring core, Tephra

©2019. Japan Geoscience Union. All Right Reserved.

[E] Oral | H (Human Geosciences)：H-CG Complex & General

Mon. May 27, 2019 1:45 PM - 3:15 PM JST | Mon. May 27, 2019 4:45 AM - 6:15 AM UTC | 301B 3F

[H-CG26] Deltas and estuaries: multidisciplinary analyses of complex river-mouth systems

convener:Yoshiki Saito(Estuary Research Center, Shimane University), Guan-Hong Lee(Inha University), David L Dettman(University of Arizona), Kazuaki Hori(Department of Geography, Graduate School of Environmental Studies, Nagoya University), Chairperson:Yoshiki Saito(Shimane Univ/ GSJ, AIST), David Dettman(University of Arizona)

This session has foci on morphodynamics, material cycling, and sustainability in deltas and estuaries. We invite contributions that advance research on deltas and estuaries as complex river-mouth systems from modern and ancient examples, and that develop integrated frameworks for delta & estuary dynamics modeling on a broad range of temporal and spatial scales: from studies of coastal evolution over the Quaternary to small-scale sediment/material transport processes. We also invite physical processes studies based on field observations, numerical simulation and flume experiments. Finally, the conveners encourage contributions that promote data collection and sharing for both advancing science and local problem solving, that consider policy and governance issues linked to the sustainable development of deltas and estuaries, and that use in-situ and satellite data for modeling and risk assessment.

1:45 PM - 2:15 PM JST | 4:45 AM - 5:15 AM UTC

[HCG26-01] Recent Changes of the Asian Major Deltas

★Invited Papers

*Paul Liu[1] (1.North Carolina State University Raleigh)

2:15 PM - 2:30 PM JST | 5:15 AM - 5:30 AM UTC

[HCG26-02] **Matching trends in channel width, sinuosity, and depth along the fluvial to marine transition zone of tide-dominated river deltas: the need for a revision of depositional and hydraulic models**

★Invited Papers

*Marcello Gugliotta[1], Yoshiki Saito[1] (1.Shimane University)

2:30 PM - 2:45 PM JST | 5:30 AM - 5:45 AM UTC

[HCG26-03] **Effects of an Estuarine Dam on Sediment Flux Mechanisms in a Macrotidal Estuary**

Steven Miguel Figueroa[1], *Guan-Hong Lee[1] (1.Inha University)

2:45 PM - 3:00 PM JST | 5:45 AM - 6:00 AM UTC

[HCG26-04] **Late Pleistocene sedimentary evolution of the north Jiangsu coastal plain revealed by OSL dating based chronostratigraphy**

*Lei Gao[1], Hao Long[1], Ping Zhang[2], Toru Tamura[3,4], Ji Shen[1] (1.Nanjing Institute of Geography and Limnology, CAS,China, 2.Geological Survey of Jiangsu Province (GSJP), Key Lab of EFGD, Ministry of LR, China, 3.Geological Survey of Japan (GSJ), AIST, 4.Graduate School of Frontier Sciences, The University of Tokyo)

3:00 PM - 3:15 PM JST | 6:00 AM - 6:15 AM UTC

[HCG26-05] The sedimentary environments and provenance of the late Quaternary sediments, in South Yellow Sea shelf, eastern China

*Yong Yin[1] (1.School of Geography and Ocean Science, Nanjing University)

Recent Changes of the Asian Major Deltas

*Paul Liu[1]

1. North Carolina State University Raleigh

In the past 50 years, sediments from major Asian rivers have sharply decreased 80-90% due to the increased human activities (like building dams, overusing water, or sand mining) and climatic changes. Many of those river deltas have been experiencing severe coastal erosions, like the Yellow, Red, Mekong, Chao Phraya, and Indus, etc. Most of these deltas have turned from constructive growing mode to destructive declining mode, for example, the Mekong Delta has shown overall negative net land gain starting ~ 2005. Our studies also show not only the deltaic shorelines are retreating, but also some delta’s subaqueous portions are under strong erosion, such as the Yangtze, Mekong, Chao Phraya and Indus, etc.

Keywords: river delta , sediment decrease , shoreline erosion , subsidence

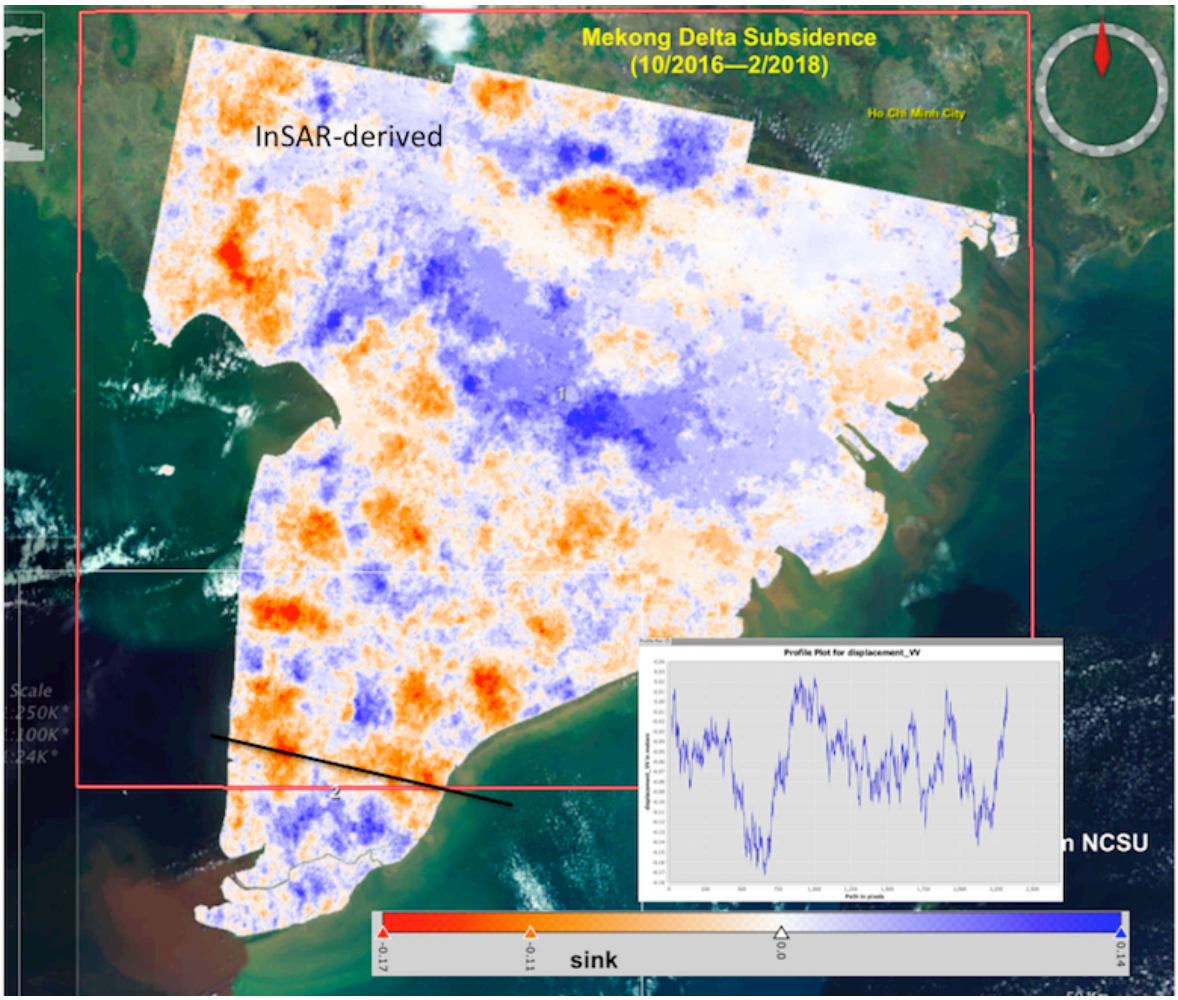

©2019. Japan Geoscience Union. All Right Reserved.

Matching trends in channel width, sinuosity, and depth along the fluvial to marine transition zone of tide-dominated river deltas: the need for a revision of depositional and hydraulic models

*Marcello Gugliotta[1], Yoshiki Saito[1]

1. Shimane University

Along their fluvial to marine transition zone, tide-dominated river deltas show upstream to downstream trends in channel width, sinuosity, and depth, which at present have been only partially reported. This review article aims to describe these morphological trends from five modern tide-dominated river deltas using original data collected from satellite images and bathymetric maps and published data from field surveys. All the studied channels show similar trends with two distinct tracts separated by areas of morphological changes. The upstream tracts are characterized by constant width, relatively high sinuosity, and seaward-increasing depth, and are mainly controlled by the fluvial dynamics. The downstream tracts are characterized by seaward-increasing width, relatively low sinuosity, and seaward-decreasing depth, and are mainly controlled by the tidal dynamics. The delineation of this morphological configuration of the channels is crucial to understand the responses of deltas to the interacting riverine and marine processes. Additionally, this has important implications for depositional and hydraulic models, and for the long-term evolution and the assessment of human-induced versus natural modifications of these systems.

©2019. Japan Geoscience Union. All Right Reserved.

Effects of an Estuarine Dam on Sediment Flux Mechanisms in a Macrotidal Estuary

Steven Miguel Figueroa[1], *Guan-Hong Lee[1]

1. Inha University

Sediment flux convergence traps sediment in many estuaries of the world coast. This sediment flux can be decomposed into a mean-flow flux and correlation flux to better understand the mechanisms driving the sediment trapping in estuaries. Humans have modified and are modifying many natural estuarine systems, however it isn’ t well understood what affects humans can have on sediment flux mechanisms and flux convergence in altered estuaries. Geum Estuary is a shallow, macrotidal estuary on the eastern Yellow Sea which has experienced tidal amplification and enhanced depositional rates following the operation of an estuarine dam since 1994. Geum Estuary thus serves as a good case for studying decomposed sediment fluxes for a shallow, macrotidal estuary affected by an estuarine dam. To quantify the sediment fluxes, we measured current and acoustic backscatter profiles at 1.5 km and 6.5 km seaward of the estuarine dam in Geum Estuary, over a period of two neap-spring cycles during which six episodic dam discharges occurred. Suspended sediment concentration (SSC) was estimated from acoustic backscatter and sediment flux was computed as the product of current velocity and SSC. The flux was decomposed into a mean-flow flux and correlation flux using 36-hr Lanczos filters. Additionally, ship-borne surveys were conducted at the two stations seaward of the estuarine dam to investigate more closely the role of dam-induced horizontal salinity gradient and vertical stratification on sediment resuspension and flocculation tidal asymmetries. Results indicated landward flux at both moorings with a negative flux gradient indicating deposition. Landward directed correlation flux was the dominant term. Its magnitude was proportional to the tidal range and tidal asymmetry and was found to occur in the bottom boundary layer. Seaward directed mean-flow fluxes were caused by the episodic dam discharges. Their magnitude was proportional to the discharge volume and was greatest in the surface layer of the water column. At the seaward station, periodic stratification occurred following the dam discharge and resulted in tidal asymmetries in resuspension and flocculation providing evidence for landward flux due to tidal straining. Overall the data confirms that the estuarine dam controls the seaward mean-flow fluxes, and these fluxes are smaller when the dam is closed. Furthermore, the proportionality of the correlation flux with tidal range provides supports that the dam enhanced the landward correlation fluxes because of the tidal amplification effect. Finally, the tidal straining effect was confirmed to occur in a macrotidal estuary with an estuarine dam.

Keywords: estuary, sediment flux, tidal straining, dam discharge, anthropocene

©2019. Japan Geoscience Union. All Right Reserved.

Late Pleistocene sedimentary evolution of the north Jiangsu coastal plain revealed by OSL dating based chronostratigraphy

*Lei Gao[1], Hao Long[1], Ping Zhang[2], Toru Tamura[3,4], Ji Shen[1]

1. Nanjing Institute of Geography and Limnology, CAS,China, 2. Geological Survey of Jiangsu Province (GSJP), Key Lab of EFGD, Ministry of LR, China, 3. Geological Survey of Japan (GSJ), AIST, 4. Graduate School of Frontier Sciences, The University of Tokyo

In the past decades, many Chinese geoscientists carried out numerous research works to investigate the sedimentary history of the Jiangsu coastal plain. However, we still have limited understanding of history prior to the Holocene because of the lack of reliable chronology. In this study, we applied quartz optically stimulated luminescence dating (OSL) techniques to determine the ages of 11 sediment samples from a 30-m-long core (EGWY02) drilled from the north Jiangsu coastal plain. The sedimentary facies of the core were identified based on observation, grain-size analysis, colors and textures of sediments. The stratigraphy of the core was then correlated to three cores collected in the adjacent area (Zhang et al., 2010; Xia and Zhang, 2018). In our core, we identified two marine transgressive events T1 and T2 at intervals of 3-5 and 21-27 m deep, respectively. The timing of T1 and T2 were dated as 7.1±0.9 ka and > 77±6 ka, respectively. The interval of T1 is overlain by a littoral sedimentary facies deposited over the last 2 ka. Three layers of “stiff clay” (SC) were identified at depths of 1-2, 8-12 and 27-30 m and are interpreted terrestrial deposits. The first SC layer was dated about 1.8±0.1 ka while the second layer was between 44±3 ka and 72±6 ka. In addition, we recognized fluvial deposits at interval of 12-21 m deep, which was dated from 72 to 77 ka. A lacustrine layer was also identified at 5-8 m deep and dated as 41-44 ka. Our OSL dating application to the core EGWY02 thus clarified that the sedimentary succession represents two transgressive episodes in relation to the last interglacial (MIS 5) and post glacial periods (MIS 1), intervened by the terrestrial environments related to the MIS 4-2. Further application of the OSL dating to the subsurface sediment cores will unveil the pre-Holocene environmental changes in the Jiangsu coastal plain, which was possibly affected by the paleo-Yangtze River.

Keywords: OSL dating, Chronostratigraphy, The north Jiangsu coastal plain , Sedimentary evolution, Late Pleistocene

©2019. Japan Geoscience Union. All Right Reserved.

The sedimentary environments and provenance of the late Quaternary sediments, in South Yellow Sea shelf, eastern China

*Yong Yin[1]

1. School of Geography and Ocean Science, Nanjing University

The late Quaternary sedimentary systems are mainly controlled by sea-level changes, sediment supply and regional subsidence. The late Quaternary source materials of South Yellow Sea shelf were controlled by Yellow and Yangtze rivers. So sediment provenance is very important not only for “source to sink (S2S)” processes but also for land-sea interaction.

The South Yellow Sea is a semi-enclosed epicontinental sea between China to the west and Korea Peninsula to the east. Since the late Quaternary, the South Yellow Sea has experienced several eustatic sea-level changes and sediment supplies alternatively from old Yellow and Yangtze Rivers. Previous work did not documented the late Quaternary environments and sediment provenance in this region. Several boreholes are used: 1) to synthesize the long term sedimentary environments since the late Quaternary; 2) to discriminate the source materials and appraise the contribution of Yellow and Yangtze rivers; 3) to evaluate the driving forces controlling the formation of South Yellow Sea shelf.

The sedimentary facies analysis indicates the South Yellow Sea shelf experienced fluvial and tidal influenced fluvial environments during MIS6. Then the fluvial environment was replaced by tidal flat, estuary and delta front environments during the transgression taking place in MIS5. Delta front environments dominated the South Yellow Sea shelf during the transgression occurred in MIS3. During MIS2, the shelf was cut by network of valleys and filled with coarse materials within the fluvial channels and fine materials beyond the channels. During the Holocene, transgression environment developed in early period followed by tidal dominated coast to shelf environments in late period in South Yellow Sea shelf and estuary to delta environments in Yangtze River mouth area.

Detrital zircon U-Pb ages were employed to analyze the provenance of source materials. By comparison of Yangtze and Yellow rivers U-Pb age spectrum, the Yangtze River is characterized by 100~300Ma and 700~900Ma zircons and Yellow River is dominated by 300~500Ma and 1800~2000Ma zircons. The zircons younger than 150Ma merely found in Yangtze affiliated sediments and the zircons between 1300 and 1600 Ma only found in Yellow River affiliated sediments. For zircons between 1800 and 2000Ma and between 2200 and 2500Ma, the particles from Yellow River are more than those from Yangtze River. The results indicate the late Quaternary sediments are mostly from the old Yangtze River and occasionally influenced by Yellow River, e.g. during some periods in MIS6 and MIS2 and Holocene.

The core-recorded strata have revealed the study area experienced the similar estuary to delta processes in MIS 5 as the Yangtze delta in the Holocene. The deltaic successions dominate the South Yellow Sea shelf during the MIS 5 and MIS 3. The source province indicates the old Yangtze attributed a lot to delta sediments. Sea-level cycles and source material supplies play an important role in the late Quaternary coast and shelf successions.

Keywords: sedimentary environment , source provenance, deltaic successions, zircon U-Pb ages

©2019. Japan Geoscience Union. All Right Reserved.

[E] Poster | H (Human Geosciences)：H-CG Complex & General

Mon. May 27, 2019 3:30 PM - 5:00 PM JST | Mon. May 27, 2019 6:30 AM - 8:00 AM UTC | Poster Hall International Exhibition Hall8, Makuhari Messe_9

[H-CG26] Deltas and estuaries: multidisciplinary analyses of complex river-mouth systems

convener:Yoshiki Saito(Estuary Research Center, Shimane University), Guan-Hong Lee(Inha University), David L Dettman(University of Arizona), Kazuaki Hori(Department of Geography, Graduate School of Environmental Studies, Nagoya University)

This session has foci on morphodynamics, material cycling, and sustainability in deltas and estuaries. We invite contributions that advance research on deltas and estuaries as complex river-mouth systems from modern and ancient examples, and that develop integrated frameworks for delta & estuary dynamics modeling on a broad range of temporal and spatial scales: from studies of coastal evolution over the Quaternary to small-scale sediment/material transport processes. We also invite physical processes studies based on field observations, numerical simulation and flume experiments. Finally, the conveners encourage contributions that promote data collection and sharing for both advancing science and local problem solving, that consider policy and governance issues linked to the sustainable development of deltas and estuaries, and that use in-situ and satellite data for modeling and risk assessment.

[HCG26-P01] Deltafront Clinoform of Abandoned Yellow River Delta in Jiangsu Province, China

*LIANGYONG ZHOU[1] (1.Qingdao Institute of Marine Geology China Geological Survey)

[HCG26-P02] Holocene evolution and Anthropocene destruction of the Krishna delta, east coast of India: delta lobe shifts, human impact, and sea-level history

Kakani Nageswara Rao[2], *Yoshiki Saito[1], K.Ch.V. Nagakumar[4], Sumiko Kubo[3], Shilpa Pandey[5], Zhen Li[6], G. Demudu[2], A.S. Rajawat[7] (1.Estuary Research Center, Shimane University, 2.Andhra University, 3.Waseda University, 4.Centre for Water Resources and Management, 5.Birbal Sahni Institute of Palaeosciences, 6.University of Victoria, 7.Space Applications Centre)

[HCG26-P03] Offset in radiocarbon ages between marine bioclast and terrestrial plant pairs in the Holocene sediments around Japan

*Nakanishi Toshimichi[1,2], Futoshi Nanayama[3,4], Atsushi Urabe[5], Kazuaki Hori[6], Wan Hong[7] (1.Kyoto Univ., 2.JAEA, 3.AIST, 4.Kumamoto Univ., 5.Niigata Univ., 6.Nagoya Univ., 7.KIGAM)

[HCG26-P04] Assessment of MEIS for Marine Spatial Planning in the Nakdong River Estuary, Busan Metropolitan City, South Korea

*Jun-Ho Lee[1], Han Jun Woo[1], Hoi-Soo Jung[1], Chan Mi Park[1] (1.Korea Institute of Ocean Science and Technology)

[HCG26-P05] Tidal changes at Asian deltas in response to future sea-level rise

*Katsuto Uehara[1] (1.Kyushu University)

[HCG26-P06] **A governing equation of non-deltaic transgressive profile: 2D numerical simulation and flume experiments**

*Junhui Wang[1,2,3], Tetsuji Muto[3] (1.China University of Petroleum (Beijing), 2.State Key Laboratory of Petroleum Resources and Prospecting, China, 3.Nagasaki University)

Deltafront Clinoform of Abandoned Yellow River Delta in Jiangsu Province, China

*LIANGYONG ZHOU[1]

1. Qingdao Institute of Marine Geology China Geological Survey

The abandoned Yellow River delta in Jiangsu province is a major sediment supplier to the South Yellow Sea and East China Sea. In this study, comparison of historical maps, two cores and three seismic profiles were used to examine its deltafront clinoform (nearshore clinoform). The original historical maps and nautical charts since AD 1750s were collected and compared after calibration, showing the accretion of the shoreline before 1855, when the Yellow River shifted to the Bohai Sea. Near Sheyang River mouth, two 20m-long cores onshore (1 m above present sea level) and offshore (6 m bellow present sea level) were on a line normal to the shoreline. Samples og both cores were dated using AMS ^{14}C and OSL(Optical Stimulated Luminescence) dating technologies. Ages in bottoms of the cores are 43000 to 44000 cal yr BP. At approximate 17.5m bellow present sea level in both cores, yellow and younger (younger than 5000 yr BP) silt sediment occurs. Several young ages in upper part of two cores were obtained, and these show a clear clinoform pattern. Furthermore, seismic profiles across the offshore core show the deltafront clinoform. The upper part weak reflector or transparent part in seismic profiles become thinner seaward and the lower part is strong reflectors. Sea bottom nearshore show a convex shape, but the seaward low gradient part show erosional gullies. The evolution of the deltafront clinoform was revealed in profiles and in plan view.

Keywords: Abandoned Yellow River Delta, Deltafront clinoform, C-14 ages, OSL ages

©2019. Japan Geoscience Union. All Right Reserved.

Holocene evolution and Anthropocene destruction of the Krishna delta, east coast of India: delta lobe shifts, human impact, and sea-level history

Kakani Nageswara Rao[2], *Yoshiki Saito[1], K.Ch.V. Nagakumar[4], Sumiko Kubo[3], Shilpa Pandey[5], Zhen Li[6], G. Demudu[2], A.S. Rajawat[7]

1. Estuary Research Center, Shimane University, 2. Andhra University, 3. Waseda University, 4. Centre for Water Resources and Management, 5. Birbal Sahni Institute of Palaeosciences, 6. University of Victoria, 7. Space Applications Centre

Holocene evolution of the Krishna delta was inferred using landform characteristics and 11 sediment cores with 59 Accelerator Mass Spectrometry ^{14}C dates. Landform assemblage in 5880 km^2area of the Krishna delta indicated the upper river-built fluvial plain and the lower marine-built beach-ridge delta plain with the maximum landwardbeach ridge located at˜30 km from the shoreline separating the two plains. Sedimentary facies and their ages showed the Holocene marine sediment overlying the Pleistocene basement and progressively thickened seaward from <10 m to 25 m below the present sea level. The basal mangrove peat layers indicated that the sea level rose from −9 m to −3 m during 8.3–6.3 cal ky BP before stabilizing at the present level around 5 cal ky BP.
Considering the spatiotemporal variations of sediment facies and sediment accumulation rates and the configuration of the palaeo beach ridges (former shorelines), we surmised five major stages in the growth of 3539 km^2area of the Krishna delta beach-ridge plain during the last 6 cal ky BP with distinct lateral and seaward migration of delta lobes (depocentre shifts). Delta progradation was accelerated in the last 500 years, forming an out-building lobate delta. However, predominant erosion along the sediment-starved Krishna delta front coast during the past 50 years, due to impoundment of the riverine inputs at the burgeoning upstream dams pushed the Krishna delta into a persistent a destruction phase after ˜6,000 years of delta progradation.

Keywords: Beach-ridge plain, Sedimentary facies, Delta lobes, Coastal erosion

©2019. Japan Geoscience Union. All Right Reserved.

Offset in radiocarbon ages between marine bioclast and terrestrial plant pairs in the Holocene sediments around Japan

*Nakanishi Toshimichi[1,2], Futoshi Nanayama[3,4], Atsushi Urabe[5], Kazuaki Hori[6], Wan Hong[7]

1. Kyoto Univ., 2. JAEA, 3. AIST, 4. Kumamoto Univ., 5. Niigata Univ., 6. Nagoya Univ., 7. KIGAM

To identify chronological and spatial changes in the radiocarbon (^{14}C) marine reservoir effects, the ^{14}C ages of eight pairs of marine bioclasts and terrestrial plants were measured from the same horizons of one core of Holocene sediments around Japan (Nakanishi et al. 2013, 2015, 2017abc). The reservoir ages ranged from 60 to 1100 years, scattered over the period 100-10,200 cal BP, which were significantly larger than the values from “prebomb” samples of known age, before AD 1955 in this area. These results indicate that the information on reservoir effects is indispensable for chronological control not only from prebomb samples but also from geological and archaeological samples. Moreover, the effects also reflects the influence of complex river-mouth systems such as deltas and estuaries. To determine the direct chronological changes of the marine reservoir effect between the Kuroshio and Tsushima Currents, radiocarbon ages from pairs of marine bioclasts and terrestrial plants were measured from the same stratigraphic horizons within three cores of Holocene sediments beneath the Sukumo Plain, Miyazaki Plain, and Oki Islands, in west Japan. Subsequently, the results were compared with values from the Oita Plain and Hakata Bay on the northern coast of Kyushu (Nakanishi et al. 2017ac), as well as the Korean Peninsula (Nakanishi et al. 2013, 2015, 2017b). The study was partially funded by the Japan Society for the Promotion of Science Kakenhi grant number 18H01310.

References

Nakanishi T, Hong W, Sung KS, Lim J. 2013. Radiocarbon reservoir effect from shell and plant pair in Holocene sediments around the Yeongsan River in Korea. *Nuclear Instruments and Methods in Physics Research B* 294: 444–51.

Nakanishi T, Hong W, Sung KS, Sung KH, Nakashima R. 2015. Offsets in radiocarbon ages between plants and shells from same horizons of coastal sediments in Korea. *Nuclear Instruments and Methods in Physics Research B* 361: 670–9.

Nakanishi T, Hong W, Shimoyama S, Sato S, Park G, Lee JG. 2017a. Radiocarbon age offset between shell and plant pairs in the Holocene sediments under the Hakata Bay, western Japan. *Radiocarbon* 59 (2): 423–34.

Nakanishi T, Hong W, Sung KS, Nakashima R, Nahm WH, Lim J, Katsuki K. 2017b. Offset in radiocarbon age between plant and shell pairs in Holocene sediment around the Mae-ho Lagoon on the eastern coast of Korea. *Quaternary International* 447: 3–12.

Nakanishi T, Takemura K, Matsuyama H, Shimoyama S, Hong W, Okuno M. 2017c. Activity of the Funai fault and radiocarbon age offsets of shell and plant pairs from the latest Pleistocene to Holocene sediments beneath the Oita Plain, western Japan. *Radiocarbon* 59(6): 1737–48.

Keywords: Radiocarbon age, Marine reservoir effect, Holocene, Kuroshio Current

©2019. Japan Geoscience Union. All Right Reserved.

Assessment of MEIS for Marine Spatial Planning in the Nakdong River Estuary, Busan Metropolitan City, South Korea

*Jun-Ho Lee[1], Han Jun Woo[1], Hoi-Soo Jung[1], Chan Mi Park[1]

1. Korea Institute of Ocean Science and Technology

The Nakdong River has a length of nearly 510 km, with a drainage basin of around 23,400 km^2 in South Korea. The Nakdong River Estuary (NRE) in Busan city is a typical example of an estuary in which the throughput is manipulated artificially. The Noksan barrage, built in 1934, blocks the flow of the West Nakdong River, and the NRE barrage was completed between 1983 and 1987 to regulate the flow of the East Nakdong River. With the construction of several huge industrial complexes on reclaimed land near the NRE barrage in the last 65 years, the hydraulic circulation in the NRE has undergone dramatic changes in river discharge and geomorphic configuration, such as the formation of a series of barrier islands. In this study, marine environmental information system (MEIS) data collected after May 2015 were applied to support marine spatial planning (MSP) in the brackish water zone of NRE. The MEIS data in NRE consists of landscape classification of sub-environments, surface sediment distributions, characteristics of suspended sediment, short-term sedimentation, stratification index analysis in channels, closed circuit television (CCTV) using 4G long term evolution (LTE), automatic weather stations (AWS) in real time, calculated residual flow (R_f), net suspended sediment loads (Q_S), and net suspended sediment flux (F_S) in main stream inlet using mooring station, *etc*. The NRE could be divided into areas continuously managed by government, marine protected areas, areas for the development of marine attractions, areas conserved for research education, and coastal areas subject to safety management, e*tc*. For MSP, it was possible to use comparative data of the characteristics of environmental changes in the estuarine watershed to prepare the NRE for the partial opening or drainage extension in 2019 to 2021. This study aims to discuss how to predict environmental change after partial or full opening in NRE barrage and use ecological-based environmental maps in the process of MSP. The development of marine spatial planning mapping in NRE is much necessary for the nation at a time when the diversity of marine use and the demand for policies regarding marine space rapidly increase.

Keywords: Barrage, Busan, Estuary, Marine Environmental Information System, Marine Spatial Planning, Nakdong River Estuary

©2019. Japan Geoscience Union. All Right Reserved.

Assessment of MEIS for Marine Spatial Planning in the Nakdong River Estuary, Busan Metropolitan City, South Korea

Jun-Ho Lee[1] · Han Jun Woo[1] · Hoi-Soo Jung[1] · Chan Mi Park[1]

[1]Korean Seas Geosystem Research Unit, Korea Institute of Ocean Science & Technology, 385 Yeongdo, Busan 49111, Republic of Korea

The Nakdong River has a length of nearly 510 km, with a drainage basin of around 23,400 km^2 in South Korea. The Nakdong River Estuary (NRE) in Busan city is a typical example of an estuary in which the throughput is manipulated artificially. The Noksan barrage, built in 1934, blocks the flow of the West Nakdong River, and the NRE barrage was completed between 1983 and 1987 to regulate the flow of the East Nakdong River. With the construction of several huge industrial complexes on reclaimed land near the NRE barrage in the last 65 years, the hydraulic circulation in the NRE has undergone dramatic changes in river discharge and geomorphic configuration, such as the formation of a series of barrier islands. In this study, marine environmental information system (MEIS) data collected after May 2015 were applied to support marine spatial planning (MSP) in the brackish water zone of NRE. The MEIS data in NRE consists of landscape classification of sub-environments, surface sediment distributions, characteristics of suspended sediment, short-term sedimentation, stratification index analysis in channels, closed circuit television (CCTV) using 4G long term evolution (LTE), automatic weather stations (AWS) in real time, calculated residual flow (R_f), net suspended sediment loads (Q_S), and net suspended sediment flux (F_S) in main stream inlet using mooring station, *etc*. The NRE could be divided into areas continuously managed by government, marine protected areas, areas for the development of marine attractions, areas conserved for research education, and coastal areas subject to safety management, *etc*. For MSP, it was possible to use comparative data of the characteristics of environmental changes in the estuarine watershed to prepare the NRE for the partial opening or drainage extension in 2019 to 2021. This study aims to discuss how to predict environmental change after partial or full opening in NRE barrage and use ecological-based environmental maps in the process of MSP. The development of marine spatial planning mapping in NRE is much necessary for the nation at a time when the diversity of marine use and the demand for policies regarding marine space rapidly increase.

©2019. Japan Geoscience Union. All Right Reserved.

Tidal changes at Asian deltas in response to future sea-level rise

*Katsuto Uehara[1]

1. Kyushu University

A numerical model has been employed to assess the impact of sea level rise on tidal regimes in the East China Sea and the South China Sea with a special interest on tidal changes at around the deltaic region where the elevation is low and coasts are vulnerable to changes in water levels. The model covers the East and South China seas as a whole with a spatial resolution of 2 minutes (approx. 3 km). A preliminary result for the East China Sea suggests recognizable changes in the amplitude of M2 tides and M2 tidal currents at region such as Hangzhou Bay, the Changjiang Estuary and Haizhou Bay when the sea-level was raised by 1 m. Off the Changjiang Estuary, for example, tidal velocity increased for more than 10 cm/s at deep channels while decreased by about 5 cm/s on shoals. These results indicate that the sea-level rise may alter equilibrium among water currents and seafloor and modify the bottom topography of large estuaries and subaquatic deltas through the induced changes in tides and tidal currents.

Keywords: tides, china sea, sea level rise

©2019. Japan Geoscience Union. All Right Reserved.

A governing equation of non-deltaic transgressive profile: 2D numerical simulation and flume experiments

*Junhui Wang[1,2,3], Tetsuji Muto[3]

1. China University of Petroleum (Beijing), 2. State Key Laboratory of Petroleum Resources and Prospecting, China, 3. Nagasaki University

An alluvial river subject to relative sea level rise has a critical length (L_{crt}), beyond which the river can no longer sustain deltaic sedimentation but behaves to develop an estuarine environment. In such cases, there occurs non-deltaic rapid transgression. It is not difficult to imagine that non-deltaic transgression is pervasive in geological records, since most of the world large rivers would have “over-extended” to as far as the shelf edges during glacial or lowstand sea level periods. The configuration of non-deltaic transgressive profiles deserves a study because (1) it would provide a criterion for identifying non-deltaic transgression in the past and thus the fact of over-extension of the feeder alluvial river, and (2) it would constrain arguments on sediment transportation to the deep-water depositional systems.

Suppose that a river has an over-extended alluvial length of L ($>>L_{crt}$). During non-deltaic transgression, all the sediment fed by the river is consumed for alluvial aggradation and thus allocated in the subaerial realm. On the assumption that the supplied sediment is evenly distributed along the river profile which is approximately regarded as linear and has an averaged slope of α, the local transgressive slope Ψcan be expressed as:

$$\Psi = \alpha L / [L - \Lambda_{2D}(1+\alpha^2)^{0.5}] \quad (1)$$

We set an x–z coordinate system (x: basinward horizontal, z: vertical) that originates from the intersection of the initial horizontal line and the hinterland profile. Let x to be positive downstream and z to be positive upward. Equation 1 can be rewritten as:

$$\Psi_{x,z} = \alpha(\gamma x+z) / [(\gamma x+z) - \Lambda_{2D}(\gamma - \alpha)] \quad (2)$$

where $\gamma$is the averaged hinterland slope.

Equation 2 can be regarded as the derivative function of the governing equation of the non-deltaic transgressive profile, which can be expressed as:

$$\partial \eta_{x,z} / \partial x = \alpha(\gamma x+z) / [(\gamma x+z) - \Lambda_{2D}(\gamma - \alpha)] \quad (3)$$

where $\eta_{x,z}$ denotes the non-deltaic transgressive profile expressed as the pathway of shoreline. Note that sediment compaction is not considered.

Equation 3 can hardly be solved analytically but by numerical simulation. The solutions that we have obtained indicate that $\eta_{x,z}$ takes a concave-upward geometry with upstream-increasing gradient.

To test our numerical model, a series of 2D physical experiments was performed at Nagasaki University. The experiments were conducted using a 4 m-long and 2.0 cm-wide, open flume, from the upstream end of which sediment and water were fed at constant rates. Before each experimental run, we built a sufficiently long river profile inside the flume, to model the initial over-extended alluvial river ($L >> L_{crt}$). The initial river lengths were different by runs (L_0, ranging from 120–350 cm) and were set to be within a range of 0.139–0.158 (α). The hinterland slope was set as a constant value of 0.612 (γ). In each run, there occurred non-deltaic transgression as soon as base level started to rise.

©2019. Japan Geoscience Union. All Right Reserved.

Any of the resulting profiles of non-deltaic transgression shows a concave-upward geometry. The downstream end of the profile was tangent to the initial river profile (thus $\alpha \sim \Psi$). To the upstream, Ψ gradually increased, and approached a value as large as γ when the alluvial river was sufficiently shortened. The non-deltaic transgressive profiles generated in the experiments match well with the numerical model, implying that equation 3 can account for the non-deltaic transgressive profile in nature.

Keywords: Autostratigraphy, Non-deltaic transgressive profile, Numerical simulation, Flume experiments

©2019. Japan Geoscience Union. All Right Reserved.

[E] Poster | H (Human Geosciences)：H-CG Complex & General

Mon. May 27, 2019 5:15 PM - 6:30 PM JST | Mon. May 27, 2019 8:15 AM - 9:30 AM UTC | Poster Hall International Exhibition Hall8, Makuhari Messe_16

[H-CG26] Deltas and estuaries: multidisciplinary analyses of complex river-mouth systems

convener:Yoshiki Saito(Estuary Research Center, Shimane University), Guan-Hong Lee(Inha University), David L Dettman(University of Arizona), Kazuaki Hori(Department of Geography, Graduate School of Environmental Studies, Nagoya University)

This session has foci on morphodynamics, material cycling, and sustainability in deltas and estuaries. We invite contributions that advance research on deltas and estuaries as complex river-mouth systems from modern and ancient examples, and that develop integrated frameworks for delta & estuary dynamics modeling on a broad range of temporal and spatial scales: from studies of coastal evolution over the Quaternary to small-scale sediment/material transport processes. We also invite physical processes studies based on field observations, numerical simulation and flume experiments. Finally, the conveners encourage contributions that promote data collection and sharing for both advancing science and local problem solving, that consider policy and governance issues linked to the sustainable development of deltas and estuaries, and that use in-situ and satellite data for modeling and risk assessment.

[HCG26-P01] Deltafront Clinoform of Abandoned Yellow River Delta in Jiangsu Province, China

*LIANGYONG ZHOU[1] (1.Qingdao Institute of Marine Geology China Geological Survey)

[HCG26-P02] Holocene evolution and Anthropocene destruction of the Krishna delta, east coast of India: delta lobe shifts, human impact, and sea-level history

Kakani Nageswara Rao[2], *Yoshiki Saito[1], K.Ch.V. Nagakumar[4], Sumiko Kubo[3], Shilpa Pandey[5], Zhen Li[6], G. Demudu[2], A.S. Rajawat[7] (1.Estuary Research Center, Shimane University, 2.Andhra University, 3.Waseda University, 4.Centre for Water Resources and Management, 5.Birbal Sahni Institute of Palaeosciences, 6.University of Victoria, 7.Space Applications Centre)

[HCG26-P03] Offset in radiocarbon ages between marine bioclast and terrestrial plant pairs in the Holocene sediments around Japan

*Nakanishi Toshimichi[1,2], Futoshi Nanayama[3,4], Atsushi Urabe[5], Kazuaki Hori[6], Wan Hong[7] (1.Kyoto Univ., 2.JAEA, 3.AIST, 4.Kumamoto Univ., 5.Niigata Univ., 6.Nagoya Univ., 7.KIGAM)

[HCG26-P04] Assessment of MEIS for Marine Spatial Planning in the Nakdong River Estuary, Busan Metropolitan City, South Korea

*Jun-Ho Lee[1], Han Jun Woo[1], Hoi-Soo Jung[1], Chan Mi Park[1] (1.Korea Institute of Ocean Science and Technology)

[HCG26-P05] Tidal changes at Asian deltas in response to future sea-level rise

*Katsuto Uehara[1] (1.Kyushu University)

[HCG26-P06] **A governing equation of non-deltaic transgressive profile: 2D numerical simulation and flume experiments**

*Junhui Wang[1,2,3], Tetsuji Muto[3] (1.China University of Petroleum (Beijing), 2.State Key Laboratory of Petroleum Resources and Prospecting, China, 3.Nagasaki University)

Deltafront Clinoform of Abandoned Yellow River Delta in Jiangsu Province, China

*LIANGYONG ZHOU[1]

1. Qingdao Institute of Marine Geology China Geological Survey

The abandoned Yellow River delta in Jiangsu province is a major sediment supplier to the South Yellow Sea and East China Sea. In this study, comparison of historical maps, two cores and three seismic profiles were used to examine its deltafront clinoform (nearshore clinoform). The original historical maps and nautical charts since AD 1750s were collected and compared after calibration, showing the accretion of the shoreline before 1855, when the Yellow River shifted to the Bohai Sea. Near Sheyang River mouth, two 20m-long cores onshore (1 m above present sea level) and offshore (6 m bellow present sea level) were on a line normal to the shoreline. Samples og both cores were dated using AMS ^{14}C and OSL(Optical Stimulated Luminescence) dating technologies. Ages in bottoms of the cores are 43000 to 44000 cal yr BP. At approximate 17.5m bellow present sea level in both cores, yellow and younger (younger than 5000 yr BP) silt sediment occurs. Several young ages in upper part of two cores were obtained, and these show a clear clinoform pattern. Furthermore, seismic profiles across the offshore core show the deltafront clinoform. The upper part weak reflector or transparent part in seismic profiles become thinner seaward and the lower part is strong reflectors. Sea bottom nearshore show a convex shape, but the seaward low gradient part show erosional gullies. The evolution of the deltafront clinoform was revealed in profiles and in plan view.

Keywords: Abandoned Yellow River Delta, Deltafront clinoform, C-14 ages, OSL ages

©2019. Japan Geoscience Union. All Right Reserved.

Holocene evolution and Anthropocene destruction of the Krishna delta, east coast of India: delta lobe shifts, human impact, and sea-level history

Kakani Nageswara Rao[2], *Yoshiki Saito[1], K.Ch.V. Nagakumar[4], Sumiko Kubo[3], Shilpa Pandey[5], Zhen Li[6], G. Demudu[2], A.S. Rajawat[7]

1. Estuary Research Center, Shimane University, 2. Andhra University, 3. Waseda University, 4. Centre for Water Resources and Management, 5. Birbal Sahni Institute of Palaeosciences, 6. University of Victoria, 7. Space Applications Centre

Holocene evolution of the Krishna delta was inferred using landform characteristics and 11 sediment cores with 59 Accelerator Mass Spectrometry ^{14}C dates. Landform assemblage in 5880 km^2area of the Krishna delta indicated the upper river-built fluvial plain and the lower marine-built beach-ridge delta plain with the maximum landwardbeach ridge located at˜30 km from the shoreline separating the two plains. Sedimentary facies and their ages showed the Holocene marine sediment overlying the Pleistocene basement and progressively thickened seaward from <10 m to 25 m below the present sea level. The basal mangrove peat layers indicated that the sea level rose from −9 m to −3 m during 8.3–6.3 cal ky BP before stabilizing at the present level around 5 cal ky BP.
Considering the spatiotemporal variations of sediment facies and sediment accumulation rates and the configuration of the palaeo beach ridges (former shorelines), we surmised five major stages in the growth of 3539 km^2area of the Krishna delta beach-ridge plain during the last 6 cal ky BP with distinct lateral and seaward migration of delta lobes (depocentre shifts). Delta progradation was accelerated in the last 500 years, forming an out-building lobate delta. However, predominant erosion along the sediment-starved Krishna delta front coast during the past 50 years, due to impoundment of the riverine inputs at the burgeoning upstream dams pushed the Krishna delta into a persistent a destruction phase after ˜6,000 years of delta progradation.

Keywords: Beach-ridge plain, Sedimentary facies, Delta lobes, Coastal erosion

©2019. Japan Geoscience Union. All Right Reserved.

Offset in radiocarbon ages between marine bioclast and terrestrial plant pairs in the Holocene sediments around Japan

*Nakanishi Toshimichi[1,2], Futoshi Nanayama[3,4], Atsushi Urabe[5], Kazuaki Hori[6], Wan Hong[7]

1. Kyoto Univ., 2. JAEA, 3. AIST, 4. Kumamoto Univ., 5. Niigata Univ., 6. Nagoya Univ., 7. KIGAM

To identify chronological and spatial changes in the radiocarbon (^{14}C) marine reservoir effects, the ^{14}C ages of eight pairs of marine bioclasts and terrestrial plants were measured from the same horizons of one core of Holocene sediments around Japan (Nakanishi et al. 2013, 2015, 2017abc). The reservoir ages ranged from 60 to 1100 years, scattered over the period 100-10,200 cal BP, which were significantly larger than the values from “prebomb” samples of known age, before AD 1955 in this area. These results indicate that the information on reservoir effects is indispensable for chronological control not only from prebomb samples but also from geological and archaeological samples. Moreover, the effects also reflects the influence of complex river-mouth systems such as deltas and estuaries. To determine the direct chronological changes of the marine reservoir effect between the Kuroshio and Tsushima Currents, radiocarbon ages from pairs of marine bioclasts and terrestrial plants were measured from the same stratigraphic horizons within three cores of Holocene sediments beneath the Sukumo Plain, Miyazaki Plain, and Oki Islands, in west Japan. Subsequently, the results were compared with values from the Oita Plain and Hakata Bay on the northern coast of Kyushu (Nakanishi et al. 2017ac), as well as the Korean Peninsula (Nakanishi et al. 2013, 2015, 2017b). The study was partially funded by the Japan Society for the Promotion of Science Kakenhi grant number 18H01310.

References

Nakanishi T, Hong W, Sung KS, Lim J. 2013. Radiocarbon reservoir effect from shell and plant pair in Holocene sediments around the Yeongsan River in Korea. *Nuclear Instruments and Methods in Physics Research B* 294: 444–51.

Nakanishi T, Hong W, Sung KS, Sung KH, Nakashima R. 2015. Offsets in radiocarbon ages between plants and shells from same horizons of coastal sediments in Korea. *Nuclear Instruments and Methods in Physics Research B* 361: 670–9.

Nakanishi T, Hong W, Shimoyama S, Sato S, Park G, Lee JG. 2017a. Radiocarbon age offset between shell and plant pairs in the Holocene sediments under the Hakata Bay, western Japan. *Radiocarbon* 59 (2): 423–34.

Nakanishi T, Hong W, Sung KS, Nakashima R, Nahm WH, Lim J, Katsuki K. 2017b. Offset in radiocarbon age between plant and shell pairs in Holocene sediment around the Mae-ho Lagoon on the eastern coast of Korea. *Quaternary International* 447: 3–12.

Nakanishi T, Takemura K, Matsuyama H, Shimoyama S, Hong W, Okuno M. 2017c. Activity of the Funai fault and radiocarbon age offsets of shell and plant pairs from the latest Pleistocene to Holocene sediments beneath the Oita Plain, western Japan. *Radiocarbon* 59(6): 1737–48.

Keywords: Radiocarbon age, Marine reservoir effect, Holocene, Kuroshio Current

©2019. Japan Geoscience Union. All Right Reserved.

Assessment of MEIS for Marine Spatial Planning in the Nakdong River Estuary, Busan Metropolitan City, South Korea

*Jun-Ho Lee[1], Han Jun Woo[1], Hoi-Soo Jung[1], Chan Mi Park[1]

1. Korea Institute of Ocean Science and Technology

The Nakdong River has a length of nearly 510 km, with a drainage basin of around 23,400 km^2 in South Korea. The Nakdong River Estuary (NRE) in Busan city is a typical example of an estuary in which the throughput is manipulated artificially. The Noksan barrage, built in 1934, blocks the flow of the West Nakdong River, and the NRE barrage was completed between 1983 and 1987 to regulate the flow of the East Nakdong River. With the construction of several huge industrial complexes on reclaimed land near the NRE barrage in the last 65 years, the hydraulic circulation in the NRE has undergone dramatic changes in river discharge and geomorphic configuration, such as the formation of a series of barrier islands. In this study, marine environmental information system (MEIS) data collected after May 2015 were applied to support marine spatial planning (MSP) in the brackish water zone of NRE. The MEIS data in NRE consists of landscape classification of sub-environments, surface sediment distributions, characteristics of suspended sediment, short-term sedimentation, stratification index analysis in channels, closed circuit television (CCTV) using 4G long term evolution (LTE), automatic weather stations (AWS) in real time, calculated residual flow (R_f), net suspended sediment loads (Q_S), and net suspended sediment flux (F_S) in main stream inlet using mooring station, *etc*. The NRE could be divided into areas continuously managed by government, marine protected areas, areas for the development of marine attractions, areas conserved for research education, and coastal areas subject to safety management, e*tc*. For MSP, it was possible to use comparative data of the characteristics of environmental changes in the estuarine watershed to prepare the NRE for the partial opening or drainage extension in 2019 to 2021. This study aims to discuss how to predict environmental change after partial or full opening in NRE barrage and use ecological-based environmental maps in the process of MSP. The development of marine spatial planning mapping in NRE is much necessary for the nation at a time when the diversity of marine use and the demand for policies regarding marine space rapidly increase.

Keywords: Barrage, Busan, Estuary, Marine Environmental Information System, Marine Spatial Planning, Nakdong River Estuary

©2019. Japan Geoscience Union. All Right Reserved.

Assessment of MEIS for Marine Spatial Planning in the Nakdong River Estuary, Busan Metropolitan City, South Korea

Jun-Ho Lee[1] · Han Jun Woo[1] · Hoi-Soo Jung[1] · Chan Mi Park[1]

[1]Korean Seas Geosystem Research Unit, Korea Institute of Ocean Science & Technology, 385 Yeongdo, Busan 49111, Republic of Korea

The Nakdong River has a length of nearly 510 km, with a drainage basin of around 23,400 km^2 in South Korea. The Nakdong River Estuary (NRE) in Busan city is a typical example of an estuary in which the throughput is manipulated artificially. The Noksan barrage, built in 1934, blocks the flow of the West Nakdong River, and the NRE barrage was completed between 1983 and 1987 to regulate the flow of the East Nakdong River. With the construction of several huge industrial complexes on reclaimed land near the NRE barrage in the last 65 years, the hydraulic circulation in the NRE has undergone dramatic changes in river discharge and geomorphic configuration, such as the formation of a series of barrier islands. In this study, marine environmental information system (MEIS) data collected after May 2015 were applied to support marine spatial planning (MSP) in the brackish water zone of NRE. The MEIS data in NRE consists of landscape classification of sub-environments, surface sediment distributions, characteristics of suspended sediment, short-term sedimentation, stratification index analysis in channels, closed circuit television (CCTV) using 4G long term evolution (LTE), automatic weather stations (AWS) in real time, calculated residual flow (R_f), net suspended sediment loads (Q_S), and net suspended sediment flux (F_S) in main stream inlet using mooring station, *etc*. The NRE could be divided into areas continuously managed by government, marine protected areas, areas for the development of marine attractions, areas conserved for research education, and coastal areas subject to safety management, *etc*. For MSP, it was possible to use comparative data of the characteristics of environmental changes in the estuarine watershed to prepare the NRE for the partial opening or drainage extension in 2019 to 2021. This study aims to discuss how to predict environmental change after partial or full opening in NRE barrage and use ecological-based environmental maps in the process of MSP. The development of marine spatial planning mapping in NRE is much necessary for the nation at a time when the diversity of marine use and the demand for policies regarding marine space rapidly increase.

©2019. Japan Geoscience Union. All Right Reserved.

Tidal changes at Asian deltas in response to future sea-level rise

*Katsuto Uehara[1]

1. Kyushu University

A numerical model has been employed to assess the impact of sea level rise on tidal regimes in the East China Sea and the South China Sea with a special interest on tidal changes at around the deltaic region where the elevation is low and coasts are vulnerable to changes in water levels. The model covers the East and South China seas as a whole with a spatial resolution of 2 minutes (approx. 3 km). A preliminary result for the East China Sea suggests recognizable changes in the amplitude of M2 tides and M2 tidal currents at region such as Hangzhou Bay, the Changjiang Estuary and Haizhou Bay when the sea-level was raised by 1 m. Off the Changjiang Estuary, for example, tidal velocity increased for more than 10 cm/s at deep channels while decreased by about 5 cm/s on shoals. These results indicate that the sea-level rise may alter equilibrium among water currents and seafloor and modify the bottom topography of large estuaries and subaquatic deltas through the induced changes in tides and tidal currents.

Keywords: tides, china sea, sea level rise

©2019. Japan Geoscience Union. All Right Reserved.

A governing equation of non-deltaic transgressive profile: 2D numerical simulation and flume experiments

*Junhui Wang[1,2,3], Tetsuji Muto[3]

1. China University of Petroleum (Beijing), 2. State Key Laboratory of Petroleum Resources and Prospecting, China, 3. Nagasaki University

An alluvial river subject to relative sea level rise has a critical length (L_{crt}), beyond which the river can no longer sustain deltaic sedimentation but behaves to develop an estuarine environment. In such cases, there occurs non-deltaic rapid transgression. It is not difficult to imagine that non-deltaic transgression is pervasive in geological records, since most of the world large rivers would have “over-extended” to as far as the shelf edges during glacial or lowstand sea level periods. The configuration of non-deltaic transgressive profiles deserves a study because (1) it would provide a criterion for identifying non-deltaic transgression in the past and thus the fact of over-extension of the feeder alluvial river, and (2) it would constrain arguments on sediment transportation to the deep-water depositional systems.

Suppose that a river has an over-extended alluvial length of L ($>>L_{crt}$). During non-deltaic transgression, all the sediment fed by the river is consumed for alluvial aggradation and thus allocated in the subaerial realm. On the assumption that the supplied sediment is evenly distributed along the river profile which is approximately regarded as linear and has an averaged slope of α, the local transgressive slope Ψcan be expressed as:

$$\Psi = \alpha L / [L - \Lambda_{2D}(1+\alpha^2)^{0.5}] \quad (1)$$

We set an x–z coordinate system (x: basinward horizontal, z: vertical) that originates from the intersection of the initial horizontal line and the hinterland profile. Let x to be positive downstream and z to be positive upward. Equation 1 can be rewritten as:

$$\Psi_{x,z} = \alpha(\gamma x+z) / [(\gamma x+z) - \Lambda_{2D}(\gamma - \alpha)] \quad (2)$$

where $\gamma$is the averaged hinterland slope.

Equation 2 can be regarded as the derivative function of the governing equation of the non-deltaic transgressive profile, which can be expressed as:

$$\partial \eta_{x,z} / \partial x = \alpha(\gamma x+z) / [(\gamma x+z) - \Lambda_{2D}(\gamma - \alpha)] \quad (3)$$

where $\eta_{x,z}$ denotes the non-deltaic transgressive profile expressed as the pathway of shoreline. Note that sediment compaction is not considered.

Equation 3 can hardly be solved analytically but by numerical simulation. The solutions that we have obtained indicate that $\eta_{x,z}$ takes a concave-upward geometry with upstream-increasing gradient.

To test our numerical model, a series of 2D physical experiments was performed at Nagasaki University. The experiments were conducted using a 4 m-long and 2.0 cm-wide, open flume, from the upstream end of which sediment and water were fed at constant rates. Before each experimental run, we built a sufficiently long river profile inside the flume, to model the initial over-extended alluvial river ($L >> L_{crt}$). The initial river lengths were different by runs (L_0, ranging from 120–350 cm) and were set to be within a range of 0.139–0.158 (α). The hinterland slope was set as a constant value of 0.612 (γ). In each run, there occurred non-deltaic transgression as soon as base level started to rise.

©2019. Japan Geoscience Union. All Right Reserved.

Any of the resulting profiles of non-deltaic transgression shows a concave-upward geometry. The downstream end of the profile was tangent to the initial river profile (thus $\alpha \sim \Psi$). To the upstream, Ψ gradually increased, and approached a value as large as γ when the alluvial river was sufficiently shortened. The non-deltaic transgressive profiles generated in the experiments match well with the numerical model, implying that equation 3 can account for the non-deltaic transgressive profile in nature.

Keywords: Autostratigraphy, Non-deltaic transgressive profile, Numerical simulation, Flume experiments

©2019. Japan Geoscience Union. All Right Reserved.

[E] Oral | H (Human Geosciences)：H-CG Complex & General

Mon. May 27, 2019 9:00 AM - 10:30 AM JST | Mon. May 27, 2019 12:00 AM - 1:30 AM UTC | 301B 3F

[H-CG27] Turbidity current: from triggers for the generation to the depositional and morphologic al processes

convener:Miwa Yokokawa(Osaka Institute of Technology), Hajime Naruse(Department of Geology and Mineralogy, Graduate School of Science, Kyoto University), Norihiro Izumi(Faculty of Engineering, Hokkaido University), Ken Ikehara(Institute of Geology and Geoinformation, National Institute of Advanced Industrial Science and Technology), Chairperson:Miwa Yokokawa(Osaka Institute of Technology), Norihiro Izumi(Hokkaido University)

Recent developments of field observation, physical and numerical experiments, and mathematical analysis have brought us a better understanding of the dynamics of turbidity currents and relevant morphology and bedforms. Applying new findings to rock records, more profound understanding of turbidites have been achieved. It has been found that different triggers and/or sources generate distinctive features of turbidity currents, resulting in various appearances of rock records and morphology. The integration of such new knowledge on turbidity currents is important not only from scientific but also practical points of view, such as assessments of natural hazards, and exploration of resources. This international session welcomes all kinds of approaches for the turbidity currents such as field observation, physical and numerical experiments, mathematical analysis, and studies from rock records.

9:00 AM - 9:15 AM JST | 12:00 AM - 12:15 AM UTC

[HCG27-01] Inverse analysis of turbidity currents using two dimensional shallow water model

*Hajime Naruse[1] (1.Department of Geology and Mineralogy, Graduate School of Science, Kyoto University)

9:15 AM - 9:30 AM JST | 12:15 AM - 12:30 AM UTC

[HCG27-02] Inverse Analysis of Experimental Scale Turbidity Currents by Deep Learning Neural Network

*Cai Zhirong[1], Hajime Naruse[1], Qifeng Yao[1] (1.Kyoto University)

9:30 AM - 9:45 AM JST | 12:30 AM - 12:45 AM UTC

[HCG27-03] Conditions for development of depositional submarine channels: examination by flume experiments

*Justine Poppeschi[1], Kazushi Nakata[1], Hajime Naruse[1] (1.Division of Earth and Planetary Sciences, Graduate School of Science, Kyoto University)

9:45 AM - 10:00 AM JST | 12:45 AM - 1:00 AM UTC

[HCG27-04] Cyclic steps formed by long-runout turbidity currents

*Zhuyuan Wu[1], Norihiro Izumi [1] (1.Hokkaido University)

10:00 AM - 10:15 AM JST | 1:00 AM - 1:15 AM UTC

[HCG27-05] Is surface sediment remobilization more popular mechanism for generating earthquake-induced turbidity current? Evidence of radiocarbon dates from the westernmost Nankai and Japan Trench subduction zones

*Ken Ikehara[1], Toshiya Kanamatsu[3], Tobias Schwestermann[2], Arata Kioka[2], Michael Strasser[2] (1.Institute of Geology and Geoinformation, National Institute of Advanced Industrial Science and Technology, 2.Universität Innsbruck, 3.Japan Agency for Marine-Earth Science and Technology)

10:15 AM - 10:30 AM JST | 1:15 AM - 1:30 AM UTC

[HCG27-06] Shallow-subsurface event stratigraphy along the hadal trench axis of the Japan Trench

*A. Kioka[1], T. Schwestermann[1], J. Moernaut[1], K. Ikehara[2], T. Kanamatsu[3], M. Strasser[1,4] (1.Universität Innsbruck, Austria, 2.GSJ-AIST, Japan, 3.JAMSTEC, Japan, 4.MARUM-U. Bremen, Germany)

Inverse analysis of turbidity currents using two dimensional shallow water model

*Hajime Naruse[1]

1. Department of Geology and Mineralogy, Graduate School of Science, Kyoto University

Quantitative reconstruction of flow properties from turbidites is a long-standing problem in deep-sea sedimentology. If this is realized, magnitudes of past hazardous events may be estimated from geologic records containing seismo-(tsunami-)generated turbidites. Also, entire geometry of turbidite reservoir can be inferred by flow reconstruction. Thus, inverse analysis of turbidity currents contributes to disaster-risk assessment, and is of economic importance. Here we propose a new methodology to reconstruct flow properties of turbidity currents from three-dimensional geometry of deposits. In this method, a two-dimensional shallow-water model of turbidity currents was employed as the forward model. Numerical simulation was repeated to obtain horizontal distribution of thickness of turbidites under various initial conditions, and then this synthetic data set was used for supervised training of a deep-learning neural network (DNN). After the training phase finished, DNN properly estimated initial conditions of turbidity currents (e.g. initial flow height, velocity, etc.) from artificial test data set that was also produced from the forward model. To summarize, the machine learning produced the inverse model of turbidity currents that can estimate paleo-hydraulic conditions from synthetic or ancient turbidites. In previous methods, the computational cost of two dimensional model was too high to be employed as the forward model for turbidite inversion. On the other hand, our methodology can reconstruct initial conditions of turbidity currents instantaneously. Although production of the training data set requires 1000s times repetition of calculation, the problem of calculation efficiency can be easily solved by using PC cluster. In future study, it is expected to apply the new methodology to actual turbidites measured in 3D seismic profiles or by high-resolution sampling on modern sea floor.

Keywords: sediment gravity flow, turbidite, inverse analysis, machine learning

©2019. Japan Geoscience Union. All Right Reserved.

Inverse Analysis of Experimental Scale Turbidity Currents by Deep Learning Neural Network

*Cai Zhirong[1], Hajime Naruse[1], Qifeng Yao[1]

1. Kyoto University

In this study, inverse analysis of turbidite deposited in flume experiments will be performed using a new machine learning method. The results of inverse analysis will serve to verify the accuracy of the machine learning method.

Understanding of the hydraulic conditions of turbidity current remains limited due to its destructive nature and its unpredictable occurrences. Thus, the inverse analysis of turbidity currents from ancient deposits of submarine fans is required for estimating the conditions of flows in the natural environments.

In the past, inverse modeling of turbidity currents was done in a trial and error fashion by adjusting initial conditions of numerical models, which is high in calculation load, making such technique very expensive and highly impractical. Naruse (2017 AGU Fall Meeting) developed a completely new method for inverse analysis of turbidity currents using a deep learning neural network. In this method, training data is generated by a numerical model, and a neural network for reconstructing hydraulic conditions of turbidity currents from turbidite is produced by machine learning of the training dataset. However, the validity of this new inverse model has not yet been tested in actual deposits. Therefore, this study aims to verify the method by flume experiments.

Currently, the initial conditions of a dataset produced by a flume experiment sized forward model program is used to test the applicability of the neural network method when applied to flume experiment size data. Three thousand sets of training data were fed into the neural network as training data. Another two hundred separate cases were used as test data to verify the accuracy of prediction by the neural network. The result shows initial flow velocity can be predicted relatively accurately. The initial concentrations of the finer grain size class and the initial flow height was partially reconstructed. The flow duration, the coarser grain size classes and the slopes within the flume could not be predicted. After tuning of the neural network and the forward model, the neural network trained for flume sized data will be applied to flume experiment results.

Keywords: Machine Learning, Flume Experiment, Turbidite

©2019. Japan Geoscience Union. All Right Reserved.

Conditions for development of depositional submarine channels: examination by flume experiments

*Justine Poppeschi[1], Kazushi Nakata[1], Hajime Naruse[1]

1. Division of Earth and Planetary Sciences, Graduate School of Science, Kyoto University

Although submarine channels are ubiquitously observed in various submarine fans, it is also known that submarine fans lacking continuous leveed channels are common depending on regions. However, the governing parameters to determine this diversity in developments of leveed channels has not been clarified yet. This is because there has been no previous researches that successfully reproduced depositional leveed channel topography in experimental flumes. Therefore, the formative conditions of depositional submarine channels have not been clarified yet. Here, we conducted flume experiments, aiming to reproduce depositional submarine channels for understanding their formative conditions. As a result, we succeeded to form experimental topography that resemble natural depositional submarine channels showing a ceiling river structure with levees in all five experiments. Comparing the experimental topography with the actual submarine fans, the relative depth of the experimental channel was slightly shallow, but features such as the spatial variation of the channel width showed similar trends to those of the actual submarine channels. Thus, we imply that purely depositional submarine channels can be formed without presence of precursor of erosive features. Furthermore, experimental conditions of this study were in the region where the previous study predicted that submarine channels cannot be formed, suggesting that further investigation is needed to discover the governing parameters for developments of submarine leveed channels.

Keywords: turbidity currents, flume experiment, submarine fan

©2019. Japan Geoscience Union. All Right Reserved.

Cyclic steps formed by long-runout turbidity currents

*Zhuyuan Wu[1], Norihiro Izumi [1]

1. Hokkaido University

It has been found that a variety of submarine morphology such as submarine fans, submarine rivers, and submarine canyons, has been formed by turbidity currents which travel relatively long distance (long-run out turbidity currents). The long-run out turbidity currents have a number of features similar to open channel flow. They have an equilibrium (or quasi-equilibrium at least) state, and are accompanied by hydraulic jumps when they transition from supercritical to subcritical flow regimes. In this research, with the use of the assumption that an equilibrium state can be achieved in the high-concentrated lower layer near the bottom of long-run out turbidity currents, we propose an analytical model with the use of the layer-averaged governing equations, which reproduces cyclic steps with relatively long wavelengths accompanied by periodic internal hydraulic jumps.

Integrating the Reynolds-averaged Navier-Stokes equations and continuity equation over the high concentrated lower layer, we obtain the boundary layer approximated (layer-averaged) momentum and continuity equations. In the integration, it is possible to simplify the governing equations by ignoring the entertainment from the top of the high concentrated lower layer with the assumption that the Reynolds stress becomes almost zero and the shear stress almost vanishes there. In addition to the momentum equations and continuity equation, we employ the diffusion/dispersion equation of suspended sediment, and the continuity equation of sediment (Exner equation).

The unknown variables in the problem are four: the velocity, the layer thickness, the layer-averaged suspended sediment concentration, and the bed elevation. The governing equations are the layer-averaged momentum and continuity equations, the layer-averaged diffusion/dispersion equation of suspended sediment, and the continuity equation of sediment (Exner equation). The boundary conditions for this problem are that the momentum has to be continuous before and after each hydraulic jump. More specifically, the velocity and the layer thickness have to satisfy the jump condition before and after each jump. In addition, the suspended sediment concentration has to be continuous at the jump.

We solve the problem numerically, and obtain the wavelengths of steps. The wavelength of a long-run out turbidity current is determined by the thickness of the high-concentration layer near the bottom. It is shown that the wavelengths obtained in the analysis agree relatively well with the observation.

Keywords: cyclic steps, turbidity currents, submarine bedform

©2019. Japan Geoscience Union. All Right Reserved.

Is surface sediment remobilization more popular mechanism for generating earthquake-induced turbidity current? Evidence of radiocarbon dates from the westernmost Nankai and Japan Trench subduction zones

*Ken Ikehara[1], Toshiya Kanamatsu[3], Tobias Schwestermann[2], Arata Kioka[2], Michael Strasser[2]

1. Institute of Geology and Geoinformation, National Institute of Advanced Industrial Science and Technology, 2. Universität Innsbruck, 3. Japan Agency for Marine-Earth Science and Technology

Deep-sea turbidite has been used for reconstructing past large earthquake history. Surface sediment remobilization is a relatively new idea for generating earthquake-induced turbidite, although submarine landslide has been considered as major mechanism for earthquake-induced turbidite deposition. Surface sediment remobilization has been reported from the Chilean lakes, forearc slopes along the Nankai and Japan Trench subduction zones. However, the detailed mechanism of surface sediment resuspension, remobilization and initiation of turbidity current is still unknown. For better understanding of the mechanism, it is important to understand the spatio-temporal occurrence of surface sediment remobilization. We obtained some cores from a small basin on the forearc slope in Hyuga-nada off Kyushu, and the Japan Trench floor. Fine-grained turbidites were found in the cores. Paired radiocarbon dates of the turbidite muds and hemipelagic muds between the turbidites show only small age differences. This indicates that it is unnecessary to occur bathymetry-scale (with >several meters bathymetric change) submarine landslides by earthquake ground shaking for generation of the turbidites. Large surface sediment resuspension by earthquake ground shaking at the sedimented slope near the depositional area (basin) is thought to be an important process for repeated deposition of earthquake-induced turbidites in the basin.

Keywords: surface sediment remobilization, turbidite, earthquake, radiocarbon dating

©2019. Japan Geoscience Union. All Right Reserved.

Shallow-subsurface event stratigraphy along the hadal trench axis of the Japan Trench

*A. Kioka[1], T. Schwestermann[1], J. Moernaut[1], K. Ikehara[2], T. Kanamatsu[3], M. Strasser[1,4]

1. Universität Innsbruck, Austria, 2. GSJ-AIST, Japan, 3. JAMSTEC, Japan, 4. MARUM-U. Bremen, Germany

The giant AD 2011 Tohoku-oki earthquake has been documented to remobilize a wide area of surface sediment, redistributing from the slope into the >7 km deep Japan Trench forming distinct event deposits in hadal terminal basins (Ikehara et al., 2016; Kioka et al., 2019). Other than the 2011 earthquake, similarly large earthquakes are historically known along the Japan Trench, and respective deposits have been described in recent studies from cores retrieved from the Japan Trench (Ikehara et al., 2016). Yet, little is understood about (i) the temporal and spatial distribution of event deposits along the entire trench axis, (ii) how the spatial extent may link to the rupture area of historically-reported earthquakes, and (iii) whether older deposits may indicate prehistoric large earthquakes along the Japan Trench. We herein study dm-scale vertical resolution subbottom profiler data acquired during 2012–2018 using PARASOUND and TOPAS recording systems installed on R/Vs Sonne and Shinsei-Maru over the entire Japan Trench area (36.0˚–40.5˚N), in order to investigate the event-stratigraphic distribution of acoustically-transparent layers that represent sediment remobilization event deposits. The subbottom profiler data generally record well up to ~40 m below the seafloor. Transparent bodies of the upper ~10 m correlate well to event layers reported from sediment cores linked to major historic earthquake such as the AD 2011 Tohoku-oki, AD 1454 Kyotoku, and AD 869 Jogan events. Mapping of these event deposits in the spatially-extensive subbottom profiler data allows to study the spatial distribution of these events and its comparison to their reconstructed rupture areas. Furthermore, the lower part of the hitherto only acoustically-imaged stratigraphic succession of isolated trench-floor basins along the Japan Trench also documents several thick acoustically-transparent bodies. Preliminary interpretation suggests several of the bodies could be event deposits triggered by old large earthquakes. While ground-truth of this interpretation and absolute dating requires long coring efforts in the ultra-deep Japan Trench, our study yields relative stratigraphic information and quantitative constraints of along strike variation of sediment volumes redistributed by episodic events along the Tohoku seismogenic margin.

Keywords: Japan Trench, Hadal zone, Event deposit, Bathymetry, Subbottom profiler (SBP)

©2019. Japan Geoscience Union. All Right Reserved.

[E] Oral | H (Human Geosciences)：H-CG Complex & General

Mon. May 27, 2019 10:45 AM - 12:15 PM JST | Mon. May 27, 2019 1:45 AM - 3:15 AM UTC | 301B 3F

[H-CG27] Turbidity current: from triggers for the generation to the depositional and morphologic al processes

convener:Miwa Yokokawa(Osaka Institute of Technology), Hajime Naruse(Department of Geology and Mineralogy, Graduate School of Science, Kyoto University), Norihiro Izumi(Faculty of Engineering, Hokkaido University), Ken Ikehara(Institute of Geology and Geoinformation, National Institute of Advanced Industrial Science and Technology), Chairperson:Hajime Naruse(Kyoto University), Ken Ikehara(AIST)

Recent developments of field observation, physical and numerical experiments, and mathematical analysis have brought us a better understanding of the dynamics of turbidity currents and relevant morphology and bedforms. Applying new findings to rock records, more profound understanding of turbidites have been achieved. It has been found that different triggers and/or sources generate distinctive features of turbidity currents, resulting in various appearances of rock records and morphology. The integration of such new knowledge on turbidity currents is important not only from scientific but also practical points of view, such as assessments of natural hazards, and exploration of resources. This international session welcomes all kinds of approaches for the turbidity currents such as field observation, physical and numerical experiments, mathematical analysis, and studies from rock records.

10:45 AM - 11:07 AM JST | 1:45 AM - 2:07 AM UTC

[HCG27-07] Canyon changes caused by an earthquake-triggered turbidity current in the 2016 M7.8 Kaikōura Earthquake, New Zealand

★Invited Papers

*Joshu J Mountjoy[1], Jamie D Howarth[2], Alan R Orpin[1], Philip M Barnes[1], David A Bowden[1], Ashley A Rowden[1], Alexander C. G. Schimel[1], Caroline Holden[3], Huw J Horgan[2], Scott D Nodder[1], Jayson R Patton[4], Geoffroy Lamarche[1,5], Matt Gerstenberger[3], Aaron Micallef[6], Arne Pallentin[1], Tim Kane[1] (1.NIWA, Wellington. New Zealand, 2.VUW, Wellington. New Zealand, 3.GNS Science, Lower Hutt. New Zealand, 4.HSU, Arcata CA. USA, 5.UoA, Auckland. New Zealand, 6.UoM, Msida. Malta)

11:07 AM - 11:29 AM JST | 2:07 AM - 2:29 AM UTC

[HCG27-08] Far More Prolonged Deep-sea Turbidity Currents triggered by typhoon and earthquake in the Gaoping Submarine Canyon

★Invited Papers

*Yanwei Zhang[1], Zhifei Liu[1], Yulong Zhao[1], Xiaodong Zhang[1] (1.Tongji University)

11:29 AM - 11:51 AM JST | 2:29 AM - 2:51 AM UTC

[HCG27-09] Filling the gap between turbidity current processes and products in British Columbia fjords

★Invited Papers

*Sophie Hage[1,2,3] (1.School of Ocean and Earth Sciences, University of Southampton, United Kingdom, 2.National Oceanography Centre Southampton, United Kingdom, 3.Department of Geography, Durham University, United Kingdom)

11:51 AM - 12:13 PM JST | 2:51 AM - 3:13 AM UTC

[HCG27-10] Sediment transfer from shelf to abyss through giant ganyons and valleys system in deep-sea carbonate slopes (Bahamas)

★Invited Papers

*Thierry Mulder[1], Hervé Gillet[1], Vincent Hanquiez[1], Audrey Recouvreur[1], Kelly Fauquembergue[1], Johan Le Goff[2], John J.G. Reijmer[2], Emmanuelle Ducassou[1], Margot Joumes, Thibault Cavailhes[1], Elsa Tournadour[5], Jean Borgomano[3], Emmanuelle Poli[4] (1.University of Bordeaux, UMR CNRS 5805 EPOC, Allée Geoffroy Saint Hilaire, Pessac, France, 2.King Fahd Univ. of Petroleum. and Minerals, Dhahran, Saudi

Arabia., 3.Aix Marseille University, CNRS, IRD, Collège de France, CEREGE, Aix-en-Provence, France., 4.Total, CSTJF, avenue Larribau, Pau, France, 5.Ifremer, Centre de Brest, Plouzané)

12:13 PM - 12:15 PM JST | 3:13 AM - 3:15 AM UTC

Discussion

Canyon changes caused by an earthquake-triggered turbidity current in the 2016 M7.8 Kaikōura Earthquake, New Zealand

*Joshu J Mountjoy[1], Jamie D Howarth[2], Alan R Orpin[1], Philip M Barnes[1], David A Bowden[1], Ashley A Rowden[1], Alexander C. G. Schimel[1], Caroline Holden[3], Huw J Horgan[2], Scott D Nodder[1], Jayson R Patton[4], Geoffroy Lamarche[1,5], Matt Gerstenberger[3], Aaron Micallef[6], Arne Pallentin[1], Tim Kane[1]

1. NIWA, Wellington. New Zealand, 2. VUW, Wellington. New Zealand, 3. GNS Science, Lower Hutt. New Zealand, 4. HSU, Arcata CA. USA, 5. UoA, Auckland. New Zealand, 6. UoM, Msida. Malta

Based on repeat seafloor measurements and samples we show that the M_w 7.8 November 2016 Kaikōura earthquake (New Zealand) triggered widespread landslides in a large-scale bedrock submarine canyon. These landslides initiated a powerful “canyon-flushing” event and turbidity current that travelled > 680 km along one of the world’s longest deep-sea channels, the Hikurangi Channel. To our knowledge these observations provide the first direct quantification of seafloor landscape change and large-scale sediment transport associated with an earthquake-triggered full canyon flushing event. Our results augment observations from smaller scale turbidites confined to large submarine canyons (e.g. repeat surveying in Monterey Canyon) that move stored material within canyons but do not export sediment to the deep ocean or erode into underlying substrate. The inter-event period for the Kaikōura Canyon flushing event, calculated from back analysis of triggering strong ground motion, is ~140 years. Combined with observed erosion into bedrock this indicates a canyon incision rate of 40 mm y^{-1}, substantially higher than most terrestrial rivers. Significant geomorphic change occurred within the canyon including erosion up to 60m depth in the upper canyon, scour hole formation, and down canyon movement of mega-scale bedforms constructed of gravel-boulder sized sediments. The event synchronously transferred 850 Mt of sediment and 7 Mt organic carbon to the deep ocean. Our observations demonstrate that earthquake-triggered canyon flushing is a primary driver of submarine canyon development and material transfer from active continental margins to the deep ocean.

Keywords: submarine canyon, earthquake, multibeam bathymetry, submarine landslide, seafloor erosion

©2019. Japan Geoscience Union. All Right Reserved.

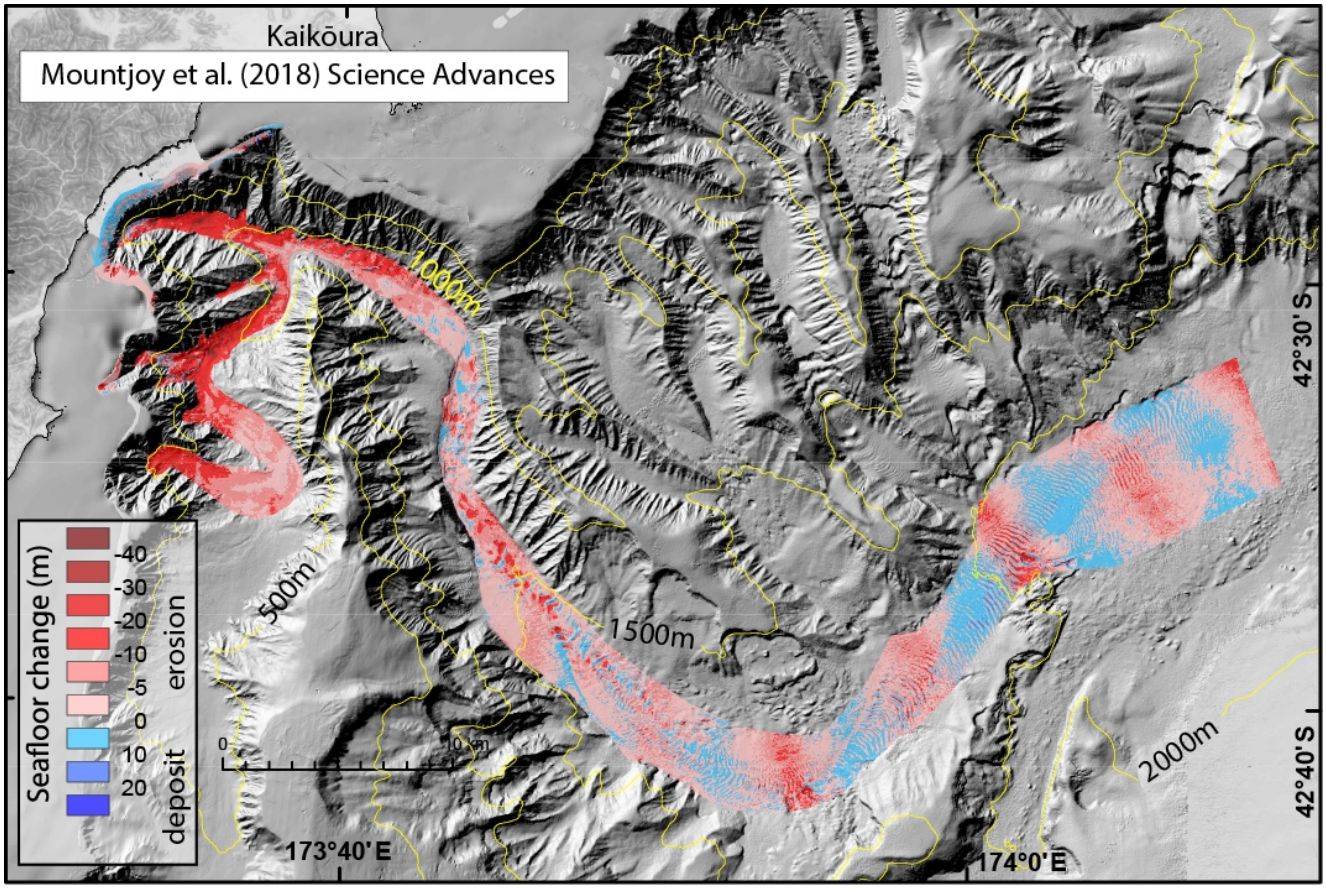

©2019. Japan Geoscience Union. All Right Reserved.

Far More Prolonged Deep-sea Turbidity Currents triggered by typhoon and earthquake in the Gaoping Submarine Canyon

*Yanwei Zhang[1], Zhifei Liu[1], Yulong Zhao[1], Xiaodong Zhang[1]

1. Tongji University

Submarine turbidity currents are argued to deliver more sediment along their long-runout propagation than other dynamic processes from shelf to deep sea. The *in situ* temporal and spatial features of turbidity currents are urgently required for a better quantitative constraints on sediment transport and deposition in the deep sea. Here, we document yearlong direct monitoring of turbidity currents in the middle reach at a water depth of 1265 m and the lower reach at 2425 m on the margin of the Gaoping Submarine Canyon off Taiwan, which has the wettest typhoons and active earthquakes. Both the two moorings (~35 km apart) were equipped with sediment traps and various sensors to collect particles consecutively with 18 days interval and to record velocity, sediment concentration, temperature and salinity with 20 min interval. Seven turbidity currents are identified consistently at these two reaches with enhanced sediment flux, which was recorded by a time-series sediment trap at 30 m above the seafloor. By combining the atmospheric measurements and earthquake data, four turbidity currents are triggered by the four powerful typhoons crossed Taiwan during typhoon season in boreal summer 2015, and one event is attributed to the M_L 6.5 Kaohsiung earthquake in southern Taiwan in February 2016. The two types of turbidity currents associated with individual typhoon and earthquake show a sustained duration ranging from 9 to 41 days, far more prolonged than the longest documented deep-sea turbidity currents (~10 days) in other locations. The flow velocity observed on the margin (~0.2 m/s) is much weaker than that in the thalweg of the canyon (> 5.8 m/s) inferred from the break of cables. For the first time, our observation provides the variability of the timing and hydrographic properties of the turbidity currents triggered by individual mechanisms for better constraints on flow capacity and sediment redistribution.

Keywords: in situ mooring observation, prolonged turbidity currents, typhoon and earthquake

©2019. Japan Geoscience Union. All Right Reserved.

Filling the gap between turbidity current processes and products in British Columbia fjords

*Sophie Hage[1,2,3]

1. School of Ocean and Earth Sciences, University of Southampton, United Kingdom, 2. National Oceanography Centre Southampton, United Kingdom, 3. Department of Geography, Durham University, United Kingdom

Turbidity currents are one of the volumetrically most important processes to transfer sediments from land to sea. Fast-moving, powerful turbidity currents can damage seafloor infrastructure and carve submarine channels. These submarine channels feed deep sea fans, which are the largest sediment accumulations on Earth. Such huge sediment accumulations sequester organic carbon over geologic timescales and are thus thought to play a role in the global carbon cycle. Despite the global significance of turbidity currents, the link between flow processes (e.g. triggering mechanisms, seafloor erosion) and depositional products is still poorly constrained. This lack of knowledge is mainly due to the difficulty to monitor flows and to directly sample the associated deposits to these flows. Here we present direct observations of turbidity currents and their deposits in two Canadian fjords: Howe Sound and Bute Inlet in British Columbia. As these two fjords are connected at their head to glacier-fed rivers, they are excellent sites to study the transport and fate of particles from land to submarine sites. Using these new observations, this talk will cover three research themes: 1) How do dilute river plumes generate turbidity currents? 2) What is the depositional architecture/facies resulting from supercritical turbidity currents and crescentic bedforms? 3) How are organic carbon mixtures distributed in turbidites and what are the implications for the carbon cycle?

Keywords: turbidity current, turbidite, organic carbon, crescentic bedforms

©2019. Japan Geoscience Union. All Right Reserved.

Sediment transfer from shelf to abyss through giant ganyons and valleys system in deep-sea carbonate slopes (Bahamas)

*Thierry Mulder[1], Hervé Gillet[1], Vincent Hanquiez[1], Audrey Recouvreur[1], Kelly Fauquembergue[1], Johan Le Goff[2], John J.G. Reijmer[2], Emmanuelle Ducassou[1], Margot Joumes, Thibault Cavailhes[1], Elsa Tournadour[5], Jean Borgomano[3], Emmanuelle Poli[4]

1. University of Bordeaux, UMR CNRS 5805 EPOC, Allée Geoffroy Saint Hilaire, Pessac, France, 2. King Fahd Univ. of Petroleum. and Minerals, Dhahran, Saudi Arabia., 3. Aix Marseille University, CNRS, IRD, Collège de France, CEREGE, Aix-en-Provence, France., 4. Total, CSTJF, avenue Larribau, Pau, France, 5. Ifremer, Centre de Brest, Plouzané

Bahamas are one of the rare present-day study areas in the world that allows to understand carbonate particle transfer from platform to deep-sea. A lot of ancient (DSDP/ODP, Bacar cruises) and recent (Carambar Cruises) dataset have been collected from 30 m to 5,000 m water depth. It includes high-resolution multibeam mapping, backscatter imaging, very-high resolution seismics and gravity cores. These new high-resolution data expose in great details the deep-water sedimentary system in the southern part of Exuma Sound (ES) and the northern part of Little Bahama Bank (LBB, Bahamas). The data reveal the detailed and complex morphology of giant valleys like the Great and Little Abaco canyons (GAC and LAC) along the LBB slope, the Great Bahama Canyon between LBB and Eleuthera Island, being the deepest canyon in the world, and the Exuma Valley/Canyon in the ES area. In all cases, present-day off-bank transport is initiated by two ways: (1) When a cold atmospheric front occurs, high-density, cold surface water sinks and entrains fine-grained particles through density cascading. This process is at the origin of the deposition of the Holocene Prograding Wedge that began to form 13.6 ka ago with a maximum growing at 4 ka when the platform was flooded. (2) During hurricanes when the fine-grained particles deposited on the shelf are resuspended and pushed off the platform through tidal passes. There, acceleration of tidal currents generates tidal flushing. On the LBB smooth slopes, coarse-grained particles (ooids and bioclasts) are trapped in tidal deltas and only fine-grained carbonate particles reach the upper slope. In Exuma area, steeper slopes allow transfer of coarse-grained particles that reach the ES slope and finally supply coarse-grained (bioclasts-rich) turbidity currents and concentrated/hyperconcentrated flows that are channeled down to the Atlantic Abyssal Plain though giant valleys. Along the valley, they form classical spill-over levee deposits. Four of these large valleys extending parallel to the shelf are presented. They all probably extend along structural directions. In GAC, finely-grained sediments originate essentially from the canyon flanks, driven by sediment slides as well as many secondary slope gullies and smaller tributaries. In LAC, gullies directly drain the upper LBB slope providing coarser particles. In the Exuma Valley/Canyon, a part of the material comes from the slope of adjacent islands and cays through small-scale gravity processes and mass failures. A substantial part of the sediments also originate from along-slope sediment flow erosion. In all areas, the valleys abruptly turn into deep canyons incising the Bahama Escarpment (BE). The canyons link the LBB and ES sedimentary systems to the deep abyssal plain of the Western North Atlantic where water depth exceeds 5,000 m. The transition occurs through major knickpoints with outsized chutes exceeding several hundred of meters in height. The sudden transformation from a wide valley to a deep narrow canyon occurs as a result of flow erosion of the underlying lower Cretaceous carbonate platform stack. Huge hydraulic jumps as well as enormous and permanent plunge pools and related deposits were identified at the transition. Dissolution processes in the carbonate deposits may also play a part in the formation of theses outsized plunge pools. In ES, the high kinetic flow energy constrained by narrow and deeply incised canyon formed a wide fan-shaped channel-levee complex on the abyssal plain. The latter is made up of coarse-grained carbonate turbidites and concentrated density-flow deposits that are mixed with fine-grained siliciclastics transported along

©2019. Japan Geoscience Union. All Right Reserved.

the BE by the energetic Western Boundary Undercurrent. Conversely the canyon mouth of the LBB system only reveals a small channeled lobe. Seismic data on this system at water depth > 4500 show the distalmost deposits are younger than mid-Miocene, suggesting that the activity of the canyon is very recent.

Keywords: Turbidity currents, Carbonate slope, giant canyons, Bahamas, Plunge pools

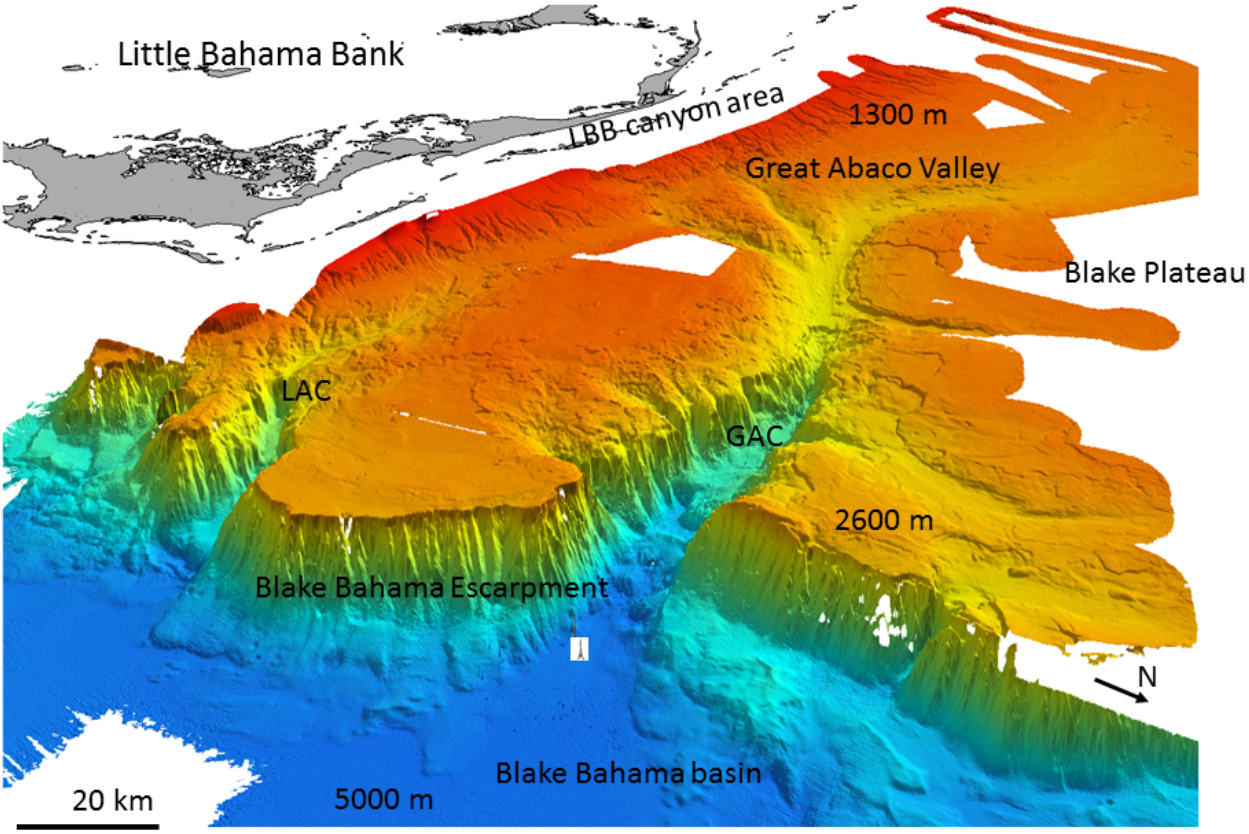

©2019. Japan Geoscience Union. All Right Reserved.

[E] Poster | H (Human Geosciences)：H-CG Complex & General

Mon. May 27, 2019 5:15 PM - 6:30 PM JST | Mon. May 27, 2019 8:15 AM - 9:30 AM UTC | Poster Hall International Exhibition Hall8, Makuhari Messe_17

[H-CG27] Turbidity current: from triggers for the generation to the depositional and morphologic al processes

convener:Miwa Yokokawa(Osaka Institute of Technology), Hajime Naruse(Department of Geology and Mineralogy, Graduate School of Science, Kyoto University), Norihiro Izumi(Faculty of Engineering, Hokkaido University), Ken Ikehara(Institute of Geology and Geoinformation, National Institute of Advanced Industrial Science and Technology)

Recent developments of field observation, physical and numerical experiments, and mathematical analysis have brought us a better understanding of the dynamics of turbidity currents and relevant morphology and bedforms. Applying new findings to rock records, more profound understanding of turbidites have been achieved. It has been found that different triggers and/or sources generate distinctive features of turbidity currents, resulting in various appearances of rock records and morphology. The integration of such new knowledge on turbidity currents is important not only from scientific but also practical points of view, such as assessments of natural hazards, and exploration of resources. This international session welcomes all kinds of approaches for the turbidity currents such as field observation, physical and numerical experiments, mathematical analysis, and studies from rock records.

[HCG27-P01] The Huapinghsu Canyon (SW East China Sea): morphology and sedimentary processes

*Cheng-Shing Chiang[1], Ho-Shing Yu[2] (1.National Museum of Natural Science, Taiwan, 2.Institute of Oceanography, National Taiwan University, Taipei, Taiwan)

[HCG27-P02] Towards understanding the seismic history of the Nankai Trough using fine-grained turbidites

*Natsumi Okutsu[1], Juichiro Ashi[1], Asuka Yamaguchi[1] (1.The University of Tokyo)

[HCG27-P03] Flood-induced sediment gravity-flow deposits in varved diatomites

*Hana Sasaki[1], Yoshiro Ishihara[2] (1.Graduate School of Science, Fukuoka University, 2.Department of Science, Fukuoka University)

[HCG27-P04] Features of parallel lamination in turbidite sandstones in the Upper Cretaceous Izumi Group in the southern part of the Awaji Island, southwest Japan

*Akane Okuda[1], Hajime Naruse[1] (1.Division of Earth and Planetary Sciences, Graduate school of Science, Kyoto University)

[HCG27-P05] Sediment wave formation on slope base environments: an example of the Neogene Aoshima Formation, Miyazaki Prefecture, Southwest Japan

Shiori Iwao[1], Yuri Onishi[2], *Yoshiro Ishihara[1], Miwa Yokokawa[3] (1.Department of Earth System Science Faculty of Science, Fukuoka University, 2.OYO Corporation, 3.Lab. of Geoenvironment, Osaka Institute of Technology)

[HCG27-P06] A flume experiment on sedimentary structures and grain size distribution of cyclic steps formed by surge-type turbidity currents

*Miwa Yokokawa[1], Kazunori Fujita[1], Isamu Mori[1], Robert Fernandez[2], Matt Czapiga[3], John Berrens[4], Jeffrey Kwang[4], Kensuke Naito[4], Gary Parker[4], Norihiro Izumi[5], Hajime Naruse[6] (1.Osaka Institute of Technology, 2.University of Hull, 3.Technical University of Delft, 4.University of Illinois, 5.Hokkaido University, 6.Kyoto University)

The Huapinghsu Canyon (SW East China Sea): morphology and sedimentary processes

*Cheng-Shing Chiang[1], Ho-Shing Yu[2]

1. National Museum of Natural Science, Taiwan, 2. Institute of Oceanography, National Taiwan University, Taipei, Taiwan

The Haupinghsu Canyon (also known as the Mienhua Canyon) is a multi-head submarine canyon which indents the shelf in the southwestern part of the East China Sea. Using seismic reflection sections and bathymetric mapping, we reveal erosive sedimentary processes responsible for entrenched thalweg and sediment dispersal of the canyon that are closely related to turbidity currents in the canyon during the late Pleistocene. The canyon system consists of three distinct units: (1) tributary canyon heads which cut into the shelf, (2) wide trough cut by entrenched thalweg, and (3) narrow V-shaped canyon with steep walls on the slope.

The Haupinghsu Canyon head incises into the shelf for a relatively long distance of about 100 km. During the last lowstand of the East China Shelf the canyon head was located in an area with sediment supply close to the paleo-river mouths. The second segment of the upper reach is dominated by a deeply incised canyon pathway with trough-like morphology. Canyon morphology is interpreted as a result of erosive sediment flows along the entrenched thalweg that caused downcutting into the canyon floor. We infer that erosive flows in the canyon resulted from hyperpycnal currents at the river mouths during periods of lowstand sea level. Moreover, sediment-gravity flows may be generated from the collapse of V-shaped canyon walls that may be over-steepened by tectonic deformation.

Keywords: Haupinghsu Canyon, turbidity current, East China Sea

©2019. Japan Geoscience Union. All Right Reserved.

Towards understanding the seismic history of the Nankai Trough using fine-grained turbidites

*Natsumi Okutsu[1], Juichiro Ashi[1], Asuka Yamaguchi[1]

1. The University of Tokyo

Turbidites are deposits of a turbidity current triggered by slope failure, earthquakes and floods. To obtain paleoseismic records using marine sediments, the extent of the turbidite distribution area and age are generally used. Characteristics and sedimentary process of turbidites assumed to be varied by the scale of seismic motion, seafloor topography and composition of sediments. Therefore, understanding and compiling the characteristics of turbidites distributed in each sea region is important to estimate paleoseismic records using turbidites. However, in the Nankai Trough, much less work has been done on paleoseismology using turbidites. This study aims to obtain the fundamental data of fine-grained turbidites, and apply it to reconstruct the seismic history in the Nankai Trough.
Samples are multi-cores and piston cores collected from off Kumano and Hyuga, the Nankai Trough. Main samples are obtained from small slope-basins with pin-point accuracy. Based on its sedimentary structure and magnetic susceptibility, fine-grained turbidites are identified in off Kumano sample and in off Hyuga. In off Kumano sample, coarse silt layer(we named this KL2 unit), silt layer (KL3, KL4) and a thick homogeneous clay layer from the bottom to the top of the upper unit can be identified as fine-grained turbidites. More specifically, KL2 unit shows low CT value, which cannot be shown in X-ray CT image and has Fe peak in XRF core scanner profile. KL3, KL4 unit shows high CT value and has Ca peak in XRF core scanner profile. Although X-ray CT image can be useful tool to identify the fine-grained turbidites, it may lead to misunderstanding the basement of fine-grained turbidites. C-14 radiocarbon dating of the foraminifera, the individual sediment layer interval is 160 years, which is almost agreed with past earthquake recurrence intervals. Also some obtained ages matches with historicalearthaquake age. In off Hyuga sample, characteristics of XRF core scanner profile such as Ca, Fe are different from that of Kumano, which can be affected by volcanic products. Since one of the sampling sites off Hyuga is located at the terrace of the foot of the Oyodo Knoll and topographically isolated from direct sediment path through river, the turbidite deposition is inferred to be triggered by seismic shaking. The youngest C-14 age obtained from this samplewas 11,000 cal yr BP, it cannot be compared to historicalearthquake age. Average earthquake recurrence is estimated to be 700 years, which is longer than other regions in the Nankai Trough.

Keywords: turbidites, turbidity currents, The Nankai Trough

©2019. Japan Geoscience Union. All Right Reserved.

Flood-induced sediment gravity-flow deposits in varved diatomites

*Hana Sasaki[1], Yoshiro Ishihara[2]

1. Graduate School of Science, Fukuoka University, 2. Department of Science, Fukuoka University

Based on differences between inflows and lake water, lacustrine sediment gravity-flows induced by floods can classified as hyperpycnal flows along the bottom of lakes, homopycnal flows mixed with lake water, and hypopycnal flows that spread along lake surfaces. Lacustrine sediment gravity-flow deposits that show an inversely grading unit overlain by a normally grading unit have been recognized as hyperpycnites. A depositional model is presented where the lower inversely grading unit is deposited during an increasing phase of the flow followed by the upper normally grading unit overlaying in a decreasing phase of the flow. That process based sedimentary model established in marine environments has been applied to sandy inflow deposits of lakes. However, there are only a few reports of fine-grained hyperpycnites, and there is no consideration of lateral facies changes associated with sediment processes of silty hyperpycnites. Also, there is no observation associated with homopycnites and hypopycnites, although these deposits are expected in a depositional setting, including hyperpycnite. In this study, we described detailed sedimentary facies of hyperpycnite, homopycnite, and hypopycnite from lacustrine varved deposits considering their sedimentary processes. We examined several formations including the Hiruzenbara Formation in Maniwa City, Okayama Prefecture, which can easily be used to define flood- and slope-failure deposits. The formation deposited in the paleo-Hiruzenbara Lake includes varved diatomite with more than 95% fossil diatoms. Therefore, inflow materials can be easily identified in the formation. Fine-grained hyperpycnites identified in this study show a set of normally grading and inversely grading units or a normal grading unit. As previously discussed, it is suggested that these deposits are deposited in an increasing phase of inflow followed by a decreasing phase of inflow. The deposit of a normally grading unit is deposited from a flow completely eroding the lower unit. Due to the occurrence of rip-up clasts, the lower inversely grading unit might erode the lower layer; whereas, the upper normally grading unit is suggested to be dominated by more depositional flows that have a higher organic matter content. Hyperpycnites tend to thin out toward the downstream ward and change their sedimentary facies with the occurrence of rip-up clasts and organic matter. Fine-grained homopycnite and hypopycnite are present as structureless thin deposits of less than 1 mm composed of inflows of fine materials with no erosion. These deposits have lower organic matter content than hyperpycnites and do not include rip-up clasts. It is possible that flows of these deposits mixed with the lake water or were spread along the lake surface, after which the materials slowly settled. Thin fine-grained homopycnites and hypopycnites do not exhibit any sedimentary facies change over several kilometers, except in cases where they are pinched out.

Keywords: lacustrine deposit, sediment gravity-flow deposit, hyperpycnite, homopycnite, hypopycnite, varved diatomite

©2019. Japan Geoscience Union. All Right Reserved.

Features of parallel lamination in turbidite sandstones in the Upper Cretaceous Izumi Group in the southern part of the Awaji Island, southwest Japan

*Akane Okuda[1], Hajime Naruse[1]

1. Division of Earth and Planetary Sciences, Graduate school of Science, Kyoto University

Parallel lamination is a common structure in sedimentary rocks, which characterizes Bouma T_b division of turbidites. Recent studies of flume experiments suggested that characteristics of parallel lamination vary depending on rates of bed aggradation. That is, the clarity of lamination decreases as rate of bed aggradation increases, and formation of parallel lamination is suppressed under very high bed-aggradation rate (>4 cm/min). However, it has not been examined that variation in features of parallel lamination corresponding to results of flume experiments can be observed in actual turbidite sandstones. In this study, we analyzed microtextures of parallel lamination in the upper part of turbidite sandstones taken from the Upper Cretaceous Izumi Group in soutern part of the Awaji Island, and compared the observed features with the experimental results.

The Izumi Group was subdivided into three lithological parts; the northern marginal part, main part, and southern part. The main part of Izumi Group consists of alternating beds of sandstone, mudstone and conglomerate, and has been interpreted as submarine fan deposits. The turbidite sundstones was sampled from Anaga and Kita-ama formations of the main part of the Izumi Group. The intervals of laminae and oscillation of the grain-size distribution in parallel lamination of turbidite sandstones were measured by automated image analyses.

As a result, it was suggested that parallel lamination in turbidite sandstones can be classified into two types A and B. Type A lamination shows the abrupt change in grain-size at the boundary between laminae, while Type B shows gradual change. In naked eye observation, the former lamination is clearly recognized and the later lamina is unclear. The type B lamination occurs dominantly in turbidites observed in the study area.

Comparing with existing results of flume experiments, we interpret that two types of parallel lamination reflect difference in bed-aggradation rates. In general, the rate of bed-aggradation due to depositti on from turbidity current decreases with time. The fact that the occurrence of Type A lamination is limited in the upper interval of turbidites implies that there is a threshold value of bed-aggradation rate to from Type A parallel lamination. In future, to reconstruct quantitative paleo-flow conditions from characteristics of parallel lamination, we will examine the process and conditions of formation of parallel lamination by the model calculation with further analysis of actual turbidite sandstones.

Keywords: turbidite, parallel lamination, formative condition

©2019. Japan Geoscience Union. All Right Reserved.

Sediment wave formation on slope base environments: an example of the Neogene Aoshima Formation, Miyazaki Prefecture, Southwest Japan

Shiori Iwao[1], Yuri Onishi[2], *Yoshiro Ishihara[1], Miwa Yokokawa[3]

1. Department of Earth System Science Faculty of Science, Fukuoka University, 2. OYO Corporation, 3. Lab. of Geoenvironment, Osaka Institute of Technology

Sediment waves with a wavelength of a few hundred meters and an amplitude of a few meters are observed in a turbidite succession of the uppermost part of the Neogene Aoshima Formation, Miyazaki Group. Sediment waves, a type of large sedimentary bedform in deep-sea environments, are frequently observed on levees and in channels of modern, deep-sea floors, and shallow subsurface areas. The Aoshima Formation is suggested to have been deposited on a slope-to-basin area offshore of a fan delta. However, because a turbidite succession of the Aoshima Formation shows a rather monotonous, detailed, and precise depositional setting, the sedimentary waves have not been clarified. To clarify why the sediment waves were in the limited area and horizon of the Aoshima Formation, sedimentary logs were measured at turbidite successions, including upcurrent and downcurrent regions of the sediment waves. Also, the sedimentary logs were carefully correlated together and sedimentary facies of the succession were analysed. The results are as follows: (1) Sediment gravity-flow deposits of the sediment wave horizon have relatively variable thickness. Facies could only be traced between a few hundred meters, even though most sediment gravity-flow deposits of the Aoshima Formation can trace more than 10 km along the paleocurrent directions. In addition, sediment gravity-flow deposits in the sediment wave horizon can trace between the upcurrent and downcurrent sections, except for an interval of the sediment wave formation. (2) Rare, thick sediment gravity-flow deposits including slump-fold beds are observed just under the downcurrent area of the sediment wave horizon. (3) Sediment gravity-flow deposits overlaying the beds, including slump-folds, are relatively thicker than other areas. (4) Sediment gravity-flow deposits in the sediment wave interval show oblique paleocurrent directions against sediment gravity-flow deposits in the upcurrent and downcurrent regions. (5) Small-scale slumping deposits are located at the most downcurrent part of the sediment wave. Results (1) to (3) suggest that the sediment waves of the Aoshima Formation developed on an upcurrent area of a slope change-point near the slope base. Also, results (4) and (5) suggest that the sediment waves were in a depositional channel on the slope base.

Keywords: turbidite, sediment wave, Aoshima Formation

©2019. Japan Geoscience Union. All Right Reserved.

A flume experiment on sedimentary structures and grain size distribution of cyclic steps formed by surge-type turbidity currents

*Miwa Yokokawa[1], Kazunori Fujita[1], Isamu Mori[1], Robert Fernandez[2], Matt Czapiga[3], John Berrens[4], Jeffrey Kwang[4], Kensuke Naito[4], Gary Parker[4], Norihiro Izumi[5], Hajime Naruse[6]

1. Osaka Institute of Technology, 2. University of Hull, 3. Technical University of Delft, 4. University of Illinois, 5. Hokkaido University, 6. Kyoto University

In the submarine canyon and the vicinity, continuous step-like morphology is often observed. Many of them are inferred to be formed by turbidity currents. In this study we investigate the sedimentary structures and grain size distribution of cyclic steps formed by surge-type turbidity currents in an experimental flume. Two kinds of plastic particles, whose grain-size distributions differ from each other, were used in this study to observe grain size distribution and sedimentary structures of the cyclic steps, with an eye to application to sediment waves in the modern sea floor and in the rock record.
The experiment was conducted at the Hydrosystems Laboratory of University of Illinois, Urbana-Champaign (UIUC). In the experiment, a flume, which is 14.5 m long, 0.5 m deep and 0.1m wide was suspended in a larger tank, tilted at 2.5 degrees. Salt water (density: 1.17 g/cm^3) and two kinds of plastic particles (specific gravity: 1.5, D_{50}: 68 μm, 206 μm) were mixed at a weight ratio of 20:1:1 in the head tank, and then introduced into the flume as a slurry. In Case A, slurry filling the entire volume of the head tank, 58.7 L (5.87 L/cm), was supplied for single surge, which took 40 seconds to flow out. We repeated 40 such surges. In Case B, slurry filling half the volume of the head tank, 27.4 L (2.74 L/cm), was supplied for each surge, which took 10 seconds to flow out; we repeated 80 surges. The total amount of supplied sediment was about the same in both cases. The flow rate per unit time gradually decreased during a single surge.
At the end of each series, 4 steps were formed in the two series. Those steps moved upstream during the series of pulse runs. The mean values of wave steepness of the resulting steps were 0.06 and 0.05. The sedimentary structures observed in the cyclic steps of these experiments were mainly laminae gently dipping toward the upstream side. These laminae were truncated at the downstream side of the step. Moreover, the grain size analysis of the cyclic steps showed that D_{50} of the surface sediments tended to decrease toward the downstream, with the tendency being more prominent as the total discharge of the surge increased. It was also found that the D_{50} on the downstream side is smaller than on the upstream side of each step. This distribution is inferred to be caused by a hydraulic jump at the upstream side of each step.

Keywords: Cyclic steps, Surge-type turbidity currents, Flume experiments

©2019. Japan Geoscience Union. All Right Reserved.

[J] Poster | S (Solid Earth Sciences)：S-GD Geodesy

Mon. May 27, 2019 10:45 AM - 12:15 PM JST | Mon. May 27, 2019 1:45 AM - 3:15 AM UTC | Poster Hall International Exhibition Hall8, Makuhari Messe_1

[S-GD03] Geodesy General Contributions/Global Geodetic Observing System

convener:Koji Matsuo(Geospatial Information Authority of Japan), Yusuke Yokota(Institute of Industrial Science, The University of Tokyo), Takahiro Wakasugi(Geospatial Information Authority of Japan)

In this session, general contributions from all areas of geodesy are welcomed. Topics of interest will include but not limited to recent advances in measurement techniques, reference frame realization, earth rotation or earth tide. In addition, this session also provides a forum for discussing GGOS (Global Geodetic Observing System) related observation programs, advancement of geodetic techniques, collaboration among various organizations in the world. Topics will include improvements of observing system and data analysis, participations in global programs, global reference frames and geodesy's contributions to society.

[SGD03-P01] The Study of Sky Condition Prediction and Combination Efficiency Estimation about Multi-GNSS

*Chieh-Ting Chou[1], Yi-Shan - Li[2], Yen-Te - Li[1], Wan-Yu - Yu[1] (1.Department of Environmental Information and Engineering, CCIT, National Defense University, Graduate Student, 2.Department of Environmental Information and Engineering, CCIT, National Defense University, Assistant Professor)

[SGD03-P02] Research on the development of rapid and accurate GNSS routine analysis system (2)

*Hiroyuki Nakagawa[1] (1.The Geospatial Information Authority of Japan)

[SGD03-P03] Characteristics of the Tenryu-Funagira laser extensometer and its detection ability of slow slips

*Akio Katsumata[1], Akiteru Takamori[2], Akito Araya[2] (1.Meteorological Research Institute, Japan Meteorological Agency, 2.Earthquake Research Institute, University of Tokyo)

[SGD03-P04] Performance evaluation of laser strainmeters

*Akiteru Takamori[1], Akito Araya[1], Akio Katsumata[2], Wataru Morii[3], Kouseki Miyo[4], Masatake Ohashi[4] (1.Earthquake Research Institute, University of Tokyo, 2.Meteorological Research Institute, 3.Disaster Prevention Research Institute, Kyoto University, 4.Institute for Cosmic Ray Research, University of Tokyo)

[SGD03-P05] Calculation Method of the Tidal Love Numbers with the Fluid Core Resonance of the Solid Earth

*Yuji Harada[1,2], Shuhei Okubo[3] (1.State Key Laboratory of Lunar and Planetary Science, Space Science Institute, Macau University of Science and Technology, 2.Ocean Hemisphere Research Center, Earthquake Research Institute, University of Tokyo, 3.Center for High Energy Geophysics Research, Earthquake Research Institute, University of Tokyo)

[SGD03-P06] Integrating PSInSAR and Hydrogeophysical Methods for the Characterization of a Earth fissure in the eastern Beijing plain

*Menglin Zhao[1], juan wang[1], wang xu[1], bing hu[1], yisheng chen[1] (1.Capitai Normal University)

The Study of Sky Condition Prediction and Combination Efficiency Estimation about Multi-GNSS

*Chieh-Ting Chou[1], Yi-Shan - Li[2], Yen-Te - Li[1], Wan-Yu - Yu[1]

1. Department of Environmental Information and Engineering, CCIT, National Defense University, Graduate Student,
2. Department of Environmental Information and Engineering, CCIT, National Defense University, Assistant Professor

The Global Navigation Satellite System (GNSS) is widely used in military and civilian applications because of the high-precision services of positioning, velocity and time-of-flight (PVT) at any time and any place. At present, GNSS include the GPS of the United States, the GLONASS of Russia, the Galileo of European Union and the Beidou of China. Due to the rapid development and diversity of GNSS, the positioning efficiency of multi-GNSS is an important information for user reference when surveying.

In this study, the sky condition of the project area is predicted by the STK software. It is expected that the best location and period of observation can be provided to improve the observation efficiency according to simulated calculate the satellite geometric distribution and satellite visible number. Based on mentioned above, the observation efficiency can be improved. In addition, this study conducts a study on the positioning effectiveness of GNSS by actual observation data through different combination of satellite systems, ephemeris and weathers. In the discussion of sky condition prediction, the prediction is successfully carried out. In the discussion of GNSS combination, the results show that the GPS satellite system is relatively stable and highly accurate compared to other satellite systems. The relative positioning accuracy of multi-GNSS with GPS satellite system compared to without GPS system can improve 14ppm. In the discussion of different ephemeris, the short baselines can produce consistent results with relative accuracy in either broadcast or precision ephemeris. In the discussion of weathers, the relative accuracy of observations on a sunny day can be improved by 4ppm compared to a rainy day.

Keywords: GNSS, sky condition prediction, combination efficiency

©2019. Japan Geoscience Union. All Right Reserved.

Research on the development of rapid and accurate GNSS routine analysis system (2)

*Hiroyuki Nakagawa[1]

1. The Geospatial Information Authority of Japan

The Geospatial Information Authority of Japan (GSI) routinely analyzes GNSS data obtained by GEONET and monitoring crustal deformation all over Japan. The results are used as fundamental data in the field of such as evaluating earthquake activity or monitoring volcanic activity.

However, depending on the timing of earthquake occurrence or speed of deformation of mountain body, even up-to-date GEONET routine analysis do not always have enough rapidness or time resolution. New analysis method that is more rapid and with higher time resolution are required.

Therefore, we focused on Precise Point Positioning with Ambiguity Resolution, or PPP-AR. With corrective information called Fractional Cycle Bias (FCB) as well as precise orbit and clock information of GNSS satellites, PPP-AR can calculate position for each site as accurate as those derived by interferometric analysis. A key feature is that the position of the stations in every epoch can be calculated rapidly with small calculation load. In addition, PPP-AR does not need fixed reference station. That has advantage when crustal deformation occurs over wide area by large earthquake and it is difficult to find the point that is not subjected to the deformation.

Thus, GSI has started a three-year research project since the April of 2017. In this project, we will develop more rapid and accurate GNSS analysis method based on PPP-AR and make prototype system implementing this method envisioning future GEONET routine analysis. The goal of this research is developing analysis method that can routinely and stably obtain the solution of one-second interval with typical repeatability of about 1cm in horizontal component within about two hours after data acquisition.

In 2018, we perform test analysis of 31 days from Jul. 12 to Aug. 12, 2018 using prototype system under development. Twenty-four hour time series of 1 sec. interval from 0 hour to 0 hour of next day was calculated for al GEONET station once a day, and evaluated estimated satellite orbit and clock, and resulted GEONET time series solutions. First, as an evaluation of quality of estimated satellite orbits and clocks, RMS of estimated orbits with respect to IGS final orbit and RMS of estimated clocks with respect to CODE clock were calculated. As a tentative result, RMS of orbit is about 2.7cm for GPS and about 8.8cm for GLONASS, and RMS of clock is about 4.15ns for GPS and about 6.02ns for GLONASS. Next, as a evaluation of repeatability of GEONET time-series solutions, we calculate a frequency distribution of standard deviation of horizontal coordinate time series. Then, frequency distribution peak is located at a bin from 1.0 to 1.2cm of standard deviation and almost 25% of all time series are fall into this bin. On the other hand, only 21% of time series has standard deviation less than 1cm, which is target of this research project. Time series with standard deviation less than 1.4cm accounts for about 68%.

In this presentation, we will consider the reason and a way to improve the quality of estimated orbit/clock and time series solution.

Keywords: GNSS, PPP-AR, GEONET routine analysis, GEONET

©2019. Japan Geoscience Union. All Right Reserved.

©2019. Japan Geoscience Union. All Right Reserved.

Characteristics of the Tenryu-Funagira laser extensometer and its detection ability of slow slips

*Akio Katsumata[1], Akiteru Takamori[2], Akito Araya[2]

1. Meteorological Research Institute, Japan Meteorological Agency, 2. Earthquake Research Institute, University of Tokyo

Katsumata et al. (2010) installed a long-baseline laser extensometer in Funagira tunnel in Hamamatsu, Shizuoka Pref. Its baseline length is 400 m. Short-term slow-slips were detected with the extensometer. From spectral analysis, it was shown that a long-term slow-slip can be detected with the laser extensometer earlier than the GNSS network. However. iodine-stabilized He-Ne laser, which was used formerly, had a relatively short life time. It was difficult to continue observation for more than several years. We replaced the stabilized laser with the iodine-stabilized YAG laser developed by Araya et al. (2002), and started observation from March, 2018. The sampling rate was changed from 1 kS/s to 10 kS/s to catch up fast phase change due to quick strain change.
We compared the obtained data with that previously obtained with He-Ne laser. It was found that the atmospheric pressure response and tidal response were not changed. However, trend was changed. Trend of about 10^{-7} strain/year was previously observed. No such trend is observed currently. A trend change was observed before and after the 2011 Tohoku earthquake. The trend might be affected by local condition. We compared spectrum levels of the detrended previous and current data. The spectrum level was almost the same over a period range from 0.1 s to several months.
Ide et al. (2007) presented a scaling law of slow earthquakes, in which seismic moment is proportional to event duration. It is considered that strain rate would be the same level regardless of its seismic moment based on the scaling law. Katsumata et al. (2001) showed that the Tenry-Funagira laser extensometer would detect strain change with strain rate the same as those of short-term slow-slips in a day. If there were a slow-slip of one day duration, the Tenryu-Funagira laser extensometer could detect it.

Keywords: Laser extensometer, iodine-stabilized laser, slow-slip observation

©2019. Japan Geoscience Union. All Right Reserved.

Performance evaluation of laser strainmeters

*Akiteru Takamori[1], Akito Araya[1], Akio Katsumata[2], Wataru Morii[3], Kouseki Miyo[4], Masatake Ohashi[4]

1. Earthquake Research Institute, University of Tokyo, 2. Meteorological Research Institute, 3. Disaster Prevention Research Institute, Kyoto University, 4. Institute for Cosmic Ray Research, University of Tokyo

We have constructed four laser strainmeters which are in operation to observe Earth’ s strain in underground sites in Japan. The strainmeters are asymmetric Michelson interferometers implemented with a long main arm (ranging from 100 m to 1.5 km, depending on deployment) that follows ground motion and a short reference arm (shorter than 1 m) which is mounted on a stable platform isolated from the ground. The ground strain is observed by detecting phase difference of the two beams that enter and return from these arms. Due to the sensitivity of the phase difference to laser frequency caused by the mismatch of the arm lengths, the laser frequency needs to be stabilized to maintain high resolution of the instruments in long term. For this purpose, we developed a laser frequency stabilization system that locks a Nd:YAG laser to one of the iodine absorption lines, with the designed stability of 10e-13 to 10e-12. In order to evaluate the performance of the strainmeters, we have been studying stability of the lasers by comparing equivalent systems in situ. The details and results of the experiments are presented together with the estimated performance of the strainmeters.

Keywords: laser strainmeter, frequency stabilized laser

©2019. Japan Geoscience Union. All Right Reserved.

Calculation Method of the Tidal Love Numbers with the Fluid Core Resonance of the Solid Earth

*Yuji Harada[1,2], Shuhei Okubo[3]

1. State Key Laboratory of Lunar and Planetary Science, Space Science Institute, Macau University of Science and Technology, 2. Ocean Hemisphere Research Center, Earthquake Research Institute, University of Tokyo, 3. Center for High Energy Geophysics Research, Earthquake Research Institute, University of Tokyo

Effect of non-rigidity of the solid Earth exerted on the Earth’ s tide and rotation is of importance for understanding dynamical behavior of the core and mantle. The influence of the fluid core on the solid tide is predictable based on Sasao et al.’ s theory (i.e., the SOS theory). In the present study, we show a couple of new ideas so as to simply estimate the Love numbers describing the tidal deformation by means of the SOS theory, and report the results. One of them is how to compute the independent solutions of the radial functions in the solid layer (i.e., the y functions), where we show that it become unnecessary to calculate a part of the solutions in doing numerical integration of the y functions. The other is how to compute those in the liquid layer (i.e., the q functions), where we show that it become unnecessary to calculate the vertical derivative of density in integrating the q functions.

Keywords: Earth's Tide, Earth's Rotation, Earth's Interior

©2019. Japan Geoscience Union. All Right Reserved.

Integrating PSInSAR and Hydrogeophysical Methods for the Characterization of a Earth fissure in the eastern Beijing plain

*Menglin Zhao[1], juan wang[1], wang xu[1], bing hu[1], yisheng chen[1]

1. Capitai Normal University

Modern Earth fissure, ranging from renewed displacement on 1-km-long fault scarps to 9.8-km-long tension cracks, occur in the eastern part of Beijing plain. Most of the failures closely parallel the pre-existing Medio-Pleistocene fault zone. The pattern of earth fissure and the relation to the inferred fault remain controversial. An integrated project, including PSInSAR, geophysical and trenching methods, has been conducted to characterize the formation of earth fissure. The results indicate that this earth fissure was caused by groundwater-level decline rather than natural tectonism. In addition, it is the first time to accurate the initiation and terminal Location of pumping-induced earth fissures within the fault zone.

Keywords: PSInSAR, earth fissure, Hydrogeophysical, fault scarps

Integrating PSInSAR and Hydrogeophysical Methods for the Characterization of a Earth fissure in the eastern Beijing plain

Wang Xu[1] Yisheng Chen[1] ·Bing Hu[1] ·Juan Wang[1] Menglin Zhao[1] Youquan Zhang[1]

Abstract

Modern Earth fissure, ranging from renewed displacement on 1-km-long fault scarps to 9.8-km-long tension cracks, occur in the eastern part of Beijing plain. Most of the failures closely parallel the pre-existing Medio-Pleistocene fault zone. The pattern of earth fissure and the relation to the inferred fault remain controversial. An integrated project, including PSInSAR, geophysical and trenching methods, has been conducted to characterize the formation of earth fissure. The results indicate that this earth fissure was caused by groundwater-level decline rather than natural tectonism. In addition, it is the first time to accurate the initiation and terminal Location of pumping-induced earth fissures within the fault zone.

Keywords: *PSInSAR; earth fissure; Hydrogeophysical;* fault scarps*;* groundwater *; trenching.*

©2019. Japan Geoscience Union. All Right Reserved.

[J] Poster | S (Solid Earth Sciences)：S-GD Geodesy

Mon. May 27, 2019 5:15 PM - 6:30 PM JST | Mon. May 27, 2019 8:15 AM - 9:30 AM UTC | Poster Hall International Exhibition Hall8, Makuhari Messe_18

[S-GD03] Geodesy General Contributions/Global Geodetic Observing System

convener:Koji Matsuo(Geospatial Information Authority of Japan), Yusuke Yokota(Institute of Industrial Science, The University of Tokyo), Takahiro Wakasugi(Geospatial Information Authority of Japan)

In this session, general contributions from all areas of geodesy are welcomed. Topics of interest will include but not limited to recent advances in measurement techniques, reference frame realization, earth rotation or earth tide. In addition, this session also provides a forum for discussing GGOS (Global Geodetic Observing System) related observation programs, advancement of geodetic techniques, collaboration among various organizations in the world. Topics will include improvements of observing system and data analysis, participations in global programs, global reference frames and geodesy's contributions to society.

[SGD03-P01] The Study of Sky Condition Prediction and Combination Efficiency Estimation about Multi-GNSS

*Chieh-Ting Chou[1], Yi-Shan - Li[2], Yen-Te - Li[1], Wan-Yu - Yu[1] (1.Department of Environmental Information and Engineering, CCIT, National Defense University, Graduate Student, 2.Department of Environmental Information and Engineering, CCIT, National Defense University, Assistant Professor)

[SGD03-P02] Research on the development of rapid and accurate GNSS routine analysis system (2)

*Hiroyuki Nakagawa[1] (1.The Geospatial Information Authority of Japan)

[SGD03-P03] Characteristics of the Tenryu-Funagira laser extensometer and its detection ability of slow slips

*Akio Katsumata[1], Akiteru Takamori[2], Akito Araya[2] (1.Meteorological Research Institute, Japan Meteorological Agency, 2.Earthquake Research Institute, University of Tokyo)

[SGD03-P04] Performance evaluation of laser strainmeters

*Akiteru Takamori[1], Akito Araya[1], Akio Katsumata[2], Wataru Morii[3], Kouseki Miyo[4], Masatake Ohashi[4] (1.Earthquake Research Institute, University of Tokyo, 2.Meteorological Research Institute, 3.Disaster Prevention Research Institute, Kyoto University, 4.Institute for Cosmic Ray Research, University of Tokyo)

[SGD03-P05] Calculation Method of the Tidal Love Numbers with the Fluid Core Resonance of the Solid Earth

*Yuji Harada[1,2], Shuhei Okubo[3] (1.State Key Laboratory of Lunar and Planetary Science, Space Science Institute, Macau University of Science and Technology, 2.Ocean Hemisphere Research Center, Earthquake Research Institute, University of Tokyo, 3.Center for High Energy Geophysics Research, Earthquake Research Institute, University of Tokyo)

[SGD03-P06] Integrating PSInSAR and Hydrogeophysical Methods for the Characterization of a Earth fissure in the eastern Beijing plain

*Menglin Zhao[1], juan wang[1], wang xu[1], bing hu[1], yisheng chen[1] (1.Capitai Normal University)

The Study of Sky Condition Prediction and Combination Efficiency Estimation about Multi-GNSS

*Chieh-Ting Chou[1], Yi-Shan - Li[2], Yen-Te - Li[1], Wan-Yu - Yu[1]

1. Department of Environmental Information and Engineering, CCIT, National Defense University, Graduate Student,
2. Department of Environmental Information and Engineering, CCIT, National Defense University, Assistant Professor

The Global Navigation Satellite System (GNSS) is widely used in military and civilian applications because of the high-precision services of positioning, velocity and time-of-flight (PVT) at any time and any place. At present, GNSS include the GPS of the United States, the GLONASS of Russia, the Galileo of European Union and the Beidou of China. Due to the rapid development and diversity of GNSS, the positioning efficiency of multi-GNSS is an important information for user reference when surveying.

In this study, the sky condition of the project area is predicted by the STK software. It is expected that the best location and period of observation can be provided to improve the observation efficiency according to simulated calculate the satellite geometric distribution and satellite visible number. Based on mentioned above, the observation efficiency can be improved. In addition, this study conducts a study on the positioning effectiveness of GNSS by actual observation data through different combination of satellite systems, ephemeris and weathers. In the discussion of sky condition prediction, the prediction is successfully carried out. In the discussion of GNSS combination, the results show that the GPS satellite system is relatively stable and highly accurate compared to other satellite systems. The relative positioning accuracy of multi-GNSS with GPS satellite system compared to without GPS system can improve 14ppm. In the discussion of different ephemeris, the short baselines can produce consistent results with relative accuracy in either broadcast or precision ephemeris. In the discussion of weathers, the relative accuracy of observations on a sunny day can be improved by 4ppm compared to a rainy day.

Keywords: GNSS, sky condition prediction, combination efficiency

©2019. Japan Geoscience Union. All Right Reserved.

Research on the development of rapid and accurate GNSS routine analysis system (2)

*Hiroyuki Nakagawa[1]

1. The Geospatial Information Authority of Japan

The Geospatial Information Authority of Japan (GSI) routinely analyzes GNSS data obtained by GEONET and monitoring crustal deformation all over Japan. The results are used as fundamental data in the field of such as evaluating earthquake activity or monitoring volcanic activity.

However, depending on the timing of earthquake occurrence or speed of deformation of mountain body, even up-to-date GEONET routine analysis do not always have enough rapidness or time resolution. New analysis method that is more rapid and with higher time resolution are required.

Therefore, we focused on Precise Point Positioning with Ambiguity Resolution, or PPP-AR. With corrective information called Fractional Cycle Bias (FCB) as well as precise orbit and clock information of GNSS satellites, PPP-AR can calculate position for each site as accurate as those derived by interferometric analysis. A key feature is that the position of the stations in every epoch can be calculated rapidly with small calculation load. In addition, PPP-AR does not need fixed reference station. That has advantage when crustal deformation occurs over wide area by large earthquake and it is difficult to find the point that is not subjected to the deformation.

Thus, GSI has started a three-year research project since the April of 2017. In this project, we will develop more rapid and accurate GNSS analysis method based on PPP-AR and make prototype system implementing this method envisioning future GEONET routine analysis. The goal of this research is developing analysis method that can routinely and stably obtain the solution of one-second interval with typical repeatability of about 1cm in horizontal component within about two hours after data acquisition.

In 2018, we perform test analysis of 31 days from Jul. 12 to Aug. 12, 2018 using prototype system under development. Twenty-four hour time series of 1 sec. interval from 0 hour to 0 hour of next day was calculated for al GEONET station once a day, and evaluated estimated satellite orbit and clock, and resulted GEONET time series solutions. First, as an evaluation of quality of estimated satellite orbits and clocks, RMS of estimated orbits with respect to IGS final orbit and RMS of estimated clocks with respect to CODE clock were calculated. As a tentative result, RMS of orbit is about 2.7cm for GPS and about 8.8cm for GLONASS, and RMS of clock is about 4.15ns for GPS and about 6.02ns for GLONASS. Next, as a evaluation of repeatability of GEONET time-series solutions, we calculate a frequency distribution of standard deviation of horizontal coordinate time series. Then, frequency distribution peak is located at a bin from 1.0 to 1.2cm of standard deviation and almost 25% of all time series are fall into this bin. On the other hand, only 21% of time series has standard deviation less than 1cm, which is target of this research project. Time series with standard deviation less than 1.4cm accounts for about 68%.

In this presentation, we will consider the reason and a way to improve the quality of estimated orbit/clock and time series solution.

Keywords: GNSS, PPP-AR, GEONET routine analysis, GEONET

©2019. Japan Geoscience Union. All Right Reserved.

©2019. Japan Geoscience Union. All Right Reserved.

Characteristics of the Tenryu-Funagira laser extensometer and its detection ability of slow slips

*Akio Katsumata[1], Akiteru Takamori[2], Akito Araya[2]

1. Meteorological Research Institute, Japan Meteorological Agency, 2. Earthquake Research Institute, University of Tokyo

Katsumata et al. (2010) installed a long-baseline laser extensometer in Funagira tunnel in Hamamatsu, Shizuoka Pref. Its baseline length is 400 m. Short-term slow-slips were detected with the extensometer. From spectral analysis, it was shown that a long-term slow-slip can be detected with the laser extensometer earlier than the GNSS network. However. iodine-stabilized He-Ne laser, which was used formerly, had a relatively short life time. It was difficult to continue observation for more than several years. We replaced the stabilized laser with the iodine-stabilized YAG laser developed by Araya et al. (2002), and started observation from March, 2018. The sampling rate was changed from 1 kS/s to 10 kS/s to catch up fast phase change due to quick strain change.
We compared the obtained data with that previously obtained with He-Ne laser. It was found that the atmospheric pressure response and tidal response were not changed. However, trend was changed. Trend of about 10^{-7} strain/year was previously observed. No such trend is observed currently. A trend change was observed before and after the 2011 Tohoku earthquake. The trend might be affected by local condition. We compared spectrum levels of the detrended previous and current data. The spectrum level was almost the same over a period range from 0.1 s to several months.
Ide et al. (2007) presented a scaling law of slow earthquakes, in which seismic moment is proportional to event duration. It is considered that strain rate would be the same level regardless of its seismic moment based on the scaling law. Katsumata et al. (2001) showed that the Tenry-Funagira laser extensometer would detect strain change with strain rate the same as those of short-term slow-slips in a day. If there were a slow-slip of one day duration, the Tenryu-Funagira laser extensometer could detect it.

Keywords: Laser extensometer, iodine-stabilized laser, slow-slip observation

©2019. Japan Geoscience Union. All Right Reserved.

Performance evaluation of laser strainmeters

*Akiteru Takamori[1], Akito Araya[1], Akio Katsumata[2], Wataru Morii[3], Kouseki Miyo[4], Masatake Ohashi[4]

1. Earthquake Research Institute, University of Tokyo, 2. Meteorological Research Institute, 3. Disaster Prevention Research Institute, Kyoto University, 4. Institute for Cosmic Ray Research, University of Tokyo

We have constructed four laser strainmeters which are in operation to observe Earth’ s strain in underground sites in Japan. The strainmeters are asymmetric Michelson interferometers implemented with a long main arm (ranging from 100 m to 1.5 km, depending on deployment) that follows ground motion and a short reference arm (shorter than 1 m) which is mounted on a stable platform isolated from the ground. The ground strain is observed by detecting phase difference of the two beams that enter and return from these arms. Due to the sensitivity of the phase difference to laser frequency caused by the mismatch of the arm lengths, the laser frequency needs to be stabilized to maintain high resolution of the instruments in long term. For this purpose, we developed a laser frequency stabilization system that locks a Nd:YAG laser to one of the iodine absorption lines, with the designed stability of 10e-13 to 10e-12. In order to evaluate the performance of the strainmeters, we have been studying stability of the lasers by comparing equivalent systems in situ. The details and results of the experiments are presented together with the estimated performance of the strainmeters.

Keywords: laser strainmeter, frequency stabilized laser

©2019. Japan Geoscience Union. All Right Reserved.

Calculation Method of the Tidal Love Numbers with the Fluid Core Resonance of the Solid Earth

*Yuji Harada[1,2], Shuhei Okubo[3]

1. State Key Laboratory of Lunar and Planetary Science, Space Science Institute, Macau University of Science and Technology, 2. Ocean Hemisphere Research Center, Earthquake Research Institute, University of Tokyo, 3. Center for High Energy Geophysics Research, Earthquake Research Institute, University of Tokyo

Effect of non-rigidity of the solid Earth exerted on the Earth’ s tide and rotation is of importance for understanding dynamical behavior of the core and mantle. The influence of the fluid core on the solid tide is predictable based on Sasao et al.’ s theory (i.e., the SOS theory). In the present study, we show a couple of new ideas so as to simply estimate the Love numbers describing the tidal deformation by means of the SOS theory, and report the results. One of them is how to compute the independent solutions of the radial functions in the solid layer (i.e., the y functions), where we show that it become unnecessary to calculate a part of the solutions in doing numerical integration of the y functions. The other is how to compute those in the liquid layer (i.e., the q functions), where we show that it become unnecessary to calculate the vertical derivative of density in integrating the q functions.

Keywords: Earth's Tide, Earth's Rotation, Earth's Interior

©2019. Japan Geoscience Union. All Right Reserved.

Integrating PSInSAR and Hydrogeophysical Methods for the Characterization of a Earth fissure in the eastern Beijing plain

*Menglin Zhao[1], juan wang[1], wang xu[1], bing hu[1], yisheng chen[1]

1. Capitai Normal University

Modern Earth fissure, ranging from renewed displacement on 1-km-long fault scarps to 9.8-km-long tension cracks, occur in the eastern part of Beijing plain. Most of the failures closely parallel the pre-existing Medio-Pleistocene fault zone. The pattern of earth fissure and the relation to the inferred fault remain controversial. An integrated project, including PSInSAR, geophysical and trenching methods, has been conducted to characterize the formation of earth fissure. The results indicate that this earth fissure was caused by groundwater-level decline rather than natural tectonism. In addition, it is the first time to accurate the initiation and terminal Location of pumping-induced earth fissures within the fault zone.

Keywords: PSInSAR, earth fissure, Hydrogeophysical, fault scarps

Integrating PSInSAR and Hydrogeophysical Methods for the Characterization of a Earth fissure in the eastern Beijing plain

Wang Xu[1] Yisheng Chen[1] ·Bing Hu[1] ·Juan Wang[1] Menglin Zhao[1] Youquan Zhang[1]

Abstract

Modern Earth fissure, ranging from renewed displacement on 1-km-long fault scarps to 9.8-km-long tension cracks, occur in the eastern part of Beijing plain. Most of the failures closely parallel the pre-existing Medio-Pleistocene fault zone. The pattern of earth fissure and the relation to the inferred fault remain controversial. An integrated project, including PSInSAR, geophysical and trenching methods, has been conducted to characterize the formation of earth fissure. The results indicate that this earth fissure was caused by groundwater-level decline rather than natural tectonism. In addition, it is the first time to accurate the initiation and terminal Location of pumping-induced earth fissures within the fault zone.

Keywords: *PSInSAR; earth fissure; Hydrogeophysical;* fault scarps*;* groundwater *; trenching.*

©2019. Japan Geoscience Union. All Right Reserved.

[J] Oral | S (Solid Earth Sciences)：S-GD Geodesy

Mon. May 27, 2019 1:45 PM - 3:15 PM JST | Mon. May 27, 2019 4:45 AM - 6:15 AM UTC | 304 3F

[S-GD03] Geodesy General Contributions/Global Geodetic Observing System

convener:Koji Matsuo(Geospatial Information Authority of Japan), Yusuke Yokota(Institute of Industrial Science, The University of Tokyo), Takahiro Wakasugi(Geospatial Information Authority of Japan), Chairperson:Kensuke Kokado(GSI of Japan), Yusuke Yokota

In this session, general contributions from all areas of geodesy are welcomed. Topics of interest will include but not limited to recent advances in measurement techniques, reference frame realization, earth rotation or earth tide. In addition, this session also provides a forum for discussing GGOS (Global Geodetic Observing System) related observation programs, advancement of geodetic techniques, collaboration among various organizations in the world. Topics will include improvements of observing system and data analysis, participations in global programs, global reference frames and geodesy's contributions to society.

1:45 PM - 1:50 PM JST | 4:45 AM - 4:50 AM UTC

Introduction

1:50 PM - 2:05 PM JST | 4:50 AM - 5:05 AM UTC

[SGD03-01] Activities and future perspective of GGOS Working Group Japan

*Basara Miyahara[1] (1.GSI of Japan)

2:05 PM - 2:20 PM JST | 5:05 AM - 5:20 AM UTC

[SGD03-02] Discussion

*Koji Matsuo[1] (1.Geospatial Information Authority of Japan)

2:20 PM - 2:35 PM JST | 5:20 AM - 5:35 AM UTC

[SGD03-03] VLBI-GNSS Co-location Survey at the Ishioka Geodetic Observing Station

*Saho Matsumoto[1], Michiko Umei[1], Haruka Ueshiba[1], Shinobu Kurihara[1], Tadao Kikkawa[1], Takahiro Wakasugi[1] (1.GSI of Japan)

2:35 PM - 2:50 PM JST | 5:35 AM - 5:50 AM UTC

[SGD03-04] **Research of Crustal Deformation Model for Next Version of Japanese Geodetic Datum**

*Kensuke Kokado[1] (1.GSI of Japan)

2:50 PM - 3:05 PM JST | 5:50 AM - 6:05 AM UTC

[SGD03-05] Construction of a laser-strainmeter network for accurate seismic and geodetic observations

*Akito Araya[1], Akiteru Takamori[1], Wataru Morii[2], Akio Katsumata[3], Akio Kobayashi[3], Takeo Ito[4], Takashi Okuda[4], Makoto Okubo[5] (1.Earthquake Research Institute, University of Tokyo, 2.Disaster Prevention Research Institute, Kyoto University, 3.Meteorological Research Institute, Japan Meteorological Agency, 4.Graduate School of Environmental Studies, Nagoya University, 5.Natural Science Cluster, Kochi University)

3:05 PM - 3:15 PM JST | 6:05 AM - 6:15 AM UTC

Discussion

Activities and future perspective of GGOS Working Group Japan

*Basara Miyahara[1]

1. GSI of Japan

Global Geodetic Observing System (GGOS) is a fundamental framework for integration of global geodetic observations such as GNSS, VLBI, SLR, DORIS, gravity measurements and so on. The main objective of the system is to measure and monitor shape, rotation, gravity field of the earth and its changes. GGOS integrates various international organizations related geodetic observation such as International GNSS Service (IGS), International VLBI Service for Geodesy and Astrometry (IVS), International Laser Ranging Service (ILRS) and so on in order to coordinate and promote global geodetic observations. International Terrestrial Reference Frame (ITRF) which is a de-facto standard for Global Geodetic Reference Frame (GGRF), reference frame for earth’s shape and variation which was endorsed by the United Nations General Assembly in 2015, is also one of the main achievements of GGOS observation. GGOS is essential basic infrastructure for measuring and monitoring of earth’s shape and its change.
The objective of GGOS, that is to continue to measure and monitor earth’s shape and its change can be possible only with continuous global geodetic observation with high quality and enough spatial coverage. Such observation cannot be possible without continuous geodetic observation by countries all over the world. Therefore, several agencies in Japan such as Geospatial Information Authority of Japan (GSI), Japan Coast Guard, National Institute of Information and Communications, National Astronomical Observatory of Japan, National Institute of Polar Research, and Japan Aerospace Exploration Agency have been individually conducting geodetic observation such as GNSS, VLBI and SLR in Japan and Antarctica, and participating in global geodetic observation through international organizations such as IGS, IVS, and ILRS and so on. Several researchers with universities have also participated in the organizations as chairs and board members. In addition, we established a working group on GGOS, GGOS-WG of Japan under IAG Subcommittee in Science Council of Japan in 2013 in order to facilitate information sharing and strengthen collaboration between the agencies for further contribution to GGOS. The WG submitted a status report of geodetic observatories of Japan to GGOS in 2014 and updated it in 2017. The WG has also held a session on GGOS at annual meetings of Japan Geoscience Union (JpGU) since 2015. The theme of GGOS has also added in annual meeting of the Geodetic Society of Japan since 2018. Furthermore, GGOS invited the WG as the first GGOS Affiliate, which is a regional component of GGOS aiming to strengthen regional participation to GGOS and the WG has participated in and contributed to activities of GGOS from regional and national perspectives. As the first GGOS Affiliate, the WG hosted the GGOS annual meeting, GGOS Days 2018 in Tsukuba, Japan and discussed the future activities of GGOS for more strengthened collaboration between GGOS and the WG. In the meeting, current status and issues of network, observation, products and standard were discussed activities of three of four Focus Areas, 1. Unified Height System, 2. Geohazards, 4. Geodetic Space Weather were reported. Some members also reported the possibility of establishment of new GGOS affiliates in DACH countries, Scandinavia, Latin America and North America. The members agreed on the new WG in GGOS which will work on DOI of geodetic data. An update of GGOS guide book was also discussed in the meeting. In addition to the above activities, the WG organized special issue on GGOS in Journal of the Geodetic Society of Japan and also developed a Japanese brochure of GGOS in 2018 to facilitate understanding of the role and significance of GGOS for science and society. In 2018, some members of the WG participated in several international conferences related to GGOS and facilitated exchange of the latest information on geodetic observation. In 2019, we will continue sharing of information and strengthening collaboration in Japan and strengthen collaboration between GGOS and GGOS-WG of Japan.

©2019. Japan Geoscience Union. All Right Reserved.

Keywords: GGOS, GGRF

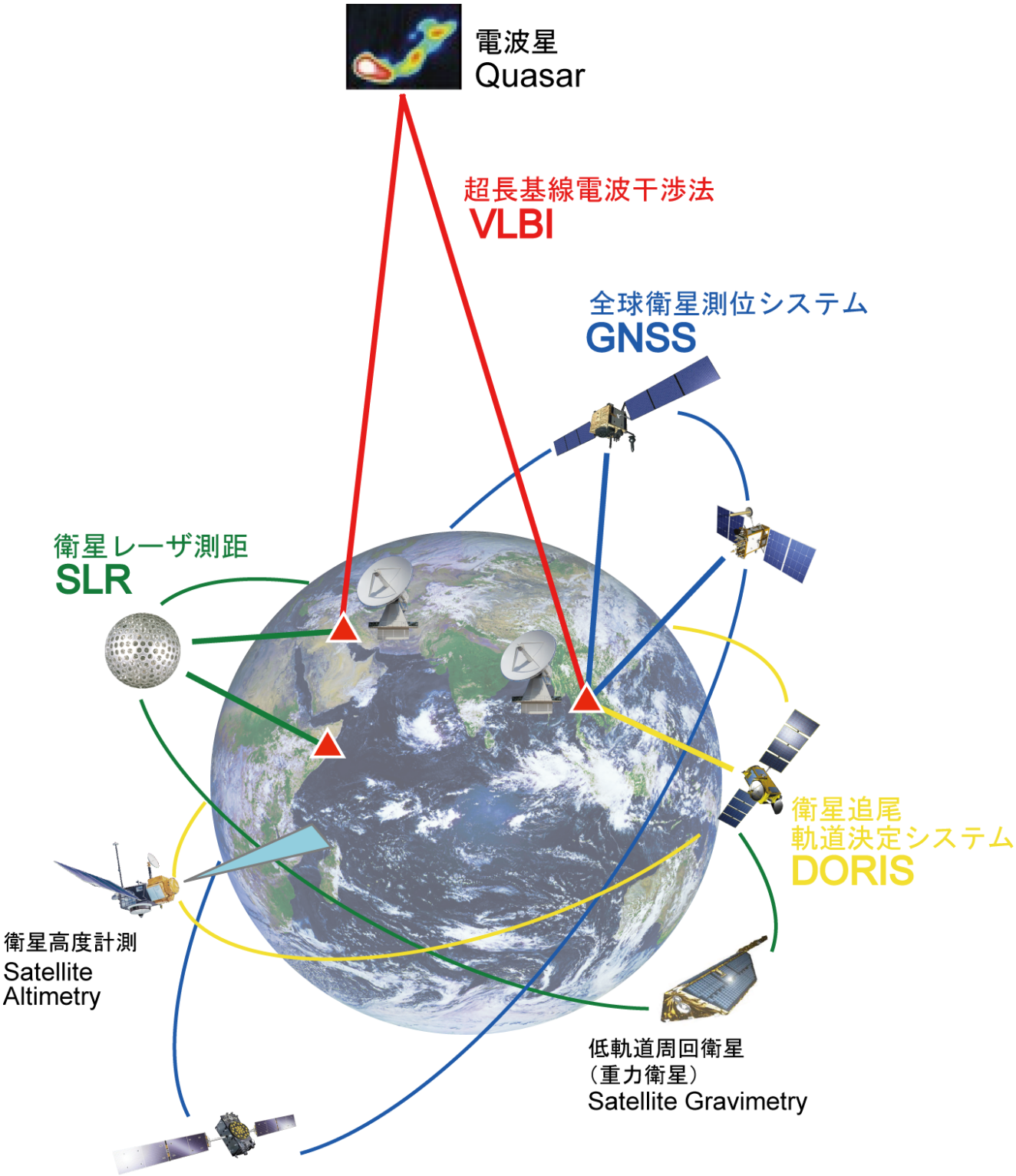

©2019. Japan Geoscience Union. All Right Reserved.

Discussion

*Koji Matsuo[1]

1. Geospatial Information Authority of Japan

We provide a forum for discussion on today's presentation and any topics related to geodesy and GGOS.

Keywords: Discussion

©2019. Japan Geoscience Union. All Right Reserved.

VLBI-GNSS Co-location Survey at the Ishioka Geodetic Observing Station

*Saho Matsumoto[1], Michiko Umei[1], Haruka Ueshiba[1], Shinobu Kurihara[1], Tadao Kikkawa[1], Takahiro Wakasugi[1]

1. GSI of Japan

The International Terrestrial Reference Frame (ITRF) is realized by a combination of four space geodetic observing techniques (VLBI, SLR, GNSS and DORIS), where VLBI contributes in determining scale and EOP, and SLR contributes in determining scale and the center of mass. To perform this combination, it is necessary that relative coordinates between these space geodetic observing stations are precisely known at co-location sites.

The Ishioka Geodetic Observing Station operates the two space geodetic observing stations, VLBI and GNSS. Ishioka station is a fundamental site on a geodetic perspective since the VLBI station is one of the VGOS (VLBI Global Observing System) stations which is promoted by IVS (International VLBI Service for Geodesy and Astrometry) as the next-generation standards, and the GNSS station "ISHI" is registered as one of the IGS (International GNSS Service) sites. To measure the relative coordinate between the VLBI invariant point (IVP) and the GNSS reference point, we conducted the co-location survey in November 2018 in Ishioka station. In this survey, we adopted two methods to determine the IVP. One is "outside method" where we observe the target attached on the antenna movable part (near the counterweight) with "Total Station" at the reference pillars installed around the antenna. The other is "inside method" where we observe the targets attached near the IVP from the inside of the antenna cabin. "Inside method" was adopted for the first time in Ishioka station so we discussed the way of observation, computation and evaluation of error.

In this talk, we will report a co-location survey result in November 2018 and discuss details on two different methods.

Keywords: VLBI, Co-location survey, Local tie vector, ITRF, GNSS

©2019. Japan Geoscience Union. All Right Reserved.

Research of Crustal Deformation Model for Next Version of Japanese Geodetic Datum

*Kensuke Kokado[1]

1. GSI of Japan

Geospatial Information Authority of Japan (GSI) maintains the Japanese horizontal and vertical datum reference system and provides the accurate positions of control points including GNSS CORSs (Continuously Operating Reference Stations) as basic survey result based on the reference system. By utilizing the survey results as the reference position of various surveys and maps, people can receive location information service which positions are aligned with each other nationwide. Along with the progress of Global Navigation Satellite System (GNSS) and the satellite positioning techniques in recent years, it is expected that location information service will be developed using the high accuracy GNSS positioning.

However, there is some gaps due to the crustal deformation between the position of the survey results such as map and the measurement position of the GNSS positioning, which will be used in location information service. Therefore it is necessary to correct the crustal deformation that occurred between the reference date of map and the measurement date of the GNSS positioning in order to match the measurement position by GNSS with the map.

In order to properly correct the above gaps due to the crustal deformation, GSI plans to develop advanced correction system instead of the existing semi-dynamic correction system. For the system development, we have been researching the crustal deformation model considering not only steady crustal deformation but also postseismic deformation of the 2011 Tohoku-Oki earthquake or coseismic deformation of the other earthquakes caused along an active inland faults.

In this presentation, we will focus on the postseismic deformation of 2011 Tohoku-Oki earthquake among the contents of the research, and report the progress of the research to create the crustal deformation model in the Tohoku region.

Keywords: Geodetic Datum, Crustal Deformation, Deformation Model, GNSS positiong

©2019. Japan Geoscience Union. All Right Reserved.

Construction of a laser-strainmeter network for accurate seismic and geodetic observations

*Akito Araya[1], Akiteru Takamori[1], Wataru Morii[2], Akio Katsumata[3], Akio Kobayashi[3], Takeo Ito[4], Takashi Okuda[4], Makoto Okubo[5]

1. Earthquake Research Institute, University of Tokyo, 2. Disaster Prevention Research Institute, Kyoto University, 3. Meteorological Research Institute, Japan Meteorological Agency, 4. Graduate School of Environmental Studies, Nagoya University, 5. Natural Science Cluster, Kochi University

Laser interferometers are widely used for precise measurements of displacement with reference to wavelength of light. As their geophysical application, a laser strainmeter is used for measuring deformation of the ground by sensing distance between two separated points, enabling to detect small strain changes over wide frequency range [1]. The advantages of the laser strainmeter over conventional strainmeters using mechanical references are high resolution with a long baseline, resonance-free response of optical reference, and low-drift detection using stabilized laser wavelength. Apart from the instrumental detectability, local noise sources, such as changes in temperature, air pressure, and ground water level, will affect both the instrument and the ground, and should be properly evaluated to examine the measured strain data. For this purpose, we constructed a network of laser strainmeters deployed at three underground sites in Japan: Kamioka (Gifu Pref.), Inuyama (Aichi Pref.), and Tenryu-Funagira (Shizuoka Pref.). These strain data are analyzed to evaluate performance of instruments installed at these sites as well as to identify common geophysical signals.

At Kamioka site, two laser strainmeters with baselines of 100m and 1500m are in operation [2, 3]. At Inuyama and Tenryu-Funagira sites, a 30-m strainmeter and a 400-m one are installed, respectively [4]. These strainmeters clearly detect earth tides, and their amplitudes are consistent with the calculation based on the tidal force, the standard Earth's model, and the topographic effects around the sites. Using the site effects, coseismic strain steps observed by the strainmeter network are compared with fault parameters estimated from seismic observations and the detectability of the fault mechanisms using the strainmeter network is estimated. For long-term strain changes, local disturbances of the sites and detectability of the network are estimated using GNSS data. In the presentation, we discuss detectability of the strainmeter network for seismic and geodetic signals and prospects for monitoring crustal activities using long-baseline laser strainmeters.

References

[1] V. Vali, R. S. Krogstad, and R. W. Moss, Laser interferometer for earth strain measurements, Rev. Sci. Instrum., 36, 1352, 1965.

[2] A. Araya, A. Takamori, W. Morii, K. Miyo, M. Ohashi, K. Hayama, T. Uchiyama, S. Miyoki, and Y. Saito, Design and operation of a 1500-m laser strainmeter installed at an underground site in Kamioka, Japan, Earth, Planets and Space, 69:77, 2017.

©2019. Japan Geoscience Union. All Right Reserved.

[3] T. Akutsu, M. Ando, S. Araki, A. Araya, T. Arima et al., Construction of KAGRA: an underground gravitational-wave observatory, Prog. Theor. Exp. Phys., 013F01, 2018.

[4] A. Araya, T. Kunugi, Y. Fukao, I. Yamada, N. Suda, S. Maruyama, N. Mio, and S. Moriwaki, Iodine-stabilized Nd:YAG laser applied to a long-baseline interferometer for wideband earth strain observations, Rev. Sci. Instrum., 73, 6, 2434-2439, 2002.

Keywords: strainmeter, laser, crustal deformation, Kamioka, Inuyama, Tenryu-Funagira

©2019. Japan Geoscience Union. All Right Reserved.

[J] Oral | S (Solid Earth Sciences)：S-GD Geodesy

Mon. May 27, 2019 3:30 PM - 5:00 PM JST | Mon. May 27, 2019 6:30 AM - 8:00 AM UTC | 304 3F

[S-GD03] Geodesy General Contributions/Global Geodetic Observing System

convener:Koji Matsuo(Geospatial Information Authority of Japan), Yusuke Yokota(Institute of Industrial Science, The University of Tokyo), Takahiro Wakasugi(Geospatial Information Authority of Japan), Chairperson:Yuji Harada(Macau University of Science and Technology), Koji Matsuo

In this session, general contributions from all areas of geodesy are welcomed. Topics of interest will include but not limited to recent advances in measurement techniques, reference frame realization, earth rotation or earth tide. In addition, this session also provides a forum for discussing GGOS (Global Geodetic Observing System) related observation programs, advancement of geodetic techniques, collaboration among various organizations in the world. Topics will include improvements of observing system and data analysis, participations in global programs, global reference frames and geodesy's contributions to society.

3:30 PM - 3:35 PM JST | 6:30 AM - 6:35 AM UTC

Introduction

3:35 PM - 3:50 PM JST | 6:35 AM - 6:50 AM UTC

[SGD03-06] UNAVCO GNSS Data: Real-time High-rate Streams, Geodetic Earthquake Magnitudes, Cloud Computing and Future Machine Learning Frameworks

*David A Phillips[1], Kathleen Hodgkinson[1], David Mencin[1], Charles Meertens[1], Thomas Herring[2], Walter Szeliga[3], Timothy Melbourne[3], Mark Murray[4], Glen Mattioli[1], Christine Puskas[1] (1.UNAVCO, Inc. Boulder, 2.Massachusetts Institute of Technology, 3.Central Washington University, 4.USGS)

3:50 PM - 4:05 PM JST | 6:50 AM - 7:05 AM UTC

[SGD03-07] **On application of GNSS-techniques for early tsunami warning in the Sea of Japan**

*Grigorii Viktorovich Nechaev[1,2,3], Nikolai Shestakov[2,3], Hiroaki Takahashi[1], Mako Ohzono[1] (1.Institute of Seismology and Volcanology, Graduate Schooll of Science, Hokkaido University, 2.Far Eastern Federal University, 3.Institute for Applied Mathematics FEB RAS)

4:05 PM - 4:20 PM JST | 7:05 AM - 7:20 AM UTC

[SGD03-08] Measurements of occurrence of solar conjunction with the orbits of Asian QZSS/IGSO satellites

Cancelled

*Fujinobu Takahashi[1] (1.Yokohama National University)

4:20 PM - 4:35 PM JST | 7:20 AM - 7:35 AM UTC

[SGD03-09] Sea level evaluation in northern Australian coast

*Yuta Tokui[1], Kosuke Heki[1] (1.Hokkaido University)

4:35 PM - 4:50 PM JST | 7:35 AM - 7:50 AM UTC

[SGD03-10] Implications from geomagnetic observation for the interannual fluctuations of Earth rotation

*Seiki Asari[1], Masanori Kurihara[1], Kenji Morinaga[1], Shingo Nagamachi[1] (1.Kakioka Magnetic Observatory, Japan Meteorological Agency)

4:50 PM - 5:00 PM JST | 7:50 AM - 8:00 AM UTC

Discussion

UNAVCO GNSS Data: Real-time High-rate Streams, Geodetic Earthquake Magnitudes, Cloud Computing and Future Machine Learning Frameworks

*David A Phillips[1], Kathleen Hodgkinson[1], David Mencin[1], Charles Meertens[1], Thomas Herring[2], Walter Szeliga[3], Timothy Melbourne[3], Mark Murray[4], Glen Mattioli[1], Christine Puskas[1]

1. UNAVCO, Inc. Boulder, 2. Massachusetts Institute of Technology, 3. Central Washington University, 4. USGS

UNAVCO provides a diverse suite of geodetic data, derived products and cyberinfrastructure services to support the geodetic community, Earth science research and education. We present here an overview of recent developments related to real-time GNSS data streams, GNSS earthquake magnitude estimation, a new project focusing on machine learning for geoscience and hazards research, and cloud based GNSS data analysis experiments. UNAVCO operates the National Earth Science Geodetic Facility through a cooperative agreement with the U.S. National Science Foundation (NSF) and NASA.

Real-time (<2 seconds) high-rate (1 Hz) GNSS (RT-GNSS) data streams are now provided from ~900 UNAVCO sites. Streams include raw data in BINEX and RTCM3, and PPP solutions in ITRF2008 via Trimble PIVOT RTX software. Most UNAVCO RT-GNSS sites are within the Network of the Americas (NOTA). NOTA, which includes the historic Plate Boundary Observatory (PBO) network, is an extensive network of GNSS reference stations and other geophysical instruments in the United States, Mexico, Central America, the Caribbean and parts of South America. The network advances research into Earth systems from the core to the atmosphere. Recent advances include improved plate tectonic models, understanding earthquakes and slow slip/episodic tremor, measuring surface water load, deciphering ionospheric dynamics and measuring changes in permafrost. Beyond research the network provides information for earthquake and tsunami early warning systems (EWS), severe weather and space weather forecasts, volcanic activity alerts, drought and flood monitoring and other risk assessments. UNAVCO data are open access; an objective of the geodetic community is to enhance data access and data use for global hazard risk reduction.

Following an earthquake, RT-GNSS data streams can record peak ground displacement (PGD) measurements from long-period surface waves and provide a source-scaling relation that does not saturate with event magnitude. “Geodetic magnitudes” derived from RT-GNSS data can be estimated within seconds to minutes after an earthquake, and can improve earthquake and tsunami EWS. Dynamic displacements estimated in real time show reasonable agreement with post-processed estimates. And while individual position estimates have large errors, RT-GNSS solutions offer excellent operational potential for EWS, including the use of PGD to directly invert for finite-fault solutions. We will show PGD and geodetic magnitude estimate results from recent earthquakes including the 2018-11-30 Mw 7.0 Anchorage, Alaska earthquake. PGD’s from this earthquake were calculated automatically from the RT-GNSS displacement traces, which were large enough and recorded by enough sites to determine that, using GNSS data only, the event was ~M7 within 120s.

As the number of RT-GNSS sites increases, the volume of data and the complexity of automated analysis increase as well. When other data streams are factored in, such as seismic, ocean bottom pressure and satellite radar, the shear volume and complexity of these data streams, coupled with the need to model, analyze and assess hazards in a matter of only minutes, makes geophysical applications to hazards early

©2019. Japan Geoscience Union. All Right Reserved.

warning a Big Data problem. To address this, UNAVCO is collaborating in an NSF project called "GeoSCIFramework: Scalable Real-time Streaming Analytics and Machine Learning for Geoscience and Hazards Research." This project unites computer scientists and geoscientists to develop a data framework for generalized real-time streaming analytics and machine learning for geoscience and hazards research. The goals of this project, which was just initiated, will be presented.

In addition to real-time products, UNAVCO also provides post-processed position time series and velocities from 2000+ GNSS stations. These products are based on daily solutions generated using GIPSY PPP and GAMIT/GLOBK double-difference network software. This software is currently run on local computing clusters. As part of an NSF funded project called GeoSciCloud, we are testing our GIPSY and GAMIT workflows in two cloud computing environments: Amazon Web Services and NSF's Extreme Science and Engineering Discovery Environment (XSEDE). The IRIS seismic data facility is a collaborative partner on this project and conducted similar experiments using seismic software and data. We summarize our latest findings from these cloud computing experiments including performance and cost relative to local systems.

Keywords: Geodesy, GNSS, Real-Time Data, EWS

©2019. Japan Geoscience Union. All Right Reserved.

On application of GNSS-techniques for early tsunami warning in the Sea of Japan

*Grigorii Viktorovich Nechaev[1,2,3], Nikolai Shestakov[2,3], Hiroaki Takahashi[1], Mako Ohzono[1]

1. Institute of Seismology and Volcanology, Graduate Schooll of Science, Hokkaido University, 2. Far Eastern Federal University, 3. Institute for Applied Mathematics FEB RAS

Tsunami hazard threatens an extensive coastlines located in the seismically active areas. About 250000 persons were killed by tsunami only with the beginning of 21th century. Thus, the problem of reliable early tsunami warning is very important nowadays.
The most of working tsunami early warning systems (TEWS) are based on seismic methods that often cannot provide a reliable and accurate warning due to different reasons. The GNSS-based TEWS recently has been developed and they are free of many shortcomings of seismic methods. Such systems utilize coseismic shifts measured by onshore GNSS-networks for tsunami modeling. The TEWS operating now, for example, REGARD [Kawamoto S. et al., 2017], are mainly focused on detection of huge Mw8-9 class subduction zone earthquakes. They are not designed to process relatively small events, which can produce coseismic displacements less than 10 cm, despite on RTX-techniques or recently developed methods [Fratarcangeli F. et al., 2018], which can detect site position changes of 1-2 cm in horizontal and 3-4 cm in vertical components. However, devastating tsunamis regularly appear in the Japan Sea. They are caused by shallow thrust seismic events with magnitudes Mw6.2-7.8. These quakes generate tsunamis more effectively than Pacific ones with the same magnitude.The epicenters of tsunamigenic earthquakes are distributed along the western coast of Honshu, south-west of Hokkaido and Sakhalin Islands. Nevertheless, tectonics and seismicity of the Japan Seahaven't been sufficiently investigated still and tsunamigenic seismic events can occur along the north-western margin of the sea. For example, the potentially tsunamigenic Mw˜6 shallow seismic event occurred near the northeastern coast of Primorye on Nov. 11, 1990.
In this work we explored: 1) the capacity of GNSS-based TEWS application using data about historical Mw 6.2-7.8 Japan Sea crustal seismic events. The appropriate coseismic displacement fields were calculated and analyzed. Possible hypothetic tsunamigenic seismic sources were also considered; 2) the optimal GNSS-site distribution for earthquake source parameters obtaining based on existing and prospective GNSS-networks configuration in the region.
We obtained, that historical tsunamigenic earthquakes occurred along the eastern margin of the Japan Sea induced coseismic displacements ranging from 1 cm to a few decimeters through the northern Honshu and western Hokkaido. Even 1964 Oga-oki, Mw7.0 event caused up to 4 cm surface offsets on the Honshu Island coast. Southwestern Sakhalin Island are also might be affected by centimeter level coseismic movement invoked by the shallow Mw 6.2-7.3 earthquakes appeared in the north of the Sea of Japan and Tatar strait. Hypothetical events with Mw > 7.5 and located in the north-west of the sea may excite displacement varying from 1 to 4 cm in Russian Primorye and Hokkaido Island. A set of inversion tests lead us to a conclusion that GEONET GNSS-network might be used to model tsunamigenic earthquake sources with Mw>7.0-7.8 distributed along the eastern margin of the Japan Sea. Working and prospective GNSS-networks located along the western coast of the sea and Sakhalin Island might be involved into processing of seismic events with Mw ≧ 7.3 appeared in the northern part of the sea.

This work was partially supported by the RFBR grant No. 17-55-53110 and JREX Fellowship.

©2019. Japan Geoscience Union. All Right Reserved.

Keywords: tsunami early warning, GNSS

©2019. Japan Geoscience Union. All Right Reserved.

Measurements of occurrence of solar conjunction with the orbits of Asian QZSS/IGSO satellites

*Fujinobu Takahashi[1]

1. Yokohama National University

On the space PNT in the 20th century, the MEO satellite system represented by GPS space segment of USA has played a major role. In the 21st century, Japan's QZSS (Michibiki) satellite system and IGSO space segment of China and India are now appearing. The feature of the MEO satellite system is a scheme that the positioning accuracy is determined by randomly selecting MEO satellites above the elevation limit and by the satellites combination of smaller DOP. This is one of the stochastic based on the group of the randomly selected satellites, rather than the orbital theory of the satellite. Meanwhile the orbital motions of QZSS/IGSO of new 21st century are very slow over the respective earth regions. The more theoretical methods using satellite orbit models are available and the more reproducible analytic methods are possible. The author will report the measuring results of the orbital motion and the solar conjunctions of Asian QZSS/IGSO satellites over more than a year.

Keywords: QZSS, IGSO, PNT

©2019. Japan Geoscience Union. All Right Reserved.

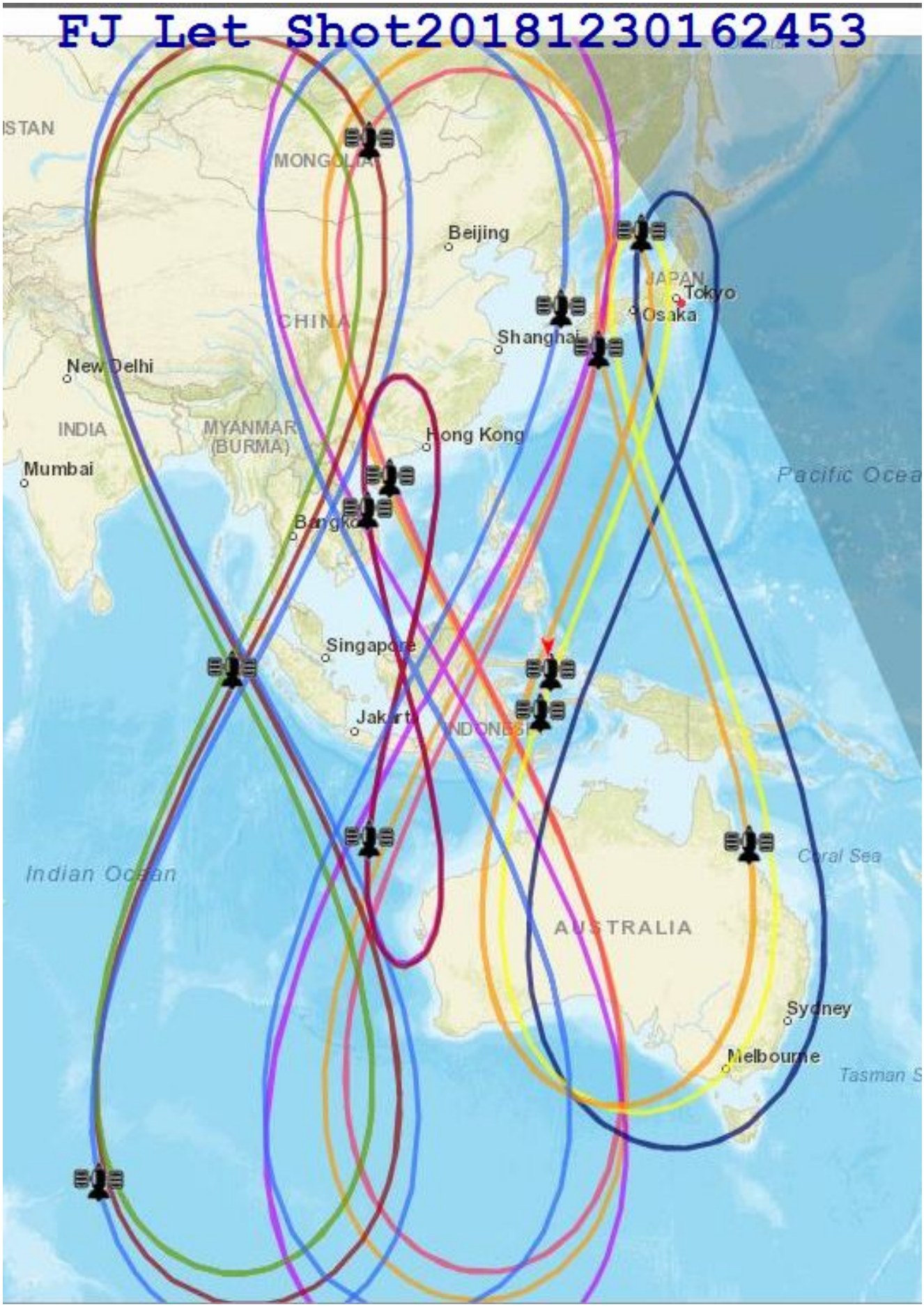

©2019. Japan Geoscience Union. All Right Reserved.

Sea level evaluation in northern Australian coast

*Yuta Tokui[1], Kosuke Heki[1]

1. Hokkaido University

Sea surface heights (SSH) are observed by satellite ocean altimetry, and it changes by two major causes. They are barystatic changes e.g. inflow of melt water from land ice, and thermal expansion of sea water, and they can be observed by GRACE and Argo floats, respectively. The three quantities behave differently from region to region, and their mutual link is important to understand regional characteristic of oceans. Here we study sea level changes in northern Australian coast (consisting of the Arafura, Timor, and Solomon Seas and the Gulf of Carpentaria). This region is characterized by large seasonal changes in SSH and gravity, and influenced by multiple climate changes such as ENSO (El Nino and Southern Oscillation) and IOD (Indian Ocean Dipole). First, we compare three changes (altimetric, thermosteric and gravity) to evaluate sea level budget. We found that SSH changes mainly come from steric changes excluding Gulf of Carpentaria where barystatic changes prevail. Next, we use the Empirical Orthogonal Functions (EOF) approach to identify the major modes of the seasonal and interannual variability. Seasonal changes in SSH are strong in Gulf of Carpentaria. The 1 st EOF of gravity indicates that main seasonal change occur in phase in the land and the sea. We also found that long-term precipitation variability appears as the 2nd EOF. The EOF analysis further showed that non-seasonal altimetric and gravity changes are driven mainly by climate changes, mainly ENSO in SSH and PDO in gravity.

Keywords: Altimeter, GRACE, Argo float, SSH, ENSO

©2019. Japan Geoscience Union. All Right Reserved.

Implications from geomagnetic observation for the interannual fluctuations of Earth rotation

*Seiki Asari[1], Masanori Kurihara[1], Kenji Morinaga[1], Shingo Nagamachi[1]

1. Kakioka Magnetic Observatory, Japan Meteorological Agency

Kakioka Magnetic Observatory has a history of magnetic observation over as long time as more then a century. It has supported a progress of scietific researches and industry by providing accurate data, developing observation technology, certifying measurement instruments, as well as playing a geodetic role as a magnetic reference station of Japan. The observatory is even increasingly expected to stay as one of world's principal observatories, with the increase of demands for prompt data issuance to serve as reference for the recent satellite magnetic observations.

Geomagnetic variations consist of different components with varying sources and timescales. The accumulation of enormous amount of data from the recent satellite observations in the late years have drawn attentions to the interannual variations of the geomagnetic main field originating in Earth core. These variations had not been well recognised, with their tiny signals hidden by the magnetic perturbations from the magnetosphere. If these signals are resolved more clearly, they can be a precious key to reveal the interannual phenomena in Earth fluid core such as hydromagnetic waves. Imaging of the core fluid flow relies entirely on mangetic observations, as the seismic and gravitational observations do not provide high enough sensitivity, while the net fluctuations of the core may be analysed by using Earth rotation variation.

Currently, monthly mean database for the past half century has been under construction at Kakioka Magnetic Observatory such that they are optimised for better identifying the interannual main field variations. It has been found that approximately 70 percent of the external field perturbations can be eliminated from monthly data at any observatories at low- and mid-latitudes. A better mapping of the fluid core flow may be possible for even longer period. In this presentation, a report for the progress and prospect is given, together with discussion on implications for the interannual Earth rotation fluctuations through the core flow map imaged from magnetic observations. A spatiotemporal features of the westward core fluid jet at the polar region in the northern hemisphere, which may be responsible for both the rapid changes in both the geomagnetic main field and the length-of-day.

Keywords: Earth rotation, Geomagnetic field, Interannual variation, Angular momentum, Core

©2019. Japan Geoscience Union. All Right Reserved.

[E] Poster | S (Solid Earth Sciences)：S-SS Seismology

Mon. May 27, 2019 1:45 PM - 3:15 PM JST | Mon. May 27, 2019 4:45 AM - 6:15 AM UTC | Poster Hall International Exhibition Hall8, Makuhari Messe_5

[S-SS07] Rigorous Seismicity Modelling and Hypothesis Testing

convener:Jiancang Zhuang(Institute of Statistical Mathematics), Danijel Schorlemmer(GFZ German Research Centre for Geosciences), Matt Gerstenberger(GNS Science), Hiroshi Tsuruoka(Earthquake Research Institute, Tokyo Univ.)

Probabilistic models have been developed for describing, analyzing, and forecasting seismicity since more than 100 years and, with the advent of large-scale digital networks, in high resolution during the last 30 years. These models include recurrence and stress-release models for long-term earthquake hazard assessment, and short-term models describing earthquake clustering, e.g. the ETAS model. Some models have become standard tools in seismic hazard assessment. However, the overall probabilities remain on the low end and the uncertainties of the forecasts are not well described. Rigorous data-based development and testing of models will help further improving forecasting power and accuracy of these models. Similarly, new hypotheses shall be evaluated rigorously using some existing model as the null hypothesis model or in dedicated tests addressing the hypothesis directly. In this context, the Collaboratory for the Study of Earthquake Predictability and its Japan branch provides the necessary testing capabilities for rigorous and unbiased evaluation of models and hypotheses. This session focuses on research that increases information on seismicity, being with respect to a reference model or as an independent hypothesis. We solicit contributions of model developments and hypothesis formulation based on the increased understanding of the physical process of earthquakes, such as the preparation and rupture processes of the earthquake source and the interaction between earthquakes and tectonic environments. We also welcome development and implementation of improved statistical methods for testing and validating physical hypotheses based on observed data. In particular, we welcome contributions about model- or hypothesis-test experiments that could be implemented in the Japan testing center.

[SSS07-P01] Development of Physics-based Ground Motion Simulation in A Hybrid Approach and Applications to Seismic Hazard Assessment in Taiwan

*Ming-Che Hsieh[1], Yin-Tung Yen[1], Kuo-Fong Ma[2,3] (1.Disaster Prevention Technology Research Center, Sinotech Engineering Consultants (Inc.), Taiwan, 2.Department of Earth Sciences, National Central University, Taiwan, 3.Earthquake-Disaster & Risk Evaluation and Management Center, National Central University, Taiwan)

[SSS07-P02] Increasing Earthquake Forecast Testability - CSEP Future Developments

*Danijel Schorlemmer[1], Naoshi Hirata[2], Fabrice Cotton[1], Matt Gerstenberger[3], Thomas Jordan[7], Warner Marzocchi[4], William Savran[7], Maximilian Werner[5], Stefan Wiemer[6], Thomas Beutin[1], David D Jackson[8], Philip Maechling[7], Sum Mak[1], Kazuyoshi Nanjo[9], Yosihiko Ogata[10], David Rhoades[3], Hiroshi Tsuruoka[2], Graeme Weatherill[1], Jiancang Zhuang[10] (1.GFZ German Research Centre for Geosciences, 2.Earthquake Research Institute, University of Tokyo, Japan, 3.GNS Science, Lower Hutt, New Zealand, 4.University of Naples, Naples, Italy, 5.University of Bristol, Bristol, United Kingdom, 6.ETH Zurich, Zurich, Switzerland, 7.University of Southern California, Los Angeles, USA, 8.University of California Los Angeles, Los Angeles, USA, 9.University of Shizuoka, Shizuoka, Japan, 10.Institute of Statistical Mathematics, Tachikawa, Japan)

[SSS07-P03] Precision versus uncertainty in regional seismic hazard mapping

*Matt Gerstenberger[1], Danijel Schorlemmer[2] (1.GNS Science, 2.GFZ-Potsdam)

[SSS07-P04] An extreme value analysis of seismograms designed for early forecast of aftershocks

*Kaoru Sawazaki[1] (1.National Research Institute for Earth Science and Disaster Resilience)

[SSS07-P05] **Spatio-temporal clustering of successive earthquakes: data analyses of global data.**

*THYSTERE MATONDO BANTIDI[1], Takeshi Nishimura[1] (1.Tohoku University)

[SSS07-P06] Kanto 3 month testing class results of CSEP Japan

*Hiroshi Tsuruoka[1], Naoshi Hirata[1] (1.Earthquake Research Institute, Tokyo Univ.)

[SSS07-P07] Long-term earthquake risk in North China estimated from a modern catalogue

Ziyao Xiong[2], *Jiancang Zhuang[1], Shiyong Zhou[2] (1.Institute of Statistical Mathematics, 2.Peking University)

[SSS07-P08] **Distributions of focal mechanisms in background seismicity and earthquake clusters in Japan**

*Jiancang Zhuang[1,2], Eri Maita[2] (1.Institute of Statistical Mathematics, 2.Graduate University for Advanced Studies)

[SSS07-P09] New Ground Motion Prediction Equations for Western Saudi Arabia

*Ryota Kiuchi[1,2], Walter Mooney[1], Hani Zahran[3] (1.U.S. Geological Survey, 2.Disaster Prevenetion Research Institute, Kyoto University, 3.Saudi Geological Survey)

[SSS07-P10] Study on the spatial and temporal change of velocity structure before and after 2003 Chengkung earthquake, Taiwan

*TING YA LIANG[1], Wen-Yen Chang[1,2,3], Strong Wen[4] (1.National DONG HWA University, 2.Eastern Taiwan Earthquake Research Center, 3.National Center for Research on Earthquake Engineering, 4.National Chung Cheng University)

Development of Physics-based Ground Motion Simulation in A Hybrid Approach and Applications to Seismic Hazard Assessment in Taiwan

*Ming-Che Hsieh[1], Yin-Tung Yen[1], Kuo-Fong Ma[2,3]

1. Disaster Prevention Technology Research Center, Sinotech Engineering Consultants (Inc.), Taiwan, 2. Department of Earth Sciences, National Central University, Taiwan, 3. Earthquake-Disaster & Risk Evaluation and Management Center, National Central University, Taiwan

Damages to engineering structures by an earthquake depend on the entire time history of the ground motion, which is affected by a number of factors including source-rupture process, seismic-wave velocity structure, topographic relief, and local site condition. To quantitatively assess these effects to ground motion, physics-based ground motion simulation is a powerful tool which enables rigorous modeling of each effect and their coupling. In this study, we present a recent-developed physics-based ground motion simulator in generating broadband seismograms for seismic hazard assessment. The simulator is essentially based on a hybrid approach in which long-period synthetics are calculated by the efficient 3-D strain Green’ s tensor (SGT) and short-period synthetics are modeled by the stochastic method. Physical effects of (1) source slip distribution, (2) seismic wave propagation, (3) surface topography and (4) site amplification are taken into account. This hybrid approach has been validated by the 2016 M_W6.6 Meinong earthquake in southern Taiwan and reveals good potential for engineering applications. We also carried out simulations to model rupture scenarios of seismogenic structure and subduction zone sources. Output full waveform and ground motion parameters, e.g. peak ground acceleration (PGA) and 1.0-s-period spectral acceleration (SA1.0), have been further implemented to risk estimation, and even earthquake drill. Our result shows the ground motion simulator has the potential for earthquake scenario modeling and hazard assessment.

Keywords: Ground motion simulation, Seismic hazard assessment, Strain Green’ s tensor, Stochastic method

©2019. Japan Geoscience Union. All Right Reserved.

Increasing Earthquake Forecast Testability - CSEP Future Developments

*Danijel Schorlemmer[1], Naoshi Hirata[2], Fabrice Cotton[1], Matt Gerstenberger[3], Thomas Jordan[7], Warner Marzocchi[4], William Savran[7], Maximilian Werner[5], Stefan Wiemer[6], Thomas Beutin[1], David D Jackson[8], Philip Maechling[7], Sum Mak[1], Kazuyoshi Nanjo[9], Yosihiko Ogata[10], David Rhoades[3], Hiroshi Tsuruoka[2], Graeme Weatherill[1], Jiancang Zhuang[10]

1. GFZ German Research Centre for Geosciences, 2. Earthquake Research Institute, University of Tokyo, Japan, 3. GNS Science, Lower Hutt, New Zealand, 4. University of Naples, Naples, Italy, 5. University of Bristol, Bristol, United Kingdom, 6. ETH Zurich, Zurich, Switzerland, 7. University of Southern California, Los Angeles, USA, 8. University of California Los Angeles, Los Angeles, USA, 9. University of Shizuoka, Shizuoka, Japan, 10. Institute of Statistical Mathematics, Tachikawa, Japan

The Collaboratory for the Study of Earthquake Predictability (CSEP) has expanded over the years to many different testing areas hosted at multiple testing centers. Hundreds of earthquake forecast models have been submitted to CSEP and are being tested. New testing metrics were developed and implemented and a lot of progress was made to establish CSEP as an institution that cannot be ignored when issuing earthquake forecasts. Its rigor and independence became the standard in evaluating earthquake forecasts and in reporting on the results.

In the framework of the testing activities of the Global Earthquake Model, one line of expanding the capabilities of CSEP was developed at GFZ Potsdam. The group there applied the mechanisms that CSEP introduced to earthquake forecast models to the area of intensity prediction equations (IPEs) and ground-motion prediction equations (GMPEs). The first truly prospective tests were carried out on IPEs for Italy and also on GMPEs for Japan and New Zealand. This new set of tests helped CSEP move into the hazard domain and increase the relevance of its results to the hazard community. Finally, the group at GFZ Potsdam has also conducted the first prospective test of the US national seismic hazard maps.

Although these tests have been successful and well-received, they have also shown the limitations of the CSEP approach. Many aspects of seismic hazard or earthquake forecasting remain inherently untestable if only the model forecasts are tested and not the model ingredients. We propose to continue along the lines of the GFZ Potsdam developments and create new areas of activity for CSEP, namely targeted experiments that cannot be conducted with the current CSEP software system. As part of the eGSIM (European Ground Shaking Intensity Models) service, we will introduce permanent testing of IPEs and GMPEs to the testing center to establish strong performance records to be used in hazard models. Further targeted experiments include the predictive power of b-values, discrimination of foreshocks for short-term forecasting, as well as a deeper look into precursory
phenomena applying CSEP-style rigorous testing. We support including testability in future hazard models or their components to move to better testable seismic hazard models. Finally, to expand into the risk domain, we will test exposure models against new and independent data.

Keywords: Seismicity, Forecasting, Testing

©2019. Japan Geoscience Union. All Right Reserved.

Precision versus uncertainty in regional seismic hazard mapping

*Matt Gerstenberger[1], Danijel Schorlemmer[2]

1. GNS Science, 2. GFZ-Potsdam

Regional and national seismic hazard mapping efforts have increasingly pursued more detailed and precise models and outputs, particularly in terms of source characterisation and modelling. With increasing precision comes increasing uncertainty. In recent years much attention has been paid to modelling uncertainty in ground-motion models and including this in seismic hazard modelling. However, much less effort has been made to quantify and model uncertainty in seismic source characterisation. This raises two questions: 1) is increasing precision appropriate when uncertainty remains poorly quantified? 2) what is the optimal balance between precision and uncertainty? Ultimately the answer to this depends on the end-uses of the models and the implications of increasing uncertainty with increasing precision. Here we explore some of the main sources of uncertainty in seismic source characterisation such as incomplete and limited records of earthquake occurrence in paleoseismic data and earthquake catalogues, non-stationarity of seismicity and the poisson assumption, fault source characterisation and so-called moment balancing. We pay particular focus to uncertainties in estimating hazard in less seismically active regions and the implications for building design guidance.

Keywords: Seismic hazard, PSHA, uncertainty

©2019. Japan Geoscience Union. All Right Reserved.

An extreme value analysis of seismograms designed for early forecast of aftershocks

*Kaoru Sawazaki[1]

1. National Research Institute for Earth Science and Disaster Resilience

Conventional aftershock forecasting has been operated through applying the Gutenberg-Richter and Omori-Utsu laws to an earthquake catalog. However, catalog's quality is influenced by detectability of earthquake signals (P or S waves), which causes degradation of the catalog in the early stage after a large earthquake and at regions which are sparsely covered by seismograph network. This eventually causes the catalog's nonuniformity and limitation of the forecasting performance.

In this study, we propose a new approach designed for high-performance early aftershock forecasting without using earthquake catalog. Instead, we use a continuous seismogram recorded at each station. First, we pick the maximum amplitude of the seismogram obtained in every assigned time interval (e.g., 1 minute). This picking process can be completely automated and is rarely affected by overlap of multiple seismic signals occurring in approximately the same time. We empirically derive a probability distribution (PD) that accounts for the frequency of the maximum amplitudes. This PD is essentially a non-stationary extreme value distribution derived from the generalized Pareto distribution (GPD) and the Omori-Utsu type temporal decay. We optimize three parameters that control the PD shape (K_a: parameter that controls whole aftershock activity, p_a: parameter that controls temporal decay of the aftershock frequency, m: parameter that controls power-law decay of the maximum amplitude) by applying the maximum likelihood estimation to the observed maximum amplitudes. By extrapolating the optimized PD, we estimate the number of maximum amplitudes that will exceed a threshold value within arbitral time interval in the future. The proposed approach provides forecast of peak ground motion at each station rather than magnitude, which is directly desired for public use. Moreover, the forecasted peak ground motion may automatically incorporate many factors that cannot be described by a simple ground motion attenuation model (e.g., site amplification, radiation pattern, rupture directivity, and so on).

We apply the proposed method to 25 Hi-net seismograms recorded the 2016 Kumamoto earthquakes in Japan. We set the learning periods every one hour after the mainshock (Mj7.3), and set the forecasting period within 24 hours after the end of each learning period. We find that parameters K_a and m become temporally stable within a few hours after the mainshock at many stations. On the other hand, the parameter p_a temporally varies more probably because the induced seismicity at northeast area (Aso and Oita regions) strongly affects the apparent temporal decay rate of the amplitudes. Within 3 hours after the mainshock, the forecasted number of the maximum amplitudes exceeding 10^{-4} m/s is within 0.5 to 2.0 times the actual observation for about 80 % of the used stations. For the threshold amplitude of 10^{-3} m/s, on the other hand, the forecasted number tends to overestimate, probably due to saturation of seismograms by both artificial and physical reasons.

Keywords: extreme value analysis, aftershock forecasting, peak ground motion

©2019. Japan Geoscience Union. All Right Reserved.

Spatio-temporal clustering of successive earthquakes: data analyses of global data.

*THYSTERE MATONDO BANTIDI[1], Takeshi Nishimura[1]

1. Tohoku University

Spatio-temporal clustering of seismicity is an interesting phenomenon in the earthquake generation process. We investigate the earthquakes closely occurring in space and time, which have been sometimes observed at various regions. A recent example is *Mw*6.5 earthquake at Hinagu active fault on April 14, 2016, followed by a *Mw*7.3 at Futagawa active fault on April 16. The present study analyzes moderate and large earthquakes to clarify characteristics of such successive occurrence of earthquakes.

We use the Global Centroid Moment Tensor catalog for the period from 1976 to 2016. Earthquakes with moment magnitudes (*Mw*) of larger or equal to 5.0 and with depths less than or equal to 70 km are analyzed. The earthquakes that occur within some horizontal distance ranges (Δd*:* from 10 to 500 km*)*, and lapse times (Δt=30, 180 and 365 days*)* from the occurrence of each target earthquake is grouped in a cluster, and the number of clusters are counted.

The results show that cumulative numbers of clusters almost constantly increase in the logarithmic scale with increasing Δt, and the number of clusters increases constantly in general with increasing Δd. For example, for the *Mw* 5.0 –5.5, the cumulative number of clusters at Δd*=100* km are 3177, 4525 and 4808, respectively, for Δt of 30, 180 and 365 days.

To examine whether or not these successive earthquakes occur randomly, in other words, whether or not these successive earthquakes occur under some physical conditions, we compare the observed results with simulations in which earthquakes are set to randomly occur in time. The results show that the observed cumulative numbers of clusters are larger than those of simulation in short distance ranges. The former gradually approach to the latter with increasing the horizontal distance, and merge into a same number at a distance, which is defined as “triggering distance” in the present study. As Δt increases, the occurrence probability decreases and approaches to the normal condition in which the occurrence time intervals of earthquakes obey a Poisson distribution. For example, the triggering distances of Mw5.0-5.5 are 420 km and 66 km, respectively, for Δt*=30* days and *365* days. The results obtained by changing the parameters related to the spatial and temporal distributions of aftershock show no significant difference in the number of clusters and triggering distances.

Keywords: Clustering, Successive earthquakes, Triggering distance

©2019. Japan Geoscience Union. All Right Reserved.

Kanto 3 month testing class results of CSEP Japan

*Hiroshi Tsuruoka[1], Naoshi Hirata[1]

1. Earthquake Research Institute, Tokyo Univ.

We report about 3 month testing class results of Kanto test region of CSEP Japan. We show the results of three models: RI10K, HISTETAS5PA and HISTETAS5PA1205. HISTETAS5 PA1205 is a model submitted to the Japan test center after the Tohoku-oki earthquake. The test results are about 40 rounds evaluated from 1 November 2009.

From the standard test results of CSEP, RI10K did not pass the S-test in the round of 2017/5 / 1-8 / 1. In addition, there were some rounds that did not pass N-Test in all models when the number of observed earthquakes was relatively small. Calculating the average of information gain values per earthquake for each model in all rounds was 1.419, 1.168, 1.162 for HISTETAS5PA1205, HISTETAS5PA, and RI10K respectively. Regarding the forecast of the number of earthquakes, HISTETA5PA1205 predicts the number of observation earthquakes well.

From the results of multiple rounds, forecast number of earthquakes improvement directly leads to improvement of an earthquake forecast model. Moreover, a model characteristic can be showed well by evaluating the spatial forecast performance and the performance of forecast number of earthquakes.

Keywords: Earthquake Predictability, CSEP

©2019. Japan Geoscience Union. All Right Reserved.

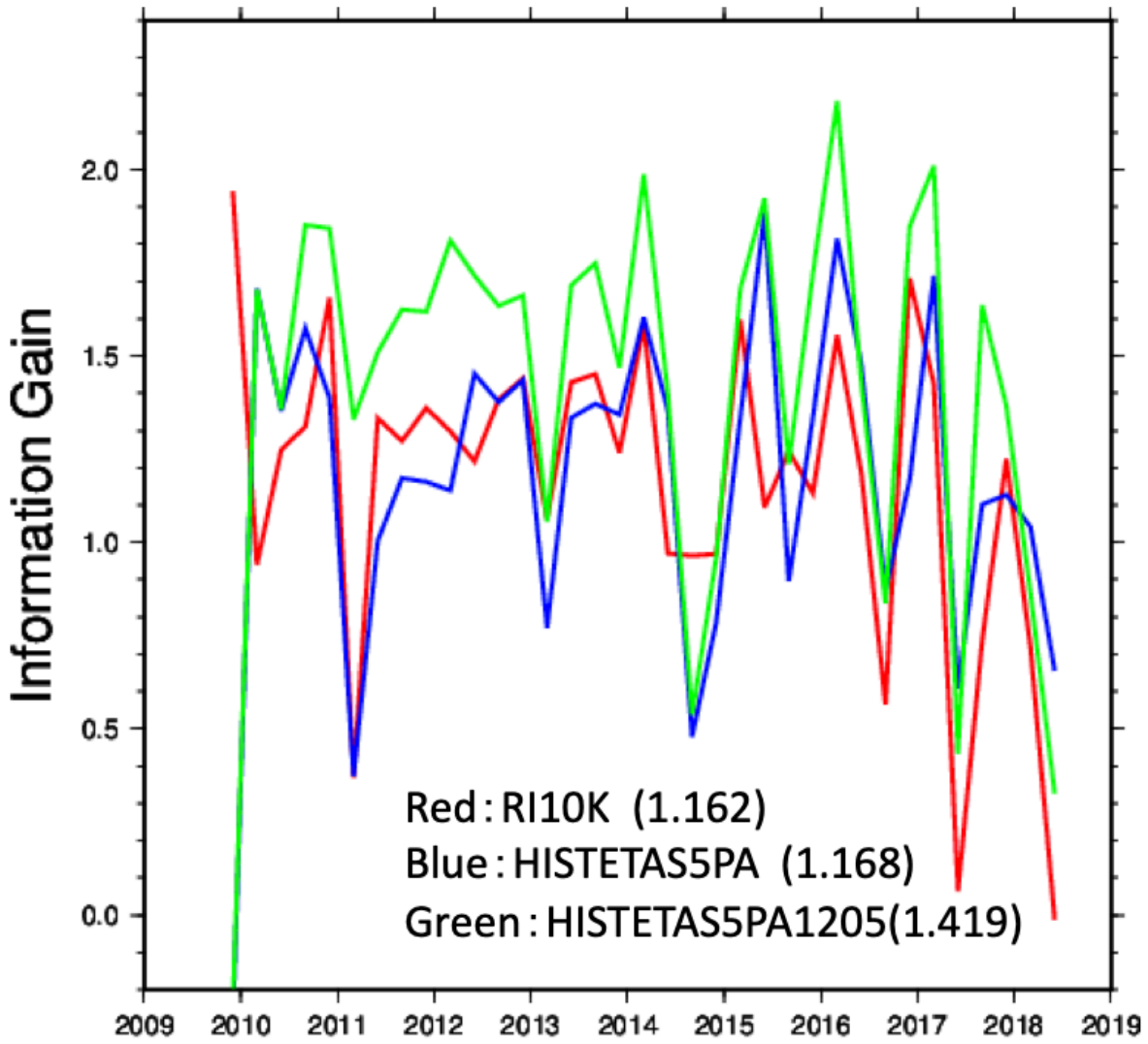

©2019. Japan Geoscience Union. All Right Reserved.

Long-term earthquake risk in North China estimated from a modern catalogue

Ziyao Xiong[2], *Jiancang Zhuang[1], Shiyong Zhou[2]

1. Institute of Statistical Mathematics, 2. Peking University

In this study, to obtain optimal estimates of the earthquake hazard in North China based on the modern earthquake catalogue, we used two variable kernel function estimation methods and two spatial tessellation methods to calculate the total and background seismic spatial occurrence rates for the study area.

The first problem of this study is to derive the best estimate of the long-term earthquake risk in North China. To address the first problem, we use the kernel function estimation methods of Stock and Smith (2002) and Zhuang et al. (2002), the Bayesian Delaunay-Tessellation Smoothing Method used by Ogata (ODTB) (2003, 2004), and ICVT to estimate the total earthquake hazard for North China. The results were compared and analyzed through the cross-validation method, to ensure accurate reflection of the seismic activity in North China. The sophisticated ODTB method is more stable than the others, but is relatively expensive, in terms of computation demands, while Zhuang et al.’ s kernel estimate and the new ICVT method are able to provide reasonable estimates and easier to implement.

For the second problem, of b-value, we use Ogata’ s method (2004, 2015) based on free nodes, to calculate the *b*-value spatial distribution. We expect that the obtained results of the spatial distribution of seismic risk and *b*-value provide a reference for the evaluation and prediction of large earthquakes and stress distribution in the study area.

For the third problem, we use two methods to estimate background seismic rates, and compare the results. The first method uses the result of the background seismic event probability, calculated by the epidemic-type aftershock sequence (ETAS) model (Zhuang et al., 2002; Zhuang, 2011), to simulate the background seismic risk distribution. The second method is to calculate the spatial distribution of earthquake hazard by using the HIST-ETAS model (Ogata, 2004).

Using comparative analyses and simulation experiments, we show that all of methods give similar spatial patterns of seismic occurrences.

Keywords: seismic risk, tessellation, background seismicity, ETAS model

©2019. Japan Geoscience Union. All Right Reserved.

Distributions of focal mechanisms in background seismicity and earthquake clusters in Japan

*Jiancang Zhuang[1,2], Eri Maita[2]

1. Institute of Statistical Mathematics, 2. Graduate University for Advanced Studies

This study tries to find the probability distributions of focal mechanisms in background seismicity and earthquake clusters in Japan by analyzing F-net data. To describe the probability distribution, each focal mechanism is discomposed as the result of a rotation about a particular pole starting from a reference focal mechanism. In this study, DC4 symmetry is considered, i.e., either nodal-plane can be the fault plane and the two sides of the fault plane are distinguishable.

To separate the background and clustering seismicity, we fit the space-time ETAS model (e.g., Zhuang et al, 2011) to the earthquakes with magnitude 4.2+ from 1997 to 2017 in the F-net catalog, and use the stochastic declustering method to estimate the background probabilities that each event is a background event and the triggered probabilities that each event is triggered by other events.

For the background events, the reference focal mechanism is taken as the average focal mechanism in each area, calculated by the method in Kagan (2014). The ration angles between a background event and the mean focal mechanisms at *(x, y)* is reconstructed by

$\zeta(\Delta) \propto \sum_j \phi_j I$(Rotation angle betwen *j* and the mean focal mechanism is within $(\Delta-\delta, \Delta+\delta)$),

where *j* runs over all background events near *x,y,* δ is a small number, and ϕj is the background probability estimated from fitting the space-time ETAS model. For the triggered events, the reference focal mechanism is naturally taken the focal mechanism of the event which triggers it. The rotation angles between the parent event and its direct offspring are reconstructed by

$\xi(\Delta) \propto \sum_{i,j} \rho_{i,j} I$(Rotation angle betwen *i* and *j* is within $(\Delta-\delta, \Delta+\delta)$) .

where *i* and *j* run over all the event pairs in the catalog, ρij is the probability that event *j* is triggered by event *i* estimated based on the ETAS model.

We find that the rotation poles are almost uniformly distributed. The reconstructed results for the rotation angles are shown in Figure 1.

Figure 1 (a) mean focal mechanisms of background seismicity in Japan. (b) Reconstructed distribution of rotation angles for focal mechanisms in the background seismicity and triggered seismicity.

References:

Zhuang J., (2011) , *Next-day earthquake forecasts for the Japan region generated by the ETAS model*. **Earth Planets Space**, 63, 207-216. doi:10.5047/eps.2010.12.010.

Kagan Y.Y. and Jackson D. D. (2014) Statistical earthquake focal mechanism forecasts. **Geophys. J. Int.** 197, 620–629. doi: 10.1093/gji/ggu015.

©2019. Japan Geoscience Union. All Right Reserved.

Keywords: earthquake focal mechanism, probability distribution, earthquake cluster, background seismcity, ETAS model

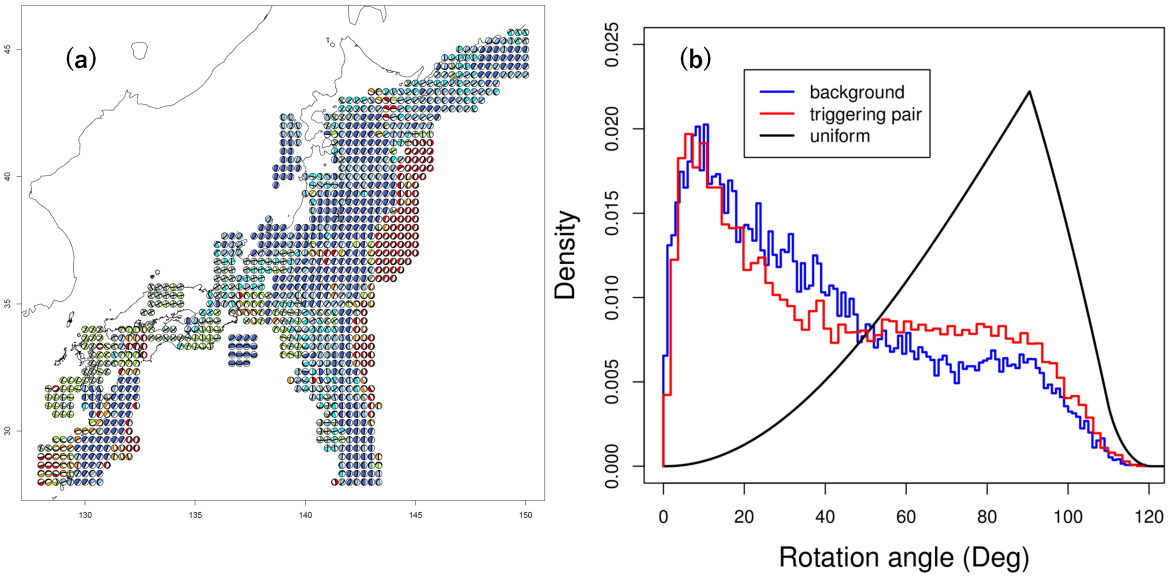

©2019. Japan Geoscience Union. All Right Reserved.

New Ground Motion Prediction Equations for Western Saudi Arabia

*Ryota Kiuchi[1,2], Walter Mooney[1], Hani Zahran[3]

1. U.S. Geological Survey, 2. Disaster Prevenetion Research Institute, Kyoto University, 3. Saudi Geological Survey

We developed Ground Motion Prediction Equations (GMPEs) for western Saudi Arabia using 2770 selected records of PGA and PGV from 177 earthquakes of magnitude 3.0 –5.4, recorded at 58 stations in the distance range from 1 km to 400 km. Our GMPEs are developed based on one of the NGA-West2 Project GMPEs (Boore et al., 2014) by employing a mixed effects regression model.

Saudi Arabia is surrounded by several active tectonic regions, including an extension in the Red Sea and left-lateral strike-slip motion in the Gulf of Aqaba and along the Dead Sea Transform Fault (DSTF). In this area, multiple seismic swarms in and around volcanic fields, also known as harrats, have been detected over the past several decades (El-Isa and Shanti, 1989). The most recent large earthquake swarm in the region, which included more than 30,000 earthquakes, occurred from April to June 2009 beneath the volcanic field of Harrat Lunayyir in northwestern Saudi Arabia. The strongest seismic activity occurred May 13-19, 2009 and consisted of events M > 4 (Pallister et al., 2010). The largest earthquake occurred on May 19th, ML 5.4 as estimated by the SGS (Saudi Geological Survey) and Mw 5.7 by the USGS.

The NGA-West2 project used as a reference model mainly consists of shallow crustal earthquakes in active tectonic regions, rather than extensional earthquakes, such as those observed in Saudi Arabia. This deficiency is corrected by calculating a magnitude scaling of the new Saudi Arabia GMPEs compared to those of Boore et al. (2014). Furthermore, there is a clear difference in distance scaling for the Arabian GMPEs in comparison with the NGA-West2 GMPEs. This difference is especially significant at large distances and is mainly due to lower anelastic attenuation in the crystalline crust of western Saudi Arabia. Our empirical data demonstrate that the GMPEs presented here are in good agreement with observed earthquake ground motions in western Saudi Arabia.

Keywords: GMPE, Saudi Arabia, Seismic Hazard

©2019. Japan Geoscience Union. All Right Reserved.

Study on the spatial and temporal change of velocity structure before and after 2003 Chengkung earthquake, Taiwan

*TING YA LIANG[1], Wen-Yen Chang[1,2,3], Strong Wen[4]

1. National DONG HWA University, 2. Eastern Taiwan Earthquake Research Center, 3. National Center for Research on Earthquake Engineering, 4. National Chung Cheng University

Taiwan is located in the plate converge zone, in which the Longitudinal Valley(LV) is the suture zone between the Eurasian Plate and Philippine Sea Plate. The collision process yields two nearly parallel major fault systems: the Central Range fault (CRF) and the Longitudinal Valley fault(LVF). The Chihshang fault is a creeping thrust fault, which is located in the southern section of the LVF in eastern Taiwan. According to geodetic survey, this fault moves to northwest at a rate approximately 2–3 cm/yr. There were two significant earthquakes occurred nearby the Chihshang fault, the 1951 M7.1 Hualien-Taitung earthquake and the 2003 M6.4 Chengkung earthquake. In this study, the spatial and temporal variations of velocity structure before and after 2003 Chengkung earthquake were obtained through the tomography inversion beneath the southern segment of the Longitudinal Valley. The damping least-square technique and 3D ray tracing scheme were adopted to calculate the most appropriate solution and obtain the velocity structures. The results showed that the Vp values exhibit less significant variations than the parameters Vs and Vp/Vs ratio. But the Vs structures show larger variation after the 2003 mainshock. These results imply that Vp/Vs ratios began to increase before the mainshock, at the hanging wall of the Chihshang fault, which may be related to the increasing density of microcracks and fluid. Previous studies has shown that high Vp/Vs ratio may lead to cracks generating and fluid migration, which can result in changing rock volume and produce partial compensation. Therefore, our results not only give better understanding the seismogenic structures in the ES Taiwan, but also allow us to detect variations of physical parameters caused by crack propagating in stratum during the strong earthquake sequence. Hence, this study shows that the results from temporal and spatial variation of Vp/Vs values in the southern segment of the LVF could allow us to assess the seismic hazard potential in this area, and further explore the relationship between the seismicity and the rheology of fault plane. Finally, long-term monitoring of fault activities will contribute to the research of future earthquake early warning.

Keywords: spatial and temporal variations, Vp/Vs ratio

©2019. Japan Geoscience Union. All Right Reserved.

[E] Poster | S (Solid Earth Sciences)：S-SS Seismology

Mon. May 27, 2019 5:15 PM - 6:30 PM JST | Mon. May 27, 2019 8:15 AM - 9:30 AM UTC | Poster Hall International Exhibition Hall8, Makuhari Messe_19

[S-SS07] Rigorous Seismicity Modelling and Hypothesis Testing

convener:Jiancang Zhuang(Institute of Statistical Mathematics), Danijel Schorlemmer(GFZ German Research Centre for Geosciences), Matt Gerstenberger(GNS Science), Hiroshi Tsuruoka(Earthquake Research Institute, Tokyo Univ.)

Probabilistic models have been developed for describing, analyzing, and forecasting seismicity since more than 100 years and, with the advent of large-scale digital networks, in high resolution during the last 30 years. These models include recurrence and stress-release models for long-term earthquake hazard assessment, and short-term models describing earthquake clustering, e.g. the ETAS model. Some models have become standard tools in seismic hazard assessment. However, the overall probabilities remain on the low end and the uncertainties of the forecasts are not well described. Rigorous data-based development and testing of models will help further improving forecasting power and accuracy of these models. Similarly, new hypotheses shall be evaluated rigorously using some existing model as the null hypothesis model or in dedicated tests addressing the hypothesis directly. In this context, the Collaboratory for the Study of Earthquake Predictability and its Japan branch provides the necessary testing capabilities for rigorous and unbiased evaluation of models and hypotheses. This session focuses on research that increases information on seismicity, being with respect to a reference model or as an independent hypothesis. We solicit contributions of model developments and hypothesis formulation based on the increased understanding of the physical process of earthquakes, such as the preparation and rupture processes of the earthquake source and the interaction between earthquakes and tectonic environments. We also welcome development and implementation of improved statistical methods for testing and validating physical hypotheses based on observed data. In particular, we welcome contributions about model- or hypothesis-test experiments that could be implemented in the Japan testing center.

[SSS07-P01] Development of Physics-based Ground Motion Simulation in A Hybrid Approach and Applications to Seismic Hazard Assessment in Taiwan

*Ming-Che Hsieh[1], Yin-Tung Yen[1], Kuo-Fong Ma[2,3] (1.Disaster Prevention Technology Research Center, Sinotech Engineering Consultants (Inc.), Taiwan, 2.Department of Earth Sciences, National Central University, Taiwan, 3.Earthquake-Disaster & Risk Evaluation and Management Center, National Central University, Taiwan)

[SSS07-P02] Increasing Earthquake Forecast Testability - CSEP Future Developments

*Danijel Schorlemmer[1], Naoshi Hirata[2], Fabrice Cotton[1], Matt Gerstenberger[3], Thomas Jordan[7], Warner Marzocchi[4], William Savran[7], Maximilian Werner[5], Stefan Wiemer[6], Thomas Beutin[1], David D Jackson[8], Philip Maechling[7], Sum Mak[1], Kazuyoshi Nanjo[9], Yosihiko Ogata[10], David Rhoades[3], Hiroshi Tsuruoka[2], Graeme Weatherill[1], Jiancang Zhuang[10] (1.GFZ German Research Centre for Geosciences, 2.Earthquake Research Institute, University of Tokyo, Japan, 3.GNS Science, Lower Hutt, New Zealand, 4.University of Naples, Naples, Italy, 5.University of Bristol, Bristol, United Kingdom, 6.ETH Zurich, Zurich, Switzerland, 7.University of Southern California, Los Angeles, USA, 8.University of California Los Angeles, Los Angeles, USA, 9.University of Shizuoka, Shizuoka, Japan, 10.Institute of Statistical Mathematics, Tachikawa, Japan)

[SSS07-P03] Precision versus uncertainty in regional seismic hazard mapping

*Matt Gerstenberger[1], Danijel Schorlemmer[2] (1.GNS Science, 2.GFZ-Potsdam)

[SSS07-P04] An extreme value analysis of seismograms designed for early forecast of aftershocks

*Kaoru Sawazaki[1] (1.National Research Institute for Earth Science and Disaster Resilience)

[SSS07-P05] **Spatio-temporal clustering of successive earthquakes: data analyses of global data.**

*THYSTERE MATONDO BANTIDI[1], Takeshi Nishimura[1] (1.Tohoku University)

[SSS07-P06] Kanto 3 month testing class results of CSEP Japan

*Hiroshi Tsuruoka[1], Naoshi Hirata[1] (1.Earthquake Research Institute, Tokyo Univ.)

[SSS07-P07] Long-term earthquake risk in North China estimated from a modern catalogue

Ziyao Xiong[2], *Jiancang Zhuang[1], Shiyong Zhou[2] (1.Institute of Statistical Mathematics, 2.Peking University)

[SSS07-P08] **Distributions of focal mechanisms in background seismicity and earthquake clusters in Japan**

*Jiancang Zhuang[1,2], Eri Maita[2] (1.Institute of Statistical Mathematics, 2.Graduate University for Advanced Studies)

[SSS07-P09] New Ground Motion Prediction Equations for Western Saudi Arabia

*Ryota Kiuchi[1,2], Walter Mooney[1], Hani Zahran[3] (1.U.S. Geological Survey, 2.Disaster Prevenetion Research Institute, Kyoto University, 3.Saudi Geological Survey)

[SSS07-P10] Study on the spatial and temporal change of velocity structure before and after 2003 Chengkung earthquake, Taiwan

*TING YA LIANG[1], Wen-Yen Chang[1,2,3], Strong Wen[4] (1.National DONG HWA University, 2.Eastern Taiwan Earthquake Research Center, 3.National Center for Research on Earthquake Engineering, 4.National Chung Cheng University)

Development of Physics-based Ground Motion Simulation in A Hybrid Approach and Applications to Seismic Hazard Assessment in Taiwan

*Ming-Che Hsieh[1], Yin-Tung Yen[1], Kuo-Fong Ma[2,3]

1. Disaster Prevention Technology Research Center, Sinotech Engineering Consultants (Inc.), Taiwan, 2. Department of Earth Sciences, National Central University, Taiwan, 3. Earthquake-Disaster & Risk Evaluation and Management Center, National Central University, Taiwan

Damages to engineering structures by an earthquake depend on the entire time history of the ground motion, which is affected by a number of factors including source-rupture process, seismic-wave velocity structure, topographic relief, and local site condition. To quantitatively assess these effects to ground motion, physics-based ground motion simulation is a powerful tool which enables rigorous modeling of each effect and their coupling. In this study, we present a recent-developed physics-based ground motion simulator in generating broadband seismograms for seismic hazard assessment. The simulator is essentially based on a hybrid approach in which long-period synthetics are calculated by the efficient 3-D strain Green’ s tensor (SGT) and short-period synthetics are modeled by the stochastic method. Physical effects of (1) source slip distribution, (2) seismic wave propagation, (3) surface topography and (4) site amplification are taken into account. This hybrid approach has been validated by the 2016 M_W6.6 Meinong earthquake in southern Taiwan and reveals good potential for engineering applications. We also carried out simulations to model rupture scenarios of seismogenic structure and subduction zone sources. Output full waveform and ground motion parameters, e.g. peak ground acceleration (PGA) and 1.0-s-period spectral acceleration (SA1.0), have been further implemented to risk estimation, and even earthquake drill. Our result shows the ground motion simulator has the potential for earthquake scenario modeling and hazard assessment.

Keywords: Ground motion simulation, Seismic hazard assessment, Strain Green’ s tensor, Stochastic method

©2019. Japan Geoscience Union. All Right Reserved.

Increasing Earthquake Forecast Testability - CSEP Future Developments

*Danijel Schorlemmer[1], Naoshi Hirata[2], Fabrice Cotton[1], Matt Gerstenberger[3], Thomas Jordan[7], Warner Marzocchi[4], William Savran[7], Maximilian Werner[5], Stefan Wiemer[6], Thomas Beutin[1], David D Jackson[8], Philip Maechling[7], Sum Mak[1], Kazuyoshi Nanjo[9], Yosihiko Ogata[10], David Rhoades[3], Hiroshi Tsuruoka[2], Graeme Weatherill[1], Jiancang Zhuang[10]

1. GFZ German Research Centre for Geosciences, 2. Earthquake Research Institute, University of Tokyo, Japan, 3. GNS Science, Lower Hutt, New Zealand, 4. University of Naples, Naples, Italy, 5. University of Bristol, Bristol, United Kingdom, 6. ETH Zurich, Zurich, Switzerland, 7. University of Southern California, Los Angeles, USA, 8. University of California Los Angeles, Los Angeles, USA, 9. University of Shizuoka, Shizuoka, Japan, 10. Institute of Statistical Mathematics, Tachikawa, Japan

The Collaboratory for the Study of Earthquake Predictability (CSEP) has expanded over the years to many different testing areas hosted at multiple testing centers. Hundreds of earthquake forecast models have been submitted to CSEP and are being tested. New testing metrics were developed and implemented and a lot of progress was made to establish CSEP as an institution that cannot be ignored when issuing earthquake forecasts. Its rigor and independence became the standard in evaluating earthquake forecasts and in reporting on the results.

In the framework of the testing activities of the Global Earthquake Model, one line of expanding the capabilities of CSEP was developed at GFZ Potsdam. The group there applied the mechanisms that CSEP introduced to earthquake forecast models to the area of intensity prediction equations (IPEs) and ground-motion prediction equations (GMPEs). The first truly prospective tests were carried out on IPEs for Italy and also on GMPEs for Japan and New Zealand. This new set of tests helped CSEP move into the hazard domain and increase the relevance of its results to the hazard community. Finally, the group at GFZ Potsdam has also conducted the first prospective test of the US national seismic hazard maps.

Although these tests have been successful and well-received, they have also shown the limitations of the CSEP approach. Many aspects of seismic hazard or earthquake forecasting remain inherently untestable if only the model forecasts are tested and not the model ingredients. We propose to continue along the lines of the GFZ Potsdam developments and create new areas of activity for CSEP, namely targeted experiments that cannot be conducted with the current CSEP software system. As part of the eGSIM (European Ground Shaking Intensity Models) service, we will introduce permanent testing of IPEs and GMPEs to the testing center to establish strong performance records to be used in hazard models. Further targeted experiments include the predictive power of b-values, discrimination of foreshocks for short-term forecasting, as well as a deeper look into precursory
phenomena applying CSEP-style rigorous testing. We support including testability in future hazard models or their components to move to better testable seismic hazard models. Finally, to expand into the risk domain, we will test exposure models against new and independent data.

Keywords: Seismicity, Forecasting, Testing

©2019. Japan Geoscience Union. All Right Reserved.

Precision versus uncertainty in regional seismic hazard mapping

*Matt Gerstenberger[1], Danijel Schorlemmer[2]

1. GNS Science, 2. GFZ-Potsdam

Regional and national seismic hazard mapping efforts have increasingly pursued more detailed and precise models and outputs, particularly in terms of source characterisation and modelling. With increasing precision comes increasing uncertainty. In recent years much attention has been paid to modelling uncertainty in ground-motion models and including this in seismic hazard modelling. However, much less effort has been made to quantify and model uncertainty in seismic source characterisation. This raises two questions: 1) is increasing precision appropriate when uncertainty remains poorly quantified? 2) what is the optimal balance between precision and uncertainty? Ultimately the answer to this depends on the end-uses of the models and the implications of increasing uncertainty with increasing precision. Here we explore some of the main sources of uncertainty in seismic source characterisation such as incomplete and limited records of earthquake occurrence in paleoseismic data and earthquake catalogues, non-stationarity of seismicity and the poisson assumption, fault source characterisation and so-called moment balancing. We pay particular focus to uncertainties in estimating hazard in less seismically active regions and the implications for building design guidance.

Keywords: Seismic hazard, PSHA, uncertainty

©2019. Japan Geoscience Union. All Right Reserved.

An extreme value analysis of seismograms designed for early forecast of aftershocks

*Kaoru Sawazaki[1]

1. National Research Institute for Earth Science and Disaster Resilience

Conventional aftershock forecasting has been operated through applying the Gutenberg-Richter and Omori-Utsu laws to an earthquake catalog. However, catalog's quality is influenced by detectability of earthquake signals (P or S waves), which causes degradation of the catalog in the early stage after a large earthquake and at regions which are sparsely covered by seismograph network. This eventually causes the catalog's nonuniformity and limitation of the forecasting performance.

In this study, we propose a new approach designed for high-performance early aftershock forecasting without using earthquake catalog. Instead, we use a continuous seismogram recorded at each station. First, we pick the maximum amplitude of the seismogram obtained in every assigned time interval (e.g., 1 minute). This picking process can be completely automated and is rarely affected by overlap of multiple seismic signals occurring in approximately the same time. We empirically derive a probability distribution (PD) that accounts for the frequency of the maximum amplitudes. This PD is essentially a non-stationary extreme value distribution derived from the generalized Pareto distribution (GPD) and the Omori-Utsu type temporal decay. We optimize three parameters that control the PD shape (K_a: parameter that controls whole aftershock activity, p_a: parameter that controls temporal decay of the aftershock frequency, m: parameter that controls power-law decay of the maximum amplitude) by applying the maximum likelihood estimation to the observed maximum amplitudes. By extrapolating the optimized PD, we estimate the number of maximum amplitudes that will exceed a threshold value within arbitral time interval in the future. The proposed approach provides forecast of peak ground motion at each station rather than magnitude, which is directly desired for public use. Moreover, the forecasted peak ground motion may automatically incorporate many factors that cannot be described by a simple ground motion attenuation model (e.g., site amplification, radiation pattern, rupture directivity, and so on).

We apply the proposed method to 25 Hi-net seismograms recorded the 2016 Kumamoto earthquakes in Japan. We set the learning periods every one hour after the mainshock (Mj7.3), and set the forecasting period within 24 hours after the end of each learning period. We find that parameters K_a and m become temporally stable within a few hours after the mainshock at many stations. On the other hand, the parameter p_a temporally varies more probably because the induced seismicity at northeast area (Aso and Oita regions) strongly affects the apparent temporal decay rate of the amplitudes. Within 3 hours after the mainshock, the forecasted number of the maximum amplitudes exceeding 10^{-4} m/s is within 0.5 to 2.0 times the actual observation for about 80 % of the used stations. For the threshold amplitude of 10^{-3} m/s, on the other hand, the forecasted number tends to overestimate, probably due to saturation of seismograms by both artificial and physical reasons.

Keywords: extreme value analysis, aftershock forecasting, peak ground motion

©2019. Japan Geoscience Union. All Right Reserved.

Spatio-temporal clustering of successive earthquakes: data analyses of global data.

*THYSTERE MATONDO BANTIDI[1], Takeshi Nishimura[1]

1. Tohoku University

Spatio-temporal clustering of seismicity is an interesting phenomenon in the earthquake generation process. We investigate the earthquakes closely occurring in space and time, which have been sometimes observed at various regions. A recent example is *Mw*6.5 earthquake at Hinagu active fault on April 14, 2016, followed by a *Mw*7.3 at Futagawa active fault on April 16. The present study analyzes moderate and large earthquakes to clarify characteristics of such successive occurrence of earthquakes.

We use the Global Centroid Moment Tensor catalog for the period from 1976 to 2016. Earthquakes with moment magnitudes (*Mw*) of larger or equal to 5.0 and with depths less than or equal to 70 km are analyzed. The earthquakes that occur within some horizontal distance ranges (Δd*:* from 10 to 500 km*)*, and lapse times (Δt=30, 180 and 365 days*)* from the occurrence of each target earthquake is grouped in a cluster, and the number of clusters are counted.

The results show that cumulative numbers of clusters almost constantly increase in the logarithmic scale with increasing Δt, and the number of clusters increases constantly in general with increasing Δd. For example, for the *Mw* 5.0 –5.5, the cumulative number of clusters at Δd*=100* km are 3177, 4525 and 4808, respectively, for Δt of 30, 180 and 365 days.

To examine whether or not these successive earthquakes occur randomly, in other words, whether or not these successive earthquakes occur under some physical conditions, we compare the observed results with simulations in which earthquakes are set to randomly occur in time. The results show that the observed cumulative numbers of clusters are larger than those of simulation in short distance ranges. The former gradually approach to the latter with increasing the horizontal distance, and merge into a same number at a distance, which is defined as “triggering distance” in the present study. As Δt increases, the occurrence probability decreases and approaches to the normal condition in which the occurrence time intervals of earthquakes obey a Poisson distribution. For example, the triggering distances of Mw5.0-5.5 are 420 km and 66 km, respectively, for Δt*=30* days and *365* days. The results obtained by changing the parameters related to the spatial and temporal distributions of aftershock show no significant difference in the number of clusters and triggering distances.

Keywords: Clustering, Successive earthquakes, Triggering distance

©2019. Japan Geoscience Union. All Right Reserved.

Kanto 3 month testing class results of CSEP Japan

*Hiroshi Tsuruoka[1], Naoshi Hirata[1]

1. Earthquake Research Institute, Tokyo Univ.

We report about 3 month testing class results of Kanto test region of CSEP Japan. We show the results of three models: RI10K, HISTETAS5PA and HISTETAS5PA1205. HISTETAS5 PA1205 is a model submitted to the Japan test center after the Tohoku-oki earthquake. The test results are about 40 rounds evaluated from 1 November 2009.

From the standard test results of CSEP, RI10K did not pass the S-test in the round of 2017/5 / 1-8 / 1. In addition, there were some rounds that did not pass N-Test in all models when the number of observed earthquakes was relatively small. Calculating the average of information gain values per earthquake for each model in all rounds was 1.419, 1.168, 1.162 for HISTETAS5PA1205, HISTETAS5PA, and RI10K respectively. Regarding the forecast of the number of earthquakes, HISTETA5PA1205 predicts the number of observation earthquakes well.

From the results of multiple rounds, forecast number of earthquakes improvement directly leads to improvement of an earthquake forecast model. Moreover, a model characteristic can be showed well by evaluating the spatial forecast performance and the performance of forecast number of earthquakes.

Keywords: Earthquake Predictability, CSEP

©2019. Japan Geoscience Union. All Right Reserved.

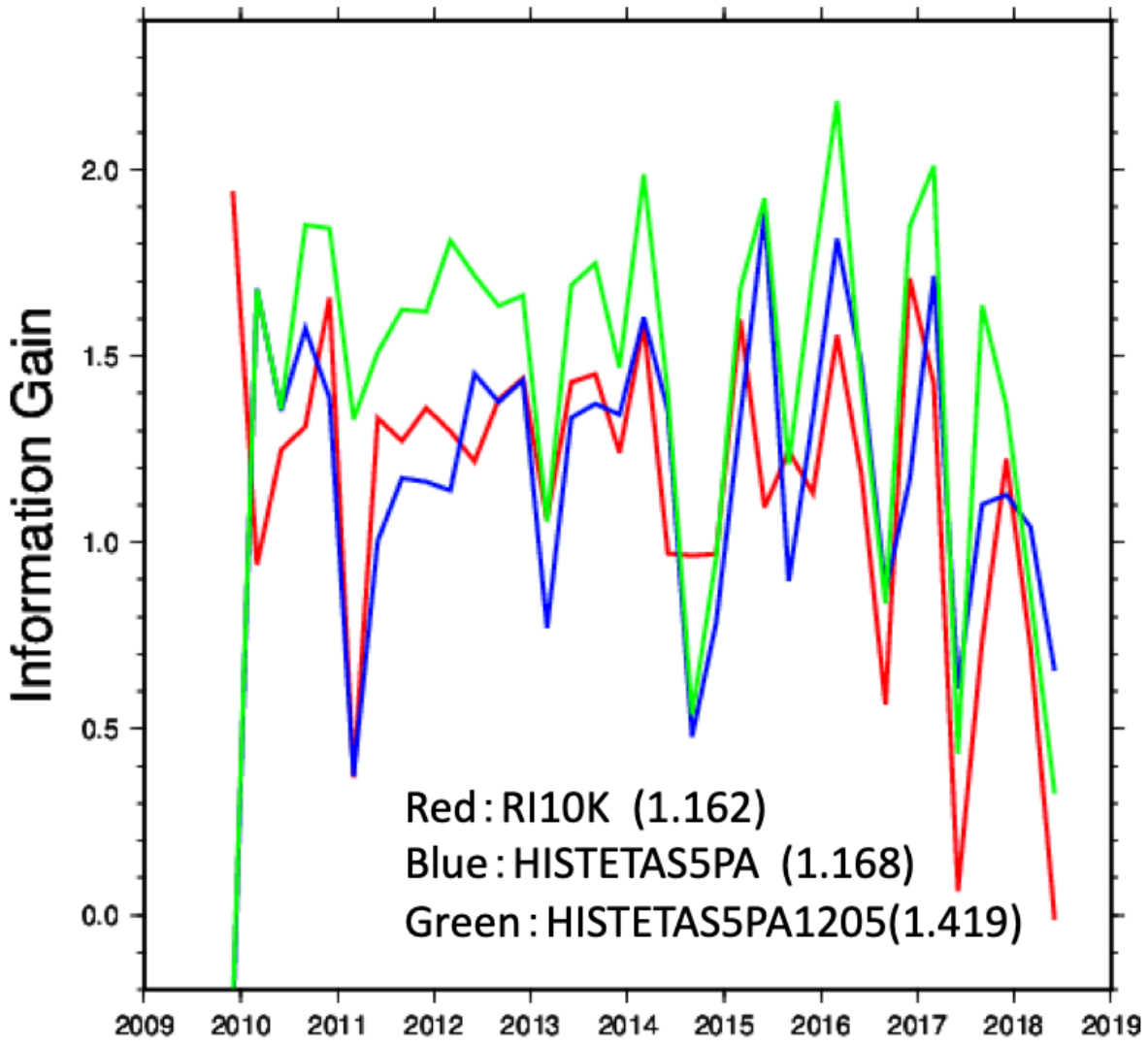

©2019. Japan Geoscience Union. All Right Reserved.

Long-term earthquake risk in North China estimated from a modern catalogue

Ziyao Xiong[2], *Jiancang Zhuang[1], Shiyong Zhou[2]

1. Institute of Statistical Mathematics, 2. Peking University

In this study, to obtain optimal estimates of the earthquake hazard in North China based on the modern earthquake catalogue, we used two variable kernel function estimation methods and two spatial tessellation methods to calculate the total and background seismic spatial occurrence rates for the study area.

The first problem of this study is to derive the best estimate of the long-term earthquake risk in North China. To address the first problem, we use the kernel function estimation methods of Stock and Smith (2002) and Zhuang et al. (2002), the Bayesian Delaunay-Tessellation Smoothing Method used by Ogata (ODTB) (2003, 2004), and ICVT to estimate the total earthquake hazard for North China. The results were compared and analyzed through the cross-validation method, to ensure accurate reflection of the seismic activity in North China. The sophisticated ODTB method is more stable than the others, but is relatively expensive, in terms of computation demands, while Zhuang et al.’ s kernel estimate and the new ICVT method are able to provide reasonable estimates and easier to implement.

For the second problem, of b-value, we use Ogata’ s method (2004, 2015) based on free nodes, to calculate the *b*-value spatial distribution. We expect that the obtained results of the spatial distribution of seismic risk and *b*-value provide a reference for the evaluation and prediction of large earthquakes and stress distribution in the study area.

For the third problem, we use two methods to estimate background seismic rates, and compare the results. The first method uses the result of the background seismic event probability, calculated by the epidemic-type aftershock sequence (ETAS) model (Zhuang et al., 2002; Zhuang, 2011), to simulate the background seismic risk distribution. The second method is to calculate the spatial distribution of earthquake hazard by using the HIST-ETAS model (Ogata, 2004).

Using comparative analyses and simulation experiments, we show that all of methods give similar spatial patterns of seismic occurrences.

Keywords: seismic risk, tessellation, background seismicity, ETAS model

©2019. Japan Geoscience Union. All Right Reserved.

Distributions of focal mechanisms in background seismicity and earthquake clusters in Japan

*Jiancang Zhuang[1,2], Eri Maita[2]

1. Institute of Statistical Mathematics, 2. Graduate University for Advanced Studies

This study tries to find the probability distributions of focal mechanisms in background seismicity and earthquake clusters in Japan by analyzing F-net data. To describe the probability distribution, each focal mechanism is discomposed as the result of a rotation about a particular pole starting from a reference focal mechanism. In this study, DC4 symmetry is considered, i.e., either nodal-plane can be the fault plane and the two sides of the fault plane are distinguishable.

To separate the background and clustering seismicity, we fit the space-time ETAS model (e.g., Zhuang et al, 2011) to the earthquakes with magnitude 4.2+ from 1997 to 2017 in the F-net catalog, and use the stochastic declustering method to estimate the background probabilities that each event is a background event and the triggered probabilities that each event is triggered by other events.

For the background events, the reference focal mechanism is taken as the average focal mechanism in each area, calculated by the method in Kagan (2014). The ration angles between a background event and the mean focal mechanisms at *(x, y)* is reconstructed by

$\zeta(\Delta) \propto \sum_j \phi_j I$(Rotation angle betwen *j* and the mean focal mechanism is within $(\Delta-\delta, \Delta+\delta)$),

where *j* runs over all background events near *x,y,* δ is a small number, and ϕj is the background probability estimated from fitting the space-time ETAS model. For the triggered events, the reference focal mechanism is naturally taken the focal mechanism of the event which triggers it. The rotation angles between the parent event and its direct offspring are reconstructed by

$\xi(\Delta) \propto \sum_{i,j} \rho_{i,j} I$(Rotation angle betwen *i* and *j* is within $(\Delta-\delta, \Delta+\delta)$) .

where *i* and *j* run over all the event pairs in the catalog, ρij is the probability that event *j* is triggered by event *i* estimated based on the ETAS model.

We find that the rotation poles are almost uniformly distributed. The reconstructed results for the rotation angles are shown in Figure 1.

Figure 1 (a) mean focal mechanisms of background seismicity in Japan. (b) Reconstructed distribution of rotation angles for focal mechanisms in the background seismicity and triggered seismicity.

References:

Zhuang J., (2011) , *Next-day earthquake forecasts for the Japan region generated by the ETAS model*. **Earth Planets Space**, 63, 207-216. doi:10.5047/eps.2010.12.010.

Kagan Y.Y. and Jackson D. D. (2014) Statistical earthquake focal mechanism forecasts. **Geophys. J. Int.** 197, 620–629. doi: 10.1093/gji/ggu015.

©2019. Japan Geoscience Union. All Right Reserved.

Keywords: earthquake focal mechanism, probability distribution, earthquake cluster, background seismcity, ETAS model

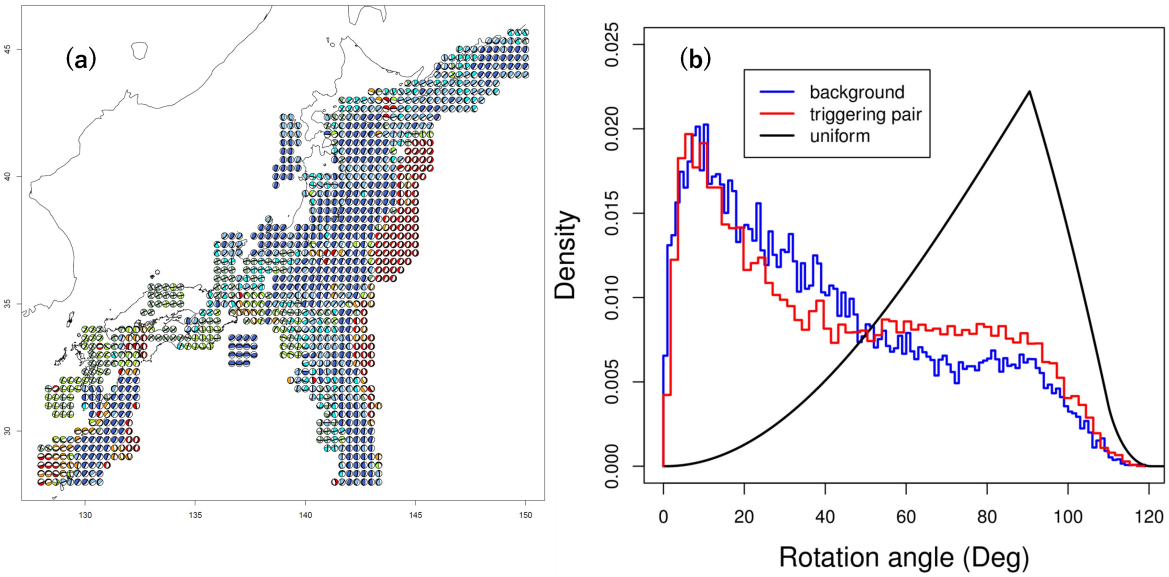

©2019. Japan Geoscience Union. All Right Reserved.

New Ground Motion Prediction Equations for Western Saudi Arabia

*Ryota Kiuchi[1,2], Walter Mooney[1], Hani Zahran[3]

1. U.S. Geological Survey, 2. Disaster Prevenetion Research Institute, Kyoto University, 3. Saudi Geological Survey

We developed Ground Motion Prediction Equations (GMPEs) for western Saudi Arabia using 2770 selected records of PGA and PGV from 177 earthquakes of magnitude 3.0 –5.4, recorded at 58 stations in the distance range from 1 km to 400 km. Our GMPEs are developed based on one of the NGA-West2 Project GMPEs (Boore et al., 2014) by employing a mixed effects regression model.

Saudi Arabia is surrounded by several active tectonic regions, including an extension in the Red Sea and left-lateral strike-slip motion in the Gulf of Aqaba and along the Dead Sea Transform Fault (DSTF). In this area, multiple seismic swarms in and around volcanic fields, also known as harrats, have been detected over the past several decades (El-Isa and Shanti, 1989). The most recent large earthquake swarm in the region, which included more than 30,000 earthquakes, occurred from April to June 2009 beneath the volcanic field of Harrat Lunayyir in northwestern Saudi Arabia. The strongest seismic activity occurred May 13-19, 2009 and consisted of events M > 4 (Pallister et al., 2010). The largest earthquake occurred on May 19th, ML 5.4 as estimated by the SGS (Saudi Geological Survey) and Mw 5.7 by the USGS.

The NGA-West2 project used as a reference model mainly consists of shallow crustal earthquakes in active tectonic regions, rather than extensional earthquakes, such as those observed in Saudi Arabia. This deficiency is corrected by calculating a magnitude scaling of the new Saudi Arabia GMPEs compared to those of Boore et al. (2014). Furthermore, there is a clear difference in distance scaling for the Arabian GMPEs in comparison with the NGA-West2 GMPEs. This difference is especially significant at large distances and is mainly due to lower anelastic attenuation in the crystalline crust of western Saudi Arabia. Our empirical data demonstrate that the GMPEs presented here are in good agreement with observed earthquake ground motions in western Saudi Arabia.

Keywords: GMPE, Saudi Arabia, Seismic Hazard

©2019. Japan Geoscience Union. All Right Reserved.

Study on the spatial and temporal change of velocity structure before and after 2003 Chengkung earthquake, Taiwan

*TING YA LIANG[1], Wen-Yen Chang[1,2,3], Strong Wen[4]

1. National DONG HWA University, 2. Eastern Taiwan Earthquake Research Center, 3. National Center for Research on Earthquake Engineering, 4. National Chung Cheng University

Taiwan is located in the plate converge zone, in which the Longitudinal Valley(LV) is the suture zone between the Eurasian Plate and Philippine Sea Plate. The collision process yields two nearly parallel major fault systems: the Central Range fault (CRF) and the Longitudinal Valley fault(LVF). The Chihshang fault is a creeping thrust fault, which is located in the southern section of the LVF in eastern Taiwan. According to geodetic survey, this fault moves to northwest at a rate approximately 2–3 cm/yr. There were two significant earthquakes occurred nearby the Chihshang fault, the 1951 M7.1 Hualien-Taitung earthquake and the 2003 M6.4 Chengkung earthquake. In this study, the spatial and temporal variations of velocity structure before and after 2003 Chengkung earthquake were obtained through the tomography inversion beneath the southern segment of the Longitudinal Valley. The damping least-square technique and 3D ray tracing scheme were adopted to calculate the most appropriate solution and obtain the velocity structures. The results showed that the Vp values exhibit less significant variations than the parameters Vs and Vp/Vs ratio. But the Vs structures show larger variation after the 2003 mainshock. These results imply that Vp/Vs ratios began to increase before the mainshock, at the hanging wall of the Chihshang fault, which may be related to the increasing density of microcracks and fluid. Previous studies has shown that high Vp/Vs ratio may lead to cracks generating and fluid migration, which can result in changing rock volume and produce partial compensation. Therefore, our results not only give better understanding the seismogenic structures in the ES Taiwan, but also allow us to detect variations of physical parameters caused by crack propagating in stratum during the strong earthquake sequence. Hence, this study shows that the results from temporal and spatial variation of Vp/Vs values in the southern segment of the LVF could allow us to assess the seismic hazard potential in this area, and further explore the relationship between the seismicity and the rheology of fault plane. Finally, long-term monitoring of fault activities will contribute to the research of future earthquake early warning.

Keywords: spatial and temporal variations, Vp/Vs ratio

©2019. Japan Geoscience Union. All Right Reserved.

[E] Oral | S (Solid Earth Sciences)：S-SS Seismology

Mon. May 27, 2019 3:30 PM - 5:00 PM JST | Mon. May 27, 2019 6:30 AM - 8:00 AM UTC | A10 TOKYO BAY MAKUHARI HALL

[S-SS07] Rigorous Seismicity Modelling and Hypothesis Testing

convener:Jiancang Zhuang(Institute of Statistical Mathematics), Danijel Schorlemmer(GFZ German Research Centre for Geosciences), Matt Gerstenberger(GNS Science), Hiroshi Tsuruoka(Earthquake Research Institute, Tokyo Univ.), Chairperson:Matthew Gerstenberger(GNS Science, New Zealand), Danijel Schorlemmer(GFZ-Potsdam, Germany)

Probabilistic models have been developed for describing, analyzing, and forecasting seismicity since more than 100 years and, with the advent of large-scale digital networks, in high resolution during the last 30 years. These models include recurrence and stress-release models for long-term earthquake hazard assessment, and short-term models describing earthquake clustering, e.g. the ETAS model. Some models have become standard tools in seismic hazard assessment. However, the overall probabilities remain on the low end and the uncertainties of the forecasts are not well described. Rigorous data-based development and testing of models will help further improving forecasting power and accuracy of these models. Similarly, new hypotheses shall be evaluated rigorously using some existing model as the null hypothesis model or in dedicated tests addressing the hypothesis directly. In this context, the Collaboratory for the Study of Earthquake Predictability and its Japan branch provides the necessary testing capabilities for rigorous and unbiased evaluation of models and hypotheses. This session focuses on research that increases information on seismicity, being with respect to a reference model or as an independent hypothesis. We solicit contributions of model developments and hypothesis formulation based on the increased understanding of the physical process of earthquakes, such as the preparation and rupture processes of the earthquake source and the interaction between earthquakes and tectonic environments. We also welcome development and implementation of improved statistical methods for testing and validating physical hypotheses based on observed data. In particular, we welcome contributions about model- or hypothesis-test experiments that could be implemented in the Japan testing center.

3:30 PM - 3:45 PM JST | 6:30 AM - 6:45 AM UTC

[SSS07-01] Improving medium-term earthquake forecasts by compensating the EEPAS model for the time-lag

★Invited Papers

David Rhoades[1], Christophersen Annemarie[1], *Matt Gerstenberger[1] (1.GNS Science)

3:45 PM - 4:00 PM JST | 6:45 AM - 7:00 AM UTC

[SSS07-02] Earthquake probability forecast incorporating non-seismic data

*Peng Han[1], Jiancang Zhuang[2], Yosihiko Ogata[2], Katsumi Hattori[3] (1.Southern University of Science and Technology, Shenzhen, China, 2.The Institute of Statistical Mathematics, Tokyo, Japan , 3.Chiba University, Chiba, Japan)

4:00 PM - 4:15 PM JST | 7:00 AM - 7:15 AM UTC

[SSS07-03] Extended versions of the space-time ETAS model and application to the 2016 Kumamoto earthquake sequence

★Invited Papers

*YICUN GUO[1], Jiancang Zhuang[1], Yosihiko Ogata[1] (1.The Institute of Statistical Mathematics, Tokyo, Japan)

4:15 PM - 4:30 PM JST | 7:15 AM - 7:30 AM UTC

[SSS07-04] CSEP Japan results and future developments

*Naoshi Hirata[1], Hiroshi Tsuruoka[1], Danijel Schorlemmer[3], Jiancang Zhuang[2] (1.Earthquake Research Institute, the University of Tokyo, 2.Institute of Statistical Mathematics, 3.GFZ German Research Centre for Geosciences)

4:30 PM - 4:45 PM JST | 7:30 AM - 7:45 AM UTC

[SSS07-05] From the studies of historical earthquakes to the implication of single fault to multiple fault segments ruptures in seismic hazard analysis

★Invited Papers

*Kuo-Fong Ma[1,2,3], Mingshen Yen[1], Yiwun Liao[1], Henyi Su[2] (1.Earthquake - Disaster & Risk Evaluation and Managment (E-DREaM) Center, National Central University, Taiwan, ROC, 2.Department of Earth Sciences, National Central University, Taiwan, ROC, 3.Institute of Earth Sciences, Academia Sinica, Taiwan, ROC)

4:45 PM - 5:00 PM JST | 7:45 AM - 8:00 AM UTC

[SSS07-06] **High resolution space-time models forecasting 3D seismicity beneath the Greater Tokyo Area**

★Invited Papers

*Yosihiko Ogata[1,2], Koichi Katsura, Hiroshi Tsuruoka[2], Naoshi Hirata[2] (1.Research Organization of Information and Systems, The Institute of Statistical Mathematics, 2.Earthquake Research Institute, The University of Tokyo)

Improving medium-term earthquake forecasts by compensating the EEPAS model for the time-lag

David Rhoades[1], Christophersen Annemarie[1], *Matt Gerstenberger[1]

1. GNS Science

The “Every Earthquake a Precursor According to Scale” (EEPAS) model treats every earthquake as a precursor of larger earthquakes to follow it in the medium term. Each earthquake contributes a transient increment to the expected rate of earthquake occurrence in its vicinity, based on empirical predictive scaling relations associated with the precursory scale increase phenomenon. Incomplete information on precursory earthquakes causes the EEPAS model to under-predict the expected number of earthquakes when forecasting across a time-lag. We modify EEPAS to compensate for the time-lag when calculating future forecasts. Given a set of model parameters, the completeness of precursory information can be expressed as a function of the target earthquake magnitude and the time-lag. The EEPAS model has a time-varying component and a background component. We consider two end-members for compensating the model for incompleteness: one entirely in the background component, and the other entirely in the time-varying component. We estimate an optimal mixture of these two end-members for time-lags out to 12 years using several different versions of the EEPAS model and subsets of the New Zealand earthquake catalogue to which EEPAS was previously fitted. Performance is checked on an independent test period. The optimal compensated model having increasingly high information gains over the original EEPAS model with increasing time-lags. Using catalogue data complete to 2018, the compensated models forecast increased annual probabilities of earthquake occurrence above magnitude thresholds from 6.0 to 8.0 in central New Zealand in the period 2019-2030 relative to the preceding period 2008-2018.

Keywords: earthquake forecasting, EEPAS, hypothesis testing, New Zealand

©2019. Japan Geoscience Union. All Right Reserved.

Earthquake probability forecast incorporating non-seismic data

*Peng Han[1], Jiancang Zhuang[2], Yosihiko Ogata[2], Katsumi Hattori[3]

1. Southern University of Science and Technology, Shenzhen, China, 2. The Institute of Statistical Mathematics, Tokyo, Japan , 3. Chiba University, Chiba, Japan

This study aims to develop statistical models for earthquake temporal occurrences based on both earthquake catalogs and other geophysical observations. As an example, the seismomagnetic signals at Kakioka (KAK) station are utilized to illustrate the modeling strategies, because previous studies suggest they might contain certain precursory information of local sizable earthquakes. Self-exciting, external-exciting, and combined models modified from Ogata’ s LIN-LIN algorithm have been applied to forecast the occurrences of M>4.05 earthquakes within 100 km from the KAK station. The self-exciting and external-exciting models perform significantly better than the Poisson Model, implying there are explanatory power in earthquake catalogs and magnetic anomalies, respectively. The combined model, which integrates information from catalogs and magnetic observations, is greatly superior to any of the other three models. Additional tests show that external exciting component derived from the magnetic data is not post-seismic in character, and is more likely to cooperate with large earthquakes. The combined model proposed in this study could also be useful to incorporate other non-catalog observations and may have potential value in improving Time-dependent hazard maps for operational forecasting.

Keywords: Probabilistic forecasting, Seismomagnetic, Modelling and interpretation, Japan

©2019. Japan Geoscience Union. All Right Reserved.

Extended versions of the space-time ETAS model and application to the 2016 Kumamoto earthquake sequence

*YICUN GUO[1], Jiancang Zhuang[1], Yosihiko Ogata[1]

1. The Institute of Statistical Mathematics, Tokyo, Japan

We proposed an extended version of the space-time ETAS model which simultaneously incorporates focal depths and rupture geometries of large earthquakes. The depth component is decoupled from earthquake hypocenters and assumed to follow the Beta distribution. This 3D-hypocenter finite-source ETAS model is applied to the 2016 Kumamoto earthquake sequence. Results from other versions of ETAS models are also obtained as comparisons. To model the dynamically triggered seismicity in Yufuin-Beppu region, an extended source which is more than two times' length of the ruptured fault of the Kumamoto mainshock is taken as its triggering source. Our results show that about 11.2% of the total seismicity is the background rate. Within the triggering source of mainshock, proportions of earthquakes being recognized as direct aftershocks of two foreshocks and the mainshock are 3.6%, 2.7%, and 23.3%, respectively. The reconstructed patterns of aftershock productivity show significant migrations in space and time. In near field (10km from slip > 1m areas), the decay of aftershock productivity follows an inverse power law of distance, verifying that aftershocks occur as an effect of stress changes imparted by the mainshock. Areas of high aftershock productivity form complementary patterns for coseismic slips, meaning that aftershocks contribute to the postseismic relaxation process.

Keywords: ETAS model, aftershock productivity, dynamic triggering

©2019. Japan Geoscience Union. All Right Reserved.

CSEP Japan results and future developments

*Naoshi Hirata[1], Hiroshi Tsuruoka[1], Danijel Schorlemmer[3], Jiancang Zhuang[2]

1. Earthquake Research Institute, the University of Tokyo, 2. Institute of Statistical Mathematics, 3. GFZ German Research Centre for Geosciences

An earthquake predictability experiment based on the Collaboratory for the Study of Earthquake Predictability (CSEP) had started in Japan in November 2009 and ten years have passed. In Japan, three test regions and four testing classes were set up, and more than 160 models are evaluated at the Japan test center operated by Earthquake Research Institute.

Tohoku-oki earthquake occurred immediately after the start of the experiment, and the results of the model’ s forecast were not good, but after that there was a recovery trend. However, it was also found that the model performance improved by model modification considering the influence of the Tohoku-oki earthquake. We also found that the forecast of the number of earthquakes is relatively difficult in many models.

Evaluation of the forecast result is carried out by N-test, M-Test, S-Test, L-test which are the CSEP standard tests, but for comparison between models, log likelihood and information gain (or probability gain) is direct and effective.

Ten years have passed since the experiment was started, testing center hardware replacement are required and some models are required modification about dimension of array according to increase of learning data. In addition, test classes in the current experiment forecasting magnitude 4 or 5 are set, it is necessary to set test classes to forecast larger magnitude such as 6 or 7.

Keywords: Earthquake Predictability, CSEP

©2019. Japan Geoscience Union. All Right Reserved.

From the studies of historical earthquakes to the implication of single fault to multiple fault segments ruptures in seismic hazard analysis

*Kuo-Fong Ma[1,2,3], Mingshen Yen[1], Yiwun Liao[1], Henyi Su[2]

1. Earthquake - Disaster & Risk Evaluation and Managment (E-DREaM) Center, National Central University, Taiwan, ROC, 2. Department of Earth Sciences, National Central University, Taiwan, ROC, 3. Institute of Earth Sciences, Academia Sinica, Taiwan, ROC

Historically, significant crustal damaging earthquakes in Taiwan mostly were from complicated fault system rather than from a single fault segment, which was not incorporated in the seismic hazard analysis of TEM PSHA2015, but, included in current developed new seismic hazard map of TEM PSHA2019. The 1906 M7.1 Meishan earthquake, recently, had been resolved to be from a fault system of blind NE strike thrust with EW surface breaching fault (one of the identified seismogenic structures). And, the 1935 M7.1 was occurred with bilateral rupture from a blind fault to strike-slip mechanism to the south and thrusting mechanism to the north. We employed the rupture kinematic modeling to the historical geodetic data with comparison to the intensity pattern to understand the possible involvement of the fault system. In addition to the damaging earthquakes from seismic active region, an ancient 1604 M7.5-M8.0 Quanchao damaging Earthquake in southeastern coast China region was also explored from literature intensity to understand the seismic potential of less seismic active regime in Taiwan strait. These historical and past events suggest that a single fault segment evaluation for seismic hazard might be inadequate. But, we have not yet had solution to solve this inadequacy to pin down the partition of slip rate within an identified fault system. We examined the fault rupture system from kinematic and dynamic modeling of the historical events, and examined the possible partition in slip rate for the fault segments in this identified fault system. We, further then compare its influence to the estimation of seismic hazard analysis. For development in PSHA and its application, we suggest the importance of resolving historical damaging earthquakes from modern developed seismology to seismic hazard assessment and risk management.

Keywords: fault system, seismic hazard analysis

©2019. Japan Geoscience Union. All Right Reserved.

High resolution space-time models forecasting 3D seismicity beneath the Greater Tokyo Area

*Yosihiko Ogata[1,2], Koichi Katsura, Hiroshi Tsuruoka[2], Naoshi Hirata[2]

1. Research Organization of Information and Systems, The Institute of Statistical Mathematics, 2. Earthquake Research Institute, The University of Tokyo

We propose an extended 3D epidemic-type aftershock sequence (ETAS) models of longitude, latitude and depth for short-term forecasts beneath the Metropolitan area (south Kanto region), Japan; this model also takes account of the induced effects by the 2011 Tohoku-Oki earthquake of magnitude 9.0 (M9). Specifically, we use some location-dependent coefficients in the 3D space; which is called as a hierarchical model. Similarly, we consider 3D location-dependent b-value for the Gutenberg-Richter law. In such modeling, we use linear interpolation on each of the 3D Delaunay tetrahedra of the hypocenters to estimate high resolution images in zones where hypocenters are dense. Based on the hypocenter catalog for a century period, we solve the location dependent parameters including the background seismicity rates, the self-exciting (aftershock) productivity rates, and the M9 induced productivity rate. The optimally inverted 3D spatial images of such characteristic parameters represent quite informative seismicity patterns such as in shallow crust and on the surface of subducting plates. In particular, the location-dependent external triggering factor shows the zones where the induced effect took place intensely by the M9 earthquake beneath the region.

Keywords: Akaike Bayesian Information Criterion (ABIC), Earthquake forecast, Extended 3D hierarchical space-time ETAS model, Induced seismicity, Tohoku-Oki Earthquake of M9

©2019. Japan Geoscience Union. All Right Reserved.

[J] Oral | S (Solid Earth Sciences)：S-SS Seismology

Mon. May 27, 2019 1:45 PM - 3:15 PM JST | Mon. May 27, 2019 4:45 AM - 6:15 AM UTC | A09 TOKYO BAY MAKUHARI HALL

[S-SS11] Seismic wave propagation: Theory and Application

convener:Kiwamu Nishida(Earthquake Research Institute, University of Tokyo), Kazuya Shiraishi(Japan Agency for Marine-Earth Science and Technology), Takao Nibe(JAPEX), Kaoru Sawazaki(National Research Institute for Earth Science and Disaster Resilience), Chairperson:Tsutomu Takahashi(JAMSTEC)

Seismic wave propagation provides rich information of earth's heterogeneities and the excitation sources. In order to extract the information, integrated studies are needed among mathematical/numerical studies based on the wave theory, miniature physical experiments using rock specimens, and practical data analyses. Furthermore, it is greatly beneficial to conduct comparative studies of various kinds of waves, such as elastic, acoustic, traveling ionospheric disturbances, and oceanic waves. This session widely invites presentations about the theories and applications related to seismic and other geophysical waves.

1:45 PM - 2:00 PM JST | 4:45 AM - 5:00 AM UTC

[SSS11-01] Power Spectrum of Random Heterogeneity of the Solid Earth

*Haruo Sato[1] (1.Tohoku Unvieristy)

2:00 PM - 2:15 PM JST | 5:00 AM - 5:15 AM UTC

[SSS11-02] Estimation of spatio-temporal changes of seismic scattering property associated with the 2008 Iwate-Miyagi Nairiku earthquake from sparse modeling of seismic ambient noise CCFs

*Takashi Hirose[1], Hisashi Nakahara[1], Takeshi Nishimura[1], Michel Campillo[2] (1.Graduate School of Science, Tohoku University, 2.University Grenoble Alpes, CNRS, ISTerre)

2:15 PM - 2:30 PM JST | 5:15 AM - 5:30 AM UTC

[SSS11-03] Surface roughness of the Philippine Sea plate at Nankai subduction zone

*Tsutomu Takahashi[1], Ayako Nakanishi[1], Shuichi Kodaira[1], Yoshiyuki Kaneda[2] (1.JAMSTEC, 2.Kagawa University)

2:30 PM - 2:45 PM JST | 5:30 AM - 5:45 AM UTC

[SSS11-04] Source location of volcanic earthquakes and tremors at Sakurajima volcano based on seismic correlation

*Theodorus Permana[1], Takeshi Nishimura[1], Hisashi Nakahara[1] (1.Solid Earth Physics Laboratory, Department of Geophysics, Graduate School of Science, Tohoku University)

2:45 PM - 3:00 PM JST | 5:45 AM - 6:00 AM UTC

[SSS11-05] **Crustal Structure Investigation in Northern Taiwan - Localized Wavefield Inversion of TAIGER T6 Wide Angle Refraction/Reflection Data**

*Fandy Adji Fachtony[1], How-wei Chen[1] (1.Institute of Geophysics, National Central University)

3:00 PM - 3:15 PM JST | 6:00 AM - 6:15 AM UTC

[SSS11-06] Self-organized criticality induced by randomness in block-spring models and the Gutenberg=Richter law

*Hidetsugu Sakaguchi [1] (1.Kyushi University)

Power Spectrum of Random Heterogeneity of the Solid Earth

*Haruo Sato[1]

1. Tohoku Unvieristy

Recent observations focusing on scattering of seismic waves revealed the existence of random heterogeneities in the solid earth medium. The radiative transfer theory (RTT) has been often used for the study of the propagation and scattering of wavelet intensities. For the statistical characterization of the power spectral density function (PSDF) of the random fractional fluctuation of velocity inhomogeneities in a 3-D space, we use von Karman type with three parameters: the RMS fractional velocity fluctuation, the characteristic length, and the order of the modified Bessel function of the second kind. This model leads to a power-law decay of PSDF at wavenumbers higher than the corner.

We compile reported statistical parameters of the lithosphere and the mantle based on various types of measurements. Reported exponents of wavenumber are distributed between -3 and -4, where many of them are close to -3. Reported RMS fractional fluctuations are of the order of 0.01 -- 0.1 in the crust and the upper mantle. Reported characteristic lengths distribute very widely. In order to grasp the spectral characteristics, eliminating strong heterogeneity data and the lower mantle data, we have plotted all the reported PSDFs of the crust and the upper mantle against wavenumber for a very wide range.

We find that the envelope of those PSDFs is well approximated by the -3rd power of wavenumber. In theory, we need to re-examine the applicable range of the Born approximation in the RTT when the wavenumber of a wavelet is much higher than the corner. In observation, we will have to measure carefully the PSDF on both sides of the corner. It is interesting to study what kinds of geophysical processes created the observed power-law spectral envelope in different scales and in different portions of the solid earth medium.

Keywords: Seismic waves, Velocity structure, Crust, Mantle, Random media, Scattering

©2019. Japan Geoscience Union. All Right Reserved.

Estimation of spatio-temporal changes of seismic scattering property associated with the 2008 Iwate-Miyagi Nairiku earthquake from sparse modeling of seismic ambient noise CCFs

*Takashi Hirose[1], Hisashi Nakahara[1], Takeshi Nishimura[1], Michel Campillo[2]

1. Graduate School of Science, Tohoku University, 2. University Grenoble Alpes, CNRS, ISTerre

In recent years, spatial distributions of seismic velocity and/or seismic scattering property changes associated with volcanic activities and earthquakes have been investigated by linear least-squares inversions using seismic ambient noise cross-correlation functions (CCFs) and sensitivity kernels (e.g., Obermann et al., 2013; Obermann et al., 2014). However, spatial distributions of medium changes are not easily estimated in the regions where only a small number of stations are set up. Here, we use sparse modeling (L_1 norm regularization) to estimate model parameters for a small data set (e.g., Tibshirani, 1996), and evaluate the minimum number of stations for these studies. We apply the sparse modeling to the 2008 M_w 6.9 Iwate-Miyagi Nairiku earthquake that occurred on 14 June 2008, and estimate the spatial distribution of seismic scattering property changes from decoherence (waveform changes) data of seismic ambient noise CCFs. Since we have enough seismic stations, we can compare the results from the sparse modeling and those from an ordinary linear least-squares inversion with L_2 norm regularization which has been widely used to solve linearized problems.

Seismic ambient noise CCFs were calculated at 0.5-1 Hz band for the pairs among 17 Hi-net stations during the years of 2007 and 2008. We firstly calculate decoherence values between reference CCFs (Jan-Dec, 2007) and target CCFs in two time periods of May 1 to June 13 (Period I) and June 15 to July 31 (Period II) in 2008, respectively. We then calculate the differences of decoherence values of Period I and Period II, and use them as observed decoherences. Totally, 450 observed decoherence values are analyzed. Finally, we divide the study area into 63 small cells with a size of $0.15^\circ \times 0.15^\circ$ and estimate scattering coefficient changes, Δg, for each small cell by comparing the observed and synthesized decoherence values. Here, we estimate synthesized decoherence values using 2-D decorrelation kernels (Margerin et al., 2016).

The result from the linear least-squares inversion with L_2 norm regularization shows that large Δg values are estimated around the epicenter of the main shock. The region of the largest Δg value is located at the south of the epicenter also from the sparse modeling. The maximum Δg value is about 0.035 km^{-1}, which is almost equivalent to the total scattering coefficient at this region. To know a minimum number of stations for the estimation, we selected the stations which locate within 30 km, 40 km, and 50 km from the epicenter (5, 7, and 13 stations, respectively), and conducted the same estimations for each case using the sparse modeling. We confirmed that 7 stations were necessary to recover the similar result.

The regions with large Δg values are well correlated with the region where large peak ground acceleration and large seismic velocity decreases are obtained (Takagi et al., 2012; Hobiger et al., 2014). This consistency suggests that strong motion by the main shock introduce not only large seismic velocity decreases but also large seismic scattering property changes in the shallow medium at the south of the epicenter. The sparse modeling will be useful to locate a change region of seismic scattering property changes from a sparse seismic network with several seismic stations.

©2019. Japan Geoscience Union. All Right Reserved.

Acknowledgements: We would like to thank the High Sensitivity Seismograph Network (Hi-net), NIED for providing the waveform data used in the present study.

Keywords: sparse modeling, seismic scattering property change, Iwate-Miyagi Nairiku earthquake, seismic interferometry

©2019. Japan Geoscience Union. All Right Reserved.

Surface roughness of the Philippine Sea plate at Nankai subduction zone

*Tsutomu Takahashi[1], Ayako Nakanishi[1], Shuichi Kodaira[1], Yoshiyuki Kaneda[2]

1. JAMSTEC, 2. Kagawa University

Seismic fault surfaces have roughness over a broad spatial scale range. In this study, we measured surface roughness of subducting Philippine Sea plate along several seismic survey lines at Nankai trough. Surface geometry of the subducting plate have been estimated by analyzing both the wide-angle refraction and high-resolution seismic-reflection surveys by Nakanishi et al. (2018). They estimated velocity structures from the former data with consideration for travel times of reflected waves from the top of the Philippine Sea plate of the latter data. Uncertainties of their geometry of the Philippine Sea plate can be examined by the uncertainties of velocity structures in the overriding continental plate.
First, we examined the P-wave velocity structures in the continental plate. Power spectra of the velocity fluctuations obey a power-law at small wavenumbers. We also find a clear decrease of power spectral density at larger wavenumbers. Cutoff wavenumber of this change almost corresponds to the inverse of receiver interval. Such decrease of power spectral density is probably caused by a spatial smoothness constraint of velocity estimation. Then, we examined the surface geometries at wavenumbers smaller than the cutoff wavenumber. Power spectra of surface geometries shows self-affine property. We applied bandpass filters for geometry data and mapped the root mean squared amplitudes of filtered geometries as surface roughness. Roughness is large at Hyuga-nada, and becomes small near the trough-axis off south of Shikoku. The small roughness area off Shikoku shows low activity of regular and slow earthquakes. Meanwhile, Hyuga-nada area shows high activity of low frequency earthquakes (Yamashita et al. 2015). Since surface roughness is relevant to a small-scale stress concentration on faults, this result implies an importance of surface roughness for seismicity.

Acknowledgement
This study was supported by “Research Project for Compound Disaster Mitigation on the Great Earthquakes and Tsunamis around the Nankai Trough Region” of the Ministry of Education, Culture, Sports, Science and Technology (MEXT) of Japan.

Keywords: surface roughness, Philippine Sea plate, velocity inhomogeneity, self-affine

©2019. Japan Geoscience Union. All Right Reserved.

Source location of volcanic earthquakes and tremors at Sakurajima volcano based on seismic correlation

*Theodorus Permana[1], Takeshi Nishimura[1], Hisashi Nakahara[1]

1. Solid Earth Physics Laboratory, Department of Geophysics, Graduate School of Science, Tohoku University

Precise source locations of volcanic tremors and earthquakes are one of the most basic information that is important to understand the volcanic process. The spatio-temporal changes of these source locations may provide insights into the eruption mechanism and the movement of volcanic fluids. However, the determination of those source locations is quite challenging due to the difficulties to distinguish their seismic phases and precisely measure the arrival times. Recently, we developed a hypocenter determination method for volcanic earthquakes and tremor, which adopts seismic interferometry processing technique for calculating cross-correlation functions (CCFs) and the source-scanning algorithm (SSA) (Permana et al., in preparation). Here, we apply our method to observed data recorded at Sakurajima volcano. We first locate volcano-tectonic earthquakes (VTs) and evaluate the location errors by comparing the results with the hypocenters determined by a phase-picking method. Then, we locate volcanic tremors and discuss their source locations, which cannot be obtained from phase-picking methods due to indistinguishable phase arrivals.

We analyze VTs that occurred during a rapid dike intrusion on August 15, 2015. Our result shows the hypocenters are distributed beneath the Mt. Minamidake mainly at 0-4 km depths. Our source locations are consistent with the hypocenters obtained by using the method of Hirata and Matsuura (1987), and the errors are estimated to be 2 km or less.

We determine the source locations of two kinds of tremors occurred on August 22-25, 2017. The first is a 13.5 hours long continuous tremor accompanying Strombolian eruptions on August 22-23. The second is a series of intermittent tremors that are recorded following the explosion earthquakes associated with Vulcanian eruptions which followed the continuous tremor. We calculate the CCFs at 1-3 Hz by using 20 s time windows with 19 s overlap for these tremors and stacked them to obtain average CCFs. Our results show that the source locations of the first 6 hours of continuous tremor, which are determined every 10 minutes, are located beneath Mt. Minamidake at depths from about 3 km to below the active crater. The sources of the following continuous tremor are located at shallower depths, from about 2 km depth to the ground surface on the southern flank of Mt. Minamidake. The sources of 61 segments of the intermittent tremors are densely distributed at 0-2 km depth beneath Mt. Minamidake.

The observed tremors are related to the eruptive activities at Sakurajima volcano and their sources are expected to be located at the eruptive conduit. Our estimated sources are distributed at the shallow depths beneath the active craters within the estimated errors. Therefore, our results show the prospect of our method as an alternative for tremor source location determination and volcano monitoring. The depth range of our results for continuous tremor also coincides with the previous studies on the generation depth of volcanic earthquakes.

Keywords: volcanic earthquakes, volcanic tremor, source location, cross-correlation, hypocenter

©2019. Japan Geoscience Union. All Right Reserved.

Crustal Structure Investigation in Northern Taiwan - Localized Wavefield Inversion of TAIGER T6 Wide Angle Refraction/Reflection Data

*Fandy Adji Fachtony[1], How-wei Chen[1]

1. Institute of Geophysics, National Central University

TAIGER T6 transects is one of the four crustal-scale Wide Angle Refraction/Reflection (WARR) survey lines under **TA**iwan **I**ntegrated **GE**odynamics **R**esearch (TAIGER) project conducted in 2008 in Taiwan. The north main array consist of four shot points (N1, N2, N3, and N4) across northern Taiwan from west to east. A total of 456 geophones deployed with receiver interval of ~200m on average. However, the recorded data suffers from crooked survey line geometry, uneven shot energy, noise level and currently available poorly defined 3D reference velocity model. Near-surface static effects caused by the irregular source and receiver spacing, strong lateral velocity variations and rapid topography changes produce apparent 3D wave propagation so that the standard seismic data processing or travel-time inversion could not be fully applied. To compensate above-mentioned drawbacks, Localized Slant Stack Transformation (LSST) for data pre-processing was applied to separate signal from interfering noise that has big amplitude and minor T-X curve difference. LSST is slowness and offset range-based plane wave destruction and construction techniques. The pros and cons of LSST will be discussed for TAIGER-T6 line.
For stable wavefield inversion, sufficient spatial sampling and events enhancement is essential. Wavefield inversion utilize the complete-cycle of wavelet information without picking compared to tomography study that rely on the travel time picks with potential reading errors. Velocity estimation is performed via wavefield transformation from τ-p data domain to τ-p-z solution domain through downward continuation and the application of imaging condition ($\tau = 0$). Ray tracing is performed for quality control and to quantify the separated static effects produced from source, receiver and velocity changes. Feasibility studies of three crustal scale synthetic models containing: (1) flat layers without topographic, (2) flat layers with topographic, (3) laterally varying topographic velocity models. Synthetic data is produced from Specfem2D computations. Effects of source and/or receiver static, velocity variation, and the combination of all were studied. Wavefield inversion is stable for all test models. Inverted 1D velocity becomes less smooth when static effects are included with and without static corrections. Real data implementation for all shots were cross-checked through numerical travel-time curve with acceptable error bound. Furthermore, the bottoming point of each ray through seismic ray tracing can be mapped along with the velocity information to construct quasi-2D velocity model. Inverted velocity depth profile from wavefield inversion provide higher resolution compared to the existing tomography velocity model across northern Taiwan area.

Keywords: Localized Slant Stack, TAIGER Project, Wiechert-Herglotz Inversion, Vespagram

©2019. Japan Geoscience Union. All Right Reserved.

Self-organized criticality induced by randomness in block-spring models and the Gutenberg=Richter law

*Hidetsugu Sakaguchi [1]

1. Kyushi University

The Block-spring model is a simple mathematical model for earthquakes proposed by Burridge and Knopoff. Later, Carlson and Langer performed numerical simulations of a uniform block-spring model with velocity-weakening friction. They found that the slip-size distribution obeys a power law in a small scale. Their model exhibits a kind of spatio-temporal chaos and the slip size distribution is dur to the chaotic behavior. Many authors studied a variety of block-spring models. In this presentation, we will show numerical results of a block-spring model with quenched randomness in the velocity-strengthening friction. When the pulling force is stationary, there is a continuous transition from a state pinned by the quenched randomness to a sliding state. When the external force is applied through a spring, the pinning and sliding repeat randomly. The effective pulling force fluctuates around the critical value of the pinning-depinning transition. The phase transition is self-organiized even if the parameter is not controlled. As a result of the criticality, the slip size distribution obeys a power law. We consider that the power law is caused by the self-organized criticality to the pinning-depinning transition in the random media. Our model is related to the asperity theory in that the spatial inhomogeneity is important.

Keywords: block-spring model, power law, pinning transition, self-organized criticality

©2019. Japan Geoscience Union. All Right Reserved.

[J] Oral | S (Solid Earth Sciences)：S-SS Seismology

Mon. May 27, 2019 3:30 PM - 5:00 PM JST | Mon. May 27, 2019 6:30 AM - 8:00 AM UTC | A09 TOKYO BAY MAKUHARI HALL

[S-SS11] Seismic wave propagation: Theory and Application

convener:Kiwamu Nishida(Earthquake Research Institute, University of Tokyo), Kazuya Shiraishi(Japan Agency for Marine-Earth Science and Technology), Takao Nibe(JAPEX), Kaoru Sawazaki(National Research Institute for Earth Science and Disaster Resilience), Chairperson:Kiwamu Nishida(東京大学地震研究所)

Seismic wave propagation provides rich information of earth's heterogeneities and the excitation sources. In order to extract the information, integrated studies are needed among mathematical/numerical studies based on the wave theory, miniature physical experiments using rock specimens, and practical data analyses. Furthermore, it is greatly beneficial to conduct comparative studies of various kinds of waves, such as elastic, acoustic, traveling ionospheric disturbances, and oceanic waves. This session widely invites presentations about the theories and applications related to seismic and other geophysical waves.

3:30 PM - 3:45 PM JST | 6:30 AM - 6:45 AM UTC

[SSS11-07] Land-Atmosphere Interaction in the low-frequency seismic band and inversion for shallow elasticity structure

*Toshiro Tanimoto[1], Jiong Wang[1] (1.Department of Earth Science, University of California, Santa Barbara, CA93106, USA)

3:45 PM - 4:00 PM JST | 6:45 AM - 7:00 AM UTC

[SSS11-08] Noise correlation analysis of S-net records

*Ryota Takagi[1], Genti Toyokuni[1], Mare Yamamoto[1] (1.Research Center for Prediction of Earthquakes and Volcanic Eruptions, Graduate School of Science, Tohoku University)

4:00 PM - 4:15 PM JST | 7:00 AM - 7:15 AM UTC

[SSS11-09] Atmospheric waves from the gas explosion in Sapporo on December 16, 2018, recorded by seismometers

*Kazunori Yoshizawa[1] (1.Faculty of Science, Hokkaido University)

4:15 PM - 4:30 PM JST | 7:15 AM - 7:30 AM UTC

[SSS11-10] Time-lapse monitoring of seismic velocity associated with the 2011 Shinmoedake eruption using seismic interferometry

*Kiwamu Nishida[1], Yuta Mizutani[1] (1.Earthquake Research Institute, University of Tokyo)

4:30 PM - 4:45 PM JST | 7:30 AM - 7:45 AM UTC

[SSS11-11] Temporal variations of seismic velocity and azimuthal anisotropy in near-surface rock and soil at KiK-net downhole array sites

*Taka'aki Taira[1], Li-Wei Chen[1], Hiroe Miyake[2] (1.Berkeley Seismological Laboratory, University of California, Berkeley, 2.The University of Tokyo)

4:45 PM - 5:00 PM JST | 7:45 AM - 8:00 AM UTC

[SSS11-12] **Denoising Ambient Seismic Field Correlation Functions with Deep Autoencoders**

*Loic Viens[1], Chris Van Houtte[2] (1.Disaster Prevention Research Institute, Kyoto University, 2.GNS Science)

Land-Atmosphere Interaction in the low-frequency seismic band and inversion for shallow elasticity structure

*Toshiro Tanimoto[1], Jiong Wang[1]

1. Department of Earth Science, University of California, Santa Barbara, CA93106, USA

For frequencies below 0.05 Hz, except for the hum signals generated by ocean waves, the atmosphere is the main source of seismic noise. Some characteristics of atmosphere-generated seismic noise have been reported (e.g., Zürn et al., 2007; Zürn and Wielandt, 2007) but recent data from co-located pressure and seismic sensors allow us to improve our understanding of this interaction. We report our analysis of data from the EarthScope Transportable Array (TA) and some global permanent stations that are equipped with pressure and seismic sensors.

We first point out that coherence between surface pressure and vertical seismic data shows two broad peaks, a lower frequency one that rises below about 0.002 Hz and a higher frequency peak that reaches its maximum about 0.02 Hz. There is a minimum of coherence between them at about 0.003-0.004 Hz.

We noted that there is basically no phase-shift between pressure and vertical seismic displacement for the lower frequency peak while there is a 180-degree phase shift between pressure and vertical displacement for the higher frequency peak at about 0.02 Hz. Two peaks show a completely opposite relationship between pressure and vertical displacement. The zero phase-shift for the lower frequency peak is consistent with the mass-attraction effect due to density perturbations in the atmosphere and the 180-degree phase shift for the peak about 0.02 Hz is consistent with elastic deformation caused by surface pressure.

They suggest that these are two competing forces generated by the atmosphere, one that tends to attract the sensor mass upward by density perturbations in the atmosphere and the other that tends to push down the ground due to high pressure. The mass-attraction effect wins for the lower frequency peak and the ground deformation effect wins for frequencies above 0.01 Hz. The existence of the minimum between the two peaks indicates that relative size of these forces switches at about 0.003-0.004 Hz (already pointed out by Zürn and Wielandt, 2007).

The size of the higher frequency peak (at about 0.02 Hz) is strongly influenced by the elasticity of near-surface materials; at many sites with STS-1 sensors, this high frequency peak is often hard to identify as the sites are mostly at hard-rock sites, meaning there is little deformation due to atmospheric pressure. On the other hand, some EarthScope TA sites are at soft sediment sites and show a large (and dominant) peak at about 0.02 Hz. For such soft sites, we can derive shallow structure from pressure and seismic data.

We will present an inversion scheme to invert data from this higher frequency peak. Basic data are the ratios between vertical seismic data to pressure data and also between horizontal seismic data to pressure data for frequencies between 0.005 Hz and 0.05 Hz. The method is an iterative nonlinear inversion from a starting model using depth sensitivity kernels that are computed at each iteration step. The framework of inversion is similar to surface-wave phase velocity inversion. The product is a layered elasticity structure beneath a co-located station.

©2019. Japan Geoscience Union. All Right Reserved.

Keywords: Land-Atmosphere Interaction, Shallow elasticity structure, Inversion of pressure and seismic data

©2019. Japan Geoscience Union. All Right Reserved.

Noise correlation analysis of S-net records

*Ryota Takagi[1], Genti Toyokuni[1], Mare Yamamoto[1]

1. Research Center for Prediction of Earthquakes and Volcanic Eruptions, Graduate School of Science, Tohoku University

We applied noise correlation analysis to continuous records of Seafloor Observation Network for Earthquakes and Tsunamis along the Japan Trench (S-net) to estimate crustal structure beneath the offshore region of northeast Japan. We used three-component records from 2017 to 2018 provided by National Research Institute for Earth Science and Disaster Resilience (NIED) and converted wavefoms from XYZ to UNE components. We analyzed accelerometer records because signal-to-noise ratio of accelerometer is higher than that of velocity sensor in the periods longer than a few seconds. The noise cross-correlation functions show periodic pulses every 60 seconds and a single pulse at zero lag. The periodic pulses and zero lag pulse can be attributed to coherent periodic noise and random noise, respectively, due to electric perturbation in instruments. The periodic noise depends on station, component, and time period. The random noise appears to be common only within stations along the same cable lines. We removed the periodic noise by computing cross-correlation functions of the difference waveforms between the records of one day and the records of one day before. The cable-dependent random noise was removed by fitting an empirical function to cross-correlation functions in the frequency domain. The noise reduction and staking within station separation bins enable us to extract Rayleigh and Love waves up to about 30 seconds. In the shorter period than 10 seconds, we found multiple modes of Rayleigh waves with group velocities of about 1.5 km/s and 0.3 km/s, which may have energy in ocean layer and sediment. In addition, we found Rayleigh waves propagating from coastal stations to deep offshore stations at the period around 4 seconds, whereas Rayleigh waves mainly propagate from deep offshore stations to coastal stations at the period around 8 seconds. The extracted surface waves may be useful to estimate crustal structure beneath the offshore region along the Japan trench.

Acknowledgement: We used continuous records of S-net managed by NIED. We thank NIED for providing the data.

Keywords: S-net, Seismic interferometry, Ambient noise, Noise correlation, Surface wave, Japan trench

©2019. Japan Geoscience Union. All Right Reserved.

Atmospheric waves from the gas explosion in Sapporo on December 16, 2018, recorded by seismometers

*Kazunori Yoshizawa[1]

1. Faculty of Science, Hokkaido University

A large gas explosion occurred in Hiragishi, Sapporo, on December 16, 2018, which blew up a two-story building in the hypocenter with more than 50 injured, although no casualty was reported miraculously. Damages to window glasses of neighboring buildings were reported in the radius of about 100 meters around the hypocenter due to strong blast waves from the explosion.

The infrasound waves from this explosion have been recorded in several seismometers installed on the ground surface of Ishikari Lowland (including the one in the campus of Hokkaido University) even at stations more than 60 kilometers away from the hypocenter, which has traveled with a speed of about 330 m/s. It is well known that atmospheric infrasound waves from large volcanic eruptions and/or meteor blast can travel very long distances, which can be observed with broad-band seismometers. Although this explosion in Sapporo is much smaller than such natural phenomena, the observed seismic records are likely to be caused by the air-earth coupled ground motions due to the infrasound waves from the explosion.

The observed infrasound/acoustic signals from this explosion cannot be observed in seismometers installed underground in and around Sapporo. Also, we cannot see any clear elastic wave (P-wave or surface waves) from this explosion. Only several seismometers installed on the ground surface have recorded the infrasound signals that are characterized by strong spectral peaks in a frequency range between 5 and 30 Hz. We can also identify the directional dependence of the observed waveforms; i.e., the amplitudes of infrasound signals are more attenuated and scattered in the north of hypocenter. This may be affected by winds and/or propagation paths, in particular, the urban area of Sapporo with tall buildings spared over the north of hypocenter.

Keywords: infrasound, atmospheric wave, seismometer, gas explosion

©2019. Japan Geoscience Union. All Right Reserved.

Time-lapse monitoring of seismic velocity associated with the 2011 Shinmoedake eruption using seismic interferometry

*Kiwamu Nishida[1], Yuta Mizutani[1]

1. Earthquake Research Institute, University of Tokyo

In recent years, the number of applications of seismic interferometry is increasing. In the analysis, the cross-correlation function between ambient noise records of a pair of stations can be regarded as a virtual seismic waveform recorded at one station when the source is placed at the other station. Since, in any time period, the seismic velocity around the station pair can be estimated from the cross-correlation function calculated without an earthquake, the seismic interferometry has been applied in many studies to monitor the temporal change of the seismic velocity. A number of studies have monitored the seismic velocity change in the volcanic region with seismic interferometry and detected the temporal change in seismic velocity associated with the eruption (Brenguier et al., 2008; Rivet et al., 2015). Inferred seismic velocity changes in the volcanic region frequently show the seasonal variations, which were caused by precipitation. The amplitude of seasonal fluctuation has the same order of magnitude of velocity change associated with the eruption. Therefore, in order to detect the transient velocity change accompanying the eruption, it is important to evaluate the seasonal fluctuation due to precipitation quantitatively and remove it appropriately from the estimated seismic velocity change. In this study, seismic interferometry was applied to a seismic array around Shinmoedake to monitor the seismic velocity change, aiming at detecting the velocity change associated with the Shinmoedake eruption in 2011. First, a cross-correlation function was calculated for each pair of stations using continuous ambient noise data for 8 years from May 2010 to April 2018. The stretching method (Sens-Schönfelder and Wegler, 2006) was applied to the calculated cross-correlation function to estimate the temporal change of the seismic velocity. From the estimated seismic velocity change by the stretching method, the seasonal variation affected by precipitation was detected as in the previous study (Wang et al., 2017). Therefore, the effect of precipitation was quantitatively evaluated using pore pressure model (Roeloffs, 1988; Talwani et al., 2007). After the effect of precipitation was subtracted, the seismic velocity change associated with the eruption was detected in several pairs. In order to constrain locations of the seismic velocity change in space, the horizontal and depth sensitivity kernel was calculated. The kernels suggested that structural changes would not occur in the depth of 1-3 km in the southeastern side and in the depth of 1-2 km in the northwestern side of Shinmoedake.

Keywords: seismic interferometry

©2019. Japan Geoscience Union. All Right Reserved.

Temporal variations of seismic velocity and azimuthal anisotropy in near-surface rock and soil at KiK-net downhole array sites

*Taka'aki Taira[1], Li-Wei Chen[1], Hiroe Miyake[2]

1. Berkeley Seismological Laboratory, University of California, Berkeley, 2. The University of Tokyo

Measuring stress and damage induced seismic velocity and anisotropy in crustal structure and their temporal behaviors provide insights into the underlying mechanisms of healing processes and its evolution, which would lead to a better understanding of earthquake cycle. We analyze three-component surface and borehole seismic data collected by KiK-net (Kiban-Kyoshin Net) to explore temporal variations in P- and S-wave velocity and S-wave azimuthal anisotropy (strength of anisotropy and polarization direction of the fast S wave) through coda wave interferometry. Our preliminary focus is on Hokkaido sites that experienced ground motion from the 2003 magnitude (M) 8.3 Tokachi-Oki and the 2018 M 6.0 Hokkaido Eastern Iburi earthquakes. Following Chen et al. (2017, EPSL), we analyzed all available KiK-net seismic waveforms in a frequency band of 1-15 Hz from 1997 through 2018 (more than 700 events) and evaluated seismic velocity and azimuthal anisotropy between surface and borehole sensors at 22 KiK-net sites. Median P- and S-wave velocity stacked by all measurements at each site are good agreement with them obtained from borehole logging data provided by NIED (National Research Institute for Earth Science and Disaster Resilience). We find that a number of KiK-net sites recording peak ground acceleration (PGA) higher than ~500 cm/s^2 (at surface sensor) exhibit clear S-wave velocity reductions following the 2018 Hokkaido Eastern Iburi mainshock. Station IBUH03 (located at Atuma town) also shows a sudden decrease of S-wave velocity following the 2003 Tokachi-Oki earthquake (PGA = ~350 cm cm/s^2 at station IBUH03). Reductions of S-wave velocity were about 6.5% for both mainshocks. However, there are a number of differences between two earthquakes. Our preliminary analysis suggests that the polarization direction of fast S-wave was systematically changed from 50 degrees to 10 degrees (measured clockwise from the north) following the 2018 earthquake and no notable change of P-wave velocity was observed. On the other hand, for the Hokkaido earthquake case, station IBUH03 appears to have a large variability in the polarization direction and displays a P-wave velocity reduction of about 4.5%. Our observation suggests a temporally increase of randomly oriented fractures following the 2003 Tokachi-Oki earthquake and also may suggest that the stress changes from the 2018 Hokkaido Eastern Iburi earthquake created water-saturated cracks oriented at ~10 degrees from north.

©2019. Japan Geoscience Union. All Right Reserved.

Denoising Ambient Seismic Field Correlation Functions with Deep Autoencoders

*Loic Viens[1], Chris Van Houtte[2]

1. Disaster Prevention Research Institute, Kyoto University, 2. GNS Science

In the last decade, seismic interferometry has become an established technique for monitoring the temporal changes of the Earth’s physical properties. This technique relies on measuring time shifts of seismic waves present in Green’s functions, which are generally approximated by cross-correlating 1-h long ambient seismic field records at two stations. To increase the accuracy of the phase information of hourly cross-correlation functions, pre-processing is generally applied to the recorded ambient seismic field, such as 1-bit normalization and/or pre-whitening. Despite this, hourly cross correlation functions often need to be stacked over a few hours/days to increase their signal-to-noise ratio and measure reliable phase shifts. We introduce a new technique for improving the time resolution of seismic monitoring, which denoises cross-correlation functions using deep autoencoders. Autoencoders are composed of an encoding function, which computes a compressed representation of the input data, and a decoding function which reconstructs a simplified representation of the input data. Both the encoder and decoder parts are composed of a stack of densely-connected neural network layers. Such an algorithm can be trained to denoise corrupted versions of their inputs, which in our case are correlation functions with low signal-to-noise ratio. We apply our deep denoising autoencoder on synthetic and real single-station cross-correlation functions computed from a few MeSO-net stations located in the Tokyo Metropolitan area. The denoised waveforms allow us to compute more precise relative velocity change (dv/v) than with the raw waveforms. The great advantage of this technique is that the algorithm can be trained within a few seconds and can be used to denoise near-real-time data, which could be useful for volcano monitoring.

Keywords: Seismic noise, Deep Autoencoders, Green's function

©2019. Japan Geoscience Union. All Right Reserved.

[J] Oral | S (Solid Earth Sciences)：S-SS Seismology

Mon. May 27, 2019 9:00 AM - 10:30 AM JST | Mon. May 27, 2019 12:00 AM - 1:30 AM UTC | Convention Hall A 2F

[S-SS13] Strong Ground Motion and Earthquake Disaster

convener:Masayuki Kuriyama(Central Research Institute of Electric Power Industry), Kazuhiro Somei(Geo-Research Institute), Chairperson:Nobuyuki Morikawa(National Research Institute for Earth Science and Disaster Resilience), Ryoichi Nakamura(Earthquake Research Institute, The University of Tokyo)

Strong ground motion has social impacts as it induces earthquake disasters. We solicit contribution on any seismological topics related to strong ground motion that includes, but are not limited to, source processes, wave propagation, and site effects. We also welcome contribution on earthquake related disaster mitigation.

9:00 AM - 9:15 AM JST | 12:00 AM - 12:15 AM UTC

[SSS13-25] Determination of dynamic characteristics of existing buildings at various site conditions in Eskisehir, Turkey

*Onur Kaplan[1], Seiji Tsuno[2], Hiroaki Yamanaka[3], Mehmet Safa Arslan[4], Oguz Ozel[4] (1.Eskisehir Technical University, 2.Railway Technical Research Institute , 3.Tokyo Institute of Technology , 4.Istanbul University)

9:15 AM - 9:30 AM JST | 12:15 AM - 12:30 AM UTC

[SSS13-26] ICDP DSeis 10: Near-field Observations for the M5.5 Orkney, South Africa Earthquake

Tatsunari Yasutomi[1], *James Mori[1], Hiroshi Ogasawara[2] (1.Earthquake Hazards Division, Disaster Prevention Research Institute, Kyoto University, 2.Ritsumeikan University)

9:30 AM - 9:45 AM JST | 12:30 AM - 12:45 AM UTC

[SSS13-27] Number of earthquakes from seismic activity model of the national seismic hazard maps for Japan

*Nobuyuki Morikawa[1], Junichi Miyakoshi[2], Hiroyuki Fujiwara[1] (1.National Research Institute for Earth Science and Disaster Resilience, 2.Ohsaki Research Institute, Inc.)

9:45 AM - 10:00 AM JST | 12:45 AM - 1:00 AM UTC

[SSS13-28] Comparative examination of the Probabilistic Seismic Hazard Maps in Japan with observed maximum seismic intensities for various periods

*Takamoto Muneta[1], Kazuki Koketsu[1] (1.Earthquake Research Institute, The University of Tokyo)

10:00 AM - 10:15 AM JST | 1:00 AM - 1:15 AM UTC

[SSS13-29] A Study on the Ground Motion Characteristics close to the Basin Edge

Ryota Hamabe[2], *Shinichi Matsushima[1], Takashi Azuma[3], Florent De Martin[4] (1.Disaster Prevention Research Institute, Kyoto University, 2.Graduate School of Engineering, Kyoto University, 3.National Institute of Advanced Industrial Science and Technology, 4.French Geological Survey)

10:15 AM - 10:30 AM JST | 1:15 AM - 1:30 AM UTC

[SSS13-30] Spectrum Characteristics of MeSO-net seismograms – Effect of Underground Installation -

*Ryoichi Nakamura[1], Hiroshi Tsuruoka[1], Aitaro Kato[1], Shin'ichi Sakai[1], Naoshi Hirata[1], Takahiro Shiina[1] (1.Earthquake Research Institute, The University of Tokyo)

Determination of dynamic characteristics of existing buildings at various site conditions in Eskisehir, Turkey

*Onur Kaplan[1], Seiji Tsuno[2], Hiroaki Yamanaka[3], Mehmet Safa Arslan[4], Oguz Ozel[4]

1. Eskisehir Technical University, 2. Railway Technical Research Institute , 3. Tokyo Institute of Technology , 4. Istanbul University

The fundamental vibration period of a building is a crucial parameter for earthquake engineering. The equivalent seismic lateral force is determined from a design spectrum in most static design methods. Accordingly, the earthquake force is a function of the fundamental vibration period of the building. The fundamental period of an existing building can be determined by both forced and ambient vibration measurements. In this study, ambient vibration measurements were conducted at 17 existing buildings including different structural styles (masonry and reinforced concrete) and heights (7 to about 65 meters) which are located at different site conditions in Eskisehir, Turkey. In ambient vibration measurements, two accelerometers were placed on the top of the buildings and one accelerometer was placed on the ground. The fundamental vibration periods and the dampings of the measured buildings were evaluated. The fundamental vibration periods of the buildings were evaluated by picking the peaks of the spectral ratios of Fourier spectra on the top floor of buildings to those on the ground. The dampings of the measured buildings were estimated by fitting the spectral ratios calculated using a single degree of freedom system to the spectral ratios observed, in the process of trial and error (Iwata and Tsuno, 2013). In order to understand the site conditions near the buildings, array microtremor observations by small-scale arrays of 1.5 to 16 meters were performed on the free field. SPAC method was used to obtain the phase velocities of Rayleigh waves and the S-wave velocity profiles were estimated using those phase velocities in the inversion technique. Tsuno et al. (2018) derived an equation of T=0.016H from 10 building measurements carried out in Eskisehir, Turkey. In this study, 7 more measurements were added to the previous measurements of Tsuno et al. (2018) thus, according to findings of this study, the equation of T=0.0165H was proposed to estimate the fundamental vibration period (T, in seconds) of an existing building in Eskisehir, Turkey with respect to its height (H, in meters). This equation is still in need to improve with additional measurements, which could represent most of the building heights in the Eskisehir building inventory. The calculated dampings of the measured buildings have a general tendency that the higher the buildings, the smaller the dampings.

Acknowledgment

This study is supported by the Joint Research Project under the Bilateral Program of the Japan Society for the Promotion of Science (JSPS) and The Scientific and Technological Research Council of Turkey (TUBITAK) under Grant TUBITAK 116Y524.

References

Iwata, N., and Tsuno, S. (2013). Estimation of vibration characteristics and seismic responses of railway viaducts using microtremors data. In *Proceedings of the 11th SEGJ International Symposium, Yokohama, Japan, 18-21 November 2013* (pp. 286-289).

Tsuno, S., Yamanaka, H., Kaplan, O., Arslan, M. S. and Ozel, O. (2018). Characteristics of building vibrations estimated in various site conditions in Eskisehir, Turkey. In *Proceedings of the 13th SEGJ International Symposium, Tokyo, Japan, 12-14 November 2018.*

©2019. Japan Geoscience Union. All Right Reserved.

Keywords: Ambient Vibration Measurement, Fundamental Vibration Period, Damping, Array Microtremor Observation

©2019. Japan Geoscience Union. All Right Reserved.

ICDP DSeis 10: Near-field Observations for the M5.5 Orkney, South Africa Earthquake

Tatsunari Yasutomi[1], *James Mori[1], Hiroshi Ogasawara[2]

1. Earthquake Hazards Division, Disaster Prevention Research Institute, Kyoto University, 2. Ritsumeikan University

We examined the near-field records for the 2014 Orkney earthquake (M5.5) to infer source properties for this moderate-sized earthquake. The event was the largest recent earthquake associated with the deep gold mines of the region. Different from usual normal-faulting events that are induced on known structures of the mines, the M5.5 earthquake took place significantly below the mining horizon with a strike-slip mechanism on an unknown geologic structure. Seismic activity close to the Moab Khotsong and Great Noligwa mines is very well monitored by instruments installed on the surface and in the mine tunnels. The high sample-rate (6 khz) geophones installed in the mine at depths of 1 to 3 km provide high-quality recordings of the mainshock and aftershocks.

The waveforms show that there is a small foreshock (about M1.8) located 1.6 km south of the mainshock hypocenter and at 0.6 sec before the mainshock. There is no evidence of any unusual character of the foreshock, or any significant deformation between the foreshock and mainshock.

Using lower frequency (<2.0 hz) data, the nearfield waveforms can be modeled using a finite fault slip inversion. The results show a slip distribution with two main patches of larger slip, which are located a few kilometers to the north and to the south of the hypocenter. The area of the fault plane is relatively large for a M5 earthquake and this gives a rather small static stress drop.

Keywords: Orkney earthquake, South Africa, slip inverstion

©2019. Japan Geoscience Union. All Right Reserved.

Number of earthquakes from seismic activity model of the national seismic hazard maps for Japan

*Nobuyuki Morikawa[1], Junichi Miyakoshi[2], Hiroyuki Fujiwara[1]

1. National Research Institute for Earth Science and Disaster Resilience, 2. Ohsaki Research Institute, Inc.

In this paper, as a part of the verification of the probabilistic national seismic hazard maps for Japan, we compare the earthquake occurrence ratio from seismic activity model in the national seismic hazard maps for Japan and that from earthquake catalog data.
As the number of earthquakes from seismic activity model of the national seismic hazard maps for Japan 2018 version, the expected value in 30 years is calculated for each magnitude and expressed by the cumulative number of earthquakes. The procedure is as follows.
1. For earthquakes with nonstationary seismic activity model adopted, set the probability of occurrence of earthquake in 30 years from January 2018 as the expected value of the number of earthquakes.
2. Earthquakes in Nankai Trough (M8-9 class), in Sagami Trough (M8-class), Mega-earthquake along the Kuril trench, and large plate-boundary earthquakes in Tokachi-oki and Nemruo-oki, the whole 30 years of the earthquake occurrence probability by the weight of each occurrence pattern as the expected value of the earthquake number in 30 years, respectively.
3. For the earthquakes in which the Poisson process is adopted, use the 30 year earthquake number based on the occurrence frequency of earthquakes.
Here, we prepare three datasets of cumulative earthquake number. The first is based on the “average case”, the second is based on the “maximum case”, and the third is based on the “averaged hazard” models.
For the earthquake catalog to be compared, we combine earthquakes with M 6.0 or more from 1885 to 1925 by Utsu (1982) and Japan Meteorological Agency earthquake data of M 5.0 or more from 1926 to 2010. At this time, aftershocks are removed according to the same rules as the national seismic hazard maps for Japan.
For shallow crustal earthquakes, the number of earthquakes from the model and the catalog are consistent at less than M 7.0 for the “average case”, and are consistent at less than M 7.7 for the “maximum case”. However, on a larger magnitude, there is a tendency for the model to have a smaller number of earthquakes. For earthquakes in Philippine Sea Plate, the number of earthquakes from the model and the catalog are consistent at M 8.0 and below. However, on a larger magnitude, the number of earthquakes in the model is extremely large. This is caused by the modeling of the large occurrence probability based on the time predictable model for the Nankai Trough earthquake. The number of earthquakes from the “average hazard” model decreases at M 8.0 or more. For earthquakes in the Pacific plate, the number of earthquakes from the model and the catalog are consistent at less than M 7.0. However, on a larger magnitude, the number of earthquakes from the model is somewhat larger. For M 7.8 and more, the model has changed based on the new long-term evaluation of earthquakes along the Kuril Trench by Headquarters for Earthquake Research Promotion of Japan, and the increase in number of earthquakes is also affecting.
On the other hand, when the period of the earthquake catalog is expanded until 2015, after the 2011 great Tohoku earthquake, the number of earthquakes from the model becomes smaller than that from the catalog for earthquakes in the Pacific and Philippine Sea plates. This is due to a large number of aftershocks and induced earthquakes of the 2011 Tohoku earthquake. How to incorporate the earthquake catalog after the great Tohoku earthquake into the seismic activity model in the seismic hazard assessment is a very important task.

©2019. Japan Geoscience Union. All Right Reserved.

Keywords: National seismic hazard maps for Japan, Seismic activity model, Earthquake catalog, The 2011 great Tohoku earthquake, Verification

©2019. Japan Geoscience Union. All Right Reserved.

Comparative examination of the Probabilistic Seismic Hazard Maps in Japan with observed maximum seismic intensities for various periods

*Takamoto Muneta[1], Kazuki Koketsu[1]

1. Earthquake Research Institute, The University of Tokyo

The accuracy of the Probabilistic Seismic Hazard Maps in Japan (PSHMJ), which is being published by the Headquarters for Earthquake Research Promotion of the Japanese government, was examined by comparing the observed maximum seismic intensities with the PSHMJ. Miyazawa and Mori (2009) compared those only for about 500 years from 1498, and Kondo (2017) compared those for 30 years from 1890, 1920, 1950, or 1980. However, in this study, we compared those for 30, 60, 90, and 120 years from 1890, to show how the accuracy varies for various periods.

Following Kondo (2017), for synthetic seismic intensities, we combined the hazard curves in the engineering bedrocks for PSHMJ (Miyakoshi et al., 2016), the site amplification factors (Wakamatsu and Matsuoka, 2013), and the relationship of seismic intensities and peak ground velocities (Midorikawa et al., 1999; Fujimoto and Midorikawa, 2005). As in Miyazawa and Mori (2009), the Poisson distribution was assumed, and phenomena of return periods of 30, 60, 90, and 120 years were related to those with probabilities of exceedance in 30 years of 64, 45, 28, and 22%, respectively. Observed seismic intensities were derived from the JMA seismic intensity database (Ishigaki and Takagi, 2000; Ishigaki, 2007) and the reports of large earthquakes between 1944 and 1964 (Usami, 1985; Harada et al., 2016). The derived dataset consists of observed seismic intensities at 110 points. This observed dataset was compared with the synthetic seismic intensities at the corresponding points in PSHMJ.

As an index of the comparison, we first calculated the root mean square of differences between observed and synthetic seismic intensities. The results are 1.2, 0.8, 0.7, and 0.7 for return periods of 30, 60, 90, and 120 years, respectively. Since large earthquakes, which can lead to large seismic intensities, are phenomena happening once in several hundred years (plate boundary earthquakes) or once in several thousand years, it is expected that a smaller root mean square is obtained for a longer return period. The above results mostly meet this expectation, but they do not approach 0.4 to 0.5 for a return period of 500 years (Miyazawa and Mori, 2009) being saturated at 0.7 for 90 and 120 years. We secondly performed regression analyses, and similar saturation was also found. For example, the small number of observed seismic intensities can cause this problem, and therefore it will be considered further.

Acknowledgments: J. Miyakoshi provided the hazard curves, and T. Kondo provided computer codes etc. Discussion with J. Miyakoshi and H. Fujiwara is helpful for this study.

Keywords: probabilistic seismic hazard map, observed maximun seismic intensity, return period

©2019. Japan Geoscience Union. All Right Reserved.

A Study on the Ground Motion Characteristics close to the Basin Edge

Ryota Hamabe[2], *Shinichi Matsushima[1], Takashi Azuma[3], Florent De Martin[4]

1. Disaster Prevention Research Institute, Kyoto University, 2. Graduate School of Engineering, Kyoto University, 3. National Institute of Advanced Industrial Science and Technology, 4. French Geological Survey

The 1995 Kobe Earthquake brought significant damage around the Kobe area in Japan. It was notable that a “Damage Belt” with an area with a width of 1km and length of 20km was formed. The main cause of this phenomenon was called the “Basin-Edge Effect”, which is a result of the constructive interference of seismic waves owing to the basin edge structure, i.e. the interference between the direct S-wave propagating upward and the basin-induced/diffracted surface waves propagating laterally. Therefore, this phenomenon should not limited to the Kobe area. In this study, we conduct a ground response analysis at sites close to the basin edge, assuming various types of basin structures, to understand the influence of the subsurface structure to the characteristics of the ground motion close to the basin edge. Also, the observed microtremor Horizontal-to-Vertical spectral ratio (MHVR) will be used to understand the relation between the shape of the MHVR and the basin edge shape. A method to estimate the region of amplification of ground motion due to the Basin-Edge effect at the basin edge estimated from MHVRs will be introduced.

Keywords: Basin-Edge effect, Basin edge, Amplification factor, Horizontal-to-Vertical spectral ratio

©2019. Japan Geoscience Union. All Right Reserved.

Spectrum Characteristics of MeSO-net seismograms –Effect of Underground Installation -

*Ryoichi Nakamura[1], Hiroshi Tsuruoka[1], Aitaro Kato[1], Shin'ichi Sakai[1], Naoshi Hirata[1], Takahiro Shiina[1]

1. Earthquake Research Institute, The University of Tokyo

1. Introduction

In the Kanto district, high-density seismographs with about 300 accelerometers by MeSO-net have been deployed, and records from 2008 have been accumulated. By analyzing the MeSO-net records integrating with those obtained in K-NET and KiK-net, which is operated near the ground surface, it will able to largely improve structural images in seismic attenuation. However, MeSO-net is installed at a depth of 20 m and there is a problem to integrate records obtained at the surface. In this study, we investigated relative amplification factors among MeSO-net sites and compared the factors to those estimated at the surface sites, K-NET and KiK-net.

2. Method and Data

Observation records which are obtained at two closely located sites by the same earthquake have almost the same propagation paths, so the difference of the two site records can represent a difference of site amplifications because effects of source radiation and attenuation along paths are canceled out. Based on this idea, some studies have been investigated relative amplification factors between the sites. Recently, Ikeura and Kato (2011) proposed a new method that regards site pairs as a network and estimates relative ground amplification factors by using least squares method within the network.

In this study, the relative amplification factors in MeSO-net was examined by using the Ikeura and Kato's method. In order to compare with the amplification factors on the surface, the ground record of K-NET and KiK-net was also included in the analysis. The ARTB method (Herman, 1980) was used for least squares estimation. A distance between sites to pair is 10 km or short. The Fourier spectrum of every 1 Hz from 1 Hz to 10 Hz were used for the data. The strong motion records of MeSO-net from 2011 to 2015 and K-NET/KiK-net from 1996 to July 2016 were selected. Earthquakes with Mj 4 or more and depths less than 200 km were used. We only adopted records which the maximum acceleration amplitude is 100 Gal or less to exclude the nonlinearity effects resulted in strong ground motion. Finally, we used site pairs of 962,422 with 394 observation sites of 394, which include MeSO-net site of 297.

3. Results

In this study, first, we performed numerical experiments to vilify the validity of results given by the ARTB. The geometries of site and earthquake used in the experiments are the same to the actual investigation. After 50 times iteration, it is confirmed that synthesized dataset well reproduce the relative site amplifications assumed in artificially.

Then, we conducted 100 times iteration for the actual observation records to obtain the relative ground amplification. Fig.1 shows an example of the result at 5 Hz. Here we compare the relationship with the average S wave velocity to 30m depth (AVS 30) provided from the JSHIS. The amplification factors at the

©2019. Japan Geoscience Union. All Right Reserved.

ground surface (K-NET and KiK-net) is about 3 times larger than that at the underground (MeSO-net) on average. The amplification rate tends to decrease with increasing velocities of the AVS 30. This trend is consistent with the relationship for the PGV data expected based on Fujimoto and Midorikawa (2006) (black solid line in Fig. 1).

We confirmed that the residuals in the attenuation tomographic inversion can be greatly reduced by giving the relative amplification factors obtained in this study as a priori information.

4. Conclusions

Relative amplifications of ground motion were investigated for observation sites of the MeSO-net, K-NET and KiK-net by using the site-pair network and the least squares method. As a result, it was found that amplification factor in the MeSO-net of which seismographs are deployed at the underground, 20 m depth, is about 1/3 comparing with those of ground surface recorded in the K-NET and KiK -net on average.

Keywords: MeSO-net, Relative Amplification Factor

©2019. Japan Geoscience Union. All Right Reserved.

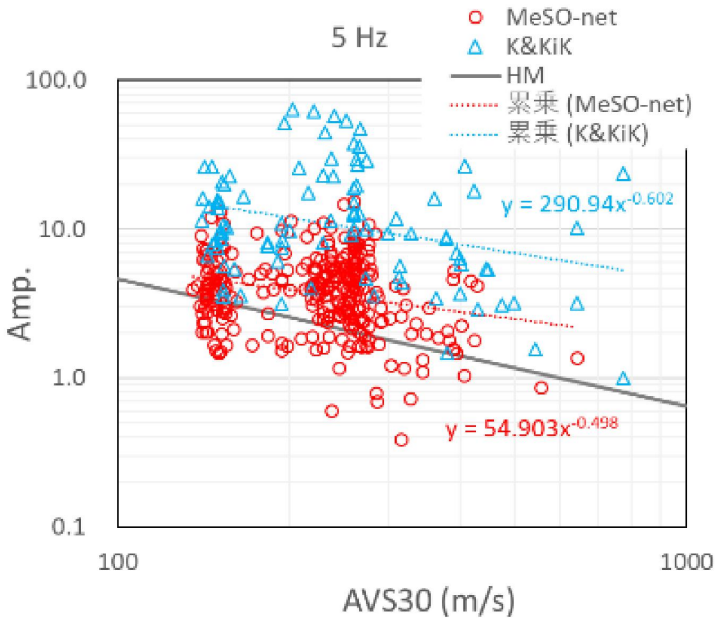

Fig.1 Relation between relative amplification factors at 5 Hz and AVS30 by JSHIS
△ : K-NET・KiK-net (free surface) ○ : MeSO-net(underground G.L.-20 m)
HM : Relation between PGV and AVS30 by Fujimoto and Midorikawa(2006)

©2019. Japan Geoscience Union. All Right Reserved.

[J] Oral | S (Solid Earth Sciences)：S-SS Seismology

Mon. May 27, 2019 10:45 AM - 12:15 PM JST | Mon. May 27, 2019 1:45 AM - 3:15 AM UTC | Convention Hall A 2F

[S-SS13] Strong Ground Motion and Earthquake Disaster

convener:Masayuki Kuriyama(Central Research Institute of Electric Power Industry), Kazuhiro Somei(Geo-Research Institute), Chairperson:Yasumaro Kakehi(Department of Planetology, Graduate School of Science, Kobe University), Hisashi Nakahara(Solid Earth Physics Laboratory, Department of Geophysics, Graduate School of Science, Tohoku University)

Strong ground motion has social impacts as it induces earthquake disasters. We solicit contribution on any seismological topics related to strong ground motion that includes, but are not limited to, source processes, wave propagation, and site effects. We also welcome contribution on earthquake related disaster mitigation.

10:45 AM - 11:00 AM JST | 1:45 AM - 2:00 AM UTC

[SSS13-31] Interpretation of attenuation of high-frequency waves from the intraslab, interplate, and outer-rise earthqukakes of Northeastern Japan

*Yasumaro Kakehi[1], Yu Ogasawara[1] (1.Graduate School of Science, Kobe University)

11:00 AM - 11:15 AM JST | 2:00 AM - 2:15 AM UTC

[SSS13-32] **Effect analysis of soil interlayer on seismic dynamic response and failure mode of metro station structure**

*Shuai Huang[1], Yuejun Lyu[1], Yanju Peng[1] (1.Institute of Crustal Dynamics,China Earthquake Administration)

11:15 AM - 11:30 AM JST | 2:15 AM - 2:30 AM UTC

[SSS13-33] **Investigation on the Applicability of V_{S30} Estimation Models for the Beijing Plain Area**

*Yi Fang, Yanju Peng, Zhijie Jiang

11:30 AM - 11:45 AM JST | 2:30 AM - 2:45 AM UTC

[SSS13-34] Early prediction of PGA and Sa using ANN

*Ting Yu Hsu[1] (1.Taiwan Tech)

11:45 AM - 12:00 PM JST | 2:45 AM - 3:00 AM UTC

[SSS13-35] Analysis of strong-motion acceleration records based on the Generalized Pareto distribution

*Hisashi Nakahara[1] (1.Solid Earth Physics Laboratory, Department of Geophysics, Graduate School of Science, Tohoku University)

12:00 PM - 12:15 PM JST | 3:00 AM - 3:15 AM UTC

Discussion

Interpretation of attenuation of high-frequency waves from the intraslab, interplate, and outer-rise earthqukakes of Northeastern Japan

*Yasumaro Kakehi[1], Yu Ogasawara[1]

1. Graduate School of Science, Kobe University

Previous studies (e.g. Tsumura et al., 2000) have shown the backarc side of Northeastern Japan has lower Q-value than the forearc side and remarkably low-Q zones exist just beneath and slightly backarc-side of the volcanic front. On the backarc side, high-frequency seismic waves attenuate due to the low-Q medium, and the contrast is seen between the high-frequency wave amplitudes on the backarc side and those of the forearc side, where such attenuation does not occur. In this study, characteristics of the spatial distribution of peak ground acceleration and the attenuation relation from 3 types of earthquakes: intraslab, interplate, and outer-rise earthquakes, are investigated using high-density strong motion data of NIED K-NET and KiK-net. The number of studied earthquakes is 15 in total. The most clear contrast between the forearc and backarc sides is seen in the intraslab earthquakes with deep focal depths, and the contrast is also clear in the outer-rise earthquakes though the contrast is not so clear as that in the intraslab earthquakes. On the other hand, the contrast is observed also in the interplate earthquakes, but it is less clear than that in the outer-rise earthquakes. The length of seismic wave path propagating in the low-Q region on the backarc side is long in the case of intraslab earthquakes with deep focal depths, and in the case of interplate and outer-rise earthquakes, both of which have shallow focal depths, the lengths of seismic wave path are shorter than the case of intraslab earthqukaes and are approximately the same. Therefore, it is reasonable that the contrast in outer-rise earthquakes is less clear than that in intraslab eartgquake. It is incomprehensible, however, that the contrast in interplate earthquakes is less clear than that in outer-rise earthquakes. To understand this mystery, we newly take the contribution of the attenuation due to the geometrical spreading factor into consideration. In case of interplate earthquakes whose epicenters are close to the land, the curvature of hypocentral distance contors in the land area (where the observation stations are located) is large. Therefore, attenuation due to the geometric spreading factor is large at the northern and southern ends of the Northeastern Japan arc, where hypocentral distances are large than those in the central part of the island arc, the amplitude difference between the forearch and backarc sides is masked. On the other hand, in case of outer-rise earthquake whose epicenter is far away from the land, the curvature of hypocentral distance contors in the land area is very small and the geometrical spreading factor hardly varies throughout the Northeastern Japan arc. Therefore, the mask effect due to the geometric spreading factor at the norther and southern ends of the Northeastern Japan arc does not work effectively. That is, due to the mask effect of the geometric spreading factor, the contrast between the forearc and backarc sides in interplate earthquakes becomes less clear than that in outer-rise earthquakes, where the mask effect does not work. Furthermore, as to the PGA attenuation relation, an apparent effect appears in the case of outer-rise earthquakes that makes the amplitude difference between the forearc and the backarc sides apparently emphasized than it is, as pointed out by Ogasawara and Kakehi (2018, SSJ Fall Meeting). Thus, the difference of the contrast of seismic shaking on the forearc side and that of the backarc side of Northeastern Japan due to the 3 types of earthquakes is interpreted unifiedly by considering the following 3 factors: (1) the length of seismic wave path propagating in the low-Q region, (2) the mask effect due to the geometrical spreading factor, and (3) the apparent effect in the case of outer-rise earthquakes whose hypocentral distances are systematically large.

©2019. Japan Geoscience Union. All Right Reserved.

Keywords: intraslab earthquake, interplate earthquake, outer-rise earthquake, attenuation of seismic waves

©2019. Japan Geoscience Union. All Right Reserved.

Effect analysis of soil interlayer on seismic dynamic response and failure mode of metro station structure

*Shuai Huang[1], Yuejun Lyu[1], Yanju Peng[1]

1. Institute of Crustal Dynamics,China Earthquake Administration

When the metro station structure is built in the site with weak interlayer, the metro station structure shows different patterns of destruction. In this article, based on the nonlinear elastic-plastic finite element model for metro station, considering the structure-soil dynamic interaction, the influence laws of the weak interlayer on the dynamic response and failure mode of the metro station structure under near and far-field earthquakes are studied. We found that the weak interlayer in the middle of the metro station has the greatest effect on the displacement, dynamic amplification factor and internal force of the metro station which leads to the poor anti-seismic performance of the metro station structure, and the metro station is more vulnerable to damage under near-field earthquake. When there is a middle interlayer, the maximum horizontal displacement of the metro station increases 63% at most compared to no interlayer under near-field earthquake. The interlayer below the metro station has a minimal impact on the dynamic amplification factor which shows that the existence of the interlayer below the metro station could reduce the vibration of the metro station to a certain extent. At last, indoor shaking table test for metro station was done, through which we determined the position of initial failure and the failure mode of the metro station structure under earthquake, and shaking table test results demonstrate the validation of the numerical simulation results.

Keywords: weak interlayer, metro station, near and far-field earthquakes, shaking table test, failure mode

©2019. Japan Geoscience Union. All Right Reserved.

Investigation on the Applicability of V_{S30} Estimation Models for the Beijing Plain Area

*Yi Fang, Yanju Peng, Zhijie Jiang

Using three models which respectively are bottom-layer constant velocity model, velocity gradient model and the extrapolation model with the travel-time averaged shear-wave velocities at two different depths, we investigate the data from 460 boreholes in Beijing plain area that the shear-wave velocity profile reaches at least 30 m. Through a detailed research, we found that the last method can estimate V_{S30} with high accuracy. It does not need any regression analysis to derive empirical relations from a large number of data. Meanwhile, this method is not regionally dependent, and has a remarkable improvement in the accuracy, therefore, it is potentially useful for many parts of the world including Beijing. It provides a basis for site classification, and then extends its application to evaluation of site effect in a rapid assessment of earthquake damage, thus being worth to be extensively applied.

Keywords: Vs30 , Estimation Models, Beijing Plain Area

©2019. Japan Geoscience Union. All Right Reserved.

Early prediction of PGA and Sa using ANN

*Ting Yu Hsu[1]

1. Taiwan Tech

In order to perform on-site earthquake early warning, in this study, we develop a novel approach to predict the peak ground acceleration (PGA) and pseudo-spectral acceleration (Sa) using the first few seconds of P-wave features. The Fourier spectrum amplitude (FSA) and phase (FSP) are handled separately and then combined together to predict the acceleration time history, then the PGA and Sa can be estimated accordingly. The FSA is predicted using the artificial neural network (ANN) with the predominant period, peak acceleration amplitude, peak velocity amplitude, peak displacement amplitude, cumulative absolute velocity, integral of the squared velocity, and FSA of the first three seconds of P-wave as input. The mean and standard deviation of the group delay time of phase spectrum of each separated frequency range decomposed by wavelet transform is employed as the prediction target, then the FSP can be generated using these mean and standard deviation of the group delay time. The FSP is predicted using another ANN model using similar P-wave features as the FSA ANN model. The earthquake records of the Taiwan Strong Motion Instrumentation Program from 1992 to 2006 were used to train and validate the proposed approach, and the promising accuracy of PGA and Sa prediction is obtained.

Keywords: Peak Ground Acceleration, Pseudo-spectral Acceleration, Artificial Neural Network

©2019. Japan Geoscience Union. All Right Reserved.

Analysis of strong-motion acceleration records based on the Generalized Pareto distribution

*Hisashi Nakahara[1]

1. Solid Earth Physics Laboratory, Department of Geophysics, Graduate School of Science, Tohoku University

Owing to K-NET and KiK-net managed by NIED, high-quality strong ground motion data have been accumulating in Japan in these two decades. Analyzing these data set, I investigate the upper limit of ground accelerations of near-field strong motion records in Japan. I apply the Generalized Pareto distribution (GPD) to amplitude distributions of ground accelerations exceeding given threshold levels, and estimate the parameters of GPD. Especially, the shape parameter of GPD is very important for this purpose. If the shape parameter is negative, an upper limit exists in the distribution. If the shape parameter is greater or equal to 0, there is no upper limit.

Among the strong motion database from K-NET and KiK-net, I select 98 strong motion records whose peak ground accelerations exceed 1g. I finally use 77 strong motion records after eliminating records contaminated by other events like aftershocks and those whose duration times are too short to have enough data. Positive values and negative values of ground accelerations are independently analyzed. I use the absolute value for the negative amplitude. Changing the threshold value of ground acceleration from 10 to 300 gal, I fit GPD to the data exceeding the threshold, and estimate the minimum threshold over which the estimated parameters of GPD (the shape parameter, the scale parameter, and the mean excess) will not change much. I also confirm the goodness of fit of GPD by checking P-P plots and Q-Q plots visually.

GPD explains amplitude distributions of 77 acceleration records. For the positive amplitudes of accelerations, 48 records show the upper limits. For the negative amplitudes of accelerations, 53 records show the limits. In total, about 70 % records show the limit in ground accelerations. The range of the limit is mostly smaller than about 6000gal. However, a few results with very small negative shape parameters suggest much larger limits. These results should be regarded practically as no limits. For the rest of about 30 % records, the existence of the limit is not statistically supported. However, there should be the upper limit in ground accelerations from the viewpoint of physics. So it is necessary to clarify reasons why about 30 % records do not suggest the upper limit in ground acceleration.

Acknowledgment:

I used strong motion records obtained by K-NET and KiK-net, NIED.

Keywords: Strong motion, peak ground acceleration, generalized Pareto distribution

©2019. Japan Geoscience Union. All Right Reserved.

[J] Poster | S (Solid Earth Sciences)：S-SS Seismology

Mon. May 27, 2019 3:30 PM - 5:00 PM JST | Mon. May 27, 2019 6:30 AM - 8:00 AM UTC | Poster Hall International Exhibition Hall8, Makuhari Messe_10

[S-SS13] Strong Ground Motion and Earthquake Disaster

convener:Masayuki Kuriyama(Central Research Institute of Electric Power Industry), Kazuhiro Somei(Geo-Research Institute)

Strong ground motion has social impacts as it induces earthquake disasters. We solicit contribution on any seismological topics related to strong ground motion that includes, but are not limited to, source processes, wave propagation, and site effects. We also welcome contribution on earthquake related disaster mitigation.

[SSS13-P01] Observation of Aftershock due to the 2018 Hokkaido Eastern Iburi Earthquake and Microtremor observation in the Damaged Area

*Isamu Nishimura[1], Tatsuya Noguchi[2], Yusuke Ono[2], Masanori Kohno[2], Keishin Hibi[1] (1.Graduate School of Sustainability Science,Tottori Univercity,Department of Engineering,Social Systems and Civil Engineering Program, 2.Department of Engineering Tottori Univercity)

[SSS13-P02] **Nonlinear site amplification for high intensity ground motions during the 2018 Mw 6.6 Hokkaido eastern Iburi earthquake**

*Yadab Prasad Dhakal[1], Takashi Kunugi[1], Takeshi Kimura[1], Wataru Suzuki[1], Shin Aoi[1] (1.National Research Institute for Earth Science and Disaster Resilience (NIED))

[SSS13-P03] Microtremor array measurements at strong motion recording stations, HKD127 and IBUH01, in 2018 Hokkaido Iburi earthquake.

*Takuto Kogawa[1], Koji Tokimatsu[1], Izuru Okawa[1], Hitoshi Tanaka[1], Kentaro Motoki[2] (1.TOKYO SOIL RESEARCH CO.,LTD., 2.KOBORI RESEARCH COMPLEX INC.)

[SSS13-P04] Subsurface structure model based at diffuse-field theory in Oiwake region: Simultaneous inversion analysis on adjacent two sites

*Moeko Koie[1], Kentaro Motoki[1], Kenichi Kato[1], Takuto Kogawa[2] (1.KOBORI RESEARCH COMPLEX INC., 2.TOKYO SOIL RESEARCH CO., LTD.)

[SSS13-P05] Exploration of the velocity structure model in the Mukawa town, damaged area during the 2018 Hokkaido eastern Iburi earthquake

*Michiko Shigefuji[1], Nobuo TAKAI[2], Jun Horita[3], Shingo Nomoto[3], Takahiro Maeda[4], Hiroaki Takahashi[2], Masayoshi Ichiyanagi[2], Hiroaki Yamanaka[5], Kosuke Chimoto[5], Seiji Tsuno[6], Masahiro Korenaga[6], Nobuyuki Yamada[7] (1.Kyushu University, 2.Hokkaido University, 3.Geo-Technical Research Co.,Ltd, 4.National Research Institute for Earth Science and Disaster Resilience, 5.Tokyo Institute of Technology, 6.Railway Technical Research Institute, 7.Kochi University)

[SSS13-P06] Source Process of the 2018 Hokkaido Eastern Iburi Earthquake Inferred from Strong Motion Data and Green's Functions Based on Three-Dimensional Velocity Structure Model

*Kimiyuki Asano[1], Tomotaka Iwata[1] (1.Disaster Prevention Research Institute, Kyoto University)

[SSS13-P07] Source process of the 2018 Hokkaido Eastern Iburi earthquake derived from strong motion data

*Hisahiko Kubo[1], Wataru Suzuki[1], Asako Iwaki[1], Shin Aoi[1], Haruko Sekiguchi[2] (1.National Research Institute for Earth Science and Disaster Resilience, 2.DPRI, Kyoto University)

[SSS13-P08] Broadband ground-motion simulation of the 2018 Hokkaido Eastern Iburi earthquake

*Asako Iwaki[1], Nobuyuki Morikawa[1], Takahiro Maeda[1], Hisahiko Kubo[1], Hiroyuki Fujiwara[1] (1.National Research Institute for Earth Science and Disaster Resilience)

[SSS13-P09] **Estimation of 1D S-wave velocity structures in Kumamoto plain and Mashiki town using a waveform inversion of S-wave**

*Kengo Muroi[1], Hiroaki Yamanaka[1], Kosuke Chimoto[1], Seiji Tsuno[2], Masahiro Korenaga[2], Hiroe Miyake[3], Nobuyuki Yamada[4] (1.Tokyo Institute of Technology, 2.Railway Technical Research Institute, 3.The University of Tokyo, 4.Kochi University)

[SSS13-P10] Investigation to estimate high-frequency Empirical Green's tensor derivatives (EGTD) using aftershocks for the 2016 Kumamoto earthquake

*Sayumi Yoshida[1], Horike Masanori [1], Ken Miyakoshi[2] (1.HANSHIN CONSULTANTS Co., Ltd., 2.Geo-Research Institute)

[SSS13-P11] Estimation of Site Amplification Characteristics in Kumamoto plain by Spectral Separation Analysis Using Aftershock Records of the 2016 Kumamoto Earthquake

*Tomomi Iida[1], Hiroaki Yamanaka[1], Kosuke Chimoto[1], Daiki Shinoyama[8], Seiji Tsuno[5], Masahiro Korenaga[5], Nobuyuki Yamada[7], Hiroe Miyake[6], Tatsuo Kanno[3], Michiko Shigefuji[3], Masayuki Yoshimi[2], Shinichi Matsushima[4], Hiroshi Kawase[4], Kimiyuki Asano[4], Tomotaka Iwata[4] (1.Tokyo institute of Technology, 2.National Institute of Advanced Industrial Science and Technology, 3.Kyushu University, 4.Kyoto University, 5.Railway Technical Research Institute, 6.The University of Tokyo, 7.Kochi Unicersity, 8.Central Research Institute of Electric Power Industry)

[SSS13-P12] Kinematic and dynamic source models of the 2016 Mj6.4 Kumamoto third large earthquake

*Kunikazu Yoshida[1], Ken Miyakoshi[1] (1.Geo-Research Institute)

[SSS13-P13] Source rupture process and strong motion generation area assuming the curved fault model for the 2003 northern Miyagi prefecture earthquake

*Kazuhiro Somei[1], Ken Miyakoshi[1], Yujia Guo[1] (1.Geo-Research Institute)

[SSS13-P14] Estimation of source rupture process during the 2018 Shimane-ken seibu earthquake using strong motion data

*Susumu Kurahashi[1], Ken Miyakoshi[2] (1.Aichi Institute of Technology, 2.Geo-Research Institute)

[SSS13-P15] An estimation of SMGA of M6 class earthquakes based on strong motion records near the source regions

*Kentaro Motoki[1], Kenichi Kato[1], Tetsuo Shiota[2] (1.Kobori Research Complex, 2.Shikoku Electric Power Company)

[SSS13-P16] Difference in short-period level between the surface and buried fault rupture crustal earthquake in Japan

*Shohei Yoshida[1], Takao Kagawa[1], Tatsuya Noguchi[1] (1.Graduate School of Engineering, Tottori University)

[SSS13-P17] Probabilistic seismic hazard assessment of response spectra for whole Japan (part 1: Selection of ground motion prediction equations)

*Nobuyuki Morikawa[1], Junichi Miyakoshi[2], Hiroyuki Fujiwara[1] (1.National Research Institute for Earth Science and Disaster Resilience, 2.Ohsaki Research Institute, Inc.)

[SSS13-P18] Probabilistic seismic hazard assessment of response spectra for whole Japan (part 2: Probabilistic seismic hazard assessment)

*Junichi Miyakoshi[1], Takeshi Morii[1], Nobuyuki Morikawa[2], Hiroyuki Fujiwara[2] (1.Ohsaki Research Institute, Inc., 2.National Research Institute for Earth Science and Disaster Resilience)

[SSS13-P19] **Simulation of Long-period Ground Motion around The Fujikawa-kako Fault Zone during the 2018 Northern Osaka Earthquake**

*Seina Hashimoto[1], Hiroaki Yamanaka[1], Kosuke Chimoto[1], Masahiro Korenaga[2], Seiji Tsuno[2], Hiroe Miyake[3], Shigeki Senna[4] (1.Tokyo Institute of Technology School of Enviroment and Society, 2.Railway Technical Research Institute, 3.The University of Tokyo, 4.National Research Institute for Earth Science and Disaster Prevention)

[SSS13-P20] Site amplification factors for KiK-net stations in and around Ibaraki Prefecture estimated by the coda normalization method

*Jun Kawahara[1], Takahiro Nakamura[1], Takuji Yamada[1] (1.Graduate School of Science and Engineering, Ibaraki University)

[SSS13-P21] Estimation of earthquake ground level in Horinouchi area in the 2014 Northern Nagano earthquake

*RYOTA KAWAI[1], Hiroaki Yamanaka[1], Kosuke Chimoto[1], Seiji Tsuno[2], Masahiro Korenaga[2] (1.Interdisciplinary Graduate School of Science and Engineering,Tokyo institute of Technology, 2.Railway Technical Research Institute)

[SSS13-P22] Ground type classification for strong ground motion prediction based on characteristics of phase-velocity curves from microtremor explorations

*Atsushi Wakai[1], Shigeki Senna[1], Hisanori Matsuyama[2], Yatagai Atsushi[2], Yoshiaki Inagaki[2], Hiroyuki Fujiwara[2] (1.National Research Institute for Earth Science and Disaster Prevention, 2.OYO Corporation)

[SSS13-P23] **Establishment of the Underground Structure Model for Seismic Damage Estimation**

*Shigeki Senna[1], Atsushi Wakai[1], Hiroyuki Fujiwara[1] (1.National Research Institute for Earth Science and Disaster Resilience)

[SSS13-P24] Consideration of liquefaction damage rate based on liquefaction damage in recent years

*Shigeki Senna[1], Ozawa Kyoko[1] (1.National Research Institute for Earth Science and Disaster Resilience)

[SSS13-P25] Estimation of surface earthquake record at MeSO-NET observation points

*Shigeki Senna[1], Atsushi Wakai[1] (1.National Research Institute for Earth Science and Disaster Resilience)

[SSS13-P26] Possibility of estimating phase velocity of Love wave using Horizontal components in microtremor array surveys in the case of Nishio

*Kotoyo Tsuchida[1], Masanori Horike[1], Koji Yamada[1], Masaki Suehiro[1], Sayumi Yoshida[1] (1.HANSHIN CONSULTANTS COMPANY LIMITED)

[SSS13-P27] Enhancement of shallow velocity structure models based on array microtremor explorations for Tokai region, Central Japan

*Atsushi Wakai[1], Shigeki Senna[1], Yatagai Atsushi[2], Yoshiaki Inagaki[2], Hisanori Matsuyama[2], Hiroyuki Fujiwara[1] (1.National Research Institute for Earth Science and Disaster Prevention, 2.OYO Corporation)

[SSS13-P28] Validation of seismic bedrock structure model in the Shimousa region, Chibe prefecture, Japanusing seismic interferometry to strong motion

*Kosuke Chimoto[1], Hiroaki Yamanaka[1] (1.Tokyo Institute of Technology)

[SSS13-P29] Microtremor survey for subsurface velocity structure of Saga plain

*Masayuki Yoshimi[1], Michiko Shigefuji[2], Tadashi Maruyama[1] (1.Geological Survey of Japan, AIST, 2.Kyushu University)

[SSS13-P30] Densely microtremor observation to estimation of subsurface structure in Hane and Kute area, Ohda City, Shimane Prefecture, Japan

*Tatsuya Noguchi[1], Yoshito Yamaguchi, Yuhei Morita, Isamu Nishimura[1], Shohei Yoshida[1], Takao Kagawa[1] (1.Department of Management of Social Systems and Civil Engineering, Civil Engineering Course Graduate School of Engineering, Tottori University)

[SSS13-P31] Densely microtremor observation to estimation of subsurface structure in Nishizono and Yura area, Hokuei Town, Tottori Prefecture, Japan

*Tatsuya Noguchi[1], Katsuya Tomeoku, Isamu Nishimura[1], Shohei Yoshida[1], Takao Kagawa[1] (1.Department of Management of Social Systems and Civil Engineering, Civil Engineering Course Graduate School of Engineering, Tottori University)

[SSS13-P32] Seismic reflection survey in the Kathmandu Valley, Nepal.

*Kota Koshika[1], Yusuke Kawasaki[1], Om Pradhan[1], Masato Yamamoto[1], Dai Nobuoka[1], Yoshikazu Matsubara[1], Hisanori Matsuyama[1], Monika Jha[2], Chintan Timisina[2], Suresh Shrestha[2], Mukunda Bhattarai[2], Dinesh Nepali[2], Soma Nath Sapkota[2], Hiroe Miyake[3], Kazuki Koketsu[3] (1.OYO Corporation, 2.Department of Mines and Geology, 3.Earthquake Research Institute, University of Tokyo)

[SSS13-P33] Broadband Microtremor Array Exploration at and around Tribhuvan International Airport, Kathmandu, Nepal

*Toshiaki Yokoi[1], Takumi Hayashida[1], Mukunda Bhattarai[2], Tara Pokharel[2], Suresh Shrestha[2], Chintan Timsina[2], Sunita Bhatarrai[2], Dinesh Nepali[2] (1.International Institute of Seismology and Earthquake Engineering, Building Research Institute, Japan, 2.Department of Mines and Geology, Ministry of Industry, Commerce and Supplies, Nepal)

[SSS13-P34] Distribution of average S-wave velocities by small-scale (5 to 15 meters) microtremor arrays in and around Hue City, Thua Thien-Hue province, Vietnam

*Ikuo Cho[1], Makoto OKUBO[2] (1.National Institute of Advanced Industrial Science and Technology, 2.Kochi University)

[SSS13-P35] Microtremor Array Exploration in the Syiah Kuala University, Banda Aceh, Indonesia

*Makoto OKUBO[1] (1.Natural Science Cluster, Kochi University)

[SSS13-P36] **Turkey-Japan Joint Project on Modeling of Geological Structures for Strong Ground Motion Simulations due to Crustal Earthquakes in Eskisehir Basin, Turkey, by Using Seismic Interferometry Method**

*Mehmet Safa Arslan[1], Kosuke Chimoto[2], Asim Oguz Ozel[1], Hiroaki Yamanaka[2] (1.ISTANBUL UNIVERSITY-CERRAHPASA, 2.TOKYO INSTITUTE OF TECHNOLOGY)

[SSS13-P37] **Nonlinear Ground Motion Response During the 2016 Meinong Taiwan Earthquake**

*Kuo-Liang Wen[1], Chun-Te Chen[2] (1.National Central University, Department of Earth Sciences, 2.Academia Sinica, Institute of Earth Sciences)

[SSS13-P38] Earthquake damage of the 2017 Pohang earthquake in South Korea

*Mikyung Choi[1], Sun-Cheon Park[1], Dong-Hyo Sohn[1], Seolhan You[1], Jongsun Sun[1], Seongheum Cho[1], Duk-Kee Lee[1] (1. Korea Meteorological Administration)

Observation of Aftershock due to the 2018 Hokkaido Eastern Iburi Earthquake and Microtremor observation in the Damaged Area

*Isamu Nishimura[1], Tatsuya Noguchi[2], Yusuke Ono[2], Masanori Kohno[2], Keishin Hibi[1]

1. Graduate School of Sustainability Science,Tottori Univercity,Department of Engineering,Social Systems and Civil Engineering Program, 2. Department of Engineering Tottori Univercity

To investigate a cause of serious damages of the 2018 Hokkaido Eastern Iburi Earthquake, we observed microtremors and aftershocks at a landslide area and around strong ground motion observation stations. As a result, S-wave velocity structures were estimated at all observation sites. It was found that thickness of the volcanic ash layer (S-wave velocity:75-130 m/s) is 10m. Especially, it is suggested that two layers of volcanic ash layer have caused a landslide in the Shikanuma and Atsuma sites. It was found that the H / V spectral ratio of microtremor corresponds to the thickness of volcanic ash. The spectral amplitude of the H / V of the orthogonal direction component of the mountain ridge line became larger than that of the parallel direction component.

Keywords: Microtremor observation, landslide, H / V spectral ratio, S-wave velocity, subsurface abstraction

©2019. Japan Geoscience Union. All Right Reserved.

Nonlinear site amplification for high intensity ground motions during the 2018 Mw 6.6 Hokkaido eastern Iburi earthquake

*Yadab Prasad Dhakal[1], Takashi Kunugi[1], Takeshi Kimura[1], Wataru Suzuki[1], Shin Aoi[1]

1. National Research Institute for Earth Science and Disaster Resilience (NIED)

Large peak ground accelerations (PGAs) exceeding 1g on both the horizontal and vertical components were recorded at a fault distance of about 25 km during the September 6, 2018, Mw 6.6 Hokkaido eastern Iburi earthquake. Explaining the large PGAs at the distance for the magnitude of the event requires detailed investigation of the site response and source radiations. At several sedimentary sites, peak ground velocities (PGVs) exceeding 100 cm/s were recorded. Comparison of the observed PGAs and PGVs with the ground motion prediction equations (GMPEs) by Si and Midorikawa (1999) revealed that the observed data, especially the PGVs, were substantially larger at fault distances smaller than about 40-50 km, while the data at longer distances showed little or no trend different from the GMPEs. This motivated us to examine the site response during the earthquake. We processed many small amplitude (PGAs between 5 and 20 cm/s/s) accelerograms from earthquakes that occurred prior to the mainshock (the Mw 6.6 event) at sixteen KiK-net sites, and compared the surface-to-borehole spectral ratios between the small-amplitude ground motions from prior earthquakes and large-amplitude ground motions recorded during the mainshock. The comparison suggested that the sites at short distances where PGVs were underestimated, sustained various degrees of nonlinear site response, and the recovery is still undergoing at some of the sites based on similar analysis of aftershock recordings. Nonlinear site amplification has been known for a long time for the reduction of short-period ground motion amplitudes at a soil site during strong input motions compared with the weak input motions. Another commonly reported effect of nonlinear site response is the shift of predominant frequency to lower one. This second effect was found to be very prominent during the mainshock at soil sites and smaller distances, which caused stronger amplification at relatively longer-periods resulting into large PGVs and large JMA intensities. At the site of largest PGA, the ground motions were amplified by an order of magnitude at the new predominant frequency during the mainshock. We also analyzed the horizontal-to-vertical (H-to-V) spectral ratios at K-NET sites where PGAs were larger than 200 cm/s/s. We found that the K-NET sites also experienced larger degree of nonlinear site response at sites of larger PGAs. Based on the above analysis, the nonlinear site amplification could be one of the major reasons for the high intensity ground motions that were underestimated at the smaller distances by the GMPEs. Moreover, two sites (IBUH01: KiK-net; HKD127: K-NET), which were closely located, recorded vertical PGAs exceeding 1g for the up going motions at the surface, and the recordings showed asymmetric waveforms and amplitudes characteristics to the nonlinear site response reported during a few earthquakes in the past. A few sites having lower vertical PGAs were also suspected of being experienced nonlinear site response on vertical motions. Finally, we derived an ad-hoc equation to correct for the nonlinear site amplification in the prediction of horizontal PGVs with respect to the GMPE by Si and Midorikawa (1999). The results indicated that the stronger input motions may induce larger changes in PGVs at the surface than that for a proportional change in the shallow S-wave velocities (Dhakal et al. 2019).

Reference:

Dhakal YP, Kunugi T, Kimura T, Suzuki W, Aoi S (2019) Peak ground motions and characteristics of nonlinear site response during the 2018 Mw 6.6, Hokkaido eastern Iburi earthquake. Earth, Planets and Space (submitted)

©2019. Japan Geoscience Union. All Right Reserved.

Si H, Midorikawa S (1999) New attenuation relations for peak ground acceleration and velocity considering effects of fault type and site condition. Journal of Structural and Construction Engineering Transactions of AIJ 523:63–70

Keywords: Soil nonlinearity, 2018 Iburi earthquake, PGA, PGV, Spectral ratios

©2019. Japan Geoscience Union. All Right Reserved.

Microtremor array measurements at strong motion recording stations, HKD127 and IBUH01, in 2018 Hokkaido Iburi earthquake.

*Takuto Kogawa[1], Koji Tokimatsu[1], Izuru Okawa[1], Hitoshi Tanaka[1], Kentaro Motoki[2]

1. TOKYO SOIL RESEARCH CO.,LTD., 2. KOBORI RESEARCH COMPLEX INC.

1.Introduction

An earthquake of Mj6.7 occurred at 3:07 on September 6, 2018, in the Eastern part of the Hokkaido Iburi region. High seismic intensities (SI) of upper 6 and 7 were observed during this earthquake, even though the hypocenter of the earthquake was at the depth of 37 km. The amplification of surface ground was considered as one of the main factors that contributed such high SI. In order to estimate the ground amplification of the near surface ground, microtremor array measurements were conducted at six strong motion recording stations that observed SI upper 6 or 7.
In this presentation, we focused on two stations, HKD127 and IBUH01, because there was a difference in SI in spite that the two stations closely located. So we will show the result of analysis for these two sites.

2.Microtremor array measurement

The shape of the microtremor array used was an equilateral triangle. The vertical components were measured at three vertex points as well as the center of the array, in addition to the two horizontal components at the center. The measurements with a radius of 10m or less were made for each station, whereas those with a radius of 25m or more were made once around the two stations and used for both, because the distance between the two is as close as about 100m.

3.Analysis

A dispersion curve was determined from stationary part of microtremor array data based on SPAC method, and calculated H/V spectra from the three component microtremors observed at the center. The shear wave velocity profiles of the two stations were then back-calculated by the genetic algorithm using both observed dispersion curve and H/V spectra. The influence of higher modes of Rayleigh and Love waves was considered for the observed H/V spectra but neglected for the observed dispersion curve.

Keywords: Microtremor Array Measurement, H/V Spectra, Dispersion Curve, 2018 Hokkaido Iburi earthquake, Velocity Structure

©2019. Japan Geoscience Union. All Right Reserved.

Subsurface structure model based at diffuse-field theory in Oiwake region: Simultaneous inversion analysis on adjacent two sites

*Moeko Koie[1], Kentaro Motoki[1], Kenichi Kato[1], Takuto Kogawa[2]

1. KOBORI RESEARCH COMPLEX INC., 2. TOKYO SOIL RESEARCH CO., LTD.

During the 2018 Hokkaido Eastern Iburi Earthquake, 6.7 seismic intensity was observed in KiK-net Oiwake. On the other hand, observed seismic intensity at K-NET Oiwake, which is 100m away from the KiK-net, was 6.4. The amplitude of response spectra at KiK-net were higher near the predominant period than those at K-NET. The reason for the difference between their seismic intensity seems to be thought of due to the difference of their subsurface structure. In this study, we deduce subsurface structure models at the two sites by H/V inversion based on diffuse-field theory and estimate amplification factor at the sites.

To select the earthquakes for inversion analysis, we set the conditions such as occurrence before the main shock, less PGA than 100 cm/s^2, and higher ratio of epicentral distance to depth of hypocenter than 2. We used the average H/V of the selected earthquakes for observed H/V. In the calculation of H/V, we use the square-root of sum of squares of NS and EW component for horizontal component. The period at the peak observed H/V at K-NET Oiwake is shorter than that at KiK-net. The difference between their observed H/V is small in longer period range than 2 seconds.

Because of the adjacent of the sites and similarity of observed H/V in the long period, we set the deep part of structure at the 2 sites to be in common and search for shallow part of that individually. In order to make the deep part of structure in common, we adopted simultaneous inversion analysis at the two sites. We used the hybrid heuristic method and set the range of search based on the model of PS logging and J-SHIS. We searched for the thickness for the deep structure and S wave velocity for the shallow structure.

As a result of inversion analysis, we could deduce subsurface structure models which accorded with the observed H/V. The depth up to engineering bedrock of deduced K-NET model is 7m, and that at KiK-net is 20m. AVS30 at K-NET is 278m/s, whereas that at KiK-net is 243m/s. On the whole, S wave velocity at KiK-net in shallow part is lower than that at K-NET. We calculated the amplification factor of the shallow part, which was searched individually. The first natural period of amplification factor at KiK-net is 0.31s and that at K-NET is 0.20s. The predominant period of response spectra at KiK-net’ s (0.53s) is also longer than K-NET (0.48s). Because both of the natural and the predominant period at K-NET are shorter than those at KiK-net, the difference between subsurface structures might cause that of the amplitude of the main shock. However, the predominant period of the main shock is longer than the natural period at both sites, which seems to be influenced by nonlinear effect of the subsurface soil.

We will study about a cause of the difference of seismic intensity considering nonlinear effect of the subsurface soil.

Keywords: The 2018 Hokkaido Eastern Iburi Earthquake, Diffuse-field theory, H/V inversion, Subsurface structure

©2019. Japan Geoscience Union. All Right Reserved.

Exploration of the velocity structure model in the Mukawa town, damaged area during the 2018 Hokkaido eastern Iburi earthquake

*Michiko Shigefuji[1], Nobuo TAKAI[2], Jun Horita[3], Shingo Nomoto[3], Takahiro Maeda[4], Hiroaki Takahashi[2], Masayoshi Ichiyanagi[2], Hiroaki Yamanaka[5], Kosuke Chimoto[5], Seiji Tsuno[6], Masahiro Korenaga[6], Nobuyuki Yamada[7]

1. Kyushu University, 2. Hokkaido University, 3. Geo-Technical Research Co.,Ltd, 4. National Research Institute for Earth Science and Disaster Resilience, 5. Tokyo Institute of Technology, 6. Railway Technical Research Institute, 7. Kochi University

The 2018 Hokkaido eastern Iburi earthquake (M_w 6.6, focal depth=37 km) occurred on 6 September 2018 at the Hidaka arc-arc collision zone, Hokkaido, Japan. The many building damages by strong ground motion were concentrated around K-NET Mukawa strong motion observation station (HKD126). Strong motion records had strong power in 1-2 second periods of the response spectrum to destroy the timber frame buildings. It is an important examination to know the cause of the generation of this destructive strong motion.

To understand the site effects of this strong motion, we estimate the velocity structure models by using the microtremor array and multichannel analysis of surface wave measurements at three sites; around HKD126 site, a hillside site located about 6 km north from HKD126, and midpoint between both sites. We carried out the microtremor array measurements (R=1-2000 m) on 14-16 December 2018. We used servo type velocity sensor (Le-3D/5s) and 24-bit data logger (DATAMARK LS-7000XT) with GPS time calibration. At small arrays (R<~10 m), we used moving coil accelerometer (JEP-6A3, 10V/g). The fundamental Rayleigh wave phase velocity is examined with the spatial autocorrelation method. We also carried out a multichannel analysis of surface wave to emphasize the high-frequency side phase velocity. We set 24 channel 4.5 Hz geophones in interval 1 m with GEODE and 10 kg wood hammer. The phase velocity is examined with the Frequency-wavenumber method. The shear wave velocity structure models are estimated to fit the dispersion curve of the fundamental mode of Rayleigh wave using the genetic algorithm inversion method (Yamanaka and Ishida, 1998). The phase velocity data of the large array (R=2000 m) were used in common to the three sites.

Comparing the velocity structures, the Vs=1300 m/s layer’s depth of HKD126 is shallower than the hillside site ones and midpoint depth is mid of both. This tendency of depth variation is the same as the seismic bedrock and subsurface structure depth variation of AIST model (Yoshida *et al.*, 2007) and J-SHIS V2 model (Fujiwara *et al.*, 2012). On the other hand, about the shallow part, engineering bedrock depth of hillside site is shallower than the HKD126. The midpoint’s seismic bedrock is mid for the others, however, the surface soft soil deposit is detected as richer than the HKD126. These features of the shallow part structure's variation are able to confirm by the surface geology or Vs30 values of J-SHIS.

Acknowledgements: A part of this study was supported by the Grant-in-Aid for Scientific Research No. 18K19952 and 17H06215 from MEXT of Japan, and MEXT of Japan’s Earthquake and Volcano Hazards Observation and Research Program.

Keywords: The 2018 Hokkaido eastern Iburi earthquake, Velocity structure model, Microtremor measurement, MASW

©2019. Japan Geoscience Union. All Right Reserved.

©2019. Japan Geoscience Union. All Right Reserved.

Source Process of the 2018 Hokkaido Eastern Iburi Earthquake Inferred from Strong Motion Data and Green's Functions Based on Three-Dimensional Velocity Structure Model

*Kimiyuki Asano[1], Tomotaka Iwata[1]

1. Disaster Prevention Research Institute, Kyoto University

The source rupture process of the 2018 Hokkaido Eastern Iburi earthquake (M_{JMA} 6.7) was analyzed by the kinematic waveform inversion using strong motion data. Since this earthquake occurred close to the Hidaka Collision Zone and the Ishikari Lowland, the crustal and sedimentary basin structure of surrounding region is rather complex. Thus, we tried to use a three-dimensional velocity structure model to compute theoretical Green's functions. We used the Japan Integrated Velocity Structure Model (JIVSM; Koketsu *et al.*, 2012), and the Green's functions were computed by the three-dimensional finite difference method. The source fault model with strike-angle variation was set by referring to the spatial distribution of early aftershocks and the Global CMT solution. The source rupture process was estimated by the multiple time-window kinematic waveform inversion method (e.g., Hartzell and Heaton, 1983). The observed data for the inversion was strong-motion velocity waveforms in 0.04–0.5 Hz at K-NET, KiK-net and F-net stations. The rupture starting point was assumed to be at the hypocenter located by JMA at a depth of 37 km. The strong motion stations were selected based on the result of forward ground motion simulation of an Mw 4.1 aftershock occurring on September 14, 2018.
The estimated source model has small slip in the vicinity of the hypocenter, but significant slip is found in the depth range from about 22 km to 32 km. The rupture mainly propagated toward shallow and southwest direction. Considering crustal structure in this region (e.g., Iwasaki et al., 2004; Kita et al., 2012), the large slip area (asperity) is located in the middle-to-lower crust, and its rupture does not reach the upper crust. The depth range of significant slip is consistent with the spatial distribution of early aftershocks. Later aftershocks occurring in shallower depth are thought to occur outside the mainshock's source fault.

Acknowledgements: Strong motion data from K-NET, KiK-net and F-net (NIED) and JMA unified hypocenter catalog were used in this study. This study was supported by the Grant-in-Aid for Special Purposes 18K19952 (PI: Prof. Hiroaki Takahashi at Hokkaido University) from MEXT.

Keywords: the 2018 Hokkaido Eastern Iburi earthquake, strong motion data, source rupture process, three-dimensional velocity structure model

©2019. Japan Geoscience Union. All Right Reserved.

Source process of the 2018 Hokkaido Eastern Iburi earthquake derived from strong motion data

*Hisahiko Kubo[1], Wataru Suzuki[1], Asako Iwaki[1], Shin Aoi[1], Haruko Sekiguchi[2]

1. National Research Institute for Earth Science and Disaster Resilience, 2. DPRI, Kyoto University

The 2018 Hokkaido Eastern Iburi earthquake (M_{jma} 6.7) struck southern Hokkaido, Japan on September 6, 2018 (JST). This earthquake caused strong ground motions over southern Hokkaido with a maximum seismic intensity of 7 on the JMA scale and a maximum PGA of over 1500 cm/s/s. In this study, we estimate the source process of this earthquake using strong motion waveforms.
For source-process analysis of this event, we develop a curved fault model based on the spatial distribution of aftershocks. This curved fault model consists of multiple planes, each with a width of 20 km, a common dip angle (65 degree), and a common top depth (approximately 22 km). The common dip angle refers to the moment tensor analysis of F-net. The strike angle of the planes smoothly changes along the strike direction: the strike angle is 15˚ at the north part, 340˚ at the central part, and 40˚ at the south part. The rupture starting point is set to the hypocenter determined by JMA. The curved fault model is divided into 15 subfaults along the strike direction and 10 subfaults along the dip direction.
We use velocity waveforms at 20 stations of K-NET and KiK-net, F-net of NIED. The waveforms are band-pass filtered between 0.05 and 0.5 Hz, resampled to 10 Hz, and windowed from 1 s before S-wave arrival for 25 s.
Green's functions are calculated with the discrete wavenumber method (Bouchon 1981) and the reflection/transmission matrix method (Kennett and Kerry 1979) assuming 1-D velocity structure models. The structure models are obtained for each station from the 3-D structure model (Fujiwara et al. 2009). Logging information is also used for the KiK-net station. To consider the rupture propagation effect, 25 point-sources are uniformly distributed over each subfault in the calculation of Green’ s functions.
The multi-time-window linear waveform inversion method (Olson and Apsel 1982; Hartzell and Heaton 1983) is used in this study. The slip time history of each subfault is discretized using eight smoothed ramp functions (time windows) progressively delayed by 0.4 s and having a duration of 0.8 s each. The triggering velocity of first time window is set to 1.4 km/s to minimize the data-fit residual. Two orthogonal slips of each time window at each subfault are derived by minimizing the difference between the observed and synthetic waveforms using the non-negative least-squares scheme (Lawson and Hanson 1974). The slip angle is allowed to vary centered at 107˚, which is the rake angle of the F-net analysis. In addition, we impose a spatiotemporal smoothing constraint on slips (Sekiguchi et al. 2000).
In the estimated source model, the large slips are found at approximately 30 km depth in the up-dip direction from the hypocenter. In the first 6 s, the rupture grows slowly around the hypocenter with small slips. Then, the rupture developed with the large moment release between 6 s and 12 s in the large slip area. The large slip area does not overlap with the active aftershock area

Keywords: 2018 Hokkaido Eastern Iburi earthquake, Source process, Strong ground motion

©2019. Japan Geoscience Union. All Right Reserved.

Broadband ground-motion simulation of the 2018 Hokkaido Eastern Iburi earthquake

*Asako Iwaki[1], Nobuyuki Morikawa[1], Takahiro Maeda[1], Hisahiko Kubo[1], Hiroyuki Fujiwara[1]

1. National Research Institute for Earth Science and Disaster Resilience

1. Introduction

The 2018 Hokkaido Eastern Iburi earthquake (M_{JMA}6.7) was an inland crustal earthquake at a focal depth of approximately 35 km. This earthquake brought strong ground motion to the southern Hokkaido, causing JMA seismic intensity of 6+ and 7 above the fault and nearby, and 6- in the city of Sapporo. The seismicity around the source region reaches to deeper region compared to other inland areas in Japan (HERP 2018). Inland crustal earthquakes at this depth have not been considered by the current ground-motion prediction procedure in Japan. Therefore it is necessary to examine whether the strong ground motion from this earthquake can be modeled by the conventional procedure.

2. Broadband ground-motion simulation

We conducted broadband ground-motion simulation using the characterized source model based on the “recipe” for strong motion prediction (HERP 2017), aiming to reproduce the observed ground motion. A planner fault is set referring to the fault slip model by Kubo et al. (2019, this meeting) with the length and width of 28km and 22km, respectively, in the lower crust. Rupture starting point is set to 35 km, and a single asperity is set several km shallower than the rupture starting point on the fault plane. Source parameters are derived by the recipe for inland crustal earthquakes. We call this source model the reference source model.

Broadband ground motion time-series on the engineering bedrock is computed using the J-SHIS v2 3D velocity model (Fujiwara et al. 2009, 2012). We employed a hybrid technique of the 3D finite-difference method (Aoi et al. 2004) and the stochastic Green’s function method (Dan and Sato 1998) superposed in time domain at the period of 1 s. JMA seismic intensity (I_{JMA}) on the ground surface is derived by using the empirical relationships between V_{S30}, PGV and I_{JMA} (Fujimoto and Midorikawa 2005, 2006).

Main features of the velocity waveforms in long-period range (> 1s), amplitude and travel time of the main phases, are found to be consistent with observed records at many observation stations. On the other hand, I_JMA on the ground surface systematically underestimated the observation. Although this underestimation can be attributed to many factors including the source and velocity models, since our simulation results underestimates the observation at all points in short-period component, we first examine the effect of the source parameters that mainly affects the ground-motion level of short-period components. The short-period level, or the source spectral amplitude level at short period, of this earthquake estimated by Tomozawa et al. (2018, SSJ) is 1 –2 times larger, depending on the dataset, than the empirical relation by Dan et al. (2001) which is employed in the recipe. Referring to their result, we set another source model that has smaller size of asperity and consequently higher short-period level, 1.5 times larger than the empirical relation of Dan et al. (2001). I_{JMA} computed with this source model was more consistent with the observation compared to the reference source model.

3. Summary

Broadband ground-motion simulations were conducted for this earthquake using the characterized source models. It was found that the ground motion computed with higher value of short-period level compared to the empirical relation for the ordinary inland crustal earthquake was more consistent with the observed ground motion. It maybe reflecting the feature of the earthquake source characterized by

©2019. Japan Geoscience Union. All Right Reserved.

the depth or the tectonic condition.
We will further study on the source characteristics and site response characteristics in order to better explain the strong ground motion records.

Acknowledgments: We used strong motion data provided by JMA, Hokkaido, the city of Sapporo, and NIED.

Keywords: the 2018 Hokkaido Eastern Iburi earthquake, strong ground motion, broadband ground-motion simulation, inland crustal earthquake

©2019. Japan Geoscience Union. All Right Reserved.

Estimation of 1D S-wave velocity structures in Kumamoto plain and Mashiki town using a waveform inversion of S-wave

*Kengo Muroi[1], Hiroaki Yamanaka[1], Kosuke Chimoto[1], Seiji Tsuno[2], Masahiro Korenaga[2], Hiroe Miyake[3], Nobuyuki Yamada[4]

1. Tokyo Institute of Technology, 2. Railway Technical Research Institute, 3. The University of Tokyo, 4. Kochi University

The 2016 Kumamoto earthquakes are crustal earthquakes caused by inland active faults with damage of many wooden houses to the focal area. In this study, we revised the previous subsurface structural model, using the observed ground motion records during aftershocks of the earthquakes, on the purpose of evaluating strong ground motion in damaged area during the main shock. Furthermore, we reproduced the strong motion of main shock, using the revised subsurface structural model.
First, we conducted 3-D finite difference simulations during aftershocks of the 2016 Kumamoto earthquakes, using previous subsurface structural model by Headquarters for Earthquake Research Promotion. We used the aftershock with an Mj of 5.5 and a depth of 10km on April 19 assuming a homogeneous fault model. From the comparison of the observed waveforms and the calculated waveforms in Mashiki, we found that the qualitative characteristics seen in the observed waveforms can be reproduced. However, we found it difficult to reproduce the detailed characteristics, such as the amplitude and phase.
Therefore, we tuned the 1-D subsurface structural models just beneath the observation sites by an inversion analysis, using waveforms of the observed initial S-wave during aftershocks. We estimated a 1-D velocity model minimizing misfit of mean squares between amplitudes of the observed waveforms and the calculated waveforms by a 1-D simulation using the discrete wavenumber method. We estimated the 1-D velocity structures at 36 observation sites in Kumamoto plain and Mashiki town during the aftershocks. We could well explain the characteristics of the observed waveforms, compared with the calculated waveforms using the previous subsurface structural model.
Finally, we conducted a simulation of the ground motion for the main shock, using the revised subsurface structural model. We used the source model by Kubo et al. (2016) and site amplification factors of J-SHIS in order to consider the effect of the amplification of the shallow soil. The calculated J.M.A seismic intensity distribution underestimated the observed seismic intensity at the center of Mashiki town and the calculated waveform at Mashiki town hall was 3 to 4 times smaller than the observed waveform. On the other hand, the calculated waveforms at K-net Kumamoto and KiK-net Mashiki are similar characteristics of the observed waveforms. These results show that the revised subsurface structure was reasonable in the Kumamoto plain, but we need to reconstruct further more the subsurface structural model beneath the center of Mashiki town.

Keywords: The 2016 Kumamoto Earthquakes, Waveform Inversion, 1D S-wave Velocity Structure, Simulation of Ground Motion

©2019. Japan Geoscience Union. All Right Reserved.

Investigation to estimate high-frequency Empirical Green’s tensor derivatives (EGTD) using aftershocks for the 2016 Kumamoto earthquake

*Sayumi Yoshida[1], Horike Masanori [1], Ken Miyakoshi[2]

1. HANSHIN CONSULTANTS Co., Ltd., 2. Geo-Research Institute

1) Introduction
Green’s tensor derivatives play a key role for evaluation and prediction of strong ground motions and for surveys of the velocity and damping structures. However, it is difficult to generate high-frequency (above 1Hz) Green’s tensor derivatives using numerical approaches for want of fine geological structure models. Plicka and Zahradnik (1998) proposed a method for estimation of Empirical Green’s tensor derivatives (EGTDs) using multiple small earthquakes. EGTDs does not require the structural model along propagation paths for their estimation and is possible to calculate high-frequency ground motions for any focal mechanism. In this study, we investigate the conditions required (focal mechanism, grouping radius, applicable frequency) to obtain high-frequency EGTDs, using aftershocks of the 2016 Kumamoto earthquake.
2) Data and method
The size of the aftershocks ranges between the magnitudes 2 and 4. The focal mechanism, such as the strike, the dip angle, and the rake angle, and the source parameters of radiated spectra, such as the seismic moment and the corner frequency, are required for the estimation of EGTDs. The focal mechanism was obtained from the sign of P-wave first motions and the source parameters were obtained from the Fourier spectra of S-wave motions, assuming the model.
We first set the grouped aftershocks located within a sphere with a certain radius. Then, we estimated 3 EGTDs for 3-component ground motions from the grouped aftershocks by the approach developed by Plicka and Zahradnik (1998). Finally, we evaluated the accuracy of the estimated EGTDs by the correlation coefficients between observed seismic recordings of the grouped aftershocks and those calculated using the estimated EGTD for the 3- component ground motions. We furthermore evaluate the accuracy of EGTDs by investigating whether they can reproduce seismic waveforms of the aftershocks which are not contained in the group.
3) Results
Accurate EGTDs up to 2 Hz can be stably estimated from most groups with the radius of 1km, having the correlation coefficients over 0.8. Also, these EGTDs can reproduce the seismic motions of the aftershock that is not contained in the group. In the meantime, the correlation coefficients calculated from the estimated EGTDs up to 4Hz are not always not high values over 0.8 even for the groups with the radius 0.5 km. These results suggest that estimation of EGTDs up to the frequency higher than 2Hz requires accurate focal mechanism and source parameters of the radiated spectra. Thus, we will improve them, for example, using the Genetic algorithm.
4) Acknowledgement
In this study, we use event waveform data provided by NIED (Hi-net).

Keywords: Empirical Green’s tensor, 2016 Kumamoto earthquake, high-frequency

©2019. Japan Geoscience Union. All Right Reserved.

Estimation of Site Amplification Characteristics in Kumamoto plain by Spectral Separation Analysis Using Aftershock Records of the 2016 Kumamoto Earthquake

*Tomomi Iida[1], Hiroaki Yamanaka[1], Kosuke Chimoto[1], Daiki Shinoyama[8], Seiji Tsuno[5], Masahiro Korenaga[5], Nobuyuki Yamada[7], Hiroe Miyake[6], Tatsuo Kanno[3], Michiko Shigefuji[3], Masayuki Yoshimi[2], Shinichi Matsushima[4], Hiroshi Kawase[4], Kimiyuki Asano[4], Tomotaka Iwata[4]

1. Tokyo institute of Technology, 2. National Institute of Advanced Industrial Science and Technology, 3. Kyushu University, 4. Kyoto University, 5. Railway Technical Research Institute, 6. The University of Tokyo, 7. Kochi Unicersity, 8. Central Research Institute of Electric Power Industry

The 2016 Kumamoto earthquake contains a foreshock with an Mj of 6.5 on April 14 and the main shock with an Mj of 7.3 on April 16. The earthquakes generated ground motions with a seismic intensity of 7 on the Japan Meteorological Agency scale twice in Mashiki, Kumamoto, Japan and many wooden houses were collapsed. In this study we estimated site amplification characteristics in Kumamoto plain by using ground motion records at strong motion stations of K-NET, KiK-net, seismic intensity-meters stations by local governments and aftershock observation stations by Yamanaka et al. (2016) through a spectral inversion technique. We choose the OITH08 station as the referential site in the inversion. The estimated frequency dependent Q and the source characteristics by the spectral inversion technique show similar features to those from previous studies (e.g. Somei et al, 2018). The site amplifications in the alluvium plain show large values in a frequency range of 0.5-2.0Hz. At high frequency the site amplifications of the mountain are larger than those of the plain area. We estimated S-wave velocity structures in Kumamoto plain by an inverse analysis of the site amplifications. The sediments are large in central area of the Kumamoto plain.
Acknowledgements: This work was conducted as a part of the Comprehensive Study on the Futagawa-Hinagu fault zone after the 2016 Kumamoto earthquake, MEXT.

Keywords: Spectral inversion technique, the 2016 Kumamoto Earthquake, Site Amplification

©2019. Japan Geoscience Union. All Right Reserved.

Kinematic and dynamic source models of the 2016 Mj6.4 Kumamoto third large earthquake

*Kunikazu Yoshida[1], Ken Miyakoshi[1]

1. Geo-Research Institute

We make a kinematic source model of the 2016 Mj6.4 earthquake (2016 Apr. 15, 00:03 JST) which is a third large event during the 2016 Kumamoto earthquake sequence and dynamic source models based on the result of the kinematic model.

The kinematic model is made by inverting the strong-motion data obtained from K-NET, KiK-net, JMA and local government were used. The data were windowed for 18 s, starting at P-wave arrival time, and band-pass-filtered between 0.05 to 1.0 Hz (periods of 1-20 s) for waveform inversion. The accelerograms were integrated into ground velocities. Theoretical Green's functions are calculated using the discrete wavenumber method (Bouchon, 1981) and the Reflection/Transmission coefficient matrix method (Kennett and Kerry, 1979) using a stratified medium. We assumed individual one-dimensional velocity structure model for each station by using waveform modelling with small earthquake records (Yoshida et al., 2017). The event locations were relocated using double-difference method by Uchide et al. (2016). We used multi-time-window linear waveform inversion procedure (e.g., Hartzell and Heaton, 1983) in which the moment-release distribution is discretized in both space and time. The length and width of the fault plane was assumed to be 12 km and 10.5 km, respectively. The fault plane is divided into subfaults of 1.5 km ×1.5 km. The moment function of each subfault was represented by a series of six smoothed ramp functions in the 0.4 second interval. The first time-window triggering velocity (V_{FT}) was determined as 2.4 km/s, which was searched between 2.0 and 2.6 km/s based on residual of the waveform fits.

The estimated source model indicated 1.2 ×10^{18} Nm (Mw6.0) of the total moment release and 0.3 m average slip. One rectangular asperity and a high slip/moment rate area (HRA, Yoshida et al., 2017) patches with the average slip of 0.7 m were identified on the shallow part of the fault plane. The slip of the background area is 0.1 m.

We attempt to make dynamic rupture models based on the kinematic model. Stress drop distribution of the kinematic model was calculated (Okada, 1992). The average static stress drops were 3.9 MPa (asperity) or 4.9 MPa (HRA) and 1.0 MPa for the background. Effective stress was taken from the stress parameters estimated from SMGA (Kurahashi et al., 2017). The effective stresses were adjusted as 5.1 MPa (Asperity) or 6.3 MPa (HRA) to rupture over the entire fault. We conducted dynamic rupture simulations using the patched stress drop distribution obtained from the kinematic model (Figure left-bottom). We assumed slip-weakening law with uniform critical distances of 0.1 m, based on Dc’’ (Fukuyama and Mikumo, 2007) of about 0.15 m at KMMH14. The simulation results show that the final slips and total moments well agree with the ones of the kinematic model. Nevertheless, small slips and high slip rate on the top margin of the patches, and supershear rupture propagation on the further of the patch were found. We expect examination of some dynamic parameters, such as critical slip distances, to improve simulation results.

Acknowledgements: We used strong motion data of K-NET, KiK-net, JMA and Mifune town. We thank Dr. Uchide (AIST) to provide the relocated hypocenter location data. This study was based on the 2018 research project ‘Examination for uncertainty of strong ground motion prediction for inland crustal

©2019. Japan Geoscience Union. All Right Reserved.

earthquakes' by the Secretariat of Nuclear Regulation Authority (NRA), Japan.

Keywords: 2016 Kumamoto earthquake, source process, dynamic simulation

Kinematic model

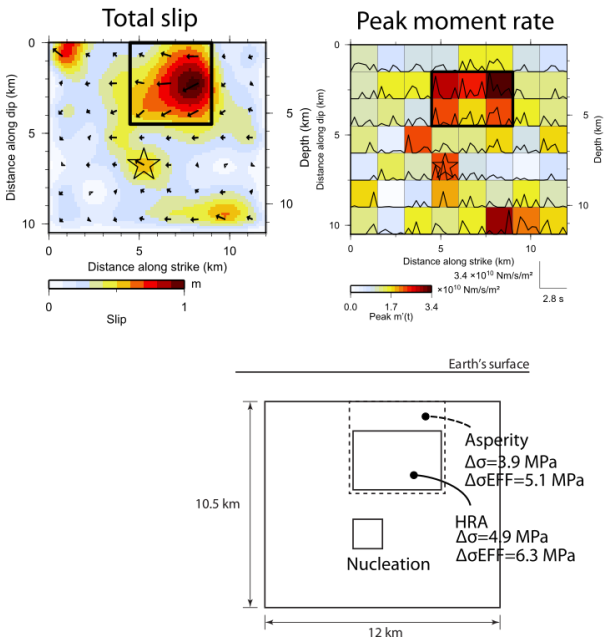

Dynamic simulation

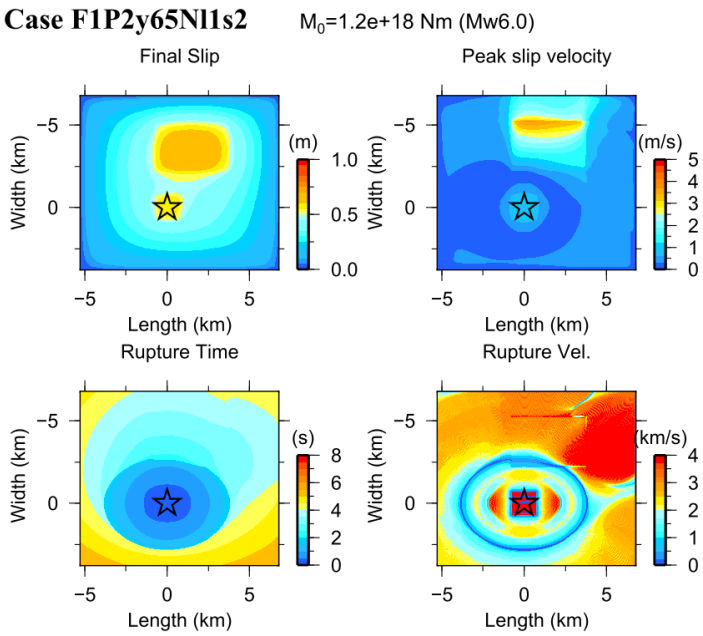

©2019. Japan Geoscience Union. All Right Reserved.

Source rupture process and strong motion generation area assuming the curved fault model for the 2003 northern Miyagi prefecture earthquake

*Kazuhiro Somei[1], Ken Miyakoshi[1], Yujia Guo[1]

1. Geo-Research Institute

At 07:13 on 26 July 2003 (JST), a shallow inland crustal earthquake (M_{JMA}6.4) with reverse faulting occurred in the northern Miyagi prefecture, north-east Japan. From the strong ground motion records in 0.05-0.5 Hz, the kinematic source rupture processes assuming a two-segment fault model have been estimated by waveform inversion method (e.g., Hikima and Koketsu, 2004). They showed large slips around 1.0 m occurred in a shallow part of the northern segment. However, surface breaks caused by this earthquake were not found along the source area by field surveys (e.g., Imaizumi et al., 2003). Since the shallow large slip area was identified between the north and the south segment, it is reasonable in estimating robust slip distribution to consider the more realistic fault plane with bending zone rather than a simple two-segment fault plane. Actually, the precisely relocated hypocenters of aftershocks were located along a curved plane dipping westward to north-westward (Okada et al., 2003). In this study, we investigate the source rupture process assuming the curved source fault, and estimate the strong motion generation areas (SMGAs; Miyake et al., 2003), in order to discuss the broadband ground motion generation processes during this event.

First, we employed the multi-time window linear waveform inversion method by using the strong motion waveforms (0.1-1.0Hz) recorded by K-NET, KiK-net, and JMA stations around the source area. From the observational information of relocated aftershock distribution and geological structure, the assumed curved fault model was composed of two planar segments (north and south segments) set by Hikima and Koketsu (2004) with transitional part that smoothly connect the north with south segment. The length, width, and shallowest top depth of fault model were 20 km, 11 km, and 0.59 km, respectively. This curved fault model was divided into 220 subfaults of 1.0 ×1.0 km. The temporal moment release history from each subfault was expressed by a series of 6 smoothed ramp functions with a rise time of 1.0 sec separated by 0.5 sec. The first-time window triggering velocity (FTWTV) was 2.8 km/s given by the smallest misfit solution. The theoretical Green’ s function was calculated by using the discrete wavenumber integration method (Bouchon, 1981) with the reflection and transmission matrix (Kennett and Kerry, 1979) assuming a 1D velocity structure model. The velocity structure model of each station was given by referring the Somei et al. (2018) or Petukhin and Miyakoshi (2006).

Second, the SMGAs were constructed based on the forward simulations using the empirical Green’ s function method (Irikura.1986) in the frequency range 0.3-10 Hz. The locations of rupture starting points and rupture times for two SMGAs were fixed by using the onset times of first and second S-wave packets in observations. Scaling parameters N and C were obtained based on the source spectral ratio analysis. The best set of parameters for SMGAs, such as the size, rupture velocity, rise time, and rupture starting point inside the SMGA, were determined by a grid searching to minimize the residual function of waveform fitting between observations and synthetics.

The principal findings from the source inversion and SMGA modeling are following. 1) The large slip area whose maximum slip of 0.93 m was concentrated in the transitional segment, where is north of the

©2019. Japan Geoscience Union. All Right Reserved.

hypocenter. The top depth of characterized asperity area (Somerville et al., 1999) was 3.07 km, which is deeper than that of Hikima and Koketsu (2004) model. The size of asperity area was 35 km^2, which is comparable to that expected by empirical scaling relationship (Somerville et al., 1999). 2) High peak moment ate areas (HRA; Yoshida and Miyakoshi, 2013), which implied the large slip velocity, were characterized with a size of 29 km^2 near the edge of the asperity area. 3) Synthetic ground motions generated from two SMGAs with a size of 24 km^2 identified close to the HRAs explained well the observations in a broadband frequency range. 4) The stress drops of two SMGAs were 13.7 MPa, which are comparable to those estimated for past large inland crustal earthquakes in Japan.

Acknowledgements: This study was based on the 2018 research project ‘Examination for uncertainty of strong ground motion prediction for inland crustal earthquakes’ by the Secretariat of Nuclear Regulation Authority (NRA), Japan.

Keywords: The 2003 northern Miyagi prefecture earthquake, Curved fault, Source inversion, Strong motion generation area, Empirical Green’s function method

©2019. Japan Geoscience Union. All Right Reserved.

Estimation of source rupture process during the 2018 Shimane-ken seibu earthquake using strong motion data

*Susumu Kurahashi[1], Ken Miyakoshi[2]

1. Aichi Institute of Technology, 2. Geo-Research Institute

1. Introduction

The 2018 Shimane-ken seibu earthquake (Mw5.6) occurred in the western part of Shimane-prefecture, Japan, on April 9, 2018. The maximum seismic intensity with 5 upper was observed at Ohta city. PGA of 564 gal is observed at the SMN006 station. We estimated the source process of this earthquake by the waveform inversion using the strong motion data.

2. Estimation of rupture area from the waveform inversion

We analyzed the slip distribution during this earthquake using the multi-time window linear waveform inversion method (Sekiguchi et al., 2000). The data sets used for the inversion analysis were velocity waveforms of S-waves parts at 13 stations (KiK-net, K-NET). The Green's functions were calculated using the one-dimensional velocity structure models by the discrete wavenumber method (Bouchon, 1981) with the reflection and transmission matrix method (Kennett and Kerry, 1979) at the stations. A fault plane was assumed referring to the aftershock distribution and the moment tensor solution determined by F-net data.

First, in order to estimate the rupture area, we analyzed the waveform inversion in target frequency 0.1-0.5Hz. The fault plane is divided into 36 subfaults of 2.0km×2.0km. The temporal moment release history from each subfault is modeled by a series of 3 smoothed-ramp-functions with a rise time of 1.0 second each separated by 0.5 second. The estimated rupture area was trimmed by criteria of Somerville et al. (1999). The trimming result removes one column of the north edge of rupture area. Seismic moment, area, rupture velocity and average slip are estimated 4.67 $\times 10^{17}$Nm,126km^2, 2.7km/s and 0.11m, respectively. The rupture area was approximately three times larger than the scaling relationship of rupture area vs seismic moment from Irikura and Miyake (2001).

3. Extraction of asperity from the waveform inversion results

Next, in order to extract of asperity from slip distribution, we analyzed the waveform inversion in the frequency range of 0.1-1.0Hz. The rupture area is divided into 56 subfaults of 1.5km×1.5km. The temporal moment release history from each subfault is modeled by a series of 6 smoothed-ramp-functions with a rise time of 0.6 second each separated by 0.3 second. A large slip area is constructed in the proximity of the hypocenter.
The asperity and high rate area (HRA) were extracted from the slip distribution by the criterion of Somerville et al. (1999) and Yoshida et al. (2005), respectively. Seismic moment and area are estimated 2.23×1017Nm and 27km2, respectively. The area and location of the asperity and the HRA are estimated to be almost the same. On the other hands, the asperity was overestimated in comparison with the scaling relationship of asperity are vs seismic moment from Irikura and Miyake (2001).

4. Conclusion

©2019. Japan Geoscience Union. All Right Reserved.

We estimated source process of the 2018 Shimane-ken seibu earthquake (Mw 5.6) form the waveform inversion using the strong motion data. The asperity and the HRA of this earthquake are collocated with nearly the same area. On the other hands, the rupture area and the asperity were overestimated corresponding to scaling law from Irikura and Miyake (2001). The rupture area data of earthquake of Mw6 class vary widely in the scaling law from Irikura and Miyake (2001). Therefore, it is necessary to consider about earthquake of Mw6 class.

Acknowledgements. Seismic waveform data of the K-NET and KiK-net were used. This study was based on the 2018 research project 'Examination for uncertainth of strong ground motion prediction for inland crustal earthquakes').

Keywords: The 2018 Shimane-ken seibu earthquake, source rupture process, strong ground motion

©2019. Japan Geoscience Union. All Right Reserved.

An estimation of SMGA of M6 class earthquakes based on strong motion records near the source regions

*Kentaro Motoki[1], Kenichi Kato[1], Tetsuo Shiota[2]

1. Kobori Research Complex, 2. Shikoku Electric Power Company

High amplitude earthquake motions exceeding 1 G have been observed when M6 class earthquakes occurred for a couple of decades. In the 2004 Rumoi earthquake (M6.1), two SMGAs in the vicinity of the strong motion station caused high amplitude earthquake motions (Maeda and Sasatani , 2008, Motoki et al., 2015). For M6 class earthquakes, which are difficult to set up fault models to be used for strong ground motion prediction, we thought that accumulating information such as stress drop and area of SMGA gave useful information for setting ground motion level for future earthquakes. In this report, we inverted SMGA for the 2011 Ibaraki-ken Hokubu earthquake.

We used empirical Green's function method (EGF) to invert SMGA. Unknown parameters in this inversion were the location of SMGA trigger point, stress drop ratio c, the number of superposition N, length of SMGA, rupture velocity in SMGA, starting rupture time of SMGA, rise time, and random numbers giving the rupture fluctuation to weaken artificial periodicity. For inverse analysis of SMGA, we used a hybrid heuristic method (Yamanaka, 2007), which could solve nonlinear problems and did not require an initial model.

For an inversion of SMGA, we selected 4 stations (IBRH13, IBRH14, IBR001 and FKS014) where the influence of nonlinearity in subsurface soil during the main shock might be small based on degree of nonlinear site response proposed by Noguchi and Sasatani (2011). We also selected 7 earthquakes as element earthquakes for empirical Green’ s function. We performed 7 inversion analyses using each element earthquake record.

Corner frequencies of the element earthquakes were evaluated by means of genetic algorithm so as to minimize the sum of residuals between the observed source spectral ratio and the source spectrum ratio function assumed ω-square model in the frequency domain. We set the search range for an inversion of SMGA, by referring to the previous source model (JMA, 2017) and c and N expected from the observed source spectral ratio. In this inversion M_0 and A, which means radiant amplitude in a short period range, were constrained not to exceed the value estimated by F-net and the value obtained from the source spectral ratio, respectively. The acceleration envelope shapes, the displacement waveform, and the Fourier amplitude were used as the objective function for an inversion.

Assuming one SMGA, the inverted SMGA could explain the earthquake motions near the source region. The SMGA location were good agreement with the large slip area in the previous models (JMA, 2017 and Hikima, 2017), which were used long period motions for their inversions.

Furthermore, in order to confirm the validity of the inverted SMGA from a theoretical aspect, we performed numerical simulation for the down-hall station at IBRH13 using the theoretical Green’ s function analysis (Hisada and Bielak, 2003). The simulated motions successfully reproduced the pulse wave and the response spectra of the observed motions.

We compared the area of SMGA estimated in this study with the relation of M_0 –area of SMGA according

©2019. Japan Geoscience Union. All Right Reserved.

to Miyake et al. (2003). The result of this study is smaller than that of relation by Miyake et al. One factor that caused this difference is thought to be due to the difference in idea of modeling. As mentioned above, M_0 of the SMGA in this study corresponded to a third of M_0 evaluated by F-net. Meanwhile, the SMGA of Miyake et al. (2003) had set the SMGA to include all of the M_0. It can be consider that the larger M_0 of SMGA has the larger area of SMGA. On this issue, we think that it is important to apply other earthquakes and accumulate data, and we will analyze SMGA of the 2013 Tochigi-ken Hokubu earthquake.

Keywords: Strong motion generation area, M6 class earthquake, Inversion, Empirical Green's function method

©2019. Japan Geoscience Union. All Right Reserved.

Difference in short-period level between the surface and buried fault rupture crustal earthquake in Japan

*Shohei Yoshida[1], Takao Kagawa[1], Tatsuya Noguchi[1]

1. Graduate School of Engineering, Tottori University

Appearance of surface fault rupture in inland crustal earthquake affects significantly on ground motion characteristics. Somerville(2003) indicated that observed ground motions from buried rupture earthquakes are larger than those from surface fault rupture earthquakes in period range around 1.0 second. Kagawa *et al.*(2004) explained that the differences are mainly caused in seismic source characteristics of fault ruptures, such as peak slip rate and stress drop between shallow and deep region. The Headquarters for Earthquake Research Promotion compiled a method for strong motion prediction (recipe). Short-period level as a parameter of the recipe is an important factor that affects generation of short-period ground motion. Due to the difference in ground motion characteristics between surface and buried fault rupture, the short-period level may also be different between the two rupture types. In this study, we organize short-period levels that evaluated characteristic source models by empirical Green's function method, and investigated empirical relations between short-period level and seismic moment for both surface and buried fault rupture crustal earthquake in Japan.

Somerville, P. G.(2003) : Physics of the Earth and Planetary Interior, 137, pp.201-212.
Kagawa et al.(2004) : Earth planet and space, 56, 3-14.

Keywords: Inand crustal earthquake, Surface fault rupture, Seismic source characteristics, Short-period level

©2019. Japan Geoscience Union. All Right Reserved.

Probabilistic seismic hazard assessment of response spectra for whole Japan (part 1: Selection of ground motion prediction equations)

*Nobuyuki Morikawa[1], Junichi Miyakoshi[2], Hiroyuki Fujiwara[1]

1. National Research Institute for Earth Science and Disaster Resilience, 2. Ohsaki Research Institute, Inc.

The seismic intensity or peak velocity is used in the probabilistic national seismic hazard maps for Japan. However, seismic hazard assessment of response spectra is useful in seismic risk assessment and engineering field. In this study, we try to assess seismic hazard of the response spectra by using the seismic activity model in the national seismic hazard maps for Japan. In this paper, we mention selection of ground motion prediction equations (GMPEs) used in the assessment, and the results are shown in the next report.
In Douglas (2019), 290 GMPEs for spectral ordinates published after 1973 are summarized, of which about 50 are derived from strong-motion records mainly observed in Japan. The 2003 Tokachi-oki earthquake was the first magnitude 8-class earthquake in the world where strong-motion records observed by the nation-wide dense networks, K-NET and KiK-net. It is very important to use the GMPE obtained using the record of the 2003 earthquake, because the contribution of large subduction earthquakes on seismic hazard assessment in Japan is extremely large. In this study, we carry out the assessment of 5%-damped acceleration response spectra whose period is shorter than 5 seconds all over Japan on the engineering bedrock (Vs=400m/s). So we select GMPEs that satisfy the following conditions.
a. It has been published as a peer-reviewed paper.
b. It was derived from records mainly observed in Japan, including records of the 2003 Tokachi-oki earthquake.
c. It is included peak acceleration and 5% damped acceleration response spectra whose period ranges from 0.1 to 5 seconds and can evaluate on the engineering bedrock.
d. It is possible to consider the difference of source and path characteristics in earthquake type (crustal, subduction plate-boundary, and subduction intra-plate).
e. It is modeled anomalous seismic intensity distribution.
f. It does not target specific earthquakes or observation points only.
g. It is used records of magnitude 9-class mega-earthquake.
As the result, two sets of GMPEs by Morikawa and Fujiwara (2013) and Zhao et al. (2016) were selected. However, with regard to the above condition g, it is inevitable that the uncertainties concerning the applicability to the earthquakes in Nankai trough are large because both GMPEs are used records the 2011 Tohoku great earthquake only for magnitude 9-class. In order to consider such uncertainty, we decide to add the latest GMPE, Goda and Atkinson (2009)’s, that satisfies other conditions.
The difference is large in the short distance or mega-earthquake, which number of records is quite few, among three GMPEs. By the way, the dataset for deriving the GMPE is constructed by each researchers. As the result,
1. Methods of filtering applied to observed waveforms and definition of horizontal maximum amplitude are different each other.
2. The magnitude and fault model selected are different for each other.
3. Indicators related to site amplification, such as site class and Vs30, are not unified.
This situation makes it impossible to compare among GMPEs under exactly the same conditions. This is not limited to the three GMPEs selected here, but is a problem common to all Japanese GMPEs that do not have derived from the same dataset. In seismic hazard assessment including mega-earthquakes and very close distance to the source fault with quite few observation records, it is necessary to use multiple

©2019. Japan Geoscience Union. All Right Reserved.

GMPEs in consideration of epistemic uncertainty. In case of seismic hazard assessment targeting a specific site, there is also the idea that each GMPE is weighted based on consistency with observation records. However, in order to evaluate its consistency, it is necessary to construct a unified standard dataset and to use GMPEs derived based on it that can be compare under the same conditions.

Keywords: Seismic hazard assessment, Response spectra, Peak acceleration, Ground motion prediction equation

©2019. Japan Geoscience Union. All Right Reserved.

Probabilistic seismic hazard assessment of response spectra for whole Japan (part 2: Probabilistic seismic hazard assessment)

*Junichi Miyakoshi[1], Takeshi Morii[1], Nobuyuki Morikawa[2], Hiroyuki Fujiwara[2]

1. Ohsaki Research Institute, Inc., 2. National Research Institute for Earth Science and Disaster Resilience

The seismic intensity or peak velocity is used in the probabilistic national seismic hazard maps for Japan. However, seismic hazard assessment of response spectra is useful in seismic risk assessment and engineering field. In this study, we try to assess seismic hazard of the response spectra by using the seismic activity model in the national seismic hazard maps for Japan. In this paper, the seismic hazard assessment results of the response spectra are shown using the selected ground motion prediction equations (GMPEs) in the previous report.
Three GMPEs are used: Morikawa and Fujiwara (2013), Goda and Atkinson (2009), Zhao et al. (2016). When evaluating seismic hazards for Japan, it is difficult to evaluate only by one GMPE, so it is necessary to select multiple GMPEs as a branch of the logic tree.
Based on the hazard curve of the response value with respect to the natural period, a uniform hazard spectrum (UHS) is calculated by connecting response spectra that have the same excess probability for each natural period. We calculate UHS at 6 cities (Sapporo, Sendai, Tokyo, Nagoya, Osaka, Fukuoka) by using the seismic activity model in the national seismic hazard maps for Japan.
As an example of the result, we are shown uniform hazard spectra for 39%, 10%, 5%, and 2% probability of exceedance occurring within 50 years from the present for all seismic activity models in Sapporo and Tokyo using GMPE by Morikawa and Fujiwara (2013). In the uniform hazard spectra, we can confirm the difference between the seismic hazard level of Sapporo and Tokyo. Also, the degree of influence of the seismic category for each natural period for a 10% probability of exceedance occurring within 50 years from the present is shown. By using the seismic activity model in the national seismic hazard maps for Japan in this way, it becomes possible to grasp the difference of the seismic hazard in the region for each natural period. In addition, we assess seismic hazard of standard peak acceleration in the world.

Keywords: Seismic hazard assessment, Response spectra, Peak acceleration, Ground motion prediction equation

©2019. Japan Geoscience Union. All Right Reserved.

Simulation of Long-period Ground Motion around The Fujikawa-kako Fault Zone during the 2018 Northern Osaka Earthquake

*Seina Hashimoto[1], Hiroaki Yamanaka[1], Kosuke Chimoto[1], Masahiro Korenaga[2], Seiji Tsuno[2], Hiroe Miyake[3], Shigeki Senna[4]

1. Tokyo Institute of Technology School of Enviroment and Society, 2. Railway Technical Research Institute, 3. The University of Tokyo, 4. National Research Institute for Earth Science and Disaster Prevention

Abstract

The Fujikawa-kako fault zone is an active fault that is suggested to be associated with the Nankai Trough in Suruga Bay, and the activity interval of this fault is a relatively high as compared to the other general active faults. Furthermore, this area is so important for the transportation network for our lives near this fault zone. A high-reliable prediction of strong ground motion in this area is important in earthquake disaster prevention in the area. In this study, we have installed strong motion observation instruments in Fujinomiya City and Fuji City to acquire strong motion records during small earthquakes since April 2018. From the earthquake records obtained at the observation points, it was found that the duration of the shaking was as long as nearly 2 minutes, and the long period component was dominant in the 2018 Northern Osaka Earthquake with a magnitude of 6.1. Then, using the deep S-wave velocity structure model of J-SHIS, we conducted seismic motion simulation of Northern Osaka Earthquake. We also assumed appoint source model, based on the CMT solution released by the Meteorological Agency. First, we compared the synthetic waveform of the rock site (YMNH10) with the observed one. The calculated waveform had similar characteristics of the observed waveform. By using the snapshots, we found that the major phases observed mainly in this area were surface waves with a north-south oriented wavefront arriving a right after the S wave arrival. We also found the later phases arriving from the southwestern part of Yamanashi Prefecture where the depth of the seismic bedrock is suddenly increases. On the other hand, the reproducibility of the observed frequency characteristics in the vicinity of Shizuoka City was low in a period range of 3-20 seconds. We need further improvement in the S-wave velocity model of the sedimentary layers.

Acknowledgements

A part of this study was carried out as an integrated research project for observation for the Fujikawa estuary fault zone by Ministry of Education, Culture, Sports, Science and Technology-Japan.

Keywords: The Fujikawa-kako Fault Zone , the 2018 Northern Osaka Earthquake, Simulation of Long-period Ground Motion , strong motion observation

©2019. Japan Geoscience Union. All Right Reserved.

Site amplification factors for KiK-net stations in and around Ibaraki Prefecture estimated by the coda normalization method

*Jun Kawahara[1], Takahiro Nakamura[1], Takuji Yamada[1]

1. Graduate School of Science and Engineering, Ibaraki University

It is empirically known that the spatial distribution of the coda wave energy from a local earthquake is nearly uniform for long lapse times. The coda normalization method is a method of separating source, path, and site effects from coda wave records, based on this empirical characteristic (Sato et al., 2012). There are many studies on the evaluation of site amplification factors based on the coda normalization method (e.g., Takahashi et al. 2005; Takemoto et al., 2012). However, little attention has been paid on the magnitude of the variability of amplification factors estimated for different earthquakes in an identical region.

We applied the method to the strong-motion records for 21 KiK-net stations and F-net TSK (Tsukuba) station in and around Ibaraki Prefecture. We used the records of 31 earthquakes with 4.7≦Mw≦6.4, which were classified into four groups depending on their locations. Stations with the epicentral distances less than 100 km were chosen for each earthquake, and the seismograms for lapse times greater than twice the direct S-wave travel time at the farthest station were used in the analysis. We selected TSK as the reference station for which the site amplification is expected to be low, and we obtained the amplification factor for each KiK-net station relative to TSK. We also calculated the geometric mean of the factors for each earthquake group.

We obtained the following results. (1) The low-frequency (0.5 to 1 Hz) amplification factors were apparently correlated with both basement depths and geological ages. It is consistent with previous studies such as Takemoto et al. (2012). (2) At the stations with shallow basement in the northern areas, the variability of the amplification factors among the earthquakes was small irrespectively of frequencies, and the geometric means of the factors for four earthquake groups were nearly the same. (3) At the stations with deep basement in the southern areas, the variability of the amplification factors among the earthquakes was relatively large, and the geometric means of the factors for four earthquake groups were somewhat different. (4) The geometric standard deviations of the amplification factors were apparently correlated with both basement depths and geological ages. (5) There appears no clear relationship between the amplification factors and the hypocentral distances for most stations. It supports the empirical assumption that the spatial distribution of the coda wave energy is nearly uniform.

Acknowledgment.
We used the strong-motion records form KiK-net and F-net and the data of basement depths from J-SHIS (National Research Institute for Earth Science and Disaster Resilience).

Keywords: site amplification factor, coda normalization method, Ibaraki Prefecture

©2019. Japan Geoscience Union. All Right Reserved.

Estimation of earthquake ground level in Horinouchi area in the 2014 Northern Nagano earthquake

*RYOTA KAWAI[1], Hiroaki Yamanaka[1], Kosuke Chimoto[1], Seiji Tsuno[2], Masahiro Korenaga[2]

1. Interdisciplinary Graduate School of Science and Engineering,Tokyo institute of Technology, 2. Railway Technical Research Institute

The 2014 Northern Nagano Earthquake with Mj of 6.7 occurred on 22 November 2014. The JMA maximum intensity of 6 lower was observed in Otari village and Ogawa village. However, heavy damage was observed in Horinouchi and Mikkaichiba areas which are 5km away from the strong observation point with intensity of 5 higher. One of the reasons for the heady damage is low seismic performance of the damaged houses as reported in JAEE's team. However, strong motion features of main shock are not fully understood in the area... In this study, we estimated the ground motions in the damaged areas to know the reasons of the damage.

After the main shock, Chimoto et. al (2015) observed aftershock records around the damaged areas In this study, we analyzed these records with records observed at strong motion stations using the spectral inversion technique. This technique can divide ground motion spectra into site, source and propagation effects. We used records from 59 earthquakes including aftershocks between JMA magnitudes of 2.4 and 5.8, and the main shock. During strong shaking like the main shock, nonlinear behavior of soil layers can be observed. Thus, we set three conditions for the data selection in this inversion analysis.

1) For earthquake records with PGAs less than 100 gal except for the main shock,

2) the main shock records with PGAs less than 100 gal have site effects as same to those of weak shock,

3) the main shock records with PGAs more than 100 gal has site effects that are different from those of the weak motions. Under these conditions, different site effects for the weak motion and the main shock are estimated at the observation stations with PGAs more than 100gal during the main shock.

We investigated the relation of the estimated site effect for the weak shaking and the main shock at the observation stations. The differences of these site effects can be caused by the nonlinearity of the soft soil. Therefore, in this study, we defined Ra(f) as an ration of the site effect for the main shock to that of weak shaking. We investigated the relationship between this Ra and the S wave velocity profiles by our microtremor surveys. At the observation stations with PGAs of 400 gal during the main shock, it was found that the Ra is similar for the sites with similar average S wave velocities up to a depth of 10 m (hereafter, Vs 10). The Vs10 in Horinouchi area is 165m/s, and VS10 in Ogawa village is 151m/s. Therefore, it is indicated that Ras in Horinouchi area and Ogawa village are the same.

The spectra characteritics of the main shock at basement was calculated from the source effect of the main shock and the propagation effect, estimated by spectrum inversion. Furthermore, we estimated the site effect of the main shock in Horinouchi area from the site effect of weak shaking and Ra of Ogawa village for estimating the spectral features of the main shock in Horinouchi area by these multiplications of these factors.

As a result, it was found that the estimated earthquake ground motion level was about 2 times stronger

©2019. Japan Geoscience Union. All Right Reserved.

than the strong motion observation stations at a period of 1-1.5 seconds, which has large effects on the wooden houses. We also found that this motion is classified to a seismic intensity of 6 upper on the JMA scale. On the other hand, the estimated spectral power in this study is about 1/4 to 1/2 of the strong motion spectrum of past destructive earthquakes observed in areas with heavy damage of the wooden building.

From these discussions we have concluded that ground motion at periods of 1-1.5 seconds were slightly larger than the surrounding observation stations. However the low earthquake resistance of the damaged building in Horinouchi area must be also included in one of the reasons of the damage.

Keywords: Spectral inversion technique, 2014 Northern Nagano earthquake, Nonlinear site effect, Building damage

©2019. Japan Geoscience Union. All Right Reserved.

Ground type classification for strong ground motion prediction based on characteristics of phase-velocity curves from microtremor explorations

*Atsushi Wakai[1], Shigeki Senna[1], Hisanori Matsuyama[2], Yatagai Atsushi[2], Yoshiaki Inagaki[2], Hiroyuki Fujiwara[2]

1. National Research Institute for Earth Science and Disaster Prevention, 2. OYO Corporation

For the purpose of strong ground motion evaluation and prediction, subsurface velocity structures in sedimentary layers have ever been modeled and sophisticated for Kanto, Tokai and Kumamoto region in the national investigation conducted by SIP (Cross-ministerial Strategic Innovation Promotion Program) of Council for Science, Technology and innovation.

There, spatially dense array-microtremor explorations also have been conducted at more than 27,500 sites in the regions, as of February 2019. They consist of miniature and irregular array measurements made at interval of about 1 km and standard-sized array ones made at interval of about 5 km. As a result, shallow S-wave velocity structures were modeled in detail, which can affect ground amplification, building and human damage.

In this study, regarding characteristics of phase-velocity (hereinafter called Pv) curves from array microtremor explorations, it was attempted to investigate relationships with geomorphologic land classification [Wakamatsu et al., 2013] and geological constitution of ground.

Pv curves can be usually obtained 2Hz to 30Hz in frequency from miniature and irregular array microtremor explorations. In general, Pv in higher frequency corresponds to velocity structures in the depth of a few of meters to 10 meters and that in lower frequency corresponds to those in the depth of dozens of meters below ground surface. Here, Pv at wave length of 40 meters or C40 [Konno et al., 2000] was extracted and made use of at each microtremor measurement site. C40 can be regarded as AVS30.

As a result, useful information was able to be acquired to model subsurface velocity structures in addition to new knowledge which was not able to be obtained from only bore-hole exploration data. Also, C40s vary due to different-sized plains and different sedimentary environment despite the same geomorphologic land classification. This presentation will report the results in detail.

Keywords: Ground type classification, phase-velocity curve, microtremor exploration, strong ground motion

©2019. Japan Geoscience Union. All Right Reserved.

Establishment of the Underground Structure Model for Seismic Damage Estimation

*Shigeki Senna[1], Atsushi Wakai[1], Hiroyuki Fujiwara[1]

1. National Research Institute for Earth Science and Disaster Resilience

1.Introduction
To develop subsurface structure models for estimating earthquake damage on a real-time basis, we studied subsurface models capable of evaluating ground motion characteristics at a broad range of frequencies. We combined a shallow subsurface model and a deep subsurface model by collecting boring data and soil property data, which are crucial for explaining the ground motion in the vicinity of each period (0.5 to 2.0s), as such ground motion affects soil both near the surface and deep in the ground. In this study, we developed a widearea subsurface structure model (250m grid cell) and a more detailed subsurface model (50m grid cell), as well as a microtremor measurement system and a subsurface structure information management system to support model development. A brief description of each of the following themes will be provided in the sections below.

(1) Construction of wide-area subsurface models for estimating earthquake damage
(2) Understanding of ground motion characteristics and development of a microtremor observation system
(3) Development of a construction technique for a detailed subsurface model through public-private collaboration

2. Construction of Wide-Area Subsurface Models for Estimating Earthquake Damage
Wide-area subsurface models were constructed for the entire Kanto and Tokai regions. Here, we will mainly report on the progress made with the model for the Kanto and Tokai area. To develop a shallow subsurface model, we primarily used approximately 440,000 sets of boring data gathered by NIED. We created an initial integrated model for shallow and deep subsurfaces by combining this shallow subsurface model with an existing deep subsurface model (J-SHIS) and adjusting the engineering bedrock. Records compiled by K-NET, KiK-net, JMA, and local governments were used as seismic observation records. To gather continuous microtremor data, two types of observation techniques, namely miniature and irregular arrays and large arrays (R = 25 to 800 m), were used at approximately 20,000 and 800 points, respectively.

3. Understanding Ground Motion Characteristics and Development of a Microtremor Observation System
To obtain a large number of microtremor array measurements and ensure that results are managed effectively until the results of analysis are produced, it is necessary to minimize and simplify the steps required to collect observation data, analyze them, and evaluate the results. To achieve these goals, we developed a mechanism that can perform all the steps quickly, including on-site data sorting and analysis while minimizing human error. More specifically, we developed i-Bido, which transmits data between seismometers and computers, tablets, and other computing devices without corrupting the data while preserving its quality, and sends the data to the database described below.

4. Development of a Construction Technique for a Detailed Subsurface Model Through Public-Private Collaboration
Our goal is to construct detailed subsurface models with 50m grid cells capable of predicting liquefaction

©2019. Japan Geoscience Union. All Right Reserved.

and landslides while accounting for factors such as ground irregularity and artificial sites, using both public and private boring data, building confirmation applications, topographical information, old topographic maps, and other data. A slope map developed by the Geospatial Information Man-made structures were excluded. The distribution of small artificial valley fills that could not be identified by topographical maps derived from an algorithm for calculating and comparing slopes was obtained. Finally, the buffer region was applied to the water systems identified from the results of water system analysis to develop a model. The model is consistent with the distribution of large-scale artificial sites and also appears to show small artificial sites.

Keywords: subsurface velocity structure, bore-hole, array microtremor, strong ground motion

©2019. Japan Geoscience Union. All Right Reserved.

Consideration of liquefaction damage rate based on liquefaction damage in recent years

*Shigeki Senna[1], Ozawa Kyoko[1]

1. National Research Institute for Earth Science and Disaster Resilience

1. Introduction
In the 2011 off the Pacific coast of Tohoku Earthquake, liquefaction occurred in an extremely large area from the Tohoku region to the Kanto region, and a large number of liquefaction damage was confirmed in Kumamoto City and Aso City in the 2016 Kumamoto earthquake. In The past, the authors examined the rate of liquefaction in recent years of liquefaction and showed that the difference in the rate of liquefaction in the Tohoku-Pacific Ocean earthquake and other earthquakes was explained by the effects of the duration of the seismic motion. However, this creation of anation, liquefaction hazard map is difficult, and there is grouping based on the history of the microtopography of 250 m mesh and the regional classification method for this regionality consideration. the improvement of the high accuracy of the liquefaction rate prediction equation by setting the area ratio of the area and the subdivision of the micro-topography division, etc. by using topography and elevation data. We also collected information on building damage and investigated the rate of liquefaction damage.

2. Collected and maintained data
The 2011 off the Pacific coast of Tohoku Earthquake and the 2016 Kumamoto earthquake liquefaction Point by local surveys and aerial images, A re-reading of the sand point was performed from high sight point of the geographical institute immediately after the earthquake. we have created a detailed data set of about 50 m and about 25 m mesh units as well as the data set of approximate 250 m mesh units that have been prepared so far.
In addition, the following data were also prepared.

(1) Average elevation, average gradient, and ratio of high data for each mesh size (250 m, 50 m, 25 m) based on 10 MDEM data.
(2) Topographic classification data for each mesh size based on land use classification data based on the above data, we investigated the liquefaction incidence and the area ratio from the relationship between the data and the liquefaction point.
(3) We collected damage information such as slope and settlement of buildings in the 2011 off the Pacific coast of Tohoku Earthquake and the 2016 Kumamoto earthquake, and investigated the relationship with the incidence rate.

3. Investigation of liquefaction generation rate and area ratio
With regard to liquefaction incidence, data on liquefaction occurrence rates of the 2011 off the Pacific coast of Tohoku Earthquake and the 2016 Kumamoto Earthquake are summed up and the measured seismic intensity and maximum velocity fragility are calculated for each micro-topography classification using the least squares method and maximum likelihood Method and cluster analysis was carried out to group the micro topographical classification. As a result, it was able to be grouped into four new groups different from the micro topography group classified based on the liability to liquefaction by a previous study. For each group, the possibility of group subdivision was examined by comparing with average elevation, average gradient, specific height data etc. of each mesh. As a result of examination, it was found that the liquefaction occurrence rate has extremely high correlation with the specific height in any of the

©2019. Japan Geoscience Union. All Right Reserved.

micro topography classifications, and it is highly likely that the above four groups can be further subdivided. Regarding the liquefaction area ratio, assuming that 25 m mesh is the minimum unit, if there is even one sand in the mesh, it is assumed that the whole mesh is liquefied. Regarding the areal ratio, because there was no clear correlation with the measured seismic intensity and the maximum velocity in all the micro topographical classifications, the average value of the area ratio was calculated for each micro topographical classification. For the sake of simplicity, this study summarizes the final liquefaction occurrence rate by multiplying the liquefaction occurrence rate and liquefaction area rate shown above. In addition, we examined the relationship between seismic intensity, maximum speed and liquefaction occurrence rate for slope and settlement of building damage caused by liquefaction.

4. Conclusion (future plans)
The liquefaction incidence rate calculation formula (florality) examined in this study will be compared with building damage damage distribution data in the future, and the validity of the results will be verified.

Keywords: liquefaction, strong motion, phase-velocity curves

©2019. Japan Geoscience Union. All Right Reserved.

Estimation of surface earthquake record at MeSO-NET observation points

*Shigeki Senna[1], Atsushi Wakai[1]

1. National Research Institute for Earth Science and Disaster Resilience

1. Introduction
In this research, in order to predict the state of shake of the ground surface with high precision from the data of the underground seismometer installed at the depth of 20 m of MeSO-net, microtremor observation at each observation point and temporary observation at the surface By observation, we evaluate the ground amplification characteristics and estimate the S wave velocity structure of the ground. As research and development items for that, 1. Acquisition of surface earthquake record and estimation of amplification characteristics at MeSO-net observation point, 2. Estimation of geophysical properties such as microtremor array observation and S wave velocity structure.The following section introduces efforts for each item.

2. Acquisition of surface earthquake records and estimation of amplification characteristics at MeSO-net observation point
In this item, in order to estimate the ground-to-ground spectral amplification factor for each observation point by temporary seismic observation at the MeSo-net observation point, it was conducted at all MeSO-net observation points (297sites) There. The observation period is 2 to 3 months per point, and observation is completed at 60 points. For each target observation point, one seismometer (JU 310 and JU 410 manufactured by Hakusan Kogyo Co., Ltd.) having the same sensor as the MeSO-net seismograph was used. In addition, the sampling frequency at the time of data acquisition was set to 200 Hz and the range was set to ±4.0G (± 1.0 G for JU 310) for JU410. Amplification characteristics are calculated by calculating the Fourier spectrum for each component from the seismic waveform obtained in the ground and the surface at each observation point, applying a bandpass filter of 0.1 to 10 Hz, smoothing in a logarithmic window, The ratio was taken. As a result, the difference in amplification characteristics between the relatively hard Rohm plateau sites and the soft backward swamp and natural embankment sites.

3. Microtremor array observation and estimation of ground physical property values such as S wave velocity structure
To verify the ground amplification characteristics of the previous section and make it possible to assume the shake even under strong ground motion, microtremor array observation to obtain the S wave velocity structure of about 50 m underground was carried out. Microtremor observation purchased a three component seismometer/ microtremor observation device (JU410) with the same sensor characteristics as the MeSO-net seismograph. Using them, microtremor array observation is carried out just above 296 points of the target MeSO-net observation point. In the fine motion array, we deployed a 4-point extremely small array with an array radius of 60 cm and a 3-point irregular array with about 5 to 15 m on each side, and observation was done for about 15 minutes at the same time. In addition, the ground physical property values such as the S wave velocity structure were estimated using inverse analysis methods such as extraction of amplification characteristics of AVS30 etc. (C40), direct curve transformation method of dispersion curve, inverse analysis and the like. As in the previous section, the difference between the characteristics of the relatively hard Rohm and the soft backward swamp are clear.

©2019. Japan Geoscience Union. All Right Reserved.

4. Conclusion
Based on the seismic observations and microtremor observations carried out up to the previous section, we will consider the ground amplification factor considering the period in the future, but we will consider the past ground model (SIP) of the existing Kanto region We will further improve the S wave velocity structure model using the shallow / deep integrated subsurface structure model of the Kanto region implemented in the real-time earthquake damage estimation) and estimate the highly accurate seismic motion at 250 m mesh interval The goal is to do.

Keywords: earthquake observation, microtremor, subsurface velocity structure

©2019. Japan Geoscience Union. All Right Reserved.

Possibility of estimating phase velocity of Love wave using Horizontal components in microtremor array surveys in the case of Nishio

*Kotoyo Tsuchida[1], Masanori Horike[1], Koji Yamada[1], Masaki Suehiro[1], Sayumi Yoshida[1]

1. HANSHIN CONSULTANTS COMPANY LIMITED

1) Introduction

The S wave velocity structure of sediments is the most important factor for amplification of earthquake motions. In recent years, microtremor array surveys have been popularized because the S wave velocity structures can be estimated by simple measurements and at a low cost. For example, Horike (1985) inferred the S wave velocity from f-k spectra estimated array microtremors and Aki (1957) and Okada (2003) also inferred them from the spatial autocorrelation functions (SPAC). These approaches use vertical microtremor array recordings and discard horizontal-component recordings. As is well known, the phase velocity of Rayleigh waves is influenced not only by the S-wave velocity structure but also by the P-wave velocity structure, while that of Love wave is influenced by the S-wave velocity structure alone. Therefore, it is expected that S wave velocity structure can be obtained clearly by estimating the velocity structure using the dispersion of the Love wave. Several approaches are developed for inference of the phase velocity of Love waves, for example f-k method by Tsuchida et al (2016), SPAC and CCA method by Tada et al (2010; using the microtremor array analysis tool "BIDO 2.0" software). The aim of this study is to compare the phase velocities obtained using the same arrays.

2) Observation and data

For this comparison, we implemented microtremor measurement in Nishio City, Aichi Prefecture, using different-size array composed of 7 stations. At each station 3-component velocity sensors were installed. Microtremor recording were acquired at a sampling interval of 0.005s for 30 minutes. This site is suitable for this comparison, because there is much information about geotechnical and geological property.

3) Results

At the present, the phase velocity by the f-k method is estimated, but it is still in the process of analysis. Therefore, by the day of the presentation, we will proceed with the remains to do.

Keywords: microtremor array surveys, Love wave, Horizontal components

©2019. Japan Geoscience Union. All Right Reserved.

Enhancement of shallow velocity structure models based on array microtremor explorations for Tokai region, Central Japan

*Atsushi Wakai[1], Shigeki Senna[1], Yatagai Atsushi[2], Yoshiaki Inagaki[2], Hisanori Matsuyama[2], Hiroyuki Fujiwara[1]

1. National Research Institute for Earth Science and Disaster Prevention, 2. OYO Corporation

1. Introduction
For sophistication of strong ground motion prediction, it is important to model subsurface velocity structure so that earthquake ground motions can be evaluated in broadband period from 0.1 s to 10 s. Therefore, it is indispensable to combine shallow and deep velocity structure models which have ever been constructed separately and to constructed subsurface velocity structure models so that earthquake observation records can be reproduced.

We have ever modeled subsurface velocity structure for Kanto, Tokai and Kumamoto region in the national investigation conducted by SIP (Cross-ministerial Strategic Innovation Promotion Program), “reinforcement of resilient disaster prevention and mitigation function” of Council for Science, Technology and innovation.

This study attempted to sophisticate shallow geological and soil structure models in initial subsurface velocity structure ones from seismic bedrock to ground surface which had been constructed for Tokai region (Shizuoka, Gifu, Aichi and Mie pref.) last year. It was based on results of a great number of array microtremor explorations. This report will introduce outline of array microtremor exploration, sophistication process of shallow velocity structure models and characteristics of ground motion.

2. miniature and irregular array microtremor exploration
About microtremor measurements, array observations were conducted in lowland and plateau of Tokai region. It consists of 4-point miniature array with a radius of 60 centi-meters and 3-point irregular array from 5 to more than 10 meters on a side. These measurements were made on the road and near seismic ground-motion stations such as K-NET and KiK-net. The total number of measurement sites has reached about five thousand and nine hundred, as of February in 2019. In addition, the measurement was conducted for around 15 minutes per site at intervals of 1km using JU210/215 or JU410 which was an all-in-one microtremor measurement unit [Senna et al., 2008]. And sampling frequency was set at 200Hz.

About analysis of miniature and irregular array microtremor data, we evaluated one-dimensional S-wave velocity structure using shallow velocity structure exploration method based on microtremor measurements. The method has been proposed and advanced in recent researches [Cho et al., 2013]. The analysis was made using a microtremor analysis tool such as “BIDO” or “Microtremor Array Tools [Cho et al., 2016].”

3. Improvement of initial shallow velocity structure models based on results of array microtremor explorations
Last year, initial shallow velocity structures were modeled using the existing bore-hole data and surface geological data. In basis of results of miniature and irregular array microtremor exploration, 1-dimensional S-wave velocity structures in the initial models were modified at each microtremor measurement point. And then, they were interpolated spatially by means of Kriging method and three-dimensional shallow

©2019. Japan Geoscience Union. All Right Reserved.

velocity structures were modeled.

On the improved models in this study and the conventional models based on geomorphologic land classification [Wakamatsu et al., 2013], ground amplification index was compared in spatial distribution. From a general viewpoint, the improved models have wider areas with large amplification in lowlands and they tend to have large local variation in ground amplification. In addition, for the improved models, distribution of ground amplification rates was evaluated by each period in basis of 1-dimensional multiple reflection theory. Amplification rates seem to be larger in different areas by each period.

4. Summary and future challenge
In this study, initial shallow velocity structure models, which were constructed based on a lot of bore-hole and geological data, were enhanced for Tokai region using results of array microtremor explorations. Also, it can be suggested that it is important to evaluate ground motion characteristics using both of amplification and period characteristics. In the close future, improved subsurface velocity structure models will be validated using moderate seismic records at strong-motion stations.

Keywords: S-wave velocity structure, shallow ground, array microtremor exploration, strong ground motion

©2019. Japan Geoscience Union. All Right Reserved.

Validation of seismic bedrock structure model in the Shimousa region, Chibe prefecture, Japan using seismic interferometry to strong motion

*Kosuke Chimoto[1], Hiroaki Yamanaka[1]

1. Tokyo Institute of Technology

Green’s function is estimated using autocorrelation of strong motions by seismic interferometry, and the depth to the seismic bedrock is estimated in sedimentary basins (Yoshimoto et al., 2009; Watanabe et al., 2011, Shiraishi et al., 2016). Oren and Nowack (2017) observed clear Reflected waves by applying spectral whitening to the autocorrelation of ambient noise. Chimoto and Yamanaka (2018) applied this method to the autocorrelation of strong motions and observed reflected wave from seismic bedrock by estimating the Green’s function in the sedimentary layers. We apply this method in the Shimousa region, Chiba prefecture, Japan to estimate autocorrelation using strong motions. Validation of 3D S-wave velocity structure model was attempted based on the spatial variation of reflected waves from seismic bedrock in the region.

Number of autocorrelations without the selection of strong motions enhance the clear reflected wave (Chimoto and Yamanaka, 2018). We used all the strong motions observed in the period of January 2008 to Jun 2018 observed at the strong motion stations of K-NET and KiK-net installed in the Shimousa region. After removal of offset of the strong motion, horizontal components are rotated to the transverse component. Spectral whitening is applied to the power spectrum and inverse Fourier transform provides autocorrelation function after the bandpass filtering. The range of bandpass filter is important to estimate the expected reflected waves from sedimentary layers (Chimoto and Yamanaka, 2018). We used the range of 0.5-2.0Hz to estimate the reflected wave from the seismic bedrock. Theoretical Green’s function for the validation of the model was calculated by Haskell method using 1D structure model extracted from the 3D J-SHIS deep structure model.

We observe the distinct reflected waves from the seismic bedrock in the autocorrelation functions estimated in the Shimousa region, Chiba prefecture. Two-way travel time of the reflected wave at KiK-net Narita station is 3 seconds and that is 3.5 seconds at K-NET Narita station. These values are almost consistent to those of the theoretical Green’s functions, while slight faster arrivals are observed. On the other hand, the stations located north and east to Narita exhibit several arrivals in the autocorrelations and the reflected wave from the seismic bedrock becomes weak. The travel time is faster than Narita. The reflected waves from the seismic bedrock at the stations located west to Narita appears later than 4 seconds, meaning the deeper bedrock than Narita. The southern part to Narita, central part of Chiba prefecture, shows the two-way times of later than 6 seconds, suggesting the deepest bedrock structure. This fact is consistent with the previous 3D models in the Kanto basin. We thus captured the spatial variation of the seismic bedrock from the estimation of autocorrelations of the strong motions in the Shimousa region, Chiba prefecture. The characteristics of spatial variation was similar to that of previously proposed 3D models. However, it is highly expected for the accurate modeling by tuning the slight difference between the autocorrelation function and the theoretical Green’s function.
We used the records observed at K-NET and KiK-net by National Research Institute for Earth Science and Disaster Resilience and deep structure model of Japan Seismic Hazard Information Station.

Keywords: Seismic interferometry, Autocorrelation function, Strong motion, Seismic bedrock structure model, Shimousa

©2019. Japan Geoscience Union. All Right Reserved.

©2019. Japan Geoscience Union. All Right Reserved.

Microtremor survey for subsurface velocity structure of Saga plain

*Masayuki Yoshimi[1], Michiko Shigefuji[2], Tadashi Maruyama[1]

1. Geological Survey of Japan, AIST, 2. Kyushu University

Saga plain, located in northern Kyushu island, is quite flat lowland facing south to the Ariake Sea. An active fault zone is recognized at the northern boundary of the plain. If the fault zone activates, strong ground motion will hit whole the plain. To assess possible earthquake hazards, subsurface structure of the plain has to be revealed.

We conducted microtremor array measurements in the plain to investigate the S-wave velocity of the sediment layers and spatial variation of the bedrock depth. Four locations for the survey are chosen along the P-wave reflection survey line (Maruyama et al. 2017) and its extension toward south. Array aperture of the measurements at each location is set about 10 to 500 meters enabling to estimate the subsurface velocity structure down to about 1 km. Four velocity sensors (Tokyo sokushin, SE-321) are deployed at each array to compose equilateral array with a center point. Phase velocity of the Rayleigh wave are estimated using vertical component data of the microtremor by SAPC and V-method (Cho et al. 2004, Tada et al., 2007). The results will be shown.

Keywords: microtremor array survey, S-wave velocity structure, Saga plain

©2019. Japan Geoscience Union. All Right Reserved.

Densely microtremor observation to estimation of subsurface structure in Hane and Kute area, Ohda City, Shimane Prefecture, Japan

*Tatsuya Noguchi[1], Yoshito Yamaguchi, Yuhei Morita, Isamu Nishimura[1], Shohei Yoshida[1], Takao Kagawa[1]

1. Department of Management of Social Systems and Civil Engineering, Civil Engineering Course Graduate School of Engineering, Tottori University

An earthquake (Mj6.1) occurred in vicinity Ohda City western Shimane Prefecture in Japan on April 9, 2018. Densely microtremor observations were carried out to estimate the characteristic of ground motion in the damage area, Hane and Kute area, Ohda City. A distribution of the predominant period of microtremor H/V spectra and S-wave velocity structures were obtained from observation data. As a result, it was found that maximum thickness of the weak soil subsurface layer is 40m and a short period component of predominant period about 0.2-0.4 seconds may have influenced structural damage.

Keywords: microtremor observation, characteristics of ground motion, subsurface structure, 2018 eastern Shimane prefecture earthquake

©2019. Japan Geoscience Union. All Right Reserved.

Densely microtremor observation to estimation of subsurface structure in Nishizono and Yura area, Hokuei Town, Tottori Prefecture, Japan

*Tatsuya Noguchi[1], Katsuya Tomeoku, Isamu Nishimura[1], Shohei Yoshida[1], Takao Kagawa[1]

1. Department of Management of Social Systems and Civil Engineering, Civil Engineering Course Graduate School of Engineering, Tottori University

Densely microtremor observations were carried out to estimate a characteristic of ground motion and subsurface structure in the damage area due to 2016 central Tottori Prefecture earthquake, Yura and Nishizono area, Hokuei Town, Tottori Prefecutre. Microtremor H/V spectra and a distribution of the predominant period and underground structure models were obtained, and grasped the characteristic of ground motion based on this result. As a result, it was found that a difference of the subsurface structure depth to about 20m and a short period component of predominant period less than 0.5 seconds may have influenced structural damage.

Keywords: microtremor observation, characteristics of ground motion, subsurface structure, 2016 central Tottori prefecture earthquake

©2019. Japan Geoscience Union. All Right Reserved.

Seismic reflection survey in the Kathmandu Valley, Nepal.

*Kota Koshika[1], Yusuke Kawasaki[1], Om Pradhan[1], Masato Yamamoto[1], Dai Nobuoka[1], Yoshikazu Matsubara[1], Hisanori Matsuyama[1], Monika Jha[2], Chintan Timisina[2], Suresh Shrestha[2], Mukunda Bhattarai[2], Dinesh Nepali[2], Soma Nath Sapkota[2], Hiroe Miyake[3], Kazuki Koketsu[3]

1. OYO Corporation, 2. Department of Mines and Geology, 3. Earthquake Research Institute, University of Tokyo

On the April 25, 2015, earthquake of magnitude 7.8 Mw (USGS, 2015) struck in the 78 km north west of Kathmandu (Gorkha Earthquake) and major after shock of magnitude 7.3 Mw, with epicenter about 80 km north east of Kathmandu cases heavy damage in the Kathmandu Valley (KV). It was thought that the damage in the KV was particularly great, due to the underground structure of the KV.

We conducted gravity survey in the KV as part of the SATREPS projects in 2017. The shape of the gravity basement of the whole KV was estimated (Pradhan et al.,2018).

We conducted seismic reflection survey to clarify the detailed basement of the KV and the upper sedimentary structure in 2018. Survey lines were set up at Tribhuvan International Airport (TIA) where depth of gravity basement greatly changes and Nepal Agricultural Research Council (NARC) where deep gravity basement was estimated. Survey line length is about 4km (TIA) and 1km (NARC). Enviro Vibe (IVI, Inc.) was used as a seismic source.

The shape of the basement obtained by the seismic reflection survey and the shape of the gravity basement match well and the structure of the sedimentary layer in the basin was also revealed. These are the world's first results visually showing the underground structure in the KV and are expected to greatly contribute to future earthquake disaster prevention.

Keywords: Kathmandu Valley, seismic reflection survey

©2019. Japan Geoscience Union. All Right Reserved.

Broadband Microtremor Array Exploration at and around Tribhuvan International Airport, Kathmandu, Nepal

*Toshiaki Yokoi[1], Takumi Hayashida[1], Mukunda Bhattarai[2], Tara Pokharel[2], Suresh Shrestha[2], Chintan Timsina[2], Sunita Bhatarrai[2], Dinesh Nepali[2]

1. International Institute of Seismology and Earthquake Engineering, Building Research Institute, Japan, 2. Department of Mines and Geology, Ministry of Industry, Commerce and Supplies, Nepal

Strong ground motion of long duration and long predominant period around four seconds were observed during the 2015 Gorkha earthquake at the central part of the Kathmandu Valley (KTV), Nepal (Dixit et al. 2015, Bhattarai et al. 2015, Takai et al. 2016, Rajaure et al. 2017), a tectonic basin formed during the Himalayan orogeny due to the collision of the Indian plate to the Eurasian plate (e.g., Sakai et al. 2016). Aimed to reveal the cause of this phenomenon and to make possible the seismic hazard assessment considering on the structure of deep sedimentary layers, the research group to which the authors belong (Group3-SATREPS) has conducted the deep exploration by deploying microtremor arrays (Maximum inter station distance about 1400 m) at few sites using four sets of broadband seismographs (CMG40T, Guralp) for estimating the shear wave velocity structure of deep sediments from Dec. 2016 to Feb. 2018, together with shallow exploration using 2 Hz seismometers (L22D, Sercel) and 4.5 Hz geophones (GS11D, GeoSpace) (Yokoi et al. 2018, SSJ-Fall). In KTV as a whole, the gravity survey had been performed in 2017 by the OYO corp. team which belongs the same research group (Pradhan et al. 2018 (JpGU)) and the reflection survey has been conducted Nov. 2018 by OYO corp. also at the Tribhuvan International Airport (TIA) and at the National Agriculture Research Institute (NARI) located at around 2 km SW of TIA. The deep structure of KTV is gradually getting revealed (Koshika et al. 2019 (JpGU) submitted).
In this poster session, we will report the results of analysis of the microtremor array exploration at and around TIA and NAST, and a hard rock site (Chobar) that we have conducted Dec. 2018 following the above mentioned activities.
The attached figure shows the configuration of observation sites and a summary of the dispersion curves of Rayleigh waves. In the legend, *BDR* (red circles) shows the results given by Hayashida et al. (2018, SSJ-Fall) using tele-seismic surface waves, *CHB* (red “x” s): the phase velocities estimated on the outcropped bedrock of the Chobar hill. *SDB*: Singhadurbar, DMG: Department of Mines and Geology-Narayanhiti Royal Palace Museum, *TEKU*: Teku Gas well of DMG, *KIR*: Kirtipur Campus of the Tribhuvan Univ., *BLJ*: Department of Nepal Bureau of Standard and Metrology at Balaju, *GAU*: Gaucharan, *TIA*: Tribhuvan International Airport, *NAST*: National Academy of Science and Technology-National Agriculture Research Institute.
Acknowledgements: This study was supported by Japan Science and Technology Agency (JST) and Japan International Cooperation Agency (JICA) under the “Science and Technology Research Partnership for Sustainable Development (SATREPS): Integrated Research on Great Earthquakes and Disaster Mitigation in Nepal Himalaya (FY2016-2020)”.

Keywords: Gorkha earthquake, Kathmandu Valley, Broadband Microtremor Array Exploration

©2019. Japan Geoscience Union. All Right Reserved.

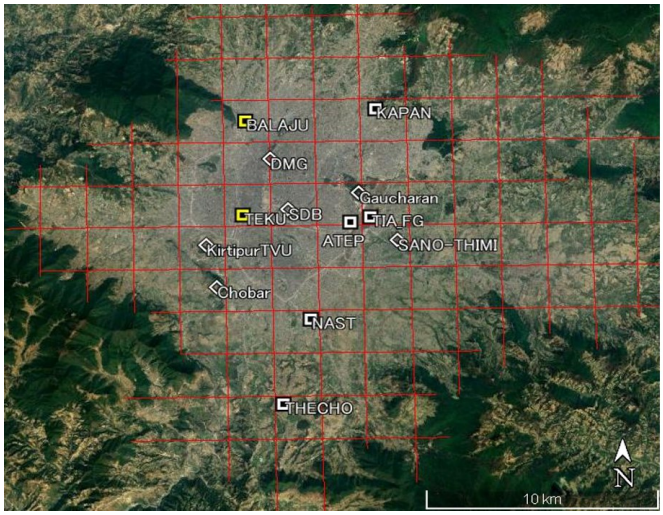

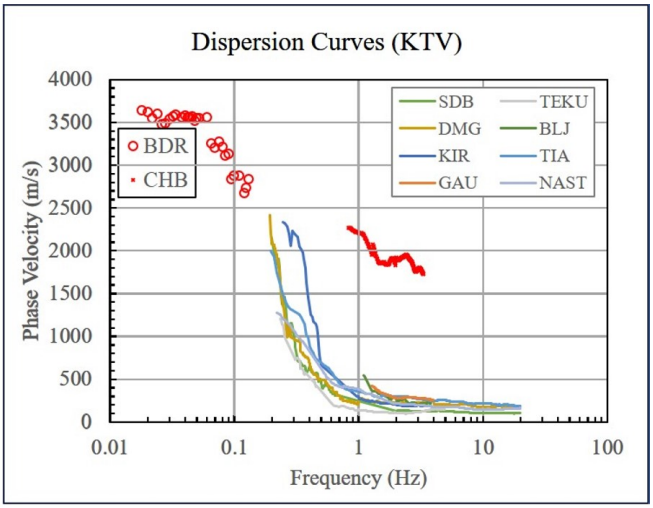

©2019. Japan Geoscience Union. All Right Reserved.

Distribution of average S-wave velocities by small-scale (5 to 15 meters) microtremor arrays in and around Hue City, Thua Thien-Hue province, Vietnam

*Ikuo Cho[1], Makoto OKUBO[2]

1. National Institute of Advanced Industrial Science and Technology, 2. Kochi University

We are promoting earthquake hazard assessment for safe operation of hydroelectric power generation and protection of world cultural heritage for Hue City, Thua Thien-Hue Province, Vietnam. This is a collaborative research with Dr. Nguyen Anh Duong at Vietnam Academy of Science and Technology (VAST). As a part of this research project, we conducted multiple small-scale microtremor array observations in that area and evaluated the distribution of shallow average S-wave velocities.

We began this microtremor research with providing a technical support to researchers at VAST. First, the authors conducted a microtremor array observation at four sites in and around the Hanoi City on 20th and 21st October, 2017, as a practical training of microtremor observation. On the premise of applying the SPAC method, we deployed linear-shaped arrays with a length of about 30 m using a three-component servo-velocimeter. We recorded microtremors for 1 to 2 hours at each site. Since the authors brought two seismometers (three-component servo-accelerometers) from Japan, we deployed two-point arrays along with their array at intervals of 5 to 30 m, and compared the analysis results with those from the VAST observation apparatuses.

On the next step, the VAST research team and the authors conducted microtremor array observations at seven sites in Hue City on 17-19th March, 2018. At each site we deployed triangle-shaped arrays with side lengths of 5 m and 15 m. We also deployed a linear array with a length of 12 m. Those arrays consisted of 4.5 Hz vertical geophones. In addition to this, we deployed two-point arrays with two seismometers brought from Japan. We set the observation durations from about 30 minutes to 1 hour at each site. There were existing subsurface data by refraction surveys at these sites, and therefore, we compared our analysis results with them. As a result, the analysis results of microtremors were consistent with those existing data.

Through the above preparatory period, the VAST research team conducted microtremor array observations at 126 sites in and around the Hue City (observation area of about 11km x 14 km) in a period from June to July 2018 (19 days in total). More specifically, they deployed triangular arrays with side lengths of 5 m and 15 m at 89 sites and a linear array with a length of 12 m at 37 sites. Vertical 4.5Hz geophones were used to consist seismic arrays. The observation duration was set to 30 minutes at each site.

We applied the SPAC method to the array data thus obtained and identified the Rayleigh-wave phase velocities. We read the phase velocities with the wavelengths of 13 m, 25 m and 40 m and interpreted them as average S-wave velocities to the depths of 10 m, 20 m, and 30 m, respectively. The spatial distribution of average S-wave velocities thus obtained is consistent with the geological map in and around the Hue City. In near future, we will improve the accuracy of soil evaluations by adding H/V spectral data at each site of array observation.

©2019. Japan Geoscience Union. All Right Reserved.

Keywords: microtremor, array, surface wave, Vietnam

©2019. Japan Geoscience Union. All Right Reserved.

Microtremor Array Exploration in the Syiah Kuala University, Banda Aceh, Indonesia

*Makoto OKUBO[1]

1. Natural Science Cluster, Kochi University

We deployed microtremor array survey at Syiah Kuala University in Banda Aceh, Indonesia to clarify a seismic amplification by subsurface S-wave structure. Banda Aceh, located at northern end of Sumatra island, was seriously damaged by the tsunami caused by the 2004 Sumatra earthquake. At the tsunami evacuation, we first have to consider the safe route that does not corrupted, damaged and flooded. Therefore, we plan to understand the seismic amplification distribution as fundamental material. Our results will be available to make a future plan to reconstruction/renovate architectures.

We visited to Banda Aceh at January, 2019, and carried out microtremor exploration using with linear array and triangle array at 17 sites. We used are three 5 Hz geophones and one 1 kHz sampling GPS synchronised data logger for survey. In the case of triangle array, we always used 1.7 m side length. This side length is corresponding to 1.0 m array radius. In the other case, that is linear array, distances of each sensors (A, B, and C) are, A-B:1.7 m, B-C:2.7 m, and A-C:4.4 m. We Assumed these lengths are the array radius for each exploration, and applied SPAC method (*c.f.* Aki 1957). We used a tool, as known as BIDO2.0 (Cho, 2010) to analyze recorded waveforms and estimate dispersion curves.

By using obtained dispersion curves, we determined 3 averaged S wave velocities and roughly velocity structure. Roughly velocity structure was estimated by simple conversion method by using 1/2 wavelength law with linear array's dispersion curves. And three Averaged S-wave velocities AVS10, AVS20 and AVS30 were estimated from the Rayleigh wave phase velocities corresponding to the wave length of 13 m, 25 m and 40 m, respectively. By a preliminary analysis, we obtained result that a thicker low S-wave velocity layer exists along the river and the coastline. This result implies that plain part of Banda Aceh was developed on the old delta made by river and sea. This situation of subsurface structure will be strongly affect to the seismic amplification.

We will discuss in detail at the presentation.

Acknowledgements:
We thanks to Dr. Muksin Umar, Ms. Wiwik and Mr. Arif, they were attended and cooperated to our microtremor array survey in Syiah Kuala University. This study is supported by JSPS KAKENHI Grant Number 17H0457751.

Keywords: Microtremor, Array exploration, Subsurface S-wave velocity structure

©2019. Japan Geoscience Union. All Right Reserved.

Turkey-Japan Joint Project on Modeling of Geological Structures for Strong Ground Motion Simulations due to Crustal Earthquakes in Eskisehir Basin, Turkey, by Using Seismic Interferometry Method

*Mehmet Safa Arslan[1], Kosuke Chimoto[2], Asim Oguz Ozel[1], Hiroaki Yamanaka[2]

1. ISTANBUL UNIVERSITY-CERRAHPASA, 2. TOKYO INSTITUTE OF TECHNOLOGY

Understanding the seismic hazard of specific area, depends on the regional 2D/3D underground structure on wave propagation. In the frame of the bilateral project between Turkey and Japan, we aim at observing ground motion parameters, crustal activities, underground structures, and improvement of seismic hazard maps. The seismic interferometry method (SIM) is one of the tools to investigate the surface-wave propagation. The method goals to obtain green’ s function (GF) by using ambient noise data. Cross-correlations (CC) between the two pairs of stations’ continuous records, reveal GF and provide group and phase velocities of surface waves. We analyze one-year vertical component broadband data from 8 stations deployed and affiliated with ANANET (Eskisehir Anadolu University Local Seismic Network). Interstation distances between the designated stations are in the range of ~23-139 km. After getting the CC functions, group velocity dispersion curves will be obtained for selected correlation paths in particular to address the azimuthal dependence of the velocity field. Averaging the dispersion curves, in other saying analyzing the group velocities and waveforms typical of these observations, we attempt to estimate the S-wave velocity structure model inside the Eskisehir basin. This study is supported by the Joint Research Project under the Bilateral Program of the Japan Society for the Promotion of Science (JSPS) and The Scientific and Technological Research Council of Turkey (TUBITAK) under Grant TUBITAK 116Y524.

Keywords: seismic interferometry, cross correlation function, S-wave structure, group velocities, Turkey

©2019. Japan Geoscience Union. All Right Reserved.

Nonlinear Ground Motion Response During the 2016 Meinong Taiwan Earthquake

*Kuo-Liang Wen[1], Chun-Te Chen[2]

1. National Central University, Department of Earth Sciences, 2. Academia Sinica, Institute of Earth Sciences

The Meinong Taiwan earthquake occurred on February 6, 2016, at 03:57 (UTC+8) with M_L 6.6. The strong ground motion induced the soil liquefaction in Sinshih and Annan districts. To investigate the nonlinear site response during Meinong mainshock, the degree of nonlinear site response (DNL) which summation of the horizontal to vertical spectral ratios (HVSR) differences between weak-motions and Meinong mainshock records from the Taiwan Strong Motion Instrumentation Program (TSMIP) network are calculated. We compare the DNL values with the ground motion parameters such as peak ground acceleration (PGA), peak ground velocity (PGV), and also the ratio between PGV and Vs30. The DNL shows a positive correlation with ground motion intensity, particular with PGV, and the surface site conditions also leading the DNL strength. We also applied a stochastic method for modeling the ground motion of the Meinong earthquake with site correction by the HVSR of weak and strong motions respectively. The percentage of PGA reduction calculated in this study can be an indicator of the spatial distribution of the degree of nonlinear soil effects of the 2016 Meinong Taiwan earthquake.

Keywords: Meinong earthquake, nonlinear site response, HVSR

©2019. Japan Geoscience Union. All Right Reserved.

Earthquake damage of the 2017 Pohang earthquake in South Korea

*Mikyung Choi[1], Sun-Cheon Park[1], Dong-Hyo Sohn[1], Seolhan You[1], Jongsun Sun[1], Seongheum Cho[1], Duk-Kee Lee[1]

1. Korea Meteorological Administration

Pohang earthquake with a magnitude of ML 5.4 occurred on November 15, 2017. This earthquake caused more damage than the 2016 Gyeongju earthquake (ML 5.8). Modified Mercalli intensities were assigned from residential property damage report in the Pohang area. Major damage type was wall crack of building. Maximum intensity was MMI VIII. Result of damage analysis from damage report reveals that the main damage area was distributed within a radius of about 20 km distance from the epicenter. And sand and mud volcanoes were observed in many places.
Between 16 November and 31 December 2017, 10 temporary seismic stations were deployed to record aftershocks and site effect of the Pohang earthquake. Ground motion generated by an earthquake is controlled by several factors, such as source characteristics, propagation path, surface geology, topography. Using recordings of aftershocks, we analyzed the ground motion at two seismic stations near the epicenter and another two seismic stations located on sedimentary rock and bedrock. We compared amplitude and predominant frequencies of ground motion with damage analysis results. Mapping and characterization of the damage for this earthquake is an opportunity to provide useful information on the damage of future possible earthquake in South Korea.

Keywords: Pohang earthquake, earthquake damage, ground motion

©2019. Japan Geoscience Union. All Right Reserved.

[J] Poster | S (Solid Earth Sciences)：S-SS Seismology

Mon. May 27, 2019 5:15 PM - 6:30 PM JST | Mon. May 27, 2019 8:15 AM - 9:30 AM UTC | Poster Hall International Exhibition Hall8, Makuhari Messe_20

[S-SS13] Strong Ground Motion and Earthquake Disaster

convener:Masayuki Kuriyama(Central Research Institute of Electric Power Industry), Kazuhiro Somei(Geo-Research Institute)

Strong ground motion has social impacts as it induces earthquake disasters. We solicit contribution on any seismological topics related to strong ground motion that includes, but are not limited to, source processes, wave propagation, and site effects. We also welcome contribution on earthquake related disaster mitigation.

[SSS13-P01] Observation of Aftershock due to the 2018 Hokkaido Eastern Iburi Earthquake and Microtremor observation in the Damaged Area

*Isamu Nishimura[1], Tatsuya Noguchi[2], Yusuke Ono[2], Masanori Kohno[2], Keishin Hibi[1] (1.Graduate School of Sustainability Science,Tottori Univercity,Department of Engineering,Social Systems and Civil Engineering Program, 2.Department of Engineering Tottori Univercity)

[SSS13-P02] Nonlinear site amplification for high intensity ground motions during the 2018 Mw 6.6 Hokkaido eastern Iburi earthquake

*Yadab Prasad Dhakal[1], Takashi Kunugi[1], Takeshi Kimura[1], Wataru Suzuki[1], Shin Aoi[1] (1.National Research Institute for Earth Science and Disaster Resilience (NIED))

[SSS13-P03] Microtremor array measurements at strong motion recording stations, HKD127 and IBUH01, in 2018 Hokkaido Iburi earthquake.

*Takuto Kogawa[1], Koji Tokimatsu[1], Izuru Okawa[1], Hitoshi Tanaka[1], Kentaro Motoki[2] (1.TOKYO SOIL RESEARCH CO.,LTD., 2.KOBORI RESEARCH COMPLEX INC.)

[SSS13-P04] Subsurface structure model based at diffuse-field theory in Oiwake region: Simultaneous inversion analysis on adjacent two sites

*Moeko Koie[1], Kentaro Motoki[1], Kenichi Kato[1], Takuto Kogawa[2] (1.KOBORI RESEARCH COMPLEX INC., 2.TOKYO SOIL RESEARCH CO., LTD.)

[SSS13-P05] Exploration of the velocity structure model in the Mukawa town, damaged area during the 2018 Hokkaido eastern Iburi earthquake

*Michiko Shigefuji[1], Nobuo TAKAI[2], Jun Horita[3], Shingo Nomoto[3], Takahiro Maeda[4], Hiroaki Takahashi[2], Masayoshi Ichiyanagi[2], Hiroaki Yamanaka[5], Kosuke Chimoto[5], Seiji Tsuno[6], Masahiro Korenaga[6], Nobuyuki Yamada[7] (1.Kyushu University, 2.Hokkaido University, 3.Geo-Technical Research Co.,Ltd, 4.National Research Institute for Earth Science and Disaster Resilience, 5.Tokyo Institute of Technology, 6.Railway Technical Research Institute, 7.Kochi University)

[SSS13-P06] Source Process of the 2018 Hokkaido Eastern Iburi Earthquake Inferred from Strong Motion Data and Green's Functions Based on Three-Dimensional Velocity Structure Model

*Kimiyuki Asano[1], Tomotaka Iwata[1] (1.Disaster Prevention Research Institute, Kyoto University)

[SSS13-P07] Source process of the 2018 Hokkaido Eastern Iburi earthquake derived from strong motion data

*Hisahiko Kubo[1], Wataru Suzuki[1], Asako Iwaki[1], Shin Aoi[1], Haruko Sekiguchi[2] (1.National Research Institute for Earth Science and Disaster Resilience, 2.DPRI, Kyoto University)

[SSS13-P08] Broadband ground-motion simulation of the 2018 Hokkaido Eastern Iburi earthquake

*Asako Iwaki[1], Nobuyuki Morikawa[1], Takahiro Maeda[1], Hisahiko Kubo[1], Hiroyuki Fujiwara[1] (1.National Research Institute for Earth Science and Disaster Resilience)

[SSS13-P09] **Estimation of 1D S-wave velocity structures in Kumamoto plain and Mashiki town using a waveform inversion of S-wave**

*Kengo Muroi[1], Hiroaki Yamanaka[1], Kosuke Chimoto[1], Seiji Tsuno[2], Masahiro Korenaga[2], Hiroe Miyake[3], Nobuyuki Yamada[4] (1.Tokyo Institute of Technology, 2.Railway Technical Research Institute, 3.The University of Tokyo, 4.Kochi University)

[SSS13-P10] Investigation to estimate high-frequency Empirical Green's tensor derivatives (EGTD) using aftershocks for the 2016 Kumamoto earthquake

*Sayumi Yoshida[1], Horike Masanori [1], Ken Miyakoshi[2] (1.HANSHIN CONSULTANTS Co., Ltd., 2.Geo-Research Institute)

[SSS13-P11] Estimation of Site Amplification Characteristics in Kumamoto plain by Spectral Separation Analysis Using Aftershock Records of the 2016 Kumamoto Earthquake

*Tomomi Iida[1], Hiroaki Yamanaka[1], Kosuke Chimoto[1], Daiki Shinoyama[8], Seiji Tsuno[5], Masahiro Korenaga[5], Nobuyuki Yamada[7], Hiroe Miyake[6], Tatsuo Kanno[3], Michiko Shigefuji[3], Masayuki Yoshimi[2], Shinichi Matsushima[4], Hiroshi Kawase[4], Kimiyuki Asano[4], Tomotaka Iwata[4] (1.Tokyo institute of Technology, 2.National Institute of Advanced Industrial Science and Technology, 3.Kyushu University, 4.Kyoto University, 5.Railway Technical Research Institute, 6.The University of Tokyo, 7.Kochi Unicersity, 8.Central Research Institute of Electric Power Industry)

[SSS13-P12] Kinematic and dynamic source models of the 2016 Mj6.4 Kumamoto third large earthquake

*Kunikazu Yoshida[1], Ken Miyakoshi[1] (1.Geo-Research Institute)

[SSS13-P13] Source rupture process and strong motion generation area assuming the curved fault model for the 2003 northern Miyagi prefecture earthquake

*Kazuhiro Somei[1], Ken Miyakoshi[1], Yujia Guo[1] (1.Geo-Research Institute)

[SSS13-P14] Estimation of source rupture process during the 2018 Shimane-ken seibu earthquake using strong motion data

*Susumu Kurahashi[1], Ken Miyakoshi[2] (1.Aichi Institute of Technology, 2.Geo-Research Institute)

[SSS13-P15] An estimation of SMGA of M6 class earthquakes based on strong motion records near the source regions

*Kentaro Motoki[1], Kenichi Kato[1], Tetsuo Shiota[2] (1.Kobori Research Complex, 2.Shikoku Electric Power Company)

[SSS13-P16] Difference in short-period level between the surface and buried fault rupture crustal earthquake in Japan

*Shohei Yoshida[1], Takao Kagawa[1], Tatsuya Noguchi[1] (1.Graduate School of Engineering, Tottori University)

[SSS13-P17] Probabilistic seismic hazard assessment of response spectra for whole Japan (part 1: Selection of ground motion prediction equations)

*Nobuyuki Morikawa[1], Junichi Miyakoshi[2], Hiroyuki Fujiwara[1] (1.National Research Institute for Earth Science and Disaster Resilience, 2.Ohsaki Research Institute, Inc.)

[SSS13-P18] Probabilistic seismic hazard assessment of response spectra for whole Japan (part 2: Probabilistic seismic hazard assessment)

*Junichi Miyakoshi[1], Takeshi Morii[1], Nobuyuki Morikawa[2], Hiroyuki Fujiwara[2] (1.Ohsaki Research Institute, Inc., 2.National Research Institute for Earth Science and Disaster Resilience)

[SSS13-P19] **Simulation of Long-period Ground Motion around The Fujikawa-kako Fault Zone during the 2018 Northern Osaka Earthquake**

*Seina Hashimoto[1], Hiroaki Yamanaka[1], Kosuke Chimoto[1], Masahiro Korenaga[2], Seiji Tsuno[2], Hiroe Miyake[3], Shigeki Senna[4] (1.Tokyo Institute of Technology School of Enviroment and Society, 2.Railway Technical Research Institute, 3.The University of Tokyo, 4.National Research Institute for Earth Science and Disaster Prevention)

[SSS13-P20] Site amplification factors for KiK-net stations in and around Ibaraki Prefecture estimated by the coda normalization method

*Jun Kawahara[1], Takahiro Nakamura[1], Takuji Yamada[1] (1.Graduate School of Science and Engineering, Ibaraki University)

[SSS13-P21] Estimation of earthquake ground level in Horinouchi area in the 2014 Northern Nagano earthquake

*RYOTA KAWAI[1], Hiroaki Yamanaka[1], Kosuke Chimoto[1], Seiji Tsuno[2], Masahiro Korenaga[2] (1.Interdisciplinary Graduate School of Science and Engineering,Tokyo institute of Technology, 2.Railway Technical Research Institute)

[SSS13-P22] Ground type classification for strong ground motion prediction based on characteristics of phase-velocity curves from microtremor explorations

*Atsushi Wakai[1], Shigeki Senna[1], Hisanori Matsuyama[2], Yatagai Atsushi[2], Yoshiaki Inagaki[2], Hiroyuki Fujiwara[2] (1.National Research Institute for Earth Science and Disaster Prevention, 2.OYO Corporation)

[SSS13-P23] **Establishment of the Underground Structure Model for Seismic Damage Estimation**

*Shigeki Senna[1], Atsushi Wakai[1], Hiroyuki Fujiwara[1] (1.National Research Institute for Earth Science and Disaster Resilience)

[SSS13-P24] Consideration of liquefaction damage rate based on liquefaction damage in recent years

*Shigeki Senna[1], Ozawa Kyoko[1] (1.National Research Institute for Earth Science and Disaster Resilience)

[SSS13-P25] Estimation of surface earthquake record at MeSO-NET observation points

*Shigeki Senna[1], Atsushi Wakai[1] (1.National Research Institute for Earth Science and Disaster Resilience)

[SSS13-P26] Possibility of estimating phase velocity of Love wave using Horizontal components in microtremor array surveys in the case of Nishio

*Kotoyo Tsuchida[1], Masanori Horike[1], Koji Yamada[1], Masaki Suehiro[1], Sayumi Yoshida[1] (1.HANSHIN CONSULTANTS COMPANY LIMITED)

[SSS13-P27] Enhancement of shallow velocity structure models based on array microtremor explorations for Tokai region, Central Japan

*Atsushi Wakai[1], Shigeki Senna[1], Yatagai Atsushi[2], Yoshiaki Inagaki[2], Hisanori Matsuyama[2], Hiroyuki Fujiwara[1] (1.National Research Institute for Earth Science and Disaster Prevention, 2.OYO Corporation)

[SSS13-P28] Validation of seismic bedrock structure model in the Shimousa region, Chibe prefecture, Japanusing seismic interferometry to strong motion

*Kosuke Chimoto[1], Hiroaki Yamanaka[1] (1.Tokyo Institute of Technology)

[SSS13-P29] Microtremor survey for subsurface velocity structure of Saga plain

*Masayuki Yoshimi[1], Michiko Shigefuji[2], Tadashi Maruyama[1] (1.Geological Survey of Japan, AIST, 2.Kyushu University)

[SSS13-P30] Densely microtremor observation to estimation of subsurface structure in Hane and Kute area, Ohda City, Shimane Prefecture, Japan

*Tatsuya Noguchi[1], Yoshito Yamaguchi, Yuhei Morita, Isamu Nishimura[1], Shohei Yoshida[1], Takao Kagawa[1] (1.Department of Management of Social Systems and Civil Engineering, Civil Engineering Course Graduate School of Engineering, Tottori University)

[SSS13-P31] Densely microtremor observation to estimation of subsurface structure in Nishizono and Yura area, Hokuei Town, Tottori Prefecture, Japan

*Tatsuya Noguchi[1], Katsuya Tomeoku, Isamu Nishimura[1], Shohei Yoshida[1], Takao Kagawa[1] (1.Department of Management of Social Systems and Civil Engineering, Civil Engineering Course Graduate School of Engineering, Tottori University)

[SSS13-P32] Seismic reflection survey in the Kathmandu Valley, Nepal.

*Kota Koshika[1], Yusuke Kawasaki[1], Om Pradhan[1], Masato Yamamoto[1], Dai Nobuoka[1], Yoshikazu Matsubara[1], Hisanori Matsuyama[1], Monika Jha[2], Chintan Timisina[2], Suresh Shrestha[2], Mukunda Bhattarai[2], Dinesh Nepali[2], Soma Nath Sapkota[2], Hiroe Miyake[3], Kazuki Koketsu[3] (1.OYO Corporation, 2.Department of Mines and Geology, 3.Earthquake Research Institute, University of Tokyo)

[SSS13-P33] Broadband Microtremor Array Exploration at and around Tribhuvan International Airport, Kathmandu, Nepal

*Toshiaki Yokoi[1], Takumi Hayashida[1], Mukunda Bhattarai[2], Tara Pokharel[2], Suresh Shrestha[2], Chintan Timsina[2], Sunita Bhatarrai[2], Dinesh Nepali[2] (1.International Institute of Seismology and Earthquake Engineering, Building Research Institute, Japan, 2.Department of Mines and Geology, Ministry of Industry, Commerce and Supplies, Nepal)

[SSS13-P34] Distribution of average S-wave velocities by small-scale (5 to 15 meters) microtremor arrays in and around Hue City, Thua Thien-Hue province, Vietnam

*Ikuo Cho[1], Makoto OKUBO[2] (1.National Institute of Advanced Industrial Science and Technology, 2.Kochi University)

[SSS13-P35] Microtremor Array Exploration in the Syiah Kuala University, Banda Aceh, Indonesia

*Makoto OKUBO[1] (1.Natural Science Cluster, Kochi University)

[SSS13-P36] **Turkey-Japan Joint Project on Modeling of Geological Structures for Strong Ground Motion Simulations due to Crustal Earthquakes in Eskisehir Basin, Turkey, by Using Seismic Interferometry Method**

*Mehmet Safa Arslan[1], Kosuke Chimoto[2], Asim Oguz Ozel[1], Hiroaki Yamanaka[2] (1.ISTANBUL UNIVERSITY-CERRAHPASA, 2.TOKYO INSTITUTE OF TECHNOLOGY)

[SSS13-P37] **Nonlinear Ground Motion Response During the 2016 Meinong Taiwan Earthquake**

*Kuo-Liang Wen[1], Chun-Te Chen[2] (1.National Central University, Department of Earth Sciences, 2.Academia Sinica, Institute of Earth Sciences)

[SSS13-P38] Earthquake damage of the 2017 Pohang earthquake in South Korea

*Mikyung Choi[1], Sun-Cheon Park[1], Dong-Hyo Sohn[1], Seolhan You[1], Jongsun Sun[1], Seongheum Cho[1], Duk-Kee Lee[1] (1. Korea Meteorological Administration)

Observation of Aftershock due to the 2018 Hokkaido Eastern Iburi Earthquake and Microtremor observation in the Damaged Area

*Isamu Nishimura[1], Tatsuya Noguchi[2], Yusuke Ono[2], Masanori Kohno[2], Keishin Hibi[1]

1. Graduate School of Sustainability Science,Tottori Univercity,Department of Engineering,Social Systems and Civil Engineering Program, 2. Department of Engineering Tottori Univercity

To investigate a cause of serious damages of the 2018 Hokkaido Eastern Iburi Earthquake, we observed microtremors and aftershocks at a landslide area and around strong ground motion observation stations. As a result, S-wave velocity structures were estimated at all observation sites. It was found that thickness of the volcanic ash layer (S-wave velocity:75-130 m/s) is 10m. Especially, it is suggested that two layers of volcanic ash layer have caused a landslide in the Shikanuma and Atsuma sites. It was found that the H / V spectral ratio of microtremor corresponds to the thickness of volcanic ash. The spectral amplitude of the H / V of the orthogonal direction component of the mountain ridge line became larger than that of the parallel direction component.

Keywords: Microtremor observation, landslide, H / V spectral ratio, S-wave velocity, subsurface abstraction

©2019. Japan Geoscience Union. All Right Reserved.

Nonlinear site amplification for high intensity ground motions during the 2018 Mw 6.6 Hokkaido eastern Iburi earthquake

*Yadab Prasad Dhakal[1], Takashi Kunugi[1], Takeshi Kimura[1], Wataru Suzuki[1], Shin Aoi[1]

1. National Research Institute for Earth Science and Disaster Resilience (NIED)

Large peak ground accelerations (PGAs) exceeding 1g on both the horizontal and vertical components were recorded at a fault distance of about 25 km during the September 6, 2018, Mw 6.6 Hokkaido eastern Iburi earthquake. Explaining the large PGAs at the distance for the magnitude of the event requires detailed investigation of the site response and source radiations. At several sedimentary sites, peak ground velocities (PGVs) exceeding 100 cm/s were recorded. Comparison of the observed PGAs and PGVs with the ground motion prediction equations (GMPEs) by Si and Midorikawa (1999) revealed that the observed data, especially the PGVs, were substantially larger at fault distances smaller than about 40-50 km, while the data at longer distances showed little or no trend different from the GMPEs. This motivated us to examine the site response during the earthquake. We processed many small amplitude (PGAs between 5 and 20 cm/s/s) accelerograms from earthquakes that occurred prior to the mainshock (the Mw 6.6 event) at sixteen KiK-net sites, and compared the surface-to-borehole spectral ratios between the small-amplitude ground motions from prior earthquakes and large-amplitude ground motions recorded during the mainshock. The comparison suggested that the sites at short distances where PGVs were underestimated, sustained various degrees of nonlinear site response, and the recovery is still undergoing at some of the sites based on similar analysis of aftershock recordings. Nonlinear site amplification has been known for a long time for the reduction of short-period ground motion amplitudes at a soil site during strong input motions compared with the weak input motions. Another commonly reported effect of nonlinear site response is the shift of predominant frequency to lower one. This second effect was found to be very prominent during the mainshock at soil sites and smaller distances, which caused stronger amplification at relatively longer-periods resulting into large PGVs and large JMA intensities. At the site of largest PGA, the ground motions were amplified by an order of magnitude at the new predominant frequency during the mainshock. We also analyzed the horizontal-to-vertical (H-to-V) spectral ratios at K-NET sites where PGAs were larger than 200 cm/s/s. We found that the K-NET sites also experienced larger degree of nonlinear site response at sites of larger PGAs. Based on the above analysis, the nonlinear site amplification could be one of the major reasons for the high intensity ground motions that were underestimated at the smaller distances by the GMPEs. Moreover, two sites (IBUH01: KiK-net; HKD127: K-NET), which were closely located, recorded vertical PGAs exceeding 1g for the up going motions at the surface, and the recordings showed asymmetric waveforms and amplitudes characteristics to the nonlinear site response reported during a few earthquakes in the past. A few sites having lower vertical PGAs were also suspected of being experienced nonlinear site response on vertical motions. Finally, we derived an ad-hoc equation to correct for the nonlinear site amplification in the prediction of horizontal PGVs with respect to the GMPE by Si and Midorikawa (1999). The results indicated that the stronger input motions may induce larger changes in PGVs at the surface than that for a proportional change in the shallow S-wave velocities (Dhakal et al. 2019).

Reference:

Dhakal YP, Kunugi T, Kimura T, Suzuki W, Aoi S (2019) Peak ground motions and characteristics of nonlinear site response during the 2018 Mw 6.6, Hokkaido eastern Iburi earthquake. Earth, Planets and Space (submitted)

©2019. Japan Geoscience Union. All Right Reserved.

Si H, Midorikawa S (1999) New attenuation relations for peak ground acceleration and velocity considering effects of fault type and site condition. Journal of Structural and Construction Engineering Transactions of AIJ 523:63–70

Keywords: Soil nonlinearity, 2018 Iburi earthquake, PGA, PGV, Spectral ratios

©2019. Japan Geoscience Union. All Right Reserved.

Microtremor array measurements at strong motion recording stations, HKD127 and IBUH01, in 2018 Hokkaido Iburi earthquake.

*Takuto Kogawa[1], Koji Tokimatsu[1], Izuru Okawa[1], Hitoshi Tanaka[1], Kentaro Motoki[2]

1. TOKYO SOIL RESEARCH CO.,LTD., 2. KOBORI RESEARCH COMPLEX INC.

1.Introduction

An earthquake of Mj6.7 occurred at 3:07 on September 6, 2018, in the Eastern part of the Hokkaido Iburi region. High seismic intensities (SI) of upper 6 and 7 were observed during this earthquake, even though the hypocenter of the earthquake was at the depth of 37 km. The amplification of surface ground was considered as one of the main factors that contributed such high SI. In order to estimate the ground amplification of the near surface ground, microtremor array measurements were conducted at six strong motion recording stations that observed SI upper 6 or 7.
In this presentation, we focused on two stations, HKD127 and IBUH01, because there was a difference in SI in spite that the two stations closely located. So we will show the result of analysis for these two sites.

2.Microtremor array measurement

The shape of the microtremor array used was an equilateral triangle. The vertical components were measured at three vertex points as well as the center of the array, in addition to the two horizontal components at the center. The measurements with a radius of 10m or less were made for each station, whereas those with a radius of 25m or more were made once around the two stations and used for both, because the distance between the two is as close as about 100m.

3.Analysis

A dispersion curve was determined from stationary part of microtremor array data based on SPAC method, and calculated H/V spectra from the three component microtremors observed at the center. The shear wave velocity profiles of the two stations were then back-calculated by the genetic algorithm using both observed dispersion curve and H/V spectra. The influence of higher modes of Rayleigh and Love waves was considered for the observed H/V spectra but neglected for the observed dispersion curve.

Keywords: Microtremor Array Measurement, H/V Spectra, Dispersion Curve, 2018 Hokkaido Iburi earthquake, Velocity Structure

©2019. Japan Geoscience Union. All Right Reserved.

Subsurface structure model based at diffuse-field theory in Oiwake region: Simultaneous inversion analysis on adjacent two sites

*Moeko Koie[1], Kentaro Motoki[1], Kenichi Kato[1], Takuto Kogawa[2]

1. KOBORI RESEARCH COMPLEX INC., 2. TOKYO SOIL RESEARCH CO., LTD.

During the 2018 Hokkaido Eastern Iburi Earthquake, 6.7 seismic intensity was observed in KiK-net Oiwake. On the other hand, observed seismic intensity at K-NET Oiwake, which is 100m away from the KiK-net, was 6.4. The amplitude of response spectra at KiK-net were higher near the predominant period than those at K-NET. The reason for the difference between their seismic intensity seems to be thought of due to the difference of their subsurface structure. In this study, we deduce subsurface structure models at the two sites by H/V inversion based on diffuse-field theory and estimate amplification factor at the sites.

To select the earthquakes for inversion analysis, we set the conditions such as occurrence before the main shock, less PGA than 100 cm/s^2, and higher ratio of epicentral distance to depth of hypocenter than 2. We used the average H/V of the selected earthquakes for observed H/V. In the calculation of H/V, we use the square-root of sum of squares of NS and EW component for horizontal component. The period at the peak observed H/V at K-NET Oiwake is shorter than that at KiK-net. The difference between their observed H/V is small in longer period range than 2 seconds.

Because of the adjacent of the sites and similarity of observed H/V in the long period, we set the deep part of structure at the 2 sites to be in common and search for shallow part of that individually. In order to make the deep part of structure in common, we adopted simultaneous inversion analysis at the two sites. We used the hybrid heuristic method and set the range of search based on the model of PS logging and J-SHIS. We searched for the thickness for the deep structure and S wave velocity for the shallow structure.

As a result of inversion analysis, we could deduce subsurface structure models which accorded with the observed H/V. The depth up to engineering bedrock of deduced K-NET model is 7m, and that at KiK-net is 20m. AVS30 at K-NET is 278m/s, whereas that at KiK-net is 243m/s. On the whole, S wave velocity at KiK-net in shallow part is lower than that at K-NET. We calculated the amplification factor of the shallow part, which was searched individually. The first natural period of amplification factor at KiK-net is 0.31s and that at K-NET is 0.20s. The predominant period of response spectra at KiK-net’ s (0.53s) is also longer than K-NET (0.48s). Because both of the natural and the predominant period at K-NET are shorter than those at KiK-net, the difference between subsurface structures might cause that of the amplitude of the main shock. However, the predominant period of the main shock is longer than the natural period at both sites, which seems to be influenced by nonlinear effect of the subsurface soil.

We will study about a cause of the difference of seismic intensity considering nonlinear effect of the subsurface soil.

Keywords: The 2018 Hokkaido Eastern Iburi Earthquake, Diffuse-field theory, H/V inversion, Subsurface structure

©2019. Japan Geoscience Union. All Right Reserved.

Exploration of the velocity structure model in the Mukawa town, damaged area during the 2018 Hokkaido eastern Iburi earthquake

*Michiko Shigefuji[1], Nobuo TAKAI[2], Jun Horita[3], Shingo Nomoto[3], Takahiro Maeda[4], Hiroaki Takahashi[2], Masayoshi Ichiyanagi[2], Hiroaki Yamanaka[5], Kosuke Chimoto[5], Seiji Tsuno[6], Masahiro Korenaga[6], Nobuyuki Yamada[7]

1. Kyushu University, 2. Hokkaido University, 3. Geo-Technical Research Co.,Ltd, 4. National Research Institute for Earth Science and Disaster Resilience, 5. Tokyo Institute of Technology, 6. Railway Technical Research Institute, 7. Kochi University

The 2018 Hokkaido eastern Iburi earthquake (M_w 6.6, focal depth=37 km) occurred on 6 September 2018 at the Hidaka arc-arc collision zone, Hokkaido, Japan. The many building damages by strong ground motion were concentrated around K-NET Mukawa strong motion observation station (HKD126). Strong motion records had strong power in 1-2 second periods of the response spectrum to destroy the timber frame buildings. It is an important examination to know the cause of the generation of this destructive strong motion.

To understand the site effects of this strong motion, we estimate the velocity structure models by using the microtremor array and multichannel analysis of surface wave measurements at three sites; around HKD126 site, a hillside site located about 6 km north from HKD126, and midpoint between both sites. We carried out the microtremor array measurements (R=1-2000 m) on 14-16 December 2018. We used servo type velocity sensor (Le-3D/5s) and 24-bit data logger (DATAMARK LS-7000XT) with GPS time calibration. At small arrays (R<~10 m), we used moving coil accelerometer (JEP-6A3, 10V/g). The fundamental Rayleigh wave phase velocity is examined with the spatial autocorrelation method. We also carried out a multichannel analysis of surface wave to emphasize the high-frequency side phase velocity. We set 24 channel 4.5 Hz geophones in interval 1 m with GEODE and 10 kg wood hammer. The phase velocity is examined with the Frequency-wavenumber method. The shear wave velocity structure models are estimated to fit the dispersion curve of the fundamental mode of Rayleigh wave using the genetic algorithm inversion method (Yamanaka and Ishida, 1998). The phase velocity data of the large array (R=2000 m) were used in common to the three sites.

Comparing the velocity structures, the Vs=1300 m/s layer’s depth of HKD126 is shallower than the hillside site ones and midpoint depth is mid of both. This tendency of depth variation is the same as the seismic bedrock and subsurface structure depth variation of AIST model (Yoshida *et al.*, 2007) and J-SHIS V2 model (Fujiwara *et al.*, 2012). On the other hand, about the shallow part, engineering bedrock depth of hillside site is shallower than the HKD126. The midpoint’s seismic bedrock is mid for the others, however, the surface soft soil deposit is detected as richer than the HKD126. These features of the shallow part structure's variation are able to confirm by the surface geology or Vs30 values of J-SHIS.

Acknowledgements: A part of this study was supported by the Grant-in-Aid for Scientific Research No. 18K19952 and 17H06215 from MEXT of Japan, and MEXT of Japan’s Earthquake and Volcano Hazards Observation and Research Program.

Keywords: The 2018 Hokkaido eastern Iburi earthquake, Velocity structure model, Microtremor measurement, MASW

©2019. Japan Geoscience Union. All Right Reserved.

©2019. Japan Geoscience Union. All Right Reserved.

Source Process of the 2018 Hokkaido Eastern Iburi Earthquake Inferred from Strong Motion Data and Green's Functions Based on Three-Dimensional Velocity Structure Model

*Kimiyuki Asano[1], Tomotaka Iwata[1]

1. Disaster Prevention Research Institute, Kyoto University

The source rupture process of the 2018 Hokkaido Eastern Iburi earthquake (M_{JMA} 6.7) was analyzed by the kinematic waveform inversion using strong motion data. Since this earthquake occurred close to the Hidaka Collision Zone and the Ishikari Lowland, the crustal and sedimentary basin structure of surrounding region is rather complex. Thus, we tried to use a three-dimensional velocity structure model to compute theoretical Green's functions. We used the Japan Integrated Velocity Structure Model (JIVSM; Koketsu *et al.*, 2012), and the Green's functions were computed by the three-dimensional finite difference method. The source fault model with strike-angle variation was set by referring to the spatial distribution of early aftershocks and the Global CMT solution. The source rupture process was estimated by the multiple time-window kinematic waveform inversion method (e.g., Hartzell and Heaton, 1983). The observed data for the inversion was strong-motion velocity waveforms in 0.04–0.5 Hz at K-NET, KiK-net and F-net stations. The rupture starting point was assumed to be at the hypocenter located by JMA at a depth of 37 km. The strong motion stations were selected based on the result of forward ground motion simulation of an Mw 4.1 aftershock occurring on September 14, 2018.
The estimated source model has small slip in the vicinity of the hypocenter, but significant slip is found in the depth range from about 22 km to 32 km. The rupture mainly propagated toward shallow and southwest direction. Considering crustal structure in this region (e.g., Iwasaki et al., 2004; Kita et al., 2012), the large slip area (asperity) is located in the middle-to-lower crust, and its rupture does not reach the upper crust. The depth range of significant slip is consistent with the spatial distribution of early aftershocks. Later aftershocks occurring in shallower depth are thought to occur outside the mainshock's source fault.

Acknowledgements: Strong motion data from K-NET, KiK-net and F-net (NIED) and JMA unified hypocenter catalog were used in this study. This study was supported by the Grant-in-Aid for Special Purposes 18K19952 (PI: Prof. Hiroaki Takahashi at Hokkaido University) from MEXT.

Keywords: the 2018 Hokkaido Eastern Iburi earthquake, strong motion data, source rupture process, three-dimensional velocity structure model

©2019. Japan Geoscience Union. All Right Reserved.

Source process of the 2018 Hokkaido Eastern Iburi earthquake derived from strong motion data

*Hisahiko Kubo[1], Wataru Suzuki[1], Asako Iwaki[1], Shin Aoi[1], Haruko Sekiguchi[2]

1. National Research Institute for Earth Science and Disaster Resilience, 2. DPRI, Kyoto University

The 2018 Hokkaido Eastern Iburi earthquake (M_{jma} 6.7) struck southern Hokkaido, Japan on September 6, 2018 (JST). This earthquake caused strong ground motions over southern Hokkaido with a maximum seismic intensity of 7 on the JMA scale and a maximum PGA of over 1500 cm/s/s. In this study, we estimate the source process of this earthquake using strong motion waveforms.
For source-process analysis of this event, we develop a curved fault model based on the spatial distribution of aftershocks. This curved fault model consists of multiple planes, each with a width of 20 km, a common dip angle (65 degree), and a common top depth (approximately 22 km). The common dip angle refers to the moment tensor analysis of F-net. The strike angle of the planes smoothly changes along the strike direction: the strike angle is 15˚ at the north part, 340˚ at the central part, and 40˚ at the south part. The rupture starting point is set to the hypocenter determined by JMA. The curved fault model is divided into 15 subfaults along the strike direction and 10 subfaults along the dip direction.
We use velocity waveforms at 20 stations of K-NET and KiK-net, F-net of NIED. The waveforms are band-pass filtered between 0.05 and 0.5 Hz, resampled to 10 Hz, and windowed from 1 s before S-wave arrival for 25 s.
Green's functions are calculated with the discrete wavenumber method (Bouchon 1981) and the reflection/transmission matrix method (Kennett and Kerry 1979) assuming 1-D velocity structure models. The structure models are obtained for each station from the 3-D structure model (Fujiwara et al. 2009). Logging information is also used for the KiK-net station. To consider the rupture propagation effect, 25 point-sources are uniformly distributed over each subfault in the calculation of Green’ s functions.
The multi-time-window linear waveform inversion method (Olson and Apsel 1982; Hartzell and Heaton 1983) is used in this study. The slip time history of each subfault is discretized using eight smoothed ramp functions (time windows) progressively delayed by 0.4 s and having a duration of 0.8 s each. The triggering velocity of first time window is set to 1.4 km/s to minimize the data-fit residual. Two orthogonal slips of each time window at each subfault are derived by minimizing the difference between the observed and synthetic waveforms using the non-negative least-squares scheme (Lawson and Hanson 1974). The slip angle is allowed to vary centered at 107˚, which is the rake angle of the F-net analysis. In addition, we impose a spatiotemporal smoothing constraint on slips (Sekiguchi et al. 2000).
In the estimated source model, the large slips are found at approximately 30 km depth in the up-dip direction from the hypocenter. In the first 6 s, the rupture grows slowly around the hypocenter with small slips. Then, the rupture developed with the large moment release between 6 s and 12 s in the large slip area. The large slip area does not overlap with the active aftershock area

Keywords: 2018 Hokkaido Eastern Iburi earthquake, Source process, Strong ground motion

©2019. Japan Geoscience Union. All Right Reserved.

Broadband ground-motion simulation of the 2018 Hokkaido Eastern Iburi earthquake

*Asako Iwaki[1], Nobuyuki Morikawa[1], Takahiro Maeda[1], Hisahiko Kubo[1], Hiroyuki Fujiwara[1]

1. National Research Institute for Earth Science and Disaster Resilience

1. Introduction

The 2018 Hokkaido Eastern Iburi earthquake (M_{JMA}6.7) was an inland crustal earthquake at a focal depth of approximately 35 km. This earthquake brought strong ground motion to the southern Hokkaido, causing JMA seismic intensity of 6+ and 7 above the fault and nearby, and 6- in the city of Sapporo. The seismicity around the source region reaches to deeper region compared to other inland areas in Japan (HERP 2018). Inland crustal earthquakes at this depth have not been considered by the current ground-motion prediction procedure in Japan. Therefore it is necessary to examine whether the strong ground motion from this earthquake can be modeled by the conventional procedure.

2. Broadband ground-motion simulation

We conducted broadband ground-motion simulation using the characterized source model based on the “recipe” for strong motion prediction (HERP 2017), aiming to reproduce the observed ground motion. A planner fault is set referring to the fault slip model by Kubo et al. (2019, this meeting) with the length and width of 28km and 22km, respectively, in the lower crust. Rupture starting point is set to 35 km, and a single asperity is set several km shallower than the rupture starting point on the fault plane. Source parameters are derived by the recipe for inland crustal earthquakes. We call this source model the reference source model.

Broadband ground motion time-series on the engineering bedrock is computed using the J-SHIS v2 3D velocity model (Fujiwara et al. 2009, 2012). We employed a hybrid technique of the 3D finite-difference method (Aoi et al. 2004) and the stochastic Green’s function method (Dan and Sato 1998) superposed in time domain at the period of 1 s. JMA seismic intensity (I_{JMA}) on the ground surface is derived by using the empirical relationships between V_{S30}, PGV and I_{JMA} (Fujimoto and Midorikawa 2005, 2006).

Main features of the velocity waveforms in long-period range (> 1s), amplitude and travel time of the main phases, are found to be consistent with observed records at many observation stations. On the other hand, I_JMA on the ground surface systematically underestimated the observation. Although this underestimation can be attributed to many factors including the source and velocity models, since our simulation results underestimates the observation at all points in short-period component, we first examine the effect of the source parameters that mainly affects the ground-motion level of short-period components. The short-period level, or the source spectral amplitude level at short period, of this earthquake estimated by Tomozawa et al. (2018, SSJ) is 1 –2 times larger, depending on the dataset, than the empirical relation by Dan et al. (2001) which is employed in the recipe. Referring to their result, we set another source model that has smaller size of asperity and consequently higher short-period level, 1.5 times larger than the empirical relation of Dan et al. (2001). I_{JMA} computed with this source model was more consistent with the observation compared to the reference source model.

3. Summary

Broadband ground-motion simulations were conducted for this earthquake using the characterized source models. It was found that the ground motion computed with higher value of short-period level compared to the empirical relation for the ordinary inland crustal earthquake was more consistent with the observed ground motion. It maybe reflecting the feature of the earthquake source characterized by

©2019. Japan Geoscience Union. All Right Reserved.

the depth or the tectonic condition.
We will further study on the source characteristics and site response characteristics in order to better explain the strong ground motion records.

Acknowledgments: We used strong motion data provided by JMA, Hokkaido, the city of Sapporo, and NIED.

Keywords: the 2018 Hokkaido Eastern Iburi earthquake, strong ground motion, broadband ground-motion simulation, inland crustal earthquake

©2019. Japan Geoscience Union. All Right Reserved.

Estimation of 1D S-wave velocity structures in Kumamoto plain and Mashiki town using a waveform inversion of S-wave

*Kengo Muroi[1], Hiroaki Yamanaka[1], Kosuke Chimoto[1], Seiji Tsuno[2], Masahiro Korenaga[2], Hiroe Miyake[3], Nobuyuki Yamada[4]

1. Tokyo Institute of Technology, 2. Railway Technical Research Institute, 3. The University of Tokyo, 4. Kochi University

The 2016 Kumamoto earthquakes are crustal earthquakes caused by inland active faults with damage of many wooden houses to the focal area. In this study, we revised the previous subsurface structural model, using the observed ground motion records during aftershocks of the earthquakes, on the purpose of evaluating strong ground motion in damaged area during the main shock. Furthermore, we reproduced the strong motion of main shock, using the revised subsurface structural model.
First, we conducted 3-D finite difference simulations during aftershocks of the 2016 Kumamoto earthquakes, using previous subsurface structural model by Headquarters for Earthquake Research Promotion. We used the aftershock with an Mj of 5.5 and a depth of 10km on April 19 assuming a homogeneous fault model. From the comparison of the observed waveforms and the calculated waveforms in Mashiki, we found that the qualitative characteristics seen in the observed waveforms can be reproduced. However, we found it difficult to reproduce the detailed characteristics, such as the amplitude and phase.
Therefore, we tuned the 1-D subsurface structural models just beneath the observation sites by an inversion analysis, using waveforms of the observed initial S-wave during aftershocks. We estimated a 1-D velocity model minimizing misfit of mean squares between amplitudes of the observed waveforms and the calculated waveforms by a 1-D simulation using the discrete wavenumber method. We estimated the 1-D velocity structures at 36 observation sites in Kumamoto plain and Mashiki town during the aftershocks. We could well explain the characteristics of the observed waveforms, compared with the calculated waveforms using the previous subsurface structural model.
Finally, we conducted a simulation of the ground motion for the main shock, using the revised subsurface structural model. We used the source model by Kubo et al. (2016) and site amplification factors of J-SHIS in order to consider the effect of the amplification of the shallow soil. The calculated J.M.A seismic intensity distribution underestimated the observed seismic intensity at the center of Mashiki town and the calculated waveform at Mashiki town hall was 3 to 4 times smaller than the observed waveform. On the other hand, the calculated waveforms at K-net Kumamoto and KiK-net Mashiki are similar characteristics of the observed waveforms. These results show that the revised subsurface structure was reasonable in the Kumamoto plain, but we need to reconstruct further more the subsurface structural model beneath the center of Mashiki town.

Keywords: The 2016 Kumamoto Earthquakes, Waveform Inversion, 1D S-wave Velocity Structure, Simulation of Ground Motion

©2019. Japan Geoscience Union. All Right Reserved.

Investigation to estimate high-frequency Empirical Green’s tensor derivatives (EGTD) using aftershocks for the 2016 Kumamoto earthquake

*Sayumi Yoshida[1], Horike Masanori [1], Ken Miyakoshi[2]

1. HANSHIN CONSULTANTS Co., Ltd., 2. Geo-Research Institute

1) Introduction
Green’s tensor derivatives play a key role for evaluation and prediction of strong ground motions and for surveys of the velocity and damping structures. However, it is difficult to generate high-frequency (above 1Hz) Green’s tensor derivatives using numerical approaches for want of fine geological structure models. Plicka and Zahradnik (1998) proposed a method for estimation of Empirical Green’s tensor derivatives (EGTDs) using multiple small earthquakes. EGTDs does not require the structural model along propagation paths for their estimation and is possible to calculate high-frequency ground motions for any focal mechanism. In this study, we investigate the conditions required (focal mechanism, grouping radius, applicable frequency) to obtain high-frequency EGTDs, using aftershocks of the 2016 Kumamoto earthquake.
2) Data and method
The size of the aftershocks ranges between the magnitudes 2 and 4. The focal mechanism, such as the strike, the dip angle, and the rake angle, and the source parameters of radiated spectra, such as the seismic moment and the corner frequency, are required for the estimation of EGTDs. The focal mechanism was obtained from the sign of P-wave first motions and the source parameters were obtained from the Fourier spectra of S-wave motions, assuming the model.
We first set the grouped aftershocks located within a sphere with a certain radius. Then, we estimated 3 EGTDs for 3-component ground motions from the grouped aftershocks by the approach developed by Plicka and Zahradnik (1998). Finally, we evaluated the accuracy of the estimated EGTDs by the correlation coefficients between observed seismic recordings of the grouped aftershocks and those calculated using the estimated EGTD for the 3- component ground motions. We furthermore evaluate the accuracy of EGTDs by investigating whether they can reproduce seismic waveforms of the aftershocks which are not contained in the group.
3) Results
Accurate EGTDs up to 2 Hz can be stably estimated from most groups with the radius of 1km, having the correlation coefficients over 0.8. Also, these EGTDs can reproduce the seismic motions of the aftershock that is not contained in the group. In the meantime, the correlation coefficients calculated from the estimated EGTDs up to 4Hz are not always not high values over 0.8 even for the groups with the radius 0.5 km. These results suggest that estimation of EGTDs up to the frequency higher than 2Hz requires accurate focal mechanism and source parameters of the radiated spectra. Thus, we will improve them, for example, using the Genetic algorithm.
4) Acknowledgement
In this study, we use event waveform data provided by NIED (Hi-net).

Keywords: Empirical Green’s tensor, 2016 Kumamoto earthquake, high-frequency

©2019. Japan Geoscience Union. All Right Reserved.

Estimation of Site Amplification Characteristics in Kumamoto plain by Spectral Separation Analysis Using Aftershock Records of the 2016 Kumamoto Earthquake

*Tomomi Iida[1], Hiroaki Yamanaka[1], Kosuke Chimoto[1], Daiki Shinoyama[8], Seiji Tsuno[5], Masahiro Korenaga[5], Nobuyuki Yamada[7], Hiroe Miyake[6], Tatsuo Kanno[3], Michiko Shigefuji[3], Masayuki Yoshimi[2], Shinichi Matsushima[4], Hiroshi Kawase[4], Kimiyuki Asano[4], Tomotaka Iwata[4]

1. Tokyo institute of Technology, 2. National Institute of Advanced Industrial Science and Technology, 3. Kyushu University, 4. Kyoto University, 5. Railway Technical Research Institute, 6. The University of Tokyo, 7. Kochi Unicersity, 8. Central Research Institute of Electric Power Industry

The 2016 Kumamoto earthquake contains a foreshock with an Mj of 6.5 on April 14 and the main shock with an Mj of 7.3 on April 16. The earthquakes generated ground motions with a seismic intensity of 7 on the Japan Meteorological Agency scale twice in Mashiki, Kumamoto, Japan and many wooden houses were collapsed. In this study we estimated site amplification characteristics in Kumamoto plain by using ground motion records at strong motion stations of K-NET, KiK-net, seismic intensity-meters stations by local governments and aftershock observation stations by Yamanaka et al. (2016) through a spectral inversion technique. We choose the OITH08 station as the referential site in the inversion. The estimated frequency dependent Q and the source characteristics by the spectral inversion technique show similar features to those from previous studies (e.g. Somei et al, 2018). The site amplifications in the alluvium plain show large values in a frequency range of 0.5-2.0Hz. At high frequency the site amplifications of the mountain are larger than those of the plain area. We estimated S-wave velocity structures in Kumamoto plain by an inverse analysis of the site amplifications. The sediments are large in central area of the Kumamoto plain.
Acknowledgements: This work was conducted as a part of the Comprehensive Study on the Futagawa-Hinagu fault zone after the 2016 Kumamoto earthquake, MEXT.

Keywords: Spectral inversion technique, the 2016 Kumamoto Earthquake, Site Amplification

©2019. Japan Geoscience Union. All Right Reserved.

Kinematic and dynamic source models of the 2016 Mj6.4 Kumamoto third large earthquake

*Kunikazu Yoshida[1], Ken Miyakoshi[1]

1. Geo-Research Institute

We make a kinematic source model of the 2016 Mj6.4 earthquake (2016 Apr. 15, 00:03 JST) which is a third large event during the 2016 Kumamoto earthquake sequence and dynamic source models based on the result of the kinematic model.

The kinematic model is made by inverting the strong-motion data obtained from K-NET, KiK-net, JMA and local government were used. The data were windowed for 18 s, starting at P-wave arrival time, and band-pass-filtered between 0.05 to 1.0 Hz (periods of 1-20 s) for waveform inversion. The accelerograms were integrated into ground velocities. Theoretical Green's functions are calculated using the discrete wavenumber method (Bouchon, 1981) and the Reflection/Transmission coefficient matrix method (Kennett and Kerry, 1979) using a stratified medium. We assumed individual one-dimensional velocity structure model for each station by using waveform modelling with small earthquake records (Yoshida et al., 2017). The event locations were relocated using double-difference method by Uchide et al. (2016). We used multi-time-window linear waveform inversion procedure (e.g., Hartzell and Heaton, 1983) in which the moment-release distribution is discretized in both space and time. The length and width of the fault plane was assumed to be 12 km and 10.5 km, respectively. The fault plane is divided into subfaults of 1.5 km ×1.5 km. The moment function of each subfault was represented by a series of six smoothed ramp functions in the 0.4 second interval. The first time-window triggering velocity (V_{FT}) was determined as 2.4 km/s, which was searched between 2.0 and 2.6 km/s based on residual of the waveform fits.

The estimated source model indicated 1.2 ×10^{18} Nm (Mw6.0) of the total moment release and 0.3 m average slip. One rectangular asperity and a high slip/moment rate area (HRA, Yoshida et al., 2017) patches with the average slip of 0.7 m were identified on the shallow part of the fault plane. The slip of the background area is 0.1 m.

We attempt to make dynamic rupture models based on the kinematic model. Stress drop distribution of the kinematic model was calculated (Okada, 1992). The average static stress drops were 3.9 MPa (asperity) or 4.9 MPa (HRA) and 1.0 MPa for the background. Effective stress was taken from the stress parameters estimated from SMGA (Kurahashi et al., 2017). The effective stresses were adjusted as 5.1 MPa (Asperity) or 6.3 MPa (HRA) to rupture over the entire fault. We conducted dynamic rupture simulations using the patched stress drop distribution obtained from the kinematic model (Figure left-bottom). We assumed slip-weakening law with uniform critical distances of 0.1 m, based on Dc’’ (Fukuyama and Mikumo, 2007) of about 0.15 m at KMMH14. The simulation results show that the final slips and total moments well agree with the ones of the kinematic model. Nevertheless, small slips and high slip rate on the top margin of the patches, and supershear rupture propagation on the further of the patch were found. We expect examination of some dynamic parameters, such as critical slip distances, to improve simulation results.

Acknowledgements: We used strong motion data of K-NET, KiK-net, JMA and Mifune town. We thank Dr. Uchide (AIST) to provide the relocated hypocenter location data. This study was based on the 2018 research project ‘Examination for uncertainty of strong ground motion prediction for inland crustal

©2019. Japan Geoscience Union. All Right Reserved.

earthquakes' by the Secretariat of Nuclear Regulation Authority (NRA), Japan.

Keywords: 2016 Kumamoto earthquake, source process, dynamic simulation

Kinematic model

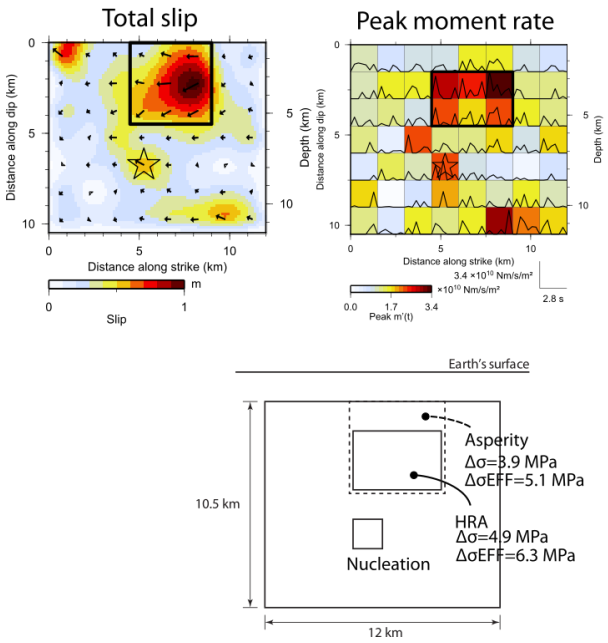

Dynamic simulation

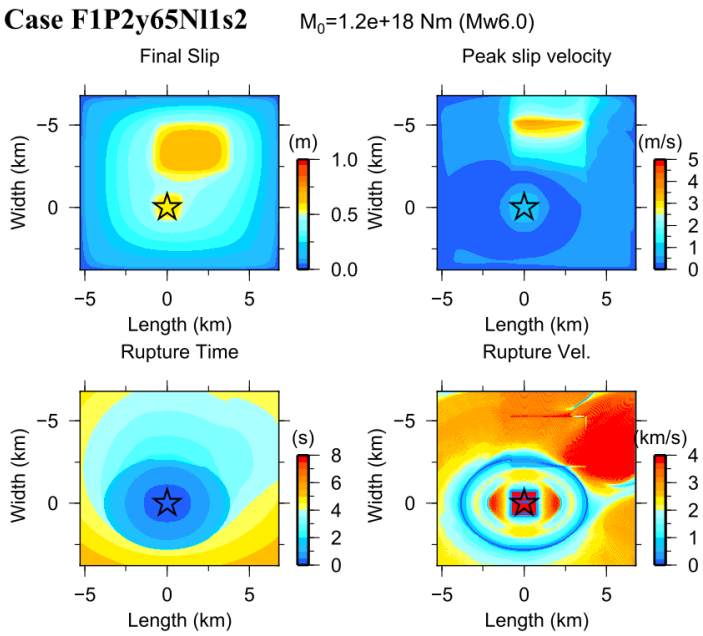

©2019. Japan Geoscience Union. All Right Reserved.

Source rupture process and strong motion generation area assuming the curved fault model for the 2003 northern Miyagi prefecture earthquake

*Kazuhiro Somei[1], Ken Miyakoshi[1], Yujia Guo[1]

1. Geo-Research Institute

At 07:13 on 26 July 2003 (JST), a shallow inland crustal earthquake (M_{JMA}6.4) with reverse faulting occurred in the northern Miyagi prefecture, north-east Japan. From the strong ground motion records in 0.05-0.5 Hz, the kinematic source rupture processes assuming a two-segment fault model have been estimated by waveform inversion method (e.g., Hikima and Koketsu, 2004). They showed large slips around 1.0 m occurred in a shallow part of the northern segment. However, surface breaks caused by this earthquake were not found along the source area by field surveys (e.g., Imaizumi et al., 2003). Since the shallow large slip area was identified between the north and the south segment, it is reasonable in estimating robust slip distribution to consider the more realistic fault plane with bending zone rather than a simple two-segment fault plane. Actually, the precisely relocated hypocenters of aftershocks were located along a curved plane dipping westward to north-westward (Okada et al., 2003). In this study, we investigate the source rupture process assuming the curved source fault, and estimate the strong motion generation areas (SMGAs; Miyake et al., 2003), in order to discuss the broadband ground motion generation processes during this event.

First, we employed the multi-time window linear waveform inversion method by using the strong motion waveforms (0.1-1.0Hz) recorded by K-NET, KiK-net, and JMA stations around the source area. From the observational information of relocated aftershock distribution and geological structure, the assumed curved fault model was composed of two planar segments (north and south segments) set by Hikima and Koketsu (2004) with transitional part that smoothly connect the north with south segment. The length, width, and shallowest top depth of fault model were 20 km, 11 km, and 0.59 km, respectively. This curved fault model was divided into 220 subfaults of 1.0 ×1.0 km. The temporal moment release history from each subfault was expressed by a series of 6 smoothed ramp functions with a rise time of 1.0 sec separated by 0.5 sec. The first-time window triggering velocity (FTWTV) was 2.8 km/s given by the smallest misfit solution. The theoretical Green’ s function was calculated by using the discrete wavenumber integration method (Bouchon, 1981) with the reflection and transmission matrix (Kennett and Kerry, 1979) assuming a 1D velocity structure model. The velocity structure model of each station was given by referring the Somei et al. (2018) or Petukhin and Miyakoshi (2006).

Second, the SMGAs were constructed based on the forward simulations using the empirical Green’ s function method (Irikura.1986) in the frequency range 0.3-10 Hz. The locations of rupture starting points and rupture times for two SMGAs were fixed by using the onset times of first and second S-wave packets in observations. Scaling parameters N and C were obtained based on the source spectral ratio analysis. The best set of parameters for SMGAs, such as the size, rupture velocity, rise time, and rupture starting point inside the SMGA, were determined by a grid searching to minimize the residual function of waveform fitting between observations and synthetics.

The principal findings from the source inversion and SMGA modeling are following. 1) The large slip area whose maximum slip of 0.93 m was concentrated in the transitional segment, where is north of the

©2019. Japan Geoscience Union. All Right Reserved.

hypocenter. The top depth of characterized asperity area (Somerville et al., 1999) was 3.07 km, which is deeper than that of Hikima and Koketsu (2004) model. The size of asperity area was 35 km^2, which is comparable to that expected by empirical scaling relationship (Somerville et al., 1999). 2) High peak moment ate areas (HRA; Yoshida and Miyakoshi, 2013), which implied the large slip velocity, were characterized with a size of 29 km^2 near the edge of the asperity area. 3) Synthetic ground motions generated from two SMGAs with a size of 24 km^2 identified close to the HRAs explained well the observations in a broadband frequency range. 4) The stress drops of two SMGAs were 13.7 MPa, which are comparable to those estimated for past large inland crustal earthquakes in Japan.

Acknowledgements: This study was based on the 2018 research project ‘Examination for uncertainty of strong ground motion prediction for inland crustal earthquakes’ by the Secretariat of Nuclear Regulation Authority (NRA), Japan.

Keywords: The 2003 northern Miyagi prefecture earthquake, Curved fault, Source inversion, Strong motion generation area, Empirical Green’s function method

©2019. Japan Geoscience Union. All Right Reserved.

Estimation of source rupture process during the 2018 Shimane-ken seibu earthquake using strong motion data

*Susumu Kurahashi[1], Ken Miyakoshi[2]

1. Aichi Institute of Technology, 2. Geo-Research Institute

1. Introduction

The 2018 Shimane-ken seibu earthquake (Mw5.6) occurred in the western part of Shimane-prefecture, Japan, on April 9, 2018. The maximum seismic intensity with 5 upper was observed at Ohta city. PGA of 564 gal is observed at the SMN006 station. We estimated the source process of this earthquake by the waveform inversion using the strong motion data.

2. Estimation of rupture area from the waveform inversion

We analyzed the slip distribution during this earthquake using the multi-time window linear waveform inversion method (Sekiguchi et al., 2000). The data sets used for the inversion analysis were velocity waveforms of S-waves parts at 13 stations (KiK-net, K-NET). The Green's functions were calculated using the one-dimensional velocity structure models by the discrete wavenumber method (Bouchon, 1981) with the reflection and transmission matrix method (Kennett and Kerry, 1979) at the stations. A fault plane was assumed referring to the aftershock distribution and the moment tensor solution determined by F-net data.

First, in order to estimate the rupture area, we analyzed the waveform inversion in target frequency 0.1-0.5Hz. The fault plane is divided into 36 subfaults of 2.0km×2.0km. The temporal moment release history from each subfault is modeled by a series of 3 smoothed-ramp-functions with a rise time of 1.0 second each separated by 0.5 second. The estimated rupture area was trimmed by criteria of Somerville et al. (1999). The trimming result removes one column of the north edge of rupture area. Seismic moment, area, rupture velocity and average slip are estimated 4.67 $\times 10^{17}$Nm,126km^2, 2.7km/s and 0.11m, respectively. The rupture area was approximately three times larger than the scaling relationship of rupture area vs seismic moment from Irikura and Miyake (2001).

3. Extraction of asperity from the waveform inversion results

Next, in order to extract of asperity from slip distribution, we analyzed the waveform inversion in the frequency range of 0.1-1.0Hz. The rupture area is divided into 56 subfaults of 1.5km×1.5km. The temporal moment release history from each subfault is modeled by a series of 6 smoothed-ramp-functions with a rise time of 0.6 second each separated by 0.3 second. A large slip area is constructed in the proximity of the hypocenter.
The asperity and high rate area (HRA) were extracted from the slip distribution by the criterion of Somerville et al. (1999) and Yoshida et al. (2005), respectively. Seismic moment and area are estimated 2.23×1017Nm and 27km2, respectively. The area and location of the asperity and the HRA are estimated to be almost the same. On the other hands, the asperity was overestimated in comparison with the scaling relationship of asperity are vs seismic moment from Irikura and Miyake (2001).

4. Conclusion

©2019. Japan Geoscience Union. All Right Reserved.

We estimated source process of the 2018 Shimane-ken seibu earthquake (Mw 5.6) form the waveform inversion using the strong motion data. The asperity and the HRA of this earthquake are collocated with nearly the same area. On the other hands, the rupture area and the asperity were overestimated corresponding to scaling law from Irikura and Miyake (2001). The rupture area data of earthquake of Mw6 class vary widely in the scaling law from Irikura and Miyake (2001). Therefore, it is necessary to consider about earthquake of Mw6 class.

Acknowledgements. Seismic waveform data of the K-NET and KiK-net were used. This study was based on the 2018 research project 'Examination for uncertainth of strong ground motion prediction for inland crustal earthquakes').

Keywords: The 2018 Shimane-ken seibu earthquake, source rupture process, strong ground motion

©2019. Japan Geoscience Union. All Right Reserved.

An estimation of SMGA of M6 class earthquakes based on strong motion records near the source regions

*Kentaro Motoki[1], Kenichi Kato[1], Tetsuo Shiota[2]

1. Kobori Research Complex, 2. Shikoku Electric Power Company

High amplitude earthquake motions exceeding 1 G have been observed when M6 class earthquakes occurred for a couple of decades. In the 2004 Rumoi earthquake (M6.1), two SMGAs in the vicinity of the strong motion station caused high amplitude earthquake motions (Maeda and Sasatani , 2008, Motoki et al., 2015). For M6 class earthquakes, which are difficult to set up fault models to be used for strong ground motion prediction, we thought that accumulating information such as stress drop and area of SMGA gave useful information for setting ground motion level for future earthquakes. In this report, we inverted SMGA for the 2011 Ibaraki-ken Hokubu earthquake.

We used empirical Green's function method (EGF) to invert SMGA. Unknown parameters in this inversion were the location of SMGA trigger point, stress drop ratio c, the number of superposition N, length of SMGA, rupture velocity in SMGA, starting rupture time of SMGA, rise time, and random numbers giving the rupture fluctuation to weaken artificial periodicity. For inverse analysis of SMGA, we used a hybrid heuristic method (Yamanaka, 2007), which could solve nonlinear problems and did not require an initial model.

For an inversion of SMGA, we selected 4 stations (IBRH13, IBRH14, IBR001 and FKS014) where the influence of nonlinearity in subsurface soil during the main shock might be small based on degree of nonlinear site response proposed by Noguchi and Sasatani (2011). We also selected 7 earthquakes as element earthquakes for empirical Green’ s function. We performed 7 inversion analyses using each element earthquake record.

Corner frequencies of the element earthquakes were evaluated by means of genetic algorithm so as to minimize the sum of residuals between the observed source spectral ratio and the source spectrum ratio function assumed ω-square model in the frequency domain. We set the search range for an inversion of SMGA, by referring to the previous source model (JMA, 2017) and c and N expected from the observed source spectral ratio. In this inversion M_0 and A, which means radiant amplitude in a short period range, were constrained not to exceed the value estimated by F-net and the value obtained from the source spectral ratio, respectively. The acceleration envelope shapes, the displacement waveform, and the Fourier amplitude were used as the objective function for an inversion.

Assuming one SMGA, the inverted SMGA could explain the earthquake motions near the source region. The SMGA location were good agreement with the large slip area in the previous models (JMA, 2017 and Hikima, 2017), which were used long period motions for their inversions.

Furthermore, in order to confirm the validity of the inverted SMGA from a theoretical aspect, we performed numerical simulation for the down-hall station at IBRH13 using the theoretical Green’ s function analysis (Hisada and Bielak, 2003). The simulated motions successfully reproduced the pulse wave and the response spectra of the observed motions.

We compared the area of SMGA estimated in this study with the relation of M_0 –area of SMGA according

©2019. Japan Geoscience Union. All Right Reserved.

to Miyake et al. (2003). The result of this study is smaller than that of relation by Miyake et al. One factor that caused this difference is thought to be due to the difference in idea of modeling. As mentioned above, M_0 of the SMGA in this study corresponded to a third of M_0 evaluated by F-net. Meanwhile, the SMGA of Miyake et al. (2003) had set the SMGA to include all of the M_0. It can be consider that the larger M_0 of SMGA has the larger area of SMGA. On this issue, we think that it is important to apply other earthquakes and accumulate data, and we will analyze SMGA of the 2013 Tochigi-ken Hokubu earthquake.

Keywords: Strong motion generation area, M6 class earthquake, Inversion, Empirical Green's function method

©2019. Japan Geoscience Union. All Right Reserved.

Difference in short-period level between the surface and buried fault rupture crustal earthquake in Japan

*Shohei Yoshida[1], Takao Kagawa[1], Tatsuya Noguchi[1]

1. Graduate School of Engineering, Tottori University

Appearance of surface fault rupture in inland crustal earthquake affects significantly on ground motion characteristics. Somerville(2003) indicated that observed ground motions from buried rupture earthquakes are larger than those from surface fault rupture earthquakes in period range around 1.0 second. Kagawa *et al.*(2004) explained that the differences are mainly caused in seismic source characteristics of fault ruptures, such as peak slip rate and stress drop between shallow and deep region. The Headquarters for Earthquake Research Promotion compiled a method for strong motion prediction (recipe). Short-period level as a parameter of the recipe is an important factor that affects generation of short-period ground motion. Due to the difference in ground motion characteristics between surface and buried fault rupture, the short-period level may also be different between the two rupture types. In this study, we organize short-period levels that evaluated characteristic source models by empirical Green's function method, and investigated empirical relations between short-period level and seismic moment for both surface and buried fault rupture crustal earthquake in Japan.

Somerville, P. G.(2003) : Physics of the Earth and Planetary Interior, 137, pp.201-212.
Kagawa et al.(2004) : Earth planet and space, 56, 3-14.

Keywords: Inand crustal earthquake, Surface fault rupture, Seismic source characteristics, Short-period level

©2019. Japan Geoscience Union. All Right Reserved.

Probabilistic seismic hazard assessment of response spectra for whole Japan (part 1: Selection of ground motion prediction equations)

*Nobuyuki Morikawa[1], Junichi Miyakoshi[2], Hiroyuki Fujiwara[1]

1. National Research Institute for Earth Science and Disaster Resilience, 2. Ohsaki Research Institute, Inc.

The seismic intensity or peak velocity is used in the probabilistic national seismic hazard maps for Japan. However, seismic hazard assessment of response spectra is useful in seismic risk assessment and engineering field. In this study, we try to assess seismic hazard of the response spectra by using the seismic activity model in the national seismic hazard maps for Japan. In this paper, we mention selection of ground motion prediction equations (GMPEs) used in the assessment, and the results are shown in the next report.
In Douglas (2019), 290 GMPEs for spectral ordinates published after 1973 are summarized, of which about 50 are derived from strong-motion records mainly observed in Japan. The 2003 Tokachi-oki earthquake was the first magnitude 8-class earthquake in the world where strong-motion records observed by the nation-wide dense networks, K-NET and KiK-net. It is very important to use the GMPE obtained using the record of the 2003 earthquake, because the contribution of large subduction earthquakes on seismic hazard assessment in Japan is extremely large. In this study, we carry out the assessment of 5%-damped acceleration response spectra whose period is shorter than 5 seconds all over Japan on the engineering bedrock (Vs=400m/s). So we select GMPEs that satisfy the following conditions.
a. It has been published as a peer-reviewed paper.
b. It was derived from records mainly observed in Japan, including records of the 2003 Tokachi-oki earthquake.
c. It is included peak acceleration and 5% damped acceleration response spectra whose period ranges from 0.1 to 5 seconds and can evaluate on the engineering bedrock.
d. It is possible to consider the difference of source and path characteristics in earthquake type (crustal, subduction plate-boundary, and subduction intra-plate).
e. It is modeled anomalous seismic intensity distribution.
f. It does not target specific earthquakes or observation points only.
g. It is used records of magnitude 9-class mega-earthquake.
As the result, two sets of GMPEs by Morikawa and Fujiwara (2013) and Zhao et al. (2016) were selected. However, with regard to the above condition g, it is inevitable that the uncertainties concerning the applicability to the earthquakes in Nankai trough are large because both GMPEs are used records the 2011 Tohoku great earthquake only for magnitude 9-class. In order to consider such uncertainty, we decide to add the latest GMPE, Goda and Atkinson (2009)’s, that satisfies other conditions.
The difference is large in the short distance or mega-earthquake, which number of records is quite few, among three GMPEs. By the way, the dataset for deriving the GMPE is constructed by each researchers. As the result,
1. Methods of filtering applied to observed waveforms and definition of horizontal maximum amplitude are different each other.
2. The magnitude and fault model selected are different for each other.
3. Indicators related to site amplification, such as site class and Vs30, are not unified.
This situation makes it impossible to compare among GMPEs under exactly the same conditions. This is not limited to the three GMPEs selected here, but is a problem common to all Japanese GMPEs that do not have derived from the same dataset. In seismic hazard assessment including mega-earthquakes and very close distance to the source fault with quite few observation records, it is necessary to use multiple

©2019. Japan Geoscience Union. All Right Reserved.

GMPEs in consideration of epistemic uncertainty. In case of seismic hazard assessment targeting a specific site, there is also the idea that each GMPE is weighted based on consistency with observation records. However, in order to evaluate its consistency, it is necessary to construct a unified standard dataset and to use GMPEs derived based on it that can be compare under the same conditions.

Keywords: Seismic hazard assessment, Response spectra, Peak acceleration, Ground motion prediction equation

©2019. Japan Geoscience Union. All Right Reserved.

Probabilistic seismic hazard assessment of response spectra for whole Japan (part 2: Probabilistic seismic hazard assessment)

*Junichi Miyakoshi[1], Takeshi Morii[1], Nobuyuki Morikawa[2], Hiroyuki Fujiwara[2]

1. Ohsaki Research Institute, Inc., 2. National Research Institute for Earth Science and Disaster Resilience

The seismic intensity or peak velocity is used in the probabilistic national seismic hazard maps for Japan. However, seismic hazard assessment of response spectra is useful in seismic risk assessment and engineering field. In this study, we try to assess seismic hazard of the response spectra by using the seismic activity model in the national seismic hazard maps for Japan. In this paper, the seismic hazard assessment results of the response spectra are shown using the selected ground motion prediction equations (GMPEs) in the previous report.
Three GMPEs are used: Morikawa and Fujiwara (2013), Goda and Atkinson (2009), Zhao et al. (2016). When evaluating seismic hazards for Japan, it is difficult to evaluate only by one GMPE, so it is necessary to select multiple GMPEs as a branch of the logic tree.
Based on the hazard curve of the response value with respect to the natural period, a uniform hazard spectrum (UHS) is calculated by connecting response spectra that have the same excess probability for each natural period. We calculate UHS at 6 cities (Sapporo, Sendai, Tokyo, Nagoya, Osaka, Fukuoka) by using the seismic activity model in the national seismic hazard maps for Japan.
As an example of the result, we are shown uniform hazard spectra for 39%, 10%, 5%, and 2% probability of exceedance occurring within 50 years from the present for all seismic activity models in Sapporo and Tokyo using GMPE by Morikawa and Fujiwara (2013). In the uniform hazard spectra, we can confirm the difference between the seismic hazard level of Sapporo and Tokyo. Also, the degree of influence of the seismic category for each natural period for a 10% probability of exceedance occurring within 50 years from the present is shown. By using the seismic activity model in the national seismic hazard maps for Japan in this way, it becomes possible to grasp the difference of the seismic hazard in the region for each natural period. In addition, we assess seismic hazard of standard peak acceleration in the world.

Keywords: Seismic hazard assessment, Response spectra, Peak acceleration, Ground motion prediction equation

©2019. Japan Geoscience Union. All Right Reserved.

Simulation of Long-period Ground Motion around The Fujikawa-kako Fault Zone during the 2018 Northern Osaka Earthquake

*Seina Hashimoto[1], Hiroaki Yamanaka[1], Kosuke Chimoto[1], Masahiro Korenaga[2], Seiji Tsuno[2], Hiroe Miyake[3], Shigeki Senna[4]

1. Tokyo Institute of Technology School of Enviroment and Society, 2. Railway Technical Research Institute, 3. The University of Tokyo, 4. National Research Institute for Earth Science and Disaster Prevention

Abstract

The Fujikawa-kako fault zone is an active fault that is suggested to be associated with the Nankai Trough in Suruga Bay, and the activity interval of this fault is a relatively high as compared to the other general active faults. Furthermore, this area is so important for the transportation network for our lives near this fault zone. A high-reliable prediction of strong ground motion in this area is important in earthquake disaster prevention in the area. In this study, we have installed strong motion observation instruments in Fujinomiya City and Fuji City to acquire strong motion records during small earthquakes since April 2018. From the earthquake records obtained at the observation points, it was found that the duration of the shaking was as long as nearly 2 minutes, and the long period component was dominant in the 2018 Northern Osaka Earthquake with a magnitude of 6.1. Then, using the deep S-wave velocity structure model of J-SHIS, we conducted seismic motion simulation of Northern Osaka Earthquake. We also assumed appoint source model, based on the CMT solution released by the Meteorological Agency. First, we compared the synthetic waveform of the rock site (YMNH10) with the observed one. The calculated waveform had similar characteristics of the observed waveform. By using the snapshots, we found that the major phases observed mainly in this area were surface waves with a north-south oriented wavefront arriving a right after the S wave arrival. We also found the later phases arriving from the southwestern part of Yamanashi Prefecture where the depth of the seismic bedrock is suddenly increases. On the other hand, the reproducibility of the observed frequency characteristics in the vicinity of Shizuoka City was low in a period range of 3-20 seconds. We need further improvement in the S-wave velocity model of the sedimentary layers.

Acknowledgements

A part of this study was carried out as an integrated research project for observation for the Fujikawa estuary fault zone by Ministry of Education, Culture, Sports, Science and Technology-Japan.

Keywords: The Fujikawa-kako Fault Zone , the 2018 Northern Osaka Earthquake, Simulation of Long-period Ground Motion , strong motion observation

©2019. Japan Geoscience Union. All Right Reserved.

Site amplification factors for KiK-net stations in and around Ibaraki Prefecture estimated by the coda normalization method

*Jun Kawahara[1], Takahiro Nakamura[1], Takuji Yamada[1]

1. Graduate School of Science and Engineering, Ibaraki University

It is empirically known that the spatial distribution of the coda wave energy from a local earthquake is nearly uniform for long lapse times. The coda normalization method is a method of separating source, path, and site effects from coda wave records, based on this empirical characteristic (Sato et al., 2012). There are many studies on the evaluation of site amplification factors based on the coda normalization method (e.g., Takahashi et al. 2005; Takemoto et al., 2012). However, little attention has been paid on the magnitude of the variability of amplification factors estimated for different earthquakes in an identical region.

We applied the method to the strong-motion records for 21 KiK-net stations and F-net TSK (Tsukuba) station in and around Ibaraki Prefecture. We used the records of 31 earthquakes with 4.7≦Mw≦6.4, which were classified into four groups depending on their locations. Stations with the epicentral distances less than 100 km were chosen for each earthquake, and the seismograms for lapse times greater than twice the direct S-wave travel time at the farthest station were used in the analysis. We selected TSK as the reference station for which the site amplification is expected to be low, and we obtained the amplification factor for each KiK-net station relative to TSK. We also calculated the geometric mean of the factors for each earthquake group.

We obtained the following results. (1) The low-frequency (0.5 to 1 Hz) amplification factors were apparently correlated with both basement depths and geological ages. It is consistent with previous studies such as Takemoto et al. (2012). (2) At the stations with shallow basement in the northern areas, the variability of the amplification factors among the earthquakes was small irrespectively of frequencies, and the geometric means of the factors for four earthquake groups were nearly the same. (3) At the stations with deep basement in the southern areas, the variability of the amplification factors among the earthquakes was relatively large, and the geometric means of the factors for four earthquake groups were somewhat different. (4) The geometric standard deviations of the amplification factors were apparently correlated with both basement depths and geological ages. (5) There appears no clear relationship between the amplification factors and the hypocentral distances for most stations. It supports the empirical assumption that the spatial distribution of the coda wave energy is nearly uniform.

Acknowledgment.
We used the strong-motion records form KiK-net and F-net and the data of basement depths from J-SHIS (National Research Institute for Earth Science and Disaster Resilience).

Keywords: site amplification factor, coda normalization method, Ibaraki Prefecture

©2019. Japan Geoscience Union. All Right Reserved.

Estimation of earthquake ground level in Horinouchi area in the 2014 Northern Nagano earthquake

*RYOTA KAWAI[1], Hiroaki Yamanaka[1], Kosuke Chimoto[1], Seiji Tsuno[2], Masahiro Korenaga[2]

1. Interdisciplinary Graduate School of Science and Engineering,Tokyo institute of Technology, 2. Railway Technical Research Institute

The 2014 Northern Nagano Earthquake with Mj of 6.7 occurred on 22 November 2014. The JMA maximum intensity of 6 lower was observed in Otari village and Ogawa village. However, heavy damage was observed in Horinouchi and Mikkaichiba areas which are 5km away from the strong observation point with intensity of 5 higher. One of the reasons for the heady damage is low seismic performance of the damaged houses as reported in JAEE's team. However, strong motion features of main shock are not fully understood in the area... In this study, we estimated the ground motions in the damaged areas to know the reasons of the damage.

After the main shock, Chimoto et. al (2015) observed aftershock records around the damaged areas In this study, we analyzed these records with records observed at strong motion stations using the spectral inversion technique. This technique can divide ground motion spectra into site, source and propagation effects. We used records from 59 earthquakes including aftershocks between JMA magnitudes of 2.4 and 5.8, and the main shock. During strong shaking like the main shock, nonlinear behavior of soil layers can be observed. Thus, we set three conditions for the data selection in this inversion analysis.

1) For earthquake records with PGAs less than 100 gal except for the main shock,

2) the main shock records with PGAs less than 100 gal have site effects as same to those of weak shock,

3) the main shock records with PGAs more than 100 gal has site effects that are different from those of the weak motions. Under these conditions, different site effects for the weak motion and the main shock are estimated at the observation stations with PGAs more than 100gal during the main shock.

We investigated the relation of the estimated site effect for the weak shaking and the main shock at the observation stations. The differences of these site effects can be caused by the nonlinearity of the soft soil. Therefore, in this study, we defined Ra(f) as an ration of the site effect for the main shock to that of weak shaking. We investigated the relationship between this Ra and the S wave velocity profiles by our microtremor surveys. At the observation stations with PGAs of 400 gal during the main shock, it was found that the Ra is similar for the sites with similar average S wave velocities up to a depth of 10 m (hereafter, Vs 10). The Vs10 in Horinouchi area is 165m/s, and VS10 in Ogawa village is 151m/s. Therefore, it is indicated that Ras in Horinouchi area and Ogawa village are the same.

The spectra characteritics of the main shock at basement was calculated from the source effect of the main shock and the propagation effect, estimated by spectrum inversion. Furthermore, we estimated the site effect of the main shock in Horinouchi area from the site effect of weak shaking and Ra of Ogawa village for estimating the spectral features of the main shock in Horinouchi area by these multiplications of these factors.

As a result, it was found that the estimated earthquake ground motion level was about 2 times stronger

©2019. Japan Geoscience Union. All Right Reserved.

than the strong motion observation stations at a period of 1-1.5 seconds, which has large effects on the wooden houses. We also found that this motion is classified to a seismic intensity of 6 upper on the JMA scale. On the other hand, the estimated spectral power in this study is about 1/4 to 1/2 of the strong motion spectrum of past destructive earthquakes observed in areas with heavy damage of the wooden building.

From these discussions we have concluded that ground motion at periods of 1-1.5 seconds were slightly larger than the surrounding observation stations. However the low earthquake resistance of the damaged building in Horinouchi area must be also included in one of the reasons of the damage.

Keywords: Spectral inversion technique, 2014 Northern Nagano earthquake, Nonlinear site effect, Building damage

©2019. Japan Geoscience Union. All Right Reserved.

Ground type classification for strong ground motion prediction based on characteristics of phase-velocity curves from microtremor explorations

*Atsushi Wakai[1], Shigeki Senna[1], Hisanori Matsuyama[2], Yatagai Atsushi[2], Yoshiaki Inagaki[2], Hiroyuki Fujiwara[2]

1. National Research Institute for Earth Science and Disaster Prevention, 2. OYO Corporation

For the purpose of strong ground motion evaluation and prediction, subsurface velocity structures in sedimentary layers have ever been modeled and sophisticated for Kanto, Tokai and Kumamoto region in the national investigation conducted by SIP (Cross-ministerial Strategic Innovation Promotion Program) of Council for Science, Technology and innovation.

There, spatially dense array-microtremor explorations also have been conducted at more than 27,500 sites in the regions, as of February 2019. They consist of miniature and irregular array measurements made at interval of about 1 km and standard-sized array ones made at interval of about 5 km. As a result, shallow S-wave velocity structures were modeled in detail, which can affect ground amplification, building and human damage.

In this study, regarding characteristics of phase-velocity (hereinafter called Pv) curves from array microtremor explorations, it was attempted to investigate relationships with geomorphologic land classification [Wakamatsu et al., 2013] and geological constitution of ground.

Pv curves can be usually obtained 2Hz to 30Hz in frequency from miniature and irregular array microtremor explorations. In general, Pv in higher frequency corresponds to velocity structures in the depth of a few of meters to 10 meters and that in lower frequency corresponds to those in the depth of dozens of meters below ground surface. Here, Pv at wave length of 40 meters or C40 [Konno et al., 2000] was extracted and made use of at each microtremor measurement site. C40 can be regarded as AVS30.

As a result, useful information was able to be acquired to model subsurface velocity structures in addition to new knowledge which was not able to be obtained from only bore-hole exploration data. Also, C40s vary due to different-sized plains and different sedimentary environment despite the same geomorphologic land classification. This presentation will report the results in detail.

Keywords: Ground type classification, phase-velocity curve, microtremor exploration, strong ground motion

©2019. Japan Geoscience Union. All Right Reserved.

Establishment of the Underground Structure Model for Seismic Damage Estimation

*Shigeki Senna[1], Atsushi Wakai[1], Hiroyuki Fujiwara[1]

1. National Research Institute for Earth Science and Disaster Resilience

1.Introduction
To develop subsurface structure models for estimating earthquake damage on a real-time basis, we studied subsurface models capable of evaluating ground motion characteristics at a broad range of frequencies. We combined a shallow subsurface model and a deep subsurface model by collecting boring data and soil property data, which are crucial for explaining the ground motion in the vicinity of each period (0.5 to 2.0s), as such ground motion affects soil both near the surface and deep in the ground. In this study, we developed a widearea subsurface structure model (250m grid cell) and a more detailed subsurface model (50m grid cell), as well as a microtremor measurement system and a subsurface structure information management system to support model development. A brief description of each of the following themes will be provided in the sections below.

(1) Construction of wide-area subsurface models for estimating earthquake damage
(2) Understanding of ground motion characteristics and development of a microtremor observation system
(3) Development of a construction technique for a detailed subsurface model through public-private collaboration

2. Construction of Wide-Area Subsurface Models for Estimating Earthquake Damage
Wide-area subsurface models were constructed for the entire Kanto and Tokai regions. Here, we will mainly report on the progress made with the model for the Kanto and Tokai area. To develop a shallow subsurface model, we primarily used approximately 440,000 sets of boring data gathered by NIED. We created an initial integrated model for shallow and deep subsurfaces by combining this shallow subsurface model with an existing deep subsurface model (J-SHIS) and adjusting the engineering bedrock. Records compiled by K-NET, KiK-net, JMA, and local governments were used as seismic observation records. To gather continuous microtremor data, two types of observation techniques, namely miniature and irregular arrays and large arrays (R = 25 to 800 m), were used at approximately 20,000 and 800 points, respectively.

3. Understanding Ground Motion Characteristics and Development of a Microtremor Observation System
To obtain a large number of microtremor array measurements and ensure that results are managed effectively until the results of analysis are produced, it is necessary to minimize and simplify the steps required to collect observation data, analyze them, and evaluate the results. To achieve these goals, we developed a mechanism that can perform all the steps quickly, including on-site data sorting and analysis while minimizing human error. More specifically, we developed i-Bido, which transmits data between seismometers and computers, tablets, and other computing devices without corrupting the data while preserving its quality, and sends the data to the database described below.

4. Development of a Construction Technique for a Detailed Subsurface Model Through Public-Private Collaboration
Our goal is to construct detailed subsurface models with 50m grid cells capable of predicting liquefaction

©2019. Japan Geoscience Union. All Right Reserved.

and landslides while accounting for factors such as ground irregularity and artificial sites, using both public and private boring data, building confirmation applications, topographical information, old topographic maps, and other data. A slope map developed by the Geospatial Information Man-made structures were excluded. The distribution of small artificial valley fills that could not be identified by topographical maps derived from an algorithm for calculating and comparing slopes was obtained. Finally, the buffer region was applied to the water systems identified from the results of water system analysis to develop a model. The model is consistent with the distribution of large-scale artificial sites and also appears to show small artificial sites.

Keywords: subsurface velocity structure, bore-hole, array microtremor, strong ground motion

©2019. Japan Geoscience Union. All Right Reserved.

Consideration of liquefaction damage rate based on liquefaction damage in recent years

*Shigeki Senna[1], Ozawa Kyoko[1]

1. National Research Institute for Earth Science and Disaster Resilience

1. Introduction
In the 2011 off the Pacific coast of Tohoku Earthquake, liquefaction occurred in an extremely large area from the Tohoku region to the Kanto region, and a large number of liquefaction damage was confirmed in Kumamoto City and Aso City in the 2016 Kumamoto earthquake. In The past, the authors examined the rate of liquefaction in recent years of liquefaction and showed that the difference in the rate of liquefaction in the Tohoku-Pacific Ocean earthquake and other earthquakes was explained by the effects of the duration of the seismic motion. However, this creation of anation, liquefaction hazard map is difficult, and there is grouping based on the history of the microtopography of 250 m mesh and the regional classification method for this regionality consideration. the improvement of the high accuracy of the liquefaction rate prediction equation by setting the area ratio of the area and the subdivision of the micro-topography division, etc. by using topography and elevation data. We also collected information on building damage and investigated the rate of liquefaction damage.

2. Collected and maintained data
The 2011 off the Pacific coast of Tohoku Earthquake and the 2016 Kumamoto earthquake liquefaction Point by local surveys and aerial images, A re-reading of the sand point was performed from high sight point of the geographical institute immediately after the earthquake. we have created a detailed data set of about 50 m and about 25 m mesh units as well as the data set of approximate 250 m mesh units that have been prepared so far.
In addition, the following data were also prepared.

(1) Average elevation, average gradient, and ratio of high data for each mesh size (250 m, 50 m, 25 m) based on 10 MDEM data.
(2) Topographic classification data for each mesh size based on land use classification data based on the above data, we investigated the liquefaction incidence and the area ratio from the relationship between the data and the liquefaction point.
(3) We collected damage information such as slope and settlement of buildings in the 2011 off the Pacific coast of Tohoku Earthquake and the 2016 Kumamoto earthquake, and investigated the relationship with the incidence rate.

3. Investigation of liquefaction generation rate and area ratio
With regard to liquefaction incidence, data on liquefaction occurrence rates of the 2011 off the Pacific coast of Tohoku Earthquake and the 2016 Kumamoto Earthquake are summed up and the measured seismic intensity and maximum velocity fragility are calculated for each micro-topography classification using the least squares method and maximum likelihood Method and cluster analysis was carried out to group the micro topographical classification. As a result, it was able to be grouped into four new groups different from the micro topography group classified based on the liability to liquefaction by a previous study. For each group, the possibility of group subdivision was examined by comparing with average elevation, average gradient, specific height data etc. of each mesh. As a result of examination, it was found that the liquefaction occurrence rate has extremely high correlation with the specific height in any of the

©2019. Japan Geoscience Union. All Right Reserved.

micro topography classifications, and it is highly likely that the above four groups can be further subdivided. Regarding the liquefaction area ratio, assuming that 25 m mesh is the minimum unit, if there is even one sand in the mesh, it is assumed that the whole mesh is liquefied. Regarding the areal ratio, because there was no clear correlation with the measured seismic intensity and the maximum velocity in all the micro topographical classifications, the average value of the area ratio was calculated for each micro topographical classification. For the sake of simplicity, this study summarizes the final liquefaction occurrence rate by multiplying the liquefaction occurrence rate and liquefaction area rate shown above. In addition, we examined the relationship between seismic intensity, maximum speed and liquefaction occurrence rate for slope and settlement of building damage caused by liquefaction.

4. Conclusion (future plans)
The liquefaction incidence rate calculation formula (florality) examined in this study will be compared with building damage damage distribution data in the future, and the validity of the results will be verified.

Keywords: liquefaction, strong motion, phase-velocity curves

©2019. Japan Geoscience Union. All Right Reserved.

Estimation of surface earthquake record at MeSO-NET observation points

*Shigeki Senna[1], Atsushi Wakai[1]

1. National Research Institute for Earth Science and Disaster Resilience

1. Introduction
In this research, in order to predict the state of shake of the ground surface with high precision from the data of the underground seismometer installed at the depth of 20 m of MeSO-net, microtremor observation at each observation point and temporary observation at the surface By observation, we evaluate the ground amplification characteristics and estimate the S wave velocity structure of the ground. As research and development items for that, 1. Acquisition of surface earthquake record and estimation of amplification characteristics at MeSO-net observation point, 2. Estimation of geophysical properties such as microtremor array observation and S wave velocity structure.The following section introduces efforts for each item.

2. Acquisition of surface earthquake records and estimation of amplification characteristics at MeSO-net observation point
In this item, in order to estimate the ground-to-ground spectral amplification factor for each observation point by temporary seismic observation at the MeSo-net observation point, it was conducted at all MeSO-net observation points (297sites) There. The observation period is 2 to 3 months per point, and observation is completed at 60 points. For each target observation point, one seismometer (JU 310 and JU 410 manufactured by Hakusan Kogyo Co., Ltd.) having the same sensor as the MeSO-net seismograph was used. In addition, the sampling frequency at the time of data acquisition was set to 200 Hz and the range was set to ±4.0G (± 1.0 G for JU 310) for JU410. Amplification characteristics are calculated by calculating the Fourier spectrum for each component from the seismic waveform obtained in the ground and the surface at each observation point, applying a bandpass filter of 0.1 to 10 Hz, smoothing in a logarithmic window, The ratio was taken. As a result, the difference in amplification characteristics between the relatively hard Rohm plateau sites and the soft backward swamp and natural embankment sites.

3. Microtremor array observation and estimation of ground physical property values such as S wave velocity structure
To verify the ground amplification characteristics of the previous section and make it possible to assume the shake even under strong ground motion, microtremor array observation to obtain the S wave velocity structure of about 50 m underground was carried out. Microtremor observation purchased a three component seismometer/ microtremor observation device (JU410) with the same sensor characteristics as the MeSO-net seismograph. Using them, microtremor array observation is carried out just above 296 points of the target MeSO-net observation point. In the fine motion array, we deployed a 4-point extremely small array with an array radius of 60 cm and a 3-point irregular array with about 5 to 15 m on each side, and observation was done for about 15 minutes at the same time. In addition, the ground physical property values such as the S wave velocity structure were estimated using inverse analysis methods such as extraction of amplification characteristics of AVS30 etc. (C40), direct curve transformation method of dispersion curve, inverse analysis and the like. As in the previous section, the difference between the characteristics of the relatively hard Rohm and the soft backward swamp are clear.

©2019. Japan Geoscience Union. All Right Reserved.

4. Conclusion
Based on the seismic observations and microtremor observations carried out up to the previous section, we will consider the ground amplification factor considering the period in the future, but we will consider the past ground model (SIP) of the existing Kanto region We will further improve the S wave velocity structure model using the shallow / deep integrated subsurface structure model of the Kanto region implemented in the real-time earthquake damage estimation) and estimate the highly accurate seismic motion at 250 m mesh interval The goal is to do.

Keywords: earthquake observation, microtremor, subsurface velocity structure

©2019. Japan Geoscience Union. All Right Reserved.

Possibility of estimating phase velocity of Love wave using Horizontal components in microtremor array surveys in the case of Nishio

*Kotoyo Tsuchida[1], Masanori Horike[1], Koji Yamada[1], Masaki Suehiro[1], Sayumi Yoshida[1]

1. HANSHIN CONSULTANTS COMPANY LIMITED

1) Introduction

The S wave velocity structure of sediments is the most important factor for amplification of earthquake motions. In recent years, microtremor array surveys have been popularized because the S wave velocity structures can be estimated by simple measurements and at a low cost. For example, Horike (1985) inferred the S wave velocity from f-k spectra estimated array microtremors and Aki (1957) and Okada (2003) also inferred them from the spatial autocorrelation functions (SPAC). These approaches use vertical microtremor array recordings and discard horizontal-component recordings. As is well known, the phase velocity of Rayleigh waves is influenced not only by the S-wave velocity structure but also by the P-wave velocity structure, while that of Love wave is influenced by the S-wave velocity structure alone. Therefore, it is expected that S wave velocity structure can be obtained clearly by estimating the velocity structure using the dispersion of the Love wave. Several approaches are developed for inference of the phase velocity of Love waves, for example f-k method by Tsuchida et al (2016), SPAC and CCA method by Tada et al (2010; using the microtremor array analysis tool "BIDO 2.0" software). The aim of this study is to compare the phase velocities obtained using the same arrays.

2) Observation and data

For this comparison, we implemented microtremor measurement in Nishio City, Aichi Prefecture, using different-size array composed of 7 stations. At each station 3-component velocity sensors were installed. Microtremor recording were acquired at a sampling interval of 0.005s for 30 minutes. This site is suitable for this comparison, because there is much information about geotechnical and geological property.

3) Results

At the present, the phase velocity by the f-k method is estimated, but it is still in the process of analysis. Therefore, by the day of the presentation, we will proceed with the remains to do.

Keywords: microtremor array surveys, Love wave, Horizontal components

©2019. Japan Geoscience Union. All Right Reserved.

Enhancement of shallow velocity structure models based on array microtremor explorations for Tokai region, Central Japan

*Atsushi Wakai[1], Shigeki Senna[1], Yatagai Atsushi[2], Yoshiaki Inagaki[2], Hisanori Matsuyama[2], Hiroyuki Fujiwara[1]

1. National Research Institute for Earth Science and Disaster Prevention, 2. OYO Corporation

1. Introduction
For sophistication of strong ground motion prediction, it is important to model subsurface velocity structure so that earthquake ground motions can be evaluated in broadband period from 0.1 s to 10 s. Therefore, it is indispensable to combine shallow and deep velocity structure models which have ever been constructed separately and to constructed subsurface velocity structure models so that earthquake observation records can be reproduced.

We have ever modeled subsurface velocity structure for Kanto, Tokai and Kumamoto region in the national investigation conducted by SIP (Cross-ministerial Strategic Innovation Promotion Program), “reinforcement of resilient disaster prevention and mitigation function” of Council for Science, Technology and innovation.

This study attempted to sophisticate shallow geological and soil structure models in initial subsurface velocity structure ones from seismic bedrock to ground surface which had been constructed for Tokai region (Shizuoka, Gifu, Aichi and Mie pref.) last year. It was based on results of a great number of array microtremor explorations. This report will introduce outline of array microtremor exploration, sophistication process of shallow velocity structure models and characteristics of ground motion.

2. miniature and irregular array microtremor exploration
About microtremor measurements, array observations were conducted in lowland and plateau of Tokai region. It consists of 4-point miniature array with a radius of 60 centi-meters and 3-point irregular array from 5 to more than 10 meters on a side. These measurements were made on the road and near seismic ground-motion stations such as K-NET and KiK-net. The total number of measurement sites has reached about five thousand and nine hundred, as of February in 2019. In addition, the measurement was conducted for around 15 minutes per site at intervals of 1km using JU210/215 or JU410 which was an all-in-one microtremor measurement unit [Senna et al., 2008]. And sampling frequency was set at 200Hz.

About analysis of miniature and irregular array microtremor data, we evaluated one-dimensional S-wave velocity structure using shallow velocity structure exploration method based on microtremor measurements. The method has been proposed and advanced in recent researches [Cho et al., 2013]. The analysis was made using a microtremor analysis tool such as “BIDO” or “Microtremor Array Tools [Cho et al., 2016].”

3. Improvement of initial shallow velocity structure models based on results of array microtremor explorations
Last year, initial shallow velocity structures were modeled using the existing bore-hole data and surface geological data. In basis of results of miniature and irregular array microtremor exploration, 1-dimensional S-wave velocity structures in the initial models were modified at each microtremor measurement point. And then, they were interpolated spatially by means of Kriging method and three-dimensional shallow

©2019. Japan Geoscience Union. All Right Reserved.

velocity structures were modeled.

On the improved models in this study and the conventional models based on geomorphologic land classification [Wakamatsu et al., 2013], ground amplification index was compared in spatial distribution. From a general viewpoint, the improved models have wider areas with large amplification in lowlands and they tend to have large local variation in ground amplification. In addition, for the improved models, distribution of ground amplification rates was evaluated by each period in basis of 1-dimensional multiple reflection theory. Amplification rates seem to be larger in different areas by each period.

4. Summary and future challenge
In this study, initial shallow velocity structure models, which were constructed based on a lot of bore-hole and geological data, were enhanced for Tokai region using results of array microtremor explorations. Also, it can be suggested that it is important to evaluate ground motion characteristics using both of amplification and period characteristics. In the close future, improved subsurface velocity structure models will be validated using moderate seismic records at strong-motion stations.

Keywords: S-wave velocity structure, shallow ground, array microtremor exploration, strong ground motion

©2019. Japan Geoscience Union. All Right Reserved.

Validation of seismic bedrock structure model in the Shimousa region, Chibe prefecture, Japan using seismic interferometry to strong motion

*Kosuke Chimoto[1], Hiroaki Yamanaka[1]

1. Tokyo Institute of Technology

Green’s function is estimated using autocorrelation of strong motions by seismic interferometry, and the depth to the seismic bedrock is estimated in sedimentary basins (Yoshimoto et al., 2009; Watanabe et al., 2011, Shiraishi et al., 2016). Oren and Nowack (2017) observed clear Reflected waves by applying spectral whitening to the autocorrelation of ambient noise. Chimoto and Yamanaka (2018) applied this method to the autocorrelation of strong motions and observed reflected wave from seismic bedrock by estimating the Green’s function in the sedimentary layers. We apply this method in the Shimousa region, Chiba prefecture, Japan to estimate autocorrelation using strong motions. Validation of 3D S-wave velocity structure model was attempted based on the spatial variation of reflected waves from seismic bedrock in the region.

Number of autocorrelations without the selection of strong motions enhance the clear reflected wave (Chimoto and Yamanaka, 2018). We used all the strong motions observed in the period of January 2008 to Jun 2018 observed at the strong motion stations of K-NET and KiK-net installed in the Shimousa region. After removal of offset of the strong motion, horizontal components are rotated to the transverse component. Spectral whitening is applied to the power spectrum and inverse Fourier transform provides autocorrelation function after the bandpass filtering. The range of bandpass filter is important to estimate the expected reflected waves from sedimentary layers (Chimoto and Yamanaka, 2018). We used the range of 0.5-2.0Hz to estimate the reflected wave from the seismic bedrock. Theoretical Green’s function for the validation of the model was calculated by Haskell method using 1D structure model extracted from the 3D J-SHIS deep structure model.

We observe the distinct reflected waves from the seismic bedrock in the autocorrelation functions estimated in the Shimousa region, Chiba prefecture. Two-way travel time of the reflected wave at KiK-net Narita station is 3 seconds and that is 3.5 seconds at K-NET Narita station. These values are almost consistent to those of the theoretical Green’s functions, while slight faster arrivals are observed. On the other hand, the stations located north and east to Narita exhibit several arrivals in the autocorrelations and the reflected wave from the seismic bedrock becomes weak. The travel time is faster than Narita. The reflected waves from the seismic bedrock at the stations located west to Narita appears later than 4 seconds, meaning the deeper bedrock than Narita. The southern part to Narita, central part of Chiba prefecture, shows the two-way times of later than 6 seconds, suggesting the deepest bedrock structure. This fact is consistent with the previous 3D models in the Kanto basin. We thus captured the spatial variation of the seismic bedrock from the estimation of autocorrelations of the strong motions in the Shimousa region, Chiba prefecture. The characteristics of spatial variation was similar to that of previously proposed 3D models. However, it is highly expected for the accurate modeling by tuning the slight difference between the autocorrelation function and the theoretical Green’s function.
We used the records observed at K-NET and KiK-net by National Research Institute for Earth Science and Disaster Resilience and deep structure model of Japan Seismic Hazard Information Station.

Keywords: Seismic interferometry, Autocorrelation function, Strong motion, Seismic bedrock structure model, Shimousa

©2019. Japan Geoscience Union. All Right Reserved.

©2019. Japan Geoscience Union. All Right Reserved.

Microtremor survey for subsurface velocity structure of Saga plain

*Masayuki Yoshimi[1], Michiko Shigefuji[2], Tadashi Maruyama[1]

1. Geological Survey of Japan, AIST, 2. Kyushu University

Saga plain, located in northern Kyushu island, is quite flat lowland facing south to the Ariake Sea. An active fault zone is recognized at the northern boundary of the plain. If the fault zone activates, strong ground motion will hit whole the plain. To assess possible earthquake hazards, subsurface structure of the plain has to be revealed.

We conducted microtremor array measurements in the plain to investigate the S-wave velocity of the sediment layers and spatial variation of the bedrock depth. Four locations for the survey are chosen along the P-wave reflection survey line (Maruyama et al. 2017) and its extension toward south. Array aperture of the measurements at each location is set about 10 to 500 meters enabling to estimate the subsurface velocity structure down to about 1 km. Four velocity sensors (Tokyo sokushin, SE-321) are deployed at each array to compose equilateral array with a center point. Phase velocity of the Rayleigh wave are estimated using vertical component data of the microtremor by SAPC and V-method (Cho et al. 2004, Tada et al., 2007). The results will be shown.

Keywords: microtremor array survey, S-wave velocity structure, Saga plain

©2019. Japan Geoscience Union. All Right Reserved.

Densely microtremor observation to estimation of subsurface structure in Hane and Kute area, Ohda City, Shimane Prefecture, Japan

*Tatsuya Noguchi[1], Yoshito Yamaguchi, Yuhei Morita, Isamu Nishimura[1], Shohei Yoshida[1], Takao Kagawa[1]

1. Department of Management of Social Systems and Civil Engineering, Civil Engineering Course Graduate School of Engineering, Tottori University

An earthquake (Mj6.1) occurred in vicinity Ohda City western Shimane Prefecture in Japan on April 9, 2018. Densely microtremor observations were carried out to estimate the characteristic of ground motion in the damage area, Hane and Kute area, Ohda City. A distribution of the predominant period of microtremor H/V spectra and S-wave velocity structures were obtained from observation data. As a result, it was found that maximum thickness of the weak soil subsurface layer is 40m and a short period component of predominant period about 0.2-0.4 seconds may have influenced structural damage.

Keywords: microtremor observation, characteristics of ground motion, subsurface structure, 2018 eastern Shimane prefecture earthquake

©2019. Japan Geoscience Union. All Right Reserved.

Densely microtremor observation to estimation of subsurface structure in Nishizono and Yura area, Hokuei Town, Tottori Prefecture, Japan

*Tatsuya Noguchi[1], Katsuya Tomeoku, Isamu Nishimura[1], Shohei Yoshida[1], Takao Kagawa[1]

1. Department of Management of Social Systems and Civil Engineering, Civil Engineering Course Graduate School of Engineering, Tottori University

Densely microtremor observations were carried out to estimate a characteristic of ground motion and subsurface structure in the damage area due to 2016 central Tottori Prefecture earthquake, Yura and Nishizono area, Hokuei Town, Tottori Prefecutre. Microtremor H/V spectra and a distribution of the predominant period and underground structure models were obtained, and grasped the characteristic of ground motion based on this result. As a result, it was found that a difference of the subsurface structure depth to about 20m and a short period component of predominant period less than 0.5 seconds may have influenced structural damage.

Keywords: microtremor observation, characteristics of ground motion, subsurface structure, 2016 central Tottori prefecture earthquake

©2019. Japan Geoscience Union. All Right Reserved.

Seismic reflection survey in the Kathmandu Valley, Nepal.

*Kota Koshika[1], Yusuke Kawasaki[1], Om Pradhan[1], Masato Yamamoto[1], Dai Nobuoka[1], Yoshikazu Matsubara[1], Hisanori Matsuyama[1], Monika Jha[2], Chintan Timisina[2], Suresh Shrestha[2], Mukunda Bhattarai[2], Dinesh Nepali[2], Soma Nath Sapkota[2], Hiroe Miyake[3], Kazuki Koketsu[3]

1. OYO Corporation, 2. Department of Mines and Geology, 3. Earthquake Research Institute, University of Tokyo

On the April 25, 2015, earthquake of magnitude 7.8 Mw (USGS, 2015) struck in the 78 km north west of Kathmandu (Gorkha Earthquake) and major after shock of magnitude 7.3 Mw, with epicenter about 80 km north east of Kathmandu cases heavy damage in the Kathmandu Valley (KV). It was thought that the damage in the KV was particularly great, due to the underground structure of the KV.

We conducted gravity survey in the KV as part of the SATREPS projects in 2017. The shape of the gravity basement of the whole KV was estimated (Pradhan et al.,2018).

We conducted seismic reflection survey to clarify the detailed basement of the KV and the upper sedimentary structure in 2018. Survey lines were set up at Tribhuvan International Airport (TIA) where depth of gravity basement greatly changes and Nepal Agricultural Research Council (NARC) where deep gravity basement was estimated. Survey line length is about 4km (TIA) and 1km (NARC). Enviro Vibe (IVI, Inc.) was used as a seismic source.

The shape of the basement obtained by the seismic reflection survey and the shape of the gravity basement match well and the structure of the sedimentary layer in the basin was also revealed. These are the world's first results visually showing the underground structure in the KV and are expected to greatly contribute to future earthquake disaster prevention.

Keywords: Kathmandu Valley, seismic reflection survey

©2019. Japan Geoscience Union. All Right Reserved.

Broadband Microtremor Array Exploration at and around Tribhuvan International Airport, Kathmandu, Nepal

*Toshiaki Yokoi[1], Takumi Hayashida[1], Mukunda Bhattarai[2], Tara Pokharel[2], Suresh Shrestha[2], Chintan Timsina[2], Sunita Bhatarrai[2], Dinesh Nepali[2]

1. International Institute of Seismology and Earthquake Engineering, Building Research Institute, Japan, 2. Department of Mines and Geology, Ministry of Industry, Commerce and Supplies, Nepal

Strong ground motion of long duration and long predominant period around four seconds were observed during the 2015 Gorkha earthquake at the central part of the Kathmandu Valley (KTV), Nepal (Dixit et al. 2015, Bhattarai et al. 2015, Takai et al. 2016, Rajaure et al. 2017), a tectonic basin formed during the Himalayan orogeny due to the collision of the Indian plate to the Eurasian plate (e.g., Sakai et al. 2016). Aimed to reveal the cause of this phenomenon and to make possible the seismic hazard assessment considering on the structure of deep sedimentary layers, the research group to which the authors belong (Group3-SATREPS) has conducted the deep exploration by deploying microtremor arrays (Maximum inter station distance about 1400 m) at few sites using four sets of broadband seismographs (CMG40T, Guralp) for estimating the shear wave velocity structure of deep sediments from Dec. 2016 to Feb. 2018, together with shallow exploration using 2 Hz seismometers (L22D, Sercel) and 4.5 Hz geophones (GS11D, GeoSpace) (Yokoi et al. 2018, SSJ-Fall). In KTV as a whole, the gravity survey had been performed in 2017 by the OYO corp. team which belongs the same research group (Pradhan et al. 2018 (JpGU)) and the reflection survey has been conducted Nov. 2018 by OYO corp. also at the Tribhuvan International Airport (TIA) and at the National Agriculture Research Institute (NARI) located at around 2 km SW of TIA. The deep structure of KTV is gradually getting revealed (Koshika et al. 2019 (JpGU) submitted).
In this poster session, we will report the results of analysis of the microtremor array exploration at and around TIA and NAST, and a hard rock site (Chobar) that we have conducted Dec. 2018 following the above mentioned activities.
The attached figure shows the configuration of observation sites and a summary of the dispersion curves of Rayleigh waves. In the legend, *BDR* (red circles) shows the results given by Hayashida et al. (2018, SSJ-Fall) using tele-seismic surface waves, *CHB* (red “x” s): the phase velocities estimated on the outcropped bedrock of the Chobar hill. *SDB*: Singhadurbar, DMG: Department of Mines and Geology-Narayanhiti Royal Palace Museum, *TEKU*: Teku Gas well of DMG, *KIR*: Kirtipur Campus of the Tribhuvan Univ., *BLJ*: Department of Nepal Bureau of Standard and Metrology at Balaju, *GAU*: Gaucharan, *TIA*: Tribhuvan International Airport, *NAST*: National Academy of Science and Technology-National Agriculture Research Institute.
Acknowledgements: This study was supported by Japan Science and Technology Agency (JST) and Japan International Cooperation Agency (JICA) under the “Science and Technology Research Partnership for Sustainable Development (SATREPS): Integrated Research on Great Earthquakes and Disaster Mitigation in Nepal Himalaya (FY2016-2020)”.

Keywords: Gorkha earthquake, Kathmandu Valley, Broadband Microtremor Array Exploration

©2019. Japan Geoscience Union. All Right Reserved.

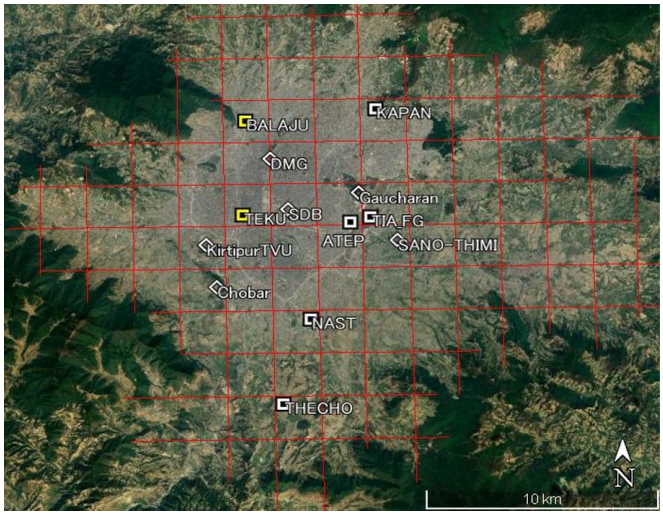

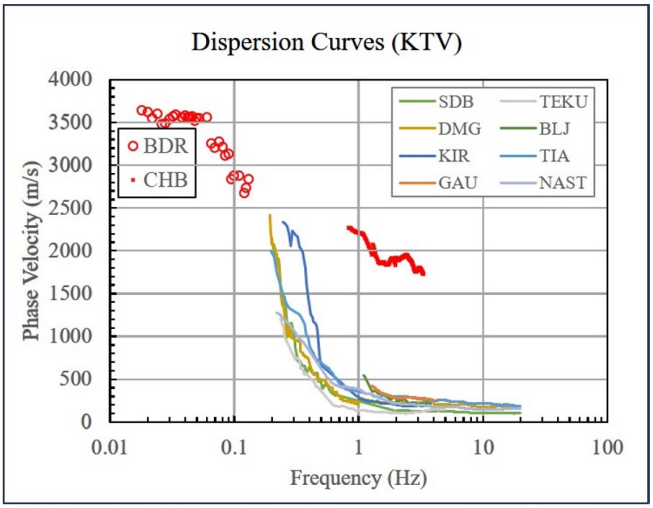

©2019. Japan Geoscience Union. All Right Reserved.

Distribution of average S-wave velocities by small-scale (5 to 15 meters) microtremor arrays in and around Hue City, Thua Thien-Hue province, Vietnam

*Ikuo Cho[1], Makoto OKUBO[2]

1. National Institute of Advanced Industrial Science and Technology, 2. Kochi University

We are promoting earthquake hazard assessment for safe operation of hydroelectric power generation and protection of world cultural heritage for Hue City, Thua Thien-Hue Province, Vietnam. This is a collaborative research with Dr. Nguyen Anh Duong at Vietnam Academy of Science and Technology (VAST). As a part of this research project, we conducted multiple small-scale microtremor array observations in that area and evaluated the distribution of shallow average S-wave velocities.

We began this microtremor research with providing a technical support to researchers at VAST. First, the authors conducted a microtremor array observation at four sites in and around the Hanoi City on 20th and 21st October, 2017, as a practical training of microtremor observation. On the premise of applying the SPAC method, we deployed linear-shaped arrays with a length of about 30 m using a three-component servo-velocimeter. We recorded microtremors for 1 to 2 hours at each site. Since the authors brought two seismometers (three-component servo-accelerometers) from Japan, we deployed two-point arrays along with their array at intervals of 5 to 30 m, and compared the analysis results with those from the VAST observation apparatuses.

On the next step, the VAST research team and the authors conducted microtremor array observations at seven sites in Hue City on 17-19th March, 2018. At each site we deployed triangle-shaped arrays with side lengths of 5 m and 15 m. We also deployed a linear array with a length of 12 m. Those arrays consisted of 4.5 Hz vertical geophones. In addition to this, we deployed two-point arrays with two seismometers brought from Japan. We set the observation durations from about 30 minutes to 1 hour at each site. There were existing subsurface data by refraction surveys at these sites, and therefore, we compared our analysis results with them. As a result, the analysis results of microtremors were consistent with those existing data.

Through the above preparatory period, the VAST research team conducted microtremor array observations at 126 sites in and around the Hue City (observation area of about 11km x 14 km) in a period from June to July 2018 (19 days in total). More specifically, they deployed triangular arrays with side lengths of 5 m and 15 m at 89 sites and a linear array with a length of 12 m at 37 sites. Vertical 4.5Hz geophones were used to consist seismic arrays. The observation duration was set to 30 minutes at each site.

We applied the SPAC method to the array data thus obtained and identified the Rayleigh-wave phase velocities. We read the phase velocities with the wavelengths of 13 m, 25 m and 40 m and interpreted them as average S-wave velocities to the depths of 10 m, 20 m, and 30 m, respectively. The spatial distribution of average S-wave velocities thus obtained is consistent with the geological map in and around the Hue City. In near future, we will improve the accuracy of soil evaluations by adding H/V spectral data at each site of array observation.

©2019. Japan Geoscience Union. All Right Reserved.

Keywords: microtremor, array, surface wave, Vietnam

©2019. Japan Geoscience Union. All Right Reserved.

Microtremor Array Exploration in the Syiah Kuala University, Banda Aceh, Indonesia

*Makoto OKUBO[1]

1. Natural Science Cluster, Kochi University

We deployed microtremor array survey at Syiah Kuala University in Banda Aceh, Indonesia to clarify a seismic amplification by subsurface S-wave structure. Banda Aceh, located at northern end of Sumatra island, was seriously damaged by the tsunami caused by the 2004 Sumatra earthquake. At the tsunami evacuation, we first have to consider the safe route that does not corrupted, damaged and flooded. Therefore, we plan to understand the seismic amplification distribution as fundamental material. Our results will be available to make a future plan to reconstruction/renovate architectures.

We visited to Banda Aceh at January, 2019, and carried out microtremor exploration using with linear array and triangle array at 17 sites. We used are three 5 Hz geophones and one 1 kHz sampling GPS synchronised data logger for survey. In the case of triangle array, we always used 1.7 m side length. This side length is corresponding to 1.0 m array radius. In the other case, that is linear array, distances of each sensors (A, B, and C) are, A-B:1.7 m, B-C:2.7 m, and A-C:4.4 m. We Assumed these lengths are the array radius for each exploration, and applied SPAC method (*c.f.* Aki 1957). We used a tool, as known as BIDO2.0 (Cho, 2010) to analyze recorded waveforms and estimate dispersion curves.

By using obtained dispersion curves, we determined 3 averaged S wave velocities and roughly velocity structure. Roughly velocity structure was estimated by simple conversion method by using 1/2 wavelength law with linear array's dispersion curves. And three Averaged S-wave velocities AVS10, AVS20 and AVS30 were estimated from the Rayleigh wave phase velocities corresponding to the wave length of 13 m, 25 m and 40 m, respectively. By a preliminary analysis, we obtained result that a thicker low S-wave velocity layer exists along the river and the coastline. This result implies that plain part of Banda Aceh was developed on the old delta made by river and sea. This situation of subsurface structure will be strongly affect to the seismic amplification.

We will discuss in detail at the presentation.

Acknowledgements:
We thanks to Dr. Muksin Umar, Ms. Wiwik and Mr. Arif, they were attended and cooperated to our microtremor array survey in Syiah Kuala University. This study is supported by JSPS KAKENHI Grant Number 17H0457751.

Keywords: Microtremor, Array exploration, Subsurface S-wave velocity structure

©2019. Japan Geoscience Union. All Right Reserved.

Turkey-Japan Joint Project on Modeling of Geological Structures for Strong Ground Motion Simulations due to Crustal Earthquakes in Eskisehir Basin, Turkey, by Using Seismic Interferometry Method

*Mehmet Safa Arslan[1], Kosuke Chimoto[2], Asim Oguz Ozel[1], Hiroaki Yamanaka[2]

1. ISTANBUL UNIVERSITY-CERRAHPASA, 2. TOKYO INSTITUTE OF TECHNOLOGY

Understanding the seismic hazard of specific area, depends on the regional 2D/3D underground structure on wave propagation. In the frame of the bilateral project between Turkey and Japan, we aim at observing ground motion parameters, crustal activities, underground structures, and improvement of seismic hazard maps. The seismic interferometry method (SIM) is one of the tools to investigate the surface-wave propagation. The method goals to obtain green’ s function (GF) by using ambient noise data. Cross-correlations (CC) between the two pairs of stations’ continuous records, reveal GF and provide group and phase velocities of surface waves. We analyze one-year vertical component broadband data from 8 stations deployed and affiliated with ANANET (Eskisehir Anadolu University Local Seismic Network). Interstation distances between the designated stations are in the range of ~23-139 km. After getting the CC functions, group velocity dispersion curves will be obtained for selected correlation paths in particular to address the azimuthal dependence of the velocity field. Averaging the dispersion curves, in other saying analyzing the group velocities and waveforms typical of these observations, we attempt to estimate the S-wave velocity structure model inside the Eskisehir basin. This study is supported by the Joint Research Project under the Bilateral Program of the Japan Society for the Promotion of Science (JSPS) and The Scientific and Technological Research Council of Turkey (TUBITAK) under Grant TUBITAK 116Y524.

Keywords: seismic interferometry, cross correlation function, S-wave structure, group velocities, Turkey

©2019. Japan Geoscience Union. All Right Reserved.

Nonlinear Ground Motion Response During the 2016 Meinong Taiwan Earthquake

*Kuo-Liang Wen[1], Chun-Te Chen[2]

1. National Central University, Department of Earth Sciences, 2. Academia Sinica, Institute of Earth Sciences

The Meinong Taiwan earthquake occurred on February 6, 2016, at 03:57 (UTC+8) with M_L 6.6. The strong ground motion induced the soil liquefaction in Sinshih and Annan districts. To investigate the nonlinear site response during Meinong mainshock, the degree of nonlinear site response (DNL) which summation of the horizontal to vertical spectral ratios (HVSR) differences between weak-motions and Meinong mainshock records from the Taiwan Strong Motion Instrumentation Program (TSMIP) network are calculated. We compare the DNL values with the ground motion parameters such as peak ground acceleration (PGA), peak ground velocity (PGV), and also the ratio between PGV and Vs30. The DNL shows a positive correlation with ground motion intensity, particular with PGV, and the surface site conditions also leading the DNL strength. We also applied a stochastic method for modeling the ground motion of the Meinong earthquake with site correction by the HVSR of weak and strong motions respectively. The percentage of PGA reduction calculated in this study can be an indicator of the spatial distribution of the degree of nonlinear soil effects of the 2016 Meinong Taiwan earthquake.

Keywords: Meinong earthquake, nonlinear site response, HVSR

©2019. Japan Geoscience Union. All Right Reserved.

Earthquake damage of the 2017 Pohang earthquake in South Korea

*Mikyung Choi[1], Sun-Cheon Park[1], Dong-Hyo Sohn[1], Seolhan You[1], Jongsun Sun[1], Seongheum Cho[1], Duk-Kee Lee[1]

1. Korea Meteorological Administration

Pohang earthquake with a magnitude of ML 5.4 occurred on November 15, 2017. This earthquake caused more damage than the 2016 Gyeongju earthquake (ML 5.8). Modified Mercalli intensities were assigned from residential property damage report in the Pohang area. Major damage type was wall crack of building. Maximum intensity was MMI VIII. Result of damage analysis from damage report reveals that the main damage area was distributed within a radius of about 20 km distance from the epicenter. And sand and mud volcanoes were observed in many places.
Between 16 November and 31 December 2017, 10 temporary seismic stations were deployed to record aftershocks and site effect of the Pohang earthquake. Ground motion generated by an earthquake is controlled by several factors, such as source characteristics, propagation path, surface geology, topography. Using recordings of aftershocks, we analyzed the ground motion at two seismic stations near the epicenter and another two seismic stations located on sedimentary rock and bedrock. We compared amplitude and predominant frequencies of ground motion with damage analysis results. Mapping and characterization of the damage for this earthquake is an opportunity to provide useful information on the damage of future possible earthquake in South Korea.

Keywords: Pohang earthquake, earthquake damage, ground motion

©2019. Japan Geoscience Union. All Right Reserved.

[J] Oral | S (Solid Earth Sciences)：S-EM Earth's Electromagnetism

Mon. May 27, 2019 9:00 AM - 10:30 AM JST | Mon. May 27, 2019 12:00 AM - 1:30 AM UTC | 304 3F

[S-EM19] Electromagnetic Induction in the Earth and Planetary Interiors, and Tectono-Electromagnetism

convener:Koki Aizawa(Institute of Seismology and Volcanology, Faculty of Sciences, Kyushu University), Tetsuo Matsuno(Kobe Ocean Bottom Exploration Center, Kobe University), Chairperson:Tetsuo Matsuno, Koki Aizawa

This session welcomes papers on electromagnetism in the Earth and planetary interiors. The topics include but not limited to electromagnetic phenomena associated with earthquakes and volcanism, electrical conductivity structure, laboratory experiments, results of simulations, new equipment for observation, and methods of data analysis.

9:00 AM - 9:15 AM JST | 12:00 AM - 12:15 AM UTC

[SEM19-01] Repeated measurements of the Self-Potential at Akita-Yakeyama, Iwate and Kurikoma volcanoes

*Shin'ya Sakanaka[1], Yasiaki Sawada[3], Kenta Kato[2], Inoue Yusuke[1], Kobayashi Takuya[1], Ryuichi Takei[1], YUYA TADA[2], Muhammad Faizul Nizam Bin Zainudin[2], Tomoya Moriwaki[2] (1.Graduate school of International Resource Sciences, Akita University, 2.Faculty of International Resource Sciences, Akita University, 3.Faculty of International Resource Sciences, Akita University (gradusted in 2018))

9:15 AM - 9:30 AM JST | 12:15 AM - 12:30 AM UTC

[SEM19-02] Evaluation of surface conductivity of unsaturated Berea sandstone and porous glasses

*Ryosuke Umezawa[1], Makoto Katsura[1], Satoru Nakashima[1] (1.Department of Earth and Space Science, Graduate School of Science, Osaka University)

9:30 AM - 9:45 AM JST | 12:30 AM - 12:45 AM UTC

[SEM19-03] Observational and theoretical waveforms of electromagnetic signals generated by the motional induction effect before the arrival of seismic waves

*Ken'ichi Yamazaki[1] (1.Disaster Prevention Research Institute, Kyoto University)

9:45 AM - 10:00 AM JST | 12:45 AM - 1:00 AM UTC

[SEM19-04] Effect of reference data on geomagnetic transfer functions

*Shinya Sato[1], Tada-nori Goto[1] (1.Kyoto Univesity, Graduate School of Engineering)

10:00 AM - 10:15 AM JST | 1:00 AM - 1:15 AM UTC

[SEM19-05] Reliability estimation of magnetotelluric inversion result based on the Principle Component Analysis and Markov Chain Monte-Carlo method

Hisatoshi Koji[1], *Tada-nori Goto[1] (1.Graduate School of Engineering, Kyoto University)

10:15 AM - 10:30 AM JST | 1:15 AM - 1:30 AM UTC

[SEM19-06] Probing one-dimensional electrical anisotropy in the oceanic upper mantle from seafloor magnetotelluric array data

*Tetsuo Matsuno[1], Kiyoshi Baba[2], Hisashi Utada[2] (1.Kobe Ocean Bottom Exploration Center, Kobe University, 2.Earthquake Research Institute, The University of Tokyo)

Repeated measurements of the Self-Potential at Akita-Yakeyama, Iwate and Kurikoma volcanoes

*Shin'ya Sakanaka[1], Yasiaki Sawada[3], Kenta Kato[2], Inoue Yusuke[1], Kobayashi Takuya[1], Ryuichi Takei[1], YUYA TADA[2], Muhammad Faizul Nizam Bin Zainudin[2], Tomoya Moriwaki[2]

1. Graduate school of International Resource Sciences, Akita University, 2. Faculty of International Resource Sciences, Akita University, 3. Faculty of International Resource Sciences, Akita University (gradusted in 2018)

We will report the SP (Self-Potential) anomalies at Akita-Yakeyama, Iwate, and Kurikomayama volcanoes. They are active volcanoes along the boundary of Akita and Iwate prefectures and their volcanic activities are relatively high recently.

SP measurements and SP anomalies at those volcanoes were reported by some researchers. We are still carrying out the SP measurements there repeatedly so as to monitor the activities of the volcanoes.

We conducted the SP measurements along the mountain trail from Tamagawa hot spring to Goshougake hot spring at Akita-Yakeyama in 2007 and 2017. At Mt. Iwate the SP measurements were conducted along the Yakebashiri trail up to the summit in 1999, 2004 and 2017. At northern part of Mt. Kurikoma we walked from the Nagorigahara moor, went through the summit and returned back anti-clockwised along the trail with SP electrodes in 2018. The result of the previous SP measurement in Kurikoma volcano can be found in the part of the Aizawa (2010) and we can investigate the time-lapse SP anomalies on these volcanoes.

We adopted the leap-frog measurement method with a 50 m cable, copper-copper sulfate electrodes, and a digital multi-meter (voltmeter). The latitude and longitude data were recorded by the handy GPS receiver (like as Garmin product). Although in the measurements of the leap-frog method might be easily piled up each error of the measured value at a site, a short cable can be easier handled than a longer cable over the length of a couple of kilometers using by the total-potential measurement method. The long and thin cable is sometimes cut apart by animals or human beings and unfortunately we have to return back to the cut point all the way to fix it.

On the compiling the SP data in different years we draw the SP curves along the cumulated distance. Since the cumulated distances of the SP measurements are sometimes up to several kilometers, the lengths of the cumulated distance are sometimes different by more than 100 m in the data of the respective years. We measure the SP on the same mountain trail but the end of the cable at each measurement is not always at the same point and the SP paths are slightly different in year to year on the measurements. This is the reason why the difference of the cumulated distance in different years. The problem might be happened also with the measurements of the total-potential method. To solve it, we set a model path with the function of the cumulated distance on the trail map in advance and the measured site were relocated (projected) onto the model path referred by GPS locations. After that we successfully and comfortably compare the SP data on the same trails.

At Akita-Yakeyama and Iwate volcanoes, we cannot find out the outstanding time variations of SP anomalies but the acquired SP data can be use the monitor the active volcanoes.

©2019. Japan Geoscience Union. All Right Reserved.

Keywords: self potential, active volcano, leap frog method, copper-copper sulfate electrode, Akita-Yakeyama volcano, Iwate volcano

©2019. Japan Geoscience Union. All Right Reserved.

Evaluation of surface conductivity of unsaturated Berea sandstone and porous glasses

*Ryosuke Umezawa[1], Makoto Katsura[1], Satoru Nakashima[1]

1. Department of Earth and Space Science, Graduate School of Science, Osaka University

Electrical conduction of rocks composed of insulating minerals are known to depend on degree of water saturation, distribution of pore water, pore size and pore structure. Electrical conduction in rocks is considered to be composed of conductions in bulk water and on mineral surfaces. The electrical double layer (EDL), a layer with adsorbed ions on mineral surfaces (Stern layer) and gradients of ion concentrations (diffuse layer), has thickness characteristic length of the diffuse layer (Debye length). Surface conduction becomes important, when bulk water in rock pore decreases, such as in unsaturated rocks and less porous rocks with thin grain boundary water. Since quantification of dissolved ions in rocks with thin grain boundaries is difficult, quantitative description of surface conduction remains poor.
In this study, in order to examine surface conduction with known dissolved ion concentrations, electrical conductivity of a sandstone and porous glasses were measured for varying water saturation and ion concentrations. Berea sandstone (predominant pore diameter: about 40 μm) and Shirasu porous glass (SPG) membranes (SPG technology; uniform pore sizes: 1.0, 0.5, and 0.2 μm) were saturated with aqueous solutions having varying NaCl concentrations (0, 0.001, 0.01, 0.1 mol L^{-1}). Electrical conductivity values were measured for frequencies from 0.1 Hz to 1 MHz while drying.
Effects of surface conduction of Berea sandstone and SPG membranes were compared by their specific surface conductivity values, which were evaluated by conduction models using surface complexation model, and were discussed in relation to water film thickness and Debye length.

Keywords: Water saturation, electrical conductivity, ion concentration, Debye length, surface conductivity

©2019. Japan Geoscience Union. All Right Reserved.

Observational and theoretical waveforms of electromagnetic signals generated by the motional induction effect before the arrival of seismic waves

*Ken'ichi Yamazaki[1]

1. Disaster Prevention Research Institute, Kyoto University

Earthquake ruptures and consequent ground motions generates variations in the electromagnetic (EM) field by means of variety of conversion processes in the Earth’s crust. The generated EM signals are referred to as seismo-EM signals. Some of the earlier works have reported seismo-EM signals that are observed prior to the arrival of seismic waves [e.g. Iyemori et al. 1996 (JGG); Honkura et al. 2002 (EPS); Okubo et al. 2011 (EPSL)], which are sometimes referred to as “early seismo-EM signals”. Theoretical calculations have been conducted to identify the generation mechanisms of the observed seismo-EM signals assuming some of candidate conversion mechanisms including the electrokinetic effect [Haartsen and Pride 1997 (JGR)], the motional induction effect [Gao et al. 2014 (JGR)], the piezomagnetic effect [Yamazaki 2016 (GJI)] and the piezoelectric effect [Ogawa and Utada 2000a (PEPI), 2000b (EPS)]. However, definitive answers have not been obtained, particularly for the case of early seismo-EM signals.

The objective of this work is to compare theoretical time-series of seismo-EM signals arising from the motional induction effect with observational one by means of simple numerical models. In an earlier work, Gao et al. [2014] consider the same problem by assuming uniform full-space model with analytical solutions. Their results imply that theoretical early seismo-EM signals in this situation are far smaller than observed ones. In the present work, I consider a model composed from conductive half-space that represents the Earth’s crust and another half-space that represents the air as an insulator. In frequency domain, governing equations in this situation are reduced to ordinary differential equations by applying the Hankel transform, which can be solved analytically. Seismo-EM Solutions of the original equations are then obtained after the inverse Hankel transform. Time-series of seismo-EM signals are then obtained after the inverse Fourier transform.

The comparisons between observed and theoretical seismo-EM variations are performed for two cases: one is the phenomena observed at the time of 1999 Izmit earthquake, Turkey [Honkura et al. 2002], and the other is that observed at the time of 2008 Iwate-Miyagi earthquake, Japan [Okubo et al. 2011]. Early seismo-EM signals observed for these two earthquakes have different characters. For the case of Izmit earthquake, signals appeared only after seismic waves reach close to the observational site. In contrast, for the case of Iwate-Miyagi earthquake, EM signals emerges just after the onset of seismic ruptures. Numerical calculations assuming the motional induction effect reasonably account the feature of signals for the Izmit earthquake, but do not account that for the Iwate-Miyagi earthquake.

Keywords: electromagnetic field, motional induction effect, seismic ground motion

©2019. Japan Geoscience Union. All Right Reserved.

Effect of reference data on geomagnetic transfer functions

*Shinya Sato[1], Tada-nori Goto[1]

1. Kyoto Univesity, Graduate School of Engineering

It is well-known that inter-station transfer functions (TFs), which are derived generally using two sites (as following Schmucker 1984; Neska 2006), are effected by source field. Also, we sometimes use three sites for deriving TFs in order to reduce the noises mixed in geomagnetic data. These 2 or 3 sites-based TFs have been used for evaluating the spatial characteristics of source field. However, the 3 sites-based TFs (i.e., using site 1, site 2 and reference site) do not always reflect the source field’s condition between site 1 and site 2, and can possibly be effected by the source field’ characteristics at reference site. Also, the evaluation of source field’s condition at time-frequency domain (i.e., at the stage of spectra or spectrograms) will be more accurate. Therefore, for the evaluation we used Multi-Channel Nonnegative Matrix Factorization (MC-NMF, suggested by Sato and Goto 2018), which can extract components included in several geomagnetic spectrograms. Moreover, we derived the condition of geomagnetic events’ spatial-characteristics, which triggers the effect of reference data on 3 sites-based TFs. In order to verify that the TFs are effected by the reference site, we derived the temporal changes in 3 sites-based TFs replacing the reference sites. As a result, we founded that the TFs changed not only temporally but dependent on the reference site and the interpretation of source field’s spatial characteristics was different dependent on the reference site. For exposing the cause, we evaluated the spatial-characteristics of geomagnetic events using MC-NMF. The evaluated spatial-characteristics of geomagnetic events were corresponding with the condition triggering the effect of reference data on TFs as mentioned above. We succeeded to expose the cause of TFs’ variation triggered by reference data evaluating the spatial-characteristics of geomagnetic events at time-frequency domain. Using TFs together with MC-NMF, the interpretation of source-field’s spatial characteristics will be with high accuracy.

Keywords: Spatial characteristics of source field, Inter-station Transfer Function, Remote reference

©2019. Japan Geoscience Union. All Right Reserved.

Reliability estimation of magnetotelluric inversion result based on the Principle Component Analysis and Markov Chain Monte-Carlo method

Hisatoshi Koji[1], *Tada-nori Goto[1]

1. Graduate School of Engineering, Kyoto University

Magnetotelluric (MT) method is used for detection of electrical conductive materials such as fluid, clay, partial melt and so on. Subsurface resistivity structure is generally estimated by an inverse algorism, based on the least-square scheme using observed apparent resistivity and phase. The reliability of the optimal model in the inversion procedure should be discussed together with seeking the “better” model having the lower data misfit than the optimal model. However, the sophisticated method is not well developed for the magnetotelluric survey, except for the simple test based on a number of forward modeling, constrained inversions and so on, or simple visualization of sensitivity of model parameters. In this study, for a quantitative visualization of reliability of optimal model parameters, we propose a new way of the numerical test of the model based on the Markov Chain Monte-Carlo (MCMC) methods. Since the MCMC cannot solve a number of unknowns in model parameters, we adopted the principle component analysis (PCA) to reduce unknowns in the model obtained by MT inversion code. First, for testing the PCA ability in subsurface image analysis, various two-dimensional (2-D) resistivity models are decomposed by PCA. As a result, we succeeded to extract the “major features” of 2-D resistivity model, especially by using first to third principle components. Then, we tested the MCMC algorithm with changing parameters of “major features” of 2-D model, such as its resistivity, width, thickness, horizontal and vertical locations. In a case of a simple two-prism model, we confirmed that the reliability of low and high resistive anomalies are shown in the probability density functions obtained by MCMC. We also found that some parameters (e.g., thickness and resistivity of an anomalous body) indicate a tread-off relationship as mentioned in the previous studies, and also found the reliable range of parameters even under the trade-off. We then applied this technique to the magnetotelluric data obtained at a field experiment. In consequence, anomalies in the optimal model are detected properly by PCA, and the reliable range of model parameters based on the MCMC method are similar to those inferred by the conventional forward calculations. We conclude that our proposed method can be widely applied to magnetotelluric exploration, even to the three-dimensional inversion.

Keywords: Principle Component Analysis, Markov Chain Monte-Carlo method, Magnetotelluric Inversion

©2019. Japan Geoscience Union. All Right Reserved.

Probing one-dimensional electrical anisotropy in the oceanic upper mantle from seafloor magnetotelluric array data

*Tetsuo Matsuno[1], Kiyoshi Baba[2], Hisashi Utada[2]

1. Kobe Ocean Bottom Exploration Center, Kobe University, 2. Earthquake Research Institute, The University of Tokyo

Electrical anisotropy in the oceanic upper mantle provides important clues on mantle structure and dynamics if it is confirmed from seafloor magnetotelluric (MT) data. Here we try to probe electrical (azimuthal) anisotropy in the oceanic upper mantle by analyzing recent seafloor MT array data from the northwestern Pacific at 130-145 Ma seafloor. We propose a method, in which an isotropic 1-D model is first obtained from seafloor MT data through iterative correction for topographic distortion, then anisotropic properties are inferred as deviations from the isotropic 1-D model. We investigate the performance of this method through synthetic forward modeling and inversion, using plausible anisotropic 1-D models and actual 3-D bathymetry and topography for the target area. Synthetic tests reveal that the method can detect the electrical anisotropy in the conductive upper mantle or the electrical asthenosphere. We also compare the performance by using two rotational invariant impedances and two topographic correction equations. An application of the method to two seafloor MT array data in the northwestern Pacific reveal anisotropic inversion models, showing the possible presence of electrical anisotropy in two layers in a conductive mantle of <100 Ω-m at 50-250 km depth. Anisotropic signals are larger in shallower layers for both array areas, while anisotropic azimuths (or most conductive directions) and depths to the two layers are different for two array areas even at similar seafloor ages with the horizontal distance of ~1,000 km. Most conductive directions mostly align rather to directions of past seafloor spreading or their perpendicular directions, than a direction of current plate motion and are inconsistent with fastest directions of seismic azimuthal anisotropy. The electrical anisotropic signals may dominantly result from mantle dynamics in array-scale (~500 km or over), like small-scale convection and the formation of seafloor in the past, over in Pacific basin scale.

©2019. Japan Geoscience Union. All Right Reserved.

[J] Oral | S (Solid Earth Sciences)：S-EM Earth's Electromagnetism

Mon. May 27, 2019 10:45 AM - 12:15 PM JST | Mon. May 27, 2019 1:45 AM - 3:15 AM UTC | 304 3F

[S-EM19] Electromagnetic Induction in the Earth and Planetary Interiors, and Tectono-Electromagnetism

convener:Koki Aizawa(Institute of Seismology and Volcanology, Faculty of Sciences, Kyushu University), Tetsuo Matsuno(Kobe Ocean Bottom Exploration Center, Kobe University), Chairperson:Koki Aizawa, Tetsuo Matsuno

This session welcomes papers on electromagnetism in the Earth and planetary interiors. The topics include but not limited to electromagnetic phenomena associated with earthquakes and volcanism, electrical conductivity structure, laboratory experiments, results of simulations, new equipment for observation, and methods of data analysis.

10:45 AM - 11:00 AM JST | 1:45 AM - 2:00 AM UTC

[SEM19-07] The Analysis of magnetotelluric sounding data on Kikai submarine caldera.

*Toki Hirose[1], Tetsuo Matsuno[2,1], Nobukazu Seama[1,2], Yuki Okizono[4], Hiroshi Ichihara[3], Hiroko Sugioka[1,2], Yoshiyuki Tatsumi[2,1] (1.Department of Planetology, Graduate School of Science, Kobe University, 2.Kobe ocean Bottom Exploration Center, Kobe University, 3.Graduate school of environmental studies, Nagoya University, 4.Department of Planetology, Faculty of Science, Kobe University)

11:00 AM - 11:15 AM JST | 2:00 AM - 2:15 AM UTC

[SEM19-08] Role of Fluids in the earthquake generation: The Nagamachi-Rifu reverse fault, NE Honshu, Japan

*Sabri Bulent Tank[1], Yasuo Ogawa[2] (1.Bogazici University, 2.Tokyo Institute of Technology)

11:15 AM - 11:30 AM JST | 2:15 AM - 2:30 AM UTC

[SEM19-09] Audio-frequency Magnetotelluric Survey of the Tsuyama-hoppou Fault, Yamasaki Fault Zone, southwest Japan.

*Satoru Yamaguchi[1], Daisuke Takakuwa[2], Akira Mimura[1], Kazuki Fkue[1], Shigehiro Katoh[3], Hideki Murakami[4], Shinichi Takakura[5] (1.Department of Geosciences, Graduate School of Science, Osaka City University, 2.Faculty of Science, Osaka City University, 3.The Museum of Nature and Human Activities, 4.Science and Technology Unit, Research and Education Faculty, Kochi University, 5.Geological Survey of Japan, Institute of Advanced Industrial Science and Technology)

11:30 AM - 11:45 AM JST | 2:30 AM - 2:45 AM UTC

[SEM19-10] Three dimensional resistivity structure around the focal region of the 2016 Kumamoto earthquakes

*Koki Aizawa[1], Hisashi Asaue[2], Katsuaki Koike[3], Shinichi Takakura[4], Toru Yoshinaga[10], Makoto Uyeshima[5], Takao Koyama[5], Ryokei Yoshimura[7], Ken'ichi Yamazaki[7], Shintaro Komatsu[7], Yusuke Yamashita[7], Hiroshi Ichihara[9], Mitsuru Utsugi[8], Kaori Tsukamoto[12], Dan Muramatsu[12], Yoshiko Teguri[1,11], Kazunari Uchida[1], Hideaki Hase[6], Azusa Shito[1], Satoshi Matsumoto[1], Takeshi Matsushima[1], Hiroshi Shimizu[1] (1.Institute of Seismology and Volcanology, Faculty of Sciences, Kyushu University, 2.Laboratory on Innovative Techniques for Infrastructures, Kyoto University, 3.Environmental Geosphere Engineering, Department of Urban Management, Graduate School of Engineering, Kyoto University, 4.Geological Survey of Japan, National Institute of Advanced Industrial Science and Technology, 5.Earthquake Research Institute, University of Tokyo, 6.GERD, 7.Disaster Prevention Research Institute, Kyoto University, 8.Aso Volcanological Laboratory, Institute for Geothermal Sciences, Graduate School of Science, Kyoto University, 9.Earthquake and Volcano Research Center, Graduate School of Environmental Studies, Nagoya University, 10.Kumamoto University, 11.Japan Meteorological Agency, 12.Department of Earth and Planetary Sciences, Graduate School of Science, Kyushu University)

11:45 AM - 12:00 PM JST | 2:45 AM - 3:00 AM UTC

[SEM19-11] **A research report on the fundamental investigations of an electrical resistivity structure beneath Chugoku and Shikoku regions, southwestern Japan(2018)**

*Ichiro Shiozaki[1], Tomofumi Uto[1], Makoto Uyeshima[2], Hiroshi Hataoka[3], Yasuo Ikezoe[3], Shinji Yamamoto[3], Tatsuya Noguchi[1], Daiki Furuichi[4], Yuki Murayama[4], Kohei Matsushita[4], Hideki Murakami[5], Naoto Oshiman[6], Yoshihisa Iio[6], Kazuya Ando[7] (1.Graduate School of Engineering, Tottori University, 2.Earthquake Research Institute, The University of Tokyo, 3.Technical Department, Tottori University, 4.Faculty of Engineering, Tottori University, 5.Research and Education Faculty , Kochi University, 6.Disaster Prevention Research Institute, Kyoto University, 7.San'in Kaigan Geopark Museum of the Earth and Sea)

12:00 PM - 12:15 PM JST | 3:00 AM - 3:15 AM UTC

[SEM19-12] Fluid distribution beneath central and southern Kyushu imaged by 3-D electrical resistivity model

*Maki Hata[1], Hiroshi Munekane[2], Hisashi Utada[1], Tsuneomi Kagiyama[3] (1.Earthquake Research Institute, the University of Tokyo , 2.Geospatial Information Aurhotiry of Japan, 3.Aso Geopark Promotion Council)

The Analysis of magnetotelluric sounding data on Kikai submarine caldera.

*Toki Hirose[1], Tetsuo Matsuno[2,1], Nobukazu Seama[1,2], Yuki Okizono[4], Hiroshi Ichihara[3], Hiroko Sugioka[1,2], Yoshiyuki Tatsumi[2,1]

1. Department of Planetology, Graduate School of Science, Kobe University, 2. Kobe ocean Bottom Exploration Center, Kobe University, 3. Graduate school of environmental studies, Nagoya University, 4. Department of Planetology, Faculty of Science, Kobe University

Kikai submarine caldera locates on the south waters of Kagoshima. The caldera was formed after super eruption on 7.3ka, and have formed huge lava dome since the eruption(Tatsumi et al., 2018). A main aim of this study is to determine the electrical resistivity structure beneath the Kikai caldera, and estimate the distriution of melt, magma chamber and thermal anomaly. As one step to the main aim, this study presents the results of calculations of apparent resistivity and phase, and estimating 1D inversion resistivity structure models after their correction for topographic distortion.
Measurements of the time variations of electric and magnetic fields at the seafloor were conducted at 10 sites with a sample rate of 8 Hz for about 20 days. At the four of those after the surveys, measurements were switched to the sample period of 60 s for about half year. Observed data with sample rate of 8 Hz were processed as followings: (1) downsampled to 1 Hz, (2) corrected by comparing the instrument clocks with GPS time, (3) detrended for longer-periods than 1 day, and (4) corrected instrument inclines. The instrument coordinates were transformed to geographic coordinate system. After these processing, we extracted the data without noises which attribute to the shaking of instrument and calculated magnetotelluric(MT) inpedances, apparent resistivity, and phase using the BIRRP method(Chave and Thomson, 2004). Kanoya magnetic observatory was used as the magnetic remote reference.
Estimated apparent resistivities were characterized with respect to periods and elements, whose characteristics are commonly found at all the sites. With respect to periods, off-diagonal apparent resistivity ranges 1Ωm to 10Ωm at the periods of 21s, and increases to 10Ωm to 100Ωm at a longer periods of 1024s. As for elements, diagonal elements are smaller than non-diagonal elements by a degree of magnitude. Estimated phases were characterized by xy and yx elements that are within the range of the first quadrant and the third quadrant respectively.
Effect of topography on MT impedances are modeled with with FS3D(Baba and Seama, 2002). Using The results of FS3D and the method of removing of topographic distortion(Nolasco et al., 1998), MT impedance are corrected for bathymetry. Using the corrected MT impedance, the 1D electrical resistivity structure models at the observation sites are estimated by OCCAM1D inversion program(Constable et al., 1987). The 1-D structure models are compared to 3-D electrical resistivity structure model(Matsuno et al., presented at this meeting) .

Keywords: magnetotelluric, Kikai caldera, 1D inversion

©2019. Japan Geoscience Union. All Right Reserved.

Role of Fluids in the earthquake generation: The Nagamachi-Rifu reverse fault, NE Honshu, Japan

*Sabri Bulent Tank[1], Yasuo Ogawa[2]

1. Bogazici University, 2. Tokyo Institute of Technology

The Japanese island arc was drastically influenced by the occurence of the 2011 Tohoku-Oki earthquake (M9) which also effected the volcanic activity and modified the local seismicity both of which are proven to be related to crustal fluid distribution. Therefore, for understanding the dynamic behavior of the region and for making further comparisons, developing an electrical conductivity model that enables to image the fluid’ s presence and capacity by means of analyses based on high-quality magnetotellurics data collected prior to the Tohoku-Oki earthquake at 61 sounding locations near the Nagamachi-Rifu Fault, Northeast Honshu, Japan, became an important task. Magnetotelluric data collected along three profiles that orthogonally cross the almost NE-SW geo-electric strike were used to image the epicentral region of this active reverse fault and its vicinity. State-of-the-art three-dimensional data-space inversion schemes were applied on the wide-band magnetotellurics data to map the fluid-rich and/or -depleted zones. Inversions included 0.3 Ohmm cells with realistic bathymetry on both sides of the initial model representing the Japan Sea in the west and Pacific Ocean in the east to realize the ocean effect. Resulting models were compared with prior and post seismicity of the main event.

Keywords: Magnetotellurics, Nagamachi-Rifu fault, Fluids

©2019. Japan Geoscience Union. All Right Reserved.

Audio-frequency Magnetotelluric Survey of the Tsuyama-hoppou Fault, Yamasaki Fault Zone, southwest Japan.

*Satoru Yamaguchi[1], Daisuke Takakuwa[2], Akira Mimura[1], Kazuki Fkue[1], Shigehiro Katoh[3], Hideki Murakami[4], Shinichi Takakura[5]

1. Department of Geosciences, Graduate School of Science, Osaka City University, 2. Faculty of Science, Osaka City University, 3. The Museum of Nature and Human Activities, 4. Science and Technology Unit, Research and Education Faculty, Kochi University, 5. Geological Survey of Japan, Institute of Advanced Industrial Science and Technology

The Yamasaki fault zone (YFZ) is a ~80 km long, typical left-lateral strike-slip fault zone extending WNW from eastern part Okayama prefecture to southeastern part of Hyogo prefecture. The YFZ consists of the Nagisen fault zone, the main part of the YFZ, and the Kusadani Fault. The Nagisen fault zone show different features in fault activity (e.g. general strike, mean slip rate, the latest event) and seismic activity. Fewer earthquakes are occurred around the Nagisen fault zone compared with around the main part of the YFZ, and the Kusadani Fault.
Earthquake Research Committee (2013) reported that the Nagisen fault zone consists of the Nagisen Fault and Tsuyama-hoppou Fault (abbreviated as TYN Fault here after) and Okada *et al*. (2016) further divided the Nagisen Fault into the Koegatawa Fault, Nagiike Fault, and Nagisen Fault (we referred to them as Nagisen Fault Group here after) and reported fault displacement is recognized along the Nagisen Fault Group. While the TYN Fault is classified into the fault of Certainty II and Degree of activity C, and is annotated as “no fault activity after Middle Pleistocene is recognized” (The Research Group for Active Faults of Japan, 1991). That is, the TYN Fault is still an unknown fault and further survey is required.
Fukue *et al*. (2018) made a magnetotelluric (MT) survey using an audio-frequency MT (AMT) method, which is suitable for revealing shallow part (0 - 2 km in depth) with high spatial resolution, along the line across the Nagiike and Nagisen Faults, then established the two-dimensional resistivity model (NGS model). They pointed out that the Nagiike Fault is recognized as an clear resistivity boundary but that the Nagisen Fault is not recognized in the model.
Aiming to reveal subsurface structure of the unknow TYN Fault, we made an AMT survey along the line of ~4 km long across the TYN Fault and determined the two-dimensional resistivity model along the line. In this paper, we present outline of observation, procedures of data & model analysis, and the resistivity model, then discuss the subsurface structure of the TYN Fault comparing the NGS model.

Keywords: Yamasaki Fault Zone, Tsuyama-hoppou Fault, active fault, resistivity, Magnetotellurics

©2019. Japan Geoscience Union. All Right Reserved.

Three dimensional resistivity structure around the focal region of the 2016 Kumamoto earthquakes

*Koki Aizawa[1], Hisashi Asaue[2], Katsuaki Koike[3], Shinichi Takakura[4], Toru Yoshinaga[10], Makoto Uyeshima[5], Takao Koyama[5], Ryokei Yoshimura[7], Ken'ichi Yamazaki[7], Shintaro Komatsu[7], Yusuke Yamashita[7], Hiroshi Ichihara[9], Mitsuru Utsugi[8], Kaori Tsukamoto[12], Dan Muramatsu[12], Yoshiko Teguri[1,11], Kazunari Uchida[1], Hideaki Hase[6], Azusa Shito[1], Satoshi Matsumoto[1], Takeshi Matsushima[1], Hiroshi Shimizu[1]

1. Institute of Seismology and Volcanology, Faculty of Sciences, Kyushu University, 2. Laboratory on Innovative Techniques for Infrastructures, Kyoto University, 3. Environmental Geosphere Engineering, Department of Urban Management, Graduate School of Engineering, Kyoto University, 4. Geological Survey of Japan, National Institute of Advanced Industrial Science and Technology, 5. Earthquake Research Institute, University of Tokyo, 6. GERD, 7. Disaster Prevention Research Institute, Kyoto University, 8. Aso Volcanological Laboratory, Institute for Geothermal Sciences, Graduate School of Science, Kyoto University, 9. Earthquake and Volcano Research Center, Graduate School of Environmental Studies, Nagoya University, 10. Kumamoto University, 11. Japan Meteorological Agency, 12. Department of Earth and Planetary Sciences, Graduate School of Science, Kyushu University

In December 2018, we have conducted broad-band magnetotelluric (MT) observation around Hinagu fault and Uto Peninsula, which are close to the focal regions of the 2016 M_{JMA} 7.3 Kumamoto earthquakes. Since the resistivity structure of these regions are not well imaged by the previous 3-D inversion by using the 80 MT sites (Aizawa et al., 2017, Sgepss fall meeting), we acquired the new data by using the Metronix ADU-07 system and the telluric loggers (NT System Design ELOG1K). We will present new 3-D resistivity structure and argue its relationship to the hypocenters that are relocated by using the double difference method and 3-D seismic velocity structure (Shito et al., 2017, GRL).

Acknowledgment

We are greatly indebted to the land owners for their permission for field campaigns. The geomagnetic data used for the remote-reference processing were provided by the Kakioka Geomagnetic Observatory of JMA. This work is partly supported by MEXT KAKENHI Grant Number JP16H06298, the Ministry of Education, Culture, Sports, Science and Technology of Japan under its Earthquake and Volcano Hazards Observation and Research Program, and Earthquake Research Institute, The University of Tokyo under Joint Usage Program.

Keywords: resistivity structure, magnetotellurics, Kumamoto earthquake

©2019. Japan Geoscience Union. All Right Reserved.

A research report on the fundamental investigations of an electrical resistivity structure beneath Chugoku and Shikoku regions, southwestern Japan(2018)

*Ichiro Shiozaki[1], Tomofumi Uto[1], Makoto Uyeshima[2], Hiroshi Hataoka[3], Yasuo Ikezoe[3], Shinji Yamamoto[3], Tatsuya Noguchi[1], Daiki Furuichi[4], Yuki Murayama[4], Kohei Matsushita[4], Hideki Murakami[5], Naoto Oshiman[6], Yoshihisa Iio[6], Kazuya Ando[7]

1. Graduate School of Engineering, Tottori University, 2. Earthquake Research Institute, The University of Tokyo, 3. Technical Department, Tottori University, 4. Faculty of Engineering, Tottori University, 5. Research and Education Faculty , Kochi University, 6. Disaster Prevention Research Institute, Kyoto University, 7. San'in Kaigan Geopark Museum of the Earth and Sea

In order to contribute to a reduction in damage caused by earthquakes and volcanic eruptions, heterogeneities of crustal and upper mantle structure should be clarified based on fundamental investigations of electrical resistivity structure in Chugoku and Shikoku regions, southwestern Japan arc.
Our research group has shown that there is a clear relationship between resistivity and seismicity in the San'in and Shikoku regions. In the eastern part of San'in region, it was found that a conductive area exists in the deep crust part under the seismic region, which is a resistive area, along with the seismic activity area stretching nearly in the east and west direction. Assuming that inland earthquakes occur because of local stress concentration caused by heterogeneity beneath a seismic activity band(Iio, 2009), it is necessary to improve spatial data and to clarify the heterogeneity in this area hereafter.
On the other hand, in the Shikoku district, it was suggested that the distinctive low resistivity region exists in the upper crust mainly from the survey results in the outer belt, and that there is a clear relation between the low resistivity and low seismicity in the central and the western area. In order to understand the earthquake phenomenon, it is important to clarify the generation environment and the principle as well as the activity style of the slow earthquake (Obara(2017)).
In this background, a Magnitude (M6.6) Earthquake in the Central Tottori Prefecture on October 21, 2016 occurred. In order to elucidate the heterogeneous structure of the lower crust beneath the seisimic region, we set up several survey lines across the central focal region of the Chubu region to carry out wideband MT observation at 12 sites in the observations gap area around this region.
By integrating the existing MT data, we tried model analysis using the program code of Ogawa and Uchida (1996) assuming that this region had a two-dimensional structure of EW strike direction harmonious with the seismic active band. According to the 2D model, we confirmed the southern limit of the low resistivity part existing in the deep crust of the focal region.
In the Chugoku and Shikoku district, we aimed to determine the 3D resistivity structure as a whole, and as in the 2017 research, 1D Occam inversion analysis based on determinant impedance was performed and integrated with existing MT data to estimate the preliminary spatial resistivity structure distribution. As a result, in San'in region, it is generally harmonious with the former studies, the low resistivity region in the deep crust continues to exist in the east-west direction with a certain scale.
In the Shikoku district, the resistivity in the mid crust shows the existence of a relative high/low resistivity boundary in the vicinity of the MTL is prominent, consistent with the existing research. Although there is a observation gap on the Seto Inland Sea side, continuity to the south of the low resistivity region of the San'in region is suggested with respect to the northern extension of the high resistivity crust. Moreover, when we look at the correspondence with the epicentral distribution of the crustal earthquake at this depth, there is clear correspondence with the high resistivity region in the north side of inner zone around

©2019. Japan Geoscience Union. All Right Reserved.

the Median Tectonic Line. This relevance is common knowledge with that in the San'in region.
Acknowledgments : This study was supported by the Ministry of Education, Culture, Sports, Science and Technology (MEXT) of Japan, under its Observation and Research Program for Prediction of Earthquakes and Volcanic Eruptions, and also supported by 2018 Tottori Prefecture Environmental academic research promotion promotion project. We would like to express sincere gratitude for the Nittetsu Mining Consultants Co. Ltd. kindly let us use their continuous geomagnetic records as remote references. We used joint research equipment of Kyoto University Disaster Prevention Research Institute for observation of this research.

Keywords: electrical resistivity, Chugoku and Shikoku regions, fundamental investigations

©2019. Japan Geoscience Union. All Right Reserved.

Fluid distribution beneath central and southern Kyushu imaged by 3-D electrical resistivity model

*Maki Hata[1], Hiroshi Munekane[2], Hisashi Utada[1], Tsuneomi Kagiyama[3]

1. Earthquake Research Institute, the University of Tokyo , 2. Geospatial Information Aurhotiry of Japan, 3. Aso Geopark Promotion Council

The island of Kyushu is characterized by a high concentration of active Quaternary volcanoes along a volcanic front of N30˚E–S30˚W associated with the subduction of the Philippine Sea Plate. Some of the active volcanoes exist in southern Kyushu (the southern volcanic region), whereas no volcano exists in central Kyushu (the non-volcanic region). Most of volcanoes in the southern volcanic region exist in the Kagoshima Graben, whose formation was created with ejecting huge pyroclastic flows by the Quaternary volcanism. The Kirishima volcano group appears in Kakuto-Kobayashi caldera on the northern edge of the graben. Shinmoe-dake of the Kirishima volcano group experienced a magmatic eruption of the VEI 3 in 2011 and ash emissions in March 2018. Moreover, Iwo-yama of the Kirishima volcano group experienced hot material ejections in April 2018. Besides, Sakurajima volcano in the southern part of the graben has experienced 153–1,355 small eruptions per year for the last 10 years (the Japanese Meteorological Agency).
The Philippine Sea Plate, whose subduction involves the formation of the volcanic island of Kyushu, in and around Kyushu is classified into three portions: a younger portion, an older portion, and the other part of the Kyushu–Palau Ridge between the two portions. A non-volcanic region distributes in central Kyushu above a junction where the three portions of the subducting Philippine Sea Plate contact with each other. Owing to the subduction of the Philippine Sea Plate, moment magnitude 7-class thrust earthquakes have repeatedly occurred in the Hyuga-nada, lying offshore of the southeast Kyushu. In addition, recent studies using continuous global-navigation-satellite-system data have revealed that long-term slow slip events and short-term slow slip events occur in the Hyuga-nada. Besides, most of the earthquakes in the land area occur along three tectonic lines: Oita-Kumamoto tectonic line, Usuki-Yatsushiro tectonic line and Butsuzo tectonic line.
Fluid distribution in the mantle wedge is an essential factor for the seismic activity and magmatism leading to volcanic activity. Electromagnetic sounding data have high sensitivity to a few percent of interconnected fluids (aqueous fluid and melt). In this study, we generated a three-dimensional (3-D) electrical resistivity model by inverting magnetotelluric data, which covers the active southern volcanic region and the non-volcanic region, to examine the fluid distribution in the mantle wedge beneath Kyushu. We find three important conductive features in the 3-D model. A magma system and a fluid system imaged as two vertical conductors relating to slab-derived fluid, which exist along the volcanic front beneath the southern volcanic region and the non-volcanic region, respectively. The other conductor, relating to the presence of slab-derived fluid and serpentinite in the mantle wedge, appears at a blank area of the slow slip events.

Keywords: 3-D electrical resistivity model, Fluid distribution, magmatism, seismic activity, mantle wedge

©2019. Japan Geoscience Union. All Right Reserved.

[J] Poster | S (Solid Earth Sciences)：S-EM Earth's Electromagnetism

Mon. May 27, 2019 3:30 PM - 5:00 PM JST | Mon. May 27, 2019 6:30 AM - 8:00 AM UTC | Poster Hall International Exhibition Hall8, Makuhari Messe_11

[S-EM19] Electromagnetic Induction in the Earth and Planetary Interiors, and Tectono-Electromagnetism

convener:Koki Aizawa(Institute of Seismology and Volcanology, Faculty of Sciences, Kyushu University), Tetsuo Matsuno(Kobe Ocean Bottom Exploration Center, Kobe University)

This session welcomes papers on electromagnetism in the Earth and planetary interiors. The topics include but not limited to electromagnetic phenomena associated with earthquakes and volcanism, electrical conductivity structure, laboratory experiments, results of simulations, new equipment for observation, and methods of data analysis.

[SEM19-P01] Effects of absolute humidity on contact resistance between dry rock sample surface and electrodes

*Takeshi Suzuki[1], Ryokei Yoshimura[2], Ken'ichi Yamazaki[2], Naoto Oshiman[2] (1.Graduate School of Science, Kyoto University, 2.Disaster Prevention Research Institute, Kyoto University)

[SEM19-P02] Japanese geomagnetic field variation model based on the IGRF (2): modeling on the oblique Mercator projection

*Tsutomu Ogawa[1] (1.Earthquake Research Institute, the University of Tokyo)

[SEM19-P03] Examination of criteria to remove the influence of the Sq-field variations from electromagnetic field spectra for a better estimation of regional electromagnetic responses

*RUIBAI LI[1], Hisayoshi Shimizu[1], Kiyoshi Baba[1], Hisashi Utada[1] (1.Earthquake Research Institute, the University of Tokyo)

[SEM19-P04] **Study on long-term variation of geoelectric field observation**

*Ren Ozeki[1], Ikuko Fujii[1] (1.Japan Meteorological Agency)

[SEM19-P05] Deep electrical conductivity structure of Eastern Marmara, Turkey by long period magnetotellurics

*Sabri Bulent Tank[1], Naoto Oshiman[2], Mustafa Karas[1], Ryokei Yoshimura[2], Yasuo Ogawa[3] (1.Bogazici University, 2.Kyoto University, 3.Tokyo Institute of Technology)

[SEM19-P06] Audio-frequency magnetotelluric survey on the northern edifice of the Kurikoma volcano, northeast of Japan

*Kobayashi Takuya[1], Shin'ya Sakanaka[1], Tomoki Tsutsui[1], Muhammad Faizul Nizam Bin Zinudin[1], Inoue Yusuke[1], Kenta Kato[1], Tomoya Moriwaki[1], YUYA TADA[1], Ryuichi Takei[1] (1.Akita University)

[SEM19-P07] A three-dimensional crustal electrical resistivity model beneath southern Tohoku district, NE Japan

*Aoi Motoyama[1], Yasuo Ogawa[2], Makoto Uyeshima[3], Koichi Asamori[4], Toshihiro Uchida[5], Hideaki Hase[6], Takao Koyama[3], Shin'ya Sakanaka[7], Yusuke Yamaya[5], Koki Aizawa[8], Masahiro Ichiki[1] (1.Graduate school of science, Tohoku university, 2.Volcanic Fluid Research Center, School of Science, Tokyo Institute of Technology, 3.Earthquake research institute, the university of Tokyo, 4.Japan Atomic Energy Agency, 5.National institute of advanced industrial science and technology, 6. Geothermal Energy Research & Development Co., Ltd, 7.Graduate School of International Resource Sciences Department of Earth Resource Engineering and Environmental Science, Akita University, 8.Graduate school of science, Kyusyu university)

[SEM19-P08] Magnetotelluric survey on the northern foot of Meakandake volcano

*Tomohiro Inoue[1], Takeshi Hashimoto[1] (1.Institute of Seismology and Volcanology, Faculty of Science, Hokkaido University)

[SEM19-P09] Hydrothermal system of Kuttara Volcanic Group inferred from 3D resistivity modeling (2)

*Ryo Tanaka[1], Midori Hayakawa[2], Takeshi Hashimoto[1], Wataru Kanda[3], Yuichi Morita[4], Hiroshi Aoyama[1], Makoto Uyeshima[4] (1.Institute of Seismology and Volcanology, Hokkaido University, 2.Mitsui Oil Exploration Co., Ltd. Geothermal Business Division, 3.Volcanic Fluid Research Center, School of Science, Tokyo Institute of Technology, 4.Earthquake Research Institute, The University of Tokyo)

[SEM19-P10] 3D magnetic structure of Aso volcano

*Mitsuru Utsugi[1] (1.Aso Volcanological Laboratory, Institute for Geothermal Sciences, Graduate School of Science, Kyoto University)

[SEM19-P11] The piezomagnetic field produced by an ellipsoidal pressure source: A preliminary result

*Yoichi Sasai[1] (1.Earthquake Prediction Research Center, Institute of Oceanic Research and Development, Tokai University)

Effects of absolute humidity on contact resistance between dry rock sample surface and electrodes

*Takeshi Suzuki[1], Ryokei Yoshimura[2], Ken'ichi Yamazaki[2], Naoto Oshiman[2]

1. Graduate School of Science, Kyoto University, 2. Disaster Prevention Research Institute, Kyoto University

Resistivity measurements of rock under various conditions are essential for accurately interpreting geoelectromagnetic survey results. However, the contact resistance between the rock sample and measuring electrodes is a problem in measuring the resistivity of a rock sample. Because the measurement of high contact resistance on the dry rock surface is particularly difficult, its characteristics have not been well studied.
In order to investigate the characteristics of contact resistance, we have developed a measurement method of high contact resistance. By using the method, we measured high contact resistance between the dry granite surface and the electrode made of conductive epoxy. Considering the interaction between atmospheric moisture and rock samples, the contact resistance was repeatedly measured under different humidity conditions.
We confirmed the contact resistance decreased with increasing absolute humidity. A clear relationship exists between contact resistance and absolute humidity, and the relationship was approximated by an exponential function. This result suggests that increasing the contact area between the electrode and the rock surface with rising humidity. Moisture in the atmosphere may have caused improvement of contact condition by filling the microscopic gap in the contact surface.

Keywords: contact resistance, atmospheric Moisture, absolute humidity, contact area, conductive epoxy, granite

©2019. Japan Geoscience Union. All Right Reserved.

Japanese geomagnetic field variation model based on the IGRF (2): modeling on the oblique Mercator projection

*Tsutomu Ogawa[1]

1. Earthquake Research Institute, the University of Tokyo

For geomagnetic field variation observations around tectonic areas to detect the variations related to tectonic activities in Japan, geomagnetic field model or geomagnetic field variation model around Japan with high accuracy is indispensable as a reference field. The geomagnetic field variation model around Japan proposed by Abe and Miyahara (2015) using the principal component analysis of geomagnetic data is a statistical model but not a physical model of the field variation, for the vector field model is not in general divergence-free. The model also lacked the error estimation for arbitrary positions. The present study evaluates the new geomagnetic field variation model around Japan which corrects the following two points in the model by Ogawa (2018, JpGU) which attempted to overcome the difficulties in the previous work: 1) the geomagnetic field variation is expressed in the Cartesian coordinate system on the map using the oblique Mercator projection of the Japanese island arc along NE-SW direction with a great ellipse centered and oriented along the direction, instead of the Mercator projection, and 2) annual variations in the model residuals of data which correlate with sensor temperature variations at the geoelectromagnetic continuous measurement stations of GIAJ are removed.

The new geomagnetic field variation model is expressed with the magnetic scalar potential by a cubic polynomial with respect to the coordinates in the coordinate system with its origin on the ground in the SE area of Ishikawa prefecture, expressing the difference of the 1-day geomagnetic data at 5 observatories of JMA and GIAJ and 10 stations of GIAJ from the IGRF, between 2005 and 2014. By obtaining the time series of expansion coefficients using the robust least square technique, the model shows the following features: 1) the mean of the model residuals amounts to 1.28nT, 2) by the leave-one-out cross-validation, the mean of the prediction error amounts to 1.94nT, 3) the mean of the prediction error at all the observation points obtained by the propagation of the jackknife standard error of expansion coefficients amounts to 1.16nT, as large as the mean of the model residuals, and 4) the mean of the prediction errors at Chichijima station of JMA, data of which are unused for the model, because of the large distance of the station from the principal part of the Japanese island arc, amounts to 5.06nT.

The mean prediction error along the principal part of the Japanese island arc estimated using the propagation of the jackknife standard errors of estimated expansion coefficients amounts at most to about 2nT for the horizontal two components and about 3nT for the vertical component, respectively. The present geomagnetic field variation model around Japan has the accuracy of a few nT for the principal part of the Japanese island arc.

Keywords: Geomagnetic field variation model, oblique Mercator projection, Leave-one-out cross-validation, jackknife standard error

©2019. Japan Geoscience Union. All Right Reserved.

Examination of criteria to remove the influence of the Sq-field variations from electromagnetic field spectra for a better estimation of regional electromagnetic responses

*RUIBAI LI[1], Hisayoshi Shimizu[1], Kiyoshi Baba[1], Hisashi Utada[1]

1. Earthquake Research Institute, the University of Tokyo

Electromagnetic (EM) responses such as magnetotelluric (MT) impedance and geomagnetic depth sounding (GDS) response (or tipper) in the period range between several minutes to one day are used to study the electrical conductivity in the upper mantle. Spatially uniform and quasi-random magnetic field variations due to geomagnetic disturbances are considered as the source field in regional EM induction studies using the EM responses. However, the magnetic field variations in the period range from to seconds (mixed excitation band, or ME band) contain those with different spatial structure such as the solar quiet (Sq) daily variations and those induced by the ocean tide. Careful treatment of EM field data is necessary to estimate responses in the ME band that reflect actual conductivity structure. For example, Baba et al. (2010) estimated the EM responses in the period range from to seconds using a method based on Fourier transform after removing line spectra of EM field variations at periods of Sq field variations that include the higher harmonics and constituents of ocean tides. However, it was shown that the estimated responses in the ME band still included the influence of Sq field variations (Shimizu et al., 2011).

In this study we try to estimate EM responses that are less influenced by the Sq field variations. We employed line spectra of EM field obtained by using Sompi method, so called wave element (or namiso) (e.g., Kumazawa et al.,1990, Asakawa eta al.,1988), to estimate the EM responses in order to avoid the influence of the Sq field variations that could be contained in continuous spectra. Also, three conditions are applied to select appropriate wave elements from observed ones for EM response estimations. First is to select wave elements of which eastward component have common phase or that close to each other at two stations. This can avoid wave elements influenced by the Sq field variations since their westward propagation causes systematic phase difference of the magnetic field for supposed longitude difference and apparent period, which is determined by the longitudinal wave number of the variation. Second is to select magnetic field spectra that are linearly polarized in horizontal-vertical plane, because that influenced by the Sq field variations are expected to be more elliptically polarized in the plane than those suitable for regional EM response estimation. Ellipticity of the polarization ellipse is used to apply the condition. Third is to select those which have small ratio of the vertical to the horizontal magnetic field components, because the Sq field variations contain significant vertical magnetic field component that can cause larger amplitude of tipper than those from plane wave. It was confirmed that estimated phase difference, ellipticity, and vertical to horizontal field ratio showed a signature of Sq field variations in the ME band but not at a period shorter than seconds.

In this presentation, we are going to show the characteristics of the observed phase difference, ellipticity, and vertical to horizontal field ratio with respect to the period. Criteria to apply the conditions are assumed based on theoretical estimate of the magnetic field due to Sq principle mode and the induced field in assumed one dimensional Earth. The EM responses obtained by applying each condition are shown and the improvement or influence in the obtained responses, as a result, are discussed quantitatively.

©2019. Japan Geoscience Union. All Right Reserved.

Asakawa, E., et al. (1988). *J. Geomagn. Geoelec.,*40: 447-463.

Baba, K., et al. (2010).*Phys. Earth planet. Inter.,*183: 44-62.

Kumazawa, M., et al. (1990). *Geophys. J. Int.,*101: 613-630.

Shimizu, H., et al. (2011). *Geophys. J. Int.,*186: 193-206.

©2019. Japan Geoscience Union. All Right Reserved.

Study on long-term variation of geoelectric field observation

*Ren Ozeki[1], Ikuko Fujii[1]

1. Japan Meteorological Agency

Kakioka Magnetic Observatory, Japan Meteorological Agency, has observed the geomagnetic and geoelectric fields for several decades at Kakioka, Kanoya and Memambetsu. Vitage differences between two electrodes are observed in the geoelectric field observation. The baseline length is about 200-300m and the electrodes are installed at 3m deep. The data of the geoelectric field are used worldwide as a unique data set to investigate induced electric fields for last several decades.It is slightly troublesome for us to use the geoelectric field data set by Kakioka Magnetic Observatory because the geoelectric fields at three sites shows long-term variations and especially the north-south component of the geoelectric field at Kakioka clearly changes.Although some studies (e.g., Morinaga and Toya, 2015; Okawa et al., 1995) reported that this long-term variation is related to rain, details of how this long-term variation occurs are still unknown. This study aims to reveal the cause of the long-term variation.
Based on Morinaga and Toya (2015) and Fujii et al.(2007), we focus on geological structures around the electrode at the south end of the north-south line at Kakioka. We infer the geological structure from the distribution of the electrical resistivity.
The electrical prospecting was applied to an area of 20m x 20m with the south electrode as the center. Observations were conducted in March, May and October giving 7 observation lines around the south electrode, 2 lines around the east electrode, and 1 line around a boring hole (fig.1). Apparent resistivity was estimated from the observed currents and voltage differences.
We assume that the subsurface structure is one-dimensional and three layers are stratified. An optimal model of the resistivity distribution was obtained by inversion. All lines show a high resistivity layer at the surface followed by a low resistivity layer and then a high resistivity layer at the bottom. The thickness of the first layer is increased eastward from the south electrode.
The optimal model was compared with a boring profile obtained near the investigated area. We interpret that the resistive surface layer is permeable top soil and the second conductive layer is impermeable clay(Figure 2).We suspect that rain water flows on the top of clay to the east and the south electrode suffers from larger amount of water than the other electrodes.

Keywords: geoelectric field observation, electrical prospecting

©2019. Japan Geoscience Union. All Right Reserved.

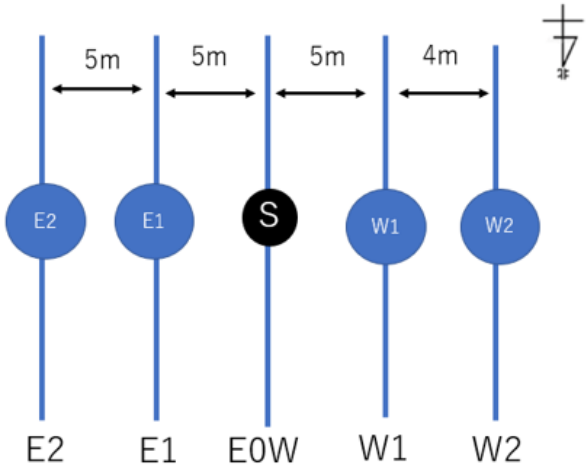

Figure 1

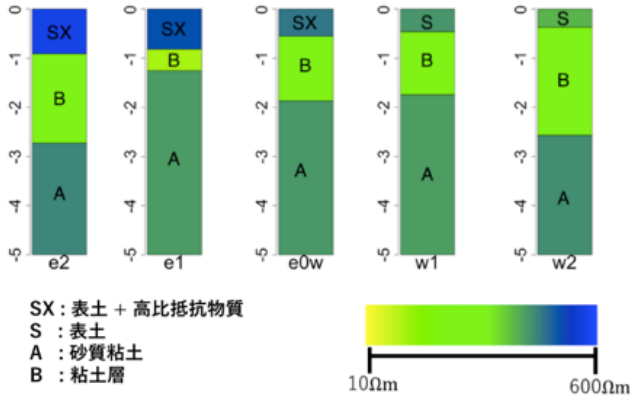

Figure 2

©2019. Japan Geoscience Union. All Right Reserved.

Deep electrical conductivity structure of Eastern Marmara, Turkey by long period magnetotellurics

*Sabri Bulent Tank[1], Naoto Oshiman[2], Mustafa Karas[1], Ryokei Yoshimura[2], Yasuo Ogawa[3]

1. Bogazici University, 2. Kyoto University, 3. Tokyo Institute of Technology

The electrical resistivity structure of a 100 km x 100 km region at northwestern Anatolia was examined by using long period magnetotelluric data with the aim to image the geo-electrical features at the lower crust and upper mantle. The electromagnetic impedance tensor elements were obtained for eighteen sounding locations within a period range of 20-13000 seconds. The soundings were distributed over the epicentral region of the 1999 Izmit earthquake and its vicinity including the Pontides in the north, Intra-Pontid transition zone and Sakarya Continent in the south. Three-dimensional data-space inversions of the long period magnetotellurics data were performed iteratively to achieve the electrical resistivity structure. In order to determine and overcome the complexities caused by the coast effect that arise due to presence of the conductive Black Sea, the dimensionality of the magnetotellurics data were examined in detail by means of induction arrows and phase tensor ellipses. These complexities may have transpired due to the seismically active branches of the North Anatolian Fault and presence of the Intra-Pontide Suture, too. The final resistivity models revealed a low resistivity zone trapped between two highly resistive blocks of Istanbul Zone in the north and Sakarya Continent in the south. This low conductivity zone coincides with the two main branches of the North Anatolian Fault and may be promoting the seismic activity in both of the branches.

Keywords: Magnetotellurics, North Anatolian Fault, Izmit earthquake, Fluids

©2019. Japan Geoscience Union. All Right Reserved.

Audio-frequency magnetotelluric survey on the northern edifice of the Kurikoma volcano, northeast of Japan

*Kobayashi Takuya[1], Shin'ya Sakanaka[1], Tomoki Tsutsui[1], Muhammad Faizul Nizam Bin Zinudin[1], Inoue Yusuke[1], Kenta Kato[1], Tomoya Moriwaki[1], YUYA TADA[1], Ryuichi Takei[1]

1. Akita University

Now we focus the Kurikoma volcano closely at the triple junction of borders of Akita, Iwate and Miyagi prefectures, northeast of Japan. The eruption style of the Kurikoma volcano is magma eruption and phreatic eruption. The Kurikoma volcano is one of important active volcanos and its most recent striking activity was a phreatic eruption in 1944. The site of 1994 eruption is now remained as a crater lake called Lake Showa. Besides the Lake Showa, volcanic gas is even now emitted upstream of a gorge called Jigoku-dani. So far the several researches have reported 2- and 3-dimensional resistivity structures of the crust including the Kurikoma volcano (e.g. Mishina, 2009; Ichihara et al., 2014). Mishina (2009) firstly reported the 2-dimensional resistivity structure targeting the deep volcanic fluid beneath the Kurikoma volcano. The result of Mishina (2009) suggested the existence of volcanic fluid at the depth of several kilometers under the volcanic structure. In this study, we aim to find the structure which becomes the key to the occurrence of the phreatic eruption from the shallow resistivity structure directly under the Kurikoma volcano obtained by AMT survey.

We carried out an AMT survey across a high temperature upstream of a gorge from August to November 2018. This method uses magnetotelluric responses derived from variations in the natural audio-frequency band (approximately 1 to 10^4 Hz) of the electromagnetic field to estimate the resistivity structure in an area down to a depth of a few kilometers. The AMT data were collected at thirteen locations. Two components of the electric field and three components of the magnetic field were recorded for 3 to 24 h overnight using a Phoenix Geophysics MTU-5A system (Phoenix Geophysics Ltd., Toronto, ON, Canada). In this study, the concept of phase tensor (Caldwell et al., 2004) and induction vector (Parkinson, 1962) was used to evaluate the dimensionality of structure and the characteristic of resistivity distribution. From the results of the phase tensor, the skew angle was less than 5 degree and the ellipticity was less than 0.2 in the range of frequencies higher than 10 Hz. Therefore, it is suggested that the structure around 1 km below the subsurface is a relatively homogeneous structure. Also, in the frequency range lower than 10 Hz, the direction of the induction vectors tends to point towards a lava dome called Tsurugi-dake.

The 2D inversion model with TM-mode data was constructed using the inversion code developed by Ogawa and Uchida (1996). Only the data with small phase-tensor skew angles (< 5 degrees) were used in the 2D inversion in this study, because the data with large skew angles are inconsistent with the 2D structure assumed in the area.

The final model has three characteristic features. The first is that the low resistivity region (C1) beneath the fumarolic area and hot spring zone. The second is that high resistivity zone (R1) is distributed in the lower layer of the low resistivity region (C1) immediately below the high temperature fumarolic area (Jigoku-dani, Iwo-yama and Yuge-yama). It is suggested that the high resistivity zone (R1) is a high temperature body or a steam dominant region because high temperature fumarolic area exposes the surface of the ground. The third is the existence of a relatively high resistivity zone (R2) is located in the lower layer of the eastern part of the low resistivity region (C1). Since the phreatic eruption crater traces are distributed in the eastern part of the east west cross section, it is suggested that R2 is a trace of activities of the phreatic eruption in the past.

©2019. Japan Geoscience Union. All Right Reserved.

Keywords: Resistivity structure, AMT, Kurikoma volcano, Phreatic eruption, Hydrothermal system

©2019. Japan Geoscience Union. All Right Reserved.

A three-dimensional crustal electrical resistivity model beneath southern Tohoku district, NE Japan

*Aoi Motoyama[1], Yasuo Ogawa[2], Makoto Uyeshima[3], Koichi Asamori[4], Toshihiro Uchida[5], Hideaki Hase[6], Takao Koyama[3], Shin'ya Sakanaka[7], Yusuke Yamaya[5], Koki Aizawa[8], Masahiro Ichiki[1]

1. Graduate school of science, Tohoku university, 2. Volcanic Fluid Research Center, School of Science, Tokyo Institute of Technology, 3. Earthquake research institute, the university of Tokyo, 4. Japan Atomic Energy Agency, 5. National institute of advanced industrial science and technology, 6. Geothermal Energy Research & Development Co., Ltd, 7. Graduate School of International Resource Sciences Department of Earth Resource Engineering and Environmental Science, Akita University, 8. Graduate school of science, Kyusyu university

On the basis of seismological and geodetic results, Hasegawa et al. (2005) proposed a vertical crustal model profile in the across-arc direction beneath Tohoku district. In the model, the magma and/or fluid reservoir lies in the lower crust beneath Ou backbone range running along the central arc of Tohoku district. On the other hand, Uyeshima et al. (2016) recently modeled a two-dimensional (2-D) crustal electrical resistivity profile in which there are three distinguished conductors in the lower crust, that is, beneath the fore-arc, volcanic front and back-arc of southern Tohoku district. The fore-arc conductor underlies the seismicity beneath around Iwaki city activated after 2011 Tohoku-oki earthquake. However, another 2-D resistivity profile 50 km northwards parallel to the Uyeshima et al’ s one shows no distinguished fore-arc conductor, but volcanic front and back-arc conductors (Motoyama et al., 2018). These results indicate geofluids rise up beneath a part of fore-arc beneath southern Tohoku district. Moreover, a part of back-arc of the southern Tohoku district may have conductive lower crust. Because previous resistivity models are limited to 2-D, we estimated a 3-D resistivity model beneath southern Tohoku district with compiling previous magnetotelluirc (MT) data, and discussed geofluids distribution beneath fore-arc and back-arc.

We compiled electromagnetic data at 118 sites and reassessed all MT responses and geomagnetic transfer functions. The $\Phi_{2,}$ square root of determinant of phase tensor (Caldwell et al., 2004), shows high values in the northern part of back-arc, and in the southern part of fore-arc and of Ou backbone range 10-100 s period range.

To estimate 3-D resistivity model, we used WSINV3D_MPI inversion code (Siripunvaraporn & Egbert, 2009). So far, we have estimated a preliminary model using only MT responses. A vertical model profile in the across-arc direction shows an oblique conductor from deeper crust beneath back-arc to shallower crust beneath Ou backbone range. On the other hand, almost all forearc has high resistivities in the crust. The map view of resistivity profile at 22.5 km depth shows a conductor distributes beneath from Murakami city of back-arc to Koriyama city of Ou backbone range. The calculation is still running by using both MT responses and geomagnetic transfer functions, and we will show the results and discussion in this presentation.

Keywords: Magnetotellurics, geofluids

©2019. Japan Geoscience Union. All Right Reserved.

Magnetotelluric survey on the northern foot of Meakandake volcano

*Tomohiro Inoue[1], Takeshi Hashimoto[1]

1. Institute of Seismology and Volcanology, Faculty of Science, Hokkaido University

We performed a broadband MT survey in the northern part of Mt. Meakandake in August and September in 2018. Mt. Meakandake is one of the active volcanoes in the southwestern part of Akan caldera in eastern Hokkaido. Recently, a remarkable ground inflation has been reported on the northeastern foot of Meakandake. We planned a magnetotelluric survey to investigate the electrical structure across the deformation source. In this study, we describe the features of our MT data and show the 1-D models as a preliminary modeling.

The Geospatial Information Authority of Japan (2018) reported a remarkable crustal inflation on the basis of the GNSS observation and InSAR analysis from late 2016 through 2017. They modeled the deformation as an opening of the sill-like crack (about 11 km long and 2 km wide) at a depth of about 6 km on the northeastern foot of Meakandake. As the estimated deformation source was large, we considered that it might be imaged as a low resistivity anomaly, if it was related to magma or hydrothermal system. Investigating the subsurface structure across such an extensive inflation source will also contribute to understanding the magma plumbing system of the Akan area. Around Meakandake, a MT survey was previously conducted in the eastern area as a part of the Geothermal Development Promotion Survey (NEDO, 1992). More recently, an AMT survey was performed across the summit along a NE-SW direction as a part of volcano study of Meakandake (Takahashi et al., 2018). However, because of the limited sounding depths, the electrical structure near the above-mentioned deformation source has not been clarified yet.

Therefore, in this study, we newly deployed twelve broadband-MT sites along a NW-SE trending survey line across the longer side of the inflation source on the northern to eastern foot of the volcano. We used four set of the MTU-5/5A system (Phoenix Geophysics) for the campaign. We acquired the time series of the electric field in two components and the magnetic field in three components for 3 to 7 days for each site. In calculating the response functions, we used the SSMT2000 software and applied the remote reference processing using the magnetic field data Sawauchi in Iwate Prefecture that was provided by Nittetsu Mining Consultants Co., Ltd.

Contrary to our first expectation, the induction vectors and phase tensors suggested an electrical regional strike of N60ºW, which was almost parallel to the survey line. Thus, in this study, we sought a provisional 1-D modelling instead of the 2-D analysis in an unpreferable direction. We estimated 1-D resistivity structures using the Occam’s inversion (Constable et al., 1987), in which we used the ssq impedance (Szarka and Menvielle, 1997; Rung-Arunwan et al., 2016) as the input data. In this inversion, we only used a frequency range, in which the responses showed approximately a 1-D feature.

The inverted 1-D models exhibited a distinct low resistivity layer (1-10 Ωm, hereinafter called, C1) at depths around a few hundred meters at all sites. In addition, at the sites in the SE half of the survey line, another low resistivity layer of approximately 10 Ωm (hereinafter called, C2) was found at a depth around 2-4 km.

According to the NEDO (1992)’s borehole logs that were drilled at about 1 km east of our survey line,

©2019. Japan Geoscience Union. All Right Reserved.

the low resistivity layer C1, which is common to all the sites, is likely to correspond with the volcanic tuff layers in the Miocene indicating weak alteration with montmorillonite and/or chlorite. Meanwhile, the deeper low–resistivity layer C2 is recognized only at the locations near the above–mentioned inflation source. In addition, C2 is shallower at the sites near the inflation source. For this reason, we suspect that C2 has some relation to the inflation source, although their depths are different. We note that the interpretations are tentative since they are based on the 1–D modeling, and further evaluation is needed through a 3–D modeling in the future.

Keywords: Magnetotelluric, Meakandake, resistivity

©2019. Japan Geoscience Union. All Right Reserved.

Hydrothermal system of Kuttara Volcanic Group inferred from 3D resistivity modeling (2)

*Ryo Tanaka[1], Midori Hayakawa[2], Takeshi Hashimoto[1], Wataru Kanda[3], Yuichi Morita[4], Hiroshi Aoyama[1], Makoto Uyeshima[4]

1. Institute of Seismology and Volcanology, Hokkaido University, 2. Mitsui Oil Exploration Co., Ltd. Geothermal Business Division, 3. Volcanic Fluid Research Center, School of Science, Tokyo Institute of Technology, 4. Earthquake Research Institute, The University of Tokyo

Estimation of the volcanic hydrothermal system that is composed of an alteration zone, a fluid upflow zone and a heat source, is a key feature in assessing the potential of phreatic eruptions. Magnetotelluric (MT) method is one of the effective ways of estimating such hydrothermal system since it has the sensitivity to hydrothermal fluid and hydrothermal alteration zones. We performed the MT survey at Kuttara Volcano Group, northern Japan, to evaluate imminence of phreatic eruption.

Kuttara Volcanic Group is a basaltic to andesitic volcanic complex in southwestern Hokkaido, northern Japan. Kuttara volcano was formed by several silicic explosive eruptions and construction of an andesitic stratovolcano built up from ca. 80 to 40 ka. Lake Kuttara is a caldera lake formed by a violent explosive eruption at ca. 40 ka (Katsui et al., 1988; Moriizumi,1998). Noboribetsu volcano, post-caldera volcanism on the western foot of the stratovolcano at ca. 15 ka, formed Hiyoriyama cryptodome and Jigokudani geothermal field. We can see weak plumes (110–140 ºC; maximum height of ca. 50 m) near the top of Hiyoriyama cryptdome. We also see hot spring areas around Kuttara volcano at Noboribetsu, Carls, and Kojo-hama.

Although some previous studies (Goto and Johmori, 2011, 2013, 2015) revealed 2-D resistivity cross sections by CSAMT and TDEM methods at Kuttara volcano, they did not image deeper than about 1km. In this study, we carried out a broadband MT survey in 2017 at 49 stations in the area of 20x20 km wide and estimated 3-D resistivity structure of Kuttara Volcanic Group. We used ModEM (Egbert and Kelbert, 2012) as the 3-D inversion code, using a model space containing topography and sea bottom relieves. Responses at twelve periods between 0.00521 and 512 s were selected as the input data of the inversion. Error floors of 5% for the diagonal components of the impedance and 10% for the tippers and non-diagonal components of the impedance were given to avoid too much weighting for these data in the inversion process. Two-step inversion was applied, in which only the tippers were inverted at first, and subsequently, only the impedances were inverted. We already presented preliminary results at JpGU 2018 (Hayakawa et al., 2018). In this presentation, we discuss the results through the sensitivity check. We performed the sensitivity check by measuring the change in RMS due to disturbance of resistivity value in the focusing area.

We summarized the key features of the modeling results as follows. (1) The near-surface resistivity distribution is in good agreement with the surface geology. The resistivity was relatively high (100 to1000 Ωm) on northern and eastern to southern flanks of Kuttara Volcano, where volcanic deposits such as andesite lava flows covered the surface. (2) A low resistivity zone is imaged beneath Noboribetsu hot spring and a columnar low resistivity zone reached to the bottom of Lake Kuttara from the depth. These low resistivity zones indicate hydrothermal system in the Kuttara-Noboribetsu area. Low resistivity layer is also imaged just below Carls hot spring. However, this low resistivity layer is not sensitive in our inversion since this layer is very thin. (3) Relatively high resistivity zone beneath Lake Kuttara also has insufficient

©2019. Japan Geoscience Union. All Right Reserved.

sensitivity. This result indicates we have to perform more dense survey around Lake Kuttara to discuss whether magma or hydrothermal reservoir exist beneath Lake Kuttara or not. Our study is the first 3-D MT modeling for Kuttara Volcanic Group and further detailed comparison to geology, hydrology, drilling data, and hydrothermal simulation is necessary to better understand the current and to assess the potential of phreatic eruptions at Kuttara Volcanic Group.

Keywords: resistivity structure, Three-dimensional modeling, volcanic hydrothermal system

©2019. Japan Geoscience Union. All Right Reserved.

3D magnetic structure of Aso volcano

*Mitsuru Utsugi[1]

1. Aso Volcanological Laboratory, Institute for Geothermal Sciences, Graduate School of Science, Kyoto University

On Aso volcano, some aeromagnetic survey was conducted in previously to reveal the subsurface magnetic structure of the volcanic bodies, on 2001 (Tanaka et al., 2001), 2004 and 2004 (Tanaka et al., 2006) and 2006 (Utsugi et al., 2007). On this study, we tried to re-analyze these previous data, and tried to obtain detailed subsurface 3D magnetic structure of Aso volcano.

To the previous observed data, the processing of the IGRF correction and trend surface analysis were applied. Further, the process of the upward continuation (Nakatsuka and Okuma, 2005) was applied, and obtained the magnetic data on regular grid above the ground surface. Using this data as an input, the magnetization intensity distribution inside the volcanic bodies was determined by L1 norm regularized magnetic inversion. For this process, we divided the summit area of Aso volcano of about 5 x 5 km and the depth of 2.5 km into small blocks of 80 x 80 x 40, and determined the magnetization of each block. At this time, it was assumed that the magnetization was constant in each block, and the direction of magnetization was parallel to the current direction of the earth's magnetic field. In this presentation, detailed results of our magnetic inversion will be introduced.

Keywords: Aso volcano, 3D magnetic structure, 3D magnetic inversion

©2019. Japan Geoscience Union. All Right Reserved.

The piezomagnetic field produced by an ellipsoidal pressure source: A preliminary result

*Yoichi Sasai[1]

1. Earthquake Prediction Research Center, Institute of Oceanic Research and Development, Tokai University

Sasai (1986) formulated the piezomagnetic potential produced by a single force operative at a point, which was called the fundamental piezomagnetic potential (FPP). As an application example, he obtained the piezomagnetic field associated with a uniform circular load or the dam-magnetic effect. He also suggested that the FPP should be applicable to an ellipsoidal pressure source based on Eshelby's (1957) elastic inclusion theory. However, such an attempt has not been completed yet. Davis (1986) pointed out that the surface deformation observed at Kilauea volcano, Hawaii, could not be fully explained by the simple Mogi model and applied Eshelby's solution to find the best-fit ellipsoidal pressure source. He gave the displacement field only at the ground surface, while we need the one within the entire elastic half-space. Seo and Mura (1979) had formulated the displacement field due to the ellipsoidal inclusions with uniform dilatational eigenstrains, which was useful in some subjects in the metallography. Their model is also applicable to the magma reservoir in a shallow depth. When we consider the piezomagntic effect in the shallow crust, we must take into account the Curie point isotherm, i.e. an elastic half-space with a uniformly magnetized top layer. According to the representation theorem of the piezomagnetic field (Sasai, 1991), the potential is given by the surface integral with respect to the displacement and its normal derivatives. We discriminate three cases, i.e. Case I: the Curie surface (H) lies below the ellipsoid, Case II: H intersects the ellipsoid, and Case III: H lies above the ellipsoid. Here we obtained the solution for the simplist case (III).

Davis, P. M., 1986, J. Geophys. Res., 91, 7429-7438.
Eshelby, J. D., 1957, Proc. Roy. Soc., London, Ser. A, 376-396.
Seo, K. and T. Mura, 1979, J. Appl. Mech., 46, 568-572.
Sasai, Y., 1986, J. Geomag. Geoelectr., 38, 949-969.
Sasai, Y., 1991, Bull. Earthq. Res. Inst., Univ. Tokyo, 66, 585-722.

Keywords: Piezomagnetic effect, Ellipsoidal pressure source, Curie point isotherm, Representation theorem of the piezomagnetic field

©2019. Japan Geoscience Union. All Right Reserved.

[J] Poster | S (Solid Earth Sciences)：S-EM Earth's Electromagnetism

Mon. May 27, 2019 5:15 PM - 6:30 PM JST | Mon. May 27, 2019 8:15 AM - 9:30 AM UTC | Poster Hall International Exhibition Hall8, Makuhari Messe_21

[S-EM19] Electromagnetic Induction in the Earth and Planetary Interiors, and Tectono-Electromagnetism

convener:Koki Aizawa(Institute of Seismology and Volcanology, Faculty of Sciences, Kyushu University), Tetsuo Matsuno(Kobe Ocean Bottom Exploration Center, Kobe University)

This session welcomes papers on electromagnetism in the Earth and planetary interiors. The topics include but not limited to electromagnetic phenomena associated with earthquakes and volcanism, electrical conductivity structure, laboratory experiments, results of simulations, new equipment for observation, and methods of data analysis.

[SEM19-P01] Effects of absolute humidity on contact resistance between dry rock sample surface and electrodes

*Takeshi Suzuki[1], Ryokei Yoshimura[2], Ken'ichi Yamazaki[2], Naoto Oshiman[2] (1.Graduate School of Science, Kyoto University, 2.Disaster Prevention Research Institute, Kyoto University)

[SEM19-P02] Japanese geomagnetic field variation model based on the IGRF (2): modeling on the oblique Mercator projection

*Tsutomu Ogawa[1] (1.Earthquake Research Institute, the University of Tokyo)

[SEM19-P03] Examination of criteria to remove the influence of the Sq-field variations from electromagnetic field spectra for a better estimation of regional electromagnetic responses

*RUIBAI LI[1], Hisayoshi Shimizu[1], Kiyoshi Baba[1], Hisashi Utada[1] (1.Earthquake Research Institute, the University of Tokyo)

[SEM19-P04] **Study on long-term variation of geoelectric field observation**

*Ren Ozeki[1], Ikuko Fujii[1] (1.Japan Meteorological Agency)

[SEM19-P05] Deep electrical conductivity structure of Eastern Marmara, Turkey by long period magnetotellurics

*Sabri Bulent Tank[1], Naoto Oshiman[2], Mustafa Karas[1], Ryokei Yoshimura[2], Yasuo Ogawa[3] (1.Bogazici University, 2.Kyoto University, 3.Tokyo Institute of Technology)

[SEM19-P06] Audio-frequency magnetotelluric survey on the northern edifice of the Kurikoma volcano, northeast of Japan

*Kobayashi Takuya[1], Shin'ya Sakanaka[1], Tomoki Tsutsui[1], Muhammad Faizul Nizam Bin Zinudin[1], Inoue Yusuke[1], Kenta Kato[1], Tomoya Moriwaki[1], YUYA TADA[1], Ryuichi Takei[1] (1.Akita University)

[SEM19-P07] A three-dimensional crustal electrical resistivity model beneath southern Tohoku district, NE Japan

*Aoi Motoyama[1], Yasuo Ogawa[2], Makoto Uyeshima[3], Koichi Asamori[4], Toshihiro Uchida[5], Hideaki Hase[6], Takao Koyama[3], Shin'ya Sakanaka[7], Yusuke Yamaya[5], Koki Aizawa[8], Masahiro Ichiki[1] (1.Graduate school of science, Tohoku university, 2.Volcanic Fluid Research Center, School of Science, Tokyo Institute of Technology, 3.Earthquake research institute, the university of Tokyo, 4.Japan Atomic Energy Agency, 5.National institute of advanced industrial science and technology, 6. Geothermal Energy Research & Development Co., Ltd, 7.Graduate School of International Resource Sciences Department of Earth Resource Engineering and Environmental Science, Akita University, 8.Graduate school of science, Kyusyu university)

[SEM19-P08] Magnetotelluric survey on the northern foot of Meakandake volcano

*Tomohiro Inoue[1], Takeshi Hashimoto[1] (1.Institute of Seismology and Volcanology, Faculty of Science, Hokkaido University)

[SEM19-P09] Hydrothermal system of Kuttara Volcanic Group inferred from 3D resistivity modeling (2)

*Ryo Tanaka[1], Midori Hayakawa[2], Takeshi Hashimoto[1], Wataru Kanda[3], Yuichi Morita[4], Hiroshi Aoyama[1], Makoto Uyeshima[4] (1.Institute of Seismology and Volcanology, Hokkaido University, 2.Mitsui Oil Exploration Co., Ltd. Geothermal Business Division, 3.Volcanic Fluid Research Center, School of Science, Tokyo Institute of Technology, 4.Earthquake Research Institute, The University of Tokyo)

[SEM19-P10] 3D magnetic structure of Aso volcano

*Mitsuru Utsugi[1] (1.Aso Volcanological Laboratory, Institute for Geothermal Sciences, Graduate School of Science, Kyoto University)

[SEM19-P11] The piezomagnetic field produced by an ellipsoidal pressure source: A preliminary result

*Yoichi Sasai[1] (1.Earthquake Prediction Research Center, Institute of Oceanic Research and Development, Tokai University)

Effects of absolute humidity on contact resistance between dry rock sample surface and electrodes

*Takeshi Suzuki[1], Ryokei Yoshimura[2], Ken'ichi Yamazaki[2], Naoto Oshiman[2]

1. Graduate School of Science, Kyoto University, 2. Disaster Prevention Research Institute, Kyoto University

Resistivity measurements of rock under various conditions are essential for accurately interpreting geoelectromagnetic survey results. However, the contact resistance between the rock sample and measuring electrodes is a problem in measuring the resistivity of a rock sample. Because the measurement of high contact resistance on the dry rock surface is particularly difficult, its characteristics have not been well studied.
In order to investigate the characteristics of contact resistance, we have developed a measurement method of high contact resistance. By using the method, we measured high contact resistance between the dry granite surface and the electrode made of conductive epoxy. Considering the interaction between atmospheric moisture and rock samples, the contact resistance was repeatedly measured under different humidity conditions.
We confirmed the contact resistance decreased with increasing absolute humidity. A clear relationship exists between contact resistance and absolute humidity, and the relationship was approximated by an exponential function. This result suggests that increasing the contact area between the electrode and the rock surface with rising humidity. Moisture in the atmosphere may have caused improvement of contact condition by filling the microscopic gap in the contact surface.

Keywords: contact resistance, atmospheric Moisture, absolute humidity, contact area, conductive epoxy, granite

©2019. Japan Geoscience Union. All Right Reserved.

Japanese geomagnetic field variation model based on the IGRF (2): modeling on the oblique Mercator projection

*Tsutomu Ogawa[1]

1. Earthquake Research Institute, the University of Tokyo

For geomagnetic field variation observations around tectonic areas to detect the variations related to tectonic activities in Japan, geomagnetic field model or geomagnetic field variation model around Japan with high accuracy is indispensable as a reference field. The geomagnetic field variation model around Japan proposed by Abe and Miyahara (2015) using the principal component analysis of geomagnetic data is a statistical model but not a physical model of the field variation, for the vector field model is not in general divergence-free. The model also lacked the error estimation for arbitrary positions. The present study evaluates the new geomagnetic field variation model around Japan which corrects the following two points in the model by Ogawa (2018, JpGU) which attempted to overcome the difficulties in the previous work: 1) the geomagnetic field variation is expressed in the Cartesian coordinate system on the map using the oblique Mercator projection of the Japanese island arc along NE-SW direction with a great ellipse centered and oriented along the direction, instead of the Mercator projection, and 2) annual variations in the model residuals of data which correlate with sensor temperature variations at the geoelectromagnetic continuous measurement stations of GIAJ are removed.

The new geomagnetic field variation model is expressed with the magnetic scalar potential by a cubic polynomial with respect to the coordinates in the coordinate system with its origin on the ground in the SE area of Ishikawa prefecture, expressing the difference of the 1-day geomagnetic data at 5 observatories of JMA and GIAJ and 10 stations of GIAJ from the IGRF, between 2005 and 2014. By obtaining the time series of expansion coefficients using the robust least square technique, the model shows the following features: 1) the mean of the model residuals amounts to 1.28nT, 2) by the leave-one-out cross-validation, the mean of the prediction error amounts to 1.94nT, 3) the mean of the prediction error at all the observation points obtained by the propagation of the jackknife standard error of expansion coefficients amounts to 1.16nT, as large as the mean of the model residuals, and 4) the mean of the prediction errors at Chichijima station of JMA, data of which are unused for the model, because of the large distance of the station from the principal part of the Japanese island arc, amounts to 5.06nT.

The mean prediction error along the principal part of the Japanese island arc estimated using the propagation of the jackknife standard errors of estimated expansion coefficients amounts at most to about 2nT for the horizontal two components and about 3nT for the vertical component, respectively. The present geomagnetic field variation model around Japan has the accuracy of a few nT for the principal part of the Japanese island arc.

Keywords: Geomagnetic field variation model, oblique Mercator projection, Leave-one-out cross-validation, jackknife standard error

©2019. Japan Geoscience Union. All Right Reserved.

Examination of criteria to remove the influence of the Sq-field variations from electromagnetic field spectra for a better estimation of regional electromagnetic responses

*RUIBAI LI[1], Hisayoshi Shimizu[1], Kiyoshi Baba[1], Hisashi Utada[1]

1. Earthquake Research Institute, the University of Tokyo

Electromagnetic (EM) responses such as magnetotelluric (MT) impedance and geomagnetic depth sounding (GDS) response (or tipper) in the period range between several minutes to one day are used to study the electrical conductivity in the upper mantle. Spatially uniform and quasi-random magnetic field variations due to geomagnetic disturbances are considered as the source field in regional EM induction studies using the EM responses. However, the magnetic field variations in the period range from to seconds (mixed excitation band, or ME band) contain those with different spatial structure such as the solar quiet (Sq) daily variations and those induced by the ocean tide. Careful treatment of EM field data is necessary to estimate responses in the ME band that reflect actual conductivity structure. For example, Baba et al. (2010) estimated the EM responses in the period range from to seconds using a method based on Fourier transform after removing line spectra of EM field variations at periods of Sq field variations that include the higher harmonics and constituents of ocean tides. However, it was shown that the estimated responses in the ME band still included the influence of Sq field variations (Shimizu et al., 2011).

In this study we try to estimate EM responses that are less influenced by the Sq field variations. We employed line spectra of EM field obtained by using Sompi method, so called wave element (or namiso) (e.g., Kumazawa et al.,1990, Asakawa eta al.,1988), to estimate the EM responses in order to avoid the influence of the Sq field variations that could be contained in continuous spectra. Also, three conditions are applied to select appropriate wave elements from observed ones for EM response estimations. First is to select wave elements of which eastward component have common phase or that close to each other at two stations. This can avoid wave elements influenced by the Sq field variations since their westward propagation causes systematic phase difference of the magnetic field for supposed longitude difference and apparent period, which is determined by the longitudinal wave number of the variation. Second is to select magnetic field spectra that are linearly polarized in horizontal-vertical plane, because that influenced by the Sq field variations are expected to be more elliptically polarized in the plane than those suitable for regional EM response estimation. Ellipticity of the polarization ellipse is used to apply the condition. Third is to select those which have small ratio of the vertical to the horizontal magnetic field components, because the Sq field variations contain significant vertical magnetic field component that can cause larger amplitude of tipper than those from plane wave. It was confirmed that estimated phase difference, ellipticity, and vertical to horizontal field ratio showed a signature of Sq field variations in the ME band but not at a period shorter than seconds.

In this presentation, we are going to show the characteristics of the observed phase difference, ellipticity, and vertical to horizontal field ratio with respect to the period. Criteria to apply the conditions are assumed based on theoretical estimate of the magnetic field due to Sq principle mode and the induced field in assumed one dimensional Earth. The EM responses obtained by applying each condition are shown and the improvement or influence in the obtained responses, as a result, are discussed quantitatively.

©2019. Japan Geoscience Union. All Right Reserved.

Asakawa, E., et al. (1988). *J. Geomagn. Geoelec.,*40: 447-463.

Baba, K., et al. (2010).*Phys. Earth planet. Inter.,*183: 44-62.

Kumazawa, M., et al. (1990). *Geophys. J. Int.,*101: 613-630.

Shimizu, H., et al. (2011). *Geophys. J. Int.,*186: 193-206.

©2019. Japan Geoscience Union. All Right Reserved.

Study on long-term variation of geoelectric field observation

*Ren Ozeki[1], Ikuko Fujii[1]

1. Japan Meteorological Agency

Kakioka Magnetic Observatory, Japan Meteorological Agency, has observed the geomagnetic and geoelectric fields for several decades at Kakioka, Kanoya and Memambetsu. Vitage differences between two electrodes are observed in the geoelectric field observation. The baseline length is about 200-300m and the electrodes are installed at 3m deep. The data of the geoelectric field are used worldwide as a unique data set to investigate induced electric fields for last several decades.It is slightly troublesome for us to use the geoelectric field data set by Kakioka Magnetic Observatory because the geoelectric fields at three sites shows long-term variations and especially the north-south component of the geoelectric field at Kakioka clearly changes.Although some studies (e.g., Morinaga and Toya, 2015; Okawa et al., 1995) reported that this long-term variation is related to rain, details of how this long-term variation occurs are still unknown. This study aims to reveal the cause of the long-term variation.
Based on Morinaga and Toya (2015) and Fujii et al.(2007), we focus on geological structures around the electrode at the south end of the north-south line at Kakioka. We infer the geological structure from the distribution of the electrical resistivity.
The electrical prospecting was applied to an area of 20m x 20m with the south electrode as the center. Observations were conducted in March, May and October giving 7 observation lines around the south electrode, 2 lines around the east electrode, and 1 line around a boring hole (fig.1). Apparent resistivity was estimated from the observed currents and voltage differences.
We assume that the subsurface structure is one-dimensional and three layers are stratified. An optimal model of the resistivity distribution was obtained by inversion. All lines show a high resistivity layer at the surface followed by a low resistivity layer and then a high resistivity layer at the bottom. The thickness of the first layer is increased eastward from the south electrode.
The optimal model was compared with a boring profile obtained near the investigated area. We interpret that the resistive surface layer is permeable top soil and the second conductive layer is impermeable clay(Figure 2).We suspect that rain water flows on the top of clay to the east and the south electrode suffers from larger amount of water than the other electrodes.

Keywords: geoelectric field observation, electrical prospecting

©2019. Japan Geoscience Union. All Right Reserved.

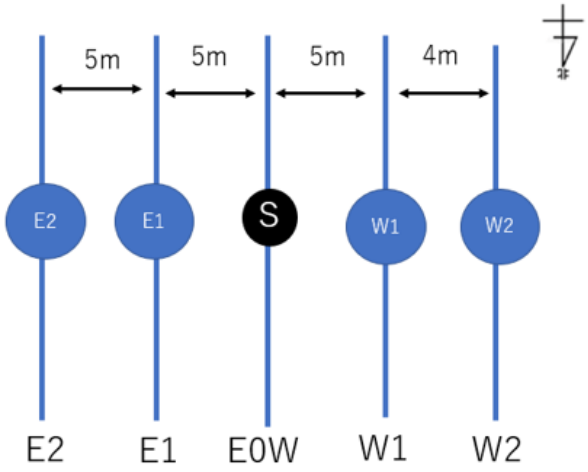

Figure 1

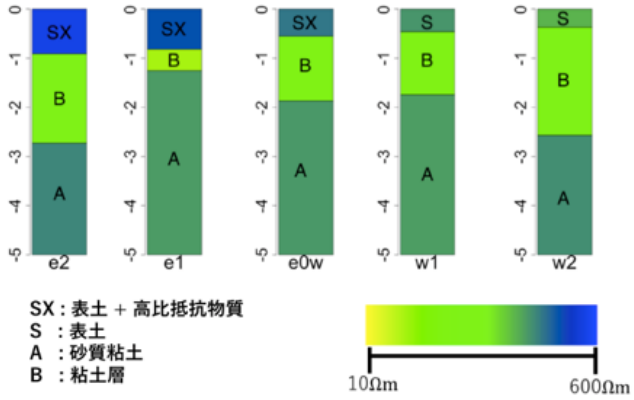

Figure 2

©2019. Japan Geoscience Union. All Right Reserved.

Deep electrical conductivity structure of Eastern Marmara, Turkey by long period magnetotellurics

*Sabri Bulent Tank[1], Naoto Oshiman[2], Mustafa Karas[1], Ryokei Yoshimura[2], Yasuo Ogawa[3]

1. Bogazici University, 2. Kyoto University, 3. Tokyo Institute of Technology

The electrical resistivity structure of a 100 km x 100 km region at northwestern Anatolia was examined by using long period magnetotelluric data with the aim to image the geo-electrical features at the lower crust and upper mantle. The electromagnetic impedance tensor elements were obtained for eighteen sounding locations within a period range of 20-13000 seconds. The soundings were distributed over the epicentral region of the 1999 Izmit earthquake and its vicinity including the Pontides in the north, Intra-Pontid transition zone and Sakarya Continent in the south. Three-dimensional data-space inversions of the long period magnetotellurics data were performed iteratively to achieve the electrical resistivity structure. In order to determine and overcome the complexities caused by the coast effect that arise due to presence of the conductive Black Sea, the dimensionality of the magnetotellurics data were examined in detail by means of induction arrows and phase tensor ellipses. These complexities may have transpired due to the seismically active branches of the North Anatolian Fault and presence of the Intra-Pontide Suture, too. The final resistivity models revealed a low resistivity zone trapped between two highly resistive blocks of Istanbul Zone in the north and Sakarya Continent in the south. This low conductivity zone coincides with the two main branches of the North Anatolian Fault and may be promoting the seismic activity in both of the branches.

Keywords: Magnetotellurics, North Anatolian Fault, Izmit earthquake, Fluids

©2019. Japan Geoscience Union. All Right Reserved.

Audio-frequency magnetotelluric survey on the northern edifice of the Kurikoma volcano, northeast of Japan

*Kobayashi Takuya[1], Shin'ya Sakanaka[1], Tomoki Tsutsui[1], Muhammad Faizul Nizam Bin Zinudin[1], Inoue Yusuke[1], Kenta Kato[1], Tomoya Moriwaki[1], YUYA TADA[1], Ryuichi Takei[1]

1. Akita University

Now we focus the Kurikoma volcano closely at the triple junction of borders of Akita, Iwate and Miyagi prefectures, northeast of Japan. The eruption style of the Kurikoma volcano is magma eruption and phreatic eruption. The Kurikoma volcano is one of important active volcanos and its most recent striking activity was a phreatic eruption in 1944. The site of 1994 eruption is now remained as a crater lake called Lake Showa. Besides the Lake Showa, volcanic gas is even now emitted upstream of a gorge called Jigoku-dani. So far the several researches have reported 2- and 3-dimensional resistivity structures of the crust including the Kurikoma volcano (e.g. Mishina, 2009; Ichihara et al., 2014). Mishina (2009) firstly reported the 2-dimensional resistivity structure targeting the deep volcanic fluid beneath the Kurikoma volcano. The result of Mishina (2009) suggested the existence of volcanic fluid at the depth of several kilometers under the volcanic structure. In this study, we aim to find the structure which becomes the key to the occurrence of the phreatic eruption from the shallow resistivity structure directly under the Kurikoma volcano obtained by AMT survey.

We carried out an AMT survey across a high temperature upstream of a gorge from August to November 2018. This method uses magnetotelluric responses derived from variations in the natural audio-frequency band (approximately 1 to 10^4 Hz) of the electromagnetic field to estimate the resistivity structure in an area down to a depth of a few kilometers. The AMT data were collected at thirteen locations. Two components of the electric field and three components of the magnetic field were recorded for 3 to 24 h overnight using a Phoenix Geophysics MTU-5A system (Phoenix Geophysics Ltd., Toronto, ON, Canada). In this study, the concept of phase tensor (Caldwell et al., 2004) and induction vector (Parkinson, 1962) was used to evaluate the dimensionality of structure and the characteristic of resistivity distribution. From the results of the phase tensor, the skew angle was less than 5 degree and the ellipticity was less than 0.2 in the range of frequencies higher than 10 Hz. Therefore, it is suggested that the structure around 1 km below the subsurface is a relatively homogeneous structure. Also, in the frequency range lower than 10 Hz, the direction of the induction vectors tends to point towards a lava dome called Tsurugi-dake.

The 2D inversion model with TM-mode data was constructed using the inversion code developed by Ogawa and Uchida (1996). Only the data with small phase-tensor skew angles (< 5 degrees) were used in the 2D inversion in this study, because the data with large skew angles are inconsistent with the 2D structure assumed in the area.

The final model has three characteristic features. The first is that the low resistivity region (C1) beneath the fumarolic area and hot spring zone. The second is that high resistivity zone (R1) is distributed in the lower layer of the low resistivity region (C1) immediately below the high temperature fumarolic area (Jigoku-dani, Iwo-yama and Yuge-yama). It is suggested that the high resistivity zone (R1) is a high temperature body or a steam dominant region because high temperature fumarolic area exposes the surface of the ground. The third is the existence of a relatively high resistivity zone (R2) is located in the lower layer of the eastern part of the low resistivity region (C1). Since the phreatic eruption crater traces are distributed in the eastern part of the east west cross section, it is suggested that R2 is a trace of activities of the phreatic eruption in the past.

©2019. Japan Geoscience Union. All Right Reserved.

Keywords: Resistivity structure, AMT, Kurikoma volcano, Phreatic eruption, Hydrothermal system

©2019. Japan Geoscience Union. All Right Reserved.

A three-dimensional crustal electrical resistivity model beneath southern Tohoku district, NE Japan

*Aoi Motoyama[1], Yasuo Ogawa[2], Makoto Uyeshima[3], Koichi Asamori[4], Toshihiro Uchida[5], Hideaki Hase[6], Takao Koyama[3], Shin'ya Sakanaka[7], Yusuke Yamaya[5], Koki Aizawa[8], Masahiro Ichiki[1]

1. Graduate school of science, Tohoku university, 2. Volcanic Fluid Research Center, School of Science, Tokyo Institute of Technology, 3. Earthquake research institute, the university of Tokyo, 4. Japan Atomic Energy Agency, 5. National institute of advanced industrial science and technology, 6. Geothermal Energy Research & Development Co., Ltd, 7. Graduate School of International Resource Sciences Department of Earth Resource Engineering and Environmental Science, Akita University, 8. Graduate school of science, Kyusyu university

On the basis of seismological and geodetic results, Hasegawa et al. (2005) proposed a vertical crustal model profile in the across-arc direction beneath Tohoku district. In the model, the magma and/or fluid reservoir lies in the lower crust beneath Ou backbone range running along the central arc of Tohoku district. On the other hand, Uyeshima et al. (2016) recently modeled a two-dimensional (2-D) crustal electrical resistivity profile in which there are three distinguished conductors in the lower crust, that is, beneath the fore-arc, volcanic front and back-arc of southern Tohoku district. The fore-arc conductor underlies the seismicity beneath around Iwaki city activated after 2011 Tohoku-oki earthquake. However, another 2-D resistivity profile 50 km northwards parallel to the Uyeshima et al’ s one shows no distinguished fore-arc conductor, but volcanic front and back-arc conductors (Motoyama et al., 2018). These results indicate geofluids rise up beneath a part of fore-arc beneath southern Tohoku district. Moreover, a part of back-arc of the southern Tohoku district may have conductive lower crust. Because previous resistivity models are limited to 2-D, we estimated a 3-D resistivity model beneath southern Tohoku district with compiling previous magnetotelluirc (MT) data, and discussed geofluids distribution beneath fore-arc and back-arc.

We compiled electromagnetic data at 118 sites and reassessed all MT responses and geomagnetic transfer functions. The $\Phi_{2,}$ square root of determinant of phase tensor (Caldwell et al., 2004), shows high values in the northern part of back-arc, and in the southern part of fore-arc and of Ou backbone range 10-100 s period range.

To estimate 3-D resistivity model, we used WSINV3D_MPI inversion code (Siripunvaraporn & Egbert, 2009). So far, we have estimated a preliminary model using only MT responses. A vertical model profile in the across-arc direction shows an oblique conductor from deeper crust beneath back-arc to shallower crust beneath Ou backbone range. On the other hand, almost all forearc has high resistivities in the crust. The map view of resistivity profile at 22.5 km depth shows a conductor distributes beneath from Murakami city of back-arc to Koriyama city of Ou backbone range. The calculation is still running by using both MT responses and geomagnetic transfer functions, and we will show the results and discussion in this presentation.

Keywords: Magnetotellurics, geofluids

©2019. Japan Geoscience Union. All Right Reserved.

Magnetotelluric survey on the northern foot of Meakandake volcano

*Tomohiro Inoue[1], Takeshi Hashimoto[1]

1. Institute of Seismology and Volcanology, Faculty of Science, Hokkaido University

We performed a broadband MT survey in the northern part of Mt. Meakandake in August and September in 2018. Mt. Meakandake is one of the active volcanoes in the southwestern part of Akan caldera in eastern Hokkaido. Recently, a remarkable ground inflation has been reported on the northeastern foot of Meakandake. We planned a magnetotelluric survey to investigate the electrical structure across the deformation source. In this study, we describe the features of our MT data and show the 1-D models as a preliminary modeling.

The Geospatial Information Authority of Japan (2018) reported a remarkable crustal inflation on the basis of the GNSS observation and InSAR analysis from late 2016 through 2017. They modeled the deformation as an opening of the sill-like crack (about 11 km long and 2 km wide) at a depth of about 6 km on the northeastern foot of Meakandake. As the estimated deformation source was large, we considered that it might be imaged as a low resistivity anomaly, if it was related to magma or hydrothermal system. Investigating the subsurface structure across such an extensive inflation source will also contribute to understanding the magma plumbing system of the Akan area. Around Meakandake, a MT survey was previously conducted in the eastern area as a part of the Geothermal Development Promotion Survey (NEDO, 1992). More recently, an AMT survey was performed across the summit along a NE-SW direction as a part of volcano study of Meakandake (Takahashi et al., 2018). However, because of the limited sounding depths, the electrical structure near the above-mentioned deformation source has not been clarified yet.

Therefore, in this study, we newly deployed twelve broadband-MT sites along a NW-SE trending survey line across the longer side of the inflation source on the northern to eastern foot of the volcano. We used four set of the MTU-5/5A system (Phoenix Geophysics) for the campaign. We acquired the time series of the electric field in two components and the magnetic field in three components for 3 to 7 days for each site. In calculating the response functions, we used the SSMT2000 software and applied the remote reference processing using the magnetic field data Sawauchi in Iwate Prefecture that was provided by Nittetsu Mining Consultants Co., Ltd.

Contrary to our first expectation, the induction vectors and phase tensors suggested an electrical regional strike of N60ºW, which was almost parallel to the survey line. Thus, in this study, we sought a provisional 1-D modelling instead of the 2-D analysis in an unpreferable direction. We estimated 1-D resistivity structures using the Occam’s inversion (Constable et al., 1987), in which we used the ssq impedance (Szarka and Menvielle, 1997; Rung-Arunwan et al., 2016) as the input data. In this inversion, we only used a frequency range, in which the responses showed approximately a 1-D feature.

The inverted 1-D models exhibited a distinct low resistivity layer (1-10 Ωm, hereinafter called, C1) at depths around a few hundred meters at all sites. In addition, at the sites in the SE half of the survey line, another low resistivity layer of approximately 10 Ωm (hereinafter called, C2) was found at a depth around 2-4 km.

According to the NEDO (1992)’s borehole logs that were drilled at about 1 km east of our survey line,

©2019. Japan Geoscience Union. All Right Reserved.

the low resistivity layer C1, which is common to all the sites, is likely to correspond with the volcanic tuff layers in the Miocene indicating weak alteration with montmorillonite and/or chlorite. Meanwhile, the deeper low–resistivity layer C2 is recognized only at the locations near the above–mentioned inflation source. In addition, C2 is shallower at the sites near the inflation source. For this reason, we suspect that C2 has some relation to the inflation source, although their depths are different. We note that the interpretations are tentative since they are based on the 1–D modeling, and further evaluation is needed through a 3–D modeling in the future.

Keywords: Magnetotelluric, Meakandake, resistivity

©2019. Japan Geoscience Union. All Right Reserved.

Hydrothermal system of Kuttara Volcanic Group inferred from 3D resistivity modeling (2)

*Ryo Tanaka[1], Midori Hayakawa[2], Takeshi Hashimoto[1], Wataru Kanda[3], Yuichi Morita[4], Hiroshi Aoyama[1], Makoto Uyeshima[4]

1. Institute of Seismology and Volcanology, Hokkaido University, 2. Mitsui Oil Exploration Co., Ltd. Geothermal Business Division, 3. Volcanic Fluid Research Center, School of Science, Tokyo Institute of Technology, 4. Earthquake Research Institute, The University of Tokyo

Estimation of the volcanic hydrothermal system that is composed of an alteration zone, a fluid upflow zone and a heat source, is a key feature in assessing the potential of phreatic eruptions. Magnetotelluric (MT) method is one of the effective ways of estimating such hydrothermal system since it has the sensitivity to hydrothermal fluid and hydrothermal alteration zones. We performed the MT survey at Kuttara Volcano Group, northern Japan, to evaluate imminence of phreatic eruption.

Kuttara Volcanic Group is a basaltic to andesitic volcanic complex in southwestern Hokkaido, northern Japan. Kuttara volcano was formed by several silicic explosive eruptions and construction of an andesitic stratovolcano built up from ca. 80 to 40 ka. Lake Kuttara is a caldera lake formed by a violent explosive eruption at ca. 40 ka (Katsui et al., 1988; Moriizumi,1998). Noboribetsu volcano, post-caldera volcanism on the western foot of the stratovolcano at ca. 15 ka, formed Hiyoriyama cryptodome and Jigokudani geothermal field. We can see weak plumes (110–140 ºC; maximum height of ca. 50 m) near the top of Hiyoriyama cryptdome. We also see hot spring areas around Kuttara volcano at Noboribetsu, Carls, and Kojo-hama.

Although some previous studies (Goto and Johmori, 2011, 2013, 2015) revealed 2-D resistivity cross sections by CSAMT and TDEM methods at Kuttara volcano, they did not image deeper than about 1km. In this study, we carried out a broadband MT survey in 2017 at 49 stations in the area of 20x20 km wide and estimated 3-D resistivity structure of Kuttara Volcanic Group. We used ModEM (Egbert and Kelbert, 2012) as the 3-D inversion code, using a model space containing topography and sea bottom relieves. Responses at twelve periods between 0.00521 and 512 s were selected as the input data of the inversion. Error floors of 5% for the diagonal components of the impedance and 10% for the tippers and non-diagonal components of the impedance were given to avoid too much weighting for these data in the inversion process. Two-step inversion was applied, in which only the tippers were inverted at first, and subsequently, only the impedances were inverted. We already presented preliminary results at JpGU 2018 (Hayakawa et al., 2018). In this presentation, we discuss the results through the sensitivity check. We performed the sensitivity check by measuring the change in RMS due to disturbance of resistivity value in the focusing area.

We summarized the key features of the modeling results as follows. (1) The near-surface resistivity distribution is in good agreement with the surface geology. The resistivity was relatively high (100 to1000 Ωm) on northern and eastern to southern flanks of Kuttara Volcano, where volcanic deposits such as andesite lava flows covered the surface. (2) A low resistivity zone is imaged beneath Noboribetsu hot spring and a columnar low resistivity zone reached to the bottom of Lake Kuttara from the depth. These low resistivity zones indicate hydrothermal system in the Kuttara-Noboribetsu area. Low resistivity layer is also imaged just below Carls hot spring. However, this low resistivity layer is not sensitive in our inversion since this layer is very thin. (3) Relatively high resistivity zone beneath Lake Kuttara also has insufficient

©2019. Japan Geoscience Union. All Right Reserved.

sensitivity. This result indicates we have to perform more dense survey around Lake Kuttara to discuss whether magma or hydrothermal reservoir exist beneath Lake Kuttara or not. Our study is the first 3-D MT modeling for Kuttara Volcanic Group and further detailed comparison to geology, hydrology, drilling data, and hydrothermal simulation is necessary to better understand the current and to assess the potential of phreatic eruptions at Kuttara Volcanic Group.

Keywords: resistivity structure, Three-dimensional modeling, volcanic hydrothermal system

©2019. Japan Geoscience Union. All Right Reserved.

3D magnetic structure of Aso volcano

*Mitsuru Utsugi[1]

1. Aso Volcanological Laboratory, Institute for Geothermal Sciences, Graduate School of Science, Kyoto University

On Aso volcano, some aeromagnetic survey was conducted in previously to reveal the subsurface magnetic structure of the volcanic bodies, on 2001 (Tanaka et al., 2001), 2004 and 2004 (Tanaka et al., 2006) and 2006 (Utsugi et al., 2007). On this study, we tried to re-analyze these previous data, and tried to obtain detailed subsurface 3D magnetic structure of Aso volcano.

To the previous observed data, the processing of the IGRF correction and trend surface analysis were applied. Further, the process of the upward continuation (Nakatsuka and Okuma, 2005) was applied, and obtained the magnetic data on regular grid above the ground surface. Using this data as an input, the magnetization intensity distribution inside the volcanic bodies was determined by L1 norm regularized magnetic inversion. For this process, we divided the summit area of Aso volcano of about 5 x 5 km and the depth of 2.5 km into small blocks of 80 x 80 x 40, and determined the magnetization of each block. At this time, it was assumed that the magnetization was constant in each block, and the direction of magnetization was parallel to the current direction of the earth's magnetic field. In this presentation, detailed results of our magnetic inversion will be introduced.

Keywords: Aso volcano, 3D magnetic structure, 3D magnetic inversion

©2019. Japan Geoscience Union. All Right Reserved.

The piezomagnetic field produced by an ellipsoidal pressure source: A preliminary result

*Yoichi Sasai[1]

1. Earthquake Prediction Research Center, Institute of Oceanic Research and Development, Tokai University

Sasai (1986) formulated the piezomagnetic potential produced by a single force operative at a point, which was called the fundamental piezomagnetic potential (FPP). As an application example, he obtained the piezomagnetic field associated with a uniform circular load or the dam-magnetic effect. He also suggested that the FPP should be applicable to an ellipsoidal pressure source based on Eshelby's (1957) elastic inclusion theory. However, such an attempt has not been completed yet. Davis (1986) pointed out that the surface deformation observed at Kilauea volcano, Hawaii, could not be fully explained by the simple Mogi model and applied Eshelby's solution to find the best-fit ellipsoidal pressure source. He gave the displacement field only at the ground surface, while we need the one within the entire elastic half-space. Seo and Mura (1979) had formulated the displacement field due to the ellipsoidal inclusions with uniform dilatational eigenstrains, which was useful in some subjects in the metallography. Their model is also applicable to the magma reservoir in a shallow depth. When we consider the piezomagntic effect in the shallow crust, we must take into account the Curie point isotherm, i.e. an elastic half-space with a uniformly magnetized top layer. According to the representation theorem of the piezomagnetic field (Sasai, 1991), the potential is given by the surface integral with respect to the displacement and its normal derivatives. We discriminate three cases, i.e. Case I: the Curie surface (H) lies below the ellipsoid, Case II: H intersects the ellipsoid, and Case III: H lies above the ellipsoid. Here we obtained the solution for the simplist case (III).

Davis, P. M., 1986, J. Geophys. Res., 91, 7429-7438.
Eshelby, J. D., 1957, Proc. Roy. Soc., London, Ser. A, 376-396.
Seo, K. and T. Mura, 1979, J. Appl. Mech., 46, 568-572.
Sasai, Y., 1986, J. Geomag. Geoelectr., 38, 949-969.
Sasai, Y., 1991, Bull. Earthq. Res. Inst., Univ. Tokyo, 66, 585-722.

Keywords: Piezomagnetic effect, Ellipsoidal pressure source, Curie point isotherm, Representation theorem of the piezomagnetic field

©2019. Japan Geoscience Union. All Right Reserved.

[E] Oral | S (Solid Earth Sciences)：S-IT Science of the Earth's Interior & Techtonophysics

Mon. May 27, 2019 9:00 AM - 10:30 AM JST | Mon. May 27, 2019 12:00 AM - 1:30 AM UTC | A10 TOKYO BAY MAKUHARI HALL

[S-IT21] Interaction and Coevolution of the Core and Mantle in the Earth and Planets

convener:Kenji Kawai(Department of Earth and Planetary Science, School of Science, University of Tokyo), Tsuyoshi Iizuka(University of Tokyo), Kenji Ohta(Department of Earth and Planetary Sciences, Tokyo Institute of Technology), Taku Tsuchiya(Geodynamics Research Center, Ehime University), Chairperson:Anselme Borgeaud, Taku Tsuchiya

Recent observational and experimental investigations have significantly advanced our understanding of the structure and constituent materials of the deep Earth. Yet, even fundamental properties intimately linked with formation and evolution of the planet, such as details of the chemical heterogeneity in the mantle and light elements dissolved in the core, remained unclear. Seismological evidence has suggested a vigorous convection in the lower mantle, whereas geochemistry has suggested the presence of stable regions there that hold ancient chemical signatures. The amounts of radioactive isotopes that act as heat sources and drive dynamic behaviors of the deep Earth are also still largely unknown. We provide an opportunity to exchange the achievements and ideas, and encourage persons who try to elucidate these unsolved issues of the core-mantle evolution using various methods, including high-pressure and high-temperature experiments, high-precision geochemical and paleomagnetic analyses, high-resolution geophysical observations, geo-neutrino observations, and large-scale numerical simulations. Papers stimulating an interdisciplinary collaboration relating to establishment of the Japan-SEDI community are also welcomed.

9:00 AM - 9:15 AM JST | 12:00 AM - 12:15 AM UTC

[SIT21-01] The role of stishovite as a deep nitrogen carrier indicated from high-pressure and high-temperature experiments

*Ko Fukuyama[1], Hiroyuki Kagi[1], Toru Inoue[2,3], Toru Shimei[3], Sho Kakizawa[3], Shunichi Hishita[4], Yuji Sano[5], Naoto Takahata[5] (1.Geochemical Research Center, Graduate School of Science, The University of Tokyo, 2.Department of Earth and Planetary Systems Science, Graduate School of Science, Hiroshima University, 3.Geodynamics Research Center, Ehime University, 4.National Institute for Materials Science, 5.Atmosphere and Ocean Research Institute, The University of Tokyo)

9:15 AM - 9:30 AM JST | 12:15 AM - 12:30 AM UTC

[SIT21-02] 3-D P- and S-velocity structure of the D″ layer beneath Central America and the Caribbean using waveform inversion

★Invited Papers

*Anselme F. E. Borgeaud[1,2], Kenji Kawai[1], Robert J. Geller[1] (1.Department of Earth and Planetary Science, Graduate School of Science, University of Tokyo, 2.Institute of Earth Sciences, Academia Sinica)

9:30 AM - 9:45 AM JST | 12:30 AM - 12:45 AM UTC

[SIT21-03] Uniaxial deformation experiments of bridgmanite using D-111 type high pressure apparatus

★Invited Papers

*Noriyoshi Tsujino[1], Daisuke Yamazaki[1], Yu Nishihara[2] (1.Institute for Planetary Materials, Okayama University, 2.Geodynamics Research Center, Ehime University)

9:45 AM - 10:00 AM JST | 12:45 AM - 1:00 AM UTC

[SIT21-04] Waveform inversion for 3D anisotropic structure in D″ beneath the Northern Pacific: Constraints on mineralogy and flow in the lowermost mantle

*Yuki Suzuki[1], Kenji Kawai[1], Robert J. Geller[1] (1.Department of Earth and Planetary Sciences, School of Science,The University of Tokyo)

10:00 AM - 10:15 AM JST | 1:00 AM - 1:15 AM UTC

[SIT21-05] Maximum water solubility of bridgmanite under the Earth's lower mantle conditions

*Sho Kakizawa[1], Toru Inoue[1,2,3], Ryotaro Abe[1], Minami Kuroda[4], Naoya Sakamoto[5], Hisayoshi Yurimoto[4,5,6] (1.Geodynamics Reseach Center, Ehime University, 2.Graduate School of Science, Hiroshima University, 3.Hiroshima Institute of Plate Convergence Region Research, 4.Graduate School of Science, Hokkaido University, 5.Creative Research Institution, Hokkaido University, 6.Institute of Space and Astronautical Science, Japan Aerospace Exploration Agency)

10:15 AM - 10:30 AM JST | 1:15 AM - 1:30 AM UTC

[SIT21-06] Origin and role of lost continents

*Shigenori Maruyama[1], Kenji Kawai[2], Steeve Gréaux[3], Taku Tsuchiya[3], Dapeng Zhao[4] (1.Earth-Life Science Institute, Tokyo Institute of Technology, 2.Department of Earth and Planetary Science, School of Science, University of Tokyo, 3.Ehime University, 4.Department of Geophysics, Tohoku University)

The role of stishovite as a deep nitrogen carrier indicated from high-pressure and high-temperature experiments

*Ko Fukuyama[1], Hiroyuki Kagi[1], Toru Inoue[2,3], Toru Shimei[3], Sho Kakizawa[3], Shunichi Hishita[4], Yuji Sano[5], Naoto Takahata[5]

1. Geochemical Research Center, Graduate School of Science, The University of Tokyo, 2. Department of Earth and Planetary Systems Science, Graduate School of Science, Hiroshima University, 3. Geodynamics Research Center, Ehime University, 4. National Institute for Materials Science, 5. Atmosphere and Ocean Research Institute, The University of Tokyo

Nitrogen occupies about 80% in the Earth's atmosphere and is one of essential elements of life. For these reasons, nitrogen is an important volatile element in various aspects of geoscience, including climates (e.g. Goldblatt et al., 2009; Wordsworth and Pierrehumbert, 2013) and the origin of life. However, we couldn't have still understood details of behavior or cycle of nitrogen in the Earth's interior. For example, it is known that the amount of nitrogen in deep Earth is more depleted than that of other volatile elements (Marty, 2012). This is called "missing" nitrogen and suggested to be caused by nitrogen stored in the upper mantle, the mantle transition zone, and the lower mantle through magma ocean from experimental researches (e.g., Li et al., 2013; Yoshioka et al., 2018). However, only two experiments corresponding to the lower mantle were conducted in the previous study (Yoshioka et al., 2018). In addition, subducting slab have played important role for volatile cycle into the deep Earth.

In this research, in order to investigate how much nitrogen is incorporated into stishovite which can carry nitrogen to the lower mantle, we conducted high-pressure and high-temperature experiments using multi-anvil apparatus installed at Geodynamics Research Center, Ehime University. All experimental pressure conditions were 27 GPa and temperature conditions ranged from 1400 ℃ to 1700 ℃. Fe-FeO buffer was used to control the redox state equal to the lower mantle. Nitrogen in recovered samples were analyzed using NanoSIMS installed at Atmosphere and Ocean Research Institute, The University of Tokyo. Nitrogen implanted standard samples were prepared in order to estimate nitrogen solubility in silicate minerals at National Institute for Materials Science.

A series of experimental results revealed that stishovite can incorporate 39-418 ppm nitrogen which is higher than nitrogen solubility in bridgmanite (5-50 ppm nitrogen solubility reported by Yoshioka et al. (2018)). Stishovite is mainly formed by the transition of nitrogen-rich sedimentary rocks transported to the lower mantle via subducting slabs. Our study suggests that nitrogen would continue to be supplied to the lower mantle via subducting slabs since when the plate tectonics had begun. This implies that "hidden" nitrogen reservoir was formed in the lower mantle approximately 4 billion years ago. Furthermore, this " hidden" nitrogen reservoir may play a role in decreasing high-concentration nitrogen which had enhanced greenhouse effect in the early atmosphere (Goldblatt et al., 2009) to the present nitrogen concentration level. Thus, our experimental results support the young faint Sun paradox explained by high-concentration nitrogen in the early Earth (e.g. Goldblatt et al., 2009; Wordsworth and Pierrehumbert, 2013) and suggest that "missing" nitrogen has been caused by forming a "hidden" nitrogen reservoir in the lower mantle.

Keywords: "Missing" nitrogen, Deep nitrogen cycle, Plate techtonics, Stishovite, The faint young Sun paradox

©2019. Japan Geoscience Union. All Right Reserved.

©2019. Japan Geoscience Union. All Right Reserved.

3-D P- and S-velocity structure of the D″ layer beneath Central America and the Caribbean using waveform inversion

*Anselme F. E. Borgeaud[1,2], Kenji Kawai[1], Robert J. Geller[1]

1. Department of Earth and Planetary Science, Graduate School of Science, University of Tokyo, 2. Institute of Earth Sciences, Academia Sinica

We present 3-D P- and S-velocity models of the lowermost mantle (0–400 km above the core-mantle boundary) beneath Central America and the Caribbean inferred from waveform inversion of a large dataset of ~16,000 USArray waveforms data. The origin of seismic velocity anomalies in the D″ region, e.g., thermal, chemical, or due to the phase transition from Bridgemanite (brg) to post-perovskite (pPv), is still debated. Insights into the origin of velocity anomalies can be obtained by comparison of P- and S-velocity models (Wentzcovitch et al. 2006). Previous tomographic studies have reported large S-to-P velocity ratio in the lowermost mantle based mainly on normal modes, which can constrain the large-scale structure of the mantle (e.g., Masters et al. 2000; Koelemeijer et al. 2018). There are, however, few local high-resolution models of the 3-D P- and S-velocity structure of the lowermost mantle due to the difficulty of measuring the arrival-time of the small-amplitude PcP phase. Since waveform inversion does not require measuring arrival times, it might provide a more robust way of using the PcP phase to constrain the high-resolution structure of the lowermost mantle. In this study, we use ~7000 transverse component and ~7000 vertical component records from ~38 intermediate and deep-focus earthquakes in South-America recorded at USArray stations between 2004–2015. The records are cut ~10 s before the arrival of the P (S) phase, and ~40 s after the arrival of the PcP (ScS) phase. Resolution tests shows that we can resolve separately the P- and S-velocity structure of the lowermost mantle on scales less than ~300 km. Our preliminary results show a relatively good correlation between S- and P-wave anomalies on small-scales, with a large S-to-P velocity ratio in the range 100–300 km above the CMB, and a smaller ratio 0–100 km above the CMB, in general agreement with the results of Koelemeijer et al. (2018).

Keywords: Waveform inversion, Lowermost mantle

©2019. Japan Geoscience Union. All Right Reserved.

Uniaxial deformation experiments of bridgmanite using D-111 type high pressure apparatus

*Noriyoshi Tsujino[1], Daisuke Yamazaki[1], Yu Nishihara[2]

1. Institute for Planetary Materials, Okayama University, 2. Geodynamics Research Center, Ehime University

One dimensional viscosity models of the Earth’s mantle proposed by geophysical observations suggested that the lower mantle had the largest viscosity in the Earth’s mantle. In order to understand mantle dynamics in the Earth’s interior, it is important to know the viscosity of the Earth’s lower mantle. However, there are large variations of viscosity in the lower mantle between suggested models because of limitation of locations for geophysical observations. Therefore it is important to determine viscosity of lower mantle minerals by high pressure experiments in order to discuss mantle dynamics. Bridgmanite would be the most abundant mineral in the lower mantle. This mineral could dominate the lower mantle viscosity. In this study, we conducted in-situ stress-strain measurements of uniaxial deformation experiments of bridgmanite aggregate using D-111 type high pressure apparatus.
In-situ measurements were conducted using MAX III with D111 type guide block at PF-AR NE7A beam line. Mg-pure bridgmanite aggregates were used as starting material. Experimental conditions are 1473-1673 K and 24-27 GPa. WC second cubic anvils with cone (6.5˚) to take 2D X-ray diffraction, was used along X-ray path. Two-dimensional X-ray diffraction patterns were corrected for 240 s using flat panel detector. To calculate pressure and the stress magnitude of bridgmanite, (112) X-ray diffraction peaks were used. Strain of bridgmanite was measured by X-ray radiographies taken using an imaging system composed of a YAG crystal and a CMOS camera.
Largest strain was reached to approximately 20 %. It is confirmed that strain rate can be well controlled using stroke speed of differential rams. Steady state creep were observed at 1473 K –1673 K and 5 $\times 10^{-6}$ –3.8 $\times 10^{-5}$ /s. At normalized strain (10^{-5} /s), the creep strength of bridgmanite in this study is the largest in constituent mantle minerals reported by D-DAI apparatus.

Keywords: Bridgmanite, Deformation experiments, Creep strength

©2019. Japan Geoscience Union. All Right Reserved.

Waveform inversion for 3D anisotropic structure in D″ beneath the Northern Pacific: Constraints on mineralogy and flow in the lowermost mantle

*Yuki Suzuki[1], Kenji Kawai[1], Robert J. Geller[1]

1. Department of Earth and Planetary Sciences, School of Science,The University of Tokyo

The D″ region is the lowermost several hundred km of the mantle immediately above the core-mantle boundary (CMB) and its base is in contact with the liquid outer core composed of iron alloy. Since the D″ region is the thermal boundary layer (TBL) at the base of the Earth's mantle, and the solidus of its constituent materials is thought to be close to the mantle geotherm, vertical and lateral variations of temperature and chemical composition associated with the Earth's thermal evolution are expected. Since chemically and thermally distinct subducted slabs would interact with the hot TBL above the CMB, and disturb the lowermost mantle, understanding the thermal and chemical evolution processes of the D″ region under subduction zones is essential to better understand the Earth's evolution.
The D″ region beneath the northern Pacific is of particular geodynamical interest because the paleo-Izanagi and present Pacific plates have been subducting beneath the northwestern margin of Laurentia since ~250 million years ago (Müller et al. 2016), which implies that paleoslabs could have reached the lowermost mantle. Suzuki et al. (2016) inferred the detailed three-dimensional S-velocity structure in the lowermost 400 km of the mantle beneath the northern Pacific. They hypothesized a prominent sheet-like lateral high-velocity, interpreted as paleoslabs, and a prominent low-velocity anomaly block immediately above the CMB below the high-velocity anomalies, which they interpreted as a TBL. In order to verify the above hypothesis and obtain geodynamical information, we infer 3D anisotropic structure beneath the northern Pacific in this study.
We conduct waveform inversion (Kawai et al. 2014) to infer the variation of the values of the TI (transverse isotropic, i.e. radial anisotropic) elastic constants L and N (Note that L is related to V_{SV} and N is related to V_{SH} when the shear wave propagates horizontally) straightforwardly in the lowermost mantle beneath the Northern Pacific, using a total of ~18,000 (~9,000 transverse and ~9,000 radial component) broadband body-wave seismograms. We used deep- and intermediate-focus events recorded at epicentral distances 70 to100 degrees at seismic stations of the USArray. The data are filtered in the period range of 20 to 200 s (i.e. 0.005 to 0.05 Hz) using a Butterworth bandpass filter. By using an S/ScS time window which is sensitive to the D″ structure we could image small-scale structure with finer resolution than previous tomographic studies.
The observed anisotropy is interpreted as due to the deformation-induced alignment of crystal caused by mantle flow for either Mg-perovskite (Mg-Pv), Mg-post-Perovskite (Mg-pPv), Ferro-periclase (Fp) or a combination thereof. In order to relate the flow geometry to the anisotropic geometry, we assume the dominant glide system and elastic constants of each mineral under the lowermost mantle condition based on high pressure experiment and theoretical calculation studies (e.g., Tsujino et al. 2016, Yamazaki et al. 2006 for deformation experiments; Wentzcovich et al. 2006 for ab initio calculation). We interpret the inferred 3D anisotropic structure based on above assumption, and we find the horizontal flow which could be related to subducted paleo-slabs is dominant in this region, and we also find vertical flow which could be related to the plume induced by slab sinking.

Keywords: the lowermost mantle, waveform inversion, anisotropy, D" region

©2019. Japan Geoscience Union. All Right Reserved.

©2019. Japan Geoscience Union. All Right Reserved.

Maximum water solubility of bridgmanite under the Earth's lower mantle conditions

*Sho Kakizawa[1], Toru Inoue[1,2,3], Ryotaro Abe[1], Minami Kuroda[4], Naoya Sakamoto[5], Hisayoshi Yurimoto[4,5,6]

1. Geodynamics Reseach Center, Ehime University, 2. Graduate School of Science, Hiroshima University, 3. Hiroshima Institute of Plate Convergence Region Research, 4. Graduate School of Science, Hokkaido University, 5. Creative Research Institution, Hokkaido University, 6. Institute of Space and Astronautical Science, Japan Aerospace Exploration Agency

The Earth initially contained ~2 wt% H_2O, if it was formed by the mixture of C1 chondrite and enstatite chondrite [Ringwood, 1977]. However, the mass of the Earth's ocean is only 0.02 wt% of that of the Earth. Thus, most of the H_2O or molecular H may have been lost from the Earth since then, or it may still be stored in the Earth's deep interior. Water significantly influences the physical and chemical properties of the mantle minerals and rocks. Therefore, it is important to clarify the effect of water to understand the evolution and dynamics of the Earth. A part of water in the deep mantle can be dissolved in nominally anhydrous minerals. Wadsleyite and ringwoodite which are the major constituent minerals in the mantle transition zone, can contain ~2-3 wt% H_2O [e.g., Inoue et al., 1995; Kohlstedt et al., 1996]. On the other hand, water solubility of bridgmanite which is the most abundant mineral in the lower mantle, is a matter of debate [e.g., Bolfan-Casanova et al., 2004; Murakami et al., 2003]. Recently, Al-bearing hydrous bridgmanite contained ~0.8 wt% water was synthesized by Inoue et al. (under review). This report suggests that lower mantle can become a water reservoir in the Earth. However, the effects of pressure and Fe content on maximum water solubility of Al-bearing bridgmanite have not been clarified yet.
To determine the maximum water solubility of Al-bearing hydrous bridgmanite, high pressure and high temperature experiments were conducted under the conditions of 25-48 GPa and 1600℃. The starting materials were prepared by the mixtures of MgO, SiO_2, $Mg(OH)_2$, and $Al(OH)_3$ reagents with clinochlore [$Mg_5Al_2Si_3O_{10}(OH)_8$], Fe-bearing natural chlorite [$Mg_{4.9}Al_{1.6}Si_{3.2}Fe_{0.3}O_{10}(OH)_8$], and Fe-bearing hydrous pyrolite compositions. The water contents of the recovered run products were measured by SIMS. The water contents of Al-bearing hydrous bridgmanite increased with increasing pressure, at least up to 48 GPa. This is considered to occur the following two hydrous coupling substitutions with increasing pressure: $Si^{4+} = Al^{3+} + H^+$ and $2Mg^{2+} = Al^{3+} + H^+ + V_{Mg}$. These substitutions were dominant at low Al content, and Tschermak substitution ($Mg^{2+} + Si^{4+} = 2Al^{3+}$) became dominant with increasing Al content above Al = ~0.1 per formula unit (pfu, O = 3). The water content decreased as a result of Tschermak substitution, thus the maximum water solubility of bridgmanite is expected to be about 1.0 wt% at Al = ~0.1 pfu. In addition, the water solubility of Al-bearing hydrous bridgmanite decreased in the presence of Fe, and it became clear that it depends on the amount of Al and Fe in bridgmanite. Because of these properties, the maximum water solubility of bridgmanite in pyrolite and MORB are expected to be ~0.1 and ~0.2 wt%, respectively. When ringwoodite with high H_2O content is subducted to the lower mantle, the dehydration would occur at the top of the lower mantle. The dehydrated water should decrease melting temperature of the surrounding rocks and generates magma. Moreover, when chlorite dominant rock with high Al and low Fe content is subducted to the lower mantle, water heterogeneity would be predicted in the lower mantle, because the water content of bridgmanite generated by chlorite is significantly higher than that generated by pyrolite.

Keywords: deep mantle, lower mantle, bridgmanite, water

©2019. Japan Geoscience Union. All Right Reserved.

©2019. Japan Geoscience Union. All Right Reserved.

Origin and role of lost continents

*Shigenori Maruyama[1], Kenji Kawai[2], Steeve Gréaux[3], Taku Tsuchiya[3], Dapeng Zhao[4]

1. Earth-Life Science Institute, Tokyo Institute of Technology, 2. Department of Earth and Planetary Science, School of Science, University of Tokyo, 3. Ehime University, 4. Department of Geophysics, Tohoku University

<Purpose>

Continental crust had long been regarded that it cannot subduct into mantle forever because of lower density. If so, the Earth must have extraordinary thick continental crust over 300km in thickness. But, of course, not. We elucidate where continental curst has gone?

<Method>

Recently, on-going process of direct subduction of island arcs off Japan was reported (Yamamoto et al., 2007), as well as tectonic erosion of hanging wall of continental crust (von Huene and Scholl, 1991), the physical process by numerical simulation (Ichikawa et al., 2009), the presence of abundant TTG materials in MTZ (Kawai et al., 2013), and spatial distribution of the second continents in the MTZ over the world (Maruyama et al., 2008).

<Result>

We revealed continental curst is subducted into mantle and accumulated as “lost continent”. The estimated mass of the lost continent in MTZ (depth range of 520-660km) is 7.5 times more than total volume of TTG crust on the surface Kawai et al (2009; 2013), and the existing material is expected to be TTG, not MORB or harzuburgite based on seismology. Kawai et al. (2007) also predicted that D” layer ca. 300km thick right above CMB could be another lost continent, which anorthosite and KREEP dominated. However, this idea cannot explain reasonable enough that the density of KREEP basalt is close to that of surrounding peridotites. According to more recent estimate by Greaux et al. (2018), lost continent on CMB is expected to be fractionated KREEP and anorthosite. If KREEP lower crust of the Hadean continent subducted and segregated at 660km depth, these material could be falling preferentially into lower mantle, and they must have been accumulated on the CMB.

<Discussion>

It is pointed out that those lost continents may have played critical role for the thermal history of Earth, because most radiogenic elements such as U, Th, and K were predominantly concentrated into the primordial continents, whereas these elements were rare in the mantle. Radiogenic elements contained in lost continents must have contributed as the heat generator of the inner Earth and controlled thermal history of the Earth. One of the most significant next research targets is to conduct the quantitative estimates of lost continent. The idea of lost continents would change the concept of mantle dynamics.

Keywords: KREEP basalt, Lost continent, mantle dynamics

©2019. Japan Geoscience Union. All Right Reserved.

[E] Oral | S (Solid Earth Sciences)：S-IT Science of the Earth's Interior & Techtonophysics

Mon. May 27, 2019 10:45 AM - 12:15 PM JST | Mon. May 27, 2019 1:45 AM - 3:15 AM UTC | A10 TOKYO BAY MAKUHARI HALL

[S-IT21] Interaction and Coevolution of the Core and Mantle in the Earth and Planets

convener:Kenji Kawai(Department of Earth and Planetary Science, School of Science, University of Tokyo), Tsuyoshi Iizuka(University of Tokyo), Kenji Ohta(Department of Earth and Planetary Sciences, Tokyo Institute of Technology), Taku Tsuchiya(Geodynamics Research Center, Ehime University), Chairperson:Kenji Ohta, Riko Iizuka

Recent observational and experimental investigations have significantly advanced our understanding of the structure and constituent materials of the deep Earth. Yet, even fundamental properties intimately linked with formation and evolution of the planet, such as details of the chemical heterogeneity in the mantle and light elements dissolved in the core, remained unclear. Seismological evidence has suggested a vigorous convection in the lower mantle, whereas geochemistry has suggested the presence of stable regions there that hold ancient chemical signatures. The amounts of radioactive isotopes that act as heat sources and drive dynamic behaviors of the deep Earth are also still largely unknown. We provide an opportunity to exchange the achievements and ideas, and encourage persons who try to elucidate these unsolved issues of the core-mantle evolution using various methods, including high-pressure and high-temperature experiments, high-precision geochemical and paleomagnetic analyses, high-resolution geophysical observations, geo-neutrino observations, and large-scale numerical simulations. Papers stimulating an interdisciplinary collaboration relating to establishment of the Japan-SEDI community are also welcomed.

10:45 AM - 11:00 AM JST | 1:45 AM - 2:00 AM UTC

[SIT21-07] Thermal conductivity anomaly in spin-crossover ferropericlase under lower mantle conditions

★Invited Papers

*Zhongqing Wu[1] (1.University of Science and Technology of China)

11:00 AM - 11:15 AM JST | 2:00 AM - 2:15 AM UTC

[SIT21-08] Discussion

*Kenji Ohta[1] (1.Department of Earth and Planetary Sciences, Tokyo Institute of Technology)

11:15 AM - 11:30 AM JST | 2:15 AM - 2:30 AM UTC

[SIT21-09] ***Ab initio* anharmonic lattice dynamics for Fe-bearing lower mantle minerals**

*Haruhiko Dekura[1], Taku Tsuchiya[1] (1.Geodynamics Research Center, Ehime University)

11:30 AM - 11:45 AM JST | 2:30 AM - 2:45 AM UTC

[SIT21-10] **Measurements of high pressure-temperature thermal conductivity of the Earth's lower mantle minerals in a laser-heated diamond anvil cell**

*Kenji Ohta[1], Akira Hasegawa[1,2], Takashi Yagi[2], Yoshiyuki Okuda[1], Koutarou Onga[1], Kei Hirose[3,4], Yasuo Ohishi[5] (1.Department of Earth and Planetary Sciences, Tokyo Institute of Technology, 2.National Metrology Institute of Japan, National Institute of Advanced Industrial Science and Technology, 3.Earth-Life Science Institute, Tokyo Institute of Technology, 4.Department of Earth and Planetary Science, The University of Tokyo, 5.Japan Synchrotron Radiation Research Institute)

11:45 AM - 12:00 PM JST | 2:45 AM - 3:00 AM UTC

[SIT21-11] Is there evidence for a paleo-LLSVP beneath Eurasia?: Implications for the origin of the Siberian Traps

*Tsubasa Ue[1], Yuki Suzuki[1], Kenji Kawai[1] (1.Department of Earth and Planetary Sciences, Graduate School of Science, The University of Tokyo)

12:00 PM - 12:15 PM JST | 3:00 AM - 3:15 AM UTC

[SIT21-12] Possible compositional region of Al-bearing anhydrous bridgmanite

*Toru Inoue[1,2], Masamichi Noda[2], Sho Kakizawa[2] (1.Department of Earth and Planetary Systems Science, Graduate School of Science, Hiroshima University, 2.Geodynamics Research Center, Ehime University)

Thermal conductivity anomaly in spin-crossover ferropericlase under lower mantle conditions

*Zhongqing Wu[1]

1. University of Science and Technology of China

Thermal conductivity of the mantle minerals is one of the key parameters that control mantle convection. The heat flux from the core, which is determined by the heat conductivity of the thin layer overlying the core-mantle boundary (CMB), is critical to the understanding of many processes such as the Earth’s evolution, mantle convection, and geodynamo. Iron in ferropericlase experiences a spin crossover from a high spin to a low spin under lower mantle conditions, which generates anomalies in many properties such as the heat capacity and sound velocity (Wu et al., 2009, 2013). Since the thermal conductivity is proportional to the heat capacity and the square of the sound velocity, the spin-state crossover of iron in the lower mantle minerals may profoundly affect the lattice thermal conductivity of the lower mantle. However, knowledge of the spin-crossover effect on the lattice thermal conductivity is very limited.

Here, I found that the spin crossover completely changes the conventional pressure and temperature dependences of the thermal conductivity. The pressure dependence of the thermal conductivity of ferropericlase will show a double-valley feature across the spin-crossover region. Thermal conductivity of ferropericalse may increase with the temperature in some temperature region. The spin crossover can explain the anomalous reduction in thermal conductivity of ferropericlase observed recently by Ohta et al (2017) in the spin crossover region. The unusual effect of spin crossover on the thermal conductivity can be expected in other minerals with spin crossover. Since the spin-crossover region of ferropericlase covers the CMB conditions, the spin crossover effect needs serious consideration when estimating the thermal conductivity at the core-mantle boundary

Wu, Z., J. F. Justo, C. R. S. da Silva, S. de Gironcoli, and R. M. Wentzcovitch (2009), Anomalous thermodynamic properties in ferropericlase throughout its spin crossover transition, *Phys. Rev. B*, *80*(1), 014409.

Wu, Z. Q., J. F. Justo, and R. M. Wentzcovitch (2013), Elastic Anomalies in a Spin-Crossover System: Ferropericlase at Lower Mantle Conditions, *Phys. Rev. Lett.*, *110*(22).

Ohta, K., T. Yagi, K. Hirose, and Y. Ohishi (2017), Thermal conductivity of ferropericlase in the Earth's lower mantle, Earth and Planetary Science Letters, 465, 29-37.

©2019. Japan Geoscience Union. All Right Reserved.

Discussion

*Kenji Ohta[1]

1. Department of Earth and Planetary Sciences, Tokyo Institute of Technology

Discussion

©2019. Japan Geoscience Union. All Right Reserved.

Ab initio anharmonic lattice dynamics for Fe-bearing lower mantle minerals

*Haruhiko Dekura[1], Taku Tsuchiya[1]

1. Geodynamics Research Center, Ehime University

Determination of lattice thermal conductivity (κ_{lat}) of lower mantle (LM) minerals is a key to understanding the dynamics and evolution of the earth’ s deep interior. Some recent experimental studies have shown that κ_{lat} of MgO and $MgSiO_3$ bridgmanite (Brg) are substantially reduced by Fe incorporation (Manthilake et al., 2012; Goncharov et al., 2015; Ohta et al., 2017; Hsieh et al., 2017). In contrast, Okuda et al. (2017) reported a very different result on Brg with a marginal effect of Fe. Besides, the effect of Fe on $MgSiO_3$ post-perovskite (PPv) has never been reported. Therefore, in this study, we investigate κ_{lat} of Fe-bearing LM minerals (ferropericlase (FP), Brg, and PPv) in the LM pressure and temperature conditions, based on the *ab initio* anharmonic lattice dynamics techniques with fully solving the phonon Boltzmann transport equation (Dekura and Tsuchiya, 2017) combined with the internally consistent LDA+*U* technique for more precisely describing the Fe-O bond (Wang et al., 2015). Calculations demonstrate strong negative solid solution effects of low-spin Fe on κ_{lat} of FP and high-spin Fe on κ_{lat} of Brg and PPv, as a linear decrease in log κ_{lat} of FP with increasing the Fe concentration. Our detailed analyses indicate that such strong effects occur primarily due to the substantial changes in harmonic properties and are found to be Brg > PPv >FP. The present results improve the conventional estimation of the effective LM conductivity (e.g., Stacey 1992). It is estimated to be ~2-3 $Wm^{-1}K^{-1}$ for the pyrolytic aggregate (FP + Brg) and ~4-5 $Wm^{-1}K^{-1}$ (FP+PPv) at 136 GPa and 4000 K, which are ~60-80% smaller than the conventional value of 10 $Wm^{-1}K^{-1}$.

Keywords: Lower mantle minerals, Lattice thermal conductivity , First-principles calculation

©2019. Japan Geoscience Union. All Right Reserved.

Measurements of high pressure-temperature thermal conductivity of the Earth's lower mantle minerals in a laser-heated diamond anvil cell

*Kenji Ohta[1], Akira Hasegawa[1,2], Takashi Yagi[2], Yoshiyuki Okuda[1], Koutarou Onga[1], Kei Hirose[3,4], Yasuo Ohishi[5]

1. Department of Earth and Planetary Sciences, Tokyo Institute of Technology, 2. National Metrology Institute of Japan, National Institute of Advanced Industrial Science and Technology, 3. Earth-Life Science Institute, Tokyo Institute of Technology, 4. Department of Earth and Planetary Science, The University of Tokyo, 5. Japan Synchrotron Radiation Research Institute

The thermal transport properties of the Earth's constituents are important information to understand thermal evolution and the heat budget of the Earth. Thus, the experimental determination of thermal conductivity of deep Earth materials are required. The diamond anvil cell (DAC) is capable of accessing the pressure-temperature conditions of the Earth's deep interior, and is compatible with laser optical techniques. The pulsed light heating thermoreflectance (TR) method has been applied to a DAC in order to measure thermal conductivity and diffusivity of condensed material [1,2]. This TR with DAC method successfully obtained the thermal conductivity of the Earth's lower mantle minerals to the pressure condition equal to the Earth's core-mantle boundary (135 GPa) but at room temperature [3]. To extend measurable temperature range, the TR method may be combined with a laser-heated DAC (LHDAC) technique that is able to generate the pressure-temperature condition equivalent to the center of the Earth.

We recently developed a new instrument to measure the thermal diffusivity (and thus thermal conductivity) of sample *in-situ* at high pressure and temperature based on the combination of the TR method and the LHDAC system. We use a double-sided high-power CW laser heating technique to generate stable high temperature conditions of sample in a DAC. A pulsed pump laser and a CW probe laser are also irradiated to the sample to determine heat diffusion time through the sample via the thermoreflectance phenomena. Details of the thermoreflectance technique in a DAC may be found in our previous studies [2]. Using the developed method, we measured the thermal conductivity of the main minerals in the Earth's lower mantle, MgO periclase, $MgSiO_3$ bridgmanite, post-perovskite and $CaSiO_3$ perovskite *in-situ* at high pressures and high temperatures. These are the first experimental demonstrations of thermal conductivity of the lower mantle minerals at the conditions below the mid-part of the Earth's lower mantle. The new thermal conductivity measurement system will shed light on the controversial thermal transport properties of the Earth's deep interior [4].

References:[1] Hsieh, W.-P. et al., *Phys. Rev. B*, **80**, 180302 (2009).[2] Yagi, T. et al., *Meas. Sci. Technol.,* **22**, 024011 (2011). [3] Okuda, Y. et al., *Earth Planet. Sci. Lett.*, **474**, 25–31 (2017). [4] Kavner, A. and Rainey, E.S.G., *Deep Earth: Physics and Chemistry of the Lower Mantle and Core*, 31–42 (2016).

Keywords: Thermal conductivity, Lower mantle, High P-T experiment

©2019. Japan Geoscience Union. All Right Reserved.

Is there evidence for a paleo-LLSVP beneath Eurasia?: Implications for the origin of the Siberian Traps

*Tsubasa Ue[1], Yuki Suzuki[1], Kenji Kawai[1]

1. Department of Earth and Planetary Sciences, Graduate School of Science, The University of Tokyo

The massive eruption during the latest Permian, which precipitated the Earth's most severe known extinction event, is one of the largest known volcanic events on Earth. However, the cause of the active volcanism remains incompletely understood. Recent seismological analysis has revealed that currently active volcanoes are related to seismic low-velocity anomalies which are almost vertically continuous from the core-mantle boundary (CMB) to shallow depths. Here we infer the seismic velocity structure beneath Eurasia in order to confirm whether formerly active volcanism is also related to a mantle upwelling.

We apply the 3-D localized waveform inversion methods to about 5,500 transverse-component of broadband body-wave seismograms observed at Japan for 3 intermediate and deep earthquakes occurred in Europe, European stations for 116 events occurred beneath the western Pacific subduction zone and Canadian stations for 5 events occurred beneath the Hindu Kush. We use waveform data obtained from the National Research Institute for Earth Science and Disaster Prevention (NIED), Observation & Research Facilities for European Seismology (ORFEUS) and Canadian National Data Centre (CNDC).

We found a high-velocity anomaly about 100 km above the CMB beneath Lake Baikal and two low-velocity anomalies immediately above the CMB beneath the cities of Perm and Irkutsk, Russia, respectively. Plate reconstructions show there are some large igneous provinces (LIPs) and slab remnants beneath Eurasia. Our results suggest two scenarios: one where two low-velocity anomalies used to be united and larger than present size but divided and weakened by the subducted cold slab and another where two low-velocity anomalies were originally separated with each other and became different LIPs. In either case, our findings suggest that the cause of a massive eruption during the latest Permian was a plume upwelling from the CMB.

Keywords: D″, Waveform inversion, Perm Anomaly, LIPs, S velocity structure

©2019. Japan Geoscience Union. All Right Reserved.

Possible compositional region of Al-bearing anhydrous bridgmanite

*Toru Inoue[1,2], Masamichi Noda[2], Sho Kakizawa[2]

1. Department of Earth and Planetary Systems Science, Graduate School of Science, Hiroshima University, 2. Geodynamics Research Center, Ehime University

Bridgmanite should be a major constituent mineral in the Earth's lower mantle, and Irifune (1994) reported that bridgmanite can incorporate almost Al_2O_3 component in lower mantle. The Al substitution mechanism is supposed to be complicated, because there are two types of Al substitution mechanisms in anhydrous bridgmanite, Tschermak and oxygen vacancy substitutions (e.g. Kojitani et al., 2007). However, the pure Tschermak and oxygen vacancy substitutions bridgmanite has not been reported so far in low Al content, when we checked the previous studies carefully (e.g. Irifune et al, 1996; Kubo and Akaogi, 2000). The previous studies have used powder samples as the starting materials, so we considered that the absorbed water may affect the results, because we have a knowledge of the possible existence of hydrous bridgmanite which has a water content of ~0.8 wt%. Therefore, we tried to investigate the possible existence of the Al substitution mechanism in bridgmanite as a function of Al content in extremely anhydrous condition.

The high pressure experiments were conducted at 28 GPa and 1600-1700℃ for 1 hour using a Kawai type apparatus. Some different Al content samples were prepared as the starting materials along the ideal substitution line of Tschermak and oxygen vacancy substitutions, respectively. Glass rods were used as the starting materials to eliminate the absorbed water on the sample surface. Moreover, the glass rods were enclosed in a rhenium capsule to prevent the water incorporation from the surrounding cell assembly. In addition, all parts of the cell assembly were dried just before the synthesis experiments. The chemical compositions of the starting materials were examined by SEM-EDS, and the recovered samples were identified by X-ray and neutron (in J-PARC) diffractions and SEM-EDS.

Our results show that it is possible to exist both Tschermak and oxygen vacancy substitution bridgmanites in low Al content in anhydrous condition. The maximum Al content for pure oxygen vacancy substitution bridgmanite was ~0.025 pfu in total cation of 2, and the existence of oxygen vacancy substitution component was restricted to be less than Al=~0.1 pfu. The present result combining with our previous study in hydrous condition, shows that hydration in Al-bearing bridgmanite should occur easily if hydrogen exists in the system (lower mantle) in pyrolite (MgO-excess) composition. Thus the large deviation from the Tschermak substitution in the previous studies mainly should come from the hydration from the absorbed water.

Keywords: lower mantle, bridgmanite, Al2O3 component, anhydrous condition, hydrous condition

©2019. Japan Geoscience Union. All Right Reserved.

[E] Oral | S (Solid Earth Sciences)：S-IT Science of the Earth's Interior & Techtonophysics

Mon. May 27, 2019 1:45 PM - 3:15 PM JST | Mon. May 27, 2019 4:45 AM - 6:15 AM UTC | A10 TOKYO BAY MAKUHARI HALL

[S-IT21] Interaction and Coevolution of the Core and Mantle in the Earth and Planets

convener:Kenji Kawai(Department of Earth and Planetary Science, School of Science, University of Tokyo), Tsuyoshi Iizuka(University of Tokyo), Kenji Ohta(Department of Earth and Planetary Sciences, Tokyo Institute of Technology), Taku Tsuchiya(Geodynamics Research Center, Ehime University), Chairperson:Hitoshi Gomi, Tsuyoshi Iizuka

Recent observational and experimental investigations have significantly advanced our understanding of the structure and constituent materials of the deep Earth. Yet, even fundamental properties intimately linked with formation and evolution of the planet, such as details of the chemical heterogeneity in the mantle and light elements dissolved in the core, remained unclear. Seismological evidence has suggested a vigorous convection in the lower mantle, whereas geochemistry has suggested the presence of stable regions there that hold ancient chemical signatures. The amounts of radioactive isotopes that act as heat sources and drive dynamic behaviors of the deep Earth are also still largely unknown. We provide an opportunity to exchange the achievements and ideas, and encourage persons who try to elucidate these unsolved issues of the core-mantle evolution using various methods, including high-pressure and high-temperature experiments, high-precision geochemical and paleomagnetic analyses, high-resolution geophysical observations, geo-neutrino observations, and large-scale numerical simulations. Papers stimulating an interdisciplinary collaboration relating to establishment of the Japan-SEDI community are also welcomed.

1:45 PM - 2:00 PM JST | 4:45 AM - 5:00 AM UTC

[SIT21-13] Evolution of the Earth mantle and its possible interaction with core: view from olivine and its inclusions study

★Invited Papers

*Alexander V Sobolev[1], Valentina G. Batanova[2] (1.ISTerre Institute of Earth Sciences, 2.Vernadsky Institute of Geochemistry and Analytical Chemistry, Russian Academy of Sciences, Kosygina str. 19, Moscow 119991, Russia.)

2:00 PM - 2:15 PM JST | 5:00 AM - 5:15 AM UTC

[SIT21-14] Discussion

*Tsuyoshi Iizuka[1] (1.University of Tokyo)

2:15 PM - 2:30 PM JST | 5:15 AM - 5:30 AM UTC

[SIT21-15] Ultralow-velocity zones possibly explained by light element-enriched iron compounds

*Liang Yuan[1], Eiji Ohtani[1], Xiang Wu[2], Shengxuan Huang[3], Daijo Ikuta[1], Tatsuya Sakamaki[1], Seiji Kamada[1], Hiroshi Fukui[4,5], Satoshi Tsutsui[6], Hiroshi Uchiyama[6], Daisuke Ishikawa[5,6], Naohisa Hirao[6], Alfred Q. R. Baron[5] (1.Department of Earth and Planetary Materials Science, Graduate School of Science, Tohoku University, Sendai 980-8578, Japan, 2.State Key Laboratory of Geological Processes and Mineral Resources, China University of Geosciences, Wuhan 430074, China, 3.Key Laboratory of Orogenic Belts and Crustal Evolution, MOE, Peking University and School of Earth and Space Sciences, Peking University, Beijing 100871, China, 4.Center for Novel Material Science under Multi-Extreme Conditions, Graduate School of Material Science, University of Hyogo, Hyogo 678-1297, Japan, 5.Materials Dynamics Laboratory, RIKEN SPring-8 Center, Hyogo 679-5148, Japan, 6.Japan Synchrotron Radiation Research Institute (JASRI), SPring-8, Hyogo, 679-5198, Japan)

2:30 PM - 2:45 PM JST | 5:30 AM - 5:45 AM UTC

[SIT21-16] High-precision $^{142}W/^{144}W$ ratios of oceanic island basalts and Large Igneous Province basalts.

Asako Takamasa[1], *Katsuhiko Suzuki[1], Yusuke Fukami[2], Tsuyoshi Iizuka[3] (1.Research and Development Center for Submarine Resources, Japan Agency for Marine-Earth Science and Technology, 2.Department

of Subsurface Geobiological Analysis and Research, Japan Agency for Marine-Earth Science and Technology, 3.Graduate School of Science, The University of Tokyo)

2:45 PM - 3:00 PM JST | 5:45 AM - 6:00 AM UTC

[SIT21-17] **Some technological developments in high temperature generation using KMA and precise melting/phase relations of minerals and rocks under deep mantle conditions**

*Tetsuo Irifune[1,2], Youmo Zhou[1], Takeshi Arimoto[1], Hideharu Kuwahara[1], Ryuichi Nomura[3], Masayuki Nishi[1], Momoko Yamaguchi[1], Yoshinori Tange[4], Takahiro Kuribayashi[5], Zhaodong Liu[6] (1.Geodynamics Research Center, Ehime University, 2.Eearth Life Science Institute, Tokyo Institute of Technology, 3.Hakubi Center/ Graduate School of Human and Environmental Studies, Kyoto University, 4.Research & Utilization Division, Japan Synchrotron Research Institute, 5.Graduate School of Science, Tohoku University, 6.Institute of Super Hard Materials, Jilin University)

3:00 PM - 3:15 PM JST | 6:00 AM - 6:15 AM UTC

[SIT21-18] Zr isotope constraints on early Earth differentiation

*Tsuyoshi Iizuka[1], Keita Itano[1], Shinji Yamamoto[2] (1.University of Tokyo, 2.Yokohama National University)

Evolution of the Earth mantle and its possible interaction with core: view from olivine and its inclusions study

*Alexander V Sobolev[1], Valentina G. Batanova[2]

1. ISTerre Institute of Earth Sciences, 2. Vernadsky Institute of Geochemistry and Analytical Chemistry, Russian Academy of Sciences, Kosygina str. 19, Moscow 119991, Russia.

The rate and style of mantle convection, as well as production and recycling of crust into the mantle, control the evolution of the Earth. Present knowledge of mantle evolution is mostly restricted to the Phanerozoic, for which fresh mantle-derived lavas and relevant geophysical data are available. Information about the Precambrian mantle comes almost entirely from the compositions of altered rocks, which lack data on the contents of mobile and volatile elements and their isotopes. Such data are crucial for geodynamic reconstructions and understanding of surface rock recycling into the deep mantle. Fortunately, this information is preserved within inclusions of melt in relicts of olivine phenocrysts in komatiites.

In this presentation we will address the compositional evolution of the terrestrial mantle, from the Archean to the Phanerozoic, using compositions and temperatures of primary mantle-derived melts reconstructed from the study of melt inclusions and host olivine. We will report an extensive range of geochemical parameters, including mobile and volatile element (Pb, B, Rb, Ba, Sr, Cl, S, H2O, CO2) concentrations and isotopic compositions of H in homogenized melt inclusions and the elemental compositions of host olivines and inclusions of spinel. We will present data for komatiites and picrites that originated at different depths and cratons between 3.3 and 0.09 Ga. We will apply published and new models to constrain the temperatures and compositions of their mantle sources to relate our observations to the evolution of mantle convection and plate tectonics. We will, therefore, address the following issues: the rate of crustal growth and recycling through time; the timing of the onset of large-scale subduction and plate tectonics; the concentration and origin of H2O and halogens in the deep mantle, and the extent (if any) of core-mantle interaction.

We will present evidence of the significant excess of H2O and Cl in the mantle sources of komatiites and will show that hydrogen isotope composition of komatiites is significantly more depleted in deuterium than all surface reservoirs and typical mantle but resembles that in dehydrated subducted slabs. We will demonstrate temporal trends of Pb/Ce and oxygen fugacity of primary komatiite melts.

Our results suggest that lithosphere recycling into the deep mantle, arguably via subduction, started before 3.3 Ga and interaction of mantle and core probably took place all this time.

©2019. Japan Geoscience Union. All Right Reserved.

Discussion

*Tsuyoshi Iizuka[1]

1. University of Tokyo

Discussion

©2019. Japan Geoscience Union. All Right Reserved.

Ultralow-velocity zones possibly explained by light element-enriched iron compounds

*Liang Yuan[1], Eiji Ohtani[1], Xiang Wu[2], Shengxuan Huang[3], Daijo Ikuta[1], Tatsuya Sakamaki[1], Seiji Kamada[1], Hiroshi Fukui[4,5], Satoshi Tsutsui[6], Hiroshi Uchiyama[6], Daisuke Ishikawa[5,6], Naohisa Hirao[6], Alfred Q. R. Baron[5]

1. Department of Earth and Planetary Materials Science, Graduate School of Science, Tohoku University, Sendai 980-8578, Japan, 2. State Key Laboratory of Geological Processes and Mineral Resources, China University of Geosciences, Wuhan 430074, China, 3. Key Laboratory of Orogenic Belts and Crustal Evolution, MOE, Peking University and School of Earth and Space Sciences, Peking University, Beijing 100871, China, 4. Center for Novel Material Science under Multi-Extreme Conditions, Graduate School of Material Science, University of Hyogo, Hyogo 678-1297, Japan, 5. Materials Dynamics Laboratory, RIKEN SPring-8 Center, Hyogo 679-5148, Japan, 6. Japan Synchrotron Radiation Research Institute (JASRI), SPring-8, Hyogo, 679-5198, Japan

The core–mantle boundary (CMB) is the most fundamental chemical discontinuity in the Earth. Recent experiments showed that, when water meets iron at the CMB, hydrogen-bearing iron peroxide FeO_2H_x can be produced. The results indicate that water can interact with iron metal very differently than it does on the surface of the earth. Seismic waves speeds in this hydrogen bearing iron peroxide are much slower compared with lower-mantle silicate solid phases, and therefore it may help explain the seismic anomalies at the CMB.

Given the steep geothermal gradient across the CMB, the hydrogen-bearing iron peroxide FeO_2H_x likely undergoes high-temperature decomposition into anhydrous iron oxides (e.g., Fe_2O_3) and fluids. We measured the sound velocity of Fe_2O_3 post-perovskite (ppv) through inelastic X-ray scattering up to 132 GPa and 1,800 K, relevant to the lowermost mantle. Combined with first-principles investigations, we are able to show that Fe_2O_3 ppv has very low sound velocities and strong anisotropy with respect to lower-mantle silicates. Therefore, both hydrogen-bearing iron peroxide FeO_2H_x and post-perovskite Fe_2O_3 are candidate phases for ultralow-velocity zones at the CMB.

Funding acknowledgment: This work was supported by the JSPS Japanese–German Graduate Externship.

Keywords: Core–mantle boundary, Ultralow-velocity zones, Light elements, Iron compounds

©2019. Japan Geoscience Union. All Right Reserved.

High-precision $^{142}W/^{144}W$ ratios of oceanic island basalts and Large Igneous Province basalts.

Asako Takamasa[1], *Katsuhiko Suzuki[1], Yusuke Fukami[2], Tsuyoshi Iizuka[3]

1. Research and Development Center for Submarine Resources, Japan Agency for Marine-Earth Science and Technology, 2. Department of Subsurface Geobiological Analysis and Research, Japan Agency for Marine-Earth Science and Technology, 3. Graduate School of Science, The University of Tokyo

Among five W isotopes, ^{182}W is a product of b-decay of ^{182}Hf with the relatively short half life of 8.9 m.y. As Hf and W are lithophile and siderophile, respectively, the ^{182}Hf-^{182}W radiometric system could constrain metal-silicate (core-mantle) differentiation, especially core segregation, in the very early Earth system because of its large fractionation between metal-silicate and the short half life of ^{182}Hf. Recent improvements of analytical techniques of W isotope analyses using TIMS and MC-ICP-MS equipped with a desolvating device allow to obtain highly precise $^{182}W/^{184}W$ ratios of terrestrial rocks. These led to findings of $m^{182}W$ anomalies (mostly positive) in old komatiites (2.4 –3.8 Ga) and young volcanic rocks with positive anomalies of 12 Ma Ontong Java Plateau and 6 Ma Baffin Bay (Rizo et al., 2016) and with negative anomalies of those such as the Loihi and Samoa basalts (Mundl et al., 2017). Recently, Kruijer and Kleine (2018) proposed that the ^{182}W excesses for an OJP sample by Rizo et al. (2016) may result from the nuclear field shift effect leading to defect of ^{183}W, as the NTIMS analyses utilized a double normalization involving the $^{183}W/^{184}W$ ratio.

In our study, high-precision W isotope ratio measurement with MC-ICP-MS (Thermo co. Ltd., NEPTUNE PLUS) equipped with desolvating nebulizer (ARIDAS II) following the chemical separation using both cation and anion exchange resin has been developed. We have measured the W standard solution (SRM 3163) and obtained the isotopic compositions with a precision of ±5ppm. However, the standard solution, which was processed by the cation or anion exchange chemistry in the same way as for rock samples, has systematic $^{182}W/^{184}W$ drift of -5ppm, which was also observed by Willbold et al. (2011) and Kruijer and Kleine (2018). This shift likely resulted from the nuclear field shift effect as mentioned by Kruijer and Kleine (2018). Therefore, we corrected the measured W isotope ratios of samples with the standard solution processed by the same method as that of the samples. This technique led to obtaining of the W isotopic compositions with reproducibility of several ppm. We have obtained negative $\mu^{182}W$ for the basalts with the high $^{3}He/^{4}He$ isotopic composition from the Loihi, Hawaii, through the developed analytical method. This result is consistent with that of Mundl et al., (2017). As the Earth’s core should have a negative $\mu^{182}W$ value of ca. -210, the Loihi sample we analyzed probably contains a component with a signature of core-mantle interaction. We have obtained the high-precision W isotope data for the fresh drilled basalts from Louisville. Louisville is known to have been originated from the primordial deep mantle source. We will discuss the obtained results and the early evolution of the deep mantle.

Acknowledgement –JSPS Grant-in-Aid has supported this project. We are grateful to M. Kawamura for experimental help and Y. Orihashi, T. Hanyu, M. Tejada for providing samples.

Keywords: tungsten isotope, core-mantle interaction

©2019. Japan Geoscience Union. All Right Reserved.

Some technological developments in high temperature generation using KMA and precise melting/phase relations of minerals and rocks under deep mantle conditions

*Tetsuo Irifune[1,2], Youmo Zhou[1], Takeshi Arimoto[1], Hideharu Kuwahara[1], Ryuichi Nomura[3], Masayuki Nishi[1], Momoko Yamaguchi[1], Yoshinori Tange[4], Takahiro Kuribayashi[5], Zhaodong Liu[6]

1. Geodynamics Research Center, Ehime University, 2. Eearth Life Science Institute, Tokyo Institute of Technology, 3. Hakubi Center/ Graduate School of Human and Environmental Studies, Kyoto University, 4. Research & Utilization Division, Japan Synchrotron Research Institute, 5. Graduate School of Science, Tohoku University, 6. Institute of Super Hard Materials, Jilin University

Technological developments in stable and homogeneous high temperature generation have been made using conventional $LaCrO_3$ or Re heater for Kawai-type multianvil apparatus (KMA) with tungusten carbide (WC) and sintered diamond (SD) anvils. For WC-KMA, stable temeperature generation to ~3000 K has been achieved under the pressures up to ~27 GPa mainly for quench experiments. Temperatures of ~2000-2300 K have been produced stably for 20-180 minutes at pressures to ~65 GPa for *in situ* X-ray measurements using SD-KMA, in addition to the *ex situ* experiments.

Some experimental studies for precise determination of subsolidus and melting phase relations have successfully been made for some simple mineral systems, such as $MgSiO_3$-Al_2O_3, $MgSiO_3$-$FeSiO_3$, $MgSiO_3$-$CaSiO_3$, $CaSiO_3$-SiO_2, Al_2O_3-SiO_2, $KAlSi_3O_8$-$NaAlSi_3O_8$, Al_2SiO_5, $Ca_3Al_2Si_3O_{12}$, etc. at temperatures near and above the typical geotherm at pressures corresponding to those of the mantle transition region to the middle part of the lower mantle. These studies have provided firm experimental databases for the mineralogy of the deep mantle, and also led to findings of some new high-pressure phases stable only under the very high-temperture conditions. Melting and associated partioning of some key trace elements in more complex chemical compositions have also been conducted under the pressures of the uppermost lower manlte to constrain the differentiation and evolution of the deep mantle.

Keywords: lower mantle, multianvil apparatus, melting relations, phase relations, high pressure and high temperature experiment, technological development

©2019. Japan Geoscience Union. All Right Reserved.

Zr isotope constraints on early Earth differentiation

*Tsuyoshi Iizuka[1], Keita Itano[1], Shinji Yamamoto[2]

1. University of Tokyo, 2. Yokohama National University

The radionuclide 92Nb decays to 92Zr with a half-life of 37 Ma [1]. Because Nb and Zr can fractionate from each other during partial melting of the mantle and mineral crystallization as well as metal-silicate differentiation, Nb-Zr isotope systematics can potentially place chronological constraints on early planetary differentiation. Considering the initial abundance of 92Nb in the solar system (92Nb/93Nb = 1.7 ×10-5), yet, the possible Zr isotopic variation on the Earth would be highly restricted [2]. For instance, even a 4.53 Ga reservoir having a Nb/Zr ratio four times higher than that of CHUR is expected to display a 92Zr anomaly of only +10 ppm. Such reservoir with an elevated Nb/Zr ratio might be formed if Fe-Ti oxide and sulfide minerals presented as a liquidus phase during differentiation on the infant Earth.
Here we report our search for a Zr isotopic vestige of early Earth differentiation using ancient terrestrial zircons. Zirconium isotopic ratios in single zircon grains were measured using MC-ICP-MS with the desolvating nebulization technique, which allows us to achieve analytical precision of ±˜10 ppm. So far, the high-precision Zr isotopic analysis has been applied to detrital zircons with ages up to 4.3 Ga from the Jack Hills in the Yilgarn Craton, Western Australia and igneous zircons from the 4.0–3.6 Ga orthogneisses in the Acasta Gneiss Complex, northwestern Canada. These Acasta rock samples were previously studied for zircon Lu–Hf isotope systematics and the results indicated that their magmatic sources contained Hadean crustal components [3]. Our Zr isotopic data for the Jack Hills and Acasta zircons display no 92Zr anomalies larger than 10 ppm. By combining the Hf isotopic data for these zircon grain, we indicate the development of a 4.5 Ga enriched reservoir on the Earth that had a Lu/Hf of 0.07 and a Nb/Zr less than 0.4. Such reservoir could form via fractional crystallization processes within the shallow or upper mantle.
[1] Holden (1990) Pure Appl. Chem. 62, 941–958. [2] Iizuka et al. (2016) Earth Planet. Sci. Lett. 439, 172–181. [3] Iizuka et al. (2009) Chem. Geol. 259, 230–239.

Keywords: Hadean, magma ocean, Zr isotopes, zircon

©2019. Japan Geoscience Union. All Right Reserved.

[E] Poster | S (Solid Earth Sciences)：S-IT Science of the Earth's Interior & Techtonophysics

Mon. May 27, 2019 3:30 PM - 5:00 PM JST | Mon. May 27, 2019 6:30 AM - 8:00 AM UTC | Poster Hall International Exhibition Hall8, Makuhari Messe_12

[S-IT21] Interaction and Coevolution of the Core and Mantle in the Earth and Planets

convener:Kenji Kawai(Department of Earth and Planetary Science, School of Science, University of Tokyo), Tsuyoshi Iizuka(University of Tokyo), Kenji Ohta(Department of Earth and Planetary Sciences, Tokyo Institute of Technology), Taku Tsuchiya(Geodynamics Research Center, Ehime University)

Recent observational and experimental investigations have significantly advanced our understanding of the structure and constituent materials of the deep Earth. Yet, even fundamental properties intimately linked with formation and evolution of the planet, such as details of the chemical heterogeneity in the mantle and light elements dissolved in the core, remained unclear. Seismological evidence has suggested a vigorous convection in the lower mantle, whereas geochemistry has suggested the presence of stable regions there that hold ancient chemical signatures. The amounts of radioactive isotopes that act as heat sources and drive dynamic behaviors of the deep Earth are also still largely unknown. We provide an opportunity to exchange the achievements and ideas, and encourage persons who try to elucidate these unsolved issues of the core-mantle evolution using various methods, including high-pressure and high-temperature experiments, high-precision geochemical and paleomagnetic analyses, high-resolution geophysical observations, geo-neutrino observations, and large-scale numerical simulations. Papers stimulating an interdisciplinary collaboration relating to establishment of the Japan-SEDI community are also welcomed.

[SIT21-P01] Sample-scale compositional variation of the Inada granite, Ibaraki, Japan -toward the reduction of geoneutrino flux estimation errors from the Japanese crust-

★Invited Papers

*Kenta Ueki[1], Minami Kazuki[2], Tsuyoshi Iizuka[3], Sanshiro Enomoto[4], Hiroyuki Tanaka[2] (1.Japan Agency for Marine-Earth Science and Technology, 2.Earthquake Research Institute, University of Tokyo, 3.Department of Earth and Planetary Science, University of Tokyo, 4.Center for Experimental Nuclear Physics and Astrophysics, University of Washington)

[SIT21-P02] Towards a better estimation of the temperature distribution beneath the Japanese Islands

*Akiko Tanaka[1], Makoto Yamano[2], Hideki Hamamoto[3], Shusaku Goto[4], Takumi Matsumoto[5] (1.Geological Survey of Japan, National Institute of Advanced Industrial Science and Technology, 2.Earthquake Research Institute, The University of Tokyo, 3.Center for Environmental Science in Saitama, 4.Institute for Geo-Resources and Environment National Institute of Advanced Industrial Science and Technology, 5.National Research Institute for Earth Science and Disaster Resilience)

[SIT21-P03] The estimation of the neutrino flux from the crust of the Japanese islands using the geochemical database

*Satoru Haraguchi[1], Kenta Ueki[1], Hikaru Iwamori[1,2,3] (1.Japan Agency for Marine-Earth Science and Technology, 2.Earthquake Research Institute, the University of Tokyo, 3.Tokyo Institute of Technology)

[SIT21-P04] Viscosity of potassium titanosilicate melt at high pressure

*Akio Suzuki[1] (1.Department of Earth Science, Graduate School of Science, Tohoku University)

[SIT21-P05] Lattice thermal conductivity of wadsleyite and ringwoodite at the mantle transition zone pressures

*seiji kimura[1], Kenji Ohta[6], Takaaki Kawazoe[2], Kei Hirose[3], Hiroyuki Kagi[4], Takashi Yagi[5] (1.Department of Earth and Planetary Sciences Tokyo Institute of Technology, 2.Department of Earth and Planetary Systems Science, Hiroshima University, 3.Earth-Life Science Institute, Tokyo Institute of Technology, 4.Geochemical Research Center, Graduate School of Science, University of Tokyo, 5.National Institute of Advanced Industrial Science and Technology, 6.Department of Earth and Planetary Sciences, Tokyo Institute of Technology)

[SIT21-P06] In-situ X-ray observations of the olivine-spinel transformation under shear deformation: preliminary results on the reaction-induced weakening

*Tomoaki Kubo[1], Moriyama Kazuya[1], Yuichiro Mori[1], Masahiro Imamura[1], Sanae Koizumi[2], Yu Nishihara[3], Akio Suzuki[4], Yuji Higo[5] (1.Kyushu Univ., 2.ERI, 3.GRC Ehime Univ., 4.Tohoku Univ., 5.JASRI)

[SIT21-P07] Internally resistive heated diamond anvil cell experiments with metal encapsulated minerals

*YAMAMOTO TOMONARI[1], Kenji Ohta[1], Sho Suehiro[1], Hayato Inoue[1] (1.Tokyo Institute of Technology)

[SIT21-P08] Shear deformation on post-spinel

*Daisuke Yamazaki[1], Noriyoshi Tsujino[1], Yu Nishihara[2] (1.Institute for Planetary Materials, Okayama University, 2.GRC, Ehime University)

[SIT21-P09] **Lattice thermal conductivity of $CaSiO_3$ perovskite at high pressures and high temperatures**

*Kotaro Onga[1], Kenji Ohta[1], Akira Hasegawa[1,2], Takashi Yagi[2], Kei Hirose[3,4], Yasuo Ohishi[5] (1.Department of Earth and Planetary Sciences, Tokyo Institute of Technology, 2.National Institute of Advanced Industrial Science and Technology, 3.Earth-Life Science Institute, Tokyo Institute of Technology, 4.Department of Earth and Planetary Science, The University of Tokyo, 5.Japan Synchrotron Radiation Research Institute)

[SIT21-P10] **Polycrystalline diamond sintered from ultradispersed nanodiamonds**

*Masayuki Nishi[1,2], Koichiro Yamamoto[1], Youmo Zhou[1], Tetsuo Irifune[2,1] (1.Geodynamics Research Center, Ehime University, 2.Earth-Life Science Institute, Tokyo Institute of Technology)

[SIT21-P11] Thermal conductivity measurements on iron and MgO periclase at high pressure and high temperature similar to the Earth's mid-lower mantle conditions

*Akira Hasegawa[1,2], Kenji Ohta[2], Takashi Yagi[1], Kei Hirose[3,4] (1.National Institute of Advanced Industrial Science and Technology, 2.Tokyo Institude of Technology, 3.Earth-Life Science Institute, Tokyo Institude of Technology, 4.The University of Tokyo)

[SIT21-P12] Azimuthal anisotropy in the lowermost mantle beneath Philippine from ScS-S times

*Satoru Tanaka[1] (1.Department of Deep Earth Structure and Dynamics Research Japan Agency for Marine-Earth Science and Technology)

[SIT21-P13] Detailed 3-D S-velocity structure within D" at the western Pacific LLSVP margin: smaller scale plumes and paleoslabs

*Yuki Suzuki[1], Kenji Kawai[1], Robert J. Geller[1], Satoru Tanaka[2], Weerachai Siripuvaraporn[3], Songkhun Boonchaisuku[3], Noisagool Sutthipong[3], Yasushi Ishihara[2], Taweoon Kim, Koji MIYAKAWA[4], Nozomu Takeuchi[4] (1.The University of Tokyo, 2.Japan Agency for Marine-Earth Science and Technology, 3.Mahidol University, 4.Earthquake Research Institute, The University of Tokyo)

[SIT21-P14] Possible interaction between the core and mantle inferred from a core surface flow model

*Masaki Matsushima[1] (1.Department of Earth and Planetary Sciences, School of Science, Tokyo Institute of Technology)

[SIT21-P15] Determination of the noble gas partition coefficients between metal-silicate melts under high-pressure and high-temperature conditions

*Tomotaka Tanaka[1], Hideharu Kuwahara[2], Satoshi Kishi[1], Ryuichi Nomura[3], Kenji Mibe[5], Hiroyuki Kagi[4], Shigehiko Tateno[6], Hirochika Sumino[1] (1.Department of Basic Science, Graduate School of Arts and

Sciences, The University of Tokyo , 2.Geodynamics Research Center, Ehime University, 3.Kyoto University, 4.Geochemical Research Center, Graduate School of Science, University of Tokyo, 5.Earthquake Research Institute, University of Tokyo, 6.Earth-Life Science Institute, Tokyo Institute of Technology)

[SIT21-P16] **Measurement of T-dependent electrical resistivity of solid and liquid Fe and Pt at fixed P**

*Innocent Ezenwa[1], Takashi Yoshino[1] (1.Institute for Planetary Materials, Okayama University)

[SIT21-P17] Ancient, highly depleted mantle constrained by Re-Os isotope and highly-siderophile element compositions of French Polynesian xenoliths

*Norikatsu Akizawa[1], Akira Ishikawa[2], Katsuhiko Suzuki[3], Tetsu Kogiso[4] (1.Atmosphere and Ocean Research Institute, The University of Tokyo, 2.Department of Earth and Planetary Sciences, Tokyo Institute of Technology, 3.Research and Development Center for Submarine Resources, Japan Agency for Marine-Earth Science and Technology (JAMSTEC), 4.Graduate School of Human and Environmental Studies, Kyoto University)

[SIT21-P18] First-principles prediction of hydrogen partitioning between the core and mantle

*Atsuroh Ohba[1], Taku Tsuchiya[1] (1.Ehime University Geodynamics Research Center)

[SIT21-P19] Microvolume stable isotope measuremetns and its applicaiton for high-pressure high-temperature experimental run products

*Madhusoodhan Satish-Kumar[1], Shinnosuke Aoyama[1] (1.Department of Geology, Faculty of Science, Niigata University)

[SIT21-P20] Electrical resistivity of hcp Fe-Si alloys at high pressure and temperature

*Hayato Inoue[1], Sho Suehiro[1], Kenji Ohta[1], Kei Hirose[2,3], Yasuo Ohishi[4] (1.Department of Earth and Planetary Sciences, Tokyo Institute of Technology, 2.Earth-Life Science Institute, Tokyo Institute of Technology, 3.Department of Earth and Planetary Science, The University of Tokyo, 4.Japan Synchrotron Radiation Research Institute)

[SIT21-P21] Electrical resistivity and thermal conductivity of fcc Fe: Implications for the Mercury's core

★Invited Papers

*Hitoshi Gomi[1], Takashi Yoshino[1] (1.Okayama University)

[SIT21-P22] Lateral heterogeneity in the lowermost outer core (F layer) of the Earth revealed by seismic analyses

*Toshiki Ohtaki[1], Satoshi Kaneshima[2], Taku Tsuchiya[3] (1.Geological Survey of Japan, National Institute of Advanced Industrial Science and Technology (AIST), 2.Department of Earth and Planetary Sciences, Kyushu University, 3.Geodynamics Research Center, Ehime University)

[SIT21-P23] Flows and light element distribution in the outer core associated with heterogeneous growth of the inner core of the Earth

*Shin-ichi Takehiro[1], Youhei SASAKI[2] (1.Research Institute for Mathematical Sciences, Kyoto University, 2.Department of Mathematics, Kyoto University)

[SIT21-P24] Sharpness of the hemispherical boundary in the inner core beneath the northern Pacific

*Ryohei Iritani[1], Hitoshi Kawakatsu[1], Nozomu Takeuchi[1] (1.Earthquake Research Institute, Univ. of Tokyo)

[SIT21-P25] Stable carbon isotope fractionation in Fe-C system from first principles

*Haruhiko Dekura[1], Taku Tsuchiya[1] (1.Geodynamics Research Center, Ehime University)

Sample-scale compositional variation of the Inada granite, Ibaraki, Japan -toward the reduction of geoneutrino flux estimation errors from the Japanese crust-

*Kenta Ueki[1], Minami Kazuki[2], Tsuyoshi Iizuka[3], Sanshiro Enomoto[4], Hiroyuki Tanaka[2]

1. Japan Agency for Marine-Earth Science and Technology, 2. Earthquake Research Institute, University of Tokyo, 3. Department of Earth and Planetary Science, University of Tokyo, 4. Center for Experimental Nuclear Physics and Astrophysics, University of Washington

Geoneutrio observed at anti-neutrino observatory "KamLAND" in Kamioka (Hida City, Gifu Prefecture), enables us to directly observe the abundance of radiogenic elements in the deep earth. As crustal rocks exhibit a high concentration of geoneutrino producing radiogenic elements (Uranium and Thorium) than mantle rocks, we have to subtract the contribution of geoneutrino from the Japanese crust from the observation value in Kamioka to estimate geoneutrino flux from core and mantle. For the purpose, we estimated the 3D distribution of uranium and thorium in the Japanese crust by the stochastic modeling using the seismic velocity structure, geological information and geochemical database for the Japanese crustal rock. Geoneutrino flux calculated using the compositional map exhibits a very large error (up to 80%) at present.
We found that information on the compositional heterogeneity (spatial correlation) of various length scale, such as of the single rock suite scale (km to m scale), and sample scale (cm to mm scale) are essential to reduce the estimation error of crustal geoneutrino flux as small as the observation error of the geoneutrino on KamLAND. Therefore, we conducted a grid sampling of the granite of Inada, Ibaraki prefecture, to obtain quantitative knowledge on the small scale compositional heterogeneity. Samples (about 500g) were divided into several centimeter scale split (about 25g). Based on the compositional variations between small splits from one sample, we discuss the small scale sample wise compositional variation. Whole rock chemical composition of each small split was analyzed using XRF. Also, we conducted surface analysis using an ED-XRF to evaluate the spatial distribution of elements in each split. As a result, even within a single sample (about 500g), a compositional variation of about several% at maximum was observed. This result indicates that when conducting the analysis based on the rock chemical composition considering the spatial context, it is necessary to properly evaluate the sample scale heterogeneity, in addition to the tectonic scale, the rock suite scale, and microscopic scale.Also, this result will contribute to the reduction of the estimation error of geoneutrino from the Japanese crust.

Keywords: Geoneutrino, Granite, Rock chemical composition

©2019. Japan Geoscience Union. All Right Reserved.

Towards a better estimation of the temperature distribution beneath the Japanese Islands

*Akiko Tanaka[1], Makoto Yamano[2], Hideki Hamamoto[3], Shusaku Goto[4], Takumi Matsumoto[5]

1. Geological Survey of Japan, National Institute of Advanced Industrial Science and Technology, 2. Earthquake Research Institute, The University of Tokyo, 3. Center for Environmental Science in Saitama, 4. Institute for Geo-Resources and Environment National Institute of Advanced Industrial Science and Technology, 5. National Research Institute for Earth Science and Disaster Resilience

To improve our understanding of the thermal evolution and structure of the deep Earth, it is necessary to know the shallow part of them. Surface heat flow provides important constraint on it. However, the number of heat flow data is limited and spatially very inhomogeneous and even in regions with measurements the data quality varies. For this reason, we have been working on compiling a comprehensive database of heat flow, thermal conductivity, and geothermal gradient. In 2004, Geological Survey of Japan published a digital geoscience map entitled "Geothermal Gradient and Heat Flow Data in and around Japan", which contains heat flow data in the northwestern Pacific area (from 0 to 60°N and from 120 to 160°E) and geothermal gradient data in and around Japan. In 2019, we will be releasing database entitled "Thermal Data Collection in and around Japan", which contains continuously updated of geothermal gradient and heat flow data and adds thermal conductivity data in and around Japan. Thermal conductivity data were compiled from published data and site-specific reports, and measured using the archived cores. This database offers considerable improvements over the previous version released in 2004, and will be published and available at https://www.gsj.jp/en/database/db-portal/index.html. It presents an opportunity to revisit the thermal state of the lithosphere along with other geophysical/geochemical constraints on heat flow extrapolation.

Keywords: heat flow, thermal conductivity, geothermal gradient

©2019. Japan Geoscience Union. All Right Reserved.

The estimation of the neutrino flux from the crust of the Japanese islands using the geochemical database

*Satoru Haraguchi[1], Kenta Ueki[1], Hikaru Iwamori[1,2,3]

1. Japan Agency for Marine-Earth Science and Technology, 2. Earthquake Research Institute, the University of Tokyo, 3. Tokyo Institute of Technology

Geoneutrino observed at the anti-neutrino observatory "KamLAND" at Kamioka allows us to obtain information on the amount and distribution of radiogenic elements (uranium and thorium) in the deep mantle and crust.. It is necessary to divide the contribution from Japanese from the observed neutrino flux on closely to precisely estimate the quantity of U, Th of the earth deep earth because such radiogenic elements exhibit high concentration in the crust. Previous estimation of the crust origin geoneutrino was estimated based on the relatively simple chemical assumption on the compositional variation and spatial distribution. However, the radioactive elements of the Japanese crustal rock are distributed with very wide compositional range with complex spatial distribution. Therefore, it is necessary to estimate spatial distribution of radioactive element in the Japanese crust for the precisely measurement of geoneutrino from Japanese crust. In addition, petrogical and geochemical structure of the Japanese crust of are fundamental information for understanding seismic activity, volcanic activity and tectonism. The analysis of the spatial variation of the chemical composition of the Japanese Islands crust is important in discussing about the evolution history of the Japanese Islands and the chemical evolution in the subduction zone.

In this study, we utilize DODAI to improve the estimation error of geoneutrino from the Japanese crust (Takeuchi et al., 2019). We published the database “DODAI” which compiled geochemical data published by the Japanese domestic journals and bulletins in the journal of the Geological Society of Japan (Haraguchi et al., 2018). This database incorporates the precise sampling position of individual geochemical data using an electronic map. Resolution of the positional information were improved drastically.
The "DODAI" database covers whole area of Japanese Islands with highly precise positional information is useful for data analysis and modeling. The geochemistry database with highly precise positional information is useful for modeling of the geochemical structure of the solid earth. In this study, we present the potential of the DODAI database and geoneutrion in the analysis of the geochemical structures of Japanese crust, as well as the deep earth.

Keywords: neutrino, geochemical database, geochemical structure of crust and mantle

©2019. Japan Geoscience Union. All Right Reserved.

Viscosity of potassium titanosilicate melt at high pressure

*Akio Suzuki[1]

1. Department of Earth Science, Graduate School of Science, Tohoku University

Viscosity of silicate melt is a fundamental property, which controls volcanic processes, including rates of melt extraction, ascent, and magma mixing. Titanium oxide is contained less than 10 wt% in terrestrial magmatic liquids, however, some lunar magmas contains it over 10 wt%. The addition of titanium to silicate melt affects on the properties such as viscosity, density, and compressibility. Especially the pressure dependence of viscosity is of great interest, because magma is generated in the planetary interiors. The aim of this study is to measure the viscosity of K2TiSi4O11 melt at high pressures to estimate the influence of the pressure-induced structural change of melt.
We performed in situ falling sphere viscometry in the pressure range from 1.3 to 7.4 GPa, by using the MAX-III high pressure apparatus at BL14C2 and NE7A beamlines at Photon Factory in KEK, Tsukuba, Japan. A falling platinum sphere in the melt was monitored by using an X-ray CCD camera with a YAG:Ce fluorescence screen. We observed that the viscosity of KTS4 melt decreased up to 3.3 GPa. In contrast, the pressure dependence in viscosity was not observed above 3.3 GPa. Based on XANES spectra of K2TiSi4O11 glasses quenched under high pressure, Paris et al. (1994) showed that the coordination number of titanium increased with increasing pressure. The present study suggests that the melt becomes depolymerized by the coordination change of titanium under high pressure.

Keywords: magma, viscosity, high pressure

©2019. Japan Geoscience Union. All Right Reserved.

Lattice thermal conductivity of wadsleyite and ringwoodite at the mantle transition zone pressures

*seiji kimura[1], Kenji Ohta[6], Takaaki Kawazoe[2], Kei Hirose[3], Hiroyuki Kagi[4], Takashi Yagi[5]

1. Department of Earth and Planetary Sciences Tokyo Institute of Technology, 2. Department of Earth and Planetary Systems Science, Hiroshima University, 3. Earth-Life Science Institute, Tokyo Institute of Technology, 4. Geochemical Research Center, Graduate School of Science, University of Tokyo, 5. National Institute of Advanced Industrial Science and Technology, 6. Department of Earth and Planetary Sciences, Tokyo Institute of Technology

The lattice thermal conductivities of wadsleyite (Wd) and ringwoodite (Rw), which predominantly occupy the Earth's mantle transition zone, are important transport properties to understand the dynamics and thermal structure of the mantle. In particular, the temperature in the subducting slab is mainly controlled by the thermal conduction of Wd and Rw. Wd and Rw are both thought to preserve a large amount of hydrogen ions, thus should play an important role as the main water reservoir in the Earth. Furthermore, it has been reported that the hydration affects the physical properties of minerals including thermal conductivity, and it is necessary to measure the lattice thermal conductivity of Wd and Rw considering their water content. However, so far, the reported lattice thermal conductivities of Wd and Rw has not been considered their water content (Xu et al., 2004). Here we measured the room temperature lattice thermal conductivity of $(Mg_{0.89}Fe_{0.11})_2SiO_4$ Wd and $(Mg_{0.91}Fe_{0.09})_2SiO_4$ Rw up to 27 GPa, respectively, to clarify their hydration dependence using the pulsed light heating thermoreflectance technique in a diamond anvil cell.The obtained results show similar pressure dependence of the lattice thermal conductivity to the previous study (Xu et al., 2004). However, the absolute values of the thermal conductivity are different; the lattice conductivities of hydrous Wd and Rd are ~52% and ~40% lower than the results of Xu et al. (2004), respectively. Our results suggest strong water content dependence of lattice thermal conductivities of Wd and Rw, implying that the water content in the mantle minerals is key factor for calculating the thermal structure in a subducting slab, mantle dynamics.

Keywords: wadsleyite, ringwoodite, mantle transition zone, hydrous minerals, thermal conductivity

©2019. Japan Geoscience Union. All Right Reserved.

In-situ X-ray observations of the olivine-spinel transformation under shear deformation: preliminary results on the reaction-induced weakening

*Tomoaki Kubo[1], Moriyama Kazuya[1], Yuichiro Mori[1], Masahiro Imamura[1], Sanae Koizumi[2], Yu Nishihara[3], Akio Suzuki[4], Yuji Higo[5]

1. Kyushu Univ., 2. ERI, 3. GRC Ehime Univ., 4. Tohoku Univ., 5. JASRI

It has been suggested that high-pressure transformations cause rheological weakening and large deformation of subducting slabs in mantle transition zone (MTZ) . However, there have been few direct experimental evidences so far largely because of the difficulties in quantitative deformation experiments under such conitions. Here we report preliminary results on the olivine-spinel transformation experiments under shear deformation upto MTZ pressures. D-111 (DT-cup) type high-pressure deformation apparatus was newly used for this purpose combined with high-energy synchrotron mono X-rays (50-60 keV) at Photon Factory (PFAR NE7 beamline), which enables in-situ observations of interactions between transformation and creep behaviors. Sintered Mg_2SiO_4 forsterite was first deformed at 15-25 GPa at 600˚C in shear, and subsequently heated to higher temperatures (~0.2˚C/s) to cause the olivine-spinel transformation under shear deformation. The transformation started at much lower temperatures under shear deformation (~900-1100˚C depending on the overpressure from the phase boundary) compared to that without deformation (~1400˚C), suggesting that the shear deformation enhances the olivine-spinel transition rate. The shear strain rate in the sample monitored by X-ray radiography was ~3-4 x 10^{-6} (s^{-1}) at 600˚C, and increased up to ~2-3 x 10^{-4} (s^{-1}) with ramping temperatures even keeping the anvil displacement rate constant (200 micron/h). We observed that the shear weakening does not occur at the same temperature, but reflects on the initiation of the olivine transition. Also, the weakening effects become significant at larger overpressures (and low T). This implies that the weakening of the shear zone induced by the grain-size reduction due to the olivine-spinel transition, however further evidences from microstructural observations are necessary. We plan to install 8-ch acoustic emission measurement system attached with D-111 apparatus to capture the transformation-induced shear instabitiy. Results of D-DIA shear deformation study on the olivine-spinel transition in Fe_2SiO_4 will also be presented and compared with those of the D-111 study in Mg_2SiO_4 .

©2019. Japan Geoscience Union. All Right Reserved.

Internally resistive heated diamond anvil cell experiments with metal encapsulated minerals

*YAMAMOTO TOMONARI[1], Kenji Ohta[1], Sho Suehiro[1], Hayato Inoue[1]

1. Tokyo Institute of Technology

Heating technique is crucial for *in-situ* high pressure-temperature (*P-T*) studies into the physical and chemical properties of minerals in the diamond anvil cell (DAC) under deep Earth's conditions. External resistive heating methods that use resistive heaters such as AlChrom-O wire and graphite surrounding the DAC or just the diamonds (Dubrovinskaia and Dubrovinsky, 2003; Du et al., 2013). This approach creates a homogeneous temperature field in the sample chamber but limits the maximum temperature of about 1200℃ due to graphitization of diamond anvils. Double-sided laser heating with a DAC generates the *P-T* conditions corresponding to the center of the Earth's (Tateno et al., 2010). However, tightly focused laser beams, instabilities in output laser power and misalignment of the focused beams on the sample surface result in significant temperature variation within the sample in the DAC. Internally resistive heated DAC is an effective heating method to overcome the temperature limitation of external heated DAC and the significant temperature gradients experienced in conventional laser-heated DAC (e.g., Zha and Bassett, 2003). However, the internally resistive heated DAC is mostly applied to metal sample to study the properties of the planetary metallic core despite this technique could be applicable to an insulating mineral.

In this study, we modified the internally resistive heated DAC technique for nonmetallic material. We developed a microfabrication technique for total metal encapsulation of the nonmetallic sample. The sample encapsulated by platinum was loaded in DAC with thermal insulator and connected with two electrical leads to make electrical circuit for resistive heating. We confirmed very stable and homogeneous heating for insulating sample at 30 GPa to 2450 K in the modified internally resistive heated DAC. The highest temperature which this method can generate depends on the metal heater encapsulating the sample. This method offers a larger heating volume with more stable and uniform temperature than laser heating and at temperatures much greater than those that can be generated by external resistive heating methods.

References

Dubrovinskaia, N., & Dubrovinsky, L. (2003). Whole-cell heater for the diamond anvil cell. *Review of Scientific Instruments*, *74*(7), 3433-3437.

Du, Z., Miyagi, L., Amulele, G., & Lee, K. K. (2013). Efficient graphite ring heater suitable for diamond-anvil cells to 1300 K. *Review of Scientific Instruments*, *84*(2), 024502.

Tateno, S., Hirose, K., Ohishi, Y., & Tatsumi, Y. (2010). The structure of iron in Earth's inner core. *Science* , *330*(6002), 359-361.

Zha, C. S., & Bassett, W. A. (2003). Internal resistive heating in diamond anvil cell for in situ X-ray diffraction and Raman scattering. *Review of scientific instruments*, *74*(3), 1255-1262.

©2019. Japan Geoscience Union. All Right Reserved.

Keywords: Internally resistive heated diamond anvil cell, high pressure-temperature experiments

©2019. Japan Geoscience Union. All Right Reserved.

Shear deformation on post-spinel

*Daisuke Yamazaki[1], Noriyoshi Tsujino[1], Yu Nishihara[2]

1. Institute for Planetary Materials, Okayama University, 2. GRC, Ehime University

Earth’ s lower mantle is mainly composed of ferro-periclase and bridgmanite. The viscosity of ferro-periclase is considered to be 2-3 orders of magnitude lower than that of bridgmanite. Such large discrepancy in viscosity may cause the significant effect of microstructure of the aggregate of bridgmanite and ferro-periclase on bulk viscosity. For example, bulk viscosity is low when the interconnected weak layer structure is formed, whereas bulk viscosity is as high as the viscosity of bridgmanite when the load bearing framework structure is formed [1].

Microstructural evolution from the load bearing framework structure to the interconnected weak layer structure in post-spinel phase (mixture of bridgmanite and ferro-periclase) during deformation was previously reported based on the rotational Drickamer apparatus [2]. This results suggests the important viscosity reduction during deformation in the lower mantle. We therefore considered that more detailed and precise experiments are necessary to discuss the lower mantle rheology quantitatively.

Deformation experiments under the lower mantle conditions can be conducted by using D111-type deformation Kawai-type high pressure apparatus. This apparatus was previously installed at UCL followed by PF-AR and Misasa. In this study, we use these apparatus for the deformation on post-spinel phase.

Starting material for deformation experiment was well-sintered aggregate of bridgmanite and ferro-periclase synthesized at 24 GPa and 1873 K. For the simple shear deformation, we used 45 degree cut design. In in-situ X-ray experiments at PF-AR, we used tapered and coned anvils for X-ray paths. On the other hand, in “quench” experiments at Misasa, we used a simple cubic anvils (TEL=2.0 mm). All deformation experiments were performed with constant D-rams displacement rate.
We deformed sample up to shear strain of ~0.8 with the 0.4 mm displacements of D-rams. SEM observation on the recovered sample by SEM shows that there is no significant evolution in microstructure, indicating that viscosity reduction is not expected with shear deformation to gamma~1. [1] D. Yamazaki, S. Karato: Am. Mineral., **86**, 385 (2001). [2] J. Girard et al.: Science, **351**, 144 (2016).

©2019. Japan Geoscience Union. All Right Reserved.

Lattice thermal conductivity of $CaSiO_3$ perovskite at high pressures and high temperatures

*Kotaro Onga[1], Kenji Ohta[1], Akira Hasegawa[1,2], Takashi Yagi[2], Kei Hirose[3,4], Yasuo Ohishi[5]

1. Department of Earth and Planetary Sciences, Tokyo Institute of Technology, 2. National Institute of Advanced Industrial Science and Technology, 3. Earth-Life Science Institute, Tokyo Institute of Technology, 4. Department of Earth and Planetary Science, The University of Tokyo, 5. Japan Synchrotron Radiation Research Institute

Laboratory measurements of thermal conductivity of deep Earth materials provide important information on the dynamics and thermal evolution of the mantle and the core. $CaSiO_3$ perovskite (CaPv) is a constituent of pyrolitic lower mantle and of the subducting oceanic crust at depth greater than 560 km. In recent years, there are many reports of the laboratory-based lower mantle thermal conductivity profiles, but the thermal conductivity of CaPv has never been measured and included in the models [1,2,3,4,5] . CaPv is an unquenchable high-pressure phase at ambient conditions, and temperature-induced structure change from tetragonal to cubic occurs at around 500 K [6]. Therefore, *in-situ* high pressure and temperature X-ray diffraction (XRD) and thermal conductivity measurements are required to determine the thermal conductivity of CaPv in the Earth’ s deep interior.
In this study, we determined the thermal conductivity of CaPv at about 50 GPa and high temperature to 1950 K by a combination of synchrotron XRD measurements and the pulsed light heating thermoreflectance technique. Based on our experimental results, we consider the effect of the presence of CaPv on the thermal conductivity of the pyrolitic lower mantle and the subducting oceanic crust.

Reference: [1] Manthilake, G. et al., *Proc National Acad Sci.* **108,** 17901–17904 (2011). [2] Ohta, K. et al., *Earth Planet Sc. Lett.* **349,**109–115 (2012). [3] Ohta, K. et al., *Earth Planet Sc. Lett.* **465,** 29–37 (2017). [4] Okuda, Y. et al., *Earth Planet Sc. Lett.* **474,** 25–31 (2017). [5] Hsieh, W.-P. et al., J. Geophys. Res. Solid Earth 122, 4900-4917 (2017). [6] Komabayashi, T. et al., *Earth Planet Sc. Lett.* **260,** 564–569 (2007).

Keywords: CaPv, thermal conductivity, lower mantle

©2019. Japan Geoscience Union. All Right Reserved.

Polycrystalline diamond sintered from ultradispersed nanodiamonds

*Masayuki Nishi[1,2], Koichiro Yamamoto[1], Youmo Zhou[1], Tetsuo Irifune[2,1]

1. Geodynamics Research Center, Ehime University, 2. Earth-Life Science Institute, Tokyo Institute of Technology

NPD is a binder-less nanodiamond aggregate (~50 nm) synthesized by direct conversion of graphite under high pressure and temperature [1]. Although NPD has extremely high hardness exceeding that of single-crystalline diamond, it is difficult to obtain the large size of the NPD above 1 cm^3, because extreme high pressure conditions are required. Here we show nanodiamond polyclystalline sintered from ultradispersive nanodiamond under relatively moderate pressure and temperature conditions.

We used a multi-anvil apparatus to sinter the nanodiamonds at 8-15 GPa and 1600-2300˚C, where the diamond is thermodynamically stabilized. The starting materials were enclosed in metal capsules. The microstructures and chemical compositions of the recovered samples were examined using a field-emission scanning electron microscope with energy-dispersive X-ray spectroscopy. Well-sintered polycrystalline were subjected to the Knoop indentation test to evaluate its hardness.

We succeeded in recovering the well-sintered polycrystalline diamonds with grain size of ~10-30 nm in some runs (Figure 1). Full width at half maximum of XRD peaks decreased with increasing temperature due to the grain growth of diamond particles. The color, hardness, and grain size of the sintered polycrystalline changed depending on the capsule materials as well as the pressure and temperature conditions. These features might be affected by the porosity, the grain size, and the impurities. Further studies are required to synthesize the polycrystalline with high hardness comparable to NPD.

References: [1] T. Irifune, A. Kurio, S. Sakamoto, T. Inoue, H. Sumiya., *Nature*, **421**, 599 (2003).

Keywords: multianvil apparatus, nanodiamond, NPD

©2019. Japan Geoscience Union. All Right Reserved.

Thermal conductivity measurements on iron and MgO periclase at high pressure and high temperature similar to the Earth’s mid-lower mantle conditions

*Akira Hasegawa[1,2], Kenji Ohta[2], Takashi Yagi[1], Kei Hirose[3,4]

1. National Institute of Advanced Industrial Science and Technology, 2. Tokyo Institude of Technology, 3. Earth-Life Science Institute, Tokyo Institude of Technology, 4. The University of Tokyo

The thermal transport properties of the Earth’s constituents are important information to constrain the thermal evolution and the heat budget of the Earth. In particular, the thermal conductivity of the core, the largest heat source of the Earth, and the lower mantle, occupying more than half the volume of the whole Earth, are indispensable.

In recent years, thermal conductivity measurement on the sample inside the diamond anvil cell has been carried out utilizing the thermoreflectance phenomenon, the reflectance of metal changes slightly due to the temperature perturbation of several kelvin (e.g. Hsieh et al., 2009 Phys Rev B; Yagi et al., 2011 Meas Sci Technol). However, the reported temperature condition is far from that in Earth’s interior.

In this study, we combined the pulsed light heating thermoreflectance method with high power CW laser heating to obtain the thermal conductivity of material *in-situ* at high pressures and temperatures. As a result of test measurement for Pt, we obtained thermal conductivities of Pt up to 60 GPa and 2000 K, which is in good agreement with the measured values using flash heating method in a laser heated diamond anvil cell (McWilliams et al., 2015 Phys Earth Planet In).

The thermal conductivities of iron and MgO periclase were measured up to 60 GPa and 1700 K with this developed system. We found that the obtained thermal conductivities of iron and MgO have negative temperature dependence, and are consistent with the literatures (Fe: Konôpková et al., 2016 Nature; Ohta et al., 2016 Nature, MgO; Manthilake et al., 2011 Proc National Acad Sci; Dekura and Tsuchiya, 2017 Phys Rev B). The newly developed system here would be a powerful tool to examine the thermal conductivity of Earth’s deep interior.

Keywords: thermal conductivity, laser heated diamond anvil cell, pulsed light heating thermoreflectance method, lower mantle, core

©2019. Japan Geoscience Union. All Right Reserved.

Azimuthal anisotropy in the lowermost mantle beneath Philippine from ScS-S times

*Satoru Tanaka[1]

1. Department of Deep Earth Structure and Dynamics Research Japan Agency for Marine-Earth Science and Technology

Introduction: Seismic anisotropy in the lowermost mantle has been detected by splitting of diffracted S and ScS phases, the discrepancy of shear wave splitting of SKS and SKKS, to date. In many cases, the propagation direction of such seismic waves is restricted due to the combination of sources and receivers. Thus, the azimuthal anisotropy using ray paths passing in multi-directions has been rarely discussed. Now, seismic networks and large-scale seismic arrays have been increasing especially in the eastern Asia where there are also many earthquakes. It is a good opportunity to examine an azimuthal variation of travel times passing through the outside of the Pacific Large Low Shear Velocity Province, where the existence of anisotropy in the lowermost mantle is expected.

Data and Method: I used the seismograms of earthquakes occurred in Mariana, east China, Indonesia, and Vanuatu that are record with the seismic stations belonging to IRIS GSN and PASSCAL, Thai Metrological Department, F-net, JISNET, NECESSArray. This geometry gives a good condition that the mid-points of seismic ray paths are located near Philippine with various azimuths.I measured ScS–S differential travel times using a waveform cross-correlation method, which can effectively cancel the heterogeneity in the crust and upper mantle and the uncertainty of hypocenters. The differential travel times are compared with theoretical travel times by PREM with correction of physical dispersion due to anelasticity for the typical period of 10 s, that for ellipticity of the Earth, finally I obtained about 500 residuals. Even though I used the differential travel times, the ScS–S residuals show the large scattering and the correlation with the residuals of S travel times are much larger than that of ScS phases. This means that the raw ScS–S residuals are affected by heterogeneity in the upper part of the lower mantle where only S waves are propagated. Thus, we applied the further corrections using 3D mantle heterogeneity models.

Results and Discussion: We used S-wave 3D models of S16U6L8, S4BL16, S40RTS, SEMUCB-WM, and a P-wave 3D model of GAP-P4 with conversion rate dlnVs/dlnVp=1.7. I found that the scatter of the ScS–S residuals are much improved and that the correlation coefficient between the residuals of ScS–S and ScS are increased and that between ScS–S and S are much reduced when the GAP-P4 model are used for the correction, probably due to its high spatial resolution in the upper lower mantle. As a result, only the ScS–S residuals corrected with the modified GAP-P4 can be used to infer seismic anisotropy in the lowermost mantle.

Then I fitted cos 2qand cos 4qcurves with least square to obtain the characteristics of the azimuthal variation of the ScS–S residuals, clearly indicating that cos 2qcomponent is significant with the fastest direction (the minimum ScS–S) is along ESE-WNW (N110˚E). This can be explained if [100] axis of post-perovskite is oriented vertically and the direction of [001] axis is ESE-WNW for the incident angle of 45˚. The S-wave fastest direction is nearly parallel to the plate motion directions of the Philippine Sea plate and Sunda block. The amplitude of the azimuthal variation in the ScS–S residual is ±1.1 s, which corresponds to 1.7 % anisotropy if we assume the D” thickness of 300 km based on the previous studies on the D” discontinuity.

©2019. Japan Geoscience Union. All Right Reserved.

Keywords: lowermost mantle, seismic anisotropy

©2019. Japan Geoscience Union. All Right Reserved.

Detailed 3-D S-velocity structure within D" at the western Pacific LLSVP margin: smaller scale plumes and paleoslabs

*Yuki Suzuki[1], Kenji Kawai[1], Robert J. Geller[1], Satoru Tanaka[2], Weerachai Siripuvaraporn[3], Songkhun Boonchaisuku[3], Noisagool Sutthipong[3], Yasushi Ishihara[2], Taweoon Kim, Koji MIYAKAWA[4], Nozomu Takeuchi[4]

1. The University of Tokyo, 2. Japan Agency for Marine-Earth Science and Technology, 3. Mahidol University, 4. Earthquake Research Institute, The University of Tokyo

Global tomographic models of shear velocity have shown two large-scale low shear velocity provinces (LLSVPs) in D″ beneath the Pacific and Africa. It has been controversial whether these LLSVPs are due to thermal effects, chemical effects, or their combination. The nature and origin of the LLSVPs are of fundamental importance since each of the proposed geodynamical scenarios carries different implications for the thermal, chemical and dynamical evolution of the Earth. Previous seismological studies based on travel-time analysis or forward modeling inferred a sharp-sided velocity contrast of the Pacific LLSVP beneath the western Pacific and suggested that the LLSVP is chemically distinct, although the suggested structures of the western edge of the Pacific LLSVP different from each other. To better understand the origin of LLSVPs, it is essential to infer the detailed three-dimensional (3-D) velocity structure within LLSVP beneath the western Pacific. We recently deployed a seismic array stations in Thailand (Thai Seismic Array—TSAR). We assemble waveforms recorded by TSAR as well as other networks such as TM, AU, MM, and MY, allowing us to sample a wider region than previous studies. We conducted waveform inversion using ~5,300 transverse component records of this dataset for the detailed 3-D shear velocity structure in the lowermost 400 km of the mantle beneath the western Pacific. The inferred model shows a low-velocity anomaly immediately above the core-mantle boundary (CMB) and high-velocity anomalies extending vertically from 400 km to the CMB. Taken into account the previous geodynamical simulation studies, the size of the inferred low velocity anomaly suggests a thermal plume rather than a chemical anomaly. The location of the high velocity anomaly in D″ is consistent with the paleo-Izanagi plate subduction boundary about 200 Ma. This implies that a cold paleo-slab produces the strong lateral velocity contrast at the western edge of the western Pacific LLSVP. Hence, we conclude that the western margin of the Pacific LLSVP and its sharp velocity boundary can be explained mainly by thermal effects, and this implies that the lowermost mantle would be well-mixed and the Pacific LLSVP would not be geochemical reservoir.

Keywords: D" region, Pacific LLSVP, Waveform Inversion, Thai Seismic Array (TSAR)

©2019. Japan Geoscience Union. All Right Reserved.

Possible interaction between the core and mantle inferred from a core surface flow model

*Masaki Matsushima[1]

1. Department of Earth and Planetary Sciences, School of Science, Tokyo Institute of Technology

Fluid flow in the Earth's liquid outer core is responsible for the dynamo action by which the geomagnetic field is generated and maintained. The fluid flow can be estimated from geomagnetic field data, such as spatial distribution of geomagnetic field and its temporal change referred to as secular variations. This implies that spatial and temporal variations of fluid flow in the core provide information on any interaction between the core and mantle. To investigate possible core-mantle interaction, a core surface flow model is obtained from a geomagnetic field model, COV-OBS.x1 (Gillet et al., 2015) using the method of Matsushima (2015). That is, inside a viscous boundary layer at the core-mantle boundary (CMB), magnetic diffusion is assumed to significantly contribute to temporal change of geomagnetic field, and the radial dependence of core flow is expressed in terms of a spiral similar to the Ekman spiral. Below the boundary layer, magnetic diffusion is neglected as in the frozen-flux approximation, and the tangentially magnetostrophic constraint is imposed on the flow.

Any inhomogeneous structure, such as temperature or heat flux, at the CMB is likely to have a strong effect on the core flow. The inhomogeneity successively influences the flow pattern. Therefore, average of fluid flow is expected to show possible core-mantle interaction. Hence, fluid flows inside and below the boundary layer are averaged over the time from 1840 to 2015 covered by the COV-OBS.x1 model. However, mean amplitudes of upwelling and downwelling flows as well as mean horizontal flows are found to be smaller than those at respective times. This result suggests that possible thermal heterogeneity due to the lowermost mantle structure has little effect on the core surface flow; that is, compositional convection is dominant in the Earth's outer core. It should be noted, however, that there is a noticeable upwelling flow corresponding to a counterclockwise vortex beneath the south of Africa, and that the location is just outside the tangent cylinder, an imaginary cylinder parallel to the rotational axis and attached to the equator of the inner core. This may indicate that the vortex corresponds to an edge of columnar convective motion, although the other edge in the northern hemisphere is unclear.

Keywords: core-mantle interaction, core surface flow

©2019. Japan Geoscience Union. All Right Reserved.

Determination of the noble gas partition coefficients between metal-silicate melts under high-pressure and high-temperature conditions

*Tomotaka Tanaka[1], Hideharu Kuwahara[2], Satoshi Kishi[1], Ryuichi Nomura[3], Kenji Mibe[5], Hiroyuki Kagi[4], Shigehiko Tateno[6], Hirochika Sumino[1]

1. Department of Basic Science, Graduate School of Arts and Sciences, The University of Tokyo , 2. Geodynamics Research Center, Ehime University, 3. Kyoto University, 4. Geochemical Research Center, Graduate School of Science, University of Tokyo, 5. Earthquake Research Institute, University of Tokyo, 6. Earth-Life Science Institute, Tokyo Institute of Technology

Analyses of ocean island basalts reveal a geochemical reservoir characterized by unradiogenic, “primordial” noble gas signatures (e.g., high $^{3}He/^{4}He$ and low $^{40}Ar/^{36}Ar$ ratios), likely residing in the deep mantle. There has been much debate about the area holding the “primordial” noble gases deep in the Earth (Porcelli & Ballentine, 2002), including that the “primordial” noble gasses have been retained in the deepest region of the mantle since 4.4 Ga (Mukhopadhyay, 2012), or in the core since the core-mantle separation (Trieloff & Kunz, 2005; Bouhifd et al., 2013). However, the validity of latter strongly depends on the quantity of noble gases the core incorporates during accretion and can hold in the present day.

In order to investigate noble gas partitioning behavior between the core and mantle, noble gases were dissolved into metal-silicate melts under high temperature and pressure conditions, and then the samples were quenched, recovered, and analyzed for noble gas concentrations. Sample synthesis was performed at the Geodynamics Research Center, Ehime University. Noble-gas doped silicate glass and iron were melted and equilibrated under high pressure and temperature (3-6 GPa, 1700 and 1800 ˚C) using a multianvil apparatus. The sample capsule was cut and the polished surface of the section was investigated with scanning electron microscope and Raman spectroscopy. The chemical compositions of silicate and metal phases were determined with electron microprobe. And then, the noble gases in the silicate phase were extracted by an ultraviolet laser ablation apparatus and analyzed using a noble gas mass spectrometer at the University of Tokyo.

From the Raman spectra, it was found that crystallization (clinopyroxene) had occurred in samples synthesized at pressures of 6 GPa or higher, indicating that the sample quenching was not enough rapid. There is a possibility that noble gas may not be contained much in the crystallized part because a previous study showed that noble gas content in pyroxene crystal is smaller than those in glass (melt) by about 10^{-4} (Heber *et al.*, 2007). The noble gas concentrations in silicate glass phase are fairly homogeneous, even where a crack is formed during quenching. In future we will measure the noble gases in the iron part and determine the partition coefficient of the noble gases.

References: Bouhifd et al, *Nature Geoscience*. **6**, 982-986, 2013; Mukhopadhyay, *Nature* **486**, 101-104, 2012; Porcelli & Ballentine, *Rev. Mineral. Geochem.* **47**, 411-480, 2002; Trieloff & Kunz, *Phys. Earth Planet. Inter.* **148**, 13-38, 2005; Herber *et al*, *Geochim. Cosmochim. Acta*. **71**, 1041-1061, 2007

©2019. Japan Geoscience Union. All Right Reserved.

Measurement of T-dependent electrical resistivity of solid and liquid Fe and Pt at fixed P

*Innocent Ezenwa[1], Takashi Yoshino[1]

1. Institute for Planetary Materials, Okayama University

Knowledge of the thermal and electrical conductivity of solid and liquid Fe and its relevant alloys at P and T conditions is essential for understanding the cooling history of planetary cores and modelling their dynamo. The general understanding of the electrical transport properties of the transition metals at lower P will perhaps give insight in understanding Fe behavior at the inaccessible planetary core conditions. Theoretical investigation has suggested that the electrical and thermal conductivity of solid and liquid Fe at Earth’ s core conditions are similar in value (Wagle and Steinle-Neumann, (2017). At ambient T, experimental investigation showed that hcp ε -phase of Fe becomes paramagnetic at ~18GPa while Pt is paramagnetic and crystalize fcc at ambient conditions. Since Fe and Pt have an unfilled *d*-band electronic structure and at high P both exhibits closed packed crystal structures, experimental determination of the transport properties of molten Pt at lower P conditions is important for understanding the behavior of molten Fe preceding ε -phase at ~80 GPa. We develop a technique and cell design for the investigation of the electrical resistivity of metals that keeps it free from contamination using multianvil press. And, we report measurements on Fe and Pt. The sample was kept pure by making the electrodes and the sample the same composition while the thermocouple (TC) is placed close to the sample and taking through the gasket. The major challenge of TC breakage during compression and/or heating was overcome by shielding the TC with a cylindrical hollow coiling ring made of the same composition as the TC leads. The use of current polarity reversal to eliminate biased voltage as deployed in previous studies was adopted. On Fe and Pt, resistivity increases and decreases with T and P respectively, was observed. On melting, Fe result at 3 GPa agrees with very recent data by Silber et al. (2018) which showed an increasing difference in the resistivity value of solid and liquid with increasing P. While, Pt resistivity at 3 GPa appears constant comparable to its 1 atm value.

Keywords: Electrical resistivity, Thermal Conductivity, Iron Fe

©2019. Japan Geoscience Union. All Right Reserved.

Ancient, highly depleted mantle constrained by Re-Os isotope and highly-siderophile element compositions of French Polynesian xenoliths

*Norikatsu Akizawa[1], Akira Ishikawa[2], Katsuhiko Suzuki[3], Tetsu Kogiso[4]

1. Atmosphere and Ocean Research Institute, The University of Tokyo, 2. Department of Earth and Planetary Sciences, Tokyo Institute of Technology, 3. Research and Development Center for Submarine Resources, Japan Agency for Marine-Earth Science and Technology (JAMSTEC), 4. Graduate School of Human and Environmental Studies, Kyoto University

Mantle xenoliths, which are fragmented mantle material trapped by ascending magma, can provide lithological and geochemical information of the inaccessible mantle. In order to better understand the lithological and geochemical characteristics of the mantle, we conducted extensive sampling of mantle xenoliths throughout French Polynesia archipelago: Tahiti, Moorea, and Rurutu islands. We collected a total of 42 mantle xenoliths: 1 lherzolite, 14 harzburgites, 22 dunites, 3 wehrlites, and 2 orthopyroxenites. Here, we present whole-rock rhenium-osmium isotope and highly-siderophile element (Os, Ir, Ru, Pt, Pd, and Re) compositions in addition to whole-rock major-element compositions. Osmium isotope ratio ($^{187}Os/^{188}Os$) of the mantle xenoliths ranges from 0.1172 to 0.1464, where the harzburgites show a statistical bimodal distribution with unradiogenic ($^{187}Os/^{188}Os < 0.125$) and radiogenic ($^{187}Os/^{188}Os > 0.125$) compositions. The harzburgites with unradiogenic $^{187}Os/^{188}Os$ are depleted with regards to whole-rock major-element compositions (< 1.22 wt% Al_2O_3), and chondrite-normalized patterns of highly-siderophile elements. Considering the lithological variation of the mantle xenoliths used herein, the mantle is considerably heterogeneous beneath French Polynesia archipelago. In particular, the contrasting isotopic compositions of the harzburgites suggest different mantle reservoirs with unradiogenic and radiogenic $^{187}Os/^{188}Os$ compositions. We propose a possibility that the harzburgites with unradiogenic $^{187}Os/^{188}Os$ are impinged mantle material beneath normal oceanic lithosphere due probably to ascending plumes.

Keywords: Harzburgite, Dunite, PGE, TIMS, ICP-MS, Whole-rock chemical composition

©2019. Japan Geoscience Union. All Right Reserved.

First-principles prediction of hydrogen partitioning between the core and mantle

*Atsuroh Ohba[1], Taku Tsuchiya[1]

1. Ehime University Geodynamics Research Center

Some recent studies have reported high-P,T hydrous minerals which are stable at the core mantle boundary (CMB) pressure (Sano et al., 2008; Ohhira et al., 2016; Nishi et al., 2017). In order to elucidate the water circulation in the Earth's interior, experiments on the reaction between iron and hydrous minerals or water were also conducted (Iizuka-Oku et al., 2016; Mao et al., 2018; Clesi et al., 2018). However, the partition of hydrogen reported is different in different studies. In this study, we try estimating hydrogen partitioning between molten silicate and liquid iron under the CMB conditions based on the first principles calculation method combined with thermodynamic integration similar to our previous study (Xiong et al., 2018). Here, we assume following the exchange reaction of water between liquid iron and molten silicate is expressed as follows
(16MgSiO3+H2O) + 50Fe ⇔16MgSiO3 + (50Fe+H2O)
as a first example with ensuring the charge neutrality. Here, reaction free energy is calculated by the thermodynamic integration molecular dynamics method (Taniuchi & Tsuchiya, 2018). In the moment, simulations suggest that water prefer liquid iron. Now, additional computations are ongoing for improving numerical accuracy. The mechanism dissolving water into liquid iron is also investigated.

©2019. Japan Geoscience Union. All Right Reserved.

Microvolume stable isotope measuremetns and its applicaiton for high-pressure high-temperature experimental run products

*Madhusoodhan Satish-Kumar[1], Shinnosuke Aoyama[1]

1. Department of Geology, Faculty of Science, Niigata University

Light elements are very important in deep earth processes. Its composition in the lower mantle and core is still not well constrained. Stable isotope composition can be effectively used as an independent proxy. Although isotope fractionation in the deep earth occur in a narrow range, the volume of light element content in the mantle and core are extremely high, which can effectively cause significant natural isotopic compositional variations. It is necessary to accurately measure the isotope composition accurately in micro to nanomole scales, because the high-pressure experimental run products are small in volume. Recent studies have predicted the presence of isotope fractionation even at lower mantle and core *P-T* conditions, especially in magma ocean environment and during the core segregation. Despite the necessity of the micro-volume stable isotope measurement, there is always a tradeoff between the accuracy and the sample size.

At Niigata University, a MAT-253 mass spectrometer (Thermo Fisher Scientific) was installed through the MEXT Grant-in-Aid for Scientific Research on Innovative Areas. Carbon and oxygen isotopic compositions are measured using $CO_2$and multiple sulfur isotopic composition are measured using SF_6gas. A new micro-volume inlet system was installed and fundamental parameters such as pressure effect and capillary flow effect were tested. Using the micro-volume inlet system the minimum volume required for analysis is 1 micro-mole sample gas, and the precession for carbon and oxygen isotopic composition are better than 0.1‰. The precession for sulfur isotopes is ±0.3‰ and ±0.01‰ (1s) for $\delta^{34}S$ and $D^{33}S$, respectively, based on the repeated analyses of standard Ag_2S (IAEA S-1).Multiple sulfur isotope measurement system consists of 1) curie point pyrolyzer for rapid conversion of small volume samples to SF_6gas, 2) vacuum line system for pumping out non-condensable gasses, 3) gas chromatograph for purifying the SF_6gas and 4) micro-volume inlet system for introduction of sample gas to ionization chamber.
Multiple sulfur isotope ratios experimental run products were measured using the new system. Metal phases were separated and sulfur was extracted using Cr(II) reduction method [6]. Preliminary results indicate that S isotope fractionations occur in the pressure range of 3–5 GPa, under high-temperature conditions corresponding to the magma ocean environment. The negative $\delta^{34}S$ of mantle, can hence be explained by sulfur isotope fractionation in a magma ocean environment. Sulfur isotope measurements were also carried out on granitoid samples from the Archean with sulfide sulfur showing positive $\delta^{34}S$ values. Mass independent isotope fractionation, expressed as $\Delta^{33}S$, was also observed, suggesting that sulfur in the mantle alone cannot explain these variations. The incorporation of surface sulfur from sedimentary rocks and seawater is proposed.

Keywords: HPHT experiments, Micro-volume stable isotope measurements, Sulfur isotopes

©2019. Japan Geoscience Union. All Right Reserved.

Electrical resistivity of hcp Fe-Si alloys at high pressure and temperature

*Hayato Inoue[1], Sho Suehiro[1], Kenji Ohta[1], Kei Hirose[2,3], Yasuo Ohishi[4]

1. Department of Earth and Planetary Sciences, Tokyo Institute of Technology, 2. Earth-Life Science Institute, Tokyo Institute of Technology, 3. Department of Earth and Planetary Science, The University of Tokyo, 4. Japan Synchrotron Radiation Research Institute

Silicon (Si) has been repeatedly suggested to be the major light element in the Earth’ s core that mainly consists of iron [1]. Alloying the light element(s) affects a variety of physical properties of iron. Electrical and thermal conductivities strongly constrain the dynamics and thermal evolution of Earth’ s core and these parameters are linked by the Wiedemann-Franz law ($\kappa = \sigma LT$; κ : thermal conductivity, σ : electrical conductivity, L: Lorenz number, T: absolute temperature). However, measurements of electrical and thermal conductivities under static condition at extremely high pressures (P) and temperature (T) are limited for pure iron [2], [3]. The estimates of the core conductivity considering the effect of light element(s) have been done based on the resistivity saturation model, but the validity of the model at the core condition is unclear [4], [5].
In this study, we examined electrical resistivity (the reciprocal of electrical conductivity) of Fe-2, 4 and 6.5 wt.%Si at high P-T conditions in an internally-heated diamond anvil cell (IHDAC) up to 99 GPa and 2910 K. Our results of electrical resistivity of hcp Fe-Si alloys showed its nonlinear temperature dependence, indicating the occurrence of the resistivity saturation. The resistivity saturation in Fe-Si alloys observed in this study supports the notion of high core conductivity and resulting molten lowermost mantle and young inner core.

References: [1] Poirier: *Phys. Earth Planet. Inter.* **85**, 319-337 (1994).;[2] Ohta et al.: *Nature* **534**, 95–98 (2016).;[3] Konôpková et al.: *Nature* **534**, 99–101 (2016).;[4] Gomi et al.: *Phys. Earth Planet. Inter.* **224**, 88–103 (2013).;[5] Gomi et al.: *Earth Planet. Sci. Lett.* **451**, 51–61 (2016).

Keywords: Electrical conductivity, Thermal conductivity, Earth's core

©2019. Japan Geoscience Union. All Right Reserved.

Electrical resistivity and thermal conductivity of fcc Fe: Implications for the Mercury's core

*Hitoshi Gomi[1], Takashi Yoshino[1]

1. Okayama University

The Mercury's magnetic field may be sustained by the geodynamo motion in the liquid Fe core. However, its strength is about 1% of that of Earth. This weak magnetic field may implies a partly stratified core. Gomi et al. (2013) pointed out that the geometry of the thermal stratification depends critically on the depth dependency of the thermal conductivity. In this study, we conducted first-principles calculations on the face-centered cubic (fcc) Fe to constrain the electrical resistivity and the thermal conductivity of the Mercury's core.

We calculated the electrical resistivity and the thermal conductivity of fcc Fe by means of the Korringa-Kohn-Rostoker method combined with the coherent potential approximation (KKR-CPA) (Akai, 1989). The CPA was adopted to treat the disorder effects due to the atomic vibrations and the magnetic fluctuations on the electronic band structure (Glasbrenner et al., 2014; Ebert et al., 2015; Kou and Akai, 2018). Within the alloy analogy model, the thermal atomic displacements were represented by a discrete set of N_v displacement vectors $\Delta R_v(T)$, where $|\Delta R_v(T)|=\sqrt{<u^2>}$ is the root mean square displacement of atoms, which is based on the Debye model without zero point vibration. The lattice parameter and the Debye temperature are obtained from the equation of state of fcc Fe (Tsujino et al., 2013). In addition to the non-magnetic state, the magnetic disorder was simulated by the local magnetic disorder (LMD) approach. The conductivity was calculated by the Kubo-Greenwood formula with the vertex correction.

The calculated electrical resistivities and thermal conductivities with LMD state are consistent with the literature data at 0 GPa (Ho et al., 1972; 1983), whereas the non-magnetic results show smaller resistivity and larger thermal conductivity. This suggests the importance of the magnetic scattering at low pressures. However, our calculation predicts that the magnetic contribution banishes at higher pressures than 20 GPa. Figure 1 compares the present results and previous experiments (gray broken line; Secco and Scholoessin, 1989, gray square; Deng et al., 2013, open diamond; Pommier, 2018, black circle; Silber et al., 2018) on the electrical resistivity at ~5 GPa. Note that, within the fcc stability field, previous measurements have a large variation. Our calculated resistivity values are between Secco and Scholoessin (1989) and Silber et al. (2018).

We further calculated the electrical resistivity and the thermal conductivity of fcc Fe up to 50 GPa and 3000 K. The thermal conductivity increases with increasing pressure and temperature. This means that, if the inner core is absent, the thermal stratification starts from the bottom, and, after the onset of the inner core, a thick thermal stratified layer may develop at the top of the fluid core (Gomi et al., 2013).

Keywords: electrical resistivity, thermal conductivity, Mercury, core, thermal stratification

©2019. Japan Geoscience Union. All Right Reserved.

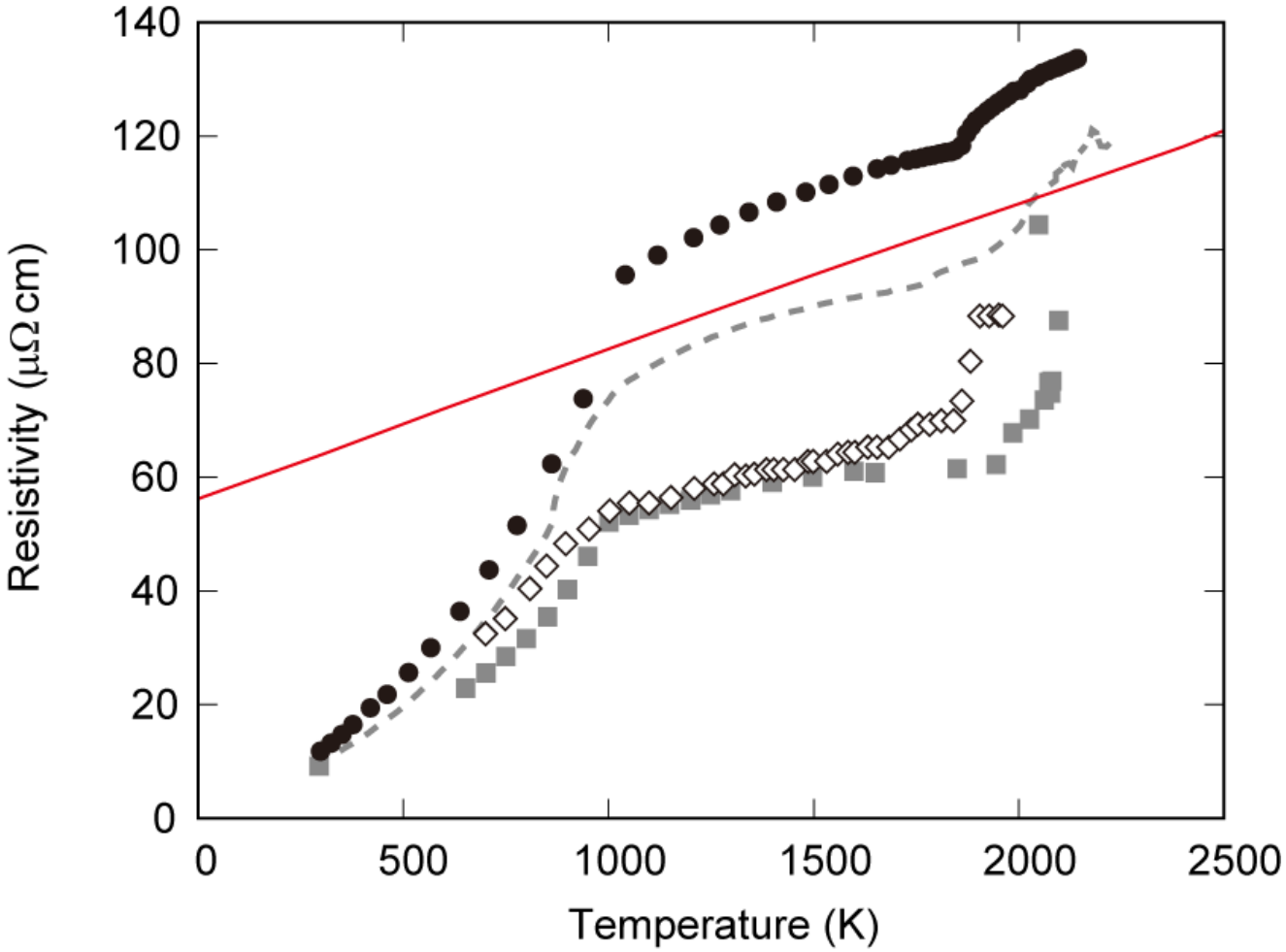

©2019. Japan Geoscience Union. All Right Reserved.

Lateral heterogeneity in the lowermost outer core (F layer) of the Earth revealed by seismic analyses

*Toshiki Ohtaki[1], Satoshi Kaneshima[2], Taku Tsuchiya[3]

1. Geological Survey of Japan, National Institute of Advanced Industrial Science and Technology (AIST), 2. Department of Earth and Planetary Sciences, Kyushu University, 3. Geodynamics Research Center, Ehime University

We have determined seismic velocity structures of the lowermost outer core (F layer) beneath Northeast Pacific and Australia (Ohtaki and Kaneshima, 2015; Ohtaki et al., 2018), and found that the F layer is seismologically heterogeneous. These structures were obtained using a combination of two observations. First one is differential traveltimes between waves that reflect at the inner core boundary (ICB) and that graze the boundary; the second is dispersion (frequency dependence of velocity) of the grazing wave.

Our results show a somewhat strange velocity profile in the F layer beneath Australia, which has a lower-velocity-gradient layer than that of the Preliminary Reference Earth Model (PREM; Dziewonski and Anderson, 1981) on the ICB, and a higher-gradient layer just above the layer. Recent advance in high pressure research enables seismologists to translate lateral seismic velocity variation to relative chemical abundance in the outer core condition. Based on the results of Ichikawa and Tsuchiya (e.g., 2018), we showed light-element enrichment there. This result suggests that lighter fluid exists beneath Australia in the lowermost part of the liquid core, although the outer core is low-viscosity fluid.

The solid inner core of the Earth has quasi-hemispherical structure (e.g., Tanaka and Hamaguchi, 1997). As the origin of this hemispherical structure, uneven growth of the inner core has been proposed (e.g., Aubert et al., 2008; Alboussière et al., 2010; Monnereau et al., 2010). When the liquid in the outer core solidifies at the inner core surface, excess light element is partitioned to residue because the solid inner core is poorer in light elements compared with the liquid outer core. Thus, the uneven growth of the inner core is tied with an uneven release of the light elements to the F layer, which may be related to our results of the heterogeneous F layer. Then, a question arises: this heterogeneity has hemispherical structure like the inner core or local one?

We have not answered it yet because the survey areas of the above studies are restricted. Furthermore, other studies focusing F-layer velocity are not so many. Souriau (2015) determined lateral variations of velocity in the lower outer core using traveltimes of waves that turn there, and suggested that heterogeneity in F has degree-one feature. We also determined the seismic structure of the F layer beneath Antarctica using amplitude ratios between waves that turn just above the inner core and that get into the inner core. Although the resolution and reliability of structure obtained using amplitude ratios is lower than those using the method of our recent papers, the structure beneath Antarctica has a much lower velocity gradient in the F layer compared with PREM. Such a lower gradient is close to the model beneath Australia.

In this paper, we will show the summary of the heterogeneous F-layer structures of velocity and chemical abundance at this stage.

References

Alboussière, T., R. Deguen, and M. Melzani (2010), *Nature*, *466*, 744–747, doi:10.1038/nature09257.

©2019. Japan Geoscience Union. All Right Reserved.

Aubert, J., H. Amit, G. Hulot, and P. Olson (2008), *Nature*, *454*, 758–761, doi:10.1038/nature07109.
Dziewonski, A. M., and D. L. Anderson (1981), *Phys. Earth Planet. Inter.*, 25, 297–356, doi:10.1016/0031-9201(81)90046-7.
Monnereau, M., M. Calvet, L. Margerin, and A. Souriau (2010), *Science*, *328*, 1014–1017, doi:10.1126/science.1186212.
Ichikawa, H., and T. Tsuchiya (2018), J. Geography, 127, 631-646 (in Japanese with English abstract).
Ohtaki, T., S. Kaneshima, and K. Kanjo (2012), *J. Geophys. Res.*, 117, B03312, doi:10.1029/2011JB008717.
Ohtaki, T., and S. Kaneshima (2015), *J. Geophys. Res. Solid Earth*, 120, 7572–7586, doi:10.1002/2015JB012140.
Ohtaki, T., S. Kaneshima, H. Ichikawa, and T. Tsuchiya (2018), *J. Geophys. Res. Solid Earth*, doi:10.1029/2018JB015857.
Tanaka, S., and H. Hamaguchi (1997), *J. Geophys. Res.*, *102*, 2925–2938, doi:10.1029/96JB03187.

Keywords: F layer, lowermost outer core, Heterogeneity of the outer core, Light element concentration in the F layer beneath Australia

©2019. Japan Geoscience Union. All Right Reserved.

Flows and light element distribution in the outer core associated with heterogeneous growth of the inner core of the Earth

*Shin-ichi Takehiro[1], Youhei SASAKI[2]

1. Research Institute for Mathematical Sciences, Kyoto University, 2. Department of Mathematics, Kyoto University

Recent seismological observations suggest longitudinal heterogeneity of seismological wave velocity of the inner core of the Earth, which stimulates a discussion that phase change at the inner core boundary (ICB) does not occur uniformly in the horizontal directions. It is simply supposed from this suggestion that temperature is lower and concentration of light element is higher just above the solidification hemisphere at ICB, and vice versa. The heterogeneous structure of the inner core and thermodynamic properties just above ICB in the outer core is expected to be correlated, however, more recent analysis shows that distribution of seismological wave velocity anomaly does not correspond to longitudinal heterogeneity of the inner core.

There are two kinds of mechanisms explaining heterogeneous growth of the inner core. One of the mechanisms is that the heterogeneous thermal condition at the core mantle boundary (CMB) drives horizontal thermal convection which induces non-uniform temperature distribution at ICB. However, since this study uses co-density, which combines density variations by temperature and light element concentration, it cannot find distribution of the light elements just above ICB. Another mechanism is that hydrodynamic instability of the inner core surrounded by the phase boundary causes translational motion inside the inner core. However, since the theory assumes homogeneous light element distribution in the outer core, it is not clear this mechanism can explain the light element distribution above ICB.

In this study, by using a rotating spherical shell model in which temperature and light element concentration are independent variables, we perform numerical experiments of thermal and compositional convection related to two kinds of mechanisms. Obtained distributions of light element concentration are compared with the distribution of seismological wave velocity anomaly, and plausible dynamical regimes of thermal and compositional convection in the outer core are discussed.

Keywords: Heterogeneity, Inner core, Core-mantle boundary

©2019. Japan Geoscience Union. All Right Reserved.

Sharpness of the hemispherical boundary in the inner core beneath the northern Pacific

*Ryohei Iritani[1], Hitoshi Kawakatsu[1], Nozomu Takeuchi[1]

1. Earthquake Research Institute, Univ. of Tokyo

The hemispherical heterogeneity in the topmost of the Earth’ s inner core, faster velocity and higher attenuation in the eastern hemisphere and slower velocity and weaker attenuation in the western hemisphere, has been revealed by seismological studies. However, how the transition structure between two hemispheres looks like has not been known because of the difficulty to analyze complex core-sensitive data and the limitation of earthquake and seismic array distribution. In this study, we apply the array-based waveform inversion (Iritani et al., 2014) to core phase data that propagate beneath the northern Pacific, and investigate the nature of the transition structure in this region.Dataset used in this study consists of two directional event-station pairs, seismograms observed by the permanent European stations for events at Fiji-Tonga region, and USArray for events near Indonesia. We analyze the broadband vertical component of core phase data containing PKIKP and PKP phases (i.e. the epicentral distance between 145 –155 degree). Resultant analyzed waveforms for EU stations and USArray are 2,108 and 1,172 traces respectively.
In the analysis, waveform inversion approach is employed for each event data to measure traveltime and attenuation in the inner core. As a result, traveltime anomalies observed by EU stations show obvious positive anomaly suggesting mainly propagating the eastern hemisphere, while traveltimes observed by USAray show relatively smaller (or no) anomalies suggesting effects from both of hemispheres. On the other hand, attenuation parameters for both arrays show similar trend that suggests high attenuation corresponding to the eastern hemisphere. To investigate a hemispherical transition boundary in the sampled region, we conduct a ray theory based forward modeling of traveltimes by changing a shape of boundary from meridian boundary to eyeball shaped boundary, and its position. We compute root-mean-square (RMS) of residual between observations and theoretical traveltimes computed with each boundary model. Then, an eyeball shaped boundary, that is located at longitude of 158°W on the equatorial line and latitude of 80°N at the northernmost point, obtained as the preferred boundary model. Finally, we investigate a sharpness of the boundary by varying a width of hemispherical transition. We assume linear variation from the eastern and western hemisphere in a given width and compute RMS. As a result, a width of 600 km at the surface of the inner core shows smaller RMS than sharp boundary. Geophysical significance of this finding will be further discussed.

Keywords: Inner core, Waveform inversion

©2019. Japan Geoscience Union. All Right Reserved.

Stable carbon isotope fractionation in Fe-C system from first principles

*Haruhiko Dekura[1], Taku Tsuchiya[1]

1. Geodynamics Research Center, Ehime University

Carbon is the fourth most abundant element in the solar system and likely one of the constituent light elements in the Earth’s core. Determination of its equilibrium isotope fractionation factor (α) under high pressure (P) and temperature (T) is a key for understanding chemical evolution such as the whole Earth carbon distributions and the amount in the Earth’s core (e.g., Kumar et al., 2011). Because experimental measurement of the isotope fractionation remains technically challenging at the deep mantle condition, attempts to evaluate the α among mantle minerals by first-principles calculations have been made in recent years (e.g., Huang et al., 2014). Recently, our group initiated the theoretical determination of the α in the Fe-C system in the Earth’s deep interior with a full ab initio approach based on the density-functional theory. We performed ab initio lattice dynamics calculations for diamond and iron-carbide (hexagonal Fe7C3) having the two stable carbon isotopes (12C and 13C). The α between the two phases were then determined by using the Gibbs free energies calculated at P ~300 GPa and T ~2000-6000 K. The obtained $10^3 \ln \alpha$ dia-Fe7C3 is found to vary with T from ~+8‰ (2000 K) to ~+5‰ (6000 K). This result indicates that the Fe7C3 is enriched in the heavier isotope (13C) compared with diamond. This trend is qualitatively consistent with low-pressure experimental observations (Kumar et al., 2011).

Keywords: Isotope fractionation, First-principles calculation

©2019. Japan Geoscience Union. All Right Reserved.

[E] Poster | S (Solid Earth Sciences)：S-IT Science of the Earth's Interior & Techtonophysics

Mon. May 27, 2019 5:15 PM - 6:30 PM JST | Mon. May 27, 2019 8:15 AM - 9:30 AM UTC | Poster Hall International Exhibition Hall8, Makuhari Messe_22

[S-IT21] Interaction and Coevolution of the Core and Mantle in the Earth and Planets

convener:Kenji Kawai(Department of Earth and Planetary Science, School of Science, University of Tokyo), Tsuyoshi Iizuka(University of Tokyo), Kenji Ohta(Department of Earth and Planetary Sciences, Tokyo Institute of Technology), Taku Tsuchiya(Geodynamics Research Center, Ehime University)

Recent observational and experimental investigations have significantly advanced our understanding of the structure and constituent materials of the deep Earth. Yet, even fundamental properties intimately linked with formation and evolution of the planet, such as details of the chemical heterogeneity in the mantle and light elements dissolved in the core, remained unclear. Seismological evidence has suggested a vigorous convection in the lower mantle, whereas geochemistry has suggested the presence of stable regions there that hold ancient chemical signatures. The amounts of radioactive isotopes that act as heat sources and drive dynamic behaviors of the deep Earth are also still largely unknown. We provide an opportunity to exchange the achievements and ideas, and encourage persons who try to elucidate these unsolved issues of the core-mantle evolution using various methods, including high-pressure and high-temperature experiments, high-precision geochemical and paleomagnetic analyses, high-resolution geophysical observations, geo-neutrino observations, and large-scale numerical simulations. Papers stimulating an interdisciplinary collaboration relating to establishment of the Japan-SEDI community are also welcomed.

[SIT21-P01] Sample-scale compositional variation of the Inada granite, Ibaraki, Japan -toward the reduction of geoneutrino flux estimation errors from the Japanese crust-

★Invited Papers

*Kenta Ueki[1], Minami Kazuki[2], Tsuyoshi Iizuka[3], Sanshiro Enomoto[4], Hiroyuki Tanaka[2] (1.Japan Agency for Marine-Earth Science and Technology, 2.Earthquake Research Institute, University of Tokyo, 3.Department of Earth and Planetary Science, University of Tokyo, 4.Center for Experimental Nuclear Physics and Astrophysics, University of Washington)

[SIT21-P02] Towards a better estimation of the temperature distribution beneath the Japanese Islands

*Akiko Tanaka[1], Makoto Yamano[2], Hideki Hamamoto[3], Shusaku Goto[4], Takumi Matsumoto[5] (1.Geological Survey of Japan, National Institute of Advanced Industrial Science and Technology, 2.Earthquake Research Institute, The University of Tokyo, 3.Center for Environmental Science in Saitama, 4.Institute for Geo-Resources and Environment National Institute of Advanced Industrial Science and Technology, 5.National Research Institute for Earth Science and Disaster Resilience)

[SIT21-P03] The estimation of the neutrino flux from the crust of the Japanese islands using the geochemical database

*Satoru Haraguchi[1], Kenta Ueki[1], Hikaru Iwamori[1,2,3] (1.Japan Agency for Marine-Earth Science and Technology, 2.Earthquake Research Institute, the University of Tokyo, 3.Tokyo Institute of Technology)

[SIT21-P04] Viscosity of potassium titanosilicate melt at high pressure

*Akio Suzuki[1] (1.Department of Earth Science, Graduate School of Science, Tohoku University)

[SIT21-P05] Lattice thermal conductivity of wadsleyite and ringwoodite at the mantle transition zone pressures

*seiji kimura[1], Kenji Ohta[6], Takaaki Kawazoe[2], Kei Hirose[3], Hiroyuki Kagi[4], Takashi Yagi[5] (1.Department of Earth and Planetary Sciences Tokyo Institute of Technology, 2.Department of Earth and Planetary Systems Science, Hiroshima University, 3.Earth-Life Science Institute, Tokyo Institute of Technology, 4.Geochemical Research Center, Graduate School of Science, University of Tokyo, 5.National Institute of Advanced Industrial Science and Technology, 6.Department of Earth and Planetary Sciences, Tokyo Institute of Technology)

[SIT21-P06] In-situ X-ray observations of the olivine-spinel transformation under shear deformation: preliminary results on the reaction-induced weakening

*Tomoaki Kubo[1], Moriyama Kazuya[1], Yuichiro Mori[1], Masahiro Imamura[1], Sanae Koizumi[2], Yu Nishihara[3], Akio Suzuki[4], Yuji Higo[5] (1.Kyushu Univ., 2.ERI, 3.GRC Ehime Univ., 4.Tohoku Univ., 5.JASRI)

[SIT21-P07] Internally resistive heated diamond anvil cell experiments with metal encapsulated minerals

*YAMAMOTO TOMONARI[1], Kenji Ohta[1], Sho Suehiro[1], Hayato Inoue[1] (1.Tokyo Institute of Technology)

[SIT21-P08] Shear deformation on post-spinel

*Daisuke Yamazaki[1], Noriyoshi Tsujino[1], Yu Nishihara[2] (1.Institute for Planetary Materials, Okayama University, 2.GRC, Ehime University)

[SIT21-P09] **Lattice thermal conductivity of $CaSiO_3$ perovskite at high pressures and high temperatures**

*Kotaro Onga[1], Kenji Ohta[1], Akira Hasegawa[1,2], Takashi Yagi[2], Kei Hirose[3,4], Yasuo Ohishi[5] (1.Department of Earth and Planetary Sciences, Tokyo Institute of Technology, 2.National Institute of Advanced Industrial Science and Technology, 3.Earth-Life Science Institute, Tokyo Institute of Technology, 4.Department of Earth and Planetary Science, The University of Tokyo, 5.Japan Synchrotron Radiation Research Institute)

[SIT21-P10] **Polycrystalline diamond sintered from ultradispersed nanodiamonds**

*Masayuki Nishi[1,2], Koichiro Yamamoto[1], Youmo Zhou[1], Tetsuo Irifune[2,1] (1.Geodynamics Research Center, Ehime University, 2.Earth-Life Science Institute, Tokyo Institute of Technology)

[SIT21-P11] Thermal conductivity measurements on iron and MgO periclase at high pressure and high temperature similar to the Earth's mid-lower mantle conditions

*Akira Hasegawa[1,2], Kenji Ohta[2], Takashi Yagi[1], Kei Hirose[3,4] (1.National Institute of Advanced Industrial Science and Technology, 2.Tokyo Institude of Technology, 3.Earth-Life Science Institute, Tokyo Institude of Technology, 4.The University of Tokyo)

[SIT21-P12] Azimuthal anisotropy in the lowermost mantle beneath Philippine from ScS-S times

*Satoru Tanaka[1] (1.Department of Deep Earth Structure and Dynamics Research Japan Agency for Marine-Earth Science and Technology)

[SIT21-P13] Detailed 3-D S-velocity structure within D" at the western Pacific LLSVP margin: smaller scale plumes and paleoslabs

*Yuki Suzuki[1], Kenji Kawai[1], Robert J. Geller[1], Satoru Tanaka[2], Weerachai Siripuvaraporn[3], Songkhun Boonchaisuku[3], Noisagool Sutthipong[3], Yasushi Ishihara[2], Taweoon Kim, Koji MIYAKAWA[4], Nozomu Takeuchi[4] (1.The University of Tokyo, 2.Japan Agency for Marine-Earth Science and Technology, 3.Mahidol University, 4.Earthquake Research Institute, The University of Tokyo)

[SIT21-P14] Possible interaction between the core and mantle inferred from a core surface flow model

*Masaki Matsushima[1] (1.Department of Earth and Planetary Sciences, School of Science, Tokyo Institute of Technology)

[SIT21-P15] Determination of the noble gas partition coefficients between metal-silicate melts under high-pressure and high-temperature conditions

*Tomotaka Tanaka[1], Hideharu Kuwahara[2], Satoshi Kishi[1], Ryuichi Nomura[3], Kenji Mibe[5], Hiroyuki Kagi[4], Shigehiko Tateno[6], Hirochika Sumino[1] (1.Department of Basic Science, Graduate School of Arts and

Sciences, The University of Tokyo , 2.Geodynamics Research Center, Ehime University, 3.Kyoto University, 4.Geochemical Research Center, Graduate School of Science, University of Tokyo, 5.Earthquake Research Institute, University of Tokyo, 6.Earth-Life Science Institute, Tokyo Institute of Technology)

[SIT21-P16] **Measurement of T-dependent electrical resistivity of solid and liquid Fe and Pt at fixed P**

*Innocent Ezenwa[1], Takashi Yoshino[1] (1.Institute for Planetary Materials, Okayama University)

[SIT21-P17] Ancient, highly depleted mantle constrained by Re-Os isotope and highly-siderophile element compositions of French Polynesian xenoliths

*Norikatsu Akizawa[1], Akira Ishikawa[2], Katsuhiko Suzuki[3], Tetsu Kogiso[4] (1.Atmosphere and Ocean Research Institute, The University of Tokyo, 2.Department of Earth and Planetary Sciences, Tokyo Institute of Technology, 3.Research and Development Center for Submarine Resources, Japan Agency for Marine-Earth Science and Technology (JAMSTEC), 4.Graduate School of Human and Environmental Studies, Kyoto University)

[SIT21-P18] First-principles prediction of hydrogen partitioning between the core and mantle

*Atsuroh Ohba[1], Taku Tsuchiya[1] (1.Ehime University Geodynamics Research Center)

[SIT21-P19] Microvolume stable isotope measuremetns and its applicaiton for high-pressure high-temperature experimental run products

*Madhusoodhan Satish-Kumar[1], Shinnosuke Aoyama[1] (1.Department of Geology, Faculty of Science, Niigata University)

[SIT21-P20] Electrical resistivity of hcp Fe-Si alloys at high pressure and temperature

*Hayato Inoue[1], Sho Suehiro[1], Kenji Ohta[1], Kei Hirose[2,3], Yasuo Ohishi[4] (1.Department of Earth and Planetary Sciences, Tokyo Institute of Technology, 2.Earth-Life Science Institute, Tokyo Institute of Technology, 3.Department of Earth and Planetary Science, The University of Tokyo, 4.Japan Synchrotron Radiation Research Institute)

[SIT21-P21] Electrical resistivity and thermal conductivity of fcc Fe: Implications for the Mercury's core

★Invited Papers

*Hitoshi Gomi[1], Takashi Yoshino[1] (1.Okayama University)

[SIT21-P22] Lateral heterogeneity in the lowermost outer core (F layer) of the Earth revealed by seismic analyses

*Toshiki Ohtaki[1], Satoshi Kaneshima[2], Taku Tsuchiya[3] (1.Geological Survey of Japan, National Institute of Advanced Industrial Science and Technology (AIST), 2.Department of Earth and Planetary Sciences, Kyushu University, 3.Geodynamics Research Center, Ehime University)

[SIT21-P23] Flows and light element distribution in the outer core associated with heterogeneous growth of the inner core of the Earth

*Shin-ichi Takehiro[1], Youhei SASAKI[2] (1.Research Institute for Mathematical Sciences, Kyoto University, 2.Department of Mathematics, Kyoto University)

[SIT21-P24] Sharpness of the hemispherical boundary in the inner core beneath the northern Pacific

*Ryohei Iritani[1], Hitoshi Kawakatsu[1], Nozomu Takeuchi[1] (1.Earthquake Research Institute, Univ. of Tokyo)

[SIT21-P25] Stable carbon isotope fractionation in Fe-C system from first principles

*Haruhiko Dekura[1], Taku Tsuchiya[1] (1.Geodynamics Research Center, Ehime University)

Sample-scale compositional variation of the Inada granite, Ibaraki, Japan -toward the reduction of geoneutrino flux estimation errors from the Japanese crust-

*Kenta Ueki[1], Minami Kazuki[2], Tsuyoshi Iizuka[3], Sanshiro Enomoto[4], Hiroyuki Tanaka[2]

1. Japan Agency for Marine-Earth Science and Technology, 2. Earthquake Research Institute, University of Tokyo, 3. Department of Earth and Planetary Science, University of Tokyo, 4. Center for Experimental Nuclear Physics and Astrophysics, University of Washington

Geoneutrio observed at anti-neutrino observatory "KamLAND" in Kamioka (Hida City, Gifu Prefecture), enables us to directly observe the abundance of radiogenic elements in the deep earth. As crustal rocks exhibit a high concentration of geoneutrino producing radiogenic elements (Uranium and Thorium) than mantle rocks, we have to subtract the contribution of geoneutrino from the Japanese crust from the observation value in Kamioka to estimate geoneutrino flux from core and mantle. For the purpose, we estimated the 3D distribution of uranium and thorium in the Japanese crust by the stochastic modeling using the seismic velocity structure, geological information and geochemical database for the Japanese crustal rock. Geoneutrino flux calculated using the compositional map exhibits a very large error (up to 80%) at present.
We found that information on the compositional heterogeneity (spatial correlation) of various length scale, such as of the single rock suite scale (km to m scale), and sample scale (cm to mm scale) are essential to reduce the estimation error of crustal geoneutrino flux as small as the observation error of the geoneutrino on KamLAND. Therefore, we conducted a grid sampling of the granite of Inada, Ibaraki prefecture, to obtain quantitative knowledge on the small scale compositional heterogeneity. Samples (about 500g) were divided into several centimeter scale split (about 25g). Based on the compositional variations between small splits from one sample, we discuss the small scale sample wise compositional variation. Whole rock chemical composition of each small split was analyzed using XRF. Also, we conducted surface analysis using an ED-XRF to evaluate the spatial distribution of elements in each split. As a result, even within a single sample (about 500g), a compositional variation of about several% at maximum was observed. This result indicates that when conducting the analysis based on the rock chemical composition considering the spatial context, it is necessary to properly evaluate the sample scale heterogeneity, in addition to the tectonic scale, the rock suite scale, and microscopic scale.Also, this result will contribute to the reduction of the estimation error of geoneutrino from the Japanese crust.

Keywords: Geoneutrino, Granite, Rock chemical composition

©2019. Japan Geoscience Union. All Right Reserved.

Towards a better estimation of the temperature distribution beneath the Japanese Islands

*Akiko Tanaka[1], Makoto Yamano[2], Hideki Hamamoto[3], Shusaku Goto[4], Takumi Matsumoto[5]

1. Geological Survey of Japan, National Institute of Advanced Industrial Science and Technology, 2. Earthquake Research Institute, The University of Tokyo, 3. Center for Environmental Science in Saitama, 4. Institute for Geo-Resources and Environment National Institute of Advanced Industrial Science and Technology, 5. National Research Institute for Earth Science and Disaster Resilience

To improve our understanding of the thermal evolution and structure of the deep Earth, it is necessary to know the shallow part of them. Surface heat flow provides important constraint on it. However, the number of heat flow data is limited and spatially very inhomogeneous and even in regions with measurements the data quality varies. For this reason, we have been working on compiling a comprehensive database of heat flow, thermal conductivity, and geothermal gradient. In 2004, Geological Survey of Japan published a digital geoscience map entitled "Geothermal Gradient and Heat Flow Data in and around Japan", which contains heat flow data in the northwestern Pacific area (from 0 to 60°N and from 120 to 160°E) and geothermal gradient data in and around Japan. In 2019, we will be releasing database entitled "Thermal Data Collection in and around Japan", which contains continuously updated of geothermal gradient and heat flow data and adds thermal conductivity data in and around Japan. Thermal conductivity data were compiled from published data and site-specific reports, and measured using the archived cores. This database offers considerable improvements over the previous version released in 2004, and will be published and available at https://www.gsj.jp/en/database/db-portal/index.html. It presents an opportunity to revisit the thermal state of the lithosphere along with other geophysical/geochemical constraints on heat flow extrapolation.

Keywords: heat flow, thermal conductivity, geothermal gradient

©2019. Japan Geoscience Union. All Right Reserved.

The estimation of the neutrino flux from the crust of the Japanese islands using the geochemical database

*Satoru Haraguchi[1], Kenta Ueki[1], Hikaru Iwamori[1,2,3]

1. Japan Agency for Marine-Earth Science and Technology, 2. Earthquake Research Institute, the University of Tokyo, 3. Tokyo Institute of Technology

Geoneutrino observed at the anti-neutrino observatory "KamLAND" at Kamioka allows us to obtain information on the amount and distribution of radiogenic elements (uranium and thorium) in the deep mantle and crust.. It is necessary to divide the contribution from Japanese from the observed neutrino flux on closely to precisely estimate the quantity of U, Th of the earth deep earth because such radiogenic elements exhibit high concentration in the crust. Previous estimation of the crust origin geoneutrino was estimated based on the relatively simple chemical assumption on the compositional variation and spatial distribution. However, the radioactive elements of the Japanese crustal rock are distributed with very wide compositional range with complex spatial distribution. Therefore, it is necessary to estimate spatial distribution of radioactive element in the Japanese crust for the precisely measurement of geoneutrino from Japanese crust. In addition, petrogical and geochemical structure of the Japanese crust of are fundamental information for understanding seismic activity, volcanic activity and tectonism. The analysis of the spatial variation of the chemical composition of the Japanese Islands crust is important in discussing about the evolution history of the Japanese Islands and the chemical evolution in the subduction zone.

In this study, we utilize DODAI to improve the estimation error of geoneutrino from the Japanese crust (Takeuchi et al., 2019). We published the database “DODAI” which compiled geochemical data published by the Japanese domestic journals and bulletins in the journal of the Geological Society of Japan (Haraguchi et al., 2018). This database incorporates the precise sampling position of individual geochemical data using an electronic map. Resolution of the positional information were improved drastically.
The "DODAI" database covers whole area of Japanese Islands with highly precise positional information is useful for data analysis and modeling. The geochemistry database with highly precise positional information is useful for modeling of the geochemical structure of the solid earth. In this study, we present the potential of the DODAI database and geoneutrion in the analysis of the geochemical structures of Japanese crust, as well as the deep earth.

Keywords: neutrino, geochemical database, geochemical structure of crust and mantle

©2019. Japan Geoscience Union. All Right Reserved.

Viscosity of potassium titanosilicate melt at high pressure

*Akio Suzuki[1]

1. Department of Earth Science, Graduate School of Science, Tohoku University

Viscosity of silicate melt is a fundamental property, which controls volcanic processes, including rates of melt extraction, ascent, and magma mixing. Titanium oxide is contained less than 10 wt% in terrestrial magmatic liquids, however, some lunar magmas contains it over 10 wt%. The addition of titanium to silicate melt affects on the properties such as viscosity, density, and compressibility. Especially the pressure dependence of viscosity is of great interest, because magma is generated in the planetary interiors. The aim of this study is to measure the viscosity of K2TiSi4O11 melt at high pressures to estimate the influence of the pressure-induced structural change of melt.
We performed in situ falling sphere viscometry in the pressure range from 1.3 to 7.4 GPa, by using the MAX-III high pressure apparatus at BL14C2 and NE7A beamlines at Photon Factory in KEK, Tsukuba, Japan. A falling platinum sphere in the melt was monitored by using an X-ray CCD camera with a YAG:Ce fluorescence screen. We observed that the viscosity of KTS4 melt decreased up to 3.3 GPa. In contrast, the pressure dependence in viscosity was not observed above 3.3 GPa. Based on XANES spectra of K2TiSi4O11 glasses quenched under high pressure, Paris et al. (1994) showed that the coordination number of titanium increased with increasing pressure. The present study suggests that the melt becomes depolymerized by the coordination change of titanium under high pressure.

Keywords: magma, viscosity, high pressure

©2019. Japan Geoscience Union. All Right Reserved.

Lattice thermal conductivity of wadsleyite and ringwoodite at the mantle transition zone pressures

*seiji kimura[1], Kenji Ohta[6], Takaaki Kawazoe[2], Kei Hirose[3], Hiroyuki Kagi[4], Takashi Yagi[5]

1. Department of Earth and Planetary Sciences Tokyo Institute of Technology, 2. Department of Earth and Planetary Systems Science, Hiroshima University, 3. Earth-Life Science Institute, Tokyo Institute of Technology, 4. Geochemical Research Center, Graduate School of Science, University of Tokyo, 5. National Institute of Advanced Industrial Science and Technology, 6. Department of Earth and Planetary Sciences, Tokyo Institute of Technology

The lattice thermal conductivities of wadsleyite (Wd) and ringwoodite (Rw), which predominantly occupy the Earth's mantle transition zone, are important transport properties to understand the dynamics and thermal structure of the mantle. In particular, the temperature in the subducting slab is mainly controlled by the thermal conduction of Wd and Rw. Wd and Rw are both thought to preserve a large amount of hydrogen ions, thus should play an important role as the main water reservoir in the Earth. Furthermore, it has been reported that the hydration affects the physical properties of minerals including thermal conductivity, and it is necessary to measure the lattice thermal conductivity of Wd and Rw considering their water content. However, so far, the reported lattice thermal conductivities of Wd and Rw has not been considered their water content (Xu et al., 2004). Here we measured the room temperature lattice thermal conductivity of $(Mg_{0.89}Fe_{0.11})_2SiO_4$ Wd and $(Mg_{0.91}Fe_{0.09})_2SiO_4$ Rw up to 27 GPa, respectively, to clarify their hydration dependence using the pulsed light heating thermoreflectance technique in a diamond anvil cell.The obtained results show similar pressure dependence of the lattice thermal conductivity to the previous study (Xu et al., 2004). However, the absolute values of the thermal conductivity are different; the lattice conductivities of hydrous Wd and Rd are ~52% and ~40% lower than the results of Xu et al. (2004), respectively. Our results suggest strong water content dependence of lattice thermal conductivities of Wd and Rw, implying that the water content in the mantle minerals is key factor for calculating the thermal structure in a subducting slab, mantle dynamics.

Keywords: wadsleyite, ringwoodite, mantle transition zone, hydrous minerals, thermal conductivity

©2019. Japan Geoscience Union. All Right Reserved.

In-situ X-ray observations of the olivine-spinel transformation under shear deformation: preliminary results on the reaction-induced weakening

*Tomoaki Kubo[1], Moriyama Kazuya[1], Yuichiro Mori[1], Masahiro Imamura[1], Sanae Koizumi[2], Yu Nishihara[3], Akio Suzuki[4], Yuji Higo[5]

1. Kyushu Univ., 2. ERI, 3. GRC Ehime Univ., 4. Tohoku Univ., 5. JASRI

It has been suggested that high-pressure transformations cause rheological weakening and large deformation of subducting slabs in mantle transition zone (MTZ) . However, there have been few direct experimental evidences so far largely because of the difficulties in quantitative deformation experiments under such conitions. Here we report preliminary results on the olivine-spinel transformation experiments under shear deformation upto MTZ pressures. D-111 (DT-cup) type high-pressure deformation apparatus was newly used for this purpose combined with high-energy synchrotron mono X-rays (50-60 keV) at Photon Factory (PFAR NE7 beamline), which enables in-situ observations of interactions between transformation and creep behaviors. Sintered Mg_2SiO_4 forsterite was first deformed at 15-25 GPa at 600˚C in shear, and subsequently heated to higher temperatures (~0.2˚C/s) to cause the olivine-spinel transformation under shear deformation. The transformation started at much lower temperatures under shear deformation (~900-1100˚C depending on the overpressure from the phase boundary) compared to that without deformation (~1400˚C), suggesting that the shear deformation enhances the olivine-spinel transition rate. The shear strain rate in the sample monitored by X-ray radiography was ~3-4 x 10^{-6} (s^{-1}) at 600˚C, and increased up to ~2-3 x 10^{-4} (s^{-1}) with ramping temperatures even keeping the anvil displacement rate constant (200 micron/h). We observed that the shear weakening does not occur at the same temperature, but reflects on the initiation of the olivine transition. Also, the weakening effects become significant at larger overpressures (and low T). This implies that the weakening of the shear zone induced by the grain-size reduction due to the olivine-spinel transition, however further evidences from microstructural observations are necessary. We plan to install 8-ch acoustic emission measurement system attached with D-111 apparatus to capture the transformation-induced shear instabitiy. Results of D-DIA shear deformation study on the olivine-spinel transition in Fe_2SiO_4 will also be presented and compared with those of the D-111 study in Mg_2SiO_4 .

©2019. Japan Geoscience Union. All Right Reserved.

Internally resistive heated diamond anvil cell experiments with metal encapsulated minerals

*YAMAMOTO TOMONARI[1], Kenji Ohta[1], Sho Suehiro[1], Hayato Inoue[1]

1. Tokyo Institute of Technology

Heating technique is crucial for *in-situ* high pressure-temperature (*P-T*) studies into the physical and chemical properties of minerals in the diamond anvil cell (DAC) under deep Earth's conditions. External resistive heating methods that use resistive heaters such as AlChrom-O wire and graphite surrounding the DAC or just the diamonds (Dubrovinskaia and Dubrovinsky, 2003; Du et al., 2013). This approach creates a homogeneous temperature field in the sample chamber but limits the maximum temperature of about 1200℃ due to graphitization of diamond anvils. Double-sided laser heating with a DAC generates the *P-T* conditions corresponding to the center of the Earth's (Tateno et al., 2010). However, tightly focused laser beams, instabilities in output laser power and misalignment of the focused beams on the sample surface result in significant temperature variation within the sample in the DAC. Internally resistive heated DAC is an effective heating method to overcome the temperature limitation of external heated DAC and the significant temperature gradients experienced in conventional laser-heated DAC (e.g., Zha and Bassett, 2003). However, the internally resistive heated DAC is mostly applied to metal sample to study the properties of the planetary metallic core despite this technique could be applicable to an insulating mineral.

In this study, we modified the internally resistive heated DAC technique for nonmetallic material. We developed a microfabrication technique for total metal encapsulation of the nonmetallic sample. The sample encapsulated by platinum was loaded in DAC with thermal insulator and connected with two electrical leads to make electrical circuit for resistive heating. We confirmed very stable and homogeneous heating for insulating sample at 30 GPa to 2450 K in the modified internally resistive heated DAC. The highest temperature which this method can generate depends on the metal heater encapsulating the sample. This method offers a larger heating volume with more stable and uniform temperature than laser heating and at temperatures much greater than those that can be generated by external resistive heating methods.

References

Dubrovinskaia, N., & Dubrovinsky, L. (2003). Whole-cell heater for the diamond anvil cell. *Review of Scientific Instruments*, *74*(7), 3433-3437.

Du, Z., Miyagi, L., Amulele, G., & Lee, K. K. (2013). Efficient graphite ring heater suitable for diamond-anvil cells to 1300 K. *Review of Scientific Instruments*, *84*(2), 024502.

Tateno, S., Hirose, K., Ohishi, Y., & Tatsumi, Y. (2010). The structure of iron in Earth's inner core. *Science* , *330*(6002), 359-361.

Zha, C. S., & Bassett, W. A. (2003). Internal resistive heating in diamond anvil cell for in situ X-ray diffraction and Raman scattering. *Review of scientific instruments*, *74*(3), 1255-1262.

©2019. Japan Geoscience Union. All Right Reserved.

Keywords: Internally resistive heated diamond anvil cell, high pressure-temperature experiments

©2019. Japan Geoscience Union. All Right Reserved.

Shear deformation on post-spinel

*Daisuke Yamazaki[1], Noriyoshi Tsujino[1], Yu Nishihara[2]

1. Institute for Planetary Materials, Okayama University, 2. GRC, Ehime University

Earth’ s lower mantle is mainly composed of ferro-periclase and bridgmanite. The viscosity of ferro-periclase is considered to be 2-3 orders of magnitude lower than that of bridgmanite. Such large discrepancy in viscosity may cause the significant effect of microstructure of the aggregate of bridgmanite and ferro-periclase on bulk viscosity. For example, bulk viscosity is low when the interconnected weak layer structure is formed, whereas bulk viscosity is as high as the viscosity of bridgmanite when the load bearing framework structure is formed [1].

Microstructural evolution from the load bearing framework structure to the interconnected weak layer structure in post-spinel phase (mixture of bridgmanite and ferro-periclase) during deformation was previously reported based on the rotational Drickamer apparatus [2]. This results suggests the important viscosity reduction during deformation in the lower mantle. We therefore considered that more detailed and precise experiments are necessary to discuss the lower mantle rheology quantitatively.

Deformation experiments under the lower mantle conditions can be conducted by using D111-type deformation Kawai-type high pressure apparatus. This apparatus was previously installed at UCL followed by PF-AR and Misasa. In this study, we use these apparatus for the deformation on post-spinel phase.

Starting material for deformation experiment was well-sintered aggregate of bridgmanite and ferro-periclase synthesized at 24 GPa and 1873 K. For the simple shear deformation, we used 45 degree cut design. In in-situ X-ray experiments at PF-AR, we used tapered and coned anvils for X-ray paths. On the other hand, in “quench” experiments at Misasa, we used a simple cubic anvils (TEL=2.0 mm). All deformation experiments were performed with constant D-rams displacement rate.
We deformed sample up to shear strain of ~0.8 with the 0.4 mm displacements of D-rams. SEM observation on the recovered sample by SEM shows that there is no significant evolution in microstructure, indicating that viscosity reduction is not expected with shear deformation to gamma~1. [1] D. Yamazaki, S. Karato: Am. Mineral., **86**, 385 (2001). [2] J. Girard et al.: Science, **351**, 144 (2016).

©2019. Japan Geoscience Union. All Right Reserved.

Lattice thermal conductivity of $CaSiO_3$ perovskite at high pressures and high temperatures

*Kotaro Onga[1], Kenji Ohta[1], Akira Hasegawa[1,2], Takashi Yagi[2], Kei Hirose[3,4], Yasuo Ohishi[5]

1. Department of Earth and Planetary Sciences, Tokyo Institute of Technology, 2. National Institute of Advanced Industrial Science and Technology, 3. Earth-Life Science Institute, Tokyo Institute of Technology, 4. Department of Earth and Planetary Science, The University of Tokyo, 5. Japan Synchrotron Radiation Research Institute

Laboratory measurements of thermal conductivity of deep Earth materials provide important information on the dynamics and thermal evolution of the mantle and the core. $CaSiO_3$ perovskite (CaPv) is a constituent of pyrolitic lower mantle and of the subducting oceanic crust at depth greater than 560 km. In recent years, there are many reports of the laboratory-based lower mantle thermal conductivity profiles, but the thermal conductivity of CaPv has never been measured and included in the models [1,2,3,4,5] . CaPv is an unquenchable high-pressure phase at ambient conditions, and temperature-induced structure change from tetragonal to cubic occurs at around 500 K [6]. Therefore, *in-situ* high pressure and temperature X-ray diffraction (XRD) and thermal conductivity measurements are required to determine the thermal conductivity of CaPv in the Earth’ s deep interior.
In this study, we determined the thermal conductivity of CaPv at about 50 GPa and high temperature to 1950 K by a combination of synchrotron XRD measurements and the pulsed light heating thermoreflectance technique. Based on our experimental results, we consider the effect of the presence of CaPv on the thermal conductivity of the pyrolitic lower mantle and the subducting oceanic crust.

Reference: [1] Manthilake, G. et al., *Proc National Acad Sci.* **108,** 17901–17904 (2011). [2] Ohta, K. et al., *Earth Planet Sc. Lett.* **349,**109–115 (2012). [3] Ohta, K. et al., *Earth Planet Sc. Lett.* **465,** 29–37 (2017). [4] Okuda, Y. et al., *Earth Planet Sc. Lett.* **474,** 25–31 (2017). [5] Hsieh, W.-P. et al., J. Geophys. Res. Solid Earth 122, 4900-4917 (2017). [6] Komabayashi, T. et al., *Earth Planet Sc. Lett.* **260,** 564–569 (2007).

Keywords: CaPv, thermal conductivity, lower mantle

©2019. Japan Geoscience Union. All Right Reserved.

Polycrystalline diamond sintered from ultradispersed nanodiamonds

*Masayuki Nishi[1,2], Koichiro Yamamoto[1], Youmo Zhou[1], Tetsuo Irifune[2,1]

1. Geodynamics Research Center, Ehime University, 2. Earth-Life Science Institute, Tokyo Institute of Technology

NPD is a binder-less nanodiamond aggregate (~50 nm) synthesized by direct conversion of graphite under high pressure and temperature [1]. Although NPD has extremely high hardness exceeding that of single-crystalline diamond, it is difficult to obtain the large size of the NPD above 1 cm^3, because extreme high pressure conditions are required. Here we show nanodiamond polyclystalline sintered from ultradispersive nanodiamond under relatively moderate pressure and temperature conditions.

We used a multi-anvil apparatus to sinter the nanodiamonds at 8-15 GPa and 1600-2300˚C, where the diamond is thermodynamically stabilized. The starting materials were enclosed in metal capsules. The microstructures and chemical compositions of the recovered samples were examined using a field-emission scanning electron microscope with energy-dispersive X-ray spectroscopy. Well-sintered polycrystalline were subjected to the Knoop indentation test to evaluate its hardness.

We succeeded in recovering the well-sintered polycrystalline diamonds with grain size of ~10-30 nm in some runs (Figure 1). Full width at half maximum of XRD peaks decreased with increasing temperature due to the grain growth of diamond particles. The color, hardness, and grain size of the sintered polycrystalline changed depending on the capsule materials as well as the pressure and temperature conditions. These features might be affected by the porosity, the grain size, and the impurities. Further studies are required to synthesize the polycrystalline with high hardness comparable to NPD.

References: [1] T. Irifune, A. Kurio, S. Sakamoto, T. Inoue, H. Sumiya., *Nature*, **421**, 599 (2003).

Keywords: multianvil apparatus, nanodiamond, NPD

©2019. Japan Geoscience Union. All Right Reserved.

Thermal conductivity measurements on iron and MgO periclase at high pressure and high temperature similar to the Earth’s mid-lower mantle conditions

*Akira Hasegawa[1,2], Kenji Ohta[2], Takashi Yagi[1], Kei Hirose[3,4]

1. National Institute of Advanced Industrial Science and Technology, 2. Tokyo Institude of Technology, 3. Earth-Life Science Institute, Tokyo Institude of Technology, 4. The University of Tokyo

The thermal transport properties of the Earth’s constituents are important information to constrain the thermal evolution and the heat budget of the Earth. In particular, the thermal conductivity of the core, the largest heat source of the Earth, and the lower mantle, occupying more than half the volume of the whole Earth, are indispensable.

In recent years, thermal conductivity measurement on the sample inside the diamond anvil cell has been carried out utilizing the thermoreflectance phenomenon, the reflectance of metal changes slightly due to the temperature perturbation of several kelvin (e.g. Hsieh et al., 2009 Phys Rev B; Yagi et al., 2011 Meas Sci Technol). However, the reported temperature condition is far from that in Earth’s interior.

In this study, we combined the pulsed light heating thermoreflectance method with high power CW laser heating to obtain the thermal conductivity of material *in-situ* at high pressures and temperatures. As a result of test measurement for Pt, we obtained thermal conductivities of Pt up to 60 GPa and 2000 K, which is in good agreement with the measured values using flash heating method in a laser heated diamond anvil cell (McWilliams et al., 2015 Phys Earth Planet In).

The thermal conductivities of iron and MgO periclase were measured up to 60 GPa and 1700 K with this developed system. We found that the obtained thermal conductivities of iron and MgO have negative temperature dependence, and are consistent with the literatures (Fe: Konôpková et al., 2016 Nature; Ohta et al., 2016 Nature, MgO; Manthilake et al., 2011 Proc National Acad Sci; Dekura and Tsuchiya, 2017 Phys Rev B). The newly developed system here would be a powerful tool to examine the thermal conductivity of Earth’s deep interior.

Keywords: thermal conductivity, laser heated diamond anvil cell, pulsed light heating thermoreflectance method, lower mantle, core

©2019. Japan Geoscience Union. All Right Reserved.

Azimuthal anisotropy in the lowermost mantle beneath Philippine from ScS-S times

*Satoru Tanaka[1]

1. Department of Deep Earth Structure and Dynamics Research Japan Agency for Marine-Earth Science and Technology

Introduction: Seismic anisotropy in the lowermost mantle has been detected by splitting of diffracted S and ScS phases, the discrepancy of shear wave splitting of SKS and SKKS, to date. In many cases, the propagation direction of such seismic waves is restricted due to the combination of sources and receivers. Thus, the azimuthal anisotropy using ray paths passing in multi-directions has been rarely discussed. Now, seismic networks and large-scale seismic arrays have been increasing especially in the eastern Asia where there are also many earthquakes. It is a good opportunity to examine an azimuthal variation of travel times passing through the outside of the Pacific Large Low Shear Velocity Province, where the existence of anisotropy in the lowermost mantle is expected.

Data and Method: I used the seismograms of earthquakes occurred in Mariana, east China, Indonesia, and Vanuatu that are record with the seismic stations belonging to IRIS GSN and PASSCAL, Thai Metrological Department, F-net, JISNET, NECESSArray. This geometry gives a good condition that the mid-points of seismic ray paths are located near Philippine with various azimuths.I measured ScS–S differential travel times using a waveform cross-correlation method, which can effectively cancel the heterogeneity in the crust and upper mantle and the uncertainty of hypocenters. The differential travel times are compared with theoretical travel times by PREM with correction of physical dispersion due to anelasticity for the typical period of 10 s, that for ellipticity of the Earth, finally I obtained about 500 residuals. Even though I used the differential travel times, the ScS–S residuals show the large scattering and the correlation with the residuals of S travel times are much larger than that of ScS phases. This means that the raw ScS–S residuals are affected by heterogeneity in the upper part of the lower mantle where only S waves are propagated. Thus, we applied the further corrections using 3D mantle heterogeneity models.

Results and Discussion: We used S-wave 3D models of S16U6L8, S4BL16, S40RTS, SEMUCB-WM, and a P-wave 3D model of GAP-P4 with conversion rate dlnVs/dlnVp=1.7. I found that the scatter of the ScS–S residuals are much improved and that the correlation coefficient between the residuals of ScS–S and ScS are increased and that between ScS–S and S are much reduced when the GAP-P4 model are used for the correction, probably due to its high spatial resolution in the upper lower mantle. As a result, only the ScS–S residuals corrected with the modified GAP-P4 can be used to infer seismic anisotropy in the lowermost mantle.

Then I fitted cos 2qand cos 4qcurves with least square to obtain the characteristics of the azimuthal variation of the ScS–S residuals, clearly indicating that cos 2qcomponent is significant with the fastest direction (the minimum ScS–S) is along ESE-WNW (N110˚E). This can be explained if [100] axis of post-perovskite is oriented vertically and the direction of [001] axis is ESE-WNW for the incident angle of 45˚. The S-wave fastest direction is nearly parallel to the plate motion directions of the Philippine Sea plate and Sunda block. The amplitude of the azimuthal variation in the ScS–S residual is ±1.1 s, which corresponds to 1.7 % anisotropy if we assume the D” thickness of 300 km based on the previous studies on the D” discontinuity.

©2019. Japan Geoscience Union. All Right Reserved.

Keywords: lowermost mantle, seismic anisotropy

©2019. Japan Geoscience Union. All Right Reserved.

Detailed 3-D S-velocity structure within D" at the western Pacific LLSVP margin: smaller scale plumes and paleoslabs

*Yuki Suzuki[1], Kenji Kawai[1], Robert J. Geller[1], Satoru Tanaka[2], Weerachai Siripuvaraporn[3], Songkhun Boonchaisuku[3], Noisagool Sutthipong[3], Yasushi Ishihara[2], Taweoon Kim, Koji MIYAKAWA[4], Nozomu Takeuchi[4]

1. The University of Tokyo, 2. Japan Agency for Marine-Earth Science and Technology, 3. Mahidol University, 4. Earthquake Research Institute, The University of Tokyo

Global tomographic models of shear velocity have shown two large-scale low shear velocity provinces (LLSVPs) in D″ beneath the Pacific and Africa. It has been controversial whether these LLSVPs are due to thermal effects, chemical effects, or their combination. The nature and origin of the LLSVPs are of fundamental importance since each of the proposed geodynamical scenarios carries different implications for the thermal, chemical and dynamical evolution of the Earth. Previous seismological studies based on travel-time analysis or forward modeling inferred a sharp-sided velocity contrast of the Pacific LLSVP beneath the western Pacific and suggested that the LLSVP is chemically distinct, although the suggested structures of the western edge of the Pacific LLSVP different from each other. To better understand the origin of LLSVPs, it is essential to infer the detailed three-dimensional (3-D) velocity structure within LLSVP beneath the western Pacific. We recently deployed a seismic array stations in Thailand (Thai Seismic Array—TSAR). We assemble waveforms recorded by TSAR as well as other networks such as TM, AU, MM, and MY, allowing us to sample a wider region than previous studies. We conducted waveform inversion using ~5,300 transverse component records of this dataset for the detailed 3-D shear velocity structure in the lowermost 400 km of the mantle beneath the western Pacific. The inferred model shows a low-velocity anomaly immediately above the core-mantle boundary (CMB) and high-velocity anomalies extending vertically from 400 km to the CMB. Taken into account the previous geodynamical simulation studies, the size of the inferred low velocity anomaly suggests a thermal plume rather than a chemical anomaly. The location of the high velocity anomaly in D″ is consistent with the paleo-Izanagi plate subduction boundary about 200 Ma. This implies that a cold paleo-slab produces the strong lateral velocity contrast at the western edge of the western Pacific LLSVP. Hence, we conclude that the western margin of the Pacific LLSVP and its sharp velocity boundary can be explained mainly by thermal effects, and this implies that the lowermost mantle would be well-mixed and the Pacific LLSVP would not be geochemical reservoir.

Keywords: D" region, Pacific LLSVP, Waveform Inversion, Thai Seismic Array (TSAR)

©2019. Japan Geoscience Union. All Right Reserved.

Possible interaction between the core and mantle inferred from a core surface flow model

*Masaki Matsushima[1]

1. Department of Earth and Planetary Sciences, School of Science, Tokyo Institute of Technology

Fluid flow in the Earth's liquid outer core is responsible for the dynamo action by which the geomagnetic field is generated and maintained. The fluid flow can be estimated from geomagnetic field data, such as spatial distribution of geomagnetic field and its temporal change referred to as secular variations. This implies that spatial and temporal variations of fluid flow in the core provide information on any interaction between the core and mantle. To investigate possible core-mantle interaction, a core surface flow model is obtained from a geomagnetic field model, COV-OBS.x1 (Gillet et al., 2015) using the method of Matsushima (2015). That is, inside a viscous boundary layer at the core-mantle boundary (CMB), magnetic diffusion is assumed to significantly contribute to temporal change of geomagnetic field, and the radial dependence of core flow is expressed in terms of a spiral similar to the Ekman spiral. Below the boundary layer, magnetic diffusion is neglected as in the frozen-flux approximation, and the tangentially magnetostrophic constraint is imposed on the flow.

Any inhomogeneous structure, such as temperature or heat flux, at the CMB is likely to have a strong effect on the core flow. The inhomogeneity successively influences the flow pattern. Therefore, average of fluid flow is expected to show possible core-mantle interaction. Hence, fluid flows inside and below the boundary layer are averaged over the time from 1840 to 2015 covered by the COV-OBS.x1 model. However, mean amplitudes of upwelling and downwelling flows as well as mean horizontal flows are found to be smaller than those at respective times. This result suggests that possible thermal heterogeneity due to the lowermost mantle structure has little effect on the core surface flow; that is, compositional convection is dominant in the Earth's outer core. It should be noted, however, that there is a noticeable upwelling flow corresponding to a counterclockwise vortex beneath the south of Africa, and that the location is just outside the tangent cylinder, an imaginary cylinder parallel to the rotational axis and attached to the equator of the inner core. This may indicate that the vortex corresponds to an edge of columnar convective motion, although the other edge in the northern hemisphere is unclear.

Keywords: core-mantle interaction, core surface flow

©2019. Japan Geoscience Union. All Right Reserved.

Determination of the noble gas partition coefficients between metal-silicate melts under high-pressure and high-temperature conditions

*Tomotaka Tanaka[1], Hideharu Kuwahara[2], Satoshi Kishi[1], Ryuichi Nomura[3], Kenji Mibe[5], Hiroyuki Kagi[4], Shigehiko Tateno[6], Hirochika Sumino[1]

1. Department of Basic Science, Graduate School of Arts and Sciences, The University of Tokyo , 2. Geodynamics Research Center, Ehime University, 3. Kyoto University, 4. Geochemical Research Center, Graduate School of Science, University of Tokyo, 5. Earthquake Research Institute, University of Tokyo, 6. Earth-Life Science Institute, Tokyo Institute of Technology

Analyses of ocean island basalts reveal a geochemical reservoir characterized by unradiogenic, “primordial” noble gas signatures (e.g., high $^{3}He/^{4}He$ and low $^{40}Ar/^{36}Ar$ ratios), likely residing in the deep mantle. There has been much debate about the area holding the “primordial” noble gases deep in the Earth (Porcelli & Ballentine, 2002), including that the “primordial” noble gasses have been retained in the deepest region of the mantle since 4.4 Ga (Mukhopadhyay, 2012), or in the core since the core-mantle separation (Trieloff & Kunz, 2005; Bouhifd et al., 2013). However, the validity of latter strongly depends on the quantity of noble gases the core incorporates during accretion and can hold in the present day.

In order to investigate noble gas partitioning behavior between the core and mantle, noble gases were dissolved into metal-silicate melts under high temperature and pressure conditions, and then the samples were quenched, recovered, and analyzed for noble gas concentrations. Sample synthesis was performed at the Geodynamics Research Center, Ehime University. Noble-gas doped silicate glass and iron were melted and equilibrated under high pressure and temperature (3-6 GPa, 1700 and 1800 ˚C) using a multianvil apparatus. The sample capsule was cut and the polished surface of the section was investigated with scanning electron microscope and Raman spectroscopy. The chemical compositions of silicate and metal phases were determined with electron microprobe. And then, the noble gases in the silicate phase were extracted by an ultraviolet laser ablation apparatus and analyzed using a noble gas mass spectrometer at the University of Tokyo.

From the Raman spectra, it was found that crystallization (clinopyroxene) had occurred in samples synthesized at pressures of 6 GPa or higher, indicating that the sample quenching was not enough rapid. There is a possibility that noble gas may not be contained much in the crystallized part because a previous study showed that noble gas content in pyroxene crystal is smaller than those in glass (melt) by about 10^{-4} (Heber *et al.*, 2007). The noble gas concentrations in silicate glass phase are fairly homogeneous, even where a crack is formed during quenching. In future we will measure the noble gases in the iron part and determine the partition coefficient of the noble gases.

References: Bouhifd et al, *Nature Geoscience*. **6**, 982-986, 2013; Mukhopadhyay, *Nature* **486**, 101-104, 2012; Porcelli & Ballentine, *Rev. Mineral. Geochem.* **47**, 411-480, 2002; Trieloff & Kunz, *Phys. Earth Planet. Inter.* **148**, 13-38, 2005; Herber *et al*, *Geochim. Cosmochim. Acta*. **71**, 1041-1061, 2007

©2019. Japan Geoscience Union. All Right Reserved.

Measurement of T-dependent electrical resistivity of solid and liquid Fe and Pt at fixed P

*Innocent Ezenwa[1], Takashi Yoshino[1]

1. Institute for Planetary Materials, Okayama University

Knowledge of the thermal and electrical conductivity of solid and liquid Fe and its relevant alloys at P and T conditions is essential for understanding the cooling history of planetary cores and modelling their dynamo. The general understanding of the electrical transport properties of the transition metals at lower P will perhaps give insight in understanding Fe behavior at the inaccessible planetary core conditions. Theoretical investigation has suggested that the electrical and thermal conductivity of solid and liquid Fe at Earth’ s core conditions are similar in value (Wagle and Steinle-Neumann, (2017). At ambient T, experimental investigation showed that hcp ε -phase of Fe becomes paramagnetic at ~18GPa while Pt is paramagnetic and crystalize fcc at ambient conditions. Since Fe and Pt have an unfilled *d*-band electronic structure and at high P both exhibits closed packed crystal structures, experimental determination of the transport properties of molten Pt at lower P conditions is important for understanding the behavior of molten Fe preceding ε -phase at ~80 GPa. We develop a technique and cell design for the investigation of the electrical resistivity of metals that keeps it free from contamination using multianvil press. And, we report measurements on Fe and Pt. The sample was kept pure by making the electrodes and the sample the same composition while the thermocouple (TC) is placed close to the sample and taking through the gasket. The major challenge of TC breakage during compression and/or heating was overcome by shielding the TC with a cylindrical hollow coiling ring made of the same composition as the TC leads. The use of current polarity reversal to eliminate biased voltage as deployed in previous studies was adopted. On Fe and Pt, resistivity increases and decreases with T and P respectively, was observed. On melting, Fe result at 3 GPa agrees with very recent data by Silber et al. (2018) which showed an increasing difference in the resistivity value of solid and liquid with increasing P. While, Pt resistivity at 3 GPa appears constant comparable to its 1 atm value.

Keywords: Electrical resistivity, Thermal Conductivity, Iron Fe

©2019. Japan Geoscience Union. All Right Reserved.

Ancient, highly depleted mantle constrained by Re-Os isotope and highly-siderophile element compositions of French Polynesian xenoliths

*Norikatsu Akizawa[1], Akira Ishikawa[2], Katsuhiko Suzuki[3], Tetsu Kogiso[4]

1. Atmosphere and Ocean Research Institute, The University of Tokyo, 2. Department of Earth and Planetary Sciences, Tokyo Institute of Technology, 3. Research and Development Center for Submarine Resources, Japan Agency for Marine-Earth Science and Technology (JAMSTEC), 4. Graduate School of Human and Environmental Studies, Kyoto University

Mantle xenoliths, which are fragmented mantle material trapped by ascending magma, can provide lithological and geochemical information of the inaccessible mantle. In order to better understand the lithological and geochemical characteristics of the mantle, we conducted extensive sampling of mantle xenoliths throughout French Polynesia archipelago: Tahiti, Moorea, and Rurutu islands. We collected a total of 42 mantle xenoliths: 1 lherzolite, 14 harzburgites, 22 dunites, 3 wehrlites, and 2 orthopyroxenites. Here, we present whole-rock rhenium-osmium isotope and highly-siderophile element (Os, Ir, Ru, Pt, Pd, and Re) compositions in addition to whole-rock major-element compositions. Osmium isotope ratio ($^{187}Os/^{188}Os$) of the mantle xenoliths ranges from 0.1172 to 0.1464, where the harzburgites show a statistical bimodal distribution with unradiogenic ($^{187}Os/^{188}Os < 0.125$) and radiogenic ($^{187}Os/^{188}Os > 0.125$) compositions. The harzburgites with unradiogenic $^{187}Os/^{188}Os$ are depleted with regards to whole-rock major-element compositions (< 1.22 wt% Al_2O_3), and chondrite-normalized patterns of highly-siderophile elements. Considering the lithological variation of the mantle xenoliths used herein, the mantle is considerably heterogeneous beneath French Polynesia archipelago. In particular, the contrasting isotopic compositions of the harzburgites suggest different mantle reservoirs with unradiogenic and radiogenic $^{187}Os/^{188}Os$ compositions. We propose a possibility that the harzburgites with unradiogenic $^{187}Os/^{188}Os$ are impinged mantle material beneath normal oceanic lithosphere due probably to ascending plumes.

Keywords: Harzburgite, Dunite, PGE, TIMS, ICP-MS, Whole-rock chemical composition

©2019. Japan Geoscience Union. All Right Reserved.

First-principles prediction of hydrogen partitioning between the core and mantle

*Atsuroh Ohba[1], Taku Tsuchiya[1]

1. Ehime University Geodynamics Research Center

Some recent studies have reported high-P,T hydrous minerals which are stable at the core mantle boundary (CMB) pressure (Sano et al., 2008; Ohhira et al., 2016; Nishi et al., 2017). In order to elucidate the water circulation in the Earth's interior, experiments on the reaction between iron and hydrous minerals or water were also conducted (Iizuka-Oku et al., 2016; Mao et al., 2018; Clesi et al., 2018). However, the partition of hydrogen reported is different in different studies. In this study, we try estimating hydrogen partitioning between molten silicate and liquid iron under the CMB conditions based on the first principles calculation method combined with thermodynamic integration similar to our previous study (Xiong et al., 2018). Here, we assume following the exchange reaction of water between liquid iron and molten silicate is expressed as follows
(16MgSiO3+H2O) + 50Fe ⇔16MgSiO3 + (50Fe+H2O)
as a first example with ensuring the charge neutrality. Here, reaction free energy is calculated by the thermodynamic integration molecular dynamics method (Taniuchi & Tsuchiya, 2018). In the moment, simulations suggest that water prefer liquid iron. Now, additional computations are ongoing for improving numerical accuracy. The mechanism dissolving water into liquid iron is also investigated.

©2019. Japan Geoscience Union. All Right Reserved.

Microvolume stable isotope measuremetns and its applicaiton for high-pressure high-temperature experimental run products

*Madhusoodhan Satish-Kumar[1], Shinnosuke Aoyama[1]

1. Department of Geology, Faculty of Science, Niigata University

Light elements are very important in deep earth processes. Its composition in the lower mantle and core is still not well constrained. Stable isotope composition can be effectively used as an independent proxy. Although isotope fractionation in the deep earth occur in a narrow range, the volume of light element content in the mantle and core are extremely high, which can effectively cause significant natural isotopic compositional variations. It is necessary to accurately measure the isotope composition accurately in micro to nanomole scales, because the high-pressure experimental run products are small in volume. Recent studies have predicted the presence of isotope fractionation even at lower mantle and core *P-T* conditions, especially in magma ocean environment and during the core segregation. Despite the necessity of the micro-volume stable isotope measurement, there is always a tradeoff between the accuracy and the sample size.

At Niigata University, a MAT-253 mass spectrometer (Thermo Fisher Scientific) was installed through the MEXT Grant-in-Aid for Scientific Research on Innovative Areas. Carbon and oxygen isotopic compositions are measured using $CO_2$and multiple sulfur isotopic composition are measured using SF_6gas. A new micro-volume inlet system was installed and fundamental parameters such as pressure effect and capillary flow effect were tested. Using the micro-volume inlet system the minimum volume required for analysis is 1 micro-mole sample gas, and the precession for carbon and oxygen isotopic composition are better than 0.1‰. The precession for sulfur isotopes is ±0.3‰ and ±0.01‰ (1s) for $\delta^{34}S$ and $D^{33}S$, respectively, based on the repeated analyses of standard Ag_2S (IAEA S-1).Multiple sulfur isotope measurement system consists of 1) curie point pyrolyzer for rapid conversion of small volume samples to SF_6gas, 2) vacuum line system for pumping out non-condensable gasses, 3) gas chromatograph for purifying the SF_6gas and 4) micro-volume inlet system for introduction of sample gas to ionization chamber.
Multiple sulfur isotope ratios experimental run products were measured using the new system. Metal phases were separated and sulfur was extracted using Cr(II) reduction method [6]. Preliminary results indicate that S isotope fractionations occur in the pressure range of 3–5 GPa, under high-temperature conditions corresponding to the magma ocean environment. The negative $\delta^{34}S$ of mantle, can hence be explained by sulfur isotope fractionation in a magma ocean environment. Sulfur isotope measurements were also carried out on granitoid samples from the Archean with sulfide sulfur showing positive $\delta^{34}S$ values. Mass independent isotope fractionation, expressed as $\Delta^{33}S$, was also observed, suggesting that sulfur in the mantle alone cannot explain these variations. The incorporation of surface sulfur from sedimentary rocks and seawater is proposed.

Keywords: HPHT experiments, Micro-volume stable isotope measurements, Sulfur isotopes

©2019. Japan Geoscience Union. All Right Reserved.

Electrical resistivity of hcp Fe-Si alloys at high pressure and temperature

*Hayato Inoue[1], Sho Suehiro[1], Kenji Ohta[1], Kei Hirose[2,3], Yasuo Ohishi[4]

1. Department of Earth and Planetary Sciences, Tokyo Institute of Technology, 2. Earth-Life Science Institute, Tokyo Institute of Technology, 3. Department of Earth and Planetary Science, The University of Tokyo, 4. Japan Synchrotron Radiation Research Institute

Silicon (Si) has been repeatedly suggested to be the major light element in the Earth’ s core that mainly consists of iron [1]. Alloying the light element(s) affects a variety of physical properties of iron. Electrical and thermal conductivities strongly constrain the dynamics and thermal evolution of Earth’ s core and these parameters are linked by the Wiedemann-Franz law ($\kappa = \sigma LT$; κ : thermal conductivity, σ : electrical conductivity, L: Lorenz number, T: absolute temperature). However, measurements of electrical and thermal conductivities under static condition at extremely high pressures (P) and temperature (T) are limited for pure iron [2], [3]. The estimates of the core conductivity considering the effect of light element(s) have been done based on the resistivity saturation model, but the validity of the model at the core condition is unclear [4], [5].
In this study, we examined electrical resistivity (the reciprocal of electrical conductivity) of Fe-2, 4 and 6.5 wt.%Si at high P-T conditions in an internally-heated diamond anvil cell (IHDAC) up to 99 GPa and 2910 K. Our results of electrical resistivity of hcp Fe-Si alloys showed its nonlinear temperature dependence, indicating the occurrence of the resistivity saturation. The resistivity saturation in Fe-Si alloys observed in this study supports the notion of high core conductivity and resulting molten lowermost mantle and young inner core.

References: [1] Poirier: *Phys. Earth Planet. Inter.* **85**, 319-337 (1994).;[2] Ohta et al.: *Nature* **534**, 95–98 (2016).;[3] Konôpková et al.: *Nature* **534**, 99–101 (2016).;[4] Gomi et al.: *Phys. Earth Planet. Inter.* **224**, 88–103 (2013).;[5] Gomi et al.: *Earth Planet. Sci. Lett.* **451**, 51–61 (2016).

Keywords: Electrical conductivity, Thermal conductivity, Earth's core

©2019. Japan Geoscience Union. All Right Reserved.

Electrical resistivity and thermal conductivity of fcc Fe: Implications for the Mercury's core

*Hitoshi Gomi[1], Takashi Yoshino[1]

1. Okayama University

The Mercury's magnetic field may be sustained by the geodynamo motion in the liquid Fe core. However, its strength is about 1% of that of Earth. This weak magnetic field may implies a partly stratified core. Gomi et al. (2013) pointed out that the geometry of the thermal stratification depends critically on the depth dependency of the thermal conductivity. In this study, we conducted first-principles calculations on the face-centered cubic (fcc) Fe to constrain the electrical resistivity and the thermal conductivity of the Mercury's core.

We calculated the electrical resistivity and the thermal conductivity of fcc Fe by means of the Korringa-Kohn-Rostoker method combined with the coherent potential approximation (KKR-CPA) (Akai, 1989). The CPA was adopted to treat the disorder effects due to the atomic vibrations and the magnetic fluctuations on the electronic band structure (Glasbrenner et al., 2014; Ebert et al., 2015; Kou and Akai, 2018). Within the alloy analogy model, the thermal atomic displacements were represented by a discrete set of N_v displacement vectors $\Delta R_v(T)$, where $|\Delta R_v(T)|=\sqrt{<u^2>}$ is the root mean square displacement of atoms, which is based on the Debye model without zero point vibration. The lattice parameter and the Debye temperature are obtained from the equation of state of fcc Fe (Tsujino et al., 2013). In addition to the non-magnetic state, the magnetic disorder was simulated by the local magnetic disorder (LMD) approach. The conductivity was calculated by the Kubo-Greenwood formula with the vertex correction.

The calculated electrical resistivities and thermal conductivities with LMD state are consistent with the literature data at 0 GPa (Ho et al., 1972; 1983), whereas the non-magnetic results show smaller resistivity and larger thermal conductivity. This suggests the importance of the magnetic scattering at low pressures. However, our calculation predicts that the magnetic contribution banishes at higher pressures than 20 GPa. Figure 1 compares the present results and previous experiments (gray broken line; Secco and Scholoessin, 1989, gray square; Deng et al., 2013, open diamond; Pommier, 2018, black circle; Silber et al., 2018) on the electrical resistivity at ~5 GPa. Note that, within the fcc stability field, previous measurements have a large variation. Our calculated resistivity values are between Secco and Scholoessin (1989) and Silber et al. (2018).

We further calculated the electrical resistivity and the thermal conductivity of fcc Fe up to 50 GPa and 3000 K. The thermal conductivity increases with increasing pressure and temperature. This means that, if the inner core is absent, the thermal stratification starts from the bottom, and, after the onset of the inner core, a thick thermal stratified layer may develop at the top of the fluid core (Gomi et al., 2013).

Keywords: electrical resistivity, thermal conductivity, Mercury, core, thermal stratification

©2019. Japan Geoscience Union. All Right Reserved.

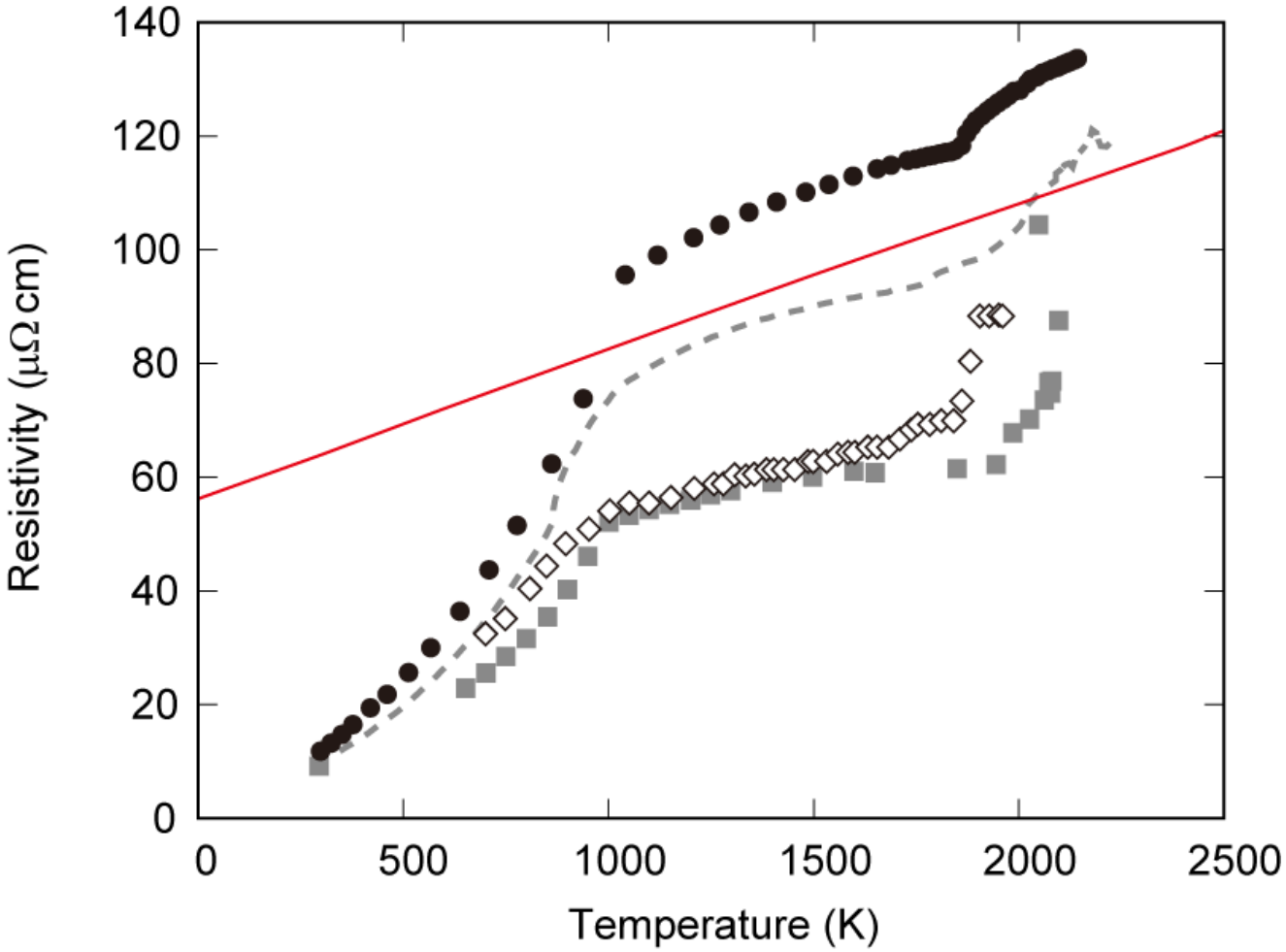

©2019. Japan Geoscience Union. All Right Reserved.

Lateral heterogeneity in the lowermost outer core (F layer) of the Earth revealed by seismic analyses

*Toshiki Ohtaki[1], Satoshi Kaneshima[2], Taku Tsuchiya[3]

1. Geological Survey of Japan, National Institute of Advanced Industrial Science and Technology (AIST), 2. Department of Earth and Planetary Sciences, Kyushu University, 3. Geodynamics Research Center, Ehime University

We have determined seismic velocity structures of the lowermost outer core (F layer) beneath Northeast Pacific and Australia (Ohtaki and Kaneshima, 2015; Ohtaki et al., 2018), and found that the F layer is seismologically heterogeneous. These structures were obtained using a combination of two observations. First one is differential traveltimes between waves that reflect at the inner core boundary (ICB) and that graze the boundary; the second is dispersion (frequency dependence of velocity) of the grazing wave.

Our results show a somewhat strange velocity profile in the F layer beneath Australia, which has a lower-velocity-gradient layer than that of the Preliminary Reference Earth Model (PREM; Dziewonski and Anderson, 1981) on the ICB, and a higher-gradient layer just above the layer. Recent advance in high pressure research enables seismologists to translate lateral seismic velocity variation to relative chemical abundance in the outer core condition. Based on the results of Ichikawa and Tsuchiya (e.g., 2018), we showed light-element enrichment there. This result suggests that lighter fluid exists beneath Australia in the lowermost part of the liquid core, although the outer core is low-viscosity fluid.

The solid inner core of the Earth has quasi-hemispherical structure (e.g., Tanaka and Hamaguchi, 1997). As the origin of this hemispherical structure, uneven growth of the inner core has been proposed (e.g., Aubert et al., 2008; Alboussière et al., 2010; Monnereau et al., 2010). When the liquid in the outer core solidifies at the inner core surface, excess light element is partitioned to residue because the solid inner core is poorer in light elements compared with the liquid outer core. Thus, the uneven growth of the inner core is tied with an uneven release of the light elements to the F layer, which may be related to our results of the heterogeneous F layer. Then, a question arises: this heterogeneity has hemispherical structure like the inner core or local one?

We have not answered it yet because the survey areas of the above studies are restricted. Furthermore, other studies focusing F-layer velocity are not so many. Souriau (2015) determined lateral variations of velocity in the lower outer core using traveltimes of waves that turn there, and suggested that heterogeneity in F has degree-one feature. We also determined the seismic structure of the F layer beneath Antarctica using amplitude ratios between waves that turn just above the inner core and that get into the inner core. Although the resolution and reliability of structure obtained using amplitude ratios is lower than those using the method of our recent papers, the structure beneath Antarctica has a much lower velocity gradient in the F layer compared with PREM. Such a lower gradient is close to the model beneath Australia.

In this paper, we will show the summary of the heterogeneous F-layer structures of velocity and chemical abundance at this stage.

References

Alboussière, T., R. Deguen, and M. Melzani (2010), *Nature*, *466*, 744–747, doi:10.1038/nature09257.

©2019. Japan Geoscience Union. All Right Reserved.

Aubert, J., H. Amit, G. Hulot, and P. Olson (2008), *Nature*, *454*, 758–761, doi:10.1038/nature07109.
Dziewonski, A. M., and D. L. Anderson (1981), *Phys. Earth Planet. Inter.*, 25, 297–356, doi:10.1016/0031-9201(81)90046-7.
Monnereau, M., M. Calvet, L. Margerin, and A. Souriau (2010), *Science*, *328*, 1014–1017, doi:10.1126/science.1186212.
Ichikawa, H., and T. Tsuchiya (2018), J. Geography, 127, 631-646 (in Japanese with English abstract).
Ohtaki, T., S. Kaneshima, and K. Kanjo (2012), *J. Geophys. Res.*, 117, B03312, doi:10.1029/2011JB008717.
Ohtaki, T., and S. Kaneshima (2015), *J. Geophys. Res. Solid Earth*, 120, 7572–7586, doi:10.1002/2015JB012140.
Ohtaki, T., S. Kaneshima, H. Ichikawa, and T. Tsuchiya (2018), *J. Geophys. Res. Solid Earth*, doi:10.1029/2018JB015857.
Tanaka, S., and H. Hamaguchi (1997), *J. Geophys. Res.*, *102*, 2925–2938, doi:10.1029/96JB03187.

Keywords: F layer, lowermost outer core, Heterogeneity of the outer core, Light element concentration in the F layer beneath Australia

©2019. Japan Geoscience Union. All Right Reserved.

Flows and light element distribution in the outer core associated with heterogeneous growth of the inner core of the Earth

*Shin-ichi Takehiro[1], Youhei SASAKI[2]

1. Research Institute for Mathematical Sciences, Kyoto University, 2. Department of Mathematics, Kyoto University

Recent seismological observations suggest longitudinal heterogeneity of seismological wave velocity of the inner core of the Earth, which stimulates a discussion that phase change at the inner core boundary (ICB) does not occur uniformly in the horizontal directions. It is simply supposed from this suggestion that temperature is lower and concentration of light element is higher just above the solidification hemisphere at ICB, and vice versa. The heterogeneous structure of the inner core and thermodynamic properties just above ICB in the outer core is expected to be correlated, however, more recent analysis shows that distribution of seismological wave velocity anomaly does not correspond to longitudinal heterogeneity of the inner core.

There are two kinds of mechanisms explaining heterogeneous growth of the inner core. One of the mechanisms is that the heterogeneous thermal condition at the core mantle boundary (CMB) drives horizontal thermal convection which induces non-uniform temperature distribution at ICB. However, since this study uses co-density, which combines density variations by temperature and light element concentration, it cannot find distribution of the light elements just above ICB. Another mechanism is that hydrodynamic instability of the inner core surrounded by the phase boundary causes translational motion inside the inner core. However, since the theory assumes homogeneous light element distribution in the outer core, it is not clear this mechanism can explain the light element distribution above ICB.

In this study, by using a rotating spherical shell model in which temperature and light element concentration are independent variables, we perform numerical experiments of thermal and compositional convection related to two kinds of mechanisms. Obtained distributions of light element concentration are compared with the distribution of seismological wave velocity anomaly, and plausible dynamical regimes of thermal and compositional convection in the outer core are discussed.

Keywords: Heterogeneity, Inner core, Core-mantle boundary

©2019. Japan Geoscience Union. All Right Reserved.

Sharpness of the hemispherical boundary in the inner core beneath the northern Pacific

*Ryohei Iritani[1], Hitoshi Kawakatsu[1], Nozomu Takeuchi[1]

1. Earthquake Research Institute, Univ. of Tokyo

The hemispherical heterogeneity in the topmost of the Earth’ s inner core, faster velocity and higher attenuation in the eastern hemisphere and slower velocity and weaker attenuation in the western hemisphere, has been revealed by seismological studies. However, how the transition structure between two hemispheres looks like has not been known because of the difficulty to analyze complex core-sensitive data and the limitation of earthquake and seismic array distribution. In this study, we apply the array-based waveform inversion (Iritani et al., 2014) to core phase data that propagate beneath the northern Pacific, and investigate the nature of the transition structure in this region.Dataset used in this study consists of two directional event-station pairs, seismograms observed by the permanent European stations for events at Fiji-Tonga region, and USArray for events near Indonesia. We analyze the broadband vertical component of core phase data containing PKIKP and PKP phases (i.e. the epicentral distance between 145 –155 degree). Resultant analyzed waveforms for EU stations and USArray are 2,108 and 1,172 traces respectively.
In the analysis, waveform inversion approach is employed for each event data to measure traveltime and attenuation in the inner core. As a result, traveltime anomalies observed by EU stations show obvious positive anomaly suggesting mainly propagating the eastern hemisphere, while traveltimes observed by USAray show relatively smaller (or no) anomalies suggesting effects from both of hemispheres. On the other hand, attenuation parameters for both arrays show similar trend that suggests high attenuation corresponding to the eastern hemisphere. To investigate a hemispherical transition boundary in the sampled region, we conduct a ray theory based forward modeling of traveltimes by changing a shape of boundary from meridian boundary to eyeball shaped boundary, and its position. We compute root-mean-square (RMS) of residual between observations and theoretical traveltimes computed with each boundary model. Then, an eyeball shaped boundary, that is located at longitude of 158°W on the equatorial line and latitude of 80°N at the northernmost point, obtained as the preferred boundary model. Finally, we investigate a sharpness of the boundary by varying a width of hemispherical transition. We assume linear variation from the eastern and western hemisphere in a given width and compute RMS. As a result, a width of 600 km at the surface of the inner core shows smaller RMS than sharp boundary. Geophysical significance of this finding will be further discussed.

Keywords: Inner core, Waveform inversion

©2019. Japan Geoscience Union. All Right Reserved.

Stable carbon isotope fractionation in Fe-C system from first principles

*Haruhiko Dekura[1], Taku Tsuchiya[1]

1. Geodynamics Research Center, Ehime University

Carbon is the fourth most abundant element in the solar system and likely one of the constituent light elements in the Earth’s core. Determination of its equilibrium isotope fractionation factor (α) under high pressure (P) and temperature (T) is a key for understanding chemical evolution such as the whole Earth carbon distributions and the amount in the Earth’s core (e.g., Kumar et al., 2011). Because experimental measurement of the isotope fractionation remains technically challenging at the deep mantle condition, attempts to evaluate the α among mantle minerals by first-principles calculations have been made in recent years (e.g., Huang et al., 2014). Recently, our group initiated the theoretical determination of the α in the Fe-C system in the Earth’s deep interior with a full ab initio approach based on the density-functional theory. We performed ab initio lattice dynamics calculations for diamond and iron-carbide (hexagonal Fe7C3) having the two stable carbon isotopes (12C and 13C). The α between the two phases were then determined by using the Gibbs free energies calculated at P ~300 GPa and T ~2000-6000 K. The obtained $10^3 \ln \alpha$ dia-Fe7C3 is found to vary with T from ~+8‰ (2000 K) to ~+5‰ (6000 K). This result indicates that the Fe7C3 is enriched in the heavier isotope (13C) compared with diamond. This trend is qualitatively consistent with low-pressure experimental observations (Kumar et al., 2011).

Keywords: Isotope fractionation, First-principles calculation

©2019. Japan Geoscience Union. All Right Reserved.

[J] Oral | S (Solid Earth Sciences)：S-GL Geology

Mon. May 27, 2019 9:00 AM - 10:30 AM JST | Mon. May 27, 2019 12:00 AM - 1:30 AM UTC | A09 TOKYO BAY MAKUHARI HALL

[S-GL28] Regional geology and tectonics

convener:Makoto Otsubo(Geological Survey of Japan, Research Institute of Earthquake and Volcano Geology), Jun Hosoi(Geological Survey of Japan, Institute of Geology and Geoinformation, AIST), Chairperson:Makoto Otsubo(Research Institute of Earthquake and Volcano Geology, Geological Survey of Japan)

The main aim of this session is to discuss geologic structure and tectonic history of East Asia, especially of Japanese Islands, on the basis of the recent results of geology and other earth sciences.

9:00 AM - 9:15 AM JST | 12:00 AM - 12:15 AM UTC

[SGL28-01] Lithology and zircon U-Pb geochronology of Paleoproterozoic and Paleozoic granitic complex in Maizuru Terrane from Tsuwano area, Shimane Prefecture, SW Japan

*Kosuke Kimura[1], Yasutaka Hayasaka[1], Tomoyuki Shibata[1], Kenta Kawaguchi[1], Hiroshi Fujiwara[1] (1.Hiroshima University)

9:15 AM - 9:30 AM JST | 12:15 AM - 12:30 AM UTC

[SGL28-02] Tectonic significance of new Zircon U-Pb ages of sedimentary complexes in the northern Hidaka Belt, central Hokkaido, northern Japan

*Futoshi Nanayama[1,5], Toru Yamasaki[1], Jun Tajika[2], Hideki Iwano[3], Tohru Danhara[3], Takafumi Hirata[4] (1.Geological Survey of Japan, AIST, 2.Docon Co. Ltd, 3.Kyoto Fission-Track Co.Ltd, 4.Tokyo Univ., 5.CWMD, Kumamoto Univ.)

9:30 AM - 9:45 AM JST | 12:30 AM - 12:45 AM UTC

[SGL28-03] New age constraints and tectonic significance of Late Oligocene marine biosiliceous deposits in the Hidaka Belt, northeastern Hokkaido, northern Japan

*Futoshi Nanayama[1,6], Hiroshi Kurita[2], Toru Yamasaki[1], Jun Tajika[3], Hideki Iwano[4], Tohru Danhara[4], Takafumi Hirata[5] (1.Geological Survey of Japan, AIST, 2.Niigata Univ., 3.Docon Co. Ltd, 4.Kyoto Fission-Track Co. Ltd, 5.Tokyo Univ., 6.CWMD, Kumamoto Univ.)

9:45 AM - 10:00 AM JST | 12:45 AM - 1:00 AM UTC

[SGL28-04] Late Cretaceous sea-level changes and tectonic history recorded in the forearc sedimentary successions of the Northeast Japan

*Jun Arimoto[1], Reishi Takashima[2], Hiroshi Nishi[2], Yuji Orihashi[3], Toshiro Yamanaka[4] (1.Department of Earth Science, Graduate School of Science, Tohoku University, 2.The Center for Academic Resources and Archives, Tohoku University, 3.Department of Earth and Environmental Sciences, Graduate School of Hirosaki University, 4.Tokyo University of Marine Science and Technology)

10:00 AM - 10:15 AM JST | 1:00 AM - 1:15 AM UTC

[SGL28-05] Paleo-stress analysis in coherent zone, an exhumed Cretacesou accretionary complex, Shimanto Belt, in Konan city and Geisei villege, Kochi prefecture, SW Japan

*Makoto Hashiguchi[1], Yoshitaka Hashimoto[1] (1.Kochi University)

10:15 AM - 10:30 AM JST | 1:15 AM - 1:30 AM UTC

[SGL28-06] Relationship between accretion of limestone blocks and subduction tectonics in Japan

*Koji Wakita[1] (1.Yamaguchi University)

Lithology and zircon U-Pb geochronology of Paleoproterozoic and Paleozoic granitic complex in Maizuru Terrane from Tsuwano area, Shimane Prefecture, SW Japan

*Kosuke Kimura[1], Yasutaka Hayasaka[1], Tomoyuki Shibata[1], Kenta Kawaguchi[1], Hiroshi Fujiwara[1]

1. Hiroshima University

Maizuru Terrane is geographically distributed from Oshima Peninsula of Fukui Prefecture to western Shimane Prefecture, Southwest Japan. Maizuru Terrane is divided into three subzones, the Northern zone, Central zone, and Southern zone. Northern zone is mainly composed of granitic rocks and metamorphic rocks that derived from continental crust, and Siluro-Devonian granitoids have been reported from Maizuru-Oe area which is the type locality of the Maizuru Terrane (Fujii et al., 2008; Tsutsumi et al., 2014). Recently, Kimura et al. (2018) reported granitic complex from Tsuwano area, Shimane Prefecture. This complex contains not only Paleozoic granitoid that show same age of the Maizuru granite but also the late Paleoproterozoic granitoid and orthogneiss those are unreported so far from the basement rock distributed in Honshu island.

The granitic complex occurs in Tsuwano area is distributed discontinuously along with the northern margin of Maizuru Terrane, and about 2 km long. This complex occurs as lenticular blocks in a narrow zone of several hundred meters in width. This complex is mainly composed of granitic rocks and mafic rocks that intruded into granitic rocks, and suffered cataclasis in the major part. From the viewpoint of their age and lithology, this granitic complex could be divided into three groups, which are as follows:

1) early Paleoproterozoic metaquartzite: Quartz completely recrystallized and doesn’t show the dust rim. Grain boundary shows sutured texture. Detrital zircon grains show reddish brown color and rounded shape. Zircon U-Pb concordant ages are only older than 2.4 Ga, and the probability density curve shows two large peaks around 2.5 Ga and 2.7 Ga.

2) late Paleoproterozoic granitoids and orthogneiss: These rocks are most common in the granitic complex. These rocks show various lithology. Orthogneiss show banded structure and granoblastic texture. Zircon grains show reddish brown color and core-rim structure, and zircon U-Pb ages range 1.85-1.83 Ga. Furthermore, 2.8-2.05 Ga inherited ages are also yielded.

3) early Paleozoic rocks: These Paleozoic rocks are less in amount than Paleoproterozoic rocks in Tsuwano area. Paleozoic rocks are subdivided into plutonic rocks and volcaniclastic rocks. Plutonic rocks are leucocratic granodiorite and metagabbro. Their zircon U-Pb ages range from 423-411 Ma. On the other hand, volcaniclastic rock is felsic tuff that shows light brown to light greenish gray color, and this lithology varies from glassy to crystalline. Zircon U-Pb ages range from 424-413 Ma.

Metaquartzite have only older than 2.4 Ga concordant ages in spite of 1.85 Ga rocks are most common in this granitic complex. Therefore, the sedimentation age of metaquartzite is considered to be between 2.4

©2019. Japan Geoscience Union. All Right Reserved.

to 1.85 Ga. On the other hand, detrital monazite and zircon ages reported from orthoquartzite pebble that occur in the conglomerate layer of Tetori and Muro groups show 1.8 Ga peak (Yokoyama et al., 2002; Hisada et al., 2010). Therefore, metaquartzite occur in Tsuwano area have a different origin that of these orthoquartzite pebbles.

Ages of 2.7, 2.5 and 1.8 Ga that measured from metaquartzite and late Paleoproterozoic rocks are consistent with similar rocks reported from North China Craton.

Zircon U-Pb ages of early Paleozoic rocks range from ca. 424-411 Ma. These ages and occurrence of this granitic complex are consistent with that of Northern zone from Maizuru-Oe area. Therefore, the granitic complex of Tsuwano area can be compared with Northern zone of Maizuru Terrane.

Reference: Fujii et al. (2008) Island Arc, 17, 322-341. Tsutsumi et al. (2014) JMPS, 101, 289-298. Kimura et al. (2018) 125th Annu. Meet. Geol. Soc. Japan, Abstr, R5-O-23. Yokoyama et al. (2002) Research Report of the Mesozoic Tetori Group in the Tedori River Area, Ishikawa Prefecture, 57-70. Hisada et al. (2010) JpGU Meeting 2010 Abstr., SGL046-03.

Keywords: Inner Zone of Southwest Japan, Tsuwano area, Northern zone of Maizuru Terrane, Paleoproterozoic granitoid, Zircon U-Pb age, North China Craton

©2019. Japan Geoscience Union. All Right Reserved.

Tectonic significance of new Zircon U-Pb ages of sedimentary complexes in the northern Hidaka Belt, central Hokkaido, northern Japan

*Futoshi Nanayama[1,5], Toru Yamasaki[1], Jun Tajika[2], Hideki Iwano[3], Tohru Danhara[3], Takafumi Hirata[4]

1. Geological Survey of Japan, AIST, 2. Docon Co. Ltd, 3. Kyoto Fission-Track Co.Ltd, 4. Tokyo Univ., 5. CWMD, Kumamoto Univ.

The Hidaka belt in the central axis zone of Hokkaido has been one of the areas where geological research is most delayed in Japan, and their depositional ages and tectonic settings were not clear untill now. It has been considered as late Cretaceous accretionary complex like the Shimato belt in southwestern Japan. In this study, zircon particles are extracted from turbidite sandston beds of eastern Rurochi Formation, central Kamiokoppe Formation and western Iwaonai Flysch and zircon U-Pb ages were measured by LA-ICP-MS method. As a result, age values of 52.4 ±0.5 Ma from Rurochi Formation, 54.9 ±0.3 Ma from Kamiokoppe Formation and 47.3 ±0.5 Ma from Iwaonai Flysch were obtained respectively. Looking down the entire Hidaka belt including the age data of the southern part of the Hidaka belt reported by Nanayama et al. (2018), the following four points have been clarified.
(1) Clastic rocks (Hidaka Supergroup) distributed in the Hidaka belt are within the age of Paleocene ~ early Eocene.
(2) The Hidaka belt is distributed widely across the east-west width of more than 100 km. However, its internal structure and age differences are not clear, and it can not be explained by the accretionary growth model which becomes younger in the eastward.
(3) There is no significant age difference in the eruption age of the three bands of in situ basalts (N-MORB) recognized in the Hidaka belt (Miyashita et al., 1997), and if this is explained by the ridge subduction model, It can be explained only one event.
(4) The Hidaka Supergroup was a sedimentary body mainly composed of turbidite facies filled in the sea area between the Paleo-Japan arc and the Paleo-Kuril arc in Paleocene ~ early Eocene age. After 47 Ma, according to the joining of two arc-trench systems, significant deformation was occurred it. So, it is considered to be "collision complex".

This work was supported by JSPS KAKENHI Grant Number 16K05585.

(References) Kiminami et al., 1986, Monog. Assoc. Geol. Collab., no. 31, 137-155. Miyashita et al., 1997, Mem. Geol. Soc., Japan, no. 47, 307-323.Nanayama et al., 1993, Palaeogeography, Palaeoclinatology, Palaeoecology, 105, 53-69. Nanayama et al., 2018, Island Arc, 27, e12233. Tajika, 1989, Chikyu monthly, 11, 323-327.

Keywords: Depositional age, Hidaka Belt, Hidaka Supergroup, LA-ICP-MS, zircon U-Pb age, collision complex

©2019. Japan Geoscience Union. All Right Reserved.

New age constraints and tectonic significance of Late Oligocene marine biosiliceous deposits in the Hidaka Belt, northeastern Hokkaido, northern Japan

*Futoshi Nanayama[1,6], Hiroshi Kurita[2], Toru Yamasaki[1], Jun Tajika[3], Hideki Iwano[4], Tohru Danhara[4], Takafumi Hirata[5]

1. Geological Survey of Japan, AIST, 2. Niigata Univ., 3. Docon Co. Ltd, 4. Kyoto Fission-Track Co. Ltd, 5. Tokyo Univ., 6. CWMD, Kumamoto Univ.

The Tatsuushi Formation distributed in the Kitami-Monbetsu area consisted of siliceous mudstone, and has been incorporated into the Hidaka Supergroup along associated with the surrounding the Uenkotan and Rurochi Formations (Tajika and Iwata, 1994). In this study, the depositional age of the Tatsuushi Formation was examined by three methods. Detrital zircon grains are separated from turbidite sandstone and a U-Pb age of 27.2 ±0.1 Ma is obtained by the LA-ICP-MS method. Dinoflagellate cysts indicate late Oligocene and early Miocene, respectively. Therefore, the U-Pb age is shown as the depositional age of this formation. The depositional age of the Hidaka Supergroup has been reported Paleocene to Early Eocene so far. Therefore, it is difficult to include this formation in Hidaka Supergroup. The Tatsuushi Formation can be compared to the Erimo Formation in the soutjern Hidaka Belt (Kurita and Kusunoki, 1997) and the lower part of the Tsubetsu and Kawakami Groups based on their depositional ages and affinity of the lithology (Kurita et al., 1998) distributed along the Abashiri tectonic line as the right-lateral strike-slip fault since late Oligocene. These siliceous mudstones may have been formed by the upwelling flow caused by the bottom deepwater brought from the Sea of Okhotsk by the opening of the Kuril basin.

This work was supported by JSPS KAKENHI Grant Number 16K05585.

(References) Kurita and Kusunoki, 1997, Jour. Geol. Soc. Japan, 103, 1179-1182. Kurita et al., 1998, Research reports of JAPEX Research Center, no. 13, 11-31. Tajika and Iwata, 1994, Chikyu monthly, 16, 495-499.

Keywords: LA-ICP-MS U-Pb age, late Oligocene to early Miocene, Tatsuushi Formation, Hidaka Belt, Hidaka Supergroup, Dinoflagellate cysts

©2019. Japan Geoscience Union. All Right Reserved.

Late Cretaceous sea-level changes and tectonic history recorded in the forearc sedimentary successions of the Northeast Japan

*Jun Arimoto[1], Reishi Takashima[2], Hiroshi Nishi[2], Yuji Orihashi[3], Toshiro Yamanaka[4]

1. Department of Earth Science, Graduate School of Science, Tohoku University, 2. The Center for Academic Resources and Archives, Tohoku University, 3. Department of Earth and Environmental Sciences, Graduate School of Hirosaki University, 4. Tokyo University of Marine Science and Technology

Elucidating tectonic history of the Cretaceous East Asian continental margin provides us essential information to understand the origin of modern Japanese islands and paleo-biogeography of terrestrial fauna and flora, with implications for connection with the Eurasia continent. One of the keys to reconstruct the geologic history of the NE Japan is the Upper Cretaceous to Paleogene siliciclastic sedimentary successions that filled a N-S trending large fore-arc basin (the Yezo forearc basin) along the Pacific margin. The Futaba, Kuji, and Yezo groups are known as representative strata among these successions, and have been well studied. Especially the Kuji and Futaba groups were accumulated in shallow-marine and non-marine environments, and their facies changes were reflected by relative sea-level changes attributed to global eustacy and regional tectonic uplift/subsidence. The previous studies for these two groups, however, have not fully made it clear that the observed depositional changes were derived from local tectonic effects or global eustatic sea-level changes due to lack of precise age controls. To address this issue, here we provide the latest age model of the Kuji Group and partly revised regional sequence stratigraphic correlation. Comparing our age-calibrated depositional sequences of the Kuji Group with an available global sea-level reconstruction would separates the influence of eustacy from that of regional tectonics which formed the Yezo forearc basin sedimentary successions.

The Kuji Group is distributed along the northeastern coastal area of the Iwate prefecture. The group mainly comprises sandy siltstone, coaly mudstone, sandstone and conglomerate, with intercalated coal and felsic tuff beds. The total thickness is over 700 m. It unconformably overlies the pre-Cretaceous accretionary complex and lower Cretaceous granitoids, and is unconformably overlain by the Paleogene siliciclastic succession. The Kuji Group is divided into three lithostratigraphic units: the Tamagawa (marine and non-marine), Kunitan (marine), and Sawayama (non-marine) formations, in ascending order. The overall succession consists of at least four largely upward-fining sequences. Previous studies on sedimentary facies analysis divided them into five depositional sequences derived from the third-order sea level change (DS1 to DS5) (Ref. 1).

The newly established age model, based on carbon isotope stratigraphy and U–Pb ages, indicates that the depositional sequences in the Kuji Group is correlated with the middle Turonian to middle Campanian stages. The DS2 to DS4 in the Kuji group are likely coeval with the depositional sequences of the adjacent Futaba Group (the Coniacian to Santonian stages) (Ref. 2). Relative sea-level changes recognized in the DS1 to DS4 are mostly consistent with the second- and third-order global eustatcy (Ref. 3). In contrast, the DS5, equivalent to the Sawayama Formation of the Kuji Group, represents lowstand systems tract (non-marine fluvial facies) with maximum thickness of 200 m. Similarly, development of shallower facies is implied in the Hakobuchi Formation (the Campanian stage; Ref. 4) of the Yezo Group, accumulated in the northern sub-basin. These coeval relative sea-level falls are apparently inconsistent with contemporaneous global transgressive trend, and thus are interpreted to reflect basin-wide uplift of the forearc region in the early Campanian. Here we provide a new constraint for the age of the major tectonic event occurred in the Late Cretaceous East Asian continental margin, possibly related to the change in

©2019. Japan Geoscience Union. All Right Reserved.

subducting oceanic plate motion (e.g. Ref. 5).

References

*1. Mitsuzuka, S., Ando, H., 2016, *123th Ann. Meet. Geol. Soc. Japan, Abstr.*, 205. *2. Ando, H. et al., 1995, *Jour. Tokyo Geogr. Soc.* 104, 284–303. *3. Haq, B., 2014, *Glob. Planet. Change* 113, 44–58. *4. Tsujino, Y., 2009, *Jour. Geol. Soc. Japan* 115, 122–129. *5. Ando, H., 2003, *Jour. Asian Earth Sci.* 21, 921–935.

Keywords: Late Cretaceous, Northeast Japan, forearc basin, Kuji Group, Sequence stratigraphy, tectonics

©2019. Japan Geoscience Union. All Right Reserved.

Paleo-stress analysis in coherent zone, an exhumed Cretacesou accretionary complex, Shimanto Belt, in Konan city and Geisei villege, Kochi prefecture, SW Japan

*Makoto Hashiguchi[1], Yoshitaka Hashimoto[1]

1. Kochi University

Stress state in a subduction zone can be exchanged between reverse-fault and normal-fault regimes with an earthquake cycle. A similar change in paleostresses has been also obtained in some exhumed accretionary complexes (e.g., Hashimoto et al., 2014). However, most of previous studies in exhumed accretionary complexes cover only mélange zones exposed to the coastline. Therefore, in this study, we examine the paleostress change in a coherent zone. In order to investigate a spatial relationship, we analyzed the paleostress in the coherent zone adjacent to a mélange zone.

The study area is in Konan City, Yasu Town and Geisei Village in Kochi Prefecture, Southwest Japan where the Cretaceous northern Shimanto Belt is cropped out. The geology of the study area is composed of the coherent and mélange zones in the northern and the southern sides, respectively. The coherent zone consists mainly of alternating layers of sandstone and mudstone. The strike and dip of bedding are about N 37 ˚E and 75 ˚S, respectively. The age of the coherent zone has been reported as Cenomanian–Campanian (100 Ma–72 Ma) from microfossils (Taira et al., 1988). As a result of the micro-fault analysis, six stress state (stress 1, 2, 3, 4, 5, and 6) were obtained. Four stresses (stress 1, 3, 5, and 6) could be reasonbale because many unique faults, which are micro-faults with misfit angle of less than 30 degree only in individual stress state, are found. Stress 2 and stress 4 are not treated as reasonable stress solutions because the number of the unique fault is small. Stress 1 and stress 3 are the reverse-fault stress regimes. Stress 5 is obscured for fault types. Stress 6 is a normal-fault stress regime.

In order to constrain stress magnitude, stress polygon was employed. Furthermore, a liner function between SHmax and Shmin can be obtained from the estimated paleo-stress, which can be drawn in the stress polygon. Sv is calculated from density and paleo-maximum depth (5.5 km from vitrinite reflectance). Stress magnitude would be constrained from the overlapping area between the stress polygon and the liner function. According to the results, the stress for the reverse fault regimes is larger than that for the normal fault stress regime. In addition, assuming that the reverse fault changed to a normal fault, the validity of the difference of shear stress (stress drop) was examined. The stress drop is estimated from the difference in the radius of Mohr circles ((SHmax - Shmin) / 2) between the normal fault and the reverse fault stress regimes. The stress drops between stress 1 (reverse fault) and stress 6 (normal fault) ranges, and stress 3 (reverse fault) and stress 6 (normal fault) range 1.8-14.0 MPa and 43 - 63 MPa, respectively. Susan L. et al. (2018) showd the distribution of stress drops from geophysical observations in trench type earthquakes rangeing approximately 0.01–100 MPa. The stress drops obtained from our results are consistent with the range of 0.01-100 MPa. Therefore, it is possible for our results to be related to earthquake cycles.

In conclusion, we would like to emphasize that the exchange of stress accompanying earthquake cycles occurs even in the coherent zone as the same as that observed in mélange zones based on the differences in stress magnitude between the reverse and normal fault stress regimes and the reasonable range of stress drop. The interpretation that the exchange of stress observed in the mélange zone and

©2019. Japan Geoscience Union. All Right Reserved.

also in the coherent zone implies that the exchange in stress state could be recorded after the mélange zone were located adjacent to coherent zonet. In other words, it is suggested that the micro-faults we examined in this study were activated within an accretionary wedge at the critical stress states.

Keywords: Paleo-stress analysis, accretionary complex, Shimanto Belt

©2019. Japan Geoscience Union. All Right Reserved.

Relationship between accretion of limestone blocks and subduction tectonics in Japan

*Koji Wakita[1]

1. Yamaguchi University

Detailed mechanism for accretion of limestone and basalt is not elucidated yet. Seamount collapse occurs in the tectonic erosion convergent margin such as the Japan trench, but the seamount accretion does not happen in accretionary convergent margin such as the Nankai trough. How are the limestone and basalt blocks preserved in accretionary complexes? The key to understand the reason of accretion of limestone and basalt is the tectono-stratigraphic position of limestone and basalt blocks. In the most of the Japanese accretionary complexes, limestone and basalt blocks occur in the youngest unit of each complex. The cessation of the development of the accretionary complex must be associated with the special tectonic setting, which caused less supply of detrital materials from the provenance area. Flat slab subduction is one of the candidates to cause the less igneous activities in the provenance area. The flat subduction may be caused by the subduction and accretion of buoyant body such as ocean plateau. This subduction and accretion of oceanic plateau caused the cessation of accretionary process, and may have allowed to preserve limestone and basalt block in the accretionary complexes in Japan.

Keywords: limestone, accretionary complex, oceanic plateau

©2019. Japan Geoscience Union. All Right Reserved.

[J] Oral | S (Solid Earth Sciences)：S-GL Geology

Mon. May 27, 2019 10:45 AM - 12:15 PM JST | Mon. May 27, 2019 1:45 AM - 3:15 AM UTC | A09 TOKYO BAY MAKUHARI HALL

[S-GL28] Regional geology and tectonics

convener:Makoto Otsubo(Geological Survey of Japan, Research Institute of Earthquake and Volcano Geology), Jun Hosoi(Geological Survey of Japan, Institute of Geology and Geoinformation, AIST), Chairperson:Jun Hosoi(Geological Survey of Japan)

The main aim of this session is to discuss geologic structure and tectonic history of East Asia, especially of Japanese Islands, on the basis of the recent results of geology and other earth sciences.

10:45 AM - 11:00 AM JST | 1:45 AM - 2:00 AM UTC

[SGL28-07] Discovery of faulted basin margin from the middle Miocene Tottori Grope, Tottori Prefecture, Southwest Japan and its significance

*Yuta Maruyma[1] (1.Shimane Umiversity)

11:00 AM - 11:15 AM JST | 2:00 AM - 2:15 AM UTC

[SGL28-08] Fault activity during Quaternary Period off the Shimane Peninsula based on the profiles acquired by the high-resolution seismic survey

*Masaaki Tanaka[1], Norihiro Matsuda[1], Masaru Nakamura[1], Yuichi Shimizu[1], Masanori Shimazaki[2], Kazuhito Hatakeyama[2] (1.The Chugoku Electric Power Co., Inc., 2.Sogo Geophysical Exploration Co., Ltd.)

11:15 AM - 11:30 AM JST | 2:15 AM - 2:30 AM UTC

[SGL28-09] Paleomagnetic directions of early Miocene sediments in central Japan and tectonic implications

*Hiroyuki Hoshi[1], Takuro Matsuo[2] (1.Department of Earth Sciences, Aichi University of Education, 2.Aichi Prefectural Kariya High School)

11:30 AM - 11:45 AM JST | 2:30 AM - 2:45 AM UTC

[SGL28-10] Revised Cenozoic chronostratigraphy and tectonics in the Yatsuo Area, Toyama Prefecture, central Japan

*Takeshi Nakajima[1], Hideki Iwano[2], Tohru Danhara[2], Tohru Yamashita[2], Yukio Yanagisawa[1], Yoshihiro Tanimura[3], Mahito Watanabe[1], Takayuki Sawaki[1], Satoshi Nakanishi[4], Hiroyuki Mitsuishi[4], Okiyuki Yamashina[4], Seiichi Imahori[5] (1.Geological Survey of Japan, National Institute of Advanced Industrial Science and Technology, 2.Kyoto Fission-Track Co., Ltd., 3.National Museum of Nature and Science, 4.JX Nippon Oil & Gas Exploration Corporation, 5.JX Nippon Oil & Gas Exploration Technical Services Corporation)

11:45 AM - 12:15 PM JST | 2:45 AM - 3:15 AM UTC

Discussion

Discovery of faulted basin margin from the middle Miocene Tottori Grope, Tottori Prefecture, Southwest Japan and its significance

*Yuta Maruyma[1]

1. Shimane Umiversity

Some Miocene sedimentary basins in the San’in region extend N-S or NE-SW and, have been called the indentation of sedimentary basins. Several studies speculated that these basins were aulacogenes formed in association with the Japan Sea opening event, or extensional basins opened parallel to the rifting axis before the rotation of Southwest Japan. The little sedimentary geological and chronological studies for this type of sedimentary basins remain their evolution to have been still unknown. The precise reconstruction of evolution of these sedimentary basins leads to understanding of the deformation of Southwest Japan crust associated with the Japan Sea opening event and thus to know the concrete Japan Sea opening process. The geological information in the marginal part of such type of basin fills is indispensable in order to elucidate their evolution.

A sedimentary basin, extending almost N-S and called the Tottori Indentation, is spread in the eastern part of Tottori Prefecture, Southwest Japan. Because the sediments of this basin have not been suffered from extensive intrusion of the volcanic rocks in its southeastern part, unlike the other basin fills in the Shimane Prefecture, this is an ideal sediment succession as the target of the sedimentary basin analysis in order to know the evolution of this type of sedimentary basins. The present study conducted geological survey of the Tottori Group using a conventional sedimentary geological method (facies analysis) for reconstruction of the sedimentary environment of the southeastern part of the Tottori Group (Iwami Formation).
The Iwami Formation of the Tottori Group is made up from the Entsuji Conglomerate and Sandstone Member (EM) and Fuganji Mudstone Member (FM). The FM contains both freshwater and marine mudstones. New faults with large displacement on and near the boundary with the underlying rocks are discovered. One represents the boundary between the granitic rock and the EM sandstone with thin vertical veneer of the deformed Kawabara Volcanic Rock Member of the underlying Yazu Formation along the fault. The other is running within the EM sandstone. The presence of gravels of debris fall origin in the FM mudstone near the fault and the talus deposits together with the presence of the deformed Yazu Formation along the fault imply that the fault started to be activated after the Kawabara Member phase and may have been active during the Fuganji period to have formed the slope along the fault. As the result, the block to the west of the fault subsided to have formed a lacustrine basin. Another faults are also expected along the boundary between the basement rock or the Yazu Formation and the Iwami Formation based on the presence of small slump structures indicating a slope that dipped away from the boundary in the southeastern part of the group. Additional study is necessary in order to elucidate the basin type (e.g. strike slip basin or half graben) and to determine the specific timing of basin generation. The present study is financially supported by the Grant-in-aid for scientific research from the San’in Kaigan UNESCO Global Geopark Promotion Council.

Keywords: Tottori Group, Middle Miocene, Sedimentary basin, Japan Sea opening event

©2019. Japan Geoscience Union. All Right Reserved.

Fault activity during Quaternary Period off the Shimane Peninsula based on the profiles acquired by the high-resolution seismic survey

*Masaaki Tanaka[1], Norihiro Matsuda[1], Masaru Nakamura[1], Yuichi Shimizu[1], Masanori Shimazaki[2], Kazuhito Hatakeyama[2]

1. The Chugoku Electric Power Co., Inc., 2. Sogo Geophysical Exploration Co., Ltd.

A number of faults are shown off the Shimane Peninsula by Tamaki *et al.* (1982), Japan Coast Guard (1991, 1992), Tokuyama *et al.* (2001) and others. The Chugoku Electric Power Co., Inc. (Energia) carried out seismic reflection survey by using mainly Sparker in 1981 in the area including some faults described by the above-mentioned authors. The investigated area was about 60 kilometers long along the shoreline and about 30 kilometers long perpendicular to the shoreline. Seismic survey lines were deployed at the interval of about 1 to 4 kilometers in it. Since then, Energia has continually been investigating to grasp more detailed locations and characteristics of the faults in the area by using the latest technology such as multi-channel seismic system and so on. Furthermore, Energia has referred to the concepts of sequence stratigraphy in its interpretation to improve the reliability of the evaluation for fault activity. Government organization MLIT, Cabinet Office and MEXT referred to the Energia's fault evaluation in their document published in 2014.

Structures found off the Shimane Peninsula mostly extend ENE-WSW, forming reverse faults and flexures. Ito and Arato (1999) and others indicate that the stress field off the San-in district was north-south compression during Late Miocene epoch and has been east-west compression since Pliocene epoch, and many folds and reverse faults extending ENE-WSW in this region were developed during Miocene epoch. Therefore, most faults off the Shimane Peninsula are considered to develop around Late Miocene epoch under the north-south compression stress field and end their activity by Latest Miocene epoch. However, Middle to Upper Pliocene (Unit-B) off the Shimane Peninsula is distributed in a narrow area, and it is also extremely thin. These factors have made the evaluation for fault activity during Quaternary period difficult.

On the basis of the above information, we conducted seismic survey in 2014 by using various sound sources off the Shimane Peninsula to grasp the detailed geological structure from shallow to deep. We also conducted bottom sampling for dating on the seismic line at about 7 kilometers off the coast of Kashima town in Matsue city. The samples collected in Unit-A were analyzed by tephrochronology and radiocarbon dating. As a result, we found the Sanbe-Unnan (SUn : about 50ka. Machida and Arai, 2011) tephra and a few samples dated as Late Pleistocene. This shows that most Unit-A is possibly Upper Pleistocene except its surface portion. We confirm that the conventional sparker profiles cannot distinguish Unit-A in more detail, but the high-resolution profiles acquired by multi-channel boomer system can distinguish it into more units : Middle to Upper Pleistocene and Holocene.
From the above, we confirm that faults existing within the area where Middle to Upper Pleistocene, have been inactive at least since Late Pleistocene epoch. Pleistocene possibly exist much more widely compared to the previous interpretation off the Shimane Peninsula. Additional multi-channel high-resolution boomer seismic survey may contribute to reveal the detailed fault activity under the east-west compressive stress field in Quaternary period.

Keywords: offshore area of the Shimane Peninsula, seismic profile, bottom sampling, tectonic evolution, Quaternary period, fault

©2019. Japan Geoscience Union. All Right Reserved.

©2019. Japan Geoscience Union. All Right Reserved.

Paleomagnetic directions of early Miocene sediments in central Japan and tectonic implications

*Hiroyuki Hoshi[1], Takuro Matsuo[2]

1. Department of Earth Sciences, Aichi University of Education, 2. Aichi Prefectural Kariya High School

We present new paleomagnetic data obtained from early Miocene (~18-17 Ma) sediments in three areas (Iwamura, Tengudana and Niinotoge) in central Japan. Oriented cores consisting mainly of mudstones and intercalated fine felsic tuffs were collected at more than 50 sites. Stepwise thermal demagnetization of both natural and isothermal remanent magnetizations suggests magnetite as a main magnetic carrier, with possible presence of greigite in rock samples from some sites. Site-mean directions of characteristic remanent magnetization components are all reverse polarity, suggesting deposition within the same reverse polarity chron, probably Chron C5Dr. Declinations of the site-mean directions are mostly southwesterly and deflected clockwise from the expected direction, indicating clockwise rotation after deposition. These declinations are similar to those from early Miocene and older rocks of the main part of the SW Japan arc, while they are significantly different from the undeflected paleomagnetic direction from Tomikusa, located 10-20 km northeast of Niinotoge. Thus, the Iwamura, Tengudana and Niinotoge areas are located on the main part of the SW Japan arc. It is suggested that the main part of the SW Japan arc has its eastern "rotational" boundary with a differentially rotated piece of crust between Niinotoge and Tomikusa.

Keywords: central Japan, early Miocene, paleomagnetism, rock magnetism, tectonic rotation

©2019. Japan Geoscience Union. All Right Reserved.

Revised Cenozoic chronostratigraphy and tectonics in the Yatsuo Area, Toyama Prefecture, central Japan

*Takeshi Nakajima[1], Hideki Iwano[2], Tohru Danhara[2], Tohru Yamashita[2], Yukio Yanagisawa[1], Yoshihiro Tanimura[3], Mahito Watanabe[1], Takayuki Sawaki[1], Satoshi Nakanishi[4], Hiroyuki Mitsuishi[4], Okiyuki Yamashina[4], Seiichi Imahori[5]

1. Geological Survey of Japan, National Institute of Advanced Industrial Science and Technology, 2. Kyoto Fission-Track Co., Ltd., 3. National Museum of Nature and Science, 4. JX Nippon Oil & Gas Exploration Corporation, 5. JX Nippon Oil & Gas Exploration Technical Services Corporation

Cenozoic chronostratigraphy of the Yatsuo Area in Toyama Prefecture is revised based on U-Pb and fission-track (FT) dating on the same zircon grains from tuff beds using LA-ICP-MS, mineralogical analysis of tuff beds and diatom biostratigraphy. The results reveal followings. Syn-rift volcanism (the Iwaine Formation) started at around 17.5 Ma. The Ikahama unconformity between the syn-rift Higashibessho Formation and the post-rift Tenguyama Formation was a relatively short duration (c. 0.5 m.y.) tectonic event around 15 Ma. The Otogawa Formation unconformably overlying the Tenguyama Formation is divided into Middle Miocene (Serravallian) lower portion and Late Miocene upper portion with a possible unconformity between them. The age of the Mita Formation ranges from 4 to 2 Ma and unconformably overlies the Otogawa Formation. Local correlation of a key tuff bed MT2 in the Mita Formation in previous reports was misleading and needs to be reassessed.

Facies and sequence stratigraphic analysis of the lowermost Nirehara Formation clarifies that the Nirehara Formation comprises many depositional cycles formed by sea level or lake level fluctuation in a coastal or lacustrine fan delta environment. The results also suggest that the Nirehara Formation was formed in an early rift basin, which is overlain by the syn-rift Yatsuo Group with an unconformity. Detrital zircon U-Pb and FT dating of sandstone in the Nirehara Formation suggests that possible source of sandstone was the Nohi Rhyolite.

Regional correlation of onshore and offshore Cenozoic chronostratigraphy in the Hokuriku district shows multistage rifting during Oligocene-Middle Miocene opening of the Sea of Japan. The regional correlation also suggests that post-rifting compressive tectonics was also incremental associated with fluctuation of strength and direction of compressive stress fields.

Keywords: Cenozoic, chronostratigraphy, U-Pb dating, Fission-Track dating, diatom, tectonics

©2019. Japan Geoscience Union. All Right Reserved.

[J] Poster | S (Solid Earth Sciences)：S-GL Geology

Mon. May 27, 2019 3:30 PM - 5:00 PM JST | Mon. May 27, 2019 6:30 AM - 8:00 AM UTC | Poster Hall International Exhibition Hall8, Makuhari Messe_13

[S-GL28] Regional geology and tectonics

convener:Makoto Otsubo(Geological Survey of Japan, Research Institute of Earthquake and Volcano Geology), Jun Hosoi(Geological Survey of Japan, Institute of Geology and Geoinformation, AIST)

The main aim of this session is to discuss geologic structure and tectonic history of East Asia, especially of Japanese Islands, on the basis of the recent results of geology and other earth sciences.

[SGL28-P01] **Petrogenesis of Oligocene to Miocene volcanic rocks in the Tonami area, central Japan: temporal evolution of continental- to island-arc volcanism during the Japan Sea opening**

*Raiki Yamada[1], Toshiro Takahashi[2], Hayato Ueda[2] (1.Graduate school of science and technology, Niigata University, 2.Faculty of Science, Niigata University)

[SGL28-P02] Geology and post mid-Miocene tectonics of the Ogawa basin and the Atogura Nappe

*Akira Ono

[SGL28-P03] Paleostress transition estimated from small-scale deformation structures of the Sanbagawa metamorphic rocks in the Nagatoro area, Saitama Prefecture, central Japan

*Minami Nakamura[1], Aiko Takada[1,2], Hideo Takagi[1] (1.Waseda University , 2.Japan Petroleum Exploration Co., Ltd.)

[SGL28-P04] Estimation of the paleostress directions using “new dyke method” from the microcracks in the Tanzawa Tonalite

*Misaki Tomioka[1], Hideo Takagi[1] (1.Waseda University)

[SGL28-P05] Ring faults topographically discovered in the Tono-Kurihashi granitic plutonic masses by using a cnstant vertical exaggeration stereoscopic map of slope, Kitakami massif

*Nobuo Doi[1], Michio Shirasawa[2], Ryuzo Yokoyama[2] (1.Research Center for Regional Disaster Management, Iwate University, 2.Yokoyama Geo-Spatial Information Laboratory Co., Ltd.)

[SGL28-P06] **The Maizuru tectonic zone (MTZ), its formation and rearrangement as revealed by new zircon chronology data**

*Yasutaka Hayasaka[1], Kosuke Kimura[1] (1.Graduate School of Science, Hiroshima University)

[SGL28-P07] **Erosional features of Soma Slope Channel, off Miyagi, Japan**

*Jih-Hsin Chang[1], Takahiko Inoue[1], Ayanori Misawa[1], Kohsaku Arai[1] (1.Geological Survey of Japan, National Institute of Advanced Industrial and Science Technology.)

[SGL28-P08] Preliminary Analysis Result for the Integrated Lineament Map in South Korea

*Hong-Jin Lee[1], Kyoungtae Ko[2], You Hong Kihm[2] (1.Geoscience Platfrom Division, Korea Institute of Geoscience and Mineral Resources, 2.Geology Division, Korea Institute of Geoscience and Mineral Resources)

[SGL28-P09] **Seismicity along the Moradabad Basement Fault in the Central Ganga Plain: A Geological and Geophysical approach**

*ANKIT GUPTA[1], Pitambar Pati[1], Chinmay Dash[1] (1.Indian Institute of Technology Roorkee)

[SGL28-P10] Petrological and geochronological studies of the volcanic rocks in the Muslim Bagh area, Pakistan

*Masanari Arao[1,2], Takeshi Imayama[1], Koshi Yagi[3], Chiaki Ikawa[3], Yoshihiro Sawada[4], Rehanul Haq Siddiqui[5], Said Rahim Khan[5] (1.Research Institute of Natural Sciences, Okayama University of Science, 2.Faculty of Biosphere - Geosphere Science, Okayama University of Science, 3.Hiruzen Institute for Geology and Chronology, 4.Emeritus Professor of Shimane University, 5.Geoscience Laboratory, Geological Survey of Pakistan)

Petrogenesis of Oligocene to Miocene volcanic rocks in the Tonami area, central Japan: temporal evolution of continental- to island-arc volcanism during the Japan Sea opening

*Raiki Yamada[1], Toshiro Takahashi[2], Hayato Ueda[2]

1. Graduate school of science and technology, Niigata University, 2. Faculty of Science, Niigata University

The Japan islands was torn from the continent to form island-arc by spreading of the Japan Sea in Late Oligocene to Early Miocene. Basaltic to rhyolitic active volcanism occurred in the Japan arc during the Japan Sea opening. Since many researchers have targeted mainly mafic volcanic rocks for petrological study, petrological and geochemical studies on Oligocene to Miocene rhyolites are not still enough. Therefore, we examined Oligocene to Miocene volcanic rocks, including Chattian to Aquitanian and Burdigalian to Langhian rhyolites, on the basis of petrology and geochemistry.

Oligocene to Miocene strata consist of the Tori Conglomerate, Usunaka Moonstone Rhyolite, and the Iwaine and Iozen formations, in stratigraphically ascending order (Sudo, 1979; Ganzawa, 1983), the study area, Nanto City, Toyama Prefecture. The Tori Conglomerate is composed of conglomerate and sandstone, whereas the others are composed of volcanic and pyroclastic rocks; the Usunaka Moonstone Rhyolite, and the Iwaine and Iozen formations consist of rhyolitic welded tuff, andesites (lava and pyroclastic rocks), and rhyolites (lava and pyroclastic rocks), respectively. In this study, weighted averages of ^{238}U–^{206}Pb ages of 22.4 ±0.7 and 16.3 ±0.6 Ma are obtained from zircons in the Usunaka Moonstone Rhyolite (welded tuff) and the Iozen Formation (aphyric lava; the same outcrop as FU06 of Ganzawa (1983)). These ages indicate formation ages of the rhyolites, because they are consistent with K–Ar (Yamasaki and Miyajima, 1970; Ueda and Aoki, 1970) or fission track ages (Ganzawa, 1983), whose blocking temperatures are much lower than zircon U–Pb age.

Following petrogenesis of Oligocene to Miocene volcanic rocks is considered by whole-rock chemical compositions (major and trace elements, and Sr–Nd isotopes) and comparison with other studies. The Usunaka Moonstone Rhyolite (25–22 Ma) is alkalic rhyolite showing intermediate compositions between continental rifts and continental-arcs, and its magma was S-type and relatively dry. Therefore, it is continental-arc rift-type rhyolite, and mafic magma in subduction zone would have melted crustal materials derived from sedimentary rocks. Andesitic volcanism of the Iwaine Formation can be divided into two stages (e.g., Yamada and Yamada, 2018); amphibole-bearing andesite (high Sr andesite; 19–18 Ma?) and two pyroxene andesites (18–16.5 Ma?). Amphibole-bearing andesite is low-SiO_2 adakite (Martin et al., 2005) generated by partial melting of mantle wedge matasomatised by adakitic melt formed by slab melting. Two pyroxene andesites, who and equivalent beds have the large distribution in the Hokuriku region, are continental-arc type tholeiites, and their compositions suggest AFC (assimilation and fractional crystallization). The Iozen Formation (16.5–15.0 Ma) has intermediate chemical compositions between continental- and island-arcs, and its magma was I-type and had high water content. The Iozen Formation got primitively dacitic to rhyolitic composition, and almost only fractional crystallization occurred in magma chamber. High-temperature state, which had continued since the Iwaine Formation, in mantle wedge would had caused crustal melting.

Above genesis of Oligocene to Miocene volcanic rock in the study suggests that high temperature was kept in mantle wedge and continental crust during the back-arc spreading and that tectonic settings changed as time went on; continental-arc rift, continental-arc, and continental- to island-arc. This reflect that the Japan arc developed from continental- to island-arc through the Japan Sea opening, a back-arc formation.

©2019. Japan Geoscience Union. All Right Reserved.

Ganzawa, Y. (1983) *Jour. Geol. Soc. Japan*, **89**, 271–286.
Sudo, S. (1979) *Mem. Geol. Soc. Japan*, no. 17, 187–194.
Ueda, Y. and Aoki, K. (1970) *Jour. Japan Assoc. Mineral. Petrol. Econ. Geol.*, **63**, 28–29.
Yamada and Yamada (2018) *Sci. Rep. Niigata Univ., Geol.*, **33**, 25–40.
Yamasaki, M. and Miyajima, Y. (1970) *Jour. Japan Assoc. Mineral. Petrol. Econ. Geol.*, **63**, 22–27

Keywords: Japan Sea opening, volcanic rocks, rhyolite, petrology, zircon U-Pb age

©2019. Japan Geoscience Union. All Right Reserved.

Geology and post mid-Miocene tectonics of the Ogawa basin and the Atogura Nappe

*Akira Ono

The Sanbagawa Belt in the Kanto Mountains consists of the Sanbagawa Unit, Mikabu Unit and Atogura Nappe which are piling up in this order. The Atogura Nappe is widely distributed in the Yorii-Ogawa area. The main part of the Atogura Nappe is surrounded by autochthonous pre-Cretaceous geological units with high angle faults. The Atogura Nappe is unconformably overlaid by the early Miocene deposits in the Ogawa basin (Figure 1). The early Miocene Ogawa basin was a low mountainous area. The sea invaded, and conglomerates and sandstones of the Kozono Formation deposited. As the sea level rise further, mudstones of the Arakawa Formation deposited. Then the Miocene deposits and the Atogura Nappe were subjected to upheaval tectonics. Small rock masses of the Mikabu Unit in the Atogura Nappe are evidence for the post-early Miocene uplifts.

Gently dipping Miocene strata are distributed in the western part of the Ogawa basin which is divided into three areas, i.e., Notake, Iida and Central areas. Basement rocks of these areas are Yorii Formation, Atogura Formation and Kinshozan quartzdiorite, resepectively. In the Notake area, sandstones and conglomerates are widely distributed, and are overlaid by mudstones of the Arakawa Formation. The sandstone below the mudstone is about 3 m in thickness. The depth of the basement rock is unknown in the Notake area. However, judging from shallow Miocene valleys in the Ogawa basin, the thickness of the Kozono Formation may be about 50 - 100m. Miocene conglomerates are mainly composed of many large rounded granite clasts (open red circle in Figure 1). The provenance of the granite clasts appears to be the Ryoke Nappe located between the ridge lines rB and rC (Figure 1). Small Miocene deposits are exposed at three locations in the northeastern part of the Notake area. Miocene coarse sandstones unconformably overlie the Paleogene mudstones of the Yorii Formation at the northernmost exposure. The sandstones of about 10m in thickness are conformably overlaid by the Miocene mudstones. The boundary between the Kozono and Arakawa Formations is located at the altitude of about 140m in the Notake area.

In the Central area, Kinshozan quartz diorite is exposed widely, and is unconformably overlaid by sandstones of the Kozono Formation. In the Iida area, conglomerates are distributed near basement rocks (Figure 1, black circles), which mainly consist of clasts of chert, sandstone and mudstone. On the other hand, mudstones are widely exposed in hills and plains with low altitudes.

Figures 1A, 1B and 1C are schematic geological sections across the N-S direction of the western part of the Ogawa basin. Figure 1A is based on the assumption of slight post-Miocene uplift. On the other hand significant post-Miocene uplifts and tilting movements are assumed for Figure 1B. Judging from many exposures of the unconformity, early Miocene and present-day earth surfaces are close to each other in many localities (Figure 1C). Moreover, thin gently dipping Miocene deposits widely overlie the various rocks of the Atogura Nappe. These geological facts suggest that the Atogura Nappe and Miocene deposits were subjected to no remarkable tectonics after early Miocene. However, the quartz diorite in the Central area was subjected to upheaval tectonics. It is in contact with Miocene strata by high angle faults. However, early Miocene sandstones overlying the quartz diorite are distributed rather widely. Moreover, the Mikabu Unit is not exposed anywhere. Hence, no remarkable uplift occurred in the Central area. Contrary to the Central area small three blocks of Mikabu greenstones in the FujiYama area suggest a significant uplift of the Mikabu Unit. However, small exposures of Miocene sandstones are evidence for weak uplifts of the Atogura Nappe in the FujiYama area.

©2019. Japan Geoscience Union. All Right Reserved.

Keywords: Kanto Mountains, Ogawa basin, early Miocene, Atogura Nappe, Kozono Fm., Arakawa Fm.

Figure 1

Geological map of the Yorii-Ogawa area

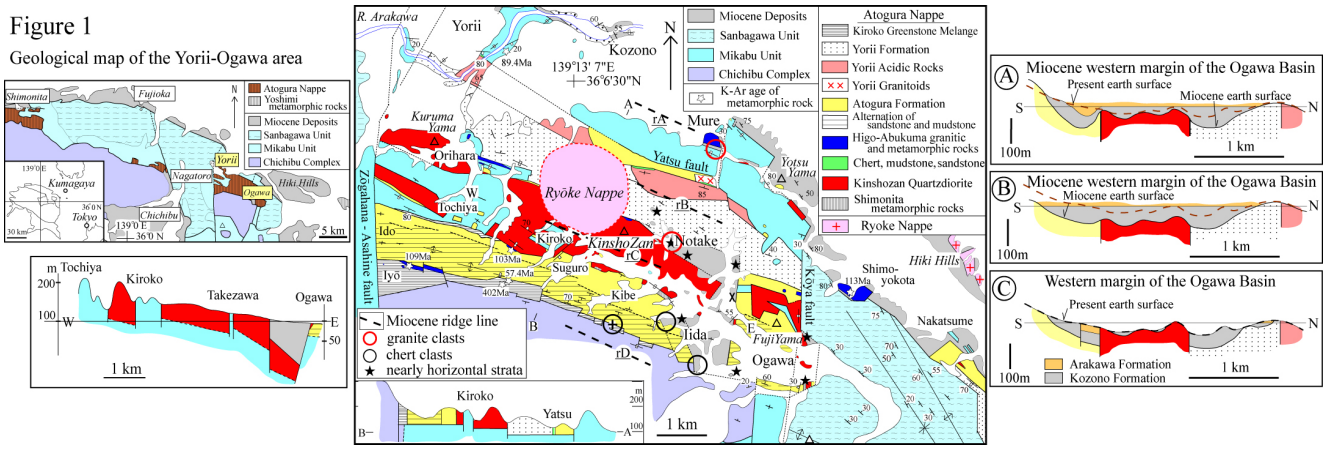

©2019. Japan Geoscience Union. All Right Reserved.

Paleostress transition estimated from small-scale deformation structures of the Sanbagawa metamorphic rocks in the Nagatoro area, Saitama Prefecture, central Japan

*Minami Nakamura[1], Aiko Takada[1,2], Hideo Takagi[1]

1. Waseda University , 2. Japan Petroleum Exploration Co., Ltd.

Low-grade metamorphic rocks of the Sanbagawa belt are well exposed in the Nagatoro area, Saitama Prefecture, where deformation structures such as folds, kink bands, faults, and mineral veins are well developed. Uemura and Kanesaki (1989) described deformed small structures in detail in the Nagatoro area, and reported that deformation stages (D1~D5) can be divided by cutting relationship. In low-ductility phase, contractional kink bands (D4 stage) were formed prior to extensional kink bands, small faults, and mineral veins (D5 stage). However, few studies have focused on the paleostress fields of D4 and D5 stages forming these structures. This study aims to determine the paleostress fields and to study its detailed deformation history of the Sanbagawa metamorphic rocks of in the Nagatoro area using paleostress analytical methods after Yamaji et al. (2006), and Yamaji and Sato (2011). We measured the attitudes (and slip directions) of 27 kink bands, 17 small faults, and 202 white mineral (quartz and/or calcite) veins to determine the paleostress fields. By using the Hough transform method (Yamaji et al., 2006), contractional kink bands (D4 stage) are indicated to have been subjected to Stress D4 (σ_1: 216˚/18˚, σ_3: 54˚/71˚), while the extensional kink bands and small faults (D5 stage) to the two different stresses; Stress D5-1 (σ_1: 180˚/79˚, σ_3: 47˚/8˚), and Stress D5-2 (σ_1: 33˚/32˚, σ_3: 211˚/58˚). These results are also consistent with those of paleostress analysis using the quartz veins (D5 stage). Furthermore, the stress analysis using calcite twins in the veins indicates that deformation structures in D5 stage were subjected to Stress D5-1 prior to Stress D5-2. These results imply that the Sanbagawa metamorphic rocks in the Nagatoro area have experienced the transition of three paleostress fields from D4 through D5-1 to D5-2 stages. Considering the mean ductility of each small structure and the deformation temperature (around 200 ˚C: Burkhard, 1993) estimated from the geometrical characteristics of calcite deformation twin, these small structures are sequentially formed at the time of exhumation of the Sanbagawa metamorphic rocks.

Keywords: Sanbagawa metamorphic belt, kink band, mineral vein, fault, paleostress analysis

©2019. Japan Geoscience Union. All Right Reserved.

Estimation of the paleostress directions using “new dyke method” from the microcracks in the Tanzawa Tonalite

*Misaki Tomioka[1], Hideo Takagi[1]

1. Waseda University

The Tanzawa Tonalite intruded around 5-4 Ma (Tani et al. 2010) is located in the South Fossa Magna region that records the collision of Izu-Bonin Arc against the Honshu Arc. The paleostress direction has been estimated from the analysis of microcracks in quartz grains in the Tonalite (Sato and Takagi, 2010). Healed microcracks (HC) forming the plane of fluid inclusions are considered that they had formed just after the intrusion using fluid inclusion thermometry, and sealed microcracks (SC) had formed after HC formation by crosscutting relationship. The orientations of both HC and SC indicate that σ_{Hmax} keeps around N-S~NNE-SSW direction. Recently, Yamaji et al. (2010), and Yamaji and Sato (2011) developed new method of grouping the orientations of dikes or veins (cracks) recording different stress field, and then to determine σ_1, σ_2, σ_3 axes of each group and stress ratios by fitting mixed Bingham distribution (Bingham, 1974) (hereinafter called “new dyke method”). In this study, we estimated the paleostress using “new dyke method” for oriented samples used by Sato and Takagi (2010) to make it clear whether the σ_{Hmax} is σ_1 or σ_2.
We measured strikes and dips of intracrystalline HC and SC using U-stage, and then analysed the distribution using “new dyke method” and the correction developed by Kanai et al. (2014) to determine σ_1, σ_2 and σ_3.
As a result, the dominant stress directions for 16 points (HC) and for 22 points (SC) indicate that σ_1 for HC and SC concentrates in vertical and NE-SW direction, respectively. With correcting 10° clockwise rotation by paleomagnetic research (Kanamaru and Takahashi, 2005), the paleostress orientation results should be vertical around 4Ma, and in NNE-SSW direction after 4Ma. Accordingly, the σ_{Hmax} evaluated by HCs after Sato and Takagi (2010) is actually σ_2, and this vertical stress seems to reflect the stress caused by the lifting in vertical direction along with subduction of Philippine Sea Plate placing the volcanic islands on it. On the other hand, the NNE-SSW direction of σ_1 estimated by SCs can be explained by the collision of relatively large blocks that might be the Izu Peninsula collided around 1 Ma.

References:
Bingham, C., 1974, *Annals of Statistics. 2*, **6**, 1201-1225.
Kanai, T., Yamaji, A. and Takagi, H., 2014, *Jour. Geol.*, **120**, 23-35.
Kanamaru, T., Takahashi, M., 2005, *Jour. Geol.,* **111**, 458-475.
Sato, T. and Takagi, H., 2010, *Jour. Geol.*, **116**, 309-320.
Tani, K, Dunkley, D. J, Kimura, J., Wysoczanski, R. J , Yamada, K. and Tatsumi, Y., 2010, *Geology*, **38**, 215–218.
Yamaji, A., Sato, K. and Tonai, S., 2010, *Jour. Struct. Geol.,* **32**, 1137-1146.
Yamaji, A. and Sato, K., 2011, *Jour. Struct. Geol.,* **33**, 1148-1157.

©2019. Japan Geoscience Union. All Right Reserved.

Ring faults topographically discovered in the Tono-Kurihashi granitic plutonic masses by using a cnstant vertical exaggeration stereoscopic map of slope, Kitakami massif

*Nobuo Doi[1], Michio Shirasawa[2], Ryuzo Yokoyama[2]

1. Research Center for Regional Disaster Management, Iwate University, 2. Yokoyama Geo-Spatial Information Laboratory Co., Ltd.

The Tono-Kurihashi granitic plutonic masses, the largest pluton in the Kitakami massif, were surveyed topographically by using a constant vertical exaggeration stereoscopic map of slope(CVES map)in scale 1/100,000 which was published by Yokoyama *et al*. (2012). Three ring fault systems about 11-13km in diameter were found out from Tono and Kurihashi plutonic masses. A granite porphyry intruded along the RF in the northern Tono plutonic mass. The ring fault system shows the deep structure of cauldron.
The northern Tono plutonic mass was composed of two granitic plutonic masses with different age (Nishimura *et al*., 1999). They have the different topographic features of plateau and hill, respectively, with steep slope and knick points between them. The old plutonic mass became hard because of recrystallization by the intrusion of new pluton, and remained as a plateau.
Many parallel faults, which were no extension into the Paleozoic wall rocks and the new plutonic mass, were also found out in the Tono-Kurihashi plutonic masses. Therefore, it was estimated that there was a long time between the old and new plutonic intrusions.

Keywords: Tono-Kurihashi granitic plutonic masses, CVES map, ring fault, parallel fault, knick point, cauldron

©2019. Japan Geoscience Union. All Right Reserved.

The Maizuru tectonic zone (MTZ), its formation and rearrangement as revealed by new zircon chronology data

*Yasutaka Hayasaka[1], Kosuke Kimura[1]

1. Graduate School of Science, Hiroshima University

In the Pre-Cretaceous terranes of Inner Zone of SW Japan showing low-angle piled nappe structure, only Maizuru zone shows a continuous narrow zonal arrangement. Therefore, the Pre-Cretaceous basement of the adjacent area is separated north and south by this zone. The Maizuru zone characterized by melange-like disrupted terrane with exotic blocks of plutonic complex called "Yakuno rocks" and has often been called Maizuru tectonic zone (MTZ) for that reason. MTZ is divided into three subzones, Northern, Central and Southern zones by their lithologies in its typical Maizuru area. The Southern Maizuru zone consists mainly of Yakuno ophiolite originated from the Permian intra-oceanic island arc and back-arc basin crust that occurred in the early Carboniferous oceanic crust, and the Central Maizuru zone consists of clastic rocks deposited in the back-arc basin.[1] In significant contrast with those two subzones, the Northern Maizuru zone is composed mainly of deformed granitic rocks with subordinate amount of pelitic gneiss, metagabbro and metadolerite indicating an affinity of a matured continental crust. [2] Zircon U-Pb ages of 441.9 ±2.8 Ma, 424-405 Ma, 291.6 ±4.3 Ma, and 249-243 Ma have been reported from granitic rocks of the Northern Maizuru zone of Type area so far. [3] [4] After that, granite mylonites of 488.7 ±0.9 Ma, 449.3 ±3.6 Ma, 323-301 Ma were also found in the Kume area of Okayama Prefecture 120 km west of the Type area. According to the age of intrusion, inherited ages, mode of occurrence and their similar geological setting, the Siluro–Devonian granites of the Northern zone can be correlated with the Khanka massif, southern Primorye, Russia.

Recently, we found granitic rocks showing zircon U-Pb ages of the Paleoproterozoic Era from the western end of MTZ in the Tsuwano area of Shimane Prefecture. [5] These granitic rocks exist as lenticular blocks in a narrow zone of 150 to 300 m in width. Zircon U-Pb ages are 1836 ±17 Ma for orthogneiss and 1853 ±14 Ma for tonalite, while that of granodiorite is 415.2 ±2.5 Ma. Paleoproterozoic zircon grains often contain inherited 2800-2100 Ma core. Furthermore, these rocks are accompanied by meta-quartzite blocks containing detrital zircon with two age clusters at around 2500 Ma and 2700 Ma. These Paleoproterozoic rocks are considered to be the exotic blocks originated from the North China Craton on the basis of their age affinity. In Tsuwano area, this narrow zone is embedded in the Permian strata and Jurassic accretionary complex and its metamorphic equivalents. Such a structure is anomalous to the piled nappe structure of the Pre-Cretaceous Terranes of SW Japan. As in response to the east-west change of dominant age of the Northern Maizuru zone, the age spectra of the detrital zircon of the adjacent Permo-Triassic strata in the MTZ also dominates the ages of 500-400 Ma in the eastern part, and the ages at around 1800 Ma dominates in the west. We consider that these blocks in the Northern Maizuru zone were displaced by the lateral fault movement along the northern boundary of MTZ.

[1] M. Fujii, Y. Hayasaka, K. Terada, Island Arc, 17(2008) 322-341.

[2] Y. Hayasaka, K. Ikeda, T. Shisido, M. Ishizuka, Shimamoto et al. (eds.) *Tectonics and Metamorphism (The Hara Volume),*SOUBUN Co. Ltd. (1996) 134-44 (in Japanese with English abstract).

[3] K. Ikeda, Y. Hayasaka, Jour. Min., Petrol. and Economic Geol. 89 (1994), 443–54 (in Japanese with

©2019. Japan Geoscience Union. All Right Reserved.

English abstract).

[4] K. Kimura, Y. Hayasaka, T. Shibata, K. Kawaguchi, H. Fujiwara, Jour. Geol. Soc. Japan (2019) *in press*(in Japanese with English abstract).
[5] Y. Tsutsumi, K. Yokoyama, S.A. Kasatkin, S.A., V.V. Golozubov, Jour. Min. Petrol. Sci 109 (2014) 97-102.

Keywords: Maizuru tectonic zone, Inner zone of Southwest Japan, Paleoproterozoic, zircon U-Pb age, Tsuwano area, Shimane Prefecture, North China cartoon

©2019. Japan Geoscience Union. All Right Reserved.

Erosional features of Soma Slope Channel, off Miyagi, Japan

*Jih-Hsin Chang[1], Takahiko Inoue[1], Ayanori Misawa[1], Kohsaku Arai[1]

1. Geological Survey of Japan, National Institute of Advanced Industrial and Science Technology.

Located at the boundary between Pacific Plate and North America Plate, Tohoku (NE Japan) is the forearc slope of the active subduction zone, featuring as a tectonically active margin. In the central part off Tohoku, the bathymetric data off Miyagi show that there is a channel (Soma Slope Channel) connecting shallow marine (< 500 m) and slope terrace (>1000 m). The reflection seismic data across the Soma Slope Channel show more than 10 U-shaped and V-shaped reflectors, suggesting that channelized features and filling of the channels. Besides, the channel-shaped reflectors became shallower toward north, suggesting a series of northward migration of the Soma Slope Channel. The reflection seismic data along the axis of the Soma Slope Channel show a several regional erosional surfaces and could be regarded as stratigraphic sequences boundaries. The ages of these stratigraphic sequences boundaries derived from exploration well (MITI Soma-oki) indicates that this slope channel system is likely to develop during Pliocene-Pleistocene. It seems that the Pliocene-Pleistocene sequence are thick and the Miocene-age strata are generally deep south of the Soma Slope Channel, while Pliocene-Pleistocene sequence are thinner and the Miocene-age strata are shallower north of the Soma Slope Channel. Whether the Soma Slope Channel is structural-dominated or sedimentary-dominated as well as the mechanism of channel migration will be discussed in this study.

Keywords: submarine channel, Tohoku, Japan

©2019. Japan Geoscience Union. All Right Reserved.

Preliminary Analysis Result for the Integrated Lineament Map in South Korea

*Hong-Jin Lee[1], Kyoungtae Ko[2], You Hong Kihm[2]

1. Geoscience Platfrom Division, Korea Institute of Geoscience and Mineral Resources, 2. Geology Division, Korea Institute of Geoscience and Mineral Resources

The geological lineament reflects the characteristics of various geological parameters and scale etc. In order to obtain more reliable analysis results, it is necessary to integrate the results from several experts' opinions. In this study, we used previous lineament data in the Korean Peninsula from the Korea Institute of Geoscience and Mineral Resources (KIGAM) and obtained new lineament data from the field geologists such as structural geologist, paleoseismologist, and geomophologist. To ensure the reliability of the newly lineament analysis data, we used high-resolution satellite images and hill-shade relief maps which were constructed by a digital elevation model from the National Geographic Information Institute of Korea (NGII). In the prevailing direction analysis from the acquired lineament data, the NNE-SSW direction was the most dominant, but the ENE-WSE and NNW-SSE directions also showed highly frequency depending on the experts. Different lineament analysis results based on the same data are interpreted as a result of subjective experience and analytical criteria from each expert. Therefore, it is necessary to establish integrated criteria and consider various geographical data for the publication of reliable nation-wide lineament map.

Keywords: geological lineament, integrated map, density map

©2019. Japan Geoscience Union. All Right Reserved.

©2019. Japan Geoscience Union. All Right Reserved.

Seismicity along the Moradabad Basement Fault in the Central Ganga Plain: A Geological and Geophysical approach

*ANKIT GUPTA[1], Pitambar Pati[1], Chinmay Dash[1]

1. Indian Institute of Technology Roorkee

The basement of Indo-Gangetic plain is characterized by various fault bounded ridges and troughs. These Basement faults have great influence on the Ganga Plain tectonics. In response to the stress generated along the Himalaya these basement faults propagate surface ward and affect the sediment cover. This results in the form of Earthquakes along these basement faults. The present study shows several field evidences of surface deformation caused by the Moradabad basement fault. Soft sediment deformation structures (seismites) and surface faults are found at four different locations on the trace of the Moradabad basement fault in the upper Ganga Plain. Ground Penetrating Radar (GPR) survey across the fault also provides evidence of shallow subsurface deformations. The epicenters of historical earthquakes are concentrated along the Moradabad basement fault. The deformations can be attributed to possible pre-historic earthquake events associated with Moradabad basement fault as other impulsive stresses like slope instability, flood surges and rapid sediment deposition are absent. Close association of these secondary faults and deformation structures with the Moradabad basement fault indicate their origin is due to the stress release along this fault generated by Himalayan tectonics.

Keywords: Ganga Plain, Neotectonics, Basement Fault

©2019. Japan Geoscience Union. All Right Reserved.

Petrological and geochronological studies of the volcanic rocks in the Muslim Bagh area, Pakistan

*Masanari Arao[1,2], Takeshi Imayama[1], Koshi Yagi[3], Chiaki Ikawa[3], Yoshihiro Sawada[4], Rehanul Haq Siddiqui[5], Said Rahim Khan[5]

1. Research Institute of Natural Sciences, Okayama University of Science, 2. Faculty of Biosphere - Geosphere Science, Okayama University of Science, 3. Hiruzen Institute for Geology and Chronology, 4. Emeritus Professor of Shimane University, 5. Geoscience Laboratory, Geological Survey of Pakistan

Several type volcanic rocks occurred in the Muslim Bagh (MB) area, which were developed mainly in the Cretaceous period at a continental active margin of the northwestern India subcontinent: Bibai-basalt intruded into the sediment from the Indian subcontinent, Bagh Complex(BC) consisting of melange and basalt-chert unit, and metamorphosed basalts in the Muslim Bagh Ophiolite (MBO) sequence. However, the division among these volcanic rocks is insufficient in terms of whole rock composition, mineral composition, and mineral assemblage. Radiolarians age of the chart layer in the BC implies that tholeiitic basalt in the BC formed during late Jurassic (Sawada et al., 1995), but there are no direct geochronological data for tholeiitic basalt. In addition, hornblende K-Ar age 82-67 Ma reported from meta-dolerite and gabbro in the MBO (Sawada et al., 1995) is unclear whether formation or metamorphic ages. In this study, whole-rock composition, mineral composition, and K-Ar age were investigated to understand the origin and ages of volcanic rocks in the MB area. According to SiO_2-(Na_2O+K_2O) discrimination diagram, the Bibai-basalt and a part of BC-basalt belong to alkali rock series (Alk.), whereas the MBO basalt and the other BC-basalt belong to non-alkali rock series. The latter series were classified into tholeiitic rock series (Tho.) based on FeO*/MgO-SiO_2 diagram. The Harker diagram indicate that the Bibai and BC(Alk.) basalts were rich in Ti and Nb, whereas the BC(Tho.)-basalt was rich in Cr. Alkali series rocks include abundant alkali feldspar, in contrast to plagioclase in non-alkali series rocks. The more metamorphic grade in the MBO-basalt increases, the more anorthite content in plagioclase and Mg/(Mg+Fe^{2+})ratio in hornblende increase. The Bibai-basalt contains Ti-clinopyroxene and Ti-amphibole, and the BC-basalt includes Ca-clinopyroxene. Based on these occurrences, the volcanic rocks in this study area are divided into four types. The BC (Tho.)-basalt yielded the K-Ar feldspar ages of ca. 78 Ma and ca. 51 Ma, which is significantly younger than the late Jurassic previously considered. The former age represents the formation age, whereas the latter age from altered sample may represent the timing of accretion or an apparent age affected by argon loss. The MBO-basalt mainly yielded the K-Ar amphibole ages from 78 Ma to 71 Ma with one exceptional age of ca. 99 Ma. The ca. 78-71 Ma ages are interpreted as the formation age, because there are no clear differences between low-grade and high-grade metamorphosed samples. These ages are also similar with the U-Pb zircon age of ca. 80 Ma obtained from plagiogranite in the MBO (Kakar et al., 2012). The ca. 99 Ma age older than other samples may attribute to the influence by excess argon. The similarities in whole-rock composition and formation ages between the MBO-basalt and BC (Tho.)-basalt implies that the BC(Tho.)-basalt was originally formed with the MBO-basalt. Then, the MBO-basalt experienced the metamorphism during obduction of ophiolite, whereas the BC(Tho.)-basalt was accreted to Indian continent without the metamorphism.
Reference: Sawada et al., 1995, GSP, 12, 73-80; Kakar et al., 2012 Geology, 40, 1099-1102

Keywords: Pakistan, Volcanic rocks, The Whole rock composition, K-Ar age

©2019. Japan Geoscience Union. All Right Reserved.

[J] Poster | S (Solid Earth Sciences)：S-GL Geology

Mon. May 27, 2019 5:15 PM - 6:30 PM JST | Mon. May 27, 2019 8:15 AM - 9:30 AM UTC | Poster Hall International Exhibition Hall8, Makuhari Messe_23

[S-GL28] Regional geology and tectonics

convener:Makoto Otsubo(Geological Survey of Japan, Research Institute of Earthquake and Volcano Geology), Jun Hosoi(Geological Survey of Japan, Institute of Geology and Geoinformation, AIST)

The main aim of this session is to discuss geologic structure and tectonic history of East Asia, especially of Japanese Islands, on the basis of the recent results of geology and other earth sciences.

[SGL28-P01] **Petrogenesis of Oligocene to Miocene volcanic rocks in the Tonami area, central Japan: temporal evolution of continental- to island-arc volcanism during the Japan Sea opening**

*Raiki Yamada[1], Toshiro Takahashi[2], Hayato Ueda[2] (1.Graduate school of science and technology, Niigata University, 2.Faculty of Science, Niigata University)

[SGL28-P02] Geology and post mid-Miocene tectonics of the Ogawa basin and the Atogura Nappe

*Akira Ono

[SGL28-P03] Paleostress transition estimated from small-scale deformation structures of the Sanbagawa metamorphic rocks in the Nagatoro area, Saitama Prefecture, central Japan

*Minami Nakamura[1], Aiko Takada[1,2], Hideo Takagi[1] (1.Waseda University , 2.Japan Petroleum Exploration Co., Ltd.)

[SGL28-P04] Estimation of the paleostress directions using “new dyke method” from the microcracks in the Tanzawa Tonalite

*Misaki Tomioka[1], Hideo Takagi[1] (1.Waseda University)

[SGL28-P05] Ring faults topographically discovered in the Tono-Kurihashi granitic plutonic masses by using a cnstant vertical exaggeration stereoscopic map of slope, Kitakami massif

*Nobuo Doi[1], Michio Shirasawa[2], Ryuzo Yokoyama[2] (1.Research Center for Regional Disaster Management, Iwate University, 2.Yokoyama Geo-Spatial Information Laboratory Co., Ltd.)

[SGL28-P06] **The Maizuru tectonic zone (MTZ), its formation and rearrangement as revealed by new zircon chronology data**

*Yasutaka Hayasaka[1], Kosuke Kimura[1] (1.Graduate School of Science, Hiroshima University)

[SGL28-P07] **Erosional features of Soma Slope Channel, off Miyagi, Japan**

*Jih-Hsin Chang[1], Takahiko Inoue[1], Ayanori Misawa[1], Kohsaku Arai[1] (1.Geological Survey of Japan, National Institute of Advanced Industrial and Science Technology.)

[SGL28-P08] Preliminary Analysis Result for the Integrated Lineament Map in South Korea

*Hong-Jin Lee[1], Kyoungtae Ko[2], You Hong Kihm[2] (1.Geoscience Platfrom Division, Korea Institute of Geoscience and Mineral Resources, 2.Geology Division, Korea Institute of Geoscience and Mineral Resources)

[SGL28-P09] **Seismicity along the Moradabad Basement Fault in the Central Ganga Plain: A Geological and Geophysical approach**

*ANKIT GUPTA[1], Pitambar Pati[1], Chinmay Dash[1] (1.Indian Institute of Technology Roorkee)

[SGL28-P10] Petrological and geochronological studies of the volcanic rocks in the Muslim Bagh area, Pakistan

*Masanari Arao[1,2], Takeshi Imayama[1], Koshi Yagi[3], Chiaki Ikawa[3], Yoshihiro Sawada[4], Rehanul Haq Siddiqui[5], Said Rahim Khan[5] (1.Research Institute of Natural Sciences, Okayama University of Science, 2.Faculty of Biosphere - Geosphere Science, Okayama University of Science, 3.Hiruzen Institute for Geology and Chronology, 4.Emeritus Professor of Shimane University, 5.Geoscience Laboratory, Geological Survey of Pakistan)

Petrogenesis of Oligocene to Miocene volcanic rocks in the Tonami area, central Japan: temporal evolution of continental- to island-arc volcanism during the Japan Sea opening

*Raiki Yamada[1], Toshiro Takahashi[2], Hayato Ueda[2]

1. Graduate school of science and technology, Niigata University, 2. Faculty of Science, Niigata University

The Japan islands was torn from the continent to form island-arc by spreading of the Japan Sea in Late Oligocene to Early Miocene. Basaltic to rhyolitic active volcanism occurred in the Japan arc during the Japan Sea opening. Since many researchers have targeted mainly mafic volcanic rocks for petrological study, petrological and geochemical studies on Oligocene to Miocene rhyolites are not still enough. Therefore, we examined Oligocene to Miocene volcanic rocks, including Chattian to Aquitanian and Burdigalian to Langhian rhyolites, on the basis of petrology and geochemistry.

Oligocene to Miocene strata consist of the Tori Conglomerate, Usunaka Moonstone Rhyolite, and the Iwaine and Iozen formations, in stratigraphically ascending order (Sudo, 1979; Ganzawa, 1983), the study area, Nanto City, Toyama Prefecture. The Tori Conglomerate is composed of conglomerate and sandstone, whereas the others are composed of volcanic and pyroclastic rocks; the Usunaka Moonstone Rhyolite, and the Iwaine and Iozen formations consist of rhyolitic welded tuff, andesites (lava and pyroclastic rocks), and rhyolites (lava and pyroclastic rocks), respectively. In this study, weighted averages of ^{238}U–^{206}Pb ages of 22.4 ±0.7 and 16.3 ±0.6 Ma are obtained from zircons in the Usunaka Moonstone Rhyolite (welded tuff) and the Iozen Formation (aphyric lava; the same outcrop as FU06 of Ganzawa (1983)). These ages indicate formation ages of the rhyolites, because they are consistent with K–Ar (Yamasaki and Miyajima, 1970; Ueda and Aoki, 1970) or fission track ages (Ganzawa, 1983), whose blocking temperatures are much lower than zircon U–Pb age.

Following petrogenesis of Oligocene to Miocene volcanic rocks is considered by whole-rock chemical compositions (major and trace elements, and Sr–Nd isotopes) and comparison with other studies. The Usunaka Moonstone Rhyolite (25–22 Ma) is alkalic rhyolite showing intermediate compositions between continental rifts and continental-arcs, and its magma was S-type and relatively dry. Therefore, it is continental-arc rift-type rhyolite, and mafic magma in subduction zone would have melted crustal materials derived from sedimentary rocks. Andesitic volcanism of the Iwaine Formation can be divided into two stages (e.g., Yamada and Yamada, 2018); amphibole-bearing andesite (high Sr andesite; 19–18 Ma?) and two pyroxene andesites (18–16.5 Ma?). Amphibole-bearing andesite is low-SiO_2 adakite (Martin et al., 2005) generated by partial melting of mantle wedge matasomatised by adakitic melt formed by slab melting. Two pyroxene andesites, who and equivalent beds have the large distribution in the Hokuriku region, are continental-arc type tholeiites, and their compositions suggest AFC (assimilation and fractional crystallization). The Iozen Formation (16.5–15.0 Ma) has intermediate chemical compositions between continental- and island-arcs, and its magma was I-type and had high water content. The Iozen Formation got primitively dacitic to rhyolitic composition, and almost only fractional crystallization occurred in magma chamber. High-temperature state, which had continued since the Iwaine Formation, in mantle wedge would had caused crustal melting.

Above genesis of Oligocene to Miocene volcanic rock in the study suggests that high temperature was kept in mantle wedge and continental crust during the back-arc spreading and that tectonic settings changed as time went on; continental-arc rift, continental-arc, and continental- to island-arc. This reflect that the Japan arc developed from continental- to island-arc through the Japan Sea opening, a back-arc formation.

©2019. Japan Geoscience Union. All Right Reserved.

Ganzawa, Y. (1983) *Jour. Geol. Soc. Japan*, **89**, 271–286.
Sudo, S. (1979) *Mem. Geol. Soc. Japan*, no. 17, 187–194.
Ueda, Y. and Aoki, K. (1970) *Jour. Japan Assoc. Mineral. Petrol. Econ. Geol.*, **63**, 28–29.
Yamada and Yamada (2018) *Sci. Rep. Niigata Univ., Geol.*, **33**, 25–40.
Yamasaki, M. and Miyajima, Y. (1970) *Jour. Japan Assoc. Mineral. Petrol. Econ. Geol.*, **63**, 22–27

Keywords: Japan Sea opening, volcanic rocks, rhyolite, petrology, zircon U-Pb age

©2019. Japan Geoscience Union. All Right Reserved.

Geology and post mid-Miocene tectonics of the Ogawa basin and the Atogura Nappe

*Akira Ono

The Sanbagawa Belt in the Kanto Mountains consists of the Sanbagawa Unit, Mikabu Unit and Atogura Nappe which are piling up in this order. The Atogura Nappe is widely distributed in the Yorii-Ogawa area. The main part of the Atogura Nappe is surrounded by autochthonous pre-Cretaceous geological units with high angle faults. The Atogura Nappe is unconformably overlaid by the early Miocene deposits in the Ogawa basin (Figure 1). The early Miocene Ogawa basin was a low mountainous area. The sea invaded, and conglomerates and sandstones of the Kozono Formation deposited. As the sea level rise further, mudstones of the Arakawa Formation deposited. Then the Miocene deposits and the Atogura Nappe were subjected to upheaval tectonics. Small rock masses of the Mikabu Unit in the Atogura Nappe are evidence for the post-early Miocene uplifts.

Gently dipping Miocene strata are distributed in the western part of the Ogawa basin which is divided into three areas, i.e., Notake, Iida and Central areas. Basement rocks of these areas are Yorii Formation, Atogura Formation and Kinshozan quartzdiorite, resepectively. In the Notake area, sandstones and conglomerates are widely distributed, and are overlaid by mudstones of the Arakawa Formation. The sandstone below the mudstone is about 3 m in thickness. The depth of the basement rock is unknown in the Notake area. However, judging from shallow Miocene valleys in the Ogawa basin, the thickness of the Kozono Formation may be about 50 - 100m. Miocene conglomerates are mainly composed of many large rounded granite clasts (open red circle in Figure 1). The provenance of the granite clasts appears to be the Ryoke Nappe located between the ridge lines rB and rC (Figure 1). Small Miocene deposits are exposed at three locations in the northeastern part of the Notake area. Miocene coarse sandstones unconformably overlie the Paleogene mudstones of the Yorii Formation at the northernmost exposure. The sandstones of about 10m in thickness are conformably overlaid by the Miocene mudstones. The boundary between the Kozono and Arakawa Formations is located at the altitude of about 140m in the Notake area.

In the Central area, Kinshozan quartz diorite is exposed widely, and is unconformably overlaid by sandstones of the Kozono Formation. In the Iida area, conglomerates are distributed near basement rocks (Figure 1, black circles), which mainly consist of clasts of chert, sandstone and mudstone. On the other hand, mudstones are widely exposed in hills and plains with low altitudes.

Figures 1A, 1B and 1C are schematic geological sections across the N-S direction of the western part of the Ogawa basin. Figure 1A is based on the assumption of slight post-Miocene uplift. On the other hand significant post-Miocene uplifts and tilting movements are assumed for Figure 1B. Judging from many exposures of the unconformity, early Miocene and present-day earth surfaces are close to each other in many localities (Figure 1C). Moreover, thin gently dipping Miocene deposits widely overlie the various rocks of the Atogura Nappe. These geological facts suggest that the Atogura Nappe and Miocene deposits were subjected to no remarkable tectonics after early Miocene. However, the quartz diorite in the Central area was subjected to upheaval tectonics. It is in contact with Miocene strata by high angle faults. However, early Miocene sandstones overlying the quartz diorite are distributed rather widely. Moreover, the Mikabu Unit is not exposed anywhere. Hence, no remarkable uplift occurred in the Central area. Contrary to the Central area small three blocks of Mikabu greenstones in the FujiYama area suggest a significant uplift of the Mikabu Unit. However, small exposures of Miocene sandstones are evidence for weak uplifts of the Atogura Nappe in the FujiYama area.

©2019. Japan Geoscience Union. All Right Reserved.

Keywords: Kanto Mountains, Ogawa basin, early Miocene, Atogura Nappe, Kozono Fm., Arakawa Fm.

Figure 1

Geological map of the Yorii-Ogawa area

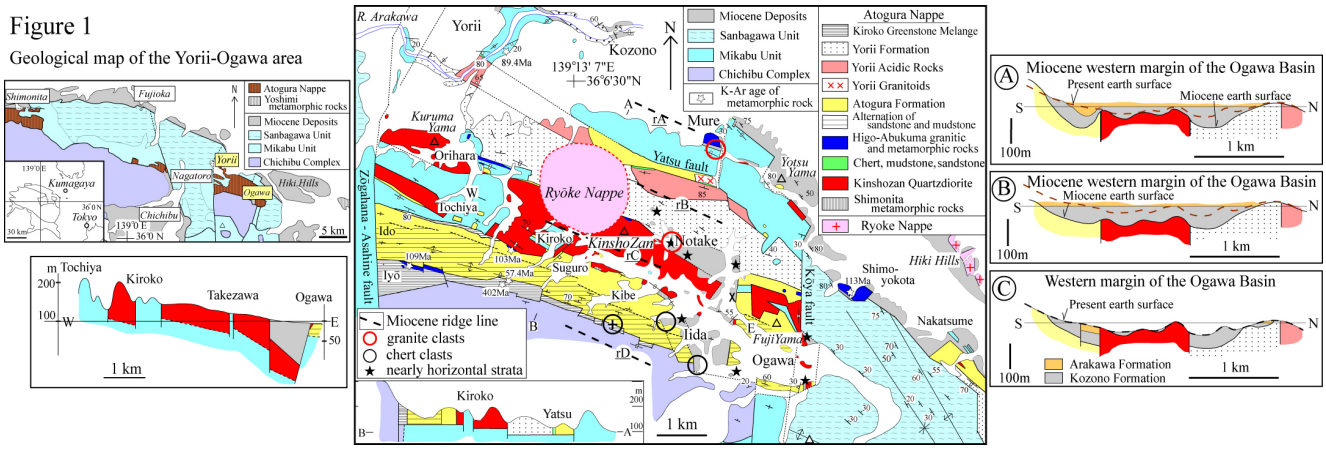

©2019. Japan Geoscience Union. All Right Reserved.

Paleostress transition estimated from small-scale deformation structures of the Sanbagawa metamorphic rocks in the Nagatoro area, Saitama Prefecture, central Japan

*Minami Nakamura[1], Aiko Takada[1,2], Hideo Takagi[1]

1. Waseda University , 2. Japan Petroleum Exploration Co., Ltd.

Low-grade metamorphic rocks of the Sanbagawa belt are well exposed in the Nagatoro area, Saitama Prefecture, where deformation structures such as folds, kink bands, faults, and mineral veins are well developed. Uemura and Kanesaki (1989) described deformed small structures in detail in the Nagatoro area, and reported that deformation stages (D1~D5) can be divided by cutting relationship. In low-ductility phase, contractional kink bands (D4 stage) were formed prior to extensional kink bands, small faults, and mineral veins (D5 stage). However, few studies have focused on the paleostress fields of D4 and D5 stages forming these structures. This study aims to determine the paleostress fields and to study its detailed deformation history of the Sanbagawa metamorphic rocks of in the Nagatoro area using paleostress analytical methods after Yamaji et al. (2006), and Yamaji and Sato (2011). We measured the attitudes (and slip directions) of 27 kink bands, 17 small faults, and 202 white mineral (quartz and/or calcite) veins to determine the paleostress fields. By using the Hough transform method (Yamaji et al., 2006), contractional kink bands (D4 stage) are indicated to have been subjected to Stress D4 (σ_1: 216˚/18˚, σ_3: 54˚/71˚), while the extensional kink bands and small faults (D5 stage) to the two different stresses; Stress D5-1 (σ_1: 180˚/79˚, σ_3: 47˚/8˚), and Stress D5-2 (σ_1: 33˚/32˚, σ_3: 211˚/58˚). These results are also consistent with those of paleostress analysis using the quartz veins (D5 stage). Furthermore, the stress analysis using calcite twins in the veins indicates that deformation structures in D5 stage were subjected to Stress D5-1 prior to Stress D5-2. These results imply that the Sanbagawa metamorphic rocks in the Nagatoro area have experienced the transition of three paleostress fields from D4 through D5-1 to D5-2 stages. Considering the mean ductility of each small structure and the deformation temperature (around 200 ˚C: Burkhard, 1993) estimated from the geometrical characteristics of calcite deformation twin, these small structures are sequentially formed at the time of exhumation of the Sanbagawa metamorphic rocks.

Keywords: Sanbagawa metamorphic belt, kink band, mineral vein, fault, paleostress analysis

©2019. Japan Geoscience Union. All Right Reserved.

Estimation of the paleostress directions using “new dyke method” from the microcracks in the Tanzawa Tonalite

*Misaki Tomioka[1], Hideo Takagi[1]

1. Waseda University

The Tanzawa Tonalite intruded around 5-4 Ma (Tani et al. 2010) is located in the South Fossa Magna region that records the collision of Izu-Bonin Arc against the Honshu Arc. The paleostress direction has been estimated from the analysis of microcracks in quartz grains in the Tonalite (Sato and Takagi, 2010). Healed microcracks (HC) forming the plane of fluid inclusions are considered that they had formed just after the intrusion using fluid inclusion thermometry, and sealed microcracks (SC) had formed after HC formation by crosscutting relationship. The orientations of both HC and SC indicate that σ_{Hmax} keeps around N-S~NNE-SSW direction. Recently, Yamaji et al. (2010), and Yamaji and Sato (2011) developed new method of grouping the orientations of dikes or veins (cracks) recording different stress field, and then to determine σ_1, σ_2, σ_3 axes of each group and stress ratios by fitting mixed Bingham distribution (Bingham, 1974) (hereinafter called “new dyke method”). In this study, we estimated the paleostress using “new dyke method” for oriented samples used by Sato and Takagi (2010) to make it clear whether the σ_{Hmax} is σ_1 or σ_2.
We measured strikes and dips of intracrystalline HC and SC using U-stage, and then analysed the distribution using “new dyke method” and the correction developed by Kanai et al. (2014) to determine σ_1, σ_2 and σ_3.
As a result, the dominant stress directions for 16 points (HC) and for 22 points (SC) indicate that σ_1 for HC and SC concentrates in vertical and NE-SW direction, respectively. With correcting 10° clockwise rotation by paleomagnetic research (Kanamaru and Takahashi, 2005), the paleostress orientation results should be vertical around 4Ma, and in NNE-SSW direction after 4Ma. Accordingly, the σ_{Hmax} evaluated by HCs after Sato and Takagi (2010) is actually σ_2, and this vertical stress seems to reflect the stress caused by the lifting in vertical direction along with subduction of Philippine Sea Plate placing the volcanic islands on it. On the other hand, the NNE-SSW direction of σ_1 estimated by SCs can be explained by the collision of relatively large blocks that might be the Izu Peninsula collided around 1 Ma.

References:
Bingham, C., 1974, *Annals of Statistics. 2*, **6**, 1201-1225.
Kanai, T., Yamaji, A. and Takagi, H., 2014, *Jour. Geol.*, **120**, 23-35.
Kanamaru, T., Takahashi, M., 2005, *Jour. Geol.,* **111**, 458-475.
Sato, T. and Takagi, H., 2010, *Jour. Geol.*, **116**, 309-320.
Tani, K, Dunkley, D. J, Kimura, J., Wysoczanski, R. J , Yamada, K. and Tatsumi, Y., 2010, *Geology*, **38**, 215–218.
Yamaji, A., Sato, K. and Tonai, S., 2010, *Jour. Struct. Geol.,* **32**, 1137-1146.
Yamaji, A. and Sato, K., 2011, *Jour. Struct. Geol.,* **33**, 1148-1157.

©2019. Japan Geoscience Union. All Right Reserved.

Ring faults topographically discovered in the Tono-Kurihashi granitic plutonic masses by using a cnstant vertical exaggeration stereoscopic map of slope, Kitakami massif

*Nobuo Doi[1], Michio Shirasawa[2], Ryuzo Yokoyama[2]

1. Research Center for Regional Disaster Management, Iwate University, 2. Yokoyama Geo-Spatial Information Laboratory Co., Ltd.

The Tono-Kurihashi granitic plutonic masses, the largest pluton in the Kitakami massif, were surveyed topographically by using a constant vertical exaggeration stereoscopic map of slope(CVES map)in scale 1/100,000 which was published by Yokoyama *et al*. (2012). Three ring fault systems about 11-13km in diameter were found out from Tono and Kurihashi plutonic masses. A granite porphyry intruded along the RF in the northern Tono plutonic mass. The ring fault system shows the deep structure of cauldron.
The northern Tono plutonic mass was composed of two granitic plutonic masses with different age (Nishimura *et al*., 1999). They have the different topographic features of plateau and hill, respectively, with steep slope and knick points between them. The old plutonic mass became hard because of recrystallization by the intrusion of new pluton, and remained as a plateau.
Many parallel faults, which were no extension into the Paleozoic wall rocks and the new plutonic mass, were also found out in the Tono-Kurihashi plutonic masses. Therefore, it was estimated that there was a long time between the old and new plutonic intrusions.

Keywords: Tono-Kurihashi granitic plutonic masses, CVES map, ring fault, parallel fault, knick point, cauldron

©2019. Japan Geoscience Union. All Right Reserved.

The Maizuru tectonic zone (MTZ), its formation and rearrangement as revealed by new zircon chronology data

*Yasutaka Hayasaka[1], Kosuke Kimura[1]

1. Graduate School of Science, Hiroshima University

In the Pre-Cretaceous terranes of Inner Zone of SW Japan showing low-angle piled nappe structure, only Maizuru zone shows a continuous narrow zonal arrangement. Therefore, the Pre-Cretaceous basement of the adjacent area is separated north and south by this zone. The Maizuru zone characterized by melange-like disrupted terrane with exotic blocks of plutonic complex called "Yakuno rocks" and has often been called Maizuru tectonic zone (MTZ) for that reason. MTZ is divided into three subzones, Northern, Central and Southern zones by their lithologies in its typical Maizuru area. The Southern Maizuru zone consists mainly of Yakuno ophiolite originated from the Permian intra-oceanic island arc and back-arc basin crust that occurred in the early Carboniferous oceanic crust, and the Central Maizuru zone consists of clastic rocks deposited in the back-arc basin.[1] In significant contrast with those two subzones, the Northern Maizuru zone is composed mainly of deformed granitic rocks with subordinate amount of pelitic gneiss, metagabbro and metadolerite indicating an affinity of a matured continental crust. [2] Zircon U-Pb ages of 441.9 ±2.8 Ma, 424-405 Ma, 291.6 ±4.3 Ma, and 249-243 Ma have been reported from granitic rocks of the Northern Maizuru zone of Type area so far. [3] [4] After that, granite mylonites of 488.7 ±0.9 Ma, 449.3 ±3.6 Ma, 323-301 Ma were also found in the Kume area of Okayama Prefecture 120 km west of the Type area. According to the age of intrusion, inherited ages, mode of occurrence and their similar geological setting, the Siluro–Devonian granites of the Northern zone can be correlated with the Khanka massif, southern Primorye, Russia.

Recently, we found granitic rocks showing zircon U-Pb ages of the Paleoproterozoic Era from the western end of MTZ in the Tsuwano area of Shimane Prefecture. [5] These granitic rocks exist as lenticular blocks in a narrow zone of 150 to 300 m in width. Zircon U-Pb ages are 1836 ±17 Ma for orthogneiss and 1853 ±14 Ma for tonalite, while that of granodiorite is 415.2 ±2.5 Ma. Paleoproterozoic zircon grains often contain inherited 2800-2100 Ma core. Furthermore, these rocks are accompanied by meta-quartzite blocks containing detrital zircon with two age clusters at around 2500 Ma and 2700 Ma. These Paleoproterozoic rocks are considered to be the exotic blocks originated from the North China Craton on the basis of their age affinity. In Tsuwano area, this narrow zone is embedded in the Permian strata and Jurassic accretionary complex and its metamorphic equivalents. Such a structure is anomalous to the piled nappe structure of the Pre-Cretaceous Terranes of SW Japan. As in response to the east-west change of dominant age of the Northern Maizuru zone, the age spectra of the detrital zircon of the adjacent Permo-Triassic strata in the MTZ also dominates the ages of 500-400 Ma in the eastern part, and the ages at around 1800 Ma dominates in the west. We consider that these blocks in the Northern Maizuru zone were displaced by the lateral fault movement along the northern boundary of MTZ.

[1] M. Fujii, Y. Hayasaka, K. Terada, Island Arc, 17(2008) 322-341.

[2] Y. Hayasaka, K. Ikeda, T. Shisido, M. Ishizuka, Shimamoto et al. (eds.) *Tectonics and Metamorphism (The Hara Volume),*SOUBUN Co. Ltd. (1996) 134-44 (in Japanese with English abstract).

[3] K. Ikeda, Y. Hayasaka, Jour. Min., Petrol. and Economic Geol. 89 (1994), 443–54 (in Japanese with

©2019. Japan Geoscience Union. All Right Reserved.

English abstract).

[4] K. Kimura, Y. Hayasaka, T. Shibata, K. Kawaguchi, H. Fujiwara, Jour. Geol. Soc. Japan (2019) *in press*(in Japanese with English abstract).
[5] Y. Tsutsumi, K. Yokoyama, S.A. Kasatkin, S.A., V.V. Golozubov, Jour. Min. Petrol. Sci 109 (2014) 97-102.

Keywords: Maizuru tectonic zone, Inner zone of Southwest Japan, Paleoproterozoic, zircon U-Pb age, Tsuwano area, Shimane Prefecture, North China cartoon

©2019. Japan Geoscience Union. All Right Reserved.

Erosional features of Soma Slope Channel, off Miyagi, Japan

*Jih-Hsin Chang[1], Takahiko Inoue[1], Ayanori Misawa[1], Kohsaku Arai[1]

1. Geological Survey of Japan, National Institute of Advanced Industrial and Science Technology.

Located at the boundary between Pacific Plate and North America Plate, Tohoku (NE Japan) is the forearc slope of the active subduction zone, featuring as a tectonically active margin. In the central part off Tohoku, the bathymetric data off Miyagi show that there is a channel (Soma Slope Channel) connecting shallow marine (< 500 m) and slope terrace (>1000 m). The reflection seismic data across the Soma Slope Channel show more than 10 U-shaped and V-shaped reflectors, suggesting that channelized features and filling of the channels. Besides, the channel-shaped reflectors became shallower toward north, suggesting a series of northward migration of the Soma Slope Channel. The reflection seismic data along the axis of the Soma Slope Channel show a several regional erosional surfaces and could be regarded as stratigraphic sequences boundaries. The ages of these stratigraphic sequences boundaries derived from exploration well (MITI Soma-oki) indicates that this slope channel system is likely to develop during Pliocene-Pleistocene. It seems that the Pliocene-Pleistocene sequence are thick and the Miocene-age strata are generally deep south of the Soma Slope Channel, while Pliocene-Pleistocene sequence are thinner and the Miocene-age strata are shallower north of the Soma Slope Channel. Whether the Soma Slope Channel is structural-dominated or sedimentary-dominated as well as the mechanism of channel migration will be discussed in this study.

Keywords: submarine channel, Tohoku, Japan

©2019. Japan Geoscience Union. All Right Reserved.

Preliminary Analysis Result for the Integrated Lineament Map in South Korea

*Hong-Jin Lee[1], Kyoungtae Ko[2], You Hong Kihm[2]

1. Geoscience Platfrom Division, Korea Institute of Geoscience and Mineral Resources, 2. Geology Division, Korea Institute of Geoscience and Mineral Resources

The geological lineament reflects the characteristics of various geological parameters and scale etc. In order to obtain more reliable analysis results, it is necessary to integrate the results from several experts' opinions. In this study, we used previous lineament data in the Korean Peninsula from the Korea Institute of Geoscience and Mineral Resources (KIGAM) and obtained new lineament data from the field geologists such as structural geologist, paleoseismologist, and geomophologist. To ensure the reliability of the newly lineament analysis data, we used high-resolution satellite images and hill-shade relief maps which were constructed by a digital elevation model from the National Geographic Information Institute of Korea (NGII). In the prevailing direction analysis from the acquired lineament data, the NNE-SSW direction was the most dominant, but the ENE-WSE and NNW-SSE directions also showed highly frequency depending on the experts. Different lineament analysis results based on the same data are interpreted as a result of subjective experience and analytical criteria from each expert. Therefore, it is necessary to establish integrated criteria and consider various geographical data for the publication of reliable nation-wide lineament map.

Keywords: geological lineament, integrated map, density map

©2019. Japan Geoscience Union. All Right Reserved.

©2019. Japan Geoscience Union. All Right Reserved.

Seismicity along the Moradabad Basement Fault in the Central Ganga Plain: A Geological and Geophysical approach

*ANKIT GUPTA[1], Pitambar Pati[1], Chinmay Dash[1]

1. Indian Institute of Technology Roorkee

The basement of Indo-Gangetic plain is characterized by various fault bounded ridges and troughs. These Basement faults have great influence on the Ganga Plain tectonics. In response to the stress generated along the Himalaya these basement faults propagate surface ward and affect the sediment cover. This results in the form of Earthquakes along these basement faults. The present study shows several field evidences of surface deformation caused by the Moradabad basement fault. Soft sediment deformation structures (seismites) and surface faults are found at four different locations on the trace of the Moradabad basement fault in the upper Ganga Plain. Ground Penetrating Radar (GPR) survey across the fault also provides evidence of shallow subsurface deformations. The epicenters of historical earthquakes are concentrated along the Moradabad basement fault. The deformations can be attributed to possible pre-historic earthquake events associated with Moradabad basement fault as other impulsive stresses like slope instability, flood surges and rapid sediment deposition are absent. Close association of these secondary faults and deformation structures with the Moradabad basement fault indicate their origin is due to the stress release along this fault generated by Himalayan tectonics.

Keywords: Ganga Plain, Neotectonics, Basement Fault

©2019. Japan Geoscience Union. All Right Reserved.

Petrological and geochronological studies of the volcanic rocks in the Muslim Bagh area, Pakistan

*Masanari Arao[1,2], Takeshi Imayama[1], Koshi Yagi[3], Chiaki Ikawa[3], Yoshihiro Sawada[4], Rehanul Haq Siddiqui[5], Said Rahim Khan[5]

1. Research Institute of Natural Sciences, Okayama University of Science, 2. Faculty of Biosphere - Geosphere Science, Okayama University of Science, 3. Hiruzen Institute for Geology and Chronology, 4. Emeritus Professor of Shimane University, 5. Geoscience Laboratory, Geological Survey of Pakistan

Several type volcanic rocks occurred in the Muslim Bagh (MB) area, which were developed mainly in the Cretaceous period at a continental active margin of the northwestern India subcontinent: Bibai-basalt intruded into the sediment from the Indian subcontinent, Bagh Complex(BC) consisting of melange and basalt-chert unit, and metamorphosed basalts in the Muslim Bagh Ophiolite (MBO) sequence. However, the division among these volcanic rocks is insufficient in terms of whole rock composition, mineral composition, and mineral assemblage. Radiolarians age of the chart layer in the BC implies that tholeiitic basalt in the BC formed during late Jurassic (Sawada et al., 1995), but there are no direct geochronological data for tholeiitic basalt. In addition, hornblende K-Ar age 82-67 Ma reported from meta-dolerite and gabbro in the MBO (Sawada et al., 1995) is unclear whether formation or metamorphic ages. In this study, whole-rock composition, mineral composition, and K-Ar age were investigated to understand the origin and ages of volcanic rocks in the MB area. According to SiO_2-(Na_2O+K_2O) discrimination diagram, the Bibai-basalt and a part of BC-basalt belong to alkali rock series (Alk.), whereas the MBO basalt and the other BC-basalt belong to non-alkali rock series. The latter series were classified into tholeiitic rock series (Tho.) based on FeO*/MgO-SiO_2 diagram. The Harker diagram indicate that the Bibai and BC(Alk.) basalts were rich in Ti and Nb, whereas the BC(Tho.)-basalt was rich in Cr. Alkali series rocks include abundant alkali feldspar, in contrast to plagioclase in non-alkali series rocks. The more metamorphic grade in the MBO-basalt increases, the more anorthite content in plagioclase and Mg/(Mg+Fe^{2+})ratio in hornblende increase. The Bibai-basalt contains Ti-clinopyroxene and Ti-amphibole, and the BC-basalt includes Ca-clinopyroxene. Based on these occurrences, the volcanic rocks in this study area are divided into four types. The BC (Tho.)-basalt yielded the K-Ar feldspar ages of ca. 78 Ma and ca. 51 Ma, which is significantly younger than the late Jurassic previously considered. The former age represents the formation age, whereas the latter age from altered sample may represent the timing of accretion or an apparent age affected by argon loss. The MBO-basalt mainly yielded the K-Ar amphibole ages from 78 Ma to 71 Ma with one exceptional age of ca. 99 Ma. The ca. 78-71 Ma ages are interpreted as the formation age, because there are no clear differences between low-grade and high-grade metamorphosed samples. These ages are also similar with the U-Pb zircon age of ca. 80 Ma obtained from plagiogranite in the MBO (Kakar et al., 2012). The ca. 99 Ma age older than other samples may attribute to the influence by excess argon. The similarities in whole-rock composition and formation ages between the MBO-basalt and BC (Tho.)-basalt implies that the BC(Tho.)-basalt was originally formed with the MBO-basalt. Then, the MBO-basalt experienced the metamorphism during obduction of ophiolite, whereas the BC(Tho.)-basalt was accreted to Indian continent without the metamorphism.
Reference: Sawada et al., 1995, GSP, 12, 73-80; Kakar et al., 2012 Geology, 40, 1099-1102

Keywords: Pakistan, Volcanic rocks, The Whole rock composition, K-Ar age

©2019. Japan Geoscience Union. All Right Reserved.

[J] Poster | S (Solid Earth Sciences)：S-VC Volcanology

Mon. May 27, 2019 10:45 AM - 12:15 PM JST | Mon. May 27, 2019 1:45 AM - 3:15 AM UTC | Poster Hall International Exhibition Hall8, Makuhari Messe_2

[S-VC35] Mitigation of volcanic disasters - basic and applied researches

convener:Shinji Takarada(Geological Survey of Japan, National Institute of Advanced Industrial Science and Technology), Mitsuhiro Yoshimoto(Mount Fuji Research Institute, Yamanashi Prefectural Government), Yasuhiro Ishimine(Research and Education Center for Natural Hazards, Kagoshima University), Tomohiro Kubo(National Research Institute for Earth Science and Disaster Prevention)

Volcanic disasters are caused by wide range of volcanic phenomena including ash fall, pyroclastic flow, debris avalanche, lahar, and lava flow. To mitigate volcanic disasters, wide range of technologies including simulation, data processing on GIS, and communication techniques are required. Researches on volcanic hazards mapping, eruption scenarios, and probabilistic eruption assessments are getting important. This session invites presentations and broad reviews related to these topics. Contributions on database technology, case studies of social and school educations, and specific examples of eruption crisis events are also encouraged.

[SVC35-P01] Oil paintings describing the 1914 Sakurajima eruption

*Satoko Murotani[1] (1.National Museum of Nature and Science)

[SVC35-P02] Constructing and utilizing digitized volcanic hazardmap database

*Yuhki Kohno[1], Tomohiro Kubo[1], Yosuke Miyagi[1], Toshikazu Tanada[1] (1.National Research Institute for Earth Science and Disaster Resilience)

[SVC35-P03] Pyroclastic fall simulation using Tephra2 and JRA-55

*Hisashi Sasaki[1], Shunsuke Miura[1], Shino Naruke[1] (1.Asia Air Survey Co., Ltd.)

[SVC35-P04] Research on observation method of volcanic ash-fall accumulation using spaceborne SAR

*Taku Ozawa[1], Eisuke Fujita[1] (1.National Research Institute for Earth Science and Disaster Resilience)

[SVC35-P05] Method for estimation of debris flow runout in the volcanic area

*Yusuke Yamazaki[1], Naoki Fujimura[1], Sakiko Tetsuka[1], Masaki Mizuno[1], Yasuo Ishii[1], Toshihiro Kikui[2], Shinya Yoshida[2], Yuki Igarashi[2], Takao Yamakoshi[2] (1.Public Works Research Institute, 2.STC)

[SVC35-P06] On the H_2S concentration continuous observation at Kurikoma volcano

*Hideyuki Itoh[1], Yasumichi Yamamoto[2], Kenji OOba[2], Morio Tsuji[1], Takeshi Ohba[3] (1.Faculty of policy studies, Iwate prefectural University, 2.JMS INc, 3.Tokai University)

Oil paintings describing the 1914 Sakurajima eruption

*Satoko Murotani[1]

1. National Museum of Nature and Science

The National Museum of Nature and Science (NMNS) possesses three oil paintings describing the 1914 Sakurajima eruption. These oil paintings were drawn by “Nanto Omure” and “Kanehide Yamashita”. They were disciples of “Seiki Kuroda” who was an oil painter representing Japan. One of these was drawn at the request of Prof. Fusakichi Omori. The status immediately after eruption painted with oil paints is eloquent the violence of volcanic smokes and thunders.

These pictures originally were hung in the Seismological Institute of the Imperial University. Now, these pictures do not have the frame, and were incurred dirty or moldy due to deterioration over time. So we restored and framed these oil paintings. For people who aren’t unfamiliar with science, we would be happy if these oil paintings become interested in historical volcanic eruption as a work of art, rather than as an educational tool for science.

Keywords: The 1914 Sakurajima eruption, oil printing, Fusakichi Omori, Seiki Kuroda, Nanto Omure, Kanehide Yamashita

©2019. Japan Geoscience Union. All Right Reserved.

Constructing and utilizing digitized volcanic hazardmap database

*Yuhki Kohno[1], Tomohiro Kubo[1], Yosuke Miyagi[1], Toshikazu Tanada[1]

1. National Research Institute for Earth Science and Disaster Resilience

National Research Institute for Earth Science and Disaster Resilience (NIED) has published “Volcanic Hazard Maps of Japan –Second Edition” recording whole volcanic hazard maps or hazard mitigation plans of 40 active volcanoes issued from 1983 to 2013. After that, volcanic hazardmaps are required under law to be prepared in each volcanic area in Japan since the 2014 eruption of Ontake volcano. NIED has been compiling and digitizing volcanic hazard information published by each Volcano Disaster Management Council established for 50 continuously monitored volcanoes in Japan. In this presentation, we report the progress of the project and examples of utilization for the digitized data.
Each digitized volcanic hazard information, with shapefile format, are converted into image data such as tile data in order to be useful on WebGIS as a layer. We are preparing online map to show easier the hazard information to residents or tourists in the volcanic area. The map will be expected as a promotion tool to the residents regarding volcanic disaster since calm period as well as a hazard map available online in emergencies, and it should be available to anytime, anyone and anywhere. Additionally we try to make tool analysing how many disasters have been possible to occur at each area where is divided into a several mesh over a target volcanic area on the map, applying Kubo et al.(2003). It may help users can recognize volcanic risks having possibility to occur at the place they are (or will be) by the information of each mesh.
We will welcome for discussion about how the way of effective expression of volcanic hazard information toward the target people or utilization of the information materials.

Keywords: digitized volcano hazard map, WebGIS

©2019. Japan Geoscience Union. All Right Reserved.

Pyroclastic fall simulation using Tephra2 and JRA-55

*Hisashi Sasaki[1], Shunsuke Miura[1], Shino Naruke[1]

1. Asia Air Survey Co., Ltd.

We present an example using Tephra2 and Japan Meteorological Agency's 55-year long-term reanalysis data (hereinafter abbreviated as JRA-55) for the pyroclastic fall simulation. The characteristics of JRA - 55 are that there is uniform data throughout Japan and there is no missing data. It is easy to reproduce the eruption that occurred after 1958 using Tephra2 and JRA-55. It is also effective for creating volcanic hazard maps and probability maps.

Keywords: pyroclastic fall simulation , the Japanese 55-year Reanalysis, hazard map, probability map

©2019. Japan Geoscience Union. All Right Reserved.

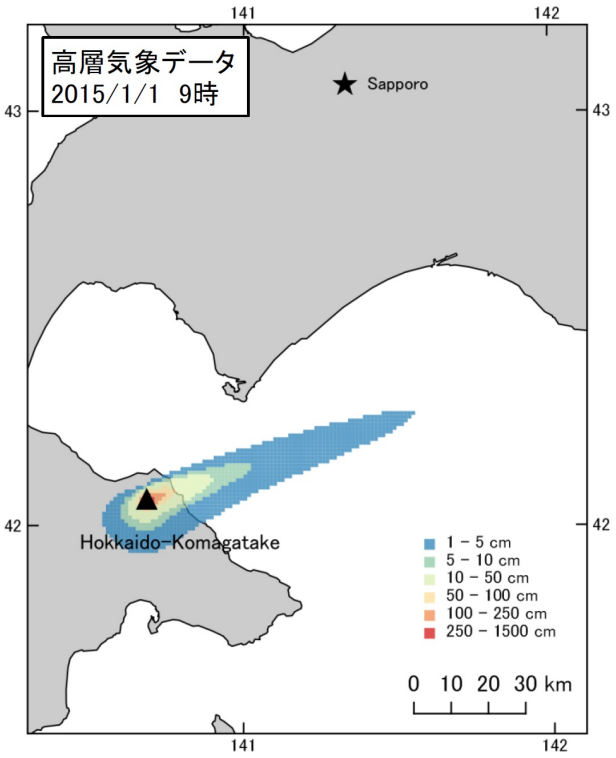

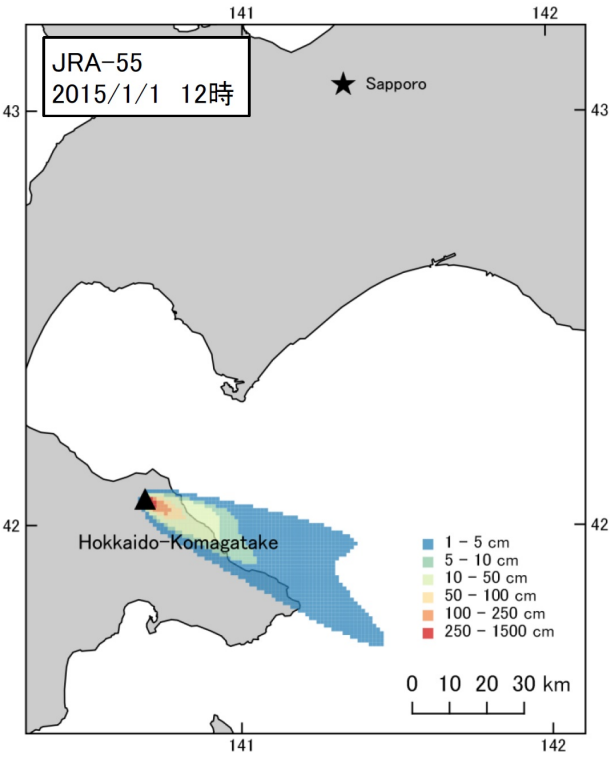

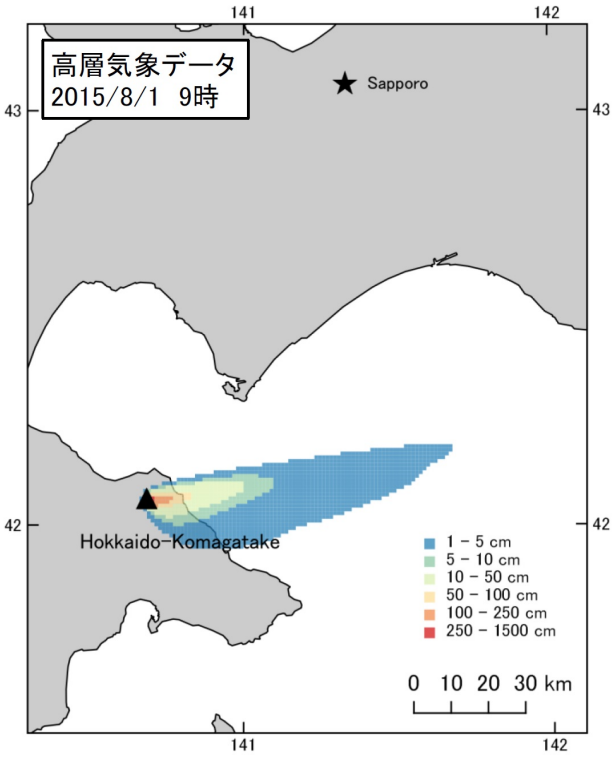

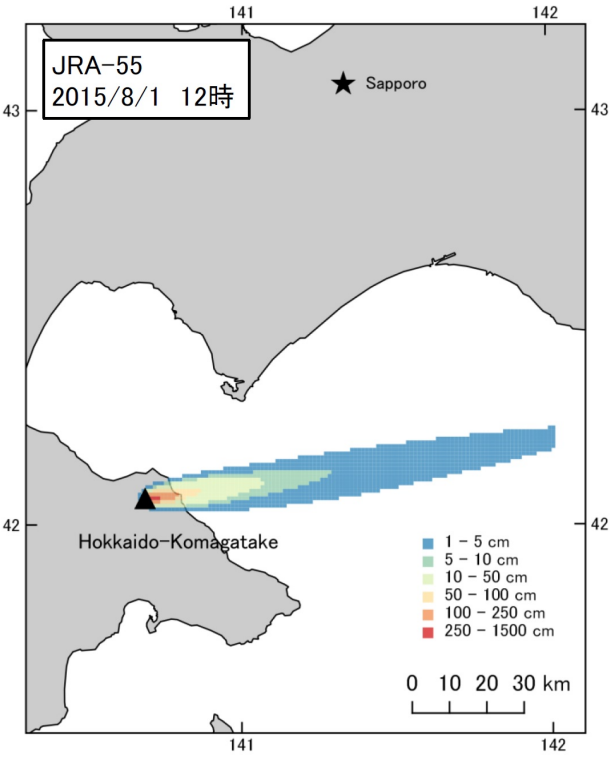

©2019. Japan Geoscience Union. All Right Reserved.

Research on observation method of volcanic ash-fall accumulation using spaceborne SAR

*Taku Ozawa[1], Eisuke Fujita[1]

1. National Research Institute for Earth Science and Disaster Resilience

Volcanic ash often causes heavy disaster due to debris flow. To mitigate such disaster, rapid observation of the volcanic ash distribution and forecast of debris flow from such observation are important. However, rapid observation of the volcanic ash distribution has been carried out mainly by on-site survey, and it is difficult to observe it rapidly. Then development of more rapid observation method are required. As one of solutions resolving such problem, utilization of satellite remote sensing technique is expected. Then, we began research on observation method of volcanic ash distribution using spaceborne SAR in “Cross-ministerial Strategis Innovation Promotion Program (SIP)-2nd season” as one of development items. In this presentation, we show results related to this development and explain the overview of this project.

In this development, we use InSAR coherence analysis. In InSAR results, clear fringes are seen if the coherence is high. On the other hand, noise is dominant if the coherence is low, and fringe becomes unclear. Generally, loss of coherence (decorrelation) is caused by difference of radar scatter at the pixel for InSAR pair. In a result from an interferometric pair including the eruption occurrence, decorrelation due to radar scatter change caused by volcanic ash accumulation is generally seen around the crater. For example, we analyzed PALSAR-2 InSAR pairs acquired before and after the Kuchinoerabujima eruption on January 17, 2019 and revealed that decorrelation area due to volcanic ash accumulation was seen within the range of about 1 km from the Shin-dake crater. Furthermore, decorrelation area extended to a range of about 1.5 km along the southwest and northwest valleys, which is consistent with the direction of pyroclastic flow.

Additionally, we analyzed InSAR pairs for December 18, 2018 and January 29, 2019 eruptions, and revealed the similar decorrelation around the crater. However, they were obviously small relative to that for January 17, 2019 eruption. Especially, that for January 17, 2019 eruption was limited to the vicinity of the crater. Thus, we could clearly see the difference in the volcanic ash accumulation area from InSAR coherence analysis.

If the relation between decorrelation and the amount of volcanic ash accumulation becomes clear quantitatively, the amount of volcanic ash accumulation will be obtained from InSAR coherence analysis. Then, in this development, we estimate decorrelation only due to volcanic ash accumulation, using a temporal coherence change model without volcanic ash effect constructed from InSAR coherence time-series analysis. Furthermore, we estimate coefficient converting coherence to the amount of volcanic ash accumulation from case studies. However, coherence basically saturates easily and thin accumulation of volcanic ash is difficult to detect, and therefore, it is difficult to detect the spatial distribution of volcanic ash accumulation. So, we attempt to estimate spatial distribution of volcanic ash accumulation by combining InSAR coherence analysis and ash-fall simulation in this development.

Keywords: ash-fall distribution, SAR, coherence

©2019. Japan Geoscience Union. All Right Reserved.

Method for estimation of debris flow runout in the volcanic area

*Yusuke Yamazaki[1], Naoki Fujimura[1], Sakiko Tetsuka[1], Masaki Mizuno[1], Yasuo Ishii[1], Toshihiro Kikui[2], Shinya Yoshida[2], Yuki Igarashi[2], Takao Yamakoshi[2]

1. Public Works Research Institute, 2. STC

Debris flows often occur even with a small amount of rainfall after a volcanic eruption. For disaster prevention and mitigation of debris flows in the volcanic mountainous areas, hazard maps and warning - evacuation systems are necessary. As basic information for such disaster prevention and mitigation, it is important to predict timings and areas of flood and sediment provided by debris flows in the volcanic areas after the eruptions.
Regarding debris flows associated with rainfalls after the volcanic eruptions, the authors assume that volcanic ash decreases the hydraulic conductivity of the topsoil layer of the basin slopes. Then surface flow occurs and volcanic ash deposited on the river channel easily becomes saturated by water. The saturated volcanic deposits result in flowing as debris flows because the deposits lose their stability by saturation. In order to analyze these, we observe rainfall events, soil moisture, surface flow, and ground surface conditions on a slope of two square meters in Arimura River basin in Sakurajima Island. Also, at the Arimura River No. 3 dam, the depth, surface velocity and load of the debris flow are continuously measured. In this presentation, we analyze these observation results and report the occurrence mechanism of surface flow and the flow mechanism of debris flows.
As a result of verifying the momentum conservation law of debris flows based on the measurements of the water depth, surface flow velocity and load data in Arimura River No. 3 dam, it seems appropriate. Although conditions for simulation such as spatial distribution of the depth of volcanic deposit, grain size distribution, runout path were determined by trial and errors, the results of simulation of the flow processes of the debris flows showed that simulated temporal changes in depth and velocity were closed to measured ones. As a future task, it is still necessary to obtain the information for spatial distribution of the depth of volcanic deposit, grain size distribution, runout path of the debris flows.

Keywords: volcanic area, debris flow

©2019. Japan Geoscience Union. All Right Reserved.

On the H_2S concentration continuous observation at Kurikoma volcano

*Hideyuki Itoh[1], Yasumichi Yamamoto[2], Kenji OOba[2], Morio Tsuji[1], Takeshi Ohba[3]

1. Faculty of policy studies, Iwate prefectural University, 2. JMS INc, 3. Tokai University

urikoma volcano is active volcano located on junction of miyagi, akita, iwate prefectures. Phreatic explosion occurred in 1944 and 1744, it generated acid water descended on the iwai river triggered by phreatic explosion.

Active fumaroles can have been observed along the ohjigoku-dani valley and showa crater, especially, trails are maintained along ohjigoku-dani valley, and many climbers are exposed to volcanic gas.

We installed the environmental h_2s sensors which called “odalog” (http://www.jmsystem.co.jp/kazan/odalog.html) in order to ascertain concentration of h_2s along the trail and beside the showa crater during june, 6 to october, 3, 2018.

The result of our observation, high concentration h_2s gas can been observed, especially, instantaneous maximum concentration can have been observed 334ppm at showa crater, and 38ppm at ohjigoku-dani valley. It is necessary to take immediate measures against volcanic gas for climbers.

Keywords: Kurikoma Volcano, H2S gas, continuous observation, climer care

©2019. Japan Geoscience Union. All Right Reserved.

[J] Poster | S (Solid Earth Sciences)：S-VC Volcanology

Mon. May 27, 2019 5:15 PM - 6:30 PM JST | Mon. May 27, 2019 8:15 AM - 9:30 AM UTC | Poster Hall International Exhibition Hall8, Makuhari Messe_24

[S-VC35] Mitigation of volcanic disasters - basic and applied researches

convener:Shinji Takarada(Geological Survey of Japan, National Institute of Advanced Industrial Science and Technology), Mitsuhiro Yoshimoto(Mount Fuji Research Institute, Yamanashi Prefectural Government), Yasuhiro Ishimine(Research and Education Center for Natural Hazards, Kagoshima University), Tomohiro Kubo(National Research Institute for Earth Science and Disaster Prevention)

Volcanic disasters are caused by wide range of volcanic phenomena including ash fall, pyroclastic flow, debris avalanche, lahar, and lava flow. To mitigate volcanic disasters, wide range of technologies including simulation, data processing on GIS, and communication techniques are required. Researches on volcanic hazards mapping, eruption scenarios, and probabilistic eruption assessments are getting important. This session invites presentations and broad reviews related to these topics. Contributions on database technology, case studies of social and school educations, and specific examples of eruption crisis events are also encouraged.

[SVC35-P01] Oil paintings describing the 1914 Sakurajima eruption

*Satoko Murotani[1] (1.National Museum of Nature and Science)

[SVC35-P02] Constructing and utilizing digitized volcanic hazardmap database

*Yuhki Kohno[1], Tomohiro Kubo[1], Yosuke Miyagi[1], Toshikazu Tanada[1] (1.National Research Institute for Earth Science and Disaster Resilience)

[SVC35-P03] Pyroclastic fall simulation using Tephra2 and JRA-55

*Hisashi Sasaki[1], Shunsuke Miura[1], Shino Naruke[1] (1.Asia Air Survey Co., Ltd.)

[SVC35-P04] Research on observation method of volcanic ash-fall accumulation using spaceborne SAR

*Taku Ozawa[1], Eisuke Fujita[1] (1.National Research Institute for Earth Science and Disaster Resilience)

[SVC35-P05] Method for estimation of debris flow runout in the volcanic area

*Yusuke Yamazaki[1], Naoki Fujimura[1], Sakiko Tetsuka[1], Masaki Mizuno[1], Yasuo Ishii[1], Toshihiro Kikui[2], Shinya Yoshida[2], Yuki Igarashi[2], Takao Yamakoshi[2] (1.Public Works Research Institute, 2.STC)

[SVC35-P06] On the H_2S concentration continuous observation at Kurikoma volcano

*Hideyuki Itoh[1], Yasumichi Yamamoto[2], Kenji OOba[2], Morio Tsuji[1], Takeshi Ohba[3] (1.Faculty of policy studies, Iwate prefectural University, 2.JMS INc, 3.Tokai University)

Oil paintings describing the 1914 Sakurajima eruption

*Satoko Murotani[1]

1. National Museum of Nature and Science

The National Museum of Nature and Science (NMNS) possesses three oil paintings describing the 1914 Sakurajima eruption. These oil paintings were drawn by “Nanto Omure” and “Kanehide Yamashita”. They were disciples of “Seiki Kuroda” who was an oil painter representing Japan. One of these was drawn at the request of Prof. Fusakichi Omori. The status immediately after eruption painted with oil paints is eloquent the violence of volcanic smokes and thunders.

These pictures originally were hung in the Seismological Institute of the Imperial University. Now, these pictures do not have the frame, and were incurred dirty or moldy due to deterioration over time. So we restored and framed these oil paintings. For people who aren’t unfamiliar with science, we would be happy if these oil paintings become interested in historical volcanic eruption as a work of art, rather than as an educational tool for science.

Keywords: The 1914 Sakurajima eruption, oil printing, Fusakichi Omori, Seiki Kuroda, Nanto Omure, Kanehide Yamashita

©2019. Japan Geoscience Union. All Right Reserved.

Constructing and utilizing digitized volcanic hazardmap database

*Yuhki Kohno[1], Tomohiro Kubo[1], Yosuke Miyagi[1], Toshikazu Tanada[1]

1. National Research Institute for Earth Science and Disaster Resilience

National Research Institute for Earth Science and Disaster Resilience (NIED) has published “Volcanic Hazard Maps of Japan –Second Edition” recording whole volcanic hazard maps or hazard mitigation plans of 40 active volcanoes issued from 1983 to 2013. After that, volcanic hazardmaps are required under law to be prepared in each volcanic area in Japan since the 2014 eruption of Ontake volcano. NIED has been compiling and digitizing volcanic hazard information published by each Volcano Disaster Management Council established for 50 continuously monitored volcanoes in Japan. In this presentation, we report the progress of the project and examples of utilization for the digitized data.
Each digitized volcanic hazard information, with shapefile format, are converted into image data such as tile data in order to be useful on WebGIS as a layer. We are preparing online map to show easier the hazard information to residents or tourists in the volcanic area. The map will be expected as a promotion tool to the residents regarding volcanic disaster since calm period as well as a hazard map available online in emergencies, and it should be available to anytime, anyone and anywhere. Additionally we try to make tool analysing how many disasters have been possible to occur at each area where is divided into a several mesh over a target volcanic area on the map, applying Kubo et al.(2003). It may help users can recognize volcanic risks having possibility to occur at the place they are (or will be) by the information of each mesh.
We will welcome for discussion about how the way of effective expression of volcanic hazard information toward the target people or utilization of the information materials.

Keywords: digitized volcano hazard map, WebGIS

©2019. Japan Geoscience Union. All Right Reserved.

Pyroclastic fall simulation using Tephra2 and JRA-55

*Hisashi Sasaki[1], Shunsuke Miura[1], Shino Naruke[1]

1. Asia Air Survey Co., Ltd.

We present an example using Tephra2 and Japan Meteorological Agency's 55-year long-term reanalysis data (hereinafter abbreviated as JRA-55) for the pyroclastic fall simulation. The characteristics of JRA - 55 are that there is uniform data throughout Japan and there is no missing data. It is easy to reproduce the eruption that occurred after 1958 using Tephra2 and JRA-55. It is also effective for creating volcanic hazard maps and probability maps.

Keywords: pyroclastic fall simulation , the Japanese 55-year Reanalysis, hazard map, probability map

©2019. Japan Geoscience Union. All Right Reserved.

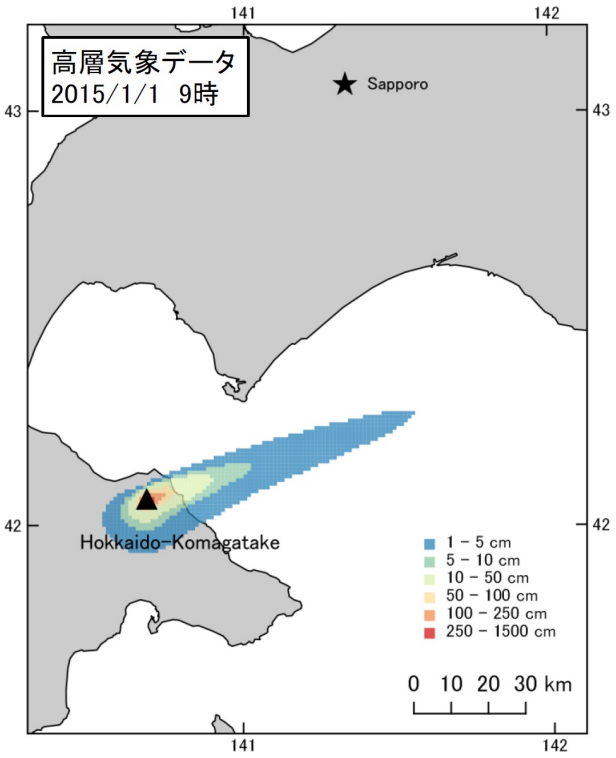

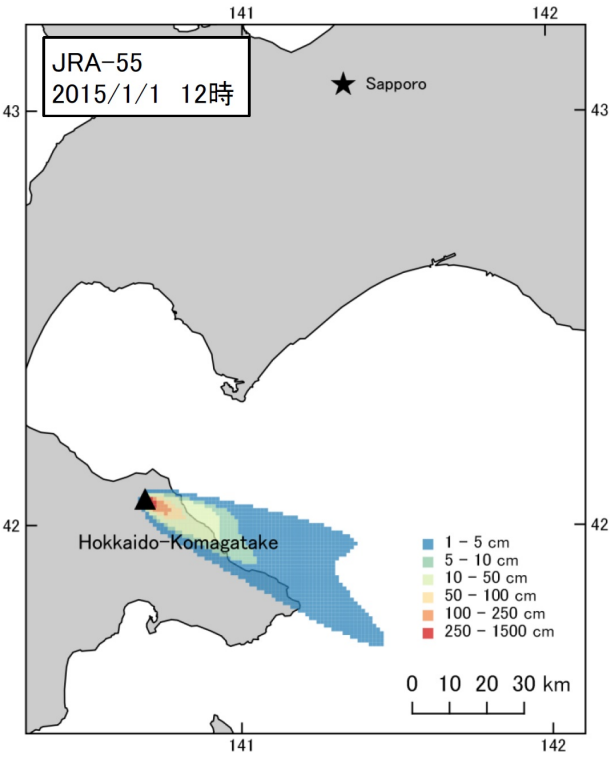

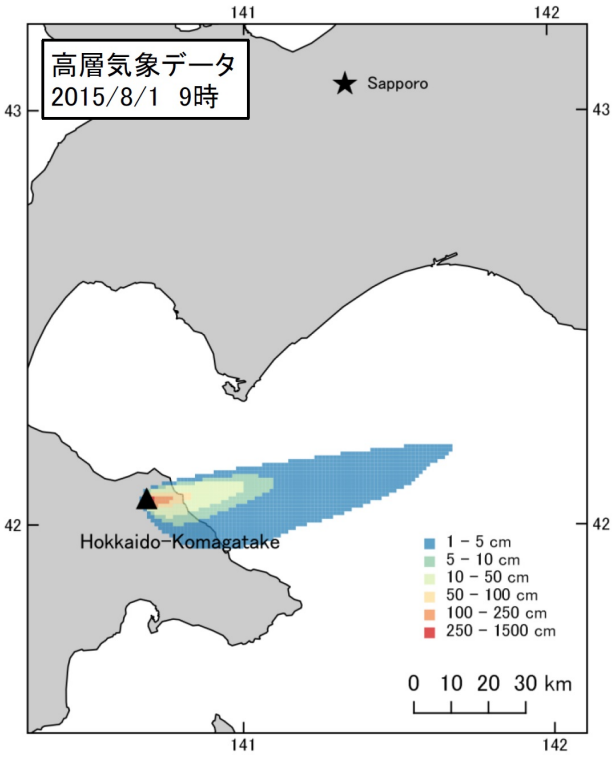

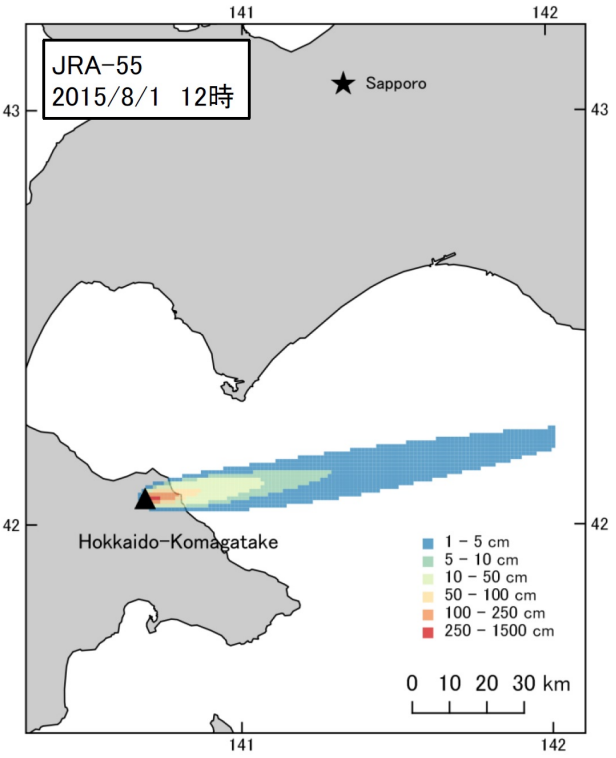

©2019. Japan Geoscience Union. All Right Reserved.

Research on observation method of volcanic ash-fall accumulation using spaceborne SAR

*Taku Ozawa[1], Eisuke Fujita[1]

1. National Research Institute for Earth Science and Disaster Resilience

Volcanic ash often causes heavy disaster due to debris flow. To mitigate such disaster, rapid observation of the volcanic ash distribution and forecast of debris flow from such observation are important. However, rapid observation of the volcanic ash distribution has been carried out mainly by on-site survey, and it is difficult to observe it rapidly. Then development of more rapid observation method are required. As one of solutions resolving such problem, utilization of satellite remote sensing technique is expected. Then, we began research on observation method of volcanic ash distribution using spaceborne SAR in “Cross-ministerial Strategis Innovation Promotion Program (SIP)-2nd season” as one of development items. In this presentation, we show results related to this development and explain the overview of this project.

In this development, we use InSAR coherence analysis. In InSAR results, clear fringes are seen if the coherence is high. On the other hand, noise is dominant if the coherence is low, and fringe becomes unclear. Generally, loss of coherence (decorrelation) is caused by difference of radar scatter at the pixel for InSAR pair. In a result from an interferometric pair including the eruption occurrence, decorrelation due to radar scatter change caused by volcanic ash accumulation is generally seen around the crater. For example, we analyzed PALSAR-2 InSAR pairs acquired before and after the Kuchinoerabujima eruption on January 17, 2019 and revealed that decorrelation area due to volcanic ash accumulation was seen within the range of about 1 km from the Shin-dake crater. Furthermore, decorrelation area extended to a range of about 1.5 km along the southwest and northwest valleys, which is consistent with the direction of pyroclastic flow.

Additionally, we analyzed InSAR pairs for December 18, 2018 and January 29, 2019 eruptions, and revealed the similar decorrelation around the crater. However, they were obviously small relative to that for January 17, 2019 eruption. Especially, that for January 17, 2019 eruption was limited to the vicinity of the crater. Thus, we could clearly see the difference in the volcanic ash accumulation area from InSAR coherence analysis.

If the relation between decorrelation and the amount of volcanic ash accumulation becomes clear quantitatively, the amount of volcanic ash accumulation will be obtained from InSAR coherence analysis. Then, in this development, we estimate decorrelation only due to volcanic ash accumulation, using a temporal coherence change model without volcanic ash effect constructed from InSAR coherence time-series analysis. Furthermore, we estimate coefficient converting coherence to the amount of volcanic ash accumulation from case studies. However, coherence basically saturates easily and thin accumulation of volcanic ash is difficult to detect, and therefore, it is difficult to detect the spatial distribution of volcanic ash accumulation. So, we attempt to estimate spatial distribution of volcanic ash accumulation by combining InSAR coherence analysis and ash-fall simulation in this development.

Keywords: ash-fall distribution, SAR, coherence

©2019. Japan Geoscience Union. All Right Reserved.

Method for estimation of debris flow runout in the volcanic area

*Yusuke Yamazaki[1], Naoki Fujimura[1], Sakiko Tetsuka[1], Masaki Mizuno[1], Yasuo Ishii[1], Toshihiro Kikui[2], Shinya Yoshida[2], Yuki Igarashi[2], Takao Yamakoshi[2]

1. Public Works Research Institute, 2. STC

Debris flows often occur even with a small amount of rainfall after a volcanic eruption. For disaster prevention and mitigation of debris flows in the volcanic mountainous areas, hazard maps and warning - evacuation systems are necessary. As basic information for such disaster prevention and mitigation, it is important to predict timings and areas of flood and sediment provided by debris flows in the volcanic areas after the eruptions.
Regarding debris flows associated with rainfalls after the volcanic eruptions, the authors assume that volcanic ash decreases the hydraulic conductivity of the topsoil layer of the basin slopes. Then surface flow occurs and volcanic ash deposited on the river channel easily becomes saturated by water. The saturated volcanic deposits result in flowing as debris flows because the deposits lose their stability by saturation. In order to analyze these, we observe rainfall events, soil moisture, surface flow, and ground surface conditions on a slope of two square meters in Arimura River basin in Sakurajima Island. Also, at the Arimura River No. 3 dam, the depth, surface velocity and load of the debris flow are continuously measured. In this presentation, we analyze these observation results and report the occurrence mechanism of surface flow and the flow mechanism of debris flows.
As a result of verifying the momentum conservation law of debris flows based on the measurements of the water depth, surface flow velocity and load data in Arimura River No. 3 dam, it seems appropriate. Although conditions for simulation such as spatial distribution of the depth of volcanic deposit, grain size distribution, runout path were determined by trial and errors, the results of simulation of the flow processes of the debris flows showed that simulated temporal changes in depth and velocity were closed to measured ones. As a future task, it is still necessary to obtain the information for spatial distribution of the depth of volcanic deposit, grain size distribution, runout path of the debris flows.

Keywords: volcanic area, debris flow

©2019. Japan Geoscience Union. All Right Reserved.

On the H_2S concentration continuous observation at Kurikoma volcano

*Hideyuki Itoh[1], Yasumichi Yamamoto[2], Kenji OOba[2], Morio Tsuji[1], Takeshi Ohba[3]

1. Faculty of policy studies, Iwate prefectural University, 2. JMS INc, 3. Tokai University

urikoma volcano is active volcano located on junction of miyagi, akita, iwate prefectures. Phreatic explosion occurred in 1944 and 1744, it generated acid water descended on the iwai river triggered by phreatic explosion.

Active fumaroles can have been observed along the ohjigoku-dani valley and showa crater, especially, trails are maintained along ohjigoku-dani valley, and many climbers are exposed to volcanic gas.

We installed the environmental h_2s sensors which called “odalog” (http://www.jmsystem.co.jp/kazan/odalog.html) in order to ascertain concentration of h_2s along the trail and beside the showa crater during june, 6 to october, 3, 2018.

The result of our observation, high concentration h_2s gas can been observed, especially, instantaneous maximum concentration can have been observed 334ppm at showa crater, and 38ppm at ohjigoku-dani valley. It is necessary to take immediate measures against volcanic gas for climbers.

Keywords: Kurikoma Volcano, H2S gas, continuous observation, climer care

©2019. Japan Geoscience Union. All Right Reserved.

[J] Oral | S (Solid Earth Sciences)：S-VC Volcanology

Mon. May 27, 2019 1:45 PM - 3:15 PM JST | Mon. May 27, 2019 4:45 AM - 6:15 AM UTC | 105 1F

[S-VC35] Mitigation of volcanic disasters - basic and applied researches

convener:Shinji Takarada(Geological Survey of Japan, National Institute of Advanced Industrial Science and Technology), Mitsuhiro Yoshimoto(Mount Fuji Research Institute, Yamanashi Prefectural Government), Yasuhiro Ishimine(Research and Education Center for Natural Hazards, Kagoshima University), Tomohiro Kubo(National Research Institute for Earth Science and Disaster Prevention), Chairperson:Tomohiro Kubo(防災科学技術研究所), Shinji Takarada(Geological Survey of Japan/AIST)

Volcanic disasters are caused by wide range of volcanic phenomena including ash fall, pyroclastic flow, debris avalanche, lahar, and lava flow. To mitigate volcanic disasters, wide range of technologies including simulation, data processing on GIS, and communication techniques are required. Researches on volcanic hazards mapping, eruption scenarios, and probabilistic eruption assessments are getting important. This session invites presentations and broad reviews related to these topics. Contributions on database technology, case studies of social and school educations, and specific examples of eruption crisis events are also encouraged.

1:45 PM - 2:00 PM JST | 4:45 AM - 5:00 AM UTC

[SVC35-01] A working hypothesis for source craters and sequence of the 1707 Hoei eruption of Fuji Volcano, Japan

*Masato Koyama[1] (1.Shizuoka Univ.)

2:00 PM - 2:15 PM JST | 5:00 AM - 5:15 AM UTC

[SVC35-02] Consideration of the formation process of Mt.Hoei, Fuji volcano

*Akira Baba[1], Toshitsugu Fujii[1], Tatsuro Chiba[2], Mitsuhiro Yoshimoto[1], Fumikatsu NISHIZAWA[1], Hidetoshi Shibuya[3] (1.Mount Fuji Research Institute, 2.Asia Air Survey Co., Ltd., 3.Department of Earth and Environmental Sciences, Faculty of Advanced Science and Technology, Kumamoto University)

2:15 PM - 2:30 PM JST | 5:15 AM - 5:30 AM UTC

[SVC35-03] Airborne LiDAR Bathymetry reveals underwater topography of Lake Motosu - The level of water raised by lava inflow -

*Tatsuro Chiba[1], Sin-ichi kaneta[1], Makoto Ohashi[1] (1.Asia Air Survey Co., Ltd.)

2:30 PM - 2:45 PM JST | 5:30 AM - 5:45 AM UTC

[SVC35-04] Volcano monitoring using satellite thermal infrared imagery of CIRC (Compact Infrared Camera)

*Yuki Takakura[1], Koji Nakau[1], Junichiro Ishizawa[1] (1.Japan Aerospace Exploration Agency)

2:45 PM - 3:00 PM JST | 5:45 AM - 6:00 AM UTC

[SVC35-05] Impact absorption properties of wooden buildings roof subjected to ballistic block collision

*Kohei Tateyama[1], Hiroyuki Yamada[2], Mitsuhiro Yoshimoto[3], Ryo Honda[3], Toshitsugu Fujii[3] (1.Ritsumeikan University, 2.National defense academy, 3.Mount Fuji Research Institute, Yamanashi Prefectural Government)

3:00 PM - 3:15 PM JST | 6:00 AM - 6:15 AM UTC

[SVC35-06] Distribution of ballistic ejecta of the phreatic eruption at Kusatsu-Shirane volcano, on 23 Jan, 2018, part 2

*Mitsuhiro Yoshimoto[1], Ryuta FURUKAWA[2,3], Yoshihiro Ishizuka[2], Yusuke Minami[2], Masashi NAGAI[4], Shuichi Hosokawa[3], Ryo Honda[1], Taisuke Yasuda[1], Akihiko Terada[5], Tatsuji Nishizawa[5], Yasuhiro Ishimine[6], Kenichi Arai[7], Hisashi Sasaki[7], Shino Naruke[7], Yuko Sekiguchi[3], Takahiro Yanada[3], Yasuo Ishizaki[8], Nobuko Kametani[8], Fukashi Maeno[9] (1.Mount Fuji Research Institute, Yamanashi Prefectural Government, 2.Geological Survey of Japan, National Institute of Advanced Industrial Science and

Technology, 3.Japan Meteorological Agency, 4.Volcano Research Department, National Research Institute for Earth Science and Disaster Resilience, 5.Volcanic Fluid Research Center, Tokyo Institute of Technology, 6.Research and Education Center for Natural Hazards, Kagoshima University, 7.Asia Air Survey Co., Ltd., 8. Graduate School of Science and Engineering, University of Toyama, 9.Earthquake Research Institute, University of Tokyo)

A working hypothesis for source craters and sequence of the 1707 Hoei eruption of Fuji Volcano, Japan

*Masato Koyama[1]

1. Shizuoka Univ.

The 1707 Hoei eruption, one of the most voluminous and violent eruptions of Fuji Volcano, has been considered to have occurred from the NW-SE trending three craters (Hoei craters) on the southeastern flank of the volcano and to have made the bulge (Hoei mound) at the edge of the craters. The Akaiwa rock, located near the summit of the Hoei mound, has been thought to be an outcrop of older strata, which have unconformable relationship with overlying deposits.
On the basis of careful geomorphological and geological survey including SfM(Structure from Motion) technology with UAV photos, the strata exposed on the Akaiwa rock are revealed to be part of the proximal deposits of the Hoei eruption. Moreover, another NW-SE eruptive fissure is estimated to have opened between the Hoei mound and the Gotenniwa Higashi pyroclastic cone in the initial stage of the Hoei eruption and to have been buried by the subsequent eruptive deposits from the Hoei craters. The hypothesis of this fissure can resolve the problem thatlocation of a source crater of the basal pumice layer of the distal Hoei pyroclastic deposits is still unclear.

Keywords: Fuji Volcano, 1707 Hoei eruption, source craters, Hoei mound, eruption sequence, working hypothesis

©2019. Japan Geoscience Union. All Right Reserved.

宝永火口周辺の地形・地質の新たな解釈（作業仮説）

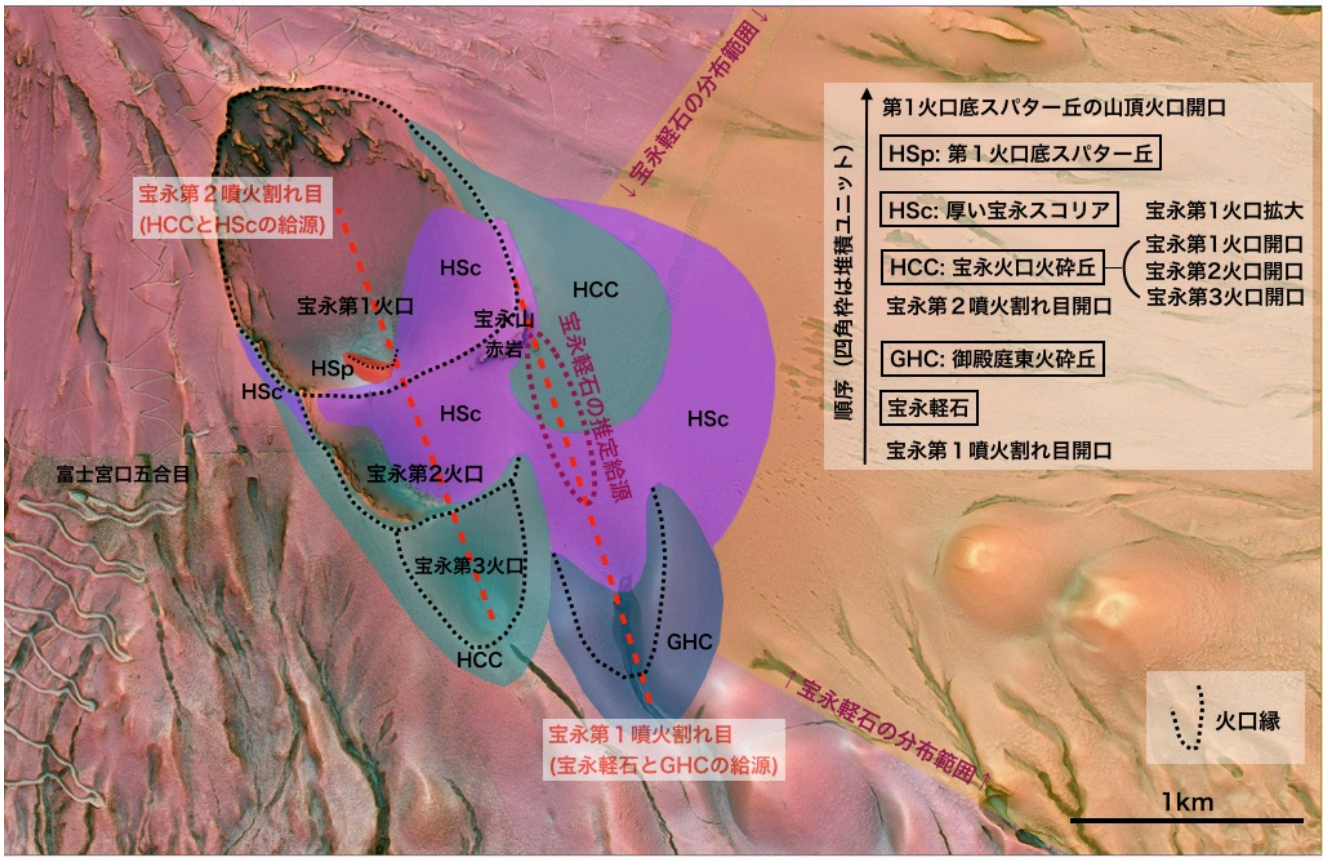

背景図：国交省富士砂防事務所・(株)アジア航測

©2019. Japan Geoscience Union. All Right Reserved.

Consideration of the formation process of Mt.Hoei, Fuji volcano

*Akira Baba[1], Toshitsugu Fujii[1], Tatsuro Chiba[2], Mitsuhiro Yoshimoto[1], Fumikatsu NISHIZAWA[1], Hidetoshi Shibuya[3]

1. Mount Fuji Research Institute, 2. Asia Air Survey Co., Ltd., 3. Department of Earth and Environmental Sciences, Faculty of Advanced Science and Technology, Kumamoto University

It is important to review the sequence of each eruption in the past in order to mitigate volcanic hazard in the future. Especially the Hoei eruption is regarded to be important because it represents large scale explosive eruption that is rare in the eruptive history of Fuji volcano, but may cause extensive disaster in the metropolitan area. Mt.Hoei has been considered to be protuberance formed during the Hoei eruption and to be composed of Old Fuji formation (Tsuya, 1955). The protuberance has been considered as a kind of bulge accompanied by lateral intrusion of degassed magma (Miyaji et al., 2011). Koyama (2018) suggested the bulge by intrusion of magma could cause sector collapse and the evacuation plan for such sector collapse should be made. In this presentation, we will discuss the genesis and the formation process of Mt.Hoei based on new data obtained from geological survey, geochemical analysis and palaeomagnetic measurements of the constituents of Mt. Hoei and the ultraproximal deposits of Hoei eruption.

Mt.Hoei located at the northeast of Hoei craters, consists of pyroclastic rocks including mainly dense blackish-grey scoriaceous lapilli, spatters, volcanic bombs capturing gabbro and gabbroic fragments. From these observations, microscopy, whole rock chemical composition analysis, palaeomagnetic measurements and XRD analysis results, Mt.Hoei (Akaiwa) is presumed that ultraproximal fall and surge deposits by phreatomagmatic eruptions, compared with Ho-Ⅲ(Stage 2) of Miyaji et al.,(2011) from petrography and chemical composition. In addition, 2nd and 3rd crater ridge, the wall of the erosion valley of Gotenniwa consists of fallout deposits of Hoei eruption, corresponding to Ho- Ⅰ to Ⅲ(Stage 1) of Miyaji et al.,(2011). Although the white and banded pumice layer cannot be confirmed at the base of the erosion valley of Gotenniwa at the present moment, the deposits show a gradual compositional change from andesite to the basalt (SiO_2 = 62.8 to 52.2 wt%) upward. The paleomagnetic directions obtained from the spatter cone in the 1st crater of Hoei, the deposit around the summit of Mt.Hoei and the fallout deposit at erosion valley of Gotenniwa coincides with 1707 A.D.of the paleomagnetic secular variation curve (JRFM 2K.1).

We estimated the formation process of Mt.Hoei based on these new findings, isopach maps of Hoei eruption(Miyaji et al., 2011), the model of magmatic development of Hoei eruption (Fujii, 2007 ; Yasuda et al.,2015), and historical records and drawings (Koyama, 2009). Mt.Hoei is not a bulge caused by the magmatic intrusion, but a pyroclastic cone of Hoei eruption formed in only 9 days.

1. The basaltic magmas contacted and mixed with the dacitic magma, white-banded pumice squirted from the vicinity of the 1st crater and was swept in the east direction by the westerlies (December 16th around 10 to 17 o'clock, Unit A, B of Miyaji et al.,(2011)).
2. As the crater expanded, the side of the mountain of the first crater was also scraped off, and abundant accessory materials were ejected in the east-south direction together with the essentials, and deposited near crater to form Mt.Hoei (December 17th before daylight, Unit C ~ F of Miyaji et al, (2011)).
3. The vent transitioned to the 2nd crater due to the landslide at the 1st crater edge or expansion of the vent. (December 17 to 19 th, Unit G ~ I of Miyaji et al, (2011))
4. The vent transitioned to the 1st crater due to the accessory materials of landslide were gradually ejected, Mt.Hoei (Akaiwa) was formed by intermittent phreatomagmatic eruptions (December 19-25 th, Unit J ~ M of Miyaji et al, (2011)).

©2019. Japan Geoscience Union. All Right Reserved.

5. As crater is restricted to the 1st crater, inflow of accessory materials stopped and Plinian eruption of basaltic magma continued for 6 days and ended (December 25 - 30 th, Unit N ~ Q of Miyaji et al, (2011)).

Keywords: Fuji volcano, Mt.Hoei, formation process, hazard map

©2019. Japan Geoscience Union. All Right Reserved.

Airborne LiDAR Bathymetry reveals underwater topography of Lake Motosu
- The level of water raised by lava inflow -

*Tatsuro Chiba[1], Sin-ichi kaneta[1], Makoto Ohashi[1]

1. Asia Air Survey Co., Ltd.

1. Introduction

Lake Motosu is a dammed lake located northwest of Mt. Fuji, the elevation of the lake is about 900m. Aokigahara lava flow, which is occurred by the eruption of 864 AD, flood into the lake, and the northeast lake shoreline is seen like cut off by the truncated arc. Though regarding the characteristics of this lava flow, there is a study by Obata and Unno (1999), no survey of the shallow part of the lake had been conducted. Generally, the level of lake water is the possibility of rising up by the entry of a large amount of debris or lava flows. Of course, it is not a kind of transient phenomenon like Tsunami, but the possibility to rise permanently because of the bottom of the lake getting shallow. Airborne LiDAR Bathymetry measurement was carried out in order to investigate whether the level of water of Motosu Lake changes during Aokigahara lave flow entry, and the results are as bellows.

2. Airborne LiDAR Bathymetry

Airborne LiDAR Bathymetry, as follows ALB, is a measurement method aiming to measure depth and topography of shallow water along river and coast. The equipment used in this research consists of two pair of laser ranging systems for ground measurement using NIR laser and underwater measurement using visible range (532nm). The measurable depth depends upon the transparency of the object greatly. It was expected to be measurable up to 15m depth since Lake Motosu has high transparency throughout the year and is visible around 14-16m depth. The measurement carried out on 9th September 2017. Since the area terrain is heavily rough, Helicopter, which is easy to control flight height, is used and flew 11 courses.

3. Bathymetry

For ALB measurement, the position of the aircraft is determined by kinematic GNSS survey based upon GNSS-based Control Station, objective terrain of the ground and the seafloor are measured by both the data of the initial navigation device and the two channels of laser ranging device. The density of point-clouds was 10 to 100 points/m^2 on land and 1 to 5 points/m^2 on water. The maximum water depth was measured to be 11-15m. Based on pon point-clouds data, the topography of the lake bottom is totally different between the northern and southern measurement range. On the northern side, unique irregularities of Aokigahara lava can be seen from land to underwater. There is no change between the border of the surface of the lake and reach to around 15m continuously. On the other side, the topography of the southern side of the lacustrine terrace, there can be seen slightly higher hill than the seafloor closer to the lakeshore. Not less than two stages of rectangular flat surface can be seen on the northern slope of the hill.

4. Conclusion

On the northern side of the measurement range, there found lava topography divergent like branch coral and split on the center part, and there found red oxidized portion, so it is clear that the lava landscape was deposited on land (Obata and Unno, 1999). Continuously tracking terrain similar to this topography

©2019. Japan Geoscience Union. All Right Reserved.

to 15m water depth suggests that the level of water at the time of lava flow was at least 15m lower than the current one. Underwater archeology surveys are also conducted around the southern lacustrine terrace (Kamikuissiki Village Board of Education, 1999). Relics including turtle type earthenware have been ensured so far, most of relics were identified as the age of the beginning of the early stage of Kofun Period. Many of them are completed and it seems to have been submerged since there is no inconsistency that the time is the invasion time of Aokigahara lava flow in the Heian era. It is to be wished that the detailed investigation confirms the red oxidized portion of the underwater lava topography and the research of the possibility of flat surface to be the construction of the submerged village in the future.

Reference

Sumie Obata and Susumu Umino (1999) Morphology of A. D. 864 Aokigahara Lava Flow Exposed on the Coast of Motosuko Lake, Fuji Volcano, Bulletin of the Volcanological Society of Japan, 44, 201-206,
Kami-Kuichiichi Village Board of Education (2004) Survey Report on Lake Motosu bottom site.
Shinichi Kaneta, Tatsuro Chiba (2017) Topographic measurements of Lake Motosu lake by ALB, http://www.rssj.or.jp/wp-content/uploads/2018/08/u05_64_h30.pdf

Keywords: LiDAR, lava flow, bathymnetry, water level change

©2019. Japan Geoscience Union. All Right Reserved.

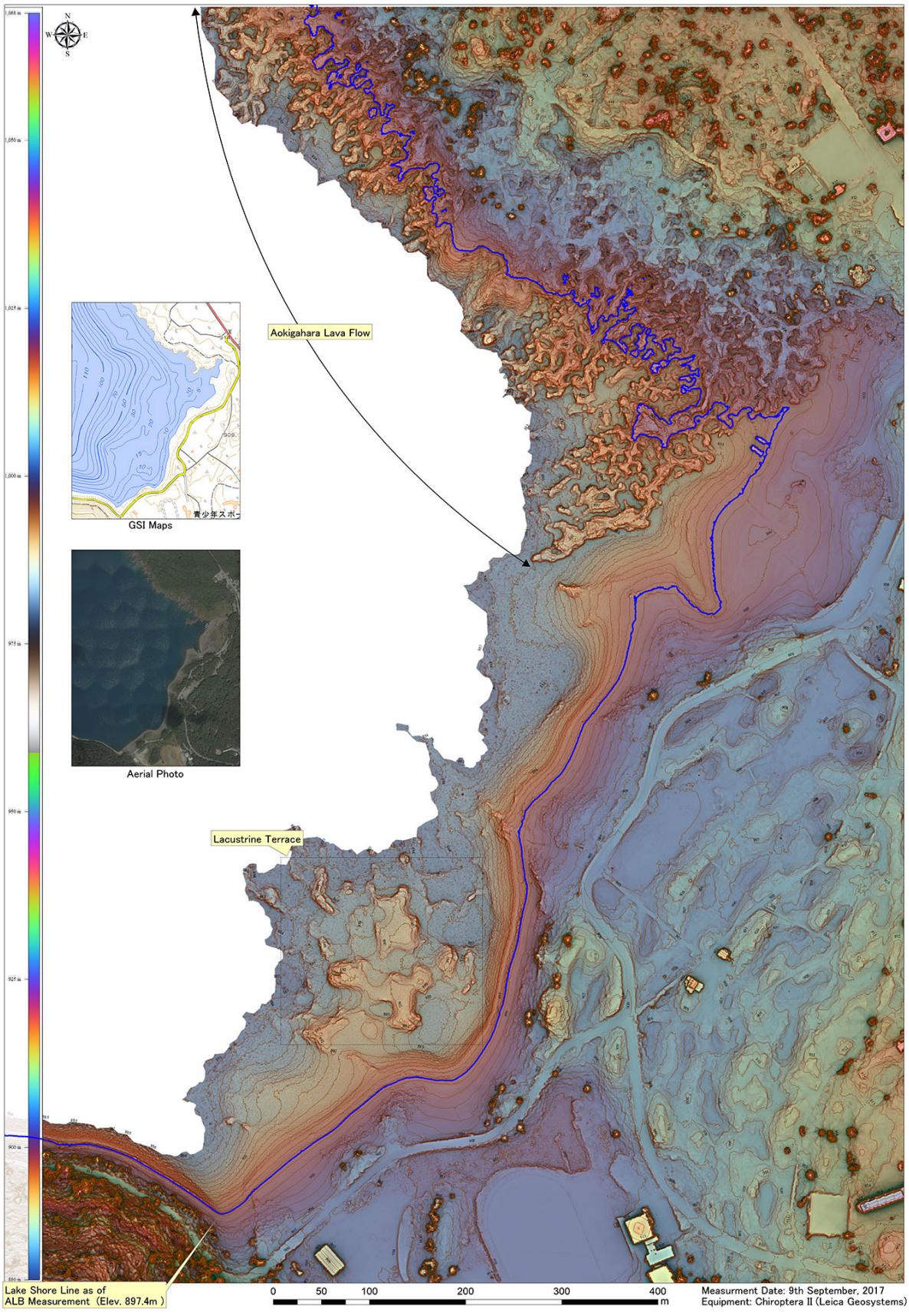

©2019. Japan Geoscience Union. All Right Reserved.

Volcano monitoring using satellite thermal infrared imagery of CIRC (Compact Infrared Camera)

*Yuki Takakura[1], Koji Nakau[1], Junichiro Ishizawa[1]

1. Japan Aerospace Exploration Agency

Although volcanic activities are monitored by various approaches, it is difficult to observe some volcanoes in Japan using ground equipment (e.g. remote islands or submarine volcanos). In such case, satellite imagery is one of the powerful tools to monitor them. Satellite can observe extensive area simultaneously, including many volcanos. Thus, we can capture geothermal activities; lava flow, pyroclastic flow or heat of crater even at night.

To prevent or to mitigate volcanic disaster, the disaster management agencies needs ready-to-use dataset; information extracted from satellite imagery. Therefore, we developed “Volcano Monitoring System” (released in Sep 2018; https://kazan.jaxa.jp/); which system provides such information and visualized satellite infrared imagery of CIRC and other satellites. CIRC is uncooled microbolometer thermal infrared sensor for the earth observation and it is on board ALOS-2 satellite (Advanced Land Observing Satellite 2). On the Volcano Monitoring System, we can browse satellite RGB or infrared imagery as a map and get the variation of volcanic activity’s indices automatically extracted from satellite imagery. To produce concrete indices for volcano monitoring, we are studying several approaches of satellite infrared data processing in cooperation with the disaster management agencies. In such study, we are focusing on 12 volcanoes which are defined among us. In this presentation, we introduce “Volcano Monitoring System” and some volcanic events captured by CIRC.

Keywords: Satellite, Infrared, Volcanic disasters

©2019. Japan Geoscience Union. All Right Reserved.

Impact absorption properties of wooden buildings roof subjected to ballistic block collision

*Kohei Tateyama[1], Hiroyuki Yamada[2], Mitsuhiro Yoshimoto[3], Ryo Honda[3], Toshitsugu Fujii[3]

1. Ritsumeikan University, 2. National defense academy, 3. Mount Fuji Research Institute, Yamanashi Prefectural Government

Volcanic disasters include various factors such as eruption, lava flow, pyroclastic flow, debris avalanche, debris flow and so on. Especially, at the phreatic eruption of Mt. Ontake in September 27, 2014, most of the damages were caused by clashes of ballistic block. In order to prevent these damages, it is suggested that evacuation to a mountain hut is effective. Thus, evaluation of impact absorption properties for wooden buildings (e.g. mountain hut) against ballistic block collision is necessary. Previously, we reported the protective abilities of as-built wooden buildings, which were reinforced with high performance fabric using aramid fiber. In addition, the penetration boundary energy for a 15 mm thick wooden building roof was reported. However, the impact absorption properties of various type wooden buildings has not been clarified enough. Therefore, in this study, impact absorption properties of wooden buildings roof subjected to ballistic block collision was experimentally investigated.

A collision test was carried out at the velocity of 10 to 90 m/s using a large scale launching system. In this system, a projectile was accelerated by compressed air and then collided with the target. The projectile velocity was measured using two lasers and light receiving parts. In many cases, size of the ballistic block is almost the fist size (ϕ100 mm) under phreatic eruption. Therefore, Vitrified whetstone similar to the common ballistic block (density: 2400 kg/m^3) was used as the projectile, and the diameter was determined ϕ90 mm (mass: 2.66 kg). For the target, typical wooden roof structure (e.g. cedar boards, waterproof sheet, galvalume steel plate and cedar rafter) was used. Two types of thickness of cedar board (15 mm and 18 mm) were prepared. The thickness of the waterproof sheet and galvalume steel plate were 1.0 mm and 0.4 mm, respectively. The dimensions of the specimen were 600 mm ×600 mm. The components were fixed with nails and its spacing was approximately 150 mm. In addition, specimens in which two cedar plates were superimposed was also prepared. There are two kinds of superimposing methods: a ” staggered structure “ that is alternately superimposed on one another, and a "cross structure" in which plates are orthogonalized.

Collision test results revealed penetration boundary energies of 15 mm and 18 mm specimens, respectively. In previous study, it was shown the maximum collision energy of volcanic ballistic block (ϕ 2-64 mm) was 1700 J (in the case of ϕ64mm, 100 m/s), and average collision energy was less than approximately 1200J in many cases. From the result, it was revealed that the roof of cedar board having a thickness of 15 mm and 18 mm could prevent penetration of volcanic ballistic block. In addition, it was found that by superimposing the cedar boards, impact absorption properties can be improved simply. At the time of superimposition, the impact absorption properties was hardly improved in the ” staggered structure”. However, in the "cross structure", it was confirmed that the impact absorption properties were greatly improved. From this it was found that the "cross structure" is better when reinforcing by simple superimposition.

Keywords: ballistic block collision, Impact absorption, wooden buildings roof

©2019. Japan Geoscience Union. All Right Reserved.

Distribution of ballistic ejecta of the phreatic eruption at Kusatsu-Shirane volcano, on 23 Jan, 2018, part 2

*Mitsuhiro Yoshimoto[1], Ryuta FURUKAWA[2,3], Yoshihiro Ishizuka[2], Yusuke Minami[2], Masashi NAGAI[4], Shuichi Hosokawa[3], Ryo Honda[1], Taisuke Yasuda[1], Akihiko Terada[5], Tatsuji Nishizawa[5], Yasuhiro Ishimine[6], Kenichi Arai[7], Hisashi Sasaki[7], Shino Naruke[7], Yuko Sekiguchi[3], Takahiro Yanada[3], Yasuo Ishizaki[8], Nobuko Kametani[8], Fukashi Maeno[9]

1. Mount Fuji Research Institute, Yamanashi Prefectural Government, 2. Geological Survey of Japan, National Institute of Advanced Industrial Science and Technology, 3. Japan Meteorological Agency, 4. Volcano Research Department, National Research Institute for Earth Science and Disaster Resilience, 5. Volcanic Fluid Research Center, Tokyo Institute of Technology, 6. Research and Education Center for Natural Hazards, Kagoshima University, 7. Asia Air Survey Co., Ltd., 8. Graduate School of Science and Engineering, University of Toyama, 9. Earthquake Research Institute, University of Tokyo

Moto-Shirane volcano, which is part of Kusatsu-Shirane volcano, erupted on 23 January 2018 after 1500 years dormancy. One parson died and 11 other people were injured by the ballistic ejecta of this phreatic eruption. We report the results of a survey on the distribution of ballistic rocks around the crater and climbing trails and ski courses on May 10 - 12, 2018 and October 23 - 25, 2018.The maximum size of the ballistic rocks was measured at a total of 191 sites and the number density of the rocks (>64mm) was measured at a total of 64 sites. Ballistic rocks of the eruption are distributed within 500 meters around the main crater and is mainly distributed from north to northeast. The maximum size of ballistic rock was 4.8 m which fell to the western crater rim, and near the main crater was 3.4 m. The flight-distance of ballistic rocks with a major axis of about 20 cm, 50 cm, 100 cm, 200 cm are 400 to 650 m, 400 m, 350 m, 150 m, respectively. It suggests that the initial velocity of ballistic rocks of each size is different.

Keywords: ballistic ejecta, Kusatsu-Shirane volcano, phreatic eruption

©2019. Japan Geoscience Union. All Right Reserved.

[J] Oral | S (Solid Earth Sciences)：S-VC Volcanology

Mon. May 27, 2019 3:30 PM - 5:00 PM JST | Mon. May 27, 2019 6:30 AM - 8:00 AM UTC | 105 1F

[S-VC35] Mitigation of volcanic disasters - basic and applied researches

convener:Shinji Takarada(Geological Survey of Japan, National Institute of Advanced Industrial Science and Technology), Mitsuhiro Yoshimoto(Mount Fuji Research Institute, Yamanashi Prefectural Government), Yasuhiro Ishimine(Research and Education Center for Natural Hazards, Kagoshima University), Tomohiro Kubo(National Research Institute for Earth Science and Disaster Prevention), Chairperson:Mitsuhiro Yoshimoto(山梨県富士山科学研究所), Yasuhiro Ishimine(鹿児島大学地域防災教育研究センター)

Volcanic disasters are caused by wide range of volcanic phenomena including ash fall, pyroclastic flow, debris avalanche, lahar, and lava flow. To mitigate volcanic disasters, wide range of technologies including simulation, data processing on GIS, and communication techniques are required. Researches on volcanic hazards mapping, eruption scenarios, and probabilistic eruption assessments are getting important. This session invites presentations and broad reviews related to these topics. Contributions on database technology, case studies of social and school educations, and specific examples of eruption crisis events are also encouraged.

3:30 PM - 3:45 PM JST | 6:30 AM - 6:45 AM UTC

[SVC35-07] Developing Ash-fall impact forecasting content.

*Tomohiro Kubo[1], Yosuke Miyagi[1], Setsuya Nakada[1], Eisuke Fujita[1], Masamitsu Miyamura[1] (1.National Research Institute for Earth Science and Disaster Prevention)

3:45 PM - 4:00 PM JST | 6:45 AM - 7:00 AM UTC

[SVC35-08] New Websites and a Pamphlet of IVHHN

*Yasuhiro Ishimine[1] (1.Research and Education Center for Natural Hazards, Kagoshima University)

4:00 PM - 4:15 PM JST | 7:00 AM - 7:15 AM UTC

[SVC35-09] State of river water pollution derived from the recent volcanic activity of Mt Iwo-Yama, Kirishima volcanoes

*Yoshikazu Kikawada[1], Haruka Yamamoto[2], Wei Deng, Megumi Fukai (1.Faculty of Science and Technology, Sophia University, 2.Graduate School of Science and Technology, Sophia University)

4:15 PM - 4:30 PM JST | 7:15 AM - 7:30 AM UTC

[SVC35-10] Development of information tools for evacuation and rescue in the event of volcanic disaster

*Yosuke Miyagi[1], Setsuya Nakada[1], Tomohiro Kubo[1], Mitsuhiro Yoshimoto[2], Ryo Honda[2] (1.National Research Institute for Earth Science and Disaster Resilience, 2.Mount Fuji Research Institute, Yamanashi Prefectural Government)

4:30 PM - 4:45 PM JST | 7:30 AM - 7:45 AM UTC

[SVC35-11] **Ignimbrite, tephra-fall, caldera and fatalities of major volcanoes in the East and Southeast Asia**

*Shinji Takarada[1], Joel Calupas Bandibas[1] (1.Geological Survey of Japan, AIST)

4:45 PM - 5:00 PM JST | 7:45 AM - 8:00 AM UTC

[SVC35-12] On the climber’s attitudes to the Volcanic mitigation for active volcanoes.

*Hideyuki Itoh[1], Chizuru Totani[2], Mizuho Arai[2] (1.Faculty of policy studies, Iwate prefectural University, 2.Asia air Survey, Co.Ltd.)

Developing Ash-fall impact forecasting content.

*Tomohiro Kubo[1], Yosuke Miyagi[1], Setsuya Nakada[1], Eisuke Fujita[1], Masamitsu Miyamura[1]

1. National Research Institute for Earth Science and Disaster Prevention

The falling ash is expected to cause extensive damage over a wide area, because the ash widely spread out. For example, the highway road was closed to traffic due to falling ash, because the falling ash causes a car slip accident. In Mt.Aso 2016 Eruption, the Aso-shi lost power, because the ash fall an electric power substation. On the other hand, the wooden houses may be collapsed by over volcanic ash load. In addition, the buildings that are constructed by Reinforced Concrete or Steel such as a hospital, an office or a city hall are not collapsed, but the building equipment on the roof supposes to be damaged by the falling ash. Thus, we research the impact of the building equipment function due to falling ash by experimental study.

We report the experimental result of a cooling tower by falling ash. In addition, we report the prototype ash-fall impact forecasting content for the infrastructure and the building equipment, based on the Central Disaster Management Council report and the experimental result.

Keywords: ash-fall, damage estimation, volcano disaster countermeasure, experiment, building equipment

©2019. Japan Geoscience Union. All Right Reserved.

New Websites and a Pamphlet of IVHHN

*Yasuhiro Ishimine[1]

1. Research and Education Center for Natural Hazards, Kagoshima University

I will present an outline of new websites and a pamphlet of International Volcanic Health Hazard Network (= IVHHN), both of which have been translated into Japanese by the author. IVHHN is an IAVCEI commission which has been launched in 2003 and focuses on research and dissemination of information on volcanic health hazards. Dr. Claire Horwell and some other leading members of IVHHN have conducted a research project entitled “A New Evidence Base for Respiratory Health Interventions in Volcanic Eruption Crises”, which is called HIVE project for short, with a grant from Enhancing Learning and Research for Humanitarian Assistance (ELRHA), a global charity organization in 2015-2018. IVHHN has revised its websites and published in August 2018 to include new outcomes obtained from HIVE project. It is notable that the new websites include the guideline on recommended facemasks for respiratory protection during ashfall on the basis of the field research in Indonesia, Mexico and Japan carried out as a part of HIVE project. The guideline advises residents to stay indoors to reduce exposure to volcanic ash if possible and wear a well-fitting industry-certified facemask such as a N95 mask, or a DS2 mask, which is Japanese standard equivalent to N95, when they are cleaning up volcanic ash or stay outdoors for a long time. The guideline also mentions that industry-certified facemasks are not usually designed to fit children’s face, and thus, they are not effective for children. The new IVHHN websites add the guideline and some other scientific protocols for assessing volcanic health hazard. They also adopt a responsive layout to works well on smartphones. The websites also contain three new videos which describe the experience of coping with volcanic ash, how to protect yourself from breathing ash and how to properly fit a facemask. Subtitles are available in English by clicking on the CC button or you can switch to Spanish or Bahasa in the Settings button. They are also available on YouTube and Vimeo. As the author has been a member of IVHHN since 2005 and managed Japanese IVHHN website. he translated the revised English websites into Japanese and published in January 2019. The new Japanese pages is published newly obtained internet domain at http://www.ivhhn.jp/, while the Japanese website has been published at http://www.geocities.jp/ychojp/ivhhn/ for twelve years. The author printed 2,000 copies of the Japanese version IVHHN guideline on the protection from breathing volcanic ash as a pamphlet. A half of the copies were distributed at the general disaster drill on large-scale eruptions of Sakurajima held on 12 January 2019.IVHHN now prepare for another guideline on the health effects of volcanic gases, which has already been reviewed by the author and some other members of an IVHHN expert panel. The author also provides IVHHN with some photos of fumaroles taken at volcanic areas in Japan.

Keywords: IVHHN, HIVE, Mask

©2019. Japan Geoscience Union. All Right Reserved.

State of river water pollution derived from the recent volcanic activity of Mt Iwo-Yama, Kirishima volcanoes

*Yoshikazu Kikawada[1], Haruka Yamamoto[2], Wei Deng, Megumi Fukai

1. Faculty of Science and Technology, Sophia University, 2. Graduate School of Science and Technology, Sophia University

Mt Iwo-Yama belonging to the Kirishima Volcanoes erupted in 2018 for the first time in 250 years. The recent activity of the volcano has a profound effect on the regional economy, especially in the fields of agriculture and tourism. With the phreatic eruption in April 2018, muddy thermal water spouted out from the newly opened vents resulting pollution in the downstream river. As a result, about 1,400 farmers in the downstream area abandoned rice cultivation in 2018.
The muddy water from the newly opened vents is strongly acidic and high in the concentrations of chloride and sulfate with a remarkable amount of arsenic and some kinds of heavy metals. The mud from the vents is mainly composed of grayish argillaceous particles and elemental sulfur suggesting that it is originated from highly-altered zone related to the geothermal reservoir beneath the volcano.
The vents are still busy gushing the muddy thermal water and vapor/steam as of mid-February 2019, ten months after the eruptive events. Based on our continuous investigation, the overflowing water from the vents is constantly strongly acidic (pH <1) and contains a relatively high concentration of arsenic, although the overflow rate is not constant and changes on occasion. The results of our latest chemical analysis show the water contains around 5 mg/L arsenic. Besides, the spring water in the west flank area of the volcano, which is one of the headwaters of the local river, has become strongly acidic with a rise of volcanic activity. That spring water is also one of the reasons for water pollution in the downstream. As a result, even recently the river water pollution in the foot of the volcano is sometimes reported. The river water pollution thus remains as a problem to be solved both environmentally and economically.

Keywords: Iwo-Yama, Kirishima Volcanoes, Ebino Highland, river water pollution, arsenic

©2019. Japan Geoscience Union. All Right Reserved.

Development of information tools for evacuation and rescue in the event of volcanic disaster

*Yosuke Miyagi[1], Setsuya Nakada[1], Tomohiro Kubo[1], Mitsuhiro Yoshimoto[2], Ryo Honda[2]

1. National Research Institute for Earth Science and Disaster Resilience, 2. Mount Fuji Research Institute, Yamanashi Prefectural Government

Integrated Program for Next Generation Volcano Research (IPNGVR) conducted by Ministry of Education, Culture, Sports, Science and Technology, Japan started in 2016. This project takes notice to not only observation and prediction researches but also research for countermeasure technology of volcano disasters. National Research Institute for Earth Science and Disaster Resilience (NIED) has been in charge of one of the main theme which is named “Development of countermeasure technology for volcano disasters”. In this theme, we develop an information tool for volcano disasters, in which we consider disaster management personnel in local governments as users, and we try to provide appropriate information for them in both the event of disaster and normal times.

In the tragic disaster of Ontake Volcano in 2014, it was difficult for local governments to grasp whereabouts of climbers and to conduct rescue and search for victims. Even recently, climbers can approach to an active vent in many volcanoes in Japan, for example Mt. Fuji, it is quite important to grasp whereabouts of climbers in the event of disaster for proper decision of rescue and search. Experiments to acquire data of climbers in Mt. Fuji have conducted since 2015, named “Mt. Fuji Challenge”. Mt. Fuji is active volcano and gets more than 200,000 of visitors including climbers from all over the world each year. In experiments, we distribute beacons to climbers and receivers which are set in mountain trails detect signals from the beacons, then we can grasp the number and location of climbers who have the beacons. Numbers of beacon which we distributed were 2,300 in 2017 and 14,000 in 2018.

The tool developed in our research use the data from the above experiments as input data, and visualize on GIS software. As a result, it is possible to grasp whereabouts of climbers on map information, including trails, shelters and hazard information from hazard map. Even in normal times, information from the tool can be used for evacuation plans, including establishment of shelters or evacuation routes, instituted by local governments. And, by combining with hazard simulations, we can infer casualties in the event of disaster.
In this presentation, we introduce a summary of the experiments in Mt. Fuji in 2018, and report a progress of the development of the tool.

Keywords: Next Generation Volcano Research, countermeasure technology for volcanic disaster, Mt. Fuji Challenge

©2019. Japan Geoscience Union. All Right Reserved.

Ignimbrite, tephra-fall, caldera and fatalities of major volcanoes in the East and Southeast Asia

*Shinji Takarada[1], Joel Calupas Bandibas[1]

1. Geological Survey of Japan, AIST

Large-scale caldera-forming eruption can cause major destruction within 10 to several 100-km radius from the erupting volcano. The information about the area affected by ignimbrite and tephra falls and size of caldera are useful for future volcanic hazard assessment. Hence, the compilation of data about the distribution of ignimbrite and tephra fall, shape and size of caldera and fatalities caused by volcanic eruptions in East and Southeast Asia is very important.

The G-EVER Promotion Team of the Geological Survey of Japan, AIST is implementing the Asia-Pacific region earthquake and volcanic hazards mapping project, which compiles earthquake source regions, active faults, tephra falls, caldera, ignimbrite, and fatalities caused by earthquake and volcanic events, in collaborations with geohazard research institutes in the Asia-Pacific region. The G-EVER Promotion Team published the 1:10M Eastern Asia Earthquake and Volcanic Hazards Information Map in 2016 (Takarada et al., 2016). The contents of the map can also be viewed or downloaded using the Asia-Pacific Region Earthquake and Volcanic Hazard Information System at http://ccop-geoinfo.org/G-EVER/. The distribution of ignimbrite and tephra fall, shape of caldera and fatality data are updated and available on the site in 2019.

Ignimbrite: The distribution of large-scale ignimbrites (VEI>6) in East and Southeast Asia are compiled. Ignimbrites data are obtained from 19 volcanic caldera-forming eruptions in the region such as Toba 74 ka, Changbaishan 946AD, Tambora 1815AD, Rinjani-Samalas 1257AD, Aso-4, Aso-3, Aira-Ito, Kikai-Koya, Kikai-Nagase, Ata, Toya, Shikotsu 4.6 ka, Kutcharo I, Kutcharo IV, Krakatau 1883AD, Rabaul 7c, Pinatubo 1991AD, Hakone-Tokyo, and Towada-Hachinohe.

Tephra falls: The distribution of large-scale tephra falls (VEI>6) in East and Southeast Asia are compiled. Tephra falls data are obtained from 24 volcanic caldera-forming eruptions in the region such as Toba 74 ka, B-Tm 946AD, Tambora 1815AD, Rinjani-Samalas, Krakatau 1883AD, Rabaul 7c, Pinatubo 1991AD, Long Island 1660AD, Witori-Kimbe2, Ulleung-Oki and Ulleung-Yamato.

Caldera: The shape of major calderas (VEI>6) in East and Southeast Asia are compiled. There are 23 caldera data obtained from volcanoes such as Toba, Tambora, Aso, Aira, Kikai, Ata, Toya, Shikotu, Akan, Kutcharo, Taal, Krakatau, Rinjani-Samalas, Pinatubo, Rabaul, Long Island, Dakataua, Wiroti, Billy Michel, Towada, Mashu, and Moekeshi.

Fatalities: The number of volcanic eruption fatalities and their causes (i.e. pyroclastic flow, debris avalanche, tephra fall, lahar, tsunami, volcanic gas and other reasons) since 1400AD in East and Southeast Asia are complied. The 13 events at 9 volcanoes in Papua New Guinea, 3 events at 2 volcanoes in Solomon Islands, 6 events at 3 volcanoes in Vanuatu, 74 events at 27 volcanoes in Indonesia, 20 events at 6 volcanoes in the Philippines and 36 events at 21 volcanoes in Japan (152 events at 67 volcanoes in total) were compiled.

The data in ESRI shapefile and other formats are available for download at the Asia-Pacific Region

©2019. Japan Geoscience Union. All Right Reserved.

Earthquake and Volcanic Hazard Information System site. The same data with detailed explanation are also available from GSJ open file report. The data are very useful for the various volcanic hazard assessment undertakings.

Figure: Distribution of ignimbrite and shape of Pinatubo caldera after its eruption in 1991AD (Base map provided by the ArcGIS software is used).

Keywords: Ignimbrite, Tephra Fall, Caldera, Fatality, Hazard

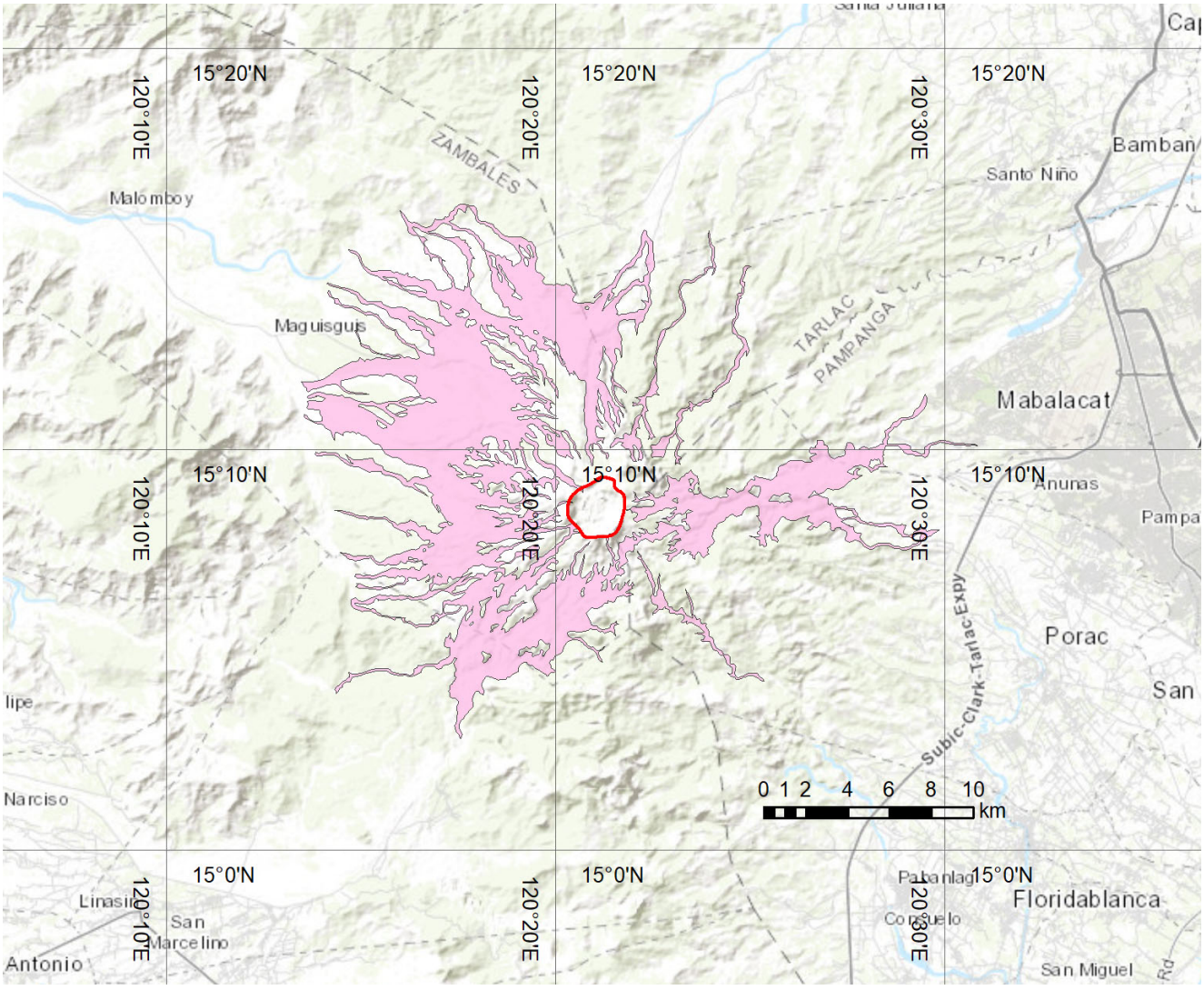

©2019. Japan Geoscience Union. All Right Reserved.

On the climber’ s attitudes to the Volcanic mitigation for active volcanoes.

*Hideyuki Itoh[1], Chizuru Totani[2], Mizuho Arai[2]

1. Faculty of policy studies, Iwate prefectural University, 2. Asia air Survey, Co.Ltd.

Following the Ontake disaster on September 27,2014, the act on active volcano special measures law was revised in 2015, local governments well informed of hazardous area, items for smooth alert evacuation by distributing volcanic hazard map. On the other hand, it is hard to say that the method of transmitting volcanic disaster information to climber is sufficiently under the present circumstances, it is urgent to provide information smoothly in emergency and evacuation method.

We carried out questionnaire survey on the climber in order to know the attitudes to the volcanic mitigation for active volcanoes. 74 respondents were collected at Kurikoma volcano, and 84 respondents were collected at Akita-Komagadake volcano.

At the result, climber in Akita –Komagadake, more than 62 percent of respondents visited from both Iwate and Akita prefecture, whereas in Kurikoma volcano, 56 percent of respondents visited from Kanto area by the large –scale bus with a sightseeing tour.

More than 67 percent of climbers have not issued climbing notifications in both volcanoes.
It is clear that the 40 percent of respondents in Kurikoma volcano, 25 percent of respondents in Akita –Komagadake climber are not recognized where they are climbing as active volcano, and eruption alert level is not also well understood.

©2019. Japan Geoscience Union. All Right Reserved.

[J] Poster | S (Solid Earth Sciences)：S-VC Volcanology

Mon. May 27, 2019 10:45 AM - 12:15 PM JST | Mon. May 27, 2019 1:45 AM - 3:15 AM UTC | Poster Hall International Exhibition Hall8, Makuhari Messe_3

[S-VC38] Active Volcanism

convener:Yuta Maeda(Nagoya University), Takahiro Miwa(National research institute for earth science and disaster prevention), Takeshi Nishimura(Department of Geophysics, Graduate School of Science, Tohoku University)

This session discusses various aspects of active volcanisms including, but not limited to, recent and historical eruptions, various phenomena associated with the volcanic activities, underground structures of the volcanoes, and developments of new instruments based on geophysical, geochemical, geological, and multidiscipline approaches. We also welcome studies on understanding and predicting the transitions of the eruptive activities from observational, theoretical, and experimental approaches.

[SVC38-P01] The structure of Showa-Shinzan Yaneyama Usu by seismic reflection surveys

*Ryuichi Takei[1], Tomoki Tsutsui[1,2], Yuya Tada[2], Tomoya Moriwaki[2], Yosuke Aoki[3], Hiroshi Aoyama[4], Go Maruyama[5] (1.Graduate School of International Resource Sciences, The University of Akita, 2.Faculty of International Resource Sciences, The University of Akita, 3.Earthquake Research Institute, The University of Tokyo, 4.Graduate school of Science, The University of Hokkaido, 5.Marutec Co., Ltd.)

[SVC38-P02] Ground deformation associated with the 2014-2015 and the 2018-2019 volcanic activities at Azumayama

*Jun Okada[1], Shigeo Matsuura[2], Katsuya Ohmi[2], Takuya Yamamura[2], Yu Nihara[3], Susumu Seki[3] (1.Volcanology Research Department (Sendai Office), Meteorological Research Institute, JMA, 2.Seismology and Volcanology Division, Sendai Regional Headquarters, JMA, 3.Regional Volcanic Observation and Warning Center, Sendai Regional Headquarters, JMA)

[SVC38-P03] BP-type and BT-type volcanic earthquakes in Azumayama

*Yusuke Yoshigai[1], Yuichi Morita[2], Katsuya Ohmi[3], Yu Nihara[4], Tsukasa Kobayashi[1] (1.Volcanological Division, Japan Meteorological Agency, 2.Earthquake Research Institute, University of Tokyo, 3.Seismology and Volcanology Division, Sendai Regional Headquarters, Japan Meteorological Agency, 4.Regional Volcanic Observation and Warning Center, Sendai Regional Headquarters, Japan Meteorological Agency)

[SVC38-P04] The occurrence and petrology of the fine-grained pyroclastic materials of the Futatsudake-Shibukawa eruption in Haruna volcano.

*Teruyoshi Maruyama[1], Yuki Suzuki[2] (1.Department of Earth Sciences, School of Education , Waseda University, 2.Department of Earth Sciences, Faculty of Education and Integrated Arts of Sciences, Waseda University)

[SVC38-P05] The occurrence and petrology of the block and ash flow deposit from the Futatsudake-Shibukawa eruption, Haruna volcano

*Yuki Suzuki[1], Ryouto Fukushima[2] (1.Department of Earth Sciences, Faculty of Education and Integrated Arts of Sciences, Waseda University, 2.Department of Earth Sciences, School of Education, Waseda University)

[SVC38-P06] Report of Volcanic Activity at Kusatsu-Shiranesan in 2018

*Tsukasa Kobayashi[1], Koji Kato[1], Koichi Suemine[1], Kazuhiro Kimura[1], Yusuke Yoshigai[1], Yasuo Ogawa[2], Kenji Nogami[2], Wataru Kanda[2], Akihiko Terada[2] (1.Volcanological Division, Japan Meteorological Agency, 2.Volcanic Fluid Research Center, Tokyo Institute of Technology)

[SVC38-P07] Noble gas isotope composition of fumaroles and hydrothermal gases around Kusatsu-Shirane volcano

*Kotaro Toyama[1], Hirochika Sumino[1], Kaori Kawana[1], Yoshihide Akiyama[1], Takeshi Ohba[2], Muga Yaguchi[3], Akihiko Terada[4] (1.Department of Basic Science, Graduate School of Arts and Sciences, The University of Tokyo, 2.Department of chemistry, School of Science, Tokia University, 3.Meteorological Research Institute, 4.Volcanic Fluid Research Center, Tokyo Institute of Technology)

[SVC38-P08] Self-potential and geomagnetic total intensity observations at Motoshirane volcano after the 2018 eruption

*Akira Yamazaki[1], Hideki Iino[1], Tatsurou Tanaka[1] (1.Kakioka Magnetic Observatory)

[SVC38-P09] Eruption processes of the 3rd and 4th stage of Niigata-Yakeyama Volcano, Japan, inferred from microlite texture and chemical composition

*Takumi Yoshida[1], Takeshi Saito[1] (1.Shinshu University)

[SVC38-P10] Estimation of subsurface structure of Shinyu crater lake, Tateyama Caldera, based on the water level and seismic observation data

*Ryohei Kawaguchi[1], Naoko Saito[2], Shin'ya Onizawa[1] (1.Meteorological Research Institute, 2.Toyama local Meteorological office, Japan Meteorological Agency)

[SVC38-P11] Real time monitoring of underground temperature in Jigokudani, Midagahara volcano using LPWA devices

*Tohru Watanabe[1], Toyama branch NTT West[2] (1.Gradudate School of Science and Engineering, University of Toyama, 2.Nippon Telegraph and Telephone West Corporation)

[SVC38-P12] Varying chemical and isotopic compositions of fumarolic gases from the summit and from the 1962-63 eruptive vents at Yakedake Volcano, Japan

*Takeshi Saito[1], Shun Sawamura[2], Kazuhiro Amita[3], Taketoshi Mishima[4], Shinji Ohsawa[4] (1.Institute of Science, Academic Assembly School of Science and Technology, Shinshu University, 2.Graduate School of Science and Technology, Shinshu University, 3.Graduate School of Engineering Science, Akita University, 4.Beppu Geothermal Research Laboratory, Institute for Geothermal Sciences, Graduate School of Science, Kyoto University)

[SVC38-P13] Eruption age determination of the latest two lava flows and characteristics of volcaniclastic materials from the recent activity of Yokodake Volcano, Japan

*Hiroya Nitta[1], Takeshi Saito[1], Yorinao Shitaoka[2] (1.Shinshu University of Science and Technology, 2.Department of Environment System, Faculty of Geo-environmental Science, Rissho University)

[SVC38-P14] Estimating the date of the 2007 eruption of Mount Ontake Volcano using waveform correlation

*Shuhei Nishijima[1], Toshiko Terakawa[1], Shinichiro Horikawa[1] (1.Graduate School of Environmental Studies, Nagoya University)

[SVC38-P15] Seismic activity beneath Mt. Ontake volcano before and after the 2007 and 2014 eruptions

*Yoshiko Yamanaka[1], Shinichiro Horikawa[1], Yuta Maeda[1] (1.Graduate School of Encironmental Studies, University of NAGOYA)

[SVC38-P16] Effect of rain and snowmelt correction of tiltmeter data
- Application example for Ontakesan Volcano -

*Kazuhiro Kimura[1,5], Katsuhisa Kawashima[2], Takane Matsumoto[2], Akihiko SASAKI[4], Tsutomu Iyobe[3], Junichi Miyamura[1], Masaki Nakahashi[1] (1.Japan Meteorological Agency, 2.Research Institute for Natural Hazards and Disaster Recovery, Niigata University, 3.Faculty of Engineering, Kyoto University,

4.Department of Geography and Environmental Studies, Kokushikan University, 5.Graduate School Science and Technology, Niigata University)

[SVC38-P17] **Spatial Variation of b-value around Mt. Fuji influenced by the Eastern Shizuoka Earthquake of 15 March 2011**

*Takumi Murakoshi[1], Tomonari Miyashita[2] (1.National Defense Academy, 2.JASDF)

[SVC38-P18] Present condition of submarged volcano, Teishi Knoll, off Ito, Eastern Izu Peninsula

*Toshiro Yamanaka[1], Yoshifumi Kawada[2], Takuro Noguchi[3], Mayumi Hatta[3], Kei Okamura[3] (1.Tokyo Univ. Marine Science and Technology, 2.Tohoku University, 3.Kochi University)

[SVC38-P19] Descriptions and age of volcanic products before the caldera formation in the northern part of Izu-Oshima, off Tokyo, Pacific Ocean

*Satoshi Terayama[1], Takehiko Suzuki[1], Makoto Kobayashi[2] (1.Tokyo Metropolitan University, 2.Research Center for Volcanic Hazards and Their Mitigation, Tokyo Metropolitan University)

[SVC38-P20] Time change of p-value by Schuster method using earthquakes around Izu-Ohsima summit

*Hiroyuki Takayama[1] (1.Volcanological Division 1st labolatory, Meteorological Research Institute)

[SVC38-P21] Standard stratigraphy and characteristic properties of late Quaternary tephras on the Niijima-island: Report of geochemistry and refractive indices of volcanic glass shards, orthopyroxene, hornblende, and cummingtonite

*Kaori Aoki[1], Makoto Kobayashi[1], Fumikatsu NISHIZAWA[1,2], Masanori Murata[1], Daisuke Ishimura[1], Takehiko Suzuki[1] (1.Research Center for Volcanic Hazards and Their Mitigation, Tokyo Metropolitan University, 2.Mount Fuji Research Institute, Yamanashi Prefectural Government)

[SVC38-P22] **Tephrostratigraphy and its eruption history of the Latest Activity in the Kozushima Volcano, the Izu Islands**

*Makoto Kobayashi[1], Masanori Murata[1], Fumikatsu NISHIZAWA[2], Takehiko Suzuki[1,3] (1.Research Center for Volcanic Hazards and their mitigations, Tokyo Metropolitan Univ., 2.Fuji Research Institute, Yamanashi Prefectural Government, 3.Department of Geography, Tokyo Metropolitan Univ.)

[SVC38-P23] Characteristics of hypocenter distribution connected with velocity structures in and around Miyakejima, Kozushima and Hachijojima volcanoes

*Hiroko Hagiwara[1], Hidefumi Watanabe[1] (1.Tokyo Metroplitan Government)

[SVC38-P24] Deformation of Miyakejima volcano measured by GNSS campaign observation (2013-2015)

*Haruna Watanabe[1], Takeshi Matsushima[2], Miyo Fukui, Atsushi Watanabe[3], Jun Oikawa[3], Takashi OKUDA[4], Taku Ozawa[5], Yosuke Miyagi[5] (1.Department of Earth and Planetary Sciences, Graduate School of Science, Kyushu University, 2.Institute of Seismology and Volcanology, Faculty of Sciences, Kyushu University, 3.Earthquake Research Institute, University of Tokyo, 4.Earthquake and Volcanology Research Center, 5.National Research Institute for Earth Science and Disaster Resilience)

[SVC38-P25] Characteristic properties of distal and proximal tephras in the Mikurajima Island, Izu Islands.

*Tomohiro Tano[1], Takehiko Suzuki[1,2], Makoto Kobayashi[2], Masanori Murata[2] (1.Faculty of Urban Environmental Sciences, Tokyo Metropolitan University, 2.Research Center for Volcanic Hazards and Their Mitigation, Tokyo Metropolitan University)

[SVC38-P26] Pseudo thermal anomalies in the shortwave infrared bands of the Himawari-8 AHI and their correction for volcano thermal observation

*Takayuki Kaneko[1], ATSUSHI YASUDA[1], Yoshizaki Yoshito[2], Takasaki Kenji[3], Yoshiaki HONDA[4] (1.Earthquake Research Institute, University of Tokyo, 2.Meteorological Satellite Center, Japan Meteorological Agency, 3.Japan Fisheries Research and Education Agency, 4.Center for Environmental Remote Sensing, Chiba University)

[SVC38-P27] Shallow earthquakes in Unzen Volcano inferred from dense seismic observation and resistivity structure

*Hashimoto Tasuku[1], Koki Aizawa[2], Takeshi Matsushima[2], Hiroshi Shimizu[2], Yuto Hayashida[1], Yuhei Yuasa[1], Kaori Tsukamoto[1], Yuto Yamamoto[3], Kanta Miyano[3], Megumi Kamizono[1], Satoshi Matsumoto[2] (1.Department of Earth and Planetary Sciences, Graduate School of Science, Kyushu University, 2.Institute of Seismology and Volcanology, Faculty of Science, Kyushu University, 3.Department of Earth and Planetary Sciences, School of Science, Kyushu University)

[SVC38-P28] Characteristics of shallow volcanic earthquakes beneath the summit of Unzen Volcano

*Kanta Miyano[1], Hiroshi Shimizu[2], Takeshi Matsushima[2], Satoshi Matsumoto[2], Koki Aizawa[2], Hashimoto Tasuku[3], Yuto Hayashida[3], Yuhei Yuasa[3] (1.Department of Earth and Planetary Sciences, School of Science, Kyushu University, 2.Institute of Seismology and Volcanology, Faculty of Science, Kyushu University, 3.Department of Earth and Planetary Sciences, Graduate School of Science, Kyushu University)

[SVC38-P29] Pyroclastic deposits and the stratigraphy on the outcrop to north east from Mt.Unzen

*Daisuke Nagai[1] (1.Mt.Unzen disaster memorial hall)

[SVC38-P30] Relative gravity changes in Aso Volcano (Kumamoto Prefecture) observed from 2015 to 2018

*Yusuke Miyauchi[1], Takahito Kazama[1], Yoichi Fukuda[1], Shin Yoshikawa[2], Takahiro Ohkura[2], Jun Nishijima[3], Yasuhiro Fujimitsu[3] (1.Graduate School of Science, Kyoto University, 2.Aso Volcanological Laboratory, Kyoto University, 3.Graduate School of Engineering, Kyushu University)

[SVC38-P31] Precise leveling survey in Aso volcano, 2018

*Takahiro Ohkura[1], Shin Yoshikawa[1], Hiroyuki Inoue[1], Akihiko Yokoo[1], Mitsuru Utsugi[1], Keigo Yamamoto[2], Kazunari Uchida[4], Yuta Maeda[5], Shinichiro Horikawa[5], Kenjiro Matsuhiro[5], Takashi OKUDA[5], Kazushi Tanoue[5], Fumiaki Kimata[7], Masayuki Murase[6], Hitoshi Mori[6], Taketoshi Mishima[3], Shintaro Komatsu[2], Masaki Takaya[3], Jun Oikawa[8], Kyoka Ishii[3], Yusuke Miyauchi[3], Ikuma Kimura[3], Masaki Uchida[3], Kazuho Nakai[3], Kosei Takishita[3], Keita Chiba[4], Hashimoto Tasuku[4], Yoshinosuke Kamiya[4], Yuto Yamamoto[4] (1.Aso Volcanological Laboratory, Institute for Geothermal Sciences, Graduate School of Science, Kyoto University, 2.DPRI, Kyoto University, 3.Graduate School of Science, Kyoto University, 4.Graduate School of Science, Kyushu University, 5.Graduate School, Nagoya University, 6.College of Human and Society, Nihon University, 7.TRIES, 8.ERI,Univ.of Tokyo)

[SVC38-P32] Magma evolution during the Aso-3 caldera-forming eruption cycle deduced from the chemistry of plagioclase phenocrysts

*yuki matsukida[1], Tsuyoshi Iizuka[1], Takayuki Ushikubo[2], Kenji Shimizu[2], Nobuo Geshi[3], Isoji MIYAGI[3], Morihisa Hamada[2] (1.the University of Tokyo, 2.Japan Agency for Marine-Earth and Science Technology, 3.The National Institute of Advanced Industrial Science and Technology)

[SVC38-P33] Relationship between duration of eruption tremor and eruption volume

*Azusa Mori[1], Hiroyuki Kumagai[1] (1.Nagoya University Environmental Studies)

[SVC38-P34] Crustal deformation accompanied with the eruption of Shinmoe-dake in early March 2018

*Tsuyoshi Watanabe[1], Takashi Yokota[1], Susumu Kurahashi[1], Kenta Enomoto[1] (1.Aichi Institute of Technology)

[SVC38-P35] Sources under Iwo-yama, Kirishima Volcanoes derived from GNSS observation and Precise leveling survey.

*Yuki Koga[1], Takeshi Matsushima[2], Kazunari Uchida[2], Dan Muramatsu[1], Yuichi Iwasa[1] (1.Department of Earth and Planetary Sciences, Graduate School of Science, Kyushu university , 2.Institute of Seismology and Volcanology, Faculty of Science, Kyushu University)

[SVC38-P36] Regional vertical deformation around Aira caldera from GNSS data

*Kazuho Nakai[1], Masato Iguchi[2], Takahiro Ohkura[3] (1.Division of Earth and Planetary Sciences, Graduate School of Science, Kyoto University, 2.Sakurajima Volcano Research Center, Disaster Prevention Research Institute, Kyoto University, 3.Aso Volcanological Laboratory, Institute for Geothermal Sciences, Graduate School of Science, Kyoto University)

[SVC38-P37] Vertical ground deformation in Sakurajima volcano measured by precise leveling survey (during Nov. 2017 - Nov. 2018)

*Keigo Yamamoto[1], Takeshi Matsushima[2], Shin Yoshikawa[3], Hiroyuki Inoue[3], Tadaomi Sonoda[1], Kosei Takishita[1], Kazuho Nakai[1], Masaki Uchida[3], Ryo Oyanagi[3], Yoshinosuke Kamiya[2], Takahiro Ohkura[3] (1.Disaster Prevention Research Institute, Kyoto University, 2.Fuculty of Sciences, Kyushu University, 3.Gruduate School of Science, Kyoto University)

[SVC38-P38] Spatiotemporal gravity variations from the 1990s in Sakurajima Volcano, revealed by repeated relative gravity measurements

*Ryo Oyanagi[1], Takahito Kazama[1], Keigo Yamamoto[2], Hiromitsu Oshima[3], Kazumi Okada[3], Tadaomi Sonoda[2], Masato Iguchi[2] (1.Graduate School of Science, Kyoto University, 2.DPRI, Kyoto University, 3.ISV, Hokkaido University)

[SVC38-P39] Investigation into the crater of Sakurajima volcano during eruption using UAV

*Shunsuke Miura[1], Takumi Mochiduki[1], Kouji Fujita[1], Toshihiro Urayama[1], Hisashi Sasaki[1], Tatsuro Chiba[1] (1.Asia Air Survey Co.,Ltd)

[SVC38-P40] **Seismic refraction and wide-angle reflection experiment in southern Kyushu, Japan: (3) the 2018 exploration report**

*Hiroki Miyamachi[1], Hiroaki Takahashi[2], Hiroshi Aoyama[2], Mako Ohzono[2], Takahiro Shiina[6], Masamitsu Takada[2], Masayoshi Ichiyanagi[2], Teruhiro Yamaguchi[2], Yuki Susukida[2], Saito Kazuma[2], Chihiro Ito[2], Yoshio Murai[2], Tatsuya Nakagaki[2], Tomoki Tsutsui[3], Ryuichi Takei[3], Yuuya Tada[3], Mare Yamamoto[4], Satoshi Hirahara[4], Takashi NAKAYAMA[4], Ryosuke Azuma[4], Syuichi Suzuki[4], Toshinori Sato[5], Eiji Kurashimo[6], Miwako Ando[6], Shinichi Tanaka[6], Satoshi Ikezawa[6], Tomoaki Yamada[6], Kazuo Nakahigashi[7], Yuta Maeda[8], Shinichiro Horikawa[8], Kenjirou Matsuhiro[8], Takashi OKUDA[8], Shuhei Tsuji[8], Naoki Sogawa[8], Hiroshi Katao[9], Takuo Shibutani[9], Tsutomu Miura[9], Nakagawa Jun[9], Itaru Yoneda[9], Takeshi Tameguri[9], Kosei Takishita[9], Kazuho Nakai[9], Yusuke Yamashita[9], Takeshi Matsushima[10], Kazunari Uchida[10], Rintaro Miyamachi[10], Hiroshi Yakiwara[1], Shuichiro Hirano[1], Takeshi Kubo[1], Kenyu Sakao[1] (1.Kagoshima University, 2.Hokkaido University, 3.Akita University, 4.Tohoku University, 5.Chiba University, 6.University of Tokyo, 7.Tokyo University of Marine Science and Technology, 8.Nagoya University, 9.Kyoto University, 10.Kyushu University)

[SVC38-P41] Flow and emplacement mechanism of Koya Ignimbrite

*Keiko Suzuki-Kamata[1], Reina NAKAOKA[1], Tomomi Yamane[2] (1.Kobe Ocean-Bottom Exploration Center , 2.Department of Planetology, Graduate School of Science, Kobe University)

[SVC38-P42] Investigating Origin of landslide-like bathymetric feature at southern Mt.Kaimon using bathymetric and multichannel seismic reflection surveys

*hiroto yamaguchi[1], Satoshi Shimizu[2], Hikaru Iwamaru[2], Mamoru Sano[2], Nobukazu Seama[3,2], Misaki Horiuchi[3], Tetsuo Matsuno[2,3], Yoshiyuki Tatsumi[2,3] (1.Department of Planetology, Faculty of Science, Kobe university, 2.Kobe ocean-bottom exploration center, 3.Department of Planetology, Graduate School of Science, Kobe university)

[SVC38-P43] Occurrence and distribution of pyroclastic fall deposits of Kuchinoerabujima volcano 2018-2019 eruption

*Masashi NAGAI[1], Shojiro Nakagawa[2], Yu Iriyama[1], Takahiro Miwa[1], Toshikazu Tanada[1], Hideki Ueda[1], Setsuya Nakada[1] (1.Volcano Research Department, National Research Institute for Earth Science and Disaster Resilience, 2.Yakushima Chigaku Club)

[SVC38-P44] Ground Deformation around Domestic Active Volcanoes detected by InSAR of ALOS-2/PALSAR-2

*Takafumi Taniguchi[1], Isao Kageyama[1], Okuyama Satoshi[2], Shinobu Ando[2] (1.Japan Meteorological Agency, 2.Meteorological Research Institute)

[SVC38-P45] **Volcano-hydrothermal inflation revealed by the spatial variation of stress field at the Tatun Volcano Group, northern Taiwan**

*Hsin-Chieh Pu[1], Cheng-Horng Lin[2,3,4,5], Ya-Ju Hsu[2], Li-Chin Chang[3] (1.Central Weather Bureau, Taiwan, ROC., 2.Institute of Earth Sciences, Academia Sinica, Taipei, Taiwan, ROC., 3.Taiwan Volcano Observatory at Tatun, Taipei, Taiwan, ROC., 4. Department of Geosciences, National Taiwan University, Taipei 10617, Taiwan, ROC., 5.National Center for Research on Earthquake Engineering, National Applied Research Laboratories, Taipei, Taiwan, ROC.)

[SVC38-P46] Topographic change and crustal deformation associated with December 2018 eruption of Krakatau volcano in Indonesia

*Hiroshi Yarai[1], Tomokazu Kobayashi[1], Shinya Yamada[1] (1.GSI of Japan)

The structure of Showa-Shinzan Yaneyama Usu by seismic reflection surveys

*Ryuichi Takei[1], Tomoki Tsutsui[1,2], Yuya Tada[2], Tomoya Moriwaki[2], Yosuke Aoki[3], Hiroshi Aoyama[4], Go Maruyama[5]

1. Graduate School of International Resource Sciences, The University of Akita, 2. Faculty of International Resource Sciences, The University of Akita, 3. Earthquake Research Institute, The University of Tokyo, 4. Graduate school of Science, The University of Hokkaido, 5. Marutec Co., Ltd.

Reflection seismic surveys at Usu-Showashinzan-Yaneyama was conducted in order to, estimate the shallow structure of the lava-dome base. Usu-Showashinzan is a young volcano formed in 1943-1945. It is characterized by consisting of a lava dome structure with top elevation of about 406.9m and a bun-shaped plateau called Yaneyama. Various geophysical explorations and geological surveys have been carried out in Showa-Shinzan until now, and the formation process and the supply route of magma have been discussed. However, the details of structure beneath Yaneyama are still unknown.
Total of 4 lines were conducted in 2017 and 2018 with 2 lines each, and seismic data were acquired. Two observation lines (Y17 and Y18) were set in the east-west direction on the east foot of the lava dome and two (G17 and G18) in the Guren-valley on the southwest foot of the lava dome. Both survey lines (Y17, G17) were conducted in 2017 with 24 receivers with using a hammer of 6.3kg as the seismic source. Other survey lines (Y18, G18) conducted in 2018 with 48 receivers with using a tamping rammer (MT-55L by Mikasa Industries) as the seismic source. Split-spread method was applied in all seismic lines. The receiver interval was 4m for Y lines and 3m for G lines. SU (Seismic Un*x) software was used for the seismic reflection analysis of the acquired seismograms. For 2018 lines with using tamping rammer, preprocessing is necessary before analysis of seismic reflection. That is based on the principle “SOSIE” (Yokokawa et.al. 1983).
As the result, the time sections on all the survey lines were obtained. Especially, in the G18 line, reflection profile down to 100m depth, which shows gentle valley structure in the middle of the line down to 80m depth and there is almost horizontal boundary at 100m depth.
The refraction tomography analysis and considering previous researches are going to be conducted.

Keywords: Seismic reflection survey, Showa-Shinzan

©2019. Japan Geoscience Union. All Right Reserved.

Ground deformation associated with the 2014-2015 and the 2018-2019 volcanic activities at Azumayama

*Jun Okada[1], Shigeo Matsuura[2], Katsuya Ohmi[2], Takuya Yamamura[2], Yu Nihara[3], Susumu Seki[3]

1. Volcanology Research Department (Sendai Office), Meteorological Research Institute, JMA, 2. Seismology and Volcanology Division, Sendai Regional Headquarters, JMA, 3. Regional Volcanic Observation and Warning Center, Sendai Regional Headquarters, JMA

Azumayama is a basaltic to andesitic active volcano located in the volcanic front on the Tohoku (NE Japan) Arc. Historical eruptions occurred mainly in and around O-ana crater in the south flank of Issaikyosan. No eruption occurred for more than 40 years after the last one on December 1977. However, various volcanic phenomena have been observed in recent years. Repeated GPS surveys revealed local inflation-deflation around O-ana crater which plays in a cycle of 2-3-year and corresponds to the increase-decrease of seismicity during 2003-2009. Yoshida *et al.* (2012) estimated the pressure source 200 to 600 meters beneath the O-ana crater. This shows a good agreement with the thermal demagnetization source studied by Yamazaki *et al.* (2010). Monochromatic earthquakes were observed when fumarolic activity of O-ana crater was high during 2008-2011 (e.g. Ueki *et al.*, 2010). By analyzing the frequencies of these earthquakes Torimoto (2016) is beginning to understand the characteristics of shallow hydrothermal systems, a potential hotbed for phreatic eruptions. In more recent years, there are two volcanic unrests such as the 2014-2015 and the 2018-2019 activities. JMA released “Near-crater Warning” and raised Volcanic Alert Level from 1 to 2 on December 2014 and September 2018, respectively.

The start of the 2014-2015 activity can be marked by the slight tilt change at Jododaira station, 750m ESE from O-ana Crater. It showed East-downward ground deformation since late July 2014. Continuous GNSS measurements also captured local inflation around Issaikyosan since September 2014. Seismic activity started on middle October and culminated from December 2014 to middle January 2015. Similarly, the 2018-2019 activity can be recognized by the tilt data of Jododaira. A slow East-downward ground deformation started since May 2018. The tilting rate was significantly increased after the occurrence of the volcanic tremor on 22 July 2018 and remained almost constant (at least at the time of writing). Continuous GNSS data suggested also an inflation of the volcanic edifice since May 2018. The shallow seismicity started since middle August 2018 and remained active (at least at the time of writing).

Strong similarity exists in deformation characteristics between the 2014-2015 and the 2018-2019 activities, that is the dilatational ground deformation, both preceded to the activation of shallow seismicity. Except for the beginning of the activities tilting is maintained with almost the same rate and direction for more than several months. However, several discrepancies should be remarked: (1) Volcanic tremors are more frequent in the 2018-2019 than the 2014-2015. (2) The 2018-2019 activity may be triggered by a remarkable coincidental tilt change (about 1 micro radian at Jododaira station) and the associated volcanic tremor on 22 July 2018. (3) Slight tilt changes which may suggest a deep deflation of Azumayama were clearly observed at distant stations on the foot of Adatarayama, a neighboring volcano in the 2018-2019. These observational evidences may indicate the different volcanic processes in both activities. Regarding (3), other field observation results such as both the increase of SO_2/H_2S since late July 2018 and the enlargement of geothermal areas around O-ana crater can be triggered by the intermittent injection of volcanic fluids (e.g. hot volcanic gasses) from the depth of Azumayama. Results of both tilt and continuous GNSS observations will be presented in the session.

©2019. Japan Geoscience Union. All Right Reserved.

Keywords: Azumayama, deformation, GNSS, tiltmeters, volcanic earthquakes

©2019. Japan Geoscience Union. All Right Reserved.

BP-type and BT-type volcanic earthquakes in Azumayama

*Yusuke Yoshigai[1], Yuichi Morita[2], Katsuya Ohmi[3], Yu Nihara[4], Tsukasa Kobayashi[1]

1. Volcanological Division, Japan Meteorological Agency, 2. Earthquake Research Institute, University of Tokyo, 3. Seismology and Volcanology Division, Sendai Regional Headquarters, Japan Meteorological Agency, 4. Regional Volcanic Observation and Warning Center, Sendai Regional Headquarters, Japan Meteorological Agency

At Azumayama located on the prefectural boundary between Yamagata and Fukushima prefectures, volcanic tremors occurred on 22 July 2018. Changes in tiltmeter data from Joudodaira Station (around 1 km ESE of the Oana crater) indicated ground deformation with a remarkable rising trend in the direction toward the crater. Volcanic seismicity has mostly remained at high levels since August 2018, and volcanic activity has remained at high levels. Japan Meteorological Agency (JMA) issued a Near-crater Warning on 13 September and raised the Volcanic Alert Level from 1 (Potential for increased activity) to 2 (Do not approach the crater).

There are mainly three types of volcanic earthquakes in the vicinity of the Oana crater: the BH-type in which the dominant frequency is high, the BL-type in which the dominant frequency is low, and the BP-type / BT-type with the harmonic waveform. These volcanic earthquakes occur roughly at depths of less than 1 km.

From July to October 2018, BH-type earthquakes mainly occurred, and the proportion of BL-type earthquakes and BP-type / BT-type earthquakes slightly increased in November. After that, the proportion of the BL-type earthquakes decreased, but the proportion of the BP-type / BT-type earthquakes further increased. The proportion of the BP-type / BT-type earthquakes to the whole volcanic earthquakes is 25% in November and 50% since December, and it continues high levels. The BP-type / BT-type earthquakes that occurred after July 2018 have various types of characteristics, such as damped harmonic oscillators with a single frequency peak seen in the BP-type / BT-type earthquakes occurred from 2010 to 2011, damped harmonic oscillators with multiple frequency peaks and those with high-frequency earthquake near the beginning of the earthquake, and no systematic change of the dominant frequency can be observed. In this presentation, we introduce what we found as the results of focusing on waveform shape and amplitude ratio for the BP-type / BT-type earthquakes that occurred after July 2018.

In this research, under the agreement on collaboration and cooperation in the field of seismic / volcanic disaster prevention research between Earthquake Research Institute (ERI), the University of Tokyo and Seismology and Volcanology Department, JMA, I used facilities of ERI and discussed with the people of ERI. I express my gratitude to everyone involved.

Keywords: Azumayama, Volcanic Earthquake, N-type Earthquake

©2019. Japan Geoscience Union. All Right Reserved.

The occurrence and petrology of the fine-grained pyroclastic materials of the Futatsudake-Shibukawa eruption in Haruna volcano.

*Teruyoshi Maruyama[1], Yuki Suzuki[2]

1. Department of Earth Sciences, School of Education , Waseda University, 2. Department of Earth Sciences, Faculty of Education and Integrated Arts of Sciences, Waseda University

Haruna volcano is an active volcano of Quaternary which is located in the southern end of the NE Japan arc. Haruna volcano has 500000 years active time. Geshi and Takeuchi (2012) showed the activity is classified into older period (500-240ka), and newer period (45ka-) following activity halt of about 200,000 years. The newest activity in Haruna volcano is Shibukawa eruption (late 5th to early 6th century) and Ikaho eruption (late 6th to early 7th century), both of which occurred at the location of present Futatsudake (ages by Geshi and Oishi (2011)). Occurrences of ejecta from two eruption, as described in Soda (1989), indicate the different manner of pyroclastic flow generation; explosive destruction of the lava dome in the Shibukawa eruption, while column collapse in the Ikaho eruption. Suzuki and Nakada (2007) carried out detailed petrological study for the Ikaho eruption. They proposed mush-like felsic magma was remobilized by the injection of mafic magma. The important point in the eruption triggering was that mixed magma and heated magma with considerably lower viscosity than the original mush-like magma opened the vent, resulting in the decompression of whole felsic magma reservoir. However, no study has revealed the magma plumbing system and the eruption triggering process of the Shibukawa eruption. For the purpose of understanding these points, we have conducted the petrological study of the Shibukawa eruption. In particular, in this research, in order to clarify the progress of eruption and the temporal change of the erupted magma, fine-grained pyroclastic materials were studied rather than pumice blocks in the block and ash flow (BAF).

We sampled fine-grained pyroclastic deposits at four sites locating at the northeastern to eastern foot of Haruna volcano. All sites locate at the periphery of BAF mapped in Soda (1989). Therefore, our investigated sites correspond to the region where pyroclastic surge deposit emplaces (example of Unzen 1991-1995 eruption; Fujii and Nakada, 1999). We could observe the basal part of fine-grained pyroclastic material in three sites. In all sites, the strata were divided into multiple units according to their facies. The juvenile pumice clasts, the coarse part of the deposit, had variation in color (white, gray, light gray). We measured whole rock compositions of the pumice samples and found they are felsic andesite (SiO_2 =60.7-61.9wt.%; N=22). Thin sections were prepared for ten representative pumices and one volcanic ash sample. It is necessary to study the volcanic ash sample, because it is not possible to discuss the change in magma composition from lower to the upper layer, only with the pumice clasts for which whole-rock chemical analyses were performed. The phenocryst phases (Pl+Opx+Am+Fe-Ti Ox) in all samples form aggregates, so when they crystallized, they were in equilibrium. We observed free crystals (Pl+Opx+Am), pumice particles, and lava particles in the thin sections of volcanic ash. All thin sections of pumice and ash include the dusty zone of Pl, so these products resulted from either through magma mixing (between felsic and mafic magmas) or the heating of felsic magma by the mafic magma. In four out of five samples of gray pumice, breakdown reaction rims of amphibole and groundmass crystals were confirmed, so magma that formed gray pumice likely underwent a different ascending process in conduit, in comparison with the magma that formed white pumice.

Suzuki and Fukushima (2019, this conference) studied pumice blocks in the BAF from the Futatsudake-Shibukawa eruption. This result is similar to our result. Therefore, we infer magmas formed these two products was homogeneous in magma chamber. The original pyroclastic flow was separated into rock mass flow and pyroclastic surge as they descended river valleys, resulting in simultaneous

©2019. Japan Geoscience Union. All Right Reserved.

emplacement of the BAF and fine-grained pyroclastic materials at different distances from the river valleys.

Keywords: Haruna volcano, Block and ash flow, Pyroclastic surge, Magma mixing, Heating from hotter magma, Eruption trigger

©2019. Japan Geoscience Union. All Right Reserved.

The occurrence and petrology of the block and ash flow deposit from the Futatsudake-Shibukawa eruption, Haruna volcano

*Yuki Suzuki[1], Ryouto Fukushima[2]

1. Department of Earth Sciences, Faculty of Education and Integrated Arts of Sciences, Waseda University, 2. Department of Earth Sciences, School of Education, Waseda University

Haruna volcano is located in the southern end of the NE Japan arc. The latest two eruptions occurred at Futatsudake; Shibukawa eruption in late 5th to early 6th century (0.4 DRE km^3), and Ikaho eruption in late 6th to early 7th century (0.99 DRE km^3)(ages from Geshi and Oishi, 2011; volumes from Yamamoto, 2013). Suzuki and Nakada (2007) conducted petrological study of Ikaho eruption to reveal eruption triggering process. First, injection of mafic magma into the mush-like felsic magma generated mixed magma and heated felsic magma. Then, these low viscosity magmas opened the conduit and vent, resulting in the decompression of whole reservoir. It is indispensable to study two eruptions from a continuous view point, because two eruptions occurred from the same place at an interval of only several decades.

The outcrops of the Shibukawa eruption are categorized into those consisting of block-and-ash-flow (BAF) deposit (this presentation) and those consisting of fine pyroclasts derived from pyroclastic surge and phreatic explosion (Maruyama and Suzuki, 2019; this conference). Outcrops of BAF deposit locate in the vicinity of river valleys, while outcrops of fine pyroclasts locate away from the valleys. The BAF deposit includes relatively large (up to 30cm) juvenile pumiceous blocks, allowing more precise determination of bulk composition of erupted magma than the fine pyroclastic deposit. We investigated four outcrops, two of which locate along Owagawa and Noborisawagawa in the NE flank of the volcano, and two of which locate along Haruna-Shirakawa in the SE flank. Geshi and Oishi (2011) recently clarified the BAF deposit in the SE flank is the product of the Shibukawa eruption by the carbon dating. At some outcrops, BAF deposit could be divided into subunits by the existence of intercalated ash deposit. In any outcrop/subunit, juvenile blocks were classified into white, gray and dark gray. In some blocks, parts with different colors are in stripes or irregularly mixed.

The pumice blocks are homogeneous felsic andesite with 60.6-61.7 wt.% SiO_2(N=21). There is no systematic difference in the composition between the NE and SE flanks. In Unzen 1991-1995 eruption, the composition of the erupted magma changed with time, and there was a temporal change in the flow direction of the pyroclastic flow (Nakada and Motomura, 1999). The present data of Shibukawa eruption show no tendency like that. In the representative six samples covering the pumice color variation, Hb, Opx, Pl, Qtz and Fe-Ti oxides present as phenocryst phase. But, Qtz is quite rare, as we observed only one crystal in 8 thin sections. Phenocryst phases other than Qtz form aggregate, indicating they crystallized in equilibrium. Dusty zone was observed in the plagioclase rim, showing that the melt became undifferentiated just prior to the eruption, due to 1) mixing with hotter magma, or 2) heating by hotter magma. There is no change in whole rock composition and phenocryst assemblage with pumice block color. The different color is likely to be caused by different amount of groundmass crystal (Gardner*et al.*, 1998). The breakdown of Hb was observed only in dark gray blocks.

The felsic endmember magma of the Ikaho eruption erupted as white pumice (60 to 62 wt.% SiO_2). The white pumices contain phenocrysts of Hb, Opx, Pl and Fe-Ti oxides. Therefore, it is highly probable that the felsic magma similar to that in Ikaho eruption was active in the Shibukawa eruption. In the Ikaho eruption, ejecta with obvious characteristics of magma mixing (gray pumice and lava, down to 57.5 wt.% SiO_2) have been confirmed. It means that the mixing ratio of the high-temperature magma in the Shibukawa eruption (even if it happened) was very small. In the future, as well as exploring the eruption

©2019. Japan Geoscience Union. All Right Reserved.

triggering process of the Shibukawa eruption in detail, we need to investigate phenocrysts derived from the felsic magma for the Ikaho eruption. They might record the effects of heating and mixing by high-temperature magma, which occurred several decades before the eruption.

Keywords: Haruna volcano, Block and ash flow deposit, Mush-like felsic magma , Eruption trigger, Magma mixing, Heating from hotter magma

©2019. Japan Geoscience Union. All Right Reserved.

Report of Volcanic Activity at Kusatsu-Shiranesan in 2018

*Tsukasa Kobayashi[1], Koji Kato[1], Koichi Suemine[1], Kazuhiro Kimura[1], Yusuke Yoshigai[1], Yasuo Ogawa[2], Kenji Nogami[2], Wataru Kanda[2], Akihiko Terada[2]

1. Volcanological Division, Japan Meteorological Agency, 2. Volcanic Fluid Research Center, Tokyo Institute of Technology

Kusatsu-Shiranesan is the active volcano located in north-eastern Gunma-pref. Japan Meteorological Agency (JMA) monitors Kusatsu-Shiranesan volcanic activity. A group of pyroclastic cones, including Shiranesan, Ainomine, and Motoshiranesan, which stretch from the north to the south, are located in its highest western area. Latest magmatic eruption occurred about 3,000 years ago. All recent eruptions were occurred in the area around Yugama and Motoshiranesan area, and these eruptions were phreatic explosions.

In January 2018, phreatic explosion occurred at Motoshiranesan area. In April, volcanic seismicity in shallow areas beneath the Yugama crater increased. We report volcanic activity at Kusatsu-Shiranesan in 2018.

A phreatic explosion occurred at 10:02 on 23 January 2018 at the northern and western area of Kagamiike-kita cone in Motoshiranesan. Before the eruption, volcanic tremor occurred from 09:59, and significant tilt changes which indicate the upward of Motoshiranesan direction was obserbed by tiltmeter installed around Yugama crater by the Tokyo Institute of Technology. At around 10:02, low frequency earthquake was observed, and these tilt signals turned to the downward to the Motoshiranesan direction. After the eruption, a very small volcanic earthquake (BH-type earthquake) occurred frequently in a shallow place near Kagamiike-kita cone, but it gradually declined.
In late April 2018, earthquakes around shallow part of Yugama crater rapidly increased, and crustal deformation indicating the expansion of the shallow part around Yugama began to be observed with the tiltmeter installed around Yugama crater.By the geomagnetic observation, the variation of geomagnetic total intensity indicating thermal demagnetization was observed from April.
In early September, the volcanic earthquake activity decreased somewhat and the tiltmeter variation also became smaller. But on September 28, again the earthquake around the Yugama increased rapidly. And crustal deformation similar to April was observed by the tiltmeter installed around Yugama. After that, earthquake activity decreased gradually, but continued in January 2019.

Analysis result of GNSS continuous observation date from 2014 to 2015, in which period seismicity around Yugama crater was high, indicates the expansion of the deep part of northwest area of Kusatsu-Shiranesan. Similar changes was observed at several observation points in 2018.

We would like to thank Kakioka Magnetic Observatory, JMA for the use of his observation and analysis data.

Keywords: Kusatsu-Shiranesan, phreatic explosion, earthquake activity, ground deformation, variation of geomagnetic total intensity

©2019. Japan Geoscience Union. All Right Reserved.

Noble gas isotope composition of fumaroles and hydrothermal gases around Kusatsu-Shirane volcano

*Kotaro Toyama[1], Hirochika Sumino[1], Kaori Kawana[1], Yoshihide Akiyama[1], Takeshi Ohba[2], Muga Yaguchi[3], Akihiko Terada[4]

1. Department of Basic Science, Graduate School of Arts and Sciences, The University of Tokyo, 2. Department of chemistry, School of Science, Tokia University, 3. Meteorological Research Institute, 4. Volcanic Fluid Research Center, Tokyo Institute of Technology

Mount Kusatsu-Shirane, an active stratovolcano consisting of three pyroclastic cones (from north to south, Mt. Shirane, Mt. Ainomine, and Mt. Motoshirane) erupted on 23 January 2018 at Mt. Motoshirane. This eruption was a phreatic eruption, which often occur without magma movement. Therefore, there is no or very small precursor geophysical signals. In contrast, the chemical and isotopic compositions of volcanic gases can change reflecting pressure rise of a gas reservoir which caused the phreatic eruption. Especially, helium isotope ratio ($^3He/^4He$) is regarded as a useful tracer for the volcanic activity, because it exhibits unique values corresponding to the origin (e.g., 7-8 Ra in the mantle and < 0.1 Ra in the curst, where 1 Ra denotes atmospheric $^3He/^4He$ ratio of 1.4×10^{-6} [1]). Some studies have reported pre-eruptive $^3He/^4He$ anomalies, suggesting the increase of supply of the magmatic helium into the hydrothermal system preceding eruption [2,3].

We report the noble gas (He, Ne, Ar) isotopes of fumaroles and hot-spring gases collected from 9 sites around Kusatsu-Shirane volcano during 2014 and 2018. The measured $^3He/^4He$ ratios were corrected for atmospheric contamination based on $^4He/^{20}Ne$ ratios. The air-corrected $^3He/^4He$ ratio of Sesshogawara fumarole, located on 2 km east of the 2018 phreatic vent, had been constant at 7.0-7.5 Ra during 2014 and 24 January 2018, and dropped to 6.5 Ra on 13 February 2018. The $^3He/^4He$ ratio increased to 7.6 Ra on 21 May 2018 and has been constant at about 7.5 Ra. The $^3He/^4$ He ratios of bubbling gases of Kusatsu-Yubatake hot spring, which located on 5 km east of the 2018 phreatic vent, had been constant at 6.5-6.9 Ra during 2014 and 12 February 2018, decreased to 6.0 Ra on 3 June 2018, and then increased to 7.5 Ra on 6 August 2018. The $^3He/^4$ He ratios of Hoshimata fumarole, which located on 3 km west of the 2018 phreatic vent, increased from 6.2 Ra to 7.3 Ra during 2 March 2018 and 19 June 2018. The trends observed in these sites seem to be associated with the 2018 eruption with different time lags, which may reflect the migration distance from the 2018 phreatic vent to the sites.

In Kusatsu-Shirane area, two hydrothermal reservoirs, one of which is located beneath Yugama crater of Mt. Shirane and the other is located beneath Mt. Motoshirane (between Ainomine and Mt. Motoshirane), have been proposed [4]. The $^3He/^4He$ ratios (7.2-8.1 Ra) of Kitagawa fumaroles on the northern flank of Mt. Shirane near the Yugama crater, may reflect the values of the gases derived from the hydrothermal reservoir beneath Mt. Shirane. On the other hand, the lower $^3He/^4He$ ratios observed in Sesshogawara, Kusatsu-Yubatake and Hoshimata after the eruption may result from another contribution from a reservoir having lower $^3He/^4He$ ratios (less than 6.5 Ra), which could be attributed to the hydrothermal reservoir beneath Mt. Motoshirane. The reservoir beneath Mt. Motoshirane may be enriched in radiogenic ^4He derived from the crust, because Mt. Motoshirane has not erupted for last 1500 years [5].

It has been proposed that the 2018 eruption was caused by sealing of gas pathway from magma to the hydrothermal reservoir beneath Mt. Shirane [4]. This would result in decrease of supply of magmatic gas with high $^3He/^4He$ ratio to Sesshogawara, Kusatsu-Yubatake, and Hoshimata. Therefore, the low $^3He/^4He$

©2019. Japan Geoscience Union. All Right Reserved.

ratios observed in these sites after the 2018 eruption may reflect relative increase of the contribution of gas supplied from the Mt. Motoshirane hydrothermal reservoir. In contrast, the high and relatively constant $^{3}He/^{4}He$ ratios at all of the sites since August 2018 suggest that the gas from the reservoir beneath Mt. Shirane is dominant. Ohba et al. [4] proposed that supply of magmatic gas to the Mt. Motoshirane reservoir increased before the eruption as a result of the sealing of gas pathway from magma to the Mt. Shirane reservoir, and that it caused high fluid pressure of the reservoir and subsequent phreatic eruption at Mt. Motoshirane. This implies that $^{3}He/^{4}He$ ratio of the Mt. Motoshirane reservoir also increased from a lower value to a higher value less than 6.5 Ra before the eruption. Although further study is necessary to constrain $^{3}He/^{4}He$ ratios of the reservoirs, the remarkable temporal $^{3}He/^{4}He$ variation after the eruption can be accounted for by the change in mixing ratio of the gases from the two reservoirs.

References: [1] Ozima and Podosek (2002) Noble Gas Geochemistry.; [2] Padrón et al. (2013) Geol.; [3]Paonita et al. (2016) Geol.; [4]Ohba et al. (2018) JpGU2018, SVC41-38.; [5]Nigorikawa et al. (2016) JpGU, SVC48-11.

Keywords: Noble gas , Volcanic gas, Kusatsu-Shirane volcano, Volcanic eruption, Temporal variation

©2019. Japan Geoscience Union. All Right Reserved.

Self-potential and geomagnetic total intensity observations at Motoshirane volcano after the 2018 eruption

*Akira Yamazaki[1], Hideki Iino[1], Tatsurou Tanaka[1]

1. Kakioka Magnetic Observatory

A phreatic eruption occurred at Kusatsu-Shirane volcano (Motoshirane volcano) on January 23, 2018, and some impact craters were formed on the Kagami-ike crater floor and the Kagami-ike northern crater. After the eruption, the temporarily activated seismic activity near the crater has declined, and the fumarolic activity has ceased after late February 2018. In order to estimate geothermal status after the eruption, we carried out self-potential (SP) and geomagnetic total intensity observations at Motoshirane volcano. Measurements of the SP were conducted at about 130 points around the summit of Motoshirane volcano from June 30 to July 2, 2018. Copper-Copper sulfate electrodes were used, the measurement interval was about 50 m, and the measurement was carried out by the so-called full potential method. We applied -1.3mV/m as correlation coefficient for correction of the topographic effect to all the SP measurement stations. The coefficient was obtained from a clear negative correlation (-1.3 mV/m) between the elevation and the potential in the survey line on the eastern slope of the Kagami-ike. As a result of the SP, we detected a positive anomaly, 200~500mV in magnitude, developing around the summit of Motoshirane volcano. By comparison of the result of the 4th Joint Observation of Kusatsu-Shirane Volcano in 2003, we found temporal variations of the SP near Kagami-ike northern crater which may have been caused by the eruption. As for the geomagnetic total intensity observation, we selected ten repetitive observation stations around the summit of Motoshirane volcano, and carried out first observation in June 2018 (June 28-30). Following the first observation, we carried out repeated observation in August (August 28-29) and October (October 7). As a result, no significant changes in the geomagnetic total intensity in the period from June to October, 2018. It suggests that rapid thermal demagnetization or magnetization by cooling does not occur at underground of Motoshirane volcano.

Keywords: Kusatsu-Shirane volcano, Motoshirane volcano, Self-potential observation, Geomagnetic total intensity observation, Thermal demagnetization

©2019. Japan Geoscience Union. All Right Reserved.

Eruption processes of the 3rd and 4th stage of Niigata-Yakeyama Volcano, Japan, inferred from microlite texture and chemical composition

*Takumi Yoshida[1], Takeshi Saito[1]

1. Shinshu University

Niigata-Yakeyama volcano, which belongs to the Myoko volcano group, is one of the most active and youngest volcanoes in Japan. In the 3rd stage of Yakeyama activity, Maeyama lava flows and Hayakawa pyroclastic flows were generated to the northern slope of the volcano. In the 4th stage activity, Yakeyama lava flows, which forms present lava dome at the summit, and Otani pyroclastic flows were effused. Otani pyroclastic flow deposit contains well-vesiculated lavas, while lavas from Hayakawa pyroclastic flow are poorly-vesiculated. In this study, groundmass textural analysis of the eruptive products at the 4th stage was carried out. Chemical composition of plagioclase phenocrysts and microlites of the eruptive products at the 3rd and 4th stage were analyzed in order to examine the eruption process of the 3rd and 4th stage of Yakeyama volcano.

Microlite number density (MND) and crystallinity of plagioclase in Otani pyroclastic flow deposits were obtained from groundmass textural analysis. Our results indicated that Otani pyroclastic flows showed lower MND and intermediate crystallinity compared with Hayakawa pyroclastic flow deposits. As a result of chemical composition analysis, phenocryst in the samples of the 3rd stage activity shows An#(Ca/Ca+Na) =0.65~0.84. Microlite of andesite of Maeyama lava flow has an average An# of 0.61, which is lower than that of dacite lava of Maeyama Lava flow (average An# =0.54). Phenocryst of the 4th stage activity has An# =0.45~0.89. Microlite of Yakeyama lava flow and Otani pyroclastic flow have average An# of 0.63 and 0.62, respectively. The An# of plagioclase microlite becomes lower with decreasing crystal size.

Plagioclase microlite becomes lower An# with higher degree of H2O exsolution due to decompression (e.g. Nakamura, 2011). Our results suggest that microlite in dacite lava of Maeyama lava flow has undergone high decompression compared with andesite lava of Maeyama lava flow. However, there were little difference between plagioclase microlite of lava flow and that of pyroclastic flow samples. Eruptive products of the 4th eruption have relatively homogeneous SiO2 composition. Plagioclase microlite of Otani pyroclastic flow deposit, showing lower MND and higher An# than Hayakawa pyroclastic flow, may be crystallized under a condition of lower undercooling. Another possibility is that rapid vesiculation and H2O exsolution may proceed before microlite crystallization and prevent from decreasing An#.

Keywords: Niigata-Yakeyama, Yakeyama lava flow, Otani pyroclastic flow, Maeyama lava flow, Hayakawa pyroclastic flow, Plagioclase microlite

©2019. Japan Geoscience Union. All Right Reserved.

Estimation of subsurface structure of Shinyu crater lake, Tateyama Caldera, based on the water level and seismic observation data

*Ryohei Kawaguchi[1], Naoko Saito[2], Shin'ya Onizawa[1]

1. Meteorological Research Institute, 2. Toyama local Meteorological office, Japan Meteorological Agency

Shinyu, located in the Tateyama caldera is a crater lake with the diameter of about 40 m and the depth of about 5.6 m. The water level of Shinyu is maintained by the influx of hot water from vents at the bottom of Shinyu. Shinyu had continued the full water level for decades, but periodic geyser activity was reported from 2014 which has the period of 0-20 days (Fukui et al 2018). In order to investigate the activity of the water level change in Shinyu, we installed water level meter and seismometer around Shinyu from June to October in 2017 and 2018. In this study, we estimate the underground structure of Shinyu based on the temporal changes of water level and seismic data.

The water level change was observed by a bubble type water level meter which has a sampling period of 10 minutes. In addition, a seismometer was installed at about 20 m from the Shinyu. The seismic data was recorded with a sampling frequency of 100 Hz.

During the observation period, we were able to obtain the water level change data of 7 cycles in 2017 and 8 cycles in 2018, respectively. For the preliminary analysis, we examined the periods of water level changes, dividing the water level change cycle into four categories, dry-up, rising in the water level, full water level, and descent in the water level. As a result, the period of the dry-up is about 3 days, the rise in water level is about 4.5 days, the full water is 0 to 20 days and the descent in water level is about 0.5 days. The period of raising and decent of the water levels were almost constant for each cycle. During the rising and full of the water level, rising of hot water with gas bubbles were observed by the image of Shinyu surface taken by time-lapse camera. The amplitudes level of seismometer data was clearly different between the period of rising and full of water level and the period of dry-up and decent of water level. These indicate that geyser activity of Shinyu is occurred by boiling of hot water in the water reservoir located below the Shinyu.
When the shape of Shinyu is conical and the flux of the hot water drop under the Shinyu is constant, the flux of dropping hot water is estimated about 0.06 m^3/s by the size of Shinyu and the period of the descent of water level. According the data of water level meter, the rate of water level descent were 1.2-2.5 $\times 10^{-3}$ m/s. From these data, the radius of cylindrical pipe assuming below the Shinyu was estimated to be 2.8-4.0 m. We also report on the result of comparing the time scale of water level changes using the observed data and simulation result based on the previous geyser model.

Keywords: Shinyu, Tateyama caldera, geyser

©2019. Japan Geoscience Union. All Right Reserved.

Real time monitoring of underground temperature in Jigokudani, Midagahara volcano using LPWA devices

*Tohru Watanabe[1], Toyama branch NTT West[2]

1. Gradudate School of Science and Engineering, University of Toyama, 2. Nippon Telegraph and Telephone West Corporation

Jigokudani is an active geothermal area in Midagahara volcano, Toyama prefecture, central Japan. It was formed as a result of repeated phreatic eruptions over 40,000 years. Increased volcanic activity in this area has been observed since 2011. In order to detect a precursory signal of a phreatic eruption, seismicity, observations should be conducted on seismicity, ground deformation, geothermal activity, volcanic gas, etc. A real time monitoring system of underground temperature using LPWA (Low Power, Wide Area) devices has been tested since 30 August 2018. An LPWA device (NHR, SS05-ST) is composed of thermometer and transmitter (LoRaWAN). 10 devices were deployed in Jigokudani. Temperature sensors (thermocouples) were placed at the depth of 50 cm. Transmitters send temperature data every 30 minutes to a gateway to the internet situated in Hotel Tateyama. The distances from the gateway to LPWA devices are within 1 km. Underground temperatures can be monitored on internet devices. Since Jigokudani has a heavy snowfall in winter, 7 devices were removed and 3 devices were left to test in winter. Though temperature data could be received until December 2018, no data could be received since then. Transmitters of around 50 cm high above the ground must be covered with snow. During summer and fall, LPWA devices are useful for real time monitoring.

Keywords: underground temperature, LPWA, real time monitoring

©2019. Japan Geoscience Union. All Right Reserved.

Varying chemical and isotopic compositions of fumarolic gases from the summit and from the 1962-63 eruptive vents at Yakedake Volcano, Japan

*Takeshi Saito[1], Shun Sawamura[2], Kazuhiro Amita[3], Taketoshi Mishima[4], Shinji Ohsawa[4]

1. Institute of Science, Academic Assembly School of Science and Technology, Shinshu University, 2. Graduate School of Science and Technology, Shinshu University, 3. Graduate School of Engineering Science, Akita University, 4. Beppu Geothermal Research Laboratory, Institute for Geothermal Sciences, Graduate School of Science, Kyoto University

Since the latest phreatic eruption in 1962-1963, Yakedake volcano has remained dormant, but fumarolic activity around the summit area has continued steadily during the past hundred years. Recently, temperature, chemical, and isotopic compositions of fumarolic gases discharged from the summit fumaroles were ascertained for 2013-2017 (Saito et al., 2019). This time, fumarolic gases discharged from the 1962-63 eruptive vents, which locate about 300m north of the summit, were collected and chemical and isotopic compositions were analyzed. We compared our results from the 1962-63 eruptive vents with those from the summit fumaroles in order to evaluate the formation of volcanic hydrothermal system beneath the volcano.

Discharge temperatures of the fumaroles around the 1962-63 vents were 95-100˚C: slightly lower temperatures than those from the summit fumaroles but higher than the boiling temperature at the elevation. Chemical analysis revealed that fumarolic gases from the 1962-63 vents contain lower amounts of SO_2 than the summit fumaroles. Higher CO_2/total S ratio and lower apparent equilibrium temperatures of the 1962-63 fumaroles coincide with lower discharge temperatures. On the other hand, the 1962-63 fumaroles show higher He/Ar ratio than the summit fumaroles, suggesting higher contribution of magmatic fluid.

The isotopic compositions of water (D, ^{18}O) show that the fumarolic fluids from the summit fumaroles were probably formed by mixing of the magmatic fluids and local meteoric water. The isotopic compositions of the 1962-63 fumaroles show much lower values not only than the summit fumaroles but than local meteoric water, suggesting that the fluids suffered isotopic fractionation due to evaporation of the fumarolic gases.

Our results possibly indicate that volcanic hydrothermal system beneath the summit region differ from that under the 1962-63 vents.

©2019. Japan Geoscience Union. All Right Reserved.

Eruption age determination of the latest two lava flows and characteristics of volcaniclastic materials from the recent activity of Yokodake Volcano, Japan

*Hiroya Nitta[1], Takeshi Saito[1], Yorinao Shitaoka[2]

1. Shinshu University of Science and Technology, 2. Department of Environment System, Faculty of Geo-environmental Science, Rissho University

Yokodake volcano, which effused nine lava flows (Y1~Y9), is the only active volcano belonging to Yatsugatake volcano groups in central Japan. Eruption ages of Y1-Y8 lava were not determined distinctively. To evaluate the latest activity of Yokodake volcano, we carried out paleomagnetic studies and tried to estimate the eruption ages of the Y8 and Y9 lava flows. However, several candidates for paleomagnetic ages were remained (Nitta and Saito, 2018, JPGU; Nitta and Saito, 2018, fall meeting of the volcanological society of Japan). In this study, we applied thermoluminescence (TL) dating for Y8 and Y9 lava and viscous remanent magnetization (VRM) dating for Y9 lava. In addition, the volcaniclastic layers were found just above the Y9 lava and around the surface of the summit region. We will report characteristics of the volcaniclastic layers, discussing the recent activities of this volcano.

TL dating was performed by using poly-minerals (ca 10~50 μm) sample extracted from Y8 and Y9 lava. TL age of Y8 sample was 3.3 ±1.2 ka. Y9 lava sample didn't emit TL intensity. As for Y9 lava, we tried to estimate the age using VRM. However, the estimated ages were widely scattered. We conclude eruption age of the Y8 lava is ca. 3.3 ka, which is consistent with our previous paleomagnetic age of 3.35~3.85ka. On the other hand, five eruption ages of Y9 lava (0.60 ka, 1.80 ka, 1.90~1.95 ka, 2.20~2.25 ka, 2.4~2.45 ka) are still remained.

We recognized light gray volcanic ash deposit just above Y9 lava which composed of sand to silt size and contained carbonaceous material. It may be comparable to NYk-1 tephra (Okuno, 1995). Four volcaniclastic layers were found at summit region and the lower layer is a possibility of being correlated with NYk-2 tephra (2.35~2.15 cal ka BP; Okuno and Kobayashi, 2010). Two volcaniclastic layers above NYk-2 tephra seem to be derived from Yokodake volcano, suggesting at least two volcanic eruptions were occurred after NYk-2 tephra eruption.

Keywords: Yokodake Volcano, Latest lava, Eruption age determination, TL dating, Volcaniclastic materials from the recent activity

©2019. Japan Geoscience Union. All Right Reserved.

Estimating the date of the 2007 eruption of Mount Ontake Volcano using waveform correlation

*Shuhei Nishijima[1], Toshiko Terakawa[1], Shinichiro Horikawa[1]

1. Graduate School of Environmental Studies, Nagoya University

Mt. Ontake volcano erupted on late March, 2007. However, we do not know the exact time of the eruption with a Volcanic Explosivity Index 0 because of little visual evidence. I tried to estimate the date of the 2007 eruption, using a waveform correlation method. A previous study reports that focal mechanisms of volcanic earthquakes associated with the latest eruption in 2014 changed from normal/strike-slip faulting with east-west tension to reverse faulting with east-west compression. Based on this fact, I selected 10 and 8 volcanic events for the pre- and the post-periods of the 2014 eruption as template events. I applied the technique to continuous seismic waveforms from 22 December 2006 to 31 March 2007. I detected 2375 (pre-eruption type) and 1659 (post-eruption type) events corresponding to the pre- and the post-eruption events, respectively. I found that events with east-west tension (pre-eruption type) became active at the early stage until a very long period (VLP) event occurred on 25 January, and during the period from 5 to 19 February. On the other hand, the activity of events with east-west compression (post-eruption type) became dominant for 11 days after the VLP event occurred, and during the period from 20 February to 24 March. Subsequently, neither type of events became dominant. The activity of pre-eruption type events synchronized with the period when the length of the baseline in the east-west direction across Mt. Ontake increased. This suggests that events of pre-eruption type are related to the magma intrusion process beneath the volcano. The activation of events of post-eruption type following to the VLP event, which is well modeled by a tensile crack with a strike of N20W, may be related to contraction processes after the event released water vapor from the volcano. Based on the changes in types of detected events as well as the seismicity, I concluded that Mt. Ontake would have erupted on 20 February or between 11 and 12 March, 2007.

Keywords: volcano, Matched Filter Method

©2019. Japan Geoscience Union. All Right Reserved.

Seismic activity beneath Mt. Ontake volcano before and after the 2007 and 2014 eruptions

*Yoshiko Yamanaka[1], Shinichiro Horikawa[1], Yuta Maeda[1]

1. Graduate School of Encironmental Studies, University of NAGOYA

We developed a portable seismic telemetry system. This system is compact size, and the consumption electricity is small (Horikawa et al., 2017VSJ). From October 2017 performance test of this system has been carried out in the summit region of Mt. Ontake volcano. 10 seismic observations were installed. We determined seismic activity around Mount Ontake volcano by using those 10 summit observations and the seismic networks of Nagoya University and Japan Meteorological Agency, and obtained station corrections. Most of earthquakes were located beneath the craters of the 2014 eruption, and those depths were close in sea level or were shallower. The seismic activity is almost distributed on a straight line at -1.5km from 0km in depth and spreads through the northeast-southwest direction at around -1.5km (Yamanaka et al., 2018JpGU).

We try to determine seismicity linked to the 2007 and 2014 eruption of the Mount Ontake by using obtained station corrections. Before the 2014 eruption, earthquakes occurred from 1.0 km to -0.6 km linearly. This seismic activity is on an extension line of the 2017-2018 linear activity. After the 2014 eruption, earthquakes spread in the north and south direction from around -0.6 km in depth. The seismic activity gradually become shallow and extended to the current seismic activity. The events before the 2007 eruption also occurred from 3.0 km to 0 km on an extension line of the 2017-2018 linear activity. It is considered that some kind of fluid has risen through almost the same passage at the 2007 and 2014 eruptions.

Keywords: Mt. Ontake, Seismic activity

©2019. Japan Geoscience Union. All Right Reserved.

Effect of rain and snowmelt correction of tiltmeter data - Application example for Ontakesan Volcano -

*Kazuhiro Kimura[1,5], Katsuhisa Kawashima[2], Takane Matsumoto[2], Akihiko SASAKI[4], Tsutomu Iyobe[3], Junichi Miyamura[1], Masaki Nakahashi[1]

1. Japan Meteorological Agency, 2. Research Institute for Natural Hazards and Disaster Recovery, Niigata University, 3. Faculty of Engineering, Kyoto University, 4. Department of Geography and Environmental Studies, Kokushikan University, 5. Graduate School Science and Technology, Niigata University

Japan Meteorological Agency(JMA) installed a tiltmeter about 3km southeast of Mt. Ontake in 2010. A clear tilt change was observed northwest upward from several minutes before the 2014 phreatic eruption and northwest downward after the eruption. Kimura and Nakahashi (2015) applied the rain correction method using the tank model and precipitation data to the tiltmeter data of east-west component of the summer (From June to October), and they detected the small tilt change of west rising from September 10, 2014 when the earthquake activity became active. However, the similar tilt change of west rising has been confirmed several times and it has not been able to remove the influence of snowmelt in the spring (From March to May).

Miyamura et al. (2017) developed the rain and snowmelt correction method that adds the snow-tank to the tank model by Kimura et al. (2015) that uses snowmelt amount data as input values in addition to the precipitation data. They applied this method to the tiltmeter data of east-west component, and they confirmed that the influence of snowmelt in the spring was removed from the tiltmeter data. We used a method using a TR model that uses temparature and solar radiation as indices with reference to Matsumoto et al. (2010). Because there is not the continuous meteorological observation data for a long time near the tiltmeter (altitude 2195 m), they used the meteorological observation data at Kaidakogen (altitude 1130 m) closest to the tiltmeter (about 11.5km). In order to consider the difference between the two meteorological observation data, they compared with the meteorological observation data at Kaidakogen and the meteorological data near the tiltmeter observed by Kawashima et al. (2016).

There is a large seasonal changes from spring to summer every year for the tiltmeter data of north-south component. We applied the method of Miyamura et al (2017) to the tiltmeter data of north-south component, and it is able to remove this seasonal changes. Focusing on the 2014 phreatic eruption of Mt. Ontake, we detected the tilt change of north rising from the mid August 2014. In other words, the tilt change began north rising from the mid August 2014, and turned to northwest rising from around September 10. Similar tilt change could not be confirmed during the reserch period (April 2011 - September 2017).

We considered this tilt change while related to two previous studies. First, with reference to hypocenters before and after the eruption by Kato et al (2015), assuming an open crack model with NNW-SSE strike and moving its upper end from the 2 km to 1 km depth. As a result, we were able to confirm the tilt change pattern from north rising to northwest rising. Next, Miyaoka and Takagi (2016) applied the stacking method to the GNSS baseline length data, they detected that the change of the long baseline began from the middle of August and the change of the short baseline began from the beginning of September. They inferred that the pressure source migrated to a shallower region from a deeper region. The results of these previous studies are consistent with the tilt change applied the rain and snowmelt correction method to the tiltmeter data, and are considered to indicate the effectiveness of this method.

©2019. Japan Geoscience Union. All Right Reserved.

Keywords: Tiltmeter, Mt. Ontake, rainfall, snowmelt

©2019. Japan Geoscience Union. All Right Reserved.

Spatial Variation of b-value around Mt. Fuji influenced by the Eastern Shizuoka Earthquake of 15 March 2011

*Takumi Murakoshi[1], Tomonari Miyashita[2]

1. National Defense Academy, 2. JASDF

The Eastern Shizuoka earthquake occurred on March 15, 2011 (Mj6.4). The hypocenter of the earthquake was approximately 6 km southwest of Mt. Fuji’ s peak at a subsurface depth of about 15 km. Estimating spatial variation of the b-value of the Gutenberg–Richter relation is important in the examination of time and spatial changes in volcanic and seismic activity after large earthquakes. This study aims to evaluate changes in seismic activity after the 2011 Eastern Shizuoka earthquake using the spatial variation of the b-value. Hypocentral data from July 2001 to December 2017 was obtained from the JMA catalog. As a result, the b-value for earthquakes around Mt. Fuji was significantly smaller during the period after the 2011 Eastern Shizuoka earthquake than during the period from July 2001 through February 2011, and it continued to gradually recover after the Eastern Shizuoka earthquake.

Keywords: b-value, Mt. Fuji, 2011 Eastern Shizuoka Earthquake

©2019. Japan Geoscience Union. All Right Reserved.

Present condition of submarged volcano, Teishi Knoll, off Ito, Eastern Izu Peninsula

*Toshiro Yamanaka[1], Yoshifumi Kawada[2], Takuro Noguchi[3], Mayumi Hatta[3], Kei Okamura[3]

1. Tokyo Univ. Marine Science and Technology, 2. Tohoku University, 3. Kochi University

Teishi Knoll is a submerged volcano belonging to Eastern Izu volcanic zone and located c. 4 km east off the coastline of Ito City, Eastern Izu Peninsula. The volcano erupted in July, 1989, then the cone shaped knoll with a crater on the summit was formed. The Japan Meteorological Agency has reported that the Eastern Izu volcanic zone is composed of some small volcanoes including scoria cones, tuff rings, maars, and lava domes, erupted on land and many submerged volcanoes distributed densely on the seafloor off the coast. Detail of the submerged volcanoes has been unknown yet. The volcanoes have been considered to distribute on several lines of northwest-southeast direction reflecting the stress field of this area. Previous activities of the volcanic zone have been reported; Ohmuroyama Volcano was formed by eruption about 4 ka, Kawago-daira Volcano was formed about 3.2 ka, and Iwanoyama-Iwoyama volcanic chain was formed by a fissure eruption about 2.7 ka. The last eruption of the volcano belonging to the zone is considered the Teishi eruption in 1989.

In Japan there are confirmed 110 active volcanoes, 12 volcanoes of them are located below sea surface. Such submerged volcanoes have not been observed continuously due to its difficulty by visual observation, therefore, those volcanoes have not ranked according their activity by Japan Meteorological Agency. Therefore, we started observation of Teishi volcano in December, 2017, for evaluation whether active magma supply is still continuing or the intrusive magma causing of 1989 eruption is just cooling. Geochemical (water chemistry) and geophysical (heat-flow) observation has been done using training vessels of TUMSAT every half year.

We have not accumulated enough data yet, measurements of geothermal gradient were performed every time. For calculation of the heat-flow it is required the temperature record of the bottom water, so we started long-term temperature observation on the seafloor from the last December. On the other hand, chemistry of the bottom water in the crater showed slight positive anomaly of dissolved inorganic carbon and significant positive anomaly of manganese relative to the bottom water obtained from outside of the crater. Those chemical anomalies suggest that any thermal activity is still alive in the volcano.

Keywords: Teishi Knoll, Submerged volcano, Activity, Chemical flux, Heat flow

©2019. Japan Geoscience Union. All Right Reserved.

Descriptions and age of volcanic products before the caldera formation in the northern part of Izu-Oshima, off Tokyo, Pacific Ocean

*Satoshi Terayama[1], Takehiko Suzuki[1], Makoto Kobayashi[2]

1. Tokyo Metropolitan University, 2. Research Center for Volcanic Hazards and Their Mitigation, Tokyo Metropolitan University

Introduction

Izu-Oshima Volcano erupted in 1986 is an active volcano that will erupt in near future. The volcano has been studied for a long time, and many studies has been conducted (Nakamura, 1964; Koyama and Hayakawa, 1996; Kawanabe, 2012 and so on). However, most previous studies focused on ″Syn-and post-caldera volcano″ (Kawanabe, 1998) after the caldera formation of Izu-Oshima Volcano. There are few studies discussed ″Younger Edifice of Pre-caldera volcano″. In this study, the purpose is to investigate the volcanic products of Younger Edifice of Pre-caldera volcano and older period with little investigation and to clarify the eruption history. The description of the volcanic products should be important in considering prediction of volcanic eruption and volcanic disaster prevention.

The study site is a coast called Goishihama located between the Chigasaki and Kazehayasaki capes in the northernmost part of Izu-Oshima. At the site volcanic products are exposed on the coasted cliff with a width of about 1 km and a height of about 30-40 m. Volcanic products that can be observed along Goishihama are described by Isshiki (1984), who reported mainly volcanic product of ″Okata volcano″ and ″Older Edifice of Pre-caldera volcano″. However, its description is limited, and description and discussion of fall-out tephra have not been done. In this study, we investigated volcanic products that are exposed on the sea cliff of Goishihama. As a result, some new views on the observable layer were obtained.

Results

The fall-out tephra group composed of 31 eruptive products is named ″Goishihama fall-out tephra group″. We sampled black humus buried soil from three horizon in ″Goishihama fall-out tephra group″ and determined the radiocarbon age. Ages are 11076-10713, 12027-11747, 18117-17803 cal BP in descending order. Therefore, it was revealed that ″Goishihama fall-out tephra group″ is the volcanic products of ″Younger Edifice of Pre-caldera volcano″ after 20 ka. Isshiki(1984) showed no description of the volcanic products of ″Younger Edifice of Pre-caldera volcano″ at Goishihama. As a future issue, it is necessary to correlate Goishihama with 95 fall-out of O1 to O95 distributed mainly in southwest part of the island by Tazawa (1980).

In addition, a fine white pumice with a diameter of about 1 mm was found slightly in the ″Goishihama fall-out tephra group″. After sampling the layer, we washed and observed it with a microscope, colorless and transparent pumice type volcanic glass shards were discovered. The chemical composition of the volcanic glass was measured, that is, SiO_2=78.07 wt.%, CaO=0.61 wt.%, FeO=0.75 wt.%, Al_2O_3=12.74 wt.%, K_2O=3.29 wt.%, showing a rhyolitic tephra. Therefore, it is not a tephra from the Izu-Oshima volcano formed by basaltic magma. The source of this rhyolitic tephra seems to be Kozushima Volcano or Niijima Volcano. These results suggest that ″Goishihama fall-out tephra group″ is the products of ″Younger Edifice of Pre-caldera volcano″ and that this rhyolitic tephra can be compared with O55 (Niijima Miyatsukayama tephra) (Saito et al., 2007). Thus, in this study, a new radio carbon age was obtained from Goishihama, and a rhyolitic tephra was newly discovered. The future issue is to correlate tephra in the outcrop of this study site with those in other outcrops, and it is needed to confirm the correlating of rhyolitic tephra.

©2019. Japan Geoscience Union. All Right Reserved.

Keywords: Izu-Oshima Volcano, volcanic products, Niijima Miyatukayama tephra, radiocarbon dating

©2019. Japan Geoscience Union. All Right Reserved.

Time change of p-value by Schuster method using earthquakes around Izu-Ohsima summit

*Hiroyuki Takayama[1]

1. Volcanological Division 1st labolatory, Meteorological Research Institute

Morita et al.(2016) and Morita et al.(2017) consider relation between volcanic earthquakes in Izu-Ohsima island and earth tide. Takayama et al.(2018) divide Izu-Oshima into 5 area and calculate p-value and consider relation between earthquakes and earth tide.

We use Schuster method (Schuster (1897)) whether occurrence of earthquake relate earth tide or not. This method is check null hypothesis of no correlation between earthquake occurrence and earth tide. Specifically, we set tide phase angle of earthquake occurrence as Di,

$$R=(\sum \cos Di)^2+(\sum \sin Di)^2$$

$$p=\exp(-R/N)$$

we test relation between earthquake occurrence and earth tide by this p-value. P-value falls in 0 to 1. If p-value is nearly 0, we reject null hypothesis. We calculate tide phase angle to each tidal component. In this research, we use principal lunar semi-diurnal tide (after this, we abbreviate M2).

In principal, if earthquake catalogue contain swarm, we can’ t calculate precise p-value. So, we avoid this problem to decluster catalogue.

In this study, we investigate time change of p-value in summit earthquakes. Detection capability of JMA catalogue in summit area is magnitude 0.0. After we decluster this catalogue, p-value is 0.011. So, we divide summit earthquake by time and calculate p-value of M2 in each group.

Specifically, we use JMA catalogue from April 2002 to January 2017. We pick up earthquakes of Izu-Ohsima summit. The number of earthquakes larger than magnitude 0.0 is 1084. After declusterd, the number of earthquakes is 901. We pick up 100 earthquakes from declusterd catalogue. We calculate p-value by M2 in 801 earthquake lists.
As a result, p-value increase and decrease periodically in time. Maximum is 0.98, minimum is 0.0030. If we select standard of rejection of null hypothesis as 0.05, periods of p-value less than this standard are around 2006, around 2010 and around 2014. Morita et al.(2017) suggest that release of volatile component from magma increase when earthquakes correlate earth tide. In the above three periods, release of volatile component increase possible. Also, Morita et al.(2017) suggest that release of volatile component from magma increase from 2013. This coincide with 2014 period.

©2019. Japan Geoscience Union. All Right Reserved.

Keywords: volcanic earthquake, earth tide, p-value

©2019. Japan Geoscience Union. All Right Reserved.

Standard stratigraphy and characteristic properties of late Quaternary tephras on the Niijima-island: Report of geochemistry and refractive indices of volcanic glass shards, orthopyroxene, hornblende, and cummingtonite

*Kaori Aoki[1], Makoto Kobayashi[1], Fumikatsu NISHIZAWA[1,2], Masanori Murata[1], Daisuke Ishimura[1], Takehiko Suzuki[1]

1. Research Center for Volcanic Hazards and Their Mitigation, Tokyo Metropolitan University, 2. Mount Fuji Research Institute, Yamanashi Prefectural Government

Tokyo Metropolis has the twenty-three wards, the Tama district, and the islands area. The population of the islands area is 25,353 (1st January 2019). The islands area, namely, the Izu-Ogasawara Islands consist of 21 volcanoes (islands and submarine volcanoes), excluding some islands. For residents in this area, volcanic disasters are always the threat. Accordingly, to integrate the fundamental information for preventing volcanic disasters, we investigate the history of volcanic activities, the pattern of each eruption, and the mass volume of erupted tephras and try to establish the high-resolution tephrochronology (Kobayashi *et al.*, 2019a,b). This project focuses on establishing the database of tephras collected form each island of the Izu Islands and their petrographic description and geochemical data. Also, it is likely that such tephra across the sea would deposit in the hemipelagic sediment around volcanic islands. Our tephra database of the Izu Islands has been a powerful tool to identify the source of marine tephra bearing in drilled core CK09-03,C9010E collected at the site of 100 km east from the Izu Island, off the Boso Peninsula (Aoki et al., 2019). Today, we present the petrographic and geochemical characters of many tephras provided through volcanic activities of the Niijima island during late Quaternary.

At the Daisan-yama, Fujimi Touge, and Miyatsukayama on Niijima island, and also Jinaijima off 1.6km west of Niijima island, we have recognized 21 eruptive events at least, including some tephras derived from off-island (Kobayashi *et al.*, 2019a). Kobayashi et al. (2019a) recognized as Niijima Origin tephra felsic magma events and mafic magma events on Nijjima islnad. On the island, as widespread marker tephra, AT and K-Ah tephra were detected. After tephra samples were washed by the ultrasonic cleaner, we collected the description of petrographic characters, major-element chemistry determined by EDS and refractive indices (RI) of volcanic glass shards, orthopyroxene, hornblende, and cummingtonite in each tephra. Generally, felsic tephra derived from vents on the Niijima island include often a small amount scoria grain. Most felsic tephras consist of felsic volcanic glass shards, and including plagioclase, quartz (including β-quartz), orthopyroxene, hornblende, cummingtonite, and occasionally biotite. The characteristic fact of Niijima Origin tephra is that RIs of heavy minerals (orthopyroxene and hornblende) has broad variations. Especially, RIs of orthopyroxene in Akasakimine tephra series, Miyatsukayama tephra series, and Miyatsukayama Nannbu tephra series show the bimodal or trimodal histograms within the limit of 1.700-1.730, including high RIs over 1.730 slightly, considered as close to ferrosilite. Also, there is the tendency that RIs of hornblende in Akasakimine tephra series and Miyatsukayama tephra series show the bimodal histograms or broad variations within the limit of 1.663-1.688. On the other hand, RIs of cummingtonite in Niijima Origin tephra during 60 ka show the unimodal histograms within the limit of 1.658-1.669. RIs of felsic volcanic glass shards in Niijima Origin tephra show within the limit of 1.492-1.501. By comparison that common range of RIs on Quaternary tephra in Japan is 1.501-1.505 (Machida and Arai, 1992), RIs of Niijima Origin tephra would be classified to lower RI groups in Japanese Quaternary tephras.

©2019. Japan Geoscience Union. All Right Reserved.

The content of SiO_2 in volcanic glass shards is 77.7-78.2 wt%, Na_2O+K_2O is 7.2-7.7 wt% generally, excluding some tephra which range is within the limit of 7.0-8.3 wt%. The content of FeO* is 0.7-1.0 wt% and high-SiO_2 is harmonious to the lower RIs of volcanic glass shards (Furuta *et al.*,1986; Kikkawa, 1990).

Keywords: Izu, Niijima, tephrochronology, petrographic characters, major-element composition

©2019. Japan Geoscience Union. All Right Reserved.

Tephrostratigraphy and its eruption history of the Latest Activity in the Kozushima Volcano, the Izu Islands

*Makoto Kobayashi[1], Masanori Murata[1], Fumikatsu NISHIZAWA[2], Takehiko Suzuki[1,3]

1. Research Center for Volcanic Hazards and their mitigations, Tokyo Metropolitan Univ., 2. Fuji Research Institute, Yamanashi Prefectural Government, 3. Department of Geography, Tokyo Metropolitan Univ.

In this study, we defined the younger eruptive activity since the eruptive event of Chichibuyama A tephra (ca. 22–26 ka; Suga et al., 1992, 2003) composed of pyroclastic deposits from the southern part of Kozushima covering the whole island as "the Latest Activity". In order to establish the tephrostratigraphy during this period, we are aiming to construct more detailed eruption history of Kozushima Volcano.
As a result of the topographical interpretation using DEM, we recognized Tenjo-san edifice (pyroclastic cone and lava domes), Kobeyama-Hanadateyama volcanic chain (lava domes) and Kushigamine (pyroclastic cone) as younger volcanic landforms presumably formed by the Latest Activity.

In addition, according to the geological survey, we recognized deposits associated with eight eruptions events in minimum. At Loc. 16 in the north part of Nachi-san, northern Kozushima, we recognized pyroclastic surge deposit composed of alternate layers such as pumice, volcanic lapilli and coarse ash so on (no. 16-1; Tenjo-san Tephra (AD 838)), fall-out deposit including altered volcanic blocks and lapillus (no. 16-2), medium to fine fall-out ash deposit (ca. 10 cm in thickness) containing pumice clasts (no. 16-3), densely scattered zone composed of scoria clasts with diameter of several mm (no. 16-4) and densely scatter zone composed of coarse volcanic ash (no. 16-5) in descending order. On the other hand, at the Akabane-tunnel (Loc. 4) in southern Kozushima, Tenjo-san tephra (no. 4-1), densely scattered zone composed of coarse ash (no. 4-2), medium to fine volcanic ash deposit (ca. 3 cm in thickness) containing pumices (no. 4-3), densely scattered zone composed of scoria clasts with diameter of several mm (no. 4-4), fine volcanic ash deposit with a thickness of ca. 9 cm (no. 4-5) and pyroclastic surge deposit composed of alternated layers such as volcanic lapilli and coarse ash (no. 4-6) in descending order. Widespread tephra of K-Ah was detected between no. 4-2 and no. 4-3. Among these eruption deposits, it is suggested that the eruption of no. 16-2 occurred around central to northern part of Kozushima because these deposits distributed only these areas. In contrast, medium to fine air fall ash deposits (no. 16-3 and no. 4-3) containing pumices and fall-out fine ash deposit (no. 4-5) are very prominent layers, then, we are deeming these deposits as widespread tephras originated by relatively larger eruptions. ^{14}C datings for charcoal scattered in tephric loess or humus soil just below tephra layer were applied. ^{14}C ages are 1300±20 yr BP under the fall-out ash deposit correlated with the no.16-2 (Loc. 15; 262 m lava dome), 5790±30 yr BP at top of the no. 4-2, 8850±30 yr BP and 9390±30 yr BP above and below the no. 4-3, respectively, and 12030±30 yr BP just under the no. 4-6. Considering the calendar years and tephrostratigraphic relation, the ages of tephras during Latest Activity comprises five eruptions of ca. 1.1-1.2 ka (no. 16-2), ca. 7.5 ka (no.16-3 and no. 4-3), ca. 10 ka (no. 4-4) and ca.13.5 ka (no. 4-6).

Currently, we are further collecting data on mineral compositions, the refractive indexes and the major element compositions of volcanic glass shards for each tephra, and we are studying from the viewpoint of correlation with eruption deposits from Kobeyama-Hanadateyama volcanic chain, and Niijima Volcano origin tephra (Miyatsukayama, Shikinejima and Miyatsuikayama South: Kobayashi et al., 2018). In the presentation on the day, we will report the eruption history of the Latest Activity of Kozushima Volcano based on the results of these studies.

©2019. Japan Geoscience Union. All Right Reserved.

Keywords: tephrostratigraphy, 14C age, eruption history, Kozushima Volcano

©2019. Japan Geoscience Union. All Right Reserved.

Characteristics of hypocenter distribution connected with velocity structures in and around Miyakejima, Kozushima and Hachijojima volcanoes

*Hiroko Hagiwara[1], Hidefumi Watanabe[1]

1. Tokyo Metroplitan Government

The aim of this study was to examine the characteristics of seismic activities in association with the seismic velocity structures in and around the Izu islands. We focused on three seismic activities, the swarm off the west coast of Miyakejima on April 2013, the swarm off the northeast coast of Kozushima on April 2018 and the low frequency earthquakes beneath Hachijojima from 2003 to 2018. To construct the 3-D velocity structure models for Miyakejima and Kozushima we used the data of the swarm accompanied with the 2000 Miyakejima eruption, while for Hachijojima we used the data from 2003 to 2018 based on the Izu islands volcanic observation system. These travel times were adopted to the tomographic inversion method (Zhang and Thurber, 2003). The relocated precise hypocenters on the velocity imaging maps revealed an interesting relationship between seismicity and structure. In the target region, both Miyakejima and Kozushima swarms occur at 5-10 km and 2-6 km depth, in the border of high-velocity zones adjacent to or underlain by the low-velocity zones in figure 1 and figure 2. Their swarm regions were located nearby the two end sides of the 2000 swarm, where the huge seismic activity occurred repeatedly. That suggests the upward moving of magmatic fluids. In contrast, the Hachijojima earthquakes occur at 10-14 km depth in the middle-velocity area around a high-velocity zone in figure 3. This high-velocity zone is supposed to be somewhat cold body beneath Nishiyama volcano in Hachijojima. We interpret that the former low-velocity zones consist of hot magmatic materials and the latter high-velocity zone consists of the solidified volcanic body. On the basis of three case studies, it is suggested that volcanic fluids derived from hot magma or solidified magma caused the upper or surrounding seismic activities through complex crack systems.

Keywords: seismic activity, velocity structure, volcanic fluid, Miyakejima, Kozushima, Hachijojima

©2019. Japan Geoscience Union. All Right Reserved.

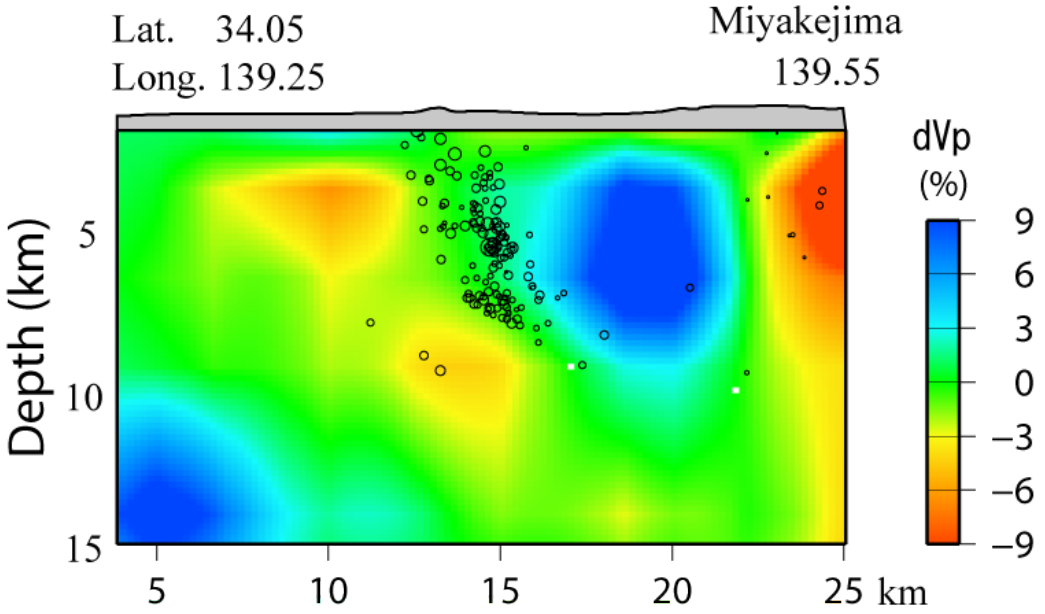

Fig. 1. E-W cross section of the dVp and relocated seismicity near Miyakejima.

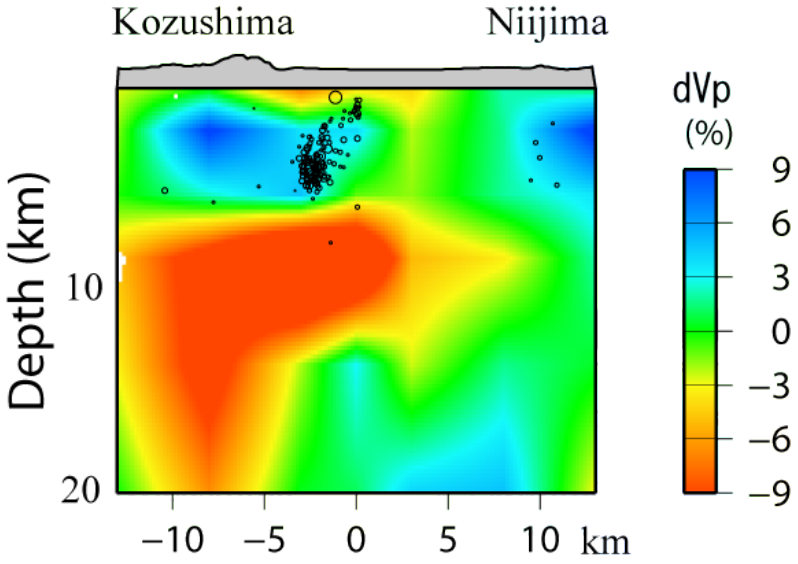

Fig. 2. Cross section of the dVp and relocated seismicity near Kozusima along the axis passing through Kozushima and Niijima.

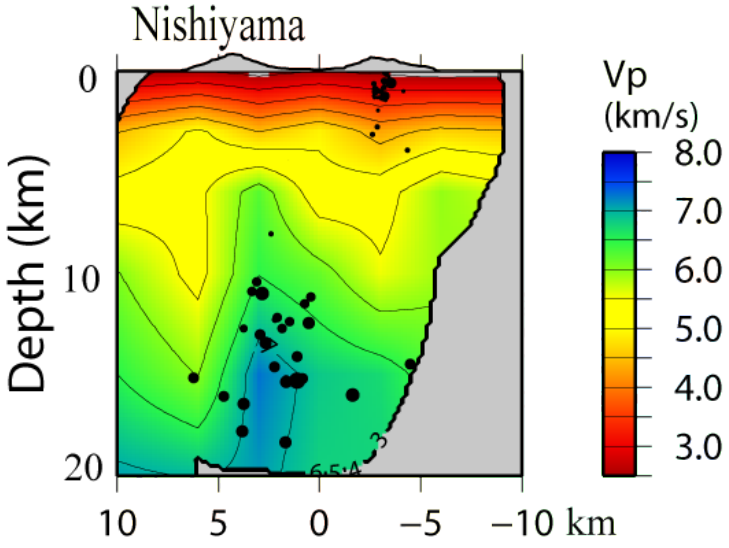

Fig. 3. Cross section of the Vp and relocated seismicity along the long axis of Hachijojima.

©2019. Japan Geoscience Union. All Right Reserved.

©2019. Japan Geoscience Union. All Right Reserved.

Deformation of Miyakejima volcano measured by GNSS campaign observation (2013-2015)

*Haruna Watanabe[1], Takeshi Matsushima[2], Miyo Fukui, Atsushi Watanabe[3], Jun Oikawa[3], Takashi OKUDA[4], Taku Ozawa[5], Yosuke Miyagi[5]

1. Department of Earth and Planetary Sciences, Graduate School of Science, Kyushu University, 2. Institute of Seismology and Volcanology, Faculty of Sciences, Kyushu University, 3. Earthquake Research Institute, University of Tokyo, 4. Earthquake and Volcanology Research Center, 5. National Research Institute for Earth Science and Disaster Resilience

Miyakejima is an active volcano located about 180 km south of Tokyo, and since the 20th century it erupted at intervals of about 20 years (1940, 1962, 1983, and 2000). Fukui et al. (2015) conducted GNSS campaign observations and estimated the pressure source of Miyakejima from 2011 to 2013. Therefore, in this research, we estimated the crustal deformation of Miyakejima from 2013 to 2015, the position of the pressure source and the volume change, and estimate the temporal change of the pressure source of Miyakejima.

We conducted GNSS campaign observations at 15 reference points arranged so as to be distributed almost evenly throughout Miyakejima from 2 September to 6 September 2013 and from 31 August to 4 September 2015. We used the data obtained from this GNSS campaign observation and the data for the same period of continuous observation points established by the Geospatial Information Authority of Japan etc. In order to analyze the obtained data, the coordinate value of the observation point for each year was obtained using RTKLIBver.2.4.2 software (Takasu et al., 2007).

The pressure source was estimated based on horizontal displacement from 2013 to 2015. The optimum value of the variation was obtained by using MaGCAP-V software (Meteorological Research Institute, 2008) for analyzing crustal activity for volcano. Although the positions of the pressure sources have not changed significantly from 2011 to 2013, it is presumed that the pressure source at the depth of about 0.3~8 km continues to contract and the pressure source at the depth of about 13 km continues to expand.

This work is partly supported by MEXT under Earthquake and Volcano Hazards Observation and Research Program, and also supported by Earthquake Research Institute, The University of Tokyo under Joint Usage Program.

Keywords: Miyakejima, GNSS observation

©2019. Japan Geoscience Union. All Right Reserved.

Characteristic properties of distal and proximal tephras in the Mikurajima Island, Izu Islands.

*Tomohiro Tano[1], Takehiko Suzuki[1,2], Makoto Kobayashi[2], Masanori Murata[2]

1. Faculty of Urban Environmental Sciences, Tokyo Metropolitan University, 2. Research Center for Volcanic Hazards and Their Mitigation, Tokyo Metropolitan University

Mikurajima of the Izu Islands is the stratovolcano island and located at 200 km south of Tokyo. The latest volcanic activity is about 6,300 years ago, there is no eruption activities in history. Mikurajima volcano is characterized by high occurrence frequency of andesite in volcanic front on the Izu arc(Isshiki,1980). Study on tephras distributed in the Mikurajima volcano has been reported by Sugihara & Shimada(1999),and Sekiguchi et al.(2001).They reported 6 tephra in Mikurajima island.(From the top Kozushima Tenzyosan:A.D.838,Iz-Kt,latest eruption of Mikurajima volcano:Mk-3,Kikai-Akahoya:7.3ka(Machida & Arai,2003),red scoria originated Mikurajima:Mk-2,rhyolithic tephra with unknown source:Mk-G, and fall pumice Mikurajima volcano tephra:Mk-1).The latest tephra of Mikurajima volcano:Mk-3,erupted from the lava dome in the southeastern in part of the islands(Sugihara & Shimada,1999).However, comparison/identification is insufficient of tephra compared to Iz-Kt. So it is necessary to compare and examine the Niijima Mukaiyama tephra(A.D.886,Iz-Mk).
They are rhyolithic tephra and indicated SiO2=77-79 wt.%. They erupted same age and constituent minerals and the refractive index of volcanic glasses are similar. So difficult to identify in distal place. Recently both can be distinguished by content of K2O in volcanic glasses. Iz-Kt indicated high K2O content compared with Iz-Mk. Both tephras are important indicator tephra widely distributed in the Izu islands. So it is important to clarify Iz-Kt distribution on Mikurajima.
In this research, we report on the tephras confirmed in Mikurajima. We found 18 tephras on Mikurajima island, and 4 tephras are confirmed(Iz-Kt,Mk-1,2,3).
1)The tephra confirmed Iz-Kt in previous study, we performed refractive index measurement by RIMS2000 and principal component analysis by SEM-EDS for volcanic grasses. This tephra present cryptotephra in topsoil. This glasses is pumice type and reflective index indicated n=1.496-497.Principal component:SiO2=77.0-78.5 wt.%,Al2O3=12.5-13.0 wt.%,FeO=0.5-1.3 wt.%,CaO=0.2-1.7 wt.%,K2O=2.7-3.9 wt.% and Na2O=3.6-4.6 wt.%.Iz-Kt and Iz-Mk confirmed on the Izu islands,they shows 3.8 wt% and 3.5 wt.% K2O content, respectively. So this tephra confirmed Iz-Kt.
2)For the latest tephra on Mikurajima volcano Mk-3,it is bad foaming yellow pumice between black volcanic sand.Maximum particle size of pumice is 10cm and maximum layer thickness is over 200cm.The lithophasies of MK-3 shows Prinian eruption.However,the detail of Mk-3 are unknown and under consideration.We performed principal component analysis as well.As a result,SiO2=62.3-70.7 wt.%,Al2O3=14.8-21.0 wt.%,FeO=2.2-3.8 wt.%,CaO=4.1-7.5 wt.%,K2O=0.3-0.9 wt.%,Na2O=3.8-4.4 wt.%.The values indicate andesite-dacite.
As a future work,to find and confirmed indicator tephra originated another volcano (like Iz-Kt and Mk-G).By comparing and identifying indicator tephra, I believe that we provide new distribute axis and age axis for history of eruption history in Mikurajima and tephra in the Izu Islands.And it is important to grasp detail of Mk-3 which is the latest eruption of Mikurajima volcano in order to grasp the volcanic activity of Mikurajima.

Keywords: Izu Islands, Mikurajima volcano, volcanin activity history, Kozushima Tenzyosan Tephra

©2019. Japan Geoscience Union. All Right Reserved.

Pseudo thermal anomalies in the shortwave infrared bands of the Himawari-8 AHI and their correction for volcano thermal observation

*Takayuki Kaneko[1], ATSUSHI YASUDA[1], Yoshizaki Yoshito[2], Takasaki Kenji[3], Yoshiaki HONDA[4]

1. Earthquake Research Institute, University of Tokyo, 2. Meteorological Satellite Center, Japan Meteorological Agency, 3. Japan Fisheries Research and Education Agency, 4. Center for Environmental Remote Sensing, Chiba University

Volcanic eruptions bring high-temperature gas or magma to the surface. Therefore, thermal observations of volcanic eruptions can be used to investigate the timeline of eruptive sequences. Eruptive activity includes processes that can change over short periods of time, which is sometimes related to the eruptive mode or the timing of its transitions. If we could observe short-term eruptive processes by detecting thermal changes, this would be beneficial for analyzing the eruptive sequence of volcanoes. Himawari-8 is a meteorological geostationary satellite operating above the equator at a longitude of 140.7 deg E and carrying a newly developed sensor, the Advanced Himawari Imager (AHI). With its improved performance, the Himawari-8 AHI enables the collection of high-frequency thermal observations that had never been obtained before. However, while observing volcanoes with the AHI, we noticed a frequent thermal anomaly in the nighttime 1.6-um and 2.3-um images. Because this anomaly occurred regardless of volcanic activity, it was considered to be a pseudo thermal anomaly. In-depth examination of the AHI observation data for several inactive volcanoes showed that the pseudo thermal anomaly was often seen around the vernal and autumn eclipse periods, and its in?uence persisted for about 6 months of each year. Further, daily variation of the anomaly peaked when it was midnight in the areas around 140 deg E. At this time and position, the AHI was facing the sun, suggesting that the anomaly was caused by stray light. We devised a correction method by assuming that the observed thermal radiance in a pixel consists of components from the radiating volcanic ground surface and stray light contamination. The latter can be estimated using values from nearby inactive pixels. Thus, the component from the radiating volcanic ground surface can be obtained by subtracting the estimated stray light from the observed thermal radiance. We evaluated the validity of this method using data from the 2017 Nishinoshima eruption and found that it satisfactorily removed the stray light component. An adoption of this correction allowed us to use all nighttime 1.6-um and 2.3-um images obtained by the AHI, half of which were formerly unusable due to the degradation caused by stray light.

Keywords: observation data correction, thermal anomaly, volcanoes

©2019. Japan Geoscience Union. All Right Reserved.

Shallow earthquakes in Unzen Volcano inferred from dense seismic observation and resistivity structure

*Hashimoto Tasuku[1], Koki Aizawa[2], Takeshi Matsushima[2], Hiroshi Shimizu[2], Yuto Hayashida[1], Yuhei Yuasa[1], Kaori Tsukamoto[1], Yuto Yamamoto[3], Kanta Miyano[3], Megumi Kamizono[1], Satoshi Matsumoto[2]

1. Department of Earth and Planetary Sciences, Graduate School of Science, Kyushu University, 2. Institute of Seismology and Volcanology, Faculty of Science, Kyushu University, 3. Department of Earth and Planetary Sciences, School of Science, Kyushu University

Unzen volcano is a stratovolcano located in central part of the Shimabara peninsula of Kyushu Island, Japan. During the eruption periods 1991-1995, the seismicity was vigorous at shallow level beneath the Heisein-Shinzan lava dome (Umakoshi et al., 2001), then the number of shallow earthquakes decreased significantly after the eruptions. However, since 2010, the number of shallow earthquakes have been increasing steadily beneath Mt. Fugen and Heiseishinzan lava dome (Japan Metrological Agency (JMA)). The most of the hypocenters were estimated 1 to 2 km below sea level, while importantly, several earthquakes were located above sea level since February 2017. The P-wave arrivals of the earthquakes above sea level show the downward motion at all stations of JMA, MLIT, and Kyushu university. The coda, which shows relatively longer period oscillation, continues approximately 20 to 30 seconds. According to JMA, this type of shallowest earthquakes has occurred 5 times in 2018. Mildon et al. (2016) reported the similar non-DC earthquakes at Krafla volcano, Iceland, and suggested closing clacks model to explain the observation.

In order to explore the shallow earthquake activity beneath Unzen volcano, we established (1) 12 seismic stations around Mt. Fugen and Heisei-Shinzan lava dome in August, 2018. In addition, (2) broad-band magnetotelluric (MT) observation was conducted in October and November, 2018 to estimate subsurface resistivity structure. We recorded telluric fields at 12 sites around Mt. Fugen and Heisei-Shinzen lava dome, and recorded MT fields at two sites at the mid flank of the Unzen volcano. The main purpose of this study is to investigate the relationship between the shallow earthquakes and volcanic fluids beneath Unzen volcano. In particular, the locations and initial motions of the shallowest earthquakes are investigated. We will present the preliminary analysis of the shallow earthquakes obtained from the dense seismic records, and the preliminary resistivity structure.

Keywords: volcanic tectonic earthquake, Unzen Volcano

©2019. Japan Geoscience Union. All Right Reserved.

Characteristics of shallow volcanic earthquakes beneath the summit of Unzen Volcano

*Kanta Miyano[1], Hiroshi Shimizu[2], Takeshi Matsushima[2], Satoshi Matsumoto[2], Koki Aizawa[2], Hashimoto Tasuku[3], Yuto Hayashida[3], Yuhei Yuasa[3]

1. Department of Earth and Planetary Sciences, School of Science, Kyushu University, 2. Institute of Seismology and Volcanology, Faculty of Science, Kyushu University, 3. Department of Earth and Planetary Sciences, Graduate School of Science, Kyushu University

Unzen Volcano is located in the central part of the Shimabara peninsula, western Kyushu, Japan. The last eruption took place in 1990-1995, and a lava dome complex was formed during the eruption. High level seismicity was observed before and during the eruption. In particular, isolated tremor occurred in the volcanic edifice above sea level preceding the lava dome emergence (Shimizu et al., 1992). Predominant frequencies of the isolated tremor’ s waveforms were comparatively low (2 - 4 Hz) and the duration was long (30 - 180 s). Moreover, extremely-shallow earthquakes occurred beneath the growing lava dome. Unzen Volcano has been in dormancy since the end of the 1990-1995 eruption. However, shallow volcanic earthquakes have been observed below the summit since 2010, and the hypocenters are determined by Japan Meteorological Agency (JMA) and Institute of Seismology and Volcanology, Kyushu University (SEVO). In order to reveal the generation mechanism of these earthquakes, we investigated the characteristics of the hypocenters and wave forms.

First, we relocated the hypocenters of these earthquakes from Jan. 1 to Sep. 7 2018. The relocated hypocenters are distributed beneath the lava dome and Mt. Fugen, and they are classified into 3 groups. Focal depths of Group 2 and 3 are located 1km and 2km below sea level under Mt. Fugen, while Group 1 (three earthquakes in this period) locates above sea level beneath the lava dome. The first motions of P-waves for Group 1 are all “down” in this study, and the duration times are longer than those of Group 2 and 3.

Next, we calculated particle motions of these earthquakes using relocated hypocenters. The result indicates that the earthquakes of Group 2 and 3 have clear P and S phases, which are similar to tectonic earthquakes. On the other hand, no obvious S phase is recognized in the seismograms of Group 1.

Spectral analysis shows that the seismograms of Group 1 are lacking in high frequency components and the low frequency (2 - 5 Hz) is dominant compared with Group 2 and 3.

We will discuss candidates for the source mechanism of these earthquakes based on the results of wave form analyses.

Keywords: Unzen, volcanic earthquake, particle motion, spectral analysis

©2019. Japan Geoscience Union. All Right Reserved.

Pyroclastic deposits and the stratigraphy on the outcrop to north east from Mt.Unzen

*Daisuke Nagai[1]

1. Mt.Unzen disaster memorial hall

Pyroclastic flows occurred at many times during formation of lava dome on the Heisei eruption of Mt.Unzen. There were some studies of pyroclastic flows on Mt. Unzen (Kobayashi and Kato, 1985). After the Heisei erupyion many studies reported about it (Kobayashi and Nakada, 1991, Watanabe and Hoshizumi, 1995). It is important about understanding the characteristics of the volcano from the past activities. In this study, the pyroclastic deposits and the stratigraphy 150ka on Mt.Unzen be reported.

Keywords: active volcano, pyroclastic flow, stratigrahy

©2019. Japan Geoscience Union. All Right Reserved.

Relative gravity changes in Aso Volcano (Kumamoto Prefecture) observed from 2015 to 2018

*Yusuke Miyauchi[1], Takahito Kazama[1], Yoichi Fukuda[1], Shin Yoshikawa[2], Takahiro Ohkura[2], Jun Nishijima[3], Yasuhiro Fujimitsu[3]

1. Graduate School of Science, Kyoto University, 2. Aso Volcanological Laboratory, Kyoto University, 3. Graduate School of Engineering, Kyushu University

Gravity measurement is one of the most effective methods to understand mass variations due to volcanism. In Aso Volcano, Kumamoto Prefecture, spatiotemporal gravity variations have been monitored by repeated relative gravity measurements every several years since 1964 (Yoshikawa et al., 2009). Gravity data was frequently collected 3-4 times every year during the active period of Aso Volcano from 2011 to 2016 and revealed spatiotemporal variations in hydrothermal mass under the volcano (Sofyan et al., 2016). However, any gravity data has not been collected after March 2016 due to Kumamoto Earthquake which occurred in April 2016. Since the volcanism became quieter after a phreatic explosion was observed in October 2016, a series of volcanic activities including the quiet period should be discussed in terms of mass variations to predict future volcanic activities. In order to monitor gravity changes in Aso Volcano after the volcanically active period, we repeated relative gravity measurements in May, August and November 2017, and in March, May, August and November 2018. We measured relative gravity values at gravity points around Aso Volcano using CG5 relative gravimeters owned by Kyushu University and Aso Volcanological Laboratory (CG5-KYU and CG5-AVL, respectively) and a LaCoste relative gravimeter G680 owned by Graduate School of Science, Kyoto University (LC-G680). We also collected continuous gravity data using CG5-AVL at the AVL station even when it was not used for the campaign gravity measurements, in order to understand the long-term instrumental drift. A gravity value relative to AVL was obtained for each point and survey, by correcting the effects of instrumental height, tide, instrumental drift, and scaling factor. The spatiotemporal absolute gravity data was then calculated, using the absolute gravity values measured at reference stations. We finally estimated the spatial distributions of the absolute gravity change around Aso Volcano before and after Kumamoto Earthquake. We found that the absolute gravity increased at the gravity points around the Aso crater. Since this absolute gravity change includes the effect of crustal deformation due to Kumamoto Earthquake, we subtracted the effect from the absolute gravity values using the quasi-vertical deformation data derived from the InSAR analyses (Geospatial Information Authority of Japan) and the typical gravity gradient value of -0.2 mGal/m. We found that the residual of the absolute gravity change still increases by up to 0.1 mGal at the areas of Kusa-senri and the Naka-dake crater, which implies mass accumulation under these areas. In the future, we will model time variations of the volcanic mass distributions in the volcano and compare them with the spherical pressure source proposed by the leveling data (Sudo et al., 2016). In addition, the gravity data should be repeatedly obtained and reprocessed more accurately, by considering the spatial variation of the gravity gradient value and correcting the effect of ground deformation using the continuous GNSS data.

Keywords: gravity change, crustal deformation, mass variation, Aso Volcano

©2019. Japan Geoscience Union. All Right Reserved.

Precise leveling survey in Aso volcano, 2018

*Takahiro Ohkura[1], Shin Yoshikawa[1], Hiroyuki Inoue[1], Akihiko Yokoo[1], Mitsuru Utsugi[1], Keigo Yamamoto[2], Kazunari Uchida[4], Yuta Maeda[5], Shinichiro Horikawa[5], Kenjiro Matsuhiro[5], Takashi OKUDA[5], Kazushi Tanoue[5], Fumiaki Kimata[7], Masayuki Murase[6], Hitoshi Mori[6], Taketoshi Mishima[3], Shintaro Komatsu[2], Masaki Takaya[3], Jun Oikawa[8], Kyoka Ishii[3], Yusuke Miyauchi[3], Ikuma Kimura[3], Masaki Uchida[3], Kazuho Nakai[3], Kosei Takishita[3], Keita Chiba[4], Hashimoto Tasuku[4], Yoshinosuke Kamiya[4], Yuto Yamamoto[4]

1. Aso Volcanological Laboratory, Institute for Geothermal Sciences, Graduate School of Science, Kyoto University, 2. DPRI, Kyoto University, 3. Graduate School of Science, Kyoto University, 4. Graduate School of Science, Kyushu University, 5. Graduate School, Nagoya University, 6. College of Human and Society, Nihon University, 7. TRIES, 8. ERI,Univ.of Tokyo

In Aso volcano, leveling survey has been conducted since 1937 by Kyoto University. As a result of these surveys, subsidence in Kusasenri about 3km west-southwest of Naka-dake crater has been observed. And this subsidence was considered to be caused by a contraction source located at about 3km west of Naka-dake crater with a depth of 4 to 6 km (Sudo et al. 2006). A seismic tomography study showed a low velocity zone of a 2 to 3 km diameter located at a depth of 6km in Kusasenri (Sudo and Kong, 2001), almost in accordance with the position of contraction source. Therefore, this low velocity zone is considered to correspond to a magma chamber.
We conducted a first-order leveling survey at Aso volcano during the period from Sep.30 to Oct.6 2018, for the first time since 2012 and after the 2016 Kumamoto Earthquake. As a result, mean square errors of the conducted survey were ranging from ±0.18 to ±0.21 mm/km.
From the obtained survey data, we calculated the relative height of each bench mark referred to a bench mark (960701A) which corresponds to GEONET 960701 GNSS station, located at the south-western foot of central cones of Aso volcano. We also calculated the height difference of 960701A between September 2012 and September 2018, using F3 solutions of GEONET, resulting in the vertical displacements of the benchmarks during the period from September 2012 to September 2018.
It was found that the obtained displacements show ground accordance with 2.5-D surface deformation of the 2016 Kumamoto earthquake detected by SAR interferometry. Therefore, we can conclude that the vertical displacements in Aso volcano detected by leveling survey are attributed to the surface deformation during the 2018 Kumamoto Earthquake.

Keywords: Aso volcano, Crustal deformation, the 2016 Kumamoto earthquake

©2019. Japan Geoscience Union. All Right Reserved.

Magma evolution during the Aso-3 caldera-forming eruption cycle deduced from the chemistry of plagioclase phenocrysts

*yuki matsukida[1], Tsuyoshi Iizuka[1], Takayuki Ushikubo[2], Kenji Shimizu[2], Nobuo Geshi[3], Isoji MIYAGI[3], Morihisa Hamada[2]

1. the University of Tokyo, 2. Japan Agency for Marine-Earth and Science Technology, 3. The National Institute of Advanced Industrial Science and Technology

Title

Magma evolution during the Aso-3 caldera-forming eruption cycle deduced from the chemistry of plagioclase phenocrysts

Author

Yuki Matsukida, Tsuyoshi Iizuka, Takayuki Ushikubo, Kenji Shimizu, Nobuo Geshi,

Isoji Miyagi, Morihisa Hamada

Introduction

Caldera-forming eruptions are the most destructive type of volcanic activity and exert a great influence on the Earth’ s surface. Therefore, the underlying magmatic mechanism leading to caldera-forming eruptions is of fundamental importance in volcanology. The Aso volcano is the largest (18×25 km in diameter) caldera in the southwestern Japan Island Arc and formed through four large eruption cycles. In this study, we have investigated the evolution of magmas that erupted during the second youngest cycle among the four cycles, the Aso-3 cycle at 123 ka. It ejected >150 km^3 of pyroclasts that are divided into the following four units in stratigraphic ascending order: 3W, a plinian pumice fall deposit; 3A, a pumice flow deposit containing dominantly aphyric pumice and glassy ash; 3B, a scoria flow deposit characterized by abundant aphyric scoria; and 3C, a scoria flow deposit consisting mainly of porphyritic scoria and glassy ash matrix.

On the basis of major and trace element compositions and Sr-Nd-Pb isotope ratios of whole rocks as well as phenocrysts, Kaneko et al. (2015) argued that the pre-eruptive magma chamber was chemically stratified from a mafic lower part to a felsic upper part. The previous study further estimated water contents in the melts using the hygrometer based on plagioclase-melt partitioning of anorthite-albite components (Lange et al., 2009), but the estimates have large uncertainty. Here we determined hydrogen contents of plagioclase phenocrysts. By combining the hydrogen contents with major and trace element compositions of the plagioclase phenocrysts, this study aims to better understand pre-eruptive magma evolution and water behavior of the Aso-3 cycle.

Methods

Plagioclase as well as pyroxene and oxide mineral phenocrysts were separated from pumices of 3W, an obsidian clast of 3A, a welded clast of 3B, and a pumice clast of 3C. Major and trace elements in phenocrysts were quantified by electron probe microanalyzer (EPMA) and laser ablation-inductively

©2019. Japan Geoscience Union. All Right Reserved.

coupled plasma-mass spectrometry (LA-ICP-MS), respectively. In LA-ICP-MS analysis, Ca contents measured by EPMA were used for internal standard normalization. OH contents in plagioclase phenocrysts were determined by secondary ion mass spectrometry (SIMS).

Results

Anorthite contents (#An) of plagioclase phenocrysts are variable even in individual units, but show the systematic increase in ascending order, consistent with the results of Kaneko et al. (2015). REE patterns of plagioclase and pyroxene show positive and negative Eu anomalies, respectively. Plagioclase Ce content degreases as #An increases (Figure 1). On the other hand, OH contents in plagioclase phenocrysts are significantly higher in 3W (~250 ppm) as compared to the others (<50 ppm) (Figure 2).

Discussion

OH contents in a plagioclase phenocryst of 3W are significantly higher than those of 3A-C, nevertheless Ce contents of plagioclase are not significantly different between 3W and 3A. Considering that the partition coefficients of Ce between anhydrous major minerals and melt are similar to those of OH, this finding suggests that H_2O was lost from the melt through gas exsolution or fractional crystallization of hydrous minerals. Alternatively, given the fast diffusion of hydrogen relative to Ce in plagioclase, it may be attributed to secondary loss of hydrogen from plagioclase phenocrysts of 3A-C during welding processes. From the observation of thin sections of 3W and 3A, however, microlite was rarely observed, suggesting that the secondary thermal effects would be restricted for both 3W and 3A. Furthermore, little hydrous phenocrysts have been observed from ejecta of the Aso-3 cycle. Therefore, the results of this study suggest that gas exsolution and degassing occurred between the eruptions of 3W and 3A.

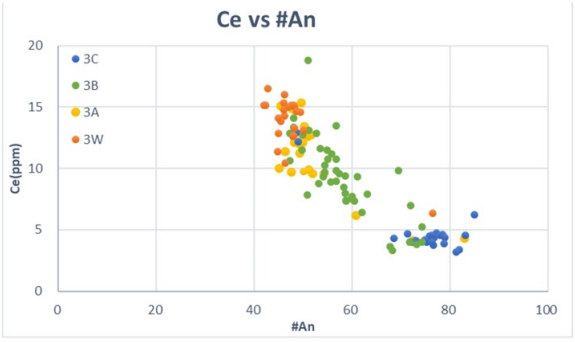

Figure 1 Ce vs anorthite contents for plagioclase phenocrysts

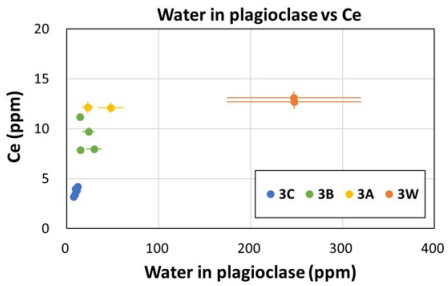

Figure 2 Water vs Ce contents for plagioclase phenocrysts (The water contents were calculated from hydrogen concentrations in the phenocrysts)

©2019. Japan Geoscience Union. All Right Reserved.

Relationship between duration of eruption tremor and eruption volume

*Azusa Mori[1], Hiroyuki Kumagai[1]

1. Nagoya University Environmental Studies

We studied the high-frequency seismic signals of eruption tremors during recent eruptions at various volcanoes and quantified their seismic source amplitudes (A_s) and cumulative source amplitudes (I_s) in the 5–10 Hz based on the assumption of isotropic *S*-wave radiation. A_s and I_s correspond to the maximum and the cumulative value of amplitudes at the source during eruption tremor. We previously found that the power law relations between A_s and I_s holds for eruption tremors. We also found the proportional relation between eruption rate and A_s for eruption tremors by comparing seismic and geodetic data during sub-Plinian eruptions at Kirishima. In this study, we further investigated time variations of eruption tremors and found the scaling relation between duration of eruption tremor and eruption volume.

We calculated the envelope width (p) using the estimated values of A_s and I_s and investigated the relation between p and I_s. p is defined as I_s/A_s and can be used as a parameter of duration (T) of a seismic envelope waveform (Kumagai et al., JGR, 2018). We found that p is proportional to 0.4 power of I_s. We also found that envelope waveforms of eruption tremors in 5–10 Hz have the following features; the amplitudes of envelope waveforms gradually increase, remain roughly constant during a certain period, and gradually decrease to the noise level. Moreover, p tends to increase with A_s. These envelope waveforms can be approximated as trapezoids, where A_s and T correspond to their height and lower base, respectively. We found that the ratios of upper to lower bases for these envelope waveforms are roughly constant. In this case, the proportionality between p and T holds. Based on the relation between eruption rate and A_s, eruption volume (V) is proportional to I_s. Therefore, the relation between p and I_s as shown above indicates that T is proportional to 0.4 power of V. We found that this proportional relation is consistent with the estimates of T and V for various Plinian eruptions compiled by Mastin et al. (JVGR, 2009). This indicates that the scaling relation between duration of eruption tremor and eruption volume in Plinian eruptions holds over a wide range of eruption size.

©2019. Japan Geoscience Union. All Right Reserved.

Crustal deformation accompanied with the eruption of Shinmoe-dake in early March 2018

*Tsuyoshi Watanabe[1], Takashi Yokota[1], Susumu Kurahashi[1], Kenta Enomoto[1]

1. Aichi Institute of Technology

Shinmoe-dake is a part of Kirishima volcano group composed of 20 Quaternary volcanoes located in southern Kyushu, Japan, erupted on 19 January 2011. This eruption began with a phreatomagmatic event including atmospheric vibration and eventually developed to subplinian eruptions within a week. From GNSS data, position and volume change of the magma chamber were estimated to be about 5 km to the northwest of the top of Shinmoe-dake at a depth of 8-9 km and 1.3×10^7 m^3. Shinmoe-dake erupted on 11 October 2017 after an interval of six years, however, this eruption ended in a week. While the extension of baseline length between the sites across Mt. Kirishima has been detected by GNSS observation since July 2017, indicating the possibility of magma accumulation. Eventually, the extension of baseline length led to eruption on 1 March 2018. In this study, in order to clarify the mechanism of the volcanic eruption, we investigated the crustal deformation accompanied with a series of volcanic activities occurred in early March 2018 at Shinmoe-dake by using GNSS data, then estimated the position of the magma chamber.

For the study, GEONET F3 solutions obtained by GNSS observation sites located mainly in the Kyushu district from 1 January 2013 to 25 March 2018 were used. Firstly, common mode bias was removed from time series of GEONET F3 solutions according to the method of Wdowinski et al. (1997). Secondly, visco-elastic deformation due to the 2016 Kumamoto earthquake was corrected by using a code of Fukahata and Matsu’ura (2005, 2006). In this time, we used the co-seismic fault model of Geospatial Information Authority of Japan (GSI, 2016) and calculated the visco-elastic deformation, where the calculation was conducted on the condition that an elastic material with thickness of 25 km lies on a Maxwell visco-elastic half-space with viscosity of 2×10^{18} Pas. Thirdly, to estimate elastic deformation due to subduction of the Philippine Sea plate (PH), we reproduced the upper surface of the PH by 170 rectangular faults based on the result of Hirose et al. (2008) and estimated coupling ratio. The Green’s functions of rectangular faults were calculated by the formula of Okada (1985). Using horizontal and vertical velocities of GEONET 150 sites between 1 January 2013 and 31 March 2016, we conducted a back-slip inversion analysis with smoothing constraint of coupling ratio among the adjacent faults. Assuming the interplate coupling obtained by the analysis continues after July 2017, we corrected the effect of the plate subduction from original data. After completing three processes above mentioned, finally, the positions of the magma chambers were estimated in two periods: inflation phase (1 July 2017–28 February 2018) and deflation phase (14 February 2018–25 March 2018) by using the Mogi’s model. We selected 7 GEONET sites located around Shinmoe-dake and estimated the positions of Mogi sources (longitude, latitude, and depth) corresponding to the two phases by performing a grid search in the ranges of 130.6-131.1˚every 0.001˚for longitude, 31.7-32.1˚every 0.001˚for latitude, and 4-15 km every 0.1 km for depth. The volume change of the Mogi sources were assumed to be 1.6×10^7 m^3 in the inflation phase and -0.7×10^7 m^3 in the deflation phase, according to the results of Japan Meteorological Agency (JMA). The result showed that the positions of the magma sources were estimated not to be just under the top of Shinmoe-dake but to be about 6-7 km to the northwest of it at a depth of 7-12 km. Although our result is generally consistent with that of JMA, the depth of the magma sources in the inflation phase was estimated to be approximately 4 km deep part. For the next step, we investigate the effects of topography and heterogeneous structure on crustal deformation.

©2019. Japan Geoscience Union. All Right Reserved.

Keywords: Shinmoe-dake, GNSS data, visco-elastic deformation due to the 2016 Kumamoto earthquake, elastic deformation by subduction of the Philippine Sea plate, estimation of magma chambers

©2019. Japan Geoscience Union. All Right Reserved.

Sources under Iwo-yama, Kirishima Volcanoes derived from GNSS observation and Precise leveling survey.

*Yuki Koga[1], Takeshi Matsushima[2], Kazunari Uchida[2], Dan Muramatsu[1], Yuichi Iwasa[1]

1. Department of Earth and Planetary Sciences, Graduate School of Science, Kyushu university , 2. Institute of Seismology and Volcanology, Faculty of Science, Kyushu University

At Iwo-yama that active volcano located in Ebino kogen volcanic area of Kirishima Volcanoes, fumarolic activity has risen again from December 2015 after dozen year's silence and suddenly increasing of seismicity (50 times and more a day) and volcanic tremors was observed several times. And phreatic eruption occurred in April 2018. Morita (2018) inferred inflation spherical pressure source as Mogi source from leveling survey between June 2015 and December 2015. The source's depth is about 700m beneath Iwo-yama and the source was considered that correspond with bottom of conductive layer inferred clay layer from MT survey (Tsukamoto et al., 2018). But, leveling can detect vertical displacement only and the inferred source is not considered horizontal displacement. So, we will improve pressure source inferred from leveling adding detect horizontal displacement from GNSS observation in this study.

As result of the observation, radial crustal deformation was detected several months before the occurrence of the phreastic eruption and after the eruption occurred. Estimating those displacement using an elevation-modified Mogi model, volume increse of the pressure source located at 700m depth below Iwo-yama was estimated. The depth of this pressure source coincided with the depth of the clay layer and it was found that the pressure source had expanded under the clay layer before the eruption occurred. But, for the GNSS observation point of the edifice before eruption, displacement which can’t be explained by the pressure source under the clay layer has been detected. This displacement is thought to be due to the rise of hot water to the shallow part as the pressure source under the clay layer expands.

We conducted GNSS continuous observation point around Iwo-yama established by Japan Meteorological Agency to verify the pressure source under the clay layer. As a result, displacements which can’t be explained by this model detected at these observation points. Using the GNSS continuous observation points throughout Kirishima, we estimated the pressure source of this displacement. Then, we could estimate the spherical pressure source located 7 km deep in the vicinity of Ebino-dake. This model is consistent with the source of crustal deformation before and after the eruption of Shinmoe-dake volcano in 2011 estimated by Nakao et al. (2018). Therefore, those displacement is thought to be due to volume change of magma chamber of Shinmoe-dake. In conclusion, the crustal deformation around Iwo-yama is due to these three sources, spherical pressure source under clay layer, displacement due to hot water rising to shallow part of Iwo-yama, magma chamber of Shinmoe-dake.

Keywords: Iwo-yama, GNSS observation, Precise leveling survey

©2019. Japan Geoscience Union. All Right Reserved.

GNSS 観測と精密水準測量から推定される霧島硫黄山の地下圧力源
Sources under Iwo-yama, Kirishima Volcanoes derived from GNSS observation and Precise leveling survey.

*古賀 勇輝[1]、松島 健[2]、内田 和也[2]、村松 弾[1]、岩佐 優一[1]
*Yuki Koga[1], Takeshi Matsushima[2], Kazunari Uchida[2], Dan Muramatsu[1], Yuichi Iwasa[1]
1. 九州大学大学院理学府地球惑星科学専攻、2. 九州大学大学院理学研究院附属地震火山観測研究センター
1. Department of Earth and Planetary Sciences, Graduate School of Science, Kyushu University, 2. Institute of Seismology and Volcanology, Faculty of Science, Kyushu University

At Iwo-yama that active volcano located in Ebino kogen volcanic area of Kirishima Volcanoes, fumarolic activity has risen again from December 2015 after dozen year's silence and suddenly increasing of seismicity (50 times and more a day) and volcanic tremors was observed several times. And phreatic eruption occurred in April 2018. Morita (2018) inferred inflation spherical pressure source as Mogi source from leveling survey between June 2015 and December 2015. The source's depth is about 700m beneath Iwo-yama and the source was considered that correspond with bottom of conductive layer inferred clay layer from MT survey (Tsukamoto et al., 2018). But, leveling can detect vertical displacement only and the inferred source is not considered horizontal displacement. So, we will improve pressure source inferred from leveling adding detect horizontal displacement from GNSS observation in this study.

As result of the observation, radial crustal deformation was detected several months before the occurrence of the phreastic eruption and after the eruption occurred. Estimating those displacement using an elevation-modified Mogi model, volume increse of the pressure source located at 700m depth below Iwo-yama was estimated. The depth of this pressure source coincided with the depth of the clay layer and it was found that the pressure source had expanded under the clay layer before the eruption occurred. But, for the GNSS observation point of the edifice before eruption, displacement which can't be explained by the pressure source under the clay layer has been detected. This displacement is thought to be due to the rise of hot water to the shallow part as the pressure source under the clay layer expands.

We conducted GNSS continuous observation point around Iwo-yama established by Japan Meteorological Agency to verify the pressure source under the clay layer. As a result, displacements which can't be explained by this model detected at these observation points. Using the GNSS continuous observation points throughout Kirishima, we estimated the pressure source of this displacement. Then, we could estimate the spherical pressure source located 7 km deep in the vicinity of Ebino-dake. This model is consistent with the source of crustal deformation before and after the eruption of Shinmoe-dake volcano in 2011 estimated by Nakao et al. (2018). Therefore, those displacement is thought to be due to volume change of magma chamber of Shinmoe-dake. In conclusion, the crustal deformation around Iwo-yama is due to these three sources, spherical pressure source under clay layer, displacement due to hot water rising to shallow part of Iwo-yama, magma chamber of Shinmoe-dake.

This work was partly supported by MEXT under Integrated Program for Next Generation Volcano Research and Human Resource Development, and under Earthquake and Volcano Hazards Observation and Research Program.Also it was suppoerted by ERI, The University of Tokyo under Joint Usage Program.

キーワード：硫黄山、GNSS 測量、水準測量
Keyword：Iwo-yama, GNSS observation, Precise leveling survey

©2019. Japan Geoscience Union. All Right Reserved.

Regional vertical deformation around Aira caldera from GNSS data

*Kazuho Nakai[1], Masato Iguchi[2], Takahiro Ohkura[3]

1. Division of Earth and Planetary Sciences, Graduate School of Science, Kyoto University, 2. Sakurajima Volcano Research Center, Disaster Prevention Research Institute, Kyoto University, 3. Aso Volcanological Laboratory, Institute for Geothermal Sciences, Graduate School of Science, Kyoto University

We investigated regional ground deformation around Aira caldera by analyzing vertical displacement observed by GNSS.

We used daily coordinate data from F3 solutions of GEONET stations in Kyusyu for periods from 1998 to 1999 and 2015 to 2016 when the ground uplift rate was larger than 18 mm/yr at 960719 station (North of Sakurajima). In order to increase number of stations, we analyzed RINEX data around Aira caldera and Sakurajima observed by Kyoto University and obtained daily coordinate data calculated based on the coordinates of the F3 solution of the GEONET stations closest to each observation point by using RTKLIB Ver. 2.4.2. The vertical displacement rate was estimated by removing the coseismic or antenna change steps and the annual and semiannual components. The ground deformation close to Kirishima volcano was affected by the pressure source located about 9 km beneath the Karakuni-dake (Nakao et al. 2013). We removed these effects causing inflation of the pressure source.

The ground within a radius of 20 km from the center of Aira caldera was uplifted in the both periods. The amount of uplift near the center of Aira caldera is larger than that in distant region and the largest uplift of station (25 mm/yr in 1998-1999 and 20 mm/yr in 2015-2016) was obtained at northern part of Sakurajima. In contrast, the ground subsidence was detected at distances from 20 to 30 km away from the center of the caldera during the period in 1998-1999 and from 30 to 40 km during the period in 2015-2016. The amounts of subsidence were about 3 mm/yr in the both periods.

We applied a model of dual source of Mogi-type (Mogi, 1958) to the ground deformation. In the period of 1998-1999, an inflation source was obtained at a depth of 10 km and a deflation source at a depth of 14 km beneath the Aira caldera. The amounts of volume change were estimated at about $+1.8\times10^7$ m^3 and -1.5×10^7 m^3, respectively. Similarly, in the period of 2015-2016, an inflation source was obtained at a depth of 10 km and a deflation source at a depth of 30 km. The amounts of volume change were estimated at about $+1.5\times10^7$ m^3 and -3.3×10^7 m^3, respectively. The order of volume change of the inflation source is almost same as the deflation source in the both periods.

The spatial distribution of the vertical displacement rate can be explained by the shallow inflation source and the deep deflation source. The shallow inflation source coincide with A-source beneath the Aira caldera (Hotta et al. 2016) corresponding to magma reservoir. Considering similarity of the volume changes, magma seems to move from to the shallow magma reservoir around 10 km deep from a deeper part.

Keywords: Aira caldera, Global Navigation Satellite System, vertical deformation

©2019. Japan Geoscience Union. All Right Reserved.

Vertical ground deformation in Sakurajima volcano measured by precise leveling survey (during Nov. 2017 - Nov. 2018)

*Keigo Yamamoto[1], Takeshi Matsushima[2], Shin Yoshikawa[3], Hiroyuki Inoue[3], Tadaomi Sonoda[1], Kosei Takishita[1], Kazuho Nakai[1], Masaki Uchida[3], Ryo Oyanagi[3], Yoshinosuke Kamiya[2], Takahiro Ohkura[3]

1. Disaster Prevention Research Institute, Kyoto University, 2. Fuculty of Sciences, Kyushu University, 3. Gruduate School of Science, Kyoto University

We conducted the precise leveling survey in Sakurajima volcano, southwest Japan in November 2018, in order to evaluate the vertical ground deformation associated with the recent eruptive activity of the volcano. The leveling routes measured in this survey are about 21 km long in total, including Sakurajima western flank route and Sakurajima northern flank route. These leveling routes were measured during the period from November 12 to 29. As a result of the preparatory calibrations and careful measurements, mean square errors of the conducted survey were achieved with a good accuracy ranging from ±0.18 to ± 0.25 mm/km.
From the measured data, we calculated the relative height of each benchmark referring to the reference benchmark BM.S.17 which is located at the western coast of Sakurajima. The calculated relative heights of the benchmarks were then compared with those of the previous survey conducted in November 2017 (Yamamoto et al., 2018), resulting in the relative vertical displacements of the benchmarks during the period from November 2017 to November 2018.
The resultant displacements indicate the ground subsidence (-6.2 mm at maximum) at benchmarks around the central part of Sakurajima. The ground subsidence is also detected at benchmarks along Sakurajima northern flank route, suggesting that the inflation of the magma reservoir beneath Aira caldera was not remarkable during the period between November 2017 and November 2018. From the preliminary analysis based on a spherical source model (Mogi, 1958), the deflation source is located beneath Minamidake crater. The results indicate that the pressure decrease is suggested at the magma reservoir beneath Minamidake caused by the eruptive magma ejection.

Keywords: Sakurajima volcano, precise leveling survey, vertical ground deformation

©2019. Japan Geoscience Union. All Right Reserved.

Spatiotemporal gravity variations from the 1990s in Sakurajima Volcano, revealed by repeated relative gravity measurements

*Ryo Oyanagi[1], Takahito Kazama[1], Keigo Yamamoto[2], Hiromitsu Oshima[3], Kazumi Okada[3], Tadaomi Sonoda[2], Masato Iguchi[2]

1. Graduate School of Science, Kyoto University, 2. DPRI, Kyoto University, 3. ISV, Hokkaido University

Gravity observation is one of the most effective methods to detect spatiotemporal mass variations in volcanoes. In and around Sakurajima Volcano, relative gravity measurements were first started in 1975 and have been repeated 20 times until 2018. The long-term gravity variations from 1975 to 1992 was modeled by Kazama et al. (2018), to understand volcanic mass variations associated with active eruptions at the Minami-dake summit during the same period. They showed that the relative gravity increase in Sakurajima cannot be fully explained by two spherical deflation sources, which were expected from the leveling data. Instead, they found that the gravity increase can be modeled by an additional point mass of 6.0 E+10 kg/yr at 5 km depth under the Kita-dake summit. However, Kazama et al. (2018) modeled the volcanic mass distributions only from 1975 to 1992, and mass distributions during the subsequent period from the late 1990s to the 2010s should be modeled as well to understand present mass accumulating processes and forecast future volcanic activities of Sakurajima Volcano.

We therefore analyzed the GPS and relative gravity data obtained from the late 1990s to the 2010s, to model the long-term pressure and mass sources under Sakurajima Volcano as follows. We first subtracted the effect of tectonic crustal deformation in the southern Kyushu Island from the horizontal displacement data of the GEONET F3 solution, using the method of Takayama and Yoshida (2007). We also reproduced the residual horizontal displacement data by a spherical pressure source of Mogi (1958), assuming the inflation of a magma reservoir located under Aira Caldera; in this calculation, several parameters about the location and volume change of the pressure source were determined by the grid search method so as to most reproduce the horizontal displacement data. The inflation source was calculated to be located at 9 km depth under the center of Aira caldera with the inflation rate of 5.5 E+6 m3/yr. However, this inflation source never agrees with the gravity increase observed in Sakurajima volcano after the late 1990s, because the source inflation and consequent ground uplift leads to the gravity decrease (Hagiwara, 1977).

After correcting the effect of the inflating pressure source, the observed gravity values were found to increase at rates of +7.49 and +1.61 microGal/yr at S110 (located at the summit of Sakurajima) and S16 (located at the western foot of Sakurajima), respectively. We thus calculated theoretical gravity variations in Sakurajima Volcano by assuming a point mass under the center of the volcano, so as to explain the observed gravity increase; in this calculation, the parameters about the depth and mass increase were determined with the trial-and-error method. The point mass was estimated to be located at 3.3 km depth below sea level with a mass increasing rate of 2.3 E+10 kg/yr. This result implies that the mass accumulation continues under Sakurajima Volcano even now, although the present accumulating rate reduced by less than half compared with that from the 1970s to the former 1990s. We will sophisticate the pressure/mass source models in the future, to reveal the mass redistribution processes associated with volcanic activities of Sakurajima Volcano.

Keywords: Sakurajima Volcano, relative gravity, crustal deformation, mass variation, magma, hydrology

©2019. Japan Geoscience Union. All Right Reserved.

Investigation into the crater of Sakurajima volcano during eruption using UAV

*Shunsuke Miura[1], Takumi Mochiduki[1], Kouji Fujita[1], Toshihiro Urayama[1], Hisashi Sasaki[1], Tatsuro Chiba[1]

1. Asia Air Survey Co.,Ltd

1. Intoroduction
Measuring the active crater topography can obtain important information on volcanologically and disaster prevention, but the flight over the crater is risky involved in the eruption and is dangerous. The Minamidake crater of Sakurajima has repeated vigorous eruptions over a long period of time, and the topography change is intense. The Minamidake crater has A crater and B crater, and on the east slope there is Showa crater. Ministry of Land, Infrastructure, Transport and Tourism has regularly conducted airborne laser surveying to clarify the geometry shape. However, airborne laser surveying has become difficult due to the activation of eruption activity. Especially it was difficult to measure the topography of Minamidake crater, west of the Showa crater. Therefore, in this study, in order to grasp detailed crater circumstances of Minamidake crater and Showa crater on Sakurajima, we tried near-field photographing by UAV and terrain measurement utilizing SfM / MVS.

2. Investigation of Showa crater and Minamidake crater of Sakurajima by UAV
The UAV used is Matrice 210 (manufactured by DJI), and the installed camera is ZENMUSE X4S (visible light) and ZENMUSE XT2 (thermal infrared). DJI's UAV has an altitude limit of 500 m above ground level from the takeoff and landing point as a safety measure. For this reason, the takeoff and landing site was the upper stream of the Amida River (around 600 m altitude) outside the entry restriction. The photographing by UAV was performed three times in total, about 15 minutes using the moving picture photographing method.In UAV photographing of visible light, we were able to confirm the state inside the Showa crater, which is unknown by the surveillance camera at the foot. On the other hand, inside the Minamidake crater, due to the influence of the plume, it was impossible to photograph clearly. In the thermal infrared photography, resolution as much as visible light could not be obtained, but we could confirm the movement of the plume inside the Minamidake crater. Moreover, in the thermal infrared, it was possible to capture a high resolution movie rather than photographing with a helicopter, and at Showa crater the stratification of the crater wall could also be confirmed.

3. Create 3D model and orthoimage
An image was cut out from the movie of the visible light that was shot, and an orthoimage of 0.5 m resolution of the Showa crater and a 3D model were made by SfM / MVS. Actually the Showa crater was almost stopped, except for some fumaroles, it was possible to clearly shoot the crater bottom. On the other hand, the Minamidake crater was greatly affected by the plume, a lot of clouds appeared above the crater, and the crater bottom was unknown. We are going to try SfM / MVS analysis using measurement results of thermal infrared with less influence of plume compared with visible light.

4. Conclusion
In order to eliminate the influence of the plume and to obtain a clearer image, it is thought that low-altitude flight to the crater's sky or inside the crater is necessary. Currently, since images are recorded on the SD card, collection after returning is a major premise, but in the future it is desirable to create models from images obtained by wireless communication.

©2019. Japan Geoscience Union. All Right Reserved.

Acknowledgments
This work was supported by the Japanese Ministry of Education, Culture, Sorts, Science and Technology under a grant from the Integrated Program for Next Generation Volcano Research and Human Resource Development. Regarding entry into the takeoff and landing site, I would like to thank you for providing the cooperation and permission of Kyoto University and Kagoshima Forest Management Office, here.

Keywords: UAV, Active Volcano, SfM/MVS, Thermal infrared image

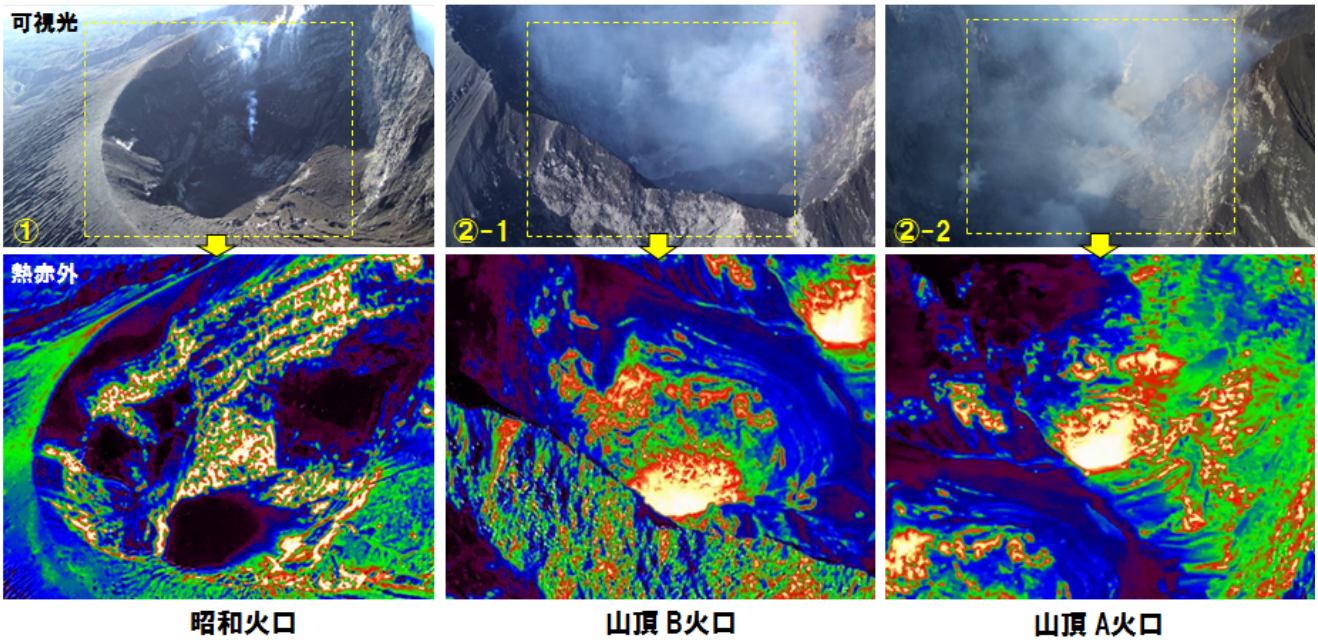

©2019. Japan Geoscience Union. All Right Reserved.

Seismic refraction and wide-angle reflection experiment in southern Kyushu, Japan: (3) the 2018 exploration report

*Hiroki Miyamachi[1], Hiroaki Takahashi[2], Hiroshi Aoyama[2], Mako Ohzono[2], Takahiro Shiina[6], Masamitsu Takada[2], Masayoshi Ichiyanagi[2], Teruhiro Yamaguchi[2], Yuki Susukida[2], Saito Kazuma[2], Chihiro Ito[2], Yoshio Murai[2], Tatsuya Nakagaki[2], Tomoki Tsutsui[3], Ryuichi Takei[3], Yuuya Tada[3], Mare Yamamoto[4], Satoshi Hirahara[4], Takashi NAKAYAMA[4], Ryosuke Azuma[4], Syuichi Suzuki[4], Toshinori Sato[5], Eiji Kurashimo[6], Miwako Ando[6], Shinichi Tanaka[6], Satoshi Ikezawa[6], Tomoaki Yamada[6], Kazuo Nakahigashi[7], Yuta Maeda[8], Shinichiro Horikawa[8], Kenjirou Matsuhiro[8], Takashi OKUDA[8], Shuhei Tsuji[8], Naoki Sogawa[8], Hiroshi Katao[9], Takuo Shibutani[9], Tsutomu Miura[9], Nakagawa Jun[9], Itaru Yoneda[9], Takeshi Tameguri[9], Kosei Takishita[9], Kazuho Nakai[9], Yusuke Yamashita[9], Takeshi Matsushima[10], Kazunari Uchida[10], Rintaro Miyamachi[10], Hiroshi Yakiwara[1], Shuichiro Hirano[1], Takeshi Kubo[1], Kenyu Sakao[1]

1. Kagoshima University, 2. Hokkaido University, 3. Akita University, 4. Tohoku University, 5. Chiba University, 6. University of Tokyo, 7. Tokyo University of Marine Science and Technology, 8. Nagoya University, 9. Kyoto University, 10. Kyushu University

[1] Primary Objective

Southern Kyushu is a typical island arc region: subduction of Philippine Sea plate under Kyushu off Hyuganada with high seismic activity, the Aira caldera with active volcanic activity, the extending Okinawa trough, and the East China Sea. Our project is aimed at clarifying the detailed velocity structure of the crust beneath southern Kyushu and recognizing interactions with crustal activities in these regions.
It is also concerned about the occurrence of large-scale eruptions at the Aira caldera larger than the 1914 Taisho eruption in Sakurajima volcano. Accordingly, we also intend to reveal the caldera structure of the Aira caldera in order to deepen the understanding of the present magma supply system beneath the Aira caldera.
This reports an outline of the second seismic exploration carried out in November 2018.

[2] Report of Seismic Exploration in 2018

For our purpose mentioned above, we carried out the first seismic exploration in November 2017, which consists of 9 shot points with charges of about 200 kg dynamite in the land area and 906 temporary seismic stations including 42 OBSs along about 165 km long profile running transversely across the Osumi Peninsula, the central part of the Aira caldera, the Satsuma Peninsula, the Koshiki Strait and the Koshiki Islands.
The second seismic exploration was carried out in November 2018. In this 2018 exploration, 872 temporary seismic stations were deployed along the 2017 seismic main profile. The equipment at each station is same as that in 2017. In addition, we widely deployed 49 seismic temporary stations with a 4.5 Hz three components seismometerand a portable data logger ”GSX” in Sakurajima volcano in order to estimate the 3-D velocity structure beneath the volcano.
In the 2018 exploration, artificial explosions by the seismic air-gun blasting system(6000 cubic inches) were applied at 50m or 100m intervals along the sea profiles (Profile-B, Profile-D, Profile-F, Profile-H). We successfully observed the seismic refraction and reflection signals generated from the air-gun in a distance range of more than 20 km. We also introduced 4 big vibrator vehicles in the land area, which vibrates continuously during about 4 hours at the fixed locations. In addition, we carried out the seismic reflection profiling with 5 km long profile in the northeastern area in Sakurajima volcano.

©2019. Japan Geoscience Union. All Right Reserved.

Acknowledgement : This project is mainly funded by the Kyushu Electric Power Co., Inc. The JGI Inc. conducted the artificial explosions, and the Hanshin Consultants Co., Ltd shared a part of the temporary seismic observation.

Keywords: velocity structure, southern Kyushu

©2019. Japan Geoscience Union. All Right Reserved.

Flow and emplacement mechanism of Koya Ignimbrite

*Keiko Suzuki-Kamata[1], Reina NAKAOKA[1], Tomomi Yamane[2]

1. Kobe Ocean-Bottom Exploration Center , 2. Department of Planetology, Graduate School of Science, Kobe University

Koya ignimbrite sourced from Kikai caldera 7.3 ka and traveled across the sea to reach the adjacent islands and the mainland of south Kyushu 40-90 km distant. Proximal facies of Koya ignimbrite, called Takeshima pyroclastic-flow deposit, comprise two or more flow units with a maximum thickness of 30 m, but the distal deposits collectively called Koya ignimbrite are consist of one flow unit and are exclusively very thin. Lag Breccia of Koya ignimbrite is recognized as layer 2b of 5 m thick on Takeshima and layer 1 of 2 m thick on Satsuma-Iwo Jima.

Koya ignimbrite contains essential pumices and volcanic glasses, both exhibiting a bimodal compositional distribution, e.g., ~60 and ~70 wt.% SiO_2 (Fujihara and Suzuki-Kamata, 2013). In addition to the silicic component, reflecting contribution the mafic component increases upwards from the basal to middle level of the deposit, and this vertical variation likely indicates progressive aggradation of pyroclasts. Koya ignimbrite overlies the ground layer consisting of crystal and fine pumice 1~5cm thick, and segregation pipe is commonly recognized in the ignimbrite in distributed area. The pyroclastic-surge deposit showing cross lamination overlies the ignimbrite on south of Osumi Peninsula. The surge deposit is rich in the mafic component, and suggests that the surge is formed at the late stage of ignimbrite eruption.

Koya ignimbrite distributes from the shoreline to the highland 1900m above sea level in Yakushima. Koya ignimbrite shows different lithofacies depending on altitude, which is thick and massive deposit more than severeal meters thick at lower area, and thin less than 50cm and composed of layer 1 at the base at higher altitude of 1600m above sea level. Mafic component is contained from the base of Koya ignimbrite in the north-west area on Yakushima both the lower area and the higher area, but mafic component increases upwards from the basal to middle level of the deposit in south-west area of Yakusima as same as Kyushu, Kuchinoerabujima and Tanegashima. This suggests that the earlier Koya ignimbrite climbing up the mountain area flows back due to the gravity in the north-west area and deposited thick at the lower area.

While silicic component can be recognized throughout the ignimbrite, mafic component exist only at the upper level of it at Tanegashima. The early phase products of Koya ignimbrite eruption reached to Tanegashima because this vertical variation is equal to that of the ignimbrites on proximal area, Satsuma Peninsula and Osumi Peninsula (Fujihara and Suzuki-Kamata, 2013). Lower contents of mafic component from upper most level compared with that of Osumi Peninsula suggest that the flows which contain abundant in mafic component occured at the later phase of the ignimbrite eruption cannot reach to Tanegashima. This is conformable the fact that the ignimbrites on Osumi Peninsula are thicker than that of Tanegashima. Based on above, it is estimated that Koya ignimbrite lost a great many amount of pyroclasts in the sea during traveling across the sea and the Koya ignimbrite widely lies on the sea floor around Kikai caldera. Koya ignimbrite became the low aspect ratio ignimbrite after passing the sea area, and low density pyroclastic surge was formed in the mountain area reflecting the topography.

Keywords: low-aspect ratio ignimbrite, Koya ignimbrite, Kikai caldera

©2019. Japan Geoscience Union. All Right Reserved.

©2019. Japan Geoscience Union. All Right Reserved.

Investigating Origin of landslide-like bathymetric feature at southern Mt.Kaimon using bathymetric and multichannel seismic reflection surveys

*hiroto yamaguchi[1], Satoshi Shimizu[2], Hikaru Iwamaru[2], Mamoru Sano[2], Nobukazu Seama[3,2], Misaki Horiuchi[3], Tetsuo Matsuno[2,3], Yoshiyuki Tatsumi[2,3]

1. Department of Planetology, Faculty of Science, Kobe university, 2. Kobe ocean-bottom exploration center, 3. Department of Planetology, Graduate School of Science, Kobe university

The existence of a landslide-like bathymetric feature is reported (Japan Coast Guard, 2007) to the south of Mt.Kaimon volcano that started eruption at the shallow sea area about 4400 years ago. We conducted the multichannel seismic reflection and bathymetric surveys in March and October 2018 using T/S 'Fukae-maru' to investigate how the landslide-like bathymetric feature was formed and where the source was if it was formed by a landslide. The bathymetric data (Figure) are used to make hill-shade map, slope map and terrain ruggedness index map, which characterize bathymetric features. We acquired seismic reflection data sets along eleven survey lines across the landslide-like bathymetric feature (green lines in Figure), which allows us to provide eleven seismic reflection profiles. The seismic reflection profiles indicate that there is a clear reflection boundary, which divide into two areas: The lower layers below the reflection boundary observed at large area and were not affected by stress. Many reverse faults and folds in the upper layers above the reflection boundary with its thickness of about 70m, which were formed by horizontally compressional stress. The analysis of the reflection profiles and the bathymetric lead to, divide the landslide-like bathymetric feature area into four areas. We name each area North-Eastern, South-Eastern, Central and Western part, which shows characteristic features as bellows:

・North-Eastern part; this area is large rugged sea bottom and slope. In the reflection profile, the boundary of upper and lower layers is not so clear. Deeper layers are not observed.

・South-Eastern part; this part is little rugged sea bottom and slope. In the reflection profile, there are some reverse faults and the fault strikes are East-West direction. Stratified structures are also found in spots.

・Central part; this part is the least rugged sea bottom and slope of four area. In the reflection profile, there are a lot of reverse faults. The fault strikes are always North-northwest-South-southeast direction. Stratified structures are found at eastern and western edge.

・Western part; this part is not as large as North-Eastern part, but large rugged sea bottom and slope. In the reflection profile, there are many (but less than Central part) reverse faults, and the fault strikes are North-South.

These characteristic features duggest that an event sweeping the ocean bottom was occurred at northern North-Eastern part, and directions the sweeping landslide are moving in south and west-southwest. It is because deeper layers are effected by collapse at North-eastern part, compressional stress is estimated by faults and folds (direction at the eastern part is North-South and at the central-western part is East-West) and bathymetric feature is more rugged at the eastern part.

Keywords: seismic reflection, ocean bottom topography, Kaimondake

©2019. Japan Geoscience Union. All Right Reserved.

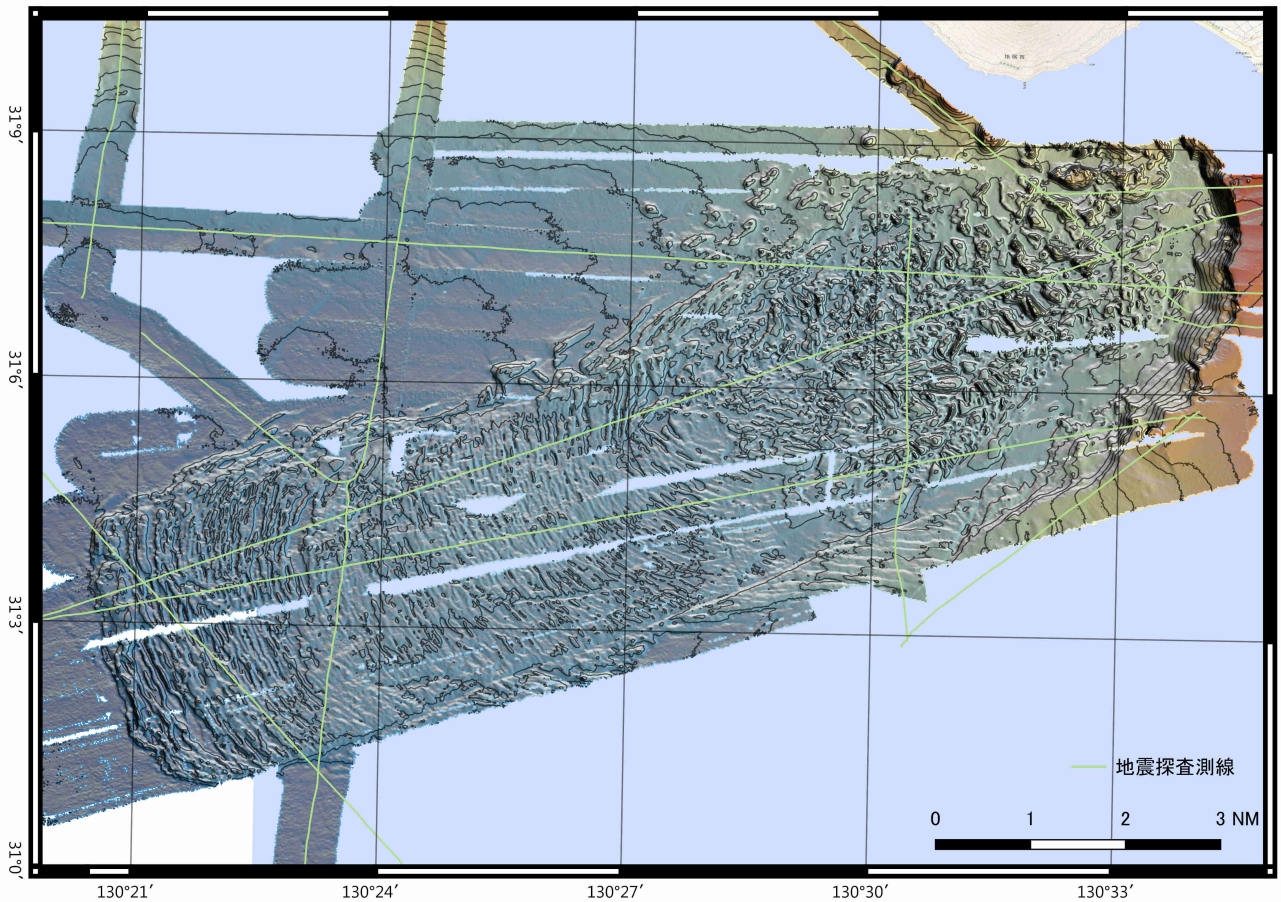

国土地理院の電子地形図（タイル）に海底地形図と反射波地震探査の測線を追記して掲載

©2019. Japan Geoscience Union. All Right Reserved.

Occurrence and distribution of pyroclastic fall deposits of Kuchinoerabujima volcano 2018-2019 eruption

*Masashi NAGAI[1], Shojiro Nakagawa[2], Yu Iriyama[1], Takahiro Miwa[1], Toshikazu Tanada[1], Hideki Ueda[1], Setsuya Nakada[1]

1. Volcano Research Department, National Research Institute for Earth Science and Disaster Resilience, 2. Yakushima Chigaku Club

At Kuchierabujima volcano, eruption began intermittently from October 21, 2018. Relatively large eruptions such as Yakushima and Tanegashima Islands adjacent to the east side of Kuchinoerabujima Island are observed on December 18 and 28, 2018, January 17 and 29, 2019. The ash fall distribution survey was conducted on three eruptions excluding the December 28 eruption where the ash fall axis was in the southeast direction and ash fall on the land was small. In Kuchinoerabujima Island, we conducted an investigation in early February, 2019. We also used information provided by Japan Meteorological Agency Kuchinoerabujima Volcano Disaster Prevention Liaison Office and interviews with local residents.

The Ash fall deposits on Yakushima and Tanegashima Islands are all light gray to reddish light gray colored sandy to silty volcanic ash layers, the component are mainly composed of lithic fragments and hydrothermal altered fragments and small amount of fresh vitreous rock fragments. At the eruption of January 17, 2019 where the largest one during a series of eruptions, on the ash fall axis extending to the east, 400 g/m^2 of ash deposited in the northwestern part of Yakushima Island, 100 g/m^2 in the northeast part, and 20 g/m^2 in the southern tip part of Tanegashima Island. Part of the deposit had the characteristics that ash particles fell as mud rain. In the northern part of Yakushima Island, fine lapilli was also included, and the maximum particle diameter tended to be larger on the north side than the ash fall axis. The deviation between the axis of ash fall axis and the axis of maximum particle diameter distribution can be explained by the difference in wind direction and wind speed at altitude. In Kuchinoerabujima Island, there was an ash fall axis from the summit crater to the southeast direction as total air fall deposit of the series of eruptions, and a deposit amount of about 12 kg/m^2 was confirmed at a distance of about 1.5 km. The layer corresponding to the eruption on January 17 is coarse deposit contains lapilli with long diameter of about 5 cm or more.

The amounts of air fall deposits were obtained by the method of Fierstein and Nathenson (1992) using average deposition density of 1000 kg/m^3. Based on the distribution data of distant deposits such as Yakushima Island, they are estimated to be ca.29,000 tons on the December 18, 2018 eruption, ca.62,000 tons for the January 17, 2019 eruption, and ca.14,000 tons for the January 29, 2019 eruption. These are smaller than the amount of air fall deposit of May 29, 2015 eruption estimated in the same method, ca.120,000 tons. When adding the depositional mass data of Kuchinoerabujima which is the proximal area to these distal data, the total of air fall deposits from December 2018 to January 2019 is estimated to be about 130,000 tons.

Keywords: tephra, phreatic eruption, Phreatomagmatic eruption, eruption column, Ryukyu arc

©2019. Japan Geoscience Union. All Right Reserved.

Ground Deformation around Domestic Active Volcanoes detected by InSAR of ALOS-2/PALSAR-2

*Takafumi Taniguchi[1], Isao Kageyama[1], Okuyama Satoshi[2], Shinobu Ando[2]

1. Japan Meteorological Agency, 2. Meteorological Research Institute

Monitoring of volcanic activity by observing ground deformation is one of useful means to understand signs of eruption such as accumulation and migration of magma. Japan Meteorological Agency (JMA) monitors volcanic activity by tiltmeter, light wave distance measuring equipment and GNSS around volcanoes. However, there are some problems only using these ground-based observation methods. Observable ground deformation is restricted to point information such as the tilt at the observation point and relative position between observation points. Also, it is difficult to install and maintain observation device at an isolated island such as Nishinoshima volcano. It is important to grasp surface ground deformation around volcanoes using not only ground-based observation but also satellite data like SAR (Synthetic Aperture Rader). In this presentation, we mainly report on the analysis results of the long-term pair (2015 to 2018) around the domestic active volcanoes.

Some of PALSAR-2 data were prepared by the Japan Aerospace Exploration Agency (JAXA) via Coordinating Committee for the Prediction of Volcanic Eruption (CCPVE) as part of the project ‘ALOS-2 Domestic Demonstration on Disaster Management Application’ of the Volcano Working Group. Also, we used some of PALSAR-2 data that are shared within PALSAR Interferometry Consortium to Study our Evolving Land surface (PIXEL). PALSAR-2 data belongs to JAXA. We would like to thank Dr.Ozawa (NIED) for the use of his RINC software. In the process of the InSAR, we used Digital Ellipsoidal Height Model (DEHM) based on ‘the digital elevation map 10m-mesh’ provided by GSI, and Generic Mapping Tools (P.Wessel and W.H.F.Smith, 1999) to prepare illustrations.

Keywords: ALOS-2/PALSAR-2, InSAR, Domestic Active Volcano

©2019. Japan Geoscience Union. All Right Reserved.

Volcano-hydrothermal inflation revealed by the spatial variation of stress field at the Tatun Volcano Group, northern Taiwan

*Hsin-Chieh Pu[1], Cheng-Horng Lin[2,3,4,5], Ya-Ju Hsu[2], Li-Chin Chang[3]

1. Central Weather Bureau, Taiwan, ROC., 2. Institute of Earth Sciences, Academia Sinica, Taipei, Taiwan, ROC., 3. Taiwan Volcano Observatory at Tatun, Taipei, Taiwan, ROC., 4. Department of Geosciences, National Taiwan University, Taipei 10617, Taiwan, ROC., 5. National Center for Research on Earthquake Engineering, National Applied Research Laboratories, Taipei, Taiwan, ROC.

To investigate the volcanic behaviors, the Taiwan Volcano Observatory at Tatun has deployed a dense seismic network in the Tatun Volcano Group (TVG), where the government and business metropolis-Taipei city is bounded and various phenomenon related to volcano-hydrothermal activity were found. This network is composed of 40 seismic stations for covering an area of ~10 km by ~10 km. Based on the seismic data recorded by this network, we have solved an extremely huge number of 1,016 earthquake focal mechanisms with depths less 5 km from 2012 to 2017. Then the detailed spatial variations of the local stress field near the surface are firstly inverted from these focal mechanisms. Overall, local earthquakes were dominated by both the sub-horizontal extensional stress striking ESE-WNW and sub-vertical compressional stress. In detail, the orientations of extensional stress formed the abnormal pattern of a couple of semi curves around the Dayoukeng area. In this particular area of Dayoukeng, the magnitude of compressional stress at the sub-vertical component was stronger than the others principle stresses based on the significantly lower ∅values in local than the surrounding area. We ascribe these local variations to an inflating phenomenon buried in the Dayoukeng area. This inflating mechanism should be induced by the volcano-hydrothermal fluid. The current volcano-hydrothermal activity represented by inflation is principally concentrated at the Dayoukeng area and disturbs the faulting behaviors of local earthquakes in the TVG.

Keywords: focal mechanism, stress field, Tatun volcano group, inflation

©2019. Japan Geoscience Union. All Right Reserved.

Topographic change and crustal deformation associated with December 2018 eruption of Krakatau volcano in Indonesia

*Hiroshi Yarai[1], Tomokazu Kobayashi[1], Shinya Yamada[1]

1. GSI of Japan

Krakatau volcano is located in the Sunda Strait between Java Island of Indonesia and Sumatra Island. A high tsunami occurred on this Sunda Strait on December 22, 2018, causing major damage. It is estimated that this tsunami was caused by the collapse of Krakatau volcano. Therefore, in order to grasp the topography change of Krakatau volcano, we analyzed SAR intensity image observed by the Japanese earth observation satellite "Daichi 2" (ALOS-2) before and after the eruption. As a result of the analysis, a clear topographic change was observed in the southwestern part of the island on December 24 after eruption. It is thought that the southwestern part of the island collapsed by this 24th.

Furthermore, for capturing crustal deformation before and after the eruption, SAR interferometry was carried out using Daichi-2 SAR data. As a result, the displacement of the LOS's distance increased in the islands surrounding the Anaku Krakatau Island. Although the characteristic of the change suggests contraction centered around the Anak and Krakatau Island, it is not isotropic but it extends somewhat north and south. Therefore, the source may not be a simple mogi source.

Keywords: Krakatau volcano, volcanic collapse,, crustal deformation, SAR

©2019. Japan Geoscience Union. All Right Reserved.

[J] Poster | S (Solid Earth Sciences)：S-VC Volcanology

Mon. May 27, 2019 5:15 PM - 6:30 PM JST | Mon. May 27, 2019 8:15 AM - 9:30 AM UTC | Poster Hall International Exhibition Hall8, Makuhari Messe_25

[S-VC38] Active Volcanism

convener:Yuta Maeda(Nagoya University), Takahiro Miwa(National research institute for earth science and disaster prevention), Takeshi Nishimura(Department of Geophysics, Graduate School of Science, Tohoku University)

This session discusses various aspects of active volcanisms including, but not limited to, recent and historical eruptions, various phenomena associated with the volcanic activities, underground structures of the volcanoes, and developments of new instruments based on geophysical, geochemical, geological, and multidiscipline approaches. We also welcome studies on understanding and predicting the transitions of the eruptive activities from observational, theoretical, and experimental approaches.

[SVC38-P01] The structure of Showa-Shinzan Yaneyama Usu by seismic reflection surveys

*Ryuichi Takei[1], Tomoki Tsutsui[1,2], Yuya Tada[2], Tomoya Moriwaki[2], Yosuke Aoki[3], Hiroshi Aoyama[4], Go Maruyama[5] (1.Graduate School of International Resource Sciences, The University of Akita, 2.Faculty of International Resource Sciences, The University of Akita, 3.Earthquake Research Institute, The University of Tokyo, 4.Graduate school of Science, The University of Hokkaido, 5.Marutec Co., Ltd.)

[SVC38-P02] Ground deformation associated with the 2014-2015 and the 2018-2019 volcanic activities at Azumayama

*Jun Okada[1], Shigeo Matsuura[2], Katsuya Ohmi[2], Takuya Yamamura[2], Yu Nihara[3], Susumu Seki[3] (1.Volcanology Research Department (Sendai Office), Meteorological Research Institute, JMA, 2.Seismology and Volcanology Division, Sendai Regional Headquarters, JMA, 3.Regional Volcanic Observation and Warning Center, Sendai Regional Headquarters, JMA)

[SVC38-P03] BP-type and BT-type volcanic earthquakes in Azumayama

*Yusuke Yoshigai[1], Yuichi Morita[2], Katsuya Ohmi[3], Yu Nihara[4], Tsukasa Kobayashi[1] (1.Volcanological Division, Japan Meteorological Agency, 2.Earthquake Research Institute, University of Tokyo, 3.Seismology and Volcanology Division, Sendai Regional Headquarters, Japan Meteorological Agency, 4.Regional Volcanic Observation and Warning Center, Sendai Regional Headquarters, Japan Meteorological Agency)

[SVC38-P04] The occurrence and petrology of the fine-grained pyroclastic materials of the Futatsudake-Shibukawa eruption in Haruna volcano.

*Teruyoshi Maruyama[1], Yuki Suzuki[2] (1.Department of Earth Sciences, School of Education , Waseda University, 2.Department of Earth Sciences, Faculty of Education and Integrated Arts of Sciences, Waseda University)

[SVC38-P05] The occurrence and petrology of the block and ash flow deposit from the Futatsudake-Shibukawa eruption, Haruna volcano

*Yuki Suzuki[1], Ryouto Fukushima[2] (1.Department of Earth Sciences, Faculty of Education and Integrated Arts of Sciences, Waseda University, 2.Department of Earth Sciences, School of Education, Waseda University)

[SVC38-P06] Report of Volcanic Activity at Kusatsu-Shiranesan in 2018

*Tsukasa Kobayashi[1], Koji Kato[1], Koichi Suemine[1], Kazuhiro Kimura[1], Yusuke Yoshigai[1], Yasuo Ogawa[2], Kenji Nogami[2], Wataru Kanda[2], Akihiko Terada[2] (1.Volcanological Division, Japan Meteorological Agency, 2.Volcanic Fluid Research Center, Tokyo Institute of Technology)

[SVC38-P07] Noble gas isotope composition of fumaroles and hydrothermal gases around Kusatsu-Shirane volcano

*Kotaro Toyama[1], Hirochika Sumino[1], Kaori Kawana[1], Yoshihide Akiyama[1], Takeshi Ohba[2], Muga Yaguchi[3], Akihiko Terada[4] (1.Department of Basic Science, Graduate School of Arts and Sciences, The University of Tokyo, 2.Department of chemistry, School of Science, Tokia University, 3.Meteorological Research Institute, 4.Volcanic Fluid Research Center, Tokyo Institute of Technology)

[SVC38-P08] Self-potential and geomagnetic total intensity observations at Motoshirane volcano after the 2018 eruption

*Akira Yamazaki[1], Hideki Iino[1], Tatsurou Tanaka[1] (1.Kakioka Magnetic Observatory)

[SVC38-P09] Eruption processes of the 3rd and 4th stage of Niigata-Yakeyama Volcano, Japan, inferred from microlite texture and chemical composition

*Takumi Yoshida[1], Takeshi Saito[1] (1.Shinshu University)

[SVC38-P10] Estimation of subsurface structure of Shinyu crater lake, Tateyama Caldera, based on the water level and seismic observation data

*Ryohei Kawaguchi[1], Naoko Saito[2], Shin'ya Onizawa[1] (1.Meteorological Research Institute, 2.Toyama local Meteorological office, Japan Meteorological Agency)

[SVC38-P11] Real time monitoring of underground temperature in Jigokudani, Midagahara volcano using LPWA devices

*Tohru Watanabe[1], Toyama branch NTT West[2] (1.Gradudate School of Science and Engineering, University of Toyama, 2.Nippon Telegraph and Telephone West Corporation)

[SVC38-P12] Varying chemical and isotopic compositions of fumarolic gases from the summit and from the 1962-63 eruptive vents at Yakedake Volcano, Japan

*Takeshi Saito[1], Shun Sawamura[2], Kazuhiro Amita[3], Taketoshi Mishima[4], Shinji Ohsawa[4] (1.Institute of Science, Academic Assembly School of Science and Technology, Shinshu University, 2.Graduate School of Science and Technology, Shinshu University, 3.Graduate School of Engineering Science, Akita University, 4.Beppu Geothermal Research Laboratory, Institute for Geothermal Sciences, Graduate School of Science, Kyoto University)

[SVC38-P13] Eruption age determination of the latest two lava flows and characteristics of volcaniclastic materials from the recent activity of Yokodake Volcano, Japan

*Hiroya Nitta[1], Takeshi Saito[1], Yorinao Shitaoka[2] (1.Shinshu University of Science and Technology, 2.Department of Environment System, Faculty of Geo-environmental Science, Rissho University)

[SVC38-P14] Estimating the date of the 2007 eruption of Mount Ontake Volcano using waveform correlation

*Shuhei Nishijima[1], Toshiko Terakawa[1], Shinichiro Horikawa[1] (1.Graduate School of Environmental Studies, Nagoya University)

[SVC38-P15] Seismic activity beneath Mt. Ontake volcano before and after the 2007 and 2014 eruptions

*Yoshiko Yamanaka[1], Shinichiro Horikawa[1], Yuta Maeda[1] (1.Graduate School of Encironmental Studies, University of NAGOYA)

[SVC38-P16] Effect of rain and snowmelt correction of tiltmeter data
- Application example for Ontakesan Volcano -

*Kazuhiro Kimura[1,5], Katsuhisa Kawashima[2], Takane Matsumoto[2], Akihiko SASAKI[4], Tsutomu Iyobe[3], Junichi Miyamura[1], Masaki Nakahashi[1] (1.Japan Meteorological Agency, 2.Research Institute for Natural Hazards and Disaster Recovery, Niigata University, 3.Faculty of Engineering, Kyoto University,

4.Department of Geography and Environmental Studies, Kokushikan University, 5.Graduate School Science and Technology, Niigata University)

[SVC38-P17] **Spatial Variation of b-value around Mt. Fuji influenced by the Eastern Shizuoka Earthquake of 15 March 2011**

*Takumi Murakoshi[1], Tomonari Miyashita[2] (1.National Defense Academy, 2.JASDF)

[SVC38-P18] Present condition of submarged volcano, Teishi Knoll, off Ito, Eastern Izu Peninsula

*Toshiro Yamanaka[1], Yoshifumi Kawada[2], Takuro Noguchi[3], Mayumi Hatta[3], Kei Okamura[3] (1.Tokyo Univ. Marine Science and Technology, 2.Tohoku University, 3.Kochi University)

[SVC38-P19] Descriptions and age of volcanic products before the caldera formation in the northern part of Izu-Oshima, off Tokyo, Pacific Ocean

*Satoshi Terayama[1], Takehiko Suzuki[1], Makoto Kobayashi[2] (1.Tokyo Metropolitan University, 2.Research Center for Volcanic Hazards and Their Mitigation, Tokyo Metropolitan University)

[SVC38-P20] Time change of p-value by Schuster method using earthquakes around Izu-Ohsima summit

*Hiroyuki Takayama[1] (1.Volcanological Division 1st labolatory, Meteorological Research Institute)

[SVC38-P21] Standard stratigraphy and characteristic properties of late Quaternary tephras on the Niijima-island: Report of geochemistry and refractive indices of volcanic glass shards, orthopyroxene, hornblende, and cummingtonite

*Kaori Aoki[1], Makoto Kobayashi[1], Fumikatsu NISHIZAWA[1,2], Masanori Murata[1], Daisuke Ishimura[1], Takehiko Suzuki[1] (1.Research Center for Volcanic Hazards and Their Mitigation, Tokyo Metropolitan University, 2.Mount Fuji Research Institute, Yamanashi Prefectural Government)

[SVC38-P22] **Tephrostratigraphy and its eruption history of the Latest Activity in the Kozushima Volcano, the Izu Islands**

*Makoto Kobayashi[1], Masanori Murata[1], Fumikatsu NISHIZAWA[2], Takehiko Suzuki[1,3] (1.Research Center for Volcanic Hazards and their mitigations, Tokyo Metropolitan Univ., 2.Fuji Research Institute, Yamanashi Prefectural Government, 3.Department of Geography, Tokyo Metropolitan Univ.)

[SVC38-P23] Characteristics of hypocenter distribution connected with velocity structures in and around Miyakejima, Kozushima and Hachijojima volcanoes

*Hiroko Hagiwara[1], Hidefumi Watanabe[1] (1.Tokyo Metroplitan Government)

[SVC38-P24] Deformation of Miyakejima volcano measured by GNSS campaign observation (2013-2015)

*Haruna Watanabe[1], Takeshi Matsushima[2], Miyo Fukui, Atsushi Watanabe[3], Jun Oikawa[3], Takashi OKUDA[4], Taku Ozawa[5], Yosuke Miyagi[5] (1.Department of Earth and Planetary Sciences, Graduate School of Science, Kyushu University, 2.Institute of Seismology and Volcanology, Faculty of Sciences, Kyushu University, 3.Earthquake Research Institute, University of Tokyo, 4.Earthquake and Volcanology Research Center, 5.National Research Institute for Earth Science and Disaster Resilience)

[SVC38-P25] Characteristic properties of distal and proximal tephras in the Mikurajima Island, Izu Islands.

*Tomohiro Tano[1], Takehiko Suzuki[1,2], Makoto Kobayashi[2], Masanori Murata[2] (1.Faculty of Urban Environmental Sciences, Tokyo Metropolitan University, 2.Research Center for Volcanic Hazards and Their Mitigation, Tokyo Metropolitan University)

[SVC38-P26] Pseudo thermal anomalies in the shortwave infrared bands of the Himawari-8 AHI and their correction for volcano thermal observation

*Takayuki Kaneko[1], ATSUSHI YASUDA[1], Yoshizaki Yoshito[2], Takasaki Kenji[3], Yoshiaki HONDA[4] (1.Earthquake Research Institute, University of Tokyo, 2.Meteorological Satellite Center, Japan Meteorological Agency, 3.Japan Fisheries Research and Education Agency, 4.Center for Environmental Remote Sensing, Chiba University)

[SVC38-P27] Shallow earthquakes in Unzen Volcano inferred from dense seismic observation and resistivity structure

*Hashimoto Tasuku[1], Koki Aizawa[2], Takeshi Matsushima[2], Hiroshi Shimizu[2], Yuto Hayashida[1], Yuhei Yuasa[1], Kaori Tsukamoto[1], Yuto Yamamoto[3], Kanta Miyano[3], Megumi Kamizono[1], Satoshi Matsumoto[2] (1.Department of Earth and Planetary Sciences, Graduate School of Science, Kyushu University, 2.Institute of Seismology and Volcanology, Faculty of Science, Kyushu University, 3.Department of Earth and Planetary Sciences, School of Science, Kyushu University)

[SVC38-P28] Characteristics of shallow volcanic earthquakes beneath the summit of Unzen Volcano

*Kanta Miyano[1], Hiroshi Shimizu[2], Takeshi Matsushima[2], Satoshi Matsumoto[2], Koki Aizawa[2], Hashimoto Tasuku[3], Yuto Hayashida[3], Yuhei Yuasa[3] (1.Department of Earth and Planetary Sciences, School of Science, Kyushu University, 2.Institute of Seismology and Volcanology, Faculty of Science, Kyushu University, 3.Department of Earth and Planetary Sciences, Graduate School of Science, Kyushu University)

[SVC38-P29] Pyroclastic deposits and the stratigraphy on the outcrop to north east from Mt.Unzen

*Daisuke Nagai[1] (1.Mt.Unzen disaster memorial hall)

[SVC38-P30] Relative gravity changes in Aso Volcano (Kumamoto Prefecture) observed from 2015 to 2018

*Yusuke Miyauchi[1], Takahito Kazama[1], Yoichi Fukuda[1], Shin Yoshikawa[2], Takahiro Ohkura[2], Jun Nishijima[3], Yasuhiro Fujimitsu[3] (1.Graduate School of Science, Kyoto University, 2.Aso Volcanological Laboratory, Kyoto University, 3.Graduate School of Engineering, Kyushu University)

[SVC38-P31] Precise leveling survey in Aso volcano, 2018

*Takahiro Ohkura[1], Shin Yoshikawa[1], Hiroyuki Inoue[1], Akihiko Yokoo[1], Mitsuru Utsugi[1], Keigo Yamamoto[2], Kazunari Uchida[4], Yuta Maeda[5], Shinichiro Horikawa[5], Kenjiro Matsuhiro[5], Takashi OKUDA[5], Kazushi Tanoue[5], Fumiaki Kimata[7], Masayuki Murase[6], Hitoshi Mori[6], Taketoshi Mishima[3], Shintaro Komatsu[2], Masaki Takaya[3], Jun Oikawa[8], Kyoka Ishii[3], Yusuke Miyauchi[3], Ikuma Kimura[3], Masaki Uchida[3], Kazuho Nakai[3], Kosei Takishita[3], Keita Chiba[4], Hashimoto Tasuku[4], Yoshinosuke Kamiya[4], Yuto Yamamoto[4] (1.Aso Volcanological Laboratory, Institute for Geothermal Sciences, Graduate School of Science, Kyoto University, 2.DPRI, Kyoto University, 3.Graduate School of Science, Kyoto University, 4.Graduate School of Science, Kyushu University, 5.Graduate School, Nagoya University, 6.College of Human and Society, Nihon University, 7.TRIES, 8.ERI,Univ.of Tokyo)

[SVC38-P32] Magma evolution during the Aso-3 caldera-forming eruption cycle deduced from the chemistry of plagioclase phenocrysts

*yuki matsukida[1], Tsuyoshi Iizuka[1], Takayuki Ushikubo[2], Kenji Shimizu[2], Nobuo Geshi[3], Isoji MIYAGI[3], Morihisa Hamada[2] (1.the University of Tokyo, 2.Japan Agency for Marine-Earth and Science Technology, 3.The National Institute of Advanced Industrial Science and Technology)

[SVC38-P33] Relationship between duration of eruption tremor and eruption volume

*Azusa Mori[1], Hiroyuki Kumagai[1] (1.Nagoya University Environmental Studies)

[SVC38-P34] Crustal deformation accompanied with the eruption of Shinmoe-dake in early March 2018

*Tsuyoshi Watanabe[1], Takashi Yokota[1], Susumu Kurahashi[1], Kenta Enomoto[1] (1.Aichi Institute of Technology)

[SVC38-P35] Sources under Iwo-yama, Kirishima Volcanoes derived from GNSS observation and Precise leveling survey.

*Yuki Koga[1], Takeshi Matsushima[2], Kazunari Uchida[2], Dan Muramatsu[1], Yuichi Iwasa[1] (1.Department of Earth and Planetary Sciences, Graduate School of Science, Kyushu university , 2.Institute of Seismology and Volcanology, Faculty of Science, Kyushu University)

[SVC38-P36] Regional vertical deformation around Aira caldera from GNSS data

*Kazuho Nakai[1], Masato Iguchi[2], Takahiro Ohkura[3] (1.Division of Earth and Planetary Sciences, Graduate School of Science, Kyoto University, 2.Sakurajima Volcano Research Center, Disaster Prevention Research Institute, Kyoto University, 3.Aso Volcanological Laboratory, Institute for Geothermal Sciences, Graduate School of Science, Kyoto University)

[SVC38-P37] Vertical ground deformation in Sakurajima volcano measured by precise leveling survey (during Nov. 2017 - Nov. 2018)

*Keigo Yamamoto[1], Takeshi Matsushima[2], Shin Yoshikawa[3], Hiroyuki Inoue[3], Tadaomi Sonoda[1], Kosei Takishita[1], Kazuho Nakai[1], Masaki Uchida[3], Ryo Oyanagi[3], Yoshinosuke Kamiya[2], Takahiro Ohkura[3] (1.Disaster Prevention Research Institute, Kyoto University, 2.Fuculty of Sciences, Kyushu University, 3.Gruduate School of Science, Kyoto University)

[SVC38-P38] Spatiotemporal gravity variations from the 1990s in Sakurajima Volcano, revealed by repeated relative gravity measurements

*Ryo Oyanagi[1], Takahito Kazama[1], Keigo Yamamoto[2], Hiromitsu Oshima[3], Kazumi Okada[3], Tadaomi Sonoda[2], Masato Iguchi[2] (1.Graduate School of Science, Kyoto University, 2.DPRI, Kyoto University, 3.ISV, Hokkaido University)

[SVC38-P39] Investigation into the crater of Sakurajima volcano during eruption using UAV

*Shunsuke Miura[1], Takumi Mochiduki[1], Kouji Fujita[1], Toshihiro Urayama[1], Hisashi Sasaki[1], Tatsuro Chiba[1] (1.Asia Air Survey Co.,Ltd)

[SVC38-P40] **Seismic refraction and wide-angle reflection experiment in southern Kyushu, Japan: (3) the 2018 exploration report**

*Hiroki Miyamachi[1], Hiroaki Takahashi[2], Hiroshi Aoyama[2], Mako Ohzono[2], Takahiro Shiina[6], Masamitsu Takada[2], Masayoshi Ichiyanagi[2], Teruhiro Yamaguchi[2], Yuki Susukida[2], Saito Kazuma[2], Chihiro Ito[2], Yoshio Murai[2], Tatsuya Nakagaki[2], Tomoki Tsutsui[3], Ryuichi Takei[3], Yuuya Tada[3], Mare Yamamoto[4], Satoshi Hirahara[4], Takashi NAKAYAMA[4], Ryosuke Azuma[4], Syuichi Suzuki[4], Toshinori Sato[5], Eiji Kurashimo[6], Miwako Ando[6], Shinichi Tanaka[6], Satoshi Ikezawa[6], Tomoaki Yamada[6], Kazuo Nakahigashi[7], Yuta Maeda[8], Shinichiro Horikawa[8], Kenjirou Matsuhiro[8], Takashi OKUDA[8], Shuhei Tsuji[8], Naoki Sogawa[8], Hiroshi Katao[9], Takuo Shibutani[9], Tsutomu Miura[9], Nakagawa Jun[9], Itaru Yoneda[9], Takeshi Tameguri[9], Kosei Takishita[9], Kazuho Nakai[9], Yusuke Yamashita[9], Takeshi Matsushima[10], Kazunari Uchida[10], Rintaro Miyamachi[10], Hiroshi Yakiwara[1], Shuichiro Hirano[1], Takeshi Kubo[1], Kenyu Sakao[1] (1.Kagoshima University, 2.Hokkaido University, 3.Akita University, 4.Tohoku University, 5.Chiba University, 6.University of Tokyo, 7.Tokyo University of Marine Science and Technology, 8.Nagoya University, 9.Kyoto University, 10.Kyushu University)

[SVC38-P41] Flow and emplacement mechanism of Koya Ignimbrite

*Keiko Suzuki-Kamata[1], Reina NAKAOKA[1], Tomomi Yamane[2] (1.Kobe Ocean-Bottom Exploration Center , 2.Department of Planetology, Graduate School of Science, Kobe University)

[SVC38-P42] Investigating Origin of landslide-like bathymetric feature at southern Mt.Kaimon using bathymetric and multichannel seismic reflection surveys

*hiroto yamaguchi[1], Satoshi Shimizu[2], Hikaru Iwamaru[2], Mamoru Sano[2], Nobukazu Seama[3,2], Misaki Horiuchi[3], Tetsuo Matsuno[2,3], Yoshiyuki Tatsumi[2,3] (1.Department of Planetology, Faculty of Science, Kobe university, 2.Kobe ocean-bottom exploration center, 3.Department of Planetology, Graduate School of Science, Kobe university)

[SVC38-P43] Occurrence and distribution of pyroclastic fall deposits of Kuchinoerabujima volcano 2018-2019 eruption

*Masashi NAGAI[1], Shojiro Nakagawa[2], Yu Iriyama[1], Takahiro Miwa[1], Toshikazu Tanada[1], Hideki Ueda[1], Setsuya Nakada[1] (1.Volcano Research Department, National Research Institute for Earth Science and Disaster Resilience, 2.Yakushima Chigaku Club)

[SVC38-P44] Ground Deformation around Domestic Active Volcanoes detected by InSAR of ALOS-2/PALSAR-2

*Takafumi Taniguchi[1], Isao Kageyama[1], Okuyama Satoshi[2], Shinobu Ando[2] (1.Japan Meteorological Agency, 2.Meteorological Research Institute)

[SVC38-P45] **Volcano-hydrothermal inflation revealed by the spatial variation of stress field at the Tatun Volcano Group, northern Taiwan**

*Hsin-Chieh Pu[1], Cheng-Horng Lin[2,3,4,5], Ya-Ju Hsu[2], Li-Chin Chang[3] (1.Central Weather Bureau, Taiwan, ROC., 2.Institute of Earth Sciences, Academia Sinica, Taipei, Taiwan, ROC., 3.Taiwan Volcano Observatory at Tatun, Taipei, Taiwan, ROC., 4. Department of Geosciences, National Taiwan University, Taipei 10617, Taiwan, ROC., 5.National Center for Research on Earthquake Engineering, National Applied Research Laboratories, Taipei, Taiwan, ROC.)

[SVC38-P46] Topographic change and crustal deformation associated with December 2018 eruption of Krakatau volcano in Indonesia

*Hiroshi Yarai[1], Tomokazu Kobayashi[1], Shinya Yamada[1] (1.GSI of Japan)

The structure of Showa-Shinzan Yaneyama Usu by seismic reflection surveys

*Ryuichi Takei[1], Tomoki Tsutsui[1,2], Yuya Tada[2], Tomoya Moriwaki[2], Yosuke Aoki[3], Hiroshi Aoyama[4], Go Maruyama[5]

1. Graduate School of International Resource Sciences, The University of Akita, 2. Faculty of International Resource Sciences, The University of Akita, 3. Earthquake Research Institute, The University of Tokyo, 4. Graduate school of Science, The University of Hokkaido, 5. Marutec Co., Ltd.

Reflection seismic surveys at Usu-Showashinzan-Yaneyama was conducted in order to, estimate the shallow structure of the lava-dome base. Usu-Showashinzan is a young volcano formed in 1943-1945. It is characterized by consisting of a lava dome structure with top elevation of about 406.9m and a bun-shaped plateau called Yaneyama. Various geophysical explorations and geological surveys have been carried out in Showa-Shinzan until now, and the formation process and the supply route of magma have been discussed. However, the details of structure beneath Yaneyama are still unknown.
Total of 4 lines were conducted in 2017 and 2018 with 2 lines each, and seismic data were acquired. Two observation lines (Y17 and Y18) were set in the east-west direction on the east foot of the lava dome and two (G17 and G18) in the Guren-valley on the southwest foot of the lava dome. Both survey lines (Y17, G17) were conducted in 2017 with 24 receivers with using a hammer of 6.3kg as the seismic source. Other survey lines (Y18, G18) conducted in 2018 with 48 receivers with using a tamping rammer (MT-55L by Mikasa Industries) as the seismic source. Split-spread method was applied in all seismic lines. The receiver interval was 4m for Y lines and 3m for G lines. SU (Seismic Un*x) software was used for the seismic reflection analysis of the acquired seismograms. For 2018 lines with using tamping rammer, preprocessing is necessary before analysis of seismic reflection. That is based on the principle “SOSIE” (Yokokawa et.al. 1983).
As the result, the time sections on all the survey lines were obtained. Especially, in the G18 line, reflection profile down to 100m depth, which shows gentle valley structure in the middle of the line down to 80m depth and there is almost horizontal boundary at 100m depth.
The refraction tomography analysis and considering previous researches are going to be conducted.

Keywords: Seismic reflection survey, Showa-Shinzan

©2019. Japan Geoscience Union. All Right Reserved.

Ground deformation associated with the 2014-2015 and the 2018-2019 volcanic activities at Azumayama

*Jun Okada[1], Shigeo Matsuura[2], Katsuya Ohmi[2], Takuya Yamamura[2], Yu Nihara[3], Susumu Seki[3]

1. Volcanology Research Department (Sendai Office), Meteorological Research Institute, JMA, 2. Seismology and Volcanology Division, Sendai Regional Headquarters, JMA, 3. Regional Volcanic Observation and Warning Center, Sendai Regional Headquarters, JMA

Azumayama is a basaltic to andesitic active volcano located in the volcanic front on the Tohoku (NE Japan) Arc. Historical eruptions occurred mainly in and around O-ana crater in the south flank of Issaikyosan. No eruption occurred for more than 40 years after the last one on December 1977. However, various volcanic phenomena have been observed in recent years. Repeated GPS surveys revealed local inflation-deflation around O-ana crater which plays in a cycle of 2-3-year and corresponds to the increase-decrease of seismicity during 2003-2009. Yoshida *et al.* (2012) estimated the pressure source 200 to 600 meters beneath the O-ana crater. This shows a good agreement with the thermal demagnetization source studied by Yamazaki *et al.* (2010). Monochromatic earthquakes were observed when fumarolic activity of O-ana crater was high during 2008-2011 (e.g. Ueki *et al.*, 2010). By analyzing the frequencies of these earthquakes Torimoto (2016) is beginning to understand the characteristics of shallow hydrothermal systems, a potential hotbed for phreatic eruptions. In more recent years, there are two volcanic unrests such as the 2014-2015 and the 2018-2019 activities. JMA released “Near-crater Warning” and raised Volcanic Alert Level from 1 to 2 on December 2014 and September 2018, respectively.

The start of the 2014-2015 activity can be marked by the slight tilt change at Jododaira station, 750m ESE from O-ana Crater. It showed East-downward ground deformation since late July 2014. Continuous GNSS measurements also captured local inflation around Issaikyosan since September 2014. Seismic activity started on middle October and culminated from December 2014 to middle January 2015. Similarly, the 2018-2019 activity can be recognized by the tilt data of Jododaira. A slow East-downward ground deformation started since May 2018. The tilting rate was significantly increased after the occurrence of the volcanic tremor on 22 July 2018 and remained almost constant (at least at the time of writing). Continuous GNSS data suggested also an inflation of the volcanic edifice since May 2018. The shallow seismicity started since middle August 2018 and remained active (at least at the time of writing).

Strong similarity exists in deformation characteristics between the 2014-2015 and the 2018-2019 activities, that is the dilatational ground deformation, both preceded to the activation of shallow seismicity. Except for the beginning of the activities tilting is maintained with almost the same rate and direction for more than several months. However, several discrepancies should be remarked: (1) Volcanic tremors are more frequent in the 2018-2019 than the 2014-2015. (2) The 2018-2019 activity may be triggered by a remarkable coincidental tilt change (about 1 micro radian at Jododaira station) and the associated volcanic tremor on 22 July 2018. (3) Slight tilt changes which may suggest a deep deflation of Azumayama were clearly observed at distant stations on the foot of Adatarayama, a neighboring volcano in the 2018-2019. These observational evidences may indicate the different volcanic processes in both activities. Regarding (3), other field observation results such as both the increase of SO_2/H_2S since late July 2018 and the enlargement of geothermal areas around O-ana crater can be triggered by the intermittent injection of volcanic fluids (e.g. hot volcanic gasses) from the depth of Azumayama. Results of both tilt and continuous GNSS observations will be presented in the session.

©2019. Japan Geoscience Union. All Right Reserved.

Keywords: Azumayama, deformation, GNSS, tiltmeters, volcanic earthquakes

©2019. Japan Geoscience Union. All Right Reserved.

BP-type and BT-type volcanic earthquakes in Azumayama

*Yusuke Yoshigai[1], Yuichi Morita[2], Katsuya Ohmi[3], Yu Nihara[4], Tsukasa Kobayashi[1]

1. Volcanological Division, Japan Meteorological Agency, 2. Earthquake Research Institute, University of Tokyo, 3. Seismology and Volcanology Division, Sendai Regional Headquarters, Japan Meteorological Agency, 4. Regional Volcanic Observation and Warning Center, Sendai Regional Headquarters, Japan Meteorological Agency

At Azumayama located on the prefectural boundary between Yamagata and Fukushima prefectures, volcanic tremors occurred on 22 July 2018. Changes in tiltmeter data from Joudodaira Station (around 1 km ESE of the Oana crater) indicated ground deformation with a remarkable rising trend in the direction toward the crater. Volcanic seismicity has mostly remained at high levels since August 2018, and volcanic activity has remained at high levels. Japan Meteorological Agency (JMA) issued a Near-crater Warning on 13 September and raised the Volcanic Alert Level from 1 (Potential for increased activity) to 2 (Do not approach the crater).

There are mainly three types of volcanic earthquakes in the vicinity of the Oana crater: the BH-type in which the dominant frequency is high, the BL-type in which the dominant frequency is low, and the BP-type / BT-type with the harmonic waveform. These volcanic earthquakes occur roughly at depths of less than 1 km.

From July to October 2018, BH-type earthquakes mainly occurred, and the proportion of BL-type earthquakes and BP-type / BT-type earthquakes slightly increased in November. After that, the proportion of the BL-type earthquakes decreased, but the proportion of the BP-type / BT-type earthquakes further increased. The proportion of the BP-type / BT-type earthquakes to the whole volcanic earthquakes is 25% in November and 50% since December, and it continues high levels. The BP-type / BT-type earthquakes that occurred after July 2018 have various types of characteristics, such as damped harmonic oscillators with a single frequency peak seen in the BP-type / BT-type earthquakes occurred from 2010 to 2011, damped harmonic oscillators with multiple frequency peaks and those with high-frequency earthquake near the beginning of the earthquake, and no systematic change of the dominant frequency can be observed. In this presentation, we introduce what we found as the results of focusing on waveform shape and amplitude ratio for the BP-type / BT-type earthquakes that occurred after July 2018.

In this research, under the agreement on collaboration and cooperation in the field of seismic / volcanic disaster prevention research between Earthquake Research Institute (ERI), the University of Tokyo and Seismology and Volcanology Department, JMA, I used facilities of ERI and discussed with the people of ERI. I express my gratitude to everyone involved.

Keywords: Azumayama, Volcanic Earthquake, N-type Earthquake

©2019. Japan Geoscience Union. All Right Reserved.

The occurrence and petrology of the fine-grained pyroclastic materials of the Futatsudake-Shibukawa eruption in Haruna volcano.

*Teruyoshi Maruyama[1], Yuki Suzuki[2]

1. Department of Earth Sciences, School of Education , Waseda University, 2. Department of Earth Sciences, Faculty of Education and Integrated Arts of Sciences, Waseda University

Haruna volcano is an active volcano of Quaternary which is located in the southern end of the NE Japan arc. Haruna volcano has 500000 years active time. Geshi and Takeuchi (2012) showed the activity is classified into older period (500-240ka), and newer period (45ka-) following activity halt of about 200,000 years. The newest activity in Haruna volcano is Shibukawa eruption (late 5th to early 6th century) and Ikaho eruption (late 6th to early 7th century), both of which occurred at the location of present Futatsudake (ages by Geshi and Oishi (2011)). Occurrences of ejecta from two eruption, as described in Soda (1989), indicate the different manner of pyroclastic flow generation; explosive destruction of the lava dome in the Shibukawa eruption, while column collapse in the Ikaho eruption. Suzuki and Nakada (2007) carried out detailed petrological study for the Ikaho eruption. They proposed mush-like felsic magma was remobilized by the injection of mafic magma. The important point in the eruption triggering was that mixed magma and heated magma with considerably lower viscosity than the original mush-like magma opened the vent, resulting in the decompression of whole felsic magma reservoir. However, no study has revealed the magma plumbing system and the eruption triggering process of the Shibukawa eruption. For the purpose of understanding these points, we have conducted the petrological study of the Shibukawa eruption. In particular, in this research, in order to clarify the progress of eruption and the temporal change of the erupted magma, fine-grained pyroclastic materials were studied rather than pumice blocks in the block and ash flow (BAF).

We sampled fine-grained pyroclastic deposits at four sites locating at the northeastern to eastern foot of Haruna volcano. All sites locate at the periphery of BAF mapped in Soda (1989). Therefore, our investigated sites correspond to the region where pyroclastic surge deposit emplaces (example of Unzen 1991-1995 eruption; Fujii and Nakada, 1999). We could observe the basal part of fine-grained pyroclastic material in three sites. In all sites, the strata were divided into multiple units according to their facies. The juvenile pumice clasts, the coarse part of the deposit, had variation in color (white, gray, light gray). We measured whole rock compositions of the pumice samples and found they are felsic andesite (SiO_2 =60.7-61.9wt.%; N=22). Thin sections were prepared for ten representative pumices and one volcanic ash sample. It is necessary to study the volcanic ash sample, because it is not possible to discuss the change in magma composition from lower to the upper layer, only with the pumice clasts for which whole-rock chemical analyses were performed. The phenocryst phases (Pl+Opx+Am+Fe-Ti Ox) in all samples form aggregates, so when they crystallized, they were in equilibrium. We observed free crystals (Pl+Opx+Am), pumice particles, and lava particles in the thin sections of volcanic ash. All thin sections of pumice and ash include the dusty zone of Pl, so these products resulted from either through magma mixing (between felsic and mafic magmas) or the heating of felsic magma by the mafic magma. In four out of five samples of gray pumice, breakdown reaction rims of amphibole and groundmass crystals were confirmed, so magma that formed gray pumice likely underwent a different ascending process in conduit, in comparison with the magma that formed white pumice.

Suzuki and Fukushima (2019, this conference) studied pumice blocks in the BAF from the Futatsudake-Shibukawa eruption. This result is similar to our result. Therefore, we infer magmas formed these two products was homogeneous in magma chamber. The original pyroclastic flow was separated into rock mass flow and pyroclastic surge as they descended river valleys, resulting in simultaneous

©2019. Japan Geoscience Union. All Right Reserved.

emplacement of the BAF and fine-grained pyroclastic materials at different distances from the river valleys.

Keywords: Haruna volcano, Block and ash flow, Pyroclastic surge, Magma mixing, Heating from hotter magma, Eruption trigger

©2019. Japan Geoscience Union. All Right Reserved.

The occurrence and petrology of the block and ash flow deposit from the Futatsudake-Shibukawa eruption, Haruna volcano

*Yuki Suzuki[1], Ryouto Fukushima[2]

1. Department of Earth Sciences, Faculty of Education and Integrated Arts of Sciences, Waseda University, 2. Department of Earth Sciences, School of Education, Waseda University

Haruna volcano is located in the southern end of the NE Japan arc. The latest two eruptions occurred at Futatsudake; Shibukawa eruption in late 5th to early 6th century (0.4 DRE km^3), and Ikaho eruption in late 6th to early 7th century (0.99 DRE km^3)(ages from Geshi and Oishi, 2011; volumes from Yamamoto, 2013). Suzuki and Nakada (2007) conducted petrological study of Ikaho eruption to reveal eruption triggering process. First, injection of mafic magma into the mush-like felsic magma generated mixed magma and heated felsic magma. Then, these low viscosity magmas opened the conduit and vent, resulting in the decompression of whole reservoir. It is indispensable to study two eruptions from a continuous view point, because two eruptions occurred from the same place at an interval of only several decades.

The outcrops of the Shibukawa eruption are categorized into those consisting of block-and-ash-flow (BAF) deposit (this presentation) and those consisting of fine pyroclasts derived from pyroclastic surge and phreatic explosion (Maruyama and Suzuki, 2019; this conference). Outcrops of BAF deposit locate in the vicinity of river valleys, while outcrops of fine pyroclasts locate away from the valleys. The BAF deposit includes relatively large (up to 30cm) juvenile pumiceous blocks, allowing more precise determination of bulk composition of erupted magma than the fine pyroclastic deposit. We investigated four outcrops, two of which locate along Owagawa and Noborisawagawa in the NE flank of the volcano, and two of which locate along Haruna-Shirakawa in the SE flank. Geshi and Oishi (2011) recently clarified the BAF deposit in the SE flank is the product of the Shibukawa eruption by the carbon dating. At some outcrops, BAF deposit could be divided into subunits by the existence of intercalated ash deposit. In any outcrop/subunit, juvenile blocks were classified into white, gray and dark gray. In some blocks, parts with different colors are in stripes or irregularly mixed.

The pumice blocks are homogeneous felsic andesite with 60.6-61.7 wt.% SiO_2(N=21). There is no systematic difference in the composition between the NE and SE flanks. In Unzen 1991-1995 eruption, the composition of the erupted magma changed with time, and there was a temporal change in the flow direction of the pyroclastic flow (Nakada and Motomura, 1999). The present data of Shibukawa eruption show no tendency like that. In the representative six samples covering the pumice color variation, Hb, Opx, Pl, Qtz and Fe-Ti oxides present as phenocryst phase. But, Qtz is quite rare, as we observed only one crystal in 8 thin sections. Phenocryst phases other than Qtz form aggregate, indicating they crystallized in equilibrium. Dusty zone was observed in the plagioclase rim, showing that the melt became undifferentiated just prior to the eruption, due to 1) mixing with hotter magma, or 2) heating by hotter magma. There is no change in whole rock composition and phenocryst assemblage with pumice block color. The different color is likely to be caused by different amount of groundmass crystal (Gardner*et al.*, 1998). The breakdown of Hb was observed only in dark gray blocks.

The felsic endmember magma of the Ikaho eruption erupted as white pumice (60 to 62 wt.% SiO_2). The white pumices contain phenocrysts of Hb, Opx, Pl and Fe-Ti oxides. Therefore, it is highly probable that the felsic magma similar to that in Ikaho eruption was active in the Shibukawa eruption. In the Ikaho eruption, ejecta with obvious characteristics of magma mixing (gray pumice and lava, down to 57.5 wt.% SiO_2) have been confirmed. It means that the mixing ratio of the high-temperature magma in the Shibukawa eruption (even if it happened) was very small. In the future, as well as exploring the eruption

©2019. Japan Geoscience Union. All Right Reserved.

triggering process of the Shibukawa eruption in detail, we need to investigate phenocrysts derived from the felsic magma for the Ikaho eruption. They might record the effects of heating and mixing by high-temperature magma, which occurred several decades before the eruption.

Keywords: Haruna volcano, Block and ash flow deposit, Mush-like felsic magma , Eruption trigger, Magma mixing, Heating from hotter magma

©2019. Japan Geoscience Union. All Right Reserved.

Report of Volcanic Activity at Kusatsu-Shiranesan in 2018

*Tsukasa Kobayashi[1], Koji Kato[1], Koichi Suemine[1], Kazuhiro Kimura[1], Yusuke Yoshigai[1], Yasuo Ogawa[2], Kenji Nogami[2], Wataru Kanda[2], Akihiko Terada[2]

1. Volcanological Division, Japan Meteorological Agency, 2. Volcanic Fluid Research Center, Tokyo Institute of Technology

Kusatsu-Shiranesan is the active volcano located in north-eastern Gunma-pref. Japan Meteorological Agency (JMA) monitors Kusatsu-Shiranesan volcanic activity. A group of pyroclastic cones, including Shiranesan, Ainomine, and Motoshiranesan, which stretch from the north to the south, are located in its highest western area. Latest magmatic eruption occurred about 3,000 years ago. All recent eruptions were occurred in the area around Yugama and Motoshiranesan area, and these eruptions were phreatic explosions.

In January 2018, phreatic explosion occurred at Motoshiranesan area. In April, volcanic seismicity in shallow areas beneath the Yugama crater increased. We report volcanic activity at Kusatsu-Shiranesan in 2018.

A phreatic explosion occurred at 10:02 on 23 January 2018 at the northern and western area of Kagamiike-kita cone in Motoshiranesan. Before the eruption, volcanic tremor occurred from 09:59, and significant tilt changes which indicate the upward of Motoshiranesan direction was obserbed by tiltmeter installed around Yugama crater by the Tokyo Institute of Technology. At around 10:02, low frequency earthquake was observed, and these tilt signals turned to the downward to the Motoshiranesan direction. After the eruption, a very small volcanic earthquake (BH-type earthquake) occurred frequently in a shallow place near Kagamiike-kita cone, but it gradually declined.
In late April 2018, earthquakes around shallow part of Yugama crater rapidly increased, and crustal deformation indicating the expansion of the shallow part around Yugama began to be observed with the tiltmeter installed around Yugama crater.By the geomagnetic observation, the variation of geomagnetic total intensity indicating thermal demagnetization was observed from April.
In early September, the volcanic earthquake activity decreased somewhat and the tiltmeter variation also became smaller. But on September 28, again the earthquake around the Yugama increased rapidly. And crustal deformation similar to April was observed by the tiltmeter installed around Yugama. After that, earthquake activity decreased gradually, but continued in January 2019.

Analysis result of GNSS continuous observation date from 2014 to 2015, in which period seismicity around Yugama crater was high, indicates the expansion of the deep part of northwest area of Kusatsu-Shiranesan. Similar changes was observed at several observation points in 2018.

We would like to thank Kakioka Magnetic Observatory, JMA for the use of his observation and analysis data.

Keywords: Kusatsu-Shiranesan, phreatic explosion, earthquake activity, ground deformation, variation of geomagnetic total intensity

©2019. Japan Geoscience Union. All Right Reserved.

Noble gas isotope composition of fumaroles and hydrothermal gases around Kusatsu-Shirane volcano

*Kotaro Toyama[1], Hirochika Sumino[1], Kaori Kawana[1], Yoshihide Akiyama[1], Takeshi Ohba[2], Muga Yaguchi[3], Akihiko Terada[4]

1. Department of Basic Science, Graduate School of Arts and Sciences, The University of Tokyo, 2. Department of chemistry, School of Science, Tokia University, 3. Meteorological Research Institute, 4. Volcanic Fluid Research Center, Tokyo Institute of Technology

Mount Kusatsu-Shirane, an active stratovolcano consisting of three pyroclastic cones (from north to south, Mt. Shirane, Mt. Ainomine, and Mt. Motoshirane) erupted on 23 January 2018 at Mt. Motoshirane. This eruption was a phreatic eruption, which often occur without magma movement. Therefore, there is no or very small precursor geophysical signals. In contrast, the chemical and isotopic compositions of volcanic gases can change reflecting pressure rise of a gas reservoir which caused the phreatic eruption. Especially, helium isotope ratio ($^3He/^4He$) is regarded as a useful tracer for the volcanic activity, because it exhibits unique values corresponding to the origin (e.g., 7-8 Ra in the mantle and < 0.1 Ra in the curst, where 1 Ra denotes atmospheric $^3He/^4He$ ratio of 1.4×10^{-6} [1]). Some studies have reported pre-eruptive $^3He/^4He$ anomalies, suggesting the increase of supply of the magmatic helium into the hydrothermal system preceding eruption [2,3].

We report the noble gas (He, Ne, Ar) isotopes of fumaroles and hot-spring gases collected from 9 sites around Kusatsu-Shirane volcano during 2014 and 2018. The measured $^3He/^4He$ ratios were corrected for atmospheric contamination based on $^4He/^{20}Ne$ ratios. The air-corrected $^3He/^4He$ ratio of Sesshogawara fumarole, located on 2 km east of the 2018 phreatic vent, had been constant at 7.0-7.5 Ra during 2014 and 24 January 2018, and dropped to 6.5 Ra on 13 February 2018. The $^3He/^4He$ ratio increased to 7.6 Ra on 21 May 2018 and has been constant at about 7.5 Ra. The $^3He/^4$ He ratios of bubbling gases of Kusatsu-Yubatake hot spring, which located on 5 km east of the 2018 phreatic vent, had been constant at 6.5-6.9 Ra during 2014 and 12 February 2018, decreased to 6.0 Ra on 3 June 2018, and then increased to 7.5 Ra on 6 August 2018. The $^3He/^4$ He ratios of Hoshimata fumarole, which located on 3 km west of the 2018 phreatic vent, increased from 6.2 Ra to 7.3 Ra during 2 March 2018 and 19 June 2018. The trends observed in these sites seem to be associated with the 2018 eruption with different time lags, which may reflect the migration distance from the 2018 phreatic vent to the sites.

In Kusatsu-Shirane area, two hydrothermal reservoirs, one of which is located beneath Yugama crater of Mt. Shirane and the other is located beneath Mt. Motoshirane (between Ainomine and Mt. Motoshirane), have been proposed [4]. The $^3He/^4He$ ratios (7.2-8.1 Ra) of Kitagawa fumaroles on the northern flank of Mt. Shirane near the Yugama crater, may reflect the values of the gases derived from the hydrothermal reservoir beneath Mt. Shirane. On the other hand, the lower $^3He/^4He$ ratios observed in Sesshogawara, Kusatsu-Yubatake and Hoshimata after the eruption may result from another contribution from a reservoir having lower $^3He/^4He$ ratios (less than 6.5 Ra), which could be attributed to the hydrothermal reservoir beneath Mt. Motoshirane. The reservoir beneath Mt. Motoshirane may be enriched in radiogenic ^4He derived from the crust, because Mt. Motoshirane has not erupted for last 1500 years [5].

It has been proposed that the 2018 eruption was caused by sealing of gas pathway from magma to the hydrothermal reservoir beneath Mt. Shirane [4]. This would result in decrease of supply of magmatic gas with high $^3He/^4He$ ratio to Sesshogawara, Kusatsu-Yubatake, and Hoshimata. Therefore, the low $^3He/^4He$

©2019. Japan Geoscience Union. All Right Reserved.

ratios observed in these sites after the 2018 eruption may reflect relative increase of the contribution of gas supplied from the Mt. Motoshirane hydrothermal reservoir. In contrast, the high and relatively constant $^{3}He/^{4}He$ ratios at all of the sites since August 2018 suggest that the gas from the reservoir beneath Mt. Shirane is dominant. Ohba et al. [4] proposed that supply of magmatic gas to the Mt. Motoshirane reservoir increased before the eruption as a result of the sealing of gas pathway from magma to the Mt. Shirane reservoir, and that it caused high fluid pressure of the reservoir and subsequent phreatic eruption at Mt. Motoshirane. This implies that $^{3}He/^{4}He$ ratio of the Mt. Motoshirane reservoir also increased from a lower value to a higher value less than 6.5 Ra before the eruption. Although further study is necessary to constrain $^{3}He/^{4}He$ ratios of the reservoirs, the remarkable temporal $^{3}He/^{4}He$ variation after the eruption can be accounted for by the change in mixing ratio of the gases from the two reservoirs.

References: [1] Ozima and Podosek (2002) Noble Gas Geochemistry.; [2] Padrón et al. (2013) Geol.; [3]Paonita et al. (2016) Geol.; [4]Ohba et al. (2018) JpGU2018, SVC41-38.; [5]Nigorikawa et al. (2016) JpGU, SVC48-11.

Keywords: Noble gas , Volcanic gas, Kusatsu-Shirane volcano, Volcanic eruption, Temporal variation

©2019. Japan Geoscience Union. All Right Reserved.

Self-potential and geomagnetic total intensity observations at Motoshirane volcano after the 2018 eruption

*Akira Yamazaki[1], Hideki Iino[1], Tatsurou Tanaka[1]

1. Kakioka Magnetic Observatory

A phreatic eruption occurred at Kusatsu-Shirane volcano (Motoshirane volcano) on January 23, 2018, and some impact craters were formed on the Kagami-ike crater floor and the Kagami-ike northern crater. After the eruption, the temporarily activated seismic activity near the crater has declined, and the fumarolic activity has ceased after late February 2018. In order to estimate geothermal status after the eruption, we carried out self-potential (SP) and geomagnetic total intensity observations at Motoshirane volcano. Measurements of the SP were conducted at about 130 points around the summit of Motoshirane volcano from June 30 to July 2, 2018. Copper-Copper sulfate electrodes were used, the measurement interval was about 50 m, and the measurement was carried out by the so-called full potential method. We applied -1.3mV/m as correlation coefficient for correction of the topographic effect to all the SP measurement stations. The coefficient was obtained from a clear negative correlation (-1.3 mV/m) between the elevation and the potential in the survey line on the eastern slope of the Kagami-ike. As a result of the SP, we detected a positive anomaly, 200~500mV in magnitude, developing around the summit of Motoshirane volcano. By comparison of the result of the 4th Joint Observation of Kusatsu-Shirane Volcano in 2003, we found temporal variations of the SP near Kagami-ike northern crater which may have been caused by the eruption. As for the geomagnetic total intensity observation, we selected ten repetitive observation stations around the summit of Motoshirane volcano, and carried out first observation in June 2018 (June 28-30). Following the first observation, we carried out repeated observation in August (August 28-29) and October (October 7). As a result, no significant changes in the geomagnetic total intensity in the period from June to October, 2018. It suggests that rapid thermal demagnetization or magnetization by cooling does not occur at underground of Motoshirane volcano.

Keywords: Kusatsu-Shirane volcano, Motoshirane volcano, Self-potential observation, Geomagnetic total intensity observation, Thermal demagnetization

©2019. Japan Geoscience Union. All Right Reserved.

Eruption processes of the 3rd and 4th stage of Niigata-Yakeyama Volcano, Japan, inferred from microlite texture and chemical composition

*Takumi Yoshida[1], Takeshi Saito[1]

1. Shinshu University

Niigata-Yakeyama volcano, which belongs to the Myoko volcano group, is one of the most active and youngest volcanoes in Japan. In the 3rd stage of Yakeyama activity, Maeyama lava flows and Hayakawa pyroclastic flows were generated to the northern slope of the volcano. In the 4th stage activity, Yakeyama lava flows, which forms present lava dome at the summit, and Otani pyroclastic flows were effused. Otani pyroclastic flow deposit contains well-vesiculated lavas, while lavas from Hayakawa pyroclastic flow are poorly-vesiculated. In this study, groundmass textural analysis of the eruptive products at the 4th stage was carried out. Chemical composition of plagioclase phenocrysts and microlites of the eruptive products at the 3rd and 4th stage were analyzed in order to examine the eruption process of the 3rd and 4th stage of Yakeyama volcano.

Microlite number density (MND) and crystallinity of plagioclase in Otani pyroclastic flow deposits were obtained from groundmass textural analysis. Our results indicated that Otani pyroclastic flows showed lower MND and intermediate crystallinity compared with Hayakawa pyroclastic flow deposits. As a result of chemical composition analysis, phenocryst in the samples of the 3rd stage activity shows An#(Ca/Ca+Na) =0.65~0.84. Microlite of andesite of Maeyama lava flow has an average An# of 0.61, which is lower than that of dacite lava of Maeyama Lava flow (average An# =0.54). Phenocryst of the 4th stage activity has An# =0.45~0.89. Microlite of Yakeyama lava flow and Otani pyroclastic flow have average An# of 0.63 and 0.62, respectively. The An# of plagioclase microlite becomes lower with decreasing crystal size.

Plagioclase microlite becomes lower An# with higher degree of H2O exsolution due to decompression (e.g. Nakamura, 2011). Our results suggest that microlite in dacite lava of Maeyama lava flow has undergone high decompression compared with andesite lava of Maeyama lava flow. However, there were little difference between plagioclase microlite of lava flow and that of pyroclastic flow samples. Eruptive products of the 4th eruption have relatively homogeneous SiO2 composition. Plagioclase microlite of Otani pyroclastic flow deposit, showing lower MND and higher An# than Hayakawa pyroclastic flow, may be crystallized under a condition of lower undercooling. Another possibility is that rapid vesiculation and H2O exsolution may proceed before microlite crystallization and prevent from decreasing An#.

Keywords: Niigata-Yakeyama, Yakeyama lava flow, Otani pyroclastic flow, Maeyama lava flow, Hayakawa pyroclastic flow, Plagioclase microlite

©2019. Japan Geoscience Union. All Right Reserved.

Estimation of subsurface structure of Shinyu crater lake, Tateyama Caldera, based on the water level and seismic observation data

*Ryohei Kawaguchi[1], Naoko Saito[2], Shin'ya Onizawa[1]

1. Meteorological Research Institute, 2. Toyama local Meteorological office, Japan Meteorological Agency

Shinyu, located in the Tateyama caldera is a crater lake with the diameter of about 40 m and the depth of about 5.6 m. The water level of Shinyu is maintained by the influx of hot water from vents at the bottom of Shinyu. Shinyu had continued the full water level for decades, but periodic geyser activity was reported from 2014 which has the period of 0-20 days (Fukui et al 2018). In order to investigate the activity of the water level change in Shinyu, we installed water level meter and seismometer around Shinyu from June to October in 2017 and 2018. In this study, we estimate the underground structure of Shinyu based on the temporal changes of water level and seismic data.

The water level change was observed by a bubble type water level meter which has a sampling period of 10 minutes. In addition, a seismometer was installed at about 20 m from the Shinyu. The seismic data was recorded with a sampling frequency of 100 Hz.

During the observation period, we were able to obtain the water level change data of 7 cycles in 2017 and 8 cycles in 2018, respectively. For the preliminary analysis, we examined the periods of water level changes, dividing the water level change cycle into four categories, dry-up, rising in the water level, full water level, and descent in the water level. As a result, the period of the dry-up is about 3 days, the rise in water level is about 4.5 days, the full water is 0 to 20 days and the descent in water level is about 0.5 days. The period of raising and decent of the water levels were almost constant for each cycle. During the rising and full of the water level, rising of hot water with gas bubbles were observed by the image of Shinyu surface taken by time-lapse camera. The amplitudes level of seismometer data was clearly different between the period of rising and full of water level and the period of dry-up and decent of water level. These indicate that geyser activity of Shinyu is occurred by boiling of hot water in the water reservoir located below the Shinyu.
When the shape of Shinyu is conical and the flux of the hot water drop under the Shinyu is constant, the flux of dropping hot water is estimated about 0.06 m^3/s by the size of Shinyu and the period of the descent of water level. According the data of water level meter, the rate of water level descent were 1.2-2.5 $\times 10^{-3}$ m/s. From these data, the radius of cylindrical pipe assuming below the Shinyu was estimated to be 2.8-4.0 m. We also report on the result of comparing the time scale of water level changes using the observed data and simulation result based on the previous geyser model.

Keywords: Shinyu, Tateyama caldera, geyser

©2019. Japan Geoscience Union. All Right Reserved.

Real time monitoring of underground temperature in Jigokudani, Midagahara volcano using LPWA devices

*Tohru Watanabe[1], Toyama branch NTT West[2]

1. Gradudate School of Science and Engineering, University of Toyama, 2. Nippon Telegraph and Telephone West Corporation

Jigokudani is an active geothermal area in Midagahara volcano, Toyama prefecture, central Japan. It was formed as a result of repeated phreatic eruptions over 40,000 years. Increased volcanic activity in this area has been observed since 2011. In order to detect a precursory signal of a phreatic eruption, seismicity, observations should be conducted on seismicity, ground deformation, geothermal activity, volcanic gas, etc. A real time monitoring system of underground temperature using LPWA (Low Power, Wide Area) devices has been tested since 30 August 2018. An LPWA device (NHR, SS05-ST) is composed of thermometer and transmitter (LoRaWAN). 10 devices were deployed in Jigokudani. Temperature sensors (thermocouples) were placed at the depth of 50 cm. Transmitters send temperature data every 30 minutes to a gateway to the internet situated in Hotel Tateyama. The distances from the gateway to LPWA devices are within 1 km. Underground temperatures can be monitored on internet devices. Since Jigokudani has a heavy snowfall in winter, 7 devices were removed and 3 devices were left to test in winter. Though temperature data could be received until December 2018, no data could be received since then. Transmitters of around 50 cm high above the ground must be covered with snow. During summer and fall, LPWA devices are useful for real time monitoring.

Keywords: underground temperature, LPWA, real time monitoring

©2019. Japan Geoscience Union. All Right Reserved.

Varying chemical and isotopic compositions of fumarolic gases from the summit and from the 1962-63 eruptive vents at Yakedake Volcano, Japan

*Takeshi Saito[1], Shun Sawamura[2], Kazuhiro Amita[3], Taketoshi Mishima[4], Shinji Ohsawa[4]

1. Institute of Science, Academic Assembly School of Science and Technology, Shinshu University, 2. Graduate School of Science and Technology, Shinshu University, 3. Graduate School of Engineering Science, Akita University, 4. Beppu Geothermal Research Laboratory, Institute for Geothermal Sciences, Graduate School of Science, Kyoto University

Since the latest phreatic eruption in 1962-1963, Yakedake volcano has remained dormant, but fumarolic activity around the summit area has continued steadily during the past hundred years. Recently, temperature, chemical, and isotopic compositions of fumarolic gases discharged from the summit fumaroles were ascertained for 2013-2017 (Saito et al., 2019). This time, fumarolic gases discharged from the 1962-63 eruptive vents, which locate about 300m north of the summit, were collected and chemical and isotopic compositions were analyzed. We compared our results from the 1962-63 eruptive vents with those from the summit fumaroles in order to evaluate the formation of volcanic hydrothermal system beneath the volcano.

Discharge temperatures of the fumaroles around the 1962-63 vents were 95-100˚C: slightly lower temperatures than those from the summit fumaroles but higher than the boiling temperature at the elevation. Chemical analysis revealed that fumarolic gases from the 1962-63 vents contain lower amounts of SO_2 than the summit fumaroles. Higher CO_2/total S ratio and lower apparent equilibrium temperatures of the 1962-63 fumaroles coincide with lower discharge temperatures. On the other hand, the 1962-63 fumaroles show higher He/Ar ratio than the summit fumaroles, suggesting higher contribution of magmatic fluid.

The isotopic compositions of water (D, ^{18}O) show that the fumarolic fluids from the summit fumaroles were probably formed by mixing of the magmatic fluids and local meteoric water. The isotopic compositions of the 1962-63 fumaroles show much lower values not only than the summit fumaroles but than local meteoric water, suggesting that the fluids suffered isotopic fractionation due to evaporation of the fumarolic gases.

Our results possibly indicate that volcanic hydrothermal system beneath the summit region differ from that under the 1962-63 vents.

©2019. Japan Geoscience Union. All Right Reserved.

Eruption age determination of the latest two lava flows and characteristics of volcaniclastic materials from the recent activity of Yokodake Volcano, Japan

*Hiroya Nitta[1], Takeshi Saito[1], Yorinao Shitaoka[2]

1. Shinshu University of Science and Technology, 2. Department of Environment System, Faculty of Geo-environmental Science, Rissho University

Yokodake volcano, which effused nine lava flows (Y1~Y9), is the only active volcano belonging to Yatsugatake volcano groups in central Japan. Eruption ages of Y1-Y8 lava were not determined distinctively. To evaluate the latest activity of Yokodake volcano, we carried out paleomagnetic studies and tried to estimate the eruption ages of the Y8 and Y9 lava flows. However, several candidates for paleomagnetic ages were remained (Nitta and Saito, 2018, JPGU; Nitta and Saito, 2018, fall meeting of the volcanological society of Japan). In this study, we applied thermoluminescence (TL) dating for Y8 and Y9 lava and viscous remanent magnetization (VRM) dating for Y9 lava. In addition, the volcaniclastic layers were found just above the Y9 lava and around the surface of the summit region. We will report characteristics of the volcaniclastic layers, discussing the recent activities of this volcano.

TL dating was performed by using poly-minerals (ca 10~50 μm) sample extracted from Y8 and Y9 lava. TL age of Y8 sample was 3.3 ±1.2 ka. Y9 lava sample didn't emit TL intensity. As for Y9 lava, we tried to estimate the age using VRM. However, the estimated ages were widely scattered. We conclude eruption age of the Y8 lava is ca. 3.3 ka, which is consistent with our previous paleomagnetic age of 3.35~3.85ka. On the other hand, five eruption ages of Y9 lava (0.60 ka, 1.80 ka, 1.90~1.95 ka, 2.20~2.25 ka, 2.4~2.45 ka) are still remained.

We recognized light gray volcanic ash deposit just above Y9 lava which composed of sand to silt size and contained carbonaceous material. It may be comparable to NYk-1 tephra (Okuno, 1995). Four volcaniclastic layers were found at summit region and the lower layer is a possibility of being correlated with NYk-2 tephra (2.35~2.15 cal ka BP; Okuno and Kobayashi, 2010). Two volcaniclastic layers above NYk-2 tephra seem to be derived from Yokodake volcano, suggesting at least two volcanic eruptions were occurred after NYk-2 tephra eruption.

Keywords: Yokodake Volcano, Latest lava, Eruption age determination, TL dating, Volcaniclastic materials from the recent activity

©2019. Japan Geoscience Union. All Right Reserved.

Estimating the date of the 2007 eruption of Mount Ontake Volcano using waveform correlation

*Shuhei Nishijima[1], Toshiko Terakawa[1], Shinichiro Horikawa[1]

1. Graduate School of Environmental Studies, Nagoya University

Mt. Ontake volcano erupted on late March, 2007. However, we do not know the exact time of the eruption with a Volcanic Explosivity Index 0 because of little visual evidence. I tried to estimate the date of the 2007 eruption, using a waveform correlation method. A previous study reports that focal mechanisms of volcanic earthquakes associated with the latest eruption in 2014 changed from normal/strike-slip faulting with east-west tension to reverse faulting with east-west compression. Based on this fact, I selected 10 and 8 volcanic events for the pre- and the post-periods of the 2014 eruption as template events. I applied the technique to continuous seismic waveforms from 22 December 2006 to 31 March 2007. I detected 2375 (pre-eruption type) and 1659 (post-eruption type) events corresponding to the pre- and the post-eruption events, respectively. I found that events with east-west tension (pre-eruption type) became active at the early stage until a very long period (VLP) event occurred on 25 January, and during the period from 5 to 19 February. On the other hand, the activity of events with east-west compression (post-eruption type) became dominant for 11 days after the VLP event occurred, and during the period from 20 February to 24 March. Subsequently, neither type of events became dominant. The activity of pre-eruption type events synchronized with the period when the length of the baseline in the east-west direction across Mt. Ontake increased. This suggests that events of pre-eruption type are related to the magma intrusion process beneath the volcano. The activation of events of post-eruption type following to the VLP event, which is well modeled by a tensile crack with a strike of N20W, may be related to contraction processes after the event released water vapor from the volcano. Based on the changes in types of detected events as well as the seismicity, I concluded that Mt. Ontake would have erupted on 20 February or between 11 and 12 March, 2007.

Keywords: volcano, Matched Filter Method

©2019. Japan Geoscience Union. All Right Reserved.

Seismic activity beneath Mt. Ontake volcano before and after the 2007 and 2014 eruptions

*Yoshiko Yamanaka[1], Shinichiro Horikawa[1], Yuta Maeda[1]

1. Graduate School of Encironmental Studies, University of NAGOYA

We developed a portable seismic telemetry system. This system is compact size, and the consumption electricity is small (Horikawa et al., 2017VSJ). From October 2017 performance test of this system has been carried out in the summit region of Mt. Ontake volcano. 10 seismic observations were installed. We determined seismic activity around Mount Ontake volcano by using those 10 summit observations and the seismic networks of Nagoya University and Japan Meteorological Agency, and obtained station corrections. Most of earthquakes were located beneath the craters of the 2014 eruption, and those depths were close in sea level or were shallower. The seismic activity is almost distributed on a straight line at -1.5km from 0km in depth and spreads through the northeast-southwest direction at around -1.5km (Yamanaka et al., 2018JpGU).

We try to determine seismicity linked to the 2007 and 2014 eruption of the Mount Ontake by using obtained station corrections. Before the 2014 eruption, earthquakes occurred from 1.0 km to -0.6 km linearly. This seismic activity is on an extension line of the 2017-2018 linear activity. After the 2014 eruption, earthquakes spread in the north and south direction from around -0.6 km in depth. The seismic activity gradually become shallow and extended to the current seismic activity. The events before the 2007 eruption also occurred from 3.0 km to 0 km on an extension line of the 2017-2018 linear activity. It is considered that some kind of fluid has risen through almost the same passage at the 2007 and 2014 eruptions.

Keywords: Mt. Ontake, Seismic activity

©2019. Japan Geoscience Union. All Right Reserved.

Effect of rain and snowmelt correction of tiltmeter data - Application example for Ontakesan Volcano -

*Kazuhiro Kimura[1,5], Katsuhisa Kawashima[2], Takane Matsumoto[2], Akihiko SASAKI[4], Tsutomu Iyobe[3], Junichi Miyamura[1], Masaki Nakahashi[1]

1. Japan Meteorological Agency, 2. Research Institute for Natural Hazards and Disaster Recovery, Niigata University, 3. Faculty of Engineering, Kyoto University, 4. Department of Geography and Environmental Studies, Kokushikan University, 5. Graduate School Science and Technology, Niigata University

Japan Meteorological Agency(JMA) installed a tiltmeter about 3km southeast of Mt. Ontake in 2010. A clear tilt change was observed northwest upward from several minutes before the 2014 phreatic eruption and northwest downward after the eruption. Kimura and Nakahashi (2015) applied the rain correction method using the tank model and precipitation data to the tiltmeter data of east-west component of the summer (From June to October), and they detected the small tilt change of west rising from September 10, 2014 when the earthquake activity became active. However, the similar tilt change of west rising has been confirmed several times and it has not been able to remove the influence of snowmelt in the spring (From March to May).

Miyamura et al. (2017) developed the rain and snowmelt correction method that adds the snow-tank to the tank model by Kimura et al. (2015) that uses snowmelt amount data as input values in addition to the precipitation data. They applied this method to the tiltmeter data of east-west component, and they confirmed that the influence of snowmelt in the spring was removed from the tiltmeter data. We used a method using a TR model that uses temparature and solar radiation as indices with reference to Matsumoto et al. (2010). Because there is not the continuous meteorological observation data for a long time near the tiltmeter (altitude 2195 m), they used the meteorological observation data at Kaidakogen (altitude 1130 m) closest to the tiltmeter (about 11.5km). In order to consider the difference between the two meteorological observation data, they compared with the meteorological observation data at Kaidakogen and the meteorological data near the tiltmeter observed by Kawashima et al. (2016).

There is a large seasonal changes from spring to summer every year for the tiltmeter data of north-south component. We applied the method of Miyamura et al (2017) to the tiltmeter data of north-south component, and it is able to remove this seasonal changes. Focusing on the 2014 phreatic eruption of Mt. Ontake, we detected the tilt change of north rising from the mid August 2014. In other words, the tilt change began north rising from the mid August 2014, and turned to northwest rising from around September 10. Similar tilt change could not be confirmed during the reserch period (April 2011 - September 2017).

We considered this tilt change while related to two previous studies. First, with reference to hypocenters before and after the eruption by Kato et al (2015), assuming an open crack model with NNW-SSE strike and moving its upper end from the 2 km to 1 km depth. As a result, we were able to confirm the tilt change pattern from north rising to northwest rising. Next, Miyaoka and Takagi (2016) applied the stacking method to the GNSS baseline length data, they detected that the change of the long baseline began from the middle of August and the change of the short baseline began from the beginning of September. They inferred that the pressure source migrated to a shallower region from a deeper region. The results of these previous studies are consistent with the tilt change applied the rain and snowmelt correction method to the tiltmeter data, and are considered to indicate the effectiveness of this method.

©2019. Japan Geoscience Union. All Right Reserved.

Keywords: Tiltmeter, Mt. Ontake, rainfall, snowmelt

©2019. Japan Geoscience Union. All Right Reserved.

Spatial Variation of b-value around Mt. Fuji influenced by the Eastern Shizuoka Earthquake of 15 March 2011

*Takumi Murakoshi[1], Tomonari Miyashita[2]

1. National Defense Academy, 2. JASDF

The Eastern Shizuoka earthquake occurred on March 15, 2011 (Mj6.4). The hypocenter of the earthquake was approximately 6 km southwest of Mt. Fuji’ s peak at a subsurface depth of about 15 km. Estimating spatial variation of the b-value of the Gutenberg–Richter relation is important in the examination of time and spatial changes in volcanic and seismic activity after large earthquakes. This study aims to evaluate changes in seismic activity after the 2011 Eastern Shizuoka earthquake using the spatial variation of the b-value. Hypocentral data from July 2001 to December 2017 was obtained from the JMA catalog. As a result, the b-value for earthquakes around Mt. Fuji was significantly smaller during the period after the 2011 Eastern Shizuoka earthquake than during the period from July 2001 through February 2011, and it continued to gradually recover after the Eastern Shizuoka earthquake.

Keywords: b-value, Mt. Fuji, 2011 Eastern Shizuoka Earthquake

©2019. Japan Geoscience Union. All Right Reserved.

Present condition of submarged volcano, Teishi Knoll, off Ito, Eastern Izu Peninsula

*Toshiro Yamanaka[1], Yoshifumi Kawada[2], Takuro Noguchi[3], Mayumi Hatta[3], Kei Okamura[3]

1. Tokyo Univ. Marine Science and Technology, 2. Tohoku University, 3. Kochi University

Teishi Knoll is a submerged volcano belonging to Eastern Izu volcanic zone and located c. 4 km east off the coastline of Ito City, Eastern Izu Peninsula. The volcano erupted in July, 1989, then the cone shaped knoll with a crater on the summit was formed. The Japan Meteorological Agency has reported that the Eastern Izu volcanic zone is composed of some small volcanoes including scoria cones, tuff rings, maars, and lava domes, erupted on land and many submerged volcanoes distributed densely on the seafloor off the coast. Detail of the submerged volcanoes has been unknown yet. The volcanoes have been considered to distribute on several lines of northwest-southeast direction reflecting the stress field of this area. Previous activities of the volcanic zone have been reported; Ohmuroyama Volcano was formed by eruption about 4 ka, Kawago-daira Volcano was formed about 3.2 ka, and Iwanoyama-Iwoyama volcanic chain was formed by a fissure eruption about 2.7 ka. The last eruption of the volcano belonging to the zone is considered the Teishi eruption in 1989.

In Japan there are confirmed 110 active volcanoes, 12 volcanoes of them are located below sea surface. Such submerged volcanoes have not been observed continuously due to its difficulty by visual observation, therefore, those volcanoes have not ranked according their activity by Japan Meteorological Agency. Therefore, we started observation of Teishi volcano in December, 2017, for evaluation whether active magma supply is still continuing or the intrusive magma causing of 1989 eruption is just cooling. Geochemical (water chemistry) and geophysical (heat-flow) observation has been done using training vessels of TUMSAT every half year.

We have not accumulated enough data yet, measurements of geothermal gradient were performed every time. For calculation of the heat-flow it is required the temperature record of the bottom water, so we started long-term temperature observation on the seafloor from the last December. On the other hand, chemistry of the bottom water in the crater showed slight positive anomaly of dissolved inorganic carbon and significant positive anomaly of manganese relative to the bottom water obtained from outside of the crater. Those chemical anomalies suggest that any thermal activity is still alive in the volcano.

Keywords: Teishi Knoll, Submerged volcano, Activity, Chemical flux, Heat flow

©2019. Japan Geoscience Union. All Right Reserved.

Descriptions and age of volcanic products before the caldera formation in the northern part of Izu-Oshima, off Tokyo, Pacific Ocean

*Satoshi Terayama[1], Takehiko Suzuki[1], Makoto Kobayashi[2]

1. Tokyo Metropolitan University, 2. Research Center for Volcanic Hazards and Their Mitigation, Tokyo Metropolitan University

Introduction

Izu-Oshima Volcano erupted in 1986 is an active volcano that will erupt in near future. The volcano has been studied for a long time, and many studies has been conducted (Nakamura, 1964; Koyama and Hayakawa, 1996; Kawanabe, 2012 and so on). However, most previous studies focused on ″Syn-and post-caldera volcano″ (Kawanabe, 1998) after the caldera formation of Izu-Oshima Volcano. There are few studies discussed ″Younger Edifice of Pre-caldera volcano″. In this study, the purpose is to investigate the volcanic products of Younger Edifice of Pre-caldera volcano and older period with little investigation and to clarify the eruption history. The description of the volcanic products should be important in considering prediction of volcanic eruption and volcanic disaster prevention.

The study site is a coast called Goishihama located between the Chigasaki and Kazehayasaki capes in the northernmost part of Izu-Oshima. At the site volcanic products are exposed on the coasted cliff with a width of about 1 km and a height of about 30-40 m. Volcanic products that can be observed along Goishihama are described by Isshiki (1984), who reported mainly volcanic product of ″Okata volcano″ and ″Older Edifice of Pre-caldera volcano″. However, its description is limited, and description and discussion of fall-out tephra have not been done. In this study, we investigated volcanic products that are exposed on the sea cliff of Goishihama. As a result, some new views on the observable layer were obtained.

Results

The fall-out tephra group composed of 31 eruptive products is named ″Goishihama fall-out tephra group″. We sampled black humus buried soil from three horizon in ″Goishihama fall-out tephra group″ and determined the radiocarbon age. Ages are 11076-10713, 12027-11747, 18117-17803 cal BP in descending order. Therefore, it was revealed that ″Goishihama fall-out tephra group″ is the volcanic products of ″Younger Edifice of Pre-caldera volcano″ after 20 ka. Isshiki(1984) showed no description of the volcanic products of ″Younger Edifice of Pre-caldera volcano″ at Goishihama. As a future issue, it is necessary to correlate Goishihama with 95 fall-out of O1 to O95 distributed mainly in southwest part of the island by Tazawa (1980).

In addition, a fine white pumice with a diameter of about 1 mm was found slightly in the ″Goishihama fall-out tephra group″. After sampling the layer, we washed and observed it with a microscope, colorless and transparent pumice type volcanic glass shards were discovered. The chemical composition of the volcanic glass was measured, that is, SiO_2=78.07 wt.%, CaO=0.61 wt.%, FeO=0.75 wt.%, Al_2O_3=12.74 wt.%, K_2O=3.29 wt.%, showing a rhyolitic tephra. Therefore, it is not a tephra from the Izu-Oshima volcano formed by basaltic magma. The source of this rhyolitic tephra seems to be Kozushima Volcano or Niijima Volcano. These results suggest that ″Goishihama fall-out tephra group″ is the products of ″Younger Edifice of Pre-caldera volcano″ and that this rhyolitic tephra can be compared with O55 (Niijima Miyatsukayama tephra) (Saito et al., 2007). Thus, in this study, a new radio carbon age was obtained from Goishihama, and a rhyolitic tephra was newly discovered. The future issue is to correlate tephra in the outcrop of this study site with those in other outcrops, and it is needed to confirm the correlating of rhyolitic tephra.

©2019. Japan Geoscience Union. All Right Reserved.

Keywords: Izu-Oshima Volcano, volcanic products, Niijima Miyatukayama tephra, radiocarbon dating

©2019. Japan Geoscience Union. All Right Reserved.

Time change of p-value by Schuster method using earthquakes around Izu-Ohsima summit

*Hiroyuki Takayama[1]

1. Volcanological Division 1st labolatory, Meteorological Research Institute

Morita et al.(2016) and Morita et al.(2017) consider relation between volcanic earthquakes in Izu-Ohsima island and earth tide. Takayama et al.(2018) divide Izu-Oshima into 5 area and calculate p-value and consider relation between earthquakes and earth tide.

We use Schuster method (Schuster (1897)) whether occurrence of earthquake relate earth tide or not. This method is check null hypothesis of no correlation between earthquake occurrence and earth tide. Specifically, we set tide phase angle of earthquake occurrence as Di,

$$R=(\sum \cos Di)^2+(\sum \sin Di)^2$$

$$p=\exp(-R/N)$$

we test relation between earthquake occurrence and earth tide by this p-value. P-value falls in 0 to 1. If p-value is nearly 0, we reject null hypothesis. We calculate tide phase angle to each tidal component. In this research, we use principal lunar semi-diurnal tide (after this, we abbreviate M2).

In principal, if earthquake catalogue contain swarm, we can’ t calculate precise p-value. So, we avoid this problem to decluster catalogue.

In this study, we investigate time change of p-value in summit earthquakes. Detection capability of JMA catalogue in summit area is magnitude 0.0. After we decluster this catalogue, p-value is 0.011. So, we divide summit earthquake by time and calculate p-value of M2 in each group.

Specifically, we use JMA catalogue from April 2002 to January 2017. We pick up earthquakes of Izu-Ohsima summit. The number of earthquakes larger than magnitude 0.0 is 1084. After declusterd, the number of earthquakes is 901. We pick up 100 earthquakes from declusterd catalogue. We calculate p-value by M2 in 801 earthquake lists.
As a result, p-value increase and decrease periodically in time. Maximum is 0.98, minimum is 0.0030. If we select standard of rejection of null hypothesis as 0.05, periods of p-value less than this standard are around 2006, around 2010 and around 2014. Morita et al.(2017) suggest that release of volatile component from magma increase when earthquakes correlate earth tide. In the above three periods, release of volatile component increase possible. Also, Morita et al.(2017) suggest that release of volatile component from magma increase from 2013. This coincide with 2014 period.

©2019. Japan Geoscience Union. All Right Reserved.

Keywords: volcanic earthquake, earth tide, p-value

©2019. Japan Geoscience Union. All Right Reserved.

Standard stratigraphy and characteristic properties of late Quaternary tephras on the Niijima-island: Report of geochemistry and refractive indices of volcanic glass shards, orthopyroxene, hornblende, and cummingtonite

*Kaori Aoki[1], Makoto Kobayashi[1], Fumikatsu NISHIZAWA[1,2], Masanori Murata[1], Daisuke Ishimura[1], Takehiko Suzuki[1]

1. Research Center for Volcanic Hazards and Their Mitigation, Tokyo Metropolitan University, 2. Mount Fuji Research Institute, Yamanashi Prefectural Government

Tokyo Metropolis has the twenty-three wards, the Tama district, and the islands area. The population of the islands area is 25,353 (1st January 2019). The islands area, namely, the Izu-Ogasawara Islands consist of 21 volcanoes (islands and submarine volcanoes), excluding some islands. For residents in this area, volcanic disasters are always the threat. Accordingly, to integrate the fundamental information for preventing volcanic disasters, we investigate the history of volcanic activities, the pattern of each eruption, and the mass volume of erupted tephras and try to establish the high-resolution tephrochronology (Kobayashi *et al.*, 2019a,b). This project focuses on establishing the database of tephras collected form each island of the Izu Islands and their petrographic description and geochemical data. Also, it is likely that such tephra across the sea would deposit in the hemipelagic sediment around volcanic islands. Our tephra database of the Izu Islands has been a powerful tool to identify the source of marine tephra bearing in drilled core CK09-03,C9010E collected at the site of 100 km east from the Izu Island, off the Boso Peninsula (Aoki et al., 2019). Today, we present the petrographic and geochemical characters of many tephras provided through volcanic activities of the Niijima island during late Quaternary.

At the Daisan-yama, Fujimi Touge, and Miyatsukayama on Niijima island, and also Jinaijima off 1.6km west of Niijima island, we have recognized 21 eruptive events at least, including some tephras derived from off-island (Kobayashi *et al.*, 2019a). Kobayashi et al. (2019a) recognized as Niijima Origin tephra felsic magma events and mafic magma events on Nijjima islnad. On the island, as widespread marker tephra, AT and K-Ah tephra were detected. After tephra samples were washed by the ultrasonic cleaner, we collected the description of petrographic characters, major-element chemistry determined by EDS and refractive indices (RI) of volcanic glass shards, orthopyroxene, hornblende, and cummingtonite in each tephra. Generally, felsic tephra derived from vents on the Niijima island include often a small amount scoria grain. Most felsic tephras consist of felsic volcanic glass shards, and including plagioclase, quartz (including β-quartz), orthopyroxene, hornblende, cummingtonite, and occasionally biotite. The characteristic fact of Niijima Origin tephra is that RIs of heavy minerals (orthopyroxene and hornblende) has broad variations. Especially, RIs of orthopyroxene in Akasakimine tephra series, Miyatsukayama tephra series, and Miyatsukayama Nannbu tephra series show the bimodal or trimodal histograms within the limit of 1.700-1.730, including high RIs over 1.730 slightly, considered as close to ferrosilite. Also, there is the tendency that RIs of hornblende in Akasakimine tephra series and Miyatsukayama tephra series show the bimodal histograms or broad variations within the limit of 1.663-1.688. On the other hand, RIs of cummingtonite in Niijima Origin tephra during 60 ka show the unimodal histograms within the limit of 1.658-1.669. RIs of felsic volcanic glass shards in Niijima Origin tephra show within the limit of 1.492-1.501. By comparison that common range of RIs on Quaternary tephra in Japan is 1.501-1.505 (Machida and Arai, 1992), RIs of Niijima Origin tephra would be classified to lower RI groups in Japanese Quaternary tephras.

©2019. Japan Geoscience Union. All Right Reserved.

The content of SiO_2 in volcanic glass shards is 77.7-78.2 wt%, Na_2O+K_2O is 7.2-7.7 wt% generally, excluding some tephra which range is within the limit of 7.0-8.3 wt%. The content of FeO* is 0.7-1.0 wt% and high-SiO_2 is harmonious to the lower RIs of volcanic glass shards (Furuta *et al.*,1986; Kikkawa, 1990).

Keywords: Izu, Niijima, tephrochronology, petrographic characters, major-element composition

©2019. Japan Geoscience Union. All Right Reserved.

Tephrostratigraphy and its eruption history of the Latest Activity in the Kozushima Volcano, the Izu Islands

*Makoto Kobayashi[1], Masanori Murata[1], Fumikatsu NISHIZAWA[2], Takehiko Suzuki[1,3]

1. Research Center for Volcanic Hazards and their mitigations, Tokyo Metropolitan Univ., 2. Fuji Research Institute, Yamanashi Prefectural Government, 3. Department of Geography, Tokyo Metropolitan Univ.

In this study, we defined the younger eruptive activity since the eruptive event of Chichibuyama A tephra (ca. 22–26 ka; Suga et al., 1992, 2003) composed of pyroclastic deposits from the southern part of Kozushima covering the whole island as "the Latest Activity". In order to establish the tephrostratigraphy during this period, we are aiming to construct more detailed eruption history of Kozushima Volcano.
As a result of the topographical interpretation using DEM, we recognized Tenjo-san edifice (pyroclastic cone and lava domes), Kobeyama-Hanadateyama volcanic chain (lava domes) and Kushigamine (pyroclastic cone) as younger volcanic landforms presumably formed by the Latest Activity.

In addition, according to the geological survey, we recognized deposits associated with eight eruptions events in minimum. At Loc. 16 in the north part of Nachi-san, northern Kozushima, we recognized pyroclastic surge deposit composed of alternate layers such as pumice, volcanic lapilli and coarse ash so on (no. 16-1; Tenjo-san Tephra (AD 838)), fall-out deposit including altered volcanic blocks and lapillus (no. 16-2), medium to fine fall-out ash deposit (ca. 10 cm in thickness) containing pumice clasts (no. 16-3), densely scattered zone composed of scoria clasts with diameter of several mm (no. 16-4) and densely scatter zone composed of coarse volcanic ash (no. 16-5) in descending order. On the other hand, at the Akabane-tunnel (Loc. 4) in southern Kozushima, Tenjo-san tephra (no. 4-1), densely scattered zone composed of coarse ash (no. 4-2), medium to fine volcanic ash deposit (ca. 3 cm in thickness) containing pumices (no. 4-3), densely scattered zone composed of scoria clasts with diameter of several mm (no. 4-4), fine volcanic ash deposit with a thickness of ca. 9 cm (no. 4-5) and pyroclastic surge deposit composed of alternated layers such as volcanic lapilli and coarse ash (no. 4-6) in descending order. Widespread tephra of K-Ah was detected between no. 4-2 and no. 4-3. Among these eruption deposits, it is suggested that the eruption of no. 16-2 occurred around central to northern part of Kozushima because these deposits distributed only these areas. In contrast, medium to fine air fall ash deposits (no. 16-3 and no. 4-3) containing pumices and fall-out fine ash deposit (no. 4-5) are very prominent layers, then, we are deeming these deposits as widespread tephras originated by relatively larger eruptions. ^{14}C datings for charcoal scattered in tephric loess or humus soil just below tephra layer were applied. ^{14}C ages are 1300±20 yr BP under the fall-out ash deposit correlated with the no.16-2 (Loc. 15; 262 m lava dome), 5790±30 yr BP at top of the no. 4-2, 8850±30 yr BP and 9390±30 yr BP above and below the no. 4-3, respectively, and 12030±30 yr BP just under the no. 4-6. Considering the calendar years and tephrostratigraphic relation, the ages of tephras during Latest Activity comprises five eruptions of ca. 1.1-1.2 ka (no. 16-2), ca. 7.5 ka (no.16-3 and no. 4-3), ca. 10 ka (no. 4-4) and ca.13.5 ka (no. 4-6).

Currently, we are further collecting data on mineral compositions, the refractive indexes and the major element compositions of volcanic glass shards for each tephra, and we are studying from the viewpoint of correlation with eruption deposits from Kobeyama-Hanadateyama volcanic chain, and Niijima Volcano origin tephra (Miyatsukayama, Shikinejima and Miyatsuikayama South: Kobayashi et al., 2018). In the presentation on the day, we will report the eruption history of the Latest Activity of Kozushima Volcano based on the results of these studies.

©2019. Japan Geoscience Union. All Right Reserved.

Keywords: tephrostratigraphy, 14C age, eruption history, Kozushima Volcano

©2019. Japan Geoscience Union. All Right Reserved.

Characteristics of hypocenter distribution connected with velocity structures in and around Miyakejima, Kozushima and Hachijojima volcanoes

*Hiroko Hagiwara[1], Hidefumi Watanabe[1]

1. Tokyo Metroplitan Government

The aim of this study was to examine the characteristics of seismic activities in association with the seismic velocity structures in and around the Izu islands. We focused on three seismic activities, the swarm off the west coast of Miyakejima on April 2013, the swarm off the northeast coast of Kozushima on April 2018 and the low frequency earthquakes beneath Hachijojima from 2003 to 2018. To construct the 3-D velocity structure models for Miyakejima and Kozushima we used the data of the swarm accompanied with the 2000 Miyakejima eruption, while for Hachijojima we used the data from 2003 to 2018 based on the Izu islands volcanic observation system. These travel times were adopted to the tomographic inversion method (Zhang and Thurber, 2003). The relocated precise hypocenters on the velocity imaging maps revealed an interesting relationship between seismicity and structure. In the target region, both Miyakejima and Kozushima swarms occur at 5-10 km and 2-6 km depth, in the border of high-velocity zones adjacent to or underlain by the low-velocity zones in figure 1 and figure 2. Their swarm regions were located nearby the two end sides of the 2000 swarm, where the huge seismic activity occurred repeatedly. That suggests the upward moving of magmatic fluids. In contrast, the Hachijojima earthquakes occur at 10-14 km depth in the middle-velocity area around a high-velocity zone in figure 3. This high-velocity zone is supposed to be somewhat cold body beneath Nishiyama volcano in Hachijojima. We interpret that the former low-velocity zones consist of hot magmatic materials and the latter high-velocity zone consists of the solidified volcanic body. On the basis of three case studies, it is suggested that volcanic fluids derived from hot magma or solidified magma caused the upper or surrounding seismic activities through complex crack systems.

Keywords: seismic activity, velocity structure, volcanic fluid, Miyakejima, Kozushima, Hachijojima

©2019. Japan Geoscience Union. All Right Reserved.

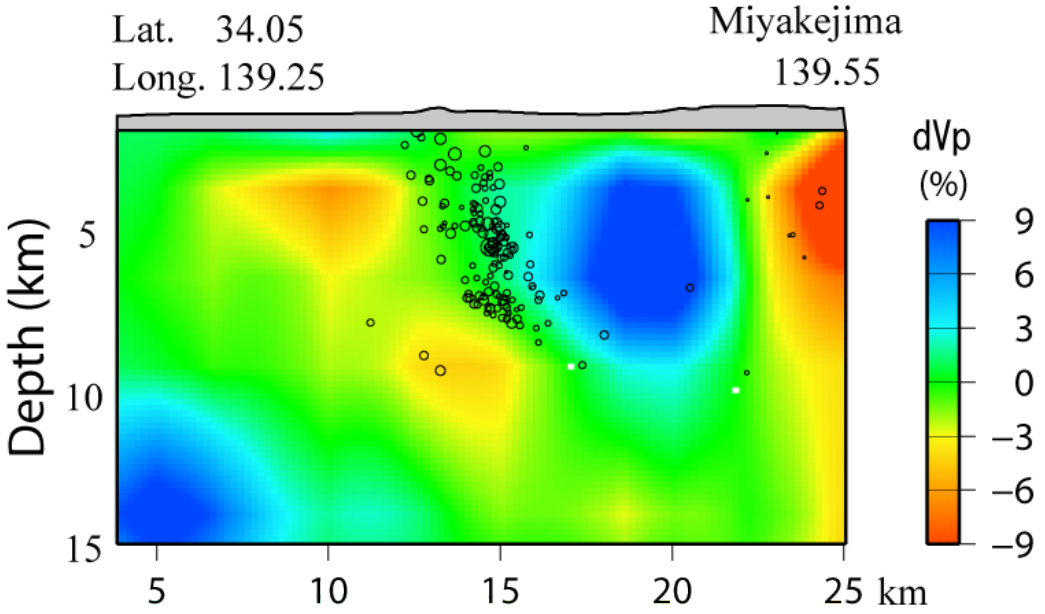

Fig. 1. E-W cross section of the dVp and relocated seismicity near Miyakejima.

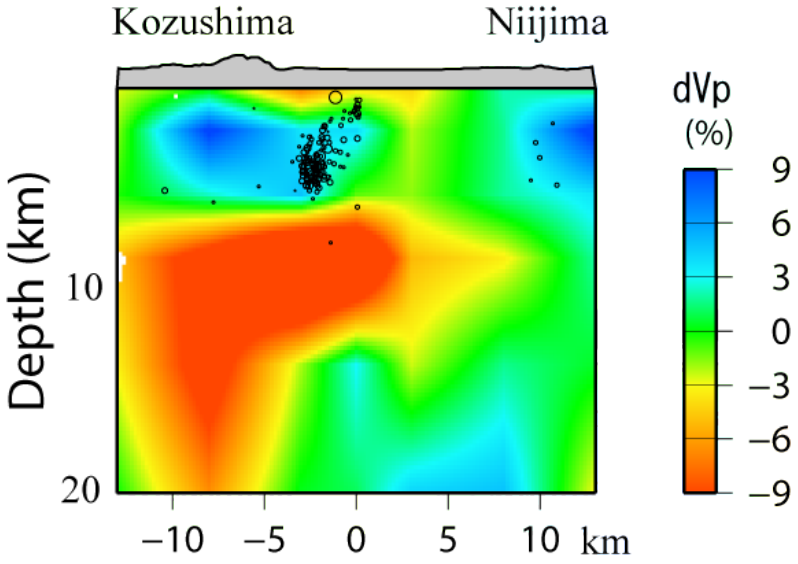

Fig. 2. Cross section of the dVp and relocated seismicity near Kozusima along the axis passing through Kozushima and Niijima.

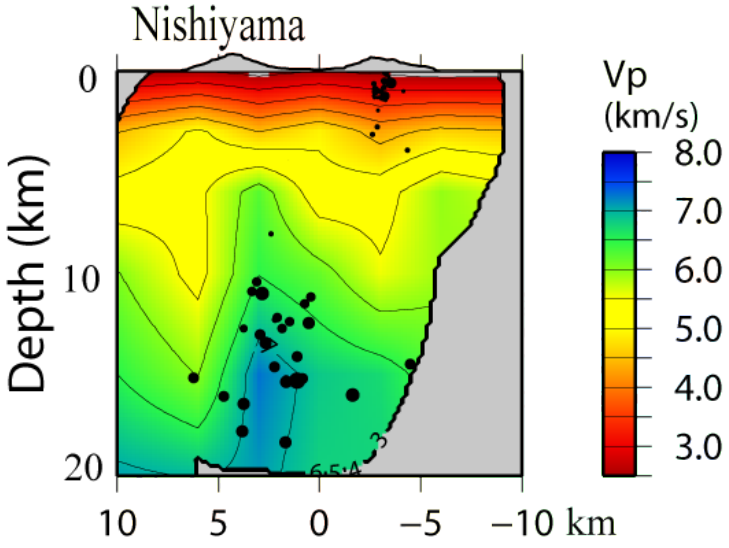

Fig. 3. Cross section of the Vp and relocated seismicity along the long axis of Hachijojima.

©2019. Japan Geoscience Union. All Right Reserved.

©2019. Japan Geoscience Union. All Right Reserved.

Deformation of Miyakejima volcano measured by GNSS campaign observation (2013-2015)

*Haruna Watanabe[1], Takeshi Matsushima[2], Miyo Fukui, Atsushi Watanabe[3], Jun Oikawa[3], Takashi OKUDA[4], Taku Ozawa[5], Yosuke Miyagi[5]

1. Department of Earth and Planetary Sciences, Graduate School of Science, Kyushu University, 2. Institute of Seismology and Volcanology, Faculty of Sciences, Kyushu University, 3. Earthquake Research Institute, University of Tokyo, 4. Earthquake and Volcanology Research Center, 5. National Research Institute for Earth Science and Disaster Resilience

Miyakejima is an active volcano located about 180 km south of Tokyo, and since the 20th century it erupted at intervals of about 20 years (1940, 1962, 1983, and 2000). Fukui et al. (2015) conducted GNSS campaign observations and estimated the pressure source of Miyakejima from 2011 to 2013. Therefore, in this research, we estimated the crustal deformation of Miyakejima from 2013 to 2015, the position of the pressure source and the volume change, and estimate the temporal change of the pressure source of Miyakejima.

We conducted GNSS campaign observations at 15 reference points arranged so as to be distributed almost evenly throughout Miyakejima from 2 September to 6 September 2013 and from 31 August to 4 September 2015. We used the data obtained from this GNSS campaign observation and the data for the same period of continuous observation points established by the Geospatial Information Authority of Japan etc. In order to analyze the obtained data, the coordinate value of the observation point for each year was obtained using RTKLIBver.2.4.2 software (Takasu et al., 2007).

The pressure source was estimated based on horizontal displacement from 2013 to 2015. The optimum value of the variation was obtained by using MaGCAP-V software (Meteorological Research Institute, 2008) for analyzing crustal activity for volcano. Although the positions of the pressure sources have not changed significantly from 2011 to 2013, it is presumed that the pressure source at the depth of about 0.3~8 km continues to contract and the pressure source at the depth of about 13 km continues to expand.

This work is partly supported by MEXT under Earthquake and Volcano Hazards Observation and Research Program, and also supported by Earthquake Research Institute, The University of Tokyo under Joint Usage Program.

Keywords: Miyakejima, GNSS observation

©2019. Japan Geoscience Union. All Right Reserved.

Characteristic properties of distal and proximal tephras in the Mikurajima Island, Izu Islands.

*Tomohiro Tano[1], Takehiko Suzuki[1,2], Makoto Kobayashi[2], Masanori Murata[2]

1. Faculty of Urban Environmental Sciences, Tokyo Metropolitan University, 2. Research Center for Volcanic Hazards and Their Mitigation, Tokyo Metropolitan University

Mikurajima of the Izu Islands is the stratovolcano island and located at 200 km south of Tokyo. The latest volcanic activity is about 6,300 years ago, there is no eruption activities in history. Mikurajima volcano is characterized by high occurrence frequency of andesite in volcanic front on the Izu arc(Isshiki,1980). Study on tephras distributed in the Mikurajima volcano has been reported by Sugihara & Shimada(1999),and Sekiguchi et al.(2001).They reported 6 tephra in Mikurajima island.(From the top Kozushima Tenzyosan:A.D.838,Iz-Kt,latest eruption of Mikurajima volcano:Mk-3,Kikai-Akahoya:7.3ka(Machida & Arai,2003),red scoria originated Mikurajima:Mk-2,rhyolithic tephra with unknown source:Mk-G, and fall pumice Mikurajima volcano tephra:Mk-1).The latest tephra of Mikurajima volcano:Mk-3,erupted from the lava dome in the southeastern in part of the islands(Sugihara & Shimada,1999).However, comparison/identification is insufficient of tephra compared to Iz-Kt. So it is necessary to compare and examine the Niijima Mukaiyama tephra(A.D.886,Iz-Mk).
They are rhyolithic tephra and indicated SiO2=77-79 wt.%. They erupted same age and constituent minerals and the refractive index of volcanic glasses are similar. So difficult to identify in distal place. Recently both can be distinguished by content of K2O in volcanic glasses. Iz-Kt indicated high K2O content compared with Iz-Mk. Both tephras are important indicator tephra widely distributed in the Izu islands. So it is important to clarify Iz-Kt distribution on Mikurajima.
In this research, we report on the tephras confirmed in Mikurajima. We found 18 tephras on Mikurajima island, and 4 tephras are confirmed(Iz-Kt,Mk-1,2,3).
1)The tephra confirmed Iz-Kt in previous study, we performed refractive index measurement by RIMS2000 and principal component analysis by SEM-EDS for volcanic grasses. This tephra present cryptotephra in topsoil. This glasses is pumice type and reflective index indicated n=1.496-497.Principal component:SiO2=77.0-78.5 wt.%,Al2O3=12.5-13.0 wt.%,FeO=0.5-1.3 wt.%,CaO=0.2-1.7 wt.%,K2O=2.7-3.9 wt.% and Na2O=3.6-4.6 wt.%.Iz-Kt and Iz-Mk confirmed on the Izu islands,they shows 3.8 wt% and 3.5 wt.% K2O content, respectively. So this tephra confirmed Iz-Kt.
2)For the latest tephra on Mikurajima volcano Mk-3,it is bad foaming yellow pumice between black volcanic sand.Maximum particle size of pumice is 10cm and maximum layer thickness is over 200cm.The lithophasies of MK-3 shows Prinian eruption.However,the detail of Mk-3 are unknown and under consideration.We performed principal component analysis as well.As a result,SiO2=62.3-70.7 wt.%,Al2O3=14.8-21.0 wt.%,FeO=2.2-3.8 wt.%,CaO=4.1-7.5 wt.%,K2O=0.3-0.9 wt.%,Na2O=3.8-4.4 wt.%.The values indicate andesite-dacite.
As a future work,to find and confirmed indicator tephra originated another volcano (like Iz-Kt and Mk-G).By comparing and identifying indicator tephra, I believe that we provide new distribute axis and age axis for history of eruption history in Mikurajima and tephra in the Izu Islands.And it is important to grasp detail of Mk-3 which is the latest eruption of Mikurajima volcano in order to grasp the volcanic activity of Mikurajima.

Keywords: Izu Islands, Mikurajima volcano, volcanin activity history, Kozushima Tenzyosan Tephra

©2019. Japan Geoscience Union. All Right Reserved.

Pseudo thermal anomalies in the shortwave infrared bands of the Himawari-8 AHI and their correction for volcano thermal observation

*Takayuki Kaneko[1], ATSUSHI YASUDA[1], Yoshizaki Yoshito[2], Takasaki Kenji[3], Yoshiaki HONDA[4]

1. Earthquake Research Institute, University of Tokyo, 2. Meteorological Satellite Center, Japan Meteorological Agency, 3. Japan Fisheries Research and Education Agency, 4. Center for Environmental Remote Sensing, Chiba University

Volcanic eruptions bring high-temperature gas or magma to the surface. Therefore, thermal observations of volcanic eruptions can be used to investigate the timeline of eruptive sequences. Eruptive activity includes processes that can change over short periods of time, which is sometimes related to the eruptive mode or the timing of its transitions. If we could observe short-term eruptive processes by detecting thermal changes, this would be beneficial for analyzing the eruptive sequence of volcanoes. Himawari-8 is a meteorological geostationary satellite operating above the equator at a longitude of 140.7 deg E and carrying a newly developed sensor, the Advanced Himawari Imager (AHI). With its improved performance, the Himawari-8 AHI enables the collection of high-frequency thermal observations that had never been obtained before. However, while observing volcanoes with the AHI, we noticed a frequent thermal anomaly in the nighttime 1.6-um and 2.3-um images. Because this anomaly occurred regardless of volcanic activity, it was considered to be a pseudo thermal anomaly. In-depth examination of the AHI observation data for several inactive volcanoes showed that the pseudo thermal anomaly was often seen around the vernal and autumn eclipse periods, and its in?uence persisted for about 6 months of each year. Further, daily variation of the anomaly peaked when it was midnight in the areas around 140 deg E. At this time and position, the AHI was facing the sun, suggesting that the anomaly was caused by stray light. We devised a correction method by assuming that the observed thermal radiance in a pixel consists of components from the radiating volcanic ground surface and stray light contamination. The latter can be estimated using values from nearby inactive pixels. Thus, the component from the radiating volcanic ground surface can be obtained by subtracting the estimated stray light from the observed thermal radiance. We evaluated the validity of this method using data from the 2017 Nishinoshima eruption and found that it satisfactorily removed the stray light component. An adoption of this correction allowed us to use all nighttime 1.6-um and 2.3-um images obtained by the AHI, half of which were formerly unusable due to the degradation caused by stray light.

Keywords: observation data correction, thermal anomaly, volcanoes

©2019. Japan Geoscience Union. All Right Reserved.

Shallow earthquakes in Unzen Volcano inferred from dense seismic observation and resistivity structure

*Hashimoto Tasuku[1], Koki Aizawa[2], Takeshi Matsushima[2], Hiroshi Shimizu[2], Yuto Hayashida[1], Yuhei Yuasa[1], Kaori Tsukamoto[1], Yuto Yamamoto[3], Kanta Miyano[3], Megumi Kamizono[1], Satoshi Matsumoto[2]

1. Department of Earth and Planetary Sciences, Graduate School of Science, Kyushu University, 2. Institute of Seismology and Volcanology, Faculty of Science, Kyushu University, 3. Department of Earth and Planetary Sciences, School of Science, Kyushu University

Unzen volcano is a stratovolcano located in central part of the Shimabara peninsula of Kyushu Island, Japan. During the eruption periods 1991-1995, the seismicity was vigorous at shallow level beneath the Heisein-Shinzan lava dome (Umakoshi et al., 2001), then the number of shallow earthquakes decreased significantly after the eruptions. However, since 2010, the number of shallow earthquakes have been increasing steadily beneath Mt. Fugen and Heiseishinzan lava dome (Japan Metrological Agency (JMA)). The most of the hypocenters were estimated 1 to 2 km below sea level, while importantly, several earthquakes were located above sea level since February 2017. The P-wave arrivals of the earthquakes above sea level show the downward motion at all stations of JMA, MLIT, and Kyushu university. The coda, which shows relatively longer period oscillation, continues approximately 20 to 30 seconds. According to JMA, this type of shallowest earthquakes has occurred 5 times in 2018. Mildon et al. (2016) reported the similar non-DC earthquakes at Krafla volcano, Iceland, and suggested closing clacks model to explain the observation.

In order to explore the shallow earthquake activity beneath Unzen volcano, we established (1) 12 seismic stations around Mt. Fugen and Heisei-Shinzan lava dome in August, 2018. In addition, (2) broad-band magnetotelluric (MT) observation was conducted in October and November, 2018 to estimate subsurface resistivity structure. We recorded telluric fields at 12 sites around Mt. Fugen and Heisei-Shinzen lava dome, and recorded MT fields at two sites at the mid flank of the Unzen volcano. The main purpose of this study is to investigate the relationship between the shallow earthquakes and volcanic fluids beneath Unzen volcano. In particular, the locations and initial motions of the shallowest earthquakes are investigated. We will present the preliminary analysis of the shallow earthquakes obtained from the dense seismic records, and the preliminary resistivity structure.

Keywords: volcanic tectonic earthquake, Unzen Volcano

©2019. Japan Geoscience Union. All Right Reserved.

Characteristics of shallow volcanic earthquakes beneath the summit of Unzen Volcano

*Kanta Miyano[1], Hiroshi Shimizu[2], Takeshi Matsushima[2], Satoshi Matsumoto[2], Koki Aizawa[2], Hashimoto Tasuku[3], Yuto Hayashida[3], Yuhei Yuasa[3]

1. Department of Earth and Planetary Sciences, School of Science, Kyushu University, 2. Institute of Seismology and Volcanology, Faculty of Science, Kyushu University, 3. Department of Earth and Planetary Sciences, Graduate School of Science, Kyushu University

Unzen Volcano is located in the central part of the Shimabara peninsula, western Kyushu, Japan. The last eruption took place in 1990-1995, and a lava dome complex was formed during the eruption. High level seismicity was observed before and during the eruption. In particular, isolated tremor occurred in the volcanic edifice above sea level preceding the lava dome emergence (Shimizu et al., 1992). Predominant frequencies of the isolated tremor’ s waveforms were comparatively low (2 - 4 Hz) and the duration was long (30 - 180 s). Moreover, extremely-shallow earthquakes occurred beneath the growing lava dome. Unzen Volcano has been in dormancy since the end of the 1990-1995 eruption. However, shallow volcanic earthquakes have been observed below the summit since 2010, and the hypocenters are determined by Japan Meteorological Agency (JMA) and Institute of Seismology and Volcanology, Kyushu University (SEVO). In order to reveal the generation mechanism of these earthquakes, we investigated the characteristics of the hypocenters and wave forms.

First, we relocated the hypocenters of these earthquakes from Jan. 1 to Sep. 7 2018. The relocated hypocenters are distributed beneath the lava dome and Mt. Fugen, and they are classified into 3 groups. Focal depths of Group 2 and 3 are located 1km and 2km below sea level under Mt. Fugen, while Group 1 (three earthquakes in this period) locates above sea level beneath the lava dome. The first motions of P-waves for Group 1 are all “down” in this study, and the duration times are longer than those of Group 2 and 3.

Next, we calculated particle motions of these earthquakes using relocated hypocenters. The result indicates that the earthquakes of Group 2 and 3 have clear P and S phases, which are similar to tectonic earthquakes. On the other hand, no obvious S phase is recognized in the seismograms of Group 1.

Spectral analysis shows that the seismograms of Group 1 are lacking in high frequency components and the low frequency (2 - 5 Hz) is dominant compared with Group 2 and 3.

We will discuss candidates for the source mechanism of these earthquakes based on the results of wave form analyses.

Keywords: Unzen, volcanic earthquake, particle motion, spectral analysis

©2019. Japan Geoscience Union. All Right Reserved.

Pyroclastic deposits and the stratigraphy on the outcrop to north east from Mt.Unzen

*Daisuke Nagai[1]

1. Mt.Unzen disaster memorial hall

Pyroclastic flows occurred at many times during formation of lava dome on the Heisei eruption of Mt.Unzen. There were some studies of pyroclastic flows on Mt. Unzen (Kobayashi and Kato, 1985). After the Heisei erupyion many studies reported about it (Kobayashi and Nakada, 1991, Watanabe and Hoshizumi, 1995). It is important about understanding the characteristics of the volcano from the past activities. In this study, the pyroclastic deposits and the stratigraphy 150ka on Mt.Unzen be reported.

Keywords: active volcano, pyroclastic flow, stratigrahy

©2019. Japan Geoscience Union. All Right Reserved.

Relative gravity changes in Aso Volcano (Kumamoto Prefecture) observed from 2015 to 2018

*Yusuke Miyauchi[1], Takahito Kazama[1], Yoichi Fukuda[1], Shin Yoshikawa[2], Takahiro Ohkura[2], Jun Nishijima[3], Yasuhiro Fujimitsu[3]

1. Graduate School of Science, Kyoto University, 2. Aso Volcanological Laboratory, Kyoto University, 3. Graduate School of Engineering, Kyushu University

Gravity measurement is one of the most effective methods to understand mass variations due to volcanism. In Aso Volcano, Kumamoto Prefecture, spatiotemporal gravity variations have been monitored by repeated relative gravity measurements every several years since 1964 (Yoshikawa et al., 2009). Gravity data was frequently collected 3-4 times every year during the active period of Aso Volcano from 2011 to 2016 and revealed spatiotemporal variations in hydrothermal mass under the volcano (Sofyan et al., 2016). However, any gravity data has not been collected after March 2016 due to Kumamoto Earthquake which occurred in April 2016. Since the volcanism became quieter after a phreatic explosion was observed in October 2016, a series of volcanic activities including the quiet period should be discussed in terms of mass variations to predict future volcanic activities. In order to monitor gravity changes in Aso Volcano after the volcanically active period, we repeated relative gravity measurements in May, August and November 2017, and in March, May, August and November 2018. We measured relative gravity values at gravity points around Aso Volcano using CG5 relative gravimeters owned by Kyushu University and Aso Volcanological Laboratory (CG5-KYU and CG5-AVL, respectively) and a LaCoste relative gravimeter G680 owned by Graduate School of Science, Kyoto University (LC-G680). We also collected continuous gravity data using CG5-AVL at the AVL station even when it was not used for the campaign gravity measurements, in order to understand the long-term instrumental drift. A gravity value relative to AVL was obtained for each point and survey, by correcting the effects of instrumental height, tide, instrumental drift, and scaling factor. The spatiotemporal absolute gravity data was then calculated, using the absolute gravity values measured at reference stations. We finally estimated the spatial distributions of the absolute gravity change around Aso Volcano before and after Kumamoto Earthquake. We found that the absolute gravity increased at the gravity points around the Aso crater. Since this absolute gravity change includes the effect of crustal deformation due to Kumamoto Earthquake, we subtracted the effect from the absolute gravity values using the quasi-vertical deformation data derived from the InSAR analyses (Geospatial Information Authority of Japan) and the typical gravity gradient value of -0.2 mGal/m. We found that the residual of the absolute gravity change still increases by up to 0.1 mGal at the areas of Kusa-senri and the Naka-dake crater, which implies mass accumulation under these areas. In the future, we will model time variations of the volcanic mass distributions in the volcano and compare them with the spherical pressure source proposed by the leveling data (Sudo et al., 2016). In addition, the gravity data should be repeatedly obtained and reprocessed more accurately, by considering the spatial variation of the gravity gradient value and correcting the effect of ground deformation using the continuous GNSS data.

Keywords: gravity change, crustal deformation, mass variation, Aso Volcano

©2019. Japan Geoscience Union. All Right Reserved.

Precise leveling survey in Aso volcano, 2018

*Takahiro Ohkura[1], Shin Yoshikawa[1], Hiroyuki Inoue[1], Akihiko Yokoo[1], Mitsuru Utsugi[1], Keigo Yamamoto[2], Kazunari Uchida[4], Yuta Maeda[5], Shinichiro Horikawa[5], Kenjiro Matsuhiro[5], Takashi OKUDA[5], Kazushi Tanoue[5], Fumiaki Kimata[7], Masayuki Murase[6], Hitoshi Mori[6], Taketoshi Mishima[3], Shintaro Komatsu[2], Masaki Takaya[3], Jun Oikawa[8], Kyoka Ishii[3], Yusuke Miyauchi[3], Ikuma Kimura[3], Masaki Uchida[3], Kazuho Nakai[3], Kosei Takishita[3], Keita Chiba[4], Hashimoto Tasuku[4], Yoshinosuke Kamiya[4], Yuto Yamamoto[4]

1. Aso Volcanological Laboratory, Institute for Geothermal Sciences, Graduate School of Science, Kyoto University, 2. DPRI, Kyoto University, 3. Graduate School of Science, Kyoto University, 4. Graduate School of Science, Kyushu University, 5. Graduate School, Nagoya University, 6. College of Human and Society, Nihon University, 7. TRIES, 8. ERI,Univ.of Tokyo

In Aso volcano, leveling survey has been conducted since 1937 by Kyoto University. As a result of these surveys, subsidence in Kusasenri about 3km west-southwest of Naka-dake crater has been observed. And this subsidence was considered to be caused by a contraction source located at about 3km west of Naka-dake crater with a depth of 4 to 6 km (Sudo et al. 2006). A seismic tomography study showed a low velocity zone of a 2 to 3 km diameter located at a depth of 6km in Kusasenri (Sudo and Kong, 2001), almost in accordance with the position of contraction source. Therefore, this low velocity zone is considered to correspond to a magma chamber.
We conducted a first-order leveling survey at Aso volcano during the period from Sep.30 to Oct.6 2018, for the first time since 2012 and after the 2016 Kumamoto Earthquake. As a result, mean square errors of the conducted survey were ranging from ±0.18 to ±0.21 mm/km.
From the obtained survey data, we calculated the relative height of each bench mark referred to a bench mark (960701A) which corresponds to GEONET 960701 GNSS station, located at the south-western foot of central cones of Aso volcano. We also calculated the height difference of 960701A between September 2012 and September 2018, using F3 solutions of GEONET, resulting in the vertical displacements of the benchmarks during the period from September 2012 to September 2018.
It was found that the obtained displacements show ground accordance with 2.5-D surface deformation of the 2016 Kumamoto earthquake detected by SAR interferometry. Therefore, we can conclude that the vertical displacements in Aso volcano detected by leveling survey are attributed to the surface deformation during the 2018 Kumamoto Earthquake.

Keywords: Aso volcano, Crustal deformation, the 2016 Kumamoto earthquake

©2019. Japan Geoscience Union. All Right Reserved.

Magma evolution during the Aso-3 caldera-forming eruption cycle deduced from the chemistry of plagioclase phenocrysts

*yuki matsukida[1], Tsuyoshi Iizuka[1], Takayuki Ushikubo[2], Kenji Shimizu[2], Nobuo Geshi[3], Isoji MIYAGI[3], Morihisa Hamada[2]

1. the University of Tokyo, 2. Japan Agency for Marine-Earth and Science Technology, 3. The National Institute of Advanced Industrial Science and Technology

Title

Magma evolution during the Aso-3 caldera-forming eruption cycle deduced from the chemistry of plagioclase phenocrysts

Author

Yuki Matsukida, Tsuyoshi Iizuka, Takayuki Ushikubo, Kenji Shimizu, Nobuo Geshi,

Isoji Miyagi, Morihisa Hamada

Introduction

Caldera-forming eruptions are the most destructive type of volcanic activity and exert a great influence on the Earth’ s surface. Therefore, the underlying magmatic mechanism leading to caldera-forming eruptions is of fundamental importance in volcanology. The Aso volcano is the largest (18×25 km in diameter) caldera in the southwestern Japan Island Arc and formed through four large eruption cycles. In this study, we have investigated the evolution of magmas that erupted during the second youngest cycle among the four cycles, the Aso-3 cycle at 123 ka. It ejected >150 km^3 of pyroclasts that are divided into the following four units in stratigraphic ascending order: 3W, a plinian pumice fall deposit; 3A, a pumice flow deposit containing dominantly aphyric pumice and glassy ash; 3B, a scoria flow deposit characterized by abundant aphyric scoria; and 3C, a scoria flow deposit consisting mainly of porphyritic scoria and glassy ash matrix.

On the basis of major and trace element compositions and Sr-Nd-Pb isotope ratios of whole rocks as well as phenocrysts, Kaneko et al. (2015) argued that the pre-eruptive magma chamber was chemically stratified from a mafic lower part to a felsic upper part. The previous study further estimated water contents in the melts using the hygrometer based on plagioclase-melt partitioning of anorthite-albite components (Lange et al., 2009), but the estimates have large uncertainty. Here we determined hydrogen contents of plagioclase phenocrysts. By combining the hydrogen contents with major and trace element compositions of the plagioclase phenocrysts, this study aims to better understand pre-eruptive magma evolution and water behavior of the Aso-3 cycle.

Methods

Plagioclase as well as pyroxene and oxide mineral phenocrysts were separated from pumices of 3W, an obsidian clast of 3A, a welded clast of 3B, and a pumice clast of 3C. Major and trace elements in phenocrysts were quantified by electron probe microanalyzer (EPMA) and laser ablation-inductively

©2019. Japan Geoscience Union. All Right Reserved.

coupled plasma-mass spectrometry (LA-ICP-MS), respectively. In LA-ICP-MS analysis, Ca contents measured by EPMA were used for internal standard normalization. OH contents in plagioclase phenocrysts were determined by secondary ion mass spectrometry (SIMS).

Results

Anorthite contents (#An) of plagioclase phenocrysts are variable even in individual units, but show the systematic increase in ascending order, consistent with the results of Kaneko et al. (2015). REE patterns of plagioclase and pyroxene show positive and negative Eu anomalies, respectively. Plagioclase Ce content degreases as #An increases (Figure 1). On the other hand, OH contents in plagioclase phenocrysts are significantly higher in 3W (~250 ppm) as compared to the others (<50 ppm) (Figure 2).

Discussion

OH contents in a plagioclase phenocryst of 3W are significantly higher than those of 3A-C, nevertheless Ce contents of plagioclase are not significantly different between 3W and 3A. Considering that the partition coefficients of Ce between anhydrous major minerals and melt are similar to those of OH, this finding suggests that H_2O was lost from the melt through gas exsolution or fractional crystallization of hydrous minerals. Alternatively, given the fast diffusion of hydrogen relative to Ce in plagioclase, it may be attributed to secondary loss of hydrogen from plagioclase phenocrysts of 3A-C during welding processes. From the observation of thin sections of 3W and 3A, however, microlite was rarely observed, suggesting that the secondary thermal effects would be restricted for both 3W and 3A. Furthermore, little hydrous phenocrysts have been observed from ejecta of the Aso-3 cycle. Therefore, the results of this study suggest that gas exsolution and degassing occurred between the eruptions of 3W and 3A.

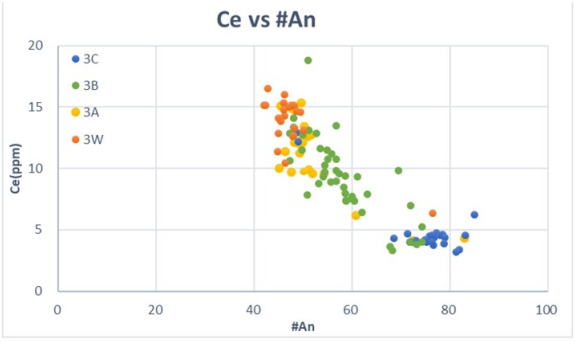

Figure 1 Ce vs anorthite contents for plagioclase phenocrysts

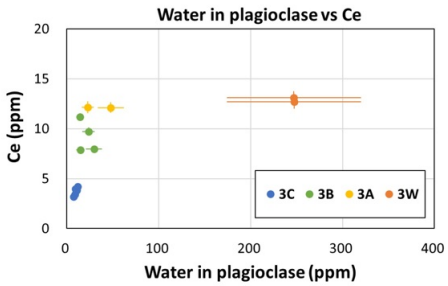

Figure 2 Water vs Ce contents for plagioclase phenocrysts (The water contents were calculated from hydrogen concentrations in the phenocrysts)

©2019. Japan Geoscience Union. All Right Reserved.

Relationship between duration of eruption tremor and eruption volume

*Azusa Mori[1], Hiroyuki Kumagai[1]

1. Nagoya University Environmental Studies

We studied the high-frequency seismic signals of eruption tremors during recent eruptions at various volcanoes and quantified their seismic source amplitudes (A_s) and cumulative source amplitudes (I_s) in the 5–10 Hz based on the assumption of isotropic *S*-wave radiation. A_s and I_s correspond to the maximum and the cumulative value of amplitudes at the source during eruption tremor. We previously found that the power law relations between A_s and I_s holds for eruption tremors. We also found the proportional relation between eruption rate and A_s for eruption tremors by comparing seismic and geodetic data during sub-Plinian eruptions at Kirishima. In this study, we further investigated time variations of eruption tremors and found the scaling relation between duration of eruption tremor and eruption volume.

We calculated the envelope width (p) using the estimated values of A_s and I_s and investigated the relation between p and I_s. p is defined as I_s/A_s and can be used as a parameter of duration (T) of a seismic envelope waveform (Kumagai et al., JGR, 2018). We found that p is proportional to 0.4 power of I_s. We also found that envelope waveforms of eruption tremors in 5–10 Hz have the following features; the amplitudes of envelope waveforms gradually increase, remain roughly constant during a certain period, and gradually decrease to the noise level. Moreover, p tends to increase with A_s. These envelope waveforms can be approximated as trapezoids, where A_s and T correspond to their height and lower base, respectively. We found that the ratios of upper to lower bases for these envelope waveforms are roughly constant. In this case, the proportionality between p and T holds. Based on the relation between eruption rate and A_s, eruption volume (V) is proportional to I_s. Therefore, the relation between p and I_s as shown above indicates that T is proportional to 0.4 power of V. We found that this proportional relation is consistent with the estimates of T and V for various Plinian eruptions compiled by Mastin et al. (JVGR, 2009). This indicates that the scaling relation between duration of eruption tremor and eruption volume in Plinian eruptions holds over a wide range of eruption size.

©2019. Japan Geoscience Union. All Right Reserved.

Crustal deformation accompanied with the eruption of Shinmoe-dake in early March 2018

*Tsuyoshi Watanabe[1], Takashi Yokota[1], Susumu Kurahashi[1], Kenta Enomoto[1]

1. Aichi Institute of Technology

Shinmoe-dake is a part of Kirishima volcano group composed of 20 Quaternary volcanoes located in southern Kyushu, Japan, erupted on 19 January 2011. This eruption began with a phreatomagmatic event including atmospheric vibration and eventually developed to subplinian eruptions within a week. From GNSS data, position and volume change of the magma chamber were estimated to be about 5 km to the northwest of the top of Shinmoe-dake at a depth of 8-9 km and 1.3×10^7 m^3. Shinmoe-dake erupted on 11 October 2017 after an interval of six years, however, this eruption ended in a week. While the extension of baseline length between the sites across Mt. Kirishima has been detected by GNSS observation since July 2017, indicating the possibility of magma accumulation. Eventually, the extension of baseline length led to eruption on 1 March 2018. In this study, in order to clarify the mechanism of the volcanic eruption, we investigated the crustal deformation accompanied with a series of volcanic activities occurred in early March 2018 at Shinmoe-dake by using GNSS data, then estimated the position of the magma chamber.

For the study, GEONET F3 solutions obtained by GNSS observation sites located mainly in the Kyushu district from 1 January 2013 to 25 March 2018 were used. Firstly, common mode bias was removed from time series of GEONET F3 solutions according to the method of Wdowinski et al. (1997). Secondly, visco-elastic deformation due to the 2016 Kumamoto earthquake was corrected by using a code of Fukahata and Matsu’ura (2005, 2006). In this time, we used the co-seismic fault model of Geospatial Information Authority of Japan (GSI, 2016) and calculated the visco-elastic deformation, where the calculation was conducted on the condition that an elastic material with thickness of 25 km lies on a Maxwell visco-elastic half-space with viscosity of 2×10^{18} Pas. Thirdly, to estimate elastic deformation due to subduction of the Philippine Sea plate (PH), we reproduced the upper surface of the PH by 170 rectangular faults based on the result of Hirose et al. (2008) and estimated coupling ratio. The Green’s functions of rectangular faults were calculated by the formula of Okada (1985). Using horizontal and vertical velocities of GEONET 150 sites between 1 January 2013 and 31 March 2016, we conducted a back-slip inversion analysis with smoothing constraint of coupling ratio among the adjacent faults. Assuming the interplate coupling obtained by the analysis continues after July 2017, we corrected the effect of the plate subduction from original data. After completing three processes above mentioned, finally, the positions of the magma chambers were estimated in two periods: inflation phase (1 July 2017–28 February 2018) and deflation phase (14 February 2018–25 March 2018) by using the Mogi’s model. We selected 7 GEONET sites located around Shinmoe-dake and estimated the positions of Mogi sources (longitude, latitude, and depth) corresponding to the two phases by performing a grid search in the ranges of 130.6-131.1˚every 0.001˚for longitude, 31.7-32.1˚every 0.001˚for latitude, and 4-15 km every 0.1 km for depth. The volume change of the Mogi sources were assumed to be 1.6×10^7 m^3 in the inflation phase and -0.7×10^7 m^3 in the deflation phase, according to the results of Japan Meteorological Agency (JMA). The result showed that the positions of the magma sources were estimated not to be just under the top of Shinmoe-dake but to be about 6-7 km to the northwest of it at a depth of 7-12 km. Although our result is generally consistent with that of JMA, the depth of the magma sources in the inflation phase was estimated to be approximately 4 km deep part. For the next step, we investigate the effects of topography and heterogeneous structure on crustal deformation.

©2019. Japan Geoscience Union. All Right Reserved.

Keywords: Shinmoe-dake, GNSS data, visco-elastic deformation due to the 2016 Kumamoto earthquake, elastic deformation by subduction of the Philippine Sea plate, estimation of magma chambers

©2019. Japan Geoscience Union. All Right Reserved.

Sources under Iwo-yama, Kirishima Volcanoes derived from GNSS observation and Precise leveling survey.

*Yuki Koga[1], Takeshi Matsushima[2], Kazunari Uchida[2], Dan Muramatsu[1], Yuichi Iwasa[1]

1. Department of Earth and Planetary Sciences, Graduate School of Science, Kyushu university , 2. Institute of Seismology and Volcanology, Faculty of Science, Kyushu University

At Iwo-yama that active volcano located in Ebino kogen volcanic area of Kirishima Volcanoes, fumarolic activity has risen again from December 2015 after dozen year's silence and suddenly increasing of seismicity (50 times and more a day) and volcanic tremors was observed several times. And phreatic eruption occurred in April 2018. Morita (2018) inferred inflation spherical pressure source as Mogi source from leveling survey between June 2015 and December 2015. The source's depth is about 700m beneath Iwo-yama and the source was considered that correspond with bottom of conductive layer inferred clay layer from MT survey (Tsukamoto et al., 2018). But, leveling can detect vertical displacement only and the inferred source is not considered horizontal displacement. So, we will improve pressure source inferred from leveling adding detect horizontal displacement from GNSS observation in this study.

As result of the observation, radial crustal deformation was detected several months before the occurrence of the phreastic eruption and after the eruption occurred. Estimating those displacement using an elevation-modified Mogi model, volume increse of the pressure source located at 700m depth below Iwo-yama was estimated. The depth of this pressure source coincided with the depth of the clay layer and it was found that the pressure source had expanded under the clay layer before the eruption occurred. But, for the GNSS observation point of the edifice before eruption, displacement which can’t be explained by the pressure source under the clay layer has been detected. This displacement is thought to be due to the rise of hot water to the shallow part as the pressure source under the clay layer expands.

We conducted GNSS continuous observation point around Iwo-yama established by Japan Meteorological Agency to verify the pressure source under the clay layer. As a result, displacements which can’t be explained by this model detected at these observation points. Using the GNSS continuous observation points throughout Kirishima, we estimated the pressure source of this displacement. Then, we could estimate the spherical pressure source located 7 km deep in the vicinity of Ebino-dake. This model is consistent with the source of crustal deformation before and after the eruption of Shinmoe-dake volcano in 2011 estimated by Nakao et al. (2018). Therefore, those displacement is thought to be due to volume change of magma chamber of Shinmoe-dake. In conclusion, the crustal deformation around Iwo-yama is due to these three sources, spherical pressure source under clay layer, displacement due to hot water rising to shallow part of Iwo-yama, magma chamber of Shinmoe-dake.

Keywords: Iwo-yama, GNSS observation, Precise leveling survey

©2019. Japan Geoscience Union. All Right Reserved.

GNSS 観測と精密水準測量から推定される霧島硫黄山の地下圧力源
Sources under Iwo-yama, Kirishima Volcanoes derived from GNSS observation and Precise leveling survey.

*古賀 勇輝[1]、松島 健[2]、内田 和也[2]、村松 弾[1]、岩佐 優一[1]
*Yuki Koga[1], Takeshi Matsushima[2], Kazunari Uchida[2], Dan Muramatsu[1], Yuichi Iwasa[1]
1. 九州大学大学院理学府地球惑星科学専攻、2. 九州大学大学院理学研究院附属地震火山観測研究センター
1. Department of Earth and Planetary Sciences, Graduate School of Science, Kyushu University, 2. Institute of Seismology and Volcanology, Faculty of Science, Kyushu University

At Iwo-yama that active volcano located in Ebino kogen volcanic area of Kirishima Volcanoes, fumarolic activity has risen again from December 2015 after dozen year's silence and suddenly increasing of seismicity (50 times and more a day) and volcanic tremors was observed several times. And phreatic eruption occurred in April 2018. Morita (2018) inferred inflation spherical pressure source as Mogi source from leveling survey between June 2015 and December 2015. The source's depth is about 700m beneath Iwo-yama and the source was considered that correspond with bottom of conductive layer inferred clay layer from MT survey (Tsukamoto et al., 2018). But, leveling can detect vertical displacement only and the inferred source is not considered horizontal displacement. So, we will improve pressure source inferred from leveling adding detect horizontal displacement from GNSS observation in this study.

As result of the observation, radial crustal deformation was detected several months before the occurrence of the phreastic eruption and after the eruption occurred. Estimating those displacement using an elevation-modified Mogi model, volume increse of the pressure source located at 700m depth below Iwo-yama was estimated. The depth of this pressure source coincided with the depth of the clay layer and it was found that the pressure source had expanded under the clay layer before the eruption occurred. But, for the GNSS observation point of the edifice before eruption, displacement which can't be explained by the pressure source under the clay layer has been detected. This displacement is thought to be due to the rise of hot water to the shallow part as the pressure source under the clay layer expands.

We conducted GNSS continuous observation point around Iwo-yama established by Japan Meteorological Agency to verify the pressure source under the clay layer. As a result, displacements which can't be explained by this model detected at these observation points. Using the GNSS continuous observation points throughout Kirishima, we estimated the pressure source of this displacement. Then, we could estimate the spherical pressure source located 7 km deep in the vicinity of Ebino-dake. This model is consistent with the source of crustal deformation before and after the eruption of Shinmoe-dake volcano in 2011 estimated by Nakao et al. (2018). Therefore, those displacement is thought to be due to volume change of magma chamber of Shinmoe-dake. In conclusion, the crustal deformation around Iwo-yama is due to these three sources, spherical pressure source under clay layer, displacement due to hot water rising to shallow part of Iwo-yama, magma chamber of Shinmoe-dake.

This work was partly supported by MEXT under Integrated Program for Next Generation Volcano Research and Human Resource Development, and under Earthquake and Volcano Hazards Observation and Research Program.Also it was suppoerted by ERI, The University of Tokyo under Joint Usage Program.

キーワード：硫黄山、GNSS 測量、水準測量
Keyword：Iwo-yama, GNSS observation, Precise leveling survey

©2019. Japan Geoscience Union. All Right Reserved.

Regional vertical deformation around Aira caldera from GNSS data

*Kazuho Nakai[1], Masato Iguchi[2], Takahiro Ohkura[3]

1. Division of Earth and Planetary Sciences, Graduate School of Science, Kyoto University, 2. Sakurajima Volcano Research Center, Disaster Prevention Research Institute, Kyoto University, 3. Aso Volcanological Laboratory, Institute for Geothermal Sciences, Graduate School of Science, Kyoto University

We investigated regional ground deformation around Aira caldera by analyzing vertical displacement observed by GNSS.

We used daily coordinate data from F3 solutions of GEONET stations in Kyusyu for periods from 1998 to 1999 and 2015 to 2016 when the ground uplift rate was larger than 18 mm/yr at 960719 station (North of Sakurajima). In order to increase number of stations, we analyzed RINEX data around Aira caldera and Sakurajima observed by Kyoto University and obtained daily coordinate data calculated based on the coordinates of the F3 solution of the GEONET stations closest to each observation point by using RTKLIB Ver. 2.4.2. The vertical displacement rate was estimated by removing the coseismic or antenna change steps and the annual and semiannual components. The ground deformation close to Kirishima volcano was affected by the pressure source located about 9 km beneath the Karakuni-dake (Nakao et al. 2013). We removed these effects causing inflation of the pressure source.

The ground within a radius of 20 km from the center of Aira caldera was uplifted in the both periods. The amount of uplift near the center of Aira caldera is larger than that in distant region and the largest uplift of station (25 mm/yr in 1998-1999 and 20 mm/yr in 2015-2016) was obtained at northern part of Sakurajima. In contrast, the ground subsidence was detected at distances from 20 to 30 km away from the center of the caldera during the period in 1998-1999 and from 30 to 40 km during the period in 2015-2016. The amounts of subsidence were about 3 mm/yr in the both periods.

We applied a model of dual source of Mogi-type (Mogi, 1958) to the ground deformation. In the period of 1998-1999, an inflation source was obtained at a depth of 10 km and a deflation source at a depth of 14 km beneath the Aira caldera. The amounts of volume change were estimated at about $+1.8\times10^7$ m^3 and -1.5×10^7 m^3, respectively. Similarly, in the period of 2015-2016, an inflation source was obtained at a depth of 10 km and a deflation source at a depth of 30 km. The amounts of volume change were estimated at about $+1.5\times10^7$ m^3 and -3.3×10^7 m^3, respectively. The order of volume change of the inflation source is almost same as the deflation source in the both periods.

The spatial distribution of the vertical displacement rate can be explained by the shallow inflation source and the deep deflation source. The shallow inflation source coincide with A-source beneath the Aira caldera (Hotta et al. 2016) corresponding to magma reservoir. Considering similarity of the volume changes, magma seems to move from to the shallow magma reservoir around 10 km deep from a deeper part.

Keywords: Aira caldera, Global Navigation Satellite System, vertical deformation

©2019. Japan Geoscience Union. All Right Reserved.

Vertical ground deformation in Sakurajima volcano measured by precise leveling survey (during Nov. 2017 - Nov. 2018)

*Keigo Yamamoto[1], Takeshi Matsushima[2], Shin Yoshikawa[3], Hiroyuki Inoue[3], Tadaomi Sonoda[1], Kosei Takishita[1], Kazuho Nakai[1], Masaki Uchida[3], Ryo Oyanagi[3], Yoshinosuke Kamiya[2], Takahiro Ohkura[3]

1. Disaster Prevention Research Institute, Kyoto University, 2. Fuculty of Sciences, Kyushu University, 3. Gruduate School of Science, Kyoto University

We conducted the precise leveling survey in Sakurajima volcano, southwest Japan in November 2018, in order to evaluate the vertical ground deformation associated with the recent eruptive activity of the volcano. The leveling routes measured in this survey are about 21 km long in total, including Sakurajima western flank route and Sakurajima northern flank route. These leveling routes were measured during the period from November 12 to 29. As a result of the preparatory calibrations and careful measurements, mean square errors of the conducted survey were achieved with a good accuracy ranging from ±0.18 to ± 0.25 mm/km.
From the measured data, we calculated the relative height of each benchmark referring to the reference benchmark BM.S.17 which is located at the western coast of Sakurajima. The calculated relative heights of the benchmarks were then compared with those of the previous survey conducted in November 2017 (Yamamoto et al., 2018), resulting in the relative vertical displacements of the benchmarks during the period from November 2017 to November 2018.
The resultant displacements indicate the ground subsidence (-6.2 mm at maximum) at benchmarks around the central part of Sakurajima. The ground subsidence is also detected at benchmarks along Sakurajima northern flank route, suggesting that the inflation of the magma reservoir beneath Aira caldera was not remarkable during the period between November 2017 and November 2018. From the preliminary analysis based on a spherical source model (Mogi, 1958), the deflation source is located beneath Minamidake crater. The results indicate that the pressure decrease is suggested at the magma reservoir beneath Minamidake caused by the eruptive magma ejection.

Keywords: Sakurajima volcano, precise leveling survey, vertical ground deformation

©2019. Japan Geoscience Union. All Right Reserved.

Spatiotemporal gravity variations from the 1990s in Sakurajima Volcano, revealed by repeated relative gravity measurements

*Ryo Oyanagi[1], Takahito Kazama[1], Keigo Yamamoto[2], Hiromitsu Oshima[3], Kazumi Okada[3], Tadaomi Sonoda[2], Masato Iguchi[2]

1. Graduate School of Science, Kyoto University, 2. DPRI, Kyoto University, 3. ISV, Hokkaido University

Gravity observation is one of the most effective methods to detect spatiotemporal mass variations in volcanoes. In and around Sakurajima Volcano, relative gravity measurements were first started in 1975 and have been repeated 20 times until 2018. The long-term gravity variations from 1975 to 1992 was modeled by Kazama et al. (2018), to understand volcanic mass variations associated with active eruptions at the Minami-dake summit during the same period. They showed that the relative gravity increase in Sakurajima cannot be fully explained by two spherical deflation sources, which were expected from the leveling data. Instead, they found that the gravity increase can be modeled by an additional point mass of 6.0 E+10 kg/yr at 5 km depth under the Kita-dake summit. However, Kazama et al. (2018) modeled the volcanic mass distributions only from 1975 to 1992, and mass distributions during the subsequent period from the late 1990s to the 2010s should be modeled as well to understand present mass accumulating processes and forecast future volcanic activities of Sakurajima Volcano.

We therefore analyzed the GPS and relative gravity data obtained from the late 1990s to the 2010s, to model the long-term pressure and mass sources under Sakurajima Volcano as follows. We first subtracted the effect of tectonic crustal deformation in the southern Kyushu Island from the horizontal displacement data of the GEONET F3 solution, using the method of Takayama and Yoshida (2007). We also reproduced the residual horizontal displacement data by a spherical pressure source of Mogi (1958), assuming the inflation of a magma reservoir located under Aira Caldera; in this calculation, several parameters about the location and volume change of the pressure source were determined by the grid search method so as to most reproduce the horizontal displacement data. The inflation source was calculated to be located at 9 km depth under the center of Aira caldera with the inflation rate of 5.5 E+6 m3/yr. However, this inflation source never agrees with the gravity increase observed in Sakurajima volcano after the late 1990s, because the source inflation and consequent ground uplift leads to the gravity decrease (Hagiwara, 1977).

After correcting the effect of the inflating pressure source, the observed gravity values were found to increase at rates of +7.49 and +1.61 microGal/yr at S110 (located at the summit of Sakurajima) and S16 (located at the western foot of Sakurajima), respectively. We thus calculated theoretical gravity variations in Sakurajima Volcano by assuming a point mass under the center of the volcano, so as to explain the observed gravity increase; in this calculation, the parameters about the depth and mass increase were determined with the trial-and-error method. The point mass was estimated to be located at 3.3 km depth below sea level with a mass increasing rate of 2.3 E+10 kg/yr. This result implies that the mass accumulation continues under Sakurajima Volcano even now, although the present accumulating rate reduced by less than half compared with that from the 1970s to the former 1990s. We will sophisticate the pressure/mass source models in the future, to reveal the mass redistribution processes associated with volcanic activities of Sakurajima Volcano.

Keywords: Sakurajima Volcano, relative gravity, crustal deformation, mass variation, magma, hydrology

©2019. Japan Geoscience Union. All Right Reserved.

Investigation into the crater of Sakurajima volcano during eruption using UAV

*Shunsuke Miura[1], Takumi Mochiduki[1], Kouji Fujita[1], Toshihiro Urayama[1], Hisashi Sasaki[1], Tatsuro Chiba[1]

1. Asia Air Survey Co.,Ltd

1. Intoroduction
Measuring the active crater topography can obtain important information on volcanologically and disaster prevention, but the flight over the crater is risky involved in the eruption and is dangerous. The Minamidake crater of Sakurajima has repeated vigorous eruptions over a long period of time, and the topography change is intense. The Minamidake crater has A crater and B crater, and on the east slope there is Showa crater. Ministry of Land, Infrastructure, Transport and Tourism has regularly conducted airborne laser surveying to clarify the geometry shape. However, airborne laser surveying has become difficult due to the activation of eruption activity. Especially it was difficult to measure the topography of Minamidake crater, west of the Showa crater. Therefore, in this study, in order to grasp detailed crater circumstances of Minamidake crater and Showa crater on Sakurajima, we tried near-field photographing by UAV and terrain measurement utilizing SfM / MVS.

2. Investigation of Showa crater and Minamidake crater of Sakurajima by UAV
The UAV used is Matrice 210 (manufactured by DJI), and the installed camera is ZENMUSE X4S (visible light) and ZENMUSE XT2 (thermal infrared). DJI's UAV has an altitude limit of 500 m above ground level from the takeoff and landing point as a safety measure. For this reason, the takeoff and landing site was the upper stream of the Amida River (around 600 m altitude) outside the entry restriction. The photographing by UAV was performed three times in total, about 15 minutes using the moving picture photographing method.In UAV photographing of visible light, we were able to confirm the state inside the Showa crater, which is unknown by the surveillance camera at the foot. On the other hand, inside the Minamidake crater, due to the influence of the plume, it was impossible to photograph clearly. In the thermal infrared photography, resolution as much as visible light could not be obtained, but we could confirm the movement of the plume inside the Minamidake crater. Moreover, in the thermal infrared, it was possible to capture a high resolution movie rather than photographing with a helicopter, and at Showa crater the stratification of the crater wall could also be confirmed.

3. Create 3D model and orthoimage
An image was cut out from the movie of the visible light that was shot, and an orthoimage of 0.5 m resolution of the Showa crater and a 3D model were made by SfM / MVS. Actually the Showa crater was almost stopped, except for some fumaroles, it was possible to clearly shoot the crater bottom. On the other hand, the Minamidake crater was greatly affected by the plume, a lot of clouds appeared above the crater, and the crater bottom was unknown. We are going to try SfM / MVS analysis using measurement results of thermal infrared with less influence of plume compared with visible light.

4. Conclusion
In order to eliminate the influence of the plume and to obtain a clearer image, it is thought that low-altitude flight to the crater's sky or inside the crater is necessary. Currently, since images are recorded on the SD card, collection after returning is a major premise, but in the future it is desirable to create models from images obtained by wireless communication.

©2019. Japan Geoscience Union. All Right Reserved.

Acknowledgments
This work was supported by the Japanese Ministry of Education, Culture, Sorts, Science and Technology under a grant from the Integrated Program for Next Generation Volcano Research and Human Resource Development. Regarding entry into the takeoff and landing site, I would like to thank you for providing the cooperation and permission of Kyoto University and Kagoshima Forest Management Office, here.

Keywords: UAV, Active Volcano, SfM/MVS, Thermal infrared image

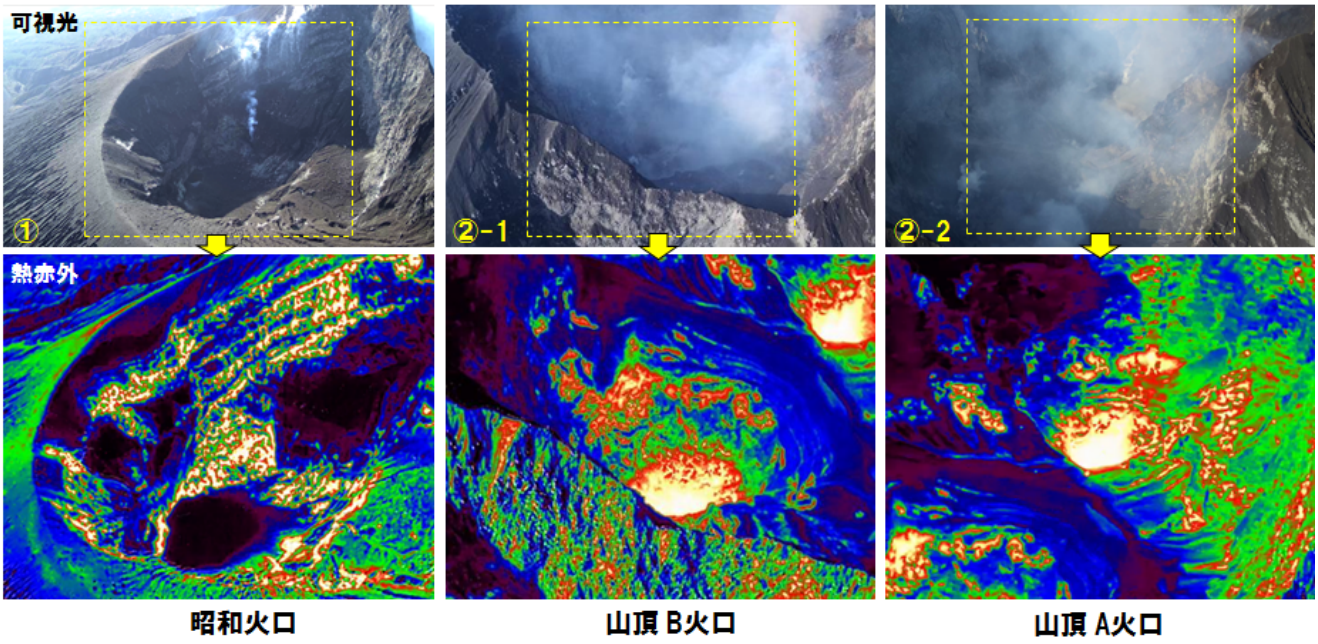

©2019. Japan Geoscience Union. All Right Reserved.

Seismic refraction and wide-angle reflection experiment in southern Kyushu, Japan: (3) the 2018 exploration report

*Hiroki Miyamachi[1], Hiroaki Takahashi[2], Hiroshi Aoyama[2], Mako Ohzono[2], Takahiro Shiina[6], Masamitsu Takada[2], Masayoshi Ichiyanagi[2], Teruhiro Yamaguchi[2], Yuki Susukida[2], Saito Kazuma[2], Chihiro Ito[2], Yoshio Murai[2], Tatsuya Nakagaki[2], Tomoki Tsutsui[3], Ryuichi Takei[3], Yuuya Tada[3], Mare Yamamoto[4], Satoshi Hirahara[4], Takashi NAKAYAMA[4], Ryosuke Azuma[4], Syuichi Suzuki[4], Toshinori Sato[5], Eiji Kurashimo[6], Miwako Ando[6], Shinichi Tanaka[6], Satoshi Ikezawa[6], Tomoaki Yamada[6], Kazuo Nakahigashi[7], Yuta Maeda[8], Shinichiro Horikawa[8], Kenjirou Matsuhiro[8], Takashi OKUDA[8], Shuhei Tsuji[8], Naoki Sogawa[8], Hiroshi Katao[9], Takuo Shibutani[9], Tsutomu Miura[9], Nakagawa Jun[9], Itaru Yoneda[9], Takeshi Tameguri[9], Kosei Takishita[9], Kazuho Nakai[9], Yusuke Yamashita[9], Takeshi Matsushima[10], Kazunari Uchida[10], Rintaro Miyamachi[10], Hiroshi Yakiwara[1], Shuichiro Hirano[1], Takeshi Kubo[1], Kenyu Sakao[1]

1. Kagoshima University, 2. Hokkaido University, 3. Akita University, 4. Tohoku University, 5. Chiba University, 6. University of Tokyo, 7. Tokyo University of Marine Science and Technology, 8. Nagoya University, 9. Kyoto University, 10. Kyushu University

[1] Primary Objective

Southern Kyushu is a typical island arc region: subduction of Philippine Sea plate under Kyushu off Hyuganada with high seismic activity, the Aira caldera with active volcanic activity, the extending Okinawa trough, and the East China Sea. Our project is aimed at clarifying the detailed velocity structure of the crust beneath southern Kyushu and recognizing interactions with crustal activities in these regions.
It is also concerned about the occurrence of large-scale eruptions at the Aira caldera larger than the 1914 Taisho eruption in Sakurajima volcano. Accordingly, we also intend to reveal the caldera structure of the Aira caldera in order to deepen the understanding of the present magma supply system beneath the Aira caldera.
This reports an outline of the second seismic exploration carried out in November 2018.

[2] Report of Seismic Exploration in 2018

For our purpose mentioned above, we carried out the first seismic exploration in November 2017, which consists of 9 shot points with charges of about 200 kg dynamite in the land area and 906 temporary seismic stations including 42 OBSs along about 165 km long profile running transversely across the Osumi Peninsula, the central part of the Aira caldera, the Satsuma Peninsula, the Koshiki Strait and the Koshiki Islands.
The second seismic exploration was carried out in November 2018. In this 2018 exploration, 872 temporary seismic stations were deployed along the 2017 seismic main profile. The equipment at each station is same as that in 2017. In addition, we widely deployed 49 seismic temporary stations with a 4.5 Hz three components seismometerand a portable data logger ”GSX” in Sakurajima volcano in order to estimate the 3-D velocity structure beneath the volcano.
In the 2018 exploration, artificial explosions by the seismic air-gun blasting system(6000 cubic inches) were applied at 50m or 100m intervals along the sea profiles (Profile-B, Profile-D, Profile-F, Profile-H). We successfully observed the seismic refraction and reflection signals generated from the air-gun in a distance range of more than 20 km. We also introduced 4 big vibrator vehicles in the land area, which vibrates continuously during about 4 hours at the fixed locations. In addition, we carried out the seismic reflection profiling with 5 km long profile in the northeastern area in Sakurajima volcano.

©2019. Japan Geoscience Union. All Right Reserved.

Acknowledgement : This project is mainly funded by the Kyushu Electric Power Co., Inc. The JGI Inc. conducted the artificial explosions, and the Hanshin Consultants Co., Ltd shared a part of the temporary seismic observation.

Keywords: velocity structure, southern Kyushu

©2019. Japan Geoscience Union. All Right Reserved.

Flow and emplacement mechanism of Koya Ignimbrite

*Keiko Suzuki-Kamata[1], Reina NAKAOKA[1], Tomomi Yamane[2]

1. Kobe Ocean-Bottom Exploration Center , 2. Department of Planetology, Graduate School of Science, Kobe University

Koya ignimbrite sourced from Kikai caldera 7.3 ka and traveled across the sea to reach the adjacent islands and the mainland of south Kyushu 40-90 km distant. Proximal facies of Koya ignimbrite, called Takeshima pyroclastic-flow deposit, comprise two or more flow units with a maximum thickness of 30 m, but the distal deposits collectively called Koya ignimbrite are consist of one flow unit and are exclusively very thin. Lag Breccia of Koya ignimbrite is recognized as layer 2b of 5 m thick on Takeshima and layer 1 of 2 m thick on Satsuma-Iwo Jima.

Koya ignimbrite contains essential pumices and volcanic glasses, both exhibiting a bimodal compositional distribution, e.g., ~60 and ~70 wt.% SiO_2 (Fujihara and Suzuki-Kamata, 2013). In addition to the silicic component, reflecting contribution the mafic component increases upwards from the basal to middle level of the deposit, and this vertical variation likely indicates progressive aggradation of pyroclasts. Koya ignimbrite overlies the ground layer consisting of crystal and fine pumice 1~5cm thick, and segregation pipe is commonly recognized in the ignimbrite in distributed area. The pyroclastic-surge deposit showing cross lamination overlies the ignimbrite on south of Osumi Peninsula. The surge deposit is rich in the mafic component, and suggests that the surge is formed at the late stage of ignimbrite eruption.

Koya ignimbrite distributes from the shoreline to the highland 1900m above sea level in Yakushima. Koya ignimbrite shows different lithofacies depending on altitude, which is thick and massive deposit more than severeal meters thick at lower area, and thin less than 50cm and composed of layer 1 at the base at higher altitude of 1600m above sea level. Mafic component is contained from the base of Koya ignimbrite in the north-west area on Yakushima both the lower area and the higher area, but mafic component increases upwards from the basal to middle level of the deposit in south-west area of Yakusima as same as Kyushu, Kuchinoerabujima and Tanegashima. This suggests that the earlier Koya ignimbrite climbing up the mountain area flows back due to the gravity in the north-west area and deposited thick at the lower area.

While silicic component can be recognized throughout the ignimbrite, mafic component exist only at the upper level of it at Tanegashima. The early phase products of Koya ignimbrite eruption reached to Tanegashima because this vertical variation is equal to that of the ignimbrites on proximal area, Satsuma Peninsula and Osumi Peninsula (Fujihara and Suzuki-Kamata, 2013). Lower contents of mafic component from upper most level compared with that of Osumi Peninsula suggest that the flows which contain abundant in mafic component occured at the later phase of the ignimbrite eruption cannot reach to Tanegashima. This is conformable the fact that the ignimbrites on Osumi Peninsula are thicker than that of Tanegashima. Based on above, it is estimated that Koya ignimbrite lost a great many amount of pyroclasts in the sea during traveling across the sea and the Koya ignimbrite widely lies on the sea floor around Kikai caldera. Koya ignimbrite became the low aspect ratio ignimbrite after passing the sea area, and low density pyroclastic surge was formed in the mountain area reflecting the topography.

Keywords: low-aspect ratio ignimbrite, Koya ignimbrite, Kikai caldera

©2019. Japan Geoscience Union. All Right Reserved.

©2019. Japan Geoscience Union. All Right Reserved.

Investigating Origin of landslide-like bathymetric feature at southern Mt.Kaimon using bathymetric and multichannel seismic reflection surveys

*hiroto yamaguchi[1], Satoshi Shimizu[2], Hikaru Iwamaru[2], Mamoru Sano[2], Nobukazu Seama[3,2], Misaki Horiuchi[3], Tetsuo Matsuno[2,3], Yoshiyuki Tatsumi[2,3]

1. Department of Planetology, Faculty of Science, Kobe university, 2. Kobe ocean-bottom exploration center, 3. Department of Planetology, Graduate School of Science, Kobe university

The existence of a landslide-like bathymetric feature is reported (Japan Coast Guard, 2007) to the south of Mt.Kaimon volcano that started eruption at the shallow sea area about 4400 years ago. We conducted the multichannel seismic reflection and bathymetric surveys in March and October 2018 using T/S 'Fukae-maru' to investigate how the landslide-like bathymetric feature was formed and where the source was if it was formed by a landslide. The bathymetric data (Figure) are used to make hill-shade map, slope map and terrain ruggedness index map, which characterize bathymetric features. We acquired seismic reflection data sets along eleven survey lines across the landslide-like bathymetric feature (green lines in Figure), which allows us to provide eleven seismic reflection profiles. The seismic reflection profiles indicate that there is a clear reflection boundary, which divide into two areas: The lower layers below the reflection boundary observed at large area and were not affected by stress. Many reverse faults and folds in the upper layers above the reflection boundary with its thickness of about 70m, which were formed by horizontally compressional stress. The analysis of the reflection profiles and the bathymetric lead to, divide the landslide-like bathymetric feature area into four areas. We name each area North-Eastern, South-Eastern, Central and Western part, which shows characteristic features as bellows:

・North-Eastern part; this area is large rugged sea bottom and slope. In the reflection profile, the boundary of upper and lower layers is not so clear. Deeper layers are not observed.

・South-Eastern part; this part is little rugged sea bottom and slope. In the reflection profile, there are some reverse faults and the fault strikes are East-West direction. Stratified structures are also found in spots.

・Central part; this part is the least rugged sea bottom and slope of four area. In the reflection profile, there are a lot of reverse faults. The fault strikes are always North-northwest-South-southeast direction. Stratified structures are found at eastern and western edge.

・Western part; this part is not as large as North-Eastern part, but large rugged sea bottom and slope. In the reflection profile, there are many (but less than Central part) reverse faults, and the fault strikes are North-South.

These characteristic features duggest that an event sweeping the ocean bottom was occurred at northern North-Eastern part, and directions the sweeping landslide are moving in south and west-southwest. It is because deeper layers are effected by collapse at North-eastern part, compressional stress is estimated by faults and folds (direction at the eastern part is North-South and at the central-western part is East-West) and bathymetric feature is more rugged at the eastern part.

Keywords: seismic reflection, ocean bottom topography, Kaimondake

©2019. Japan Geoscience Union. All Right Reserved.

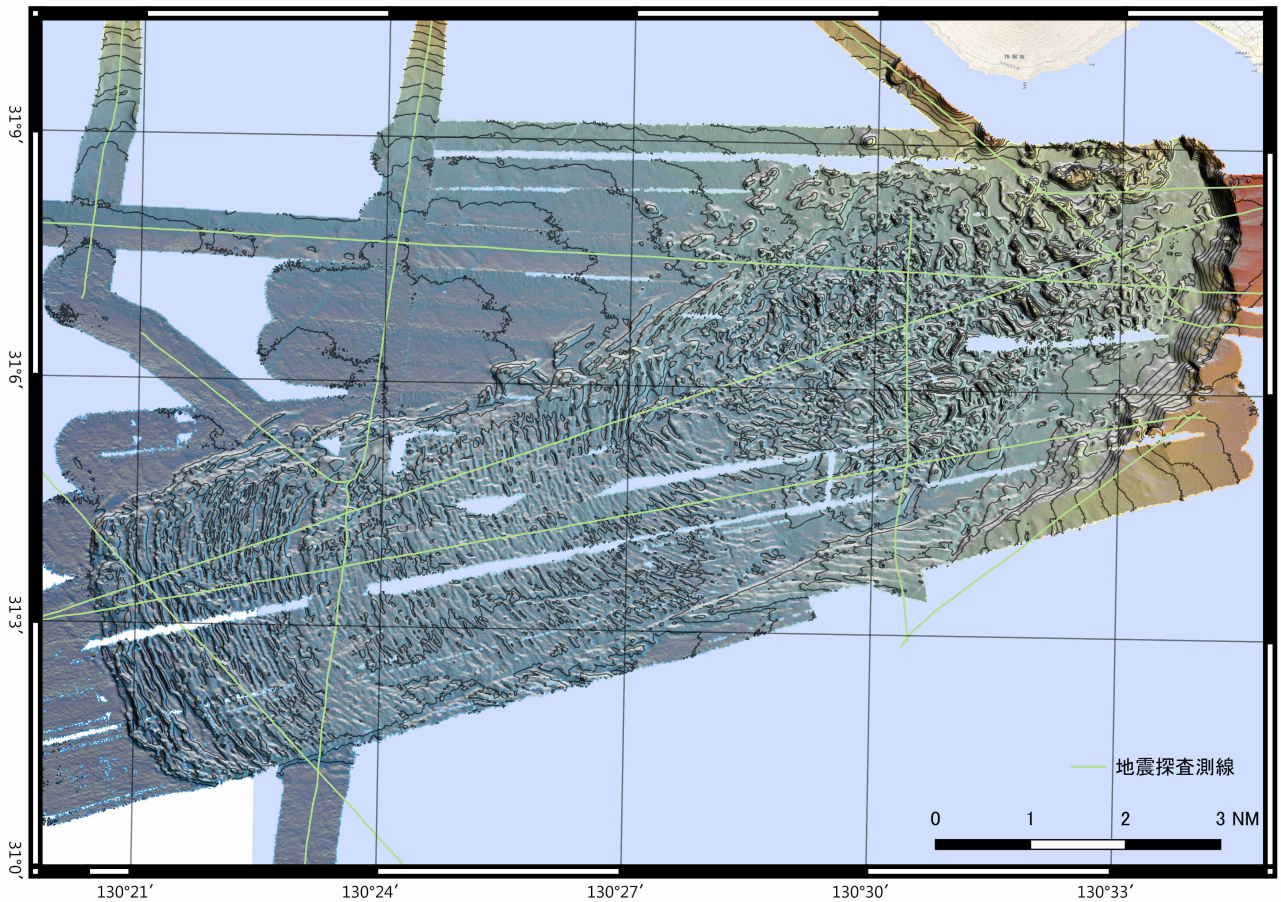

国土地理院の電子地形図（タイル）に海底地形図と反射波地震探査の測線を追記して掲載

©2019. Japan Geoscience Union. All Right Reserved.

Occurrence and distribution of pyroclastic fall deposits of Kuchinoerabujima volcano 2018-2019 eruption

*Masashi NAGAI[1], Shojiro Nakagawa[2], Yu Iriyama[1], Takahiro Miwa[1], Toshikazu Tanada[1], Hideki Ueda[1], Setsuya Nakada[1]

1. Volcano Research Department, National Research Institute for Earth Science and Disaster Resilience, 2. Yakushima Chigaku Club

At Kuchierabujima volcano, eruption began intermittently from October 21, 2018. Relatively large eruptions such as Yakushima and Tanegashima Islands adjacent to the east side of Kuchinoerabujima Island are observed on December 18 and 28, 2018, January 17 and 29, 2019. The ash fall distribution survey was conducted on three eruptions excluding the December 28 eruption where the ash fall axis was in the southeast direction and ash fall on the land was small. In Kuchinoerabujima Island, we conducted an investigation in early February, 2019. We also used information provided by Japan Meteorological Agency Kuchinoerabujima Volcano Disaster Prevention Liaison Office and interviews with local residents.

The Ash fall deposits on Yakushima and Tanegashima Islands are all light gray to reddish light gray colored sandy to silty volcanic ash layers, the component are mainly composed of lithic fragments and hydrothermal altered fragments and small amount of fresh vitreous rock fragments. At the eruption of January 17, 2019 where the largest one during a series of eruptions, on the ash fall axis extending to the east, 400 g/m^2 of ash deposited in the northwestern part of Yakushima Island, 100 g/m^2 in the northeast part, and 20 g/m^2 in the southern tip part of Tanegashima Island. Part of the deposit had the characteristics that ash particles fell as mud rain. In the northern part of Yakushima Island, fine lapilli was also included, and the maximum particle diameter tended to be larger on the north side than the ash fall axis. The deviation between the axis of ash fall axis and the axis of maximum particle diameter distribution can be explained by the difference in wind direction and wind speed at altitude. In Kuchinoerabujima Island, there was an ash fall axis from the summit crater to the southeast direction as total air fall deposit of the series of eruptions, and a deposit amount of about 12 kg/m^2 was confirmed at a distance of about 1.5 km. The layer corresponding to the eruption on January 17 is coarse deposit contains lapilli with long diameter of about 5 cm or more.

The amounts of air fall deposits were obtained by the method of Fierstein and Nathenson (1992) using average deposition density of 1000 kg/m^3. Based on the distribution data of distant deposits such as Yakushima Island, they are estimated to be ca.29,000 tons on the December 18, 2018 eruption, ca.62,000 tons for the January 17, 2019 eruption, and ca.14,000 tons for the January 29, 2019 eruption. These are smaller than the amount of air fall deposit of May 29, 2015 eruption estimated in the same method, ca.120,000 tons. When adding the depositional mass data of Kuchinoerabujima which is the proximal area to these distal data, the total of air fall deposits from December 2018 to January 2019 is estimated to be about 130,000 tons.

Keywords: tephra, phreatic eruption, Phreatomagmatic eruption, eruption column, Ryukyu arc

©2019. Japan Geoscience Union. All Right Reserved.

Ground Deformation around Domestic Active Volcanoes detected by InSAR of ALOS-2/PALSAR-2

*Takafumi Taniguchi[1], Isao Kageyama[1], Okuyama Satoshi[2], Shinobu Ando[2]

1. Japan Meteorological Agency, 2. Meteorological Research Institute

Monitoring of volcanic activity by observing ground deformation is one of useful means to understand signs of eruption such as accumulation and migration of magma. Japan Meteorological Agency (JMA) monitors volcanic activity by tiltmeter, light wave distance measuring equipment and GNSS around volcanoes. However, there are some problems only using these ground-based observation methods. Observable ground deformation is restricted to point information such as the tilt at the observation point and relative position between observation points. Also, it is difficult to install and maintain observation device at an isolated island such as Nishinoshima volcano. It is important to grasp surface ground deformation around volcanoes using not only ground-based observation but also satellite data like SAR (Synthetic Aperture Rader). In this presentation, we mainly report on the analysis results of the long-term pair (2015 to 2018) around the domestic active volcanoes.

Some of PALSAR-2 data were prepared by the Japan Aerospace Exploration Agency (JAXA) via Coordinating Committee for the Prediction of Volcanic Eruption (CCPVE) as part of the project ‘ALOS-2 Domestic Demonstration on Disaster Management Application’ of the Volcano Working Group. Also, we used some of PALSAR-2 data that are shared within PALSAR Interferometry Consortium to Study our Evolving Land surface (PIXEL). PALSAR-2 data belongs to JAXA. We would like to thank Dr.Ozawa (NIED) for the use of his RINC software. In the process of the InSAR, we used Digital Ellipsoidal Height Model (DEHM) based on ‘the digital elevation map 10m-mesh’ provided by GSI, and Generic Mapping Tools (P.Wessel and W.H.F.Smith, 1999) to prepare illustrations.

Keywords: ALOS-2/PALSAR-2, InSAR, Domestic Active Volcano

©2019. Japan Geoscience Union. All Right Reserved.

Volcano-hydrothermal inflation revealed by the spatial variation of stress field at the Tatun Volcano Group, northern Taiwan

*Hsin-Chieh Pu[1], Cheng-Horng Lin[2,3,4,5], Ya-Ju Hsu[2], Li-Chin Chang[3]

1. Central Weather Bureau, Taiwan, ROC., 2. Institute of Earth Sciences, Academia Sinica, Taipei, Taiwan, ROC., 3. Taiwan Volcano Observatory at Tatun, Taipei, Taiwan, ROC., 4. Department of Geosciences, National Taiwan University, Taipei 10617, Taiwan, ROC., 5. National Center for Research on Earthquake Engineering, National Applied Research Laboratories, Taipei, Taiwan, ROC.

To investigate the volcanic behaviors, the Taiwan Volcano Observatory at Tatun has deployed a dense seismic network in the Tatun Volcano Group (TVG), where the government and business metropolis-Taipei city is bounded and various phenomenon related to volcano-hydrothermal activity were found. This network is composed of 40 seismic stations for covering an area of ~10 km by ~10 km. Based on the seismic data recorded by this network, we have solved an extremely huge number of 1,016 earthquake focal mechanisms with depths less 5 km from 2012 to 2017. Then the detailed spatial variations of the local stress field near the surface are firstly inverted from these focal mechanisms. Overall, local earthquakes were dominated by both the sub-horizontal extensional stress striking ESE-WNW and sub-vertical compressional stress. In detail, the orientations of extensional stress formed the abnormal pattern of a couple of semi curves around the Dayoukeng area. In this particular area of Dayoukeng, the magnitude of compressional stress at the sub-vertical component was stronger than the others principle stresses based on the significantly lower ∅values in local than the surrounding area. We ascribe these local variations to an inflating phenomenon buried in the Dayoukeng area. This inflating mechanism should be induced by the volcano-hydrothermal fluid. The current volcano-hydrothermal activity represented by inflation is principally concentrated at the Dayoukeng area and disturbs the faulting behaviors of local earthquakes in the TVG.

Keywords: focal mechanism, stress field, Tatun volcano group, inflation

©2019. Japan Geoscience Union. All Right Reserved.

Topographic change and crustal deformation associated with December 2018 eruption of Krakatau volcano in Indonesia

*Hiroshi Yarai[1], Tomokazu Kobayashi[1], Shinya Yamada[1]

1. GSI of Japan

Krakatau volcano is located in the Sunda Strait between Java Island of Indonesia and Sumatra Island. A high tsunami occurred on this Sunda Strait on December 22, 2018, causing major damage. It is estimated that this tsunami was caused by the collapse of Krakatau volcano. Therefore, in order to grasp the topography change of Krakatau volcano, we analyzed SAR intensity image observed by the Japanese earth observation satellite "Daichi 2" (ALOS-2) before and after the eruption. As a result of the analysis, a clear topographic change was observed in the southwestern part of the island on December 24 after eruption. It is thought that the southwestern part of the island collapsed by this 24th.

Furthermore, for capturing crustal deformation before and after the eruption, SAR interferometry was carried out using Daichi-2 SAR data. As a result, the displacement of the LOS's distance increased in the islands surrounding the Anaku Krakatau Island. Although the characteristic of the change suggests contraction centered around the Anak and Krakatau Island, it is not isotropic but it extends somewhat north and south. Therefore, the source may not be a simple mogi source.

Keywords: Krakatau volcano, volcanic collapse,, crustal deformation, SAR

©2019. Japan Geoscience Union. All Right Reserved.

[J] Oral | S (Solid Earth Sciences)：S-VC Volcanology

Mon. May 27, 2019 3:30 PM - 5:00 PM JST | Mon. May 27, 2019 6:30 AM - 8:00 AM UTC | IC 2F

[S-VC38] Active Volcanism

convener:Yuta Maeda(Nagoya University), Takahiro Miwa(National research institute for earth science and disaster prevention), Takeshi Nishimura(Department of Geophysics, Graduate School of Science, Tohoku University), Chairperson:Takehiko Suzuki, Maya Yasui

This session discusses various aspects of active volcanisms including, but not limited to, recent and historical eruptions, various phenomena associated with the volcanic activities, underground structures of the volcanoes, and developments of new instruments based on geophysical, geochemical, geological, and multidiscipline approaches. We also welcome studies on understanding and predicting the transitions of the eruptive activities from observational, theoretical, and experimental approaches.

3:30 PM - 3:45 PM JST | 6:30 AM - 6:45 AM UTC

[SVC38-01] Tephrochoronology in the southwest part of basaltic Izu-oshima volcanic island during last 20,000 years, off Tokyo, Pacific Ocean

*Takehiko Suzuki[1], Satoshi Terayama[1], Jun Matsukaze[1], Yuichi Kato[1] (1.Faculty of Urban Environmental Sciences, Tokyo Metropolitan University)

3:45 PM - 4:00 PM JST | 6:45 AM - 7:00 AM UTC

[SVC38-02] **Tephrostratigraphy at Daisan-yama and Jinai-jima, and correlation with eruption deposits from Mamashitaura Volcanoes in Niijima Volcano, Izu-islands**

*Makoto Kobayashi[1], Masanori Murata[1], Kaori Aoki[1], Daisuke Ishimura[1,2], Takehiko Suzuki[1,2] (1.Research Center for Volcanic Hazards and Their Mitigations, Tokyo Metropolitan Univ., 2.Department of Geography, Tokyo Metropolitan Univ.)

4:00 PM - 4:15 PM JST | 7:00 AM - 7:15 AM UTC

[SVC38-03] Constration of pre-eruptive process using crystal clot: A case study of Unzen 1991-95 eruption

*Kurumi Iwahashi[1], ATSUSHI YASUDA[1] (1.Earthquake Research Institute,The University of Tokyo)

4:15 PM - 4:30 PM JST | 7:15 AM - 7:30 AM UTC

[SVC38-04] Petrological study of Pinatubo 1991 eruption ~ Discussions of magma plumbing model~

*Tomohisa Tamura[1,2], Mitsuhiro Nakagawa[2] (1.West Japan Engineering Consultants, Inc., 2.Earth and Planetary System Science, Hokkaido University)

4:30 PM - 4:45 PM JST | 7:30 AM - 7:45 AM UTC

[SVC38-05] Rediscovery of the Higuruma Debris Avalanche Deposit in Asama-Kurofu Volcano

*Maya Yasui[1], Masaki Takahashi[1], Tatsuo Kanamaru[1] (1.College of Humanities and Sciences, Nihon University)

4:45 PM - 5:00 PM JST | 7:45 AM - 8:00 AM UTC

Discussion

Tephrochoronology in the southwest part of basaltic Izu-oshima volcanic island during last 20,000 years, off Tokyo, Pacific Ocean

*Takehiko Suzuki[1], Satoshi Terayama[1], Jun Matsukaze[1], Yuichi Kato[1]

1. Faculty of Urban Environmental Sciences, Tokyo Metropolitan University

The Izu-oshima volcano (110 km SSW of Tokyo) in northern Izu-Bonin Arc, is one of the most active Quaternary volcanoes in Japan. This volcano originating from basaltic magma has frequently erupted; that is, 12 times of major eruptions occurred after 2 ka. Studies of its eruption history have been carried out by Nakamura (1964), Kawanabe (2012) and so on. However, precise ages of eruption preceding the caldera formation occurred at 1.8 ka have not been determined. Here, we re-examine the chronological framework of eruption history of the Younger Edifice of pre-caldera.

Fall-out tephras are typically exposed along so-called Great Cut of Beds in SW part of the island. Previous studies by Tazawa (1990) and Uesugi et al. (1994) have described this outcrop, numbering each tephra layer using serial numbers (O1–95 and Osb96–127). All tephras except O55 and O58 are proximal fall-out tephras composed of scoriaceous lapilli and/or scoriaceous ash. Due to the large number of tephras and lithological similarity, it is difficult to confirm each tephra defined by previous studies except several characteristic ones such as O95, O58, and O55. O55 and O58 are rhyolitic tephras from Nijima island and Omuro-dashi submarine depression, respectively (Saito et al., 2007).

Uesugi et al. (1994) estimated the age of the lowest tephra to be 25 ka or older by using 15 radiocarbon ages. However, this estimation is not reliable because it was determined using two oldest conventional radiocarbon ages (non-calibration) of 14–13 ka for the same horizon (just above O64) and under the assumption that the frequency of the tephra occurrence (154 years interval) is constant.
In this study, radiocarbon dating was performed for organic tephric loess collected from 9 horizons above O55 and 16 under O55. The oldest radiocarbon age is 18,598–18,287 cal BP, determined at the horizon 4 m below O95. The age of O95, the most prominent scoria fall deposit, is most likely to be 16–17 ka judging from several radiocarbon ages. It is 2400–3700 years younger than the estimated age (19.4–19.7 ka) by Uesugi et al. (1994). We also recognized widespread K-Ah tephra using volcanic glass geochemistry. Two radiocarbon ages determined at 45 cm above and 55 cm below K-Ah are 6,882–6,747 cal BP and 8167–8021 cal BP, respectively. These ages are concordant with revised age of K-Ah (7,307–7,196 cal yrs BP; McLean et al., 2018), indicating the age of horizon detected K-Ah is older than estimated age of 6,330±85 yBP by Uesugi et al. (1994). These results indicate that the interval between O95 and K-Ah is shorter (67–75%) than previous estimation, suggesting higher frequent occurrence of the eruptions in this period.

Keywords: Izu-oshima, eruption history, carbon dating

©2019. Japan Geoscience Union. All Right Reserved.

Tephrostratigraphy at Daisan-yama and Jinai-jima, and correlation with eruption deposits from Mamashitaura Volcanoes in Niijima Volcano, Izu-islands

*Makoto Kobayashi[1], Masanori Murata[1], Kaori Aoki[1], Daisuke Ishimura[1,2], Takehiko Suzuki[1,2]

1. Research Center for Volcanic Hazards and Their Mitigations, Tokyo Metropolitan Univ., 2. Department of Geography, Tokyo Metropolitan Univ.

In this study, we established tephrostratigraphy at both sites of Daisen-yama and Jinai-jima, and correlated with eruption deposits from Mamashitaura volcanoes based on the characteristics of the mineral compositions, the refractive indexes and major chemical element compositions of the volcanic glass shards. We are aiming to clear long-term eruption history of Niijima volcano.
We recognized deposits associated with at least 20 eruption deposit events at Daisan-yama and Jinai-jima. Based on the stratification of widespread tephra AT, it is considered that the history of the explosive eruption of Niijima volcano and the surrounding volcanoes during late Quaternary (past about 50,000 years) are preserved at these sites. At the both sites, as the ca. 20ka tephra layers, there are coarse fall-out ash deposits containing accretionary lapilli (N), fine fall-out ash deposits (P; Kozushima-Chichibuyama A (Suga et al., 1992)), AT, fine fall-out ash deposits containing pumices (S; Kozushima-Chichibuyama B (Suga et al., 1992)), pyroclastic surge deposits that squeezes phalanx of pumices with diameter several cm (T), fall-out ash deposits containing volcanic lapilli and pumices (V) and pyroclastic surge deposits (X) in descending orders. At Jinai-jima, as lower tephra layers, there are pyroclastic deposit containing many altered volcanic lapilli and blocks (Y) and pyroclastic surge deposit (Z) covering Jinai-jima lava.
Ito and Isobe (2007) suggested that eruption deposits from Mamashitaura Volcanoes were divided into upper Mamashitaura Volcano (cummingtonite rhyolite; ca. 20 ka) and lower Mamashitaura Volcano (biotite rhyolite; >ca. 35 ka) based on the difference of mineral compositions, paleo-soil layers and ^{14}C ages of charcoals contained therein. We recognized that upper Mamashitaura Volcano deposits composed of pyroclastic surge and pyroclastic cone deposits including rhyolite blocks and lapilli, that the lower layer contained more altered brown volcanic breccia (basalt?). On the other hand, lower Mamashitaura Volcanoes deposits composed of pyroclastic flow and pyroclastic surge deposits with a thickness of 20 m or more, and the debris flow containing many volcanic blocks covering them.
We collected data mineral compositions, refractive indexes and major chemical element compositions of glass shards for Daisan-yama and Jinai-jima tephras (T, V, X etc.) and Mamashitaura Volcano deposits. Tephra-T contains many minerals of hornblende and cummingtonite, and is characterized by refractive indexes (1.497-1.500), K_2O contents (3.0-3.3 wt.%) and CaO contents (0.7-1.0 wt %). These characteristics closely resemble features of some of upper Mamashitaura Volcano deposits. On the other hand, the lower tephras V and X are similar to lower Mamashitaura Volcano deposits in point of contain biotite in addition to hornblende and cummingtonite, but the refractive indexes and CaO contents of the volcanic glass shards are significantly different. This suggests that it is difficult to correlation them.
As a result of currently in progress, it is highly likely that T-tephra is eruption deposits from upper Mamashitaura Volcano, and it is appropriate to think that the age is 30,000 to several thousand years ago. On the other hand, we can’ t recognize eruption deposits from the lower Mamashitaura Volcano at Daisan-yama and Jinai-jima.

©2019. Japan Geoscience Union. All Right Reserved.

Keywords: Daisan-yama, Jinai-jima, Mamashitaura Volcano, Niijima Volcano

©2019. Japan Geoscience Union. All Right Reserved.

Constration of pre-eruptive process using crystal clot: A case study of Unzen 1991-95 eruption

*Kurumi Iwahashi[1], ATSUSHI YASUDA[1]

1. Earthquake Research Institute,The University of Tokyo

1.Introduction

Magma mixing is thought to be the major eruption triggers of arc volcanoes. This process can control whether magmas will erupt or stall in the crust. However, magma mixing processes have not been revealed well. Therefore, it is important to reveal mixing process at magma reservoir.
For this purpose, we focus on Unzen 1991-95 eruption. This eruption is characterized by continuous growth of dacitic lava domes and pyroclastic flows caused by collapse of the lava domes. During the eruption, two vulcanian eruptions were recognized. Previous studies proposed that magma mixing between nearly aphyric, mafic and crystal-rich, silicic end-members occurred in the magma chamber (e.g., Sato et al., 1999). Because there are lots of geophysical and geological studies, this eruption is suitable for getting more detailed information about pre-eruptive processes.
Recent studies demonstrated that igneous amphiboles are powerful tools to constrain pre-eruptive magmatic conditions (e.g., Ridolfi and Renzulli, 2012; Putirka, 2016). For example, empirical equations relating temperature and SiO_2 content of co-existing melt with amphibole composition were proposed by Putirka (2016). By using these equations, we can constrain physicochemical conditions of melts in which individual phenocryst crystallized.
Our previous results suggest that the 1991-95 magma was formed by three-component mixing, in which contribution of the newly-recognized 3rd endmember magma (MT magma) (Iwahashi et al., JpGU2018).
Products of 1991-95 eruption often contain crystal clots. They consist of amphibole, plagioclase and Fe-Ti oxides. Because magma reservoir of Unzen volcano is thought to be mushy (e.g., Nakamnura et al., 1995), crystal clots are possible to be part of mushy magma reservoir. Therefore, in this study, we expect to get more detailed information about pre-eruptive process of 1991-95 eruption using crystal clots in addition to amphibole phenocrysts.

2.Methods

We used 11 dacitic samples erupted at different times during the 1991-95 eruption. All of these samples contain crystal clots. They are composed of amphiboles, plagioclases, Fe-Ti oxides and interstitial glass. The major element compositions of amphibole phenocrysts and constituent minerals and glasses in crystal clots were measured by using EPMA at ERI, University of Tokyo.

3.Results

Amphiboles in crystal clots are classified into four types; Type A, Type B, Type C, Type D. Amphibooles of Type A has zonal structure, Type B has reaction rim, Type C has both zonal structure and reaction rim and Type D is almost homogenous. These amphiboles are classified magnesiohornblende and tchermakite based on their compositions. There is an apparent compositional gap between these two clusters. Crystallization temperatures are estimated to be ~750-800ºC and ~850-950ºC for magnesiohornblendes and tchermakites, respectively. Amphiboles in crystal clots reveal temperatures of ~750-800ºC. Estimated SiO_2 contents of melts coexisted with amphiboles (SiO_2^{melt}) are ~66-73wt.% and ~60-67wt.% for magnesiohornblendes and tchermakites, respectively. On the other hand, SiO_2 contents of interstitial melts are ~68-72wt.%. Almost all plagioclases in crystal clots have oscillatory zoned texture. An content (=100*Ca/Ca+Na) of these rim are 60-75.

©2019. Japan Geoscience Union. All Right Reserved.

4.Discussion

H_2O saturation depth estimated for the interstitial melt compositions are consistent with that of main magma chamber in which the silicic endmember magma was thought to be stored.
On the other hand, zonal texture of amphibole often cut by other crystals and this implies that MT magma reservoir may present before 1991-95 eruption. In addition, comparison of temperatures estimated by amphiboles with phase diagram by Noguchi et al.(2008) indicate that there may be almost no plagioclases in MT magma reservoir.
In addition to these results below, we plan to present some new picture of pre-eruptive process at 1991-95 eruption and MT magma reservoir.

Keywords: pre-eruptive process, crystal clot, amphibole

©2019. Japan Geoscience Union. All Right Reserved.

Petrological study of Pinatubo 1991 eruption ~ Discussions of magma plumbing model~

*Tomohisa Tamura[1,2], Mitsuhiro Nakagawa[2]

1. West Japan Engineering Consultants, Inc., 2. Earth and Planetary System Science, Hokkaido University

Introduction

Pinatubo volcano which locates at Northern Luzon island, Philippines caused cataclysmic eruption on June 15, 1991. This eruption includes the four main eruptive products, dome lava andesite on June 7 (J7-LD), basaltic mafic enclave in J7-LD (J7-ME), andesitic scoria from first Plinian eruption on June 12 (J12-P) and dacite pumice from climactic Plinian eruption on June 15 (J15-C). J15-C is separated into two types which constitute gray, precise and phenocryst-poor pumice (J15-CP) and white, bubbly and phenocryst-rich pumice (J15-CR). There are many petrological studies of Pinatubo volcano 1991 eruption, and magma plumbing model of this eruption is established by Pallister*et al.* (1996). Their model indicates magma mixing that andesitic magma is generated by mixing between felsic magma and mafic magma in magma reservoir. However, we carry out whole rock and mineral compositions of 1991 products in detail, and obtain the new findings of magma plumbing model of 1991 eruption.

Analytical methods

We made many thin sections and observed them under polarizing microscope, and counted the modal compositions of phenocrysts.Whole rock and mineral compositions were determined by X-ray fluorescence (XRF) and Scanning electron microscope / Wavelength dispersive X-ray spectroscopy (SEM-WDS) at Hokkaido University, respectively.

Results and Discussions

1991 products mainly include plagioclase and amphibole phenocrysts, and there is a few olivine, clinopyroxene, biotite, quartz and opaque minerals. For Harker diagram of major elements, all products stand in a straight line and it means magma mixing trend. J15-C composition, however, has compositional variation and another trend which crosses the mixing trend. J7-LD and J12-P also have slightly crossed compositional variation. This crossed trend and compositional variation are clearly confirmed in K_2O and Rb contents. The contents of amphibole and biotite which include many potassium do not relate the compositional variation. Therefore, felsic magma of Pinatubo volcano has had the compositional heterogeneous before mafic magma injected into felsic magma reservoir.

Plagioclase and amphibole cores have wide compositional range. According to calculating the equilibrium melt compositions from plagioclase and amphibole cores, we estimate the two felsic endmember that are less-evolved melt, D1 and more-evolved melt, D2. Their melt compositions correspond with glass compositions hosted in melt inclusions of plagioclase and amphibole crystals. Above discussion indicates that felsic magma has the heterogenous, and we estimate that the heterogeneous felsic magma was generated by mixing between D1 and D2.

For minerals of 1991 products, normal and reversal zonings coexist and are repeated from line profile analyses. The melt composition and temperature of magma were heterogeneous and convection occurred in magma reservoir because the composition of plagioclase depends on the melt composition and temperature of magma.

Conclusions

The compositional variation of dacitic magma is consistent with one of minerals, plagioclase and amphibole, for example. The felsic magma has compositional heterogeneous before mafic magma injection, and two different compositional endmember magma coexist (D1 and D2). The continuous compositions of felsic magma were generated between D1 and D2 because of the convection in magma

©2019. Japan Geoscience Union. All Right Reserved.

reservoir. Before 1991 eruption, mafic magma injected into the heterogeneous felsic magma and mixed together, so that andesitic magma which has slightly compositional variation was generated.

Acknowledgements
We thank John Pallister, Cascade Volcano Observatory, US Geological Survey and Takehiro Koyaguchi, Earthquake Research Institute, The University of Tokyo for providing the samples used in this study.

Keywords: Pinatubo volcano, Heterogeneous of silicic magma, Magma mixing

©2019. Japan Geoscience Union. All Right Reserved.

Rediscovery of the Higuruma Debris Avalanche Deposit in Asama-Kurofu Volcano

*Maya Yasui[1], Masaki Takahashi[1], Tatsuo Kanamaru[1]

1. College of Humanities and Sciences, Nihon University

Asama-Kurofu volcano experienced a large-scale sector collapse in its later stage indicated by a horse-shoe shaped caldera and debris avalanche deposit in the distal flank. The area immediately east of the collapsed caldera is occupied by younger volcanic edifices of Hotokeiwa and Maekake. The medial area that is a flank slope of the former Kurofu is thickly covered with the younger deposits from Hotokeiwa and Maekake. Therefore, few information was available for the distribution and thickness of the debris avalanche deposit. Hummocky topography develops on the eastern area of Maekake and Hotokeiwa volcanoes. Geological survey especially in the valley bottom in the hummocky area in the Gunma Prefecture Asama Dairy Farm, the Nagakurayama National Forest, and its vicinity was carried out in this study. Outcrops of the deposits those occurrences were typical of debris avalanche were occasionally found in the valley bottom. In addition, 50-meter deep borehole core sample was taken on the ENE flank slope of Maekake volcano. This is a part of the “integrated program for next generation volcano research and human resource development” supported by ministry of education, culture, sports, science and technology, Japan. Thick debris avalanche deposit of 27 meters was recognized in the lower half of the borehole core sample. That is, weakly stratified and partly solidified tuff breccia that is characterized by heterogeneous matrix and occasional mega-blocks is observed. Whole-rock chemical analyses of the blocks from these deposits show that they are the same as those of the Asama-Kurofu and Asama-Sennin volcanoes. The distribution of “Higuruma debris avalanche” was shown on Yagi (1936) ‘s geologic map but few descriptions were made about it. The deposit confirmed in this study corresponds to the Higuruma debris avalanche and the description including thickness will be a clue for understanding the scale of the sector collapse.

Keywords: Asama volcano, debris avalanche deposit, sector collapse

©2019. Japan Geoscience Union. All Right Reserved.

[J] Oral | S (Solid Earth Sciences)：S-VC Volcanology

Mon. May 27, 2019 9:00 AM - 10:30 AM JST | Mon. May 27, 2019 12:00 AM - 1:30 AM UTC | IC 2F

[S-VC39] Hydrothermal systems of volcanoes

convener:Yasuhiro Fujimitsu(Department of Earth Resources Engineering, Faculty of Engineering, Kyushu University), Wataru Kanda(Volcanic Fluid Research Center, School of Science, Tokyo Institute of Technology), Takeshi Ohba(Department of chemistry, School of Science, Tokia University), Chairperson:Yasuhiro Fujimitsu(Faculty of Engineering, Kyushu University), Takeshi Ohba, Wataru Kanda

There is a diversity of hydrothermal systems between magmas and the ground surface in various geoscientific environments. Understanding of the hydrothermal systems contributes to understanding of the earth systems, and is essential for utilization of geothermal energy and prediction of volcanic eruption. In this session, we will discuss the topics on subsurface structures and heat and fluid flows of "hydrothermal systems of volcanoes" from the perspectives of geophysics, geochemistry, geology and geothermal reservoir engineering. Any research approaches, theoretical, observational and experimental, are welcome.

9:00 AM - 9:15 AM JST | 12:00 AM - 12:15 AM UTC

[SVC39-01] Hydrothermal system of Tokachidake volcano, Japan: Examination from multi-disciplinary surveys

*Ryo Takahashi[1], Noritoshi Okazaki[1], Makoto Tamura[1] (1.Geological Survey of Hokkaido, Hokkaido Research Organization)

9:15 AM - 9:30 AM JST | 12:15 AM - 12:30 AM UTC

[SVC39-02] Fumarole and hot spring activities after the 2015 eruption of Hakone Volcano and their relationships with the seismicity and crustal deformation

*Kazutaka Mannen[1], Masatake Harada[1], Yohei Yukutake[1], George Kikugawa[1] (1.Hot Springs Research Institute of Kanagawa Prefecture)

9:30 AM - 9:45 AM JST | 12:30 AM - 12:45 AM UTC

[SVC39-03] A possible geothermal source at around 4 km depth estimated by the seismic observation in Ibusuki geothermal area

*Junzo Kasahara[1,3], Yoko Hasada[2,1], Hiroyasu Kuzume[1] (1.ENAA, 2.Daiwa Exploration and Consulting Co., 3.Shizuoka Univ.)

9:45 AM - 10:00 AM JST | 12:45 AM - 1:00 AM UTC

[SVC39-04] Time variation in the chemical and isotopic composition of fumarolic gases at Kusatsu-Shirane volcano Japan

*Takeshi Ohba[1], Muga Yaguchi[2], Nozomi Numanami[1], Kotaro Toyama[3], Hirochika Sumino[3], Urumu Tsunogai[4], Masanori Ito[4], Ryo Shingubara[4] (1.Department of chemistry, School of Science, Tokia University, 2.Meteorological Research Institute, JMA, 3.The University of Tokyo Graduate School of Arts and Sciences Department of Basic Science, 4.Nagoya University Graduate School of Environmental Studies)

10:00 AM - 10:15 AM JST | 1:00 AM - 1:15 AM UTC

[SVC39-05] Behavior of Arsenic and Mercury related to hydrothermal activities in Kirishima, Satsuma Iwojima, and Yamagawa, Kyushu Japan

*Motoya Habuchi[1], Harue Masuda[1], Tsuyoshi Shintani[1], Shuzo Furuya[1], Keigo Mori[1], Jun-ichiro Ishibashi[2], Takeshi Matsushima[2], Akinori Takeuchi[3], Syogo Oshima[4], Reo Ikawa[5] (1.Osaka City University, 2.Kyushu University, 3.National Institute for Environmental Studies, 4.West Japan Engineering Consultants, Inc., 5.National Institute of Advanced Industrial Science and Technology)

10:15 AM - 10:30 AM JST | 1:15 AM - 1:30 AM UTC

[SVC39-06] The chemical composition of thermal waters from spring and hot pool at Mt. Iwoyama of Kirishima volcano

*Muga Yaguchi[1], Takeshi Ohba[2], Kotaro Toyama[3], Fukuoka Regional Headquarters JMA[4], Kagoshima Meteorological Office JMA[4] (1.Meteorological Research Institute, 2.Tokai University, 3.Graduate School of the University of Tokyo, 4.Japan Meteorological Agency)

Hydrothermal system of Tokachidake volcano, Japan: Examination from multi-disciplinary surveys

*Ryo Takahashi[1], Noritoshi Okazaki[1], Makoto Tamura[1]

1. Geological Survey of Hokkaido, Hokkaido Research Organization

Tokachidake volcano, located in central Hokkaido, Japan, has had intermittent magmatic eruptions during the 20th century. Recently, increases in seismic activity, ground inflation around the active craters and chemical changes of thermal waters are observed, and hence, a magmatic eruption in the near future is of concern. The 1926 eruption induced a large-scale lahar (Taisho lahar). Uesawa (2014) proposed that large amounts of thermal water were released as a hydrothermal surge from the interior of the volcanic edifice, expanding the scale of the Taisho lahar. In addition, chemical and thermal changes related to volcanic activity were observed in thermal waters around the volcano (Takahashi et al., 2015). These phenomena are deeply related to hydrothermal systems. Therefore, to detect precursor activities precisely at Tokachidake volcano, we should understand the subvolcanic hydrothermal systems. In this study, we performed multi-disciplinary surveys, such as magnetotelluric (MT) survey, geological investigations and thermal water and fumarolic gas observations, to examine the subvolcanic hydrothermal systems.

We performed MT survey at 13 stations along an NW-SE survey line across the volcano, and detected several conductive zones in the edifice. A conductive zone was detected at more than 3–4 km depth beneath the summit crater area (deep conductive zone). Volcanic earthquakes did not occur in this conductive zone, but their hypocenters were distributed surrounding the zone. This would indicate that the outer margin of the conductive zone is coincident with the brittle-ductile transition zone. Another conductive zone is distributed at 300–1,500 m depth beneath the summit crater area (shallow conductive zone).

In order to discuss the shallow hydrothermal system, we investigated phreatic ejecta, the 1926 debris avalanche deposits and accessory ejecta, all of which record subsurface hydrothermal environments. As a result, we revealed that an alteration zone with a pyrophyllite+quartz assemblage occurs at depths of >500 m beneath the crater area (Takahashi & Yahata, 2018). This zone reflects a high-temperature environment (200–300 ˚C). Also, fumarolic gas observations suggest that high-temperature (200–300 ˚C) hydrothermal systems exist the shallow subsurface. We can consider that the shallow hydrothermal system inferred from these investigations is coincident with the shallow conductive zone detected by MT survey.

We have observed the thermal waters around Tokachidake volcano over a period of more than three decades. At Fukiage spa area, thermal waters caused chemical and thermal changes by the supply of the magmatic NaCl-type thermal water associated with the increase in volcanic activity (Takahashi et al., 2015). A distribution area of the NaCl-type thermal water around magma would be detected as a conductive zone because thermal waters with high temperature and high NaCl concentration show high conductivity. Thus, we can consider that the deep conductive zone is interpreted as a distribution area of the NaCl-type thermal water.
In consequence of multi-disciplinary surveys at Tokachidake volcano, we revealed the subvolcanic hydrothermal systems. We should continue careful observations and revise the model to understand more precisely the volcanic activity of the volcano.

©2019. Japan Geoscience Union. All Right Reserved.

Keywords: Tokachidake volcano, hydrothermal system, magnetotelluric survey

©2019. Japan Geoscience Union. All Right Reserved.

Fumarole and hot spring activities after the 2015 eruption of Hakone Volcano and their relationships with the seismicity and crustal deformation

*Kazutaka Mannen[1], Masatake Harada[1], Yohei Yukutake[1], George Kikugawa[1]

1. Hot Springs Research Institute of Kanagawa Prefecture

A very small phreatic eruption occurred at Hakone volcano in 2015. Before the eruption, in Owakudani, where the eruption center formed, there has been no significant fumarole activity; however, more than 20 craters and fumaroles formed associated with the eruption and they still remain active. We have routinely measured the steam temperatures emitted from the fumaroles and analyzed chemical composition of hot spring and surface waters every two weeks since we were permitted to enter the eruption center. In this presentation, we show the temporal changes and its relationship with the seismic activity and crustal deformation.

1. Steam temperature of fumaroles
Among the more than 20 fumaroles, we have measured 10 fumaroles that are significant and accessible (Mannen et al., 2019). We have only two stable fumaroles named 15-12 (since May 1, 2017) and 16-1 (since January 11, 2018) for routine measurement.

The temperature of 15-12 was higher than 150 ºC before August 2017. However, the temperature lowered gradually up to 120 ºC until the late 2018. The temperature of 16-1 was approximately 140 ºC when we started measurement. However, the steam temperature also lowered gradually and marked 130 ºC in the late 2018.

On the other hand, fumaroles named 15-1 and 15-14B continuously emit high temperature steams and higher than 150 ºC even in the late 2018 without significant decline although steam vents of these fumaroles are unstable and migrate frequently. We suppose that the steam temperature and emission are on decline since detection of high temperature steam is getting difficult and extinction of fumarolic activity is common recently. The highest temperature ever recorded was 162.0 ºC from 15-1 observed on August 23, 2017.

2. Chemical composition of hot springs and surface waters
In Owakudani area, we routinely correct and analyze waters from 13 sources including natural springs, stream water and artificial hot springs, which is made by mixing of steam emitted from steam well and water (Kikugawa et al., 2019). The stream water, watershed of which includes the eruption center, shows high Cl content associated with the 2015 volcanic unrest ($Cl/SO_4 > 1.0$; Mannen et al. 2018). The Cl concentration lowered to the background level ($Cl/SO_4 \sim 0.2$) until early 2017; however, increased slightly from November 2017 to January 2018 ($Cl/SO_4 \sim 0.3$). The artificial hot springs from No. 52 steam well also showed significant rise of electric conductivity and Cl content and decline of pH.

Our measurement of volcanic gas from underfloor of a building in Owakudani shows continuous decline of CO_2/H_2S ratio after the eruption. The decline rate seemed to lower in 2017; however, it was not clear. On the other hand, Daita et al. (2018) reported that CO_2/H_2S ratio of volcanic gas from Kamiyu, north of Owakudani showed rise from around June 2017.

©2019. Japan Geoscience Union. All Right Reserved.

3. Seismicity and crustal deformation in 2017
In Hakone volcano, earthquake swarm, deep low frequency earthquakes and increase of baseline length across the volcano have observed before increase of geothermal activity (Harada et al. 2018; Mannen et al. 2018). After the 2015 eruption, there has been no earthquake swarm; however, there were slight increase of seismicity from the late April to the early May in 2017 beneath Mt. Kintoki (Yukutake et al. 2018). Before the earthquake swarm, in the mid-April, deep low frequency earthquakes (DLF) was found active by matched filter method (Yukutake, 2017). The baseline length across Hakone volcano started to increase from the early May in 2017 and ended in the late November of the year with total stretch of 12 mm (the total stretch during the 2015 eruption and unrest was 21 mm). In the period, there is no significant change in steam temperature. Increase of hydrothermal activity was implied by the changes in chemical compositions of artificial hot spring water and surface water in the late April and in November respectively.

The observed trend of the weak change in 2017 are similar to that of the volcanic unrests in 2013 and 2015. We thus suppose that there was a small increase of volcanic activity in 2017. Comparing to the changes in 2013 and 2015, seismicity and stretch rate of the baseline in 2017 are notably lower. Daita et al (2018) also pointed out that the increase in CO2/H2S ratio in 2017 was significantly lower than that observed in 2013 and 2015. Such differences observed in 2017 may imply that the magma-hydrothermal system of Hakone volcano has altered by the 2015 eruption (Daita et al, 2018).

Keywords: Hakone, Deep low frequency earthquake, inflation of edifice, fumarole, hot springs, volcanic activity

©2019. Japan Geoscience Union. All Right Reserved.

A possible geothermal source at around 4 km depth estimated by the seismic observation in Ibusuki geothermal area

*Junzo Kasahara[1,3], Yoko Hasada[2,1], Hiroyasu Kuzume[1]

1. ENAA, 2. Daiwa Exploration and Consulting Co., 3. Shizuoka Univ.

Introduction: The Medipolis is located in Ibusuki geothermal area, Japan. There are three geothermal boreholes in the field. The geothermal characteristics of the boreholes were studied by NEDO (2008-2010). The IK-1 borehole is commercially used for the electric power generation. The IK-4 is used for observation. The depths of three boreholes are around 1,500 m. The temperature of the boreholes was approximately 250˚C around the 900 m-depth and the production depth for the steam is around 1,200 m. The temperature model by NEDO (2008-2010) proposes a hot reservoir around the NE direction of IK-1 and IK-4 boreholes although it is not confirmed by real drillings.

To know the precise geothermal characteristics of this field, we conducted a seismic observation by a fiber-optic distributed acoustic sensor (DAS) and ground surface seismometers in November 2018.

Field observation: We installed 20 sets of 3C seismometers along the 2 km-long EW line and deployed a fiber-optic cable for the DAS and distributed temperature (DTS) measurements down to 977 m depth. We measured the temperature and seismic signals using the same fiber-optic cable for DAS and DTS. The total DAS observation period is 4.5 days. The interval of ground surface seismometers is approximately 100 m. We observed seven natural earthquakes by DAS and surface seismometers. The largest observed earthquake is M5.2 which occurred west of Tanegashima with 123 km focal depth. The temperature of the IK-4 was measured as 264˚C by DTS at the 914 m depth.

Observed waveforms: The first arrivals of the M5.2 earthquake measured by DAS are traveling from the 977 m depth to the wellhead with the velocity of 4 km/s~3 km/s. There are no evident reflections from the deeper zone than 1,000 m. In addition, any evident attenuation of seismic waves is not identified in the high temperature zone around the 914 m-depth.

Surface seismometers show unusual waveform characteristics. Although the amplitudes of the P-wave first arrivals of M5.2 earthquake on vertical seismometers are small, the EW and the NS seismometers show small P first arrivals and succeeding large amplitude phase with a second delay. Because this phase is recognized only on EW and NS components, this phase is possibly P-to-S converted phase. The aftershocks of the M5.2 Tanegashima also showed similar waveforms as those of the M5.2 event. Other earthquakes also showed similar characteristics on the horizontal components.

Interpretation of P-to-S converted phase: We examined the cause of estimated P-to-S conversion. The delay time from the P first arrival to the P-to-S converted phase is estimated as ~0.8 s. We assumed a low Vp/Vs zone at the 4 km-depth with 500 m thick and calculated synthetic waveforms generated by deep seismic sources corresponding to natural earthquakes. The seismic velocity profile estimated by the DAS observation is used in the calculation. The models can explain the observed characteristics such as small P amplitude and large P-to-S converted phase on horizontal components, when incident seismic wave is slightly oblique to the low Vp/Vs zone. We also estimated borehole waveforms and ground surface waveforms.

©2019. Japan Geoscience Union. All Right Reserved.

Discussion and conclusions: According to the simulation, there is a chance to prove the presence of the low Vs zone at the 4 km-depth. Because the temperature around ~900 m is 264˚C, the low Vs zone might be useful for a future geothermal energy source. For either case, more detailed study of the proposed low Vs zone is required.

Acknowledgements: This study is supported by the New Energy and Industrial Technology Development Organization (NEDO). Medipolis Energy Co. kindly allowed the use of their IK-4 geothermal well for this study. Mr. Kimura provided us with the Schlumberger hDVS measurements. WELMA Co. provided us with the borehole fiber-optic system and measurement of temperatures in the borehole. The staff of West Japan Engineering Consultants, Inc., helped us during the field study.

Keywords: Geothermal field, Seismic wave, Vp/Vs, P-to-S conversion, Geothermal reservoir, Passive seismic source

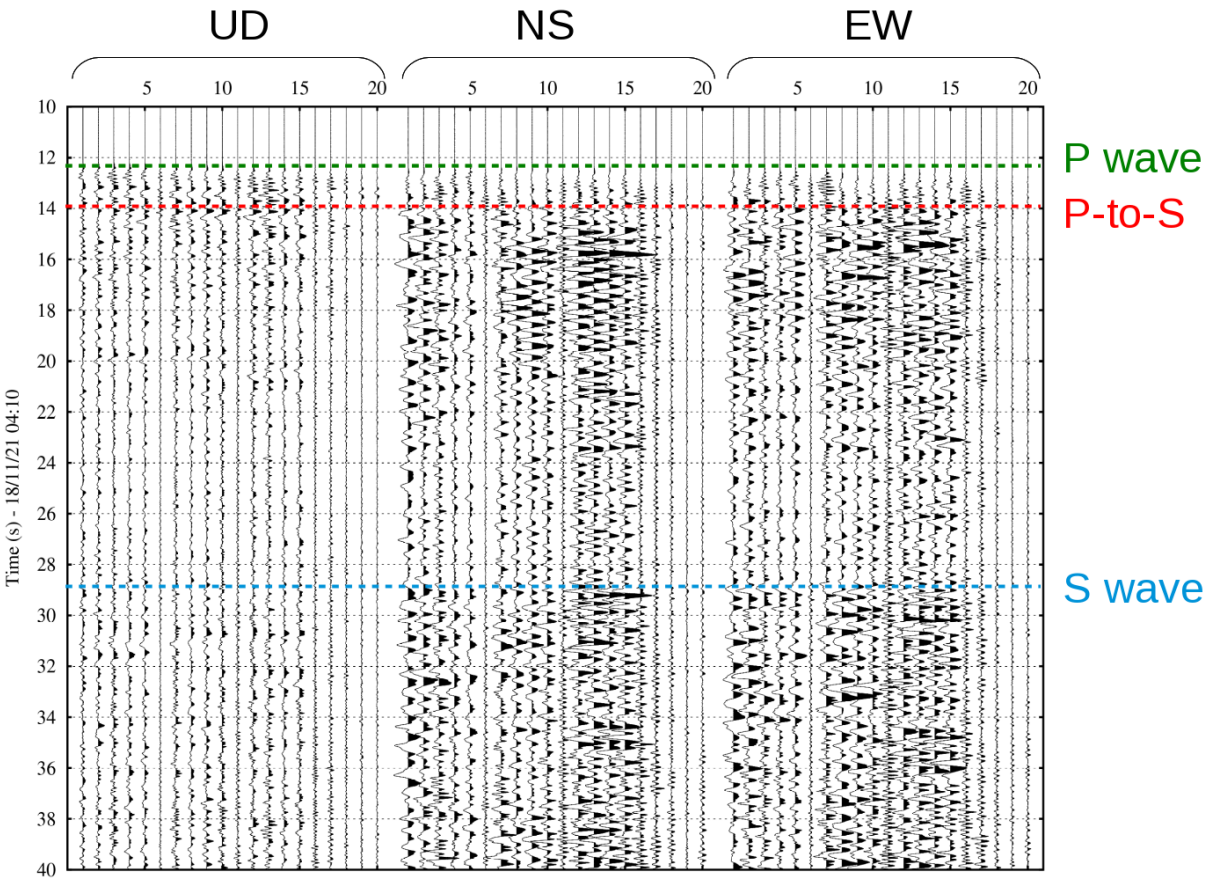

The seismic records of M5.2 Tanegashima earthquake obtained by the surface seismometers. The labels on the horizonal axis are the station numbers and the station interval is approximately 100 m. The vertical axis is time in seconds. The horizontal dotted lines denote arrival times for P, P-to-S, S waves, respectively.

©2019. Japan Geoscience Union. All Right Reserved.

Time variation in the chemical and isotopic composition of fumarolic gases at Kusatsu-Shirane volcano Japan

*Takeshi Ohba[1], Muga Yaguchi[2], Nozomi Numanami[1], Kotaro Toyama[3], Hirochika Sumino[3], Urumu Tsunogai[4], Masanori Ito[4], Ryo Shingubara[4]

1. Department of chemistry, School of Science, Tokia University, 2. Meteorological Research Institute, JMA, 3. The University of Tokyo Graduate School of Arts and Sciences Department of Basic Science, 4. Nagoya University Graduate School of Environmental Studies

At Kusatsu-Shirane volcano Japan, the intense seismic activity took place in 2014 and 2018. To investigate the relationship between the activity and the chemistry of fumarolic gas, the gas samples have been repeatedly analyzed. A monotonic decrease in CO2/H2O, He/H2O and N2/H2O ratios since July 2014 to November 2017 suggests the decline of magmatic component. On contrary CH4/H2O ratio significantly increased during the seismically quiet period, suggesting the reduced condition in hydrothermal system favoring to the formation of CH4. The high N2/He ratio in the quiet period suggests the addition of component originating in crustal rock hosting hydrothermal system. The N2/He ratio in 2018 was definitely lower than the ratio in 2014, indicating the evolution of magma brought by the degassing. The δD(H2O), δ18O(H2O) and CO2/H2O ratio of fumarolic gas were modeled with the following processes; the generation of vapor phase after the mixing between magmatic gas and a cold groundwater with meteoric origin, the addition of vapor phase with meteoric origin, and the partial condensation of water vapor near surface. Only a single magmatic gas is necessary for the above modeling.

©2019. Japan Geoscience Union. All Right Reserved.

Behavior of Arsenic and Mercury related to hydrothermal activities in Kirishima, Satsuma Iwojima, and Yamagawa, Kyushu Japan

*Motoya Habuchi[1], Harue Masuda[1], Tsuyoshi Shintani[1], Shuzo Furuya[1], Keigo Mori[1], Jun-ichiro Ishibashi[2], Takeshi Matsushima[2], Akinori Takeuchi[3], Syogo Oshima[4], Reo Ikawa[5]

1. Osaka City University, 2. Kyushu University, 3. National Institute for Environmental Studies, 4. West Japan Engineering Consultants, Inc., 5. National Institute of Advanced Industrial Science and Technology

Arsenic and mercury behave in similar manners during migration from the deep to the surface of the Earth with magmatic and associating hydrothermal activities. In this study, we sampled total 57 hydrothermal and local meteoric waters from Kirishima, Satsuma-Iwojima and Yamagawa in November 2017 to December 2018 to trace the migration processes of arsenic and mercury related to the volcanic and its associating hydrothermal activities. We analyzed concentrations of major components, arsenic and mercury and hydrogen and oxygen isotope ratios.
The highest temperature of hydrothermal water, which was taken from the craters phreatically exploded in the April 2018, was 94.5 ˚C and the pH was 0.8-1.7. The maximum concentrations of chloride ion and sulfate ion were 300 mM and 190 mM, and the positively linear relationship between these two components indicated the simple mixing of acidic hydrothermal fluid and local meteoric water. In many high temperature hydrothermal waters, $\delta^{2}H$ and $\delta^{18}O$ were in the range of magmatic water, -25 to -5‰ and +4 to +9 ‰. Total arsenic concentration in the hydrothermal waters was 1210-4640 μg/l, which had a positively linear relationship with sulfate ion concentration. Dissolved and suspended total mercury concentrations in hydrothermal waters were 0.5-85 ng/l and 0.5-826 ng/l, respectively. Since highly mercury concentrated hydrothermal water also contained high arsenic, these were derived from the same magmatic fluid. Chloride and sulfate ion concentrations of hot spring waters derived from fumarole in Kirishima and Kurinodake were < 0.2 mM and 26 mM at the maximum. Total arsenic concentration was 0.58-24 μg/l, and total suspended mercury concentration was 1980 ng/l at the maximum. Hot spring waters in Satsuma Iwojima and Yamakawa,contained high total arsenic concentration when the seawater directly infiltrated and the highest concentration was 2500 μg/l for the one of hot spring water in Satsuma Iwojima. In these areas, the highest total dissolved mercury concentration was 177 ng/l for a hot spring water with pH of 1.4 in Satuma Iwojima. Both arsenic and mercury are rising up from the deep with magmatic fluid. However, the two elements may behave differently along the migration path; mercury moves preferentially with vapor and removed from the water during flowing path on the surface, while arsenic preferentially behaves with hydrothermal water and remains as a dissolved phase in the surface water.

Keywords: magmatic fluids, Iwo-yama, phreatic eruption, hydrogen and oxygen isotope ratios of water

©2019. Japan Geoscience Union. All Right Reserved.

The chemical composition of thermal waters from spring and hot pool at Mt. Iwoyama of Kirishima volcano

*Muga Yaguchi[1], Takeshi Ohba[2], Kotaro Toyama[3], Fukuoka Regional Headquarters JMA[4], Kagoshima Meteorological Office JMA[4]

1. Meteorological Research Institute, 2. Tokai University, 3. Graduate School of the University of Tokyo, 4. Japan Meteorological Agency

Mt. Iwoyama of Kirishima volcanic complex is an active volcano where fumarolic activity restarted in December 2015 at summit crater. After the restart of the fumaroles, volcanic activities at the surface, such as the expansion of fumarolic area, the appearance of thermal springs and water quality changes in springs around Mt Iwoyama have been observed. In April 2018, small phreatic eruptions occurred at the south of the summit and west flank of Mt. Iwoyama, and boiling hot pools have appeared in some of the newly created craters after the eruptions. In this study, the chemical composition of water samples collected from a natural spring site on the west flank of Mt. Iwoyama and hot pools in the newly created craters have been analyzed to obtain information for evaluation of volcanic activity at this mountain.

Between August 2016 to March 2018 (about a month before the eruption), the Cl/SO_4 of the spring water increased from 0.07 to 0.9. About a month after the eruption, the ratio increased to 1.6 as of May 2018, and remain between 1.2 and 1.6 since then to January 2019.

Cl/SO_4 molar ratio of hot water pool in one of the southern craters was 1.3 in May 2018 and 1.8-2.3 in January 2019. The ratio of hot water pool in the western crater was 1.3 in July 2018, 1.9 in October 2018 and 2.2 in January 2019. The increase of Cl/SO_4 molar ratio may be caused by several reasons, for example, the ascent of volatile-rich magma or chemical composition change of volatiles along with the progress of degassing.

Keywords: Mt. Iwoyama of Kirishimayama volcano, Thermal water, Chemical composition

©2019. Japan Geoscience Union. All Right Reserved.

[J] Oral | S (Solid Earth Sciences)：S-VC Volcanology

Mon. May 27, 2019 10:45 AM - 12:15 PM JST | Mon. May 27, 2019 1:45 AM - 3:15 AM UTC | IC 2F

[S-VC39] Hydrothermal systems of volcanoes

convener:Yasuhiro Fujimitsu(Department of Earth Resources Engineering, Faculty of Engineering, Kyushu University), Wataru Kanda(Volcanic Fluid Research Center, School of Science, Tokyo Institute of Technology), Takeshi Ohba(Department of chemistry, School of Science, Tokia University), Chairperson:Yasuhiro Fujimitsu(Faculty of Engineering, Kyushu University), Takeshi Ohba, Wataru Kanda

There is a diversity of hydrothermal systems between magmas and the ground surface in various geoscientific environments. Understanding of the hydrothermal systems contributes to understanding of the earth systems, and is essential for utilization of geothermal energy and prediction of volcanic eruption. In this session, we will discuss the topics on subsurface structures and heat and fluid flows of "hydrothermal systems of volcanoes" from the perspectives of geophysics, geochemistry, geology and geothermal reservoir engineering. Any research approaches, theoretical, observational and experimental, are welcome.

10:45 AM - 11:00 AM JST | 1:45 AM - 2:00 AM UTC

[SVC39-07] Re-examination of origin of the variety in magmatic-hydrothermal fluids

*Hiroshi Shinohara[1] (1.Geological Survey of Japan, AIST)

11:00 AM - 11:15 AM JST | 2:00 AM - 2:15 AM UTC

[SVC39-08] **Constraining electrical resistivity structure of volcanoes using multiphase flow modelling: an example of Miyake-jima**

*Marceau Gresse[1], Makoto Uyeshima[1], Takao Koyama[1], Maki Hata[1], Hideaki Hase[2], Koki Aizawa[3], Yusuke Yamaya[4], Yoichi Sasai[5], Jacques Zlotnicki[6], Tawat Rung-Arunwan[1], Hideki Ueda[7] (1.Earthquake Research Institute, The University of Tokyo, Tokyo, Japan, 2.Geothermal Energy Research & Development Co., Ltd., Tokyo, Japan, 3.Institute of Seismology and Volcanology, Faculty of Science, Kyushu University, Fukuoka, Japan., 4.Planning Division, National Institute of Advanced Industrial Science and Technology, Tokyo, Japan, 5.Earthquake Prediction Research Centre, Tokai University, Shizuoka, Japan, 6.CNRS, OPGC-UMR6524, Aubière, France, 7.National Research Institute for Earth Science and Disaster Resilience, Tsukuba, Japan)

11:15 AM - 11:30 AM JST | 2:15 AM - 2:30 AM UTC

[SVC39-09] MT survey and 3-D resistivity structure in the Niseko area, southwestern Hokkaido

*Makoto Tamura[1], Toru Mogi[2], Junna Kanahiro[2], Daisuke Oka[1], Junya Maruyama[1], Takahiro Suzuki[1], Noritoshi Okazaki[1] (1.Geological Survey of Hokkaido, Hokkaido Research Organization, 2.Division of Sustainable Resource Engineering, Fucluty of Engineering, Hokkaido University)

11:30 AM - 11:45 AM JST | 2:30 AM - 2:45 AM UTC

[SVC39-10] **Hydrothermal fluid activity of the Tatun Volcano Group, Taiwan, revealed by self-potentials and seismicity**

*Hong-Jia Chen[1], Zhi-Xian Yang[1], Chien-Chih Chen[1,2], Cheng-Horng Lin[3,4] (1.Department of Earth Sciences, National Central University, Taiwan., 2.Earthquake-Disaster & Risk Evaluation and Management, National Central University, Taoyuan, Taiwan., 3.Institute of Earth Sciences, Academia Sinica, Taipei, Taiwan., 4.Taiwan Volcano Observatory at Tatun, Taipei, Taiwan.)

11:45 AM - 12:00 PM JST | 2:45 AM - 3:00 AM UTC

[SVC39-11] Utilizing the electrical conductivity distribution to unravel the hydrothermal system beneath Mt.Hasan composite volcano and its vicinity, southwest Cappodocia, Turkey

*Sabri Bulent Tank[1], Mustafa Karas[1] (1.Bogazici University)

12:00 PM - 12:15 PM JST | 3:00 AM - 3:15 AM UTC

[SVC39-12] Three-dimensional Magnetotelluric Inversion to map geothermal structures in Eburru Geothermal field, Kenya.

*JUSTUS MAITHYA[1], Yasuhiro FUJIMITSU[2] (1.Graduate School of Engineering, Department of Earth Resources Engineering, Kyushu University, 2.Faculty of Engineering, Department of Earth Resources Engineering, Kyushu University)

Re-examination of origin of the variety in magmatic-hydrothermal fluids

*Hiroshi Shinohara[1]

1. Geological Survey of Japan, AIST

A variety of magmatic-hydrothermal fluids, including volcanic gases, hot spring waters and geothermal waters, is created from a magma and we will re-evaluate those origins with particular interest on variation of Cl/S ratios. Giggenbach (1996) classified fluids in a magmatic-hydrothermal system as 1) Acid Cl-SO_4 water, 2) Neutral NaCl water, 3) Bicarbonate water and 4) Steam heated acid SO_4 waters. The acid Cl-SO_4 waters are formed by condensation of magmatic gases discharged from a magma. The neutral NaCl waters are formed from the acid water through neutralization and S-mineral deposition due to water-rock interaction at lowering temperature. The bicarbonate waters and acid SO_4 waters are formed by mixing of CO_2 or H_2S derived from vapor separation of a deep hydrothermal system with meteoric water or the neutral NaCl waters. The principal differentiation process is the neutralization and S-mineral deposition of the acid Cl-SO_4 water under a temperature gradient to create the neutral NaCl water. However, we also need to consider other factors than the temperature dependence.

Water-rock reactions also have pressure dependent. HCl content in hydrothermal fluids has a negative pressure dependence; a hydrothermal solution has a larger HCl content at a lower pressure than at a higher pressure (Shinohara and Fujimoto, 1996; Botcharnikov et al., 2015). The pressure dependence implies that hydrothermal fluids discharged from a magma at a high pressure tend to have less acid than volcanic gases discharge at the surface. The average Cl/S ratio of the Japanese volcanic gases is about 0.2 (Shinohara 2013), whereas the ratio is about 0.5 in melt inclusion of basaltic magmas and is about 10 in those of silicic magmas. Therefore, a hydrothermal fluid formed by a complete solidification of the magma will have Cl/S ratio much larger than those of volcanic gases or the acid Cl-SO_4 waters. These evidences suggest that the acid Cl-SO_4 waters and the neutral NaCl waters have distinct origins with different condition of a magma degassing. Compilation of chemical compositions of hot spring waters and hydrothermal waters in Japan show a clear two frequency peaks of acid and near neutral pH with a gap at pH 4-5 (Muraoka et al., 2007). This pH distribution also suggests that the distinct origin of the two types of the hydrothermal fluids.

Keywords: volcanic gas, hot spring, geothermal fluids

©2019. Japan Geoscience Union. All Right Reserved.

Constraining electrical resistivity structure of volcanoes using multiphase flow modelling: an example of Miyake-jima

*Marceau Gresse[1], Makoto Uyeshima[1], Takao Koyama[1], Maki Hata[1], Hideaki Hase[2], Koki Aizawa[3], Yusuke Yamaya[4], Yoichi Sasai[5], Jacques Zlotnicki[6], Tawat Rung-Arunwan[1], Hideki Ueda[7]

1. Earthquake Research Institute, The University of Tokyo, Tokyo, Japan, 2. Geothermal Energy Research & Development Co., Ltd., Tokyo, Japan, 3. Institute of Seismology and Volcanology, Faculty of Science, Kyushu University, Fukuoka, Japan., 4. Planning Division, National Institute of Advanced Industrial Science and Technology, Tokyo, Japan, 5. Earthquake Prediction Research Centre, Tokai University, Shizuoka, Japan, 6. CNRS, OPGC-UMR6524, Aubière, France, 7. National Research Institute for Earth Science and Disaster Resilience, Tsukuba, Japan

Measuring the electrical resistivity of rocks is a powerful and reliable method used to investigate volcanic edifices at depth. The electrical resistivity has two main contributions: (i) the conduction in the bulk pore fluid, associated to saturation, the ionic strength, and temperature of pore water, and (ii) the surface conductivity, related to the formation of secondary minerals. In volcanic environments, these two contributions are controlled by numerous interactions between hydrology, geology, tectonic settings and magmatic forcing. As a consequence, the evaluation of electrical resistivity images is strongly non-unique, and its interpretation remains complex.

Here, we propose a new approach to address this issue. First, we performed a 3-D electrical resistivity imagery of the Miyake-jima volcano using Magnetotellurics. Next, we combined the resistivity model obtained with hypocenters distribution. We revealed the sharp boundary between the saturated and unsaturated region, and a large conductive hydrothermal system connected to the main fumarolic area through a fractured region. Finally, we created a multiphase flow model of the volcano that constrains the resistivity model in term of temperature, fluid content and alteration.

Keywords: Hydrothermal system, Magnetotellurics, Miyake-jima, multiphase flow, electrical resistivity, alteration

©2019. Japan Geoscience Union. All Right Reserved.

MT survey and 3-D resistivity structure in the Niseko area, southwestern Hokkaido

*Makoto Tamura[1], Toru Mogi[2], Junna Kanahiro[2], Daisuke Oka[1], Junya Maruyama[1], Takahiro Suzuki[1], Noritoshi Okazaki[1]

1. Geological Survey of Hokkaido, Hokkaido Research Organization, 2. Division of Sustainable Resource Engineering, Fucluty of Engineering, Hokkaido University

In the Niseko area, southwestern Hokkaido, there are many volcanoes distributed along East-West direction that is so called “Niseko volcanic group”. And many hot springs are distributed around Iwaonupuri and Niseko-Annupuri volcano. Recently, geothermal explorations for energy development have been performed in this area.
During such situation, we are carrying out the priority research “Modelling of geothermal structure and assessment of geothermal resource potentials in the Niseko area” for sustainable application of geothermal resources. In this presentation, we show the MT survey and the 3-D resistivity structure analysis result as a part of this research.
We performed wideband MT survey at 18 stations in 2017 and 24 stations in 2018 around the Niseko area. Five components of electromagnetic fields were measured by ADU-07e and ADU-08e (manufactured by Metronix Geophisics). We obtained 32Hz data that was recorded for more than 5 days, 1024Hz data that was recorded more than 5 nights (1:00-5:00 : LT) and 32kHz data that was recorded one hour. Horizontal components of magnetic field data recorded at Ookura Vil., Yamagata Pref. were used for the remote reference processing of 32Hz and 1024Hz data. For 32kHz sampled data, we measured data at the same time in multiple stations for the remote reference processing. Also, we performed noise elimination processing for 50Hz electrical power lines.
MT responses at the frequency band of 12288-0.000488Hz were estimated using the robust time series processing code BIRRP (Chave and Thomson, 2004). Furthermore, we tried to obtain a 3-D resistivity structure with the aid of the ModEM inversion scheme (Egbert and Kelbert, 2012). Topographic effects might strongly affect the MT impedances because the survey area is located from the top to the foot of the volcano. In order to consider the topography into the 3D inversion, we used inland DEM data of 10m spacing provided by Geospatial Information Authority of Japan, and the seabed data of 500m spacing provided by Japan Coast Guard. Three-dimensional inversion was performed using four components of the tensor impedance from the field records.
In the results, we detected several conductive zones. A conductive zone was detected from the surface to several kilometers depth beneath the Iwaonupuri volcano. This would indicate volcanic hydrothermal system or hydrothermal rock alteration area. Also, we detected conductive zones around Ooyunuma Pond that is a hot spring bog, and southern foot of the Niseko-Annupuri volcano area where many hot springs are distributed. These conductive zones would indicate thermal water aquifers or related altered area.

Acknowledgement
The MT equipments (ADU-07) were used by Joint Usage Program in Earthquake Research Institute, University of Tokyo. Also, we used Magnetic field data of Geothermal Energy Research & Development CO., Ltd., for remote reference processing. We would like to thank these institutions.

Keywords: Niseko volcanic group, Magnetotelluric survey, resistivity structure, 3-D modeling

©2019. Japan Geoscience Union. All Right Reserved.

Hydrothermal fluid activity of the Tatun Volcano Group, Taiwan, revealed by self-potentials and seismicity

*Hong-Jia Chen[1], Zhi-Xian Yang[1], Chien-Chih Chen[1,2], Cheng-Horng Lin[3,4]

1. Department of Earth Sciences, National Central University, Taiwan., 2. Earthquake-Disaster & Risk Evaluation and Management, National Central University, Taoyuan, Taiwan., 3. Institute of Earth Sciences, Academia Sinica, Taipei, Taiwan., 4. Taiwan Volcano Observatory at Tatun, Taipei, Taiwan.

The objective of our research was to unravel the evolutions of the hydrothermal activities in the Tatun Volcano Group, Taiwan. We observed the significant variations of monthly earthquake counts, daily cumulative earthquake counts, and self-potential power spectral densities (PSDs) after April 21, 2016, providing strong evidence to identify hydrothermal fluid activities. This was further confirmed by the simulated electrical impedances using the resistivity forward modeling. Thus, an upward hydrothermal fluid movement is required to generate weaker PSDs of self-potentials at different frequencies. Herein, we concluded that geoelectric monitoring, along with seismic monitoring, help to understand the evolution of a hydrothermal system beneath a volcanic region.

Keywords: Hydrothermal fluid, Tatun Volcano, self-potential

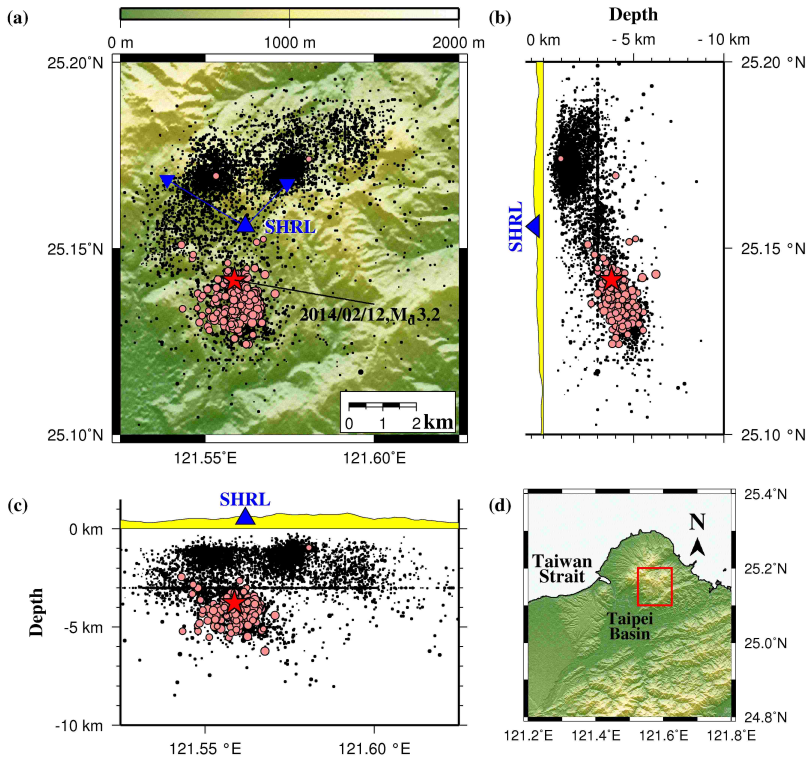

©2019. Japan Geoscience Union. All Right Reserved.

Utilizing the electrical conductivity distribution to unravel the hydrothermal system beneath Mt.Hasan composite volcano and its vicinity, southwest Cappodocia, Turkey

*Sabri Bulent Tank[1], Mustafa Karas[1]

1. Bogazici University

The electrical conductivity structure in the vicinity of Mt.Hasan composite volcano at Central Anatolia, Turkey was imaged by means of wide-band magnetotellurics data collected at 38 sounding locations and three-dimensional numerical modeling. The primary aim in this study was to decipher the major elements that drive a hydrothermal system beneath study area in detail. Therefore, following the dimensionality analyses performed by plotting induction arrows and phase tensor ellipses, the electromagnetic impedance data were numerically modeled in the data-space for imaging (i) the shallow and (ii) the deep electric structure with different frequency tables. While the former approach, provided information on the the thickness of a surficial (surface-to-2 km) and widespread welded ignimbrite layer, the latter approach, revealed the geometry of the deeper two layers beneath the ignimbrites that make up the clay cap. These layers that are found on the top of one another are interpreted as smectite (<10 Ohmm) and smectite-illite mixed (<10-15 Ohmm) layers. And finally beneath the smectite and smectite-illite layers, there is a cone-shaped anomaly (10 –60 Ohmm) that may have been serving as a reservoir for different vents in the area.

Keywords: Magnetotellurics, Volcanology, Hydrothermal systems, Mt.Hasan

©2019. Japan Geoscience Union. All Right Reserved.

Three-dimensional Magnetotelluric Inversion to map geothermal structures in Eburru Geothermal field, Kenya.

*JUSTUS MAITHYA[1], Yasuhiro FUJIMITSU[2]

1. Graduate School of Engineering, Department of Earth Resources Engineering, Kyushu University, 2. Faculty of Engineering, Department of Earth Resources Engineering, Kyushu University

To explore the geothermal system in Eburru geothermal field in an attempt to delineate possible heat sources and fluid flow pathways governing the system, 107 Magnetotelluric (MT) soundings were deployed in the field. The MT data was analyzed using phase tensor to determine the dimensionality of the subsurface resistivity structure. These data were inverted to a fully three-dimensional resistivity model. Overall, the inverted resistivity model fits the MT data very well as evidenced by the data misfit curves. Consequently, 2-D inversion were carried out and a joint interpretation was made on the basis of the two models. The preferred 3-D model images a resistive top layer overlying a very conductive layer (~ 10 ohm.m) interpreted as the hydrothermally altered clay cap of the system and a moderate resistivity layer (about 30 ohm.m). These layers are underlain by a higher resistivity zone (~ 100 ohm.m). To characterize the resistivity structure in the field, resistivity profiles were extracted from the 3-D model in order to cut across the known geological structures. The profiles analysed show a deep reaching conductive channel connecting two conductors located at ~ 1 km from the surface and at a depth of ~ 4 km. This channel can be interpreted as potential path way used by geothermal fluid to migrate to the surface and manifests as fumaroles and hot spring. The occurrence of fumaroles along faults suggests leakage of steam where the cap is likely to have been cut by the faults. The resultant 3-D resistivity models are generally similar to the two-dimensional (2-D) inversion models, however, the deeper portion of the 3-D model seems to be more realistic than that of the 2-D model.

Keywords: Eburru geothermal field , Magnetotelluric, 3-D Inversion, Resistivity, 2-D inversion

©2019. Japan Geoscience Union. All Right Reserved.

[J] Poster | S (Solid Earth Sciences)：S-VC Volcanology

Mon. May 27, 2019 3:30 PM - 5:00 PM JST | Mon. May 27, 2019 6:30 AM - 8:00 AM UTC | Poster Hall International Exhibition Hall8, Makuhari Messe_14

[S-VC39] Hydrothermal systems of volcanoes

convener:Yasuhiro Fujimitsu(Department of Earth Resources Engineering, Faculty of Engineering, Kyushu University), Wataru Kanda(Volcanic Fluid Research Center, School of Science, Tokyo Institute of Technology), Takeshi Ohba(Department of chemistry, School of Science, Tokia University)

There is a diversity of hydrothermal systems between magmas and the ground surface in various geoscientific environments. Understanding of the hydrothermal systems contributes to understanding of the earth systems, and is essential for utilization of geothermal energy and prediction of volcanic eruption. In this session, we will discuss the topics on subsurface structures and heat and fluid flows of "hydrothermal systems of volcanoes" from the perspectives of geophysics, geochemistry, geology and geothermal reservoir engineering. Any research approaches, theoretical, observational and experimental, are welcome.

[SVC39-P01] Changes in the chemistry of spring water related to the recent volcanic activity of Mt Iwo-Yama, Kirishima volcanic area

*Haruka Yamamoto[1], Yoshikazu Kikawada[2], Megumi Fukai, Wei Deng (1.Graduated school of Fuculty of Sience and Technology Sophia University, 2.Fuculty of Sience and Technology Sophia University)

[SVC39-P02] Hydrothermal circulation process related to phreatic eruption of Iwo-Yama at Kirishima volcanoes

*Keigo Mori[1], Harue Masuda[1], Tsuyoshi Shintani[1], Motoya Habuchi[1], Syuzou Furuya[1], Jun-ichiro Ishibashi[2], Takeshi Matsushima[2], Syogo Oshima[3], Reo Ikawa[4] (1.Osaka City University, 2.Kyushu University, 3.West Japan Engineering Consultants, Inc., 4.AIST)

[SVC39-P03] Determination on the stable isotopic compositions of H_2O in a volcanic plume

*Masanori Ito[1], Urumu Tsunogai[1], Koji U Takahashi[2], Fumiko Nakagawa[1] (1.Nagoya University, Graduate School of Environmental Studies, 2.Geological Survey of Japan, National Institute of Advanced Industrial Science and Technology)

[SVC39-P04] **Radon measurements at Aso volcano: an experimental automatic radon station operative within the proximal zone of Nakadake**

*Corrado CIGOLINI[1], Shin Yoshikawa[2], Tomo Shibata[3], Marco Laiolo[1], Diego Coppola[1] (1.Department of Earth Sciences, University of Torino, Italy, 2.Aso Volcanological Laboratory, Kyoto University, Japan, 3.Institute for Geothermal Sciences, Graduate school of Science, Kyoto University, Japan)

[SVC39-P05] Evolution of the hydrothermal system of Aso volcano during the 2014-2016 eruption period, as inferred by the ACTIVE observations

*Takuto Minami[1], Mitsuru Utsugi[2], Hisashi Utada[1], Tsuneomi Kagiyama[3] (1.Ocean Hemisphere Research Institute, Earthquake Research Institute,The University of Tokyo, 2.Aso Volcanological Laboratory, Institute for Geothremal Sciences, Graduate School of Science, Kyoto University, 3.Aso Geopark Promotion Council)

[SVC39-P06] 3-D Inversion of Magnetotelluric data from the Aluto-Langano Geothermal Field, Ethiopia

*Dejene Bekele[1], Yasuhiro FUJIMITSU[2] (1.Graduate School of Engineering, Department of Cooperative Resources Engineering, Kyushu University, 2.Faculty of Engineering, Department of Earth Resources Engineering, Kyushu University)

[SVC39-P07] Interpretation of Gravity Data to Delineate the Geothermal Reservoir Extent and Assess the Geothermal Resource in the Municipality of Isa, Southern Kyushu, Japan

*CARLOS OSMIN POCASANGRE[1], Yasuhiro Fujimitsu[1], Jun Nishijima[1] (1.Department of Earth Resources Engineering, Kyushu University)

[SVC39-P08] Conductive and convective heat fluxes inferred from temperature profile of a borehole in Izu-Oshima volcano

*Shin'ya Onizawa[1] (1.Volcanology Research Department, Meteorological Research Institute, JMA)

[SVC39-P09] Numerical model of the hydrothermal system at the Akakura Caldera in Kurikoma Area

*Yasuhiro Fujimitsu[1], Daichi Yoshioka[2] (1.Department of Earth Resources Engineering, Faculty of Engineering, Kyushu University, 2.Department of Earth Resources Engineering, Graduate School of Engineering, Kyushu University)

Changes in the chemistry of spring water related to the recent volcanic activity of Mt Iwo-Yama, Kirishima volcanic area

*Haruka Yamamoto[1], Yoshikazu Kikawada[2], Megumi Fukai, Wei Deng

1. Graduated school of Fuculty of Sience and Technology Sophia University, 2. Fuculty of Sience and Technology Sophia University

Mt Iwo-Yama is an active volcano in the Kirishima volcanic area. The west flank of the volcano is known as the Ebino Highland. The volcano erupted in April 2018 for the first time in 250 years. The vents have opened with the phreatic eruptions and then formed boiling muddy pools. In this study, we discuss the current status of the volcanic activity of Mt Iwo-Yama based on the water chemistry of muddy crater lakes and the springs in the Ebino Highland.

We collected the sample water repeatedly from the muddy crater lakes at the summit area (V1) and the west flank (V2). The former one is the vent opened on April 19th, 2018 and the latter one is that opened on April 26th, 2018. In addition, we also collected repeatedly the specific spring water located along the small stream in the Ebino Highland. We labeled the spring water as S1 to S4 in the order of distance from the summit area. The collected water samples were chemically analyzed in our laboratory.

The V1 and V2 water contain extremely high concentrations of chloride and sulfate ions. Those two are very acidic, and the pH of them sometimes show the value lower than unity. These are considered that thermal water is supplied from the geothermal reservoir directly. At this writing, although the estimated temperatures for both reservoirs of V1 and V2 by the quartz geothermometer are over 200 deg-C, the temperature for V2 is a little higher than that of V1.

The fluctuations of Cl/SO4 ratio at S1, S2 and S3 are similar to that of V2. Also, the fluctuation of the ratio at S4, which is most far from the summit among the four, seems to be similar to these with 1- month time lag. From this, it is suggested that these springs in the Ebino Highland are affected by the geothermal activity related to V2. The concentration of dissolved chemical components and water temperature at S1 changed from an increasing trend to decreasing trend in August 2018. Conversely, these at S4 are on an increasing trend since September 2018.

The volcanic activity of Mt Iwo-Yama is remained to be active. Based on the water chemistry, the temperature of the geothermal system seems to be higher in the west flank area, that is the Ebino Highland area, than the summit area. The changes in the water chemistry of the hot springs suggesting the rise of thermal activity in the Ebino Highland have been observed. Further, the new fumaroles were opened in the west flank area since autumn 2018. In conclusion, it is considered that the geothermal activity of Mt Iwo-Yama is expanding from the summit area to the west flank area. This means that the thermal activity in the Ebino Highland area will become more active, and the fumarolic area will expand to the western part of the Ebino highland.

Keywords: Kirishima Iwo-Yama

©2019. Japan Geoscience Union. All Right Reserved.

Hydrothermal circulation process related to phreatic eruption of Iwo-Yama at Kirishima volcanoes

*Keigo Mori[1], Harue Masuda[1], Tsuyoshi Shintani[1], Motoya Habuchi[1], Syuzou Furuya[1], Jun-ichiro Ishibashi[2], Takeshi Matsushima[2], Syogo Oshima[3], Reo Ikawa[4]

1. Osaka City University, 2. Kyushu University, 3. West Japan Engineering Consultants, Inc., 4. AIST

A phreatic eruption occurred on a south crater of Iwo-yama, Kirishima active volcano, on April 19, 2018, and active hydrothermal activities including fumarole and high temperature water outflow have continued until now. We analyzed major chemical compositions of waters sampled on the 12th and 13th October 2018 in order to clarify the hydrothermal systems beneath the Iwo-yama related to the phreatic eruption. Water temperature, pH, ORP, and EC were measured *in situ* using electrodes. Na^+ and K^+ were quantified using an atomic absorption spectrophotometer, and Si, As, Al^{3+}, Mn^{2+}, and Fe^{2+} were analyzed by ICP-MS. Ca^{2+} and Mg^{2+} were quantified by EDTA titration, while those of some samples by ICP-MS. Alkalinity was analyzed by neutralization titration. F^-, Cl^-, Br^-, NO_3^-, PO_4^{3-} and SO_4^{2-} were analyzed by ion chromatography. Hydrogen and oxygen isotope ratios of waters were analyzed by cavity ring down spectrophotometry.
The temperature and pH of erupting hot waters in the south and west craters were 70~ 97 ℃ and 1.3 ~ 2.1, respectively. The temperature and pH of low temperature springs in the northeastern wetland out of the craters were about 20 ℃ and 2.2 ~ 5.2. Cl^- and SO_4^{2-} concentrations ranged within 1000 ~ 8000 ppm and 2,000 to 10,000 ppm for hot waters and 3 ~ 300 ppm and 10 to 1100 ppm for low temperature spring waters. Positively linear relationship indicated the same origin of between concentrations of Cl^- and SO_4^{2-}. The d^2H and $d^{18}O$ of the highest Cl^- and SO_4^{2-} concentrated water were -18 ‰and -4.0 ‰, indicating high contribution of magmatic water. Strongly acidic water was formed by oxidation of magmatic components due to mixing of meteoric water in the groundwater aquifer. The all analyzed waters can be explained simple mixing of the above high temperature water with local meteoric water. It is notable that up to about 3000 ppb As was confirmed in the hot water.
The silica geothermometer indicated the highest temperature of 262 ˚C for the hot water containing the highest Cl^- concentration, suggesting the aquifer temperature is higher than that. The formation of high temperature water in the groundwater aquifer must be related to the phreatic eruption.

Keywords: geothermometer, hydrogen and oxygen isotope

©2019. Japan Geoscience Union. All Right Reserved.

Determination on the stable isotopic compositions of H_2O in a volcanic plume

*Masanori Ito[1], Urumu Tsunogai[1], Koji U Takahashi[2], Fumiko Nakagawa[1]

1. Nagoya University, Graduate School of Environmental Studies, 2. Geological Survey of Japan, National Institute of Advanced Industrial Science and Technology

The fumarolic H_2O occupied more than 80% of volatiles ejected from volcanic fumaroles (volcanic gases). The origin of fumarolic H_2O is either magma (magmatic water) or groundwater (meteoric water). Because of the significant differences in the isotopic ratios (δ D and δ^{18}O) of H_2O between magmatic water and meteoric water, we can differentiate the origins of fumarolic H_2O (magmatic water or meteoric water), if we can determine the isotopic ratios of fumarolic H_2O from those in volcanic plumes during a volcanic eruption. This is extremely useful for us to differentiate the mechanism of each volcanic eruption, magmatic eruption or phreatic eruption.
In this study, we determined the isotopic ratios of H_2O in a volcanic plume that had been ejected from accessible fumaroles to confirm whether the isotopic ratios (δ D and δ^{18}O) estimated from plume H_2O is consistent with those of fumarolic H_2O or not.
The samples were taken in Hakone volcano from 2014 to 2018. We collected around 20 volcanic plume samples into pre-evacuated glass bottle (ca. 1000 ml) during each sampling, while changing the distances from the fumarole. Besides, we also collected the fumarolic H_2O through condensation using a cold trap. The isotopic ratios (δ D and δ^{18}O) of plume H_2O showed strong linear correlation (R^2 = 0.9 or more) with the reciprocal of H_2O concentration. The isotopic ratios (δ D and δ^{18}O) estimated as the intercept of the linear correlation found in the plume H_2O was consistent with fumarolic H_2O. We concluded that we can estimate the stable isotopic ratios of fumarolic H_2O remotely using those in plume H_2O.
This study was supported by MEXT Scientific Research Program grants “Integrated Program for Next Generation Volcano Research and Human Resource Development”.

Keywords: Volcanic gases, Stable isotopic compositions, Cavity Ring-Down Sectroscopy

©2019. Japan Geoscience Union. All Right Reserved.

Radon measurements at Aso volcano: an experimental automatic radon station operative within the proximal zone of Nakadake

*Corrado CIGOLINI[1], Shin Yoshikawa[2], Tomo Shibata[3], Marco Laiolo[1], Diego Coppola[1]

1. Department of Earth Sciences, University of Torino, Italy, 2. Aso Volcanological Laboratory, Kyoto University, Japan, 3. Institute for Geothermal Sciences, Graduate school of Science, Kyoto University, Japan

Radon measurements at Aso Volcano first started on May 2015 and persisted until January 2016. They were resumed on August 2017 and they are currently on-going. Radon data have been collected by means of an in-soil automatic station located at about 1.06 km from the active crater (crater 1) together with soil temperatures (measured at the sampling site and 1 m below) and local atmospheric parameters (JMA).
During earlier measurements Aso volcano was affected by a sporadic explosive activity, which marked the ceasing of a Strombolian phase, and was followed by moderate phreatomagmatic events. Radon measurements been compared with ground-based and satellite thermal data, the latter collected by the MIROVA system. Radon concentrations were fluctuating from 300 to about 1100 Bq/m^3 during May-July 2015, and they reached a minimum two weeks before the strong degassing that occurred at the beginning of August. On August 8, 2015 the Volcanic Radiative Power (VRP) detected by MIROVA was slightly below 1 MW. Since then there has been an increasing trend in Radon emissions (up to about 900 Bq/m^3) that preceded the strong phreatic explosion of September 14. By the end of September, a new increasing trend reached a relative maximum (up to 1900 Bq/m^3) one week before the explosion of the 23 of October 2015. Then, radon data persistently fluctuated well above 900 Bq/m^3. This time span was accompanied by a general decrease of the detected thermal anomalies which were nearly coeval with the replenishment of the crater lake.
During 2017 radon emissions reached their relative maxima (up to 1380 Bq/m3) during fall-winter, whereas in 2018 the higher peak reaches 1450 Bq/m3 during the early fall (October 3). Several peaks seems to be correlated with the thermal gradient at the measurement site. However, some other peaks appear somehow coeval with some thermal anomalies in the crater area detected by the MIROVA system. Among these the one that occurred on May 15 that touched 1250 Bq/m3 and preceded the drastic increase in temperature of the South wall (up to 715 ˚C, according to JMA data). Two other minor anomalous peaks were recorded on June 13 and July 29, both were well above 800 Bq/m3. A systematic analysis of all radon data shows that radon emissions, in absence of anomalous spikes, are inversely correlated with soil temperatures and that the contribution of atmospheric pressure marginally affect radon emissions. The spectrum of the radon signal shows the existence of both diurnal and semidiurnal peaks, typically observed during continuous radon measurements. Future work should be concentrated in the attempt to better correlate radon emissions with the changes in volcanic activity, including the effects of environmental parameters on the radon signal.

Keywords: Radon , radon signal, radon anomalies/peaks, environmental parameters

©2019. Japan Geoscience Union. All Right Reserved.

Evolution of the hydrothermal system of Aso volcano during the 2014-2016 eruption period, as inferred by the ACTIVE observations

*Takuto Minami[1], Mitsuru Utsugi[2], Hisashi Utada[1], Tsuneomi Kagiyama[3]

1. Ocean Hemisphere Research Institute, Earthquake Research Institute,The University of Tokyo, 2. Aso Volcanological Laboratory, Institute for Geothremal Sciences, Graduate School of Science, Kyoto University, 3. Aso Geopark Promotion Council

Electrical resistivity structures provide important information about hydrothermal systems of volcanos. Previous studies using the magnetotelluric method have revealed shallow resistivity structures associated with conductive cap rocks underlain by hydrothermal reservoirs (e.g. Nurhasan et al. 2006). However, evolution of such a hydrothermal system over volcanic eruptions has never been understood in detail.

We have intermittently conducted observations of an electromagnetic volcano monitoring system, ACTIVE (Utada et al. 2007), in Aso volcano for about half a decade. ACTIVE system consists of transmitter dipoles for controlled-source electric currents and an array of induction-coil receivers for measuring the vertical component of the induced magnetic field dependent on the subsurface resistivity structure. ACTIVE system in Aso volcano recently succeeded in detecting temporal variation in the resistivity structure over the magmatic eruptions that started in November 2014 and ceased in May 2015 (hereafter referred to as the magmatic eruption period (MEP)). In our previous study, three-dimensional inversions for the two sets of ACTIVE responses obtained in August 2014 and August 2015 revealed (1) a broad increase in resistivity ~400 m below the bottom of the first Nakadake crater and (2) a decrease in resistivity ~100 m beneath the western rim of the crater (Minami et al. 2018). Both changes in resistivity presumably originated before MEP because the corresponding variation in the ACTIVE response happened mainly between the two observation campaigns in August 2014 and just after the starting of MEP, say, on November 26, 2015. The decrease of resistivity at shallow level implies presence of a temporal fluid reservoir which appeared prior to MEP and possibly contributed to the phreatomagmatic eruptions in September 2015 and October 2016. We are now analyzing the ACTIVE responses after MEP to resolve evolution of the hydrothermal system of Aso volcano over the active period spanning from November 2014 to October 2016.

In the presentation, we comprehensively discuss evolution of the hydrothermal system of Aso volcano from August 2014 to August 2017, including MEP from August 2014 to May 2015 and the two phreatomagmatic eruption events in September 2015 and in October 2016, by using ACTIVE data sets.

Keywords: Aso, volcano, ACTIVE, resistivity, temporal variation

©2019. Japan Geoscience Union. All Right Reserved.

3-D Inversion of Magnetotelluric data from the Aluto-Langano Geothermal Field, Ethiopia

*Dejene Bekele[1], Yasuhiro FUJIMITSU[2]

1. Graduate School of Engineering, Department of Cooperative Resources Engineering, Kyushu University, 2. Faculty of Engineering, Department of Earth Resources Engineering, Kyushu University

The Main Ethiopian rift valley hosts a number of geothermal prospected area, which is known to be actively deforming with reoccurring periods of uplift and setting. One of the regions where the prospected area is confirmed by drilling is the Aluto-Langano geothermal area. Aluto area is situated in the Main Ethiopian rift valley system bounded by latitude 7.60˚-7.96˚ N and longitude 38.68˚-38.92˚ E. This field has been studied by the Geological Survey of Ethiopia (GSE) since1980s, and these studies subsequently led to the drilling of 10 exploration wells. This field is currently developed with a Binary power plant of a 7.2 MWe installed capacity. From the results of various regional geoscientific studies in this part of the Ethiopian rift, the area of Aluto-Langano geothermal field was observed to have relatively higher exploitable geothermal potential in Ethiopia. However, more studies are required in order to obtain more information about the subsurface structure and heat source below the Aluto volcanic complex (AVC) and to delineate the parameters of the geothermal reservoir in the area. To address this, Electro Consultant (ELC) and GSE carried out magnetotelluric surveys in the Aluto-Langano geothermal field in 2009 and 2015 respectively. This study combines the two surveys done covering the whole Aluto volcanic complex with a total of 166 MT stations. The MT data was processed and used in the construction of a 3-D MT inversion model, which was then interpreted alongside the available geological information. The dimensionality analysis of MT data was carried out based on the strike and dimensions of the resistivity distribution around the MT sites, by plotting the Phase tensor for each MT site for the frequency range of 10^{4} -10^{-3} Hz. Most of the maps of phase tensor exhibit 3-D structures, hence need for 3-D inversion. In order to get 3-D conductivity models of the subsurface, the MT data were inverted in the period range of 10^{-3}–10^{4}s at uniform distributed discrete periods using the ModEM code. The resultant 3-D resistivity model shows a highly conductive zone with a diameter of around 10 km in the center of the Aluto volcanic complex at depths between 800–2500 m. The identified resistivity distribution corresponds very well to the conceptual reservoir model of a high-enthalpy geothermal system with its mushroom shaped zoning comprising a resistive up-flow zone overlain by a conductive clay cap. From well data analysis it is known that the conductive cap at Aluto is related to rock units and therefore, eliciting the origin of the heat source and delineating the subsurface structure in the study area. The 3-D resistivity model images the resistivity structure in the study area hence showing the origin of Aluto heat sources and delineating the location of faults and fracture system. In particular, the cap rock zones of the geothermal reservoir system by studying low resistivity zones at relatively shallow depths are important in selecting future drilling targets.

Keywords: Aluto-Langano, 3-D Inversion, Magnetetolluric, Ethiopia

©2019. Japan Geoscience Union. All Right Reserved.

Interpretation of Gravity Data to Delineate the Geothermal Reservoir Extent and Assess the Geothermal Resource in the Municipality of Isa, Southern Kyushu, Japan

*CARLOS OSMIN POCASANGRE[1], Yasuhiro Fujimitsu[1], Jun Nishijima[1]

1. Department of Earth Resources Engineering, Kyushu University

The municipality of Isa is located in the southern part of Kyushu Island, and it is considered one of the wealthiest places in Japan because one of the most important gold mines is found in this area, Hishikari mine. Additionally, there are many hydrothermal manifestations, e.g., Hishikari, Yunoo, Kawanami, and Kintaro hot springs, which can be exploited by the community as an electric power source. Until now, the geothermal resource has not been used for power generation purpose although Geological Survey of Japan had carried out some preliminary geothermal assessments, which show that the power potential density is between 10 and 20 kW/km^2. To calibrate the previous value, first, this study attempts to analyze and interpret the gravity data for delineating the geothermal reservoir boundary and the assessment of geothermal resource. Accordingly, the corresponding researchers conducted 2-D and 3-D gravity modeling in the current research. This modeling is an essential stage of the complete gravity analysis in the region, because the filtering gravity methods, i.e., Horizontal-Derivative and Tilt-Derivative, can quickly detect steep gradients and indicate the location of faults or geological boundaries, however, they cannot estimate geological structure depth and shape. For this purpose, an area of 10 x 10 km was selected and analyzed considering a Bouguer Density of 2.45 g/cm^3. The Bouguer Anomaly result shows a high value at the center, which extends 5.61 km^2 wide and could represent the probable geothermal resource. According to the Kagoshima geological map, volcanic and sedimentary rocks are the dominant type of rocks in this area. Cretaceous Shimanto group controls the fundamental structure of the deepest element. This arrangement is typically composed of sandstone, shale, acidic tuff with subordinate conglomerates, and their alterations, also Pliocene volcanic rocks and alluvial deposits. Similarly, Kakuto and Okuchi Basin, which are located at east and west respectively, control the region. The 2-D gravity modeling was carried out requiring a density contrast between the two assumed layers, i.e., the basement and the low-density deposit, and thus a value of 0.4 g/cm^3 was assigned. Likewise, the horizontal size of the cells was set at 100 m. The profile trending NW- SE shows a significant depression 400 m to 700 m deep located next to Hishikari hot spring. In this way, the hydrothermal fluids might be flowing up to the surface forming altered rocks and hot springs by using a possible geological fault. For a better understanding of the region, the authors also carried out 3-D gravity modeling. The result shows an area which has density values below 2.4 g/cm^3 and the zone NE-SW direction that starts at the Uonogoe area and ends at the Yamada area. Besides, a large anomaly located in the central area that has density values above 2.5 g/cm^3 is evident. This anomaly represents the hydrothermal alteration zone that hosts the propylitic altered rocks having precious minerals such as gold and silver. Between these evidenced zones, we could infer the location of the geothermal reserve which has an area of 4.06 km^2. Integrating past research reports carried out by NEDO, using the Volumetric method with the calculated geothermal reserve area, and a Monte Carlo simulation, we estimated a geothermal power potential of 90 kW (22.5 kW/km^2) for 20 years. Nevertheless, this result needs to be corrected by further geoscientific investigations including inversion modelings.

Keywords: Isa region, gravity data, propylitic alteration, hot springs, gravity modeling, geothermal power assessment

©2019. Japan Geoscience Union. All Right Reserved.

©2019. Japan Geoscience Union. All Right Reserved.

Conductive and convective heat fluxes inferred from temperature profile of a borehole in Izu-Oshima volcano

*Shin'ya Onizawa[1]

1. Volcanology Research Department, Meteorological Research Institute, JMA

A 1,000 m-deep borehole was drilled at the western rim of the caldera of Izu-Oshima volcano by Earthquake Research Institute, University of Tokyo in 1998. Temperature profiles of deep borehole provide information of subsurface heat and groundwater flows, which are clues to understand structure of geothermal fluid systems in volcanic and geothermal areas. Here, conducive and convective heat fluxes of Izu-Oshima volcano are estimated by using the temperature profile data.

A wellhead altitude of the borehole is 547 m, so as that the bottom depth is 453 m bsl. The borehole penetrates main strata in this area. Above the sea level, the edifice is mainly composed of the alternation of scoria, lava and volcanic ash (“Post-caldera” and “Pre-caldera younger edifice”). Tuff breccias become dominant approximately below the sea level (“Pre-caldera older edifice”). “The basement”, which comprises altered volcanic and volcaniclastic sedimentary rocks, appears from 250 m bsl. to the well bottom (Nakada *et al.* 1999).

Groundwater level is 36 m asl. Thus, about 500 m of a thick unsaturated zone develops above the level. Characteristics of the ground temperature profile are divided at the groundwater level. In the unsaturated zone, 16-17 degC of a constant temperature continues at depths of ca. 50-350 m (ca. 500-200 m asl.). From 200 m asl. to the groundwater level, the temperature gradient gradually increases. This downward convex pattern of the temperature profile implies a strong downward flow of meteoric water infiltrating into the unsaturated volcanic edifice. At the groundwater level, the temperature is about 37 degC. Below the level, ca. 0.28 degC/m of a steep temperature gradient is observed, reaching 173.3 degC at the well bottom. The gradient is not constant but seems to be two upward convex patterns implying upward flows of groundwater.

The temperature profile in the saturated zone below the groundwater level was analyzed. The temperature gradients seem to depend on the lithology. Therefore, correction of lithology should be conducted to quantitatively extract information on the convective heat fluxes. Since a bulk density has been inferred by borehole gravimeter measurements in intervals of about 10 m, the porosity for each depth can be calculated by assuming densities of the rock without pore and water filling the pore. The bulk thermal conductivity for each depth was calculated by a relationship proposed for porous basaltic rocks by Robertson (1988).

The temperature profile data were analyzed by assuming a one-dimensional steady vertical groundwater flow. The model was applied to two depth ranges; 1) upper part of the Pre-caldera older edifice, and 2)

©2019. Japan Geoscience Union. All Right Reserved.

the basement. In the upper part of the Pre-caldera older edifice, *Pe* = 0.91 of the Péclet number was obtained, suggesting the convective heat flux is comparable to the conductive heat flux. The estimated conductive and convective heat fluxes and the Darcy velocity are 0.45 –0.56 W/m^2, 0.41 –0.51 W/m^2 and (1.42-1.78)*10^{-6} m/s, respectively. In the basement layer, as compared to the upper part of the older edifice of pre-caldera, *Pe=0.31-0.41* of smaller Péclet numbers were obtained, suggesting that the conductive heat flux is dominant. The conductive and convective heat fluxes and the Darcy velocity are 0.32 –0.39 W/m^2, 0.12 –0.13 W/m^2 and (4.71-4.98)*10^{-7} m/s, respectively.

Honda *et al.* (1979) inferred 0.2 W/m^2 of the conductive heat flux at the depth of 500-700 m (within the basement layer) at the northwestern coastal area. The estimated flux is about three times of the averaged terrestrial heat flux. The conductive heat flux within the basement layer in the caldera region inferred by this study is one and a half times to twice of the flux at the coastal area. The convective flux is added to this. When these heat fluxes are applied to 100 km^2 of the area (approximately whole the island scale), the total heat flow is estimated as to be 20-51 MW.

Keywords: Izu-Oshima volcano, temperature profile, heat flux, groundwater

©2019. Japan Geoscience Union. All Right Reserved.

Numerical model of the hydrothermal system at the Akakura Caldera in Kurikoma Area

*Yasuhiro Fujimitsu[1], Daichi Yoshioka[2]

1. Department of Earth Resources Engineering, Faculty of Engineering, Kyushu University, 2. Department of Earth Resources Engineering, Graduate School of Engineering, Kyushu University

The Akakura Caldera is located at the southern part of Kurikoma Area, and is one of the old calderas in Tohoku District. It was formed by the huge pyroclastic flow about 3 million years ago. This study conducts numerical simulations of the hydrothermal system development that is modeled after the Akakura Caldera. In the numerical modeling, the structures such as a magma chamber that was associated with the formation of the caldera structure (Magma 1), high permeable fracture zone associated with a reverse fault and a circular fracture, impermeable layers filled with quartz and fracture clouds were considered and emplacement of a magma chamber that generated the post-caldera volcanic activity of 0.8 to 1.4 Ma (Magma 2) was also included. The calculation period was 3 million years from the emplacement of Magma 1 to the present and Magma 2 was emplaced 2.2 million years after the emplacement of Magma 1. The initial temperature of Magmas 1 and 2 was set as 1000 deg C. For the size of Magma 2, two kinds of diameter (2.5 km and 3.5 km) were adopted for the modeling. As a result, it was indicated that a supercritical geothermal fluid region still remains at the depth of 5 km until about 100 thousands years after the emplacement of Magma 2. It is inferred that a high enthalpy hydrothermal system can exist at a piston-cylinder type caldera with a post-caldera volcanic activity like the Akakura Caldera until about 10 thousands years after the commencement of the post-caldera volcanic activity.

Keywords: hydrothermal system, numerical modeling, caldera

©2019. Japan Geoscience Union. All Right Reserved.

[J] Poster | S (Solid Earth Sciences)：S-VC Volcanology

Mon. May 27, 2019 5:15 PM - 6:30 PM JST | Mon. May 27, 2019 8:15 AM - 9:30 AM UTC | Poster Hall International Exhibition Hall8, Makuhari Messe_26

[S-VC39] Hydrothermal systems of volcanoes

convener:Yasuhiro Fujimitsu(Department of Earth Resources Engineering, Faculty of Engineering, Kyushu University), Wataru Kanda(Volcanic Fluid Research Center, School of Science, Tokyo Institute of Technology), Takeshi Ohba(Department of chemistry, School of Science, Tokia University)

There is a diversity of hydrothermal systems between magmas and the ground surface in various geoscientific environments. Understanding of the hydrothermal systems contributes to understanding of the earth systems, and is essential for utilization of geothermal energy and prediction of volcanic eruption. In this session, we will discuss the topics on subsurface structures and heat and fluid flows of "hydrothermal systems of volcanoes" from the perspectives of geophysics, geochemistry, geology and geothermal reservoir engineering. Any research approaches, theoretical, observational and experimental, are welcome.

[SVC39-P01] Changes in the chemistry of spring water related to the recent volcanic activity of Mt Iwo-Yama, Kirishima volcanic area

*Haruka Yamamoto[1], Yoshikazu Kikawada[2], Megumi Fukai, Wei Deng (1.Graduated school of Fuculty of Sience and Technology Sophia University, 2.Fuculty of Sience and Technology Sophia University)

[SVC39-P02] Hydrothermal circulation process related to phreatic eruption of Iwo-Yama at Kirishima volcanoes

*Keigo Mori[1], Harue Masuda[1], Tsuyoshi Shintani[1], Motoya Habuchi[1], Syuzou Furuya[1], Jun-ichiro Ishibashi[2], Takeshi Matsushima[2], Syogo Oshima[3], Reo Ikawa[4] (1.Osaka City University, 2.Kyushu University, 3.West Japan Engineering Consultants, Inc., 4.AIST)

[SVC39-P03] Determination on the stable isotopic compositions of H_2O in a volcanic plume

*Masanori Ito[1], Urumu Tsunogai[1], Koji U Takahashi[2], Fumiko Nakagawa[1] (1.Nagoya University, Graduate School of Environmental Studies, 2.Geological Survey of Japan, National Institute of Advanced Industrial Science and Technology)

[SVC39-P04] Radon measurements at Aso volcano: an experimental automatic radon station operative within the proximal zone of Nakadake

*Corrado CIGOLINI[1], Shin Yoshikawa[2], Tomo Shibata[3], Marco Laiolo[1], Diego Coppola[1] (1.Department of Earth Sciences, University of Torino, Italy, 2.Aso Volcanological Laboratory, Kyoto University, Japan, 3.Institute for Geothermal Sciences, Graduate school of Science, Kyoto University, Japan)

[SVC39-P05] Evolution of the hydrothermal system of Aso volcano during the 2014-2016 eruption period, as inferred by the ACTIVE observations

*Takuto Minami[1], Mitsuru Utsugi[2], Hisashi Utada[1], Tsuneomi Kagiyama[3] (1.Ocean Hemisphere Research Institute, Earthquake Research Institute,The University of Tokyo, 2.Aso Volcanological Laboratory, Institute for Geothremal Sciences, Graduate School of Science, Kyoto University, 3.Aso Geopark Promotion Council)

[SVC39-P06] 3-D Inversion of Magnetotelluric data from the Aluto-Langano Geothermal Field, Ethiopia

*Dejene Bekele[1], Yasuhiro FUJIMITSU[2] (1.Graduate School of Engineering, Department of Cooperative Resources Engineering, Kyushu University, 2.Faculty of Engineering, Department of Earth Resources Engineering, Kyushu University)

[SVC39-P07] Interpretation of Gravity Data to Delineate the Geothermal Reservoir Extent and Assess the Geothermal Resource in the Municipality of Isa, Southern Kyushu, Japan

*CARLOS OSMIN POCASANGRE[1], Yasuhiro Fujimitsu[1], Jun Nishijima[1] (1.Department of Earth Resources Engineering, Kyushu University)

[SVC39-P08] Conductive and convective heat fluxes inferred from temperature profile of a borehole in Izu-Oshima volcano

*Shin'ya Onizawa[1] (1.Volcanology Research Department, Meteorological Research Institute, JMA)

[SVC39-P09] Numerical model of the hydrothermal system at the Akakura Caldera in Kurikoma Area

*Yasuhiro Fujimitsu[1], Daichi Yoshioka[2] (1.Department of Earth Resources Engineering, Faculty of Engineering, Kyushu University, 2.Department of Earth Resources Engineering, Graduate School of Engineering, Kyushu University)

Changes in the chemistry of spring water related to the recent volcanic activity of Mt Iwo-Yama, Kirishima volcanic area

*Haruka Yamamoto[1], Yoshikazu Kikawada[2], Megumi Fukai, Wei Deng

1. Graduated school of Fuculty of Sience and Technology Sophia University, 2. Fuculty of Sience and Technology Sophia University

Mt Iwo-Yama is an active volcano in the Kirishima volcanic area. The west flank of the volcano is known as the Ebino Highland. The volcano erupted in April 2018 for the first time in 250 years. The vents have opened with the phreatic eruptions and then formed boiling muddy pools. In this study, we discuss the current status of the volcanic activity of Mt Iwo-Yama based on the water chemistry of muddy crater lakes and the springs in the Ebino Highland.

We collected the sample water repeatedly from the muddy crater lakes at the summit area (V1) and the west flank (V2). The former one is the vent opened on April 19th, 2018 and the latter one is that opened on April 26th, 2018. In addition, we also collected repeatedly the specific spring water located along the small stream in the Ebino Highland. We labeled the spring water as S1 to S4 in the order of distance from the summit area. The collected water samples were chemically analyzed in our laboratory.

The V1 and V2 water contain extremely high concentrations of chloride and sulfate ions. Those two are very acidic, and the pH of them sometimes show the value lower than unity. These are considered that thermal water is supplied from the geothermal reservoir directly. At this writing, although the estimated temperatures for both reservoirs of V1 and V2 by the quartz geothermometer are over 200 deg-C, the temperature for V2 is a little higher than that of V1.

The fluctuations of Cl/SO4 ratio at S1, S2 and S3 are similar to that of V2. Also, the fluctuation of the ratio at S4, which is most far from the summit among the four, seems to be similar to these with 1- month time lag. From this, it is suggested that these springs in the Ebino Highland are affected by the geothermal activity related to V2. The concentration of dissolved chemical components and water temperature at S1 changed from an increasing trend to decreasing trend in August 2018. Conversely, these at S4 are on an increasing trend since September 2018.

The volcanic activity of Mt Iwo-Yama is remained to be active. Based on the water chemistry, the temperature of the geothermal system seems to be higher in the west flank area, that is the Ebino Highland area, than the summit area. The changes in the water chemistry of the hot springs suggesting the rise of thermal activity in the Ebino Highland have been observed. Further, the new fumaroles were opened in the west flank area since autumn 2018. In conclusion, it is considered that the geothermal activity of Mt Iwo-Yama is expanding from the summit area to the west flank area. This means that the thermal activity in the Ebino Highland area will become more active, and the fumarolic area will expand to the western part of the Ebino highland.

Keywords: Kirishima Iwo-Yama

©2019. Japan Geoscience Union. All Right Reserved.

Hydrothermal circulation process related to phreatic eruption of Iwo-Yama at Kirishima volcanoes

*Keigo Mori[1], Harue Masuda[1], Tsuyoshi Shintani[1], Motoya Habuchi[1], Syuzou Furuya[1], Jun-ichiro Ishibashi[2], Takeshi Matsushima[2], Syogo Oshima[3], Reo Ikawa[4]

1. Osaka City University, 2. Kyushu University, 3. West Japan Engineering Consultants, Inc., 4. AIST

A phreatic eruption occurred on a south crater of Iwo-yama, Kirishima active volcano, on April 19, 2018, and active hydrothermal activities including fumarole and high temperature water outflow have continued until now. We analyzed major chemical compositions of waters sampled on the 12th and 13th October 2018 in order to clarify the hydrothermal systems beneath the Iwo-yama related to the phreatic eruption. Water temperature, pH, ORP, and EC were measured *in situ* using electrodes. Na^+ and K^+ were quantified using an atomic absorption spectrophotometer, and Si, As, Al^{3+}, Mn^{2+}, and Fe^{2+} were analyzed by ICP-MS. Ca^{2+} and Mg^{2+} were quantified by EDTA titration, while those of some samples by ICP-MS. Alkalinity was analyzed by neutralization titration. F^-, Cl^-, Br^-, NO_3^-, PO_4^{3-} and SO_4^{2-} were analyzed by ion chromatography. Hydrogen and oxygen isotope ratios of waters were analyzed by cavity ring down spectrophotometry.
The temperature and pH of erupting hot waters in the south and west craters were 70~ 97 ℃ and 1.3 ~ 2.1, respectively. The temperature and pH of low temperature springs in the northeastern wetland out of the craters were about 20 ℃ and 2.2 ~ 5.2. Cl^- and SO_4^{2-} concentrations ranged within 1000 ~ 8000 ppm and 2,000 to 10,000 ppm for hot waters and 3 ~ 300 ppm and 10 to 1100 ppm for low temperature spring waters. Positively linear relationship indicated the same origin of between concentrations of Cl^- and SO_4^{2-}. The d^2H and $d^{18}O$ of the highest Cl^- and SO_4^{2-} concentrated water were -18 ‰and -4.0 ‰, indicating high contribution of magmatic water. Strongly acidic water was formed by oxidation of magmatic components due to mixing of meteoric water in the groundwater aquifer. The all analyzed waters can be explained simple mixing of the above high temperature water with local meteoric water. It is notable that up to about 3000 ppb As was confirmed in the hot water.
The silica geothermometer indicated the highest temperature of 262 ˚C for the hot water containing the highest Cl^- concentration, suggesting the aquifer temperature is higher than that. The formation of high temperature water in the groundwater aquifer must be related to the phreatic eruption.

Keywords: geothermometer, hydrogen and oxygen isotope

©2019. Japan Geoscience Union. All Right Reserved.

Determination on the stable isotopic compositions of H_2O in a volcanic plume

*Masanori Ito[1], Urumu Tsunogai[1], Koji U Takahashi[2], Fumiko Nakagawa[1]

1. Nagoya University, Graduate School of Environmental Studies, 2. Geological Survey of Japan, National Institute of Advanced Industrial Science and Technology

The fumarolic H_2O occupied more than 80% of volatiles ejected from volcanic fumaroles (volcanic gases). The origin of fumarolic H_2O is either magma (magmatic water) or groundwater (meteoric water). Because of the significant differences in the isotopic ratios (δ D and δ^{18}O) of H_2O between magmatic water and meteoric water, we can differentiate the origins of fumarolic H_2O (magmatic water or meteoric water), if we can determine the isotopic ratios of fumarolic H_2O from those in volcanic plumes during a volcanic eruption. This is extremely useful for us to differentiate the mechanism of each volcanic eruption, magmatic eruption or phreatic eruption.
In this study, we determined the isotopic ratios of H_2O in a volcanic plume that had been ejected from accessible fumaroles to confirm whether the isotopic ratios (δ D and δ^{18}O) estimated from plume H_2O is consistent with those of fumarolic H_2O or not.
The samples were taken in Hakone volcano from 2014 to 2018. We collected around 20 volcanic plume samples into pre-evacuated glass bottle (ca. 1000 ml) during each sampling, while changing the distances from the fumarole. Besides, we also collected the fumarolic H_2O through condensation using a cold trap. The isotopic ratios (δ D and δ^{18}O) of plume H_2O showed strong linear correlation (R^2 = 0.9 or more) with the reciprocal of H_2O concentration. The isotopic ratios (δ D and δ^{18}O) estimated as the intercept of the linear correlation found in the plume H_2O was consistent with fumarolic H_2O. We concluded that we can estimate the stable isotopic ratios of fumarolic H_2O remotely using those in plume H_2O.
This study was supported by MEXT Scientific Research Program grants “Integrated Program for Next Generation Volcano Research and Human Resource Development”.

Keywords: Volcanic gases, Stable isotopic compositions, Cavity Ring-Down Sectroscopy

©2019. Japan Geoscience Union. All Right Reserved.

Radon measurements at Aso volcano: an experimental automatic radon station operative within the proximal zone of Nakadake

*Corrado CIGOLINI[1], Shin Yoshikawa[2], Tomo Shibata[3], Marco Laiolo[1], Diego Coppola[1]

1. Department of Earth Sciences, University of Torino, Italy, 2. Aso Volcanological Laboratory, Kyoto University, Japan, 3. Institute for Geothermal Sciences, Graduate school of Science, Kyoto University, Japan

Radon measurements at Aso Volcano first started on May 2015 and persisted until January 2016. They were resumed on August 2017 and they are currently on-going. Radon data have been collected by means of an in-soil automatic station located at about 1.06 km from the active crater (crater 1) together with soil temperatures (measured at the sampling site and 1 m below) and local atmospheric parameters (JMA).
During earlier measurements Aso volcano was affected by a sporadic explosive activity, which marked the ceasing of a Strombolian phase, and was followed by moderate phreatomagmatic events. Radon measurements been compared with ground-based and satellite thermal data, the latter collected by the MIROVA system. Radon concentrations were fluctuating from 300 to about 1100 Bq/m^3 during May-July 2015, and they reached a minimum two weeks before the strong degassing that occurred at the beginning of August. On August 8, 2015 the Volcanic Radiative Power (VRP) detected by MIROVA was slightly below 1 MW. Since then there has been an increasing trend in Radon emissions (up to about 900 Bq/m^3) that preceded the strong phreatic explosion of September 14. By the end of September, a new increasing trend reached a relative maximum (up to 1900 Bq/m^3) one week before the explosion of the 23 of October 2015. Then, radon data persistently fluctuated well above 900 Bq/m^3. This time span was accompanied by a general decrease of the detected thermal anomalies which were nearly coeval with the replenishment of the crater lake.
During 2017 radon emissions reached their relative maxima (up to 1380 Bq/m3) during fall-winter, whereas in 2018 the higher peak reaches 1450 Bq/m3 during the early fall (October 3). Several peaks seems to be correlated with the thermal gradient at the measurement site. However, some other peaks appear somehow coeval with some thermal anomalies in the crater area detected by the MIROVA system. Among these the one that occurred on May 15 that touched 1250 Bq/m3 and preceded the drastic increase in temperature of the South wall (up to 715 ˚C, according to JMA data). Two other minor anomalous peaks were recorded on June 13 and July 29, both were well above 800 Bq/m3. A systematic analysis of all radon data shows that radon emissions, in absence of anomalous spikes, are inversely correlated with soil temperatures and that the contribution of atmospheric pressure marginally affect radon emissions. The spectrum of the radon signal shows the existence of both diurnal and semidiurnal peaks, typically observed during continuous radon measurements. Future work should be concentrated in the attempt to better correlate radon emissions with the changes in volcanic activity, including the effects of environmental parameters on the radon signal.

Keywords: Radon , radon signal, radon anomalies/peaks, environmental parameters

©2019. Japan Geoscience Union. All Right Reserved.

Evolution of the hydrothermal system of Aso volcano during the 2014-2016 eruption period, as inferred by the ACTIVE observations

*Takuto Minami[1], Mitsuru Utsugi[2], Hisashi Utada[1], Tsuneomi Kagiyama[3]

1. Ocean Hemisphere Research Institute, Earthquake Research Institute,The University of Tokyo, 2. Aso Volcanological Laboratory, Institute for Geothremal Sciences, Graduate School of Science, Kyoto University, 3. Aso Geopark Promotion Council

Electrical resistivity structures provide important information about hydrothermal systems of volcanos. Previous studies using the magnetotelluric method have revealed shallow resistivity structures associated with conductive cap rocks underlain by hydrothermal reservoirs (e.g. Nurhasan et al. 2006). However, evolution of such a hydrothermal system over volcanic eruptions has never been understood in detail.

We have intermittently conducted observations of an electromagnetic volcano monitoring system, ACTIVE (Utada et al. 2007), in Aso volcano for about half a decade. ACTIVE system consists of transmitter dipoles for controlled-source electric currents and an array of induction-coil receivers for measuring the vertical component of the induced magnetic field dependent on the subsurface resistivity structure. ACTIVE system in Aso volcano recently succeeded in detecting temporal variation in the resistivity structure over the magmatic eruptions that started in November 2014 and ceased in May 2015 (hereafter referred to as the magmatic eruption period (MEP)). In our previous study, three-dimensional inversions for the two sets of ACTIVE responses obtained in August 2014 and August 2015 revealed (1) a broad increase in resistivity ~400 m below the bottom of the first Nakadake crater and (2) a decrease in resistivity ~100 m beneath the western rim of the crater (Minami et al. 2018). Both changes in resistivity presumably originated before MEP because the corresponding variation in the ACTIVE response happened mainly between the two observation campaigns in August 2014 and just after the starting of MEP, say, on November 26, 2015. The decrease of resistivity at shallow level implies presence of a temporal fluid reservoir which appeared prior to MEP and possibly contributed to the phreatomagmatic eruptions in September 2015 and October 2016. We are now analyzing the ACTIVE responses after MEP to resolve evolution of the hydrothermal system of Aso volcano over the active period spanning from November 2014 to October 2016.

In the presentation, we comprehensively discuss evolution of the hydrothermal system of Aso volcano from August 2014 to August 2017, including MEP from August 2014 to May 2015 and the two phreatomagmatic eruption events in September 2015 and in October 2016, by using ACTIVE data sets.

Keywords: Aso, volcano, ACTIVE, resistivity, temporal variation

©2019. Japan Geoscience Union. All Right Reserved.

3-D Inversion of Magnetotelluric data from the Aluto-Langano Geothermal Field, Ethiopia

*Dejene Bekele[1], Yasuhiro FUJIMITSU[2]

1. Graduate School of Engineering, Department of Cooperative Resources Engineering, Kyushu University, 2. Faculty of Engineering, Department of Earth Resources Engineering, Kyushu University

The Main Ethiopian rift valley hosts a number of geothermal prospected area, which is known to be actively deforming with reoccurring periods of uplift and setting. One of the regions where the prospected area is confirmed by drilling is the Aluto-Langano geothermal area. Aluto area is situated in the Main Ethiopian rift valley system bounded by latitude 7.60˚-7.96˚ N and longitude 38.68˚-38.92˚ E. This field has been studied by the Geological Survey of Ethiopia (GSE) since1980s, and these studies subsequently led to the drilling of 10 exploration wells. This field is currently developed with a Binary power plant of a 7.2 MWe installed capacity. From the results of various regional geoscientific studies in this part of the Ethiopian rift, the area of Aluto-Langano geothermal field was observed to have relatively higher exploitable geothermal potential in Ethiopia. However, more studies are required in order to obtain more information about the subsurface structure and heat source below the Aluto volcanic complex (AVC) and to delineate the parameters of the geothermal reservoir in the area. To address this, Electro Consultant (ELC) and GSE carried out magnetotelluric surveys in the Aluto-Langano geothermal field in 2009 and 2015 respectively. This study combines the two surveys done covering the whole Aluto volcanic complex with a total of 166 MT stations. The MT data was processed and used in the construction of a 3-D MT inversion model, which was then interpreted alongside the available geological information. The dimensionality analysis of MT data was carried out based on the strike and dimensions of the resistivity distribution around the MT sites, by plotting the Phase tensor for each MT site for the frequency range of 10^{4} -10^{-3} Hz. Most of the maps of phase tensor exhibit 3-D structures, hence need for 3-D inversion. In order to get 3-D conductivity models of the subsurface, the MT data were inverted in the period range of 10^{-3}–10^{4}s at uniform distributed discrete periods using the ModEM code. The resultant 3-D resistivity model shows a highly conductive zone with a diameter of around 10 km in the center of the Aluto volcanic complex at depths between 800–2500 m. The identified resistivity distribution corresponds very well to the conceptual reservoir model of a high-enthalpy geothermal system with its mushroom shaped zoning comprising a resistive up-flow zone overlain by a conductive clay cap. From well data analysis it is known that the conductive cap at Aluto is related to rock units and therefore, eliciting the origin of the heat source and delineating the subsurface structure in the study area. The 3-D resistivity model images the resistivity structure in the study area hence showing the origin of Aluto heat sources and delineating the location of faults and fracture system. In particular, the cap rock zones of the geothermal reservoir system by studying low resistivity zones at relatively shallow depths are important in selecting future drilling targets.

Keywords: Aluto-Langano, 3-D Inversion, Magnetetolluric, Ethiopia

©2019. Japan Geoscience Union. All Right Reserved.

Interpretation of Gravity Data to Delineate the Geothermal Reservoir Extent and Assess the Geothermal Resource in the Municipality of Isa, Southern Kyushu, Japan

*CARLOS OSMIN POCASANGRE[1], Yasuhiro Fujimitsu[1], Jun Nishijima[1]

1. Department of Earth Resources Engineering, Kyushu University

The municipality of Isa is located in the southern part of Kyushu Island, and it is considered one of the wealthiest places in Japan because one of the most important gold mines is found in this area, Hishikari mine. Additionally, there are many hydrothermal manifestations, e.g., Hishikari, Yunoo, Kawanami, and Kintaro hot springs, which can be exploited by the community as an electric power source. Until now, the geothermal resource has not been used for power generation purpose although Geological Survey of Japan had carried out some preliminary geothermal assessments, which show that the power potential density is between 10 and 20 kW/km^2. To calibrate the previous value, first, this study attempts to analyze and interpret the gravity data for delineating the geothermal reservoir boundary and the assessment of geothermal resource. Accordingly, the corresponding researchers conducted 2-D and 3-D gravity modeling in the current research. This modeling is an essential stage of the complete gravity analysis in the region, because the filtering gravity methods, i.e., Horizontal-Derivative and Tilt-Derivative, can quickly detect steep gradients and indicate the location of faults or geological boundaries, however, they cannot estimate geological structure depth and shape. For this purpose, an area of 10 x 10 km was selected and analyzed considering a Bouguer Density of 2.45 g/cm^3. The Bouguer Anomaly result shows a high value at the center, which extends 5.61 km^2 wide and could represent the probable geothermal resource. According to the Kagoshima geological map, volcanic and sedimentary rocks are the dominant type of rocks in this area. Cretaceous Shimanto group controls the fundamental structure of the deepest element. This arrangement is typically composed of sandstone, shale, acidic tuff with subordinate conglomerates, and their alterations, also Pliocene volcanic rocks and alluvial deposits. Similarly, Kakuto and Okuchi Basin, which are located at east and west respectively, control the region. The 2-D gravity modeling was carried out requiring a density contrast between the two assumed layers, i.e., the basement and the low-density deposit, and thus a value of 0.4 g/cm^3 was assigned. Likewise, the horizontal size of the cells was set at 100 m. The profile trending NW- SE shows a significant depression 400 m to 700 m deep located next to Hishikari hot spring. In this way, the hydrothermal fluids might be flowing up to the surface forming altered rocks and hot springs by using a possible geological fault. For a better understanding of the region, the authors also carried out 3-D gravity modeling. The result shows an area which has density values below 2.4 g/cm^3 and the zone NE-SW direction that starts at the Uonogoe area and ends at the Yamada area. Besides, a large anomaly located in the central area that has density values above 2.5 g/cm^3 is evident. This anomaly represents the hydrothermal alteration zone that hosts the propylitic altered rocks having precious minerals such as gold and silver. Between these evidenced zones, we could infer the location of the geothermal reserve which has an area of 4.06 km^2. Integrating past research reports carried out by NEDO, using the Volumetric method with the calculated geothermal reserve area, and a Monte Carlo simulation, we estimated a geothermal power potential of 90 kW (22.5 kW/km^2) for 20 years. Nevertheless, this result needs to be corrected by further geoscientific investigations including inversion modelings.

Keywords: Isa region, gravity data, propylitic alteration, hot springs, gravity modeling, geothermal power assessment

©2019. Japan Geoscience Union. All Right Reserved.

©2019. Japan Geoscience Union. All Right Reserved.

Conductive and convective heat fluxes inferred from temperature profile of a borehole in Izu-Oshima volcano

*Shin'ya Onizawa[1]

1. Volcanology Research Department, Meteorological Research Institute, JMA

A 1,000 m-deep borehole was drilled at the western rim of the caldera of Izu-Oshima volcano by Earthquake Research Institute, University of Tokyo in 1998. Temperature profiles of deep borehole provide information of subsurface heat and groundwater flows, which are clues to understand structure of geothermal fluid systems in volcanic and geothermal areas. Here, conducive and convective heat fluxes of Izu-Oshima volcano are estimated by using the temperature profile data.

A wellhead altitude of the borehole is 547 m, so as that the bottom depth is 453 m bsl. The borehole penetrates main strata in this area. Above the sea level, the edifice is mainly composed of the alternation of scoria, lava and volcanic ash (“Post-caldera” and “Pre-caldera younger edifice”). Tuff breccias become dominant approximately below the sea level (“Pre-caldera older edifice”). “The basement”, which comprises altered volcanic and volcaniclastic sedimentary rocks, appears from 250 m bsl. to the well bottom (Nakada *et al.* 1999).

Groundwater level is 36 m asl. Thus, about 500 m of a thick unsaturated zone develops above the level. Characteristics of the ground temperature profile are divided at the groundwater level. In the unsaturated zone, 16-17 degC of a constant temperature continues at depths of ca. 50-350 m (ca. 500-200 m asl.). From 200 m asl. to the groundwater level, the temperature gradient gradually increases. This downward convex pattern of the temperature profile implies a strong downward flow of meteoric water infiltrating into the unsaturated volcanic edifice. At the groundwater level, the temperature is about 37 degC. Below the level, ca. 0.28 degC/m of a steep temperature gradient is observed, reaching 173.3 degC at the well bottom. The gradient is not constant but seems to be two upward convex patterns implying upward flows of groundwater.

The temperature profile in the saturated zone below the groundwater level was analyzed. The temperature gradients seem to depend on the lithology. Therefore, correction of lithology should be conducted to quantitatively extract information on the convective heat fluxes. Since a bulk density has been inferred by borehole gravimeter measurements in intervals of about 10 m, the porosity for each depth can be calculated by assuming densities of the rock without pore and water filling the pore. The bulk thermal conductivity for each depth was calculated by a relationship proposed for porous basaltic rocks by Robertson (1988).

The temperature profile data were analyzed by assuming a one-dimensional steady vertical groundwater flow. The model was applied to two depth ranges; 1) upper part of the Pre-caldera older edifice, and 2)

©2019. Japan Geoscience Union. All Right Reserved.

the basement. In the upper part of the Pre-caldera older edifice, *Pe* = 0.91 of the Péclet number was obtained, suggesting the convective heat flux is comparable to the conductive heat flux. The estimated conductive and convective heat fluxes and the Darcy velocity are 0.45 –0.56 W/m^2, 0.41 –0.51 W/m^2 and (1.42-1.78)*10^{-6} m/s, respectively. In the basement layer, as compared to the upper part of the older edifice of pre-caldera, *Pe=0.31-0.41* of smaller Péclet numbers were obtained, suggesting that the conductive heat flux is dominant. The conductive and convective heat fluxes and the Darcy velocity are 0.32 –0.39 W/m^2, 0.12 –0.13 W/m^2 and (4.71-4.98)*10^{-7} m/s, respectively.

Honda *et al.* (1979) inferred 0.2 W/m^2 of the conductive heat flux at the depth of 500-700 m (within the basement layer) at the northwestern coastal area. The estimated flux is about three times of the averaged terrestrial heat flux. The conductive heat flux within the basement layer in the caldera region inferred by this study is one and a half times to twice of the flux at the coastal area. The convective flux is added to this. When these heat fluxes are applied to 100 km^2 of the area (approximately whole the island scale), the total heat flow is estimated as to be 20-51 MW.

Keywords: Izu-Oshima volcano, temperature profile, heat flux, groundwater

©2019. Japan Geoscience Union. All Right Reserved.

Numerical model of the hydrothermal system at the Akakura Caldera in Kurikoma Area

*Yasuhiro Fujimitsu[1], Daichi Yoshioka[2]

1. Department of Earth Resources Engineering, Faculty of Engineering, Kyushu University, 2. Department of Earth Resources Engineering, Graduate School of Engineering, Kyushu University

The Akakura Caldera is located at the southern part of Kurikoma Area, and is one of the old calderas in Tohoku District. It was formed by the huge pyroclastic flow about 3 million years ago. This study conducts numerical simulations of the hydrothermal system development that is modeled after the Akakura Caldera. In the numerical modeling, the structures such as a magma chamber that was associated with the formation of the caldera structure (Magma 1), high permeable fracture zone associated with a reverse fault and a circular fracture, impermeable layers filled with quartz and fracture clouds were considered and emplacement of a magma chamber that generated the post-caldera volcanic activity of 0.8 to 1.4 Ma (Magma 2) was also included. The calculation period was 3 million years from the emplacement of Magma 1 to the present and Magma 2 was emplaced 2.2 million years after the emplacement of Magma 1. The initial temperature of Magmas 1 and 2 was set as 1000 deg C. For the size of Magma 2, two kinds of diameter (2.5 km and 3.5 km) were adopted for the modeling. As a result, it was indicated that a supercritical geothermal fluid region still remains at the depth of 5 km until about 100 thousands years after the emplacement of Magma 2. It is inferred that a high enthalpy hydrothermal system can exist at a piston-cylinder type caldera with a post-caldera volcanic activity like the Akakura Caldera until about 10 thousands years after the commencement of the post-caldera volcanic activity.

Keywords: hydrothermal system, numerical modeling, caldera

©2019. Japan Geoscience Union. All Right Reserved.

[J] Oral | S (Solid Earth Sciences)：S-TT Technology & Techniques

Mon. May 27, 2019 10:45 AM - 12:15 PM JST | Mon. May 27, 2019 1:45 AM - 3:15 AM UTC | 303 3F

[S-TT45] Synthetic Aperture Radar

convener:Youhei Kinoshita(University of Tsukuba), Yu Morishita(Geospatial Information Authority of Japan), Shoko Kobayashi(Tamagawa University), Takahiro Abe(Earth Observation Research Center, Japan Aerospace Exploration Agency), Chairperson:Shoko Kobayashi(Tamagawa University), Kazuya Ishitsuka(Kyoto University)

ALOS-2 and Sentinel-1A and 1B, which have highly enhanced capacity compared to previous SAR satellites, were launched in 2014, and their utilization has been widely expanding as the data has accumulated for approximately four years. Other long-operating SAR satellites like TerraSAR-X and Cosmo-SkyMed also contribute to expanding the SAR utilization. Now we are facing a new and abundant era of the satellite SAR, along with a worldwide trend to an open and free data policy of satellite data, with next-generation advanced SAR satellite plans by several countries, and with several plans to construct SAR constellations by private sectors. In addition, SAR technologies with other platforms, such as ground-based SAR with high temporal resolution and UAV (Unmanned Aerial Vehicle) SAR with flexible operability, have also been developed and used for various targets. These facts indicate that the SAR utilization has become widespread in both basic researches (e.g., earth science) and diverse applications (e.g., disaster prevention and forest monitoring). In this session, we would like to widely invite research and application results with regard to SAR, sharing our knowledge and having a discussion for the advancement of the SAR utilization.

10:45 AM - 11:00 AM JST | 1:45 AM - 2:00 AM UTC

[STT45-01] Extraction of ground changes near the crater by the eruption of Kilauea volcano.

*Fujiyama Kaho[1], Masanobu Shimada[1], Yuki Kimoto[1], Kenta Yoshioka[1] (1.TokyoDenki University)

11:00 AM - 11:15 AM JST | 2:00 AM - 2:15 AM UTC

[STT45-02] ALOS-2 observation of the 2017 Sefidsang earthquake, northeastern Iran: a blind shallow-dipping thrust event near the Eastern Kopeh Dagh

*Nematollah Ghayournajarkar[1], Yo Fukushima[2] (1.Graduate School of Science, Tohoku University, 2.International Research Institute of Disaster Science, Tohoku University)

11:15 AM - 11:30 AM JST | 2:15 AM - 2:30 AM UTC

[STT45-03] **InSAR ground displacements and slip distribution associated with secondary fault slips of the 2016 Kumamoto earthquake**

*Yo Fukushima[1], Daisuke Ishimura[2] (1.International Research Institute of Disaster Science, Tohoku University, 2.Department of Geology, Tokyo Metropolitan University)

11:30 AM - 11:45 AM JST | 2:30 AM - 2:45 AM UTC

[STT45-04] Surface displacements at the Kumamoto plain using persistent scatterer interferometry and comparison with groundwater levels

*Kazuya Ishitsuka[1], Takeshi Tsuji[2] (1.Kyoto Univ., 2.Kyushu Univ.)

11:45 AM - 12:00 PM JST | 2:45 AM - 3:00 AM UTC

[STT45-05] Forest fire detection in the low biomass dry forest with JICA-JAXA Forest Early Warning System in the Tropics (JJ-FAST).

*Manabu Watanabe[1], Christian Naohide koyama[1], Masato Hayashi[2], Izumi Nagatani[2], Takeo Tadono[2], Masanobu Shimada[1,2] (1.School of Science and Engineering, Tokyo denki university, 2.JAXA/EORC)

12:00 PM - 12:15 PM JST | 3:00 AM - 3:15 AM UTC

[STT45-06] Nominal operation results of Japanese ALOS-2

★Invited Papers

*Shinichi Sobue[1] (1.Japan Aerospace Exploration Agency)

Extraction of ground changes near the crater by the eruption of Kilauea volcano.

*Fujiyama Kaho[1], Masanobu Shimada[1], Yuki Kimoto[1], Kenta Yoshioka[1]

1. TokyoDenki University

Synthetic Aperture Radar, SAR, is a sensor that irradiates radio waves (microwaves) and receives radio waves reflected and returned from the ground surface.

It is characterized that SAR can observe the target regardless of weather and day and night. Even when the plume is blowing hard, SAR signal can penetrate through the clouds and smokes and can observe the crater.

The Kilauea volcano to be investigated is one of the five shield volcanoes that made up the Island of Hawaii on Hawaii Island. It is an active volcano that is presumed to have formed about 600,000 years ago, and is presumed that it appeared on the sea surface about 100 thousand years ago and the eruption is still continuing, but the eruption of 2018 stopped the flow of the lava did. The Kilauea is known for its calm eruption, but since 1983 it continues to erupt almost continuously, depending on the direction of the lava flow, lava may swallow the settlement and destroy the settlement.

This research will detect the deformation of the volcanic mountain by using the interferometric SAR technique. INSAR uses two types of data with different times and finds variates from the differential distance between from the satellite to the target (phase difference).

Using this method, we measure the crustal deformation with accuracy of several mm to several cm by capturing the variation near the crater of Kilauea volcano which can not be investigated locally. We will quantitatively evaluate the crustal deformation around the crater using image data of two periods including the eruption occurrence period from October 9, 2014 to July 31, 2018.

As a result, the crater was subsided by 6.5 cm from November 25, 2014 to March 27, 2018 in the ascending orbit, and it was subsided by 9 cm during the period from October 9, 2014 to December 14, 2017 in descending orbit.

As a future task, since we observed fluctuations in the north direction other than vertical component fluctuations in the crater, we plan to conduct research including the relation with the ground characteristics of Hawaii Island.

Keywords: INSAR

©2019. Japan Geoscience Union. All Right Reserved.

ALOS-2 observation of the 2017 Sefidsang earthquake, northeastern Iran: a blind shallow-dipping thrust event near the Eastern Kopeh Dagh

*Nematollah Ghayournajarkar[1], Yo Fukushima[2]

1. Graduate School of Science, Tohoku University, 2. International Research Institute of Disaster Science, Tohoku University

The Iranian plateau is deformed between the converging Arabian and Eurasian plates. Their convergence is principally taken up by the active Makran subduction zone to the South, in addition to shortening and strike-slip faulting accommodated by crustal structures, which are non-uniformly distributed in several continental deformation domains such as the Zagros, Alborz and Kopeh Dagh mountain ranges. During the last decade, several studies carried out in the Zagros, Alborz and central Iran have produced a better understanding of active deformation in these zones. Conversely, such detailed studies are less common in northeast Iran.
Indeed, despite all the efforts made by previous workers to shed light on active tectonics in northeast Iran, this region still suffers from a lack of detailed structural and kinematics data and should be considered as a concealed segment in the geodynamic puzzle of the Arabia-Eurasia collision. This matter is made worse by the facts that northeast Iran is the second populated region and one of the most seismically active deformation domains in the country that has experienced at least nine large earthquakes (M >= 7) during the last six centuries (Tchalenko, 1975; Ambraseys and Melville, 1982; Berberian and Yeats, 1999, 2001).
On 5 April 2017, an Mw 6.1 earthquake occurred in the northeastern region of Iran, about 90 km southeast of the city of Mashhad, the second most populous city in Iran with a population of over 3 million people. The epicenter (35.776 N, 60.436 E, USGS) was at a remote mountainous area, about 30 km northeast of the Sefidsang district where approximately 5000 people live, and the depth was about 13 km. This earthquake raised an opportunity to study the deformation pattern in the SE of the Kopeh Dagh Mountains.
Space geodetic observations of ground deformation provide important data to investigate the seismogenic fault and the subsurface deformation mechanics. Here we used ALOS-2 synthetic aperture radar data to produce SAR interferograms using the GMTSAR software (Sandwell et al., 2010) to investigate coseismic and postseismic deformation associated with the 2017 Sefidsang earthquake. The ascending and descending interferograms were produced and both indicate thrust-dominated slip that is consistent with seismic data sets, with the maximum line-of-sight coseismic displacement of 9.9 and 13 cm, respectively. The obtained coseismic deformation maps have good consistency with Sentinel-1 interferograms that showed maximum line-of-sight displacement of 10.5 and 13.7 cm for ascending and descending interferograms, respectively (Xu et al., 2018).
We also used ascending SAR data acquired on 2017/06/24 to 2018/12/22 for evaluating the postseismic deformation caused by this earthquake. The produced interferogram does not show any displacement more than the noise level (~1 cm).

Keywords: InSAR, Northeastern Iran, Kopeh Dagh, Sefidsang earthquake

©2019. Japan Geoscience Union. All Right Reserved.

InSAR ground displacements and slip distribution associated with secondary fault slips of the 2016 Kumamoto earthquake

*Yo Fukushima[1], Daisuke Ishimura[2]

1. International Research Institute of Disaster Science, Tohoku University, 2. Department of Geology, Tokyo Metropolitan University

By using interferometric synthetic aperture radar (InSAR) and field reconnaissance surveys, activation of numerous secondary faults associated with the occurrence of the 2016 Kumamoto earthquake has been identified (e.g., Fujiwara et al., 2016, EPS). In this study, we investigated the characteristics of the displacements of secondary faults around the Miyaji district, Aso, within the Aso caldera, and further inverted for the slip distribution of the secondary faults.

In this study, we used RINC software (Ozawa et al., 2016, EPS) to produce three interferograms with different line-of-sight directions, and unwrapped with SNAPHU (Chen and Zebker, 2000). The unwrapped interferograms are “un-referenced”, and each of them contains an unknown offset. The offset values were estimated using the daily coordinates data (F3 solution) of the GEONET network provided by the Geospatial Information Authority of Japan, and are subtracted from the interferograms. Finally, displacements along three line-of-sight directions are decomposed into EW, NS, and UD components, and EW and NS components were further used to derive the horizontal displacements in N50E direction, parallel to the secondary faults in Miyaji. The main characteristics of the ground displacements are as follows. (1) Two strands of parallel displacement discontinuity traces, corresponding to the surface fault, are observed, with a separation of around 0.8 km. (2) The length of the northern and southern strands of traces are around 1.3 km and 2.3 km. (3) Each of the two strands of traces are composed of multiple en-echelon traces. (4) The fault displacements of the northern strand were up to 5 cm for both vertical (northern side downward) and right-lateral directions. (5) The fault displacements of the southern strand were up to 8cm for vertical (northern side downward) and 10cm for right-lateral directions.

Next, we simultaneously estimated the slip distribution and geometry of the two faults (Fukushima et al., 2013, 2018), after removing long wavelength displacements by polynomial fitting. As for the fault geometry, we assumed that the top of the faults reach the averaged location of the fault strands and we set the dip angles as model parameters. We conducted non-negative least squares inversion for the fault slip, prohibiting reverse and left-lateral faulting based on the observed ground displacements. Two types of inversions were made on the assumption of the rake angle; one is assuming a uniform rake angle for all the fault elements, and the other is solving for the vertical and left-lateral slips. The two types of inversions both succeeded in explaining the ground displacement data, so we adopted the result of the simpler model with uniform rake angle as our preferred model.

In our preferred model, two faults dip northward with the southern one having a lower angle (48 degrees) than the northern one (67 degrees), making two faults merge at a depth of approximately 1.3 km. The lower limit of the slip area on the southern fault coincided the merging depth of 1.3 km, and the maximum slip of 25 cm was obtained at a depth of approximately 0.7 km. The slip on the northern fault was limited to shallower than 0.4 km with smaller slips of up to 12 cm.

Acknowledgements
This study used the PALSAR-2 data shared among PIXEL (PALSAR Interferometry Consortium to Study out

©2019. Japan Geoscience Union. All Right Reserved.

Evolving Land surface), originally provided from Japan Aerospace Exploration Agency (JAXA) through a joint research contract with the Earthquake Research Institute (ERI) of the University of Tokyo. A part of this study was conducted under a special joint research project of ERI. We are grateful to Dr. Taku Ozawa for the RINC software, and to the Geospatial Information Authority of Japan for letting us use the daily coordinates (F3 solution) derived from the GEONET network.

Keywords: Synthetic Aperture Radar Interferometry, Kumamoto Earthquake, Secondary Fault

©2019. Japan Geoscience Union. All Right Reserved.

Surface displacements at the Kumamoto plain using persistent scatterer interferometry and comparison with groundwater levels

*Kazuya Ishitsuka[1], Takeshi Tsuji[2]

1. Kyoto Univ., 2. Kyushu Univ.

After the 2016 Kumamoto earthquake, change in groundwater levels has been observed at the Kumamoto plain, which is likely associated with the alteration of the aquifer system by the earthquake. Surface displacement can occur due to groundwater level changes at a confined aquifer because pore pressure changes lead to the deformation of its granular skeleton. Persistent scatterer interferometry (PSI) using a satellite imaging is a powerful method to estimate spatial and temporal pattern of surface displacements. In this study, we estimated surface displacement at the Kumamoto plain from May 2016 to June 2017 using PSI analysis of ALOS-2/PALSAR-2 images. Moreover, we compared the displacement pattern in the period after the earthquake with the displacement from Jan. 2007 to Jan. 2011 using ALOS/PALSAR images.

As a result of analysis, we estimated surface displacement with the magnitude of about 2-3 cm along the Futagawa and Hinagu fault systems. We interpreted that the displacements along the fault traces were due to the afterslip. On the other hand, we also found surface displacements apart from the fault traces. For example, surface uplift up to 4 cm/year was observed during about 1 year after the earthquake around the west flank of Aso volcano. The displacement began several months after the earthquake, and generally correlated with the areas of groundwater level increased. Since the displacement pattern was not observed in ALOS/PALSAR results, we speculated that the displacement was induced by the groundwater level changes by the earthquake. In addition, we estimated the skeletal storage coefficients from surface displacements and groundwater levels, and found that the coefficients differed by the earthquake at several locations, indicating the temporal alteration of permeability or compressibility of the aquifer. Our results demonstrate the effectiveness of the surface displacement monitoring combined with groundwater level data at the aquifer system.

Acknowledgements: The ALOS-2/PALSAR-2 level 1.1 data used in this study were provided by the PIXEL (PALSAR Interferometry Consortium to Study our Evolving Land Surface) group in cooperative research with the Earthquake Research Institute, University of Tokyo. The ALOS-2/PALSAR-2 data belongs to the Japan Aerospace Exploration Agency. The groundwater level data used in this study were measured by several public institutes, and the data were corrected by the working group in Japan Association of Groundwater Hydrology.

Keywords: Surface displacement, the Kumamoto plain, change in groundwater levels

©2019. Japan Geoscience Union. All Right Reserved.

Forest fire detection in the low biomass dry forest with JICA-JAXA Forest Early Warning System in the Tropics (JJ-FAST).

*Manabu Watanabe[1], Christian Naohide koyama[1], Masato Hayashi[2], Izumi Nagatani[2], Takeo Tadono[2], Masanobu Shimada[1,2]

1. School of Science and Engineering, Tokyo denki university, 2. JAXA/EORC

JICA-JAXA Forest Early Warning System in the Tropics (JJ-FAST, [1]) is first and only one SAR-based deforestation detection system monitoring tropical forest globally. The JJ-FAST started from November 2016, and has a merit to operate not only in dry season, but also in rainy season. The current system uses change of gamma_0 for deforestation detection. Watanabe et al. [2] pointed out the JJ-FAST detected not only the deforestation sites, but also detected severely damaged forest fire sites occurred in a dense forest. In this paper, detectability of forest fire in the low biomass dry forest with JJ-FAST system were examined.

JJ-FAST detected 168 deforestation sites between Nov. 11 and Dec. 23, 2018 in South Africa. MODIS burned area product [3] obtained between Oct. 10 and Dec. 31, 2018 were overlapped and confirmed that the almost all the polygons detected by the JJ-FAST deforestation detection algorithm were overlapped with the burned area detected by MODIS. The forest fire area were also identified by Sentinel-2 data. BBC news [4] reported severe wildfire occurred in George, South Africa on Oct. 30, and the area was also coincident with the one detected by the JJ-FAST algorithm. The JJ-FAST algorithm also detected 82 deforestation sites in Mozambique between Aug. 13 and Nov. 5, 2018. These sites were also overlapped with the MODIS burned area. From these facts, we concluded that the current JJ-FAST deforestation detection algorithm could detected severely damaged forest fire area in the low biomass dry forest. It is known that forest fire in dense forest is detected by increase of radar backscattering in HH polarization [2]. This is explained that forest fire makes forest canopy dry and induces more double bounce scattering, implying the increase of backscattering in HH polarization. In the case of low biomass dry forest, forest fire makes forest canopy dry and induces lower volume scattering in a tree canopy layer, implying the decrease of backscattering in HV. The decrease of volume scattering also occurred in the dense forest. But higher density of burned trees left on the ground still induces brighter radar reflection in HV and make it difficult to detects the forest fire sites in HV polarization.

[1] JJ-FAST, http://www.eorc.jaxa.jp/jjfast/jj_index.html, accessed on February 17, 2019

[2] Manabu Watanabe, et al., A possibility of forest fire site detection by JJ-FAST system

[3] https://modis.gsfc.nasa.gov/data/dataprod/mod45.php, accessed on Feb. 17, 2019

[4] https://www.bbc.com/news/world-africa-46029553, accessed on Feb. 17, 2019

Keywords: Forest monitoring, Deforestation detection, PALSAR-2

©2019. Japan Geoscience Union. All Right Reserved.

Nominal operation results of Japanese ALOS-2

*Shinichi Sobue[1]

1. Japan Aerospace Exploration Agency

The Advanced Land Observing Satellite-2 (ALOS-2) was successfully launched on 24th May 2014. The mission sensor of ALOS-2 is the Phased Array type L-band Synthetic Aperture Radar-2 called PALSAR-2 which is the state of the art L-band SAR system. Until now after the successful completion of initial checkout after launching, ALOS-2 has been contributed to a lot of emergency observations for natural disasters, not only in Japan but also in the world. Furthermore, based on the Basic Observation Scenario (BOS) of ALOS-2, 10m global map data and other mode data are routinely collected and archived. This paper describes the results of ALOS-2 operation in nominal operation phase.

Keywords: ALOS-2, nominal operation

©2019. Japan Geoscience Union. All Right Reserved.

[J] Oral | S (Solid Earth Sciences)：S-TT Technology & Techniques

Mon. May 27, 2019 1:45 PM - 3:15 PM JST | Mon. May 27, 2019 4:45 AM - 6:15 AM UTC | 303 3F

[S-TT45] Synthetic Aperture Radar

convener:Youhei Kinoshita(University of Tsukuba), Yu Morishita(Geospatial Information Authority of Japan), Shoko Kobayashi(Tamagawa University), Takahiro Abe(Earth Observation Research Center, Japan Aerospace Exploration Agency), Chairperson:Yohei Kinoshita(RESTEC), Takahiro Abe(JAXA)

ALOS-2 and Sentinel-1A and 1B, which have highly enhanced capacity compared to previous SAR satellites, were launched in 2014, and their utilization has been widely expanding as the data has accumulated for approximately four years. Other long-operating SAR satellites like TerraSAR-X and Cosmo-SkyMed also contribute to expanding the SAR utilization. Now we are facing a new and abundant era of the satellite SAR, along with a worldwide trend to an open and free data policy of satellite data, with next-generation advanced SAR satellite plans by several countries, and with several plans to construct SAR constellations by private sectors. In addition, SAR technologies with other platforms, such as ground-based SAR with high temporal resolution and UAV (Unmanned Aerial Vehicle) SAR with flexible operability, have also been developed and used for various targets. These facts indicate that the SAR utilization has become widespread in both basic researches (e.g., earth science) and diverse applications (e.g., disaster prevention and forest monitoring). In this session, we would like to widely invite research and application results with regard to SAR, sharing our knowledge and having a discussion for the advancement of the SAR utilization.

1:45 PM - 2:00 PM JST | 4:45 AM - 5:00 AM UTC

[STT45-07] Estimation of velocity distribution of Shirase Glacier derived from SAR data obtained by ERS-1/2 tandem mission

*Koichiro Doi[1,2], Yuichi Aoyama[1,2], Kazuki Nakamura[3], Tsutomu Yamanokuchi[4], Kazuo Shibuya[1] (1.National Institute of Polar Research, 2.SOKENDAI, 3.College of Engineering, Nihon University, 4.RESTEC)

2:00 PM - 2:15 PM JST | 5:00 AM - 5:15 AM UTC

[STT45-08] Heavy rainfall-induced displacement of more than 2.5m in the Kushiro Marsh in 2016, detected by ALOS-2 SAR

*Satoshi Fujiwara[1], Yu Morishita[1], Takayuki Nakano[1], Yuji Miura[1], Yasuaki Kakiage[1], MURAMATSU Hiroki[1], Hiroshi Une[1] (1.GSI of Japan)

2:15 PM - 2:30 PM JST | 5:15 AM - 5:30 AM UTC

[STT45-09] Surface deformation of Asama Volcano, Japan, detected by time-series InSAR combining persistent and distributed scatterers, 2014-2018

*Yosuke Aoki[1], Xiaowen Wang[1] (1.Earthquake Research Institute, University of Tokyo)

2:30 PM - 2:45 PM JST | 5:30 AM - 5:45 AM UTC

[STT45-10] Improvement of Airborne L-band-SAR (Pi-SAR-L2) Coherence by Pixel by Pixel Resampling

*Makoto Murakami[1], Masato Furuya[1], Taku Ozawa[4], Youichiro Takada[1], Yosuke Aoki[3], Masanobu Shimada[2], Shohei Narita[1] (1.Hokkaido University, 2.Tokyo Denki University, School of Science and engineerring, 3.Earthquake Research Institute, The University of Tokyo, 4. National Research Institute for Earth Science and Disaster Resilience)

2:45 PM - 3:00 PM JST | 5:45 AM - 6:00 AM UTC

[STT45-11] Ionospheric delay estimation in SAR interferometry: Significance of the method using the split-spectrum double-difference interferogram

*Taku Ozawa[1] (1.National Research Institute for Earth Science and Disaster Resilience)

3:00 PM - 3:15 PM JST | 6:00 AM - 6:15 AM UTC

[STT45-12] Detecting surface displacement accosiated with the 2018 slow slip event around Boso peninsla by use of Sentinel-1 InSAR with atmospheric correction

*Youhei Kinoshita[1], Tadahiro Nimura[1], Ryoichi Furuta[1] (1.RESTEC, Remote Sensing Technology Center of Japan)

Estimation of velocity distribution of Shirase Glacier derived from SAR data obtained by ERS-1/2 tandem mission

*Koichiro Doi[1,2], Yuichi Aoyama[1,2], Kazuki Nakamura[3], Tsutomu Yamanokuchi[4], Kazuo Shibuya[1]

1. National Institute of Polar Research, 2. SOKENDAI, 3. College of Engineering, Nihon University, 4. RESTEC

Shirase Glacier is one of the fastest flowing ice stream in Antarctica flowing into the southernmost of Lutzow-Holm Bay in Dronning Maud Land, East Antarctica. It is important to clarify the spatial flow rate distribution with a high resolution to investigate causes of the fast flow and the temporal flow rate changes. In order to make a high resolution flow velocity map, we apply a usual interferometric Synthetic Aperture Radar (InSAR) technique to the obtained data. However, since flowing velocity of the ice stream is greater than 2 km/year (Nakamura et al., 2007, Aoyama et al., 2016), it is difficult to estimate the flow velocity by applying an InSAR technique to the ordinal repeat cycle SAR mission data.

Tandem mission by European Satellite of Remote sensing (ERS)-1/2 was conducted in 1996 and 1999. In this tandem mission, ERS-2 had flown after ERS-1 in the same orbit with an interval of one day, and many InSAR pairs with one day temporal baseline were obtained through the mission.

We successfully obtained two SAR interferograms over Shirase Glacier using this tandem mission InSAR pairs acquired at 1996/06/02-1996/06/03 and 1999/11/14-1999/11/15. We estimated surface displacements along range direction (direction of radar illumination) by applying differential InSAR (DInSAR) with a TanDEM-X 90m DEM (Rizzoli et al., 2017) to remove topographic phase. We also estimated displacements along azimuth direction (direction perpendicular to range direction) by applying a split beam interferometry (SBI) (Bechor and Zebker, 2006) technique to the two InSAR pairs. By combining the range and azimuth displacements, spatial flow velocity distributions can be derived with a high resolution.

In the presentation, we will show two dimensional flow velocity maps with a resolution of approximately 20 m at the two periods and discuss spatial and temporal velocity changes. We will also compare the obtained flow velocity with those by in-situ GNSS measurements in the glacier.

Keywords: Shirase Glacier, flow velocity map, ERS-1/2 tandem mission, DInSAR, SBI

©2019. Japan Geoscience Union. All Right Reserved.

Heavy rainfall-induced displacement of more than 2.5m in the Kushiro Marsh in 2016, detected by ALOS-2 SAR

*Satoshi Fujiwara[1], Yu Morishita[1], Takayuki Nakano[1], Yuji Miura[1], Yasuaki Kakiage[1], MURAMATSU Hiroki[1], Hiroshi Une[1]

1. GSI of Japan

The Kushiro Marsh in eastern Hokkaido is the largest wetland in Japan. Monitoring changes in environmental conditions is important to support preservation of the wetland. In the summer of 2016, Hokkaido was affected by several typhoons and suffered record-breaking heavy rainfall. We constructed ~50 ALOS-2 SAR interferograms, covering the Kushiro Marsh for the period 2014 to 2018, including the summer of 2016. A time series of vertical displacement of the wetland detected by the interferograms corresponded with water level changes in the rivers in the wetland. This implied that the SAR data had successfully detected the height change of the water surface in the wetland. Between August 6, 2016 and September 5, 2016, an area of the wetland (~1 km) to the southeast of Akanuma shifted ~2.7 m horizontally in the downstream direction, which coincided with a large and rapid increase in the water level caused by the heavy rains. This large displacement remained after the water level decreased. Prior to this large horizontal shift, an uplift of ~10 cm was identified in almost the same region. This uplift might have been caused by the leaking of groundwater from the basement of the Akanuma pond, and implied that the peat layer, which had a thickness of several meters floated slightly, like a floating islands, possibly causing the large horizontal shift.

Reference

Fujiwara et al. (2019): Heavy rainfall-induced displacement of more than 2.5m in the Kushiro Marsh in 2016, detected by ALOS-2 SAR, *Journal of Geography (Chigaku Zasshi)*.

Keywords: Kushiro Marsh, environment of wetland, underground water, heavy rainfall, surface displacement, ALOS-2

©2019. Japan Geoscience Union. All Right Reserved.

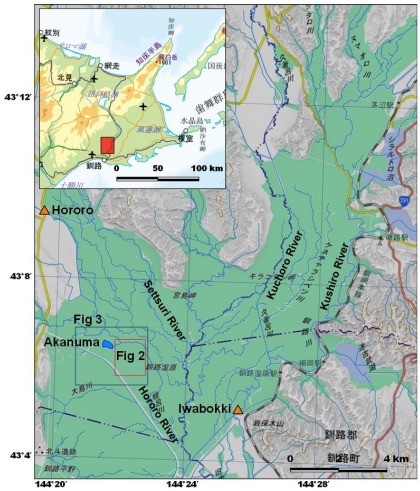

Fig 1 Map of the Kushiro Marsh.
The light green areas denote the wetlands. The red rectangles denotes the area shown in Fig 2, and the dark blue rectangle corresponds to the area shown in Fig 3.

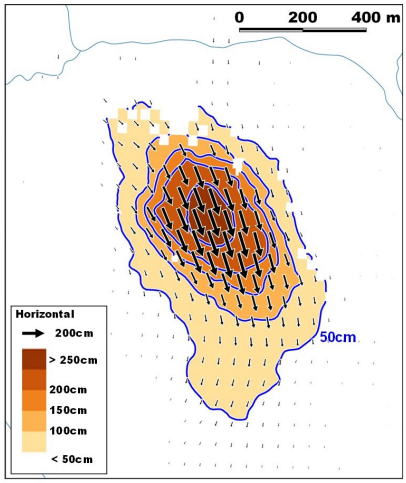

Fig 2 Horizontal displacement to the southeast of Akanuma in the summer of 2016 detected by ALOS-2 SAR.

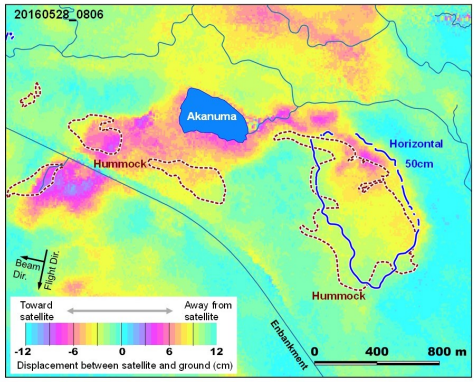

Fig 3 ALOS-2 SAR interferogram of around Akanuma. The blue line denotes the area with large horizontal displacement (>50cm). The brown broken lines denote hummocks.

©2019. Japan Geoscience Union. All Right Reserved.

Surface deformation of Asama Volcano, Japan, detected by time-series InSAR combining persistent and distributed scatterers, 2014-2018

*Yosuke Aoki[1], Xiaowen Wang[1]

1. Earthquake Research Institute, University of Tokyo

Asama volcano, located in Central Japan, is one of the most active volcanoes in Japan. Surface deformation at Asama volcano has rarely been documented because of its high topography and snow cover at the summit. In this study, we present first Interferometric Synthetic Aperture Radar (InSAR) observation of ground deformation of Asama volcano with 120 Sentinel-1 SAR images from both ascending and descending tracks and 20 ALOS-2 images from a descending track acquired between 2014 and 2018. We exploited both persistent and distributed scatterers to overcome SAR signal decorrelation and applied the three-dimensional unwrapping method to retrieval displacement time series efficiently. Our observations reveal asymmetric deformation at Asama volcano with two main deformation regions at the northeast and southeast flanks of the volcano, respectively. The northeast flank (NEF) exhibits line-of-sight (LOS) extensions in all the three SAR datasets with maximum velocities of 14, 10, and 12 mm/year for the descending ALOS-2, ascending and descending Sentinel-1 measurements, respectively. The southeast flank (SEF) shows LOS extension in the ascending observations and LOS shortening in the descending observations with velocities between -12 and 9 mm/year, respectively. Decomposition of the LOS displacements reveals nearly pure vertical subsidence at the NEF, while the SEF also shows an evident eastward component other than vertical subsidence. Comparisons of the vertical subsidence at two continuous GPS stations near the summit crater with our InSAR observations indicate small discrepancies smaller than 3 mm/year. We interpret that the subsidence at the NEF is primarily due to the cooling contraction of pyroclastic deposits emplaced in the 1783 eruption, and the SEF is susceptible to flank instability. The asymmetric deformation of the volcano may also be related to the hydrothermal activity that is controlled by the underground structure of the volcano. This study highlights that much more efforts should be taken to monitor the slope instability of Asama volcano in the future.

Keywords: Synthetic Aperture Radar, Time-series analysis, Thermal contraction

©2019. Japan Geoscience Union. All Right Reserved.

Improvement of Airborne L-band-SAR (Pi-SAR-L2) Coherence by Pixel by Pixel Resampling

*Makoto Murakami[1], Masato Furuya[1], Taku Ozawa[4], Youichiro Takada[1], Yosuke Aoki[3], Masanobu Shimada[2], Shohei Narita[1]

1. Hokkaido University, 2. Tokyo Denki University, School of Science and engineerring, 3. Earthquake Research Institute, The University of Tokyo, 4. National Research Institute for Earth Science and Disaster Resilience

1. Introduction

Although Airborne SAR is advantageous in terms of flexibility of flight path direction and observation scheduling, the deviation from the flight path linearity due to the perturbation by wind irregularity makes interferometry difficult. We have been working on a development of L band airplane SAR interferometric technique with an aim to use it for volcanic deformation monitoring. The most effective way to improve the coherence between 2 airborne observations is precise coregistration of the slave image against the master image. We here present a new method of precise coregistraion for airborne SAR interferometry using pixel by pixel resampling capability of RINC software package developed by Taku Ozawa at NIED. We demonstrate the usefulness of this technique utilizing airborne repeat path SAR data acquired by JAXA’ s airborne L-band SAR system (pi-sar-l2) over southern Kyushu volcanoes (Sakurajima volcano, Kirishima volcano and Unzen volcano) .

2. The classic coregistration method

Because the flight path of satellite is relatively smooth, the coregistration between master and slave images based on two dimensional quadratic function fitting is sufficient. Our interferometric process for airborne SAR started with the same technique. However, our preliminary tests suggested the insufficiency of this classic method for airborne SAR failing to faithfully follow high frequency component of pixel offset caused by irregularity of the airplane flight path due to the wind fluctuations especially in along-track direction.

3. Precise coregistration method using pixel by pixel matching technique

©2019. Japan Geoscience Union. All Right Reserved.

To improve the effectiveness of coresistration, we employ an additional step to fit the two dimensional pixel offset field after the primary fitting using a quadratic function. In the process of the additional fitting for the the primary fitting residuals, we use an empirical smooth function fitting capability of Matlab software package. Thus we calculate the offset values between master and slave for every pixel of master image and then we carry out coregistration using pixel by pixel resampling capability of RINC software package. This additional procedure significantly improves the coherence as we see below.

3. Demonstration of Usefulness of New method using data over Kirishima volcano

We tested the usefulness of the new method for the repeat path SAR data acquired on 2014 and 2016 over the Kirishima volcano complex. The figure shows the comparison of the coherence between the results of classic and new methods. The area of good coherence increases significantly in the image derived by the new method in the right hand, where brighter colorization corresponds to better coherence. The improvement of the lower half of the image is obvious. Although there still remain stripes of worse coherence which run in the direction perpendicular to the azimuthal axis, the width of those stripes is reduced. This bad coherency seems to be caused by abrupt change of flight speed of the airplane. In this particular observation, our target is Iwoyama dome which is a nest of recent phreatic activity, and the coherence there is actually greatly improved by the new method resulting in better understanding of the ongoing inflation mechanism which will be reported elsewise. In the presentation, we will show the test results using other data sets and discuss the usefulness of the new methods.

Credits: We used RINC (Ver. 0. 36) developed by Dr. Taku Ozawa and Geospatial Information Authority of Japan height data for SAR interferometric processing. This study was supported by the Ministry of Education, Culture, Sports, Science and Technology (MEXT) of Japan, under its Earthquake and Volcano Hazards Observation and Research Program.

Keywords: Airborne SAR, SAR Interferometry, Crustal Deformation

©2019. Japan Geoscience Union. All Right Reserved.

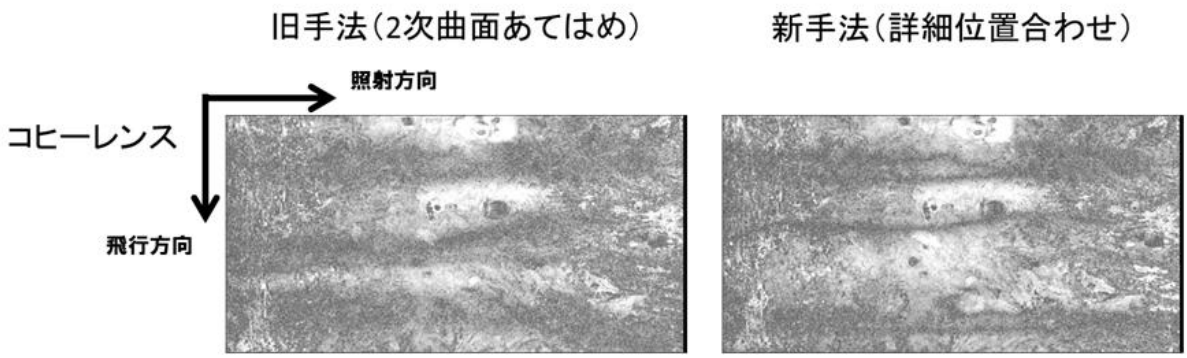

図　EW軌道データ（2014-2016）に対するリサンプル新旧手法の比較.
コヒーレンスは，明るいピクセルほど干渉性が高い．全体的に干渉性が上がっているが，特に，画像の下半分で改善が顕著である.

©2019. Japan Geoscience Union. All Right Reserved.

Ionospheric delay estimation in SAR interferometry: Significance of the method using the split-spectrum double-difference interferogram

*Taku Ozawa[1]

1. National Research Institute for Earth Science and Disaster Resilience

Split-spectrum method is used as a useful method in reducing the ionospheric delay which is one of the major error factors in SAR interferometry (e.g., Brcic et al., 2010; Rosen et al., 2010; Gomba et al., 2016). This method divides chirp signal of SAR into high and low bands, and generates interferograms for each bands. The ionospheric delay and crustal deformation components are extracted from them. Generally, the ionospheric delay component phai,iono can be estimated from

$\Phi_{iono}=f_L f_H(\Phi_L f_H - \Phi_H f_L)/(f_0(f_H^2-f_L^2))$ -(1)

where f0, fl, fh are center frequencies of full, lower, and higher bands. phai,l phai,h are phase differences of interferograms for lower and higher bands. Empirically, for interferometric pairs with high coherence, the ionospheric delay component can be accurately estimated from this equation. However, that with low coherence, the accuracy degrades mainly due to the difficulty of unwrapping. Then Wegmüller et al. (2018) proposed the method using following equation,

$\Phi_{iono}=A\Phi_0 + B(\Phi_H-\Phi_L)$ -(2)

where phai,0 is phase difference of full-band interferogram, and A, B are coefficient derived from center frequencies. In general, the better coherence is obtained for interferometric pair with wider bandwidth, and therefore the first term is relatively easier to unwrap than that with divided frequencies. Since the second term falls within the value of $-\pi$ to $+\pi$ in most cases, it is possible to easily obtain the phase difference. Furthermore, since A is approximately 0.5, equation (2) can be approximated to

$2\Phi_{iono}=\Phi_0 + 2B(\Phi_H-\Phi_L)$ -(3)

As mentioned before, the second term can easily estimate the phase difference, and then it is possible to obtain an interferogram showing only the ionospheric delay component without unwrapping.

Now, we are developing ionospheric delay estimation tools based on the above three equations. In this presentation, we describe the results of test analysis on several pairs using tools under development. In this analysis, SAR images divided the band in half are used. For high and low frequency pairs, interferograms are generated. After removing orbital and topographic fringes, the spectrum filter (Goldstein and Werner, 1998) is applied to them. From these interferograms, ionospheric delay is estimated using each equation. An outlier removing filter and a Gaussian filter are applied to ionospheric delay image.

First, as a pair with relatively high coherence, the interferometric pair of ALOS-2/PALSAR-2 images which observed Azuma-yama on September 9, 2014 and August 11, 2015 was analyzed. About this pair, almost the same results were obtained from analysis using each equation. However, as a result from interferometric pair which observed on March 7, 2016 and April 18, 2016, included large crustal deformation associated with the 2016 Kumamoto earthquake, differences were obtained in results from analysis using each equation. In particular, in the analysis using Eq. (1), the unwrapping error in the vicinity of the fault seems to have a big influence. In manual analysis, if the error is correctly masked, it is considered that roughly the same result as equation (2) is obtained. In a result from equation (3), the ionospheric delay component was obtained even in the vicinity of the fault. However, in other interfering pairs with particularly poor coherence, the ionospheric delay could not be properly estimated by the analysis using Equation (3) in some cases.

Although there are few analysis cases at the present time and more case analysis is required, it is generally felt that the method based on equation (2) can estimate the ionosphere delay with relatively high

©2019. Japan Geoscience Union. All Right Reserved.

accuracy. However, in cases where large crustal deformation are included such that unwrapping is difficult, the method based on equation (3) may be better. It may be necessary to select a method which is appropriate for a case.

Keywords: SAR, ionospheric delay, crustal deformation

©2019. Japan Geoscience Union. All Right Reserved.

Detecting surface displacement accosiated with the 2018 slow slip event around Boso peninsla by use of Sentinel-1 InSAR with atmospheric correction

*Youhei Kinoshita[1], Tadahiro Nimura[1], Ryoichi Furuta[1]

1. RESTEC, Remote Sensing Technology Center of Japan

The slow slip, also denoted as the slow eathquake, is known to release accumulated strain energy with no or slight seismic wave radiation. The slow slip is usually detected by highly accurate geophysical measurements such as the Global Navigation Satellite System (GNSS) and seismometers because of very small surface deformation on the order of millimeters to centimeters, and small ground oscillation (named as a tremor). Until now, several papers reported slow slip events, for example, at Tokai area (e.g. Yamamoto et al. 2005, EPS; Ozawa et al. 2016, EPS), Cascadia (e.g. Dragert et al. 2004, EPS; Hawthorne and Bartlow 2018, JGR), and Nankai Trough (e.g. Kobayashi 2017, EPS; Ozawa 2017, EPS). The area around Boso Peninsla is also a location where slow slip events have occuered with intervals of several years (Fukuda 2018, JGR). However, most of the reffered papers here used GNSS observations that have a limitation of low spatial resolution (Usually a few tens of kilometers between ground stations). In this study we conducted the InSAR analysis to detect the surface displacement accosiated with the 2018 slow slip event near the Boso peninsla by use of Sentinel-1 observations and numerically-derived atmospheric models.

In the InSAR andalysis we used Sentinel-1 TOPS IW data with three satellite paths (path 39, 141, and 46). Paths 39 and 141 are ascending direction and path 46 is descending direction. The interferometric analysis was conducted by GAMMA software with the 1-arcsecond SRTM DEM for the topographic fringe simulation. All of the InSAR pairs have absolute perpendicular baselines below 200m, indicating most InSAR pairs showed good coherence. Because the expected surface displacement has an amplitude of 2cm or below (by GNSS observations), we performed the stacking analysis for each paths to enhance the detectability of line-of-sight (LOS) displacements. In addition, we applied the MSM-based atmospheric delay correction to each interferograms to further increase the detectability of the surface displacement signal.

The stacking result showed that the surface displacement signal with an amplitude of approximately 1 cm in the LOS direction was clearly detected in path 141. The displacement signal extended spatially to approximately 20 km in both north-south and east-west direction. The spatial distribution and amplitude of InSAR-detected displacement was consistent with the GNSS observation. On the other hand, There were no clear displacement signal in the stacked interferogram in paths 39 and 46. This would be due to the significant atmospheric delay effect in several interferograms of these paths. Therefore we only used the stacking interferogram in path 141 for the fault modeling.

We also performed the assessment of the atmospheric delay correction effectiveness. Phase standard deviations (SDs) calculated on the area outside of the expected displacement signal clearly showed the effectiveness of the atmospheric delay correction. Before the correction, SDs of the stacked interferograms were 5.9 cm, 7.5 cm, and 4.2 cm for paths 39, 46, and 141, respectively, which decreased to 2.7 cm, 4.6 cm, and 1.6 cm after the correction. Although the spatial and temporal resolutions of MSM were 10 km and 3 hours that were not significant for the InSAR atmospheric delay modeling, it showed good performance for the InSAR stacking.

Based on the derived displacement signal in path 141, we performed a forward modeling to estimate preliminary fault parameters using the simple Okada fault model. The estimated fault model suggested

©2019. Japan Geoscience Union. All Right Reserved.

that the upper-left corner of the fault was located at 140.8 degrees in longitude and 34.98 degrees in latitude with the depth of 15 km, which was consistent with the boundary of the Phillipine plate. The fault length and width were set to 50 km and 30 km with the dip angle of 18 degrees. The estimated slip amount was 13 cm with the rake of 105 degrees, which was equivalent to the moment magnitude of 6.6.

Keywords: InSAR, Atmospheric delay correction, Slow Slip

©2019. Japan Geoscience Union. All Right Reserved.

[J] Poster | S (Solid Earth Sciences)：S-TT Technology & Techniques

Mon. May 27, 2019 3:30 PM - 5:00 PM JST | Mon. May 27, 2019 6:30 AM - 8:00 AM UTC | Poster Hall International Exhibition Hall8, Makuhari Messe_15

[S-TT45] Synthetic Aperture Radar

convener:Youhei Kinoshita(University of Tsukuba), Yu Morishita(Geospatial Information Authority of Japan), Shoko Kobayashi(Tamagawa University), Takahiro Abe(Earth Observation Research Center, Japan Aerospace Exploration Agency)

ALOS-2 and Sentinel-1A and 1B, which have highly enhanced capacity compared to previous SAR satellites, were launched in 2014, and their utilization has been widely expanding as the data has accumulated for approximately four years. Other long-operating SAR satellites like TerraSAR-X and Cosmo-SkyMed also contribute to expanding the SAR utilization. Now we are facing a new and abundant era of the satellite SAR, along with a worldwide trend to an open and free data policy of satellite data, with next-generation advanced SAR satellite plans by several countries, and with several plans to construct SAR constellations by private sectors. In addition, SAR technologies with other platforms, such as ground-based SAR with high temporal resolution and UAV (Unmanned Aerial Vehicle) SAR with flexible operability, have also been developed and used for various targets. These facts indicate that the SAR utilization has become widespread in both basic researches (e.g., earth science) and diverse applications (e.g., disaster prevention and forest monitoring). In this session, we would like to widely invite research and application results with regard to SAR, sharing our knowledge and having a discussion for the advancement of the SAR utilization.

[STT45-P01] Development of InSAR tropospheric phase delay correction system at MRI (2nd report)

*Okuyama Satoshi[1], Shinobu Ando[1], Toshiki Shimbori[1] (1.Meteorological Research Institute)

[STT45-P02] Mitigation of atmospheric delay in InSAR for fair estimate of crustal deformation at Azumayama volcano

*Kana Abe[1], Yoshiko Ogawa[1], Yasuhiro Hisada[1], Hirohide Demura[1], Taku Ozawa[2], Satoshi Miura[3], Akira Kusakabe[1], Takehiro Arai[1] (1.The University of Aizu, 2.National Research Institute for Earth Science and Disaster Resilience, 3.Graduate School of Science, Tohoku University)

[STT45-P03] Unusual displacement observed in InSAR analysis results of fumarolic area of active volcanos: An example of the Kamiyu district in Hakone Volcano

*Ryosuke Doke[1], Kazuhiro Itadera[1] (1.Hot Springs Research Institute of Kanagawa Prefecture)

[STT45-P04] Detection of Deformation Signals at Mud Volcanoes in Semau Island, Indonesia

*Naufal Setiawan[1], Masato Furuya[1] (1.Hokkaido University)

[STT45-P05] Extraction of supraglacial lakes on debris-covered glacier using ALOS-2/PALSAR-2

Chikako Kinefuchi[2], *Chiyuki Narama[1], Tsutomu Yamanokuchi[3], Takeo Tadono[4] (1.Niigata University, Program of Field Research in the Environmental Sciences, 2.Graduate School of Science and Technology, Niigata University, 3.RESTEC, 4.JAXA)

[STT45-P06] **Observation of the water level fluctuation at Ozegahara by ALOS-2/PALSAR-2**

*Wataru Iwatate[1], Masanobu Shimada[1] (1.Tokyo Denki University)

[STT45-P07] The steady crustal deformation around the Omaezaki, Sionomisaki, Muroto and Ashizuri, using InSAR time-series analysis 2

*Shinobu Ando[1], Akio Kobayashi[1] (1.Seismology and Tsunami Research Department, Meteorological Research Institute)

[STT45-P08] Evaluation of InSAR analysis result using pipe strain gauge data in Otari village, Nagano prefecture, Japan

*Tomoya Kiyosawa[1], Hiroshi, P. Sato[2] (1.Department of Geography, Graduate School of Science and Technology, Nihon University , 2.College of Humanities and Science, Nihon University)

[STT45-P09] DEM creation using ALOS / PALSAR interferometric SAR and its accuracy evaluation.

*takahashi koya[1], Masanobu Shimada[1] (1.tokyo denki university)

[STT45-P10] Approach to monitoring ground deformation using InSAR time series analysis all over Japan

*Kyonosuke Hayahsi[1], Tatsuya Yamashita[1], Masaki Kuwahara[1], Masaki Honda[1], Kazuki Sakai[1], Hiroshi Munekane[1], Tomokazu Kobayashi[1] (1.GSI of Japan)

Development of InSAR tropospheric phase delay correction system at MRI (2nd report)

*Okuyama Satoshi[1], Shinobu Ando[1], Toshiki Shimbori[1]

1. Meteorological Research Institute

Introduction

SAR Interferometry is a technique which utilize the phase information of the SAR images to detect surface displacement which took place between two observations. However, its result contains the effect of medium between the antenna and the target such as tropospheric delay. Conventional method to correct tropospheric delay is proposed by Fujiwara et al. (1999), which assumes that the delay is a function of topographic height. On the other hand, correction using numerical weather model, which is independent data from SAR interferogram, is also proposed (Hobiger et al., 2008; Ozawa and Shimizu, 2010). We started the development of tropospheric delay correction system in MRI and reported our preliminary result (Okuyama et al., 2018). In our preliminary analysis, we calculated zenith delay and projected it on line-of-sight of the SAR observation. As an improvement, we replaced this by the integration of refractivity along line-of-sight of the SAR observation.

System composition

Our correction system consists of three units: 1) read grid point values (NuSDaS format) and interpolate in time to generate gridded data at the observation time, 2) calculate refractivity at each gridpoint, and 3) integrate refractivity to calculate the delay at each pixel in the interferogram. This composition allows us to replace each unit separately. For example, when new weather model is released, we replace unit 1) only, leaving the rest of the units unchanged.

Difference from preliminary result

We corrected interferogram of PALSAR-2 (path125/frame660, 2015/1/4 - 2015/8/16) using JMA-MA (Meso Analysis) data by both (A) projecting zenith delay on line-of-sight and (B) integrating the refractivity along line-of-sight. As stated above, tropospheric delay tends to have strong correlation between topography. Thus, we use correlation coefficient between phase and topographic height as a measure of correction quality. We obtained correlation coefficient of -0.431 for original interferogram, -0.097 for correction (A), and -0.047 for correction (B).
The difference between (A) and (B) shows correlation between delay and topography, however its factor shows horizontal variation. This is caused by the horizontal variation of the refractivity. The maximum difference between (A) and (B) is -2.1 radians.

Future direction

We will develop the support for other model types such as JMA-LA (Local Analysis) or JMA-GA (Global Analysis) as next step and validate the algorithm of interpolation/refractivity.

Acknowledgement

PALSAR-2 level 1.1 data are shared among PIXEL (PALSAR Interferometry Consortium to Study our Evolving Land surface) and provided from JAXA under a cooperative research contract with ERI, Univ., Tokyo. The ownership of PALSAR-2 data belongs to JAXA.

©2019. Japan Geoscience Union. All Right Reserved.

Keywords: SAR interferometry, atmospheric delay, numerical weather model

©2019. Japan Geoscience Union. All Right Reserved.

Mitigation of atmospheric delay in InSAR for fair estimate of crustal deformation at Azumayama volcano

*Kana Abe[1], Yoshiko Ogawa[1], Yasuhiro Hisada[1], Hirohide Demura[1], Taku Ozawa[2], Satoshi Miura[3], Akira Kusakabe[1], Takehiro Arai[1]

1. The University of Aizu, 2. National Research Institute for Earth Science and Disaster Resilience, 3. Graduate School of Science, Tohoku University

Azumayama volcano is one of the five active volcanoes in Fukushima prefecture which is now issued volcanic alert level 2. Since 2014 winter, the volcano had/has been issued the level 1 and 2 repeatedly according to the situation. It is the most active volcano in the Fukushima pref. We have been working to clarify time-series of crustal deformation at Azumayama volcano.

Abe et al. [2017, JpGU] conducted InSAR (Interferometric Synthetic Aperture Radar) analysis using ALOS2 (Advanced Land Observing Satellite 2)/PALSAR2 (Phased Array L-band Synthetic Aperture Radar-2) data and estimated crustal deformation around Azumayama volcano . However, some of the results showed subsidence at the west of Azumayama which would be due to atmospheric delay and ionospheric delay.

In this study, we attempted to correct atmospheric delay and ionospheric delay in InSAR analysis using three numerical weather models: MSM (MesoScale Model), LFM (Local Forecast model) and WRF (Weather Research and Forecasting). WRF is created by using MSM data to improve resolution of time. Then we tried to estimate the amount of crustal deformation more precisely from 2014 fall to 2017 fall after applying atmospheric correction. Eight of the ALOS2/PALSAR2 data were used for the InSAR analysis. We evaluated the InSAR results after performing each atmospheric correction based on each numerical model and compare them quantitatively and select suitable weather model among the three.

Artifacts and false fringe in InSAR results seem to be reduced. Comparing InSAR analysis results with the value of GNSS (Global Navigation Satellite System) analysis at ground stations, correction by LFM and WRF showed similar trend better than that by MSM. Numerical weather models with higher resolutions seem effective in correcting atmospheric delay in InSAR. Uplift and subsidence at the Oana crater and subsidence in the western part of Azumayama were detected during 2014 fall - 2015 summer and 2015 summer - 2015 fall, respectively, which reflect actual deformation.

Keywords: Azumayama, crustal deformation, volcano, SAR, numerical weather model

©2019. Japan Geoscience Union. All Right Reserved.

Unusual displacement observed in InSAR analysis results of fumarolic area of active volcanos: An example of the Kamiyu district in Hakone Volcano

*Ryosuke Doke[1], Kazuhiro Itadera[1]

1. Hot Springs Research Institute of Kanagawa Prefecture

In this presentation, we report on the characteristics and causes of displacements observed in the InSAR analysis results of ALOS-2/PALSAR-2 data for the fumarolic area in the Kamiyu area of the Hakone volcano.

The Kamiyu fumarolic area is in the northern slope of the central cone of the Hakone volcano and located about 500m north of the Owakudani fumarolic area that had phreatic eruptions in 2015. The Kamiyu fumarolic area was formed around 2003 after the 2001 swarm earthquake occurred at the Hakone Volcano (Tsujiuchi et al., 2003). The most active fumarole in the Kamiyu area is the area called E region, which was activated after the earthquake swarm induced by the 2011 Tohoku Earthquake (Yukutake et al., 2011; Harada et al., 2012). The scale of the E region is about 200m north to south and about 150m east to west. Moreover, the heat flux from the E region is estimated to be 7 to 8 MW (Mannen et al., 2018).

The observation by ALOS-2/PALSAR-2 for the Hakone volcano has been carried out repeatedly, mainly in four orbits, and each orbit is performed almost once every several months. From October 2014 to the end of 2018, data from descending orbit with right looking angles were obtained 22, and 15 scenes in Path 18 and 19, respectively, and data from ascending orbit with right looking angles were obtained 11 scenes in Paths 125 and 126, respectively. In this study, we performed DInSAR analysis with the latest interference pairs for all these data and clarified the displacement of the ground surface in the Kamiyu E region.

In the observation from the east side (Paths 18, 19), the Kamiyu E region displaced about 3 to 5 cm toward the satellite with respect to a reference point outside the fumarolic area during about four years. Moreover, in the observation from the west side (Paths 125, 126) displaced about 10 to 13 cm away from the satellite during the same period. These results suggest that the E region steadily displaces in the northeast direction in the long term, which also coincides with the inclination direction of the E region so that it is considered that the landslide displacement is occurring.

On the other hand, the analysis results of Paths 18 and 19 observed from the east side show the seasonal displacement that the area moved toward the satellite in the summer seasons and away from the satellite in winter seasons. In Paths 125 and 126 observed from the west side, such seasonal displacement is not observed, but these Paths have few observations in the summer and cannot judge the actual seasonal displacement. One of the possible causes of this seasonal displacement is a seasonal change in contrast between the vapor amount inside of the fumarolic area and that of the outside. The amount of water vapor near the ground changes seasonally outside of the fumarolic area whereas it is almost saturated throughout the year in the fumarolic area. Such contrast between the summer and winter is possibly affecting the DInSAR results. Another possible cause is an effect of the difference of soil moisture between summer and winter season because the fumarolic area is almost bare land and surface scattering is more dominant than forest area. Other factors are also conceivable, but we are considering the possibilities to evaluate the fumarolic activities from this seasonal displacement, in addition to accurately evaluate the

©2019. Japan Geoscience Union. All Right Reserved.

landslide movement in the fumarolic area.

ALOS-2/PALSAR-2 data were provided by JAXA via the Coordinating Committee for the Prediction of Volcanic Eruption as part of the project, “ALOS Domestic Demonstration on Disaster Management Application,” of the Volcano Working Group. The original ALOS-2/PALSAR-2 data belong to JAXA.

Keywords: InSAR, active volcano, fumarolic area, Hakone Volcano

©2019. Japan Geoscience Union. All Right Reserved.

Detection of Deformation Signals at Mud Volcanoes in Semau Island, Indonesia

*Naufal Setiawan[1], Masato Furuya[1]

1. Hokkaido University

Mud volcanoes are associated with fluid and solid material vertical extrusion from its source layer (mud reservoir). The size and shape of the mud volcanoes throughout the world are diverse. Furthermore, the reason behind this event is difference in each region but predominantly occurred at convergent plate margins. To date, the most mud extrusion known is in the Mediterranian Sea and Tethyan belt (including Azerbaijan, south Greece, Iran, and Turkmenistan).

Semau Island, located in Timor area of Indonesia, is one of the islands where the northern margin of Australian continental plate meets Banda sea plate. Previous geologic map identified Semau island hosted six mud volcanoes with no description in its size [Barber, et al. 1986], and some of them erupt only mud, whereas others produce mud with an admixture of liquid hydrocarbons [Kholodov. 2002].

In order to detect any possible deformation signals in the mud volcanoes in this region, we applied InSAR method. Twenty four (24) ascending images and ten (10) descending images of ALOS/PALSAR data spanning from 2006 to 2011 were acquired. Because our research area is not covered by single observation image, we concatenate the consecutive frame number. To enhance the processing step in GAMMA software, the oceanic areas and some part of other islands that not our interest were cropped to focus on Semau Island. Interferograms of ALOS/PALSAR dataset were consist of eleven (11) ascending pairs and four (4) descending pairs. Then, using AW3D30 DEM data we tried to remove topographic fringe. During the processing, images were multi-looked in range and azimuth by 2 and 6 respectively. While the oversampling in the azimuth direction can be avoided due to the effect of azimuth slope is limited, range oversampling by a factor of two is needed for good quality of interferogram. This procedure is to avoid uncorrelated contributions that arise in the spectral cross-correlation from interferogram generation. Finally, we applied low order polynomial to mitigate the effects of long wavelength phase trends in our interferograms.

The deformation signal is hardly detected in the majority of the data pairs, due to the unwrapping errors in some pairs and also probably due to the small size of mud volcanoes. Despite low coherence in the possible mud extrusion source, in two image pairs, we detected the possible signal from the mud volcano area that is identical to the location described from the previous geologic map. However, since the geologic map from the previous study was derived from aerial photograph interpretation and the signal detection is in slope area, further research is needed to confirm if it is related to active mud volcanism or simply a landslide signal.

Keywords: Mud volcanoes, InSAR, Landslide

©2019. Japan Geoscience Union. All Right Reserved.

Extraction of supraglacial lakes on debris-covered glacier using ALOS-2/PALSAR-2

Chikako Kinefuchi[2], *Chiyuki Narama[1], Tsutomu Yamanokuchi[3], Takeo Tadono[4]

1. Niigata University, Program of Field Research in the Environmental Sciences, 2. Graduate School of Science and Technology, Niigata University, 3. RESTEC, 4. JAXA

In the eastern part of the Himalaya (eastern Nepal and Bhutan), large drainages occur from supraglacial lakes on debris-covered glaciers when large lake connects to englacial network (Komori et al., 2012; Rounce et al., 2016; Miles et al., 2018). In the Himalaya, it is difficult to monitor the variations of supraglacial lakes during summer, because most optical satellite images are covered by cloud due to Indian monsoon. It is possible to investigate supraglacial lake under cloud using ALOS-2/PALSAR-2 of microwave sensor. However, backscatter of supraglacial lake differs in relief conditions on debris-covered glacier, and ice cliff and depression also have lower backscatter. In this study, we try to extract supraglacial lakes correctly using ALOS-2/PALSAR-2 data analysis.

Keywords: supraglacial lake, debris-covered glacier, ALOS-2/PALSAR-2, relief amount

©2019. Japan Geoscience Union. All Right Reserved.

Observation of the water level fluctuation at Ozegahara by ALOS-2/PALSAR-2

*Wataru Iwatate[1], Masanobu Shimada[1]

1. Tokyo Denki University

The SAR can measure the phase and the amplitude of the reflected wave from the surface object. This phase contains information on the round trip distance from the antenna to the surface of the earth in general, and more precisely the fraction of the above distance off the wave length. By differenciating two individual measurements, it can detect a slight distance difference. By using this InSAR technique, we can see the change of the Earth's surface due to earthquakes and volcanic eruptions in a visible form. On the water surface such as river, sea, lake, it is always moving by waves, so it is difficult to measure in places where the reflecting surface is not constant. However, in wetlands where grass and reeds are growing on top, the radar signal emitted to the water surface may reflect back from the grass and reeds, and return to the satellite.

Therefore, our research themes were defined to verify the possibility of observation on the water level change during two different observations. The target area was selected from the Honjou's largest Ozasegahara in wetlands. This Ozegahara is located in the Oze National Park, around the border areas of Fukushima, Tochigi Prefecture, Gunma, and Niigata Prefectures, and it is composed of 2,000 m class mountains. The observation was carried out using the period from September 2014 to May 2018 of PALSAR - 2 installed in JAXA 's Daichi 2 (ALOS 2). Since it is told that the water level of Ozegahara decreases, if the numerical value obtained by using the interference SAR technique shows a decrease, we can verify the possibility of observation on the water surface. In fact, we got an average of about -6.6 cm as a annual decreases. Comparing rainfall, etc., we can see that the water level goes down, and it was possible to show that the water level observation in the wetland zone is possible.

As future developments, it is conceivable to conduct verification in terms of accuracy from the possibility. One way to do this is to observe it using GPS or water gauge.

Keywords: Interferometry, ALOS-2, PALSAR-2

©2019. Japan Geoscience Union. All Right Reserved.

The steady crustal deformation around the Omaezaki, Sionomisaki, Muroto and Ashizuri, using InSAR time-series analysis 2

*Shinobu Ando[1], Akio Kobayashi[1]

1. Seismology and Tsunami Research Department, Meteorological Research Institute

At the Meteorological Research Institute, we are working on detection of crustal deformation using satellite SAR data as a method to detect changes in locked part such as slow slips and pre-slips at the plate boundary.

Especially focusing on the large-scale earthquake of the Nankai-Trough which is concerned about the occurrence in the near future, near the cape from Tokai to Shikoku which is close to the subduction zone of the plate and is thought to be susceptible to the change of the fixation state Analysis was conducted as an object.

We carried out InSAR time series for ALOS/PALSAR data to detect the steady crustal deformation around the cape from Tokai to Shikoku. As a result, we confirmed that the result of InSAR time series analysis correspond to GNSS data (Ando et al., 2018).

In this report, we tried to analysis for these data using InSAR time series analysis because of the archive data of ALOS-2/PALSAR-2 (operation period: 2014 -) has been adequately accumulated. In this analysis, interferograms were generated using RINC software (Ozawa et al., 2016), and then we carried out InSAR time series analysis about these data by SBAS method using GIAnT software (Agram et al., 2011). The data of each area used for the analysis is as follows.

Omaezaki: path 19 (18 scenes) and path 126 (11 scenes),

Shionomisaki: path 20 (16 scenes) and path 128 (11 scenes),

Muroto: path 21 (14 scenes) and path 128 (10 scenes),

Ashizuri: path 22 (14 scenes) and path 129 (10 scenes).

In principle, we used all data in which the archive exists for analysis in any path, but recalculated after excluding data which is clearly an error by checking the analysis result. The cumulative displacement result of Omaezaki (path 19) is shown in Fig.1.

As a result, we detected the elongation of displacement around the cape and shortening of displacement in the inland. The trends of these displacement distributions are similar to those of ALOS/PALSAR. In this presentation, we also report on the comparison with the GNSS observation results in the analysis area.

Some of PALSAR-2 data we used were provided by the Japan Aerospace Exploration Agency (JAXA) via the 6th ALOS-2 research announcement (RA-6). PALSAR-2 data belongs to JAXA. In the process of the InSAR, we used Digital Ellipsoidal Height Model (DEHM) based on the digital elevation map 10m-mesh provided by Geospatial Information Authority of Japan (GSI), and Generic Mapping Tools (P.Wessel and W.H.F.Smith, 1999) to prepare illustrations.

©2019. Japan Geoscience Union. All Right Reserved.

Keywords: ALOS-2/PALSAR-2, TS–InSAR, crustal deformation, Nankai-Trough

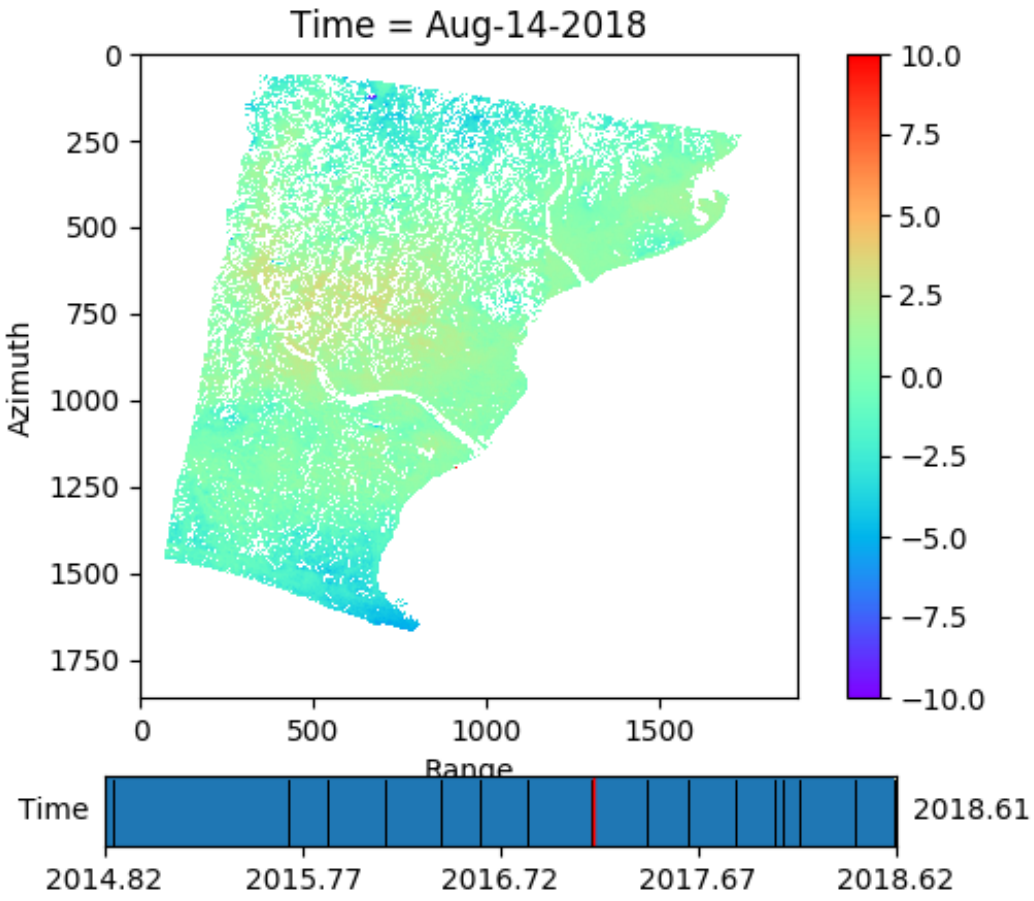

©2019. Japan Geoscience Union. All Right Reserved.

Evaluation of InSAR analysis result using pipe strain gauge data in Otari village, Nagano prefecture, Japan

*Tomoya Kiyosawa[1], Hiroshi, P. Sato[2]

1. Department of Geography, Graduate School of Science and Technology, Nihon University , 2. College of Humanities and Science, Nihon University

In order to detect landslide surface deformation, InSAR (Synthetic Aperture Radar interferometry) images were produced and interpreted in the study area of Ahara area in Otari Villege, Nagano Prefecure in Japan. The images were produced from time-series ALOS-2/PALSAR-2 data, taken from September 2014 to March 2018. More than 50 InSAR images were produced; however, at most four images gave good coherence available to interpret and detect the deformation. The one was taken on and the three were after Kamishiro Fault earthquake (M 6.7) on 22 Nov 2014. As a result of images interpretation, westwards deformation was detected up to ca. 2.5 cm and 4.5 cm along LoS (line of sight) on and after the earthquake, respectively.

To take measures against landslide disaster, Nagano Prefecture installed pipe type strain gauge in Ahara area, and the measured strain data were used to evaluate the image-detected deformation. As a result, at the slip layer of 8-m depth from the ground, the strain gauge measured 13 μST on the earthquake and it also indicated westward deformation. Empirically, strain over ca. 20,000 μST cuts electric measurement cables, and this strain is known to be equal to 2-3 cm deformation under the ground. Therefore, 13 μST is thought to be correspondent to 0.0013 cm deformation. Thus, the image-detected deformation itself was proved by the gauge-measured strain data and westward deformation direction was harmonized with the gauge-measured strain data. However, it was found that the image-detected deformation amount is 2,000 times larger than the strain gauge-calculated deformation amount.

Focusing on the deformation after the earthquake, as the observation periods of the images were not overlapped with measurement period of the strain gauge, assuming that the deformation proceeds at uniform speed in landslide body, then, both data were compared in daily mean deformation speed. The image-detected speed was calculated as 0.025-0.064 cm/day, and strain gauge-detected speed 0.000083 cm/day was calculated from 58 μST. It was found that the image-detected deformation speed is 300-780 times larger than the strain gauge-calculated speed. We think that this difference is attributed to the fact that InSAR measured the deformation not on the ground but along LoS distance and strain gauge measured the deformation not on the ground but under the ground. Furthermore, we think that the reason of more difference of the deformation amount on the earthquake than after the earthquake is that the image on the earthquake includes the deformation not only by landslide surface deformation but also crustal deformation by the earthquake.

Keywords: PALSAR-2, Landslide, InSAR

©2019. Japan Geoscience Union. All Right Reserved.

DEM creation using ALOS / PALSAR interferometric SAR and its accuracy evaluation.

*takahashi koya[1], Masanobu Shimada[1]

1. tokyo denki university

Digital Elevation Model (DEM) is a digital representation of the terrain on the ground surface, with the ground surface divided into equally spaced squares and the elevation of the center point of the square is given. In general, it expresses the surface of the earth that does not include vegetation, buildings, bridges, etc. DEM is often used in geographic information systems and is used as basic data in creating a three-dimensional map on a computer. There are several methods of making DEM, such as parallax measurement that combines optical pictures observed from multiple directions, interference processing of synthetic aperture radar, airborne laser surveying to find height using a laser mounted on an aircraft, etc. In this study We will prepare DEM by Synthetic Aperture Radar (SAR) and study related errors. DEM is created using synthetic aperture radar installed in ALOS and compared with DEM of Geographical Survey Institute. We measured the error, calculated the difference from the theoretical value, and evaluated its effectiveness. As a result, DEM creation by SAR was conducted for Hatoyama cho Higashi-gun (forest, residential area, Tabata), and the difference from the theoretical value occurred several centimeters to several tens of meters, but the average error was 9.94 m Therefore, through this study, we believe that practicality of DEM creation by SAR is sufficient.

Keywords: SAR, Digital Elevation Model

©2019. Japan Geoscience Union. All Right Reserved.

Approach to monitoring ground deformation using InSAR time series analysis all over Japan

*Kyonosuke Hayahsi[1], Tatsuya Yamashita[1], Masaki Kuwahara[1], Masaki Honda[1], Kazuki Sakai[1], Hiroshi Munekane[1], Tomokazu Kobayashi[1]

1. GSI of Japan

GSI (Geospatial Information Authority Japan) has been monitoring ground deformation all over Japan with ALOS-2 data by applying two-pass Differential Synthetic Aperture Radar Interferometry (D-InSAR) method. The two-pass D-InSAR method is a procedure to extract deformation that occurred between two observations from two radar images obtained from two observations. The two-pass D-InSAR method is susceptible to errors due to tropospheric disturbances, ionospheric disturbances, and change of the ground surface such as vegetation, which can be obstacles in detecting small ground deformations. Tropospheric disturbances and ionospheric disturbances may be reduced by Ray-tracing algorithm using numerical weather prediction model data (Kobayashi et al., 2014) and Split-Spectrum method (Gomba et al., 2016), respectively. However, it is still a challenging task to detect the ground deformation less than several centimeters with two-pass D-InSAR method.
Recently, InSAR time series analysis has been developed where a number of images are processed and statistically analyzed to extract deformations with enhanced accuracies. Persistent Scatter Interferometry method (PSI method) and Small Baseline Subset algorithm method (SBAS method) are typical examples of InSAR time series analysis. GSI has been developed the InSAR time series analysis system (GSITSA) which includes PSI method and SBAS method (Kobayashi et al., 2018). Kobayashi et al., (2018) compared the result of InSAR time series analysis with levering data of same period in subsidence area and showed that with InSAR time series analysis one could detect ground deformation with a velocity of 1 cm / year or less. Thus ground deformation detection capability of InSAR time series analysis is better than that of the two-pass D-InSAR method, and the analysis should be useful for monitoring ground deformation all over Japan more accurately. Furthermore, with Advanced Land Observing Stellite-4 (ALOS-4) that is planned for launch in the 2020 fiscal year, the observation frequency will be increased by five-fold compared to that of ALOS-2, and the InSAR time series analysis should be more applicable.
With this background, we investigated the characteristics of PSI method and SBAS method using GSITSA for consideration of introducing InSAR time series analysis into our future strategy for ground deformation monitoring. In this study, we conducted InSAR time series analysis with ALOS-2 data for Niigata Plain and Tsugaru Plain as examples of land subsidence area, and Mt. Kirishima (Mt. Iwoyama) and Mt. Usu as examples of active volcano area, respectively. In InSAR time series analysis, we were able to detect similar ground deformation in the areas where ground deformation were detected by the two-pass D-InSAR method. In addition, we were able to detect some ground deformation of about 1 cm per year that could not be detected with the two-pass D-InSAR method.
In this presentation, we will show the results of comparison between PSI method and SBAS method, and discuss the optimal analysis strategy focusing on spatial scale and vegetation.
"Acknowledgment"
ALOS-2 data were provided from the Volcano Working Group under a cooperative research contract with JAXA (Japan Aerospace Exploration Agency). The ownership of ALOS-2 data belongs to JAXA.

Keywords: "DAICHI-2"(ALOS-2), SAR, Volcanic activity, Ground deformation

©2019. Japan Geoscience Union. All Right Reserved.

[J] Poster | S (Solid Earth Sciences)：S-TT Technology & Techniques

Mon. May 27, 2019 5:15 PM - 6:30 PM JST | Mon. May 27, 2019 8:15 AM - 9:30 AM UTC | Poster Hall International Exhibition Hall8, Makuhari Messe_27

[S-TT45] Synthetic Aperture Radar

convener:Youhei Kinoshita(University of Tsukuba), Yu Morishita(Geospatial Information Authority of Japan), Shoko Kobayashi(Tamagawa University), Takahiro Abe(Earth Observation Research Center, Japan Aerospace Exploration Agency)

ALOS-2 and Sentinel-1A and 1B, which have highly enhanced capacity compared to previous SAR satellites, were launched in 2014, and their utilization has been widely expanding as the data has accumulated for approximately four years. Other long-operating SAR satellites like TerraSAR-X and Cosmo-SkyMed also contribute to expanding the SAR utilization. Now we are facing a new and abundant era of the satellite SAR, along with a worldwide trend to an open and free data policy of satellite data, with next-generation advanced SAR satellite plans by several countries, and with several plans to construct SAR constellations by private sectors. In addition, SAR technologies with other platforms, such as ground-based SAR with high temporal resolution and UAV (Unmanned Aerial Vehicle) SAR with flexible operability, have also been developed and used for various targets. These facts indicate that the SAR utilization has become widespread in both basic researches (e.g., earth science) and diverse applications (e.g., disaster prevention and forest monitoring). In this session, we would like to widely invite research and application results with regard to SAR, sharing our knowledge and having a discussion for the advancement of the SAR utilization.

[STT45-P01] Development of InSAR tropospheric phase delay correction system at MRI (2nd report)

*Okuyama Satoshi[1], Shinobu Ando[1], Toshiki Shimbori[1] (1.Meteorological Research Institute)

[STT45-P02] Mitigation of atmospheric delay in InSAR for fair estimate of crustal deformation at Azumayama volcano

*Kana Abe[1], Yoshiko Ogawa[1], Yasuhiro Hisada[1], Hirohide Demura[1], Taku Ozawa[2], Satoshi Miura[3], Akira Kusakabe[1], Takehiro Arai[1] (1.The University of Aizu, 2.National Research Institute for Earth Science and Disaster Resilience, 3.Graduate School of Science, Tohoku University)

[STT45-P03] Unusual displacement observed in InSAR analysis results of fumarolic area of active volcanos: An example of the Kamiyu district in Hakone Volcano

*Ryosuke Doke[1], Kazuhiro Itadera[1] (1.Hot Springs Research Institute of Kanagawa Prefecture)

[STT45-P04] Detection of Deformation Signals at Mud Volcanoes in Semau Island, Indonesia

*Naufal Setiawan[1], Masato Furuya[1] (1.Hokkaido University)

[STT45-P05] Extraction of supraglacial lakes on debris-covered glacier using ALOS-2/PALSAR-2

Chikako Kinefuchi[2], *Chiyuki Narama[1], Tsutomu Yamanokuchi[3], Takeo Tadono[4] (1.Niigata University, Program of Field Research in the Environmental Sciences, 2.Graduate School of Science and Technology, Niigata University, 3.RESTEC, 4.JAXA)

[STT45-P06] **Observation of the water level fluctuation at Ozegahara by ALOS-2/PALSAR-2**

*Wataru Iwatate[1], Masanobu Shimada[1] (1.Tokyo Denki University)

[STT45-P07] The steady crustal deformation around the Omaezaki, Sionomisaki, Muroto and Ashizuri, using InSAR time-series analysis 2

*Shinobu Ando[1], Akio Kobayashi[1] (1.Seismology and Tsunami Research Department, Meteorological Research Institute)

[STT45-P08] Evaluation of InSAR analysis result using pipe strain gauge data in Otari village, Nagano prefecture, Japan

*Tomoya Kiyosawa[1], Hiroshi, P. Sato[2] (1.Department of Geography, Graduate School of Science and Technology, Nihon University , 2.College of Humanities and Science, Nihon University)

[STT45-P09] DEM creation using ALOS / PALSAR interferometric SAR and its accuracy evaluation.

*takahashi koya[1], Masanobu Shimada[1] (1.tokyo denki university)

[STT45-P10] Approach to monitoring ground deformation using InSAR time series analysis all over Japan

*Kyonosuke Hayahsi[1], Tatsuya Yamashita[1], Masaki Kuwahara[1], Masaki Honda[1], Kazuki Sakai[1], Hiroshi Munekane[1], Tomokazu Kobayashi[1] (1.GSI of Japan)

Development of InSAR tropospheric phase delay correction system at MRI (2nd report)

*Okuyama Satoshi[1], Shinobu Ando[1], Toshiki Shimbori[1]

1. Meteorological Research Institute

Introduction

SAR Interferometry is a technique which utilize the phase information of the SAR images to detect surface displacement which took place between two observations. However, its result contains the effect of medium between the antenna and the target such as tropospheric delay. Conventional method to correct tropospheric delay is proposed by Fujiwara et al. (1999), which assumes that the delay is a function of topographic height. On the other hand, correction using numerical weather model, which is independent data from SAR interferogram, is also proposed (Hobiger et al., 2008; Ozawa and Shimizu, 2010). We started the development of tropospheric delay correction system in MRI and reported our preliminary result (Okuyama et al., 2018). In our preliminary analysis, we calculated zenith delay and projected it on line-of-sight of the SAR observation. As an improvement, we replaced this by the integration of refractivity along line-of-sight of the SAR observation.

System composition

Our correction system consists of three units: 1) read grid point values (NuSDaS format) and interpolate in time to generate gridded data at the observation time, 2) calculate refractivity at each gridpoint, and 3) integrate refractivity to calculate the delay at each pixel in the interferogram. This composition allows us to replace each unit separately. For example, when new weather model is released, we replace unit 1) only, leaving the rest of the units unchanged.

Difference from preliminary result

We corrected interferogram of PALSAR-2 (path125/frame660, 2015/1/4 - 2015/8/16) using JMA-MA (Meso Analysis) data by both (A) projecting zenith delay on line-of-sight and (B) integrating the refractivity along line-of-sight. As stated above, tropospheric delay tends to have strong correlation between topography. Thus, we use correlation coefficient between phase and topographic height as a measure of correction quality. We obtained correlation coefficient of -0.431 for original interferogram, -0.097 for correction (A), and -0.047 for correction (B).
The difference between (A) and (B) shows correlation between delay and topography, however its factor shows horizontal variation. This is caused by the horizontal variation of the refractivity. The maximum difference between (A) and (B) is -2.1 radians.

Future direction

We will develop the support for other model types such as JMA-LA (Local Analysis) or JMA-GA (Global Analysis) as next step and validate the algorithm of interpolation/refractivity.

Acknowledgement

PALSAR-2 level 1.1 data are shared among PIXEL (PALSAR Interferometry Consortium to Study our Evolving Land surface) and provided from JAXA under a cooperative research contract with ERI, Univ., Tokyo. The ownership of PALSAR-2 data belongs to JAXA.

©2019. Japan Geoscience Union. All Right Reserved.

Keywords: SAR interferometry, atmospheric delay, numerical weather model

©2019. Japan Geoscience Union. All Right Reserved.

Mitigation of atmospheric delay in InSAR for fair estimate of crustal deformation at Azumayama volcano

*Kana Abe[1], Yoshiko Ogawa[1], Yasuhiro Hisada[1], Hirohide Demura[1], Taku Ozawa[2], Satoshi Miura[3], Akira Kusakabe[1], Takehiro Arai[1]

1. The University of Aizu, 2. National Research Institute for Earth Science and Disaster Resilience, 3. Graduate School of Science, Tohoku University

Azumayama volcano is one of the five active volcanoes in Fukushima prefecture which is now issued volcanic alert level 2. Since 2014 winter, the volcano had/has been issued the level 1 and 2 repeatedly according to the situation. It is the most active volcano in the Fukushima pref. We have been working to clarify time-series of crustal deformation at Azumayama volcano.

Abe et al. [2017, JpGU] conducted InSAR (Interferometric Synthetic Aperture Radar) analysis using ALOS2 (Advanced Land Observing Satellite 2)/PALSAR2 (Phased Array L-band Synthetic Aperture Radar-2) data and estimated crustal deformation around Azumayama volcano . However, some of the results showed subsidence at the west of Azumayama which would be due to atmospheric delay and ionospheric delay.

In this study, we attempted to correct atmospheric delay and ionospheric delay in InSAR analysis using three numerical weather models: MSM (MesoScale Model), LFM (Local Forecast model) and WRF (Weather Research and Forecasting). WRF is created by using MSM data to improve resolution of time. Then we tried to estimate the amount of crustal deformation more precisely from 2014 fall to 2017 fall after applying atmospheric correction. Eight of the ALOS2/PALSAR2 data were used for the InSAR analysis. We evaluated the InSAR results after performing each atmospheric correction based on each numerical model and compare them quantitatively and select suitable weather model among the three.

Artifacts and false fringe in InSAR results seem to be reduced. Comparing InSAR analysis results with the value of GNSS (Global Navigation Satellite System) analysis at ground stations, correction by LFM and WRF showed similar trend better than that by MSM. Numerical weather models with higher resolutions seem effective in correcting atmospheric delay in InSAR. Uplift and subsidence at the Oana crater and subsidence in the western part of Azumayama were detected during 2014 fall - 2015 summer and 2015 summer - 2015 fall, respectively, which reflect actual deformation.

Keywords: Azumayama, crustal deformation, volcano, SAR, numerical weather model

©2019. Japan Geoscience Union. All Right Reserved.

Unusual displacement observed in InSAR analysis results of fumarolic area of active volcanos: An example of the Kamiyu district in Hakone Volcano

*Ryosuke Doke[1], Kazuhiro Itadera[1]

1. Hot Springs Research Institute of Kanagawa Prefecture

In this presentation, we report on the characteristics and causes of displacements observed in the InSAR analysis results of ALOS-2/PALSAR-2 data for the fumarolic area in the Kamiyu area of the Hakone volcano.

The Kamiyu fumarolic area is in the northern slope of the central cone of the Hakone volcano and located about 500m north of the Owakudani fumarolic area that had phreatic eruptions in 2015. The Kamiyu fumarolic area was formed around 2003 after the 2001 swarm earthquake occurred at the Hakone Volcano (Tsujiuchi et al., 2003). The most active fumarole in the Kamiyu area is the area called E region, which was activated after the earthquake swarm induced by the 2011 Tohoku Earthquake (Yukutake et al., 2011; Harada et al., 2012). The scale of the E region is about 200m north to south and about 150m east to west. Moreover, the heat flux from the E region is estimated to be 7 to 8 MW (Mannen et al., 2018).

The observation by ALOS-2/PALSAR-2 for the Hakone volcano has been carried out repeatedly, mainly in four orbits, and each orbit is performed almost once every several months. From October 2014 to the end of 2018, data from descending orbit with right looking angles were obtained 22, and 15 scenes in Path 18 and 19, respectively, and data from ascending orbit with right looking angles were obtained 11 scenes in Paths 125 and 126, respectively. In this study, we performed DInSAR analysis with the latest interference pairs for all these data and clarified the displacement of the ground surface in the Kamiyu E region.

In the observation from the east side (Paths 18, 19), the Kamiyu E region displaced about 3 to 5 cm toward the satellite with respect to a reference point outside the fumarolic area during about four years. Moreover, in the observation from the west side (Paths 125, 126) displaced about 10 to 13 cm away from the satellite during the same period. These results suggest that the E region steadily displaces in the northeast direction in the long term, which also coincides with the inclination direction of the E region so that it is considered that the landslide displacement is occurring.

On the other hand, the analysis results of Paths 18 and 19 observed from the east side show the seasonal displacement that the area moved toward the satellite in the summer seasons and away from the satellite in winter seasons. In Paths 125 and 126 observed from the west side, such seasonal displacement is not observed, but these Paths have few observations in the summer and cannot judge the actual seasonal displacement. One of the possible causes of this seasonal displacement is a seasonal change in contrast between the vapor amount inside of the fumarolic area and that of the outside. The amount of water vapor near the ground changes seasonally outside of the fumarolic area whereas it is almost saturated throughout the year in the fumarolic area. Such contrast between the summer and winter is possibly affecting the DInSAR results. Another possible cause is an effect of the difference of soil moisture between summer and winter season because the fumarolic area is almost bare land and surface scattering is more dominant than forest area. Other factors are also conceivable, but we are considering the possibilities to evaluate the fumarolic activities from this seasonal displacement, in addition to accurately evaluate the

©2019. Japan Geoscience Union. All Right Reserved.

landslide movement in the fumarolic area.

ALOS-2/PALSAR-2 data were provided by JAXA via the Coordinating Committee for the Prediction of Volcanic Eruption as part of the project, “ALOS Domestic Demonstration on Disaster Management Application,” of the Volcano Working Group. The original ALOS-2/PALSAR-2 data belong to JAXA.

Keywords: InSAR, active volcano, fumarolic area, Hakone Volcano

©2019. Japan Geoscience Union. All Right Reserved.

Detection of Deformation Signals at Mud Volcanoes in Semau Island, Indonesia

*Naufal Setiawan[1], Masato Furuya[1]

1. Hokkaido University

Mud volcanoes are associated with fluid and solid material vertical extrusion from its source layer (mud reservoir). The size and shape of the mud volcanoes throughout the world are diverse. Furthermore, the reason behind this event is difference in each region but predominantly occurred at convergent plate margins. To date, the most mud extrusion known is in the Mediterranian Sea and Tethyan belt (including Azerbaijan, south Greece, Iran, and Turkmenistan).

Semau Island, located in Timor area of Indonesia, is one of the islands where the northern margin of Australian continental plate meets Banda sea plate. Previous geologic map identified Semau island hosted six mud volcanoes with no description in its size [Barber, et al. 1986], and some of them erupt only mud, whereas others produce mud with an admixture of liquid hydrocarbons [Kholodov. 2002].

In order to detect any possible deformation signals in the mud volcanoes in this region, we applied InSAR method. Twenty four (24) ascending images and ten (10) descending images of ALOS/PALSAR data spanning from 2006 to 2011 were acquired. Because our research area is not covered by single observation image, we concatenate the consecutive frame number. To enhance the processing step in GAMMA software, the oceanic areas and some part of other islands that not our interest were cropped to focus on Semau Island. Interferograms of ALOS/PALSAR dataset were consist of eleven (11) ascending pairs and four (4) descending pairs. Then, using AW3D30 DEM data we tried to remove topographic fringe. During the processing, images were multi-looked in range and azimuth by 2 and 6 respectively. While the oversampling in the azimuth direction can be avoided due to the effect of azimuth slope is limited, range oversampling by a factor of two is needed for good quality of interferogram. This procedure is to avoid uncorrelated contributions that arise in the spectral cross-correlation from interferogram generation. Finally, we applied low order polynomial to mitigate the effects of long wavelength phase trends in our interferograms.

The deformation signal is hardly detected in the majority of the data pairs, due to the unwrapping errors in some pairs and also probably due to the small size of mud volcanoes. Despite low coherence in the possible mud extrusion source, in two image pairs, we detected the possible signal from the mud volcano area that is identical to the location described from the previous geologic map. However, since the geologic map from the previous study was derived from aerial photograph interpretation and the signal detection is in slope area, further research is needed to confirm if it is related to active mud volcanism or simply a landslide signal.

Keywords: Mud volcanoes, InSAR, Landslide

©2019. Japan Geoscience Union. All Right Reserved.

Extraction of supraglacial lakes on debris-covered glacier using ALOS-2/PALSAR-2

Chikako Kinefuchi[2], *Chiyuki Narama[1], Tsutomu Yamanokuchi[3], Takeo Tadono[4]

1. Niigata University, Program of Field Research in the Environmental Sciences, 2. Graduate School of Science and Technology, Niigata University, 3. RESTEC, 4. JAXA

In the eastern part of the Himalaya (eastern Nepal and Bhutan), large drainages occur from supraglacial lakes on debris-covered glaciers when large lake connects to englacial network (Komori et al., 2012; Rounce et al., 2016; Miles et al., 2018). In the Himalaya, it is difficult to monitor the variations of supraglacial lakes during summer, because most optical satellite images are covered by cloud due to Indian monsoon. It is possible to investigate supraglacial lake under cloud using ALOS-2/PALSAR-2 of microwave sensor. However, backscatter of supraglacial lake differs in relief conditions on debris-covered glacier, and ice cliff and depression also have lower backscatter. In this study, we try to extract supraglacial lakes correctly using ALOS-2/PALSAR-2 data analysis.

Keywords: supraglacial lake, debris-covered glacier, ALOS-2/PALSAR-2, relief amount

©2019. Japan Geoscience Union. All Right Reserved.

Observation of the water level fluctuation at Ozegahara by ALOS-2/PALSAR-2

*Wataru Iwatate[1], Masanobu Shimada[1]

1. Tokyo Denki University

The SAR can measure the phase and the amplitude of the reflected wave from the surface object. This phase contains information on the round trip distance from the antenna to the surface of the earth in general, and more precisely the fraction of the above distance off the wave length. By differenciating two individual measurements, it can detect a slight distance difference. By using this InSAR technique, we can see the change of the Earth's surface due to earthquakes and volcanic eruptions in a visible form. On the water surface such as river, sea, lake, it is always moving by waves, so it is difficult to measure in places where the reflecting surface is not constant. However, in wetlands where grass and reeds are growing on top, the radar signal emitted to the water surface may reflect back from the grass and reeds, and return to the satellite.

Therefore, our research themes were defined to verify the possibility of observation on the water level change during two different observations. The target area was selected from the Honjou's largest Ozasegahara in wetlands. This Ozegahara is located in the Oze National Park, around the border areas of Fukushima, Tochigi Prefecture, Gunma, and Niigata Prefectures, and it is composed of 2,000 m class mountains. The observation was carried out using the period from September 2014 to May 2018 of PALSAR - 2 installed in JAXA 's Daichi 2 (ALOS 2). Since it is told that the water level of Ozegahara decreases, if the numerical value obtained by using the interference SAR technique shows a decrease, we can verify the possibility of observation on the water surface. In fact, we got an average of about -6.6 cm as a annual decreases. Comparing rainfall, etc., we can see that the water level goes down, and it was possible to show that the water level observation in the wetland zone is possible.

As future developments, it is conceivable to conduct verification in terms of accuracy from the possibility. One way to do this is to observe it using GPS or water gauge.

Keywords: Interferometry, ALOS-2, PALSAR-2

©2019. Japan Geoscience Union. All Right Reserved.

The steady crustal deformation around the Omaezaki, Sionomisaki, Muroto and Ashizuri, using InSAR time-series analysis 2

*Shinobu Ando[1], Akio Kobayashi[1]

1. Seismology and Tsunami Research Department, Meteorological Research Institute

At the Meteorological Research Institute, we are working on detection of crustal deformation using satellite SAR data as a method to detect changes in locked part such as slow slips and pre-slips at the plate boundary.

Especially focusing on the large-scale earthquake of the Nankai-Trough which is concerned about the occurrence in the near future, near the cape from Tokai to Shikoku which is close to the subduction zone of the plate and is thought to be susceptible to the change of the fixation state Analysis was conducted as an object.

We carried out InSAR time series for ALOS/PALSAR data to detect the steady crustal deformation around the cape from Tokai to Shikoku. As a result, we confirmed that the result of InSAR time series analysis correspond to GNSS data (Ando et al., 2018).

In this report, we tried to analysis for these data using InSAR time series analysis because of the archive data of ALOS-2/PALSAR-2 (operation period: 2014 -) has been adequately accumulated. In this analysis, interferograms were generated using RINC software (Ozawa et al., 2016), and then we carried out InSAR time series analysis about these data by SBAS method using GIAnT software (Agram et al., 2011). The data of each area used for the analysis is as follows.

Omaezaki: path 19 (18 scenes) and path 126 (11 scenes),

Shionomisaki: path 20 (16 scenes) and path 128 (11 scenes),

Muroto: path 21 (14 scenes) and path 128 (10 scenes),

Ashizuri: path 22 (14 scenes) and path 129 (10 scenes).

In principle, we used all data in which the archive exists for analysis in any path, but recalculated after excluding data which is clearly an error by checking the analysis result. The cumulative displacement result of Omaezaki (path 19) is shown in Fig.1.

As a result, we detected the elongation of displacement around the cape and shortening of displacement in the inland. The trends of these displacement distributions are similar to those of ALOS/PALSAR. In this presentation, we also report on the comparison with the GNSS observation results in the analysis area.

Some of PALSAR-2 data we used were provided by the Japan Aerospace Exploration Agency (JAXA) via the 6th ALOS-2 research announcement (RA-6). PALSAR-2 data belongs to JAXA. In the process of the InSAR, we used Digital Ellipsoidal Height Model (DEHM) based on the digital elevation map 10m-mesh provided by Geospatial Information Authority of Japan (GSI), and Generic Mapping Tools (P.Wessel and W.H.F.Smith, 1999) to prepare illustrations.

©2019. Japan Geoscience Union. All Right Reserved.

Keywords: ALOS-2/PALSAR-2, TS–InSAR, crustal deformation, Nankai-Trough

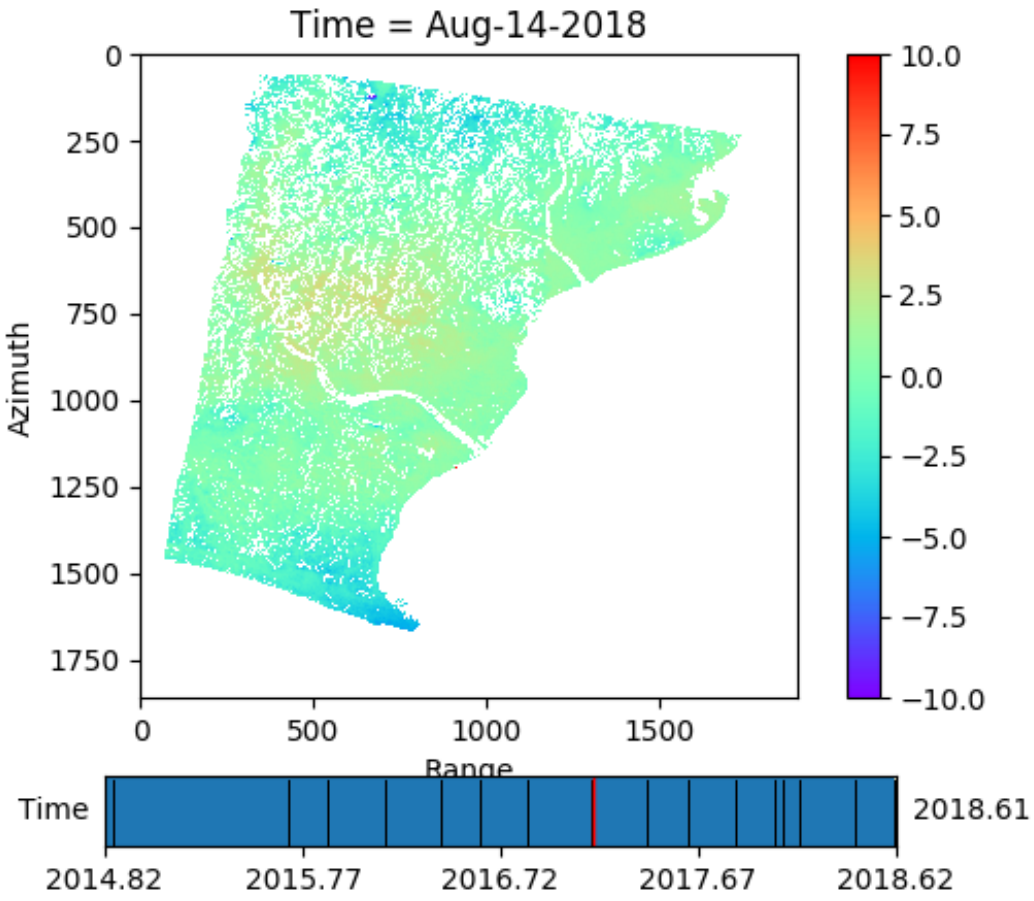

©2019. Japan Geoscience Union. All Right Reserved.

Evaluation of InSAR analysis result using pipe strain gauge data in Otari village, Nagano prefecture, Japan

*Tomoya Kiyosawa[1], Hiroshi, P. Sato[2]

1. Department of Geography, Graduate School of Science and Technology, Nihon University , 2. College of Humanities and Science, Nihon University

In order to detect landslide surface deformation, InSAR (Synthetic Aperture Radar interferometry) images were produced and interpreted in the study area of Ahara area in Otari Villege, Nagano Prefecure in Japan. The images were produced from time-series ALOS-2/PALSAR-2 data, taken from September 2014 to March 2018. More than 50 InSAR images were produced; however, at most four images gave good coherence available to interpret and detect the deformation. The one was taken on and the three were after Kamishiro Fault earthquake (M 6.7) on 22 Nov 2014. As a result of images interpretation, westwards deformation was detected up to ca. 2.5 cm and 4.5 cm along LoS (line of sight) on and after the earthquake, respectively.

To take measures against landslide disaster, Nagano Prefecture installed pipe type strain gauge in Ahara area, and the measured strain data were used to evaluate the image-detected deformation. As a result, at the slip layer of 8-m depth from the ground, the strain gauge measured 13 μST on the earthquake and it also indicated westward deformation. Empirically, strain over ca. 20,000 μST cuts electric measurement cables, and this strain is known to be equal to 2-3 cm deformation under the ground. Therefore, 13 μST is thought to be correspondent to 0.0013 cm deformation. Thus, the image-detected deformation itself was proved by the gauge-measured strain data and westward deformation direction was harmonized with the gauge-measured strain data. However, it was found that the image-detected deformation amount is 2,000 times larger than the strain gauge-calculated deformation amount.

Focusing on the deformation after the earthquake, as the observation periods of the images were not overlapped with measurement period of the strain gauge, assuming that the deformation proceeds at uniform speed in landslide body, then, both data were compared in daily mean deformation speed. The image-detected speed was calculated as 0.025-0.064 cm/day, and strain gauge-detected speed 0.000083 cm/day was calculated from 58 μST. It was found that the image-detected deformation speed is 300-780 times larger than the strain gauge-calculated speed. We think that this difference is attributed to the fact that InSAR measured the deformation not on the ground but along LoS distance and strain gauge measured the deformation not on the ground but under the ground. Furthermore, we think that the reason of more difference of the deformation amount on the earthquake than after the earthquake is that the image on the earthquake includes the deformation not only by landslide surface deformation but also crustal deformation by the earthquake.

Keywords: PALSAR-2, Landslide, InSAR

©2019. Japan Geoscience Union. All Right Reserved.

DEM creation using ALOS / PALSAR interferometric SAR and its accuracy evaluation.

*takahashi koya[1], Masanobu Shimada[1]

1. tokyo denki university

Digital Elevation Model (DEM) is a digital representation of the terrain on the ground surface, with the ground surface divided into equally spaced squares and the elevation of the center point of the square is given. In general, it expresses the surface of the earth that does not include vegetation, buildings, bridges, etc. DEM is often used in geographic information systems and is used as basic data in creating a three-dimensional map on a computer. There are several methods of making DEM, such as parallax measurement that combines optical pictures observed from multiple directions, interference processing of synthetic aperture radar, airborne laser surveying to find height using a laser mounted on an aircraft, etc. In this study We will prepare DEM by Synthetic Aperture Radar (SAR) and study related errors. DEM is created using synthetic aperture radar installed in ALOS and compared with DEM of Geographical Survey Institute. We measured the error, calculated the difference from the theoretical value, and evaluated its effectiveness. As a result, DEM creation by SAR was conducted for Hatoyama cho Higashi-gun (forest, residential area, Tabata), and the difference from the theoretical value occurred several centimeters to several tens of meters, but the average error was 9.94 m Therefore, through this study, we believe that practicality of DEM creation by SAR is sufficient.

Keywords: SAR, Digital Elevation Model

©2019. Japan Geoscience Union. All Right Reserved.

Approach to monitoring ground deformation using InSAR time series analysis all over Japan

*Kyonosuke Hayahsi[1], Tatsuya Yamashita[1], Masaki Kuwahara[1], Masaki Honda[1], Kazuki Sakai[1], Hiroshi Munekane[1], Tomokazu Kobayashi[1]

1. GSI of Japan

GSI (Geospatial Information Authority Japan) has been monitoring ground deformation all over Japan with ALOS-2 data by applying two-pass Differential Synthetic Aperture Radar Interferometry (D-InSAR) method. The two-pass D-InSAR method is a procedure to extract deformation that occurred between two observations from two radar images obtained from two observations. The two-pass D-InSAR method is susceptible to errors due to tropospheric disturbances, ionospheric disturbances, and change of the ground surface such as vegetation, which can be obstacles in detecting small ground deformations. Tropospheric disturbances and ionospheric disturbances may be reduced by Ray-tracing algorithm using numerical weather prediction model data (Kobayashi et al., 2014) and Split-Spectrum method (Gomba et al., 2016), respectively. However, it is still a challenging task to detect the ground deformation less than several centimeters with two-pass D-InSAR method.
Recently, InSAR time series analysis has been developed where a number of images are processed and statistically analyzed to extract deformations with enhanced accuracies. Persistent Scatter Interferometry method (PSI method) and Small Baseline Subset algorithm method (SBAS method) are typical examples of InSAR time series analysis. GSI has been developed the InSAR time series analysis system (GSITSA) which includes PSI method and SBAS method (Kobayashi et al., 2018). Kobayashi et al., (2018) compared the result of InSAR time series analysis with levering data of same period in subsidence area and showed that with InSAR time series analysis one could detect ground deformation with a velocity of 1 cm / year or less. Thus ground deformation detection capability of InSAR time series analysis is better than that of the two-pass D-InSAR method, and the analysis should be useful for monitoring ground deformation all over Japan more accurately. Furthermore, with Advanced Land Observing Stellite-4 (ALOS-4) that is planned for launch in the 2020 fiscal year, the observation frequency will be increased by five-fold compared to that of ALOS-2, and the InSAR time series analysis should be more applicable.
With this background, we investigated the characteristics of PSI method and SBAS method using GSITSA for consideration of introducing InSAR time series analysis into our future strategy for ground deformation monitoring. In this study, we conducted InSAR time series analysis with ALOS-2 data for Niigata Plain and Tsugaru Plain as examples of land subsidence area, and Mt. Kirishima (Mt. Iwoyama) and Mt. Usu as examples of active volcano area, respectively. In InSAR time series analysis, we were able to detect similar ground deformation in the areas where ground deformation were detected by the two-pass D-InSAR method. In addition, we were able to detect some ground deformation of about 1 cm per year that could not be detected with the two-pass D-InSAR method.
In this presentation, we will show the results of comparison between PSI method and SBAS method, and discuss the optimal analysis strategy focusing on spatial scale and vegetation.
"Acknowledgment"
ALOS-2 data were provided from the Volcano Working Group under a cooperative research contract with JAXA (Japan Aerospace Exploration Agency). The ownership of ALOS-2 data belongs to JAXA.

Keywords: "DAICHI-2"(ALOS-2), SAR, Volcanic activity, Ground deformation

©2019. Japan Geoscience Union. All Right Reserved.

[J] Oral | S (Solid Earth Sciences)：S-TT Technology & Techniques

Mon. May 27, 2019 1:45 PM - 3:15 PM JST | Mon. May 27, 2019 4:45 AM - 6:15 AM UTC | A08 TOKYO BAY MAKUHARI HALL

[S-TT46] Seismic Big Data Analysis Based on the State-of-the-Art of Bayesian Statistics

convener:Hiromichi Nagao(Earthquake Research Institute, The University of Tokyo), Aitaro Kato(Earthquake Research Institute, the University of Tokyo), Takuto Maeda(Graduate School of Science and Technology, Hirosaki University), Keisuke Yano(The university of Tokyo), Chairperson:Nana Yoshimitsu(Earthquake Research Institute, The University of Tokyo), Takeru Matsuda(Graduate School of Information Science and Technology, The University of Tokyo)

Recently, a big seismic database has been being constructed that collects data of vibrators implemented in such as buildings, lifelines and smartphones, in addition to seismic data of the conventional continuous/temporal dense seismic observation arrays. Development of methodologies and algorithms, which are inadequate at this moment, optimized to comprehensively analyze the seismic big data is essential in order to utilize the big database as much as possible for prevention/mitigation of earthquake disasters and clarification of earthquake phenomena. On the other hand, recent progress of Bayesian statistics is significant, which is the mathematical basis of various methodologies, such as machine learning, especially deep learning, to extract valuable information from big data. The state-of-the-art of Bayesian statistics is expected to substantially advance seismic big data analyses.
This session mainly accepts presentations that focus on analyses of seismic big data, especially related to analysis methods based on Bayesian statistics such as machine learning, sparse modeling and data assimilation, and their applications to real seismic data. Presentations related to mathematical or statistical theories beneficial to data analyses, feasibility studies of algorithms eventually applicable to real seismic data, and the current status of seismic observations and analysis results are also highly welcome.

1:45 PM - 2:00 PM JST | 4:45 AM - 5:00 AM UTC

[STT46-01] A bad inversion result suggests bad modeling

★Invited Papers

*Yukitoshi Fukahata[1], Yuji Yagi[2] (1.Disaster Prevention Research Institute, Kyoto University, 2.Graduate School of Life and Environmental Sciences, University of Tsukuba)

2:00 PM - 2:15 PM JST | 5:00 AM - 5:15 AM UTC

[STT46-02] A seismic wavefield estimation in a dense seismograph network: An optimization for the MeSO-net

*Takahiro Shiina[1], Takuto Maeda[2], Masayuki Kano[3], Aitaro Kato[1], Naoshi Hirata[1] (1.Earthquake Research Institute, The University of Tokyo, 2.Graduate School of Science and Technology, Hirosaki University, 3.Graduate school of science, Tohoku University)

2:15 PM - 2:30 PM JST | 5:15 AM - 5:30 AM UTC

[STT46-03] Uncertainty quantification based on 4DVar data assimilation for massive simulation models

*Shin-ichi Ito[1], Masayuki Kano[2], Hiromichi Nagao[1] (1.The University of Tokyo, 2.Tohoku University)

2:30 PM - 2:45 PM JST | 5:30 AM - 5:45 AM UTC

[STT46-04] Bayesian approach for statistical modeling and forecasting of aftershock activities

★Invited Papers

*Takahiro Omi[1] (1.Institue of Industrial Science, the University of Tokyo)

2:45 PM - 3:00 PM JST | 5:45 AM - 6:00 AM UTC

[STT46-05] Bias Correction for the Distribution of Aftershocks Within Short-Term Period Immediately After Large Main Shock

*Kosuke Morikawa[1], Hiromichi Nagao[2], Shin-ichi Ito[2], Shin'ichi Sakai[2], Naoshi Hirata[2] (1.Osaka University, 2.Earthquake Research Institute, The University of Tokyo)

3:00 PM - 3:15 PM JST | 6:00 AM - 6:15 AM UTC

[STT46-06] Deep-learning-based Earthquake Detection for Continuous Seismic Network Records

*Keisuke Yano[1], Takahiro Shiina[2], Sumito Kurata[1], Aitaro Kato[2], Fumiyasu Komaki[1], Shin'ichi Sakai[2], Naoshi Hirata[2] (1.Graduate School of Information Science and Technology, The University of Tokyo, , 2.Earthquake Research Institute, The University of Tokyo)

A bad inversion result suggests bad modeling

*Yukitoshi Fukahata[1], Yuji Yagi[2]

1. Disaster Prevention Research Institute, Kyoto University, 2. Graduate School of Life and Environmental Sciences, University of Tsukuba

Bayesian inference is a powerful tool in inversion analyses of geophysical problems. In Bayesian inference, we always encounter a problem in determining the relative weight between observed data and prior information. ABIC (Akaike's Bayesian Information Criterion) gives an objective solution to this problem by maximizing the marginal likelihood for the relative weight. In principle, ABIC gives us an inverse solution that mostly follows observed data when we have enough amounts of data with good accuracy, and gives us an inverse solution that mostly follows prior information when observed data are insufficient and/or inaccurate.

In inversion analyses using ABIC, we do not manually adjust the relative weight. Hence, geophysically unrealistic results are quite easily obtained. Because of that, someone may think that inversion analyses using ABIC is difficult in dealing with or even unreliable. However, this is an excellent point of ABIC. If we obtain a geophysically unrealistic result, this implies that some problems are hidden in this analysis.

In this talk, we show some examples of the invention of inversion methods inspired by ABIC, including the discovery of the importance of modeling errors. As shown by these examples, we can get closer to the true solution not by manually adjusting the relative weight to obtain a seemingly good-looking result, but by determining the relative weight statistically. It is a harder way to determine the relative weight statistically, but we should pursue this way to understand geophysical problems more appropriately.

Keywords: Inversion analysis, ABIC, slip distribution of earthquakes

©2019. Japan Geoscience Union. All Right Reserved.

A seismic wavefield estimation in a dense seismograph network: An optimization for the MeSO-net

*Takahiro Shiina[1], Takuto Maeda[2], Masayuki Kano[3], Aitaro Kato[1], Naoshi Hirata[1]

1. Earthquake Research Institute, The University of Tokyo, 2. Graduate School of Science and Technology, Hirosaki University, 3. Graduate school of science, Tohoku University

MeSO-net (Metropolitan Seismic Observation network) is a dense seismograph network deployed in and around Tokyo, Japan [Kasahara et al., 2009; Sakai and Hirata, 2009]. Station separation of the MeSO-net is about 5 km on average and ~2 km at the densest area. Recently, some reconstructing method of seismic wavefield in such dense seismograph networks have been developed [e.g., Langston, 2007; Kano et al., 2017]. Kano et al. [2017] proposed a wavefield imaging method based on the data assimilation: they demonstrated the reconstructions of wavefield up to ~1 Hz using the MeSO-net. Their method can simultaneously determine layered structures and location of the hypocenter. Seismic wave gradiometry (SWG) method is also well known as another method for estimating 2D seismic wavefield. The SWG method has low computational cost and can apply to observations without assumptions of hypocenter and structural heterogeneity. Therefore, the SWG method will be useful for monitoring wavefield and investigating ground motions without source data as prior information.
We adopt the SWG method developed by Maeda et al. [2016] to estimate seismic wavefield within the MeSO-net. In this method, amplitude and its spatial gradients of seismic wave at grid points are estimated from observed amplitude at surrounding stations. Interpolation coefficients used for the estimation are determined by the weighted least squares technique and are only depended on a grid-station distance.
In order to optimize the interpolation coefficient, we perform the analysis based on numerical modeling. The finite difference modeling, the OpenSWPC [Maeda et al., 2017], is used to simulate seismic waves at any grid points and sites of which locations correspond to the MeSO-net stations. For the simulated waveforms, we adopt bandpass filter of 0.1-0.2 Hz which is lower than the upper-limit frequency of our numerical modeling, ~0.25 Hz. Then, we synthesize waveform at a grid point from simulated ones at surrounding sites by the SWG method. As the weighting function imposing to the least square, we assume the 2D Gaussian form with respecting to the grid-station distance. The 2D Gaussian weight is characterized by the lengths in two orthogonal axes, long and short arms, and a rotation angle of the short axis in the clockwise direction from the north. The ” optimization” in this study is to find the three parameters which maximize the three-components cross-correlation coefficient between the SWG-synthesize and the simulated waveforms at the grid point. We investigate the parameters by the grid search technique.
We carry out the numerical simulations for hypocenters of 12 directions with 30 degree interval. The hypocenters are located at a depth of 10 km and a distance of 150 km from the center of the MeSO-net. In this case, the determined Gaussian weight realize the highest reproducibility of the seismic wavefield for wave incidence from an arbitrary direction. The obtained Gaussian weights mark small and isotropic shapes near the central area of the MeSO-net, whereas they mark large and elliptical shapes around edges of the network. These shapes of the optimum weight would represent the configuration of the MeSO-net stations and demonstrate that the high-reproducible area of seismic waveform is expanded. Moreover, we confirmed that the accuracy of the seismic wavefield estimation can improve when selecting the interpolation coefficients coinciding with the incoming direction of the seismic waves.

Keywords: Seismic wavefield, Seismic wave gradiometry, MeSO-net

©2019. Japan Geoscience Union. All Right Reserved.

©2019. Japan Geoscience Union. All Right Reserved.

Uncertainty quantification based on 4DVar data assimilation for massive simulation models

*Shin-ichi Ito[1], Masayuki Kano[2], Hiromichi Nagao[1]

1. The University of Tokyo, 2. Tohoku University

Data assimilation (DA) is a fundamental computational technique that integrates numerical simulation models and observation data on the basis of Bayesian statistics. Originally developed for meteorology, especially weather forecasting, DA is now an accepted technique in various scientific fields. One key issue that remains controversial is the implementation of DA in massive simulation models under the constraints of limited computation time and resources. This work proposes a DA technique based on a four dimensional variational (4DVar) method for massive autonomous models that produces optimum estimates and their uncertainties within reasonable computation time and resource constraints. The uncertainties are given as several elements of an inverse Hessian matrix, which is the covariance matrix of a normal distribution that approximates the target posterior probability density function in the neighborhood of the optimum. The proposed method based on a second-order adjoint method allows us to directly evaluate the elements of the inverse Hessian matrix without computing all of its elements. Some numerical tests assuming a massive simulation model confirm that the proposed method works well and enables us to evaluate the uncertainties of the parameters involved in the assumed model faster than the conventional DA approaches. Such information regarding uncertainty is valuable, as it can be used to optimize the design of experiments.

Keywords: Bayesian statistics, Data assimilation, Uncertainty quantification

©2019. Japan Geoscience Union. All Right Reserved.

Bayesian approach for statistical modeling and forecasting of aftershock activities

*Takahiro Omi[1]

1. Institue of Industrial Science, the University of Tokyo

A large earthquake triggers a considerable number of aftershocks, which potentially cause additional damage in the affected area. It is therefore important to forecast aftershock activities as early as possible after a main shock. A basic method for forecasting aftershocks was proposed in 1989. However, for practical application of aftershock forecasting, we have to additionally consider (i) the missing of early aftershocks (ii) the forecast uncertainty. We consider such features by taking Bayesian statistical approach. In this talk, we briefly explain our forecasting method and demonstrate its utility.

Keywords: aftershock activity, probabilistic forecasting, bayesian statistics

©2019. Japan Geoscience Union. All Right Reserved.

Bias Correction for the Distribution of Aftershocks Within Short-Term Period Immediately After Large Main Shock

*Kosuke Morikawa[1], Hiromichi Nagao[2], Shin-ichi Ito[2], Shin'ichi Sakai[2], Naoshi Hirata[2]

1. Osaka University, 2. Earthquake Research Institute, The University of Tokyo

The main shock of a large earthquake often makes it difficult to identify a number of subsequent aftershocks. Knowing the distribution of magnitudes and arrival times of the aftershocks is essential to figure out the characteristics of the sequence of earthquakes, which enables us to predict the frequency of earthquakes depending on space and time. Such the distribution of aftershocks should be estimated within a couple of days eventually since most of the large aftershocks occur within one day from the main shock. However, an exact count of all aftershocks right after a main shock is very hard due to large signal-to-noise ratio, so that an estimated distribution of the aftershocks is usually biased.

An adoption of a likelihood that incorporates models of the detection rate of aftershocks can be a solution to correct the bias, but the simultaneous dependency on both magnitudes and arrival times of the aftershocks makes this difficult. Thus using nonparametric models for the detection rate is unrealistic though misspecification of the model may lead to a severe biased estimator.

In this study, we propose two detection rate models that are individually conditional on the magnitudes and the arrival times. The Generalized Moments of Methods (GMM)-type estimator overcomes the difficulty in estimation due to the imcompletely defined joint distribution. With the use of prior information, the distribution of the aftershocks can be effectively estimated within short-time period.

Keywords: Magnitude frequency, Marked point process, Geoscience

©2019. Japan Geoscience Union. All Right Reserved.

Deep-learning-based Earthquake Detection for Continuous Seismic Network Records

*Keisuke Yano[1], Takahiro Shiina[2], Sumito Kurata[1], Aitaro Kato[2], Fumiyasu Komaki[1], Shin'ichi Sakai[2], Naoshi Hirata[2]

1. Graduate School of Information Science and Technology, The University of Tokyo, , 2. Earthquake Research Institute, The University of Tokyo

Over the last decade, continuous seismic data have been enormously acquired on seismic networks consisting of multiple sensors at distributed locations. Analyzing these data efficiently and thoroughly offers substantial benefits to seismology. The first important step in the analysis is earthquake detection, that is, detecting earthquakes in continuous massive datasets.

In this talk, we present a deep-learning-based scheme for earthquake detection from continuous records in a seismic network. We work with a convolutional neural network (CNN), which is one of the most powerful supervised learning techniques, to capture features discriminating between earthquakes and noises. Our scheme has an advantage of utilizing multiple stations in a seismic network to discriminate between earthquakes and noises.

We apply our scheme to continuous data on Metropolitan Seismic Observation network (MeSO-net) from September 4, 2011 to September 16, 2011. We show our scheme improves on CNNs based on few stations especially in preventing mis-detection. In addition, the trained network in the last fully connected layer has quasi-sparsity, by which we identify features important for CNN to recognize earthquakes.

Keywords: Seismology, Deep learning

©2019. Japan Geoscience Union. All Right Reserved.

[J] Poster | S (Solid Earth Sciences)：S-TT Technology & Techniques

Mon. May 27, 2019 3:30 PM - 5:00 PM JST | Mon. May 27, 2019 6:30 AM - 8:00 AM UTC | Poster Hall International Exhibition Hall8, Makuhari Messe_16

[S-TT46] Seismic Big Data Analysis Based on the State-of-the-Art of Bayesian Statistics

convener:Hiromichi Nagao(Earthquake Research Institute, The University of Tokyo), Aitaro Kato(Earthquake Research Institute, the University of Tokyo), Takuto Maeda(Graduate School of Science and Technology, Hirosaki University), Keisuke Yano(The university of Tokyo)

Recently, a big seismic database has been being constructed that collects data of vibrators implemented in such as buildings, lifelines and smartphones, in addition to seismic data of the conventional continuous/temporal dense seismic observation arrays. Development of methodologies and algorithms, which are inadequate at this moment, optimized to comprehensively analyze the seismic big data is essential in order to utilize the big database as much as possible for prevention/mitigation of earthquake disasters and clarification of earthquake phenomena. On the other hand, recent progress of Bayesian statistics is significant, which is the mathematical basis of various methodologies, such as machine learning, especially deep learning, to extract valuable information from big data. The state-of-the-art of Bayesian statistics is expected to substantially advance seismic big data analyses.
This session mainly accepts presentations that focus on analyses of seismic big data, especially related to analysis methods based on Bayesian statistics such as machine learning, sparse modeling and data assimilation, and their applications to real seismic data. Presentations related to mathematical or statistical theories beneficial to data analyses, feasibility studies of algorithms eventually applicable to real seismic data, and the current status of seismic observations and analysis results are also highly welcome.

[STT46-P01] P-wave Polarity Determination of Waveform Data Observed in Western Japan, Using Deep Learning

*Shota Hara[1], Yukitoshi Fukahata[2], Yoshihisa Iio[2] (1.Division of Earth and Planetary Sciences, Graduate School of Science, Kyoto University, 2.Disaster Prevention Research Institute, Kyoto University)

[STT46-P02] Trans-dimensional Bayesian inversion for a radially anisotropic S-wave velocity model in the crust and upper mantle: Application to the Australian continent

*Toru Taira[1], Kazunori Yoshizawa[2] (1.Graduate School of Science, Hokkaido University, 2.Faculty of Science, Hokkaido University)

[STT46-P03] Seismic wavefield imaging based on dense seismic networks using replica exchange Monte Carlo method

*Masayuki Kano[1], Hiromichi Nagao[2,3], Kenji Nagata[4,5], Shin-ichi Ito[2,3], Kei Hasegawa[2], Shin'ichi Sakai[2], Shigeki Nakagawa[2], Muneo Hori[2], Naoshi Hirata[2] (1.Graduate school of science, Tohoku University, 2.Earthquake Research Institute, The University of Tokyo, 3.Graduate School of Information Science and Technology, The University of Tokyo, 4.AIST, 5.Japan Science and Technology Agency)

[STT46-P04] Bayesian oscillator decomposition for seismic data

*Takeru Matsuda[1] (1.The University of Tokyo)

[STT46-P05] Uncertainty evaluation of source parameter estimates by MCMC in Oklahoma

*Nana Yoshimitsu[1], Takuto Maeda[2], William Ellsworth[3] (1.The University of Tokyo, Earthquake Research Institute, 2.Hirosaki University, 3.Stanford Univerisy)

P-wave Polarity Determination of Waveform Data Observed in Western Japan, Using Deep Learning

*Shota Hara[1], Yukitoshi Fukahata[2], Yoshihisa Iio[2]

1. Division of Earth and Planetary Sciences, Graduate School of Science, Kyoto University, 2. Disaster Prevention Research Institute, Kyoto University

In order to determine focal mechanisms of earthquakes, it is necessary to determine first-motion polarities of P-wave. Researches on various automatic determination algorithms has been developed, but the performance of conventional algorithms has been significantly lower than that of human experts. Therefore, check by human experts is commonly needed, when we apply an automatic determination algorithm to observed waveform data. In this study, we develop a model of the convolutional neural network (CNN) that can determine P-wave first-motion polarities of seismic waveforms, in which P-wave arrival times determined by human experts are given beforehand. We use about 130 thousand 250 Hz and about 40 thousand 100 Hz waveform data observed in the San-in and the northern Kinki area, western Japan, to train and test the CNN. The P-wave polarities determined by the CNN have the accuracy of about 98 % for the 250 Hz data and about 95 % for the 100 Hz data. To examine the regional dependence, we divide seismic waveform data according to the observational area and trained the CNN using the data of one region, and applied the CNN to the data of the other region. As a result, the accuracy was different only by about 2 %. This means that there is almost no need to retrain the CNN by region.

Keywords: Machine Learning, Deep Learning, First-motion Polarity Determination

©2019. Japan Geoscience Union. All Right Reserved.

Trans-dimensional Bayesian inversion for a radially anisotropic S-wave velocity model in the crust and upper mantle: Application to the Australian continent

*Toru Taira[1], Kazunori Yoshizawa[2]

1. Graduate School of Science, Hokkaido University, 2. Faculty of Science, Hokkaido University

The velocity structure and discontinuities in the upper mantle, such as Lithosphere-Asthenosphere Boundary (LAB) and Mid-Lithosphere Discontinuity (MLD), have been investigated through a number of seismological studies, in which both body and surface waves have been employed. Many studies using body waves have extracted information on the upper mantle from the later arrivals of teleseismic body waves by deconvolving the vertical component from the horizontal components, which produces "receiver functions". While they are good at constraining impedance contrasts across the discontinuities, they are not sensitive to the absolute velocity. In contrast, surface waves enable us to recover the absolute velocity, though sharp velocity jumps cannot be resolved due to their lower frequency content (< 0.05Hz). In view of such different sensitivities of receiver functions and surface waves, the joint inversions of body and surface waves will be the most effective approach to the accurate estimation of seismic velocity structures in the crust and upper mantle.

In this study, we develop a new method for non-linear joint inversion of Ps receiver functions and multi-mode Rayleigh and Love surface waves using trans-dimensional Bayesian formulation, following the earlier works by Bodin et al., (2012, JGR). This trans-dimensional approach allows us to constrain the complexity of earth model with little a priori information, in which the number of model parameters (e.g. number of layers) can also be treated as a part of unknowns. The reversible-jump Markov Chain Monte Carlo approach (Green, 1995, Biometrika) is used to sample models with variable dimension in proportion to the posterior distribution of the Earth models. Assuming that data errors follow the Gaussian distribution, we also estimate the variances of the data errors at the same time. Such an approach is called 'Hierarchical Bayes' (e.g. Malinverno and Briggs, 2004, Geophysics), in which the overfitting of the models can be prevented. Parallel Tempering method (e.g. Sambridge, 2014, GJI) is also incorporated in our inversions, which makes the model samplings more efficient enabling us to extend the parameter search ranges.

With this method, we jointly inverted the Ps receiver function, multi-mode Rayleigh and Love dispersion curves from Yoshizawa (2014, PEPI) for a radially anisotropic 1-D shear velocity model under Global Seismographic Network (GSN) stations in Australia. Our preliminary result for the WRAB station in the central Australia implies the existence of two MLDs with negative and positive velocity jumps at around 90 km and 150 km depths, respectively, and LAB at around 220km depth. The depths of MLDs are consistent with an earlier receiver function study by Ford et al. (2010, EPSL) and such multiple MLDs are also reported by another study in North America (Calo et al., 2016, EPSL). Our estimated LAB depth at 220 km is deeper than that from the earlier surface wave study (Yoshizawa & Kennett, 2015, GRL), in which the Lithosphere-Asthenosphere Boundary under cratons is supposed to be a smooth transition. Still, we can still see the common feature of strong radial anisotropy (SH>SV) in the asthenospheric depth below 220 km, indicating the effects of strong shear flow under the fast-moving Australian continent.

©2019. Japan Geoscience Union. All Right Reserved.

Keywords: Bayesian inversion, receiver function, surface wave, higher mode, lithosphere, asthenosphere

©2019. Japan Geoscience Union. All Right Reserved.

Seismic wavefield imaging based on dense seismic networks using replica exchange Monte Carlo method

*Masayuki Kano[1], Hiromichi Nagao[2,3], Kenji Nagata[4,5], Shin-ichi Ito[2,3], Kei Hasegawa[2], Shin'ichi Sakai[2], Shigeki Nakagawa[2], Muneo Hori[2], Naoshi Hirata[2]

1. Graduate school of science, Tohoku University, 2. Earthquake Research Institute, The University of Tokyo, 3. Graduate School of Information Science and Technology, The University of Tokyo, 4. AIST, 5. Japan Science and Technology Agency

In recent years, dense seismic observation networks have been constructed. For example, the Metropolitan Seismic Observation network called MeSO-net has been observing ground motions since 2011 with the average intervals of ~5 km in the Tokyo metropolitan located on the Kanto sedimentary basin, Japan. Utilizing seismograms of MeSO-net, we have developed a wavefield reconstruction method by simultaneously estimating subsurface velocity structures and source locations using replica exchange Monte Carlo (REMC) method [Kano et al. 2017, GJI, JGR]. The reconstructed wavefield can be used as input ground motions to simulate seismic response of infrastructure for the purpose of rapid evaluation of seismic hazards. In this presentation, we will summarize the REMC-based wavefield estimation method and discuss future developments and applications of the method.

Keywords: MeSO-net, Replica exchange Monte Carlo, Seismic wavefield imaging

©2019. Japan Geoscience Union. All Right Reserved.

Bayesian oscillator decomposition for seismic data

*Takeru Matsuda[1]

1. The University of Tokyo

Many time series including seismic data are naturally considered as a superposition of several oscillators. Matsuda and Komaki (2017a,b) proposed a Bayesian statistical method for decomposing time series data into oscillators by using Gaussian linear state space models. For example, this method can be used to extract neural oscillators (such as alpha, beta, and gamma) from neuroimaging data. In this study, we apply this method to seismic data and investigate the extracted oscillators.

Keywords: Bayesian statistics, state space model, data assimilation

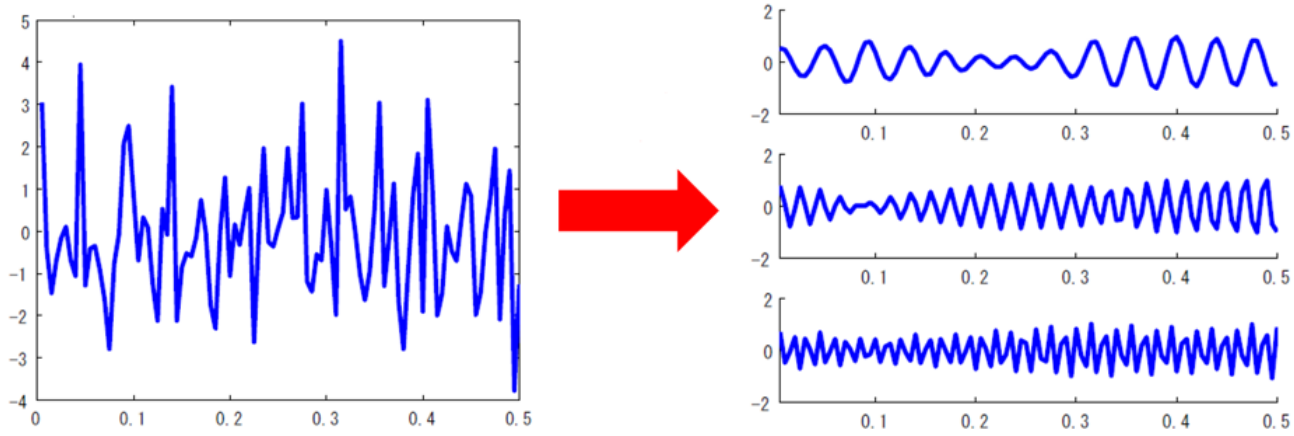

©2019. Japan Geoscience Union. All Right Reserved.

Uncertainty evaluation of source parameter estimates by MCMC in Oklahoma

*Nana Yoshimitsu[1], Takuto Maeda[2], William Ellsworth[3]

1. The University of Tokyo, Earthquake Research Institute, 2. Hirosaki University, 3. Stanford Univerisy

Stress drop is important parameter to understand earthquake source characteristics and to improve hazard assessment. Many studies use the spectral ratio method to measure the moment ratio and two corner frequencies by comparing theoretical and observed spectral ratio in the frequency domain and obtain the stress drop. Accurate stress drop estimates are difficult to make because it depends on the accuracy of the three parameters. The Markov Chain Monte Carlo (MCMC) method is effective to estimate high dimensional parameters. In this study, we evaluate the uncertainty of the estimation and trade-off among parameters from a statistical perspective.

We analyzed five clusters of events near Cushing, Oklahoma, each containing a M 4+ event. Empirical Green’ s function events used as the denominator all locate within 2 km of the target event. We analyzed 5.12 seconds of the time-aligned seismogram from twice the S wave arrival time. Spectral ratios between a large event ($M_L > 4$) and small events were formed by stacking all stations to remove path effects. Then, analyzed spectral ratios between event pairs using the Metropolis-Hastings algorithm to estimate moment ratio and two corner frequencies for the Brune model. We updated the value of moment ratio and two corner frequencies with 300,000 iterations which first 100,000 calculations was ignored as burn-in.

In most cases, the distribution of the sampling showed ellipsoidal shape in the 3D parameter space. We searched the axial direction of the sampling distribution by principal component analysis (PCA), and estimated loadings of the principal component and contribution rate. Some spectral ratio showed irregular shape from ideal shape because of small magnitude difference or contamination by noise. The percentage of the contribution rate indicates how well the sampling distribution is explained by each component. The contribution rate of the first principal component with irregular shape of the spectral ratio was lower than 80 % while it was higher than 80 % with normal shape of the spectral ratio. The loadings among three parameters and three principal components also showed different pattern in the case of normal shape and irregular shape of the spectral ratio. These different trend of the contribution rate and the loadings indicates different pattern of the sampling distribution of a spectral ratio that have irregular shape. Thus, the combination of MCMC and PCA analysis have a possibility that to automatically classify spectral ratios which have irregular shape and ideal shape.

Keywords: Stress Drop, MCMC

©2019. Japan Geoscience Union. All Right Reserved.

[J] Poster | S (Solid Earth Sciences)：S-TT Technology & Techniques

Mon. May 27, 2019 5:15 PM - 6:30 PM JST | Mon. May 27, 2019 8:15 AM - 9:30 AM UTC | Poster Hall International Exhibition Hall8, Makuhari Messe_28

[S-TT46] Seismic Big Data Analysis Based on the State-of-the-Art of Bayesian Statistics

convener:Hiromichi Nagao(Earthquake Research Institute, The University of Tokyo), Aitaro Kato(Earthquake Research Institute, the University of Tokyo), Takuto Maeda(Graduate School of Science and Technology, Hirosaki University), Keisuke Yano(The university of Tokyo)

Recently, a big seismic database has been being constructed that collects data of vibrators implemented in such as buildings, lifelines and smartphones, in addition to seismic data of the conventional continuous/temporal dense seismic observation arrays. Development of methodologies and algorithms, which are inadequate at this moment, optimized to comprehensively analyze the seismic big data is essential in order to utilize the big database as much as possible for prevention/mitigation of earthquake disasters and clarification of earthquake phenomena. On the other hand, recent progress of Bayesian statistics is significant, which is the mathematical basis of various methodologies, such as machine learning, especially deep learning, to extract valuable information from big data. The state-of-the-art of Bayesian statistics is expected to substantially advance seismic big data analyses.
This session mainly accepts presentations that focus on analyses of seismic big data, especially related to analysis methods based on Bayesian statistics such as machine learning, sparse modeling and data assimilation, and their applications to real seismic data. Presentations related to mathematical or statistical theories beneficial to data analyses, feasibility studies of algorithms eventually applicable to real seismic data, and the current status of seismic observations and analysis results are also highly welcome.

[STT46-P01] P-wave Polarity Determination of Waveform Data Observed in Western Japan, Using Deep Learning

*Shota Hara[1], Yukitoshi Fukahata[2], Yoshihisa Iio[2] (1.Division of Earth and Planetary Sciences, Graduate School of Science, Kyoto University, 2.Disaster Prevention Research Institute, Kyoto University)

[STT46-P02] Trans-dimensional Bayesian inversion for a radially anisotropic S-wave velocity model in the crust and upper mantle: Application to the Australian continent

*Toru Taira[1], Kazunori Yoshizawa[2] (1.Graduate School of Science, Hokkaido University, 2.Faculty of Science, Hokkaido University)

[STT46-P03] Seismic wavefield imaging based on dense seismic networks using replica exchange Monte Carlo method

*Masayuki Kano[1], Hiromichi Nagao[2,3], Kenji Nagata[4,5], Shin-ichi Ito[2,3], Kei Hasegawa[2], Shin'ichi Sakai[2], Shigeki Nakagawa[2], Muneo Hori[2], Naoshi Hirata[2] (1.Graduate school of science, Tohoku University, 2.Earthquake Research Institute, The University of Tokyo, 3.Graduate School of Information Science and Technology, The University of Tokyo, 4.AIST, 5.Japan Science and Technology Agency)

[STT46-P04] Bayesian oscillator decomposition for seismic data

*Takeru Matsuda[1] (1.The University of Tokyo)

[STT46-P05] Uncertainty evaluation of source parameter estimates by MCMC in Oklahoma

*Nana Yoshimitsu[1], Takuto Maeda[2], William Ellsworth[3] (1.The University of Tokyo, Earthquake Research Institute, 2.Hirosaki University, 3.Stanford Univerisy)

P-wave Polarity Determination of Waveform Data Observed in Western Japan, Using Deep Learning

*Shota Hara[1], Yukitoshi Fukahata[2], Yoshihisa Iio[2]

1. Division of Earth and Planetary Sciences, Graduate School of Science, Kyoto University, 2. Disaster Prevention Research Institute, Kyoto University

In order to determine focal mechanisms of earthquakes, it is necessary to determine first-motion polarities of P-wave. Researches on various automatic determination algorithms has been developed, but the performance of conventional algorithms has been significantly lower than that of human experts. Therefore, check by human experts is commonly needed, when we apply an automatic determination algorithm to observed waveform data. In this study, we develop a model of the convolutional neural network (CNN) that can determine P-wave first-motion polarities of seismic waveforms, in which P-wave arrival times determined by human experts are given beforehand. We use about 130 thousand 250 Hz and about 40 thousand 100 Hz waveform data observed in the San-in and the northern Kinki area, western Japan, to train and test the CNN. The P-wave polarities determined by the CNN have the accuracy of about 98 % for the 250 Hz data and about 95 % for the 100 Hz data. To examine the regional dependence, we divide seismic waveform data according to the observational area and trained the CNN using the data of one region, and applied the CNN to the data of the other region. As a result, the accuracy was different only by about 2 %. This means that there is almost no need to retrain the CNN by region.

Keywords: Machine Learning, Deep Learning, First-motion Polarity Determination

©2019. Japan Geoscience Union. All Right Reserved.

Trans-dimensional Bayesian inversion for a radially anisotropic S-wave velocity model in the crust and upper mantle: Application to the Australian continent

*Toru Taira[1], Kazunori Yoshizawa[2]

1. Graduate School of Science, Hokkaido University, 2. Faculty of Science, Hokkaido University

The velocity structure and discontinuities in the upper mantle, such as Lithosphere-Asthenosphere Boundary (LAB) and Mid-Lithosphere Discontinuity (MLD), have been investigated through a number of seismological studies, in which both body and surface waves have been employed. Many studies using body waves have extracted information on the upper mantle from the later arrivals of teleseismic body waves by deconvolving the vertical component from the horizontal components, which produces "receiver functions". While they are good at constraining impedance contrasts across the discontinuities, they are not sensitive to the absolute velocity. In contrast, surface waves enable us to recover the absolute velocity, though sharp velocity jumps cannot be resolved due to their lower frequency content (< 0.05Hz). In view of such different sensitivities of receiver functions and surface waves, the joint inversions of body and surface waves will be the most effective approach to the accurate estimation of seismic velocity structures in the crust and upper mantle.

In this study, we develop a new method for non-linear joint inversion of Ps receiver functions and multi-mode Rayleigh and Love surface waves using trans-dimensional Bayesian formulation, following the earlier works by Bodin et al., (2012, JGR). This trans-dimensional approach allows us to constrain the complexity of earth model with little a priori information, in which the number of model parameters (e.g. number of layers) can also be treated as a part of unknowns. The reversible-jump Markov Chain Monte Carlo approach (Green, 1995, Biometrika) is used to sample models with variable dimension in proportion to the posterior distribution of the Earth models. Assuming that data errors follow the Gaussian distribution, we also estimate the variances of the data errors at the same time. Such an approach is called 'Hierarchical Bayes' (e.g. Malinverno and Briggs, 2004, Geophysics), in which the overfitting of the models can be prevented. Parallel Tempering method (e.g. Sambridge, 2014, GJI) is also incorporated in our inversions, which makes the model samplings more efficient enabling us to extend the parameter search ranges.

With this method, we jointly inverted the Ps receiver function, multi-mode Rayleigh and Love dispersion curves from Yoshizawa (2014, PEPI) for a radially anisotropic 1-D shear velocity model under Global Seismographic Network (GSN) stations in Australia. Our preliminary result for the WRAB station in the central Australia implies the existence of two MLDs with negative and positive velocity jumps at around 90 km and 150 km depths, respectively, and LAB at around 220km depth. The depths of MLDs are consistent with an earlier receiver function study by Ford et al. (2010, EPSL) and such multiple MLDs are also reported by another study in North America (Calo et al., 2016, EPSL). Our estimated LAB depth at 220 km is deeper than that from the earlier surface wave study (Yoshizawa & Kennett, 2015, GRL), in which the Lithosphere-Asthenosphere Boundary under cratons is supposed to be a smooth transition. Still, we can still see the common feature of strong radial anisotropy (SH>SV) in the asthenospheric depth below 220 km, indicating the effects of strong shear flow under the fast-moving Australian continent.

©2019. Japan Geoscience Union. All Right Reserved.

Keywords: Bayesian inversion, receiver function, surface wave, higher mode, lithosphere, asthenosphere

©2019. Japan Geoscience Union. All Right Reserved.

Seismic wavefield imaging based on dense seismic networks using replica exchange Monte Carlo method

*Masayuki Kano[1], Hiromichi Nagao[2,3], Kenji Nagata[4,5], Shin-ichi Ito[2,3], Kei Hasegawa[2], Shin'ichi Sakai[2], Shigeki Nakagawa[2], Muneo Hori[2], Naoshi Hirata[2]

1. Graduate school of science, Tohoku University, 2. Earthquake Research Institute, The University of Tokyo, 3. Graduate School of Information Science and Technology, The University of Tokyo, 4. AIST, 5. Japan Science and Technology Agency

In recent years, dense seismic observation networks have been constructed. For example, the Metropolitan Seismic Observation network called MeSO-net has been observing ground motions since 2011 with the average intervals of ~5 km in the Tokyo metropolitan located on the Kanto sedimentary basin, Japan. Utilizing seismograms of MeSO-net, we have developed a wavefield reconstruction method by simultaneously estimating subsurface velocity structures and source locations using replica exchange Monte Carlo (REMC) method [Kano et al. 2017, GJI, JGR]. The reconstructed wavefield can be used as input ground motions to simulate seismic response of infrastructure for the purpose of rapid evaluation of seismic hazards. In this presentation, we will summarize the REMC-based wavefield estimation method and discuss future developments and applications of the method.

Keywords: MeSO-net, Replica exchange Monte Carlo, Seismic wavefield imaging

©2019. Japan Geoscience Union. All Right Reserved.

Bayesian oscillator decomposition for seismic data

*Takeru Matsuda[1]

1. The University of Tokyo

Many time series including seismic data are naturally considered as a superposition of several oscillators. Matsuda and Komaki (2017a,b) proposed a Bayesian statistical method for decomposing time series data into oscillators by using Gaussian linear state space models. For example, this method can be used to extract neural oscillators (such as alpha, beta, and gamma) from neuroimaging data. In this study, we apply this method to seismic data and investigate the extracted oscillators.

Keywords: Bayesian statistics, state space model, data assimilation

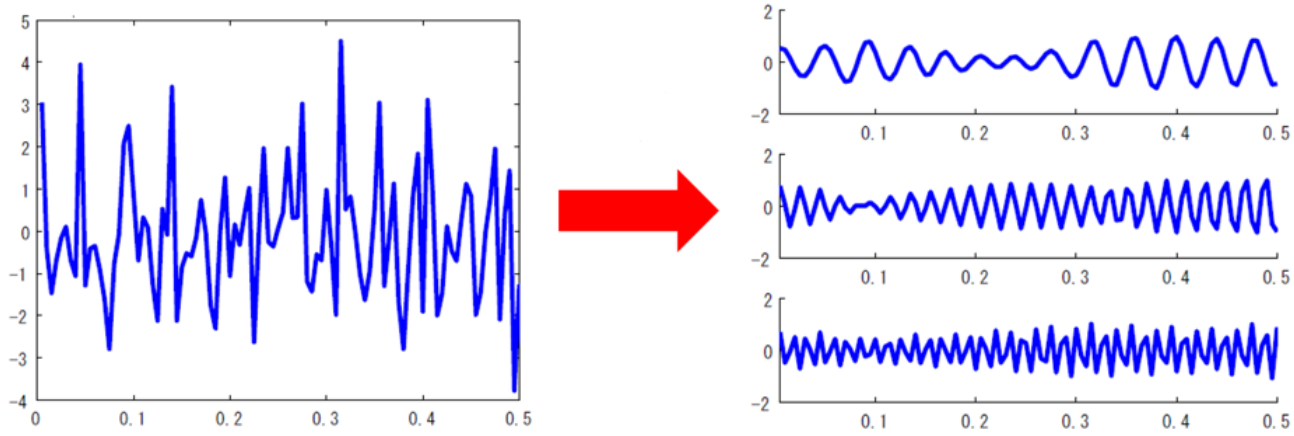

©2019. Japan Geoscience Union. All Right Reserved.

Uncertainty evaluation of source parameter estimates by MCMC in Oklahoma

*Nana Yoshimitsu[1], Takuto Maeda[2], William Ellsworth[3]

1. The University of Tokyo, Earthquake Research Institute, 2. Hirosaki University, 3. Stanford Univerisy

Stress drop is important parameter to understand earthquake source characteristics and to improve hazard assessment. Many studies use the spectral ratio method to measure the moment ratio and two corner frequencies by comparing theoretical and observed spectral ratio in the frequency domain and obtain the stress drop. Accurate stress drop estimates are difficult to make because it depends on the accuracy of the three parameters. The Markov Chain Monte Carlo (MCMC) method is effective to estimate high dimensional parameters. In this study, we evaluate the uncertainty of the estimation and trade-off among parameters from a statistical perspective.

We analyzed five clusters of events near Cushing, Oklahoma, each containing a M 4+ event. Empirical Green’ s function events used as the denominator all locate within 2 km of the target event. We analyzed 5.12 seconds of the time-aligned seismogram from twice the S wave arrival time. Spectral ratios between a large event ($M_L > 4$) and small events were formed by stacking all stations to remove path effects. Then, analyzed spectral ratios between event pairs using the Metropolis-Hastings algorithm to estimate moment ratio and two corner frequencies for the Brune model. We updated the value of moment ratio and two corner frequencies with 300,000 iterations which first 100,000 calculations was ignored as burn-in.

In most cases, the distribution of the sampling showed ellipsoidal shape in the 3D parameter space. We searched the axial direction of the sampling distribution by principal component analysis (PCA), and estimated loadings of the principal component and contribution rate. Some spectral ratio showed irregular shape from ideal shape because of small magnitude difference or contamination by noise. The percentage of the contribution rate indicates how well the sampling distribution is explained by each component. The contribution rate of the first principal component with irregular shape of the spectral ratio was lower than 80 % while it was higher than 80 % with normal shape of the spectral ratio. The loadings among three parameters and three principal components also showed different pattern in the case of normal shape and irregular shape of the spectral ratio. These different trend of the contribution rate and the loadings indicates different pattern of the sampling distribution of a spectral ratio that have irregular shape. Thus, the combination of MCMC and PCA analysis have a possibility that to automatically classify spectral ratios which have irregular shape and ideal shape.

Keywords: Stress Drop, MCMC

©2019. Japan Geoscience Union. All Right Reserved.

[E] Oral | S (Solid Earth Sciences)：S-CG Complex & General

Mon. May 27, 2019 3:30 PM - 5:00 PM JST | Mon. May 27, 2019 6:30 AM - 8:00 AM UTC | A07 TOKYO BAY MAKUHARI HALL

[S-CG49] Hard-Rock Drilling Science: From Continental to Deep Sea Drilling, and Oman Project

convener:Katsuyoshi Michibayashi(Department of Earth and Planetary Sciences, Nagoya University), Eiichi TAKAZAWA(Department of Geology, Faculty of Science, Niigata University), Norikatsu Akizawa(Department of Ocean Floor Geoscience, Atmosphere and Ocean Research Institute, The University of Tokyo), Chairperson:Katsuyoshi Michibayashi

The Oman Drilling Project (OmDP) has completed to drill numerous hard-rock cores within ancient oceanic lithosphere and the underlying subduction zone of the Samail ophiolite in Oman, with support from ICDP, IODP, Japan Society for the Promotion of Science, the Sloan Foundation's Deep Carbon Observatory, US, and European research agencies. Moreover, a number of IODP expeditions have focused on hard-rock drilling over the last several years including Expedition 352 in 2014, which drilled the volcanic sequence associated with subduction initiation in the Bonin fore-arc, Expedition 357, which drilled the Lost City hydrothermal field, Expedition 360, which drilled the lithosphere associated with ultraslow-spreading at the Southwest Indian Ridge in 2016, and Expedition 366, which drilled the serpentinite seamounts in the Mariana fore-arc. In this session, we invite presentations on the scientific results of hard-rock drilling at these and other sites. We also invite related presentations on oceanic lithosphere, island arc formation, and any other significant issue that could be addressed by future hard-rock drilling. This includes marine studies of oceanic lithosphere and on-land geological investigations of ophiolites, accreted arcs, and subduction complexes. The session is intended to be interdisciplinary, including the fields of geophysics, geochemistry, petrology, engineering, and biology.

3:30 PM - 3:45 PM JST | 6:30 AM - 6:45 AM UTC

[SCG49-01] Geochemical and Geochronological Constraints on the Origin and Emplacement of the East Taiwan Ophiolite: Implication for Subduction Initiation of the South China Sea.

*Chiou-ting Lin[1], Ron A. Harris[2], Wei-dong Sun[1], Guo-liang Zhang[1] (1.Center of Deep Sea Research, Institute of Oceanology, Chinese Academy of Sciences, 2.Department of Geology, Brigham Young University)

3:45 PM - 4:05 PM JST | 6:45 AM - 7:05 AM UTC

[SCG49-02] Towards a complete profile of hydrothermal alteration in the lower oceanic crust and uppermost mantle; Insights from the Oman Drilling Project and ChikyuOman2017 and 2018

★Invited Papers

*Damon A H Teagle[1], Michelle Harris[2], Gretchen Früh-Green[3], Eiichi TAKAZAWA[4], Katsuyoshi Michibayashi[5], Peter B Kelemen[6], Oman Drilling Project Science Team[1] (1.Ocean & Earth Science, National Oceanography Centre Southampton, University of Southampton, SO14-3ZH, Southampton, UK, 2.School of Geography, Earth and Environmental Sciences, Plymouth University, UK, 3.Earth Sciences, ETH Zürich, Switzerland, 4.Geology, Niigata University, Japan, 5.Earth and Planetary Sciences, Nagoya University, Japan, 6.LDEO, Columbia University, New York, USA)

4:05 PM - 4:25 PM JST | 7:05 AM - 7:25 AM UTC

[SCG49-03] Peridotite alteration in OmanDP cores

★Invited Papers

*Peter B Kelemen[1], Juan Carlos de Obeso[1], Craig Manning[2], Marguerite Godard[3], Wolfgang Bach[4], Merry Yue Cai[1], Saebyul Choe[5], Judith Coggon[6], Eric Ellison[7], Alireza Eslami[8], Katy Evans[9], Michelle Harris[10], Wolf-Achim Kahl[4], Jürg Matter[6], Katsu Michibayashi[11], Keichi Okazaki[12], Philippe Pézard[3], Damon A.H. Teagle[6], Alexis Templeton[7], OmanDP Oman Drilling Project Science Team (1.LDEO, 2.UCLA, 3.U. Montpellier, 4.U. Bremen, 5.AMNH, 6.U. Southampton, 7.U. Colorado, 8.U. Tehran, 9.Curtin U., 10.U. Plymouth, 11.Nagoya U., 12.JAMSTEC)

4:25 PM - 4:40 PM JST | 7:25 AM - 7:40 AM UTC

[SCG49-04] Low-salinity aqueous fluid inclusions in dolomite veins of a listvenite of Oman Drilling Project Phase 1

*Tatsuhiko Kawamoto[1], Hiroki Sato[2], Toma Takahashi[3], Juan Miguel Guotana[4], Tomoaki Morishita[4], Peter B Kelemen[5], Jude Ann Coggon[6], Michelle Harris[7], Juerg Michael Matter[6], Katsuyoshi Michibayashi[8], Eiichi TAKAZAWA[9], Damon A H Teagle[6], The Oman Drilling Project Phase 1 Science Party (1.Department of Geoscience, Faculty of Science, Shizuoka University, 2.Faculty of Science, Kyoto University, 3.Faculty of Geosciences and Civil Engineering, Kanazawa University, 4.Division of Natural Sciences, Graduate School of Natural Science and Technology, Kanazawa University, 5.Lamont-Doherty Earth Observatory, Columbia University, 6.School of Ocean and Earth Science, National Oceanography Centre Southampton, University of Southampton, 7.School of Geography, Earth and Environmental Sciences, Plymouth University, 8.Department of Earth Planetary Sciences, Graduate School of Environmental Studies, Nagoya University, 9.Institute of Science and Technology, Niigata University)

4:40 PM - 5:00 PM JST | 7:40 AM - 8:00 AM UTC

[SCG49-05] Hydration and development of fracture network within oceanic lower crust: an evidence from CM1A of Oman Drilling

★Invited Papers

*Atsushi Okamoto[1], Kazuki Yosida[1], Ryosuke Oyanagi[2], Oman Drilling Project Phase 2 Science Party[3] (1.Graduate School of Environmental Studies, 2.JAMSTEC, 3.Oman Drillng Project Phase 2 Science Party)

Geochemical and Geochronological Constraints on the Origin and Emplacement of the East Taiwan Ophiolite: Implication for Subduction Initiation of the South China Sea.

*Chiou-ting Lin[1], Ron A. Harris[2], Wei-dong Sun[1], Guo-liang Zhang[1]

1. Center of Deep Sea Research, Institute of Oceanology, Chinese Academy of Sciences, 2. Department of Geology, Brigham Young University

The East Taiwan Ophiolite (ETO) occurs as blocks and thrust sheets associated with the Lichi Mélange in the Coastal Range of eastern Taiwan. The blocks consist of serpentinized harzburgite, serpentinite breccia, gabbro, dikes of dolerite and plagiogranite, pillow basalts, and red clay within a mud- and serpentinite-rich mélange matrix. New U-Pb zircon dating of a pegmatite gabbro yields a weighted mean age of 16.65±0.20 Ma. This age is earlier than the North Luzon Arc, but overlaps with the late–stage spreading of the South China Sea. ETO glassy basalt has low K_2O, MgO and high CaO contents, similar to MORB. REE and trace element patterns show both N-MORB patterns with LREE depletion and E-MORB patterns with slight LREE enrichment. A few samples show slight depletion in Nb-Ta, and Ti and enrichment in Rb, Ba, U and Sr, indicating a hint of subduction influence. Most ETO basalt plots within the overlapping fields of N-MORB and BABB on Ti-V, Cr-Y, Nb/Yb- Th/Yb and Hf/3-Th-Ta discrimination diagrams. The geochemical compositions of the ETO basalt are emblematic of mid-ocean ridge or back-arc lava, and the Pb isotope values are similar to those of MORB of the South China Sea from IODP Expedition 349. We interpret ETO basalt as fragments of the subducted South China Sea basement that were scrapped off and accreted to the Luzon forearc during the process of subduction initiation along the nascent Manila Trench. Blocks of mantle material in the mélange may originate from the upper plate of the arc-continent collision and were mixed with lower plate crustal material in a subduction channel now represented by the Lichi Mélange.

Keywords: East Taiwan Ophiolite, Lichi Mélange, South China Sea, back-arc basin, subduction initiation, arc-continent collision

©2019. Japan Geoscience Union. All Right Reserved.

Towards a complete profile of hydrothermal alteration in the lower oceanic crust and uppermost mantle; Insights from the Oman Drilling Project and ChikyuOman2017 and 2018

*Damon A H Teagle[1], Michelle Harris[2], Gretchen Früh-Green[3], Eiichi TAKAZAWA[4], Katsuyoshi Michibayashi[5], Peter B Kelemen[6], Oman Drilling Project Science Team[1]

1. Ocean & Earth Science, National Oceanography Centre Southampton, University of Southampton, SO14-3ZH, Southampton, UK, 2. School of Geography, Earth and Environmental Sciences, Plymouth University, UK, 3. Earth Sciences, ETH Zürich, Switzerland, 4. Geology, Niigata University, Japan, 5. Earth and Planetary Sciences, Nagoya University, Japan, 6. LDEO, Columbia University, New York, USA

Drilling a continuous section through the lower oceanic crust and into the uppermost mantle has been an unfulfilled scientific ambition for more than 60 years since before the development of plate tectonics. Although an imperfect analogue of in situ, intact ocean crust, the 96 Ma Samail ophiolite of Oman is the largest and best preserved on-land exposure of ancient ocean crust that formed in some type of fast spreading ocean ridge, in the Tethyan ocean shortly before its obduction on to the Arabian margin. Offset drilling by Oman Drilling Project has now sampled critical intervals of the mid to lower oceanic crust and the uppermost mantle preserved in the Samail ophiolite. In a series of 400 m-deep diamond-cored boreholes the Oman Drilling Project has made with near 100 % rates of recovery, continuous objective observations from the lower sheeted dikes and the dike-gabbro transition zone (Hole GT3A), the mid-crustal transition from foliated to layered cumulate gabbros (Hole GT2A), deep layered gabbros including mineralised fault zones (Hole GT1A), and across the crust-mantle transition from layered gabbros through dunites into residual harzburgites of the Samail upper mantle (Holes CM1A and CM2B). Observations of drillcore, complemented by instrumental (e.g., X-ray CT, Infrared scanning) and geophysical wireline logging, now provide the opportunity to objectively quantify the conditions and extent of seawater-rock exchange in the mid to lower oceanic crust and uppermost mantle. These new observations will lead to better understand the role and influence of deep hydrothermal circulation on the accretion of the lower oceanic crust and the improved quantification of geochemical and isotopic exchanges between the oceans and new crust formed at mid-ocean ridges.

Keywords: ocean crust, hydrothermal alteration, ophiolite, Oman Drilling Project

©2019. Japan Geoscience Union. All Right Reserved.

Peridotite alteration in OmanDP cores

*Peter B Kelemen[1], Juan Carlos de Obeso[1], Craig Manning[2], Marguerite Godard[3], Wolfgang Bach[4], Merry Yue Cai[1], Saebyul Choe[5], Judith Coggon[6], Eric Ellison[7], Alireza Eslami[8], Katy Evans[9], Michelle Harris[10], Wolf-Achim Kahl[4], Jürg Matter[6], Katsu Michibayashi[11], Keichi Okazaki[12], Philippe Pézard[3], Damon A.H. Teagle[6], Alexis Templeton[7], OmanDP Oman Drilling Project Science Team

1. LDEO, 2. UCLA, 3. U. Montpellier, 4. U. Bremen, 5. AMNH, 6. U. Southampton, 7. U. Colorado, 8. U. Tehran, 9. Curtin U., 10. U. Plymouth, 11. Nagoya U., 12. JAMSTEC

Here we present some preliminary results constraining peridotite alteration in cores from several Oman Drilling Project (OmanDP) boreholes, from the Samail ophiolite in the Sultanate of Oman. Hole BT1B in Wadi Mansah east of Fanjah was drilled through 200 m of fully carbonated and/or serpentinized peridotites of the mantle wedge, through the basal thrust of the ophiolite, into the metamorphic sole. Holes BA1B, BA3A and BA4A were drilled into extensively serpentinized peridotite of the eastern Wadi Tayin massif.

Fully carbonated peridotites (listvenites) and serpentinites of Hole BT1B reflect carbonation and hydration by fluids rising from the Cretaceous subduction zone at the base of the ophiolite, at about 100° C (Falk & Kelemen GCA 2015). Though there is extensive, 0.01-10 m scale chemical variation, the average, volatile-free composition of the listvenites is almost identical to that of partially serpentinized harzburgites throughout the ophiolite mantle section. This observation and thermodynamic modeling indicate that, during addition of CO2, H2O, Ca and K from subduction zone fluids, Mg/Fe/Si ratios were nearly unchanged, suggesting very minor export of dissolved, major elements. In turn, this requires a large increase in solid volume. One possibility is that major volume expansion occurred at a serpentinization front, perhaps advancing via reaction-driven cracking, followed by smaller amounts of expansion at the carbonation front. Observed mineral parageneses and thermodynamic modeling require relatively CO2-rich aqueous fluids, and perhaps an exsolved, CO2-dominated fluid. CO2 contents were higher than for fluids in equilibrium with underlying metasediments at any likely depth for formation of the observed listvenite, and thus suggest that fluids derived from higher temperature and pressure devolatilization migrated up the subduction zone to this site.

Highly serpentinized peridotites from Holes BA1B, BA3A and BA4A record steep chemical gradients, with sharply decreasing f(O2) and f(CO2) downhole, beginning at the present-day erosional surface. Moreover, inferred conditions based on mineral parageneses are consistent with present-day borehole water compositions. Oxygen fugacity reaches the limit for H2 production from H2O at < 100 meters below the surface. These borehole observations are consistent with previous observations (14C in carbonates, reduced sulfides, oxides and metals, highly alkaline and reduced fluids, H2 gas) and thermodynamic modeling indicating that carbonation and serpentinization-related redox reactions are ongoing. Given experimental data suggesting that serpentinization of olivine is slow, evidence for low temperature “serpentinization” raises interesting questions about natural rates, and the nature of reactants and products, in the present-day weathering environment.

Keywords: Global carbon cycle, Oman Drilling Project, Peridotite weathering, Serpentinization, Carbon mineralization aka mineral carbonation, Natural production of H2 hydrogen gas

©2019. Japan Geoscience Union. All Right Reserved.

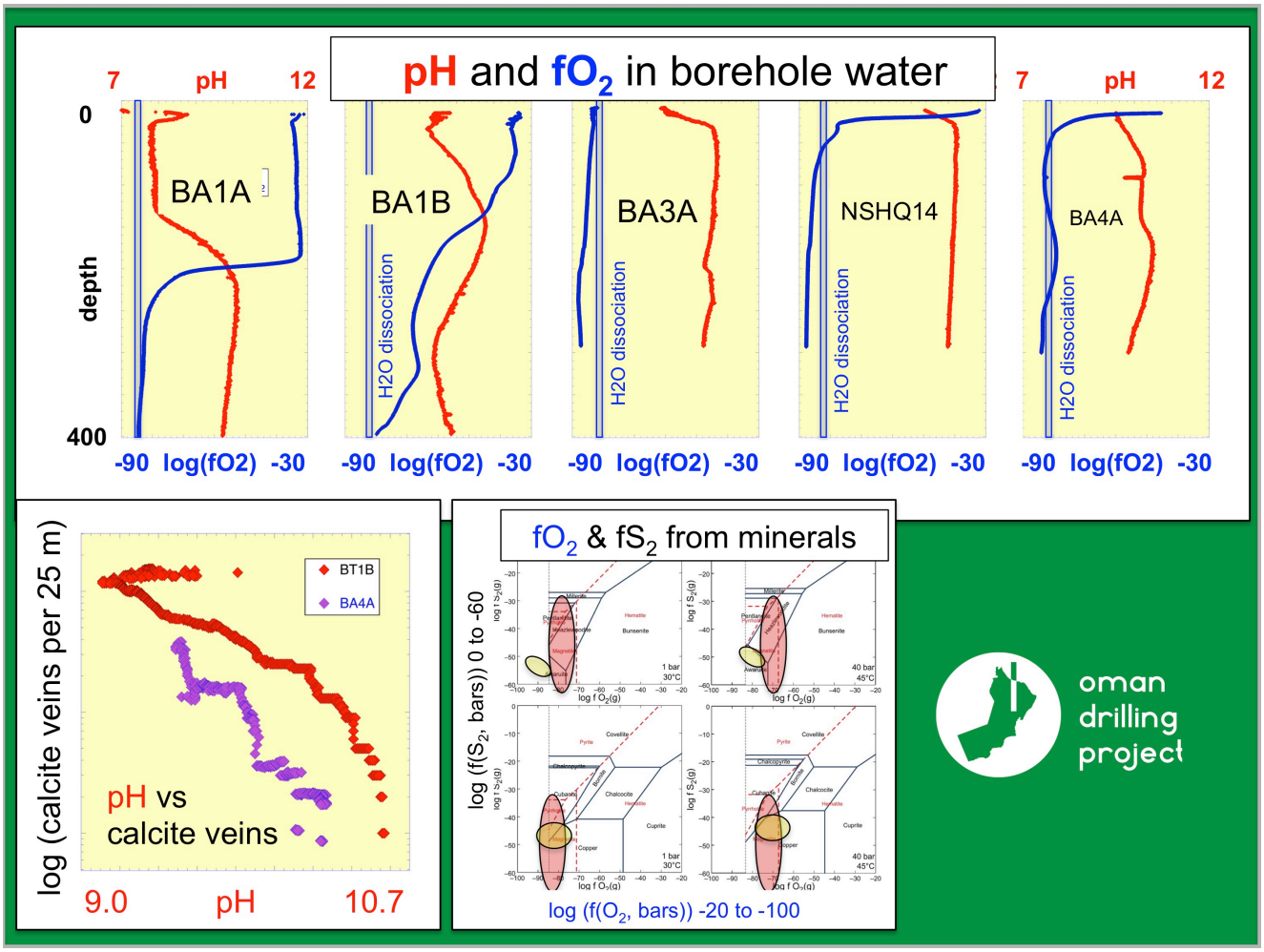

©2019. Japan Geoscience Union. All Right Reserved.

Low-salinity aqueous fluid inclusions in dolomite veins of a listvenite of Oman Drilling Project Phase 1

*Tatsuhiko Kawamoto[1], Hiroki Sato[2], Toma Takahashi[3], Juan Miguel Guotana[4], Tomoaki Morishita[4], Peter B Kelemen[5], Jude Ann Coggon[6], Michelle Harris[7], Juerg Michael Matter[6], Katsuyoshi Michibayashi[8], Eiichi TAKAZAWA[9], Damon A H Teagle[6], The Oman Drilling Project Phase 1 Science Party

1. Department of Geoscience, Faculty of Science, Shizuoka University, 2. Faculty of Science, Kyoto University, 3. Faculty of Geosciences and Civil Engineering, Kanazawa University, 4. Division of Natural Sciences, Graduate School of Natural Science and Technology, Kanazawa University, 5. Lamont-Doherty Earth Observatory, Columbia University, 6. School of Ocean and Earth Science, National Oceanography Centre Southampton, University of Southampton, 7. School of Geography, Earth and Environmental Sciences, Plymouth University, 8. Department of Earth Planetary Sciences, Graduate School of Environmental Studies, Nagoya University, 9. Institute of Science and Technology, Niigata University

There are numerous gas and liquid, two-phase inclusions in dolomite crystals in a white-green-colored listvenite recovered through Oman Drilling Project Phase 1 (specimen name z68w). Most of the fluid inclusions are tiny, <6 micrometer across and seems to be too small to provide detectable Raman spectra of fluids. Fluid inclusions >6 micrometer across in dolomite provide Raman spectra of H_2O, but they become dark possibly due to destruction during the cooling processes and usually prohibit from observation of melting ices. So far, Raman microscopy indicated that they are filled with H_2O and do not detect any other gasses such as CH_4 or CO_2. Melting temperature of ice in the tiny fluid inclusions, on a Linkam THM600 heating stage with a Nikon 100X objective lens indicates that they are filled with saline fluids with 1.1 ±0.5 wt% NaCl equivalent (n=42, Figure 1), which is much lower than that of seawater (3.5 wt% NaCl). Homogenization temperature of vapor-liquid suggests that the fluid inclusions were formed at temperature >139 ±31˚C (n=8, Figure 2). The fluid inclusions are mainly in dolomite veins, which cut magnesite and quartz (Figure 3, Raman mapping of magnesite, quartz, and dolomite). The present data indicate that low-salinity aqueous fluids were available during the crystallization of dolomite veins after the formation of magnesite-quartz assemblage. If seawater carries carbon to form listvenite from peridotite or serpentinite, the present low-salinity data suggest that chlorine needs to be absorbed by some phases during the fluid migration or be diluted by mixing with meteoric water.

Keywords: seawater, carbon cycling, serpentinite, serpentine, carbonate, carbonation

©2019. Japan Geoscience Union. All Right Reserved.

Figure 1 Histogram of salinity.

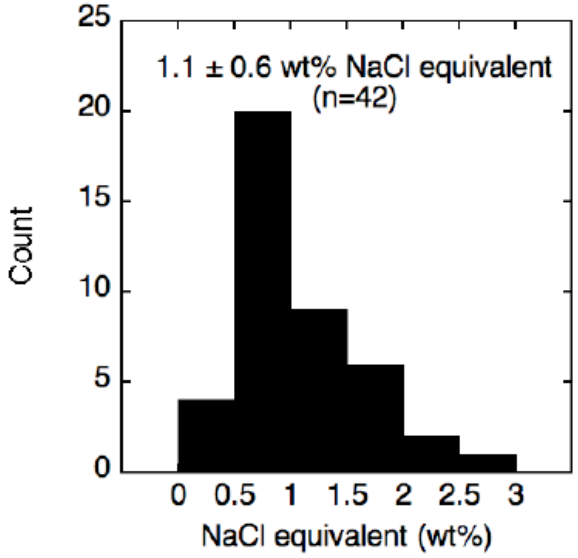

Figure 2 Homogenization T vs salinity.

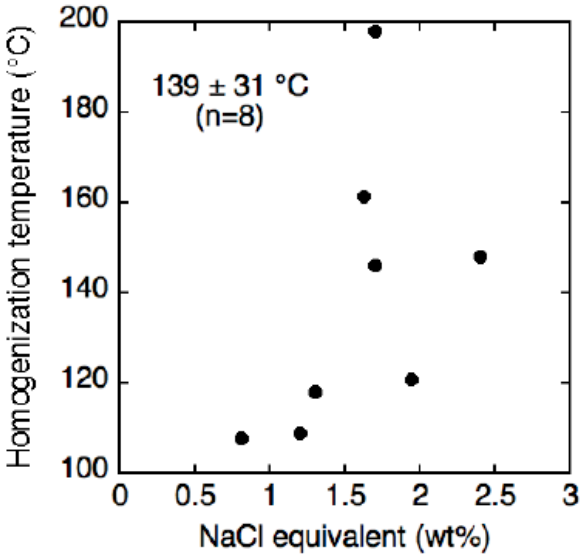

Figure 3 Microphotograph of a listvenite under transparent light (7.5mm wide) and Raman mapping images showing the distribution of magnesite, quartz, and dolomite.

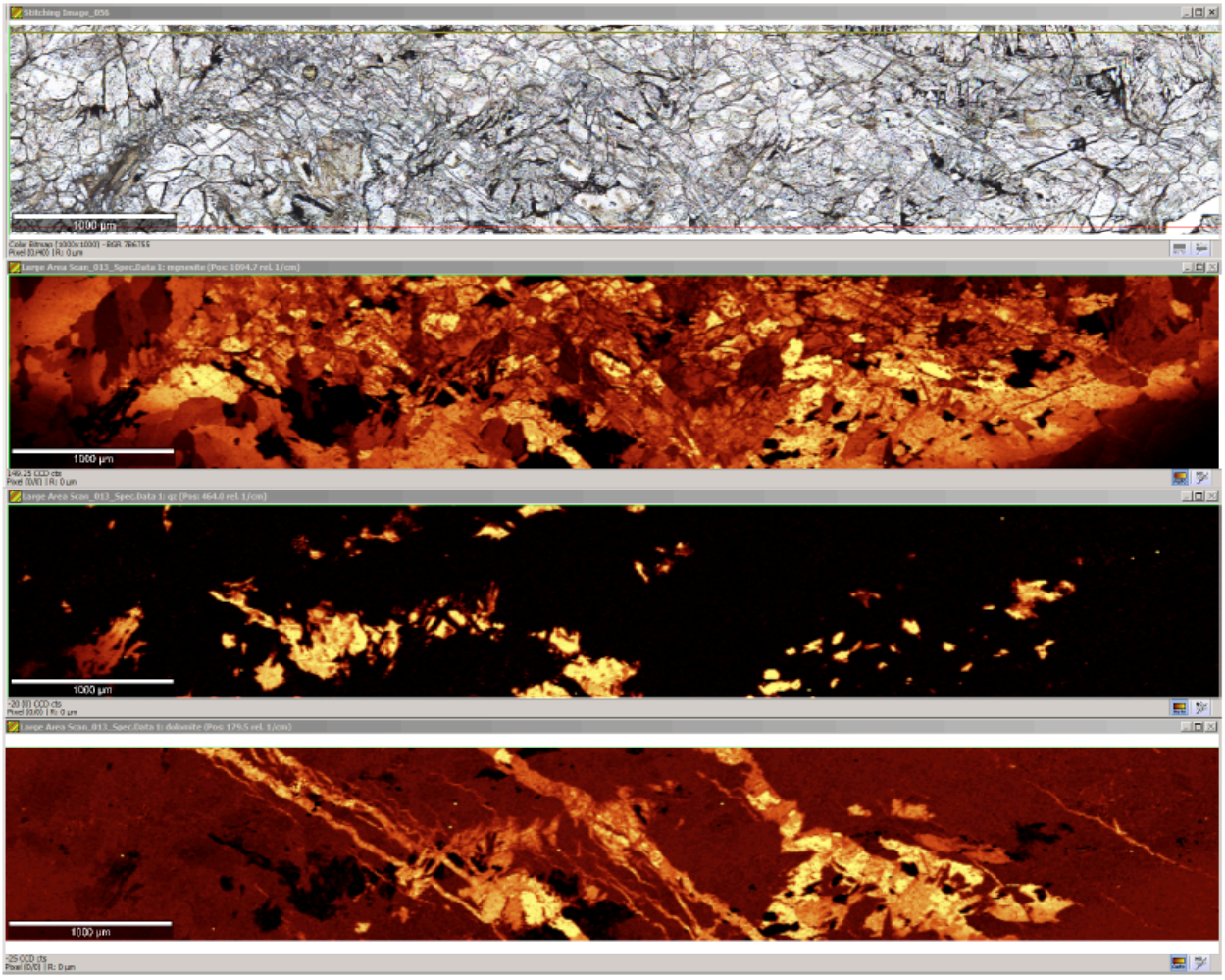

©2019. Japan Geoscience Union. All Right Reserved.

Hydration and development of fracture network within oceanic lower crust: an evidence from CM1A of Oman Drilling

*Atsushi Okamoto[1], Kazuki Yosida[1], Ryosuke Oyanagi[2], Oman Drilling Project Phase 2 Science Party[3]

1. Graduate School of Environmental Studies, 2. JAMSTEC, 3. Oman Drillng Project Phase 2 Science Party

The rate and extent of hydration of oceanic lithosphere are of special importance for understanding of the global water budget, the physical properties of crust-mantle boundary and potential limit of microbial activities in the crusts. It has been suggested that Moho transition zone and uppermost mantle has been highly serpentinized. If the fluid source for serpentinization is seawater, the fluid infiltration through the “less permeable” lower crust should occur. In this study, we report the nature of serpentinization in olivine within the lower crusts that was recovered from the CM1A site of the Oman Drilling Project, and discuss the relationship between hydration, fluid flow and fracturing based on the modeling of distinct element method (DEM).

The gabbroic rocks of the lower crust showed layer structures composed of light and dark colored layers with few to several tens millimeter thickness. The former is mainly composed of plagioclase and clinopyroxnene and the latter is enriched in olivine. The olivine grains were serpentinized with forming mesh-like textures, and the extent of serpentinization increases with increasing the modal abundance of olivine. The serpentine veins within the olivine grains do not always contain brucite, and show the zoning of Al, indicating an influx of silica and aluminum from plagioclase during serpentinization. The large amount of magnetite was formed in the serpentine mesh veins, indicating that olivine with high Fe content (Mg# = ~0.82) effectively produce hydrogen compared to the common mantle peridotite (Mg# = ~0.9). Radial cracks, which are filled with chlorite, are also developed around the serpentinized olivine grains. These features indicated that the reaction-induced fracturing occurred as the force of crystallization exceeds the tensile strength of the matrix minerals as suggested by the previous studies (Jamtveit et al., 2008; Kelemen and Hirth, 2012). It is also noted that fractures in olivine tends to developed in horizontal direction (parallel to the gabbroic layering) whereas those with in the plagioclase developed in vertical direction.

We conducted the DEM simulation on serpentinization in layered gabbro, which treats the reaction, advective fluid flow and fracturing, and the reaction rate is defined as a function of fluid pressure (Okamoto and Shimizu, 2015; Shimizu and Okamoto, 2016). The model reproduces a simultaneous development of contrasting fracture patterns inside and outside of the olivine grains, and shows the development of fracture network connecting the olivine grains, and shows the positive feedback of serpentinization, fracturing and permeability enhancement in vertical direction. These results indicate that the reaction-induced fracturing play essential roles on the fluid infiltration through the lower crusts and mantle hydration.

References

Kelemen, P.B., Hirth, G., 2012. Earth Planet Sci Let, 81-89. Jamtveit B., Malthe-Sorenssen, A., Kostenko, O., 2008. Earth Planet Sci Let, 267, 620-627. Okamoto, A., Shimizu, H., 2015. Earth Planet Sci Let, 417, 9-18. Shimizu, H., Okamoto, A., 2016. Contrib Mineral Petrol, 171, 73.

©2019. Japan Geoscience Union. All Right Reserved.

Keywords: layered gabbro, distinct element method, serpentinization, Oman Drilling Project, reaction induced fracturing

©2019. Japan Geoscience Union. All Right Reserved.

[J] Oral | S (Solid Earth Sciences)：S-CG Complex & General

Mon. May 27, 2019 9:00 AM - 10:30 AM JST | Mon. May 27, 2019 12:00 AM - 1:30 AM UTC | A05 TOKYO BAY MAKUHARI HALL

[S-CG56] Ocean Floor Geosciences

convener:Kyoko Okino(Atmosphere and Ocean Research Institute, The University of Tokyo), Chairperson:Arata Kioka, Atsushi Noda

Most of Earth's volcanism and much of its tectonic activity occur on and beneath the seafloor. Various phenomena on the seafloor are closely linked to plate tectonics, Earth and atmosphere. Seafloor rocks and sediments record Earth's evolution and heat and material fluxes on the Earth. Ocean Floor Geosciences session covers a broad range of research on LIPs, crustal movement and structure etc. Any fields of research and approach are welcomed. The session aims to encourage discussion among scientists from different study fields and to integrate our understanding of ocean floor. The session is co-chaired by K. Tadokoro (Nagoya Univ.), O. Ishizuka (AIST), T. Toki (Univ. Ryukyus), and N. Takahashi (JAMSTEC).

9:00 AM - 9:15 AM JST | 12:00 AM - 12:15 AM UTC

[SCG56-25] Observational plans of the South Sandwich Arc by R/V Hakuho Maru: Toward understanding formation and evolution of the world southernmost arc-trench system

*Asuka Yamaguchi[1], Kenichiro Tani[2], Minoru Ikehara[3] (1.Atomosphere and Ocean Research Institute, The University of Tokyo, 2.National Museum of Nature and Science, 3.Center for Advanced Marine Core Research, Kochi University)

9:15 AM - 9:30 AM JST | 12:15 AM - 12:30 AM UTC

[SCG56-26] Seismic imaging of the source zone of the 2011 Tohoku-oki earthquake

*Dapeng Zhao[1], Xin Liu[1] (1.Department of Geophysics, Tohoku University)

9:30 AM - 9:45 AM JST | 12:30 AM - 12:45 AM UTC

[SCG56-27] Drastic export of organic carbon to hadal trench driven by megathrust earthquake

*A. Kioka[1], T. Schwestermann[1], J. Moernaut[1], K. Ikehara[2], T. Kanamatsu[3], C. M. McHugh[4], C. dos Santos Ferreira[5], G. Wiemer[5], N. Haghipour[6], A. J. Kopf[5], T. I. Eglinton[6], M. Strasser[1,5] (1.Universität Innsbruck, Austria, 2.GSJ-AIST, Japan, 3.JAMSTEC, Japan, 4.Queens-CUNY, USA, 5.MARUM-U. Bremen, Germany, 6.ETH Zürich, Switzerland)

9:45 AM - 10:00 AM JST | 12:45 AM - 1:00 AM UTC

[SCG56-28] How do trench-fill sediments subduct under the accretionary wedge?

*Atsushi Noda[1], Hiroaki Koge[2], Yasuhiro Yamada[3], Ayumu Miyakawa[1], Juichiro Ashi[2] (1.National Institute of Advanced Industrial Science and Technology, 2.Atomosphere and Ocean Research Institute, The University of Tokyo, 3.Japan Agency for Marine-Earth Science and Technology)

10:00 AM - 10:15 AM JST | 1:00 AM - 1:15 AM UTC

[SCG56-29] Formation process of a slope basin in the Nankai Accretionary prism reconstructed from high-resolution SBP integrated with core data of ODP Site 1175 and Site 1176

*Yuichi Okuma[1], Asuka Yamaguchi[1], Hiroaki Koge[1], Rina Fukuchi[1], Juichiro Ashi[1] (1.Atmosphere and Ocean Research Institute, the University of Tokyo)

10:15 AM - 10:30 AM JST | 1:15 AM - 1:30 AM UTC

[SCG56-30] About the turbidity current considered that it occurred in the northern Suruga Bay, Central Japan by the typhoon No.24. -The traces of the accidents and the phenomenon at the sea floor detected the OBSs Array-

*Nakao Nagisa[1], Hisatoshi Baba[2], Hiroshi Sato[3], Kayoko Tsuruga[4], Izumi Sakamoto[2], Takahito Nishimiya[5], Masanao Shinohara[3], Shintaro Abe[6] (1.Tokai University, 2.Department of Marine and Earth Science, Tokai University, 3.Earthquake Research Institute, University of Tokyo, 4.Tokyo University of

Marine Science and Technology, 5.Meteorological Research Institute, Japan Meteorological Agency, 6.Association for the Development of Earthquake Prediction)

Observational plans of the South Sandwich Arc by R/V Hakuho Maru: Toward understanding formation and evolution of the world southernmost arc-trench system

*Asuka Yamaguchi[1], Kenichiro Tani[2], Minoru Ikehara[3]

1. Atomosphere and Ocean Research Institute, The University of Tokyo, 2. National Museum of Nature and Science, 3. Center for Advanced Marine Core Research, Kochi University

The South Sandwich arc-trench system, located in between South America and Antarctica, is one of the unexplored subduction zones of the world. It was originated in Mesozoic fragmentation of Gondwana, and Neogene westward subduction of South American plate causes formation of South Sandwich volcanic arc and back-arc opening of West and East Scotia Sea. The formation of Scotia Sea is closely related to the opening of Drake Passage Gateway, and thus it caused the development of the Antarctic Circumpolar Current and affected the earth’ s climate. However, detail back-arc opening process of Scotia Sea is poorly understood. Sediment accumulated in the South Sandwich Trench is expected to contain large amount of diatom and IRD (ice-rafted debris), but the nature of the sediment in the trench is unknown because of the lack of sediment cores.
On 2019 December-2020 January, R/V Hakuho Maru will visit the South Sandwich Arc and Weddell Sea as a part of around the world cruise for her 30th anniversary. During this cruise, we plan to take 1) dredge samples of forearc high of South Sandwich Arc possibly recording initiation process of oceanic island arc, as well as 2) sediment cores in South Sandwich Trench as an input to a subduction zone in polar region. By comparing the findings during this cruise to accumulated knowledge on backarc-arc-trench system around Japan, we try to understand the formation and evolution of the world southernmost arc-trench system.

©2019. Japan Geoscience Union. All Right Reserved.

Seismic imaging of the source zone of the 2011 Tohoku-oki earthquake

*Dapeng Zhao[1], Xin Liu[1]

1. Department of Geophysics, Tohoku University

The great 2011 Tohoku-oki earthquake (*Mw* 9.0) is the best-documented megathrust earthquake in the world, but its causal mechanism is still in controversy because of the poor state of knowledge on the nature of the megathrust zone. *Zhao et al*. (2011) used seismic tomography to study structural heterogeneity in the megathrust zone and suggested that lateral structural variations atop the subducting Pacific slab, such as the subducted seafloor topography, seamounts and sediments, affected nucleation of the 2011 Tohoku-oki earthquake. In contrast, *Bassett et al*. (2016) used residual topography and gravity data to constrain the Tohoku forearc structure and proposed that variations in the forearc lithology of the overriding Okhotsk plate were the main cause of along-strike variations of the Tohoku-oki slip behavior. In this work we constrain the structure of the Tohoku forearc using seismic tomography, residual topography and gravity data. We apply a tomographic method (*Zhao et al*., 2002) to invert 144,354 *P*-wave arrival-time data recorded at 382 permanent seismic stations in Tohoku from 4760 local shallow and intermediate depth earthquakes that occurred during January 2000 to June 2016.

Our results reveal a close relationship between structural heterogeneities in and around the megathrust zone and rupture processes of the 2011 Tohoku-oki earthquake (*Liu and Zhao*, 2018). Its mainshock nucleated in an off-Miyagi area with high seismic velocity, low seismic attenuation and strong seismic coupling, indicating a large asperity (or a cluster of asperities) in the Tohoku megathrust zone. Strong coseismic high-frequency radiations also occurred in high-velocity patches, whereas large afterslips took plate in low-velocity areas, which may reflect changes in fault friction and lithological variations. These results indicate that structural anomalies in and around the Tohoku megathrust originate from both the upper Okhotsk plate and the lower Pacific plate, which controlled the generation and rupture processes of the 2011 Tohoku-oki earthquake. This huge earthquake was caused by collision of harder rocks in both the upper and lower plates.

This work sheds new light on the causal mechanism of megathrust earthquakes. It also suggests that the location of a future great earthquake may be pinpointed by investigating the detailed structure of the megathrust zone.

In this presentation, we will also show our new results obtained by adding the data recorded by the S-net that has been installed in the eastern Japan forearc region under the Pacific Ocean.

References

Bassett, D., D. Sandwell, Y. Fialko, A. Watts (2016) Upper-plate controls on co-seismic slip in the 2011 magnitude 9.0 Tohoku-oki earthquake. *Nature* **531,** 92-96.

Liu, X., D. Zhao (2018) Upper and lower plate controls on the great 2011 Tohoku-oki earthquake. *Science Advances* **4**, eaat4396.

Zhao, D., Z. Huang, N. Umino, A. Hasegawa, H. Kanamori (2011) Structural heterogeneity in the

©2019. Japan Geoscience Union. All Right Reserved.

megathrust zone and mechanism of the 2011 Tohoku-oki earthquake (Mw 9.0). *Geophys. Res. Lett.* **38,** L17308.

Zhao, D., O.P. Mishra, R. Sanda (2002) Influence of fluids and magma on earthquakes: seismological evidence. *Phys. Earth Planet. Inter.* **132,** 249-267.

Keywords: The great Tohoku-oki earthquake, seismic tomography, Earthquake mechanism

©2019. Japan Geoscience Union. All Right Reserved.

Drastic export of organic carbon to hadal trench driven by megathrust earthquake

*A. Kioka[1], T. Schwestermann[1], J. Moernaut[1], K. Ikehara[2], T. Kanamatsu[3], C. M. McHugh[4], C. dos Santos Ferreira[5], G. Wiemer[5], N. Haghipour[6], A. J. Kopf[5], T. I. Eglinton[6], M. Strasser[1,5]

1. Universität Innsbruck, Austria, 2. GSJ-AIST, Japan, 3. JAMSTEC, Japan, 4. Queens-CUNY, USA, 5. MARUM-U. Bremen, Germany, 6. ETH Zürich, Switzerland

Despite a growing understanding of pivotal role of the carbon cycle in governing the Earth system, the nature and quantification of carbon supply to hadal environments remains poorly constrained. The giant 2011 Tohoku-oki earthquake has been inferred to remobilise fine-grained, young surface sediment enriched in organic matter from the slope into the >7 km deep Japan Trench. Yet, this hypothesis and assessment of its significance for the carbon cycle has been hindered by limited data density and resolution in the hadal zone. Here we combine new high-resolution bathymetry data with subbottom profiler images and sediment cores taken during 2012–2016, in order to map for the first time the spatial extent of the earthquake-triggered event deposit along the hadal Japan Trench. We quantify a sediment volume of ~0.2 km^3 deposited from spatially-widespread remobilisation of young surficial seafloor slope sediments triggered by the 2011 earthquake and its aftershock sequence. The mapped volume and organic carbon content in sediment cores encompassing the 2011 event reveals that this single tectonic event delivered >1 Tg of organic carbon to the hadal trench. This carbon is comparable to high carbon fluxes described for other Earth system processes, shedding new light on the impact of large earthquakes on long-term carbon cycling in the deep sea.

Keywords: Hadal zone, Japan Trench, Organic carbon, Carbon cycle, Sediment remobilization, The 2011 Tohoku-oki Earthquake

©2019. Japan Geoscience Union. All Right Reserved.

How do trench-fill sediments subduct under the accretionary wedge?

*Atsushi Noda[1], Hiroaki Koge[2], Yasuhiro Yamada[3], Ayumu Miyakawa[1], Juichiro Ashi[2]

1. National Institute of Advanced Industrial Science and Technology, 2. Atomosphere and Ocean Research Institute, The University of Tokyo, 3. Japan Agency for Marine-Earth Science and Technology

Ancient exhumed accretionary complexes sometimes have combinations of low-grade accretionary rocks from trench-fill turbidites, high-pressure/low-temperature metamorphic rocks including psammitic schists, and forearc basin deposits composed of sandy submarine fan deposits, whose provenance and depositional ages are similar to each other. For example of the southwestern Japan, sandstones in the Shimanto Accretionary Complex and psammitic schists in the Sanbagawa Metamorphic Complex are derived from terrigenous trench-fill deposits showing the similar geochemical and geochronological characteristics each other; the former is composed of accretionary rocks at the shallow part of the subduction zone and the latter comprises metamorphic rocks subducted to deeper than 10~km. Generally, at accretionary-type subduction zones, because weak layers within sediments deposited on the oceanic plate are used as a decollement, the lower pelagic and hemipelagic sediments can subduct beneath accretionary wedge through the subduction channel, but the upper terrigenous sediments are accreted at the toe of the wedge. Growth of accretionary wedge enabled to develop a forearc basin between the wedge and the backstop. At tectonically erosive subduction zones, most of the trench-fill sediments can subduct beneath the frontal prisms, but accretionary wedge cannot be grew at the same time. Therefore, it is difficult to explain coexistence of growth of accretionary wedge derived from coarse-grained trench-fill sediments and subduction of them deeper than seismogenic zone at the same time. In this study, we attempt to identify an importance of seafloor roughness for transportation of trench-fill sediments to deep during subduction. For this purpose, we conducted sandbox analogue experiments by using an unfixed rigid backstop on a subduction channel with the cases of smooth surface (Exp. A) and rough surface representing a seamount or ridge on subducting lower plate (Exp. B). The results of Exp. A showed progressive thickening of the accretionary wedge pushed the backstop down, meaning stepping down of the decollement and narrowing the subduction channel. On the other hand, Exp. B showed a subducting seamount lifted up the backstop, stepped up the d{\'e}collement, and then widened the subduction channel. Subduction of a rigid material like a chain of seamounts is a possible mechanism to open subduction channels for transportation of terrigenous sediments from the trench to high-pressure condition. Significant sediment supply to the trench and rough surface of subducting oceanic plate are required to enable subduction of protolith of HP-LT metamorphic rocks, accretion of trench-fill sediments at the shallow part, and formation of forearc basin simultaneously.

Keywords: Subduction zone, Accretionary wedge, High-pressure/low-temperature metamorphic rocks, Forearc basin, Seamount, trench-fill sediments

©2019. Japan Geoscience Union. All Right Reserved.

Formation process of a slope basin in the Nankai Accretionary prism reconstructed from high-resolution SBP integrated with core data of ODP Site 1175 and Site 1176

*Yuichi Okuma[1], Asuka Yamaguchi[1], Hiroaki Koge[1], Rina Fukuchi[1], Juichiro Ashi[1]

1. Atmosphere and Ocean Research Institute, the University of Tokyo

Upper plates of subduction zones record various phenomena associated with plate subduction. Geological records of slope basins overrapping accretionary prisms are useful to reconstruct tectonic activities of decollements and/or splay faults. In general, low-frequency sources are preferred for seismic reflection profiling to avoid attenuation in the water. However, low-frequency sources permit limited resolution of profiles due to trade-off relationship of frequency and resolution. For this reason, only limited studies focused on detail structures of the shallow portion of the deep-sea slope basins (e.g., Tsuji et al., 2014, *EPS*). In this study, we conducted interpretation of subsurface structures and reconstructed the formation process of the slope basin on the Nankai accretionary prism using high-resolution cross section images obtained by deep towed subbottom profiler on the R/V Hakuho-maru KH-16-5 cruise around the Nankai Trough off Muroto. This slope basin is located at 80 kilometers to southwest of the cape Muroto and a depth of 3000 m, and 8 kilometers long in northwest-southeast and 6.5 kilometers long in northeast-southwest forming an ellipse shape. An obvious strike-slip fault including normal-slip orientation at 1 kilometer seaward from the basin and a splay fault at 2 kilometers from the strike-slip fault are confirmed by Underwood et al. (2003, *JSR*), there is a high possibility that the basin records those activities. Moreover, Kodaira et al. (2000, *Science*) reported the existence of a subducted seamount at north of the slope basin, which means that subduction of this seamount had an impact on formation of the basin. Two cores from Site 1175 and Site 1176 were obtained by Ocean Drilling Program (ODP) Leg 190 around the basin, we also compared the result of interpretation to depositional structures and age. The high-resolution cross section shows a splay fault, strike-slip fault and hillock associated with minor faults including a strike-slip fault with reverse fault component at the center of the hillock. In the landward region from the strike-slip fault on the hillock, structures indicating relative subsidence of landward margin of the basin were confirmed. Additionally, basin strata show the evidence of landward migration of a depocenter in that region, which is coincident with the structures in the seismic profiles (Shipboard Scientific Party, 2001). The dip angle near the Site 1175 increase with depth, which suggest continuous tilting. Only normal faults exist in the landward region from the top of the hillock. Especially, four normal faults getting through to the seafloor are attributed to successive faulting because the displacement of those faults increase with depth. In addition, landslide deposit flowed from landward slopes is ascertained in the cross section. On the other hand, the reverse fault group being part of a splay fault is included in the trenchward region from the strike slip fault. The subbottom profile shows the evidence of obvious reverse and normal faulting around that region. Notably, reverse faulting is dominant in trenchward-half of the hillock, although no faults are getting through to the seafloor. The reflecting surfaces correspond with volcanic ash or sand layers by comparison both reflection surfaces and stratigraphic succession of cores on the Site 1175 and Site1175. Depositional age from analysis of ash suggest that the tilting in landward region from the strike-slip fault was getting low in activity and calmed within 28 ka. It is difficult to presume the moment of initiation of tilting due to depth limit of SBP, however, the basin already started tilting when the 105 ka surface deposited because that tilting of the surface confirmed around Site 1175. Additionally, the number of faults cutting surface younger than 28 ka is less than those cutting older than that surface, and no faults except the well-developed strike-slip fault at the center of the hillock reach the

©2019. Japan Geoscience Union. All Right Reserved.

seafloor. Therefore, those results indicate that a high likelihood of that the tilting at shallow portion of the basin caused by faulting of the splay fault, and suggest that the tilting had initiated before deposition of 105 ka surface and stopped by 28 ka at the latest. In this way, deep towed SBP integrated with core data has a great potential for reconstructing high time-resolution basin growth and fault activity.

Keywords: Slope basins, Accretionary prism, Sub-bottom profiler

©2019. Japan Geoscience Union. All Right Reserved.

About the turbidity current considered that it occurred in the northern Suruga Bay, Central Japan by the typhoon No.24. -The traces of the accidents and the phenomenon at the sea floor detected the OBSs Array-

*Nakao Nagisa[1], Hisatoshi Baba[2], Hiroshi Sato[3], Kayoko Tsuruga[4], Izumi Sakamoto[2], Takahito Nishimiya[5], Masanao Shinohara[3], Shintaro Abe[6]

1. Tokai University, 2. Department of Marine and Earth Science, Tokai University, 3. Earthquake Research Institute, University of Tokyo, 4. Tokyo University of Marine Science and Technology, 5. Meteorological Research Institute, Japan Meteorological Agency, 6. Association for the Development of Earthquake Prediction

In August 2018, Structural exploration based on "The integrated research project for the Fujikawa fault zone" began in the northern Suruga Bay. We installed 18 pop-up type Ocean Bottom Seismographs (OBSs) in this survey line (from Shimizu to Heda). In addition, we installed 4 OBSs in other survey lines for the observation of seismic activities around the Suruga Bay.

The typhoon No.24 passed off in the vicinity of the Suruga Bay from September 30th to October 1st 2018. After passing off that, various accidents of OBS occurred. Those accidents of OBS are as follows:

1. 4 OBSs drifted on the coast.

2. The movement of the installation position of the 2 OBSs was confirmed.

3. 1 OBS did not have a transponder response and it was missing.

4. The two OBSs have a transponder response, but they do not pop-up.

From this and the above, in this study, we considered OBS to have an accidentally due to a phenomenon occurred at the seafloor in the northern part of Suruga Bay by typhoon 24.

We analyzed using seismic wave, submarine topography and mud and considered them.

・According to the waveform record obtained by OBS, the accidenty spread from the central part of Suruga Bay of the extension of the Fujikawa estuary.

・It was a tilt that caused turbidity flow to occur by hanging from the Fujikawa estuary to the survey line.

・When the bottom sampling was done at the installation point and recovery point, the same particle size was present.

From the above,the cause of the accidenty in the OBS in the northern Suruga Bay is presumed to have flowed into the Suruga bay, where the sediments originating from the Fujikawa streamed OBSs.

©2019. Japan Geoscience Union. All Right Reserved.

From this, there is a high possibility that a turbid flow has occurred in northern Suruga Bay.

Keywords: Suruga Bay, OBS, turbidity current

©2019. Japan Geoscience Union. All Right Reserved.

[J] Poster | S (Solid Earth Sciences)：S-CG Complex & General

Mon. May 27, 2019 3:30 PM - 5:00 PM JST | Mon. May 27, 2019 6:30 AM - 8:00 AM UTC | Poster Hall International Exhibition Hall8, Makuhari Messe_17

[S-CG56] Ocean Floor Geosciences

convener:Kyoko Okino(Atmosphere and Ocean Research Institute, The University of Tokyo)

Most of Earth's volcanism and much of its tectonic activity occur on and beneath the seafloor. Various phenomena on the seafloor are closely linked to plate tectonics, Earth and atmosphere. Seafloor rocks and sediments record Earth's evolution and heat and material fluxes on the Earth. Ocean Floor Geosciences session covers a broad range of research on LIPs, crustal movement and structure etc. Any fields of research and approach are welcomed. The session aims to encourage discussion among scientists from different study fields and to integrate our understanding of ocean floor. The session is co-chaired by K. Tadokoro (Nagoya Univ.), O. Ishizuka (AIST), T. Toki (Univ. Ryukyus), and N. Takahashi (JAMSTEC).

[SCG56-P01] Signature of plume-ridge interaction on bathymetry and geochemistry along mid-ocean ridges: Insights from the Réunion Plume and Central Indian Ridge

*Clement Vincent[1], Jung-Woo Park[1], Sang-Mook Lee[1], Jonguk Kim[2], Sang-Joon Pak[2] (1.Seoul National University, 2.Korea Institute of Ocean Science and Technology)

[SCG56-P02] Spreading rate and its stability of Chile Ridge near the Chile Triple Junction

*Takanori Ishihara[1], Takeshi Matsumoto[1] (1.Ryukyu university)

[SCG56-P03] Newly Mapped Seamounts on the Antarctic Plate off Southern Chile

*Toshiya Fujiwara[1], Natsue Abe[2], Naomi Harada[3], Mirai MR16-09 Leg 2 Shipboard Science Party (1.Research and Development Center for Earthquake and Tsunami, Japan Agency for Marine-Earth Science and Technology, 2.Research and Development Center for Ocean Drilling Science, 3.Research and Development Center for Global Change)

[SCG56-P04] Surface-ship gravimetry on board MR16-09 Cruise by R/V MIRAI - Characteristrics of gravity anomaly around the Chile Triple Junction

*Takeshi Matsumoto[1], Takanori Ishihara[1] (1.Faculty of Science, University of the Ryukyus)

[SCG56-P05] Magnetic and Magnetotelluric surveys across the Afar depression, transition between continental rifting and sea-floor spreading

*Ryokei Yoshimura[1], Naoto Ishikawa[2], Tesfaye Kidane[3], Shin-ichi Kagashima[4], Nobutatsu Mochizuki[5], Ameha Atnafu Muluneh[3], Kirika Kitagawa[4], Taito Ikema[6] (1.Disaster Prevention Research Institute, Kyoto University, 2.Graduate School of Human and Environmental Studies, Kyoto University, 3.Addis Ababa University, 4.Faculty of Science, Yamagata University, 5.Priority Organization for Innovation and Excellence, Kumamoto University, 6.Faculty of Science, Kyoto University)

[SCG56-P06] Evolution of oceanic core complexes in the Shikoku Basin: when backarc basins cease to open

*Kyoko Okino[1], Yasuhiko Ohara[2,3], Masakazu Fujii[4], Tomoko Hanyu[1] (1.Atmosphere and Ocean Research Institute, The University of Tokyo, 2.Japan Coast Guard, 3.Japan Agency for Marine-Earth Science and Technology, 4.National Institute of Polar Research)

[SCG56-P07] Thermal evolution of the Lanzo orogenic peridotite massif in western Alps: implications on thermal structure near subcontinental lithosphere-asthenosphere boundary

*Tomo Aoki[1], Kazuhito Ozawa[1], Jean-Louis Bodinier[3], Françoise Boudier[2] (1.The University of Tokyo, 2.Montpellier 2 University, 3.Geosciences Montpellier)

[SCG56-P08] Comparison of the back-arc basins of the South and the Central Ryukyus in the northwest Pacific

*Kohsaku Arai[1], Ayanori Misawa[1], Takahiko Inoue[1] (1.Institute of Geology and Geoinformation, National Institute of Advanced Industrial and Technology)

[SCG56-P09] Geochemistry and zircon U-Pb ages of mafic rocks in the Mikabu and Sorachi-Yezo belts: Comparison with the Shatsky Rise

*Naoto Kimura[1], Yuji Ichiyama[1], Shohei Takahashi[1], Hisatoshi Ito[2], Akihiro Tamura[3], Tomoaki Morishita[3] (1.Chiba University, 2.Central Research Institute of Electric Power Industry, 3.Kanazawa University)

[SCG56-P10] Submersible magnetics reveals relationship between off-axis volcanism and hydrothermal systems of the Kairei and Yokoniwa fields at the Central Indian Ridge

*Masakazu Fujii[1], Kyoko Okino[2] (1.National Institute of Polar Research and SOKENDAI, 2.Atmosphere and Ocean Research Institute, The University of Tokyo)

[SCG56-P11] Shipboard magnetic and gravity surveys around the Iheya North Knoll and the Iheya Minor Ridge in the Mid-Okinawa Trough: Preliminary results of KR18-14 Leg1/Leg2 cruises

*Kazuya Kitada[1], Takafumi Kasaya[1], Hisanori Iwamoto[1], Yoshifumi Nogi[2] (1.Japan Agency for Marine-Earth Science and Technology, 2.National Institute of Polar Research)

[SCG56-P12] A shallow scientific drilling at Higashi Ensei Hydrothermal Field, Okinawa Trough

*Hidenori Kumagai[1], Takafumi Kasaya[1], Shuhei Totsuka[2], Shinsuke Kawagucci[1], Hideaki Machiyama[1], Koichi Iijima[1], Hirofumi Yamamoto[1], junji kaneko[1], Yusuke Ohta[3], Shohei Albert Tomita[3], Shogo Komori[4] (1.Japan Agency for Marine-Earth Science and Technology, 2.Kyushu Univ., 3.Kyoto Univ., 4.AIST)

[SCG56-P13] Mineralogical and geochemical study of sediment cores collected from the Gondou hydrothermal field in the Okinawa Trough

*Jun-ichiro Ishibashi[1,2], Shuhei Totsuka[2], Akihi Tsutsumi[2], Naru Tsukamoto[2], Yusuke Kira[2], Kazuhiko Shimada[1], Toru Yamasaki[3], Ken Ikehara[3], Toshiro Nagase[4], Yutaro Takaya[5,9], Kei Ikehata[6], Takashi Goto[7], Chitaro Gouzu[7], Ryuichi Shinjo[8], Hideaki Machiyama[9], Koichi Iijima[9], Hirofumi Yamamoto[9], Hidenori Kumagai[9] (1.Department of Earth and Planetary Sciences, Kyushu University, 2.Graduate School of Science, Kyushu University, 3.National Institute of Advanced Industrial Science and Technology, 4.Tohoku University Museum, 5.School of Creative Science and Enginerring, Waseda University, 6.Faculty of Life and Environmental Sciences, University of Tsukuba, 7.Hiruzen Institute for Geology and Chronology, 8.Faculty of Science, University of the Ryukyus, 9.Japan Agency for Marine-Earth Science and Technology)

[SCG56-P14] New type of self-potential anomaly observed near a hydrothermal site of Oomuro-dashi volcano, Izu-Ogasawara arc

*Yoshifumi Kawada[1,2], Takafumi Kasaya[2] (1.International Research Institute of Disaster Science, Tohoku University, 2.Japan Agency for Marine-Earth Science and Technology)

[SCG56-P15] Numerical simulation of submarine hydrothermal ore-deposits due to a coupled process of fluid migration and reactive geochemical transport

*Claudia Fujita[1], Hajime Yamamoto[1], Jun-ichiro Ishibashi[2], Takeshi Tsuji[3] (1.Taisei Corporation, 2. Department of Earth and Planetary Sciences, Faculty of Science, Kyushu University, 3.Department of Earth Resources Engineering, Faculty of Science, Kyushu University)

[SCG56-P16] Mineral composition and grain size distribution of REY-rich mud in the Minamitorishima EEZ: Implication for formation process of extremely REY-rich mud

*Sakai Takumi[1], Erika Tanaka[1], Kazutaka Yasukawa[1,2], Junichiro Ohta[2,1], Koichiro Fujinaga[2,1], Kentaro Nakamura[1], Yasuhiro Kato[3,1,2] (1.Department of Systems Innovation, School of Engineering, University of

Tokyo, 2.Ocean Resources Research Center for Next Generation, Chiba Institute of Technology, 3.Frontier Research Center for Energy and Resources, School of Engineering, The University of Tokyo)

[SCG56-P17] **Geochemical and morphological features of manganese micronodules in REY-rich mud within the Minamitorishima EEZ, western North Pacific Ocean**

*Satoshi Kino[1], Kazutaka Yasukawa[1,2], Keishiro Azami[1], Erika Tanaka[1], Koichiro Fujinaga[2,1], Kentaro Nakamura[1], Yasuhiro Kato[1,2] (1.Department of Systems Innovation, School of Engineering, University of Tokyo, 2.Ocean Resources Research Center for Next Generation, Chiba Institute of Technology)

[SCG56-P18] Seafloor sediment thickness around the Japan and Kurile trenches obtained by traveltime analysis for PS converted wave recoded by ocean bottom seismograms

*Ryosuke Azuma[1], Genti Toyokuni[1], Ryota Takagi[1], Syuichi Suzuki[1], Makiko Sato[1], Takashi NAKAYAMA[1], Naoki Uchida[1], Ryota Hino[1] (1.Recearch Center for Prediction of Earthquake and Volcanic Eruption, Graduate School of Science, Tohoku University)

[SCG56-P19] Examination of critical taper theory based on bathymetry data in subduction zones

*Hiroaki Koge[1], Juichiro Ashi[1], Jin-Oh Park[1] (1.Atmosphere and Ocean Research Institute, The University of Tokyo)

[SCG56-P20] Active structures of the Sagami Bay Fault by high-resolution sub-bottom profiling and pin-point core sampling

*Juichiro Ashi[1], Asuka Yamaguchi[2], Natsumi Okutsu[1], Ayanori Misawa[3] (1.Graduate School of Frontier Sciences, The University of Tokyo, 2.Atmosphere and Ocean Research Institute, The University of Tokyo, 3.National Institute of Advanced Industrial Science and Technology)

[SCG56-P21] Fault Distribution and Structural Characteristic in the Nankai Trough Area, Japan

*Rei Arai[1], Narumi Takahashi[1], Minako Katsuyama[1], Shigeyoshi Tanaka[1], Hiromi Kamata[1], Tomoyuki Sato[2], Takahiko Inoue[2], Yoshiyuki Kaneda[3] (1.Japan Agency for Marine-Earth Science and Technology, 2.National Institute of Advanced Industrial Science and Technology, 3.Kagawa University)

[SCG56-P22] Seismicity in the central Ryukyu Trench by the Ocean Bottom Seismometers

*Ren Yakabu[1], Mamoru Nakamura[1], Yusuke Yamashita[2], Masanao Shinohara[3], Tomoaki Yamada[3], Hajime Shiobara[3], Kimihiro Mochizuki[3] (1.University of the Ryukyus, 2.DPRI, Kyoto University, 3.ERI, Tokyo University)

[SCG56-P23] Seismic structure of subducted Philippine Sea plate beneath Kyushu inferred from Po/So waves

*Azusa Shito[1] (1.Institute of Seismology and Volcanology, Kyushu University)

[SCG56-P24] Slope failure features and their distribution in the forearc off northwestern Sumatra

*Kenji Hirata[1], Toshiya Fujiwara[2], Ayanori Misawa[3], Kohsaku Arai[3] (1.National Research Institue for Earth Science and Diaster resilience, 2.Japan Agency for Marine-Earth Science and Technology, 3.National Institute of Advanced Industrial Science and Technology)

[SCG56-P25] Origin and migration of fluid in the Sumatra subduction input: application of a geochronological method using a long-lived radioisotope of dissolved iodine

*Satoko Owari[1], Hitoshi Tomaru[1] (1.Chiba university)

[SCG56-P26] Challenge to Future Deep-Water Mapping: Unmanned Bathymetric Survey Competition "Shell Ocean Discovery XPRIZE"

*MASANAO SUMIYOSHI[1] (1.Hydrographic and Oceanographic Department, Japan Coast Guard)

[SCG56-P27] Prototype of deep-sea ocean bottom pressure recorder with self-calibration capability using “A-0-A” approach for detection of long-term crustal deformation

*Yusaku Ohta[1], Ryota Hino[1], Syuichi Suzuki[1], Makiko Sato[1], Yui Nishimagi[1], Hiroaki Kajikawa[2], Tokihiko Kobata[2] (1.Research Center for Prediction of Earthquakes and Volcanic Eruptions, Graduate School of Science, Tohoku University, 2.National Metrology Institute of Japan, National Institute of Advanced Industrial Science and Technology)

[SCG56-P28] Noise reduction and surface wave array dispersion measurements applied to NOMan's broadband OBS data

*Yuki Kawano[1], Takehi Isse[1], Hitoshi Kawakatsu[1], Akiko Takeo[1], Hajime Shiobara[1] (1.Earthquake Research Institute, The University of Tokyo)

[SCG56-P29] High-tech dredge system for abyssal bedrock research; dredge system with acoustic real time monitoring on deep sea floor.

*Teruaki Ishii[1], Yukihiro - Kida[2], Izumi - Sakamoto[3], Shiki - - Machida[4] (1.Center for Integrated Research and Education of Natural Hazards, Sizuoka University, 2.JAMSTEC, 3.Toukai University, 4.Chiba Institute of Technology)

[SCG56-P30] Construction of Database System on Offshore Faults around Japan

*Hiromi Kamata[1], Narumi Takahashi[1,2], Shigeyoshi Tanaka[1], Rei Arai[1], Minako Katsuyama[1], Ayako Nakanishi[1], Hiroyuki Fujiwara[2], Tsuneo Ohsumi[2], Takahiko Inoue[3], Tomoyuki Sato[3], Yoshiyuki Kaneda[4] (1.Japan Agency for Marine-Earth Science and Technology, 2.National Research Institute for Earth Science and Disaster Resilience, 3.National Institute of Advanced Industrial Science and Technology, 4.Kagawa University)

[SCG56-P31] **An integration method for multiple sets of seafloor backscatter intensity data**

*Shiki Machida[1,2], Taichi Sato[3], Kazutaka Yasukawa[2] (1.Ocean Resources Research Center for Next Generation, Chiba Institute of Technology, 2.University of Tokyo, 3.AIST)

[SCG56-P32] A precise calculation of average depth for ETOPO1

*Yasushi Harada[1], Sae Horiuchi[1] (1.School of Marine Science and Technology, Tokai University)

Signature of plume-ridge interaction on bathymetry and geochemistry along mid-ocean ridges: Insights from the Réunion Plume and Central Indian Ridge

*Clement Vincent[1], Jung-Woo Park[1], Sang-Mook Lee[1], Jonguk Kim[2], Sang-Joon Pak[2]

1. Seoul National University, 2. Korea Institute of Ocean Science and Technology

Plume-ridge interaction is an important thermal and geological process, which results in various physical and chemical anomalies along a significant length of the global mid-ocean ridges system. Despite numerous studies, some remaining questions to be solved are origin and mechanisms of geochemical variations and their possible influence on the morphology of mid-ocean ridges. The Central Indian Ridge, with a slow to intermediate spreading rate, provides an ideal opportunity to explore distant plume-ridge interactions. Presently, the ridge is moving away from the hotspot. The hotspot which started at the Deccan Traps (65 Ma) is presently 1000 km away from the Central Indian Ridge, at the Réunion Island. Paleogeographic reconstruction suggests that the hotspot crossed the middle part of the Central Indian Ridge (MCIR) between 8˚S and 17˚S at ~34 Ma. Studies suggest that the plume material that flows into the Central Indian Ridge is more or less concentrated around 19˚S, to the south of Marie Celeste Fracture Zone (MCFZ). In addition, recent geochemical study show southward-increasing gradient in Réunion mantle component between 14˚S and 18˚S north of MCFZ. The detailed mechanism of the plume interaction on the MCIR is in debate. In this study, we revisited the MCIR with additional Nd, Sr and Pb isotope analyses and ship-board high-resolution bathymetry data to constrain the influence of the Ré union plume on geochemistry and bathymetry of the MCIR. The results show that the geochemical anomaly observed between 14˚S and 18˚S are found only in the northern part of segments and subsegments, and these enrichments correlate with the shallow axial bathymetry. The localized geochemical and bathymetric anomalies can be ascribed to a hotspot leading edge effect where the hotspot leading segments are offset in the direction of the plume and are more influenced by the plume materials. It appears that discontinuities such as transform faults and the non-transform discontinuities influence the flow of mantle plume material into the ridge, and that the proximity of the ridge to the hotspot plays an important role in the plume-ridge interaction.

Keywords: Plume-ridge interaction, Reunion Plume, Central Indian Ridge, MORB

©2019. Japan Geoscience Union. All Right Reserved.

Spreading rate and its stability of Chile Ridge near the Chile Triple Junction

*Takanori Ishihara[1], Takeshi Matsumoto[1]

1. Ryukyu university

Chile triple junction (CTJ) is located at 46°13'S, 75°13'W off the coast of Chile and is composed of Nazca plate, Antarctic plate and South America plate, forming a ridge-trench-trench type triple junction. Chile ridge that is an active spreading ridge is subducting under the South America plate at CTJ and is the only ridge system that is currently subducting under trench in the world. Therefore this area is an important target to study the behavior of the active ridge just before subduction. And also, the mechanism and a possible driving force of the active ridge subduction are also to be studied by subsurface structure, age, development history, and so on through marine geophysical survey. The authors analysed total geomagnetic data from the tracks along the segments and attempted to obtain seafloor spreading rate at each segment and seafloor age from magnetic anomaly, and spreading stability in this area by the magnetic N/R boundary strikes derived from the three component magnetic data. Both the total force and the three-component magnetic data for this study were obtained from MR16-09 cruise by R/V MIRAI, Leg1 and Leg2. Marine Trackline data that were achived in National Geophysical Data Center were also used supplementarily. Seafloor spreading rate decrease is shown along almost all the tracks close to the trench, and comparison of several track data along the Segment SCR1 shows the same characteristics that spreading rate along the southern track is slower than that along the northern track. Moreover, the result from the other segments show that SCR1’s spreading rate (about3.0cm/yr) is higher than SCR3’s one (about 2.0cm/yr). These results show spreading rate is decreasing as the ridge is close to the trench. This mightbe due to declining of igneous activity and reduction of magma supply rate near the trench as Matsumoto et al (2013) showed. The reason why the young seafloor subducts early is that increasing of slab pull force caused by thickening of the oceanic lithosphere by cooling with closing the trench. Magnetic N/R boundary strike shows almost uniform trends, except near Guamblin fracture zone, so spreading stability is attained on the whole.

©2019. Japan Geoscience Union. All Right Reserved.

Newly Mapped Seamounts on the Antarctic Plate off Southern Chile

*Toshiya Fujiwara[1], Natsue Abe[2], Naomi Harada[3], Mirai MR16-09 Leg 2 Shipboard Science Party

1. Research and Development Center for Earthquake and Tsunami, Japan Agency for Marine-Earth Science and Technology, 2. Research and Development Center for Ocean Drilling Science, 3. Research and Development Center for Global Change

We conducted bathymetry, gravity, and magnetic survey of seamounts on the Antarctic Plate off southern Chile in the R/V Mirai MR16-09 Leg 2 cruise (January 20 - February 5, 2017: Puerto Montt - Punta Arenas). The survey including transit was an unprecedented opportunity to collect data in the regions of the Pacific Ocean where it has been sparsely surveyed.

A SeaBeam 3012 multibeam echo sounder was used for the bathymetric survey. The Micro-G LaCoste and Romberg S-116 shipboard gravity meter, a Geometrics G-882 cesium towing magnetometer, and a Tierra Tecnica SFG1214 shipboard three-component magnetometer were used for the gravity and magnetic surveys, respectively. Unfortunately, dredge rock sampling and seismic reflection survey was not conducted.

The seamounts are located on the Antarctic Plate. The mid-ocean ridge (Chile Ridge) was considered to be already subducted beneath the South American Plate. Magnetic Anomaly 6a was identified by Cande et al. (1982) on the seafloor in the vicinity of the seamounts. The crustal age around the seamounts is 18 Ma according to Muller et al. (2008). We observed magnetic anomaly stripes with amplitudes of about 400 nT, therefore, we will examine the crustal age and the seafloor spreading rate.

Since the seafloor was covered with a sedimentary layer, abyssal hills and their strikes could not be identified. The largest seamount was located at 51˚00'S, 79˚25'W. The seamount has a major axis of about 17 km, a minor axis of 10 km, and the strike of the major axis is N45˚W. The water depth of the base of the seamount is about 3900 m and the shallowest depth is about 2900 m, thus the relative height is about 1000 m. The seamount was surrounded by a moat with the maximum deep of 100 m. The basal area is about 160 square kilometers and the volume above the seafloor is about 70 cubic kilometers. The seamounts have calderas, and the depth and the diameter of the largest seamount are 200 m and 2.5 km, respectively.

The existence of the largest seamount was estimated by satellite altimetry and gravity observations. The relative height was estimated to be 364 m (Kim and Wessel (2011) seamount catalogue, ID: KW-05846). However, the accurate estimation of such a small seamount is difficult. We observed free-air gravity anomaly of about +20 mGal at the base of the seamount, and of about +50 mGal over the top of the seamount, thus the peak-to-trough amplitude of the gravity anomaly was 30 mGal. The gravity anomaly due to the seamount with 20 mGal larger amplitude was observed compared with a satellite-based gravity anomaly (Sandwell et al., 2014).

Keywords: Off Chile, Antarctic Plate, Seamount, Bathymetry, Gravity Anomaly, Magnetic Anomaly

©2019. Japan Geoscience Union. All Right Reserved.

Surface-ship gravimetry on board MR16-09 Cruise by R/V MIRAI - Characteristrics of gravity anomaly around the Chile Triple Junction

*Takeshi Matsumoto[1], Takanori Ishihara[1]

1. Faculty of Science, University of the Ryukyus

MR16-09 cruise by R/V MIRAI traversed the Southeast Pacific and the Western Pacific from December 2016 to March 2017, with the portcall at Fiji, Chile, New Zealand and Mutsu. Gravity measurement was also carried out during the whole cruise except for within the EEZ of other countries.
During Leg2 of this cruise, the Segment SCR1 of the Chile Ridge, an active spreading ridge producing the Nazca plate and the Antarctica plate, was also surveyed in order to detect the characteristics of the gravity anomaly due to the subduction of the active mid-oceanic ridge below the South American Plate at the Chile Trench at the Chile Triple Junction (CTJ) located off Taitao Peninsula on the west coast of Chile.
The shipboard gravimeter used for the survey was a relative measurement system. Micro-g LaCoste air-sea gravity meter S-116 is equipped on board MIRAI. Normally, ‘gravity tie’ is carried out during the portcall at the wharf and the gravity base stations nearby where absolute value of gravity is known in order to obtain the absolute gravity value during the cruise. However, it was difficult to obtain accurate values after correcting the drift of the gravimeter because gravity tie was carried out only at 3 stations at the beginning (Shimizu), at the end (Sekinehama) and during the cruise (Punta Arenas). Therefore, correction of the value at the gravity measurement points on the survey lines was carried out using the latest global gravity 1’ grid data (Sandwell et al., 2014, Sandwell et al., 2013, Sandwell et al., 2009) derived from satellite altimetry data etc.

Let the grid intervals in the x and y directions of the grid data be dx and dy, respectively. Let g11, g21, g12, g22 be the gravitational values at the four corner points of this area (approximated by a rectangle) enclosed by x1, x2 (x1 < x2) for x-coordinate and y1, y2 (y1 > y2) for y-coordinate. The linearly interpolated value at the point (x, y) within this the area is

g1 = g11 * (x2 - x) * (y1 - y)

g2 = g21 * (x - x1) * (y1 - y)

g3 = g12 * (x2 - x) * (y - y2)

g4 = g22 * (x - x1) * (y - y2)

Then,

g = (g1 + g2 + g3 + g4) / (dx * dy).

Based on the difference between the gravity values obtained by this interpolation and the measured values, the drift rate at each leg was determined as,

Leg 1: 0.216 mgal/day

Leg 2: 0.520 mgal/day

©2019. Japan Geoscience Union. All Right Reserved.

Leg 3: -0.599 mgal/day

Leg 4: 0.562 mgal/day.

The measured gravity was corrected using these drift rates to obtain the final free air anomalies during the cruise.

Bouguer anomaly along the 3 survey lines on the Segment SCR1 (including the CTJ) of the Chile Ridge off the Chilean west coast was obtained by the two-dimensional calculation (assuming that the same seafloor topography and sub-seafloor structure are continuous along the trench/ridge axis direction) by use of the profiles of free air anomaly and seafloor topography along these survey lines. Regardless of the topographic undulation on the western side of the ridge/trench, the Bouguer anomaly decreased relatively uniformly towards the trench/ridge axis. This pattern is similar to that of the normal trenches and mid-ocean ridges. The rate of decrease as approaching the trench is about 1.5~2 mgal/km in the Western Pacific trench, <0.1 mgal/km for the Mid-Atlantic Ridge. However, the result of the current gravity survey shows that the decrease rate is 0.4~0.8 mgal/km.

In addition, geophysical traverses across the Tonga-Kermadec arc-trench, the southern East Pacific Rise (Leg1), the Bellingshausen Sea, the Amundsen Sea, the Eltanin-Udintzev fracture zones (Leg3), the South Fiji Basin, the Solomon arc-trench, and the West Caroline Plateau were obtained during the cruise.

Keywords: Chile Triple Junction, Gravity Anomaly, R/V MIRAI

©2019. Japan Geoscience Union. All Right Reserved.

Magnetic and Magnetotelluric surveys across the Afar depression, transition between continental rifting and sea-floor spreading

*Ryokei Yoshimura[1], Naoto Ishikawa[2], Tesfaye Kidane[3], Shin-ichi Kagashima[4], Nobutatsu Mochizuki[5], Ameha Atnafu Muluneh[3], Kirika Kitagawa[4], Taito Ikema[6]

1. Disaster Prevention Research Institute, Kyoto University, 2. Graduate School of Human and Environmental Studies, Kyoto University, 3. Addis Ababa University, 4. Faculty of Science, Yamagata University, 5. Priority Organization for Innovation and Excellence, Kumamoto University, 6. Faculty of Science, Kyoto University

The Afar area (Ethiopia) is well known as one of continental rifts transitioning to oceanic spreading centers. In order to delineate subsurface electric properties and document an initial stage of the formation process of magnetic stripes, we carried out wideband magnetotelluric (MT) measurements and ground magnetic survey along a common profile in 2016 and 2017. This profile, approximately 55km long, cuts across the Dabbahu rift in the Afar Depression. In magnetic survey on foot, we recorded total magnetic fields at 2.4 meters above the ground every 4 seconds by utilizing GSM-19 Overhauser magnetometer (GEM systems). In MT survey, we obtained electromagnetic and electric data at 14 sites using MTU-5A (Phoenix Geophysics) and ELOG1K-PHX (NT system design) systems. In this presentation, we will introduce the outline of our project and show results of magnetic and MT surveys.

Keywords: Afar depression, sea-floor spreading, magnetotelluric survey, magnetic survey

©2019. Japan Geoscience Union. All Right Reserved.

Evolution of oceanic core complexes in the Shikoku Basin: when backarc basins cease to open

*Kyoko Okino[1], Yasuhiko Ohara[2,3], Masakazu Fujii[4], Tomoko Hanyu[1]

1. Atmosphere and Ocean Research Institute, The University of Tokyo, 2. Japan Coast Guard, 3. Japan Agency for Marine-Earth Science and Technology, 4. National Institute of Polar Research

How and why backarc basins cease to open is one of the unsolved questions in plate tectonics. The Shikoku Basin is a typical backarc basin, that was formed behind the proto Izu-Bonin arc and stopped opening at ca.15 Ma. The post-spreading volcanism has formed a series of seamounts along the remnant spreading axis in the northern basin, whereas multiple oceanic core complexes have developed just before the spreading stop in the southern basin. Oceanic core complexes (OCC) are exposed lower crust and/or upper mantle materials along detachment faults, that are supposed to develop when melt supply rate M (=magmatic accommodation / plate separation) is around 0.5. The OCC is, therefore, a good indicator for temporal variation of melt supply when the backarc system died. During Yokosuka YK18-07 and Hakuho-maru KH-18-02 cruises in 2018 summer, we conducted the geophysical mapping (multibeam bathymetry, scalar and vector magnetics, and gravity) of an OCC at 23°50’ N, 138°50’ E in the southernmost Shikoku Basin and its adjusting areas. The OCC is tentatively named Mado Megamullion. We compiled these new datasets and previously collected data and analyzed detailed bathymetry and magnetic and gravity anomalies. In this presentation, we show the results and discuss the structure and evolutionary process of this OCC and its implications for demise of backarc opening system.

The Mado Megamulliion is about 20 km square domed high, located at the intersection of remnant ridge segment and transform fault. Its surface is characterized prominent corrugations parallel to flow lines. The mantle Bouguer anomaly is about 20mGal higher than the surroundings. This observation is consistent with the fact that high-density gabbro and peridotite samples were recovered both by Shinkai6500 dive in YK18-07 and dredge hauls in KH-18-02. A part of recovered rock samples show the deformation structure, suggesting that the surface of this OCC is a detachment fault surface. Magnetic anomaly distribution shows generally linear, positive and negative bands over the OCC as same as in the well-ordered abyssal hill area, suggesting continuous crust formation from ridge segments. The widths of lineations are, however, longer at the OCC, indicating clear asymmetric spreading during detachment faulting. The spreading asymmetry is often observed over world OCC areas. The equivalent magnetization value seems to be positively shifted, that may suggest the effect of induced magnetization of OCC massif. The result of vector magnetic field analysis shows clear, strong and ridge-parallel magnetic boundaries in well-ordered abyssal hill areas, that is consistent with normal seafloor spreading and block model. In contrast, the clear, systematic magnetic boundaries don’t exist. The estimated three dimensionality is not so strong. Within the rift valley south of the Mado Megamullion, a small domed high with high Bouguer anomaly exists. This is likely NTO (non-transform offset) massif, previously reported along mid-ocean ridges. Another corrugated surface is observed at neighboring segment, that shows typical detachment surface morphology but are not accompanied by gravity anomalies.
The structure and evolutionary process of the Mado Megamullion and the adjacent OCC-like massifs infer the temporal variation of melt supply on the final stage of backarc opening. Multiple core complexes including world largest Godzilla Megamullion are distributed along the Parece Vela Rift, south of the study area. The integrated analysis of these OCCs is a key to understand the demise of backarc systems.

©2019. Japan Geoscience Union. All Right Reserved.

Keywords: backarc opening, oceanic lithosphere, oceanic core complex

©2019. Japan Geoscience Union. All Right Reserved.

Thermal evolution of the Lanzo orogenic peridotite massif in western Alps: implications on thermal structure near subcontinental lithosphere-asthenosphere boundary

*Tomo Aoki[1], Kazuhito Ozawa[1], Jean-Louis Bodinier[3], Françoise Boudier[2]

1. The University of Tokyo, 2. Montpellier 2 University, 3. Geosciences Montpellier

Lithosphere-asthenosphere boundary (LAB) is a zone where heat, momentum, and materials are exchanged between conductive mantle and underlying convective mantle, and plays an important role in plate tectonics (McKenzie & Priestley, 2005; Fischer et al., 2010; Kawakatsu & Utada, 2017). Its internal structure and dynamic behavior are, however, far from understood. This study addresses this issue on the basis of petrological study of an orogenic peridotite complex. Lanzo massif in the western Alps, Northern Italy. We attempt to clarify temporal change of internal thermal structure of the complex during exhumation, from which the original thermal structures before exhumation may be estimated.
Lanzo massif is one of the largest mantle exposure thought to be a subcontinental lithospheric mantle exhumed related to the opening of the Jurassic Piedmont Sea between European continent and Adriatic continent, following slow spreading of the Atlantic mid ocean ridge (Müntener & Piccardo, 2003). The massif consists dominantly of plagioclase-bearing lherzolite, stable at the pressure lower than 1GPa, with subordinate amount of mafic rocks occurring as layers or dikes (Bodinier, 1988; Bodinier et al., 1991). The Lanzo massif divided into three bodies on the basis of petrographic characteristics: north, central and south. Previous studies argued that the northern part represents subcontinental lithospheric mantle and that the southern part may be of asthenospher origin (Bodinier, 1988; Bodinier et al. 1991). Therefore, the complex may represent a zone of lithosphere-asthenosphere boundary and can provide information on processes operated there (Bodinier, 1988; Bodinier et al., 1991; Kaczmarek & Müntener, 2008).
We examined plagioclase-bearing lherzolite collected from 16 localities covering the entire massif. Systematic variations of microstructures and mineral chemical compositions were confirmed, which is principally consistent with previous studies (Bodinier, 1988; Bodinier et al., 1991). All constituent minerals show chemical heterogeneity on grain scales, which is regarded as record of various processes the rocks underwent. Grain-scale zonings of Al and Ca in pyroxene, fluorescence-corrected Ca in olivine adjacent to pyroxenes, Cr and Al in spinel adjacent to plagioclase, and Ca and Na in plagioclase suggest that monotonous cooling and decompression accompanied by deformation occurred during decompression of the Lanzo massif. We quantified the space-dependent thermal history of Lanzo by using Ca-in-orthopyroxene geothermometer after Lindsley (1983) and Ca-in-olivine geothermometers calibrated on the basis of experimental results of Köhler & Brey (1990). All the estimated temperatures decrease from the southern body towards the northern body. The calculated temperatures were critically examined if they represent closure temperatures or a condition at which Lanzo resided for a certain period of time. The grain-scale zoning patterns indicate that the temperatures from core of orthopyroxene recorded a long residence, whereas those from rim of pyroxenes and both core and rim of olivine represent closure temperatures (Tc) at various timings during monotonous cooling. The decrease in temperatures of pyroxene cores from the south to the north by ~60K may represent a geotherm near LAB zone. All the Tc decrease from the north to the south and the difference of temperatures between the core and rim of orthopyroxene increases from the southern body to the northern body. This suggests that the cooler and probably shallower northern body cooled at slower rate at a wide temperature range (Tc=700-1100˚C) than the hotter and probably deeper southern body. A thermal gradient recorded in the Lanzo massif is estimated to be ~6K/km, which is greater than those estimated for deep subcontinental

©2019. Japan Geoscience Union. All Right Reserved.

lithosphere at steady thermal state (Mckenzie et al., 2005). We speculate that the high geotherm might have caused by thermal perturbation from asthenosphere.

Keywords: lithosphere-asthenosphere boundary, mantle peridotite, thermal structure

©2019. Japan Geoscience Union. All Right Reserved.

Comparison of the back-arc basins of the South and the Central Ryukyus in the northwest Pacific

*Kohsaku Arai[1], Ayanori Misawa[1], Takahiko Inoue[1]

1. Institute of Geology and Geoinformation, National Institute of Advanced Industrial and Technology

The Ryukyu Arc, which extend for over 1200 km along the east coast of Asia from Kyushu to Taiwan, and the associated Ryukyu Trench, are products of the subduction of the Philippine Sea Plate (PSP) beneath the Eurasian Plate. The PSP is subducting northwestward beneath the Eurasian Plate at a convergence rate of 4–9 cm/yr (Seno et al., 1993). The major islands of the Ryukyu Arc are considered the forearc highs.
The Okinawa Trough is a back-arc basin located beside of the Ryukyu Arc that was formed in the late Miocene (Gungor et al., 2012) or the late Pliocene–early Pleistocene (Sibuet et al., 1998). Formation of the Okinawa Trough was a key geological event associated with complex tectonics and changes in the topographic configuration of the Ryukyu Arc. Geological Survey of Japan (GSJ), AIST has started the marine geological mapping project around Ryukyu Arc since the 2008 FY. Multi-channel (16 ch or 32 ch) high-resolution seismic profiles were acquired during these cruises by the GI-gun (355cu. inch) systems. In our investigation into the deformation of the Ryukyu Arc using the high-density seismic profiles, we found that the normal faults parallel to the trench axis are well developed on the back-arc side of the arc. Slope of northern off the Southern Ryukyu (Miyako-jima and Ishigaki-jima) is simply downthrown to the axis of Okinawa Trough and reach to 2000 m in depth. In the other hand, the Central Ryukyu, northwestern off the Okinawa-jima is characterized by the small basin structure which accompanies with active normal faults. The faults show ENE-WSW strike and dip to the north with clear half graben structure. We present the tectonics of these structure compare the back-arc basins of the South Ryukyu with the Central Ryukyu.

Keywords: Ryukyu Arc, back-arc basin, Quaternary, seismic reflection survey, MCS

©2019. Japan Geoscience Union. All Right Reserved.

Geochemistry and zircon U-Pb ages of mafic rocks in the Mikabu and Sorachi-Yezo belts: Comparison with the Shatsky Rise

*Naoto Kimura[1], Yuji Ichiyama[1], Shohei Takahashi[1], Hisatoshi Ito[2], Akihiro Tamura[3], Tomoaki Morishita[3]

1. Chiba University, 2. Central Research Institute of Electric Power Industry, 3. Kanazawa University

Large igneous provinces (LIPs) are large volcanic edifices on the Earth, such as oceanic plateaus and continental traps. It is commonly believed that LIPs are formed by large-scale magmatism caused by the upwelling of unusually hot mantle plume from the deep mantle (e.g., Coffin and Eldholm, 1994). Therefore, the genesis and formation mechanisms of LIPs is crucial to understand the dynamics of the Earth’s interior and episodic global events. Recent studies have revealed that the fragments of accreted oceanic plateaus are preserved in orogenic belts as ophiolites and accretionary complexes (e.g., Kerr et al., 2000; Ichiyama et al., 2014). The investigation of accreted oceanic plateaus will help to enhance our understanding of LIPs.

The Mikabu belt in SW Japan and Sorachi-Yezo belt in central Hokkaido, North Japan contain large accreted fragments of a paleo-oceanic plateau (Kimura et al., 1994). Recently, Ichiyama et al. (2014) proposed that the Mikabu and Sorachi-Yezo picrites with highly magnesian olivine phenocrysts (up to Fo_{94}) were produced by an unusually hot mantle plume. They also suggested that these picrites are derived from the Late Jurassic oceanic plateau (hereafter named “Mikabu-Sorachi plateau”) formed on the Izanagi plate, which was possibly produced together with the Shatsky Rise at the Pacific-Izanagi-Farallon triple junction in the Pacific Ocean. However, the geochronological and geochemical comparison between the Mikabu-Sorachi and Shatsky Rise has been poorly constrained.

The Mikabu and Sorachi-Yezo mafic rocks are geochemically divided into depleted (D)-type and enriched (E)-type in the same manner as the picrites. The D-type is depleted in light rare earth elements (LREE), whereas the E-type is relatively enriched in LREE. These types were produced by higher degrees of partial melting (30-50%) than MORB. The U-Pb zircon analyses of gabbroic rocks in both belts yield the weighted mean $^{206}Pb/^{238}U$ zircon ages of 153.1-146.3 Ma for the Mikabu rocks and 146.2 and 137.6 Ma for the Sorachi-Yezo rocks.

A wide geochemical variety of basalts were recovered from the Shatsky Rise during the IODP Expedition 324 (Expedition 324 Scientists, 2010; Sano et al., 2012). The U1349-type and Normal-type basalts of the Shatsky Rise are closely similar in geochemical composition to the Mikabu-Sorachi D-type and E-type rocks, respectively. The radiometric ages of the Shastky Rise basalts show 144.6-133.9 Ma (Mahoney et al., 2005; Geldmacher et al., 2014). The magnetic anomaly lineations of the Shatsky Rise exhibit that the formation of the rise started at M21 (about 147 Ma). The zircon U-Pb ages of the Mikabu-Sorachi mafic rocks are almost coeval with the formation ages of the Shatsky Rise. However, the older radiometric ages than 147 Ma are shown in this study. Recently, Sawada et al. (2019) also report the zircon U-Pb age of 154.6 Ma for the Mikabu metabasite from the Toba area.

The magnetic anomaly lineation of M29 (about 157 Ma) drawn at the southwest of the Shatsky Rise implies that the triple junction was already present at 157 Ma. The Mikabu-Sorachi plateau was produced on the Izanagi plate before the Shatsky Rise at the triple junction. The igneous rocks in the Mikabu-Sorachi belt possibly record the information on initiation mechanisms of the triple junction and

©2019. Japan Geoscience Union. All Right Reserved.

initial stages of LIPs formation in the paleo-Pacific Ocean.

Keywords: Mikabu belt, Sorachi-Yezo belt, Shatsky Rise, zircon U-Pb age, Large igneous provinces (LIPs), mantle plume

©2019. Japan Geoscience Union. All Right Reserved.

Submersible magnetics reveals relationship between off-axis volcanism and hydrothermal systems of the Kairei and Yokoniwa fields at the Central Indian Ridge

*Masakazu Fujii[1], Kyoko Okino[2]

1. National Institute of Polar Research and SOKENDAI, 2. Atmosphere and Ocean Research Institute, The University of Tokyo

The Kairei (KHF) and Yokoniwa hydrothermal fields (YHF)are hosted in mafic as well as ultramafic rocks distributed at an off-axis volcanic knoll of the Central Indian Ridge. Despite intensive investigations, their geological and geophysical background is still debated. Here, we show the results of near-seafloor magnetic anomaly surveys conducted using a submersible. We investigated the bulk magnetization of the hydrothermally altered zone and the surrounding lava flows and evaluated their intensities compared with previously reported values at axial areas of seafloor spreading environments. The KHF is characterized by low coherence between observed and modeled anomalies and low values of magnetization. This result suggests that magnetic minerals within basaltic lava flows were likely altered by hydrothermal fluid circulation. The variation pattern in the observed magnetic anomalies above the lava flows is in phase with that of the modeled magnetic anomalies for the simple assumption that the magnetization direction is parallel to the geomagnetic field. This result suggests that these lava flows preserve normal magnetic polarity corresponding to the Brunhes Chron. The estimated magnetic-anomaly-derived absolute magnetizations (MADAM) show a reasonable correlation with the natural remanent magnetizations of rock samples collected from the seafloor of the same region; their relationship is consistent with previously reported datasets from the Mariana Trough and Mid-Atlantic Ridge. The estimated MADAM intensity reaches 20 A/m in the study area, which is clearly greater than those of previously reported off-axis areas, suggesting that recent volcanic eruption may have occurred in these off-axis areas. The high magnetization distributions are commonly observed at the bottoms of the western slope from the KHF and YHF. This finding provides new insight into the distribution of highly magnetized lava flows in the off-axis areas and indicates the distribution of recent off-axis volcanic activities, which is potentially linked to the sub-seafloor hydrothermal circulation.

Keywords: Central Indian Ridge, Seafloor hydrothermal system, Near-seafloor magnetic anomaly

©2019. Japan Geoscience Union. All Right Reserved.

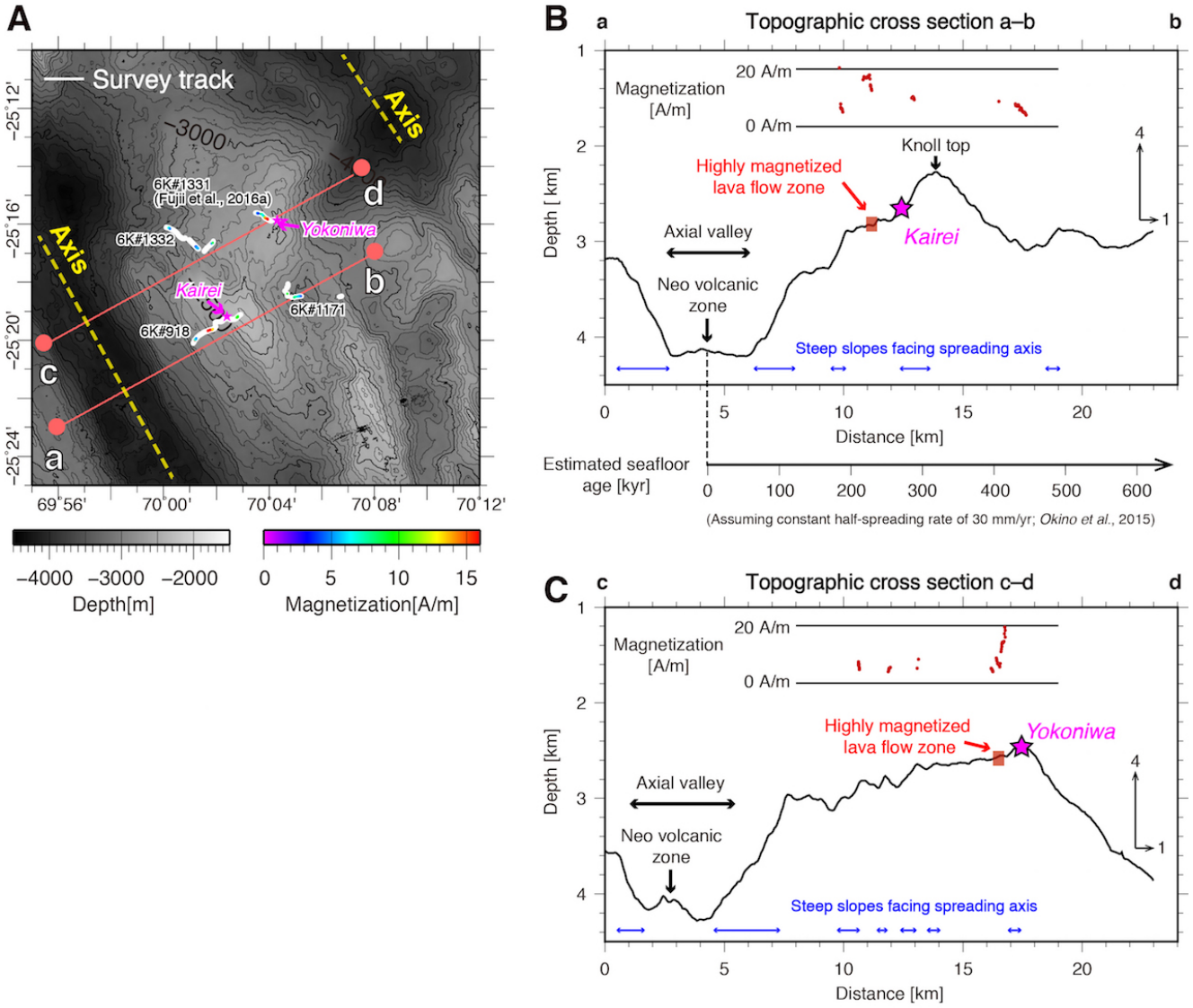

©2019. Japan Geoscience Union. All Right Reserved.

Shipboard magnetic and gravity surveys around the Iheya North Knoll and the Iheya Minor Ridge in the Mid-Okinawa Trough: Preliminary results of KR18-14 Leg1/Leg2 cruises

*Kazuya Kitada[1], Takafumi Kasaya[1], Hisanori Iwamoto[1], Yoshifumi Nogi[2]

1. Japan Agency for Marine-Earth Science and Technology, 2. National Institute of Polar Research

The Okinawa Trough, an active back-arc basin behind the Ryukyu trench, exhibits active rifting associated with extension of the continental margin. In the Mid-Okinawa Trough, more than 10 hydrothermal vent sites belonging to relatively large hydrothermal vent fields at the Iheya North Knoll, the Iheya Minor Ridge, the Izena Hole and etc., were discovered by previous studies (e.g., Halbach et al., 1989; Sakai et al., 1990; Momma et al., 1996; Kasaya et al., 2015; Nakamura et al., 2015). Although shipboard magnetic and gravity surveys are too low in resolution to investigate the hydrothermal sites, they are important for understanding the geological background of the hydrothermal systems across an entire region. As for the area off Kumejima Island in the Okinawa Trough, Kitada et al. (2018) revealed the characteristics of the submarine volcanic activity around a hydrothermal area by using dense magnetic and gravity data. In order to characterize sub-seafloor structures and the spatial distribution of the submarine volcanic activity around the Iheya North Knoll and the Iheya Minor Ridge, we conducted detailed magnetic and gravity surveys with a line spacing of 0.5 nmi aboard research vessel Kairei during the KR18-14 Leg1 and Leg2 cruises from October to November 2018. Additionally, we also compiled magnetic, gravity and bathymetric data which were collected during previous cruises by the Japan Agency for Marine-Earth Science and Technology (JAMSTEC) over the recent years. Magnetization intensities were estimated from observed magnetic anomalies, without applying annihilator. Bouguer gravity anomalies were calculated from free-air anomalies obtained. The distribution of magnetization intensity and variation in Bouguer gravity anomalies revealed the characteristics of submarine volcanic activity. Most of the knolls in the area show a relatively high magnetization (~1.0 to ~3.0 A/M) corresponding to the individual submarine knolls. Higher Bouguer gravity anomalies (~45 to ~55 mgal) implying the lower crustal thickness were observed in the Iheya graben. The knolls including the Iheya Minor Ridge, elongated in the ENE-WSW direction parallel to the graben, exhibit the ENE-WSW trending magnetization distribution with relatively high positive intensities, so volcanism appears to be constrained by normal faults forming the rift structure. On the other hand, the Iheya North Knoll have a relatively low magnetization of ~-1.0 to ~0.0 A/M with less variation of the magnetization. Although the data are sparse (the line spacing of ~1.5 to ~2 nmi), low magnetization (~1.5 A/M) with no prominent magnetic signature was also observed in the Izena Hole. Moreover, these knolls are located on the area where the Bouguer gravity anomaly is changed from ~30 to ~10 mgal and ~45 to ~30 mgal, respectively. The magmatism associated with submarine volcanic activity and back-arc rifting will be discussed based on the results obtained from these dense surveys.

Keywords: Okinawa Trough, backarc rifting, hydrothermal systems, magnetic anomaly, gravity anomaly

©2019. Japan Geoscience Union. All Right Reserved.

A shallow scientific drilling at Higashi Ensei Hydrothermal Field, Okinawa Trough

*Hidenori Kumagai[1], Takafumi Kasaya[1], Shuhei Totsuka[2], Shinsuke Kawagucci[1], Hideaki Machiyama[1], Koichi Iijima[1], Hirofumi Yamamoto[1], junji kaneko[1], Yusuke Ohta[3], Shohei Albert Tomita[3], Shogo Komori[4]

1. Japan Agency for Marine-Earth Science and Technology, 2. Kyushu Univ., 3. Kyoto Univ., 4. AIST

A shallow seabed drilling was performed in February 2019 at Higashi Ensei Hydrothermal Field, Northern Okinawa Trough (Cruise ID: KM19-E01). Two localities were selected to investigate natures of sub-seafloor lithology with and without self-potential anomaly (SP anomaly) measured by near-bottom AUV survey. Here such a SP anomaly is to be resulted from a sub-seafloor orebody consisted of mainly sulfides. A seabed drilling apparatus, BMS (Boring machine system, Cellula Robotics Ltd.), was deployed twice from R/V Kaimei. At the first drilling in the cruise, the drilled hole reached to a formation 44m beneath the seafloor but stopped there due to significant venting through the drilled hole. Volcaniclastics with and without sulfide blocks or veins were sampled even poor recovery in the shallow part of the hole. Contrasting to it, the second drilled hole reached to 10 m beneath the seafloor where intact mafic-intermediate lava flow, i.e. volcanic basement, was sampled. In the second hole, little sulfide were retrieved except orange-colored one, probably realgar associating with orpiment and stibnite, in the first core, shallower than 1.5mbsf. On board IP measurement both as well as standard MSCL and visual core description were performed for the cores from the first hole. Further, an ROV dive observation was conducted within 16.5 hours after the drilling of the first hole. An exotic white sediment was recognized in the vicinity of the hole, similarly to the IODP exp.331 at Iheya-North Knoll, and successfully sampled. In this presentation, retrieved drilled samples as well as those sampled by ROV will be reported.

Keywords: A seabed driling system, Self-potential anomaly, An exotic white sediment around the drilled hole

©2019. Japan Geoscience Union. All Right Reserved.

Mineralogical and geochemical study of sediment cores collected from the Gondou hydrothermal field in the Okinawa Trough

*Jun-ichiro Ishibashi[1,2], Shuhei Totsuka[2], Akihi Tsutsumi[2], Naru Tsukamoto[2], Yusuke Kira[2], Kazuhiko Shimada[1], Toru Yamasaki[3], Ken Ikehara[3], Toshiro Nagase[4], Yutaro Takaya[5,9], Kei Ikehata[6], Takashi Goto[7], Chitaro Gouzu[7], Ryuichi Shinjo[8], Hideaki Machiyama[9], Koichi Iijima[9], Hirofumi Yamamoto[9], Hidenori Kumagai[9]

1. Department of Earth and Planetary Sciences, Kyushu University, 2. Graduate School of Science, Kyushu University, 3. National Institute of Advanced Industrial Science and Technology, 4. Tohoku University Museum, 5. School of Creative Science and Enginerring, Waseda University, 6. Faculty of Life and Environmental Sciences, University of Tsukuba, 7. Hiruzen Institute for Geology and Chronology, 8. Faculty of Science, University of the Ryukyus, 9. Japan Agency for Marine-Earth Science and Technology

Intense hydrothermal activity associated with sulfide mineralization had been observed in the Gondou field, which is located at the seafloor around a water depth of 1330-1470 mbsl (meters below the sea level) at the western flank of the Daisan-Kume Knoll (Minami and Ohara, 2017; Ishikawaet al., 2016). Scientific drilling was performed by J-MARES during the SIP Integrated Ocean Resource Surveying System JM17-04 Cruise from October to November, 2017. Sediment cores were obtained from 5 sites in Southern area of the Gondou field by drilling using BMS (Benthic Multi-coring System) installed on *Shincho-maru*. Mineralogy and geochemistry of the obtained cores were studied based on VCD (Visual Core Description), microscopic observation, XRD (X-ray diffractometer) analysis, and electron probe microanalyzer (EPMA) analysis.
Most part of the obtained sediment, except for the surface hemipelagic sediment within a few mbsf (meters below the seafloor), was hydrothermally altered intensely. Abundant occurrence of illite (or illite/smectite mixed-layer mineral) was observed, which is common signature among hydrothermal alteration in hydrothermal fields in the Okinawa Trough. Whereas, occurrence of chlorite was limitedly recognized within a layer of 5-15 m thickness in each site. Kaolin minerals were identified in altered pumiceous volcaniclastic sediment in two sites. These specific occurrences may reflect subseafloor fluid migration of distinctive chemistry, based on the idea that chlorite formation would be related to interaction with heated seater-derived fluid while kaolin minerals formation would be related to interaction with acidic fluid. Occurrence of sulfate minerals such as anhydrite and barite is also limited, which may provide another information about subseafloor fluid migration.

Acknowledgements
This study was conducted under the framework of the Next-Generation Technology for Ocean Resources Exploration Project, Cross-ministerial Strategic Innovation Promotion Program (SIP) funded by the Japanese cabinet office. The sediment cores used in this study were provided from J-MARES (Research and Development Partnership for Next Generation Technology of Marine Resources Survey).

Keywords: seafloor massive sulfide deposits, seafloor scientific drilling, hydrothermal alteration

©2019. Japan Geoscience Union. All Right Reserved.

New type of self-potential anomaly observed near a hydrothermal site of Oomuro-dashi volcano, Izu-Ogasawara arc

*Yoshifumi Kawada[1,2], Takafumi Kasaya[2]

1. International Research Institute of Disaster Science, Tohoku University, 2. Japan Agency for Marine-Earth Science and Technology

Using a deep-towed electrode array, we identified a pair of positive and negative self-potential anomalies observed near an active hydrothermal field associated with a quarterly rhyolitic volcano, Oomuro-dashi, Izu-Ogasawara arc. Results with different rowed directions, the magnitude of both anomalies is of the order of millivolt. The negative anomaly is located immediately above the most active area; the positive self-potential anomaly is located a few hundreds of meters away from the most active hydrothermal area, where no apparent hydrothermal activity has been detected. The discovery of the positive self-potential anomaly in marine environments is probably the first time.

The origin of the negative self-potential anomalies may be explained by the geo-battery mechanism (Sato and Mooney, 1960), in which the presence of a conductive ore body crossing the redox gradient results in the upward electron transfer to give a negative self-potential anomaly above the body. Oxidized materials near the seafloor are reduced. In other words, an ore body near the seafloor behaves as a cathode. We have reported negative self-potential anomalies many times above hydrothermal areas of other sites (e.g., Sato et al., 2017; Kawada and Kasaya, 2017, 2018).

The origin of this newly founded positive self-potential anomaly is problematic. One possibility is that an anode of the geo-battery, where reduced materials are oxidized, is exhumed near to the seafloor. If this is true, shallow drilling or piston coring may confirm signals from oxidized chemical reactions around an anode. This is important for the understanding of the geo-battery because its anode is usually located far below the seafloor and cannot be accessed easily. Another possibility is the streaming potential, which is caused by a local charge imbalance due to the flow of electrolytes in the pore space. Although this mechanism is estimated to be minor in marine environments, a positive self-potential anomaly of the order of one millivolt may not be immediately rejected above an area of upward fluid flow. However, the area of this positive self-potential anomaly is away from the active hydrothermal site, where upward fluid discharge is expected.

Keywords: geophysical exploration, marine resource, ore deposit, redox reaction, hydrothermal circulation

©2019. Japan Geoscience Union. All Right Reserved.

Numerical simulation of submarine hydrothermal ore-deposits due to a coupled process of fluid migration and reactive geochemical transport

*Claudia Fujita[1], Hajime Yamamoto[1], Jun-ichiro Ishibashi[2], Takeshi Tsuji[3]

1. Taisei Corporation, 2. Department of Earth and Planetary Sciences, Faculty of Science, Kyushu University, 3. Department of Earth Resources Engineering, Faculty of Science, Kyushu University

Submarine hydrothermal ore-deposits are known to be rich in metal resources and are to be found abundant around the Japanese islands. In recent years, several studies (mostly field surveys) had been carried out and a lot of data on chemical, physical and biological properties of compounds have been gathered especially for hydrothermal fields in the Okinawa Trough. However, the mechanism of formation (hydrothermal fluid flow in combination with geochemical reaction) of these deposits is not yet clearly understood.

Hydrothermal ore-deposits are formed by precipitation of metal elements from hydrothermal fluid due to rapid cooling around the seafloor where the fluid discharges. Contrary to the hydrothermal systems in the mid-ocean ridges, hydrothermal systems in the Okinawa Trough has a fluid discharge region at the seafloor in sediment-rich environment. The sediment is often composed of two components; one is hemipelagic sediment possibly transported from the continental margin and the other is volcaniclastic sediment derived from felsic volcanism in the vicinity. Because these two components have quite different permeability, it is expected complicated fluid migration within the discharge region.

In this study, we investigated the above process using a numerical code TOUGHREACT V3.0 –OMP, which is for coupled non-isothermal multiphase fluid flow and geochemical reactive transport. A 2-dimensional radial model with the radius of 5 km and a depth of 1 km below the seafloor was chosen to represent a sufficient area of the discharge region around the hydrothermal vent. The center of the radial model represented a fluid conduit (10 cm diameter) where the venting hydrothermal fluid of 300 ˚C ascends from basal to the seafloor, with a flow rate of ~1000 t/day. Almost all model parameters are chosen based on available results of geophysical survey of the Iheya hydrothermal fields in the Okinawa Trough[1)]. The geological structures were set as having diverse permeability from 1×10^{-10} m^2 to 1×10^{-16} m^2, which reflects alternating pumiceous volcaniclastics layer and hemipelagic sediment layer. The initial thermal gradient was set to 4.8 ˚C/100 m. The top boundary (seafloor) was set to constant pressure condition (20 MPa) and a basal heat flux was also imposed at the bottom (5.6×10^{6} W/m^2), assuming a pumice thermal conductivity of 0.96 W-m/˚C.

The geochemical setting included initial concentrations of primary species, as, for instance, Na^{+}, SO_4^{-2}, H_4SiO_4, Ca^{+2}, S^{-2}, Zn^{+2}, HCO_3^{-} or NH_3 for seawater and hydrothermal fluid separately. Chemical reaction including precipitation of minerals) caused by mixing of the both fluids and cooling was considered in this setting. In order to simulate accumulation of mineral precipitations to form hydrothermal deposits over a long-time duration (an order of thousands of years), the numerical simulation was conducted for 10000 years.

As a result, the following features were clarified: First, high velocity venting hydrothermal fluid ascends to the seafloor through the fluid conduit at the center of the model, whereas nearby cold water percolates downward from the seafloor and convection occurs. Second, among the alternating layer structure, preferential horizontal flow is obvious for layers with high permeability, which resulted in primary sulfide precipitation with a lateral extend.

These results are likely to be consistent to recent field studies during scientific drilling into the submarine

©2019. Japan Geoscience Union. All Right Reserved.

hydrothermal fields in the Okinawa Trough, Japan.
This study was conducted in co-operation with Kyushu University as a part of the “Next-Generation Technology for Ocean Resources Exploration (Zipangu-in-the-Ocean Project)”, a sub-topic of the Cross-ministerial Strategic Innovation Promotion Program (SIP) led by the Cabinet Office's Council for Science, Technology and Innovation.

1)Tsuji, T., Takai, K., Oiwane, H., Nakamura, Y., Masaki, Y., Kumagai, H., ... Kuramoto, S. (2012). Hydrothermal fluid flow system around the Iheya North Knoll in the mid-Okinawa trough based on seismic reflection data. Journal of Volcanology and Geothermal Research, 213-214, 41-50, doi:10.1016/j.jvolgeores.2011.11.007

Keywords: submarine hydrothermal ore deposit, hydrothermal convection, TOUGHREACT, coupled hydrothermalfluid flow with reactive geochemical transport

©2019. Japan Geoscience Union. All Right Reserved.

Mineral composition and grain size distribution of REY-rich mud in the Minamitorishima EEZ: Implication for formation process of extremely REY-rich mud

*Sakai Takumi[1], Erika Tanaka[1], Kazutaka Yasukawa[1,2], Junichiro Ohta[2,1], Koichiro Fujinaga[2,1], Kentaro Nakamura[1], Yasuhiro Kato[3,1,2]

1. Department of Systems Innovation, School of Engineering, University of Tokyo, 2. Ocean Resources Research Center for Next Generation, Chiba Institute of Technology, 3. Frontier Research Center for Energy and Resources, School of Engineering, The University of Tokyo

In 2011, it was reported that deep-sea sediments containing high concentrations of rare-earth elements and yttrium (REY) are widely distributed in the Pacific Ocean, and can constitute a new mineral resource for the industrially critical elements [1]. Moreover, the “extremely REY-rich mud” containing more than 5,000 ppm of total REY (ΣREY) was discovered within the Japanese exclusive economic zome (EEZ) around Minamitorishima Island [2], and various researches to reveal a detailed spatial distribution of the extremely REY-rich mud has been carried out [3]. However, the formation mechanism(s) of the extremely REY-rich mud have not been completely elucidated yet.

Recently, based on multi-elemental compositions of 49 piston core samples collected from the Minamitorishima EEZ, it was confirmed that the deep-sea sediments in the area could be classified into nine sedimentary units based on characteristic chemical compositions [4]. This chemostratigraphy indicated that there are at least three “ΣREY peaks” containing 2,000 ppm of ΣREY in the Minamitorishima EEZ [4]. A previous study targeting the extremely REY-rich mud corresponding to the 1st ΣREY peak (i.e, the shallowest ΣREY peak in the chemostratigraphy) demonstrated that grain sizes of biogenic Ca-phosphate (BCP) and authigenic phillipsite were largest in the horizon with the maximum ΣREY concentration, based on analyses of mineral composition and grain size distribution [5]. However, whether this feature is common in all of the ΣREY peak units remains uncertain. In addition, no systematic investigation of relationships between each chemostratigraphic unit and mineral composition and grain size distribution has been carried out.

Here, we aimed to characterize each chemostratigraphic unit from the perspectives of the mineral composition and grain size distribution, and also to provide a constraint on the formation process of the extremely REY-rich mud. We selected 80 sediment samples from the 17 piston cores collected within the Minamitorishima EEZ to cover all units of the chemostratigraphy. The mineral composition was estimated by microscopic observation following the standard protocols of the International Ocean Discovery Program. The grain size distribution was measured by using laser diffraction spectroscopy. As the result, we revealed systematic variations in mineral composition and grain size distribution of each chemostratigraphic unit, and confirmed that grain sizes of BCP and phillipsite in all the ΣREY peak units were coarser (i.e., more enriched in silt- to sand-sized fractions) than other units. The increased sizes of BCP grains as a common feature of the ΣREY peaks imply that a grain-size sorting by enhanced bottom currents concentrated coarse BCP grains on the seafloor and contributed to the formation of extremely REY-rich mud for multiple times throughout the sedimentary history of the area.

Reference

©2019. Japan Geoscience Union. All Right Reserved.

[1] Kato et al. (2011) Nature Geoscience, 4, 535–539.

[2] Iijima et al. (2016) Geochemical Journal, 50, 557–573.

[3] Takaya et al. (2018) Scientific Reports, 8, 5763.

[4] Tanaka et al. Submitted to Ore Geology Reviews.

[5] Ohta et al. (2016) Geochemical Journal, 50, 591–603.

Keywords: REY-rich mud, grain size distribution, mineral composition, chemostratigraphy, deep-sea sediments

©2019. Japan Geoscience Union. All Right Reserved.

Geochemical and morphological features of manganese micronodules in REY-rich mud within the Minamitorishima EEZ, western North Pacific Ocean

*Satoshi Kino[1], Kazutaka Yasukawa[1,2], Keishiro Azami[1], Erika Tanaka[1], Koichiro Fujinaga[2,1], Kentaro Nakamura[1], Yasuhiro Kato[1,2]

1. Department of Systems Innovation, School of Engineering, University of Tokyo, 2. Ocean Resources Research Center for Next Generation, Chiba Institute of Technology

Manganese micronodules are small grains (< 1 mm) composed of manganese oxides, and constitute one of the important components of pelagic sediments. The micronodules show high contents of various heavy metals, especially of some redox-sensitive transition metals [1]. In addition to chemical compositions, the abundance and texture of micronodules can be affected by sedimentation rates and/or redox conditions of the sediment column [1, 2]. Therefore, the micronodules have been regarded as a useful indicator of the sedimentary environment.

Recently, deep-sea sediment extremely enriched in rare-earth elements and yttrium (REY) was discovered within the Japanese exclusive economic zone (EEZ) around Minamitorishima Island [3]. Previous studies reported that the extremely REY-rich mud contains significant amounts of biogenic calcium phosphate, which is a main host of REY, and phillipsite grains [3, 4]. In addition to them, manganese micronodules were also recognized in the sediment column, which were especially abundant in the extremely REY-rich layer [3, 4]. However, detailed features of the micronodules in the REY-rich mud within the Minamitorishima EEZ have not been investigated yet. Manganese micronodules in the REY-rich mud are about μm –mm ferromanganese oxides. Because their abundance and chemical compositions are considered to reflect respectively the sedimentation rate and redox conditions when they were buried [4], the micronodules can provide important constraints on the depositional environment of the REY-rich mud.

In this study, therefore, to characterize the manganese micronodules in the REY-rich mud within the Minamitorishima EEZ, we implemented (1) microscopic observations of the shape, surface texture, and relative abundance of the micronodules, and (2) bulk chemical analysis of them by using ICP-MS. We compared the geochemical features of the micronodules with those of macronodules both on the seafloor of the Minamitorishima EEZ, and also with those of macro- and micronodules in other areas.

The Minamitorishima micronodules are generally characterized by diagenetic features, although showing a compositional shift towards hydrogenetic features in some samples. Based on the integration of the observational and analytical results, we will discuss the possible changes in the sedimentary environment (e.g., sedimentation rates and redox conditions) involving the formation of the extremely REY-rich mud.

References

[1] Pattan (1993) Marin Geology 113, 331-344

[2] Svalnov et al. (2017) Oceanology 57, 3, 424-438

©2019. Japan Geoscience Union. All Right Reserved.

[3] Iijima et al. (2016) Geochemical Journal 50, 557-573.

[4] Ohta et al. (2016) Geochemical Journal 50, 591-603.

Keywords: manganese micronodules, REY-rich mud, Minamitorishima EEZ, bulk chemical composition, morphology

©2019. Japan Geoscience Union. All Right Reserved.

Seafloor sediment thickness around the Japan and Kurile trenches obtained by traveltime analysis for PS converted wave recoded by ocean bottom seismograms

*Ryosuke Azuma[1], Genti Toyokuni[1], Ryota Takagi[1], Syuichi Suzuki[1], Makiko Sato[1], Takashi NAKAYAMA[1], Naoki Uchida[1], Ryota Hino[1]

1. Recearch Center for Prediction of Earthquake and Volcanic Eruption, Graduate School of Science, Tohoku University

seafloor observation network for earthquake and tsunamis has been working in the Japan and Kurile trench subduction zones since 2016 (S-net, installed by National Research Institute for Earth Science and Disaster Resilience). The seismograms recorded by such the ocean bottom observatories are very useful for a precise hypocenter estimation. On the other hand, to obtain precise location results, it is also necessary to take suitable correction for traveltime delay due to the presence of the thick low-velocity sediments below sites, because the thickness of sediments differs with sites.

This study aims to estimate thickness of the sedimentary layer below the sites of the S-net and pop-up-type ocean bottom seismometers (OBSs). We then focused on traveltime difference between direct P-waves and PS waves converted at the sedimentary basement.

In the analysis, we first estimated a sensor direction based on gravitational acceleration and particle motions of teleseismic surface waves on accelerograms and then transformed components of velocity waveforms from XYZ to UD, NS and EW (Takagi et al., this meeting). Next, we picked PS arrivals on horizontal components of velocity records, for thirty of intraslab earthquakes observed at twenty of the S-net sites located on the outer slope of the Kurile and Japan trenches and the landward slope of the Kurile trench (off Nemuro). As a result, we obtained PS-P traveltime difference of ~1.4 s at the most of sites, ~1.6 s near the Japan and Kurile trenches junction, and 1.8 and 2.7 s on the lower and upper portions of the landward slope of the Kurile trench. Considering the standard deviation of PS-P of ~0.15 s at each site, our result suggests that PS-P traveltimes at the junction and other trench-outer region differs significantly while that variation between neighbor sites seems to be small.

The obtained PS-P traveltime differences for the outer-trench sites is consistent with those by seismic surveys (1.0–1.5 s, Kodaira et al., 2014; Fujie et al., 2016) and OBS observations (0.9–1.2 s, Hino et al., 2009) at the outer rise of the Japan trench. Therefore, picked PS arrivals on the S-net records in this study coincide with those by the previous studies. Assuming a Vp/Vs ratio of 8.0 and an average Vp of 2.0 km/s in the sediments estimated by the wide-angle seismic surveys (Kodaira et al., 2014; Fujie et al., 2016) at the Japan and Kurile trench-outer rise regions, sediments thickness below the S-net sites would be 350~400 m, which is also consistent with results of the seismic reflection section (Kodaira et al., 2014; Fujie et al., 2016). By further analysis for PS converted wave at the inner-trench sites of OBSs and S-net besides off Nemuro, we will investigate the distribution of thickness of the sedimentary layer in the forearc region of the east Japan.

Acknowledgements: We used waveform data from S-net by NIED.

©2019. Japan Geoscience Union. All Right Reserved.

Keywords: PS converted-wave traveltime analysis, Sedimentary-layer thickness, Ocean bottom seismograph (S-net and pop-up type OBS)

©2019. Japan Geoscience Union. All Right Reserved.

Examination of critical taper theory based on bathymetry data in subduction zones

*Hiroaki Koge[1], Juichiro Ashi[1], Jin-Oh Park[1]

1. Atmosphere and Ocean Research Institute, The University of Tokyo

The fold-and-thrust belts and submarine accretionary wedges lie along compressive plate boundaries. The critical taper model has been recognized to be the most appropriate theory that describes the first-order mechanics of these structures. Applying the critical taper model in the subduction zones, we can estimate the frictional coefficient of the plate boundary fault with only simple topographical parameters from the cross-section. Thus, this model has been also used in discussions related to earthquakes.
However, in the critical taper model, the following two problems could be pointed out when acquiring the topographic parameters. 1) It is impossible to apply the critical taper model to the area without seismic cross-section. 2) In the depth conversion in the seismic cross-section, the depth of the plate boundary fault largely depends on the velocity model and affects the estimation of the décollement dip angle β. Thus, it is unreliable in terms of accurate comparison. Therefore, when comparing the result with various velocity models, the reliability is low in terms of accurate comparison.
Therefore, in this research, we developed a new method to obtain the topographical parameters only from bathymetry data instead of the seismic cross-section. We verified the validity of the method from the results, with comparing the result from the décollement dip angle β obtained from the seismic cross-sections and the result from the trench seaward slope angle β obtained from the bathymetry. We check the validity of the new method using the Nankai Trough as the target area. In the Nankai Trough, many seismic cross-sections have been acquired for the disaster mitigation of the large earthquake, and the observation based on various methods such as seismic waves or GPS has proceeded. Thus, it should be easy for acquiring the topographical parameters and interpreting the result of the critical taper model.
We found the theoretical blind spot of the critical taper model in the condition of the subduction zone under the sea. When a high pore pressure ratio is assumed for the whole wedge, the effect of β on the result is very small for the effective friction coefficient. Therefore, it is sufficiently possible to discuss the frictional distribution of the plate boundary fault with only the bathymetry data. It is although necessary to pay attention to relatively large error up to about 20%. Since the bathymetry data is spatially densely acquired data, it was possible to calculate the friction distribution of the shallow plate boundary fault along the trench axis in the high density.
As a preliminary interpretation of the results with the bathymetrical critical taper model , this metho is considered to be effective to contribute to earthquake/tsunami disaster mitigation in sea areas where seismic activity segments are not sufficiently studied.

Keywords: subduction zone, critical taper model, Japan Trench, Nankai Trough

©2019. Japan Geoscience Union. All Right Reserved.

Active structures of the Sagami Bay Fault by high-resolution sub-bottom profiling and pin-point core sampling

*Juichiro Ashi[1], Asuka Yamaguchi[2], Natsumi Okutsu[1], Ayanori Misawa[3]

1. Graduate School of Frontier Sciences, The University of Tokyo, 2. Atmosphere and Ocean Research Institute, The University of Tokyo, 3. National Institute of Advanced Industrial Science and Technology

Seafloor knolls called the Okinoyama Bank Chain are aligned in the eastern slope of the NW trending Sagami Trough. Existence of the Sagami Tectonic Line is estimated at the slope base and interpreted as a tectonic boundary of a subdution zone (Kimura, 1973, Kagaku). Ohkochi (1990, Chigaku Zasshi) reported active faults and an anticlinal fold based on seismic profiles. An eastward dipping reflector is recognized at the southeastern extension of the Kozu-Matsuda Fault by onshore-offshore integrated seismic imaging and interpreted as a splay fault of the plate boundary fault (Sato et al., 2010, Annual Meeting abstract of the Geological Society of Japan). However, Deformation of shallow sediment recording recent activity has not been clarified. The purpose of this study is to reveal recent fault activity by high resolution subbottom survey and sediment sampling. We carried out deep towed subbottom survey and pinpoint sediment sampling by remotely operqated vehicle NSS in the southwest slope of the Misaki Knoll during the Hakuho-maru cruises KH-10-3, KH-11-9 and KH-16-5. NSS can take piston cores at pinpoint accuracy by four propeller thrusters, video cameras and a payload fuck. Deep towed subbottom survey can obtain high resolution subsurface structure by pinging 1.1 to 1.6 kHz chirp frequency and receiving near the seafloor. Subbottom profiles across the southwest slope base of the Miura Knoll show a reflector suggesting a fault plane at the scarp base. The reflector dips 30 degree to northeast. Although the hanging wall shows structureless, the foot wall exhibits horizontal reflectors or chaotic suggesting talus deposit. We successfully obtained a 6-meter-long core after confirming a dipping reflector of a possible fault plane. The upper 1.2 meters of the core sample consists of alternation of dark green silty mud and pebbly mud with shell fragments of Calyptogena fossils. Thin silt layers are intercalated with dark green clay at about 15 cm intervals. A 5-mm thick zone, which suggesting a fault plane and consists of silty mud and granule size clasts, is recognized at 2.25 m from the core top. This zone, dipping 30 degree toward north to east after paleomagnetic restoration, is interpreted to correspond to the reflector of the fault plane on subbottom profiles. We also present shallow subsurface structures around the Miura Knoll.

Keywords: active fault, talus deposit, active fold

©2019. Japan Geoscience Union. All Right Reserved.

Fault Distribution and Structural Characteristic in the Nankai Trough Area, Japan

*Rei Arai[1], Narumi Takahashi[1], Minako Katsuyama[1], Shigeyoshi Tanaka[1], Hiromi Kamata[1], Tomoyuki Sato[2], Takahiko Inoue[2], Yoshiyuki Kaneda[3]

1. Japan Agency for Marine-Earth Science and Technology, 2. National Institute of Advanced Industrial Science and Technology, 3. Kagawa University

As part of “The Comprehensive Evaluation of Offshore Fault Information Project” by the Ministry of Education, Culture, Sports, Science and Technology, JAMSTEC has conducted collecting marine seismic reflection/refraction data, bathymetric data, well data acquired within the Japan EEZ and surrounding areas, and assembling a database to serve data for future scientific research.

Data includes 1) seismic reflection/refraction data acquired by JAMSTEC, AIST(Japan Geological Survey), and Japan Coastal Guard for purposes of geological investigation and research, and 2) seismic reflection data acquired for purposes of oil and gas exploration by Ministry of Economy, Trade and Industry and Japanese oil companies.

Since 2D multichannel seismic reflection were acquired and processed according to survey standards of the early era to the recent, the original data were re-processed by applying the state-of-the-art data processing methods to obtain unified high-quality seismic profile which capable of interpreting subsurface structures and fault morphology. Within the Nankai Trough and the Izu-Ogasawara area more than 180,000 km of 2D single/multichannel data and 4,800 km^2 of 3D multichannel data was collected to set for geological interpretation.

To identify a fault which caused earthquakes in geological history, a seismic profile must show not only geomorphological feature but also subsurface displacement or flexure in sedimentary layers and bed rocks. In order to determine the fault surface and morphology, the same structure must exist on other successive profiles, and bathymetric data also helps to trace lineament caused by fault activities.
The Nankai Trough is a part of plate boundaries where the Philippine Sea Plate subducts beneath the overlying the Eurasian Plate, and seismic reflection/refraction studied have been conducted to reveal the structure of the plate boundary and to understand the mechanics of seismic hazards. This project allows to use widely acquired data from scientific purposes to economic purposes in the Nankai Trough area, and as a result, the preliminary fault distribution on the area has been mapped. Offshore of Hamamatsu, Shizuoka Pref., seismic reflection profile shows compressive structures of the two known fault zones, the Enshu fault system and the Kodaiba fault system, which extends to offshore of Shima, Mie pref. Seismic reflection profiles which cross the trough shows that the beneath the forearc basin deposits and the old accretional prism a seismic reflector that dips landward iles just above the oceanic crust. This reflector is known as the spray fault (e.g. Park et al., 2002) and can be traced in other profile, with length of more than 50km.Off the Shikoku island to Hyuganada, seismic reflection data show very complex structures such as subsiding of a seamounts and ridges or mud domes which form along faults.

Keywords: Nankai Trough, offshore fault, seismic reflection survey

©2019. Japan Geoscience Union. All Right Reserved.

Seismicity in the central Ryukyu Trench by the Ocean Bottom Seismometers

*Ren Yakabu[1], Mamoru Nakamura[1], Yusuke Yamashita[2], Masanao Shinohara[3], Tomoaki Yamada[3], Hajime Shiobara[3], Kimihiro Mochizuki[3]

1. University of the Ryukyus, 2. DPRI, Kyoto University, 3. ERI, Tokyo University

We investigated the seismicity in the central Ryukyu Trench from the island of Amami to Okinawa between January 2015 and September 2016. Five ocean-bottom seismometers (OBSs) and 20 short-period seismometers of the Japan Meteorological Agency (JMA) were used. We analyzed the events with JMA magnitude over 3.0, which occurred near the trench running from Amami to Okinawa. The P and S arrivals were selected using the WIN system.

Subsequently, we determined the hypocenters. To achieve this, we first revised the 1-D velocity structure model in this region. For the velocity structure in the island arc area, we calculated the 1-D velocity structure with the Joint Hypocenter Determination method using the software VELEST (Kissling et al., 1994). We implemented the original model (JMA2001) first, then we adopted the revised model for the calculation of the travel time to the JMA stations. For the velocity structure beneath the OBSs, we built the velocity model based on a refraction survey performed near Okinawa (Kodaira et al., 1996; Nishizawa et al., 2017). Subsequently, we selected the PS-P time differences at each OBS station and computed the sediment layer correction. Using these values, we adopted the hypocenter determination modifying the software hypomh.

In addition, we investigated the seismicity for the earthquake swarm that occurred near the trench axis from May to June 2016. The swarm began with a M 5.7 earthquake at 12:44 (JST) on May 27th, 2016. We identified the P-S time difference of the earthquakes which were recorded at the NS02 of the OBS station from April 1st to May 27th, 2016.

The relocated hypocenters were shallower compared to those in the JMA catalog by 20-30 km, on average. The change in the depth is larger (approximately 60 km) near the trench axis. The relocated epicenters changed slightly with respect to the JMA epicenters in almost area near the trench. However, the relocated epicenters in the south of Okinawa moved trench-ward compared with the JMA epicenters.

In the P-S time diagram of the period preceding the 2016 earthquake swarm, we identified events with short-duration of P-S times approximately 12 h before the start of the swarm. Although this would constitute a foreshock activity of the swarm, it had not been recorded by the JMA seismic network. This suggests that the earthquake swarm had a precursor activity.

Keywords: Ocean Bottom Seismometer, Ryukyu Trench, Earthquake Swarm

©2019. Japan Geoscience Union. All Right Reserved.

Seismic structure of subducted Philippine Sea plate beneath Kyushu inferred from Po/So waves

*Azusa Shito[1]

1. Institute of Seismology and Volcanology, Kyushu University

Po/So waves are oceanic Pn/Sn phases that are characterized by their high-frequency (f>2.5 Hz) content, long-duration, and great travel distances (up to 3000km) through the oceanic lithosphere [e.g., Linehan, 1940; Walker, 1977, 1982]. In our previous study [Shito et al., 2013], we demonstrated that Po/So waves develop from the multiple forward scatterings of P and S waves in oceanic lithosphere due to the laminated small-scale heterogeneities. Shito et al. [2015] analyzed Po/So waves in the Philippine Sea Plate, which consists of three regions with different lithospheric ages. They found that Po/So waves propagate more effectively in older regions and demonstrated that the increase in propagation efficiency of Po/So waves depending on the age of the oceanic lithosphere can be qualitatively explained by thickening of the oceanic lithosphere including small-scale heterogeneities and a reduction in the intrinsic attenuation. This study showed that Po/So waves are powerful tool to explore structural variations of the oceanic lithosphere.

Recently, such structural variations (e.g., thickness) of the incoming oceanic lithosphere are supposed to affect seismic and volcanic activity of the subduction zone [Yamamoto et al., 2013; Shibata et al., 2014]. However, it is poorly known that such structural variations of the oceanic lithosphere remain or dissipate after the subduction. In this study, we investigate the structural variations of the subducted Philippine Sea plate by using Po/So waves. We analyze Po/So waves from the earthquakes (mb>3.0, depth>50 km) that occurred in the subducted Philippine Sea slab beneath Kyushu. We compare Po/So waves propagating through different portion of the subducted Philippine Sea Plate and discuss the relation between observed features (velocity and energy) of the Po/So waves and the structural variations of the Philippine Sea plate. We verify that Po/So waves trace deeper extension of Kyushu-Palau Ridge (KPR) that is subducting beneath the Hyuga-nada region.

Acknowledgments
The data analyzed in this study were obtained from Hi-net (NIED) stations in Kyushu. The source parameters of the earthquakes were provided by JMA. This work was supported by JSPS KAKENHI Grant Number JP18K03807.

Keywords: Po/So waves, Philippine Sea Plate, Kyushu-Palau Ridge

©2019. Japan Geoscience Union. All Right Reserved.

Slope failure features and their distribution in the forearc off northwestern Sumatra

*Kenji Hirata[1], Toshiya Fujiwara[2], Ayanori Misawa[3], Kohsaku Arai[3]

1. National Research Institue for Earth Science and Diaster resilience, 2. Japan Agency for Marine-Earth Science and Technology, 3. National Institute of Advanced Industrial Science and Technology

In Feb. 2005 and Oct. 2009, we conducted multi-narrow beam bathymetric (MNB) surveys during NT05-02 cruise with R/V Natsushima (NT05-02 scientific party, scientific party,http://www.jamstec.go.jp/jamstec-e/sumatra/ natsushima/bm/contents.html)and KY09-09 cruise with R/V KAIYO (Hirata et al.,2012, JAMSTEC report), respectively. Apporox. 1 degree angular intervals of multi narrow beams with both the R/Vs makes us possible to retrieve detailed bathymetry with high resolution of ~35 meters in azimuthal direction for seafloor of ~2000 meters in water depth beneath ship tracks. Hirata et al. integrated these multi-narrow beam bathymetric data to construct detailed bathymetric data (grid data of ~37 meters interval for the surveyed area with ~50 km x ~100 km, surrounded by latitudes 3˚50’ N and 5˚00’ N, and longitudes 93˚10’ E and 94˚10’ E). In this study, we identify slope failure features in the forearc region off the northwestern Sumatra, and discuss its spatial distribution in terms of the geological processes.

To identify bathymetric features clearly, we make four kinds of maps as follows; slope angle map, slope angle change map, slope (direction) azimuth map, as well as plain bathymetric map. Slope angle is defined by arctangent of dz/ds, where z is the water depth and s is unit distance vector projected the steepest descending direction on horizontal plain. Slope angle change is defined by arctangent of second derivative of a unit distance vector s. Slope (direction) azimuth is defined by arctangent of dx/dy, where x and y are due east and due north components, respectively, of unit distance vector projected the steepest descending direction on horizontal plain. As a sample, we show figures consisting of slope angle map ((b) in Fig), slope angle change map (c), slope (direction) azimuth map (d) as well as plain bathymetric map (a) for a small rectangular region in the forearc off northwest Sumatra. We finally interpret such kinds of maps to identify slope failure features, etc (e).

We can identify the upper portion of slope failure structures with an elevation difference of about 1 km which bounded the western edge of the outer arc high, although we cannot retrieve bathymetry of the Sumatra Trench at ~ 4500 meters water depth because the multi-narrow beam survey systems can sounding up to less than 3000 meters. The slope failure structures are created by several to more than ten of successive landslides in the region shown in Fig. The landslide features show uneroded and sharp crowns, implying that the landslide features nearby the Sumatra Trench are created “recently” in geological time scale. Slope failure features with weak to strong rounded crowns come to appear as our sample point migrates landward. This can be explained from the formation process of the outer arc high off northwestern Sumatra ; thick, upper sedimentary layers in the top of subducting Indo-Australia plate that are stripped off at the toe of the forearc obduct onto the outer arc high so that accretional process proceeds (Mosher et al.,2008, Mar.Geol.; Misawa et al., 2014, EPSL).This means that landward (eastward) of the outer arc high is accreted older than its seaward (westward).

©2019. Japan Geoscience Union. All Right Reserved.

On the one hand, there are exceptions to such a geological rule; we can find several slope failure features with uneroded, sharp crowns in a landward region where many slope failure features with weak and strong rounded crowns exist (e.g., two slope failure structures with a width of ~ 1 km around a location of4° 06’ N, 93°39’ E). These relatively fresh failure structures existing landward of the outer arc high possibly relate to recent activation of major thrusts proposed in the outer arc high off northwest Sumatra (Hirata et al., 2010, AGU).

Keywords: Sumatra, forearc, outer arc high, slope failure, submarine landslide

©2019. Japan Geoscience Union. All Right Reserved.

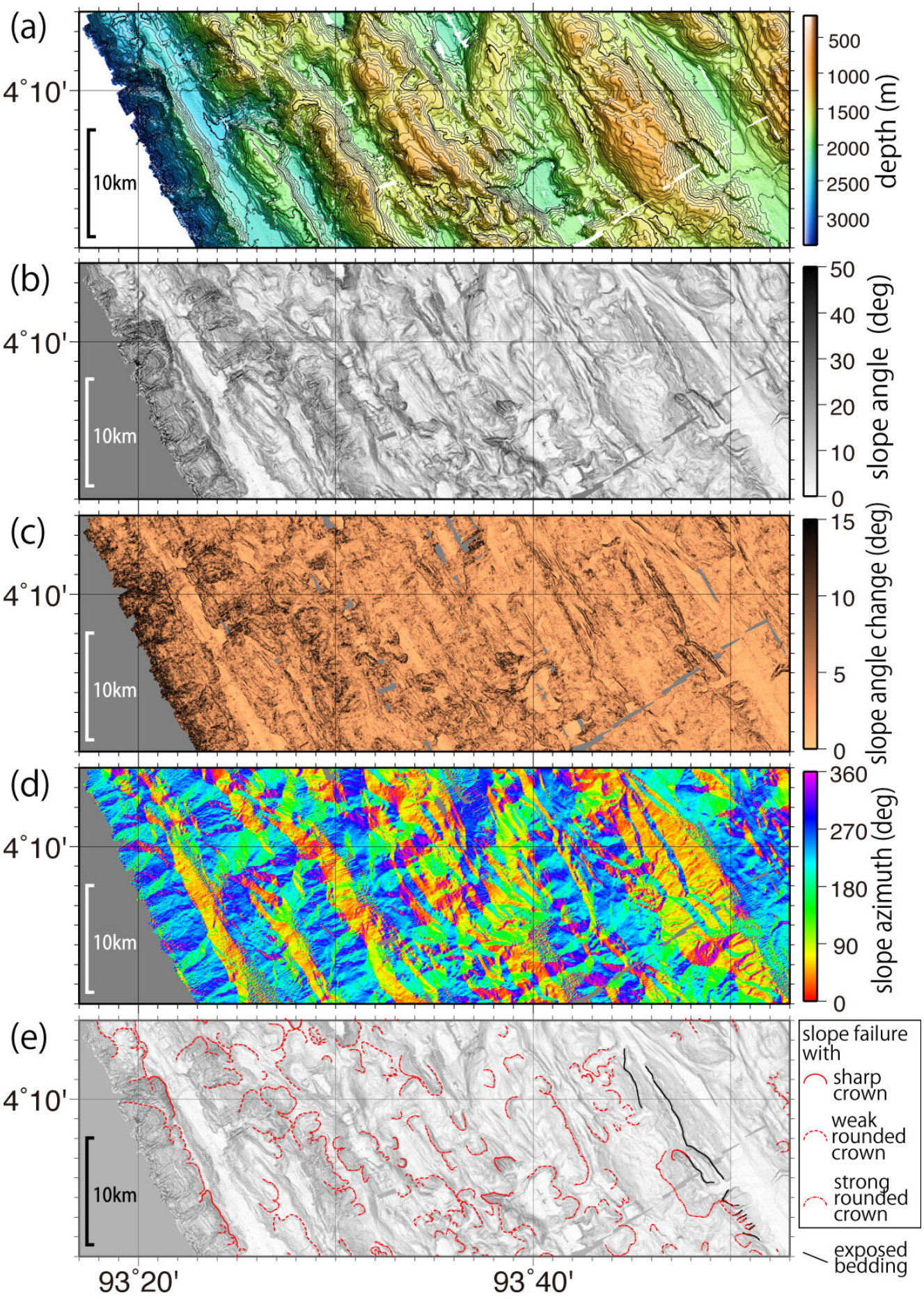

©2019. Japan Geoscience Union. All Right Reserved.

Origin and migration of fluid in the Sumatra subduction input: application of a geochronological method using a long-lived radioisotope of dissolved iodine

*Satoko Owari[1], Hitoshi Tomaru[1]

1. Chiba university

Iodine has a strong biophilic character and is highly enriched in organic matter in the marine environment. Organic matter is decomposed by thermogenic and microbial processes during the sedimentation and releases iodine into the interstitial water. Iodine has one stable isotope (^{127}I) and one long-lived radio isotope (^{129}I) with the half-life of 15.7 Myr. Therefore, the ^{129}I/^{127}I ratio of marine interstitial water has been used for identifying the origin of fluid. We applied iodine geochronology to the interstitial waters extracted from the deep drilling cores recovered by IODP Exp. 362, where Sumatra subduction input sediments develop more than 1400 m without major fractures. The concentration and isotopic ratio (^{129}I/^{127}I) of iodine dissolved in the interstitial water were analyzed in order to characterize the source and potential age of iodine prior to the subduction and examine the basic geological factors controlling the fluid migration in the input sediment body.

Concentrations of iodine and methane increase and TOC decreases toward 200 meters below seafloor (mbsf) and 1250 mbsf, which indicate degradation of organic matter around that depth and subsequent release of iodine and methane into the interstitial water. Iodine gradient is controlled by the degradation of iodine-rich organic matter microbially in shallow sediment (at 200 mbsf) and geothermally in deep sediment (at 1250 mbsf), respectively. The ^{129}I/^{127}I ratios between 0 and 400 mbsf vary between 300 $\times 10^{-15}$ and 800 $\times 10^{-15}$, and the lowest ratio of 300×10^{-15} is found at 175 mbsf. There are some thick sand layers > 60 meters between 0 and 400 mbsf. These porous layers transport allochthonous dissolved iodine and interstitial water, which are relatively old. However ^{129}I/^{127}I of 1300×10^{-15} at 67 mbsf corresponding to the sediment age of 3 Ma at 200 mbsf which is the zone of degradation of organic matter. ^{129}I/^{127}I between 400 to 1480 mbsf decrease from 700 $\times 10^{-15}$ to 400×10^{-15}, resulting from mixing with deep (old) iodine and shallow (young) iodine. In the input sediment, iodine gradient is strongly controlled by degradation of organic matter and the migration is controlled by vertical diffusion which indicates poor fluid migration or slow migration rate. However, the horizontal advection/migration of interstitial water is significant within the thick-porous sandy layers.

Keywords: 129I, Iodine geochronology, Interstitial water, Sumatra subduction input, IODP Exp.362

©2019. Japan Geoscience Union. All Right Reserved.

Challenge to Future Deep-Water Mapping: Unmanned Bathymetric Survey Competition "Shell Ocean Discovery XPRIZE"

*MASANAO SUMIYOSHI[1]

1. Hydrographic and Oceanographic Department, Japan Coast Guard

Unmanned survey technology is utilized in the world of bathymetric survey in the present age, when unmanned technologies are developing in various fields. Especially Autonomous Underwater Vehicle (AUV) is actively used in order to acquire high resolution bathymetric data in the deep waters. The technological innovation is needed to further advance the unmanned and automated deep-water mapping, including AUV operations of launch and retrieval. In order to encourage such innovation, an international competition of unmanned deep-water mapping, "Shell Ocean Discovery XPRIZE" has been held for 3 years.
The University of New Hampshire actively develops many hydrographic and oceanographic survey technologies that will open a new era, and as a part of these efforts GEBCO-NF Alumni Team challenges the international unmanned deep-water competition. The author has been strongly pushing the research and development of technology of bathymetric survey for this challenge as a member of this team, who was studying abroad to this university until 2017 to learn the latest hydrographic survey technologies.
This team had passed through Round 1 (semi-final: ~ 2000 m) held in November 2017, and challenged Round 2 (final: ~ 4000 m) as one of the finalists in the last November. In this paper, we report our efforts and achievements of the GEBCO-NF Alumni team, including those in Round 2.

Keywords: Shell Ocean Discovery XPRIZE, GEBCO-NF Alumni Team, Unmanned/Autonomous Technologies (USV, AUV), Bathymetric Survey, Multibeam Echosounder (MBES), Synthetic Aperture Sonar (SAS)

©2019. Japan Geoscience Union. All Right Reserved.

Prototype of deep-sea ocean bottom pressure recorder with self-calibration capability using “A-0-A” approach for detection of long-term crustal deformation

*Yusaku Ohta[1], Ryota Hino[1], Syuichi Suzuki[1], Makiko Sato[1], Yui Nishimagi[1], Hiroaki Kajikawa[2], Tokihiko Kobata[2]

1. Research Center for Prediction of Earthquakes and Volcanic Eruptions, Graduate School of Science, Tohoku University, 2. National Metrology Institute of Japan, National Institute of Advanced Industrial Science and Technology

Ocean bottom pressure gauge (OBP) can continuously observe the vertical crustal deformation in the seafloor. However, a nature of long-term drift of pressure sensors causes a serious problem in detection of the long-term crustal deformation. A possible approach to remove the sensor drift on the sea-floor is to use a dead-weight tester as the pressure standard to make in-situ calibration on the seafloor by periodically switching between the ambient pressure and the reference pressure (Sasagawa et al. 2016). Recently, an alternative approach, an “A-0-A” method, using the internal pressure of the instrument housing as the reference pressure was proposed (e.g. Wilcock et al., 2018). We investigated the long-term drift behavior and ability of “A-0-A” method by a laboratory experiment using dead-weight tester as a pressure standard (e.g. Nishimagi et al. AGU fall meeting, 2018). We regard the reading at high applied pressure as ambient pressure point (“A”) and that at atmospheric pressure as zero-point (“0”). Although the residual time series between the “A” and “0”, however, showed small discrepancy, we found drift characteristics of “A” and “0” are basically similar to each other.

Based on these laboratory experiment results, we have started to develop a proto-type of ocean bottom pressure recorder with self-calibration capability using “A-0-A” approach for deep-water (up to 7,000 m) deployment. We install all the equipments including a pressure sensor in a 17-in glass sphere. To measure both of the internal and external (water) pressure by a single sensor, we adopt 3-way a ball valve controlled by an electric actuator in front of the sensor, as in the previous self-calibrating system using a dead-weight tester. The actuator is operated by the microcomputer to switch by arbitrary interval. We also install alternative barometer to compare the internal pressure value recorded by the pressure sensor. The development is still under way, and we will show more detail characteristic of the prototype system and its potential abilites.

©2019. Japan Geoscience Union. All Right Reserved.

Noise reduction and surface wave array dispersion measurements applied to NOMan's broadband OBS data

*Yuki Kawano[1], Takehi Isse[1], Hitoshi Kawakatsu[1], Akiko Takeo[1], Hajime Shiobara[1]

1. Earthquake Research Institute, The University of Tokyo

To achieve better performance of broadband ocean bottom seismometer (BBOBS) survey, we applied noise reduction analysis and dispersion measurements to the vertical component seismograms of the Normal Oceanic Mantle (NOMan) project arrays, which are previously analyzed by Takeo et al. (2018). Our noise reduction targets on the tilt noise that is significant for low-frequency (<0.1 Hz) BBOBS vertical records. Tilt noise is generated by the seafloor current which flows pass the BBOBS. It originally only dominates horizontal records, but the misalignment between the seismic sensor's vertical axis and gravitational direction allows projection of noisy horizontal tilt noise onto vertical records. Hence, vertical tilt noise can be estimated from the transfer function between horizontal and vertical records (Crawford and Webb, 2000). We developed a noise reduction method which is suitable for Japanese BBOBS based on the approach of Crawford and Webb (2000) and Bell et al. (2015). By performing noise reduction analysis, we achieved about 20 dB noise reduction at the frequency lower than 50 mHz and extracted lots of buried seismic signals. To verify the effect of noise reduction analysis, we compared array dispersion measurement results which derived from tilt noise removed and non-removed data. Using the method of Takeo et al. (2018), we measured average phase velocity and azimuthal anisotropy of fundamental mode Rayleigh waves to estimate isotropic and azimuthally anisotropic Vsv (βv) profiles. The results show that tilt noise removed data can provide us with more precise low-frequency measurements and the better-constrained structure at a depth of 80 km or deeper. Our results indicate that noise reduction preprocessing is important for improving Japanese BBOBS analysis.

Keywords: broadband ocean bottom seismometer, tilt noise, low frequency, surface wave array measurement

©2019. Japan Geoscience Union. All Right Reserved.

High-tech dredge system for abyssal bedrock research; dredge system with acoustic real time monitoring on deep sea floor.

*Teruaki Ishii[1], Yukihiro - Kida[2], Izumi - Sakamoto[3], Shiki -- Machida[4]

1. Center for Integrated Research and Education of Natural Hazards, Sizuoka University, 2. JAMSTEC, 3. Toukai University, 4. Chiba Institute of Technology

It is very important to recover geological samples including hard rocks and soft materials from ocean floor to investigate bedrocks itself as well as sea floor environment on the basis of the material scientific aspects. Dredge haul methods being a simple and easy way with low costs, have been widely used for recovering the bedrocks. One of author (TI) has been working on the dredge hauls during about 40 years on the several Japanese and American Research Vessels (R/Vs), that is, R/V Tansei Maru, R/V Hakuho Maru, R/V Yokosuka, and R/V Kairei as well as R/V Atlantis-II, R/V Melville (2 times), R/V Moana Wave, and R/V Thomas Thompson, respectively. He has been proposing the (1) ORI-TI type dredge system, which has been improved and still improving on the basis of the better ideas gathered from the above mentioned all cruises. The dredge systems in the US Research Vessels have been continuing the conventional and basic technical methods, that is, box type chin-bag dredge (within or without fishing net) and using tension-meter as well as pinger.

On the other hand, Japanese scientists have been recently improving the traditional dredge systems with active introduction of high technique, for example, (2) transponder system and/or (3) deep sea TV camera system during dredge hauls. (4) new underwater acoustic transmission system of real-time TV-image.

(1)ORI-TI (Ocean Research Institute T. Ishii) type dredge system is composed of box type chain-bag dredge with steel bucket which can recover any sea bottom material including hard rocks as well as sand, mud and organisms(Ishii, 2017).

(2)Acoustic transponder attached on the dredge wire can mention real-time position of the dredge system on monitor showing pre-surveyed bathymetric map in the navigation room, This system helps safe and reliable rock sampling (Machida et al, 2011).

(3) Box-cage type dredge with installed deep sea TV camera system can record occurrence of bed rocks during dredge hauls (Sakamoto et al, 2017).

(4) New underwater acoustic transmission system of real-time TV -image with every 2 second from Shinkai 6500 to R/V Yokosuka put to practical use (Sakurai, 2018) on the basis of the new underwater acoustic communication system (Kida et al, 2018). If we can get low price (about USD$10,000) above mentioned system in a near future, it will be applied to the dredge hauls with real-time monitor on the sea bottom. The author (T.I.) assumes that its application fields are very wide; piston core, mooring system, ocean bottom seismometer, net fishing etc.

Reference

Kida, Yukihiro, Mitsuyasu Deguchi, and Takuya Shimura.(2018): Experimental result for a high-rate underwater acoustic communication in deep sea for a manned submersible SHINKAI 6500, J. Marine Acoust. Soc. Jpn., 45 (4),197-207.

©2019. Japan Geoscience Union. All Right Reserved.

ISHII, Teruaki (2017):Evolution of dredge system from low to high technological equipment--Improvement of dredge system toward advanced material science on bedrocks--, Fukada Geological Institute Annual Report, 18, 29-48 (in Japanese with English abstract).

Sakamoto, Izumi, Satsuki Iijima, Yamato Monma, and Kenichirou Tani (2017) :Dredge “Satsuki” system with Deep Sea Camera, ① her development and function, Blue Earth Symposium 2017 (JAMSTEC) abstract BE17-12 (in Japanese).

Machida, Shiki, Yutaka Matsuura, Natsue Abe, and Teruaki Ishii (2011):Rock sampling from the ocean floor using transponder-based real-time monitoring of the dredge system, JAMSTEC Rep. Res. Dev,13, 89-105 (in Japanese with English abstract).

Keywords: abyssal bedrocks, high-tech dredge system, ORI-TI type dredge, dredge transponder, deep sea dredge VTR, underwater acoustic transmission system

©2019. Japan Geoscience Union. All Right Reserved.

Construction of Database System on Offshore Faults around Japan

*Hiromi Kamata[1], Narumi Takahashi[1,2], Shigeyoshi Tanaka[1], Rei Arai[1], Minako Katsuyama[1], Ayako Nakanishi[1], Hiroyuki Fujiwara[2], Tsuneo Ohsumi[2], Takahiko Inoue[3], Tomoyuki Sato[3], Yoshiyuki Kaneda[4]

1. Japan Agency for Marine-Earth Science and Technology, 2. National Research Institute for Earth Science and Disaster Resilience, 3. National Institute of Advanced Industrial Science and Technology, 4. Kagawa University

JAMSTEC has performed the project for “Comprehensive Evaluation of Offshore Fault Information” sponsored by the Ministry of Education, Culture, Sports, Science and Technology (MEXT) since FY2013. The project consists of three themes named “Sub-theme 1” gathering various kinds of existing geological/geophysical information and constructing offshore fault database system (DB), “Sub-theme 2” re-processing seismic data and interpreting offshore faults based on unified evaluation standard, and “Sub-theme 3” building offshore fault models conducted by NIED.

In Sub-theme 1, JAMSTEC has obtained or borrowed huge volumes of multi-channel seismic (MCS)/single-channel seismic (SCS) reflection data and ocean bottom seismometer (OBS) refraction data surveyed around Japan from various organizations including national research institutes and private enterprises, and has collected seismic velocity information, bathymetry data etc. After the quality check of these data, they are made into a database and unitary management of them are carried out. The final output of Sub-theme 1 is an offshore fault DB comprising the data sets of collected/re-processed seismic data and overall offshore fault information provided by Sub-theme 2 and Sub-theme 3. In Sub-theme 2, the past old-fashioned MCS data have been re-processed applying the latest sophisticated technology with de-multiple filtering and noise suppression for obtaining the high resolution profile of these seismic sections. Using the MCS/SCS data, offshore faults around Japan have been identified based on unified evaluation standard. Some geological horizons and a plate boundary have been also interpreted to model subsurface geometry and 3D velocity structure. The final output of Sub-theme 2 is to delineate the spatial distribution and continuity of identified faults on the high resolution bathymetric map such as a red relief image map, and to organize their features/parameters such as type, length, dipping direction, extension etc. after the seismic time–depth conversion using 3D velocity structure model. The 3D velocity structure has been modeled using collected OBS refraction data, velocity analysis results in MCS re-processing and some available published data. In Sub-theme 3, NIED has built the offshore fault models based on a fault information catalog completed by Sub-theme 2. The model validation for historical earthquake source faults with the magnitude over seven has been also conducted through ground motion and tsunami simulations.

This poster presentation focuses on the offshore fault DB constructed by Sub-theme 1 of the project. JAMSTEC has finished the clarification of faults in the Sea of Japan, and around the sea area of the Nansei Islands and Izu-Ogasawara Islands by FY2017. We are currently working on the interpretation of subsurface structure and fault distribution in the Nankai Trough area, and continue to register MCS/SCS reflection time/depth sectional figures, 3D velocity models, NIED’s fault models and their parameters into the DB sequentially. The trial operation of the DB has been also done at the subcommittee of the Headquarters for Earthquake Research Promotion of MEXT. The DB is highly expected to become a useful tool that contribute to tsunami hazard evaluation and disaster management conducted by Japanese government and local authorities, and that improve the public awareness against disaster prevention.

©2019. Japan Geoscience Union. All Right Reserved.

We would like to express our acknowledgements to Ministry of Economy, Trade and Industry (METI), Japan Oil, Gas and Metals National Corporation (JOGMEC), Japan Coast Guard (JCG), Geospatial Information Authority of Japan (GSI), AIST, Akita Prefecture, Okinawa Prefecture, University of Tokyo, Toyama University, Inpex Corporation and Japan Petroleum Exploration Co.,Ltd. (JAPEX) for providing the geological/geophysical data.

Keywords: Offshore Fault, Seismic Data, 3D Velocity Structure, Fault Model, Database

©2019. Japan Geoscience Union. All Right Reserved.

An integration method for multiple sets of seafloor backscatter intensity data

*Shiki Machida[1,2], Taichi Sato[3], Kazutaka Yasukawa[2]

1. Ocean Resources Research Center for Next Generation, Chiba Institute of Technology, 2. University of Tokyo, 3. AIST

Acoustic backscattering of the seafloor is thought to provide a useful signal representing the existence of hard materials, such as lava flows with ferromanganese crust along the slope of seamount or knoll [1, 2], and ferromanganese nodules on the seafloor [3]. Previous investigations using vessel-equipped multi-narrow beam echo sounder (MBES) [1–3] identified variations of distributions over an area of tens or hundreds of square kilometres. Therefore, vessel-equipped MBES can provide a more economical exploration for vast areas than that provided by underwater apparatuses such as a deep-towed side scan sonar. However, a disadvantage inhibiting its use is that the different physical and technical parameters, such as sounder characteristics, observation period, and processing, yield different absolute values of backscatter intensity for the same area. As a solution, we propose a generally applicable method for obtaining the widespread distribution of deep-sea solid materials using a combination of several datasets of vessel-equipped MBES.

The Japanese exclusively economic zone (EEZ) around Minamitorishima Island in the western North Pacific is the best candidate area in which to analyse vessel-equipped multibeam backscatter data. This is due to the fact that several research cruises, operated by the Japan Agency for Marine-Earth Science and Technology (JAMSTEC), have obtained multiple sets of backscatter data, combined with bathymetry mapping. These data were obtained with an identical MBES (SeaBeam 3012. multibeam system) for each of the four cruises of *R/V Mirai*(MR14-E02, MR15-E01 Legs 2 and 3, and MR15-02) in 2014 and 2015, and with the other MBES (SeaBeam 2112.004 multibeam system) during a cruise of *R/V Yokosuka* (YK10-05) in 2010.

We identified two important components for successfully integrating several sets of backscatter intensity data collected by vessel-equipped MBES, as follows. (1) The folding points in the trend of the second-order differential values of the histogram of backscatter data correspond to the boundaries between different types of geology, e.g. barren pelagic sediment and dense ferromanganese nodules. (2) These thresholds each indicate that the same geologic boundaries appear at similar intervals in the histogram, even if the absolute values of intensity are different for each dataset. In particular, this latter component ensures linear fitting of the thresholds used to adjust each dataset to the arbitrary standard data. We need the confirmation of the geographical distributions of the identified boundary intensities between the different datasets. In this presentation, we will show an example of data integration for nine datasets to map the backscatter intensity of a region of approximately 155,500 km^2in the Japanese EEZ around Minamitorishima Island.

References: [1] Hirano et al. (2006) *Science***313**, 1426–1428. [1] Hirano et al. (2016) *Mar. Geol.***373**, 39–48. [3] Machida et al. (2016) *Geochem. J.***50**, 539–555.

©2019. Japan Geoscience Union. All Right Reserved.

Keywords: backscatter intensity, multi-narrow beam echo sounder, Minamitorishima EEZ

©2019. Japan Geoscience Union. All Right Reserved.

A precise calculation of average depth for ETOPO1

*Yasushi Harada[1], Sae Horiuchi[1]

1. School of Marine Science and Technology, Tokai University

NOAA calculated global ocean average depth as -3688m (https://www.ngdc.noaa.gov/mgg/global/etopo1_ocean_volumes.html) , but in their method, there are deviations for distribution of sampling points, especially at high latitude area. Generally, perfect uniform sampling points are needed to calculate precise average depth using digital elevation data such as ETOPO1.

We tried a different method for creating uniform sampling points on spherical surface. Yamaji(2001) created this software called GSS generator(GSS). The GSS makes almost perfect uniform sampling points on sphere, but not on WGS84 ellipsoid. Therefore we compared the two methods, and performed a statistical analysis for both methods.

We found that the two methods produced similar average depth values and the errors, and that the average depth of ETOPO1 is 3685.9 ±0.5m and about 2m shallower than NOAA’s 3688m value.

Keywords: ETOPO1, average depth, GSS Generator

©2019. Japan Geoscience Union. All Right Reserved.

[J] Poster | S (Solid Earth Sciences)：S-CG Complex & General

Mon. May 27, 2019 5:15 PM - 6:30 PM JST | Mon. May 27, 2019 8:15 AM - 9:30 AM UTC | Poster Hall International Exhibition Hall8, Makuhari Messe_29

[S-CG56] Ocean Floor Geosciences

convener:Kyoko Okino(Atmosphere and Ocean Research Institute, The University of Tokyo)

Most of Earth's volcanism and much of its tectonic activity occur on and beneath the seafloor. Various phenomena on the seafloor are closely linked to plate tectonics, Earth and atmosphere. Seafloor rocks and sediments record Earth's evolution and heat and material fluxes on the Earth. Ocean Floor Geosciences session covers a broad range of research on LIPs, crustal movement and structure etc. Any fields of research and approach are welcomed. The session aims to encourage discussion among scientists from different study fields and to integrate our understanding of ocean floor. The session is co-chaired by K. Tadokoro (Nagoya Univ.), O. Ishizuka (AIST), T. Toki (Univ. Ryukyus), and N. Takahashi (JAMSTEC).

[SCG56-P01] Signature of plume-ridge interaction on bathymetry and geochemistry along mid-ocean ridges: Insights from the Réunion Plume and Central Indian Ridge

*Clement Vincent[1], Jung-Woo Park[1], Sang-Mook Lee[1], Jonguk Kim[2], Sang-Joon Pak[2] (1.Seoul National University, 2.Korea Institute of Ocean Science and Technology)

[SCG56-P02] Spreading rate and its stability of Chile Ridge near the Chile Triple Junction

*Takanori Ishihara[1], Takeshi Matsumoto[1] (1.Ryukyu university)

[SCG56-P03] Newly Mapped Seamounts on the Antarctic Plate off Southern Chile

*Toshiya Fujiwara[1], Natsue Abe[2], Naomi Harada[3], Mirai MR16-09 Leg 2 Shipboard Science Party (1.Research and Development Center for Earthquake and Tsunami, Japan Agency for Marine-Earth Science and Technology, 2.Research and Development Center for Ocean Drilling Science, 3.Research and Development Center for Global Change)

[SCG56-P04] Surface-ship gravimetry on board MR16-09 Cruise by R/V MIRAI - Characteristrics of gravity anomaly around the Chile Triple Junction

*Takeshi Matsumoto[1], Takanori Ishihara[1] (1.Faculty of Science, University of the Ryukyus)

[SCG56-P05] Magnetic and Magnetotelluric surveys across the Afar depression, transition between continental rifting and sea-floor spreading

*Ryokei Yoshimura[1], Naoto Ishikawa[2], Tesfaye Kidane[3], Shin-ichi Kagashima[4], Nobutatsu Mochizuki[5], Ameha Atnafu Muluneh[3], Kirika Kitagawa[4], Taito Ikema[6] (1.Disaster Prevention Research Institute, Kyoto University, 2.Graduate School of Human and Environmental Studies, Kyoto University, 3.Addis Ababa University, 4.Faculty of Science, Yamagata University, 5.Priority Organization for Innovation and Excellence, Kumamoto University, 6.Faculty of Science, Kyoto University)

[SCG56-P06] **Evolution of oceanic core complexes in the Shikoku Basin: when backarc basins cease to open**

*Kyoko Okino[1], Yasuhiko Ohara[2,3], Masakazu Fujii[4], Tomoko Hanyu[1] (1.Atmosphere and Ocean Research Institute, The University of Tokyo, 2.Japan Coast Guard, 3.Japan Agency for Marine-Earth Science and Technology, 4.National Institute of Polar Research)

[SCG56-P07] Thermal evolution of the Lanzo orogenic peridotite massif in western Alps: implications on thermal structure near subcontinental lithosphere-asthenosphere boundary

*Tomo Aoki[1], Kazuhito Ozawa[1], Jean-Louis Bodinier[3], Françoise Boudier[2] (1.The University of Tokyo, 2.Montpellier 2 University, 3.Geosciences Montpellier)

[SCG56-P08] Comparison of the back-arc basins of the South and the Central Ryukyus in the northwest Pacific

*Kohsaku Arai[1], Ayanori Misawa[1], Takahiko Inoue[1] (1.Institute of Geology and Geoinformation, National Institute of Advanced Industrial and Technology)

[SCG56-P09] Geochemistry and zircon U-Pb ages of mafic rocks in the Mikabu and Sorachi-Yezo belts: Comparison with the Shatsky Rise

*Naoto Kimura[1], Yuji Ichiyama[1], Shohei Takahashi[1], Hisatoshi Ito[2], Akihiro Tamura[3], Tomoaki Morishita[3] (1.Chiba University, 2.Central Research Institute of Electric Power Industry, 3.Kanazawa University)

[SCG56-P10] Submersible magnetics reveals relationship between off-axis volcanism and hydrothermal systems of the Kairei and Yokoniwa fields at the Central Indian Ridge

*Masakazu Fujii[1], Kyoko Okino[2] (1.National Institute of Polar Research and SOKENDAI, 2.Atmosphere and Ocean Research Institute, The University of Tokyo)

[SCG56-P11] Shipboard magnetic and gravity surveys around the Iheya North Knoll and the Iheya Minor Ridge in the Mid-Okinawa Trough: Preliminary results of KR18-14 Leg1/Leg2 cruises

*Kazuya Kitada[1], Takafumi Kasaya[1], Hisanori Iwamoto[1], Yoshifumi Nogi[2] (1.Japan Agency for Marine-Earth Science and Technology, 2.National Institute of Polar Research)

[SCG56-P12] A shallow scientific drilling at Higashi Ensei Hydrothermal Field, Okinawa Trough

*Hidenori Kumagai[1], Takafumi Kasaya[1], Shuhei Totsuka[2], Shinsuke Kawagucci[1], Hideaki Machiyama[1], Koichi Iijima[1], Hirofumi Yamamoto[1], junji kaneko[1], Yusuke Ohta[3], Shohei Albert Tomita[3], Shogo Komori[4] (1.Japan Agency for Marine-Earth Science and Technology, 2.Kyushu Univ., 3.Kyoto Univ., 4.AIST)

[SCG56-P13] Mineralogical and geochemical study of sediment cores collected from the Gondou hydrothermal field in the Okinawa Trough

*Jun-ichiro Ishibashi[1,2], Shuhei Totsuka[2], Akihi Tsutsumi[2], Naru Tsukamoto[2], Yusuke Kira[2], Kazuhiko Shimada[1], Toru Yamasaki[3], Ken Ikehara[3], Toshiro Nagase[4], Yutaro Takaya[5,9], Kei Ikehata[6], Takashi Goto[7], Chitaro Gouzu[7], Ryuichi Shinjo[8], Hideaki Machiyama[9], Koichi Iijima[9], Hirofumi Yamamoto[9], Hidenori Kumagai[9] (1.Department of Earth and Planetary Sciences, Kyushu University, 2.Graduate School of Science, Kyushu University, 3.National Institute of Advanced Industrial Science and Technology, 4.Tohoku University Museum, 5.School of Creative Science and Enginerring, Waseda University, 6.Faculty of Life and Environmental Sciences, University of Tsukuba, 7.Hiruzen Institute for Geology and Chronology, 8.Faculty of Science, University of the Ryukyus, 9.Japan Agency for Marine-Earth Science and Technology)

[SCG56-P14] New type of self-potential anomaly observed near a hydrothermal site of Oomuro-dashi volcano, Izu-Ogasawara arc

*Yoshifumi Kawada[1,2], Takafumi Kasaya[2] (1.International Research Institute of Disaster Science, Tohoku University, 2.Japan Agency for Marine-Earth Science and Technology)

[SCG56-P15] Numerical simulation of submarine hydrothermal ore-deposits due to a coupled process of fluid migration and reactive geochemical transport

*Claudia Fujita[1], Hajime Yamamoto[1], Jun-ichiro Ishibashi[2], Takeshi Tsuji[3] (1.Taisei Corporation, 2. Department of Earth and Planetary Sciences, Faculty of Science, Kyushu University, 3.Department of Earth Resources Engineering, Faculty of Science, Kyushu University)

[SCG56-P16] Mineral composition and grain size distribution of REY-rich mud in the Minamitorishima EEZ: Implication for formation process of extremely REY-rich mud

*Sakai Takumi[1], Erika Tanaka[1], Kazutaka Yasukawa[1,2], Junichiro Ohta[2,1], Koichiro Fujinaga[2,1], Kentaro Nakamura[1], Yasuhiro Kato[3,1,2] (1.Department of Systems Innovation, School of Engineering, University of

Tokyo, 2.Ocean Resources Research Center for Next Generation, Chiba Institute of Technology, 3.Frontier Research Center for Energy and Resources, School of Engineering, The University of Tokyo)

[SCG56-P17] **Geochemical and morphological features of manganese micronodules in REY-rich mud within the Minamitorishima EEZ, western North Pacific Ocean**

*Satoshi Kino[1], Kazutaka Yasukawa[1,2], Keishiro Azami[1], Erika Tanaka[1], Koichiro Fujinaga[2,1], Kentaro Nakamura[1], Yasuhiro Kato[1,2] (1.Department of Systems Innovation, School of Engineering, University of Tokyo, 2.Ocean Resources Research Center for Next Generation, Chiba Institute of Technology)

[SCG56-P18] Seafloor sediment thickness around the Japan and Kurile trenches obtained by traveltime analysis for PS converted wave recoded by ocean bottom seismograms

*Ryosuke Azuma[1], Genti Toyokuni[1], Ryota Takagi[1], Syuichi Suzuki[1], Makiko Sato[1], Takashi NAKAYAMA[1], Naoki Uchida[1], Ryota Hino[1] (1.Recearch Center for Prediction of Earthquake and Volcanic Eruption, Graduate School of Science, Tohoku University)

[SCG56-P19] Examination of critical taper theory based on bathymetry data in subduction zones

*Hiroaki Koge[1], Juichiro Ashi[1], Jin-Oh Park[1] (1.Atmosphere and Ocean Research Institute, The University of Tokyo)

[SCG56-P20] Active structures of the Sagami Bay Fault by high-resolution sub-bottom profiling and pin-point core sampling

*Juichiro Ashi[1], Asuka Yamaguchi[2], Natsumi Okutsu[1], Ayanori Misawa[3] (1.Graduate School of Frontier Sciences, The University of Tokyo, 2.Atmosphere and Ocean Research Institute, The University of Tokyo, 3.National Institute of Advanced Industrial Science and Technology)

[SCG56-P21] Fault Distribution and Structural Characteristic in the Nankai Trough Area, Japan

*Rei Arai[1], Narumi Takahashi[1], Minako Katsuyama[1], Shigeyoshi Tanaka[1], Hiromi Kamata[1], Tomoyuki Sato[2], Takahiko Inoue[2], Yoshiyuki Kaneda[3] (1.Japan Agency for Marine-Earth Science and Technology, 2.National Institute of Advanced Industrial Science and Technology, 3.Kagawa University)

[SCG56-P22] Seismicity in the central Ryukyu Trench by the Ocean Bottom Seismometers

*Ren Yakabu[1], Mamoru Nakamura[1], Yusuke Yamashita[2], Masanao Shinohara[3], Tomoaki Yamada[3], Hajime Shiobara[3], Kimihiro Mochizuki[3] (1.University of the Ryukyus, 2.DPRI, Kyoto University, 3.ERI, Tokyo University)

[SCG56-P23] Seismic structure of subducted Philippine Sea plate beneath Kyushu inferred from Po/So waves

*Azusa Shito[1] (1.Institute of Seismology and Volcanology, Kyushu University)

[SCG56-P24] Slope failure features and their distribution in the forearc off northwestern Sumatra

*Kenji Hirata[1], Toshiya Fujiwara[2], Ayanori Misawa[3], Kohsaku Arai[3] (1.National Research Institue for Earth Science and Diaster resilience, 2.Japan Agency for Marine-Earth Science and Technology, 3.National Institute of Advanced Industrial Science and Technology)

[SCG56-P25] Origin and migration of fluid in the Sumatra subduction input: application of a geochronological method using a long-lived radioisotope of dissolved iodine

*Satoko Owari[1], Hitoshi Tomaru[1] (1.Chiba university)

[SCG56-P26] Challenge to Future Deep-Water Mapping: Unmanned Bathymetric Survey Competition "Shell Ocean Discovery XPRIZE"

*MASANAO SUMIYOSHI[1] (1.Hydrographic and Oceanographic Department, Japan Coast Guard)

[SCG56-P27] Prototype of deep-sea ocean bottom pressure recorder with self-calibration capability using “A-0-A” approach for detection of long-term crustal deformation

*Yusaku Ohta[1], Ryota Hino[1], Syuichi Suzuki[1], Makiko Sato[1], Yui Nishimagi[1], Hiroaki Kajikawa[2], Tokihiko Kobata[2] (1.Research Center for Prediction of Earthquakes and Volcanic Eruptions, Graduate School of Science, Tohoku University, 2.National Metrology Institute of Japan, National Institute of Advanced Industrial Science and Technology)

[SCG56-P28] Noise reduction and surface wave array dispersion measurements applied to NOMan's broadband OBS data

*Yuki Kawano[1], Takehi Isse[1], Hitoshi Kawakatsu[1], Akiko Takeo[1], Hajime Shiobara[1] (1.Earthquake Research Institute, The University of Tokyo)

[SCG56-P29] High-tech dredge system for abyssal bedrock research; dredge system with acoustic real time monitoring on deep sea floor.

*Teruaki Ishii[1], Yukihiro - Kida[2], Izumi - Sakamoto[3], Shiki - - Machida[4] (1.Center for Integrated Research and Education of Natural Hazards, Sizuoka University, 2.JAMSTEC, 3.Toukai University, 4.Chiba Institute of Technology)

[SCG56-P30] Construction of Database System on Offshore Faults around Japan

*Hiromi Kamata[1], Narumi Takahashi[1,2], Shigeyoshi Tanaka[1], Rei Arai[1], Minako Katsuyama[1], Ayako Nakanishi[1], Hiroyuki Fujiwara[2], Tsuneo Ohsumi[2], Takahiko Inoue[3], Tomoyuki Sato[3], Yoshiyuki Kaneda[4] (1.Japan Agency for Marine-Earth Science and Technology, 2.National Research Institute for Earth Science and Disaster Resilience, 3.National Institute of Advanced Industrial Science and Technology, 4.Kagawa University)

[SCG56-P31] **An integration method for multiple sets of seafloor backscatter intensity data**

*Shiki Machida[1,2], Taichi Sato[3], Kazutaka Yasukawa[2] (1.Ocean Resources Research Center for Next Generation, Chiba Institute of Technology, 2.University of Tokyo, 3.AIST)

[SCG56-P32] A precise calculation of average depth for ETOPO1

*Yasushi Harada[1], Sae Horiuchi[1] (1.School of Marine Science and Technology, Tokai University)

Signature of plume-ridge interaction on bathymetry and geochemistry along mid-ocean ridges: Insights from the Réunion Plume and Central Indian Ridge

*Clement Vincent[1], Jung-Woo Park[1], Sang-Mook Lee[1], Jonguk Kim[2], Sang-Joon Pak[2]

1. Seoul National University, 2. Korea Institute of Ocean Science and Technology

Plume-ridge interaction is an important thermal and geological process, which results in various physical and chemical anomalies along a significant length of the global mid-ocean ridges system. Despite numerous studies, some remaining questions to be solved are origin and mechanisms of geochemical variations and their possible influence on the morphology of mid-ocean ridges. The Central Indian Ridge, with a slow to intermediate spreading rate, provides an ideal opportunity to explore distant plume-ridge interactions. Presently, the ridge is moving away from the hotspot. The hotspot which started at the Deccan Traps (65 Ma) is presently 1000 km away from the Central Indian Ridge, at the Réunion Island. Paleogeographic reconstruction suggests that the hotspot crossed the middle part of the Central Indian Ridge (MCIR) between 8˚S and 17˚S at ~34 Ma. Studies suggest that the plume material that flows into the Central Indian Ridge is more or less concentrated around 19˚S, to the south of Marie Celeste Fracture Zone (MCFZ). In addition, recent geochemical study show southward-increasing gradient in Réunion mantle component between 14˚S and 18˚S north of MCFZ. The detailed mechanism of the plume interaction on the MCIR is in debate. In this study, we revisited the MCIR with additional Nd, Sr and Pb isotope analyses and ship-board high-resolution bathymetry data to constrain the influence of the Ré union plume on geochemistry and bathymetry of the MCIR. The results show that the geochemical anomaly observed between 14˚S and 18˚S are found only in the northern part of segments and subsegments, and these enrichments correlate with the shallow axial bathymetry. The localized geochemical and bathymetric anomalies can be ascribed to a hotspot leading edge effect where the hotspot leading segments are offset in the direction of the plume and are more influenced by the plume materials. It appears that discontinuities such as transform faults and the non-transform discontinuities influence the flow of mantle plume material into the ridge, and that the proximity of the ridge to the hotspot plays an important role in the plume-ridge interaction.

Keywords: Plume-ridge interaction, Reunion Plume, Central Indian Ridge, MORB

©2019. Japan Geoscience Union. All Right Reserved.

Spreading rate and its stability of Chile Ridge near the Chile Triple Junction

*Takanori Ishihara[1], Takeshi Matsumoto[1]

1. Ryukyu university

Chile triple junction (CTJ) is located at 46°13'S, 75°13'W off the coast of Chile and is composed of Nazca plate, Antarctic plate and South America plate, forming a ridge-trench-trench type triple junction. Chile ridge that is an active spreading ridge is subducting under the South America plate at CTJ and is the only ridge system that is currently subducting under trench in the world. Therefore this area is an important target to study the behavior of the active ridge just before subduction. And also, the mechanism and a possible driving force of the active ridge subduction are also to be studied by subsurface structure, age, development history, and so on through marine geophysical survey. The authors analysed total geomagnetic data from the tracks along the segments and attempted to obtain seafloor spreading rate at each segment and seafloor age from magnetic anomaly, and spreading stability in this area by the magnetic N/R boundary strikes derived from the three component magnetic data. Both the total force and the three-component magnetic data for this study were obtained from MR16-09 cruise by R/V MIRAI, Leg1 and Leg2. Marine Trackline data that were achived in National Geophysical Data Center were also used supplementarily. Seafloor spreading rate decrease is shown along almost all the tracks close to the trench, and comparison of several track data along the Segment SCR1 shows the same characteristics that spreading rate along the southern track is slower than that along the northern track. Moreover, the result from the other segments show that SCR1’s spreading rate (about3.0cm/yr) is higher than SCR3’s one (about 2.0cm/yr). These results show spreading rate is decreasing as the ridge is close to the trench. This mightbe due to declining of igneous activity and reduction of magma supply rate near the trench as Matsumoto et al (2013) showed. The reason why the young seafloor subducts early is that increasing of slab pull force caused by thickening of the oceanic lithosphere by cooling with closing the trench. Magnetic N/R boundary strike shows almost uniform trends, except near Guamblin fracture zone, so spreading stability is attained on the whole.

©2019. Japan Geoscience Union. All Right Reserved.

Newly Mapped Seamounts on the Antarctic Plate off Southern Chile

*Toshiya Fujiwara[1], Natsue Abe[2], Naomi Harada[3], Mirai MR16-09 Leg 2 Shipboard Science Party

1. Research and Development Center for Earthquake and Tsunami, Japan Agency for Marine-Earth Science and Technology, 2. Research and Development Center for Ocean Drilling Science, 3. Research and Development Center for Global Change

We conducted bathymetry, gravity, and magnetic survey of seamounts on the Antarctic Plate off southern Chile in the R/V Mirai MR16-09 Leg 2 cruise (January 20 - February 5, 2017: Puerto Montt - Punta Arenas). The survey including transit was an unprecedented opportunity to collect data in the regions of the Pacific Ocean where it has been sparsely surveyed.

A SeaBeam 3012 multibeam echo sounder was used for the bathymetric survey. The Micro-G LaCoste and Romberg S-116 shipboard gravity meter, a Geometrics G-882 cesium towing magnetometer, and a Tierra Tecnica SFG1214 shipboard three-component magnetometer were used for the gravity and magnetic surveys, respectively. Unfortunately, dredge rock sampling and seismic reflection survey was not conducted.

The seamounts are located on the Antarctic Plate. The mid-ocean ridge (Chile Ridge) was considered to be already subducted beneath the South American Plate. Magnetic Anomaly 6a was identified by Cande et al. (1982) on the seafloor in the vicinity of the seamounts. The crustal age around the seamounts is 18 Ma according to Muller et al. (2008). We observed magnetic anomaly stripes with amplitudes of about 400 nT, therefore, we will examine the crustal age and the seafloor spreading rate.

Since the seafloor was covered with a sedimentary layer, abyssal hills and their strikes could not be identified. The largest seamount was located at 51˚00'S, 79˚25'W. The seamount has a major axis of about 17 km, a minor axis of 10 km, and the strike of the major axis is N45˚W. The water depth of the base of the seamount is about 3900 m and the shallowest depth is about 2900 m, thus the relative height is about 1000 m. The seamount was surrounded by a moat with the maximum deep of 100 m. The basal area is about 160 square kilometers and the volume above the seafloor is about 70 cubic kilometers. The seamounts have calderas, and the depth and the diameter of the largest seamount are 200 m and 2.5 km, respectively.

The existence of the largest seamount was estimated by satellite altimetry and gravity observations. The relative height was estimated to be 364 m (Kim and Wessel (2011) seamount catalogue, ID: KW-05846). However, the accurate estimation of such a small seamount is difficult. We observed free-air gravity anomaly of about +20 mGal at the base of the seamount, and of about +50 mGal over the top of the seamount, thus the peak-to-trough amplitude of the gravity anomaly was 30 mGal. The gravity anomaly due to the seamount with 20 mGal larger amplitude was observed compared with a satellite-based gravity anomaly (Sandwell et al., 2014).

Keywords: Off Chile, Antarctic Plate, Seamount, Bathymetry, Gravity Anomaly, Magnetic Anomaly

©2019. Japan Geoscience Union. All Right Reserved.

Surface-ship gravimetry on board MR16-09 Cruise by R/V MIRAI - Characteristrics of gravity anomaly around the Chile Triple Junction

*Takeshi Matsumoto[1], Takanori Ishihara[1]

1. Faculty of Science, University of the Ryukyus

MR16-09 cruise by R/V MIRAI traversed the Southeast Pacific and the Western Pacific from December 2016 to March 2017, with the portcall at Fiji, Chile, New Zealand and Mutsu. Gravity measurement was also carried out during the whole cruise except for within the EEZ of other countries.
During Leg2 of this cruise, the Segment SCR1 of the Chile Ridge, an active spreading ridge producing the Nazca plate and the Antarctica plate, was also surveyed in order to detect the characteristics of the gravity anomaly due to the subduction of the active mid-oceanic ridge below the South American Plate at the Chile Trench at the Chile Triple Junction (CTJ) located off Taitao Peninsula on the west coast of Chile.
The shipboard gravimeter used for the survey was a relative measurement system. Micro-g LaCoste air-sea gravity meter S-116 is equipped on board MIRAI. Normally, ‘gravity tie’ is carried out during the portcall at the wharf and the gravity base stations nearby where absolute value of gravity is known in order to obtain the absolute gravity value during the cruise. However, it was difficult to obtain accurate values after correcting the drift of the gravimeter because gravity tie was carried out only at 3 stations at the beginning (Shimizu), at the end (Sekinehama) and during the cruise (Punta Arenas). Therefore, correction of the value at the gravity measurement points on the survey lines was carried out using the latest global gravity 1’ grid data (Sandwell et al., 2014, Sandwell et al., 2013, Sandwell et al., 2009) derived from satellite altimetry data etc.

Let the grid intervals in the x and y directions of the grid data be dx and dy, respectively. Let g11, g21, g12, g22 be the gravitational values at the four corner points of this area (approximated by a rectangle) enclosed by x1, x2 (x1 < x2) for x-coordinate and y1, y2 (y1 > y2) for y-coordinate. The linearly interpolated value at the point (x, y) within this the area is

g1 = g11 * (x2 - x) * (y1 - y)

g2 = g21 * (x - x1) * (y1 - y)

g3 = g12 * (x2 - x) * (y - y2)

g4 = g22 * (x - x1) * (y - y2)

Then,

g = (g1 + g2 + g3 + g4) / (dx * dy).

Based on the difference between the gravity values obtained by this interpolation and the measured values, the drift rate at each leg was determined as,

Leg 1: 0.216 mgal/day

Leg 2: 0.520 mgal/day

©2019. Japan Geoscience Union. All Right Reserved.

Leg 3: -0.599 mgal/day

Leg 4: 0.562 mgal/day.

The measured gravity was corrected using these drift rates to obtain the final free air anomalies during the cruise.

Bouguer anomaly along the 3 survey lines on the Segment SCR1 (including the CTJ) of the Chile Ridge off the Chilean west coast was obtained by the two-dimensional calculation (assuming that the same seafloor topography and sub-seafloor structure are continuous along the trench/ridge axis direction) by use of the profiles of free air anomaly and seafloor topography along these survey lines. Regardless of the topographic undulation on the western side of the ridge/trench, the Bouguer anomaly decreased relatively uniformly towards the trench/ridge axis. This pattern is similar to that of the normal trenches and mid-ocean ridges. The rate of decrease as approaching the trench is about 1.5~2 mgal/km in the Western Pacific trench, <0.1 mgal/km for the Mid-Atlantic Ridge. However, the result of the current gravity survey shows that the decrease rate is 0.4~0.8 mgal/km.

In addition, geophysical traverses across the Tonga-Kermadec arc-trench, the southern East Pacific Rise (Leg1), the Bellingshausen Sea, the Amundsen Sea, the Eltanin-Udintzev fracture zones (Leg3), the South Fiji Basin, the Solomon arc-trench, and the West Caroline Plateau were obtained during the cruise.

Keywords: Chile Triple Junction, Gravity Anomaly, R/V MIRAI

©2019. Japan Geoscience Union. All Right Reserved.

Magnetic and Magnetotelluric surveys across the Afar depression, transition between continental rifting and sea-floor spreading

*Ryokei Yoshimura[1], Naoto Ishikawa[2], Tesfaye Kidane[3], Shin-ichi Kagashima[4], Nobutatsu Mochizuki[5], Ameha Atnafu Muluneh[3], Kirika Kitagawa[4], Taito Ikema[6]

1. Disaster Prevention Research Institute, Kyoto University, 2. Graduate School of Human and Environmental Studies, Kyoto University, 3. Addis Ababa University, 4. Faculty of Science, Yamagata University, 5. Priority Organization for Innovation and Excellence, Kumamoto University, 6. Faculty of Science, Kyoto University

The Afar area (Ethiopia) is well known as one of continental rifts transitioning to oceanic spreading centers. In order to delineate subsurface electric properties and document an initial stage of the formation process of magnetic stripes, we carried out wideband magnetotelluric (MT) measurements and ground magnetic survey along a common profile in 2016 and 2017. This profile, approximately 55km long, cuts across the Dabbahu rift in the Afar Depression. In magnetic survey on foot, we recorded total magnetic fields at 2.4 meters above the ground every 4 seconds by utilizing GSM-19 Overhauser magnetometer (GEM systems). In MT survey, we obtained electromagnetic and electric data at 14 sites using MTU-5A (Phoenix Geophysics) and ELOG1K-PHX (NT system design) systems. In this presentation, we will introduce the outline of our project and show results of magnetic and MT surveys.

Keywords: Afar depression, sea-floor spreading, magnetotelluric survey, magnetic survey

©2019. Japan Geoscience Union. All Right Reserved.

Evolution of oceanic core complexes in the Shikoku Basin: when backarc basins cease to open

*Kyoko Okino[1], Yasuhiko Ohara[2,3], Masakazu Fujii[4], Tomoko Hanyu[1]

1. Atmosphere and Ocean Research Institute, The University of Tokyo, 2. Japan Coast Guard, 3. Japan Agency for Marine-Earth Science and Technology, 4. National Institute of Polar Research

How and why backarc basins cease to open is one of the unsolved questions in plate tectonics. The Shikoku Basin is a typical backarc basin, that was formed behind the proto Izu-Bonin arc and stopped opening at ca.15 Ma. The post-spreading volcanism has formed a series of seamounts along the remnant spreading axis in the northern basin, whereas multiple oceanic core complexes have developed just before the spreading stop in the southern basin. Oceanic core complexes (OCC) are exposed lower crust and/or upper mantle materials along detachment faults, that are supposed to develop when melt supply rate M (=magmatic accommodation / plate separation) is around 0.5. The OCC is, therefore, a good indicator for temporal variation of melt supply when the backarc system died. During Yokosuka YK18-07 and Hakuho-maru KH-18-02 cruises in 2018 summer, we conducted the geophysical mapping (multibeam bathymetry, scalar and vector magnetics, and gravity) of an OCC at 23°50’ N, 138°50’ E in the southernmost Shikoku Basin and its adjusting areas. The OCC is tentatively named Mado Megamullion. We compiled these new datasets and previously collected data and analyzed detailed bathymetry and magnetic and gravity anomalies. In this presentation, we show the results and discuss the structure and evolutionary process of this OCC and its implications for demise of backarc opening system.

The Mado Megamulliion is about 20 km square domed high, located at the intersection of remnant ridge segment and transform fault. Its surface is characterized prominent corrugations parallel to flow lines. The mantle Bouguer anomaly is about 20mGal higher than the surroundings. This observation is consistent with the fact that high-density gabbro and peridotite samples were recovered both by Shinkai6500 dive in YK18-07 and dredge hauls in KH-18-02. A part of recovered rock samples show the deformation structure, suggesting that the surface of this OCC is a detachment fault surface. Magnetic anomaly distribution shows generally linear, positive and negative bands over the OCC as same as in the well-ordered abyssal hill area, suggesting continuous crust formation from ridge segments. The widths of lineations are, however, longer at the OCC, indicating clear asymmetric spreading during detachment faulting. The spreading asymmetry is often observed over world OCC areas. The equivalent magnetization value seems to be positively shifted, that may suggest the effect of induced magnetization of OCC massif. The result of vector magnetic field analysis shows clear, strong and ridge-parallel magnetic boundaries in well-ordered abyssal hill areas, that is consistent with normal seafloor spreading and block model. In contrast, the clear, systematic magnetic boundaries don’t exist. The estimated three dimensionality is not so strong. Within the rift valley south of the Mado Megamullion, a small domed high with high Bouguer anomaly exists. This is likely NTO (non-transform offset) massif, previously reported along mid-ocean ridges. Another corrugated surface is observed at neighboring segment, that shows typical detachment surface morphology but are not accompanied by gravity anomalies.
The structure and evolutionary process of the Mado Megamullion and the adjacent OCC-like massifs infer the temporal variation of melt supply on the final stage of backarc opening. Multiple core complexes including world largest Godzilla Megamullion are distributed along the Parece Vela Rift, south of the study area. The integrated analysis of these OCCs is a key to understand the demise of backarc systems.

©2019. Japan Geoscience Union. All Right Reserved.

Keywords: backarc opening, oceanic lithosphere, oceanic core complex

©2019. Japan Geoscience Union. All Right Reserved.

Thermal evolution of the Lanzo orogenic peridotite massif in western Alps: implications on thermal structure near subcontinental lithosphere-asthenosphere boundary

*Tomo Aoki[1], Kazuhito Ozawa[1], Jean-Louis Bodinier[3], Françoise Boudier[2]

1. The University of Tokyo, 2. Montpellier 2 University, 3. Geosciences Montpellier

Lithosphere-asthenosphere boundary (LAB) is a zone where heat, momentum, and materials are exchanged between conductive mantle and underlying convective mantle, and plays an important role in plate tectonics (McKenzie & Priestley, 2005; Fischer et al., 2010; Kawakatsu & Utada, 2017). Its internal structure and dynamic behavior are, however, far from understood. This study addresses this issue on the basis of petrological study of an orogenic peridotite complex. Lanzo massif in the western Alps, Northern Italy. We attempt to clarify temporal change of internal thermal structure of the complex during exhumation, from which the original thermal structures before exhumation may be estimated.
Lanzo massif is one of the largest mantle exposure thought to be a subcontinental lithospheric mantle exhumed related to the opening of the Jurassic Piedmont Sea between European continent and Adriatic continent, following slow spreading of the Atlantic mid ocean ridge (Müntener & Piccardo, 2003). The massif consists dominantly of plagioclase-bearing lherzolite, stable at the pressure lower than 1GPa, with subordinate amount of mafic rocks occurring as layers or dikes (Bodinier, 1988; Bodinier et al., 1991). The Lanzo massif divided into three bodies on the basis of petrographic characteristics: north, central and south. Previous studies argued that the northern part represents subcontinental lithospheric mantle and that the southern part may be of asthenospher origin (Bodinier, 1988; Bodinier et al. 1991). Therefore, the complex may represent a zone of lithosphere-asthenosphere boundary and can provide information on processes operated there (Bodinier, 1988; Bodinier et al., 1991; Kaczmarek & Müntener, 2008).
We examined plagioclase-bearing lherzolite collected from 16 localities covering the entire massif. Systematic variations of microstructures and mineral chemical compositions were confirmed, which is principally consistent with previous studies (Bodinier, 1988; Bodinier et al., 1991). All constituent minerals show chemical heterogeneity on grain scales, which is regarded as record of various processes the rocks underwent. Grain-scale zonings of Al and Ca in pyroxene, fluorescence-corrected Ca in olivine adjacent to pyroxenes, Cr and Al in spinel adjacent to plagioclase, and Ca and Na in plagioclase suggest that monotonous cooling and decompression accompanied by deformation occurred during decompression of the Lanzo massif. We quantified the space-dependent thermal history of Lanzo by using Ca-in-orthopyroxene geothermometer after Lindsley (1983) and Ca-in-olivine geothermometers calibrated on the basis of experimental results of Köhler & Brey (1990). All the estimated temperatures decrease from the southern body towards the northern body. The calculated temperatures were critically examined if they represent closure temperatures or a condition at which Lanzo resided for a certain period of time. The grain-scale zoning patterns indicate that the temperatures from core of orthopyroxene recorded a long residence, whereas those from rim of pyroxenes and both core and rim of olivine represent closure temperatures (Tc) at various timings during monotonous cooling. The decrease in temperatures of pyroxene cores from the south to the north by ~60K may represent a geotherm near LAB zone. All the Tc decrease from the north to the south and the difference of temperatures between the core and rim of orthopyroxene increases from the southern body to the northern body. This suggests that the cooler and probably shallower northern body cooled at slower rate at a wide temperature range (Tc=700-1100˚C) than the hotter and probably deeper southern body. A thermal gradient recorded in the Lanzo massif is estimated to be ~6K/km, which is greater than those estimated for deep subcontinental

©2019. Japan Geoscience Union. All Right Reserved.

lithosphere at steady thermal state (Mckenzie et al., 2005). We speculate that the high geotherm might have caused by thermal perturbation from asthenosphere.

Keywords: lithosphere-asthenosphere boundary, mantle peridotite, thermal structure

©2019. Japan Geoscience Union. All Right Reserved.

Comparison of the back-arc basins of the South and the Central Ryukyus in the northwest Pacific

*Kohsaku Arai[1], Ayanori Misawa[1], Takahiko Inoue[1]

1. Institute of Geology and Geoinformation, National Institute of Advanced Industrial and Technology

The Ryukyu Arc, which extend for over 1200 km along the east coast of Asia from Kyushu to Taiwan, and the associated Ryukyu Trench, are products of the subduction of the Philippine Sea Plate (PSP) beneath the Eurasian Plate. The PSP is subducting northwestward beneath the Eurasian Plate at a convergence rate of 4–9 cm/yr (Seno et al., 1993). The major islands of the Ryukyu Arc are considered the forearc highs.
The Okinawa Trough is a back-arc basin located beside of the Ryukyu Arc that was formed in the late Miocene (Gungor et al., 2012) or the late Pliocene–early Pleistocene (Sibuet et al., 1998). Formation of the Okinawa Trough was a key geological event associated with complex tectonics and changes in the topographic configuration of the Ryukyu Arc. Geological Survey of Japan (GSJ), AIST has started the marine geological mapping project around Ryukyu Arc since the 2008 FY. Multi-channel (16 ch or 32 ch) high-resolution seismic profiles were acquired during these cruises by the GI-gun (355cu. inch) systems. In our investigation into the deformation of the Ryukyu Arc using the high-density seismic profiles, we found that the normal faults parallel to the trench axis are well developed on the back-arc side of the arc. Slope of northern off the Southern Ryukyu (Miyako-jima and Ishigaki-jima) is simply downthrown to the axis of Okinawa Trough and reach to 2000 m in depth. In the other hand, the Central Ryukyu, northwestern off the Okinawa-jima is characterized by the small basin structure which accompanies with active normal faults. The faults show ENE-WSW strike and dip to the north with clear half graben structure. We present the tectonics of these structure compare the back-arc basins of the South Ryukyu with the Central Ryukyu.

Keywords: Ryukyu Arc, back-arc basin, Quaternary, seismic reflection survey, MCS

©2019. Japan Geoscience Union. All Right Reserved.

Geochemistry and zircon U-Pb ages of mafic rocks in the Mikabu and Sorachi-Yezo belts: Comparison with the Shatsky Rise

*Naoto Kimura[1], Yuji Ichiyama[1], Shohei Takahashi[1], Hisatoshi Ito[2], Akihiro Tamura[3], Tomoaki Morishita[3]

1. Chiba University, 2. Central Research Institute of Electric Power Industry, 3. Kanazawa University

Large igneous provinces (LIPs) are large volcanic edifices on the Earth, such as oceanic plateaus and continental traps. It is commonly believed that LIPs are formed by large-scale magmatism caused by the upwelling of unusually hot mantle plume from the deep mantle (e.g., Coffin and Eldholm, 1994). Therefore, the genesis and formation mechanisms of LIPs is crucial to understand the dynamics of the Earth’s interior and episodic global events. Recent studies have revealed that the fragments of accreted oceanic plateaus are preserved in orogenic belts as ophiolites and accretionary complexes (e.g., Kerr et al., 2000; Ichiyama et al., 2014). The investigation of accreted oceanic plateaus will help to enhance our understanding of LIPs.

The Mikabu belt in SW Japan and Sorachi-Yezo belt in central Hokkaido, North Japan contain large accreted fragments of a paleo-oceanic plateau (Kimura et al., 1994). Recently, Ichiyama et al. (2014) proposed that the Mikabu and Sorachi-Yezo picrites with highly magnesian olivine phenocrysts (up to Fo_{94}) were produced by an unusually hot mantle plume. They also suggested that these picrites are derived from the Late Jurassic oceanic plateau (hereafter named “Mikabu-Sorachi plateau”) formed on the Izanagi plate, which was possibly produced together with the Shatsky Rise at the Pacific-Izanagi-Farallon triple junction in the Pacific Ocean. However, the geochronological and geochemical comparison between the Mikabu-Sorachi and Shatsky Rise has been poorly constrained.

The Mikabu and Sorachi-Yezo mafic rocks are geochemically divided into depleted (D)-type and enriched (E)-type in the same manner as the picrites. The D-type is depleted in light rare earth elements (LREE), whereas the E-type is relatively enriched in LREE. These types were produced by higher degrees of partial melting (30-50%) than MORB. The U-Pb zircon analyses of gabbroic rocks in both belts yield the weighted mean $^{206}Pb/^{238}U$ zircon ages of 153.1-146.3 Ma for the Mikabu rocks and 146.2 and 137.6 Ma for the Sorachi-Yezo rocks.

A wide geochemical variety of basalts were recovered from the Shatsky Rise during the IODP Expedition 324 (Expedition 324 Scientists, 2010; Sano et al., 2012). The U1349-type and Normal-type basalts of the Shatsky Rise are closely similar in geochemical composition to the Mikabu-Sorachi D-type and E-type rocks, respectively. The radiometric ages of the Shastky Rise basalts show 144.6-133.9 Ma (Mahoney et al., 2005; Geldmacher et al., 2014). The magnetic anomaly lineations of the Shatsky Rise exhibit that the formation of the rise started at M21 (about 147 Ma). The zircon U-Pb ages of the Mikabu-Sorachi mafic rocks are almost coeval with the formation ages of the Shatsky Rise. However, the older radiometric ages than 147 Ma are shown in this study. Recently, Sawada et al. (2019) also report the zircon U-Pb age of 154.6 Ma for the Mikabu metabasite from the Toba area.

The magnetic anomaly lineation of M29 (about 157 Ma) drawn at the southwest of the Shatsky Rise implies that the triple junction was already present at 157 Ma. The Mikabu-Sorachi plateau was produced on the Izanagi plate before the Shatsky Rise at the triple junction. The igneous rocks in the Mikabu-Sorachi belt possibly record the information on initiation mechanisms of the triple junction and

©2019. Japan Geoscience Union. All Right Reserved.

initial stages of LIPs formation in the paleo-Pacific Ocean.

Keywords: Mikabu belt, Sorachi-Yezo belt, Shatsky Rise, zircon U-Pb age, Large igneous provinces (LIPs), mantle plume

©2019. Japan Geoscience Union. All Right Reserved.

Submersible magnetics reveals relationship between off-axis volcanism and hydrothermal systems of the Kairei and Yokoniwa fields at the Central Indian Ridge

*Masakazu Fujii[1], Kyoko Okino[2]

1. National Institute of Polar Research and SOKENDAI, 2. Atmosphere and Ocean Research Institute, The University of Tokyo

The Kairei (KHF) and Yokoniwa hydrothermal fields (YHF)are hosted in mafic as well as ultramafic rocks distributed at an off-axis volcanic knoll of the Central Indian Ridge. Despite intensive investigations, their geological and geophysical background is still debated. Here, we show the results of near-seafloor magnetic anomaly surveys conducted using a submersible. We investigated the bulk magnetization of the hydrothermally altered zone and the surrounding lava flows and evaluated their intensities compared with previously reported values at axial areas of seafloor spreading environments. The KHF is characterized by low coherence between observed and modeled anomalies and low values of magnetization. This result suggests that magnetic minerals within basaltic lava flows were likely altered by hydrothermal fluid circulation. The variation pattern in the observed magnetic anomalies above the lava flows is in phase with that of the modeled magnetic anomalies for the simple assumption that the magnetization direction is parallel to the geomagnetic field. This result suggests that these lava flows preserve normal magnetic polarity corresponding to the Brunhes Chron. The estimated magnetic-anomaly-derived absolute magnetizations (MADAM) show a reasonable correlation with the natural remanent magnetizations of rock samples collected from the seafloor of the same region; their relationship is consistent with previously reported datasets from the Mariana Trough and Mid-Atlantic Ridge. The estimated MADAM intensity reaches 20 A/m in the study area, which is clearly greater than those of previously reported off-axis areas, suggesting that recent volcanic eruption may have occurred in these off-axis areas. The high magnetization distributions are commonly observed at the bottoms of the western slope from the KHF and YHF. This finding provides new insight into the distribution of highly magnetized lava flows in the off-axis areas and indicates the distribution of recent off-axis volcanic activities, which is potentially linked to the sub-seafloor hydrothermal circulation.

Keywords: Central Indian Ridge, Seafloor hydrothermal system, Near-seafloor magnetic anomaly

©2019. Japan Geoscience Union. All Right Reserved.

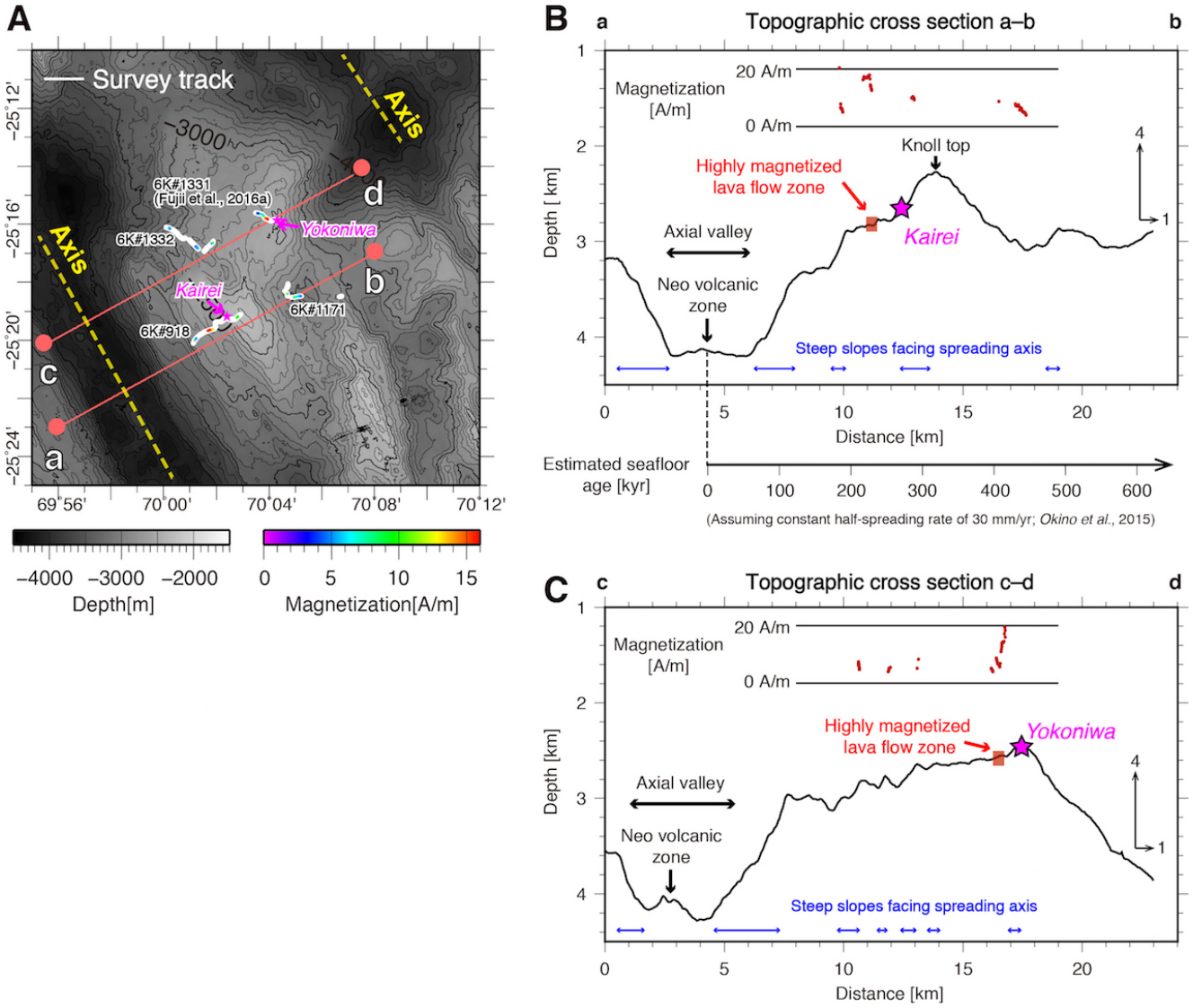

©2019. Japan Geoscience Union. All Right Reserved.

Shipboard magnetic and gravity surveys around the Iheya North Knoll and the Iheya Minor Ridge in the Mid-Okinawa Trough: Preliminary results of KR18-14 Leg1/Leg2 cruises

*Kazuya Kitada[1], Takafumi Kasaya[1], Hisanori Iwamoto[1], Yoshifumi Nogi[2]

1. Japan Agency for Marine-Earth Science and Technology, 2. National Institute of Polar Research

The Okinawa Trough, an active back-arc basin behind the Ryukyu trench, exhibits active rifting associated with extension of the continental margin. In the Mid-Okinawa Trough, more than 10 hydrothermal vent sites belonging to relatively large hydrothermal vent fields at the Iheya North Knoll, the Iheya Minor Ridge, the Izena Hole and etc., were discovered by previous studies (e.g., Halbach et al., 1989; Sakai et al., 1990; Momma et al., 1996; Kasaya et al., 2015; Nakamura et al., 2015). Although shipboard magnetic and gravity surveys are too low in resolution to investigate the hydrothermal sites, they are important for understanding the geological background of the hydrothermal systems across an entire region. As for the area off Kumejima Island in the Okinawa Trough, Kitada et al. (2018) revealed the characteristics of the submarine volcanic activity around a hydrothermal area by using dense magnetic and gravity data. In order to characterize sub-seafloor structures and the spatial distribution of the submarine volcanic activity around the Iheya North Knoll and the Iheya Minor Ridge, we conducted detailed magnetic and gravity surveys with a line spacing of 0.5 nmi aboard research vessel Kairei during the KR18-14 Leg1 and Leg2 cruises from October to November 2018. Additionally, we also compiled magnetic, gravity and bathymetric data which were collected during previous cruises by the Japan Agency for Marine-Earth Science and Technology (JAMSTEC) over the recent years. Magnetization intensities were estimated from observed magnetic anomalies, without applying annihilator. Bouguer gravity anomalies were calculated from free-air anomalies obtained. The distribution of magnetization intensity and variation in Bouguer gravity anomalies revealed the characteristics of submarine volcanic activity. Most of the knolls in the area show a relatively high magnetization (~1.0 to ~3.0 A/M) corresponding to the individual submarine knolls. Higher Bouguer gravity anomalies (~45 to ~55 mgal) implying the lower crustal thickness were observed in the Iheya graben. The knolls including the Iheya Minor Ridge, elongated in the ENE-WSW direction parallel to the graben, exhibit the ENE-WSW trending magnetization distribution with relatively high positive intensities, so volcanism appears to be constrained by normal faults forming the rift structure. On the other hand, the Iheya North Knoll have a relatively low magnetization of ~-1.0 to ~0.0 A/M with less variation of the magnetization. Although the data are sparse (the line spacing of ~1.5 to ~2 nmi), low magnetization (~1.5 A/M) with no prominent magnetic signature was also observed in the Izena Hole. Moreover, these knolls are located on the area where the Bouguer gravity anomaly is changed from ~30 to ~10 mgal and ~45 to ~30 mgal, respectively. The magmatism associated with submarine volcanic activity and back-arc rifting will be discussed based on the results obtained from these dense surveys.

Keywords: Okinawa Trough, backarc rifting, hydrothermal systems, magnetic anomaly, gravity anomaly

©2019. Japan Geoscience Union. All Right Reserved.

A shallow scientific drilling at Higashi Ensei Hydrothermal Field, Okinawa Trough

*Hidenori Kumagai[1], Takafumi Kasaya[1], Shuhei Totsuka[2], Shinsuke Kawagucci[1], Hideaki Machiyama[1], Koichi Iijima[1], Hirofumi Yamamoto[1], junji kaneko[1], Yusuke Ohta[3], Shohei Albert Tomita[3], Shogo Komori[4]

1. Japan Agency for Marine-Earth Science and Technology, 2. Kyushu Univ., 3. Kyoto Univ., 4. AIST

A shallow seabed drilling was performed in February 2019 at Higashi Ensei Hydrothermal Field, Northern Okinawa Trough (Cruise ID: KM19-E01). Two localities were selected to investigate natures of sub-seafloor lithology with and without self-potential anomaly (SP anomaly) measured by near-bottom AUV survey. Here such a SP anomaly is to be resulted from a sub-seafloor orebody consisted of mainly sulfides. A seabed drilling apparatus, BMS (Boring machine system, Cellula Robotics Ltd.), was deployed twice from R/V Kaimei. At the first drilling in the cruise, the drilled hole reached to a formation 44m beneath the seafloor but stopped there due to significant venting through the drilled hole. Volcaniclastics with and without sulfide blocks or veins were sampled even poor recovery in the shallow part of the hole. Contrasting to it, the second drilled hole reached to 10 m beneath the seafloor where intact mafic-intermediate lava flow, i.e. volcanic basement, was sampled. In the second hole, little sulfide were retrieved except orange-colored one, probably realgar associating with orpiment and stibnite, in the first core, shallower than 1.5mbsf. On board IP measurement both as well as standard MSCL and visual core description were performed for the cores from the first hole. Further, an ROV dive observation was conducted within 16.5 hours after the drilling of the first hole. An exotic white sediment was recognized in the vicinity of the hole, similarly to the IODP exp.331 at Iheya-North Knoll, and successfully sampled. In this presentation, retrieved drilled samples as well as those sampled by ROV will be reported.

Keywords: A seabed driling system, Self-potential anomaly, An exotic white sediment around the drilled hole

©2019. Japan Geoscience Union. All Right Reserved.

Mineralogical and geochemical study of sediment cores collected from the Gondou hydrothermal field in the Okinawa Trough

*Jun-ichiro Ishibashi[1,2], Shuhei Totsuka[2], Akihi Tsutsumi[2], Naru Tsukamoto[2], Yusuke Kira[2], Kazuhiko Shimada[1], Toru Yamasaki[3], Ken Ikehara[3], Toshiro Nagase[4], Yutaro Takaya[5,9], Kei Ikehata[6], Takashi Goto[7], Chitaro Gouzu[7], Ryuichi Shinjo[8], Hideaki Machiyama[9], Koichi Iijima[9], Hirofumi Yamamoto[9], Hidenori Kumagai[9]

1. Department of Earth and Planetary Sciences, Kyushu University, 2. Graduate School of Science, Kyushu University, 3. National Institute of Advanced Industrial Science and Technology, 4. Tohoku University Museum, 5. School of Creative Science and Enginerring, Waseda University, 6. Faculty of Life and Environmental Sciences, University of Tsukuba, 7. Hiruzen Institute for Geology and Chronology, 8. Faculty of Science, University of the Ryukyus, 9. Japan Agency for Marine-Earth Science and Technology

Intense hydrothermal activity associated with sulfide mineralization had been observed in the Gondou field, which is located at the seafloor around a water depth of 1330-1470 mbsl (meters below the sea level) at the western flank of the Daisan-Kume Knoll (Minami and Ohara, 2017; Ishikawaet al., 2016). Scientific drilling was performed by J-MARES during the SIP Integrated Ocean Resource Surveying System JM17-04 Cruise from October to November, 2017. Sediment cores were obtained from 5 sites in Southern area of the Gondou field by drilling using BMS (Benthic Multi-coring System) installed on *Shincho-maru*. Mineralogy and geochemistry of the obtained cores were studied based on VCD (Visual Core Description), microscopic observation, XRD (X-ray diffractometer) analysis, and electron probe microanalyzer (EPMA) analysis.
Most part of the obtained sediment, except for the surface hemipelagic sediment within a few mbsf (meters below the seafloor), was hydrothermally altered intensely. Abundant occurrence of illite (or illite/smectite mixed-layer mineral) was observed, which is common signature among hydrothermal alteration in hydrothermal fields in the Okinawa Trough. Whereas, occurrence of chlorite was limitedly recognized within a layer of 5-15 m thickness in each site. Kaolin minerals were identified in altered pumiceous volcaniclastic sediment in two sites. These specific occurrences may reflect subseafloor fluid migration of distinctive chemistry, based on the idea that chlorite formation would be related to interaction with heated seater-derived fluid while kaolin minerals formation would be related to interaction with acidic fluid. Occurrence of sulfate minerals such as anhydrite and barite is also limited, which may provide another information about subseafloor fluid migration.

Acknowledgements
This study was conducted under the framework of the Next-Generation Technology for Ocean Resources Exploration Project, Cross-ministerial Strategic Innovation Promotion Program (SIP) funded by the Japanese cabinet office. The sediment cores used in this study were provided from J-MARES (Research and Development Partnership for Next Generation Technology of Marine Resources Survey).

Keywords: seafloor massive sulfide deposits, seafloor scientific drilling, hydrothermal alteration

©2019. Japan Geoscience Union. All Right Reserved.

New type of self-potential anomaly observed near a hydrothermal site of Oomuro-dashi volcano, Izu-Ogasawara arc

*Yoshifumi Kawada[1,2], Takafumi Kasaya[2]

1. International Research Institute of Disaster Science, Tohoku University, 2. Japan Agency for Marine-Earth Science and Technology

Using a deep-towed electrode array, we identified a pair of positive and negative self-potential anomalies observed near an active hydrothermal field associated with a quarterly rhyolitic volcano, Oomuro-dashi, Izu-Ogasawara arc. Results with different rowed directions, the magnitude of both anomalies is of the order of millivolt. The negative anomaly is located immediately above the most active area; the positive self-potential anomaly is located a few hundreds of meters away from the most active hydrothermal area, where no apparent hydrothermal activity has been detected. The discovery of the positive self-potential anomaly in marine environments is probably the first time.

The origin of the negative self-potential anomalies may be explained by the geo-battery mechanism (Sato and Mooney, 1960), in which the presence of a conductive ore body crossing the redox gradient results in the upward electron transfer to give a negative self-potential anomaly above the body. Oxidized materials near the seafloor are reduced. In other words, an ore body near the seafloor behaves as a cathode. We have reported negative self-potential anomalies many times above hydrothermal areas of other sites (e.g., Sato et al., 2017; Kawada and Kasaya, 2017, 2018).

The origin of this newly founded positive self-potential anomaly is problematic. One possibility is that an anode of the geo-battery, where reduced materials are oxidized, is exhumed near to the seafloor. If this is true, shallow drilling or piston coring may confirm signals from oxidized chemical reactions around an anode. This is important for the understanding of the geo-battery because its anode is usually located far below the seafloor and cannot be accessed easily. Another possibility is the streaming potential, which is caused by a local charge imbalance due to the flow of electrolytes in the pore space. Although this mechanism is estimated to be minor in marine environments, a positive self-potential anomaly of the order of one millivolt may not be immediately rejected above an area of upward fluid flow. However, the area of this positive self-potential anomaly is away from the active hydrothermal site, where upward fluid discharge is expected.

Keywords: geophysical exploration, marine resource, ore deposit, redox reaction, hydrothermal circulation

©2019. Japan Geoscience Union. All Right Reserved.

Numerical simulation of submarine hydrothermal ore-deposits due to a coupled process of fluid migration and reactive geochemical transport

*Claudia Fujita[1], Hajime Yamamoto[1], Jun-ichiro Ishibashi[2], Takeshi Tsuji[3]

1. Taisei Corporation, 2. Department of Earth and Planetary Sciences, Faculty of Science, Kyushu University, 3. Department of Earth Resources Engineering, Faculty of Science, Kyushu University

Submarine hydrothermal ore-deposits are known to be rich in metal resources and are to be found abundant around the Japanese islands. In recent years, several studies (mostly field surveys) had been carried out and a lot of data on chemical, physical and biological properties of compounds have been gathered especially for hydrothermal fields in the Okinawa Trough. However, the mechanism of formation (hydrothermal fluid flow in combination with geochemical reaction) of these deposits is not yet clearly understood.

Hydrothermal ore-deposits are formed by precipitation of metal elements from hydrothermal fluid due to rapid cooling around the seafloor where the fluid discharges. Contrary to the hydrothermal systems in the mid-ocean ridges, hydrothermal systems in the Okinawa Trough has a fluid discharge region at the seafloor in sediment-rich environment. The sediment is often composed of two components; one is hemipelagic sediment possibly transported from the continental margin and the other is volcaniclastic sediment derived from felsic volcanism in the vicinity. Because these two components have quite different permeability, it is expected complicated fluid migration within the discharge region.

In this study, we investigated the above process using a numerical code TOUGHREACT V3.0 –OMP, which is for coupled non-isothermal multiphase fluid flow and geochemical reactive transport. A 2-dimensional radial model with the radius of 5 km and a depth of 1 km below the seafloor was chosen to represent a sufficient area of the discharge region around the hydrothermal vent. The center of the radial model represented a fluid conduit (10 cm diameter) where the venting hydrothermal fluid of 300 ˚C ascends from basal to the seafloor, with a flow rate of ~1000 t/day. Almost all model parameters are chosen based on available results of geophysical survey of the Iheya hydrothermal fields in the Okinawa Trough[1)]. The geological structures were set as having diverse permeability from 1×10^{-10} m^2 to 1×10^{-16} m^2, which reflects alternating pumiceous volcaniclastics layer and hemipelagic sediment layer. The initial thermal gradient was set to 4.8 ˚C/100 m. The top boundary (seafloor) was set to constant pressure condition (20 MPa) and a basal heat flux was also imposed at the bottom (5.6×10^{6} W/m^2), assuming a pumice thermal conductivity of 0.96 W-m/˚C.

The geochemical setting included initial concentrations of primary species, as, for instance, Na^{+}, SO_4^{-2}, H_4SiO_4, Ca^{+2}, S^{-2}, Zn^{+2}, HCO_3^{-} or NH_3 for seawater and hydrothermal fluid separately. Chemical reaction including precipitation of minerals) caused by mixing of the both fluids and cooling was considered in this setting. In order to simulate accumulation of mineral precipitations to form hydrothermal deposits over a long-time duration (an order of thousands of years), the numerical simulation was conducted for 10000 years.

As a result, the following features were clarified: First, high velocity venting hydrothermal fluid ascends to the seafloor through the fluid conduit at the center of the model, whereas nearby cold water percolates downward from the seafloor and convection occurs. Second, among the alternating layer structure, preferential horizontal flow is obvious for layers with high permeability, which resulted in primary sulfide precipitation with a lateral extend.

These results are likely to be consistent to recent field studies during scientific drilling into the submarine

©2019. Japan Geoscience Union. All Right Reserved.

hydrothermal fields in the Okinawa Trough, Japan.
This study was conducted in co-operation with Kyushu University as a part of the “Next-Generation Technology for Ocean Resources Exploration (Zipangu-in-the-Ocean Project)”, a sub-topic of the Cross-ministerial Strategic Innovation Promotion Program (SIP) led by the Cabinet Office's Council for Science, Technology and Innovation.

1)Tsuji, T., Takai, K., Oiwane, H., Nakamura, Y., Masaki, Y., Kumagai, H., ... Kuramoto, S. (2012). Hydrothermal fluid flow system around the Iheya North Knoll in the mid-Okinawa trough based on seismic reflection data. Journal of Volcanology and Geothermal Research, 213-214, 41-50, doi:10.1016/j.jvolgeores.2011.11.007

Keywords: submarine hydrothermal ore deposit, hydrothermal convection, TOUGHREACT, coupled hydrothermalfluid flow with reactive geochemical transport

©2019. Japan Geoscience Union. All Right Reserved.

Mineral composition and grain size distribution of REY-rich mud in the Minamitorishima EEZ: Implication for formation process of extremely REY-rich mud

*Sakai Takumi[1], Erika Tanaka[1], Kazutaka Yasukawa[1,2], Junichiro Ohta[2,1], Koichiro Fujinaga[2,1], Kentaro Nakamura[1], Yasuhiro Kato[3,1,2]

1. Department of Systems Innovation, School of Engineering, University of Tokyo, 2. Ocean Resources Research Center for Next Generation, Chiba Institute of Technology, 3. Frontier Research Center for Energy and Resources, School of Engineering, The University of Tokyo

In 2011, it was reported that deep-sea sediments containing high concentrations of rare-earth elements and yttrium (REY) are widely distributed in the Pacific Ocean, and can constitute a new mineral resource for the industrially critical elements [1]. Moreover, the “extremely REY-rich mud” containing more than 5,000 ppm of total REY (ΣREY) was discovered within the Japanese exclusive economic zome (EEZ) around Minamitorishima Island [2], and various researches to reveal a detailed spatial distribution of the extremely REY-rich mud has been carried out [3]. However, the formation mechanism(s) of the extremely REY-rich mud have not been completely elucidated yet.

Recently, based on multi-elemental compositions of 49 piston core samples collected from the Minamitorishima EEZ, it was confirmed that the deep-sea sediments in the area could be classified into nine sedimentary units based on characteristic chemical compositions [4]. This chemostratigraphy indicated that there are at least three “ΣREY peaks” containing 2,000 ppm of ΣREY in the Minamitorishima EEZ [4]. A previous study targeting the extremely REY-rich mud corresponding to the 1st ΣREY peak (i.e, the shallowest ΣREY peak in the chemostratigraphy) demonstrated that grain sizes of biogenic Ca-phosphate (BCP) and authigenic phillipsite were largest in the horizon with the maximum ΣREY concentration, based on analyses of mineral composition and grain size distribution [5]. However, whether this feature is common in all of the ΣREY peak units remains uncertain. In addition, no systematic investigation of relationships between each chemostratigraphic unit and mineral composition and grain size distribution has been carried out.

Here, we aimed to characterize each chemostratigraphic unit from the perspectives of the mineral composition and grain size distribution, and also to provide a constraint on the formation process of the extremely REY-rich mud. We selected 80 sediment samples from the 17 piston cores collected within the Minamitorishima EEZ to cover all units of the chemostratigraphy. The mineral composition was estimated by microscopic observation following the standard protocols of the International Ocean Discovery Program. The grain size distribution was measured by using laser diffraction spectroscopy. As the result, we revealed systematic variations in mineral composition and grain size distribution of each chemostratigraphic unit, and confirmed that grain sizes of BCP and phillipsite in all the ΣREY peak units were coarser (i.e., more enriched in silt- to sand-sized fractions) than other units. The increased sizes of BCP grains as a common feature of the ΣREY peaks imply that a grain-size sorting by enhanced bottom currents concentrated coarse BCP grains on the seafloor and contributed to the formation of extremely REY-rich mud for multiple times throughout the sedimentary history of the area.

Reference

©2019. Japan Geoscience Union. All Right Reserved.

[1] Kato et al. (2011) Nature Geoscience, 4, 535–539.

[2] Iijima et al. (2016) Geochemical Journal, 50, 557–573.

[3] Takaya et al. (2018) Scientific Reports, 8, 5763.

[4] Tanaka et al. Submitted to Ore Geology Reviews.

[5] Ohta et al. (2016) Geochemical Journal, 50, 591–603.

Keywords: REY-rich mud, grain size distribution, mineral composition, chemostratigraphy, deep-sea sediments

©2019. Japan Geoscience Union. All Right Reserved.

Geochemical and morphological features of manganese micronodules in REY-rich mud within the Minamitorishima EEZ, western North Pacific Ocean

*Satoshi Kino[1], Kazutaka Yasukawa[1,2], Keishiro Azami[1], Erika Tanaka[1], Koichiro Fujinaga[2,1], Kentaro Nakamura[1], Yasuhiro Kato[1,2]

1. Department of Systems Innovation, School of Engineering, University of Tokyo, 2. Ocean Resources Research Center for Next Generation, Chiba Institute of Technology

Manganese micronodules are small grains (< 1 mm) composed of manganese oxides, and constitute one of the important components of pelagic sediments. The micronodules show high contents of various heavy metals, especially of some redox-sensitive transition metals [1]. In addition to chemical compositions, the abundance and texture of micronodules can be affected by sedimentation rates and/or redox conditions of the sediment column [1, 2]. Therefore, the micronodules have been regarded as a useful indicator of the sedimentary environment.

Recently, deep-sea sediment extremely enriched in rare-earth elements and yttrium (REY) was discovered within the Japanese exclusive economic zone (EEZ) around Minamitorishima Island [3]. Previous studies reported that the extremely REY-rich mud contains significant amounts of biogenic calcium phosphate, which is a main host of REY, and phillipsite grains [3, 4]. In addition to them, manganese micronodules were also recognized in the sediment column, which were especially abundant in the extremely REY-rich layer [3, 4]. However, detailed features of the micronodules in the REY-rich mud within the Minamitorishima EEZ have not been investigated yet. Manganese micronodules in the REY-rich mud are about μm –mm ferromanganese oxides. Because their abundance and chemical compositions are considered to reflect respectively the sedimentation rate and redox conditions when they were buried [4], the micronodules can provide important constraints on the depositional environment of the REY-rich mud.

In this study, therefore, to characterize the manganese micronodules in the REY-rich mud within the Minamitorishima EEZ, we implemented (1) microscopic observations of the shape, surface texture, and relative abundance of the micronodules, and (2) bulk chemical analysis of them by using ICP-MS. We compared the geochemical features of the micronodules with those of macronodules both on the seafloor of the Minamitorishima EEZ, and also with those of macro- and micronodules in other areas.

The Minamitorishima micronodules are generally characterized by diagenetic features, although showing a compositional shift towards hydrogenetic features in some samples. Based on the integration of the observational and analytical results, we will discuss the possible changes in the sedimentary environment (e.g., sedimentation rates and redox conditions) involving the formation of the extremely REY-rich mud.

References

[1] Pattan (1993) Marin Geology 113, 331-344

[2] Svalnov et al. (2017) Oceanology 57, 3, 424-438

©2019. Japan Geoscience Union. All Right Reserved.

[3] Iijima et al. (2016) Geochemical Journal 50, 557-573.

[4] Ohta et al. (2016) Geochemical Journal 50, 591-603.

Keywords: manganese micronodules, REY-rich mud, Minamitorishima EEZ, bulk chemical composition, morphology

©2019. Japan Geoscience Union. All Right Reserved.

Seafloor sediment thickness around the Japan and Kurile trenches obtained by traveltime analysis for PS converted wave recoded by ocean bottom seismograms

*Ryosuke Azuma[1], Genti Toyokuni[1], Ryota Takagi[1], Syuichi Suzuki[1], Makiko Sato[1], Takashi NAKAYAMA[1], Naoki Uchida[1], Ryota Hino[1]

1. Recearch Center for Prediction of Earthquake and Volcanic Eruption, Graduate School of Science, Tohoku University

seafloor observation network for earthquake and tsunamis has been working in the Japan and Kurile trench subduction zones since 2016 (S-net, installed by National Research Institute for Earth Science and Disaster Resilience). The seismograms recorded by such the ocean bottom observatories are very useful for a precise hypocenter estimation. On the other hand, to obtain precise location results, it is also necessary to take suitable correction for traveltime delay due to the presence of the thick low-velocity sediments below sites, because the thickness of sediments differs with sites.

This study aims to estimate thickness of the sedimentary layer below the sites of the S-net and pop-up-type ocean bottom seismometers (OBSs). We then focused on traveltime difference between direct P-waves and PS waves converted at the sedimentary basement.

In the analysis, we first estimated a sensor direction based on gravitational acceleration and particle motions of teleseismic surface waves on accelerograms and then transformed components of velocity waveforms from XYZ to UD, NS and EW (Takagi et al., this meeting). Next, we picked PS arrivals on horizontal components of velocity records, for thirty of intraslab earthquakes observed at twenty of the S-net sites located on the outer slope of the Kurile and Japan trenches and the landward slope of the Kurile trench (off Nemuro). As a result, we obtained PS-P traveltime difference of ~1.4 s at the most of sites, ~1.6 s near the Japan and Kurile trenches junction, and 1.8 and 2.7 s on the lower and upper portions of the landward slope of the Kurile trench. Considering the standard deviation of PS-P of ~0.15 s at each site, our result suggests that PS-P traveltimes at the junction and other trench-outer region differs significantly while that variation between neighbor sites seems to be small.

The obtained PS-P traveltime differences for the outer-trench sites is consistent with those by seismic surveys (1.0–1.5 s, Kodaira et al., 2014; Fujie et al., 2016) and OBS observations (0.9–1.2 s, Hino et al., 2009) at the outer rise of the Japan trench. Therefore, picked PS arrivals on the S-net records in this study coincide with those by the previous studies. Assuming a Vp/Vs ratio of 8.0 and an average Vp of 2.0 km/s in the sediments estimated by the wide-angle seismic surveys (Kodaira et al., 2014; Fujie et al., 2016) at the Japan and Kurile trench-outer rise regions, sediments thickness below the S-net sites would be 350~400 m, which is also consistent with results of the seismic reflection section (Kodaira et al., 2014; Fujie et al., 2016). By further analysis for PS converted wave at the inner-trench sites of OBSs and S-net besides off Nemuro, we will investigate the distribution of thickness of the sedimentary layer in the forearc region of the east Japan.

Acknowledgements: We used waveform data from S-net by NIED.

©2019. Japan Geoscience Union. All Right Reserved.

Keywords: PS converted-wave traveltime analysis, Sedimentary-layer thickness, Ocean bottom seismograph (S-net and pop-up type OBS)

©2019. Japan Geoscience Union. All Right Reserved.

Examination of critical taper theory based on bathymetry data in subduction zones

*Hiroaki Koge[1], Juichiro Ashi[1], Jin-Oh Park[1]

1. Atmosphere and Ocean Research Institute, The University of Tokyo

The fold-and-thrust belts and submarine accretionary wedges lie along compressive plate boundaries. The critical taper model has been recognized to be the most appropriate theory that describes the first-order mechanics of these structures. Applying the critical taper model in the subduction zones, we can estimate the frictional coefficient of the plate boundary fault with only simple topographical parameters from the cross-section. Thus, this model has been also used in discussions related to earthquakes.
However, in the critical taper model, the following two problems could be pointed out when acquiring the topographic parameters. 1) It is impossible to apply the critical taper model to the area without seismic cross-section. 2) In the depth conversion in the seismic cross-section, the depth of the plate boundary fault largely depends on the velocity model and affects the estimation of the décollement dip angle β. Thus, it is unreliable in terms of accurate comparison. Therefore, when comparing the result with various velocity models, the reliability is low in terms of accurate comparison.
Therefore, in this research, we developed a new method to obtain the topographical parameters only from bathymetry data instead of the seismic cross-section. We verified the validity of the method from the results, with comparing the result from the décollement dip angle β obtained from the seismic cross-sections and the result from the trench seaward slope angle β obtained from the bathymetry. We check the validity of the new method using the Nankai Trough as the target area. In the Nankai Trough, many seismic cross-sections have been acquired for the disaster mitigation of the large earthquake, and the observation based on various methods such as seismic waves or GPS has proceeded. Thus, it should be easy for acquiring the topographical parameters and interpreting the result of the critical taper model.
We found the theoretical blind spot of the critical taper model in the condition of the subduction zone under the sea. When a high pore pressure ratio is assumed for the whole wedge, the effect of β on the result is very small for the effective friction coefficient. Therefore, it is sufficiently possible to discuss the frictional distribution of the plate boundary fault with only the bathymetry data. It is although necessary to pay attention to relatively large error up to about 20%. Since the bathymetry data is spatially densely acquired data, it was possible to calculate the friction distribution of the shallow plate boundary fault along the trench axis in the high density.
As a preliminary interpretation of the results with the bathymetrical critical taper model , this metho is considered to be effective to contribute to earthquake/tsunami disaster mitigation in sea areas where seismic activity segments are not sufficiently studied.

Keywords: subduction zone, critical taper model, Japan Trench, Nankai Trough

©2019. Japan Geoscience Union. All Right Reserved.

Active structures of the Sagami Bay Fault by high-resolution sub-bottom profiling and pin-point core sampling

*Juichiro Ashi[1], Asuka Yamaguchi[2], Natsumi Okutsu[1], Ayanori Misawa[3]

1. Graduate School of Frontier Sciences, The University of Tokyo, 2. Atmosphere and Ocean Research Institute, The University of Tokyo, 3. National Institute of Advanced Industrial Science and Technology

Seafloor knolls called the Okinoyama Bank Chain are aligned in the eastern slope of the NW trending Sagami Trough. Existence of the Sagami Tectonic Line is estimated at the slope base and interpreted as a tectonic boundary of a subdution zone (Kimura, 1973, Kagaku). Ohkochi (1990, Chigaku Zasshi) reported active faults and an anticlinal fold based on seismic profiles. An eastward dipping reflector is recognized at the southeastern extension of the Kozu-Matsuda Fault by onshore-offshore integrated seismic imaging and interpreted as a splay fault of the plate boundary fault (Sato et al., 2010, Annual Meeting abstract of the Geological Society of Japan). However, Deformation of shallow sediment recording recent activity has not been clarified. The purpose of this study is to reveal recent fault activity by high resolution subbottom survey and sediment sampling. We carried out deep towed subbottom survey and pinpoint sediment sampling by remotely operqated vehicle NSS in the southwest slope of the Misaki Knoll during the Hakuho-maru cruises KH-10-3, KH-11-9 and KH-16-5. NSS can take piston cores at pinpoint accuracy by four propeller thrusters, video cameras and a payload fuck. Deep towed subbottom survey can obtain high resolution subsurface structure by pinging 1.1 to 1.6 kHz chirp frequency and receiving near the seafloor. Subbottom profiles across the southwest slope base of the Miura Knoll show a reflector suggesting a fault plane at the scarp base. The reflector dips 30 degree to northeast. Although the hanging wall shows structureless, the foot wall exhibits horizontal reflectors or chaotic suggesting talus deposit. We successfully obtained a 6-meter-long core after confirming a dipping reflector of a possible fault plane. The upper 1.2 meters of the core sample consists of alternation of dark green silty mud and pebbly mud with shell fragments of Calyptogena fossils. Thin silt layers are intercalated with dark green clay at about 15 cm intervals. A 5-mm thick zone, which suggesting a fault plane and consists of silty mud and granule size clasts, is recognized at 2.25 m from the core top. This zone, dipping 30 degree toward north to east after paleomagnetic restoration, is interpreted to correspond to the reflector of the fault plane on subbottom profiles. We also present shallow subsurface structures around the Miura Knoll.

Keywords: active fault, talus deposit, active fold

©2019. Japan Geoscience Union. All Right Reserved.

Fault Distribution and Structural Characteristic in the Nankai Trough Area, Japan

*Rei Arai[1], Narumi Takahashi[1], Minako Katsuyama[1], Shigeyoshi Tanaka[1], Hiromi Kamata[1], Tomoyuki Sato[2], Takahiko Inoue[2], Yoshiyuki Kaneda[3]

1. Japan Agency for Marine-Earth Science and Technology, 2. National Institute of Advanced Industrial Science and Technology, 3. Kagawa University

As part of “The Comprehensive Evaluation of Offshore Fault Information Project” by the Ministry of Education, Culture, Sports, Science and Technology, JAMSTEC has conducted collecting marine seismic reflection/refraction data, bathymetric data, well data acquired within the Japan EEZ and surrounding areas, and assembling a database to serve data for future scientific research.

Data includes 1) seismic reflection/refraction data acquired by JAMSTEC, AIST(Japan Geological Survey), and Japan Coastal Guard for purposes of geological investigation and research, and 2) seismic reflection data acquired for purposes of oil and gas exploration by Ministry of Economy, Trade and Industry and Japanese oil companies.

Since 2D multichannel seismic reflection were acquired and processed according to survey standards of the early era to the recent, the original data were re-processed by applying the state-of-the-art data processing methods to obtain unified high-quality seismic profile which capable of interpreting subsurface structures and fault morphology. Within the Nankai Trough and the Izu-Ogasawara area more than 180,000 km of 2D single/multichannel data and 4,800 km^2 of 3D multichannel data was collected to set for geological interpretation.

To identify a fault which caused earthquakes in geological history, a seismic profile must show not only geomorphological feature but also subsurface displacement or flexure in sedimentary layers and bed rocks. In order to determine the fault surface and morphology, the same structure must exist on other successive profiles, and bathymetric data also helps to trace lineament caused by fault activities.
The Nankai Trough is a part of plate boundaries where the Philippine Sea Plate subducts beneath the overlying the Eurasian Plate, and seismic reflection/refraction studied have been conducted to reveal the structure of the plate boundary and to understand the mechanics of seismic hazards. This project allows to use widely acquired data from scientific purposes to economic purposes in the Nankai Trough area, and as a result, the preliminary fault distribution on the area has been mapped. Offshore of Hamamatsu, Shizuoka Pref., seismic reflection profile shows compressive structures of the two known fault zones, the Enshu fault system and the Kodaiba fault system, which extends to offshore of Shima, Mie pref. Seismic reflection profiles which cross the trough shows that the beneath the forearc basin deposits and the old accretional prism a seismic reflector that dips landward iles just above the oceanic crust. This reflector is known as the spray fault (e.g. Park et al., 2002) and can be traced in other profile, with length of more than 50km.Off the Shikoku island to Hyuganada, seismic reflection data show very complex structures such as subsiding of a seamounts and ridges or mud domes which form along faults.

Keywords: Nankai Trough, offshore fault, seismic reflection survey

©2019. Japan Geoscience Union. All Right Reserved.

Seismicity in the central Ryukyu Trench by the Ocean Bottom Seismometers

*Ren Yakabu[1], Mamoru Nakamura[1], Yusuke Yamashita[2], Masanao Shinohara[3], Tomoaki Yamada[3], Hajime Shiobara[3], Kimihiro Mochizuki[3]

1. University of the Ryukyus, 2. DPRI, Kyoto University, 3. ERI, Tokyo University

We investigated the seismicity in the central Ryukyu Trench from the island of Amami to Okinawa between January 2015 and September 2016. Five ocean-bottom seismometers (OBSs) and 20 short-period seismometers of the Japan Meteorological Agency (JMA) were used. We analyzed the events with JMA magnitude over 3.0, which occurred near the trench running from Amami to Okinawa. The P and S arrivals were selected using the WIN system.

Subsequently, we determined the hypocenters. To achieve this, we first revised the 1-D velocity structure model in this region. For the velocity structure in the island arc area, we calculated the 1-D velocity structure with the Joint Hypocenter Determination method using the software VELEST (Kissling et al., 1994). We implemented the original model (JMA2001) first, then we adopted the revised model for the calculation of the travel time to the JMA stations. For the velocity structure beneath the OBSs, we built the velocity model based on a refraction survey performed near Okinawa (Kodaira et al., 1996; Nishizawa et al., 2017). Subsequently, we selected the PS-P time differences at each OBS station and computed the sediment layer correction. Using these values, we adopted the hypocenter determination modifying the software hypomh.

In addition, we investigated the seismicity for the earthquake swarm that occurred near the trench axis from May to June 2016. The swarm began with a M 5.7 earthquake at 12:44 (JST) on May 27th, 2016. We identified the P-S time difference of the earthquakes which were recorded at the NS02 of the OBS station from April 1st to May 27th, 2016.

The relocated hypocenters were shallower compared to those in the JMA catalog by 20-30 km, on average. The change in the depth is larger (approximately 60 km) near the trench axis. The relocated epicenters changed slightly with respect to the JMA epicenters in almost area near the trench. However, the relocated epicenters in the south of Okinawa moved trench-ward compared with the JMA epicenters.

In the P-S time diagram of the period preceding the 2016 earthquake swarm, we identified events with short-duration of P-S times approximately 12 h before the start of the swarm. Although this would constitute a foreshock activity of the swarm, it had not been recorded by the JMA seismic network. This suggests that the earthquake swarm had a precursor activity.

Keywords: Ocean Bottom Seismometer, Ryukyu Trench, Earthquake Swarm

©2019. Japan Geoscience Union. All Right Reserved.

Seismic structure of subducted Philippine Sea plate beneath Kyushu inferred from Po/So waves

*Azusa Shito[1]

1. Institute of Seismology and Volcanology, Kyushu University

Po/So waves are oceanic Pn/Sn phases that are characterized by their high-frequency (f>2.5 Hz) content, long-duration, and great travel distances (up to 3000km) through the oceanic lithosphere [e.g., Linehan, 1940; Walker, 1977, 1982]. In our previous study [Shito et al., 2013], we demonstrated that Po/So waves develop from the multiple forward scatterings of P and S waves in oceanic lithosphere due to the laminated small-scale heterogeneities. Shito et al. [2015] analyzed Po/So waves in the Philippine Sea Plate, which consists of three regions with different lithospheric ages. They found that Po/So waves propagate more effectively in older regions and demonstrated that the increase in propagation efficiency of Po/So waves depending on the age of the oceanic lithosphere can be qualitatively explained by thickening of the oceanic lithosphere including small-scale heterogeneities and a reduction in the intrinsic attenuation. This study showed that Po/So waves are powerful tool to explore structural variations of the oceanic lithosphere.

Recently, such structural variations (e.g., thickness) of the incoming oceanic lithosphere are supposed to affect seismic and volcanic activity of the subduction zone [Yamamoto et al., 2013; Shibata et al., 2014]. However, it is poorly known that such structural variations of the oceanic lithosphere remain or dissipate after the subduction. In this study, we investigate the structural variations of the subducted Philippine Sea plate by using Po/So waves. We analyze Po/So waves from the earthquakes (mb>3.0, depth>50 km) that occurred in the subducted Philippine Sea slab beneath Kyushu. We compare Po/So waves propagating through different portion of the subducted Philippine Sea Plate and discuss the relation between observed features (velocity and energy) of the Po/So waves and the structural variations of the Philippine Sea plate. We verify that Po/So waves trace deeper extension of Kyushu-Palau Ridge (KPR) that is subducting beneath the Hyuga-nada region.

Acknowledgments
The data analyzed in this study were obtained from Hi-net (NIED) stations in Kyushu. The source parameters of the earthquakes were provided by JMA. This work was supported by JSPS KAKENHI Grant Number JP18K03807.

Keywords: Po/So waves, Philippine Sea Plate, Kyushu-Palau Ridge

©2019. Japan Geoscience Union. All Right Reserved.

Slope failure features and their distribution in the forearc off northwestern Sumatra

*Kenji Hirata[1], Toshiya Fujiwara[2], Ayanori Misawa[3], Kohsaku Arai[3]

1. National Research Institue for Earth Science and Diaster resilience, 2. Japan Agency for Marine-Earth Science and Technology, 3. National Institute of Advanced Industrial Science and Technology

In Feb. 2005 and Oct. 2009, we conducted multi-narrow beam bathymetric (MNB) surveys during NT05-02 cruise with R/V Natsushima (NT05-02 scientific party, scientific party,http://www.jamstec.go.jp/jamstec-e/sumatra/ natsushima/bm/contents.html)and KY09-09 cruise with R/V KAIYO (Hirata et al.,2012, JAMSTEC report), respectively. Apporox. 1 degree angular intervals of multi narrow beams with both the R/Vs makes us possible to retrieve detailed bathymetry with high resolution of ~35 meters in azimuthal direction for seafloor of ~2000 meters in water depth beneath ship tracks. Hirata et al. integrated these multi-narrow beam bathymetric data to construct detailed bathymetric data (grid data of ~37 meters interval for the surveyed area with ~50 km x ~100 km, surrounded by latitudes 3˚50’ N and 5˚00’ N, and longitudes 93˚10’ E and 94˚10’ E). In this study, we identify slope failure features in the forearc region off the northwestern Sumatra, and discuss its spatial distribution in terms of the geological processes.

To identify bathymetric features clearly, we make four kinds of maps as follows; slope angle map, slope angle change map, slope (direction) azimuth map, as well as plain bathymetric map. Slope angle is defined by arctangent of dz/ds, where z is the water depth and s is unit distance vector projected the steepest descending direction on horizontal plain. Slope angle change is defined by arctangent of second derivative of a unit distance vector s. Slope (direction) azimuth is defined by arctangent of dx/dy, where x and y are due east and due north components, respectively, of unit distance vector projected the steepest descending direction on horizontal plain. As a sample, we show figures consisting of slope angle map ((b) in Fig), slope angle change map (c), slope (direction) azimuth map (d) as well as plain bathymetric map (a) for a small rectangular region in the forearc off northwest Sumatra. We finally interpret such kinds of maps to identify slope failure features, etc (e).

We can identify the upper portion of slope failure structures with an elevation difference of about 1 km which bounded the western edge of the outer arc high, although we cannot retrieve bathymetry of the Sumatra Trench at ~ 4500 meters water depth because the multi-narrow beam survey systems can sounding up to less than 3000 meters. The slope failure structures are created by several to more than ten of successive landslides in the region shown in Fig. The landslide features show uneroded and sharp crowns, implying that the landslide features nearby the Sumatra Trench are created “recently” in geological time scale. Slope failure features with weak to strong rounded crowns come to appear as our sample point migrates landward. This can be explained from the formation process of the outer arc high off northwestern Sumatra ; thick, upper sedimentary layers in the top of subducting Indo-Australia plate that are stripped off at the toe of the forearc obduct onto the outer arc high so that accretional process proceeds (Mosher et al.,2008, Mar.Geol.; Misawa et al., 2014, EPSL).This means that landward (eastward) of the outer arc high is accreted older than its seaward (westward).

©2019. Japan Geoscience Union. All Right Reserved.

On the one hand, there are exceptions to such a geological rule; we can find several slope failure features with uneroded, sharp crowns in a landward region where many slope failure features with weak and strong rounded crowns exist (e.g., two slope failure structures with a width of ~ 1 km around a location of4° 06’ N, 93°39’ E). These relatively fresh failure structures existing landward of the outer arc high possibly relate to recent activation of major thrusts proposed in the outer arc high off northwest Sumatra (Hirata et al., 2010, AGU).

Keywords: Sumatra, forearc, outer arc high, slope failure, submarine landslide

©2019. Japan Geoscience Union. All Right Reserved.

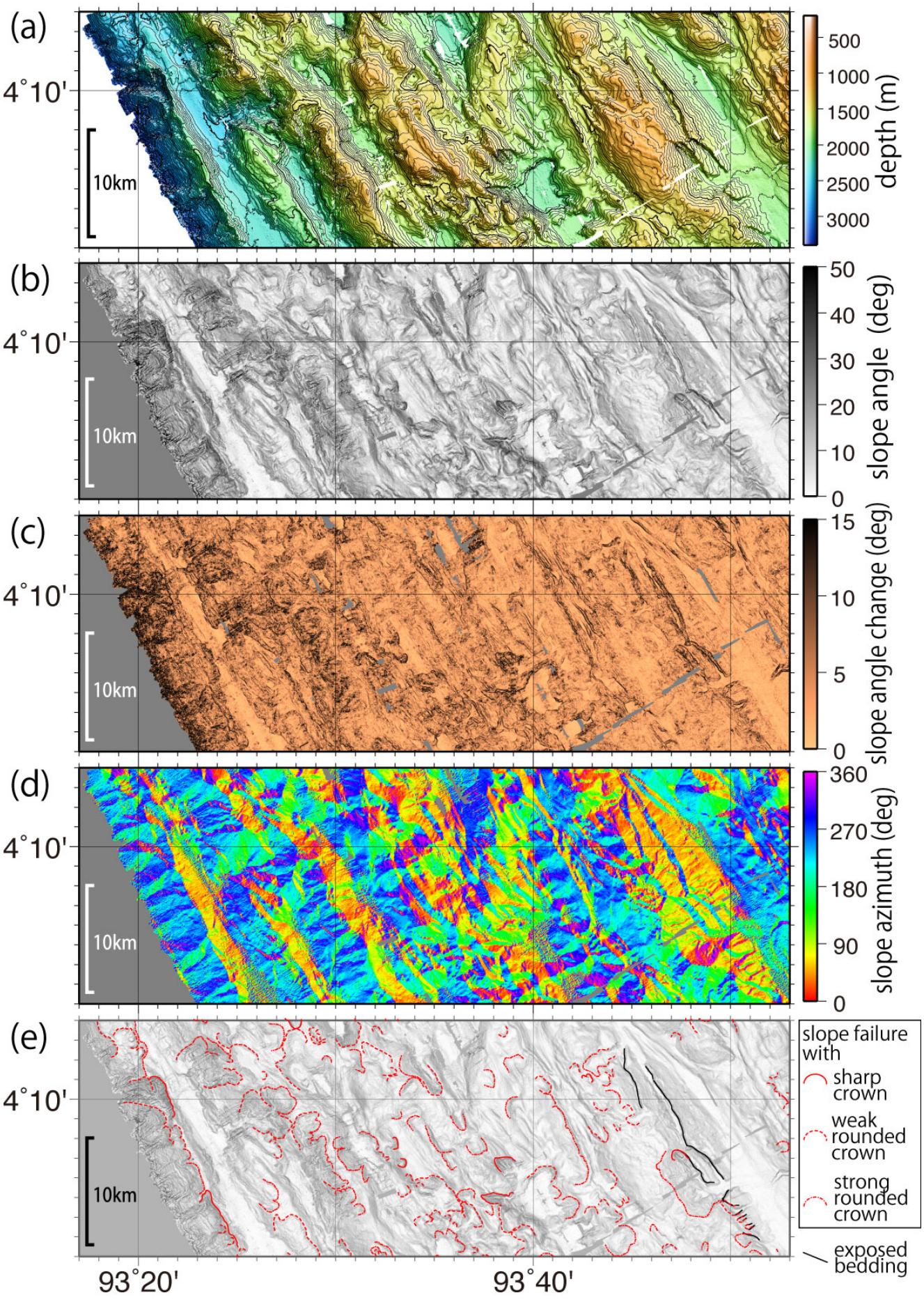

©2019. Japan Geoscience Union. All Right Reserved.

Origin and migration of fluid in the Sumatra subduction input: application of a geochronological method using a long-lived radioisotope of dissolved iodine

*Satoko Owari[1], Hitoshi Tomaru[1]

1. Chiba university

Iodine has a strong biophilic character and is highly enriched in organic matter in the marine environment. Organic matter is decomposed by thermogenic and microbial processes during the sedimentation and releases iodine into the interstitial water. Iodine has one stable isotope (^{127}I) and one long-lived radio isotope (^{129}I) with the half-life of 15.7 Myr. Therefore, the ^{129}I/^{127}I ratio of marine interstitial water has been used for identifying the origin of fluid. We applied iodine geochronology to the interstitial waters extracted from the deep drilling cores recovered by IODP Exp. 362, where Sumatra subduction input sediments develop more than 1400 m without major fractures. The concentration and isotopic ratio (^{129}I/^{127}I) of iodine dissolved in the interstitial water were analyzed in order to characterize the source and potential age of iodine prior to the subduction and examine the basic geological factors controlling the fluid migration in the input sediment body.

Concentrations of iodine and methane increase and TOC decreases toward 200 meters below seafloor (mbsf) and 1250 mbsf, which indicate degradation of organic matter around that depth and subsequent release of iodine and methane into the interstitial water. Iodine gradient is controlled by the degradation of iodine-rich organic matter microbially in shallow sediment (at 200 mbsf) and geothermally in deep sediment (at 1250 mbsf), respectively. The ^{129}I/^{127}I ratios between 0 and 400 mbsf vary between 300 $\times 10^{-15}$ and 800 $\times 10^{-15}$, and the lowest ratio of 300×10^{-15} is found at 175 mbsf. There are some thick sand layers > 60 meters between 0 and 400 mbsf. These porous layers transport allochthonous dissolved iodine and interstitial water, which are relatively old. However ^{129}I/^{127}I of 1300×10^{-15} at 67 mbsf corresponding to the sediment age of 3 Ma at 200 mbsf which is the zone of degradation of organic matter. ^{129}I/^{127}I between 400 to 1480 mbsf decrease from 700 $\times 10^{-15}$ to 400×10^{-15}, resulting from mixing with deep (old) iodine and shallow (young) iodine. In the input sediment, iodine gradient is strongly controlled by degradation of organic matter and the migration is controlled by vertical diffusion which indicates poor fluid migration or slow migration rate. However, the horizontal advection/migration of interstitial water is significant within the thick-porous sandy layers.

Keywords: 129I, Iodine geochronology, Interstitial water, Sumatra subduction input, IODP Exp.362

©2019. Japan Geoscience Union. All Right Reserved.

Challenge to Future Deep-Water Mapping: Unmanned Bathymetric Survey Competition "Shell Ocean Discovery XPRIZE"

*MASANAO SUMIYOSHI[1]

1. Hydrographic and Oceanographic Department, Japan Coast Guard

Unmanned survey technology is utilized in the world of bathymetric survey in the present age, when unmanned technologies are developing in various fields. Especially Autonomous Underwater Vehicle (AUV) is actively used in order to acquire high resolution bathymetric data in the deep waters. The technological innovation is needed to further advance the unmanned and automated deep-water mapping, including AUV operations of launch and retrieval. In order to encourage such innovation, an international competition of unmanned deep-water mapping, "Shell Ocean Discovery XPRIZE" has been held for 3 years.
The University of New Hampshire actively develops many hydrographic and oceanographic survey technologies that will open a new era, and as a part of these efforts GEBCO-NF Alumni Team challenges the international unmanned deep-water competition. The author has been strongly pushing the research and development of technology of bathymetric survey for this challenge as a member of this team, who was studying abroad to this university until 2017 to learn the latest hydrographic survey technologies.
This team had passed through Round 1 (semi-final: ~ 2000 m) held in November 2017, and challenged Round 2 (final: ~ 4000 m) as one of the finalists in the last November. In this paper, we report our efforts and achievements of the GEBCO-NF Alumni team, including those in Round 2.

Keywords: Shell Ocean Discovery XPRIZE, GEBCO-NF Alumni Team, Unmanned/Autonomous Technologies (USV, AUV), Bathymetric Survey, Multibeam Echosounder (MBES), Synthetic Aperture Sonar (SAS)

©2019. Japan Geoscience Union. All Right Reserved.

Prototype of deep-sea ocean bottom pressure recorder with self-calibration capability using “A-0-A” approach for detection of long-term crustal deformation

*Yusaku Ohta[1], Ryota Hino[1], Syuichi Suzuki[1], Makiko Sato[1], Yui Nishimagi[1], Hiroaki Kajikawa[2], Tokihiko Kobata[2]

1. Research Center for Prediction of Earthquakes and Volcanic Eruptions, Graduate School of Science, Tohoku University, 2. National Metrology Institute of Japan, National Institute of Advanced Industrial Science and Technology

Ocean bottom pressure gauge (OBP) can continuously observe the vertical crustal deformation in the seafloor. However, a nature of long-term drift of pressure sensors causes a serious problem in detection of the long-term crustal deformation. A possible approach to remove the sensor drift on the sea-floor is to use a dead-weight tester as the pressure standard to make in-situ calibration on the seafloor by periodically switching between the ambient pressure and the reference pressure (Sasagawa et al. 2016). Recently, an alternative approach, an “A-0-A” method, using the internal pressure of the instrument housing as the reference pressure was proposed (e.g. Wilcock et al., 2018). We investigated the long-term drift behavior and ability of “A-0-A” method by a laboratory experiment using dead-weight tester as a pressure standard (e.g. Nishimagi et al. AGU fall meeting, 2018). We regard the reading at high applied pressure as ambient pressure point (“A”) and that at atmospheric pressure as zero-point (“0”). Although the residual time series between the “A” and “0”, however, showed small discrepancy, we found drift characteristics of “A” and “0” are basically similar to each other.

Based on these laboratory experiment results, we have started to develop a proto-type of ocean bottom pressure recorder with self-calibration capability using “A-0-A” approach for deep-water (up to 7,000 m) deployment. We install all the equipments including a pressure sensor in a 17-in glass sphere. To measure both of the internal and external (water) pressure by a single sensor, we adopt 3-way a ball valve controlled by an electric actuator in front of the sensor, as in the previous self-calibrating system using a dead-weight tester. The actuator is operated by the microcomputer to switch by arbitrary interval. We also install alternative barometer to compare the internal pressure value recorded by the pressure sensor. The development is still under way, and we will show more detail characteristic of the prototype system and its potential abilites.

©2019. Japan Geoscience Union. All Right Reserved.

Noise reduction and surface wave array dispersion measurements applied to NOMan's broadband OBS data

*Yuki Kawano[1], Takehi Isse[1], Hitoshi Kawakatsu[1], Akiko Takeo[1], Hajime Shiobara[1]

1. Earthquake Research Institute, The University of Tokyo

To achieve better performance of broadband ocean bottom seismometer (BBOBS) survey, we applied noise reduction analysis and dispersion measurements to the vertical component seismograms of the Normal Oceanic Mantle (NOMan) project arrays, which are previously analyzed by Takeo et al. (2018). Our noise reduction targets on the tilt noise that is significant for low-frequency (<0.1 Hz) BBOBS vertical records. Tilt noise is generated by the seafloor current which flows pass the BBOBS. It originally only dominates horizontal records, but the misalignment between the seismic sensor's vertical axis and gravitational direction allows projection of noisy horizontal tilt noise onto vertical records. Hence, vertical tilt noise can be estimated from the transfer function between horizontal and vertical records (Crawford and Webb, 2000). We developed a noise reduction method which is suitable for Japanese BBOBS based on the approach of Crawford and Webb (2000) and Bell et al. (2015). By performing noise reduction analysis, we achieved about 20 dB noise reduction at the frequency lower than 50 mHz and extracted lots of buried seismic signals. To verify the effect of noise reduction analysis, we compared array dispersion measurement results which derived from tilt noise removed and non-removed data. Using the method of Takeo et al. (2018), we measured average phase velocity and azimuthal anisotropy of fundamental mode Rayleigh waves to estimate isotropic and azimuthally anisotropic Vsv (βv) profiles. The results show that tilt noise removed data can provide us with more precise low-frequency measurements and the better-constrained structure at a depth of 80 km or deeper. Our results indicate that noise reduction preprocessing is important for improving Japanese BBOBS analysis.

Keywords: broadband ocean bottom seismometer, tilt noise, low frequency, surface wave array measurement

©2019. Japan Geoscience Union. All Right Reserved.

High-tech dredge system for abyssal bedrock research; dredge system with acoustic real time monitoring on deep sea floor.

*Teruaki Ishii[1], Yukihiro - Kida[2], Izumi - Sakamoto[3], Shiki -- Machida[4]

1. Center for Integrated Research and Education of Natural Hazards, Sizuoka University, 2. JAMSTEC, 3. Toukai University, 4. Chiba Institute of Technology

It is very important to recover geological samples including hard rocks and soft materials from ocean floor to investigate bedrocks itself as well as sea floor environment on the basis of the material scientific aspects. Dredge haul methods being a simple and easy way with low costs, have been widely used for recovering the bedrocks. One of author (TI) has been working on the dredge hauls during about 40 years on the several Japanese and American Research Vessels (R/Vs), that is, R/V Tansei Maru, R/V Hakuho Maru, R/V Yokosuka, and R/V Kairei as well as R/V Atlantis-II, R/V Melville (2 times), R/V Moana Wave, and R/V Thomas Thompson, respectively. He has been proposing the (1) ORI-TI type dredge system, which has been improved and still improving on the basis of the better ideas gathered from the above mentioned all cruises. The dredge systems in the US Research Vessels have been continuing the conventional and basic technical methods, that is, box type chin-bag dredge (within or without fishing net) and using tension-meter as well as pinger.

On the other hand, Japanese scientists have been recently improving the traditional dredge systems with active introduction of high technique, for example, (2) transponder system and/or (3) deep sea TV camera system during dredge hauls. (4) new underwater acoustic transmission system of real-time TV-image.

(1)ORI-TI (Ocean Research Institute T. Ishii) type dredge system is composed of box type chain-bag dredge with steel bucket which can recover any sea bottom material including hard rocks as well as sand, mud and organisms(Ishii, 2017).

(2)Acoustic transponder attached on the dredge wire can mention real-time position of the dredge system on monitor showing pre-surveyed bathymetric map in the navigation room, This system helps safe and reliable rock sampling (Machida et al, 2011).

(3) Box-cage type dredge with installed deep sea TV camera system can record occurrence of bed rocks during dredge hauls (Sakamoto et al, 2017).

(4) New underwater acoustic transmission system of real-time TV -image with every 2 second from Shinkai 6500 to R/V Yokosuka put to practical use (Sakurai, 2018) on the basis of the new underwater acoustic communication system (Kida et al, 2018). If we can get low price (about USD$10,000) above mentioned system in a near future, it will be applied to the dredge hauls with real-time monitor on the sea bottom. The author (T.I.) assumes that its application fields are very wide; piston core, mooring system, ocean bottom seismometer, net fishing etc.

Reference

Kida, Yukihiro, Mitsuyasu Deguchi, and Takuya Shimura.(2018): Experimental result for a high-rate underwater acoustic communication in deep sea for a manned submersible SHINKAI 6500, J. Marine Acoust. Soc. Jpn., 45 (4),197-207.

©2019. Japan Geoscience Union. All Right Reserved.

ISHII, Teruaki (2017):Evolution of dredge system from low to high technological equipment--Improvement of dredge system toward advanced material science on bedrocks--, Fukada Geological Institute Annual Report, 18, 29-48 (in Japanese with English abstract).

Sakamoto, Izumi, Satsuki Iijima, Yamato Monma, and Kenichirou Tani (2017) :Dredge “Satsuki” system with Deep Sea Camera, ① her development and function, Blue Earth Symposium 2017 (JAMSTEC) abstract BE17-12 (in Japanese).

Machida, Shiki, Yutaka Matsuura, Natsue Abe, and Teruaki Ishii (2011):Rock sampling from the ocean floor using transponder-based real-time monitoring of the dredge system, JAMSTEC Rep. Res. Dev,13, 89-105 (in Japanese with English abstract).

Keywords: abyssal bedrocks, high-tech dredge system, ORI-TI type dredge, dredge transponder, deep sea dredge VTR, underwater acoustic transmission system

©2019. Japan Geoscience Union. All Right Reserved.

Construction of Database System on Offshore Faults around Japan

*Hiromi Kamata[1], Narumi Takahashi[1,2], Shigeyoshi Tanaka[1], Rei Arai[1], Minako Katsuyama[1], Ayako Nakanishi[1], Hiroyuki Fujiwara[2], Tsuneo Ohsumi[2], Takahiko Inoue[3], Tomoyuki Sato[3], Yoshiyuki Kaneda[4]

1. Japan Agency for Marine-Earth Science and Technology, 2. National Research Institute for Earth Science and Disaster Resilience, 3. National Institute of Advanced Industrial Science and Technology, 4. Kagawa University

JAMSTEC has performed the project for “Comprehensive Evaluation of Offshore Fault Information” sponsored by the Ministry of Education, Culture, Sports, Science and Technology (MEXT) since FY2013. The project consists of three themes named “Sub-theme 1” gathering various kinds of existing geological/geophysical information and constructing offshore fault database system (DB), “Sub-theme 2” re-processing seismic data and interpreting offshore faults based on unified evaluation standard, and “Sub-theme 3” building offshore fault models conducted by NIED.

In Sub-theme 1, JAMSTEC has obtained or borrowed huge volumes of multi-channel seismic (MCS)/single-channel seismic (SCS) reflection data and ocean bottom seismometer (OBS) refraction data surveyed around Japan from various organizations including national research institutes and private enterprises, and has collected seismic velocity information, bathymetry data etc. After the quality check of these data, they are made into a database and unitary management of them are carried out. The final output of Sub-theme 1 is an offshore fault DB comprising the data sets of collected/re-processed seismic data and overall offshore fault information provided by Sub-theme 2 and Sub-theme 3. In Sub-theme 2, the past old-fashioned MCS data have been re-processed applying the latest sophisticated technology with de-multiple filtering and noise suppression for obtaining the high resolution profile of these seismic sections. Using the MCS/SCS data, offshore faults around Japan have been identified based on unified evaluation standard. Some geological horizons and a plate boundary have been also interpreted to model subsurface geometry and 3D velocity structure. The final output of Sub-theme 2 is to delineate the spatial distribution and continuity of identified faults on the high resolution bathymetric map such as a red relief image map, and to organize their features/parameters such as type, length, dipping direction, extension etc. after the seismic time–depth conversion using 3D velocity structure model. The 3D velocity structure has been modeled using collected OBS refraction data, velocity analysis results in MCS re-processing and some available published data. In Sub-theme 3, NIED has built the offshore fault models based on a fault information catalog completed by Sub-theme 2. The model validation for historical earthquake source faults with the magnitude over seven has been also conducted through ground motion and tsunami simulations.

This poster presentation focuses on the offshore fault DB constructed by Sub-theme 1 of the project. JAMSTEC has finished the clarification of faults in the Sea of Japan, and around the sea area of the Nansei Islands and Izu-Ogasawara Islands by FY2017. We are currently working on the interpretation of subsurface structure and fault distribution in the Nankai Trough area, and continue to register MCS/SCS reflection time/depth sectional figures, 3D velocity models, NIED’s fault models and their parameters into the DB sequentially. The trial operation of the DB has been also done at the subcommittee of the Headquarters for Earthquake Research Promotion of MEXT. The DB is highly expected to become a useful tool that contribute to tsunami hazard evaluation and disaster management conducted by Japanese government and local authorities, and that improve the public awareness against disaster prevention.

©2019. Japan Geoscience Union. All Right Reserved.

We would like to express our acknowledgements to Ministry of Economy, Trade and Industry (METI), Japan Oil, Gas and Metals National Corporation (JOGMEC), Japan Coast Guard (JCG), Geospatial Information Authority of Japan (GSI), AIST, Akita Prefecture, Okinawa Prefecture, University of Tokyo, Toyama University, Inpex Corporation and Japan Petroleum Exploration Co.,Ltd. (JAPEX) for providing the geological/geophysical data.

Keywords: Offshore Fault, Seismic Data, 3D Velocity Structure, Fault Model, Database

©2019. Japan Geoscience Union. All Right Reserved.

An integration method for multiple sets of seafloor backscatter intensity data

*Shiki Machida[1,2], Taichi Sato[3], Kazutaka Yasukawa[2]

1. Ocean Resources Research Center for Next Generation, Chiba Institute of Technology, 2. University of Tokyo, 3. AIST

Acoustic backscattering of the seafloor is thought to provide a useful signal representing the existence of hard materials, such as lava flows with ferromanganese crust along the slope of seamount or knoll [1, 2], and ferromanganese nodules on the seafloor [3]. Previous investigations using vessel-equipped multi-narrow beam echo sounder (MBES) [1–3] identified variations of distributions over an area of tens or hundreds of square kilometres. Therefore, vessel-equipped MBES can provide a more economical exploration for vast areas than that provided by underwater apparatuses such as a deep-towed side scan sonar. However, a disadvantage inhibiting its use is that the different physical and technical parameters, such as sounder characteristics, observation period, and processing, yield different absolute values of backscatter intensity for the same area. As a solution, we propose a generally applicable method for obtaining the widespread distribution of deep-sea solid materials using a combination of several datasets of vessel-equipped MBES.

The Japanese exclusively economic zone (EEZ) around Minamitorishima Island in the western North Pacific is the best candidate area in which to analyse vessel-equipped multibeam backscatter data. This is due to the fact that several research cruises, operated by the Japan Agency for Marine-Earth Science and Technology (JAMSTEC), have obtained multiple sets of backscatter data, combined with bathymetry mapping. These data were obtained with an identical MBES (SeaBeam 3012. multibeam system) for each of the four cruises of *R/V Mirai*(MR14-E02, MR15-E01 Legs 2 and 3, and MR15-02) in 2014 and 2015, and with the other MBES (SeaBeam 2112.004 multibeam system) during a cruise of *R/V Yokosuka* (YK10-05) in 2010.

We identified two important components for successfully integrating several sets of backscatter intensity data collected by vessel-equipped MBES, as follows. (1) The folding points in the trend of the second-order differential values of the histogram of backscatter data correspond to the boundaries between different types of geology, e.g. barren pelagic sediment and dense ferromanganese nodules. (2) These thresholds each indicate that the same geologic boundaries appear at similar intervals in the histogram, even if the absolute values of intensity are different for each dataset. In particular, this latter component ensures linear fitting of the thresholds used to adjust each dataset to the arbitrary standard data. We need the confirmation of the geographical distributions of the identified boundary intensities between the different datasets. In this presentation, we will show an example of data integration for nine datasets to map the backscatter intensity of a region of approximately 155,500 km^2in the Japanese EEZ around Minamitorishima Island.

References: [1] Hirano et al. (2006) *Science***313**, 1426–1428. [1] Hirano et al. (2016) *Mar. Geol.***373**, 39–48. [3] Machida et al. (2016) *Geochem. J.***50**, 539–555.

©2019. Japan Geoscience Union. All Right Reserved.

Keywords: backscatter intensity, multi-narrow beam echo sounder, Minamitorishima EEZ

©2019. Japan Geoscience Union. All Right Reserved.

A precise calculation of average depth for ETOPO1

*Yasushi Harada[1], Sae Horiuchi[1]

1. School of Marine Science and Technology, Tokai University

NOAA calculated global ocean average depth as -3688m (https://www.ngdc.noaa.gov/mgg/global/etopo1_ocean_volumes.html) , but in their method, there are deviations for distribution of sampling points, especially at high latitude area. Generally, perfect uniform sampling points are needed to calculate precise average depth using digital elevation data such as ETOPO1.

We tried a different method for creating uniform sampling points on spherical surface. Yamaji(2001) created this software called GSS generator(GSS). The GSS makes almost perfect uniform sampling points on sphere, but not on WGS84 ellipsoid. Therefore we compared the two methods, and performed a statistical analysis for both methods.

We found that the two methods produced similar average depth values and the errors, and that the average depth of ETOPO1 is 3685.9 ±0.5m and about 2m shallower than NOAA’s 3688m value.

Keywords: ETOPO1, average depth, GSS Generator

©2019. Japan Geoscience Union. All Right Reserved.

[J] Oral | S (Solid Earth Sciences)：S-CG Complex & General

Mon. May 27, 2019 10:45 AM - 12:15 PM JST | Mon. May 27, 2019 1:45 AM - 3:15 AM UTC | A05 TOKYO BAY MAKUHARI HALL

[S-CG60] Investigation of inputs to subduction zones: Influence of tectonic processes on the incoming plate

convener:Makoto Yamano(Earthquake Research Institute, the University of Tokyo), Tomoaki Morishita(School of Geoscience and Civil Engineering, College of Science and Technology, Kanazawa University), Gou Fujie(Japan Agency for Marine-Earth Science and Technology), Chairperson:Shigeaki Ono(Japan Agency for Marine-Earth Science and Technology)

Various tectonic processes occur on the seaward side of the trench associated with bending of the incoming oceanic plate, e.g., fracturing of oceanic crust, infiltration of water, and intraplate volcanism. Investigation of these processes and their influence on the incoming plate provides important information on the boundary condition at the trench, inputs to subduction zones. Variation in inputs should significantly affect geophysical/geological phenomena around the plate interface and geochemical cycles in subduction zones. We welcome contributions from a broad range of earth science (geophysics, geology, petrology, and so on) discussing topics related to inputs to subduction zones such as occurrence of tectonic processes due to bending of the incoming plate, modification of the incoming plate by the processes, relationship between the processes and the inherited structure of the incoming plate, and influence of the processes on the subduction plate interface. We hope discussions are made on studies of a variety of subduction zones, including the Japan Trench and the Nankai Trough, and comparative studies among different subduction zones.

10:45 AM - 11:00 AM JST | 1:45 AM - 2:00 AM UTC

[SCG60-01] Geophysical-petrological studies of the Chile triple junction and their significance: MIRAI research cruise MR-1806Leg2

*Masataka Kinoshita[1,5], Hikaru Iwamori[1,5], Tomoaki Nishikawa[2], Ryo Anma[3], Sofia Lagarrigue[4], Natsue Abe[5], Yuka Yokoyama[6], Andres Veloso Espinosa[4], Alessandra Isabella Rivero Cortes[7], Gabriela Pia Lazcano Prado[7], Ivan Andres Arriagada Bascuñan[7], Satoru Haraguchi[5], Kosuke Ota[9], Yuji Orihashi[8], Kaishi Nakao[8], Shogo Numata[8], Hajime Shiobara[1], Hiroko Sugioka[10], Aki Ito[5], Nicolás Pérez-Estay[11] (1.Earthquake Research Institute, University of Tokyo, 2.DPRI, Kyoto Univ., 3.Tokushima Univ., 4.Pontificia Universidad Catolica de Chile, 5.JAMSTEC, 6.Tokai Univ., 7.Andres Bello University, 8.Hirosaki Univ., 9.AORI, Univ. Tokyo, 10.Graduate School of Science, Kobe Univ., 11.Ministerio de relaciones exteriores, Chile)

11:00 AM - 11:15 AM JST | 2:00 AM - 2:15 AM UTC

[SCG60-02] Heat flow measurement on the seaward side of the Kuril Trench off Hokkaido

*Kouta Sasaki[1], Makoto Yamano[1], Yoshifumi Kawada[2], Masataka Kinoshita[1], Kiichiro Kawamura[3] (1.Earthquake Research Institute, the University of Tokyo, 2.International Research Institute of Disaster Science, Tohoku University, 3.Yamaguchi University)

11:15 AM - 11:30 AM JST | 2:15 AM - 2:30 AM UTC

[SCG60-03] Comparison of experimental and intermediate-depth earthquake b-value: difference in hydration degree of the oceanic mantle between Tohoku and Hokkaido

★Invited Papers

*Saeko Kita[1], Thomas P. Ferrand[2] (1.International Institute of Seismology and Earthquake Engineering, BRI, 2.ERI, University of Tokyo)

11:30 AM - 11:45 AM JST | 2:30 AM - 2:45 AM UTC

[SCG60-04] Variations in bend faulting and the nature of the incoming oceanic plate off northeast Japan arc

*Gou Fujie[1], Koichiro Obana[1], Yojiro Yamamoto[1], Tomoaki Yamada[2], Takehi Isse[2], Shuichi Kodaira[1], Seiichi Miura[1] (1.Japan Agency for Marine-Earth Science and Technology, 2.Earthquake Research Institute, Univ. of Tokyo)

11:45 AM - 12:00 PM JST | 2:45 AM - 3:00 AM UTC

[SCG60-05] Seismicity in the trench-outer rise region off Fukushima and Ibaraki, southern Japan Trench

*Koichiro Obana[1], Gou Fujie[1], Yojiro Yamamoto[1], Yuka Kaiho[1], Yasuyuki Nakamura[1], Seiichi Miura[1], Tsutomu Takahashi[1], Shuichi Kodaira[1] (1.Research and Development Center for Earthquake and Tsunami, Japan Agency for Marine-Earth Science and Technology)

12:00 PM - 12:15 PM JST | 3:00 AM - 3:15 AM UTC

[SCG60-06] Influence of water–rock interactions on the strength of outer-rise faults

★Invited Papers

*Ken-ichi Hirauchi[1] (1.Department of Geosciences, Faculty of Science, Shizuoka University)

Geophysical-petrological studies of the Chile triple junction and their significance: MIRAI research cruise MR-1806Leg2

*Masataka Kinoshita[1,5], Hikaru Iwamori[1,5], Tomoaki Nishikawa[2], Ryo Anma[3], Sofia Lagarrigue[4], Natsue Abe[5], Yuka Yokoyama[6], Andres Veloso Espinosa[4], Alessandra Isabella Rivero Cortes[7], Gabriela Pia Lazcano Prado[7], Ivan Andres Arriagada Bascuñan[7], Satoru Haraguchi[5], Kosuke Ota[9], Yuji Orihashi[8], Kaishi Nakao[8], Shogo Numata[8], Hajime Shiobara[1], Hiroko Sugioka[10], Aki Ito[5], Nicolás Pérez-Estay[11]

1. Earthquake Research Institute, University of Tokyo, 2. DPRI, Kyoto Univ., 3. Tokushima Univ., 4. Pontificia Universidad Catolica de Chile, 5. JAMSTEC, 6. Tokai Univ., 7. Andres Bello University, 8. Hirosaki Univ., 9. AORI, Univ. Tokyo, 10. Graduate School of Science, Kobe Univ., 11. Ministerio de relaciones exteriores, Chile

The Chile triple junction (CTJ) is a unique place where a spreading center of mid-ocean ridge is subducting near the Taitao peninsula. Around CTJ, presence of high heat flow on the continental slope (Cande et al., 1987, J. Geophys. Res.) and near-trench young granitic rocks on the Taitao peninsula (Anma and Orihashi, 2013, Geochem. J.) suggests the thermal and petrological impact of subducting ridge on the continental side. The tectonic history of the southeast Pacific since early Cenozoic to the present suggests that ridge subduction continuously occurred along the Chile trench, which migrated northward (Cande and Leslie, 1986, J. Geophys. Res.), which can contribute to growth of the continental crust (Iwamori, 2000, EPSL).
In January 2019, the MR18-06 cruise Leg 2 was conducted at the Chile Triple Junction, as a part of 'EPIC' expedition by using R.V Mirai of JAMSTEC. During the leg, we completed 4 SCS lines, 6 piston coring, 6 heat flow measurements, 2 dredges, and underway geophysics observations, as well as deployment of 13 OBSs. The primary object of heat flow measurement at CTJ is to better constrain the thermal regime around CTJ by adding new data right above CTJ. The key question is whether CTJ is thermally dominated by ridge activity (magmatic, tectonic, and/or hydrothermal) or by subduction initiation (tectonic thickening, accretion, and/or erosion). The ultimate goal is to model the temperature at the plate interface from the heat flow and other data, and to infer how the thermal regime at CTJ contributes the seismogenic behavior at the M~9 megathrust zone.
Our preliminary analysis shows high and variable heat flow around CTJ. It is generally consistent with previous heat flow along line 751 (Cande et al., 1987). With SCS and piston core data, a reasonable thermal model can be constructed around CTJ. (Acknowledgment) we thank the Hydrographic Department of Chile (SHOA), for allowing to enter the Chilean EEZ and territory for our survey.

Keywords: heat flow, Chile Triple Junction

©2019. Japan Geoscience Union. All Right Reserved.

Heat flow measurement on the seaward side of the Kuril Trench off Hokkaido

*Kouta Sasaki[1], Makoto Yamano[1], Yoshifumi Kawada[2], Masataka Kinoshita[1], Kiichiro Kawamura[3]

1. Earthquake Research Institute, the University of Tokyo, 2. International Research Institute of Disaster Science, Tohoku University, 3. Yamaguchi University

To understand thermal structure of subduction zone, heat flow on the surface of incoming oceanic plate serves as an important boundary condition. On the surface of oceanic plate, observed value of heat flow is generally consistent with prediction of the plate cooling model (e.g., Stein and Stein, 1992). Yamano et al. (2014) revealed extensive high heat flow anomaly on the seaward side of the Japan Trench, where the very old Pacific plate (~135 Myr) subducts beneath northeast Japan, and some possible causes of the anomaly have been examined. Fujie et al. (2013, 2015) pointed out seismic velocity structure anomalies in the crust and the uppermost mantle seaward of the Japan and Kuril trenches and attributed them to increase in water content as a result of bending of the incoming oceanic plate. Kawada et al. (2014) examined influence of hydrothermal circulation in a permeable layer in the oceanic crust as a possible source of the high heat flow anomaly. They showed that hydrothermal circulation in the permeable layer thickening toward the trench axis in concordance with the seismic velocity anomaly pumps up heat efficiently and raises heat flow on the seafloor.

Infiltration of water into the crust is inferred seaward of the Kuril Trench as well based on the seismic velocity anomaly. Nakanishi (2011) argued that the direction of bending-related faults on the oceanward slope of the Kuril and Japan trenches is well correlated with the angle between the trench axis and the ancient spreading ridge axis, which varies along the trenches. It is also speculated that the trench-ridge angle is a major controlling factor of incoming plate hydration (Fujie et al., 2018). These studies suggest that it is indispensable to examine heat flow distribution seaward of the Kuril Trench, where few data have been obtained, for investigation of water and heat transport processes associated with plate bending.

In this study, we conducted heat flow measurement on the seaward of the Kuril trench off Hokkaido on KH-18-5 cruise of R/V Hakuho-maru. We measured geothermal gradient with a 3 m long temperature probe at eight sites and with a piston corer at four sites within about 120 km of the trench axis. We attempted penetration of the temperature probe several times at each site at intervals of 300 to 500 m. Few penetrations were successful within 60 km of the trench axis probably because thick layers of volcanic ash prevented the probe from penetrating into the sediment. Thermal conductivity was measured on piston core samples.

Most of the obtained 25 new heat flow values are roughly consistent with typical values for ocean basins older than 100 Myr (~50 mW/m^2), while high heat flow, 90 to 100 mW/m^2, was observed at one station about 70 km from the trench axis. This result indicates that the degree of heat flow anomaly on the seaward side of the Kuril Trench is lower than that in the counterpart of the Japan Trench.

Keywords: heat flow, Kuril Trench, oceanic crust, hydrothermal circulation, Japan Trench, Pacific plate

©2019. Japan Geoscience Union. All Right Reserved.

Comparison of experimental and intermediate-depth earthquake b-value: difference in hydration degree of the oceanic mantle between Tohoku and Hokkaido

*Saeko Kita[1], Thomas P. Ferrand[2]

1. International Institute of Seismology and Earthquake Engineering, BRI, 2. ERI, University of Tokyo

We examine b-values of the lower-plane events than beneath Tohoku. Using the acoustic emission (AE) experimental result, the b-values for intermediate-depth intraslab earthquakes in the Pacific slab beneath the Tohoku and Hokkaido regions, northeastern Japan and find a difference in the b-values of lower-plane events in the double seismic zone. Lower-plane events reveal significantly larger b-values beneath Tohoku (0.96) than Hokkaido (0.86), implying that the brittle deformation beneath Hokkaido is more localized and leads to higher ratio of relatively large lower-plane events by Ferrand et al. [2017, Nature Communications], we also found that the b-values for experimental earthquakes increase with increasing antigorite content in serpentinized peridotite. A comparison of experimental and natural earthquake b-values implies that lower- plane peridotite is more hydrated beneath the Tohoku region, which is consistent with the difference in oceanic-plate velocity structures near the trench identified in Ocean Bottom Seismometer studies off Tohoku and Hokkaido by Fujie et al. [2017, Nature communications]. Since the density of fracture zones offshore Tohoku is larger than offshore Hokkaido, the extent of hydration of the oceanic mantle beneath Tohoku could be larger than beneath Hokkaido.

Keywords: intraslab earthquake, b-value, Acoustic emission , Wadati-Benioff zone, oceanic mantle, peridotite

©2019. Japan Geoscience Union. All Right Reserved.

Variations in bend faulting and the nature of the incoming oceanic plate off northeast Japan arc

*Gou Fujie[1], Koichiro Obana[1], Yojiro Yamamoto[1], Tomoaki Yamada[2], Takehi Isse[2], Shuichi Kodaira[1], Seiichi Miura[1]

1. Japan Agency for Marine-Earth Science and Technology, 2. Earthquake Research Institute, Univ. of Tokyo

As the inputs to subduction zone, the nature of the incoming oceanic plate, such as relief, thermal state, lithology, and the water content, affects subduction zone processes, including arc magmatism and interplate and intraplate seismic activities. Thus, regional variations in the nature of the incoming oceanic plate have a potential to cause regional variations in such subduction zone processes.

To reveal the nature of the incoming oceanic plate and its regional variations off northeastern Japan arc, we have conducted extensive controlled-source seismic experiments at the northwestern margin of the oceanic Pacific plate. First, we conducted seismic experiments at around the junction of the Kuril and Japan trenches. We observed seismic structural changes owing to the plate bending-related faults just prior to subduction at both trenches and found the structural changes caused by bend faulting are more significant in the Japan trench side than that in the Kuril Trench side, indicating that plate hydration before subduction is remarkably higher in the Japan Trench than in the Kuril Trench. These observed differences can be explained by the type of the bend faults, newly created faults (Japan Trench) or reactivated abyssal-hill faults (Kuril Trench). As the type of bend faults are determined by the angle between the current trench and the ancient spreading ridge, this angle is one of key factors controlling the hydration of the incoming oceanic plate.

In 2017 and 2018, we conducted additional seismic experiment at the trench-outer rise areas of the southern Japan Trench off Fukushima. This was our first seismic survey in the trench-outer rise region of the southern Japan trench. The strike of the Japan trench differs between the northern part and the southern part, indicating that the angle between the current trench axis and the ancient spreading ridge also differs between the northern part and the southern part. In addition, unlike the northern part of the Japan trench, a large seamount chain exists in the trench-outer rise region of the southern Japan Trench. The primary aim of our new seismic survey in the southern part of the Japan Trench is to clarify the differences between the northern and the southern part of the Japan trenches.

We applied traveltime tomographic inversion to the wide-angle reflection and refraction seismic data and developed a P-wave velocity (Vp) model. The obtained Vp model clearly shows the reduction in Vp near the trench axis caused by bend faulting. The Vp reduction patterns are closely akin to that in the northern Japan trench area. The angle between the current trench and the ancient ridge axis differs between the northern and the southern Japan trench, but the type of bend faults are the same. Our new observation confirmed that the type of bend faults is a key controlling factor on the bend faulting and plate hydration prior to subduction.

In addition to the structural changes caused by bend faulting, we observed curious features in crustal Vp structure. In the area far from the trench axis off Fukushima, our Vp model shows velocity reversal within the oceanic crust which is suggested by the "shadow zones" of the crustal refractions. We have observed similar velocity reversal within the oceanic crust in the areas far off Iwate, but not in the areas far off Miyagi. These observations suggest that the oceanic crust are intrinsically inhomogeneous in the

©2019. Japan Geoscience Union. All Right Reserved.

northwestern part of the Pacific plate.

In this presentation, we will show the variations in the Vp model in the northwestern part of the Pacific plate including the structural changes caused by bend faulting and the velocity reversal within the crust, and discuss the possible impact as the subduction inputs.

Keywords: outer rise, controlled-source seismic survey, oceaic plate

©2019. Japan Geoscience Union. All Right Reserved.

Seismicity in the trench-outer rise region off Fukushima and Ibaraki, southern Japan Trench

*Koichiro Obana[1], Gou Fujie[1], Yojiro Yamamoto[1], Yuka Kaiho[1], Yasuyuki Nakamura[1], Seiichi Miura[1], Tsutomu Takahashi[1], Shuichi Kodaira[1]

1. Research and Development Center for Earthquake and Tsunami, Japan Agency for Marine-Earth Science and Technology

After the 2011 Tohoku-oki earthquake, seismicity within the incoming Pacific plate is active in the trench-outer rise region along the Japan Trench. These earthquakes were characterized by normal-faulting focal mechanisms and could provide information about potential source faults of large outer-rise normal-faulting earthquakes. We have conducted earthquake observations in the southern part of the Japan Trench, off Fukushima and Ibaraki region(36º—38º N) by using ocean bottom seismographs (OBSs). The observations were conducted from March to July, 2017. We have deployed 35 OBSs including 14 ultra-deep type OBSs, which can be deployed in the trench-axis area where the maximum water depth was about 7800 m. Earthquakes were detected from continuous OBS records and phase arrival times were picked manually. Then, we relocated earthquakes by using double-difference tomography technique. In the tomography analysis, we used the initial velocity model based on an active seismic study conducted in the study area. Finally, we have obtained hypocenter location of about 1400 earthquakes. We also estimated focal mechanisms by using P-wave first-motion polarities in vertical component seismograms. The results show several linear earthquake clusters in the trench-outer rise region extended in roughly N-S and NNE-SSW directions. Pre-dominance of the normal-faulting focal mechanisms indicate that the earthquakes in the trench-outer rise region were explained by bending-related normal-faulting. The earthquake cluster oriented N-S direction was almost parallel to the strike of the northern Japan Trench, whereas NNE-SSW oriented linear clusters were almost parallel to the strike of the southern Japan Trench. Although the strike of the Japan trench changes from N-S in the north to NNE-SSW in the south at around 38º N, linear clusters parallel to both directions suggest existence of the complicated fault system in the trench-outer rise region in this area. Previous OBS observations along the Japan Trench showed that there was almost no seismicity along the plate boundary and within the overriding plate closed to the trench axis. The trench landward seismicity close to the trench axis observed only within the subducting Pacific plate. However, shallow earthquakes, which could occur along the plate boundary or within the overriding plate, close to the trench axis were observed landward slope of the Japan Trench south of 36.7º N. Seafloor geodetic studies indicated that seaward motion in the landward slope along the southern part of the Japan Trench, while landward motion were observed along the central part of the Japan trench. The characteristic shallow seismicity beneath the landward slope close to the trench axis might relate to the different displacement of the trench landward slope in the southern part of the Japan Trench.

Keywords: oceanic plate, outer rise, Japan trench

©2019. Japan Geoscience Union. All Right Reserved.

Influence of water–rock interactions on the strength of outer-rise faults

*Ken-ichi Hirauchi[1]

1. Department of Geosciences, Faculty of Science, Shizuoka University

Knowledge of the amount of water stored in oceanic plates is important for understanding subduction zone water budgets (e.g., Hatakeyama et al., 2017, *Sci. Rep.*). Beneath the outer rise, the incoming oceanic plate bends down into the trench, resulting in the formation of extensional normal faults (i.e., outer-rise faults). Seismic reflection studies have shown that these normal faults penetrate into the upper mantle and act as a permeable fluid pathway. How deep outer-rise faults can develop primarily depends on the depth extent of strain localization within the oceanic lithosphere. Infiltration of seawater into outer-rise faults may promote the growth of mechanically weak hydrous phases such as talc and serpentines, perhaps leading to further strain localization. In order to understand effects of water–rock interactions on the strength of the upper mantle, I have conducted high-pressure deformation experiments on simulated peridotite fault gouges in the presence of hydrothermal water (Hirauchi et al., 2016, *Nat. Commun.*). I found that at a temperature of 500˚C and a confining pressure of 1 GPa, the development of talc-bearing, localized shear zones leads to an order-of-magnitude reduction in strength. This finding indicates that water–rock interactions along outer-rise faults play a role in deepening the fault depth and increasing water budgets in the oceanic upper mantle.

Keywords: outer-rise faults, fault strength, hydrous minerals

©2019. Japan Geoscience Union. All Right Reserved.

[J] Oral | S (Solid Earth Sciences)：S-CG Complex & General

Mon. May 27, 2019 1:45 PM - 3:15 PM JST | Mon. May 27, 2019 4:45 AM - 6:15 AM UTC | A05 TOKYO BAY MAKUHARI HALL

[S-CG60] Investigation of inputs to subduction zones: Influence of tectonic processes on the incoming plate

convener:Makoto Yamano(Earthquake Research Institute, the University of Tokyo), Tomoaki Morishita(School of Geoscience and Civil Engineering, College of Science and Technology, Kanazawa University), Gou Fujie(Japan Agency for Marine-Earth Science and Technology), Chairperson:Makoto Yamano(Earthquake Research Institute, University of Tokyo)

Various tectonic processes occur on the seaward side of the trench associated with bending of the incoming oceanic plate, e.g., fracturing of oceanic crust, infiltration of water, and intraplate volcanism. Investigation of these processes and their influence on the incoming plate provides important information on the boundary condition at the trench, inputs to subduction zones. Variation in inputs should significantly affect geophysical/geological phenomena around the plate interface and geochemical cycles in subduction zones. We welcome contributions from a broad range of earth science (geophysics, geology, petrology, and so on) discussing topics related to inputs to subduction zones such as occurrence of tectonic processes due to bending of the incoming plate, modification of the incoming plate by the processes, relationship between the processes and the inherited structure of the incoming plate, and influence of the processes on the subduction plate interface. We hope discussions are made on studies of a variety of subduction zones, including the Japan Trench and the Nankai Trough, and comparative studies among different subduction zones.

1:45 PM - 2:00 PM JST | 4:45 AM - 5:00 AM UTC

[SCG60-07] Seismic image of the incoming oceanic crust entering the central part of the Japan Trench: structural variation caused by petite-spot, bend fault and seamount

*Shuichi Kodaira[1,2], Akane Ohira[1,2], Gou Fujie[1], Tetsuo No[1], Yasuyuki Nakamura[1], Yuka Kaiho[1], Seiichi Miura[1] (1.R&D Center for Earthquake and Tsunami Japan Agency for Marine-Earth Science and Technology, 2.Graduate School of Environment and Information Sciences, Yokohama National University)

2:00 PM - 2:15 PM JST | 5:00 AM - 5:15 AM UTC

[SCG60-08] Dependence of calculation parameters on tsunami height from the outer-rise earthquakes

*Toshitaka Baba[1], Naotaka YAMAMOTO CHIKASADA[2], Yasuyuki Nakamura[3], Gou Fujie[3], Koichiro Obana[3], Seiichi Miura[3], Shuichi Kodaira[3] (1.Graduate School of Science and Technology, Tokushima University, 2.National Research Institute for Earth Science and Disaster Resilience, 3.Japan Agency for Marine-Earth Science and Technology)

2:15 PM - 2:30 PM JST | 5:15 AM - 5:30 AM UTC

[SCG60-09] Bathymetry data analysis and multi-channel seismic reflection survey in the 1933 Sanriku earthquake (Mw 8.4) rupture region

*Tomoko Hanyu[1], Jin-Oh Park[1], Yukari Kido[2] (1.Atmosphere and Ocean Research Institute, The University of Tokyo, 2.Japan Agency for Marine-Earth Science and Technology)

2:30 PM - 2:45 PM JST | 5:30 AM - 5:45 AM UTC

[SCG60-10] Sedimentation process and deformation process before sinking of sediment on oceanic plate: examples in northwest Pacific Ocean and Sumatra

★Invited Papers

*Kiichiro Kawamura[1] (1.Yamaguchi University)

2:45 PM - 3:00 PM JST | 5:45 AM - 6:00 AM UTC

[SCG60-11] Exploring more asthenospheric melt: the preliminary report of KS-18-9 cruise, R/V Shinseimaru

*Naoto Hirano[1], Taku Yutani[2,1], Yuki Katsuragi[1], Jeffrey Anthony Oalmann[3], Fidel Costa Rodriguez[3], KS-18-9 Onboard Scientific Party (1.Tohoku University, 2.University of Bayreuth, 3.Nanyang Technological University)

3:00 PM - 3:15 PM JST | 6:00 AM - 6:15 AM UTC

[SCG60-12] Inputs of Argon on oceanic plate at subduction zones

*Shigeaki Ono[1] (1.Japan Agency for Marine-Earth Science and Technology)

Seismic image of the incoming oceanic crust entering the central part of the Japan Trench: structural variation caused by petite-spot, bend fault and seamount

*Shuichi Kodaira[1,2], Akane Ohira[1,2], Gou Fujie[1], Tetsuo No[1], Yasuyuki Nakamura[1], Yuka Kaiho[1], Seiichi Miura[1]

1. R&D Center for Earthquake and Tsunami Japan Agency for Marine-Earth Science and Technology, 2. Graduate School of Environment and Information Sciences, Yokohama National University

The structure of an incoming oceanic plate influences various seismic behavior in subduction zones. In the outer-rise region of the Japan Trench, young intraplate volcanism, called “petit-spot” volcanism, has been reported (e.g., Hirano et al., 2006). However, to date, only a few geophysical studies have focused on petit-spot volcanism and its modifying effects on the structure of the oceanic crust. In 2017, Japan Agency for Marine-Earth Science and Technology (JAMSTEC) conducted an active-source seismic survey in the trench-outer-rise region of the Japan Trench during cruise KM17-05 of R/V *Kaimei* (Ohira et al., 2018). For refraction studies, a large tuned airgun array with a total volume of 10,600 cubic inches was towed at 10 m depth and fired every 100 m. The seismic data were recorded on 40 OBSs deployed along a 100-km-long line (line A4) with a spacing of 2 km. The multi-channel seismic (MCS) reflection data were collected by R/V *Kairei* using a 6,000-m-long, 444-channel streamer cable during cruise KR11-05 and KR15-07. On the MCS reflection section, we imaged opaque reflections at the top of the oceanic crust and a weak or absent Moho reflection under petit-spot volcanoes. The P-wave velocity model obtained from first-arrival traveltime tomography showed the large velocity reduction at the top of the oceanic crust near petit-spot volcanoes. This velocity reduction can be interpreted as fractures, hydration, and high porosity associated with petit-spot volcanic activity, as well as by the development of bend faulting (e.g., Fujie et al., 2018) and ancient fractures (Fujie et al., 2016). Our results suggest that petit-spot volcanism is one of the contributing factors leading to structural variation and modification of the incoming oceanic plate prior to its subduction. In 2018, additional new seismic reflection data from 25 –50 km interval of profiles were acquired during cruise KM18-06 of R/V Kaimei to cover the outer-rise region from 38°N to 36°N at the south of the petit-spot region. The new data provide along-strike structural variations attributed to petite-spot, bend fault and seamount.

Keywords: Japan Trench, Outer-rise, Seismic survey

©2019. Japan Geoscience Union. All Right Reserved.

Dependence of calculation parameters on tsunami height from the outer-rise earthquakes

*Toshitaka Baba[1], Naotaka YAMAMOTO CHIKASADA[2], Yasuyuki Nakamura[3], Gou Fujie[3], Koichiro Obana[3], Seiichi Miura[3], Shuichi Kodaira[3]

1. Graduate School of Science and Technology, Tokushima University, 2. National Research Institute for Earth Science and Disaster Resilience, 3. Japan Agency for Marine-Earth Science and Technology

Huge subduction zone earthquakes often induced outer-rise earthquakes occurring on the sea side from the trench axis. An outer-rise earthquake of M8 class which becomes a pair of the 2011 Tohoku earthquake has not yet been occurred. We should pay much attention on the next outer-rise earthquakes and resulting tsunamis in the Japan Trench. A data base (DB) retrieval type system is common for real-time tsunami prediction. It is necessary to incorporate various kinds of earthquake scenarios into DB without deficiencies. However, we have no clear answer to questions such as to how many every kilometer to be set in the depth of the fault stored in the DB in order to guarantee the prediction accuracy of a tsunami. Therefore, in this study, sensitivity analysis of calculation parameters was carried out for tsunamis caused by the outer-rise earthquakes.

We set nine basic fault models of the outer-rise earthquakes with reference to the results of crustal structure surveys and ocean bottom seismic observations. Each basic fault model was composed of multiple small subfaults of about 20 km in length, and the top end of the small subfaults were all set to be 0.1 km under the seafloor, the slope angle was 60 ˚, and the rake angle was 270 ˚. The strike angle of the subfaults were based on seafloor topography and crustal structure surveys. Magnitude (M) of the modeled outer-rise earthquake was calculated from the total fault length (L) using an outer-rise earthquake scaling law complied by Álvarez-Gómez et al. (2012). The fault width (W) was constrained at the lower end of the seismogenic layer, but it was given as L/W = 1 until reaching the lower end. The thickness of the seismogenic layer was set at 35 km. Slip amount was calculated from the fault area and M. Crustal deformation due to the faulting was calculated assuming a semi-infinite homogeneous elastic medium (Okada, 1985). The initial sea surface distribution was obtained considering the effect of tsunami excitation by horizontal movement of the slope (Tanioka and Satake, 1996) and the hydraulic filter (Kajiura, 1963) on the calculated seafloor crustal deformation. For tsunami calculations, the nonlinear shallow water equations were solved on a finite difference scheme.

Tsunamis were calculated by changing the calculation parameters and methods of the basic model one by one. The investigated cases were when using the dip angle of (1) 45 ˚or (2) 75 ˚against the dip angle of 60 ˚of the basic model, (3) when using the model approximated by single subfault, (4) when ignoring the effect of horizontal movement of the slope , (5) when ignoring the hydraulic filter, (6) when using different fault scaling laws, and (7) when using the nonlinear dispersive equations in the tsunami calculations. For the coastal tsunami height, the residuals from the basic model were evaluated by the root mean square error normalized by average tsunami height (NRMSE).

In this study, the difference in the coastal maximum tsunami height between the basic model and the derived model was large when (6) the fault scaling law was different (NRMSE ~ 0.50). This is followed by (7) without dispersion (NRMSE = 0.28), (5) without hydraulic filter (NRMSE = 0.21), (1)(2) when using the different dip angle in the subfault (NEMSE ~ 0.15), and (3) when approximating with a single fault (NRMSE = 0.10). Since the outer rise earthquake is a high-angle fault occurring in the relatively flat ocean, the effect of horizontal movement of the slope is relatively small (NRMSE = 0.025).

This research is supported by Grant-in-Aid for Scientific Research 15H05718.

©2019. Japan Geoscience Union. All Right Reserved.

Keywords: Outer rise earthquake, Tsunami, Numerical simulation

©2019. Japan Geoscience Union. All Right Reserved.

Bathymetry data analysis and multi-channel seismic reflection survey in the 1933 Sanriku earthquake (Mw 8.4) rupture region

*Tomoko Hanyu[1], Jin-Oh Park[1], Yukari Kido[2]

1. Atmosphere and Ocean Research Institute, The University of Tokyo, 2. Japan Agency for Marine-Earth Science and Technology

In the northern part of the Japan Trench, the 1933 Showa-Sanriku earthquake (Mw 8.4), a normal-faulting earthquake such as large tensional outer-rise earthquake, occurred 37 yr after the 1896 Meiji-Sanriku tsunami earthquake (Mw 8.0) that ruptured plate-interface. Both earthquakes generated tsunamis that caused serious damages along the Sanriku coast of northeast Japan. As such, similar large-scale outer-rise earthquake is predicted to occur after the 2011 Tohoku-Oki earthquake (Mw 9.0). However, evolution process of the outer-rise earthquake fault has been poorly understood so far. From seismological data, Kanamori (1971) indicated that the faulting, with the average slippage on the fault plane, dipping 45˚ towards N 90˚W, amounts to 3.3 m, took place over the entire thickness of the lithosphere that caused the Showa-Sanriku earthquake. However, the large fault that penetrated from seafloor to upper mantle has not been identified yet. In order to obtain detailed images of the normal faults that cause the outer-rise earthquakes of the Japan Trench, we will carry out a multi-channel seismic reflection survey using R/V Shinsei-maru in April 2019. Before the survey, fine scale bathymetry data sets (90 meters grid), which were compiled and provided by JAMSTEC (after Kido et al., 2011), are used for the analysis of seafloor structure. In this study, we applied second-order differentiation to detect the horst-graben structures with slope at a steep angle.

The characteristics of horst-graben structures and inherited seafloor spreading fabric in our study are well concordant to those of Nakanishi (2011). In the region between 37.5˚N–40˚N, the horst-graben structures with trend of N20˚E–N30˚E are sometime broken continuity by the abyssal hills with trend of N50˚E–N70˚E and fault structures with trend of N20˚W. In a part of this region, between 38˚N–39˚N, was considered that this region was formed as a result of the ridge propagation (Nakanishi, 2011). The structure boundary on the crustal surface and Moho is observed by the OBS survey (Fujie et al., 2016) that located at a fracture zone associated with the ridge propagation, although the length of the distorted crustal surface and Moho across the fracture zone is extended about 60 km. Note that, Nakanishi (2011) suggested that the fault structures with trend of N20˚W are inherited seafloor spreading fabric and reactivated by the subduction. On the other hand, Kobayashi et al. (1998) interpreted that these faults are formed by the orientation change of the plate strength which is caused by the trend change of the trench axis from south to north along the Japan Trench. A few faults with slope angle of more than 50 degrees are recognized, but there is lack of continuity. Around the 39.5˚ N, continuous horst-graben structures with slope angle of about 30 degrees are confirmed. These continuous horst-graben structures have average vertical displacement of about 200 m. The longest horst-graben structure has length of about 250 km, and the northern portion of this fault reaches the hypocenter of Showa-Sanriku earthquake. It remains uncertain whether this structure is actually continuous or just apparently continuous. Because of the overlying sediment and lower resolution than that of seismic reflection data, the accurate slope angle and vertical displacement could not be obtained from only the bathymetry data. While, the large horst-graben structures could be detected by the bathymetry data and analysis of the bathymetric data is useful for planning the observation lines and pick-up the specific observation data set from the database. We will present the results of the bathymetry data analysis and preliminary results of the multi-channel seismic reflection survey in April 2019, and discuss the normal fault behavior associated with the outer-rise earthquakes.

©2019. Japan Geoscience Union. All Right Reserved.

Keywords: Japan Trench, Outer-rise, Normal fault associated with the outer-rise earthquakes, Bathymetry data, Multi-channel seismic reflection survey

©2019. Japan Geoscience Union. All Right Reserved.

Sedimentation process and deformation process before sinking of sediment on oceanic plate: examples in northwest Pacific Ocean and Sumatra

*Kiichiro Kawamura[1]

1. Yamaguchi University

The sediments covering subducting oceanic plate are pressed into continents. Sometimes it forms an accretionary prism, and they may collapse into submarine landslides in some cases. Also, it may become a fault zone during the further subducting process. Thus, the sediment on the subducting oceanic plate plays an important role in the continental deformation process in the subduction zones. From the above viewpoint, it is a currently required research topic to compare sedimentological, mineralogical and mechanical characteristics of sediment on the subducting plate before and after subducting. In this paper, I report the characteristics of sediments before subducting in the Northwest Pacific and off Sumatra in detail.

As a sedimentary feature, in the northwest Pacific, the effect of the bottom current is large, and it appears in sediments and ocean bathymetry as shown below. In this area, the Pacific plate is subducting into the Izu-Ogasawara Trench on the south part, the Japan Trench and the Kuril Trench in the northern part. In this area, a strong north - south bottom current along the trench axis has been observed at about 6000 m in water depth (Lee et al., 2003, etc), from the north to the south on the land side (Owens and Warren, 2001). Furthermore, in the deep ocean of the Pacific Ocean, flow from west to east is reported (Fujio and Yanagimoto, 2005).

18 sediment samples have been collected using a 4-m piston corer system. The samples are composed mainly of diatomaceous hemipelagic clay and volcanic ash layers. The volcanic ash layer is dated using the glass refractive index measurement. Various sedimentary structures are found in the clay layer, and in particular, on the trench axis, eroded surfaces are seen, suggesting the influence of bottom currents along the trench axis. The effect of the bottom current also is detected in the magnetic susceptibility anisotropy data. In addition, it is suggested that topographical features by the bottom current is also found from an asymmetric depression and/or moat (depth of several tens of meters, width of several kilometers) around a knoll. Thus, from sediments and submarine topography, The sediment and topographic features would suggest that we could understand the predominant bottom current directions in the northwest Pacific during the geological time scale of several thousand years.

As a mechanical feature, burial consolidation and/or diagenesis are one of the important processes in sediments before subducting. It is known that when deposits are consolidated during burial, dehydration progresses in response to stress and the microstructure gradually changes accordingly. They are called to be a card house structure in the shallow part, a book house structure in the middle part, and a shale-like (preferred horizontally orientation) structure in the deep part. They would be proceed by creeping by particle rotation and sliding and are generally considered to be secondary consolidation that occurs after primary compaction caused by reduction of excess pore fluid pressure. Burial consolidation causes gradual hardening of sediments, but the rate of change of its mechanical properties varies depending on various factors such as deposition rate, geothermal gradient, pore water chemical composition, particle composition. For example, the shale-like structure occurs at an void ratio of about 1.0 in the input

©2019. Japan Geoscience Union. All Right Reserved.

sediments of the Izu-Ogasawara trench and occurs at about 0.5 off Sumatra. In addition, in the Izu-Ogasawara Trench and the input sediments off the coast of Sumatra, various deformation structures of the normal fault system are observed as a deformed structure before subducting.

By clarifying the sedimentary features such as the input sediments and the surrounding seabed topography, it is possible to interpret the difference of the deposition rate, the distribution area of the layer thickness of the sediment and so on. In addition, the mechanical characteristics represent the pre-additional deformation process before subducting, that is, in the area where the accretionary prism body is developing. The detailed characteristics of the sediments before subducting as described above will be important information for comparing deposits after subducting.

Keywords: Input sediments, Northwest Pacific, Sumatra

©2019. Japan Geoscience Union. All Right Reserved.

Exploring more asthenospheric melt: the preliminary report of KS-18-9 cruise, R/V Shinseimaru

*Naoto Hirano[1], Taku Yutani[2,1], Yuki Katsuragi[1], Jeffrey Anthony Oalmann[3], Fidel Costa Rodriguez[3], KS-18-9 Onboard Scientific Party

1. Tohoku University, 2. University of Bayreuth, 3. Nanyang Technological University

The petit-spot magmas originate from the asthenosphere, ascending along the flexed zone of the outer-rise prior to plate subduction (Hirano *et al.*, 2006, *Science* 313, 1426; Valentine & Hirano, 2010, *Geology* 38, 55; Yamamoto *et al.*, 2014, *Geology* 42, 967; Machida *et al.*, 2015, *EPSL* 426, 267). This forms a unique opportunity to examine the asthenosphere below the ocean in a region outside of the well-examined but spatially restricted areas of MORs and hotspots. Recent researches, however, indicates that most of petit-spot erupted on concavely flexed plate are highly reacted with the depleted lithosphere during the magma ascending to surface. Geochemical composition of entrained xenolith from depleted mantle is disturbed by wall-rock interaction (Pilet *et al.*, 2016, *Nature Geosci.* 9, 898). From the observation that silica-poor alkaline melt is shifted to silica-rich subalkaline melts as a result of metasomatic interaction with lithospheric peridotite, the wall-rock interaction with silica-poor and strongly alkaline melts produces melts such as the majority of those at petit-spot lavas in NW Pacific (Pilet *et al.*, 2008, *Science* 320, 916). Experimental studies conducted by Machida *et al.* (2017, *Nature Comm.* 8, 14302), moreover, reported that the NW Pacific petit-spot melts were last equilibrated with peridotite at 1.5–2 GPa corresponding to the mid-depth or lower part of NW Pacific lithosphere as well. The melt fractionation must occur at depths greater than the mid-lithosphere because the geobarometer of peridotitic xenoliths shows the deepest 43 km (Yamamoto *et al.*, 2014) in spite of the lack of olivine phenocrysts. The most of petit-spot magma fractionated in mid- or lower lithosphere with some metasomatic reactions with depleted mantle at lower lithosphere during the magma-ascending to surface.

We newly discovered the directly ascending petit-spot melt from asthenosphere (Sato *et al.*, 2018, *Int'l. Geol. Rev.* 60, 1231). The lavas, silica-poor and strongly alkaline with phenocrystic olivines, are completely discriminated from the majority of previously reported petit-spot. They selectively erupt atop the outer-rise wherein the lithosphere behaves entirely in an extensional regime during the ascent of melt from asthenosphere. We conducted several dredge samplings in order to access the asthenosphere more directly, by the research cruise KS-18-9, R/V *Shinseimaru*, in August 2018, supported by AORI, Tokyo University, and the JSPS Japanese-German Graduate Externship. Special thanks to shipboard scientific party (S. Machida, N. Akizawa, T. Ishii, A. Matsumoto, M. Kaneko, Y. Sato, Y. Nakano, T. Yutani, K. Azami, S. Sakai, Y. Katsuragi), captain A. Tsuji, and crews on KS18-09, R/V Shinsei.

The petit-spot rocks are dredged at a lava field displayed by multibeam survey without any topographic highs, which are small blocks surrounding very fresh glass with less palagonitic alteration and manganese coating, implying the lavas are quite young. The quenched glass rinds were analysed for major and trace elements by an electoron microprobe at University of Bayreuth, Germany (co-work with T. Yutani), and an inductively coupled plasma–mass spectrometer (LA-ICP-MS) at Nanyang Technological University, Singapore (co-work with F. Rodriguez, J. Oalmann, Y. Katsuragi), respectively. As we gained "directly ascending petit-spots" from several volcanoes on this cruise, it is possible to recognize their source and melting process from their geochemical variations. The strongly alkaline lavas, directly ascending petit-spot, show clear trend in Zr/Hf, Sm/Hf ratios and HREEs, implying the carbonatite addition with the depth in source mantle. We present here the several processes of lithospheric flexure, metasomatized

©2019. Japan Geoscience Union. All Right Reserved.

lithosphere, magma-fractionation, and finally, upwelling directly from asthenosphere occur prior to trench-oceanward slope, which would be significant components into the incoming oceanic plate.

Keywords: petit-spot, asthenosphere, Pacific plate, alkali-basalt, outer rise

©2019. Japan Geoscience Union. All Right Reserved.

Inputs of Argon on oceanic plate at subduction zones

*Shigeaki Ono[1]

1. Japan Agency for Marine-Earth Science and Technology

It is known that noble gases are key tracers to understand the evolution of the mantle because of their inertness nature and isotope variations. However, a mechanism of recycle of noble gases in the deep mantle is still open question. Argon is one of noble gases and has three isotopes, ^{36}Ar, ^{38}Ar, and ^{40}Ar. Holland and Ballentine [2006] proposed that Ar from the mantle is identical to seawater component. This indicates that the seawater recycling dominates a behavior of Ar in the mantle. In contrast, the systematic analysis for noble gases indicates that ocean island basalt has a primordial signature which is different from atmosphere component [Mukhopadhyay 2012]. The recycling of Ar between the Earth’s surface and the deep mantle has been discussed using the isotope data of noble gases. However, it is difficult to understand a mechanism of recycling of Ar because of a lack of knowledge for physical and chemical properties of Ar at high pressure and high temperature.

In this study, we used density functional theory to investigate the melting temperature and thermal pressure of Ar. We also performed the high-pressure experiments to determine the room-temperature equation of state for Ar. The combination of the first-principles molecular dynamics calculations and the high-pressure experiments led us to determine reliable physical properties, such as the equation of state and the melting temperature, over a wide range of pressures and temperatures.

The equation of state of Ar has been investigated to 382 GPa and 3000 K using the diamond anvil cell experiments and the first-principles molecular dynamics method. A large volume dependence of the thermal pressure of Ar was revealed at pressures higher than 200 GPa. A significant temperature dependence of the calculated effective Grüneisen parameters was confirmed at high pressures. This indicates that the conventional approach to analyze thermal properties using the Mie-Grüneisen approximation is likely to have a significant uncertainty in determining the equation of state for Ar, and that an intrinsic anharmonicity should be considered to analyze the equation of state. A melting temperature of Ar was estimated from calculation data, and a significant pressure dependence was confirmed. If the pressure-temperature path of the subducted slab is lower than critical condition, ~750 K and ~7.5 GPa, solid Ar can be carried down into the deep mantle. Melting of solid Ar in the upwelling mantle plume occurs at the bottom of the transition zone.

Keywords: Argon, Oceanic plate, Mantle, Equation of state

©2019. Japan Geoscience Union. All Right Reserved.

[J] Poster | S (Solid Earth Sciences)：S-CG Complex & General

Mon. May 27, 2019 3:30 PM - 5:00 PM JST | Mon. May 27, 2019 6:30 AM - 8:00 AM UTC | Poster Hall International Exhibition Hall8, Makuhari Messe_18

[S-CG60] Investigation of inputs to subduction zones: Influence of tectonic processes on the incoming plate

convener:Makoto Yamano(Earthquake Research Institute, the University of Tokyo), Tomoaki Morishita(School of Geoscience and Civil Engineering, College of Science and Technology, Kanazawa University), Gou Fujie(Japan Agency for Marine-Earth Science and Technology)

Various tectonic processes occur on the seaward side of the trench associated with bending of the incoming oceanic plate, e.g., fracturing of oceanic crust, infiltration of water, and intraplate volcanism. Investigation of these processes and their influence on the incoming plate provides important information on the boundary condition at the trench, inputs to subduction zones. Variation in inputs should significantly affect geophysical/geological phenomena around the plate interface and geochemical cycles in subduction zones. We welcome contributions from a broad range of earth science (geophysics, geology, petrology, and so on) discussing topics related to inputs to subduction zones such as occurrence of tectonic processes due to bending of the incoming plate, modification of the incoming plate by the processes, relationship between the processes and the inherited structure of the incoming plate, and influence of the processes on the subduction plate interface. We hope discussions are made on studies of a variety of subduction zones, including the Japan Trench and the Nankai Trough, and comparative studies among different subduction zones.

[SCG60-P01] Tsunami Simulations of the 2006 and 2007 Kuril Earthquakes

Cancelled

*Keiji Akai[1] (1.Graduate School of Advanced Technology and Science, Tokushima University)

[SCG60-P02] The variation of seismic attributes about incoming oceanic crust in Nankai Trough using multi-channel seismic reflection data

*Mikiya Yamashita[1], Seiichi Miura[1], Ayako Nakanishi[1], Jin-Oh Park[2], Shuichi Kodaira[1] (1.Japan Agency for Marine-Earth Science and Technology, 2.Department of Ocean Floor Geoscience, Atmosphere and Ocean Research Institute, The University of Tokyo)

[SCG60-P03] Bending-Related Topographic Structures of the Subducting Plate in the Southeastern Pacific Ocean

*Reno Kotate[1], Masao Nakanishi[2] (1.Chiba University Graduate School Science and Engineering Dvision of Earth and Environmental Scienes Department of Earth Sciences, 2.Chiba University Graduate School Faculty of Science)

[SCG60-P04] Detailed tectonic structure of the Japan Trench subduction zone off Miyagi by 2D pre-stack depth migration imaging

*GUO CHEN[1], Jin-Oh Park[1] (1.The University of Tokyo)

[SCG60-P05] Conductive zone of incoming Pacific Plate in the outer rise region off Japan trench

*Shinya Sato[1], Tada-nori Goto[1], Takafumi Kasaya[2], Hiroshi Ichihara[3], Makoto Yamano[4] (1.Kyoto Univesity, Graduate School of Engineering, 2.Japan Agency for Marine-Earth Science and Technology, 3.Nagoya University, Graduate School of Environmental Studies, 4.University of Tokyo, Earthquake Research Institute)

[SCG60-P06] Geochemical variations of the asthenosphere inferred from the geochemistry of petit-spot lavas in the NW Pacific plate

*Yuki Katsuragi[1], Naoto Hirano[1], Kenji Shimizu[2], Fidel Costa[3], Jaffrey Oalmann[3], Taku Yutani[1] (1.Tohoku University, 2.Kochi Core Center, Kochi University / JAMSTEC, 3.Nanyang Technological University)

Tsunami Simulations of the 2006 and 2007 Kuril Earthquakes

*Keiji Akai[1]

1. Graduate School of Advanced Technology and Science, Tokushima University

On November 15, 2006, an earthquake (Mw8.3) occurred off the Kuril Islands (the 2006 Kuril earthquake). Following tsunami was observed in the coastal region in Japan, Hawaii and North, Central and South America. About 2 month later, on January 13, 2007, another earthquake (Mw8.1) occurred and the tsunami was also observed (the 2007 Kuril earthquake). At the 2006 Kuril earthquake, tsunami warning had been cancelled in Japan before the maximum wave arrived. After the 2010 Chile Maule tsunami and the 2011 Tohoku tsunamis, technology simulating far-field tsunami was well developed including effect of elastic deformation of the Earth during tsunami propagation. In this study, using the new simulation method for the far-field tsunami, we revisited at the 2006 and 2007 Kuril earthquakes. The new simulation method has not been validated on tsunami cause by the outer-rise earthquakes, so that, especially, we focus on the 2007 Kuril earthquake because it was an outer-rise event.

In the tsunami calculations, tsunami sources were calculated by fault parameters from IISEE HP and Fujii and Satake (2008) with analytical solution using homogeneous elastic media. Tsunami propagations were solved by nonlinear shallow water equations with effects of dispersion, elastic loading and sea water density stratification on a finite difference scheme. We used GEBCO data resampled by 5 arc-min. and time step with of 5 s to calculate tsunami for 24 hours. The calculated tsunamis were compared with observed data by DARTs. As the results, the 2006 Kuril tsunami had been well modelled at the DART observation points in terms of arrival time and the maximum amplitude. However, for the 2007 Kuril tsunami, the agreement between the calculated and observed data were not good as the 2006 Kuril tsunami. The misfit became large as the lapse of time. This discrepancy may be caused by insufficient resolution of bathymetric data because the outer-rise earthquakes generate tsunami shorter wavelength than that of the subduction zone earthquakes.

Keywords: Outer-rise earthquake, Kuril earthquakes, Tsunami simulation

©2019. Japan Geoscience Union. All Right Reserved.

The variation of seismic attributes about incoming oceanic crust in Nankai Trough using multi-channel seismic reflection data

*Mikiya Yamashita[1], Seiichi Miura[1], Ayako Nakanishi[1], Jin-Oh Park[2], Shuichi Kodaira[1]

1. Japan Agency for Marine-Earth Science and Technology, 2. Department of Ocean Floor Geoscience, Atmosphere and Ocean Research Institute, The University of Tokyo

The physical properties of seismic reflection profiles include many geological information with tectonic setting. Nankai Trough is one of the best places to reveal the characteristics about plate boundary of subducting oceanic plate for understanding the large disaster earthquake because there are many exploration data. Japan Agency for Marine-Earth Science and Technology carried out high-resolution multi-channel seismic reflection (MCS) survey in Shikoku Basin along the Nankai Trough by using R/V Kaiyo with high-resolution portable system in 2012 and 2014. To reveal the characteristics of the subducting oceanic plate is important to evaluate the property of plate boundary for understanding the large disaster earthquake. We evaluate not only structure of MCS profiles, but also the variations of reflection strength about the top of oceanic crust of incoming plate.

MCS profiles of lines KY12-4 and SB01 were obtained along the Nankai Trough. These data were valuable for case study by comparison about physical properties from seismic attribute of top of oceanic crust. In order to extract the physical properties from the reflector of top of oceanic crust, we apply seismic attributes analysis for these data. Seismic attributes are measured from seismic data that can be analyzed in order to enhance information that might be well understanding in a traditional seismic image (Tarner et al. 1979). The seismic envelope attributes often use the reflection strength of the reflector (e.g. Tsuji et al. 2007). The envelope of seismic attributes means the envelope of seismic signal. These attributes are good for looking at packages of amplitudes. We select the second derivative of single envelope as reflection strength of top of oceanic crust. Although calculated seismic attributes of reflection strength indicate the high intensities in the central part of Shikoku Basin, the west and east part of Shikoku Basin where is initial stage of spreading of Shikoku Basin have the small intensities. This suggests that the reflection strength of top of oceanic crust is affected by the created condition of oceanic crust. We also discuss about the relationship between the reflection strength of top of oceanic crust and the thickness of sediments of Shikoku Basin.
This study is part of 'Research project for compound disaster mitigation on the great earthquakes and tsunamis around the Nankai trough region' funded by Ministry of Education, Culture, Sports, Science and Technology, Japan.

©2019. Japan Geoscience Union. All Right Reserved.

Bending-Related Topographic Structures of the Subducting Plate in the Southeastern Pacific Ocean

*Reno Kotate[1], Masao Nakanishi[2]

1. Chiba University Graduate School Science and Engineering Dvision of Earth and Environmental Scienes Department of Earth Sciences, 2. Chiba University Graduate School Faculty of Science

Oceanic plates bend near trenches before subduction. The bending causes elongated topographic structures such as ridges and escarpments on the incoming oceanic plate. The elongated topographic structures facilitate the infiltration of seawater into the oceanic plate. The amount of water in the subducting plate is one of the important properties controlling subduction. Therefore, the study of bending-related topographic structures on the incoming plate is one of the imperative studies of the subduction zone.

The strike of bending-related topographic structures on the oceanward trench slopes is parallel to the trench axis or inherited seafloor spreading fabric (Kobayashi et al.,1995,1998). Nakanishi (2017) pointed out the following rule for the topographic structures.

1. Most of bending-related topographic structures near the trenches in the northwestern Pacific Ocean are limited to less than about 80 km from the trench axis.

2. Seafloor spreading fabric is reactivated where the angle between the fabric and trench axis is less than about 30˚.

3. The above rules are not applicable to curved trenches and trenches near seamounts or other volcanic edifices constructed by off-ridge volcanism.

To find out that the above rule is appropriate to the whole trenches in the southeastern margin of the Pacific Ocean, we made the bathymetric maps and described the bending-related topographic structures from Middle America Trench to Peru-Chile Trench.

The bending-related topographic structures are limited to less than 60 km from the trench axis for the Peru Trench and the northern part of the Peru-Chile Trench. In the southern part of Peru-Chile Trench, elongated topographic structures parallel to the magnetic anomaly lineation are confirmed more than 150 km from the trench axis. The throw of the structures doesn’ t increase toward the trench axis, implying that it is difficult to distinguish the structures are made by reactivation of seafloor spreading fabric. Elongated topographic structures in the Middle America Trench are found more than 250 km from the trench axis. The structures are parallel to the magnetic anomaly lineations. The throw of the structures starts to increase from the distance of 150 km to the trench axis. This indicates that the elongated structures are grown by reactivation of seafloor spreading fabric and the bending-related topographic structures are limited to less than 150 km from the trench axis in the Middle America Trench.

The bending-related topographic structures in the Middle America Trench and the southern part of the Peru Trench are parallel to the magnetic anomaly lineations. The angle between the structures and the trench axis is less than 30˚. The bending-related topographic structures in the northern parts of the Peru and Peru-Chile Trenches are parallel to the trench axis. The angle between the structures and the trench

©2019. Japan Geoscience Union. All Right Reserved.

axis is more than 30˚. Our study concluded that the rule proposed by Nakanishi (2017) is applicable to the trenches of the southeastern margin in the Pacific Ocean.

Keywords: plate bending, Bending-related fault topography, abyssal hill, subduction zone

©2019. Japan Geoscience Union. All Right Reserved.

Detailed tectonic structure of the Japan Trench subduction zone off Miyagi by 2D pre-stack depth migration imaging

*GUO CHEN[1], Jin-Oh Park[1]

1. The University of Tokyo

The 2011 Tohoku earthquake (Mw 9.0) has been extensively examined by many geophysical data from state-of-the-art observational networks deployed both globally and locally. There were lots of studies to investigate the tectonic structure of the 2011 coseismic rupture zone. However, there were a few detailed seismic reflection images about both shallow and deep structure, because of the complicated geologic structure. In order to figure out detailed geologic structure and P-wave velocity modelof the Japan Trenchsubduction zone off Miyagi, northeast Japan, we tried to do 2D pre-stack depth migration (PSDM) imaging using multi-channel seismic (MCS) reflection data acrossthe2011 Tohoku coseismic rupture zone. Pre-processing to get CDP gathers with high S/N ratio includes trace editing, pre-filtering, spherical divergence correction, debubbling, deghosting, and surface-related multiple attenuation (SRMA).After air gun shots, a main pulse and following bubble oscillations were recorded, even though the air gun was tuned. In order to suppress the periodic bubble oscillations, we designed debubble filter. We used shot gather data with gain, trace header modification, sort and static application to extract the bubble signature from the raw MCS data, eventually producing a filter with ~30 Hz bubble waveform.In marine MCS data acquisition, source (air gun) and receiver (streamer cable) ghosts are recorded as notches in power spectrum. These secondary wavefield usually corrupts the raw data, depending on offset, time and geologic dip. We designed deghost filter to reduce the source and receiver ghosts. Like no other time before, we used both horizon-based tomography and grid-based tomography during the PSDM processing. Horizon-based tomography and grid-based tomography are global approaches which involve a solution of simultaneous set of equations for calculating the updating parameters of the velocity-depth model. In the horizon-based tomography, we built a depth-velocity model along which the residuals were picked, and updated both the depth surfaces and velocity of each layer. The updates are calculated at equally spaced spline nodes and then interpolated. After the horizon-based tomography, we inputted this velocity section into 2D auto-picker and calculated the QC semblance for defining a complete depth surface and updated for velocity at equally spaced points on a 2D grid. We recognize a bright reflector as the topmost oceanic crust (i.e., plate interface) of the Pacific plate subducting beneath the overlying Okhotsk plate, which can be traceable to more than 100 km landward from the Japan Trench axis. The seaward Pacific plate is characterized by horst and graben structure with normal faults. A strong reflector of Moho discontinuity, which is observed beneath the oceanic crust before subduction, is also observed even after subduction of the Pacific plate, up to more than 100 km landward from the Japan Trench axis. In the upper plate, we identify the Neogene sedimentary layer overlying the Cretaceous erosional unconformity, andseverallargereversefaultsdevelopingwithin theCretaceous basement. The backstop interface showshigh amplitude and negative polarityreflection that may be indicative offluid-rich fault. We observe a reflection of Arc Moho at depth of about 20 km. We can also observe megalens structure along plate interface at about 15-20 km depth, which is similar in Costa Rica subduction zone.

©2019. Japan Geoscience Union. All Right Reserved.

Conductive zone of incoming Pacific Plate in the outer rise region off Japan trench

*Shinya Sato[1], Tada-nori Goto[1], Takafumi Kasaya[2], Hiroshi Ichihara[3], Makoto Yamano[4]

1. Kyoto Univesity, Graduate School of Engineering, 2. Japan Agency for Marine-Earth Science and Technology, 3. Nagoya University, Graduate School of Environmental Studies, 4. University of Tokyo, Earthquake Research Institute

Various geophysical surveys have been operated in order to expose the subsurface structure of incoming Pacific plate in the outer rise region off Japan trench. One of the targets is existence of water in the plate, and two geophysical surveys (seismic surveys and heat flow measurements), which were conducted independently, in the outer rise region reported recently the possibility of water existence in the plate. The seismic surveys (e.g., Fujie et al., 2016; Fujie et al., 2018) visualized the subsurface structure indicating low velocity in the oceanic crust and below the boundary between crust and lithosphere (i.e., Moho) although there are high pressures. Also, the heat flow measurements (e.g., Yamano and Kawada, 2017) reported high heat-flow anomalies in the region, and suggested the possibilities that the anomalies were triggered by the water through the permeable layer in the plate. However, the existence of water in the deep portion below the oceanic crust has not been well known, and the source of water is now being discussed. A marine magnetotelluric (MT) survey was conducted in the outer rise region with distant of 100 –200 km from the Japan trench. This survey' s target is to verify the existence of water in the oceanic mantle visualizing the subsurface resistivity structure. We recorded electromagnetic data (MT data) for the analysis of subsurface resistivity structure at four locations with water depth of about 5500 m. Unfortunately, one of four data failed to record the MT data appropriately, and the other data included large noises, whose source were possibly the instruments themselves. We applied the noise-reduction method based on Frequency Domain Independent Component Analysis (Sato et al., 2017) for the estimation of MT responses at the three sites. The resistivity structure was visualized using a 2D inversion code by Uchida and Ogawa (1993) from the derived MT responses. The visualized structure showed two features: i) the boundary between resistive lithosphere and conductive asthenosphere and ii) the conductive zones below the oceanic crust. At the presentation, we will not only show them but discuss the source of conductive zones based on electromagnetic environment, whose model includes the effect of trench or coast.

Keywords: Outer rise region off Japan trench, Conductive zone, Marine magnetotelluric survey

©2019. Japan Geoscience Union. All Right Reserved.

Geochemical variations of the asthenosphere inferred from the geochemistry of petit-spot lavas in the NW Pacific plate

*Yuki Katsuragi[1], Naoto Hirano[1], Kenji Shimizu[2], Fidel Costa[3], Jaffrey Oalmann[3], Taku Yutani[1]

1. Tohoku University, 2. Kochi Core Center, Kochi University / JAMSTEC, 3. Nanyang Technological University

The low seismic velocity and high electrical conductivity of the asthenosphere may be due to the presence of volatile materials (e.g. CO_2 and H_2O) (e.g. Gairrard et al., 2008; Hirschmann, 2010). Recently, the so-called “petit-spot volcanism” which is characterized by submarine eruptions that occur in oceanic plates in response to lithospheric flexures, has been proposed to result from melts directly ascending from the asthenosphere (Hirano et al., 2006; Sato et al., 2018). The lava samples (foidite to trachybasalt) show high vesicularity despite the eruption occurring under high hydrostatic pressure at approximately 6000 meters below sea level (Sato et al., 2018). Here we discuss the volatile, bulk, and Sr-Nd isotopic compositions of quenched glass rinds of petit-spot lavas from the NW Pacific plate, supported by the JSPS Japanese-German Graduate Externship.

The glass has higher volatile contents (H_2O, CO_2, and halogens) than most MORBs and lacks chlorine alteration by seawater. Some samples are clearly oversaturated in CO_2 and H_2O at 60 MPa, which is the submarine hydrostatic pressure. The glass also shows negative anomalies of Zr, Hf and Ti, implying that there is a carbonatitic component in the mantle source. Moreover, Nd and Sr isotope ratios, and some geochemical trends with volatile elements indicate that the magma was derived from an EM1-like mantle component. Therefore, the compositions of the petit-spot lavas can possibly be explained by mixing of DMM and recycled EM1 material with carbonates. The degree of EM1 signature for each eruptive location gradually decreases toward the trench. We suggest that the variation of volatile compositions and Sr-Nd isotopic systematics of petit-spot magmas reflect their temporal and spatial transition in the asthenosphere along the NW Pacific plate track.

Keywords: petit-spot basalt, asthenosphere, volatile elements

©2019. Japan Geoscience Union. All Right Reserved.

[J] Poster | S (Solid Earth Sciences)：S-CG Complex & General

Mon. May 27, 2019 5:15 PM - 6:30 PM JST | Mon. May 27, 2019 8:15 AM - 9:30 AM UTC | Poster Hall International Exhibition Hall8, Makuhari Messe_30

[S-CG60] Investigation of inputs to subduction zones: Influence of tectonic processes on the incoming plate

convener:Makoto Yamano(Earthquake Research Institute, the University of Tokyo), Tomoaki Morishita(School of Geoscience and Civil Engineering, College of Science and Technology, Kanazawa University), Gou Fujie(Japan Agency for Marine-Earth Science and Technology)

Various tectonic processes occur on the seaward side of the trench associated with bending of the incoming oceanic plate, e.g., fracturing of oceanic crust, infiltration of water, and intraplate volcanism. Investigation of these processes and their influence on the incoming plate provides important information on the boundary condition at the trench, inputs to subduction zones. Variation in inputs should significantly affect geophysical/geological phenomena around the plate interface and geochemical cycles in subduction zones. We welcome contributions from a broad range of earth science (geophysics, geology, petrology, and so on) discussing topics related to inputs to subduction zones such as occurrence of tectonic processes due to bending of the incoming plate, modification of the incoming plate by the processes, relationship between the processes and the inherited structure of the incoming plate, and influence of the processes on the subduction plate interface. We hope discussions are made on studies of a variety of subduction zones, including the Japan Trench and the Nankai Trough, and comparative studies among different subduction zones.

[SCG60-P01] Tsunami Simulations of the 2006 and 2007 Kuril Earthquakes

*Keiji Akai[1] (1.Graduate School of Advanced Technology and Science, Tokushima University)

[SCG60-P02] The variation of seismic attributes about incoming oceanic crust in Nankai Trough using multi-channel seismic reflection data

*Mikiya Yamashita[1], Seiichi Miura[1], Ayako Nakanishi[1], Jin-Oh Park[2], Shuichi Kodaira[1] (1.Japan Agency for Marine-Earth Science and Technology, 2.Department of Ocean Floor Geoscience, Atmosphere and Ocean Research Institute, The University of Tokyo)

[SCG60-P03] Bending-Related Topographic Structures of the Subducting Plate in the Southeastern Pacific Ocean

*Reno Kotate[1], Masao Nakanishi[2] (1.Chiba University Graduate School Science and Engineering Dvision of Earth and Environmental Scienes Department of Earth Sciences, 2.Chiba University Graduate School Faculty of Science)

[SCG60-P04] **Detailed tectonic structure of the Japan Trench subduction zone off Miyagi by 2D pre-stack depth migration imaging**

*GUO CHEN[1], Jin-Oh Park[1] (1.The University of Tokyo)

[SCG60-P05] Conductive zone of incoming Pacific Plate in the outer rise region off Japan trench

*Shinya Sato[1], Tada-nori Goto[1], Takafumi Kasaya[2], Hiroshi Ichihara[3], Makoto Yamano[4] (1.Kyoto Univesity, Graduate School of Engineering, 2.Japan Agency for Marine-Earth Science and Technology, 3.Nagoya University, Graduate School of Environmental Studies, 4.University of Tokyo, Earthquake Research Institute)

[SCG60-P06] Geochemical variations of the asthenosphere inferred from the geochemistry of petit-spot lavas in the NW Pacific plate

*Yuki Katsuragi[1], Naoto Hirano[1], Kenji Shimizu[2], Fidel Costa[3], Jaffrey Oalmann[3], Taku Yutani[1] (1.Tohoku University, 2.Kochi Core Center, Kochi University / JAMSTEC, 3.Nanyang Technological University)

Tsunami Simulations of the 2006 and 2007 Kuril Earthquakes

*Keiji Akai[1]

1. Graduate School of Advanced Technology and Science, Tokushima University

On November 15, 2006, an earthquake (Mw8.3) occurred off the Kuril Islands (the 2006 Kuril earthquake). Following tsunami was observed in the coastal region in Japan, Hawaii and North, Central and South America. About 2 month later, on January 13, 2007, another earthquake (Mw8.1) occurred and the tsunami was also observed (the 2007 Kuril earthquake). At the 2006 Kuril earthquake, tsunami warning had been cancelled in Japan before the maximum wave arrived. After the 2010 Chile Maule tsunami and the 2011 Tohoku tsunamis, technology simulating far-field tsunami was well developed including effect of elastic deformation of the Earth during tsunami propagation. In this study, using the new simulation method for the far-field tsunami, we revisited at the 2006 and 2007 Kuril earthquakes. The new simulation method has not been validated on tsunami cause by the outer-rise earthquakes, so that, especially, we focus on the 2007 Kuril earthquake because it was an outer-rise event.

In the tsunami calculations, tsunami sources were calculated by fault parameters from IISEE HP and Fujii and Satake (2008) with analytical solution using homogeneous elastic media. Tsunami propagations were solved by nonlinear shallow water equations with effects of dispersion, elastic loading and sea water density stratification on a finite difference scheme. We used GEBCO data resampled by 5 arc-min. and time step with of 5 s to calculate tsunami for 24 hours. The calculated tsunamis were compared with observed data by DARTs. As the results, the 2006 Kuril tsunami had been well modelled at the DART observation points in terms of arrival time and the maximum amplitude. However, for the 2007 Kuril tsunami, the agreement between the calculated and observed data were not good as the 2006 Kuril tsunami. The misfit became large as the lapse of time. This discrepancy may be caused by insufficient resolution of bathymetric data because the outer-rise earthquakes generate tsunami shorter wavelength than that of the subduction zone earthquakes.

Keywords: Outer-rise earthquake, Kuril earthquakes, Tsunami simulation

©2019. Japan Geoscience Union. All Right Reserved.

The variation of seismic attributes about incoming oceanic crust in Nankai Trough using multi-channel seismic reflection data

*Mikiya Yamashita[1], Seiichi Miura[1], Ayako Nakanishi[1], Jin-Oh Park[2], Shuichi Kodaira[1]

1. Japan Agency for Marine-Earth Science and Technology, 2. Department of Ocean Floor Geoscience, Atmosphere and Ocean Research Institute, The University of Tokyo

The physical properties of seismic reflection profiles include many geological information with tectonic setting. Nankai Trough is one of the best places to reveal the characteristics about plate boundary of subducting oceanic plate for understanding the large disaster earthquake because there are many exploration data. Japan Agency for Marine-Earth Science and Technology carried out high-resolution multi-channel seismic reflection (MCS) survey in Shikoku Basin along the Nankai Trough by using R/V Kaiyo with high-resolution portable system in 2012 and 2014. To reveal the characteristics of the subducting oceanic plate is important to evaluate the property of plate boundary for understanding the large disaster earthquake. We evaluate not only structure of MCS profiles, but also the variations of reflection strength about the top of oceanic crust of incoming plate.

MCS profiles of lines KY12-4 and SB01 were obtained along the Nankai Trough. These data were valuable for case study by comparison about physical properties from seismic attribute of top of oceanic crust. In order to extract the physical properties from the reflector of top of oceanic crust, we apply seismic attributes analysis for these data. Seismic attributes are measured from seismic data that can be analyzed in order to enhance information that might be well understanding in a traditional seismic image (Tarner et al. 1979). The seismic envelope attributes often use the reflection strength of the reflector (e.g. Tsuji et al. 2007). The envelope of seismic attributes means the envelope of seismic signal. These attributes are good for looking at packages of amplitudes. We select the second derivative of single envelope as reflection strength of top of oceanic crust. Although calculated seismic attributes of reflection strength indicate the high intensities in the central part of Shikoku Basin, the west and east part of Shikoku Basin where is initial stage of spreading of Shikoku Basin have the small intensities. This suggests that the reflection strength of top of oceanic crust is affected by the created condition of oceanic crust. We also discuss about the relationship between the reflection strength of top of oceanic crust and the thickness of sediments of Shikoku Basin.
This study is part of 'Research project for compound disaster mitigation on the great earthquakes and tsunamis around the Nankai trough region' funded by Ministry of Education, Culture, Sports, Science and Technology, Japan.

©2019. Japan Geoscience Union. All Right Reserved.

Bending-Related Topographic Structures of the Subducting Plate in the Southeastern Pacific Ocean

*Reno Kotate[1], Masao Nakanishi[2]

1. Chiba University Graduate School Science and Engineering Dvision of Earth and Environmental Scienes Department of Earth Sciences, 2. Chiba University Graduate School Faculty of Science

Oceanic plates bend near trenches before subduction. The bending causes elongated topographic structures such as ridges and escarpments on the incoming oceanic plate. The elongated topographic structures facilitate the infiltration of seawater into the oceanic plate. The amount of water in the subducting plate is one of the important properties controlling subduction. Therefore, the study of bending-related topographic structures on the incoming plate is one of the imperative studies of the subduction zone.

The strike of bending-related topographic structures on the oceanward trench slopes is parallel to the trench axis or inherited seafloor spreading fabric (Kobayashi et al.,1995,1998). Nakanishi (2017) pointed out the following rule for the topographic structures.

1. Most of bending-related topographic structures near the trenches in the northwestern Pacific Ocean are limited to less than about 80 km from the trench axis.

2. Seafloor spreading fabric is reactivated where the angle between the fabric and trench axis is less than about 30˚.

3. The above rules are not applicable to curved trenches and trenches near seamounts or other volcanic edifices constructed by off-ridge volcanism.

To find out that the above rule is appropriate to the whole trenches in the southeastern margin of the Pacific Ocean, we made the bathymetric maps and described the bending-related topographic structures from Middle America Trench to Peru-Chile Trench.

The bending-related topographic structures are limited to less than 60 km from the trench axis for the Peru Trench and the northern part of the Peru-Chile Trench. In the southern part of Peru-Chile Trench, elongated topographic structures parallel to the magnetic anomaly lineation are confirmed more than 150 km from the trench axis. The throw of the structures doesn’ t increase toward the trench axis, implying that it is difficult to distinguish the structures are made by reactivation of seafloor spreading fabric. Elongated topographic structures in the Middle America Trench are found more than 250 km from the trench axis. The structures are parallel to the magnetic anomaly lineations. The throw of the structures starts to increase from the distance of 150 km to the trench axis. This indicates that the elongated structures are grown by reactivation of seafloor spreading fabric and the bending-related topographic structures are limited to less than 150 km from the trench axis in the Middle America Trench.

The bending-related topographic structures in the Middle America Trench and the southern part of the Peru Trench are parallel to the magnetic anomaly lineations. The angle between the structures and the trench axis is less than 30˚. The bending-related topographic structures in the northern parts of the Peru and Peru-Chile Trenches are parallel to the trench axis. The angle between the structures and the trench

©2019. Japan Geoscience Union. All Right Reserved.

axis is more than 30˚. Our study concluded that the rule proposed by Nakanishi (2017) is applicable to the trenches of the southeastern margin in the Pacific Ocean.

Keywords: plate bending, Bending-related fault topography, abyssal hill, subduction zone

©2019. Japan Geoscience Union. All Right Reserved.

Detailed tectonic structure of the Japan Trench subduction zone off Miyagi by 2D pre-stack depth migration imaging

*GUO CHEN[1], Jin-Oh Park[1]

1. The University of Tokyo

The 2011 Tohoku earthquake (Mw 9.0) has been extensively examined by many geophysical data from state-of-the-art observational networks deployed both globally and locally. There were lots of studies to investigate the tectonic structure of the 2011 coseismic rupture zone. However, there were a few detailed seismic reflection images about both shallow and deep structure, because of the complicated geologic structure. In order to figure out detailed geologic structure and P-wave velocity modelof the Japan Trenchsubduction zone off Miyagi, northeast Japan, we tried to do 2D pre-stack depth migration (PSDM) imaging using multi-channel seismic (MCS) reflection data acrossthe2011 Tohoku coseismic rupture zone. Pre-processing to get CDP gathers with high S/N ratio includes trace editing, pre-filtering, spherical divergence correction, debubbling, deghosting, and surface-related multiple attenuation (SRMA).After air gun shots, a main pulse and following bubble oscillations were recorded, even though the air gun was tuned. In order to suppress the periodic bubble oscillations, we designed debubble filter. We used shot gather data with gain, trace header modification, sort and static application to extract the bubble signature from the raw MCS data, eventually producing a filter with ~30 Hz bubble waveform.In marine MCS data acquisition, source (air gun) and receiver (streamer cable) ghosts are recorded as notches in power spectrum. These secondary wavefield usually corrupts the raw data, depending on offset, time and geologic dip. We designed deghost filter to reduce the source and receiver ghosts. Like no other time before, we used both horizon-based tomography and grid-based tomography during the PSDM processing. Horizon-based tomography and grid-based tomography are global approaches which involve a solution of simultaneous set of equations for calculating the updating parameters of the velocity-depth model. In the horizon-based tomography, we built a depth-velocity model along which the residuals were picked, and updated both the depth surfaces and velocity of each layer. The updates are calculated at equally spaced spline nodes and then interpolated. After the horizon-based tomography, we inputted this velocity section into 2D auto-picker and calculated the QC semblance for defining a complete depth surface and updated for velocity at equally spaced points on a 2D grid. We recognize a bright reflector as the topmost oceanic crust (i.e., plate interface) of the Pacific plate subducting beneath the overlying Okhotsk plate, which can be traceable to more than 100 km landward from the Japan Trench axis. The seaward Pacific plate is characterized by horst and graben structure with normal faults. A strong reflector of Moho discontinuity, which is observed beneath the oceanic crust before subduction, is also observed even after subduction of the Pacific plate, up to more than 100 km landward from the Japan Trench axis. In the upper plate, we identify the Neogene sedimentary layer overlying the Cretaceous erosional unconformity, andseverallargereversefaultsdevelopingwithin theCretaceous basement. The backstop interface showshigh amplitude and negative polarityreflection that may be indicative offluid-rich fault. We observe a reflection of Arc Moho at depth of about 20 km. We can also observe megalens structure along plate interface at about 15-20 km depth, which is similar in Costa Rica subduction zone.

©2019. Japan Geoscience Union. All Right Reserved.

Conductive zone of incoming Pacific Plate in the outer rise region off Japan trench

*Shinya Sato[1], Tada-nori Goto[1], Takafumi Kasaya[2], Hiroshi Ichihara[3], Makoto Yamano[4]

1. Kyoto Univesity, Graduate School of Engineering, 2. Japan Agency for Marine-Earth Science and Technology, 3. Nagoya University, Graduate School of Environmental Studies, 4. University of Tokyo, Earthquake Research Institute

Various geophysical surveys have been operated in order to expose the subsurface structure of incoming Pacific plate in the outer rise region off Japan trench. One of the targets is existence of water in the plate, and two geophysical surveys (seismic surveys and heat flow measurements), which were conducted independently, in the outer rise region reported recently the possibility of water existence in the plate. The seismic surveys (e.g., Fujie et al., 2016; Fujie et al., 2018) visualized the subsurface structure indicating low velocity in the oceanic crust and below the boundary between crust and lithosphere (i.e., Moho) although there are high pressures. Also, the heat flow measurements (e.g., Yamano and Kawada, 2017) reported high heat-flow anomalies in the region, and suggested the possibilities that the anomalies were triggered by the water through the permeable layer in the plate. However, the existence of water in the deep portion below the oceanic crust has not been well known, and the source of water is now being discussed. A marine magnetotelluric (MT) survey was conducted in the outer rise region with distant of 100 –200 km from the Japan trench. This survey' s target is to verify the existence of water in the oceanic mantle visualizing the subsurface resistivity structure. We recorded electromagnetic data (MT data) for the analysis of subsurface resistivity structure at four locations with water depth of about 5500 m. Unfortunately, one of four data failed to record the MT data appropriately, and the other data included large noises, whose source were possibly the instruments themselves. We applied the noise-reduction method based on Frequency Domain Independent Component Analysis (Sato et al., 2017) for the estimation of MT responses at the three sites. The resistivity structure was visualized using a 2D inversion code by Uchida and Ogawa (1993) from the derived MT responses. The visualized structure showed two features: i) the boundary between resistive lithosphere and conductive asthenosphere and ii) the conductive zones below the oceanic crust. At the presentation, we will not only show them but discuss the source of conductive zones based on electromagnetic environment, whose model includes the effect of trench or coast.

Keywords: Outer rise region off Japan trench, Conductive zone, Marine magnetotelluric survey

©2019. Japan Geoscience Union. All Right Reserved.

Geochemical variations of the asthenosphere inferred from the geochemistry of petit-spot lavas in the NW Pacific plate

*Yuki Katsuragi[1], Naoto Hirano[1], Kenji Shimizu[2], Fidel Costa[3], Jaffrey Oalmann[3], Taku Yutani[1]

1. Tohoku University, 2. Kochi Core Center, Kochi University / JAMSTEC, 3. Nanyang Technological University

The low seismic velocity and high electrical conductivity of the asthenosphere may be due to the presence of volatile materials (e.g. CO_2 and H_2O) (e.g. Gairrard et al., 2008; Hirschmann, 2010). Recently, the so-called “petit-spot volcanism” which is characterized by submarine eruptions that occur in oceanic plates in response to lithospheric flexures, has been proposed to result from melts directly ascending from the asthenosphere (Hirano et al., 2006; Sato et al., 2018). The lava samples (foidite to trachybasalt) show high vesicularity despite the eruption occurring under high hydrostatic pressure at approximately 6000 meters below sea level (Sato et al., 2018). Here we discuss the volatile, bulk, and Sr-Nd isotopic compositions of quenched glass rinds of petit-spot lavas from the NW Pacific plate, supported by the JSPS Japanese-German Graduate Externship.

The glass has higher volatile contents (H_2O, CO_2, and halogens) than most MORBs and lacks chlorine alteration by seawater. Some samples are clearly oversaturated in CO_2 and H_2O at 60 MPa, which is the submarine hydrostatic pressure. The glass also shows negative anomalies of Zr, Hf and Ti, implying that there is a carbonatitic component in the mantle source. Moreover, Nd and Sr isotope ratios, and some geochemical trends with volatile elements indicate that the magma was derived from an EM1-like mantle component. Therefore, the compositions of the petit-spot lavas can possibly be explained by mixing of DMM and recycled EM1 material with carbonates. The degree of EM1 signature for each eruptive location gradually decreases toward the trench. We suggest that the variation of volatile compositions and Sr-Nd isotopic systematics of petit-spot magmas reflect their temporal and spatial transition in the asthenosphere along the NW Pacific plate track.

Keywords: petit-spot basalt, asthenosphere, volatile elements

©2019. Japan Geoscience Union. All Right Reserved.

[J] Oral | S (Solid Earth Sciences)：S-CG Complex & General

Mon. May 27, 2019 1:45 PM - 3:15 PM JST | Mon. May 27, 2019 4:45 AM - 6:15 AM UTC | Convention Hall A 2F

[S-CG61] Dynamics in mobile belts

convener:Yukitoshi Fukahata(Disaster Prevention Research Institute, Kyoto University), Toru Takeshita(Department of Natural History Sciences, Graduate School of Science, Hokkaido University), Hikaru Iwamori(Geochemical Evolution Research Program, Japan Agency for Marine-Earth Science and Technology), Chairperson:Toru Takeshita, Kenta Kobayashi

The dynamic behaviours of mobile belts are expressed across a wide range of time scales, from the seismic and volcanic events that impact society during our lifetimes, to orogeny and the formation of large-scale fault systems which can take place over millions of years. Deformation occurs on length scales from microscopic fracture and flow to macroscopic deformation to plate-scale tectonics. To gain a physical understanding of the dynamics of mobile belts, we must determine the relationships between deformation and the driving stresses due to plate motion and other causes, which are connected through the rheological properties of the materials. To understand the full physical system, an integration of geophysics, geomorphology, and geology is necessary, as is the integration of observational, theoretical and experimental approaches. In addition, because rheological properties are greatly affected by fluids in the crust and fluid chemical reactions, petrological and geochemical approaches are also important. After the 2011 great Tohoku-oki earthquake, large-scale changes in seismic activity and regional scale crustal deformation were observed, making present-day Japan a unique natural laboratory for the study of the dynamics of mobile belts. This session welcomes presentations from different disciplines, such as seismology, geodesy, tectonic geomorphology, structural geology, petrology, and hydrology, as well as interdisciplinary studies, that relate to the dynamic behaviours of mobile belts.

1:45 PM - 2:00 PM JST | 4:45 AM - 5:00 AM UTC

[SCG61-01] Fault zone development in the West Tottori area, Japan

*Kenta Kobayashi[1] (1.Department of Geology, Faculty of Science, Niigata University)

2:00 PM - 2:15 PM JST | 5:00 AM - 5:15 AM UTC

[SCG61-02] **Inerastic deformation around focal area of the 2000 Western Tottori EQ (M7.3) detected by “0.1 manten” Hyper Dense Seismic Observation (2)**

★Invited Papers

*Satoshi Matsumoto[1], Yoshihisa Iio[2], Shin'ichi Sakai[3], Aitaro Kato[3], Takuo Shibutani[2], Yuto Hayashida[4], Group for 0.1 manten Hyper dense seismic observation (1.Institute of Seismology and Volcanology, Faculty of Sciences, Kyushu University, 2.Disaster Prevention Reasearch Institute, Kyoto University, 3.Earthquake Research Institute, University of Tokyo, 4.Graduate School of Science, Kyushu University)

2:15 PM - 2:30 PM JST | 5:15 AM - 5:30 AM UTC

[SCG61-03] Non-double couple micro-earthquakes in the focal area of the 2000 Western Tottori earthquake (M7.3) by "0.1 manten" hyper dense seismic observation

*Yuto Hayashida[1], Satoshi Matsumoto[2], Yoshihisa Iio[3], Shin'ichi Sakai[4], Aitaro Kato[4], Group for "0.1 Manten" hyper dense seismic observation Group registration (1.Department of Earth and Planetary Sciences, Graduate School of Science, Kyushu University, 2.Institute of Seismology and Volcanology, Faculty of Sciences, Kyushu University, 3.Disater Prevention Research Institute, Kyoto University, 4.Earthquake Research Institute, the University of Tokyo)

2:30 PM - 2:45 PM JST | 5:30 AM - 5:45 AM UTC

[SCG61-04] Stress field in the Western Tottori and Western Shimane regions deduced by the dense seismic observations

*Yoshihisa Iio[1], Manten seicmic observation group, Manten seismic observation group in the Western Tottori region (1.Disater Prevention Research Institute, Kyoto University)

2:45 PM - 3:00 PM JST | 5:45 AM - 6:00 AM UTC

[SCG61-05] Modeling the spatiotemporal change in stress field around Hinagu fault zone through the 2016 Kumamoto earthquake sequence, in central Kyushu, Japan

*Ayaho Mitsuoka[1], Satoshi Matsumoto[2], Azusa Shito[2], Yusuke Yamashita[3], Manami Nakamoto[4], Masahiro Miyazaki[3], Shin'ichi Sakai[5], Yoshihisa Iio[3], Group for urgent joint seismic observation of the 2016 Kumamoto earthquake (1.Department of Earth and Planetary Sciences, Graduate School of Science, Kyushu University, 2.Institute of Seismology and Volcanology, Faculty of Sciences, Kyushu University, 3.Disaster Prevention Research Institute, Kyoto University, 4.Association for the Development of Earthquake Prediction, 5.Earthquake Research Institute, The University of Tokyo)

3:00 PM - 3:15 PM JST | 6:00 AM - 6:15 AM UTC

[SCG61-06] **Development of the Median Tectonic Line Fault zone in Mie Prefecture, Southwest Japan : A Possible Interpretation for Strain Localization and Softening**

*Toru Takeshita[1], Dong Van Bui[1], Thomas Anthony Czertowicz[1], Shun Arai[2], Takafumi Yamamoto[3], Jun-ichi Ando[3], Norio Shigematsu[4], Koichiro Fujimoto[5] (1.Department of Natural History Sciences, Graduate School of Science, Hokkaido University, 2.Department of Earth Science, Graduate School of Science, Tohoku University, 3.Department of Earth and Planetary Systems Science, Hiroshima University, 4.AIST, 5.Tokyo Gakugei University)

Fault zone development in the West Tottori area, Japan

*Kenta Kobayashi[1]

1. Department of Geology, Faculty of Science, Niigata University

Several kinds of investigations were carried out in the NW-SE trending aftershock area of the 2000 Tottori-ken Seibu earthquake (Mj7.3) and along the Nichinanko lineament (L=15km) which runs the SW of the aftershock area. The earthquake occurred in a place where no active fault is identified, with the exception of some short lineaments (e.g. Kanayama lineament: L=2km) in the direction of NW-SE. After the earthquake, many NW-SE to WNW-ESE trending surface ruptures were found in the aftershock area (e.g. Ryokusuien in central part of the area). They indicated sinistral slip sense. On the other hand, brittle fault rock zones are distributed in Late Cretaceous to Paleogene granitic rocks. Miocene rhyolite, basalt-andesite and aplite dikes intrude the granitic rocks, also deformed along the faults. Most fault planes with WNW strike indicate sinistral slip, and most of those with ENE strike show dextral slip. The determined paleo stress field is strike slip type of N-S tension, congruents with the 2000 Tottori-ken Seibu earthquake. However, along a few fault planes with WNW strike the early dextral slip is detected (e.g. Ryokusuien). Brittle fault rock zones are also distributed along the NW-SE trending Nichinanko lineament. Along the lineament, a wider mixture zone is formed. Fault planes with NW strike indicate sinistral slip.

XRD analysis showed that the gouge in the central part of the aftershock area is mainly composed of illite and chlorite (Kobayashi et al., 2006; Manaka et al., 2012), while the gouges in the NW and SE parts of the aftershock area (Kaneki et al., 2019) and those along the Nichinanko lineament (Manaka et al., 2012) are rich in halloysite. Chemical processes are different between these fault rock zones. In the central part of the aftershock area, most gouges were formed at a higher temperature than the neighborhood. On the other hand, the latest gouge is rich in smectite at Ryokusuien.

These facts suggest that the maturity of the fault zone along the aftershock area has been a low level, WNW strike fault planes (R1 shears) and ENE strike fault planes (R2 shears) formed predominantly. Therefore, the early kinematic (dextral) and chemical (illite-chlorite forming hydrothermal alteration) processes are remained. On the other hand, the activity along the Nichinanko lineament has been a higher level in a shallower depth (halloysite-smectite forming environment), NW strike fault planes (Y surfaces) formed predominantly, the remarkable Nichinanko lineament developed. In addition, the Komachi-Ohdani lineament system (L=12km) which runs the NE of the aftershock area also developed. How these fault zones have developed over a long period of time will be discussed.

Keywords: Tottori Prefecture, active fault, fault rocks, earthquake

©2019. Japan Geoscience Union. All Right Reserved.

Inerastic deformation around focal area of the 2000 Western Tottori EQ (M7.3) detected by “0.1 manten” Hyper Dense Seismic Observation (2)

*Satoshi Matsumoto[1], Yoshihisa Iio[2], Shin'ichi Sakai[3], Aitaro Kato[3], Takuo Shibutani[2], Yuto Hayashida[4], Group for 0.1 manten Hyper dense seismic observation

1. Institute of Seismology and Volcanology, Faculty of Sciences, Kyushu University, 2. Disaster Prevention Reasearch Institute, Kyoto University, 3. Earthquake Research Institute, University of Tokyo, 4. Graduate School of Science, Kyushu University

Seismic observation with high resolution and sensitivity is a key to solve a question how the crust deforms inelastically and accumulate stress in the seismogenic zone. We have completed a seismic observation for one year at one thousand sites (0.1 Manten seismic observation) in an aftershock area of the 2000 Western Tottori earthquake (M7.3). The seismic network with radius of about 18 km covered entire aftershock area of the M7.3 event. Automatic-detecting procedure was applied to the seismograms in order to detect small earthquakes. Over 5000 events of natural earthquakes were obtained during the observation. Sensitivity of the network is high and its detection limit for small earthquake was about magnitude of -1.0. Focal mechanism of the earthquake with magnitude range below zero could be determined. In this study, we showed inelastic deformation due to seismic activity of the small earthquake around the fault of the main shock.
The detected aftershock activity is higher at north of the large slip area of the main shock than at other area. Taking into account the activity just after the main shock, we found inelastic strain rate inferred from the aftershock reveals spatial heterogeneous distribution. The rate is smaller than inverse of the lapse time from the main shock, indicating that inelastic deformation due to the aftershock continue long duration compared with other part of the fault. This area corresponds to the hypocentral area of the preceding activity toward the main shock of the Western Tottori earthquake. These suggests that the high inelastic strain rate area at the north of the asperity of the main shock behaved as low strength area relaxing stress at the part and resulted stress loading to the asperity. Comparing the rate with it estimated from the preceding activity to the main shock, the rate at present is similar order to one before the mainshock. It suggests a possibility that loading processes exists below the low-decay rate zone where seismic activity observed prior to the main shock.

©2019. Japan Geoscience Union. All Right Reserved.

Non-double couple micro-earthquakes in the focal area of the 2000 Western Tottori earthquake (M7.3) by "0.1 manten" hyper dense seismic observation

*Yuto Hayashida[1], Satoshi Matsumoto[2], Yoshihisa Iio[3], Shin'ichi Sakai[4], Aitaro Kato[4], Group for "0.1 Manten" hyper dense seismic observation Group registration

1. Department of Earth and Planetary Sciences, Graduate School of Science, Kyushu University, 2. Institute of Seismology and Volcanology, Faculty of Sciences, Kyushu University, 3. Disater Prevention Research Institute, Kyoto University, 4. Earthquake Research Institute, the University of Tokyo

Earthquakes with non-double couple (NDC) component could provide information such as geometric fault complexity, tensile failure, and fluid flow in faulting.

In this study, we found definite micro-earthquakes with NDC in the aftershock area of the 2000 Western Tottori earthquake (M 7.3) based on polarity analysis for first P-wave motion data from “0.1 manten” hyper dense seismic observation. The observation composed of a thousand seismic stations successfully provided with high resolution focal mechanisms of a lot of micro-earthquakes in the area.

We attempted to model the events with NDC by tensile-shear faulting, shear-tensile faulting, and multiple events with pure double couple focal mechanisms. We analyzed 8 events that distributes the entire after shock area.

Plausible models for the events occurring at shallower and deeper depth are the faulting with tensile crack and the multiple shear faulting models, respectively. The results suggest that fluid contributes to the crack opening at the shallow part. In contrast, fluid pressure does not sufficient to open tensile crack at the deep part. Therefore, the depth of the boundary may relate to the pressure of fluid at the earthquake fault. In addition, the events with large NDC component were located around co-seismic large slip area of the mainshock of the Western Tottori earthquake. This suggests that fluid exits around the co-seismic slip area.

Keywords: non-double couple earthquake, focal mechanism, the 2000 Western Tottori earthquake

©2019. Japan Geoscience Union. All Right Reserved.

Stress field in the Western Tottori and Western Shimane regions deduced by the dense seismic observations

*Yoshihisa Iio[1], Manten seicmic observation group, Manten seismic observation group in the Western Tottori region

1. Disater Prevention Research Institute, Kyoto University

We estimate the stress field in the Western Tottori and Western Shimane regions by precisely analyzing focal mechanisms from dense seismic observations installed in and around the seismic belt in the San-in district, Japan. In this region, we installed a Manten seismic observation network with 50 high-gain short period seismometers in 2009, and another Manten seismic observation network with 81 high-gain short period seismometers in 2015. In this study, we utilize data from these Manten seismic observation networks and nearby permanent seismic stations, and also those obtained by the group for the dense aftershock observations of the 2000 Western Tottori Prefecture earthquake. It was inferred by previous studies that the azimuths of the maximum compressional stress axis in the seismic belt are oriented in a WNW–ESE direction, while they are aligned in almost the EW direction i in the south of the seismic belt, in the inland plate along the Nankai Trough. This spatial change in the stress field in and around the seismic belt was qualitatively explained by the aseismic slip in a ductile fault zone in the lower crust beneath the seismic belt. The results obtained in this study are summarized as follows. In the region from the aftershock area of the Western Tottori prefecture earthquake to the vicinity of Sanbe-san, rotation of $\sigma 1$ direction was observed. On the south side of the region, the direction of $\sigma 1$ is N 90 ˚E to N 110 ˚E, whereas in the region it is N 100 ˚E to N 140 ˚E, which is a rotation of 20 to 30 ˚. Rotation is large on the west side of the aftershock area of the Western Tottori prefecture earthquake and in the vicinity of Sanbe-san and small between them. In the area around the Shinji Rift zone on the north side of this area, although the number of data is small, the direction of $\sigma 1$ is N 120 ˚E to N 140 ˚E, and the rotation is the largest among the entire area. In this way, in this area, the rotation of the direction of $\sigma 1$ is seen in the central part of the San-in earthquake zone, and among them, the rotation is locally large in the west side of the aftershock area of the Western Tottori prefecture earthquake and in the vicinity of Sanbe-san. In addition, $\sigma 1$ turns greatly around the Shinji Rift zone north of the seismic belt.

In the lower crust beneath the vicinity of the seismic belt, a low velocity zone of about 50 km in width is estimated at a depth of 25 km (Tsuda et al., 2017). In the upper crust, large low velocity anomalies are seen along the Shinji Rift Belt. The stress field in this area may be formed by shortening in the orthogonal direction of the Shinji groove belt in addition to the slow slip immediately beneath the seismic belt Kawanishi et al. (2009) estimated the stress field with the seismic zone as a region, but it became clear that there is an internal structure in it.

Keywords: stress, lower crust, focal mechanism, intraplate earthquake, seicmic observation

©2019. Japan Geoscience Union. All Right Reserved.

Modeling the spatiotemporal change in stress field around Hinagu fault zone through the 2016 Kumamoto earthquake sequence, in central Kyushu, Japan

*Ayaho Mitsuoka[1], Satoshi Matsumoto[2], Azusa Shito[2], Yusuke Yamashita[3], Manami Nakamoto[4], Masahiro Miyazaki[3], Shin'ichi Sakai[5], Yoshihisa Iio[3], Group for urgent joint seismic observation of the 2016 Kumamoto earthquake

1. Department of Earth and Planetary Sciences, Graduate School of Science, Kyushu University, 2. Institute of Seismology and Volcanology, Faculty of Sciences, Kyushu University, 3. Disaster Prevention Research Institute, Kyoto University, 4. Association for the Development of Earthquake Prediction, 5. Earthquake Research Institute, The University of Tokyo

For a purpose of understanding physical process of earthquake generation, knowledge of stress condition around a fault is required. We estimated stress field and discussed its spatiotemporal change around Hinagu fault zone that was the hypocentral area of the 2016 Kumamoto earthquake sequence.
The 2016 Kumamoto earthquake sequence occurred around Hinagu and Futagawa fault zones in Kumamoto prefecture, central Kyushu Island, Japan. The largest foreshock with Mj 6.5 (Mj: magnitude by Japan Metrological Agency) on April 14, 2016 was located Hinagu fault zone. The mainshock (Mj 7.3) generated slip at both Hinagu and Futagawa fault on April 16, 2016. After that, many earthquakes occurred around these faults until now.
In this study, we estimated the spatiotemporal change in the deviatoric stress field and its differential stress. For discussing the temporal change in the target region, we divided time sequence into three periods: (1) prior to the sequence (i.e. before Mj 6.5 event), (2) between the foreshock and the mainshock, and (3) after the mainshock. We compared the deviatoric stress fields with the co-seismic stress change by faulting of this sequence. From focal mechanism solutions from January 1, 1993 to December 31, 2017, we estimated the deviatoric stress field using the method by Matsumoto [2016]. We adopted fault slip models of the fore- and mainshock, which is the slip distribution projected result by Asano and Iwata [2016] on the fault geometries determined from the distribution of hypocenters. We performed a grid search procedure for the differential stress at each spatial block with horizontal size of 0.05˚in latitude and longitude, and 5 km in depth.
As a result, we captured the stress condition in the both period (1) and (3). Before the foreshock (i.e. period (1)), the differential stress around the fore- and mainshock faults is higher than the other region, its value is from several MPa to several tens of MPa. On the other hand, the differential stress in south area of Hinagu fault zone ranges from about 0.1 to 1 MPa. We found the foreshock and mainshock occurred in the state of high differential stress.
After the mainshock (i.e. period (3)), the spatial heterogeneity of the differential stress still remained. However, the differential stress at the area around the hypocenters of the fore- and mainshock is about half of that before the foreshock. At the southeast area of Hinagu fault, the differential stress is about twice of that before, so potential of occurring earthquake becomes relatively high compared with the prior state to this sequence.

Keywords: 2016 Kumamoto earthquake, stress field, fault strength

©2019. Japan Geoscience Union. All Right Reserved.

Development of the Median Tectonic Line Fault zone in Mie Prefecture, Southwest Japan : A Possible Interpretation for Strain Localization and Softening

*Toru Takeshita[1], Dong Van Bui[1], Thomas Anthony Czertowicz[1], Shun Arai[2], Takafumi Yamamoto[3], Jun-ichi Ando[3], Norio Shigematsu[4], Koichiro Fujimoto[5]

1. Department of Natural History Sciences, Graduate School of Science, Hokkaido University, 2. Department of Earth Science, Graduate School of Science, Tohoku University, 3. Department of Earth and Planetary Systems Science, Hiroshima University, 4. AIST, 5. Tokyo Gakugei University

We have investigated the development of the Median Tectonic Line (MTL) fault zone in the upper-plate Ryoke granitoids in Mie Prefecture, southwest Japan. In the study area, although c. 80 m thick cataclasite develops in direct proximity to the MTL, mylonitic rocks were pervasively formed before the formation of cataclasite, which can be divided into protomylonite distributed from the MTL to the point 300 m north from it and mylonite distributed from the latter point to the one at c. 800 m further north from the MTL. However, in the protomylonite zone, ultramylonite with the thickness up to c. 50 m is developed in direct proximity to the MTL, which occur as clasts in the cataclasite zone. We also have found that the protomylonite originates from tonalite, while the mylonite originates from granite. Hence, the boundary between the protomylonite and mylonite exactly coincides with the protolith boundary.

We analyze both microstructures and c-axis fabrics in recrystallized quartz grains from the protomylonite and mylonite zones along the MTL. In the protomylonite, sizes of recrystallized grains formed by subgrain rotation (SGR) recrystallization are low ranging between 7-14 microns. In particular, in the ultramylonite, the recrystallized grain sizes ranges between 4-11 microns. The quartz c-axis fabrics mostly show a Y-maximum pattern. On the other hand, the mylonite zone can be divided into two subzones in terms of quartz microstructures. In the subzone from 300 m to 490 m from the MTL, the microstructures are characterized by elongated grains (S-type) with finer recrystallized grain sizes varying between 11-20 microns formed by SGR. On the other hand, in the zone from 490 m to 800 m from the MTL, the microstructures are characterized by relatively equant grains (P-type) with coarser recrystallized grain sizes varying between 49-107 microns and lobate grain boundaries formed by grain-boundary migration (GBM) recrystallization. In both mylonite subzones, a Y-maximum quartz c-axis fabric dominates.

We further analyze microstructures of K-feldspar, and infer deformation temperatures based on the two-feldspar geothermometry after Stormer (1975) and Stormer and Whitney (1985) in the mylonite zone which originated from granite. While K-feldspar porphyroclasts are broken in the S-type mylonite subzone, they are plastically deformed to a sigma shape in the P-type mylonite subzone. Myrmekite pervasively develops at the periphery of K-feldspar porphyroclasts from the entire mylonite zone. Using the chemical compositions of K-feldspar and plagioclase in myrmekite, we infer the deformation temperatures in the mylonite zone. At the northernmost P-type mylonite subzone, the deformation temperatures are calculated at 500 ˚C, which decrease to 400 ˚C at the boundary between the P- and S-type mylonite subzones, and further decrease in the S-type mylonite zone, ranging between 350-400 ˚C.

Plastic deformation is dominant in the granite than in the tonalite at higher temperatures than 500 ˚C, leading to the formation of mylonite in the former area alone, perhaps because granite including abundant K-feldspar is rheologically weaker than tonalite. Subsequently, with decreasing temperature,

©2019. Japan Geoscience Union. All Right Reserved.

plastic deformation becomes localized in the southern part of the mylonite zone. At 400 ˚C, only the S-type mylonite subzone continues to deform, and the protomylonite starts to deform at higher stresses than in the S-type mylonite subzone. With further decreasing temperatures, the plastic deformation of S-type mylonite subzone is abandoned at 350 ˚C, and the further plastic deformation only occurs in the ultramylonite at 300-350 ˚C, leading to the formation of very fine-recrystallized quartz grains and type-I crossed girdle quartz c-axis fabric with R-maxima, which is further followed by cataclasis. We currently do not have a good idea on why the zone of plastic deformation suddenly jumps from the southernmost S-type mylonite subzone, which is 300 m apart from the MTL, to the protomylonite zone in direct proximity to the present MTL, forming ultramylonite. However, since a type-I crossed girdle quartz c-axis fabric with R-maxima is developed in the ultramylonite, it can be inferred that water weakening of quartz either by decreasing the strength of slip systems or facilitating dynamic recrystallization occurs in the protomylonite zone, which could have been caused by infiltration of water along newly formed fractures.

Keywords: Median Tectonic Line, mylonite, quartz c-axis fabric

©2019. Japan Geoscience Union. All Right Reserved.

[J] Oral | S (Solid Earth Sciences)：S-CG Complex & General

Mon. May 27, 2019 3:30 PM - 5:00 PM JST | Mon. May 27, 2019 6:30 AM - 8:00 AM UTC | Convention Hall A 2F

[S-CG61] Dynamics in mobile belts

convener:Yukitoshi Fukahata(Disaster Prevention Research Institute, Kyoto University), Toru Takeshita(Department of Natural History Sciences, Graduate School of Science, Hokkaido University), Hikaru Iwamori(Geochemical Evolution Research Program, Japan Agency for Marine-Earth Science and Technology), Chairperson:Tomomi Okada, Ryosuke Ando(Graduate School of Science, University of Tokyo)

The dynamic behaviours of mobile belts are expressed across a wide range of time scales, from the seismic and volcanic events that impact society during our lifetimes, to orogeny and the formation of large-scale fault systems which can take place over millions of years. Deformation occurs on length scales from microscopic fracture and flow to macroscopic deformation to plate-scale tectonics. To gain a physical understanding of the dynamics of mobile belts, we must determine the relationships between deformation and the driving stresses due to plate motion and other causes, which are connected through the rheological properties of the materials. To understand the full physical system, an integration of geophysics, geomorphology, and geology is necessary, as is the integration of observational, theoretical and experimental approaches. In addition, because rheological properties are greatly affected by fluids in the crust and fluid chemical reactions, petrological and geochemical approaches are also important. After the 2011 great Tohoku-oki earthquake, large-scale changes in seismic activity and regional scale crustal deformation were observed, making present-day Japan a unique natural laboratory for the study of the dynamics of mobile belts. This session welcomes presentations from different disciplines, such as seismology, geodesy, tectonic geomorphology, structural geology, petrology, and hydrology, as well as interdisciplinary studies, that relate to the dynamic behaviours of mobile belts.

3:30 PM - 3:45 PM JST | 6:30 AM - 6:45 AM UTC

[SCG61-07] What caused the Main Himalayan Thrust (MHT) to ramp? Insights from analogue and numerical models

*Subhajit Ghosh[1,2], Arijit Laik[2], Santanu Bose[2,3], Nibir Mandal[4] (1.Earthquake Research Institute, The University of Tokyo, 1-1-1 Yayoi, Bunkyo-Ku, Tokyo 113-0032, 2.Department of Geology, University of Calcutta, 35, Ballygunge Circular Road, Kolkata 700019, India, 3.Department of Geology, Presidency University, 86/1 College Street, Kolkata 700073, India, 4.Department of Geological Sciences, Jadavpur University, Kolkata 700032, India)

3:45 PM - 4:00 PM JST | 6:45 AM - 7:00 AM UTC

[SCG61-08] Control of fault weakening on the structural styles of underthrusting-dominated non-cohesive tectonic wedges

*Arthur Bauville[1], Mikito Furuichi[1] (1.Department of Mathematical Science and Advanced Techology, JAMSTEC)

4:00 PM - 4:15 PM JST | 7:00 AM - 7:15 AM UTC

[SCG61-09] Complexity of the 2016 *M* 7.8 Kaikoura, New Zealand, earthquake from seismic observation: inferences of overpressured fluid involvement

*Tomomi Okada[1], Satoshi Matsumoto[2], Yoshihisa Iio[3], Federica Lanza[4], Clifford H Thurber[4], Miu Matsuno[1], Yuta Kawamura[2], Tadashi Sato[1], Stephen C Bannister[5], John Ristau[5], Martha K Savage[6], John Townend[6], Jarg Petttinga[7], Francesca Ghisetti[8], Richard H Sibson[9] (1.Research Center for Prediction of Earthquakes and Volcanic Eruptions, Graduate School of Science, Tohoku University, 2. Institute of Seismology and Volcanology, Faculty of Sciences, Kyushu University, 3. Disater Prevention Research Institute, Kyoto University, 4.University of Wisconsin-Madison, U.S.A., 5.GNS Science, New Zealand, 6.Victoria University of Wellington, New Zealand, 7.University of Canterbury, New Zealand, 8.TerraGeoLogica, New Zealand, 9.University of Otago, New Zealand)

4:15 PM - 4:30 PM JST | 7:15 AM - 7:30 AM UTC

[SCG61-10] Dynamic Rupture Simulation Reproduces Spontaneous Multifault Rupture and Arrest During the 2016 Mw 7.9 Kaikoura Earthquake

*Ryosuke Ando[1], Yoshihiro Kaneko[2] (1.Graduate School of Science, University of Tokyo, 2.GNS science)

4:30 PM - 4:45 PM JST | 7:30 AM - 7:45 AM UTC

[SCG61-11] Ductile deformation explains the physics of friction and genesis of earthquakes

*James Daniel Paul Moore[1], Stefan Nielsen[2], Lars N Hansen[3] (1.Earth Observatory of Singapore, 2.University of Durham, 3.University of Oxford)

4:45 PM - 5:00 PM JST | 7:45 AM - 8:00 AM UTC

[SCG61-12] The seismic moment, stress drop, and strain energy release for the rupture of asperities

*Mitsuhiro Matsu'ura[1] (1.Institute of Statistical Mathematics)

What caused the Main Himalayan Thrust (MHT) to ramp? Insights from analogue and numerical models

*Subhajit Ghosh[1,2], Arijit Laik[2], Santanu Bose[2,3], Nibir Mandal[4]

1. Earthquake Research Institute, The University of Tokyo, 1-1-1 Yayoi, Bunkyo-Ku, Tokyo 113-0032, 2. Department of Geology, University of Calcutta, 35, Ballygunge Circular Road, Kolkata 700019, India, 3. Department of Geology, Presidency University, 86/1 College Street, Kolkata 700073, India, 4. Department of Geological Sciences, Jadavpur University, Kolkata 700032, India

Occurrence of any conspicuous ramp on the low angle basal detachment causes hindrance on the overall wedge progression and behaves as an asperity by localizing stress in the inter-seismic gaps. The mid-crustal ramp on the Main Himalayan Thrust (MHT) results in strain partitioning by focusing seismicity, including 2015 magnitude 7.8 Gorkha earthquake in the central Nepal Himalaya. However, the ramp structure is laterally discontinuous; even absent in some parts of the Himalaya (e.g. western Bhutan). Interestingly, it has been widely shown that the geometry of the basal detachment (in terms of presence or absence or geographic location of the ramp) provides first order control on the along strike variations in the structure, topography, low-temperature thermochronological ages, precipitation, exhumation and erosion patterns. Motivated by the absence of any mechanical explanation for these peculiar observations, we compare physical and numerical experiments with the geology of the frontal eastern Himalaya to show how the mechanically weak coal bearing Gondwana horizon controls the position of the basal detachment in space and time. Our modelling results confirm that the initial spatial distribution of the Gondwana horizon strongly influences the position of the mid-crustal ramp at different geographic location which resulted in segmented MHT structure (Fig. 1). The numerical modelling largely validates the physical experiments and explains the rock uplift and river incision pattern recorded in the Nepal Himalaya.

Keywords: mid-crustal ramp, Main Himalayan megathrust, seismicity asperity, Basal friction, Analog sandbox, Numerical model Underground

©2019. Japan Geoscience Union. All Right Reserved.

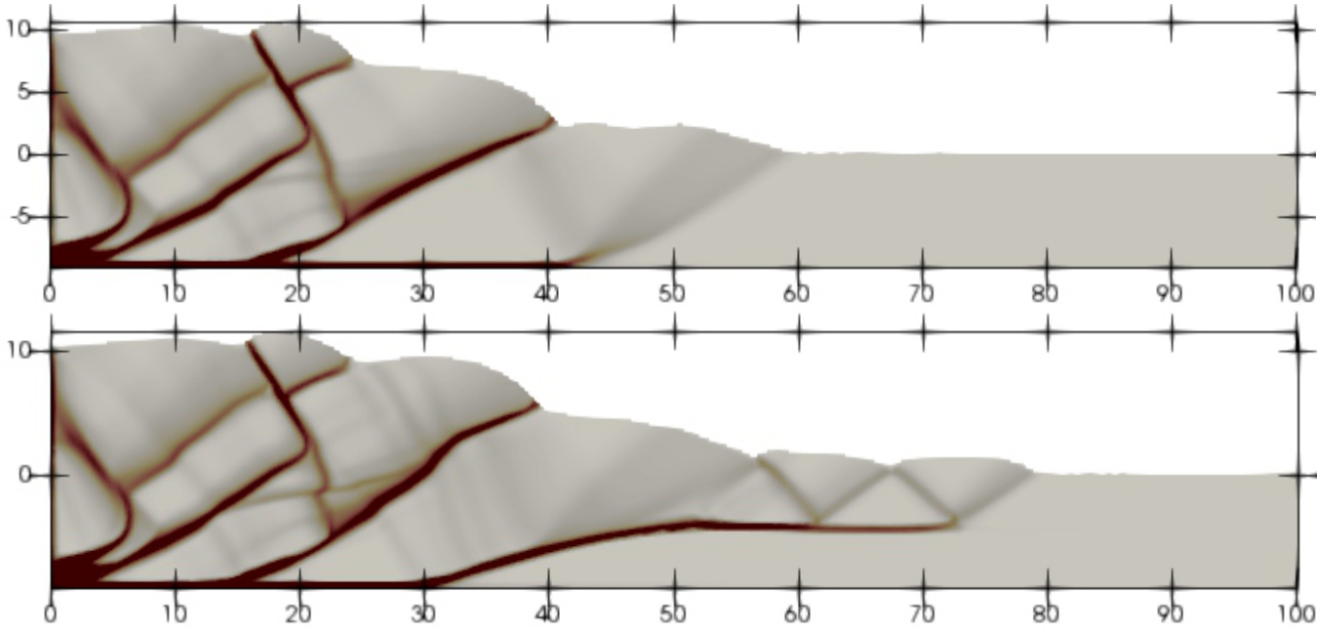

Fig. 1 Numerical sandbox simulation with visco-plastic rheology. Sequential thrust progression in a model containing a weak zone (Φ_W = 10°). The weak zone shifted the thrust progression to a shallower depth. Plastic strain mapping clearly marks the location of ramping of the basal detachment.

©2019. Japan Geoscience Union. All Right Reserved.

Control of fault weakening on the structural styles of underthrusting-dominated non-cohesive tectonic wedges

*Arthur Bauville[1], Mikito Furuichi[1]

1. Department of Mathematical Science and Advanced Techology, JAMSTEC

Underthrusting is a typical process at compressive margins responsible for nappe stacking and sediment subduction. Despite being essential for orogenesis, and the subduction cycle, the mechanics of underthrusting is still incompletely understood. The critical taper theory predicts that underthrusting occurs only in the limit where $\mu_b'=\mu'$, with μ' and μ_b' the inner and basal effective coefficient of friction, respectively. Paradoxically, in nature, underthrusting is associated with weak faults. For instance, at erosive subduction margins, sediments are dragged in subduction, while normal faulting in the middle prism suggests the plate boundary is weak. Wang et al., (2010) have proposed that dynamic fault strength variations during the earthquake cycle can reconcile these observations. In their model, underthrusting occurs during earthquakes when the fault is strong and normal faulting occurs in the prism during the interseismic period when the fault is weak. However, recent evidence (Gao and Wang, 2016) suggests that plate boundaries are relatively weak also during earthquakes.
In this contribution, we investigate the control of permanent fault weakening on the dynamics of a strong-based ($\mu_b'=\mu'$,) non-cohesive tectonic wedge. We control the wedge material strength by a spatially constant fluid overpressure factor (λ^*, and fault strength by a strain weakening factor (χ). We investigated the problem in two steps. First, we used the critical taper theory to determine a mechanical mode diagram that predicts structural styles. This diagram is deduced from the function $\Delta\alpha(\beta,\chi,\lambda^*)$ which is the difference in taper angle at a given β, between the compressively critical taper of a strong-based wedge and the extensionally critical taper of a weak-based wedge ($\mu_b'=(1-\chi)\mu'$). Then, we performed numerical simulations of accretionary wedge formation to establish the characteristics of these structural styles regarding wedge and fault geometry. We determined there is a continuum of structural styles with three end-members occurring at the theoretically determined mechanical mode transitions.

Style 1 is characterized by thin tectonic slices and little to no underthrusting.
Style 2 is characterized by thick slices and nappe stacking.
Style 3 is characterized by the complete underthrusting of the incoming sediments.

The model gives a mechanical explanation that reconciles underthrusting with weak faults. In agreement with observations, the model predicts the occurrence of style 2 in strong-based sandbox experiment. Finally, we argue that style 3 is triggered by any mechanism, such as material weakening, erosion or sedimentation, that limits the surface angle such that the incoming material is always significantly under-critical.

Keywords: Accretionary prism, Underthrusting, Critical taper theory, Numerical simulations

©2019. Japan Geoscience Union. All Right Reserved.

Complexity of the 2016 *M* 7.8 Kaikoura, New Zealand, earthquake from seismic observation: inferences of overpressured fluid involvement

*Tomomi Okada[1], Satoshi Matsumoto[2], Yoshihisa Iio[3], Federica Lanza[4], Clifford H Thurber[4], Miu Matsuno[1], Yuta Kawamura[2], Tadashi Sato[1], Stephen C Bannister[5], John Ristau[5], Martha K Savage[6], John Townend[6], Jarg Petttinga[7], Francesca Ghisetti[8], Richard H Sibson[9]

1. Research Center for Prediction of Earthquakes and Volcanic Eruptions, Graduate School of Science, Tohoku University, 2. Institute of Seismology and Volcanology, Faculty of Sciences, Kyushu University, 3. Disater Prevention Research Institute, Kyoto University, 4. University of Wisconsin-Madison, U.S.A., 5. GNS Science, New Zealand, 6. Victoria University of Wellington, New Zealand, 7. University of Canterbury, New Zealand, 8. TerraGeoLogica, New Zealand, 9. University of Otago, New Zealand

The *M* 7.8 Kaikoura earthquake occurred in the northern South Island on 3 Nov., 2016, involving the rupture of > 20 faults. To understand the complexity of the Kaikoura earthquake, details of fault geometry, seismic velocity distribution and stress field are necessary. We have undertaken seismic tomography and stress tensor inversion using focal mechanisms along the c. 200 km length of the rupture zone.

Data from both 51 temporary stations and 22 GEONET stations were collected from March 2011 to December 2017. Hypocenter locations and the three-dimensional velocity structure were determined using the method of Zhang and Thurber (2003 and 2006).

The hypocenter of the Kaikoura earthquake and aftershocks near the Kekerengu fault locate along lineaments where seismic velocity changes horizontally.

In the uppermost crust, lower velocities occur beneath the Emu Plain and Cape Campbell. Higher velocities occur in and around Kaikoura.
In the middle to lower crust, high Vp/Vs occurs not only in and around the hypocenter but also along the northern part of the rupture zone.
In the lowermost crustal or uppermost mantle, high Vp occurs east of the Kekerengu fault and south of the Hope fault and beneath the Canterbury plains faults. This high Vp likely corresponds to the Pacific plate.

These complexities in the seismic velocity structure may relate to the multi-rupture character of the Kaikoura earthquake. In particular, spatial correlations between rupture areas and high Vp/Vs suggests the involvement of overpressured fluid in the nucleation and propagation of rupture segments, which is also supported by the reactivation of unfavourably oriented strike-slip ruptures, many lying at c.70˚ to regional sigma-one stress trajectories.

Keywords: 2016 Kaikoura earthquake

©2019. Japan Geoscience Union. All Right Reserved.

Dynamic Rupture Simulation Reproduces Spontaneous Multifault Rupture and Arrest During the 2016 Mw 7.9 Kaikoura Earthquake

*Ryosuke Ando[1], Yoshihiro Kaneko[2]

1. Graduate School of Science, University of Tokyo, 2. GNS science

The 2016 Kaikoura (New Zealand) earthquake is characterized as one of the most complex multifault rupture events ever observed. We perform dynamic rupture simulations to evaluate to what extent relatively simple forward models accounting for realistic fault geometry can explain the characteristics of coseismic observations. Without fine parameter tuning, our model reproduces many observed features including the multifault rupture, overall slip distribution and direction, and the locations of the maximum slip and rupture arrest. In particular, our model shows spontaneous arrest of dynamic rupture at the both ends of the ruptured fault system due to smaller prestress levels expected from a regional tectonic stress field. Both the simulated and the observationally inferred source time functions show similar double peaks with a larger second peak. The results illuminate the importance of the 3-D fault geometry in understanding the dynamics of complex multifault rupture.

Keywords: Dynamic rupture, Boundary integral equation method, Fault geometry

©2019. Japan Geoscience Union. All Right Reserved.

Ductile deformation explains the physics of friction and genesis of earthquakes

*James Daniel Paul Moore[1], Stefan Nielsen[2], Lars N Hansen[3]

1. Earth Observatory of Singapore, 2. University of Durham, 3. University of Oxford

Seismic hazard presents a significant global threat to both life and property, with increased urbanisation in the twenty-first century only intensifying the risk as populations concentrate near fault lines. It is therefore imperative to develop a clear understanding of the physical origins of earthquakes, with their associated hazards, and use that knowledge to work towards building more resilient societies. To this end, we show that ductile deformation on contact regions within fault zones explains the physics of fault friction, and the genesis of earthquakes. We find the empirical framework of rate-and-state friction may be derived from grain-scale creep processes, and that earthquakes are the macroscopic manifestation of ductile deformation at microscopic contacting regions. The governing equations are well behaved at low slip rates, the seismogenic layer emerges as a consequence of the pressure-temperature dependence of ductile creep processes, and we offer an explanation for the temporal distribution of earthquake clustering.

The physical origins of the laws of friction that govern the genesis of earthquakes have long been the subject of discussion and debate. Here we demonstrate that the empirical framework of rate-and-state friction is a natural consequence of grain-scale processes, and that fault slip is the macroscopic manifestation of creep on contact asperities, modulated by grain-size processes, at the microscopic scale.We find that common rate-and-state parameters derived from laboratory data and geodetic observations are entirely commensurate with known flow laws: diffusion creep, dislocation-accommodated grain-boundary sliding, and dislocation creep. Additionally, we find that the temperature, grain size, and stress dependence of these flow laws naturally give rise to the full spectrum of fault behaviour from stable creep, through slow slip and tremor, to bilateral ruptures. In particular a seismogenic layer emerges spontaneously from the interplay of these creep mechanisms, for which the stability is primarily determined by the grain-size dependence of the active flow law. Our framework unifies the work of friction experiments for localised deformation and flow laws governing distributed deformation, whilst simultaneously addressing a number of shortcomings of the Dieterich-Ruina form of rate-and-state friction, such as the non-physical divergence as the sliding velocity tends to zero. We present very close equivalence between rate-and-state friction and established flow laws, and provide an explanation for the emergence of the seismogenic layer.

Keywords: Earthquake, Friction, Rheology

©2019. Japan Geoscience Union. All Right Reserved.

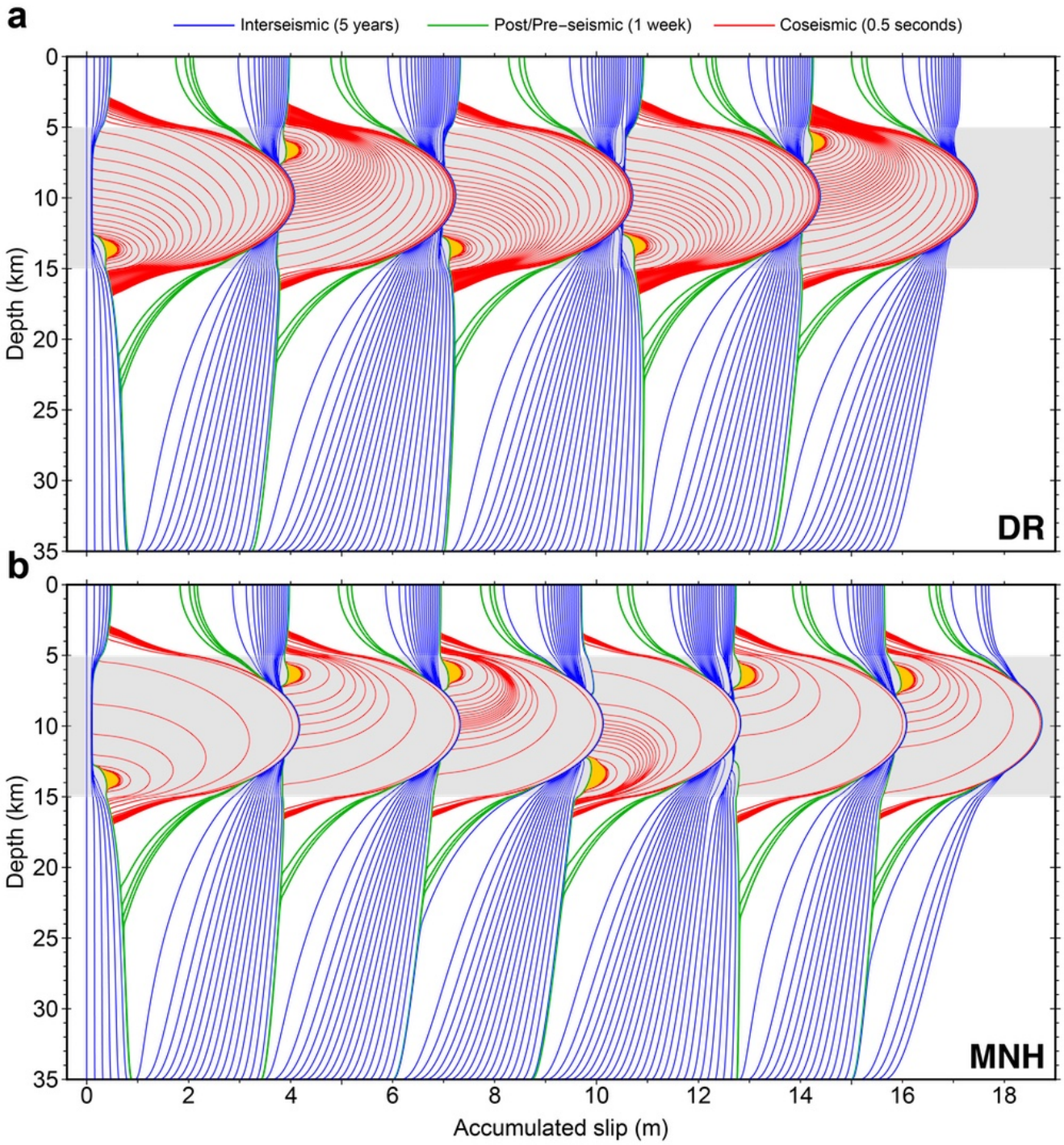

©2019. Japan Geoscience Union. All Right Reserved.

The seismic moment, stress drop, and strain energy release for the rupture of asperities

*Mitsuhiro Matsu'ura[1]

1. Institute of Statistical Mathematics

Seismic moment and stress drop are known as the most fundamental physical quantities characterizing seismic events. The seismic moment of an event is clearly defined as the product of its rupture area (S), average fault slip (D), and the rigidity of the surrounding elastic medium (Aki, 1966; Kostrov, 1974), but the stress drop is not (Madariaga, 1979), which depends on adopted source models. In the simplest case of a circular crack model with uniform stress drop, the stress drop is proportional to D and the inverse of the square root of S, and so independent of seismic moment (e.g., Kanamori & Anderson, 1975). However, with the simplest model, Nadeau & Johnson (1998) found a clear dependence of average stress drop on seismic moment from a detailed analysis of repeating earthquakes along the Parkfield segment of SAF. This empirical scaling relationship for average stress drop is contrary to what is commonly assumed in seismology: that is the stress drop is independent of earthquake size.

Since then, many seismologists (e.g., Sammis & Rice, 2001; Anooshehpoor & Brune, 2001; Beeler, Lockner & Hickman, 2001; Johnson & Nadeau, 2002) tried to explain the observed size-dependence of stress drop by theoretically considering the loading and rupture processes of asperities, but didn't succeed. The size-dependence of stress drop seems to result from an inappropriate assumption for background slip rates [1]. Aside from that, in these theoretical studies, the asperity is modeled as a completely locked small patch surrounded by freely creeping zones. In such modeling, steady tectonic loading causes stress singularity just inside the locked patch and broad slip-deficit distribution on the surrounding freely creeping zones. The rupture of the asperity suddenly releases the concentrated stress at the small locked patch and causes fault slip so as to cancel the slip deficit distributed on the surrounding zones without stress drop. Even in such a case, we can clearly define the seismic moment by multiplying the integral of coseismic slip over the whole fault plane by the rigidity of the surrounding medium. In contrast, the definition of average stress drop is multiple (Noda, Lapusta & Kanamori, 2013), which suggests that the static stress drop on fault may not be the fundamental physical quantity.

Recently, on the basis of theoretical consideration to the equation of motion in continuum mechanics, we derived a fundamental equation that the volume integral of static stress changes caused by a seismic event over the whole elastic region is mathematically equivalent to its moment tensor [2]. Applying the fundamental equation to the energetics of shear faulting, we can obtain a quantitative relationship between the work done for shear faulting and the change in elastic strain energy in the surrounding region. This means that we should use the volume integral of static stress changes or the total strain energy change as the fundamental physical quantity characterizing seismic events.

References:
[1] Matsu'ura, M., Nomura, S., Ogata, Y., & Uchida, N. (2017), Reciprocal relationship between seismically estimated slip rates and geodetically estimated slip-deficit rates at plate interfaces: Physical interpretation and logical consequence, IAG-IASPEI 2017 Meeting, J05, Kobe, Japan.
[2] Matsu'ura, M., Noda, A., & Terakawa, T. (2018), Two different representations of moment tensor and the energetics of shear faulting, 10th ACES International Worlshop, O24-3, Awaji Island, Japan.

©2019. Japan Geoscience Union. All Right Reserved.

Keywords: Seismic moment, Stress drop, Strain energy release, Asperity model

©2019. Japan Geoscience Union. All Right Reserved.

[E] Poster | B (Biogeosciences)：B-BG Biogeosciences & Geosphere-Biosphere Interactions

Mon. May 27, 2019 1:45 PM - 3:15 PM JST | Mon. May 27, 2019 4:45 AM - 6:15 AM UTC | Poster Hall International Exhibition Hall8, Makuhari Messe_6

[B-BG01] Elemental cycling in terrestrial and coastal ecosystems- Carbon and Nitrogen perspectives

convener:Punyasloke Bhadury(Indian Institute of Science Education and Research Kolkata)

Biogeochemical cycling of carbon and nitrogen hold the key to cropping cycle, monsoonal patterns and climate globally. Biological communities that make up the biosphere are essential for cycling of carbon and nitrogen and their functions are regulated by numerous factors including redox conditions, trace metal availability, and energy sources. At the same time temporal and spatial variability of biological communities such as those observed in microbes strongly affect the rate of carbon and nitrogen cycling in various environments including land and marine systems. In this session, submissions are welcomed from scientists including early career scientists working on various aspects of carbon and nitrogen cycling across terrestrial, coastal and oceanic environments. Submissions are also encouraged addressing challenges related to estimation of carbon and nitrogen budgets representing local, regional and global scales.

[BBG01-P01] Forest-CEW: A Forest Ecosystems Model for Carbon-Energy-Water Processes.

*Zhenghong Tan[1] (1.Hainan University China)

[BBG01-P02] **Interdependent Dynamics of LAI-ET across Roofing Landscapes: the Mongolian and Tibetan Plateaus**

*Li Tian[1] (1.Institute of Geographic Sciences and Natural Resources Research, Chinese Academy of Sciences)

[BBG01-P03] **Particle Phase Organic compounds (PAHs and VOCs) at Two Big Cities (Dhaka and Rajshahi) in Bangladesh**

*Islam Nazrul nazrulislam6727@gmail.com[1], Tanzina Tul Karim[1], Rasheda Nahida[1], Nusrat Mousume[1], Farha Jeba[1], Abdus Salam[1] (1.Department of Chemistry, University of Dhaka, Dhaka-1000, Bangladesh)

[BBG01-P04] **Diversity and activity of diazotrophs in the coastal waters of Southeastern Arabian Sea (SEAS)**

*JABIR THAJUDEEN[1], Mohamed Hatha Abdullah (1.Cochin University of Science and Technology India)

[BBG01-P05] **Bloom of *Palmerina hardmaniana*, a marine centric planktonic diatom in a coastal mangrove ecosystem- implication for coastal carbon cycling**

*Punyasloke Bhadury[1] (1.Centre for Climate and Environmental Studies and Department of Biological Sciences, Indian Institute of Science Education and Research Kolkata)

[BBG01-P06] Dynamics of Carbon and Nitrogen influx in large river system: Isotopic study from river Ganga, India

*Anurag Kumar[1], Prasanta Sanyal[1,2], Punyasloke Bhadury[3,2] (1.Department of Earth Sciences, Indian Institute of Science Education and Research Kolkata, Mohanpur 741246, India, 2.Centre for Climate and Environmental studies, Indian Institute of Science Education and Research Kolkata, Mohanpur 741246, India, 3.Department of Biological Sciences, Indian Institute of Science Education and Research Kolkata, Mohanpur 741246, India)

Forest-CEW: A Forest Ecosystems Model for Carbon-Energy-Water Processes.

*Zhenghong Tan[1]

1. Hainan University China

Forest ecosystem models (FEM) are essential tools for studying the forest carbon budget, which is an important subject in the global climate change studies. Although using FEM has a long history and there exist many types of FEM, new models are still being developed for special uses. This presentation introduces Forest-CEW, a forest ecosystems model for carbon-energy-water processes. The model is aimed at having a structure that can be configured flexibly for different forest ecosystems, a graphic interface for inexperienced users, and a command execution mode for experts. The time scale of the model is at the hourly level. Model validation using the data from Tomakomai flux research site (asiaflux.net/index.php?page_id=113) shows that the model can well reconstruct major ecosystem variables including net ecosystem exchange, soil temperature and water content. We also compared Forest-CEW with those include in the TDE ecosystem model intercomparison (cdiac.ess-dive.lbl.gov/epubs/tdemodel/models.html) and the results show that its performance is among the best of the 13 models.

Keywords: Model, Forest Ecosystem, Carbon, Water, Energy

©2019. Japan Geoscience Union. All Right Reserved.

Interdependent Dynamics of LAI-ET across Roofing Landscapes: the Mongolian and Tibetan Plateaus

*Li Tian[1]

1. Institute of Geographic Sciences and Natural Resources Research, Chinese Academy of Sciences

The Mongolian and Tibetan Plateaus have experienced higher-than-global average warming in recent decades, resulting in many significant changes in ecosystem structure and function. Among them are Leaf area index (LAI) and evapotranspiration (ET) that play a fundamental role in shaping many causes and consequences of land surface processes and climate. Here, we focused on the spatiotemporal changes of the LAI, ET and their relationships on these two roofing landscapes. Based on the MODIS products from 2000 through 2014. We found that there existed a general positive relationship between LAI and ET on the Mongolia Plateau (MP), while there was not synergy on the Tibetan Plateau (TP).

Overall, 49.38% (50.62%) of land areas on the TP experienced significant increased (decreased) in LAI, while 94.92% (5.09%) on the MP. For the ET, the increased land area was 21.70% (124.10×10^3 km^2) on the TP and 88.01% (341.60×10^3 km^2) on the MP. More importantly, the relationships varied substantially across the space and over time, with mismatches found in some parts of the landscapes. Substantial additional efforts with observational and/or experimental investigations are need to explore the relationships, including the influences of vegetation characteristics and disturbances.

Keywords: ET, LAI, Eurasian continent, alpine, land surface process

©2019. Japan Geoscience Union. All Right Reserved.

Particle Phase Organic compounds (PAHs and VOCs) at Two Big Cities (Dhaka and Rajshahi) in Bangladesh

*Islam Nazrul nazrulislam6727@gmail.com[1], Tanzina Tul Karim[1], Rasheda Nahida[1], Nusrat Mousume[1], Farha Jeba[1], Abdus Salam[1]

1. Department of Chemistry, University of Dhaka, Dhaka-1000, Bangladesh

Particle Phase Organic compounds (PAHs and VOCs) at Two Big Cities (Dhaka and Rajshahi) in Bangladesh

Md. Nazrul Islam[1*], Tanzina Tul Karim, Rasheda Nahida, Nusrut Mousume, Farha Jeba, and Abdus Salam[2*]

Department of Chemistry, University of Dhaka, Dhaka 1000, Bangladesh

Corresponding Author: [1] nazrulislam6727@gmail.com, Tel: +8801717672748; [2*] asalam@gmail.com, Tel: +880117061160

Atmospheric pollution has a significant impact on human health, climate change, agriculture, and ecosystem. Air quality and the climate change is the top most concern of the World Health Organization (WHO, 2019). Bangladesh is a rapidly developing country with kinds of environmental problems. It became the top most country in the world for the human deaths due to environmental pollution, which was accounted about 27% of the total death (Lancet, 207). Only air pollution caused two thirds of these deaths (Lancet, 2017). Dhaka along with Narayanganj and Gazipur are the top ranking cities in the World for the air pollution (WHO, 2014). Volatile organic compounds (VOCs) and poly aromatic hydrocarbons (PAHs) are the major organic pollutants in the atmosphere. Until now there is no information of VOCs and PAHs regarding their occurrences, sources, seasonal variation and health impact in Bangladesh. In this study we have collected particulate matters samples on quartz filters with a low volume sampler at two big cities in Bangladesh (Capital Dhaka and North West City Rajshahi) from January 2015 to February 2019. Individual organic compounds were extracted with acetone and n-hexane from the particulate matter loaded filters. The chemical analysis was done with Gas Chromatography (GC)-Mass spectrometry (MS). The analyzed organic compounds were naphthalene, anthracene, diazinon, deltramethrin, pyrabenxoime, pyrazosulfuran, prophenophos butachlor, propiconazole, cymoxanil, cypermethrin, lamda cyhalothrin, dimethoate, chloropyriphos, carbofuran, metalaxyl, pentane, hexane, propene, isobutene, 1,3-butadiene, dichloroflouromethane, ethanol, benzene, toluene, ethylbenzene, xylene, styrene, 1,2,3trimethylbenzene, isoprene, cyclopentane, and cyclohexane. Positive matrix factorization (PMF) and air mass trajectory analysis were done for source characterization. Health risk assessment and life time cancer risk (LCR)

©2019. Japan Geoscience Union. All Right Reserved.

were determined with US EPA based model. The elevated concentrations of the determined compounds at both Dhaka and Rajshahi were observed; Dhaka values were slightly higher than Rajshahi. The concentrations of determined compounds were higher during the winter months basically December to February and lower during the monsoon period in the month of July. PMF model revealed that the sources of organic compounds in Bangladesh were diesel exhaust, coal and biomass burning, industry and gasoline exhaust. Ethyl benzene, dichlorouflouromethane, 1,2,3-trimethylbenzene have the potential carcinogenic impact.

Key words: Particle Phase Organics, PAHs, VOCs, PMF, Health Risk Assessment

Keywords: Particle Phase Organics, PAHs and VOCs, PMF and Health Risk Assessment

©2019. Japan Geoscience Union. All Right Reserved.

Diversity and activity of diazotrophs in the coastal waters of Southeastern Arabian Sea (SEAS)

*JABIR THAJUDEEN[1], Mohamed Hatha Abdullah

1. Cochin University of Science and Technology India

In marine environments availability of nitrogen (N2) limits the primary productivity. Nitrogen fixing bacteria (diazotrophs) could convert atmospheric nitrogen to ammonium thereby providing significant input of new nitrogen into the ocean. The knowledge about their diversity, distribution and physiological activity are limited in tropical coastal marine environments. In this study, we determined diversity of nitrogen fixing bacteria and the nitrogen fixation rate through *nifH* based clone library analysis and 15N2 bubble method respectively. We encountered *Trichodesmium*bloom and diatom diazotrophic associations along the coastal environments of SEAS. Nitrogen fixation rate in the coastal waters were varied from 0.15 to 1.02 nmolN/L/h. *Trichodesmium*bloom in the Arabian Sea during pre-monsoon season showed higher nitrogen fixation rate of 3.6 nmolN/L/h. Clone library analysis revealed that 19 Operational Taxonomic Units (OTUs) of nitrogen fixing bacteria were observed from the coastal waters SEAS. The OTUs were related to 7 OTUs of cyanobacteria and 12 OTUs of heterotrophic diazotrophs. Major cyanobacterial OTUs are closely similar to *Trichodesmium*sp., *Richelia*sp., *Synechocystis*sp.. Major heterotrophic diazotrophs belonged to alpha-, beta-, gamma-, epislon-, proteobacteria and firmicutes. Gamma proteobacterial clones were dominating among heterotrophic diazotrophs in the coastal water column of south eastern Arabian Sea. Nitrogen fixation rate in the water column were significantly correlated with dissolved Fe (R^2= 0.66, p= 0.05) and phosphorous (R^2= 0.49, p= 0.05), which revealed these are the major factors controlling nitrogen fixation process in the coastal environments of SEAS.

Keywords: Nitrogen fixation , diazotrophs, Fe, SEAS

©2019. Japan Geoscience Union. All Right Reserved.

Bloom of *Palmerina hardmaniana*, a marine centric planktonic diatom in a coastal mangrove ecosystem- implication for coastal carbon cycling

*Punyasloke Bhadury[1]

1. Centre for Climate and Environmental Studies and Department of Biological Sciences, Indian Institute of Science Education and Research Kolkata

Large celled diatoms play an important role in export of carbon in coastal ecosystems. In the Sundarbans mangrove ecosystem located on the delta of Ganga-Brahmaputra-Meghna riverine systems and facing the coastal Bay of Bengal, a bloom of *Palmerina hardmaniana* (Greville) Hasle was tracked in 2015. The bloom of this centric diatom species was tracked from April- July, 2015 in Sundarbans Biological Observatory Time Series (SBOTS) site of Sundarbans. During pre-bloom (April) dissolved oxygen (DO) concentration was 6.82 mg/L while during bloom (May-June) DO concentration decreased to 3.83 mg/L. This also coincided with Chlorophyll-a concentration which ranged from 0.22-6.28 mg/L during the study period, with highest concentration of 6.28 mg/L in bloom period and overwhelmingly dominated by cells belonging to *Palmerina hardmaniana* (40.8 X 10^4 cells/L). In total 72 phytoplankton species were observed from April-July, 2015 in SBOTS site. The frustules of *Palmerina hardmaniana* ranged from 291-358 μm in length and from 195 to 260 μm in width. Based on *rbc*L phylogeny of RuBISCO, the dominance of *P. hardmaniana* was also confirmed. Increased air and surface water temperatures in SBOTS site showed significant correlation with observed cell abundance of *P. hardmaniana* with the onset of bloom. This is the first report of *P. hardmaniana* bloom in the coastal Sundarbans mangrove ecosystem. Therefore, understanding the physiological success of this centric diatom species in relation to dynamic environmental conditions has consequences for tracking export of carbon by centric diatoms in coastal water and resulting implications for coastal carbon cycling.

Keywords: diatom, phytoplankton bloom, mangrove, carbon cycling

©2019. Japan Geoscience Union. All Right Reserved.

Dynamics of Carbon and Nitrogen influx in large river system: Isotopic study from river Ganga, India

*Anurag Kumar[1], Prasanta Sanyal[1,2], Punyasloke Bhadury[3,2]

1. Department of Earth Sciences, Indian Institute of Science Education and Research Kolkata, Mohanpur 741246, India, 2. Centre for Climate and Environmental studies, Indian Institute of Science Education and Research Kolkata, Mohanpur 741246, India, 3. Department of Biological Sciences, Indian Institute of Science Education and Research Kolkata, Mohanpur 741246, India

Freshwater flux transport large amount of carbon (dissolved and particulate, organic and inorganic) and nitrogen (Dissolved) from continent into the ocean, contributing significantly to the global carbon and nitrogen cycle. The present sources and sinks of naturally as well as anthropogenically produced C and N compounds in the global carbon and nitrogen cycle remains enigmatic. Among the carbon sources in the river ecosystem, the dissolved inorganic carbon (DIC) constitute major component of carbon influx from land to ocean. These fluxes are significantly influenced by the terrestrial and estuary processes. The isotopic composition of DIC can be used to understand the sources and cycling of carbon in rivers and estuaries. In this study, $d^{13}C$ of DIC in river water of Ganga has been used to understand the dissolved inorganic carbon sources into the river. The river Ganga (2500 km) is the largest river of the Indian subcontinent which originates from the Gangotri glacier and drains into Bay of Bengal through its vast delta in the Sunderban. The $d^{13}C_{DIC}$ of river water were measured from source (Gomukh) to sink (Bay of Bengal) of the river Ganga for pre and post-monsoon period. The seasonal variation in the $d^{13}C_{DIC}$ shows enriched isotopic values in pre-monsoon compared to post-monsoon samples, indicating increased biological activities in the riverine system during pre-monsoon. A varied enrichment factor in the $d^{13}C_{DIC}$ values were observed for upper, middle and lower stretch of the river Ganga which might be indicating different sources contributing water in different stretch of the river Ganga. The $d^{18}O$ value of river water, ground water and rain water were used to delineate the different sources of water into the river Ganga. The water budget of the river Ganga shows high glacier melt in the upper stretch, high ground water influx in middle stretch and high rain water input in lower stretch of the river Ganga.

On similar note, the dissolved form of nitrogen in river water (NO_3^-) also significantly impacts the riverine as well as costal ecosystem. The increased influx of nitrate changes the competition between species causing disruption in the biological diversity. The lower stretch of the river Ganga receives maximum rain water input; therefore the region becomes prone to pollutant as result of surface runoff from the catchment areas. The isotopic composition of dissolved nitrate in water can be used to delineate the sources of NO_3^- into the riverine system. The $d^{15}N$ and $d^{18}O$ of the dissolved nitrate in river water from the lower stretch (Kolkata) of the river Ganga indicates the input of anthropogenic activities (pollutant) to river water. The data indicates manure from septic pipe lines as major source of dissolved nitrate present in the river Ganga.

Keywords: DIC, Ganga river, nitrate isotope, India

©2019. Japan Geoscience Union. All Right Reserved.

[E] Poster | B (Biogeosciences)：B-BG Biogeosciences & Geosphere-Biosphere Interactions

Mon. May 27, 2019 5:15 PM - 6:30 PM JST | Mon. May 27, 2019 8:15 AM - 9:30 AM UTC | Poster Hall International Exhibition Hall8, Makuhari Messe_31

[B-BG01] Elemental cycling in terrestrial and coastal ecosystems- Carbon and Nitrogen perspectives

convener:Punyasloke Bhadury(Indian Institute of Science Education and Research Kolkata)

Biogeochemical cycling of carbon and nitrogen hold the key to cropping cycle, monsoonal patterns and climate globally. Biological communities that make up the biosphere are essential for cycling of carbon and nitrogen and their functions are regulated by numerous factors including redox conditions, trace metal availability, and energy sources. At the same time temporal and spatial variability of biological communities such as those observed in microbes strongly affect the rate of carbon and nitrogen cycling in various environments including land and marine systems. In this session, submissions are welcomed from scientists including early career scientists working on various aspects of carbon and nitrogen cycling across terrestrial, coastal and oceanic environments. Submissions are also encouraged addressing challenges related to estimation of carbon and nitrogen budgets representing local, regional and global scales.

[BBG01-P01] Forest-CEW: A Forest Ecosystems Model for Carbon-Energy-Water Processes.

*Zhenghong Tan[1] (1.Hainan University China)

[BBG01-P02] **Interdependent Dynamics of LAI-ET across Roofing Landscapes: the Mongolian and Tibetan Plateaus**

*Li Tian[1] (1.Institute of Geographic Sciences and Natural Resources Research, Chinese Academy of Sciences)

[BBG01-P03] **Particle Phase Organic compounds (PAHs and VOCs) at Two Big Cities (Dhaka and Rajshahi) in Bangladesh**

*Islam Nazrul nazrulislam6727@gmail.com[1], Tanzina Tul Karim[1], Rasheda Nahida[1], Nusrat Mousume[1], Farha Jeba[1], Abdus Salam[1] (1.Department of Chemistry, University of Dhaka, Dhaka-1000, Bangladesh)

[BBG01-P04] **Diversity and activity of diazotrophs in the coastal waters of Southeastern Arabian Sea (SEAS)**

*JABIR THAJUDEEN[1], Mohamed Hatha Abdullah (1.Cochin University of Science and Technology India)

[BBG01-P05] **Bloom of *Palmerina hardmaniana*, a marine centric planktonic diatom in a coastal mangrove ecosystem- implication for coastal carbon cycling**

*Punyasloke Bhadury[1] (1.Centre for Climate and Environmental Studies and Department of Biological Sciences, Indian Institute of Science Education and Research Kolkata)

[BBG01-P06] Dynamics of Carbon and Nitrogen influx in large river system: Isotopic study from river Ganga, India

*Anurag Kumar[1], Prasanta Sanyal[1,2], Punyasloke Bhadury[3,2] (1.Department of Earth Sciences, Indian Institute of Science Education and Research Kolkata, Mohanpur 741246, India, 2.Centre for Climate and Environmental studies, Indian Institute of Science Education and Research Kolkata, Mohanpur 741246, India, 3.Department of Biological Sciences, Indian Institute of Science Education and Research Kolkata, Mohanpur 741246, India)

Forest-CEW: A Forest Ecosystems Model for Carbon-Energy-Water Processes.

*Zhenghong Tan[1]

1. Hainan University China

Forest ecosystem models (FEM) are essential tools for studying the forest carbon budget, which is an important subject in the global climate change studies. Although using FEM has a long history and there exist many types of FEM, new models are still being developed for special uses. This presentation introduces Forest-CEW, a forest ecosystems model for carbon-energy-water processes. The model is aimed at having a structure that can be configured flexibly for different forest ecosystems, a graphic interface for inexperienced users, and a command execution mode for experts. The time scale of the model is at the hourly level. Model validation using the data from Tomakomai flux research site (asiaflux.net/index.php?page_id=113) shows that the model can well reconstruct major ecosystem variables including net ecosystem exchange, soil temperature and water content. We also compared Forest-CEW with those include in the TDE ecosystem model intercomparison (cdiac.ess-dive.lbl.gov/epubs/tdemodel/models.html) and the results show that its performance is among the best of the 13 models.

Keywords: Model, Forest Ecosystem, Carbon, Water, Energy

©2019. Japan Geoscience Union. All Right Reserved.

Interdependent Dynamics of LAI-ET across Roofing Landscapes: the Mongolian and Tibetan Plateaus

*Li Tian[1]

1. Institute of Geographic Sciences and Natural Resources Research, Chinese Academy of Sciences

The Mongolian and Tibetan Plateaus have experienced higher-than-global average warming in recent decades, resulting in many significant changes in ecosystem structure and function. Among them are Leaf area index (LAI) and evapotranspiration (ET) that play a fundamental role in shaping many causes and consequences of land surface processes and climate. Here, we focused on the spatiotemporal changes of the LAI, ET and their relationships on these two roofing landscapes. Based on the MODIS products from 2000 through 2014. We found that there existed a general positive relationship between LAI and ET on the Mongolia Plateau (MP), while there was not synergy on the Tibetan Plateau (TP).

Overall, 49.38% (50.62%) of land areas on the TP experienced significant increased (decreased) in LAI, while 94.92% (5.09%) on the MP. For the ET, the increased land area was 21.70% (124.10×10^3 km^2) on the TP and 88.01% (341.60×10^3 km^2) on the MP. More importantly, the relationships varied substantially across the space and over time, with mismatches found in some parts of the landscapes. Substantial additional efforts with observational and/or experimental investigations are need to explore the relationships, including the influences of vegetation characteristics and disturbances.

Keywords: ET, LAI, Eurasian continent, alpine, land surface process

©2019. Japan Geoscience Union. All Right Reserved.

Particle Phase Organic compounds (PAHs and VOCs) at Two Big Cities (Dhaka and Rajshahi) in Bangladesh

*Islam Nazrul nazrulislam6727@gmail.com[1], Tanzina Tul Karim[1], Rasheda Nahida[1], Nusrat Mousume[1], Farha Jeba[1], Abdus Salam[1]

1. Department of Chemistry, University of Dhaka, Dhaka-1000, Bangladesh

Particle Phase Organic compounds (PAHs and VOCs) at Two Big Cities (Dhaka and Rajshahi) in Bangladesh

Md. Nazrul Islam[1*], Tanzina Tul Karim, Rasheda Nahida, Nusrut Mousume, Farha Jeba, and Abdus Salam[2*]

Department of Chemistry, University of Dhaka, Dhaka 1000, Bangladesh

Corresponding Author: [1] nazrulislam6727@gmail.com, Tel: +8801717672748; [2*] asalam@gmail.com, Tel: +880117061160

Atmospheric pollution has a significant impact on human health, climate change, agriculture, and ecosystem. Air quality and the climate change is the top most concern of the World Health Organization (WHO, 2019). Bangladesh is a rapidly developing country with kinds of environmental problems. It became the top most country in the world for the human deaths due to environmental pollution, which was accounted about 27% of the total death (Lancet, 207). Only air pollution caused two thirds of these deaths (Lancet, 2017). Dhaka along with Narayanganj and Gazipur are the top ranking cities in the World for the air pollution (WHO, 2014). Volatile organic compounds (VOCs) and poly aromatic hydrocarbons (PAHs) are the major organic pollutants in the atmosphere. Until now there is no information of VOCs and PAHs regarding their occurrences, sources, seasonal variation and health impact in Bangladesh. In this study we have collected particulate matters samples on quartz filters with a low volume sampler at two big cities in Bangladesh (Capital Dhaka and North West City Rajshahi) from January 2015 to February 2019. Individual organic compounds were extracted with acetone and n-hexane from the particulate matter loaded filters. The chemical analysis was done with Gas Chromatography (GC)-Mass spectrometry (MS). The analyzed organic compounds were naphthalene, anthracene, diazinon, deltramethrin, pyrabenxoime, pyrazosulfuran, prophenophos butachlor, propiconazole, cymoxanil, cypermethrin, lamda cyhalothrin, dimethoate, chloropyriphos, carbofuran, metalaxyl, pentane, hexane, propene, isobutene, 1,3-butadiene, dichloroflouromethane, ethanol, benzene, toluene, ethylbenzene, xylene, styrene, 1,2,3trimethylbenzene, isoprene, cyclopentane, and cyclohexane. Positive matrix factorization (PMF) and air mass trajectory analysis were done for source characterization. Health risk assessment and life time cancer risk (LCR)

©2019. Japan Geoscience Union. All Right Reserved.

were determined with US EPA based model. The elevated concentrations of the determined compounds at both Dhaka and Rajshahi were observed; Dhaka values were slightly higher than Rajshahi. The concentrations of determined compounds were higher during the winter months basically December to February and lower during the monsoon period in the month of July. PMF model revealed that the sources of organic compounds in Bangladesh were diesel exhaust, coal and biomass burning, industry and gasoline exhaust. Ethyl benzene, dichlorouflouromethane, 1,2,3-trimethylbenzene have the potential carcinogenic impact.

Key words: Particle Phase Organics, PAHs, VOCs, PMF, Health Risk Assessment

Keywords: Particle Phase Organics, PAHs and VOCs, PMF and Health Risk Assessment

©2019. Japan Geoscience Union. All Right Reserved.

Diversity and activity of diazotrophs in the coastal waters of Southeastern Arabian Sea (SEAS)

*JABIR THAJUDEEN[1], Mohamed Hatha Abdullah

1. Cochin University of Science and Technology India

In marine environments availability of nitrogen (N2) limits the primary productivity. Nitrogen fixing bacteria (diazotrophs) could convert atmospheric nitrogen to ammonium thereby providing significant input of new nitrogen into the ocean. The knowledge about their diversity, distribution and physiological activity are limited in tropical coastal marine environments. In this study, we determined diversity of nitrogen fixing bacteria and the nitrogen fixation rate through *nifH* based clone library analysis and 15N2 bubble method respectively. We encountered *Trichodesmium*bloom and diatom diazotrophic associations along the coastal environments of SEAS. Nitrogen fixation rate in the coastal waters were varied from 0.15 to 1.02 nmolN/L/h. *Trichodesmium*bloom in the Arabian Sea during pre-monsoon season showed higher nitrogen fixation rate of 3.6 nmolN/L/h. Clone library analysis revealed that 19 Operational Taxonomic Units (OTUs) of nitrogen fixing bacteria were observed from the coastal waters SEAS. The OTUs were related to 7 OTUs of cyanobacteria and 12 OTUs of heterotrophic diazotrophs. Major cyanobacterial OTUs are closely similar to *Trichodesmium*sp., *Richelia*sp., *Synechocystis*sp.. Major heterotrophic diazotrophs belonged to alpha-, beta-, gamma-, epislon-, proteobacteria and firmicutes. Gamma proteobacterial clones were dominating among heterotrophic diazotrophs in the coastal water column of south eastern Arabian Sea. Nitrogen fixation rate in the water column were significantly correlated with dissolved Fe (R^2= 0.66, p= 0.05) and phosphorous (R^2= 0.49, p= 0.05), which revealed these are the major factors controlling nitrogen fixation process in the coastal environments of SEAS.

Keywords: Nitrogen fixation , diazotrophs, Fe, SEAS

©2019. Japan Geoscience Union. All Right Reserved.

Bloom of *Palmerina hardmaniana*, a marine centric planktonic diatom in a coastal mangrove ecosystem- implication for coastal carbon cycling

*Punyasloke Bhadury[1]

1. Centre for Climate and Environmental Studies and Department of Biological Sciences, Indian Institute of Science Education and Research Kolkata

Large celled diatoms play an important role in export of carbon in coastal ecosystems. In the Sundarbans mangrove ecosystem located on the delta of Ganga-Brahmaputra-Meghna riverine systems and facing the coastal Bay of Bengal, a bloom of *Palmerina hardmaniana* (Greville) Hasle was tracked in 2015. The bloom of this centric diatom species was tracked from April- July, 2015 in Sundarbans Biological Observatory Time Series (SBOTS) site of Sundarbans. During pre-bloom (April) dissolved oxygen (DO) concentration was 6.82 mg/L while during bloom (May-June) DO concentration decreased to 3.83 mg/L. This also coincided with Chlorophyll-a concentration which ranged from 0.22-6.28 mg/L during the study period, with highest concentration of 6.28 mg/L in bloom period and overwhelmingly dominated by cells belonging to *Palmerina hardmaniana* (40.8 X 10^4 cells/L). In total 72 phytoplankton species were observed from April-July, 2015 in SBOTS site. The frustules of *Palmerina hardmaniana* ranged from 291-358 μm in length and from 195 to 260 μm in width. Based on *rbc*L phylogeny of RuBISCO, the dominance of *P. hardmaniana* was also confirmed. Increased air and surface water temperatures in SBOTS site showed significant correlation with observed cell abundance of *P. hardmaniana* with the onset of bloom. This is the first report of *P. hardmaniana* bloom in the coastal Sundarbans mangrove ecosystem. Therefore, understanding the physiological success of this centric diatom species in relation to dynamic environmental conditions has consequences for tracking export of carbon by centric diatoms in coastal water and resulting implications for coastal carbon cycling.

Keywords: diatom, phytoplankton bloom, mangrove, carbon cycling

©2019. Japan Geoscience Union. All Right Reserved.

Dynamics of Carbon and Nitrogen influx in large river system: Isotopic study from river Ganga, India

*Anurag Kumar[1], Prasanta Sanyal[1,2], Punyasloke Bhadury[3,2]

1. Department of Earth Sciences, Indian Institute of Science Education and Research Kolkata, Mohanpur 741246, India, 2. Centre for Climate and Environmental studies, Indian Institute of Science Education and Research Kolkata, Mohanpur 741246, India, 3. Department of Biological Sciences, Indian Institute of Science Education and Research Kolkata, Mohanpur 741246, India

Freshwater flux transport large amount of carbon (dissolved and particulate, organic and inorganic) and nitrogen (Dissolved) from continent into the ocean, contributing significantly to the global carbon and nitrogen cycle. The present sources and sinks of naturally as well as anthropogenically produced C and N compounds in the global carbon and nitrogen cycle remains enigmatic. Among the carbon sources in the river ecosystem, the dissolved inorganic carbon (DIC) constitute major component of carbon influx from land to ocean. These fluxes are significantly influenced by the terrestrial and estuary processes. The isotopic composition of DIC can be used to understand the sources and cycling of carbon in rivers and estuaries. In this study, $d^{13}C$ of DIC in river water of Ganga has been used to understand the dissolved inorganic carbon sources into the river. The river Ganga (2500 km) is the largest river of the Indian subcontinent which originates from the Gangotri glacier and drains into Bay of Bengal through its vast delta in the Sunderban. The $d^{13}C_{DIC}$ of river water were measured from source (Gomukh) to sink (Bay of Bengal) of the river Ganga for pre and post-monsoon period. The seasonal variation in the $d^{13}C_{DIC}$ shows enriched isotopic values in pre-monsoon compared to post-monsoon samples, indicating increased biological activities in the riverine system during pre-monsoon. A varied enrichment factor in the $d^{13}C_{DIC}$ values were observed for upper, middle and lower stretch of the river Ganga which might be indicating different sources contributing water in different stretch of the river Ganga. The $d^{18}O$ value of river water, ground water and rain water were used to delineate the different sources of water into the river Ganga. The water budget of the river Ganga shows high glacier melt in the upper stretch, high ground water influx in middle stretch and high rain water input in lower stretch of the river Ganga.

On similar note, the dissolved form of nitrogen in river water (NO_3^-) also significantly impacts the riverine as well as costal ecosystem. The increased influx of nitrate changes the competition between species causing disruption in the biological diversity. The lower stretch of the river Ganga receives maximum rain water input; therefore the region becomes prone to pollutant as result of surface runoff from the catchment areas. The isotopic composition of dissolved nitrate in water can be used to delineate the sources of NO_3^- into the riverine system. The $d^{15}N$ and $d^{18}O$ of the dissolved nitrate in river water from the lower stretch (Kolkata) of the river Ganga indicates the input of anthropogenic activities (pollutant) to river water. The data indicates manure from septic pipe lines as major source of dissolved nitrate present in the river Ganga.

Keywords: DIC, Ganga river, nitrate isotope, India

©2019. Japan Geoscience Union. All Right Reserved.

[E] Oral | B (Biogeosciences)：B-BG Biogeosciences & Geosphere-Biosphere Interactions

Mon. May 27, 2019 3:30 PM - 5:00 PM JST | Mon. May 27, 2019 6:30 AM - 8:00 AM UTC | 201A 2F

[B-BG01] Elemental cycling in terrestrial and coastal ecosystems- Carbon and Nitrogen perspectives

convener:Punyasloke Bhadury(Indian Institute of Science Education and Research Kolkata), Chairperson:Punyasloke Bhadury(Indian Institute of Science Education and Research Kolkata)

Biogeochemical cycling of carbon and nitrogen hold the key to cropping cycle, monsoonal patterns and climate globally. Biological communities that make up the biosphere are essential for cycling of carbon and nitrogen and their functions are regulated by numerous factors including redox conditions, trace metal availability, and energy sources. At the same time temporal and spatial variability of biological communities such as those observed in microbes strongly affect the rate of carbon and nitrogen cycling in various environments including land and marine systems. In this session, submissions are welcomed from scientists including early career scientists working on various aspects of carbon and nitrogen cycling across terrestrial, coastal and oceanic environments. Submissions are also encouraged addressing challenges related to estimation of carbon and nitrogen budgets representing local, regional and global scales.

3:30 PM - 3:35 PM JST | 6:30 AM - 6:35 AM UTC

Introduction

3:35 PM - 4:00 PM JST | 6:35 AM - 7:00 AM UTC

[BBG01-01] **Modelling nitrogen and carbon cycles in Hooghly estuary along with adjacent mangrove ecosystem**

★Invited Papers

*Santanu Ray[1] (1.Systems ecology and ecological modelling laboratory, Dept. of Zoology, Visva-Bharati University, Santiniketan 731235, India)

4:00 PM - 4:15 PM JST | 7:00 AM - 7:15 AM UTC

[BBG01-02] ^{17}O-rich nitrate as a tracer for constraining nitrogen transformations in coastal sediments

*Chawalit Charoenpong[1,2], Scott D Wankel[2], Carolyn Buchwald[3,2], Wiebke Ziebis[4] (1.Chulalongkorn University, 2.Woods Hole Oceanographic Institution, 3.Dalhousie University, 4.University of Southern California)

4:15 PM - 4:30 PM JST | 7:15 AM - 7:30 AM UTC

[BBG01-03] **Exploring changes in bacterioplankton community structure in response to tannic acid, a major component of litterfall, in a mangrove ecosystem: a laboratory mesocosm approach**

*Anwesha Ghosh[1] (1.Integrative Tax Microb Ecol Res Group, Dept. of Biol Sci, IISERK)

4:30 PM - 4:45 PM JST | 7:30 AM - 7:45 AM UTC

[BBG01-04] **Diel variations of dissolved inorganic carbon in the Pearl River plume and the northern South China Sea shelf upwelling during summer**

*Wei-Jen Huang[1], Kai-Jung Kao[1], Yu-Shih Lin[1], James T. Liu[1], Chen-Tung Arthur Chen[1] (1.National Sun Yat-sen University)

4:45 PM - 5:00 PM JST | 7:45 AM - 8:00 AM UTC

[BBG01-05] **Spatial and vertical variations of carbon and nitrogen isotopes of larch forest and NDVI in Eastern Siberia**

*Aleksandr Nogovitcyn[1], Atsuko Sugimoto[2], Ruslan Shakhmatov[1], Tomoki Morozumi[1], Shunsuke Tei[2], Yumiko Miyamoto[2], Trofim Maximov[3,4] (1.Graduate School of Environmental Science, Hokkaido University, Sapporo, Hokkaido, Japan, 2.Arctic Research Center, Hokkaido University, Sapporo,

Hokkaido, Japan, 3.Institute for Biological Problems of Cryolithozone, Siberian Blanch of Russian Academy of Sciences, Yakutsk, Yakutia, Russia, 4.International Center for Biogeoscience Educational and Scientific Trainings (BEST), North-Eastern Federal University, Yakutsk, Yakutia, Russia)

Modelling nitrogen and carbon cycles in Hooghly estuary along with adjacent mangrove ecosystem

*Santanu Ray[1]

1. Systems ecology and ecological modelling laboratory, Dept. of Zoology, Visva-Bharati University, Santiniketan 731235, India

Hooghly estuary of India is very rich in natural resources and receives large amountof nutrients through litterfall from adjacent mangrove forest. Nitrogen and carbon as important nutrients occur in various forms and plays a crucial role in the regulation of productivity in this estuarine system. Modelling of nitrogen and carbon dynamics from mangrove litterfall and particularly the release of dissolved inorganic nitrogen and carbon in this estuarine system is important because of their roles in augmenting growth of phytoplankton and other higher plants and all other biological components of grazing food chain. Considering the importance of nitrogen and cabron, two dynamic models both with seven compartmentsare proposed. In these models, nitrogen and carbon of the mangrove litterfall are considered as source and its conversion into different organic and inorganic forms are considered as state variables. Some physical and chemical factors and also rate parameters such as nitrogen fraction of litter biomass, litter biomass, redox potential, soil temperature, conversion rates of nitrogen of one form to another form, phytoplankton uptake rate of dissolved inorganic nitrogen and carbon, dissolved oxygen, water temperature and water pH are considered as graph-time functions in this model. These data are collected over two years from field works and experiments. Other rate parameters are calibrated following standard procedure. Sensitivity analysis is performed before calibration. Model simulation results are properly validated with observed data. Sensitivity analysis reveals that the leaching rate of soil organic nitrogen to total organic nitrogen of water and loss rate of soil organic nitrogen as humic acid and fulvic acids are very sensitive parameters in this system. Redox potential plays an important role in the conversion of soil total nitrogen to soil inorganic nitrogen whereas soil temperature is considered to be key factor regulating the microbial activity for the conversion of soil organic nitrogen to soil inorganic nitrogen. Similarly inwater, total organic nitrogen of water including dissolved organic nitrogen and particulate organic nitrogen is dependent on soil organic nitrogen. The dissolved organic nitrogen, particulate organic nitrogen and soil inorganic nitrogen ultimately get converted into dissolved inorganic nitrogen and accumulated in water which is taken by phytoplankton and microflora as minerals.For carbon cycle model results show seasonal variations of litterfall and which is the main source of SOC pool and ultimately transportedto the estuary. Other than litterfall, the death of organisms in soil and water enriches the SOC and POC respectively. pH of water is governing factor and depending on this factor, DIC is converted to DCO_2 and DBC, which are taken up by phytoplankton during photosynthesis. Mineralization rate of SOC to SIC and uptake rate of DCO_2 and DBC are the sensitive parameters.

Keywords: Dynamic models, litterfall, inorganic, organic, tropical estuary

©2019. Japan Geoscience Union. All Right Reserved.

Modelling nitrogen and carbon cycles in Hooghly estuary along with adjacent mangrove ecosystem

Santanu Ray
[1]Ecological Modelling Laboratory, Department of Zoology, Visva-Bharati University, Santiniketan 731235, India
[2]Department of Environmental Science, Burdwan University, Burdwan, India

Abstract

Hooghly estuary of India is very rich in natural resources and receives large amountof nutrients through litterfall from adjacent mangrove forest. Nitrogen and carbon as important nutrients occur in various forms and plays a crucial role in the regulation of productivity in this estuarine system. Modelling of nitrogen and carbon dynamics from mangrove litterfall and particularly the release of dissolved inorganic nitrogen and carbon in this estuarine system is important because of their roles in augmenting growth of phytoplankton and other higher plants and all other biological components of grazing food chain. Considering the importance of nitrogen and cabron, two dynamic models both with seven compartmentsare proposed. In these models, nitrogen and carbon of the mangrove litterfall are considered as source and its conversion into different organic and inorganic forms are considered as state variables. Some physical and chemical factors and also rate parameters such as nitrogen fraction of litter biomass, litter biomass, redox potential, soil temperature, conversion rates of nitrogen of one form to another form, phytoplankton uptake rate of dissolved inorganic nitrogen and carbon, dissolved oxygen, water temperature and water pH are considered as graph-time functions in this model. These data are collected over two years from field works and experiments. Other rate parameters are calibrated following standard procedure. Sensitivity analysis is performed before calibration. Model simulation results are properly validated with observed data. Sensitivity analysis reveals that the leaching rate of soil organic nitrogen to total organic nitrogen of water and loss rate of soil organic nitrogen as humic acid and fulvic acids are very sensitive parameters in this system. Redox potential plays an important role in the conversion of soil total nitrogen to soil inorganic nitrogen whereas soil temperature is considered to be key factor regulating the microbial activity for the conversion of soil organic nitrogen to soil inorganic nitrogen. Similarly inwater, total organic nitrogen of water including dissolved organic nitrogen and particulate organic nitrogen is dependent on soil organic nitrogen. The dissolved organic nitrogen, particulate organic nitrogen and soil inorganic nitrogen ultimately get converted into dissolved inorganic nitrogen and accumulated in water which is taken by phytoplankton and microflora as minerals.For carbon cycle model results show seasonal variations of litterfall and which is the main source of SOC pool and ultimately transportedto the estuary. Other than litterfall, the death of organisms in soil and water enriches the SOC and POC respectively. pH of water is governing factor and depending on this factor, DIC is converted to DCO_2 and DBC, which are taken up by phytoplankton during photosynthesis. Mineralization rate of SOC to SIC and uptake rate of DCO_2 and DBC are the sensitive parameters

Keywords: Dynamic models; litterfall; inorganic; organic; tropical estuary

©2019. Japan Geoscience Union. All Right Reserved.

^{17}O-rich nitrate as a tracer for constraining nitrogen transformations in coastal sediments

*Chawalit Charoenpong[1,2], Scott D Wankel[2], Carolyn Buchwald[3,2], Wiebke Ziebis[4]

1. Chulalongkorn University, 2. Woods Hole Oceanographic Institution, 3. Dalhousie University, 4. University of Southern California

Coastal sediments are often replete in organic matter and exhibit sharp gradient in redox conditions. In addition, the oxic-anoxic interfaces are often around a few centimeters if not less below the sediment surface. This make this environment poised to harbor both oxidative and reductive nitrogen transformations. As such, the use of a single or a couple of isotope-labeling tracers to determine the rates of these many processes might suffer from the systems being underconstrained. In this work, we demonstrate how naturally-occurring, ^{17}O-rich nitrate can aid in the studying these complex systems through the ability to follow the transformations of added nitrate (NO_3^-) into other different pools of N-species and closely investigate the triple isotopic compositions (δ^{15}N, δ^{18}O, and Δ^{17}O). While we followed five different pools of N-species namely NO_3^-, NO_2^-, N_2O, NH_4^+, and total reduced N (NH_4^+ plus DON), we chose to focus this work on the intermediate nitrite, NO_2^-. For all intact flow-through core incubations done on the sediments collected from Sylt Island, Germany, sediments acted as sources for NO_2^- in all experimental manipulations including sediment type, dissolved oxygen level, and NO_3^- loading. Unlike in the environments that are solely driven by reductive processes where the changes in δ^{15}N and δ^{18}O are coupled, the co-occurrence of both oxic and anoxic in the sediments such as ones from this study cause the δ^{15}N and δ^{18}O to decouple primarily because O is often subject to more processes than N. By using three isotope systems along with the change in concentrations, we demonstrate how we can use a natural abundance appraoch and rely on a series of mathematical equations to solve for different N transformation rates.

Keywords: nitrogen, isotope, 17O, sediments

©2019. Japan Geoscience Union. All Right Reserved.

©2019. Japan Geoscience Union. All Right Reserved.

Exploring changes in bacterioplankton community structure in response to tannic acid, a major component of litterfall, in a mangrove ecosystem: a laboratory mesocosm approach

*Anwesha Ghosh[1]

1. Integrative Tax Microb Ecol Res Group, Dept. of Biol Sci, IISERK

Litterfall constitutes a major source of allochthonous matter for bacterioplankton communities in estuarine mangroves. Tannic acid, an abundant component of mangrove litterfall, leaches out and contributes substantially to DOC and DOM pools of the adjacent estuaries. About 50% of mangrove litterfall maybe degraded and channelized into the marine microbial loop. Estuarine conditions of Sundarbans, world’ s largest contiguous mangrove, was mimicked in a laboratory mescocosm set-up using barrels to understand the influence of tannic acid on bacterioplankton communities. Estuarine water from a station, Stn3 of Sundarbans Biological Observatory Time Series (SBOTS) was enriched with tannic acid and the change in functional bacterioplankton community structure was analysed on the start (Day 0), intermediate (Day 7) and end (Day 15) of the experiment. Bacterioplankton community structure was elucidated by sequencing the V3-V4 region of 16S rRNA on an Illumina MiSeq platform. Concentration of tannic acid, gallic acid, trace elements, dissolved nutrients such as nitrate and *ortho* -phosphate along with hydrological parameters were determined on a daily basis. Degradation of tannic acid was tracked by decrease in concentration of tannic acid and generation of gallic acid, one of the final products of tannic acid degradation. Tannic acid was shown to significantly affect the concentration of dissolved nitrate and trace elements in the barrels. Proteobacteria was found to be the most dominant bacterial phylum in Control and tannic acid enriched barrels (Barrel 1 and 2) on Day 0. With the progression of experiment, the abundance of Proteobacteria decreased significantly in the Control barrel indicating the dependence of this phylum on steady flux of nutrients. The abundance of Proteobacteria in the tannic acid enriched barrels remained high indicating that members of Proteobacteria may be capable of using tannic acid as a source of carbon and nitrogen. Tannic acid appeared to inhibit other bacterioplankton phyla including Actinobacteria, Acidobacteria and Verrucomicrobia that existed in large abundance in the Control barrel on Day 15 but were absent in the tannic acid enriched barrels. At class level, Bacteroides was found to be present in highest abundance in the tannic acid enriched barrels. Bacteroides are capable of breaking down tannic acid using tannase as an enzyme. This experiment indicated that bacterioplankton communities of Sundarbans could harbour genes necessary for breakdown of complex components of litterfall and recycle them into the marine microbial loop. Breakdown of tannic acid could influence the marine nitrogen and carbon cycling by releasing DON and DOC respectively into the adjacent estuaries. An understanding of the breakdown of tannic acid and other components of mangrove litterfall and its influence on the resident biological communities of estuarine mangroves could be essential for our understanding of functioning of coastal ecosystems.

Keywords: bacterioplankton, mangrove, litterfall

©2019. Japan Geoscience Union. All Right Reserved.

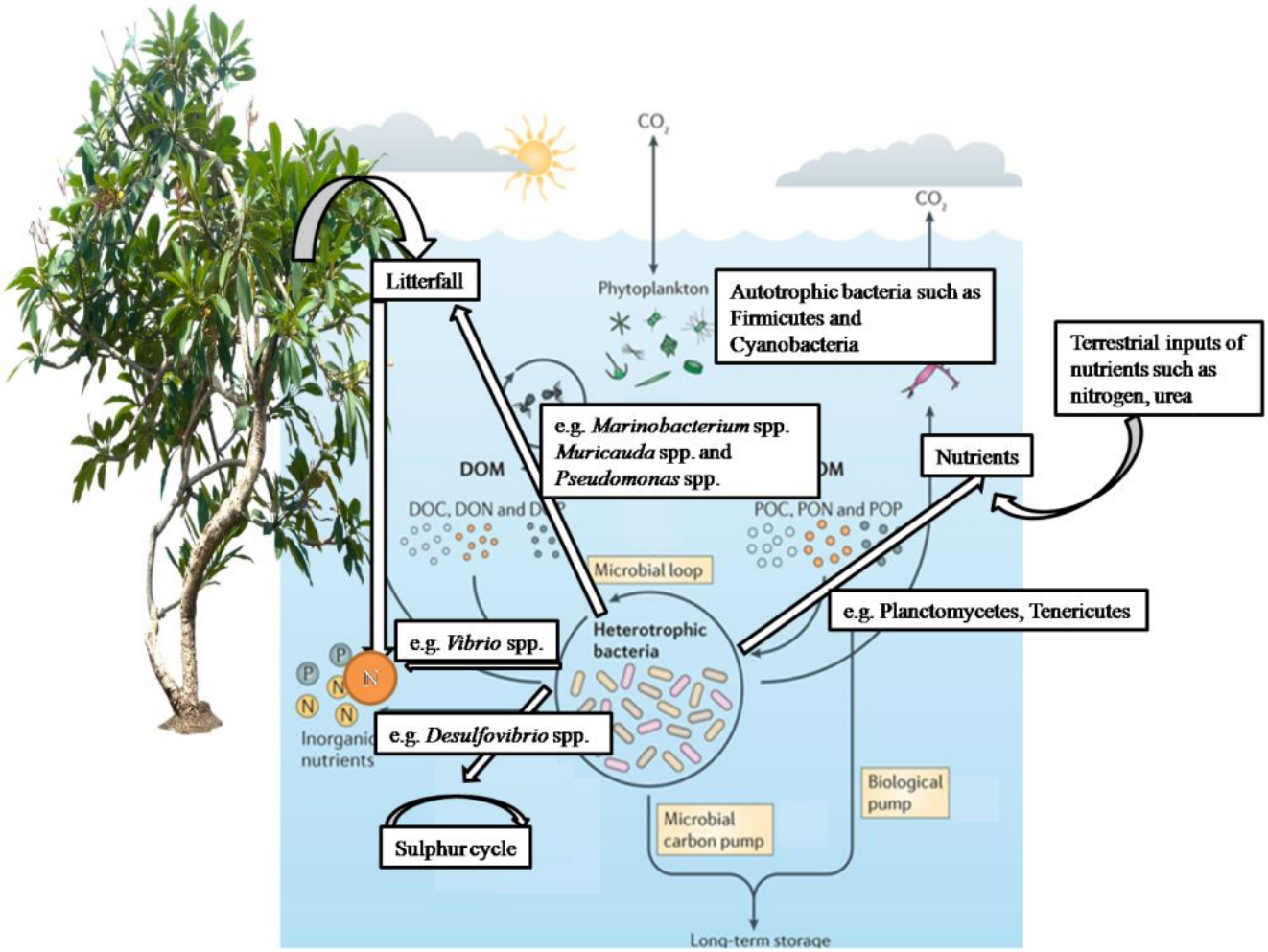

©2019. Japan Geoscience Union. All Right Reserved.

Diel variations of dissolved inorganic carbon in the Pearl River plume and the northern South China Sea shelf upwelling during summer

*Wei-Jen Huang[1], Kai-Jung Kao[1], Yu-Shih Lin[1], James T. Liu[1], Chen-Tung Arthur Chen[1]

1. National Sun Yat-sen University

Strong river-to-sea mixing, stratification, and coastal eutrophication are usually observed on a plume dominated-continental shelf, but the effects of diel variations and upwelling on the carbonate system are still unclear on the northern South China Sea continental shelf. The Pearl River plume and upwelling at the northern South China Sea were surveyed at the near-field (1 day), the mid-field (6 days), and the far-field sites (1day) along the plume trajectory. We sampled total alkalinity (TA) and dissolved inorganic carbon (DIC) and calculated buffer capacity at the near-surface and near-bottom waters. We also estimated primary productivity (PP, based on $d^{13}C$) at the near-field site and calculated net community productivity (NCP) in the mid-field site after removing the mixing effect. At this plume-upwelling hybrid system, lower salinity, TA, and DIC value and higher buffer capacity and NCP were observed in the near-surface water than the values in the near-bottom water. A good correlation between the common logarithm of light intensity and PP was observed; suggesting that the diel variation of PP was dominated by day-night light cycle. Moreover, the changes of net biological uptake (36% to 76%) were higher than the changes of salinities (3% to 8%) during the subsurface upwelling (from development, maxima, and decline stages at the middle-field site). We suggest that respiration-associated biological activities in addition to PP and physical mixing dominated the near-surface water during subsurface upwelling. Finally, at this coupled plume and upwelling system, the diel variation of carbonate system can be dominated by PP induced by periodic sunlight cycle and further affected by respiration strengthened by intensive upwelling.

Keywords: Pearl River plume, inorganic carbon, upwelling, CO2

©2019. Japan Geoscience Union. All Right Reserved.

Spatial and vertical variations of carbon and nitrogen isotopes of larch forest and NDVI in Eastern Siberia

*Aleksandr Nogovitcyn[1], Atsuko Sugimoto[2], Ruslan Shakhmatov[1], Tomoki Morozumi[1], Shunsuke Tei[2], Yumiko Miyamoto[2], Trofim Maximov[3,4]

1. Graduate School of Environmental Science, Hokkaido University, Sapporo, Hokkaido, Japan, 2. Arctic Research Center, Hokkaido University, Sapporo, Hokkaido, Japan, 3. Institute for Biological Problems of Cryolithozone, Siberian Blanch of Russian Academy of Sciences, Yakutsk, Yakutia, Russia, 4. International Center for Biogeoscience Educational and Scientific Trainings (BEST), North-Eastern Federal University, Yakutsk, Yakutia, Russia

Under a global climate change, taiga forest ecosystem is expected to change. Tree ring data obtained at northeast Siberian Taiga indicated tree growth decrease during warm climate (Tei et al., 2014), consequently primary production may decrease in the future. As tools for monitoring ecosystem changes, stable isotope of carbon $\delta^{13}C$ and nitrogen $\delta^{15}N$ are widely applied in ecological research. The $\delta^{13}C$ is a common proxy for water use efficiency in plants, and the $\delta^{15}N$ is for nitrogen availability that is important because boreal forest on permafrost is usually poor in the nitrogen (Popova et al., 2013).

Observations were conducted at Spasskaya Pad forest station (62˚25’ N, 129˚62’ E) near Yakutsk, Russia. The forest is usually dry, but after the extreme wet event in 2007, wet sites were distributed in the forest. Transect (60m x 510m) with 30m x 30m plots, in total 33, was set including dry sites and wet sites, to obtain needle samples from 104 trees at the height of 5-6 m were obtained in order to investigate spatial variations in $\delta^{13}C$, $\delta^{15}N$, and N contents. These spatial variations were compared with satellite-derived Normalized difference vegetation index (NDVI) using Landsat images with the resolution of 30 m. Lower NDVI and lower foliar N content were observed at wet sites than those at dry sites. A high $\delta^{13}C$ and high $\delta^{15}N$ were also observed at a wet site. After extreme wet event happened, ecosystem (and N availability) changes and NDVI also changes. We also obtained the needles from two trees at different heights in a jungle gym to investigate the vertical variations in $\delta^{13}C$ and $\delta^{15}N$. There were large differences in $\delta^{13}C$, $\delta^{15}N$ and N contents vertically.

Tei, S., A. Sugimoto, H. Yonenobu, T. Ohta, T. C. Maximov. Growth and physiological responses of larch trees to climate changes deduced from tree-ring widths and $\delta^{13}C$ at two forest sites in eastern Siberia. *Polar Science*, 8, 183-195, doi:10.1016/j.polar.2013.12.002, 2014

Popova A.S., N. Tokuchi, N. Ohte, M.U. Ueda, K. Osaka, T.Ch. Maximov and A. Sugimoto. Nitrogen availability in the taiga forest ecosystem of northeastern Siberia. *Soil Science and Plant Nutrition*, 59, 427-441, doi:10.1080/00380768.2013.772495, 2013

Keywords: taiga (boreal) forest, NDVI, carbon isotope, nitrogen isotope

©2019. Japan Geoscience Union. All Right Reserved.

[E] Oral | M (Multidisciplinary and Interdisciplinary)：M-IS Intersection

Mon. May 27, 2019 9:00 AM - 10:30 AM JST | Mon. May 27, 2019 12:00 AM - 1:30 AM UTC | A07 TOKYO BAY MAKUHARI HALL

[M-IS02] Drilling Earth Science

convener:Yasuhiro Yamada(Japan Agency for Marine-Earth Science and Technology (JAMSTEC), R&D Center for Ocean Drilling Science (ODS)), Yumiko Harigane(Geological Survey of Japan, National Institute of Advanced Industrial Science and Technology (AIST)), Azumi Kuroyanagi(Tohoku University Museum, The Center for Academic Resources and Archives, Tohoku University), Kosei E. Yamaguchi(Toho University and NASA Astrobiology Institute), Chairperson:Azumi Kuroyanagi(Tohoku University), Kan Hsiung(JAMSTEC)

"Earth Drilling Science" session aims to exchange the latest information and scientific achievements in Ocean/Continental drilling projects and to promote the interdisciplinary science. The session covers a wide range of drilling sciences, earth dynamics, environments, and the drilling-related technologies. The overview of the recent IODP cruises as well as future projects of any types of scientific drilling will be reported.

9:00 AM - 9:15 AM JST | 12:00 AM - 12:15 AM UTC

[MIS02-01] Planktonic foraminiferal biostratigraphy in the South China Sea IODP Exp. 367 U 1499

*Akira Furusawa[1], Hiroki Hayashi[1] (1.Interdisciplinary Graduate School of Science and Engineering, Shimane University)

9:15 AM - 9:30 AM JST | 12:15 AM - 12:30 AM UTC

[MIS02-02] High heat with slow cooling of rift margin in the South China Sea, IODP Exp.368

*Arito Sakaguchi[1,2], Nobuaki Osono[1], Keita Nakano[1] (1.Yamaguchi Univ., 2.JAMSTEC)

9:30 AM - 9:45 AM JST | 12:30 AM - 12:45 AM UTC

[MIS02-03] Abundant ferromanganese microparticles in oxic pelagic sediments (IODP Exp. 329)

*Go-Ichiro Uramoto[1,2], Yuki Morono[2], Naotaka Tomioka[2], Shigeyuki Wakaki[2], Ryoichi Nakada[2], Rota Wagai[3], Kentaro Uesugi[4], Akihisa Takeuchi[4], Masato Hoshino[4], Yoshio Suzuki[4,5], Satoshi Mitsunobu[6], Fumito Shiraishi[7], Hiroki Suga[5], Yasuo Takeichi[8], Yoshio Takahashi[5], Fumio Inagaki[2] (1.Kochi University, 2.Japan Agency for Marine-Earth Science and Technology, 3.National Agriculture and Food Research Organization, 4.Japan Synchrotron Radiation Research Institute, 5.University of Tokyo, 6.Ehime University, 7.Hiroshima University, 8.High Energy Accelerator Research Organization)

9:45 AM - 10:00 AM JST | 12:45 AM - 1:00 AM UTC

[MIS02-04] **Regional stratigraphic framework, Gas Hydrate occurrence and distribution of National Gas Hydrate Program Expedition 02 (NGHP-02) Area-B, offshore eastern India**

*KanHsi Hsiung[1], Saneatsu Saito[1], Toshiya Kanamatsu[1], Yoshinori Sanada[1], Yasuhiro Yamada[1], KYAW MOE[1], Yohei Hamada[1], Yasuyuki Nakamura[1], HungYu Wu[1] (1.Japan Agency for Marine-Earth Science and Technology)

10:00 AM - 10:15 AM JST | 1:00 AM - 1:15 AM UTC

[MIS02-05] Fluid flow and diagenetic process in frontal thrust zone off Cape Muroto in the Nankai Trough

*Akira Ijiri[1], Shigeyuki Wakaki[1], Yoshiro Nishio[2], Yohei Hamada[1], Tsuyoshi Ishikawa[1], Fumio Inagaki[1] (1.Japan Agency for Marine-Earth Science and Technology, 2.Kochi University)

10:15 AM - 10:30 AM JST | 1:15 AM - 1:30 AM UTC

[MIS02-06] Recent progress and perspective on paleomagnetism by means of deep-sea drilling

*Toshitsugu Yamazaki[1], Yuhji Yamamoto[2], Toshiya Kanamatsu[3], Yuho Kumagai[4], Norihiro Nakamura[4] (1.Atmosphere and Ocean Research Institute, The University of Tokyo, 2.Center for Advanced Marine Core

Research, Kochi University, 3.Japan Agency for Marine-Earth Science and Technology, 4.Tohoku University)

Planktonic foraminiferal biostratigraphy in the South China Sea IODP Exp. 367 U 1499

*Akira Furusawa[1], Hiroki Hayashi[1]

1. Interdisciplinary Graduate School of Science and Engineering, Shimane University

In the IODP Exp. 367 voyage in the South China Sea, I certified several floating foraminiferal biostratigraphy from the core catcher sample in shipboard analysis when I carried on research as a micro-paleontologist. I finished the voyage and brought the sample home and examined the more detailed chronology using buoyant foraminiferal fossils based on the samples obtained from the excavated U 1499 core.

Keywords: International Ocean Discovery Program: IODP, Planktonic foraminiferal biostratigraphy

©2019. Japan Geoscience Union. All Right Reserved.

High heat with slow cooling of rift margin in the South China Sea, IODP Exp.368

*Arito Sakaguchi[1,2], Nobuaki Osono[1], Keita Nakano[1]

1. Yamaguchi Univ., 2. JAMSTEC

The cooling rate of the crust may depend on thermal setting including heat source, heat transportation system and thermal properties. The heat flow of the ocean plate decreases with reversed root of the plate age, and this implies that the plate tectonics is thermo dynamic system. Thermal analysis can be applied to more complex tectonic region such as marginal sea and continental divisions.

The IODP Exp. 368 has carried out at the Paleogene South China Sea, and the sediment must record thermal history of the formation of rift margin. The site U1501 is located at the most landward outer margin high of the continent-ocean transition of the rift zone. It is expected that the sediment records thermal history of initial stage of rifting. During the cruise, early Oligocene to late Eocene sediment was cored to 697 m, and high geothermal gradient of 81.4˚C/km was obtained using in-situ temperature measurement (Jian et al., 2018). The terrigenous sediment of this core includes many vitrinite fragment, and its reflectance is sensitive geo-thermometer for sediment.

The result of vitrinite reflectance from 0.21 to 0.34 % are obtained from 340 to 510 mbsf. The estimated maximum paleo-temperature is from approximately 27 to 70˚C, and obtained paleo-geothermal gradient is >250˚C/km. This is higher than present measurement value, and quite higher than world average value of the crust. In case of hot basement covers with thin sediment, apparent geo-thermal gradient gets higher, and thickening history of sediment can be measured from the deposition rate of 11mm/Ky in average (Jian et al., 2018). To satisfy the obtained vitrinite reflectance profile, this site must cool by 2.8% in million years. This cooling rate is much slower than general rate of reversed root of the plate age. This might be due to heat being transferred for a long time or being warmed by the cover sediment layer.

Keywords: Rift margin, heat flow, cooling rate, Joides Resolution, vitrinite reflectance, South China Sea

©2019. Japan Geoscience Union. All Right Reserved.

Abundant ferromanganese microparticles in oxic pelagic sediments (IODP Exp. 329)

*Go-Ichiro Uramoto[1,2], Yuki Morono[2], Naotaka Tomioka[2], Shigeyuki Wakaki[2], Ryoichi Nakada[2], Rota Wagai[3], Kentaro Uesugi[4], Akihisa Takeuchi[4], Masato Hoshino[4], Yoshio Suzuki[4,5], Satoshi Mitsunobu[6], Fumito Shiraishi[7], Hiroki Suga[5], Yasuo Takeichi[8], Yoshio Takahashi[5], Fumio Inagaki[2]

1. Kochi University, 2. Japan Agency for Marine-Earth Science and Technology, 3. National Agriculture and Food Research Organization, 4. Japan Synchrotron Radiation Research Institute, 5. University of Tokyo, 6. Ehime University, 7. Hiroshima University, 8. High Energy Accelerator Research Organization

Manganese is the third most abundant metallic element, after iron and titanium, in the Earth’ s crust, and ferromanganese minerals are sensitive to changes in redox condition. Assessing the formation and preservation of ferromanganese minerals is important for understanding the global marine cycles of manganese and numerous associated trace elements. The most extensive manganese mineral deposits occur on abyssal plains, including those below open-ocean gyres. However, the extent of ferromanganese minerals buried in subseafloor sediments remains unclear. During the Integrated Ocean Drilling Program (IODP) Expedition 329, we drilled the entire sedimentary sequence at 6 sites in the ultra-oligotrophic region of the South Pacific Gyre (SPG), where dissolved O_2 and aerobic microbial communities are present from the seafloor to the sediment-basement interface [1]. By using high-resolution imaging techniques, we found abundant (10^8-10^9 particles cm^{-3}) micrometer-scale ferromanganese mineral particles (Mn-microparticles) in the oxic pelagic clays of the South Pacific Gyre [2]. Furthermore, we established microparticle separation technique by the combined use of density concentration and flowcytometer/particles sorting techniques. Major and trace element compositional analyses revealed that iron and manganese were the major components of Mn-microparticles, while they also contained rare-earth elements. From the number of Mn-microparticles per unit volume of sediment and the global distribution of oxic pelagic clays, we estimated the number of Mn-microparticles to be 1.5-8.8 $\times 10^{28}$ particles, which accounted for 1.28-7.62 Tt of manganese. This estimate is at least 2 orders of magnitude larger than the manganese budget for manganese nodules and manganese crusts on the seafloor. Along with the examination of manganese input, formation, and preservation, this study provides new insights into the global budget of metallic elements in the abundant Mn-microparticles present in deep subseafloor environments.

[1] D’ Hondt, S., Inagaki, F., Zarikian, C. A., Abrams, L. J., Dubois, N., Engelhardt, T., Evans, H., Ferdelman, T., Gribsholt, B., Harris, R. N., Hoppie, B. W., Hyun, J.-H., Kallmeyer, J., Kim. J., Lynch, J. E., McKinley, C. C., Mitsunobu, S., Morono, Y., Murray, R. W., Pockalny, R., Sauvage, J., Shimono, T., Shiraishi, F., Smith, D. C., Smith-Duque, C., Spivack, A. J., Steinsbu, B. O., Suzuki, Y., Szpak, M., Toffin, L., Uramoto, G., Yamaguchi, T. Y., Zhang, G., Zhang, X.-H., and Ziebis, W. Presence of oxygen and aerobic communities from seafloor to basement in deep-sea sediment. *Nature Geosciences,* 8(4), 299-304, 2015.
[2] Uramoto, G.-I., Morono, Y., Tomioka, N., Wakaki, S., Wagai, R., Uesugi, K., Takeuchi, A., Hoshino, M., Suzuki, Y., Shiraishi, F., Mitsunobu, S., Suga, H., Nakada, R., Takeichi, Y., Takahashi, Y., and Inagaki, F., Significant contribution of subseafloor microparticles to the global manganese budget. *Nature Communications*. **10**, 400, https://doi.org/10.1038/s41467-019-08347-2, 2019

Keywords: Mn-microparticle, oxic pelagic clay, IODP Exp. 329

©2019. Japan Geoscience Union. All Right Reserved.

Regional stratigraphic framework, Gas Hydrate occurrence and distribution of National Gas Hydrate Program Expedition 02 (NGHP-02) Area-B, offshore eastern India

*KanHsi Hsiung[1], Saneatsu Saito[1], Toshiya Kanamatsu[1], Yoshinori Sanada[1], Yasuhiro Yamada[1], KYAW MOE[1], Yohei Hamada[1], Yasuyuki Nakamura[1], HungYu Wu[1]

1. Japan Agency for Marine-Earth Science and Technology

Gas hydrates, one of the important resources for the future energy, are abundant in nature existing in a wide variety of forms in land and marine environments. Krishna-Godavari Basin was formed along the rifted eastern continental margin of India in the Late Jurassic to Early Cretaceous, receiving amount sediments with numerous tilted fault blocks and growth faults. The offshore Krishna–Godavari Basin is considered a potential gas hydrate province as well as the presence of bottom-simulating-reflectors. The Indian National Gas Hydrate Program Expedition 02 (NGHP-02) was designed to study the occurrence of gas hydrate along the margin. Area-B of NGHP-02 contains important world-class gas hydrate accumulations and represent ideal sites for the consideration of future gas hydrate production testing. The primary goal was to explore for highly saturated gas hydrate occurrences and distribution in seismic reflectors that would become targets for future production tests.

Twelve holes were logged and measured with logging-while-drilling (LWD) and five holes were cored in Area-B of NGHP-02. This study summarized the log- and litho-units in Area-B and establish the Integrated-Units A, B and C based on the data from twelve LWD and five coring sites in Area-B. Most of the downhole log and core inferred gas hydrate occurrences are in the Late Miocene Integrated-Unit B with several sets of reservoir sections exhibiting favorable conditions for hosting gas hydrate. Based on the core-log-seismic integration, the LWD and coring results in Area-B helped to understand the geological significance of sequence stratigraphy in Krishna-Godavari Basin and identified the occurrence of gas hydrate. The thickness variations associated with the Reflectors R1 and R2 are possibly associated with the development anticlinal structure and are likely related to syn-sedimentary growth of the folding structures. Major gas hydrate zones exist in and around the Reflectors R1 and R2 near the BSR depth, and mostly have coincident with the fractures and mass-transport deposits. The Hydrate-bearing intervals can be identified by resistivity and sonic velocity logs and classified into pore-filling type, fracture-filling type, and a mixture of pore- and fracture-filling types based on borehole image characteristics. In addition, the spatial distribution of gas hydrate in the Reflectors R1 and R2 reservoirs is highly influenced by the anticlinal structure.

Keywords: NGHP-02, Krishna-Godavari Basin, Logging-while-drilling, Gas hydrate occurrence, Core-log facies analysis, D/V Chikyu

©2019. Japan Geoscience Union. All Right Reserved.

Fluid flow and diagenetic process in frontal thrust zone off Cape Muroto in the Nankai Trough

*Akira Ijiri[1], Shigeyuki Wakaki[1], Yoshiro Nishio[2], Yohei Hamada[1], Tsuyoshi Ishikawa[1], Fumio Inagaki[1]

1. Japan Agency for Marine-Earth Science and Technology, 2. Kochi University

During the International Ocean Discovery Program (IODP) Expedition 370 “Temperature Limit of the Deep Biosphere off Muroto” (T-Limit) in 2016, the drilling was conducted at the protothrust zone in the Nankai Trough off Cape Muroto by using the D/V *Chikyu*, which penetrated the plate boundary fault (dé collement) between 758.2 and 796.4 meters below seafloor (mbsf) and recovered the accretionary deposits down to the basement. Expedition 370 aimed to explore the limits of subseafloor life and the biosphere where temperature exceeds the known temperature maximum of microbial life (~120ºC) at the sediment/basement interface at ~1.2 km below seafloor. Within the protothrust zone, it is thought that deep sourced water and energy, which are necessary for maintaining microbial activities, are supplied by fluid flow through faults. In order to clarify the origin and migration paths of the fluid, we analyzed the stable hydrogen and oxygen isotopic composition of water (δD and δ^{18}O), the isotopic compositions of $^{87}Sr/^{86}Sr$ and $^{7}Li/^{6}Li$ ratios of the porewaters, and compared those isotopic compositions to the chemical compositions of porewater analyzed on-board. The previous study of the in-situ strength of sediments using drilling parameters shows that there are mechanically strong (potential impermeable layers) and weak (potential fluid pathway) zones at 602–648 mbsf and 800–1050 mbsf, respectively. The especially weak zone is observed between 836 and 870 mbsf. The concentration of chloride ion (Cl^-) suddenly decreases from 530 mM at ~600 mbsf to 480 mM at ~660 mbsf, below which it slightly decreases with depth and shows the minimum value of 450 mM at around ~950 mbsf. The concentration again increases from ~460 mM at ~1000 mbsf to ~550 mM, which is similar to the seawater value, at 1126 mbsf (just above the basement rock). The decrease of Cl^-concentration suggests that the dilution of the original porewater by the addition of fresh water. The depth profiles of δD and δ^{18}O show the trends corresponding to that of Cl^-. The δD value scatters in the range from −12 to −8‰ between 600 and 940 mbsf, and shows the minimum value of −12‰ around ~940 mbsf, below which it increases to −4‰ at 1126 mbsf. The δ^{18}O value increases from −4‰ at ~600 mbsf to −1.5‰ at ~800 mbsf with depth. Then the value increases to −0.6‰ at ~960 mbsf. Below the depth, it decreases to −1.2‰ at 1126 mbsf. The decrease of δD and increase of δ^{18}O accompanied with the depletion of Cl^-between ~600 and ~1000 mbsf suggest the addition of freshwater derived from in-situ clay mineral dehydration and the lateral fluid flow. The sharp decrease of the Cl^-concentration between ~600 and ~650 mbsf suggests that the sediments at this interval is a boundary of low permeability, corresponding to the mechanically strong zone estimated by the drilling parameters. Around décollement (758.2–796.4 mbsf), no remarkable changes were observed in chemical compositions in porewater. Instead, the vicinity of ~900 to ~1000 mbsf, where the lowest Cl^-concentration was observed, is probably associated with the main fluid pathway at present. On the other hand, the depth profiles of the isotopic compositions of Sr and Li as well as their concentrations were not corresponding to that of the Cl^-concentration. The maximum concentrations of Sr and Li, ~620 μM and ~790 μM, respectively, were observed at ~1080 mbsf, together with the high $^{87}Sr/^{86}Sr$ and the lowest $^{7}Li/^{6}Li$ ratio. The high concentration of Li and low δ^{7}Li around ~1080 mbsf indicate that the fluid was experienced by relatively high temperature conditions; i.e., presumably the deep sourced fluid. The discrepancy between the depth profile of $Cl^-$and those of Li and Sr suggests that there is (or was) another fluid pathway at the vicinity around ~1080 mbsf.

©2019. Japan Geoscience Union. All Right Reserved.

Keywords: ptotothrust zone, fluid flow, porewater chemistry

©2019. Japan Geoscience Union. All Right Reserved.

Recent progress and perspective on paleomagnetism by means of deep-sea drilling

*Toshitsugu Yamazaki[1], Yuhji Yamamoto[2], Toshiya Kanamatsu[3], Yuho Kumagai[4], Norihiro Nakamura[4]

1. Atmosphere and Ocean Research Institute, The University of Tokyo, 2. Center for Advanced Marine Core Research, Kochi University, 3. Japan Agency for Marine-Earth Science and Technology, 4. Tohoku University

We review recent progress of paleomagnetism using deep-sea drilling cores since the beginning of IODP in 2003, in particular for estimations of paleomagnetic-field intensity (paleointensity) from sediments, and discuss problems to be resolved and perspectives.

For the establishment of the high-resolution relative paleointensity stack for the last 1.5 m.y., sediment cores of Exp. 303/306 from the North Atlantic were utilized. While only few records were available before about 3 m.y. previously, some Eocene to Miocene relative paleointensity records were obtained from the cores in the east equatorial Pacific taken during Exp. 320/321. Applicability of relative paleointensity to inter-core correlations and age estimations has extended to older ages accordingly. On the other hand, contamination of sediment lithological variations induced by paleoclimate changes, in particular fluctuations of the proportion of biogenic and terrigenous magnetites, to paleointensity estimations has become widely recognized. It is urgently necessary to resolve this problem and recover reliable long-term paleointensity records for tackling fundamental issues in geomagnetism such as possible dependence of field intensity to the length of polarity intervals and a possible relation between Earth’s orbital parameters and the geomagnetic field. Better understanding of the role of biogenic magnetite in remanent magnetization acquisition processes is important to solve the contamination problem. Information on the variations of time-averaged field in 10^5 to 10^6 year time-scales is also important for geomagnetism. Departure from the geocentric axial dipole (GAD) field of these time-scales may reflect boundary conditions of the geodynamo at the core-mantle boundary. The departure from GAD emerges as inclination anomalies in sediment cores. IODP cores may be useful for such studies although little studied before.

Acquisition of long deep-sea sediment cores is still required for obtaining continuous paleomagnetic records of Miocene and older ages, and IODP will continue to be the only means for this. Paleointensity estimations from sediments of older ages are hindered by dissolution of magnetite by reductive diagenesis; as sediments are buried deeper, reductive diagenesis becomes more serious. Successful expeditions resulted from the strategic selections of drilling sites; for example, the sediments of target ages are not covered with thick younger sediments (Exp. 320/321), and sediments in relatively oxic environments exist even buried under thick sediments (drift sediments of Exp. 363). Recently, the importance of silicate-hosted magnetic minerals as a carrier of remanent magnetization of sediments becomes recognized; they could escape from dissolution even in anoxic conditions. We need to revisit anoxic sediment cores to investigate the possibility for recovering paleomagnetic records from such sediments. Previously paleomagnetists just discarded them without detailed studies.

Keywords: paleomagnetism, paleointensity, IODP

©2019. Japan Geoscience Union. All Right Reserved.

[E] Oral | M (Multidisciplinary and Interdisciplinary)：M-IS Intersection

Mon. May 27, 2019 10:45 AM - 12:15 PM JST | Mon. May 27, 2019 1:45 AM - 3:15 AM UTC | A07 TOKYO BAY MAKUHARI HALL

[M-IS02] Drilling Earth Science

convener:Yasuhiro Yamada(Japan Agency for Marine-Earth Science and Technology (JAMSTEC), R&D Center for Ocean Drilling Science (ODS)), Yumiko Harigane(Geological Survey of Japan, National Institute of Advanced Industrial Science and Technology (AIST)), Azumi Kuroyanagi(Tohoku University Museum, The Center for Academic Resources and Archives, Tohoku University), Kosei E. Yamaguchi(Toho University and NASA Astrobiology Institute), Chairperson:Kosei Yamaguchi(Toho University), Yasuhiro Yamada(JAMSTEC)

"Earth Drilling Science" session aims to exchange the latest information and scientific achievements in Ocean/Continental drilling projects and to promote the interdisciplinary science. The session covers a wide range of drilling sciences, earth dynamics, environments, and the drilling-related technologies. The overview of the recent IODP cruises as well as future projects of any types of scientific drilling will be reported.

10:45 AM - 11:00 AM JST | 1:45 AM - 2:00 AM UTC

[MIS02-07] Patterns in natural fractures during transitions between stress regimes

*Nikita Dubinya[1] (1.The Schmidt Institute of Physics of the Earth of the Russian Academy of Sciences)

11:00 AM - 11:15 AM JST | 2:00 AM - 2:15 AM UTC

[MIS02-08] ICDP DSeis 1: Introduction into JpGU 2019 papers on Drilling into Seismogenic zones of M2.0-5.5 earthquakes in South African gold mines

*Hiroshi Ogasawara[1], Bennie Liebenberg[2], Martin Ziegler[3], Yasuo Yabe[4], Ray Durrheim[5], Musa Manzi[5], Tullis C Onstott[6], Thomas Weirsberg[7] (1.Faculty of Science and Engineering, Ritsumeikan University, 2.Moab Khotsong mine, South Africa, 3.ETH, Zurich Dep. Earth Sciences, 4.Graduate School of Science, Tohoku Univ., 5.Univ. Witwatersrand, School of Geoscience, South Africa, 6.Princeton Univ., Dept. Geoscience, USA, 7.GFZ, Potzdam, Germany)

11:15 AM - 11:30 AM JST | 2:15 AM - 2:30 AM UTC

[MIS02-09] ICDP DSeis 2: Preliminary results of physical property measurement and XRD analysis of the M5.5 fault material recovered from DSeis Project

*Tetsuro Hirono[1], Yuki Yukoyama[1], Shunya Kaneki[2], Hiroshi Ogasawara[3], Yasuo Yabe[4], Takuya Matsuzaki[5], Yuhji Yamamoto[5], Hidekazu Tokuyama[5], Tullis C. Onstott[6], Martin Ziegler[7], Durrheim Ray[8], Esterhuizen van Heerden[9], Bennie Liebenberg[9], The ICDP DSeis team (1.Department of Earth and Space Science, Graduate School of Science, Osaka University, 2.Disaster Prevention Research Institute, Kyoto University, 3.Ritsumeikan University, 4.Tohoku University, 5.Center for Advanced Marine Core Research, Kochi University, 6.Princeton University, 7.ETH Zurich, 8.Witwatersrand University, 9.Moab Khotsong mine)

11:30 AM - 11:45 AM JST | 2:30 AM - 2:45 AM UTC

[MIS02-10] ICDP DSeis 3: Spatial variation in stress state in the source region of Orkeny earthqauke (M5.5) based on analyses of the ICDP-DSeis borehole cores

*Yasuo Yabe[1], Akimasa Ishida[2], Kosuke Sugimura[2], Kanematsu Makoto[2], Mitsuya Higashi[2], Shunsuke YOSHIDA[2], Bennie Liebenberg[7], Takatoshi Ito[3], Akio Funato[5], Bryan Watson[6], Raymond Durrheim[4], Hiroshi Ogasawara[2] (1.Research Center for Prediction of Earthquakes and Volcanic Eruptions, Graduate School of Science, Tohoku University, 2.Faculty of Science and Engeneer, Ritsumeikan University, 3.Institute of Fluid Science, Tohoku University, 4.School of Geoscience, University of the Witwatersrand, 5.Fukada Geological Institute, 6.School of Mining Engeneering, University of the Witwatersrand, 7.Moab Khotsong mine)

11:45 AM - 12:00 PM JST | 2:45 AM - 3:00 AM UTC

[MIS02-11] Applications of DCDA method for in-situ crustal stress measurement - Rock core samples from NIED seismic observation wells -

*Kentaro Omura[1], Weiren Lin[2], Takatoshi Ito[3], Akio Funato[4] (1.National Research Institute for Earth Science and Disaster Resilience, 2.Graduate School of Engineering, Kyoto University, 3.Institute of Fluid Science, Tohoku University, 4.Fukada Geological Institute)

12:00 PM - 12:15 PM JST | 3:00 AM - 3:15 AM UTC

[MIS02-12] Temperature depth profile in a 700 m deep vertical borehole in Aso volcanic zone

*Weiren Lin[1], Susumu Shibutani[1,2], Koichiro Sado[2], Nana Kamiya[1], Tatsuhiro Sugimoto[1], Terasu Sano[1], Kazuya Ishitsuka[1], Xiaoqiu Yang[4], Aiming Lin[3] (1.Graduate School of Engineering, Kyoto University, 2.Chiken Sogo Consultants Co., Ltd., 3.Graduate School of Science, Kyoto University, 4.South China Sea Institute of Oceanology, Chinese Academy of Sciences)

Patterns in natural fractures during transitions between stress regimes

*Nikita Dubinya[1]

1. The Schmidt Institute of Physics of the Earth of the Russian Academy of Sciences

The study is aimed at analysis of transitions between different stress regimes –Normal Fault, Strike-Slip and Reverse Fault following Anderson’s classification –in terms of natural shear fractures corresponding to each regime. The study is mostly focused on spatial orientations of shear fractures emerging at each stress regime.

It is clear that not all natural fractures existing in a rock mass have the same response to changes in surrounding stresses. Some fractures are considered to be critically stressed in the given stress state which means that a small increase in differential stress (difference between maximum and minimum principal stresses) leads to fracture growth. The fracture is considered as critically stressed if shear stress acting on its plane exceeds normal stress multiplied by internal fraction coefficient of the medium. Normal and shear stresses are calculated from principal stresses’ values and fracture spatial orientation with regard to stress tensor principal axes. That means that for any given stress tensor one is capable of obtaining all the possible spatial orientations of critically stressed fractures.

In the current paper this problem is solved for different stress states for obtaining the typical patterns of fractures’ spatial orientations when stresses are varied considerably enough to change the stress regime. Figure 1 represents a transition between Normal Fault and Strike-Slip regimes: a series of contours on Wolff nets serve as borderlines for poles to critically stressed fractures’ planes. Each color represents its own triad of principal stresses (tables provide necessary match between color and stresses’ values); maximum horizontal stress σ_H is assumed to act in North-South direction. Minimum horizontal stress σ_h and vertical stress σ_V are fixed at the values of 10 and 50 MPa respectively, while transition is caused by increase in σ_H magnitude from 10 to 160 MPa. During the first stage of transition (fig. 1(A), σ_H is between 10 and 30 MPa) poles to fractures tend to gather in Eastern and Western parts of the stereonet. On the second stage (fig. 1(B), σ_H is between 40 and 90 MPa) fractures’ orientation remains stable with slight increase observed in east-northeast, west-northwest, west-southwest, and east-southeast directions. This tendency continues at final stage of transition (fig. 1(C), σ_H is between 100 and 120 MPa) where four main areas typical for Strike-Slip fracture orientation emerge. The same analysis may be completed for other analogous transitions with two fixed principal stresses and one being varied.

Transition between stress regimes may also be observed if principal axes of stress tensor rotate with principal stresses’ magnitudes remaining constant. This scenario may take place near Earth's surface or near large faults due to changes in principal stresses' trajectories. Figure 2 represents transition from Normal Fault to Strike-Slip with principal stresses being fixed at 50, 20, and 10 MPa, while angle ϕ –angle between maximum principal stress direction and vertical –is varied between 0 and 90 degrees. Blue lines still serve as borderlines for the orientations of critically stressed fractures in each case; circles represent the directions of principal stresses (red for maximum, yellow for intermediate, and green for minimum principal stress). It should be noted that lower hemisphere Lambert equal area stereonet is used in this case.

Analogous constructions may be completed for any given stress tensor broadening the understanding of natural fractures’ patterns and their relation to stress geomechanics providing a possibility to solve the

©2019. Japan Geoscience Union. All Right Reserved.

inverse problem of in-situ stresses estimation and their changes near geological structures utilizing the previously developed methods. As a result, some problems of drilling in vicinity of faults - one of primary objects for scientific drilling - may be solved, reducing the drilling risks and costs.

Keywords: Critically stressed fractures, Stress regimes, Stereonet, Drilling near faults

©2019. Japan Geoscience Union. All Right Reserved.

Fig. 1

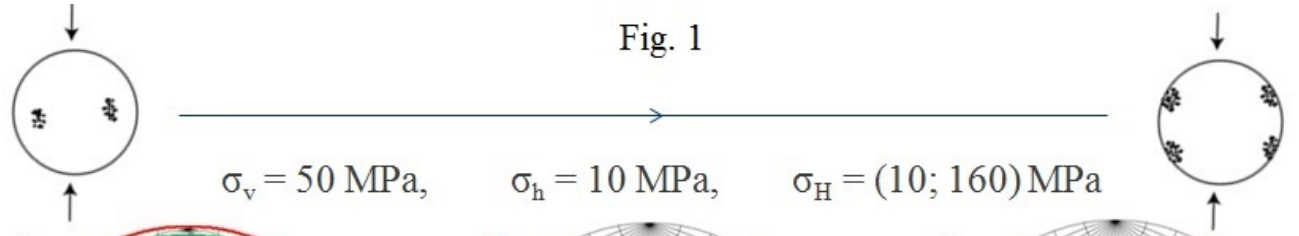

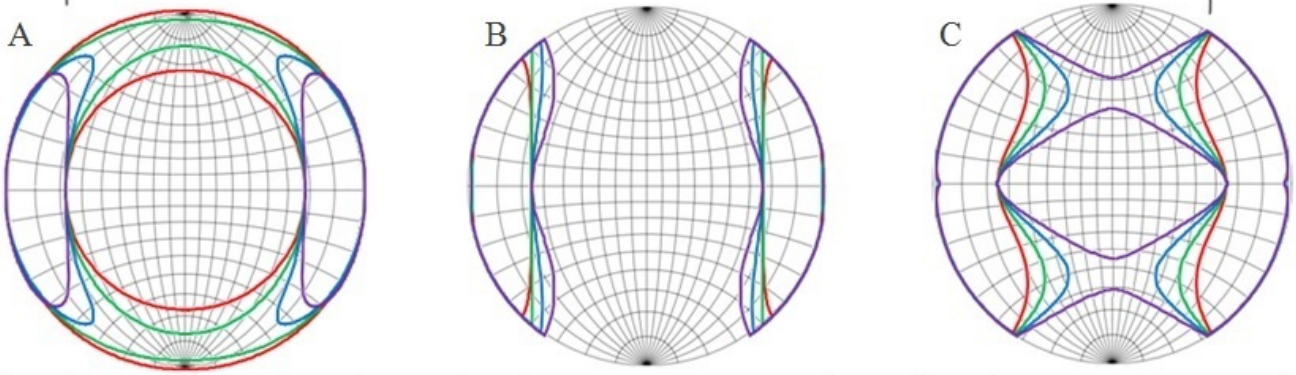

A	σ_H [MPa]
	10
	15
	20
	30

B	σ_H [MPa]
	40
	50
	70
	90

C	σ_H [MPa]
	100
	120
	140
	160

Fig. 2

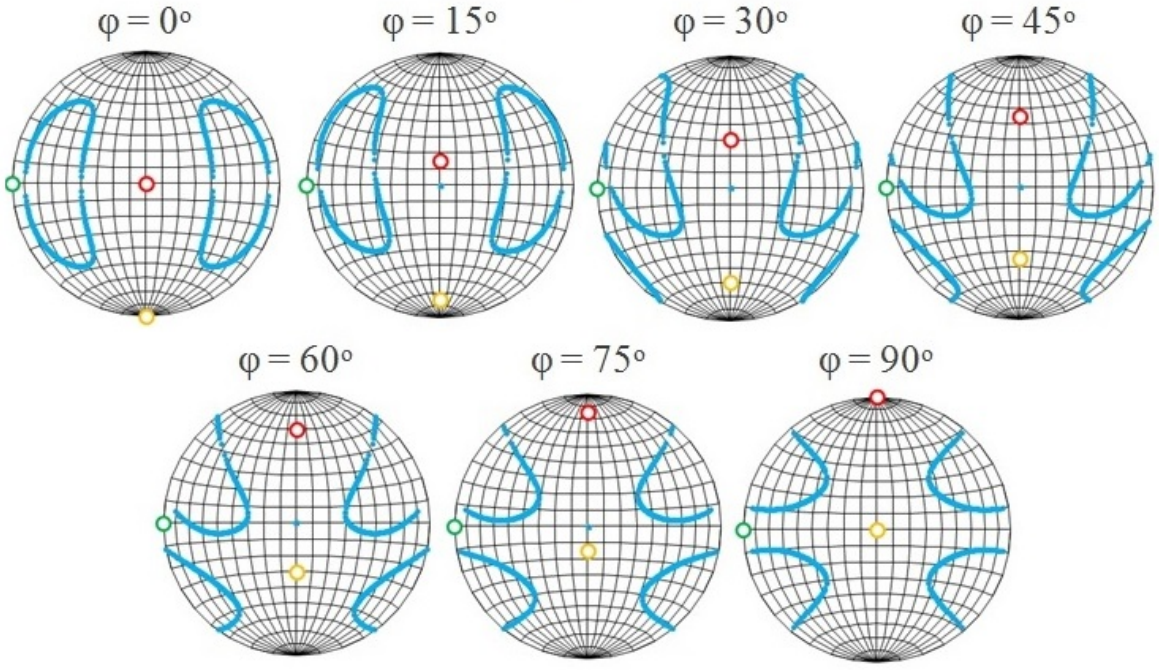

©2019. Japan Geoscience Union. All Right Reserved.

ICDP DSeis 1: Introduction into JpGU 2019 papers on Drilling into Seismogenic zones of M2.0-5.5 earthquakes in South African gold mines

*Hiroshi Ogasawara[1], Bennie Liebenberg[2], Martin Ziegler[3], Yasuo Yabe[4], Ray Durrheim[5], Musa Manzi[5], Tullis C Onstott[6], Thomas Weirsberg[7]

1. Faculty of Science and Engineering, Ritsumeikan University, 2. Moab Khotsong mine, South Africa, 3. ETH, Zurich Dep. Earth Sciences, 4. Graduate School of Science, Tohoku Univ., 5. Univ. Witwatersrand, School of Geoscience, South Africa, 6. Princeton Univ., Dept. Geoscience, USA, 7. GFZ, Potzdam, Germany

The 2014-2019 ICDP Science plan states: “reaching the depths of the seismogenic zone where earthquakes nucleate has always been a challenge for fault-zone drilling projects” (Mori and Ellsworth, 2013). However, during 2016-2018, we could recover cores with a total length of about 1.6 km from seismogenic zones ahead of mining faces, M3.5 and M5.5 earthquakes by drilling collared from depths of 1.0 to 3.3 km below surface in deep South African gold mines. The drilling targets had been already elucidated by tens of near-field seismic sensors. Talc, biotite, and amorphous were found at the M5.5 fault intersection (Kaneki et al. SSJ 2018).

The reliable measurement of the magnitude and orientation of stress at depth is a significant challenge (Brodsky et al., 2009). However, we overcame the difficulty. We intersected hypersaline water where geomicrobiologists started water and gas monitoring.

This paper reviews the scientific drilling and associated activities and briefly introduces the other reports (ICDP DSeis 2-10) presented in JpGU 2019 as shown below:

Hirono et al. (ICDP DSeis 2) ICDP DSeis 2: Preliminary results of physical property measurement

and XRD analysis of the M5.5 fault material recovered from DSeis Project,

Yabe et al. (ICDP DSeis 3) on the spatial variation of stress in the seismogenic zones,

Yoshida et al. (poster; ICDP DSeis 4): drilling, core logging, and in-hole geophysical logging of ICDP DSeis drilling into the M5.5 aftershock zones in a South African gold mines.

Sugimura et al. (poster) ICDP DSeis 5: Diametrical Core Deformation Analysis of the M5.5 aftershock zone core - stress concentration at reflective intrusives and transition in stress regimes.

Kanematsu et al (poster) ICDP DSeis 6: Deformation Rate Analysis of the M5.5 aftershock zone core - stress concentration at reflective intrusives.
Higashi et al. (poster) ICDP DSeis 7: compilation of stress information and comparison with calculated stresses in the M5.5 aftershock zones,

Noda et al. (poster) ICDP DSeis 8: the M5.5 fault structure and reflective intrusives in legacy 3D seismic

©2019. Japan Geoscience Union. All Right Reserved.

reflection data

Tadokoro et al. (poster) ICDP DSeis 9: streaks in the M5.5 aftershocks potentially located on highly stressed intrusive

Mori et al. ICDP DSeis 10: Near-field Observations for the M5.5 Orkney, South Africa Earthquake

Acknowledgement: The DSeis team includes co-authors of the papers ICDP DSeis 2-9 and members shown at https://www.icdp-online.org/projects/world/africa/orkney-s-africa/details/. We thank Harmony Gold, Anglogold Ashanthi, Lesedi, Digital Surveying, OHMS, Seismogen, 3D Geoscience. ICDP, JSPS, SA NRF, MEXT Japan, US NSF, German DRF, and Ritsumeikan Univ. financially support the project.

Keywords: ICDP DSeis, Seismogenic zone drilling, South African gold mines

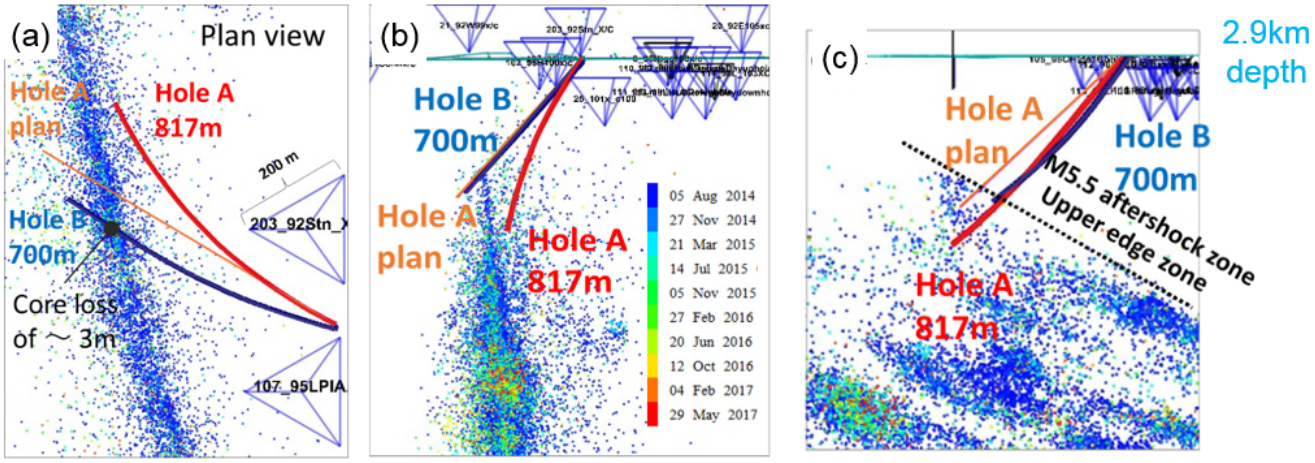

©2019. Japan Geoscience Union. All Right Reserved.

ICDP DSeis 2: Preliminary results of physical property measurement and XRD analysis of the M5.5 fault material recovered from DSeis Project

*Tetsuro Hirono[1], Yuki Yukoyama[1], Shunya Kaneki[2], Hiroshi Ogasawara[3], Yasuo Yabe[4], Takuya Matsuzaki[5], Yuhji Yamamoto[5], Hidekazu Tokuyama[5], Tullis C. Onstott[6], Martin Ziegler[7], Durrheim Ray[8], Esterhuizen van Heerden[9], Bennie Liebenberg[9], The ICDP DSeis team

1. Department of Earth and Space Science, Graduate School of Science, Osaka University, 2. Disaster Prevention Research Institute, Kyoto University, 3. Ritsumeikan University, 4. Tohoku University, 5. Center for Advanced Marine Core Research, Kochi University, 6. Princeton University, 7. ETH Zurich, 8. Witwatersrand University, 9. Moab Khotsong mine

Drilling into seismogenic zones of M2.0-M5.5 earthquakes in deep South Africa gold mines (DSeis Project) was undertaken in 2017–2018 near Orkney, South Africa, to understand principal mechanism of earthquakes nucleate and propagate. Drilling at two main holes, Hole A (817 m) and Hole B (700 m), was completed at the Moab Khotsong mine, and the latter hole penetrated the fault zone that slipped at the 2014 M5.5 earthquake. Fault-related material and its surrounding host rocks were successfully recovered from the hole, and the samples were analyzed in the Center for Advanced Marine Core Research, Kochi University, Japan. The main damaged zone is characterized by highly fragmented fault breccia with high amount of talc and amorphous material, which is likely to related to recent earthquake event. Nondestructive continuous measurements of physical properties (X-ray CT image, density, magnetic susceptibility, and natural gamma ray) are in progress. We will show the preliminary results about the characteristics of the M5.5 fault zone and its implication for generation of the M5.5 earthquake.

Keywords: Deep fault drilling, ICDP

©2019. Japan Geoscience Union. All Right Reserved.

ICDP DSeis 3: Spatial variation in stress state in the source region of Orkeny earthqauke (M5.5) based on analyses of the ICDP-DSeis borehole cores

*Yasuo Yabe[1], Akimasa Ishida[2], Kosuke Sugimura[2], Kanematsu Makoto[2], Mitsuya Higashi[2], Shunsuke YOSHIDA[2], Bennie Liebenberg[7], Takatoshi Ito[3], Akio Funato[5], Bryan Watson[6], Raymond Durrheim[4], Hiroshi Ogasawara[2]

1. Research Center for Prediction of Earthquakes and Volcanic Eruptions, Graduate School of Science, Tohoku University, 2. Faculty of Science and Engeneer, Ritsumeikan University, 3. Institute of Fluid Science, Tohoku University, 4. School of Geoscience, University of the Witwatersrand, 5. Fukada Geological Institute, 6. School of Mining Engeneering, University of the Witwatersrand, 7. Moab Khotsong mine

The Orkney earthquake (M5.5), South Africa, occurred on 5 August 2014 beneath a deep gold mine, of which the deepest mining horizon is ~3 km depth from ground surface. Hypocenter of the Orkney earthquake and the shallowest aftershocks were located at ~5 km and ~3.5 km depths from ground surface. Therefore, the ICDP-DSeis project was devised to investigate the geological, geomechanical and geochemical environments in and around the source region of the Orkney earthquake. Two 800 m-long boreholes (Holes A and B) were drilled from a drilling site established on a tunnel at a depth of 2.8 km in the mine. While Hole A reached the seismogenic depth, it did not intersect the aftershock cluster. Hole B success fully penetrated to the aftershock cluster. Borehole cores were almost fully recovered from these holes, though they were not oriented during drilling. Therefore, the core orientation was determined by comparing in-hole optical images and unrolled core images in this study. Then, Diametrical Core Deformation Analysis (DCDA, Funato and Ito, 2017) and Deformation Rate Analysis (DRA, Yamamoto et al., 1990) were applied to borehole cores to evaluate a spatial variation in stress state in and around the aftershock cluster. Finally, a numerical elastic model in which the depth variations along Hole A and B were reproduced was developed to understand a spatial distribution of stress state in and around the aftershock cluster that extended along upper extension of the source fault of the Orkney earthquake.

Acknowledgement. This study was supported by ICDP, JSPS-NRF bilateral research project, JSPS Core-to-Core program, Ritsumeikan University and the Ministry of Education, Culture, Sports, Science and Technology (MEXT) of Japan, under its Earthquake and Volcano Hazards Observation and Research Program. The authors thank Harmony Gold Ltd. for kindly providing an opportunity of drilling from Moab Khotsong mine.

Keywords: ICDP-DSeis, Stress measurement, DRA, DCDA, Deep mines in South Africa

©2019. Japan Geoscience Union. All Right Reserved.

Applications of DCDA method for in-situ crustal stress measurement - Rock core samples from NIED seismic observation wells -

*Kentaro Omura[1], Weiren Lin[2], Takatoshi Ito[3], Akio Funato[4]

1. National Research Institute for Earth Science and Disaster Resilience, 2. Graduate School of Engineering, Kyoto University, 3. Institute of Fluid Science, Tohoku University, 4. Fukada Geological Institute

In-situ crustal stress is an important factor to understand earthquake mechanism and tectonic activities. However, the reliable in-situ stress data seems to be poor related with seismic or strain observation data. We tried to apply the DCDA (Diametrical Core Deformation Analysis) method for in-situ crustal stress measurement using boring rock core samples. DCDA method measures the circumferential diameter variation and elastic constants of core sample without complicate procedures in the borehole. We expect the method can be applied to old-time boring rock cores from seismic observation wells, and we may collect global in-situ crustal stress data in Japan island.
We used recovered hard rock cores from 7 Hi-net obsevation wells of NIED (more than 10 years ago) from the depth about 100m - 200m (one is from the depth of 2000m). The circumferential core diameter variation was measured by an especially designed apparatus that consists of an optical micrometer, a pair of motor-driven rollers and a data processing system (Funato and Ito, 2017, IJRMMS). We got the sine curves of circumferential diameter variation associated with stress relief. However, in some cases, we got the sine curve of circumferential diameter variation obviously related petrogical suructure of sedimetary rocks.The data suggest that the DCDA method is applicable to boring cores from shallow seismic obsevation wells, except for sedimetary rock cores.

Keywords: DCDA method, in-sitsu crustal stress, rock core, seismic observation well

©2019. Japan Geoscience Union. All Right Reserved.

Temperature depth profile in a 700 m deep vertical borehole in Aso volcanic zone

*Weiren Lin[1], Susumu Shibutani[1,2], Koichiro Sado[2], Nana Kamiya[1], Tatsuhiro Sugimoto[1], Terasu Sano[1], Kazuya Ishitsuka[1], Xiaoqiu Yang[4], Aiming Lin[3]

1. Graduate School of Engineering, Kyoto University, 2. Chi-ken Sogo Consultants Co., Ltd., 3. Graduate School of Science, Kyoto University, 4. South China Sea Institute of Oceanology, Chinese Academy of Sciences

Temperature profile measurements in scientific-drilling boreholes and determination of heat flow from the measured temperature profiles are important approaches to understand the temperature distribution and thermal structure around volcanic regions and seismogenic fault zones. A scientific-drilling borehole down to ~700 m deep was penetrated through the Futagawa Fault ruptured during the 2016 Mw 7.1 Kumamoto, Japan earthquake in Aso volcanic region. To obtain the fundamental features of the temperature profile in the borehole, we repeated measurements of temperature depth profile totally four times, i.e., once per two –three months from the borehole penetration was completed in March 2018. As a preliminary result, the temperature depth profile showed a popular trend between depth ranges of 200 –310 m and 430 –650 m where the formation temperature may not be influenced by weather and seasonal temperature change on surface. The temperature in the two depth ranges linearly increased with depth increasing, and showed a geothermal gradient of ~55 ˚C/km. This geothermal gradient is much higher than the global average geothermal gradient 20 –30 ˚C/km, being considered reasonable in a volcanic region. However, a very unexpected temperature distribution feature was observed in the depth range of 310 –430 m. The temperature was almost the same in the ~120 m depth interval; and the geothermal gradient was only ~1 ˚C/km. To make sure if this special temperature distribution is a natural phenomenon, we will continuous our temperature measurements and monitoring in the borehole.

Keywords: Drilling , Temperature, Geothermal gradient

©2019. Japan Geoscience Union. All Right Reserved.

[E] Oral | M (Multidisciplinary and Interdisciplinary)：M-IS Intersection

Mon. May 27, 2019 1:45 PM - 3:15 PM JST | Mon. May 27, 2019 4:45 AM - 6:15 AM UTC | A07 TOKYO BAY MAKUHARI HALL

[M-IS02] Drilling Earth Science

convener:Yasuhiro Yamada(Japan Agency for Marine-Earth Science and Technology (JAMSTEC), R&D Center for Ocean Drilling Science (ODS)), Yumiko Harigane(Geological Survey of Japan, National Institute of Advanced Industrial Science and Technology (AIST)), Azumi Kuroyanagi(Tohoku University Museum, The Center for Academic Resources and Archives, Tohoku University), Kosei E. Yamaguchi(Toho University and NASA Astrobiology Institute), Chairperson:Yumiko Harigane(産総研), Natsue Abe(R&D Center for Ocean Drilling Science, JAMSTEC)

"Earth Drilling Science" session aims to exchange the latest information and scientific achievements in Ocean/Continental drilling projects and to promote the interdisciplinary science. The session covers a wide range of drilling sciences, earth dynamics, environments, and the drilling-related technologies. The overview of the recent IODP cruises as well as future projects of any types of scientific drilling will be reported.

1:45 PM - 2:00 PM JST | 4:45 AM - 5:00 AM UTC

[MIS02-13] Estimation of Shear Stress and Lithology Prediction Using Machine Learning and Surface Drilling Data

Tomoya Inoue[1], *Ryuta Tanaka[1], Junya Ishiwata[1] (1.Japan Agency for Marine-Earth Science and Technology)

2:00 PM - 2:15 PM JST | 5:00 AM - 5:15 AM UTC

[MIS02-14] Overview of drilling of crust-mantle boundary of Oman ophiolite: the ICDP Oman Drilling Project

*Eiichi TAKAZAWA[1,4], Damon A H Teagle[2], Katsuyoshi Michibayashi[3], Yoshihiko Tamura[4], Jude Ann Coggon[2], Juerg Matter[2], Peter B Kelemen[5], Oman Drilling Project Phase 2 Science Party (1.Department of Geology, Faculty of Science, Niigata University, 2.University of Sauthampton, 3.Nagoya University, 4.JAMSTEC, 5.Columbia University)

2:15 PM - 2:30 PM JST | 5:15 AM - 5:30 AM UTC

[MIS02-15] Geophysical Logging of Crust-Mantle boundary at Oman Ophiolite

*Yasuhiro Yamada[1], Kyaw Moe[1], Philippe Pezard[2], Juerg Matter[3], OmanDP Science Party (1.Japan Agency for Marine-Earth Science and Technology (JAMSTEC), 2.Géosciences Montpellier, Université de Montpellier, 3.Southampton University)

2:30 PM - 2:45 PM JST | 5:30 AM - 5:45 AM UTC

[MIS02-16] Overview of the physical property measurements, ChikyuOman 2017 and 2018: Crust and Mantle sections from ICDP Oman Drilling Project Phase I and II

*Natsue Abe[1], Keishi Okazaki[1,11], Ikuo Katayama[2], Kohei Hatakeyama[2], Yuya Akamatsu[2], Benoit Ildefonse[3], Ole Ivar ulven[4], Gilbert Hong[5], Wenlu Zhu[6], Benoit Cordonnier[4], Katsuyoshi Michibayashi[7], Eiichi TAKAZAWA[8], Michell Harris[12], Damon Teagle[10], Peter Kelemen[9], Marguerite Goddard[3], Jurg Matter[10], Jude Coggon[10], The Oman Drilling Project Science Party (1.Japan Agency for Marine-Earth Science and Technology, 2.Hiroshima University, 3.Universitè de Montpellier, 4.University of Oslo, 5.Seoul National University, 6.University of Maryland, 7.Nagoya University, 8.Niigata University, 9.Columbia University, 10.University of Southampton, 11.Kanazawa University, 12.Polymouth University)

2:45 PM - 3:00 PM JST | 5:45 AM - 6:00 AM UTC

[MIS02-17] Exploring the deep subseafloor biosphere and biogeochemical carbon cycling beneath the Arctic ocean

*Fumio Inagaki[1], Steffen Leth Jørgensen[2], Rolf Birger Pedersen[2] (1.Japan Agency for Marine-Earth Science and Technology (JAMSTEC), 2.Department of Earth Science, University of Bergen, Norway)

3:00 PM - 3:15 PM JST | 6:00 AM - 6:15 AM UTC
Discussion

Estimation of Shear Stress and Lithology Prediction Using Machine Learning and Surface Drilling Data

Tomoya Inoue[1], *Ryuta Tanaka[1], Junya Ishiwata[1]

1. Japan Agency for Marine-Earth Science and Technology

Introduction

JAMSTEC operates the scientific deep-sea drilling vessel Chikyu. Chikyu conducted the Japan Trench Fast Drilling Program (JFAST) for study on the Tohoku earthquake. Chikyu has also started to conduct the Nankai Trough Seismogenic Zone Experiment (NanTroSEIZE).
The main purpose of the scientific drillings is to obtain core samples from sediment layers under the seabed. However, we are facing the situation that we cannot have enough core samples because the operation philosophy defines that core samples are generally assigned for a lot of separate examinations including geological, chemical, and biological examinations. It is also the reason that the coring operations are conducted at spots. This means that analyzed data, for example the shear stress, can be obtained just at spot(s).
As one of the primary goals of scientific drilling is to evaluate sediment properties, it is highly beneficial to obtain the properties of drilling layers and to characterize the lithology over the full drilling depth during drilling operations. Even an approximation of these properties could potentially provide valuable information for conducting coring operations.

Methods/Procedure

A previous study attempted to discuss the properties of sediment layers using surface drilling data, and estimated the shear stress of the sediment. In this study, we first summarize the method applied in the previous paper for estimating the torque at the drill bit, which leads to estimation of shear stress of sediment layer from the surface measured drilling data for NanTroSEIZE deep riser drilling operation.
The surface drilling data was obtatined using the surface drilling data acquisition system that we developed. The surface drilling data includes the torque of the power swivel (HPS torque) that is equipmenti to provide a torque and rotation to the drillstring. This HPS torque includes not only the drilling torque but also other torques such as friction toque between riser and drill pipe, and mechanical torque inside HPS. This paper proposes to estimate the drilling torque at the drill bit from the surface drilling data by removing other torques based the torque during a “bottom’s” up operations.
We also used machine-learning approaches to predict the lithology, where learning data was created from surface drilling data and lithology information from core samples obtained during past scientific drilling operations. Machine learning was then applied using neural network algorithms by tuning L1 regularization coefficient and the number of layers to create a predictive model. This paper discusses the preliminary attempt to predict the lithology using machine-learning approaches for NanTroSEIZE and JFAST data.

Result/Conclusions

We presented a method for estimating the drilling torque, which was compared to downhole-measured data with logging while drilling (LWD). The result of the calculation shows that the drilling torque at the bit differed from the surface measured torque, where this difference increased with increasing drilling depth. In addition, the estimated drilling torque was validated using downhole-measured torque data obtained from LWD operations. Although the deviation of the mean values between the drilling torque and the downhole measured torque was large, our method is considered valid from the viewpoint of correcting

©2019. Japan Geoscience Union. All Right Reserved.

the characteristics of the depth for the surface measured torque.
This study also presented the lithilogy predicution from machine learning approaches. Preliminary results were presented using NanTroSEIZE and JFAST data including surface drilling data and core sample data. The prediction performance obtained from the generated neural networks indicated that the lithology properties could be predicted by machine learning approaches as an interpolation problem; however, the prediction is sensitive to the structure and parameters of the neural network, along with the selection of training data due to the small learning dataset. In addition, it can be difficult to clearly classify the lithology from core samples as the core sometimes contains several rock types, leading to uncertain classification. We will continue to study lithology prediction using machine-learning methods in future studies.

Acknowledgments
This research was partially supported by a Grant-in-Aid for Scientific Research (B) [grant number 16H04610].

Keywords: surface drilling data, lithology prediction, machine Learning, shear stress, ocean drilling

©2019. Japan Geoscience Union. All Right Reserved.

Overview of drilling of crust-mantle boundary of Oman ophiolite: the ICDP Oman Drilling Project

*Eiichi TAKAZAWA[1,4], Damon A H Teagle[2], Katsuyoshi Michibayashi[3], Yoshihiko Tamura[4], Jude Ann Coggon[2], Juerg Matter[2], Peter B Kelemen[5], Oman Drilling Project Phase 2 Science Party

1. Department of Geology, Faculty of Science, Niigata University, 2. University of Sauthampton, 3. Nagoya University, 4. JAMSTEC, 5. Columbia University

From the winter of 2017 to 2018 the drilling of crust-mantle transition zone (MTZ) was conducted at Wadi Zeeb (CM1&2 sites) in Wadi Tayin massif by the International Continental Scientific Drilling ProgramOman Drilling Project [6]. The MTZ of Oman ophiolite has been characterized by thick dunites accompanied by thin veins or clots of plagioclase and clinopyroxene and several centimeters to meters thick gabbro sills and wehrlite intrusions. The origin of MTZ is still under debate [2-5]. To clarify this origin, more detailed research by continuous core through MTZ is necessary.

Geological mapping on ground associated with information from the recovered cores in CM1&2 sites the thickness of the MTZ is estimated as about 150 m. The upper and lower boundaries of the MTZ has a strike in the east-west direction, and it is inclined about 30 degrees south. In the summer of 2018, the drilled cores were carefully described by scientists on the deep-sea drilling vessel "CHIKYU". The stratigraphy has been divided into four igneous sequences based on the abundance of different lithologies: Layered Gabbro Sequence, Dunite Sequence, Dunite with Gabbro Sequence, and Mantle Sequence. Dunite Sequence and Dunite with Gabbro Sequence are summarized as Crust - Mantle Transition.

Hole CM1A is inclined 60˚ northward. The upper 160 m of the core is the Layered Gabbro Sequence, mostly composed of olivine gabbro, interlayered with gabbro and a small amount of wehrlite, dunite, anorthosite and troctolite. From 160 to 310 m the Crust-Mantle Transition is divided into an upper 90 m Dunite Sequence and a lower 60 m Dunite with Gabbro Sequence containing small lenses of gabbro, troctolite and wehrlite. The dunites are highly serpentinized, and rodingite and diopsidite commonly replace minor gabbroic rocks in these sequences. The lower 80 m of the hole is the Mantle Sequence, with alternating layers of dunite and increasingly abundant, residual mantle harzburgite.

Hole CM2B is a vertical hole located 400 m north of CM1A, and samples the Crust-Mantle Transition and the Mantle Sequence. As in CM1A, the transition is divided into an upper Dunite Sequence and a lower Dunite with Gabbro Sequence. In contrast to Hole CM1A, a small amount of olivine has escaped complete serpentinization in the lower portions of the CM2B transition zone. In the Mantle Sequence, harzburgite is dominant. Dunite accounts for about 25% of this Sequence, less than in CM1A. The lowermost peridoties in Hole CM2B are strongly altered to talc+carbonate.

[1] Boudier and Nicolas, 1995, J. Petrol., 36, 777-796, [2] Pallister and Hopson, 1981, J. Geophys. Res., 86, 2593-2644, [3] Kelemen et al., 1995, Nature, 375, 747-753, [4] Abily and Ceuleneer, 2013, Geology, 41, 67-70, [5] Rospabé et al., 2017, Geol. Soc. Am., Data Rep. 2017139, [6] Kelemen et al., 2013, Scientific Drilling, 15, 64-71.

Keywords: Oman ophiolite, ICDP, Oman Drilling Project, crust-mantle transition, Moho Transition Zone

©2019. Japan Geoscience Union. All Right Reserved.

©2019. Japan Geoscience Union. All Right Reserved.

Geophysical Logging of Crust-Mantle boundary at Oman Ophiolite

*Yasuhiro Yamada[1], Kyaw Moe[1], Philippe Pezard[2], Juerg Matter[3], OmanDP Science Party

1. Japan Agency for Marine-Earth Science and Technology (JAMSTEC), 2. Géosciences Montpellier, Université de Montpellier, 3. Southampton University

The boundary between the crust and mantle is a horizon that human being can reach in the Earth interior. The nature of this surface has been proposed from viewpoints of petrology, geochemistry and geophysics, and the answer needs to wait until future scientific drilling.

The Samail ophiolite exposed in Oman is one of most well-known surface exposures of the exhumed lowest part of the oceanic crust and upper part of mantle.

The Oman Drilling Project (OmanDP) drilled 12 holes at 7 sites in this ophiolite from 2016 to 2018, and has conducted a comprehensive borehole geophysical survey as logging operation in most of these holes in 2017 and 2018. The data acquired include: electrical resistivity, spectral gamma ray, magnetic susceptibility, full waveform sonic, optical / acoustic / resistivity borehole wall imaging. The extensive logging operation also includes high-definition spectroscopy measurements that contribute to further geochemical investigations. The outline of these datasets and our preliminary analysis will be presented.

Keywords: oceanic crust, upper oceanic mantle, borehole geophysics, alteration

©2019. Japan Geoscience Union. All Right Reserved.

Overview of the physical property measurements, ChikyuOman 2017 and 2018: Crust and Mantle sections from ICDP Oman Drilling Project Phase I and II

*Natsue Abe[1], Keishi Okazaki[1,11], Ikuo Katayama[2], Kohei Hatakeyama[2], Yuya Akamatsu[2], Benoit Ildefonse[3], Ole Ivar ulven[4], Gilbert Hong[5], Wenlu Zhu[6], Benoit Cordonnier[4], Katsuyoshi Michibayashi[7], Eiichi TAKAZAWA[8], Michell Harris[12], Damon Teagle[10], Peter Kelemen[9], Marguerite Goddard[3], Jurg Matter[10], Jude Coggon[10], The Oman Drilling Project Science Party

1. Japan Agency for Marine-Earth Science and Technology, 2. Hiroshima University, 3. Universitè de Montpellier, 4. University of Oslo, 5. Seoul National University, 6. University of Maryland, 7. Nagoya University, 8. Niigata University, 9. Columbia University, 10. University of Southampton, 11. Kanazawa University, 12. Polymouth University

We report physical property measurements of core samples from the Samail ophiolite in Oman, drilled by the ICDP Oman Drilling Project. Onboard core logging was conducted on D/V Chikyu for 4 months in total in the summers of 2017 and 2018. We analyzed 4 holes (GT1A, GT2A, GT3A and BT1B) in 2017, and 5 holes (CM1A, CM2B, BA1B, BA3A and BA4A) in 2018. The total core length of those 9 holes is about 3200 m. Cores from Holes GT1A and GT2A in the lower crust section of the ophiolite are mainly composed of gabbros (gabbro and olivine gabbro), with small amounts of ultramafic rocks (wehrlite and dunite), whereas those from Hole GT3A at the boundary between the sheeted dikes and gabbro are mainly composed of basalt and diabase, followed by gabbros (gabbro, olivine gabbro and oxide gabbro). Minor felsic trondhjemite and tonalite dikes intrude the mafic rocks. In contrast, Hole BT1B penetrated from mantle section through the basal thrust and into the metamorphic sole. The CM holes were drilled through the crust-mantle transition, from gabbroic lower crust, through dunite with minor gabbros, and in to residual mantle harzburgite. BA holes were taken from the mantle section and are composed of dunite and harzburgite intruded by minor gabbroic and pyroxenite dikes. Ultramafic rocks at both sites were extensively serpentinized, but the names of igneous protoliths are used here.

Whole-round data, including X-ray CT images, natural gamma radiation (NGR), gamma ray attenuation (GRA) density, magnetic susceptibility (MS), P-wave velocity (Vp) and noncontact electrical resistivity were obtained. Split core color spectroscopy data were also collected. Magnetic susceptibility, electrical resistivity under both nominally dry and brine-saturated conditions, P-wave velocity, bulk/grain density, porosity and thermal conductivity were measured in discrete samples. Nearly 100% core recovery allowed us to take a large data set of petrophysical data on the cores from Oman ophiolite including fault zones and highly altered intervals.
Generally, gabbroic rock types have higher density, P-wave velocity, and electrical resistivity, and lower porosity than ultramafic lithologies. Serpentinized dunite have lower density, P-wave velocity and electrical resistivity, and higher porosity than serpentinized harzburgite, and these physical properties are correlated with magnetic susceptibility, probably due to crystallization of magnetite during alteration. Average X-ray CT values are also correlated with many other physical properties in most lithologies.

Keywords: ICDP, D/V Chikyu, Oman Drilling Project, ophiolite, oceanic crust

©2019. Japan Geoscience Union. All Right Reserved.

Exploring the deep subseafloor biosphere and biogeochemical carbon cycling beneath the Arctic ocean

*Fumio Inagaki[1], Steffen Leth Jørgensen[2], Rolf Birger Pedersen[2]

1. Japan Agency for Marine-Earth Science and Technology (JAMSTEC), 2. Department of Earth Science, University of Bergen, Norway

Despite the Arctic cryosphere is the most sensitive and vulnerable to the global environmental change, the nature of deep subseafloor arctic environments remains largely unknown. Active processes on the drastic climate change, including the anthropogenic global warming and subsequent ice melt, are presumably similar to those mechanisms that formed some of the major hydrocarbon resources we presently use, deeply buried in the subseafloor sediment over millions of years at high atmospheric CO_2 and global warm conditions. Continuing to advance understanding of the natural analogues beneath the Arctic ocean through scientific drilling is a powerful approach for the discoveries and understanding of life and Earth co-operating systems, and consequently will illuminate the possible resilience and sustainable strategies adopted by human society towards the future. Here, we are keenly interested in the Arctic deep biosphere and biogeochemical carbon cycling, which presumably be tightly associated with tectonics and biotic/abiotic processes through paleoceanographic events of seawater stagnations, perturbations and fertilizations in the Paleogene to Cretaceous period, and perhaps still continuing in situ over geologic time. How is diagenetic activity and microbial diversity linked to variability in Cenozoic climate and environmental changes? To what degree is carbon diagenesis linked to biotic/abiotic and tectonic processes? What fluid flow and energy transformation processes support microbial activity in situ and govern carbon sink in the Arctic sedimentary basin? How does alternation of deep oceanic crust contribute to microbial life and biogeochemical carbon cycling in the shallower habitat? In addition, what is the nature of the Arctic basement? These important scientific issues on the most climate-sensitive place on Earth remain to be explored, but using the *Chikyu*' s riser-drilling and onboard facilities, it can be addressed by the state-of-the-art interdisciplinary analyses of core samples and the long-term borehole observatory.

Keywords: Arctic ocean, scientific ocean drilling, deep subseafloor biosphere, biogeochemical carbon cycle

©2019. Japan Geoscience Union. All Right Reserved.

[E] Poster | M (Multidisciplinary and Interdisciplinary)：M-IS Intersection

Mon. May 27, 2019 3:30 PM - 5:00 PM JST | Mon. May 27, 2019 6:30 AM - 8:00 AM UTC | Poster Hall International Exhibition Hall8, Makuhari Messe_19

[M-IS02] Drilling Earth Science

convener:Yasuhiro Yamada(Japan Agency for Marine-Earth Science and Technology (JAMSTEC), R&D Center for Ocean Drilling Science (ODS)), Yumiko Harigane(Geological Survey of Japan, National Institute of Advanced Industrial Science and Technology (AIST)), Azumi Kuroyanagi(Tohoku University Museum, The Center for Academic Resources and Archives, Tohoku University), Kosei E. Yamaguchi(Toho University and NASA Astrobiology Institute)

"Earth Drilling Science" session aims to exchange the latest information and scientific achievements in Ocean/Continental drilling projects and to promote the interdisciplinary science. The session covers a wide range of drilling sciences, earth dynamics, environments, and the drilling-related technologies. The overview of the recent IODP cruises as well as future projects of any types of scientific drilling will be reported.

[MIS02-P01] Utilization and curation of frozen core samples in IODP and implementation of the Nagoya Protocol in ocean drilling science

*Nan XIAO[1] (1.Japan Agency for Marine Earthe Science and Technology)

[MIS02-P02] In-situ rock strength calculated from drilling parameters. Comparison of results from various sites.

*Adam Wspanialy[1], Yasuhiro Yamada[1], Saneatsu Saito[1], KYAW MOE[1] (1.Japan Agency for Marine-Earth Science and Technology)

[MIS02-P03] Interaction between submarine landslides and subseafloor sedimentary microbiome: Chikyu SCORE Expedition 910 off Cape Erimo

*Tatsuhiko Hoshino[1], Go-Ichiro Uramoto[2], Satoshi Tonai[2], Yuki Morono[1], Akira Ijiri[1], Shino Suzuki[1], Yusuke Kubo[1], Fumio Inagaki[1], Chikyu SCORE Exp. 910 Scientists . (1.Japan Agency for Marine-Earth Science and Technology, 2.Kochi University)

[MIS02-P04] High-resolution continuous records of the chemical composition of the marine sediment off Cape Erimo, Hokkaido, Japan

*Masafumi MURAYAMA[1], Shinsuke Yagyu[3], Satoshi Tonai[2], Go-Ichiro Uramoto[3], Yasuhiro Yamada[4], Fumio Inagaki[4], Yusuke Kubo[5] (1.Faculty of Agriculture and Marine Science, Kochi University, 2.Faculty of Science and Technology, Kochi University, 3.Center for Advanced Marine Core Research, Kochi University, 4.Research and Development Center for Ocean Drilling Science, JAMSTEC, 5.Center for Deep Earth Exploration, JAMSTEC)

[MIS02-P05] Thermal property measurements of core samples retrieved from Futagawa fault drilling

*Terasu Sano[1], Weiren Lin[1], Susumu Shibutani[1,2], Nana Kamiya[1], Tatsuhiro Sugimoto[1], Kazuya Ishitsuka[1], Aiming Lin[3] (1.Graduate School of Engineering, Kyoto University, 2.Chi-ken Sogo Consultants Co., Ltd.,, 3.Graduate School of Science, Kyoto University)

[MIS02-P06] Results of geotechnical tests on shallow sediment cores recovered from Lord Howe Rise, off eastern Australia: Implications for future Lord Howe Rise riser drilling

*Takamitsu Sugihara[1], Kan Aoike[1], Saneatsu Saito[2], Tatsuya Murayama[1], Kentaro Takeda[1], Takuya Onodera[3], Ayumi Sumikawa[3], Yukari Kido[1], Yoshinori Sanada[1] (1.Center for deep earth exploration, Japan Agency for Marine-Science and Technology, 2.Research and development center for ocean drilling science, Japan Agency for Marine-Science and Technology, 3.Nippon Marine Enterprises, Ltd.)

[MIS02-P07] ICDP DSeis 4: Drilling, core logging, and in-hole geophysical logging of ICDP DSeis drilling into the M5.5 aftershock zones in a South African gold mines.

*Shunsuke YOSHIDA[1], Tadokoro Ryogo[1], Kosuke Sugimura[1], Kanematsu Makoto[1], Mitsuya Higashi[1], Benni Liebenberg[2], Esterhuizen van Heerden[2], Stephen Tau[3], Siyanda Mngadi[3], Ray Durrheim[3], Martin Ziegler[4], Yusuke Mukuhira[5], Ronald Conze[6], Yasuo Yabe[7], Shunya Kaneki[8], Yuki Yokoyama[9], Nomqhele Nkosi[10], Dave Roberts[10], Sifiso Buccio[11], Hiroshi Ogasawara[1] (1.Graduate school of science and engineering, Ritsumeikan , 2.Moab Khotsong mine, Vijoenskroon, 3.Univ. Witwatersrand, School of Geoscience, 4.ETH, Zurich Dep. Earth Sciences, 5.Inst. Fluid Science, Tohoku Univ., 6.GFZ, Potzdam, 7.Graduate School of Science, Tohoku Univ., 8.Disaster Prevention Research Inst., Kyoto Univ., 9.Graduate School of Science,Osaka Univ., 10.Mandela Mining Precinct, CSIR, 11.Council for Geoscience)

[MIS02-P08] ICDP DSeis 5: Diametrical Core Deformation Analysis of the M5.5 aftershock zone core - stress concentration at reflective intrusives and transition in stress regimes.

*Kosuke Sugimura[1], Shunsuke YOSHIDA[1], Ryogo Tadokoro[1], Hiroshi Ogasawara[2], Akimasa Ishida, Yasuo Yabe[3], Takatoshi Ito[4], Akio Funato[5], Siyanda Mngadi[6], Ray Durrheim[6] (1.Graduate school of science and engineering, Ritsumeikan, 2.College of Science and Engineering, Ritsumeikan Univ., 3.Graduate School of Science, Tohoku Univ., 4.Inst. Fluid Science, Tohoku Univ., 5.Fukada Geological Institute, 6.Univ. Witwatersrand, School of Geoscience)

[MIS02-P09] ICDP DSeis 6: Deformation Rate Analysis of the M5.5 aftershock zone core - stress concentration at reflective intrusives

*Kanematsu Makoto[1], Mitsuya Higashi[1], Yasuo Yabe[2], Shuhei Abe[2], Bryan Watson[3], Ray Durrheim[3], Hiroshi Ogasawara[1] (1.Ritsumeikan Univ., 2.Tohoku Univ., 3.Univ. Witwatersrand)

[MIS02-P10] ICDP DSeis 7: compilation of stress information and comparison with calculated stresses in the M5.5 aftershock zones

*Mitsuya Higashi[1], Yasuo Yabe[2], Kosuke Sugimura[1], Akimasa Ishida, Makoto Kanematsu[1], Shunsuke YOSHIDA[1], Ryogo Tadokoro[1], Takatoshi Ito[4], Akio Funato[5], Hiroshi Ogasawara[3] (1.Graduate School of Science and Engineering, Ritsumeikan Univ., 2.Research Center for Prediction of Earthquakes and Volcanic Eruptions, Graduate School of Science, Tohoku University, 3.College of Science and Engineering, Ritsumeikan Univ., 4.Inst. Fluid Science, Tohoku Univ., 5.Fukada Geological Institute)

[MIS02-P11] ICDP DSeis 8: the M5.5 fault structure and reflective intrusives in legacy 3D seismic reflection data

*Noda Taku[1], Musa Manzi[2], Hiroyuki Ogasawara[1], Lindsay Linzer[2], Stephanie Enslin[2], Ray Durrheim[2], Hiroshi Ogasawara[1] (1.Ritsumeikan Univ., 2.Univ. Witwatersrand)

[MIS02-P12] ICDP DSeis 9: are streaks in the M5.5 aftershocks potentially located on highly stressed intrusive?

*Ryogo Tadokoro[1], Katsuya Ishibashi[2], Horiuchi Shigeki[3], Hiroshi Ogasawara[4] (1.Graduate School of Science and Engineering, Ritsumeikan Univ., 2.School of Science and Engineering, Ritsumeikan Univ., 3.Homeseismo ltd., 4.College of Science and Engineering, Ritsumeikan Univ.)

Utilization and curation of frozen core samples in IODP and implementation of the Nagoya Protocol in ocean drilling science

*Nan XIAO[1]

1. Japan Agency for Marine Earthe Science and Technology

Deep biosphere research has become one of the major scientific focuses in ocean drilling science. How to access to core samples with sufficient quality has been a changes for scientists. Currently there are two methods of accessing to deep biosphere samples which are participating in drilling expeditions and requesting samples from core repositories. The Kochi Core Center has curated deep biosphere samples that were processed aseptically and stored at deep frozen (-80 degree C) condition from more than 10 drilling expeditions. Increased scientific attention to microbiological research of the subseafloor envrionment raises the complications and concerns related to adherence to the Nagoya Protocol of the Convention on Biological Diversity (CBD). The Nagoya Protocol is an international agreement that aims to guide countries in developing standart protocols and protections for accessing biological materials, and sharing benefits derived from their utilization. Since its commencement, the Nagoya Protocol has placed international biological research, especially fieldwork, under greater political scrutiny and increased its complexity due to the variation in implementation between nations. We present the central points of the Nagoya Protocol on access and benefit-sharing (ABS) and discuss their relationship to ocean drilling research. In addition, we address the challenges faced by ocean drilling in complying with this internation convention.

Keywords: ocean drilling program, frozen core sample, Nagoya Protocol, convention on biological diversity

©2019. Japan Geoscience Union. All Right Reserved.

In-situ rock strength calculated from drilling parameters. Comparison of results from various sites.

*Adam Wspanialy[1], Yasuhiro Yamada[1], Saneatsu Saito[1], KYAW MOE[1]

1. Japan Agency for Marine-Earth Science and Technology

Drilling parameters are excellent datasets to understand in-situ physical properties of the rock. Continuous core samples along with parameters such as Torque, RPM, WOB and ROP have been collected during drilling operations. The borehole data acquisition was complemented with full LWD/MWD and wireline logging. After core delivery to surface core scratch tests have been carried out to measure Unconfined Compressive Strength (UCS). Our comprehensive approach enabled us to integrate all data and conduct detailed analysis of the in-situ subsurface physical and mechanical properties of a rock cut by a drill bit.

Here we present some results from offshore and onshore drilling experiments carried out in Japan, Oman and Australia. Methods such as Specific Energy (SE) and Equivalent Strength (EST) have been used to estimate in-situ rock properties, namely UCS and analyse drilling process.

Our results demonstrate that the calculated in-situ rock strength based on SE/EST methods correlates well with sonic derived UCS and core scratch derived UCS. Utilised methods also successfully detect fractures in the formation, show developing drilling dysfunctions such as vibration, and bit balling.

Keywords: rock strength, drilling parameters, Specific Energy

©2019. Japan Geoscience Union. All Right Reserved.

Interaction between submarine landslides and subseafloor sedimentary microbiome: Chikyu SCORE Expedition 910 off Cape Erimo

*Tatsuhiko Hoshino[1], Go-Ichiro Uramoto[2], Satoshi Tonai[2], Yuki Morono[1], Akira Ijiri[1], Shino Suzuki[1], Yusuke Kubo[1], Fumio Inagaki[1], Chikyu SCORE Exp. 910 Scientists .

1. Japan Agency for Marine-Earth Science and Technology, 2. Kochi University

During the past decades, scientific ocean drilling has explored the subseafloor sedimentary biosphere down to over 2 kilometers below seafloor (Inagaki et al., 2015). The total biomass and diversity of microbial community in the subseafloor biosphere are comparable to those in the hydrosphere (Kallmeyer et al., 2012). Taxonomic composition of subseafloor microbial communities are distinct from those of other habitats on Earth’ s surface, such as ocean and soil, inferring that adaptive evolution of microbial community to the energy-limited deep sedimentary habitats have occurred. In a previous study of bioturbated layers in surface marine sediments, it has been reported that seawater-migration by macrofauna activity during the initial depositional stage notably affected microbial community structures (Chen et al. 2017). Similarly, it can be hypothesized that submarine landslides have introduced easily degradable fresh organic matter and dissolved electron acceptors (e.g., oxygen, sulfate) to the sedimentary habitats, and consequently caused a shift of microbial communities and its function.

In 2017, we conducted the Chikyu’ s first SCORE Expedition 910 at the Hidaka Trough off Cap Erimo and obtained sediment cores down to 100 meters below the seafloor. In the core column, four intervals of deformed sediments were identified, indicating the occurrences of multiple submarine landslides in this area. In those deformed sediment intervals, we observed no clear anomaly in the profile of cell abundance, which decrease with sediment depth as generally seen in the other subserfloor sediments. In addition, pore water chemistry data do not show clear anomaly either, indicating recovery of sediment geochemistry from the turbation caused by landslides. While both profiles of microbial cell abundance and pore water geochemistry did not show anomaly in the deformed sediment intervals, the DNA-based analyses, showed some unusual appearances of microbial taxa relative to the depth, suggesting the potential migration of microbes from the upper horizons by submarine landslides.

Reference

Inagaki F, et al (2015). Science 349: 420-424; Kallmeyer J, et al (2012). Proc Natl Acad Sci U S A 109: 16213-16216; Chen X, et al (2017). Sci Rep 7: 2400.

Keywords: Chikyu SCORE, Deep biosphere, Mass transport deposit

©2019. Japan Geoscience Union. All Right Reserved.

High-resolution continuous records of the chemical composition of the marine sediment off Cape Erimo, Hokkaido, Japan

*Masafumi MURAYAMA[1], Shinsuke Yagyu[3], Satoshi Tonai[2], Go-Ichiro Uramoto[3], Yasuhiro Yamada[4], Fumio Inagaki[4], Yusuke Kubo[5]

1. Faculty of Agriculture and Marine Science, Kochi University, 2. Faculty of Science and Technology, Kochi University, 3. Center for Advanced Marine Core Research, Kochi University, 4. Research and Development Center for Ocean Drilling Science, JAMSTEC, 5. Center for Deep Earth Exploration, JAMSTEC

About 100 m sediment cores were taken from off Cape Erimo, Hokkaido, Japan on the Shallow Core Program (SCORE) by D/V Chikyu in 2017. The sedimentary sequence is intercalated with mass transport deposits caused by earthquake-triggered submarine landslides and/or climate changes. Here we report a result of high-resolution continuous geochemical composition of these cores using XRF core scanning technique.

Keywords: sediment core off Cape Erimo, XRF core scanner (ITARX), Shallow Core Program (SCORE), D/V Chikyu

©2019. Japan Geoscience Union. All Right Reserved.

Thermal property measurements of core samples retrieved from Futagawa fault drilling

*Terasu Sano[1], Weiren Lin[1], Susumu Shibutani[1,2], Nana Kamiya[1], Tatsuhiro Sugimoto[1], Kazuya Ishitsuka[1], Aiming Lin[3]

1. Graduate School of Engineering, Kyoto University, 2. Chi-ken Sogo Consultants Co., Ltd.,, 3. Graduate School of Science, Kyoto University

In 2017~2018, to retrieve rock samples from the Futagawa fault ruptured during the 2016 Kumamoto earthquake in Japan, a borehole was drilled down to 700 m depth through the fault in Mashikimachi, Kumamoto prefecture located in the southwest of the Aso volcano. In this borehole, temperature depth profile was measured from ~50 m to ~650 m below the surface (Lin et al., 2019 JpGU). As a preliminary result, an anomaly of temperature, about 1 ℃/km geothermal gradient, was found in the depth range of 310 - 430 m (Lin et al., 2019 JpGU). To examine if this this temperature anomaly comes from thermal conductivity change of the ricks, we collected rock core samples from the borehole and measured their thermal properties.

We measured density, porosity and three thermal transport properties (thermal conductivities, thermal diffusivities, specific heat capacities) of 20 cores drilled from the borehole in the depth range from 300 m to 700 m. I selected typical rock cores to cover not only the depth intervals and also all the main rock types. The rock types of cores are basal sedimentary rocks in 300 m - 353 m , andesite in 353 m - 514 m, sandstone and/or conglomerate in 514 m - 562 m, and tuff in 562 m - 700 m. Measured wet densities and porosities are 1.57 g/cm^3 - 2.02 g/cm^3, 40.0% - 47.8% for basal sedimentary rocks, 2.31 g/cm^3 - 2.95 g/cm^3, 3.1% - 25.5% for andesite, 2.29 g/cm^3 - 2.41 g/cm^3, 21.6% - 29.4% for sandstone and/or conglomerate, 1.99 g/cm^3 - 2.29 g/cm^3, 9.4 % - 35.8% for tuff. Measured thermal conductivities are 0.88 W/(mK) - 1.10 W/(mK) for basal sedimentary rocks, 1.00 W/(mK) - 1.81 W/(mK) for andesite, 1.26 W/(mK) - 1.31 W/(mK) for sandstone and/or conglomerate, 0.96 W/(mK) - 1.27 W/(mK) for tuff. And measured thermal diffusivities and specific heat capacities are 0.85 J/(g･K) - 3.46 J/(g･K) for alluvium, 0.48 m^2/s - 0.91 m^2/s, 1.36 J/(g･K) - 2.60 J/(g･K) for andesite, 0.49 m^2/s - 0.66 m^2/s, 1.95 J/(g･K) - 2.70 J/(g･K) for sandstone and/or conglomerate, 0.40 m^2/s - 0.99 m^2/s, 1.40 J/(g･K) - 2.93 J/(g･K) for tuff. From data of measured temperature of borehole and thermal conductivities of the cores, we calculated heat flow of in the borehole. Using this heat flow and thermal conductivities, we reconstructed the temperature profile in the borehole.

In this estimation, we couldn't reproduce the anomaly of measured temperature. So we conclude that the anomaly of measured temperature is not caused by the significant change of the thermal conductivity in 310 m - 430 m depth.

Keywords: Drilling, thermal properties, Temperature

©2019. Japan Geoscience Union. All Right Reserved.

Results of geotechnical tests on shallow sediment cores recovered from Lord Howe Rise, off eastern Australia: Implications for future Lord Howe Rise riser drilling

*Takamitsu Sugihara[1], Kan Aoike[1], Saneatsu Saito[2], Tatsuya Murayama[1], Kentaro Takeda[1], Takuya Onodera[3], Ayumi Sumikawa[3], Yukari Kido[1], Yoshinori Sanada[1]

1. Center for deep earth exploration, Japan Agency for Marine-Science and Technology, 2. Research and development center for ocean drilling science, Japan Agency for Marine-Science and Technology, 3. Nippon Marine Enterprises, Ltd.

Lord Howe Rise (LHR) Drilling Project (871-CPP2) is an accepted IODP drilling proposal to reconstruct Cretaceous tectonic history of northern Zealandia, designated as a Chikyu riser drilling project. In order to plan a riser drilling operation, it is important to evaluate mechanical strength and physical properties of shallow sediment (0 to 100 or 200 meters below sea floor, mbsf) for setting Blow-out Prevention (BOP) system and riser with heavy weight on the seafloor. Geotechnical core test (e.g., triaxial compressive test and consolidation test) is an essential work to directly measure rock strength and physical properties of geological materials. Therefore, the geotechnical core tests are usually conducted for the surface sediment to evaluate their mechanical and physical properties. In the LHR region, calcareous sediment is broadly and predominantly distributed, and clayey sediment is not observed in shallow sediments. In general, deep seafloor is composed of clayey sediment, and their mechanical and physical properties are well understood. However, mechanical and physical properties of calcareous sediment in both ambient and confined pressure conditions are not well known.

In this study, results of geotechnical test for shallow cores taken in the LHR region are presented, and characteristics of mechanical and physical properties (especially shear strength and permeability) are discussed.

Shallow cores for geotechnical test were taken by R/V Kairei with a gravity piston corer in KR17-15C and by D/V JOIDES Resolution with a rotary core barrel (RCB) in Expedition 371. The gravity piston coring by R/V Kairei was conducted at the proposed riser drilling sites DLHR-5A and -3A, and two cores with approximately 7 m length were taken at each site. The RCB coring by D/V JOIDES Resolution was conducted at Site U1506 in Expedition 371. A whole-round sample with 40 cm length was taken from U1506A-13R for our investigation, and depth of the whole-round sample is 116.5 mbsf. In order to measure physical and mechanical properties for the core samples, geotechnical tests of Penetrometer test, Bulk density, Grain density, Liquid limit, Plastic limit, Grain size distribution, Constant rate of strain consolidation test (CRSC test), and Triaxial compressive strength test with pore pressure measurement (Consolidated-Undrained conditions) were carried out.

Most of the tests except penetrometer test were carried out by OYO Co. Procedures of those measurements and tests were based on the regulations established by Japanese Geotechnical Society (JGS) and Japanese Industrial Standards (JIS). Those are almost the same as their regulations in the ASTM.

All of core samples are composed of calcareous ooze, and grain size distribution of the core samples shows clay size fraction (less than 5 micro meters) is dominant (more than 80 %).

©2019. Japan Geoscience Union. All Right Reserved.

Based on the bulk density data, overburden stresses were calculated and consolidation pressures corresponding to depth of 10 to 240 mbsf for the triaxial test were estimated assuming k0 compaction (k0 factor = 0.5). The result of the triaxial test show shear strength profile gradually increases with depth and is almost identical to those of clayey sediment from Kumano Basin and Nankai Trough. However, the result of the penetrometer test indicates that shear strength of calcareous ooze under ambient condition is quite lower than those of clayey sediment. This observation suggests mechanical strength of calcareous ooze is easily released with depressurizing of sediment.

Based on the result of the CRSC test, it is indicated that calcareous ooze shows no obvious preconsolidation stress, and this result is in good agreement with the result of the triaxial test mentioned above. Permeability of calcareous ooze calculated from the CRSC test results is similar to sandy sediment and the results indicate calcareous ooze is more permeable as compared with clayey sediment.

Those results will be dedicated to analysis for the riser operation in the LHR area.

Keywords: Lord Howe Rise, Riser drilling, Rock strength test, Shear strength, Permeability

©2019. Japan Geoscience Union. All Right Reserved.

ICDP DSeis 4: Drilling, core logging, and in-hole geophysical logging of ICDP DSeis drilling into the M5.5 aftershock zones in a South African gold mines.

*Shunsuke YOSHIDA[1], Tadokoro Ryogo[1], Kosuke Sugimura[1], Kanematsu Makoto[1], Mitsuya Higashi[1], Benni Liebenberg[2], Esterhuizen van Heerden[2], Stephen Tau[3], Siyanda Mngadi[3], Ray Durrheim[3], Martin Ziegler[4], Yusuke Mukuhira[5], Ronald Conze[6], Yasuo Yabe[7], Shunya Kaneki[8], Yuki Yokoyama[9], Nomqhele Nkosi[10], Dave Roberts[10], Sifiso Buccio[11], Hiroshi Ogasawara[1]

1. Graduate school of science and engineering, Ritsumeikan , 2. Moab Khotsong mine, Vijoenskroon, 3. Univ. Witwatersrand, School of Geoscience, 4. ETH, Zurich Dep. Earth Sciences, 5. Inst. Fluid Science, Tohoku Univ., 6. GFZ, Potzdam, 7. Graduate School of Science, Tohoku Univ., 8. Disaster Prevention Research Inst., Kyoto Univ., 9. Graduate School of Science,Osaka Univ., 10. Mandela Mining Precinct, CSIR, 11. Council for Geoscience

ICDP drilling into the aftershock zone of the 2014 M5.5 earthquake near Orkney, South Africa commenced on 2017 and was completed in 2018. This M5.5 earthquake started from a depth about 5 km and ruptured West Rand Group below mining horizon on unknown geological structure in a deep gold mine. The mechanism of left-lateral slip of this M5.5 earthquake contradicted normal-faulting mechanisms of typical mining-induced earthquakes on mining horizons. The upper fringe of the aftershock zone was several hundreds of meters from the deepest level of the mine. Two NQ holes were collared at a depth of 2.9 km (95 level) below surface at a deep gold mine. Hole A (817m) deviated too much to intersect the M5.5 fault but Hole B (700m) intersected the M5.5 fault. A 3-m double-tube couldn't recover the fault material much, while a 1.5m triple-tube could recover the fault material more in Hole C branched from 544 m in Hole B. Geophysical logging, core logging, and water/gas monitoring followed drilling. All the core was transported to Mandela Mining Precinct, CSIR, Johannesburg and systematically described and scanned by the ICDP DMT scanner. Some of the core were selected for core stress measurements.

In JpGU 2019 meeting, nine papers (ICDP DSeis 1-9) report on the outcomes. This poster (ICDP DSeis 4) compiles drilling, core logging, and in-hole geophysical logging of ICDP DSeis drilling into the M5.5 aftershock zones in a South African gold mines. A core orientation tool was used during drilling but not 100% reliable because there was a case that a bottom line in a core run was different by more than 90 degrees from the bottom line in the next core run. We elaborated to compare OTV image with core to carefully check the core orientation. The modified core orientation allowed us to modify the maximum stress direction that Ishida et al. (2018) measured. We could confirm good consistency with borehole breakout analysis (Richenbacher 2018; ETH master thesis). We will report on other associated outcomes. Refer other papers (ICDP DSeis 1-3, 5-9) for other related outcomes.

Acknowledgement: The DSeis team includes co-authors of the papers ICDP DSeis 2-9 and members shown at https://www.icdp-online.org/projects/world/africa/orkney-s-africa/details/. We thank Harmony Gold, Anglogold Ashanthi, Lesedi, Digital Surveying, OHMS, Seismogen, 3D Geoscience. ICDP, JSPS, SA NRF, MEXT Japan, US NSF, German DRF, and Ritsumeikan Univ. financially support the project.

©2019. Japan Geoscience Union. All Right Reserved.

©2019. Japan Geoscience Union. All Right Reserved.

ICDP DSeis 5: Diametrical Core Deformation Analysis of the M5.5 aftershock zone core - stress concentration at reflective intrusives and transition in stress regimes.

*Kosuke Sugimura[1], Shunsuke YOSHIDA[1], Ryogo Tadokoro[1], Hiroshi Ogasawara[2], Akimasa Ishida, Yasuo Yabe[3], Takatoshi Ito[4], Akio Funato[5], Siyanda Mngadi[6], Ray Durrheim[6]

1. Graduate school of science and engineering, Ritsumeikan, 2. College of Science and Engineering, Ritsumeikan Univ., 3. Graduate School of Science, Tohoku Univ., 4. Inst. Fluid Science, Tohoku Univ., 5. Fukada Geological Institute, 6. Univ. Witwatersrand, School of Geoscience

ICDP drilling into the aftershock zone of the 2014 M5.5 earthquake near Orkney, South Africa commenced on 2017 and was completed in 2018. Drilling was designed to minimize damage on core and borehole, being able to maximize core recovery. Hole A (817m) was drilled in 2017. It unfortunately didn't intersect the M5.5 fault, running eventually sub-parallel and roughly 100m from the aftershock zone. As the hole was stable we could recover almost 100% of core from the area traversing the periphery of the M5.5 aftershock zone for a distance of several hundreds of meters. Ishida et al. (2018) carried out Diametrical Core Diameter Analysis (Ito and Funato, 2017). This analysis measures the change in core diameter with roll angle around the core axis, which was caused by a relief of anisotropic stress during drilling. We used this analysis because (1) the expected stress was too high for hydrofracturing method, (2) uncertainty in stress magnitude is unavoidable in damage interpretations, (3) DSeis hole were too long for overcoring technique, and (4) DCDA is non-destructive and very easy to make if core is recovered. Ishida et al. (2018) measured 186 pieces of core from Hole A (817m collared at 2.9km depth) that were recovered near the M5.5 aftershock zone. They successfully illustrated spatial variation in differential stress in a plane perpendicular to Hole A axis. They found stress concentration at intrusives with one located at the depth of the upper fringe of the M5.5 aftershock zone. We carried out additional measurement for the remaining part of Hole A and Hole B. With additional data measured at adjacent locations, we could confirm that the stress concentration Ishida et al (2018) found at intrusives was not an outlier. We will report how Hole B that intersected the M5.5 fault differ from Hole A stress.

This is one of nine ICDP DSeis papers (ICDP DSeis 1-9) presented in JpGU 2019. Refer other papers for other topic on drilling, logging, other stress measurement, fault materials, comparison with calculated stress, legacy 3D seismic reflection data, and relocated aftershocks.

©2019. Japan Geoscience Union. All Right Reserved.

ICDP DSeis 6: Deformation Rate Analysis of the M5.5 aftershock zone core - stress concentration at reflective intrusives

*Kanematsu Makoto[1], Mitsuya Higashi[1], Yasuo Yabe[2], Shuhei Abe[2], Bryan Watson[3], Ray Durrheim[3], Hiroshi Ogasawara[1]

1. Ritsumeikan Univ., 2. Tohoku Univ., 3. Univ. Witwatersrand

ICDP drilling into the aftershock zone of the 2014 M5.5 earthquake near Orkney, South Africa commenced on 2017 and was completed in 2018. Ishida et al. (2018) and Sugimura et al. (2019; ICDP DSeis 5) report on spatial variation of differential stress in a plane perpendicular to the borehole axis. It is ideal to have different stress component especially at critical location where significant characteristics were found. Deformation Rate Analysis (Yamamoto, 2009) can measure stress in any direction although the method takes time and the specimen are not reusable for other test. So, we planned to selected samples where characteristic spatial variation was found by DCDA method (Ishida et al. 2018 and Sugimura et al. 2019). It was confirmed also in normal stress component along the borehole axis that stress was concentrated at the intrusive at about 400m.

This is one of nine ICDP DSeis papers (ICDP DSeis 1-9) presented in JpGU 2019. Refer other papers for other topics on drilling, logging, other stress measurement, fault materials, comparison with calculated stress, legacy 3D seismic reflection data, and relocated aftershocks.

Acknowledgement: The DSeis team includes co-authors of the papers ICDP DSeis 2-9 and members shown at https://www.icdp-online.org/projects/world/africa/orkney-s-africa/details/. We thank Harmony Gold, Anglogold Ashanthi, Lesedi, Digital Surveying, OHMS, Seismogen, 3D Geoscience. ICDP, JSPS, SA NRF, MEXT Japan, US NSF, German DRF, and Ritsumeikan Univ. financially support the project.

Keywords: Seismogenic zone, Stress Measurement, DRA

©2019. Japan Geoscience Union. All Right Reserved.

ICDP DSeis 7: compilation of stress information and comparison with calculated stresses in the M5.5 aftershock zones

*Mitsuya Higashi[1], Yasuo Yabe[2], Kosuke Sugimura[1], Akimasa Ishida, Makoto Kanematsu[1], Shunsuke YOSHIDA[1], Ryogo Tadokoro[1], Takatoshi Ito[4], Akio Funato[5], Hiroshi Ogasawara[3]

1. Graduate School of Science and Engineering, Ritsumeikan Univ., 2. Research Center for Prediction of Earthquakes and Volcanic Eruptions, Graduate School of Science, Tohoku University, 3. College of Science and Engineering, Ritsumeikan Univ., 4. Inst. Fluid Science, Tohoku Univ., 5. Fukada Geological Institute

ICDP drilling into the aftershock zone of the 2014 M5.5 earthquake near Orkney, South Africa commenced on 2017 and was completed in 2018. Spatial variation in stress was measured by Ishida et al. (2018) and Sugimura et al. (2019; ICDP DSeis 5) by DCDA method (Funato and Ito, 2017) and Kanematsu et al. (2019; ICDP DSeis 6). This poster reports on compilation of stress information including the other information sources and compares with calculated stress.

We first compared with a 3D stress state that Ogasawara et al. (2012) measured in 2011 at 98L (3.0 km depth from surface). We assume zero stress on surface, the measured 3D stress (normal faulting stress regime) at 3.0 km, and stress linearly increasing with depth. The calculated stress was consistent with DCDA results measured in the initial 100m section in Hole A, while inconsistent in deeper section. The calculated direction of maximum stress in a plane perpendicular to the borehole axis was also inconsistent with the measured stress information (Yoshida et al. 2019 JpGU; ICDP DSeis 5). Except for the stress concentration measured at intrusives, the measured DCDA results were systematically lower than the calculated stress. In a stress regime that caused the left-lateral horizontal slip on the M5.5 fault, horizontal stress should be larger, which will increase horizontal stress component in a plane perpendicular to the Hole A axis. This increase should decrease difference in stress in the plane perpendicular to the Hole A axis. By JpGU 2019, we will make additional effort to interpret more from the comparison between the measured and calculated stress.

This is one of nine papers (ICDP DSeis 1-9). Refer other papers for other topic on drilling, logging, other stress measurement, fault materials, legacy 3D seismic reflection data, and relocated aftershocks.

Acknowledgement: The DSeis team includes co-authors of the papers ICDP DSeis 2-9 and members shown at https://www.icdp-online.org/projects/world/africa/orkney-s-africa/details/. We thank Harmony Gold, Anglogold Ashanthi, Lesedi, Digital Surveying, OHMS, Seismogen, 3D Geoscience. ICDP, JSPS, SA NRF, MEXT Japan, US NSF, German DRF, and Ritsumeikan Univ. financially support the project.

©2019. Japan Geoscience Union. All Right Reserved.

ICDP DSeis 8: the M5.5 fault structure and reflective intrusives in legacy 3D seismic reflection data

*Noda Taku[1], Musa Manzi[2], Hiroyuki Ogasawara[1], Lindsay Linzer[2], Stephanie Enslin[2], Ray Durrheim[2], Hiroshi Ogasawara[1]

1. Ritsumeikan Univ., 2. Univ. Witwatersrand

ICDP drilling into the aftershock zone of the 2014 M5.5 earthquake near Orkney, South Africa commenced on 2017 and was completed in 2018. Hiroyuki et al. (2017 AGU) reported on legacy seismic reflection to analyze geological structures in the southern most area of the M5.5 aftershock zones. They found vertical structures in four 2-D lines that were potentially responsible for the M5.5 earthquake and illustrated cross-cutting relations of the M5.5 structure and other known faults that dislocated gold reefs more than several hundreds of meters both horizontally and vertically. Another legacy seismic reflection data which was recorded in 1996 and covered much wider area of the M5.5 aftershock zone was found. We calibrated velocity structure by tying with borehole data including DSeis Holes A and B, we found some of intrusives (sills) that Hole A and B were strong reflectors in the legacy 3D seismic reflection data.

Aftershocks located by in-mine 46 geophones are dense at the southern upper fringe, with a sharp cut-off dipping about 20 degrees to the south; some clear stripes of aftershocks are also seen, in parallel to the upper fringe (Tadokoro et al., JpGU2019, ICDP DSeis 9). It is interesting to note that the reflector (sills) are also in parallel to the upper fringe of the aftershock zone and the aftershock stripes. It is also notable that stress concentration is reported at the intrusives by Sugimura et al. (JpGU2019; ICDP DSeis 5) and Kanematsu et al. (JpGU2019; ICDP DSeis 6). Some mechanism that controls the extent of the aftershocks should exist.

This paper is one of nine papers (ICDP DSeis 1-9). Refer other papers for other topics, e.g. on drilling, logging, stress measurements and evaluation, fault materials, and relocated aftershocks.

Acknowledgement: The DSeis team includes co-authors of the papers ICDP DSeis 2-9 and members shown at https://www.icdp-online.org/projects/world/africa/orkney-s-africa/details/. We thank Harmony Gold, Anglogold Ashanthi, Lesedi, Digital Surveying, OHMS, Seismogen, 3D Geoscience. ICDP, JSPS, SA NRF, MEXT Japan, US NSF, German DRF, and Ritsumeikan Univ. financially support the project.

Keywords: ICDP DSeis, The M5.5 seismogenic zone, Seismic reflection

©2019. Japan Geoscience Union. All Right Reserved.

ICDP DSeis 9: are streaks in the M5.5 aftershocks potentially located on highly stressed intrusive?

*Ryogo Tadokoro[1], Katsuya Ishibashi[2], Horiuchi Shigeki[3], Hiroshi Ogasawara[4]

1. Graduate School of Science and Engineering, Ritsumeikan Univ., 2. School of Science and Engineering, Ritsumeikan Univ., 3. Homeseismo ltd., 4. College of Science and Engineering, Ritsumeikan Univ.

ICDP drilling into the aftershock zone of the 2014 M5.5 earthquake near Orkney, South Africa commenced on 2017 and was completed in 2018. Aftershocks located by in-mine 46 geophones are dense at the southern upper fringe, with a sharp cut-off dipping about 20 degrees to the south. Some clear stripes of aftershocks are also seen, in parallel to the upper fringe. It is interesting to note that the reflector (sills) are also in parallel to the upper fringe of the aftershock zone and the aftershock stripes. It is also notable that stress concentration is reported at the intrusives by Sugimura et al. (JpGU2019; ICDP DSeis 5) and Kanematsu et al. (JpGU2019; ICDP DSeis 6). Some mechanism that controls the extent of the aftershocks should exist.

In order to discuss further, we relocated aftershocks with the Double-Difference method (Waldhouser and Ellsworth, 2004). At the moment, we could relocate only 60 events at the upper fringe of the aftershocks. We used in-mine seismic network data of Anglogold Ashanti. P- and S- arrival times that the algorithm of Horiuchi et al. (2011) was used. A sharper alignment of aftershocks is successfully illustrated. By JpGU 2019, we will make additional efforts to extend the area of relocation to discuss more.

Acknowledgement: The DSeis team includes co-authors of the papers ICDP DSeis 2-9 and members shown at https://www.icdp-online.org/projects/world/africa/orkney-s-africa/details/. We thank Harmony Gold, Anglogold Ashanthi, Lesedi, Digital Surveying, OHMS, Seismogen, 3D Geoscience. ICDP, JSPS, SA NRF, MEXT Japan, US NSF, German DRF, and Ritsumeikan Univ. financially support the project.

©2019. Japan Geoscience Union. All Right Reserved.

[E] Poster | M (Multidisciplinary and Interdisciplinary)：M-IS Intersection

Mon. May 27, 2019 5:15 PM - 6:30 PM JST | Mon. May 27, 2019 8:15 AM - 9:30 AM UTC | Poster Hall International Exhibition Hall8, Makuhari Messe_32

[M-IS02] Drilling Earth Science

convener:Yasuhiro Yamada(Japan Agency for Marine-Earth Science and Technology (JAMSTEC), R&D Center for Ocean Drilling Science (ODS)), Yumiko Harigane(Geological Survey of Japan, National Institute of Advanced Industrial Science and Technology (AIST)), Azumi Kuroyanagi(Tohoku University Museum, The Center for Academic Resources and Archives, Tohoku University), Kosei E. Yamaguchi(Toho University and NASA Astrobiology Institute)

"Earth Drilling Science" session aims to exchange the latest information and scientific achievements in Ocean/Continental drilling projects and to promote the interdisciplinary science. The session covers a wide range of drilling sciences, earth dynamics, environments, and the drilling-related technologies. The overview of the recent IODP cruises as well as future projects of any types of scientific drilling will be reported.

[MIS02-P01] Utilization and curation of frozen core samples in IODP and implementation of the Nagoya Protocol in ocean drilling science

*Nan XIAO[1] (1.Japan Agency for Marine Earthe Science and Technology)

[MIS02-P02] In-situ rock strength calculated from drilling parameters. Comparison of results from various sites.

*Adam Wspanialy[1], Yasuhiro Yamada[1], Saneatsu Saito[1], KYAW MOE[1] (1.Japan Agency for Marine-Earth Science and Technology)

[MIS02-P03] Interaction between submarine landslides and subseafloor sedimentary microbiome: Chikyu SCORE Expedition 910 off Cape Erimo

*Tatsuhiko Hoshino[1], Go-Ichiro Uramoto[2], Satoshi Tonai[2], Yuki Morono[1], Akira Ijiri[1], Shino Suzuki[1], Yusuke Kubo[1], Fumio Inagaki[1], Chikyu SCORE Exp. 910 Scientists . (1.Japan Agency for Marine-Earth Science and Technology, 2.Kochi University)

[MIS02-P04] High-resolution continuous records of the chemical composition of the marine sediment off Cape Erimo, Hokkaido, Japan

*Masafumi MURAYAMA[1], Shinsuke Yagyu[3], Satoshi Tonai[2], Go-Ichiro Uramoto[3], Yasuhiro Yamada[4], Fumio Inagaki[4], Yusuke Kubo[5] (1.Faculty of Agriculture and Marine Science, Kochi University, 2.Faculty of Science and Technology, Kochi University, 3.Center for Advanced Marine Core Research, Kochi University, 4.Research and Development Center for Ocean Drilling Science, JAMSTEC, 5.Center for Deep Earth Exploration, JAMSTEC)

[MIS02-P05] Thermal property measurements of core samples retrieved from Futagawa fault drilling

*Terasu Sano[1], Weiren Lin[1], Susumu Shibutani[1,2], Nana Kamiya[1], Tatsuhiro Sugimoto[1], Kazuya Ishitsuka[1], Aiming Lin[3] (1.Graduate School of Engineering, Kyoto University, 2.Chi-ken Sogo Consultants Co., Ltd.,, 3.Graduate School of Science, Kyoto University)

[MIS02-P06] Results of geotechnical tests on shallow sediment cores recovered from Lord Howe Rise, off eastern Australia: Implications for future Lord Howe Rise riser drilling

*Takamitsu Sugihara[1], Kan Aoike[1], Saneatsu Saito[2], Tatsuya Murayama[1], Kentaro Takeda[1], Takuya Onodera[3], Ayumi Sumikawa[3], Yukari Kido[1], Yoshinori Sanada[1] (1.Center for deep earth exploration, Japan Agency for Marine-Science and Technology, 2.Research and development center for ocean drilling science, Japan Agency for Marine-Science and Technology, 3.Nippon Marine Enterprises, Ltd.)

[MIS02-P07] ICDP DSeis 4: Drilling, core logging, and in-hole geophysical logging of ICDP DSeis drilling into the M5.5 aftershock zones in a South African gold mines.

*Shunsuke YOSHIDA[1], Tadokoro Ryogo[1], Kosuke Sugimura[1], Kanematsu Makoto[1], Mitsuya Higashi[1], Benni Liebenberg[2], Esterhuizen van Heerden[2], Stephen Tau[3], Siyanda Mngadi[3], Ray Durrheim[3], Martin Ziegler[4], Yusuke Mukuhira[5], Ronald Conze[6], Yasuo Yabe[7], Shunya Kaneki[8], Yuki Yokoyama[9], Nomqhele Nkosi[10], Dave Roberts[10], Sifiso Buccio[11], Hiroshi Ogasawara[1] (1.Graduate school of science and engineering, Ritsumeikan , 2.Moab Khotsong mine, Vijoenskroon, 3.Univ. Witwatersrand, School of Geoscience, 4.ETH, Zurich Dep. Earth Sciences, 5.Inst. Fluid Science, Tohoku Univ., 6.GFZ, Potzdam, 7.Graduate School of Science, Tohoku Univ., 8.Disaster Prevention Research Inst., Kyoto Univ., 9.Graduate School of Science,Osaka Univ., 10.Mandela Mining Precinct, CSIR, 11.Council for Geoscience)

[MIS02-P08] ICDP DSeis 5: Diametrical Core Deformation Analysis of the M5.5 aftershock zone core - stress concentration at reflective intrusives and transition in stress regimes.

*Kosuke Sugimura[1], Shunsuke YOSHIDA[1], Ryogo Tadokoro[1], Hiroshi Ogasawara[2], Akimasa Ishida, Yasuo Yabe[3], Takatoshi Ito[4], Akio Funato[5], Siyanda Mngadi[6], Ray Durrheim[6] (1.Graduate school of science and engineering, Ritsumeikan, 2.College of Science and Engineering, Ritsumeikan Univ., 3.Graduate School of Science, Tohoku Univ., 4.Inst. Fluid Science, Tohoku Univ., 5.Fukada Geological Institute, 6.Univ. Witwatersrand, School of Geoscience)

[MIS02-P09] ICDP DSeis 6: Deformation Rate Analysis of the M5.5 aftershock zone core - stress concentration at reflective intrusives

*Kanematsu Makoto[1], Mitsuya Higashi[1], Yasuo Yabe[2], Shuhei Abe[2], Bryan Watson[3], Ray Durrheim[3], Hiroshi Ogasawara[1] (1.Ritsumeikan Univ., 2.Tohoku Univ., 3.Univ. Witwatersrand)

[MIS02-P10] ICDP DSeis 7: compilation of stress information and comparison with calculated stresses in the M5.5 aftershock zones

*Mitsuya Higashi[1], Yasuo Yabe[2], Kosuke Sugimura[1], Akimasa Ishida, Makoto Kanematsu[1], Shunsuke YOSHIDA[1], Ryogo Tadokoro[1], Takatoshi Ito[4], Akio Funato[5], Hiroshi Ogasawara[3] (1.Graduate School of Science and Engineering, Ritsumeikan Univ., 2.Research Center for Prediction of Earthquakes and Volcanic Eruptions, Graduate School of Science, Tohoku University, 3.College of Science and Engineering, Ritsumeikan Univ., 4.Inst. Fluid Science, Tohoku Univ., 5.Fukada Geological Institute)

[MIS02-P11] ICDP DSeis 8: the M5.5 fault structure and reflective intrusives in legacy 3D seismic reflection data

*Noda Taku[1], Musa Manzi[2], Hiroyuki Ogasawara[1], Lindsay Linzer[2], Stephanie Enslin[2], Ray Durrheim[2], Hiroshi Ogasawara[1] (1.Ritsumeikan Univ., 2.Univ. Witwatersrand)

[MIS02-P12] ICDP DSeis 9: are streaks in the M5.5 aftershocks potentially located on highly stressed intrusive?

*Ryogo Tadokoro[1], Katsuya Ishibashi[2], Horiuchi Shigeki[3], Hiroshi Ogasawara[4] (1.Graduate School of Science and Engineering, Ritsumeikan Univ., 2.School of Science and Engineering, Ritsumeikan Univ., 3.Homeseismo ltd., 4.College of Science and Engineering, Ritsumeikan Univ.)

Utilization and curation of frozen core samples in IODP and implementation of the Nagoya Protocol in ocean drilling science

*Nan XIAO[1]

1. Japan Agency for Marine Earthe Science and Technology

Deep biosphere research has become one of the major scientific focuses in ocean drilling science. How to access to core samples with sufficient quality has been a changes for scientists. Currently there are two methods of accessing to deep biosphere samples which are participating in drilling expeditions and requesting samples from core repositories. The Kochi Core Center has curated deep biosphere samples that were processed aseptically and stored at deep frozen (-80 degree C) condition from more than 10 drilling expeditions. Increased scientific attention to microbiological research of the subseafloor envrionment raises the complications and concerns related to adherence to the Nagoya Protocol of the Convention on Biological Diversity (CBD). The Nagoya Protocol is an international agreement that aims to guide countries in developing standart protocols and protections for accessing biological materials, and sharing benefits derived from their utilization. Since its commencement, the Nagoya Protocol has placed international biological research, especially fieldwork, under greater political scrutiny and increased its complexity due to the variation in implementation between nations. We present the central points of the Nagoya Protocol on access and benefit-sharing (ABS) and discuss their relationship to ocean drilling research. In addition, we address the challenges faced by ocean drilling in complying with this internation convention.

Keywords: ocean drilling program, frozen core sample, Nagoya Protocol, convention on biological diversity

©2019. Japan Geoscience Union. All Right Reserved.

In-situ rock strength calculated from drilling parameters. Comparison of results from various sites.

*Adam Wspanialy[1], Yasuhiro Yamada[1], Saneatsu Saito[1], KYAW MOE[1]

1. Japan Agency for Marine-Earth Science and Technology

Drilling parameters are excellent datasets to understand in-situ physical properties of the rock. Continuous core samples along with parameters such as Torque, RPM, WOB and ROP have been collected during drilling operations. The borehole data acquisition was complemented with full LWD/MWD and wireline logging. After core delivery to surface core scratch tests have been carried out to measure Unconfined Compressive Strength (UCS). Our comprehensive approach enabled us to integrate all data and conduct detailed analysis of the in-situ subsurface physical and mechanical properties of a rock cut by a drill bit.

Here we present some results from offshore and onshore drilling experiments carried out in Japan, Oman and Australia. Methods such as Specific Energy (SE) and Equivalent Strength (EST) have been used to estimate in-situ rock properties, namely UCS and analyse drilling process.

Our results demonstrate that the calculated in-situ rock strength based on SE/EST methods correlates well with sonic derived UCS and core scratch derived UCS. Utilised methods also successfully detect fractures in the formation, show developing drilling dysfunctions such as vibration, and bit balling.

Keywords: rock strength, drilling parameters, Specific Energy

©2019. Japan Geoscience Union. All Right Reserved.

Interaction between submarine landslides and subseafloor sedimentary microbiome: Chikyu SCORE Expedition 910 off Cape Erimo

*Tatsuhiko Hoshino[1], Go-Ichiro Uramoto[2], Satoshi Tonai[2], Yuki Morono[1], Akira Ijiri[1], Shino Suzuki[1], Yusuke Kubo[1], Fumio Inagaki[1], Chikyu SCORE Exp. 910 Scientists .

1. Japan Agency for Marine-Earth Science and Technology, 2. Kochi University

During the past decades, scientific ocean drilling has explored the subseafloor sedimentary biosphere down to over 2 kilometers below seafloor (Inagaki et al., 2015). The total biomass and diversity of microbial community in the subseafloor biosphere are comparable to those in the hydrosphere (Kallmeyer et al., 2012). Taxonomic composition of subseafloor microbial communities are distinct from those of other habitats on Earth’ s surface, such as ocean and soil, inferring that adaptive evolution of microbial community to the energy-limited deep sedimentary habitats have occurred. In a previous study of bioturbated layers in surface marine sediments, it has been reported that seawater-migration by macrofauna activity during the initial depositional stage notably affected microbial community structures (Chen et al. 2017). Similarly, it can be hypothesized that submarine landslides have introduced easily degradable fresh organic matter and dissolved electron acceptors (e.g., oxygen, sulfate) to the sedimentary habitats, and consequently caused a shift of microbial communities and its function.

In 2017, we conducted the Chikyu’ s first SCORE Expedition 910 at the Hidaka Trough off Cap Erimo and obtained sediment cores down to 100 meters below the seafloor. In the core column, four intervals of deformed sediments were identified, indicating the occurrences of multiple submarine landslides in this area. In those deformed sediment intervals, we observed no clear anomaly in the profile of cell abundance, which decrease with sediment depth as generally seen in the other subserfloor sediments. In addition, pore water chemistry data do not show clear anomaly either, indicating recovery of sediment geochemistry from the turbation caused by landslides. While both profiles of microbial cell abundance and pore water geochemistry did not show anomaly in the deformed sediment intervals, the DNA-based analyses, showed some unusual appearances of microbial taxa relative to the depth, suggesting the potential migration of microbes from the upper horizons by submarine landslides.

Reference

Inagaki F, et al (2015). Science 349: 420-424; Kallmeyer J, et al (2012). Proc Natl Acad Sci U S A 109: 16213-16216; Chen X, et al (2017). Sci Rep 7: 2400.

Keywords: Chikyu SCORE, Deep biosphere, Mass transport deposit

©2019. Japan Geoscience Union. All Right Reserved.

High-resolution continuous records of the chemical composition of the marine sediment off Cape Erimo, Hokkaido, Japan

*Masafumi MURAYAMA[1], Shinsuke Yagyu[3], Satoshi Tonai[2], Go-Ichiro Uramoto[3], Yasuhiro Yamada[4], Fumio Inagaki[4], Yusuke Kubo[5]

1. Faculty of Agriculture and Marine Science, Kochi University, 2. Faculty of Science and Technology, Kochi University, 3. Center for Advanced Marine Core Research, Kochi University, 4. Research and Development Center for Ocean Drilling Science, JAMSTEC, 5. Center for Deep Earth Exploration, JAMSTEC

About 100 m sediment cores were taken from off Cape Erimo, Hokkaido, Japan on the Shallow Core Program (SCORE) by D/V Chikyu in 2017. The sedimentary sequence is intercalated with mass transport deposits caused by earthquake-triggered submarine landslides and/or climate changes. Here we report a result of high-resolution continuous geochemical composition of these cores using XRF core scanning technique.

Keywords: sediment core off Cape Erimo, XRF core scanner (ITARX), Shallow Core Program (SCORE), D/V Chikyu

©2019. Japan Geoscience Union. All Right Reserved.

Thermal property measurements of core samples retrieved from Futagawa fault drilling

*Terasu Sano[1], Weiren Lin[1], Susumu Shibutani[1,2], Nana Kamiya[1], Tatsuhiro Sugimoto[1], Kazuya Ishitsuka[1], Aiming Lin[3]

1. Graduate School of Engineering, Kyoto University, 2. Chi-ken Sogo Consultants Co., Ltd.,, 3. Graduate School of Science, Kyoto University

In 2017~2018, to retrieve rock samples from the Futagawa fault ruptured during the 2016 Kumamoto earthquake in Japan, a borehole was drilled down to 700 m depth through the fault in Mashikimachi, Kumamoto prefecture located in the southwest of the Aso volcano. In this borehole, temperature depth profile was measured from ~50 m to ~650 m below the surface (Lin et al., 2019 JpGU). As a preliminary result, an anomaly of temperature, about 1 ℃/km geothermal gradient, was found in the depth range of 310 - 430 m (Lin et al., 2019 JpGU). To examine if this this temperature anomaly comes from thermal conductivity change of the ricks, we collected rock core samples from the borehole and measured their thermal properties.

We measured density, porosity and three thermal transport properties (thermal conductivities, thermal diffusivities, specific heat capacities) of 20 cores drilled from the borehole in the depth range from 300 m to 700 m. I selected typical rock cores to cover not only the depth intervals and also all the main rock types. The rock types of cores are basal sedimentary rocks in 300 m - 353 m , andesite in 353 m - 514 m, sandstone and/or conglomerate in 514 m - 562 m, and tuff in 562 m - 700 m. Measured wet densities and porosities are 1.57 g/cm^3 - 2.02 g/cm^3, 40.0% - 47.8% for basal sedimentary rocks, 2.31 g/cm^3 - 2.95 g/cm^3, 3.1% - 25.5% for andesite, 2.29 g/cm^3 - 2.41 g/cm^3, 21.6% - 29.4% for sandstone and/or conglomerate, 1.99 g/cm^3 - 2.29 g/cm^3, 9.4 % - 35.8% for tuff. Measured thermal conductivities are 0.88 W/(mK) - 1.10 W/(mK) for basal sedimentary rocks, 1.00 W/(mK) - 1.81 W/(mK) for andesite, 1.26 W/(mK) - 1.31 W/(mK) for sandstone and/or conglomerate, 0.96 W/(mK) - 1.27 W/(mK) for tuff. And measured thermal diffusivities and specific heat capacities are 0.85 J/(g･K) - 3.46 J/(g･K) for alluvium, 0.48 m^2/s - 0.91 m^2/s, 1.36 J/(g･K) - 2.60 J/(g･K) for andesite, 0.49 m^2/s - 0.66 m^2/s, 1.95 J/(g･K) - 2.70 J/(g･K) for sandstone and/or conglomerate, 0.40 m^2/s - 0.99 m^2/s, 1.40 J/(g･K) - 2.93 J/(g･K) for tuff. From data of measured temperature of borehole and thermal conductivities of the cores, we calculated heat flow of in the borehole. Using this heat flow and thermal conductivities, we reconstructed the temperature profile in the borehole.

In this estimation, we couldn't reproduce the anomaly of measured temperature. So we conclude that the anomaly of measured temperature is not caused by the significant change of the thermal conductivity in 310 m - 430 m depth.

Keywords: Drilling, thermal properties, Temperature

©2019. Japan Geoscience Union. All Right Reserved.

Results of geotechnical tests on shallow sediment cores recovered from Lord Howe Rise, off eastern Australia: Implications for future Lord Howe Rise riser drilling

*Takamitsu Sugihara[1], Kan Aoike[1], Saneatsu Saito[2], Tatsuya Murayama[1], Kentaro Takeda[1], Takuya Onodera[3], Ayumi Sumikawa[3], Yukari Kido[1], Yoshinori Sanada[1]

1. Center for deep earth exploration, Japan Agency for Marine-Science and Technology, 2. Research and development center for ocean drilling science, Japan Agency for Marine-Science and Technology, 3. Nippon Marine Enterprises, Ltd.

Lord Howe Rise (LHR) Drilling Project (871-CPP2) is an accepted IODP drilling proposal to reconstruct Cretaceous tectonic history of northern Zealandia, designated as a Chikyu riser drilling project. In order to plan a riser drilling operation, it is important to evaluate mechanical strength and physical properties of shallow sediment (0 to 100 or 200 meters below sea floor, mbsf) for setting Blow-out Prevention (BOP) system and riser with heavy weight on the seafloor. Geotechnical core test (e.g., triaxial compressive test and consolidation test) is an essential work to directly measure rock strength and physical properties of geological materials. Therefore, the geotechnical core tests are usually conducted for the surface sediment to evaluate their mechanical and physical properties. In the LHR region, calcareous sediment is broadly and predominantly distributed, and clayey sediment is not observed in shallow sediments. In general, deep seafloor is composed of clayey sediment, and their mechanical and physical properties are well understood. However, mechanical and physical properties of calcareous sediment in both ambient and confined pressure conditions are not well known.

In this study, results of geotechnical test for shallow cores taken in the LHR region are presented, and characteristics of mechanical and physical properties (especially shear strength and permeability) are discussed.

Shallow cores for geotechnical test were taken by R/V Kairei with a gravity piston corer in KR17-15C and by D/V JOIDES Resolution with a rotary core barrel (RCB) in Expedition 371. The gravity piston coring by R/V Kairei was conducted at the proposed riser drilling sites DLHR-5A and -3A, and two cores with approximately 7 m length were taken at each site. The RCB coring by D/V JOIDES Resolution was conducted at Site U1506 in Expedition 371. A whole-round sample with 40 cm length was taken from U1506A-13R for our investigation, and depth of the whole-round sample is 116.5 mbsf. In order to measure physical and mechanical properties for the core samples, geotechnical tests of Penetrometer test, Bulk density, Grain density, Liquid limit, Plastic limit, Grain size distribution, Constant rate of strain consolidation test (CRSC test), and Triaxial compressive strength test with pore pressure measurement (Consolidated-Undrained conditions) were carried out.

Most of the tests except penetrometer test were carried out by OYO Co. Procedures of those measurements and tests were based on the regulations established by Japanese Geotechnical Society (JGS) and Japanese Industrial Standards (JIS). Those are almost the same as their regulations in the ASTM.

All of core samples are composed of calcareous ooze, and grain size distribution of the core samples shows clay size fraction (less than 5 micro meters) is dominant (more than 80 %).

©2019. Japan Geoscience Union. All Right Reserved.

Based on the bulk density data, overburden stresses were calculated and consolidation pressures corresponding to depth of 10 to 240 mbsf for the triaxial test were estimated assuming k0 compaction (k0 factor = 0.5). The result of the triaxial test show shear strength profile gradually increases with depth and is almost identical to those of clayey sediment from Kumano Basin and Nankai Trough. However, the result of the penetrometer test indicates that shear strength of calcareous ooze under ambient condition is quite lower than those of clayey sediment. This observation suggests mechanical strength of calcareous ooze is easily released with depressurizing of sediment.

Based on the result of the CRSC test, it is indicated that calcareous ooze shows no obvious preconsolidation stress, and this result is in good agreement with the result of the triaxial test mentioned above. Permeability of calcareous ooze calculated from the CRSC test results is similar to sandy sediment and the results indicate calcareous ooze is more permeable as compared with clayey sediment.

Those results will be dedicated to analysis for the riser operation in the LHR area.

Keywords: Lord Howe Rise, Riser drilling, Rock strength test, Shear strength, Permeability

©2019. Japan Geoscience Union. All Right Reserved.

ICDP DSeis 4: Drilling, core logging, and in-hole geophysical logging of ICDP DSeis drilling into the M5.5 aftershock zones in a South African gold mines.

*Shunsuke YOSHIDA[1], Tadokoro Ryogo[1], Kosuke Sugimura[1], Kanematsu Makoto[1], Mitsuya Higashi[1], Benni Liebenberg[2], Esterhuizen van Heerden[2], Stephen Tau[3], Siyanda Mngadi[3], Ray Durrheim[3], Martin Ziegler[4], Yusuke Mukuhira[5], Ronald Conze[6], Yasuo Yabe[7], Shunya Kaneki[8], Yuki Yokoyama[9], Nomqhele Nkosi[10], Dave Roberts[10], Sifiso Buccio[11], Hiroshi Ogasawara[1]

1. Graduate school of science and engineering, Ritsumeikan , 2. Moab Khotsong mine, Vijoenskroon, 3. Univ. Witwatersrand, School of Geoscience, 4. ETH, Zurich Dep. Earth Sciences, 5. Inst. Fluid Science, Tohoku Univ., 6. GFZ, Potzdam, 7. Graduate School of Science, Tohoku Univ., 8. Disaster Prevention Research Inst., Kyoto Univ., 9. Graduate School of Science,Osaka Univ., 10. Mandela Mining Precinct, CSIR, 11. Council for Geoscience

ICDP drilling into the aftershock zone of the 2014 M5.5 earthquake near Orkney, South Africa commenced on 2017 and was completed in 2018. This M5.5 earthquake started from a depth about 5 km and ruptured West Rand Group below mining horizon on unknown geological structure in a deep gold mine. The mechanism of left-lateral slip of this M5.5 earthquake contradicted normal-faulting mechanisms of typical mining-induced earthquakes on mining horizons. The upper fringe of the aftershock zone was several hundreds of meters from the deepest level of the mine. Two NQ holes were collared at a depth of 2.9 km (95 level) below surface at a deep gold mine. Hole A (817m) deviated too much to intersect the M5.5 fault but Hole B (700m) intersected the M5.5 fault. A 3-m double-tube couldn't recover the fault material much, while a 1.5m triple-tube could recover the fault material more in Hole C branched from 544 m in Hole B. Geophysical logging, core logging, and water/gas monitoring followed drilling. All the core was transported to Mandela Mining Precinct, CSIR, Johannesburg and systematically described and scanned by the ICDP DMT scanner. Some of the core were selected for core stress measurements.

In JpGU 2019 meeting, nine papers (ICDP DSeis 1-9) report on the outcomes. This poster (ICDP DSeis 4) compiles drilling, core logging, and in-hole geophysical logging of ICDP DSeis drilling into the M5.5 aftershock zones in a South African gold mines. A core orientation tool was used during drilling but not 100% reliable because there was a case that a bottom line in a core run was different by more than 90 degrees from the bottom line in the next core run. We elaborated to compare OTV image with core to carefully check the core orientation. The modified core orientation allowed us to modify the maximum stress direction that Ishida et al. (2018) measured. We could confirm good consistency with borehole breakout analysis (Richenbacher 2018; ETH master thesis). We will report on other associated outcomes. Refer other papers (ICDP DSeis 1-3, 5-9) for other related outcomes.

Acknowledgement: The DSeis team includes co-authors of the papers ICDP DSeis 2-9 and members shown at https://www.icdp-online.org/projects/world/africa/orkney-s-africa/details/. We thank Harmony Gold, Anglogold Ashanthi, Lesedi, Digital Surveying, OHMS, Seismogen, 3D Geoscience. ICDP, JSPS, SA NRF, MEXT Japan, US NSF, German DRF, and Ritsumeikan Univ. financially support the project.

©2019. Japan Geoscience Union. All Right Reserved.

©2019. Japan Geoscience Union. All Right Reserved.

ICDP DSeis 5: Diametrical Core Deformation Analysis of the M5.5 aftershock zone core - stress concentration at reflective intrusives and transition in stress regimes.

*Kosuke Sugimura[1], Shunsuke YOSHIDA[1], Ryogo Tadokoro[1], Hiroshi Ogasawara[2], Akimasa Ishida, Yasuo Yabe[3], Takatoshi Ito[4], Akio Funato[5], Siyanda Mngadi[6], Ray Durrheim[6]

1. Graduate school of science and engineering, Ritsumeikan, 2. College of Science and Engineering, Ritsumeikan Univ., 3. Graduate School of Science, Tohoku Univ., 4. Inst. Fluid Science, Tohoku Univ., 5. Fukada Geological Institute, 6. Univ. Witwatersrand, School of Geoscience

ICDP drilling into the aftershock zone of the 2014 M5.5 earthquake near Orkney, South Africa commenced on 2017 and was completed in 2018. Drilling was designed to minimize damage on core and borehole, being able to maximize core recovery. Hole A (817m) was drilled in 2017. It unfortunately didn't intersect the M5.5 fault, running eventually sub-parallel and roughly 100m from the aftershock zone. As the hole was stable we could recover almost 100% of core from the area traversing the periphery of the M5.5 aftershock zone for a distance of several hundreds of meters. Ishida et al. (2018) carried out Diametrical Core Diameter Analysis (Ito and Funato, 2017). This analysis measures the change in core diameter with roll angle around the core axis, which was caused by a relief of anisotropic stress during drilling. We used this analysis because (1) the expected stress was too high for hydrofracturing method, (2) uncertainty in stress magnitude is unavoidable in damage interpretations, (3) DSeis hole were too long for overcoring technique, and (4) DCDA is non-destructive and very easy to make if core is recovered. Ishida et al. (2018) measured 186 pieces of core from Hole A (817m collared at 2.9km depth) that were recovered near the M5.5 aftershock zone. They successfully illustrated spatial variation in differential stress in a plane perpendicular to Hole A axis. They found stress concentration at intrusives with one located at the depth of the upper fringe of the M5.5 aftershock zone. We carried out additional measurement for the remaining part of Hole A and Hole B. With additional data measured at adjacent locations, we could confirm that the stress concentration Ishida et al (2018) found at intrusives was not an outlier. We will report how Hole B that intersected the M5.5 fault differ from Hole A stress.

This is one of nine ICDP DSeis papers (ICDP DSeis 1-9) presented in JpGU 2019. Refer other papers for other topic on drilling, logging, other stress measurement, fault materials, comparison with calculated stress, legacy 3D seismic reflection data, and relocated aftershocks.

©2019. Japan Geoscience Union. All Right Reserved.

ICDP DSeis 6: Deformation Rate Analysis of the M5.5 aftershock zone core - stress concentration at reflective intrusives

*Kanematsu Makoto[1], Mitsuya Higashi[1], Yasuo Yabe[2], Shuhei Abe[2], Bryan Watson[3], Ray Durrheim[3], Hiroshi Ogasawara[1]

1. Ritsumeikan Univ., 2. Tohoku Univ., 3. Univ. Witwatersrand

ICDP drilling into the aftershock zone of the 2014 M5.5 earthquake near Orkney, South Africa commenced on 2017 and was completed in 2018. Ishida et al. (2018) and Sugimura et al. (2019; ICDP DSeis 5) report on spatial variation of differential stress in a plane perpendicular to the borehole axis. It is ideal to have different stress component especially at critical location where significant characteristics were found. Deformation Rate Analysis (Yamamoto, 2009) can measure stress in any direction although the method takes time and the specimen are not reusable for other test. So, we planned to selected samples where characteristic spatial variation was found by DCDA method (Ishida et al. 2018 and Sugimura et al. 2019). It was confirmed also in normal stress component along the borehole axis that stress was concentrated at the intrusive at about 400m.

This is one of nine ICDP DSeis papers (ICDP DSeis 1-9) presented in JpGU 2019. Refer other papers for other topics on drilling, logging, other stress measurement, fault materials, comparison with calculated stress, legacy 3D seismic reflection data, and relocated aftershocks.

Acknowledgement: The DSeis team includes co-authors of the papers ICDP DSeis 2-9 and members shown at https://www.icdp-online.org/projects/world/africa/orkney-s-africa/details/. We thank Harmony Gold, Anglogold Ashanthi, Lesedi, Digital Surveying, OHMS, Seismogen, 3D Geoscience. ICDP, JSPS, SA NRF, MEXT Japan, US NSF, German DRF, and Ritsumeikan Univ. financially support the project.

Keywords: Seismogenic zone, Stress Measurement, DRA

©2019. Japan Geoscience Union. All Right Reserved.

ICDP DSeis 7: compilation of stress information and comparison with calculated stresses in the M5.5 aftershock zones

*Mitsuya Higashi[1], Yasuo Yabe[2], Kosuke Sugimura[1], Akimasa Ishida, Makoto Kanematsu[1], Shunsuke YOSHIDA[1], Ryogo Tadokoro[1], Takatoshi Ito[4], Akio Funato[5], Hiroshi Ogasawara[3]

1. Graduate School of Science and Engineering, Ritsumeikan Univ., 2. Research Center for Prediction of Earthquakes and Volcanic Eruptions, Graduate School of Science, Tohoku University, 3. College of Science and Engineering, Ritsumeikan Univ., 4. Inst. Fluid Science, Tohoku Univ., 5. Fukada Geological Institute

ICDP drilling into the aftershock zone of the 2014 M5.5 earthquake near Orkney, South Africa commenced on 2017 and was completed in 2018. Spatial variation in stress was measured by Ishida et al. (2018) and Sugimura et al. (2019; ICDP DSeis 5) by DCDA method (Funato and Ito, 2017) and Kanematsu et al. (2019; ICDP DSeis 6). This poster reports on compilation of stress information including the other information sources and compares with calculated stress.

We first compared with a 3D stress state that Ogasawara et al. (2012) measured in 2011 at 98L (3.0 km depth from surface). We assume zero stress on surface, the measured 3D stress (normal faulting stress regime) at 3.0 km, and stress linearly increasing with depth. The calculated stress was consistent with DCDA results measured in the initial 100m section in Hole A, while inconsistent in deeper section. The calculated direction of maximum stress in a plane perpendicular to the borehole axis was also inconsistent with the measured stress information (Yoshida et al. 2019 JpGU; ICDP DSeis 5). Except for the stress concentration measured at intrusives, the measured DCDA results were systematically lower than the calculated stress. In a stress regime that caused the left-lateral horizontal slip on the M5.5 fault, horizontal stress should be larger, which will increase horizontal stress component in a plane perpendicular to the Hole A axis. This increase should decrease difference in stress in the plane perpendicular to the Hole A axis. By JpGU 2019, we will make additional effort to interpret more from the comparison between the measured and calculated stress.

This is one of nine papers (ICDP DSeis 1-9). Refer other papers for other topic on drilling, logging, other stress measurement, fault materials, legacy 3D seismic reflection data, and relocated aftershocks.

Acknowledgement: The DSeis team includes co-authors of the papers ICDP DSeis 2-9 and members shown at https://www.icdp-online.org/projects/world/africa/orkney-s-africa/details/. We thank Harmony Gold, Anglogold Ashanthi, Lesedi, Digital Surveying, OHMS, Seismogen, 3D Geoscience. ICDP, JSPS, SA NRF, MEXT Japan, US NSF, German DRF, and Ritsumeikan Univ. financially support the project.

©2019. Japan Geoscience Union. All Right Reserved.

ICDP DSeis 8: the M5.5 fault structure and reflective intrusives in legacy 3D seismic reflection data

*Noda Taku[1], Musa Manzi[2], Hiroyuki Ogasawara[1], Lindsay Linzer[2], Stephanie Enslin[2], Ray Durrheim[2], Hiroshi Ogasawara[1]

1. Ritsumeikan Univ., 2. Univ. Witwatersrand

ICDP drilling into the aftershock zone of the 2014 M5.5 earthquake near Orkney, South Africa commenced on 2017 and was completed in 2018. Hiroyuki et al. (2017 AGU) reported on legacy seismic reflection to analyze geological structures in the southern most area of the M5.5 aftershock zones. They found vertical structures in four 2-D lines that were potentially responsible for the M5.5 earthquake and illustrated cross-cutting relations of the M5.5 structure and other known faults that dislocated gold reefs more than several hundreds of meters both horizontally and vertically. Another legacy seismic reflection data which was recorded in 1996 and covered much wider area of the M5.5 aftershock zone was found. We calibrated velocity structure by tying with borehole data including DSeis Holes A and B, we found some of intrusives (sills) that Hole A and B were strong reflectors in the legacy 3D seismic reflection data.

Aftershocks located by in-mine 46 geophones are dense at the southern upper fringe, with a sharp cut-off dipping about 20 degrees to the south; some clear stripes of aftershocks are also seen, in parallel to the upper fringe (Tadokoro et al., JpGU2019, ICDP DSeis 9). It is interesting to note that the reflector (sills) are also in parallel to the upper fringe of the aftershock zone and the aftershock stripes. It is also notable that stress concentration is reported at the intrusives by Sugimura et al. (JpGU2019; ICDP DSeis 5) and Kanematsu et al. (JpGU2019; ICDP DSeis 6). Some mechanism that controls the extent of the aftershocks should exist.

This paper is one of nine papers (ICDP DSeis 1-9). Refer other papers for other topics, e.g. on drilling, logging, stress measurements and evaluation, fault materials, and relocated aftershocks.

Acknowledgement: The DSeis team includes co-authors of the papers ICDP DSeis 2-9 and members shown at https://www.icdp-online.org/projects/world/africa/orkney-s-africa/details/. We thank Harmony Gold, Anglogold Ashanthi, Lesedi, Digital Surveying, OHMS, Seismogen, 3D Geoscience. ICDP, JSPS, SA NRF, MEXT Japan, US NSF, German DRF, and Ritsumeikan Univ. financially support the project.

Keywords: ICDP DSeis, The M5.5 seismogenic zone, Seismic reflection

©2019. Japan Geoscience Union. All Right Reserved.

ICDP DSeis 9: are streaks in the M5.5 aftershocks potentially located on highly stressed intrusive?

*Ryogo Tadokoro[1], Katsuya Ishibashi[2], Horiuchi Shigeki[3], Hiroshi Ogasawara[4]

1. Graduate School of Science and Engineering, Ritsumeikan Univ., 2. School of Science and Engineering, Ritsumeikan Univ., 3. Homeseismo ltd., 4. College of Science and Engineering, Ritsumeikan Univ.

ICDP drilling into the aftershock zone of the 2014 M5.5 earthquake near Orkney, South Africa commenced on 2017 and was completed in 2018. Aftershocks located by in-mine 46 geophones are dense at the southern upper fringe, with a sharp cut-off dipping about 20 degrees to the south. Some clear stripes of aftershocks are also seen, in parallel to the upper fringe. It is interesting to note that the reflector (sills) are also in parallel to the upper fringe of the aftershock zone and the aftershock stripes. It is also notable that stress concentration is reported at the intrusives by Sugimura et al. (JpGU2019; ICDP DSeis 5) and Kanematsu et al. (JpGU2019; ICDP DSeis 6). Some mechanism that controls the extent of the aftershocks should exist.

In order to discuss further, we relocated aftershocks with the Double-Difference method (Waldhouser and Ellsworth, 2004). At the moment, we could relocate only 60 events at the upper fringe of the aftershocks. We used in-mine seismic network data of Anglogold Ashanti. P- and S- arrival times that the algorithm of Horiuchi et al. (2011) was used. A sharper alignment of aftershocks is successfully illustrated. By JpGU 2019, we will make additional efforts to extend the area of relocation to discuss more.

Acknowledgement: The DSeis team includes co-authors of the papers ICDP DSeis 2-9 and members shown at https://www.icdp-online.org/projects/world/africa/orkney-s-africa/details/. We thank Harmony Gold, Anglogold Ashanthi, Lesedi, Digital Surveying, OHMS, Seismogen, 3D Geoscience. ICDP, JSPS, SA NRF, MEXT Japan, US NSF, German DRF, and Ritsumeikan Univ. financially support the project.

©2019. Japan Geoscience Union. All Right Reserved.

[J] Poster | M (Multidisciplinary and Interdisciplinary)：M-IS Intersection

Mon. May 27, 2019 1:45 PM - 3:15 PM JST | Mon. May 27, 2019 4:45 AM - 6:15 AM UTC | Poster Hall International Exhibition Hall8, Makuhari Messe_7

[M-IS08] Geopark

convener:Takayuki Ogata(Disaster Prevention Research Center for Island Regions, University of the Ryukyus), Tatsuto Aoki(School of Regional Development Studies, Kanazawa University), Noritaka Matsubara(Graduate School of Regional Resource Management, University of Hyogo), Keiichi Tadokoro(Research Center for Seismology, Volcanology and Earthquake and Volcano Research Center, Nagoya University)

This session targets interdisciplinary and multidisciplinary discussion on geopark, involving geoheritage, geodiversity, geoconservation, geotourism, sustainable development, governance, risk management, science communication and geoscientific education. These topics contribute to scientific and attractive activities in geoparks.

[MIS08-P01] The efforts of Mt.Daisetsu-Kamuymintar Geopark Project

*hideyuki kawabe[1] (1.大雪山カムイミンタラジオパーク構想推進協議会)

[MIS08-P02] Re-examination of meaning indicated by "Nigori-Sumi (Muddy and clear) Bridge"~Turbidity Characteristic of Meeting Point of the Ushikubi River and the Ozo River, in Hakusan Tedorigawa Geopark ~

*Tatsuto Aoki[1] (1.School of Regional Development Studies, Kanazawa University)

[MIS08-P03] Efforts of ‘Grant-in-aid for Science Research in San’in Kaigan UGGp’

*Suzuka Koriyama[1] (1.Sanin Kaigan Geopark Promotion Council)

[MIS08-P04] Practical applications in the Tosashimizu Geopark Plan of site monitoring by local residents: Landform change of Sakurahama Beach

*Satoru Imai[1], Hisaaki Sato[1], Yorihisa Hirano (1.Tosashimizu Geopark Promotion Council)

[MIS08-P05] Geological and geomorphological environment of the Jikumaru terraced paddy field (one of the Top 100 Terraced Paddy Fields in Japan) in the Oita Bungoono Geopark

*Toshikazu Yoshioka[1] (1.Oita Bungoono Geopark Promotion Council)

[MIS08-P06] The relationship of land utilization and vegetation at the Jikumaru terraced paddy field in the Oita Bungoono Geopark

*Miki Iwasato[1], Toshikazu Yoshioka[2] (1.Bungoono City, Trade, Industry and Tourism Division, 2.Oita Bungoono Geopark Promotion Council)

[MIS08-P07] **Outreach activities of Aso UNESCO Global Geopark**

*Tsuneomi Kagiyama[1], Kazunori Watanabe[1], Shinichiro Ikebe[1], Akinobu Ishimatsu[1], Katsunori Toyomura[2], Natsuko Kodama[1], Shuhei Takamori[1], Shino Miyakita[1] (1.Aso Geopark Promotion Council, 2.Aso Volcano Museum)

[MIS08-P08] Geoscientific Setting and Educational Significances of Yonaguni Island in the Ryukyu Arc, Eastern Asia

*Takayuki Ogata[1], Masakazu Nara[2], Makoto Otsubo[3], Tadahiro Shibata[4] (1.Disaster Prevention Research Center for Island Regions, University of the Ryukyus, 2.Sciences Unit, Natural Sciences Cluster, Research and Education Faculty, Kochi University, 3.Geological Survey of Japan, Research Institute of Earthquake and Volcano Geology, 4.The Unit of Natural Monuments, Monuments and Sites Division, Cultural Properties Department, Agency for Cultural Affaire)

The efforts of Mt.Daisetsu-Kamuymintar Geopark Project

*hideyuki kawabe[1]

1. -

In this area, we are promoting the "Mt.Daisetsu-Kamuymintar Geopark Project" ranging from Asahikawa City, Takasu Town, Higashikagura Town, Pippu Town, Tohma Town, Aibetsu Town, Kamikawa Town and Higashikawa Town.
We set up a preparatory organization by authorized municipalities and civil society in 2017, As an aiming area we joined the Japan Geopark Network as an associate member, in the background of resident activities such as "Kamuy's Earth" Geo-Tour and Geo-Forum etc. that "Association of Asahikawa Geoparks" has been doing since 2012.
We have been shifted promotion system to a council added by business organizations and others in August 2018.
In this presentation, we introduce Mt.Daisetsu-Kamuymintar Geopark Project and its efforts.

©2019. Japan Geoscience Union. All Right Reserved.

Re-examination of meaning indicated by "Nigori-Sumi (Muddy and clear) Bridge" ~Turbidity Characteristic of Meeting Point of the Ushikubi River and the Ozo River, in Hakusan Tedorigawa Geopark ~

*Tatsuto Aoki[1]

1. School of Regional Development Studies, Kanazawa University

Two main flow paths consisting the Tedori river water system that flows through the Hakusan Tedorigawa Geopark, the Ushikubi River, the main stream path, originating from the west side of Mt. Hakusan, and the Ozo River, tributary originating from the former the north of Mt. Hakusan. These two flow paths join in the vicinity of the "Nigori-Sumi Bridge" in the Seto area, then turn northward as the Tedori River. The word of "Nigori-Sumi" means "Muddiness and clearness" and this shows the difference in the turbidity between the two flow paths. On the webpage of Hakusan Tedorigawa Geopark, it is written as follows and is accompanied by photographs showing the state that high turbidity water and low water are joining.

“There is a point that the Ozo River meets the Tedori River, and only the Ozo River didn’ t settle down for a while during rugged weather, so it is sometimes possible to see a two-colored flow, muddy and clear water, at the meeting point. Thus this bridge was named Nigorisumi Bridge (nigori means muddy and sumi means clear).”

In this report, the author measured the turbidity of these two flow paths, organized the relationship with artificial river management, and re-examined the meaning of today's word of "Nigori-Sumi".

The Ushikubi River originated form Hakusan Gozengamine (2702 m), and Ozo River originated from Hakusan Onanjimine (2684 m), and joins at an altitude of 240 m near the Nigori-Sumi Bridge. The length of the flow path to the confluence point is 34.3 km for the Ushikubi River (average bed slope 71.8 ‰), and 24.5 km for the Ozo River (107.9 ‰). The Ozo River is steeper than the

Ushikubi River. Many of landslides are distributed in the both basin. However, it is believed that there was a crater of Paleo-Hakusan volcano in the Jigokudani of the Ozo River basin (Nagaoka, 1972), and severe degeneration is recognized. The Tedori dam is built in the Ushikubi River, and its flow is controlled by that dam. On the other hand, there is no artificial dam and the flow is not controlled in the Ozo River.

Five sites for water sampling are set in the basin, and sampled water immediately after the large-scale flood caused by the typhoon. As a result, immediately after large-scale flooding, the flow rate and turbidity are high in the Ozo River where the flow rate is not controlled and the geology of the catchment area is brittle. On the other hand, On the Ushikubi River controlled by a dam, water and suspended sediment are stored in the dam, so the increase in flow rate and turbidity is suppressed. As a result, in the vicinity of Nigori-Sumi bashi Bridge, the Ozo River becomes "muddy" and the Ushikubi River becomes "clear". When

©2019. Japan Geoscience Union. All Right Reserved.

time passes after flooding, the flow rate rapidly approaches the base flow rate in the Ozo River, and the contents of suspended sediment also decreases. On the contrary, in the Ushikubi River where discharge from the dam continues, the flow rate and turbidity is kept high because of the spouting water from the dam. As a result, the situation occurred where the Ushikubi River was "muddy" and the Ozo River was "clear".

Keywords: Hakusan Tedorigawa Geopark, turbidity, artificial dam

©2019. Japan Geoscience Union. All Right Reserved.

Efforts of ‘Grant-in-aid for Science Research in San’ in Kaigan UGGp’

*Suzuka Koriyama[1]

1. Sanin Kaigan Geopark Promotion Council

The San’ in Kaigan UNESCO Global Geopark is a bounded area comprising the entire municipalities of Kyotango City in Kyoto Prefecture; Toyooka City, Kami Town, and Shin’ onsen Town in Hyogo Prefecture; and Iwami Town in Tottori Prefecture; and the northern part of the municipality of Tottori City in Tottori Prefecture.
The San’ in Kaigan UGGp provides territorial cohesion as an area featuring natural scenery with a wide variety of rocks, strata, coastal landforms, and inland waterfalls and gorges, which show the span of history from the times when the Japanese Archipelago was not yet separated from the Asian Continent, through the formation of the Japan Sea, to the present. The Geopark area has also been home to unique human lifestyles based on such natural features.

In 2007, San’ in Kaigan Geopark Promotion Council was established. San’ in Kaigan Geopark was certified as a member of Japanese Geoparks Network (JGN) in 2008 and Global Geoparks Network (GGN) in 2010.

Since the foundation, grant-in-aid program for science research has been conducted. For the revalidation of GGN every four years, this research program plays the important role. This program called ‘Grant-in-aid for Science Research in San’ in Kaigan UGGp’ has been continued since 2009. Through this program, we have awarded 77 researches the grants.
On the other hand, current conditions and challenges are that the latest researches reported every year are not used enough to activate Geopark.

In this presentation, we discuss how this 10-year program had effected on San’ in Kaigan UGGp and researchers who awarded the grant.

©2019. Japan Geoscience Union. All Right Reserved.

Practical applications in the Tosashimizu Geopark Plan of site monitoring by local residents: Landform change of Sakurahama Beach

*Satoru Imai[1], Hisaaki Sato[1], Yorihisa Hirano

1. Tosashimizu Geopark Promotion Council

In order to properly manage sites in the geopark, utilizing site monitoring surveys to understand site change over time is important. The Tosashimizu Geopark Plan Committee is at the center of all monitoring surveys in Tosashimizu and the fact that it allows for many different people to easily get involved and cooperate is an advantage. However, it can be said that the term and frequency of monitoring surveys has been inadequate. As a result, the scientific value of the geosites has become beset by problems. Therefore, the Tosashimizu Geopark Plan Committee has begun to supplement its informational database with pictures and research gathered by local residents of the respective geosites. In addition, local residents have been accumulating such data before becoming involved with geopark activities. It is an important role of the Tosashimizu Geopark Plan Committee specialists to teach local residents about the scientific value of their research.
The focus of this presentation, Sakurahama beach, is a pocket beach located in central Tosashimizu. It has been renowned as a place of scenic beauty since the Edo period. It is known that flat coasts such as Sakurahama beach are easily affected by human influence and environmental changes and local residents have been aware of the reduction of the beach area over time. Also, Sakurahama beach is a spawning ground that many living organisms temporarily inhabit. Consequently, detailed monitoring studies are highly significant. One local resident, Hirano Yorihisa, takes photographs of the same area of Sakurahama beach almost every day. In those pictures, the changes in landform before and after typhoons, the change in granularity of beach sand over time, and loggerhead sea turtle hatchlings can be evidenced. This presentation will analyze the photographic records of Hirano Yorihisa and discuss the future prospects for such research.

Keywords: geopark, geosite, preservation, monitoring, sandy beach

©2019. Japan Geoscience Union. All Right Reserved.

Geological and geomorphological environment of the Jikumaru terraced paddy field (one of the Top 100 Terraced Paddy Fields in Japan) in the Oita Bungoono Geopark

*Toshikazu Yoshioka[1]

1. Oita Bungoono Geopark Promotion Council

The Jikumaru terraced paddy field in the Oita Bungoono Geopark is selected as one of the Top 100 Terraced Paddy Fields in Japan. This area is placed between the Ono and Ogata Rivers and the terraced paddy fields are developed in the small and shallow valleys. The bedrock of this area consists of the sandstone and conglomerate of the Late Cretaceous Onogawa Group Ryozen Formation. The non- to weakly welded Aso-3 and Aso-4 pyroclastic flow deposits covered over the Onogawa Group. The Aso-4 pyroclastic flow deposit along the Ono and Ogata Rivers is densely welded. It indicates the sedimentary rocks of the Onogawa Group formed small hills before the Aso-3 and Aso-4 pyroclastic flows. The pyroclastic flow deposits are thin and easy to erode. Accordingly, the small and shallow valleys where terraced paddy fields are developed are formed in this area. The formation of the Jikumaru terraced paddy field is related to the geology and geomorphology of this area and it may be one of the important elements of the Oita Bungoono Geopark.

Keywords: Jikumaru terraced paddy field, Top 100 Terraced Paddy Fields in Japan, Onogawa Group, Aso pyroclastic flow, Oita Bungoono Geopark

©2019. Japan Geoscience Union. All Right Reserved.

The relationship of land utilization and vegetation at the Jikumaru terraced paddy field in the Oita Bungoono Geopark

*Miki Iwasato[1], Toshikazu Yoshioka[2]

1. Bungoono City, Trade, Industry and Tourism Division, 2. Oita Bungoono Geopark Promotion Council

The Jikumaru terraced paddy field in the Oita Bungoono Geopark is located between Ono River and Ogata River and selected as one of the Top 100 Terraced Paddy Fields in Japan. It is suggested that there are a lot of plants for various geography in the Jikumaru terraced paddy field, so we surveyed vegetation in this area.
Result of survey, in the Jikumaru terraced paddy field, we identified 281 plants species. There were 106 plants for example *Ottelia alismoides* (L.) Pers., *Eclipta thermalis* Bunge and *Schoenoplectus hotarui* (Ohwi) Holub, at the paddy field and its ridge. Under the artificial forests of Japanese cedar trees and oak forests, various plants had grown for example *Quercus serrata* Murray subsp. var. *serrata*, *Rubus buergeri* Miq. and *Ardisia japonica* (Thunb.) Blume var. *japonica*. Planting species as *Lycoris radiata* (L'Hér.) Herb. var. *radiata* and *Hydrangeaceae*, were checked in this area.
In the Jikumaru terraced paddy field, it was found that vegetation of characterized terraced paddy field for we checked both of mountain and paddy field plants in various geography. This is shown that the Jikumaru terraced paddy field may be one of the elements on the Oita Bungoono Geopark.

Keywords: Jikumaru terraced paddy field, Top 100 Terraced Paddy Fields in Japan, Vegetation, Land utilization, Abandoned paddy fields, Oita Bungoono Geopark

©2019. Japan Geoscience Union. All Right Reserved.

Outreach activities of Aso UNESCO Global Geopark

*Tsuneomi Kagiyama[1], Kazunori Watanabe[1], Shinichiro Ikebe[1], Akinobu Ishimatsu[1], Katsunori Toyomura[2], Natsuko Kodama[1], Shuhei Takamori[1], Shino Miyakita[1]

1. Aso Geopark Promotion Council, 2. Aso Volcano Museum

Aso UNESCO Global Geopark made an action plan to clear a revalidation process by UNESCO. One of the plans was to reinforce sending an information on ourselves. Just after the 2016 Kumamoto Earthquake, we have collected records on hazards of this earthquake and eruptions in Aso Volcano, and have shown the recovering process from these hazards. In 2018, we have made some new Geo-tours reflecting these results. We also have collected more information about the earth activities causing hazards, and have made some educational programs and some SNS output. We will report some of these activities as follows.

Geo-tour:

In Tateno Gorge Geosite, we added to explain a close relation between a view of this site and Futagawa Active Fault, a part of Oita-Kumamoto Tectonic Line. In Uchinomaki Geosite, many hot springs did not work just after the Kumamoto Earthquake. We examined the reason, and could recover the hot springs. We introduced this recovering process in our tour. In Nakadake Geosite, we added to explain about phreatomagmatic explosion in October, 2016. And also we cooperated with the Ministry of the Environment to renew the explanations of the sign installed in National Park.

Educational Program:

We opened educational program on "Aso Geopark" in Aso-Chuo-High School; volcanic activity in Aso, recovering activities from Kumamoto Earthquake disaster, sightseeing in Aso and maintenance in grassland. Exhibition of Aso Volcano Museums was revised based on a recent research result. Visitors can see the crater and the observational data which indicates a volcanic activity in real time.

Activity by SNS:

We effectively use Facebook, Blog, Instagram. We introduced beautiful pictures, information performed within Aso and information on disaster mitigation, etc. We also opened the SNS pages which explain documents published by the Meteorological Agency on volcanic activity of Aso.

Keywords: Aso UNESCO Global Geopark, Outreach, SNS

©2019. Japan Geoscience Union. All Right Reserved.

Geoscientific Setting and Educational Significances of Yonaguni Island in the Ryukyu Arc, Eastern Asia

*Takayuki Ogata[1], Masakazu Nara[2], Makoto Otsubo[3], Tadahiro Shibata[4]

1. Disaster Prevention Research Center for Island Regions, University of the Ryukyus, 2. Sciences Unit, Natural Sciences Cluster, Research and Education Faculty, Kochi University, 3. Geological Survey of Japan, Research Institute of Earthquake and Volcano Geology, 4. The Unit of Natural Monuments, Monuments and Sites Division, Cultural Properties Department, Agency for Cultural Affaire

The Ryukyu Arc lies along the subduction zone between Eurasia and Philippine Sea Plates. Yonaguni Island is located in southwestern most of the Ryukyu Arc, where geological setting connects the Taiwan central range and the Luzon volcanic arc. Miocene sandstone (Yaeyama group) is broadly exposed on island surface which forms low altitude mountains and hills (maximum elevation is 231 m). The Yaeyama Group, of which sandstones show some distinct physical sedimentary structures, such as hummocky or ripple cross-stratification, suggesting deposition in shallow-marine to marginal-marine settings, is characterized by pervasive occurrences of well-preserved trace fossils. Sandstone surfaces in wave-splash zone often show a honeycomb structure (tafoni) indicating physical disintegration by salt weathering under present coastal environments with strong wind. This honeycomb geometry seems to be controlled by the horizontal and vertical distances from coast line and sea level. Pleistocene limestone (Ryukyu group) partly covers the Yaeyama group and forms uplifted marine terraces made mainly from coral reef sediments. As the permeable limestones of Ryukyu Group broadly covers the less permeable Yaeyama Group, a number of natural springs rise at the bottom of the precipitous limestone cliffs, and provide water resources and scenic landscapes. Such stratigraphical, paleontological, geomorphological and hydrological features present significant sites to study seamless geoscience. Geoscientist should discuss scientific significances for conservation of several geosites in Yonaguni Island.

Keywords: Ryukyu Arc, Eurasia Plate, Philippine Sea Plate, sandstone, weathering, Yaeyama group

©2019. Japan Geoscience Union. All Right Reserved.

[J] Poster | M (Multidisciplinary and Interdisciplinary)：M-IS Intersection

Mon. May 27, 2019 5:15 PM - 6:30 PM JST | Mon. May 27, 2019 8:15 AM - 9:30 AM UTC | Poster Hall International Exhibition Hall8, Makuhari Messe_33

[M-IS08] Geopark

convener:Takayuki Ogata(Disaster Prevention Research Center for Island Regions, University of the Ryukyus), Tatsuto Aoki(School of Regional Development Studies, Kanazawa University), Noritaka Matsubara(Graduate School of Regional Resource Management, University of Hyogo), Keiichi Tadokoro(Research Center for Seismology, Volcanology and Earthquake and Volcano Research Center, Nagoya University)

This session targets interdisciplinary and multidisciplinary discussion on geopark, involving geoheritage, geodiversity, geoconservation, geotourism, sustainable development, governance, risk management, science communication and geoscientific education. These topics contribute to scientific and attractive activities in geoparks.

[MIS08-P01] The efforts of Mt.Daisetsu-Kamuymintar Geopark Project

*hideyuki kawabe[1] (1.大雪山カムイミンタラジオパーク構想推進協議会)

[MIS08-P02] Re-examination of meaning indicated by "Nigori-Sumi (Muddy and clear) Bridge"~Turbidity Characteristic of Meeting Point of the Ushikubi River and the Ozo River, in Hakusan Tedorigawa Geopark ~

*Tatsuto Aoki[1] (1.School of Regional Development Studies, Kanazawa University)

[MIS08-P03] Efforts of ‘Grant-in-aid for Science Research in San’in Kaigan UGGp’

*Suzuka Koriyama[1] (1.Sanin Kaigan Geopark Promotion Council)

[MIS08-P04] Practical applications in the Tosashimizu Geopark Plan of site monitoring by local residents: Landform change of Sakurahama Beach

*Satoru Imai[1], Hisaaki Sato[1], Yorihisa Hirano (1.Tosashimizu Geopark Promotion Council)

[MIS08-P05] Geological and geomorphological environment of the Jikumaru terraced paddy field (one of the Top 100 Terraced Paddy Fields in Japan) in the Oita Bungoono Geopark

*Toshikazu Yoshioka[1] (1.Oita Bungoono Geopark Promotion Council)

[MIS08-P06] The relationship of land utilization and vegetation at the Jikumaru terraced paddy field in the Oita Bungoono Geopark

*Miki Iwasato[1], Toshikazu Yoshioka[2] (1.Bungoono City, Trade, Industry and Tourism Division, 2.Oita Bungoono Geopark Promotion Council)

[MIS08-P07] **Outreach activities of Aso UNESCO Global Geopark**

*Tsuneomi Kagiyama[1], Kazunori Watanabe[1], Shinichiro Ikebe[1], Akinobu Ishimatsu[1], Katsunori Toyomura[2], Natsuko Kodama[1], Shuhei Takamori[1], Shino Miyakita[1] (1.Aso Geopark Promotion Council, 2.Aso Volcano Museum)

[MIS08-P08] Geoscientific Setting and Educational Significances of Yonaguni Island in the Ryukyu Arc, Eastern Asia

*Takayuki Ogata[1], Masakazu Nara[2], Makoto Otsubo[3], Tadahiro Shibata[4] (1.Disaster Prevention Research Center for Island Regions, University of the Ryukyus, 2.Sciences Unit, Natural Sciences Cluster, Research and Education Faculty, Kochi University, 3.Geological Survey of Japan, Research Institute of Earthquake and Volcano Geology, 4.The Unit of Natural Monuments, Monuments and Sites Division, Cultural Properties Department, Agency for Cultural Affaire)

The efforts of Mt.Daisetsu-Kamuymintar Geopark Project

*hideyuki kawabe[1]

1. -

In this area, we are promoting the "Mt.Daisetsu-Kamuymintar Geopark Project" ranging from Asahikawa City, Takasu Town, Higashikagura Town, Pippu Town, Tohma Town, Aibetsu Town, Kamikawa Town and Higashikawa Town.
We set up a preparatory organization by authorized municipalities and civil society in 2017, As an aiming area we joined the Japan Geopark Network as an associate member, in the background of resident activities such as "Kamuy's Earth" Geo-Tour and Geo-Forum etc. that "Association of Asahikawa Geoparks" has been doing since 2012.
We have been shifted promotion system to a council added by business organizations and others in August 2018.
In this presentation, we introduce Mt.Daisetsu-Kamuymintar Geopark Project and its efforts.

©2019. Japan Geoscience Union. All Right Reserved.

Re-examination of meaning indicated by "Nigori-Sumi (Muddy and clear) Bridge" ~Turbidity Characteristic of Meeting Point of the Ushikubi River and the Ozo River, in Hakusan Tedorigawa Geopark ~

*Tatsuto Aoki[1]

1. School of Regional Development Studies, Kanazawa University

Two main flow paths consisting the Tedori river water system that flows through the Hakusan Tedorigawa Geopark, the Ushikubi River, the main stream path, originating from the west side of Mt. Hakusan, and the Ozo River, tributary originating from the former the north of Mt. Hakusan. These two flow paths join in the vicinity of the "Nigori-Sumi Bridge" in the Seto area, then turn northward as the Tedori River. The word of "Nigori-Sumi" means "Muddiness and clearness" and this shows the difference in the turbidity between the two flow paths. On the webpage of Hakusan Tedorigawa Geopark, it is written as follows and is accompanied by photographs showing the state that high turbidity water and low water are joining.

“There is a point that the Ozo River meets the Tedori River, and only the Ozo River didn’ t settle down for a while during rugged weather, so it is sometimes possible to see a two-colored flow, muddy and clear water, at the meeting point. Thus this bridge was named Nigorisumi Bridge (nigori means muddy and sumi means clear).”

In this report, the author measured the turbidity of these two flow paths, organized the relationship with artificial river management, and re-examined the meaning of today's word of "Nigori-Sumi".

The Ushikubi River originated form Hakusan Gozengamine (2702 m), and Ozo River originated from Hakusan Onanjimine (2684 m), and joins at an altitude of 240 m near the Nigori-Sumi Bridge. The length of the flow path to the confluence point is 34.3 km for the Ushikubi River (average bed slope 71.8 ‰), and 24.5 km for the Ozo River (107.9 ‰). The Ozo River is steeper than the

Ushikubi River. Many of landslides are distributed in the both basin. However, it is believed that there was a crater of Paleo-Hakusan volcano in the Jigokudani of the Ozo River basin (Nagaoka, 1972), and severe degeneration is recognized. The Tedori dam is built in the Ushikubi River, and its flow is controlled by that dam. On the other hand, there is no artificial dam and the flow is not controlled in the Ozo River.

Five sites for water sampling are set in the basin, and sampled water immediately after the large-scale flood caused by the typhoon. As a result, immediately after large-scale flooding, the flow rate and turbidity are high in the Ozo River where the flow rate is not controlled and the geology of the catchment area is brittle. On the other hand, On the Ushikubi River controlled by a dam, water and suspended sediment are stored in the dam, so the increase in flow rate and turbidity is suppressed. As a result, in the vicinity of Nigori-Sumi bashi Bridge, the Ozo River becomes "muddy" and the Ushikubi River becomes "clear". When

©2019. Japan Geoscience Union. All Right Reserved.

time passes after flooding, the flow rate rapidly approaches the base flow rate in the Ozo River, and the contents of suspended sediment also decreases. On the contrary, in the Ushikubi River where discharge from the dam continues, the flow rate and turbidity is kept high because of the spouting water from the dam. As a result, the situation occurred where the Ushikubi River was "muddy" and the Ozo River was "clear".

Keywords: Hakusan Tedorigawa Geopark, turbidity, artificial dam

©2019. Japan Geoscience Union. All Right Reserved.

Efforts of ‘Grant-in-aid for Science Research in San’ in Kaigan UGGp’

*Suzuka Koriyama[1]

1. Sanin Kaigan Geopark Promotion Council

The San’ in Kaigan UNESCO Global Geopark is a bounded area comprising the entire municipalities of Kyotango City in Kyoto Prefecture; Toyooka City, Kami Town, and Shin’ onsen Town in Hyogo Prefecture; and Iwami Town in Tottori Prefecture; and the northern part of the municipality of Tottori City in Tottori Prefecture.
The San’ in Kaigan UGGp provides territorial cohesion as an area featuring natural scenery with a wide variety of rocks, strata, coastal landforms, and inland waterfalls and gorges, which show the span of history from the times when the Japanese Archipelago was not yet separated from the Asian Continent, through the formation of the Japan Sea, to the present. The Geopark area has also been home to unique human lifestyles based on such natural features.

In 2007, San’ in Kaigan Geopark Promotion Council was established. San’ in Kaigan Geopark was certified as a member of Japanese Geoparks Network (JGN) in 2008 and Global Geoparks Network (GGN) in 2010.

Since the foundation, grant-in-aid program for science research has been conducted. For the revalidation of GGN every four years, this research program plays the important role. This program called ‘Grant-in-aid for Science Research in San’ in Kaigan UGGp’ has been continued since 2009. Through this program, we have awarded 77 researches the grants.
On the other hand, current conditions and challenges are that the latest researches reported every year are not used enough to activate Geopark.

In this presentation, we discuss how this 10-year program had effected on San’ in Kaigan UGGp and researchers who awarded the grant.

©2019. Japan Geoscience Union. All Right Reserved.

Practical applications in the Tosashimizu Geopark Plan of site monitoring by local residents: Landform change of Sakurahama Beach

*Satoru Imai[1], Hisaaki Sato[1], Yorihisa Hirano

1. Tosashimizu Geopark Promotion Council

In order to properly manage sites in the geopark, utilizing site monitoring surveys to understand site change over time is important. The Tosashimizu Geopark Plan Committee is at the center of all monitoring surveys in Tosashimizu and the fact that it allows for many different people to easily get involved and cooperate is an advantage. However, it can be said that the term and frequency of monitoring surveys has been inadequate. As a result, the scientific value of the geosites has become beset by problems. Therefore, the Tosashimizu Geopark Plan Committee has begun to supplement its informational database with pictures and research gathered by local residents of the respective geosites. In addition, local residents have been accumulating such data before becoming involved with geopark activities. It is an important role of the Tosashimizu Geopark Plan Committee specialists to teach local residents about the scientific value of their research.
The focus of this presentation, Sakurahama beach, is a pocket beach located in central Tosashimizu. It has been renowned as a place of scenic beauty since the Edo period. It is known that flat coasts such as Sakurahama beach are easily affected by human influence and environmental changes and local residents have been aware of the reduction of the beach area over time. Also, Sakurahama beach is a spawning ground that many living organisms temporarily inhabit. Consequently, detailed monitoring studies are highly significant. One local resident, Hirano Yorihisa, takes photographs of the same area of Sakurahama beach almost every day. In those pictures, the changes in landform before and after typhoons, the change in granularity of beach sand over time, and loggerhead sea turtle hatchlings can be evidenced. This presentation will analyze the photographic records of Hirano Yorihisa and discuss the future prospects for such research.

Keywords: geopark, geosite, preservation, monitoring, sandy beach

©2019. Japan Geoscience Union. All Right Reserved.

Geological and geomorphological environment of the Jikumaru terraced paddy field (one of the Top 100 Terraced Paddy Fields in Japan) in the Oita Bungoono Geopark

*Toshikazu Yoshioka[1]

1. Oita Bungoono Geopark Promotion Council

The Jikumaru terraced paddy field in the Oita Bungoono Geopark is selected as one of the Top 100 Terraced Paddy Fields in Japan. This area is placed between the Ono and Ogata Rivers and the terraced paddy fields are developed in the small and shallow valleys. The bedrock of this area consists of the sandstone and conglomerate of the Late Cretaceous Onogawa Group Ryozen Formation. The non- to weakly welded Aso-3 and Aso-4 pyroclastic flow deposits covered over the Onogawa Group. The Aso-4 pyroclastic flow deposit along the Ono and Ogata Rivers is densely welded. It indicates the sedimentary rocks of the Onogawa Group formed small hills before the Aso-3 and Aso-4 pyroclastic flows. The pyroclastic flow deposits are thin and easy to erode. Accordingly, the small and shallow valleys where terraced paddy fields are developed are formed in this area. The formation of the Jikumaru terraced paddy field is related to the geology and geomorphology of this area and it may be one of the important elements of the Oita Bungoono Geopark.

Keywords: Jikumaru terraced paddy field, Top 100 Terraced Paddy Fields in Japan, Onogawa Group, Aso pyroclastic flow, Oita Bungoono Geopark

©2019. Japan Geoscience Union. All Right Reserved.

The relationship of land utilization and vegetation at the Jikumaru terraced paddy field in the Oita Bungoono Geopark

*Miki Iwasato[1], Toshikazu Yoshioka[2]

1. Bungoono City, Trade, Industry and Tourism Division, 2. Oita Bungoono Geopark Promotion Council

The Jikumaru terraced paddy field in the Oita Bungoono Geopark is located between Ono River and Ogata River and selected as one of the Top 100 Terraced Paddy Fields in Japan. It is suggested that there are a lot of plants for various geography in the Jikumaru terraced paddy field, so we surveyed vegetation in this area.
Result of survey, in the Jikumaru terraced paddy field, we identified 281 plants species. There were 106 plants for example *Ottelia alismoides* (L.) Pers., *Eclipta thermalis* Bunge and *Schoenoplectus hotarui* (Ohwi) Holub, at the paddy field and its ridge. Under the artificial forests of Japanese cedar trees and oak forests, various plants had grown for example *Quercus serrata* Murray subsp. var. *serrata*, *Rubus buergeri* Miq. and *Ardisia japonica* (Thunb.) Blume var. *japonica*. Planting species as *Lycoris radiata* (L'Hér.) Herb. var. *radiata* and *Hydrangeaceae*, were checked in this area.
In the Jikumaru terraced paddy field, it was found that vegetation of characterized terraced paddy field for we checked both of mountain and paddy field plants in various geography. This is shown that the Jikumaru terraced paddy field may be one of the elements on the Oita Bungoono Geopark.

Keywords: Jikumaru terraced paddy field, Top 100 Terraced Paddy Fields in Japan, Vegetation, Land utilization, Abandoned paddy fields, Oita Bungoono Geopark

©2019. Japan Geoscience Union. All Right Reserved.

Outreach activities of Aso UNESCO Global Geopark

*Tsuneomi Kagiyama[1], Kazunori Watanabe[1], Shinichiro Ikebe[1], Akinobu Ishimatsu[1], Katsunori Toyomura[2], Natsuko Kodama[1], Shuhei Takamori[1], Shino Miyakita[1]

1. Aso Geopark Promotion Council, 2. Aso Volcano Museum

Aso UNESCO Global Geopark made an action plan to clear a revalidation process by UNESCO. One of the plans was to reinforce sending an information on ourselves. Just after the 2016 Kumamoto Earthquake, we have collected records on hazards of this earthquake and eruptions in Aso Volcano, and have shown the recovering process from these hazards. In 2018, we have made some new Geo-tours reflecting these results. We also have collected more information about the earth activities causing hazards, and have made some educational programs and some SNS output. We will report some of these activities as follows.

Geo-tour:

In Tateno Gorge Geosite, we added to explain a close relation between a view of this site and Futagawa Active Fault, a part of Oita-Kumamoto Tectonic Line. In Uchinomaki Geosite, many hot springs did not work just after the Kumamoto Earthquake. We examined the reason, and could recover the hot springs. We introduced this recovering process in our tour. In Nakadake Geosite, we added to explain about phreatomagmatic explosion in October, 2016. And also we cooperated with the Ministry of the Environment to renew the explanations of the sign installed in National Park.

Educational Program:

We opened educational program on "Aso Geopark" in Aso-Chuo-High School; volcanic activity in Aso, recovering activities from Kumamoto Earthquake disaster, sightseeing in Aso and maintenance in grassland. Exhibition of Aso Volcano Museums was revised based on a recent research result. Visitors can see the crater and the observational data which indicates a volcanic activity in real time.

Activity by SNS:

We effectively use Facebook, Blog, Instagram. We introduced beautiful pictures, information performed within Aso and information on disaster mitigation, etc. We also opened the SNS pages which explain documents published by the Meteorological Agency on volcanic activity of Aso.

Keywords: Aso UNESCO Global Geopark, Outreach, SNS

©2019. Japan Geoscience Union. All Right Reserved.

Geoscientific Setting and Educational Significances of Yonaguni Island in the Ryukyu Arc, Eastern Asia

*Takayuki Ogata[1], Masakazu Nara[2], Makoto Otsubo[3], Tadahiro Shibata[4]

1. Disaster Prevention Research Center for Island Regions, University of the Ryukyus, 2. Sciences Unit, Natural Sciences Cluster, Research and Education Faculty, Kochi University, 3. Geological Survey of Japan, Research Institute of Earthquake and Volcano Geology, 4. The Unit of Natural Monuments, Monuments and Sites Division, Cultural Properties Department, Agency for Cultural Affaire

The Ryukyu Arc lies along the subduction zone between Eurasia and Philippine Sea Plates. Yonaguni Island is located in southwestern most of the Ryukyu Arc, where geological setting connects the Taiwan central range and the Luzon volcanic arc. Miocene sandstone (Yaeyama group) is broadly exposed on island surface which forms low altitude mountains and hills (maximum elevation is 231 m). The Yaeyama Group, of which sandstones show some distinct physical sedimentary structures, such as hummocky or ripple cross-stratification, suggesting deposition in shallow-marine to marginal-marine settings, is characterized by pervasive occurrences of well-preserved trace fossils. Sandstone surfaces in wave-splash zone often show a honeycomb structure (tafoni) indicating physical disintegration by salt weathering under present coastal environments with strong wind. This honeycomb geometry seems to be controlled by the horizontal and vertical distances from coast line and sea level. Pleistocene limestone (Ryukyu group) partly covers the Yaeyama group and forms uplifted marine terraces made mainly from coral reef sediments. As the permeable limestones of Ryukyu Group broadly covers the less permeable Yaeyama Group, a number of natural springs rise at the bottom of the precipitous limestone cliffs, and provide water resources and scenic landscapes. Such stratigraphical, paleontological, geomorphological and hydrological features present significant sites to study seamless geoscience. Geoscientist should discuss scientific significances for conservation of several geosites in Yonaguni Island.

Keywords: Ryukyu Arc, Eurasia Plate, Philippine Sea Plate, sandstone, weathering, Yaeyama group

©2019. Japan Geoscience Union. All Right Reserved.

[J] Oral | M (Multidisciplinary and Interdisciplinary)：M-IS Intersection

Mon. May 27, 2019 3:30 PM - 5:00 PM JST | Mon. May 27, 2019 6:30 AM - 8:00 AM UTC | 103 1F

[M-IS08] Geopark

convener:Takayuki Ogata(Disaster Prevention Research Center for Island Regions, University of the Ryukyus), Tatsuto Aoki(School of Regional Development Studies, Kanazawa University), Noritaka Matsubara(Graduate School of Regional Resource Management, University of Hyogo), Keiichi Tadokoro(Research Center for Seismology, Volcanology and Earthquake and Volcano Research Center, Nagoya University), Chairperson:Takeyuki Ueki(Faculty of Risk and Crisis Management, Chiba Institute of Science), Marekazu OHNO(Unzen Volcanic Area Geopark promotion office), Takayuki Arima(Department of Tourism Management, Faculty of Economics, Teikyo University)

This session targets interdisciplinary and multidisciplinary discussion on geopark, involving geoheritage, geodiversity, geoconservation, geotourism, sustainable development, governance, risk management, science communication and geoscientific education. These topics contribute to scientific and attractive activities in geoparks.

3:30 PM - 3:45 PM JST | 6:30 AM - 6:45 AM UTC

[MIS08-01] Normal faults observed in the Yonaguni-jima Island, Okinawa Prefecture, southwestern Japan

*Makoto Otsubo[1], Kiyokazu Oohashi[2], Takayuki Ogata[3], Tadahiro Shibata[4] (1.Geological Survey of Japan, 2.Yamaguchi University, 3.University of the Ryukyus, 4.Agency for Cultural Affairs)

3:45 PM - 4:00 PM JST | 6:45 AM - 7:00 AM UTC

[MIS08-02] Example of Study of the Itoigawa-Shizuoka Tectonic Line using “NIED Quake map!”

*Ko Takenouchi[1], Yousuke Ibaraki[1], Takahiko Ogawara[1], Hiroshi Miyajima[1], Makoto Matsubara[2], Azusa Nishizawa[2], Shin Aoi[2], Yoshihiro Hiramatsu[3], Kazuyuki Nakagawa[4] (1.Fossa Magna Museum, 2.National Research Institute for earth Science and Disaster Resilience, 3.Kanazawa University, 4.Jiji Press)

4:00 PM - 4:15 PM JST | 7:00 AM - 7:15 AM UTC

[MIS08-03] The Opening of ‘NIED Quake map!’ and result of questionnaire survey about interest of local seismicity

*Makoto MATSUBARA[1], Azusa Nishizawa[1], Shin Aoi[1], Ko Takenouchi[2], Yoshihiro Hiramatsu[3], Kazuyuki Nakagawa[4] (1.National Research Institute for Earth Science and Disaster Resilience, 2.Fossa Magna Museum, Itoigawa City, 3.School of Geosciences and Civil Engineering, College of Science and Engineering, Kanazawa University, 4.Jiji Press)

4:15 PM - 4:30 PM JST | 7:15 AM - 7:30 AM UTC

[MIS08-04] Bandaisan Geopark's traveling exhibitions and lectures on "Debris avalanche in the world"

*Hiroshi Sato[1], Tadahide UI[2] (1.Mt.Bandai Museum, 2.CeMI)

4:30 PM - 4:45 PM JST | 7:30 AM - 7:45 AM UTC

[MIS08-05] PLANETARY SCIENCE Education in Geoparks-Science Festival for Youth Formation experiment of Izumo Plain in Shimane convention

*Kunihiro Abe[1] (1.Shimane Penunsula Shinjiko Narumi, Kuibiki Geopark Promotion Committee)

4:45 PM - 5:00 PM JST | 7:45 AM - 8:00 AM UTC

[MIS08-06] ESD in Geopark: Systems thinking and Systems competence for renovating the school curriculum of local area study.

*Ryuta YAMAMOTO[1] (1.Center for professional development of teachers Shizuoka University)

Normal faults observed in the Yonaguni-jima Island, Okinawa Prefecture, southwestern Japan

*Makoto Otsubo[1], Kiyokazu Oohashi[2], Takayuki Ogata[3], Tadahiro Shibata[4]

1. Geological Survey of Japan, 2. Yamaguchi University, 3. University of the Ryukyus, 4. Agency for Cultural Affairs

Yonaguni-jima Island, Okinawa prefecture is an island located at the westernmost tip of Japan and belongs to the Southern part of the Ryukyu arc. In Yonaguni-jima Island, many normal faults cut the Miocene Yaeyama Group and the Quaternary Ryukyu Group to make the diamond island shape. The fault found at the Sanninudai located in the southeastern part of the Yonaguni-jima Island has all parts of the fault zone; fault gouge part, fault damage zone, wall rock zone. The fault found at the Sanninudai can be activated by the stress field similar to the one in the Okinawa Trough (active back arc basin). Our results indicate that the stress field in the Yonaguni-jima Island may be different from the one in island part of the South Ryukyu arc (e.g., Miyako-jima Island and Ishigaki-jima Island). The relationship between the width of the fault zone and the length of the fault and the relationship between the total displacement and the width of the fault core are similar to them of the typical characteristics of faults. Based on our results, we discuss the possibility that the fault found at the Sanninudai is a suitable site to understand the crustal dynamics (back arc opening) of subdaction zone.

Keywords: Backarc basin, Normal fault, Okinawa Trough, Quaternary, Ryukyu Arc

©2019. Japan Geoscience Union. All Right Reserved.

Example of Study of the Itoigawa-Shizuoka Tectonic Line using “NIED Quake map!”

*Ko Takenouchi[1], Yousuke Ibaraki[1], Takahiko Ogawara[1], Hiroshi Miyajima[1], Makoto Matsubara[2], Azusa Nishizawa[2], Shin Aoi[2], Yoshihiro Hiramatsu[3], Kazuyuki Nakagawa[4]

1. Fossa Magna Museum, 2. National Research Institute for earth Science and Disaster Resilience, 3. Kanazawa University, 4. Jiji Press

1. Background
The Itoigawa Geopark in Niigata Prefecture features an educational park centered on a fault exposure of the Itoigawa-Shizuoka Tectonic Line (ISTL) called the Fossa Magna Park which was first opened in 1990. It is a roughly 10 minute walk from the main parking lots along National Route 148 to the fault exposure. One of the interpretive panels near the exposure features a QR code inviting visitors to examine the 'NIED Quake map!', a page which records seismic activity managed by the National Research Institute for Earth Science and Disaster Resilience (NIED). This report presents one example of academic study using the 'NIED Quake map' with high school students.

2. Earthquake and Fault Study Example (Private High School in Kanagawa Prefecture)
(1) Explanation of the Fossa Magna and Earthquakes (Via Outdoor Interpretive Panels)
The students learn that the ISTL forms the western fault boundary of the Fossa Magna, that has a very close connection to the formation of the Japanese Archipelago, and that the movement of faults causes earthquakes and particularly large fault movements cause the faults to reach the surface where they are called active faults, and that these movements over time form and shape the land around us.
(2) Information from 'Quake map!'
The students use their own smartphones to access the 'NIED Quake map!' site where they can observe the earthquake activity for past ten years in the Itoigawa Area. Through this the students understand the following:
There are many earthquakes occurring around us, even if we don't feel them.
There are distinct areas where earthquakes do and don't occur.
There are earthquakes which concentrate in a line or elliptical shape.
Inland earthquakes occur at depths shallower than 10 km.
There are earthquakes which occur both along and away from active faults.
Along the same active fault, there are areas that do and do not have earthquakes.
Itoigawa experiences no historically large earthquakes, so there is no active fault.
Areas which experienced historic earthquakes have a greater concentration of earthquakes.
Afterwards, the students look at the 5 year, 1 year, 30 day, weekly and 24 hour maps. On the 24 hour map they can see recent earthquakes, where many students are surprised by how many earthquakes occur without being felt.
(3) Fault Exposure
The students see that the fault exposure is crumbling and the rocks have been broken. The gaps among the fault breccia are filled with even more broken fine material (fault gouge) which can be easily depressed with a finger. In fault gouge, striations which show the direction of fault movement can be observed, so the students can understand how fault gouge was formed by the crushing of rock by fault movement. An earthquake of magnitude 7 causes a change in elevation of about 1.5 to 2 m, so the gap seen along the ISTL (over 6,000 m) can be understood to have formed over 3000-4000 fault movements. Through this the students can imagine how deep the Fossa Magna is. They can also understand how faults

©2019. Japan Geoscience Union. All Right Reserved.

expand.

3. Conclusion
The earthquake distribution map of 'NIED Quake map!' allows for visual understanding of Japan's most tectonically active places and is a valuable tool for understanding the connection between earthquakes and faults. Studying the fault exposure allows seeing only the result of geological processes, but using 'Quake map', the students get a better image of these processes and how they are continuing beneath us. Hopefully further experience in using 'Quake map' for high school students can be used to improve its use in earthquake risk reduction education.

Keywords: Itoigawa Geopark, Fossa Magna Park, Itoigawa-Shizuoka Tectonic Line, NIED Quake map!

©2019. Japan Geoscience Union. All Right Reserved.

The Opening of ‘NIED Quake map!’ and result of questionnaire survey about interest of local seismicity

*Makoto MATSUBARA[1], Azusa Nishizawa[1], Shin Aoi[1], Ko Takenouchi[2], Yoshihiro Hiramatsu[3], Kazuyuki Nakagawa[4]

1. National Research Institute for Earth Science and Disaster Resilience, 2. Fossa Magna Museum, Itoigawa City, 3. School of Geosciences and Civil Engineering, College of Science and Engineering, Kanazawa University, 4. Jiji Press

1. Introduction
The Seismological Society of Japan (SSJ) established the committee to support the activity of Geopark in order to notify people of the current condition of seismology with the same perspective of people. Geoparks are single, unified geographical areas where sites and landscapes of international geological significance are managed with a holistic concept of protection, education and sustainable development. There are many both natural and cultural heritages of earthquakes in Geoparks. However, there is also a lack of introduction to recognize the local seismicity.
National Research Institute for Earth Science and Disaster Resilience (NIED) opened the web site named as 'NIED Quake map!' to visualize the local seismicity at a geosite in July 2018. It is easy to observe current seismicity detected by Monitoring of Waves in Land and Seafloor (MOWLAS) and historical earthquakes. This shows the seismicity in central Japan around the Itoigawa Global UNESCO Geopark through the QR code on the guide plate at the Fossa Magna Park.

2. 'NIED Quake map!'
This page first shows the local seismicity in one year. The color and size show the depth and magnitude of the earthquake, respectively. The latest earthquake is shown with the star. There are volcanoes, active faults, and rivers to grasp the place. People can recognize the seismicity within the ground with seeing both the memorized large earthquakes and no feeling microearthquakes.

3. Results of views
We confirm about 20-30 accesses from the outside. In the case of the field trip by the group at Fossa Magna Park, there were 50-60 accesses.

4. Cooperation with geopark
NIED concluded the Comprehensive Partnership Agreement with Japan Geopark Network (JGN) on the use of the data and research results at the Geoparks on October 13, 2018. NIED also concluded the memorandum regarding the use of the 'NIED Quale map!' NIED plan to open web sites according to request from the Geoparks through JGN.

5. Questionnaire survey about interest of local seismicity and expansion of 'NIED Quake map!'
The committee of the SSJ gave seminars of seismology for Geoparks. We explained the use of the historical earthquakes in 2018 and conducted the questionnaire survey for regions composing the Japan Geopark Network, which consists of the UNESCO Geoparks, the Japan Geoparks, and associate members for proceeding to be Japan Geoparks. We obtained the answer from 26 Geoparks and seven associate members. We note as Geopark both Geopark and the associate members.
There are geosites of historical earthquake in 46 % of Geoparks. About 91 % of Geopark have interest in the local seismicity, however, there are some display of local seismicity in only 27 Geoparks. About 82 % Geoparks have an interest to introduction of local seismicity, however, it depends on the cost. Geoparks

©2019. Japan Geoscience Union. All Right Reserved.

only share the cost for display of local seismicity since NIED construct and manage the web site of the 'NIED Quake map!' NIED plans to construct and supply the web sites in accordance with the request from the Geoparks

Keywords: NIED Quake map!, display of local seismicity

©2019. Japan Geoscience Union. All Right Reserved.

Bandaisan Geopark's traveling exhibitions and lectures on "Debris avalanche in the world"

*Hiroshi Sato[1], Tadahide UI[2]

1. Mt.Bandai Museum, 2. CeMI

Bandaisan Geopark was built with the aim of showing visitors how the landform and people's lives were affected by the mountain collapse which occurred 2 times in 50,000 years ago and 1888. Mt. Bandai Museum is the core exhibition facility.
The year 2018 marked a turning point, 130 years after the collapse, and 30 years after the museum opened.
Since rock avalanches (debris avalanche) occur only about once in 100 years in Japanese Island, a special exhibition was held at the Museum to highlight the avalanche, which is not well known to the public. In addition, the traveling exhibition was also carried out in the volcanic museum in the whole country.
Believing that this traveling exhibition would promote cooperation and mutual understanding among the geoparks that participated in the event, we also held symposiums for public and lectures for school children.
In this presentation, the outline of planned exhibition, symposium and lectures are introduced, and the difference of understanding of volcano by region is introduced from the participant’ s questionnaire carried out in delivery lectures.

Keywords: Mt. Bandai, Geopark, Debris avalanche

©2019. Japan Geoscience Union. All Right Reserved.

PLANETARY SCIENCE Education in Geoparks-Science Festival for Youth Formation experiment of Izumo Plain in Shimane convention

*Kunihiro Abe[1]

1. Shimane Penunsula Shinjiko Narumi, Kuibiki Geopark Promotion Committee

The Shinji Lake Nakaumi Geopark, Shimane Peninsula, has been certified as a Japan Geopark for the third year. The Geopark certification in Shimane Prefecture will be second after the Oki Global Geopark. Although the popularity of the Oki Geopark has been recognized by the prefectural residents, the Shinji Lake Nakaumi is still strong in the Shimane Peninsula. In conjunction with cognitive activities, the Promotion Council is strongly required to utilize geoparks and to promote educational activities. The 18th Annual Science Festival for Youth at the Shimane Convention, the booth of the Shimane Peninsula and the Shinji Lake Nakaumi Geopark exhibited in Shimane Prefecture, the booth of the "Shinji Lake, the birth of the Izumo plain" and it is compatible to, 360 ×270 ×By making the basin topography of the Hiikawa and Shinmon River with the sand in the mold of 120cm, fixing the watering hose to the headwaters of the two rivers, and continuing watering, the sediment is gradually deposited in the waters sandwiched between the Chinese mountains and the Shimane Peninsula, according to the sedimentary experiment by running water. It is the one to understand the state that the Shinji Lake is formed with the passage of time while observing the process that the Izumo plain is done. The west side of Izumo Taisha is a plain and it is not a sea area. The effects of the eruption of Mijar volcano, located in the Kamimon Basin, cannot be ignored. Photos and materials of the Shinji Lake Nakaumi of the geopark that the Izumo plain was formed between the Shimane Peninsula and the Chugoku Mountains located in the north by the volcanic activity of Mt. Hiikawa, the Kamikadawa River, the granite of the Chugoku Mountains, and the Sanjar Mountain which formed the Izumo plain known for Tsukiji Matsu The experiment was performed while contrasting it with the rock sample.

Keywords: Shimane Peninsula and Shinjiko Nakaumi Estuary Geopark, Formation of the Izumo Plain, Deposition experiment, Watering

©2019. Japan Geoscience Union. All Right Reserved.

ESD in Geopark: Systems thinking and Systems competence for renovating the school curriculum of local area study.

*Ryuta YAMAMOTO[1]

1. Center for professional development of teachers Shizuoka University

Geopark education in Japan have much contact with school in its area. The revised national curriculum concentrated on compentence-oriented learning. Geopark have a way to adopt the competence-oriented learning in the learning field of local area study with systems thinking and systems competence.

Keywords: ESD, local area study, Systems thinking, Competence, SDGs, School Curriculum

©2019. Japan Geoscience Union. All Right Reserved.

[J] Oral | M (Multidisciplinary and Interdisciplinary)：M-IS Intersection

Mon. May 27, 2019 1:45 PM - 3:15 PM JST | Mon. May 27, 2019 4:45 AM - 6:15 AM UTC | A02 TOKYO BAY MAKUHARI HALL

[M-IS11] Aqua planetology

convener:Yasuhito Sekine(Earth-Life Science Insitute, Tokyo Institute of Technology), Tomohiro Usui(Earth-Life Science Institute, Tokyo Institute of Technology), Keisuke Fukushi(Institute of Nature & Environmental Technology, Kanazawa University), Takazo Shibuya(Japan Agency for Marine-Earth Science and Technology), Chairperson:Yasuhito Sekine(Dept. Earth & Planetary Sci., University of Tokyo), Tomohiro Usui, Takazo Shibuya(JAMSTEC)

This proposed session covers a wide range of topics related to aqua planetology, including chemical reactions involving water on planetary bodies, water-rock reactions within planetesimals, distribution of water in the early Solar system and the origin of water on terrestrial planets, hydrological and biogeochemical processes on Earth, geochemical cycles and habitability on Mars and icy moons, exploration of water in the solar system, and theory to understand how to build a habitable aqua planet.

1:45 PM - 2:00 PM JST | 4:45 AM - 5:00 AM UTC

[MIS11-01] An interior structure model of Pluto resolving its mysteries

*Shunichi Kamata[1], Francis Nimmo[2], Yasuhito Sekine[3], Kiyoshi Kuramoto[1], Naoki Noguchi[4], Jun Kimura[5], Atsushi Tani[6] (1.Hokkaido University, 2.University of California, Santa Cruz, 3.Tokyo Institute of Technology, 4.Tokushima University, 5.Osaka University, 6.Kobe University)

2:00 PM - 2:15 PM JST | 5:00 AM - 5:15 AM UTC

[MIS11-02] Isotopic measurement of gas hydrate sample simulating environment of icy satellite and icy planet: Equipment development and consideration for observation method

*Kushi Kudo[1], Atsushi Tani[1], Naohiro Yoshida[2,3] (1.Graduate School of Human Development and Environment, Kobe University, 2.Department of Chemical Science and Engineering, School of Materials and Chemical Technology, Tokyo Institute of Technology, 3.Earth–Life Science Institute)

2:15 PM - 2:30 PM JST | 5:15 AM - 5:30 AM UTC

[MIS11-03] Dynamics of icy crust of the Enceladus with tidal heating and asymmetric distribution of heat generation in the rocky core

*Kaho Harada[1,2], Takashi Nakagawa[3], Manabu Morishige[2], Shigenobu Hirose[2] (1.Keio University, 2.JAMSTEC, 3.University of Hong Kong)

2:30 PM - 2:45 PM JST | 5:30 AM - 5:45 AM UTC

[MIS11-04] Chlorine-bearing aqueous fluid at crust/mantle boundary in mid-ocean ridge hydrothermal system: a case study of crustal diopsidite from Oman ophiolite

★Invited Papers

*Norikatsu Akizawa[1], Akira Miyake[2], Akira Tsuchiyama[2] (1.Atmosphere and Ocean Research Institute, The University of Tokyo, 2.Graduate School of Science, Kyoto University)

2:45 PM - 3:00 PM JST | 5:45 AM - 6:00 AM UTC

[MIS11-05] Phase relation of the $MgSO_4$-H_2O system under high pressure

*Tadashi Kondo[1], Keita Harada[1], Miki Sirata[1], Takumi Kikegawa[2] (1.Department of Earth and Space Science, Graduate School of Science Osaka University, 2.Institute for Material Structure Science, KEK)

3:00 PM - 3:15 PM JST | 6:00 AM - 6:15 AM UTC

[MIS11-06] The Origin of Earth's Volatile Composition: Effects of Impact-induced Atmospheric Erosion and Core Formation

*Sakuraba Haruka[1], Hiroyuki Kurokawa[2], Hidenori Genda[2], Kenji Ohta[1] (1.Tokyo Institute of Technology, 2.Earth-Life Science Institute)

An interior structure model of Pluto resolving its mysteries

*Shunichi Kamata[1], Francis Nimmo[2], Yasuhito Sekine[3], Kiyoshi Kuramoto[1], Naoki Noguchi[4], Jun Kimura[5], Atsushi Tani[6]

1. Hokkaido University, 2. University of California, Santa Cruz, 3. Tokyo Institute of Technology, 4. Tokushima University, 5. Osaka University, 6. Kobe University

Investigating the mechanism maintaining a subsurface ocean is necessary to understand the condition under which aqua planets can form. Recent planetary exploration missions suggest the presence of subsurface oceans in several outer Solar System bodies. Most of them are icy satellites of giant planets, and tidal heating is considered to play a major role in maintaining their subsurface oceans. The presence of a subsurface ocean is also suggested for Pluto, though tidal heating is negligible. In order for heat-depleted Pluto to possess a subsurface ocean, thermal convection should not occur in the ice shell above the ocean, suggesting its high viscosity. This suggestion is consistent with studies of viscous relaxation of the ice shell. This may be due to a high concentration of contaminants, such as ammonia, in the ocean, resulting in an extremely low temperature ocean; however, ammonia is not observed on Pluto’ s surface, and comets, whose bulk chemistry should be similar to that of Pluto, contains ammonia only little. Thus, the reason why Pluto possesses a subsurface ocean is a mystery.

Here we propose a thin gas hydrate layer exists between the ice shell and a subsurface ocean, and it prevents freezing of a subsurface ocean. Gas hydrates act as a thermal insulator because of its low thermal conductivity. We perform numerical calculations of long-term thermal evolution and show that a warm ocean and a cold ice shell can be maintained for a long time and that the freezing of the ocean is ineffective. We also perform numerical calculations of long-term viscoelastic deformation and show that the significant viscous relaxation requires billions of years. Our proposal does not require large amounts of contaminants. Comets contain a few % of methane with respect to water, for example, and this concentration is sufficient for creating a thin gas hydrate layer prohibiting the ocean freezing. Some gas species are easily trapped in gas hydrates while others are not, and this selective trapping may explain a large difference in volatile compositions of comets and Pluto’ s surface. The subsurface ocean maintenance mechanism we propose here would also be applicable to larger icy bodies other than Pluto. In addition, our proposal may explain the diversity of surface chemistry of Kuiper Belt Objects.

Keywords: Pluto, Subsurface ocean, Gay hydrates

©2019. Japan Geoscience Union. All Right Reserved.

Isotopic measurement of gas hydrate sample simulating environment of icy satellite and icy planet: Equipment development and consideration for observation method

*Kushi Kudo[1], Atsushi Tani[1], Naohiro Yoshida[2,3]

1. Graduate School of Human Development and Environment, Kobe University, 2. Department of Chemical Science and Engineering, School of Materials and Chemical Technology, Tokyo Institute of Technology, 3. Earth–Life Science Institute

According to recently observation using Cassini, icy satellites and icy planets are known for having plume including the organic matter, liquid internal ocean and rocky crust (e.g. Porco et al. 2006; Waite et al. 2006, 2009, 2017). From this fact, extraterrestrial life is regarded as being likely to exist in icy satellites and icy planets. Especially in plume gas species, methane (CH_4) is regarded as one of the candidate of signature of biological activity due to CH_4 formation reaction by methanogen. However CH_4 gas in plume is consisted of not only microbial origin but also primitive CH_4 and hydrothermal formation and this fact does not let CH_4 detection is sufficient for conclusion for existence of biological activity by microbe. Therefore, we consider evaluation of the elementary process of CH_4 isotopic fractionation ($\delta^{13}C$, δD of CH_4) via room experiment important for isotopic observation of icy satellite and icy planet in nearly future.

In this study, we focus on CH_4 hydrate which is reservoir to produce the plume (Kieffer et al. 2006) and want to evaluate isotopic fractionation with its formation. Isotopic fractionation with hydrate formation has been found at only δD of CH_4 (~10‰) at the Earth condition (P: ~10 MPa) (e.g. Hachikubo et al. 2007, 2015; Lapham et al. 2012). In the case of condition of icy satellite and icy planet, pressure range of icy satellite and icy planet is wider than of the Earth, and therefore we need to estimate isotopic fractionation at 10–100 MPa scale. Thus we started design for cell for hydrate formation experiment at ice crust condition (P: ~150 MPa). In presentation, we will mainly introduce progress of the equipment development and observation method.

As next stage, we are also planning analyze isotopic fractionation of surface rocky core, and CH_4 translation process using 3-D flow simulation for evaluate CH_4 isotope changing in icy satellite and icy planet. We will subject to Enceladus, Europe and Triton as target.

Keywords: isotopic observation, isotopic fractionation, methane, icy satellite and icy planet, gas hydrate

©2019. Japan Geoscience Union. All Right Reserved.

Dynamics of icy crust of the Enceladus with tidal heating and asymmetric distribution of heat generation in the rocky core

*Kaho Harada[1,2], Takashi Nakagawa[3], Manabu Morishige[2], Shigenobu Hirose[2]

1. Keio University, 2. JAMSTEC, 3. University of Hong Kong

We investigate the dynamics of icy crust of the Enceladus, that is the sixth-largest moon of the Saturn, for understanding the diversity of the surface geology found from the planetary explorations. Especially, we have an interest in the ‘Tiger Stripes’ found around the south pole with heat release of 15.8 GW. The mechanism of formation of the Tiger Stripes is recognized as active terrains caused by thermal convection of icy crust driven by tidal heating. However, such active terrains caused by the tidal heating could not be explained by the tidal heating solely because they are only found around the south pole. Several researches concerning the convective dynamics of icy crust on the Enceladus have suggested some north-south asymmetries, for example in the thickness of icy crust or viscosity, but they have not been well-understood for the origin.

Here, to resolve the formation mechanism of Tiger Stripes, we propose the hypothesis on the north-south asymmetric distribution of heat producing elements in Enceladus’ s rocky core. We assume that the more heat producing elements can be concentrated into the southern hemisphere. Since, regarding the formation mechanism of the Enceladus, the rocky core would not be likely to experience the large-scale melting events such as the magma ocean, the Enceladus still tends to maintain the chemical structure of the early distribution. Hence, the current chemical structure of rocky core may be heterogeneous, which can lead to north-south asymmetric distribution of heat generation. We test the hypothesis for using a numerical model of icy crust dynamics including tidal heating and north-south asymmetric distribution of heat generation in the rocky core. For tidal heating of the icy crust, we impose an analytical solution of tidal deformation considering viscoelasticity in a thin shell on the surface (e.g., Ojakangas and Stevenson, 1989). For north-south asymmetric distribution in heat generation in the rocky core, we set the temperature of the bottom of the icy crust as 273 K in the northern hemisphere, 283 K in the southern hemisphere.

Our results indicate that heat upwelling around the south pole and heat downwelling around the north pole when we assume tidal heating and north-south asymmetric distribution of heat generation. Rather, the asymmetric distribution of heat generation is more important for finding the more active dynamics around the south pole. A quantitative test indicates that the plume heat flow coming from the south pole region is about 300 GW, which is about 20 times as large as the observational constraints (15.8 GW). This suggests that the amplitude of heterogeneous heat generation is too large. Again, although the amplitude of heat transfer of plume in southern hemisphere is too large, the geographical distribution of plumes can form the north-south asymmetric distribution of heat generation. Therefore, this hypothesis provided here would be promising to reveal the origin of the hydrogen plumes on the Enceladus found by the Cassini mission.

Keywords: Enceladus, Thermal convection, Tidal heating

©2019. Japan Geoscience Union. All Right Reserved.

Chlorine-bearing aqueous fluid at crust/mantle boundary in mid-ocean ridge hydrothermal system: a case study of crustal diopsidite from Oman ophiolite

*Norikatsu Akizawa[1], Akira Miyake[2], Akira Tsuchiyama[2]

1. Atmosphere and Ocean Research Institute, The University of Tokyo, 2. Graduate School of Science, Kyoto University

Hydrothermal circulation in the mid-ocean ridge system is responsible for elemental enrichment, and modification of original chemical composition of the oceanic crust. In recent times, deep-rooted hydrothermal circulation down to crust/mantle boundary has been introduced regarding geological investigations and numerical models. The deep-rooted hydrothermal circulation in the mid-ocean ridge system can be one of the necessary mechanisms generating plate tectonics due to mantle hydration lowering mantle viscosity. In order to assess the mechanism of the mantle hydration in the mid-ocean ridge system, chemical composition of mantle-buffered hydrothermal fluids must be characterized. Here, we present a series of intense investigations for aqueous fluid inclusions in crustal diopsidites from Oman ophiolite. The crustal diopsidite is considered as a reaction product between gabbro (lowermost crustal material) and seawater-derived hydrothermal fluids en route from the mantle to the crust. Considering that Cr-rich minerals such as chromian spinel (Cr-spinel) and chromian garnet (uvarovites) are contained in the crustal diopsidites, the hydrothermal fluids involved were enriched in Cr. A few micrometer-sized inclusion of aqueous fluid with chromian spinel grains was frozen with a nitrogen gas-cooled cold stage, and investigated with a focused ion beam equipped with a scanning electron microscope and an energy dispersive X-ray spectrometer (cryo-FIB-SEM-EDS system). The results showed that the Cr-spinel-bearing aqueous fluid inclusion contains Cl. Regarding the mass and chemical composition of the Cr-spinels in the aqueous fluid inclusion, Cr content in the aqueous fluid was estimated at ~71400 ppm. Although Cr is considered relatively insoluble in aqueous fluids, solubility of Cr depends strongly on the activity of Cl due to complexation reactions with Cl. We propose a possibility that seawater-derived hydrothermal fluids penetrated throughout the crustal section reacted with Cl-bearing magma portion. Flow direction of the hydrothermal fluids probably changed from downward to upward in response to the heat release of the magma to the hydrothermal fluid.

Keywords: cryo-FIB-SEM-EDS, fluid inclusion, hydrothermal circulation, Cr-spinel, Chromium, microthermometry

©2019. Japan Geoscience Union. All Right Reserved.

Phase relation of the $MgSO_4$-H_2O system under high pressure

*Tadashi Kondo[1], Keita Harada[1], Miki Sirata[1], Takumi Kikegawa[2]

1. Department of Earth and Space Science, Graduate School of Science Osaka University, 2. Institute for Material Structure Science, KEK

Resent planetary exploration projects suggest existence of internal ocean in the several icy satellites. Spectral analysis of surface material of such satellite indicate sulfate materials as solute in the water ocean. Salts change generally the phase relation such as melting temperature and generation of a kind of hydrate, and affects the internal structure of the satellite. For the $MgSO_4$-H_2O system, which was considered as a possible major component in internal ocean, Nakamura and Ohtani (2011) has proposed the phase relation under pressure condition up to 4.5 GPa with existence of epsomite($MgSO_4 \cdot {}_7H_2O$), and discussed a deep internal ocean in the Ganymede. However, the X-ray diffraction pattern they reported as epsomite includes many unidentified diffraction peaks. In this study, we re-examined the phase relation in the system $MgSO_4$-H_2O under pressure by optical observation, micro-Raman, X-ray diffraction at synchrotron facility. High pressure experiments was performed using diamond anvil cell(DAC) up to about 5GPa at room temperature for 5 to 25wt% $MgSO_4$ solution. The results show a quite different phase relation from Nakamura and Ohtani(2011) in $MgSO_4$-rich side and solidified phases. The eutectic composition is almost same as previous report, but pentahydrate($MgSO_4 \cdot 5H_2O$) is newly observed as coexisting phase with Ice VI-VII in solid, and also liquidus phase in $MgSO_4$-rich solution. We observed direct conversion from low-pressure pentahydrate to high-pressure pentahydrate which reported by Wang et al.(2018). We also evaluate the relative density difference between liquid and solid for all composition by gravitational method in DAC. Ice VI is always denser than liquid while hydrate is always less denser than liquid. We will discuss internal structure and evolution of icy satellite based on this new results.

Keywords: Europe, high-pressure experiment, structure of internal ocean

©2019. Japan Geoscience Union. All Right Reserved.

The Origin of Earth's Volatile Composition: Effects of Impact-induced Atmospheric Erosion and Core Formation

*Sakuraba Haruka[1], Hiroyuki Kurokawa[2], Hidenori Genda[2], Kenji Ohta[1]

1. Tokyo Institute of Technology, 2. Earth-Life Science Institute

Unveiling the origin of Earth's volatile composition is crucial for understanding how Earth developed its habitable environment. Carbon (C), nitrogen (N), and hydrogen (H) are the backbone for the chemistry of life and main components of the atmosphere and oceans (e.g., Katling & Casting, 2017). The volatiles in rocky planets are thought to have been delivered by chondritic materials. However, the elemental composition of the bulk silicate Earth (BSE) shows the depletion of C and N relative to H, a high C/N ratio, and a low C/H ratio compared to chondrites (e.g., Hirschmann, 2016; Bergin et al., 2015).

The volatiles delivered to the accreting planet were potentially lost to space by impacts or sequestered in the core. In order to understand how these processes affect the Earth's volatile composition, we modeled both the main accretion stage and the late accretion stage. The former considered the elemental partitioning between the atmosphere, MO, and metal which segregates into the core (e.g., Hirschmann, 2016; Bergin et al., 2015). The latter considered the partitioning between the atmosphere, oceans, and carbonate (the crust) (e.g., Sakuraba et al., 2019). By calculating the evolution for the range of partitioning coefficient, solubilities, and impactor properties, we evaluated how the resulting volatile composition of BSE depends on these input parameters.

As a result, we succeeded to reproduce the elemental composition of major volatile elements in current BSE from a chondritic source when we chose the appropriate parameter values. While the elemental fractionation during the main accretion ended up with the excess of N/C, the preferential loss of N from the atmosphere during the late accretion reproduced BSE's volatile pattern. During the main accretion, C was most affected by the core segregation because C is the most siderophile among the volatile elements. During the late accretion, N was most affected by the atmospheric erosion because C and H were trapped in the surface reservoirs. The different BSE's composition patterns were obtained depending on parameters such as impactor's composition, impactor's size-distribution, and element partitioning properties. Our results suggest that the current Earth's composition can be obtained by the homogeneous accretion of chondritic planetesimals.

[1] Hirschmann, (2016) *American Mineralogist*, 101, 540.
[2] Bergin et al., (2015) *Proceedings of the National Academy of Sciences*, 112, 8965.
[3] Sakuraba et al., (2019) *Icarus*, 317, 48.

Keywords: volatile composition, magma ocean, impact-induced atmospheric erosion, core formation

©2019. Japan Geoscience Union. All Right Reserved.

[J] Oral | M (Multidisciplinary and Interdisciplinary)：M-IS Intersection

Mon. May 27, 2019 3:30 PM - 5:00 PM JST | Mon. May 27, 2019 6:30 AM - 8:00 AM UTC | A02 TOKYO BAY MAKUHARI HALL

[M-IS11] Aqua planetology

convener:Yasuhito Sekine(Earth-Life Science Insitute, Tokyo Institute of Technology), Tomohiro Usui(Earth-Life Science Institute, Tokyo Institute of Technology), Keisuke Fukushi(Institute of Nature & Environmental Technology, Kanazawa University), Takazo Shibuya(Japan Agency for Marine-Earth Science and Technology), Chairperson:Yasuhito Sekine(Dept. Earth & Planetary Sci., University of Tokyo), Keisuke Fukushi, Tomohiro Usui

This proposed session covers a wide range of topics related to aqua planetology, including chemical reactions involving water on planetary bodies, water-rock reactions within planetesimals, distribution of water in the early Solar system and the origin of water on terrestrial planets, hydrological and biogeochemical processes on Earth, geochemical cycles and habitability on Mars and icy moons, exploration of water in the solar system, and theory to understand how to build a habitable aqua planet.

3:30 PM - 3:45 PM JST | 6:30 AM - 6:45 AM UTC

[MIS11-07] Finding of oxidized sulfur species in carbonates from a Martian meteorite Allan Hills 84001 using μ-XANES

*Kajitani Iori[1], Gaku Tanabe[1], Ryoichi Nakada[2], Tomohiro Usui[3], Mizuho Koike[3], Fumihiro Matsuura[4], Tetsuya Yokoyama[1] (1.Tokyo Institute of Technology, 2.Japan Agency for Marine-Earth Science and Technology, 3.Institute of Space and Astronautical Science, 4.Earth-Life Science Institute)

3:45 PM - 4:00 PM JST | 6:45 AM - 7:00 AM UTC

[MIS11-08] A study on Martian water environment based on the μ-XRF-XANES analysis for the secondary minerals formed in a nakhlite meteorite (Y 000593) vein

*Keika Suzuki[1], Hiroki Suga[1], Akira Yamaguchi[2], Tomohiro Usui[3], Oki Sekizawa[4], Kiyofumi Nitta[4], Yoshio Takahashi[1] (1.University of Tokyo, 2.National Institute of Polar Research, 3.JAXA, ISAS, 4.JASRI/SPring-8)

4:00 PM - 4:15 PM JST | 7:00 AM - 7:15 AM UTC

[MIS11-09] Influence of water and clay minerals for slope angles on Mars

*Yuhki Matsuoka[1], Ikuo Katayama[1], Rina Noguchi[2], Tomohiro Usui[2] (1.Department of Earth and Planetary Systems Science, Hiroshima University, 2.Institute of Space and Astronautical Science, Japan Aerospace Exploration Agency)

4:15 PM - 4:30 PM JST | 7:15 AM - 7:30 AM UTC

[MIS11-10] **Dark Streak Features in Mongolia: Implications for Formation Mechanisms of Recurring Slope Lineae on Mars**

*Maya Nakamura[1,2], Yasuhito Sekine[1], Keisuke Fukushi[3], Noriko Hasebe[3], Davaadorj Davaasuren[4], Yoshio Takahashi[2], Hitoshi Hasegawa[5], Takuro Ogura[6], Koki Morida[3], Tuvshin Gerelmaa[4] (1.Earth-Life Science Institute, Tokyo Institute of Technology, 2.Department of Earth and Planetary Science, The University of Tokyo, 3.Institute of Nature & Environmental Technology, Kanazawa University, 4.Department of Geography, National University of Mongolia, 5.Department of Global Environment and Disaster Prevention, Kochi University, 6.Department of Socio-Cultural Environmental Science, The University of Tokyo)

4:30 PM - 4:45 PM JST | 7:30 AM - 7:45 AM UTC

[MIS11-11] The occurrence of perchlorate salt in and around the Taklimakan Desert, China

*Haibo Qin[1,2], Shitong Yang[1], Qing Chang[3], Chihiro Miyamoto[1], Yoshio Takahashi[1] (1.Department of Earth and Planetary Science, Graduate School of Science, 2.State Key Laboratory of Environmental Geochemistry, Institute of Geochemistry, Chinese Academy of Sciences, 3.Japan Agency for Marine-Earth Science and Technology)

4:45 PM - 5:00 PM JST | 7:45 AM - 8:00 AM UTC

[MIS11-12] Measurement technique to quantify OH radicals photochemically generated on the ice surface

*Akihiro Yabushita[1], Hiroaki Nishimoto[1], Akira Harata[1] (1.Interdisciplinary Graduate School of Engineering Sciences, Kyushu University)

Finding of oxidized sulfur species in carbonates from a Martian meteorite Allan Hills 84001 using μ-XANES

*Kajitani Iori[1], Gaku Tanabe[1], Ryoichi Nakada[2], Tomohiro Usui[3], Mizuho Koike[3], Fumihiro Matsuura[4], Tetsuya Yokoyama[1]

1. Tokyo Institute of Technology, 2. Japan Agency for Marine-Earth Science and Technology, 3. Institute of Space and Astronautical Science, 4. Earth-Life Science Institute

The widespread evidence of liquid water on Mars has led to detailed studies of Martian habitable surface environments [1]. Among them is the geochemical study of carbonate in the 4-billion-year old meteorite Allan Hills (ALH) 84001 because the carbonate is interpreted to have formed from fluids in the early stage of Mars history (~4 Ga) [2]. This study examined speciation of sulfur in carbonates of ALH 84001 as a proxy to trace the chemical evolution of fluids that formed the ALH 84001 carbonates.

We conducted sulfur K-edge (2472 eV) micro X-ray absorption near edge structure (μ-XANES) analysis at BL27SU at SPring-8. X-ray beam was focused using a K-B mirror to a final spot size of 15 (H) ×15 (V) μm^2. Prior to the μ-XANES analysis, X-ray fluorescence mapping which was scanned in 20 μm step was obtained to determine the analytical spot with referring to the petrological observation and backscattered electron images using electron prove micro analyzer (EPMA).

A diagnostic signature of oxidized sulfur [S(VI)] was observed in all the analytical points, whereas X-ray absorption peaks corresponding to S(-II) and an organic sulfur (Di-n-octadecyl disulfide) were observed in some analytical spots. We propose two possible processes for the incorporation of S(VI) species in the carbonate grains of ALH 84001 on the Martian surface: (co-)precipitation of sulfate minerals with the carbonate or substitution of sulfate ion for carbonate ion (carbonate associated sulfate: CAS). The incorporation of trace amount of sulfate minerals is consistent with the widespread distribution of sulfate-bearing deposits in Noachian terranes [3]. However, any type of sulfate minerals has not been observed in the carbonate grains of ALH 84001 even using the transmission electron microscope observations [4]. On the other hand, the CAS-bearing carbonates are common on Earth, though the concentration of CAS in carbonate is typically low (~100s-1,000s ppm) [5]. We conducted thermodynamic calculations under conditions proposed to explain the ALH 84001 carbonates [6, 7]. The thermodynamic calculations indicated that sulfur mainly occurred as sulfate ion in water at Eh-pH conditions where the ALH 84001 carbonate precipitated. This result suggests a possibility that the observed S(VI) species could have occurred as CAS in the ALH 84001 carbonates under the fluid conditions ranging from 6 to 9 for pH and -0.25 to 0 for Eh (V).

[1] Klingelhöfer et al. (2004) Science 306, 1740-1745. [2] Lapen et al. (2010) Science 328, 347-351. [3] Okubo et al. (2008) Planets, 113. [4] Thomas-Keprta et al. (2009) Geochimica et Cosmochimica Acta 73, 6631-6677. [5] Matsu’ura (2016) PhD Thesis, Tokyo Institute of Technology. [6] Melwani Daswani et al. (2016) Meteoritics & Planetary Science 51, 2154-2174. [7] Fairén et al. (2004) Nature 431, 423.

Keywords: Mars, ALH 84001, μ-XANES, sulfur

©2019. Japan Geoscience Union. All Right Reserved.

A study on Martian water environment based on the μ-XRF-XANES analysis for the secondary minerals formed in a nakhlite meteorite (Y 000593) vein

*Keika Suzuki[1], Hiroki Suga[1], Akira Yamaguchi[2], Tomohiro Usui[3], Oki Sekizawa[4], Kiyofumi Nitta[4], Yoshio Takahashi[1]

1. University of Tokyo, 2. National Institute of Polar Research, 3. JAXA, ISAS, 4. JASRI/SPring-8

Martian meteorite nakhlite has attracted attention because it has various secondary mineral assemblages (such as iddingsite) formed by water-rock reaction on the Mars. The iddingsite holds physicochemical information of water when it formed on Mars. However, the formation processes of the minerals are not clear because both carbonates (precipitate under reductive alkaline conditions) and sulfates (precipitate under oxidative acidic conditions) that cannot coexist under an equilibrium condition were found. Among these minerals, sulfate minerals are considered as a terrestrial contamination in several researches in contrast to carbonate minerals accompanied with various secondary minerals such as saponite and serpentine. Here, we examined trace element distribution within the carbonate phases in Y 000593 by FE-SEM-EDS/FE-EPMA and synchrotron-based μ-XRF-XANES in order to determine the transition history of the Eh-pH conditions during the carbonate formation, which reconcile the coexistence of carbonate and sulfate phases in the iddingsite. The detailed understanding of environment (*e.g.,* fluid chemistry) allows us to give a new constraint on the physicochemical evolution of the water that altered the nakhlite body during the last ~6.5 million years.

The polished thin section (PTS: #58-1 in NIPR) of Y 000593 was used for this study. First, the identification of secondary mineral phases in the iddingsite were conducted by FE-SEM-EDS and FE-EPMA at the University of Tokyo. After that, we investigated distribution of trace elements by μ-XRF-XANES at BL37XU of SPring-8, and BL-4A/15A of KEK-PF. Subsequently, we tried to constrain the iddingsite formation environment (such as Eh-pH conditions) from the proportion of secondary minerals.

Carbonates ($FeCO_3$, $MnCO_3$, $CaCO_3$), iron oxides (FeOOH), clay minerals (Fe-rich saponite), and Si-rich vein were identified in the iddingsite from the outside to the center of vein by FE-SEM-EDS and FE-EPMA analysis. In particular, carbonate aggregates were mainly composed of $(Mn,Fe)CO_3$ and $(Ca,Fe)CO_3$. This result suggested that the iddingsite was altered by CO_2-rich reductive alkaline fluid (Eh≦0.2: pH=9.0~11) [Brookins, 1998]. The difference between distributions of Mn and Ca suggests that fluid with different Eh-pH conditions flowed several times or water condition was changed during carbonate formation because $(Mn,Fe)CO_3$ and $(Ca,Fe)CO_3$ cannot overlap in the Eh-pH diagrams ($(Mn,Fe)CO_3$ precipitate at Eh=-0.4~-0.0: pH=9.0~9.5; $(Ca,Fe)CO_3$ precipitate at Eh=-0.3~-0.1: pH=6.5~9.0). The μ-XANES analysis revealed that Cr(III) coexisted in $(Mn,Fe)CO_3$, since Cr cannot be enriched in MnO_2 in general. It is presumed that Mn precipitated originally as MnOOH, which was transformed into $MnCO_3$ in the presence of alkaline fluid. In $(Ca,Fe)CO_3$, 20% of Fe was present as FeOOH. It was implied that FeOOH is precursor of the $FeCO_3$. In addition, we detected S(VI) in the iddingsite, of which chemical species are the clay mineral adsorbent (Fe-rich saponite), $Mn^{2+}(Mn^{3+})O_4$, and $MnCO_3$ by XANES fitting. This results suggested that sulfate-bearing alkaline fluid flowed in the final stage of the iddingsite formation. Besides, its concentration decrease from the mesostasis phase. Therefore, S(VI) in the clay minerals portion related to the FeS in the mesostasis, and apart of FeS might flowed out as alkaline fluid.

©2019. Japan Geoscience Union. All Right Reserved.

From this study, we conclude that the carbonates in iddingsite formed by reductive alkaline fluid (Eh≦0.2: pH=9.0-11), opposite to sulfate formation. However, it is still not clear whether these carbonate minerals were locally formed or widespread in the nakhlite from the spatial distribution point of view. Therefore, we are trying to observe the 3D structure/elemental distribution of the iddingsite by XAFS-CT method in order to clarify the fluid path related to the formation process of the carbonate minerals.

Keywords: Mars, Martian meteorite, Synchrotron radiation X-ray analysis

©2019. Japan Geoscience Union. All Right Reserved.

Influence of water and clay minerals for slope angles on Mars

*Yuhki Matsuoka[1], Ikuo Katayama[1], Rina Noguchi[2], Tomohiro Usui[2]

1. Department of Earth and Planetary Systems Science, Hiroshima University, 2. Institute of Space and Astronautical Science, Japan Aerospace Exploration Agency

An internal frictional angle is determined from a frictional coefficient, which is largely influenced by water and clay minerals. Pore water reduces effective stress, then slope angles becomes smaller. Therefore, slope angles are approximately 25 under hydrostatic condition in contrast with ~35 under dry condition. Most mineral exhibit a constant frictional coefficient μ=0.6-0.85, whereas clay minerals are characterized by a markedly lower frictional coefficient ~0.1 at presence of water (e.g. Behnsen and Faulkner, 2012; Moore and Lockner, 2004). Since a slope angle is roughly equivalent to an internal frictional angle, it is considered that slope angles are affected to become smaller by presence of water and clay minerals including water.
Clay minerals are widely recognized on Mars (Ehlmann and Edwards, 2014) by infrared spectroscopic tools. We focus on a slope angle of Martian topography and research the areas where water might exist.

We focus on Recurring Slope Lineae (RSL) which might suggest the existence of flowing water on Mars (e.g. McEwen et al., 2011; Stillman et al., 2017). Some RSL are found in Coprates Chasma, eastern part of Valles Marineris. We compared slope angles of RSL confirmed points with not confirmed points.
We measured slope angles about 10 points in Coprates Chasma. Slope angles are 31-37 in almost all points and there is no tendency by the presence of RSL and hydroxylated silicates. Therefore, we considered that the contributions of water and clay minerals for slope angles are not prominent in Coprates Chasma.
Furthermore, we verified whether there is contribution of water for slope angles on other areas where water might exist in the same way.

Keywords: Mars, water, slope angle

©2019. Japan Geoscience Union. All Right Reserved.

Dark Streak Features in Mongolia: Implications for Formation Mechanisms of Recurring Slope Lineae on Mars

*Maya Nakamura[1,2], Yasuhito Sekine[1], Keisuke Fukushi[3], Noriko Hasebe[3], Davaadorj Davaasuren[4], Yoshio Takahashi[2], Hitoshi Hasegawa[5], Takuro Ogura[6], Koki Morida[3], Tuvshin Gerelmaa[4]

1. Earth-Life Science Institute, Tokyo Institute of Technology, 2. Department of Earth and Planetary Science, The University of Tokyo, 3. Institute of Nature & Environmental Technology, Kanazawa University, 4. Department of Geography, National University of Mongolia, 5. Department of Global Environment and Disaster Prevention, Kochi University, 6. Department of Socio-Cultural Environmental Science, The University of Tokyo

Recurring Slope Lineae (RSL) are dark, narrow features that appear and lengthen on steep (~30°) slopes in warm seasons and fade in cold seasons of Mars (e.g., McEwen et al., 2011). Although the formation mechanism of RSL is still in debate, several processes have been proposed, including liquid brine flows triggered by melting of subsurface ice (a wet process) (e.g., Stillman et al., 2016), and granular flows on slopes (a dry process) (e.g., Schmidt et al., 2017). However, neither wet nor dry processes can explain all of the observables of RSL. In especially, the wet process seems to be inconsistent with the absence of absorptions due to liquid water on RSL and the fact that RSL appear only on steep slopes (McEwen et al., 2014).

Here, we report RSL-like dark streak features in cold, arid areas of Khangai Mountains, Mongolia, on Earth. In this area, discontinuous permafrost and underground ice melt seasonally (Szuminska, 2016). We find that dark streak features in this area show seasonal variation similar to RSL on Mars. Although the slope angles of the terrestrial analogues (~10°) are shallow, the observed similarities in morphology and seasonal activity suggest that the streak features in Mongolia can be promising terrestrial analogues of RSL on Mars.

We also conducted geological survey for the terrestrial RSL analogues found in Mongolia in August 2018. By analyzing the visual images taken by a unmanned aerial vehicle, a three-dimensional topographic structure was constructed. In the geological survey, we measured water contents of soils on site on and outside the dark streak features. The mineralogical compositions and grain size distributions were measured for the collected soil samples.

Although no water flowed during the survey, dark streak features appeared in the terrestrial RSL analog sites in Mongolia. The upstream of the dark streaks are dented in a few centimeters, which becomes shallower toward the downstream. These observations suggest that erosion of surface soils occurred along with the dark streak features in the past. This view is supported by our results of the flow accumulation analysis. Although the formation of the dark streaks relate with water flow, darkening itself is not caused by the presence of liquid water. Water contents in surface soils on the dark streaks show no significant difference from those outside the streaks within errors. The surface of the dark streaks contains less bright sands and more dark silts than the surfaces outside the dark streaks. These results suggest that selective traction of the bright sand-sized grains by surface runoff results in remnant of the dark silt-sized grains on the slopes, which darkens the streak features after dryness. The required friction velocity for the traction is estimated to be ~20 mm/sec, consistent with flow rate due to melting of ground ice in the research area.

Based on the formation mechanism of the terrestrial RSL analogues, we can address the two issues in the

©2019. Japan Geoscience Union. All Right Reserved.

wet process for RSL formation on Mars; 1) no remote-sensing detection of liquid water, and 2) the fact that RSL appear only on steep slopes. At RSL sites on Mars, a thin layer of fine soils is considered to cover basaltic bedrocks on the slopes (Ruff and Christensen, 2002). If liquid brine flows due to melting of underground ice, this can remove fine sands on the slopes. Consequently, dark streak features appear on the slopes due to exposure of underlying basaltic bedrocks after dryness of brine. Given the difference in gravity between Earth and Mars, we suggest that a friction velocity of surface runoff similar to the terrestrial RSL analogs can be achieved when a slope with angle > ~25–30° on Mars, if the depth and width of water flow are same. Our results suggest that RSL on Mars would appear only on steep slopes due to its low gravity.

Keywords: Mars, Recurring Slope Lineae (RSL), Terrestrial analogues

©2019. Japan Geoscience Union. All Right Reserved.

The occurrence of perchlorate salt in and around the Taklimakan Desert, China

*Haibo Qin[1,2], Shitong Yang[1], Qing Chang[3], Chihiro Miyamoto[1], Yoshio Takahashi[1]

1. Department of Earth and Planetary Science, Graduate School of Science, 2. State Key Laboratory of Environmental Geochemistry, Institute of Geochemistry, Chinese Academy of Sciences, 3. Japan Agency for Marine-Earth Science and Technology

The formation and preservation of perchlorate (ClO_4^-) in arid and semi-arid deserts on Earth is of growing concern, because the desert could serve as a viable analog for Martian landscape where high perchlorate has been recently discovered. In this study, perchlorate in samples collected from the Taklimakan Desert, Xinjiang, NW China was extracted by water and then measured by IC-MS/MS. The Cl speciation was determined by Cl K-edge XANES analysis to provide direct spectroscopic evidences for the presence of perchlorate. Results showed that the moraine sample contains a higher perchlorate concentration and the ClO_4^-/Cl^- ratio in comparison with sand, river sediment and loess samples. Furthermore, $KClO_4$ was identified as the dominant perchlorate species in the hotspot of moraine sample by μ-XANES analysis, which is significantly different from the dominant presence of $Ca(ClO_4)_2$ and $Mg(ClO_4)_2$ species on Martial soil. This result could be explained by the lowest solubility for $KClO_4$, while other perchlorate salts would be easily leached and mobile on Earth in contrast to Mars where much lesser liquid water is present in the history and present-day. Thus, the finding in this study would provide important insights into the prevalence of perchlorate on Mars.

Keywords: perchlorate, distribution, XANES

©2019. Japan Geoscience Union. All Right Reserved.

Measurement technique to quantify OH radicals photochemically generated on the ice surface

*Akihiro Yabushita[1], Hiroaki Nishimoto[1], Akira Harata[1]

1. Interdisciplinary Graduate School of Engineering Sciences, Kyushu University

Reaction processes of many molecules are presumably involved in oxidative atoms/molecules generated by photodecomposition of molecules adsorbed on cold dust grains. Hydroxyl (OH) radicals are considered as one of them. The chemistry of OH radicals plays a key role in the radiolysis and photolysis of water-rich ices of astrochemical origin. Measurements of OH radical in water-ice in the laboratory have been done by UV, EPR, X-ray absorption, and infrared absorption measurements. However, quantification of OH radicals on the ice surface has not yet been made. In the present work, we have tried to develop the measurement technique to quantify OH radicals photochemically generated on the surface of ice film. In this technique, OH are converted to the different molecule by utilizing the chemical reaction, and monitored through reflection absorption infrared spectroscopy. We have investigated the effect of ice temperature on abundance of OH radicals on the ice surface at 8-70 K. In addition, the effect of ice surface morphology on abundance of OH radicals has been studied by preparing the amorphous solid water and polycrystalline ice. The present study experimentally shows both the temperature and surface morphology plays an important role in abundance of OH radicals on the ice surface.

Keywords: OH radical, ice, vacuum-ultraviolet light, RAIRS, surface

©2019. Japan Geoscience Union. All Right Reserved.

[J] Oral | M (Multidisciplinary and Interdisciplinary)：M-IS Intersection

Mon. May 27, 2019 10:45 AM - 12:15 PM JST | Mon. May 27, 2019 1:45 AM - 3:15 AM UTC | 201A 2F

[M-IS13] Biogeochemistry

convener:Keisuke Koba(Center for Ecological Research, Kyoto University), Hideaki Shibata(Field Science Center fot Northern Biosphere, Hokkaido University), Naohiko Ohkouchi(Japan Agency for Marine-Earth Science and Technology), Youhei Yamashita(Faculty of Environmental Earth Science, Hokkaido University), Chairperson:Keisuke Koba(Kyoto University), Yoshiyuki Inagaki, Kazumichi Fujii

Biogeochemistry is an interdisciplinary study field including ecology, geochemistry, oceanography, limnology, hydrology, soil science and environmental sciences. Respective researches have tended to be conducted separately so far. This session aims to provide a common platform for biogeochemists of different disciplines, which facilitates the interactive discussion and information exchanges for further development of biogeochemical studies.

10:45 AM - 11:00 AM JST | 1:45 AM - 2:00 AM UTC

[MIS13-01] Root meets clays: Tree root plasticity in podzolized soil

*Kazumichi Fujii[1], Naoki Makita[2], Martin Küttim[3], Shinya sugita[3] (1.Forestry and Forest Products Research Institute, 2.Shinshu University, 3.Tallinn University)

11:00 AM - 11:15 AM JST | 2:00 AM - 2:15 AM UTC

[MIS13-02] Nitrogen transformation process in newly created salt marsh in the aftermath of the 2011 Great East Japan Earthquake

*Keitaro Fukushima[1], Kazuma Hashimoto[2], Megumi Kuroiwa[3], Katsuhide Yokoyama[2], Yuichi Suwa[3] (1.Center for Ecological Research, Kyoto University, 2.Graduate School of Urban Environmental Sciences, Tokyo Metropolitan University, 3.Faculty of Science and Engineering, Chuo University)

11:15 AM - 11:30 AM JST | 2:15 AM - 2:30 AM UTC

[MIS13-03] Succession of soil nitrification potential at a glacier foreland in Svalbard

*Kentaro Hayashi[1], Yukiko Tanabe[2,3], Keisuke Ono[1], Maki Asano[4], Shohei Hattori[5], Masaki Uchida[2,3], Masahito Hayatsu[1] (1.Institute for Agro-Environmental Sciences, NARO, 2.National Institute of Polar Research, 3.SOKENDAI, 4.University of Tsukuba, 5.Tokyo Institute of Technology)

11:30 AM - 11:45 AM JST | 2:30 AM - 2:45 AM UTC

[MIS13-04] Transition of soil organic carbon in a volcanic ash soil derived from Towada volcano, Japan

*JITHYA NAWODI WIJESINGHE[1], Jun Koarashi[2], Mariko Atarashi Andoh[2], Yoko Saito Kokubu[3], Noriko Yamaguchi[4], Takashi Sase[5], Mamoru Hosono[6], Yudzuru Inoue[7], Yuki Mori[1], Syuntaro Hiradate[1] (1.Soil Science Laboratory, Faculty of Agriculture, Kyushu University, Fukuoka 819-0395, Japan, 2.Nuclear Science and Engineering Center, Japan Atomic Energy Agency, Ibaraki 319-1195, Japan, 3.Tono Geoscience Center, Japan Atomic Energy Agency,Gifu 509-5102, Japan, 4.National Agriculture and Food Research Organization, Institute for Agro-environmental Sciences, 3-1-3 Kan-nondai, Tsukuba, Ibaraki 305-8604, Japan, 5.Boreal Laboratory for Phytolith Research, Iwate 028-7302,Japan, 6.Tokyo Natural History Research Structure,Tokyo 162-0052, Japan, 7.Faculty of Applied Information Technology, Nagasaki Institute of Applied Science,Nagasaki 851-0193, Japan)

11:45 AM - 12:00 PM JST | 2:45 AM - 3:00 AM UTC

[MIS13-05] General pattern of carbon and nitrogen isotopic variation across a wide range of soils and its controlling factors

*Rota Wagai[1], Masako Kajiura[1], Yudzuru Inoue[2], Maki Asano[3], Chie Hayakawa[4] (1.NARO, Institute for Agro-Environmental Sciences, 2.Nagasaki Institute of Applied Science, 3.University of Tsukuba, 4.University of Tokyo)

12:00 PM - 12:15 PM JST | 3:00 AM - 3:15 AM UTC

[MIS13-06] Nutrient sources in some Japanese forest ecosystems: the contribution of precipitation, weathering and litter fall

*Yoshiyuki Inagaki[1], Kazumichi Fujii[1] (1.Forestry and Forest Products Research Institute)

Root meets clays: Tree root plasticity in podzolized soil

*Kazumichi Fujii[1], Naoki Makita[2], Martin Küttim[3], Shinya sugita[3]

1. Forestry and Forest Products Research Institute, 2. Shinshu University, 3. Tallinn University

Root functional traits could vary among plant species. Root traits are known to respond to a decrease in nutrient availability along with soil aging and plant succession, while root plasticity of single tree species to soil aging is still unclear on a soil profile scale. We investigated whether trees develop finer root architecture along with soil aging in coniferous forest dominated by single species (*Pinus sylvestris*) in Estonia. We measured depth distribution of root biomass and traits (specific root length and tissue density). We compared ca. 100, 300, and 500 years old soils (podzols) on two coastal dune chrnosequence that differ in abundance of soil clay or Al and Fe oxides; Hiiumaa island (facing Balt Sea) and Juminda (facing Finland Gulf), where ridge-swale topography has been developed by isostacy. On Juminda chronosequence where oxalate-extractable P (oxide-bonded) is accumulated in the shallow subsoil, fine roots are concentrated in oxide-rich soil horizons. On oxide-poor Hiiumaa chronosequence where P is translocated in the deeper soil, fine roots are concentrated in organic horizon. Tree roots could change root distribution and surface area depending on extent of P occlusion in clays or leaching in soil aging. Tree community shift toward finer root architecture along with migration of Al and Fe oxides or selection of individuals with finer root structure could occur.

Keywords: Isostacy, Fine root, Soil, Podzolization

©2019. Japan Geoscience Union. All Right Reserved.

Nitrogen transformation process in newly created salt marsh in the aftermath of the 2011 Great East Japan Earthquake

*Keitaro Fukushima[1], Kazuma Hashimoto[2], Megumi Kuroiwa[3], Katsuhide Yokoyama[2], Yuichi Suwa[3]

1. Center for Ecological Research, Kyoto University, 2. Graduate School of Urban Environmental Sciences, Tokyo Metropolitan University, 3. Faculty of Science and Engineering, Chuo University

Dissimilatory nitrate reduction to ammonium (DNRA) is one of the most important processes of nitrate removal in an anaerobic condition. The 2011 Great East Japan Earthquake and subsequent tsunami attack widely created the intertidal salt marsh along the coast due to sea water intrusion and large ground subsidence. It is necessary to elucidate the ecosystem functions of the newly created salt march. Salt marsh is located in the conjunction point of river and sea, therefore the conversion of dissolved inorganic nitrogen concentrations and forms in the salt marsh may directly impact the productivity and biodiversity of marine ecosystems. However it is still unknown that the role of this specific salt marsh in nutrient dynamics. In September 2017, the surface sediments were collected at the intertidal and subtidal points of the salt marsh, and their potential rates of denitrification, DNRA, and anaerobic ammonium oxidation (Anammox) were estimated by using a 15N tracer technique. As for the nitrate-nitrogen removal in the sediments, the rate of DNRA was ranged from 24.8 to 177 nmol g-1 h-1, while the denitrification rate was ranged from 2.9 to 32.8 nmol g-1 h-1. Our results demonstrate that the DNRA would be significantly important in nitrate removal, and it also suggests that the conversion of inorganic nitrogen form nitrate to ammonium in the salt marsh might affect the species composition of phytoplankton and the primary production in the marsh and the coastal area connected with the marsh.

Keywords: salt marsh, dissimilatory nitrate reduction to ammonium, denitrification

©2019. Japan Geoscience Union. All Right Reserved.

Succession of soil nitrification potential at a glacier foreland in Svalbard

*Kentaro Hayashi[1], Yukiko Tanabe[2,3], Keisuke Ono[1], Maki Asano[4], Shohei Hattori[5], Masaki Uchida[2,3], Masahito Hayatsu[1]

1. Institute for Agro-Environmental Sciences, NARO, 2. National Institute of Polar Research, 3. SOKENDAI, 4. University of Tsukuba, 5. Tokyo Institute of Technology

Glaciers in Svalbard particularly in the western part of the archipelago has experienced retreating since 20th century. It is concerned that the retreat has been accelerated recently. Glacier retreat on the land uncovers the ground surface under ice. This is a restart of soil genesis as the past soil was lost due to ice erosion. What does happen in nitrogen cycle of the redeveloping soil, and how does ongoing climate warming affect the redeveloping soil nitrogen cycle? In the present study, we focus on nitrification as a source of nitrate. Nitrification is a two-step microbial process consisting of ammonia oxidation to nitrite and nitrite oxidation to nitrate, in which ammonia oxidation is the rate limiting step. Nitrifiers are basically autotrophic and therefore contribute to soil nitrogen cycle from the early stage of soil genesis. It is also interesting that nitrifiers exist across the two domains, bacteria and archaea. The purposes of the present study are to investigate nitrification properties (ammonia oxidation potential [AOP] and flora of nitrifiers) and their time-series changes in the surface soil in the foreland of East Brøgger Glacier near Ny-Ålesund, Svalbard and to elucidate responses of the nitrification properties to environmental manipulations (passive warming and accompanied changes in soil moisture) using open top chambers (OTC). We have been conducting a field experiment at two permanent exclosures established by NIPR in the foreland, i.e., Site 1 (N78˚54'46", E11˚50'18") and Site 2 (N78˚54'54", E11˚49'38"). It is inferred from aerial photos that Site 1 lost its ice coverage between 1969 and 1977, and Site 2 in 1950s or 1960s. Although the foreland was abundant with rocks and stones, the surface was partly covered with mineral soil consisting of fine sand and silt. The field experiment started in July 2015. A passive warming plot and a control plot were set at each site. Twenty polyvinylchloride cores filled with 4-mm sieved and well mixed surface soil collected at each site were set at each of the warming and control plots, of which 5 cores were used to measure soil temperature and volumetric water content and the rest 15 cores were for determining nitrification properties of topsoil (0-2 cm) and subsoil (2-4 cm) collecting 3 cores every July. The field experiment will be end in the summer of 2020. AOP was determined as the nitrite production rate of soil by aerobic shaking incubation with substrate (ammonium sulfate) at 10 and 20 ˚C. Nitrifiers' flora, i.e., gene abundance and species composition of ammonia oxidizing bacteria and archaea will be identified after the completion of field experiment. Annual mean warming effects of the OTC were 0.4–0.5 ˚C at Site 1 and 0.5–0.7 ˚C at Site 2; however, stronger warming effect appeared in the snow season. OTC effects to soil moisture were moistening at the warming plots for the first year, but it turned into drying after that. The determined AOPs at Site 2 were roughly double of those at Site 1. Differences in AOP between the warming and control plots and between the topsoil and subsoil were not significant. The time-series changes in AOP were not monotonous. Meanwhile, AOPs at 20 ˚C were significantly larger than those at 10 ˚C for sites, topsoil and subsoil, and time-series changes. Annual mean soil temperatures at the two sites were from −1.5 to 0.3 ˚C, from 5 to 6 ˚C in the snowless season, and 14 ˚C as the maximum daily mean. The positive response of AOP to a high temperature of 20 ˚C implies that future climate warming accelerates soil nitrification in the foreland. Although it is early to conclude, the succession of AOP at 10 ˚C was unclear and that at 20 ˚C showed an increasing trend. This study was supported by Grants-in-Aid for Scientific Research (No. 26304018) provided by the Japan Society for the Promotion of Science. This study was also partly supported by the National Institute of Polar Research, Japan, through Project

©2019. Japan Geoscience Union. All Right Reserved.

Research No. KP309.

Keywords: Nitrification, Ammonia oxidation potential, Glacier retreat, Tundra, Arctic soil, Open top chamber

©2019. Japan Geoscience Union. All Right Reserved.

Transition of soil organic carbon in a volcanic ash soil derived from Towada volcano, Japan

*JITHYA NAWODI WIJESINGHE[1], Jun Koarashi[2], Mariko Atarashi Andoh[2], Yoko Saito Kokubu[3], Noriko Yamaguchi[4], Takashi Sase[5], Mamoru Hosono[6], Yudzuru Inoue[7], Yuki Mori[1], Syuntaro Hiradate[1]

1. Soil Science Laboratory, Faculty of Agriculture, Kyushu University, Fukuoka 819-0395, Japan, 2. Nuclear Science and Engineering Center, Japan Atomic Energy Agency, Ibaraki 319-1195, Japan, 3. Tono Geoscience Center, Japan Atomic Energy Agency,Gifu 509-5102, Japan, 4. National Agriculture and Food Research Organization, Institute for Agro-environmental Sciences, 3-1-3 Kan-nondai, Tsukuba, Ibaraki 305-8604, Japan, 5. Boreal Laboratory for Phytolith Research, Iwate 028-7302,Japan, 6. Tokyo Natural History Research Structure,Tokyo 162-0052, Japan, 7. Faculty of Applied Information Technology, Nagasaki Institute of Applied Science,Nagasaki 851-0193, Japan

Soil organic carbon (SOC) is generated from organic components by receiving biological and chemical transformations in soils. In volcanic ash soils, mean resident time of SOC is generally long, so the mechanisms of the long lives are of interest for the development of techniques for carbon sequestration in soils. In the present study, we aim to elucidate the transformation process of SOC by fractionating SOC representing the transition stage of the original organic components and characterized the SOC fractions by isotopic and nuclear magnetic resonance spectroscopic analyses.

In this study, we analyzed SOC from a buried soil layer formed between 6,200 and 9,400 cal yBP, because the SOC can be well conserved without the influence of serious human activity. In addition, the age of those buried SOC can be determined by ^{14}C analysis with high accuracy. The soil samples were collected from a buried soil horizon (six samples collected from the depth between 152 and 182 cm at 5 cm intervals) close to Towada volcano, Japan. From each of the soil sample, SOC were extracted and fractionated by precipitation with controlling pH of the extracted solution (Hiradate *et al.*, 2007), resulting in humin, humic acid, and four fulvic acid fractions (two hydrophilic fulvic acid fractions: FA_1 and FA_2, and two hydrophobic fulvic acid fractions: FA_3, and FA_{IHSS}). The SOC fractions were freeze-dried and analyzed for determining $\delta^{13}C$ and $\delta^{15}N$ values by using isotope ratio mass spectrometer and for ^{14}C dating by using accelerator mass spectrometer. Solid-state ^{13}C CPMAS NMR analysis was also conducted to investigate the structural characteristics and quantify the carbon species of the SOC fractions.

The $\delta^{13}C$ values of humic acid, FA_1, FA_2, FA_3, and FA_{IHSS} fractions were -23.85±0.36, -20.75±0.32, -21.10 ±0.38, -22.81±0.41, and -23.22 ±0.33‰, respectively, while $\delta^{15}N$ values were 3.00±0.37, 8.16±1.73, 9.66±0.54 , 4.73±0.83, and 5.20±0.54‰, respectively. The ^{14}C age of humic acid, FA_1, FA_2, FA_3, and FA_{IHSS} fractions was 6130±300, 5630±240, 5400±200, 5410±230, and 5680±260 cal yBP, respectively. Decomposition and recycling of plant residues during the transformation of SOC result in enrichment of heavier carbon and nitrogen isotopes due to preferential stabilization (Wada *et al.*, 2013). Therefore, the increase of $\delta^{13}C$ and $\delta^{15}N$ values in SOC fractions corresponds to successive transformation of SOC. The slope of the relationship between $\delta^{13}C$ and $\delta^{15}N$ values was 1.69, and the results were similar to the result of Wada *et al.* (2013), indicating successive transformation of SOC from plant organic matter to hydrophilic fulvic acid fraction. The hydrophilic fulvic acid fraction would be more microbially processed than hydrophobic fulvic acid and humic acid fractions. Because the humic acid fractions were rich in aromatic structure, they would be formed in the early stage of the formation right after C fixation by plants and chemically stabilized in the soil horizon by fire event etc. The hydrophobic fulvic acid horizons, which are less rich in aromatic C but relatively rich in aliphatic C, would be formed by microbial transformation

©2019. Japan Geoscience Union. All Right Reserved.

and stabilized by chemical and physical factor. The hydrophilic fulvic acid fractions, which are rich in *O* -alkyl C, would be microbially metabolized many times and stabilized physically in the soil horizons.

The validity of the chemical fractionation of SOC on the soil dynamics study has been discussed and sometimes regarded as questionable, but at least in our study on a buried volcanic ash soil, the chemical fractionation procedure successfully separated SOC receiving different metabolisms and having different genesis and chemical structural features.

Hiradate, S., Yonezawa, T., Takesako, H., 2007. Soil science and Plant Nutrition 57, 413-419.
Wada, E., Ishii, R., Aita, M.N., Ogawa, N. O., Kohzu, A., Hyodo, F., Yamada, Y., 2013. Ecological Research 28, 173-181.

©2019. Japan Geoscience Union. All Right Reserved.

General pattern of carbon and nitrogen isotopic variation across a wide range of soils and its controlling factors

*Rota Wagai[1], Masako Kajiura[1], Yudzuru Inoue[2], Maki Asano[3], Chie Hayakawa[4]

1. NARO, Institute for Agro-Environmental Sciences, 2. Nagasaki Institute of Applied Science, 3. University of Tsukuba, 4. University of Tokyo

Organic matter (OM) in soil represents the largest carbon pool on land. The production of CO2 via microbial degradation of soil OM therefore has a strong impact on global C cycle and anticipated global warming. Previous studies have shown that any soil holds multiple OM pools of varying stability against microbial attack. Growing number of studies suggests protective effect of specific mineral phases and mineral matrix. OM, however, interacts with soil minerals in highly complex ways including co-precipitation of organic ligands with multivalent metals at molecular scale and physical aggregation of OM with mineral particles at micron and larger scales.

Here we examined the relationship between the isotopic compositions (C-13, C-14, and N-15) and mineralogical characteristics (surface area and elemental composition, pedogenic metal oxides) among density fractions using a range of surface soils of contrasting mineralogy including volcanic soils rich in short-range-order minerals and much more weathered soils from both agricultural and natural systems. Each soil was separated into 4-7 density fractions after mechanical shaking with sodium polytungstate. From LF to higher-density fractions, We assessed how C aging is related to C13 and N15 enrichment and to what extent these isotopic variations among the fractions were controlled by the mineralogical characteristics.

Keywords: Soil, Carbon sequestration, organo-mineral interaction, stable carbon and nitrogen isotope, Radiocarbon, mineralogy

©2019. Japan Geoscience Union. All Right Reserved.

Nutrient sources in some Japanese forest ecosystems: the contribution of precipitation, weathering and litter fall

*Yoshiyuki Inagaki[1], Kazumichi Fujii[1]

1. Forestry and Forest Products Research Institute

Base cation such as calcium and potassium is important nutrient for tree growth in forest ecosystems. Major sources of base cation to forest soil are precipitation, weathering of parent material and litter fall. Weathering rate of base cation is estimated from the input from precipitation, runoff from stream and uptake by vegetation. For plant uptake two different properties, i.e., long-term accumulation in plant biomass and annual uptake should be quantified. Nutrient cycling of many Japanese forest ecosystems has been studied but information about the contribution of these sources is limited. This study compared three nutrient sources in four forest ecosystems in Japan. These forests are Oyasan (Gunma Pref.), Kamikamo (Kyoto Pref.), Kiryu (Shiga pref.) and Takatori (Kochi Pref.). We calculated nutrient budget of potassium, calcium and magnesium. The rate of rock weathering of base cation ranged from 0.22 to 4.37 kmolc ha^{-1} yr^{-1} and increased in the order of Kamigamo < Kiryu <Oyasan < Takatori. In potassium cycling, the contribution of litter fall was greater than that of weathering or precipitation. The runoff of calcium and magnesium from soil was greater in Takatori, where the rate of weathering was high. Although the rate of weathering varied substantially among forest ecosystems, the annual flux of litter fall was relatively constant. Similar calculation was applied for nitrogen cycling and the source from soil was treated as that from nitrogen accumulated during the past pedogenesis. Nitrogen input from the accumulated soil source was 36 % in Oyasan whereas that in other three forestswas 0%. Oyasan was considered as a nitrogen-saturated forest and the result of the study suggest the ecosystem relies on different nitrogen source.

Keywords: nutrient cycling, weathering, plant uptake, forest ecosystems

©2019. Japan Geoscience Union. All Right Reserved.

[J] Oral | M (Multidisciplinary and Interdisciplinary)：M-IS Intersection

Mon. May 27, 2019 1:45 PM - 3:15 PM JST | Mon. May 27, 2019 4:45 AM - 6:15 AM UTC | 201A 2F

[M-IS13] Biogeochemistry

convener:Keisuke Koba(Center for Ecological Research, Kyoto University), Hideaki Shibata(Field Science Center fot Northern Biosphere, Hokkaido University), Naohiko Ohkouchi(Japan Agency for Marine-Earth Science and Technology), Youhei Yamashita(Faculty of Environmental Earth Science, Hokkaido University), Chairperson:Keisuke Koba(Kyoto University), Yohei Yamashita, Kazuya Nishina, Kazumichi Fujii

Biogeochemistry is an interdisciplinary study field including ecology, geochemistry, oceanography, limnology, hydrology, soil science and environmental sciences. Respective researches have tended to be conducted separately so far. This session aims to provide a common platform for biogeochemists of different disciplines, which facilitates the interactive discussion and information exchanges for further development of biogeochemical studies.

1:45 PM - 2:00 PM JST | 4:45 AM - 5:00 AM UTC

[MIS13-07] Ultrahigh-resolution mass spectral analysis of dissolved organic matter in rainfall, throughfall and soil water in temperate forest stands, western Japan

*Junichiro Ide[1], Keitaro Yamase[2], Seonghun Jeong[3], Noki Makita[4], Hiroshi Nishimura[5], Keitaro Fukushima[6], Kyoichi Otsuki[7], Mizue Ohashi[8] (1.Institute of Decision Science for a Sustainable Society, Kyushu University, 2.Forestry and Forest Products Research Institute, Hyogo Prefectural Technology Center for Agriculture, Forestry and Fisheries, 3.Graduate School of Bioresources and Bioenvironmental Sciences, Kyushu University, 4.Faculty of Science, Shinshu University, 5.Research Institute for Sustainable Humanosphere, Kyoto University, 6.The Center for Ecological Research, Kyoto University, 7.Faculty of Agriculture, Kyushu University, 8.School of Human Science and Environment, University of Hyogo)

2:00 PM - 2:15 PM JST | 5:00 AM - 5:15 AM UTC

[MIS13-08] Basin-scale transport of allochthonous humic-like fluorescent dissolved organic matter by the North Pacific Intermediate water

*Youhei Yamashita[1], Jun Nishioka[2], Hajime Obata[3], Hiroshi Ogawa[3] (1.Faculty of Environmental and Earth Science, 2.Institute of Low Temperature Science, Hokkaido University, 3.Atmosphere and Ocean Research Institute, The University of Tokyo)

2:15 PM - 2:30 PM JST | 5:15 AM - 5:30 AM UTC

[MIS13-09] Bacterial contribution to dissolved organic matter in a large monomictic lake (Lake Biwa) indicated by amino acids enantiomers

*Yasuhiko T. Yamaguchi[1], Chikage Yoshimizu[2], Ichiro Tayasu[2], Keisuke Koba[3], Kazuhide Hayakawa[1] (1.Lake Biwa Environmental Research Institute, 2.Research Institute for Humanity and Nature, 3.Center for Ecological Research, Kyoto University)

2:30 PM - 2:45 PM JST | 5:30 AM - 5:45 AM UTC

[MIS13-10] High-sensitivity tracer assay for oxygen consumption rate in ocean and lakes using ^{17}O as a tracer

*Urumu Tsunogai[1], Shogo Kashiwagi[1], Masanori Ito[1], Fumiko Nakagawa[1], Chiho Sukigara[1] (1.Graduate School of Environmental Studies, Nagoya University)

2:45 PM - 3:00 PM JST | 5:45 AM - 6:00 AM UTC

[MIS13-11] Ecology of bacterioplankton inhabiting oxygenated hypolimnia of deep freshwater lakes

*Yusuke Okazaki[1] (1.National Institute of Advanced Industrial Science and Technology)

3:00 PM - 3:15 PM JST | 6:00 AM - 6:15 AM UTC

[MIS13-12] Nitrous oxide emission from the drainage and the production processes in oil palm plantation on peatland

*Kazuya Nishina[1], Lulie Melling[2], Ryuichi Hirata[1], Yoshiyuki Takahashi[1], Sakae Toyoda[3], Kotaro Terajima[3], Masayuki Itoh[4] (1.NIES National Institute of Environmental Studies, 2.SARAWAK Tropical Peat Research Institute, 3.Tokyo Institute of Technology, 4.University of Hyogo)

Ultrahigh-resolution mass spectral analysis of dissolved organic matter in rainfall, throughfall and soil water in temperate forest stands, western Japan

*Junichiro Ide[1], Keitaro Yamase[2], Seonghun Jeong[3], Noki Makita[4], Hiroshi Nishimura[5], Keitaro Fukushima[6], Kyoichi Otsuki[7], Mizue Ohashi[8]

1. Institute of Decision Science for a Sustainable Society, Kyushu University, 2. Forestry and Forest Products Research Institute, Hyogo Prefectural Technology Center for Agriculture, Forestry and Fisheries, 3. Graduate School of Bioresources and Bioenvironmental Sciences, Kyushu University, 4. Faculty of Science, Shinshu University, 5. Research Institute for Sustainable Humanosphere, Kyoto University, 6. The Center for Ecological Research, Kyoto University, 7. Faculty of Agriculture, Kyushu University, 8. School of Human Science and Environment, University of Hyogo

This study aimed to clarify alternations of the quality of dissolved organic matter (DOM) in rainwater moving through temperate forests. For this, we compared the molecular composition of dissolved organic matter (DOM) between bulk deposition (rainfall), throughfall and soil water in Japanese cypress (*Cryptomeria japonica*) and Japanese stone oak (*Lithocarpus edulis*) stands, which were regarded as coniferous and broad-leaved stands, respectively, during a rain event. Analyses of ultrahigh-resolution Fourier transform ion cyclotron resonance mass spectrometry revealed that the number of DOM molecular species detected was significantly greater in throughfall and soil water than in rainfall ($p < 0.05$). In contrast, the number of molecular species did not significantly differ between throughfall and soil water ($p > 0.05$). There were no significant differences in the number of molecular species in both throughfall and soil water between coniferous and broad-leaved stands ($p > 0.05$). These results suggest that a diverse array of DOM molecules are provided from the tree canopies and soils to the rainwater in both stands. Approximately 52%–59% of the total molecular species in throughfall samples ($n = 6$) were unique to throughfall. Additionally, approximately a half of the total molecular species in soil water samples ($n = 5$) were unique to soil water. The classification of molecular species into seven biomolecular classes using a van Krevelen diagram revealed that throughfall samples contained many of lipid and protein molecules compared to rainfall and soil water samples, whereas approximately 70% of the total molecular species in soil water were lignin-like molecules. The analysis of multidimensional scaling revealed that molecular species were significantly differentiated between rainfall, throughfall and soil water ($p < 0.05$). These results indicate that there are diverse molecules unique to throughfall and soil water and that the quality of DOM drastically changes in rainwater as it moves through temperate forests.

Keywords: Biomolecules, Carbon dynamics, Forest type, FT-ICR MS, Molecular diversity

©2019. Japan Geoscience Union. All Right Reserved.

Basin-scale transport of allochthonous humic-like fluorescent dissolved organic matter by the North Pacific Intermediate water

*Youhei Yamashita[1], Jun Nishioka[2], Hajime Obata[3], Hiroshi Ogawa[3]

1. Faculty of Environmental and Earth Science, 2. Institute of Low Temperature Science, Hokkaido University, 3. Atmosphere and Ocean Research Institute, The University of Tokyo

The levels of humic-like fluorescent dissolved organic matter (FDOM) in the open ocean generally showed nutrient-type vertical profile. In the surface water, low levels of humic-like FDOM is due to degradation by sunlight. In the dark ocean, linear relationships between levels of humic-like FDOM and apparent oxygen utilization (AOU) have been observed throughout the global ocean, indicating that humic-like FDOM is produced in situ in the ocean interior as organic matter is oxidized by microbes and is resistant to microbial degradation with time scales of thermohaline circulation.

While, it has also been observed that some plots of humic-like FDOM vs AOU in the specific water masses, namely, the North Pacific Intermediate Water (NPIW) and the North Atlantic Deep Water (NADW), seemed to deviate from the general relationship between humic-like FDOM and AOU. The previous studies showed that concentrations of lignin phenols, a unique biomarker of vascular plants, were found to be higher in the NPIW and the NADW compared with other water masses. Thus, the deviations of plots between humic-like FDOM and AOU in the NPIW and the NADW can be considered to be derived from terrestrial (allochthonous) humic-like FDOM.

In this study, we determined a basin-scale distribution of humic-like FDOM from the Sea of Okhotsk to the western subtropical North Pacific. We found the linear relationship between levels of humic-like FDOM and AOU in the deep layer (>1000 m) of the western North Pacific. While, we also found plots in the mesopelagic layer, corresponding to the NPIW, were significantly deviated from the relationship observed in the deep layer. Such distributional pattern implies that allochthonous humic-like FDOM derived from the Sea of Okhotsk is transported widely to the intermediate layer of the North Pacific by the NPIW.

Keywords: North Pacific Intermediate Water, dissolved organic matter, allochthonous

©2019. Japan Geoscience Union. All Right Reserved.

Bacterial contribution to dissolved organic matter in a large monomictic lake (Lake Biwa) indicated by amino acids enantiomers

*Yasuhiko T. Yamaguchi[1], Chikage Yoshimizu[2], Ichiro Tayasu[2], Keisuke Koba[3], Kazuhide Hayakawa[1]

1. Lake Biwa Environmental Research Institute, 2. Research Institute for Humanity and Nature, 3. Center for Ecological Research, Kyoto University

Dissolved organic matter (DOM) plays crucial roles in the biogeochemical cycles in aquatic environments. A number of past studies have strongly indicated that heterotrophic bacteria represent a major source to the ocean DOM pool, suggesting that microbial processes may underlie the mechanisms for DOM preservation ("microbial carbon pump"). In particular, enantiomeric (D/L) analysis of amino acids (AA) in DOM has been used to characterize sources of DOM, and high abundance of specific D-AA bacterial biomarkers have suggested that bacterially-sourced organic matter may be a key in formation of the ocean's recalcitrant DOM pool (e.g., McCarthy et al., 1998; Kaiser & Benner, 2008; Yamaguchi & McCarthy, 2018). In contrast to the marine environments, the distribution of D-AA bacterial biomarkers in DOM has been severely understudied in lacustrine environments. To our knowledge, there has been just one report of D-AA concentration in DOM for a freshwater lake water column (Kawasaki et al., 2013: in eutrophic Lake Kasumigaura, Japan).

Our study explores the use of D-AA bacterial biomarkers as an effective approach to estimate bacterial contribution to the DOM pools in lacustrine environments. First, we have developed a new analytical approach using GC-MS for D-AA concentration in the total DOM pool of lake water. This method can detect unusual D-AA molecules (e.g., D-Val, D-Phe, D-Tyr) together with the major four bacterial biomarkers (D-Ala, D-Glu, D-Asp, and D-Ser) which have been analyzed by the conventional HPLC method. Second, we determined vertical and seasonal variations in the D-AA concentrations of DOM in a large monomictic lake (Lake Biwa, Japan). To our knowledge, this study is the first report of D-AA concentrations of DOM in a meso/oligotrophic lake. Finally, we conducted an incubation experiment using natural microbial community in Lake Biwa to estimate the D-AA yields in freshly-produced bacterial DOM in the lake environment, which are essential for the calculation of bacterial contribution to the natural DOM pools.

From the vertical distribution of D-AA concentration during the stratified period (summer and fall), we estimated that a substantial fraction (30-40%) of the recalcitrant pool of dissolved organic carbon (DOC) is bacterial origin. In contrast, the bacterial contribution was less than 20% to the semi-labile DOC pool which accumulates in the lake epilimnion during summer. These results suggest that the "microbial carbon pump" (production of recalcitrant DOM by heterotrophic bacteria) is an important process in the biogeochemical cycles of lakes.

Keywords: Dissolved Organic Matter, Amino Acids, Enantiomers, Microbial Loop, Microbial Carbon Pump, Organic Geochemistry

©2019. Japan Geoscience Union. All Right Reserved.

High-sensitivity tracer assay for oxygen consumption rate in ocean and lakes using ^{17}O as a tracer

*Urumu Tsunogai[1], Shogo Kashiwagi[1], Masanori Ito[1], Fumiko Nakagawa[1], Chiho Sukigara[1]

1. Graduate School of Environmental Studies, Nagoya University

We newly devellopped new high-sensitivity tracer assay for oxygen consumption rate in ocean and lakes using ^{17}O as a tracer.

Keywords: oxygen consumption rate, stable isotopes, tracer assay, anoxic water, photorespiration

©2019. Japan Geoscience Union. All Right Reserved.

Ecology of bacterioplankton inhabiting oxygenated hypolimnia of deep freshwater lakes

*Yusuke Okazaki[1]

1. National Institute of Advanced Industrial Science and Technology

In marine and freshwater systems, there are 10^4–10^7 cells mL^{-1} of bacterioplankton in the water column, playing central roles in the microbial food web and biogeochemical cycling. In oligo-mesotrophic deep freshwater lakes, such as Lake Biwa, Baikal and The Laurentian Great Lakes, the hypolimnion is a dark, cold, aerobic water layer below the thermocline that accounts for a majority of the lake volume. Analogous to the deep ocean, the oxygenated hypolimnion is a realm for important biogeochemical processes, such as accumulation and decomposition of semilabile organic matter, nitrification, and methane oxidation. However, our knowledge for the diversity and ecology of the bacterioplankton in the oxygenated hypolimnion is still limited and even poorer than that in the deep ocean. To fill this gap, the present study comprehensively investigated the bacterioplankton community composition in the oxygenated hypolimnia of deep freshwater lakes.

To obtain data from lakes with varying depth, surface area, water temperature, trophic state, pH, lake origin and water retention time, 13 Japanese lakes and 7 European perialpine lakes have been sampled so far. The waters were collected vertically at the deepest point in each lake and the bacterial community composition was determined by 16S rRNA gene amplicon sequencing and catalyzed reporter deposition-fluorescence *in situ* hybridization (CARD-FISH). The result revealed that the oxygenated hypolimnion is inhabited by hypolimnion-specific bacterioplankton lineages that were phylogenetically different by phylum-level from commonly-known freshwater bacterioplankton lineages dominating in epilimnia. While most of the hypolimnion-specific lineages were uncultured and thus their eco-physiology was not well understood, the fact that they commonly predominate in global lakes suggests their importance in the microbial food web and biogeochemical cycling in deep freshwater lakes.

Among the hypolimnion-specific lineages, the CL500-11 lineage (phylum Chloroflexi) is particularly abundant, accounting for more than 10% of bacterioplankton cells in the hypolimnion in many lakes. CARD-FISH analysis revealed their relatively large cell size (1–2 μm), suggesting their contribution in biovolume is even greater. Together with the information collected from literatures and sequence databases, the results demonstrated that CL500-11 inhabit most freshwater lakes with the oxygenated hypolimnion, although their low abundances were observed in lakes with low pH, shallow depth, or short water retention time (<1 year). The results as well as metagenomic and geochemical insights from published studies allowed to hypothesize possible characteristics of substrates supporting CL500-11 growth, most likely nitrogen-rich autochthonous dissolved organic matter (DOM) ubiquitously available in the hypolimnion that may turnover within an annual timescale; for instance, DOM derived from the epilimnion transferred by winter vertical mixing, or DOM secondary produced in the hypolimnion, such as cellular debris from other microbes.

In conclusion, this study revealed that the microbial food web and biogeochemical processes in the oxygenated hypolimnia of deep freshwater lakes are driven by a specific bacterioplankton communities that have eluded previous studies only focusing on the surface waters. Future works should further investigate the ecophysiology of the individual lineages by a metagenomic-based approach or by establishment of their isolated cultures.

©2019. Japan Geoscience Union. All Right Reserved.

Keywords: Limnology, Microbial Ecology

©2019. Japan Geoscience Union. All Right Reserved.

Nitrous oxide emission from the drainage and the production processes in oil palm plantation on peatland

*Kazuya Nishina[1], Lulie Melling[2], Ryuichi Hirata[1], Yoshiyuki Takahashi[1], Sakae Toyoda[3], Kotaro Terajima[3], Masayuki Itoh[4]

1. NIES National Institute of Environmental Studies, 2. SARAWAK Tropical Peat Research Institute, 3. Tokyo Institute of Technology, 4. University of Hyogo

In South-East Asia, oil palm plantation has rapidly expanded in the past few decades even in peatland areas. In the light of nitrogen cycling, this land-use change would result in enrichment on the ecosystem N cycling due to the N fertilization for the maintaining oil palm growth and the wastewater emission from the palm mills in the plantation. Oil palm plantations converted from peat swamp forests require the drainage to keep cultivation and thus has unique hydrological characteristics. In such plantation, drainage water surface dominates up to 5% of plantation area and therefore it is important to evaluate the gas exchange between the drainage water and atmosphere.

In this study, we have conducted spatial sampling for dissolved N_2O concentration (dN_2O) in the oil palm plantation on drained peat soil in July 2018, in Sarawak, Malaysia in order to evaluate the indirect N_2O emission from palm oil plantation. We have intensively sampled the water samples from the drainage in the plantation (ca. 120 km^2) and the water samples from Raja river, which is adjacent to the plantation. 90% of samples (N = 84) in the drainage water showed over-saturation in dissolved N_2O concentration (up to 570%), suggesting that the drainage water in the oil palm plantation acts the source of N_2O to the atmosphere. The emission factor for indirect emission (EFr: i.e., dN_2O/nitrate concentration) showed relatively higher than the default EFr in IPCC. However, there were no clear linear relationships between the water qualities (including nitrate) and dN_2O. We have also analyzed the isotopic composition of dN_2O in both drainage and river samples. This analysis suggested the denitrification contributed dN_2O in the drainage water.

Keywords: Nitrous oxide, Oil palm plantation, Nitrogen stable isotope

©2019. Japan Geoscience Union. All Right Reserved.

[J] Poster | M (Multidisciplinary and Interdisciplinary)：M-IS Intersection

Mon. May 27, 2019 3:30 PM - 5:00 PM JST | Mon. May 27, 2019 6:30 AM - 8:00 AM UTC | Poster Hall International Exhibition Hall8, Makuhari Messe_20

[M-IS13] Biogeochemistry

convener:Keisuke Koba(Center for Ecological Research, Kyoto University), Hideaki Shibata(Field Science Center fot Northern Biosphere, Hokkaido University), Naohiko Ohkouchi(Japan Agency for Marine-Earth Science and Technology), Youhei Yamashita(Faculty of Environmental Earth Science, Hokkaido University)

Biogeochemistry is an interdisciplinary study field including ecology, geochemistry, oceanography, limnology, hydrology, soil science and environmental sciences. Respective researches have tended to be conducted separately so far. This session aims to provide a common platform for biogeochemists of different disciplines, which facilitates the interactive discussion and information exchanges for further development of biogeochemical studies.

[MIS13-P01] Biomolecular composition changes and biochemical processes associated with indicators of organic matter degradation

*Satoru Hobara[1], Hiroshi Ogawa[2] (1.Rakuno Gakuen University, 2.The University of Tokyo)

[MIS13-P02] Community and metabolic responses of marine bacteria to the dissolved organic matter derived from phytoplankton

*Yuya Tada[1], Koji Suzuki[2], Youhei Yamashita[2] (1. National Institute For Minamata Disease, 2.Hokkaido University)

[MIS13-P03] High production of benthic algae promoted by increased available phosphate in the Obitsu River tidal flat

*Yuzuki Takagai[1], Muneoki Yoh[1] (1.Tokyo University of Agriculture and Technology)

[MIS13-P04] High Concentration of Phosphate and its Mechanism in "Gomi-kui" and "Gata-do"

*KOWATA Satoshi[1], Muneoki Yoh[1] (1.Tokyo University of Agriculture and Technology)

[MIS13-P05] Estimation of the formation and reduction of organic mud in tidal river using sulfate ionic flux and principal component analysis

Hiroki Itamura[1], *Yoriko Yokoo[1] (1.Faculty of Science and Engineering, Doshisha University)

[MIS13-P06] Evaluating the relationship among energy, water and carbon in soil by using multi-layered land surface model, BEAMS

*Keisuke Komiyama[1], Takahiro Sasai[1] (1.Tohoku University Graduate School of Science)

Biomolecular composition changes and biochemical processes associated with indicators of organic matter degradation

*Satoru Hobara[1], Hiroshi Ogawa[2]

1. Rakuno Gakuen University, 2. The University of Tokyo

Degrading organic matter is the dominant carbon form in the Earth’ s surface, and an essential source of energy and nutrients for organisms. The availability of degrading organic matter is strongly constrained by its chemical composition. Many studies conducted for terrestrial and marine environment have found that degradation process usually lead to changes in these biomolecular compositions of organic matter. However, little is understood on its factors controlling the changes. In addition, few reports are available on the difference in features of useful indicators representing the decomposition stage. In this study, we review and compare the known degradation indicators based on biomolecules of decomposed organic matter and also develop more simple and useful indicators. We observed unidirectional increase/decrease in some of the well-analyzed amino acids in organic matter through decomposition, suggesting that it occurred regardless of short-term or long-term, and land or ocean, spatio-temporally. By investigating the amino acids increased or decreased during degradation, various biochemical processes occurring in the background of decomposition which has not been discussed were newly suggested.

Keywords: degradation indicators, Amino acids, land and ocean, Amino sugars

©2019. Japan Geoscience Union. All Right Reserved.

Community and metabolic responses of marine bacteria to the dissolved organic matter derived from phytoplankton

*Yuya Tada[1], Koji Suzuki[2], Youhei Yamashita[2]

1. National Institute For Minamata Disease, 2. Hokkaido University

Dissolved organic matter (DOM) representing one of the largest reduced carbon pools in the ocean, are strongly involved in the global biogeochemical processes. It is considered that a large part of labile DOM in the marine environments is derived from the photosynthesis and cell lysis of phytoplankton. Dissolved organic matter derived from phytoplankton (DOMP) can affect the bacterial community composition and metabolisms. However, little is known about the characteristics of DOMP, and the community and metabolic response of marine bacteria to the addition of DOMP. In this study, we analyzed amino acid composition in the DOMP-lysates from two different phytoplankton cultures, the diatom *Thalassiosira oceanica* (CCMP1005) and the haptophyte *Emiliania huxleyi* (CCMP374), and examined the community and metabolism of marine bacteria in response to these DOMP-lysates using metagenomic approaches. Amino acid analyses for the DOMP-lysates from two strains showed distinctive free amino acid (FAA) compositions, but little changes in their hydrolytic amino acid (HAA) fractions. The proportions of arginine, gamma-aminobutyric acid (GABA) and serine to the total FAAs in *E. huxleyi* were relatively higher than those in *T. oceanica*. However, glutamate and ornithine were the dominant FAAs in the DOMP-lysates from *T. oceanica*. As for the HAA, glutamate and alanine were dominant HAAs in both phytoplankton cultures. In addition, we conducted incubation experiments using natural seawater amended with the lysates from both diatom and haptophyte. Analysis of 16S rRNA genes in the metagenomic sequences revealed that community shifts of marine bacteria in response to DOMP-lysate additions. Relative abundance of *Firmicutes* increased in both DOMP treatments. *Bacteroidetes* increased in response to the addition of DOMP derived from the diatom. Metagenomics analysis of functional genes showed that the genes involved in histidine-, sulfur-, lipopolysaccharide-metabolisms, and polyamine biosynthesis increased in both DOMP treatments. In contrast, the relative abundance of genes associated with glycosaminoglycan metabolism and phosphotransferase system decreased. Fluorescent DOM analysis for initial and amended seawater showed that the fluorescence intensity of a protein-like matter from *E. huxleyi* decreased during incubation. These data suggest that the DOMP-lysates derived from phytoplankton can be a primary factor to change the community composition and metabolisms of marine bacteria, and may change the DOM characteristics in the marine environments.

Keywords: Marine bacteria, phytoplankton, Dissolved organic matter, Amino acids, Metagenome

©2019. Japan Geoscience Union. All Right Reserved.

High production of benthic algae promoted by increased available phosphate in the Obitsu River tidal flat

*Yuzuki Takagai[1], Muneoki Yoh[1]

1. Tokyo University of Agriculture and Technology

Tidal flats are an environment of high biological productivity, with many benthic organisms such as crabs and bivalves. Major primary producers in tidal ecosystems are regarded as benthic algae inhabiting on the sediment surface. So far, such a eutrophic property has been attributed to organic matter and nutrients derived from the upper stream. Here, we raise a hypothesis that photosynthesis of benthic algae is promoted by available phosphate (PO_4^{3-}) that is increased abiotically in tidal flats, which can support higher trophic level organisms. Phosphate bound to iron oxides is expected to be released accompanied with iron reduction under reductive environment, which is easily formed in sediments of tidal flats. In this study, we aimed to quantitatively show the production of benthic algae promoted by the available phosphate.

A monthly survey was conducted from June to December 2018 (except August) in a small creek beside the Obitsu River estuary in Kisarazu City, Chiba Prefecture. At two station of a downstream site (St.1) and an upper stream site (St.2) of the blind tubular creek, photosynthesis was measured by in situ light and dark chambers, and water analysis of pore water and properties of surface sediments were also determined. Phosphate concentration was measured by the molybdenum blue method, and the ammonium concentration by the indophenol blue method. The flux of phosphate and ammonium from sediments was measured from the concentration change in the chamber with time. Chl a, particle size composition and organic matter contents were measured for surface sediments.

Positive phosphate flux from the sediment surface was detected. At an upper stream site of a small creek, the dissolved oxygen flux was positive in the light condition and negative in the dark condition, showing the photosynthesis of benthic algae. The maximum photosynthesis rate (185 mg $O_2 m^{-2} h^{-1}$) was higher than previous reports. On the other hand, at a lower stream site, the dissolved oxygen flux was often negative not only under dark condition but under light condition. This fact implies that, despite high Chl a concentration and sufficient light onto the sediment surface, oxygen consumption due to organic decomposition surpassed photosynthesis. Organic contents were St.1>St.2. The particle size was smaller at St.1. The average N/P ratio of the pore water was 14 in St.2, whereas 4.8 at St.1, being much lower than the Redfield ratio. This remarkable low N/P ratio suggests the occurrence of abiotic phosphate production within the sediment at this site.

Results show that available phosphate is produced to promote the active primary production of benthic algae in this tidal creek. On the other hand, this creek showed a remarkable spatial difference in organic matter contents and N/P ratio.

©2019. Japan Geoscience Union. All Right Reserved.

High Concentration of Phosphate and its Mechanism in "Gomi-kui" and "Gata-do"

*KOWATA Satoshi[1], Muneoki Yoh[1]

1. Tokyo University of Agriculture and Technology

[Introduction]
River and creeks (waterways) network is developed in Saga plain, which has water and water storage functions. Silt from the upper stream and suspension clay carried by tidal effect are accumulated in creeks and rivers. Mud sediment in creeks has been used as a fertilizer until the spread of chemical fertilizer (Kato 1997). This work is called "Gomi-kui". On the other hand, the mud sediment deposited in the flow passage of the river tidal area such as the Rokkaku River is called "Gata-do". This has been considered to be a nutrient supply source to the Ariake Sea by solutes of nutrient (Mishima 2017). The present study hypothesized "Gomi-kui" and "Gata-do" is abundant in nutrients through a phosphate release by reduction of iron oxide in reductive sediments. We investigated to clarify this hypothesis.
[Results and Discussion]
Concentration of PO_4^{3-} in pore water of “Gata-do” increased along the flowing-down the river. The highest concentration of 73.5 μmol L^{-1} was observed at the point of 5.5 km from the river mouth (Fig. 1). This increase in PO_4^{3-} concentration was associated with the increase in clay content and the decrease in DO (Fig. 2). That is, the development of reductional environment apparently influenced the increase of PO_4^{3-} concentration. From the upstream to the 19.6 km point, the concentration of Fe^{2+} and S^{2-} in the pore water also increased. From the downstream side of 19.6 km point, however, Fe^{2+} and S^{2-} concentration decreased, while the PO_4^{3-} concentration continued to increase. A positive correlation was found between the increase in EC and the increase in PO_4^{3-} concentration ($p < 0.05$). It is likely from this result that the formation of iron sulfide (FeS) is involved in increasing the concentration of PO_4^{3-}. In the reductive sediment, PO_4^{3-} would be released in association with Fe reduction. In addition, as an effect of seawater intrusion, the reduction of SO_4^{2-} would produce abundant S^{2-} to remove Fe^{2+} as FeS. PO_4^{3-} would remain in dissolved state without being affected by Fe^{2+} (Hartzell and Jordan 2012). This mechanism is expected to contribute to high PO_4^{3-} concentration.
Similar results were observed for “Gomi-kui” mud: high PO_4^{3-} concentration, tendency of increase and decrease in Fe^{2+} and S^{2-} concentration, decrease in DO, and increase in clay content. Results suggest that phosphate concentration is remarkably incresed due to the mechanism associated with Fe reduction in “Gomi-kui” and “Gata-do”. Phosphate released from lowlying areas could be a source to coastal areas.

©2019. Japan Geoscience Union. All Right Reserved.

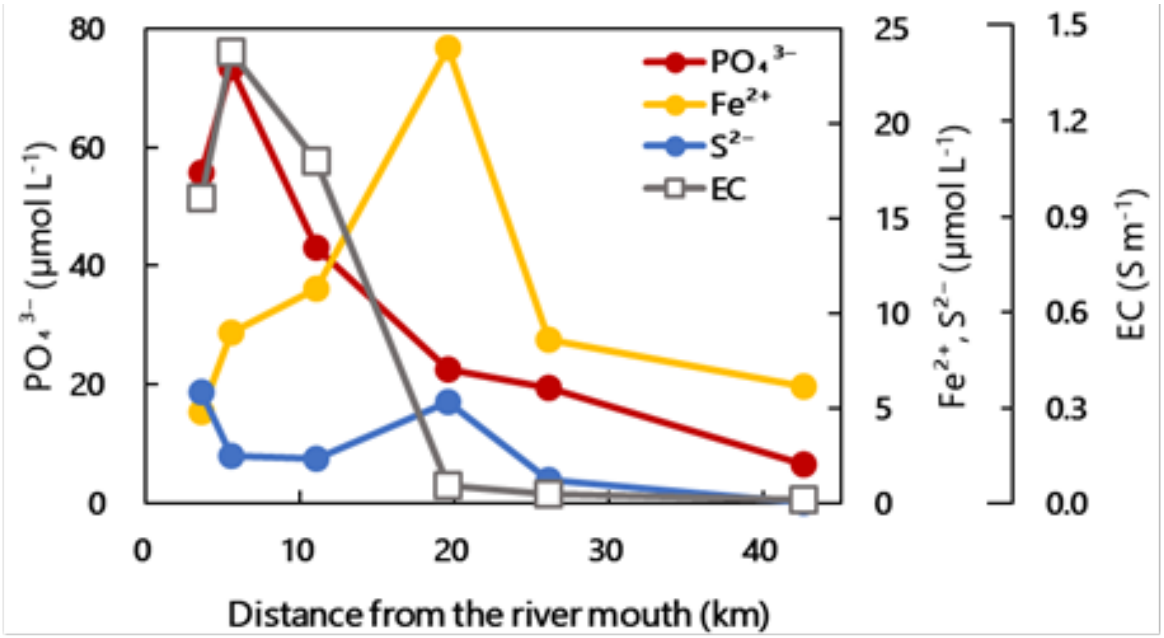

Fig.1 PO_4^{3-}, Fe^{2+}, S^{2-} concentration in pore water and EC in surface water along the flowing-down the Rokkaku

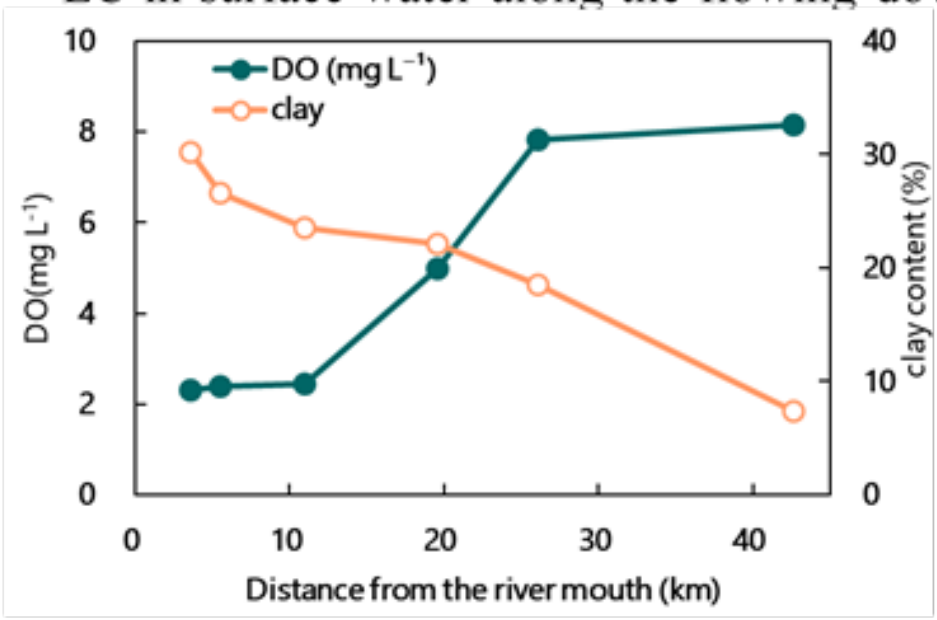

Fig.2 EC, DO in surface water and clay content of sedeiment along the flowing-down the Rokkaku River

©2019. Japan Geoscience Union. All Right Reserved.

Estimation of the formation and reduction of organic mud in tidal river using sulfate ionic flux and principal component analysis

Hiroki Itamura[1], *Yoriko Yokoo[1]

1. Faculty of Science and Engineering, Doshisha University

We determined the elemental compositions of river water and pore water in order to estimate the sites where the formation and reduction of organic mud occur in delta rivers using the principal component analysis. We collected river water and bed sediment samples at river mouth with tidal intrusion in Ota River, Hiroshima prefecture, and analyze the elemental concentrations using IC and ICP-MS.
We calculated major cations and SO_4^{2-} flux (J_{SO4}). There was positive correlation between J_{Ca} and J_{SO4}. At the sites where their J_{SO4} showed negative values, J_{SO4} had strongly positive correlation to J_{Ca}. These results demonstrate that SO_4^{2-} concentrations in pore water decreased and J_{SO4} showed negative values due to the reduction of SO_4^{2-}, therefore, the formation and reduction of organic mud could occur at those sites and SO_4^{2-} has same behavior to Ca^{2+}. We conducted the principal component analysis using eight factors such as J_{Ca}, J_{SO4}, water content, porosity, salinity, pH of pore water and concentration of Mn and Fe in pore water for the sites where their J_{SO4} showed negative values. The first principal component loadings of Fe and Mn concentrations, J_{Ca}, J_{SO4} and porosity were positive and the second principal component loadings of water content, pH, J_{SO4}, and J_{Ca} were negative, indicating that the first and second principal component are the index of redox and the formation of organic mud, respectively. The reduction of organic mud could occur at sites plotted in the range of the negative first principal component loadings and the positive second principal component loadings.

Keywords: tidal river, sulfate flux, principal component analysis, organic mud

©2019. Japan Geoscience Union. All Right Reserved.

Evaluating the relationship among energy, water and carbon in soil by using multi-layered land surface model, BEAMS

*Keisuke Komiyama[1], Takahiro Sasai[1]

1. Tohoku University Graduate School of Science

The amount of carbon released from the soil to the atmosphere is recently increasing along with climate change. One of the most focusing point is a response of soil carbon dynamics on global warming. However, since the complexity of the relationship among soil energy, water and carbon processes, we have not still understood the scientific understanding relevant to soil carbon dynamics, leading a need to more accurately develop the land surface model. Particularly, the quantitative understanding of the role of soil carbon in the subsurface layer is lacking because the importance of the surface processes has only been recognized recently. The existing models cannot sufficiently reproduce the soil carbon processes in the subsurface layer. Only few studies have focused on the response of the subsurface soil carbon to the changes in soil temperature, soil water content and freezing rate that are the key elements of soil heat and water environment. In this study, we aim to estimate the response of the soil carbon decomposition rate to the changes in soil heat and water environment of the vertically multilayered soil. By integrating an elaborate hydrological model into the existing Biosphere model integrating Eco-physiological And Mechanistic approaches using Satellite data (BEAMS) (Sasai et al., 2016), we developed a new land surface model, and estimated the 1° grid terrestrial carbon fluxes from 1982 to 2011.

As a result, the global average soil carbon decomposition rate increased throughout the model experiment period. The sensitivity experiments showed that 16% of the increasing trend resulted from the changes of the soil heat and water environment. The soil heat and water environment in the top layer (0.00m ~ 0.05m) explained 8.1%, in the middle layer (0.05m ~ 0.30m) explained 5.7%, and in the bottom layer (0.30m ~ 1.00m) explained 2.2% of the increasing trend. These results suggest that the response of the soil decomposition rate on the changes of soil heat and water environment decreases with the soil depth, so that the soil carbon below the surface layer is less affected by the changes in the soil heat and water environment than the soil carbon in the surface layer.

However, this pattern is not universal. In several regions, such as cold regions in the northern hemisphere and grassland in the southern part of Africa, the response of the bottom layer is large. We emphasize that in these regions, the role of the subsurface soil carbon is particularly important.

Keywords: terrestrial carbon cycle, land surface model, soil carbon dynamics

©2019. Japan Geoscience Union. All Right Reserved.

[J] Poster | M (Multidisciplinary and Interdisciplinary)：M-IS Intersection

Mon. May 27, 2019 5:15 PM - 6:30 PM JST | Mon. May 27, 2019 8:15 AM - 9:30 AM UTC | Poster Hall International Exhibition Hall8, Makuhari Messe_34

[M-IS13] Biogeochemistry

convener:Keisuke Koba(Center for Ecological Research, Kyoto University), Hideaki Shibata(Field Science Center fot Northern Biosphere, Hokkaido University), Naohiko Ohkouchi(Japan Agency for Marine-Earth Science and Technology), Youhei Yamashita(Faculty of Environmental Earth Science, Hokkaido University)

Biogeochemistry is an interdisciplinary study field including ecology, geochemistry, oceanography, limnology, hydrology, soil science and environmental sciences. Respective researches have tended to be conducted separately so far. This session aims to provide a common platform for biogeochemists of different disciplines, which facilitates the interactive discussion and information exchanges for further development of biogeochemical studies.

[MIS13-P01] Biomolecular composition changes and biochemical processes associated with indicators of organic matter degradation

*Satoru Hobara[1], Hiroshi Ogawa[2] (1.Rakuno Gakuen University, 2.The University of Tokyo)

[MIS13-P02] Community and metabolic responses of marine bacteria to the dissolved organic matter derived from phytoplankton

*Yuya Tada[1], Koji Suzuki[2], Youhei Yamashita[2] (1. National Institute For Minamata Disease, 2.Hokkaido University)

[MIS13-P03] High production of benthic algae promoted by increased available phosphate in the Obitsu River tidal flat

*Yuzuki Takagai[1], Muneoki Yoh[1] (1.Tokyo University of Agriculture and Technology)

[MIS13-P04] High Concentration of Phosphate and its Mechanism in "Gomi-kui" and "Gata-do"

*KOWATA Satoshi[1], Muneoki Yoh[1] (1.Tokyo University of Agriculture and Technology)

[MIS13-P05] Estimation of the formation and reduction of organic mud in tidal river using sulfate ionic flux and principal component analysis

Hiroki Itamura[1], *Yoriko Yokoo[1] (1.Faculty of Science and Engineering, Doshisha University)

[MIS13-P06] Evaluating the relationship among energy, water and carbon in soil by using multi-layered land surface model, BEAMS

*Keisuke Komiyama[1], Takahiro Sasai[1] (1.Tohoku University Graduate School of Science)

Biomolecular composition changes and biochemical processes associated with indicators of organic matter degradation

*Satoru Hobara[1], Hiroshi Ogawa[2]

1. Rakuno Gakuen University, 2. The University of Tokyo

Degrading organic matter is the dominant carbon form in the Earth’ s surface, and an essential source of energy and nutrients for organisms. The availability of degrading organic matter is strongly constrained by its chemical composition. Many studies conducted for terrestrial and marine environment have found that degradation process usually lead to changes in these biomolecular compositions of organic matter. However, little is understood on its factors controlling the changes. In addition, few reports are available on the difference in features of useful indicators representing the decomposition stage. In this study, we review and compare the known degradation indicators based on biomolecules of decomposed organic matter and also develop more simple and useful indicators. We observed unidirectional increase/decrease in some of the well-analyzed amino acids in organic matter through decomposition, suggesting that it occurred regardless of short-term or long-term, and land or ocean, spatio-temporally. By investigating the amino acids increased or decreased during degradation, various biochemical processes occurring in the background of decomposition which has not been discussed were newly suggested.

Keywords: degradation indicators, Amino acids, land and ocean, Amino sugars

©2019. Japan Geoscience Union. All Right Reserved.

Community and metabolic responses of marine bacteria to the dissolved organic matter derived from phytoplankton

*Yuya Tada[1], Koji Suzuki[2], Youhei Yamashita[2]

1. National Institute For Minamata Disease, 2. Hokkaido University

Dissolved organic matter (DOM) representing one of the largest reduced carbon pools in the ocean, are strongly involved in the global biogeochemical processes. It is considered that a large part of labile DOM in the marine environments is derived from the photosynthesis and cell lysis of phytoplankton. Dissolved organic matter derived from phytoplankton (DOMP) can affect the bacterial community composition and metabolisms. However, little is known about the characteristics of DOMP, and the community and metabolic response of marine bacteria to the addition of DOMP. In this study, we analyzed amino acid composition in the DOMP-lysates from two different phytoplankton cultures, the diatom *Thalassiosira oceanica* (CCMP1005) and the haptophyte *Emiliania huxleyi* (CCMP374), and examined the community and metabolism of marine bacteria in response to these DOMP-lysates using metagenomic approaches. Amino acid analyses for the DOMP-lysates from two strains showed distinctive free amino acid (FAA) compositions, but little changes in their hydrolytic amino acid (HAA) fractions. The proportions of arginine, gamma-aminobutyric acid (GABA) and serine to the total FAAs in *E. huxleyi* were relatively higher than those in *T. oceanica*. However, glutamate and ornithine were the dominant FAAs in the DOMP-lysates from *T. oceanica*. As for the HAA, glutamate and alanine were dominant HAAs in both phytoplankton cultures. In addition, we conducted incubation experiments using natural seawater amended with the lysates from both diatom and haptophyte. Analysis of 16S rRNA genes in the metagenomic sequences revealed that community shifts of marine bacteria in response to DOMP-lysate additions. Relative abundance of *Firmicutes* increased in both DOMP treatments. *Bacteroidetes* increased in response to the addition of DOMP derived from the diatom. Metagenomics analysis of functional genes showed that the genes involved in histidine-, sulfur-, lipopolysaccharide-metabolisms, and polyamine biosynthesis increased in both DOMP treatments. In contrast, the relative abundance of genes associated with glycosaminoglycan metabolism and phosphotransferase system decreased. Fluorescent DOM analysis for initial and amended seawater showed that the fluorescence intensity of a protein-like matter from *E. huxleyi* decreased during incubation. These data suggest that the DOMP-lysates derived from phytoplankton can be a primary factor to change the community composition and metabolisms of marine bacteria, and may change the DOM characteristics in the marine environments.

Keywords: Marine bacteria, phytoplankton, Dissolved organic matter, Amino acids, Metagenome

©2019. Japan Geoscience Union. All Right Reserved.

High production of benthic algae promoted by increased available phosphate in the Obitsu River tidal flat

*Yuzuki Takagai[1], Muneoki Yoh[1]

1. Tokyo University of Agriculture and Technology

Tidal flats are an environment of high biological productivity, with many benthic organisms such as crabs and bivalves. Major primary producers in tidal ecosystems are regarded as benthic algae inhabiting on the sediment surface. So far, such a eutrophic property has been attributed to organic matter and nutrients derived from the upper stream. Here, we raise a hypothesis that photosynthesis of benthic algae is promoted by available phosphate (PO_4^{3-}) that is increased abiotically in tidal flats, which can support higher trophic level organisms. Phosphate bound to iron oxides is expected to be released accompanied with iron reduction under reductive environment, which is easily formed in sediments of tidal flats. In this study, we aimed to quantitatively show the production of benthic algae promoted by the available phosphate.

A monthly survey was conducted from June to December 2018 (except August) in a small creek beside the Obitsu River estuary in Kisarazu City, Chiba Prefecture. At two station of a downstream site (St.1) and an upper stream site (St.2) of the blind tubular creek, photosynthesis was measured by in situ light and dark chambers, and water analysis of pore water and properties of surface sediments were also determined. Phosphate concentration was measured by the molybdenum blue method, and the ammonium concentration by the indophenol blue method. The flux of phosphate and ammonium from sediments was measured from the concentration change in the chamber with time. Chl a, particle size composition and organic matter contents were measured for surface sediments.

Positive phosphate flux from the sediment surface was detected. At an upper stream site of a small creek, the dissolved oxygen flux was positive in the light condition and negative in the dark condition, showing the photosynthesis of benthic algae. The maximum photosynthesis rate (185 mg $O_2 m^{-2} h^{-1}$) was higher than previous reports. On the other hand, at a lower stream site, the dissolved oxygen flux was often negative not only under dark condition but under light condition. This fact implies that, despite high Chl a concentration and sufficient light onto the sediment surface, oxygen consumption due to organic decomposition surpassed photosynthesis. Organic contents were St.1>St.2. The particle size was smaller at St.1. The average N/P ratio of the pore water was 14 in St.2, whereas 4.8 at St.1, being much lower than the Redfield ratio. This remarkable low N/P ratio suggests the occurrence of abiotic phosphate production within the sediment at this site.

Results show that available phosphate is produced to promote the active primary production of benthic algae in this tidal creek. On the other hand, this creek showed a remarkable spatial difference in organic matter contents and N/P ratio.

©2019. Japan Geoscience Union. All Right Reserved.

High Concentration of Phosphate and its Mechanism in "Gomi-kui" and "Gata-do"

*KOWATA Satoshi[1], Muneoki Yoh[1]

1. Tokyo University of Agriculture and Technology

[Introduction]
River and creeks (waterways) network is developed in Saga plain, which has water and water storage functions. Silt from the upper stream and suspension clay carried by tidal effect are accumulated in creeks and rivers. Mud sediment in creeks has been used as a fertilizer until the spread of chemical fertilizer (Kato 1997). This work is called "Gomi-kui". On the other hand, the mud sediment deposited in the flow passage of the river tidal area such as the Rokkaku River is called "Gata-do". This has been considered to be a nutrient supply source to the Ariake Sea by solutes of nutrient (Mishima 2017). The present study hypothesized "Gomi-kui" and "Gata-do" is abundant in nutrients through a phosphate release by reduction of iron oxide in reductive sediments. We investigated to clarify this hypothesis.
[Results and Discussion]
Concentration of PO_4^{3-} in pore water of “Gata-do” increased along the flowing-down the river. The highest concentration of 73.5 μmol L^{-1} was observed at the point of 5.5 km from the river mouth (Fig. 1). This increase in PO_4^{3-} concentration was associated with the increase in clay content and the decrease in DO (Fig. 2). That is, the development of reductional environment apparently influenced the increase of PO_4^{3-} concentration. From the upstream to the 19.6 km point, the concentration of Fe^{2+} and S^{2-} in the pore water also increased. From the downstream side of 19.6 km point, however, Fe^{2+} and S^{2-} concentration decreased, while the PO_4^{3-} concentration continued to increase. A positive correlation was found between the increase in EC and the increase in PO_4^{3-} concentration ($p < 0.05$). It is likely from this result that the formation of iron sulfide (FeS) is involved in increasing the concentration of PO_4^{3-}. In the reductive sediment, PO_4^{3-} would be released in association with Fe reduction. In addition, as an effect of seawater intrusion, the reduction of SO_4^{2-} would produce abundant S^{2-} to remove Fe^{2+} as FeS. PO_4^{3-} would remain in dissolved state without being affected by Fe^{2+} (Hartzell and Jordan 2012). This mechanism is expected to contribute to high PO_4^{3-} concentration.
Similar results were observed for “Gomi-kui” mud: high PO_4^{3-} concentration, tendency of increase and decrease in Fe^{2+} and S^{2-} concentration, decrease in DO, and increase in clay content. Results suggest that phosphate concentration is remarkably incresed due to the mechanism associated with Fe reduction in “Gomi-kui” and “Gata-do”. Phosphate released from lowlying areas could be a source to coastal areas.

©2019. Japan Geoscience Union. All Right Reserved.

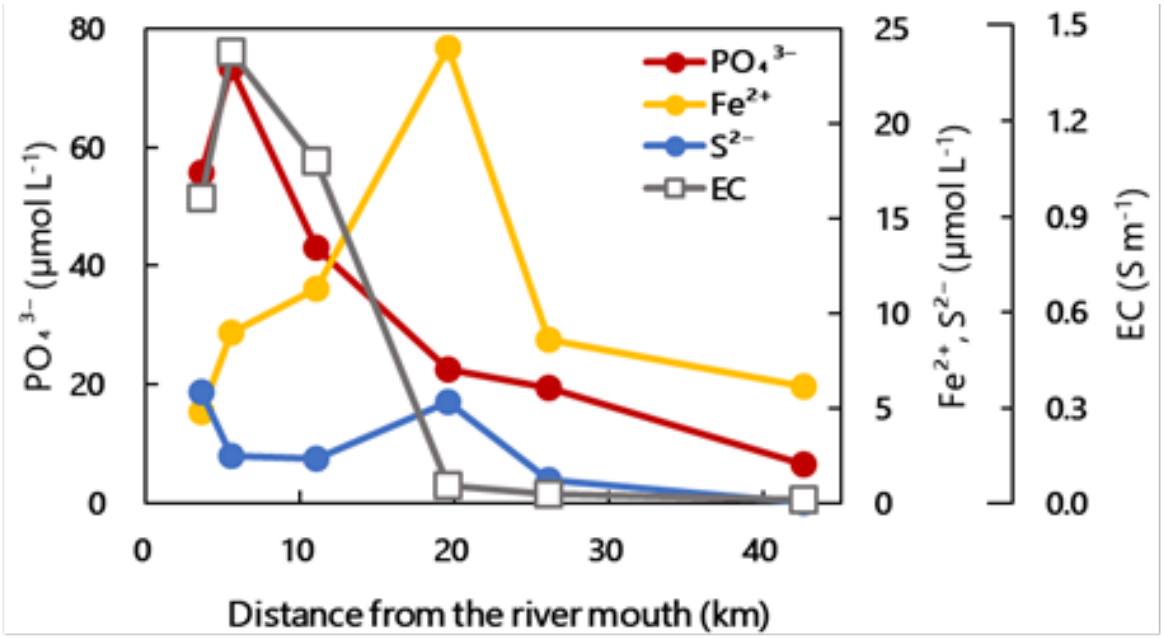

Fig.1 PO_4^{3-}, Fe^{2+}, S^{2-} concentration in pore water and EC in surface water along the flowing-down the Rokkaku

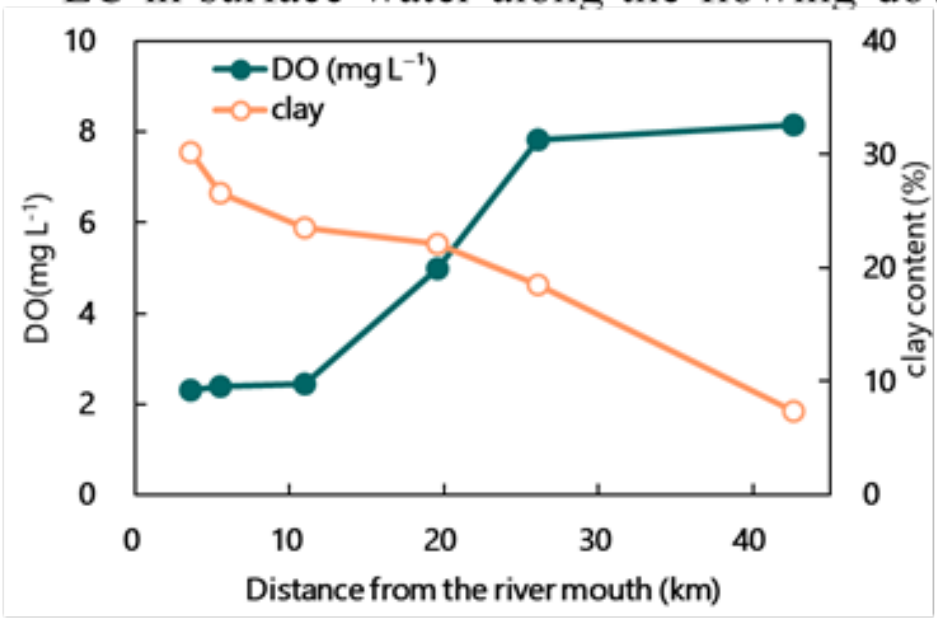

Fig.2 EC, DO in surface water and clay content of sedeiment along the flowing-down the Rokkaku River

©2019. Japan Geoscience Union. All Right Reserved.

Estimation of the formation and reduction of organic mud in tidal river using sulfate ionic flux and principal component analysis

Hiroki Itamura[1], *Yoriko Yokoo[1]

1. Faculty of Science and Engineering, Doshisha University

We determined the elemental compositions of river water and pore water in order to estimate the sites where the formation and reduction of organic mud occur in delta rivers using the principal component analysis. We collected river water and bed sediment samples at river mouth with tidal intrusion in Ota River, Hiroshima prefecture, and analyze the elemental concentrations using IC and ICP-MS.
We calculated major cations and SO_4^{2-} flux (J_{SO4}). There was positive correlation between J_{Ca} and J_{SO4}. At the sites where their J_{SO4} showed negative values, J_{SO4} had strongly positive correlation to J_{Ca}. These results demonstrate that SO_4^{2-} concentrations in pore water decreased and J_{SO4} showed negative values due to the reduction of SO_4^{2-}, therefore, the formation and reduction of organic mud could occur at those sites and SO_4^{2-} has same behavior to Ca^{2+}. We conducted the principal component analysis using eight factors such as J_{Ca}, J_{SO4}, water content, porosity, salinity, pH of pore water and concentration of Mn and Fe in pore water for the sites where their J_{SO4} showed negative values. The first principal component loadings of Fe and Mn concentrations, J_{Ca}, J_{SO4} and porosity were positive and the second principal component loadings of water content, pH, J_{SO4}, and J_{Ca} were negative, indicating that the first and second principal component are the index of redox and the formation of organic mud, respectively. The reduction of organic mud could occur at sites plotted in the range of the negative first principal component loadings and the positive second principal component loadings.

Keywords: tidal river, sulfate flux, principal component analysis, organic mud

©2019. Japan Geoscience Union. All Right Reserved.

Evaluating the relationship among energy, water and carbon in soil by using multi-layered land surface model, BEAMS

*Keisuke Komiyama[1], Takahiro Sasai[1]

1. Tohoku University Graduate School of Science

The amount of carbon released from the soil to the atmosphere is recently increasing along with climate change. One of the most focusing point is a response of soil carbon dynamics on global warming. However, since the complexity of the relationship among soil energy, water and carbon processes, we have not still understood the scientific understanding relevant to soil carbon dynamics, leading a need to more accurately develop the land surface model. Particularly, the quantitative understanding of the role of soil carbon in the subsurface layer is lacking because the importance of the surface processes has only been recognized recently. The existing models cannot sufficiently reproduce the soil carbon processes in the subsurface layer. Only few studies have focused on the response of the subsurface soil carbon to the changes in soil temperature, soil water content and freezing rate that are the key elements of soil heat and water environment. In this study, we aim to estimate the response of the soil carbon decomposition rate to the changes in soil heat and water environment of the vertically multilayered soil. By integrating an elaborate hydrological model into the existing Biosphere model integrating Eco-physiological And Mechanistic approaches using Satellite data (BEAMS) (Sasai et al., 2016), we developed a new land surface model, and estimated the 1° grid terrestrial carbon fluxes from 1982 to 2011.

As a result, the global average soil carbon decomposition rate increased throughout the model experiment period. The sensitivity experiments showed that 16% of the increasing trend resulted from the changes of the soil heat and water environment. The soil heat and water environment in the top layer (0.00m ~ 0.05m) explained 8.1%, in the middle layer (0.05m ~ 0.30m) explained 5.7%, and in the bottom layer (0.30m ~ 1.00m) explained 2.2% of the increasing trend. These results suggest that the response of the soil decomposition rate on the changes of soil heat and water environment decreases with the soil depth, so that the soil carbon below the surface layer is less affected by the changes in the soil heat and water environment than the soil carbon in the surface layer.

However, this pattern is not universal. In several regions, such as cold regions in the northern hemisphere and grassland in the southern part of Africa, the response of the bottom layer is large. We emphasize that in these regions, the role of the subsurface soil carbon is particularly important.

Keywords: terrestrial carbon cycle, land surface model, soil carbon dynamics

©2019. Japan Geoscience Union. All Right Reserved.

[J] Oral | M (Multidisciplinary and Interdisciplinary) : M-IS Intersection

Mon. May 27, 2019 9:00 AM - 10:30 AM JST | Mon. May 27, 2019 12:00 AM - 1:30 AM UTC | Convention Hall B 2F

[M-IS14] Global climate change driven by the Southern Ocean and the Antarctic Ice Sheet

convener:Osamu Seki(Institute of Low Temperature Science, Hokkaido University), Akira Oka(Atmosphere and Ocean Research Institute, The University of Tokyo), Ryu Uemura(University of the Ryukyus), Ryosuke Makabe(National Institute of Polar Research), Chairperson:Yuji Kato(Kochi University)

The Southern Ocean and Antarctic ice sheet, which are the giant reservoirs of heat, water, and materials, have a potential to play central roles in long-term global climate change. This system is composed of the following sub-systems; ice shelf which is a place of the interaction of ice sheet and ocean, flowing iceberg, seasonal sea ice zone, Antarctic bottom water which drives the thermohaline circulation, active biological production and Antarctic Circumpolar Current. These sub-systems are interacted with each other and have significant impact on changes in the global environmental system. This session aim to summarize recent observational and simulation studies from various fields relating to the past and present changes in the Antarctic Ice sheet and Southern Ocean, which are essential elements for unraveling the changes in the global climate system. Further, future science plans for understanding of the environmental changes of the Antarctic Cryosphere is also discussed.

9:00 AM - 9:25 AM JST | 12:00 AM - 12:25 AM UTC

[MIS14-01] Mass loss of the Antarctic ice sheet under the influence of ice-ocean interaction

★Invited Papers

*Shin Sugiyama[1] (1.Institute of Low Temperature Science, Hokkaido University)

9:25 AM - 9:40 AM JST | 12:25 AM - 12:40 AM UTC

[MIS14-02] Accurate chronology and climatic reconstruction around MIS 11 (interglacial period ~400,000 years ago) from Dome Fuji ice core, Antarctica

*Kenji Kawamura[1,2,3], Ikumi Oyabu[1], Shuji Aoki[4], Takakiyo Nakazawa[4], Ayako Abe-Ouchi[5,3], Fuyuki SAITO[3] (1.National Institute of Polar Research, Research Organization of Information and Systems, 2.SOKENDAI (The Graduate University of Advanced Studies), 3.JAMSTEC, 4.Tohoku University, 5.University of Tokyo)

9:40 AM - 9:55 AM JST | 12:40 AM - 12:55 AM UTC

[MIS14-03] Study on physics and layers of ice cores containing information of climate change over the past 720 k-years, and study on the "oldest ice"

*Shuji Fujita[1,2], Motohiro Hirabayashi[1], Iizuka Yoshinori[3], Hiroshi Ohno[4] (1.National Institute of Polar Research, Research Organization of Information and Systems(ROIS), 2.Department of Polar Science, The Graduate University for Advanced Studies (SOKENDAI), Japan, 3. Institute of Low Temperature Science, Hokkaido University, Japan, 4.Kitami Institute of Technology, Japan)

9:55 AM - 10:15 AM JST | 12:55 AM - 1:15 AM UTC

[MIS14-04] Reconstructions of the Antarctic Polar Front through the glacial/interglacials

★Invited Papers

*Hiroki Matsui[1], Yuji Kato[1,2], Itsuki Suto[3], Minoru Ikehara[1] (1.Center for Advanced Marine Core Research, Kochi University, 2.JSPS PD, 3.Graduate School of Environmental Studies, Nagoya University)

10:15 AM - 10:30 AM JST | 1:15 AM - 1:30 AM UTC

[MIS14-05] **Integrated observations for marine earth science in the Indian sector of the Southern Ocean: Preliminary results of R/V Hakuho-maru KH-19-1 cruise**

*Minoru Ikehara[1], Kay I. Ohshima[2], Takuya Itaki[3], Hiroshi Sato[4], Masakazu Fujii[5], Michiyo Yamamoto-Kawai[6], Hiroki Matsui[1], Takahito Ikenoue[7], . Scientific Party of R/V Hakuho-maru KH-19-1 cruise (1.Center for Advanced Marine Core Research, Kochi University, 2.ILTS, Hokkaido University, 3.GSJ, AIST, 4.Senshu

University, 5.National Institute of Polar Research, 6.Tokyo University of Marine Science and Technology, 7.Marine Ecology Research Institute)

Mass loss of the Antarctic ice sheet under the influence of ice-ocean interaction

*Shin Sugiyama[1]

1. Institute of Low Temperature Science, Hokkaido University

The Antarctic ice sheet covers 8.3% of the global land surface with a mean ice thickness of 1937 m. The mass of the ice accounts for ~90% of freshwater on the earth and has a potential of 58.3 m sea level rise. Mass change of the ice sheet has a large impact on the Antarctic and global environment since meltwater discharge affects not only sea level, but also ocean circulation and marine ecosystems. Therefore, quantification of ice sheet mass balance and understanding the driving mechanisms are crucially important.

Our understanding of the Antarctic ice sheet mass balance has been greatly improved over the last two decades. Novel satellite measurement techniques enabled us to quantify year to year variations in the mass balance, as well as to investigate key processes such as ice speed, calving and ice shelf basal melting. These new observations have shown a trend of ice sheet mass loss since 1990s. The most significant changes are observed at fast flowing glaciers and ice shelves along the coast in West Antarctica. More detailed studies strongly suggest that the mass loss is due to increasing ice shelf basal melting and ice flow acceleration. To clarify the mechanism of the observed changes, further investigations are in progress on the ice sheet and in the ocean. Study results indicate that the ice sheet is losing mass under the influence of changing ocean, and meltwater discharge is affecting the ocean environment in turn.

In this presentation, we review progress in understanding of the Antarctic ice sheet mass balance and mechanisms driving the recent mass trends. Based on the existing knowledge, we discuss future research directions required for satellite and in-situ measurements as well as numerical investigations.

Keywords: Antarctic ice sheet, Ice sheet-ocean interaction, Mass balance, Ice shelf, Sea level

©2019. Japan Geoscience Union. All Right Reserved.

Accurate chronology and climatic reconstruction around MIS 11 (interglacial period ~400,000 years ago) from Dome Fuji ice core, Antarctica

*Kenji Kawamura[1,2,3], Ikumi Oyabu[1], Shuji Aoki[4], Takakiyo Nakazawa[4], Ayako Abe-Ouchi[5,3], Fuyuki SAITO[3]

1. National Institute of Polar Research, Research Organization of Information and Systems, 2. SOKENDAI (The Graduate University of Advanced Studies), 3. JAMSTEC, 4. Tohoku University, 5. University of Tokyo

Marine Isotope Stage (MIS) 11 is characterized by long duration of glacial termination and interglacial, with higher sea level than today, despite moderate atmospheric CO_2 concentration and small variations in northern summer insolation (due to small orbital eccentricity). To investigate the roles of different forcings (e.g. orbital variations and greenhouse gases) on climate and ice sheets (sea level), paleoclimatic proxy records need to be accurately dated and precisely synchronized with each other. An accurate chronology for the past 360 ky was constructed through orbital tuning of O_2/N_2 ratio of trapped air in the Dome Fuji and Vostok ice cores with local summer insolation (Kawamura et al., 2007), and its improvement has been underway (Oyabu et al., this session). We have also been extending the O_2/N_2 chronology to older periods by analyzing the second Dome Fuji ice core, and constrain the timing and duration of the past interglacial periods.

Marine sediment cores from northern North Atlantic region exhibit millennial-scale variations, including abrupt climatic shifts and bipolar seesaw, during glacial periods and terminations in various proxy records (e.g. sea surface temperature and ice-rafted debris). By correlating the millennial-scale changes recorded in the marine sediment cores with those in the Dome Fuji ice core (CH_4 concentration and d18O of ice), it may be possible to transfer the Dome Fuji chronology to the marine cores from the North Atlantic. We first attempted to correlate planktonic $\delta^{18}O$ and IRD records from the marine core ODP 980 with the Dome Fuji CH_4 around MIS 11 and constrain the durations of interglacial periods recorded in the marine core, with some success. However, the current resolution of the Dome Fuji gas records (~2000 years on average) is not sufficient to undoubtedly identify all millennial-scale events, thus we will start new measurements to improve the resolution. In the presentation, we will show the results of the new measurements and synchronization, and discuss the timing, duration and mechanism of climatic changes over Termination V and MIS 11.

Keywords: Ice core, MIS 11, interglacial period, Dome Fuji

©2019. Japan Geoscience Union. All Right Reserved.

Study on physics and layers of ice cores containing information of climate change over the past 720 k-years, and study on the "oldest ice"

*Shuji Fujita[1,2], Motohiro Hirabayashi[1], Iizuka Yoshinori[3], Hiroshi Ohno[4]

1. National Institute of Polar Research, Research Organization of Information and Systems(ROIS), 2. Department of Polar Science, The Graduate University for Advanced Studies (SOKENDAI), Japan, 3. Institute of Low Temperature Science, Hokkaido University, Japan, 4. Kitami Institute of Technology, Japan

Purpose and Background of the Research

Ice cores collected in inland of Antarctica is one of important information sources for histories of climatic changes that occurred over 1.5 M years. At ice core drilling sites, ice is older in deeper layers; such deep layers are subject to vertical compressions by ice flow. In addition, various time-dependent metamorphic processes undergoes by influences of the geothermal heat flux. If such very deep signals are once resolved with high time resolutions, we can uncover the history of rapid climate changes. Such ice-core-based knowledge will be crucial for building strategies to make sustainable society under global warming. However, current state of our knowledge is based on limited and discrete sampling from ice cores. High resolution continuous methods for analysis has just begun in recent years. In this study, we will use cutting-edge methods for high-resolution and continuous measurements for ice cores, based on crystal physics and continuous flow analysis (CFA); we will analyze layers of ice cores spanning ca. 200,000 years and ca. 720,000 years. Based on it, we will (i) produce valuable information of the climate in the past, (ii) clarify nature of the time-dependent metamorphic processes, (iii) synchronize multiple very deep ice cores, and (iv) predict quality of information from ice cores that cover 1.5 M years.

Research Methods

At an inland site called Dome Fuji in East Antarctica, ice core researchers organized by the National Institute of Polar Research, Japan, collected ice cores covering 720,000 years. We will analyze portions of the ice cores spanning ca. 200,000 years and ca. 720,000 years. Such very old portion constitute deepest ~1000 m span within the ~3000 m-thick ice sheet. Such layers are subject to vertical compressions. In this study, key questions are as follows:
(i) Can we synchronize these very old portions of ice between to major ice cores drilled at Dome Fuji and Dome C?
(ii) How old age of ice back in time, can we clarify detailed histories of rapid changes of climate?
As actions tackling the questions, we will use two major methods to read the layered strata. One of them is to read layers of crystal textures using a method to measure dielectric permittivity tensor with the millimeter wave resonators. Spatial resolutions of this method is ~20mm. Another method is "Continuous Flow Analysis" (CFA) method to read layers of Si, Na and Ca, with a resolutions of ~10 mm.

Expected Research Achievements and Scientific Significance

First, we will produce invaluable ice core data. The data will be used to tackle the key questions. Based on the data, we will synchronize two very old ice cores at Dome Fuji and Dome C, based on collaborations of the European deep ice study community. In addition, we will examine timing difference between the climatic change records between the two ice cores. We aim to accomplish the first reliable and detailed synchronization between very old ice cores up to 720,000 years back in time. we will study change of the climatic mode over the 720,000 years. Furthermore, we will study how very old ice older than 1 M years, can be preserved near the base of the ice sheet.

©2019. Japan Geoscience Union. All Right Reserved.

Keywords: Antarctica, ice sheet, ice core, climate change, dating, paleoclimate

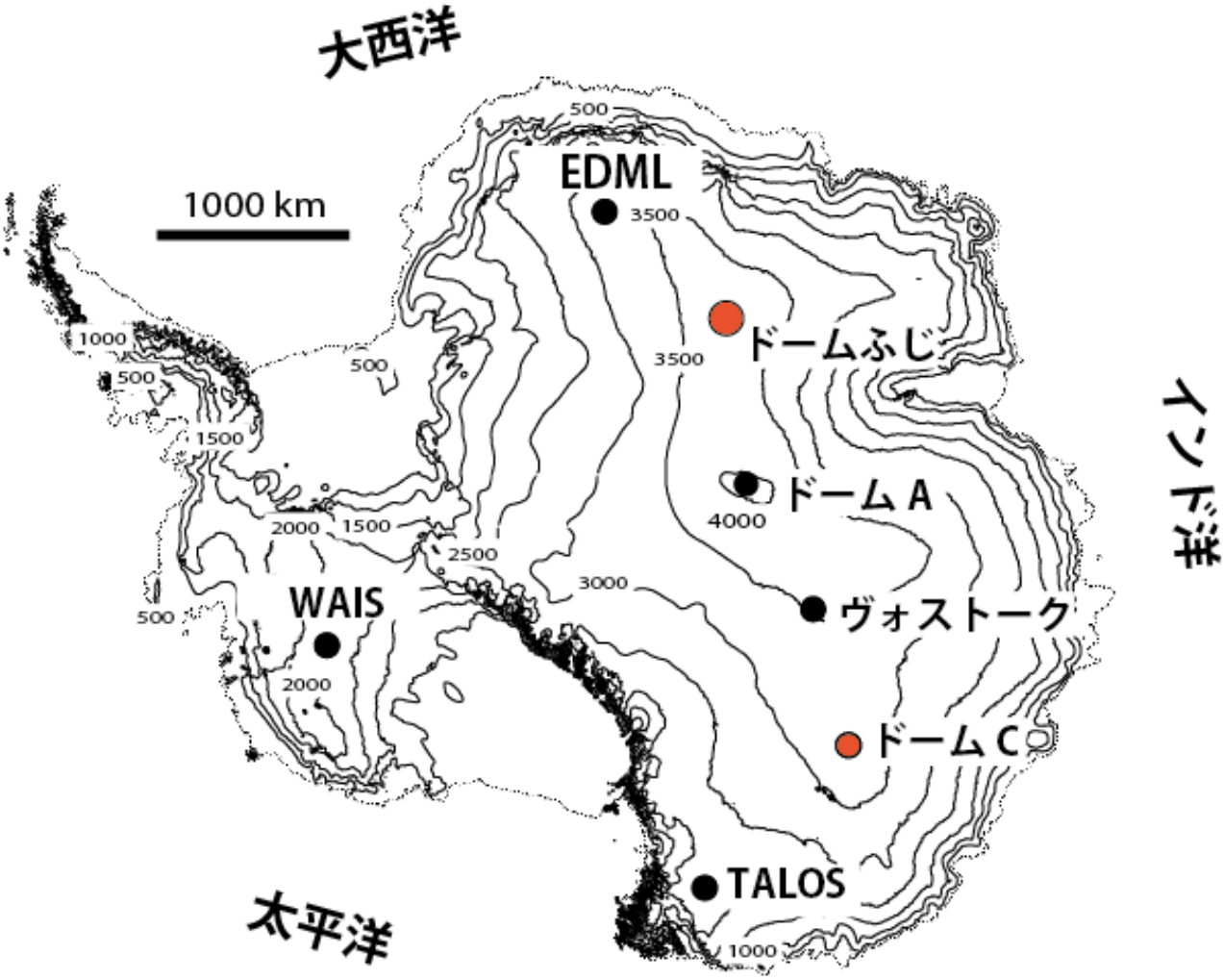

図：南極氷床上の主要な深層アイスコア掘削点

©2019. Japan Geoscience Union. All Right Reserved.

Reconstructions of the Antarctic Polar Front through the glacial/interglacials

*Hiroki Matsui[1], Yuji Kato[1,2], Itsuki Suto[3], Minoru Ikehara[1]

1. Center for Advanced Marine Core Research, Kochi University, 2. JSPS PD, 3. Graduate School of Environmental Studies, Nagoya University

Understanding the Antarctic Circumpolar Current (i.e., Antarctic Polar Front and Subantarctic front), which connects major three Oceans and major components of the Southern Ocean and Antarctic ice sheets system, is important (from past to present). Modern polar front ranges from 44˚S to 64˚S and is defined by the southern bound of strong SST gradient (>1.5˚ over 100 km) (Freeman et al., 2016). The observed PF position from 2002 to 2014 does not show discernable trend (either northward or southward) in response to the global warming. For the Last Glacial Maximum (LGM), the PF moved northward by 5 degrees (e.g., Gersonde et al., 2005). However, there is difficulty to reconstruct paleo SST gradient because of paucity of surface sediments, and the alternative definition of the PF (e.g., 4 degrees C surface isotherm) was applied (Kohfeld et al., 2013). In this presentation, we summarize current state of knowledge and obstacles of reconstruction of the PF through the glacial/interglacials. We also discuss appropriate methods to certainly track the past PF position.

Keywords: Antarctic Polar Front, Paleoceanography

©2019. Japan Geoscience Union. All Right Reserved.

Integrated observations for marine earth science in the Indian sector of the Southern Ocean: Preliminary results of R/V Hakuho-maru KH-19-1 cruise

*Minoru Ikehara[1], Kay I. Ohshima[2], Takuya Itaki[3], Hiroshi Sato[4], Masakazu Fujii[5], Michiyo Yamamoto-Kawai[6], Hiroki Matsui[1], Takahito Ikenoue[7], . Scientific Party of R/V Hakuho-maru KH-19-1 cruise

1. Center for Advanced Marine Core Research, Kochi University, 2. ILTS, Hokkaido University, 3. GSJ, AIST, 4. Senshu University, 5. National Institute of Polar Research, 6. Tokyo University of Marine Science and Technology, 7. Marine Ecology Research Institute

Integrated observations for marin earth science have been done in the Indian sector of the Southern Ocean during the KH-19-1 cruise by R/V Hakuho-maru in early 2019. Multichannel seismic (MCS) reflection and bathymetric survey were conducted at three sites on the Del Cano Rise and the Conrad Rise, and these site survey for IODP proposal 918 was successfully completed. We also obtained sediment cores from the proposed sites DCR-03A and DCR-02A, and sedimentary archives of a piston core DCR-2PC (at DCR-02A) show obviously glacial-interglacial cycles based on magnetic susceptibility and color reflectance. Various rock samples were collected by dredge observation at the Conrad Rise and the obtained materials to be used for understanding of origin of rise and tectonics in the southwest Indian Ocean. Sediment trap samples were also recovered from a site ECR-1, where is located under the biogenic silica belt south of polar front. Flux of settling particles was increased in summer, suggesting that typical seasonal change was occurred in the Southern Ocean. In addition, multichannel seismic (MCS) reflection and bathymetric survey were also done on the across transect of the deep-sea valleys off Cape Darnley, East Antarctica. By analyzing these materials and data, it is expected to advance the research leading to changes in the sedimentation process accompanying expansion and retreat of the Antarctic ice sheets and elucidation of the history of the Cape Darnley bottom water.

Keywords: Southern Ocean, paleoceanography, sea ice, Antarctic, productivity, Antarctic Bottom Water

©2019. Japan Geoscience Union. All Right Reserved.

[J] Oral | M (Multidisciplinary and Interdisciplinary) : M-IS Intersection

Mon. May 27, 2019 10:45 AM - 12:15 PM JST | Mon. May 27, 2019 1:45 AM - 3:15 AM UTC | Convention Hall B 2F

[M-IS14] Global climate change driven by the Southern Ocean and the Antarctic Ice Sheet

convener:Osamu Seki(Institute of Low Temperature Science, Hokkaido University), Akira Oka(Atmosphere and Ocean Research Institute, The University of Tokyo), Ryu Uemura(University of the Ryukyus), Ryosuke Makabe(National Institute of Polar Research), Chairperson:Sam Sherriff-Tadano(University of Tokyo)

The Southern Ocean and Antarctic ice sheet, which are the giant reservoirs of heat, water, and materials, have a potential to play central roles in long-term global climate change. This system is composed of the following sub-systems; ice shelf which is a place of the interaction of ice sheet and ocean, flowing iceberg, seasonal sea ice zone, Antarctic bottom water which drives the thermohaline circulation, active biological production and Antarctic Circumpolar Current. These sub-systems are interacted with each other and have significant impact on changes in the global environmental system. This session aim to summarize recent observational and simulation studies from various fields relating to the past and present changes in the Antarctic Ice sheet and Southern Ocean, which are essential elements for unraveling the changes in the global climate system. Further, future science plans for understanding of the environmental changes of the Antarctic Cryosphere is also discussed.

10:45 AM - 11:00 AM JST | 1:45 AM - 2:00 AM UTC

[MIS14-06] High resolution ocean temperatures reconstructions over the last glacial-interglacial in the Kerguelen region, Southern Ocean.

*Matthieu Civel[1,2], Xavier Crosta[3], Giuseppe Cortese[4], Elisabeth Michel[5], Alain Mazaud[5], Samuel Jaccard[6], Lena Thöle[6], Minoru Ikehara[1], Takuya Itaki[2] (1.Center for Advanced Marine Core Research, Kochi University, Japan, 2.Geological Survey of Japan, AIST, Tsukuba, Japan, 3.UMR 5805 CNRS EPOC, Université de Bordeaux, France, 4.GNS Science, Lower Hutt, New Zealand, 5.LSCE-IPSL, CEA-CNRS-UVSQ, 91198 Gif-sur-Yvette, France, 6.Institute of Geological Sciences & Oeschger Centre for Climate Change Research, University of Bern, Switzerland)

11:00 AM - 11:15 AM JST | 2:00 AM - 2:15 AM UTC

[MIS14-07] Present-day crustal motion and gravity change in East Antarctica: implications for the mantle viscosity and Holocene Antarctic Ice Sheet change inferred from GIA modeling

*Jun'ichi Okuno[1,2], Koichiro Doi[1,2], Yuichi Aoyama[1,2], Takeshige Ishiwa[1], Akihisa Hattori[2], Yoichi Fukuda[3] (1.National Institute of Polar Research, 2.SOKENDAI, 3.Kyoto University)

11:15 AM - 11:30 AM JST | 2:15 AM - 2:30 AM UTC

[MIS14-08] Reconstruction of the East Antarctic ice sheet variability during the last 3 myrs in the central & eastern Droning Maud Land, East Antarctica

*Yusuke Suganuma[1,2], Moto Kawamata[2], Kota Katsuki[3], Tatsuo Kanamaru[4], Heitaro Kaneda[5], Takushi Koyama[6], Tanabe Yukiko[1,2], Daisuke Shibata[7], Takeshige Ishiwa[1], Takuya Itaki[8], Jun'ichi Okuno[1,2], Osamu Seki[9], Itsuki Suto[10], Masakazu Fujii[1,2], Hideki Miura[1,2] (1.National institute of Polar Research, 2.SOKENDAI, 3.Shimane University, 4.Nihon University, 5.Chiba University, 6.Oita University, 7.Tsukuba University, 8.GSJ, AIST, 9.Hokkaido University, 10.Nagoya University)

11:30 AM - 11:45 AM JST | 2:30 AM - 2:45 AM UTC

[MIS14-09] Vertical ice flow motions obtained from year-round GNSS observations on Shirase Glacier, Antarctica

*Yuichi Aoyama[1,2], Koichiro Doi[1,2], Daisuke Hirano[3], Takeshi Tamura[1,2], Shigeru Aoki[3], Kazuo Shibuya[1] (1.National Institute of Polar Research, 2.SOKENDAI, 3.Institute of Low Temperature Science, Hokkaido University)

11:45 AM - 12:00 PM JST | 2:45 AM - 3:00 AM UTC

[MIS14-10] Operation plan and design of the Antarctic exploration AUV "MONACA"

*Hirokazu Yamagata[1], Toshihiro Maki[1], Hiroshi Yoshida[2], Yoshifumi Nogi[3] (1.Institute of Industrial Science, The University of Tokyo, 2.Japan Marine Science and Technology Center, 3.National Institute of Polar Research)

12:00 PM - 12:15 PM JST | 3:00 AM - 3:15 AM UTC

[MIS14-11] Geophysical insights into tectonic, volcanic, sedimentation, and glacial processes in Indian and Southern Oceans: Preliminary geophysical results of R/V *Hakuho-maru* KH-19-1 cruise

*Masakazu Fujii[1], Hiroshi Sato[2], Minoru Ikehara[3], Yoshifumi Nogi[1], Taichi Sato[4], Yasuyuki Nakamura[5], Eri Helen Amsler[6], Sam Sherriff-Tadano[7] (1.National Institute of Polar Research and SOKENDAI, 2.Senshu University, 3.Kochi University, 4.AIST, 5.JAMSTEC, 6.University of Bern, 7.AORI, UTokyo)

High resolution ocean temperatures reconstructions over the last glacial-interglacial in the Kerguelen region, Southern Ocean.

*Matthieu Civel[1,2], Xavier Crosta[3], Giuseppe Cortese[4], Elisabeth Michel[5], Alain Mazaud[5], Samuel Jaccard[6], Lena Thöle[6], Minoru Ikehara[1], Takuya Itaki[2]

1. Center for Advanced Marine Core Research, Kochi University, Japan, 2. Geological Survey of Japan, AIST, Tsukuba, Japan, 3. UMR 5805 CNRS EPOC, Université de Bordeaux, France, 4. GNS Science, Lower Hutt, New Zealand, 5. LSCE-IPSL, CEA-CNRS-UVSQ, 91198 Gif-sur-Yvette, France, 6. Institute of Geological Sciences & Oeschger Centre for Climate Change Research, University of Bern, Switzerland

The Southern Ocean (SO) is a place of primordial importance to the understanding of global ocean circulation as it connects the Atlantic, the Pacific and the Indian oceans and thus actively participates in global climate changes. Climate processes and variations in the Indian sector of the SO are not as well understood as processes in the Atlantic sector. This why this project documents climate variations and migrations of the Antarctic Circumpolar Current (ACC) hydrological fronts in the Kerguelen area over the last glacial-interglacial cycle. In this study sea surface temperatures (SST) are reconstructed in two sediment cores, the MD11-3353 (PFZ) and MD12-3396CQ (SAZ), with radiolarian and diatoms microfossil assemblages. By comparing the results given by these two proxies different signals were identified for surface and subsurface waters suggesting a decoupling of these two water masses in the SAZ East of the Kerguelen Plateau. But in the PFZ, both proxies showed similar results. The comparison between these results leads us to think of an influence of lower latitudes warm water in the SAZ whereas this influence is absent in the PFZ in this region.

Keywords: Southern Ocean, Radiolarian, Diatoms, Micropaleontology, Kerguelen

©2019. Japan Geoscience Union. All Right Reserved.

Present-day crustal motion and gravity change in East Antarctica: implications for the mantle viscosity and Holocene Antarctic Ice Sheet change inferred from GIA modeling

*Jun'ichi Okuno[1,2], Koichiro Doi[1,2], Yuichi Aoyama[1,2], Takeshige Ishiwa[1], Akihisa Hattori[2], Yoichi Fukuda[3]

1. National Institute of Polar Research, 2. SOKENDAI, 3. Kyoto University

Geodetic and geomorphological observations in the coastal part of Antarctica indicate the uplift trend associated with the removal mass of the Antarctic Ice Sheet (AIS) in the last deglaciation. The numerical calculations of crustal motion derived from the glacial isostatic adjustment (GIA) modeling have played the role of inferring the ice mass change of AIS from observations related to solid Earth deformation. The deglaciation histories of the AIS inferred from the comparisons between the geomorphological sea-level records, and GIA modeling shows the monotonic Holocene retreat for the AIS (e.g., Whitehouse et al., 2012). However, GNSS observations in some regions in the coastal part of Antarctica cannot be explained the amplitudes of the uplift by only glacial rebound due to the last deglaciation of the AIS. Also, recent studies (e.g., Kingslake et al., 2018) concerning bedrock topography in the margin of AIS inferred that some portions of the ice sheet might have re-advanced after retreating behind the present-day margin in mid-to-late Holocene. Therefore, this re-advance of AIS in Holocene may be caused to arise the mismatch between GNSS observations and numerical predictions. On the other hand, GNSS observations include not only the components of the GIA due to the last deglaciation and also elastic deformation due to present-day surface mass balance (e.g., Hattori et al., 2018). Similarly, this effect could cause a difference between the GNSS observations and the GIA calculations. In this presentation, we will show the crustal deformation rates and gravity changes calculated by the GIA modeling using the previously published deglaciation histories and the comparisons with these observations obtained from East Antarctica. We intend to discuss the influences of AIS mass changes and choice of mantle viscosity profile on the geodetic measurements in East Antarctica.

Keywords: Glacial Isostatic Adjustment, East Antarctica, GNSS, gravity change

©2019. Japan Geoscience Union. All Right Reserved.

Reconstruction of the East Antarctic ice sheet variability during the last 3 myrs in the central & eastern Droning Maud Land, East Antarctica

*Yusuke Suganuma[1,2], Moto Kawamata[2], Kota Katsuki[3], Tatsuo Kanamaru[4], Heitaro Kaneda[5], Takushi Koyama[6], Tanabe Yukiko[1,2], Daisuke Shibata[7], Takeshige Ishiwa[1], Takuya Itaki[8], Jun'ichi Okuno[1,2], Osamu Seki[9], Itsuki Suto[10], Masakazu Fujii[1,2], Hideki Miura[1,2]

1. National institute of Polar Research, 2. SOKENDAI, 3. Shimane University, 4. Nihon University, 5. Chiba University, 6. Oita University, 7. Tsukuba University, 8. GSJ, AIST, 9. Hokkaido University, 10. Nagoya University

Reconstructing past variability of the Antarctic ice sheets is essential to understand their stability and to anticipate their contribution to future sea level rise. However, magnitude and timing of ice sheet changes during the last several million years have not been well constrained, especially in central & eastern Droning Maud Land, East Antarctica. Recently, we have carried out several field campaigns in this area to reconstruct changes in thickness, geographical extent, and timing of retreat of the East Antarctic Ice Sheet based on the detailed geomorphological survey, cosmogenic exposure dating, and lake/shallow marine sediment records coupled with glacial isostatic adjustment modeling (GIA). In this presentation, we will introduce these recent achievements from the field campaigns and discuss scientific plans for the next few seasons.

Keywords: Giant Reservoirs - Antarctic, Solid Earth

©2019. Japan Geoscience Union. All Right Reserved.

Vertical ice flow motions obtained from year-round GNSS observations on Shirase Glacier, Antarctica

*Yuichi Aoyama[1,2], Koichiro Doi[1,2], Daisuke Hirano[3], Takeshi Tamura[1,2], Shigeru Aoki[3], Kazuo Shibuya[1]

1. National Institute of Polar Research, 2. SOKENDAI, 3. Institute of Low Temperature Science, Hokkaido University

The Antarctic ice sheet is a huge heat sink acting as a feedback controller for adjusting global warming, so a loss of its mass would cause a great impact on the global climate change. It is valuable to evaluate an Antarctic ice mass balance, which is a consequence of competition between an ice discharge and a snow accumulation. With an objective of estimating the ice discharge around Lützow-Holmbukta, East Antarctica, we have measured three-dimensional (3D) ice flow motions around a grounding line of Shirase Glacier, which is fastest and largest ice stream in Lützow-Holmbukta.

We first performed one-month GPS measurement near the calving front of Shirase Glacier in 2011/2012 austral summer. The three-dimensional position of this site was determined by the kinematic precise point positioning (kPPP) method at every 30 seconds with a 4-5-cm precision for 25 days. From the 30-s interval position, we estimated the ice flow velocity vector, the basal melting rate of the iceberg, and ocean tidal variations (Aoyama et al. 2016). Subsequently, a year-round GNSS measurement system was installed six kilometers downstream from the grounding line of Shirase Glacier at the end of Jan. 2015. By maintaining this year-round system (changing SD card and battery) every austral summer season, we have already obtained a three-years continuous data from Jan. 30, 2015 to Dec. 30, 2017.
We analyzed the time series of the three-dimensional position of this system with kPPP method. The time series revealed the ice flow motion downstream from the grounding line of Shirase Glacier during 2015-2017. Focusing on the vertical motion, there is no remarkable ocean tidal variation. And the obtained vertical flow motion shows gradually descent, then rise, again descent slope. In order to clarify whether such vertical change is local or wide area, we compared with a TanDEM-X 90m DEM (Rizzoli et al., 2017). In the presentation, we will show properties of the ice flow motion downstream the grounding line of Shirase Glacier.

Keywords: year-round GNSS measurements on Shirase Glacier, Unmanned measurement in site where access is difficult

©2019. Japan Geoscience Union. All Right Reserved.

Operation plan and design of the Antarctic exploration AUV "MONACA"

*Hirokazu Yamagata[1], Toshihiro Maki[1], Hiroshi Yoshida[2], Yoshifumi Nogi[3]

1. Institute of Industrial Science, The University of Tokyo, 2. Japan Marine Science and Technology Center, 3. National Institute of Polar Research

Autonomous Underwater Vehicles (AUVs) have been used for under-ice explorations of the Antarctic Ocean. Most of the current under ice AUVs are large and are used for the long-distance survey. Survey results of these AUVs are extremely precise, but there is a trade-off between precision and running cost and/or risk of losing AUVs.

In this presentation, the authors propose a variable and compact AUV MONACA (Mobility Oriented Nadir AntarctiC Adventurer) which can offer the necessary and sufficient compositions for various survey needs by the modular design. Development of MONACA is supported by JSPS Grant-in-Aid for Scientific Research on Innovative Areas No.4902, to measure the sea ice/shelf ice and ocean floor for research of ice sheet-ocean interaction.

MONACA is 2 m long, 230 kg weight, and it can cruise for about 8 hours. Depth rating is 1500m. The vehicle is designed to go into ice-covered oceans as far as 10 km. The flat body is filled with buoyancy materials at the top so that the battery units and main unit can be accessed from the side. The vehicle has five degrees of freedom (surge, heave, roll, pitch, and yaw) by 4 vertical thrusters and 2 horizontal thrusters. Although the survey range is limited compared with large AUVs, it can conduct a highly precise survey with lower costs.

The three missions are considered as shown in the figure. (A: Seafloor tracking, B: Ice tracking, C: Water survey in constant depth). In the missions A and B, the shape of the seafloor or the ice is mapped by a multi-beam sonar while tracking it by a probabilistic approach using a scanning sonar. The multi-beam sonar measures 480 points in the swath width of 120˚. The vehicle has two set of releasable ballasts for diving and surfacing. The vehicle is designed to follow the seafloor or ice at the reference altitude of 50 m. In the mission C, the vehicle navigates at a constant depth, measuring water quality by a CTD sensor. Resolution of the CTD sensor is Temperature = +/- 0.0001 ˚C, Conductivity = +/- 0.0001 mS / cm, Depth = 0.03 m.

In order to realize these three missions under the size limitation, MONACA has the sensor unit that can be flipped upside down. The sensor unit includes the multi-beam sonar, an INS, and a DVL. Therefore, MONACA can navigate only by the sensor unit in case there are no obstacles in the seafloor.
MONACA is currently under construction, to be launched in 2019.

Keywords: Antarctic, AUV

©2019. Japan Geoscience Union. All Right Reserved.

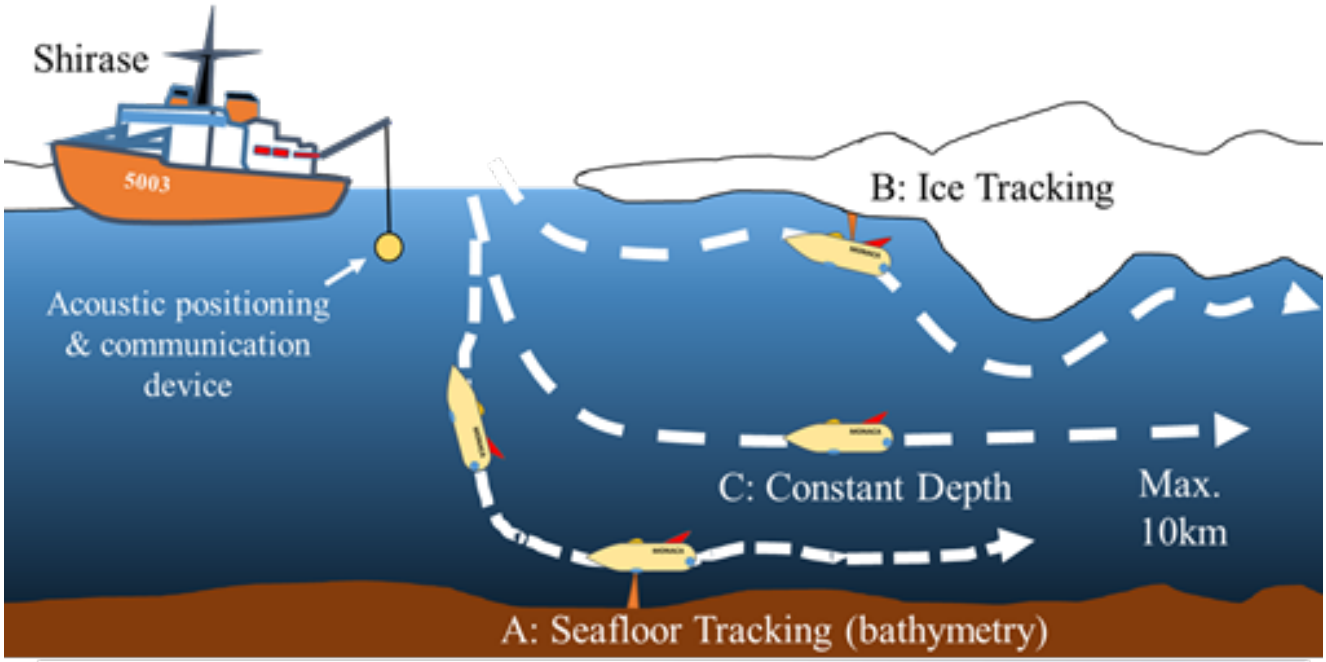

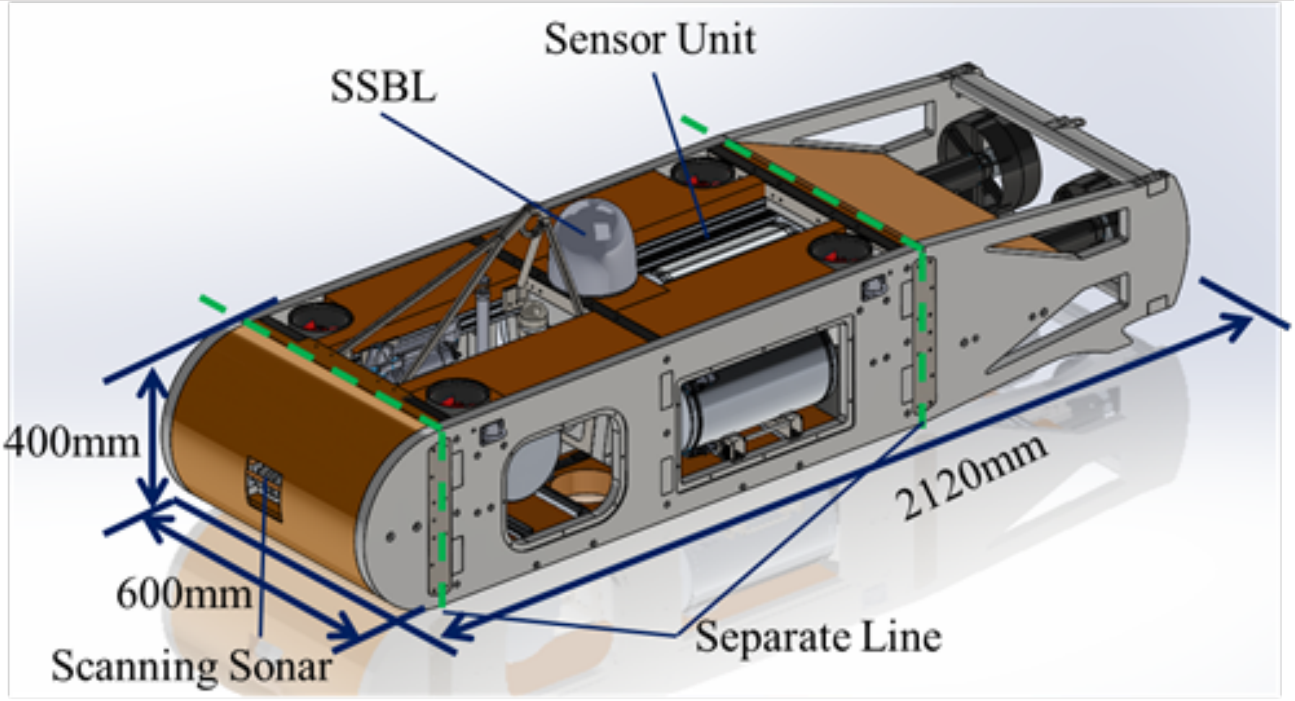

©2019. Japan Geoscience Union. All Right Reserved.

Geophysical insights into tectonic, volcanic, sedimentation, and glacial processes in Indian and Southern Oceans: Preliminary geophysical results of R/V *Hakuho-maru* KH-19-1 cruise

*Masakazu Fujii[1], Hiroshi Sato[2], Minoru Ikehara[3], Yoshifumi Nogi[1], Taichi Sato[4], Yasuyuki Nakamura[5], Eri Helen Amsler[6], Sam Sherriff-Tadano[7]

1. National Institute of Polar Research and SOKENDAI, 2. Senshu University, 3. Kochi University, 4. AIST, 5. JAMSTEC, 6. University of Bern, 7. AORI, UTokyo

The seafloor covers more than 70 percent of the solid-earth surface and has been progressively investigated since the 20th century, however most parts have not been explored because of observation difficulties in the ocean. Particularly, the seafloor of the Indian and Southern Oceans are expected to preserve significant records of paleo glacial processes and submarine volcanism as well as continental breakup and seafloor spreading. Here, we show new geophysical dataset just obtained during the R/V *Hakuho-maru*KH-19-1 cruise in early 2019. Underway geophysical mapping as well as multichannel reflection surveys and dredge rock samplings were conducted in this cruse. Specific scientific target area were set to 1) the Southwest Indian Ridge to reveal the seafloor spreading process in the Cenozoic era; 2) Conrad Rise to understand its origin and surrounding magmatism; 3) Del Cano Rise to reveal how it has been formed; 4) off Cape Darnley to reveal relationship between solid-earth processes and presently formed Antarctic bottom water; and 5) Southeast Indian Ridge to reveal the mid-ocean ridge oscillation. Multibeam bathymetry, total and vector magnetic fields, gravity, and sub-bottom profiler data were successfully acquired along the ship tracks which covers Fremantle to Mauritius in leg-1 (2 Jan to 11 Jan 2019) and Mauritius to Fremantle via mentioned target area in leg-2 (16 Jan to 12 Feb 2019). We overview preliminary geophysical results which were combined with previous *Hakuho-maru*cruises of KH-07-04, KH-09-05, KH-10-07, and KH-16-01 and data acquired during Japanese Antarctic Research Expedition by using Japanese icebreaker *Shirase*. Finally, we discuss geophysical insights into tectonic, volcanic, sedimentation, and glacial processes in Indian and Southern Oceans.

Keywords: Indian and Southern Oceans, Solid Earth processes, Marine geophysics, Hakuho-maru

©2019. Japan Geoscience Union. All Right Reserved.

[J] Oral | M (Multidisciplinary and Interdisciplinary)：M-IS Intersection

Mon. May 27, 2019 1:45 PM - 3:15 PM JST | Mon. May 27, 2019 4:45 AM - 6:15 AM UTC | Convention Hall B 2F

[M-IS14] Global climate change driven by the Southern Ocean and the Antarctic Ice Sheet

convener:Osamu Seki(Institute of Low Temperature Science, Hokkaido University), Akira Oka(Atmosphere and Ocean Research Institute, The University of Tokyo), Ryu Uemura(University of the Ryukyus), Ryosuke Makabe(National Institute of Polar Research), Chairperson:Takeshige Ishiwa(National institute of Polar Research)

The Southern Ocean and Antarctic ice sheet, which are the giant reservoirs of heat, water, and materials, have a potential to play central roles in long-term global climate change. This system is composed of the following sub-systems; ice shelf which is a place of the interaction of ice sheet and ocean, flowing iceberg, seasonal sea ice zone, Antarctic bottom water which drives the thermohaline circulation, active biological production and Antarctic Circumpolar Current. These sub-systems are interacted with each other and have significant impact on changes in the global environmental system. This session aim to summarize recent observational and simulation studies from various fields relating to the past and present changes in the Antarctic Ice sheet and Southern Ocean, which are essential elements for unraveling the changes in the global climate system. Further, future science plans for understanding of the environmental changes of the Antarctic Cryosphere is also discussed.

1:45 PM - 2:00 PM JST | 4:45 AM - 5:00 AM UTC

[MIS14-12] Simulations of glacial ocean carbon cycle with a parameterization of stratification dependence of vertical diffusivity

*Hidetaka Kobayashi[1], Akira Oka[1] (1.Atmosphere and Ocean Research Institute, The University of Tokyo)

2:00 PM - 2:15 PM JST | 5:00 AM - 5:15 AM UTC

[MIS14-13] Impacts of precession on the periodicity of climate and AMOC variabilities

*Sam Sherriff-Tadano[1] (1.Atmosphere and Ocean Research Institute, the University of Tokyo)

2:15 PM - 2:30 PM JST | 5:15 AM - 5:30 AM UTC

[MIS14-14] Warming and climate feedbacks in the southern high latitude driven by obliquity, precession-eccentricity, and atmospheric CO2

*Kanon Kino[1], Ayako Abe-Ouchi[1,2], Ryouta O'ishi[1], Fuyuki SAITO[2], Masakazu Yoshimori[1] (1.Atmosphere and Ocean Research Institute, the University of Tokyo, 2.Japan Agency for Marine-Earth Science and Technology)

2:30 PM - 2:45 PM JST | 5:30 AM - 5:45 AM UTC

[MIS14-15] Origin of Circumpolar Deep Water intruding onto the Amundsen and Bellingshausen Sea continental shelves

*Yoshihiro Nakayama[1,2], Menemenlis Dimitris[2], Hong Zhang[2], Michael Schodlok[2], Eric Rignot[2,3] (1.Institute of Low Temperature Science, Hokkaido University, 2.NASA's Jet Propulsion Laboratory, 3.Uniersity of California, Irvine)

2:45 PM - 3:00 PM JST | 5:45 AM - 6:00 AM UTC

[MIS14-16] Ocean and material circulation in the southern part of the Australian Antarctic Basin in 2018/2019 summer - preliminary results from Kaiyomaru KY18-04 cruise

*Katsuro Katsumata[1], Daisuke Hirano[2], Daiki Nomura[2], Kaihe Yamazaki[2], Yoichiro Koh[2], Masaaki Kiuchi[2], Shigeru Aoki[2], Hiroto Murase[3] (1.JAMSTEC, 2.Hokkaido Univ., 3.NRI-FSF)

3:00 PM - 3:15 PM JST | 6:00 AM - 6:15 AM UTC

[MIS14-17] Mooring observation aiming direct current measurement and quantitative evaluation of Meridional Circulation of Southern Ocean

*Kitade Yujiro[1], Kohei Mizobata[1], Kazuho Watanabe[1], Linquiao Chen[3], Gaopin Guo[3], Shigeru Aoki[2], Shyuki Ushio[4], Keishi Shimada[1], Kay I. Ohshima[2] (1.Tokyo University of Marine Science and Technology, 2.Hokkaido University, 3.Shanghi Ocean University, 4.National Institute of Polar Research)

Simulations of glacial ocean carbon cycle with a parameterization of stratification dependence of vertical diffusivity

*Hidetaka Kobayashi[1], Akira Oka[1]

1. Atmosphere and Ocean Research Institute, The University of Tokyo

Paleo-ocean reconstructions supporting the Southern Ocean hypothesis, in which carbon storage in the deep Southern Ocean increases during the glacial ages, has not been sufficiently reproduced by previous paleoclimate modeling studies. In this study, we apply salinity restoring in the Southern Ocean and a parameterization of stratification dependence of vertical diffusivity to an ocean general circulation model and attempt to reproduce oceanic properties reconstructed from paleo-ocean proxy data at the Last Glacial Maximum (LGM). An LGM simulation including the salinity restoring expresses high bottom-water salinity associated with larger sea ice production at the LGM, and reproduces the reconstructed salinity distribution. Moreover, by considering the stratification dependence of vertical diffusivity in the global ocean, the reduced vertical mixing due to enhanced salinity stratification increases ventilation ages in the intermediate to the deep ocean. As a result, more carbon is stored in the deep ocean and the vertical gradient of dissolved inorganic carbon enlarges. This redistribution of carbon reduces atmospheric carbon dioxide concentration (pCO_2). In addition, the subsequent response of carbonate compensation may amplify the glacial reduction of atmospheric pCO_2. In our presentation, we plan to report the glacial variation of atmospheric pCO_2 explained by the response of the ocean carbon cycle including carbonate compensation in numerical simulations using an ocean general circulation model.

Keywords: ocean carbon cycle, glacial-interglacial cycle, global ocean meridional overturning circulation, carbonate compensation

©2019. Japan Geoscience Union. All Right Reserved.

Impacts of precession on the periodicity of climate and AMOC variabilities

*Sam Sherriff-Tadano[1]

1. Atmosphere and Ocean Research Institute, the University of Tokyo

Over the glacial period, climate varied on centennial to millennial time scale between the warm instersadial and the cold staidial. Recent ice core and modelling studies have shown that changes in CO2 and the glacial ice sheet played a critical role in controlling the periodicity of the climate variability through affecting the Atlantic Meridional Overturning Circulation (AMOC). Here, by analysing simulation data from a climate model GFDL, it is shown that changes in insolation pattern due to changes in precession also exert a substantial impact on the periodicity of the climate and AMOC variability. Model results show that a change from a Northern Hemisphere summer solstice perihelion to winter solstice perihelion causes an increase in the periodicity of the AMOC variability from decadal to millennial. Analysis reveals that an increase of sea ice over the Northern Hemisphere and a decrease in sea ice over the Southern Ocean due to insolation changes play a role in increasing the periodicity through stabilising both the vigorous AMOC and weak AMOC. These results may have some implications in interpreting the ice core data.

Keywords: millennial time-scale climate variability, AMOC, sea ice

©2019. Japan Geoscience Union. All Right Reserved.

Warming and climate feedbacks in the southern high latitude driven by obliquity, precession-eccentricity, and atmospheric CO2

*Kanon Kino[1], Ayako Abe-Ouchi[1,2], Ryouta O'ishi[1], Fuyuki SAITO[2], Masakazu Yoshimori[1]

1. Atmosphere and Ocean Research Institute, the University of Tokyo, 2. Japan Agency for Marine-Earth Science and Technology

Polar amplification is widely known as a major characteristic of observed and simulated global warming which induced by increasing atmospheric CO2. In the southern high latitude, a study using GCM investigated climate feedback system to reproduce the warming (Lu and Cai, 2009). A latest study of the Antarctic ice core precisely analyzed phase relationship between temperature changes in the past ages and the periodic changes in the Earth’ s orbital parameters (obliquity, precession and eccentricity (Uemura et al., 2018). In this study, we use MIROC-GCM to investigate the warming in the southern high latitude due to the orbital parameter changes, and climate feedback responses. Results are compared with the doubling CO2 experiment.
We use an AGCM with slab ocean of MIROC-GCM (Hasumi and Emori, 2004) and performed experiments with (1) large obliquity, (2) large precession and the winter solstice (austral summer) at the aphelion (Maximum values in the past ages are used). A seasonal surface feedback analysis method (Lu and Cai, 2009) is also applied.
Results show that warming on the Antarctica (covered by the ice-sheet) due to the orbital parameter change is dominated by short-wave radiation which is not interrupted by cloud, in contrast that the warming due to increasing atmospheric CO2 is dominated by downward long-wave radiation. Results also show that seasonal warming and climate feedback responses on the Southern Ocean are qualitatively common in the insolation and CO2 cases, as well as warming in the Arctic Ocean; little warming in the summer with absorption of energy and large warming in the autumn and winter with releasing of the energy. The strengths of the warming are qualitatively different whether the seasonality, especially spring and early summer, of radiative forcing is favorable for sea ice melt.
We will investigate the changes of the atmospheric circulation, precipitation, and the influence of the oceanic circulation.

Keywords: GCM, Antarctica, orbital parameter, feedback

©2019. Japan Geoscience Union. All Right Reserved.

Origin of Circumpolar Deep Water intruding onto the Amundsen and Bellingshausen Sea continental shelves

*Yoshihiro Nakayama[1,2], Menemenlis Dimitris[2], Hong Zhang[2], Michael Schodlok[2], Eric Rignot[2,3]

1. Institute of Low Temperature Science, Hokkaido University, 2. NASA's Jet Propulsion Laboratory, 3. Uniersity of California, Irvine

Melting of West Antarctic ice shelves is enhanced by Circumpolar Deep Water (CDW) intruding onto the Amundsen and Bellingshausen Seas (ABS) continental shelves. Despite existing studies of cross-shelf and on-shelf CDW transports, CDW pathways onto the ABS originating from further offshore have never been investigated. Here, we investigate CDW pathways onto the ABS using a regional ocean model. Simulated CDW tracers from a zonal section across 67˚S (S04P) circulate along the Antarctic Circumpolar Current (ACC) and Ross Gyre (RG) and travel into ABS continental shelf after 3–5 years, but source locations are shifted westward by ~900 km along S04P in 2001–2006 compared to 2009–2014. We find that simulated on- and off-shelf CDW is ~0.1–0.2 ˚C warmer in the 2009–2014 case than in the 2001–2006 case together with changes in simulated ocean circulation. These differences are primarily caused by lateral, rather than surface, boundary conditions, implying that large-scale atmospheric and ocean circulations are able to control CDW pathways and thus off- and on-shelf CDW properties.

Keywords: Ice shelf-ocean interaction, Amundsen-Bellingshausen Sea, Circumpolar Deep Water (CDW)

©2019. Japan Geoscience Union. All Right Reserved.

Ocean and material circulation in the southern part of the Australian Antarctic Basin in 2018/2019 summer - preliminary results from Kaiyomaru KY18-04 cruise

*Katsuro Katsumata[1], Daisuke Hirano[2], Daiki Nomura[2], Kaihe Yamazaki[2], Yoichiro Koh[2], Masaaki Kiuchi[2], Shigeru Aoki[2], Hiroto Murase[3]

1. JAMSTEC, 2. Hokkaido Univ., 3. NRI-FSF

The Australian Antarctic Basin collects dense shelf water from the Ross Sea and off Adelie Coast along the westward-flowing Antarctic Slope Current and modifies its property through mixing before initiating the bottom branch of the meridional overturning circulations in the Indian and Pacific oceans. It is necessary to monitor the current status of the near-bottom circulation in the basin in order to understand how the recently-reported volume decrease of the Antarctic Bottom Water and changes in the atmosphere-ocean and cryosphere-ocean interactions are related. It is established that the Southern Ocean, particularly at the north of the Antarctic Circumpolar Current (ACC), acts as a sink of anthropogenic carbon through its low surface pCO2 and mode and intermediate watermass production. Then, is the south of the ACC source or sink of anthropogenic carbon with its dense shelf water production in the face of upwelling of carbon-rich deep water masses? How do these changes in the environment affect the biosphere and ecosystem in the Southern Ocean?
With these questions in mind, R/V Kaiyomaru, Japan Fishery Agency, conducted a research cruise in the basin, in proximity of its seasonal ice edge, from December 2018 to March 2019. This part of the basin has been observed by an Australian team in 1996. At the time of writing, more than 40 stations have been occupied for CTD and LADCP observations and bottle sampling, more than 80 XCTD probes have been deployed. Preliminary analysis shows the changes in the bottom water masses. The Figure below shows the CTD/LADCP/sampling stations (black dots) and XCTD deployments (crosses) for Leg1 (5 Dec 2018 to 16 Jan 2019) with AMSR2 derived ice concentration, which is a combination of west of 90E (observed on 17 Dec 2018), between 90E and 107E (24 Dec 2018) and east of 107E (31 Dec 2018). In the talk, the latest results and its outlook will be discussed.

Keywords: Shelf circulation, Bottom water formation, carbon circulation

©2019. Japan Geoscience Union. All Right Reserved.

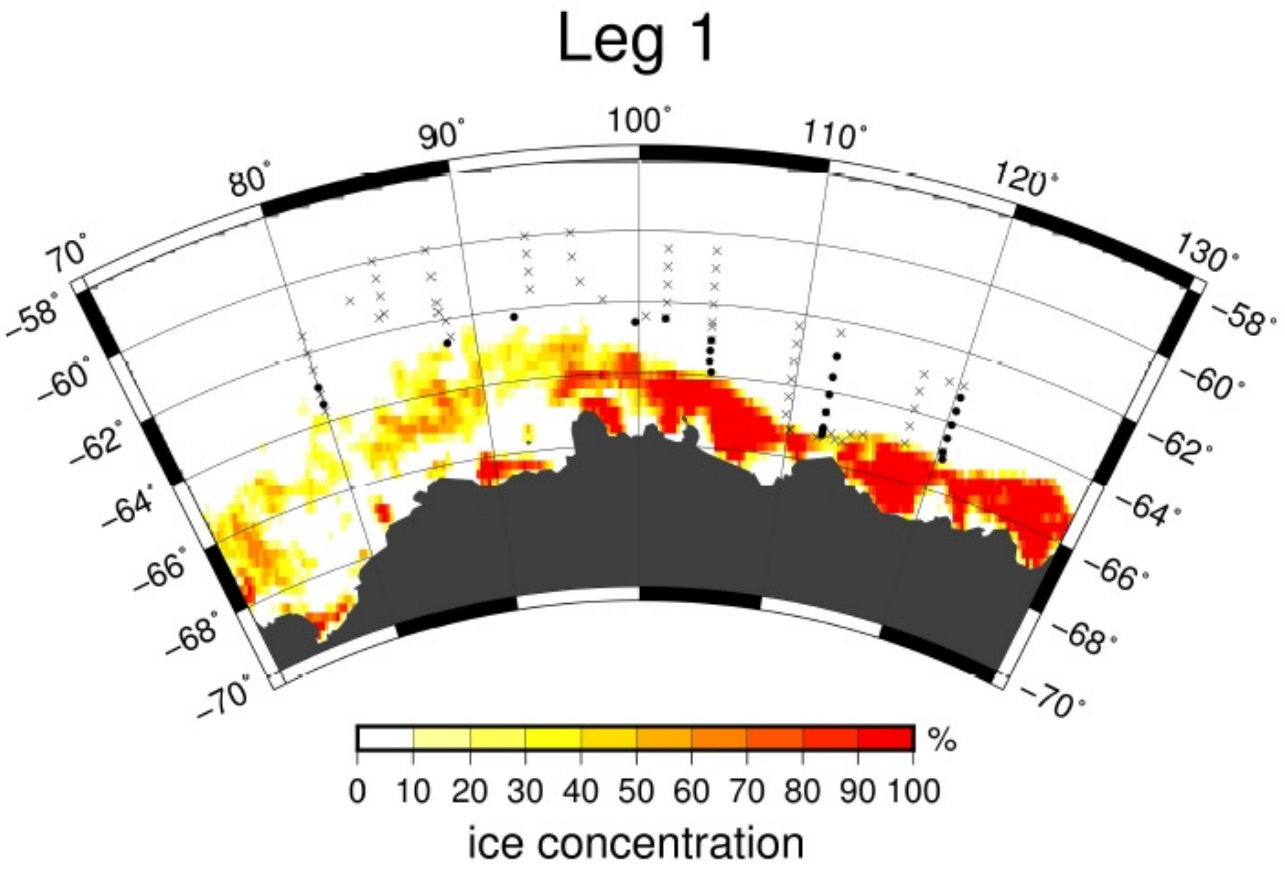

©2019. Japan Geoscience Union. All Right Reserved.

Mooring observation aiming direct current measurement and quantitative evaluation of Meridional Circulation of Southern Ocean

*Kitade Yujiro[1], Kohei Mizobata[1], Kazuho Watanabe[1], Linquiao Chen[3], Gaopin Guo[3], Shigeru Aoki[2], Shyuki Ushio[4], Keishi Shimada[1], Kay I. Ohshima[2]

1. Tokyo University of Marine Science and Technology, 2. Hokkaido University, 3. Shanghi Ocean University, 4. National Institute of Polar Research

The deep Global circulation is a large-scale thermohaline circulation over the Earth and plays an important role in maintaining a stable climate.

In recent years, as rising temperature and freshening of Antarctic bottom water is being observed in various places, in order to quantitatively understand its freshening mechanism and the flow rate and change of Southern Ocean meridional circulation, We are planning to construct a large mooring observation network.

Therefore, as the first attempt, we deployed two moorings (January 2017 - January 2018) by TR/V Umitaka-maru in order to carry out direct current measurement of Meridional circulation. At the time of deployment and recovery of mooring system, we carried out CTD observation up to the sea floor along 110 ˚E line and off Vincennes Bay. At the northern edge of the seasonal sea ice zone, station KMN (60-56 S, 110-07 E, depth of water: 4180 m), we deployed five current meters, one ADP current meter, four MicroCat-CTDs and six RBR soloTs. At KMS (63 - 32 S, 108 - 02 E, depth: 3201 m) in the vicinity of the summer divergence zone, we deployed 10 MicroCats, 3 CTs sensors, 30 soloTs. Because the top buoy of the mooring system at KMN had come up to the sea surface, the two buoys were damaged due to the overhang of the sea ice in winter, but all the sensors were successfully recovered.

Mooring revealed that a flow field suggesting the structure of circulation and periodic fluctuations due to medium-scale eddies and seasonal fluctuations. In this report, we introduce the whole of the observation, the digestive result of the moored observation. The annual averages of current velocitiy [u, v (cm / s)] obtained with 5 current meters are [2.15, -1.26] at 429 db, [1.46, - 0.88] at 859 db, 0.26, -1.26 at 1918 db, [-1.32, -0.78] at 3366 db, and [-1.65, -1.77] at 4080 db. The east-west current structure shows eastward in the upper three layers and westward in the lower two layers, indicating a reasonable zonal current velocity structure. In north - south component, it is slightly larger at the lowest layer, but in other depths it shows southward flow of about 1 cm/s. The 1 cm/s agree well with the current velocity estimated form Sverdrup transport by the wind stress field in this area.

In addition, at around 400 m depth, water masses around 2 degree considered to be the Circumpolar Deep Water were distributed, and it appeared that the temperature rose synchronously with the periodic southward current. We believe that these flow velocity structures and variations are the first approximate features of the circulation of the sea area. In addition, we investigated the fluctuation of Curl of wind stress using WindSat's wind data and found periodic period fluctuations corresponding to some of current fluctuations. In this summary, only the qualitative features which are known from the preliminary report value are described, but at the time of the presentation, other mooring data will be also added and the contents which we entered into more quantitative discussion are introduced.

©2019. Japan Geoscience Union. All Right Reserved.

Keywords: Southern Ocean, Meridional Circulation, mooring observation, wind stress

©2019. Japan Geoscience Union. All Right Reserved.

[J] Poster | M (Multidisciplinary and Interdisciplinary)：M-IS Intersection

Mon. May 27, 2019 3:30 PM - 5:00 PM JST | Mon. May 27, 2019 6:30 AM - 8:00 AM UTC | Poster Hall International Exhibition Hall8, Makuhari Messe_21

[M-IS14] Global climate change driven by the Southern Ocean and the Antarctic Ice Sheet

convener:Osamu Seki(Institute of Low Temperature Science, Hokkaido University), Akira Oka(Atmosphere and Ocean Research Institute, The University of Tokyo), Ryu Uemura(University of the Ryukyus), Ryosuke Makabe(National Institute of Polar Research)

The Southern Ocean and Antarctic ice sheet, which are the giant reservoirs of heat, water, and materials, have a potential to play central roles in long-term global climate change. This system is composed of the following sub-systems; ice shelf which is a place of the interaction of ice sheet and ocean, flowing iceberg, seasonal sea ice zone, Antarctic bottom water which drives the thermohaline circulation, active biological production and Antarctic Circumpolar Current. These sub-systems are interacted with each other and have significant impact on changes in the global environmental system. This session aim to summarize recent observational and simulation studies from various fields relating to the past and present changes in the Antarctic Ice sheet and Southern Ocean, which are essential elements for unraveling the changes in the global climate system. Further, future science plans for understanding of the environmental changes of the Antarctic Cryosphere is also discussed.

[MIS14-P01] Preliminary study on the effect of low-salinity ice melting water on biomass and composition of ice algae

*Keigo Takahashi[1], Ryosuke Makabe[2,3], Shintaro Takao[2,3], Tsuneo Odate[2,3], Masato Moteki[1,2] (1.Tokyo University of Marine Science and Technology, 2.National Institute of Polar Research, 3.The Graduate University for Advanced Studies (SOKENDAI))

[MIS14-P02] Effects of lugol's fixtation on preservation of samples for carbon and nitrogen stable isotope and molecular analyses

*Masayoshi Sano[1], Ryosuke Makabe[1,2], Ayu Yamamoto[3], Norio Kurosawa[4], Masato Moteki[2,3], Tsuneo Odate[1,2] (1.National Institute of Polar Research, 2.The Graduate University for Advanced Studies, 3.Tokyo University of Marine Science and Technology, 4.Soka University)

[MIS14-P03] The application of environmental DNA for the monitoring of Antarctic marine ecosystem

*Aiko Tachibana[1], Ryosuke Makabe[2], Masato Moteki[1] (1.Tokyo University of Marine Science and Technology, 2.National Institute of Polar Research)

[MIS14-P04] Coincidental occurrence process of frazil ice and high biomass off Amery Ice Shelf

*Yoshihiko Machimura[1], Kay I. Ohshima[2], Kazuki Nakata[3], Masato Ito[2], Yasushi Fukamachi[2,4], Ryosuke Makabe[5], Shintaro Takao[5], Sohey Nihashi[6] (1.Graduate School of Environmental Sciences, Hokkaido University, 2.Institute of Low Temperature Science, Hokkaido University, 3.Remote Sensing Technology Center of Japan, 4.Arctic Research Center, Hokkaido University, 5.National Institute of Polar Research, 6.National Institute of Technology, Tomakomai College)

[MIS14-P05] Feeding habit of the Antarctic amphipod *Themisto gaudichaudii* of Vincennes Bay (East Antarctica) during austral summer

*Junji Matsushita[1], Ryosuke Makabe[2], Masato Moteki[1] (1.Tokyo University of Marine Science and Technology, 2.National Institute of Polar Research)

[MIS14-P06] Time-series observation of subsurface chlorophyll *a* maximum in the seasonal ice zone of the Southern Ocean

*Ayuko Kagesawa[1], Masayoshi Sano[2], Shintaro Takao[1,2], Ryosuke Makabe[1,2], Kohei Mizobata[3], Norio Kurosawa[4], Masato Moteki[2,3], tuneo Odate[2] (1.The Graduate University for Advanced Studies, 2.National Institute of Polar Research, 3.Tokyo University of Marine Science and Technology, 4.Soka University)

[MIS14-P07] Seasonality in sulfur isotopic compositions of atmospheric sulfate and its implications for atmospheric sulfur cycles in East Antarctica

*Sakiko Ishino[1], Shohei Hattori[1], Joel Savarino[2], Michel Legrand[2], Susanne Preunkert[2], Bruno Jourdain[2], Francis Albarede[3], Emmanuelle Albalat[3], Naohiro Yoshida[1,4] (1.Department of Chemical Science and Engineering, School of Materials and Chemical Technology, Tokyo Institute of Technology, 2.Institut des Geoscience de l'Environnement, Université Grenoble Alpes/CNRS, 3.Ecole Normale Supérieure (LGL-TPE), 4.Earth-Life Science Institute, Tokyo Institute of Technology)

[MIS14-P08] **Penultimate glacial-interglacial transition viewed from the Dome Fuji ice core, Antarctica**

*Ikumi Oyabu[1,2], Kenji Kawamura[1,3,4], Kyotaro Kitamura[1] (1.National Institute of Polar Research, Research Organization of Information and Systems, 2.Japan Society for the Promotion of Science, 3.SOKENDAI (The Graduate University of Advanced Studies), 4.Japan Agency for Marine Science and Technology (JAMSTEC))

[MIS14-P09] Reconstruction of Antarctic ice sheet dynamics in the Last Interglacial

*Mutsumi Iizuka[1], Osamu Seki[1], Takuya Itaki[2], Tomohisa Irino[1], Minoru Ikehara[4], Saiko Sugisaki[2], Masanobu Yamamoto[1], Keiji Horikawa[5], Yuusuke Suganuma[3] (1.Hokkaido university, 2.Geological Survey of Japan, 3.National Institute of Polar Research , 4.Center for Advanced Marine Core Research, Kochi University, 5.University of Toyama)

[MIS14-P10] Pliocene CO2 concentration estimated from Southern Ocean SST

*Osamu Seki[1], Tomohiro Shimono[2] (1.Institute of Low Temperature Science, Hokkaido University, 2.Guraduate School of Environmental Science)

[MIS14-P11] **Lithogenic fluxes across a transect in the SW Indian Ocean since the last glacial inception**

*Eri Helen Amsler[1], Walter Geibert[2], Gerhard Kuhn[2], Minoru Ikehara[3], Samuel Jaccard[1] (1.Institute of Geological Sciences and Oeschger Centre for Climate Change Research, University of Bern, Switzerland, 2.Alfred-Wegener-Institut Helmholtz-Zentrum für Polar- und Meeresforschung, Bremerhaven, Germany, 3.Center for Advanced Marine Core Research, Kochi University, Kochi, Japan)

[MIS14-P12] Changes in composition of fossil diatoms from Ross Sea under gradual warming climate from MIS M2

*Saki Ishino[1], Itsuki Suto[2], Rob M. McKay[3], Laura De Santis[4], Denise K. Kluhanek[5], Expedition 374 Scientists (1.National Institute of Advanced Industrial Science and Technology, 2.Department of Earth and Planetary Sciences Graduate School of Environmental Studies, Nagoya University, 3.Victoria University, 4.Instituto Nazionale di Oceanografia e di Geofisica Sperimentale, 5.Texas A&M University)

[MIS14-P13] Geological insights into formation of Conrad Rise, Southern Ocean: Preliminary geological results of R/V *Hakuho-maru* KH-19-1 cruise

*Hiroshi Sato[1], Masakazu Fujii[2,3], Hiroki Matsui[4], Minoru Ikehara[4] (1.School of Business Administration, Senshu University, 2.NIPR, 3.SOKENDAI, 4.Center for Advanced Marine Core Research, Kochi University)

[MIS14-P14] Fossil chrysophyte cysts as a new paleoenvironmental proxy

*Yuji Kato[1,2], Itsuki Suto[1] (1.Graduate School of Environmental Studies, Nagoya University, 2.Center for Advanced Marine Core Research, Kochi University (JSPS Research Fellowship for Young Scientists))

[MIS14-P15] Spatiotemporal variability of surface mass balance along the JARE traverse route for 1991−2019

*Shun Tsutaki[1], Hideaki Motoyama[2,3], Ayako Abe-Ouchi[1,4], Shuji Fujita[2,3], Kenji Kawamura[2,3,4] (1.The University of Tokyo, 2.National Institute of Polar Research, 3.The Graduate University for Advanced Studies, 4.Japan Agency for Marine-Earth Science and Technology)

[MIS14-P16] The weathering of granitic rocks in the Sør-Rondane Mountains, East Antarctica

*Tatsuo Kanamaru[1], Yusuke Suganuma[2], hisashi Oiwane[3], Hideki Miura[2], Makoto Miura[4], Jun'ichi Okuno[2], Hideaki Hayakawa[5] (1.Department of Earth and Environmental Sciences, College of Humanities & Sciences, Nihon University, 2.National Institute of Polar Research, 3.Musuhi LLC, 4.Department of Earth and Planetary Sciences, Kanazawa University, 5.Institute for Cosmic Ray Research, University of Tokyo)

[MIS14-P17] Summary of the 2nd Year Activities of the Project on the Interaction of the solid Earth and the
Antarctic Ice Sheet:

*Yoichi Fukuda[1], Jun Nishijima[2], Takahito Kazama[1], Kazuki Nakamura[3], Koichiro Doi[4], Yusuke Suganuma[4], Jun'ichi Okuno[4], Akito Araya[5], Heitaro Kaneda[6], Yuichi Aoyama[4], Hideki Miura[4] (1.Department of Geophysics, Graduate School of Science, Kyoto University, 2.Graduate School of Engineering, Kyushu University, 3.Faculty of Engineering, Nihon University, 4.National Institute of Polar Research, 5.ERI, University of Tokyo, 6.Graduate School of Science, Chiba University)

[MIS14-P18] Late Pleistocene to Holocene sea-level change in East Antarctica revealed by glacial isostatic adjustment modeling

*Takeshige Ishiwa[1], Jun'ichi Okuno[1,2], Yusuke Suganuma[1,2], Hideki Miura[1,2] (1.National Institute of Polar Research, 2.SOKENDAI)

[MIS14-P19] An modeling study of Antarctic ice sheet of the Last Glacial Maximum and the last deglaciation

*Takashi Obase[1], Ayako Abe-Ouchi[1,2], Ralf Greve[3], Fuyuki SAITO[2] (1.Atmosphere and Ocean Research Institute, the University of Tokyo, 2.Japan Agency for Marine-Earth Science and Technology, 3.Institute of Low Temperature Science, Hokkaido University)

[MIS14-P20] Development of a coupled ice-sheet/earth rebound model for Antarctic ice-sheet simulation

*Fuyuki SAITO[1], Ayako Abe-Ouchi[2,1], Jun'ichi Okuno[3], Takashi Obase[2] (1.Japan Agency for Marine-Earth Science and Technology, 2.Atmosphere and Ocean Research Institute, University of Tokyo, 3.National Institute of Polar Research)

[MIS14-P21] Polar amplifications in the past warm periods obtained from MIROC 4m AOGCM

*Taro Higuchi[1], Ayako Abe-Ouchi[1], Wing-Le Chan[1], Sam Sherriff-Tadano[1] (1.Atmospheric and Ocean Research Institute, the University of Tokyo)

[MIS14-P22] Using a coupled AOGCM to study the Antarctic climate of the mid-Pliocene warm period

*Wing-Le Chan[1], Ayako Abe-Ouchi[1,2] (1.Atmosphere and Ocean Research Institute, The University of Tokyo, 2.National Institute of Polar Research)

[MIS14-P23] CMIP5 model analysis of future changes in ocean net primary production by focusing on different response among the individual oceans and models

*Akira Oka[1], Yuki Nakamura[1] (1.Atmosphere and Ocean Research Institute, The University of Tokyo)

[MIS14-P24] Factor analysis of the millennial time-scale climate variability in glacial periods

*Miki Akari[1], Ayako Abe-Ouchi[2], Sam Sherriff-Tadano[2] (1.Department of Earth and Planetary Science, Graduate School of Science, The University of Tokyo, 2.Atmosphere and Ocean Research Institute, the University of Tokyo)

[MIS14-P25] First continuous profiler observation of wintertime Antarctic coastal polynya

*Shigeru Aoki[1], Kazuya Ono[1], Daisuke Hirano[1], Masato Itoh[1], Tomohide Noguchi[2], Satoshi Ozawa[2] (1.Hokkaido University, 2.Marine Works Japan)

[MIS14-P26] Surface topography survey for bared rock and accumulated snow in Antarctica by Unmanned Aero Vehicle

*Yuichi Aoyama[1,2,3], Akihisa Hattori[2,3], Hajime Oishi[3,4], Koichiro Doi[1,2,3], Yoshifumi Nogi[1,2] (1.National Institute of Polar Research, 2.SOKENDAI, 3.The 59th Japanese Antarctic Research Expedition, 4.NEC Networks & System Integration Corporation)

[MIS14-P27] The analysis of long-term Mooring observation records in the northernmost area of seasonal sea ice zone in the Southern Ocean

*Kazuho Watanabe[1], Kohei Mizobata[1], Yujiro Kitade[1] (1.Tokyo University of Marine Science and Technology)

[MIS14-P28] Preliminary observation report on chlorofluorocarbons (CFCs) and sulfur hexafluoride (SF_6) off the Cape Darnley in the summer of 2019

*Yoshihiko Ohashi[1], Michiyo Yamamoto-Kawai[1], Kenichi Sasaki[2], Sayaka Kumakawa[1], Naoyuki Tamura[1], Kay I. Ohshima[3] (1.Tokyo University of Marine Science and Technology, 2.Japan Agency for Marine-Earth Science and Technology, 3.Institute of Low Temperature Science, Hokkaido University)

[MIS14-P29] Mechanism of sea-ice production variation in Amundsen Sea Polynya

*Sohey Nihashi[1], Kouta Mine[1], Kazuki Nakata[2] (1.National Institute of Technology, Tomakomai College, 2.RESTEC)

[MIS14-P30] Estimation of thin ice thickness and discrimination of ice type from AMSR2 passive microwave data

*Kazuki Nakata[1], Tamaru Naoya[1], Sohey Nihashi[2], Kay I. Ohshima[3] (1.Remote Sensing Technology Center of Japan, 2.National Institute of Technology, Tomakomai College, 3.Institute of Low Temperature Science, Hokkaido University)

Preliminary study on the effect of low-salinity ice melting water on biomass and composition of ice algae

*Keigo Takahashi[1], Ryosuke Makabe[2,3], Shintaro Takao[2,3], Tsuneo Odate[2,3], Masato Moteki[1,2]

1. Tokyo University of Marine Science and Technology, 2. National Institute of Polar Research, 3. The Graduate University for Advanced Studies (SOKENDAI)

Upon sea ice melting ice algae are subject to low salinity water, sometimes nearly freshwater, while sea ice produces a brine (high salinity). Certain taxa of ice algae, primarily diatom, increase in cell number after released in water column (seeding). Since lower salinity water deteriorates photosynthetic efficiency of ice algae, such a variability of salinity is likely to influence seeding of ice algae during melting season. However, it is not clear how biomass, abundance, composition and mortality of ice-algal community changes under different salinity conditions. To further understand the mechanism for seeding of ice algae, we conducted a shipboard experiment in the Indian Sector of the Southern Ocean during austral summer.

We collected pack ice and surface seawater in the ice edge (65º17.9’ S, 109º40.9’ E) on January 16th, 2019 during the 22nd Antarctic voyage by the training vessel *Umitaka-maru*. Sea ice was melted with different volume of filtered seawater (moderate salinity: 10.0 kg ice+90 L filtered sea water, FSW, low salinity: 8.6 kg ice+10 L FSW) to simulate different final salinity (moderate: 30.05, low: 18.00). We incubated the algal communities in seawater and two types of sea-ice melting water (moderate and low salinity conditions) under a natural light condition for 24 hours, with temperature maintained by a circulating surface seawater. Before and after the incubation, we obtained chlorophyll *a* concentration (bulk and size-fraction), Lugol-fixed samples for microscopic analysis and cell viability (live or dead).

After 24 hours, <10 μm size class of ice-algal communities in both moderate and low salinity conditions showed a significant difference in the ratio of chlorophyll *a* concentration (chl *a* fin. /chl *a* ini.) relative to the bulk and >10 μm size class (Tukey-Kramer test, Fig.). The ratio of chl *a* (mean±SD, *n*=3) in this size class was highest (moderate: 2.1±0.1, low: 1.8±0.2) among the samples. This suggests that algal community of <10 μm have an ability to acclimate to low salinity water. This study discussed the changes in species composition and abundance of the algal communities as well.

Keywords: The Southern Ocean, Ice algae, Sea ice

©2019. Japan Geoscience Union. All Right Reserved.

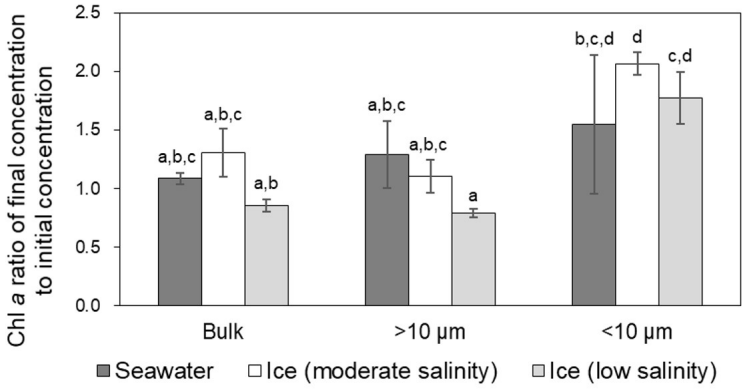

Fig. The final chlorophyll *a* concentration of bulk and size-fractionated samples relative to the initial concentration of seawater and two types of ice (moderate and low salinity). The same letters indicate no significant difference at the p=0.05 level (Tukey-Kramer test).

©2019. Japan Geoscience Union. All Right Reserved.

Effects of lugol’s fixtation on preservation of samples for carbon and nitrogen stable isotope and molecular analyses

*Masayoshi Sano[1], Ryosuke Makabe[1,2], Ayu Yamamoto[3], Norio Kurosawa[4], Masato Moteki[2,3], Tsuneo Odate[1,2]

1. National Institute of Polar Research, 2. The Graduate University for Advanced Studies, 3. Tokyo University of Marine Science and Technology, 4. Soka University

Recently, carbon and nitrogen stable isotope analysis and molecular analysis are commonly used as powerful tools in marine ecological studies including sediment trap experiments. In the southern ocean ecosystem studies, moored sediment trap samples are important to obtain information all-year around including winter season when we cannot observe directly by research vessels. Usually, collecting cups of sediment traps were filled with formalin for preventing degradation of samples during deployment periods, but formalin fixtation is not suitable for those analyses because of crosslinking and fragmantation of DNA and alteration of carbon stable isotope. On the other hand, lugol’s iodine solution is commonly used as fixatives of microzooplankton and phytoplankton samples, but its usefulness as a long term preservative of samples for stable isotope analysis and molecular analysis is still not examined. In this study, we compared carbon and nitrogen stable isotope ratios of zooplankton samples fixed by lugol’s iodine solution and other methods over 6 months and extract DNA from lugol fixed samples after 16 months preservation for examining the usefulness of lugol’s iodine solution. Samples were collected by ORI net during a cruise of training vessel *Umitaka-maru* in 2017. Collected samples were fixed by 5%, 10% lugol’s iodine seawater solution or 5% buffered formalin seawater or frozen at -80˚C on board. Samples were sorted after 1 week, 1 month, 3 months and 6 months preservation and used for stable isotope analysis. DNA was extracted from samples after 16 months preservation and amplified by PCR. In most cases, carbon stable isotope ratios were significantly different between formalin fixed samples and other samples after 1 week preservation. Nitrogen stable isotope ratios were also significantly different between formalin fixed samples and other samples after 1 month preservation. There are no significant differences in carbon and nitrogen stable isotope ratios between samples fixed by 10% lugol solution and frozen samples in all the periods. Amplification of DNA extracted from lugol fixed samples was detected by a gel electrophoresis. Thus, lugol’s fixtation is considered to be suitable for long term preservation of samples for both stable isotope analysis and molecular analysis.

Keywords: Zooplankton, Sediment trap, Stable isotope ratio, DNA, Fixation method

©2019. Japan Geoscience Union. All Right Reserved.

The application of environmental DNA for the monitoring of Antarctic marine ecosystem

*Aiko Tachibana[1], Ryosuke Makabe[2], Masato Moteki[1]

1. Tokyo University of Marine Science and Technology, 2. National Institute of Polar Research

A monitoring of biological community structure and diversity is essential to understand the global climate impact on the Antarctic marine ecosystem. Traditional biomonitoring methods typically rely on sampling methods, combined with morphology-based identification, which is time-consuming and requires sophisticated expertise. To elucidate the full impact of rapidly shifting climate on the Antarctic ecosystem, efficient and effective tools are required to understand spatial and temporal variations in biological communities. Environmental DNA (eDNA) –genomic material extracted from cells and tissue shed by organisms into environmental samples, such as soil, sediments and water –is a possible tool for rapid assessing marine biodiversity and community composition. We conducted an eDNA observation in January 2019 along the 110˚E transect off Wilkes Land, East Antarctica, by the training vessel *Umitaka-maru*, Tokyo University of Marine Science and Technology. In total, 189 samples were collected from surface to deep layers covering various water mass which was located from 40˚S to 65˚S along the 110˚E transect. We will generate DNA-based biodiversity data from these samples to produce the first comprehensive analysis of metazoan genetic diversity in the Southern Ocean. The eDNA observation and preliminary experiments are outlined here, and a future plan of analyses are discussed.

Keywords: Environmental DNA, Southern Ocean, biodiversity

©2019. Japan Geoscience Union. All Right Reserved.

Coincidental occurrence process of frazil ice and high biomass off Amery Ice Shelf

*Yoshihiko Machimura[1], Kay I. Ohshima[2], Kazuki Nakata[3], Masato Ito[2], Yasushi Fukamachi[2,4], Ryosuke Makabe[5], Shintaro Takao[5], Sohey Nihashi[6]

1. Graduate School of Environmental Sciences, Hokkaido University, 2. Institute of Low Temperature Science, Hokkaido University, 3. Remote Sensing Technology Center of Japan, 4. Arctic Research Center, Hokkaido University, 5. National Institute of Polar Research, 6. National Institute of Technology, Tomakomai College

Antarctic coastal regions are the most productive regions in the Southern Ocean and could dramatically influence global carbon cycle and ecosystems. During the austral spring, large phytoplankton blooms develop in polynyas with peak productivity occurring from December to January. According to the chlorophyll estimation from satellite, net primary production (NPP) in the Antarctic coastal polynyas rapidly declines from February to March (Arrigo et al., 2015).
Recent studies have found the regions with high biomass in Antarctic coastal regions during February-March (Lieser et al., 2015; DeJong et al., 2018). This high biomass is collaterally observed with frazil ice. Chlorophyll estimation algorithms using Moderate Resolution Imaging Spectroradiometer (MODIS) data mask pixels with high sea ice coverage to prevent the contamination by excess reflection of visible light. Therefore, the regions with high biomass collaterally observed with frazil ice have not been counted in NPP estimation in Antarctic coastal regions. These high biomass regions potentially have a large impact for global carbon cycle as the CO_2 sink. However, incidence processes and causes of frazil ice with high biomass have not been investigated in details. In this study, we focus on the regions of the Cape Darnley polynya and offshore of the Amery Ice Shelf in February and March during 2003-2011 to understand the processes and causes of high biomass collaterally observed with frazil ice.
First, we calculated Green Index from MODIS surface reflectance data obtained from the study area to identify green colored regions implicate high biomass. Second, we identified the region of frazil ice, using the algorithm that discriminates ice type between frazil ice and thin solid ice from AMSR-E passive microwave data (Nakata et al., 2019). These two analyses clearly show that the high biomass and frazil ice coincidentally occur both temporally and spatially in late summer. In particular, both of high biomass and frazil ice have a peak in their distributions at the same location about 50 km offshore of the Amery Ice Shelf in March. This is also suggesting an unknown frazil ice formation process distinctly different from a coastal polynya process.
We consider Ice Shelf Water (ISW) as a trigger of coincidental occurrence of frazil ice and high biomass. According to the CTD-tag data obtained from seals in the region off Amery Ice Shelf in late summer, ISW that is partly supercooled exists at depths of 250-400 m and the surface water is heated by solar radiation in the region from the ice shelf front to 68.3 deg. S. While in the region north of 68.2 deg. S, the surface water has reached the freezing point. Previous studies reported that ISW flows out to 50-100 km offshore from the ice shelf front and generates frazil ice at depths of 250-300 m (Dieckmann et al., 1986; Hughes et al., 2013).
To summarize the above analyses, coincidental occurence of frazil ice and high biomass is assumed to be caused by the following processes.
1. ISW is formed and flows out to the outside of Amery Ice Shelf cold cavity.
2. ISW becomes supercooled during the outflow, and frazil ice is generated.
3. Generated frazil ice gradually rises toward the surface. In the region south of 68.3deg. S, frazil ice is melted because of heated surface water. Frazil ice can appear at the surface in the region north of 68.2 deg. S, where the surface water reaches the freezing point.

©2019. Japan Geoscience Union. All Right Reserved.

4. Frazil ice scavenges phytoplankton existing in water column and carries it to the surface. Simultaneously, iron contained in ISW enhances the biological production and increases biomass. The process proposed in this study may also occur in regions just off other ice shelves. In the future, we should clarify the details of the process off Amery Ice Shelf with in-situ observation and explore the possibility of occurrence in regions off the other ice shelves.

Keywords: sea ice, polynya, ice shelf water, remote sensing, biological production

©2019. Japan Geoscience Union. All Right Reserved.

Feeding habit of the Antarctic amphipod *Themisto gaudichaudii*of Vincennes Bay (East Antarctica) during austral summer

*Junji Matsushita[1], Ryosuke Makabe[2], Masato Moteki[1]

1. Tokyo University of Marine Science and Technology, 2. National Institute of Polar Research

Amphipods are key components of macrozooplankton to link lower trophic levels to higher predators in the krill-independent food web in the Southern Ocean (SO). The carnivorous amphipod *Themisto gaudichaudii*, widely distributed in SO, is an opportunistic predator. They are known to feed on copepods, euphausiids, salps and various zooplankton in the Atlantic Ocean sector, while their food habits are poorly known in the Indian Ocean sector. This study analyzed gut contents of *T. gaudichaudii* collected along the 110˚E transect in SO in January 2019 to clarify food habit of *T. gaudichaudii*. Fecal pellet obtained from onboard experiment were supplementary used to verify the estimated food habit. We’ll preliminary demonstrate here the food web related to *T. gaudichaudii* in the Indian Ocean sector during austral summer.

Keywords: The Southern Ocean, Macrozooplankton, Amphipod

©2019. Japan Geoscience Union. All Right Reserved.

Time-series observation of subsurface chlorophyll *a* maximum in the seasonal ice zone of the Southern Ocean

*Ayuko Kagesawa[1], Masayoshi Sano[2], Shintaro Takao[1,2], Ryosuke Makabe[1,2], Kohei Mizobata[3], Norio Kurosawa[4], Masato Moteki[2,3], tuneo Odate[2]

1. The Graduate University for Advanced Studies, 2. National Institute of Polar Research, 3. Tokyo University of Marine Science and Technology, 4. Soka University

A persistent subsurface chlorophyll *a* maximum (SCM) is often found during the summer-fall season after the ice-edge bloom in the seasonal ice zone of the Southern Ocean, so that SCM would be considered important for biogeochemical cycling through the lower trophic levels. The relevant studies, however, have been qualitative in nature. This study aimed to reveal the dynamics and ecological role of the SCM in the seasonal ice zone.
We carried out Lagrangian observations using a drifter with two time-series sediment traps, an Acoustic Doppler Current Profiler (ADCP) and four sensor flames (Fig. 1). The drifter was deployed at 63.5˚S, 110.0˚E in January 14th 2019, and 5-day continuous observation was performed. In the vicinity of the drifter, 4 ship-based observations including net sampling and CTD casts were made until the drifter was recovered. Physical environments were measured by CTD, and sea water samples were collected for measurements of chlorophyll *a* (chl. *a*) concentration, nutrients, particle organic carbon, dissolved organic carbon, abundance of phytoplankton, micro-zooplankton, bacteria and nano-/pico-phytoplankton. We also conducted an incubation experiment for determining net primary production.
The temperature minimum layer, found between 37 and 52 m depth, decreased from -0.82 ºC to -1.28 ºC during the study period. The maximum chl. *a* concentration (1.0-2.0 μg/l), comparable to that in typical ice edge blooms, was observed at 40 m depth (Fig. 2). Such a high chl. *a* concentration might have important roles for food web and for material cycling. We will discuss especially on phytoplankton dynamics showing results of microscopic and chemical analyses.

Keywords: subsurface chlorophyll a maximum , the Southern Ocean

©2019. Japan Geoscience Union. All Right Reserved.

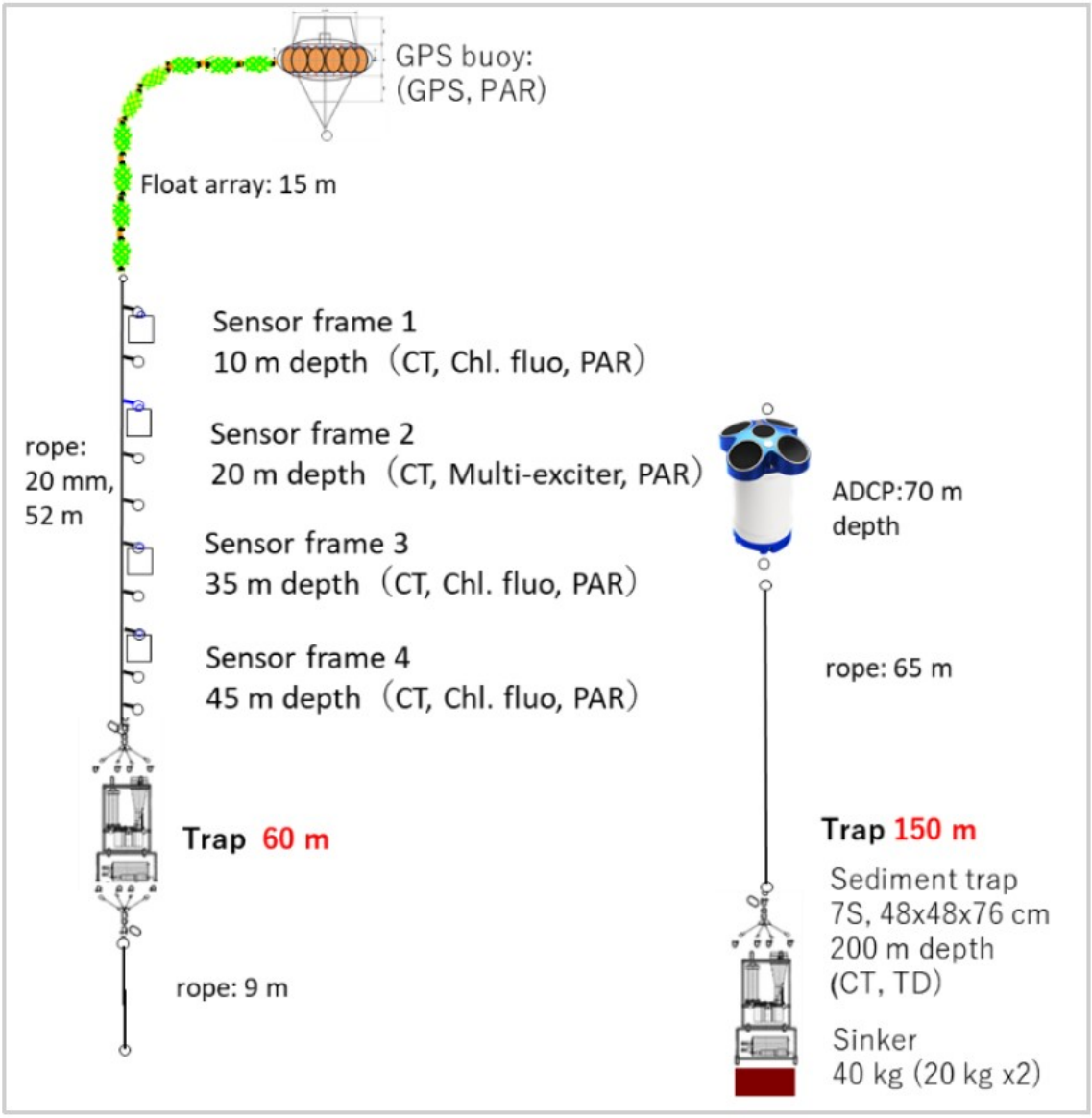

Fig. 1 A schematic image of the drifter

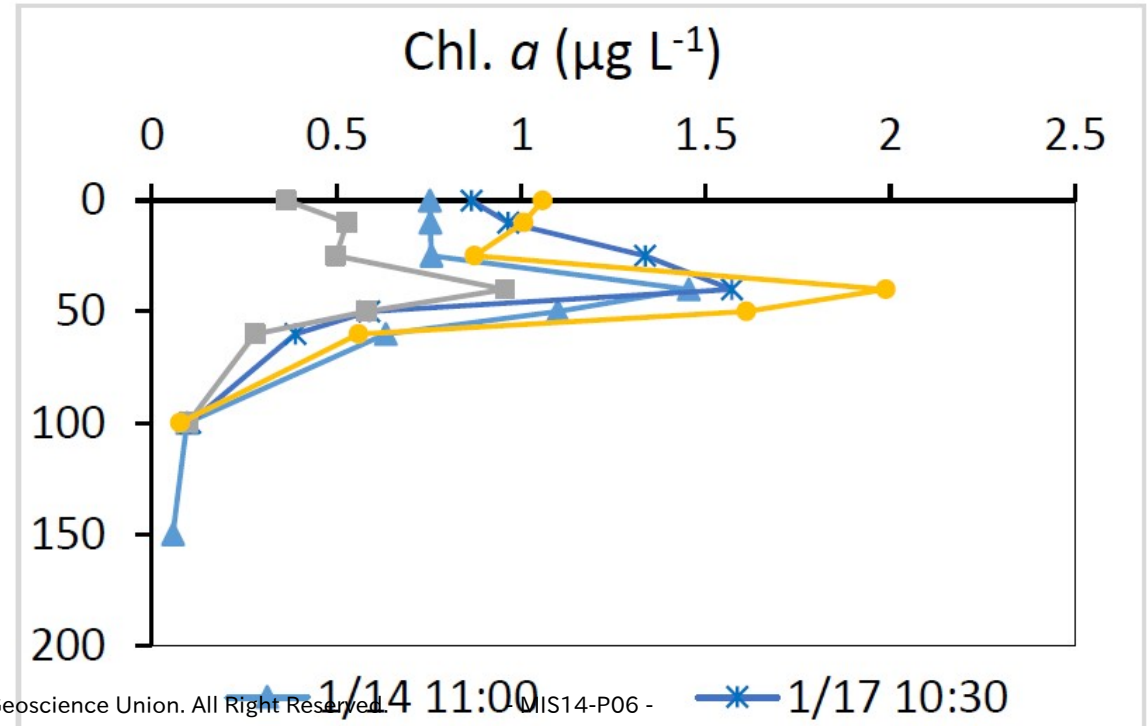

©2019. Japan Geoscience Union. All Right Reserved.

©2019. Japan Geoscience Union. All Right Reserved.

Seasonality in sulfur isotopic compositions of atmospheric sulfate and its implications for atmospheric sulfur cycles in East Antarctica

*Sakiko Ishino[1], Shohei Hattori[1], Joel Savarino[2], Michel Legrand[2], Susanne Preunkert[2], Bruno Jourdain[2], Francis Albarede[3], Emmanuelle Albalat[3], Naohiro Yoshida[1,4]

1. Department of Chemical Science and Engineering, School of Materials and Chemical Technology, Tokyo Institute of Technology, 2. Institut des Geoscience de l' Environnement, Université Grenoble Alpes/CNRS, 3. Ecole Normale Supérieure (LGL-TPE), 4. Earth-Life Science Institute, Tokyo Institute of Technology

Atmospheric sulfate in Antarctica is produced mainly from a marine biogenic sulfur compound, dimethyl sulfide. They are therefore a subject of study related to the linkage between marine biogenic activity and climate. We investigate year-round observations of sulfur isotopic compositions of atmospheric sulfate (SO_4^{2-}) at inland (Dome C) and coastal (Dumont d' Urville) sites in East Antarctica to quantify the relative importance of marine biogenic (mb) and non-marine biogenic (nmb) SO_4^{2-} for the Antarctic atmospheric sulfur cycle. The $\delta^{34}S$ values of non-sea salt sulfate showed clear seasonal variations with summer maxima and winter minima, and showed homogeneity between inland and coastal sites throughout the year. This result suggests that the isotopic fractionation through chemical reactions during transportation from coastal to inland areas insignificantly affects the observed $\delta^{34}S_{nss}$ values. The observed $\delta^{34}S_{nss}$ values are controlled mainly by the relative importance of mb-SO_4^{2-} and nmb-SO_4^{2-}. This finding, in conjunction with the SO_4^{2-} records in Antarctic ice cores, will open a perspective implying the increased relative importance of nmb-SO_4^{2-} during glacial periods. We also found a significant increase in nmb-SO_4^{2-} concentrations in November, especially for the inland site. This nmb-SO_4^{2-} increase is correlated with the ^{210}Pb concentration, suggesting the existence of long-range transport of continental nmb-SO_4^{2-} from lower latitudes to the Antarctic inland. Identification of the sources of those nmb-SO_4^{2-} will be a key step for elucidation of the linkage between Antarctic atmosphere/climate and environmental changes at lower latitudes from the past through the future.

Keywords: Sulfur isotope analysis, Sulfate aerosols, Antarctica

©2019. Japan Geoscience Union. All Right Reserved.

Penultimate glacial-interglacial transition viewed from the Dome Fuji ice core, Antarctica

*Ikumi Oyabu[1,2], Kenji Kawamura[1,3,4], Kyotaro Kitamura[1]

1. National Institute of Polar Research, Research Organization of Information and Systems, 2. Japan Society for the Promotion of Science, 3. SOKENDAI (The Graduate University of Advanced Studies), 4. Japan Agency for Marine Science and Technology (JAMSTEC)

Paleoclimatic proxies provide information about the variations of climate forcings and responses, such as atmospheric CO_2concentration, temperature and sea level, as well as their magnitudes and phase relationships. Accurate chronological constraints are particularly important for numerical simulations, both for their input and validation data, to better understand the transient behaviors of climate and ice sheets. During the last interglacial period (~130 to ~120 thousand years before present (kyr BP)), the peak global mean surface temperature was ~1 degree higher than the preindustrial period, and the global sea level was ~6 –9 m higher than today with significant contribution from the Antarctic ice sheet, whereas atmospheric CO_2levels were similar to those in the preindustrial period (Dutton et al., 2015). The last interglacial period and the preceding transition from the penultimate glacial period are important targets for the paleoclimatic research to investigate the mechanisms for warming and ice-sheet reductions. However, responses (sequences, timing or magnitude) of ice sheets, temperature or ocean circulations to climate forcing during this period are much less well understood, partly because the number of proxies and time resolution are limited, and the chronological uncertainties are relatively large. A chronology of the Dome Fuji (DF) ice core was constructed by synchronizing variations in O_2/N_2ratio of occluded air with local summer insolation (Kawamura et al., 2007), but relatively large errors were later reported around the last interglacial (Fujita et al., 2015). Here, we reanalyzed the O_2/N_2ratio of the DF core by improving the methods for sample treatment, air extraction and mass spectrometry between 57 and 165 kyr BP to revise the DF chronology. The new chronology agrees within 1.2 kyr with a radiometric (U-Th) chronology of Chinese speleothems, the whose stated error is less than 1 kyr (Cheng et al., 2009), suggesting successful improvement of our ice-core chronology. Using $\delta^{18}O$ of atmospheric O_2($\delta^{18}O_{atm}$) and CH_4records measured on the same ice samples as used for the O_2/N_2measurements, we investigate climatic variations during the penultimate glacial period and deglaciation. We found that $\delta^{18}O_{atm}$ becomes heavier while CH_4concentration increased at 138.4 kyr BP during the penultimate glacial maximum; this characteristic relationship was observed at Heinrich Event 2 (at ~24 kyr BP) during the last glacial maximum (Severinghaus et al., 2009; Rhodes et al., 2015). Other well-dated paleoclimatic records show major climatic changes around 138 kyr BP; an abrupt weakening of the Asian monsoon occurred at 138 kyr BP (Wang et al., 2008), and the onset of relative sea level rise was suggested at 139±1 kyr BP from seawater $\delta^{18}O$ of Red Sea (Grant et al., 2012) and at 137 kyr BP from U-Th dating of Tahiti fossil corals (Thomas et al., 2009). The similarity of these ages suggests that a massive iceberg discharge event occurred at ~138 kyr BP, and it marked the onset of penultimate deglaciation. Our new data may provide better chronological constraints on the climatic forcings and responses around the penultimate deglaciation and last interglacial period.

References

Dutton et al. (2015), *Science,* **349**., Kawamura, K., et al. (2007), *Nature*, **448**, 912-916., Fujita, S. et al. (2015), *Clim. Past.*,**11**, 1395-1416 ., Cheng, H. et al. (2009), *Science*, **326**, 248-252., Rhodes, R. H.et all. (2015), *Science*, **348**, 1016-1019., Severinghaus, J. P. et al., (2009), *Science*,**324**, 1431-1434., Thomas, A. L.et al. (2009), *Science*, **324**, 1186-1189., Wang, Y. et al. (2008), *Nature*, **451**, 1090-1093., Grant, K.

©2019. Japan Geoscience Union. All Right Reserved.

M., et al. (2012), *Nature*, **491**, 744-747.

Keywords: Antarctica, Ice core, Dome Fuji, deglaciation, The last interglacial

©2019. Japan Geoscience Union. All Right Reserved.

Reconstruction of Antarctic ice sheet dynamics in the Last Interglacial

*Mutsumi Iizuka[1], Osamu Seki[1], Takuya Itaki[2], Tomohisa Irino[1], Minoru Ikehara[4], Saiko Sugisaki[2], Masanobu Yamamoto[1], Keiji Horikawa[5], Yuusuke Suganuma[3]

1. Hokkaido university, 2. Geological Survey of Japan, 3. National Institute of Polar Research , 4. Center for Advanced Marine Core Research, Kochi University, 5. University of Toyama

Ongoing global warming could cause various problems in the future. One of the serious concerns is a sea level rise due to the melting of the ice sheet. Antarctic ice sheet, which hold a massive amount of fresh water was considered to be stable even if global warming progresses in the future. However, recent studies have shown that Antarctic ice sheet is more sensitive to global warming than previously thought. Therefore, it is an important to better understand extent to which Antarctic ice sheet is sensitive to global warming.

Study of past warm period proves an useful insight into the prediction of sea level rise in a future. Especially, Sea level in the last interglacial (MIS 5e), which was ~1˚C warmer than the preindustrial was estimated to be several meters higher than that of the present with the sudden and abrupt rises in sea level. This suggests significant loss of Antarctic ice sheet during MIS 5e. However, Antarctic ice sheet variability during the MIS 5e has been poorly understood. In this study, we reconstruct dynamics of Antarctic ice sheet during MIS 5e from the marine sediment core GC1407 collected from Dumont d'Urville Sea, East Antarctica (130.518˚E, 63.74˚S).

Interval of MIS 5e has been determined based on abundance of radiolaria in GC1407. Variability of iceberg discharge is reconstructed by measurement of iceberg rafted debris (IBRD) in sediments. IBRDs are found to be recognized only during MIS 5e. This suggests that the significant discharge of large icebergs possibly from Wilkes Land basin, East Antarctica happened only during warmer than present climate condition.

Keywords: Southern Ocean, Last interglacial, Antarctic icesheet

©2019. Japan Geoscience Union. All Right Reserved.

Pliocene CO2 concentration estimated from Southern Ocean SST

*Osamu Seki[1], Tomohiro Shimono[2]

1. Institute of Low Temperature Science, Hokkaido University, 2. Guraduate School of Environmental Science

Prediction of temperature change by the climate model depends on climate sensitivity, which is the temperature change associated with doubling of CO_2 concentration. The constraint on climate sensitivity is the key part in the IPCC and thus is critical for the future climate prediction. However, despite considerable efforts for constraint on climate sensitivity, the climate sensitivity still remains uncertainty. Furthermore, recent paleoclimate studies revealed that climate sensitivity depends on climate state. This highlights the necessity to know the climate sensitivity in the warmer than the present climate for the future prediction. The Pliocene Warm Period (3-4.5 million years ago) is often regarded as the best analogue of climate in the near future and thus is ideal to investigate climate sensitivity in the warm climate state. In this study, we reconstruct CO_2 concentration based on the new empirical approach (average SST in mid latitude of Southern Ocean) to estimate climate sensitivity in the Pliocene Warm Period.

Keywords: Climate sensitivity, Pliocene, carbon dioxide concentration

©2019. Japan Geoscience Union. All Right Reserved.

Lithogenic fluxes across a transect in the SW Indian Ocean since the last glacial inception

*Eri Helen Amsler[1], Walter Geibert[2], Gerhard Kuhn[2], Minoru Ikehara[3], Samuel Jaccard[1]

1. Institute of Geological Sciences and Oeschger Centre for Climate Change Research, University of Bern, Switzerland, 2. Alfred-Wegener-Institut Helmholtz-Zentrum für Polar- und Meeresforschung, Bremerhaven, Germany, 3. Center for Advanced Marine Core Research, Kochi University, Kochi, Japan

On glacial-interglacial time scale the Southern Ocean plays a prominent role in modulating climate by storing and redistributing heat, fresh water, carbon and nutrients globally. Atmospheric CO_2 is taken up by algae and sequestered in the deep ocean through the biological carbon pump. On the other hand, CO_2 is released back to the atmosphere through upwelling and vertical mixing [1]. The relative contribution of these two mechanisms controls the efficiency through which carbon can be sequestered in the ocean interior.

The effect of iron fertilization on biological productivity has previously been documented in the Atlantic and Pacific sectors of the Southern Ocean [2, 3]. During glacial periods higher input of Fe-bearing dust increased phytoplankton growth and carbon sequestration, thus leading to the drawdown of atmospheric CO_2, accounting for about half of the glacial-interglacial CO_2 amplitude [4].

Here we present ^{230}Th-normalized lithogenic fluxes in a set of marine sediment cores spanning a meridional transect in the Indian sector of the Southern Ocean further away from the Patagonian dust plume and show that increased Fe flux impacted export production patterns, contributing to the sequestration of carbon away from the atmosphere.

[1] Sigman, D. M., Boyle, E. A. (2000) Nature 407, 859-869.

[2] Martínez-Garcia, A., Sigman, D. M., Haojia, R., Anderson, R. F., Straub, M., Hodell, D. A., Jaccard, S. L., Eglinton, T. I., Haug, G. H. (2014) Science 343, 1347-1350.

[3] Lamy F., Gersonde, R., Winckler, G., Esper, O., Jaeschke, A., Kuhn, G., Ullermann, J., Martínez-Garcia, A., Lambert, F., Kilian, R. (2014) Science 343 (6169), 403-407.

[4] Hain, M. P., D. M. Sigman, and G. H. Haug (2010) Global Biogeochem. Cycles, 24, GB4023.
Please fill in your abstract text.

Keywords: Southern Ocean, Biological Pump

©2019. Japan Geoscience Union. All Right Reserved.

Changes in composition of fossil diatoms from Ross Sea under gradual warming climate from MIS M2

*Saki Ishino[1], Itsuki Suto[2], Rob M. McKay[3], Laura De Santis[4], Denise K. Kluhanek[5], Expedition 374 Scientists

1. National Institute of Advanced Industrial Science and Technology, 2. Department of Earth and Planetary Sciences Graduate School of Environmental Studies, Nagoya University, 3. Victoria University, 4. Instituto Nazionale di Oceanografia e di Geofisica Sperimentale, 5. Texas A&M University

Understanding past polar environmental changes under warming climate process will help predicting future global warming. The paleoceanographic record near Antarctic ice-proximal area provides important insight into West Antarctica Ice Sheet (WAIS) vulnerability. Antarctic sediments contain numerous fossil diatoms, which are helpful to clarify past oceanographic conditions.

International Ocean Discovery Program (IODP) Expedition 374 drilled five sites from Ross Sea continental shelf and rise to investigate WAIS evolution under warm climates. Site U1524A (74° 13.05’ S and 173° 37.98’ W, 2394 m water depth) drilled from continental rise, which lies beneath cascading Antarctic Bottom Water current, preserves high resolution Pliocene sediments. We present preliminary results of composition changes of diatom assemblages focusing on the ages from MIS M2 to warmer climate around the interval between 3.3 and 3.0 Ma. Diatom records including abundance changes in sea-ice indicator species and *Chaetoceros*resting spores contribute to evaluate the past sea-ice coverage, primary productivity, and vertical mixing in Pliocene warm condition.

Keywords: Diatom, The Southern Ocean, Paleoenvironment

©2019. Japan Geoscience Union. All Right Reserved.

Geological insights into formation of Conrad Rise, Southern Ocean: Preliminary geological results of R/V *Hakuho-maru* KH-19-1 cruise

*Hiroshi Sato[1], Masakazu Fujii[2,3], Hiroki Matsui[4], Minoru Ikehara[4]

1. School of Business Administration, Senshu University, 2. NIPR, 3. SOKENDAI, 4. Center for Advanced Marine Core Research, Kochi University

Conrad Rise is one of plateaus situated at the Indian-sector of the Southern Ocean. Origin of the rise are considered to be a sort of the Large Igneous Provinces or hotspot. Previously Borisova et al. (1996) reported alkaline igneous rocks which have similar geochemical signature to the Kelgueren Plateau. However, detailed investigations have not been performed until our recent study. We performed geological and geophysical investigations during three R/V *Hakuho-maru* cruises, KH-10-7, KH-16-1, and KH-19-1. Particularly, we had five dredge operations during KH-10-7 and KH-19-1 cruises and obtained geological (and biological) materials that have important keys to understanding the origin and development of Conrad Rise. Geological materials collected during KH-10-7 cruise had already reported by Ishizuka et al. (2011), Sato et al. (2012), and Kobayashi et al. (2013). In this presentation, we report preliminary results of recovered geological and biological materials during KH-19-1 cruise.

Two dredge operations were performed during KH-19-1 Leg 2 (16 Jan to 12 Feb 2019). Dredge site KH-19-1D4 is situated at one of peaks of unnamed small knoll that is located north of Ob seamount. Approximately 50 kg of geological and biological materials including igneous rocks, metamorphic rocks, and deep-sea coral were recovered. Dredge site KH-19-1D5 is situated at north-south trending spur on the northern slope of Ob seamount. Approximately 50 kg of materials including igneous rocks, sedimentary rocks, metamorphic rocks, deep-sea coral, and living shell were recovered.

References

Borisova et al. (1996) *Geochemistry International* **34**(6) 503-517
Sato et al. (2012) JpGU meeting 2012, SCG66-09
Ishizuka et al. (2011) 2nd Symposium on Polar Science.
Kobayashi et al. (2013) 4th Symposium on Polar Science.

Keywords: Conrad Rise, Southern Ocean, KH-19-1 cruise

©2019. Japan Geoscience Union. All Right Reserved.

Fossil chrysophyte cysts as a new paleoenvironmental proxy

*Yuji Kato[1,2], Itsuki Suto[1]

1. Graduate School of Environmental Studies, Nagoya University, 2. Center for Advanced Marine Core Research, Kochi University (JSPS Research Fellowship for Young Scientists)

Most Neogene–Quaternary sediments in the Southern Ocean have high biogenic silica contents with large amounts of siliceous microfossils including chrysophyte cysts as well as diatoms. Fossil chrysophyte cysts are considered to be potentially useful paleoenvironmental indicators, however no general consensus exists about their paleoenvironmental significance. In this study, data on fossil chrysophyte cyst abundances of late Miocene to Pliocene (ca. 9–3 Ma) age are presented from two marine sediment cores, Ocean Drilling Program Site 689 and Deep Sea Drilling Project Site 513, both located in the Atlantic sector of the Southern Ocean. Changes in the chrysophyte cyst abundances are compared to those in the diatom abundances, and the potential of fossil chrysophyte cysts as paleoceanographic indicators around the Antarctica is discussed.
As a result, similarity in the fluctuation of freshwater diatom and chrysophyte cyst abundances were observed in both sites. In addition, occurrences of chrysophyte cysts similar to previously reported ones from freshwater habitats were recognized. These results suggest that the fossil chrysophyte cysts from Sites 689 and 513 were originated from terrestrial freshwater habitats. Since freshwater input into the Southern Ocean are mainly derived from Antarctic terrestrial freshwater (i.e. meltwater of glaciers or ice sheet), fossil chrysophyte cysts in the Southern Ocean sediments can be a new useful tool to reconstruct the Antarctic Ice Sheet's fluctuation history. In addition, comparison between changes in abundance of chrysophyte cysts and the δ18O stack of benthic foraminifera (Zachos et al. 2001) shows opposite trends: matching of increases of chrysophyte cysts corresponds to decreases of δ^{18}O values (i.e. decreased ice sheet volume), which also supports the possible relationship between the fluctuations of fossil chrysophyte cysts and Antarctic Ice Sheets. On the other hand, coexistence of chrysophyte cysts and sea-ice related diatoms (e.g. 4.4–3.3 Ma at Site 689) suggests that some of the chrysophyte cysts originated from sea-ice. Further taxonomic and biogeographic studies on fossil chrysophyte cysts are needed to provide a new approach for paleoenvironmental reconstruction.

Keywords: chrysophyte cyst, diatom, Southern Ocean, microfossil

©2019. Japan Geoscience Union. All Right Reserved.

Spatiotemporal variability of surface mass balance along the JARE traverse route for 1991–2019

*Shun Tsutaki[1], Hideaki Motoyama[2,3], Ayako Abe-Ouchi[1,4], Shuji Fujita[2,3], Kenji Kawamura[2,3,4]

1. The University of Tokyo, 2. National Institute of Polar Research, 3. The Graduate University for Advanced Studies, 4. Japan Agency for Marine-Earth Science and Technology

Satellite-based observations revealed the recent mass loss of the Antarctic ice sheet, and there is concern about its influence on sea level rise. Although significant mass loss has been reported in the West Antarctica, spatial and temporal variability of surface mass balance (SMB) is poorly understood in the East Antarctica where the ice volume is more than 10 times, due to complexity in snow accumulation in space and time, resulting in relatively large uncertainty to quantify ongoing and future mass loss from the Antarctic ice sheet. Therefore, it is crucial to accurately quantify SMB in East Antarctica. SMB has been measured along the traverse route between coastal area (S16) and the inland Dome Fuji region as a part of the Japanese Antarctic Research Expedition (JARE) since 1991. Net snow accumulation was measured by the stake method at approximately 500 points every 2 km. In this study, we re-evaluate spatial and temporal variability of SMB between S16 and Dome Fuji region during the period of 1991–2019. Uncertainty of the SMB measurements is discussed by the data obtained from stake farms and stake rows along the survey route. Spatiotemporal variability of SMB is discussed with surface slope of the ice sheet as well as wind speed and direction in order to evaluate the influence of surface topography and katabatic wind blowing on the ice sheet surface on snow accumulation.

Keywords: Antarctic ice sheet, Surface mass balance

©2019. Japan Geoscience Union. All Right Reserved.

The weathering of granitic rocks in the Sør-Rondane Mountains, East Antarctica

*Tatsuo Kanamaru[1], Yusuke Suganuma[2], hisashi Oiwane[3], Hideki Miura[2], Makoto Miura[4], Jun'ichi Okuno[2], Hideaki Hayakawa[5]

1. Department of Earth and Environmental Sciences, College of Humanities & Sciences, Nihon University, 2. National Institute of Polar Research, 3. Musuhi LLC, 4. Department of Earth and Planetary Sciences, Kanazawa University, 5. Institute for Cosmic Ray Research, University of Tokyo

Weathering processes in hyper-arid and hypothermal environments are key to our understanding of geomorphological processes and landscape evolution in Antarctica. Here, we explore the weathering of granitic rocks and the associated weathering products in the Sør-Rondane Mountains of East Antarctica, to obtain quantitative information regarding the physical and chemical weathering of granitic rocks in hyper-arid and hypothermal environments. Various petrological techniques, including whole-rock chemistry, loss on ignition measurement, mineral chemistry, laser-Raman microspectroscopy, in addition to color measurement and hardness test for the rock samples, were used to analyze the physical and chemical weathering of the rocks. These measurments reveal that the weathering of granitic rocks in the Sør-Rondane Mountains of East Antarctica is controlled mainly by oxidation, including iron hydroxide formation in veins formed by the thermal expansion and contraction of rock-forming minerals, frost shattering and/or salt fretting, and Fe–Ti oxide alteration in the rock interior. Importantly, these physical and chemical weathering processes are unlikely to require a liquid water supply from the environment, and the restricted supply of liquid water and salt is the most probable explanation for the extremely slow weathering rates in the Sør-Rondane Mountains.

Keywords: Antarctica, Weathering, oxidation

©2019. Japan Geoscience Union. All Right Reserved.

Summary of the 2nd Year Activities of the Project on the Interaction of the solid Earth and the Antarctic Ice Sheet:

*Yoichi Fukuda[1], Jun Nishijima[2], Takahito Kazama[1], Kazuki Nakamura[3], Koichiro Doi[4], Yusuke Suganuma[4], Jun'ichi Okuno[4], Akito Araya[5], Heitaro Kaneda[6], Yuichi Aoyama[4], Hideki Miura[4]

1. Department of Geophysics, Graduate School of Science, Kyoto University, 2. Graduate School of Engineering, Kyushu University, 3. Faculty of Engineering, Nihon University, 4. National Institute of Polar Research, 5. ERI, University of Tokyo, 6. Graduate School of Science, Chiba University

As a part of the research project of "Giant reservoirs of heat/water/material: Global environmental changes driven by Southern Ocean and Antarctic Ice Sheet", we are involved in the research topic of "Interaction of the solid Earth and the Antarctic Ice Sheet". In this presentation, we will report the 2nd year activites of our group.
This study was partially supported by JSPS KAKENHI Grant No. 17H06321.

Keywords: Glacial Isostatic Adjustment, Ice sheet changes, Sea level rise, East Antarctica

©2019. Japan Geoscience Union. All Right Reserved.

Late Pleistocene to Holocene sea-level change in East Antarctica revealed by glacial isostatic adjustment modeling

*Takeshige Ishiwa[1], Jun'ichi Okuno[1,2], Yusuke Suganuma[1,2], Hideki Miura[1,2]

1. National Institute of Polar Research, 2. SOKENDAI

Antarctic Ice Sheet (AIS) is the most significant storage of freshwater in the Earth’ s surface and most concerned in considering future sea-level rise. Present studies attempt to assess the mass loss or gain in AIS using GNSS and satellite dataset. Moreover, past AIS variability should be considered to achieve the accurate present AIS change, since presently-observed vertical movement in Antarctica includes the effect of glacial-hydro isostasy due to past AIS variability. Glacial isostatic adjustment (GIA) modeling can provide sea-level histories in Antarctica following sea-level equation. Comparison of field-based sea-level records with predicted sea-level by GIA modeling is required to constraint past AIS histories, leading to the accurate prediction of future sea-level rise.
We document predicted sea-level change in East Antarctica by GIA modeling using several Antarctica ice-loading histories and also compare with previously reported observed sea-level records. Moreover, potential sites for future sampling to obtain observed sea-level records in East Antarctica will be presented by GIA modeling.

Keywords: Antarctic Ice Sheet, Glacial Isostatic Adjustment

©2019. Japan Geoscience Union. All Right Reserved.

An modeling study of Antarctic ice sheet of the Last Glacial Maximum and the last deglaciation

*Takashi Obase[1], Ayako Abe-Ouchi[1,2], Ralf Greve[3], Fuyuki SAITO[2]

1. Atmosphere and Ocean Research Institute, the University of Tokyo, 2. Japan Agency for Marine-Earth Science and Technology, 3. Institute of Low Temperature Science, Hokkaido University

Reconstructions indicate Antarctic ice sheet extent and volume were decreased during the last deglaciation. Sea level reconstruction of the Last Interglacial (LIG), after the penultimet deglaciation, indicate the volume of Antarctic ice sheet was smaller than the present interglacial. Climate reconstructions indicate surface temperature in the Antarctic continent and sea surface temperature in the Southern Ocean during the LIG were higher than the present interglacial. A transient climate simulation of the last deglaciation using MIROC suggests that this higher surface temperature in the Antarctic region is a result of weaker AMOC during the deglaciation and bipolar warming in the Southern Hemisphere.

In the present study, we utilize a 3-dimensional Antarctic ice sheet model (SICOPOLIS) to conduct quantitive assessment of the impact on retreat of Antarctic ice sheet during deglaciations. At first, the configuration of LGM Antarctic ice sheet is prepared using reconstructed climate and sea level changes, and is compared with reconstructions to verify the initial state of deglaciation. We will present preliminary results of Antarctic ice sheet changes of the last deglaciation using climate model outputs of the last deglaciation.

©2019. Japan Geoscience Union. All Right Reserved.

Development of a coupled ice-sheet/earth rebound model for Antarctic ice-sheet simulation

*Fuyuki SAITO[1], Ayako Abe-Ouchi[2,1], Jun'ichi Okuno[3], Takashi Obase[2]

1. Japan Agency for Marine-Earth Science and Technology, 2. Atmosphere and Ocean Research Institute, University of Tokyo, 3. National Institute of Polar Research

Feedback between changes in the ice-sheet and the earth's isostatic rebound is considered to be an important process for the evolution of the past ice-sheets in glacial cycles. We have been developing a coupled ice-sheet/earth rebound model which were applied for northern hemisphere ice sheet simulation during glacial/interglacial cycles. Earth rebound model is based on a self-gravitating visco-elastic multi-layer model developed by Okuno and Nakada (2001), while the ice-sheet model is IcIES (Abe-Ouchi 2013). The results are compared with the previous IcIES results which coupled with a simple isostatic model (i.e., a local lithosphere/relaxing asthenosphere) which is controled by two parameters (the mantle density and the time scale of isostatic response), in order to discuss the effect of more realistic visco-elastic structure of the earth.

Keywords: Antarctic ice sheet, ice sheet model, Earth rebound model

©2019. Japan Geoscience Union. All Right Reserved.

Polar amplifications in the past warm periods obtained from MIROC 4m AOGCM

*Taro Higuchi[1], Ayako Abe-Ouchi[1], Wing-Le Chan[1], Sam Sherriff-Tadano[1]

1. Atmospheric and Ocean Research Institute, the University of Tokyo

The Earth has experienced several warm periods (e.g., early Eocene and Cretaceous), which had warm climates, comparable to global warming prediction of near future due to rising CO2 concentration in the atmosphere. Paleoclimatic proxies indicate that the common characteristics of these periods are remarkable temperature amplifications in the high-latitude and polar region (Bice et al., 2003; Huber, 2008), resulting in small equator-to-polar temperature difference. However, simulations of warm periods climate using General Circulation Models tend to underestimate the polar amplifications than those suggested from geological records. The discrepancy between proxy data and climate models is one of the greatest challenges of warm climate study. Although it is important to consider the effects of the ocean circulation and vegetation feedback to reproduce the polar amplifications in the past warm periods, there were few studies using Atmosphere-Ocean coupled General Circulation Model (AOGCM). In this study, we simulate Present Day, early Eocene, and late Cretaceous climates with different CO2 levels using AOGCM MIROC 4m, additionally full-coupled with dynamic vegetation model, and get the climatology in full equilibrium with longer than 3000 years. The simulated temperatures of early Eocene and late Cretaceous experiments are compared with surface temperature reconstructions based on paleoclimatic proxies. We also investigate the difference of physical process to polar amplification between warm periods (early Eocene and late Cretaceous) and Present Day by using an energy flux analysis. Despite using the fully coupled model with paleo-configuration, the polar amplification in this study is not enough to fully reproduce proxy-indicated polar temperatures. This result implies that we need to re-verify model-performance to the polar climate in GCMs and physical feedback process to global warming due to rising greenhouse gasses in the atmosphere.

Keywords: polar amplification , paleoclimate, AOGCM

©2019. Japan Geoscience Union. All Right Reserved.

Using a coupled AOGCM to study the Antarctic climate of the mid-Pliocene warm period

*Wing-Le Chan[1], Ayako Abe-Ouchi[1,2]

1. Atmosphere and Ocean Research Institute, The University of Tokyo, 2. National Institute of Polar Research

The mid-Pliocene warm period, 3.3-3.0 million years ago, was a period of sustained warmth before global cooling occurred and a shift to repeated glacial cycles. It was also the most recent time in the history of Earth when atmospheric carbon dioxide levels were similar to those of present day. The study of this period is thus of much importance, given the growing concerns over future climate change associated with anthropogenic emissions of greenhouse gases. In particular, ice coverage in West Antarctica, as well as in Greenland, reduced significantly and there is evidence to suggest a retreat of ice sheet in the coastal areas and in the Wilkes Subglacial Basin of East Antarctica during that time.

In this study, we use the mid-resolution MIROC4m coupled atmosphere-ocean general circulation model and apply ice sheet configuration, land-sea mask and biome distribution from PRISM3 data sets, as set forth in the latest, second phase of the Pliocene Model Intercomparison Project. We conduct a series of experiments, including those which look into a range of atmospheric carbon dioxide levels given the spread in values suggested by various sources of proxy data. We show the degree of warming over Antarctica and how the precipitation responds to changes in the moisture transport.

Keywords: Antarctica, Pliocene, modeling

©2019. Japan Geoscience Union. All Right Reserved.

CMIP5 model analysis of future changes in ocean net primary production by focusing on different response among the individual oceans and models

*Akira Oka[1], Yuki Nakamura[1]

1. Atmosphere and Ocean Research Institute, The University of Tokyo

Previous modeling studies show that global primary production will decrease in the future because stratification caused by global warming reduces supply of nutrient from the deep ocean. Previous studies mainly emphasized the importance of nutrient limitation in explaining the changes in primary production; however, phytoplankton growth is actually determined by temperature limitation, light limitation and nutrient limitation. Moreover, although future changes of primary production differ depending on areas, many prior researches discuss only global mean mechanisms and it is not well understood how the mechanisms differ depending on the individual oceans. The purpose of this study is to quantitatively evaluate contribution of each limitation factor for explaining the future changes in primary production in the individual oceans by using 9 CMIP5 models. First, we calculate temperature limitation, light limitation and nutrient limitation for each model, which are not directly available from CMIP5 output data. After that, we quantitatively evaluate main drivers for changes in primary production not only for the global ocean but also for low latitudes, the North Atlantic Ocean, the North Pacific Ocean, the Arctic Ocean and the Southern Ocean, separately. By quantitative evaluation on limitation factors of primary production, we show that the future changes in primary production due to global warming is controlled by not only nutrient limitation but also warming-induced enhancement of phytoplankton growth and decreasing biomass caused by enhanced grazing. Moreover, we show that future changes in primary production and its mechanisms differ among the individual oceans.

Keywords: Ocean primary production, Global warming, CMIP5 model

©2019. Japan Geoscience Union. All Right Reserved.

Factor analysis of the millennial time-scale climate variability in glacial periods

*Miki Akari[1], Ayako Abe-Ouchi[2], Sam Sherriff-Tadano[2]

1. Department of Earth and Planetary Science, Graduate School of Science, The University of Tokyo, 2. Atmosphere and Ocean Research Institute, the University of Tokyo

It is well known that in the glacial periods, air temperature changed abruptly over the North Atlantic on millennial time-scale. It is also known that temperature changes over the Southern Ocean were opposite to the North Atlantic, called a bipolar seesaw relationship. It is suggested that changes in the strength of the Atlantic Meridional Overturning Circulation (AMOC) were closely related to such global climate changes.

In recent years, the idea that freshwater forcing causes the climate changes has been questioned. Spontaneous oscillations in AMOC can be reproduced by experiments using atmosphere-ocean coupled general circulation models (AOGCM). These studies proposed that oceanic feedbacks within the North Atlantic surface - subsurface ocean are important in inducing the spontaneous AMOC variabilities. However, the oscillation cycles shown in previous studies (Peltier and Vettoretti, 2014; Brown and Galbraith, 2016) are several hundred years, which are shorter compared to climate variabilities documented in ice core data. On the other hand, in experiments carried out with MIROC4m AOGCM under the medium glacial condition, millennial time-scale climate and AMOC variabilities are reproduced. Therefore, in this study, we analyze factors controlling the millennial time-scale climate variability obtained from MIROC4m AOGCM. Focusing on the fact that this oscillation cycle is close to the time-scale of the Southern Ocean and the bottom ocean circulation, we analyze the behavior of the Southern Ocean and the bottom ocean in detail, especially deeper than 2500 meters, in addition to oceanic feedback suggested by previous studies.

As a result, it is suggested that the density change at the bottom ocean, which is caused by changes in sea ice formation over the Southern Ocean, plays an important role in controlling the oscillation of AMOC on millennial time-scale.

Keywords: AMOC, Glacial climate, AOGCM

©2019. Japan Geoscience Union. All Right Reserved.

First continuous profiler observation of wintertime Antarctic coastal polynya

*Shigeru Aoki[1], Kazuya Ono[1], Daisuke Hirano[1], Masato Itoh[1], Tomohide Noguchi[2], Satoshi Ozawa[2]

1. Hokkaido University, 2. Marine Works Japan

Antarctic coastal polynyas are the regions where sea ice forms vigorously, leading to supply of dense abyssal water for the global ocean. Monitoring the sea state of coastal polynyas especially in winter hence has global implications. To fully understand the development of water characteristics, capturing of the whole water column is required. However, the wintertime observations of seasonal ice zone such as polynya is not abundant so far, due to the severe and variable conditions of polar oceans.

To realize a near-realtime observation of water column in coastal polynya, we deployed a tethered profiling float over the whole winter in Cape Darnley polynya, East Antarctica (bottom depth of 230 m). The tethered float was manufactured by IHI Corporation, with a temperature and salinity sensor (SBE37 of Seabird Scientific) attached.

The float observation was successful in operation for more than eight months from Feb. 26 to Nov. 13, 2017. This float was designed to park at 150 dbar depth and to surface (upto 20 dbar when sea ice is supposed to exist) at 10-day interval. During this period, 26 profiles for the water column from 180 dbar to 20 dbar were obtained. The whole 160-dbar depth range was covered by nearly half of the 26 profiles, and the total ratio of depth coverage was 81%. Comparison with a current meter record nearby (one mile distance) revealed that the minimum depth achieved did not correlate with the current speed.

The obtained record clearly revealed a seasonal development of the whole water column. While relatively warm water initially remained in the water column, significant freshening occurred and temperature decreased to the freezing point throughout the column from March to April. Then salinity gradually increased to about 35 (150 dbar) in October, successfully covering the whole cycle of sea ice production. The layer near the parking depth (between 120 dbar and 180 dbar) was covered with much higher temporal resolution, showing variations of higher frequencies.

Although the satellite data transmission was not successful due to the battery shortage, signal transmission was successful at the preparation stage. A revision of this platform will enable the monitoring of seasonal ice zone in the polar oceans, to help filling the remaining gap of the global ocean monitoring array.

Keywords: Cape Darnley polynya, Tethered profiler, mooring, Antarctica

©2019. Japan Geoscience Union. All Right Reserved.

Surface topography survey for bared rock and accumulated snow in Antarctica by Unmanned Aero Vehicle

*Yuichi Aoyama[1,2,3], Akihisa Hattori[2,3], Hajime Oishi[3,4], Koichiro Doi[1,2,3], Yoshifumi Nogi[1,2]

1. National Institute of Polar Research, 2. SOKENDAI, 3. The 59th Japanese Antarctic Research Expedition, 4. NEC Networks & System Integration Corporation

In the last decade, Gravity Recovery and Climate Experiment (GRACE) mission demonstrated an increase of surface mass in the Dronning Maud Land (DML), East Antarctica. Actually, snow accumulation has increased at Syowa Station located in DML, and its effect has been detected by superconducting gravimeter and GNSS measurements. For quantifying this effect, it is necessary to measure the distribution of the snow accumulation.
The distribution of the snow accumulation can be estimated from difference in accurate digital surface models (DSM) between the bared rock and the accumulated snow. These DSMs are derived from aerial photography byunmanned aerial vehicle (UAV) with structure from motion (SfM) analysis. In the activity of the 59th Japanese Antarctic Research Expedition (JARE59) during Dec. 2017 - Dec. 2018, some aerial photography surveys were conducted with the fixed-wing small UAV, senseFly eBee plus, and with the rotary-wing drone, DJI Inspire 2 over Syowa Station. There is a report that the eBee plus, having dual-frequency GNSS receiver, enables to generate DSM precisely without ground control point (GCP). We evaluated the accuracy of such DSM by comparing with DSM computed with GCP. We also compared with the DSM computed from aerial photography by Inspire 2 which has single-frequency GNSS for evaluating the advantage of the dual-frequency GNSS tracking. The DSMs in Langhovde, Akarui Misaki, Rundvagshetta located around Lutzow-Holmbukta are also computed from aerial photography by eBee plus.

Keywords: Unmanned aerial vehicle, Challenges for unexplored frontiers

©2019. Japan Geoscience Union. All Right Reserved.

The analysis of long-term Mooring observation records in the northernmost area of seasonal sea ice zone in the Southern Ocean

*Kazuho Watanabe[1], Kohei Mizobata[1], Yujiro Kitade[1]

1. Tokyo University of Marine Science and Technology

The meridional overturning is thought to be the contributor for the stability of the climate system via latitudinal exchange of oceanic heat in the Southern Ocean. To clarify details of the meridional overturning, mooring observations using T/RV *Umitaka-maru* were conducted by physical oceanography group mainly constructed by Tokyo University of Marine science and Technology. In this study, we analyzed the one-year record of the mooring observation and CTD measurements obtained when the mooring system was deployed and recovered.

Results from current meter analysis shows the variability (from 30-day to 90-day cycle) of ocean current. Geostrophic velocity derived from sea level anomaly map distributed by AVISO/Altimetry also shows similar variability of ocean current due to eddies. Furthermore, the location of the mooring system was far from the main axis of the Antarctic Circumpolar Current (ACC). Those results suggest us that the variability of ocean current was resulted from the mesoscale eddy field.

Even though the variability of ocean current was recoded, results also indicate the meridional overturning. The progressive vector diagram based on current meter record illustrated poleward transport at about around 400db and eastward transport at about 4000db. One-year mooring observation also revealed ocean current shear structure (about 10cm/s at about 400db and 4cm/s at about 4000db) when poleward transport was continuously captured. During poleward transport with shear structure was captured, the increase in temperature over 2.1 $^{\circ}$C from October to February at about 400db was frequently observed. Based on hydrographic data, warm water captured around 400db was identified as the Circumpolar Deep Water (CDW). Cross correlation analysis revealed that warm CDW intrusion occurred about 8-day following southward current at 400db. During the season when sea ice covered the ocean, similar event also happened but temperature at about 400db increased up to around 2°C. Our results indicate that CDW’ s southward transport is changing by seasonal and the event of mesoscale eddy passage.

Keywords: Southern ocean, Meridional circulation, Mooring observation, Mesoscale-Eddy

©2019. Japan Geoscience Union. All Right Reserved.

Preliminary observation report on chlorofluorocarbons (CFCs) and sulfur hexafluoride (SF_6) off the Cape Darnley in the summer of 2019

*Yoshihiko Ohashi[1], Michiyo Yamamoto-Kawai[1], Kenichi Sasaki[2], Sayaka Kumakawa[1], Naoyuki Tamura[1], Kay I. Ohshima[3]

1. Tokyo University of Marine Science and Technology, 2. Japan Agency for Marine-Earth Science and Technology, 3. Institute of Low Temperature Science, Hokkaido University

Antarctic Bottom Water (AABW) occupies the largest volume of water mass in the global ocean and its formation is a key process of global ocean circulation. Ohshima et al. (2013) found newly formed AABW off the Cape Darnley (Cape Darnley Bottom Water; CDBW). However, little is known about the circulation of CDBW and its time scale. To quantitatively understand the spread and circulation of CDBW, it is effective to use the chemical tracer such as chlorofluorocarbons (CFCs) and sulfur hexafluoride (SF_6). We carried out CTD observation and water sampling off the Cape Darnley in the summer of 2019. Water sampling was performed from ocean surface to the bottom at 16 Stations (along the Wild Canyon and its west). CFCs and SF_6 of the samples were measured by an analytical system developed at JAMSTEC based on Bullister and Wisegarver (2008). The concentrations of CFCs and SF_6 were significantly high near the surface (< 100 m) (CFC11 > 2.0 pmol kg^{-1}; CFC12 > 1.2 pmol kg^{-1}; SF_6 > 1.4 fmol kg^{-1}). They showed a minimum at depths of 800–1500 m and then increased to the bottom. The relatively high concentrations of CFCs and SF_6 near the bottom, together with the low temperature (< −0.4°C), reflects the spread of CDBW. At the presentation, we will discuss mean age and circulation of CDBW.

Keywords: Antarctic Bottom Water , Cape Darnley, Chemical tracer

©2019. Japan Geoscience Union. All Right Reserved.

Mechanism of sea-ice production variation in Amundsen Sea Polynya

*Sohey Nihashi[1], Kouta Mine[1], Kazuki Nakata[2]

1. National Institute of Technology, Tomakomai College, 2. RESTEC

A coastal polynya is an area of high ice production and dense water formation. This dense water is a major source of the Antarctic Bottom Water. Since winter polynya is a difficult site to observe, the mechanism of polynya formation and variation had not been understood well. About ten years ago, an algorithm was developed that uses satellite passive microwave data to detect polynyas and estimates thin ice thickness on a daily timescale. The satellite data revealed the detailed distribution and variation of polynyas (e.g., Tamura et al., 2007; 2008). Use of AMSR-E/AMSR2 data with a finer spatial resolution (about 5-6 km), can reveal the more detailed spatial distribution of polynyas. For example, it was revealed that most of coastal polynyas form on the west side of landfast ice (fast ice: stationary sea ice attached to coastal features such as shoreline and grounded icebergs). This close relationship indicates a vital role of fast ice for formation and variation of coastal polynyas (Nihashi and Ohshima, 2015; Nihashi et al., 2017). The Amundsen Sea Polynya (ASP), located in West Antarctica, is the third largest ice production area and is formed on the west side of fast ice protruding into the ocean. Thwaites Glacier adjacent to the fast ice has been suggested that a rapid melting occurs in recent decades (Rignot et al., 2008; Milio et al., 2019). Grounded icebergs that act as anchor points play an essential role in the formation of fast ice protruding into the ocean. Since the sources of an iceberg are glacier and ice sheet, the rapid melting possibly affects the formation and distribution of fast ice and accordingly adjacent polynyas.

In this study, we compare the ice production in the ASP with atmospheric parameters and fast ice extent to investigate factors for causing ice production variation. Ice production estimated from heat flux calculation with daily thin ice thickness from AMSR-E/AMSR2 data (Nihashi and Ohshima, 2015; Nihashi et al., 2017) is used. For fast ice, monthly extent detected from AMSR-E/AMSR2 data is used. We also use ice production estimated using thin ice thickness by an improved algorithm in which ice types (active frazil and thin solid ice) are considered (Nakata et al., 2019). As atmospheric data, we use ERA5.

Ice production is positively correlated with wind speed regardless of daily or monthly data with the coefficient of 0.54-0.73. Here, we use a wind component with the highest correlation; components of the wind vector are projected in all directions of every 1˚ from 0˚ (northerly wind) clockwise to 360˚, and then, correlation coefficients are calculated. The wind component is oriented to the west rather than to the offshore (north) against the land. This is a direction towards the offshore against the shoreline defined by both the land and fast ice. This result supports the analysis using only AMSR-E data (Nihashi and Ohshima, 2015). If ice production in which thin ice types are considered is used, the wind component is oriented toward further west when active frazil is dominant. This direction is to the offshore against the fast ice. Further, active frazil tends to form along fast ice. On the other hand, the wind component is northward (to the offshore against land) when thin solid ice is dominant. Multiple regression analysis is performed on the ice production using air temperature, wind speed, and fast ice extent averaged over the freezing season (May-August). Ice production can be explained by these parameters with R=0.77. This indicates that ice production in the ASP before the satellite observation era can be reproduced to some extent from atmospheric data by using this regression line. The results presented in this study suggest that fast ice plays a vital role in the formation and variation of the ASP. Continuous monitoring of Antarctic coastal polynyas and fast ice from passive microwave satellite sensor is quite meaningful understanding climate change.

©2019. Japan Geoscience Union. All Right Reserved.

Keywords: Antarctic Ocean, coastal polynya, Amundsen Sea Polynya

©2019. Japan Geoscience Union. All Right Reserved.

Estimation of thin ice thickness and discrimination of ice type from AMSR2 passive microwave data

*Kazuki Nakata[1], Tamaru Naoya[1], Sohey Nihashi[2], Kay I. Ohshima[3]

1. Remote Sensing Technology Center of Japan, 2. National Institute of Technology, Tomakomai College, 3. Institute of Low Temperature Science, Hokkaido University

Antarctic coastal polynyas (thin ice and/or low ice concentration area) are areas of high ice production due to huge heat loss to the atmosphere. Dense water formed by the high ice production is a significant source of Antarctic Bottom Water. Thin ice thickness algorithms that use satellite passive microwave data have been developed to detect coastal polynyas and estimates thin ice thickness on a daily timescale. In these algorithms, ice thickness of <20 cm is empirically estimated based on a negative correlation relationship between polarization ratio (PR) of brightness temperatures (TBs) and ice thickness (hi). However, the dispersion of the data points of PR-hi relationship was relatively large. Nakata et al. (2019) revealed that two thin ice types (active frazil and thin solid ice) cause this dispersion using AMSR-E data (2002-2011). They detected these ice types based on a PR-GR (Gradient Ratio) relationship. And thin ice thickness was estimated from PR-hi relationships for each ice type. This new thin ice algorithm can improve the accuracy of the thin-ice thickness estimation. In this study, we have examined whether this new algorithm can apply to data from AMSR2 which the successor of AMSR-E. The footprint size of AMSR2 is improved by about 85% from AMSR-E in spite of the frequency channels are the same. By adding AMSR2 data, thin-ice thickness, ice type, and ice production data set with a higher spatial resolution can be obtained from 2002 to the present.
We use TBs at 36 and 89 GHz from AMSR2 Level 1B data. The footprint sizes are 12 km ×7 km and 5 km × 3 km, respectively. Ice thickness for comparison with AMSR2 PR is derived from clear-sky thermal infrared images by MODIS with a spatial resolution of 1 km. Backscatter images acquired by C-band SAR (C-SAR) on the ESA’s Sentinel-1 satellite with a spatial resolution of 90 m are used to validate two thin ice types. We use these satellite data obtained at Ross Ice Shelf and Cape Darnley polynya areas.
AMSR2 PR-hi relationships for two ice types differs clearly as in Nakata et al. (2019). We estimate ice thickness using lines that best fit into the AMSR-E PR-hi relationships (Nakata et al., 2019) using AMSR2 data. And then, mean bias and root-mean-square error (RMSE) of the data points from the lines are calculated. The errors are slightly larger than the cases of AMSR-E data. When ice thickness is <10 cm, mean bias and RMSE for active frazil are -2.0 and 1.0 cm, respectively, while those for thin solid ice are -6.2 and 9.8 cm, respectively. For ice thickness of 10-20 cm (only for thin solid ice), the bias and RMSE are -5.9 and 9.9 cm, respectively. We also have confirmed that two ice types can be detected using AMSR2 data by a method for AMSR-E data proposed by Nakata et al. (2019). The results of this study indicate that the new thin ice algorithm for AMSR-E data can apply to the AMSR2 data.

Keywords: Thin ice thickness, Ice type, AMSR2, Coastal polynya

©2019. Japan Geoscience Union. All Right Reserved.

[J] Poster | M (Multidisciplinary and Interdisciplinary)：M-IS Intersection

Mon. May 27, 2019 5:15 PM - 6:30 PM JST | Mon. May 27, 2019 8:15 AM - 9:30 AM UTC | Poster Hall International Exhibition Hall8, Makuhari Messe_35

[M-IS14] Global climate change driven by the Southern Ocean and the Antarctic Ice Sheet

convener:Osamu Seki(Institute of Low Temperature Science, Hokkaido University), Akira Oka(Atmosphere and Ocean Research Institute, The University of Tokyo), Ryu Uemura(University of the Ryukyus), Ryosuke Makabe(National Institute of Polar Research)

The Southern Ocean and Antarctic ice sheet, which are the giant reservoirs of heat, water, and materials, have a potential to play central roles in long-term global climate change. This system is composed of the following sub-systems; ice shelf which is a place of the interaction of ice sheet and ocean, flowing iceberg, seasonal sea ice zone, Antarctic bottom water which drives the thermohaline circulation, active biological production and Antarctic Circumpolar Current. These sub-systems are interacted with each other and have significant impact on changes in the global environmental system. This session aim to summarize recent observational and simulation studies from various fields relating to the past and present changes in the Antarctic Ice sheet and Southern Ocean, which are essential elements for unraveling the changes in the global climate system. Further, future science plans for understanding of the environmental changes of the Antarctic Cryosphere is also discussed.

[MIS14-P01] Preliminary study on the effect of low-salinity ice melting water on biomass and composition of ice algae

*Keigo Takahashi[1], Ryosuke Makabe[2,3], Shintaro Takao[2,3], Tsuneo Odate[2,3], Masato Moteki[1,2] (1.Tokyo University of Marine Science and Technology, 2.National Institute of Polar Research, 3.The Graduate University for Advanced Studies (SOKENDAI))

[MIS14-P02] Effects of lugol's fixtation on preservation of samples for carbon and nitrogen stable isotope and molecular analyses

*Masayoshi Sano[1], Ryosuke Makabe[1,2], Ayu Yamamoto[3], Norio Kurosawa[4], Masato Moteki[2,3], Tsuneo Odate[1,2] (1.National Institute of Polar Research, 2.The Graduate University for Advanced Studies, 3.Tokyo University of Marine Science and Technology, 4.Soka University)

[MIS14-P03] The application of environmental DNA for the monitoring of Antarctic marine ecosystem

*Aiko Tachibana[1], Ryosuke Makabe[2], Masato Moteki[1] (1.Tokyo University of Marine Science and Technology, 2.National Institute of Polar Research)

[MIS14-P04] Coincidental occurrence process of frazil ice and high biomass off Amery Ice Shelf

*Yoshihiko Machimura[1], Kay I. Ohshima[2], Kazuki Nakata[3], Masato Ito[2], Yasushi Fukamachi[2,4], Ryosuke Makabe[5], Shintaro Takao[5], Sohey Nihashi[6] (1.Graduate School of Environmental Sciences, Hokkaido University, 2.Institute of Low Temperature Science, Hokkaido University, 3.Remote Sensing Technology Center of Japan, 4.Arctic Research Center, Hokkaido University, 5.National Institute of Polar Research, 6.National Institute of Technology, Tomakomai College)

[MIS14-P05] Feeding habit of the Antarctic amphipod *Themisto gaudichaudii* of Vincennes Bay (East Antarctica) during austral summer

*Junji Matsushita[1], Ryosuke Makabe[2], Masato Moteki[1] (1.Tokyo University of Marine Science and Technology, 2.National Institute of Polar Research)

[MIS14-P06] Time-series observation of subsurface chlorophyll *a* maximum in the seasonal ice zone of the Southern Ocean

*Ayuko Kagesawa[1], Masayoshi Sano[2], Shintaro Takao[1,2], Ryosuke Makabe[1,2], Kohei Mizobata[3], Norio Kurosawa[4], Masato Moteki[2,3], tuneo Odate[2] (1.The Graduate University for Advanced Studies, 2.National Institute of Polar Research, 3.Tokyo University of Marine Science and Technology, 4.Soka University)

[MIS14-P07] Seasonality in sulfur isotopic compositions of atmospheric sulfate and its implications for atmospheric sulfur cycles in East Antarctica

*Sakiko Ishino[1], Shohei Hattori[1], Joel Savarino[2], Michel Legrand[2], Susanne Preunkert[2], Bruno Jourdain[2], Francis Albarede[3], Emmanuelle Albalat[3], Naohiro Yoshida[1,4] (1.Department of Chemical Science and Engineering, School of Materials and Chemical Technology, Tokyo Institute of Technology, 2.Institut des Geoscience de l'Environnement, Université Grenoble Alpes/CNRS, 3.Ecole Normale Supérieure (LGL-TPE), 4.Earth-Life Science Institute, Tokyo Institute of Technology)

[MIS14-P08] **Penultimate glacial-interglacial transition viewed from the Dome Fuji ice core, Antarctica**

*Ikumi Oyabu[1,2], Kenji Kawamura[1,3,4], Kyotaro Kitamura[1] (1.National Institute of Polar Research, Research Organization of Information and Systems, 2.Japan Society for the Promotion of Science, 3.SOKENDAI (The Graduate University of Advanced Studies), 4.Japan Agency for Marine Science and Technology (JAMSTEC))

[MIS14-P09] Reconstruction of Antarctic ice sheet dynamics in the Last Interglacial

*Mutsumi Iizuka[1], Osamu Seki[1], Takuya Itaki[2], Tomohisa Irino[1], Minoru Ikehara[4], Saiko Sugisaki[2], Masanobu Yamamoto[1], Keiji Horikawa[5], Yuusuke Suganuma[3] (1.Hokkaido university, 2.Geological Survey of Japan, 3.National Institute of Polar Research , 4.Center for Advanced Marine Core Research, Kochi University, 5.University of Toyama)

[MIS14-P10] Pliocene CO2 concentration estimated from Southern Ocean SST

*Osamu Seki[1], Tomohiro Shimono[2] (1.Institute of Low Temperature Science, Hokkaido University, 2.Guraduate School of Environmental Science)

[MIS14-P11] **Lithogenic fluxes across a transect in the SW Indian Ocean since the last glacial inception**

*Eri Helen Amsler[1], Walter Geibert[2], Gerhard Kuhn[2], Minoru Ikehara[3], Samuel Jaccard[1] (1.Institute of Geological Sciences and Oeschger Centre for Climate Change Research, University of Bern, Switzerland, 2.Alfred-Wegener-Institut Helmholtz-Zentrum für Polar- und Meeresforschung, Bremerhaven, Germany, 3.Center for Advanced Marine Core Research, Kochi University, Kochi, Japan)

[MIS14-P12] Changes in composition of fossil diatoms from Ross Sea under gradual warming climate from MIS M2

*Saki Ishino[1], Itsuki Suto[2], Rob M. McKay[3], Laura De Santis[4], Denise K. Kluhanek[5], Expedition 374 Scientists (1.National Institute of Advanced Industrial Science and Technology, 2.Department of Earth and Planetary Sciences Graduate School of Environmental Studies, Nagoya University, 3.Victoria University, 4.Instituto Nazionale di Oceanografia e di Geofisica Sperimentale, 5.Texas A&M University)

[MIS14-P13] Geological insights into formation of Conrad Rise, Southern Ocean: Preliminary geological results of R/V *Hakuho-maru* KH-19-1 cruise

*Hiroshi Sato[1], Masakazu Fujii[2,3], Hiroki Matsui[4], Minoru Ikehara[4] (1.School of Business Administration, Senshu University, 2.NIPR, 3.SOKENDAI, 4.Center for Advanced Marine Core Research, Kochi University)

[MIS14-P14] Fossil chrysophyte cysts as a new paleoenvironmental proxy

*Yuji Kato[1,2], Itsuki Suto[1] (1.Graduate School of Environmental Studies, Nagoya University, 2.Center for Advanced Marine Core Research, Kochi University (JSPS Research Fellowship for Young Scientists))

[MIS14-P15] Spatiotemporal variability of surface mass balance along the JARE traverse route for 1991−2019

*Shun Tsutaki[1], Hideaki Motoyama[2,3], Ayako Abe-Ouchi[1,4], Shuji Fujita[2,3], Kenji Kawamura[2,3,4] (1.The University of Tokyo, 2.National Institute of Polar Research, 3.The Graduate University for Advanced Studies, 4.Japan Agency for Marine-Earth Science and Technology)

[MIS14-P16] The weathering of granitic rocks in the Sør-Rondane Mountains, East Antarctica

*Tatsuo Kanamaru[1], Yusuke Suganuma[2], hisashi Oiwane[3], Hideki Miura[2], Makoto Miura[4], Jun'ichi Okuno[2], Hideaki Hayakawa[5] (1.Department of Earth and Environmental Sciences, College of Humanities & Sciences, Nihon University, 2.National Institute of Polar Research, 3.Musuhi LLC, 4.Department of Earth and Planetary Sciences, Kanazawa University, 5.Institute for Cosmic Ray Research, University of Tokyo)

[MIS14-P17] Summary of the 2nd Year Activities of the Project on the Interaction of the solid Earth and the
Antarctic Ice Sheet:

*Yoichi Fukuda[1], Jun Nishijima[2], Takahito Kazama[1], Kazuki Nakamura[3], Koichiro Doi[4], Yusuke Suganuma[4], Jun'ichi Okuno[4], Akito Araya[5], Heitaro Kaneda[6], Yuichi Aoyama[4], Hideki Miura[4] (1.Department of Geophysics, Graduate School of Science, Kyoto University, 2.Graduate School of Engineering, Kyushu University, 3.Faculty of Engineering, Nihon University, 4.National Institute of Polar Research, 5.ERI, University of Tokyo, 6.Graduate School of Science, Chiba University)

[MIS14-P18] Late Pleistocene to Holocene sea-level change in East Antarctica revealed by glacial isostatic adjustment modeling

*Takeshige Ishiwa[1], Jun'ichi Okuno[1,2], Yusuke Suganuma[1,2], Hideki Miura[1,2] (1.National Institute of Polar Research, 2.SOKENDAI)

[MIS14-P19] An modeling study of Antarctic ice sheet of the Last Glacial Maximum and the last deglaciation

*Takashi Obase[1], Ayako Abe-Ouchi[1,2], Ralf Greve[3], Fuyuki SAITO[2] (1.Atmosphere and Ocean Research Institute, the University of Tokyo, 2.Japan Agency for Marine-Earth Science and Technology, 3.Institute of Low Temperature Science, Hokkaido University)

[MIS14-P20] Development of a coupled ice-sheet/earth rebound model for Antarctic ice-sheet simulation

*Fuyuki SAITO[1], Ayako Abe-Ouchi[2,1], Jun'ichi Okuno[3], Takashi Obase[2] (1.Japan Agency for Marine-Earth Science and Technology, 2.Atmosphere and Ocean Research Institute, University of Tokyo, 3.National Institute of Polar Research)

[MIS14-P21] Polar amplifications in the past warm periods obtained from MIROC 4m AOGCM

*Taro Higuchi[1], Ayako Abe-Ouchi[1], Wing-Le Chan[1], Sam Sherriff-Tadano[1] (1.Atmospheric and Ocean Research Institute, the University of Tokyo)

[MIS14-P22] Using a coupled AOGCM to study the Antarctic climate of the mid-Pliocene warm period

*Wing-Le Chan[1], Ayako Abe-Ouchi[1,2] (1.Atmosphere and Ocean Research Institute, The University of Tokyo, 2.National Institute of Polar Research)

[MIS14-P23] CMIP5 model analysis of future changes in ocean net primary production by focusing on different response among the individual oceans and models

*Akira Oka[1], Yuki Nakamura[1] (1.Atmosphere and Ocean Research Institute, The University of Tokyo)

[MIS14-P24] Factor analysis of the millennial time-scale climate variability in glacial periods

*Miki Akari[1], Ayako Abe-Ouchi[2], Sam Sherriff-Tadano[2] (1.Department of Earth and Planetary Science, Graduate School of Science, The University of Tokyo, 2.Atmosphere and Ocean Research Institute, the University of Tokyo)

[MIS14-P25] First continuous profiler observation of wintertime Antarctic coastal polynya

*Shigeru Aoki[1], Kazuya Ono[1], Daisuke Hirano[1], Masato Itoh[1], Tomohide Noguchi[2], Satoshi Ozawa[2] (1.Hokkaido University, 2.Marine Works Japan)

[MIS14-P26] Surface topography survey for bared rock and accumulated snow in Antarctica by Unmanned Aero Vehicle

*Yuichi Aoyama[1,2,3], Akihisa Hattori[2,3], Hajime Oishi[3,4], Koichiro Doi[1,2,3], Yoshifumi Nogi[1,2] (1.National Institute of Polar Research, 2.SOKENDAI, 3.The 59th Japanese Antarctic Research Expedition, 4.NEC Networks & System Integration Corporation)

[MIS14-P27] The analysis of long-term Mooring observation records in the northernmost area of seasonal sea ice zone in the Southern Ocean

*Kazuho Watanabe[1], Kohei Mizobata[1], Yujiro Kitade[1] (1.Tokyo University of Marine Science and Technology)

[MIS14-P28] Preliminary observation report on chlorofluorocarbons (CFCs) and sulfur hexafluoride (SF_6) off the Cape Darnley in the summer of 2019

*Yoshihiko Ohashi[1], Michiyo Yamamoto-Kawai[1], Kenichi Sasaki[2], Sayaka Kumakawa[1], Naoyuki Tamura[1], Kay I. Ohshima[3] (1.Tokyo University of Marine Science and Technology, 2.Japan Agency for Marine-Earth Science and Technology, 3.Institute of Low Temperature Science, Hokkaido University)

[MIS14-P29] Mechanism of sea-ice production variation in Amundsen Sea Polynya

*Sohey Nihashi[1], Kouta Mine[1], Kazuki Nakata[2] (1.National Institute of Technology, Tomakomai College, 2.RESTEC)

[MIS14-P30] Estimation of thin ice thickness and discrimination of ice type from AMSR2 passive microwave data

*Kazuki Nakata[1], Tamaru Naoya[1], Sohey Nihashi[2], Kay I. Ohshima[3] (1.Remote Sensing Technology Center of Japan, 2.National Institute of Technology, Tomakomai College, 3.Institute of Low Temperature Science, Hokkaido University)

Preliminary study on the effect of low-salinity ice melting water on biomass and composition of ice algae

*Keigo Takahashi[1], Ryosuke Makabe[2,3], Shintaro Takao[2,3], Tsuneo Odate[2,3], Masato Moteki[1,2]

1. Tokyo University of Marine Science and Technology, 2. National Institute of Polar Research, 3. The Graduate University for Advanced Studies (SOKENDAI)

Upon sea ice melting ice algae are subject to low salinity water, sometimes nearly freshwater, while sea ice produces a brine (high salinity). Certain taxa of ice algae, primarily diatom, increase in cell number after released in water column (seeding). Since lower salinity water deteriorates photosynthetic efficiency of ice algae, such a variability of salinity is likely to influence seeding of ice algae during melting season. However, it is not clear how biomass, abundance, composition and mortality of ice-algal community changes under different salinity conditions. To further understand the mechanism for seeding of ice algae, we conducted a shipboard experiment in the Indian Sector of the Southern Ocean during austral summer.

We collected pack ice and surface seawater in the ice edge (65º17.9’ S, 109º40.9’ E) on January 16th, 2019 during the 22nd Antarctic voyage by the training vessel *Umitaka-maru*. Sea ice was melted with different volume of filtered seawater (moderate salinity: 10.0 kg ice+90 L filtered sea water, FSW, low salinity: 8.6 kg ice+10 L FSW) to simulate different final salinity (moderate: 30.05, low: 18.00). We incubated the algal communities in seawater and two types of sea-ice melting water (moderate and low salinity conditions) under a natural light condition for 24 hours, with temperature maintained by a circulating surface seawater. Before and after the incubation, we obtained chlorophyll *a* concentration (bulk and size-fraction), Lugol-fixed samples for microscopic analysis and cell viability (live or dead).

After 24 hours, <10 μm size class of ice-algal communities in both moderate and low salinity conditions showed a significant difference in the ratio of chlorophyll *a* concentration (chl *a* fin. /chl *a* ini.) relative to the bulk and >10 μm size class (Tukey-Kramer test, Fig.). The ratio of chl *a* (mean±SD, *n*=3) in this size class was highest (moderate: 2.1±0.1, low: 1.8±0.2) among the samples. This suggests that algal community of <10 μm have an ability to acclimate to low salinity water. This study discussed the changes in species composition and abundance of the algal communities as well.

Keywords: The Southern Ocean, Ice algae, Sea ice

©2019. Japan Geoscience Union. All Right Reserved.

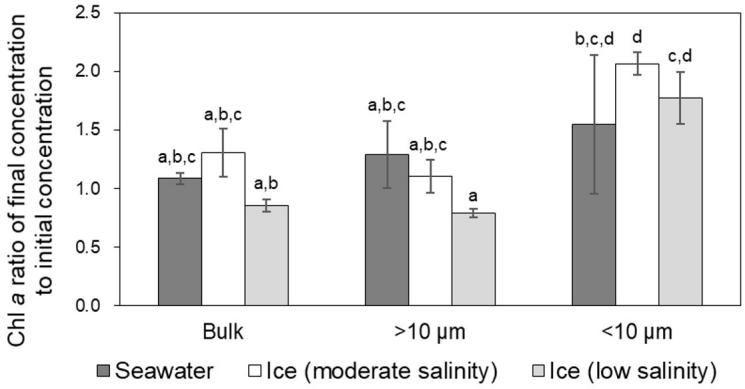

Fig. The final chlorophyll *a* concentration of bulk and size-fractionated samples relative to the initial concentration of seawater and two types of ice (moderate and low salinity). The same letters indicate no significant difference at the p=0.05 level (Tukey-Kramer test).

©2019. Japan Geoscience Union. All Right Reserved.

Effects of lugol’s fixtation on preservation of samples for carbon and nitrogen stable isotope and molecular analyses

*Masayoshi Sano[1], Ryosuke Makabe[1,2], Ayu Yamamoto[3], Norio Kurosawa[4], Masato Moteki[2,3], Tsuneo Odate[1,2]

1. National Institute of Polar Research, 2. The Graduate University for Advanced Studies, 3. Tokyo University of Marine Science and Technology, 4. Soka University

Recently, carbon and nitrogen stable isotope analysis and molecular analysis are commonly used as powerful tools in marine ecological studies including sediment trap experiments. In the southern ocean ecosystem studies, moored sediment trap samples are important to obtain information all-year around including winter season when we cannot observe directly by research vessels. Usually, collecting cups of sediment traps were filled with formalin for preventing degradation of samples during deployment periods, but formalin fixtation is not suitable for those analyses because of crosslinking and fragmantation of DNA and alteration of carbon stable isotope. On the other hand, lugol’s iodine solution is commonly used as fixatives of microzooplankton and phytoplankton samples, but its usefulness as a long term preservative of samples for stable isotope analysis and molecular analysis is still not examined. In this study, we compared carbon and nitrogen stable isotope ratios of zooplankton samples fixed by lugol’s iodine solution and other methods over 6 months and extract DNA from lugol fixed samples after 16 months preservation for examining the usefulness of lugol’s iodine solution. Samples were collected by ORI net during a cruise of training vessel *Umitaka-maru* in 2017. Collected samples were fixed by 5%, 10% lugol’s iodine seawater solution or 5% buffered formalin seawater or frozen at -80˚C on board. Samples were sorted after 1 week, 1 month, 3 months and 6 months preservation and used for stable isotope analysis. DNA was extracted from samples after 16 months preservation and amplified by PCR. In most cases, carbon stable isotope ratios were significantly different between formalin fixed samples and other samples after 1 week preservation. Nitrogen stable isotope ratios were also significantly different between formalin fixed samples and other samples after 1 month preservation. There are no significant differences in carbon and nitrogen stable isotope ratios between samples fixed by 10% lugol solution and frozen samples in all the periods. Amplification of DNA extracted from lugol fixed samples was detected by a gel electrophoresis. Thus, lugol’s fixtation is considered to be suitable for long term preservation of samples for both stable isotope analysis and molecular analysis.

Keywords: Zooplankton, Sediment trap, Stable isotope ratio, DNA, Fixation method

©2019. Japan Geoscience Union. All Right Reserved.

The application of environmental DNA for the monitoring of Antarctic marine ecosystem

*Aiko Tachibana[1], Ryosuke Makabe[2], Masato Moteki[1]

1. Tokyo University of Marine Science and Technology, 2. National Institute of Polar Research

A monitoring of biological community structure and diversity is essential to understand the global climate impact on the Antarctic marine ecosystem. Traditional biomonitoring methods typically rely on sampling methods, combined with morphology-based identification, which is time-consuming and requires sophisticated expertise. To elucidate the full impact of rapidly shifting climate on the Antarctic ecosystem, efficient and effective tools are required to understand spatial and temporal variations in biological communities. Environmental DNA (eDNA) –genomic material extracted from cells and tissue shed by organisms into environmental samples, such as soil, sediments and water –is a possible tool for rapid assessing marine biodiversity and community composition. We conducted an eDNA observation in January 2019 along the 110˚E transect off Wilkes Land, East Antarctica, by the training vessel *Umitaka-maru*, Tokyo University of Marine Science and Technology. In total, 189 samples were collected from surface to deep layers covering various water mass which was located from 40˚S to 65˚S along the 110˚E transect. We will generate DNA-based biodiversity data from these samples to produce the first comprehensive analysis of metazoan genetic diversity in the Southern Ocean. The eDNA observation and preliminary experiments are outlined here, and a future plan of analyses are discussed.

Keywords: Environmental DNA, Southern Ocean, biodiversity

©2019. Japan Geoscience Union. All Right Reserved.

Coincidental occurrence process of frazil ice and high biomass off Amery Ice Shelf

*Yoshihiko Machimura[1], Kay I. Ohshima[2], Kazuki Nakata[3], Masato Ito[2], Yasushi Fukamachi[2,4], Ryosuke Makabe[5], Shintaro Takao[5], Sohey Nihashi[6]

1. Graduate School of Environmental Sciences, Hokkaido University, 2. Institute of Low Temperature Science, Hokkaido University, 3. Remote Sensing Technology Center of Japan, 4. Arctic Research Center, Hokkaido University, 5. National Institute of Polar Research, 6. National Institute of Technology, Tomakomai College

Antarctic coastal regions are the most productive regions in the Southern Ocean and could dramatically influence global carbon cycle and ecosystems. During the austral spring, large phytoplankton blooms develop in polynyas with peak productivity occurring from December to January. According to the chlorophyll estimation from satellite, net primary production (NPP) in the Antarctic coastal polynyas rapidly declines from February to March (Arrigo et al., 2015).
Recent studies have found the regions with high biomass in Antarctic coastal regions during February-March (Lieser et al., 2015; DeJong et al., 2018). This high biomass is collaterally observed with frazil ice. Chlorophyll estimation algorithms using Moderate Resolution Imaging Spectroradiometer (MODIS) data mask pixels with high sea ice coverage to prevent the contamination by excess reflection of visible light. Therefore, the regions with high biomass collaterally observed with frazil ice have not been counted in NPP estimation in Antarctic coastal regions. These high biomass regions potentially have a large impact for global carbon cycle as the CO_2 sink. However, incidence processes and causes of frazil ice with high biomass have not been investigated in details. In this study, we focus on the regions of the Cape Darnley polynya and offshore of the Amery Ice Shelf in February and March during 2003-2011 to understand the processes and causes of high biomass collaterally observed with frazil ice.
First, we calculated Green Index from MODIS surface reflectance data obtained from the study area to identify green colored regions implicate high biomass. Second, we identified the region of frazil ice, using the algorithm that discriminates ice type between frazil ice and thin solid ice from AMSR-E passive microwave data (Nakata et al., 2019). These two analyses clearly show that the high biomass and frazil ice coincidentally occur both temporally and spatially in late summer. In particular, both of high biomass and frazil ice have a peak in their distributions at the same location about 50 km offshore of the Amery Ice Shelf in March. This is also suggesting an unknown frazil ice formation process distinctly different from a coastal polynya process.
We consider Ice Shelf Water (ISW) as a trigger of coincidental occurrence of frazil ice and high biomass. According to the CTD-tag data obtained from seals in the region off Amery Ice Shelf in late summer, ISW that is partly supercooled exists at depths of 250-400 m and the surface water is heated by solar radiation in the region from the ice shelf front to 68.3 deg. S. While in the region north of 68.2 deg. S, the surface water has reached the freezing point. Previous studies reported that ISW flows out to 50-100 km offshore from the ice shelf front and generates frazil ice at depths of 250-300 m (Dieckmann et al., 1986; Hughes et al., 2013).
To summarize the above analyses, coincidental occurence of frazil ice and high biomass is assumed to be caused by the following processes.
1. ISW is formed and flows out to the outside of Amery Ice Shelf cold cavity.
2. ISW becomes supercooled during the outflow, and frazil ice is generated.
3. Generated frazil ice gradually rises toward the surface. In the region south of 68.3deg. S, frazil ice is melted because of heated surface water. Frazil ice can appear at the surface in the region north of 68.2 deg. S, where the surface water reaches the freezing point.

©2019. Japan Geoscience Union. All Right Reserved.

4. Frazil ice scavenges phytoplankton existing in water column and carries it to the surface. Simultaneously, iron contained in ISW enhances the biological production and increases biomass. The process proposed in this study may also occur in regions just off other ice shelves. In the future, we should clarify the details of the process off Amery Ice Shelf with in-situ observation and explore the possibility of occurrence in regions off the other ice shelves.

Keywords: sea ice, polynya, ice shelf water, remote sensing, biological production

©2019. Japan Geoscience Union. All Right Reserved.

Feeding habit of the Antarctic amphipod *Themisto gaudichaudii*of Vincennes Bay (East Antarctica) during austral summer

*Junji Matsushita[1], Ryosuke Makabe[2], Masato Moteki[1]

1. Tokyo University of Marine Science and Technology, 2. National Institute of Polar Research

Amphipods are key components of macrozooplankton to link lower trophic levels to higher predators in the krill-independent food web in the Southern Ocean (SO). The carnivorous amphipod *Themisto gaudichaudii*, widely distributed in SO, is an opportunistic predator. They are known to feed on copepods, euphausiids, salps and various zooplankton in the Atlantic Ocean sector, while their food habits are poorly known in the Indian Ocean sector. This study analyzed gut contents of *T. gaudichaudii* collected along the 110˚E transect in SO in January 2019 to clarify food habit of *T. gaudichaudii*. Fecal pellet obtained from onboard experiment were supplementary used to verify the estimated food habit. We’ll preliminary demonstrate here the food web related to *T. gaudichaudii* in the Indian Ocean sector during austral summer.

Keywords: The Southern Ocean, Macrozooplankton, Amphipod

©2019. Japan Geoscience Union. All Right Reserved.

Time-series observation of subsurface chlorophyll *a* maximum in the seasonal ice zone of the Southern Ocean

*Ayuko Kagesawa[1], Masayoshi Sano[2], Shintaro Takao[1,2], Ryosuke Makabe[1,2], Kohei Mizobata[3], Norio Kurosawa[4], Masato Moteki[2,3], tuneo Odate[2]

1. The Graduate University for Advanced Studies, 2. National Institute of Polar Research, 3. Tokyo University of Marine Science and Technology, 4. Soka University

A persistent subsurface chlorophyll *a* maximum (SCM) is often found during the summer-fall season after the ice-edge bloom in the seasonal ice zone of the Southern Ocean, so that SCM would be considered important for biogeochemical cycling through the lower trophic levels. The relevant studies, however, have been qualitative in nature. This study aimed to reveal the dynamics and ecological role of the SCM in the seasonal ice zone.
We carried out Lagrangian observations using a drifter with two time-series sediment traps, an Acoustic Doppler Current Profiler (ADCP) and four sensor flames (Fig. 1). The drifter was deployed at 63.5˚S, 110.0˚E in January 14th 2019, and 5-day continuous observation was performed. In the vicinity of the drifter, 4 ship-based observations including net sampling and CTD casts were made until the drifter was recovered. Physical environments were measured by CTD, and sea water samples were collected for measurements of chlorophyll *a* (chl. *a*) concentration, nutrients, particle organic carbon, dissolved organic carbon, abundance of phytoplankton, micro-zooplankton, bacteria and nano-/pico-phytoplankton. We also conducted an incubation experiment for determining net primary production.
The temperature minimum layer, found between 37 and 52 m depth, decreased from -0.82 ºC to -1.28 ºC during the study period. The maximum chl. *a* concentration (1.0-2.0 μg/l), comparable to that in typical ice edge blooms, was observed at 40 m depth (Fig. 2). Such a high chl. *a* concentration might have important roles for food web and for material cycling. We will discuss especially on phytoplankton dynamics showing results of microscopic and chemical analyses.

Keywords: subsurface chlorophyll a maximum , the Southern Ocean

©2019. Japan Geoscience Union. All Right Reserved.

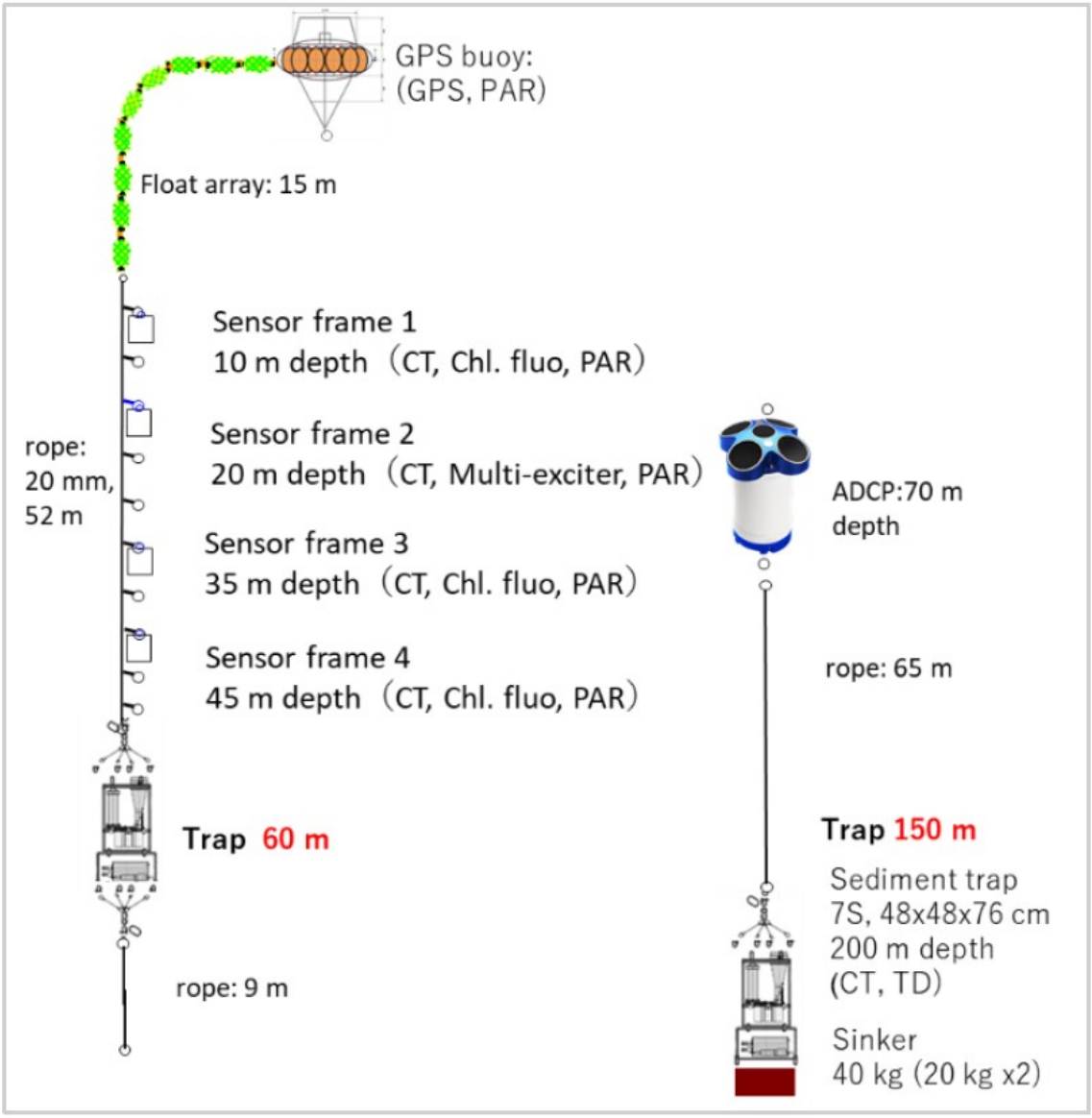

Fig. 1 A schematic image of the drifter

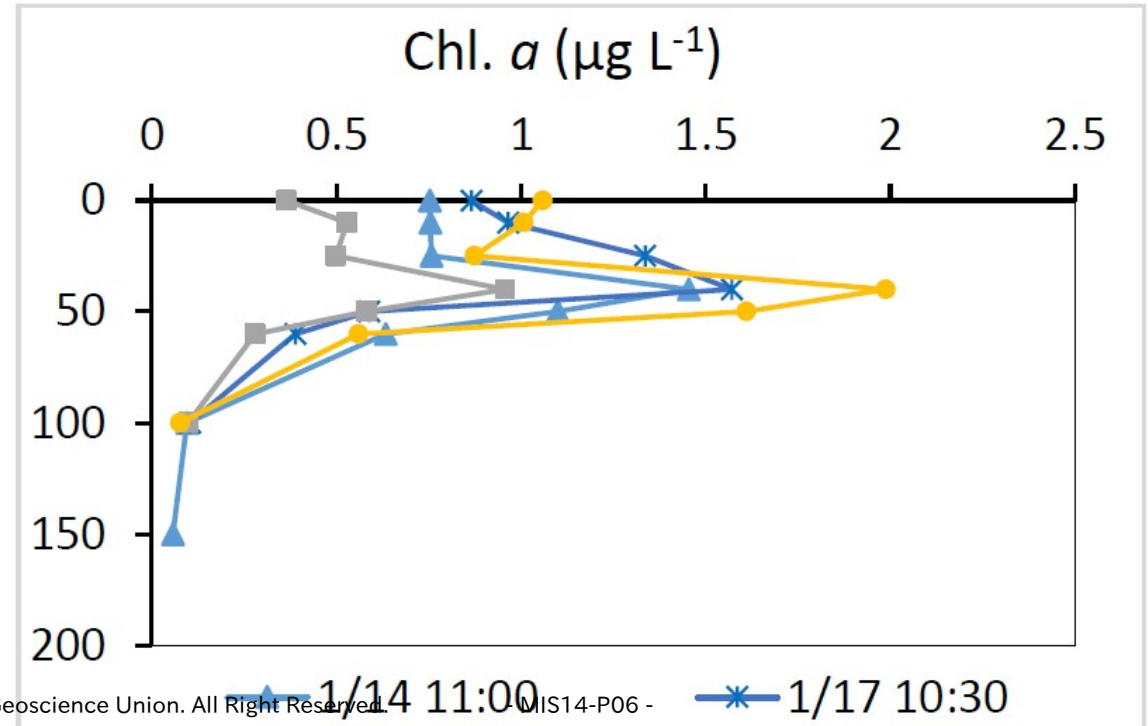

©2019. Japan Geoscience Union. All Right Reserved.

©2019. Japan Geoscience Union. All Right Reserved.

Seasonality in sulfur isotopic compositions of atmospheric sulfate and its implications for atmospheric sulfur cycles in East Antarctica

*Sakiko Ishino[1], Shohei Hattori[1], Joel Savarino[2], Michel Legrand[2], Susanne Preunkert[2], Bruno Jourdain[2], Francis Albarede[3], Emmanuelle Albalat[3], Naohiro Yoshida[1,4]

1. Department of Chemical Science and Engineering, School of Materials and Chemical Technology, Tokyo Institute of Technology, 2. Institut des Geoscience de l' Environnement, Université Grenoble Alpes/CNRS, 3. Ecole Normale Supérieure (LGL-TPE), 4. Earth-Life Science Institute, Tokyo Institute of Technology

Atmospheric sulfate in Antarctica is produced mainly from a marine biogenic sulfur compound, dimethyl sulfide. They are therefore a subject of study related to the linkage between marine biogenic activity and climate. We investigate year-round observations of sulfur isotopic compositions of atmospheric sulfate (SO_4^{2-}) at inland (Dome C) and coastal (Dumont d' Urville) sites in East Antarctica to quantify the relative importance of marine biogenic (mb) and non-marine biogenic (nmb) SO_4^{2-} for the Antarctic atmospheric sulfur cycle. The $\delta^{34}S$ values of non-sea salt sulfate showed clear seasonal variations with summer maxima and winter minima, and showed homogeneity between inland and coastal sites throughout the year. This result suggests that the isotopic fractionation through chemical reactions during transportation from coastal to inland areas insignificantly affects the observed $\delta^{34}S_{nss}$ values. The observed $\delta^{34}S_{nss}$ values are controlled mainly by the relative importance of mb-SO_4^{2-} and nmb-SO_4^{2-}. This finding, in conjunction with the SO_4^{2-} records in Antarctic ice cores, will open a perspective implying the increased relative importance of nmb-SO_4^{2-} during glacial periods. We also found a significant increase in nmb-SO_4^{2-} concentrations in November, especially for the inland site. This nmb-SO_4^{2-} increase is correlated with the ^{210}Pb concentration, suggesting the existence of long-range transport of continental nmb-SO_4^{2-} from lower latitudes to the Antarctic inland. Identification of the sources of those nmb-SO_4^{2-} will be a key step for elucidation of the linkage between Antarctic atmosphere/climate and environmental changes at lower latitudes from the past through the future.

Keywords: Sulfur isotope analysis, Sulfate aerosols, Antarctica

©2019. Japan Geoscience Union. All Right Reserved.

Penultimate glacial-interglacial transition viewed from the Dome Fuji ice core, Antarctica

*Ikumi Oyabu[1,2], Kenji Kawamura[1,3,4], Kyotaro Kitamura[1]

1. National Institute of Polar Research, Research Organization of Information and Systems, 2. Japan Society for the Promotion of Science, 3. SOKENDAI (The Graduate University of Advanced Studies), 4. Japan Agency for Marine Science and Technology (JAMSTEC)

Paleoclimatic proxies provide information about the variations of climate forcings and responses, such as atmospheric CO_2concentration, temperature and sea level, as well as their magnitudes and phase relationships. Accurate chronological constraints are particularly important for numerical simulations, both for their input and validation data, to better understand the transient behaviors of climate and ice sheets. During the last interglacial period (~130 to ~120 thousand years before present (kyr BP)), the peak global mean surface temperature was ~1 degree higher than the preindustrial period, and the global sea level was ~6 –9 m higher than today with significant contribution from the Antarctic ice sheet, whereas atmospheric CO_2levels were similar to those in the preindustrial period (Dutton et al., 2015). The last interglacial period and the preceding transition from the penultimate glacial period are important targets for the paleoclimatic research to investigate the mechanisms for warming and ice-sheet reductions. However, responses (sequences, timing or magnitude) of ice sheets, temperature or ocean circulations to climate forcing during this period are much less well understood, partly because the number of proxies and time resolution are limited, and the chronological uncertainties are relatively large. A chronology of the Dome Fuji (DF) ice core was constructed by synchronizing variations in O_2/N_2ratio of occluded air with local summer insolation (Kawamura et al., 2007), but relatively large errors were later reported around the last interglacial (Fujita et al., 2015). Here, we reanalyzed the O_2/N_2ratio of the DF core by improving the methods for sample treatment, air extraction and mass spectrometry between 57 and 165 kyr BP to revise the DF chronology. The new chronology agrees within 1.2 kyr with a radiometric (U-Th) chronology of Chinese speleothems, the whose stated error is less than 1 kyr (Cheng et al., 2009), suggesting successful improvement of our ice-core chronology. Using $\delta^{18}O$ of atmospheric O_2($\delta^{18}O_{atm}$) and CH_4records measured on the same ice samples as used for the O_2/N_2measurements, we investigate climatic variations during the penultimate glacial period and deglaciation. We found that $\delta^{18}O_{atm}$ becomes heavier while CH_4concentration increased at 138.4 kyr BP during the penultimate glacial maximum; this characteristic relationship was observed at Heinrich Event 2 (at ~24 kyr BP) during the last glacial maximum (Severinghaus et al., 2009; Rhodes et al., 2015). Other well-dated paleoclimatic records show major climatic changes around 138 kyr BP; an abrupt weakening of the Asian monsoon occurred at 138 kyr BP (Wang et al., 2008), and the onset of relative sea level rise was suggested at 139±1 kyr BP from seawater $\delta^{18}O$ of Red Sea (Grant et al., 2012) and at 137 kyr BP from U-Th dating of Tahiti fossil corals (Thomas et al., 2009). The similarity of these ages suggests that a massive iceberg discharge event occurred at ~138 kyr BP, and it marked the onset of penultimate deglaciation. Our new data may provide better chronological constraints on the climatic forcings and responses around the penultimate deglaciation and last interglacial period.

References

Dutton et al. (2015), *Science,* **349**., Kawamura, K., et al. (2007), *Nature*, **448**, 912-916., Fujita, S. et al. (2015), *Clim. Past.*,**11**, 1395-1416 ., Cheng, H. et al. (2009), *Science*, **326**, 248-252., Rhodes, R. H.et all. (2015), *Science*, **348**, 1016-1019., Severinghaus, J. P. et al., (2009), *Science*,**324**, 1431-1434., Thomas, A. L.et al. (2009), *Science*, **324**, 1186-1189., Wang, Y. et al. (2008), *Nature*, **451**, 1090-1093., Grant, K.

©2019. Japan Geoscience Union. All Right Reserved.

M., et al. (2012), *Nature*, **491**, 744-747.

Keywords: Antarctica, Ice core, Dome Fuji, deglaciation, The last interglacial

©2019. Japan Geoscience Union. All Right Reserved.

Reconstruction of Antarctic ice sheet dynamics in the Last Interglacial

*Mutsumi Iizuka[1], Osamu Seki[1], Takuya Itaki[2], Tomohisa Irino[1], Minoru Ikehara[4], Saiko Sugisaki[2], Masanobu Yamamoto[1], Keiji Horikawa[5], Yuusuke Suganuma[3]

1. Hokkaido university, 2. Geological Survey of Japan, 3. National Institute of Polar Research , 4. Center for Advanced Marine Core Research, Kochi University, 5. University of Toyama

Ongoing global warming could cause various problems in the future. One of the serious concerns is a sea level rise due to the melting of the ice sheet. Antarctic ice sheet, which hold a massive amount of fresh water was considered to be stable even if global warming progresses in the future. However, recent studies have shown that Antarctic ice sheet is more sensitive to global warming than previously thought. Therefore, it is an important to better understand extent to which Antarctic ice sheet is sensitive to global warming.

Study of past warm period proves an useful insight into the prediction of sea level rise in a future. Especially, Sea level in the last interglacial (MIS 5e), which was ~1˚C warmer than the preindustrial was estimated to be several meters higher than that of the present with the sudden and abrupt rises in sea level. This suggests significant loss of Antarctic ice sheet during MIS 5e. However, Antarctic ice sheet variability during the MIS 5e has been poorly understood. In this study, we reconstruct dynamics of Antarctic ice sheet during MIS 5e from the marine sediment core GC1407 collected from Dumont d'Urville Sea, East Antarctica (130.518˚E, 63.74˚S).

Interval of MIS 5e has been determined based on abundance of radiolaria in GC1407. Variability of iceberg discharge is reconstructed by measurement of iceberg rafted debris (IBRD) in sediments. IBRDs are found to be recognized only during MIS 5e. This suggests that the significant discharge of large icebergs possibly from Wilkes Land basin, East Antarctica happened only during warmer than present climate condition.

Keywords: Southern Ocean, Last interglacial, Antarctic icesheet

©2019. Japan Geoscience Union. All Right Reserved.

Pliocene CO2 concentration estimated from Southern Ocean SST

*Osamu Seki[1], Tomohiro Shimono[2]

1. Institute of Low Temperature Science, Hokkaido University, 2. Guraduate School of Environmental Science

Prediction of temperature change by the climate model depends on climate sensitivity, which is the temperature change associated with doubling of CO_2 concentration. The constraint on climate sensitivity is the key part in the IPCC and thus is critical for the future climate prediction. However, despite considerable efforts for constraint on climate sensitivity, the climate sensitivity still remains uncertainty. Furthermore, recent paleoclimate studies revealed that climate sensitivity depends on climate state. This highlights the necessity to know the climate sensitivity in the warmer than the present climate for the future prediction. The Pliocene Warm Period (3-4.5 million years ago) is often regarded as the best analogue of climate in the near future and thus is ideal to investigate climate sensitivity in the warm climate state. In this study, we reconstruct CO_2 concentration based on the new empirical approach (average SST in mid latitude of Southern Ocean) to estimate climate sensitivity in the Pliocene Warm Period.

Keywords: Climate sensitivity, Pliocene, carbon dioxide concentration

©2019. Japan Geoscience Union. All Right Reserved.

Lithogenic fluxes across a transect in the SW Indian Ocean since the last glacial inception

*Eri Helen Amsler[1], Walter Geibert[2], Gerhard Kuhn[2], Minoru Ikehara[3], Samuel Jaccard[1]

1. Institute of Geological Sciences and Oeschger Centre for Climate Change Research, University of Bern, Switzerland, 2. Alfred-Wegener-Institut Helmholtz-Zentrum für Polar- und Meeresforschung, Bremerhaven, Germany, 3. Center for Advanced Marine Core Research, Kochi University, Kochi, Japan

On glacial-interglacial time scale the Southern Ocean plays a prominent role in modulating climate by storing and redistributing heat, fresh water, carbon and nutrients globally. Atmospheric CO_2 is taken up by algae and sequestered in the deep ocean through the biological carbon pump. On the other hand, CO_2 is released back to the atmosphere through upwelling and vertical mixing [1]. The relative contribution of these two mechanisms controls the efficiency through which carbon can be sequestered in the ocean interior.

The effect of iron fertilization on biological productivity has previously been documented in the Atlantic and Pacific sectors of the Southern Ocean [2, 3]. During glacial periods higher input of Fe-bearing dust increased phytoplankton growth and carbon sequestration, thus leading to the drawdown of atmospheric CO_2, accounting for about half of the glacial-interglacial CO_2 amplitude [4].

Here we present ^{230}Th-normalized lithogenic fluxes in a set of marine sediment cores spanning a meridional transect in the Indian sector of the Southern Ocean further away from the Patagonian dust plume and show that increased Fe flux impacted export production patterns, contributing to the sequestration of carbon away from the atmosphere.

[1] Sigman, D. M., Boyle, E. A. (2000) Nature 407, 859-869.

[2] Martínez-Garcia, A., Sigman, D. M., Haojia, R., Anderson, R. F., Straub, M., Hodell, D. A., Jaccard, S. L., Eglinton, T. I., Haug, G. H. (2014) Science 343, 1347-1350.

[3] Lamy F., Gersonde, R., Winckler, G., Esper, O., Jaeschke, A., Kuhn, G., Ullermann, J., Martínez-Garcia, A., Lambert, F., Kilian, R. (2014) Science 343 (6169), 403-407.

[4] Hain, M. P., D. M. Sigman, and G. H. Haug (2010) Global Biogeochem. Cycles, 24, GB4023.
Please fill in your abstract text.

Keywords: Southern Ocean, Biological Pump

©2019. Japan Geoscience Union. All Right Reserved.

Changes in composition of fossil diatoms from Ross Sea under gradual warming climate from MIS M2

*Saki Ishino[1], Itsuki Suto[2], Rob M. McKay[3], Laura De Santis[4], Denise K. Kluhanek[5], Expedition 374 Scientists

1. National Institute of Advanced Industrial Science and Technology, 2. Department of Earth and Planetary Sciences Graduate School of Environmental Studies, Nagoya University, 3. Victoria University, 4. Instituto Nazionale di Oceanografia e di Geofisica Sperimentale, 5. Texas A&M University

Understanding past polar environmental changes under warming climate process will help predicting future global warming. The paleoceanographic record near Antarctic ice-proximal area provides important insight into West Antarctica Ice Sheet (WAIS) vulnerability. Antarctic sediments contain numerous fossil diatoms, which are helpful to clarify past oceanographic conditions.

International Ocean Discovery Program (IODP) Expedition 374 drilled five sites from Ross Sea continental shelf and rise to investigate WAIS evolution under warm climates. Site U1524A (74° 13.05’ S and 173° 37.98’ W, 2394 m water depth) drilled from continental rise, which lies beneath cascading Antarctic Bottom Water current, preserves high resolution Pliocene sediments. We present preliminary results of composition changes of diatom assemblages focusing on the ages from MIS M2 to warmer climate around the interval between 3.3 and 3.0 Ma. Diatom records including abundance changes in sea-ice indicator species and *Chaetoceros*resting spores contribute to evaluate the past sea-ice coverage, primary productivity, and vertical mixing in Pliocene warm condition.

Keywords: Diatom, The Southern Ocean, Paleoenvironment

©2019. Japan Geoscience Union. All Right Reserved.

Geological insights into formation of Conrad Rise, Southern Ocean: Preliminary geological results of R/V *Hakuho-maru* KH-19-1 cruise

*Hiroshi Sato[1], Masakazu Fujii[2,3], Hiroki Matsui[4], Minoru Ikehara[4]

1. School of Business Administration, Senshu University, 2. NIPR, 3. SOKENDAI, 4. Center for Advanced Marine Core Research, Kochi University

Conrad Rise is one of plateaus situated at the Indian-sector of the Southern Ocean. Origin of the rise are considered to be a sort of the Large Igneous Provinces or hotspot. Previously Borisova et al. (1996) reported alkaline igneous rocks which have similar geochemical signature to the Kelgueren Plateau. However, detailed investigations have not been performed until our recent study. We performed geological and geophysical investigations during three R/V *Hakuho-maru* cruises, KH-10-7, KH-16-1, and KH-19-1. Particularly, we had five dredge operations during KH-10-7 and KH-19-1 cruises and obtained geological (and biological) materials that have important keys to understanding the origin and development of Conrad Rise. Geological materials collected during KH-10-7 cruise had already reported by Ishizuka et al. (2011), Sato et al. (2012), and Kobayashi et al. (2013). In this presentation, we report preliminary results of recovered geological and biological materials during KH-19-1 cruise.

Two dredge operations were performed during KH-19-1 Leg 2 (16 Jan to 12 Feb 2019). Dredge site KH-19-1D4 is situated at one of peaks of unnamed small knoll that is located north of Ob seamount. Approximately 50 kg of geological and biological materials including igneous rocks, metamorphic rocks, and deep-sea coral were recovered. Dredge site KH-19-1D5 is situated at north-south trending spur on the northern slope of Ob seamount. Approximately 50 kg of materials including igneous rocks, sedimentary rocks, metamorphic rocks, deep-sea coral, and living shell were recovered.

References

Borisova et al. (1996) *Geochemistry International* **34**(6) 503-517
Sato et al. (2012) JpGU meeting 2012, SCG66-09
Ishizuka et al. (2011) 2nd Symposium on Polar Science.
Kobayashi et al. (2013) 4th Symposium on Polar Science.

Keywords: Conrad Rise, Southern Ocean, KH-19-1 cruise

©2019. Japan Geoscience Union. All Right Reserved.

Fossil chrysophyte cysts as a new paleoenvironmental proxy

*Yuji Kato[1,2], Itsuki Suto[1]

1. Graduate School of Environmental Studies, Nagoya University, 2. Center for Advanced Marine Core Research, Kochi University (JSPS Research Fellowship for Young Scientists)

Most Neogene–Quaternary sediments in the Southern Ocean have high biogenic silica contents with large amounts of siliceous microfossils including chrysophyte cysts as well as diatoms. Fossil chrysophyte cysts are considered to be potentially useful paleoenvironmental indicators, however no general consensus exists about their paleoenvironmental significance. In this study, data on fossil chrysophyte cyst abundances of late Miocene to Pliocene (ca. 9–3 Ma) age are presented from two marine sediment cores, Ocean Drilling Program Site 689 and Deep Sea Drilling Project Site 513, both located in the Atlantic sector of the Southern Ocean. Changes in the chrysophyte cyst abundances are compared to those in the diatom abundances, and the potential of fossil chrysophyte cysts as paleoceanographic indicators around the Antarctica is discussed.
As a result, similarity in the fluctuation of freshwater diatom and chrysophyte cyst abundances were observed in both sites. In addition, occurrences of chrysophyte cysts similar to previously reported ones from freshwater habitats were recognized. These results suggest that the fossil chrysophyte cysts from Sites 689 and 513 were originated from terrestrial freshwater habitats. Since freshwater input into the Southern Ocean are mainly derived from Antarctic terrestrial freshwater (i.e. meltwater of glaciers or ice sheet), fossil chrysophyte cysts in the Southern Ocean sediments can be a new useful tool to reconstruct the Antarctic Ice Sheet's fluctuation history. In addition, comparison between changes in abundance of chrysophyte cysts and the δ18O stack of benthic foraminifera (Zachos et al. 2001) shows opposite trends: matching of increases of chrysophyte cysts corresponds to decreases of δ^{18}O values (i.e. decreased ice sheet volume), which also supports the possible relationship between the fluctuations of fossil chrysophyte cysts and Antarctic Ice Sheets. On the other hand, coexistence of chrysophyte cysts and sea-ice related diatoms (e.g. 4.4–3.3 Ma at Site 689) suggests that some of the chrysophyte cysts originated from sea-ice. Further taxonomic and biogeographic studies on fossil chrysophyte cysts are needed to provide a new approach for paleoenvironmental reconstruction.

Keywords: chrysophyte cyst, diatom, Southern Ocean, microfossil

©2019. Japan Geoscience Union. All Right Reserved.

Spatiotemporal variability of surface mass balance along the JARE traverse route for 1991–2019

*Shun Tsutaki[1], Hideaki Motoyama[2,3], Ayako Abe-Ouchi[1,4], Shuji Fujita[2,3], Kenji Kawamura[2,3,4]

1. The University of Tokyo, 2. National Institute of Polar Research, 3. The Graduate University for Advanced Studies, 4. Japan Agency for Marine-Earth Science and Technology

Satellite-based observations revealed the recent mass loss of the Antarctic ice sheet, and there is concern about its influence on sea level rise. Although significant mass loss has been reported in the West Antarctica, spatial and temporal variability of surface mass balance (SMB) is poorly understood in the East Antarctica where the ice volume is more than 10 times, due to complexity in snow accumulation in space and time, resulting in relatively large uncertainty to quantify ongoing and future mass loss from the Antarctic ice sheet. Therefore, it is crucial to accurately quantify SMB in East Antarctica. SMB has been measured along the traverse route between coastal area (S16) and the inland Dome Fuji region as a part of the Japanese Antarctic Research Expedition (JARE) since 1991. Net snow accumulation was measured by the stake method at approximately 500 points every 2 km. In this study, we re-evaluate spatial and temporal variability of SMB between S16 and Dome Fuji region during the period of 1991–2019. Uncertainty of the SMB measurements is discussed by the data obtained from stake farms and stake rows along the survey route. Spatiotemporal variability of SMB is discussed with surface slope of the ice sheet as well as wind speed and direction in order to evaluate the influence of surface topography and katabatic wind blowing on the ice sheet surface on snow accumulation.

Keywords: Antarctic ice sheet, Surface mass balance

©2019. Japan Geoscience Union. All Right Reserved.

The weathering of granitic rocks in the Sør-Rondane Mountains, East Antarctica

*Tatsuo Kanamaru[1], Yusuke Suganuma[2], hisashi Oiwane[3], Hideki Miura[2], Makoto Miura[4], Jun'ichi Okuno[2], Hideaki Hayakawa[5]

1. Department of Earth and Environmental Sciences, College of Humanities & Sciences, Nihon University, 2. National Institute of Polar Research, 3. Musuhi LLC, 4. Department of Earth and Planetary Sciences, Kanazawa University, 5. Institute for Cosmic Ray Research, University of Tokyo

Weathering processes in hyper-arid and hypothermal environments are key to our understanding of geomorphological processes and landscape evolution in Antarctica. Here, we explore the weathering of granitic rocks and the associated weathering products in the Sør-Rondane Mountains of East Antarctica, to obtain quantitative information regarding the physical and chemical weathering of granitic rocks in hyper-arid and hypothermal environments. Various petrological techniques, including whole-rock chemistry, loss on ignition measurement, mineral chemistry, laser-Raman microspectroscopy, in addition to color measurement and hardness test for the rock samples, were used to analyze the physical and chemical weathering of the rocks. These measurments reveal that the weathering of granitic rocks in the Sør-Rondane Mountains of East Antarctica is controlled mainly by oxidation, including iron hydroxide formation in veins formed by the thermal expansion and contraction of rock-forming minerals, frost shattering and/or salt fretting, and Fe–Ti oxide alteration in the rock interior. Importantly, these physical and chemical weathering processes are unlikely to require a liquid water supply from the environment, and the restricted supply of liquid water and salt is the most probable explanation for the extremely slow weathering rates in the Sør-Rondane Mountains.

Keywords: Antarctica, Weathering, oxidation

©2019. Japan Geoscience Union. All Right Reserved.

Summary of the 2nd Year Activities of the Project on the Interaction of the solid Earth and the Antarctic Ice Sheet:

*Yoichi Fukuda[1], Jun Nishijima[2], Takahito Kazama[1], Kazuki Nakamura[3], Koichiro Doi[4], Yusuke Suganuma[4], Jun'ichi Okuno[4], Akito Araya[5], Heitaro Kaneda[6], Yuichi Aoyama[4], Hideki Miura[4]

1. Department of Geophysics, Graduate School of Science, Kyoto University, 2. Graduate School of Engineering, Kyushu University, 3. Faculty of Engineering, Nihon University, 4. National Institute of Polar Research, 5. ERI, University of Tokyo, 6. Graduate School of Science, Chiba University

As a part of the research project of "Giant reservoirs of heat/water/material: Global environmental changes driven by Southern Ocean and Antarctic Ice Sheet", we are involved in the research topic of "Interaction of the solid Earth and the Antarctic Ice Sheet". In this presentation, we will report the 2nd year activites of our group.
This study was partially supported by JSPS KAKENHI Grant No. 17H06321.

Keywords: Glacial Isostatic Adjustment, Ice sheet changes, Sea level rise, East Antarctica

©2019. Japan Geoscience Union. All Right Reserved.

Late Pleistocene to Holocene sea-level change in East Antarctica revealed by glacial isostatic adjustment modeling

*Takeshige Ishiwa[1], Jun'ichi Okuno[1,2], Yusuke Suganuma[1,2], Hideki Miura[1,2]

1. National Institute of Polar Research, 2. SOKENDAI

Antarctic Ice Sheet (AIS) is the most significant storage of freshwater in the Earth’ s surface and most concerned in considering future sea-level rise. Present studies attempt to assess the mass loss or gain in AIS using GNSS and satellite dataset. Moreover, past AIS variability should be considered to achieve the accurate present AIS change, since presently-observed vertical movement in Antarctica includes the effect of glacial-hydro isostasy due to past AIS variability. Glacial isostatic adjustment (GIA) modeling can provide sea-level histories in Antarctica following sea-level equation. Comparison of field-based sea-level records with predicted sea-level by GIA modeling is required to constraint past AIS histories, leading to the accurate prediction of future sea-level rise.
We document predicted sea-level change in East Antarctica by GIA modeling using several Antarctica ice-loading histories and also compare with previously reported observed sea-level records. Moreover, potential sites for future sampling to obtain observed sea-level records in East Antarctica will be presented by GIA modeling.

Keywords: Antarctic Ice Sheet, Glacial Isostatic Adjustment

©2019. Japan Geoscience Union. All Right Reserved.

An modeling study of Antarctic ice sheet of the Last Glacial Maximum and the last deglaciation

*Takashi Obase[1], Ayako Abe-Ouchi[1,2], Ralf Greve[3], Fuyuki SAITO[2]

1. Atmosphere and Ocean Research Institute, the University of Tokyo, 2. Japan Agency for Marine-Earth Science and Technology, 3. Institute of Low Temperature Science, Hokkaido University

Reconstructions indicate Antarctic ice sheet extent and volume were decreased during the last deglaciation. Sea level reconstruction of the Last Interglacial (LIG), after the penultimet deglaciation, indicate the volume of Antarctic ice sheet was smaller than the present interglacial. Climate reconstructions indicate surface temperature in the Antarctic continent and sea surface temperature in the Southern Ocean during the LIG were higher than the present interglacial. A transient climate simulation of the last deglaciation using MIROC suggests that this higher surface temperature in the Antarctic region is a result of weaker AMOC during the deglaciation and bipolar warming in the Southern Hemisphere.

In the present study, we utilize a 3-dimensional Antarctic ice sheet model (SICOPOLIS) to conduct quantitive assessment of the impact on retreat of Antarctic ice sheet during deglaciations. At first, the configuration of LGM Antarctic ice sheet is prepared using reconstructed climate and sea level changes, and is compared with reconstructions to verify the initial state of deglaciation. We will present preliminary results of Antarctic ice sheet changes of the last deglaciation using climate model outputs of the last deglaciation.

©2019. Japan Geoscience Union. All Right Reserved.

Development of a coupled ice-sheet/earth rebound model for Antarctic ice-sheet simulation

*Fuyuki SAITO[1], Ayako Abe-Ouchi[2,1], Jun'ichi Okuno[3], Takashi Obase[2]

1. Japan Agency for Marine-Earth Science and Technology, 2. Atmosphere and Ocean Research Institute, University of Tokyo, 3. National Institute of Polar Research

Feedback between changes in the ice-sheet and the earth's isostatic rebound is considered to be an important process for the evolution of the past ice-sheets in glacial cycles. We have been developing a coupled ice-sheet/earth rebound model which were applied for northern hemisphere ice sheet simulation during glacial/interglacial cycles. Earth rebound model is based on a self-gravitating visco-elastic multi-layer model developed by Okuno and Nakada (2001), while the ice-sheet model is IcIES (Abe-Ouchi 2013). The results are compared with the previous IcIES results which coupled with a simple isostatic model (i.e., a local lithosphere/relaxing asthenosphere) which is controled by two parameters (the mantle density and the time scale of isostatic response), in order to discuss the effect of more realistic visco-elastic structure of the earth.

Keywords: Antarctic ice sheet, ice sheet model, Earth rebound model

©2019. Japan Geoscience Union. All Right Reserved.

Polar amplifications in the past warm periods obtained from MIROC 4m AOGCM

*Taro Higuchi[1], Ayako Abe-Ouchi[1], Wing-Le Chan[1], Sam Sherriff-Tadano[1]

1. Atmospheric and Ocean Research Institute, the University of Tokyo

The Earth has experienced several warm periods (e.g., early Eocene and Cretaceous), which had warm climates, comparable to global warming prediction of near future due to rising CO2 concentration in the atmosphere. Paleoclimatic proxies indicate that the common characteristics of these periods are remarkable temperature amplifications in the high-latitude and polar region (Bice et al., 2003; Huber, 2008), resulting in small equator-to-polar temperature difference. However, simulations of warm periods climate using General Circulation Models tend to underestimate the polar amplifications than those suggested from geological records. The discrepancy between proxy data and climate models is one of the greatest challenges of warm climate study. Although it is important to consider the effects of the ocean circulation and vegetation feedback to reproduce the polar amplifications in the past warm periods, there were few studies using Atmosphere-Ocean coupled General Circulation Model (AOGCM). In this study, we simulate Present Day, early Eocene, and late Cretaceous climates with different CO2 levels using AOGCM MIROC 4m, additionally full-coupled with dynamic vegetation model, and get the climatology in full equilibrium with longer than 3000 years. The simulated temperatures of early Eocene and late Cretaceous experiments are compared with surface temperature reconstructions based on paleoclimatic proxies. We also investigate the difference of physical process to polar amplification between warm periods (early Eocene and late Cretaceous) and Present Day by using an energy flux analysis. Despite using the fully coupled model with paleo-configuration, the polar amplification in this study is not enough to fully reproduce proxy-indicated polar temperatures. This result implies that we need to re-verify model-performance to the polar climate in GCMs and physical feedback process to global warming due to rising greenhouse gasses in the atmosphere.

Keywords: polar amplification , paleoclimate, AOGCM

©2019. Japan Geoscience Union. All Right Reserved.

Using a coupled AOGCM to study the Antarctic climate of the mid-Pliocene warm period

*Wing-Le Chan[1], Ayako Abe-Ouchi[1,2]

1. Atmosphere and Ocean Research Institute, The University of Tokyo, 2. National Institute of Polar Research

The mid-Pliocene warm period, 3.3-3.0 million years ago, was a period of sustained warmth before global cooling occurred and a shift to repeated glacial cycles. It was also the most recent time in the history of Earth when atmospheric carbon dioxide levels were similar to those of present day. The study of this period is thus of much importance, given the growing concerns over future climate change associated with anthropogenic emissions of greenhouse gases. In particular, ice coverage in West Antarctica, as well as in Greenland, reduced significantly and there is evidence to suggest a retreat of ice sheet in the coastal areas and in the Wilkes Subglacial Basin of East Antarctica during that time.

In this study, we use the mid-resolution MIROC4m coupled atmosphere-ocean general circulation model and apply ice sheet configuration, land-sea mask and biome distribution from PRISM3 data sets, as set forth in the latest, second phase of the Pliocene Model Intercomparison Project. We conduct a series of experiments, including those which look into a range of atmospheric carbon dioxide levels given the spread in values suggested by various sources of proxy data. We show the degree of warming over Antarctica and how the precipitation responds to changes in the moisture transport.

Keywords: Antarctica, Pliocene, modeling

©2019. Japan Geoscience Union. All Right Reserved.

CMIP5 model analysis of future changes in ocean net primary production by focusing on different response among the individual oceans and models

*Akira Oka[1], Yuki Nakamura[1]

1. Atmosphere and Ocean Research Institute, The University of Tokyo

Previous modeling studies show that global primary production will decrease in the future because stratification caused by global warming reduces supply of nutrient from the deep ocean. Previous studies mainly emphasized the importance of nutrient limitation in explaining the changes in primary production; however, phytoplankton growth is actually determined by temperature limitation, light limitation and nutrient limitation. Moreover, although future changes of primary production differ depending on areas, many prior researches discuss only global mean mechanisms and it is not well understood how the mechanisms differ depending on the individual oceans. The purpose of this study is to quantitatively evaluate contribution of each limitation factor for explaining the future changes in primary production in the individual oceans by using 9 CMIP5 models. First, we calculate temperature limitation, light limitation and nutrient limitation for each model, which are not directly available from CMIP5 output data. After that, we quantitatively evaluate main drivers for changes in primary production not only for the global ocean but also for low latitudes, the North Atlantic Ocean, the North Pacific Ocean, the Arctic Ocean and the Southern Ocean, separately. By quantitative evaluation on limitation factors of primary production, we show that the future changes in primary production due to global warming is controlled by not only nutrient limitation but also warming-induced enhancement of phytoplankton growth and decreasing biomass caused by enhanced grazing. Moreover, we show that future changes in primary production and its mechanisms differ among the individual oceans.

Keywords: Ocean primary production, Global warming, CMIP5 model

©2019. Japan Geoscience Union. All Right Reserved.

Factor analysis of the millennial time-scale climate variability in glacial periods

*Miki Akari[1], Ayako Abe-Ouchi[2], Sam Sherriff-Tadano[2]

1. Department of Earth and Planetary Science, Graduate School of Science, The University of Tokyo, 2. Atmosphere and Ocean Research Institute, the University of Tokyo

It is well known that in the glacial periods, air temperature changed abruptly over the North Atlantic on millennial time-scale. It is also known that temperature changes over the Southern Ocean were opposite to the North Atlantic, called a bipolar seesaw relationship. It is suggested that changes in the strength of the Atlantic Meridional Overturning Circulation (AMOC) were closely related to such global climate changes.

In recent years, the idea that freshwater forcing causes the climate changes has been questioned. Spontaneous oscillations in AMOC can be reproduced by experiments using atmosphere-ocean coupled general circulation models (AOGCM). These studies proposed that oceanic feedbacks within the North Atlantic surface - subsurface ocean are important in inducing the spontaneous AMOC variabilities. However, the oscillation cycles shown in previous studies (Peltier and Vettoretti, 2014; Brown and Galbraith, 2016) are several hundred years, which are shorter compared to climate variabilities documented in ice core data. On the other hand, in experiments carried out with MIROC4m AOGCM under the medium glacial condition, millennial time-scale climate and AMOC variabilities are reproduced. Therefore, in this study, we analyze factors controlling the millennial time-scale climate variability obtained from MIROC4m AOGCM. Focusing on the fact that this oscillation cycle is close to the time-scale of the Southern Ocean and the bottom ocean circulation, we analyze the behavior of the Southern Ocean and the bottom ocean in detail, especially deeper than 2500 meters, in addition to oceanic feedback suggested by previous studies.

As a result, it is suggested that the density change at the bottom ocean, which is caused by changes in sea ice formation over the Southern Ocean, plays an important role in controlling the oscillation of AMOC on millennial time-scale.

Keywords: AMOC, Glacial climate, AOGCM

©2019. Japan Geoscience Union. All Right Reserved.

First continuous profiler observation of wintertime Antarctic coastal polynya

*Shigeru Aoki[1], Kazuya Ono[1], Daisuke Hirano[1], Masato Itoh[1], Tomohide Noguchi[2], Satoshi Ozawa[2]

1. Hokkaido University, 2. Marine Works Japan

Antarctic coastal polynyas are the regions where sea ice forms vigorously, leading to supply of dense abyssal water for the global ocean. Monitoring the sea state of coastal polynyas especially in winter hence has global implications. To fully understand the development of water characteristics, capturing of the whole water column is required. However, the wintertime observations of seasonal ice zone such as polynya is not abundant so far, due to the severe and variable conditions of polar oceans.

To realize a near-realtime observation of water column in coastal polynya, we deployed a tethered profiling float over the whole winter in Cape Darnley polynya, East Antarctica (bottom depth of 230 m). The tethered float was manufactured by IHI Corporation, with a temperature and salinity sensor (SBE37 of Seabird Scientific) attached.

The float observation was successful in operation for more than eight months from Feb. 26 to Nov. 13, 2017. This float was designed to park at 150 dbar depth and to surface (upto 20 dbar when sea ice is supposed to exist) at 10-day interval. During this period, 26 profiles for the water column from 180 dbar to 20 dbar were obtained. The whole 160-dbar depth range was covered by nearly half of the 26 profiles, and the total ratio of depth coverage was 81%. Comparison with a current meter record nearby (one mile distance) revealed that the minimum depth achieved did not correlate with the current speed.

The obtained record clearly revealed a seasonal development of the whole water column. While relatively warm water initially remained in the water column, significant freshening occurred and temperature decreased to the freezing point throughout the column from March to April. Then salinity gradually increased to about 35 (150 dbar) in October, successfully covering the whole cycle of sea ice production. The layer near the parking depth (between 120 dbar and 180 dbar) was covered with much higher temporal resolution, showing variations of higher frequencies.

Although the satellite data transmission was not successful due to the battery shortage, signal transmission was successful at the preparation stage. A revision of this platform will enable the monitoring of seasonal ice zone in the polar oceans, to help filling the remaining gap of the global ocean monitoring array.

Keywords: Cape Darnley polynya, Tethered profiler, mooring, Antarctica

©2019. Japan Geoscience Union. All Right Reserved.

Surface topography survey for bared rock and accumulated snow in Antarctica by Unmanned Aero Vehicle

*Yuichi Aoyama[1,2,3], Akihisa Hattori[2,3], Hajime Oishi[3,4], Koichiro Doi[1,2,3], Yoshifumi Nogi[1,2]

1. National Institute of Polar Research, 2. SOKENDAI, 3. The 59th Japanese Antarctic Research Expedition, 4. NEC Networks & System Integration Corporation

In the last decade, Gravity Recovery and Climate Experiment (GRACE) mission demonstrated an increase of surface mass in the Dronning Maud Land (DML), East Antarctica. Actually, snow accumulation has increased at Syowa Station located in DML, and its effect has been detected by superconducting gravimeter and GNSS measurements. For quantifying this effect, it is necessary to measure the distribution of the snow accumulation.
The distribution of the snow accumulation can be estimated from difference in accurate digital surface models (DSM) between the bared rock and the accumulated snow. These DSMs are derived from aerial photography byunmanned aerial vehicle (UAV) with structure from motion (SfM) analysis. In the activity of the 59th Japanese Antarctic Research Expedition (JARE59) during Dec. 2017 - Dec. 2018, some aerial photography surveys were conducted with the fixed-wing small UAV, senseFly eBee plus, and with the rotary-wing drone, DJI Inspire 2 over Syowa Station. There is a report that the eBee plus, having dual-frequency GNSS receiver, enables to generate DSM precisely without ground control point (GCP). We evaluated the accuracy of such DSM by comparing with DSM computed with GCP. We also compared with the DSM computed from aerial photography by Inspire 2 which has single-frequency GNSS for evaluating the advantage of the dual-frequency GNSS tracking. The DSMs in Langhovde, Akarui Misaki, Rundvagshetta located around Lutzow-Holmbukta are also computed from aerial photography by eBee plus.

Keywords: Unmanned aerial vehicle, Challenges for unexplored frontiers

©2019. Japan Geoscience Union. All Right Reserved.

The analysis of long-term Mooring observation records in the northernmost area of seasonal sea ice zone in the Southern Ocean

*Kazuho Watanabe[1], Kohei Mizobata[1], Yujiro Kitade[1]

1. Tokyo University of Marine Science and Technology

The meridional overturning is thought to be the contributor for the stability of the climate system via latitudinal exchange of oceanic heat in the Southern Ocean. To clarify details of the meridional overturning, mooring observations using T/RV *Umitaka-maru* were conducted by physical oceanography group mainly constructed by Tokyo University of Marine science and Technology. In this study, we analyzed the one-year record of the mooring observation and CTD measurements obtained when the mooring system was deployed and recovered.

Results from current meter analysis shows the variability (from 30-day to 90-day cycle) of ocean current. Geostrophic velocity derived from sea level anomaly map distributed by AVISO/Altimetry also shows similar variability of ocean current due to eddies. Furthermore, the location of the mooring system was far from the main axis of the Antarctic Circumpolar Current (ACC). Those results suggest us that the variability of ocean current was resulted from the mesoscale eddy field.

Even though the variability of ocean current was recoded, results also indicate the meridional overturning. The progressive vector diagram based on current meter record illustrated poleward transport at about around 400db and eastward transport at about 4000db. One-year mooring observation also revealed ocean current shear structure (about 10cm/s at about 400db and 4cm/s at about 4000db) when poleward transport was continuously captured. During poleward transport with shear structure was captured, the increase in temperature over 2.1 $^{\circ}$C from October to February at about 400db was frequently observed. Based on hydrographic data, warm water captured around 400db was identified as the Circumpolar Deep Water (CDW). Cross correlation analysis revealed that warm CDW intrusion occurred about 8-day following southward current at 400db. During the season when sea ice covered the ocean, similar event also happened but temperature at about 400db increased up to around 2°C. Our results indicate that CDW’ s southward transport is changing by seasonal and the event of mesoscale eddy passage.

Keywords: Southern ocean, Meridional circulation, Mooring observation, Mesoscale-Eddy

©2019. Japan Geoscience Union. All Right Reserved.

Preliminary observation report on chlorofluorocarbons (CFCs) and sulfur hexafluoride (SF_6) off the Cape Darnley in the summer of 2019

*Yoshihiko Ohashi[1], Michiyo Yamamoto-Kawai[1], Kenichi Sasaki[2], Sayaka Kumakawa[1], Naoyuki Tamura[1], Kay I. Ohshima[3]

1. Tokyo University of Marine Science and Technology, 2. Japan Agency for Marine-Earth Science and Technology, 3. Institute of Low Temperature Science, Hokkaido University

Antarctic Bottom Water (AABW) occupies the largest volume of water mass in the global ocean and its formation is a key process of global ocean circulation. Ohshima et al. (2013) found newly formed AABW off the Cape Darnley (Cape Darnley Bottom Water; CDBW). However, little is known about the circulation of CDBW and its time scale. To quantitatively understand the spread and circulation of CDBW, it is effective to use the chemical tracer such as chlorofluorocarbons (CFCs) and sulfur hexafluoride (SF_6). We carried out CTD observation and water sampling off the Cape Darnley in the summer of 2019. Water sampling was performed from ocean surface to the bottom at 16 Stations (along the Wild Canyon and its west). CFCs and SF_6 of the samples were measured by an analytical system developed at JAMSTEC based on Bullister and Wisegarver (2008). The concentrations of CFCs and SF_6 were significantly high near the surface (< 100 m) (CFC11 > 2.0 pmol kg^{-1}; CFC12 > 1.2 pmol kg^{-1}; SF_6 > 1.4 fmol kg^{-1}). They showed a minimum at depths of 800–1500 m and then increased to the bottom. The relatively high concentrations of CFCs and SF_6 near the bottom, together with the low temperature (< −0.4°C), reflects the spread of CDBW. At the presentation, we will discuss mean age and circulation of CDBW.

Keywords: Antarctic Bottom Water , Cape Darnley, Chemical tracer

©2019. Japan Geoscience Union. All Right Reserved.

Mechanism of sea-ice production variation in Amundsen Sea Polynya

*Sohey Nihashi[1], Kouta Mine[1], Kazuki Nakata[2]

1. National Institute of Technology, Tomakomai College, 2. RESTEC

A coastal polynya is an area of high ice production and dense water formation. This dense water is a major source of the Antarctic Bottom Water. Since winter polynya is a difficult site to observe, the mechanism of polynya formation and variation had not been understood well. About ten years ago, an algorithm was developed that uses satellite passive microwave data to detect polynyas and estimates thin ice thickness on a daily timescale. The satellite data revealed the detailed distribution and variation of polynyas (e.g., Tamura et al., 2007; 2008). Use of AMSR-E/AMSR2 data with a finer spatial resolution (about 5-6 km), can reveal the more detailed spatial distribution of polynyas. For example, it was revealed that most of coastal polynyas form on the west side of landfast ice (fast ice: stationary sea ice attached to coastal features such as shoreline and grounded icebergs). This close relationship indicates a vital role of fast ice for formation and variation of coastal polynyas (Nihashi and Ohshima, 2015; Nihashi et al., 2017). The Amundsen Sea Polynya (ASP), located in West Antarctica, is the third largest ice production area and is formed on the west side of fast ice protruding into the ocean. Thwaites Glacier adjacent to the fast ice has been suggested that a rapid melting occurs in recent decades (Rignot et al., 2008; Milio et al., 2019). Grounded icebergs that act as anchor points play an essential role in the formation of fast ice protruding into the ocean. Since the sources of an iceberg are glacier and ice sheet, the rapid melting possibly affects the formation and distribution of fast ice and accordingly adjacent polynyas.

In this study, we compare the ice production in the ASP with atmospheric parameters and fast ice extent to investigate factors for causing ice production variation. Ice production estimated from heat flux calculation with daily thin ice thickness from AMSR-E/AMSR2 data (Nihashi and Ohshima, 2015; Nihashi et al., 2017) is used. For fast ice, monthly extent detected from AMSR-E/AMSR2 data is used. We also use ice production estimated using thin ice thickness by an improved algorithm in which ice types (active frazil and thin solid ice) are considered (Nakata et al., 2019). As atmospheric data, we use ERA5.

Ice production is positively correlated with wind speed regardless of daily or monthly data with the coefficient of 0.54-0.73. Here, we use a wind component with the highest correlation; components of the wind vector are projected in all directions of every 1˚ from 0˚ (northerly wind) clockwise to 360˚, and then, correlation coefficients are calculated. The wind component is oriented to the west rather than to the offshore (north) against the land. This is a direction towards the offshore against the shoreline defined by both the land and fast ice. This result supports the analysis using only AMSR-E data (Nihashi and Ohshima, 2015). If ice production in which thin ice types are considered is used, the wind component is oriented toward further west when active frazil is dominant. This direction is to the offshore against the fast ice. Further, active frazil tends to form along fast ice. On the other hand, the wind component is northward (to the offshore against land) when thin solid ice is dominant. Multiple regression analysis is performed on the ice production using air temperature, wind speed, and fast ice extent averaged over the freezing season (May-August). Ice production can be explained by these parameters with R=0.77. This indicates that ice production in the ASP before the satellite observation era can be reproduced to some extent from atmospheric data by using this regression line. The results presented in this study suggest that fast ice plays a vital role in the formation and variation of the ASP. Continuous monitoring of Antarctic coastal polynyas and fast ice from passive microwave satellite sensor is quite meaningful understanding climate change.

©2019. Japan Geoscience Union. All Right Reserved.

Keywords: Antarctic Ocean, coastal polynya, Amundsen Sea Polynya

©2019. Japan Geoscience Union. All Right Reserved.

Estimation of thin ice thickness and discrimination of ice type from AMSR2 passive microwave data

*Kazuki Nakata[1], Tamaru Naoya[1], Sohey Nihashi[2], Kay I. Ohshima[3]

1. Remote Sensing Technology Center of Japan, 2. National Institute of Technology, Tomakomai College, 3. Institute of Low Temperature Science, Hokkaido University

Antarctic coastal polynyas (thin ice and/or low ice concentration area) are areas of high ice production due to huge heat loss to the atmosphere. Dense water formed by the high ice production is a significant source of Antarctic Bottom Water. Thin ice thickness algorithms that use satellite passive microwave data have been developed to detect coastal polynyas and estimates thin ice thickness on a daily timescale. In these algorithms, ice thickness of <20 cm is empirically estimated based on a negative correlation relationship between polarization ratio (PR) of brightness temperatures (TBs) and ice thickness (hi). However, the dispersion of the data points of PR-hi relationship was relatively large. Nakata et al. (2019) revealed that two thin ice types (active frazil and thin solid ice) cause this dispersion using AMSR-E data (2002-2011). They detected these ice types based on a PR-GR (Gradient Ratio) relationship. And thin ice thickness was estimated from PR-hi relationships for each ice type. This new thin ice algorithm can improve the accuracy of the thin-ice thickness estimation. In this study, we have examined whether this new algorithm can apply to data from AMSR2 which the successor of AMSR-E. The footprint size of AMSR2 is improved by about 85% from AMSR-E in spite of the frequency channels are the same. By adding AMSR2 data, thin-ice thickness, ice type, and ice production data set with a higher spatial resolution can be obtained from 2002 to the present.
We use TBs at 36 and 89 GHz from AMSR2 Level 1B data. The footprint sizes are 12 km ×7 km and 5 km × 3 km, respectively. Ice thickness for comparison with AMSR2 PR is derived from clear-sky thermal infrared images by MODIS with a spatial resolution of 1 km. Backscatter images acquired by C-band SAR (C-SAR) on the ESA’s Sentinel-1 satellite with a spatial resolution of 90 m are used to validate two thin ice types. We use these satellite data obtained at Ross Ice Shelf and Cape Darnley polynya areas.
AMSR2 PR-hi relationships for two ice types differs clearly as in Nakata et al. (2019). We estimate ice thickness using lines that best fit into the AMSR-E PR-hi relationships (Nakata et al., 2019) using AMSR2 data. And then, mean bias and root-mean-square error (RMSE) of the data points from the lines are calculated. The errors are slightly larger than the cases of AMSR-E data. When ice thickness is <10 cm, mean bias and RMSE for active frazil are -2.0 and 1.0 cm, respectively, while those for thin solid ice are -6.2 and 9.8 cm, respectively. For ice thickness of 10-20 cm (only for thin solid ice), the bias and RMSE are -5.9 and 9.9 cm, respectively. We also have confirmed that two ice types can be detected using AMSR2 data by a method for AMSR-E data proposed by Nakata et al. (2019). The results of this study indicate that the new thin ice algorithm for AMSR-E data can apply to the AMSR2 data.

Keywords: Thin ice thickness, Ice type, AMSR2, Coastal polynya

©2019. Japan Geoscience Union. All Right Reserved.

[J] Poster | M (Multidisciplinary and Interdisciplinary)：M-IS Intersection

Mon. May 27, 2019 1:45 PM - 3:15 PM JST | Mon. May 27, 2019 4:45 AM - 6:15 AM UTC | Poster Hall International Exhibition Hall8, Makuhari Messe_8

[M-IS15] Evolution of Pelagic Realm

convener:Atsushi Matsuoka(Department of Geology, Faculty of Science, Niigata University), Katsunori Kimoto(Japan Agency for Marine-Earth Science and Technology), Toshiyuki Kurihara(Graduate School of Science and Technology, Niigata University), Tetsuji Onoue(Earth and Environmental Sciences, Graduate School of Science and Technology, Kumamoto University)

This session focuses on the evolution of ecosystem in the pelagic realms,
including discussions on all aspects of pelagic biota covering biostratigraphy,
biochronology, evolution, and biogeography, which are important to the
reconstruction of the spatio-temporal framework in the pelagic realm.
Reconstructions of plate configuration through time are included in the scope of
 this session. Biological, geochemical, sedimentological approaches to the
pelagic environments are welcomed.

[MIS15-P01] Ichthyolith stratigraphy constraints on ages and areas of REY-rich mud deposition in the South Pacific Ocean

*Shugo Minabe[1], Kazuhide Mimura[1], Kentaro Nakamura[1], Junichiro Ohta[2,1], Kazutaka Yasukawa[1,2], Koichiro Fujinaga[2,1], Shiki Machida[2], Yasuhiro Kato[3,1,2] (1.Department of Systems Innovation, School of Engineering, The University of Tokyo, 2.Ocean Resource Research Center for Next Generation, Chiba Institute of Technology, 3.Frontier Research Center for Energy and Resources, School of Engineering, The University of Tokyo)

[MIS15-P02] Radiolarian phylogeny around the Jurassic–Cretaceous boundary

*Atsushi Matsuoka[1] (1.Department of Geology, Faculty of Science, Niigata University)

[MIS15-P03] Late Silurian and Early Devonian radiolarian assemblages from the Yokokurayama and Konomori areas in the Kurosegawa belt, Southwest Japan

*Toshiyuki Kurihara[1], Kaori Tsuchiya[2] (1.Graduate School of Science and Technology, Niigata University, 2.Faculty of Science, Niigata University)

Ichthyolith stratigraphy constraints on ages and areas of REY-rich mud deposition in the South Pacific Ocean

*Shugo Minabe[1], Kazuhide Mimura[1], Kentaro Nakamura[1], Junichiro Ohta[2,1], Kazutaka Yasukawa[1,2], Koichiro Fujinaga[2,1], Shiki Machida[2], Yasuhiro Kato[3,1,2]

1. Department of Systems Innovation, School of Engineering, The University of Tokyo, 2. Ocean Resource Research Center for Next Generation, Chiba Institute of Technology, 3. Frontier Research Center for Energy and Resources, School of Engineering, The University of Tokyo

REY-rich mud, a type of deep-sea sediment containing high concentrations of rare-earth elements and yittrium (REY), is widely distributed in the North and South Pacific Oceans [1]. It is expected to be a new resource of the critical elements that are essential for multiple high-tech devices and environment-friendly technologies. Recently, high-grade REY-rich mud layers have been discovered in the western North Pacific Ocean [2], whereas the formation process of the layers is still unclear.

Clarifying the depositional ages and areas of the high-grade REY-rich mud layers is the key to understanding their formation process. Regarding the North Pacific Ocean, the ages and areas of deposition of the high-grade REY-rich mud layers have been constrained recently [3,4]. In contrast, the ages and areas of deposition of the high-grade REY-rich mud in the South Pacific Ocean have been poorly understood, although high-grade REY-rich mud layers comparable to that in the North Pacific Ocean have been recognized [5,6].

In this study, based on the ichthyolith stratigraphy, we constrained the depositional age of high-grade REY-rich mud layers at the IODP Sites U1366 and U1370 that were drilled in the South Pacific Gyre [7]. Ichthyolith is a type of microfossil of fish teeth and denticles, which remains well even in deep-sea sediments beneath the carbonate compensation depth (CCD). Therefore, it has been used for age determination of pelagic clay with a paucity of typical age-diagnostic microfossils such as foraminifera or radiolaria [8]. We determined the depositional age of the high-grade REY-rich mud layers based on identification of more than 700 ichthyoliths contained in the sediments at Sites U1366 and U1370 and collation of them with the already known taxa associated with the ages. Based on the age data, we also located the depositional area of the layers by backtracking of plate motion. Consequently, we revealed that the depositional area of REY-rich mud during the Paleogene was significantly extended to the south of the present one. Moreover, based on the constrained depositional age, we suggest that the period of high-grade REY-rich mud deposition in the South Pacific Ocean likely continued for up to 50 million years, which is much longer than that in the North Pacific Ocean.

References

[1] Kato, Y. et al. (2011) *Nature Geoscience* **4**, 535-539.
[2] Iijima, K. et al. (2016) *Geochemical Journal* **50**, 557-573.
[3] Mimura, K. et al. (2018) *JpGU Meeting 2018*
[4] Yamamoto, K. et al. (2018) *JpGU Meeting 2018*.
[5] Nakamura, K. et al. (2017) *JpGU Meeting 2017*.
[6] Yasukawa, K. et al. (2016) *Scientific Reports* **6**, 29603.
[7] D' Hondt et al. (2011) *Proceedings of IODP Expedition 329*.

©2019. Japan Geoscience Union. All Right Reserved.

[8] Doyle, P. S., and Riedel, W. R., (1979) *Scripps institution of Oceanography*, University of California, San Diego, 1-231.

Keywords: REY-rich mud, ichthyolith, depositional age, depositional area, South Pacific Ocean

©2019. Japan Geoscience Union. All Right Reserved.

Radiolarian phylogeny around the Jurassic–Cretaceous boundary

*Atsushi Matsuoka[1]

1. Department of Geology, Faculty of Science, Niigata University

The Global Boundary Stratotype Section and Point (GSSP) of the Jurassic–Cretaceous boundary (JKB) is the last among the GSSPs in the Phanerozoic. It is defined as the base of the Berriasian Stage. Radiolarians are good candidates for defining the JKB because they are wide spread and can be found both pelagic and neritic marine environments. Pelagic sequences across the JKB have been reported in ODP/IODP sites in the western Pacific and land sections in Japan, the Philippines, southern Tibet, Iran and others. Evolutionary lineages of several radiolarian taxa across the JKB are reviewed and suitable bioevents, which are approximate to the JKB, are presented. These lineages include the radiolarian genera: *Alievium, Archaeodictyomitra, Cinguloturris, Complexapora, Crococapsa, Doliocapsa, Emiluvia, Eucyrtidiellum, Hemicryptocapsa, Hsuum, Loopus, Mirifusus, Mesovallupus, Neorelumbra, Pantanellium, Protovallupus, Protunuma, Pseudodictyomitra, Ristola, Spinosicapsa, Tethysetta, Thanarla, Vallupus, Xitus,* and *Zhamoidellum*. Among them the *Loopus–Pseudodictyomitra* lineage, the *Protovallupus –Mesovallupus–Vallupus* lineage, and *Complexapora* lineage are important phylogeny for defining the JKB.

Keywords: Jurassic–Cretaceous boundary , radiolarians, phylogeny

©2019. Japan Geoscience Union. All Right Reserved.

Late Silurian and Early Devonian radiolarian assemblages from the Yokokurayama and Konomori areas in the Kurosegawa belt, Southwest Japan

*Toshiyuki Kurihara[1], Kaori Tsuchiya[2]

1. Graduate School of Science and Technology, Niigata University, 2. Faculty of Science, Niigata University

The radiolarian biozonations for the Upper Silurian to Lower Devonian in the Kurosegawa belt, Southwest Japan, were developed by Furutani (1983), Wakamatsu et al. (1990), Aitchison et al. (1996), and Umeda (1998b), based mainly upon the studies of tuffaceous clastic strata in the Yokokurayama and Konomori areas. However, the availability of only sparse data of latest Silurian to Early Devonian radiolarians in the 1990s has hampered age assignments of the radiolarian assemblages. In addition, since most information on radiolarians from this belt has come from spot localities with poor chronostratigraphic control, little is known about faunal transition during this time period.

We recognized three radiolarian assemblages (YK-1 to 3) from fine-grained portion of an alternating tuffaceous sandstone and mudstone sequence of the Nakahata Formation (Umeda, 1998a) in the Yokokurayama area. YK-1 is characterized by diverse species of inaniguttids with a large spherical outer cortical shell (200 to 300 μm), including *Oriundogutta* (?) *kingi*, *Zadrappolus yoshikiensis*, and *Fusalfanus* (?) sp. YK-2 contains *Praespongocoelia* (?) sp. and *Futobari* (?) spp., which are somewhat similar to *Futobari solidus* in their external appearances (but they differ from *F. solidus* in the cortical shell structure and spine morphology). YK-3 is characterized by the occurrences of some inaniguttids, small spherical radiolarians with short bladed spines, and *Deflantrica solidum*. Four radiolarian assemblages (KN-1 to 4) from felsic tuff and fine-grained portion of an alternating tuffaceous sandstone and mudstone in the Konomori area. KN-1 characteristically contains *Pseudospongoprunum sagittatum*. The species compositions of KN-2 and 4 are very similar to those of YK-2 and 3, respectively, and therefore they can be correlated each other. KN-3 is characterized by *Praespongocoelia robusta* and small spherical radiolarians.

The age of KN-1 is Late Silurian based on the occurrence of *P. sagittatum* (Noble, 1994; Umeda, 1998b). Considering the species composition of YK-1, characterized by large inaniguttids, this assemblage is also Late Silurian in age. In the previous study (Umeda, 1998b), the stratigraphic interval yielding YK-2 and 3, and KN-2 to 4 was subdivided into *Futobari solidus* and *Trilonche* (?) sp. A zones; however, YK-2, KN-2, and KN-3 contain no *F. solidus*. Recently, Late Silurian (Ludlovian) chitinozoans have been reported from the type locality of *F. solidus* (Ichinotani of the Yoshiki Formation in the Hida Gaien belt: Vandenbroucke et al., 2019). Therefore, the age of these assemblages is Ludlovian or younger. The palaeoscenidiid-dominated fauna (YK-3 and KN-4) is Early Devonian in age, based on the correlation with a similar fauna of the Hida Gaien belt (Sato and Kurihara, 2018 JpGU). The result of the present study suggests that a gradual faunal change from an inaniguttid-dominated fauna to a palaeoscenidiid-dominated fauna took place some time in latest Silurian to early Devonian.

©2019. Japan Geoscience Union. All Right Reserved.

[J] Poster | M (Multidisciplinary and Interdisciplinary)：M-IS Intersection

Mon. May 27, 2019 5:15 PM - 6:30 PM JST | Mon. May 27, 2019 8:15 AM - 9:30 AM UTC | Poster Hall International Exhibition Hall8, Makuhari Messe_36

[M-IS15] Evolution of Pelagic Realm

convener:Atsushi Matsuoka(Department of Geology, Faculty of Science, Niigata University), Katsunori Kimoto(Japan Agency for Marine-Earth Science and Technology), Toshiyuki Kurihara(Graduate School of Science and Technology, Niigata University), Tetsuji Onoue(Earth and Environmental Sciences, Graduate School of Science and Technology, Kumamoto University)

This session focuses on the evolution of ecosystem in the pelagic realms,
including discussions on all aspects of pelagic biota covering biostratigraphy,
biochronology, evolution, and biogeography, which are important to the
reconstruction of the spatio-temporal framework in the pelagic realm.
Reconstructions of plate configuration through time are included in the scope of
 this session. Biological, geochemical, sedimentological approaches to the
pelagic environments are welcomed.

[MIS15-P01] Ichthyolith stratigraphy constraints on ages and areas of REY-rich mud deposition in the South Pacific Ocean

*Shugo Minabe[1], Kazuhide Mimura[1], Kentaro Nakamura[1], Junichiro Ohta[2,1], Kazutaka Yasukawa[1,2], Koichiro Fujinaga[2,1], Shiki Machida[2], Yasuhiro Kato[3,1,2] (1.Department of Systems Innovation, School of Engineering, The University of Tokyo, 2.Ocean Resource Research Center for Next Generation, Chiba Institute of Technology, 3.Frontier Research Center for Energy and Resources, School of Engineering, The University of Tokyo)

[MIS15-P02] Radiolarian phylogeny around the Jurassic–Cretaceous boundary

*Atsushi Matsuoka[1] (1.Department of Geology, Faculty of Science, Niigata University)

[MIS15-P03] Late Silurian and Early Devonian radiolarian assemblages from the Yokokurayama and Konomori areas in the Kurosegawa belt, Southwest Japan

*Toshiyuki Kurihara[1], Kaori Tsuchiya[2] (1.Graduate School of Science and Technology, Niigata University, 2.Faculty of Science, Niigata University)

Ichthyolith stratigraphy constraints on ages and areas of REY-rich mud deposition in the South Pacific Ocean

*Shugo Minabe[1], Kazuhide Mimura[1], Kentaro Nakamura[1], Junichiro Ohta[2,1], Kazutaka Yasukawa[1,2], Koichiro Fujinaga[2,1], Shiki Machida[2], Yasuhiro Kato[3,1,2]

1. Department of Systems Innovation, School of Engineering, The University of Tokyo, 2. Ocean Resource Research Center for Next Generation, Chiba Institute of Technology, 3. Frontier Research Center for Energy and Resources, School of Engineering, The University of Tokyo

REY-rich mud, a type of deep-sea sediment containing high concentrations of rare-earth elements and yittrium (REY), is widely distributed in the North and South Pacific Oceans [1]. It is expected to be a new resource of the critical elements that are essential for multiple high-tech devices and environment-friendly technologies. Recently, high-grade REY-rich mud layers have been discovered in the western North Pacific Ocean [2], whereas the formation process of the layers is still unclear.

Clarifying the depositional ages and areas of the high-grade REY-rich mud layers is the key to understanding their formation process. Regarding the North Pacific Ocean, the ages and areas of deposition of the high-grade REY-rich mud layers have been constrained recently [3,4]. In contrast, the ages and areas of deposition of the high-grade REY-rich mud in the South Pacific Ocean have been poorly understood, although high-grade REY-rich mud layers comparable to that in the North Pacific Ocean have been recognized [5,6].

In this study, based on the ichthyolith stratigraphy, we constrained the depositional age of high-grade REY-rich mud layers at the IODP Sites U1366 and U1370 that were drilled in the South Pacific Gyre [7]. Ichthyolith is a type of microfossil of fish teeth and denticles, which remains well even in deep-sea sediments beneath the carbonate compensation depth (CCD). Therefore, it has been used for age determination of pelagic clay with a paucity of typical age-diagnostic microfossils such as foraminifera or radiolaria [8]. We determined the depositional age of the high-grade REY-rich mud layers based on identification of more than 700 ichthyoliths contained in the sediments at Sites U1366 and U1370 and collation of them with the already known taxa associated with the ages. Based on the age data, we also located the depositional area of the layers by backtracking of plate motion. Consequently, we revealed that the depositional area of REY-rich mud during the Paleogene was significantly extended to the south of the present one. Moreover, based on the constrained depositional age, we suggest that the period of high-grade REY-rich mud deposition in the South Pacific Ocean likely continued for up to 50 million years, which is much longer than that in the North Pacific Ocean.

References

[1] Kato, Y. et al. (2011) *Nature Geoscience* **4**, 535-539.
[2] Iijima, K. et al. (2016) *Geochemical Journal* **50**, 557-573.
[3] Mimura, K. et al. (2018) *JpGU Meeting 2018*
[4] Yamamoto, K. et al. (2018) *JpGU Meeting 2018*.
[5] Nakamura, K. et al. (2017) *JpGU Meeting 2017*.
[6] Yasukawa, K. et al. (2016) *Scientific Reports* **6**, 29603.
[7] D' Hondt et al. (2011) *Proceedings of IODP Expedition 329*.

©2019. Japan Geoscience Union. All Right Reserved.

[8] Doyle, P. S., and Riedel, W. R., (1979) *Scripps institution of Oceanography*, University of California, San Diego, 1-231.

Keywords: REY-rich mud, ichthyolith, depositional age, depositional area, South Pacific Ocean

©2019. Japan Geoscience Union. All Right Reserved.

Radiolarian phylogeny around the Jurassic–Cretaceous boundary

*Atsushi Matsuoka[1]

1. Department of Geology, Faculty of Science, Niigata University

The Global Boundary Stratotype Section and Point (GSSP) of the Jurassic–Cretaceous boundary (JKB) is the last among the GSSPs in the Phanerozoic. It is defined as the base of the Berriasian Stage. Radiolarians are good candidates for defining the JKB because they are wide spread and can be found both pelagic and neritic marine environments. Pelagic sequences across the JKB have been reported in ODP/IODP sites in the western Pacific and land sections in Japan, the Philippines, southern Tibet, Iran and others. Evolutionary lineages of several radiolarian taxa across the JKB are reviewed and suitable bioevents, which are approximate to the JKB, are presented. These lineages include the radiolarian genera: *Alievium, Archaeodictyomitra, Cinguloturris, Complexapora, Crococapsa, Doliocapsa, Emiluvia, Eucyrtidiellum, Hemicryptocapsa, Hsuum, Loopus, Mirifusus, Mesovallupus, Neorelumbra, Pantanellium, Protovallupus, Protunuma, Pseudodictyomitra, Ristola, Spinosicapsa, Tethysetta, Thanarla, Vallupus, Xitus,* and *Zhamoidellum*. Among them the *Loopus–Pseudodictyomitra* lineage, the *Protovallupus –Mesovallupus–Vallupus* lineage, and *Complexapora* lineage are important phylogeny for defining the JKB.

Keywords: Jurassic–Cretaceous boundary , radiolarians, phylogeny

©2019. Japan Geoscience Union. All Right Reserved.

Late Silurian and Early Devonian radiolarian assemblages from the Yokokurayama and Konomori areas in the Kurosegawa belt, Southwest Japan

*Toshiyuki Kurihara[1], Kaori Tsuchiya[2]

1. Graduate School of Science and Technology, Niigata University, 2. Faculty of Science, Niigata University

The radiolarian biozonations for the Upper Silurian to Lower Devonian in the Kurosegawa belt, Southwest Japan, were developed by Furutani (1983), Wakamatsu et al. (1990), Aitchison et al. (1996), and Umeda (1998b), based mainly upon the studies of tuffaceous clastic strata in the Yokokurayama and Konomori areas. However, the availability of only sparse data of latest Silurian to Early Devonian radiolarians in the 1990s has hampered age assignments of the radiolarian assemblages. In addition, since most information on radiolarians from this belt has come from spot localities with poor chronostratigraphic control, little is known about faunal transition during this time period.

We recognized three radiolarian assemblages (YK-1 to 3) from fine-grained portion of an alternating tuffaceous sandstone and mudstone sequence of the Nakahata Formation (Umeda, 1998a) in the Yokokurayama area. YK-1 is characterized by diverse species of inaniguttids with a large spherical outer cortical shell (200 to 300 μm), including *Oriundogutta* (?) *kingi*, *Zadrappolus yoshikiensis*, and *Fusalfanus* (?) sp. YK-2 contains *Praespongocoelia* (?) sp. and *Futobari* (?) spp., which are somewhat similar to *Futobari solidus* in their external appearances (but they differ from *F. solidus* in the cortical shell structure and spine morphology). YK-3 is characterized by the occurrences of some inaniguttids, small spherical radiolarians with short bladed spines, and *Deflantrica solidum*. Four radiolarian assemblages (KN-1 to 4) from felsic tuff and fine-grained portion of an alternating tuffaceous sandstone and mudstone in the Konomori area. KN-1 characteristically contains *Pseudospongoprunum sagittatum*. The species compositions of KN-2 and 4 are very similar to those of YK-2 and 3, respectively, and therefore they can be correlated each other. KN-3 is characterized by *Praespongocoelia robusta* and small spherical radiolarians.

The age of KN-1 is Late Silurian based on the occurrence of *P. sagittatum* (Noble, 1994; Umeda, 1998b). Considering the species composition of YK-1, characterized by large inaniguttids, this assemblage is also Late Silurian in age. In the previous study (Umeda, 1998b), the stratigraphic interval yielding YK-2 and 3, and KN-2 to 4 was subdivided into *Futobari solidus* and *Trilonche* (?) sp. A zones; however, YK-2, KN-2, and KN-3 contain no *F. solidus*. Recently, Late Silurian (Ludlovian) chitinozoans have been reported from the type locality of *F. solidus* (Ichinotani of the Yoshiki Formation in the Hida Gaien belt: Vandenbroucke et al., 2019). Therefore, the age of these assemblages is Ludlovian or younger. The palaeoscenidiid-dominated fauna (YK-3 and KN-4) is Early Devonian in age, based on the correlation with a similar fauna of the Hida Gaien belt (Sato and Kurihara, 2018 JpGU). The result of the present study suggests that a gradual faunal change from an inaniguttid-dominated fauna to a palaeoscenidiid-dominated fauna took place some time in latest Silurian to early Devonian.

©2019. Japan Geoscience Union. All Right Reserved.

[J] Oral | M (Multidisciplinary and Interdisciplinary)：M-IS Intersection

Mon. May 27, 2019 3:30 PM - 5:00 PM JST | Mon. May 27, 2019 6:30 AM - 8:00 AM UTC | 302 3F

[M-IS15] Evolution of Pelagic Realm

convener:Atsushi Matsuoka(Department of Geology, Faculty of Science, Niigata University), Katsunori Kimoto(Japan Agency for Marine-Earth Science and Technology), Toshiyuki Kurihara(Graduate School of Science and Technology, Niigata University), Tetsuji Onoue(Earth and Environmental Sciences, Graduate School of Science and Technology, Kumamoto University), Chairperson:Atsushi Matsuoka, Toshiyuki Kurihara

This session focuses on the evolution of ecosystem in the pelagic realms,
including discussions on all aspects of pelagic biota covering biostratigraphy,
biochronology, evolution, and biogeography, which are important to the
reconstruction of the spatio-temporal framework in the pelagic realm.
Reconstructions of plate configuration through time are included in the scope of
 this session. Biological, geochemical, sedimentological approaches to the
pelagic environments are welcomed.

3:30 PM - 3:45 PM JST | 6:30 AM - 6:45 AM UTC

[MIS15-01] Environmental changes of the North Pacific Ocean through the Cenozoic era recorded in DSDP/ODP pelagic clay cores

*Kazuhide Mimura[1], Katsushi Yamamoto[1], Kentaro Nakamura[1], Kazutaka Yasukawa[1,2], Junichiro Ohta[2], Koichiro Fujinaga[2,1], Shiki Machida[2], Yoichi Usui[3], Yasuhiro Kato[1,2] (1.Department of Systems Innovation, School of Engineering, the University of Tokyo, 2.ORCeNG, Chiba Institute of Technology, 3.JAMSTEC)

3:45 PM - 4:00 PM JST | 6:45 AM - 7:00 AM UTC

[MIS15-02] Reconstruction of oceanic redox conditions in the Lower Jurassic (Pliensbachian–Toarcian) pelagic deep-sea bedded chert sequence of the Mino Belt, central Japan

*Katsuhito Soda[1] (1.Department of Earth and Environmental Sciences, Faculty of Science, Kumamoto University)

4:00 PM - 4:15 PM JST | 7:00 AM - 7:15 AM UTC

[MIS15-03] Conodont biostratigraphy of Anisian pelagic deep-sea sedimentary rocks deposited in the pelagic Panthalassa—Integration with radiolarian biozones—

*Shun Muto[1], Satoshi Takahashi[1], Satoshi Yamakita[2], Katsuhito Soda[3], Tetsuji Onoue[3] (1.Department of Earth and Planetary Science, Graduate School of Science, University of Tokyo, 2.Faculty of Education, University of Miyazaki, 3.Faculty of Advanced Science and Technology)

4:15 PM - 4:30 PM JST | 7:15 AM - 7:30 AM UTC

[MIS15-04] Triassic marine Os isotope record reconstructed from a pelagic chert succession, Sakahogi section, Mino Belt, southwest Japan

★Invited Papers

*Tatsuo Nozaki[1,2,3,4], Takashi Nikaido[5], Tetsuji Onoue[6], Yutaro Takaya[7,1,2,4], Keiko Sato[1], Jun-Ichi Kimura[8], Qing Chang[8], Daisuke Yamashita[6], Honami Sato[4,1], Katsuhiko Suzuki[1], Yasuhiro Kato[2,4], Atsushi Matsuoka[5] (1.JAMSTEC/R&D CSR, 2.Univ. of Tokyo, 3.Kobe Univ., 4.ChibaTech, 5.Niigata Univ., 6.Kumamoto Univ., 7.Waseda Univ., 8.JAMSTEC/D-SEG)

4:30 PM - 4:45 PM JST | 7:30 AM - 7:45 AM UTC

[MIS15-05] The preservation of radiolarians across the Jurassic-Cretaceous (J/K) boundary in the Bosso Valley section, Central Italy

*XIN LI[1], Atsushi Matsuoka[2], Angela Bertinelli[3], Marco Chiari[4] (1.State Key Laboratory of Palaeobiology and Stratigraphy, Nanjing Institute of Geology and Palaeontology, Chinese Academy of Sciences, 2.Niigata University, 3.Università degli Studi di Perugia, 4. Istituto di Geoscienze e Georisorse)

4:45 PM - 5:00 PM JST | 7:45 AM - 8:00 AM UTC

[MIS15-06] Radiolarian faunas around the Jurassic-Cretaceous boundary in the Bosso Valley section, central Italy

*Atsushi Matsuoka[1], XIN LI[2], Marco Chiari[3], Angela Bertinelli[4] (1.Department of Geology, Faculty of Science, Niigata University, 2.Nanjing Institute of Geology and Palaeontology, Chinese Academy of Sciense, 3.C.N.R., Istituto di Geoscienze e Georisorse, sede secondaria di Firenze, 4. Dipartimento di Fisica e Geologia, Università degli Studi di Perugia)

Environmental changes of the North Pacific Ocean through the Cenozoic era recorded in DSDP/ODP pelagic clay cores

*Kazuhide Mimura[1], Katsushi Yamamoto[1], Kentaro Nakamura[1], Kazutaka Yasukawa[1,2], Junichiro Ohta[2], Koichiro Fujinaga[2,1], Shiki Machida[2], Yoichi Usui[3], Yasuhiro Kato[1,2]

1. Department of Systems Innovation, School of Engineering, the University of Tokyo, 2. ORCeNG, Chiba Institute of Technology, 3. JAMSTEC

Deep-sea sediment records paleo-environmental changes thorough geologic time. Pelagic clay, one of the most common types of deep-sea sediment, is an important medium recording changes of atmospheric/oceanic circulations and surface ocean productivity that occurred in pelagic realm [1]. Despite its importance, however, less attention has been paid to the pelagic clay than to other sediments, mainly due to the two following reasons: (1) pelagic clay lacks visible features, which hampers clarifying the stratigraphic variations within pelagic clay units, (2) determining the depositional age is very difficult due to lacks of siliceous/calcareous microfossils and difficulties in identifying paleomagnetic reversals.

Our recent studies [2,3] have shown that bulk chemical composition is a very useful tool to characterize apparently homogenous pelagic clay. We previously determined bulk geochemistry of pelagic clay samples obtained from ODP sites 1149 and 1179 in the western North Pacific Ocean [2], and compared with that from LL44-GPC3 in the central North Pacific Ocean [1]. The results indicate that pelagic clay in the North Pacific is composed of common three layers, each having characteristic major- and trace-element composition [2,3]. This suggests that the problem (1) (i.e., difficulty in stratigraphic characterization) can be solved on the basis of geochemistry. Moreover, regarding the problem (2) (i.e., difficulty in age determination), we have applied biostratigraphy of ichthyolith (microfossils of fish teeth) to constraining the depositional ages of pelagic clay at sites 1149 and 1179 [3]. These achievements suggest that the problems in using pelagic clay as a recorder of paleo-environment can be overcome.

Here, we newly determined bulk chemical compositions of pelagic clay cores at DSDP sites 576, 578 and ODP Site 886, whose depositional ages were constrained [4,5]. By combining the results with our previous data, we constructed a dataset of bulk geochemistry and depositional age of pelagic clay covering a broad area in the North Pacific Ocean. The data show that the common chemostratigraphy we have reported [2,3] is truly a general feature of pelagic clay in the North Pacific Ocean. Moreover, the integration of the geochemical features and paleogeographic reconstruction suggests that the common chemostratigraphy in the North Pacific Ocean reflects the global environmental changes through the Cenozoic era.

References: [1] Kyte et al. (1993) *Geochim. Cosmochim. Acta* **57**, 1719-1740. [2] Mimura, K et al. (2017) *JpGU Meeting 2017*. [3] Mimura, K et al. (2018) *JpGU Meeting 2018*. [4] Doyle and Riedel (1985) *Init. Repts. DSDP* **86**, 349-366. [5] Ingram (1995) *Proc. ODP* **145** 399-412.

Keywords: pelagic clay, North Pacific Ocean, chemostratigraphy, paleoenvironment, Cenozoic era

©2019. Japan Geoscience Union. All Right Reserved.

Reconstruction of oceanic redox conditions in the Lower Jurassic (Pliensbachian–Toarcian) pelagic deep-sea bedded chert sequence of the Mino Belt, central Japan

*Katsuhito Soda[1]

1. Department of Earth and Environmental Sciences, Faculty of Science, Kumamoto University

The Pliensbachian-Toarcian interval in the Early Jurassic is characterized by a second-order marine mass extinction and remarkable worldwide palaeoenvironmental perturbations associated with the early Toarcian oceanic anoxic event (T-OAE). However, oceanic redox conditions and palaeoceanographic processes for redox sensitive elemental accumulation are unclear in the pelagic deep-sea realms of the Panthalassic Ocean. Here we show geochemical and multivariate statistical analyses in the pelagic deep-sea sedimentary rocks of the Panthalassic Ocean during the Pliensbachian-Toarcian. Three principal components (PC1, PC2, and PC3) in the redox sensitive elements explained 88.64% of the total variance. The PC1 represents the comprehensive redox variations, whose stratigraphic variations show euxinic-anoxic conditions across the Pliensbachian/Toarcian (Pl/To) boundary layer and the classical T-OAE. The PC2 depicts the sorption processes of Fe-Mn oxide minerals with transition elements, whose stratigraphic variations suggest few drawdowns of the transition elemental inventory after the Pl/To boundary layer. The PC3 delineates the active particulate shuttles by Fe (-Mn) oxide minerals, whose stratigraphic variations indicate the strong activation between the Pl/To boundary layer and the classical T-OAE. The statistical extraction of both the PC1 and the PC3 support the characteristic phenomena in the pelagic deep-sea realms of the Panthalassic Ocean under the relatively strong reductive conditions.

©2019. Japan Geoscience Union. All Right Reserved.

Conodont biostratigraphy of Anisian pelagic deep-sea sedimentary rocks deposited in the pelagic Panthalassa—Integration with radiolarian biozones—

*Shun Muto[1], Satoshi Takahashi[1], Satoshi Yamakita[2], Katsuhito Soda[3], Tetsuji Onoue[3]

1. Department of Earth and Planetary Science, Graduate School of Science, University of Tokyo, 2. Faculty of Education, University of Miyazaki, 3. Faculty of Advanced Science and Technology

The age of pelagic Panthalassic deep-sea sedimentary rocks such as bedded chert and claystone has been assigned based on radiolarian biozones. However, Middle Triassic radiolarian biozones of pelagic Panthalassic deep-sea strata are not precisely correlated to the standard geological timescale. In order to establish a direct correlation between the pelagic Panthalassic radiolarian biozones and the standard geological timescale, we investigated conodont biostratigraphy in two radiolarian-controlled bedded chert sections of Anisian age: the Ajiro Island section in Oita Prefecture and the Kurusu section in Aichi Prefecture. We recognised six conodont biozones in the studied sections: the upper Olenekian *Novispathodus brevissimus-Icriospathodus collinsoni* and *Triassospathodus homeri* Zones, the lower Anisian *Chiosella timorensis* Zone, the middle Anisian *Paragondolella bulgarica* Zone, the upper Anisian *Paragondolella excelsa* Zone and the uppermost Anisian to lowermost Ladinian *Paragondolella trammeri* Zone. Based on the recognition on these conodont zones, we reassessed the age of the Triassic radiolarian biozones defined by Sugiyama (1997, *Bull. Mizunami Foss. Mus.*, vol. 24, p. 79–193). Sugiyama’ s radiolarian TR 1 Zone, previously considered to be of Olenekian age, extends to the middle Anisian. The TR 2A Zone, the TR 2B Zone and the lower part of the TR 2C Zone are correlated to the middle Anisian, while the upper part of the TR 2C Zone and the lower part of the TR 3A Zone are correlated to the upper Anisian. The upper part of the TR 3A Zone and the lower part of the TR 3B Zone are probably correlative to the uppermost Anisian, but the possibility that they are correlative to the lowermost Ladinian cannot be ruled out.

Keywords: bedded chert, microbiostratigraphy, Jurassic accretionary complex

©2019. Japan Geoscience Union. All Right Reserved.

Triassic marine Os isotope record reconstructed from a pelagic chert succession, Sakahogi section, Mino Belt, southwest Japan

*Tatsuo Nozaki[1,2,3,4], Takashi Nikaido[5], Tetsuji Onoue[6], Yutaro Takaya[7,1,2,4], Keiko Sato[1], Jun-Ichi Kimura[8], Qing Chang[8], Daisuke Yamashita[6], Honami Sato[4,1], Katsuhiko Suzuki[1], Yasuhiro Kato[2,4], Atsushi Matsuoka[5]

1. JAMSTEC/R&D CSR, 2. Univ. of Tokyo, 3. Kobe Univ., 4. ChibaTech, 5. Niigata Univ., 6. Kumamoto Univ., 7. Waseda Univ., 8. JAMSTEC/D-SEG

Pelagic cherts preserved in accretionary complexes represent former seafloor sediment that can retain geochemical evidence of paleoceanographic conditions that predate the oldest extant oceanic crust. The ratio of Os isotopes in seawater, in particular, is of wide interest as a source of insight into notable geologic events such as oceanic anoxic events, rapid global warming episodes, and eruption of large igneous provinces, but marine Os isotope records from before 80 Ma are scarce. We present a record of secular variations of marine Os isotope ratios from a thick, continuous succession of Middle and Upper Triassic pelagic chert in the Sakahogi section of the Mino Belt accretionary complex.

Keywords: Chert, Re-Os isotope, Triassic, Accretionary complex, Mino Belt, Southwest Japan

©2019. Japan Geoscience Union. All Right Reserved.

The preservation of radiolarians across the Jurassic-Cretaceous (J/K) boundary in the Bosso Valley section, Central Italy

*XIN LI[1], Atsushi Matsuoka[2], Angela Bertinelli[3], Marco Chiari[4]

1. State Key Laboratory of Palaeobiology and Stratigraphy, Nanjing Institute of Geology and Palaeontology, Chinese Academy of Sciences, 2. Niigata University, 3. Università degli Studi di Perugia, 4. Istituto di Geoscienze e Georisorse

The Bosso Valley section is located near the Pianello-Cagli road and follows the Bosso River in the Umbria-Marche area of the Central Italy. The pronounced increase in abundance of *Calpionella alpina* documented at the base of *Calpionella* zone was accepted as the Jurassic–Cretaceous boundary (JKB) indicator in the Bosso Valley section. The magnetostratigraphical record of the JKB has been correlated with the *Calpionella* zone. The JKB is placed between Beds 77 and 78 (Housa et al. 2004). The Maiolica Formation, which crosses the JKB, is characterized by whitish, beige to gray colored, well-bedded limestones with abundant black to gray chert layers and chert nodules and marly intervals. Certain horizons in the Bosso Valley section yield well-preserved radiolarians, significant for the correlation of deep marine sediments. In order to establish radiolarian biostratigraphy across the JKB, detailed study was conducted to elucidate relationship between lithology and preservation of radiolarians in the Bosso Valley section.

Thin sections of 19 samples were observed to elucidate the relationship between lithology and preservation of radiolarians. Three samples of micritic limestone below the JKB (Beds 73, 75, and 77) and two samples above the JKB were collected for analyzing. The limestone samples were immersed in 10% hydrochloric acid for 30 to 60 minutes, then washed, dried and examined under a binocular microscope and a scanning electron microscope.

Radiolarians are abundant both in the chert bands or nodules and in the limestone. Preservation of radiolarians varies in different parts because of the diagenesis. Surfaces of etched limestone are observed and divided into different parts, based on the preservation of radiolarians. Radiolarians are generally calcified in the pure lime beds. Radiolarians are generally bad preserved in the chert bands or nodules. Well-preserved radiolarians are located inside the lime part near the chert bands or nodules. Primary results of radiolarian assemblages near the JKB are proposed. Limestones near chert layers or nodules in the Bosso Valley section enable radiolarian biostratigraphic study across the JKB.

Keywords: preservation, radiolarians, Jurassic-Cretaceous (J/K) boundary

©2019. Japan Geoscience Union. All Right Reserved.

Radiolarian faunas around the Jurassic-Cretaceous boundary in the Bosso Valley section, central Italy

*Atsushi Matsuoka[1], XIN LI[2], Marco Chiari[3], Angela Bertinelli[4]

1. Department of Geology, Faculty of Science, Niigata University, 2. Nanjing Institute of Geology and Palaeontology, Chinese Academy of Sciense, 3. C.N.R., Istituto di Geoscienze e Georisorse, sede secondaria di Firenze, 4. Dipartimento di Fisica e Geologia, Università degli Studi di Perugia

The Global Boundary Stratotype Section and Point (GSSP) of the Jurassic–Cretaceous boundary (JKB) is the last among the GSSPs in the Phanerozoic. It is defined as the base of the Berriasian Stage. The formal definition was decided in 2016 to use the base of the *Calpionella alpina* Subzone as the primary marker by the Berriasian Working Group in the International Subcommission on Cretaceous Stratigraphy. The definition is satisfactorily applicable for shallow marine deposits within the western Tethys, north Atlantic and central-south America. Unfortunately, the primary marker taxon cannot be found in the Pacific and circum-Pacific regions because of the limited distribution of *Calpionella*. To determine the base of the Berriasian outside of the *Calpionella* territory, alternative markers are needed.

Radiolarians are good candidates for defining the JKB because they are wide spread and can be found both shallow and deep sedimentary facies. Pelagic sequences across the JKB have been reported in ODP/IODP sites in the western Pacific and land sections in Japan, the Philippines, southern Tibet, Iran and others. Evolutionary lineages of several radiolarian taxa across the JKB are reviewed and suitable bioevents, which are approximate to the JKB, are presented. The *Loopus–Pseudodictyomitra* lineage can be the most important phylogeny for defining the JKB.

The Bosso Valley section in Umbria–Marche, central Italy, is one of potential candidates for GSSP of the JKB. The Maiolica Formation, which crosses the JKB, is characterized by whitish, beige to gray colored, well-bedded micritic limestones with abundant black to gray chert layers and nodules. Calpionellid stratigraphy and magnetostratigraphy have been studied sufficiently in the section. The base of the *Calpionella alpina* Subzone, i.e. the JKB, is placed between Beds 77 and 78. We carried out detailed field observations and careful sample collections in a 4-m interval across the JKB. Acid-etched examination of rock samples revealed that well-preserved radiolarians are recognized inside the lime part near the chert layers or nodules. Several samples of micritic limestone below and above the JKB yield well-preserved radiolarians. The result of radiolarian faunal analysis in the Bosso Valley section is presented.

Keywords: Jurassic–Cretaceous boundary , GSSP, Radiolaria

©2019. Japan Geoscience Union. All Right Reserved.

[J] Oral | M (Multidisciplinary and Interdisciplinary)：M-IS Intersection

Mon. May 27, 2019 9:00 AM - 10:30 AM JST | Mon. May 27, 2019 12:00 AM - 1:30 AM UTC | 201B 2F

[M-IS17] History X Earth and Planetary Science

convener:Yasuyuki Kano(Earthquake Research Institute, The University of Tokyo), Kei Yoshimura(Institute of Industrial Science, The University of Tokyo), Hiroaki Isobe(Faculty of Fine Arts, Kyoto City University of Arts), kiyomi iwahashi(National Institute of Japanese Literature), Chairperson:Yasuyuki Kano(東京大学 地震研究所), Kiyomi Iwahashi, Hiroaki Isobe, Kei Yoshimura, Harufumi Tamazawa

The history of modern observation in earth and planetary sciences is often far shorter compared with the timescales of their interests. Investigation of the long-term variations and occurrences of extremely rare events requires effective use of information before modern observations. Historical documents recorded by diverse kinds of authors in various situations are the important sources of such information.

Thus, historical documents have been referred in various fields of earth and planetary sciences such as seismology, climatology, meteorology and astronomy. Sharing their records, methods and experiences will be beneficial for each field and bring new insights. It is also essential to involve experienced scholars in history because one needs to carefully investigate the reliability and the context of each document in order to use it as scientific data. On the other hand, analyzing the record in the historical documents with the eyes of modern science may also bring new insights to the history scholars.

In this session we overview the studies using the historical documents in various fields of the earth and planetary sciences as well as the recent advances in related topics such as digital humanities and historical-data assimilation. The aim is to promote the communication and dialogues among the researchers in various background, and thus foster the new ideas and collaborations in the study of "History X EPS."

9:00 AM - 9:05 AM JST | 12:00 AM - 12:05 AM UTC

Introduction

9:05 AM - 9:30 AM JST | 12:05 AM - 12:30 AM UTC

[MIS17-01] Document based reconstruction of environment of forests in the Edo period

★Invited Papers

*SATOSHI SHIROUZU[1] (1.Chuogakuin University)

9:30 AM - 9:45 AM JST | 12:30 AM - 12:45 AM UTC

[MIS17-02] Studies of Babylonian Astronomical Diaries: Today and the Future

*Yasuyuki Mitsuma[1] (1.The University of Tokyo)

9:45 AM - 10:00 AM JST | 12:45 AM - 1:00 AM UTC

[MIS17-03] Characteristics of the Sunspots that Produce Large Solar Flares and the Possibility to Investigate these Events Utilizing Historical Observational Records

*Shin Toriumi[1] (1.National Astronomical Observatory of Japan)

10:00 AM - 10:15 AM JST | 1:00 AM - 1:15 AM UTC

[MIS17-04] An Approach of Environmental History to the "14th Century Crisis"

*Isahaya Yoichi[1] (1.Slavic-Eurasian Research Center, Hokkaido University)

10:15 AM - 10:30 AM JST | 1:15 AM - 1:30 AM UTC

[MIS17-05] Recovery of the Asian monsoon variations since the late 19th century by the data rescue activities in ACRE-Japan

*Jun Matsumoto[1,2], Tomoshige Inoue[1], Fumiaki Fujibe[1], Jun-Ichi Hamada[1], Taiichi Hayashi[3], Toru Terao[4], Fumie Murata[5], Hisayuki Kubota[6], Ikumi Akasaka[7], Hirotaka Kamahori[8], Nobuhiko Endo[9], Haruhiko

Yamamoto[10], Shigeru Kobayashi[11], Yoshitaka Muraji[12] (1.Deaprtment of Geography, Tokyo Metropolitan University, 2.Department of Coupled Ocean-Atmosphere-Land Processes Research, 3.Kyoto University, 4.Kagawa University, 5.Kochi University, 6.Hokkaido University, 7.Senshu University, 8.Meteorological Research Institute, 9.NARO/NIAES, 10.Yamaguchi University, 11.Osaka University, 12.EScoT)

Document based reconstruction of environment of forests in the Edo period

*SATOSHI SHIROUZU[1]

1. Chuogakuin University

Edo period is sometimes praised as the people had lived sustainably in harmony with nature. However, the people not necessarily lived sustainably. For example, excess usage of natural resources leaded to exhaustion of the resources.

There is a category of historical document called “O-Hayahi-Kakiage-Cho” or register of official forests. The “O-Hayashi” or the official forest is a forest controlled by Tokugawa shogunate or local feudal government, which could not be used by ordinary people. Maintenance of the forest was assigned to local people, “O-Hayashi-Mori” who made the register. The register contains the data such as kind or name, thickness, highlight, and number of woods. While the register itself is boring document for historians, it is a mine of data for dendrologists. The register describes a condition of the forest over a few hundred years ago, which helps dendrologists to reconstruct the environment of the forests. Dr. Yasuhiro Koyama showed that most of the official forest in northern part of Shinano province, or Nagano Prefecture, were sparse woods with Japanese red pine of 20-30 cm diameter. The official forests in the region were not green nor rich. By contrast, “Sendou-O-Hayashi” in the same region corresponds to Sakae village showed totally different environment. The forest had a spread of 13.5 ha. 70% of the woods were Japanese oak and beech. There were over 56 woods with diameter of 2 m. 1615 of woods had circumference over 3 m which corresponds the definition of “giant tree” by Ministry of the Environment. The forest was the one with a grade of Natural monuments today. It is surprising that there was such a rich forest in Japan only 200 years ago. Natural environment of Japan seemed to foster the rich forests. The rich forests have been lost because of deforestation by human. This is a good example to show the importance of human activities on condition of natural environment.

Rapid deforestation at nonofficial forests leads to exhaustion of useful woods. All the useful woods such as Japanese cedar and arborvitae had been cut down around Akiyama district until late 19 century. A historical document reported that only useless woods such as Japanese beech, oak, or chestnut remained. The people of Akiyama district demanded conifers to make wooden products such as bucket. After difficulty to obtain material, people changed their mind to use broadleaf trees and started to make bowl and plow etc. The useless woods turned to main material for production. Although they overcame the difficulty, they continued deforestation as they wrote on a document that the desire of human was limitless.

Incorrect or false descriptions are found from the close examination of the registers. There are same numbers of woods on registers recorded at different time. The person in charge seemed to alter the number for fear of meeting criticism for insufficient management. This example shows that historical records are product of “human.” The true value of historical science is to reveal the activity and society of human. The examination of historical documents on the assumption of the human nature or the procedure of information evaluation increase the value of the historical documents as data.

Keywords: history, forests, environment

©2019. Japan Geoscience Union. All Right Reserved.

©2019. Japan Geoscience Union. All Right Reserved.

Studies of Babylonian Astronomical Diaries: Today and the Future

*Yasuyuki Mitsuma[1]

1. The University of Tokyo

The presenter uses a large group of Akkadian cuneiform texts on clay tablets, the Astronomical Diaries from ancient Babylonia (mainly from Babylon) as the main source of his presentation. The text group is called ADB in this presentation. ADB is a large series of clay tablets recording astronomical and meteorological phenomena, commodity prices, level of the Euphrates, and historical events from the seventh to the first centuries BC. The clay tablets of ADB count up to over 1500, but only about 400 tablets have been published for the use of researchers. The presenter stayed in London for two years and consulted and photographed most of the unpublished tablets of ADB, which are now preserved in the British Museum. He also took photos of a considerable amount of published ADB tablets. Basesd on the photos and additional data of ADB tablets, the presenter will publish the (new and more exact) texts of published and unpublished ADB tablets. The presenter will also colloborate with some researchers and provide them with the astronomical and meteorological data of ADB, which are useful for the restoration of the ancient astronomical phenomena and climate.

Keywords: Babylonian Astronomical Diaries, Babylon, Cuneiform Scripts

©2019. Japan Geoscience Union. All Right Reserved.

Characteristics of the Sunspots that Produce Large Solar Flares and the Possibility to Investigate these Events Utilizing Historical Observational Records

*Shin Toriumi[1]

1. National Astronomical Observatory of Japan

Solar flares are the sudden releasing of magnetic energy and, among them, the energetic ones that occur around the sunspot regions may directly and indirectly affect the Earth through the enhancement of electromagnetic waves, releasing of high energy particles, and coronal mass ejection. While it is accepted that the strongest flare activity ever observed is the "Carrington event" in September 1859, in order to understand the mechanisms and trends of such extreme space-weather events, it is crucial to increase the sample number of the events with enough observational data and conduct statistical investigations. Although often these events do not have observations of sufficient data quality for modern scientific analysis, there are several ways to elucidate how and why the strong events occurred. In this presentation, we first show the morphological and magnetic characteristics of flare-productive sunspots that are revealed by observational data analysis of sunspots in Solar Cycle 24 (especially for six years from 2010) and by magnetohydrodynamic simulations to model these sunspots. Then, we introduce several research attempts to reconstruct magnetic activities by using historical documents such as sunspot drawings. Finally, we discuss the the possibility to investigate extreme space-weather events by applying our modern knowledge of flare-productive sunspots to extreme events in history.

Keywords: Solar flares, Sunspots, Historical documents

©2019. Japan Geoscience Union. All Right Reserved.

An Approach of Environmental History to the "14th Century Crisis"

*Isahaya Yoichi[1]

1. Slavic-Eurasian Research Center, Hokkaido University

This paper is an introduction to an approach of environmental history to the “14th Century Crisis.” The “14th Century Crisis” is the term for collective peril in the 14th century which is considered to be the time of transition from the Medieval Warm Period (ca. 1000–1300) to the Little Ice Age. The peril consists of cooling, natural disasters, epidemics and political upheaval such as the fall of the Mongol Empire (1206–1368). Our project embarks upon interdisciplinary collaboration between sciences (astronomy, meteorology, and seismology) and humanities (history and archival science) to elucidate an actual phase of the crisis. In the context of world history, the “14th Century Crisis” has attracted scholarly attention as the pivot that closed the multi-centered “13th Century System” across Afro-Eurasia, and paved the way for the European-centered “Modern World-System.” The grand shift, however, could not be calibrated properly without taking account of the environmental transition to the Little Ice Age. This is an introductory remark of our project aiming to shed some new light upon entangled relationships between human development and environment.

Keywords: 14th Century Crisis, Environmental History, Little Ice Age, Medieval Warm Period, History of Eurasia, Mongol Empire

©2019. Japan Geoscience Union. All Right Reserved.

Recovery of the Asian monsoon variations since the late 19th century by the data rescue activities in ACRE-Japan

*Jun Matsumoto[1,2], Tomoshige Inoue[1], Fumiaki Fujibe[1], Jun-Ichi Hamada[1], Taiichi Hayashi[3], Toru Terao[4], Fumie Murata[5], Hisayuki Kubota[6], Ikumi Akasaka[7], Hirotaka Kamahori[8], Nobuhiko Endo[9], Haruhiko Yamamoto[10], Shigeru Kobayashi[11], Yoshitaka Muraji[12]

1. Deaprtment of Geography, Tokyo Metropolitan University, 2. Department of Coupled Ocean-Atmosphere-Land Processes Research, 3. Kyoto University, 4. Kagawa University, 5. Kochi University, 6. Hokkaido University, 7. Senshu University, 8. Meteorological Research Institute, 9. NARO/NIAES, 10. Yamaguchi University, 11. Osaka University, 12. EScoT

In most of the countries in monsoon Asia, the meteorological observations by modern instruments started during their colonial period before the World War II. However, most of these old meteorological data have not been digitized yet, and have not been utilized in the past climatic change researches. Here, we will briefly introduce our recent data rescue activities mainly for the daily precipitation data in the Former British India, China, Philippines, Vietnam, and Japan for the recovery of the past Asian monsoon variations since the late 19th century as one of the activities in the ACRE (Atmospheric Circulation Reconstruction over the Earth) project. Although with the aid of the World Meteorological Organization, the National Oceanic and Atmospheric Administration archived the scanned images of huge data books all over the world, it was sometimes very difficult to read the numerals in the scanned data. The original data books/sheets are needed for the accurate digitization of the old data. Acknowledgments: Part of this study was supported by The JSPS KAKENHI (25282085,26220202,15K16283,18K19951, 18H01681), The GRENE program of the MEXT. Digitization activities of the former British India were supported by Drs. Shoichi Shige (Kyoto Univ.), Masashi Kiguchi (Univ. Tokyo), Hironari Kanamori (Nagoya Univ.), and Nozomi Kamizawa(Tokyo Metrop Univ.). They were also supported from the India Meteorological Department, the Indian Institute of Tropical Meteorology and Indian students in Pune.

Keywords: Data rescue, Precipitation, Climatic variations, Asian monsoon

©2019. Japan Geoscience Union. All Right Reserved.

[J] Oral | M (Multidisciplinary and Interdisciplinary)：M-IS Intersection

Mon. May 27, 2019 10:45 AM - 12:15 PM JST | Mon. May 27, 2019 1:45 AM - 3:15 AM UTC | 201B 2F

[M-IS17] History X Earth and Planetary Science

convener:Yasuyuki Kano(Earthquake Research Institute, The University of Tokyo), Kei Yoshimura(Institute of Industrial Science, The University of Tokyo), Hiroaki Isobe(Faculty of Fine Arts, Kyoto City University of Arts), kiyomi iwahashi(National Institute of Japanese Literature), Chairperson:Hiroaki Isobe, Kei Yoshimura, Kiyomi Iwahashi, Yasuyuki Kano(東京大学 地震研究所), Harufumi Tamazawa

The history of modern observation in earth and planetary sciences is often far shorter compared with the timescales of their interests. Investigation of the long-term variations and occurrences of extremely rare events requires effective use of information before modern observations. Historical documents recorded by diverse kinds of authors in various situations are the important sources of such information.
Thus, historical documents have been referred in various fields of earth and planetary sciences such as seismology, climatology, meteorology and astronomy. Sharing their records, methods and experiences will be beneficial for each field and bring new insights. It is also essential to involve experienced scholars in history because one needs to carefully investigate the reliability and the context of each document in order to use it as scientific data. On the other hand, analyzing the record in the historical documents with the eyes of modern science may also bring new insights to the history scholars.
In this session we overview the studies using the historical documents in various fields of the earth and planetary sciences as well as the recent advances in related topics such as digital humanities and historical-data assimilation. The aim is to promote the communication and dialogues among the researchers in various background, and thus foster the new ideas and collaborations in the study of "History X EPS."

10:45 AM - 11:00 AM JST | 1:45 AM - 2:00 AM UTC

[MIS17-06] Historical big data: integrated analysis of the past world by the workflow that bridges data structuring gaps

*Asanobu Kitamoto[1,2,3], Mika Ichino[1,2] (1.National Institute of Informatics, 2.ROIS-DS Center for Open Data in the Humanities, 3.SOKENDAI)

11:00 AM - 11:15 AM JST | 2:00 AM - 2:15 AM UTC

[MIS17-07] Felt earthquakes in Tokyo (Edo) based on historical daily records and seismic intensity data

*Kenji Satake[1] (1.Earthquake Research Institute, University of Tokyo)

11:15 AM - 11:30 AM JST | 2:15 AM - 2:30 AM UTC

[MIS17-08] Climate and social changes in ancient Japan construed by use of high resolution reconstruction of the Climate in Historical Time

*Katsunori IMAZU[1], Takeshi Nakatsuka[2] (1.OKAYAMA University Graduate School of Humanities and Social Sciences, 2.Research Institute for Humanity and Nature)

11:30 AM - 11:45 AM JST | 2:30 AM - 2:45 AM UTC

[MIS17-09] Absolute ages for huge eruptions of Towada Caldera and Baitoushan volcano in the 10th century as seen from dendrochronological studies and historical documents

*Masataka Hakozaki[1], Fusa Miyake[2], Masaki Sano[3], Katsuhiko Kimura[4], Toshio Nakamura[2], Mitsuru Okuno[5], Minoru Sakamoto[1], Takeshi Nakatsuka[6,2] (1.National Museum of Japanese History, 2.Nagoya University, 3.Waseda University, 4.Fukushima University, 5.Fukuoka University, 6.Research Institute for Humanity and Nature)

11:45 AM - 12:00 PM JST | 2:45 AM - 3:00 AM UTC

[MIS17-10] How can we activate collaborations with history and archaeology? – Lesson from Historical Climate Adaptation project

★Invited Papers

*Takeshi Nakatsuka[1,2] (1.Research Institute for Humanity and Nature, 2.Graduate School of Environmental Studies, Nagoya University)

12:00 PM - 12:15 PM JST | 3:00 AM - 3:15 AM UTC

Discussion

Historical big data: integrated analysis of the past world by the workflow that bridges data structuring gaps

*Asanobu Kitamoto[1,2,3], Mika Ichino[1,2]

1. National Institute of Informatics, 2. ROIS-DS Center for Open Data in the Humanities, 3. SOKENDAI

1. Introduction

Reconstruct and analyze the past world through the extraction and integration of information from the past books and documents –we call this type of historical research as “historical big data.” This is because this approach has the same structure and purpose with “modern big data” on the current world, and it is meaningful to extend this approach into the past world. A big obstacle, however, is in data structuring. We start from data written in Kuzushiji (cursive scripts) on historical documents to high quality data usable for computaitonal analysis of the past world. For this purpose, we need information infrastructure to support this long data structuring workflow from digitzation to quality control. Because this is difficult to automate, we need efficient data structuring workflow based on human-machine collaboration. We therefore design a workflow to convert non-structured data (e.g. image and text) to structured data (analysis-ready data) and develop information platform for humanities dataset that is reusable and verifiable.

A similar but bigger project has started in EU called “Time Machine Flagship” involving more than 200 organizations. The project is building “time machine” to move freely within spatio-temporal space, especially within the big data of cities such as Venice in Italy and Amsterdam in the Netherlands. This trend has not been incorporated in Japan and Asia, so our platform may also be an entry point for this global initiative.

2. Issues

Many research projects for reconstructing the past have been carried out, but historical big data is a different approach in terms of the following.

First, the type of data is different. For example, paleoclimate research uses any data related to climate; not only books and documents, but also traces in the nature (proxy data such as ice core and growth ring). On the other hand, historical big data limits its scope on records written by human, and focuses on developing new data structuring workflow including the interpretation of textual records.

Second, the target of discipline is different. Research in one discipline had a tendency of focusing only on a limited type of phenomena, and did not pay attention to other phenomena. Even when researchers are studying the same diary, bibliographic data or extracted data were not shared across research groups, and many researchers repeated similar tasks again and again. To solve this problem, historical big data offers data structuring workflow that is effective across disciplines, and enables research that takes advantage of data sharing.

3. Data crossing and re-interpretation

To extend the modern big data into the past, relevant issues are not only the extension of technologies

©2019. Japan Geoscience Union. All Right Reserved.

but also concepts and methodologies.

First, data crossing is a methodology to overlay different data to find unexpected relationship. A typical example is a map. By registering and overlaying data from different sources, we can take actions based on insights obtained from data. Here important challenges include the interoperability of API and sharing of terminology. To solve this challenge, we share future challenges within our research group, take advantage of the strength of each member without overlapping tasks, and develop information infrastructure maximizing the outcome within limited resources.

Second, data re-interpretation is a methodology to find effective reuse of data collected for one purpose into another purpose. A famous example in the modern big data is the case of reusing car probe data for the map showing passed routes after earthquake disasters. A same approach should be effective for historical big data. For example, is it possible to use the change of bureaucrat's directories for evaluating societal impact by climate change? Flexible imagination may lead to the creative usage of data.

4. Beyond “One Bed Multiple Dreams”

Historical big data is a multidisciplinary research. Of course, a big gap exists between humanities and science/technology, but difference within science and technology disciplines are not negligible. How to go beyond these gaps? Our basic idea is to recognize that we are in “one bed multiple dreams” situation in the sense that each member in the research group has a different dream. But at the same time, we recognize the advantages of being in one bed. For example, data and tools can be shared even if we have different dreams. After maximizing the advantages of sharing, an individual researcher tackles the reconstruction of a different part of the past world –this is the concept of historical big data research.

Keywords: Historical big data, Paleoclimate, Data structuring, Information infrastructure, Multi-disciplinary research , Historical documents

©2019. Japan Geoscience Union. All Right Reserved.

Felt earthquakes in Tokyo (Edo) based on historical daily records and seismic intensity data

*Kenji Satake[1]

1. Earthquake Research Institute, University of Tokyo

There have been three generations of collection and publication of historical materials on earthquakes. They are “Dai-Nihon Jishin Shiryo (Collection of Historical Documents on Earthquakes in Great Japan)” in 1904, “Zotei Dai-Nihon Jishin Shiryo” and “Nihon Jishin Shiryo” in 1941-1951, and “Shinshu Nihon Jishin Shiryo” in 1981-1991. On the basis of these collected materials, annual number of felt earthquakes in Tokyo (formerly Edo) was examined by Usami (1979, CCERP report) and Usami and Watanabe (2005, 2006, Historical Earthquakes). Number of felt earthquakes strongly depends on the available materials. The above collections contains some daily records of clans which documented daily weather and earthquakes, and the recorded earthquakes include small shocks or aftershocks of large damaging earthquakes. In order to discuss temporal changes of seismicity, such homogeneous records should be used. In this study, number of yearly earthquakes in several daily records are counted, and compared with seismic intensity data of Japan Meteorological Agency since 1885.

Among the daily records during the Edo period (1603-1867), “Tsugaru-han On-nikki” recorded the largest number of felt earthquakes; approximately 1550 events during 200 year period between 1668 and 1866. However, there are several years during which no earthquake was documented. The next one is “Sakaki-bara Nikki”, which documented approximately 700 events during 200 year period between 1651 and 1859. This record also contains years without any earthquake, but such years are different from those of the previous record. By merging these two daily records, there are only few years without felt earthquakes. For the earlier Edo period, “Edo-bakufu Nikki” (two different sources) cover more or less continuously from 1631 to 1707 with 680 earthquakes. In addition, several other records such as “Tsushima-han Mainichiki”, “Inaba-shi Eidai Nikki” or “Sakai-ke Shiryo” each documented more than 100 earthquakes. Yearly number of earthquakes were counted for each record, and the largest number for each year was selected. The dataset thus made contain nearly 2500 earthquakes for 241 year period (1628-1868) with annual average of about 10 events. The yearly record has several peaks in 1704 (about 60 events), in 1855 (about 50 events) and in 1649 (about 50 events). These represent aftershocks of the 1703 (31 December) Kanto earthquake, 1855 Edo earthquake and two M7 earthquakes in 1649.

Seismic intensity data since 1885 has been complied by JMA (Ishigaki and Takagi, 2000, Quarterly J. Seismology; Ishigaki, 2007, ibid), which shows that the annual number of earthquakes with intensity 1 or larger, 2 or larger, 3 or larger are 52, 16 and 5, respectively. If we assume that the seismic intensity rate is constant in the last 400 years, then the above merged historical daily data recorded felt earthquakes with intensity 2 or larger. The JMA data show that the largest number of felt earthquakes was recorded in 2011, with 148 events with intensity 2 or larger, representing aftershocks and triggered seismicity by the Tohoku earthquake. Numbers of earthquakes with intensity 2 or larger were 36 and 35 in 1923 and 1924, following the Taisho Kanto earthquake. Combining the historical data from daily records, it is concluded that the number of felt earthquakes was largest in 2011 in the last 400 years.

Keywords: Historical earthquakes, Daily records, Tokyo

©2019. Japan Geoscience Union. All Right Reserved.

Climate and social changes in ancient Japan construed by use of high resolution reconstruction of the Climate in Historical Time

*Katsunori IMAZU[1], Takeshi Nakatsuka[2]

1. OKAYAMA University Graduate School of Humanities and Social Sciences, 2. Research Institute for Humanity and Nature

This study focuses on ancient times of Japan, specifically the 8th and 9th Century in an attempt to clarify how the weather impacted societies then. Takeshi Nakatsuka developed per-annum reconstruction of climate for that period of time, which revealed that the 8th Century was, in general, relatively dry but stable, whereas the second half of the 9th Century turned to be unstable and wet, then in the 10th Century the weather changed to dry. Historical literature including Shoku Nihongi (second of the six classical Japanese history texts)、Nihon Kouki (third of the six classical Japanese history texts), Shoku Nihon Kouki (fourth of the six classical Japanese history texts), Nihon Montoku Tenno Jitsuroku (fifth of the six classical Japanese history texts), and Nihon Sandai Jitsuroku (sixth of the six classical Japanese history texts) described history of said period and included the description of the weather then. However, they are very brief and do not provide precise details as to the severity of drought, spells of rain or torrential rain. At long last, high-resolution weather reconstruction helps to bring clarity to the level of extreme dryness and humidity of summer and the damage they brought about, when we review historical documents. Additionally, the deeper understanding of the mid- to long-term weather pattern changes helps to visualize the interrelationship between the climate change and changes in the state and societies.

In this research, our interest, in particular, lies on demographic change and social system transformation in ancient times. In the early 8th Century Taiho Code was enacted and a centralized government established a political system based on the Ritsuryo Codes, which demonstrated their intent to emulate the system in China. The systems set forth by the Ritsuryo-Code-based-nation laid the foundation for the framework of Japan and played an essential role in defining the subsequent development of its history. The population that the state of the Ritsuryo Codes ruled is estimated to be around 4.5 million at the beginning of the 8th Century and approximately 5.5 million at the beginning of the 9th Century, with the average population growth rate from the 8th to 9th Century being 0.2% per annum. The population in the 17th Century, the beginning of the Edo era, is estimated as 12-18 million. The population slightly increased from the ancient times to early modern times. The yearly population increase over a course of 800 years from the mediaeval to early modern times was only 0.1-0.15% at best. Ancient Japan was frequently visited with plague and famine, which kept the nation highly fluid and vulnerable. Despite this situation, yet the population growth was at a higher rate comparing to the middle ages. This is considered due in part to a high functioning reproductive system set forth by the Ritsuryo system in which the central government exercised control over the people's lives and rice paddies and also by a relatively stable weather in the 8th Century.

Changes in Tang dynasty and Shilla, the neighboring countries of Japan, affected the Ritsuryo system in Japan, which collapsed little by little. The Ritsuryo-based-nation considerably changed from the late 9th Century to late 10th Century. These social changes were triggered by the changes in the overseas political landscape in its vicinity as well as the climate change. In the second half of the 9th Century they faced problems of the rise of non-arable rice paddies and flooding of rice fields. We are convinced that the climate change resulting in the humidity level increase of the land was at the root of these problems at that time. The Ritsuryo system started to give up on its exercise of control over its people and rice fields, thereby the reproductive system of the Ritsuryo state broke down. It was exacerbated by frequent

©2019. Japan Geoscience Union. All Right Reserved.

earthquakes, a volcano eruption, famine and pandemic, all of which occurred during the same time frame. It was a time of crisis for ancient Japan as a whole. The nation under the Ritsuryo codes established a centralized government at the beginning of the 8th Century, but in the late 9th Century and onwards it started to collapse and the central government was contracted into a dynastic state in the capital of Heiankyo.

Keywords: tree-ring oxygen isotope ratio, Ritsuryo system, population, Climate change

©2019. Japan Geoscience Union. All Right Reserved.

Absolute ages for huge eruptions of Towada Caldera and Baitoushan volcano in the 10th century as seen from dendrochronological studies and historical documents

*Masataka Hakozaki[1], Fusa Miyake[2], Masaki Sano[3], Katsuhiko Kimura[4], Toshio Nakamura[2], Mitsuru Okuno[5], Minoru Sakamoto[1], Takeshi Nakatsuka[6,2]

1. National Museum of Japanese History, 2. Nagoya University, 3. Waseda University, 4. Fukushima University, 5. Fukuoka University, 6. Research Institute for Humanity and Nature

The Towada Caldera (Aomori Prefecture / Akita Prefecture) and Baitoushan volcano (China / North Korea) each caused a huge eruption in the 10th century, respectively. These traces are clearly left behind in the stratum of the northern Japan as To-a tephra and B-Tm tephra. These two eruptions are estimated to be one of the largest in Japan and the world in the past 2000 years, respectively (Hayakawa & Koyama 1998). However, direct document records of these eruptions have not been found from any countries around the volcano. For that reason, these absolute ages had long been unknown. Also, due to uncertain age, the impact on human society and the global environment of these eruptions has not been evaluated.

Recently, the absolute age of the 10th century eruption of Baitoushan volcano was decided in AD946(Oppenheimer et al. 2017, Hakozaki et al. 2018). It was achieved by "^{14}C-spike matching" which is applied a rapidly carbon-14 increase event in AD775 discovered from tree-rings of Japanese trees (Miyake et al. 2012). And this age was also verified by the result of the oxygen isotopic dendrochronology (Kimura et al. 2017). Hayakawa and Koyama (1998) picked up this age (AD946) from descriptions suggesting distant eruptions written in a few old documents of Japan and Korea (ex. "Kofukuji-nendaiki", "Goryeosa") .

On the other hand, due to fixed in AD946 the absolute age of B-Tm, doubts occurred in the age of 10th century eruption of the Towada caldera. The 10th century eruption of Towada caldera had been estimated to be AD915 according to the description on the "Fuso Ryakuki" suggesting the eruption, and the dates of archaeological timbers buried in the lahar at Akita prefecture. Based on this age, the varves at lakes in Akita prefecture counted between To-a and B-Tm to be 14 layers, Kamite et al(2010) estimated the eruption age of Baitoushan volcano to be AD929. However, since the absolute age of B-Tm was AD946, as described above, it became clear that there was a gap of 17 years from Kamite et al's estimates. In other words, there is a possibility that the 10th century eruption of Towada caldera may be AD932. If this is correct, there is a possibility that the description of AD 915 in the "Fuso Ryakuki" indicates the eruption that occurred in volcanoes other than Towada caldera.

Recently, the oxygen isotopic dendrochronology was applied to the timbers of the fence of Tagajo site of Miyagi prefecture, and the absolute age was decided to be AD917 (Saito et al. 2018). In the archaeological survey, this fence has been thought to be built before the ash fall of To-a tephra (AD915) (Miyagi prefectural research institute of the Tagajo site 2018). The fact that the tree-ring of the AD917 was recognized in the timbers of the fence largely contradicts the estimated age (AD915) of To-a tephra. Furthermore, neither bark nor sapwood remained in these timbers, and it is clear that the logging year is later than AD917.

In this presentation, we show how the ages of timbers of Baitoushan volcano and Tagajo site determined

©2019. Japan Geoscience Union. All Right Reserved.

by two new dendrochronological methods, and what is necessary to determine the absolute age of the 10th century eruption of Towada Caldera.

Keywords: dendrochronology, 14C-spike, Baitoushan volcano, oxygen isotope, Towada Caldera, huge eruption

©2019. Japan Geoscience Union. All Right Reserved.

How can we activate collaborations with history and archaeology? –Lesson from Historical Climate Adaptation project

*Takeshi Nakatsuka[1,2]

1. Research Institute for Humanity and Nature, 2. Graduate School of Environmental Studies, Nagoya University

Introduction

Earth and planetary sciences belong to historical sciences dealing with past natural and human phenomena as well as history and archaeology. Although many inter-disciplinary researches have been conducted between them, there are a lot of problems originating from differences of their essential philosophy. Here, I will discuss how to activate collaborations with history and archaeology based on my experiences as the leader of “Historical Climate Adaptation Project” in Research Institute for Humanity and Nature (RIHN) from 2014 to 2018.

Fundamental Strategy of the Project

RIHN is an inter-university research institute, accepting many research proposals aiming to solve a global environmental problem by inter-disciplinary approaches between natural and human sciences. In the framework of RIHN, we created three steps of research strategies. 1) To reconstruct variations in past climate at annual resolution for last several millennia in Japan. 2) To compare paleoclimate data with numerous historical and archaeological archives. 3) To elucidate characteristics of societies resilient or vulnerable to climate changes by comparing many historical cases. Although I initially imaged the unidirectional data provision from paleoclimatology to history and archaeology except for the study of historical climatology, the inter-disciplinary communications actually made unexpected progress in the paleoclimatology, especially in the establishment of super-long chronology of tree-ring cellulose oxygen isotope ratio.

Results of Inter-Disciplinary Collaboration

Tree-ring cellulose oxygen isotope ratio is a novel proxy to reconstruct past summer precipitation precisely even in humid and temperate areas like Japan where traditional dendroclimatology was not very successful. We planned to establish the long-term datasets over Japan. At the beginning, historians and archaeologists were regarded as users of the data, but they actually contributed to the creation and refinement of data by various ways. After receiving the data, they answered to paleoclimatologists as follows. (1) Active provisions of excavated woods and old architectural woods for isotopic analyses. (2) Critical evaluation of the paleoclimate data from the viewpoint of history and archaeology. (3) Request to improve the resolution and extension of paleoclimate data. Paleoclimatologists welcome (1), but it was not easy to answer to (2) and (3) because such criticisms and requests are not usually originating from themselves. However, the request (3) finally made us enable the tree-ring based millennial scales climate reconstruction, by combing the tree-ring oxygen and hydrogen isotope ratios, which were validated by critical evaluations of historians and archaeologists (2). It promoted many studies in paleoclimatology, history and archaeology. However, it was not easy to elucidate “societal systems resilient to climate change” because we had not shared the research purposes between natural and human sciences.

Conclusion

©2019. Japan Geoscience Union. All Right Reserved.

The unprecedented length and precision of paleoclimate data are the results of active inter-disciplinary communications. Although the unidirectional data provision was not successful, the critical interactions improved both the data quantity and quality. On the other hand, the sharing of research philosophy between natural and human sciences was necessary to promote “real inter-disciplinary” research. In the project, I found the fact that historians and archaeologists do not usually study history to solve contemporary problems. Rather, they focus on the difference in people’s sense of values between past and present. Because the future must be different from the present as well as the past, it is very important to promote collaborations between natural scientists who seek the universality in history and human researchers who understand the diversity of history in order to make sustainable society. That was my most important finding in the project.

Keywords: Inter-disciplinary between natural and human sciences, Climate variation, Paleoclimatology, History, Archaeology, Dendrochronology

©2019. Japan Geoscience Union. All Right Reserved.

[J] Poster | M (Multidisciplinary and Interdisciplinary)：M-IS Intersection

Mon. May 27, 2019 3:30 PM - 5:00 PM JST | Mon. May 27, 2019 6:30 AM - 8:00 AM UTC | Poster Hall International Exhibition Hall8, Makuhari Messe_22

[M-IS17] History X Earth and Planetary Science

convener:Yasuyuki Kano(Earthquake Research Institute, The University of Tokyo), Kei Yoshimura(Institute of Industrial Science, The University of Tokyo), Hiroaki Isobe(Faculty of Fine Arts, Kyoto City University of Arts), kiyomi iwahashi(National Institute of Japanese Literature)

The history of modern observation in earth and planetary sciences is often far shorter compared with the timescales of their interests. Investigation of the long-term variations and occurrences of extremely rare events requires effective use of information before modern observations. Historical documents recorded by diverse kinds of authors in various situations are the important sources of such information.

Thus, historical documents have been referred in various fields of earth and planetary sciences such as seismology, climatology, meteorology and astronomy. Sharing their records, methods and experiences will be beneficial for each field and bring new insights. It is also essential to involve experienced scholars in history because one needs to carefully investigate the reliability and the context of each document in order to use it as scientific data. On the other hand, analyzing the record in the historical documents with the eyes of modern science may also bring new insights to the history scholars.

In this session we overview the studies using the historical documents in various fields of the earth and planetary sciences as well as the recent advances in related topics such as digital humanities and historical-data assimilation. The aim is to promote the communication and dialogues among the researchers in various background, and thus foster the new ideas and collaborations in the study of "History X EPS."

[MIS17-P01] Perspective of 'History X Earth and Planetary Science'

*Yasuyuki Kano[1], Hiroaki Isobe[2], Kei Yoshimura[3], Kiyomi Iwahashi[4], Harufumi Tamazawa[5,2] (1.Earthquake Research Institute, The University of Tokyo, 2.Faculty of Fine Arts, Kyoto City University of Arts, 3.Institute of Industrial Science, The University of Tokyo, 4.National Institute of Japanese Literature, 5.Disaster Prevention Research Institute, Kyoto University)

[MIS17-P02] Reexamination of intensity distribution of Japanese historical earthquakes using attenuation relation

*Yasuyuki Kano[1], Junzo Ohmura[2] (1.Earthquake Research Institute, The University of Tokyo, 2.Diasaster prevention Research institute, Kyoto University)

[MIS17-P03] Rekisuke: a system for sharing bibliographic information of historical documents through Interdisciplinary collaboration

★Invited Papers

*Mika Ichino[1,2], Yukie Hashimoto, Kooiti Masuda[3], Asanobu Kitamoto[2,1], Junpei Hirano[4] (1.Center for Open Data in the Humanities, Joint Support-Center for Data Science Research, Research Organization of Information and Systems , 2.National Institute of Informatics, 3.Tokyo Metropolitan University, 4.Faculty of Liberal Arts, Teikyo University)

[MIS17-P04] Analysis of reconstruction processes after the 1707 Hoei eruption of Fuji Volcano based on old maps

*Junzo Ohmura[1] (1.Research Institute for Earthquake Prediction, Disaster Prevention Research Institute, Kyoto University)

[MIS17-P05] Workshop of Word Survey about Earth and Planetary Phenomena by Citizen

*Harufumi Tamazawa[1,2], kiyomi iwahashi[3] (1. Disaster Prevention Research Institute Kyoto University, 2.Faculty of Fine Arts, Kyoto City University of Arts, 3.National Institute of Japanese Literature)

[MIS17-P06] Observational Data in the first half of 20th century to join modern scientific Observation and historical documents: A Usage example ob Photographic Plate of Kwasan Observatory

*Harufumi Tamazawa[1], Reizaburo Kitai[4], Hiroaki Isobe[2], Satoru UeNo[3], Takahito Sakaue[3] (1. Disaster Prevention Research Institute Kyoto University, 2.Faculty of Fine Arts, Kyoto City University of Arts, 3.Astronomical Observatory, Graduate School of Science, Kyoto University, 4.Bukkyo University)

[MIS17-P07] Climate changes and lords' control in the early modern period in Japan

*Kaoru kamatani[1], Masaki Sano[2], Takeshi Nakatsuka[3] (1.Ritsumeikan University, 2.Waseda University, 3.Research Institute for Humanity and Nature)

[MIS17-P08] Intense geomagnetic storm during Maunder minimum possibly by quiescent filament eruption

*Hiroaki Isobe[1], Yusuke Ebihara[2], Harufumi Tamazawa[1], Akito Davis Kawamura[3], Hisashi Hayakawa[4] (1.Faculty of Fine Arts, Kyoto City University of Arts, 2.Research Institute for Sustainable Humanosphere, Kyoto University, 3.Graduate School of Science, Kyoto University, 4.Graduate School of Letters, Osaka University)

[MIS17-P09] Reconstructing 1931 flood in Yangtze River basin and its application to Chinese economic history

*CHANG LIU[1], Akiyuki Kawasaki[1], Tomoko Shiroyama[2] (1.Department of Civil Engineering, Graduate School of Engineering, the University of Tokyo, 2.Department of Economics, Graduate School of Economics, the University of Tokyo)

[MIS17-P10] Seismicity Analysis Using Felt Reports and Attenuation Relation of Seismic Intensity

*Takeo Ishibe[1], Koji Iwasa[1], Mitsuko Furumura[1], Ritsuko S. Matsu'ura[1] (1.Association for the Development of Earthquake Prediction)

[MIS17-P11] Radiocarbon dating of Japanese tree rings – chronological research and Japanese calibration curve

*Minoru Sakamoto[1,2], Masataka Hakozaki[1], Takumi Mitsutani[3], Takeshi Nakatsuka[4,5] (1.National Museum of Japanese History, 2.The Graduate University for Advanced Studies, 3.Nara National Research Institute for Cultural Properties, 4.Research Institute for Humanity and Nature, 5.Nagoya University)

[MIS17-P12] Usage of Historical Documents with Scientific Understandings in the field of Solar Physics

*Akito Davis Kawamura[1], Hisashi Hayakawa[2], Harufumi Tamazawa[3], Hiroaki Isobe[3], Kazunari Shibata[1] (1.Astronomical Observatory, Kyoto University, 2.Graduate School of Letters, Osaka University, 3.Faculty of Fine Arts, Kyoto City University of Arts)

[MIS17-P13] The study of the relationship between the flood of Kitakami River and sociaty in the end of Edo period

*Daisuke Sato[1], Yoshitaka Takahashi[2] (1.International Reserch Institute of Disaster Science Tohoku University , 2.Tokyo University of Agriculture and Technology)

[MIS17-P14] Reconstruction of Historical Weather with Data Assimilation Using Old Diaries

*Kei Yoshimura[1], Panduka Neluwala[2], Mika Ichino[3], Kooiti Masuda[4], Junpei Hirano[5] (1.Institute of Industrial Science, The University of Tokyo, 2.University of Peradeniya , 3.National Institute of Informatics, 4.Tokyo Metropolitan University, 5.Teikyo University)

[MIS17-P15] Examination of data range for fitting Omori-Utsu law to temporal decay of aftershocks presented in historical materials on the 1830 Kyoto earthquake: Reason for the difference of numbers of aftershocks in the same place

*Kentaro Hattori[1], Junzo Ohmura[2], Ichiro Nakanishi[1] (1.Kyoto Univ., 2.Bukkyo Univ.)

[MIS17-P16] Tsunami trace height of the AD 1854 Ansei Tokai tsunami around the lake Hamanako inferred from historical maps

*ebina yuichi[1], Kentaro Imai[2], Yoshinobu Tsuji[3], hiroyuki iwase[4] (1.International Research Institute of Disaster Science, 2.JAMSTEC, 3.Fukuda Geological Instite, 4. (C)ECOH CORPORATION)

Perspective of 'History X Earth and Planetary Science'

*Yasuyuki Kano[1], Hiroaki Isobe[2], Kei Yoshimura[3], Kiyomi Iwahashi[4], Harufumi Tamazawa[5,2]

1. Earthquake Research Institute, The University of Tokyo, 2. Faculty of Fine Arts, Kyoto City University of Arts, 3. Institute of Industrial Science, The University of Tokyo, 4. National Institute of Japanese Literature, 5. Disaster Prevention Research Institute, Kyoto University

"History X EPS" is a title of this session as well as the name of the application area proposed for Grant-in-Aid for Scientific Research on Innovative Areas. The application area consists of 4 sub area: “Ten” (astronomy), ”Ki” (climatology and meteorology), ”Chi” (solid earth science), and ”Jin” (human and society).

Historians and researchers of earth and planetary sciences have been collaborated in the preceding projects. There are a number of projects for such interdisciplinary collaboration. Here we present prospects of "History X EPS." The scope of the session is as follows:

The history of modern observation in earth and planetary sciences is often far shorter compared with the timescales of their interests. Investigation of the long-term variations and occurrences of extremely rare events requires effective use of information before modern observations. Historical documents recorded by diverse kinds of authors in various situations are the important sources of such information.

Thus, historical documents have been referred in various fields of earth and planetary sciences such as seismology, climatology, meteorology and astronomy. Sharing their records, methods and experiences will be beneficial for each field and bring new insights. It is also essential to involve experienced scholars in history because one needs to carefully investigate the reliability and the context of each document in order to use it as scientific data. On the other hand, analyzing the record in the historical documents with the eyes of modern science may also bring new insights to the history scholars.

In this session we overview the studies using the historical documents in various fields of the earth and planetary sciences as well as the recent advances in related topics such as digital humanities and historical-data assimilation. The aim is to promote the communication and dialogues among the researchers in various background, and thus foster the new ideas and collaborations in the study of "History X EPS."

Keywords: History, Astronomy, Solar phisics, Meteorology, Seismology

©2019. Japan Geoscience Union. All Right Reserved.

Reexamination of intensity distribution of Japanese historical earthquakes using attenuation relation

*Yasuyuki Kano[1], Junzo Ohmura[2]

1. Earthquake Research Institute, The University of Tokyo, 2. Diasaster prevention Research institute, Kyoto University

Sources of historical earthquakes are usually estimated from seismic intensity distributions based on the descriptions on historical documents. Ceaseless efforts to collect historical earthquake documents leads to sourcebooks such as Dai-Nihon Jishin Shiryo (Collection of Historical Documents on Earthquakes in Great Japan) (Tayama, 1904a,b), Zotei Dai-Nihon Jishin Shiryo (Collection of Historical Documents on Earthquakes in Great Japan, Enlarged and Revised Edition) (Musha, 1941, 1943a,b), and Shinshu Nihon Jishin Shiryo (Historical Documents on Earthquakes in Japan, New Collection) (Earthquake Research Institute of the University of Tokyo, 1981-1994) etc. The location of epicenter or hypocenter, origin time, and magnitude of the historical earthquakes are estimated utilizing the descriptions in the sourcebooks. Conversion table from description of damage of building etc. to seismic intensity is used to derive seismic intensity distribution. The location and magnitudes are estimated by drawing isoseismals. The basic procedure for identification of historical earthquakes are: (1) discovery and transcription of historical documents describing earthquake, (2) estimation of intensity distribution from the description, and (3) estimation of epicenter or hypocenter and magnitude. Attenuation relation of seismic intensity can be used to (1)-(3).

Although plenty of historical earthquake documents are published as the sourcebooks mentioned above and used for preceded researches, more historical documents are necessary to know details of historical earthquakes. One possible collaboration between historians and seismologists is search for historical documents related to earthquakes. An exhaustive search for large earthquakes is sometimes hard to be done, because damaged or felt area become wide for the large earthquakes. Seismic intensity of historical earthquake can be estimated assuming attenuation relation and location and magnitude of the earthquake. We can make an effective search plan for historical documents based on the estimated seismic intensity distribution.

Various conversion tables are suggested to estimate seismic intensity of historical earthquake from damage description in historical documents. The tables correlate, for example, the extent of building damage or rate of the damage to seismic intensity. We examined the validity of a conversion table using the damage of cultural property by the earthquakes including the one occurred in northern part of Osaka. Based on the conversion table, the damage of cultural properties was converted to seismic intensity. The estimated seismic intensity is consistent with distribution of seismic intensity at the locations of the cultural properties predicted by attenuation relations.

Attenuation relation of seismic intensity can be used for estimation for location of epicenter or hypocenter. The magnitude of an earthquake can be estimated by fitting attenuation relation to spatial distribution of seismic intensity. The location and magnitude of Japanese historical earthquake are estimated using attenuation relation, which is consistent with the location and magnitude obtained by preceded studies.

Keywords: Historical earthquakes, Attenuation relation, Intensity distribution, MDPs

©2019. Japan Geoscience Union. All Right Reserved.

©2019. Japan Geoscience Union. All Right Reserved.

Rekisuke: a system for sharing bibliographic information of historical documents through Interdisciplinary collaboration

*Mika Ichino[1,2], Yukie Hashimoto, Kooiti Masuda[3], Asanobu Kitamoto[2,1], Junpei Hirano[4]

1. Center for Open Data in the Humanities, Joint Support-Center for Data Science Research, Research Organization of Information and Systems , 2. National Institute of Informatics, 3. Tokyo Metropolitan University, 4. Faculty of Liberal Arts, Teikyo University

The records of numerous historical documents in Japan have been used for research in diverse scientific fields ranging from seismology, climatology and astronomy, to humanities, social sciences and historical studies. Unfortunately, when processing and applying information found in historical documents for the purpose of scientific research, the one may encounter certain difficulties despite the instrumental observations and the born digital data which can be accessed and acquired easily. Promoting in interdisciplinary fields is one of the measures used to solve these issues related to historical documents. Even under these circumstances, the cooperation with researchers from various fields relaying on historical documents has started. It will develop into interdisciplinary collaborative research to facilitate understanding of spacio-temporal association between nature and human society with a potential to become a novel scientific field.

The processes not only include the finding, obtaining, transcribing and reading the descriptions in the documents, but also structuring, analyzing and integrating, and sharing the data. Transcribing is most difficult for scientists and engineers, because they are not always familiar with historical documents. In the first place, finding the historical documents relevant for research is not always an easy task. It might be a real challenge to identify the best one that suits our needs.

Until now, the research studies using historical documents have been progressing in separate fields, but sometimes researchers extract data from the same materials. For example, Diaries contains not only daily weather conditions, but also important records such as meteorite and earthquake events. Over the years, individual research groups have extracted and digitized the data necessary for their research field only. Sharing that data is more difficult than the information about their existence, due to the secrecy of research and intellectual property legislation.

Hence, we are focused on developing “Rekisuke”, which is a system for interdisciplinary sharing of the variety of information, experience and knowledge obtained from each individual research field. Moreover, any improvements of increasing usability, linking sources, displaying the results, user interface, and increasing the data number towards the release are in great need.

The system can thus help researchers to avoid repeating the same processes/tasks that have been already done by others. An important role of the system is to provide information about the existence and the status of the various material and data. Users can help each other in during the different phases of the process, not only finding and obtaining the data but also reading and structuring them, because it can contain descriptions of various information, such as the state of the materials (paper material, image, transcribed text data, published book, digital text data, structuring data, etc.).

It has some functions enabling the search based on particular keywords, such as weather, earthquake. One of them is a notable function to search by temporal and spatial range by using APIs developed for historical temporal and spatial. It is also helpful for libraries which need to promote their historical documents. We started the collaboration with a local library for promotion of their documents and utilization of our system.

©2019. Japan Geoscience Union. All Right Reserved.

Keywords: Historical documents, Sharing information and data, Interdisciplinary collaboration, Metadata, Paleo climatology

©2019. Japan Geoscience Union. All Right Reserved.

Analysis of reconstruction processes after the 1707 Hoei eruption of Fuji Volcano based on old maps

*Junzo Ohmura[1]

1. Research Institute for Earthquake Prediction, Disaster Prevention Research Institute, Kyoto University

Fuji erupted in 1707, and a large amount of volcanic ash was deposited at its foot. The villages in the eastern part of the Shizuoka prefecture were covered with volcanic ash of about 1 m, so the residents began removing volcanic ash. In this study, we clarified how the volcanic ash removal was carried out by using an old map. On the old map are drawn the plots filled with ash fall due to the eruption. Compared to current maps, many of the plots are found to have been in the marginal areas of slightly elevated lands and villages away from the river.

Keywords: Fuji volcano, old maps, volcanic ash, reconstruction, GIS

©2019. Japan Geoscience Union. All Right Reserved.

Workshop of Word Survey about Earth and Planetary Phenomena by Citizen

*Harufumi Tamazawa[1,2], kiyomi iwahashi[3]

1. Disaster Prevention Research Institute Kyoto University, 2. Faculty of Fine Arts, Kyoto City University of Arts, 3. National Institute of Japanese Literature

In order to find phenomena related to earth and planetary sciences such as natural disasters, weather, or astronomical phenomena from historical materials and use them, it is necessary first to read the historical materials and to accurately extract words and phrases. In particular, there are a large amount of Japanese historical materials written in "kuzushi-ji" (cursive hand), and it is indispensable how to extract accurate information from a large amount of data. In handling a large amount of data, in addition to experts, cooperation of citizens who are interested and interested in contents can not be lacked, and interest in citizen participatory research in open science in recent years is also increasing. One example of such citizen participatory research is a preceding example project called "Minna-de-Honkoku" that citizens who are interested in historical disaster histories are widely asked to interpret the historical documents using the Internet. (Kano 2017).

At the National Institute of Japaneses Literature (NIJL), as part of space weather research using historical materials, we have held a citizen participatory workshop "Aurora Hunter from History" three times from 2016 (Iwahashi & Tamazawa 2018). In the workshop, Participants survered actually seek astronomical phenomena by touching classical ceremonies and old records is with reseachers of history and astronomy. This workshop is not only a mere outreach event but also a testcase of research on natural sciences using historical document with citizen. In this report, we will present the results of the efforts and think about the possibility and meaning of citizen participation in future planetary science.

In November 2018, under the full cooperation of the Kyoto University Library, this project, which will be the 4th event, was held under the name "Aurora Hunter from History IN Kyoto" at Kyoto University. There, not only astronomical phenomena but also phenomena such as earthquakes, floods and droughts were extended to the phenomenon of natural disasters, and the research was expanded to research on earth planetary science and disaster prevention. In addition, on the day we also made a lecture on the latest research on aurora and earthquakes using historical materials and demonstrated "Minna-de-Honkoku". Also, as a new attempt, we extracted the weather information from the diary historical materials and worked on data.

Looking at the questionnaire of the participants on the day, there are a lot of participants who are interested in astronomy interest more than in the past three participants. Recruitment has been reaffirmed that the participation was triggered by many lecturers and that daily social contribution activities such as researchers' lectures are important for deepening their interest in scientific research by citizens.

From the free written part of the questionnaire, it became clear that for those with less opportunities to touch historical materials usually, they were interested in reading the historical materials written in Japanese and Chinese. On the contrary, from the people who are interested in history, I found that I was attracted by the unexpectedness that I could discover newly by reading from a different viewpoint from the viewpoint I have read so far. In other words, in a workshop with a different field collaboration type, even if it is an aggregation of citizens with different interests and interests, each interest can be found in

©2019. Japan Geoscience Union. All Right Reserved.

other fields by ingenuity of the organizer side, cooperation is obtained from a wide range It suggests the possibility.

Given the aspect of citizen participation research, the so-called open science, of citizen participatory research, in order to improve the accuracy of data extracted from citizens as natural science data, cooperation among participating experts is indispensable Being able to be accurate as data by discussing beyond its own expertise. Also, in order to capture permanent participation, we aimed for a synergistic effect of both on-line work like "reprinting at everyone" and offline workshops like "classical aurora hunter", both young and senior It is the future goal to approach approach.

This work is supported by JSPS KAKENHI Grant numbers JP18H01254 and JP18H05319.

References

K. Iwahashi & H. Tamazawa (2018) Stars and galaxies, 1, 51-65.
Y. Kano (2017): Report Kasama"63, 53-56.

Keywords: Open Science, Interdisciplinary research, Public Engagement of Science

©2019. Japan Geoscience Union. All Right Reserved.

Observational Data in the first half of 20th century to join modern scientific Observation and historical documents: A Usage example ob Photographic Plate of Kwasan Observatory

*Harufumi Tamazawa[1], Reizaburo Kitai[4], Hiroaki Isobe[2], Satoru UeNo[3], Takahito Sakaue[3]

1. Disaster Prevention Research Institute Kyoto University, 2. Faculty of Fine Arts, Kyoto City University of Arts, 3. Astronomical Observatory, Graduate School of Science, Kyoto University, 4. Bukkyo University

When surveying records of natural phenomena from historical documents and using them as scientific and academic data, it is important to understand how to compare with modern observation parameters. In order to investigate long-term fluctuations of natural phenomena seamlessly linking research using historical documents with observational data of modern science, it is also important to utilize observation data in early modern observation. In the solar observation, there are solar image data recorded by photographic plates etc from the end of the 19th century to the first half of the 20th century, and archivalization is progressing little by little.

In this report, as an example of utilizing such data, we will look at sunspot images and collation of images of chromosphere, CaK line heliograms by spectroheliography, and geomagnetism observation data in the first half of the 20th century .

Regarding the decades of the 1930s, when comparing photographic plate data of the solar CaK line heliogram photographed at Kwasan Observatory, Kyoto University, and the aa index which is one of the indicators of geomagnetic storms, it was found that geomagnetic storm of a scale exceeding -100 nT even when it occurred, it was recorded that none of sunspots, existed in nine cases. As an example, at the end of April 1933, sunspots were not seen in the Kwasan Observatory's CaK line heliogram and sunspot sketches in various places, but on May 1, a geomagnetic storm was observed in Kakioka, the aa index was about -200 nT. The advantage of the CaK line heliogram is that not only sunspots but also regions where relatively weak magnetic fields such as plague that is not visible with continuous light are distributed are visualized. This makes it possible to obtain information on the global magnetic neutral line where filaments causing coronal mass ejection can exist.

Keywords: Sunspot, Geomagnetic Storm, Data Archive

©2019. Japan Geoscience Union. All Right Reserved.

Climate changes and lords' control in the early modern period in Japan

*Kaoru kamatani[1], Masaki Sano[2], Takeshi Nakatsuka[3]

1. Ritsumeikan University, 2. Waseda University, 3. Research Institute for Humanity and Nature

Recent progress in isotope dendrochronology makes it possible to precisely reconstruct summer precipitation at an annual resolution, enabling us to study the relationship between climate changes and societal responses in the past. Our earlier study revealed that rice yields estimated from historical documents in several villages near Lake Biwa suffered from frequent flood events, which were reconstructed from tree rings. In the present study, we explore how climate changes affected governmental system of tax collection in the early modern period in Japan, by comparing the methods in tax collection between two local loads of central Japan.

Keywords: climate changes, tax, lords' control

©2019. Japan Geoscience Union. All Right Reserved.

Intense geomagnetic storm during Maunder minimum possibly by quiescent filament eruption

*Hiroaki Isobe[1], Yusuke Ebihara[2], Harufumi Tamazawa[1], Akito Davis Kawamura[3], Hisashi Hayakawa[4]

1. Faculty of Fine Arts, Kyoto City University of Arts, 2. Research Institute for Sustainable Humanosphere, Kyoto University, 3. Graduate School of Science, Kyoto University, 4. Graduate School of Letters, Osaka University

The sun occasionally undergoes the so-called grand minima, in which its magnetic activity, measured by the number of sunspots, is suppressed for decades. The most prominent grand minima, since the beginning of telescopic observations of sunspots, is the Maunder minimum (1645--1715), when the sunspots became rather scarce. The mechanism underlying the grand minima remains poorly understood as there is little observational information of the solar magnetic field at that time. In this study, we examine the records of one candidate aurora display in China and Japan during the Maunder minimum. The presence of auroras in such mid magnetic latitudes indicates the occurrence of great geomagnetic storms that are usually produced by strong solar flares. However, the records of contemporary sunspot observations from Europe suggest that, at least for the likely aurora event, there was no large sunspot that could produce a strong flare. Through simple theoretical arguments, we show that this geomagnetic storm could have been generated by a giant eruption from the spotless sun.

Keywords: magnetic storm, aurora, coronal mass ejection, solar flare, Maunder minimum, historical documents

©2019. Japan Geoscience Union. All Right Reserved.

Reconstructing 1931 flood in Yangtze River basin and its application to Chinese economic history

*CHANG LIU[1], Akiyuki Kawasaki[1], Tomoko Shiroyama[2]

1. Department of Civil Engineering, Graduate School of Engineering, the University of Tokyo, 2. Department of Economics, Graduate School of Economics, the University of Tokyo

Historical floods are receiving increased attention in flood research and in applied flood protection. One of the reasons is that they can be taken into account for the improvement of long-term data series and their statistical validation as well as for the analysis of return periods. Apart from that, analyzing the interaction between historical floods and socio-economic activities has attracted more and more interests as well. Previous research has focused on rebuilding temperature, precipitation, discharge and water level of historical floods, however, more detailed information like inundation depth and area is still required for more advanced analysis. In this research, we reconstructed the inundation condition and flood propagation process of 1931 flood in Yangtze River basin using Rainfall-Runoff-Inundation (RRI) model and carried out some primary analysis on Chinese economic history. Although the 1931 flood in Yangtze River basin is recognized as the deadliest flood ever recorded for its damage to more than 25.2 million people and 58.7 billion m^2 farmland, it is considered to be simulated by a distributed hydrological model for the first time because of data scarcity in 1930s and document loss afterwards. However, with the help from many historians, lots of valuable historical documents were found and collected, which makes the model simulation possible. For the preparation of input data of RRI model, a) 24 stations' daily precipitation data from Jan 1^{st} to Dec 31^{st} were digitized from *Monthly Meteorological Bulletin* and *Hydrological Data of Yangtze River Basin*, b) land use classification data of 2015, 2005, 1995, 1985, 1975 were collected and land use classification data of 1955, 1935 and 1915 were simulated using Artificial-Neural-Network-based-Cellular-Automata (ANN-CA) scheme. Dataset b) is further validated by military map with similarity over 60%. The model was calibrated for the discharge at Chongqing gauge station by varying the land use, soil, geometry and precipitation related parameters and then evaluated using flood investigation map. We expect that the simulation result from RRI model is especially suitable for economic history study, because the inundation depth & area were generated daily for the whole year by a 2D diffusive scheme, with which historians can analyze flood impact in more detailed time and space scale. To demonstrate this point, some primary studies were also carried out: a) validation of the number of farmers influenced by 1931 flood with inundation severity, b) analysis of the rice price fluctuation in Hunan province with the inundation time and depth. From study b), one interesting finding is that places where navigation channel was limited and blocked tended to have higher rice price, which indicated the transportation mainly to be shipping in 1930s.

Keywords: Yangtze River basin, historical flood, hydrological modeling

©2019. Japan Geoscience Union. All Right Reserved.

Seismicity Analysis Using Felt Reports and Attenuation Relation of Seismic Intensity

*Takeo Ishibe[1], Koji Iwasa[1], Mitsuko Furumura[1], Ritsuko S. Matsu'ura[1]

1. Association for the Development of Earthquake Prediction

Can felt reports of historical documents be used to estimate the source of large earthquakes or seismicity analysis during the historical period? To explore the possibility of new historical earthquake studies using felt reports, we validated the reproducibility of the spatial distribution of felt report number by using the Japan Meteorological Agency (JMA) seismic intensity database and recently-constructed attenuation relation of seismic intensity. We then established a new methodology to estimate the source area of large earthquakes based on the spatial distribution of felt report number and attenuation relation and applied it to the recent three earthquakes (2004 Niigata-Ken Chuetsu, 2008 Iwate-Miyagi, and 2011 Fukushima-Hamadori earthquakes) in order to investigate the performance of the new method. The method could successfully image the source area of these earthquakes, suggesting the possibility that the source area of historical large earthquakes can be constrained from the distribution of felt reports.

We first validated the reproducibility of felt report number using the JMA seismic intensity database and newly-constructed attenuation relation of seismic intensity by Tanaka *et al*. (2017) for approximately 2,300 shallow crustal earthquakes in 2000-2010 with the maximum intensity >3. As a result, the histogram of residuals between the calculated and observed seismic intensity showed the normal distribution with the center of approximately zero. Furthermore, the attenuation relation successfully reproduced the spatial distribution of felt report number.

We then constructed a new method imaging the source area of large earthquakes and applied it to the recent three large earthquakes. We calculated the normalized residuals between the observed and calculated number of felt reports (seismic intensity >1.5) at each grid uniformly spaced in Tohoku area, by randomly generating the earthquakes in accordance with the Gutenberg-Richter law. As for the two earthquakes (2004 and 2008 events), the source areas were successfully constrained by normalized residuals and the grids with the minimum normalized residual are well matched with the mainshock epicenters. On the other hand, the source area of the 2011 event was less imaged due to the intensive aftershocks following the 2011 Tohoku-oki earthquake. The source areas of these earthquakes were also imaged even after thinning out the observation stations.

In Japan, abundant historical documents spanning over the 1000 years remain and the source area of historical earthquakes have been traditionally estimated from the distribution of damage and casualties recorded in historical literature. However, the damage could be caused by not only a ground shaking but also tsunami, massive fire and/or landslide. In addition, the distribution of building damage is strongly controlled by the population density and elapsed years since constructed.

In some historical literature, earthquakes that were felt without any damage are also reported as well as damage description from major earthquakes, whereas these were not fully utilized except for several previous studies. The number of felt reports are strongly controlled by the elapsed time since the mainshock and distance from the source area, suggesting the possibility that the source area of these earthquakes can be constrained by the spatiotemporal distribution of felt report number. Furthermore, changes in the number of felt reports may suggest the changes in seismic activity including an occurrence

©2019. Japan Geoscience Union. All Right Reserved.

of swarm-like or triggered activity and seismic quiescence. By constructing the methodology imaging the seismicity based on felt reports in historical literature, a new development of historical earthquake studies including small to moderate earthquakes is expected.

Keywords: Felt Report, Attenuation Relation of Seismic Intensity, Seismicity Analysis

©2019. Japan Geoscience Union. All Right Reserved.

Radiocarbon dating of Japanese tree rings –chronological research and Japanese calibration curve

*Minoru Sakamoto[1,2], Masataka Hakozaki[1], Takumi Mitsutani[3], Takeshi Nakatsuka[4,5]

1. National Museum of Japanese History, 2. The Graduate University for Advanced Studies, 3. Nara National Research Institute for Cultural Properties, 4. Research Institute for Humanity and Nature, 5. Nagoya University

In order to revise radiocarbon age to calendar age, a calibration curve based on the radiocarbon ages of known age sample such as tree rings is used. Calibration curve for the northern hemisphere, IntCal, mainly depended on tree rings which had been growing in the high latitude region of the West so far. However, the latest version “IntCal19” is called upon to reflect radiocarbon ages of various regions. The authors have continued radiocarbon dating of Japanese tree rings of the past 3,000 years. Recently, from a demand for chronological research on wooden buildings as cultural properties using ^{14}C-wiggle matching, we are also focusing on the tree rings of middle to early-modern ages. In the background, there is a practical application of a new method, oxygen-isotope dendrochronology, that can be implemented in several tree species. It becomes easier to obtain tree rings with known age and accumulation of radiocarbon age is progressing rapidly.

There are some periods showing certain offset on radiocarbon ages of Japanese tree ring from IntCal. One of the regional effects is remarkable during the end of the Yayoi to the beginning of the Kofun period, and calibrated age based on IntCal shows older age than the actual age. Also, since IntCal is versatile and smooth, it is sometimes insufficient for the historic chronological research that requires high precision and accuracy. It has an obligation to reveal the behavior of the radiocarbon age of Japanese tree ring and develop domestic calibration curve to promote chronological research.

This work was one of the results of the Collaborative Research Program of the NMJH and the RIHN Research Project of the Ecohistory Program (H-05). JSPS Grant in Aid (#25282075, #18H03594) also supported our research.

Keywords: radiocarbon dating, dendrochronology, calibrated age, regional effect

©2019. Japan Geoscience Union. All Right Reserved.

Usage of Historical Documents with Scientific Understandings in the field of Solar Physics

*Akito Davis Kawamura[1], Hisashi Hayakawa[2], Harufumi Tamazawa[3], Hiroaki Isobe[3], Kazunari Shibata[1]

1. Astronomical Observatory, Kyoto University, 2. Graduate School of Letters, Osaka University, 3. Faculty of Fine Arts, Kyoto City University of Arts

The sun is the most studied star by mankind, yet our knowledge on our parent star is based on the observation of limited time scale. Solar activities have been scientifically recorded for ~400 years with sunspot and ~160 years with flares (sudden increment of light emission with energy release). Meanwhile, people have witnessed and recorded the traces of solar activities for thousands of years, which we nowadays call as aurora. By combining scientific sunspot observations and historical records of aurora, first goal of our study is to decode solar flare activities for last ~400 years.

The physical variable of interest is the flare magnitude, and we have developed an estimation method with the statistics based on modern-day solar observations. The key of this method is an observation of low latitude aurora, which is a strong indication of coronal mass ejection at the flare. By knowing the size of sunspot and the existence of coronal mass ejection, our statistical method could estimate the magnitude of the flare.

At our poster, we will discuss the potentiality and difficulty of solar physics with historical documents. We hope this poster could be a demonstration of successful collaboration of science and history.

Keywords: Solar Physics, Space Weather, Historical Documents

©2019. Japan Geoscience Union. All Right Reserved.

The study of the relationship between the flood of Kitakami River and sociaty in the end of Edo period

*Daisuke Sato[1], Yoshitaka Takahashi[2]

1. International Reserch Institute of Disaster Science Tohoku University , 2. Tokyo University of Agriculture and Technology

The purpose of this study has two focal points . First, finding the water flood in Kitakami river in the end of Edo period by reserching the historical documents include newly discovered one. Second, the relationship between the flood and social influence; foresty, fishing, and political situation.

Keywords: Kitakami River, Area study, Edo period, Historical records, Sendai Han

©2019. Japan Geoscience Union. All Right Reserved.

Reconstruction of Historical Weather with Data Assimilation Using Old Diaries

*Kei Yoshimura[1], Panduka Neluwala[2], Mika Ichino[3], Kooiti Masuda[4], Junpei Hirano[5]

1. Institute of Industrial Science, The University of Tokyo, 2. University of Peradeniya , 3. National Institute of Informatics, 4. Tokyo Metropolitan University, 5. Teikyo University

Long-term atmospheric reanalysis data is indispensable for understanding the mechanism of climate change, but the current longest data is over 130 years only. The cause of not going back further to the past is largely due to lack of direct weather observation data. However, even in the past where modern weather observation data does not exist, the daily weather information described in the ancient document may exist for a longer time. In this regard, Japan is ideal country that has kept such old weather information. In this research, we developed a method to introduce old weather information into the latest data assimilation system, investigated the effect as the constraint condition of atmospheric condition, and proposed a method to extend existing reanalysis data in the past. We constructed a system using historical weather database, global spectrum model, local ensemble transform Kalman filter as observation data, prediction model and data assimilation scheme respectively. Analog information indicating weather should be classified into about 3 to 5 categories and it is better to correspond to the cloud amount ratio and the short wave downward radiation on the ground surface. Furthermore, it is appropriate that the ensemble number is about 30 from the balance of calculation efficiency and accuracy. Using the above setting, the data assimilation result given the weather information obtained at the meteorological observatory at 18 sites, for the modern era (1990 's), is closer to the modern reanalysis than the result without any weather information. As a result, significant improvements were observed in shortwave radiation and cloud cover, and significant improvement in precipitation was confirmed. These improvements are thought to have been brought by synchronizing the modeled synoptic-scale weather patterns to the reality. Furthermore, it was confirmed that the skill of rainfall estimation was improved by adding information of “no precipitation day” to data assimilation as an observation item. Then we conducted the experiments of the 1830s and 1860s using actual ancient diary data. It was confirmed that similar seasonal change and interannual variations can be obtained compared with temperature and precipitation in the 1860s which was actually observed in Yokohama.

Keywords: old diaries, data assimilation, weather reconstruction

©2019. Japan Geoscience Union. All Right Reserved.

Examination of data range for fitting Omori-Utsu law to temporal decay of aftershocks presented in historical materials on the 1830 Kyoto earthquake: Reason for the difference of numbers of aftershocks in the same place

*Kentaro Hattori[1], Junzo Ohmura[2], Ichiro Nakanishi[1]

1. Kyoto Univ., 2. Bukkyo Univ.

We study the temporal decay of aftershock sequences of the 1830 Kyoto earthquake. Omori(1908) examined aftershock sequences including that of the 1830 Kyoto earthquake. Matsui and Oike (1997) attempted to determine epicenter of the 1830 Kyoto earthquake by using the number of felt aftershocks in time range from the main shock to the next morning in several observational areas including Kyoto. They used two different numbers as the number of felt aftershocks for Kyoto: 100 written in Banzai Rakki and 4 written in Tansui Nikki. In the case using the former number, they obtained the epicenter consistent with that obtained by Usami (1996). However, in the case using the latter number, they obtained an epicenter near the northern shore of the lake Biwa, and the epicenter is inconsistent with distribution of damage caused by the earthquake. They did not pursue the reason of the discrepancy between two numbers for Kyoto.

In order to solve the above mentioned discrepancy among the earthquake records for Kyoto, we include another record Tenpo Zakki in addition to Banzai Rakki.Both records show quite different numbers of daily aftershocks during several days, though they were written in the same place. Kitahara and Ohmura (2012) suggest that the original record was written by an officer in Nijo-jo Castle and was copied many times. They made a graph of temporal decay of daily numbers of aftershocks for a period of one month after the main shock. However, they made neither analysis of the aftershock sequences nor information evaluation of the records.

We examined carefully description of daily aftershocks in both records to know the reason for the differences of the numbers of felt aftershocks. The records show the sizes of earthquakes by the diameters of handwritten circles for each day. Comparing the diameter of standard circle for every day, we infer that writers of the records used different criterion to count the numbers of felt aftershocks.

We measure the diameter of standard circle for every day, and find the diameter changes with day. Fig.1 shows the daily variation of diameter of standard circle in the both records. The vertical axis shows the count threshold of circle diameter (arbitrary unit), and horizontal axis shows the date. Fig.1 suggests that the threshold count level used in Banzai Rakki is larger than that used in Tenpo Zakki. This result means that the number of counted aftershocks becomes smaller in Banzai Rakki than in Tenpo Zakki. The interpretation is consistent with the actual difference of the number of aftershocks in the both records. The threshold level for counting used in Banzai Rakki changes more rapidly with time than that used in Tenpo Zakki (Fig.1). Especially, the change of the threshold level from 7/3 to 7/5 is not negligible in Banzai Rakki.

The above information evaluation of the two records reveals the difference of the two records written in the same place. We fit Omori-Utsu law (Utsu, 1961) to the aftershock sequences after 7/5. We assume that the c value is 0.1 and the p values fall in about 1.2. We obtain a better fit in Tenpo Zakki (Fig.2). Our study may suggest that Tenpo Zakki may have better information quality than Banzai Rakki and the numbers of aftershocks after 7/5 should be used for study of the 1830 Kyoto earthquake.

©2019. Japan Geoscience Union. All Right Reserved.

Keywords: the 1830 Kyoto earthquake , aftershock sequence, Omori-Utsu law

©2019. Japan Geoscience Union. All Right Reserved.

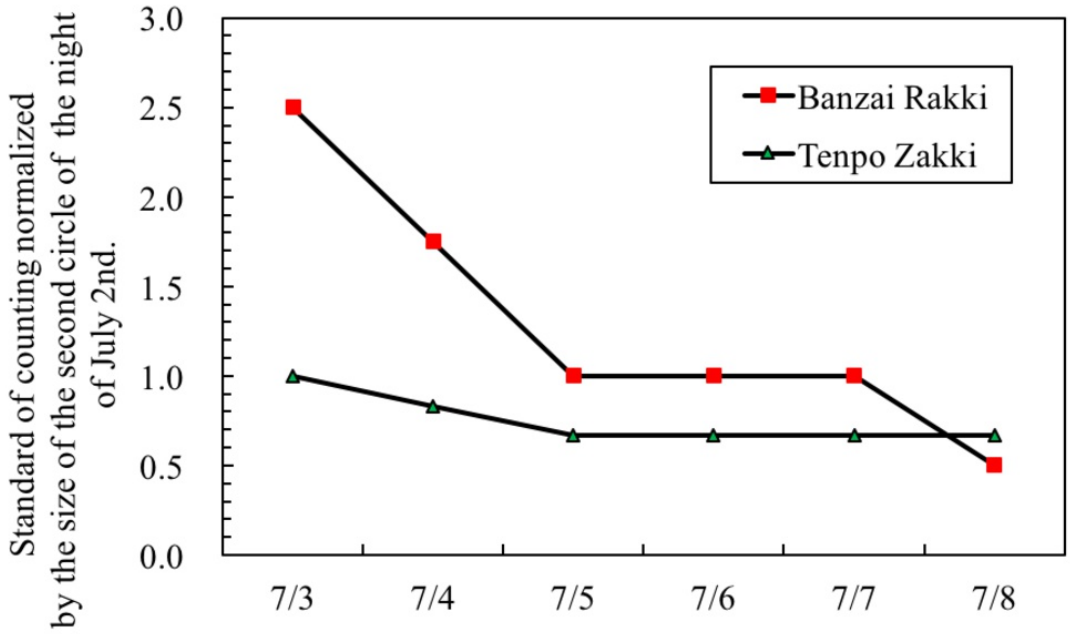

Fig.1 Comparison of two records

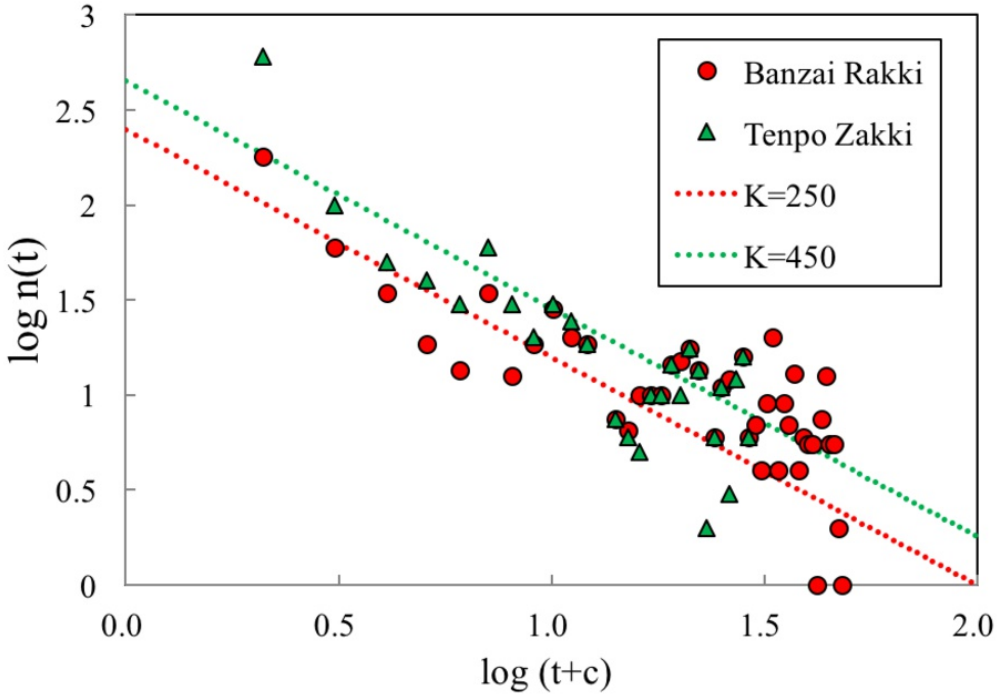

Fig. 2 Temporal decay of the aftershocks of the 1830 Kyoto earthquake with lines (p=1.2) from Omori-Utsu law (Utsu, 1961)

©2019. Japan Geoscience Union. All Right Reserved.

Tsunami trace height of the AD 1854 Ansei Tokai tsunami around the lake Hamanako inferred from historical maps

*ebina yuichi[1], Kentaro Imai[2], Yoshinobu Tsuji[3], hiroyuki iwase[4]

1. International Research Institute of Disaster Science, 2. JAMSTEC, 3. Fukuda Geological Instite, 4. (C)ECOH CORPORATION

We analyzed the trace of tsunami from historical maps "Maisaka-syuku tsunamizu" and “Ansei Tsunami saigai ezu" (in Hamamatsu museum) drawn about the tsunami damages around Hamanako in the Ansei Tokai earthquake occurred in 1854.

“Maisaka” (present Maisaka-cho Nishi-ku, Hamamatsu-shi, Shizuoka-ken) located in the “Hamanako” east shore is the area which prospered as a post town in “Tokaido”. According to "the history of Shizuoka" (1996), which was drawn by Hachiro Watanabe, who was a resident of “Maisaka” and drew the " Maisaka” tsunami figure. This picture shows that the appearance of Maisaka inundated by tsunami, or people who evacuated. On the east side of a highway, tsunami has reached to near night-lights. Moreover, in the west side, stairs around "Shigetuin" were inundated. This is a place called "Ohkonoboriba" by "Toukaido-bungen-nobe-ezu". It becomes clear that from here to several east sides of a subsidiary inn or an administration office were inundated by tsunami.

“Ansei zisin tsunami saigai ezu“ shows the time when the tsunami hits “Okuhamanako and Kiga” area and after the situation of the tsunami. Here, we can find some points reaching tsunami by considering “Himekaido” north side passes as a mark. Although seeing from the historical map, tsunami reached the front of “Kigasekisyo” but tsunami was not flooded in the barrier main part. Moreover, "Komorisawa" near "Ninomiyasya", and "Iwanesawa", near "Himekaido" were drawn as reaching points of the tsunami. Furthermore, signs that the circumference of a mountain where "Daienzi-temple" located in “Ikutagawa-river mouth-of-a-river part which flows into “Okuhama” name lake serves as a cemetery in the case of tsunami has sunk are drawn. “Dainenji Temple” in the area of mouth of “Ikutagawa River” was inundated by tsunami but only the hill used as the “Dainenji Temple Cemetery” was not. There are few documents described accurate places which was reached by the tsunami around Lake Hamanako, especially Lake Okuhamanako. However, we identified those based on historical maps. We hope that our results will contribute to future interdisciplinary research including tsunami engineering on the past great earthquakes along the Nankai Trough.

Acknowledgement
This research was supported by MEXT (“Research project for compound disaster mitigation on the great earthquakes and tsunamis around the Nankai Trough region”).

Keywords: Ansei Tokai earthquake and tsunami, Lake hamanako, historical maps

©2019. Japan Geoscience Union. All Right Reserved.

[J] Poster | M (Multidisciplinary and Interdisciplinary)：M-IS Intersection

Mon. May 27, 2019 5:15 PM - 6:30 PM JST | Mon. May 27, 2019 8:15 AM - 9:30 AM UTC | Poster Hall International Exhibition Hall8, Makuhari Messe_37

[M-IS17] History X Earth and Planetary Science

convener:Yasuyuki Kano(Earthquake Research Institute, The University of Tokyo), Kei Yoshimura(Institute of Industrial Science, The University of Tokyo), Hiroaki Isobe(Faculty of Fine Arts, Kyoto City University of Arts), kiyomi iwahashi(National Institute of Japanese Literature)

The history of modern observation in earth and planetary sciences is often far shorter compared with the timescales of their interests. Investigation of the long-term variations and occurrences of extremely rare events requires effective use of information before modern observations. Historical documents recorded by diverse kinds of authors in various situations are the important sources of such information.

Thus, historical documents have been referred in various fields of earth and planetary sciences such as seismology, climatology, meteorology and astronomy. Sharing their records, methods and experiences will be beneficial for each field and bring new insights. It is also essential to involve experienced scholars in history because one needs to carefully investigate the reliability and the context of each document in order to use it as scientific data. On the other hand, analyzing the record in the historical documents with the eyes of modern science may also bring new insights to the history scholars.

In this session we overview the studies using the historical documents in various fields of the earth and planetary sciences as well as the recent advances in related topics such as digital humanities and historical-data assimilation. The aim is to promote the communication and dialogues among the researchers in various background, and thus foster the new ideas and collaborations in the study of "History X EPS."

[MIS17-P01] Perspective of 'History X Earth and Planetary Science'

*Yasuyuki Kano[1], Hiroaki Isobe[2], Kei Yoshimura[3], Kiyomi Iwahashi[4], Harufumi Tamazawa[5,2] (1.Earthquake Research Institute, The University of Tokyo, 2.Faculty of Fine Arts, Kyoto City University of Arts, 3.Institute of Industrial Science, The University of Tokyo, 4.National Institute of Japanese Literature, 5.Disaster Prevention Research Institute, Kyoto University)

[MIS17-P02] Reexamination of intensity distribution of Japanese historical earthquakes using attenuation relation

*Yasuyuki Kano[1], Junzo Ohmura[2] (1.Earthquake Research Institute, The University of Tokyo, 2.Diasaster prevention Research institute, Kyoto University)

[MIS17-P03] Rekisuke: a system for sharing bibliographic information of historical documents through Interdisciplinary collaboration

★Invited Papers

*Mika Ichino[1,2], Yukie Hashimoto, Kooiti Masuda[3], Asanobu Kitamoto[2,1], Junpei Hirano[4] (1.Center for Open Data in the Humanities, Joint Support-Center for Data Science Research, Research Organization of Information and Systems , 2.National Institute of Informatics, 3.Tokyo Metropolitan University, 4.Faculty of Liberal Arts, Teikyo University)

[MIS17-P04] Analysis of reconstruction processes after the 1707 Hoei eruption of Fuji Volcano based on old maps

*Junzo Ohmura[1] (1.Research Institute for Earthquake Prediction, Disaster Prevention Research Institute, Kyoto University)

[MIS17-P05] Workshop of Word Survey about Earth and Planetary Phenomena by Citizen

*Harufumi Tamazawa[1,2], kiyomi iwahashi[3] (1. Disaster Prevention Research Institute Kyoto University, 2.Faculty of Fine Arts, Kyoto City University of Arts, 3.National Institute of Japanese Literature)

[MIS17-P06] Observational Data in the first half of 20th century to join modern scientific Observation and historical documents: A Usage example ob Photographic Plate of Kwasan Observatory

*Harufumi Tamazawa[1], Reizaburo Kitai[4], Hiroaki Isobe[2], Satoru UeNo[3], Takahito Sakaue[3] (1. Disaster Prevention Research Institute Kyoto University, 2.Faculty of Fine Arts, Kyoto City University of Arts, 3.Astronomical Observatory, Graduate School of Science, Kyoto University, 4.Bukkyo University)

[MIS17-P07] Climate changes and lords' control in the early modern period in Japan

*Kaoru kamatani[1], Masaki Sano[2], Takeshi Nakatsuka[3] (1.Ritsumeikan University, 2.Waseda University, 3.Research Institute for Humanity and Nature)

[MIS17-P08] Intense geomagnetic storm during Maunder minimum possibly by quiescent filament eruption

*Hiroaki Isobe[1], Yusuke Ebihara[2], Harufumi Tamazawa[1], Akito Davis Kawamura[3], Hisashi Hayakawa[4] (1.Faculty of Fine Arts, Kyoto City University of Arts, 2.Research Institute for Sustainable Humanosphere, Kyoto University, 3.Graduate School of Science, Kyoto University, 4.Graduate School of Letters, Osaka University)

[MIS17-P09] Reconstructing 1931 flood in Yangtze River basin and its application to Chinese economic history

*CHANG LIU[1], Akiyuki Kawasaki[1], Tomoko Shiroyama[2] (1.Department of Civil Engineering, Graduate School of Engineering, the University of Tokyo, 2.Department of Economics, Graduate School of Economics, the University of Tokyo)

[MIS17-P10] Seismicity Analysis Using Felt Reports and Attenuation Relation of Seismic Intensity

*Takeo Ishibe[1], Koji Iwasa[1], Mitsuko Furumura[1], Ritsuko S. Matsu'ura[1] (1.Association for the Development of Earthquake Prediction)

[MIS17-P11] Radiocarbon dating of Japanese tree rings – chronological research and Japanese calibration curve

*Minoru Sakamoto[1,2], Masataka Hakozaki[1], Takumi Mitsutani[3], Takeshi Nakatsuka[4,5] (1.National Museum of Japanese History, 2.The Graduate University for Advanced Studies, 3.Nara National Research Institute for Cultural Properties, 4.Research Institute for Humanity and Nature, 5.Nagoya University)

[MIS17-P12] Usage of Historical Documents with Scientific Understandings in the field of Solar Physics

*Akito Davis Kawamura[1], Hisashi Hayakawa[2], Harufumi Tamazawa[3], Hiroaki Isobe[3], Kazunari Shibata[1] (1.Astronomical Observatory, Kyoto University, 2.Graduate School of Letters, Osaka University, 3.Faculty of Fine Arts, Kyoto City University of Arts)

[MIS17-P13] The study of the relationship between the flood of Kitakami River and sociaty in the end of Edo period

*Daisuke Sato[1], Yoshitaka Takahashi[2] (1.International Reserch Institute of Disaster Science Tohoku University , 2.Tokyo University of Agriculture and Technology)

[MIS17-P14] Reconstruction of Historical Weather with Data Assimilation Using Old Diaries

*Kei Yoshimura[1], Panduka Neluwala[2], Mika Ichino[3], Kooiti Masuda[4], Junpei Hirano[5] (1.Institute of Industrial Science, The University of Tokyo, 2.University of Peradeniya , 3.National Institute of Informatics, 4.Tokyo Metropolitan University, 5.Teikyo University)

[MIS17-P15] Examination of data range for fitting Omori-Utsu law to temporal decay of aftershocks presented in historical materials on the 1830 Kyoto earthquake: Reason for the difference of numbers of aftershocks in the same place

*Kentaro Hattori[1], Junzo Ohmura[2], Ichiro Nakanishi[1] (1.Kyoto Univ., 2.Bukkyo Univ.)

[MIS17-P16] Tsunami trace height of the AD 1854 Ansei Tokai tsunami around the lake Hamanako inferred from historical maps

*ebina yuichi[1], Kentaro Imai[2], Yoshinobu Tsuji[3], hiroyuki iwase[4] (1.International Research Institute of Disaster Science, 2.JAMSTEC, 3.Fukuda Geological Instite, 4. (C)ECOH CORPORATION)

Perspective of 'History X Earth and Planetary Science'

*Yasuyuki Kano[1], Hiroaki Isobe[2], Kei Yoshimura[3], Kiyomi Iwahashi[4], Harufumi Tamazawa[5,2]

1. Earthquake Research Institute, The University of Tokyo, 2. Faculty of Fine Arts, Kyoto City University of Arts, 3. Institute of Industrial Science, The University of Tokyo, 4. National Institute of Japanese Literature, 5. Disaster Prevention Research Institute, Kyoto University

"History X EPS" is a title of this session as well as the name of the application area proposed for Grant-in-Aid for Scientific Research on Innovative Areas. The application area consists of 4 sub area: “Ten” (astronomy), ”Ki” (climatology and meteorology), ”Chi” (solid earth science), and ”Jin” (human and society).

Historians and researchers of earth and planetary sciences have been collaborated in the preceding projects. There are a number of projects for such interdisciplinary collaboration. Here we present prospects of "History X EPS." The scope of the session is as follows:

The history of modern observation in earth and planetary sciences is often far shorter compared with the timescales of their interests. Investigation of the long-term variations and occurrences of extremely rare events requires effective use of information before modern observations. Historical documents recorded by diverse kinds of authors in various situations are the important sources of such information.

Thus, historical documents have been referred in various fields of earth and planetary sciences such as seismology, climatology, meteorology and astronomy. Sharing their records, methods and experiences will be beneficial for each field and bring new insights. It is also essential to involve experienced scholars in history because one needs to carefully investigate the reliability and the context of each document in order to use it as scientific data. On the other hand, analyzing the record in the historical documents with the eyes of modern science may also bring new insights to the history scholars.

In this session we overview the studies using the historical documents in various fields of the earth and planetary sciences as well as the recent advances in related topics such as digital humanities and historical-data assimilation. The aim is to promote the communication and dialogues among the researchers in various background, and thus foster the new ideas and collaborations in the study of "History X EPS."

Keywords: History, Astronomy, Solar phisics, Meteorology, Seismology

©2019. Japan Geoscience Union. All Right Reserved.

Reexamination of intensity distribution of Japanese historical earthquakes using attenuation relation

*Yasuyuki Kano[1], Junzo Ohmura[2]

1. Earthquake Research Institute, The University of Tokyo, 2. Diasaster prevention Research institute, Kyoto University

Sources of historical earthquakes are usually estimated from seismic intensity distributions based on the descriptions on historical documents. Ceaseless efforts to collect historical earthquake documents leads to sourcebooks such as Dai-Nihon Jishin Shiryo (Collection of Historical Documents on Earthquakes in Great Japan) (Tayama, 1904a,b), Zotei Dai-Nihon Jishin Shiryo (Collection of Historical Documents on Earthquakes in Great Japan, Enlarged and Revised Edition) (Musha, 1941, 1943a,b), and Shinshu Nihon Jishin Shiryo (Historical Documents on Earthquakes in Japan, New Collection) (Earthquake Research Institute of the University of Tokyo, 1981-1994) etc. The location of epicenter or hypocenter, origin time, and magnitude of the historical earthquakes are estimated utilizing the descriptions in the sourcebooks. Conversion table from description of damage of building etc. to seismic intensity is used to derive seismic intensity distribution. The location and magnitudes are estimated by drawing isoseismals. The basic procedure for identification of historical earthquakes are: (1) discovery and transcription of historical documents describing earthquake, (2) estimation of intensity distribution from the description, and (3) estimation of epicenter or hypocenter and magnitude. Attenuation relation of seismic intensity can be used to (1)-(3).

Although plenty of historical earthquake documents are published as the sourcebooks mentioned above and used for preceded researches, more historical documents are necessary to know details of historical earthquakes. One possible collaboration between historians and seismologists is search for historical documents related to earthquakes. An exhaustive search for large earthquakes is sometimes hard to be done, because damaged or felt area become wide for the large earthquakes. Seismic intensity of historical earthquake can be estimated assuming attenuation relation and location and magnitude of the earthquake. We can make an effective search plan for historical documents based on the estimated seismic intensity distribution.

Various conversion tables are suggested to estimate seismic intensity of historical earthquake from damage description in historical documents. The tables correlate, for example, the extent of building damage or rate of the damage to seismic intensity. We examined the validity of a conversion table using the damage of cultural property by the earthquakes including the one occurred in northern part of Osaka. Based on the conversion table, the damage of cultural properties was converted to seismic intensity. The estimated seismic intensity is consistent with distribution of seismic intensity at the locations of the cultural properties predicted by attenuation relations.

Attenuation relation of seismic intensity can be used for estimation for location of epicenter or hypocenter. The magnitude of an earthquake can be estimated by fitting attenuation relation to spatial distribution of seismic intensity. The location and magnitude of Japanese historical earthquake are estimated using attenuation relation, which is consistent with the location and magnitude obtained by preceded studies.

Keywords: Historical earthquakes, Attenuation relation, Intensity distribution, MDPs

©2019. Japan Geoscience Union. All Right Reserved.

©2019. Japan Geoscience Union. All Right Reserved.

Rekisuke: a system for sharing bibliographic information of historical documents through Interdisciplinary collaboration

*Mika Ichino[1,2], Yukie Hashimoto, Kooiti Masuda[3], Asanobu Kitamoto[2,1], Junpei Hirano[4]

1. Center for Open Data in the Humanities, Joint Support-Center for Data Science Research, Research Organization of Information and Systems , 2. National Institute of Informatics, 3. Tokyo Metropolitan University, 4. Faculty of Liberal Arts, Teikyo University

The records of numerous historical documents in Japan have been used for research in diverse scientific fields ranging from seismology, climatology and astronomy, to humanities, social sciences and historical studies. Unfortunately, when processing and applying information found in historical documents for the purpose of scientific research, the one may encounter certain difficulties despite the instrumental observations and the born digital data which can be accessed and acquired easily. Promoting in interdisciplinary fields is one of the measures used to solve these issues related to historical documents. Even under these circumstances, the cooperation with researchers from various fields relaying on historical documents has started. It will develop into interdisciplinary collaborative research to facilitate understanding of spacio-temporal association between nature and human society with a potential to become a novel scientific field.

The processes not only include the finding, obtaining, transcribing and reading the descriptions in the documents, but also structuring, analyzing and integrating, and sharing the data. Transcribing is most difficult for scientists and engineers, because they are not always familiar with historical documents. In the first place, finding the historical documents relevant for research is not always an easy task. It might be a real challenge to identify the best one that suits our needs.

Until now, the research studies using historical documents have been progressing in separate fields, but sometimes researchers extract data from the same materials. For example, Diaries contains not only daily weather conditions, but also important records such as meteorite and earthquake events. Over the years, individual research groups have extracted and digitized the data necessary for their research field only. Sharing that data is more difficult than the information about their existence, due to the secrecy of research and intellectual property legislation.

Hence, we are focused on developing “Rekisuke”, which is a system for interdisciplinary sharing of the variety of information, experience and knowledge obtained from each individual research field. Moreover, any improvements of increasing usability, linking sources, displaying the results, user interface, and increasing the data number towards the release are in great need.

The system can thus help researchers to avoid repeating the same processes/tasks that have been already done by others. An important role of the system is to provide information about the existence and the status of the various material and data. Users can help each other in during the different phases of the process, not only finding and obtaining the data but also reading and structuring them, because it can contain descriptions of various information, such as the state of the materials (paper material, image, transcribed text data, published book, digital text data, structuring data, etc.).

It has some functions enabling the search based on particular keywords, such as weather, earthquake. One of them is a notable function to search by temporal and spatial range by using APIs developed for historical temporal and spatial. It is also helpful for libraries which need to promote their historical documents. We started the collaboration with a local library for promotion of their documents and utilization of our system.

©2019. Japan Geoscience Union. All Right Reserved.

Keywords: Historical documents, Sharing information and data, Interdisciplinary collaboration, Metadata, Paleo climatology

©2019. Japan Geoscience Union. All Right Reserved.

Analysis of reconstruction processes after the 1707 Hoei eruption of Fuji Volcano based on old maps

*Junzo Ohmura[1]

1. Research Institute for Earthquake Prediction, Disaster Prevention Research Institute, Kyoto University

Fuji erupted in 1707, and a large amount of volcanic ash was deposited at its foot. The villages in the eastern part of the Shizuoka prefecture were covered with volcanic ash of about 1 m, so the residents began removing volcanic ash. In this study, we clarified how the volcanic ash removal was carried out by using an old map. On the old map are drawn the plots filled with ash fall due to the eruption. Compared to current maps, many of the plots are found to have been in the marginal areas of slightly elevated lands and villages away from the river.

Keywords: Fuji volcano, old maps, volcanic ash, reconstruction, GIS

©2019. Japan Geoscience Union. All Right Reserved.

Workshop of Word Survey about Earth and Planetary Phenomena by Citizen

*Harufumi Tamazawa[1,2], kiyomi iwahashi[3]

1. Disaster Prevention Research Institute Kyoto University, 2. Faculty of Fine Arts, Kyoto City University of Arts, 3. National Institute of Japanese Literature

In order to find phenomena related to earth and planetary sciences such as natural disasters, weather, or astronomical phenomena from historical materials and use them, it is necessary first to read the historical materials and to accurately extract words and phrases. In particular, there are a large amount of Japanese historical materials written in "kuzushi-ji" (cursive hand), and it is indispensable how to extract accurate information from a large amount of data. In handling a large amount of data, in addition to experts, cooperation of citizens who are interested and interested in contents can not be lacked, and interest in citizen participatory research in open science in recent years is also increasing. One example of such citizen participatory research is a preceding example project called "Minna-de-Honkoku" that citizens who are interested in historical disaster histories are widely asked to interpret the historical documents using the Internet. (Kano 2017).

At the National Institute of Japaneses Literature (NIJL), as part of space weather research using historical materials, we have held a citizen participatory workshop "Aurora Hunter from History" three times from 2016 (Iwahashi & Tamazawa 2018). In the workshop, Participants survered actually seek astronomical phenomena by touching classical ceremonies and old records is with reseachers of history and astronomy. This workshop is not only a mere outreach event but also a testcase of research on natural sciences using historical document with citizen. In this report, we will present the results of the efforts and think about the possibility and meaning of citizen participation in future planetary science.

In November 2018, under the full cooperation of the Kyoto University Library, this project, which will be the 4th event, was held under the name "Aurora Hunter from History IN Kyoto" at Kyoto University. There, not only astronomical phenomena but also phenomena such as earthquakes, floods and droughts were extended to the phenomenon of natural disasters, and the research was expanded to research on earth planetary science and disaster prevention. In addition, on the day we also made a lecture on the latest research on aurora and earthquakes using historical materials and demonstrated "Minna-de-Honkoku". Also, as a new attempt, we extracted the weather information from the diary historical materials and worked on data.

Looking at the questionnaire of the participants on the day, there are a lot of participants who are interested in astronomy interest more than in the past three participants. Recruitment has been reaffirmed that the participation was triggered by many lecturers and that daily social contribution activities such as researchers' lectures are important for deepening their interest in scientific research by citizens.

From the free written part of the questionnaire, it became clear that for those with less opportunities to touch historical materials usually, they were interested in reading the historical materials written in Japanese and Chinese. On the contrary, from the people who are interested in history, I found that I was attracted by the unexpectedness that I could discover newly by reading from a different viewpoint from the viewpoint I have read so far. In other words, in a workshop with a different field collaboration type, even if it is an aggregation of citizens with different interests and interests, each interest can be found in

©2019. Japan Geoscience Union. All Right Reserved.

other fields by ingenuity of the organizer side, cooperation is obtained from a wide range It suggests the possibility.

Given the aspect of citizen participation research, the so-called open science, of citizen participatory research, in order to improve the accuracy of data extracted from citizens as natural science data, cooperation among participating experts is indispensable Being able to be accurate as data by discussing beyond its own expertise. Also, in order to capture permanent participation, we aimed for a synergistic effect of both on-line work like "reprinting at everyone" and offline workshops like "classical aurora hunter", both young and senior It is the future goal to approach approach.

This work is supported by JSPS KAKENHI Grant numbers JP18H01254 and JP18H05319.

References

K. Iwahashi & H. Tamazawa (2018) Stars and galaxies, 1, 51-65.
Y. Kano (2017): Report Kasama"63, 53-56.

Keywords: Open Science, Interdisciplinary research, Public Engagement of Science

©2019. Japan Geoscience Union. All Right Reserved.

Observational Data in the first half of 20th century to join modern scientific Observation and historical documents: A Usage example ob Photographic Plate of Kwasan Observatory

*Harufumi Tamazawa[1], Reizaburo Kitai[4], Hiroaki Isobe[2], Satoru UeNo[3], Takahito Sakaue[3]

1. Disaster Prevention Research Institute Kyoto University, 2. Faculty of Fine Arts, Kyoto City University of Arts, 3. Astronomical Observatory, Graduate School of Science, Kyoto University, 4. Bukkyo University

When surveying records of natural phenomena from historical documents and using them as scientific and academic data, it is important to understand how to compare with modern observation parameters. In order to investigate long-term fluctuations of natural phenomena seamlessly linking research using historical documents with observational data of modern science, it is also important to utilize observation data in early modern observation. In the solar observation, there are solar image data recorded by photographic plates etc from the end of the 19th century to the first half of the 20th century, and archivalization is progressing little by little.

In this report, as an example of utilizing such data, we will look at sunspot images and collation of images of chromosphere, CaK line heliograms by spectroheliography, and geomagnetism observation data in the first half of the 20th century .

Regarding the decades of the 1930s, when comparing photographic plate data of the solar CaK line heliogram photographed at Kwasan Observatory, Kyoto University, and the aa index which is one of the indicators of geomagnetic storms, it was found that geomagnetic storm of a scale exceeding -100 nT even when it occurred, it was recorded that none of sunspots, existed in nine cases. As an example, at the end of April 1933, sunspots were not seen in the Kwasan Observatory's CaK line heliogram and sunspot sketches in various places, but on May 1, a geomagnetic storm was observed in Kakioka, the aa index was about -200 nT. The advantage of the CaK line heliogram is that not only sunspots but also regions where relatively weak magnetic fields such as plague that is not visible with continuous light are distributed are visualized. This makes it possible to obtain information on the global magnetic neutral line where filaments causing coronal mass ejection can exist.

Keywords: Sunspot, Geomagnetic Storm, Data Archive

©2019. Japan Geoscience Union. All Right Reserved.

Climate changes and lords' control in the early modern period in Japan

*Kaoru kamatani[1], Masaki Sano[2], Takeshi Nakatsuka[3]

1. Ritsumeikan University, 2. Waseda University, 3. Research Institute for Humanity and Nature

Recent progress in isotope dendrochronology makes it possible to precisely reconstruct summer precipitation at an annual resolution, enabling us to study the relationship between climate changes and societal responses in the past. Our earlier study revealed that rice yields estimated from historical documents in several villages near Lake Biwa suffered from frequent flood events, which were reconstructed from tree rings. In the present study, we explore how climate changes affected governmental system of tax collection in the early modern period in Japan, by comparing the methods in tax collection between two local loads of central Japan.

Keywords: climate changes, tax, lords' control

©2019. Japan Geoscience Union. All Right Reserved.

Intense geomagnetic storm during Maunder minimum possibly by quiescent filament eruption

*Hiroaki Isobe[1], Yusuke Ebihara[2], Harufumi Tamazawa[1], Akito Davis Kawamura[3], Hisashi Hayakawa[4]

1. Faculty of Fine Arts, Kyoto City University of Arts, 2. Research Institute for Sustainable Humanosphere, Kyoto University, 3. Graduate School of Science, Kyoto University, 4. Graduate School of Letters, Osaka University

The sun occasionally undergoes the so-called grand minima, in which its magnetic activity, measured by the number of sunspots, is suppressed for decades. The most prominent grand minima, since the beginning of telescopic observations of sunspots, is the Maunder minimum (1645--1715), when the sunspots became rather scarce. The mechanism underlying the grand minima remains poorly understood as there is little observational information of the solar magnetic field at that time. In this study, we examine the records of one candidate aurora display in China and Japan during the Maunder minimum. The presence of auroras in such mid magnetic latitudes indicates the occurrence of great geomagnetic storms that are usually produced by strong solar flares. However, the records of contemporary sunspot observations from Europe suggest that, at least for the likely aurora event, there was no large sunspot that could produce a strong flare. Through simple theoretical arguments, we show that this geomagnetic storm could have been generated by a giant eruption from the spotless sun.

Keywords: magnetic storm, aurora, coronal mass ejection, solar flare, Maunder minimum, historical documents

©2019. Japan Geoscience Union. All Right Reserved.

Reconstructing 1931 flood in Yangtze River basin and its application to Chinese economic history

*CHANG LIU[1], Akiyuki Kawasaki[1], Tomoko Shiroyama[2]

1. Department of Civil Engineering, Graduate School of Engineering, the University of Tokyo, 2. Department of Economics, Graduate School of Economics, the University of Tokyo

Historical floods are receiving increased attention in flood research and in applied flood protection. One of the reasons is that they can be taken into account for the improvement of long-term data series and their statistical validation as well as for the analysis of return periods. Apart from that, analyzing the interaction between historical floods and socio-economic activities has attracted more and more interests as well. Previous research has focused on rebuilding temperature, precipitation, discharge and water level of historical floods, however, more detailed information like inundation depth and area is still required for more advanced analysis. In this research, we reconstructed the inundation condition and flood propagation process of 1931 flood in Yangtze River basin using Rainfall-Runoff-Inundation (RRI) model and carried out some primary analysis on Chinese economic history. Although the 1931 flood in Yangtze River basin is recognized as the deadliest flood ever recorded for its damage to more than 25.2 million people and 58.7 billion m^2 farmland, it is considered to be simulated by a distributed hydrological model for the first time because of data scarcity in 1930s and document loss afterwards. However, with the help from many historians, lots of valuable historical documents were found and collected, which makes the model simulation possible. For the preparation of input data of RRI model, a) 24 stations' daily precipitation data from Jan 1^{st} to Dec 31^{st} were digitized from *Monthly Meteorological Bulletin* and *Hydrological Data of Yangtze River Basin*, b) land use classification data of 2015, 2005, 1995, 1985, 1975 were collected and land use classification data of 1955, 1935 and 1915 were simulated using Artificial-Neural-Network-based-Cellular-Automata (ANN-CA) scheme. Dataset b) is further validated by military map with similarity over 60%. The model was calibrated for the discharge at Chongqing gauge station by varying the land use, soil, geometry and precipitation related parameters and then evaluated using flood investigation map. We expect that the simulation result from RRI model is especially suitable for economic history study, because the inundation depth & area were generated daily for the whole year by a 2D diffusive scheme, with which historians can analyze flood impact in more detailed time and space scale. To demonstrate this point, some primary studies were also carried out: a) validation of the number of farmers influenced by 1931 flood with inundation severity, b) analysis of the rice price fluctuation in Hunan province with the inundation time and depth. From study b), one interesting finding is that places where navigation channel was limited and blocked tended to have higher rice price, which indicated the transportation mainly to be shipping in 1930s.

Keywords: Yangtze River basin, historical flood, hydrological modeling

©2019. Japan Geoscience Union. All Right Reserved.

Seismicity Analysis Using Felt Reports and Attenuation Relation of Seismic Intensity

*Takeo Ishibe[1], Koji Iwasa[1], Mitsuko Furumura[1], Ritsuko S. Matsu'ura[1]

1. Association for the Development of Earthquake Prediction

Can felt reports of historical documents be used to estimate the source of large earthquakes or seismicity analysis during the historical period? To explore the possibility of new historical earthquake studies using felt reports, we validated the reproducibility of the spatial distribution of felt report number by using the Japan Meteorological Agency (JMA) seismic intensity database and recently-constructed attenuation relation of seismic intensity. We then established a new methodology to estimate the source area of large earthquakes based on the spatial distribution of felt report number and attenuation relation and applied it to the recent three earthquakes (2004 Niigata-Ken Chuetsu, 2008 Iwate-Miyagi, and 2011 Fukushima-Hamadori earthquakes) in order to investigate the performance of the new method. The method could successfully image the source area of these earthquakes, suggesting the possibility that the source area of historical large earthquakes can be constrained from the distribution of felt reports.

We first validated the reproducibility of felt report number using the JMA seismic intensity database and newly-constructed attenuation relation of seismic intensity by Tanaka *et al*. (2017) for approximately 2,300 shallow crustal earthquakes in 2000-2010 with the maximum intensity >3. As a result, the histogram of residuals between the calculated and observed seismic intensity showed the normal distribution with the center of approximately zero. Furthermore, the attenuation relation successfully reproduced the spatial distribution of felt report number.

We then constructed a new method imaging the source area of large earthquakes and applied it to the recent three large earthquakes. We calculated the normalized residuals between the observed and calculated number of felt reports (seismic intensity >1.5) at each grid uniformly spaced in Tohoku area, by randomly generating the earthquakes in accordance with the Gutenberg-Richter law. As for the two earthquakes (2004 and 2008 events), the source areas were successfully constrained by normalized residuals and the grids with the minimum normalized residual are well matched with the mainshock epicenters. On the other hand, the source area of the 2011 event was less imaged due to the intensive aftershocks following the 2011 Tohoku-oki earthquake. The source areas of these earthquakes were also imaged even after thinning out the observation stations.

In Japan, abundant historical documents spanning over the 1000 years remain and the source area of historical earthquakes have been traditionally estimated from the distribution of damage and casualties recorded in historical literature. However, the damage could be caused by not only a ground shaking but also tsunami, massive fire and/or landslide. In addition, the distribution of building damage is strongly controlled by the population density and elapsed years since constructed.

In some historical literature, earthquakes that were felt without any damage are also reported as well as damage description from major earthquakes, whereas these were not fully utilized except for several previous studies. The number of felt reports are strongly controlled by the elapsed time since the mainshock and distance from the source area, suggesting the possibility that the source area of these earthquakes can be constrained by the spatiotemporal distribution of felt report number. Furthermore, changes in the number of felt reports may suggest the changes in seismic activity including an occurrence

©2019. Japan Geoscience Union. All Right Reserved.

of swarm-like or triggered activity and seismic quiescence. By constructing the methodology imaging the seismicity based on felt reports in historical literature, a new development of historical earthquake studies including small to moderate earthquakes is expected.

Keywords: Felt Report, Attenuation Relation of Seismic Intensity, Seismicity Analysis

©2019. Japan Geoscience Union. All Right Reserved.

Radiocarbon dating of Japanese tree rings –chronological research and Japanese calibration curve

*Minoru Sakamoto[1,2], Masataka Hakozaki[1], Takumi Mitsutani[3], Takeshi Nakatsuka[4,5]

1. National Museum of Japanese History, 2. The Graduate University for Advanced Studies, 3. Nara National Research Institute for Cultural Properties, 4. Research Institute for Humanity and Nature, 5. Nagoya University

In order to revise radiocarbon age to calendar age, a calibration curve based on the radiocarbon ages of known age sample such as tree rings is used. Calibration curve for the northern hemisphere, IntCal, mainly depended on tree rings which had been growing in the high latitude region of the West so far. However, the latest version “IntCal19” is called upon to reflect radiocarbon ages of various regions. The authors have continued radiocarbon dating of Japanese tree rings of the past 3,000 years. Recently, from a demand for chronological research on wooden buildings as cultural properties using ^{14}C-wiggle matching, we are also focusing on the tree rings of middle to early-modern ages. In the background, there is a practical application of a new method, oxygen-isotope dendrochronology, that can be implemented in several tree species. It becomes easier to obtain tree rings with known age and accumulation of radiocarbon age is progressing rapidly.

There are some periods showing certain offset on radiocarbon ages of Japanese tree ring from IntCal. One of the regional effects is remarkable during the end of the Yayoi to the beginning of the Kofun period, and calibrated age based on IntCal shows older age than the actual age. Also, since IntCal is versatile and smooth, it is sometimes insufficient for the historic chronological research that requires high precision and accuracy. It has an obligation to reveal the behavior of the radiocarbon age of Japanese tree ring and develop domestic calibration curve to promote chronological research.

This work was one of the results of the Collaborative Research Program of the NMJH and the RIHN Research Project of the Ecohistory Program (H-05). JSPS Grant in Aid (#25282075, #18H03594) also supported our research.

Keywords: radiocarbon dating, dendrochronology, calibrated age, regional effect

©2019. Japan Geoscience Union. All Right Reserved.

Usage of Historical Documents with Scientific Understandings in the field of Solar Physics

*Akito Davis Kawamura[1], Hisashi Hayakawa[2], Harufumi Tamazawa[3], Hiroaki Isobe[3], Kazunari Shibata[1]

1. Astronomical Observatory, Kyoto University, 2. Graduate School of Letters, Osaka University, 3. Faculty of Fine Arts, Kyoto City University of Arts

The sun is the most studied star by mankind, yet our knowledge on our parent star is based on the observation of limited time scale. Solar activities have been scientifically recorded for ~400 years with sunspot and ~160 years with flares (sudden increment of light emission with energy release). Meanwhile, people have witnessed and recorded the traces of solar activities for thousands of years, which we nowadays call as aurora. By combining scientific sunspot observations and historical records of aurora, first goal of our study is to decode solar flare activities for last ~400 years.

The physical variable of interest is the flare magnitude, and we have developed an estimation method with the statistics based on modern-day solar observations. The key of this method is an observation of low latitude aurora, which is a strong indication of coronal mass ejection at the flare. By knowing the size of sunspot and the existence of coronal mass ejection, our statistical method could estimate the magnitude of the flare.

At our poster, we will discuss the potentiality and difficulty of solar physics with historical documents. We hope this poster could be a demonstration of successful collaboration of science and history.

Keywords: Solar Physics, Space Weather, Historical Documents

©2019. Japan Geoscience Union. All Right Reserved.

The study of the relationship between the flood of Kitakami River and sociaty in the end of Edo period

*Daisuke Sato[1], Yoshitaka Takahashi[2]

1. International Reserch Institute of Disaster Science Tohoku University , 2. Tokyo University of Agriculture and Technology

The purpose of this study has two focal points . First, finding the water flood in Kitakami river in the end of Edo period by reserching the historical documents include newly discovered one. Second, the relationship between the flood and social influence; foresty, fishing, and political situation.

Keywords: Kitakami River, Area study, Edo period, Historical records, Sendai Han

©2019. Japan Geoscience Union. All Right Reserved.

Reconstruction of Historical Weather with Data Assimilation Using Old Diaries

*Kei Yoshimura[1], Panduka Neluwala[2], Mika Ichino[3], Kooiti Masuda[4], Junpei Hirano[5]

1. Institute of Industrial Science, The University of Tokyo, 2. University of Peradeniya , 3. National Institute of Informatics, 4. Tokyo Metropolitan University, 5. Teikyo University

Long-term atmospheric reanalysis data is indispensable for understanding the mechanism of climate change, but the current longest data is over 130 years only. The cause of not going back further to the past is largely due to lack of direct weather observation data. However, even in the past where modern weather observation data does not exist, the daily weather information described in the ancient document may exist for a longer time. In this regard, Japan is ideal country that has kept such old weather information. In this research, we developed a method to introduce old weather information into the latest data assimilation system, investigated the effect as the constraint condition of atmospheric condition, and proposed a method to extend existing reanalysis data in the past. We constructed a system using historical weather database, global spectrum model, local ensemble transform Kalman filter as observation data, prediction model and data assimilation scheme respectively. Analog information indicating weather should be classified into about 3 to 5 categories and it is better to correspond to the cloud amount ratio and the short wave downward radiation on the ground surface. Furthermore, it is appropriate that the ensemble number is about 30 from the balance of calculation efficiency and accuracy. Using the above setting, the data assimilation result given the weather information obtained at the meteorological observatory at 18 sites, for the modern era (1990 's), is closer to the modern reanalysis than the result without any weather information. As a result, significant improvements were observed in shortwave radiation and cloud cover, and significant improvement in precipitation was confirmed. These improvements are thought to have been brought by synchronizing the modeled synoptic-scale weather patterns to the reality. Furthermore, it was confirmed that the skill of rainfall estimation was improved by adding information of “no precipitation day” to data assimilation as an observation item. Then we conducted the experiments of the 1830s and 1860s using actual ancient diary data. It was confirmed that similar seasonal change and interannual variations can be obtained compared with temperature and precipitation in the 1860s which was actually observed in Yokohama.

Keywords: old diaries, data assimilation, weather reconstruction

©2019. Japan Geoscience Union. All Right Reserved.

Examination of data range for fitting Omori-Utsu law to temporal decay of aftershocks presented in historical materials on the 1830 Kyoto earthquake: Reason for the difference of numbers of aftershocks in the same place

*Kentaro Hattori[1], Junzo Ohmura[2], Ichiro Nakanishi[1]

1. Kyoto Univ., 2. Bukkyo Univ.

We study the temporal decay of aftershock sequences of the 1830 Kyoto earthquake. Omori(1908) examined aftershock sequences including that of the 1830 Kyoto earthquake. Matsui and Oike (1997) attempted to determine epicenter of the 1830 Kyoto earthquake by using the number of felt aftershocks in time range from the main shock to the next morning in several observational areas including Kyoto. They used two different numbers as the number of felt aftershocks for Kyoto: 100 written in Banzai Rakki and 4 written in Tansui Nikki. In the case using the former number, they obtained the epicenter consistent with that obtained by Usami (1996). However, in the case using the latter number, they obtained an epicenter near the northern shore of the lake Biwa, and the epicenter is inconsistent with distribution of damage caused by the earthquake. They did not pursue the reason of the discrepancy between two numbers for Kyoto.

In order to solve the above mentioned discrepancy among the earthquake records for Kyoto, we include another record Tenpo Zakki in addition to Banzai Rakki.Both records show quite different numbers of daily aftershocks during several days, though they were written in the same place. Kitahara and Ohmura (2012) suggest that the original record was written by an officer in Nijo-jo Castle and was copied many times. They made a graph of temporal decay of daily numbers of aftershocks for a period of one month after the main shock. However, they made neither analysis of the aftershock sequences nor information evaluation of the records.

We examined carefully description of daily aftershocks in both records to know the reason for the differences of the numbers of felt aftershocks. The records show the sizes of earthquakes by the diameters of handwritten circles for each day. Comparing the diameter of standard circle for every day, we infer that writers of the records used different criterion to count the numbers of felt aftershocks.

We measure the diameter of standard circle for every day, and find the diameter changes with day. Fig.1 shows the daily variation of diameter of standard circle in the both records. The vertical axis shows the count threshold of circle diameter (arbitrary unit), and horizontal axis shows the date. Fig.1 suggests that the threshold count level used in Banzai Rakki is larger than that used in Tenpo Zakki. This result means that the number of counted aftershocks becomes smaller in Banzai Rakki than in Tenpo Zakki. The interpretation is consistent with the actual difference of the number of aftershocks in the both records. The threshold level for counting used in Banzai Rakki changes more rapidly with time than that used in Tenpo Zakki (Fig.1). Especially, the change of the threshold level from 7/3 to 7/5 is not negligible in Banzai Rakki.

The above information evaluation of the two records reveals the difference of the two records written in the same place. We fit Omori-Utsu law (Utsu, 1961) to the aftershock sequences after 7/5. We assume that the c value is 0.1 and the p values fall in about 1.2. We obtain a better fit in Tenpo Zakki (Fig.2). Our study may suggest that Tenpo Zakki may have better information quality than Banzai Rakki and the numbers of aftershocks after 7/5 should be used for study of the 1830 Kyoto earthquake.

©2019. Japan Geoscience Union. All Right Reserved.

Keywords: the 1830 Kyoto earthquake , aftershock sequence, Omori-Utsu law

©2019. Japan Geoscience Union. All Right Reserved.

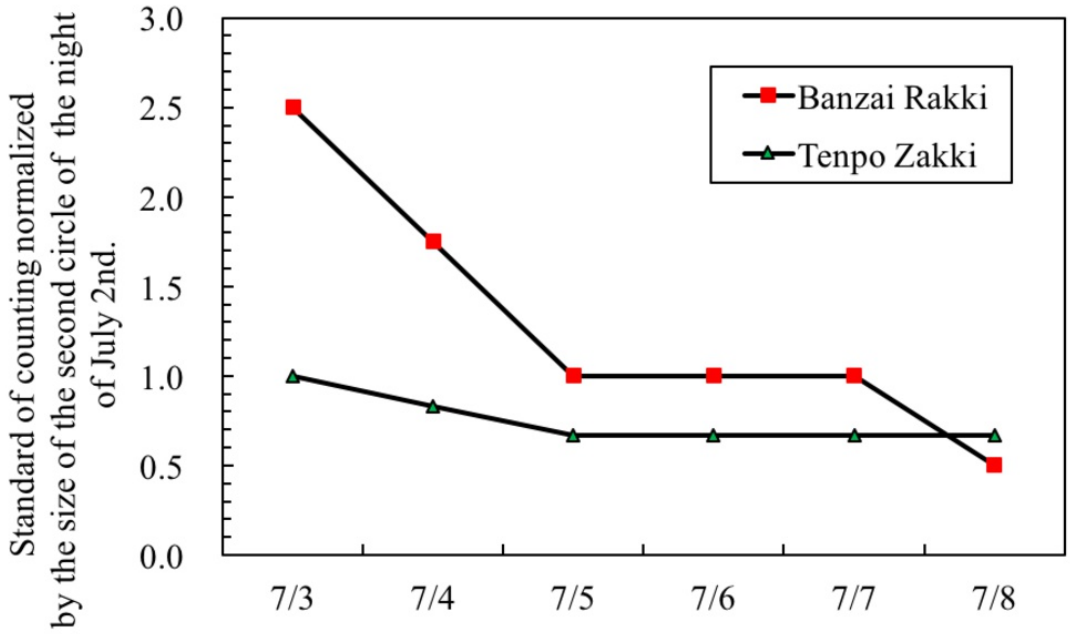

Fig.1 Comparison of two records

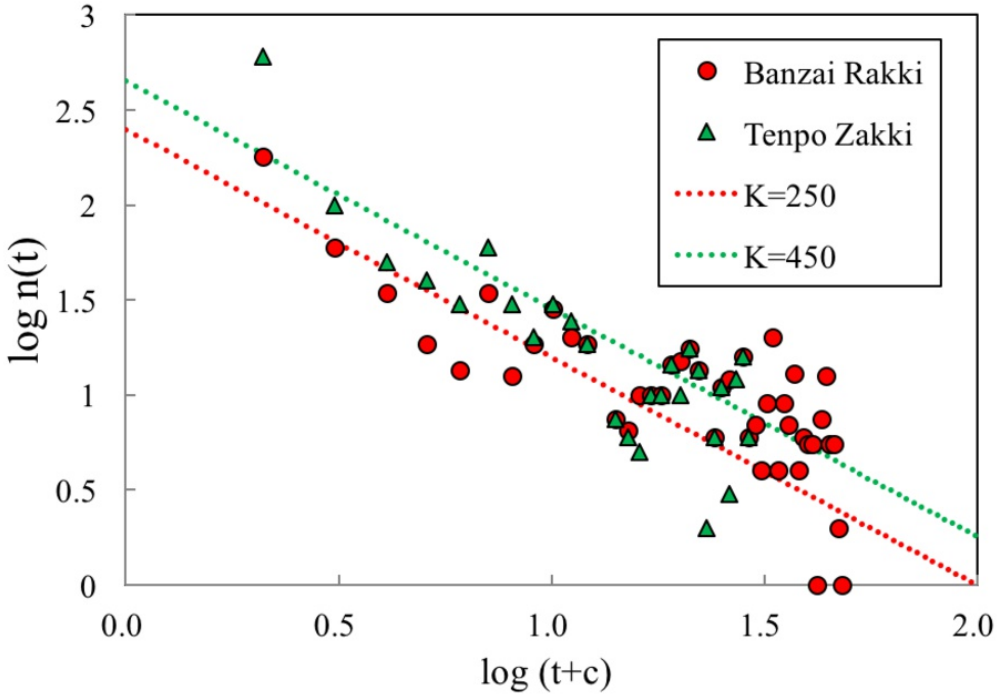

Fig. 2 Temporal decay of the aftershocks of the 1830 Kyoto earthquake with lines (p=1.2) from Omori-Utsu law (Utsu, 1961)

©2019. Japan Geoscience Union. All Right Reserved.

Tsunami trace height of the AD 1854 Ansei Tokai tsunami around the lake Hamanako inferred from historical maps

*ebina yuichi[1], Kentaro Imai[2], Yoshinobu Tsuji[3], hiroyuki iwase[4]

1. International Research Institute of Disaster Science, 2. JAMSTEC, 3. Fukuda Geological Instite, 4. (C)ECOH CORPORATION

We analyzed the trace of tsunami from historical maps "Maisaka-syuku tsunamizu" and “Ansei Tsunami saigai ezu" (in Hamamatsu museum) drawn about the tsunami damages around Hamanako in the Ansei Tokai earthquake occurred in 1854.

“Maisaka” (present Maisaka-cho Nishi-ku, Hamamatsu-shi, Shizuoka-ken) located in the “Hamanako” east shore is the area which prospered as a post town in “Tokaido”. According to "the history of Shizuoka" (1996), which was drawn by Hachiro Watanabe, who was a resident of “Maisaka” and drew the " Maisaka” tsunami figure. This picture shows that the appearance of Maisaka inundated by tsunami, or people who evacuated. On the east side of a highway, tsunami has reached to near night-lights. Moreover, in the west side, stairs around "Shigetuin" were inundated. This is a place called "Ohkonoboriba" by "Toukaido-bungen-nobe-ezu". It becomes clear that from here to several east sides of a subsidiary inn or an administration office were inundated by tsunami.

“Ansei zisin tsunami saigai ezu“ shows the time when the tsunami hits “Okuhamanako and Kiga” area and after the situation of the tsunami. Here, we can find some points reaching tsunami by considering “Himekaido” north side passes as a mark. Although seeing from the historical map, tsunami reached the front of “Kigasekisyo” but tsunami was not flooded in the barrier main part. Moreover, "Komorisawa" near "Ninomiyasya", and "Iwanesawa", near "Himekaido" were drawn as reaching points of the tsunami. Furthermore, signs that the circumference of a mountain where "Daienzi-temple" located in “Ikutagawa-river mouth-of-a-river part which flows into “Okuhama” name lake serves as a cemetery in the case of tsunami has sunk are drawn. “Dainenji Temple” in the area of mouth of “Ikutagawa River” was inundated by tsunami but only the hill used as the “Dainenji Temple Cemetery” was not. There are few documents described accurate places which was reached by the tsunami around Lake Hamanako, especially Lake Okuhamanako. However, we identified those based on historical maps. We hope that our results will contribute to future interdisciplinary research including tsunami engineering on the past great earthquakes along the Nankai Trough.

Acknowledgement
This research was supported by MEXT (“Research project for compound disaster mitigation on the great earthquakes and tsunamis around the Nankai Trough region”).

Keywords: Ansei Tokai earthquake and tsunami, Lake hamanako, historical maps

©2019. Japan Geoscience Union. All Right Reserved.

[J] Oral | M (Multidisciplinary and Interdisciplinary)：M-IS Intersection

Mon. May 27, 2019 1:45 PM - 3:15 PM JST | Mon. May 27, 2019 4:45 AM - 6:15 AM UTC | 301A 3F

[M-IS18] Geophysical fluid dynamics-Transfield approach to geoscience

convener:Keita Iga(Atmosphere and Ocean Research Institute, The University of Tokyo), Shigeo Yoshida(Department of Earth and Planetary Sciences, Faculty of Sciences, Kyushu University), Takatoshi Yanagisawa(Department of Deep Earth Structure and Dynamics Research, Japan Agency for Marine-Earth Science and Technology), Hidenori AIKI(Nagoya University), Chairperson:Kensuke Nakajima

This session on geophysical fluid dynamics is open to discussions and researches on fluid phenomena in whatever fields of earth and planetary sciences, e.g., motions in the earth and planetary interior, oceans, atmospheres, volcanoes, and the ionosphere, conducted with whatever methods. Talks intending to stimulate exchange of ideas among multiple fields of researches or those identifying concepts that are commonly applicable to wide range of geophysical fluids are especially welcome.

1:45 PM - 2:00 PM JST | 4:45 AM - 5:00 AM UTC

[MIS18-01] Axisymmetric disturbance on an axisymmetric shallow water vortex

*Toshihisa Itano[1] (1.National Defense Academy)

2:00 PM - 2:15 PM JST | 5:00 AM - 5:15 AM UTC

[MIS18-02] Numerical studies on the classification of flow regimes of the 3-D thermal convection of rotating fluids

*Masanori Kameyama[1,2] (1.Geodynamics Research Center, Ehime University, 2.Japan Agency for Marine-Earth Science and Technology)

2:15 PM - 2:30 PM JST | 5:15 AM - 5:30 AM UTC

[MIS18-03] Diffusive behavior of columnar vortices in rotating thermal convection

*Daisuke Noto[1], Yuji Tasaka[2], Takatoshi Yanagisawa[3], Yuichi Murai[2] (1.Graduate School of Engineering, Hokkaido University, 2.Faculty of Engineering, Hokkaido University, 3.Japan Agency for Marine-Earth Science and Technology)

2:30 PM - 2:45 PM JST | 5:30 AM - 5:45 AM UTC

[MIS18-04] Liquid metal flows driven by a rotating magnetic field

*Koki Sawada[1], Vladimir Galindo[2], Tobias Vogt[2], Sven Eckert[2], Yuji Tasaka[3], Yuichi Murai[3] (1.Graduate School of Engineering, Hokkaido University , 2.Helmholtz-Zentrum Dresden-Rossendorf, 3.Faculty of Engineering, Hokkaido University,)

2:45 PM - 3:00 PM JST | 5:45 AM - 6:00 AM UTC

[MIS18-05] A symmetry-breaking self-regulating dynamo generating Mercury’s anomalous magnetic field

*Futoshi Takahashi[1], Hisayoshi Shimizu[2], Hideo Tsunakawa[3] (1.Faculty of Sciences, Kyushu University, 2.Earthquake Research Institute, University of Tokyo , 3.Department of Earth and Planetary Sciences, School of Science, Tokyo Institute of Technology)

3:00 PM - 3:15 PM JST | 6:00 AM - 6:15 AM UTC

Discussion

Axisymmetric disturbance on an axisymmetric shallow water vortex

*Toshihisa Itano[1]

1. National Defense Academy

The air in an eye of a typhoon is often considered to be stratospheric origin. Indeed, the region of high equivalent potential temperature invading eyes from stratosphere can be seen in most of tropical cyclones. Therefore, we can recognize tropical cyclones are vortices where the air with low potential temperature revolves around the warm air sucked from stratosphere. Also, elliptical or polygonal deformation of an eye of a tropical cyclone can be attributed to the oscillation of the interface between such two kinds of fluids. Thus, in this study, a tropical cyclone is modeled with two layer fluids where the upper fluid touches the ground surface at the core region of the vortex, and the motion on the interface is investigated with the shallow water equations described in polar coordinate by assuming the upper fluid at rest.
An axisymmetric swirling fluid whose center is completely dried up is adopted as the basic state, where the tangential speed is assumed to be inversely proportional to the α-th power of radius. Perturbations are again set to be axisymmetric. Under these settings, the governing equations are linearized, and an eigenvalue problem is formulated after hypothesizing sinusoidal time variation with the angular frequency ω. The eigenvalues are, at first, obtained numerically by discretizing the variables with a standard staggered grid. Then, in the case of no ambient rotation, the problem is solved analytically, by applying a series expansion to the governing equations.
Results reveal the existence of modes like gravity waves. Since the amplitudes of the modes are non-zero at the inner boundary corresponding to the outer edge of the dry core, they would be responsible for the periodic expansion and contraction of an eye in an actual tropical cyclone. Moreover, quasi-steady modes with no nodes in the radial direction emerge in the case of no ambient rotation. Although numerical and analytic solutions roughly coincide with each other, a definite discrepancy is found near the dry core of the basic vortex: radial cross sections reveal that the numerical solutions tend to swing once more against the analytic solutions around there.

Keywords: eye, vortex, axisymmetric disturbance, shallow water equation

©2019. Japan Geoscience Union. All Right Reserved.

Numerical studies on the classification of flow regimes of the 3-D thermal convection of rotating fluids

*Masanori Kameyama[1,2]

1. Geodynamics Research Center, Ehime University, 2. Japan Agency for Marine-Earth Science and Technology

In this study we made a series of statistical analysis for a thermal convection in a three-dimensional Cartesian box rotating about a vertical axis, aiming at obtaining clues to readily understand the flow regimes of rotating convection. First we conducted numerical calculations of 20 cases where the values of Rayleigh number (Ra), Ekman number (Ek) and Prandtl number are systematically varied in the range of earlier studies. We confirmed that, based on the efficiency of convecting heat transfer, the flow patterns of these cases are classified into three regimes mainly depending on Ra and Ek: (i) no-rotating convection, (ii) the regime with strong effect of rotation, and (iii) that with moderate effect of rotation. In particular, we found that the change between the regimes with strong and moderate effect of rotation is associated with the change in the pattern and occurrence of Ekman pumping near the top and bottom boundaries, which can be clearly seen from the correlation between the vertical components of velocity and vorticity there. In the regime with strong effect of rotation, a strong correlation is observed in the vertical flows both away from and toward the horizontal boundaries. In the regime with moderate effect of rotation, in contrast, it is observed only in the flows departing from the boundaries. Our findings suggest that, from the viewpoint of rotating convection, the flow regime the Earth's outer core can be well identified from the observation of the correlation between the radial components of velocity and vorticity.

Keywords: thermal convection of rotating fluids, 3-D numerical experiments, Ekman pumping

©2019. Japan Geoscience Union. All Right Reserved.

Diffusive behavior of columnar vortices in rotating thermal convection

*Daisuke Noto[1], Yuji Tasaka[2], Takatoshi Yanagisawa[3], Yuichi Murai[2]

1. Graduate School of Engineering, Hokkaido University, 2. Faculty of Engineering, Hokkaido University, 3. Japan Agency for Marine-Earth Science and Technology

Rotation effect on thermal convections in a fluid layer driven between two parallel plates with temperature difference, i.e., Rayleigh-Bénard convection (RBC) is a ubiquitous to explain large scale fluid motions observed on the Earth, such as typhoon, tornadoes, and liquid metal convection inside outer core. Various approaches so far have revealed its interesting features, e.g. heat transfer enhancement at moderate rotation rate, rotation dependent flow morphologies, and so on. Especially in them, formation of vertically aligned columnar vortices is one of the most curious phenomenon. Early experimental works mentioned those chaotic behavior like vortex-vortex interactions, however, little is known about this complicated vortex dynamics.

The present study is paying attention to such vortex dynamics observable in rotating RBC. With using encapsulated thermochromic liquid crystals, long-time $O(10^3$ s) experimental visualizations of the vortices on time variations of a temperature field were conducted, and we reached two novel insights. One is horizontal diffusive motion like Brownian motion of the columnar vortices. Statistical analyses on motions of the columnar vortices elucidated various kinds of diffusive motion. Such diffusive motions strongly depend on observation timescale (vortex lifetime) and columnar vortices present anomalous diffusive motion. Another is the effect of centrifugal force even under conditions for empirically negligible small effects of centrifugal force. This is the first found thanks to our long-time observations and might give a new caution to rotating RBC studies.

Keywords: Natural convection, Rotating field, Diffusive motion, Vortex dynamics

©2019. Japan Geoscience Union. All Right Reserved.

Liquid metal flows driven by a rotating magnetic field

*Koki Sawada[1], Vladimir Galindo[2], Tobias Vogt[2], Sven Eckert[2], Yuji Tasaka[3], Yuichi Murai[3]

1. Graduate School of Engineering, Hokkaido University , 2. Helmholtz-Zentrum Dresden-Rossendorf, 3. Faculty of Engineering, Hokkaido University,

Doing experimental studies on liquid metal flows under interactions with magnetic fields is of great importance for understanding fluid dynamical phenomena including flows in planetary cores. In this research, liquid metal flows driven by a rotating magnetic field (RMF) were examined experimentally. The RMF generates eddy currents in liquid metal layers, and thus Lorentz force as the results of the interaction between the magnetic field and the current achieves the rotating flows. The fluid motions are dominated by angular velocity and magnetic strength of the RMF. In cases at which the skin effect is negligible small because of moderate angular velocity, modal transitions of the flow occur with increase of magnetic Taylor number (Ta_m), which is a dimensionless number including the angular velocity and the magnetic strength. For sufficiently small Ta_m, a quasi-two-dimensional, axisymmetric steady flow is formed. With increase of Ta_m, then, unsteady flows emerge by collapsing the symmetry. For this transition problem, theory and numerical calculation have been preceded. On the other hand, experimental approaches have essential unknows, even though there are quired to uncover the phenomena especially at higher Ta_m with stronger nonlinearity; namely, how to realize the RMF by experiment, and whether the experiment system can reproduce the flows expected by numerical simulations.

In the present experiment, we tried to produce the RMF by switching electric current in six-pair coils. A square container with aspect ratio 2 filled with eutectic of GaInSn, a liquid metal having low melting point, was arranged at the center of the coil. The GaInSn is an opaque fluid and it is impossible to be optically visualized. Ultrasonic Doppler velocimetry was used to obtain information of the flow fields. The switching frequency of the RMF was set at 50 Hz at which the skin effect did not appear, and Ta_m was modified by changing the magnetic strength. A long these methods, the flow transition depending on Ta_m was observed. As the measurement results, a stationary axial symmetric flow, that is in good agreement with the numerical simulation results, was observed under relatively small Ta_m. The increase in Reynolds number with respect to Ta_m also show reasonable agreement with the numerical simulations. Furthermore, the process of unsteady and turbulent transition in the increase of Ta_m was discussed and was compared with the numerical simulations.

Keywords: Rotating magnetic field, Liquid metal flow, Flow transition

©2019. Japan Geoscience Union. All Right Reserved.

A symmetry-breaking self-regulating dynamo generating Mercury's anomalous magnetic field

*Futoshi Takahashi[1], Hisayoshi Shimizu[2], Hideo Tsunakawa[3]

1. Faculty of Sciences, Kyushu University, 2. Earthquake Research Institute, University of Tokyo , 3. Department of Earth and Planetary Sciences, School of Science, Tokyo Institute of Technology

The discovery of Mercury's unusually axisymmetric, anomalously axially offset dipolar magnetic field shows a new regime of planetary magnetic fields. The cause of the offset dipole remains to be resolved, although some exotic models have been proposed. Since the magnetic fields of the terrestrial planets are generated by fluid motions in the liquid iron core through dynamo action, which is inevitably linked to the structure and evolution of planetary interiors, untangling why Mercury has such an anomalous field is not only crucial for understanding the internal dynamics, evolution history and origin of the planet, but also essential for establishing the general theory of planetary magnetic fields by extending our knowledge to small bodies in our solar system such as Ganymede, Moon and asteroids. In this study, we use numerical dynamo models. Convection is driven as thermo-compositional convection. A thermally stably stratified layer is imposed in the outer part of the core. It is found that the magnetic fields similar in morphology as well as strength to that of Mercury are reproduced. Also, the dynamo-generated magnetic fields act on the flow to induce interaction between equatorially symmetric and antisymmetric components, and resultantly to yield north-south asymmetric helicity. Additional runs demonstrate that the offset dipolar field cannot be maintained without the magnetic self-regulating effect. Thus, it is concluded that the symmetry breaking self-regulating effect causes the flow to generate and maintain the Mercury-like offset dipolar field.

Keywords: Mercury, Offset dipole, Dynamo, Self-regulation, Symmetry-breaking

©2019. Japan Geoscience Union. All Right Reserved.

[J] Poster | M (Multidisciplinary and Interdisciplinary)：M-IS Intersection

Mon. May 27, 2019 3:30 PM - 5:00 PM JST | Mon. May 27, 2019 6:30 AM - 8:00 AM UTC | Poster Hall International Exhibition Hall8, Makuhari Messe_23

[M-IS18] Geophysical fluid dynamics-Transfield approach to geoscience

convener:Keita Iga(Atmosphere and Ocean Research Institute, The University of Tokyo), Shigeo Yoshida(Department of Earth and Planetary Sciences, Faculty of Sciences, Kyushu University), Takatoshi Yanagisawa(Department of Deep Earth Structure and Dynamics Research, Japan Agency for Marine-Earth Science and Technology), Hidenori AIKI(Nagoya University)

This session on geophysical fluid dynamics is open to discussions and researches on fluid phenomena in whatever fields of earth and planetary sciences, e.g., motions in the earth and planetary interior, oceans, atmospheres, volcanoes, and the ionosphere, conducted with whatever methods. Talks intending to stimulate exchange of ideas among multiple fields of researches or those identifying concepts that are commonly applicable to wide range of geophysical fluids are especially welcome.

[MIS18-P01] Numerical experiments on climate of the Earth-like extrasolar planets using one-dimensional energy balance model

*Tomohiro Oonaka[1], Toru Nozawa[2] (1.Faculty of Science, Okayama University, 2.Graduate School of Natural Science and Technology,Okayama University)

[MIS18-P02] A study on disturbances with wavenumber 2 in inner-core region of tropical cyclones.

*Yuki Kawata[1], Keita Iga[1], Sho Yokota[2], Eigo Tochimoto[1] (1.Atmosphere and Ocean Research Institute, The University of Tokyo, 2.Meteorological Reseach Institute, Japan Meteorological Agency)

[MIS18-P03] Typhoon-induced vertical mixing measured by the Kuroshio Extension Observatory buoy

*Hidenori AIKI[1], Kohei Kameyama[2] (1.Institute for Space Earth Environmental Research, Nagoya University, 2.Graduate School for Environmental Studies, Nagoya University)

[MIS18-P04] A comparison between top-down and bottom-up type convective flows in a rotating spherical shell with stress-free boundaries

*Hinami Taniguchi[1], Futoshi Takahashi[1], Shin-ichi Takehiro[2] (1.Kyushu University, 2.Kyoto University)

[MIS18-P05] Oscillation of two-dimensional roll-like convection under a strong horizontal magnetic field

*Takatoshi Yanagisawa[1], Yuji Tasaka[2], Takehiro Miyagoshi[1], Ataru Sakuraba[3] (1.Department of Deep Earth Structure and Dynamics Research, Japan Agency for Marine-Earth Science and Technology, 2.Faculty of Engineering, Hokkaido University, 3.Faculty of Science, University of Tokyo)

[MIS18-P06] Two-dimensional or shallow water MHD waves on a rotating sphere with an imposed azimuthal magnetic field

*Ryosuke Nakashima[1], Shigeo Yoshida[2] (1.Department of Earth and Planetary Sciences, Graduate School of Science, Kyushu University, 2.Department of Earth and Planetary Sciences, Faculty of Science, Kyushu University)

Numerical experiments on climate of the Earth-like extrasolar planets using one-dimensional energy balance model

*Tomohiro Oonaka[1], Toru Nozawa[2]

1. Faculty of Science, Okayama University, 2. Graduate School of Natural Science and Technology,Okayama University

Recently, extrasolar planets with a mass similar to the Earth were discovered by observations. It is an important question that what kind of climate could have such an Earth-like extrasolar planet. In this study, we performed a series of numerical experiments using one-dimensional Energy Balance Model (EBM), and investigated dependence of climate of the planet on parameters such as orbital radius, obliquity angle, and rotation rate of the planets.

Assuming that the efficiency of north-south heat transport of the planet is inversely proportional to the square of its rotation rate, the steady climate state of the planet at the obliquity angle of 23.5 degrees was calculated by changing two parameters of the heat transport efficiency (that is, the rotational rate) and the orbital radius.

In the range where the heat transport efficiency is large, the orbital radius leading to the global freezing decreases with a decrease in the heat transport efficiency. On the other hand, in the range where the heat transport efficiency is small, the orbital radius leading to the global freezing increases conversely with a decrease in the heat transport efficiency. In the range where the heat transport efficiency is large, heat is efficiently transported from the equator to the pole, so the temperature difference between the equator and the pole becomes small. In this case, since the temperature in the polar region rises, it is possible to maintain the ice-free climate condition even with a smaller stellar radiation. Therefore, in this range, the orbital radius leading to global freezing decreases as the heat transport efficiency decreases. On the other hand, since heat is difficult to be transported from the equator to the pole in a range where the heat transport efficiency is small, the temperature does not rise except for the low latitude and freezes. The amount of heat accumulated in low latitude increases as the heat transport efficiency decreases. That is, the lower the heat transport efficiency, the higher the temperature at the equator. Therefore, in the range where the heat transport efficiency is small, the orbital radius leading to the global freezing increases with a decrease in the heat transport efficiency.

Keywords: frozen planet, energy balance model, habitability

©2019. Japan Geoscience Union. All Right Reserved.

A study on disturbances with wavenumber 2 in inner-core region of tropical cyclones.

*Yuki Kawata[1], Keita Iga[1], Sho Yokota[2], Eigo Tochimoto[1]

1. Atmosphere and Ocean Research Institute, The University of Tokyo, 2. Meteorological Reseach Institute, Japan Meteorological Agency

While the development mechanisms of tropical cyclones (TCs) have been investigated based on axisymmetric theories, asymmetric structures such as spiral rainbands are also observed inside them. Such asymmetric structures are explained using vortex Rossby waves (Montgomery and Kallenbach, 1997).
Wang (2002) performed idealized numerical experiments, and indicated that these asymmetric structures can be understood as convectively coupled vortex Rossby waves and that the disturbances with wavenumber 1 and 2 are important. Some previous studies have suggested that asymmetric structures have an important role in intensity changes in TCs (e.g. Yang et al., 2007). While the disturbances with wavenumber 1 have been discussed using analytic models (e.g. Ito and Kanehisa, 2013; Nishimoto and Kanehisa, 2018), disturbances with wavenumber 2, which can be observed as elliptical vortices, have been analyzed only using radar reflectivity data (e.g. Kuo, 1999) observations; dynamic environments are not examined nor sufficient numerical experiments using non-hydrostatic mesoscale models.
In this study, we focused especially on the disturbances with azimuthal wavenumber 2, and the mechanisms of its generation and maintenance processes were examined by observational data analysis, and numerical simulations with idealized settings using a non-hydrostatic mesoscale model.
First, the observational data of Typhoon Maria (TC1808) was analyzed in order to investigate asymmetric structure of the actual case. This typhoon kept its inner eyewall with an elliptic structure for a long time, whose inner-core region was observed in detail with a Doppler radar in Ishigakijima, Japan. Retrieving the wind field at 2 km altitude of the TC from the Doppler velocity data using the GBVTD analysis (Lee et al., 1999), it was confirmed that the local region of the tangential wind maximum was formed around the long axis of the ellipse. A vorticity disturbance with wavenumber 2 persisted and from the local maximum regions extended the vorticity disturbance with a filament structure to the outer direction. The results of analyses of these observational data show that this disturbance satisfies the characteristics of vortex Rossby waves.
Second, idealized numerical experiments using JMA-NHM were performed in order to investigate the formation mechanism of the asymmetric structure of TCs, which reproduced successfully a long-lasting elliptical vortex similar to Typhoon Maria. The energy budget analysis using anelastic equations revealed that the shear production and convergence terms contributed mainly to generate the asymmetric structure in the lower layer, and the buoyancy term in the middle layer. Subdividing these effective terms, it was also shown that the term of asymmetric convergence due to radial wind in the boundary layer was dominant. For a period of elliptical vortex, the convergence in the boundary layer was strong at the long axis regions of the elliptical vortex, and the mixing ratio of rainwater was large there. From these results, it is suggested that the persistent horizontal convergence in the long axis regions and the PV generation caused by the latent heat release through the vertical wind due to this convergence are important to maintain the elliptical vortex.

Keywords: vortex Rossby waves, elliptical vortex, GBVTD analysis

©2019. Japan Geoscience Union. All Right Reserved.

Typhoon-induced vertical mixing measured by the Kuroshio Extension Observatory buoy

*Hidenori AIKI[1], Kohei Kameyama[2]

1. Institute for Space Earth Environmental Research, Nagoya University, 2. Graduate School for Environmental Studies, Nagoya University

We have analyzed the consistency of the vertical profiles of temperature and salinity and air-sea fluxes as observed by the Kuroshio Extension Observatory (KEO) buoy, with an intent to improve one-dimensional turbulence closure models used in OGCMs. The advantage of the KEO buoy data is the successful measurement of extreme weather events, such as typhoons and bomb cyclones with hourly time-resolution in the past 14 years. We have selected 7 typhoons in summer-autumn and 20 bomb cyclones in winter-spring, and compared with the results of the 1D-model experiments. In our buoy-model comparison system, the effect of mesoscale eddies and internal waves has been included by referring to the observed undulation of the seasonal thermocline. Both the timing and strength of the buoy precipitation data are well reproduced by the satellite precipitation data (GSMaP). Salinity profile in the 1D-model is yet to be improved by processes other than precipitation.

©2019. Japan Geoscience Union. All Right Reserved.

A comparison between top-down and bottom-up type convective flows in a rotating spherical shell with stress-free boundaries

*Hinami Taniguchi[1], Futoshi Takahashi[1], Shin-ichi Takehiro[2]

1. Kyushu University, 2. Kyoto University

The terrestrial bodies that maintain their intrinsic magnetic fields have dynamos in the fluid cores, in which convection is developed by a certain kind of compositional/thermal buoyancy sources. In the Earth´s core, compositional buoyancy is given by light element ejection into the outer core caused by inner core growth. In other words, compositional convection occurs as a "bottom-up" type convection. In other celestial bodies, iron ejection due to solidification of iron could occur at different depth, strongly depending on temperature-pressure conditions and bulk sulfur content within the core. When iron solidification occurs at or around the core-mantle boundary, the solid iron falls downward like snow drop, that is, so-called "iron snow". The iron snow can remelt, and then the fluid motion is driven as "top-down" type convection. In this study, basic features of the flows driven by these two types of buoyancy are investigated.

For this purpose, onsets of top-down and bottom-up compositional convection in a rotating spherical shell are studied as a linear stability problem. We consider the Boussinesq fluid contained in the rotating spherical shell, of which radius ratio is 0.2. The linearized governing equations, that is, conservation equations of the momentum and mass, and the transport equation of composition, are solved as an eigenvalue problem. The adopted values of the Ekman number, Ek range from 10^{-4} to 10^{-3}. Boundary conditions are stress-free and impermeable for the velocity field, and fixed flux for composition. It is found that the critical Rayleigh numbers Rac shows an Ekman-number-dependence of $Ra_c \propto Ek^{-1.26}$ for the top-down case and $Ra_c \propto Ek^{-1.09}$ for the bottom-up one. The flows at the onsets for both the types have columnar convection owing to the effect of rotation. Motion in the top-down case is dominated by the convection outside the tangent cylinder, which is an imaginary cylinder co-axial with the rotation axis touching the inner sphere at the equator. On the other hand, the axially elongated flow structure around the surface of the tangent cylinder is formed in the bottom-up case as well as columnar flows outside the tangent cylinder. In decreasing the Ekman number, it repeats that the structure inside the cylinder appears and vanishes, and depends on the transition of critical horizontal wavenumber.

Keywords: compositional convection, linear stability analysis

©2019. Japan Geoscience Union. All Right Reserved.

Oscillation of two-dimensional roll-like convection under a strong horizontal magnetic field

*Takatoshi Yanagisawa[1], Yuji Tasaka[2], Takehiro Miyagoshi[1], Ataru Sakuraba[3]

1. Department of Deep Earth Structure and Dynamics Research, Japan Agency for Marine-Earth Science and Technology, 2. Faculty of Engineering, Hokkaido University, 3. Faculty of Science, University of Tokyo

Effects of the magnetic field, together with effects of the rotation, are important to understand coherent flow structures that should be generated in the Earth’ s outer core. To investigate the nature of liquid metal flow where a strong magnetic field exists, we studied magnetoconvection on the Rayleigh-Benard setting in which flows are driven by the temperature difference between the top and bottom boundaries, by laboratory experiments and numerical simulations. The control parameters for this setting are the Rayleigh number (Ra) and the Chandrasekhar number (Q). Ra represents the relative intensity of the buoyancy to the viscous force, while Q represents that of the Lorentz force. In applying a homogeneous magnetic field in the horizontal direction, the flow pattern tends to be a roll-like one whose axes are aligned to the direction of the magnetic field. Under a sufficiently strong magnetic field, that means high Q/Ra, an almost steady two-dimensional flow is observed even at high Ra far from the critical Ra for the onset of convective motion. The Ra corresponds to a state of developed turbulence when Q is zero or small, but significant reduction of fluctuations is observed under high Q. With reducing Q from this steady roll flow regime, an oscillatory motion of rolls is observed. The style of the oscillation shows two-dimensional signatures, that is, little difference of motion is observed in the direction of the magnetic field. On the other hand, the circulation style of rolls shows various interesting features those never observed for the well-known roll type convection near the critical Ra. It is due to the large circulation velocities of the roll-like flow. We can get to this new regime of convection by applying a strong magnetic field in the experiment, and make details of the regime clear by our numerical simulation with high resolutions.

Keywords: magnetoconvection, roll-like structure, onset of oscillation

©2019. Japan Geoscience Union. All Right Reserved.

Two-dimensional or shallow water MHD waves on a rotating sphere with an imposed azimuthal magnetic field

*Ryosuke Nakashima[1], Shigeo Yoshida[2]

1. Department of Earth and Planetary Sciences, Graduate School of Science, Kyushu University, 2. Department of Earth and Planetary Sciences, Faculty of Science, Kyushu University

Magnetohydrodynamic (MHD) waves in a thin layer on a rotating sphere with an imposed toroidal magnetic field are investigated. The system is often considered as a model of the stably stratified outermost Earth's outer core or the tachocline of the Sun. The stratification of the outermost core is suggested on the basis of seismological evidence (e.g. Helffrich and Kaneshima, 2010; Kaneshima, 2018) and interpretations of the geomagnetic variations with MHD waves (e.g. Braginsky, 1993; Buffett, 2014; Chulliat et al., 2015). In order to provide constraints on the obscure stratified layer by comparing with wavy variations in the geomagnetic field, we studied the linear waves of the two-dimensional MHD and the MHD shallow water system over a rotating sphere.

We adopt an azimuthal equatorially antisymmetric field ($B_\Phi(\theta) = B_0 \sin\theta\cos\theta$, where θ is colatitude, Φ is azimuth) as a background magnetic field. On the other hand, an equatorially symmetric field ($B_\Phi(\theta) = B_0 \sin\theta$) was assumed in Márquez-Artavia et al.(2017), whose results we replicated and reported in JpGU 2018.

Compared with previous results, the dispersion diagrams obtained with the toroidal equatorially antisymmetric field show that some fast magnetic Rossby branches remain, while slow magnetic Rossby waves disappear. Besides, a continuous spectrum is found in the range where an azimuthal phase velocity is coincident with a local Alfvén velocity divided by $\sin\theta$. Similar continuous spectra are also seen in various physical situations, including inviscid shear flow (e.g. Case, 1960; Balmforth and Morrison, 1995; Iga, 2013) and plasma oscillations (e.g. Van Kampen, 1955; Case, 1959; Barston, 1964; Sedláček, 1971). The continuous spectra are accompanied by a singular eigenfunction, which is physically meaningful only when they are integrated over the continuous spectra. Its integrated solutions generally decay with time, which is referred to as phase mixing. Unlike exponentially damped discrete modes, this decaying is proportional to negative powers of time.

In the case of the shallow water system with the antisymmetric field, discrete eigenvalues buried in the continuous spectrum is found, which include unstable modes. For the Earth-like parameters, polar trapped modes with decadal period and equatorial trapped Rossby waves with a few years period are found when the stratification is weak.

Keywords: MHD waves, MHD shallow water, toroidal magnetic field, continuous spectra, a stably stratified layer at the top of the Earth's outer core

©2019. Japan Geoscience Union. All Right Reserved.

[J] Poster | M (Multidisciplinary and Interdisciplinary)：M-IS Intersection

Mon. May 27, 2019 5:15 PM - 6:30 PM JST | Mon. May 27, 2019 8:15 AM - 9:30 AM UTC | Poster Hall International Exhibition Hall8, Makuhari Messe_38

[M-IS18] Geophysical fluid dynamics-Transfield approach to geoscience

convener:Keita Iga(Atmosphere and Ocean Research Institute, The University of Tokyo), Shigeo Yoshida(Department of Earth and Planetary Sciences, Faculty of Sciences, Kyushu University), Takatoshi Yanagisawa(Department of Deep Earth Structure and Dynamics Research, Japan Agency for Marine-Earth Science and Technology), Hidenori AIKI(Nagoya University)

This session on geophysical fluid dynamics is open to discussions and researches on fluid phenomena in whatever fields of earth and planetary sciences, e.g., motions in the earth and planetary interior, oceans, atmospheres, volcanoes, and the ionosphere, conducted with whatever methods. Talks intending to stimulate exchange of ideas among multiple fields of researches or those identifying concepts that are commonly applicable to wide range of geophysical fluids are especially welcome.

[MIS18-P01] Numerical experiments on climate of the Earth-like extrasolar planets using one-dimensional energy balance model

*Tomohiro Oonaka[1], Toru Nozawa[2] (1.Faculty of Science, Okayama University, 2.Graduate School of Natural Science and Technology,Okayama University)

[MIS18-P02] A study on disturbances with wavenumber 2 in inner-core region of tropical cyclones.

*Yuki Kawata[1], Keita Iga[1], Sho Yokota[2], Eigo Tochimoto[1] (1.Atmosphere and Ocean Research Institute, The University of Tokyo, 2.Meteorological Reseach Institute, Japan Meteorological Agency)

[MIS18-P03] Typhoon-induced vertical mixing measured by the Kuroshio Extension Observatory buoy

*Hidenori AIKI[1], Kohei Kameyama[2] (1.Institute for Space Earth Environmental Research, Nagoya University, 2.Graduate School for Environmental Studies, Nagoya University)

[MIS18-P04] A comparison between top-down and bottom-up type convective flows in a rotating spherical shell with stress-free boundaries

*Hinami Taniguchi[1], Futoshi Takahashi[1], Shin-ichi Takehiro[2] (1.Kyushu University, 2.Kyoto University)

[MIS18-P05] Oscillation of two-dimensional roll-like convection under a strong horizontal magnetic field

*Takatoshi Yanagisawa[1], Yuji Tasaka[2], Takehiro Miyagoshi[1], Ataru Sakuraba[3] (1.Department of Deep Earth Structure and Dynamics Research, Japan Agency for Marine-Earth Science and Technology, 2.Faculty of Engineering, Hokkaido University, 3.Faculty of Science, University of Tokyo)

[MIS18-P06] Two-dimensional or shallow water MHD waves on a rotating sphere with an imposed azimuthal magnetic field

*Ryosuke Nakashima[1], Shigeo Yoshida[2] (1.Department of Earth and Planetary Sciences, Graduate School of Science, Kyushu University, 2.Department of Earth and Planetary Sciences, Faculty of Science, Kyushu University)

Numerical experiments on climate of the Earth-like extrasolar planets using one-dimensional energy balance model

*Tomohiro Oonaka[1], Toru Nozawa[2]

1. Faculty of Science, Okayama University, 2. Graduate School of Natural Science and Technology,Okayama University

Recently, extrasolar planets with a mass similar to the Earth were discovered by observations. It is an important question that what kind of climate could have such an Earth-like extrasolar planet. In this study, we performed a series of numerical experiments using one-dimensional Energy Balance Model (EBM), and investigated dependence of climate of the planet on parameters such as orbital radius, obliquity angle, and rotation rate of the planets.

Assuming that the efficiency of north-south heat transport of the planet is inversely proportional to the square of its rotation rate, the steady climate state of the planet at the obliquity angle of 23.5 degrees was calculated by changing two parameters of the heat transport efficiency (that is, the rotational rate) and the orbital radius.

In the range where the heat transport efficiency is large, the orbital radius leading to the global freezing decreases with a decrease in the heat transport efficiency. On the other hand, in the range where the heat transport efficiency is small, the orbital radius leading to the global freezing increases conversely with a decrease in the heat transport efficiency. In the range where the heat transport efficiency is large, heat is efficiently transported from the equator to the pole, so the temperature difference between the equator and the pole becomes small. In this case, since the temperature in the polar region rises, it is possible to maintain the ice-free climate condition even with a smaller stellar radiation. Therefore, in this range, the orbital radius leading to global freezing decreases as the heat transport efficiency decreases. On the other hand, since heat is difficult to be transported from the equator to the pole in a range where the heat transport efficiency is small, the temperature does not rise except for the low latitude and freezes. The amount of heat accumulated in low latitude increases as the heat transport efficiency decreases. That is, the lower the heat transport efficiency, the higher the temperature at the equator. Therefore, in the range where the heat transport efficiency is small, the orbital radius leading to the global freezing increases with a decrease in the heat transport efficiency.

Keywords: frozen planet, energy balance model, habitability

©2019. Japan Geoscience Union. All Right Reserved.

A study on disturbances with wavenumber 2 in inner-core region of tropical cyclones.

*Yuki Kawata[1], Keita Iga[1], Sho Yokota[2], Eigo Tochimoto[1]

1. Atmosphere and Ocean Research Institute, The University of Tokyo, 2. Meteorological Reseach Institute, Japan Meteorological Agency

While the development mechanisms of tropical cyclones (TCs) have been investigated based on axisymmetric theories, asymmetric structures such as spiral rainbands are also observed inside them. Such asymmetric structures are explained using vortex Rossby waves (Montgomery and Kallenbach, 1997).
Wang (2002) performed idealized numerical experiments, and indicated that these asymmetric structures can be understood as convectively coupled vortex Rossby waves and that the disturbances with wavenumber 1 and 2 are important. Some previous studies have suggested that asymmetric structures have an important role in intensity changes in TCs (e.g. Yang et al., 2007). While the disturbances with wavenumber 1 have been discussed using analytic models (e.g. Ito and Kanehisa, 2013; Nishimoto and Kanehisa, 2018), disturbances with wavenumber 2, which can be observed as elliptical vortices, have been analyzed only using radar reflectivity data (e.g. Kuo, 1999) observations; dynamic environments are not examined nor sufficient numerical experiments using non-hydrostatic mesoscale models.
In this study, we focused especially on the disturbances with azimuthal wavenumber 2, and the mechanisms of its generation and maintenance processes were examined by observational data analysis, and numerical simulations with idealized settings using a non-hydrostatic mesoscale model.
First, the observational data of Typhoon Maria (TC1808) was analyzed in order to investigate asymmetric structure of the actual case. This typhoon kept its inner eyewall with an elliptic structure for a long time, whose inner-core region was observed in detail with a Doppler radar in Ishigakijima, Japan. Retrieving the wind field at 2 km altitude of the TC from the Doppler velocity data using the GBVTD analysis (Lee et al., 1999), it was confirmed that the local region of the tangential wind maximum was formed around the long axis of the ellipse. A vorticity disturbance with wavenumber 2 persisted and from the local maximum regions extended the vorticity disturbance with a filament structure to the outer direction. The results of analyses of these observational data show that this disturbance satisfies the characteristics of vortex Rossby waves.
Second, idealized numerical experiments using JMA-NHM were performed in order to investigate the formation mechanism of the asymmetric structure of TCs, which reproduced successfully a long-lasting elliptical vortex similar to Typhoon Maria. The energy budget analysis using anelastic equations revealed that the shear production and convergence terms contributed mainly to generate the asymmetric structure in the lower layer, and the buoyancy term in the middle layer. Subdividing these effective terms, it was also shown that the term of asymmetric convergence due to radial wind in the boundary layer was dominant. For a period of elliptical vortex, the convergence in the boundary layer was strong at the long axis regions of the elliptical vortex, and the mixing ratio of rainwater was large there. From these results, it is suggested that the persistent horizontal convergence in the long axis regions and the PV generation caused by the latent heat release through the vertical wind due to this convergence are important to maintain the elliptical vortex.

Keywords: vortex Rossby waves, elliptical vortex, GBVTD analysis

©2019. Japan Geoscience Union. All Right Reserved.

Typhoon-induced vertical mixing measured by the Kuroshio Extension Observatory buoy

*Hidenori AIKI[1], Kohei Kameyama[2]

1. Institute for Space Earth Environmental Research, Nagoya University, 2. Graduate School for Environmental Studies, Nagoya University

We have analyzed the consistency of the vertical profiles of temperature and salinity and air-sea fluxes as observed by the Kuroshio Extension Observatory (KEO) buoy, with an intent to improve one-dimensional turbulence closure models used in OGCMs. The advantage of the KEO buoy data is the successful measurement of extreme weather events, such as typhoons and bomb cyclones with hourly time-resolution in the past 14 years. We have selected 7 typhoons in summer-autumn and 20 bomb cyclones in winter-spring, and compared with the results of the 1D-model experiments. In our buoy-model comparison system, the effect of mesoscale eddies and internal waves has been included by referring to the observed undulation of the seasonal thermocline. Both the timing and strength of the buoy precipitation data are well reproduced by the satellite precipitation data (GSMaP). Salinity profile in the 1D-model is yet to be improved by processes other than precipitation.

©2019. Japan Geoscience Union. All Right Reserved.

A comparison between top-down and bottom-up type convective flows in a rotating spherical shell with stress-free boundaries

*Hinami Taniguchi[1], Futoshi Takahashi[1], Shin-ichi Takehiro[2]

1. Kyushu University, 2. Kyoto University

The terrestrial bodies that maintain their intrinsic magnetic fields have dynamos in the fluid cores, in which convection is developed by a certain kind of compositional/thermal buoyancy sources. In the Earth´s core, compositional buoyancy is given by light element ejection into the outer core caused by inner core growth. In other words, compositional convection occurs as a "bottom-up" type convection. In other celestial bodies, iron ejection due to solidification of iron could occur at different depth, strongly depending on temperature-pressure conditions and bulk sulfur content within the core. When iron solidification occurs at or around the core-mantle boundary, the solid iron falls downward like snow drop, that is, so-called "iron snow". The iron snow can remelt, and then the fluid motion is driven as "top-down" type convection. In this study, basic features of the flows driven by these two types of buoyancy are investigated.

For this purpose, onsets of top-down and bottom-up compositional convection in a rotating spherical shell are studied as a linear stability problem. We consider the Boussinesq fluid contained in the rotating spherical shell, of which radius ratio is 0.2. The linearized governing equations, that is, conservation equations of the momentum and mass, and the transport equation of composition, are solved as an eigenvalue problem. The adopted values of the Ekman number, Ek range from 10^{-4} to 10^{-3}. Boundary conditions are stress-free and impermeable for the velocity field, and fixed flux for composition. It is found that the critical Rayleigh numbers Rac shows an Ekman-number-dependence of $Ra_c \propto Ek^{-1.26}$ for the top-down case and $Ra_c \propto Ek^{-1.09}$ for the bottom-up one. The flows at the onsets for both the types have columnar convection owing to the effect of rotation. Motion in the top-down case is dominated by the convection outside the tangent cylinder, which is an imaginary cylinder co-axial with the rotation axis touching the inner sphere at the equator. On the other hand, the axially elongated flow structure around the surface of the tangent cylinder is formed in the bottom-up case as well as columnar flows outside the tangent cylinder. In decreasing the Ekman number, it repeats that the structure inside the cylinder appears and vanishes, and depends on the transition of critical horizontal wavenumber.

Keywords: compositional convection, linear stability analysis

©2019. Japan Geoscience Union. All Right Reserved.

Oscillation of two-dimensional roll-like convection under a strong horizontal magnetic field

*Takatoshi Yanagisawa[1], Yuji Tasaka[2], Takehiro Miyagoshi[1], Ataru Sakuraba[3]

1. Department of Deep Earth Structure and Dynamics Research, Japan Agency for Marine-Earth Science and Technology, 2. Faculty of Engineering, Hokkaido University, 3. Faculty of Science, University of Tokyo

Effects of the magnetic field, together with effects of the rotation, are important to understand coherent flow structures that should be generated in the Earth’ s outer core. To investigate the nature of liquid metal flow where a strong magnetic field exists, we studied magnetoconvection on the Rayleigh-Benard setting in which flows are driven by the temperature difference between the top and bottom boundaries, by laboratory experiments and numerical simulations. The control parameters for this setting are the Rayleigh number (Ra) and the Chandrasekhar number (Q). Ra represents the relative intensity of the buoyancy to the viscous force, while Q represents that of the Lorentz force. In applying a homogeneous magnetic field in the horizontal direction, the flow pattern tends to be a roll-like one whose axes are aligned to the direction of the magnetic field. Under a sufficiently strong magnetic field, that means high Q/Ra, an almost steady two-dimensional flow is observed even at high Ra far from the critical Ra for the onset of convective motion. The Ra corresponds to a state of developed turbulence when Q is zero or small, but significant reduction of fluctuations is observed under high Q. With reducing Q from this steady roll flow regime, an oscillatory motion of rolls is observed. The style of the oscillation shows two-dimensional signatures, that is, little difference of motion is observed in the direction of the magnetic field. On the other hand, the circulation style of rolls shows various interesting features those never observed for the well-known roll type convection near the critical Ra. It is due to the large circulation velocities of the roll-like flow. We can get to this new regime of convection by applying a strong magnetic field in the experiment, and make details of the regime clear by our numerical simulation with high resolutions.

Keywords: magnetoconvection, roll-like structure, onset of oscillation

©2019. Japan Geoscience Union. All Right Reserved.

Two-dimensional or shallow water MHD waves on a rotating sphere with an imposed azimuthal magnetic field

*Ryosuke Nakashima[1], Shigeo Yoshida[2]

1. Department of Earth and Planetary Sciences, Graduate School of Science, Kyushu University, 2. Department of Earth and Planetary Sciences, Faculty of Science, Kyushu University

Magnetohydrodynamic (MHD) waves in a thin layer on a rotating sphere with an imposed toroidal magnetic field are investigated. The system is often considered as a model of the stably stratified outermost Earth's outer core or the tachocline of the Sun. The stratification of the outermost core is suggested on the basis of seismological evidence (e.g. Helffrich and Kaneshima, 2010; Kaneshima, 2018) and interpretations of the geomagnetic variations with MHD waves (e.g. Braginsky, 1993; Buffett, 2014; Chulliat et al., 2015). In order to provide constraints on the obscure stratified layer by comparing with wavy variations in the geomagnetic field, we studied the linear waves of the two-dimensional MHD and the MHD shallow water system over a rotating sphere.

We adopt an azimuthal equatorially antisymmetric field ($B_\Phi(\theta) = B_0 \sin\theta\cos\theta$, where θ is colatitude, Φ is azimuth) as a background magnetic field. On the other hand, an equatorially symmetric field ($B_\Phi(\theta) = B_0 \sin\theta$) was assumed in Márquez-Artavia et al.(2017), whose results we replicated and reported in JpGU 2018.

Compared with previous results, the dispersion diagrams obtained with the toroidal equatorially antisymmetric field show that some fast magnetic Rossby branches remain, while slow magnetic Rossby waves disappear. Besides, a continuous spectrum is found in the range where an azimuthal phase velocity is coincident with a local Alfvén velocity divided by $\sin\theta$. Similar continuous spectra are also seen in various physical situations, including inviscid shear flow (e.g. Case, 1960; Balmforth and Morrison, 1995; Iga, 2013) and plasma oscillations (e.g. Van Kampen, 1955; Case, 1959; Barston, 1964; Sedláček, 1971). The continuous spectra are accompanied by a singular eigenfunction, which is physically meaningful only when they are integrated over the continuous spectra. Its integrated solutions generally decay with time, which is referred to as phase mixing. Unlike exponentially damped discrete modes, this decaying is proportional to negative powers of time.

In the case of the shallow water system with the antisymmetric field, discrete eigenvalues buried in the continuous spectrum is found, which include unstable modes. For the Earth-like parameters, polar trapped modes with decadal period and equatorial trapped Rossby waves with a few years period are found when the stratification is weak.

Keywords: MHD waves, MHD shallow water, toroidal magnetic field, continuous spectra, a stably stratified layer at the top of the Earth's outer core

©2019. Japan Geoscience Union. All Right Reserved.

[J] Oral | M (Multidisciplinary and Interdisciplinary)：M-IS Intersection

Mon. May 27, 2019 9:00 AM - 10:30 AM JST | Mon. May 27, 2019 12:00 AM - 1:30 AM UTC | 103 1F

[M-IS20] Mountain Science

convener:Keisuke Suzuki(Department of Environmental Sciences, Faculty of Science, Shinshu University), Yoshihiko Kariya(Department of Environmental Geography, Senshu University), Akihiko SASAKI(Department of Geography and Environmental Studies, Kokushikan University), Chiyuki Narama(Niigata University, Department of Science), Chairperson:Yoshihiko Kariya(専修大学)

Mountainous areas provide water resources to the populated downstream areas, protecting the
 diversity of ecosystem and providing tourism attraction. To access the mountain environment
 changes and mitigate the impacts of global warming influences, a cross-cutting session is
 proposed to share the scientific knowledge among various fields; such as climatology, hydrology, geography, glaciology, water/carbon/material cycle, eco-diversity, etc.

9:00 AM - 9:15 AM JST | 12:00 AM - 12:15 AM UTC

[MIS20-01] Early Holocene landslide deposits found from Mount Honita, the upper Tama River basin, west of Tokyo

*Yoshihiko Kariya[1], Koichiro Sawabe[2] (1.Department of Environmental Geography, Senshu University, 2.Japan Conservation Engineers)

9:15 AM - 9:30 AM JST | 12:15 AM - 12:30 AM UTC

[MIS20-02] The effect of understanding of mountainous terrain using 3D maps and solid model

*Jiro Komori[1] (1.Teikyo Heisei University)

9:30 AM - 9:45 AM JST | 12:30 AM - 12:45 AM UTC

[MIS20-03] Development process of Lake Naganuma in a large-scale landslide on Hachimantai Volcano

*Natsuki Sasaki[1], Toshihiko Sugai[1] (1.Graduate School of Frontier Science, the University of Tokyo)

9:45 AM - 10:00 AM JST | 12:45 AM - 1:00 AM UTC

[MIS20-04] Air and ground temperature conditions on alpine and sub-apline zone of Norikura Volcano, Northern Japanese Alps

*Akihiko SASAKI[1], Motoshi NISHIMURA[2], Keisuke Suzuki[3] (1.Department of Geography and Environmental Studies, Kokushikan University, 2.Interdisciplinary Graduate school of Science and Technology, Shinshu University, 3.Faculty of Science, Shinshu University)

10:00 AM - 10:15 AM JST | 1:00 AM - 1:15 AM UTC

[MIS20-05] Initiation and flow characteristics of debris flows on a sediment deposition zone in a mountain area

★Invited Papers

*Fumitoshi Imaizumi[1], Yuichi S. Hayakawa[2], Haruka Tsunetaka[3], Norifumi Hotta[4] (1.Faculty of Agriculture, Shizuoka University, 2.Faculty of Environmental Earth Sciences, 3.Forestry and Forest Products Research Institute, 4.Graduate School of Agricultural and Life Sciences)

10:15 AM - 10:30 AM JST | 1:15 AM - 1:30 AM UTC

[MIS20-06] Relationships between annual landform changes of the riverbed and vegetation dynamics during recent 10 years in the upper Asusa River in Kamikochi valley in the Japan Alps

★Invited Papers

*Hiroshi Shimazu[1] (1.Department of Geography, Faculty of Geo-Environmental Science, Rissho University)

Early Holocene landslide deposits found from Mount Honita, the upper Tama River basin, west of Tokyo

*Yoshihiko Kariya[1], Koichiro Sawabe[2]

1. Department of Environmental Geography, Senshu University, 2. Japan Conservation Engineers

Landslide features are common in the upper Tama River basin west of Tokyo Metropolis where sedimentary rocks derived from Mesozoic accretionary prisms are widespread. We obtained two wood fragments from landslide deposits on the northeast side of Mount Honita (710 m ASL). Radiocarbon ages of those fossils showed 10250-10189 cal BP and 10150-10057/10042-9987/9959-9704 cal BP (2sigma; OxCal4.3 with IntCal13). This result indicates that landslide occurred in the early Holocene when precipitation had increased and the elevation of riverbed had decreased in central Japan due to global changes. This situation would create morphogenetic environments prone to landslide occurrence. Although the Tachikawa Fault zone is close to Mount Honita, the age of latest paleoseismic event revealed by a trenching survey does not coincide with ages of the landslide event shown here.

Keywords: Upper Tama River basin, 14C ages, Mass movement, Landslide

©2019. Japan Geoscience Union. All Right Reserved.

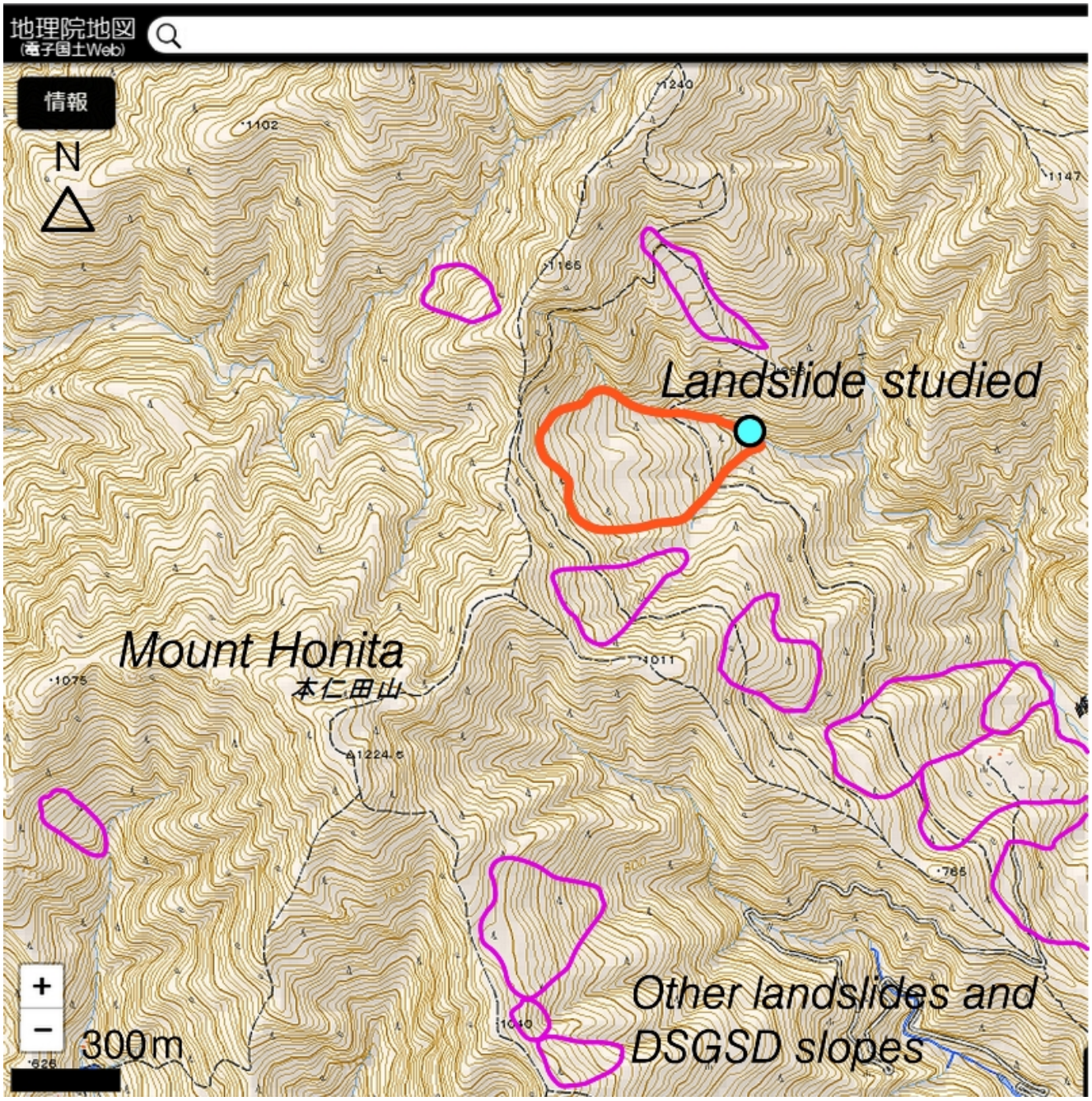

©2019. Japan Geoscience Union. All Right Reserved.

The effect of understanding of mountainous terrain using 3D maps and solid model

*Jiro Komori[1]

1. Teikyo Heisei University

The topography shows various forms by a background of the formation of the place, i.e history of geology and structural development, weathering, erosion and deposition. However, for a person without an interest and opportunity for geoscience study, it is difficult to understand the relation between the topography and background. On the other hand, it became easy to see a stereoimage of the topography without difficulty using a special relief map, 3D view on the screen and hands-on model by 3D printer. This presentation will introduce practical example and reaction of the students for understanding mountain topography.

Keywords: Red Relief Image Map, online map, 3D printer, glacial topography, landslide topography, educational effect

©2019. Japan Geoscience Union. All Right Reserved.

Development process of Lake Naganuma in a large-scale landslide on Hachimantai Volcano

*Natsuki Sasaki[1], Toshihiko Sugai[1]

1. Graduate School of Frontier Science, the University of Tokyo

In the Hachimantai volcanic group, landslide is one of the most important origins of wetland, and various types of wetlands, including lakes and peatlands, tend to coexist in a large-scale landslide (Sasaki and Sugai, 2015). Landslide wetlands commonly develop from lakes to peatlands, so the wetland types are considered to reflect their developmental stage. This study analyzed sediment cores to reconstruct the development history of Lake Naganuma formed in a large landslide of the Hachimantai volcanic group, and discussed the difference in the developmental history with Oyachi, a large peatland in the same landslide.

Lake Naganuma, which is formed in the upper part of the Komonomori landslide in the northwest of Hachimantai volcano, has an elliptical shape with a long axis in the north-south direction parallel to the scarp of the landslide, and its southern part is peatland. Drilling surveys were conducted at two sites on the long axis, and each sediment core was designated as NN1 and NN 2 from near to the water area. In NN1 core, we identified two lithostratigraphic units: NN1-Unit 1 (3.40–2.64 m depth) was organic silt; NN1-Unit 2 (2.64–0.00 m depth) was peat. In NN2 core, we recognized three lithostratigraphic units: NN2-Unit 1 (4.50–4.20 m depth) was silt with low organic content showing parallel lamination; NN2-Unit 2 (4.20–1.57 m depth) was organic silt; NN2-Unit 3 (1.57–0.00 m depth) was peat. The boundary between each unit was unclear, and their organic content gradually changed. We visually identified 5 tephra layers in NN1 core and 4 layers in NN2 core. From the result of chemical composition analysis of volcanic glasses, pumice layers at 1.05 m depth in NN1 core and at 1.10 m depth in NN2 core 2 were correlated with the To-a tephra, which is widely distributed over the northern Tohoku region as a result of the 915 AD eruption of Towada volcano. And the chemical composition of volcanic glasses at 2.22 m depth in NN1 core and at 2.87 m depth in NN2 were similar to that of the To-Cu tephra, erupted by Towada volcano at 6.2 ka.

The southern part of Lake Naganuma had developed from lake to peatland, because the organic silt layer changed to the peat layer upward in both sediment cores, and because the lower part of the organic silt layer in NN1 and the silt layer in NN2 showed parallel lamination. The lake changed to peatland before 6.2 ka, since the peat layer of NN1 contained To-Cu tephra. However, in NN2 far from the water area, To-Cu was contained in the organic silt layer below the peat layer. Moreover, the organic silt layer of NN2 was thicker, and the deposition rate between To-a and To-Cu layer was estimated about 0.35 mm/yr for NN2, while that of NN1 was about 0.27 mm/year. These suggest that fine grained soil continuously and slightly flowed into peatland around NN2 from the surrounding slopes even after terrestrialization. From the above, we concluded that Lake Naganuma had gradually filled from the upstream part and then been stable in the present state at least for over a thousand years, while peat layer formed.

Many wetlands are formed in the Komonomori landslide, and the development process of Oyachi peatland in the landslide, located about 800 m southwest of Lake Naganuma, is different from that of Lake Naganuma. Oyachi wetland was in the depression formed by a landslide activity before 8600 cal BP, and its transition from peatland to forest was interrupted at about 5500 cal BP by slope movement leading to the development of a lake that was drained by streams at about 3300 cal BP, after which a peatland environment has persisted until the present (Sasaki and Sugai, 2018). On the other hand, Lake Naganuma is more stable for a long period. These suggested that development processes and rates of wetlands are various even in a same landslide, probably depending on local slope stability rather than regional climatic

©2019. Japan Geoscience Union. All Right Reserved.

changes.

References
Sasaki, N. and Sugai, T. (2015): Distribution and Development Processes of Wetlands on Landslides in the Hachimantai Volcanic Group, NE Japan. Geographical Review of Japan Series B, 87, 103–114.
Sasaki, N. and Sugai, T. (2018): Holocene development of mountain wetlands within and outside of landslide in the Hachimantai volcanic group, northeastern Japan. Quaternary International, 471, 345–358.

Keywords: wetland, development process, landslide, Hachimantai Volcano

©2019. Japan Geoscience Union. All Right Reserved.

Air and ground temperature conditions on alpine and sub-apline zone of Norikura Volcano, Northern Japanese Alps

*Akihiko SASAKI[1], Motoshi NISHIMURA[2], Keisuke Suzuki[3]

1. Department of Geography and Environmental Studies, Kokushikan University, 2. Interdisciplinary Graduate school of Science and Technology, Shinshu University, 3. Faculty of Science, Shinshu University

In Japanese mountains, the alpine zone above the forest limit coincides with the periglacial zone, therefore the position of the forest limit and its genesis are important. The forest limit is thought to control by factors such as thermal conditions, prevailing wind, snow cover, and form and deposit of slope surfaces. We observe the air temperatures on the two sites of forest zone, where are forest limit and under limit of subalpine zone of Norikura volcano. In addition, we also observe the air temperature on an alpine zone of Fujimi-dake in Norikura volcano.
The annual mean air temperatures on the forest limit were 0.1 ℃ in 2014 and -0.3 ℃ in 2017. The warmth index (WI) on the forest limit were 19.7 ℃・months in 2014, 21.8 ℃・months in 2015, and 19.8 ℃・months in 2017, respectively. This WI value exceeds 15℃・months of Kira's WI for the forest line in Japan. This result supports the proposal that the forest line of Norikura volcano is controlled not by thermal conditions but by other factors such as the prevailing wind or snow cover.

Keywords: air temperature observation, ground temperature observation, forest limit, alpine zone, norikura volcano, Northern Japanese Alps

©2019. Japan Geoscience Union. All Right Reserved.

Initiation and flow characteristics of debris flows on a sediment deposition zone in a mountain area

*Fumitoshi Imaizumi[1], Yuichi S. Hayakawa[2], Haruka Tsunetaka[3], Norifumi Hotta[4]

1. Faculty of Agriculture, Shizuoka University, 2. Faculty of Environmental Earth Sciences, 3. Forestry and Forest Products Research Institute, 4. Graduate School of Agricultural and Life Sciences

Debris flows is a geomorphic process, which is extremely hazardous as a result of their high velocity, long travel distance, and destructive power. However, debris flow characteristics in the initiation zones, which could possibly be affected by accumulation conditions of the storage (i.e., channel gradient and volume of storage) associated with sediment supply from hillslopes and the evacuation of sediment by debris flows, are poorly understood because of the difficulty in access. Thus, we studied the influence of accumulation condition of the storage on initiation and flow characteristics of debris flow at the Ohya landslide body in Japan by periodical terrestrial laser scanning (TLS) and UAV surveys, and field monitoring. In the Ohya landslide, debris flow occurs frequently (about three or four events per year) due to the mobilization of storage Our study clarified that initiation location of the debris flow is highly affected by depth of the storage and water supply from tributaries. Partly saturated debris flow is an important hydrogeomorphic processes in the initiation zones of debris flow because of the steep terrain. The flow characteristics were affected by the volume of storage and rainfall patterns. Partly saturated flow dominated when total of the storage > 15,000 m^3, while fully saturated flow dominated when total volume of the storage < 10,000 m^3. Transition of the flow type from partly saturated flow to fully saturated flow as the surges flow down was monitored by the time lapse cameras. Therefore, debris flow characteristics in the initiation zone, which is highly affected by accumulation conditions of the storage, are sometimes different from that in the transportation and deposition zones.

Keywords: debris flow, mountainous area, sediment disasters

©2019. Japan Geoscience Union. All Right Reserved.

Relationships between annual landform changes of the riverbed and vegetation dynamics during recent 10 years in the upper Asusa River in Kamikochi valley in the Japan Alps

*Hiroshi Shimazu[1]

1. Department of Geography, Faculty of Geo-Environmental Science, Rissho University

The Azusa river is originated from Mt. Yarigatake and runs through the Kamikochi valley, whichi has the wide valley bottom instead of the mountain region. The Azusa river forms multi bar with gravelbed braided channel in the Kamikochi valley. There are patchy willow communities of *Salix arbutifolia* and *Salix rorida* in the riverbed. Kamikochi Natural History Research Group has made geomorphological maps more than 25 years, recorded annual landform changes and dynamics of vegetation. This paper discusses the relationships between landform changes and germination and destruction of willow communities.

After 2008 major channel pattern changes occurred in 2009, 2010, 2011, 2013, 2017 and 2018. Except 2009 there were heavy rain event whose daily rain fall was over 110mm in the Baiu rainy season (from June to July). In July 2009 rain observed 29 days and maximum 3 days rainfall was excess 170mm. Based on the overview images taken by interval shooting cameras placed in the study area between July 2011 and October 2016, one or two hours after beginning of rain water level rises and in heave rainfall events occurred not in the Baiu maximum water level was not high as in the event in the Baiu.

Observation of surveyed cross sections of the riverbed and distribution of vegetated area on the gravel bars shows that the channels do not move laterally. Former channels were buried by transported sediments and new channels were excavated. Although the most bars were covered with water and sediments, their surfaces were not eroded. Thus, most vegetation on the bars survived the food event. By slight lateral erosion patchy communities of willow were gradually destructed and reduction of the area. During recent ten years a new willow community germinated in a shallow ditch continues growing. The Height of the community reaches 3 meters. Another willow community germinated in 1998 and more than 20m in height continues growing, reducing its area by lateral erosion in several flood events. Isolated willow trees on the bar in the center of the riverbed survived more than 20 years impact of yearly flood flows. But some of them were washed away in the 2017 and 2018 flood events.

The landform of the riverbed of the Azusa River in Kamikochi region considerably changed by burying former channels and excavating new channels, which occurred in once in several years during heavy rainfall events in the Baiu season. After these flood events *Salix arbutifolia* germinated and form new patchy communities. Although these communities were destructed partly, they have continued growing and some of them form communities of isolated large trees. These processes form the peculiar alpine river landscape in Kamikochi area.

Keywords: riverbed, landform change, vegetation dynamics, braided channel, Azusa river, Japan Alps

©2019. Japan Geoscience Union. All Right Reserved.

[J] Oral | M (Multidisciplinary and Interdisciplinary)：M-IS Intersection

Mon. May 27, 2019 10:45 AM - 12:15 PM JST | Mon. May 27, 2019 1:45 AM - 3:15 AM UTC | 103 1F

[M-IS20] Mountain Science

convener:Keisuke Suzuki(Department of Environmental Sciences, Faculty of Science, Shinshu University), Yoshihiko Kariya(Department of Environmental Geography, Senshu University), Akihiko SASAKI(Department of Geography and Environmental Studies, Kokushikan University), Chiyuki Narama(Niigata University, Department of Science), Chairperson:Akihiko SASAKI

Mountainous areas provide water resources to the populated downstream areas, protecting the
 diversity of ecosystem and providing tourism attraction. To access the mountain environment
 changes and mitigate the impacts of global warming influences, a cross-cutting session is
 proposed to share the scientific knowledge among various fields; such as climatology, hydrology, geography, glaciology, water/carbon/material cycle, eco-diversity, etc.

10:45 AM - 11:00 AM JST | 1:45 AM - 2:00 AM UTC

[MIS20-07] Age dating of groundwater using tritium and CFCs in headwater catchments, Fukushima after the Fukushima Dai-ichi Nuclear Power Plant accident

*Koichi Sakakibara[1], Sho Iwagami[2], Maki Tsujimura[3], Yutaka Abe[4], Manami Hada[5], Ishwar Pun[6], Yuichi Onda[3,7] (1.Faculty of Science, Shinshu University, 2.Department of Disaster Prevention, Meteorology and Hydrology, Forestry and Forest Products Research Institute, 3.Faculty of Life and Environmental Sciences, University of Tsukuba, 4.Natural Environment Conservation Center, Kanagawa, 5.Graduate School of Life and Environmental Sciences, University of Tsukuba, 6.Organization for the Strategic Coordination of Research and Intellectual Property, Meiji University, 7.Center for Research in Isotopes and Environmental Dynamics, University of Tsukuba)

11:00 AM - 11:15 AM JST | 2:00 AM - 2:15 AM UTC

[MIS20-08] Hydraulic adaptation for tree height growth in tall tree species

★Invited Papers

*Wakana Azuma[1] (1.Kyoto University)

11:15 AM - 11:30 AM JST | 2:15 AM - 2:30 AM UTC

[MIS20-09] **The molecular phylogenetic structure and biogeographic history of a alpine gravel environment specific plant *Dicentra peregrina* (Papaveraceae) in Japan**

*Takahisa Ozaki[1], Hirokazu Matsuda, Koji Tojo[2] (1.Graduate School of Science and Technology, Shinshu University, 2.Biology Department, Faculty of Science, Shinshu University)

11:30 AM - 11:45 AM JST | 2:30 AM - 2:45 AM UTC

[MIS20-10] Formation process of small stands of *Abies mariesii* forest in pseudo-alpine zone on Mt. Akita-komagatake, northern Japan

*Asaka Konno[1] (1.International Research Institute of Disaster Science, Tohoku University)

11:45 AM - 12:00 PM JST | 2:45 AM - 3:00 AM UTC

[MIS20-11] Distribution of the pinas forests including a Cryptomeria japonica and its environmental factors in Echigo mountain range.

*Masatsugu YASUDA[1] (1.Asia Air Survey Co., Ltd.)

12:00 PM - 12:15 PM JST | 3:00 AM - 3:15 AM UTC

[MIS20-12] Roles of glacier microbes in alpine ecosystems of Asian high mountains: effect of cryoconite outflow on soil development in glacier forefields

★Invited Papers

*Nozomu Takeuchi[1], Masato Shiomuki[1] (1.Chiba University)

Age dating of groundwater using tritium and CFCs in headwater catchments, Fukushima after the Fukushima Dai-ichi Nuclear Power Plant accident

*Koichi Sakakibara[1], Sho Iwagami[2], Maki Tsujimura[3], Yutaka Abe[4], Manami Hada[5], Ishwar Pun[6], Yuichi Onda[3,7]

1. Faculty of Science, Shinshu University, 2. Department of Disaster Prevention, Meteorology and Hydrology, Forestry and Forest Products Research Institute, 3. Faculty of Life and Environmental Sciences, University of Tsukuba, 4. Natural Environment Conservation Center, Kanagawa, 5. Graduate School of Life and Environmental Sciences, University of Tsukuba, 6. Organization for the Strategic Coordination of Research and Intellectual Property, Meiji University, 7. Center for Research in Isotopes and Environmental Dynamics, University of Tsukuba

Groundwater age is crucial information for understanding the continuum groundwater flow system from mountain to ocean. Headwaters are origins of the terrestrial hydrological cycle and therefore important areas to understand the water resources management, material cycle, and disaster prevention. After the Fukushima Dai-ichi Nuclear Power Plant accident, concerns of radionuclide contamination of water resources have been elevated. However, the groundwater flow system including age information in radionuclide-contaminated headwaters in Japan has not been well clarified. Therefore, the objective of this study is to investigate the groundwater age and related radionuclide effect on the water resources by using multi-tracer approach in headwater catchments approximately 30 km north-west apart from the Fukushima Dai-ichi Nuclear Power Plant. Periodical field surveys were conducted from May 2011 (2 months after the disaster) to November 2012. Tritium, chlorofluorocarbon (CFCs), and stable isotopes (oxygen and hydrogen) were used as environmental tracers.
Mean groundwater age in the study areas was estimated to be ranging from 10 to 26 years by combined use of multiple CFCs concentrations. The tritium concentration in groundwater was between 1.3 TU and 6.0 TU, which supported the estimated CFCs-based groundwater age. In addition, the governing groundwater flow system was approximated by a piston flow model; however, a modern water fraction was also suggested based on the relationship between CFC-11 and CFC-12. The estimated water age and isotopic signals among the stream water, spring water, and groundwater suggested an indication of the radionuclide intrusion into the groundwater. This is consistent with the monitored ^{137}Cs concentration in the groundwater (Iwagami et al., 2017). Modern water fractions with relatively high radionuclide concentrations into groundwater possibly cause the prolonged contamination of water resources.

Keywords: tritium, CFCs, groundwater age, headwater catchment

©2019. Japan Geoscience Union. All Right Reserved.

Hydraulic adaptation for tree height growth in tall tree species

*Wakana Azuma[1]

1. Kyoto University

Forest ecosystems, one of the major elements of the mountainous area, are characterized by its complicated three-dimensional structure which is 95% occupied by canopy where cannot be reached from the ground, compared to grasslands, deserts and rocky areas (Lowman and Rinker 2004). Various life activities such as photosynthesis, transpiration, breeding, and interaction with various organisms are performed on the canopy. Canopy researches have been progressed rapidly by the development of methods for accessing treetop in recent years (Nakanishi et al. 2018).

The question of why trees can grow up so tall is simple but its discussion has continued for a long time among ecophysiological studies. Among some factors related to tree height growth being pointed out, a main factor is considered that the limitation of water transport from root to leaves at the far end (e.g. Ryan et al. 2006). While this is the beginning of theoretical research, it has not been directly measured how much actual leaves are affected by the water transport limitation in tall trees. Therefore, we accessed to crown for 100 m tall of *Sequoia sempervirens* and 50 m tall *Cryptomeria japonica* by tree climbing, and directly evaluated water relations characteristics of leaves at various heights. As a result, although the supposed influence by water limitation was not observed, the high water capacitance of treetop leaf was revealed. This results suggested that the high water capacitance of treetop leaf would compensate for the physical water transport limit at treetop (Ishii et al. 2014).

How can treetop leaves perform high water capacity? To investigate a relationship between leaf anatomy and water relations, leaves of 50 m tall C. japonica were freeze by liquid nitrogen in situ of crown before dawn and at midday, then took it back to the laboratory and sectioned with cryo-SEM for observations. As a result, it was revealed that the transfusion tissue specific to the gymnosperm, which is located between the vascular bundle and the mesophyll, reversibly stored water and shrink like a sponge. At the treetop, large number of transfusion cells contributed to maintain the physiological function by the tissue structure giving priority to the water limit compensation, and as a result, maximum tree height could be regulated by tradeoff of the resource allocation with photosynthetic structure (Azuma et al. 2016).

To elucidate the mechanism of water retention within leaves focusing on the physicochemical properties, infrared spectroscopy is conducted. By applying it to leaf cross-sections in combination with a microscope, it is possible to quantify and visualize the distribution of water and sugars which were difficult to evaluate by an anatomical method alone. Although water is treated as one kind in the present plant physiology, in actual, physicochemical studies are known that various water components exists due to a difference in hydrogen bonding. In this study, working hypothesis that water with short hydrogen bonding component could be retained to polysaccharides within leaves was discussed. (Azuma et al. 2017).

These results suggest the one of a mechanism for tree height growth in tall conifer species with a new insight that “adaptation” to the water transport limit at treetop. To elucidate the actual ecophysiological characteristics in such huge trees, more comprehensive understanding from multiple perspectives would be necessary.

References

©2019. Japan Geoscience Union. All Right Reserved.

Lowman MD, Rinker HB. 2004. Forest Canopies, Second Edition. Elsiver Academic Press, Oxford.
Nakanishi A, Azuma W, Tanaka M, Miyazaki Y, Inui Y, Science L. 2018. The opportunities and challenges of applying tree climbing techniques as a canopy access method in canopy biology. Journal of Ecological Society Japan **68**, 125–139.
Ryan MG, Phillips N, Bond BJ. 2006. The hydraulic limitation hypothesis revisited. Plant, Cell & Environment **29**, 367–381.
Ishii HR, Azuma W, Kuroda K, Sillett SC. 2014. Pushing the limits to tree height: could foliar water storage compensate for hydraulic constraints in Sequoia sempervirens? Functional Ecology **28**, 1087–1093.
Azuma W, Ishii HR, Kuroda K, Kuroda K. 2016. Function and structure of leaves contributing to increasing water storage with height in the tallest Cryptomeria japonica trees of Japan. Trees **30**, 141–152.
Azuma W, Nakashima S, Yamakita E, Ishii HR, Kuroda K. 2017. Water retained in tall Cryptomeria japonica leaves as studied by infrared micro-spectroscopy. Tree Physiology **37**.

Keywords: water relations, hydraulic architecture, canopy

©2019. Japan Geoscience Union. All Right Reserved.

The molecular phylogenetic structure and biogeographic history of a alpine gravel environment specific plant *Dicentra peregrina* (Papaveraceae) in Japan

*Takahisa Ozaki[1], Hirokazu Matsuda, Koji Tojo[2]

1. Graduate School of Science and Technology, Shinshu University, 2. Biology Department, Faculty of Science, Shinshu University

In determining the distribution area of an organism, meteorology, climate, geography, topography and geology are important factors. In particular plants are more susceptible to climate change by limitations on dispersion compared with animals, thus the relationship between climate change and geographical distributional history in the glacial-interglacial cycles have been discussed a lot. For example, a hypotheses and a pattern have been proposed about the distribution history of alpine plants in the Japanese Archipelago. During the glacial periods, their distribution area was expanded (to the more southern region), on the other hand, the distribution area shrank (to the more northern region) during the interglacial periods and survived only in the alpine areas. Regarding the geological conditions, soil nutrition, size and stability of gravels influence species composition and population dynamics. Not only environmental factors but also biological interactions play an important role. If the weather, geography and geological conditions are severe, it will be a major barrier to plants' lives. However, few cases have established the effects of habitats' environments on their distributional histories. *Dicentra peregrina* inhabiting the alpine gravel lands and represent the alpine desert plants' community. In Japan, *D. peregrina* is also called "queen of alpine plants". Such alpine gravel lands distribute scattered around the volcanoes, and also around the ridgeline areas of high altitude mountains with strong disturbances: harsh weathering and/or unstable lands' surface. Therefore, migration is strongly restricted and highly influenced by weather, geography, topography and geology, compared with other alpine plants. Thus, *D. peregrina* is a suitable targeted alpine plant to investigate the relationship between the habitat environments and the distributional history. In order to estimate their distributional history, we have conducted phylogenetic analyses of *D. peregrina* in the Japanese Archipelago. Additionally, we have also conducted the "Ecological niche modeling" to estimate distributional changes by climate changes. As a result of our phylogenetic analyses, we observed two major genetic lineages within *D. peregrina*: one is endemic to Hokkaido (Group 1), and the other was observed from wide-areas in the Japanese Archipelago (Group 2). The boundary between the two lineages was recognized within the Daisetsu Mountain Range at Central Hokkaido. In Hokkaido, Group 2 was only observed in Mt. Kaundake and Mt. Furanodake. According to some geological studies, both Mt. Kaundake and Mt. Furanodake having comparatively old origin, it is considered that they were formed before 700,000 years ago. In contrast, regarding mountains where observed the Group 1, it is considered that they were formed around 150,000 years ago. Such differences of the mountain formation ages might be affected the population dynamics of *D. peregrina* in the glacial-interglacial climate changes. The Group 2 of *D. peregrina* is highly likely migrated to the Japanese Archipelago during the last glacial period. On the other hand, the Group 1 was dispersed to the Japanese Archipelago in older period and it is considered that their distribution spread more widely in the last glacial period. Thus, these old originated mountains served as refugia during inter-glacial periods. In addition, the genetic structure of *D. peregrina* was largely different from other alpine plants, and such difference suggests the distributional history of *D. peregrina* is strongly related to geological history rather than other alpine plants.

©2019. Japan Geoscience Union. All Right Reserved.

Keywords: phylogeography, alpine Plant, alpine desert, glacial-interglacial cycles

©2019. Japan Geoscience Union. All Right Reserved.

Formation process of small stands of *Abies mariesii* forest in pseudo-alpine zone on Mt. Akita-komagatake, northern Japan

*Asaka Konno[1]

1. International Research Institute of Disaster Science, Tohoku University

The coniferous forest (largely composed of *Abies mariesii*) is presently the typical vegetation of the subalpine zone in Japan. However, around Mt. Akita-komagatake, in northern Japan, the expected predominance of *A. mariesii* is not extensively observed, and the predominant vegetation is instead the dwarf bamboo (Sasa kurilensis) grasslands and broad leaf forests. It' s called Pseudo-Alpine zone. According to pollen analysis, this vegetation is assumed to be attributed to unsatisfactory expansion of *A. mariesii* forest.

Here we clarify the formation process of small stand of the *A. mariesii* forest by its size structure and process of regeneration.

The surveyed area is located in the northern Mt. Akita-komagatake. We classified the vegetation and measured DBH (diameter at breast height) and created frequency histograms of size structure on each vegetation.

The both histograms of *A. mariesii* thick and thin forest display gradual decreasing on the small classes on the *X* axis (DBH). The maximum classes of DBH are the class of 20-30 cm on the both histograms. The decreasing is considered to be brought about by two reasons: the second generation of *A. mariesii* on 20-30 cm DBH class is not enough equipped to propagate, and there is less numbers of first generation. These results are indicated that the small stands of *A. mariesii* forest rapidly formed by second generations.

Keywords: Abies mariesii forest, formation process, Mt. Akita-komagatake, pseudo-alpine zone

©2019. Japan Geoscience Union. All Right Reserved.

Distribution of the pinas forests including a Cryptomeria japonica and its environmental factors in Echigo mountain range.

*Masatsugu YASUDA[1]

1. Asia Air Survey Co., Ltd.

Natural cedar grows in the area of southeastern part of Aizu area to Higashi Kanbara gun.
This cedar is known as the real name Cryptomeria japonica or Sanjo Sugi, a famous cultivar called Sugi or Sanjo Sugi. On a gentle slope it forms a forest that intermixes with beech and on the ridge it forms a mixed forest with the Chitose or Pinus densiflora.
Forests mixed with sugi and beech are recognized on the Sea of Japan side mainly in Akita prefecture (2018 Echigo valley), whereas forests mixed with sugi and Kitakagoyo or Pinus densiflora are not well recognized in other areas, .
Regarding vegetation in this area Matsuura (2010) says, "The most characteristic of vegetation in this area is avalanche vegetation consisting of shrub forests and grasslands formed by frequent avalanche due to heavy snow.The upper slope of the ridge An avalanche vegetation in a shrub forest from both sides, formed as a result of snow accumulation as a pine forest (Mainly for Kita gobo and Mixed Pinus densiflora in a low altitude) on a Yase ridge remains linear (Mohegan cut) It shows that it is vegetation.
By the way, the author made a survey in this area around the autumn of last year, and found that the pine forest including this cedar has relevance to snow accumulation gradient. In addition, from the viewpoint of the combination of plants, that is, from the viewpoint of plant sociology, it was also found to be strongly related to "Crobe - Kita - gobay Forest" distributed in the sub - alpine region of Japan.
We analyze these relationships, that is, the plant sociological features and the geographical relevance of the environment such as snow cover by using existing vegetation survey database and mesh climate value and report the results.

Keywords: Natural Cryptomeria japonica, Echigo mountain range, Mt. Mikagura, Snow coverage, Phytosociology, Vegetation survey database

©2019. Japan Geoscience Union. All Right Reserved.

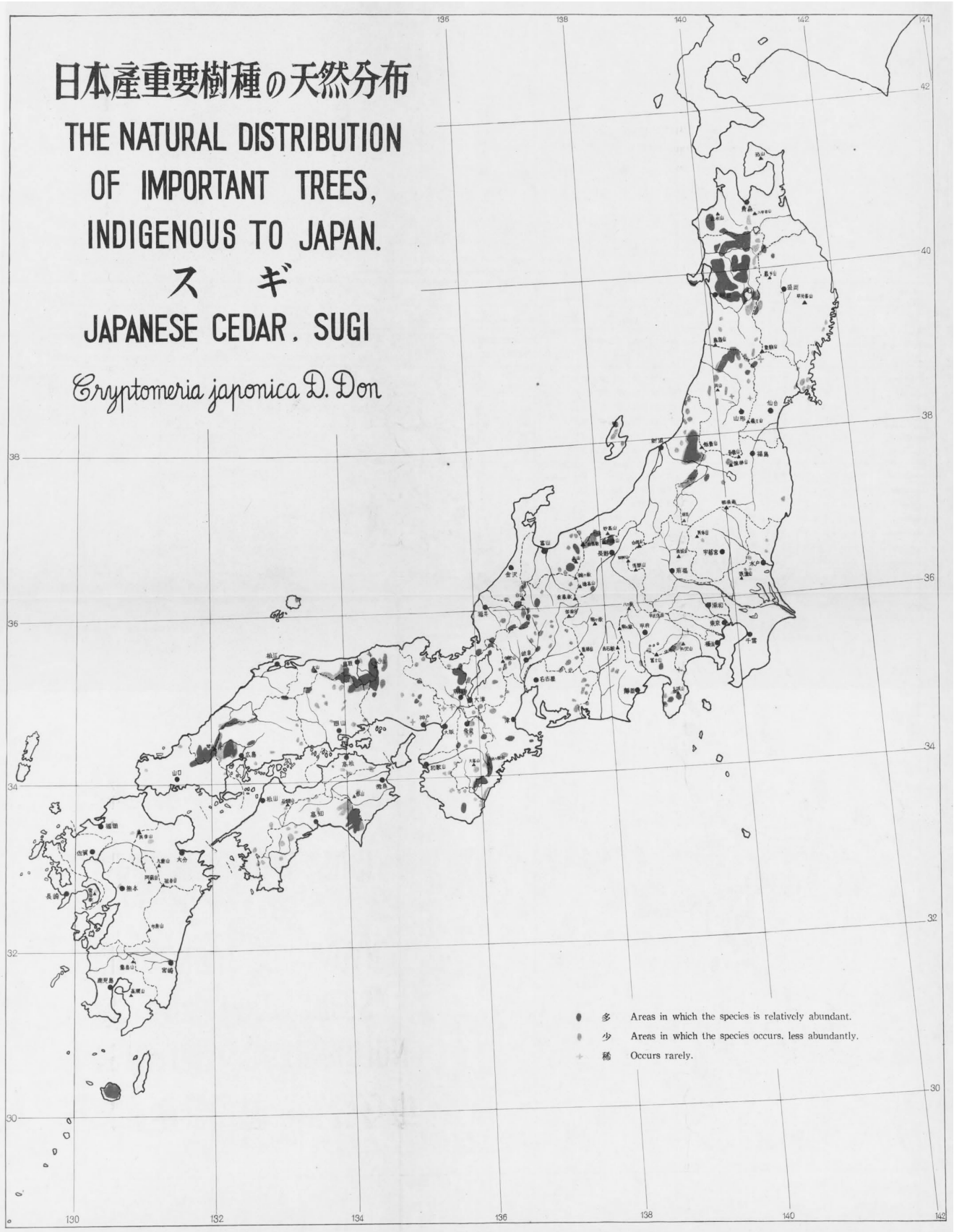

©2019. Japan Geoscience Union. All Right Reserved.

Roles of glacier microbes in alpine ecosystems of Asian high mountains: effect of cryoconite outflow on soil development in glacier forefields

*Nozomu Takeuchi[1], Masato Shiomuki[1]

1. Chiba University

The Tien Shan Mountains are one of the major mountain systems in Central Asia, extending over 2000 km, from east Uzbekistan to northeast of the Taklamakan Desert in China. The major Tien Shan peaks rise from over 4000 to 7000 m above sea level (a.s.l.). Glaciers presently exist in mountains mainly above 3500 m a.s.l. and most rivers originating from the Tien Shan glaciers flow down through the steppes and deserts surrounding the mountains. Water from the mountains has sustained the local inhabitants and ecosystems of this arid area. Recent studies revealed that there are diverse microbes living on the Tien Shan glaciers and they produce significant amounts of cryoconite, which is a small granular aggregation of microbial organic matter on the glacier ice. We found abundant cryoconite deposit along a river from glaciers, which is likely to contribute development of organic soil in the glacier forefields. Thus, biological communities living on the glaciers also play a role to maintain the alpine ecosystems and regional environments in the Tien Shan Mountains.

Keywords: cryooconite, glacier forcefields, Tienshan Mountains

©2019. Japan Geoscience Union. All Right Reserved.

[J] Oral | M (Multidisciplinary and Interdisciplinary)：M-IS Intersection

Mon. May 27, 2019 1:45 PM - 3:15 PM JST | Mon. May 27, 2019 4:45 AM - 6:15 AM UTC | 103 1F

[M-IS20] Mountain Science

convener:Keisuke Suzuki(Department of Environmental Sciences, Faculty of Science, Shinshu University), Yoshihiko Kariya(Department of Environmental Geography, Senshu University), Akihiko SASAKI(Department of Geography and Environmental Studies, Kokushikan University), Chiyuki Narama(Niigata University, Department of Science), Chairperson:Chiyuki Narama(新潟大学)

Mountainous areas provide water resources to the populated downstream areas, protecting the
 diversity of ecosystem and providing tourism attraction. To access the mountain environment
 changes and mitigate the impacts of global warming influences, a cross-cutting session is
 proposed to share the scientific knowledge among various fields; such as climatology, hydrology, geography, glaciology, water/carbon/material cycle, eco-diversity, etc.

1:45 PM - 2:00 PM JST | 4:45 AM - 5:00 AM UTC

[MIS20-13] Comparison of surface energy balance of seasonal snowcover for three sites in Japanese alpine region

*Motoshi NISHIMURA[1], Akihiko SASAKI[2], Keisuke Suzuki[3] (1.Interdisciplinary Graduate school of Science and Technology, Shinshu University, 2.Department of Geography and environmental Studies, Kokushikan University, 3.Faculty of Science, Shinshu University)

2:00 PM - 2:15 PM JST | 5:00 AM - 5:15 AM UTC

[MIS20-14] The influence of snow for the local wind system on the east slope of Mt.Norikura

*Genki Uehara[1], Keisuke Suzuki[2] (1.Graduate School of Science and Technology, Shinshu University, 2.Department of Environmental Science, Faculty of Science, Shinshu University)

2:15 PM - 2:30 PM JST | 5:15 AM - 5:30 AM UTC

[MIS20-15] Mass balance of "Avalanche-accumulation type"glaciers and perennial snow patches in Hida mountain range.

*Kenshiro Arie[1], Chiyuki Narama[2], Kotaro FUKUI[3], Hajime IIDA[3] (1.Graduate School of Science and Technology, Niigata University, 2.Faculty of Science, Niigata University, 3.Tateyama Caldera Sabo Museum)

2:30 PM - 2:45 PM JST | 5:30 AM - 5:45 AM UTC

[MIS20-16] Pattern of occurrence of sea of clouds and waterfall cloud near Mt.Nishihotakadake

★Invited Papers

*Toru Awazawa[1] (1.Faculty of Science, Shinshu University National University, Shinshu University Faculty of Science)

2:45 PM - 3:00 PM JST | 5:45 AM - 6:00 AM UTC

[MIS20-17] Review and prospect of strong local wind “Matsubori-kaze” blowing at the western foot of Mt. Aso.

★Invited Papers

*Hiroshi Matsuyama[1] (1.Graduate School of Urban Environmental Sciences, Tokyo Metropolitan University)

3:00 PM - 3:15 PM JST | 6:00 AM - 6:15 AM UTC

[MIS20-18] Two decades of mountain climate monitoring and research: lessons learned and future challenges.

*Luis Duran[1,2,3], Irene Rodríguez-Muñoz[1] (1.interMET Sistemas y Redes S.L.U. Madrid. Spain, 2.Centro de Investigación, Seguimiento y Evaluación del Parque Nacional Sierra de Guadarrama. Madrid. Spain, 3.Departamento de Física de la Tierra y Astrofísica. Facultad de Ciencias Físicas. Universidad Complutense de Madrid. Spain)

Comparison of surface energy balance of seasonal snowcover for three sites in Japanese alpine region

*Motoshi NISHIMURA[1], Akihiko SASAKI[2], Keisuke Suzuki[3]

1. Interdisciplinary Graduate school of Science and Technology, Shinshu University, 2. Department of Geography and environmental Studies, Kokushikan University, 3. Faculty of Science, Shinshu University

Process of snow and glacier ablation is one of the indicator of global climate change, so is of interest as understanding earth system. In the discussion of snow ablation process, calculating surface energy balance (SEB) is one effective method, and it is generally analysed with local meteorological observation data. SEB is sensitive to regional atmospheric conditions, therefore it often reflects in situ regional climate and surrounding environment. This presentation offers the result of regional SEB analysis in central Japanese alpine region, Kamikochi (1490 m a.s.l.), Norikura highland (1590 m a.s.l.) and Nishi-Hodaka (2355 m a.s.l.) to reveal the characteristic of SEB of seasonal snowcover in Japanese sub-alpine region. Three automatic weather stations, operated by Shinshu University, were located each targeted region in snow covered period of 2016/17 (Hydrological year). SEB analysis was conducted using surface energy balance method, and an analysis of turbulent heat flux was done using the bulk aerodynamic method. SEB analysis were conducted only snow covered period from October, 2016 to June, 2017.
The most major energy source was net shortwave radiation and negative energy flux was offered by net longwave radiation and latent heat flux in every site. Those characteristics were often reported in continental regions and high elevation areas, such as alpine region, because atmospheric condition in those regions are often cold and dry so that incoming turbulent enegy flux were restrained. The most atrractive characteristic resulted in SEB comparison is that the behavior of snowmelt energy flux in later ablation period is different in three sites. Snowpack in Nishi-Hodaka is persisted longer (untill June) than other two sites due to a lot of snowfall offered in winter, so that atmospheric condition (e.g. air temperature, specific humidity) and radiation components in later ablation period have been different from other two sites. Threrfore the different SEB properties in each site were also discovered.
Similar and diference SEB properties, which are resulted from regional climate condition and local topographic environment, among the three target sites were revealed. It is interesting that the target sites, relatively near but diferent (or same) elevation band, have each different SEB properties, so more detailed analysis of regional SEB properties are required.Comparison of surface energy balance of seasonal snowcover for three sites in Japanese alpine regionComparison of surface energy balance of seasonal snowcover for three sites in Japanese alpine region

Keywords: snow melt, alpine region, snow surface energy balance

©2019. Japan Geoscience Union. All Right Reserved.

The influence of snow for the local wind system on the east slope of Mt.Norikura

*Genki Uehara[1], Keisuke Suzuki[2]

1. Graduate School of Science and Technology, Shinshu University, 2. Department of Environmental Science, Faculty of Science, Shinshu University

On the east slope of Mt.Norikura (3026 m), there is a unique local wind system, which is thought to be influenced by the snow on the slope. In general, on the mountain regions, the nocturnal flows are down-slope and down-valley wind, while the daytime flow are up-slope and up-valley wind. However, in the Mt.Norikura on the winter-spring, the down-slope wind develop afternoon even though daytime. It is a unique local wind system. The snow on the slope of mountain is possible to play a role in the development of the unique wind system. Because a temperature of a snow surface is always near or below 0 ˚C, a downward sensible heat be formed whenever the air temperature is above 0 ˚C. The air over snow that has been cooled by a downward flux of sensible heat produce the down-slope wind in especially the late afternoon of warm, sunny days (Whiteman, 1999). We consider that the unique wind system is formed with the result of the interaction between “down-slope wind on the snow” and “up-slope wind on the no-snow surface“.

Japanese Alps including the Mt.Norikura is known as a heavy snow region, a lot of snow falls on the mountain region in winter (Suzuki, 2013). The snow surface forms a characteristic thermodynamically structure and plays important roles in the atmospheric environmental of mountain regions. However the atmospheric environment of mountain regions have not been understood sufficiently due to insufficiency of meteorological observation. In this research, We will report the relevance between a local wind system and snow on the mountain region with using the data of meteorological observation.

Keywords: mountains meteorological, thermally driven wind, snow

©2019. Japan Geoscience Union. All Right Reserved.

Mass balance of "Avalanche-accumulation type"glaciers and perennial snow patches in Hida mountain range.

*Kenshiro Arie[1], Chiyuki Narama[2], Kotaro FUKUI[3], Hajime IIDA[3]

1. Graduate School of Science and Technology, Niigata University, 2. Faculty of Science, Niigata University, 3. Tateyama Caldera Sabo Museum

In the Hida mountain range, we clarified mass balance of glaciers and perennial snow patches of ” avalanche-accumulation type" by aerial photos and SfM analysis. Comparing mass balance of the "snowdrift-acumulation type" and "avalanche-accumulation type", "avalanche-accumulation type" was more positive.

Keywords: glacier, perennial snow patch, mass balance, SfM, aerial photography

©2019. Japan Geoscience Union. All Right Reserved.

Pattern of occurrence of sea of clouds and waterfall cloud near Mt.Nishihotakadake

*Toru Awazawa[1]

1. Faculty of Science, Shinshu University National University, Shinshu University Faculty of Science

The mountain ranges of 3000 m class are connected to the spear ·Mt.Yarigatake-Mt.Hotakadake mountain range, and the mountain ranging from Mt.Nishihotakadake located at the southwest end to Mt.Yakedake, Mt.Norikuradake ridgeline is also over 2000 m. Although it is said that the atmospheric boundary layer is within 1000 meters in the temperate region, situations where the atmosphere boundary layer between Gifu prefecture and Nagano prefecture is divided by continuous mountains often occurs in this area. Under such circumstances, when moist air flows into the lower layer from the Sea of Japan side, it becomes a form that can be stopped at Gifu prefecture side. Furthermore, when an event such as subsidence inversion layer due to high pressure occurs, stratocumulus cover the sky with the reversal layer as the boundary, and a sea of clouds occurs. Analysis of the weather conditions at the time of occurrence revealed that there are some patterns in the inflow of moist air in the lower layer. We also verified the supply of lower layer wetness to maintain the generated cloud sea and the influence of solar radiation at the time of disappearance of the sea of clouds.

In addition, waterfall cloud often occurs near Nishiho Sanso, but this is due to the lowest between Nishiho Maruyama and Mt.Yakedake in the ridgeline leading from Mt.Yarigatake-Mt.Hotakadake mountain range to Mt.Yakedake. It was found that there are two patterns in the waterfall cloud seen in this mountain region. Dynamic things, such as weakening of high pressure and strengthening inflow of moist air in the lower layer, are added at the time of the occurrence of the sea of clouds, the altitude of the sea of clouds rise, and from Nishiho Maruyama - Mt.Yakedake to Nagano Prefecture side It occurs by the cloud overflowing. On a small scale, it is caused by the air rising along the slope like the cap cloud and disappearing when it goes down, but in any case, it will be between Nishiho Maruyama and Mt.Yakutake The low altitude is a major factor in the occurrence.

Keywords: Mt.Yarigatake-Mt.Hotakadake mountain range, sea of clouds, waterfall cloud, inversion layer

©2019. Japan Geoscience Union. All Right Reserved.

Review and prospect of strong local wind “Matsubori-kaze” blowing at the western foot of Mt. Aso.

*Hiroshi Matsuyama[1]

1. Graduate School of Urban Environmental Sciences, Tokyo Metropolitan University

“Matsubori-kaze” (hereafter referred to as MK) is strong local wind blowing at the western foot of Mt. Aso. It is likely to blow when a depression with warm front is located off the southwestern part of Kyushu. In this presentation, we reviewed the studies on MK and their future.

The first study that investigated MK is Hayamizu and Yamashika (1950). They observed wind speed and temperature at Tateno and Ozu from 10th to 21st November, 1949. Strong local wind blew at night when Kyushu was prevailed by an anticyclone. Because Aso-caldera is located at east, they considered cold air pooled at the caldera flew through Tateno Valley. This study was introduced in the textbook of Yoshino (1961). Yoshino (1968) investigated the distribution of wind breaks around Tateno Valley. They were densely distributed around Tateno Valley, and he estimated MK was the strongest there.

Onodera (1975) opposed to the proposed blowing mechanism of MK . He investigated the diaries of Ozu-higashi elementary school, located at the strongest area of MK. He found MK blew more frequently in spring than in autumn-winter. He also found that a depression with warm front was located at 300 km south of Kyushu when strong MK blew. Onodera (1975) concluded that the inversion layer around the top of Mt. Aso, along with the existence of warm front, was important for the occurrence and intensification of MK.

Ozu-higashi elementary school stopped keeping diaries after October 1971. Because meteorological stations were not located there, we could not know when and how MK blew after October 1971. Yoshino (1986) cited Onodera (1975), however, he still explained MK originated from cold air pooled at Aso-caldera as in Yoshino (1961).

Based on long-term meteorological and mobile observations, Kurose et al. (2002a, b) clearly distinguished two types of winds, i.e., “Aso-oroshi” (hereafter referred to as AO) and MK. Kurose et al. (2002a) found AO was outflow of cold air pooled at Aso-caldera that mainly occurred at calm night in autumn-winter. On the other hand, Kurose et al. (2002b) found MK was airflow over Mt. Aso that occurred in the specific weather condition, i.e., stable stratification was formed at lower part of the troposphere, and southeasterly wind over 10 m/s prevailed at 850 hPa level. Under this condition, the airflow over mountains converged at Tateno Valley, and its wind speed exceeded 10 m/s which usually caused damages in agriculture.

It was speculated that unique topography of Mt. Aso certainly affected MK. By using virtual topographies, Inamura et al. (2009) conducted numerical simulation using meso-scale model (RAMS). They clarified MK was composite wind of downslope wind at the southern slope of Tateno Valley as well as the gap wind through it. They also revealed that a critical layer around 850hPa was important for producing well-mixed stagnant layer and generating the strong wind beneath it.

Matsuyama et al. (2014) conducted questionnaire survey to families of the students at Ozu-higashi elementary school. Keywords in the answer sheets were summarized as “strength and mode of MK,

©2019. Japan Geoscience Union. All Right Reserved.

“agricultural damage in areas with strong winds”, and “surrendering to MK". Matsuyama (2014) also analyzed written descriptions of the students’ impressions to MK. As for children, keywords were summarized as “fear”, “outdoor experiences”, and “intellectual interest”.

Sakamoto et al. (2014) caught MK blowing on 5th to 6th April, 2013. They conducted mobile observations and investigated the spatial extent to which MK reached. They also reproduced the phenomena by RAMS. The wind speed around Ozu town was on average 1.5 times as large as that at Nishihara village, closely located south of Ozu town. RAMS revealed that fluctuation of wind speeds depended on the relation between the position of Nishihara village and hydraulic jump caused by airflow over Mt. Aso.

Based on meteorological observations, Sagawa (2017) investigated the spatial extent to which AO reached. He also compared wind speeds at Tateno and Fuketa/Uchimaki where MK is the strongest. Sagawa (2017) clarified that AO blew from Fuketa to the Kikuchi-minami fire station. Wind speeds were significantly lower at Tateno both for AO and MK. It was clearly evident during the blowing of MK.

So far, characteristics of MK have been clarified fairly well. For the occurrence of MK, wind direction and wind speed at 850 hPa (about 1500 m a.s.l.) are important information. At central cone of Mt. Aso, Aso-san Meteorological Observatory (1142.3 m a.s.l.) had been operated whose data were frequently used. However, it stopped observations on 11th December, 2017, i.e., it is impossible to use these data in the future. This is a serious damage in the study of MK.

Keywords: Mt. Aso, local wind, Matsubori-kaze, Aso-oroshi, Meteorological observations in mountains

©2019. Japan Geoscience Union. All Right Reserved.

Two decades of mountain climate monitoring and research: lessons learned and future challenges.

*Luis Duran[1,2,3], Irene Rodríguez-Muñoz[1]

1. interMET Sistemas y Redes S.L.U. Madrid. Spain, 2. Centro de Investigación, Seguimiento y Evaluación del Parque Nacional Sierra de Guadarrama. Madrid. Spain, 3. Departamento de Física de la Tierra y Astrofísica. Facultad de Ciencias Físicas. Universidad Complutense de Madrid. Spain

During the last two decades several efforts have been made in order to have an accurate assessment of climatic conditions in a mountain area in Central Spain (Peñalara Massif). A combination of in-situ measurements, statistical analysis of historical data, use of re-analyses and high resolution modeling has been done in order to overcome the difficulties inherent in such a complex terrain. The first decade has been focused on the design and operation of a mountain observational network. After some efforts, the performance achieved was satisfactory. As a result, long and homogeneous records are now available for the first time. Also, valuable technical and operational information has been gained which helped in the re-design of the network which is now in operation. In the meantime, connections between mountain meteorological phenomena and synoptic forcing has been found using weather typing methods using total column water vapor flux fields from re-analyses. The interaction between regional scale advection of humidity and orography has been identified as the leading phenomena in terms of precipitation. This finally led to the application of an orographic precipitation model giving a high resolution assessment of precipitation at this mountain area which is coherent with in-situ observations. This database opens new horizons of research since it converts point measurements into spatial fields. This comprehensive approach for researching the climate of a mountain area has proven to be effective but also brings future challenges which will be discussed here.

Keywords: Mountain climate, Mountain meteorology, Mountain weather monitoring

©2019. Japan Geoscience Union. All Right Reserved.

[J] Poster | M (Multidisciplinary and Interdisciplinary)：M-IS Intersection

Mon. May 27, 2019 3:30 PM - 5:00 PM JST | Mon. May 27, 2019 6:30 AM - 8:00 AM UTC | Poster Hall International Exhibition Hall8, Makuhari Messe_24

[M-IS20] Mountain Science

convener:Keisuke Suzuki(Department of Environmental Sciences, Faculty of Science, Shinshu University), Yoshihiko Kariya(Department of Environmental Geography, Senshu University), Akihiko SASAKI(Department of Geography and Environmental Studies, Kokushikan University), Chiyuki Narama(Niigata University, Department of Science)

Mountainous areas provide water resources to the populated downstream areas, protecting the
 diversity of ecosystem and providing tourism attraction. To access the mountain environment
 changes and mitigate the impacts of global warming influences, a cross-cutting session is
 proposed to share the scientific knowledge among various fields; such as climatology, hydrology, geography, glaciology, water/carbon/material cycle, eco-diversity, etc.

[MIS20-P01] Development of fluvial terraces and landslides since the late Pleistocene in the Shirata River basin, southeastern side of Amagi Volcano, Izu Peninsula, Japan

*Nao Tokumoto[1], Yoshihiko Kariya[2], Kuniyasu Mokudai[3] (1.Undegraduate, Senshu Univ., 2.Senshu Univ., 3.Japan Geoservice Inc.)

[MIS20-P02] Variation trends of air temperature and snow depth in the Japanese Alps

*Keisuke Suzuki[1], Akihiko SASAKI[2] (1.Faculty of Science, Shinshu University, 2.Faculty of Literature, Kokushikan University)

[MIS20-P03] Abundant tardigrades found in snow pack in Mt.Gassan in Yamagata Prefecture, Japan

*MASATO ONO[1] (1.Chiba University)

[MIS20-P04] Variation of stable isotope ratios of precipitation in the Japanese Alps Region

*Tsukasa Katsuragawa[1], Tsutomu Yamanaka[2], Akihiko SASAKI[3], Yuki Kurokumo[1], Motoshi NISHIMURA[1], Shimizu Hironori[1], Keisuke Suzuki[4] (1.Graduate School of Science and Technology,Shinshu University, 2.Faculty of Life and Environmental Sciences, University of Tsukuba, 3.Department of Geography and Environmental Studies, Kokushikan University, 4.Department of Environmental Sciences, Faculty of Science, Shinshu University)

[MIS20-P05] Probable glacier detritus found at downstream site of the Yokoo moraines in the northern Japanese Alps: its geological characteristics and implications

*Manami Ishibashi[1], Yoshihiko Kariya[2], Kuniyasu Mokudai[3] (1.Undergraduate Senshu Univ., 2.Senshu Univ., 3.Japan Geo serivice Inc.)

[MIS20-P06] Recent Geomorphological changes of rock slopes in Hakuba-Daisekkei

*Hirotaka Sugiyama[1], Chiyuki Narama[2], Hiroshi Inoue[3] (1.Graduate School of Science and Technology, Niigata University, 2.Faculty of Science, Niigata University, 3.National Reserch Institute for Earth Science and Disaster Resilience)

[MIS20-P07] Behavior of inorganic ions in air deposition and surface runoff water in an alpine headwater catchment of Mt. Norikura

*Hironori Shimizu[1], Akihiko Sasaki[2], Keisuke Suzuki[3] (1.Graduate School of Science and Technology, Shinshu University , 2.Department of Geography and Environmental Studies, Kokushikan University, 3.Faculty of Science, Shinshu University)

[MIS20-P08] Activity of gravity faults in the Tateyama caldera, Hida Mountains, during the past 55 years

*Kotaro FUKUI[1], Hajime IIDA[1] (1.Tateyama Caldera Sabo Museum)

[MIS20-P09] Community, population and genetic structures of benthic invertebrates in alpine and sub-alpine ponds of the Kamikochi area and the Yari-Hotaka Mountain Ranges

*Keisuke Inoue[1], Koji Tojo[1] (1.Biology Department, Faculty of Science, Shinshu University)

[MIS20-P10] Water and carbon use of fine root in four tree species at the forest limit

*Hikari Yahara[1], Wakana Azuma[2], Mai Kamakura[2], Naoki Makita[1] (1.Graduate School of Science and Technology Shinshu University, 2.Graduate School of Agriculture Kyoto University)

[MIS20-P11] Visible-near infrared spectral reflectance explains variations in fine root traits of woody species

*Natsuko Tanikawa[1], Tatsuro Nakaji[3], Miwa Kobatake[2], Naoki Makita[2] (1.Graduate School of Science and technology, Shinshu University, 2.Faculty of Science, Shinshu University, 3.Field Science Center for Northern Biosphere)

[MIS20-P12] Heat Balance Analysis of Cold Air Pool Formation in Kamikochi

*Sayuri Koyama[1], Motoshi NISHIMURA[2], Keisuke Suzuki[3] (1.Graduate school of science and technorogy, Shinshu University, 2.Interdisciplinary Graduate school of Science and Technology, Shinshu university, 3.Department of Environmental Sciences, Faculty of Science, Shinshu University)

[MIS20-P13] A finding of fossil trees buried in dammed-lake deposits formed by the Dondokosawa rock avalanche of the late 9th century in the Akaishi Mountains, and its significance

*Takashi Kimura[1], Ryuji Yamada[1], Yoshihiko Kariya[2] (1.National Research Institute for Earth Science and Disaster Resilience, 2.Senshu University)

[MIS20-P14] What alpine plants attract visitors in the Daisetsuzan national park, northern, Japan?

*Yukihiro Amagai[1], Kota Mameno[1,2], Hiroyuki Oguma[1], Takahiro Kubo[1] (1.National Institute for Environmental Studies, 2.Hokkaido University)

[MIS20-P15] Spatio-temporal variations of algal snow in Mt. Gassan, Yamagata prefecture, Japan

*Suzuki Takumi[1], Nozomu Takeuchi[1], Tsubasa Takahashi[1] (1.Chiba University)

[MIS20-P16] Feeding of a wingless stonefly living on snow surface in Mt. Gassan, Yamagata prefecture, Japan

*Risako Yonechi[1], Nozomu Takeuchi[1] (1.Chiba University)

[MIS20-P17] Drainage from glacial lake in Achinathang village, Ladakh Range on 4 August 2017

Maho Saotome[2], *Chiyuki Narama[1], Naoki Sakurai[2] (1.Niigata University, Program of Field Research in the Environmental Sciences, 2.Graduate School of Science and Technology, Niigata University)

[MIS20-P18] Recent glacier variations at Mt. Kenya using aerial digital image

*Chiyuki Narama[1], kenshiro Arie[2], MIZUNO KAZUHARU[3] (1.Program of Field Research in the Environmental Sciences, Niigata University , 2.Graduate School of Science and Technology, Niigata University, 3.Graduate School of Letters, Kyoto University)

Development of fluvial terraces and landslides since the late Pleistocene in the Shirata River basin, southeastern side of Amagi Volcano, Izu Peninsula, Japan

*Nao Tokumoto[1], Yoshihiko Kariya[2], Kuniyasu Mokudai[3]

1. Undegraduate, Senshu Univ., 2. Senshu Univ., 3. Japan Geoservice Inc.

This study clarified geomorphic features of debris flow-fluvial terraces and landslide complexes on the southeastern side of Amagi Volcano in Izu Peninsula, central Japan. Terrace forms can be classified into three: H, M, and L surfaces from descending altitude order. Among them, the M surface is common and its geology is unique. The M surface is composed of thick and poorly sorted angular gravel beds associated with debris flow processes. The L surface is an erosion surface of higher terraces. A longitudinal profile of the M surface seems to connect with large landslide bodies in the upper reach of stream on the volcano and to continue below the present seafloor off the mouth of such a stream. Some of large landslides show secondary movement of bodies and dissected headscarps. Furthermore, the M surface is covered by a tephra layer supplied from a nearby monogenetic volcano in 19 ka. These facts show that the M surface had been formed by debris flow events filling the stream in the late Pleistocene when the sea-level was lowered. Then an increase in precipitation in the area and a decrease in bedload supply into the stream, as well as sea level rise, would have caused down cutting of the floor of stream and created a terrace form of the M surface during the period from the latest Pleistocene to the early Holocene. Because of further down cutting, the L surface had been formed. Detailed descrption of the H surface is required in future.

Keywords: the last glacial period, fill terrace, erosional terrace, landslide, tephrochronology

©2019. Japan Geoscience Union. All Right Reserved.

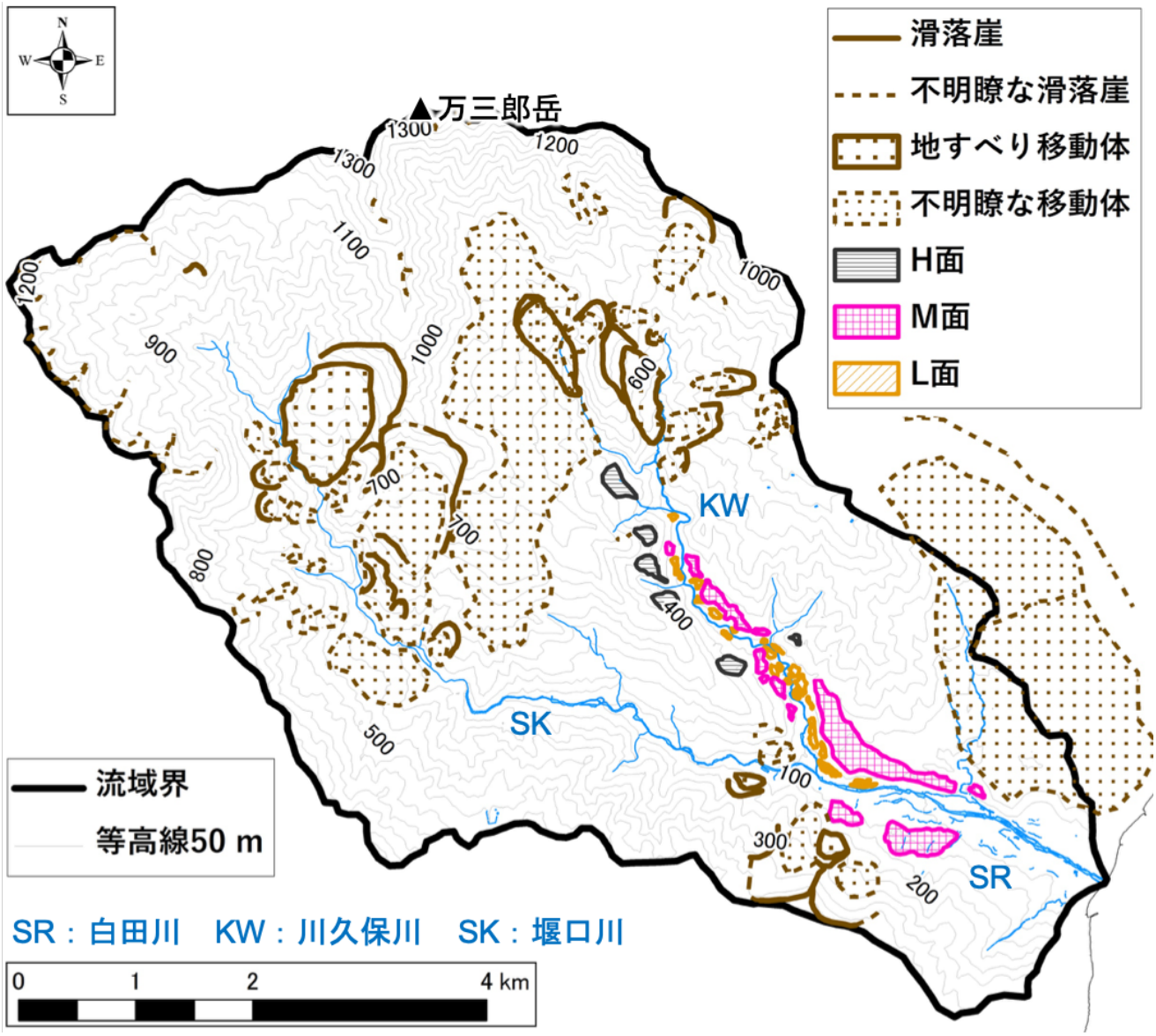

©2019. Japan Geoscience Union. All Right Reserved.

Variation trends of air temperature and snow depth in the Japanese Alps

*Keisuke Suzuki[1], Akihiko SASAKI[2]

1. Faculty of Science, Shinshu University, 2. Faculty of Literature, Kokushikan University

Mountainous areas are quite sensitive to global-scale environmental changes, such as warming. Therefore, the effects of global warming on these meteorological elements is a critical issue. We have developed a network of 14 meteorological observatories in the Japanese Alps, which have already started recording observations. The highest observation site is Mt. Yari, at 3125 m. Observation data from these sites are sent to a computer at the laboratory via a data communication mobile telephone network or phone line throughout the year. These meteorological observation data are available on the laboratory website in quasi-real time. The interannual variability of the air temperature and the snow depth in the Japanese Alps region are discussed.

Keywords: global warming, meteorological observation

©2019. Japan Geoscience Union. All Right Reserved.

Abundant tardigrades found in snow pack in Mt.Gassan in Yamagata Prefecture, Japan

*MASATO ONO[1]

1. Chiba University

Water bears are small invertebrates belonging to the phylum Tardigrada. They are typically 0.1 –1.0 mm in body length, and walk slowly with four pairs of legs. Tardigrades can shrink their body like a tun and become cryptobiosis, which enables to survive in extreme environments, such as low and high temperature, high pressure, under strong radiation. Their physiological mechanism of cryptobiosis is expected to be applied to medical and industry technologies, such as dry preservation of animal cells. They are commonly found on glaciers in polar or alpine regions. They actively live in cryoconite holes on glaciers and spend their entire lives on glaciers. In Japan, there is a heavy snow in mountainous regions due to strong monsoon westerly in winter, On the snow fields in Japan, there are various cold-tolerant organisms such as snow algae and invertebrates. However, no tardigrade has been reported on snow packs in Japan. In this study, we investigated mountain snow packs in Japan to search the presence of tardigrade and tried to reveal their life cycle.

The fieldworks were carried out on snow packs in the forest located in Mt. Gassan in Yamagata prefecture in Japan. Snow and moss samples were collected in a total of four times from April to October 2018, three times in snow season and once in no snow season. Mt. Gassan is an area with heavy snowfall in winter. Microscopic observation revealed that there were many tardigrades of the genus *Hypsibius* in surface snow. While only one species of *Hypsibius* was observed in snow samples, a total of two species including one species of the genus *Macrobiotus* were observed in moss of trees in the forest, and a total of six species were observed in moss of trees collected in no snow season. The species observed in snow is likely cold-tolerant tardigrade and preferably lives in the snow pack. Population density of tardigrades in snow was exceptionally higher on the green coloured snow due to algal blooming, but was little on white snow without algae. It was an average of 7.1×10^{3} ind L^{-1} in green snow samples. The body length distribution of tardigrades shows that the their size increased significantly from April to May in the snow pack, and the small sized larvae were observed only in the moss of trees collected in fall. Therefore, they live preferably in snow packs with green snow algae and grow up. When the snow disappears, they move to moss of trees and reproduce there. This life history seems to adapt to the area where heavy snow seasonally covers.

Keywords: Tardigrada, mountain, snow, forest

©2019. Japan Geoscience Union. All Right Reserved.

Variation of stable isotope ratios of precipitation in the Japanese Alps Region

*Tsukasa Katsuragawa[1], Tsutomu Yamanaka[2], Akihiko SASAKI[3], Yuki Kurokumo[1], Motoshi NISHIMURA[1], Shimizu Hironori[1], Keisuke Suzuki[4]

1. Graduate School of Science and Technology,Shinshu University, 2. Faculty of Life and Environmental Sciences, University of Tsukuba, 3. Department of Geography and Environmental Studies, Kokushikan University, 4. Department of Environmental Sciences, Faculty of Science, Shinshu University

We collected precipitation samples and observed meteorological condition every month from January 2011 to December 2016 at nine locations in the Japanese Alps Region (Nagano, Matsumoto, Suwa, Omachi, Sugadaira, Norikura, Kamikochi, Shigakogen, Nishihotaka). The collected water samples were brought back to the laboratory to stable isotope analysis to determineD,^{18}O and calculated d-excess. The ^{18}O in precipitation collected more than once times per month was weighted mean using the amount of precipitation and was taken as the mean monthly value. As a result of examining the seasonal variation of ^{18}O from 2011 to 2016, ^{18}O showed two peaks in spring and summer. In order to investigate the spatial variation, the coefficient of determination between latitude, longitude, altitude and ^{18}O was calculated, it clearly correlated with altitude from April to October. d-excess showed seasonal variation which is high in winter and low in summer. As a spatial variation, correlation with altitude is high in summer and correlation with longitude is high in winter. To investigate the factors that cause such variations, correlation coefficients between temperature, precipitation amount, lifting condensation level (LCL) and precipitation at δ^{18}O and d-excess at each site were calculated. Regarding δ^{18}O, it showed a positive correlation with the temperature at 8 points excluding Nishi Hodaka. Especially at 5 points of Matsumoto, Sugadaira, Omachi, Suwa, Nagano showed relatively high values. Regarding the relationship with precipitation, it showed a weak negative correlation at 6 sites excluding Omachi, Nagano and Nishi Hodaka. Regarding the relationship with LCL, there was a generally positive correlation, and particularly high correlation coefficients were found in Suwa and Nagano. From these results, it is considered that the temperature mainly contributes to δ^{18}O, and the correlation was high in Matsumoto, Sugadaira, Omachi, Suwa and Nagano, so there is a possibility that influence became strong in urban areas. The d-excess showed a negative correlation with temperature and precipitation, and there was no particularly significant relationship with LCL. The strong correlation was observed in relation to the temperature, the contribution to the fluctuation of d-excess was mainly considered to be the temperature.

Keywords: precipitation, isotope

©2019. Japan Geoscience Union. All Right Reserved.

Probable glacier detritus found at downstream site of the Yokoo moraines in the northern Japanese Alps: its geological characteristics and implications

*Manami Ishibashi[1], Yoshihiko Kariya[2], Kuniyasu Mokudai[3]

1. Undergraduate Senshu Univ., 2. Senshu Univ., 3. Japan Geo serivice Inc.

Around the upper reach of Azusa River in the northern Japanese Alps, the lowest position of a glacier snout during the late Pleistocene was known as the Yokoo-Iwagoya moraines (ca. 1700 m ASL). We revisited this widely-accepted concept of paleoglaciations in the Japanese Alps and newly found poorly-sorted angular to subangular rock clasts from the site lower than Yokoo-Iwagoya moraines (ca. 1400 m longitudinal and 50 m vertical). Rock clasts are composed of Quaternary igneous rocks that are never distributed around Yokoo. We concluded that those rock clasts were transported by a valley glacier from the higher slopes of Mount Yari-Hotaka Massif around 2800–3000 m ASL. Depositional ages of the clasts are still unknown but the Marine Isotope Stage 4 was probable.

Keywords: glaciations, the Last Glacial age, late Pleistocene, till, Japanese Alps

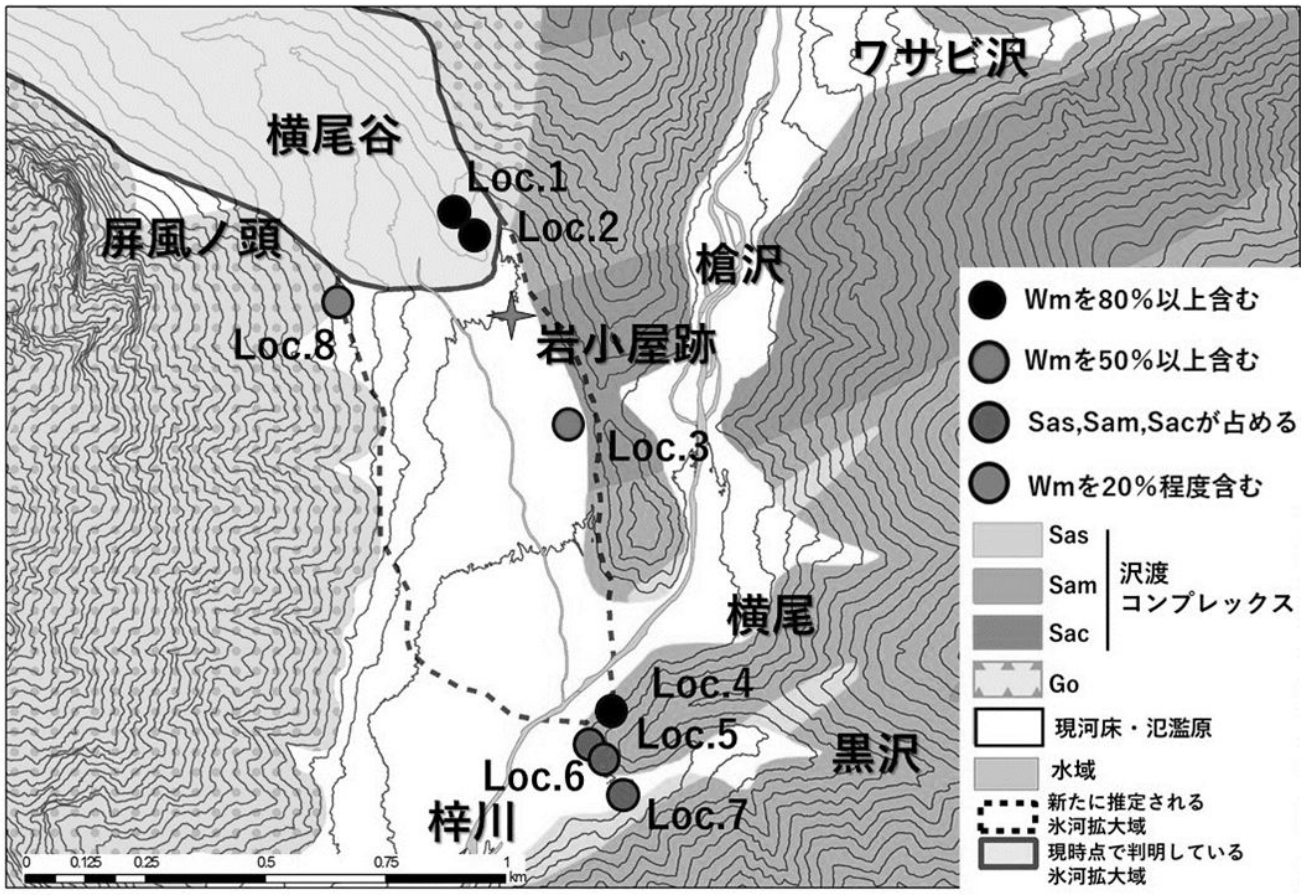

©2019. Japan Geoscience Union. All Right Reserved.

Recent Geomorphological changes of rock slopes in Hakuba-Daisekkei

*Hirotaka Sugiyama[1], Chiyuki Narama[2], Hiroshi Inoue[3]

1. Graduate School of Science and Technology, Niigata University, 2. Faculty of Science, Niigata University, 3. National Reserch Institute for Earth Science and Disaster Resilience

To understand the geomorphological characteristics of slope failure points on rock slopes of the Daisekkei valley, we investigated the surface changes of rock slopes using three-dimensional topographic models based on SfM (structure from motion) with digital aerial images from airplane, drone (Phantom4) and Cessna. Slope failure points and these surface changes were extracted by comparing three-dimensional topographic models. For large slope failure in 2005, we clarified the rock mass of 60 m height and 10 m thickness was collapsed.

Keywords: rockfall, rock failure, Hakuba-Daisekkei, aerial-photography, SfM

©2019. Japan Geoscience Union. All Right Reserved.

Behavior of inorganic ions in air deposition and surface runoff water in an alpine headwater catchment of Mt. Norikura

*Hironori Shimizu[1], Akihiko Sasaki[2], Keisuke Suzuki[3]

1. Graduate School of Science and Technology, Shinshu University , 2. Department of Geography and Environmental Studies, Kokushikan University, 3. Faculty of Science, Shinshu University

Meltwater from perennial snow patch lies on alpine catchment play an important role on the lower ecosystems as sources of fresh water during the warm season as well as rainfall, but chemical properties of air deposition and overland flow from a headwater catchment is not revealed in Japan. To characterize chemical behavior follow the rainfall and snowmelt runoff events, we studied chemical properties of stream water and air deposition during warm seasons 2016-2018, using a hydrometric and hydrochemical approaches and stable isotope of water. The study was carried out in the upper Maekawa River catchment on the east slope of Mt. Norikura, central Japan. Using an approximate curve calculated from the scatter diagrams with discharge and inorganic ion concentrations in stream water, we attempted to quantify the amount of inorganic ion dissolved in stream water during the period of August 28 to October 10, 2017.
Overland flow generation time following rainfall events was within several hours and lower surface runoff rate (up to 7%). The hydrological response properties indicate that periglacial slope overlapped by debris mainly have high water permeability and through the ground along the lava structure quickly. From the result that surface runoff rate of inorganic ions is higher than that of water amount, estimation of the amount of inorganic ions included in air deposition and surface runoff water suggest that eluviation from andesite rock contributes surface runoff amount of K^+, Mg^{2+} and Ca^{2+}. In contrast, surface runoff rate of Cl^-, NO_3^-, SO_4^{2-} were 3.9%, 2.7% and 6.5%, respectively, and it implies the dependency on air deposition for these ions dissolved in overland flow. High-frequency sampling during a rainfall event revealed that first runoff components frequently present a lower value (-19.1‰ at lowest) in $\delta^{18}O$ compared with that of stream water (-16.1‰ at lowest) during non-rainfall period. The fact that $\delta^{18}O$ of new snow obtained 2000m a.s.l. on the east slope of Mt. Norikura in January 2017 was approximately -19‰ suggests that meltwater infiltrated into the ground at early snowmelt season contribute overland flow temporarily follow rainfall input in September and October.

Keywords: headwater catchment, air deposition, perennial snow patch, stream water chemistry

©2019. Japan Geoscience Union. All Right Reserved.

Activity of gravity faults in the Tateyama caldera, Hida Mountains, during the past 55 years

*Kotaro FUKUI[1], Hajime IIDA[1]

1. Tateyama Caldera Sabo Museum

Around Mt. Murodo (2668 m) located in the northeast edge of Tateyama caldera, one of the largest collapse sites in Japan, there are several gravity faults of 300-500 m in length which seem to be the precursory phenomena of deep catastrophic collapse. The gravity faults may still move, because the mountain trail which crosses the fault moves to the caldera side year by year, but the investigation has not been carried out. In this study, the precise measurement of the movement of the fault was carried out by installing many GPS observation points around the gravity fault, and it was confirmed whether it is stable or moving at present. We clarified the change of length and width of the gravity fault for the past 55 years from the aerial photograph interpretation.

Keywords: gravity fault, Deep-seated landslides, Tateyama Caldera

©2019. Japan Geoscience Union. All Right Reserved.

Community, population and genetic structures of benthic invertebrates in alpine and sub-alpine ponds of the Kamikochi area and the Yari-Hotaka Mountain Ranges

*Keisuke Inoue[1], Koji Tojo[1]

1. Biology Department, Faculty of Science, Shinshu University

Alpine and sub-alpine ponds are considered that they pay some roles as important habitats and /or environments in mountain ecosystem. For example, they have functions as water resources for terrestrial organisms, and habitats for aquatic animals. Alpine and sub-alpine ponds have various origins, and their environments differ greatly for each origin. For aquatic animals inhabiting these ponds, differences in their environments are thought to directly effect in biota, so their environments' diversity may contribute to the creation of mountainous biodiversity. However, despite the importance of alpine and sub-alpine ponds, studies focusing on the relationship between the ponds' environments and their biodiversity have only a few cases even in high mountainous areas of Europe. Especially in the Japanese alpine ponds, there are no yet study cases. There are natural ponds, natural dammed ponds, glacier and volcanic origin ponds, and so on in the Japanese Alps, and there are good research fields for investigating the relationship between diversity of the environments and their biodiversity.

Under these circumstances, in the present study, we focused on the Kamikochi area and the Yari-Hotaka Mountain Ranges in the Japan Alps, and we have conducted analyses for the relationship between their aquatic insect fauna and the ponds' environments in alpine and sub-alpine ponds. In addition to comparing and examining the obtained community, population structure data and environmental data as habitats, the cluster analysis, the NMDS analysis, and the CCA analysis were also performed. As the result of conducting our studies of 23 ponds in total, community structures were categorized into 4 groups largely in all of our analyses. Also it was suggested that the alpine and sub-alpine aquatic insects' fauna is influenced by altitude, abundance of herbaceous plants around the shore, amount of gravels, sands and soil at the bottom of ponds. In addition, the ponds categorized into the same group, tended to be similar environments. Thus, alpine ponds with divergent environments may have important roles in the creation of mountainous biodiversity.

In addition, we also focused on the dispersal of aquatic insects inhabiting the mountain ponds. In alpine and sub-alpine mountain areas, ponds are isolated and scattered distribution. We would like to try to investigate the direction and frequency of movement and dispersion of aquatic insects between these ponds using molecular markers. As the first step, genetic analysis of the mtDNA COI region (DNA barcoding region) was performed on two caddiesflies *Pseudostenophylax ondakensis* and *Oligotricha fluvipes*, and a small diving beetle *Agabus japonicus*. As a result, in addition to that we could understand the genetic relationships in this mountain areas of *P. ondakensis*, the existence of the new haplotype which had not been observe in this area so far has been detected. Also in *A. japonicus*, in addition to that we observed individuals of the same lineage as widely distributed (i.e., from Hokkaido to Nagano), we revealed that individuals of largely genetically different lineage inhabit some alpine ponds.

Keywords: Alpine pond, Biodiversity, Community ecology

©2019. Japan Geoscience Union. All Right Reserved.

Water and carbon use of fine root in four tree species at the forest limit

*Hikari Yahara[1], Wakana Azuma[2], Mai Kamakura[2], Naoki Makita[1]

1. Graduate School of Science and Technology Shinshu University, 2. Graduate School of Agriculture Kyoto University

Tree fine roots are the primary organs for nutrient and water acquisition that is necessary for trees to survive. Trees growing at the forest limit are exposed to water stress because of drying, low temperature and soil freezing in winter. Water and carbon use strategies of fine roots may differ among tree species growing at the forest limit since it is suggested that differences in microbial-symbiosis and phylogenetic groups among tree species show a wide variation of root survival strategies. We aimed to examine the root water absorption and transport characteristics of four tree species at the forest limit (2,500 m altitude) on Mt. Norikura in Central Japan. The hydraulic conductivity, daytime water potential, respiration, morphology and anatomical traits of fine roots in deciduous broad-leaved species (*Sorbus commixta* and *Betula ermanii*) and evergreen needle-leaved species (*Abies mariesii* and *Pinus pumila*) were measured. The range of the root hydraulic conductivity was 1.17 to 4.02×10^{-4} m s^{-1} MPa^{-1}, which was significantly differed among species. In particular, *Pinus pumila* showed the highest hydraulic conductivity. The range of daytime root water potential was -0.20 to -0.12 MPa. Although there was no significant difference among species, the lowest daytime root water potential was observed in *Pinus pumila*. As a preliminary experiment, low root osmotic pressure at full turgor was estimated by pressure-volume curves in *Pinus pumila*. Therefore, the root of *Pinus pumila* might be able to absorb water actively by the low daytime water potential. We also discuss how root respiration, root morphology and anatomical traits are related to root water relations.

Keywords: water relations, fine root, hydraulic conductivity, daytime water potential, forest limit

©2019. Japan Geoscience Union. All Right Reserved.

Visible-near infrared spectral reflectance explains variations in fine root traits of woody species

*Natsuko Tanikawa[1], Tatsuro Nakaji[3], Miwa Kobatake[2], Naoki Makita[2]

1. Graduate School of Science and technology, Shinshu University, 2. Faculty of Science, Shinshu University, 3. Field Science Center for Northern Biosphere

The visible and near infrared spectroscopic information can provide powerful tools for identifying and quantifying chemical substances of soil, fruit and leaf, yet less is known about characteristics of reflectance spectroscopy for tree fine roots. In this study, we aimed to examine the effects of tree species on the reflectance of fine roots and to determine the association of the reflectance with respect to morphological, anatomical and chemical traits of fine roots of 20 species. We sampled fine roots in a cool temperate forest in Japan. The fine roots were divided into three diameter classes (0-0.5 mm, 0.5-1.0 mm, 1.0-2.0 mm). We obtained hyperspectral reflectance images at 458-2391 nm (total 376 bands by 4.1-5.8 nm interval) for fresh intact fine root for each three diameter classes. The relationships of reflectance images with average root diameter (mm), specific root length (m g^{-1}), root tissue density (g cm^{-3}), stele: cortex ratio, and carbon and nitrogen concentration (%) as each root trait were analyzed at each specific wavelength. The spectral patterns of the fresh intact root systems showed peak at four wavelength band across all woody species. Spectral reflectances at 458-1400nm were positively related to the root diameter. On the other hand, the reflectances differ among tree species. We will examine relationship the reflectance and root traits which characterized tree species. These results indicate that spectral reflectance at visible-near infrared regions can be an important determinant of species specificity of fine root traits by even fresh intact samples.

Keywords: root diameter, anatomy, morphology, chemistry

©2019. Japan Geoscience Union. All Right Reserved.

Heat Balance Analysis of Cold Air Pool Formation in Kamikochi

*Sayuri Koyama[1], Motoshi NISHIMURA[2], Keisuke Suzuki[3]

1. Graduate school of science and technorogy, Shinshu University, 2. Interdisciplinary Graduate school of Science and Technology, Shinshu university, 3. Department of Environmental Sciences, Faculty of Science, Shinshu University

Meteorological observation and heat balance analysis were conducted in Kamikochi (1490 m), Dakesawa (1600 m, 1700 m, 1800 m) and Nishi-hotakadake (2355 m), and the formation mechanism of cold air pool was clarified. The observation period is the snowy season at Kamikochi from December 6, 2016 to May 4, 2017 and from November 17, 2017 to April 16, 2018.
In this study, with referring to Dorninger et al. (2011), the cold air pools that occurred during the observation period were classified into eight tyes of the cold air pool events, undisturbed evolution, late buildup, early breakup, mixing event, temperature rise of all layers in a short time, upper disturbance, lower disturbance and short time cold air pool.
The cold air pool events occurred 28 times in April 2017 and 27 times in March 2018. However, mixing event, temperature rise of all layers in a short time, upper disturbance and lower disturbance hardly occurred in both 2016/17 and 2017/18. It is thought that Kamikochi is terrain that is difficult to generate turbulence.
The undisturbed evolution, the late buildup, and the early breakup differed in the time when the cold air pools were built and the time when they were destroyed. While the cold air pools were built, the sensible heat flux and latent heat flux were 0 W m^{-2}. The mixing event, the temperature rise of all layers in a short time and upper disturbance were different in depth of rise in temperature generated in the cold air pool and the increase amount in temperature. Regarding the sensible heat flux and latent heat flux amount, the mixing event was 5.0 W m^{-2} or more, the temperature rise of all layer in a short time was 0.5 W m^{-2} or more, and the upper disturbance was 0 W m^{-2}. The lower disturbance is the event in which a short-time increase in temperature occurs near the bottom of the basin. The cold air pools with formation time of less than 6 hours were classified as the short time cold air pool. These cold air pool events are largely responsible for the generation of clouds and the generation of turbulence by the wind, the time of occurrence and duration of clouds and wind, and the strength of turbulence are considered to be the main factors.

Keywords: Cold air pool, Heat balance

©2019. Japan Geoscience Union. All Right Reserved.

A finding of fossil trees buried in dammed-lake deposits formed by the Dondokosawa rock avalanche of the late 9th century in the Akaishi Mountains, and its significance

*Takashi Kimura[1], Ryuji Yamada[1], Yoshihiko Kariya[2]

1. National Research Institute for Earth Science and Disaster Resilience, 2. Senshu University

The Dondokosawa rock avalanche (DRA) initiated at an east-side slope of Mount Jizo, the Akaishi Mountains, the Southern Japan Alps, and traveled over 3.6 km along the mainstream of the Dondokosawa River. The displaced mass of the DRA completely blocked two parts, the outlet of a right tributary of the Dondokosawa River and the channel of the Ohdanasawa River, forming two dammed-lakes together with floodplain deposits beside the rock avalanche deposit (Kariya, 2012; Kimura *et al.*, 2018a). At these two sites, many fossil trees buried in lacustrine sediments were found by the authors. Yamada *et al.* (2018) applied the dendrochronological analysis using oxygen isotope ratios to tree-ring samples collected from two individuals (Hinoki cypress of >350 years old and Hemlock tree of >300 years old) and estimated death year of one individual to be around AD885 and that of the other to be AD888. These chronological constraints on the DRA strongly indicated that the DRA has occurred at the year of AD887 Ninna earthquake, which was one of the large ocean-trench earthquakes in Japan, or a couple of years later than the earthquake. The finding of fossil trees has a significance for not only estimating the age of the DRA but also reconstructing the paleoenvironment around the Akaishi Mountains. In this study, we present the vegetation characteristics of the Dondokosawa and the Ohdanasawa river catchments in the late 9th century, based on the tree species compositions of 41 samples analyzed in our previous studies (Kimura *et al.*, 2018b, 2019).

The sampling sites were named LLD and ULD, respectively. LLD is located at the confluence of the Dondokosawa and Ohdanasawa rivers, and has a drainage area of 8.81 km^2 with altitudes ranging from 1220 to 2780 m a.s.l. ULD is located at the outlet of the right tributary of the Dondokosawa River, and has a drainage area of 1.17 km^2 with altitudes ranging from 1470 to 2630 m a.s.l. We collected 41 samples (24 samples in LLD and 17 samples in ULD) between April 2012 and October 2017 and identified species or genus of each sample. The 24 samples in LLD include eight of Hinoki cypress (*Chamaecyparis obtusa*), seven of Hemlock tree (*Tsuga*), three of Sawara cypress (*Chamaecyparis pisifera*), two of Birch tree (*Betula*), and one each of Japanese larch (*Larix kaempferi*), Fir tree (*Abies*), Spruce tree (*Picea*) and Japanese Wingnut (*Pterocarya rhoifolia*). The other 17 samples in ULD include eight of *Tsuga*, four of *Abies*, two each of *L. kaempferi* and Willow tree (*Salix*), and one of Azalea tree (*Rhododendron*). The rates of *Tsuga* in LLD and ULD account for approx. 29% and 47%, respectively. Besides, the rate of cypress species (*C. obtusa* and *C. pisifera*) in LLD accounts for approx. 46%, while both of the two species are absent in ULD.

Although the above results are based on a limited number of samples, it is estimated as vegetation characteristics in the late 9th century, when the DRA occurred, as follows. In the Ohdanasawa River catchment, an old-growth forest dominated by Hinoki cypresses of >350 years old and Hemlock trees was established, while another old-growth forest dominated by Hemlock trees of >300 years old was established in the right tributary catchment of the Dondokosawa River. The remarkable difference in the abundance of cypress species in the two adjacent catchments suggests a possibility that the distribution of the two species has been limited within the Ohdanasawa River catchment and has not extended to the upper part of the Dondokozawa River from that time.

©2019. Japan Geoscience Union. All Right Reserved.

References:Kariya (2012) Trans. Jpn. Geomorphol. Union 33, 297-313 [in Japanese with English abstract]; Kimura *et al.* (2018a) J. Jpn. Landslide Soc. 55, 42-52 [in Japanese with English abstract]; Kimura *et al.* (2018b) JpGU2018 MGI25-P09 [in Japanese with English abstract]; Kimura *et al.* (2019) Quat. Res. 58, 65-72 [in Japanese]; Yamada *et al.* (2018) Quat. Geochr. 44, 47-54.

Keywords: Akaishi Mountains, rock avalanche , dammed-lake, fossil trees, paleoenvironment

©2019. Japan Geoscience Union. All Right Reserved.

What alpine plants attract visitors in the Daisetsuzan national park, northern, Japan?

*Yukihiro Amagai[1], Kota Mameno[1,2], Hiroyuki Oguma[1], Takahiro Kubo[1]

1. National Institute for Environmental Studies, 2. Hokkaido University

The Daisetsuzan National Park in Hokkaido northern Japan is visited by 5 million people every year, because the Taisetsu Mountains have large fields of alpine vegetation. In the alpine zone, many alpine plant species (365 species: including subspecies and variants as well as 27 Japanese endemic species) grow. However, alpine vegetation has remarkably changed, with alpine dwarf-pine (*Pinus pumila*) and dwarf-bamboo (*Sasa kurilensis*) distributions having expanded during the last decade along with significant changes in the vegetation structure. From such a background, selection of protected areas, evaluation of vulnerbility for each plant species and community type, and adaptation manegement, there are urgent problems for the conservation of biodiversity in the alpine zone. Furthermore, change of alpine vegetation can be considered to damage as tourism resources as well. Therefore, purpose of this study is to clarify the preference of visitor to alpine plant species for collecting baseline information of tourism resources as one conservation indicator.

This study was conducted at the Sugatami Station of the Daisetsuzan Asahidake Ropeway which is located at an elevation of 1600 m, and the treeline is located at an elevation of around 1400-1700m. Therefore, visitors can easily hike and watch for alpine plants in alpine area. To clarify visitors preference for alpine plant species, we distributed questionnaires to visitors at the place. Respondents were asked “what flower do you want to see (check the all plants at posted picture of 20 species)”, and socio-demographics including experiences of visiting Daisetsuzan national parks. The number of questionnaires distributed were 1201 in 6 days of August 2018, and a total of 451 respondents participated our survey. The plant pictures which were showed respondents in the questionnaire were selected from 18 typical alpine plants, which considering habitats, plant growth form, and flower color (*Trollius riederianus, Stellaria pterosperma, Primula cuneifolia, Anemone narcissiflora* var. *sachalinensis, Therorhodion camtschaticum, Lagotis yesoensis, Pentstemon frutescens, Nephrophyllidium crista-galli, Pedicularis oederi, Phyllodoce aleutica, Dicentra peregrina, Saxifraga laciniate, Trichophorum cespitosum, Drosera anglica, Gentiana jamesii, Sieversia pentapetala, Campanula chamissonis, Eriophorum*) and *P. pumila* and *S. kurilensis*.

As a result, *S. pentapetala*, *G. jamesii*, and *P. cuneifolia* are high preference, while *T. cespitosum*, *S. kurilensis*, and *P. pumila* are low. From the respondent information, repeaters had high preference to *S. pentapetala* and *D. peregrina* than first time visitor. Furthermore, we analyzed flower (15 species) and whole (20 species) morphological feature by generalized linear model (GLM) for clarify the preferred features. As a result, the high preference to flower features are: the inflorescence was flat, the number was few, and the color tended to be pink > purple > white ≧ yellow plants. And the whole features are: leaves had gloss, leaf size was small, plant height was low.
Therefore, the *S. pentapetala* is the most attractive species for many visitors, which species is necessary for secure repeaters also. The *S. pentapetala* is not a specific species in the Taisetsu Mountains, because it distributes wide area in the alpine, eastern Japan. However, in the Taisetsu Mountains, a large community is formed along the trail, resulting it represents the image of the flower garden. Therefore, as tourism resources, it is important to maintain a large flower garden and suppress the influence of the expansion of *P. pumila* and *S. kurilensis*, which low preference species. Furthermore, the popular plants

©2019. Japan Geoscience Union. All Right Reserved.

have feature that low height and few flowers from ranking based on the preference by GLM, resulting the visitors expect to see the dwarf plants just like image of alpine plants. On the other hand, we also revealed that species considered to be important as tourism resources are not necessarily consistent with rare and preferential conservation. Therefore, it is necessary to consider the balance between tourism resources and biodiversity.

Keywords: Alpine, People-plant interactions, Preference, Plant morphology, Climate change, Conservation

©2019. Japan Geoscience Union. All Right Reserved.

Spatio-temporal variations of algal snow in Mt. Gassan, Yamagata prefecture, Japan

*Suzuki Takumi[1], Nozomu Takeuchi[1], Tsubasa Takahashi[1]

1. Chiba University

Red, yellow or green colored snow due to algal blooming often appeared on the melting snow surface in the forest zone of Mt. Gassan in Yamagata Prefecture, Japan. Their distribution has been reported to be caused by physical and chemical conditions of snow surface. For example, green snow appears on eutrophic snow surfaces whereas red snow appears in poor nutrition snow surface in Antarctica. However, their temporal and spatial distributions and controlling factors are still unknown. Therefore, in this study, to clarify spatio-temporal changes of algal snow and their controlling factors, we investigated the algal biomass, pigment compositions, and nutrient conditions of colored snow of Mt.Gassan.

Snow samples were collected at 7 sites between 800 m and 1500 m above sea level along a ridge of the southern part of Mt.Ubagatake in May and June, 2018. We collected a surface snow sample from randomly selected surface at each site. The sample was preserved in a plastic bag and was melted in a laboratory. The chlorophyll a concentrations in the samples were measured with a fluorophotometer. Absorption spectra of the extracted pigments were measured with a spectrophotometer. The soluble chemical ions concentrations were measured with an ion chromatography. The samples were also observed with a microscoped.

Most of colored snow appeared in May was green snow. In June, red snow was often observed above the timber line, while orange snow was observed below the timber line. As a result of analyzing the absorption spectrum of the dye extracted from the sample, two kinds of waveforms were observed in both May and June. No major absorption was seen at any site in May. In January and June, the waveforms were found above and below the forest limit, both of which showed greater absorption than in May. Algal biomass generally increased from May to June at any sites. In addition, nitrate and phosphate ions, which are essential nutrients for algal growth, did not show any altitudinal trend, but decreased from May to June. The change of snow color from green in May to red or orange in June may be due to decrease of nutrient at the surface snow. The difference of snow color between above and below the timber line may be due to difference of solar radiation conditions.

Keywords: snow algae

©2019. Japan Geoscience Union. All Right Reserved.

Feeding of a wingless stonefly living on snow surface in Mt. Gassan, Yamagata prefecture, Japan

*Risako Yonechi[1], Nozomu Takeuchi[1]

1. Chiba University

There is a biological community on snow and ice consisting of cold-tolerant organisms. For examples, photosynthetic microbes (snow algae), heterotrophic invertebrates and bacteria are living on snow packs in Japan. Wingless stoneflies are also snowy insects commonly found in Japan. They are basically aquatic insects spending in streams when they are nymphs, but actively walks on the snow surface in winter and spring when they become adult. Wingless stoneflies in Japan have been classified into thirty species belonging to two genera (Apteroperla and Eocapnia) based on their morphological perspectives. Several species have been reported to appear on a snow surface simultaneously, however, it is still unknown that their feedings and life cycles. In this study, we reported the spatial distribution and feedings of wingless stoneflies found on snow packs in Mt. Gassan, Yamagata prefecture, Japan.
The fieldworks were conducted three times in April, May and June of 2018 in a south slope of Mt. Gassan, where heavy snow covers during winter and spring. We collected wingless stoneflies on snow surface at 13 sites in different elevations from a summit of Mt. Ubagatake (1487 m.a.s.l) down to Shizu camp site (770 m.a.s.l). We identified their species based on their body morphology using a microscope. We also analyzed carbon and nitrogen stable isotopes of the collected stonefly specimens. The stable isotopes were analyzed with an IRMS (Isotope Ratio Mass Spectrometer) at Research Institute for Humanity and Nature.
Fifty male specimens were classified into two genera. Apteroperla stoneflies were mostly found in the area above 1000 m a.s.l., conversely Eocapnia stoneflies were found in the area below 1000 m a.s.l. This suggests that the two genera have different habitats in this mountainous area. The nitrogen stable isotope of the wingless stoneflies was not significantly different between Apteroperla and Eocapnia (1.10 - 0.95‰ versus -1.63 - 1.05‰), indicating that the tropic levels of two genera are almost same. Carbon stable isotope also did not differ significantly between the two genera (-26.2‰ versus -25.7‰). However, the variance of the carbon stable isotopes of Apteroperla is smaller than that of Eocapnia (0.29‰ versus 3.00‰). This suggests that Apteroperla stoneflies have limited dietary habits while Eocapnia has broad eating habits.

Keywords: insect, alpine, ice biology

©2019. Japan Geoscience Union. All Right Reserved.

Drainage from glacial lake in Achinathang village, Ladakh Range on 4 August 2017

Maho Saotome[2], *Chiyuki Narama[1], Naoki Sakurai[2]

1. Niigata University, Program of Field Research in the Environmental Sciences, 2. Graduate School of Science and Technology, Niigata University

In the Achinatan valley of the Ladak Range, located in the northwestern part of India, a large debris flow occurred on August 4, 2017. In this disaster, this debris flow caused four victims and serious damages such as a complete collapse of bridge and field. In this study, we tried to clarify the details of drainage from glacial lake and development of debris flow in the Achinatan valley from field survey (2017-2018) and satellite image analysis.

Keywords: glacial lake, glacial lake outburst flood (GLOF), debris flow, Ladakh Range

©2019. Japan Geoscience Union. All Right Reserved.

Recent glacier variations at Mt. Kenya using aerial digital image

*Chiyuki Narama[1], kenshiro Arie[2], MIZUNO KAZUHARU[3]

1. Program of Field Research in the Environmental Sciences, Niigata University , 2. Graduate School of Science and Technology, Niigata University, 3. Graduate School of Letters, Kyoto University

The total glacier area decreased by 121.0 x 10^3 m^2 (44%) during 2004–2016 at Mt. Kenya (Prinz et al., 2018). These glaciers are estimated to extinct before 2030, implying the cessation of the longest glacier monitoring record of the tropics. In this study, we investigated mass balance of all glaciers during 2016-2018 using Pleiades satellite data and aerial digital images from Cessna.

Keywords: glacier variations, mass balance, aerial digital image, Mt. Kenya

©2019. Japan Geoscience Union. All Right Reserved.

[J] Poster | M (Multidisciplinary and Interdisciplinary)：M-IS Intersection

Mon. May 27, 2019 5:15 PM - 6:30 PM JST | Mon. May 27, 2019 8:15 AM - 9:30 AM UTC | Poster Hall International Exhibition Hall8, Makuhari Messe_39

[M-IS20] Mountain Science

convener:Keisuke Suzuki(Department of Environmental Sciences, Faculty of Science, Shinshu University), Yoshihiko Kariya(Department of Environmental Geography, Senshu University), Akihiko SASAKI(Department of Geography and Environmental Studies, Kokushikan University), Chiyuki Narama(Niigata University, Department of Science)

Mountainous areas provide water resources to the populated downstream areas, protecting the
 diversity of ecosystem and providing tourism attraction. To access the mountain environment
 changes and mitigate the impacts of global warming influences, a cross-cutting session is
 proposed to share the scientific knowledge among various fields; such as climatology, hydrology, geography, glaciology, water/carbon/material cycle, eco-diversity, etc.

[MIS20-P01] Development of fluvial terraces and landslides since the late Pleistocene in the Shirata River basin, southeastern side of Amagi Volcano, Izu Peninsula, Japan

*Nao Tokumoto[1], Yoshihiko Kariya[2], Kuniyasu Mokudai[3] (1.Undegraduate, Senshu Univ., 2.Senshu Univ., 3.Japan Geoservice Inc.)

[MIS20-P02] Variation trends of air temperature and snow depth in the Japanese Alps

*Keisuke Suzuki[1], Akihiko SASAKI[2] (1.Faculty of Science, Shinshu University, 2.Faculty of Literature, Kokushikan University)

[MIS20-P03] Abundant tardigrades found in snow pack in Mt.Gassan in Yamagata Prefecture, Japan

*MASATO ONO[1] (1.Chiba University)

[MIS20-P04] Variation of stable isotope ratios of precipitation in the Japanese Alps Region

*Tsukasa Katsuragawa[1], Tsutomu Yamanaka[2], Akihiko SASAKI[3], Yuki Kurokumo[1], Motoshi NISHIMURA[1], Shimizu Hironori[1], Keisuke Suzuki[4] (1.Graduate School of Science and Technology,Shinshu University, 2.Faculty of Life and Environmental Sciences, University of Tsukuba, 3.Department of Geography and Environmental Studies, Kokushikan University, 4.Department of Environmental Sciences, Faculty of Science, Shinshu University)

[MIS20-P05] Probable glacier detritus found at downstream site of the Yokoo moraines in the northern Japanese Alps: its geological characteristics and implications

*Manami Ishibashi[1], Yoshihiko Kariya[2], Kuniyasu Mokudai[3] (1.Undergraduate Senshu Univ., 2.Senshu Univ., 3.Japan Geo serivice Inc.)

[MIS20-P06] Recent Geomorphological changes of rock slopes in Hakuba-Daisekkei

*Hirotaka Sugiyama[1], Chiyuki Narama[2], Hiroshi Inoue[3] (1.Graduate School of Science and Technology, Niigata University, 2.Faculty of Science, Niigata University, 3.National Reserch Institute for Earth Science and Disaster Resilience)

[MIS20-P07] Behavior of inorganic ions in air deposition and surface runoff water in an alpine headwater catchment of Mt. Norikura

*Hironori Shimizu[1], Akihiko Sasaki[2], Keisuke Suzuki[3] (1.Graduate School of Science and Technology, Shinshu University , 2.Department of Geography and Environmental Studies, Kokushikan University, 3.Faculty of Science, Shinshu University)

[MIS20-P08] Activity of gravity faults in the Tateyama caldera, Hida Mountains, during the past 55 years

*Kotaro FUKUI[1], Hajime IIDA[1] (1.Tateyama Caldera Sabo Museum)

[MIS20-P09] Community, population and genetic structures of benthic invertebrates in alpine and sub-alpine ponds of the Kamikochi area and the Yari-Hotaka Mountain Ranges

*Keisuke Inoue[1], Koji Tojo[1] (1.Biology Department, Faculty of Science, Shinshu University)

[MIS20-P10] Water and carbon use of fine root in four tree species at the forest limit

*Hikari Yahara[1], Wakana Azuma[2], Mai Kamakura[2], Naoki Makita[1] (1.Graduate School of Science and Technology Shinshu University, 2.Graduate School of Agriculture Kyoto University)

[MIS20-P11] Visible-near infrared spectral reflectance explains variations in fine root traits of woody species

*Natsuko Tanikawa[1], Tatsuro Nakaji[3], Miwa Kobatake[2], Naoki Makita[2] (1.Graduate School of Science and technology, Shinshu University, 2.Faculty of Science, Shinshu University, 3.Field Science Center for Northern Biosphere)

[MIS20-P12] Heat Balance Analysis of Cold Air Pool Formation in Kamikochi

*Sayuri Koyama[1], Motoshi NISHIMURA[2], Keisuke Suzuki[3] (1.Graduate school of science and technorogy, Shinshu University, 2.Interdisciplinary Graduate school of Science and Technology, Shinshu university, 3.Department of Environmental Sciences, Faculty of Science, Shinshu University)

[MIS20-P13] A finding of fossil trees buried in dammed-lake deposits formed by the Dondokosawa rock avalanche of the late 9th century in the Akaishi Mountains, and its significance

*Takashi Kimura[1], Ryuji Yamada[1], Yoshihiko Kariya[2] (1.National Research Institute for Earth Science and Disaster Resilience, 2.Senshu University)

[MIS20-P14] What alpine plants attract visitors in the Daisetsuzan national park, northern, Japan?

*Yukihiro Amagai[1], Kota Mameno[1,2], Hiroyuki Oguma[1], Takahiro Kubo[1] (1.National Institute for Environmental Studies, 2.Hokkaido University)

[MIS20-P15] Spatio-temporal variations of algal snow in Mt. Gassan, Yamagata prefecture, Japan

*Suzuki Takumi[1], Nozomu Takeuchi[1], Tsubasa Takahashi[1] (1.Chiba University)

[MIS20-P16] Feeding of a wingless stonefly living on snow surface in Mt. Gassan, Yamagata prefecture, Japan

*Risako Yonechi[1], Nozomu Takeuchi[1] (1.Chiba University)

[MIS20-P17] Drainage from glacial lake in Achinathang village, Ladakh Range on 4 August 2017

Maho Saotome[2], *Chiyuki Narama[1], Naoki Sakurai[2] (1.Niigata University, Program of Field Research in the Environmental Sciences, 2.Graduate School of Science and Technology, Niigata University)

[MIS20-P18] Recent glacier variations at Mt. Kenya using aerial digital image

*Chiyuki Narama[1], kenshiro Arie[2], MIZUNO KAZUHARU[3] (1.Program of Field Research in the Environmental Sciences, Niigata University , 2.Graduate School of Science and Technology, Niigata University, 3.Graduate School of Letters, Kyoto University)

Development of fluvial terraces and landslides since the late Pleistocene in the Shirata River basin, southeastern side of Amagi Volcano, Izu Peninsula, Japan

*Nao Tokumoto[1], Yoshihiko Kariya[2], Kuniyasu Mokudai[3]

1. Undegraduate, Senshu Univ., 2. Senshu Univ., 3. Japan Geoservice Inc.

This study clarified geomorphic features of debris flow-fluvial terraces and landslide complexes on the southeastern side of Amagi Volcano in Izu Peninsula, central Japan. Terrace forms can be classified into three: H, M, and L surfaces from descending altitude order. Among them, the M surface is common and its geology is unique. The M surface is composed of thick and poorly sorted angular gravel beds associated with debris flow processes. The L surface is an erosion surface of higher terraces. A longitudinal profile of the M surface seems to connect with large landslide bodies in the upper reach of stream on the volcano and to continue below the present seafloor off the mouth of such a stream. Some of large landslides show secondary movement of bodies and dissected headscarps. Furthermore, the M surface is covered by a tephra layer supplied from a nearby monogenetic volcano in 19 ka. These facts show that the M surface had been formed by debris flow events filling the stream in the late Pleistocene when the sea-level was lowered. Then an increase in precipitation in the area and a decrease in bedload supply into the stream, as well as sea level rise, would have caused down cutting of the floor of stream and created a terrace form of the M surface during the period from the latest Pleistocene to the early Holocene. Because of further down cutting, the L surface had been formed. Detailed descrption of the H surface is required in future.

Keywords: the last glacial period, fill terrace, erosional terrace, landslide, tephrochronology

©2019. Japan Geoscience Union. All Right Reserved.

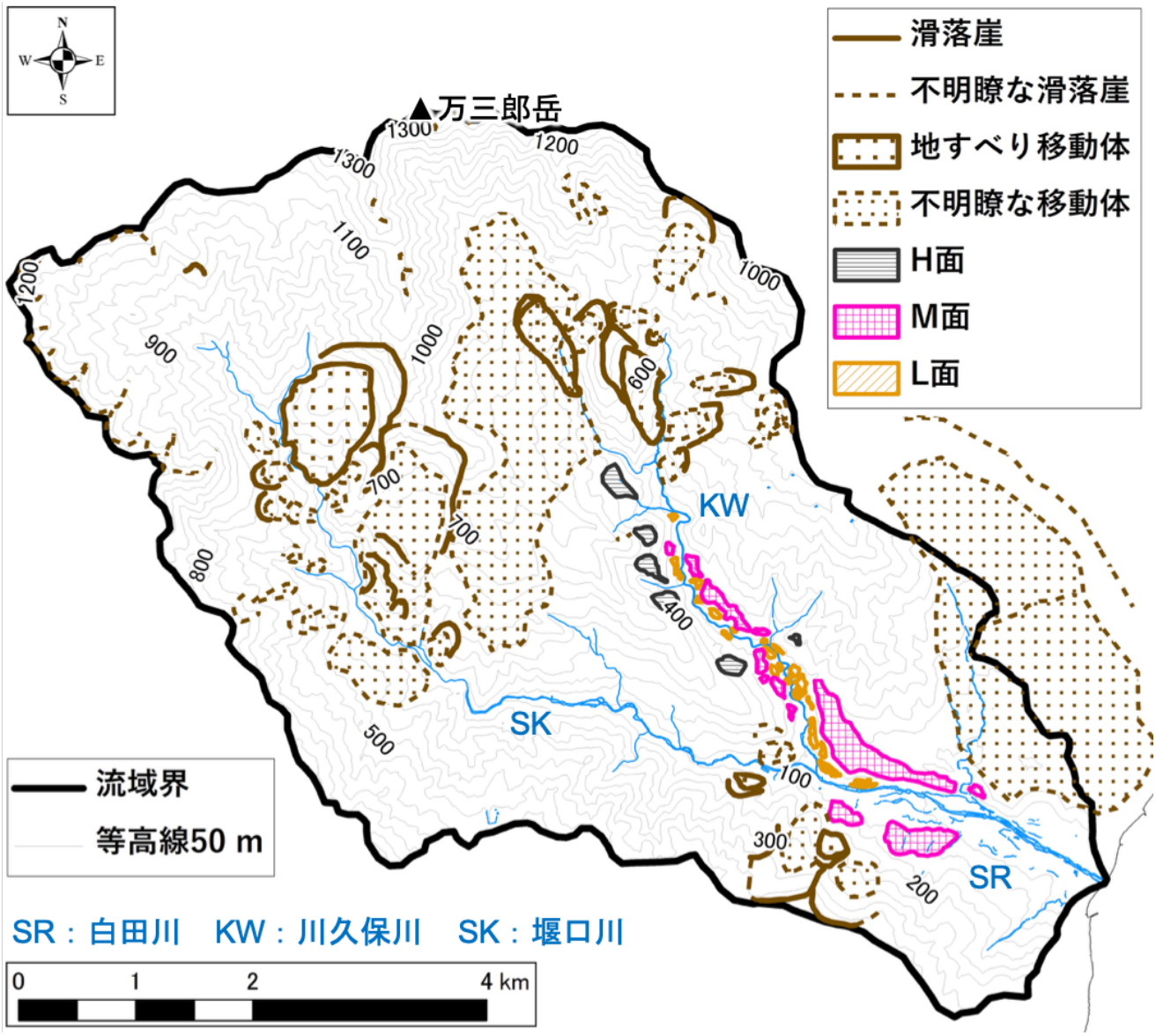

©2019. Japan Geoscience Union. All Right Reserved.

Variation trends of air temperature and snow depth in the Japanese Alps

*Keisuke Suzuki[1], Akihiko SASAKI[2]

1. Faculty of Science, Shinshu University, 2. Faculty of Literature, Kokushikan University

Mountainous areas are quite sensitive to global-scale environmental changes, such as warming. Therefore, the effects of global warming on these meteorological elements is a critical issue. We have developed a network of 14 meteorological observatories in the Japanese Alps, which have already started recording observations. The highest observation site is Mt. Yari, at 3125 m. Observation data from these sites are sent to a computer at the laboratory via a data communication mobile telephone network or phone line throughout the year. These meteorological observation data are available on the laboratory website in quasi-real time. The interannual variability of the air temperature and the snow depth in the Japanese Alps region are discussed.

Keywords: global warming, meteorological observation

©2019. Japan Geoscience Union. All Right Reserved.

Abundant tardigrades found in snow pack in Mt.Gassan in Yamagata Prefecture, Japan

*MASATO ONO[1]

1. Chiba University

Water bears are small invertebrates belonging to the phylum Tardigrada. They are typically 0.1 –1.0 mm in body length, and walk slowly with four pairs of legs. Tardigrades can shrink their body like a tun and become cryptobiosis, which enables to survive in extreme environments, such as low and high temperature, high pressure, under strong radiation. Their physiological mechanism of cryptobiosis is expected to be applied to medical and industry technologies, such as dry preservation of animal cells. They are commonly found on glaciers in polar or alpine regions. They actively live in cryoconite holes on glaciers and spend their entire lives on glaciers. In Japan, there is a heavy snow in mountainous regions due to strong monsoon westerly in winter, On the snow fields in Japan, there are various cold-tolerant organisms such as snow algae and invertebrates. However, no tardigrade has been reported on snow packs in Japan. In this study, we investigated mountain snow packs in Japan to search the presence of tardigrade and tried to reveal their life cycle.

The fieldworks were carried out on snow packs in the forest located in Mt. Gassan in Yamagata prefecture in Japan. Snow and moss samples were collected in a total of four times from April to October 2018, three times in snow season and once in no snow season. Mt. Gassan is an area with heavy snowfall in winter. Microscopic observation revealed that there were many tardigrades of the genus *Hypsibius* in surface snow. While only one species of *Hypsibius* was observed in snow samples, a total of two species including one species of the genus *Macrobiotus* were observed in moss of trees in the forest, and a total of six species were observed in moss of trees collected in no snow season. The species observed in snow is likely cold-tolerant tardigrade and preferably lives in the snow pack. Population density of tardigrades in snow was exceptionally higher on the green coloured snow due to algal blooming, but was little on white snow without algae. It was an average of 7.1×10^{3} ind L^{-1} in green snow samples. The body length distribution of tardigrades shows that the their size increased significantly from April to May in the snow pack, and the small sized larvae were observed only in the moss of trees collected in fall. Therefore, they live preferably in snow packs with green snow algae and grow up. When the snow disappears, they move to moss of trees and reproduce there. This life history seems to adapt to the area where heavy snow seasonally covers.

Keywords: Tardigrada, mountain, snow, forest

©2019. Japan Geoscience Union. All Right Reserved.

Variation of stable isotope ratios of precipitation in the Japanese Alps Region

*Tsukasa Katsuragawa[1], Tsutomu Yamanaka[2], Akihiko SASAKI[3], Yuki Kurokumo[1], Motoshi NISHIMURA[1], Shimizu Hironori[1], Keisuke Suzuki[4]

1. Graduate School of Science and Technology,Shinshu University, 2. Faculty of Life and Environmental Sciences, University of Tsukuba, 3. Department of Geography and Environmental Studies, Kokushikan University, 4. Department of Environmental Sciences, Faculty of Science, Shinshu University

We collected precipitation samples and observed meteorological condition every month from January 2011 to December 2016 at nine locations in the Japanese Alps Region (Nagano, Matsumoto, Suwa, Omachi, Sugadaira, Norikura, Kamikochi, Shigakogen, Nishihotaka). The collected water samples were brought back to the laboratory to stable isotope analysis to determineD,^{18}O and calculated d-excess. The ^{18}O in precipitation collected more than once times per month was weighted mean using the amount of precipitation and was taken as the mean monthly value. As a result of examining the seasonal variation of ^{18}O from 2011 to 2016, ^{18}O showed two peaks in spring and summer. In order to investigate the spatial variation, the coefficient of determination between latitude, longitude, altitude and ^{18}O was calculated, it clearly correlated with altitude from April to October. d-excess showed seasonal variation which is high in winter and low in summer. As a spatial variation, correlation with altitude is high in summer and correlation with longitude is high in winter. To investigate the factors that cause such variations, correlation coefficients between temperature, precipitation amount, lifting condensation level (LCL) and precipitation at δ^{18}O and d-excess at each site were calculated. Regarding δ^{18}O, it showed a positive correlation with the temperature at 8 points excluding Nishi Hodaka. Especially at 5 points of Matsumoto, Sugadaira, Omachi, Suwa, Nagano showed relatively high values. Regarding the relationship with precipitation, it showed a weak negative correlation at 6 sites excluding Omachi, Nagano and Nishi Hodaka. Regarding the relationship with LCL, there was a generally positive correlation, and particularly high correlation coefficients were found in Suwa and Nagano. From these results, it is considered that the temperature mainly contributes to δ^{18}O, and the correlation was high in Matsumoto, Sugadaira, Omachi, Suwa and Nagano, so there is a possibility that influence became strong in urban areas. The d-excess showed a negative correlation with temperature and precipitation, and there was no particularly significant relationship with LCL. The strong correlation was observed in relation to the temperature, the contribution to the fluctuation of d-excess was mainly considered to be the temperature.

Keywords: precipitation, isotope

©2019. Japan Geoscience Union. All Right Reserved.

Probable glacier detritus found at downstream site of the Yokoo moraines in the northern Japanese Alps: its geological characteristics and implications

*Manami Ishibashi[1], Yoshihiko Kariya[2], Kuniyasu Mokudai[3]

1. Undergraduate Senshu Univ., 2. Senshu Univ., 3. Japan Geo serivice Inc.

Around the upper reach of Azusa River in the northern Japanese Alps, the lowest position of a glacier snout during the late Pleistocene was known as the Yokoo-Iwagoya moraines (ca. 1700 m ASL). We revisited this widely-accepted concept of paleoglaciations in the Japanese Alps and newly found poorly-sorted angular to subangular rock clasts from the site lower than Yokoo-Iwagoya moraines (ca. 1400 m longitudinal and 50 m vertical). Rock clasts are composed of Quaternary igneous rocks that are never distributed around Yokoo. We concluded that those rock clasts were transported by a valley glacier from the higher slopes of Mount Yari-Hotaka Massif around 2800–3000 m ASL. Depositional ages of the clasts are still unknown but the Marine Isotope Stage 4 was probable.

Keywords: glaciations, the Last Glacial age, late Pleistocene, till, Japanese Alps

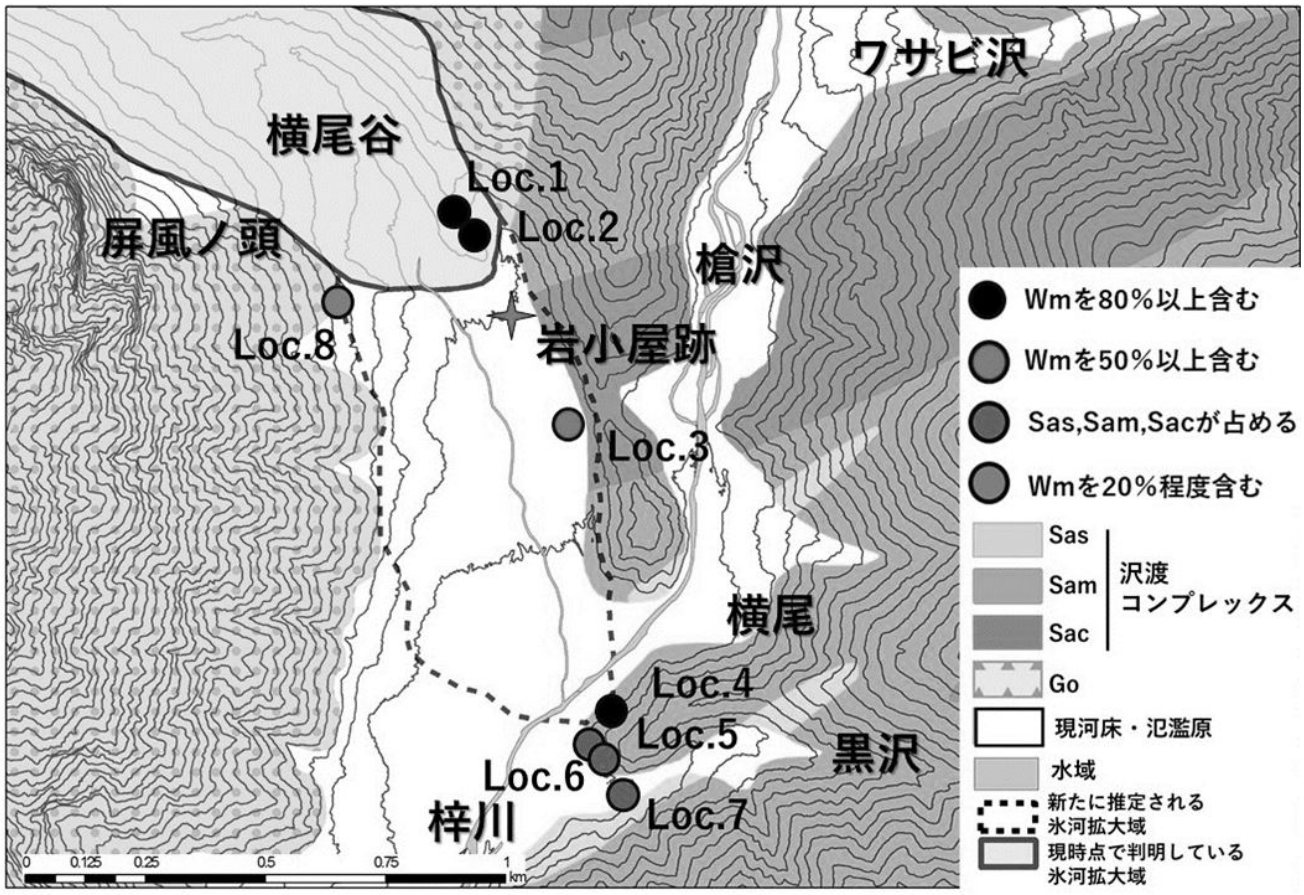

©2019. Japan Geoscience Union. All Right Reserved.

Recent Geomorphological changes of rock slopes in Hakuba-Daisekkei

*Hirotaka Sugiyama[1], Chiyuki Narama[2], Hiroshi Inoue[3]

1. Graduate School of Science and Technology, Niigata University, 2. Faculty of Science, Niigata University, 3. National Reserch Institute for Earth Science and Disaster Resilience

To understand the geomorphological characteristics of slope failure points on rock slopes of the Daisekkei valley, we investigated the surface changes of rock slopes using three-dimensional topographic models based on SfM (structure from motion) with digital aerial images from airplane, drone (Phantom4) and Cessna. Slope failure points and these surface changes were extracted by comparing three-dimensional topographic models. For large slope failure in 2005, we clarified the rock mass of 60 m height and 10 m thickness was collapsed.

Keywords: rockfall, rock failure, Hakuba-Daisekkei, aerial-photography, SfM

©2019. Japan Geoscience Union. All Right Reserved.

Behavior of inorganic ions in air deposition and surface runoff water in an alpine headwater catchment of Mt. Norikura

*Hironori Shimizu[1], Akihiko Sasaki[2], Keisuke Suzuki[3]

1. Graduate School of Science and Technology, Shinshu University , 2. Department of Geography and Environmental Studies, Kokushikan University, 3. Faculty of Science, Shinshu University

Meltwater from perennial snow patch lies on alpine catchment play an important role on the lower ecosystems as sources of fresh water during the warm season as well as rainfall, but chemical properties of air deposition and overland flow from a headwater catchment is not revealed in Japan. To characterize chemical behavior follow the rainfall and snowmelt runoff events, we studied chemical properties of stream water and air deposition during warm seasons 2016-2018, using a hydrometric and hydrochemical approaches and stable isotope of water. The study was carried out in the upper Maekawa River catchment on the east slope of Mt. Norikura, central Japan. Using an approximate curve calculated from the scatter diagrams with discharge and inorganic ion concentrations in stream water, we attempted to quantify the amount of inorganic ion dissolved in stream water during the period of August 28 to October 10, 2017.
Overland flow generation time following rainfall events was within several hours and lower surface runoff rate (up to 7%). The hydrological response properties indicate that periglacial slope overlapped by debris mainly have high water permeability and through the ground along the lava structure quickly. From the result that surface runoff rate of inorganic ions is higher than that of water amount, estimation of the amount of inorganic ions included in air deposition and surface runoff water suggest that eluviation from andesite rock contributes surface runoff amount of K^+, Mg^{2+} and Ca^{2+}. In contrast, surface runoff rate of Cl^-, NO_3^-, SO_4^{2-} were 3.9%, 2.7% and 6.5%, respectively, and it implies the dependency on air deposition for these ions dissolved in overland flow. High-frequency sampling during a rainfall event revealed that first runoff components frequently present a lower value (-19.1‰ at lowest) in $\delta^{18}O$ compared with that of stream water (-16.1‰ at lowest) during non-rainfall period. The fact that $\delta^{18}O$ of new snow obtained 2000m a.s.l. on the east slope of Mt. Norikura in January 2017 was approximately -19‰ suggests that meltwater infiltrated into the ground at early snowmelt season contribute overland flow temporarily follow rainfall input in September and October.

Keywords: headwater catchment, air deposition, perennial snow patch, stream water chemistry

©2019. Japan Geoscience Union. All Right Reserved.

Activity of gravity faults in the Tateyama caldera, Hida Mountains, during the past 55 years

*Kotaro FUKUI[1], Hajime IIDA[1]

1. Tateyama Caldera Sabo Museum

Around Mt. Murodo (2668 m) located in the northeast edge of Tateyama caldera, one of the largest collapse sites in Japan, there are several gravity faults of 300-500 m in length which seem to be the precursory phenomena of deep catastrophic collapse. The gravity faults may still move, because the mountain trail which crosses the fault moves to the caldera side year by year, but the investigation has not been carried out. In this study, the precise measurement of the movement of the fault was carried out by installing many GPS observation points around the gravity fault, and it was confirmed whether it is stable or moving at present. We clarified the change of length and width of the gravity fault for the past 55 years from the aerial photograph interpretation.

Keywords: gravity fault, Deep-seated landslides, Tateyama Caldera

©2019. Japan Geoscience Union. All Right Reserved.

Community, population and genetic structures of benthic invertebrates in alpine and sub-alpine ponds of the Kamikochi area and the Yari-Hotaka Mountain Ranges

*Keisuke Inoue[1], Koji Tojo[1]

1. Biology Department, Faculty of Science, Shinshu University

Alpine and sub-alpine ponds are considered that they pay some roles as important habitats and /or environments in mountain ecosystem. For example, they have functions as water resources for terrestrial organisms, and habitats for aquatic animals. Alpine and sub-alpine ponds have various origins, and their environments differ greatly for each origin. For aquatic animals inhabiting these ponds, differences in their environments are thought to directly effect in biota, so their environments' diversity may contribute to the creation of mountainous biodiversity. However, despite the importance of alpine and sub-alpine ponds, studies focusing on the relationship between the ponds' environments and their biodiversity have only a few cases even in high mountainous areas of Europe. Especially in the Japanese alpine ponds, there are no yet study cases. There are natural ponds, natural dammed ponds, glacier and volcanic origin ponds, and so on in the Japanese Alps, and there are good research fields for investigating the relationship between diversity of the environments and their biodiversity.

Under these circumstances, in the present study, we focused on the Kamikochi area and the Yari-Hotaka Mountain Ranges in the Japan Alps, and we have conducted analyses for the relationship between their aquatic insect fauna and the ponds' environments in alpine and sub-alpine ponds. In addition to comparing and examining the obtained community, population structure data and environmental data as habitats, the cluster analysis, the NMDS analysis, and the CCA analysis were also performed. As the result of conducting our studies of 23 ponds in total, community structures were categorized into 4 groups largely in all of our analyses. Also it was suggested that the alpine and sub-alpine aquatic insects' fauna is influenced by altitude, abundance of herbaceous plants around the shore, amount of gravels, sands and soil at the bottom of ponds. In addition, the ponds categorized into the same group, tended to be similar environments. Thus, alpine ponds with divergent environments may have important roles in the creation of mountainous biodiversity.

In addition, we also focused on the dispersal of aquatic insects inhabiting the mountain ponds. In alpine and sub-alpine mountain areas, ponds are isolated and scattered distribution. We would like to try to investigate the direction and frequency of movement and dispersion of aquatic insects between these ponds using molecular markers. As the first step, genetic analysis of the mtDNA COI region (DNA barcoding region) was performed on two caddiesflies *Pseudostenophylax ondakensis* and *Oligotricha fluvipes*, and a small diving beetle *Agabus japonicus*. As a result, in addition to that we could understand the genetic relationships in this mountain areas of *P. ondakensis*, the existence of the new haplotype which had not been observe in this area so far has been detected. Also in *A. japonicus*, in addition to that we observed individuals of the same lineage as widely distributed (i.e., from Hokkaido to Nagano), we revealed that individuals of largely genetically different lineage inhabit some alpine ponds.

Keywords: Alpine pond, Biodiversity, Community ecology

©2019. Japan Geoscience Union. All Right Reserved.

Water and carbon use of fine root in four tree species at the forest limit

*Hikari Yahara[1], Wakana Azuma[2], Mai Kamakura[2], Naoki Makita[1]

1. Graduate School of Science and Technology Shinshu University, 2. Graduate School of Agriculture Kyoto University

Tree fine roots are the primary organs for nutrient and water acquisition that is necessary for trees to survive. Trees growing at the forest limit are exposed to water stress because of drying, low temperature and soil freezing in winter. Water and carbon use strategies of fine roots may differ among tree species growing at the forest limit since it is suggested that differences in microbial-symbiosis and phylogenetic groups among tree species show a wide variation of root survival strategies. We aimed to examine the root water absorption and transport characteristics of four tree species at the forest limit (2,500 m altitude) on Mt. Norikura in Central Japan. The hydraulic conductivity, daytime water potential, respiration, morphology and anatomical traits of fine roots in deciduous broad-leaved species (*Sorbus commixta* and *Betula ermanii*) and evergreen needle-leaved species (*Abies mariesii* and *Pinus pumila*) were measured. The range of the root hydraulic conductivity was 1.17 to 4.02×10^{-4} m s^{-1} MPa^{-1}, which was significantly differed among species. In particular, *Pinus pumila* showed the highest hydraulic conductivity. The range of daytime root water potential was -0.20 to -0.12 MPa. Although there was no significant difference among species, the lowest daytime root water potential was observed in *Pinus pumila*. As a preliminary experiment, low root osmotic pressure at full turgor was estimated by pressure-volume curves in *Pinus pumila*. Therefore, the root of *Pinus pumila* might be able to absorb water actively by the low daytime water potential. We also discuss how root respiration, root morphology and anatomical traits are related to root water relations.

Keywords: water relations, fine root, hydraulic conductivity, daytime water potential, forest limit

©2019. Japan Geoscience Union. All Right Reserved.

Visible-near infrared spectral reflectance explains variations in fine root traits of woody species

*Natsuko Tanikawa[1], Tatsuro Nakaji[3], Miwa Kobatake[2], Naoki Makita[2]

1. Graduate School of Science and technology, Shinshu University, 2. Faculty of Science, Shinshu University, 3. Field Science Center for Northern Biosphere

The visible and near infrared spectroscopic information can provide powerful tools for identifying and quantifying chemical substances of soil, fruit and leaf, yet less is known about characteristics of reflectance spectroscopy for tree fine roots. In this study, we aimed to examine the effects of tree species on the reflectance of fine roots and to determine the association of the reflectance with respect to morphological, anatomical and chemical traits of fine roots of 20 species. We sampled fine roots in a cool temperate forest in Japan. The fine roots were divided into three diameter classes (0-0.5 mm, 0.5-1.0 mm, 1.0-2.0 mm). We obtained hyperspectral reflectance images at 458-2391 nm (total 376 bands by 4.1-5.8 nm interval) for fresh intact fine root for each three diameter classes. The relationships of reflectance images with average root diameter (mm), specific root length (m g^{-1}), root tissue density (g cm^{-3}), stele: cortex ratio, and carbon and nitrogen concentration (%) as each root trait were analyzed at each specific wavelength. The spectral patterns of the fresh intact root systems showed peak at four wavelength band across all woody species. Spectral reflectances at 458-1400nm were positively related to the root diameter. On the other hand, the reflectances differ among tree species. We will examine relationship the reflectance and root traits which characterized tree species. These results indicate that spectral reflectance at visible-near infrared regions can be an important determinant of species specificity of fine root traits by even fresh intact samples.

Keywords: root diameter, anatomy, morphology, chemistry

©2019. Japan Geoscience Union. All Right Reserved.

Heat Balance Analysis of Cold Air Pool Formation in Kamikochi

*Sayuri Koyama[1], Motoshi NISHIMURA[2], Keisuke Suzuki[3]

1. Graduate school of science and technorogy, Shinshu University, 2. Interdisciplinary Graduate school of Science and Technology, Shinshu university, 3. Department of Environmental Sciences, Faculty of Science, Shinshu University

Meteorological observation and heat balance analysis were conducted in Kamikochi (1490 m), Dakesawa (1600 m, 1700 m, 1800 m) and Nishi-hotakadake (2355 m), and the formation mechanism of cold air pool was clarified. The observation period is the snowy season at Kamikochi from December 6, 2016 to May 4, 2017 and from November 17, 2017 to April 16, 2018.
In this study, with referring to Dorninger et al. (2011), the cold air pools that occurred during the observation period were classified into eight tyes of the cold air pool events, undisturbed evolution, late buildup, early breakup, mixing event, temperature rise of all layers in a short time, upper disturbance, lower disturbance and short time cold air pool.
The cold air pool events occurred 28 times in April 2017 and 27 times in March 2018. However, mixing event, temperature rise of all layers in a short time, upper disturbance and lower disturbance hardly occurred in both 2016/17 and 2017/18. It is thought that Kamikochi is terrain that is difficult to generate turbulence.
The undisturbed evolution, the late buildup, and the early breakup differed in the time when the cold air pools were built and the time when they were destroyed. While the cold air pools were built, the sensible heat flux and latent heat flux were 0 W m^{-2}. The mixing event, the temperature rise of all layers in a short time and upper disturbance were different in depth of rise in temperature generated in the cold air pool and the increase amount in temperature. Regarding the sensible heat flux and latent heat flux amount, the mixing event was 5.0 W m^{-2} or more, the temperature rise of all layer in a short time was 0.5 W m^{-2} or more, and the upper disturbance was 0 W m^{-2}. The lower disturbance is the event in which a short-time increase in temperature occurs near the bottom of the basin. The cold air pools with formation time of less than 6 hours were classified as the short time cold air pool. These cold air pool events are largely responsible for the generation of clouds and the generation of turbulence by the wind, the time of occurrence and duration of clouds and wind, and the strength of turbulence are considered to be the main factors.

Keywords: Cold air pool, Heat balance

©2019. Japan Geoscience Union. All Right Reserved.

A finding of fossil trees buried in dammed-lake deposits formed by the Dondokosawa rock avalanche of the late 9th century in the Akaishi Mountains, and its significance

*Takashi Kimura[1], Ryuji Yamada[1], Yoshihiko Kariya[2]

1. National Research Institute for Earth Science and Disaster Resilience, 2. Senshu University

The Dondokosawa rock avalanche (DRA) initiated at an east-side slope of Mount Jizo, the Akaishi Mountains, the Southern Japan Alps, and traveled over 3.6 km along the mainstream of the Dondokosawa River. The displaced mass of the DRA completely blocked two parts, the outlet of a right tributary of the Dondokosawa River and the channel of the Ohdanasawa River, forming two dammed-lakes together with floodplain deposits beside the rock avalanche deposit (Kariya, 2012; Kimura *et al.*, 2018a). At these two sites, many fossil trees buried in lacustrine sediments were found by the authors. Yamada *et al.* (2018) applied the dendrochronological analysis using oxygen isotope ratios to tree-ring samples collected from two individuals (Hinoki cypress of >350 years old and Hemlock tree of >300 years old) and estimated death year of one individual to be around AD885 and that of the other to be AD888. These chronological constraints on the DRA strongly indicated that the DRA has occurred at the year of AD887 Ninna earthquake, which was one of the large ocean-trench earthquakes in Japan, or a couple of years later than the earthquake. The finding of fossil trees has a significance for not only estimating the age of the DRA but also reconstructing the paleoenvironment around the Akaishi Mountains. In this study, we present the vegetation characteristics of the Dondokosawa and the Ohdanasawa river catchments in the late 9th century, based on the tree species compositions of 41 samples analyzed in our previous studies (Kimura *et al.*, 2018b, 2019).

The sampling sites were named LLD and ULD, respectively. LLD is located at the confluence of the Dondokosawa and Ohdanasawa rivers, and has a drainage area of 8.81 km^2 with altitudes ranging from 1220 to 2780 m a.s.l. ULD is located at the outlet of the right tributary of the Dondokosawa River, and has a drainage area of 1.17 km^2 with altitudes ranging from 1470 to 2630 m a.s.l. We collected 41 samples (24 samples in LLD and 17 samples in ULD) between April 2012 and October 2017 and identified species or genus of each sample. The 24 samples in LLD include eight of Hinoki cypress (*Chamaecyparis obtusa*), seven of Hemlock tree (*Tsuga*), three of Sawara cypress (*Chamaecyparis pisifera*), two of Birch tree (*Betula*), and one each of Japanese larch (*Larix kaempferi*), Fir tree (*Abies*), Spruce tree (*Picea*) and Japanese Wingnut (*Pterocarya rhoifolia*). The other 17 samples in ULD include eight of *Tsuga*, four of *Abies*, two each of *L. kaempferi* and Willow tree (*Salix*), and one of Azalea tree (*Rhododendron*). The rates of *Tsuga* in LLD and ULD account for approx. 29% and 47%, respectively. Besides, the rate of cypress species (*C. obtusa* and *C. pisifera*) in LLD accounts for approx. 46%, while both of the two species are absent in ULD.

Although the above results are based on a limited number of samples, it is estimated as vegetation characteristics in the late 9th century, when the DRA occurred, as follows. In the Ohdanasawa River catchment, an old-growth forest dominated by Hinoki cypresses of >350 years old and Hemlock trees was established, while another old-growth forest dominated by Hemlock trees of >300 years old was established in the right tributary catchment of the Dondokosawa River. The remarkable difference in the abundance of cypress species in the two adjacent catchments suggests a possibility that the distribution of the two species has been limited within the Ohdanasawa River catchment and has not extended to the upper part of the Dondokozawa River from that time.

©2019. Japan Geoscience Union. All Right Reserved.

References:Kariya (2012) Trans. Jpn. Geomorphol. Union 33, 297-313 [in Japanese with English abstract]; Kimura *et al.* (2018a) J. Jpn. Landslide Soc. 55, 42-52 [in Japanese with English abstract]; Kimura *et al.* (2018b) JpGU2018 MGI25-P09 [in Japanese with English abstract]; Kimura *et al.* (2019) Quat. Res. 58, 65-72 [in Japanese]; Yamada *et al.* (2018) Quat. Geochr. 44, 47-54.

Keywords: Akaishi Mountains, rock avalanche , dammed-lake, fossil trees, paleoenvironment

©2019. Japan Geoscience Union. All Right Reserved.

What alpine plants attract visitors in the Daisetsuzan national park, northern, Japan?

*Yukihiro Amagai[1], Kota Mameno[1,2], Hiroyuki Oguma[1], Takahiro Kubo[1]

1. National Institute for Environmental Studies, 2. Hokkaido University

The Daisetsuzan National Park in Hokkaido northern Japan is visited by 5 million people every year, because the Taisetsu Mountains have large fields of alpine vegetation. In the alpine zone, many alpine plant species (365 species: including subspecies and variants as well as 27 Japanese endemic species) grow. However, alpine vegetation has remarkably changed, with alpine dwarf-pine (*Pinus pumila*) and dwarf-bamboo (*Sasa kurilensis*) distributions having expanded during the last decade along with significant changes in the vegetation structure. From such a background, selection of protected areas, evaluation of vulnerbility for each plant species and community type, and adaptation manegement, there are urgent problems for the conservation of biodiversity in the alpine zone. Furthermore, change of alpine vegetation can be considered to damage as tourism resources as well. Therefore, purpose of this study is to clarify the preference of visitor to alpine plant species for collecting baseline information of tourism resources as one conservation indicator.

This study was conducted at the Sugatami Station of the Daisetsuzan Asahidake Ropeway which is located at an elevation of 1600 m, and the treeline is located at an elevation of around 1400-1700m. Therefore, visitors can easily hike and watch for alpine plants in alpine area. To clarify visitors preference for alpine plant species, we distributed questionnaires to visitors at the place. Respondents were asked “what flower do you want to see (check the all plants at posted picture of 20 species)”, and socio-demographics including experiences of visiting Daisetsuzan national parks. The number of questionnaires distributed were 1201 in 6 days of August 2018, and a total of 451 respondents participated our survey. The plant pictures which were showed respondents in the questionnaire were selected from 18 typical alpine plants, which considering habitats, plant growth form, and flower color (*Trollius riederianus, Stellaria pterosperma, Primula cuneifolia, Anemone narcissiflora* var. *sachalinensis, Therorhodion camtschaticum, Lagotis yesoensis, Pentstemon frutescens, Nephrophyllidium crista-galli, Pedicularis oederi, Phyllodoce aleutica, Dicentra peregrina, Saxifraga laciniate, Trichophorum cespitosum, Drosera anglica, Gentiana jamesii, Sieversia pentapetala, Campanula chamissonis, Eriophorum*) and *P. pumila* and *S. kurilensis*.

As a result, *S. pentapetala*, *G. jamesii*, and *P. cuneifolia* are high preference, while *T. cespitosum*, *S. kurilensis*, and *P. pumila* are low. From the respondent information, repeaters had high preference to *S. pentapetala* and *D. peregrina* than first time visitor. Furthermore, we analyzed flower (15 species) and whole (20 species) morphological feature by generalized linear model (GLM) for clarify the preferred features. As a result, the high preference to flower features are: the inflorescence was flat, the number was few, and the color tended to be pink > purple > white ≧ yellow plants. And the whole features are: leaves had gloss, leaf size was small, plant height was low.
Therefore, the *S. pentapetala* is the most attractive species for many visitors, which species is necessary for secure repeaters also. The *S. pentapetala* is not a specific species in the Taisetsu Mountains, because it distributes wide area in the alpine, eastern Japan. However, in the Taisetsu Mountains, a large community is formed along the trail, resulting it represents the image of the flower garden. Therefore, as tourism resources, it is important to maintain a large flower garden and suppress the influence of the expansion of *P. pumila* and *S. kurilensis*, which low preference species. Furthermore, the popular plants

©2019. Japan Geoscience Union. All Right Reserved.

have feature that low height and few flowers from ranking based on the preference by GLM, resulting the visitors expect to see the dwarf plants just like image of alpine plants. On the other hand, we also revealed that species considered to be important as tourism resources are not necessarily consistent with rare and preferential conservation. Therefore, it is necessary to consider the balance between tourism resources and biodiversity.

Keywords: Alpine, People-plant interactions, Preference, Plant morphology, Climate change, Conservation

©2019. Japan Geoscience Union. All Right Reserved.

Spatio-temporal variations of algal snow in Mt. Gassan, Yamagata prefecture, Japan

*Suzuki Takumi[1], Nozomu Takeuchi[1], Tsubasa Takahashi[1]

1. Chiba University

Red, yellow or green colored snow due to algal blooming often appeared on the melting snow surface in the forest zone of Mt. Gassan in Yamagata Prefecture, Japan. Their distribution has been reported to be caused by physical and chemical conditions of snow surface. For example, green snow appears on eutrophic snow surfaces whereas red snow appears in poor nutrition snow surface in Antarctica. However, their temporal and spatial distributions and controlling factors are still unknown. Therefore, in this study, to clarify spatio-temporal changes of algal snow and their controlling factors, we investigated the algal biomass, pigment compositions, and nutrient conditions of colored snow of Mt.Gassan.

Snow samples were collected at 7 sites between 800 m and 1500 m above sea level along a ridge of the southern part of Mt.Ubagatake in May and June, 2018. We collected a surface snow sample from randomly selected surface at each site. The sample was preserved in a plastic bag and was melted in a laboratory. The chlorophyll a concentrations in the samples were measured with a fluorophotometer. Absorption spectra of the extracted pigments were measured with a spectrophotometer. The soluble chemical ions concentrations were measured with an ion chromatography. The samples were also observed with a microscoped.

Most of colored snow appeared in May was green snow. In June, red snow was often observed above the timber line, while orange snow was observed below the timber line. As a result of analyzing the absorption spectrum of the dye extracted from the sample, two kinds of waveforms were observed in both May and June. No major absorption was seen at any site in May. In January and June, the waveforms were found above and below the forest limit, both of which showed greater absorption than in May. Algal biomass generally increased from May to June at any sites. In addition, nitrate and phosphate ions, which are essential nutrients for algal growth, did not show any altitudinal trend, but decreased from May to June. The change of snow color from green in May to red or orange in June may be due to decrease of nutrient at the surface snow. The difference of snow color between above and below the timber line may be due to difference of solar radiation conditions.

Keywords: snow algae

©2019. Japan Geoscience Union. All Right Reserved.

Feeding of a wingless stonefly living on snow surface in Mt. Gassan, Yamagata prefecture, Japan

*Risako Yonechi[1], Nozomu Takeuchi[1]

1. Chiba University

There is a biological community on snow and ice consisting of cold-tolerant organisms. For examples, photosynthetic microbes (snow algae), heterotrophic invertebrates and bacteria are living on snow packs in Japan. Wingless stoneflies are also snowy insects commonly found in Japan. They are basically aquatic insects spending in streams when they are nymphs, but actively walks on the snow surface in winter and spring when they become adult. Wingless stoneflies in Japan have been classified into thirty species belonging to two genera (Apteroperla and Eocapnia) based on their morphological perspectives. Several species have been reported to appear on a snow surface simultaneously, however, it is still unknown that their feedings and life cycles. In this study, we reported the spatial distribution and feedings of wingless stoneflies found on snow packs in Mt. Gassan, Yamagata prefecture, Japan.
The fieldworks were conducted three times in April, May and June of 2018 in a south slope of Mt. Gassan, where heavy snow covers during winter and spring. We collected wingless stoneflies on snow surface at 13 sites in different elevations from a summit of Mt. Ubagatake (1487 m.a.s.l) down to Shizu camp site (770 m.a.s.l). We identified their species based on their body morphology using a microscope. We also analyzed carbon and nitrogen stable isotopes of the collected stonefly specimens. The stable isotopes were analyzed with an IRMS (Isotope Ratio Mass Spectrometer) at Research Institute for Humanity and Nature.
Fifty male specimens were classified into two genera. Apteroperla stoneflies were mostly found in the area above 1000 m a.s.l., conversely Eocapnia stoneflies were found in the area below 1000 m a.s.l. This suggests that the two genera have different habitats in this mountainous area. The nitrogen stable isotope of the wingless stoneflies was not significantly different between Apteroperla and Eocapnia (1.10 - 0.95‰ versus -1.63 - 1.05‰), indicating that the tropic levels of two genera are almost same. Carbon stable isotope also did not differ significantly between the two genera (-26.2‰ versus -25.7‰). However, the variance of the carbon stable isotopes of Apteroperla is smaller than that of Eocapnia (0.29‰ versus 3.00‰). This suggests that Apteroperla stoneflies have limited dietary habits while Eocapnia has broad eating habits.

Keywords: insect, alpine, ice biology

©2019. Japan Geoscience Union. All Right Reserved.

Drainage from glacial lake in Achinathang village, Ladakh Range on 4 August 2017

Maho Saotome[2], *Chiyuki Narama[1], Naoki Sakurai[2]

1. Niigata University, Program of Field Research in the Environmental Sciences, 2. Graduate School of Science and Technology, Niigata University

In the Achinatan valley of the Ladak Range, located in the northwestern part of India, a large debris flow occurred on August 4, 2017. In this disaster, this debris flow caused four victims and serious damages such as a complete collapse of bridge and field. In this study, we tried to clarify the details of drainage from glacial lake and development of debris flow in the Achinatan valley from field survey (2017-2018) and satellite image analysis.

Keywords: glacial lake, glacial lake outburst flood (GLOF), debris flow, Ladakh Range

©2019. Japan Geoscience Union. All Right Reserved.

Recent glacier variations at Mt. Kenya using aerial digital image

*Chiyuki Narama[1], kenshiro Arie[2], MIZUNO KAZUHARU[3]

1. Program of Field Research in the Environmental Sciences, Niigata University , 2. Graduate School of Science and Technology, Niigata University, 3. Graduate School of Letters, Kyoto University

The total glacier area decreased by 121.0 x 10^3 m^2 (44%) during 2004–2016 at Mt. Kenya (Prinz et al., 2018). These glaciers are estimated to extinct before 2030, implying the cessation of the longest glacier monitoring record of the tropics. In this study, we investigated mass balance of all glaciers during 2016-2018 using Pleiades satellite data and aerial digital images from Cessna.

Keywords: glacier variations, mass balance, aerial digital image, Mt. Kenya

©2019. Japan Geoscience Union. All Right Reserved.

[J] Oral | M (Multidisciplinary and Interdisciplinary)：M-IS Intersection

Mon. May 27, 2019 9:00 AM - 10:30 AM JST | Mon. May 27, 2019 12:00 AM - 1:30 AM UTC | 106 1F

[M-IS23] Planetary Volcanology

convener:Rina Noguchi(Institute of Space and Astronautical Science, Japan Aerospace Exploration Agency), Tomokatsu Morota(Graduate School of Environmental Studies, Nagoya University), Kyoko S. Kataoka(Research Institute for Natural Hazards and Disaster Recovery, Niigata University), Shizuka Otsuki(Research Institute of Earthquake and Volcano Geology, Geological Survey of Japan, Advanced Industrial Science and Technology), Chairperson:Rina Noguchi(Institute of Space and Astronautical Science, Japan Aerospace Exploration Agency), Nobuo Geshi(GSJ/AIST)

Volcanoes exist on solid planetary surface across the solar system. They tell insight into the interior, and the surface environment when they were formed and subsequent evolution. Recent high-resolution remote sensing data on extraterrestrial body allows us to analyze on outcrop scales. Now we are on the stage to share the research targets beyond fields of general volcanology and planetary science. Because some geomorphological and geological environments
in other planets are similar to those on Earth, research on volcanic geomorphology and geology on Earth will provide good terrestrial analogues to understand planetary volcanology. The aim of this session is to discuss formation history and mechanism of volcanoes across the solar system.

9:00 AM - 9:15 AM JST | 12:00 AM - 12:15 AM UTC

[MIS23-01] Growth and evolution of isolated volcanic island, Nishinoshima, Ogasawara

★Invited Papers

*Fukashi Maeno[1] (1.Earthquake Research Institute, University of Tokyo)

9:15 AM - 9:30 AM JST | 12:15 AM - 12:30 AM UTC

[MIS23-02] The style of magmatism on terrestrial planets of various sizes predicted from numerical models of mantle dynamics

*Masaki Ogawa[1] (1.Division of General Systems Studies, Graduate School of Arts and Sciences, University of Tokyo)

9:30 AM - 9:45 AM JST | 12:30 AM - 12:45 AM UTC

[MIS23-03] Lunar and Matian lava tubes and explorations to them through their skylight holes

*Junichi Haruyama[1], Takahiro Iwata[1], Yukio Yamamoto[1], Tetsuya Kaku[2,1], Wataru Miyake[2], Atsushi Kumamoto[3], Ken Ishiyama[1], yokota yasuhiro[4], Takumi Ono[2,1] (1.Japan Aerospace Exploration Agency, 2.Tokai University, 3.Tohoku University, 4.Kochi University)

9:45 AM - 10:00 AM JST | 12:45 AM - 1:00 AM UTC

[MIS23-04] Volcanic activity on Io, formation of the atmosphere, and escape of atmosphere to the magnetosphere

*Fuminori Tsuchiya[1], Ryoichi Koga[1], Mizuki Yoneda[2], Masato Kagitani[1], Kazuo Yoshioka[4], Reina Hikida[4], Go Murakami[3], Tomoki Kimura[1], Atsushi Yamazaki[3], Hajime Kita[3], Ichiro Yoshikawa[4] (1.Tohoku University, 2.Tadano, 3.ISAS/JAXA, 4.The University of Tokyo)

10:00 AM - 10:15 AM JST | 1:00 AM - 1:15 AM UTC

[MIS23-05] Cryovolcanism, a critical review

*Kei Kurita[1] (1.Earthquake Research Inst.,The University of Tokyo)

10:15 AM - 10:30 AM JST | 1:15 AM - 1:30 AM UTC

[MIS23-06] Cryovolcanisms on Solar System bodies: Observations, importance, and future perspectives

★Invited Papers

*Yasuhito Sekine[1] (1.Earth-Life Science Insitute, Tokyo Institute of Technology)

Growth and evolution of isolated volcanic island, Nishinoshima, Ogasawara

*Fukashi Maeno[1]

1. Earthquake Research Institute, University of Tokyo

The process of birth and growth of ocean islands is an interesting phenomenon in the field of geoscience in terms of the creation of new land and the creation of a place for new terrestrial life activities. Nishinoshima is a rare place on the earth that can trace the process of birth, formation and evolution of such ocean islands from various viewpoints of research fields. Meanwhile, since the eruption in the shallow sea can be a factor of maritime hazards, the establishment of investigation/observation method and risk assessment method is also an important subject. Nishinoshima is located in a place deserving to call as an isolated island, 130 km west of Chichijima, Ogasawara Islands. In November 2013, a new island was born by submarine eruption. It gradually covered the preexisted island and increased the land. A series of eruptive activities in Nishinoshima from 2013 to 2018 provided various valuable data on the birth of a new volcanic island and its growth process, and was also important as a place for practical investigation and observation of remote island volcanoes. The eruptive activity of Nishinoshima is divided into November 2013 - December 2015 (first stage), April to August 2017 (second stage), and July 2018 (third stage). Meanwhile, various surveys and observations were conducted to understand the activities of Nishinoshima. Immediately after the beginning of the eruption, the observation data from remote was the only information source, and based on analysis of high-resolution satellite images and direct observation from the airborne, the growth process of Nishinoshima was monitored, focusing on the changes in surface topography and morphology, area, volume, and discharge rate. After that, following the decline in activity at the end of 2015, comprehensive investigation of volcanic activity and biota was carried out in October 2016. In this survey, earth science and ecological scientists collaborated with each other to conduct a landing survey, in order to minimize the risk of bringing invasive species to new Nishinoshima, and lava samples were collected directly for the first time, and the seismometer and the microphone were also installed. In 2017 and 2018, Nishioshima became active again and grew larger, finally its activity ended at the end of July 2018. After 2016, surveys were conducted remotely utilizing drone and unmanned helicopter, taking images and movies of new lavas and craters, sampling eruptive products, installing and collecting loggers for ecological monitoring, magnetic survey and others were carried out, and the result enhancing our understanding of activities and evolution of Nishinoshima is being obtained. Such surveys and observations in Nishinoshima, where it is difficult to access and the perspective of conservation of primitive ecosystem is also necessary, may have common terms with surveys of extraterrestrial body surface. In this presentation, I will introduce the growth and evolution of Nishinoshima, the volcanic activity, and the methods and results of surveys carried out so far, while being conscious of the connection with planetary volcanology.

Keywords: volcanic island, Nishinoshima, remote observation, landing survey

©2019. Japan Geoscience Union. All Right Reserved.

The style of magmatism on terrestrial planets of various sizes predicted from numerical models of mantle dynamics

*Masaki Ogawa[1]

1. Division of General Systems Studies, Graduate School of Arts and Sciences, University of Tokyo

A series of numerical models of magmatism in the convecting mantle suggest that the vigor and style of mantle magmatism critically depend on the planetary size because of its effects on the elementary processes that exert control over mantle dynamics. On a small planet like the Moon, a mild magmatism continuously occurs for several hundred million years in upwelling limbs of mantle convection and then wanes, because the magmatism extracts heat-producing elements (HPEs) from the mantle. Magmatism, however, often becomes more vigorous and episodic, as observed for the Large Igneous Provinces on Mars and larger planets, because the buoyancy of the generated magma boosts the upwelling flow in the mantle that causes the magmatism itself. The convective stirring enhanced by the MMU feedback keeps the mantle rather homogeneous, despite that the vigorous magmatism due to the feedback differentiates the mantle. The effect of the MMU feedback is particularly important in Venus and the Earth where the lower mantle develops: The solid-solid phase transitions that occur at the top of the lower mantle make mantle upwelling flow pulsating, when the mantle is strongly heated by HPEs and magmatism is vigorous. This pulse or burst of hot materials from the lower mantle causes a vigorous magmatism, especially in the early mantle. Due to this vigorous magmatism, the crust enriched in HPEs recycles back to the mantle to serve as the energy source for the magmatism that continues throughout the history of the mantle. On the Earth, plate tectonics also causes magmatism and recycling of the generated crust. In contrast to Venus, this magmatism differentiates the mantle, because tectonic plates and subducting slabs stir the mantle only mildly.

Keywords: magmatism, mantle convection, planetary size, numerical simulation

©2019. Japan Geoscience Union. All Right Reserved.

Lunar and Matian lava tubes and explorations to them through their skylight holes

*Junichi Haruyama[1], Takahiro Iwata[1], Yukio Yamamoto[1], Tetsuya Kaku[2,1], Wataru Miyake[2], Atsushi Kumamoto[3], Ken Ishiyama[1], yokota yasuhiro[4], Takumi Ono[2,1]

1. Japan Aerospace Exploration Agency, 2. Tokai University, 3. Tohoku University, 4. Kochi University

Large and deep hole structures of a few tens to hundreds meter diameter and depth were discovered on Mars in the thermal emission data acquired by Mars Odyssey THEMIS and on the Moon in the SELENE (Kaguya) Terrain Camera visible image data, about 10 years ago. These are probably skylights of underlying caves produced by volcanic activities such as lava tube formation. Later, many hole structures and depression features as "pits" possibly associated to lava tubes have been identified on these celestial bodies in image data of orbiting explores. Intact lava tube existence on the Moon are also suggested by gravity measurements by GRAIL and radar sounding experiments by SELENE (Kaguya).
The role of lava tube on the formation of vast terrains expanding on the Moon and Mars are scientifically interesting, though the study has not been sufficiently done. In addition, lava tubes and their skylight holes offers prominent environments to conduct scientific examination of the history of volcanic activities on the Mars and Moon. Lava tubes on Mars and the Moon are expected to be secure shelters for humans and instruments potentially protecting from micrometeorites bombardments and cosmic ray radiations, In the next decades, therefore, Martian and lunar lava tube exploration will be executed by space agencies of countires and even private companies.
In this presentation, we would introduce recent studies of lava tubes of Mars and the Moon and their explorations.

Keywords: moon, Mars, hole, lava tube, cave

©2019. Japan Geoscience Union. All Right Reserved.

Volcanic activity on Io, formation of the atmosphere, and escape of atmosphere to the magnetosphere

*Fuminori Tsuchiya[1], Ryoichi Koga[1], Mizuki Yoneda[2], Masato Kagitani[1], Kazuo Yoshioka[4], Reina Hikida[4], Go Murakami[3], Tomoki Kimura[1], Atsushi Yamazaki[3], Hajime Kita[3], Ichiro Yoshikawa[4]

1. Tohoku University, 2. Tadano, 3. ISAS/JAXA, 4. The University of Tokyo

Jupiter's satellite Io is known as the most active volcanically active body in the solar system. The atmosphere of the satellite consists mainly of volcanic gas composed of sulfur dioxide. The molecular escaped becomes primary source of plasma in the magnetosphere of Jupiter. Here, observations of the volcanic gas escaped from satellite with the extreme ultraviolet telescope satellite, Hisaki, and a groundbased visible telescope, and observations of hot spot of Io's volcano with infrared telescopes are presented. We will discuss the formation of the satellite atmosphere, escape process of the atmospheric gas to the magnetosphere, and their relation to volcano types.

Keywords: volcano, Io, Hisaki

©2019. Japan Geoscience Union. All Right Reserved.

Cryovolcanism, a critical review

*Kei Kurita[1]

1. Earthquake Research Inst.,The University of Tokyo

Volcanoes are surface manifestation of internal activity of planets and satellites. In planetary explorations the primarily available data source would be the surface images so that the volcanoes identified on the surface are unique window into the interior. This argument is particularly significant in icy bodies of the outer solar system because exploration data are so limited except for the surface images. Up to now several types of surface morphology have been considered as a product of cryovolcanism. In this presentation I will focus on the general aspects of the cryovolcanism in comparison to the silicate volcanism and would like to emphasize the significant role of hydrate phase in cryovolcanism.

Similarities and dissimilarities between cryovolcanism and silicate volcanism: There exist a lot of similarities between ice and silicate minerals such as the rheological properties and the melting relationship. The depression of the melting point in the existence of accessary components in both systems should play an important role in promoting differentiation. The critical difference is the pressure dependence of the melting temperature and the density contrast between liquid and solid phase. Since water magma is not buoyant in the icy lithosphere this density reversal requires special mechanism for driving water magma to the surface. This situation is, however similar to the continental basalt volcanism. In the icy satellites the stress field in the outer lithosphere plays an important role. Both exogenetic origin such as tidal forcing and endogenous origin such as thermal stress and volume change driven by phase change would be

Significant role of hydrate phase in cryovolcanism: Hydrate is a common phase in the multicomponent system including H2O. It is stable at higher pressure so that it should be an important constituent phase while it decomposes near surface. This may result in explosive behavior because the decomposition is associated with generation of gas phase. Although a lot of combination of the components form various hydrate phases, there exist two planetologically significant end-members, CO2 hydrate and CH4 hydrate. These two have contrasting nature in terms of the density, which would cause different evolution path in the material differentiation.

Keywords: cryovolcanism, hydrate

©2019. Japan Geoscience Union. All Right Reserved.

Cryovolcanisms on Solar System bodies: Observations, importance, and future perspectives

*Yasuhito Sekine[1]

1. Earth-Life Science Insitute, Tokyo Institute of Technology

Cyrovolcanos are volcanos on icy planetary bodies, erupting liquids and vapors of volatiles (e.g., water, ammonia, methane, and carbon dioxide) from subsurface water reservoirs or oceans. In the Solar System, geologically-active icy moons (e.g., Enceladus, Titan, and potentially Europa) and icy dwarf planets (e.g., Ceres and Pluto) are known to possess cryovolcanisms in the past or even today.

Cryovolcanos are unique windows to reveal the physico-chemical states of the subsurface oceans of the icy bodies, which is essential to understand the thermal evolution and habitability. Morphology of cryovolcanos would be a key to constrain the physical properties (e.g., viscosity and density) of liquids in the subsurface water reservoirs. Chemical compositions of erupting materials would provide information on volatile and salt compositions of the liquids. Eruption of volatiles (e.g., methane and nitrogen) could be also a major source of atmospheric gas species and thus could have affected the surface environments.

Despite such importance, the nature of cryovolcanisms, such as formation mechanisms and eruption styles, is largely unknown. Since pure liquid water is denser than that of ice, dissolved gas species in cryolava would play a key role for its eruption through bubbling and a consequent decline in the bulk density. Dissolved gas/salt in the liquids also controls the viscosity of cryolava. Such importance of dissolved species in cryovolcanisms implies a potential similarity in the role of volatiles in silicate volcanisms on rocky planets, such as Earth. Here we review recent observations of cryovolcanos on the Solar System icy bodies by spacecrafts. We then discuss the possibility of and future perspectives for development of comparative researches between cryo- and silicate-volcanisms in the Solar System.

Keywords: icy bodies, Solar System exploration, cryovolcano

©2019. Japan Geoscience Union. All Right Reserved.

[J] Poster | M (Multidisciplinary and Interdisciplinary)：M-IS Intersection

Mon. May 27, 2019 3:30 PM - 5:00 PM JST | Mon. May 27, 2019 6:30 AM - 8:00 AM UTC | Poster Hall International Exhibition Hall8, Makuhari Messe_25

[M-IS23] Planetary Volcanology

convener:Rina Noguchi(Institute of Space and Astronautical Science, Japan Aerospace Exploration Agency), Tomokatsu Morota(Graduate School of Environmental Studies, Nagoya University), Kyoko S. Kataoka(Research Institute for Natural Hazards and Disaster Recovery, Niigata University), Shizuka Otsuki(Research Institute of Earthquake and Volcano Geology, Geological Survey of Japan, Advanced Industrial Science and Technology)

Volcanoes exist on solid planetary surface across the solar system. They tell insight into the interior, and the surface environment when they were formed and subsequent evolution. Recent high-resolution remote sensing data on extraterrestrial body allows us to analyze on outcrop scales. Now we are on the stage to share the research targets beyond fields of general volcanology and planetary science. Because some geomorphological and geological environments
in other planets are similar to those on Earth, research on volcanic geomorphology and geology on Earth will provide good terrestrial analogues to understand planetary volcanology. The aim of this session is to discuss formation history and mechanism of volcanoes across the solar system.

[MIS23-P01] **A possible method of lava flow temperature estimation by lava tube cave of Earth,Moon and Mars**

*Tsutomu Honda[1] (1.Vulcano-speleological Society)

[MIS23-P02] Process of magma eruption on the Moon

*Tomokatsu Morota[1] (1.Graduate School of Environmental Studies, Nagoya University)

[MIS23-P03] Statistical analysis of grain morphology generated under hypervelocity impact experiment as an analog of volcanic explosion

*Rina Noguchi[1], Shizuka Otsuki[2], Ayako I Suzuki, Sunao Hasegawa[1] (1.Institute of Space and Astronautical Science, Japan Aerospace Exploration Agency, 2.Geological Survey of Japan, AIST)

[MIS23-P04] Disequilibrium precipitation of salts during rapid freezing of brine: Implications for cryovolcanisms and formation of sodium carbonate of bright spots on Ceres.

*Masahiro Yoda[1,2], Yasuhito Sekine[2], Shuya Tan[1,2] (1.Department of Earth and Planetary Science, The University of Tokyo, 2.Earth-Life Science Institute, Tokyo Institute of Technology)

A possible method of lava flow temperature estimation by lava tube cave of Earth,Moon and Mars

*Tsutomu Honda[1]

1. Vulcano-speleological Society

[Introduction]In the lava flow of Miharayama of Izu Oshima eruption in 1951, the lava temperature,the lava flow thickness and the flow velocity were directly measured on the site[(1)]. Then, the temperature dependent viscosity coefficient and the yield strength were calculated [(1,2)]. In addition, the temperature dependent surface tension was measured in the laboratory by re-melting the collected sample[(3)]. In 2005, a lava tube cave called Hornito Cave was discovered under the hornito located at the crater edge. The inner and outer structure of the Hornito cave was investigated and lava yield strength and surface tension have been also identified [(4, 5, 6)]. Miharayama Hornito Cave is a representative example where lava temperature, viscosity coefficient, yield value and surface tension are identified. On the other hand, in the universe, vertical holes/pits are found in the lava zone of Moon and Mars and lava tube caves are thought to be present under the vertical hole/pit [(7, 8, 9)]. Based on the example of Mihara yama of Izu Oshima in the Earth, it seems to be possible to identify the lava temperature and viscosity coefficient from lava yield strength and surface tension obtained from lava tube shape and internal structure on the Moon and Mars. It should be considered as an important purpose of future vertical hole/pit exploration.

[Data obtained from Izu Oshima Mihara yama Hornito Cave]For Mihara yama Hornito Cave ,internal observation and the preparation of the survey map of horizontal section and longitudinal section were made [(4)]. Based on the cavity height of the lava tube cave and its slope angle, the lava yield strength f_B is estimated from $f_B = H(\rho g \sin \alpha) / 4$, the flow limitation condition of the Bingham fluid flowing in the inclined circular tube. The obtained lava yield strength was 5000 Pa[(5,6)]. This value is consistent with 4300Pa obtained by field observation of actual lava flow of 1951 of temperature ranging from 1125 to 1038[(2).] From the pitch P of the lava stalactite descending from the ceiling of the cave, the surface tension $\gamma = P^2 g \rho / 4 \pi^2$ is obtained. As the measured pitch is roughly P = 3 to 4 cm, then the surface tension is 600 to 1000 mN / m[(5,6)]. This value is consistent with extrapolated value from the temperature dependent surface tension of Izu Oshima 1951 lava measured by Yokoyama et al.,in his laboratory with the remelted sample[(3)]. This indicates that, if lava tube cave is present. it is possible to estimate the lava temperature of the eruption time, even if lava flow temperature at the past eruption is unknown.

[Application to the Moon,Mars and Future Exploration]

In the vertical hole/pit cross section images of the Moon shown by LRO, the traces such as lava flow layer thickness,lava tube cave height can be seen, so, it seems possible to identify the lava flow temperature using these traces.

For Marius Hills Hole located in the Rille-A, the yield strength can be obtained as 131 Pa from the slope angle with an average lava layer thickness of 6 m and tube cavity height of 18 m[(10)]. If the temperature dependent data of the yield strength is acquired separately, the temperature of the lava flowing through the rill-A can be estimated. Further, if we can find lava stalactite inside of the cave by future moon exploration, the temperature can be identified also by comparing the surface tension obtained from the pitch of the lava stalactite with the temperature dependent surface tension data. The viscosity coefficient can also be fixed by the temperature dependent viscosity coefficient data. Fig.1 shows a concept of estimation.

At the stage where sampling on the Moon and Mars can not be done immediately, the synthetic samples based on the chemical composition will be used to acquire the temperature dependent yield strength and surface tension data.

©2019. Japan Geoscience Union. All Right Reserved.

References:
(1)T. Minakami:Bulltin of the Earthquake Research Institute, University of Tokyo,Vol.29, pp. 487-493, 1951, (2) G. Hulme: Geophys. J. R. astr. Soc. (1974) 39, 361-383, (3) I.Yokoyama et al: Geophysical bulletin of the Hokkaido University, 24: 57-61, 1970, (4) H.Tachihara et al: Volcanic cave survey and observation report of Oshima, Tokyo, Volcanic Cave Society, 2006, (5) T.Honda: V102-001, Japan Earth and Planetary Science Joint Meeting, 2006, (6) T.Honda, et al: AMCS Bulletin 19 / SMES Boletin 7-2006, pp 185-187, Proc.X, XI, XII Internat. Symposia on Vulcanospeleology, 2008, (7) J. Haruyama, et al: Geophysical Research Letters, Vol. 36, L2 1206, 2009,
(8) M.S. Robinson et al:Planetary and Space Science 69, pp 18-27, 2012,
(9) G.E.Cushing, et al: Geophys. Res. Lett., 34, L 17201, 2007,(10) T.Honda: SVC 50-05, Japan Earth and Planetary Science Joint Meeting, 2017

Keywords: lava tube cave, Miharayama hornitocave, lava flow temperature

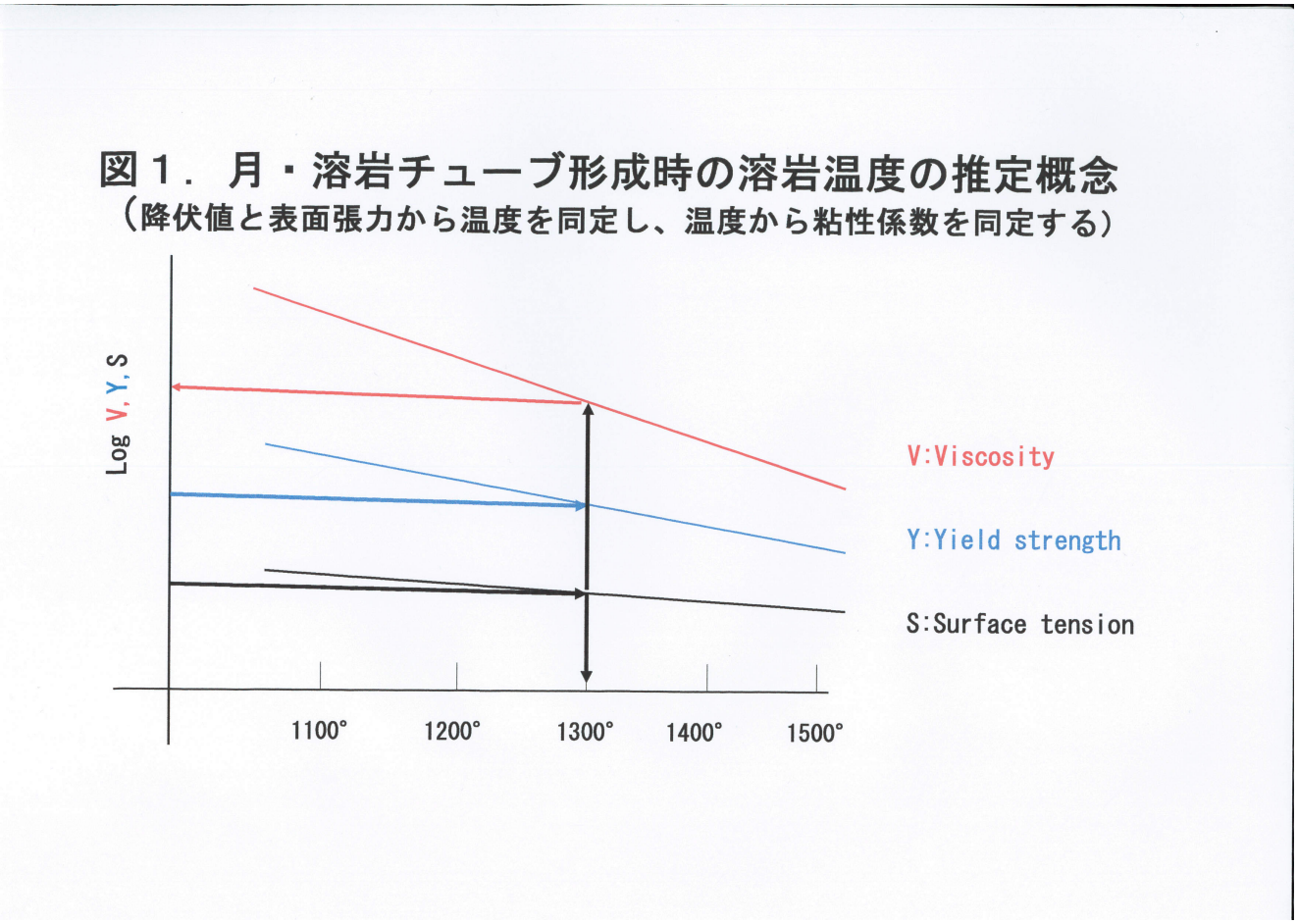

©2019. Japan Geoscience Union. All Right Reserved.

Process of magma eruption on the Moon

*Tomokatsu Morota[1]

1. Graduate School of Environmental Studies, Nagoya University

Estimates for volumes of mare basalts are essential to understand the thermal conditions of the lunar mantle and its lateral heterogeneity. We have investigated the volumes of mare basalts within farside and nearside basins using topographic and multiband image data obtained by SELENE (Kaguya). Furthermore, using the high-resolution crustal thickness model, we investigated the crustal thickness of major impact basins and its relationship with the mare volumes. Based on these results, we discuss the relationship between the mare volumes and the crustal thickness, differences between magma productions in the farside and nearside mantles, and the processes of magma ascent and eruption.

Keywords: Moon, Mare volcanism, Impact basin, Dichotomy, Magma eruption

©2019. Japan Geoscience Union. All Right Reserved.

Statistical analysis of grain morphology generated under hypervelocity impact experiment as an analog of volcanic explosion

*Rina Noguchi[1], Shizuka Otsuki[2], Ayako I Suzuki, Sunao Hasegawa[1]

1. Institute of Space and Astronautical Science, Japan Aerospace Exploration Agency, 2. Geological Survey of Japan, AIST

Natural volcanic ash is formed in several states of magma (i.e., solid or melt) and surrounding conditions (e.g., dry or wet settings). These various factors affect the morphology of ash grain. For example, in a wet setting, moss-like grains are often formed (e.g., Wohletz, 1983). Thus, grain shape of volcanic ash tells us its fragmentation process. This would be useful to estimate eruption mechanism both for on-going and historical eruptions. However, it is difficult to extract the fragmentation mechanism from the grain morphology because of the complex natural system (i.e., not by a single mechanism). Furthermore, manual verification of numbers of ash grains takes a long time and need training. To simplified these issues, we proposed a technique to measure the morphology of volcanic ash grains by using an automatic grain analyzing system (Noguchi et al., in prep.). In this study, we apply the technique to the grains formed by an impact in a laboratory in order to verify the accuracy and applicability of the technique. We used a two-stage light-gas gun in ISAS, JAXA. Grains were collected using a Styrofoam box and segregated with d-limonene. After that, we measured shape parameters and transparency using an automated grain analyzer (Morphologi G3S, Malvern Inst.) of AIST. The measured parameters of grain shape are aspect ratio, high-sensitivity circularity, convexity, and solidity. We also measured transparency of each grain. In this presentation, we show its preliminary result and indicate its applicability to returned sample from other planetary bodies such as Itokawa, Ryugu, and Phobos.

Keywords: Volcanic ash, Impact experiment, grain morphology

©2019. Japan Geoscience Union. All Right Reserved.

Disequilibrium precipitation of salts during rapid freezing of brine: Implications for cryovolcanisms and formation of sodium carbonate of bright spots on Ceres.

*Masahiro Yoda[1,2], Yasuhito Sekine[2], Shuya Tan[1,2]

1. Department of Earth and Planetary Science, The University of Tokyo, 2. Earth-Life Science Institute, Tokyo Institute of Technology

NASA's Dawn spacecraft has found geological evidence for cryovolcanoes on Ceres, the dwarf planet in the main belt. Erupted materials from Ceres' cryovolcanoes are generally bright and distribute locally over Ceres in association with floor-fractured craters and dome-like features, which have young surface ages (e.g., Buczkowski et al, 2016; Ruesch et al, 2016). The bright materials are considered to be composed mainly of sodium carbonate and ammonium salts, which are different from the average crustal compositions (a mixture of magnesium-calcium carbonates and ammonia phyllosilicates) (De Sanctis, 2016; Zambon et al, 2016). The particular compositions of bright materials could provide unique information on the formation and evolution of liquid reservoirs within Ceres.

Two possible processes have been proposed for the formation of liquid reservoirs that generate Ceres' bright spots: One is remnants of a global subsurface ocean formed in the early history of Ceres (Castillo-Rogez et al, 2018), and the other is impact-induced melting of surface materials in a recent time (Zolotov, 2017). Using thermochemical equilibrium models, Castillo-Rogez et al. (2018) suggest that freezing of an early global ocean on Ceres may not be able to generate salt materials found on bright spots. To account for the abundance and composition of salts on bright spots, Zolotov (2017) suggests extremely high concentrations of dissolved ions in localized liquid reservoirs, possibly generated by re-melting of surface due to a recent impact. These equilibrium models suggest the difficulty to form the salt compositions of the bright spots directly from freezing of an early global ocean. However, Vu et al. (2017) and Thomas et al. (2018) experimentally show the importance of kinetics in salt precipitation from rapidly freezing brine. Thomas et al. (2018) show kinetically preference of precipitation of ammonia-bearing salts upon rapid freezing of Na-NH_4-CO_3-Cl brine despite their thermochemical instability. This implies the disequilibria in salt precipitation may have played a key role to determine the salt composition of bright spots.

In the present study, we compare the results of salt precipitation using thermochemical equilibrium model of FREZCHEM with those formed by rapid freezing in laboratory experiments to evaluate the effects of disequilibria. The starting solutions are prepared based on thermochemical calculations of water-rock reactions within early Ceres. We also measure infrared spectra of the salt precipitates to compare with the observations of bright spots on Ceres.

Keywords: Cryovolcanos, Ceres, Thermochemical equilibrium

©2019. Japan Geoscience Union. All Right Reserved.

[J] Poster | M (Multidisciplinary and Interdisciplinary)：M-IS Intersection

Mon. May 27, 2019 5:15 PM - 6:30 PM JST | Mon. May 27, 2019 8:15 AM - 9:30 AM UTC | Poster Hall International Exhibition Hall8, Makuhari Messe_40

[M-IS23] Planetary Volcanology

convener:Rina Noguchi(Institute of Space and Astronautical Science, Japan Aerospace Exploration Agency), Tomokatsu Morota(Graduate School of Environmental Studies, Nagoya University), Kyoko S. Kataoka(Research Institute for Natural Hazards and Disaster Recovery, Niigata University), Shizuka Otsuki(Research Institute of Earthquake and Volcano Geology, Geological Survey of Japan, Advanced Industrial Science and Technology)

Volcanoes exist on solid planetary surface across the solar system. They tell insight into the interior, and the surface environment when they were formed and subsequent evolution. Recent high-resolution remote sensing data on extraterrestrial body allows us to analyze on outcrop scales. Now we are on the stage to share the research targets beyond fields of general volcanology and planetary science. Because some geomorphological and geological environments
in other planets are similar to those on Earth, research on volcanic geomorphology and geology on Earth will provide good terrestrial analogues to understand planetary volcanology. The aim of this session is to discuss formation history and mechanism of volcanoes across the solar system.

[MIS23-P01] **A possible method of lava flow temperature estimation by lava tube cave of Earth,Moon and Mars**

*Tsutomu Honda[1] (1.Vulcano-speleological Society)

[MIS23-P02] Process of magma eruption on the Moon

*Tomokatsu Morota[1] (1.Graduate School of Environmental Studies, Nagoya University)

[MIS23-P03] Statistical analysis of grain morphology generated under hypervelocity impact experiment as an analog of volcanic explosion

*Rina Noguchi[1], Shizuka Otsuki[2], Ayako I Suzuki, Sunao Hasegawa[1] (1.Institute of Space and Astronautical Science, Japan Aerospace Exploration Agency, 2.Geological Survey of Japan, AIST)

[MIS23-P04] Disequilibrium precipitation of salts during rapid freezing of brine: Implications for cryovolcanisms and formation of sodium carbonate of bright spots on Ceres.

*Masahiro Yoda[1,2], Yasuhito Sekine[2], Shuya Tan[1,2] (1.Department of Earth and Planetary Science, The University of Tokyo, 2.Earth-Life Science Institute, Tokyo Institute of Technology)

A possible method of lava flow temperature estimation by lava tube cave of Earth,Moon and Mars

*Tsutomu Honda[1]

1. Vulcano-speleological Society

[Introduction]In the lava flow of Miharayama of Izu Oshima eruption in 1951, the lava temperature,the lava flow thickness and the flow velocity were directly measured on the site[(1)]. Then, the temperature dependent viscosity coefficient and the yield strength were calculated [(1,2)]. In addition, the temperature dependent surface tension was measured in the laboratory by re-melting the collected sample[(3)]. In 2005, a lava tube cave called Hornito Cave was discovered under the hornito located at the crater edge. The inner and outer structure of the Hornito cave was investigated and lava yield strength and surface tension have been also identified [(4, 5, 6)]. Miharayama Hornito Cave is a representative example where lava temperature, viscosity coefficient, yield value and surface tension are identified. On the other hand, in the universe, vertical holes/pits are found in the lava zone of Moon and Mars and lava tube caves are thought to be present under the vertical hole/pit [(7, 8, 9)]. Based on the example of Mihara yama of Izu Oshima in the Earth, it seems to be possible to identify the lava temperature and viscosity coefficient from lava yield strength and surface tension obtained from lava tube shape and internal structure on the Moon and Mars. It should be considered as an important purpose of future vertical hole/pit exploration.

[Data obtained from Izu Oshima Mihara yama Hornito Cave]For Mihara yama Hornito Cave ,internal observation and the preparation of the survey map of horizontal section and longitudinal section were made [(4)]. Based on the cavity height of the lava tube cave and its slope angle, the lava yield strength f_B is estimated from $f_B = H(\rho g \sin \alpha) / 4$, the flow limitation condition of the Bingham fluid flowing in the inclined circular tube. The obtained lava yield strength was 5000 Pa[(5,6)]. This value is consistent with 4300Pa obtained by field observation of actual lava flow of 1951 of temperature ranging from 1125 to 1038[(2).] From the pitch P of the lava stalactite descending from the ceiling of the cave, the surface tension $\gamma = P^2 g \rho / 4 \pi^2$ is obtained. As the measured pitch is roughly P = 3 to 4 cm, then the surface tension is 600 to 1000 mN / m[(5,6)]. This value is consistent with extrapolated value from the temperature dependent surface tension of Izu Oshima 1951 lava measured by Yokoyama et al.,in his laboratory with the remelted sample[(3)]. This indicates that, if lava tube cave is present. it is possible to estimate the lava temperature of the eruption time, even if lava flow temperature at the past eruption is unknown.

[Application to the Moon,Mars and Future Exploration]

In the vertical hole/pit cross section images of the Moon shown by LRO, the traces such as lava flow layer thickness,lava tube cave height can be seen, so, it seems possible to identify the lava flow temperature using these traces.

For Marius Hills Hole located in the Rille-A, the yield strength can be obtained as 131 Pa from the slope angle with an average lava layer thickness of 6 m and tube cavity height of 18 m[(10)]. If the temperature dependent data of the yield strength is acquired separately, the temperature of the lava flowing through the rill-A can be estimated. Further, if we can find lava stalactite inside of the cave by future moon exploration, the temperature can be identified also by comparing the surface tension obtained from the pitch of the lava stalactite with the temperature dependent surface tension data. The viscosity coefficient can also be fixed by the temperature dependent viscosity coefficient data. Fig.1 shows a concept of estimation.

At the stage where sampling on the Moon and Mars can not be done immediately, the synthetic samples based on the chemical composition will be used to acquire the temperature dependent yield strength and surface tension data.

©2019. Japan Geoscience Union. All Right Reserved.

References:
(1)T. Minakami:Bulltin of the Earthquake Research Institute, University of Tokyo,Vol.29, pp. 487-493, 1951, (2) G. Hulme: Geophys. J. R. astr. Soc. (1974) 39, 361-383, (3) I.Yokoyama et al: Geophysical bulletin of the Hokkaido University, 24: 57-61, 1970, (4) H.Tachihara et al: Volcanic cave survey and observation report of Oshima, Tokyo, Volcanic Cave Society, 2006, (5) T.Honda: V102-001, Japan Earth and Planetary Science Joint Meeting, 2006, (6) T.Honda, et al: AMCS Bulletin 19 / SMES Boletin 7-2006, pp 185-187, Proc.X, XI, XII Internat. Symposia on Vulcanospeleology, 2008, (7) J. Haruyama, et al: Geophysical Research Letters, Vol. 36, L2 1206, 2009,
(8) M.S. Robinson et al:Planetary and Space Science 69, pp 18-27, 2012,
(9) G.E.Cushing, et al: Geophys. Res. Lett., 34, L 17201, 2007,(10) T.Honda: SVC 50-05, Japan Earth and Planetary Science Joint Meeting, 2017

Keywords: lava tube cave, Miharayama hornitocave, lava flow temperature

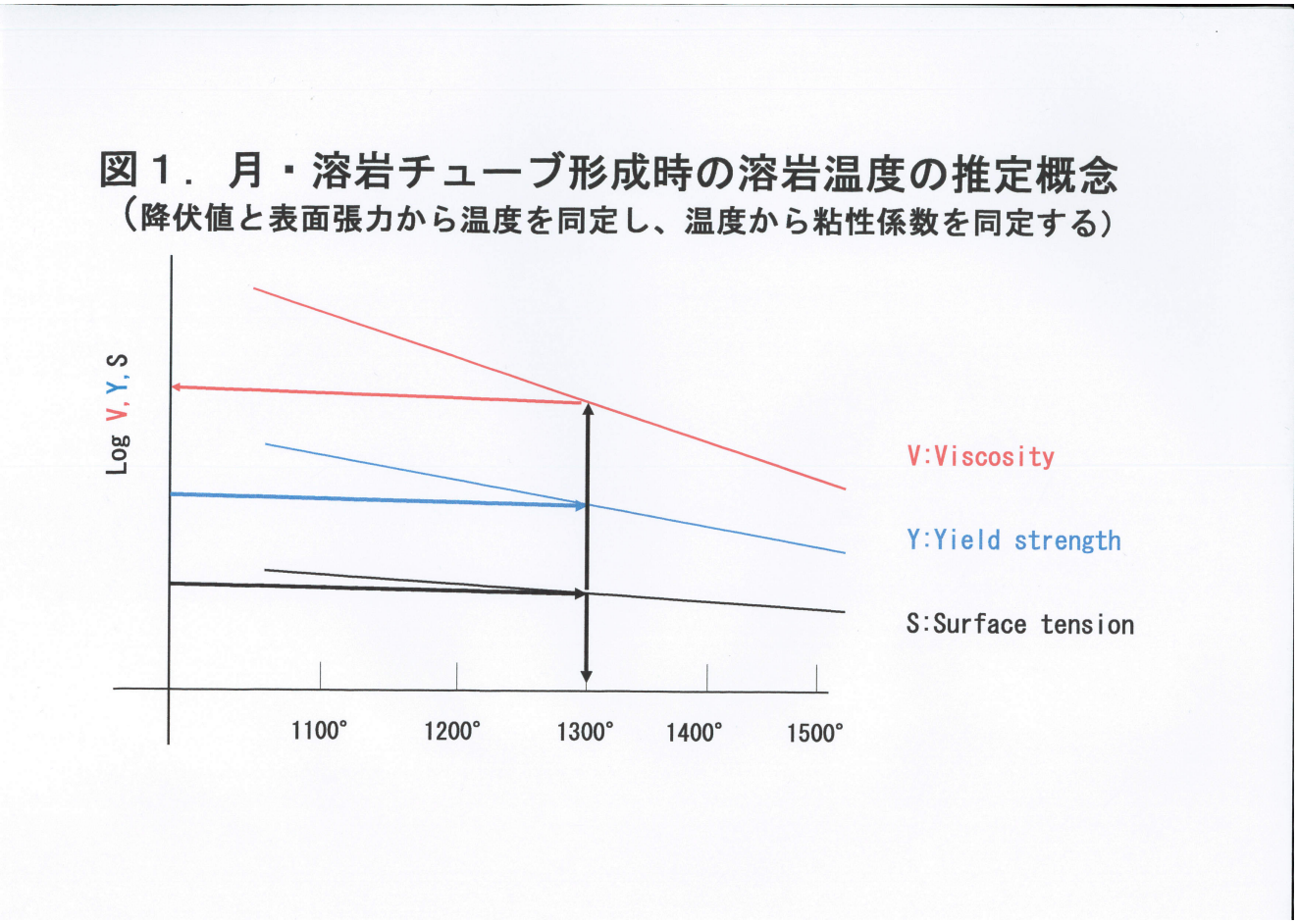

©2019. Japan Geoscience Union. All Right Reserved.

Process of magma eruption on the Moon

*Tomokatsu Morota[1]

1. Graduate School of Environmental Studies, Nagoya University

Estimates for volumes of mare basalts are essential to understand the thermal conditions of the lunar mantle and its lateral heterogeneity. We have investigated the volumes of mare basalts within farside and nearside basins using topographic and multiband image data obtained by SELENE (Kaguya). Furthermore, using the high-resolution crustal thickness model, we investigated the crustal thickness of major impact basins and its relationship with the mare volumes. Based on these results, we discuss the relationship between the mare volumes and the crustal thickness, differences between magma productions in the farside and nearside mantles, and the processes of magma ascent and eruption.

Keywords: Moon, Mare volcanism, Impact basin, Dichotomy, Magma eruption

©2019. Japan Geoscience Union. All Right Reserved.

Statistical analysis of grain morphology generated under hypervelocity impact experiment as an analog of volcanic explosion

*Rina Noguchi[1], Shizuka Otsuki[2], Ayako I Suzuki, Sunao Hasegawa[1]

1. Institute of Space and Astronautical Science, Japan Aerospace Exploration Agency, 2. Geological Survey of Japan, AIST

Natural volcanic ash is formed in several states of magma (i.e., solid or melt) and surrounding conditions (e.g., dry or wet settings). These various factors affect the morphology of ash grain. For example, in a wet setting, moss-like grains are often formed (e.g., Wohletz, 1983). Thus, grain shape of volcanic ash tells us its fragmentation process. This would be useful to estimate eruption mechanism both for on-going and historical eruptions. However, it is difficult to extract the fragmentation mechanism from the grain morphology because of the complex natural system (i.e., not by a single mechanism). Furthermore, manual verification of numbers of ash grains takes a long time and need training. To simplified these issues, we proposed a technique to measure the morphology of volcanic ash grains by using an automatic grain analyzing system (Noguchi et al., in prep.). In this study, we apply the technique to the grains formed by an impact in a laboratory in order to verify the accuracy and applicability of the technique. We used a two-stage light-gas gun in ISAS, JAXA. Grains were collected using a Styrofoam box and segregated with d-limonene. After that, we measured shape parameters and transparency using an automated grain analyzer (Morphologi G3S, Malvern Inst.) of AIST. The measured parameters of grain shape are aspect ratio, high-sensitivity circularity, convexity, and solidity. We also measured transparency of each grain. In this presentation, we show its preliminary result and indicate its applicability to returned sample from other planetary bodies such as Itokawa, Ryugu, and Phobos.

Keywords: Volcanic ash, Impact experiment, grain morphology

©2019. Japan Geoscience Union. All Right Reserved.

Disequilibrium precipitation of salts during rapid freezing of brine: Implications for cryovolcanisms and formation of sodium carbonate of bright spots on Ceres.

*Masahiro Yoda[1,2], Yasuhito Sekine[2], Shuya Tan[1,2]

1. Department of Earth and Planetary Science, The University of Tokyo, 2. Earth-Life Science Institute, Tokyo Institute of Technology

NASA's Dawn spacecraft has found geological evidence for cryovolcanoes on Ceres, the dwarf planet in the main belt. Erupted materials from Ceres' cryovolcanoes are generally bright and distribute locally over Ceres in association with floor-fractured craters and dome-like features, which have young surface ages (e.g., Buczkowski et al, 2016; Ruesch et al, 2016). The bright materials are considered to be composed mainly of sodium carbonate and ammonium salts, which are different from the average crustal compositions (a mixture of magnesium-calcium carbonates and ammonia phyllosilicates) (De Sanctis, 2016; Zambon et al, 2016). The particular compositions of bright materials could provide unique information on the formation and evolution of liquid reservoirs within Ceres.

Two possible processes have been proposed for the formation of liquid reservoirs that generate Ceres' bright spots: One is remnants of a global subsurface ocean formed in the early history of Ceres (Castillo-Rogez et al, 2018), and the other is impact-induced melting of surface materials in a recent time (Zolotov, 2017). Using thermochemical equilibrium models, Castillo-Rogez et al. (2018) suggest that freezing of an early global ocean on Ceres may not be able to generate salt materials found on bright spots. To account for the abundance and composition of salts on bright spots, Zolotov (2017) suggests extremely high concentrations of dissolved ions in localized liquid reservoirs, possibly generated by re-melting of surface due to a recent impact. These equilibrium models suggest the difficulty to form the salt compositions of the bright spots directly from freezing of an early global ocean. However, Vu et al. (2017) and Thomas et al. (2018) experimentally show the importance of kinetics in salt precipitation from rapidly freezing brine. Thomas et al. (2018) show kinetically preference of precipitation of ammonia-bearing salts upon rapid freezing of Na-NH_4-CO_3-Cl brine despite their thermochemical instability. This implies the disequilibria in salt precipitation may have played a key role to determine the salt composition of bright spots.

In the present study, we compare the results of salt precipitation using thermochemical equilibrium model of FREZCHEM with those formed by rapid freezing in laboratory experiments to evaluate the effects of disequilibria. The starting solutions are prepared based on thermochemical calculations of water-rock reactions within early Ceres. We also measure infrared spectra of the salt precipitates to compare with the observations of bright spots on Ceres.

Keywords: Cryovolcanos, Ceres, Thermochemical equilibrium

©2019. Japan Geoscience Union. All Right Reserved.

[J] Oral | M (Multidisciplinary and Interdisciplinary)：M-IS Intersection

Mon. May 27, 2019 1:45 PM - 3:15 PM JST | Mon. May 27, 2019 4:45 AM - 6:15 AM UTC | 201B 2F

[M-IS28] Fluid-sediment migration and geo-bio interaction

convener:Robert Jenkins(School of Geosciences and Civil Engineering, College of Science and Engineering, Kanazawa University), Tomohiro Toki(Faculty of Science, University of the Ryukyus), Akira Ijiri(Japan Agency for Marine-Earth Science and Technology), Takami Nobuhara(Science Education (Geology), Faculty of Education, Shizuoka University), Hiromi Kayama WATANABE(Japan Agency for Marine-Earth Science and Technology), Miho Asada(Japan Agency for Marine-Earth Science and Technology), Chairperson:Tomohiro Toki, Robert Jenkins(Kanazawa University)

Chemosynthetic communities are distributed at hydrothermal system and/or cold seep in bathal zone. They gain their energy from chemosynthetic bacteria, a symbiotic life. The chemosynthetic communities have changed in their taxonomic composition and spatial distribution through the Earth history, but the causes and background remain to be unclear.
Mud volcano is one of geological features which derives fluid nd sediment from depth to the Earth's surface and make topographic feature. It plays a role of carbon cycling connecting depth and surface, pipe of life in depth, disaster and civil engineering. Mechanism and activity of mud volcanoes, however, are not enough understood yet. Mud volcano in Japan is mostly active in offshore fields and are frequently accompanying cold seeps at around it.
Here we propose a joint session with Chemosynthetic communities and Mud volcanoes to have cross-cutting discussion between us. Topics relates to mud volcano will help discussion of evolution of communities and chemosynthetic communities will help to understand mud volcano activity along time and space. Study results for usual two sessions, for cross-cutting discussions, and from related settings are absolutely welcome.

1:45 PM - 2:00 PM JST | 4:45 AM - 5:00 AM UTC

[MIS28-01] Upper Pliocene large lucinid communities with cold-seep carbonates from the Shimajiri Group in the Miyagi-jima Island off the central part of Okinawa-jima Island, Japan

*Takami Nobuhara[1], Robert Jenkins[2], Shin-ichi Nomura[3] (1.Science Education (Geology), Faculty of Education, Shizuoka University, 2.School of Natural System, College of Science and Engineering, Kanazawa University, 3.Chiba Prefectural Kisarazu High School)

2:00 PM - 2:15 PM JST | 5:00 AM - 5:15 AM UTC

[MIS28-02] Chemosynthetic fossil community in Early Cretaceous methane seep from Yubari City, Hokkaido

*Nanami Shimazu[1], Robert Jenkins[1] (1.Kanazawa University)

2:15 PM - 2:30 PM JST | 5:15 AM - 5:30 AM UTC

[MIS28-03] Marine Snow Hypothesis: What is controling faunal composition of the methane-seep since Mesozoic?

*Robert Jenkins[1] (1.School of Geosciences and Civil Engineering, College of Science and Engineering, Kanazawa University)

2:30 PM - 2:45 PM JST | 5:30 AM - 5:45 AM UTC

[MIS28-04] *In situ* Sr isotope analysis of methane-seep carbonates: insight into ancient subseafloor fluid circulation

★Invited Papers

*Yusuke Miyajima[1], Michał Jakubowicz[2,3], Takafumi Hirata[1] (1.Geochemical Research Center, Graduate School of Science, The University of Tokyo, 2.Institute of Geoecology and Geoinformation, Adam Mickiewicz University, Poland, 3.Isotope Laboratory, Adam Mickiewicz University, Poland)

2:45 PM - 3:00 PM JST | 5:45 AM - 6:00 AM UTC

[MIS28-05] Monitoring CH_4 amounts deep inside deep-water mud volcanoes

★Invited Papers

*A. Kioka[1], T. Tsuji[2], H. Otsuka[3], J. Ashi[3] (1.Universität Innsbruck, Austria, 2.Kyushu University, Japan, 3.The University of Tokyo, Japan)

3:00 PM - 3:15 PM JST | 6:00 AM - 6:15 AM UTC

[MIS28-06] Discussion

*Robert Jenkins[1] (1.School of Natural System, College of Science and Engineering, Kanazawa University)

Upper Pliocene large lucinid communities with cold-seep carbonates from the Shimajiri Group in the Miyagi-jima Island off the central part of Okinawa-jima Island, Japan

*Takami Nobuhara[1], Robert Jenkins[2], Shin-ichi Nomura[3]

1. Science Education (Geology), Faculty of Education, Shizuoka University, 2. School of Natural System, College of Science and Engineering, Kanazawa University, 3. Chiba Prefectural Kisarazu High School

Fossil chemosynthetic lucinid communities occur with pipe- and burrow-cemented concretions from the Upper Pliocene muddy sand facies of the Shimajiri Group in the Miyagi-jima Island off the central part of Okinawa-jima Island, Japan. The outcrop is a sea-cliff wall along the west coast of Miyagi-jima Island, over 30 m high and 150 m long. The cliff consists of muddy sandstone sporadically yielding outer-shelf to upper-slope molluscan fossils, with intercalation of thin fine-grained sandstone layers. We could directly observe only the lower one-third of the cliff wall, but the fossil-lucinid occurrence seems to be restricted to about a five-meter thick horizon, which is associated with pipe- and burrow-cemented concretions.

Lucioma taiwanensis is dominant and forms shell beds and autochthonous shell clusters in matrix-supported condition. In addition “*Meganodontia*” sp., a gigantic lucinid over 10 cm in diameter, was obtained as floatstones, but all specimens are conjoined valves and maybe fell out from sites with abundant burrow-cemented concretions.

The burrow-cemented concretions look like calianassid nests in shape, irregularly sinuous to vertical to beddings, a few centimeters in diameter and over 1 m long. They amalgamated one another to form network-like clusters. The pipe concretions tend to be recognized below the network clusters of burrow-cemented types. The pipes are cylindrical and straight over 30 cm long, nearly vertical to beddings. They are composed of core calcitic cements (2 cm in diameter, -10 to -15 ‰of δ^{13}C) and surrounding dolomitic coating (4 to 5 cm thick, -20 to lower -40 ‰of δ^{13}C). The δ^{13}C value less than -30 ‰indicates methane seep influence in the sub-bottom of the lucinid community. The pipe concretions are also often recognized 5 m below the fossil lucinid horizons, which suggest that the pipe-like conduits of methane seep supported the lucinid communities.
The fossils of *Lucinoma taiwanensis* often preserve their life positions in matrices apart from the burrows and pipes. Therefore the methane-seep through focused pipe-like conduit were succeeded by into diffusive in sandy surface sediments. But some *Lucinoma* conjoined valves in life position are attached to outer walls of burrow-cemented concretions, which suggests that the burrows made contributions to promoting anaerobic oxidation of methane (AOM) and generating H_2S.

Keywords: chemosynthesis, cold seepage, Lucinidae, Okinawa, Pliocene

©2019. Japan Geoscience Union. All Right Reserved.

Chemosynthetic fossil community in Early Cretaceous methane seep from Yubari City, Hokkaido

*Nanami Shimazu[1], Robert Jenkins[1]

1. Kanazawa University

Japanese archipelagoes have rich fossil record of the methane-seep communities since the Late Cretaceous, however, the Early Cretaceous record is poorly known. Thus, we have investigated the Early Cretaceous (Albian) carbonate rocks found in Utagoesawa Creek, Yubari City, Hokkaido. The locality was previously mentioned in several papers, but the comprehensive approaches including sedimentary petrological, isotope geochemical and paleontological aspects haven't been done.

Many carbonate boulders were found along the creek and it size distribution along the creek suggest its single origin of outcrop. The carbonate rocks show mosaic textures mainly composed of micritic grayish patchy blocks. Bladed calcite and sparry calcite are filled in void spaces. Detailed observation revealed the micrites and the bladed calcites were precipitated in early diagenetic stages, and its isotopic compositions are -45.8 to -35.8 ‰VPDB for carbon and -25.4 to -17.9 ‰VPDB for oxygen.

The petrological and geochemical features indicate that carbonate rocks were formed under influence anaerobic oxidation of methane(AOM) due to the microbial activity in methane seep.

The carbonate rocks yield many bivalves, such as *Caspiconcha*, lucinids, *Nucinella*, solemyids, and thyasirids, and some hokkaidoconchid species.

Those molluscan species are well known from Cretaceous seeps in the world. No brachiopods were found from the locality. The fossil assemblage indicates that the Utagoesawa seep was fully occupied by chemosynthetic molluscan species whereas the Early Cretaceous seeps in California are characterized to have brachiopods.

Campbell and Bottjer (1995) suggested the faunal composition has been changed mainly from brachiopods to bivalves through transition between Early to Late Cretaceous. The current study indicate the phenomenon occurred only restricted in California.

Keywords: methane seep, Early Cretaceous, Chemosynthetic fossil community

©2019. Japan Geoscience Union. All Right Reserved.

Marine Snow Hypothesis: What is controling faunal composition of the methane-seep since Mesozoic?

*Robert Jenkins[1]

1. School of Geosciences and Civil Engineering, College of Science and Engineering, Kanazawa University

Fossil record of the methane-seep communities shows several interesting phenomena. One of it is the decreasing of epifaunal bivalve/brachiopod in Late Cretaceous. There are several hypotheses, e.g. “sulfate hypothesis” by Kiel (2015), are proposed to explain the situation. Here, I propose another hypothesis to explain the lacking of epifaunal bivalves/brachiopods in the Late Cretaceous. Occurring pattern of epifaunal bivalves/brachiopods through Paleozoic to Neogene is apparently corresponding to the oil resources in sedimentary rocks in each age. The oil production in the sediments are largely related to the primary production in marine, and the origin of methane is ultimately related to the organic matter in the sediment as almost same as oils. The organic matter, deposited on the sea floor, was subsequently used for the generation of methane in the anoxic condition beneath the sea floor after buried. In the case of increasing organic matter settled onto the sea floor, production of methane would be increasing, and if the organic matter decrease, the production rate of methane would be decrease. These methane is energy source for the chemosynthetic community, thus, the primary production rate at the sea surface level by the photosynthesis may control the presence/absence of epifaunal bivalve/brachiopod in seep environment. I coined this hypothesis as 'Marine Snow Hypothesis', because the particulated organic matter sinking to the sea floor is called marine snow.

Keywords: organic flux, methanogenesis, chemosynthetic community

©2019. Japan Geoscience Union. All Right Reserved.

In situ Sr isotope analysis of methane-seep carbonates: insight into ancient subseafloor fluid circulation

*Yusuke Miyajima[1], Michał Jakubowicz[2,3], Takafumi Hirata[1]

1. Geochemical Research Center, Graduate School of Science, The University of Tokyo, 2. Institute of Geoecology and Geoinformation, Adam Mickiewicz University, Poland, 3. Isotope Laboratory, Adam Mickiewicz University, Poland

Along continental margins, tectonic activities trigger subseafloor migration and seepage of geofluids enriched in methane, which sustain chemosynthesis-based biological communities on the seafloor. Depending on their source and migration pathway, seeping fluids have various elemental and isotopic signatures that provide insights into subseafloor fluid–rock interactions and material cycling. At the methane seeps, precipitation of carbonate is induced by microbial oxidation of methane and resultant production of HCO_3^- ions. The methane-seep carbonates record elemental and isotopic signals of seeping fluids in the geological past, and several studies have aimed to decode the origin and migration pathways of ancient seeping fluids using geochemical signatures of the carbonates (e.g., Jakubowicz et al., 2015, 2019).

Strontium isotope ratio ($^{87}Sr/^{86}Sr$) is one of the common tracers of fluid circulation and fluid–rock interactions, and has been applied to seep carbonates (Peckmann et al., 2001; Joseph et al., 2012; Jakubowicz et al., 2019). Methane-seep carbonates are often characterized by complex textures composed mainly of clay- or detritus-rich matrix and detritus-free void cements, the latter of which could archive Sr isotope signals of subsurface fluids distinct from near-seafloor sediments. However, millimeter- or smaller-scale cement phases are difficult to sample using the conventional microdrills without contamination from the matrix. In this study, we applied a high spatial-resolution Sr isotope analysis to cement phases of seep carbonates using laser ablation multiple collector inductively coupled plasma mass spectrometry (LA-MC-ICP-MS), in order to detect “pure” isotope signals of ancient seeping fluids. We measured the Sr isotope ratios in isopachous cements of fossil seep carbonates collected from the Hollard Mound (Middle Devonian, Morocco) and Baška (Lower Cretaceous, Czech Carpathians). Results obtained by LA-MC-ICP-MS were consistent with the isotope ratios measured previously by thermal ionization mass spectrometry coupled with microdrill sampling technique (Jakubowicz et al., 2019). We also tested the method using radial calcite cements of Upper Cretaceous seep carbonates in Hokkaido that are hosted by forearc basin sediments (Yezo Group). The Yezo Group is underlain by Jurassic to Lower Cretaceous mafic basement rocks and input of deep-sourced fluids from the basement rocks could be recorded as ^{87}Sr-depleted signals in the carbonates. Pilot results from one of the Hokkaido seep carbonates, Gakkonosawa, yielded Sr isotope ratios less-radiogenic than those for the coeval seawater, implying deep-fluid input. Exploring the ^{87}Sr-depleted signals at other Cretaceous seeps in Hokkaido would provide more insights into the deep subseafloor fluid circulation in the Cretaceous subduction zone at the eastern margin of the Eurasian Continent.

Keywords: Carbonate, Fluid flow, LA-MC-ICP-MS, Methane seep, Strontium isotopes

©2019. Japan Geoscience Union. All Right Reserved.

Monitoring CH_4 amounts deep inside deep-water mud volcanoes

*A. Kioka[1], T. Tsuji[2], H. Otsuka[3], J. Ashi[3]

1. Universität Innsbruck, Austria, 2. Kyushu University, Japan, 3. The University of Tokyo, Japan

Mud volcanoes are among the largest geological sources releasing CH_4 gas. Numerous studies have revealed their origins and compositions released from submarine mud volcanoes. Yet, quantification of the amount of gas inside submarine mud volcanoes has been challenging due to the difficulty of in situ measurements, which has hampered better evaluation for their contribution to the global methane budget. Here we provide a coupled geochemical and geophysical model that bridges bulk methane concentrations and seismic wave velocities in the mud conduit of submarine mud volcano. This model is applicable to most submarine mud volcanoes, and is able to estimate methane concentration at greater depths where methane hydrate cannot be present, using downhole logging data or seismic data. Our calculation for submarine mud volcanoes in the Eastern Mediterranean and the Nankai plate subduction zones shows that the weight fractions of gaseous and dissolved methane in total weight of sediment are 1,000--3,500 ppm within their mud conduits, which are much higher than previously expected from pore-water evidence from conventional shallow subsurface sampling. Although more definitive calculations cannot be made until the model parameters are better constrained, our approach provides an opportunity for re-estimating the global methane budget in submarine mud volcanoes, shedding new light upon the impact of submarine mud volcanism on carbon cycle.

Keywords: Submarine mud volcanoes, Methane concentration, Gaseous and dissolved methane, Chemical thermodynamics, Rock physics

©2019. Japan Geoscience Union. All Right Reserved.

Discussion

*Robert Jenkins[1]

1. School of Natural System, College of Science and Engineering, Kanazawa University

Discussion

©2019. Japan Geoscience Union. All Right Reserved.

[J] Poster | M (Multidisciplinary and Interdisciplinary)：M-IS Intersection

Mon. May 27, 2019 3:30 PM - 5:00 PM JST | Mon. May 27, 2019 6:30 AM - 8:00 AM UTC | Poster Hall International Exhibition Hall8, Makuhari Messe_26

[M-IS28] Fluid-sediment migration and geo-bio interaction

convener:Robert Jenkins(School of Geosciences and Civil Engineering, College of Science and Engineering, Kanazawa University), Tomohiro Toki(Faculty of Science, University of the Ryukyus), Akira Ijiri(Japan Agency for Marine-Earth Science and Technology), Takami Nobuhara(Science Education (Geology), Faculty of Education, Shizuoka University), Hiromi Kayama WATANABE(Japan Agency for Marine-Earth Science and Technology), Miho Asada(Japan Agency for Marine-Earth Science and Technology)

Chemosynthetic communities are distributed at hydrothermal system and/or cold seep in bathal zone. They gain their energy from chemosynthetic bacteria, a symbiotic life. The chemosynthetic communities have changed in their taxonomic composition and spatial distribution through the Earth history, but the causes and background remain to be unclear.
Mud volcano is one of geological features which derives fluid nd sediment from depth to the Earth's surface and make topographic feature. It plays a role of carbon cycling connecting depth and surface, pipe of life in depth, disaster and civil engineering. Mechanism and activity of mud volcanoes, however, are not enough understood yet. Mud volcano in Japan is mostly active in offshore fields and are frequently accompanying cold seeps at around it.
Here we propose a joint session with Chemosynthetic communities and Mud volcanoes to have cross-cutting discussion between us. Topics relates to mud volcano will help discussion of evolution of communities and chemosynthetic communities will help to understand mud volcano activity along time and space. Study results for usual two sessions, for cross-cutting discussions, and from related settings are absolutely welcome.

[MIS28-P01] An offshore mud volcano that indicates a heterogeneous subseafloor geological environment: a case study along southwest Japan

*Miho Asada[1,2], Kazuya Kitada[2] (1.JSPS Research Fellow, 2.Japan Agency for Marine-Earth Science and Technology)

[MIS28-P02] **New distribution and implication of dispersal capabililty of a deep-sea chemosymbiotic squat lobster *Shinkaia crosnieri***

*Hiromi Kayama WATANABE[1], Chong Chen[1], Tin-Yam Chan[2], Chien-Hui Yang[2], Chu-Chang Wang[3], Satoshi Mitarai[4], Hiroyuki Yamamoto[1] (1.Japan Agency for Marine-Earth Science and Technology (JAMSTEC), 2.National Taiwan Ocean University, 3.Taiwan Ocean Research Institute (TORI), 4.Okinawa Institute of Science and Technology (OIST))

[MIS28-P03] Taxonomy and diet of the *Ophryotrocha* (Annelida: Dorvilleidae) from whale- falls in the Tsukumo Bay, Japan

*Midori Suzuki[1], Robert Gwyn Jenkins[1], Shouzo Ogiso[2], Nobuo Suzuki[3] (1.Division of Environmental Science and Engineering, Graduate School of Natural Science and Technology, Kanazawa University, 2.Kanazawa university, 3.Institute of Nature and Environmental Technology, Kanazawa university)

An offshore mud volcano that indicates a heterogeneous subseafloor geological environment: a case study along southwest Japan

*Miho Asada[1,2], Kazuya Kitada[2]

1. JSPS Research Fellow, 2. Japan Agency for Marine-Earth Science and Technology

Mud volcanoes (MVs) are geological features that derive fluids and sediments from the depth to surface. Offshore MVs require continuous mud emission to maintain the shape on the seafloor against erosion (Kopf, 2002). Brown and Orange (1993) mentioned that gas is required for sediments moving up from the deep. These necessary conditions for the existence of mud volcanoes restrict the subseafloor environment beneath MV fields.

In Japan, MVs are found both on land and in offshore areas (e.g., Tajika et al., 2009; Kuramoto et al., 2001). A forearc basin, the Kumano Basin, which is bordered by the Nankai Trough along its southern edge, is a representative MV field in Japan. There are at least 14 MVs in the basin (Kuramoto et al., 2001; Morita et al., 2004; Pape et al., 2014; Asada et al., 2017). The recent morphological changes in an MV and the emission of gas bubbles from the top of the MV were discovered through acoustic investigations in the Kumano Basin in 2016 (Menapase et al., 2017), which implies that these MVs actively emit fluid and sediment on the seafloor. Additionally, a group of offshore MVs is known in the off-Tanegashima area in the southeastern part of the Kyusyu Island (Kitada et al., 2018). There are at least 14 MVs, and life moved from the MV to the seawater (Hoshino et al., 2017). Moreover, several MVs have been reported in the off-Miyazaki area of the eastern Kyusyu Island. The Hyuga-nada area, a northeastern part of the Kyusyu Island, probably holds other MVs that exhibit similar bathymetric and acoustic (backscatter) characteristics as MVs in the Kumano Basin and the off-Tanegashima areas. Only one MV candidate feature and the hardened seafloor around it have been recognized in the off-Shikoku Island; however, there are no more MVs in the area. These results indicate that there are discontinuous MV fields along southwest Japan, and there is a vast MV field over the eastern offshore area of Kyusyu Island. This indicates a heterogeneous subseafloor environment in these areas.

Within what type of subseafloor environment can MVs exist? Maintaining a continuous emission of fluid and sediment on the seafloor may restrict the subseafloor environment.
1. A budget of “fluidized mud” or continuous production of “fluidized mud” should exist under the seafloor.
- Large amounts of seawater are trapped when deposits are buried without being drained.
- Dehydration owing to clay minerals collapses the mud rock to form fluidized mud.
- Gathering fluids come along the strata and/or fault to collapse mud rock and make fluidized mud.
2. Gas is required for making intrusions, which can be a root of MVs.
- Sediment can yield enough thermogenic and/or biogenic gas.
- There is an environment for collecting enough fluid coming through the strata and/or fault.
3. Both gas and fluidized mud under the seafloor can be the origin of MVs on the seafloor. Only one of them may not lead to MVs.

The subseafloor temperature of the accretionary prism of the Kumano Basin (e.g., Marcaillow et al., 2012) satisfies the condition for the dehydration of clay minerals. The dehydration may cause the collapse of mud rock, yielding fluidized mud. Gas generation causes sediment intrusion. This fluid may flow along the strata and fault and gather together to cause MVs. As with Hyuga-nada/off-Tanegashima area, there is a

©2019. Japan Geoscience Union. All Right Reserved.

business gas field along the eastern coast of Kyusyu Island, and it may affect the area. However, in the off-Shikoku area, there is not enough subseafloor environment to generate gas and fluidized mud; this may be affected by the high-temperature subduction of the ancient plate-spreading axis in the Shikoku Basin. This subseafloor heterogeneity may be related to other geological phenomena, such as the patchy distribution of the seismogenic zone.

Keywords: Mud Volcano, offshore area along SW Japan, subseafloor environment

©2019. Japan Geoscience Union. All Right Reserved.

New distribution and implication of dispersal capabililty of a deep-sea chemosymbiotic squat lobster *Shinkaia crosnieri*

*Hiromi Kayama WATANABE[1], Chong Chen[1], Tin-Yam Chan[2], Chien-Hui Yang[2], Chu-Chang Wang[3], Satoshi Mitarai[4], Hiroyuki Yamamoto[1]

1. Japan Agency for Marine-Earth Science and Technology (JAMSTEC), 2. National Taiwan Ocean University, 3. Taiwan Ocean Research Institute (TORI), 4. Okinawa Institute of Science and Technology (OIST)

Distribution range and dispersal capability are important for conservation and understanding changing ocean. A galatheid squat lobster, *Shinkaia crosnieri*, is the dominant animas harboring epibiotic symbionts, in methane-rich deep-sea chemosynthetic environments both of hydrothermal vent and methane seep in the northwestern Pacific. Here we report that a juvenile of *S. crosnieri* inhabits in methane-poor hydrothermal vent field in the northwestern Pacific, with juveniles of another squat lobster species *Munidopsis myojinensis*, which does not have symbiontic microbes. Genetic analysis inferred that the juvenile seemed to migrate from the population in methane seep sites in South China Sea, rather than those in hydrothermal vent fields in Okinawa Trough, East China Sea. The present observation indicates that the range of dispersal of *S. crosnieri* extend north to the Myojin Knoll, while the dispersal capability is not simply correlate to horizontal distance. Furthermore, the present findings may suggest that the settlement of the vent/seep specific animal with symbionts are controlled by phylogenetic constraints rather than environmental specific factors.

Keywords: Chemosynthesis-based ecosystem, symbiotic bacteria

©2019. Japan Geoscience Union. All Right Reserved.

Taxonomy and diet of the *Ophryotrocha* (Annelida: Dorvilleidae) from whale- falls in the Tsukumo Bay, Japan

*Midori Suzuki[1], Robert Gwyn Jenkins[1], Shouzo Ogiso[2], Nobuo Suzuki[3]

1. Division of Environmental Science and Engineering, Graduate School of Natural Science and Technology, Kanazawa University, 2. Kanazawa university, 3. Institute of Nature and Environmental Technology, Kanazawa university

Decomposition of large organic-falls, e. g. sunken whale carcasses is a part of nutrient cycle (Smith et al., 2015). The decomposition is performed by not only microbes but also some animals, e. g. the polychaetes. Some polychaetes can be found from inside of decaying bone, however, roles of the polychaetes animals are poorly understood. We examined the organic carbon isotope ratio and DNA(COI) of polychaete *Ophryotrocha* (Annelida: Dorvilleidae), a species lived in the whale bone deployed in the Tsukumo Bay. They are exposed to stress in the form of high levels of hydrogen sulfide but have successfully invaded into the bone. Morphological observation revealed the species is mainly characterized by shape of jaw and we considered as new species. Phylogenetic analyses based on COI suggest that they have independently invaded into whale falls, hydrothermal vent and methane seep from normal environment for each taxon group. The examined *Ophryotrocha* sp. had the broadest $\delta^{13}C$ range (-33.8‰~-19.0‰) among other species lived on/in the bones. It indicates that some of them fed on bacterial mat such as *Beggiatoa* sp. (-37.2‰~-28.5‰) but some of them don’t. These results highlight the role of *Ophryotrocha* has diverse food source, and it would be an advantage to adapt various “extreme environment” such as vent, seep, and whale falls.

Keywords: whale-falls, Dorvilleidae, Chemosynthesis

©2019. Japan Geoscience Union. All Right Reserved.

[J] Poster | M (Multidisciplinary and Interdisciplinary)：M-IS Intersection

Mon. May 27, 2019 5:15 PM - 6:30 PM JST | Mon. May 27, 2019 8:15 AM - 9:30 AM UTC | Poster Hall International Exhibition Hall8, Makuhari Messe_41

[M-IS28] Fluid-sediment migration and geo-bio interaction

convener:Robert Jenkins(School of Geosciences and Civil Engineering, College of Science and Engineering, Kanazawa University), Tomohiro Toki(Faculty of Science, University of the Ryukyus), Akira Ijiri(Japan Agency for Marine-Earth Science and Technology), Takami Nobuhara(Science Education (Geology), Faculty of Education, Shizuoka University), Hiromi Kayama WATANABE(Japan Agency for Marine-Earth Science and Technology), Miho Asada(Japan Agency for Marine-Earth Science and Technology)

Chemosynthetic communities are distributed at hydrothermal system and/or cold seep in bathal zone. They gain their energy from chemosynthetic bacteria, a symbiotic life. The chemosynthetic communities have changed in their taxonomic composition and spatial distribution through the Earth history, but the causes and background remain to be unclear.
Mud volcano is one of geological features which derives fluid nd sediment from depth to the Earth's surface and make topographic feature. It plays a role of carbon cycling connecting depth and surface, pipe of life in depth, disaster and civil engineering. Mechanism and activity of mud volcanoes, however, are not enough understood yet. Mud volcano in Japan is mostly active in offshore fields and are frequently accompanying cold seeps at around it.
Here we propose a joint session with Chemosynthetic communities and Mud volcanoes to have cross-cutting discussion between us. Topics relates to mud volcano will help discussion of evolution of communities and chemosynthetic communities will help to understand mud volcano activity along time and space. Study results for usual two sessions, for cross-cutting discussions, and from related settings are absolutely welcome.

[MIS28-P01] An offshore mud volcano that indicates a heterogeneous subseafloor geological environment: a case study along southwest Japan

*Miho Asada[1,2], Kazuya Kitada[2] (1.JSPS Research Fellow, 2.Japan Agency for Marine-Earth Science and Technology)

[MIS28-P02] **New distribution and implication of dispersal capabililty of a deep-sea chemosymbiotic squat lobster *Shinkaia crosnieri***

*Hiromi Kayama WATANABE[1], Chong Chen[1], Tin-Yam Chan[2], Chien-Hui Yang[2], Chu-Chang Wang[3], Satoshi Mitarai[4], Hiroyuki Yamamoto[1] (1.Japan Agency for Marine-Earth Science and Technology (JAMSTEC), 2.National Taiwan Ocean University, 3.Taiwan Ocean Research Institute (TORI), 4.Okinawa Institute of Science and Technology (OIST))

[MIS28-P03] Taxonomy and diet of the *Ophryotrocha* (Annelida: Dorvilleidae) from whale- falls in the Tsukumo Bay, Japan

*Midori Suzuki[1], Robert Gwyn Jenkins[1], Shouzo Ogiso[2], Nobuo Suzuki[3] (1.Division of Environmental Science and Engineering, Graduate School of Natural Science and Technology, Kanazawa University, 2.Kanazawa university, 3.Institute of Nature and Environmental Technology, Kanazawa university)

An offshore mud volcano that indicates a heterogeneous subseafloor geological environment: a case study along southwest Japan

*Miho Asada[1,2], Kazuya Kitada[2]

1. JSPS Research Fellow, 2. Japan Agency for Marine-Earth Science and Technology

Mud volcanoes (MVs) are geological features that derive fluids and sediments from the depth to surface. Offshore MVs require continuous mud emission to maintain the shape on the seafloor against erosion (Kopf, 2002). Brown and Orange (1993) mentioned that gas is required for sediments moving up from the deep. These necessary conditions for the existence of mud volcanoes restrict the subseafloor environment beneath MV fields.

In Japan, MVs are found both on land and in offshore areas (e.g., Tajika et al., 2009; Kuramoto et al., 2001). A forearc basin, the Kumano Basin, which is bordered by the Nankai Trough along its southern edge, is a representative MV field in Japan. There are at least 14 MVs in the basin (Kuramoto et al., 2001; Morita et al., 2004; Pape et al., 2014; Asada et al., 2017). The recent morphological changes in an MV and the emission of gas bubbles from the top of the MV were discovered through acoustic investigations in the Kumano Basin in 2016 (Menapase et al., 2017), which implies that these MVs actively emit fluid and sediment on the seafloor. Additionally, a group of offshore MVs is known in the off-Tanegashima area in the southeastern part of the Kyusyu Island (Kitada et al., 2018). There are at least 14 MVs, and life moved from the MV to the seawater (Hoshino et al., 2017). Moreover, several MVs have been reported in the off-Miyazaki area of the eastern Kyusyu Island. The Hyuga-nada area, a northeastern part of the Kyusyu Island, probably holds other MVs that exhibit similar bathymetric and acoustic (backscatter) characteristics as MVs in the Kumano Basin and the off-Tanegashima areas. Only one MV candidate feature and the hardened seafloor around it have been recognized in the off-Shikoku Island; however, there are no more MVs in the area. These results indicate that there are discontinuous MV fields along southwest Japan, and there is a vast MV field over the eastern offshore area of Kyusyu Island. This indicates a heterogeneous subseafloor environment in these areas.

Within what type of subseafloor environment can MVs exist? Maintaining a continuous emission of fluid and sediment on the seafloor may restrict the subseafloor environment.
1. A budget of “fluidized mud” or continuous production of “fluidized mud” should exist under the seafloor.
- Large amounts of seawater are trapped when deposits are buried without being drained.
- Dehydration owing to clay minerals collapses the mud rock to form fluidized mud.
- Gathering fluids come along the strata and/or fault to collapse mud rock and make fluidized mud.
2. Gas is required for making intrusions, which can be a root of MVs.
- Sediment can yield enough thermogenic and/or biogenic gas.
- There is an environment for collecting enough fluid coming through the strata and/or fault.
3. Both gas and fluidized mud under the seafloor can be the origin of MVs on the seafloor. Only one of them may not lead to MVs.

The subseafloor temperature of the accretionary prism of the Kumano Basin (e.g., Marcaillow et al., 2012) satisfies the condition for the dehydration of clay minerals. The dehydration may cause the collapse of mud rock, yielding fluidized mud. Gas generation causes sediment intrusion. This fluid may flow along the strata and fault and gather together to cause MVs. As with Hyuga-nada/off-Tanegashima area, there is a

©2019. Japan Geoscience Union. All Right Reserved.

business gas field along the eastern coast of Kyusyu Island, and it may affect the area. However, in the off-Shikoku area, there is not enough subseafloor environment to generate gas and fluidized mud; this may be affected by the high-temperature subduction of the ancient plate-spreading axis in the Shikoku Basin. This subseafloor heterogeneity may be related to other geological phenomena, such as the patchy distribution of the seismogenic zone.

Keywords: Mud Volcano, offshore area along SW Japan, subseafloor environment

©2019. Japan Geoscience Union. All Right Reserved.

New distribution and implication of dispersal capabililty of a deep-sea chemosymbiotic squat lobster *Shinkaia crosnieri*

*Hiromi Kayama WATANABE[1], Chong Chen[1], Tin-Yam Chan[2], Chien-Hui Yang[2], Chu-Chang Wang[3], Satoshi Mitarai[4], Hiroyuki Yamamoto[1]

1. Japan Agency for Marine-Earth Science and Technology (JAMSTEC), 2. National Taiwan Ocean University, 3. Taiwan Ocean Research Institute (TORI), 4. Okinawa Institute of Science and Technology (OIST)

Distribution range and dispersal capability are important for conservation and understanding changing ocean. A galatheid squat lobster, *Shinkaia crosnieri*, is the dominant animas harboring epibiotic symbionts, in methane-rich deep-sea chemosynthetic environments both of hydrothermal vent and methane seep in the northwestern Pacific. Here we report that a juvenile of *S. crosnieri* inhabits in methane-poor hydrothermal vent field in the northwestern Pacific, with juveniles of another squat lobster species *Munidopsis myojinensis*, which does not have symbiontic microbes. Genetic analysis inferred that the juvenile seemed to migrate from the population in methane seep sites in South China Sea, rather than those in hydrothermal vent fields in Okinawa Trough, East China Sea. The present observation indicates that the range of dispersal of *S. crosnieri* extend north to the Myojin Knoll, while the dispersal capability is not simply correlate to horizontal distance. Furthermore, the present findings may suggest that the settlement of the vent/seep specific animal with symbionts are controlled by phylogenetic constraints rather than environmental specific factors.

Keywords: Chemosynthesis-based ecosystem, symbiotic bacteria

©2019. Japan Geoscience Union. All Right Reserved.

Taxonomy and diet of the *Ophryotrocha* (Annelida: Dorvilleidae) from whale- falls in the Tsukumo Bay, Japan

*Midori Suzuki[1], Robert Gwyn Jenkins[1], Shouzo Ogiso[2], Nobuo Suzuki[3]

1. Division of Environmental Science and Engineering, Graduate School of Natural Science and Technology, Kanazawa University, 2. Kanazawa university, 3. Institute of Nature and Environmental Technology, Kanazawa university

Decomposition of large organic-falls, e. g. sunken whale carcasses is a part of nutrient cycle (Smith et al., 2015). The decomposition is performed by not only microbes but also some animals, e. g. the polychaetes. Some polychaetes can be found from inside of decaying bone, however, roles of the polychaetes animals are poorly understood. We examined the organic carbon isotope ratio and DNA(COI) of polychaete *Ophryotrocha* (Annelida: Dorvilleidae), a species lived in the whale bone deployed in the Tsukumo Bay. They are exposed to stress in the form of high levels of hydrogen sulfide but have successfully invaded into the bone. Morphological observation revealed the species is mainly characterized by shape of jaw and we considered as new species. Phylogenetic analyses based on COI suggest that they have independently invaded into whale falls, hydrothermal vent and methane seep from normal environment for each taxon group. The examined *Ophryotrocha* sp. had the broadest $\delta^{13}C$ range (-33.8‰~-19.0‰) among other species lived on/in the bones. It indicates that some of them fed on bacterial mat such as *Beggiatoa* sp. (-37.2‰~-28.5‰) but some of them don’t. These results highlight the role of *Ophryotrocha* has diverse food source, and it would be an advantage to adapt various “extreme environment” such as vent, seep, and whale falls.

Keywords: whale-falls, Dorvilleidae, Chemosynthesis

©2019. Japan Geoscience Union. All Right Reserved.

[J] Oral | M (Multidisciplinary and Interdisciplinary)：M-GI General Geosciences, Information Geosciences & Simulations

Mon. May 27, 2019 10:45 AM - 12:15 PM JST | Mon. May 27, 2019 1:45 AM - 3:15 AM UTC | A08 TOKYO BAY MAKUHARI HALL

[M-GI33] Data-driven geosciences

convener:Tatsu Kuwatani(Japan Agency for Marine-Earth Science and Technology), Hiromichi Nagao(Earthquake Research Institute, The University of Tokyo), Kenta Ueki(Japan Agency for Marine-Earth Science and Technology), Masayuki Kano(Graduate school of science, Tohoku University), Chairperson:Kenta Ueki, Masayuki Kano(東北大学 大学院理学研究科 地球物理学専攻)

It is important to extract essential processes and structures from observed data sets in order to understand and predict the dynamic behavior of the earth and planetary systems. Recently, many powerful methodologies have been proposed to extract useful information from high-dimensional data sets in information sciences. This session aims to provide an opportunity to gather various geoscientists to have a productive discussion for interdisciplinary collaborations.

10:45 AM - 11:15 AM JST | 1:45 AM - 2:15 AM UTC

[MGI33-01] Forecasting volcanic eruption sequence based on field data and physical models

★Invited Papers

*Takehiro Koyaguchi[1], Kensuke Ishii[2], Kyle R. Anderson[3], Tomofumi Kozono[4] (1.Earthquake Research Institute, University of Tokyo, 2.Meteorological Research Institute, 3.US Geological Survey, 4.Graduate School of Science, Tohoku University)

11:15 AM - 11:30 AM JST | 2:15 AM - 2:30 AM UTC

[MGI33-02] Sparse modeling based feature selection of magmatic tectonic settings

*Kenta Ueki[1], Hideitsu Hino[2], Tatsu Kuwatani[1,3] (1.Japan Agency for Marine-Earth Science and Technology, 2.The Institute of Statistical Mathematics, 3.Japan Science and Technology Agency)

11:30 AM - 11:45 AM JST | 2:30 AM - 2:45 AM UTC

[MGI33-03] Automatic Detection of Stationary Gravity Waves in the Venus' Atmosphere Using Deep Generative Models

*Minori Narita[1], Daiki Kimura[2], Atsushi Yamazaki[3], Takeshi Imamura[1] (1.The University of Tokyo, 2.IBM Research AI, 3.ISAS/JAXA)

11:45 AM - 12:00 PM JST | 2:45 AM - 3:00 AM UTC

[MGI33-04] Fracture and mineral distribution analysis using hyper-resolution DEM and hyperspectral satellite imagery for detecting geothermal fluids paths

*Taiki Kubo[1], Hiroaki Gonnokami[1], Arie Naftali Hawu Hede[2], Mohamad Nur Heriawan[2], Irwan Iskandar[2], Katsuaki Koike[1], Sudarto Notosiswoyo[2] (1.Graduate School of Engineering, Kyoto University, 2.Bandung Institute of Technology)

12:00 PM - 12:15 PM JST | 3:00 AM - 3:15 AM UTC

[MGI33-05] **Geochemical characterization of deep-sea sediments in the western North Pacific Ocean by an integrated multivariate statistical technique**

*Kazutaka Yasukawa[1,2], Kentaro Nakamura[1], Koichiro Fujinaga[2,1], Hikaru Iwamori[3,4], Yasuhiro Kato[1,2] (1.School of Engineering, The University of Tokyo, 2.Ocean Resources Research Center for Next Generation, Chiba Institute of Technology, 3.Earthquake Research Institute, The University of Tokyo, 4.Department of Earth and Planetary Sciences, Tokyo Institute of Technology)

Forecasting volcanic eruption sequence based on field data and physical models

*Takehiro Koyaguchi[1], Kensuke Ishii[2], Kyle R. Anderson[3], Tomofumi Kozono[4]

1. Earthquake Research Institute, University of Tokyo, 2. Meteorological Research Institute, 3. US Geological Survey, 4. Graduate School of Science, Tohoku University

Volcanic eruptions often continue for more than a few months or years; the intensity and the style of eruptions remarkably change with time. It is, therefore, desired to forecast such eruption sequences on the basis of field observations during the eruptions. For this purpose, the basic idea of data assimilation is useful. The data assimilation is composed of two mathematical problems: forecasting the system evolution based on forward physical models and determining the model parameters based on inversion analyses of field observations. We are interested in how the mathematical characteristics of the forward models for volcanic eruptions affect those of their inversion problems. In this presentation, we focus on two problems: (1) the estimation of model parameters of magma plumbing system from field observations of magma discharge rate and ground deformation, and (2) the estimation of magma discharge rate of explosive eruptions from tephra-fall deposits.

The inversion problem of magma plumbing system

The eruption sequence is characterized by the evolution of magma discharge rate (Q) and chamber pressure (P) during eruption. To describe the evolution of Q and P, we formulated a model of magma plumbing system composed of a conduit and a magma chamber in elastic rocks. In this model, the effects of gas-exsolution and gas-escape on conduit flow are considered, which leads to complex features of volcanic eruptions such as a transition from a lava-dome forming eruption to an explosive eruption. The eruption style (i.e., evolution of Q and P) is sensitively dependent on model parameters related to geological and petrological conditions (e.g., volume and depth of magma chamber and magma properties). To forecast the eruption sequence, these model parameters need to be estimated from time-varying observations of Q and P through an inverse analysis.

Generally, because of the strong non-linearity of the conduit-flow model, it is mathematically and computationally difficult to investigate the influence of each observation on the estimation of the model parameters. We express the trade-off relationship between the model parameters utilizing analytical solutions of the conduit-flow model (e.g., Koyaguchi, 2005; Kozono and Koyaguchi, 2009), and show that the key parameters that affect the time evolution of P and Q are fundamentally different between explosive and effusive eruptions. Because of this difference, model parameters constrained from the observations of Q and P also depend on whether the eruption is effusive or explosive.

The inversion problem of tephra dispersion

The estimation of magma discharge rate (i.e., Q) is one of the key issues for forecasting volcanic eruption sequence. For explosive eruptions, the value of Q can be estimated from observations of tephra dispersion. The forward model of tephra dispersion is composed of the eruption column dynamics model and the advection-diffusion model. The former describes the supply rate of tephra particles from an eruption column just above the volcano as a function of altitude (referred to as the supply rate function). The latter describes the transportation of tephra particles from the source (i.e., the eruption column just

©2019. Japan Geoscience Union. All Right Reserved.

above the volcano) to the ground surface.
The above two models have distinct features in the inversion problem. The singular value decomposition (SVD) analysis indicate that the inverse problems of the advection-diffusion model is highly ill-conditioned so that the number of basis functions expressing the supply rate function is limited regardless of the number of data of tephra-fall deposits. On the other hand, the eruption column model indicates that the form of the supply rate function is strongly correlated with the eruption conditions such as Q. We, therefore, attempt to develop a method to estimate the value of Q from the supply rate function expressed by the limited number of basis functions. Some preliminary results on this problem will be presented.

Keywords: volcanic eruption, data assimilation, conduit flow model, tephra dispersal model

©2019. Japan Geoscience Union. All Right Reserved.

Sparse modeling based feature selection of magmatic tectonic settings

*Kenta Ueki[1], Hideitsu Hino[2], Tatsu Kuwatani[1,3]

1. Japan Agency for Marine-Earth Science and Technology, 2. The Institute of Statistical Mathematics, 3. Japan Science and Technology Agency

Understanding the magma generation processes and characteristic end-members in various tectonic settings is fundamental to understand the material circulation and compositional evolution of the solid Earth. Recent studies based on a machine learning approach revealed that volcanic rocks formed in different tectonic settings have unique geochemical signatures, indicating that both volcanic rock geochemistry and magma generation processes are closely connected to the tectonic setting. We present a result of a feature selection where sparse modeling approach is used. Sparse modeling is an approach in which automatically selects the smallest number of essential variables from high-dimensional data and constructs a succinct model. We used 24 elements and five isotopic ratios of igneous rocks formed in eight different tectonic settings for the feature selection of the settings. In addition to the major and trace element concentrations and isotopic ratios, we also considered combinations of elements, i.e., sum or ratio between two different elements, for the feature selection. This study uses sparse multinomial regression (SMR) approaches for feature selection. Multinomial regression is the classical linear discrimination method. Using the multinomial regression with the sparse modeling approach, a small number of essential geochemical information of tectonic settings are extracted. Based on the automatically selected features, we will discuss the geodynamical and geochemical process to derive various magmas and tectonics.

Keywords: Machine learning, Magma generation, Tectonic setting, Geochemical data

©2019. Japan Geoscience Union. All Right Reserved.

Automatic Detection of Stationary Gravity Waves in the Venus' Atmosphere Using Deep Generative Models

*Minori Narita[1], Daiki Kimura[2], Atsushi Yamazaki[3], Takeshi Imamura[1]

1. The University of Tokyo, 2. IBM Research AI, 3. ISAS/JAXA

Venus is covered with thick clouds of sulfuric acid, and the entire upper atmosphere rotates much faster than the planet itself. Recently, interhemispheric large bow-shaped structures, remaining fixed above the highland in contrast to background wind fields, were observed in long-infrared and ultraviolet images by Venus Orbiter Akatsuki. These bow-shaped structures are said to be the result of atmospheric gravity waves generated in the lower atmosphere and propagate upwards to the cloud top, which has a significant influence on the Venus' atmospheric system. Not a few bow-shaped, stationary features indicative of topographic gravity waves have been reported so far. However, to unravel where and when these structures appear frequently, we need to analyze the phenomena comprehensively, using much more data. Detection of such characteristic cloud features in images has been done by human eye in Venus research, but to detect many more cases efficiently from massive amounts of image data, we need a framework to do it automatically and robustly. Moreover, most of the bow-shaped structures in ultraviolet images are small, which is almost impossible to find out every case by our eyes.

In this study, we propose a novel approach that detects these stationary features using a deep generative model that has deep neural networks (deep learning). There are various types of such deep models nowadays; we used a variational auto-encoder (VAE) because it has reported good results in dimensionality reduction fields and been a well-known method for image reconstruction. The input and the output of VAE are set to be the same, and the network is divided into two parts, which are the encoder that converts an image to latent representation, and the decoder that reconstructs an image from given latent variables. The detection of stationary features can be seen as an anomaly detection task, which treats images that have stationary features as the anomaly class and the normal cloud image as the normal class.

We used ultraviolet (283 nm) images for this analysis. Firstly, we performed photometric correction using Minnaert Law, and averaged several images taken successively in 24 hours to highlight structures that remains still. Then we extracted features that have scales smaller than 6 degrees by high-pass filtering. Lastly, we extracted image patches from these images. Each patch has the size of 24 degrees both in latitude and longitude. We used images taken in 25 days in 2016 and 2017.

The analysis procedure is as follows. First, we train this network using only normal cloud images that do not include stationary features to let it learn its latent features. When testing, we input test images composed of both normal and anomaly (stationary feature) images, and detect anomalies based on the reconstruction loss that is calculated by the sum of the pixel-wise distance between the original image and the reconstructed image that is output from the last layer in the network. The network has five convolutional layers in the encoder and the decoder, respectively. The latent space has 32 dimensions. We used 4,000 normal cloud images as the training data, and 1,000 normal and 255 anomaly images as the test data.

We evaluated our method by calculating the area under the curve (AUC) of the receiver operating characteristic (ROC) curve. As a result, the AUC was 0.93 (maximum is 1.00), which shows that the

©2019. Japan Geoscience Union. All Right Reserved.

proposed method successfully detects stationary features. The reconstruction error of a stationary structure image is large because the network cannot reconstruct such bow-shaped structure properly. Our method can be easily applied not only to Venus but also various planetary images to detect characteristic structures.

Keywords: Venus, Deep Learning, Generative Model, Anomaly Detection, Image

©2019. Japan Geoscience Union. All Right Reserved.

Fracture and mineral distribution analysis using hyper-resolution DEM and hyperspectral satellite imagery for detecting geothermal fluids paths

*Taiki Kubo[1], Hiroaki Gonnokami[1], Arie Naftali Hawu Hede[2], Mohamad Nur Heriawan[2], Irwan Iskandar[2], Katsuaki Koike[1], Sudarto Notosiswoyo[2]

1. Graduate School of Engineering, Kyoto University, 2. Bandung Institute of Technology

From criteria of power output and temporal stability, geothermal is the most promising renewable energy for electrical generation. However, high introduction cost for geothermal power generation, in particular the cost for exploration to identify the geothermal reservoir is a main issue against the plan. Development of more accurate geothermal-resource exploration is necessary for enhancement of geothermal energy use. Detection of geothermal fluids paths including water and steam from geothermal reservoir is a major target in the exploration stage. Topographic analysis is one of the effective methods for the detection. Thus, we have generated a hyper-resolution DEM (HR-DEM) of the Wayang Windu Geothermal Field (WWGF), situated in West Java, Indonesia using UAV. HR-DEM with high spatial resolution (0.5 m) covers an area of 5 km (E–W) by 10 km (N–S) in WWGF. The lineament density map of WWGF was produced by a topographic analysis through HR-DEM. Moreover, spatial distributions of geothermal alteration minerals such as alunite, calcite, and kaolinite were mapped from an image processing of hyperspectral satellite image, Hyperion. A combination of the lineament and mineral distributions specified highly permeable zones in which the fractures and geothermal alteration minerals were concentrated. The location of high igh radon concentration by in-situ measurements correspond well with these estimated permeable zones. Therefore, the integrated analysis is expected to increase the identification accuracy of fluid paths and clarify the geothermal system in WWGF. This research is supported by JST and JICA through Science and Technology Research Partnership for Sustainable Development (SATREPS).

Keywords: alteration mineral, digital elevation model, geothermal reservoir, hyperspectral satellite image, lineament

©2019. Japan Geoscience Union. All Right Reserved.

Geochemical characterization of deep-sea sediments in the western North Pacific Ocean by an integrated multivariate statistical technique

*Kazutaka Yasukawa[1,2], Kentaro Nakamura[1], Koichiro Fujinaga[2,1], Hikaru Iwamori[3,4], Yasuhiro Kato[1,2]

1. School of Engineering, The University of Tokyo, 2. Ocean Resources Research Center for Next Generation, Chiba Institute of Technology, 3. Earthquake Research Institute, The University of Tokyo, 4. Department of Earth and Planetary Sciences, Tokyo Institute of Technology

Recently, deep-sea sediments highly enriched in rare-earth elements and yttrium (REY) were discovered within the Japanese exclusive economic zone (EEZ) surrounding Minamitorishima Island [1]. To clarify the distribution of the “extremely REY-rich mud”, eight research cruises (KR13-02, MR13-E02, KR14-02, MR14-E02, MR15-E01 Leg2, MR15-02, MR16-07, and KM17-14C) have collected 71 sediment core samples in total from 2013 to 2018. Now we have constructed a comprehensive dataset of major- and trace-element contents of 1,646 samples by X-ray fluorescence and inductively coupled plasma mass spectrometry analyses [1-8].

Here, in order to depict geochemical features of the deep-sea sediments including the extremely REY-rich mud, we applied an integrated method of k-means cluster analysis (KCA) and independent component analysis (ICA) [9] to the huge (1,646 samples x 41 elements) dataset of the deep-sea sediments in and out of the Minamitorishima EEZ. We demonstrate that the data clusters are distributed not randomly but systematically in the real space; the clusters are vertically aligned from the seafloor to depth in a specific order and thus constitute stratigraphic units defined by geochemical features. In addition, the downhole variation of an extracted independent component (IC) shows a stepwise transition across the extremely REY-enriched layer. This transition is ubiquitous in the studied area of several-hundred-kilometer wide. The geochemical clusters just below the IC transition are variable among the cores, which implies that the IC transition corresponds to an unconformity in the sediment column probably due to erosion [5, 6]. These characteristics of the spatial distributions of the geochemical clusters and ICs support a hypothesis previously proposed by Ohta et al. [10]: an enhanced bottom current caused a physical separation of sedimentary particles, or a winnowing effect, and contributed to form the extremely REY-enriched layer by a selective deposition of relatively coarse and dense grains of biogenic Ca-phosphate that significantly accumulate REY from ambient seawater.

[1] Iijima, K. et al., Geochemical Journal 50, 557-573 (2016). [2] Fujinaga, K. et al., Geochemical Journal 50, 575-590 (2016). [3] Takaya, Y. et al. Scientific Reports 8, 5763 (2018). [4] Yasukawa, K. et al., Ore Geology Reviews 102, 260-267 (2018). [5] Yasukawa, K. et al., under review. [6] Tanaka, E. et al., under review. [7] Fujinaga, K. et al., JpGU2018 SCG61-04. [8] Fujinaga, K. et al., JpGU2019. [9] Iwamori, H. et al., Geochemistry, Geophysics, Geosystems 18, 994-1012 (2017). [10] Ohta, J. et al., Geochemical Journal 50, 591-603 (2016).

Keywords: deep-sea sediment, multivariate analysis, independent component analysis, k-means cluster analysis, REY-rich mud, bulk chemical composition

©2019. Japan Geoscience Union. All Right Reserved.

[J] Poster | M (Multidisciplinary and Interdisciplinary)：M-GI General Geosciences, Information Geosciences & Simulations

Mon. May 27, 2019 1:45 PM - 3:15 PM JST | Mon. May 27, 2019 4:45 AM - 6:15 AM UTC | Poster Hall International Exhibition Hall8, Makuhari Messe_9

[M-GI33] Data-driven geosciences

convener:Tatsu Kuwatani(Japan Agency for Marine-Earth Science and Technology), Hiromichi Nagao(Earthquake Research Institute, The University of Tokyo), Kenta Ueki(Japan Agency for Marine-Earth Science and Technology), Masayuki Kano(Graduate school of science, Tohoku University)

It is important to extract essential processes and structures from observed data sets in order to understand and predict the dynamic behavior of the earth and planetary systems. Recently, many powerful methodologies have been proposed to extract useful information from high-dimensional data sets in information sciences. This session aims to provide an opportunity to gather various geoscientists to have a productive discussion for interdisciplinary collaborations.

[MGI33-P01] The geochemical database “DODAI” with high-precision location coordinates

*Satoru Haraguchi[1], Kenta Ueki[1], Kenta Yoshida[1], Tatsu Kuwatani[1,3], Mika Mohamed[1], Hikaru Iwamori[1,2,4] (1.Japan Agency for Marine-Earth Science and Technology, 2.Earthquake Research Insititute, the University of Tokyo, 3.PRESTO, 4.Tokyo Institute of Technology)

[MGI33-P02] Bayesian statistical evaluation method for detrital zircon geochronology

*Tan Furukawa[1], Tatsuki Tsujimori[1] (1.Tohoku University)

[MGI33-P03] Geochemical data processing using machine learning with artificial training data and proposal of environmental evaluation method considering natural background of heavy metals in river water in mining area

*Satoh Kenta[1], Kengo Sawayama[1], Noriyoshi Tsuchiya[1] (1.graduate school of environmental studies, Tohoku University)

[MGI33-P04] Quantitative Logging Unit Classification with Hidden Markov Model

*Suguru Yabe[1], Rina Fukuchi[2], Kenta Ueki[1], Yohei Hamada[1] (1.Japan Agency for Marine-Earth Science and Technology, 2.UTokyo AORI)

[MGI33-P05] Sparse Modeling of Nonlinear Dynamics in Heterogeneous Reactions

*Masaki Ito[1], Tatsu Kuwatani[2], Ryosuke Oyanagi[2], Toshiaki Omori[1] (1.Kobe University, 2.JAMSTEC)

[MGI33-P06] How to obtain a high-SNR EPMA map?: complementary roles of high-resolution imaging and subsequent binning

*Atsushi Yasumoto[1], Kenta Yoshida[2] (1.Hiruzen Institute of Geology and Chronlogy, 2.Japan Agency for Marine-earth Science and Technology)

[MGI33-P07] Data-driven estimation of material transfer from bulk compositions

*Tatsu Kuwatani[1,2], Kenta Yoshida[1], Kenta Ueki[1], Ryosuke Oyanagi[1], Masaoki Uno[3], Shotaro Akaho[4] (1.Japan Agency for Marine-Earth Science and Technology, 2.Japan Science and Technology Agency, 3.Graduate School of Environmental Studies, Tohoku University, 4.National Institute of Advanced Industrial Science and Technology)

The geochemical database “DODAI” with high-precision location coordinates

*Satoru Haraguchi[1], Kenta Ueki[1], Kenta Yoshida[1], Tatsu Kuwatani[1,3], Mika Mohamed[1], Hikaru Iwamori[1,2,4]

1. Japan Agency for Marine-Earth Science and Technology, 2. Earthquake Research Insititute, the University of Tokyo, 3. PRESTO, 4. Tokyo Institute of Technology

We constructed the geochemical database “DODAI” which compiled data published in the domestic journals and bulletins, and published its details recently (Haraguchi et al., 2018, J. Geol. Soc. Japan, doi: 10.5575/geosoc.2018.0027). This database has converted the sampling position of individual geochemical data into the GPS-familiar location coordinates, i.e. latitude and longitude, by image-based geocoding and improved the positional accuracy drastically compared to the previous databases.

There are some international databases of geochemical data, for example: "GEOROC" mainly involving land samples, "PetDB" mainly involving samples from seafloor. Recent progress on the data-driven science shed a light on a large number of sample data with a multitude of variables. As for heterogeneity of the mantle compositions (e.g. Iwamori et al, 2018), the world-wide scale of the geochemical structure are discussed on the basis of such databases. However, considerable number of data in these international databases provided the location coordinates only as the representative position of the geologic map of the original articles, and thus the resolution of these location data often can represent only the order of degree unit. This precision may have no problem for the discussion of world-wide scale, while interpretation in the detailed spatial scale may not be possible. The precision of location data in the “DODAI” is mostly less than 1 km, some of which have < 10m of errors, based on the spatial resolution of the map provided in the original articles. This precision allows us to correlate sample positions to the correct geological units described in the digital geologic map such as the Seamless Geological Map (AIST). We also defined a standard data format based on the metadata available in the compiled papers covering such as geographical information, sampling, and analytical methods.
In this presentation, we will show the concept and details of DODAI dataset, and discuss the potential of data-driven analysis in the geochemical study.

Keywords: geochemical database, geocoding, normalization of format

©2019. Japan Geoscience Union. All Right Reserved.

Bayesian statistical evaluation method for detrital zircon geochronology

*Tan Furukawa[1], Tatsuki Tsujimori[1]

1. Tohoku University

Over the past two decades, detrital zircon U-Pb geochronology has become an essential method not only in sedimentary provenance analyses but also in characterization of sedimentary and metamorphic strata. Although the age data has been conventionally evaluated by using relative frequency plots (here after called histograms) and density curves, the lack of statistical verification can cause miss reading of data. In order to overcome the statistical issues raised, this study proposes new statistical evaluation method for detrital zircon geochronology.
The new method is based on Bayesian statistics, adapted a theory proposed by Riihimäki and Vehtari (2014) that provides a flexible modeling for density curve using the Logistic Gaussian Process (LGP)
For introducing non-negative consistency for density curve, the logistic density transformation is performed by $p(x)=\exp(f(x))/\int\exp(f(\mathbf{s}))d\mathbf{s}$; x is age, p(x) is density curve, and f(x) is Gaussian Process; $f(x)\sim GP(0, \kappa(x,x'))$. The covariance matrix $\kappa(x,x')$ is calculated by Gaussian kernel with hyperparameters ρ and σ. For the actual computation, the logistic density transformation has integral difficulties, then, M discretized softmax function is used for approximation for it.
The likelihood function is $L(\mathbf{p}|\rho,\sigma)=\mathbf{y}^{T}\mathbf{p}$. $\mathbf{p}$ is M discretized p(x), and $\mathbf{y}$ is vector of y_i, which is the number of observations that fall within the i'th M discretized age subregion.
We have used programming language R and Stan for the MCMC computation of the statistical model above. When the number of detrital zircon data is several hundred or less, the hyperparameters of Gaussian process ρ and σ do not converge, and Bayesian estimation can not be performed. For this reason, the author estimated most plausible ρ and σ by WAIC. Using zircon data from our own data and the literature, in this presentation, we will demonstrate powerfulness of our new statistical evaluation.

Keywords: Bayesian statistics, detrital zircon geochronology, MCMC algorithm

©2019. Japan Geoscience Union. All Right Reserved.

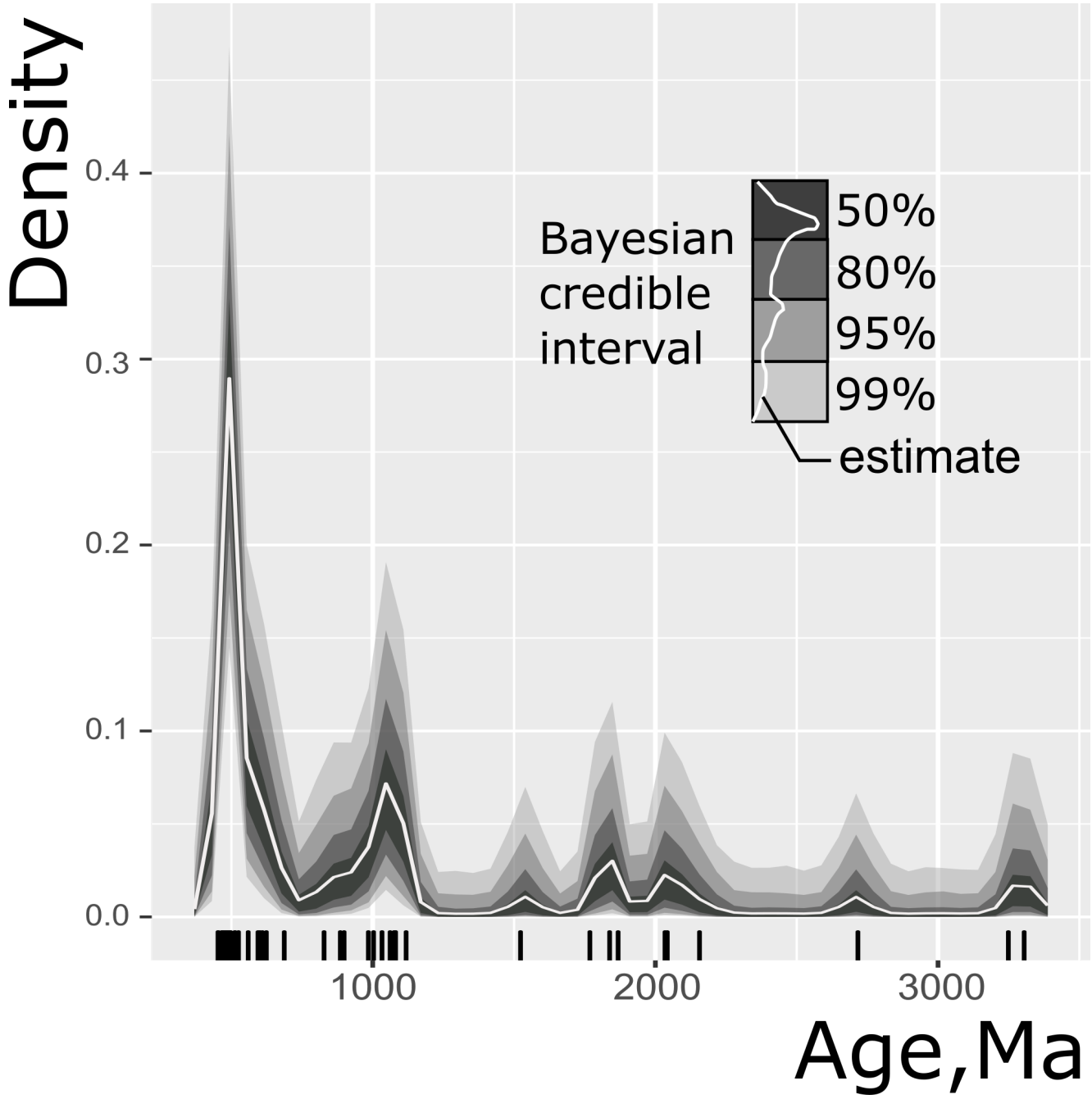

©2019. Japan Geoscience Union. All Right Reserved.

Geochemical data processing using machine learning with artificial training data and proposal of environmental evaluation method considering natural background of heavy metals in river water in mining area

*Satoh Kenta[1], Kengo Sawayama[1], Noriyoshi Tsuchiya[1]

1. graduate school of environmental studies, Tohoku University

Acid mining drainage is one of the most important sources of heavy metals in river. Environmental standards are evaluated by the effects on the Ecosystem and human body. However, the current environmental standards do not consider natural background of heavy metals, therefore the method which can evaluate the effects on the environment concerning such heavy metals is needed. Then we propose to apply machine learning to evaluation effects by heavy metals. Using natural soil data and mineral data as training data in machine learning, it will become possible to evaluate the effects concerning heavy metals naturally included in soil. However, it is very important to choose the proper training data set in machine learning. In this study, we created training data artificially. If it can be done that Verifying correctness of this artificial training data, the range of application of machine learning expands. The objective of this study is, firstly, to verify the validity of artificial training data through case study, secondly, to establish the method to evaluate effects on the environment by heavy metals considering natural background of heavy metals. Focusing on the mine area where there are effects by heavy metals has already been confirmed, we digitized the effects by mine as the evaluation score by heavy metals using Support Vector Regression (SVR) and using the element content ratio as attribute. The element content ratio of mine was used as the ore training data and the element content ratio of the area surrounding the mine was used as the training data representing heavy metals naturally included in soil. We created data of the ore training data based on literature data about the mine. Furthermore, we verified validity of the artificial data through comparing three digitized assessment of contamination by the statistical method in the area, by the previous research, and by machine learning. As a result, the evaluation score by each method increased at the same point, and it is verified that the evaluation by machine learning using artificial training data is correct. If we use machine learning using artificial training data, it may improve further development of machine learning in the geochemical data set.

Keywords: environmental evaluation, sediment, heavy metals

©2019. Japan Geoscience Union. All Right Reserved.

Quantitative Logging Unit Classification with Hidden Markov Model

*Suguru Yabe[1], Rina Fukuchi[2], Kenta Ueki[1], Yohei Hamada[1]

1. Japan Agency for Marine-Earth Science and Technology, 2. UTokyo AORI

International Ocean Discovery Program (IODP) Expeditions have drilled ocean floor to address cores and well logging data for various purposes. Expedition scientists usually define logging units by characterizing logging data, and interpret their geological meaning. Unit classifications and their geological interpretations will be useful to understand the geological formation at the drilling site. The criteria to define such the units are described in the expedition report, which is usually based on the average, the minimum, and the maximum value of logging data. However, there is no mathematical background to support the validity of unit characterization. The motivation of this study is to develop the quantitative method for log unit definition, and to find out overshadowed log-characteristics for detailed geological interpretation.

This study used Hidden Markov Model (HMM) to classify logging data into logging units. HMM is a stochastic model to classify sequential data. In HMM, each sequential step has the unobservable parameter “state”, which corresponds to the logging unit in this case. As the transition probability of the state depends on the state at previous sequential step, HMM considers Markov process. Observable data (logging data in this case) is generated stochastically following the probability distributions defined by the state at each sequential step. Transition probability of the state and data generation probability distributions for each state are parameters to be estimated. We estimated those parameters with Expectation-Maximization (EM) algorithm.

We applied HMM to four drilling sites around Japan. Two sites are located at Nankai subduction zones. In Southwest Japan, Nankai Trough Seismogenic Zone Experiment (NanTroSEIZE) project conducted a series of IODP expeditions, and large amounts of cores and well-logging data have been acquired. Among these expeditions, we used logging data from Holes C0001D and C0004B drilled during IODP Expedition 314. The other two sites are located at Japan Trench. Hole C0019B was drilled during IODP Expedition 343 as Japan Trench Fast Drilling (JFAST) project. Hole C0020A was drilled during IODP Expedition 337 as Deep Coalbed Biosphere off Shimokita. We selected in-situ electric resistivity, gamma ray, and sonic velocity (P- and S- wave) for the analysis.

For each data set, we tested the number of clusters in HMM from two to nine. We compare our results with the logging unit reported by Expedition scientists. Unit classifications with our method are usually consistent with those by Expedition scientists. However, we observed some differences or finer division of units as well. We discuss the geological meaning of our results.

Keywords: Hidden Markov Model, Clustering, Ocean Drilling Science

©2019. Japan Geoscience Union. All Right Reserved.

Sparse Modeling of Nonlinear Dynamics in Heterogeneous Reactions

*Masaki Ito[1], Tatsu Kuwatani[2], Ryosuke Oyanagi[2], Toshiaki Omori[1]

1. Kobe University, 2. JAMSTEC

Surface heterogeneous reactions are chemical reactions with conjugation of multiple phases, and they have the intrinsic nonlinearity of their dynamics caused by the effect of surface-area between different phases. We propose a sparse modeling approach for extracting nonlinear dynamics of surface heterogeneous reactions from sparse and noisy observable data. We employ sparse modeling algorithm and sequential Monte Carlo algorithm to partial observation problem, in order to simultaneously extract substantial reaction terms and surface models from a number of candidates. Using our proposed method, we show that the rate constants of dissolution and precipitation reactions, which are typical examples of surface heterogeneous reactions, necessary surface models and reaction terms underlying observable data were successfully estimated only from the observable temporal changes in the concentration of the dissolved intermediate product.

Keywords: Heterogeneous Reactions, Sparse Modeling, Nonlinear Dynamics

©2019. Japan Geoscience Union. All Right Reserved.

How to obtain a high-SNR EPMA map?: complementary roles of high-resolution imaging and subsequent binning

*Atsushi Yasumoto[1], Kenta Yoshida[2]

1. Hiruzen Institute of Geology and Chronlogy, 2. Japan Agency for Marine-earth Science and Technology

Chemical imaging is a common technique to analyze heterogeneous materials. For example in petrology, X-ray mapping with an electron probe microanalyzer (EPMA) visualizes chemical heterogeneities (so-called texture) in rocks. X-ray mapping measures signals of X-rays, and higher signal-to-noise ratio (SNR) improves clarity of heterogeneities, which is generally achieved by increasing probe current and/or dwell time of pixels (e.g., Hiroi et al., 1997). An appropriate probe current is determined by sample damages, upper limits of the detectors, and dead time. Dwell time is also determined by sample damages and available analysis time. To acquire a high-SNR image at a reasonable time, reducing total number of pixels is one plausible solution; however, spatial resolution shall become low. To overcome this trade-off, this study proposes a complementary use of short dwell time mapping and subsequent binning. The short dwell time mapping generates high-spatial-resolution and low-SNR images for observing fine textures, and the binning treatment converts the raw maps to low-spatial-resolution and high-SNR images for detecting small differences in chemistry. This approach is applicable to any imaging techniques, including EPMA, which count signals under a given dwell time.

Chemical imaging records counts of signals from multiple points, typically as orthogonal pixels. If expected counting rates are fixed for pixels, observed counts follow Poisson distribution. In EPMA mapping, this assumption is valid because counting rates of X-rays depend mostly on (1) chemistry and surface conditions of materials which are constant; and (2) on probe current, accelerating voltage, and sensitivity of detectors which are controlled by analysts. According to the reproducibility of Poisson distribution, an expected counting rate of a certain signal from a large pixel is identical to an arithmetic-mean of counting rates of the signal from pixels dividing the large pixel. In other word, a sum of counts from n-by-n pixels in m seconds each is equivalent to measuring a large pixel composed of the n-by-n pixels in mn^2 seconds. A simulation is performed on a 300-by-300 matrix of Mandelbrot set. Expected counts per second is set to squares of Mandelbrot set timed by 20. Then, a 300-by-300 map with 1 second of dwell time, and a 150-by-150 map with 4 seconds of dwell time are generated by Poisson random numbers. The 300-by-300 map has higher spatial resolutions and lower-SNR than the 150-by-150 maps. Let’s consider a binning treatment of the 300-by-300 map, i.e. combining signal intensity of each 2-by-2 pixels into one superpixel. The binned 150-by-150 map is apparently comparable to the native 150-by-150 map. This means that high-SNR (low-resolution) image can be generated subsequently from high-resolution (low-SNR) image at an arbitrary degree, if necessary. A recommended binning method is sum rather than arithmetic mean so that binned values can be modeled with Poisson distributions. For example, if a pixel value is generated by Poisson distribution, its standard deviation can be approximated as square root of the pixel value.

The proposed approach has advantages in statistical analysis dealing with mapping data. For example, cluster analysis on a map classifies pixels into a given number of groups based on similarity of pixel values. Performance of cluster analysis, such as precision and smoothness, may improve by obtaining high-SNR of pixels through binning which separates signal peaks representing different groups. Note that benefit of sum as a binning method appears in cluster analysis because Poisson-distribution-based clustering algorithm (Witten, 2011) is applicable. If pixel values follow Poisson distributions, this algorism is more

©2019. Japan Geoscience Union. All Right Reserved.

appropriate and provides better performance than k-means cluster algorism (MacQueen, 1967) which is a simple and common algorism used in variety of fields (Yasumoto et al. 2018).

Keywords: EPMA, mapping, SNR, spatial resolution

©2019. Japan Geoscience Union. All Right Reserved.

Data-driven estimation of material transfer from bulk compositions

*Tatsu Kuwatani[1,2], Kenta Yoshida[1], Kenta Ueki[1], Ryosuke Oyanagi[1], Masaoki Uno[3], Shotaro Akaho[4]

1. Japan Agency for Marine-Earth Science and Technology, 2. Japan Science and Technology Agency, 3. Graduate School of Environmental Studies, Tohoku University, 4. National Institute of Advanced Industrial Science and Technology

Material transfer of elements is the most important consequences of geological processes. However, it is difficult to estimate it, even if both compositional datasets of before and after are available. This is because the compositional data are not absolute data but relative ratio data. Isocon analysis has been widely applied as a simple and powerful standard tool for quantitative estimation of material transfer to various geoscientific problems. Despite its powerfulness, the method needs to assume the reference frame such as immobile elements or conservation of mass or volume, which relies on the researchers' intuition and experience. We propose a novel data-driven method which determines an appropriate reference frame from compositional data of multiple altered samples. In the proposed method, we use a mathematical framework, called sparse modeling, which can extract essential variables from high-dimensional datasets based on sparsity of the system. By optimizing the evaluation function, the least mobile elements are automatically selected. In this study, the effectiveness is validated and discussed using synthetic and natural sample data. The method seems to be a practical tool for estimate material transfer and it has the potential to be improved for particular problems due to its simple and flexible formulation.

Keywords: isocon, sparse modeling

©2019. Japan Geoscience Union. All Right Reserved.

[J] Poster | M (Multidisciplinary and Interdisciplinary)：M-GI General Geosciences, Information Geosciences & Simulations

Mon. May 27, 2019 5:15 PM - 6:30 PM JST | Mon. May 27, 2019 8:15 AM - 9:30 AM UTC | Poster Hall International Exhibition Hall8, Makuhari Messe_42

[M-GI33] Data-driven geosciences

convener:Tatsu Kuwatani(Japan Agency for Marine-Earth Science and Technology), Hiromichi Nagao(Earthquake Research Institute, The University of Tokyo), Kenta Ueki(Japan Agency for Marine-Earth Science and Technology), Masayuki Kano(Graduate school of science, Tohoku University)

It is important to extract essential processes and structures from observed data sets in order to understand and predict the dynamic behavior of the earth and planetary systems. Recently, many powerful methodologies have been proposed to extract useful information from high-dimensional data sets in information sciences. This session aims to provide an opportunity to gather various geoscientists to have a productive discussion for interdisciplinary collaborations.

[MGI33-P01] The geochemical database “DODAI” with high-precision location coordinates

*Satoru Haraguchi[1], Kenta Ueki[1], Kenta Yoshida[1], Tatsu Kuwatani[1,3], Mika Mohamed[1], Hikaru Iwamori[1,2,4] (1.Japan Agency for Marine-Earth Science and Technology, 2.Earthquake Research Insititute, the University of Tokyo, 3.PRESTO, 4.Tokyo Institute of Technology)

[MGI33-P02] Bayesian statistical evaluation method for detrital zircon geochronology

*Tan Furukawa[1], Tatsuki Tsujimori[1] (1.Tohoku University)

[MGI33-P03] Geochemical data processing using machine learning with artificial training data and proposal of environmental evaluation method considering natural background of heavy metals in river water in mining area

*Satoh Kenta[1], Kengo Sawayama[1], Noriyoshi Tsuchiya[1] (1.graduate school of environmental studies, Tohoku University)

[MGI33-P04] Quantitative Logging Unit Classification with Hidden Markov Model

*Suguru Yabe[1], Rina Fukuchi[2], Kenta Ueki[1], Yohei Hamada[1] (1.Japan Agency for Marine-Earth Science and Technology, 2.UTokyo AORI)

[MGI33-P05] Sparse Modeling of Nonlinear Dynamics in Heterogeneous Reactions

*Masaki Ito[1], Tatsu Kuwatani[2], Ryosuke Oyanagi[2], Toshiaki Omori[1] (1.Kobe University, 2.JAMSTEC)

[MGI33-P06] How to obtain a high-SNR EPMA map?: complementary roles of high-resolution imaging and subsequent binning

*Atsushi Yasumoto[1], Kenta Yoshida[2] (1.Hiruzen Institute of Geology and Chronlogy, 2.Japan Agency for Marine-earth Science and Technology)

[MGI33-P07] Data-driven estimation of material transfer from bulk compositions

*Tatsu Kuwatani[1,2], Kenta Yoshida[1], Kenta Ueki[1], Ryosuke Oyanagi[1], Masaoki Uno[3], Shotaro Akaho[4] (1.Japan Agency for Marine-Earth Science and Technology, 2.Japan Science and Technology Agency, 3.Graduate School of Environmental Studies, Tohoku University, 4.National Institute of Advanced Industrial Science and Technology)

The geochemical database “DODAI” with high-precision location coordinates

*Satoru Haraguchi[1], Kenta Ueki[1], Kenta Yoshida[1], Tatsu Kuwatani[1,3], Mika Mohamed[1], Hikaru Iwamori[1,2,4]

1. Japan Agency for Marine-Earth Science and Technology, 2. Earthquake Research Insititute, the University of Tokyo, 3. PRESTO, 4. Tokyo Institute of Technology

We constructed the geochemical database “DODAI” which compiled data published in the domestic journals and bulletins, and published its details recently (Haraguchi et al., 2018, J. Geol. Soc. Japan, doi: 10.5575/geosoc.2018.0027). This database has converted the sampling position of individual geochemical data into the GPS-familiar location coordinates, i.e. latitude and longitude, by image-based geocoding and improved the positional accuracy drastically compared to the previous databases.

There are some international databases of geochemical data, for example: "GEOROC" mainly involving land samples, "PetDB" mainly involving samples from seafloor. Recent progress on the data-driven science shed a light on a large number of sample data with a multitude of variables. As for heterogeneity of the mantle compositions (e.g. Iwamori et al, 2018), the world-wide scale of the geochemical structure are discussed on the basis of such databases. However, considerable number of data in these international databases provided the location coordinates only as the representative position of the geologic map of the original articles, and thus the resolution of these location data often can represent only the order of degree unit. This precision may have no problem for the discussion of world-wide scale, while interpretation in the detailed spatial scale may not be possible. The precision of location data in the “DODAI” is mostly less than 1 km, some of which have < 10m of errors, based on the spatial resolution of the map provided in the original articles. This precision allows us to correlate sample positions to the correct geological units described in the digital geologic map such as the Seamless Geological Map (AIST). We also defined a standard data format based on the metadata available in the compiled papers covering such as geographical information, sampling, and analytical methods.
In this presentation, we will show the concept and details of DODAI dataset, and discuss the potential of data-driven analysis in the geochemical study.

Keywords: geochemical database, geocoding, normalization of format

©2019. Japan Geoscience Union. All Right Reserved.

Bayesian statistical evaluation method for detrital zircon geochronology

*Tan Furukawa[1], Tatsuki Tsujimori[1]

1. Tohoku University

Over the past two decades, detrital zircon U-Pb geochronology has become an essential method not only in sedimentary provenance analyses but also in characterization of sedimentary and metamorphic strata. Although the age data has been conventionally evaluated by using relative frequency plots (here after called histograms) and density curves, the lack of statistical verification can cause miss reading of data. In order to overcome the statistical issues raised, this study proposes new statistical evaluation method for detrital zircon geochronology.
The new method is based on Bayesian statistics, adapted a theory proposed by Riihimäki and Vehtari (2014) that provides a flexible modeling for density curve using the Logistic Gaussian Process (LGP)
For introducing non-negative consistency for density curve, the logistic density transformation is performed by $p(x)=\exp(f(x))/\int\exp(f(\mathbf{s}))d\mathbf{s}$; x is age, p(x) is density curve, and f(x) is Gaussian Process; $f(x)\sim GP(0, \kappa(x,x'))$. The covariance matrix $\kappa(x,x')$ is calculated by Gaussian kernel with hyperparameters ρ and σ. For the actual computation, the logistic density transformation has integral difficulties, then, M discretized softmax function is used for approximation for it.
The likelihood function is $L(\mathbf{p}|\rho,\sigma)=\mathbf{y}^{T}\mathbf{p}$. $\mathbf{p}$ is M discretized p(x), and $\mathbf{y}$ is vector of y_i, which is the number of observations that fall within the i'th M discretized age subregion.
We have used programming language R and Stan for the MCMC computation of the statistical model above. When the number of detrital zircon data is several hundred or less, the hyperparameters of Gaussian process ρ and σ do not converge, and Bayesian estimation can not be performed. For this reason, the author estimated most plausible ρ and σ by WAIC. Using zircon data from our own data and the literature, in this presentation, we will demonstrate powerfulness of our new statistical evaluation.

Keywords: Bayesian statistics, detrital zircon geochronology, MCMC algorithm

©2019. Japan Geoscience Union. All Right Reserved.

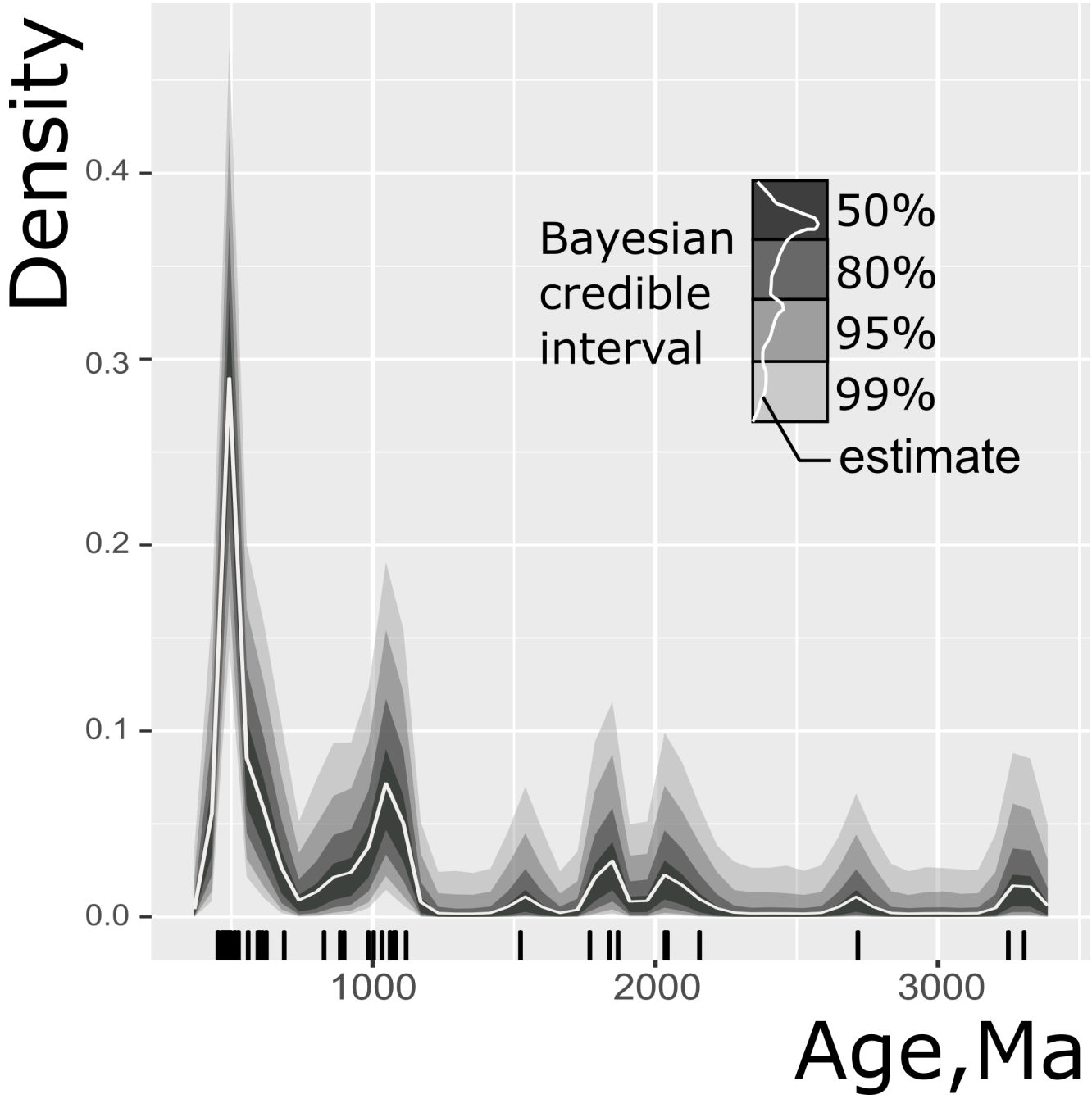

©2019. Japan Geoscience Union. All Right Reserved.

Geochemical data processing using machine learning with artificial training data and proposal of environmental evaluation method considering natural background of heavy metals in river water in mining area

*Satoh Kenta[1], Kengo Sawayama[1], Noriyoshi Tsuchiya[1]

1. graduate school of environmental studies, Tohoku University

Acid mining drainage is one of the most important sources of heavy metals in river. Environmental standards are evaluated by the effects on the Ecosystem and human body. However, the current environmental standards do not consider natural background of heavy metals, therefore the method which can evaluate the effects on the environment concerning such heavy metals is needed. Then we propose to apply machine learning to evaluation effects by heavy metals. Using natural soil data and mineral data as training data in machine learning, it will become possible to evaluate the effects concerning heavy metals naturally included in soil. However, it is very important to choose the proper training data set in machine learning. In this study, we created training data artificially. If it can be done that Verifying correctness of this artificial training data, the range of application of machine learning expands. The objective of this study is, firstly, to verify the validity of artificial training data through case study, secondly, to establish the method to evaluate effects on the environment by heavy metals considering natural background of heavy metals. Focusing on the mine area where there are effects by heavy metals has already been confirmed, we digitized the effects by mine as the evaluation score by heavy metals using Support Vector Regression (SVR) and using the element content ratio as attribute. The element content ratio of mine was used as the ore training data and the element content ratio of the area surrounding the mine was used as the training data representing heavy metals naturally included in soil. We created data of the ore training data based on literature data about the mine. Furthermore, we verified validity of the artificial data through comparing three digitized assessment of contamination by the statistical method in the area, by the previous research, and by machine learning. As a result, the evaluation score by each method increased at the same point, and it is verified that the evaluation by machine learning using artificial training data is correct. If we use machine learning using artificial training data, it may improve further development of machine learning in the geochemical data set.

Keywords: environmental evaluation, sediment, heavy metals

©2019. Japan Geoscience Union. All Right Reserved.

Quantitative Logging Unit Classification with Hidden Markov Model

*Suguru Yabe[1], Rina Fukuchi[2], Kenta Ueki[1], Yohei Hamada[1]

1. Japan Agency for Marine-Earth Science and Technology, 2. UTokyo AORI

International Ocean Discovery Program (IODP) Expeditions have drilled ocean floor to address cores and well logging data for various purposes. Expedition scientists usually define logging units by characterizing logging data, and interpret their geological meaning. Unit classifications and their geological interpretations will be useful to understand the geological formation at the drilling site. The criteria to define such the units are described in the expedition report, which is usually based on the average, the minimum, and the maximum value of logging data. However, there is no mathematical background to support the validity of unit characterization. The motivation of this study is to develop the quantitative method for log unit definition, and to find out overshadowed log-characteristics for detailed geological interpretation.

This study used Hidden Markov Model (HMM) to classify logging data into logging units. HMM is a stochastic model to classify sequential data. In HMM, each sequential step has the unobservable parameter “state”, which corresponds to the logging unit in this case. As the transition probability of the state depends on the state at previous sequential step, HMM considers Markov process. Observable data (logging data in this case) is generated stochastically following the probability distributions defined by the state at each sequential step. Transition probability of the state and data generation probability distributions for each state are parameters to be estimated. We estimated those parameters with Expectation-Maximization (EM) algorithm.

We applied HMM to four drilling sites around Japan. Two sites are located at Nankai subduction zones. In Southwest Japan, Nankai Trough Seismogenic Zone Experiment (NanTroSEIZE) project conducted a series of IODP expeditions, and large amounts of cores and well-logging data have been acquired. Among these expeditions, we used logging data from Holes C0001D and C0004B drilled during IODP Expedition 314. The other two sites are located at Japan Trench. Hole C0019B was drilled during IODP Expedition 343 as Japan Trench Fast Drilling (JFAST) project. Hole C0020A was drilled during IODP Expedition 337 as Deep Coalbed Biosphere off Shimokita. We selected in-situ electric resistivity, gamma ray, and sonic velocity (P- and S- wave) for the analysis.

For each data set, we tested the number of clusters in HMM from two to nine. We compare our results with the logging unit reported by Expedition scientists. Unit classifications with our method are usually consistent with those by Expedition scientists. However, we observed some differences or finer division of units as well. We discuss the geological meaning of our results.

Keywords: Hidden Markov Model, Clustering, Ocean Drilling Science

©2019. Japan Geoscience Union. All Right Reserved.

Sparse Modeling of Nonlinear Dynamics in Heterogeneous Reactions

*Masaki Ito[1], Tatsu Kuwatani[2], Ryosuke Oyanagi[2], Toshiaki Omori[1]

1. Kobe University, 2. JAMSTEC

Surface heterogeneous reactions are chemical reactions with conjugation of multiple phases, and they have the intrinsic nonlinearity of their dynamics caused by the effect of surface-area between different phases. We propose a sparse modeling approach for extracting nonlinear dynamics of surface heterogeneous reactions from sparse and noisy observable data. We employ sparse modeling algorithm and sequential Monte Carlo algorithm to partial observation problem, in order to simultaneously extract substantial reaction terms and surface models from a number of candidates. Using our proposed method, we show that the rate constants of dissolution and precipitation reactions, which are typical examples of surface heterogeneous reactions, necessary surface models and reaction terms underlying observable data were successfully estimated only from the observable temporal changes in the concentration of the dissolved intermediate product.

Keywords: Heterogeneous Reactions, Sparse Modeling, Nonlinear Dynamics

©2019. Japan Geoscience Union. All Right Reserved.

How to obtain a high-SNR EPMA map?: complementary roles of high-resolution imaging and subsequent binning

*Atsushi Yasumoto[1], Kenta Yoshida[2]

1. Hiruzen Institute of Geology and Chronlogy, 2. Japan Agency for Marine-earth Science and Technology

Chemical imaging is a common technique to analyze heterogeneous materials. For example in petrology, X-ray mapping with an electron probe microanalyzer (EPMA) visualizes chemical heterogeneities (so-called texture) in rocks. X-ray mapping measures signals of X-rays, and higher signal-to-noise ratio (SNR) improves clarity of heterogeneities, which is generally achieved by increasing probe current and/or dwell time of pixels (e.g., Hiroi et al., 1997). An appropriate probe current is determined by sample damages, upper limits of the detectors, and dead time. Dwell time is also determined by sample damages and available analysis time. To acquire a high-SNR image at a reasonable time, reducing total number of pixels is one plausible solution; however, spatial resolution shall become low. To overcome this trade-off, this study proposes a complementary use of short dwell time mapping and subsequent binning. The short dwell time mapping generates high-spatial-resolution and low-SNR images for observing fine textures, and the binning treatment converts the raw maps to low-spatial-resolution and high-SNR images for detecting small differences in chemistry. This approach is applicable to any imaging techniques, including EPMA, which count signals under a given dwell time.

Chemical imaging records counts of signals from multiple points, typically as orthogonal pixels. If expected counting rates are fixed for pixels, observed counts follow Poisson distribution. In EPMA mapping, this assumption is valid because counting rates of X-rays depend mostly on (1) chemistry and surface conditions of materials which are constant; and (2) on probe current, accelerating voltage, and sensitivity of detectors which are controlled by analysts. According to the reproducibility of Poisson distribution, an expected counting rate of a certain signal from a large pixel is identical to an arithmetic-mean of counting rates of the signal from pixels dividing the large pixel. In other word, a sum of counts from n-by-n pixels in m seconds each is equivalent to measuring a large pixel composed of the n-by-n pixels in mn^2 seconds. A simulation is performed on a 300-by-300 matrix of Mandelbrot set. Expected counts per second is set to squares of Mandelbrot set timed by 20. Then, a 300-by-300 map with 1 second of dwell time, and a 150-by-150 map with 4 seconds of dwell time are generated by Poisson random numbers. The 300-by-300 map has higher spatial resolutions and lower-SNR than the 150-by-150 maps. Let’s consider a binning treatment of the 300-by-300 map, i.e. combining signal intensity of each 2-by-2 pixels into one superpixel. The binned 150-by-150 map is apparently comparable to the native 150-by-150 map. This means that high-SNR (low-resolution) image can be generated subsequently from high-resolution (low-SNR) image at an arbitrary degree, if necessary. A recommended binning method is sum rather than arithmetic mean so that binned values can be modeled with Poisson distributions. For example, if a pixel value is generated by Poisson distribution, its standard deviation can be approximated as square root of the pixel value.

The proposed approach has advantages in statistical analysis dealing with mapping data. For example, cluster analysis on a map classifies pixels into a given number of groups based on similarity of pixel values. Performance of cluster analysis, such as precision and smoothness, may improve by obtaining high-SNR of pixels through binning which separates signal peaks representing different groups. Note that benefit of sum as a binning method appears in cluster analysis because Poisson-distribution-based clustering algorithm (Witten, 2011) is applicable. If pixel values follow Poisson distributions, this algorism is more

©2019. Japan Geoscience Union. All Right Reserved.

appropriate and provides better performance than k-means cluster algorism (MacQueen, 1967) which is a simple and common algorism used in variety of fields (Yasumoto et al. 2018).

Keywords: EPMA, mapping, SNR, spatial resolution

©2019. Japan Geoscience Union. All Right Reserved.

Data-driven estimation of material transfer from bulk compositions

*Tatsu Kuwatani[1,2], Kenta Yoshida[1], Kenta Ueki[1], Ryosuke Oyanagi[1], Masaoki Uno[3], Shotaro Akaho[4]

1. Japan Agency for Marine-Earth Science and Technology, 2. Japan Science and Technology Agency, 3. Graduate School of Environmental Studies, Tohoku University, 4. National Institute of Advanced Industrial Science and Technology

Material transfer of elements is the most important consequences of geological processes. However, it is difficult to estimate it, even if both compositional datasets of before and after are available. This is because the compositional data are not absolute data but relative ratio data. Isocon analysis has been widely applied as a simple and powerful standard tool for quantitative estimation of material transfer to various geoscientific problems. Despite its powerfulness, the method needs to assume the reference frame such as immobile elements or conservation of mass or volume, which relies on the researchers' intuition and experience. We propose a novel data-driven method which determines an appropriate reference frame from compositional data of multiple altered samples. In the proposed method, we use a mathematical framework, called sparse modeling, which can extract essential variables from high-dimensional datasets based on sparsity of the system. By optimizing the evaluation function, the least mobile elements are automatically selected. In this study, the effectiveness is validated and discussed using synthetic and natural sample data. The method seems to be a practical tool for estimate material transfer and it has the potential to be improved for particular problems due to its simple and flexible formulation.

Keywords: isocon, sparse modeling

©2019. Japan Geoscience Union. All Right Reserved.

[J] Oral | M (Multidisciplinary and Interdisciplinary)：M-GI General Geosciences, Information Geosciences & Simulations

Mon. May 27, 2019 3:30 PM - 5:00 PM JST | Mon. May 27, 2019 6:30 AM - 8:00 AM UTC | A08 TOKYO BAY MAKUHARI HALL

[M-GI33] Data-driven geosciences

convener:Tatsu Kuwatani(Japan Agency for Marine-Earth Science and Technology), Hiromichi Nagao(Earthquake Research Institute, The University of Tokyo), Kenta Ueki(Japan Agency for Marine-Earth Science and Technology), Masayuki Kano(Graduate school of science, Tohoku University), Chairperson:Tatsu Kuwatani(JAMSTEC), Suguru Yabe(JAMSTEC)

It is important to extract essential processes and structures from observed data sets in order to understand and predict the dynamic behavior of the earth and planetary systems. Recently, many powerful methodologies have been proposed to extract useful information from high-dimensional data sets in information sciences. This session aims to provide an opportunity to gather various geoscientists to have a productive discussion for interdisciplinary collaborations.

3:30 PM - 4:00 PM JST | 6:30 AM - 7:00 AM UTC

[MGI33-06] Markov Chain Monte Carlo: algorithms for multimodal distribution and their applications

★Invited Papers

*Yukito iba[1] (1.The Institute of Statistical Mathematics)

4:00 PM - 4:15 PM JST | 7:00 AM - 7:15 AM UTC

[MGI33-07] **Specifying rate constants and reaction path on the water-rock chemical reaction based on exchange Monte Carlo method and sparse modeling**

*Ryosuke Oyanagi[1], Tatsu Kuwatani[1], Omori Toshiaki[2] (1.Japan Agency for Marine-Earth Science and Technology, 2.Kobe University)

4:15 PM - 4:30 PM JST | 7:15 AM - 7:30 AM UTC

[MGI33-08] Superresolution of X-ray CT images of core samples for understanding the multi-scale structures of water-rock interaction

*Toshiaki Omori[1], Atsushi Okamoto[2], Katsuyoshi Michibayashi[3], Oman Drilling Project Phase 2 Science Party (1.Kobe Univ., 2.Tohoku Univ., 3.Nagoya Univ.)

4:30 PM - 4:45 PM JST | 7:30 AM - 7:45 AM UTC

[MGI33-09] 3-dimensional Fracture Network Analysis by Persistent Homology

*Miyuki Miyazawa[1], Anna Suzuki[2], Atsushi Okamoto[1], Hiroyuki Shimizu[3], Ippei Obayashi[4], Yasuaki Hiraoka[4,5], Takatoshi Ito[2] (1.Graduate School of Environmental Studies, Tohoku University, 2.Institute of Fluid Science, Tohoku University, 3.Kajima Corporation, 4.The Advanced Institute for Materials Research, Tohoku University, 5.Kyoto University)

4:45 PM - 5:00 PM JST | 7:45 AM - 8:00 AM UTC

[MGI33-10] Characteristic patterns and minimal dynamics of correlated seismicity in Japanese island region

*mitsuhiro toriumi[1] (1.Japan agency of marine science and technology)

Markov Chain Monte Carlo: algorithms for multimodal distribution and their applications

*Yukito iba[1]

1. The Institute of Statistical Mathematics

As introduction, history and software of Markov chain Monte Carlo is briefly discussed. Then, replica exchange method (parallel tempering) is explained as a useful tool for sampling multimodal distributions. It is also stressed that applications of Markov chain Monte Carlo are not rescricted to statistical physics or Bayesian computaion; it can deal with a variety of problems related to high dimensional probability, such as counting the number of discrete structures, sampling rare orbits in nonlinear dynamical systems, statistical testing under complicated null hypothesis.

Keywords: Markov Chain Monte Carlo, Replica Exchange Monte Carlo (Parallel Tempering), Bayesian modeling, rare event sampling

©2019. Japan Geoscience Union. All Right Reserved.

Specifying rate constants and reaction path on the water-rock chemical reaction based on exchange Monte Carlo method and sparse modeling

*Ryosuke Oyanagi[1], Tatsu Kuwatani[1], Omori Toshiaki[2]

1. Japan Agency for Marine-Earth Science and Technology, 2. Kobe University

Water-rock interaction in surface and subsurface environments occurs in complex multicomponent systems and involves several reactions, including element transfer. Such kinetic information is obtained by fitting a forward model into the temporal evolution of solution chemistry or the spatial pattern recorded in the rock samples, although geochemical and petrological data are essentially sparse and noisy. Therefore, the optimization of kinetic parameters sometimes fails to converge toward the global minimum due to being trapped in a local minimum.

In this study, we present a novel framework to estimate multiple reaction-rate constants from the mineral distribution pattern in a rock by using the exchange Monte Carlo method (Hukushima & Nemoto, 1997; Iba, 2001). We applied the method to the synthetic data, which includes nine unknown parameters to be estimated (Oyanagi et al., 2018). As a result, probabilistic distribution of six unknown parameters among them showed normal distributions and the proposed method could find each true parameter. However, the probabilistic distribution of others showed uniform distributions and the proposed method failed to estimate each true value because these parameters did not contribute to the observed dataset. We suggest that effective reaction paths could be extracted from mineral distribution pattern in a rock, by excluding non-effective rate constant using a sparse Modeling.

References

Hukushima K, Nemoto K (1996) Exchange Monte Carlo method and application to spin glass simulations. J Phys Soc Japan 65:1604–1608. doi: 10.1143/JPSJ.65.1604

Iba Y (2001) Extended Ensemble Monte Carlo. Int J Mod Phys C 12:623–656. doi: 10.1142/S0129183101001912

Oyanagi R, Okamoto A, Tsuchiya N (2018) Multiple Kinetic Parameterization in a Reactive Transport Model Using the Exchange Monte Carlo Method. Minerals 8:579. doi: 10.3390/min8120579

©2019. Japan Geoscience Union. All Right Reserved.

Superresolution of X-ray CT images of core samples for understanding the multi-scale structures of water-rock interaction

*Toshiaki Omori[1], Atsushi Okamoto[2], Katsuyoshi Michibayashi[3], Oman Drilling Project Phase 2 Science Party -

1. Kobe Univ., 2. Tohoku Univ., 3. Nagoya Univ.

X-ray computed tomography (CT) has become a common tool of earth sciences for the 3D imaging of various structures (layering, fractures, pores etc) of rocks. Recently, several scientific drilling projects has been carried out, and the X-ray CT of such cores provide us the 100 to 1000 m scale continuous data. However, the resolution of such X-ray CT for the cores (for example, ~0.17 mm by the X-ray CT of Drilling Chikyu) is slightly low compare to reveal the shape and geometry of mineral grains and thin fractures. In contrast, the resolution of X-ray CT in usual laboratories is high (~0.01 mm). Therefore, if we can link the high resolution X-ray CT in the lab of the limited samples to the low resolution drilling core CT data, we can obtain the valuable big data for the analyses of multi-scale structures.

For this purpose, we have tried to apply sparse superresolution techniques to the sample of serpentinezed dunite in the Moho transition zone taken by the Oman Drilling project (CM1A). We took the X-ray CT images of the samples with the voxel size of 10, 20, 40 and 80 micrometers. The X-ray CT image reveals that distribution of magnetite and spinel grains and fractures filled with serpentine. In sparse image representation framework, an image is expressed as a sparse linear combination of basis images. In learning phase, basis images are learned from multiple X-ray CT images. In superresolution phase, high resolution X-ray CT image is estimated from low resolution one through common sparse representation of basis images between high and low resolution images. By applying the sparse superresolution technique to the sample of serpentinezed dunite, we obtained results that 2x and 4x sparse superresolutions provide fine structure from low resolution X-ray image.

Keywords: Oman Drilling Project, superresolution, sparse modeling

©2019. Japan Geoscience Union. All Right Reserved.

3-dimensional Fracture Network Analysis by Persistent Homology

*Miyuki Miyazawa[1], Anna Suzuki[2], Atsushi Okamoto[1], Hiroyuki Shimizu[3], Ippei Obayashi[4], Yasuaki Hiraoka[4,5], Takatoshi Ito[2]

1. Graduate School of Environmental Studies, Tohoku University, 2. Institute of Fluid Science, Tohoku University, 3. Kajima Corporation, 4. The Advanced Institute for Materials Research, Tohoku University, 5. Kyoto University

Persistent homology (PH) based on topology is a method for capturing sizes and shapes of “holes”, that is information of connectivity. Because PH enables to quantify complex structures, automatic pattern recognition of fractures can be carried out.

Fluid flow in rocks is dominated by connectivity between fractures, so it can be expected that the relationship between fracture patterns and fluid flow can be obtained by the PH.

In this study, we quantified the images of the results from crack propagations simulation and natural mesh structures in serpentinites. The PH analysis helps to estimate the flow conditions in which the mesh structures in serpentinites were formed. And we can quantify 3D fracture structure by PH. It can be expected that PH is applied to design for geothermal reservoir by coupling PH analysis result of 3D fracture models with feature of fracture (e.g., surface area, volume, connectivity and permeability).

Keywords: Topology, Data science, Mesh structure, 3D printer

©2019. Japan Geoscience Union. All Right Reserved.

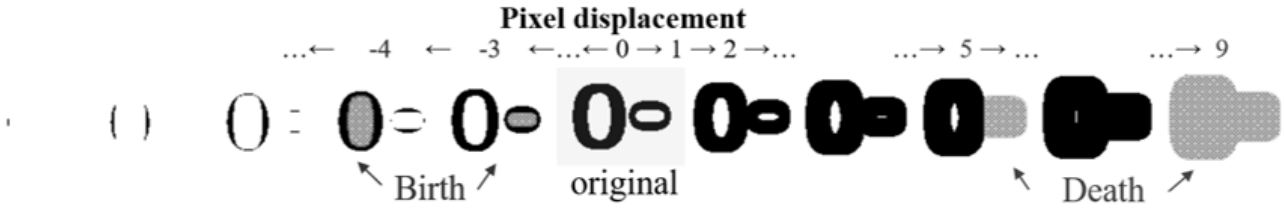

Fig.1 : Example of image analysis by persistent homology.

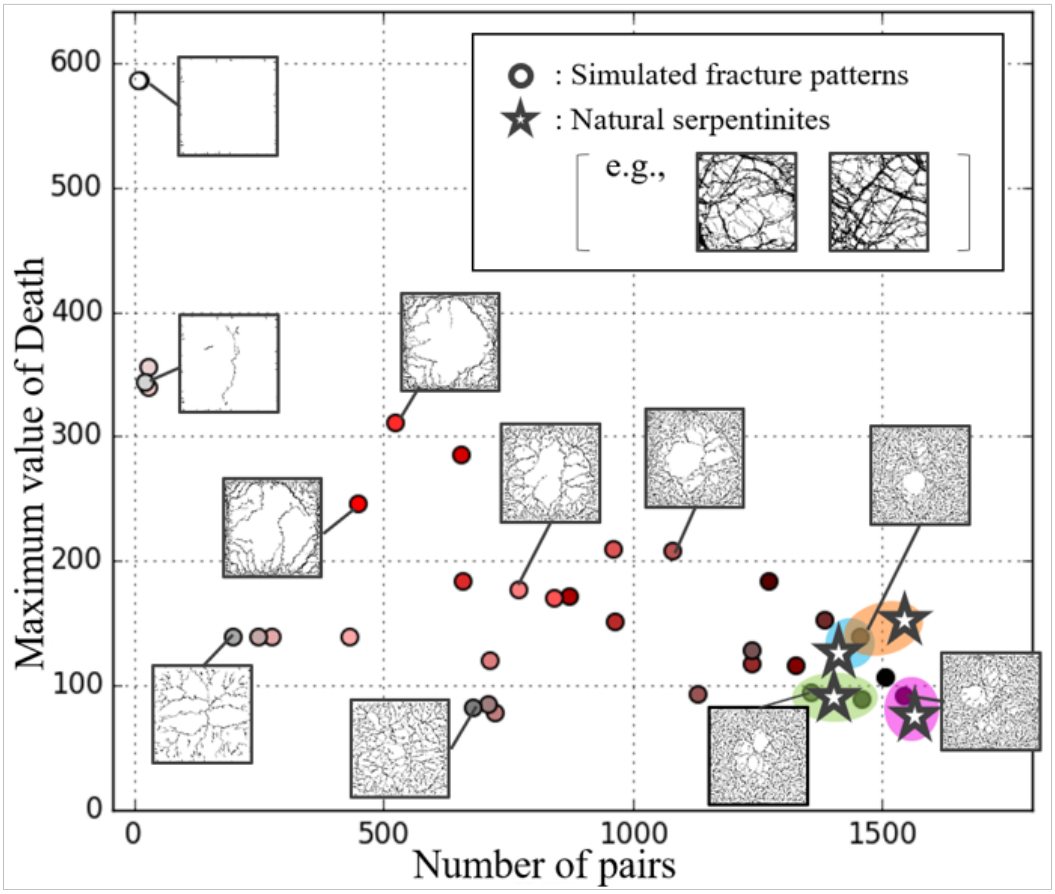

Fig.2 : PH analysis results.

©2019. Japan Geoscience Union. All Right Reserved.

Characteristic patterns and minimal dynamics of correlated seismicity in Japanese island region

*mitsuhiro toriumi[1]

1. Japan agency of marine science and technology

The seismicity rates in this study are defined as the seismic event numbers of the given volume having one degree of longitude and 2.5 degree of latitude from the surface to 30 km depth and 30 to 660km depth in the Japanese islands region. It shows that the characteristic trends of time series of strongly correlated seismicity are possibly obtained as transformed seismicity rates by SVD; the one shows the long term change, second does the periodic time series with various periodicity involving annual variation, and third does nearly Gaussian noise. The first two types of time series can be mapped as five clusters in the diagram of newly transformed seismicity rate coordinates, suggesting existence of stable nodes with annual oscilation and gaussian noises. From these stable nodes, it concludes that the minimal dynamics of the seismicity of the Japanese island region is approximated as the simple low dimensional nonlinear dynamics with semi-periodic variable as is similar to van del Pol equation.

Keywords: spatio-temporal variation of seismicity, correlated seismicity time series, minimal non-linear dynamics

©2019. Japan Geoscience Union. All Right Reserved.

[E] Oral | M (Multidisciplinary and Interdisciplinary)：M-TT Technology & Techniques

Mon. May 27, 2019 9:00 AM - 10:30 AM JST | Mon. May 27, 2019 12:00 AM - 1:30 AM UTC | 104 1F

[M-TT46] New phase of GPS/GNSS application as an integrated earth observation system

convener:Yoshinori Shoji(The Second Laboratory of Meteorological Satellite and Observation System Research Department, Meteorological Research Institute), Kaoru Ichikawa(Research Institute for Applied Mechanics, Kyushu University), Yusaku Ohta(Research Center for Prediction of Earthquakes and Volcanic Eruptions, Graduate School of Science, Tohoku University), Takuya Tsugawa(National Institute of Information and Communications Technology), Chairperson:Yusaku Ohta

GNSS has become a fundamental tool for studies on atmosphere, ionosphere, and solid earth. Ground and space-based GNSS measurements have operationally contributed to improve global and regional NWP since 2006. In recent years, studies utilizing reflected GNSS signals to derive altimetric height, surface roughness, soil moisture, snow depth, humidity or vegetation index have been evolving. Ocean-platform GNSS observations have been demonstrating their capability of real-time monitoring of maritime water vapor as well as sea level. Increasing observations provided through Multi-GNSS (GPS, GLONASS, BEIDOU, GALILEO, QZSS etc.) enhances capability of the GNSS as an integrated earth observation system.
The purpose of this session is to share the latest development of GNSS researches on monitoring the earth system and to stimulate synergetic interdisciplinary studies. Contributions on atmosphere (troposphere and ionosphere) studies, reflectometry (GNSS-R), and integrations of different observation techniques like GNSS-Acoustic measurement to monitor ocean floor positioning are welcome.

9:00 AM - 9:30 AM JST | 12:00 AM - 12:30 AM UTC

[MTT46-01] The latest status of Quasi-Zenith Satellite System (QZSS) and its future expansion

★Invited Papers

*Satoshi Kogure[1] (1.QZSS Straetegy Office, National Space Policy Secretariate, Cabinet Office)

9:30 AM - 9:45 AM JST | 12:30 AM - 12:45 AM UTC

[MTT46-02] Application of the GNSS-A for other academic fields and fundamental marine information network

*Yusuke Yokota[1], Tadashi Ishikawa[2], Shun-ichi Watanabe[2] (1.Institute of Industrial Science, The University of Tokyo, 2.Hydrographic and Oceanographic department, Japan Coast Guard)

9:45 AM - 10:00 AM JST | 12:45 AM - 1:00 AM UTC

[MTT46-03] Feasibility of the GNSS carrier phase to fault slip approach for the estimation of slip phenomena in subduction zone

*Yusuke Tanaka[1], Yusaku Ohta[1], SHINICHI MIYAZAKI[2] (1.Tohoku University, 2.Kyoto University)

10:00 AM - 10:15 AM JST | 1:00 AM - 1:15 AM UTC

[MTT46-04] Assimilation experiments of GNSS-derived ZTD and Sentinel-derived products into WRF to improve forecasts of severe rain events in Italy

*Eugenio Realini[1], Martina Lagasio[2], Luca Pulvirenti[2], Antonio Parodi[2], Andrea Gatti[1], Giulio Tagliaferro[1], Giovanna Venuti[3], Stefano Barindelli[3], Emanuele Passera[4], Alessio Rucci[4], Nazzareno Pierdicca[5], Bjorn Rommen[6] (1.Geomatics Research & Development srl, 2.CIMA Research Foundation, 3.Dept. of Civil and Environmental Engineering, Politecnico di Milano, 4.TRE Altamira srl, 5.Dept. of Information Engineering, Electronics and Telecommunications, Sapienza Univ. of Rome, 6.European Space Agency (ESA-ESTEC))

10:15 AM - 10:30 AM JST | 1:15 AM - 1:30 AM UTC

[MTT46-05] An analysis of tropospheric delays using goGPS software on all GEONET stations during the passage of Typhoon Jebi in September 2018

*Andrea Gatti[1], Eugenio Realini[1], Giulio Tagliaferro[1] (1.Geomatics Research & Development srl)

The latest status of Quasi-Zenith Satellite System (QZSS) and its future expansion

*Satoshi Kogure[1]

1. QZSS Straetegy Office, National Space Policy Secretariate, Cabinet Office

The Quasi-Zenith Satellite System (QZSS) is a regional space-based Position, Navigation and Timing (PNT) system developed and operated by Japanese government as their important national infrastructure. Three consecutive launches were successfully conducted in 2017. The official operational service has been launched since November 1, 2018. The expansion to 7 satellite constellation is now being investigated. The presentation shows the latest status of the QZSS program as well as its future expansion.

Keywords: QZSS, Space-cased Position Navigation and Timing system, GNSS

©2019. Japan Geoscience Union. All Right Reserved.

Application of the GNSS-A for other academic fields and fundamental marine information network

*Yusuke Yokota[1], Tadashi Ishikawa[2], Shun-ichi Watanabe[2]

1. Institute of Industrial Science, The University of Tokyo, 2. Hydrographic and Oceanographic department, Japan Coast Guard

The GNSS-A observation technology had detected coseismic deformation fields just above the megathrust earthquake [Sato et al., 2011, Science; Kido et al., 2011, GRL], postseismic deformations [Watanabe et al., 2014, GRL; Tomita et al., 2017, Sci. Adv.] and interseismic coupling condition [Yokota et al., 2016, Nature]. In addition, we recently upgraded the GNSS-A methodology in aspects of observation frequency and accuracy and detected a longer-term sequence of slow slip events (SSEs). The detected undersea SSEs led a new discussion about a diverse behavior of SEQs and provide many questions, i.e., their stress loading for coupling region and difference of geological condition in the SSE, other SEQs and coupling regions, to be solved by the future seafloor, submarine and onshore geophysical monitoring.

In the development process of this new GNSS-A system, new oceanographic information in km scale region was found to be extractable from the GNSS-A data [Yokota et al., 2018, MGR]. This data has features consistent and inconsistent with the JCOPE2 model [Miyazawa et al., 2009, JO], so the GNSS-A system has a potential to provide new observation data of very narrow marine region.

These observations have extremely high scientific potential from the viewpoint of seismology, earthquake disaster prevention engineering and submarine geology about megathrust subduction zones and unknown potential about new multidisciplinary aspects called the nano-scale GNSS-A oceanography and the marine GNSS meteorology. In order to promote the distribution of data to the earthquake science community and different academic fields, it is necessary to establish a simple data format and manage using doi. In particular, for carrying out long-term and stable observation, we must construct strong management and evaluation system to perform appropriately data collection and observation operation. The realization of such a solid fundamental marine observation network will also have a positive effect on new research and development.

Moreover, it is necessary to enhance the GNSS-A observation system to upgrade the observation density, continuity and real-time property for understanding the subduction zone and disaster prevention. Eventually, we should construct next-generation fundamental network that aggregates the marine information system that utilize total data in real time based on numerical simulation and data assimilation.

Keywords: GNSS-A, seafloor geodetic observation network, marine observation

©2019. Japan Geoscience Union. All Right Reserved.

Feasibility of the GNSS carrier phase to fault slip approach for the estimation of slip phenomena in subduction zone

*Yusuke Tanaka[1], Yusaku Ohta[1], SHINICHI MIYAZAKI[2]

1. Tohoku University, 2. Kyoto University

Precise detection of coseismic deformation and estimation of its source model are especially important in the case of earthquake occur in subduction zones, because it is directly related to accurate tsunami forecasting. Recent years, many researchers have tried to estimate earthquake source model and/or tsunami wave field in real-time using Global Navigation Satellite System (GNSS). However, conventional GNSS-based monitoring requires huge computational cost for positioning analysis. Using coordinate time series for observation also causes difficulty to evaluate accuracy of separation between deformation and other unknown parameters such as tropospheric delay. Additionally, current positioning analysis strongly depends on precise orbit information which is provided externally.

According to such background, we investigate the feasibility of deformation monitoring based on the GNSS carrier phase to fault slip approach for subduction zone. This method, which we call PTS (Phase To Slip) detects fault slip directly from GNSS carrier phase variation without positioning analysis. As PTS method estimates all unknown parameters in parallel, computational costs for real-time seismic monitoring can be reduced. Moreover, PTS does not require high-quality satellite orbit because it relies only on changes in azimuthal site-to-satellite ranges (Tanaka, Ohta, and Miyazaki, GRL, 2019).

Here we applied the PTS method to the largest aftershock of the 2011 Tohoku-Oki earthquake. In the analysis, we used both precise orbit provided by International GNSS Service (IGS) and broadcast orbit submitted from satellite without any network connection. As a result, we obtained very similar coseismic slip distribution in the two cases. Inferred fault slip showed clear thrust slip and was equivalent to M_w 7.8. These results well agree with the estimation based on conventional GNSS analysis such as Nishimura et al. (EPS, 2011). Calculated surface displacements also agree with independent conventional GNSS analysis result. These results indicate that the PTS method can be useful as a supplementary system of current deformation monitoring, which does not require any external information. Furthermore, once we could obtain slip distribution, we can also convert it into deformation of sea bottom, which is equivalent to initial tsunami source. Thus, our results suggest potential feasibility of PTS method for tsunami forecasting.
In the presentation, we will describe application of the PTS method to whole process of Tohoku-Oki earthquake, including its foreshock, mainshock and following aftershocks. Beside detail of its result, we will also demonstrate quantitative evaluation of parameter separation accuracy inside PTS analysis.

©2019. Japan Geoscience Union. All Right Reserved.

Assimilation experiments of GNSS-derived ZTD and Sentinel-derived products into WRF to improve forecasts of severe rain events in Italy

*Eugenio Realini[1], Martina Lagasio[2], Luca Pulvirenti[2], Antonio Parodi[2], Andrea Gatti[1], Giulio Tagliaferro[1], Giovanna Venuti[3], Stefano Barindelli[3], Emanuele Passera[4], Alessio Rucci[4], Nazzareno Pierdicca[5], Bjorn Rommen[6]

1. Geomatics Research & Development srl, 2. CIMA Research Foundation, 3. Dept. of Civil and Environmental Engineering, Politecnico di Milano, 4. TRE Altamira srl, 5. Dept. of Information Engineering, Electronics and Telecommunications, Sapienza Univ. of Rome, 6. European Space Agency (ESA-ESTEC)

The Italian peninsula is frequently struck by severe floods and flash floods causing losses of lives and significant damages every year. Improving the accuracy of rain forecasts is a fundamental goal to limit social and economic damages. Forecasts based on numerical weather prediction (NWP) models are challenged by the uncertainty related to the initial state of the atmosphere at small spatial-temporal scales. The inevitable model spin-up often results in an inaccurate simulation of the timing, the location and the severity of convective events. This challenge becomes even more relevant when the model grid spacing is approaching the kilometer scale, mainly because of the lack of high spatiotemporal resolution observations. In this scenario the STEAM (SaTellite Earth observation for Atmospheric Modelling) project, funded by the European Space Agency (ESA), has the aim of investigating to what extent GNSS-derived and Sentinel SAR-derived tropospheric delay data, as well as other Sentinel-derived products (i.e. soil moisture, soil and sea temperature, wind over sea) can be used to better understand and predict, with high spatial-temporal resolution, the atmospheric phenomena resulting in severe rain events and intense atmospheric turbulence. About 400 GNSS stations distributed throughout Italy were processed by the precise point positioning (PPP) technique, by means of the free and open source software goGPS, to estimate zenith total delay (ZTD) time series. Atmospheric phase screens (APS) were generated from Sentinel-1 observations, calibrated and converted to absolute tropospheric delays by using data from the Generic Atmospheric Correction Online Service for InSAR (GACOS). Surface soil moisture maps were retrieved from Sentinel-1 observations, by means of a multi-temporal algorithm that uses time series of Sentinel-1 data and ancillary data, such as a plant water content map, as inputs. Soil and sea temperature are directly available from ESA as level-2 products based on Sentinel-3, as well as the wind field over sea, based on Sentinel-1.
The experimental results concern two intense rainfall events and subsequent floods that occurred in Italy in Autumn 2017. The best results were obtained by assimilating the wind field (in the first test case) and the GNSS-derived ZTD (in the second test case). Promising results were achieved also by performing a combined assimilation of wind field and ZTD, and direct insertion of soil moisture. The outcomes of this study seem to confirm the synergy between high-resolution numerical weather models and a set of GNSS-derived and Sentinel-derived Earth Observation products, at least for the forecast of severe rain events.

Keywords: GNSS, SAR, Sentinel, NWP, Assimilation

©2019. Japan Geoscience Union. All Right Reserved.

An analysis of tropospheric delays using goGPS software on all GEONET stations during the passage of Typhoon Jebi in September 2018

*Andrea Gatti[1], Eugenio Realini[1], Giulio Tagliaferro[1]

1. Geomatics Research & Development srl

Nowadays, tropospheric delays estimated from GPS observations are widely used for studying weather events all over the world. Some meteorological agencies already use Zenith Tropospheric Delays (ZTD), or similar observables, by assimilation into numerical weather prediction (NWP) models; however, the increasing number of satellites from newer GNSS constellations (Galileo, QZSS, BeiDou, IRNSS), the advent of low-cost receivers and the advancement of techniques and models left space for further studies on the topic.

The new version of the open-source goGPS MATLAB software has been written to be a simple tool to perform efficient analysis of GNSS data from both geodetic and low-cost receivers. With its capability to download automatically all the resources needed by the selected algorithms, the relative easiness of use, and its flexibility with the possibility of trying different configurations in a fast way, goGPS presents itself as a convenient tool for students or researches who want to prototype new algorithms or perform studies on GNSS data.

To demonstrate the capabilities of the software, 1312 stations of the Japanese GEONET GNSS network are processed from September 2, 2018, to September 5, 2018, during the passage of Typhoon Jebi.

A 32-core machine running MATLAB 2016a and the latest beta version of goGPS 1.0 is used to process in a single parallel run the entire 4 days of the dataset. The execution performs for all the stations a multi-epoch precise point positioning (PPP) least squares (LS) adjustment in about two hours of computation time. Series of tropospheric delays and gradients are generated and used to produce maps and animations in order to observe the development of the event. Different solutions including multi-constellation results are presented and discussed.

Keywords: GNSS, Troposphere, Software, Typhoon

©2019. Japan Geoscience Union. All Right Reserved.

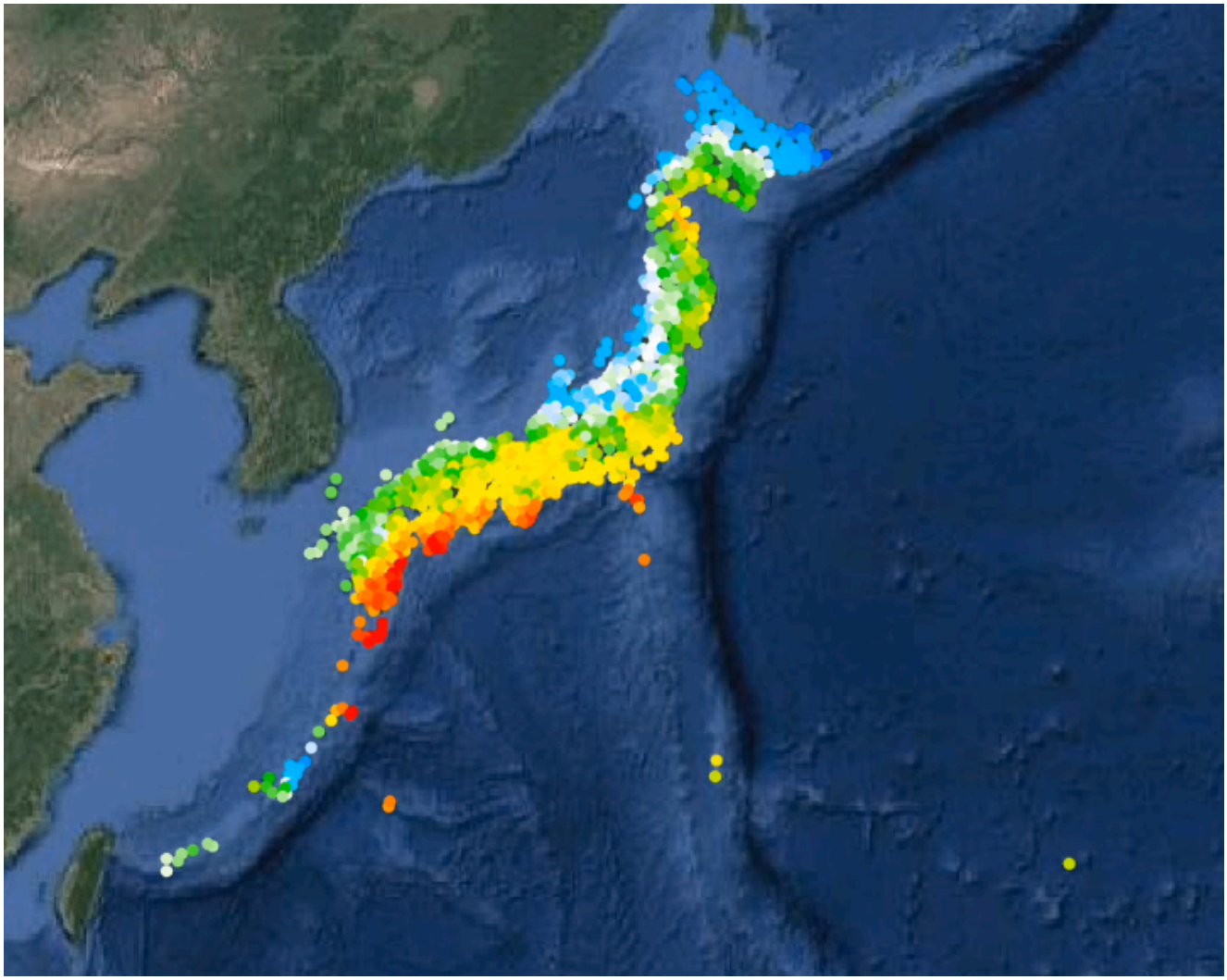

©2019. Japan Geoscience Union. All Right Reserved.

[E] Oral | M (Multidisciplinary and Interdisciplinary)：M-TT Technology & Techniques

Mon. May 27, 2019 10:45 AM - 12:15 PM JST | Mon. May 27, 2019 1:45 AM - 3:15 AM UTC | 104 1F

[M-TT46] New phase of GPS/GNSS application as an integrated earth observation system

convener:Yoshinori Shoji(The Second Laboratory of Meteorological Satellite and Observation System Research Department, Meteorological Research Institute), Kaoru Ichikawa(Research Institute for Applied Mechanics, Kyushu University), Yusaku Ohta(Research Center for Prediction of Earthquakes and Volcanic Eruptions, Graduate School of Science, Tohoku University), Takuya Tsugawa(National Institute of Information and Communications Technology), Chairperson:Takuya Tsugawa

GNSS has become a fundamental tool for studies on atmosphere, ionosphere, and solid earth. Ground and space-based GNSS measurements have operationally contributed to improve global and regional NWP since 2006. In recent years, studies utilizing reflected GNSS signals to derive altimetric height, surface roughness, soil moisture, snow depth, humidity or vegetation index have been evolving. Ocean-platform GNSS observations have been demonstrating their capability of real-time monitoring of maritime water vapor as well as sea level. Increasing observations provided through Multi-GNSS (GPS, GLONASS, BEIDOU, GALILEO, QZSS etc.) enhances capability of the GNSS as an integrated earth observation system.
The purpose of this session is to share the latest development of GNSS researches on monitoring the earth system and to stimulate synergetic interdisciplinary studies. Contributions on atmosphere (troposphere and ionosphere) studies, reflectometry (GNSS-R), and integrations of different observation techniques like GNSS-Acoustic measurement to monitor ocean floor positioning are welcome.

10:45 AM - 11:05 AM JST | 1:45 AM - 2:05 AM UTC

[MTT46-06] A new perspective of the storm-time dynamics of the ionosphere using global GNSS-TEC observation data

★Invited Papers

*Atsuki Shinbori[1], Yuichi Otsuka[1], Takuya Sori[1], Takuya Tsugawa[2], Michi Nishioka[2] (1.Institute for Space-Earth Environment Research (ISEE), Nagoya University, 2.National Institute of Information and Communications Technology (NICT))

11:05 AM - 11:20 AM JST | 2:05 AM - 2:20 AM UTC

[MTT46-07] Ionospheric space weather studies for GNSS users

*Takuya Tsugawa[1], Kornyanat Hozumi[1], Punyawi Jamjareegulgarn[2], Supnithi Pornchai [2], Susumu Saito[3], Yuichi Otsuka[3,4], Shinichi Hama[1], Takahiro Naoi[1], Mamoru Ishii[1] (1.NICT, 2.KMITL, 3.ENRI, 4.Nagoya Univ.)

11:20 AM - 11:35 AM JST | 2:20 AM - 2:35 AM UTC

[MTT46-08] QZSS geostationary satellite for ionospheric TEC observations

*Kosuke Heki[1] (1.Department of Earth and Planetary Sciences, Faculty of Science, Hokkaido University)

11:35 AM - 11:50 AM JST | 2:35 AM - 2:50 AM UTC

[MTT46-09] Precise estimation of total electron content by double-shell model using local receiver network

*Takashi Maruyama[1,2], Kornyanat Hozumi[1], Guanyi Ma[2], Qingtao Wan[2] (1.National Institute of Information and Communications Technology, 2.National Astronomical Observatories, Chinese Academy of Sciences)

11:50 AM - 12:05 PM JST | 2:50 AM - 3:05 AM UTC

[MTT46-10] Investigation of sea surface height detection by Global Navigation Satellite System Reflectometry (GNSS-R)

*Osamu Isoguchi[1], Kaoru Ichikawa[2], Yukihito Kitazawa[3] (1.RESTEC, 2.Kyushu Univ., 3.ISAS/JAXA)

12:05 PM - 12:15 PM JST | 3:05 AM - 3:15 AM UTC

[MTT46-11] Discussion

A new perspective of the storm-time dynamics of the ionosphere using global GNSS-TEC observation data

*Atsuki Shinbori[1], Yuichi Otsuka[1], Takuya Sori[1], Takuya Tsugawa[2], Michi Nishioka[2]

1. Institute for Space-Earth Environment Research (ISEE), Nagoya University, 2. National Institute of Information and Communications Technology (NICT)

The Earth’ s atmosphere is divided into four regions: troposphere, stratosphere, mesosphere and thermosphere by the temperature structure. A part of neutral gases in the mesosphere and thermosphere is ionized by solar extreme ultraviolet (EUV) radiation in a wavelength of less than 100 nm. The region having the ionized gasses (plasmas) is called the ionosphere. The height profile of the electron density in the ionosphere becomes maximum at a height of 300 km is determined by the chemical and dynamical processes in addition to the solar EUV ionization. Due to the interaction between the ionospheric electrons and electric fields of electromagnetic waves, the ionosphere gives a significant influence on the ionospheric transmissions with satellites for communications, positioning, and navigation. The ionosphere changes greatly in association with the activities of the sun, magnetosphere, and the lower atmosphere, and their ionospheric variations interfere with satellite communication and enhances satellite positioning errors in the Global Navigation Satellite System (GNSS), including GPS. The most major factor of the positioning errors is the propagation delay of GNSS signals in the ionosphere. Therefore, a global total electron content (TEC) map or ionospheric model is required to investigate global ionospheric variations associated with geomagnetic storms and lower atmospheric activities and to evaluate the ionospheric delay for GNSS positioning. A scale of the ionospheric variations (traveling ionospheric disturbances (TIDs), equatorial plasma bubbles (EPB), auroral ionospheric irregularity) is in a range between several 100 km and 1000 km. A storm enhanced density (SED) phenomena observed in the mid- and low-latitude ionosphere during the main phase of geomagnetic storms appears with a wide longitudinal extent. In order to clarify generation and propagation mechanisms of these ionospheric phenomena and to investigate their effects on the GNSS positioning, dense and wide-coverage ionospheric observations and the corresponding TEC data are needed. Under these backgrounds, we have built a global TEC database (absolute TEC, detrended TEC, and ROTI) with high time and spatial resolutions and developed a TEC data analysis system in a corroboration with NICT and the IUGONET (Inter-university Upper atmosphere Global Observation NETwork) and PWING (Study of dynamical variation of particles and waves in the inner magnetosphere using ground-based network observations) projects. For the development of the TEC database, we have collected all the available GNSS receiver data in the world. The number of the GNSS stations reaches more than 8500 in January 2019. These GNSS data are provided by the International Geoscience Services (IGS), the University NAVSTAR Consortium (UNAVCO), Scripps Orbit and Permanent Array Center (SOPAC), and other global and regional data centers (more than 50 data providers in all). In this talk, we introduce an overview of recent new scientific results of temporal and spatial variations in the ionosphere during the development and decay of geomagnetic storms as seen in the global GNSS-TEC variations.

Keywords: Global Navigation Satellite System (GNSS), Ionosphere, Geomagnetic storm, Positioning error, Total electron content (TEC), Database

©2019. Japan Geoscience Union. All Right Reserved.

Ionospheric space weather studies for GNSS users

*Takuya Tsugawa[1], Kornyanat Hozumi[1], Punyawi Jamjareegulgarn[2], Supnithi Pornchai [2], Susumu Saito[3], Yuichi Otsuka[3,4], Shinichi Hama[1], Takahiro Naoi[1], Mamoru Ishii[1]

1. NICT, 2. KMITL, 3. ENRI, 4. Nagoya Univ.

NICT has observed ionosphere using Ionosondes and GNSS receiver networks in Japan and Southeast Asia for the nowcast and forecast of the ionospheric condition.Two-dimensional ionospheric total electron content (TEC) maps have been derived from dense ground-based GNSS receiver networks and applied to studies of various ionospheric disturbances since mid-1990s. For the purpose of monitoring and researching ionospheric conditions and ionospheric space weather phenomena, we have developed TEC maps over Japan using GEONET. Currently, we are providing high-resolution two-dimensional maps of absolute TEC, detrended TEC, rate of TEC change index (ROTI), and loss-of-lock on GPS signal over Japan in real-time basis.

We have collected all the available GNSS receiver data in the world to expand the TEC observation area. To expand the two-dimensional TEC observation are with high-resolution, we have conducted Dense Regional And Worldwide International GNSS TEC observation (DRAWING-TEC) project, which consists of the three items: (1) standardizing GNSS-TEC data, (2) developing a new high-resolution TEC mapping technique, and (3) sharing the standardized TEC data or the information of GNSS receiver network. One of other effective methods to expand TEC observation area would be to use the maritime GNSS buoys.

NICT have started a new research project to validate the ionospheric effect of precise positioning technique using GNSS including quasi-zenith satellite (QZSS) since 2017. In this project, we will investigate ionospheric effects on individual positioning techniques (single frequency, DGPS, and RTK-PPP) and consider methods to mitigate and/or prevent the positioning errors under sever ionospheric conditions. We have tried to use multi-GNSS data including GPS and QZSS for routine data collection and processing. In the Southeast Asia, it is important to identify which satellite-receiver path suffers from plasma bubble structures for verifying the ionospheric effects on GNSS positioning. we have a plan to install VHF radar at Chumphon (Thailand) and multi-GNSS receivers at Chumphon, Bac Lieu (Vietnam), and Cebu (Philippines) at the magnetic equator.

Keywords: Ionosphere, GNSS, Space Weather

©2019. Japan Geoscience Union. All Right Reserved.

QZSS geostationary satellite for ionospheric TEC observations

*Kosuke Heki[1]

1. Department of Earth and Planetary Sciences, Faculty of Science, Hokkaido University

Most Global Navigation Satellite System (GNSS) satellites employ orbital periods with a half sidereal day. This makes the satellites move rapidly in the sky when observed from ground receivers. This is important in relative positioning by observing carrier phases and in estimating zenith tropospheric delays. However, measurement of ionospheric total electron content (TEC) could be done instantaneously by comparing phases of the two carrier waves, and the changes in the satellite azimuth and elevation becomes a nuisance. The change in STEC (slant TEC) comes from (1) temporal change and (2) spatial changes of ionosphere, and (3) apparent U-shaped changes coming from the elevation changes. We can mitigate (3) by using VTEC, i.e. removing the inter-frequency biases and multiplying the bias-free STEC with cosine of the line-of-sight penetration angle. Nevertheless, discrimination of (1) and (2) is difficult and becomes possible only by processing the whole data sets of dense networks. The Japanese Quasi-zenith Satellite System (QZSS) is currently composed of four satellites, 3 satellites with quasi-zenith orbits (PRN01, 02, 03) and 1 satellite with geostationary orbit (PRN07). The latter enables continuous observation of certain points in ionosphere fixed to the Earth, i.e. the changes in TEC come entirely from temporal changes.

The Japanese GEONET network GNSS receivers continuously track GPS, GLONASS, Galileo, and QZSS, and their raw data are available on line as the RINEX (Receiver independent exchange format) Ver.3.02 files. I made a software system to read them and convert the phase data to TEC time series. With TEC observations from the geostationary satellite, we could study temporal changes in ionosphere without being bothered by spatial variations. This implies certain benefits in studying ionospheric disturbances, such as LSTID (Large-Scale TID), MSTID (Medium-scale TID) (Otsuka et al., 2011), Es (sporadic-E) (Maeda & Heki, 2015), artificial ionospheric electron depletion due to launches of satellites and ballistic missiles (Hashimoto & Heki, 2018), and preseismic ionospheric anomalies (Heki, 2019). In contrast, geostationary satellites are not suitable for studying coseismic ionospheric disturbances by acoustic waves (Cahyadi & Heki, 2015) and those by volcanic eruptions (Nakashima et al., 2015). This is because stronger signals always appear in poleward line-of-sights from ground stations located at the equatorward side of the epicenters/volcanoes (Heki, 2019).

References

Cahyadi, M. N., and K. Heki (2015), Coseismic ionospheric disturbance of the large strike-slip earthquakes in North Sumatra in 2012: Mw dependence of the disturbance amplitudes, Geophys. J. Int., 200(1), 116-129.

Hashimoto, M. and K. Heki (2018), Estimation of thrust powers of missiles/rockets by GNSS-TEC observations, J. Geod. Soc. Japan, in press.

Heki, K. (2019), Ionospheric disturbances related to Earthquakes, in “Advances in Ionospheric Research: Current Understanding and Challenges”, Wiley/AGU Book, in press.

©2019. Japan Geoscience Union. All Right Reserved.

Nakashima, Y., K. Heki, A. Takeo, M. N. Cahyadi, A. Aditiya, & K. Yoshizawa (2016), Atmospheric resonant oscillations by the 2014 eruption of the Kelud volcano, Indonesia, observed with the ionospheric Total Electron Contents and seismic signal, Earth Planet. Sci. Lett., 434, 112-116.

Maeda, J. & K. Heki (2015), Morphology and dynamics of daytime mid-latitude sporadic-E plasma patches revealed by GPS total electron content observations in Japan, Earth Planets Space, 67, 89, doi:10.1186/s40623-015-0257-4.

Otsuka, Y., N. Kotake, K. Shiokawa, T. Ogawa, T. Tsugawa, & A. Saito (2011), Statistical study of mediumscale traveling ionospheric disturbances observed with a GPS receiver network in Japan, in Aeronomy of the Earth’ s Atmosphere and Ionosphere, edited by M. A. Abdu and D. Pancheva, IAGA Special Sopron Book Series 2, doi:10.1007/978-94-007-0326-1_21, Springer.

Keywords: GNSS-TEC, QZSS, ionospheric disturbance

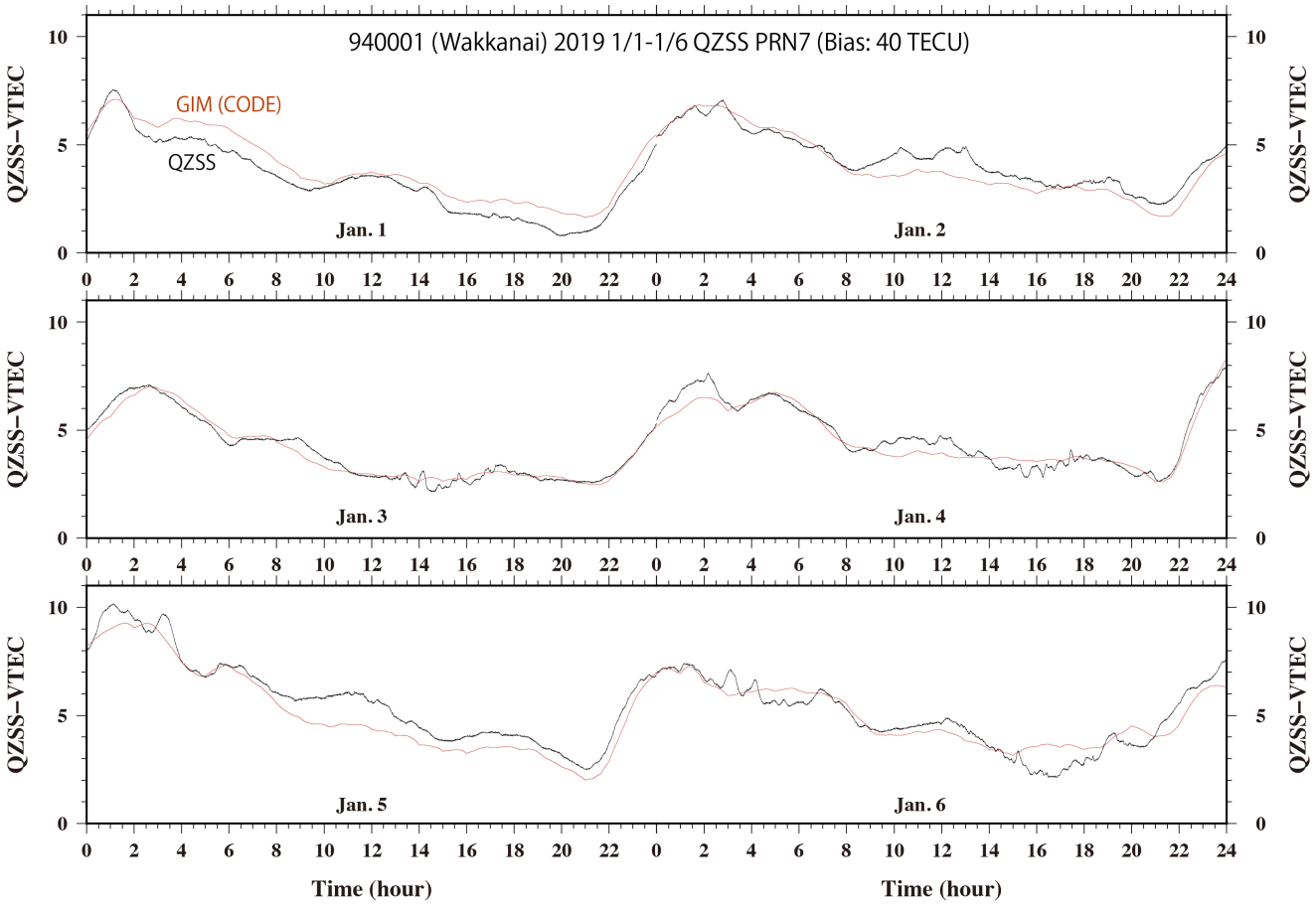

©2019. Japan Geoscience Union. All Right Reserved.

Precise estimation of total electron content by double-shell model using local receiver network

*Takashi Maruyama[1,2], Kornyanat Hozumi[1], Guanyi Ma[2], Qingtao Wan[2]

1. National Institute of Information and Communications Technology, 2. National Astronomical Observatories, Chinese Academy of Sciences

The total electron content (TEC) derived from the differential group delay of the code signals of GNSS on two frequencies has been a basic parameter in ionospheric studies. In most applications, the thin-layer approximation is used to convert the measured slant TEC to vertical TEC at the ionosphere pierce point. Usually the thin-layer height is assumed to be constant regardless of the location and time, which is unrealistic and can be a source of error in TEC estimations. This is a serious problem at low latitudes where the ionospheric height greatly varies by the action of the vertical EXB drift due to the zonal electric field and field-aligned transport due to the meridional neutral wind drag. In this paper, we parameterized the ionosphere by two thin-layers (double-shell model) at 250 and 1100 km to avoid this inconvenience. The variation of partial electron content related to each layer was approximated by the spherical harmonics expansion to minimize the error of slant TEC between the measurements and the sum of contribution from the two layers. In the harmonics expansion calculation, the longitude parameter was the sun-fixed longitude or the local time measured in angle. Thus data obtained in a whole day were used. Another problem with the conventional technique is the leveling procedure, where phase measurements with a small noise are leveled to the noisy code signal data. Therefore, noises and multipath effect on the code delay are not resolved by the leveling. To avoid this inconvenience, the leveling to the code data was not applied in our study. Instead, the total bias including instrumental (satellite and receiver) code biases and phase ambiguity for each arc (i.e., total arc bias) was determined in conjunction with TEC.
The technique was applied to datasets obtained by a local receiver network near the magnetic equator. Results were compared with those of the conventional (single) thin-layer model. A significant difference was found in the ratio of TECs at the equatorial anomaly crests and trough. The double-shell model captured the equatorial anomaly more correctly than the conventional method. Another outcome of the double-shell model was the different patterns of TEC variations at the two heights, as expected. Equatorial anomaly crests and the evening TEC bite-out at the equator were prominent in the lower shell. The TEC peak at the higher shell appeared later than the lower shell. Two shells exhibited different features of north-south asymmetry of TEC, depending on the local time. These results provide information on the ionospheric dynamics, such as the ionosphere-thermosphere coupling through the field-aligned transport and variations of the evening enhancement of zonal electric field.

Keywords: TEC, double-shell model, equatorial anomaly

©2019. Japan Geoscience Union. All Right Reserved.

Investigation of sea surface height detection by Global Navigation Satellite System Reflectometry (GNSS-R)

*Osamu Isoguchi[1], Kaoru Ichikawa[2], Yukihito Kitazawa[3]

1. RESTEC, 2. Kyushu Univ., 3. ISAS/JAXA

In recent years, the possibility of detecting ocean parameters such as sea surface height (SSH), ocean wind from the Global Navigation Satellite System reflectometry (GNSS-R) was shown. The Cyclone GNSS (CYGNSS) mission aiming to contribute to the forecast of extreme weather phenomena by observing the sea surface wind in the cyclone is in progress operating eight small satellites and ocean wind speed products are being delivered. In GNSS-R, it is theoretically possible to measure the SSH from the ellipsoid by measuring the delay of the reflected wave and the direct wave. The investigation of SSH detection using TDS-1 which was developed and operated mainly by Surrey Satellite Technology Ltd (SSTL) in the UK has been reported. Even in our group, SSH detection was performed using TDS-1 data observed near Japan and the detected ones was compared with the mean SSH constructed by the altimeter observations. It was confirmed that the SSH can be detected with an error of about 1m at observation with good conditions (antenna gain is 7.5 dBi or more). Regarding CYGNSS, SSH is not calculated as an official product and it is limited to detectability study. In this report, we used CYGNSS data to investigate SSH detection from GNSS-R like TDS-1.

The CYGNSS data used for the present study is a full resolution Delayed Doppler Map (DDM) provided as special data through the GNSS Reflectometry for Ocean Waves, Tides and Height (GROWTH) project, which is a member of NASA CYGNSS External Science Member. The size of DDM is 20 (Doppler) ×128 (Delay) bin. On the other hand, the size of the normal DDM is 11 (Doppler) ×17 (Delay) bin in the Level 1 ver 2.1 data provided by NASA's The Physical Oceanography Distributed Active Archive Center (PO.DAAC). Thus, the data are compressed to 1/2 in the doppler direction and 1/8 in the delay one. Since the resolution in the delay direction affects the range measurement, it is expected that the detection resolution by the full DDM will be improved over the usual L1 data. The data provided was data acquired mainly in the East China Sea and acquired for the purpose of demonstrating the possibility of detecting the SSH related to the large tide amplitude.

Since the provided full resolution data are those in which only a part of data on DDM is stored, L1 ver 2.1 data at the same time were collected and the positions of the transmitting GNSS satellite and the receiving CYGNSS, the position of the reflection point and the delay information of the reflection point corresponding to the full DDM were extracted to calculate the SSH. A random variation of about 6m in standard deviation was confirmed in the delay information of the reflection point, so we with calculated weighed average with the 1/e scale of 75 km after excluding the abnormal values. Based on the above information, the SSH along the reflection point was calculated and compared with the mean SSH data calculated based on the altimeter data. A large spatial error that can be approximated by a linear equation of the distance was confirmed for the difference between the two SSHs, and therefore the relative SSH was evaluated by subtracting the approximate expression. The RMS error along the 4 passes of the observation on April 18, 2018 was about 0.8 m to 1.5 m, which was almost the same accuracy as TDS-1.

In the present study, the possibility of SSH detection as a spatial relative altitude was suggested. However since the large spatial error remains, whether the SSH variation in the East China Sea with O (1 m) can be detected will be a subject for further study. In particular, since corrections to the ionosphere and the

©2019. Japan Geoscience Union. All Right Reserved.

troposphere delays have not been made at the stage of this study, it is considered necessary to estimate their influences from model data.

Keywords: GNSS-R, Sea surface height, CYGNSS

©2019. Japan Geoscience Union. All Right Reserved.

[E] Oral | M (Multidisciplinary and Interdisciplinary) | M-TT Technology & Techniques

[M-TT46] New phase of GPS/GNSS application as an integrated earth observation system

convener:Yoshinori Shoji(The Second Laboratory of Meteorological Satellite and Observation System Research Department, Meteorological Research Institute), Kaoru Ichikawa(Research Institute for Applied Mechanics, Kyushu University), Yusaku Ohta(Research Center for Prediction of Earthquakes and Volcanic Eruptions, Graduate School of Science, Tohoku University), Takuya Tsugawa(National Institute of Information and Communications Technology), Chairperson:Takuya Tsugawa
Mon. May 27, 2019 10:45 AM - 12:15 PM 104 (1F)

GNSS has become a fundamental tool for studies on atmosphere, ionosphere, and solid earth. Ground and space-based GNSS measurements have operationally contributed to improve global and regional NWP since 2006. In recent years, studies utilizing reflected GNSS signals to derive altimetric height, surface roughness, soil moisture, snow depth, humidity or vegetation index have been evolving. Ocean-platform GNSS observations have been demonstrating their capability of real-time monitoring of maritime water vapor as well as sea level. Increasing observations provided through Multi-GNSS (GPS, GLONASS, BEIDOU, GALILEO, QZSS etc.) enhances capability of the GNSS as an integrated earth observation system.
The purpose of this session is to share the latest development of GNSS researches on monitoring the earth system and to stimulate synergetic interdisciplinary studies. Contributions on atmosphere (troposphere and ionosphere) studies, reflectometry (GNSS-R), and integrations of different observation techniques like GNSS-Acoustic measurement to monitor ocean floor positioning are welcome.

12:05 PM - 12:15 PM

[MTT46-11]Discussion

©Japan Geoscience Union

[E] Poster | M (Multidisciplinary and Interdisciplinary) : M-TT Technology & Techniques

Mon. May 27, 2019 1:45 PM - 3:15 PM JST | Mon. May 27, 2019 4:45 AM - 6:15 AM UTC | Poster Hall International Exhibition Hall8, Makuhari Messe_10

[M-TT46] New phase of GPS/GNSS application as an integrated earth observation system

convener:Yoshinori Shoji(The Second Laboratory of Meteorological Satellite and Observation System Research Department, Meteorological Research Institute), Kaoru Ichikawa(Research Institute for Applied Mechanics, Kyushu University), Yusaku Ohta(Research Center for Prediction of Earthquakes and Volcanic Eruptions, Graduate School of Science, Tohoku University), Takuya Tsugawa(National Institute of Information and Communications Technology)

GNSS has become a fundamental tool for studies on atmosphere, ionosphere, and solid earth. Ground and space-based GNSS measurements have operationally contributed to improve global and regional NWP since 2006. In recent years, studies utilizing reflected GNSS signals to derive altimetric height, surface roughness, soil moisture, snow depth, humidity or vegetation index have been evolving. Ocean-platform GNSS observations have been demonstrating their capability of real-time monitoring of maritime water vapor as well as sea level. Increasing observations provided through Multi-GNSS (GPS, GLONASS, BEIDOU, GALILEO, QZSS etc.) enhances capability of the GNSS as an integrated earth observation system.
The purpose of this session is to share the latest development of GNSS researches on monitoring the earth system and to stimulate synergetic interdisciplinary studies. Contributions on atmosphere (troposphere and ionosphere) studies, reflectometry (GNSS-R), and integrations of different observation techniques like GNSS-Acoustic measurement to monitor ocean floor positioning are welcome.

[MTT46-P01] Continuous acoustic ranging from a GNSS buoy for the new method of seafloor crustal deformation measurements

*Keiichi Tadokoro[1], Natsuki Kinugasa[1], Teruyuki Kato[2], Yukihiro Terada[3], Akira Futamura[4], Kenjiro Matsuhiro[1] (1.Research Center for Seismology, Volcanology and Earthquake and Volcano Research Center, Nagoya University, 2.Hot Springs Research Institute of Kanagawa Prefecture, 3.Kochi National College of Technology, 4.National Institute of Technology, Yuge College)

[MTT46-P02] Accuracy and precision assessment of the real-time kinematic GNSS time series for moored buoy using three-axis programable moving table

*Yusaku Ohta[1], Misae Imano[1], Motoyuki Kido[2] (1.Research Center for Prediction of Earthquakes and Volcanic Eruptions, Graduate School of Science, Tohoku University, 2.IRIDeS, Tohoku University)

[MTT46-P03] GNSS-R altimetry using a Geostationary Satellite

*Kaoru Ichikawa[1], Tatsuki Okumura[2], Masanori Konda[3], Yasuyuki Baba[4] (1.Res. Inst. Appl. Mech., Kyushu Univ., 2.Dept. ESST, Interdicipl. Grad. School Eng. Sc., Kyushu Univ., 3.Graduate School of Science, Kyoto Univ., 4.Disaster Prevention Res. Inst., Kyoto Univ.)

[MTT46-P04] Estimation of typhoon wind speed using CYGNSS observations: A case study of Typhoon Lan in 2017

*Kako Shinichiro[1], Hiroyuki Tomita[2], Kaoru Ichikawa[3] (1.Graduate School of Science and Engineering, Kagoshima University, 2.Institute for Space-Earth Environment, Nagoya University, 3.Research institute for Applied Mechanics, Kyushu University)

[MTT46-P05] Ionospheric and seismic effects caused by the North Korea nuclear tests realized on 2006-2017

Nataliia Perevalova[2], *Nikolai Shestakov[1], Anna Dobrynina[3,4], Dmitry Kostylev[7], Meng Guojie[5], Wei-Wei Wu[5,6] (1.Institute for Applied Mathematics FEB RAS, Vladivostok, Russia; Far Eastern Federal University, Vladivostok, Russia, 2.Institute of Solar-Terrestrial Physics SB RAS, Irkutsk, Russia, 3.Institute of the Earth's Crust SB RAS, Irkutsk, Russia , 4.Geological institute SB RAS, Ulan-Ude, Russia , 5.Institute of Earthquake Forecasting, China Earthquake Administration, Beijing, China, 6.College of Surveying and

Geo-informatics, Tongji University, Shanghai, China, 7.Sakhalin Branch of Federal Research Center Geophysical Survey RAS, Yuzhno_Sakhalinsk, Russia)

[MTT46-P06] Relationships between Water Vapor Concentration Index derived from GNSS and Surface Wind Convergence during Localized Heavy Rainfall in Tokyo in Summer

*Yoshihito Seto[1], Yoshinori Shoji[2], Nobumitsu Tsunematsu[3], Hideo Takahashi[1] (1.Department of Geography, Graduate School of Urban Environmental Sciences, Tokyo Metropolitan University, 2.Meteorological Research Institute, 3.Tokyo Metropolitan Research Institute for Environmental Protection)

[MTT46-P07] Development of novel ground-based microwave radiometer for earth science - preliminary report-

*Ryuichi Ichikawa[1], Hideki Ujihara[1], Shinsuke Satoh[1], Jun Amagai[1], Yusaku Ohta[2], Basara Miyahara[3], Hiroshi Munekane[3], Taketo Nagasaki[4], Osamu Tajima[5], Kentaro Araki[6], Takuya Tajiri[6], Hiroshi Takiguchi[7], Takeshi Matsushima[8], Nobuo Matsushima[9], Tatsuya Momotani[10], Kenji Utsunomiya[10] (1.National Institute of Information and Communications Technology, 2.Tohoku University, 3.Geospatial Information Authority of Japan, 4.High Energy Accelerator Research Organization, 5.Kyoto University, 6.Meteorological Research Institute, JMA, 7.Japan Aerospace eXploration Agency, 8.Kyushu University, 9.National Institute of Advanced Industrial Science and Technology, 10.Japan Weather Association)

[MTT46-P08] Refractivity Distributions over the Kanto Plain Obtained by Dual-polarization Radar

*Hiromu Seko[1], Eiichi Sato[1], Hiroshi Yamauchi[2] (1.Meteorological Research Institute, 2.Japan Meteorological Agency)

[MTT46-P09] Spatial and temporal distribution of tropospheric water vapor observed by a Raman lidar and a GNSS receiver network over Shigaraki, Japan

*Masanori Yabuki[1], Toshitaka Tsuda[1], Yuya Kawano[2], Yusaku Tottori[2], Makoto Tsukamoto[2], Eiji Takeuchi[2] (1.Research Institute for Sustainable Humanosphere, Kyoto University, 2.EKO Instruments Co., Ltd.)

[MTT46-P10] **Study of the Mechanisms of Severe Thunderstorm in Tokyo Metropolitan Area using High Frequent Assimilation of GNSS and Other Ground-based Observations**

*Yoshinori Shoji[1], Tetsu Sakai[2], Ahoro Adachi[1], Satoru Yoshida[2], Tomohiro Nagai[2] (1.The Second Laboratory of Meteorological Satellite and Observation System Research Department, Meteorological Research Institute, 2.The Third Laboratory of Meteorological Satellite and Observation System Research Department, Meteorological Research Institute)

Continuous acoustic ranging from a GNSS buoy for the new method of seafloor crustal deformation measurements

*Keiichi Tadokoro[1], Natsuki Kinugasa[1], Teruyuki Kato[2], Yukihiro Terada[3], Akira Futamura[4], Kenjiro Matsuhiro[1]

1. Research Center for Seismology, Volcanology and Earthquake and Volcano Research Center, Nagoya University, 2. Hot Springs Research Institute of Kanagawa Prefecture, 3. Kochi National College of Technology, 4. National Institute of Technology, Yuge College

Our research group has been testing a measurement system for the continuous seafloor crustal deformation at a moored buoysite operated by Kochi prefecture, located 32 km off Cape Ashizuri, Japan.An acoustic transducer was fixed at about 1.7 m beneath the sea surface with a pole mounted on the buoy body.Three ocean bottom acoustic transponders had been installed around the moored point of the buoy. The acoustic signals are sequentially transmitted to these three transponders every three minutes. The recorded data on the buoy are planned to transmitted to a ground base station through a commercial communication satellite operated by Thuraya Telecommunications Company.
We performed a test for the continuous acoustic ranging between the buoy and the ocean bottom transponders from March 28 to 31 and from June 2 to July 12 (1st period), and from November 16to December 17 (2nd period) in 2018. The acoustic ranging was continuously possible throughout the above periods when power was supplied whereas it was unexpectedly terminated because of power failure during the winter season. The acoustic signals were transmitted 27,856 times in total, and the buoy-mounted acoustic ranging unit received 23,342 signals from the ocean bottom transponders. However, the acoustic data sent to the ground base station was only 12 % because of some trouble of the satellite communication modem.
The reflected signals from the buoy body and/or the seafloor sometimes contaminated the received acoustic signals; also multiple reflections inside of an anti-reflection cover attached to the buoy-mounted transducer, whose purpose is to cut off the reflection from the sea surface, were remarkable during the 1st period. The multiple reflections caused the misidentification of the direct wave from the sea-bottom units. We, therefore, removed the anti-reflection cover during the 2nd period, which remarkably reduced the confused reflections.
We coded a program for detecting the arrival time of direct acoustic wave automatically on the basis of thresholds of cross-correlation coefficient and energy ratio (the ratio of the squared amplitudes preceding and following a test point) to reduce the capacity of data transferred via satellite communication using the acoustic waveform recorded during the 1st period. The program successfully picked the correct direct wave onset for more than 99 % of the waveforms recorded during the 2nd period.

©2019. Japan Geoscience Union. All Right Reserved.

Accuracy and precision assessment of the real-time kinematic GNSS time series for moored buoy using three-axis programable moving table

*Yusaku Ohta[1], Misae Imano[1], Motoyuki Kido[2]

1. Research Center for Prediction of Earthquakes and Volcanic Eruptions, Graduate School of Science, Tohoku University, 2. IRIDeS, Tohoku University

Rapid understanding of the magnitude of large earthquakes and their associated fault dimensions are extremely important. Especially, capture of the coseismic deformation in the offshore region will be key information to understand the fault dimensions for the large interplate earthquake. Based on this background, Tohoku University and JAMSTEC are jointly developing the on-demand crustal deformation monitoring system using moored buoy system. The buoy can measure the sea-floor horizontal crustal deformation by GNSS/Acoustic technique and vertical deformation using ocean bottom pressure sensor. One of the key technology in our developed system is the real-time kinematic GNSS which can measure three-dimensional position of the buoy in real-time. In contrast, it is difficult to understand quantitatively the precision and accuracy of estimated buoy position because no reference for the position. Thus, we assess the precision and accuracy of real-time kinematic GNSS time series using programable three-axis movable table.

We have developed the single-axis precise programable movable table (Ohta et al., 2016). We expanded this developed system to three-axis. For the real-time kinematic analysis, we adopted Trimble CenterPoint RTX (hereafter, RTX) with 10Hz sampling interval. The correction message for the analysis was received via a stationary satellite. We also estimated the GNSS antenna position using very short-baseline kinematic analysis as reference solution. The developed movable table can operate single axis horizontal displacement, rotational movement, and tilt deformation. To simulate the actual buoy movement, we gave the motion to the movable table based on the actual buoy movement. We conducted the experiment in 24 hours duration.

We calculated the residual time series between obtain time series by RTX and short-baseline kinematic solution. The difference between averaged absolute position was quite good in the horizontal components which was less than 10mm. In contrast, the vertical component shows the clear discrepancy between them. RTX time series shows systemically higher than the baseline analysis which reached approximately 230mm. In contrast, the precision of the calculated residual time series was good in both of the components. Calculated standard deviations were 10-11mm and 28mm in horizontal components and vertical component, respectively. We will show the more detailed results from our experiment and discuss the ability of the real-time kinematic analysis in our developed buoy.

©2019. Japan Geoscience Union. All Right Reserved.

GNSS-R altimetry using a Geostationary Satellite

*Kaoru Ichikawa[1], Tatsuki Okumura[2], Masanori Konda[3], Yasuyuki Baba[4]

1. Res. Inst. Appl. Mech., Kyushu Univ., 2. Dept. ESST, Interdicipl. Grad. School Eng. Sc., Kyushu Univ., 3. Graduate School of Science, Kyoto Univ., 4. Disaster Prevention Res. Inst., Kyoto Univ.

The GNSS reflectometry (GNSS-R) uses GNSS signals reflected at the sea surface, which are usually eliminated as the multipath error. The reflected GNSS path received at an antenna is always longer than the direct path, so that the height of the antenna from the sea surface is geometrically determined from the excess path length. The excess path length can be either directly determined by measuring the temporal delay of the reflected signals, or indirectly estimated from interferometric cyclic modulations of the received power (often referred as signal-to-noise ratio; SNR) induced by phase differences between the direct and reflected GNSS signals. In the latter method, as the elevation angle of an earth orbiting GNSS satellite changes in time, the geometric reflection point on the sea surface temporally displaces, which results in interferometric changes of the path length during a period while the satellite is in sight. Meanwhile, for a geostationary satellite in BeiDou constellations that are always in sight, the path length changes not by the movement of the satellite but the elevation of the reflection surface, *i.e.* the sea level rise. In this study, we used the three-month time series (2016/09-11) of the 1Hz SNR of the geostationary BeiDou #02 satellite observed by a GNSS-R system deployed to the Shirahama Oceanographic Observatory Tower owned by Kyoto University (33deg, 42’ 32’’ N, 135deg, 19’ 58’’ E) at the height of ~20m. The geostationary GNSS-R altimetry observed significant flood tides when the wind speed is stably low; the 0.6m sea level rise was successfully determined by the SNR interferometry with 0.05m rms difference. However, significant interferometric SNR changes by tides were not recorded at high or low tides since at least 0.25m sea level change is required for the interferometry cycle. Consequently, the cyclic periods of the geostationary GNSS-R altimetry for tides become long (1-4 hours for 0.25m change in Shirahama), the interferometric variations were usually contaminated by SNR changes induced by the other factors such as winds. On the contrary, faster sea level changes by wave motions could be recognized by the geostationary GNSS-R altimetry, although the temporal sampling intervals of the present data were not adequate.

Keywords: GNSS-R , altimetry, BeiDou geostationary GNSS satellite

©2019. Japan Geoscience Union. All Right Reserved.

Estimation of typhoon wind speed using CYGNSS observations: A case study of Typhoon Lan in 2017

*Kako Shinichiro[1], Hiroyuki Tomita[2], Kaoru Ichikawa[3]

1. Graduate School of Science and Engineering, Kagoshima University, 2. Institute for Space-Earth Environment, Nagoya University, 3. Research institute for Applied Mechanics, Kyushu University

We conducted a case study of Typhoon Lan, which occurred in 2017, to investigate the impact of the Cyclone Global Navigation Satellite System (CYGNSS) on the estimation of extremely high wind speeds, such as those occurring during typhoons. We studied CYGNSS because it is expected to be capable of observing wind speeds in regions with extremely high wind speeds and heavy rains (i.e., typhoons) where it is difficult to perform measurements using the current microwave instrument. Firstly, we compared CYGNSS-derived wind speeds produced by NASA with those derived from AMSR2 produced by the Japan Aerospace Exploration Agency. CYGNSS was found to underestimate the wind speeds around Typhoon Lan compared with AMSR2. We then attempted to estimate the wind speeds using the leading edge slope (LES) and mean square slope (MSS) derived from the CYGNSS observations. Although the relationship between the MSS and wind speed differs depending on the wave age (Zhao and Tobe, 2003), it is difficult to estimate the wave age because this estimation is required the wind and wave speeds. We used the wave period as a substitute for the wave age since the wave period is expected to be similar to the wave age. We therefore first computed the fourth power of the wave period (T4) in line with Wang and Ichikawa (2016). Next, we classified the ocean into three regions based on T4 to investigate the relationship between the MSS and the wind speed observed by AMSR2 in each region. Finally, we approximated the curves relating the MSS to the wind speed using exponential functions in the three regions and estimated the wind speed using these curves. The comparison between the wind speeds produced by NASA and those estimated in this study demonstrated that our method can estimate high wind speeds more accurate than the CYGNSS wind speeds produced by NASA.

Keywords: CYGNSS, AMSR2, tyhoon

©2019. Japan Geoscience Union. All Right Reserved.

Ionospheric and seismic effects caused by the North Korea nuclear tests realized on 2006-2017

Nataliia Perevalova[2], *Nikolai Shestakov[1], Anna Dobrynina[3,4], Dmitry Kostylev[7], Meng Guojie[5], Wei-Wei Wu[5,6]

1. Institute for Applied Mathematics FEB RAS, Vladivostok, Russia; Far Eastern Federal University, Vladivostok, Russia, 2. Institute of Solar-Terrestrial Physics SB RAS, Irkutsk, Russia, 3. Institute of the Earth's Crust SB RAS, Irkutsk, Russia , 4. Geological institute SB RAS, Ulan-Ude, Russia , 5. Institute of Earthquake Forecasting, China Earthquake Administration, Beijing, China, 6. College of Surveying and Geo-informatics, Tongji University, Shanghai, China, 7. Sakhalin Branch of Federal Research Center Geophysical Survey RAS, Yuzhno_Sakhalinsk, Russia

Using data from GPS/GLONASS receivers and seismic networks, we studied the ionospheric and lithospheric effects caused by six underground nuclear tests realized in North Korea on 2006-2017.
To investigate the ionospheric disturbances, we analyzed data from several continuous GNSS-networks (GPS and GLONASS) operating in Asia - Western Pacific region: IGS, GEONET, FEB RAS and FEFU complex geodynamic network, a set of stations belonging to China and South Korea GNSS-networks. Sites close to the Korean Peninsula were selected for the analysis. Series of total electron content (TEC) in the ionosphere were calculated on the base of dual-frequency phase measurements of GNSS receivers. To detect disturbances caused by the nuclear tests, TEC series were filtered in the range of periods from 1 to 10 minutes. Despite the small magnitudes of seismic events associated with the nuclear tests, we were able to identify ionospheric disturbances which were most likely generated by these explosions. Such disturbances were detected for 4 out of 6 nuclear tests. The main parameters of the disturbances were determined. From our analysis we concluded that characteristics of ionospheric disturbances caused by the underground nuclear tests differed significantly from the parameters of disturbances that are usually observed after earthquakes.
For seismic analysis, we used data from the broadband seismic station networks located at distances up to 23 degrees from the Korean Peninsula: II, IC, IU, TW, JP, G, KS, and KG given by IRIS, and regional seismic network BY. The frequency content of P and surface Rayleigh waves registered by 46 broadband stations was analyzed. For some events, the P-wave frequency content showed the prevalence of low frequencies in spectra (~0.45 Hz). The peak frequencies of the surface Rayleigh waves was in the 0.05-0.45 Hz range. Preliminary analysis of the peak frequencies spatial distribution showed that the continental massive area is characterized by the relatively high frequencies (0.14-0.50 Hz) while for the areas adjacent to marginal seas the low values of peak frequencies are observed (from 0.13 Hz and less).
Acknowledgments. We are deeply indebted to Scripps Orbit and Permanent Array Center (SOPAC) for the IGS-network data, to Geospatial Information Authority of Japan for GEONET network data, to Korea Astronomy & Space Science Institute for access to GNSS data on the Korean Peninsula, CCU CC FEB RAS for access to data from the FEB RAS and FEFU complex geodynamic network; Institute of Earthquake Forecasting, China Earthquake Administration for access to GNSS data in China. The facilities of the IRIS Data Management System, and specifically the IRIS Data Management Center, and Baikal Regional Seismological Center and Sakhalin Branch of Federal Research Center Geophysical Survey RAS were used to get waveform and metadata required in this study. This work was performed with budgetary funding of Basic Research program II.16 and was also partially supported by RFBR grants 17-45-388072_p_a, 17-45-388049_ p_a, 17-55-53110_GFEN_a, 19-05-00889_a.

Keywords: North Korea nuclear tests, ionospheric and lithospheric effects, GPS/GLONASS-observations

©2019. Japan Geoscience Union. All Right Reserved.

©2019. Japan Geoscience Union. All Right Reserved.

Relationships between Water Vapor Concentration Index derived from GNSS and Surface Wind Convergence during Localized Heavy Rainfall in Tokyo in Summer

*Yoshihito Seto[1], Yoshinori Shoji[2], Nobumitsu Tsunematsu[3], Hideo Takahashi[1]

1. Department of Geography, Graduate School of Urban Environmental Sciences, Tokyo Metropolitan University, 2. Meteorological Research Institute, 3. Tokyo Metropolitan Research Institute for Environmental Protection

In recent years, short-term heavy-rainfall events that have caused severe damages such as flooding have frequently occurred in the Tokyo Metropolitan area in summer. In view of the development process of cumulonimbus clouds, the convergence of surface winds and the spatial concentration of water vapor are supposed to have taken place prior to the occurrence of heavy rainfall. This study aims to clarify the evolutionary process of short-term heavy rainfall as a contribution to short-range forecasting of heavy rainfall that occurs locally.

The relationships between the occurrence of heavy rainfall and the convergence of surface winds and water vapor concentration for heavy-rainfall cases were examined using data from July to September obtained from high-density meteorological observations in Tokyo, Japan. We used the water vapor concentration (WVC) index derived from the global navigation satellite system (GNSS) analysis as indices for the degree of divergence and convergence of water vapor in the lower troposphere (Shoji 2013).

Corresponding to heavy-rainfall areas, the convergence of surface winds tended to increase for several tens of minutes prior to the heavy rainfall. The peak time of wind convergence was observed 10–30 min before the heavy-rainfall occurrence, and the convergence continued to increase for approximately 30 min until the convergence peak time (Seto et al. 2018). Around the heavy-rainfall area, the increase in the WVC index coincided with the increase in convergence. On the other hand, it was considered that the temporal and spatial scales of the WVC index are larger than those of wind convergence. From these results, by monitoring the temporal variations and distributions of these parameters using a high-density observation network, it should be possible to predict the occurrence of heavy rainfall rapidly and accurately.

References

Seto, Y., Yokoyama, H., Nakatani, T., Ando, H., Tsunematsu, N., Shoji, Y., Kusunoki, K., Nakayama, M., Saitoh, Y. and Takahashi, H. 2018. Relationships among rainfall distribution, surface wind, and precipitable water vapor during heavy rainfall in central Tokyo in summer. J. Meteor. Soc. Japan, 96A, 35–49.

Shoji, Y. 2013. Retrieval of water vapor inhomogeneity using the Japanese nationwide GPS array and its potential for prediction of convective precipitation. J. Meteor. Soc. Japan, 91, 43–62.

Keywords: localized heavy rainfall, wind convergence, water vapor, high-density observation

©2019. Japan Geoscience Union. All Right Reserved.

Development of novel ground-based microwave radiometer for earth science -preliminary report-

*Ryuichi Ichikawa[1], Hideki Ujihara[1], Shinsuke Satoh[1], Jun Amagai[1], Yusaku Ohta[2], Basara Miyahara[3], Hiroshi Munekane[3], Taketo Nagasaki[4], Osamu Tajima[5], Kentaro Araki[6], Takuya Tajiri[6], Hiroshi Takiguchi[7], Takeshi Matsushima[8], Nobuo Matsushima[9], Tatsuya Momotani[10], Kenji Utsunomiya[10]

1. National Institute of Information and Communications Technology, 2. Tohoku University, 3. Geospatial Information Authority of Japan, 4. High Energy Accelerator Research Organization, 5. Kyoto University, 6. Meteorological Research Institute, JMA, 7. Japan Aerospace eXploration Agency, 8. Kyushu University, 9. National Institute of Advanced Industrial Science and Technology, 10. Japan Weather Association

We have started to develop a next-generation microwave radiometer to be used in millimeter-wave spectroscopy for the high-resolution and high-precision monitoring of water vapor behavior. The new radiometer will be suitable for not only space geodetic techniques such as VLBI and GNSS, but also field measurements such as monitoring volcanic activities and cumulonimbus cloud generation. The basic design concept of the new radiometer follows the previous version named KUMODeS (KEK Universal Moisture and Oxygen Detection System) developed by the High Energy Accelerator Research Organization (KEK). The KUMODeS can measure spectra using two receivers with frequency bands of 20–30 GHz and 50–60 GHz. The low-noise amplifier (LNA) of the first KUMODeS receiver and a cold calibration source are implemented in a cryostat, which is maintained at 10 K to improve the sensitivity of detecting the characteristic broad peak of water vapor at approximately 22 GHz. The second receiver is used to measure the absorption peaks of oxygen (60 GHz). We have carried out comparative measurements of precipitable water vapor (PWV) to investigate the potential of KUMODeS/PWV measurements. The preliminary results of PWV comparisons imply that KUMODeS technology will be useful for retrieving the accurate behavior of water vapor with high temporal resolution. We will implement a wide bandwidth feed of 20–60 GHz into the new system on the basis of a previous comparison study. A signal is separated into two linear orthogonal polarized signals from the feed, one is in the 20–30 GHz feed and the other in the 50–60 GHz feed, using an orthomode transducer (OMT). The wideband feed, OMT, and the LNA for each signal are cooled at 77 K using a Stirling cryocooler to improve signal-to-noise ratio. The development of a new front-end module will be completed at the end of 2019, and we are planning to implement the module in an existing dish antenna to perform validation measurements.

Keywords: GNSS, microwave radiometer, water vapor

©2019. Japan Geoscience Union. All Right Reserved.

Refractivity Distributions over the Kanto Plain Obtained by Dual-polarization Radar

*Hiromu Seko[1], Eiichi Sato[1], Hiroshi Yamauchi[2]

1. Meteorological Research Institute, 2. Japan Meteorological Agency

Temperature and water vapor near the surface play crucial roles for the generation of convection cells. However, their variations just before the generations of convection cells still are not understood completely. In this study the temporal variations of refractivity index were obtained by MRI dual-polarization Doppler radar. The features of temperature and water vapor including generation period of convection cells will be shown in this presentation. On 19th August 2017, the sea breeze invaded from Kashima-Nada and the refractivity increased along the front of the sea breeze. The scattered weak echoes that appeared around the front seem to be related with the increase of refractivity. These are the features near the surface. The comparison with other data such as GNSS PWV will be also presented.

Keywords: Observation method, Doppler radar, Refractivity index

©2019. Japan Geoscience Union. All Right Reserved.

Spatial and temporal distribution of tropospheric water vapor observed by a Raman lidar and a GNSS receiver network over Shigaraki, Japan

*Masanori Yabuki[1], Toshitaka Tsuda[1], Yuya Kawano[2], Yusaku Tottori[2], Makoto Tsukamoto[2], Eiji Takeuchi[2]

1. Research Institute for Sustainable Humanosphere, Kyoto University, 2. EKO Instruments Co., Ltd.

Understanding the spatial and temporal distributions of water vapor in the atmosphere is critical for unveiling the fundamental mechanisms of localized extreme weather events. Besides, it is highly beneficial for improving the accuracy of weather forecasts by mesoscale numerical weather prediction models. To achieve the continuous monitoring of water vapor distributions, we performed simultaneous measurements by Raman lidar in the UV-C region and a dense Global Navigation Satellite System (GNSS) network. The former is a novel technology that can be utilized for profiling the vertical distribution of the water vapor mixing ratio for twenty-four hours, while the latter can be used for detecting the horizontal distribution of precipitable water vapor. The Raman lidar employs a laser at a wavelength of 266 nm and detects the light separated into an elastic backscatter signal and vibrational Raman signals of oxygen, nitrogen, and water vapor at wavelengths of 266, 277, 284, and 295 nm, respectively. The use of these wavelengths is convenient because of the low background noise during daytime, since most of the solar radiation in the ultraviolet range below 300 nm is absorbed by the ozone layer in the stratosphere. The lidar was encased in a temperature-controlled compact container, resistant to a variety of environmental conditions. Continuous observation of water vapor profiles by lidar has been conducted at the Shigaraki MU radar observatory (34˚51’ N, 136˚06’ E, 385 m a.s.l.) since November 2017. The dense GNSS receiver network consisted of 10 dual-frequency GNSS stations which were installed with a horizontal spacing of 3-4 km near the observatory on July 2017. In this study, we present our water vapor monitoring system as well as the preliminary results on the spatio-temporal water vapor distributions in 2018.

Acknowledgements
A part of this study is supported by JSPS KAKENHI Grant Number 15H03724.

Keywords: water vapor, Raman lidar, dense GNSS network

©2019. Japan Geoscience Union. All Right Reserved.

Study of the Mechanisms of Severe Thunderstorm in Tokyo Metropolitan Area using High Frequent Assimilation of GNSS and Other Ground-based Observations

*Yoshinori Shoji[1], Tetsu Sakai[2], Ahoro Adachi[1], Satoru Yoshida[2], Tomohiro Nagai[2]

1. The Second Laboratory of Meteorological Satellite and Observation System Research Department, Meteorological Research Institute, 2. The Third Laboratory of Meteorological Satellite and Observation System Research Department, Meteorological Research Institute

Highly urbanized Tokyo metropolitan area is vulnerable to severe storms such as local torrential rainfall, thunder lightning and tornado. Recently, the number of days with thunderstorms has been increasing in Tokyo. Elucidation of the mechanism of extreme weather in Tokyo is urgent matter (Nakatani et al. 2013). To study the rolls of water vapor and wind for the rapid life-cycle (initiation, development and dissipation) of hazardous cumulus convection, we installed a mobile Raman-lidar (Sakai et al. 2018), a wind profiler, and five GNSS stations in and around Tokyo.

Using 3DVAR capability of WRF data assimilation system (WRFDA)(Barker et al. 2012) , three-dimensional atmospheric fields with 1 km horizontal resolution were produced at every 10min throughout the August 2017 and 2018. Background fields were produced by JMA nonhydrostatic model (NHM)(Saito et al. 2007). In addition to the observed data at these campaign observation instruments, Japan Meteorological Agency’ s operational surface meteorological stations, wind-profiler stations and GNSS PWV derived at dense GNSS network of Geospatial Information Authority of Japan are assimilated. We confirmed that the reproduced atmospheric fields (Temperature, humidity, and wind) showed better agreement with observations of radiosonde, lidar derived water vapor mixing ratio, and wind-profiler than background fields at altitudes lower than 2 km. Assimilation of surface meteorological observations (atmospheric pressure, temperature, humidity and wind) introduced better agreement mainly at altitude lower than 0.5 km. Inclusion of GNSS derived PWV resulted better agreement of humidity at altitude higher than 0.5 km and inclusion of wind field from wind-profiler led better agreement of wind field.

We have investigated roles of water vapor for several local heavy rainfall events occurred in Tokyo in August 2017 and 2018 and found that convergence of water vapor flux at 0.5 km altitude had intensified prior to the occurrence of torrential precipitation. Statistical and quantitative results will be discussed at the symposium.

This study is supported by JSPS KAKENHI Grants 17H00852.

Keywords: Water vapor, Data assimilation, Localized heavy rainfall

©2019. Japan Geoscience Union. All Right Reserved.

[E] Poster | M (Multidisciplinary and Interdisciplinary)：M-TT Technology & Techniques

Mon. May 27, 2019 5:15 PM - 6:30 PM JST | Mon. May 27, 2019 8:15 AM - 9:30 AM UTC | Poster Hall International Exhibition Hall8, Makuhari Messe_43

[M-TT46] New phase of GPS/GNSS application as an integrated earth observation system

convener:Yoshinori Shoji(The Second Laboratory of Meteorological Satellite and Observation System Research Department, Meteorological Research Institute), Kaoru Ichikawa(Research Institute for Applied Mechanics, Kyushu University), Yusaku Ohta(Research Center for Prediction of Earthquakes and Volcanic Eruptions, Graduate School of Science, Tohoku University), Takuya Tsugawa(National Institute of Information and Communications Technology)

GNSS has become a fundamental tool for studies on atmosphere, ionosphere, and solid earth. Ground and space-based GNSS measurements have operationally contributed to improve global and regional NWP since 2006. In recent years, studies utilizing reflected GNSS signals to derive altimetric height, surface roughness, soil moisture, snow depth, humidity or vegetation index have been evolving. Ocean-platform GNSS observations have been demonstrating their capability of real-time monitoring of maritime water vapor as well as sea level. Increasing observations provided through Multi-GNSS (GPS, GLONASS, BEIDOU, GALILEO, QZSS etc.) enhances capability of the GNSS as an integrated earth observation system.
The purpose of this session is to share the latest development of GNSS researches on monitoring the earth system and to stimulate synergetic interdisciplinary studies. Contributions on atmosphere (troposphere and ionosphere) studies, reflectometry (GNSS-R), and integrations of different observation techniques like GNSS-Acoustic measurement to monitor ocean floor positioning are welcome.

[MTT46-P01] Continuous acoustic ranging from a GNSS buoy for the new method of seafloor crustal deformation measurements

*Keiichi Tadokoro[1], Natsuki Kinugasa[1], Teruyuki Kato[2], Yukihiro Terada[3], Akira Futamura[4], Kenjiro Matsuhiro[1] (1.Research Center for Seismology, Volcanology and Earthquake and Volcano Research Center, Nagoya University, 2.Hot Springs Research Institute of Kanagawa Prefecture, 3.Kochi National College of Technology, 4.National Institute of Technology, Yuge College)

[MTT46-P02] Accuracy and precision assessment of the real-time kinematic GNSS time series for moored buoy using three-axis programable moving table

*Yusaku Ohta[1], Misae Imano[1], Motoyuki Kido[2] (1.Research Center for Prediction of Earthquakes and Volcanic Eruptions, Graduate School of Science, Tohoku University, 2.IRIDeS, Tohoku University)

[MTT46-P03] GNSS-R altimetry using a Geostationary Satellite

*Kaoru Ichikawa[1], Tatsuki Okumura[2], Masanori Konda[3], Yasuyuki Baba[4] (1.Res. Inst. Appl. Mech., Kyushu Univ., 2.Dept. ESST, Interdicipl. Grad. School Eng. Sc., Kyushu Univ., 3.Graduate School of Science, Kyoto Univ., 4.Disaster Prevention Res. Inst., Kyoto Univ.)

[MTT46-P04] Estimation of typhoon wind speed using CYGNSS observations: A case study of Typhoon Lan in 2017

*Kako Shinichiro[1], Hiroyuki Tomita[2], Kaoru Ichikawa[3] (1.Graduate School of Science and Engineering, Kagoshima University, 2.Institute for Space-Earth Environment, Nagoya University, 3.Research institute for Applied Mechanics, Kyushu University)

[MTT46-P05] Ionospheric and seismic effects caused by the North Korea nuclear tests realized on 2006-2017

Nataliia Perevalova[2], *Nikolai Shestakov[1], Anna Dobrynina[3,4], Dmitry Kostylev[7], Meng Guojie[5], Wei-Wei Wu[5,6] (1.Institute for Applied Mathematics FEB RAS, Vladivostok, Russia; Far Eastern Federal University, Vladivostok, Russia, 2.Institute of Solar-Terrestrial Physics SB RAS, Irkutsk, Russia, 3.Institute of the Earth's Crust SB RAS, Irkutsk, Russia , 4.Geological institute SB RAS, Ulan-Ude, Russia , 5.Institute of Earthquake Forecasting, China Earthquake Administration, Beijing, China, 6.College of Surveying and

Geo-informatics, Tongji University, Shanghai, China, 7.Sakhalin Branch of Federal Research Center Geophysical Survey RAS, Yuzhno_Sakhalinsk, Russia)

[MTT46-P06] Relationships between Water Vapor Concentration Index derived from GNSS and Surface Wind Convergence during Localized Heavy Rainfall in Tokyo in Summer

*Yoshihito Seto[1], Yoshinori Shoji[2], Nobumitsu Tsunematsu[3], Hideo Takahashi[1] (1.Department of Geography, Graduate School of Urban Environmental Sciences, Tokyo Metropolitan University, 2.Meteorological Research Institute, 3.Tokyo Metropolitan Research Institute for Environmental Protection)

[MTT46-P07] Development of novel ground-based microwave radiometer for earth science - preliminary report-

*Ryuichi Ichikawa[1], Hideki Ujihara[1], Shinsuke Satoh[1], Jun Amagai[1], Yusaku Ohta[2], Basara Miyahara[3], Hiroshi Munekane[3], Taketo Nagasaki[4], Osamu Tajima[5], Kentaro Araki[6], Takuya Tajiri[6], Hiroshi Takiguchi[7], Takeshi Matsushima[8], Nobuo Matsushima[9], Tatsuya Momotani[10], Kenji Utsunomiya[10] (1.National Institute of Information and Communications Technology, 2.Tohoku University, 3.Geospatial Information Authority of Japan, 4.High Energy Accelerator Research Organization, 5.Kyoto University, 6.Meteorological Research Institute, JMA, 7.Japan Aerospace eXploration Agency, 8.Kyushu University, 9.National Institute of Advanced Industrial Science and Technology, 10.Japan Weather Association)

[MTT46-P08] Refractivity Distributions over the Kanto Plain Obtained by Dual-polarization Radar

*Hiromu Seko[1], Eiichi Sato[1], Hiroshi Yamauchi[2] (1.Meteorological Research Institute, 2.Japan Meteorological Agency)

[MTT46-P09] Spatial and temporal distribution of tropospheric water vapor observed by a Raman lidar and a GNSS receiver network over Shigaraki, Japan

*Masanori Yabuki[1], Toshitaka Tsuda[1], Yuya Kawano[2], Yusaku Tottori[2], Makoto Tsukamoto[2], Eiji Takeuchi[2] (1.Research Institute for Sustainable Humanosphere, Kyoto University, 2.EKO Instruments Co., Ltd.)

[MTT46-P10] **Study of the Mechanisms of Severe Thunderstorm in Tokyo Metropolitan Area using High Frequent Assimilation of GNSS and Other Ground-based Observations**

*Yoshinori Shoji[1], Tetsu Sakai[2], Ahoro Adachi[1], Satoru Yoshida[2], Tomohiro Nagai[2] (1.The Second Laboratory of Meteorological Satellite and Observation System Research Department, Meteorological Research Institute, 2.The Third Laboratory of Meteorological Satellite and Observation System Research Department, Meteorological Research Institute)

Continuous acoustic ranging from a GNSS buoy for the new method of seafloor crustal deformation measurements

*Keiichi Tadokoro[1], Natsuki Kinugasa[1], Teruyuki Kato[2], Yukihiro Terada[3], Akira Futamura[4], Kenjiro Matsuhiro[1]

1. Research Center for Seismology, Volcanology and Earthquake and Volcano Research Center, Nagoya University, 2. Hot Springs Research Institute of Kanagawa Prefecture, 3. Kochi National College of Technology, 4. National Institute of Technology, Yuge College

Our research group has been testing a measurement system for the continuous seafloor crustal deformation at a moored buoysite operated by Kochi prefecture, located 32 km off Cape Ashizuri, Japan.An acoustic transducer was fixed at about 1.7 m beneath the sea surface with a pole mounted on the buoy body.Three ocean bottom acoustic transponders had been installed around the moored point of the buoy. The acoustic signals are sequentially transmitted to these three transponders every three minutes. The recorded data on the buoy are planned to transmitted to a ground base station through a commercial communication satellite operated by Thuraya Telecommunications Company.
We performed a test for the continuous acoustic ranging between the buoy and the ocean bottom transponders from March 28 to 31 and from June 2 to July 12 (1st period), and from November 16to December 17 (2nd period) in 2018. The acoustic ranging was continuously possible throughout the above periods when power was supplied whereas it was unexpectedly terminated because of power failure during the winter season. The acoustic signals were transmitted 27,856 times in total, and the buoy-mounted acoustic ranging unit received 23,342 signals from the ocean bottom transponders. However, the acoustic data sent to the ground base station was only 12 % because of some trouble of the satellite communication modem.
The reflected signals from the buoy body and/or the seafloor sometimes contaminated the received acoustic signals; also multiple reflections inside of an anti-reflection cover attached to the buoy-mounted transducer, whose purpose is to cut off the reflection from the sea surface, were remarkable during the 1st period. The multiple reflections caused the misidentification of the direct wave from the sea-bottom units. We, therefore, removed the anti-reflection cover during the 2nd period, which remarkably reduced the confused reflections.
We coded a program for detecting the arrival time of direct acoustic wave automatically on the basis of thresholds of cross-correlation coefficient and energy ratio (the ratio of the squared amplitudes preceding and following a test point) to reduce the capacity of data transferred via satellite communication using the acoustic waveform recorded during the 1st period. The program successfully picked the correct direct wave onset for more than 99 % of the waveforms recorded during the 2nd period.

©2019. Japan Geoscience Union. All Right Reserved.

Accuracy and precision assessment of the real-time kinematic GNSS time series for moored buoy using three-axis programable moving table

*Yusaku Ohta[1], Misae Imano[1], Motoyuki Kido[2]

1. Research Center for Prediction of Earthquakes and Volcanic Eruptions, Graduate School of Science, Tohoku University, 2. IRIDeS, Tohoku University

Rapid understanding of the magnitude of large earthquakes and their associated fault dimensions are extremely important. Especially, capture of the coseismic deformation in the offshore region will be key information to understand the fault dimensions for the large interplate earthquake. Based on this background, Tohoku University and JAMSTEC are jointly developing the on-demand crustal deformation monitoring system using moored buoy system. The buoy can measure the sea-floor horizontal crustal deformation by GNSS/Acoustic technique and vertical deformation using ocean bottom pressure sensor. One of the key technology in our developed system is the real-time kinematic GNSS which can measure three-dimensional position of the buoy in real-time. In contrast, it is difficult to understand quantitatively the precision and accuracy of estimated buoy position because no reference for the position. Thus, we assess the precision and accuracy of real-time kinematic GNSS time series using programable three-axis movable table.

We have developed the single-axis precise programable movable table (Ohta et al., 2016). We expanded this developed system to three-axis. For the real-time kinematic analysis, we adopted Trimble CenterPoint RTX (hereafter, RTX) with 10Hz sampling interval. The correction message for the analysis was received via a stationary satellite. We also estimated the GNSS antenna position using very short-baseline kinematic analysis as reference solution. The developed movable table can operate single axis horizontal displacement, rotational movement, and tilt deformation. To simulate the actual buoy movement, we gave the motion to the movable table based on the actual buoy movement. We conducted the experiment in 24 hours duration.

We calculated the residual time series between obtain time series by RTX and short-baseline kinematic solution. The difference between averaged absolute position was quite good in the horizontal components which was less than 10mm. In contrast, the vertical component shows the clear discrepancy between them. RTX time series shows systemically higher than the baseline analysis which reached approximately 230mm. In contrast, the precision of the calculated residual time series was good in both of the components. Calculated standard deviations were 10-11mm and 28mm in horizontal components and vertical component, respectively. We will show the more detailed results from our experiment and discuss the ability of the real-time kinematic analysis in our developed buoy.

©2019. Japan Geoscience Union. All Right Reserved.

GNSS-R altimetry using a Geostationary Satellite

*Kaoru Ichikawa[1], Tatsuki Okumura[2], Masanori Konda[3], Yasuyuki Baba[4]

1. Res. Inst. Appl. Mech., Kyushu Univ., 2. Dept. ESST, Interdicipl. Grad. School Eng. Sc., Kyushu Univ., 3. Graduate School of Science, Kyoto Univ., 4. Disaster Prevention Res. Inst., Kyoto Univ.

The GNSS reflectometry (GNSS-R) uses GNSS signals reflected at the sea surface, which are usually eliminated as the multipath error. The reflected GNSS path received at an antenna is always longer than the direct path, so that the height of the antenna from the sea surface is geometrically determined from the excess path length. The excess path length can be either directly determined by measuring the temporal delay of the reflected signals, or indirectly estimated from interferometric cyclic modulations of the received power (often referred as signal-to-noise ratio; SNR) induced by phase differences between the direct and reflected GNSS signals. In the latter method, as the elevation angle of an earth orbiting GNSS satellite changes in time, the geometric reflection point on the sea surface temporally displaces, which results in interferometric changes of the path length during a period while the satellite is in sight. Meanwhile, for a geostationary satellite in BeiDou constellations that are always in sight, the path length changes not by the movement of the satellite but the elevation of the reflection surface, *i.e.* the sea level rise. In this study, we used the three-month time series (2016/09-11) of the 1Hz SNR of the geostationary BeiDou #02 satellite observed by a GNSS-R system deployed to the Shirahama Oceanographic Observatory Tower owned by Kyoto University (33deg, 42’ 32’’ N, 135deg, 19’ 58’’ E) at the height of ~20m. The geostationary GNSS-R altimetry observed significant flood tides when the wind speed is stably low; the 0.6m sea level rise was successfully determined by the SNR interferometry with 0.05m rms difference. However, significant interferometric SNR changes by tides were not recorded at high or low tides since at least 0.25m sea level change is required for the interferometry cycle. Consequently, the cyclic periods of the geostationary GNSS-R altimetry for tides become long (1-4 hours for 0.25m change in Shirahama), the interferometric variations were usually contaminated by SNR changes induced by the other factors such as winds. On the contrary, faster sea level changes by wave motions could be recognized by the geostationary GNSS-R altimetry, although the temporal sampling intervals of the present data were not adequate.

Keywords: GNSS-R , altimetry, BeiDou geostationary GNSS satellite

©2019. Japan Geoscience Union. All Right Reserved.

Estimation of typhoon wind speed using CYGNSS observations: A case study of Typhoon Lan in 2017

*Kako Shinichiro[1], Hiroyuki Tomita[2], Kaoru Ichikawa[3]

1. Graduate School of Science and Engineering, Kagoshima University, 2. Institute for Space-Earth Environment, Nagoya University, 3. Research institute for Applied Mechanics, Kyushu University

We conducted a case study of Typhoon Lan, which occurred in 2017, to investigate the impact of the Cyclone Global Navigation Satellite System (CYGNSS) on the estimation of extremely high wind speeds, such as those occurring during typhoons. We studied CYGNSS because it is expected to be capable of observing wind speeds in regions with extremely high wind speeds and heavy rains (i.e., typhoons) where it is difficult to perform measurements using the current microwave instrument. Firstly, we compared CYGNSS-derived wind speeds produced by NASA with those derived from AMSR2 produced by the Japan Aerospace Exploration Agency. CYGNSS was found to underestimate the wind speeds around Typhoon Lan compared with AMSR2. We then attempted to estimate the wind speeds using the leading edge slope (LES) and mean square slope (MSS) derived from the CYGNSS observations. Although the relationship between the MSS and wind speed differs depending on the wave age (Zhao and Tobe, 2003), it is difficult to estimate the wave age because this estimation is required the wind and wave speeds. We used the wave period as a substitute for the wave age since the wave period is expected to be similar to the wave age. We therefore first computed the fourth power of the wave period (T4) in line with Wang and Ichikawa (2016). Next, we classified the ocean into three regions based on T4 to investigate the relationship between the MSS and the wind speed observed by AMSR2 in each region. Finally, we approximated the curves relating the MSS to the wind speed using exponential functions in the three regions and estimated the wind speed using these curves. The comparison between the wind speeds produced by NASA and those estimated in this study demonstrated that our method can estimate high wind speeds more accurate than the CYGNSS wind speeds produced by NASA.

Keywords: CYGNSS, AMSR2, tyhoon

©2019. Japan Geoscience Union. All Right Reserved.

Ionospheric and seismic effects caused by the North Korea nuclear tests realized on 2006-2017

Nataliia Perevalova[2], *Nikolai Shestakov[1], Anna Dobrynina[3,4], Dmitry Kostylev[7], Meng Guojie[5], Wei-Wei Wu[5,6]

1. Institute for Applied Mathematics FEB RAS, Vladivostok, Russia; Far Eastern Federal University, Vladivostok, Russia, 2. Institute of Solar-Terrestrial Physics SB RAS, Irkutsk, Russia, 3. Institute of the Earth's Crust SB RAS, Irkutsk, Russia , 4. Geological institute SB RAS, Ulan-Ude, Russia , 5. Institute of Earthquake Forecasting, China Earthquake Administration, Beijing, China, 6. College of Surveying and Geo-informatics, Tongji University, Shanghai, China, 7. Sakhalin Branch of Federal Research Center Geophysical Survey RAS, Yuzhno_Sakhalinsk, Russia

Using data from GPS/GLONASS receivers and seismic networks, we studied the ionospheric and lithospheric effects caused by six underground nuclear tests realized in North Korea on 2006-2017.
To investigate the ionospheric disturbances, we analyzed data from several continuous GNSS-networks (GPS and GLONASS) operating in Asia - Western Pacific region: IGS, GEONET, FEB RAS and FEFU complex geodynamic network, a set of stations belonging to China and South Korea GNSS-networks. Sites close to the Korean Peninsula were selected for the analysis. Series of total electron content (TEC) in the ionosphere were calculated on the base of dual-frequency phase measurements of GNSS receivers. To detect disturbances caused by the nuclear tests, TEC series were filtered in the range of periods from 1 to 10 minutes. Despite the small magnitudes of seismic events associated with the nuclear tests, we were able to identify ionospheric disturbances which were most likely generated by these explosions. Such disturbances were detected for 4 out of 6 nuclear tests. The main parameters of the disturbances were determined. From our analysis we concluded that characteristics of ionospheric disturbances caused by the underground nuclear tests differed significantly from the parameters of disturbances that are usually observed after earthquakes.
For seismic analysis, we used data from the broadband seismic station networks located at distances up to 23 degrees from the Korean Peninsula: II, IC, IU, TW, JP, G, KS, and KG given by IRIS, and regional seismic network BY. The frequency content of P and surface Rayleigh waves registered by 46 broadband stations was analyzed. For some events, the P-wave frequency content showed the prevalence of low frequencies in spectra (~0.45 Hz). The peak frequencies of the surface Rayleigh waves was in the 0.05-0.45 Hz range. Preliminary analysis of the peak frequencies spatial distribution showed that the continental massive area is characterized by the relatively high frequencies (0.14-0.50 Hz) while for the areas adjacent to marginal seas the low values of peak frequencies are observed (from 0.13 Hz and less).
Acknowledgments. We are deeply indebted to Scripps Orbit and Permanent Array Center (SOPAC) for the IGS-network data, to Geospatial Information Authority of Japan for GEONET network data, to Korea Astronomy & Space Science Institute for access to GNSS data on the Korean Peninsula, CCU CC FEB RAS for access to data from the FEB RAS and FEFU complex geodynamic network; Institute of Earthquake Forecasting, China Earthquake Administration for access to GNSS data in China. The facilities of the IRIS Data Management System, and specifically the IRIS Data Management Center, and Baikal Regional Seismological Center and Sakhalin Branch of Federal Research Center Geophysical Survey RAS were used to get waveform and metadata required in this study. This work was performed with budgetary funding of Basic Research program II.16 and was also partially supported by RFBR grants 17-45-388072_p_a, 17-45-388049_ p_a, 17-55-53110_GFEN_a, 19-05-00889_a.

Keywords: North Korea nuclear tests, ionospheric and lithospheric effects, GPS/GLONASS-observations

©2019. Japan Geoscience Union. All Right Reserved.

©2019. Japan Geoscience Union. All Right Reserved.

Relationships between Water Vapor Concentration Index derived from GNSS and Surface Wind Convergence during Localized Heavy Rainfall in Tokyo in Summer

*Yoshihito Seto[1], Yoshinori Shoji[2], Nobumitsu Tsunematsu[3], Hideo Takahashi[1]

1. Department of Geography, Graduate School of Urban Environmental Sciences, Tokyo Metropolitan University, 2. Meteorological Research Institute, 3. Tokyo Metropolitan Research Institute for Environmental Protection

In recent years, short-term heavy-rainfall events that have caused severe damages such as flooding have frequently occurred in the Tokyo Metropolitan area in summer. In view of the development process of cumulonimbus clouds, the convergence of surface winds and the spatial concentration of water vapor are supposed to have taken place prior to the occurrence of heavy rainfall. This study aims to clarify the evolutionary process of short-term heavy rainfall as a contribution to short-range forecasting of heavy rainfall that occurs locally.

The relationships between the occurrence of heavy rainfall and the convergence of surface winds and water vapor concentration for heavy-rainfall cases were examined using data from July to September obtained from high-density meteorological observations in Tokyo, Japan. We used the water vapor concentration (WVC) index derived from the global navigation satellite system (GNSS) analysis as indices for the degree of divergence and convergence of water vapor in the lower troposphere (Shoji 2013).

Corresponding to heavy-rainfall areas, the convergence of surface winds tended to increase for several tens of minutes prior to the heavy rainfall. The peak time of wind convergence was observed 10–30 min before the heavy-rainfall occurrence, and the convergence continued to increase for approximately 30 min until the convergence peak time (Seto et al. 2018). Around the heavy-rainfall area, the increase in the WVC index coincided with the increase in convergence. On the other hand, it was considered that the temporal and spatial scales of the WVC index are larger than those of wind convergence. From these results, by monitoring the temporal variations and distributions of these parameters using a high-density observation network, it should be possible to predict the occurrence of heavy rainfall rapidly and accurately.

References

Seto, Y., Yokoyama, H., Nakatani, T., Ando, H., Tsunematsu, N., Shoji, Y., Kusunoki, K., Nakayama, M., Saitoh, Y. and Takahashi, H. 2018. Relationships among rainfall distribution, surface wind, and precipitable water vapor during heavy rainfall in central Tokyo in summer. J. Meteor. Soc. Japan, 96A, 35–49.

Shoji, Y. 2013. Retrieval of water vapor inhomogeneity using the Japanese nationwide GPS array and its potential for prediction of convective precipitation. J. Meteor. Soc. Japan, 91, 43–62.

Keywords: localized heavy rainfall, wind convergence, water vapor, high-density observation

©2019. Japan Geoscience Union. All Right Reserved.

Development of novel ground-based microwave radiometer for earth science -preliminary report-

*Ryuichi Ichikawa[1], Hideki Ujihara[1], Shinsuke Satoh[1], Jun Amagai[1], Yusaku Ohta[2], Basara Miyahara[3], Hiroshi Munekane[3], Taketo Nagasaki[4], Osamu Tajima[5], Kentaro Araki[6], Takuya Tajiri[6], Hiroshi Takiguchi[7], Takeshi Matsushima[8], Nobuo Matsushima[9], Tatsuya Momotani[10], Kenji Utsunomiya[10]

1. National Institute of Information and Communications Technology, 2. Tohoku University, 3. Geospatial Information Authority of Japan, 4. High Energy Accelerator Research Organization, 5. Kyoto University, 6. Meteorological Research Institute, JMA, 7. Japan Aerospace eXploration Agency, 8. Kyushu University, 9. National Institute of Advanced Industrial Science and Technology, 10. Japan Weather Association

We have started to develop a next-generation microwave radiometer to be used in millimeter-wave spectroscopy for the high-resolution and high-precision monitoring of water vapor behavior. The new radiometer will be suitable for not only space geodetic techniques such as VLBI and GNSS, but also field measurements such as monitoring volcanic activities and cumulonimbus cloud generation. The basic design concept of the new radiometer follows the previous version named KUMODeS (KEK Universal Moisture and Oxygen Detection System) developed by the High Energy Accelerator Research Organization (KEK). The KUMODeS can measure spectra using two receivers with frequency bands of 20–30 GHz and 50–60 GHz. The low-noise amplifier (LNA) of the first KUMODeS receiver and a cold calibration source are implemented in a cryostat, which is maintained at 10 K to improve the sensitivity of detecting the characteristic broad peak of water vapor at approximately 22 GHz. The second receiver is used to measure the absorption peaks of oxygen (60 GHz). We have carried out comparative measurements of precipitable water vapor (PWV) to investigate the potential of KUMODeS/PWV measurements. The preliminary results of PWV comparisons imply that KUMODeS technology will be useful for retrieving the accurate behavior of water vapor with high temporal resolution. We will implement a wide bandwidth feed of 20–60 GHz into the new system on the basis of a previous comparison study. A signal is separated into two linear orthogonal polarized signals from the feed, one is in the 20–30 GHz feed and the other in the 50–60 GHz feed, using an orthomode transducer (OMT). The wideband feed, OMT, and the LNA for each signal are cooled at 77 K using a Stirling cryocooler to improve signal-to-noise ratio. The development of a new front-end module will be completed at the end of 2019, and we are planning to implement the module in an existing dish antenna to perform validation measurements.

Keywords: GNSS, microwave radiometer, water vapor

©2019. Japan Geoscience Union. All Right Reserved.

Refractivity Distributions over the Kanto Plain Obtained by Dual-polarization Radar

*Hiromu Seko[1], Eiichi Sato[1], Hiroshi Yamauchi[2]

1. Meteorological Research Institute, 2. Japan Meteorological Agency

Temperature and water vapor near the surface play crucial roles for the generation of convection cells. However, their variations just before the generations of convection cells still are not understood completely. In this study the temporal variations of refractivity index were obtained by MRI dual-polarization Doppler radar. The features of temperature and water vapor including generation period of convection cells will be shown in this presentation. On 19th August 2017, the sea breeze invaded from Kashima-Nada and the refractivity increased along the front of the sea breeze. The scattered weak echoes that appeared around the front seem to be related with the increase of refractivity. These are the features near the surface. The comparison with other data such as GNSS PWV will be also presented.

Keywords: Observation method, Doppler radar, Refractivity index

©2019. Japan Geoscience Union. All Right Reserved.

Spatial and temporal distribution of tropospheric water vapor observed by a Raman lidar and a GNSS receiver network over Shigaraki, Japan

*Masanori Yabuki[1], Toshitaka Tsuda[1], Yuya Kawano[2], Yusaku Tottori[2], Makoto Tsukamoto[2], Eiji Takeuchi[2]

1. Research Institute for Sustainable Humanosphere, Kyoto University, 2. EKO Instruments Co., Ltd.

Understanding the spatial and temporal distributions of water vapor in the atmosphere is critical for unveiling the fundamental mechanisms of localized extreme weather events. Besides, it is highly beneficial for improving the accuracy of weather forecasts by mesoscale numerical weather prediction models. To achieve the continuous monitoring of water vapor distributions, we performed simultaneous measurements by Raman lidar in the UV-C region and a dense Global Navigation Satellite System (GNSS) network. The former is a novel technology that can be utilized for profiling the vertical distribution of the water vapor mixing ratio for twenty-four hours, while the latter can be used for detecting the horizontal distribution of precipitable water vapor. The Raman lidar employs a laser at a wavelength of 266 nm and detects the light separated into an elastic backscatter signal and vibrational Raman signals of oxygen, nitrogen, and water vapor at wavelengths of 266, 277, 284, and 295 nm, respectively. The use of these wavelengths is convenient because of the low background noise during daytime, since most of the solar radiation in the ultraviolet range below 300 nm is absorbed by the ozone layer in the stratosphere. The lidar was encased in a temperature-controlled compact container, resistant to a variety of environmental conditions. Continuous observation of water vapor profiles by lidar has been conducted at the Shigaraki MU radar observatory (34˚51’ N, 136˚06’ E, 385 m a.s.l.) since November 2017. The dense GNSS receiver network consisted of 10 dual-frequency GNSS stations which were installed with a horizontal spacing of 3-4 km near the observatory on July 2017. In this study, we present our water vapor monitoring system as well as the preliminary results on the spatio-temporal water vapor distributions in 2018.

Acknowledgements
A part of this study is supported by JSPS KAKENHI Grant Number 15H03724.

Keywords: water vapor, Raman lidar, dense GNSS network

©2019. Japan Geoscience Union. All Right Reserved.

Study of the Mechanisms of Severe Thunderstorm in Tokyo Metropolitan Area using High Frequent Assimilation of GNSS and Other Ground-based Observations

*Yoshinori Shoji[1], Tetsu Sakai[2], Ahoro Adachi[1], Satoru Yoshida[2], Tomohiro Nagai[2]

1. The Second Laboratory of Meteorological Satellite and Observation System Research Department, Meteorological Research Institute, 2. The Third Laboratory of Meteorological Satellite and Observation System Research Department, Meteorological Research Institute

Highly urbanized Tokyo metropolitan area is vulnerable to severe storms such as local torrential rainfall, thunder lightning and tornado. Recently, the number of days with thunderstorms has been increasing in Tokyo. Elucidation of the mechanism of extreme weather in Tokyo is urgent matter (Nakatani et al. 2013). To study the rolls of water vapor and wind for the rapid life-cycle (initiation, development and dissipation) of hazardous cumulus convection, we installed a mobile Raman-lidar (Sakai et al. 2018), a wind profiler, and five GNSS stations in and around Tokyo.

Using 3DVAR capability of WRF data assimilation system (WRFDA)(Barker et al. 2012) , three-dimensional atmospheric fields with 1 km horizontal resolution were produced at every 10min throughout the August 2017 and 2018. Background fields were produced by JMA nonhydrostatic model (NHM)(Saito et al. 2007). In addition to the observed data at these campaign observation instruments, Japan Meteorological Agency’ s operational surface meteorological stations, wind-profiler stations and GNSS PWV derived at dense GNSS network of Geospatial Information Authority of Japan are assimilated. We confirmed that the reproduced atmospheric fields (Temperature, humidity, and wind) showed better agreement with observations of radiosonde, lidar derived water vapor mixing ratio, and wind-profiler than background fields at altitudes lower than 2 km. Assimilation of surface meteorological observations (atmospheric pressure, temperature, humidity and wind) introduced better agreement mainly at altitude lower than 0.5 km. Inclusion of GNSS derived PWV resulted better agreement of humidity at altitude higher than 0.5 km and inclusion of wind field from wind-profiler led better agreement of wind field.

We have investigated roles of water vapor for several local heavy rainfall events occurred in Tokyo in August 2017 and 2018 and found that convergence of water vapor flux at 0.5 km altitude had intensified prior to the occurrence of torrential precipitation. Statistical and quantitative results will be discussed at the symposium.

This study is supported by JSPS KAKENHI Grants 17H00852.

Keywords: Water vapor, Data assimilation, Localized heavy rainfall

©2019. Japan Geoscience Union. All Right Reserved.

[E] Oral | M (Multidisciplinary and Interdisciplinary)：M-TT Technology & Techniques

Mon. May 27, 2019 3:30 PM - 5:00 PM JST | Mon. May 27, 2019 6:30 AM - 8:00 AM UTC | 106 1F

[M-TT46] New phase of GPS/GNSS application as an integrated earth observation system

convener:Yoshinori Shoji(The Second Laboratory of Meteorological Satellite and Observation System Research Department, Meteorological Research Institute), Kaoru Ichikawa(Research Institute for Applied Mechanics, Kyushu University), Yusaku Ohta(Research Center for Prediction of Earthquakes and Volcanic Eruptions, Graduate School of Science, Tohoku University), Takuya Tsugawa(National Institute of Information and Communications Technology), Chairperson:Yoshinori Shoji(Meteorological Research Institute)

GNSS has become a fundamental tool for studies on atmosphere, ionosphere, and solid earth. Ground and space-based GNSS measurements have operationally contributed to improve global and regional NWP since 2006. In recent years, studies utilizing reflected GNSS signals to derive altimetric height, surface roughness, soil moisture, snow depth, humidity or vegetation index have been evolving. Ocean-platform GNSS observations have been demonstrating their capability of real-time monitoring of maritime water vapor as well as sea level. Increasing observations provided through Multi-GNSS (GPS, GLONASS, BEIDOU, GALILEO, QZSS etc.) enhances capability of the GNSS as an integrated earth observation system.
The purpose of this session is to share the latest development of GNSS researches on monitoring the earth system and to stimulate synergetic interdisciplinary studies. Contributions on atmosphere (troposphere and ionosphere) studies, reflectometry (GNSS-R), and integrations of different observation techniques like GNSS-Acoustic measurement to monitor ocean floor positioning are welcome.

3:30 PM - 3:45 PM JST | 6:30 AM - 6:45 AM UTC

[MTT46-12] Study on tropospheric delay variations extracted from a short baseline analysis and their application to meteorological observation

*Takayuki Yoshihara[1], Susumu Saito[1], Atsushi Kezuka[1], Shinji Saitoh[1] (1.Electronic Navigation Research Institute, National Institute of Maritime, Port and Aviation Technology)

3:45 PM - 4:00 PM JST | 6:45 AM - 7:00 AM UTC

[MTT46-13] Water vapor estimation using digital terrestrial broadcasting waves - Field test in Tokyo metropolitan area and trial production of small devices -

*Seiji Kawamura[1], Hiroshi HANADO[1], Hiroki Ohta[1], Yoshinobu Matsumura[2], Ryosuke Mori[2], Kazuyoshi Noda[2], Teruaki Hasegawa[2] (1.National Institute of Information and Communications Technology, 2.Socionext Inc.)

4:00 PM - 4:15 PM JST | 7:00 AM - 7:15 AM UTC

[MTT46-14] Water vapor estimation via propagation delay of 920MHz wireless communication signal

*Nobuyasu Shiga[1], Satoshi Yasuda[1], Seiji Kawamura[1], Hiroshi HANADO[1], Ryuichi Ichikawa[1], Hironori Iwai[1], Shinsuke Satoh[1] (1.National Institute of Information and communications technology)

4:15 PM - 4:30 PM JST | 7:15 AM - 7:30 AM UTC

[MTT46-15] Comparison of a water vapor observation with GPS and high sensitivity microwave radiometer, KUMODeS

*Taketo Nagasaki[1], Osamu Tajima[2], Ryuichi Ichikawa[3], Hiroshi Takiguchi[4], Kentaro Araki[5], Hiroshi Ishimoto[5] (1.High Energy Accelerator Research Organization, IPNS, 2.Kyoto University, 3.National Institute of Information and Communications Technology, 4.Japan Aerospace Exploration Agency, 5.Meteorological Research Institute)

4:30 PM - 4:45 PM JST | 7:30 AM - 7:45 AM UTC

[MTT46-16] Development and Observation of Water Vapor Raman Lidars for Localized Torrential Rainfall Prediction

*Tomohiro Nagai[1], Tetsu Sakai[1], Satoru Yoshida[1], Toshiharu Izumi[2], Sho Yokota[1], Hiromu Seko[1], Yoshinori Shoji[1], Koichi Shiraishi[3] (1.Meteorological Research Institute, Japan Meteorological Agency, 2.Japan Meteorological Agency, 3.Fukuoka University)

4:45 PM - 5:00 PM JST | 7:45 AM - 8:00 AM UTC

[MTT46-17] Study of Water Vapor Monitoring in the Open Ocean using Kinematic Precise Point Positioning

*Yoshinori Shoji[1], Teruyuki Kato[2], Yukihiro Terada[3], Toshitaka Tsuda[4], Masanori Yabuki[4] (1.The Second Laboratory of Meteorological Satellite and Observation System Research Department, Meteorological Research Institute, 2.Hot Springs Research Institute/Kanagawa Prefectural Government, 3.Natinal Institute of Technology, Kochi College, 4.Research Institute for Sustainable Humanosphere/Kyoto Unversity)

Study on tropospheric delay variations extracted from a short baseline analysis and their application to meteorological observation

*Takayuki Yoshihara[1], Susumu Saito[1], Atsushi Kezuka[1], Shinji Saitoh[1]

1. Electronic Navigation Research Institute, National Institute of Maritime, Port and Aviation Technology

This paper discusses variation of 10cm order in tropospheric delay differences between two ground-based GNSS stations, which are located with a horizontal scale of about 2km. This typical value of tropospheric delay differences is represented as a tropospheric delay difference projected to the zenith direction for a common satellite between the two stations. The variation also corresponds to an order of 50 mm/km in tropospheric delay spatial gradient. Such large differences of tropospheric delay with short baselines of several 100m had been reported in safety assessment and validation activities for aircraft high category precision approach and landing system called as GBAS (Ground-Based Augmentation System) [1,2,3]. They also reported that their temporal variations are highly correlated with the surface wind velocities under fine weather conditions.

A GBAS ground station typically has four GNSS stations with separation of several 100m each other. Electronic Navigation Research Institute (ENRI) participated in the safety assessment and validation activities, which were performed to validate draft international standards for high category GBAS. As one of the activities, ENRI developed a prototype system and installed it in New Ishigaki airport (24.40N, 124.25E). The system has the typical four GNSS stations within a horizontal scale of 400m and an additional GNSS station called as ionosphere field monitor (IFM), which is located as about 2km away from the four stations. These GNSS stations consists of dual frequency antenna and receiver and continuously collect GNSS data. Additionally, we set up a different GNSS receiver which can accept multi-RF signal inputs. Combining the receiver with Radio-over-Fiber (RoF) devices, we can use a common clock for signal processing two GNSS signals received at the both ends of the baseline with a length of 2.3km [4]. This additional system enables us to examine a tropospheric difference for each GNSS satellite without correction of difference of receiver clock drift components between two received signals although it is required to distinguish tropospheric delay differences from ionospheric effects and multipath errors using dual frequency measurements and characteristics of multipath variations [5].

In this study, we mainly examine tropospheric delay difference data with the baseline length of 2.3km, including GNSS data collected from the prototype system. Considering geometry of GNSS satellite propagation paths and observational errors, we will discuss candidate meteorological phenomena and application to future meteorological observation.

[1] K. Alexander et al., WP16, ICAO NSP/WGW, May 2014.
[2] F. Salbert et al., ICAO NSP WG1&2, Sept. 2014.
[3] S. Saito et al., Proc. of ION 2015 Pacific PNT, pp. 815-820, Honolulu, HI, April 2015.
[4] T. Yoshihara, et al., Proc. of the ION 2017 Pacific PNT, pp. 885-896, Honolulu, Hawaii, May 2017.
[5] T. Yoshihara et al., IEICE Technical Report, vol.118, no.105, pp.19-24, SANE2018-16, June 2018 (Japanese).

Keywords: GNSS, Tropospheric delay, Short baseline, Application to meteorological observation

©2019. Japan Geoscience Union. All Right Reserved.

Water vapor estimation using digital terrestrial broadcasting waves - Field test in Tokyo metropolitan area and trial production of small devices -

*Seiji Kawamura[1], Hiroshi HANADO[1], Hiroki Ohta[1], Yoshinobu Matsumura[2], Ryosuke Mori[2], Kazuyoshi Noda[2], Teruaki Hasegawa[2]

1. National Institute of Information and Communications Technology, 2. Socionext Inc.

We have developed a method to measure water vapor in horizontal direction using digital terrestrial broadcasting waves [1]. Radio waves are delayed due to water vapor through propagation. Water vapor can be estimated using propagation delay of digital terrestrial broadcasting waves. The basic idea of using propagation delay is the same as that of retrieving PWV by using GNSS. In this study, we estimate water vapor near a ground surface from the horizontal propagation delay of digital terrestrial broadcasting waves. The main features of this observation are, no need for transmitters (small and low cost due to receiving only), applicability wherever digital terrestrial broadcasting is available, and its high time resolution. Our target is to improve the accuracy of numerical weather forecast for severe weather phenomena such as localized heavy rainstorms in urban areas through data assimilation.
We have developed a real-time delay measurement system with a software-defined radio (SDR) technique, whose main components are USRP-N210 and PC (prototype). Seven measurement systems are now under operation around Tokyo metropolitan area. Although the main source of digital terrestrial broadcasting waves in Tokyo area is the Tokyo Skytree, some small radio towers that transmit Television Saitama, Chiba Television, Television Kanagawa, and do on can be also available. If plural radio waves from different radio towers are available, we can use plural base-lines to estimate water vapor. Outline of demonstration experiment in Tokyo metropolitan area and its initial results are introduced.
Small devices which can measure propagation delay using digital terrestrial broadcasting waves are now under trial production through a joint research by NICT and Socionext. These devices use FPGA for calculate propagation delay of digital terrestrial broadcasting waves. Their size and electricity consumption is smaller than those of prototype. If many small receivers are deployed, 2-D water vapor variations can be monitored with high time and space resolutions. Such a network system will contribute to increasing the accuracy of numerical weather forecast for severe weather phenomena such as localized heavy rainstorms.

Reference
[1] Kawamura, S., et al. (2017), Water vapor estimation using digital terrestrial broadcasting waves, *Radio Sci.*, *52*, 367-377, doi:10.1002/2016RS006191.

Keywords: water vapor, propagation delay, digital terrestrial broadcasting

©2019. Japan Geoscience Union. All Right Reserved.

Water vapor estimation via propagation delay of 920MHz wireless communication signal

*Nobuyasu Shiga[1], Satoshi Yasuda[1], Seiji Kawamura[1], Hiroshi HANADO[1], Ryuichi Ichikawa[1], Hironori Iwai[1], Shinsuke Satoh[1]

1. National Institute of Information and communications technology

We have developed a 920MHz wireless communication module that can measure the variation of propagation delay precisely (6mm precision) and frequently (20 times/second). We have monitored the variation of propagation delay between 2 places that are 4.25km apart with line-of-sight. The result agreed well with the estimated propagation delay using the data obtained by meteorological observation equipment. This technique is suited to monitor the distribution of surface water vapor, compared to GNSS that primarily measures the propagation delay in vertical direction.
We are seeking the right path for social impremention of this technology, aiming to provide a mean to measure the surface water vapor with high precision, high frequency and high resolution in a cost-effective way.

Keywords: water vapor estimation, space-time synchronization, propagation delay measurement, wireless communication module

©2019. Japan Geoscience Union. All Right Reserved.

Comparison of a water vapor observation with GPS and high sensitivity microwave radiometer, KUMODeS

*Taketo Nagasaki[1], Osamu Tajima[2], Ryuichi Ichikawa[3], Hiroshi Takiguchi[4], Kentaro Araki[5], Hiroshi Ishimoto[5]

1. High Energy Accelerator Research Organization, IPNS, 2. Kyoto University, 3. National Institute of Information and Communications Technology, 4. Japan Aerospace Exploration Agency, 5. Meteorological Research Institute

GPS is one of the useful technique which is using electromagnetic waves in the atmosphere. However, radio waves through the atmosphere and have a delay due to water vapor then. It is a major factor of indeterminacy in some measurement. On the other hand, as a device for identifying the amount of water vapor is a microwave radiometer.
We have developed a new microwave radiometer "KUMODeS" to detect local and sudden natural disasters such as tornadoes. This system observes radiation from water molecules present in the atmosphere (20-30 GHz band) and the emission line from the oxygen molecule (50-60 GHz band) are measured at the same time. As a result, the amount of water vapor in the atmosphere is estimated with high accuracy. As a characteristic of KUMODeS, high sensitivity (low noise) was employed as a cooling receiver by application of radio astronomical observation technology. In order to improve convenience, we employed a low-temperature(45K) calibration source in the cryostat and can be operated by remote control. And we are able to select a higher spatial resolution. We conducted long-term observations for more than half a year in Tsukuba city using KUMODeS. At the same point, we measured the amount of water vapor by GPS antenna and confirmed the validity of the observation result. In addition, we have also developed the second device that aimed at a smaller size and lower power consumption as a development of KUMODeS. In this presentation, we report the outline of the system and the results of atmospheric observation in Tsukuba City.
This research has been funded by “Program for Creating STart-ups from Advance Research and Technology (START Program)” from the Ministry of Education, Culture, Sports, Science and Technology, Japan, http://www.jst.go.jp/start/en/index.html.

Keywords: water vapor, microwave radiometer

©2019. Japan Geoscience Union. All Right Reserved.

Development and Observation of Water Vapor Raman Lidars for Localized Torrential Rainfall Prediction

*Tomohiro Nagai[1], Tetsu Sakai[1], Satoru Yoshida[1], Toshiharu Izumi[2], Sho Yokota[1], Hiromu Seko[1], Yoshinori Shoji[1], Koichi Shiraishi[3]

1. Meteorological Research Institute, Japan Meteorological Agency, 2. Japan Meteorological Agency, 3. Fukuoka University

In recent years, the way of rain has been localized and concentrated, and disasters caused by localized torrential rain are increasing accordingly. One of the causes of these rains is thought to be the continuous supply of water vapor rich air through the lower atmosphere to the area where the rainfall is occurring. Therefore, it is very important to continuously observe the vertical distribution of water vaper in the lower atmosphere on the windward side to predict the localized torrential rainfalls. Water vapor Raman lidars are developed and observations are carried out in the Tokyo metropolitan area during summer time in 2017 and 2018. The lidars are carefully designed to potentiate the measurement of the water vapor near the ground as well as to have the capability on the daytime measurement. One of the lidars has the mobility so that we could make measurement at three observational sites in the seashore of the Tokyo metropolitan area that are located on the windward side of prospective area of the heavy rain in the Tokyo metropolitan area. Feasibility study of the impact of the water vapor mixing ratio profiles taken by the lidars on the numerical experiment for the precipitation prediction was carried out. We conducted water vapor assimilation experiment with use of the water vapor mixing ratio measured with the lidars. The assimilation results indicate that water vapor distribution in the analysis field was greatly changed by water vapor assimilation in the downwind side of the lidar observation site. Furthermore, a new research project has been just started to improve quantitative precipitation forecast for heavy rains in Kyushu island of Japan by means of data assimilation of water vapor lidars.

Keywords: water vapor, lidar, heavy rain, data assimilation , weather prediction

©2019. Japan Geoscience Union. All Right Reserved.

Study of Water Vapor Monitoring in the Open Ocean using Kinematic Precise Point Positioning

*Yoshinori Shoji[1], Teruyuki Kato[2], Yukihiro Terada[3], Toshitaka Tsuda[4], Masanori Yabuki[4]

1. The Second Laboratory of Meteorological Satellite and Observation System Research Department, Meteorological Research Institute, 2. Hot Springs Research Institute/Kanagawa Prefectural Government, 3. Natinal Institute of Technology, Kochi College, 4. Research Institute for Sustainable Humanosphere/Kyoto Unversity

Japan is an archipelago located easternmost of East Asia and influenced by the East Asian monsoon, which is characterized by moist air inflow coming from the ocean that often causes heavy rainfall (Kato 2006, Tsuguti and Kato 2014, Kato 2018). From June 28 to July 8, 2018, extreme rainfall frequented western Japan to the Tokai region, wherein more than 1,000 mm, at the maximum of 1,852.5 mm, precipitation was recorded in several regions (Tsuguti et al. 2018). A press release of Japan Meteorological Agency (JMA) (JMA, 2018) attributed the event to the concentration of two massively moist air streams over western Japan and persistent upward flow. With the frequency of extreme precipitation events, water vapor monitoring over the ocean becomes one of the important issues in Japan. Shoji et al. 2009 exhibited the improvement of a heavy rainfall prediction method by assimilating precipitable water vapor (PWV) estimated via the Global Positioning System (GPS) observation network in East Asia, as well as Japan’s nationwide dense GPS network. The result insisted the importance of water vapor monitoring upstream.

Unlike ground-based fixed GNSS stations, ocean-platform (ship and buoy) GNSS measurements face difficulties in analyzing the variable antenna position simultaneously with the atmospheric delay. However, recent advancement of kinematic precise point positioning technology is beginning to overcome these difficulties. Shoji et al (2017) installed two GNSS antennas on a research vessel, the RYOFU MARU of the Japan Meteorological Agency (JMA), and conducted experimental observations to assess the GNSS derived precipitable water vapor (PWV) from October 19, 2016, to August 6, 2017. The GNSS derived PWVs showed good agreement with the radiosonde observations on the vessel (1.7 mm root mean square difference, −0.7 mm bias, and 3.6% rejection rate).

Kato et al. (2018) introduced a GNSS buoy system for a synthetic geohazard monitoring. The buoy is located about 40 km south of Cape Ashizuri, west of Shikoku, Japan. We succeeded continuous PWV retrieval from June to September 2018. Retrieved PWVs vividly captured water vapor variations associated with north-south shifting of the “BAIU” seasonal rain front and passages of heavy rainfalls and typhoons. The GNSS buoy PWVs also suggest that, compared to over land, uncertainty of water vapor field in JMA’s objective analysis is larger over the ocean (Shoji et al. 2019).

In the year of 2018, we started a new research project to monitor PWV over the ocean west of Kyushu, Japan, getting supports from eight vessels (six regular line cargo vessels, one fisheries research vessel, and one JMA’s research vessel). The purpose of this study is to assess the impact of water vapor monitoring in upward of west Japan on heavy rainfall prediction. Preliminary PWV analyses show about 3 mm rms with about -1 mm bias against JMA’s operational regional objective analysis.

Acknowledgements

The shipborne GNSS campaign observation was funded by a research grant for Mission Research for

©2019. Japan Geoscience Union. All Right Reserved.

Sustainable Humanosphere from the Research Institute for Sustainable Humanosphere (RISH) at Kyoto University, “Study on accuracy improvement of shipborne GNSS water vapor measurement.”

GNSS observation on top of a floating buoy is funded by JSPS KAKENHI Grants 16H06310. A part of this study is supported by JSPS KAKENHI Grants 17H00852.

Keywords: Water Vapor, Heavy rainfall, GNSS

©2019. Japan Geoscience Union. All Right Reserved.

[E] Poster | M (Multidisciplinary and Interdisciplinary)：M-TT Technology & Techniques

Mon. May 27, 2019 1:45 PM - 3:15 PM JST | Mon. May 27, 2019 4:45 AM - 6:15 AM UTC | Poster Hall International Exhibition Hall8, Makuhari Messe_11

[M-TT47] GEOSCIENTIFIC APPLICATIONS OF HIGH-DEFINITION TOPOGRAPHY AND GEOPHYSICAL DATA IN THE ANTHROPOCENE

convener:Yuichi S. Hayakawa(Faculty of Environmental Earth Science, Hokkaido University), Shigekazu Kusumoto(Graduate School of Science and Engineering for Research, University of Toyama), Christopher A Gomez(Kobe University Faculty of Maritime Sciences Volcanic Risk at Sea Research Group)

Recent technical developments of high-definition topographic and geophysical data acquisition have enabled us to further investigate geoscientific issues including land surface processes, subsurface structures, submarine and aerial environments, geo-ecological interactions, and disaster mitigation. Such high-definition or high-resolution data are particularly useful for studies in short-term temporal scales, and future predictions such as numerical modelings. In this session, we expect submissions on topics challenging such issues in the Anthropocene, the most recent geological era of the Earth. A range of topics would fit the session framework, including theoretical work, improvements in data acquisition, extensive data preservation and archiving, pre- and post-processing, statistical analysis, modeling, and simulation for geoscientific research and geohazard assessments in the Anthropocene. The methodological approaches may include, but not limited to, laser scanning, SfM-MVS photogrammetry, GNSS precise positioning, SAR interferometry, multi-beam sonar, and electromagnetic sensors, based on terrestrial (fixed or mobile) and aerial (UAV or manned airborne) platforms.

[MTT47-P01] High-definition topography monitoring after riverbed cultivation in the Echi River, central Japan

*Takuro Ogura[1,2], Satoshi Asano[3], Toshiaki Mizuno[3], Yoshihiro Azuma[3], Takeshi Kitai[4], Yuichi S Hayakawa[5,6], Kotaro Iizuka[6] (1.Graduate School of Frontier Sciences, The University of Tokyo, 2.Graduate School of Environmental Science, Hokkaido University, 3.Lake Biwa Environmental Research Institute , 4.Lake Biwa Museum, 5.Faculty of Environmental Earth Science, Hokkaido University, 6.Center for Spatial information Science, The University of Tokyo)

[MTT47-P02] Spatial distribution of land surface displacements in the crater of Tateyama Midagahara Volcano using high-definition topographic data

*Yuichi S. Hayakawa[1], Shigekazu Kusumoto[2], Takuro Ogura[3,4] (1.Faculty of Environmental Earth Science, Hokkaido University, 2.Graduate School of Science and Engineering for Research, University of Toyama, 3.Graduate School of Frontier Science, The University of Tokyo, 4.Graduate School of Environmental Science, Hokkaido University)

[MTT47-P03] Study on a simplified measurement of water depth and reconstruction of the riverbed form by using SfM and MVS.

*OSAWA KOTA[1], Tadafumi Niizato [2], Katsuaki Mitachi[3], Makoto Kawamura[1], Masahiro Ohkawa[1] (1.Mitsubishi Materials Techno corporation , 2.Japan Atomic Energy Agency, 3.ATOM TRANSPORT SERVICE CO., LTD)

[MTT47-P04] Ground Penetrating Radar Imaging of Moisture and Water movement in volcanic soil

*Christopher A Gomez[1] (1.Kobe University Faculty of Maritime Sciences Volcanic Risk at Sea Research Group)

[MTT47-P05] Estimating Eruptive Volumes of Mud Volcano Southwestern Taiwan by Using UAV and SfM-MVS Photogrammetry

*CHIA-YING LIU [1], Ray Y Chuang[1], Horng-Yue Chen [2] (1.Department of Geography, National Taiwan University, 2.Academia Sinica, Institute of Earth Sciences)

[MTT47-P06] Increasing temporal depth of urban Land-Use Regression Models by wind-data driven dynamic buffer generation

*Tilman Leo Hohenberger[1], King Wai Leung[1] (1.Division of Environment and Sustainability, Hong Kong University of Science and Technology)

High-definition topography monitoring after riverbed cultivation in the Echi River, central Japan

*Takuro Ogura[1,2], Satoshi Asano[3], Toshiaki Mizuno[3], Yoshihiro Azuma[3], Takeshi Kitai[4], Yuichi S Hayakawa[5,6], Kotaro Iizuka[6]

1. Graduate School of Frontier Sciences, The University of Tokyo, 2. Graduate School of Environmental Science, Hokkaido University, 3. Lake Biwa Environmental Research Institute , 4. Lake Biwa Museum, 5. Faculty of Environmental Earth Science, Hokkaido University, 6. Center for Spatial information Science, The University of Tokyo

Natural processes of erosion and deposition on riverbeds are generally limited in Japan due to large-scale public constructions including dams and banks. As a result of the construction of dams, sediment transport may dramatically decrease in the downstream area are, and the river ecosystem can also be affected. To make sediment move more vigorously, we cultivated the armored gravel riverbed with heavy machinery. We then explore the effects of riverbed cultivating by monitoring the topographic changes with high-frequency and high-definition measurements (HF-HD measurements), whereas conventional measurement technologies do not compensate spatial resolution and temporal resolution to capture the topographic change. Using UAS (Unmanned Aerial Vehicle) and SfM-MVS (Structure-from-Motion –Multi-view Stereo) photogrammetry, we found the transportation of the fixed gravels were occurring after cultivating the riverbed in 2017. The temporal and spatial resolutions of the HF-HD topographic data was approximately 2 months and 10 cm, respectively. In July 2018, water flow at 130 m^3/s was discharged from the upstream dam, and we confirmed that a part of the gravels in the cultivated area was eroded and replaced with new sediments (Fig. 1). These observations indicate that riverbed monitoring using UAV and SfM - MVS can be a practical tool for proper management of riverbeds. Applying this result, we will further clarify the relationships between the water quantity discharged from the dam and the riverbed topographic changes.

Keywords: High-definition topographic data, riverbed cultivation, UAV, SfM-MVS photogrammetry, Echi river

©2019. Japan Geoscience Union. All Right Reserved.

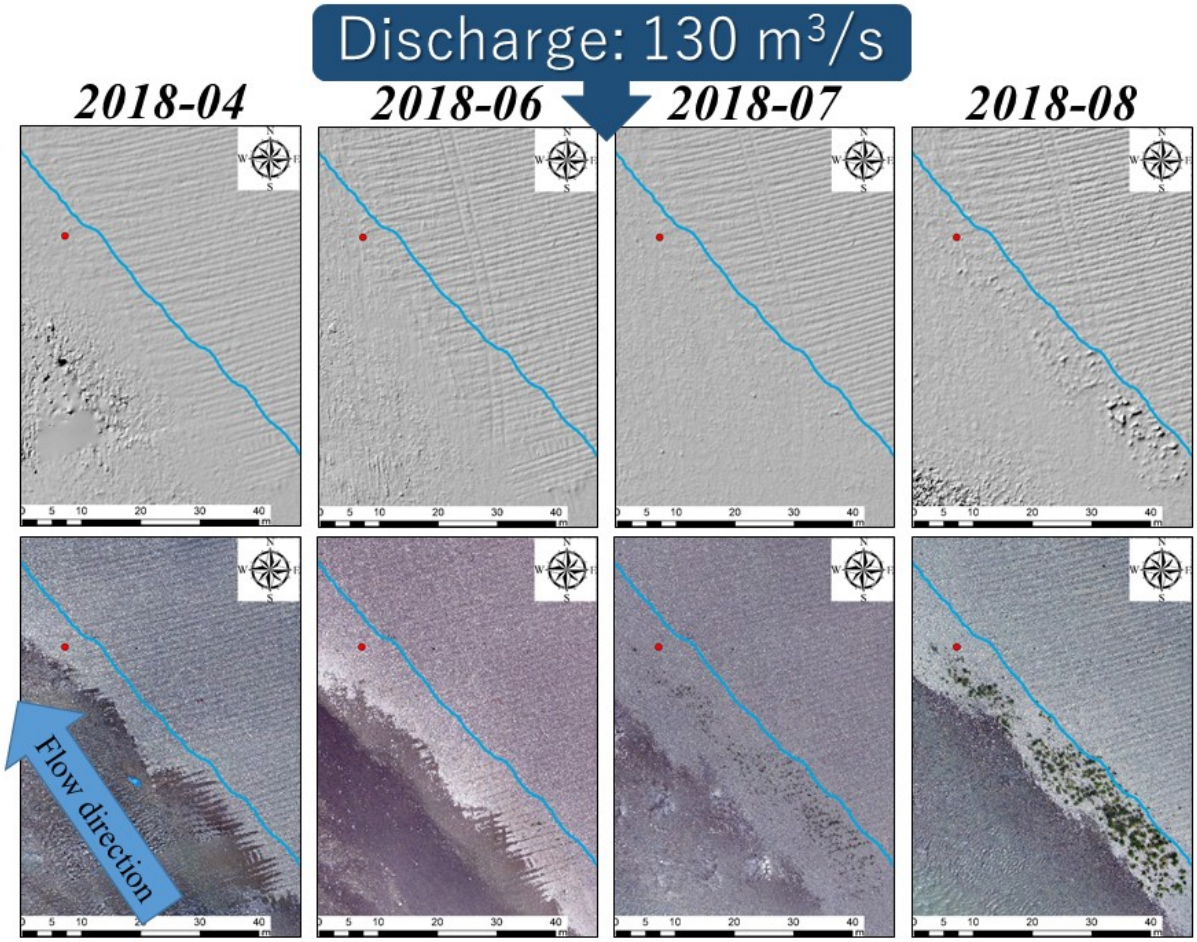

Fig.1. Hillshade images and ortho images of cultivated area.

©2019. Japan Geoscience Union. All Right Reserved.

Spatial distribution of land surface displacements in the crater of Tateyama Midagahara Volcano using high-definition topographic data

*Yuichi S. Hayakawa[1], Shigekazu Kusumoto[2], Takuro Ogura[3,4]

1. Faculty of Environmental Earth Science, Hokkaido University, 2. Graduate School of Science and Engineering for Research, University of Toyama, 3. Graduate School of Frontier Science, The University of Tokyo, 4. Graduate School of Environmental Science, Hokkaido University

Detailed monitoring of land surface displacements is crucial for the assessment of activities of a volcano, especially in its crater area. Close-range remote sensing of high-definition topographic data is advantageous in the detection of centimeter-scale ground-surface displacements in a wide spacial extent, whereas the conventional leveling method is capable of detecting millimeter-scale displacements along a measurement line. We investigated the spatial distribution of land surface displacements in the Jigoku-Dani crater area of Mt. Tateyama Midagahara Volcano in Toyama Prefecture, central Japan by high-definition topographic measurements including terrestrial laser scanning and unmanned aerial vehicle-based structure-from-motion photogrammetry. The annual measurements were performed for three years (2015 to 2017). The range of uplift detected by terrestrial laser scanning corresponds with that by leveling. Together with the analytical results of the leveling data, the spatial pattern of the uplift suggests the extent of an underground pressured zone to cause the exhumation. For the prediction of the volcanic activities, further monitoring is required to reveal the spatiotemporal patterns of the displacements.

Keywords: terrestrial laser scanning, unmanned aerial system structure-from-motion, point cloud

©2019. Japan Geoscience Union. All Right Reserved.

Study on a simplified measurement of water depth and reconstruction of the riverbed form by using SfM and MVS.

*OSAWA KOTA[1], Tadafumi Niizato [2], Katsuaki Mitachi[3], Makoto Kawamura[1], Masahiro Ohkawa[1]

1. Mitsubishi Materials Techno corporation , 2. Japan Atomic Energy Agency, 3. ATOM TRANSPORT SERVICE CO., LTD

Primary outflow process of radiocesium, which is released by the TEPCO’ s Fukushima Dai-ichi Nuclear Power Plant accident, from a forested hillslope to a mountain stream is a particulate-bond state transport. A detailed estimation of the riverbed form and sediment volume changing with time is a key issue to assess the radiocesium distribution in the forested environment. Changes in the sediment volume can be calculated from the water depth and the difference between measured water surface and reference water surface levels setting up at the initial. Conventional method for a water depth determination is a direct measurement of the stream water depth by using a scale. But it requires a lot of time and labor to evaluate the change of riverbed form and water depth in detail.
In this study, we attempted an accurate and labor-effective method to evaluate the water depth and three-dimensional (3D) structure of underwater riverbed form by applying the SfM (Structure from Motion) /MVS (Multi View Stereo) techniques and the optical image data collected on consumer-grade-camera. These images were photographed beside of the small stream located at southern part of the Abukuma Mountains, Fukushima. Light propagation properties such as attenuation or reflection influence precise reconstruction of 3D model using underwater images. This was done to reduce influence of light propagation in two steps: 1) to reduce the influence of reflection, photographing at the time of twilight using LED light and Circular PL filter. 2) to reduce the influence of attenuation, installing blue colored film on the LED light and omitting band R, G for SfM/MVS analysis. And we also photographed at the day time and reconstructed 3D model (Day Model: DM) to compare and confirm the model applying two steps (Twilight Model: TM). As a criterion for evaluation of these models, we carried out the direct measurement of water depth. Rate of estimation concordance was calculated by dividing analytical water depth by the direct measurement depth, then convert to percentage.
Discrepancy between measured and analytical results increased with depth, the rate of estimation concordances were 46 % (DM) and 73 % (TM) in the water depth of 20-25 cm, and 62 % (DM) and 93 % (TM) in 10-15 cm, respectively (Figure). Next step is an improvement of the correction and image-capturing methods to reduce the estimation errors by elimination of the light refraction on the stream water surface.

Keywords: SfM/MVS, measurement of water depth, riverbed form

©2019. Japan Geoscience Union. All Right Reserved.

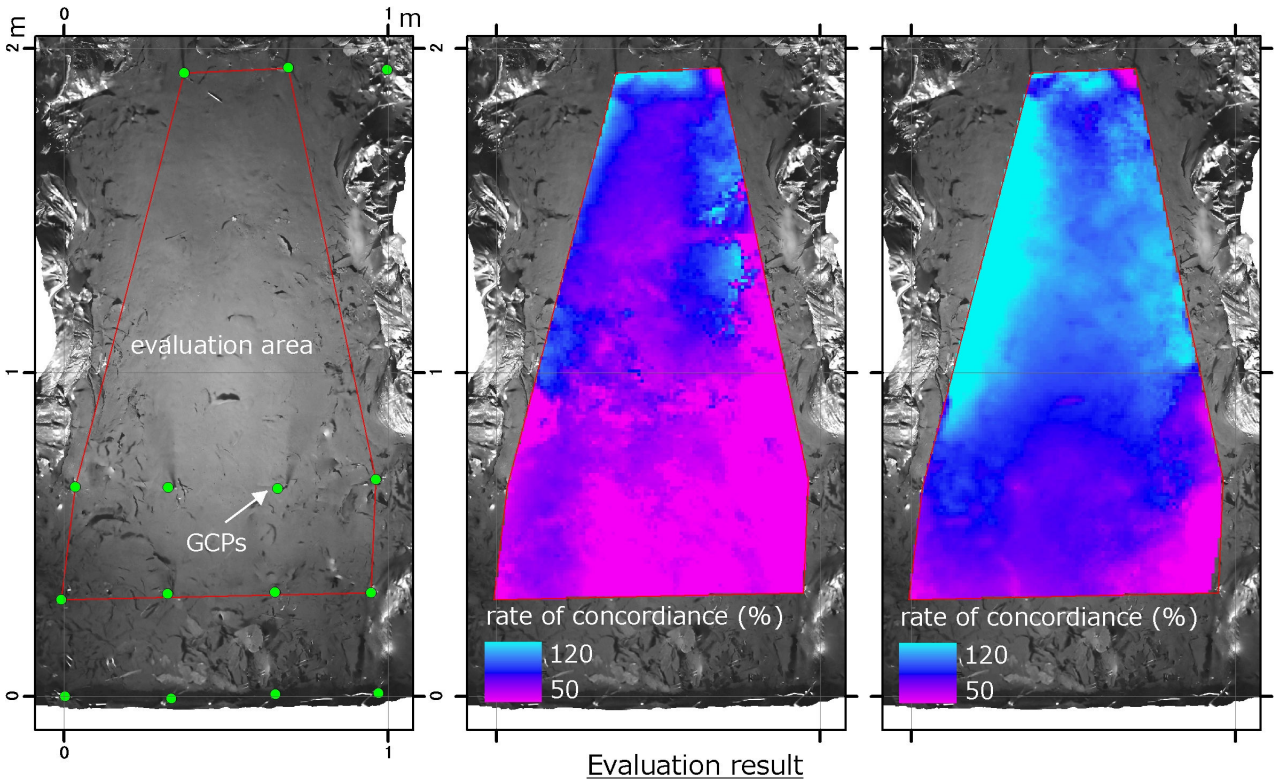

Left: Orthographic Image, Evaluation area (red polygon) and location of GCPs (green dot),
Center: Discrepancy between measured and analysis (DM),
Right: Discrepancy between measured and analysis (TM)

©2019. Japan Geoscience Union. All Right Reserved.

Ground Penetrating Radar Imaging of Moisture and Water movement in volcanic soil

*Christopher A Gomez[1]

1. Kobe University Faculty of Maritime Sciences Volcanic Risk at Sea Research Group

Ground Penetrating Radar is a non-invasive subsurface method that provides results on the dielectric properties of the ground between 0 and 30 m on average in sediments. Working from sediments from Mt Unzen in Japan, tests over the moisture content and the air content change were conducted on the material in order to infer further data during field measurement. The GPR used in the survey is a Ramac Mala mounted with an antenna of 800 Mhz and a stack signal over time. The data were processed using Matlab using data filtering and time-depth conversion, and calculation of the dielectric properties variations. The signal analysis shows that the velocity does change over time depending on the moisture content and the change in air/void ratio. For a given homogeneous material, like at volcanoes, multiplying such analysis is a step forward the development of relatable tables for various environments.

Keywords: Ground Penetrating Radar, Soil moisture content, Volcanic material

©2019. Japan Geoscience Union. All Right Reserved.

Estimating Eruptive Volumes of Mud Volcano Southwestern Taiwan by Using UAV and SfM-MVS Photogrammetry

*CHIA-YING LIU[1], Ray Y Chuang[1], Horng-Yue Chen[2]

1. Department of Geography, National Taiwan University, 2. Academia Sinica, Institute of Earth Sciences

Mud volcanoes are special geologic features occurred in tectonic areas with horizontal compression. Complete research for mud volcanos can help us to understand the interaction of the crust and surface. In Taiwan, mud volcanoes are present on-land and off-shore southwestern Taiwan around the transitional area from subduction to orogeny. Among all mud volcanoes in Taiwan, the Wandan mud volcano erupts sporadically with significantly large amount of effluent mud. However, the mechanism of the eruption remains unclear because we lack fundamental information such as eruptive volumes, duration of mud eruption, impact factors and recurrence intervals. Therefore, it is important to estimate the eruptive volumes and further to examine the spatiotemporal pattern of the Wandan mud volcano eruption. We first compile literature and newspapers for historic eruption events to estimate two groups of recurrence interval: 150-180 days for highly active period and 300-600 days for less active period.

Since the sporadic eruption make different for rapid survey by using traditional methods, we take advantage of unmanned aerial vehicles (UAV) to design a survey network specifically. Therefore, we estimate the eruptive volumes of recent eruptions for the Wandan mud volcano by using aerial images taken from UAV, and 3D models derived from the structure-from-motion (SfM) photogrammetry technique. We use RTK-GPS and leveling for horizontal and vertical measurements of ground control point, respectively. We use the SfM software to generate DSMs, point clouds, and orthophotos with cm-level accuracy. We estimate the eruptive volume by subtracting the pre-eruption DSM from the post-eruption DSM. Our results show that for the event on 15 May, 2018, the eruptive area is 12,761 m^2 and the volume is 13,106.3625 ±13.0105m^3.

Keywords: UAS, GNSS, digital surface modeling, control survey

©2019. Japan Geoscience Union. All Right Reserved.

Increasing temporal depth of urban Land-Use Regression Models by wind-data driven dynamic buffer generation

*Tilman Leo Hohenberger[1], King Wai Leung[1]

1. Division of Environment and Sustainability, Hong Kong University of Science and Technology

Land-use regression (LUR) models are commonly used as an inexpensive and easy to set-up way to predict spatial variability in air-pollution. They are successfully applied to regional and, more and more, urban settings, making use of spatial predictors such as land-use, vegetation, morphology and geography. New approaches include an improved use of wind-data for buffer-creation and predictor calculation.

Traditionally, LUR models are used to generate annual or seasonal concentration averages and are not able cover deeper temporal variability. We aim at increasing temporal depth by using a novel approach in generating dynamic buffers for predictor calculation using both monthly wind-speed and wind-direction averages. The traditional circular buffers are replaced by wedges, whose orientation and radius are bound to these meteorological variables.

Here, Hong Kong’ s diverse territory is taken as a study site, and our model is trained with 5 years data from 16 government air quality monitoring stations and deployed portable sensors network. We compare our novel approach to both traditional LUR models and a sophisticated urban chemical transport model (ADMS-Urban).

Results will highlight the opportunities in using LUR models for monthly air-quality pollution concentration as an alternative to chemical transport modelling.

Keywords: Wind, Land Use Regression, Spatial Data, Meteorology

©2019. Japan Geoscience Union. All Right Reserved.

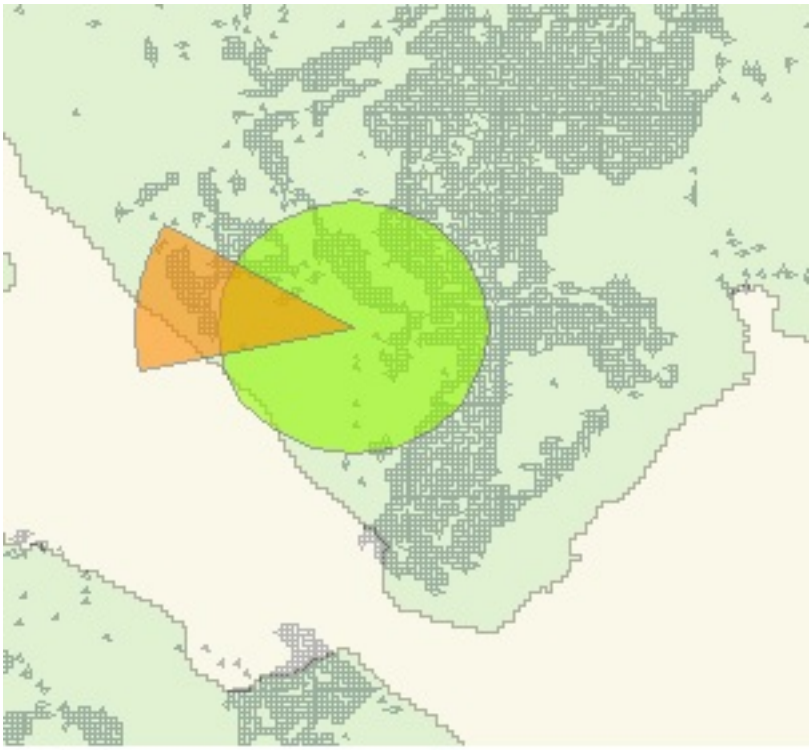

Dynamic and circular LUR buffer in Hong Kong's urban environment

©2019. Japan Geoscience Union. All Right Reserved.

[E] Poster | M (Multidisciplinary and Interdisciplinary)：M-TT Technology & Techniques

Mon. May 27, 2019 5:15 PM - 6:30 PM JST | Mon. May 27, 2019 8:15 AM - 9:30 AM UTC | Poster Hall International Exhibition Hall8, Makuhari Messe_44

[M-TT47] GEOSCIENTIFIC APPLICATIONS OF HIGH-DEFINITION TOPOGRAPHY AND GEOPHYSICAL DATA IN THE ANTHROPOCENE

convener:Yuichi S. Hayakawa(Faculty of Environmental Earth Science, Hokkaido University), Shigekazu Kusumoto(Graduate School of Science and Engineering for Research, University of Toyama), Christopher A Gomez(Kobe University Faculty of Maritime Sciences Volcanic Risk at Sea Research Group)

Recent technical developments of high-definition topographic and geophysical data acquisition have enabled us to further investigate geoscientific issues including land surface processes, subsurface structures, submarine and aerial environments, geo-ecological interactions, and disaster mitigation. Such high-definition or high-resolution data are particularly useful for studies in short-term temporal scales, and future predictions such as numerical modelings. In this session, we expect submissions on topics challenging such issues in the Anthropocene, the most recent geological era of the Earth. A range of topics would fit the session framework, including theoretical work, improvements in data acquisition, extensive data preservation and archiving, pre- and post-processing, statistical analysis, modeling, and simulation for geoscientific research and geohazard assessments in the Anthropocene. The methodological approaches may include, but not limited to, laser scanning, SfM-MVS photogrammetry, GNSS precise positioning, SAR interferometry, multi-beam sonar, and electromagnetic sensors, based on terrestrial (fixed or mobile) and aerial (UAV or manned airborne) platforms.

[MTT47-P01] High-definition topography monitoring after riverbed cultivation in the Echi River, central Japan

*Takuro Ogura[1,2], Satoshi Asano[3], Toshiaki Mizuno[3], Yoshihiro Azuma[3], Takeshi Kitai[4], Yuichi S Hayakawa[5,6], Kotaro Iizuka[6] (1.Graduate School of Frontier Sciences, The University of Tokyo, 2.Graduate School of Environmental Science, Hokkaido University, 3.Lake Biwa Environmental Research Institute , 4.Lake Biwa Museum, 5.Faculty of Environmental Earth Science, Hokkaido University, 6.Center for Spatial information Science, The University of Tokyo)

[MTT47-P02] Spatial distribution of land surface displacements in the crater of Tateyama Midagahara Volcano using high-definition topographic data

*Yuichi S. Hayakawa[1], Shigekazu Kusumoto[2], Takuro Ogura[3,4] (1.Faculty of Environmental Earth Science, Hokkaido University, 2.Graduate School of Science and Engineering for Research, University of Toyama, 3.Graduate School of Frontier Science, The University of Tokyo, 4.Graduate School of Environmental Science, Hokkaido University)

[MTT47-P03] Study on a simplified measurement of water depth and reconstruction of the riverbed form by using SfM and MVS.

*OSAWA KOTA[1], Tadafumi Niizato [2], Katsuaki Mitachi[3], Makoto Kawamura[1], Masahiro Ohkawa[1] (1.Mitsubishi Materials Techno corporation , 2.Japan Atomic Energy Agency, 3.ATOM TRANSPORT SERVICE CO., LTD)

[MTT47-P04] Ground Penetrating Radar Imaging of Moisture and Water movement in volcanic soil

*Christopher A Gomez[1] (1.Kobe University Faculty of Maritime Sciences Volcanic Risk at Sea Research Group)

[MTT47-P05] Estimating Eruptive Volumes of Mud Volcano Southwestern Taiwan by Using UAV and SfM-MVS Photogrammetry

*CHIA-YING LIU [1], Ray Y Chuang[1], Horng-Yue Chen [2] (1.Department of Geography, National Taiwan University, 2.Academia Sinica, Institute of Earth Sciences)

[MTT47-P06] Increasing temporal depth of urban Land-Use Regression Models by wind-data driven dynamic buffer generation

*Tilman Leo Hohenberger[1], King Wai Leung[1] (1.Division of Environment and Sustainability, Hong Kong University of Science and Technology)

High-definition topography monitoring after riverbed cultivation in the Echi River, central Japan

*Takuro Ogura[1,2], Satoshi Asano[3], Toshiaki Mizuno[3], Yoshihiro Azuma[3], Takeshi Kitai[4], Yuichi S Hayakawa[5,6], Kotaro Iizuka[6]

1. Graduate School of Frontier Sciences, The University of Tokyo, 2. Graduate School of Environmental Science, Hokkaido University, 3. Lake Biwa Environmental Research Institute , 4. Lake Biwa Museum, 5. Faculty of Environmental Earth Science, Hokkaido University, 6. Center for Spatial information Science, The University of Tokyo

Natural processes of erosion and deposition on riverbeds are generally limited in Japan due to large-scale public constructions including dams and banks. As a result of the construction of dams, sediment transport may dramatically decrease in the downstream area are, and the river ecosystem can also be affected. To make sediment move more vigorously, we cultivated the armored gravel riverbed with heavy machinery. We then explore the effects of riverbed cultivating by monitoring the topographic changes with high-frequency and high-definition measurements (HF-HD measurements), whereas conventional measurement technologies do not compensate spatial resolution and temporal resolution to capture the topographic change. Using UAS (Unmanned Aerial Vehicle) and SfM-MVS (Structure-from-Motion –Multi-view Stereo) photogrammetry, we found the transportation of the fixed gravels were occurring after cultivating the riverbed in 2017. The temporal and spatial resolutions of the HF-HD topographic data was approximately 2 months and 10 cm, respectively. In July 2018, water flow at 130 m^3/s was discharged from the upstream dam, and we confirmed that a part of the gravels in the cultivated area was eroded and replaced with new sediments (Fig. 1). These observations indicate that riverbed monitoring using UAV and SfM - MVS can be a practical tool for proper management of riverbeds. Applying this result, we will further clarify the relationships between the water quantity discharged from the dam and the riverbed topographic changes.

Keywords: High-definition topographic data, riverbed cultivation, UAV, SfM-MVS photogrammetry, Echi river

©2019. Japan Geoscience Union. All Right Reserved.

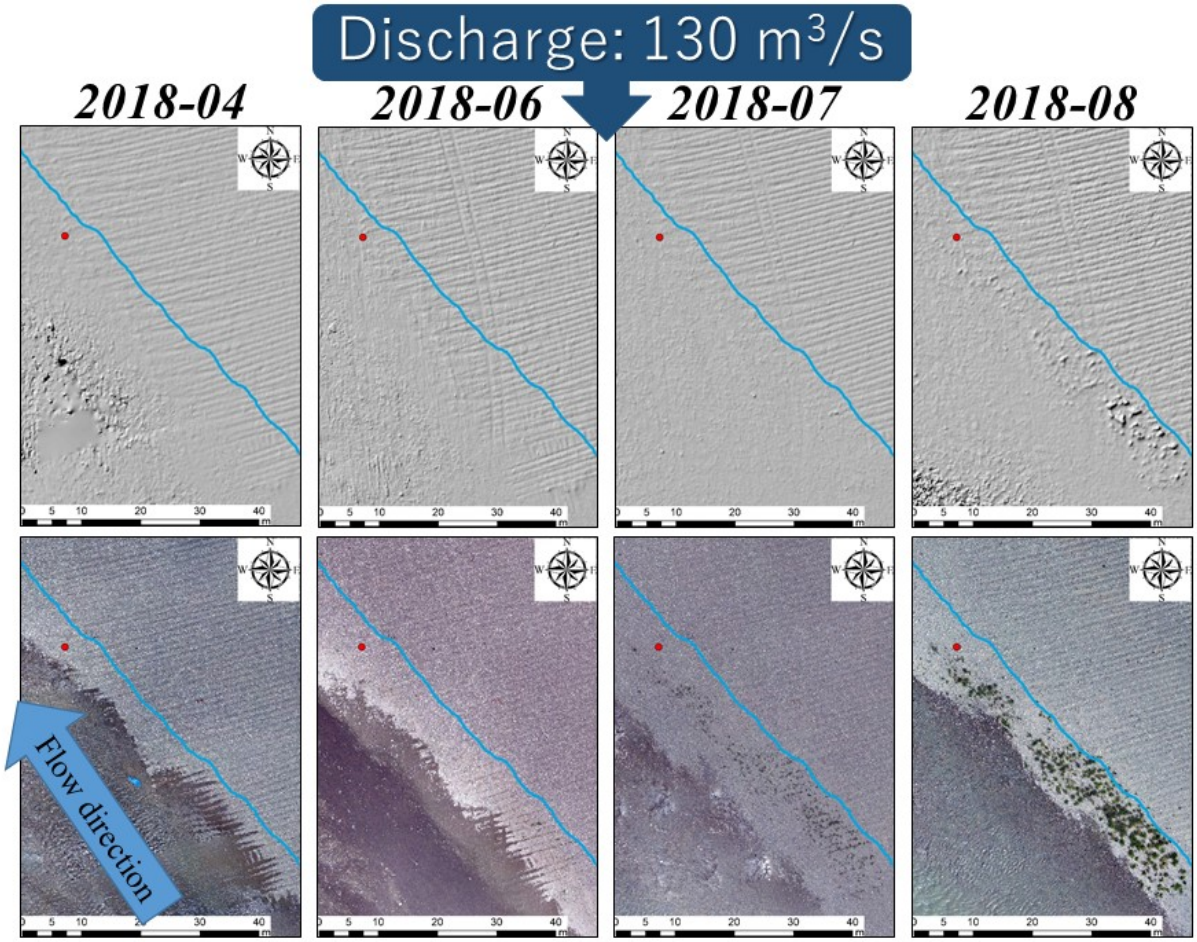

Fig.1. Hillshade images and ortho images of cultivated area.

©2019. Japan Geoscience Union. All Right Reserved.

Spatial distribution of land surface displacements in the crater of Tateyama Midagahara Volcano using high-definition topographic data

*Yuichi S. Hayakawa[1], Shigekazu Kusumoto[2], Takuro Ogura[3,4]

1. Faculty of Environmental Earth Science, Hokkaido University, 2. Graduate School of Science and Engineering for Research, University of Toyama, 3. Graduate School of Frontier Science, The University of Tokyo, 4. Graduate School of Environmental Science, Hokkaido University

Detailed monitoring of land surface displacements is crucial for the assessment of activities of a volcano, especially in its crater area. Close-range remote sensing of high-definition topographic data is advantageous in the detection of centimeter-scale ground-surface displacements in a wide spacial extent, whereas the conventional leveling method is capable of detecting millimeter-scale displacements along a measurement line. We investigated the spatial distribution of land surface displacements in the Jigoku-Dani crater area of Mt. Tateyama Midagahara Volcano in Toyama Prefecture, central Japan by high-definition topographic measurements including terrestrial laser scanning and unmanned aerial vehicle-based structure-from-motion photogrammetry. The annual measurements were performed for three years (2015 to 2017). The range of uplift detected by terrestrial laser scanning corresponds with that by leveling. Together with the analytical results of the leveling data, the spatial pattern of the uplift suggests the extent of an underground pressured zone to cause the exhumation. For the prediction of the volcanic activities, further monitoring is required to reveal the spatiotemporal patterns of the displacements.

Keywords: terrestrial laser scanning, unmanned aerial system structure-from-motion, point cloud

©2019. Japan Geoscience Union. All Right Reserved.

Study on a simplified measurement of water depth and reconstruction of the riverbed form by using SfM and MVS.

*OSAWA KOTA[1], Tadafumi Niizato [2], Katsuaki Mitachi[3], Makoto Kawamura[1], Masahiro Ohkawa[1]

1. Mitsubishi Materials Techno corporation , 2. Japan Atomic Energy Agency, 3. ATOM TRANSPORT SERVICE CO., LTD

Primary outflow process of radiocesium, which is released by the TEPCO’ s Fukushima Dai-ichi Nuclear Power Plant accident, from a forested hillslope to a mountain stream is a particulate-bond state transport. A detailed estimation of the riverbed form and sediment volume changing with time is a key issue to assess the radiocesium distribution in the forested environment. Changes in the sediment volume can be calculated from the water depth and the difference between measured water surface and reference water surface levels setting up at the initial. Conventional method for a water depth determination is a direct measurement of the stream water depth by using a scale. But it requires a lot of time and labor to evaluate the change of riverbed form and water depth in detail.
In this study, we attempted an accurate and labor-effective method to evaluate the water depth and three-dimensional (3D) structure of underwater riverbed form by applying the SfM (Structure from Motion) /MVS (Multi View Stereo) techniques and the optical image data collected on consumer-grade-camera. These images were photographed beside of the small stream located at southern part of the Abukuma Mountains, Fukushima. Light propagation properties such as attenuation or reflection influence precise reconstruction of 3D model using underwater images. This was done to reduce influence of light propagation in two steps: 1) to reduce the influence of reflection, photographing at the time of twilight using LED light and Circular PL filter. 2) to reduce the influence of attenuation, installing blue colored film on the LED light and omitting band R, G for SfM/MVS analysis. And we also photographed at the day time and reconstructed 3D model (Day Model: DM) to compare and confirm the model applying two steps (Twilight Model: TM). As a criterion for evaluation of these models, we carried out the direct measurement of water depth. Rate of estimation concordance was calculated by dividing analytical water depth by the direct measurement depth, then convert to percentage.
Discrepancy between measured and analytical results increased with depth, the rate of estimation concordances were 46 % (DM) and 73 % (TM) in the water depth of 20-25 cm, and 62 % (DM) and 93 % (TM) in 10-15 cm, respectively (Figure). Next step is an improvement of the correction and image-capturing methods to reduce the estimation errors by elimination of the light refraction on the stream water surface.

Keywords: SfM/MVS, measurement of water depth, riverbed form

©2019. Japan Geoscience Union. All Right Reserved.

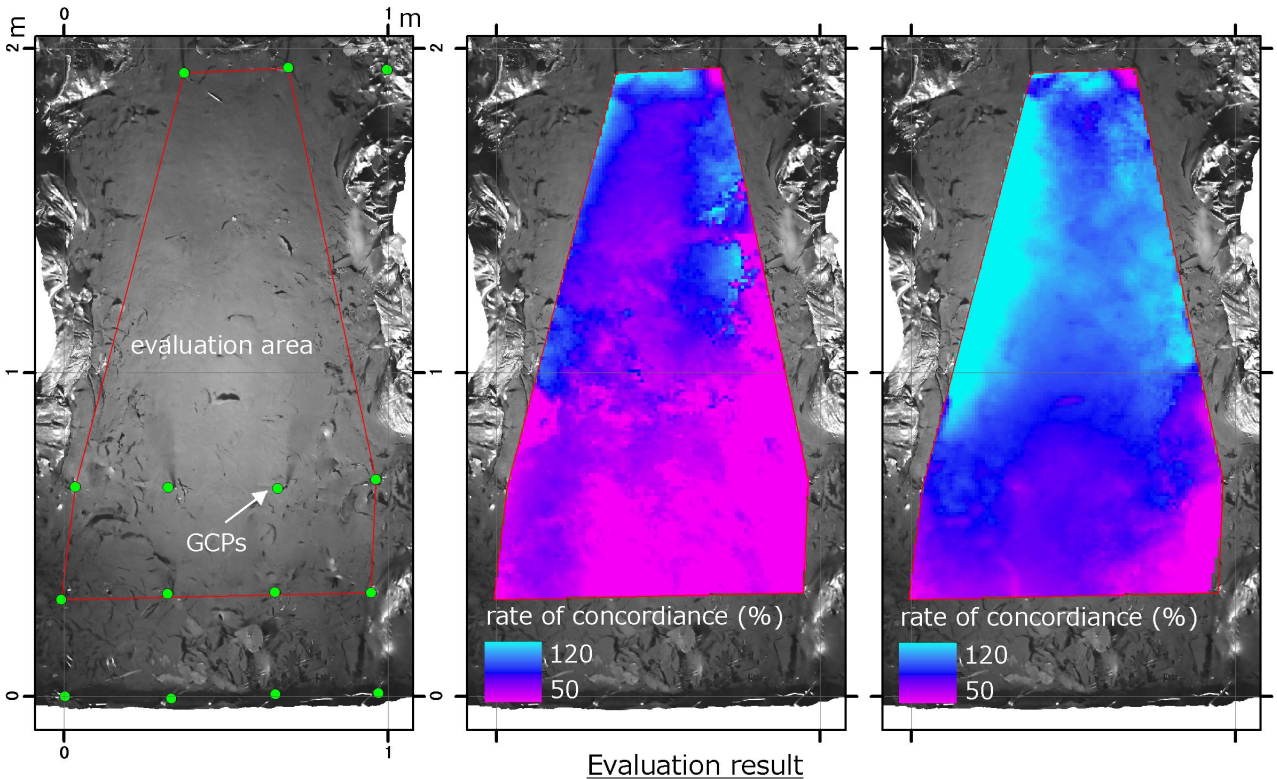

Left: Orthographic Image, Evaluation area (red polygon) and location of GCPs (green dot),
Center: Discrepancy between measured and analysis (DM),
Right: Discrepancy between measured and analysis (TM)

©2019. Japan Geoscience Union. All Right Reserved.

Ground Penetrating Radar Imaging of Moisture and Water movement in volcanic soil

*Christopher A Gomez[1]

1. Kobe University Faculty of Maritime Sciences Volcanic Risk at Sea Research Group

Ground Penetrating Radar is a non-invasive subsurface method that provides results on the dielectric properties of the ground between 0 and 30 m on average in sediments. Working from sediments from Mt Unzen in Japan, tests over the moisture content and the air content change were conducted on the material in order to infer further data during field measurement. The GPR used in the survey is a Ramac Mala mounted with an antenna of 800 Mhz and a stack signal over time. The data were processed using Matlab using data filtering and time-depth conversion, and calculation of the dielectric properties variations. The signal analysis shows that the velocity does change over time depending on the moisture content and the change in air/void ratio. For a given homogeneous material, like at volcanoes, multiplying such analysis is a step forward the development of relatable tables for various environments.

Keywords: Ground Penetrating Radar, Soil moisture content, Volcanic material

©2019. Japan Geoscience Union. All Right Reserved.

Estimating Eruptive Volumes of Mud Volcano Southwestern Taiwan by Using UAV and SfM-MVS Photogrammetry

*CHIA-YING LIU[1], Ray Y Chuang[1], Horng-Yue Chen[2]

1. Department of Geography, National Taiwan University, 2. Academia Sinica, Institute of Earth Sciences

Mud volcanoes are special geologic features occurred in tectonic areas with horizontal compression. Complete research for mud volcanos can help us to understand the interaction of the crust and surface. In Taiwan, mud volcanoes are present on-land and off-shore southwestern Taiwan around the transitional area from subduction to orogeny. Among all mud volcanoes in Taiwan, the Wandan mud volcano erupts sporadically with significantly large amount of effluent mud. However, the mechanism of the eruption remains unclear because we lack fundamental information such as eruptive volumes, duration of mud eruption, impact factors and recurrence intervals. Therefore, it is important to estimate the eruptive volumes and further to examine the spatiotemporal pattern of the Wandan mud volcano eruption. We first compile literature and newspapers for historic eruption events to estimate two groups of recurrence interval: 150-180 days for highly active period and 300-600 days for less active period.

Since the sporadic eruption make different for rapid survey by using traditional methods, we take advantage of unmanned aerial vehicles (UAV) to design a survey network specifically. Therefore, we estimate the eruptive volumes of recent eruptions for the Wandan mud volcano by using aerial images taken from UAV, and 3D models derived from the structure-from-motion (SfM) photogrammetry technique. We use RTK-GPS and leveling for horizontal and vertical measurements of ground control point, respectively. We use the SfM software to generate DSMs, point clouds, and orthophotos with cm-level accuracy. We estimate the eruptive volume by subtracting the pre-eruption DSM from the post-eruption DSM. Our results show that for the event on 15 May, 2018, the eruptive area is 12,761 m^2 and the volume is 13,106.3625 ±13.0105m^3.

Keywords: UAS, GNSS, digital surface modeling, control survey

©2019. Japan Geoscience Union. All Right Reserved.

Increasing temporal depth of urban Land-Use Regression Models by wind-data driven dynamic buffer generation

*Tilman Leo Hohenberger[1], King Wai Leung[1]

1. Division of Environment and Sustainability, Hong Kong University of Science and Technology

Land-use regression (LUR) models are commonly used as an inexpensive and easy to set-up way to predict spatial variability in air-pollution. They are successfully applied to regional and, more and more, urban settings, making use of spatial predictors such as land-use, vegetation, morphology and geography. New approaches include an improved use of wind-data for buffer-creation and predictor calculation.

Traditionally, LUR models are used to generate annual or seasonal concentration averages and are not able cover deeper temporal variability. We aim at increasing temporal depth by using a novel approach in generating dynamic buffers for predictor calculation using both monthly wind-speed and wind-direction averages. The traditional circular buffers are replaced by wedges, whose orientation and radius are bound to these meteorological variables.

Here, Hong Kong’ s diverse territory is taken as a study site, and our model is trained with 5 years data from 16 government air quality monitoring stations and deployed portable sensors network. We compare our novel approach to both traditional LUR models and a sophisticated urban chemical transport model (ADMS-Urban).

Results will highlight the opportunities in using LUR models for monthly air-quality pollution concentration as an alternative to chemical transport modelling.

Keywords: Wind, Land Use Regression, Spatial Data, Meteorology

©2019. Japan Geoscience Union. All Right Reserved.

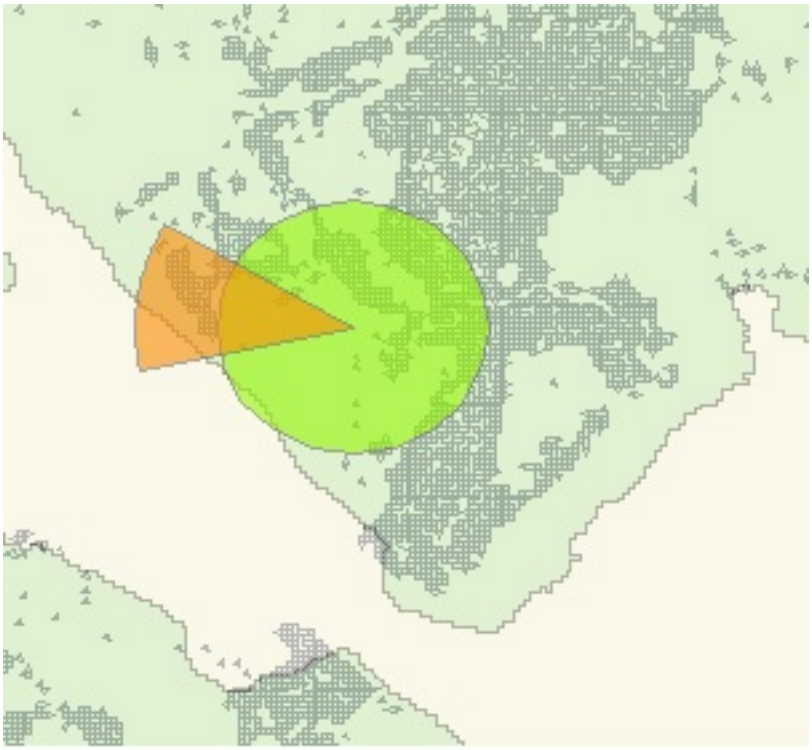

Dynamic and circular LUR buffer in Hong Kong's urban environment

©2019. Japan Geoscience Union. All Right Reserved.

[J] Poster | M (Multidisciplinary and Interdisciplinary)：M-ZZ Others

Mon. May 27, 2019 3:30 PM - 5:00 PM JST | Mon. May 27, 2019 6:30 AM - 8:00 AM UTC | Poster Hall International Exhibition Hall8, Makuhari Messe_27

[M-ZZ51] Geoscience Studies: historical, philosophical and STS studies

convener:Michiko Yajima(College of Humanity and Science, Nihon University), Shigeyuki Aoki(Faculty of Letters, Chuo University), Toshihiro Yamada(Research Fellow, Graduate School of Education, University of Tokyo), Shigeo Yoshida(Department of Earth and Planetary Sciences, Faculty of Sciences, Kyushu University)

Topics on history, philosophy and STS (science, technology and society)studies of geoscience will be discussed. Any related subject is welcome, such as history of mining, methodology of geoscience, sociology of natural hazards, and politics of environmental issues.

[MZZ51-P01] Cosmic skepticism on meaning of life

*Shigeyuki Aoki[1] (1.School of Computer Science and Engineering, University of Aizu)

[MZZ51-P02] Rethinking 'Stenonian Revolution' in stratigraphy: From *Prodromus* (1669) to 'Anthropocene'

*Toshihiro Yamada[1] (1.Research Fellow, Graduate School of Education, University of Tokyo)

[MZZ51-P03] How Edmund Naumann made the Geologic Map of Japan in 1885?

*Michiko Yajima[1] (1.College of Humanity and Science, Nihon University)

[MZZ51-P04] The role of the private sector in the formation of the meteorological observation network of Japan in the nineteenth century

*Akira Yamamoto[1] (1.Meteorological Research Institute)

[MZZ51-P05] "Thyco Brahe" in the Geology; The Compromise Models on the Plate Tectonics Revolution.

*Jun'ichi Chiba[1] (1.O-hara Business College)

[MZZ51-P06] Contributions of Tatsuro Matsumoto (1913-2009) to plate tectonics, a signifcant paradigm shift in earth sicence

*Hidehisa Mashima[1] (1.Center for Obsidian and Lithic Studies, Meiji University)

[MZZ51-P07] Online Community Responses to Volcanic Disaster: A Study of Yahoo! News Comments on the 2018 Mt. Kusatsu-Shirane eruption

*Kou Yamada[1] (1.Waseda University)

Cosmic skepticism on meaning of life

*Shigeyuki Aoki[1]

1. School of Computer Science and Engineering, University of Aizu

“Meaning of life” can be questioned in various dimensions. Most of the arguments in the present literature ask what meaning of life we can find in our individual life. So, this line of question is substantially on “meaning in life” rather than on “meaning of life”. On the contrary, cosmology or life sciences raise another type of question (or skepticism) –what on earth is the meaning of life so short? This presentation will classify various types of skepticism on individualistic meanings of life, and then discuss whether the questions on meaning of life are closed each other in each dimension.

Keywords: earth and planetary science, cosmology, philosophy

©2019. Japan Geoscience Union. All Right Reserved.

Rethinking 'Stenonian Revolution' in stratigraphy: From *Prodromus* (1669) to 'Anthropocene'

*Toshihiro Yamada[1]

1. Research Fellow, Graduate School of Education, University of Tokyo

When the Danish anatomist Nicolaus Steno (1638-1686) published his *Prodromus de solido* in 1669, it is said that the history of geology saw a revolution in stratigraphy, i.e. 'Stenonian Revolution.' My research on this topic, however, revealed that the revolution implied not only the discovery of the principles of stratigraphy but also the emergence of the concept of 'history of nature' (Spinoza suggested) and 'geo-power' (embodied in Leibniz's practice). The significance of the revolution will be discussed.

Keywords: Nicolaus Steno, stratigraphy , scientific revolution

©2019. Japan Geoscience Union. All Right Reserved.

How Edmund Naumann made the Geologic Map of Japan in 1885?

*Michiko Yajima[1]

1. College of Humanity and Science, Nihon University

German Edmund Naumann (1854-1927) came to Japan in 1875. He became the first professor of geology in the University of Tokyo, founded the Geological Survey of Japan, and made good geological reconnaissance maps of Japan. In 1885, he returned to Germany and introduced these maps at the third International Geological Congress (IGC) held in Berlin, at which they were greatly admired. The map compares favorably with any present existing geologic map. How Naumann made the good Geologic Map of Japan in 1885? Because he was not a briliant student in university days, and when he came to Japan he worked at no duty museum. And the other reason is that he knew the preliminary paper on geology in Japan writen by Guembel (1874). Guembel got stones of Japan from the International Exhibition held in Vienna in 1873.
Guembel,1874, Japanesische Gesteine, Ausland,p479, 480.

Keywords: Naumann, geologic map, Gümbel, the International Exhibition

©2019. Japan Geoscience Union. All Right Reserved.

The role of the private sector in the formation of the meteorological observation network of Japan in the nineteenth century

*Akira Yamamoto[1]

1. Meteorological Research Institute

Three names of women are recognized on the membership lists of the Meteorological Society of Japan (1882-) in the nineteenth century. At the time when the national meteorological services were under developing at the initiative of the central government, all of them are in the private sector. By following their origins and backgrounds, some role of the private sector in the formation process of the meteorological observation network in the Meiji era are described.

Keywords: meteorological observation network, history of meteorology, NONAKA Chiyoko, TONNO Kiyo, TANABE Tami, national meteorological services

©2019. Japan Geoscience Union. All Right Reserved.

"Thyco Brahe" in the Geology; The Compromise Models on the Plate Tectonics Revolution.

*Jun'ichi Chiba[1]

1. O-hara Business College

How the scientific revolutions begin, progress and finish? The plate tectonics (PT after below) revolution is the one of the example of the latest scientific revolutions which had occurred after the first definition of the word “scientific revolutions” by Thomas Kuhn, and to restore the processes of the changing mind of the geoscientists in the PT revolutions is to describe the process in detail of the driving mechanism of the scientific revolutions.

Tomari (2008) had described the PT revolution in detail from the viewpoint of scientific historiographers. He wrote the geoscientists in the PT revolution as the person who converted to new paradigm immediately (for example Seiya Uyeda, Kazuaki Nakamura and Arata Sugimura), continued refusing the new theory (Shoji Ijiri, Yukinori Fujita and Masao Minato) and other geologists who had been under the influential scientists as the way of thinking, but he did not described the processes of the conversion; changing impression and overcoming contradiction of the previous paradigm and new theory in the heart of the individual scientist. Actually, it was not the simple binary opposition such as the “immediate acceptance by the advanced mind” and “completely refusal because under arrested by the former paradigm (geosyncline theory)” but most of the heart of the geologists were “torn up” until finishing of the conversion. The author reports the example of the "compromise model" on the Japanese Islands tectonic development scenario and the orogenic movement which were shown by some geologists, in this presentation.

Toshio Kimura who was the Professor the second course of geology, faculty of science, University of Tokyo, refused that the orogenic movement by the trench subduction but accepted the sea-floor spreading as the formation theory of the surface structure of the earth continued adopting a geosyncline idea about the orogenic movement in the neighborhood of trench in the 1970s. Yujiro Ogawa who was a student of Kimura proposed a model explaining the formation process of the buck ark basin by geosyncline instead of the secondary upwelling current of the mantle wedge which caused by subducting slab. Akira Yao, the biostratigrapher of the Osaka City University had begun to think about the formation model of the lens and block-shaped limestone bed by the thrusting and folding without denying geosyncline theory in the late 1970s. In addition, there were the petrographical studies that showed a change of the magma composition in the crossing direction of island arc and an emplacement processes of ophiolite in island arc without denying geosyncline theory. Its were considered to the examples of the blended models of the PT and previous theory.

The word “compromise model” is giving a bad impression like the “opportunism”, however it may be said that it is the wrestling to adopt a new theory to conventional observation datum carefully. I think it shown the existence of the researchers who can be compared to Tycho Brahe in the Copernicus Revolution, and not a thing indicating the geologic backwardness but it express that geological tradition such as to respect the building up the foundation of by the observation fact.

Keywords: Plate Tectonics Revolution, Compromise Models, Methodology of Geology

©2019. Japan Geoscience Union. All Right Reserved.

©2019. Japan Geoscience Union. All Right Reserved.

Contributions of Tatsuro Matsumoto (1913-2009) to plate tectonics, a signifcant paradigm shift in earth sicence

*Hidehisa Mashima[1]

1. Center for Obsidian and Lithic Studies, Meiji University

Tasturo Matsumoto (1913-2009), the professor of stratigraphy of Kyushu University, was a leader of the community of geology, especially that of stratigraphy, in Japan from 1960’s to 1970’s, when the seafloor spreading hypothesis was proposed at first then the plate tectonics theory was established at the end. The paradigm shift of earth science related to plate tectonics in Japan is represented by that from the geosyncline hypothesis to the accretional prism hypothesis. Matsumoto volunteered to be the chair of international and domestic symposiums, a committeeman of an international association, the organizer of a comprehensive research program and an editor of proceedings relating to the paradigm shift in this period, which significantly encouraged Japanese earth scientists. The accretional prism model for the Shimanto Belt was proposed by Sakai, supervised by Matsumoto, and Kammera (1975) from the viewpoint of structural geology. It was the Japanese paleontological society, which Matsumoto had leverage in for a long period, that recognized the importance of studies of foraminifera by Nakaseko and his colleagues. The founding of the accretional prism model for the Shimanto, therefore, was started in the vicinity of Matsumoto. These contributions of Matsumoto were passed into silence since he didn’t like to be applauded (Mashima, 2018). His contributions therefore were not referred in recent studies of history of Japanese geology (Tomari, 2008). In this presentation, I present activities of Matsumoto relating to plate tectonics. His activities reveal that Matsumoto is the person who exerted to realize mutual understanding and collaborative alliance between researchers belonging to different disciplines of earth science.

Keywords: plate tectonics, Tatsuro Matsumoto, paradigm shift, geosyncline, accretional prism

©2019. Japan Geoscience Union. All Right Reserved.

Online Community Responses to Volcanic Disaster: A Study of Yahoo! News Comments on the 2018 Mt. Kusatsu-Shirane eruption

*Kou Yamada[1]

1. Waseda University

This work aims to summarize public real-time reaction to the publication of the news of volcanic disasters by applying a content analysis. On January 23, 2018, there was an unexpected deadly eruption of Mt. Kusatsu-Shirane, located in the Japanese central area. In order to undertake a content analysis of user-generated comments to media coverage related to this volcanic disaster, this work used 'Netnography' which means “a technique for the socio-cultural analysis of social media and online community data” (Kozinets et al. 2014:Netnographic Analysis: Understanding Culture Through Social Media Data, in The SAGE Handbook of Qualitative Data Analysis).

Online social spaces become increasingly acknowledged as important fields for quantitative and qualitative social scientific investigation because of the openness and richness of its multifarious socio-cultural sites. There are approximately 34.1 million active monthly users on Yahoo in 2016 (https://www.netratings.co.jp/news_release/2016/12/Newsrelease20161220.html). Yahoo! News is a news website and one of the most popular news aggregators in Japan. It has received about 4000 articles offered by more than 300 media companies per a day and selectively published socially-minded news from among them. In the case of Mt. Kusatsu-Shirane disaster, a large number of stories were placed on the top page with the highest priority. Therefore, Yahoo! News readers had chances to express their voice about various topics related to the volcanic disaster by posting comments. In Japan, Yahoo! News would play a huge role in shaping online opinion.

A content analysis of reader comments posted in response to twenty-two articles on Yahoo! News site, published in January 2018, was carried out. Then, about 1000 comments are randomly sampled from 4200 comments. Comments that are critical of the measures for the volcanic eruption prediction are most frequently found. A lot of commenters were commenting with experts and the Japan Meteorological Agency in mind. There is a view among commenters that experts and the Japan Meteorological Agency did not work well for the volcanic disaster. This links to the wondering whether the area around the eruption points is really safe. Approximately 10% of comments assert the belief that such accidents would be beyond human control and humans should obey the nature's activities. Moreover, in comments on whether the eruption prediction is possible, a number of comments supporting and opposing the eruption prediction research are almost equal within the error bar. The relationship between citizens and the government/experts can be severely impaired if the crisis communication is mishandled. Conclusively, the result of this study suggests an aspect of examining the public representation of the volcanic disaster. This study reveals that these comments provide any information about the volcanic risk after the Mt. Kusatsu-Shirane eruption and proposes that netnography may prove useful for building effective volcanic risk communication strategies.

Keywords: Netnography, Mitigation of volcanic disasters, content analysis

©2019. Japan Geoscience Union. All Right Reserved.

©2019. Japan Geoscience Union. All Right Reserved.

[J] Poster | M (Multidisciplinary and Interdisciplinary)：M-ZZ Others

Mon. May 27, 2019 5:15 PM - 6:30 PM JST | Mon. May 27, 2019 8:15 AM - 9:30 AM UTC | Poster Hall International Exhibition Hall8, Makuhari Messe_45

[M-ZZ51] Geoscience Studies: historical, philosophical and STS studies

convener:Michiko Yajima(College of Humanity and Science, Nihon University), Shigeyuki Aoki(Faculty of Letters, Chuo University), Toshihiro Yamada(Research Fellow, Graduate School of Education, University of Tokyo), Shigeo Yoshida(Department of Earth and Planetary Sciences, Faculty of Sciences, Kyushu University)

Topics on history, philosophy and STS (science, technology and society)studies of geoscience will be discussed. Any related subject is welcome, such as history of mining, methodology of geoscience, sociology of natural hazards, and politics of environmental issues.

[MZZ51-P01] Cosmic skepticism on meaning of life

*Shigeyuki Aoki[1] (1.School of Computer Science and Engineering, University of Aizu)

[MZZ51-P02] Rethinking 'Stenonian Revolution' in stratigraphy: From *Prodromus* (1669) to 'Anthropocene'

*Toshihiro Yamada[1] (1.Research Fellow, Graduate School of Education, University of Tokyo)

[MZZ51-P03] How Edmund Naumann made the Geologic Map of Japan in 1885?

*Michiko Yajima[1] (1.College of Humanity and Science, Nihon University)

[MZZ51-P04] The role of the private sector in the formation of the meteorological observation network of Japan in the nineteenth century

*Akira Yamamoto[1] (1.Meteorological Research Institute)

[MZZ51-P05] "Thyco Brahe" in the Geology; The Compromise Models on the Plate Tectonics Revolution.

*Jun'ichi Chiba[1] (1.O-hara Business College)

[MZZ51-P06] Contributions of Tatsuro Matsumoto (1913-2009) to plate tectonics, a signifcant paradigm shift in earth sicence

*Hidehisa Mashima[1] (1.Center for Obsidian and Lithic Studies, Meiji University)

[MZZ51-P07] Online Community Responses to Volcanic Disaster: A Study of Yahoo! News Comments on the 2018 Mt. Kusatsu-Shirane eruption

*Kou Yamada[1] (1.Waseda University)

Cosmic skepticism on meaning of life

*Shigeyuki Aoki[1]

1. School of Computer Science and Engineering, University of Aizu

“Meaning of life” can be questioned in various dimensions. Most of the arguments in the present literature ask what meaning of life we can find in our individual life. So, this line of question is substantially on “meaning in life” rather than on “meaning of life”. On the contrary, cosmology or life sciences raise another type of question (or skepticism) –what on earth is the meaning of life so short? This presentation will classify various types of skepticism on individualistic meanings of life, and then discuss whether the questions on meaning of life are closed each other in each dimension.

Keywords: earth and planetary science, cosmology, philosophy

©2019. Japan Geoscience Union. All Right Reserved.

Rethinking 'Stenonian Revolution' in stratigraphy: From *Prodromus* (1669) to 'Anthropocene'

*Toshihiro Yamada[1]

1. Research Fellow, Graduate School of Education, University of Tokyo

When the Danish anatomist Nicolaus Steno (1638-1686) published his *Prodromus de solido* in 1669, it is said that the history of geology saw a revolution in stratigraphy, i.e. 'Stenonian Revolution.' My research on this topic, however, revealed that the revolution implied not only the discovery of the principles of stratigraphy but also the emergence of the concept of 'history of nature' (Spinoza suggested) and 'geo-power' (embodied in Leibniz's practice). The significance of the revolution will be discussed.

Keywords: Nicolaus Steno, stratigraphy , scientific revolution

©2019. Japan Geoscience Union. All Right Reserved.

How Edmund Naumann made the Geologic Map of Japan in 1885?

*Michiko Yajima[1]

1. College of Humanity and Science, Nihon University

German Edmund Naumann (1854-1927) came to Japan in 1875. He became the first professor of geology in the University of Tokyo, founded the Geological Survey of Japan, and made good geological reconnaissance maps of Japan. In 1885, he returned to Germany and introduced these maps at the third International Geological Congress (IGC) held in Berlin, at which they were greatly admired. The map compares favorably with any present existing geologic map. How Naumann made the good Geologic Map of Japan in 1885? Because he was not a briliant student in university days, and when he came to Japan he worked at no duty museum. And the other reason is that he knew the preliminary paper on geology in Japan writen by Guembel (1874). Guembel got stones of Japan from the International Exhibition held in Vienna in 1873.
Guembel,1874, Japanesische Gesteine, Ausland,p479, 480.

Keywords: Naumann, geologic map, Gümbel, the International Exhibition

©2019. Japan Geoscience Union. All Right Reserved.

The role of the private sector in the formation of the meteorological observation network of Japan in the nineteenth century

*Akira Yamamoto[1]

1. Meteorological Research Institute

Three names of women are recognized on the membership lists of the Meteorological Society of Japan (1882-) in the nineteenth century. At the time when the national meteorological services were under developing at the initiative of the central government, all of them are in the private sector. By following their origins and backgrounds, some role of the private sector in the formation process of the meteorological observation network in the Meiji era are described.

Keywords: meteorological observation network, history of meteorology, NONAKA Chiyoko, TONNO Kiyo, TANABE Tami, national meteorological services

©2019. Japan Geoscience Union. All Right Reserved.

"Thyco Brahe" in the Geology; The Compromise Models on the Plate Tectonics Revolution.

*Jun'ichi Chiba[1]

1. O-hara Business College

How the scientific revolutions begin, progress and finish? The plate tectonics (PT after below) revolution is the one of the example of the latest scientific revolutions which had occurred after the first definition of the word “scientific revolutions” by Thomas Kuhn, and to restore the processes of the changing mind of the geoscientists in the PT revolutions is to describe the process in detail of the driving mechanism of the scientific revolutions.

Tomari (2008) had described the PT revolution in detail from the viewpoint of scientific historiographers. He wrote the geoscientists in the PT revolution as the person who converted to new paradigm immediately (for example Seiya Uyeda, Kazuaki Nakamura and Arata Sugimura), continued refusing the new theory (Shoji Ijiri, Yukinori Fujita and Masao Minato) and other geologists who had been under the influential scientists as the way of thinking, but he did not described the processes of the conversion; changing impression and overcoming contradiction of the previous paradigm and new theory in the heart of the individual scientist. Actually, it was not the simple binary opposition such as the “immediate acceptance by the advanced mind” and “completely refusal because under arrested by the former paradigm (geosyncline theory)” but most of the heart of the geologists were “torn up” until finishing of the conversion. The author reports the example of the "compromise model" on the Japanese Islands tectonic development scenario and the orogenic movement which were shown by some geologists, in this presentation.

Toshio Kimura who was the Professor the second course of geology, faculty of science, University of Tokyo, refused that the orogenic movement by the trench subduction but accepted the sea-floor spreading as the formation theory of the surface structure of the earth continued adopting a geosyncline idea about the orogenic movement in the neighborhood of trench in the 1970s. Yujiro Ogawa who was a student of Kimura proposed a model explaining the formation process of the buck ark basin by geosyncline instead of the secondary upwelling current of the mantle wedge which caused by subducting slab. Akira Yao, the biostratigrapher of the Osaka City University had begun to think about the formation model of the lens and block-shaped limestone bed by the thrusting and folding without denying geosyncline theory in the late 1970s. In addition, there were the petrographical studies that showed a change of the magma composition in the crossing direction of island arc and an emplacement processes of ophiolite in island arc without denying geosyncline theory. Its were considered to the examples of the blended models of the PT and previous theory.

The word “compromise model” is giving a bad impression like the “opportunism”, however it may be said that it is the wrestling to adopt a new theory to conventional observation datum carefully. I think it shown the existence of the researchers who can be compared to Tycho Brahe in the Copernicus Revolution, and not a thing indicating the geologic backwardness but it express that geological tradition such as to respect the building up the foundation of by the observation fact.

Keywords: Plate Tectonics Revolution, Compromise Models, Methodology of Geology

©2019. Japan Geoscience Union. All Right Reserved.

©2019. Japan Geoscience Union. All Right Reserved.

Contributions of Tatsuro Matsumoto (1913-2009) to plate tectonics, a signifcant paradigm shift in earth sicence

*Hidehisa Mashima[1]

1. Center for Obsidian and Lithic Studies, Meiji University

Tasturo Matsumoto (1913-2009), the professor of stratigraphy of Kyushu University, was a leader of the community of geology, especially that of stratigraphy, in Japan from 1960’s to 1970’s, when the seafloor spreading hypothesis was proposed at first then the plate tectonics theory was established at the end. The paradigm shift of earth science related to plate tectonics in Japan is represented by that from the geosyncline hypothesis to the accretional prism hypothesis. Matsumoto volunteered to be the chair of international and domestic symposiums, a committeeman of an international association, the organizer of a comprehensive research program and an editor of proceedings relating to the paradigm shift in this period, which significantly encouraged Japanese earth scientists. The accretional prism model for the Shimanto Belt was proposed by Sakai, supervised by Matsumoto, and Kammera (1975) from the viewpoint of structural geology. It was the Japanese paleontological society, which Matsumoto had leverage in for a long period, that recognized the importance of studies of foraminifera by Nakaseko and his colleagues. The founding of the accretional prism model for the Shimanto, therefore, was started in the vicinity of Matsumoto. These contributions of Matsumoto were passed into silence since he didn’t like to be applauded (Mashima, 2018). His contributions therefore were not referred in recent studies of history of Japanese geology (Tomari, 2008). In this presentation, I present activities of Matsumoto relating to plate tectonics. His activities reveal that Matsumoto is the person who exerted to realize mutual understanding and collaborative alliance between researchers belonging to different disciplines of earth science.

Keywords: plate tectonics, Tatsuro Matsumoto, paradigm shift, geosyncline, accretional prism

©2019. Japan Geoscience Union. All Right Reserved.

Online Community Responses to Volcanic Disaster: A Study of Yahoo! News Comments on the 2018 Mt. Kusatsu-Shirane eruption

*Kou Yamada[1]

1. Waseda University

This work aims to summarize public real-time reaction to the publication of the news of volcanic disasters by applying a content analysis. On January 23, 2018, there was an unexpected deadly eruption of Mt. Kusatsu-Shirane, located in the Japanese central area. In order to undertake a content analysis of user-generated comments to media coverage related to this volcanic disaster, this work used 'Netnography' which means “a technique for the socio-cultural analysis of social media and online community data” (Kozinets et al. 2014:Netnographic Analysis: Understanding Culture Through Social Media Data, in The SAGE Handbook of Qualitative Data Analysis).

Online social spaces become increasingly acknowledged as important fields for quantitative and qualitative social scientific investigation because of the openness and richness of its multifarious socio-cultural sites. There are approximately 34.1 million active monthly users on Yahoo in 2016 (https://www.netratings.co.jp/news_release/2016/12/Newsrelease20161220.html). Yahoo! News is a news website and one of the most popular news aggregators in Japan. It has received about 4000 articles offered by more than 300 media companies per a day and selectively published socially-minded news from among them. In the case of Mt. Kusatsu-Shirane disaster, a large number of stories were placed on the top page with the highest priority. Therefore, Yahoo! News readers had chances to express their voice about various topics related to the volcanic disaster by posting comments. In Japan, Yahoo! News would play a huge role in shaping online opinion.

A content analysis of reader comments posted in response to twenty-two articles on Yahoo! News site, published in January 2018, was carried out. Then, about 1000 comments are randomly sampled from 4200 comments. Comments that are critical of the measures for the volcanic eruption prediction are most frequently found. A lot of commenters were commenting with experts and the Japan Meteorological Agency in mind. There is a view among commenters that experts and the Japan Meteorological Agency did not work well for the volcanic disaster. This links to the wondering whether the area around the eruption points is really safe. Approximately 10% of comments assert the belief that such accidents would be beyond human control and humans should obey the nature's activities. Moreover, in comments on whether the eruption prediction is possible, a number of comments supporting and opposing the eruption prediction research are almost equal within the error bar. The relationship between citizens and the government/experts can be severely impaired if the crisis communication is mishandled. Conclusively, the result of this study suggests an aspect of examining the public representation of the volcanic disaster. This study reveals that these comments provide any information about the volcanic risk after the Mt. Kusatsu-Shirane eruption and proposes that netnography may prove useful for building effective volcanic risk communication strategies.

Keywords: Netnography, Mitigation of volcanic disasters, content analysis

©2019. Japan Geoscience Union. All Right Reserved.

©2019. Japan Geoscience Union. All Right Reserved.